Davson's PHYSIOLOGY OF THE EYE

FIFTH EDITION

Hugh Davson

PHYSIOLOGY OF THE EYE

PHYSIOLOGY OF THE EYE

Hugh Davson DSc (Lond)

Visiting Professor of Physiology, St. Thomas's Hospital and
Southampton University Medical Schools,
Honorary Research Fellow, King's College, London and
Fellow, University College, London

Fifth Edition

palgrave
macmillan

This edition © Hugh Davson 1990

Softcover reprint of the hardcover 5th edition 1990 978-0-333-45860-0

All rights reserved. No reproduction, copy or transmission of this publication may be made without written permission.

No paragraph of this publication may be reproduced, copied or transmitted save with written permission or in accordance with the provisions of the Copyright Act 1956 (as amended), or under the terms of any licence permitting limited copying issued by the Copyright Licensing Agency, 33–4 Alfred Place, London WC1E 7DP.

Any person who does any unauthorised act in relation to this publication may be liable to criminal prosecution and civil claims for damages.

First edition 1949
Second edition 1963
Third edition 1972
Fourth edition published by Churchill Livingstone 1980
Fifth edition 1990

Published by
THE MACMILLAN PRESS LTD
Houndmills, Basingstoke, Hampshire RG21 2XS
and London
Companies and representatives
throughout the world

Typeset by Macmillan India Ltd., Bangalore 25

Transferred to digital print 2007

British Library Cataloguing in Publication Data
Davson, Hugh, 1909–
Physiology of the eye.—5th ed.
1. Man. Eyes. Physiology
I. Title
612'.84

ISBN 978-1-349-09999-3 ISBN 978-1-349-09997-9 (eBook)
DOI 10.1007/978-1-349-09997-9

Logging, pulping and manufacturing processes are expected to conform to the environmental regulations of the country of origin.

To my fellow Academician
Professor Ljubiša Rakić

CONTENTS

Preface to the Fifth Edition xi
Acknowledgements xiii

SECTION 1 THE VEGETATIVE PHYSIOLOGY AND BIOCHEMISTRY OF THE EYE 1

1 **The Aqueous Humour and the Intraocular Pressure** 3
Anatomical relationships 7
Physiology of the vascular system 15
The aqueous humour 18
The blood-aqueous barrier 22
The blood-vitreous or blood-retinal barrier 24
Anterior and posterior chamber analysis 26
The morphology of the barriers 28
Secretion of aqueous humour 31
Electrical characteristics of retinal pigment epithelium 36
Active transport out of the eye 37
Some factors affecting rate of secretion 38
Intraocular pressure 39
The drainage of aqueous humour 40
The intraocular pressure 48
Effects of the nervous system on secretion and pressure 65

2 **The Vitreous Body** 96

3 **The Cornea** 105
Structure 105
Chemistry 108
Hydration and transparency 110
Permeability 118
Transparency of the cornea 122
Metabolism 122
Repair of damage 124
Corneal vascularization 130

4 **The Lens** 139
Development and structure 139
Transparency 145
The lens as a functional unit 145
Metabolism 153
The proteins 155
Cataract 173

SECTION 2 THE MECHANISM OF VISION 203

5 **Retinal Structure and Organization** 205
Structure 205

6 **Measurement of the Stimulus and Dioptrics of the Human Eye** 211
Photometry 211
Dioptrics 215

7 **Some General Aspects of Vision** 219
The light sense 219
The colour sense 221
Form 225
Induction 226

8 **Photochemical Aspects of Vision** 230
Ultrastructure of the rods 230
Turnover of disks 234
Ultrastructure of the cones 236
Extraction and characterization of photopigment 238
Synthesis and transport to outer segments 242
The retinal-opsin link 243
Intermediate stages in breakdown to retinal and opsin 244
The nature of the changes 246
Linkage of retinal 249
Regeneration of rhodopsin 250
Transport of retinoids 252
Comparative physiology of the pigments 254

9 **Dark Adaptation and the Minimum Visual Stimulus** 264
The dark-adaptation curve 264
Adaptation studies on single receptors 267
Some theoretical considerations 270
The absolute threshold 271
Spatial and temporal summation 274

10 **Electrophysiology of the Retina: Response to Stimulation and the Transduction Process** 279
The sensory message 279
The invertebrate eye 279
Vertebrate responses 282

11 **Electrophysiology of the Retina: Further Studies on Cold-blooded Retina** 305
The electroretinogram 313

12 **Electrophysiology of the Retina: Further Aspects** 325
Quantitative aspects of centre-surround organization 325
Classification of ganglion receptive field types 326
Some morphological correlates 334
Synaptic relationships and neuronal circuitry 336
Transmitters in the retina 343
Neuronal circuitry 352

13 **Flicker** 362
Critical fusion frequency 362
The ERG and the interpretation of flicker 363

Ganglion cell discharges 365
The visually evoked response (VER) 365
Effect of dark-adaptation 366
Size of patch and the Granit–Harper law 368
Sinusoidal wave-form 368

14 **Visual Acuity** 373
Central and peripheral viewing 373
Effects of luminance of test-object and adaptation 373
Normal visual acuity 374

15 **Wavelength Discrimination and the Theory of Colour Vision** 395
The Purkinje phenomenon 395
Wavelength discrimination 398
The Young–Helmholtz theory 399
Colour-defects 402
Absorption spectra of receptors 407
Fish pigments 409
Evolutionary significance 409
Electrophysiology of wavelength discrimination 409

16 **The Stiles–Crawford Effect, Adaptation and Photopic Sensitivity Curves** 423
Directional sensitivity of the retina 423
Adaptation and interaction of light stimuli 425
Temporal aspects 427
Spatial effects 432
Retinal electrophysiology and adaptation 437
Adaptation and the colour sense 440
Photopic sensitivity curves 441
Mesopic sensitivity curves 442

SECTION 3 VISUAL PERCEPTION 447

17 **Visual Perception: Introduction** 449
Higher integrative activity 449
Monocular perception 452
Binocular perception 462
Stereoscopic depth perception 465
Further aspects of binocular vision 476
The perception of motion 481

18 **Neurophysiology of Perception: The Higher Visual Pathways** 486
The primary visual pathway to the cerebral cortex 486
Non-geniculate targets for retinofugal input 487
Lateral geniculate body 491
Electrophysiology of the higher visual pathway 495

19 **Neurophysiology of Perception: Cortical Projection** 515
The visual cortex 515

20 **Neurophysiology of Perception: Cortical Neurones** 531

21 **Neurophysiology of Perception: Spatial Analysis** 558
Neurophysiological basis of stereopsis 558
The double pathway to higher visual centres 569

Electrophysiological aspects of visual acuity 578
Colour discrimination 587

22 Neurophysiology of Perception: Developmental Aspects of Visual Field Characteristics 603
Visual deprivation 603

23 Neurophysiology of Perception: Non-geniculostriate Pathways and the Neurones of their Central Stations 628
The superior colliculi 628
The pulvinar 635

SECTION 4 THE MUSCULAR MECHANISMS 645

24 The Extraocular Muscles and their Actions 647
Binocular movements 656
Types of movement 660
Movements during steady fixation 663

25 Nervous Control of the Eye Movements 667
The muscle fibres and their innervation 667
Some reflexes 674
Vestibular and neck proprioceptive reflexes 677
The motor neurones 685
Electromyographic studies 688
The sensory messages 689
Motor neurone discharges during movements 689
Tensions in the eye muscles 692
Coordinating centres 693
Superior colliculus 706
Cortical centres 711
The cerebellum 723
Models of control 730
Ocular and vestibular interaction 740

26 The Pupil 754
Sphincter and dilator muscles 754
The pupillary reflexes 755
Nervous pathways 758

27 Accommodation 767
Theory of accommodation 768
The change in accommodation with age (presbyopia) 771
The nervous mechanism 776

28 The Near Response 783
Convergence, accommodation and miosis 783

29 The Protective Mechanism 786
Blinking 786
Lacrimation 791

Index 809

PREFACE TO THE FIFTH EDITION

In writing this preface to the fifth edition of my *Physiology of the Eye* I am asserting the privilege of age by the indulgence in a little reminiscing. The first edition appeared some forty years ago, and was written at a time when I was teaching ocular physiology to budding ophthalmologists and orthoptists at Moorfields Hospital, and acting as examiner for the British College of Ophthalmic Opticians. The book was thus designed to be read by students in these three professional categories; in addition, of course, I hoped that students and teachers in physiology and experimental psychology would find it useful.

The first edition was, in my view, a fair presentation of the existing state of knowledge of the physiology of the eye, a field that involves several distinct disciplines, as revealed by the segregation of the book into four sections*. In making this presentation I endeavoured to be simple in my accounts so that any student with A-levels in the biological sciences would be able to follow it, but I trust that I never avoided treating the subjects in depth where there was depth; and, in looking over this first account and comparing it with the present edition, I cannot but admire the extraordinary increase in the depth of our knowledge that has resulted from the accretions of the successive decades.

Thus, the sensory electrophysiology of the visual system at the time of the first edition consisted of little more than the pioneering studies of Granit on the electroretinogram and the first single-unit studies on optic nerve fibres described by Hartline; the recording of electrical events in the actual vertebrate photoreceptor, and their interpretation, would have seemed visionary at the time. Cortical events consisted of little more than the plotting of visual fields through the analysis of the effects of lesions; and it was not until the third edition, which appeared in 1972, that I was able to begin the presentation of the studies on single units pioneered by Hubel and Wiesel. This presentation has expanded from a mere 20 pages in the third edition to some 80 pages in the fourth edition and 157 pages in the present volume.

In a similar way, the section covering the intraocular fluids, the cornea and crystalline lens, has expanded in keeping with the transformation of our knowledge from little more than vague speculations to sound theory, a transformation that has led to a real understanding of the physical bases for such clinical conditions as glaucoma, corneal opacification and vascularization, and cataract. In these last fields, covered by the general term 'Vegetative Physiology', my own researches on the eye were concentrated, so that their expansion, after I transferred my loyalties to the brain fluids in about 1953, has been a matter of peculiar satisfaction to me, and I like to think of myself and my younger colleagues at University College London, who continued these studies along lines that we had explored together, as pioneers in work that has led to such successful clinical applications.

In one field only, namely that of psychophysics, I find that I have not expanded my treatment in proportion to the large amount of experimental work that may largely be found described in the volumes of *Vision Research*. This limitation, imposed by the requirement to keep the book within the compass of a single volume, requires some apology in case I should appear to be undervaluing the contributions that this kind of experiment makes towards the understanding of higher visual functions. My excuse, then, is that Helmholtz's treatment of such visual functions as stereopsis, torsional eye movements, and the general interpretation of the visual image, remains as fundamental and as valid as it was when he published his *Physiologischen Optik*. It was this treatment that formed the basis of my first account in 1949; and, although I have added to it in the light of more modern psychophysical studies, such as those of Julesz on random-dot presentations, I have found little in the literature that has made me want to alter this first account in any fundamental way. A further reason, if not an excuse, is my own prejudice as a physiologist in favour of the direct approach; thus the validity of the Young–Helmholtz trichromatic theory, supported as it was by the psychophysical studies of Wright and Stiles, was only finally clinched by the absorptiometric and electrophysiological studies of single

* In the first three editions there was a fifth section on the Physiological Optics of the Eye. This was subsequently abandoned to make room for the rapidly expanding physiology.

photoreceptors described by Tomita, Hodgkin, Wald and Dartnall.

Finally, in the field of the control of the eye movements, once again the psychophysical approach that led to the development of models of motor control has been heavily supplemented by electrophysiological studies of the central and peripheral neurones concerned in this control; and in this case it is of especial interest that the pioneers in both aspects are the same people, notably Robinson and his colleagues.

London, 1988 H.D.

ACKNOWLEDGEMENTS

I should like to thank my colleague and friend, Dr Malcolm Segal, for valuable assistance in preparing the illustrations for this edition. Also, I gratefully acknowledge my indebtedness to the numerous authors and publishers who have granted their permission to reproduce illustrations.

Section 1

THE VEGETATIVE PHYSIOLOGY AND BIOCHEMISTRY OF THE EYE

1. THE AQUEOUS HUMOUR AND THE INTRAOCULAR PRESSURE

The Three Layers

The globe of the eye consists essentially of three coats enclosing the transparent refractive media. The outermost, protective tunic is made up of the *sclera* and *cornea*—the latter transparent; the middle coat is mainly vascular, consisting of the *choroid*, *ciliary body*, and *iris*. The innermost layer is the *retina*, containing the essential nervous elements responsible for vision—the *rods* and *cones*; it is continued forward over the ciliary body as the *ciliary epithelium*.

Dioptric Apparatus

The dioptric apparatus (Fig. 1.1) is made up of the transparent structures—the cornea, occupying the anterior sixth of the surface of the globe, and the *lens*, supported by the *zonule* which is itself attached to the ciliary body. The spaces within the eye are filled by a clear fluid, the *aqueous humour*, and a jelly, the *vitreous body*. The aqueous humour is contained in the *anterior* and *posterior chambers*, and the vitreous body in the large space behind the lens and ciliary body. The posterior chamber is the name given to the small space between the lens and iris.

The iris behaves as a diaphragm, modifying the amount of light entering the eye, whilst the ciliary body contains muscle fibres which, on contraction, increase the refractive power of the lens (accommodation). An image of external objects is formed, by means of the dioptric apparatus, on the retina, the more highly specialized portion of which is called the *fovea*.

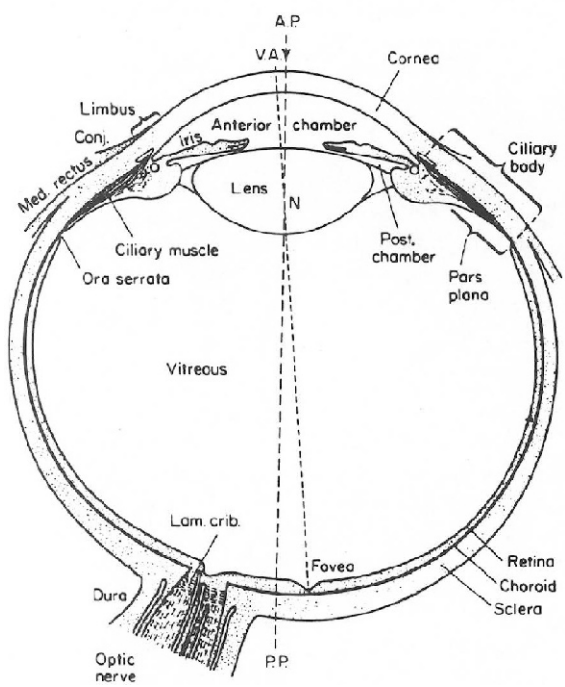

Fig. 1.1 Horizontal section of the human eye. PP, posterior pole; AP, anterior pole; VA, visual axis. (Wolff, *Anatomy of the Eye and Orbit.*)

Visual Pathway

The retina is largely made up of nervous tissue—it is an outgrowth of the central nervous system—and fibres carrying the responses of visual stimuli lead away in the *optic nerve* through a canal in the bony orbit, the *optic foramen*; the visual impulses are conveyed through the optic nerve and tract to the lateral geniculate body and thence to the cerebral cortex; on their way, the fibres carrying messages from the medial, or nasal, half of the retina cross over in the *optic chiasma*, so that the lateral geniculate body of the left side, for example, receives fibres from the temporal half of the left retina and the nasal half of the right. The nerve trunks, proximal to the chiasma, are called the *optic tracts*. This partial decussation may be regarded as a development associated with binocular vision; it will be noted that the responses to a stimulus from any one part of the visual field are carried in the same optic tract (Fig. 1.2), and the necessary motor response, whereby both eyes are directed to the same point in the field, is probably simplified by this arrangement. It will be noted also that a right-sided event, i.e. a visual stimulus arising from a point in the right half of the field, is associated with impulses passing to the left cerebral hemisphere, an arrangement common to all peripheral stimuli.

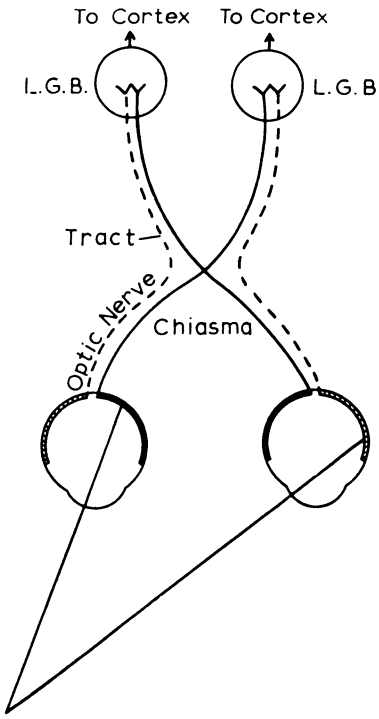

Fig. 1.2 The partial decussation of the optic pathway.

Vascular Coat

The nutrition of the eye is taken care of largely by the capillaries of the vascular coat; let us examine this structure more closely.

Choroid

The choroid is essentially a layer of vascular tissue next to the retina; it is separated from this nervous tissue by two membranes—the structureless *membrane of Bruch* and the pigment epithelium. The retina comes to an end at the ciliary body, forming the *ora serrata* (Fig. 1.3), but the vascular coat continues into the ciliary body as one of its layers, the *vessel layer*, which is separated from the eye contents by membranes—the two layers of ciliary epithelium which, viewed embryologically, are the forward continuations of the retina and its pigment epithelium, and the *lamina vitrea*, which is the continuation forward of Bruch's membrane.

Ciliary Body and Iris

The ciliary body in antero-posterior section is triangular in shape (Fig. 1.4) and has a number of processes (seventy) to which the zonule is attached; viewed from behind, these processes appear as radial ridges to which the name *corona ciliaris* has been given (Fig. 1.3). The relationship of the iris to the ciliary body is seen in Fig. 1.4; the blood vessels supplying it belong to the same system as that supplying the ciliary body. Posteriorly, the stroma is separated from the aqueous humour by the *posterior epithelium*, a double, heavily pigmented layer which may be viewed as a prolongation of the ciliary epithelial layers.

The Conjunctiva

This may be described as a vascular membrane covering the posterior segment of the eyeball that is reflected forward over the surfaces of the eyelids. The pouch formed by the lower eye-lid is termed the *conjunctival sac* and constitutes a useful cavity in which drugs, designed to pass into the bulb, may be deposited.

Nutrition

The vessels of the vascular coat nourish the internal structures of the eye; so far as the lens is concerned, this process must take place by diffusion of dissolved material from the capillaries through the aqueous humour and vitreous body. The inner (nearest the vitreous) nervous elements of the retina, however, are provided for by a functionally separate vascular system derived from the *central artery of the retina*; this artery, a branch of the *ophthalmic*, enters the globe with the optic nerve and it is its ramifications, together with the *retinal veins*, that give the fundus of the eye its characteristic appearance. The choroid, ciliary body, and iris are supplied by a separate system of arteries, also derived from the ophthalmic—the *ciliary system of arteries.*

The anterior portion of the sclera is covered by a mucous membrane, the *conjunctiva*, which is continued forward on to the inner surfaces of the lids, thus creating the *conjunctival sac.* The remainder of the sclera is enveloped by *Tenon's capsule.*

Muscle

Movements of the eye are executed by the contractions of the six extra-ocular muscles; the space between the globe and orbit being filled with the orbital fat, the movements of the eye are essentially rotations about a fixed point in space.

Nerve Supply

The essentials of the nerve supply to the eyeball are indicated in Fig. 1.5; sensory impulses (excluding, of course, the visual ones) are conveyed through the *long* and *short ciliary nerves.* The long ciliary nerves are composed mainly of the axons of nerve cells in the

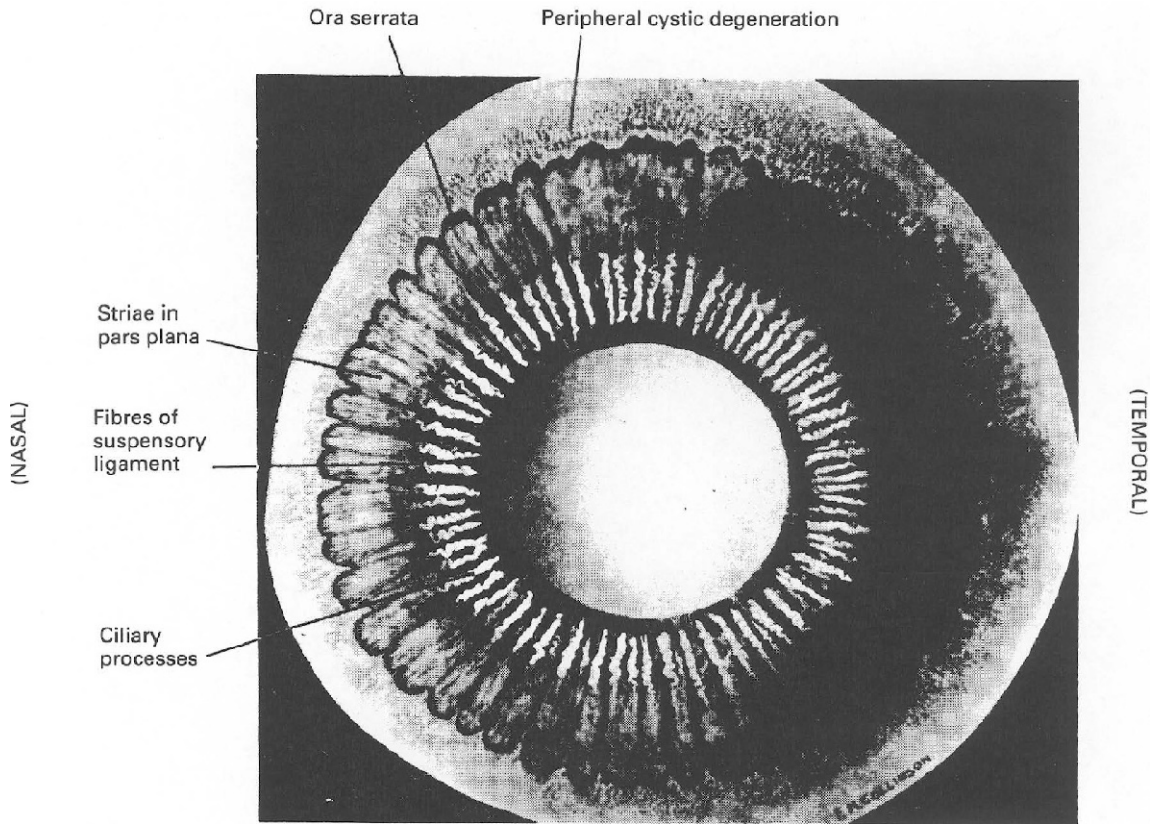

Fig. 1.3 Posterior view of the ciliary body. (Wolff, *Anatomy of the Eye and Orbit.*)

Gasserian ganglion—the ganglion of the trigeminal (N. V); they convey impulses from the iris, ciliary body, and cornea. The short ciliary nerves also contain axons of the trigeminal; they pass through a ganglion in the orbit, the *ciliary ganglion*, into the *naso-ciliary nerve*; the fibres carry impulses from all parts of the eyeball, but chiefly from the cornea.

The voluntary motor nerve supply to the extraocular muscles is through the cranial nerves III (oculomotor), IV (trochlear) and VI (abducens). Parasympathetic motor fibres to the ciliary muscle and iris travel through the lower division of N III as the *motor root* of the ciliary ganglion; post-ganglionic fibres to the muscles are contained in the short ciliary nerves.

Sympathetic fibres from the superior cervical ganglion enter the orbit as the sympathetic root of the ciliary ganglion and run in the short ciliary nerves to supply the vessels of the globe and the dilator fibres of the pupil. Other sympathetic fibres avoid the ciliary ganglion, passing through the Gasserian ganglion and entering the globe in the long ciliary nerves, whilst still others enter the globe in the adventitia of the ciliary arteries.

Additional Nerve Supplies

Figure 1.5 may be said to represent the classical view of the ciliary ganglion with its three roots; however, the work of Ruskell (1970, 1974) has revealed the existence of ocular fibres from both the facial nerve (N VII) and from the maxillary branch of the trigeminal, in addition to the nasociliary branch.

FACIAL NERVE

This represents an ocular parasympathetic pathway derived from N VII; the fibres are derived from the pterygopalatine ganglion, running as *rami orbitales* to the *retro-orbital plexus* (*top* of Fig. 1.6); the *rami oculares* find their way into the globe mainly through the long ciliary nerves and along the ciliary arteries.

MAXILLARY FIBRES

These are illustrated in Fig. 1.6, some of them entering the retro-orbital plexus which had hitherto been assumed to be entirely autonomic, and the other division represents a

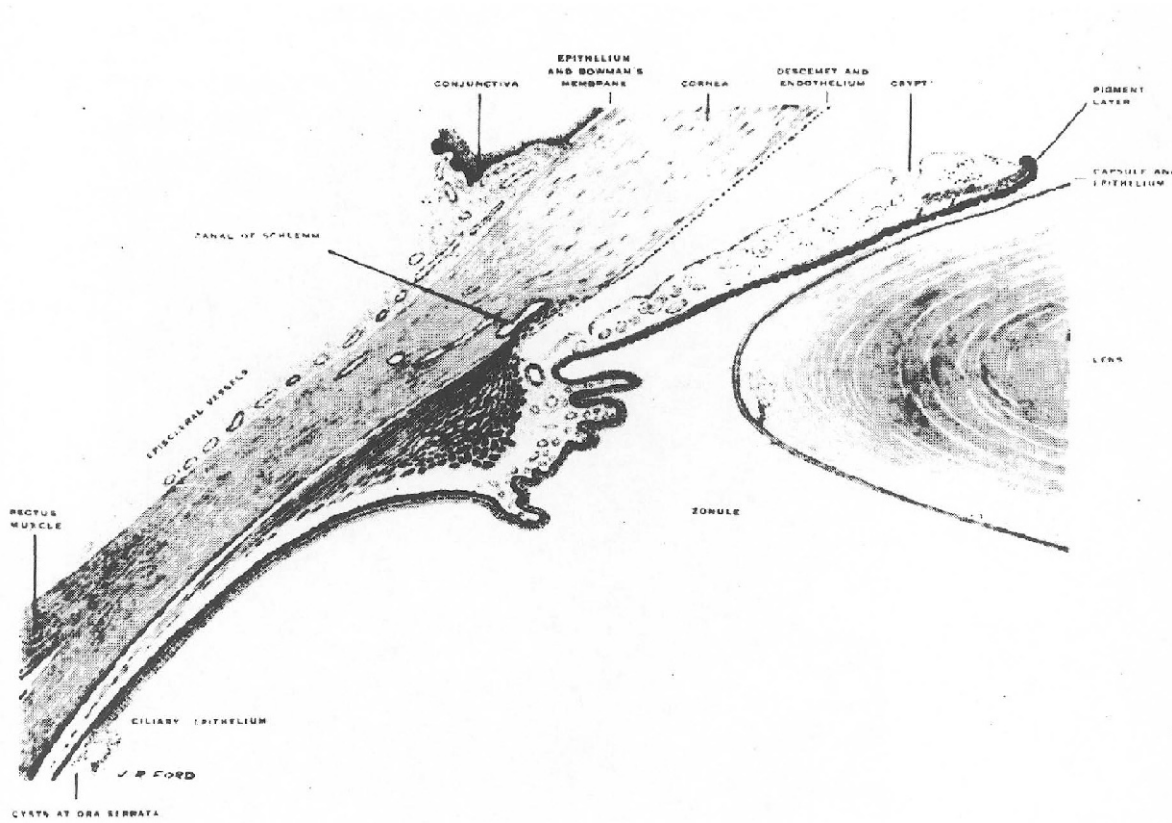

Fig. 1.4 Antero-posterior section through the anterior portion of the eye. (Wolff, *Anatomy of the Eye and Orbit.*)

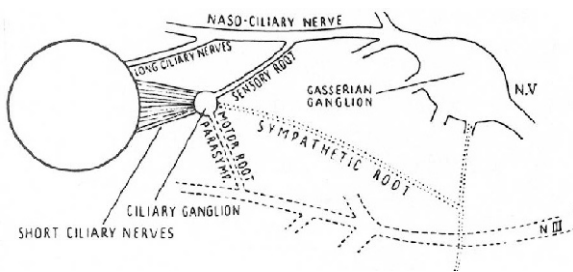

Fig. 1.5 Nervous supply to the eyeball.

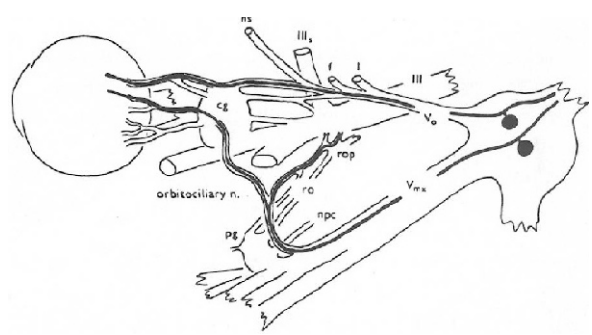

Fig. 1.6 Distribution of trigeminal nerve fibres to the eyeball. cg, ciliary ganglion; f, frontal nerve; l, lacrimal nerve; npc, nerve of the pterygoid canal; ns, nasociliary nerve; pg, pterygopalatine ganglion; ro, rami orbitales; rop, retro-orbital plexus; V_o, ophthalmic nerve; V_{mx}, maxillary nerve; III, oculomotor nerve; III_s, superior branch of oculomotor nerve. (Ruskell, *J. Anat.*)

maxillary root of the ciliary ganglion; degeneration experiments showed that the fibres passed into the globe through short ciliary nerves.

Aqueous Humour and the Intraocular Pressure

The aqueous humour is a transparent colourless fluid contained in the anterior and posterior chambers of the eye (Fig. 1.1). By inserting a hypodermic needle through the cornea, the fluid may be more or less completely withdrawn, in which case it consists of the mixed fluids from the two chambers. As Seidel (1918, 1921) first showed, the posterior fluid may be withdrawn

separately by inserting a needle through the sclera just behind the corneoscleral junction; because of the valve-like action of the iris, resting on the lens, the anterior fluid is restrained from passing backwards into the posterior chamber, so that subsequently another needle may be inserted into the anterior chamber and this anterior fluid may be withdrawn. In the cat Seidel found that the volume was some 14% of the volume of the anterior fluid, whilst in the rabbit it is about 20%, according to Copeland & Kinsey (1950). The fluids from the two chambers are of very similar composition, so that we may consider the composition of the mixed fluid when discussing the relationships between aqueous humour and blood. Thanks largely to the studies of Kinsey, however, it is now known that there are characteristic differences between the two fluids, differences that reflect their histories, the posterior fluid having been formed first and therefore exposed to diffusional exchanges with the blood in the iris for a shorter time than the anterior fluid.

ANATOMICAL RELATIONSHIPS

The nature of the aqueous humour is of fundamental interest for several reasons. There is reason to believe that it is formed continuously in the posterior chamber by the ciliary body, and that it passes through the pupil into the anterior chamber, whence it is drained away into the venous system in the angle of the anterior chamber by way of Schlemm's canal. As a circulating fluid, therefore, it must be a medium whereby the lens and cornea receive their nutrient materials. Furthermore, because it is being continuously formed, the *intraocular pressure* is largely determined by the rate of formation, the ease with which it is drained away, and by the forces behind the process of formation. To understand the nature of the fluid we must consider its chemical composition and variations of this under experimental conditions, whilst to appreciate the drainage process we must examine the detailed mircroanatomy of the structures that are concerned in this process. Since, moreover, the aqueous humour cannot be considered in isolation from the vitreous body, the posterior portion of the eyeball is also of some interest.

The Vascular Coat

The choroid, ciliary body and iris may be regarded as a vascular coat—the *uvea*—sandwiched between the protective outer coat—cornea and sclera—and the inner neuroepithelial coat—the retina and its continuation forwards as the ciliary epithelium (Fig. 1.7). This vascular coat is made up of the ramifications of the ciliary system of arteries that penetrate the globe independently of the optic nerve.

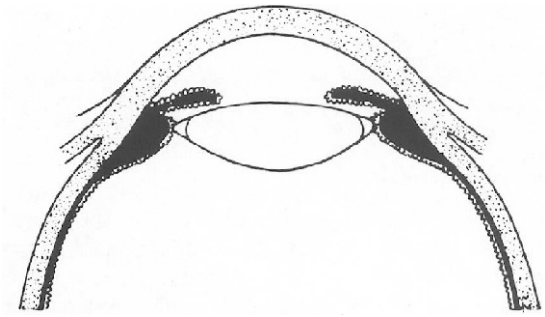

Fig. 1.7 Illustrating the uvea, or vascular coat (black), sandwiched between the sclera on the outside and the retina, ciliary epithelium, etc., on the inside.

Ciliary Arteries

The posterior ciliary arteries arise as trunks from the ophthalmic artery (Fig. 1.8), dividing into some ten to twenty branches which pierce the globe around the optic nerve. Two of them, the long posterior ciliary arteries, run forward through the choroid to the ciliary body where they anastomose with the anterior ciliary arteries[1] to form what has been incorrectly called the *major circle of the iris*; incorrectly, because the circle is actually in the ciliary body. From this circle, arteries run forward to supply the ciliary processes and iris, and backwards—as recurrent ciliary arteries—to contribute to the choroidal circulation.

By the *choroid* we mean the vascular layer between the retina and sclera; it is made up of the ramifications of the recurrent ciliary arteries, just mentioned, and of the short posterior ciliary arteries, which enter the globe around the posterior pole. The arteries break up to form a well-defined capillary layer—the *choriocapillaris*—next to the retina, but separated from this by a transparent glassy membrane—the *membrane of Bruch* or *lamina vitrea*. This

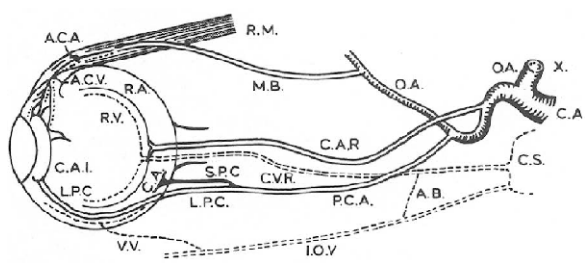

Fig. 1.8 Physiological plan of the circulation in man. OA, ophthalmic artery; MB, muscular branch; ACA, anterior ciliary artery; CAI, circulosus arteriosus iridis major; LPC, long posterior ciliary artery; SPC, short posterior ciliary artery; PCA, posterior ciliary arteries; CAR, central artery of the retina; RA, retinal artery; VV, vortex vein; IOV, inferior orbital vein; AB, anastomosing branch; CS, cavernous sinus. (Duke-Elder, *Brit. J. Ophthal.*)

capillary layer is certainly responsible for nutrition of the outer layers of the retina—pigment epithelium, rods and cones, and bipolar cells—and may also contribute to that of the innermost layer.

Venous System

The venous return is by way of two systems; the anterior ciliary veins accompany the anterior ciliary arteries, whilst the vortex veins run independently of the arterial circulation; these last are four in number, and they drain all the blood from the choroid, the iris and the ciliary processes, whilst the anterior ciliary veins drain the blood from the ciliary muscle and the superficial plexuses, which we shall describe later. According to a study by Bill (1962) only 1% of the venous return is by way of the anterior ciliary veins.

Retinal Circulation

As indicated earlier, the innermost part of the retina is supplied directly, in man, by the ramifications of the central retinal artery, a branch of the ophthalmic that penetrates the meningeal sheaths of the optic nerve in its intraorbital course and breaks up into a series of branches on the inner layer of the retina, branches that give the fundus its characteristic appearance in the ophthalmoscope. As Fig. 1.9 indicates, the central artery gives off branches that supply the optic nerve; moreover, the posterior ciliary arteries may send off branches in the region of the optic disk, forming a circle—*circle of Zinn or Haller*—which may form anastomoses with the branches of the central artery of the retina. To the extent that these anastomoses occur, the uveal and retinal vascular systems are not completely independent. Venous return from the retinal circulation is by way of the central retinal vein which, for a part of its course, runs in the subarachnoid space of the optic nerve and is thereby subjected to the intracranial pressure. For this reason, an elevated intracranial pressure may be manifest as an engorgement of the retinal veins.

So much for the general lay-out of the vascular circulation of the eye; as we have seen, the uveal circulation supplies the ciliary body and iris, the two vascular structures that come into close relationship with the aqueous humour. It is important now that we examine these structures in some detail.

Ciliary Body

In sagittal section this is a triangular body (Fig. 1.4), whilst looked at from behind it appears as a ring, some 6 mm wide in man. Where it joins the retina—the *ora serrata*—it appears smooth to the naked eye, but farther forward the inner surface is ridged, owing to the presence of some seventy to eighty *ciliary processes*, and acquires the name of *corona ciliaris* (Fig. 1.3). As the oblique section illustrated in Fig. 1.10 shows, the ciliary processes are villus-like projections of the main body, jutting into the posterior chamber. According to Baurmann (1930), the total area of these processes, in man, is some 6 cm^2 and we may look upon this expansion as subserving the secretory activity of this part of the ciliary body, since there is good reason to believe that it is here that the aqueous humour is formed. The vessel-layer of the ciliary body is similar to the choroid; it extends into each ciliary process, so that this is probably the most heavily vascularized part of the eye. Each process contains a mass of capillaries so arranged that each comes into close relationship, at some point in its course, with the surface of the epithelium. As stated above, blood from the ciliary processes is carried away by the vortex veins. In the rabbit, the ciliary processes are of two kinds—*posterior principal processes* projecting from the posterior region, and the *iridial processes*, located more anteriorly,

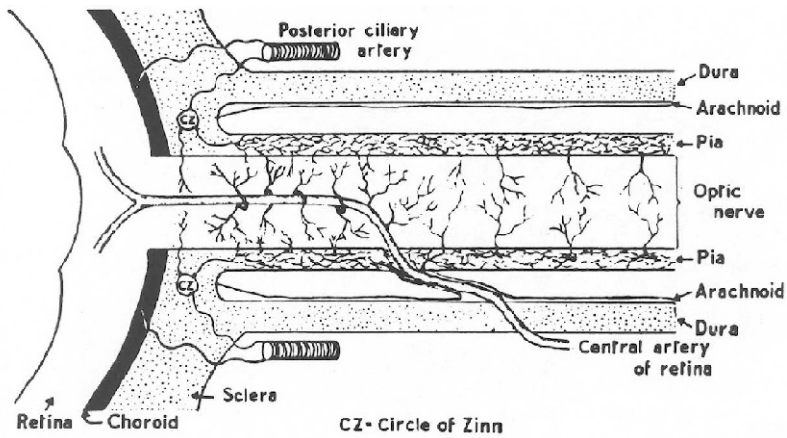

Fig. 1.9 Schematic section of the optic nerve and eyeball showing course and branches of the central retinal artery. (Singh & Dass, *Brit. J. Ophthal.*)

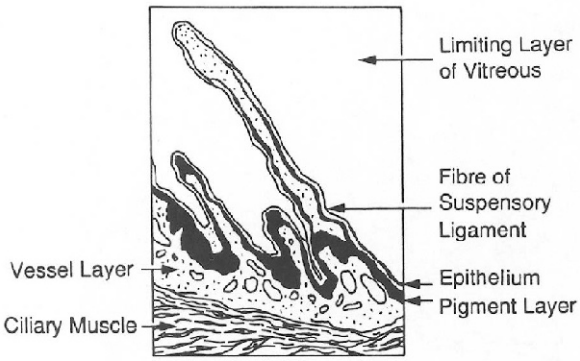

Fig. 1.10 Oblique section of the ciliary body. (After Wolff.)

and projecting towards the iris. These last have no zonular connections and may be those that are most closely concerned in production of the aqueous humour since they are the only processes to show significant morphological changes after paracentesis, according to Kozart (1968).

Ciliary Epithelium

The innermost coat, insulating the ciliary body from the aqueous humour and vitreous body, is the *ciliary epithelium*, a double layer of cells, the inner layer of which, i.e. the layer next to the aqueous humour or vitreous body, is non-pigmented, whilst the outer layer is heavily pigmented, and represents the forward continuation of the retinal pigment epithelium, whilst the unpigmented layer is the forward continuation of the neuroepithelium from which the retinal cells are derived. The cells of this epithelium, which are considered to be responsible for the secretion of the aqueous humour, have been examined in the electron microscope by several workers; a striking feature is the interdigitation of the lateral surfaces of adjacent cells, and the basal infoldings (Fig. 1.11), which are characteristic features of secretory epithelia concerned with fluid transport. The relations of the two epithelial cell layers are of importance, since the secreted aqueous humour must be derived from the blood in the stroma of the ciliary body, and thus the transport must occur across both layers. The matter will be considered in detail later in connexion with the blood-aqueous barrier, and it is sufficient to indicate now that the cells of the two layers face each other apex-to-apex, as a result of the invagination of the neuroepithelial layer during embryogenesis. Thus the *basal* aspects of the unpigmented epithelial cells face the aqueous humour, and the *basal* aspects of the pigmented cells face the ciliary stroma (Fig. 1.12).

Fig. 1.11 A section of portions of two adjacent ciliary epithelial cells of the rabbit showing complex interdigitations (B) of their boundaries. Zonular fibres (Z) can be seen in close approximation to the surface of these cells. ER, endoplasmic reticulum; M, mitochondrion. (Drawing after an electron micrograph by Pappas & Smelser, *Amer. J. Ophthal.*)

The Iris

Laminae

This is the most anterior part of the vascular coat; in a meridional section it is seen to consist of two main layers, or laminae, separated by a less dense zone, the cleft of Fuchs. As described by Freddo & Raviola (1982), the iris is covered by two epithelia which are continuations forward of the pigmented and non-pigmented layers of the ciliary body. Thus the posterior layer, facing the posterior chamber of the eye, is the continuation of the pigmented ciliary epithelial layer, and the anterior epithelium is the continuation of the non-pigmented epithelium. This anterior epithelium is referred to as myoepithelium, since the specialized basal processes of these cells make up the dilator pupillae, i.e. they behave as muscle fibres (p. 55).

The Drainage Route

We have said that the aqueous humour is most probably secreted continuously by the cells of the ciliary epi-

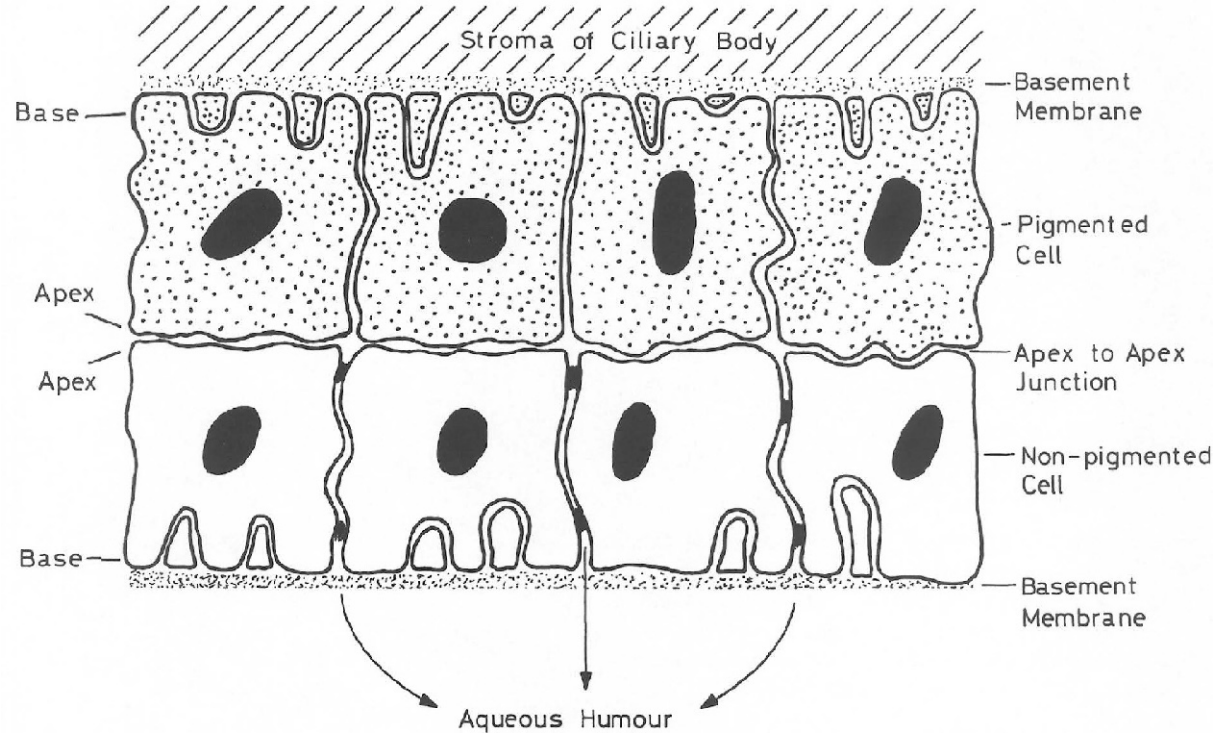

Fig. 1.12 Showing how the two layers of epithelium of the ciliary body face each other apex to apex.

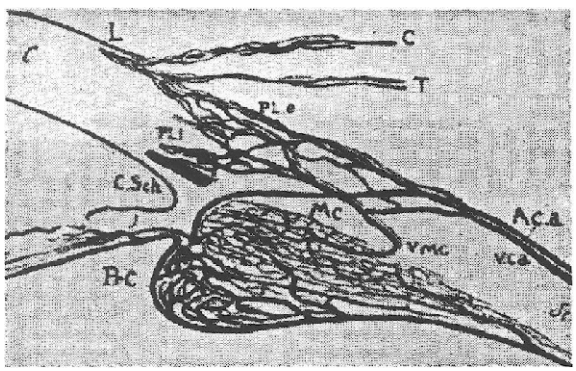

Fig. 1.13 Illustrating the canal of Schlemm and its relation to the plexuses of the anteror segment of the eye. C, conjunctival plexus; T, Tenon's capsule plexus; PLe, episcleral plexus; PLi, intrascleral plexus; Mc, ciliary muscle; VMc, vein of ciliary muscle; Ac.a, anterior ciliary artery; v.ca, anterior ciliary vein; PrC, ciliary process; *C*, cornea; c, collector; L, limbus. (Maggiore, *Ann. Ottalm.*)

thelium; to make room for the new fluid there must obviously be a continuous escape, or drainage, and this occurs by way of the *canal of Schlemm.* This is a circular canal in the corneo-sclera of the limbus (Fig. 1.4) which comes into relation with the aqueous humour on the one hand and the *intrascleral venous plexus* on the other, as illustrated by Figs 1.13 and 1.14.

The Anterior Segment Plexuses

These small vessels are of exceptional interest for the physiology of the eye, not only because they are the place where the aqueous humour is carried away, but they also represent a region that provides nutrition for the avascular corneal tissue, and subtle changes within the eye may be reflected in changes in the state of the superficial vessels that provide valuable diagnostic cues. As described by Maggiore, four layers may be differentiated; a conjunctival network surrounding the cornea at the limbus—his *conjunctival plexus*; these are visible in the living eye. A subconjuctival network particularly prominent in the region of Tenon's Capsule—his *Tenon's capsule plexus*; an *episcleral plexus* mostly composed of venous vessels originating from the confluence of small venules draining the conjunctival plexus, and an *intrascleral network* close to Schlemm's canal. Raviola (1983) has described the plexuses in the monkey and emphasizes the basic similarity with the human; the subconjunctival (Tenon's capsule) and episcleral plexuses she treated as one—the episcleral vessels. With the electron microscope

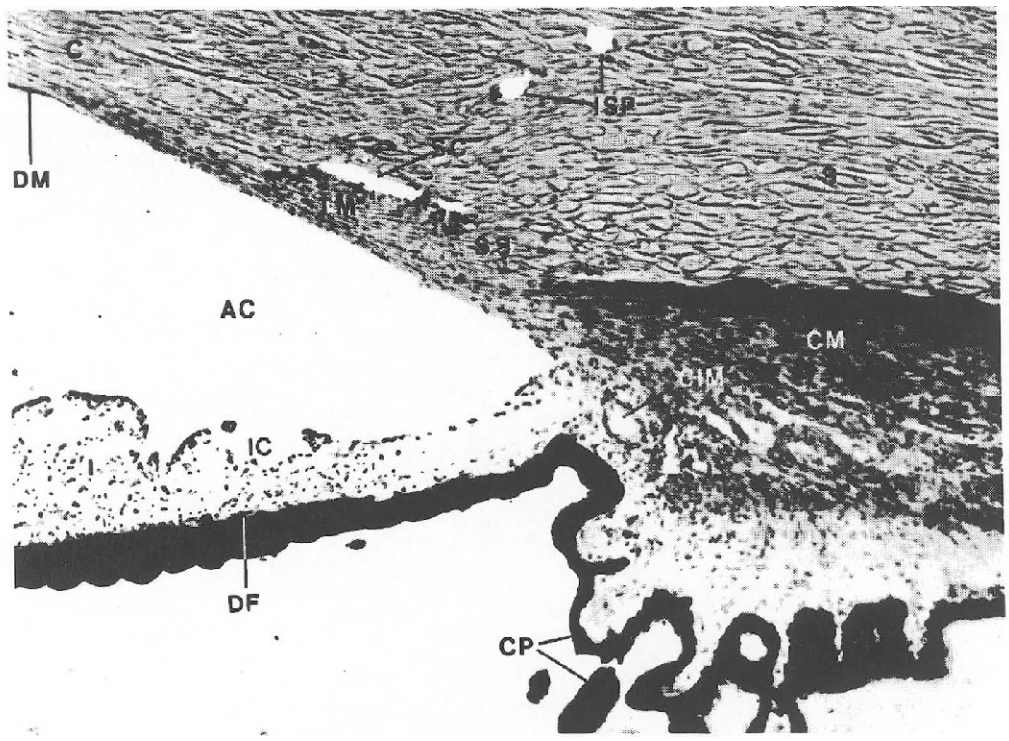

Fig. 1.14 Meridional section of the angle of the anterior chamber of human eye (× 64). C, cornea; ISP, intrascleral plexus of veins; DM, Descemet's membrane; AC, anterior chamber; I, iris; IC, iris crypts; DF, dilator fibres of the iris; CP, ciliary processes; CIM, circulus iridis major; CM, ciliary muscle; SS, scleral spur; TM, trabecular meshwork; SC, Schlemm's canal; S, sclera. (Courtesy, R. C. Tripathi.)

it was possible to show that the conjunctival and episcleral vessels were morphologically continuous, most of them being provided with simple endothelial walls with perciytes embedded in a basal lamina. Their capillary or venule nature was revealed by the ready escape of horseradish peroxidase into the surrounding tissue. Raviola described a rich plexus of lymphatic capillaries in the subconjunctival tissue.

Canal of Schlemm

The canal of Schlemm is usually represented as a ring lying in the corneo-sclera, which on cross-section (as in the meridional section of Fig. 1.14) appears as a circle or ellipse; its structure is, in fact, more complex, since it divides into several channels which, however, later reunite; hence the appearance of a cross-section varies with the position of the section. The channel, moreover, is partially interrupted by septa which probably serve a mechanical role in preventing obliteration of the canal when the pressure within the eye is very high.

The canal is essentially an endothelium-lined vessel, similar to a delicate vein; on the outside it rests on the scleral tissue whilst on the inside, nearest the aqueous humour, it is covered by a meshwork of endothelium-covered trabeculae—the *trabecular meshwork* or *pectinate ligament* (Fig. 1.15). Aqueous humour, to enter the canal, must percolate between the trabeculae and finally cross the endothelial wall.

TRABECULAR MESHWORK

An adequate understanding of the ultrastructure of the tissue in the angle of the anterior chamber, including that of Schlemm's canal, is vital for an understanding of the factors governing the resistance to flow of aqueous humour out of the eye. On meridional section the meshwork appears as a series of meridionally orientated fibres (Fig. 1.14), but on tangential section it is seen to consist of a series of flat lamellae, piled one on top of the other, the fluid-filled spaces between these lamellae being connected by holes, as illustrated schematically in Fig. 1.16. The meshwork has been divided into three parts with characteristically different ultrastructures; the innermost portion is the *uveal meshwork*; the trabeculae making up the lamellae here are finer than those of the outer or *corneoscleral meshwork* whilst the meshes are larger. Each

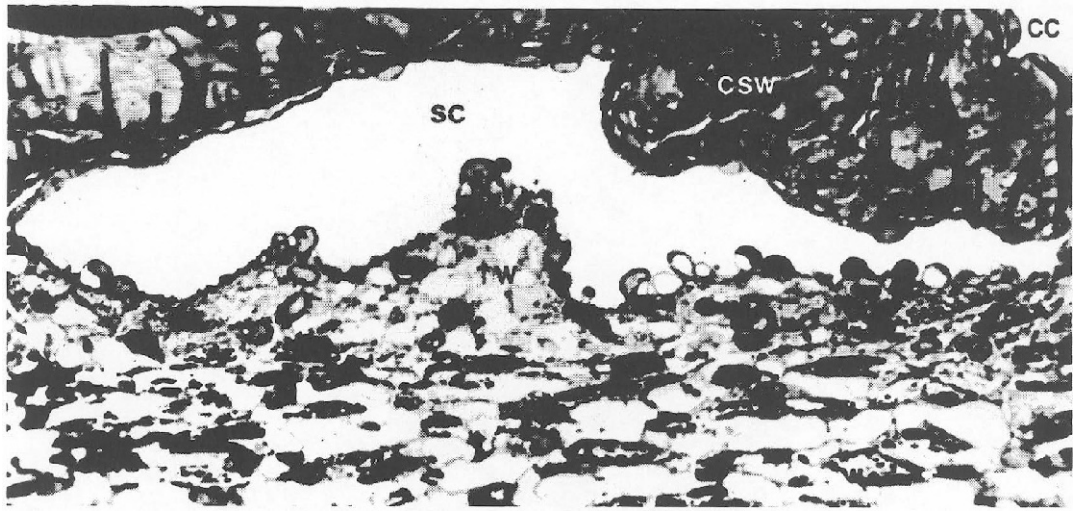

Fig. 1.15 Meridional section of Schlemm's canal and adjacent trabecular meshwork of rhesus monkey. Osmium fixed, toluidine blue stained. CC, collector channel; CSW, corneoscleral wall of Schlemm's canal; SC, Schlemm's canal; TW, trabecular wall of Schlemm's canal. Light micrograph × 750. (Courtesy, R. C. Tripathi.)

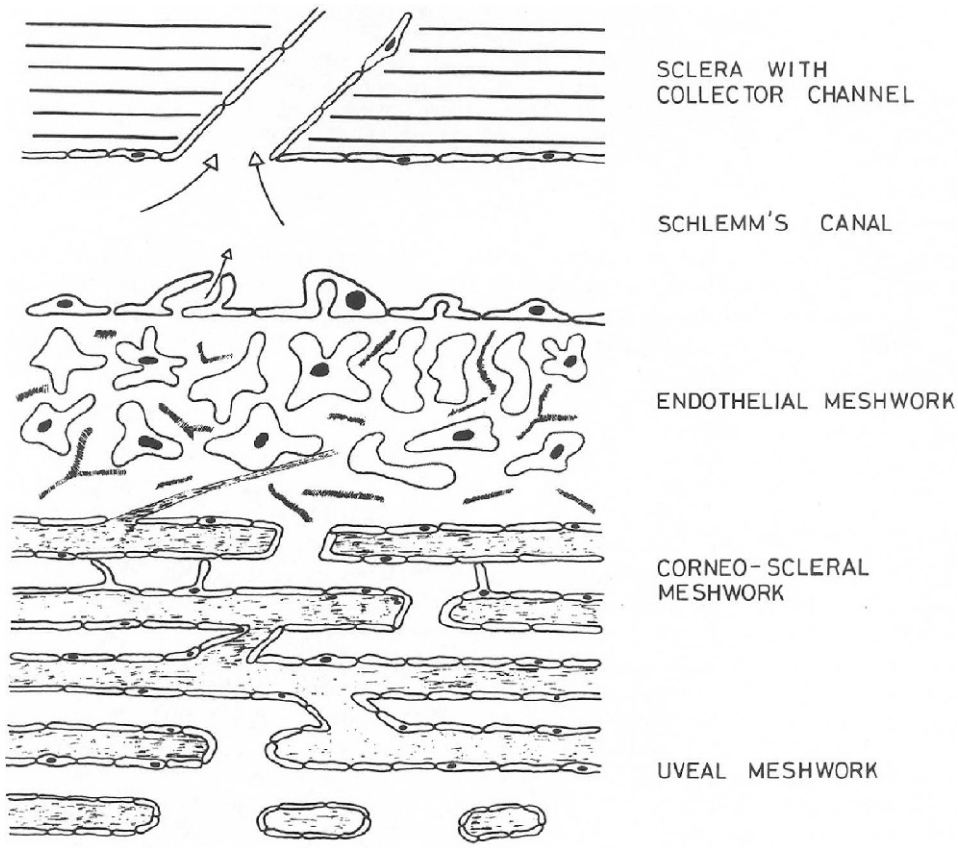

Fig. 1.16 Schematic representation of a section through chamber-angle tissue. (Bill, *Physiol. Rev.*)

lamella of the uveal meshwork is attached anteriorly to the corneal tissue at the end of Descemet's membrane, constituting *Schwalbe's ring*,[2] and posteriorly to the meridional fibres of the ciliary muscle. A pull of these fibres may well operate to open up the meshes of this trabecular structure, thereby favouring passage of fluid. The third portion, lying immediately adjacent to the canal, was described by Rohen as the *pore area*, or *pore tissue*, but is now usually referred to as the *endothelial meshwork*.

Ultrastructure As described by Tripathi (1977) the corneoscleral and outer uveal trabeculae are flattened perforated sheets orientated circumferentially parallel to the surface of the limbus. The inner 1 to 2 layers of uveal sheets are cord-like and orientated predominantly radially in a net-like fashion enclosing large spaces (Fig. 1.17). The beams constituting the meshwork are made up of collagen and of elastic tissue, covered by basement membrane material which, in turn, is completely or incompletely covered by a layer of flattened mesothelial cells. These cells exhibit both synthetic and phagocytic properties. As Fig. 1.17 shows, the trabecular meshwork forms a labyrinth of intercommunicating intra- and extra-trabecular spaces of variable size and shape, and may be likened to a coarse filter.

ENDOTHELIUM AND ADJACENT TISSUE

The endothelium of the canal consists in a single layer of cells whose lateral borders meet in either a narrow zone of apposition or in a more complex zone formed by cellular overlap or tongue-in-groove insertion (Grierson & Lee, 1975). Intercellular clefts exhibit junctional modifications which represent limited regions of apparent fusion between apposing plasma membranes, and are, in fact, gap-junctions in addition to adhering junctions. The cells rest on a basement membrane facing the *endothelial meshwork*, which may be considered to be the region lying between the basal aspect of the canal and the first layer of corneoscleral trabeculae; this is of variable thickness (8 to 16 μm).[3] The native cells constituting this region are usually orientated with their long axes parallel to the

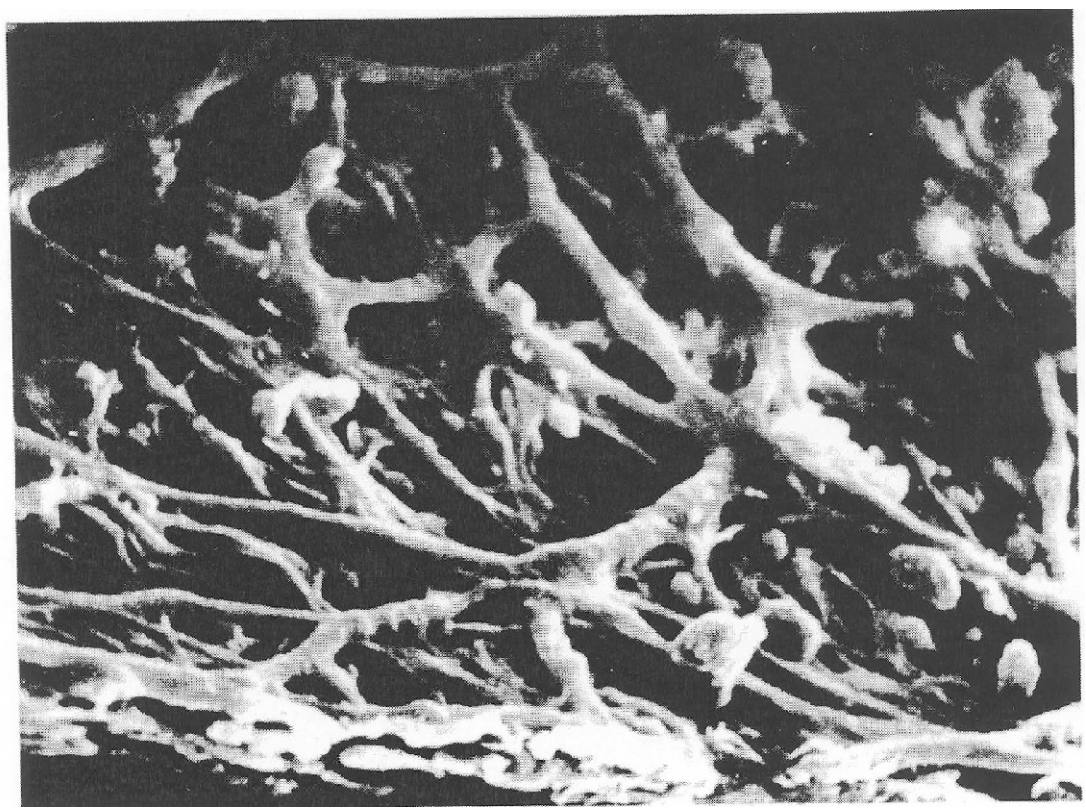

Fig. 1.17 Scanning electron micrograph of the trabecular meshwork seen from the anterior chamber aspect. The rounded beams of the inner uveal meshwork, their endothelial covering and net-like arrangement and intercommunicating inter- and trans-trabecular spaces are seen in the foreground, whereas the deeper sheet-like trabeculae seen in the background are orientated circumferentially. (Approx. × 610.) (Tripathi, *Exp. Eye Res.*)

endothelium lining the canal, and form a network by process-contacts between neighbouring cells. In the outer corneoscleral meshwork, the adjacent trabeculae are separated by narrow intertrabecular spaces, and cellular contact across these spaces is achieved through cellular processes; once again, the regions of contact show gap-type and desmosome-type junctions. A characteristic feature of the endothelial cells lining the meshwork side of the canal is the prominent vacuolization of the cells; and its significance will be considered later in relation to the mechanism of drainage.

Cribriform Meshwork Rohen (1983) has provided some extra details of the structure of the tissue immediately adjacent to Schlemm's canal, which he now calls the *cribriform meshwork*; tangential sections reveal it as containing a delicate meshwork of elastic like fibres with a predominantly equatorial orientation, and called the cribriform plexus of fibres (Fig. 1.18). The plexus appeared to be connected with the endothelium of Schlemm's canal, on the one hand, and on the other with the anterior tendons of the ciliary muscle. Thus contraction of the ciliary muscle would spread out the cribriform plexus increasing spaces between plates of fibrillar material.

As we shall see, an adequate understanding of the ultrastructure of the tissue in the drainage angle is vital for the study of the intraocular pressure.

Comparative Aspects of Drainage

Earlier anatomists tended to distinguish between the primate angle of the anterior chamber, with its canal of Schlemm, and the drainage mechanism in lower mammals, e.g. Troncoso (1942). However, the physiological studies on drainage processes in non-primates, and the recent comparative anatomical studies of Tripathi (1974), have confirmed the essential uniformity in the mechanism and site of drainage, not only amongst mammals but also in lower vertebrates including fishes, although the morphological organization of the iridocorneal angle does show interesting variations.

Angular Aqueous Plexus

Thus in primates, owing to the compact nature of the ciliary muscle, the angle is clearly defined (Fig. 1.19A), whereas in most amphibians, reptiles, birds and lower placentals it is ill defined owing to the wedge-shaped

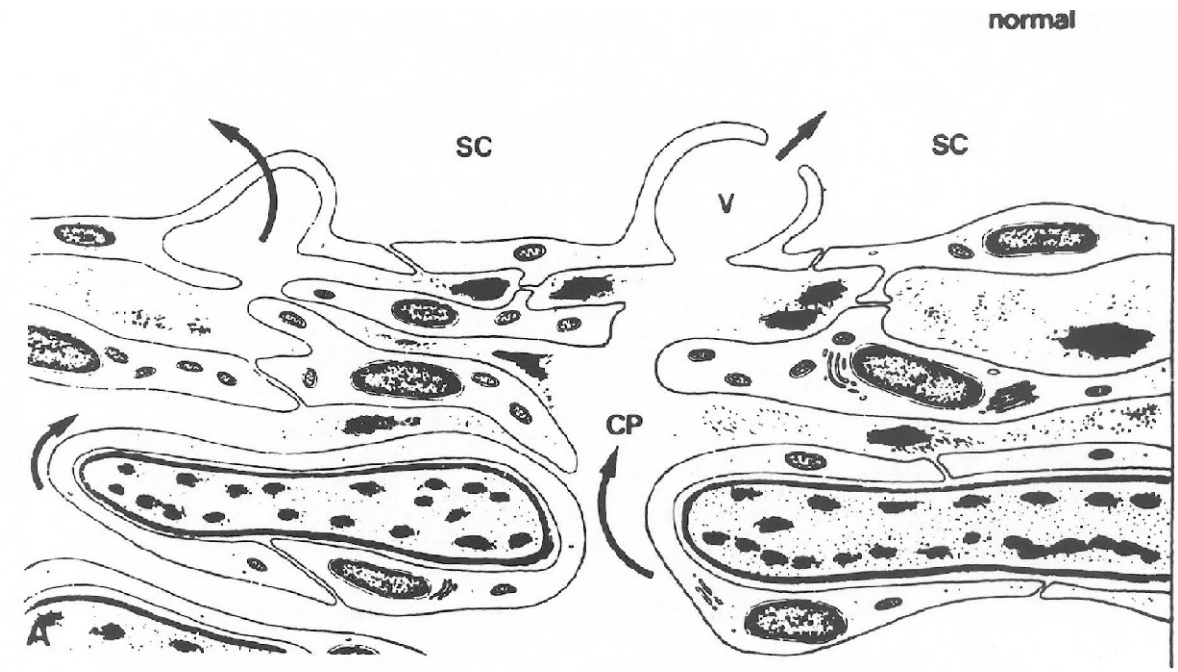

Fig. 1.18 Ultrastructure of the cribriform layer of the normal human trabecular meshwork (schematic drawing). CP, cribriform pathway; SC, Schlemm's canal; V, giant vacuole (microchannel) within the endothelial lining of Schlemm's canal. Arrows: direction of aqueous outflow. (Rohen, *Ophthalmology.*)

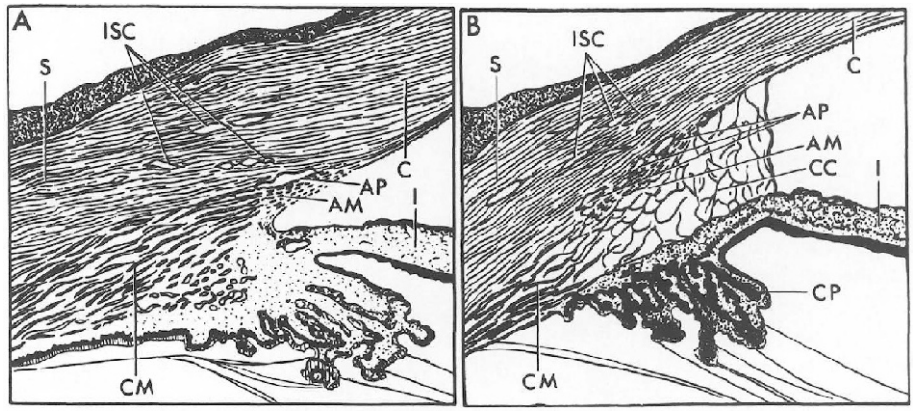

Fig. 1.19 Diagrammatic representation of the angular region of a primate (A) and a lower placental (B) showing comparative morphological organization. S, sclera; C, cornea; I, iris; AM, angular meshwork; AP, angular aqueous plexus; CM, ciliary muscle; CC, ciliary cleft; CP, ciliary processes; ISC, intrascleral collector channels. (Tripathi, *The Eye.*)

separation of the ciliary body into two leaves, one hugging the inner aspect of the sclera and the other being continuous with the fibrous base-plate of the ciliary body. The resulting *ciliary cleft* can be regarded as an extension of the anterior chamber (Fig. 1.19B); it is criss-crossed and bridged by fibro-cellular strands to form an *angular meshwork* or *pectinate ligament.*[4] The structure of this angular meshwork varies widely throughout the vertebrates. In all the species studied by Tripathi, an equivalent channel to Schlemm's canal could be discerned, and he suggested a generic term—*angular aqueous plexus*—to describe this. It is generally located on the inner aspect of the anterior sclera and sclero-cornea, and is supported partly on the anterior chamber aspect or completely surrounded by the loose tissue of the angular meshwork. As in primates, the plexus forms a circumferential structure in lower mammals, birds and many reptiles, but is more localized in amphibians and fishes. Drainage of aqueous from this plexus takes place into intra- and episcleral plexuses of veins, and in some instances also by supraciliary and suprachoroidal plexuses of veins which connect directly to the angular plexus.

CELLULAR LINING

As with the primate, the angular plexus is lined by mesothelium, the individual cells being linked by junctional complexes, whilst the large vacuoles described above for the primate eye are a universal feature, and which, on the basis of tracer studies, have been identified as representing the pathway into the channel. Thus, to quote Tripathi (1977) '. . . The normal presence of macrovacuolar structures in the mesothelial lining of the aqueous plexus in species as diverse as aquatic dogfish, arboreal pigeon and terrestrial man would suggest that the bulk flow of aqueous humour through the dynamic system of vacuolar transcellular pores is a fundamental biological mechanism of great antiquity.'

PHYSIOLOGY OF THE VASCULAR SYSTEM

The vascular circulation of the eye has attracted a great deal of interest because of its close relationship to the formation and drainage of aqueous humour. Space will not permit a detailed description of this aspect of ocular physiology, and we must be content with a few salient points.

Pulses

With the ophthalmoscope an arterial pulse may be observed in the retinal vessels; if the intraocular pressure is increased by compressing the globe the pulse may be exaggerated, since the collapse of the artery during diastole becomes greater; if the pressure is raised sufficiently, the pulse will cease, at which point the pressure in the eye is equal to the systolic pressure in the artery from which the retinal artery is derived, namely, the ophthalmic artery. The retinal veins also show a pulse; it is best seen where the large veins lie on the optic disk; it appears as a sudden emptying of this portion of the vein, progressing from the central end towards the periphery followed by a pronounced dilatation, beginning at the periphery and passing centrally. The pulse is not simply a reflexion of events taking place in the right atrium, and is closely related to ventricular systole. The rise in intraocular pressure associated with systole will tend to compress the veins; and a collapse of the latter will take place where the pressure is least, i.e. most centrally. The subsequent refilling of the vein will occur in diastole, or late in systole,

and will proceed in the reverse direction. The exact time-relationships of the pulse were established cinematographically by Serr (1937).

PATHOLOGICAL CHANGE

The rise in pressure in the eye when an artery expands is governed by the compliance of the system, i.e. the ability of the cornea-sclera to expand and the venous system to collapse and aqueous to be driven out; the exaggerated pulse in glaucoma is probably best accounted for by defective drainage of aqueous humour and the existing high intraocular pressure, which tends to reduce compliance (Friedland, 1983).

Pressures

These were studied experimentally by Seidel (1918) and later by Duke-Elder (1927); according to the latter author the following values (mmHg) are associated with an intraocular pressure of 20 mmHg:

Ophthalmic artery	99.5	Retinal vein	22.0
Retinal arteries	75.5	Intrascleral vein	21.5
		Episcleral vein	13.0

Values in normal human subjects are included in Table 1.7.

The Microcirculation of the Anterior Uvea

Before proceeding to a description of the aqueous humour, we may describe some details of the microcirculation in the ciliary processes, a description made possible by the formation of casts and subsequent examination with scanning electron-microscopy.

The Circles

Morrison & Van Buskirk (1984) showed that extensive arterial anastomoses between anterior and long posterior ciliary arteries are present in actually three localities. Thus, after leaving the rectus muscle tendons, the anterior arteries branch within the episclera to supply the episcleral plexus; adjacent anterior ciliary arteries interconnect via their lateral-most branches to form often a complete anastomotic ring within the episclera—the *episcleral circle.* Extensions of the remaining anterior branches perforate the limbal sclera to enter the ciliary muscle; the majority send multiple branches anteriorly to the root of the iris; the most lateral of these frequently anastomose with each other and with branches from the long posterior arteries to form the *intramuscular circle,*[5] which is not always complete. At the iris root arborizations from both anterior and posterior ciliary arteries form the *major circle of the iris* the arteries travelling parallel to the iris root for a short distance before terminating as ciliary process- and iris-arterioles. This circle constitutes the blood-supply to the iris and ciliary processes. Figure 1.20 illustrates the system schematically.

Anterior and Posterior Arterioles

From the major circle of the iris, arterioles are given off; in the primate two types are described, anterior and

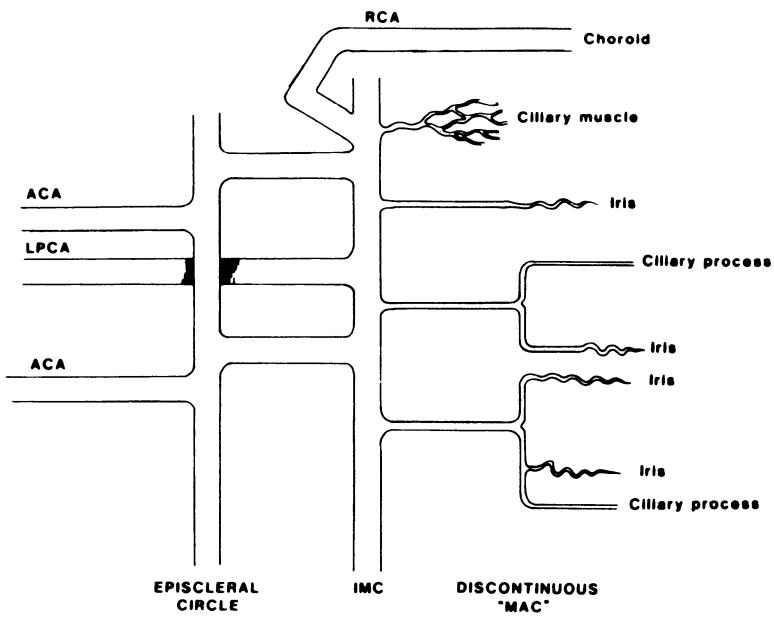

Fig. 1.20 Schematic representation of the multilevel collateral circulation in the primate anterior uvea. ACA, anterior ciliary artery; LPCA, long posterior ciliary artery; PACA, perforating anterior ciliary artery; RCA, recurrent ciliary artery; EC, episcleral circle; IMC, intramuscular circle; 'MAC', 'major arterial circle'. (Morrison & Buskirk, *Ophthalmology.*)

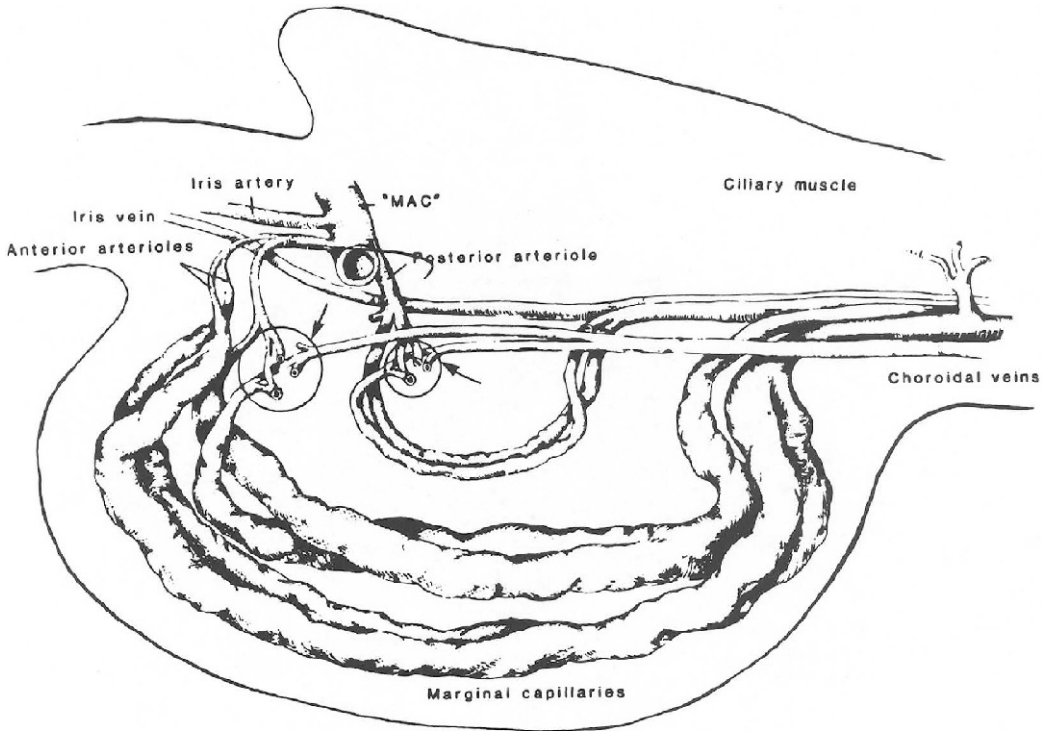

Fig. 1.21 Summary of the angioarchitecture of the primate major ciliary process, profile view. Each process is supplied by anterior and posterior arterioles radiating from the major arterial circle (MAC). The characteristically constricted anterior arterioles supply the anterior aspect of the ciliary process, forming large, irregularly dilated marginal process capillaries resembling veins and draining posteriorly into the choroidal veins. The posterior arterioles appear to be less constricted and provide posteriorly draining capillaries generally confined to the base of the process. At both levels, laterally directed arterioles form interprocess capillary networks (circled areas). From here, some capillaries re-enter the ciliary processes, thus forming interprocess communications anteriorly and connections to the adjacent minor ciliary processes (not shown) posteriorly. Other capillaries enter interprocess venous arcades (arrows), which drain directly into the choroidal veins and bypass the ciliary process entirely. The choroidal veins originate in four anterior sources: iris veins, ciliary processes, interprocess arcades, and the ciliary muscle. (Morrison & Buskirk, *Amer. J. Ophthal.*)

posterior, supplying larger, more anterior, and smaller, more posterior processes respectively. These arterioles frequently show focal constrictions, possibly the result of precapillary sphincters, that might be concerned in diverting flow of blood to the more anterior processes, considered to be more intimately concerned with fluid secretion (Hara *et al.*, 1977). Posterior arterioles lack constrictions and serve capillaries in the minor ciliary processes and the bases of the major processes (Morrison & Van Buskirk, 1984; Morrison *et al.*, 1987b). Figure 1.21 describes the detailed microvasculature of a major ciliary process in the monkey in which the separate fields of the anterior and posterior arteriolar branches are emphasized.

RABBIT

In the rabbit there is the same dichotomy, but this time the contrast is with the iridial processes, on the one hand, supplied by the anterior arteriole, and the posterior blade-like major (primary) and minor (secondary) processes; it is considered that these iridial processes, running towards the pupil behind the iris, are more closely concerned with fluid secretion. The situation is illustrated schematically in Fig. 1.22.

Some Species Variations

As classically described by Leber in man, the major circle lies in the ciliary body; from here a series of radial arterioles anastomose to terminate in an incomplete ring of a-v-anastomoses at the collarette—the minor circle of the iris. From the minor circle branches pass to the pupillary margin forming continuous capillary arcades that join vessels located posterior to the sphincter. In the rabbit the major circle lies in the mid-periphery of the *iris* and receives no contribution from the anterior ciliary artery. The same is true of guinea pigs, dog and rat. Not all radial vessels in the rabbit originate from the major circle, some being direct continuations of long posterior ciliary arteries; the minor

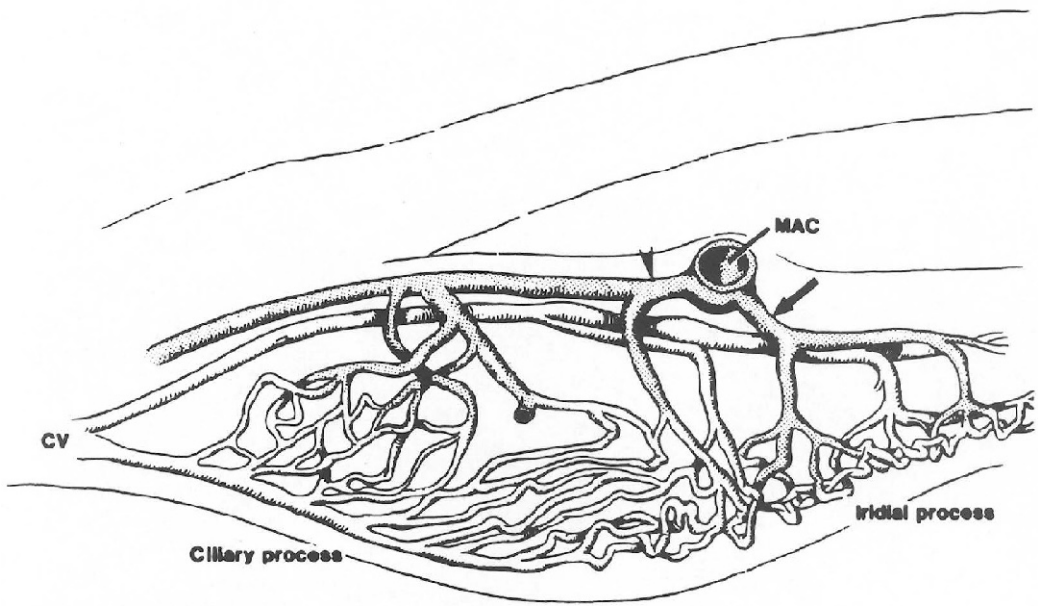

Fig. 1.22 Diagram of rabbit ciliary process microvasculature, illustrating the anterior (arrow) and posterior (arrowhead) arterioles supplying the iridial and ciliary processes, respectively. CV, choroidal veins; MAC, major arterial circle. (Morrison *et al., Invest. Ophthal.*)

circle is not prominent, but there is a well developed circle at the pupillary margin. More recent human studies have shown that portions of the major circle lie in the iris itself; the circle is not continuous and anterior ciliary arteries may not anastomose with the major circle at all but instead may contribute to the iris vasculature directly in addition to that of the episclera and ciliary muscle. Thus tenotomy, during which anterior ciliary arteries are cut, shows that these arteries provide most of the arterial supply to the iris, the major circle supplying none (Hayreh & Scott, 1978). The same is true for baboons (Wilcox *et al.*, 1980). In the monkey there is no minor circle of the iris (Freddo & Raviola, 1982).[6]

Anterior Ciliary Arteries

These are classically represented as an extraocular arterial supply to the anterior segment of the eye, contrasting with the intraocular supply from the major circle of the iris. However, Talusan & Schwartz (1981) by cinematography at 0.5 sec intervals after intravenous injection of fluorescein showed that the artery filled from within the eye, so that it was carrying blood out. The vessel was shown to be an artery, rather than a vein, as it would collapse at an externally applied pressure of 35 mmHg. Earlier Bron & Easty (1970) had described these vessels, the first to fill with fluorescein, as ciliary emissory veins. They arose in the anterior ciliary venous plexus in the outer portion of the ciliary muscle, exiting through scleral emissary foramina at a variable distance from the limbus, draining backwards over the surface of the globe to join the anterior ciliary veins. It was their bright red appearance that confused them with arteries, but this was actually a reflection of the rapid blood flow and low extraction of O_2 (Weinstein, 1950). When intraocular pressure was raised, the pressure in the anterior ciliary arteries fell (Sakimoto & Schwartz, 1984). If these vessels supply the tissue of the drainage angle, this finding may be of significance for its metabolism in glaucoma. So far as their contribution to the blood-flow of the anterior segment of the eye, i.e. iris, ciliary body and processes, Wilcox *et al.* (1980) found that this, measured by microspheres, decreased by 87% when the muscular branches of the ophthalmic artery, from which the anterior ciliary arteries are supposed to be derived, were occluded, in the primate eye.

THE AQUEOUS HUMOUR

The intraocular pressure depends primarily on the rate of secretion of aqueous humour, so that factors influencing this are of vital importance in understanding the physiology of the intraocular pressure. We may therefore pass to a consideration of the chemistry of the fluid and the dynamics of exchanges between it and the blood. These aspects, although apparently academic, are important for the full understanding of the experimental approaches to measuring the rate of secretion of the fluid and to controlling this.

Chemical Composition

The most obvious chemical difference between aqueous humour and blood plasma is to be found in the protein contents of the two fluids; in the plasma it is of the order of 6 to 7 g/100 ml, whereas in the aqueous humour it is

only 5 to 15 mg/100 ml in man and some 50 mg/100 ml in the rabbit. By concentrating the aqueous humour by modern electrophoretic techniques the proteins may be separated and identified. Such studies have shown that, although the absolute concentrations are very low, all the plasma proteins are present in the aqueous humour, so that it is reasonable to assume that they are derived from the plasma rather than synthesized during the secretory process. Table 1.1 gives an analysis of the aqueous humour and blood plasma of the rabbit, and Table 1.2 a more elaborate analysis of monkey fluids.

Non-colloidal Constituents

As the tables show, the crystalloidal composition of the aqueous humour is similar in its broad outlines to that of plasma, but there are some striking differences; thus the concentrations of ascorbate (vitamin C), pyruvate and lactate are much higher than in plasma, whilst those of urea and glucose are much less.

Table 1.1 Chemical composition of aqueous humour and blood plasma of the rabbit (after Davson, 1969)

	Aqueous humour	*Plasma*
Na	143.5	151.5
K	5.25	5.5
Ca	1.7	2.6
Mg	0.78	1.0
Cl	109.5	108.0
HCO_3	33.6	27.4
Lactate	7.4	4.3
Pyruvate	0.66	0.22
Ascorbate	0.96	0.02
Urea	7.0	9.1
Reducing value (as glucose)	6.9	8.3
Amino acids	0.17	0.12

Concentrations are expressed as millimoles per kilogramme of water.

GIBBS-DONNAN EQUILIBRIUM

The similarities between the two fluids led some earlier investigators to assume that the aqueous humour was derived from the blood plasma by a process of filtration from the capillaries of the ciliary body and iris; i.e. it was assumed that the aqueous humour was similar in origin and composition to the extracellular fluid of tissues such as skeletal muscle. If this were true, however, the ionic distributions would have to accord with the requirements of the Gibbs-Donnan equilibrium, according to which the concentrations of positive ions, e.g. Na^+ and K^+, would be greater in the plasma than in the aqueous humour, the ratio: $[Na]_{Aq}/[Na]_{Pl}$ being less than unity, whilst the reverse would hold with negative ions such as Cl^- and HCO_3^-. Moreover, the actual values of the ratios: *Concn. in Aqueous Humour/Concn. in Plasma* would have to conform to those found experimentally when plasma was dialysed against its own ultrafiltrate. In fact, however, as Table 1.3 shows, the ratios show considerable deviations from what is demanded of a plasma filtrate, and the deviations are not attributable to experimental errors. Thus with a plasma filtrate the ratio: $[Na]_{Aq}/[Na]_{Pl}$ should be 0.945 whilst it is in fact 0.96, indicating that there is an excess of 1.5% of sodium in the aqueous humour. More striking is the discrepancy of the bicarbonate ratio, which in the rabbit is 1.26 compared with a value of 1.04 demanded by the Gibbs-Donnan equilibrium. It will be noted that the dialysis-ratio for calcium is 0.65; the theoretical ratio for a divalent cation is 0.92, and the discrepancy is due to the large amount of calcium held bound to plasma proteins in unionized form. With magnesium the discrepancy is not so large, due to a smaller degree of binding.

Table 1.2 Chemical composition of aqueous humour and serum of monkeys (Gaasterland *et al.*, 1979)[7]

	Aqueous humour	*Serum*
Protein	33.3 mg/100 ml	6.2 g/100 ml
Na	152.5 meq/litre	148.3 meq/litre
K	3.9 meq/litre	4.0 meq/litre
Ca	5.3 mg/100 ml	9.4 mg/100 ml
Mg	1.9 mg/100 ml	1.8 mg/100 ml
Cl	124.8 meq/litre	107.3 meq/litre
HCO_3	27.8 meq/litre	18.8 meq/litre
Lactate	38.5 mg/100 ml	27.0 mg/100 ml
Ascorbate	20.8 mg/100 ml	0.3 mg/100 ml
Glucose	53.2 mg/100 ml	73.3 mg/100 ml
Urea nitrogen	17.2 mg/100 ml	20.5 mg/100 ml
Amino acids	1.9 mmoles/kg H_2O	2.6 mmoles/kg H_2O

Table 1.3 Values of the two distribution ratios; Concn. in Aqueous/Concn. in Plasma and Concn. in Dialysate/Concn. in Plasma. (Davson, *Physiology of the Ocular and Cerebrospinal Fluids*)

	Concn. in Aqueous	*Concn. in Dialysate*
	Concn. in Plasma	Concn. in Plasma
Na	0.96	0.945
K	0.955	0.96
Mg	0.78	0.80
Ca	0.58	0.65
Cl	1.015	1.04
HCO_3	1.26	1.04
Urea	0.87	1.00

GLUCOSE

The concentration of glucose in the aqueous humour is less than in plasma, and the concentration in the vitreous body is even lower; these differences have been ascribed to consumption within the eye by the lens, cornea and retina; this utilization may be simply demonstrated by incubating the excised eye at 37°C; within two hours all the glucose has disappeared (Bito & Salvador, 1970). It is possible that a further factor is a low concentration in the primary secretion, since the concentration of glucose in the aqueous humour of cataractous eyes is not significantly lower than normal (Pohjola, 1966).

The cerebrospinal fluid shares many characteristics with those of aqueous humour; this fluid has a much lower concentration of glucose than that of plasma, due to a primary secretion of a low-glucose fluid (Deane & Segal, 1985).

AMINO ACIDS

The relative concentrations of amino acid in the plasma aqueous humour and vitreous body depend on the particular amino acid, so that the concentration in aqueous humour may be less than, equal to, or greater than that in plasma (Fig. 1.23); the concentration in the vitreous body is always very much less than in either of the other fluids (Reddy *et al.*, 1961; Bito *et al.*, 1965). The low values in the vitreous body are not due to consumption within the eye since a non-metabolized acid, cycloleucine, shows a steady-state concentration in the vitreous body only 10% of that in plasma after intravenous injection (Reddy & Kinsey, 1963), so that an active removal of amino acid by the retina has been postulated. When the dead eye is incubated, there is a large rise in concentration of amino acids in the vitreous body, due to escape from the lens, which normally accumulates these from the aqueous humour (Bito & Salvador, 1970).

ASCORBIC ACID

The concentration of ascorbic acid in the rabbit's aqueous humour is some 18 times that in the plasma; the degree of accumulation varies with the species, being negligible in the rat and galago, but high in man, monkey, horse, guinea pig, sheep, and pig. As Kinsey (1947) showed, when the plasma level is raised, the concentration in the aqueous humour rises until a 'saturation level' is reached in the plasma, of about 3 mg/100 ml when the

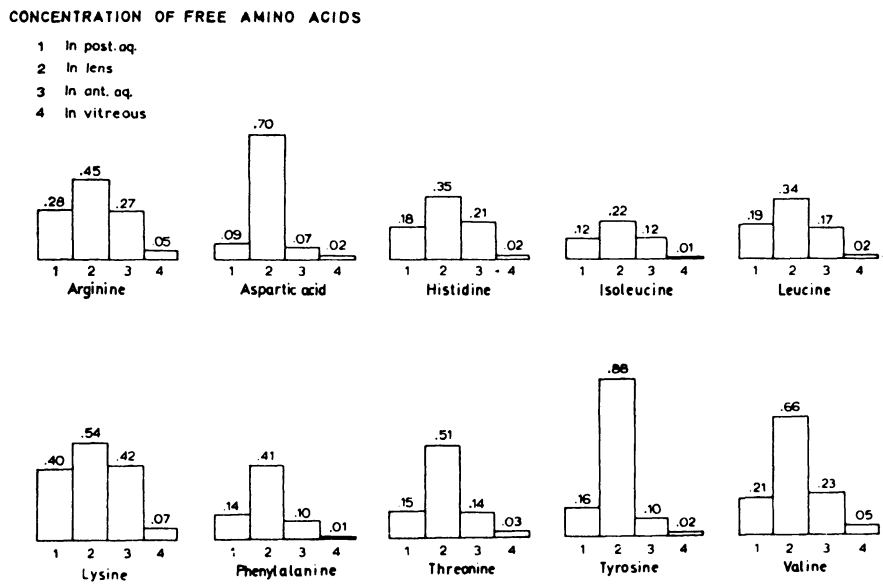

Fig. 1.23 Relative concentrations of free amino acids in lens, vitreous and aqueous humours of the rabbit eye. (After Reddy & Kinsey, *Invest. Ophthal.*)

concentration in the aqueous humour reaches some 50 mg/100 ml. Raising the plasma level beyond the saturation level causes no further rise in concentration in the aqueous humour. According to Linnér (1952) the ability of the eye to maintain this concentration of ascorbic acid depends critically on the blood-flow, so that unilateral carotid ligation causes a 17% fall in concentration on the ligatured side. Hence, under non-saturation conditions, the concentration of ascorbic acid in the aqueous humour is some measure of the rate of blood-flow through the ciliary body. When the isolated ciliary body is placed in a medium containing ascorbic acid, the tissue accumulates this to concentrations considerably higher than in the medium; D-isoascorbate competed for accumulation but glucoascorbate, containing an additional CHOH-group, had no effect (Becker, 1967). The isolated retina also accumulates ascorbic acid (Heath & Fiddick, 1966); this is true of the rat, although in this species the ocular fluids contain a very low concentration.

Significance of High Concentration In view of the great species variation in the degree of accumulation of ascorbic acid in the aqueous humour it is difficult to generalize as to its physiological role. Williams *et al.* (1984) have shown that the myeloperoxidase of polymorphonuclear leucocytes in the inflamed eye can be inhibited by ascorbic acid; thus the vitamin protects the eye from peroxides. Williams & Paterson (1987) caused inflammation by intravitreal injection of endotoxin, and found a fall in ascorbic acid level in the aqueous humour, presumably due to consumption by the leucocytes. In this connection we may note that the iris-ciliary body has catalase activity that would also help to keep the aqueous humour free of peroxides (Delamere & Williams, 1985).

Photic injury in the rat's retina may be ameliorated by ascorbic acid treatment if given before the light exposure (Li *et al.*, 1985); the vitamin probably prevents oxidation of membrane lipids of outer segments of rods (Organisciak *et al.*, 1985).

Aqueous as a Secretion

Studies along these lines have left the modern investigator in no doubt that the fluid could not have been formed by such a simple process as filtration; in consequence the aqueous humour is called a *secretion.* What is implied by this is, essentially, that in order that it should be formed from the blood plasma, something more than a mechanical filtration process that 'skims' off the proteins is necessary; the cells of the ciliary epithelium must perform work—what is called *osmotic work*—in order to produce a fluid like the aqueous humour, which is not only different from plasma but also from a filtrate of plasma or dialysate. How this happens is still a closed book; presumably the first step is the production of a plasma filtrate in the stroma of the ciliary processes; this is prevented from passing into the posterior chamber by the tightly packed cells of the ciliary epithelium. We may assume that, next, these cells abstract from this fluid the various ions and molecules that are ultimately secreted, and together with water they drive them into the posterior chamber. In making the selection, certain ions and molecules may be transferred across the cells to give higher concentrations in the secretion than in the original plasma filtrate, e.g. bicarbonate and ascorbate, whilst others are transferred at lower concentrations, e.g. calcium, urea, and so on.

Alterations of the Primary Secretion

Once formed, the composition of the fluid may well be modified by metabolic and other events taking place during its sojourn in the posterior and anterior chambers; thus the concentration of glucose could be low because the lens and cornea actually utilize it, whilst the relatively high concentrations of lactate and pyruvate could be the consequence of glycolytic activity by these structures. That this is probably true is shown by comparing the vitreous body with the aqueous humour; the vitreous body, being exposed to both lens and retina, might be expected to have an even lower concentration of glucose than that in the aqueous humour, and higher concentrations of lactate and pyruvate. In fact this is true. Moreover, if lactate and pyruvate are produced in this way, being stronger acids than carbonic acid, they will have decomposed some of the bicarbonate entering in the original secretion, so that the original concentration of bicarbonate must have been higher (and the chloride concentration lower) than that actually found, and studies of Kinsey & Reddy (1959) have shown that this is indeed true.

Species Variations

The high concentration of bicarbonate in the aqueous humour shown in Table 1.1 is not a general characteristic common to all species; thus in horse, man, cat, rabbit and guinea pig the ratios: *Concn. in Aqueous Humour/Concn. in Plasma* are 0.82, 0.93, 1.27, 1.28 and 1.35 respectively. Hence in the horse and man the concentrations of bicarbonate are *less* than what would be expected of a filtrate of plasma. Study of the chloride composition shows an inverse relationship, as we might expect, the aqueous humours with high bicarbonates having low chlorides, and *vice versa.* It would seem that the secretion of a fluid with a high concentration of bicarbonate is concerned with the buffering needs of the eye, the bicarbonate being required to neutralize the large amounts of

lactic and pyruvic acids formed by lens, retina and cornea. In animals like the rabbit and guinea pig the lens occupies a large proportion of the intraocular contents and so the buffering requirements are high; by contrast, in the horse and man the lens occupies a much smaller percentage of the contents (Davson & Luck, 1956). Wide species variations in the concentration of ascorbate in the aqueous humour are also found; thus in the horse, man, rabbit, dog, cat and rat the concentrations are about 25, 20, 25, 5, 1 and 0 mg/100 ml respectively, although the concentrations in the plasma are all of the same order, namely about 1 mg/100 ml.

THE BLOOD-AQUEOUS BARRIER

Our knowledge of the relationships between aqueous humour and plasma has been furthered by a study of the exchange of materials between the two fluids, studies of what has come to be known as the *blood-aqueous barrier*. If various substances are injected into the blood so as to establish and maintain a constant concentration in the plasma, then the rates at which the concentrations in the aqueous humour approach that of the plasma are usually very much less than occurs in such tissues of the body as skeletal muscle, liver, etc. It is because of this that we have come to speak of the 'blood-aqueous barrier', meaning that substances encounter difficulty in passing from the one fluid to the other.

Experimental Studies

Figure 1.24 illustrates the penetration of some substances into the anterior chamber of the rabbit. In general, the substances fall into three categories. First there are the very large molecules like the plasma proteins, dextrans and inulin which penetrate so slowly as to give the impression of an absolute barrier, although studies with isotopically labelled proteins leave us in no doubt that there is some, but very slow, penetration. Because the aqueous humour is constantly being drained away the concentration of these large molecules in the aqueous humour never rises very high and we may speak of a *steady-state* in which the ratio of concentrations is exceedingly low. This of course accounts for the low concentrations of plasma proteins in the aqueous humour. The second category of substance has a much smaller molecule, or may be an ion; the molecule is water-soluble, like urea, creatinine, *p*-aminohippurate, sucrose and so on. Penetration is considerably faster, usually, than that of the proteins. The third group are the lipid-soluble molecules which penetrate very rapidly; these include ethyl alcohol, various substituted thioureas, many sulphonamides. In general, the rate of penetration increases with increasing lipid-solubility, as measured by the oil-water partition coefficient. Water, although not strongly lipid-soluble, belongs to the category of rapidly penetrating substances. Again, the sugars such as glucose and galactose are insoluble in lipid solvents but they also penetrate the barrier rapidly.

Mechanism of the Barrier

We may imagine that the cells of the ciliary epithelium continually secrete a fluid, which we may call the *primary aqueous humour*, that is emptied into the posterior chamber and carried through the pupil into the anterior chamber to be finally drained away out of the eye. If a

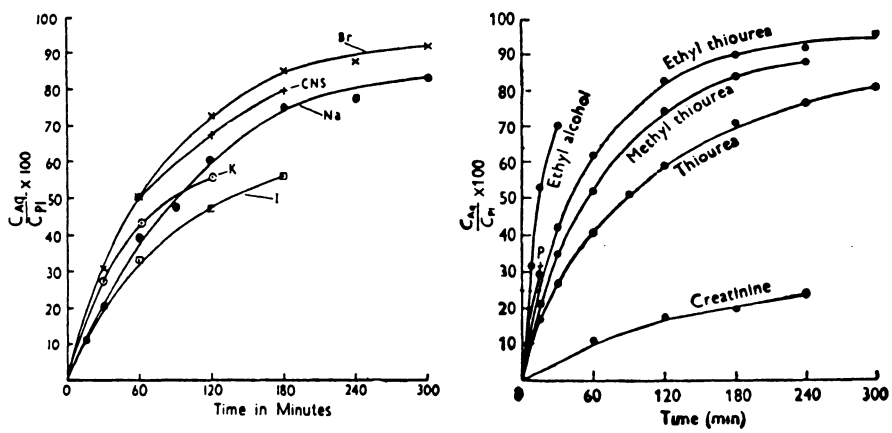

Fig. 1.24 Penetration of some non-electrolytes (*left*) and ions (*right*) into the aqueous humour of the rabbit. The concentration of the given substance in the plasma (C_{Pl}) was maintained constant, and the concentration in the aqueous humour (C_{Aq}) was determined at different times. (Davson, *Physiology of the Ocular and Cerebrospinal Fluids.*)

foreign substance, or the isotope of a normally occurring constituent of the aqueous humour, e.g. ^{24}Na, is injected into the blood it presumably equilibrates rapidly with the extracellular fluid in the ciliary processes, and thus gains ready access to the cells of the ciliary epithelium. If the substance penetrates these cells easily, then we may expect it to appear in the secretion produced by them relatively rapidly. The primary aqueous humour will therefore contain the substance in high concentration. This circumstance will favour penetration into the aqueous humour as a whole. On mixing with the fluid already present in the posterior chamber, the primary fluid will be diluted, so that it will take time for the aqueous humour as a whole to reach the concentration in the plasma, in the same way that if we were to add a coloured solution to a tank of water, removing fluid from the tank as fast as the coloured fluid was added, in time the concentration of dye in the tank would come up to that in the coloured solution, but the process would take time and be determined by the rate of flow.

Diffusion from Iris

While in the posterior and anterior chambers, however, the aqueous humour is subjected to diffusional exchanges with the blood in the iris, as illustrated in Fig. 1.25, so that if these exchanges are significant the rate at which the foreign substance comes into equilibrium with the aqueous humour is increased. There is no doubt that lipid-solubility is an important factor in determining the rapidity of these diffusional exchanges. The anterior surface of the iris is not covered by an intact epithelial or endothelial layer, so that restraint on diffusion from blood into the anterior chamber must depend on the capillaries of this tissue. That the iris offers considerable restraint to exchanges with the aqueous humour was demonstrated by Davson & Spaziani (1960), who infused artificial aqueous humour containing different solutes into the anterior chamber of the cat; under these conditions the pupil closed to a slit so that a large area of iris was exposed to the aqueous humour. If lipid-insoluble substances such as ^{24}Na, para-aminohippurate or sucrose were injected, these escaped at a rate that could be completely accounted for by bulk flow through the canal of Schlemm; even lipid-soluble substances, such as propylthiourea, did not escape much faster than sucrose.

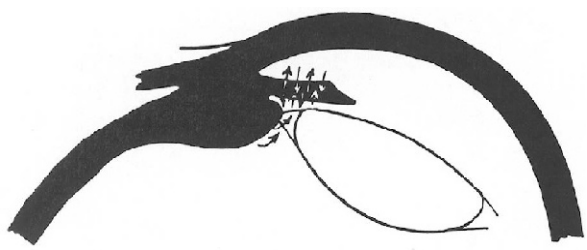

Fig. 1.25 Illustrating the diffusional exchanges between the aqueous humour in posterior and anterior chambers on the one hand and the blood plasma in the iris on the other.

Large Molecules

On the basis of this scheme, we may interpret the blood-aqueous barrier phenomena qualitatively. Thus large lipid-insoluble molecules such as the plasma proteins will probably be held back partially by the capillaries in the ciliary processes; the permeability of ciliary body capillaries to proteins is unusually high, however, (Bill, 1968b)[8] so that the main restraint will be the clefts between the unpigmented ciliary epithelial cells (p. 29). Penetration into these cells and through the clefts will be minimal, and it may be that passage across this unpigmented layer is by a process of pinocytosis or engulfment of the proteins into small vacuoles, which subsequently empty themselves into the posterior chamber (Bill, 1975). During the fluid's sojourn in the posterior and anterior chambers, additional amounts may diffuse from the iris; once again, however, the vacuolar pathway seems likely, since the capillaries of the iris are probably completely impermeable to proteins (p. 30). Because of the sluggishness of all these processes, the concentration in the aqueous humour will never build up to that pertaining in the plasma; in fact, as indicated above, the concentration-ratio never rises above about 1/200 for the plasma proteins.

Ions and Lipid-soluble Molecules

With substances such as ^{24}Na, the evidence suggests that the primary secretion contains this ion in the same concentration as in the plasma, whilst the contributions of diffusion from the iris are also significant. The overall rate of penetration into the aqueous humour is thus considerably greater than that of the proteins. With ethyl alcohol penetration is altogether more rapid because of the lipid-solubility of the molecule; this permits very rapid exchanges across the iris.

FACILITATED TRANSFER

Sugars and amino acids are relatively large and very lipid-insoluble molecules so that their penetration into the aqueous humour, which occurs relatively rapidly (Davson & Duke-Elder, 1948; Harris & Gehrsitz, 1949) is doubtless due to facilitated transport, namely the development of 'carriers' or active membrane sites that specifically react with these solutes.

Kinetic Analysis

It is not proposed to enter into a detailed mathematical analysis[9] of the process of penetration of the barrier; suffice it so say that the relation between blood, on the one hand, and aqueous humour on the other, may often be treated on the basis of a two-compartment system, the rate of equilibration being governed by a permeability constant, k. Thus

$$\text{Rate} = kA/V(C_{\text{Plasma}} - C_{\text{Aqueous}}) \qquad (1)$$

where the rate is measured by the number of molecules entering the aqueous in unit time, the C values are concentrations, A is the area of membrane exposed and V the volume of aqueous humour. A and V are not usually known, so that kA/V is combined into a transfer constant, K, with dimension t^{-1} (k has the dimensions cm sec^{-1}). If the rates inward and outward are not equal, we must use two constants, K_{In} and K_{Out}, their ratio $K_{\text{In}}/K_{\text{Out}}$ being equal to the ratio of the steady-state concentrations in the two fluids, $C_{\text{In}}/C_{\text{Out}}$. With passively diffusing substances, K_{In} and K_{Out} may be equal; however, this is not always true, because the system is not static but flowing, so that if the solute in question fails to enter the primary secretion at the same concentration as in plasma a process of 'molecular sieving' will occur leading to a steady-state concentration in the aqueous humour that may be considerably less than in the plasma. This is especially true of proteins, and probably accounts for the low concentrations of urea and amino acids in the aqueous humour compared with those in plasma. Another factor, besides passive molecular sieving, is an active transport, either directed from blood to aqueous humour, as with ascorbic acid, or in the reverse direction, as with amino acids, and para-aminohippurate.

THE BLOOD-VITREOUS OR BLOOD-RETINAL BARRIER

The passage of solutes from blood into the vitreous body has received less attention than that into the aqueous humour; as Fig. 1.26 illustrates, the system is rather more complex since solutes can diffuse from the posterior aqueous humour after crossing the blood-aqueous barrier and from the whole of the vascular system surrounding the vitreous body, i.e. the chorio-capillaris and, where this is present, the retinal circulation.

Thus the measured rate of penetration from blood into the vitreous body, which we may indicate by $k_{\text{In(v)}}$, is made up of several components. In perhaps the earliest quantitative study on the barrier Davson & Duke-Elder found the following values (min^{-1}) for aqueous humour and vitreous body:

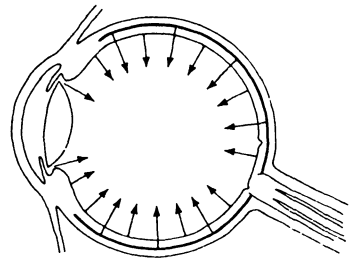

Fig. 1.26 The blood–vitreous barrier.

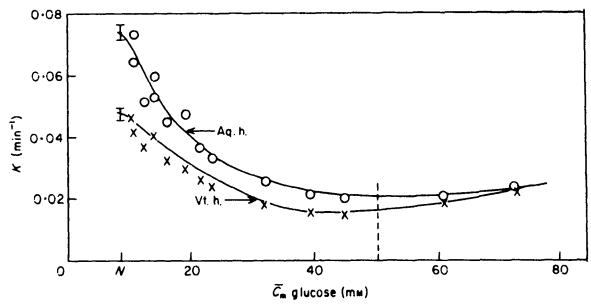

Fig. 1.27 Penetration of glucose into aqueous humour and vitreous body. Ordinates: calculated entry rate-constant. Abscissae: mean glucose concentration. (Di Mattio & Zadunaisky, *Exp. Eye Res.*)

	Aqueous humour	Vitreous body
Glucose	0.016	0.0080
Galactose	0.016	0.0069
3-Methyl glucose	0.017	0.0080
Xylose	0.017	0.0119

The generally slower rate of equilibration shown by the vitreous body could be due to a significantly higher barrier or alternatively to the different geometries of the two systems, since the area to volume ratio is highly important, and this would be unfavourable for the vitreous body. In later studies isotopically labelled sugars could be employed, when the effects of concentration on the transport-parameters could be determined. Thus Di Mattio & Zadunaisky (1981) studied penetration into aqueous humour and vitreous of rats and showed that transport of D-glucose into both fluids was carrier-mediated; D-glucose entered some six times faster than L-glucose, indicating stereospecificity of the carrier. As Fig. 1.27 shows, K for aqueous humour was greater than for vitreous body at all glucose concentrations, as found in the cat.

Fluorescein

The concentrations of fluorescein in the transparent zones of the eye, cornea, aqueous humour and vitreous

body, can be estimated with some precision with a slit-lamp fluorophotometer. The measurement of the blood-vitreal barrier by this technique has been reviewed by Ogura *et al.* (1985) who give values of 1.8×10^{-5} cm min^{-1} for inward permeability and 5.6×10^{-4} cm min^{-1} for outward permeability, a difference in inward and outward permeabilities that leads to a steady-state ratio of C_{Vitr}/C_{Plasma} of 1/31, a difference that is due to an active removal of the dye across the pigment epithelium (Cunha-Vaz & Maurice, 1967).[10]

Retinal Uptake-index

Ennis *et al.* (1982) have adapted a technique pioneered by Oldendorf for the study of the blood-brain barrier to the blood-retinal barrier; essentially the uptake by the tissue of a labelled compound, such as glucose, is compared with uptake by a reference solute that penetrates so rapidly, e.g. labelled butanol, that any variations due to changed blood-flow can be compensated. Carrier-mediated transport of glucose was confirmed and Michaelis–Menten transport constants were estimated; the K_m values were increased in streptozotocin-diabetes, a change that was viewed as an adaptation to the high blood glucose levels, so that a higher level in the blood was required to produce the same level in the tissue as that found in normal animals.

Retinal Degeneration

Rats with spontaneous retinal degeneration (RCS rats) exhibit a degeneration of visual cells and of the pigment epithelium. Di Mattio & Zadunaisky (1983) found a decreased permeability to glucose in these animals but an increased permeability to other nonelectrolytes, such as urea and sucrose. There had thus been a general breakdown of the blood-vitreous barrier reflected in an indiscriminate increase of permeability, but this was reflected in the carrier-mediated process of glucose transport being reduced, through the carriers having been inhibited in some way.

Iodate

Treatment of rabbits with iodate, which has a specific effect in damaging the cells of the pigment epithelium (Noell, 1955; Grignolo *et al.*, 1966), causes a marked decrease in electrical resistance across the retina (Noell, 1963) and an increased permeability of the blood-vitreous barrier (Davson & Hollingsworth, 1972). When the blood-brain and blood-retinal barriers were compared, Ennis & Betz (1986) found that only the blood-retinal barrier was broken down so far as penetration of sucrose was concerned. The breakdown seems to be transient due to the re-establishment of an epithelial layer (Ringvold *et al.*, 1981).

Diabetic Retinopathy

Retinal degeneration, as in diabetic retinopathy or retrolental fibroplasia, is followed by the appearance of new retinal vessels, stimulated apparently by the retinal anoxia and degeneration. This vascular proliferation is accompanied by increased permeability of the blood-retinal barrier; thus, employing an accurate quantitative technique for measuring penetration of fluorescein into the vitreous body, Lund-Andersen *et al.* (1985) found a permeability coefficient for normal human subjects of 1.1×10^{-7} cm sec^{-1}, whilst in diabetic retinopathy it was 7.1 cm sec^{-1}. Examination of the capillaries of the diabetic retina demonstrates the presence of open tight junctions (Taniguchi, 1976; Wallow & Geldner, 1980). In the case of phototoxic retinopathy in rats, the permeable capillaries are apparently the new ones that have invaded the pigment epithelium (Bellhorn *et al.*, 1980; Korte *et al.*, 1983). There are, however, early morphological evidences of pigment epithelium damage in experimental diabetes (Grimes & Laties, 1980), and in the spontaneously diabetic rat (Blair *et al.*, 1984).

Reversible Opening of Barrier

Inhalation of a high PCO_2 caused leakage of intravenously injected fluorescein into the vitreous of the rat; microscopic examination indicated that the principal mode of entry was across the pigment epithelium; the effects were reversible but were not due to changed vascular pressure (Rapoport *et al.*, 1980).

Isolated Pigment Epithelium

Pascuzzo *et al.* (1980) showed that in this preparation from the sheep, sugar tended to be transported more rapidly from choroid to retina than in the reverse direction, indicating an active transport of this metabolite from blood into retinal tissue. In the cold-blooded bull-frog, however, the transport was of the facilitated type, i.e. rapid but not requiring energy, so that it was unaffected by DNP and other metabolic inhibitors (Di Mattio & Streitman, 1986).

Amino Acids

Miller & Steinberg (1976) examined the fluxes of taurine, an amino acid that is more concentrated in the retina than any other, across the isolated frog epithelium; the outward flux, i.e. from retina to choroid, was very much greater than the inward, indicating active transport out of the retina. This somewhat surprising finding could be due to the fact that taurine is released by light stimulation, and since it is not readily metabolized, an active transport out would prevent its accumulation. The process was blocked by ouabain applied to the apical surface, so that it may well be linked with the Na^+-pump.

ACIDIC AMINO ACIDS

Glutamic and aspartic acids are probably transmitters within the retina (Chapter 11), so that their transport characteristics are of interest. Pautler & Tengerdy (1986)

studied the isolated bovine epithelium; this had a transepithelial potential of about 10 mV like that of the cold-blooded animals studied by Steinberg. Flux from retina to choroid was always some three times greater than in the reverse direction, indicating an active transport *away from the retina*; ouabain on the retina side reduced this discrepancy, indicating a dependency on Na^+-K^+-transport. The two amino acids competed with each other, indicating a common carrier mechanism.

AMINO ACID HOMEOSTASIS

In general, it appears that, although amino acids are required by the retina and must be derived from the blood, the steady-state level in the retinal extracellular fluid is maintained below that in plasma by processes of active transport. This feature has been well established in the brain-cerebrospinal fluid system, and may be regarded as the sign of homeostatic mechanisms that maintain the environment of central neurones constant and different from plasma. In the brain the same process seems to apply to glucose, the level in the cerebrospinal fluid being held well below that of the plasma by active transport mechanisms (Deane & Segal, 1985). In the retina, however, this is not true; at any rate Miller & Steinberg (1976) found no sign of asymmetrical transport of 3-*o*-methylglucose across the frog epithelium.[11]

Isolated Retinal Capillaries

It is possible by appropriate separation techniques to prepare capillaries from brain and retina homogenates; such preparations apparently retain many of their transport characteristics. Hexoses were taken up by a facilitated carrier mediated process, reminiscent of the blood-vitreous barrier; unlike transport across the pigment epithelium, however, the process seemed not to be energy dependent (Betz & Goldstein, 1980). A Na^+-dependent uptake of an amino acid analogue was observed, suggesting the ability of retinal capillaries to transport some amino acids against concentration gradients.

Bruch's Membrane

This transparent layer separating the pigment epithelium from the choriocapillaris was at one time considered to be a barrier to exchange between choroidal blood and the retina. Being acellular this is unlikely, and it may be regarded as a pair of basement membranes belonging respectively to the choroid and pigment epithelium separated by a layer of collagen which is itself divided by a thin elastic layer. Glycosaminoglycans and collagen constitute its main components; the former have been characterized by Robey & Newsome (1983) after their synthesis in organ culture. The synthesized material consisted of complexes with protein (proteoglycans) with a molecular weight of 150 000 daltons; the glycan residue, split off by papain, had a molecular weight of 44 000 daltons and consisted of 65% chondroitin and/or dermatan sulphate and 35% heparan sulphate.

ANTERIOR AND POSTERIOR CHAMBER ANALYSIS

To return to the study of the blood-aqueous barrier, it became evident when a more exact kinetic analysis was required that the penetration of a solute into the posterior and anterior chambers be measured simultaneously, largely because of the losses from the posterior chamber into the vitreous that take place when, say, we are measuring penetration of ^{22}Na from blood into the eye. The extent to which this occurs depends largely on the relative rates at which the vitreous body and aqueous humour come into equilibrium with the plasma. With lipid-soluble substances like ethyl alcohol and ethyl thiourea the discrepancy is small, and loss of material from the posterior chamber is not serious. With ^{22}Na and various other ions the losses are very significant. Figure 1.28 shows the course of penetration of ^{22}Na from plasma into anterior and posterior chambers. As we should expect, the posterior chamber tends to come into equilibrium more rapidly than the anterior chamber; the interesting feature is the crossing over of the curves, so that at the later stages the anterior chamber is ahead; this is because the posterior chamber is losing material to the vitreous body. A similar situation is found with chloride, studied with the isotope ^{36}Cl. The value of the mathematical analysis of the process of penetration is that it enables one to compute the probable character of the aqueous humour as it is primarily secreted (Kinsey & Reddy, 1959).

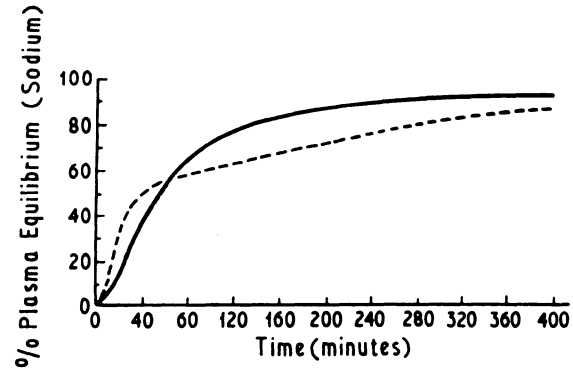

Fig. 1.28 The penetration of labelled sodium into the posterior (broken line) and anterior (full line) chambers in the rabbit. (After Kinsey & Palm, *Arch. Ophthal.*)

Posterior and Anterior Chamber Chemistry

In describing the chemistry of the aqueous humour we considered simply the fluid obtained by inserting a needle into the anterior chamber and withdrawing all the fluid; the aqueous humour so studied was a mixture of posterior and anterior fluids. When the fluids are withdrawn separately and analysed, their comparative chemistry reveals, in some measure, their different histories. Thus the bicarbonate concentration in the posterior fluid is higher than that in the anterior fluid, in the rabbit, and this is because the freshly secreted fluid has a much higher concentration than in the plasma; while in the posterior chamber, some diffuses back to the vitreous body and some is decomposed by lactic and pyruvic acids; in the anterior chamber more is decomposed by the acids formed by lens and cornea, and some diffuses back into the blood in the iris. In a similar way we can account for the circumstance that the ascorbate concentration is higher in the posterior fluid; here, the diffusion from the anterior chamber into the blood in the iris is the determining factor. With chloride the concentration is less in the posterior fluid; this is because the freshly secreted fluid has a relatively low concentration of this ion; while in the anterior chamber, chloride diffuses from the blood into the anterior fluid. Some analyses, including the vitreous body, are shown in Table 1.4.

Potassium, Magnesium and Calcium

The relative concentrations of these ions in plasma and ocular fluids have not received a great deal of attention, due, presumably, to difficulties in chemical analysis. The matter is certainly of great interest since the concentrations of these ions are very important for the functioning of the central nervous system, and they are maintained in the cerebrospinal fluid and extracellular fluid of the central nervous tissue at levels that are different from those of a plasma filtrate. Since the retina is a part of the central nervous system, and since it is exposed to the vitreous body, the concentrations of these ions in the vitreous body are of great interest; since, moreover, the vitreous body is in free communication with the aqueous humour in the posterior chamber, the concentrations in the aqueous humour are also relevant.

POTASSIUM

The situation is complicated by species variability; for example, the concentration of K^+ in the anterior aqueous humour of the dog is considerably higher than that in a plasma dialysate, whereas in the cat and rabbit it is less. Some figures from a recent paper by Bito (1970) have been collected in Table 1.5. Perhaps the most striking feature is the existence of quite large differences in concentration between the anterior and posterior halves of the vitreous

Table 1.4 Relative compositions of plasma, aqueous humours and vitreous body in the rabbit. (Reddy & Kinsey, 1960)

	Na	*Cl*	*Total CO_2*	*Ascorbate*	*Lactate*	*Glucose*
Plasma	143.0	109.0	20.6	0.04	10.3	5.7
Anterior aqueous	138.0	101.0	30.2	1.11	9.3	5.4
Posterior aqueous	136.0	96.5	37.5	1.38	9.9	5.6
Vitreous	134.0	105.0	26.0	0.46	12.0	3.0

Concentrations are expressed in millimoles per kilogramme of water.

Table 1.5 Concentrations of certain ions (mequiv/kg H_2O) in ocular fluids and plasma dialysate. (After Bito, 1970)

			Aqueous		*Vitreous*	
Species	*Ion*	*Plasma dialysate*	Ant.	Post.	Ant.	Post.
Dog	K	4.06	4.74	5.32	5.24	5.11
Cat	K	4.53	4.15	4.70	5.15	4.99
Rabbit	K	4.37	4.26	4.69	4.69	4.62
Dog	Mg	1.18	1.07	1.06	1.28	1.38
Cat	Mg	1.26	0.99	0.89	1.01	1.08
Rabbit	Mg	1.49	1.41	1.50	1.99	2.16
Dog	Ca	3.05	2.96	2.92	3.34	3.56
Cat	Ca	3.02	2.70	2.78	3.04	3.22
Rabbit	Ca	4.12	3.48	3.48	3.90	3.94

body; such differences indicate that the retina + choroid is acting as either a source or sink for the ion. Thus, in the dog, the concentration of K^+ in the posterior half is less than in the anterior half, and this is less than in the posterior aqueous humour; these gradients could be due to the retina + choroid acting as a sink for K^+, secreted by the ciliary body at a higher concentration than in a plasma filtrate. A further complicating factor is the possibility that the lens may be actively taking up K^+ at its anterior surface and releasing it at its posterior surface (Bito & Davson, 1964) and this view is supported by Kinsey's studies on transport of this ion across the lens (pump-leak hypothesis, p. 151), and the observation of Bito (1977) that, in the absence of the lens, the rabbit's vitreous has a concentration of K^+ considerably lower than in a dialysate of plasma.

MAGNESIUM

The gradients with Mg^{2+}, on the other hand, suggest that the retina plus choroid is acting as a source of this ion and this indicates that the actual concentration of Mg^{2+} immediately adjacent to the retina is even higher than in the bulk of the posterior segment of vitreous. The concentration of Mg^{2+} in the cerebrospinal fluid is likewise much higher than in a plasma dialysate (Davson, 1956) so that it seems that central nervous tissue requires a higher concentration of Mg^{2+} in its extracellular fluid than that provided by a simple filtrate of plasma.

Amino Acids

The low concentrations of amino acids in aqueous humour have been discussed earlier; the gradients of concentration between posterior aqueous and anterior vitreous, and between anterior vitreous and posterior vitreous, indicate beyond doubt that the retina is actively removing amino acids from the vitreous body; and the process has been demonstrated experimentally by Reddy *et al.* (1977a, b). These authors have shown, for example, that treatment of the sheep with iodate, which attacks the pigment epithelium specifically, actually caused the steady-state concentration of cycloleucine in the vitreous body to increase, indicating that the iodate had inhibited the active transport of the amino acid out of the eye. These authors emphasized the species variation in the steady-state distribution of amino acids in the ocular fluids; thus in the sheep the concentrations in posterior and anterior aqueous humours were always above that in the plasma, indicating an active transport inwards across the ciliary epithelium, and possibly the iris. It is possible, moreover, that the low concentrations found in many species result from the vitreous 'sink', caused by active transport across the pigment epithelium.

Water and Osmotic Exchanges

The aqueous humour and blood plasma are approximately isosmolar, with the possibility that the aqueous humour is slightly hyperosmolar. Thus exchanges of water, apart from those concerned in the formation of the fluid, are normally negligible. When the osmolarity of the blood is altered experimentally, for example by intravenous injection of a hypertonic salt solution, then there is a rapid adjustment of the osmolarity of the aqueous humour, indicating that the barrier to water is relatively slight by comparison with the barrier to salts; and this is confirmed by direct studies with labelled water. The loss of water resulting from the hypertonic injection brings about a fall in the intraocular pressure, and the effectiveness of various solutes in reducing the intraocular pressure is presumably related to the ease with which they may cross the blood-aqueous and blood-vitreous barriers. Thus, if the solute penetrates rapidly into the fluids a difference of osmotic pressure cannot be maintained for any length of time and so the loss of water will be small. For this reason sucrose or sorbitol is effective. The special effectiveness of urea, which may be used clinically to reduce intraocular pressure temporarily, is due to a relatively slow rate of penetration of the barriers, but also to the circumstance that it is not rapidly excreted by the kidneys, so that a high level may be maintained in the plasma for some time; finally, its molecular weight is low, so that from an osmotic point of view a 10% solution of urea is as effective as a 60% sucrose solution.

THE MORPHOLOGY OF THE BARRIERS

The experimental studies outlined above have revealed a restraint on the passage of many solutes from blood into aqueous humour and vitreous body; and we must now enquire into the sites of the barriers that give rise to this restraint. Thus, as indicated earlier, blood in the iris, ciliary body and choroid comes into close relations with the aqueous and vitreous humours. If relatively free and unselective exchanges are not to occur between blood and these fluids there are two possibilities; first, that a selectively permeable layer of epithelium be interposed between the stroma of the tissue and the fluids, or second, that the capillaries in the stroma be of a type similar to those found in the brain, exhibiting a high degree of selectivity and generally restraining the passage of most water-soluble compounds. In the eye, both mechanisms operate; thus the ciliary epithelium and retinal pigment epithelium separate aqueous humour and vitreous body from the stroma of the ciliary body and choroid respectively, whilst in the iris and retina the restraints to free exchanges with blood are imposed by the capillaries themselves.

Ciliary Epithelium

The blood capillaries of the ciliary body supplying the tissue immediately under the epithelium in the ciliary processes are large, like venules, and exhibit fenestrations that occupy the entire circumference of the endothelium. Capillaries with fenestrations are found to be highly permeable to all solutes, so that even plasma proteins escape into the stroma and tend to build up a high colloid osmotic pressure (Bill, 1975). Thus restraint to passage from the ciliary stroma must be determined by the ciliary epithelium, and such a restraint may be visualized by injecting into the blood a tracer that escapes from the capillaries but yet is large enough to be visualized in the electron microscope. Such a tracer is horseradish peroxidase. When Vegge (1971) injected this into the monkey he found that it rapidly filled the stroma of the ciliary body and the intercellular spaces of the pigmented layer, but was held up at the non-pigmented layer, passing along the intercellular clefts only to a restricted extent and was prevented from passing further by junctional complexes. A similar result was described by Shiose (1970) in the mouse and Uusitalo *et al.* (1973) in the rabbit.[12]

Tight Junction

When examined in thin sections in the electron microscope, the individual cells of epithelial sheets are seen to be separated from each other by a space of about 20 nm; since each cell membrane appears, at high magnification, to consist of three layers, the region of cell apposition appears as a seven-layered structure (Fig. 1.29A). At certain regions these membranes may come into much closer apposition and their constituent layers may fuse to give the tight junction, or *zonula occludens*, where the layers have been reduced to 5 (Fig. 1.29B); and it is found that electron-dense markers such as ferritin or horseradish peroxidase fail to pass through the intercellular cleft, which is therefore sealed. A membrane consisting of a layer of cells, each with its space occluded by a tight junction, would have a low permeability to solutes, and this would be manifest as a high electrical resistance.

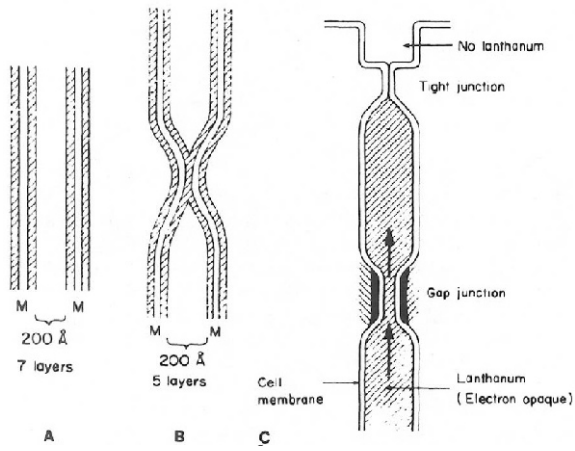

Fig. 1.29 Cell contacts. A, apposition; B, tight junction; C, tight and gap junctions in series. Cross-hatching indicates passage of La^{3+}.

Gap-junction

Another type of junction, formerly confused with and included in the category of tight junction, is the *gap-junction*; here, the outer layers of the cell membranes come into very close juxtaposition, but when a small electron-dense marker, such as lanthanum hydroxide, is employed, it is seen to pass through a narrow intercellular space of about 4 nm diameter, the outer leaflets of the cell membranes not having fused as in the tight junction (Fig. 1.29C). Thus the gap-junction constitutes a pathway for ready passage of small solutes between cells, so that an epithelium whose cells were linked by this type of junction only would be very leaky and have a low electrical resistance. Another feature of the gap-junction is that it serves to connect the two adjacent cells, so that if a dye stuff is injected into one cell the adjacent cell soon becomes coloured, due to diffusion across the gap-junction; in this way the fibres of cardiac and smooth muscle are joined, so that the tissue behaves as a syncytium.

Desmosome

A third main type of junction is the *desmosome*, or *macula adhaerens*; this serves only to hold the cells together mechanically.

JUNCTIONAL COMPLEX

In general these junctions do not occur singly but as a 'junctional complex' with the tight junction, or zonula occludens, closest to the apices of the cells.

Ciliary Junctions

Figure 1.30 illustrates the types of junction in the ciliary epithelium; it is the apices of the unpigmented cells that contain the true zonulae occludentes that act as seals restricting diffusion between the cells, so that the whole layer behaves as a single sheet of membrane-covered cytoplasm rather than a discontinuous array of cell membranes and intercellular spaces (Raviola, 1971; 1977). The gap-junctions between adjacent pigmented cells, and between pigmented and unpigmented cells, allow the tissue to behave as a syncytium, in the sense that diffusion from one cell to another is relatively unrestricted. These

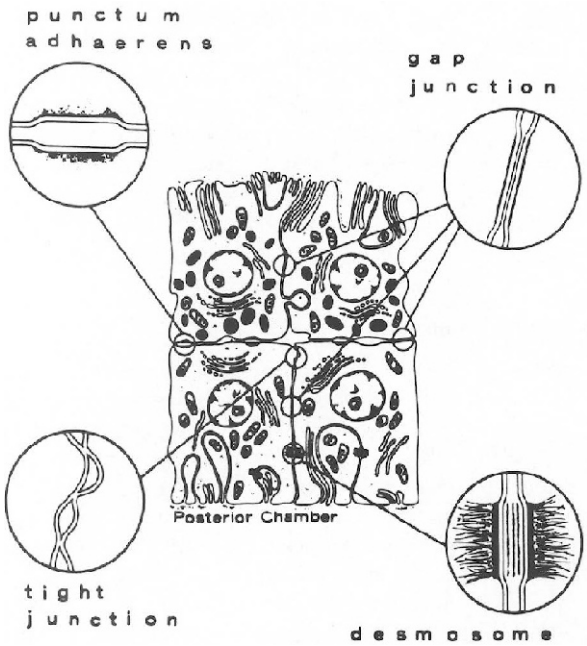

Fig. 1.30 Illustrating the intercellular junctions in the ciliary epithelium. (Raviola, *Exp. Eye Res.*)

gap-junctions have been demonstrated by Raviola (1971) and Smith & Rudt (1975) who showed that, whereas horseradish peroxidase (MW 40 000) was held up at the junctions, the smaller microperoxidase (MW 1900) did actually penetrate through the fine intercellular space at the gap-junctions between non-pigmented epithelial cells.

The Iris Barriers

As described recently by Freddo (1984), the iris of *Macaca mulatta* can be considered to be enveloped by an anterior and a posterior epithelium, the anterior epithelium being the forward continuation of the non-pigmented epithelium of the ciliary body and the posterior epithelium that of the pigmented epithelium of the ciliary body. According to whether these epithelia contain junctional complexes or not they will, or will not, act as barriers to exchange between the stroma of the iris and the aqueous humour in the anterior and posterior chambers. According to Raviola (1977) and Freddo (1984) the intercellular clefts of the posterior epithelium are sealed by tight junctions which prevent horseradish peroxidase, which diffuses from the blood vessels of the ciliary body into the stroma of the root of the iris, from passing out of the stroma into the posterior aqueous humour. Freeze-fracture showed that the occluding junctions, with 1–8 strands, were similar to those of the non-pigmented ciliary epithelium. The anterior epithelium, however, which is also called the myoepithelium since modified basal processes of the cells constitute the dilator muscle (p. 754), almost certainly does not constitute a barrier to exchanges between the iris stroma and the anterior aqueous humour. As seen in the scanning electron microscope the cells are star-shaped, and their processes interturine with those of neighbouring cells. Between the cell bodies and processes large openings are present, traversed by small bundles of connective-tissue fibres. These large holes between cells mean that there can be no barrier to free diffusion between stroma and aqueous humour (Ringvold, 1975; Raviola, 1977).

Iris Capillaries

If the anterior epithelium is highly permeable, the observed restraint to the passage of materials from the blood into the anterior chamber must be due to a restraint at the capillary endothelium, comparable with that observed in the brain (the blood-brain barrier). This is true; horseradish peroxidase (Shiose, 1971; Vegge, 1971), microperoxidase (Smith & Rudt, 1975), and the much smaller fluorescein molecule fail to escape from iris capillaries, a restricted permeability that is associated with the presence of tight junctions sealing the inter-endothelial cell clefts (Vegge, 1972a, b). Freeze-fracture analysis of the junctions by Freddo & Raviola (1982) showed that they were all tight, varying in complexity from 1–9 strands, and thus being intermediate between cerebral and striated-muscle capillaries.[13]

VESICULAR TRANSPORT

Transport of substances across a cell may be brought about by a process of endo- and exocytosis (Fig. 1.31); such a process is inefficient and usually unselective since all solutes will be uniformly engulfed at one side of the cell and ejected at the other. If, however, the cell membrane were able to attract certain specific molecules, such as immunoglobulins, to its surface, these could be selectively transported, in the sense that they would be enclosed in the membranous vesicle in preference to other large molecules without this specific binding feature. The degree to which such transport occurs across the capillary membrane is a matter of dispute (Simeonescu *et al.*, 1972; Frokjaer-Jensen, 1984). According to Raviola & Butler (1984), horseradish peroxidase, when injected into the anterior chamber, finds its way into the blood capillaries of the iris by this vesicular form of transport. When horseradish peroxidase was injected into the blood, however, there was no corresponding movement out into the stroma of the iris, suggesting a one-way type of transport which could be due to an asymmetrical distribution of reactive sites on the two sides of the capillary endothelial cell (Raviola & Butler, 1985). Thus, if horseradish peroxidase is typical of large foreign molecules, the iris may act as a scavenger for the aqueous humour, removing large unwanted molecules that, if allowed to accumulate, might reduce transparency of the ocular fluid.

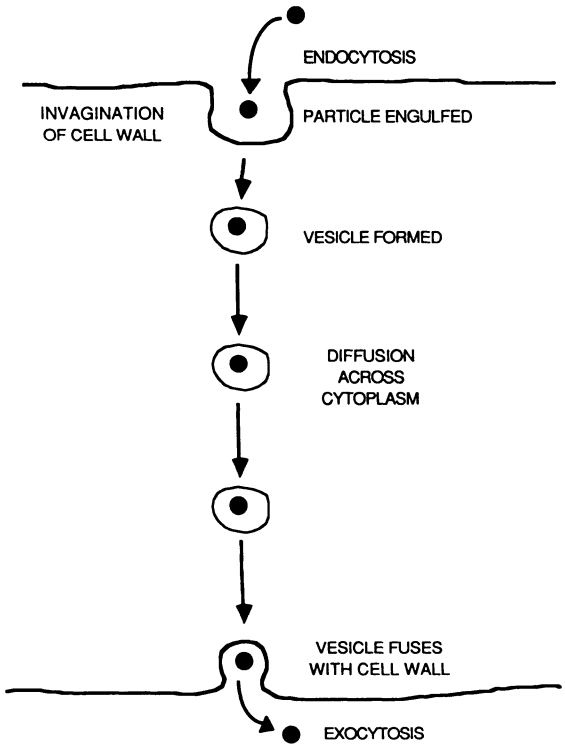

Fig. 1.31 Illustrating vesicular transport.

The Choroid and Pigment Epithelium

The choroidal capillaries are similar to those of the ciliary body, being fenestrated; and the intercellular contacts are peculiar and reminiscent of those in the liver sinusoids. Studies on passage of macromolecules from blood into the choroidal stroma indicate a high permeability (Bill, 1968b), and horseradish peroxidase passes readily into these spaces (Shiose, 1970). Thus the choroid, like the ciliary body, contains vessels that are readily permeable to the solutes of plasma, so that the observed restraint on passage of such solutes from plasma into the vitreous body must be due to the interposition of a selective membrane. Such a membrane is provided by the retinal pigment epithelium, a membrane intimately related to the layer of receptors closely apposed to it (Chapter 5). Thus, when horseradish peroxidase was injected into the vitreous body it was brought to a halt at the tight junctions between the epithelial cells (Peyman *et al.*, 1971), whilst horseradish peroxidase, injected into the blood, fails to pass beyond the stroma of the choroid, being held up at tight junctions between the pigment epithelial cells (Peyman & Bok, 1972). The junctions between pigment epithelial cells have been described by Hudspeth & Yee (1973) in the eyes of a number of species, ranging from frog to cats and monkeys; they were similar in all species, so that the frog's epithelium may be treated as typical. The junctional complex occurred about half-way down the cell, rather than at the apex, and consisted of an apical gap-junction (nearest the vitreous) and a basal desmosome or macula adhaerens, and between and overlapping these is the tight junction or zonula occludens. The presence of gap-junctions suggests electrical coupling between the cells, and this was proved by passing current through one cell and recording the electrical changes in cells at greater and greater distances away; the epithelium was clearly behaving as a syncytium.[14]

Retinal Capillaries

In those species that have a retinal circulation, in addition to the choroidal circulation, the maintenance of a blood-vitreous barrier must depend not only on a barrier between choroid and vitreous, exerted by the pigment epithelium, but also a barrier across the capillary endothelium of the retinal circulation. The retinal circulation is equivalent to the cerebral circulation, since the nervous layers of the retina are a part of the brain; in the cerebral circulation it has been demonstrated that the basis of the blood-brain barrier is the existence of tight junctions between the endothelial cells of the capillaries (Reese & Karnovsky, 1967). Shiose (1970) showed that intravenously injected horseradish peroxidase failed to pass out of retinal capillaries, in marked contrast to the capillaries of the ciliary body; the smaller microperoxidase (MW 1900 daltons) also failed to pass (Smith & Rudt, 1975).[15]

Epithelia Plus Capillaries

To conclude, then, the aqueous humour and vitreous body are insulated against free exchanges of solutes with blood by epithelial layers and, where these are lacking, by capillaries with an endothelium in which the intercellular clefts are closed by zonulae occludentes. A 'leak' in this system is probably provided by the anterior surface of the iris; solutes could diffuse out of the ciliary capillaries into the stroma of the ciliary body and from there they could diffuse to the iris root and thence into the anterior chamber. The same route in reverse is available for the uveo-scleral drainage process of Bill (p. 47).

SECRETION OF AQUEOUS HUMOUR

Active Transport

The continuous formation of a fluid that is not in thermodynamic equilibrium with the blood plasma requires the performance of work; such work is described as

active transport, and the common basis for this, whether it be the production of saliva, the secretion of gastric juices, or the reabsorption of fluid from the kidney tubule, is accomplished by the transport of one or more ions from the blood side of the system to the secreted fluid side. The osmotic gradient caused by the transport of the ion or ions leads to flow of water, and, depending on the permeability characteristics of the limiting membranes across which the transport occurs, the fluid may ultimately be isotonic, hypertonic or hypotonic. Thus the process in the eye takes place across the ciliary epithelium. In the stroma of this tissue the blood is filtered by the capillaries to produce a filtrate comparable with tissue fluid in other parts of the body; because of the high permeability of the capillaries the filtrate is by no means free from protein. The unpigmented epithelium, however, acts as a diffusional barrier to this protein and to most of the other constituents of the filtrate, so that the transport is slowed and becomes selective.

Cole's Hypothesis

The basic hypothesis, developed by Cole (1977), is that the unpigmented cells absorb selectively Na^+ from the stroma and transport it into the intercellular clefts which, as Fig. 1.32 shows, are closed at the stromal side by tight junctions but are open at the aqueous humour side; the development of hyperosmolarity in the clefts leads to osmotic flow of water from the stroma and thus to a continuous flow of fluid along the clefts. The passage of other ions may also be governed by independent active processes, e.g. Cl^-, HCO_3^-, K^+, and so on, whilst others may diffuse passively down concentration gradients established by the primary process; the same may apply to sugars and amino acids.

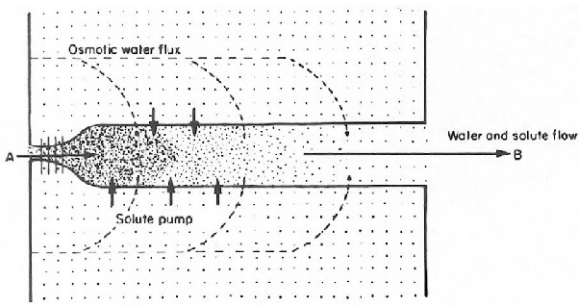

Fig. 1.32 Representation of standing gradient osmotic flow system. The system consists of a long, narrow channel, the entry to which is restricted at the left-hand end (A). The density of dots indicates the solute concentration. Solute is actively transported from the cells into the intercellular channel by a solute pump, thus making the channel-fluid hypertonic. As solute diffuses towards the open end of the channel at the right-hand side (B), water enters across the walls because of the osmotic differential. In the steady state a standing gradient will be maintained with the osmolarity decreasing from the restricted to the open end and with volume-flow directed towards the open end. In the limiting case, the emergent fluid approaches iso-osmolarity with the intracellular compartments. The arrow on the left-hand side (across the restriction) represents an element of hydraulic flow. (Cole, *Exp. Eye Res.*, modified from House, *Water Transport in Cells and Tissues.*)

Basic Considerations

Potential

Active transport of an ion is often associated with the development of a potential; thus the frog-skin, which for simplicity we may represent as a single layer of cells as in Fig. 1.33, actively transports NaCl from outside to inside even though the concentrations on both sides are maintained the same, or, if the concentration is much lower outside when the animal is in fresh water. The transport of the Na^+-ion is equivalent to an increase in its mobility in relation to the negative Cl^--ion, so that the side to which Na^+ is transported becomes positive; the difference of potential created by the separation of the ions accelerates the Cl^--ions, which are said to follow passively in the wake of the actively transported Na^+-ions; thus in a given time, because of the establishment of this potential, equal numbers of ions pass from the bulk of the outside medium to the bulk of the inside medium, and the potential is confined to the membrane. Electrodes placed in the two media will therefore register the active-transport potential, often described as a pump-potential since it results from the pumping action of metabolism on a given ion. Often the transport of Na^+ is accompanied by a transport of K^+ in the opposite direction, in which case the pump is called a Na^+-K^+-pump, the transport of Na^+ in one direction across the membrane being linked to the transport of K^+ in the reverse direction, not always in a one-for-one manner. Inhibition of the ion pump can be achieved through metabolic inhibitors, such as dinitrophenol, or by substances that exert a more specific attack

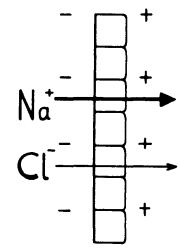

Fig. 1.33 Active transport of Na^+ across a layer of epithelium can cause a potential due to acceleration of the positive ions with respect to the passively flowing negative ions.

on the transport process such as the cardiac glycosides that inhibit an enzyme—Na^+-K^+-ATPase—that catalyses the hydrolysis of ATP whilst energizing the Na^+-K^+-pump. The effect will be to reduce, if not to inhibit entirely, the potential, but this will depend on the extent to which the measured potential is directly dependent on the ion-pump.

Short-circuit Current

Ussing & Zerahn (1951) drew attention to the importance of this current in the quantitative assessment of the active transport process. Figure 1.34 illustrates the procedure for measurement and the principle on which it is based. Ussing & Zerahn argued that, if a counter-potential was applied across the skin so as to make the potential zero, there would be no force driving Cl^- from one side of the membrane to the other if there were equal concentration on either side in the first place. The counter-potential would presumably not affect the movement of Na^+ if it was being transported as an unionized complex, so that the neutralization of the positive charges brought on to the inside of the skin by the transported Na^+ would have to be done by electrons in the external circuit. Thus the current flowing in the external circuit—*the short-circuit current*—would be equivalent to the ions carried by the active transport mechanism, *if this transport of Na^+ were the sole process generating the potential.*

This is the basis of measurements of short-circuit currents across isolated epithelia, but the interpretation becomes difficult if there is more than one active transport process, as is usually the case, so that experiments involving measurement of short-circuit current have to be supplemented by measurements of fluxes of individual ions, the effects of ion replacement in the bathing medium, and so on. The extreme situation is provided by the known existence of active transport of ions, such as Na^+, but the absence of any transepithelial potential, as with the gall-bladder. Such a system would provide no short-circuit current, but that would not mean the absence of active transport. It could mean that the pump under consideration was non-electrogenic, or that another pump, transporting an ion of opposite charge, was also electrogenic and neutralizing the effects of the first.

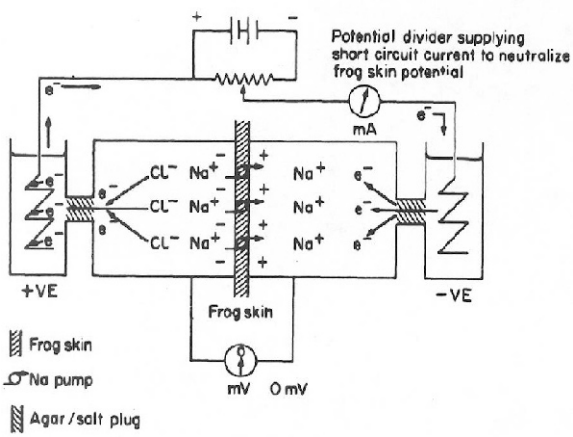

Fig. 1.34 Apparatus suitable for measuring the short-circuit current across the frog skin. The active transport of Na^+ from left to right creates a potential across the membrane due to the slower movement of Cl^--ions. If a potential is applied from a battery (top) opposing this potential, a current must flow in the external circuit such that for each ion of Na^+ transported one electron passes to neutralize it. Thus, electrons in the external circuit replace the Cl^--ions that would have moved from left to right accompanying the actively transported Na^+ ions. If, under these short-circuit conditions, the only ion being transported is Na^+, the short-circuit current is a measure of the transport of Na^+. (Davson & Segal, *Introduction to Physiology.*)

Ciliary Potential

Cole (1961) separated two fluid-filled chambers by isolated ciliary body-iris, in the typical Ussing–Zerahn apparatus, and measured a potential of some 5 mV, the aqueous humour side being positive, which he attributed to the active transport of Na^+ analogous with that across frog skin. More recent studies, however, indicate an oppositely orientated potential, the aqueous humour side being negative by 1–2 mV (Holland & Gipson, 1970; Burstein *et al.*, 1984; Krupin *et al.*, 1984; Kishida *et al.*, 1981), a potential that has been attributed to the predominance of an anion-transport system directed into the aqueous humour. Thus Kishida *et al.* (1981) found that the potential depended entirely on the presence of bicarbonate in the medium[16]; removal of Cl^- reversed the polarity, doubtless bringing into prominence the effect of a Na^+-pump. Thus Krupin *et al.* (1984) found that bicarbonate, K^+ and Na^+ were essential for the maintenance of the potential, suggesting a dependence on both cation and anion pumps; addition of ouabain to the aqueous humour side of the chamber, thereby blocking the Na^+-K^+-pump, and reducing the positivity it was creating, increased the negative potential across the epithelium.

Short-circuit Current

In view of the complexity of the system, involving as it does both anion and cation pumps, the short-circuit current provides little positive information. Holland & Gipson (1970) found that the net chloride-flux across the short-circuited epithelium was greater than the short-circuit current, indicating the involvement of positive ions in the active process. Again, Krupin *et al.* (1984) found that ouabain affected the potential when applied to either

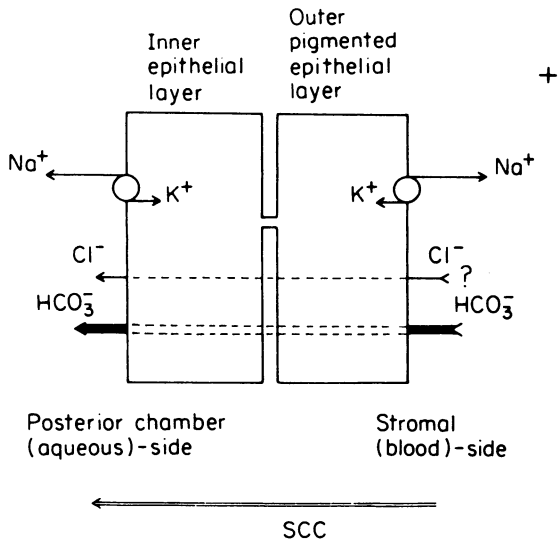

Fig. 1.35 Proposed model of rabbit ciliary epithelial transport system. (Krupin *et al.*, *Exp. Eye Res.*)

side of the epithelium, and suggested the presence of Na^+-K^+-pumps at both pigmented and non-pigmented epithelia, working against each other; the dominant, fluid-driving process would be the anion-pump driving salt into the aqueous humour (Fig. 1.35).

Transport of Na^+

Cole (1960) in the rabbit eye, blocked the escape route from the anterior chamber by inserting silicone oil into the angle, and perfused the anterior and posterior chambers through suitably placed cannulae with an isotonic mannitol solution, creating gradients of all the ions between plasma and the perfusing fluid. Na^+, K^+, and Ca^{2+} entering the fluid were estimated chemically. When a steady state was established, most of the ions entering the fluid were derived from the newly secreted aqueous humour, together with additional quantities derived from diffusion from the iris, cornea, etc. Treatment of the animal with DNP reduced the Na^+-influx by about a half, suggesting that about half the influx was due to the active secretory process. In general, Cole's studies suggested that a passive influx of Na^+, possibly by a process of filtration from the stroma across the tight junctions sealing the clefts, contributed perhaps a third of the total flow, the remainder being dependent on active transport inhibitable by DNP. However, it must be emphasized that the conditions were grossly abnormal; as we shall see, the mere presence of hypodermic needles in the anterior chamber can cause a breakdown of the blood-aqueous barrier leading to influx of material that would have been held back in the normal situation.

ATPase

The inhibition of active transport of Na^+ by the cardiac glycosides is related to the inhibition of an enzyme that catalyses the hydrolysis of ATP to ADP and phosphate; the enzyme is specifically activated by Na^+- and K^+-ions as well as Mg^{2+}, and its presence on cell membranes concerned with active transport has been visualized in the light- and electron-microscope. The localization of ATPase in the ciliary epithelium is illustrated by Fig. 1.36 where it is seen to be associated with the membranes of the unpigmented cells. Cole found that strophanthin G reduced influx of Na^+ into the anterior chamber by some 50%. Figure 1.37 illustrates the results of a study where blood-aqueous potential, aqueous humour formation, Na^+-influx and plasma sodium concentration are shown before, during, and after treatment with ouabain, another cardiac glycoside. When ouabain was injected into the vitreous humour, there was a fall in intraocular pressure, due presumably to lowered rate of secretion of aqueous humour; and the time courses of the two processes ran parallel to each other (Bonting & Becker, 1964).

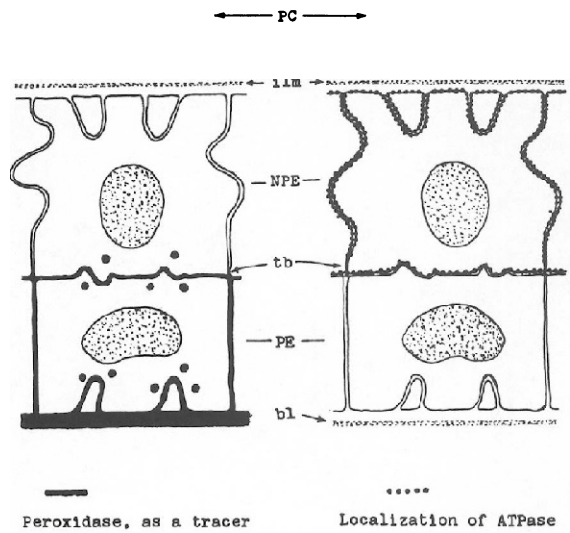

Fig. 1.36 Localization of ATPase at cell borders of the ciliary epithelium. (Shiose, *Jap. J. Ophthal.*)

Anion Transport

The inhibition of Na^+-transport by cardiac glycosides, with its concomitant reduction in the production of aqueous humour, suggest that the prime factor in secretion of fluid is this active Na^+-transport. The action of the carbonic anhydrase inhibitor, acetazolamide (Diamox), brings into prominence the importance of controlled anion transport.[17] This drug, when given systemically, lowers the intraocular pressure through a reduction in rate of secretion of aqueous humour by some 40–50%

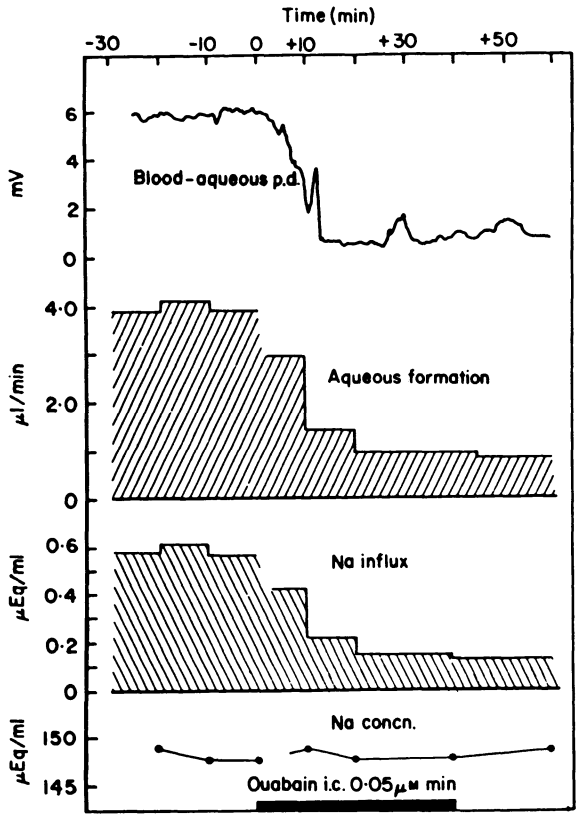

Fig. 1.37 Effects of close arterial injection of ouabain on several parameters of aqueous humour dynamics. (Cole, *Exp. Eye Res.*)

(Becker & Constant, 1955; Garg & Oppelt, 1970). According to Maren (e.g. 1977), this arises from an inhibition of the synthesis of bicarbonate by the ciliary epithelium which reduces the amount of available anion. This is not necessarily true, however, and it may be that chloride and bicarbonate are transported by anion-pumps, pumps that might easily be inhibited by the same class of substances that inhibit carbonic anhydrase. The presence of these anion-pumps is suggested by the flux and potential studies already described. This view is supported by Cousin *et al.* (1975) who have shown that sulphonamides inhibit the passive Cl^-–HCO_3^- exchange across the erythrocyte membrane; similarly Nellans *et al.* (1975) have concluded that acetazolamide inhibits a coupled Na^+–Cl^- transport across the ileum quite independently of any action on carbonic anhydrase. We may note, too, that Cl^--transport across the cornea is depressed by carbonic anhydrase inhibitors, yet there is no carbonic anhydrase in this tissue (Kitahara *et al.*, 1967).

Electrically Silent Fluxes

We have indicated that active transport of, say, Na^+, need not necessarily be associated with a potential; thus an active Cl^- transport in the same direction might well leave the system non-electrogenic, or electrically silent. Chu & Candia (1987) noted that the fluxes of Na^+ and Cl^- across the isolated iris-ciliary body preparation were greater than might have been predicted from the electrical conductance across the tissues, and they attributed this to an active transport of Cl^- in addition to Na^+.

Ultrafiltration

The tissue of the ciliary body, like other tissues, contains an extracellular fluid formed by filtration from the blood capillaries; some of this fluid might pass passively across the ciliary epithelium into the anterior chamber, bypassing the various ionic pumps presumed to act as the primary agents in producing fluid. The extent of this passive ultrafiltration will depend on the relative pressures in the stroma and anterior chamber, and on the resistance offered by the ciliary epithelium to the flow of salts and fluid across it. Evidence for some degree of ultrafiltration was provided by the study of the passage of large water-soluble molecules from blood to anterior chamber (Davson, 1953), and more decisively by Bill & Bárány (1966) who showed that a rise in pressure in the eye, artificially produced, caused a reduction in the computed rate of secretion of aqueous humour of the rabbit. This has been confirmed in the monkey by Bill (1968a) who caused a hypertension by intracameral injection of erythrocytes; the suppression corresponded to 0.06 $\mu l\,min^{-1}\,mmHg^{-1}$; thus, with a normal flow of 1.24 $\mu l\,min^{-1}$, this means that a rise of some 20 mmHg would suppress aqueous humour formation altogether. This would be only apparent, however, and Bill's observation simply indicates that, when pressure in the eye reaches a critical level, the influx by secretion is just balanced by an extra pressure-created outflux through the site of ultrafiltration.

Site of Ultrafiltration

The contribution of the iris to fluid-flow into the anterior chamber seems small or negligible (Bill, 1974), and this is attributable to the special character of the blood capillaries of this tissue which they share with the capillaries of the brain and retina, i.e. their very low permeability to ions and water. Thus we may assume that the "leaks" in the system that permit this pressure-induced flow are in the ciliary epithelium. It was considered that this epithelium belonged to the 'leaky' class, with a low electrical resistance (60 ohm cm^{-2}, according to Cole, 1966) and a

high hydraulic conductivity in the sense that flow of fluid across the epithelium under a hydrostatic difference of pressure is relatively unrestricted (Green & Pederson, 1972). On this basis Green & Pederson calculated that some 70% of the total formation of aqueous humour would be accounted for by a passive filtration due to the difference in pressure across the ciliary epithelium. Such a large fraction is quite incompatible with the observed effects of inhibitors on formation of aqueous humour, so that a value of less than 20% would be more reasonable. Brodwall & Fischbarg (1982) showed that the high hydraulic conductivities obtained by Green & Pederson were due to faulty clamping of their preparation; with a better clamped preparation Brodwall & Fischbarg obtained values of 210 μm/sec with the pressure exerted on the stromal side, and 109 μm/sec with the pressure exerted on the aqueous side, very much smaller and consistent with only a small amount of filtration under physiological conditions. In a similar way Burstein *et al.* (1984) reinvestigated the electrical resistance of the epithelium and found a value of some 1500 ohm cm^{-2}, very much greater than earlier estimates, and bringing the ciliary epithelium into the class of 'tight' epithelia, comparable with frog skin.[18]

ELECTRICAL CHARACTERISTICS OF RETINAL PIGMENT EPITHELIUM

The interest in these characteristics is not purely academic since they determine the power of the epithelium to control the microenvironment of the receptors (p. 230). They have been studied in most detail by Steinberg & Miller[19] in the bull-frog isolated tissue. As with the ciliary epithelium there is a potential difference across the epithelium, the apical or retinal side being positive to the basal or choroidal side. The characteristics of the short-circuit current, and measured fluxes of ions indicate a primary active transport of Cl^- into the choroidal stroma which may be blocked by acetazolamide, furosemide, ethacrynic acid and by reducing the bicarbonate in the medium. By mounting the epithelium on a porous filter and enclosing the system in a plastic chamber, Miller *et al.* (1982) demonstrated a net flow of fluid from retina to choroid, which was blocked by metabolic poisons. Ouabain did not affect this significantly so that the driving force was not active transport of Na^+, but presumably of Cl^- and HCO_3^-. Cyclic AMP decreased flow, suggesting the possibility of beta-adrenergic control. Clinically such a flow is of interest since disturbance of this could lead to accumulation of fluid in the subretinal space and thus to detachment of the retina.

Electrogenic Sodium Pump

Ouabain, the ATPase inhibitor and inhibitor of active sodium transport, reduces the potential across the pigment epithelium only if applied to the apical or retinal surface, suggesting the location of an electrogenic pump involved in active transport of Na^+ in the direction of choroid to retina (Fig. 1.38), confirmed by the measurement of a net flux of this ion in this direction (Miller & Steinberg, 1977). The potential was abolished by metabolic poisons or by cooling, and was highly sensitive to the concentration of K^+ in the medium (Oakley *et al.*, 1978) and thus must play an important role during the response of the receptors to light, since this is accompanied by changes of K^+-concentration in the medium (Chapter 10). Measurements of potassium transport (Miller & Steinberg, 1982) indicate an active transport in the direction retina to choroid, as would be expected of a Na^+-K^+-linked active transport process. According to Ostwald & Steinberg (1980), ATPase activity is highest on the apical side of the epithelial cell.

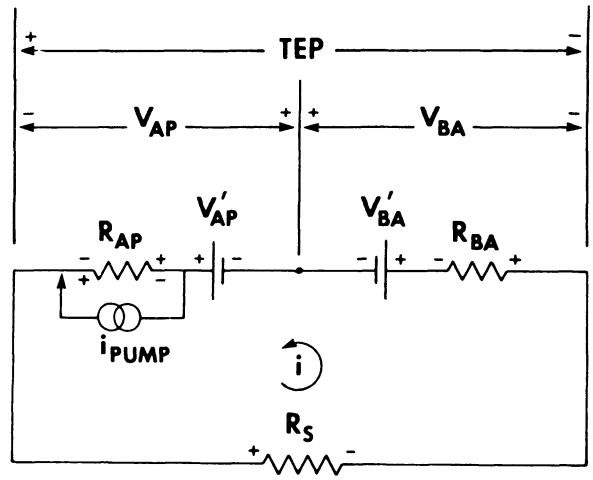

Fig. 1.38 Equivalent circuit for the retinal pigment epithelium. The apical membrane is represented by a resistor (R_{AP}) in series with a battery (V'_{AP}). Similarly, the basal membrane is represented by a resistor (R_{BA}) in series with a battery (V'_{BA}). The membrane resistances are shunted by a resistor (R_S) as described in the text. Because of the difference between V'_{AP} and V'_{BA}, a steady current (i) flows through the circuit in the counter-clockwise direction. The electrogenic pump on the apical membrane is modelled as a current source which produces a constant current (i_{pump}). As a result of current flow across the apical and basal membrane resistances, the potentials recorded across them (V_{AP} and V_{BA}, respectively) differ from the batteries (V'_{AP} and V'_{BA}, respectively). The steady potential across the tissue is called the transepithelial potential (TEP). The potentials V_{AP}, V_{BA}, and TEP are labelled with the polarity with which they were recorded. (Miller *et al.*, *J. Membrane Biol.*)

Model

Di Mattio *et al.* (1983) have represented the ionic processes in the pigment epithelium by the model of Fig. 1.39. The electrogenic ATPase-catalysed Na^+-K^+ pump tends to reduce the concentration of K^+ in the retinal fluid and is primarily responsible for the potential, with retinal positivity. Na^+-HCO_3^- and Na^+-Cl^- cotransport processes probably do not contribute to the potential but determine the flow of fluid from retina to choroid, a process inhibited by inhibitors of anion-pumps such as SITS, furosemide, acetazolamide, etc.

This model is consistent with the exhaustive studies of Miller & Farber (1984) and Hughes *et al.* (1984) on the effects of cAMP on fluid flow and electrical potential across the epithelium. Thus transport of fluid out of the retina depends on an anion-pump, whilst the concentration of K^+ in the retinal fluid is governed by the apical Na^+-K^+-pump. cAMP accelerates this latter pump, and in so doing tends to inhibit the anion-pump and thus reduces flow of fluid out of the retina.

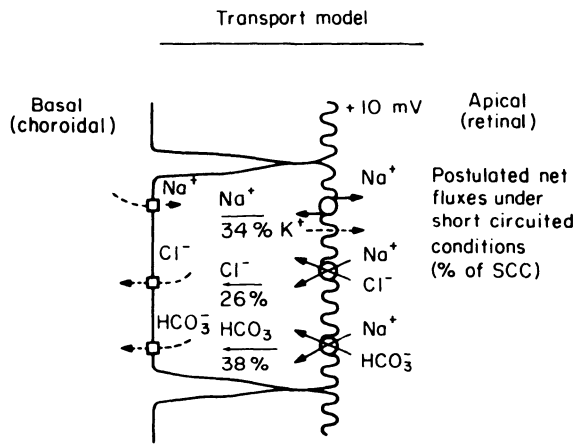

Fig. 1.39 Model of ion transport across the retinal pigment epithelium compatible with the study of Di Mattio *et al.* The small fluxes of Ca^{2+} and K^+, described by Steinberg & Miller (1973), are not included in the scheme. (Di Mattio *et al.*, *Exp. Eye Res.*)

Control of K^+-Concentration

LaCour *et al.* (1986) have described a dependence of transport of K^+ into and out of the subretinal space on the actual K^+-concentration in the subretinal fluid; thus the permeability of the retinal side of the pigment epithelium increased when the subretinal fluid concentration was reduced, and vice versa. This dependence of permeability on the ion whose concentration must be controlled provides an automatic control mechanism that cooperates with the Na^+-K^+-pump located at the retinal (apical) face of the pigment epithelium cell.

Absorption of Subretinal Fluid

Frambach & Marmor (1982), Negi & Marmor (1983) and Marmor *et al.* (1986) have made artificial retinal detachments in cats and rabbits by injecting small quantities of fluid into the subretinal space, and measured absorption-time by optical measurements of the bleb-size. Reabsorption is slowed by metabolic inhibitors, retinal hypoxia, and the substitution of the saline fluid by one made up of sucrose; thus active transport of salt is clearly the operative factor. The colloid osmotic pressure of the medium is also important so that blebs of serum were absorbed more slowly. With diffuse damage to the pigment epithelium by iodate, absorption was accelerated, presumably because of the low resistance to flow of water and salts, the driving force being now the colloid osmotic pressure difference; thus iodate did not change the rate of absorption of serum blebs, since colloid osmotic resorption was negligible.

ACTIVE TRANSPORT OUT OF THE EYE

Forbes & Becker (1960) showed that if Diodrast was injected into the vitreous body it disappeared from this into the blood but did not appear in the aqueous humour, being apparently actively removed by the ciliary epithelium and other posterior structures. *In vitro* studies on the isolated ciliary body showed that the tissue did, indeed, accumulate Diodrast and also iodide. Fluorescein was also accumulated (Stone & Wilson, 1982).

Analogy with Kidney and Liver

p-Aminohippurate is also accumulated by the ciliary body, so that there is a strong analogy with the kidney tubule. In addition to this 'kidney-type' process, there is a 'liver-type' that actively removes compounds like iodipamide, a substance typically used to measure excretion into the bile (Bárány, 1972).

Prostaglandin Transport

The physiological significance of this type of transport is revealed by Bito's studies on prostaglandins which are accumulated *in vitro* by the ciliary body (Bito, 1972). Again, when a mixture of labelled sucrose and prostaglandin was injected into the rabbit's vitreous body, only the labelled sucrose appeared in the anterior aqueous humour (Fig. 1.40), indicating that the prostaglandin was removed directly into the blood rather than through the usual drainage route. If the mixture was injected into the anterior chamber both substances disappeared at the

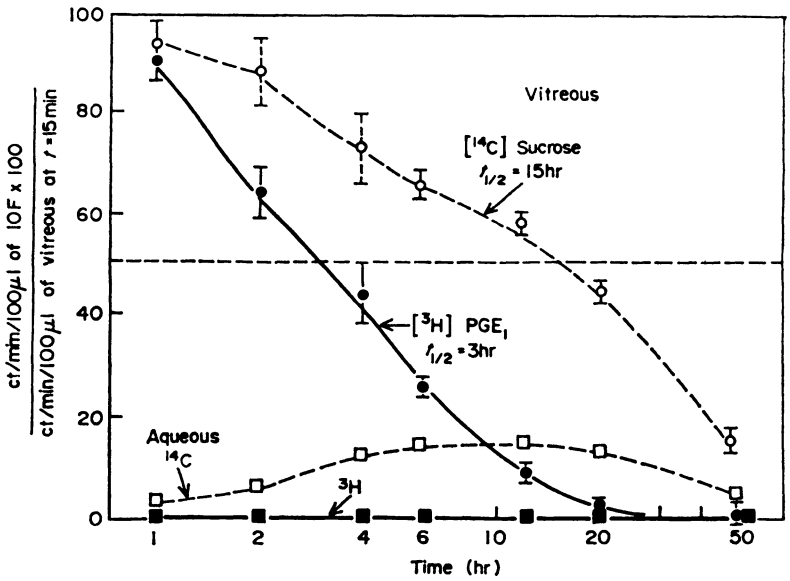

Fig. 1.40 Appearance of only ^{14}C-sucrose in aqueous humour (lower curve) after intravitreal injection of this and ^{3}H-PGE_1 and disappearance of both from vitreous (upper curves). (Bito & Salvador, *Exp. Eye Res.*)

same rate, showing that the iris is not responsible for active removal (Bito & Salvador, 1972). Bito suggested that the excretory mechanism, manifest in the active transport of *p*-aminohippurate, etc., from the eye was developed in association with a need to eliminate prostaglandins after their synthesis and liberation in the ocular tissues. Thus the eye is unlike lung in that it has a very low power of inactivation of prostaglandins, so that any removal of liberated prostaglandin would have to be achieved by the ordinary bulk flow mechanism unless supplemented by this active secretory process. That the secretory process uses the same mechanism as that involved in elimination of *p*-aminohippurate is indicated by the fact that probenecid inhibits the process (Bito & Wallenstein, 1977).[20]

SOME FACTORS AFFECTING RATE OF SECRETION

We have already seen that inhibitors of Na^+-K^+-ATPase, such as cardiac glycosides, inhibit rate of secretion of aqueous humour; the same is true of inhibitors of carbonic anhydrase, whose effects may be primarily on an anion-pump, although the interference with synthesis of bicarbonate may contribute.

Local Action of Carbonic Anhydrase Inhibitors

It was early noted that local application of acetazolamide to the eye failed to reduce rate of secretion of aqueous humour. This failure was attributed hypothetically to various causes, but the most likely was the slow penetration of the drug through the cornea, so that the concentration at the ciliary epithelium never reached the value necessary for 99% inhibition of the enzyme necessary for the effect to be observed. Maren *et al.* (1983) tested various analogues of acetazolamide, aiming at increasing lipid-solubility and lowering pK_a, two factors that would increase permeability through the membranes of the cornea. They found that bromacetazolamide with a pK_a of 6 and an ether:water partition coefficient of 25, was effective when applied locally (corresponding parameters for acetazolamide were pK_a of 7.4, and partition coefficient of 0.14). Similarly Bar-Elan *et al.* (1984) found that local application of trifluoromethazolamide reduced rate of secretion by some 31–42%, and this was accompanied by a lower intraocular pressure lasting for several hours.

Vanadate

When vanadium is in its pentavalent state, e.g. as Na_3VO_4, it is carried into the cell, probably on a phosphate-type of anion-carrier; at the cytoplasmic surface of the cell membrane it inhibits Na^+-K^+-ATPase, and thus the active transport of Na^+ and K^+ (Cantley *et al.*, 1978). A 0.5% solution applied topically to the monkey's eye lowers its intraocular pressure, presumably through inhibition of aqueous humour secretion (Becker, 1980). However, Mittag *et al.* (1984), whilst confirming the fall in intraocular pressure in the rabbit, and a reduction in rate of aqueous secretion of 33% in the monkey (Podos *et al.*, 1984), found no influence on Na^+-K^+-ATPase in the iris and ciliary body. Moreover, the accumulation of

^{48}V-labelled vanadate in the tissue, under the same conditions, was quite inadequate to have caused any inhibition of the enzyme. Thus the view that endogenous vanadate (it may be extracted from the brain; Fishman, 1979), might be a natural modulator of ATPase, i.e. might be an 'endogenous cardiac glycoside', is unsound. It is best described as a non-specific modifier of ATP-consuming enzymes, but also affecting other enzymes not involved in ATP splitting (Erdmann *et al.*, 1984), so that a simple interpretation of its action, e.g. on the eye, is difficult. Moreover, when vanadate is reduced to the 4-valency state, as occurs *in vivo*, its actions become different, so that it actually enhances the Na^+-pump due to an insulin-like stimulation.[21]

INTRAOCULAR PRESSURE

Secretion and Drainage of Aqueous Humour

Many of the effects of drugs, such as acetazolamide or vanadate, are revealed as changes in the intraocular pressure. This pressure represents a balance between the rate of secretion of aqueous humour into the posterior chamber, and the resistance to drainage from the anterior chamber. We may postpone further discussion of the action of drugs until we have described, in detail, the measurement of the rate of secretion of aqueous humour, the factors determining resistance to drainage, and the actual measurement of the intraocular pressure.

Rate of Flow of Aqueous Humour

The measurement of the rate of production (or drainage) of aqueous humour is of great interest for the study of the physiology and pathology of the eye, but unfortunately the measurement is not easy. Thus, simply placing a needle in the eye and collecting the fluid dropping out would cause a breakdown of the barrier, and the rate of production of the plasmoid aqueous humour would not be a measure of the normal rate of production. In consequence, essentially indirect methods, largely based on studies of the kinetics of penetration and escape of substances into and out of the eye, have been employed. In general, the principle on which most are based is the introduction of some material into the aqueous humour and to measure its rate of disappearance from the anterior chamber. The substance is chosen such that the rate of escape by simple diffusion into the blood stream, across the iris, is negligible by comparison with the escape in the bulk-flow of fluid through Schlemm's canal, for example, ^{131}I-labelled serum albumin, ^{14}C-labelled sucrose or inulin, and so on.

Introduction of Marker

The main experimental difficulty is the introduction of the marker into the aqueous humour without disturbing the blood-aqueous barrier; and this is extremely difficult. Thus the insertion of a hypodermic needle into the anterior chamber, however carefully executed, induces a disturbance of the blood-aqueous barrier, usually manifest by the appearance of protein in the fluid. Thus a common technique is that of anterior chamber perfusion through two needles passed through the cornea; the perfused fluid contains a 'marker', i.e. a large molecular weight substance, such as inulin, and the change in concentration of this marker, by dilution with newly secreted aqueous humour, gives a measure of the rate of secretion (see, e.g., Sperber & Bill, 1984). Jones & Maurice (1966) avoided mechanical intervention by introducing a fluorescent dye into the cornea by iontophoresis, and subsequently measuring the concentrations in cornea and aqueous humour over a period of time, making use of a fluorophotomoter.[22] Analysis of the curves gave an estimate of some 2.48 μl min^{-1} for the rabbit, corresponding to a turnover rate of some 0.0153 min^{-1}, i.e. a renewal rate of some 1.5% per minute. Johnson & Maurice (1984) improved on the technique by injecting the fluorescent dye into the vitreous body; this is a relatively innocuous method, causing no apparent interference with the normal eye physiology. With a fluorophotometer, concentrations in vitreous and aqueous were measured and the rate of secretion of aqueous humour determined. Since the fluorescein remains for weeks in the vitreous, the technique permits repeated measurements of flow-rate; in this way they confirmed the existence of a diurnal rhythm in flow-rate.[23]

Tonography

So far as measurement of rate of formation or drainage of aqueous humour is concerned, the technique of tonography, developed originally to study the resistance to drainage of aqueous humour, can be applied. Thus we may start with the equation:

$$f_o = C(P_{oc} - P_{ev}) \qquad (2)$$

where f_o is the normal rate of flow at a measured intraocular pressure, P_{oc}, and an episcleral venous pressure, P_{ev}, C being an inverse measure of the resistance to flow along the drainage route, and called the *facility*. Essentially this is an application of Poiseuille's Law of fluid-flow. Facility has the dimensions of a flow conductivity (e.g. μl min^{-1} mmHg^{-1}). To measure C, the pressure in the eye is raised by application of a weight, and the time-course of the readjustment of this pressure brought about by an extra flow of fluid out of the eye is recorded

by a suitable pressure-measuring device. Thus, as originally developed by Grant (1950), a tonometer was employed (p. 49) a device suitable for application of human studies. In animal experiments it is usual to insert a cannula into the anterior chamber and measure the steady-state pressure for given rates of flow, or alternatively, to establish different pressures and record the steady rates of flow.[24]

The average value of C found by Grant (1950; 1958) for human subjects was 0.24 $\mu l\,min^{-1}\,mmHg^{-1}$; with an average intraocular pressure of 16.4 mmHg (e.g. Weekers & Prijot, 1952) and episcleral venous pressure of 9 mmHg, we may compute a rate of flow of 1.8 $\mu l\,min^{-1}$. In the rabbit Kornbluth & Linner (1955), also using tonography, found a rate of 4 $\mu l\,min^{-1}$ or about 1.3% of the total volume per minute. Using the technique of eye cannulation, Bill & Bárány (1966) obtained a value of 1.5 to 2.0 $\mu l\,min^{-1}$ for the cynomolgus monkey.

TURNOVER RATE

The volume of aqueous humour in the eye varies enormously amongst mammalian species, from about 7 ml in the horse to less than 0.1 ml in the rat, so that we may expect the rates of formation to vary, since the most likely feature of secretion is the *rate of turnover*, expressed as fraction of the total volume in unit time. When expressed in this way, the rates are fairly uniform at about 1.5% per min (Cole, 1984).

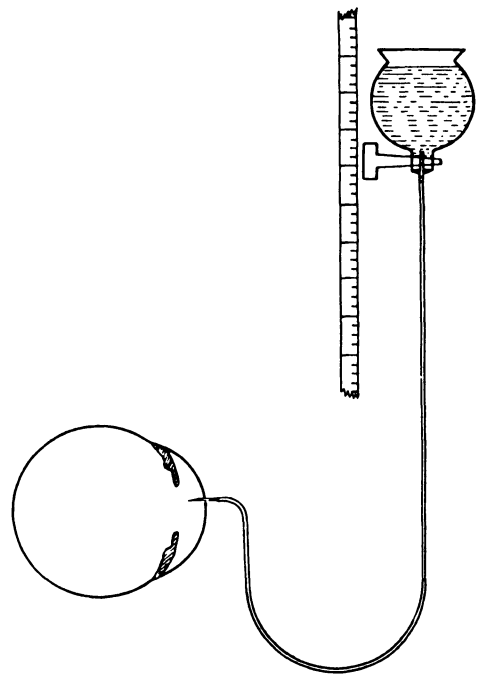

Fig. 1.41 Illustrating Seidel's apparatus.

THE DRAINAGE OF AQUEOUS HUMOUR

Experimental Study

In 1921 Seidel established beyond reasonable doubt that the aqueous humour was continually formed and drained away. He inserted a needle, connected to a reservoir containing a solution of a dye, into the anterior chamber of a rabbit (Fig. 1.41). By lowering the reservoir below the intraocular pressure a little aqueous humour was drawn into the needle and then, when the reservoir was raised, this fluid, mixed with dye, was returned to the anterior chamber. Soon the dye mixed with the rest of the fluid. Seidel observed that the dye stained the blood vessels in the surface of the globe—episcleral vessels—indicating that aqueous humour was being carried into the venous system. This passage out would only occur, however, if the pressure in the eye, determined by the height of the reservoir, was at or above 15 mmHg; when the pressure was reduced below this it was presumed that drainage of aqueous humour ceased. Since the pressure within the eye is normally above 15 mmHg, we may conclude that fluid is being continuously lost to the blood; moreover, the loss presumably depends on the existence of a pressure-gradient between the aqueous humour and the venous system. Since the episcleral vessels are derived from the anterior ciliary system, we may conclude that the dye was not being absorbed from the iris, the venous return from which is by way of the vortex veins which were uncoloured in these experiments. More recent studies, in which isotope-labelled material is introduced into the aqueous humour and the venous blood collected from both ciliary and vortex veins, have confirmed that at least 99% of drainage is by the anterior route (Bill, 1962).

Aqueous Veins

Confirmation of Seidel's view was provided in a striking manner by Ascher in 1942; when examining the superficial vessels of the globe with the slit-lamp microscope, he observed what appeared to be empty veins but they turned out to be full of aqueous humour, and he called them *aqueous veins*. Usually one of these veins could be followed till it joined a blood vessel, in which event the contents of the two vessels, aqueous humour and blood, did not mix immediately but often ran in parallel streams forming a *laminated* aqueous vein, as illustrated schematically in Fig. 1.42. These superficial vessels, full of aqueous humour, are probably derived from the deeper vessels of the intrascleral plexus, the pressure-relationships in the collectors from Schlemm's canal being such as to favour

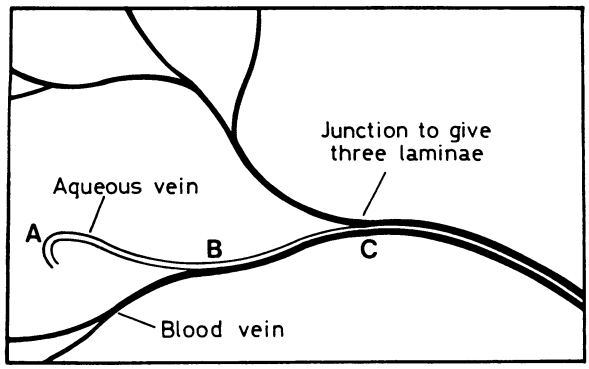

Fig. 1.42 Aqueous veins. The aqueous vein emerges from the deeper tissue and is visible at A. At B it joins a blood-vein so that the latter has two strata. At C the stratified vessel joins another vein to give three laminae. (Ascher, *Amer. J. Ophthal.*)

Fig. 1.43 Ascher's view of the origin of an aqueous vein.

displacement of blood throughout the course of the fluid to the surface of the globe as illustrated by Fig. 1.43.

Fluorescein

Goldmann (1946) proved conclusively that these vessels contained aqueous humour by injecting fluorescein intravenously. This substance passes very slowly from blood into aqueous humour so that one would not expect any vessel containing aqueous humour to fluoresce immediately after the injection, whilst vessels full of blood or plasma should do so; in fact only the blood vessels did fluoresce.

Connections

Later, Ashton (1951) identified an aqueous vein in a human eye that was about to be enucleated; a wire was tied round the vein and, after enucleation, the canal of Schlemm was injected with Neoprene. After digesting the tissue away a cast of the canal and its connecting vessels remained, and examination showed that the aqueous vein did, indeed, take origin from the canal of Schlemm. Subsequent studies of Jocson & Sears (1968), employing a silicone vulcanizing fluid, have shown that the connections of the canal of Schlemm with the vascular system are of two main kinds, large (aqueous veins) to the episcleral vessels and much finer connections to the intrascleral vessels. In addition, Rohen (1969) has described bridge-like channels running parallel with Schlemm's canal, which branch off and later rejoin it; these make connections with the intrascleral plexus.

Morphological Basis of Drainage

Giant Vacuoles

The connections between the canal of Schlemm and the vascular system have been well established since the work

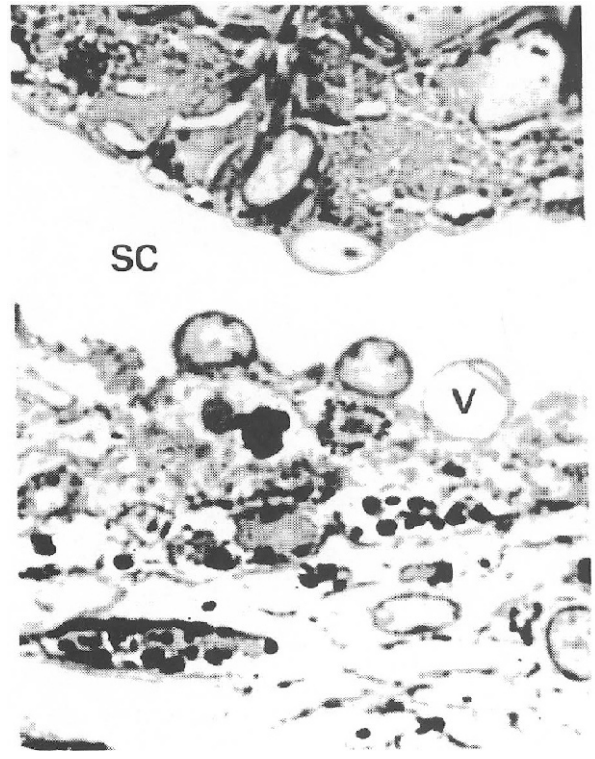

Fig. 1.44 Light photomicrograph of the trabecular wall of Schlemm's canal; the lining cells are characterized by prominent bulging nuclei and vacuolar structures (V). Note also the predominance of loosely organized cellular elements in the supporting tissue zone. SC, lumen of Schlemm's canal. Araldite section (×980). (Tripathi, *Exp. Eye Res.*)

of Maggiore; the mechanism by which fluid passes from the trabecular meshwork into the canal is not so clear. McEwan (1958) showed on hydrodynamic principles that the flow could be accounted for on the basis of a series of pores in the inner wall of the canal, and recent electron-microscopical studies have lent support to this view. Holmberg (1959) made serial sections of the trabecular tissue immediately adjacent to the canal and found channels apparently ending in vacuoles enclosed within the endothelial cells of the canal, and he considered that these vacuoles opened into the canal. Subsequent work, notably that of Kayes (1967), Tripathi (1968–1977) and Bill & Svedbergh (1972) has confirmed the existence and emphasized the significance of these giant vacuoles which are formed by the cells of the trabecular wall and cells lining the septa, recognizable even at the light-microscopical level of magnification (Fig. 1.44), and there seems little doubt they are not artefacts of fixation.

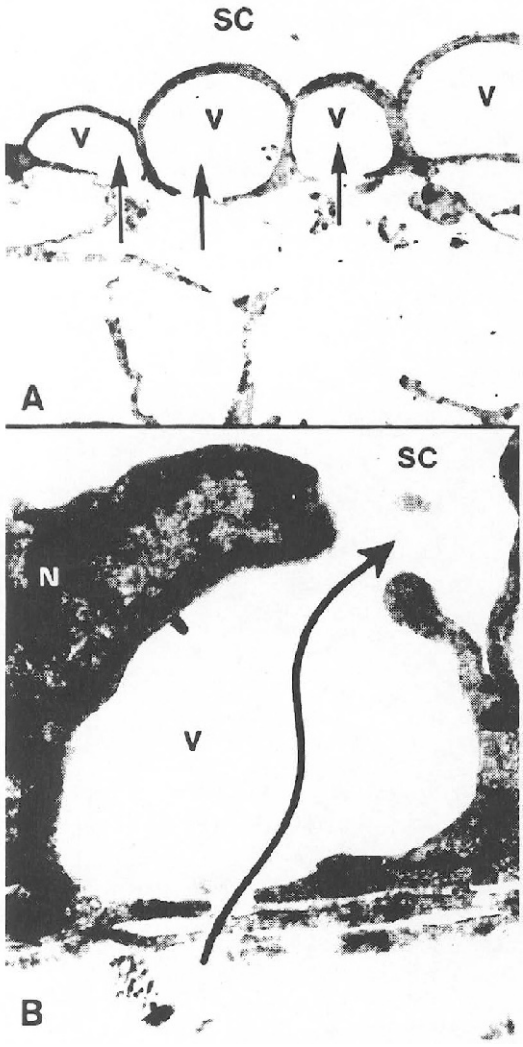

Fig. 1.45 (A) A survey electron micrograph of the cellular lining of Schlemm's canal (SC) in section showing many giant vacuoles (V). In this plane of section, many vacuoles are seen to have communication (arrow) towards the spongy subendothelial tissue containing aqueous humour. (× 3810). (B) In a given plane of section, some giant vacuoles show openings on both sides of the cell thereby constituting a vacuolar transcellular channel (continuous arrow). N, cell nucleus; SC, Schlemm's canal. (× 20 000). (Courtesy R. C. Tripathi.)

Transcellular Channels

By studying serial sections in the electron microscope it could be shown that the majority of the vacuoles were, in fact, invaginations of the basal aspect of the endothelial cell and thus may be regarded as extensions of the extracellular space into the cell, with openings measuring up to 3.5 or 4 μm on the trabecular aspect. At any given time a small proportion of these vacuoles show communications with the lumen of Schlemm's canal through smaller apical openings, in addition to the basal opening into the meshwork. Thus such a cell is, in effect, cloven into two by a channel communicating between aqueous humour in Schlemm's canal and aqueous humour in the endothelial meshwork. An example of this communication is shown in Fig. 1.45. Even more striking is the appearance of the inner (luminal) side the Schlemm's

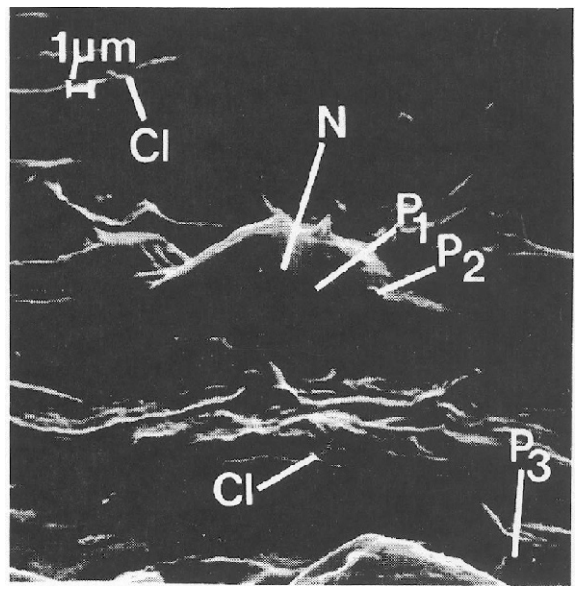

Fig. 1.46 Detail of the inner wall of Schlemm's canal. A partly collapsed bulging structure has two openings, P1 and P2. Part of the nucleus, N, can be seen through one opening. Structures most probably representing collapsed invaginations, CI, are seen at several places. P3 is also a pore. Freeze-dried preparation. (Bill & Svedbergh, *Acta Ophthal.*)

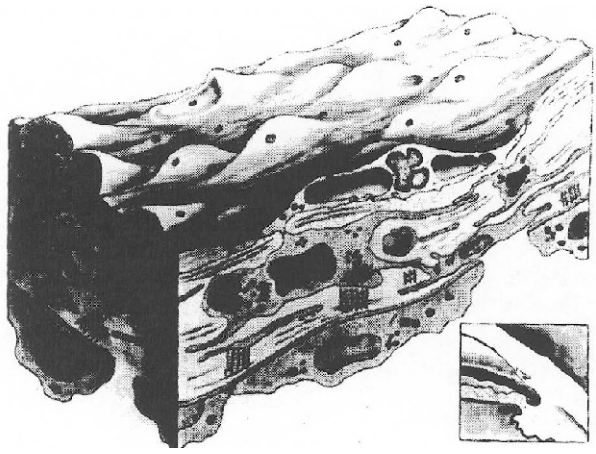

Fig. 1.47 Three-dimensional schematic drawing of endothelium lining the inner wall of Schlemm's canal and the endothelial meshwork. Endothelial cells of inner wall of Schlemm's canal are long and spindle-shaped and the nuclear portion, which often contains vacuoles, bulges into the lumen. Pores through endothelial cells are formed in flat portions of cells as well as in the wall of vacuoles opening both toward the meshwork and to the lumen of Schlemm's canal. Endothelial meshwork cells have long processes which contact those of adjacent cells forming a complicated network. These cells are often located close to the pores in the endothelial cell and are involved in 'sieving' of particles in the aqueous humour. A tiny rectangle in the Insert shows the part of the wall of Schlemm's canal that is illustrated. (Inomata *et al.*, *Amer. J. Ophthal.*)

canal as seen in the scanning electron microscope; as Fig. 1.46 shows, there are unmistakeable pores opening into the lumen.

Valvular Action

The relatively large basal openings compared with the smaller apical (luminal) openings, these last being located on the convex surface of the vacuole and usually not directly opposite the basal opening, could well provide the basis for a valvular function, flow being favoured by a pressure-gradient from aqueous humour towards the canal of Schlemm; reversal of this gradient might well cause closure of the apical openings and prevent reflux of aqueous humour into the anterior chamber. The basic concept of the structure of the angle is illustrated by Fig. 1.47 from Inomata *et al.* (1972a), the endothelial lining of Schlemm's canal, as seen from the inside by scanning electron microscopy, exhibiting depressions corresponding to the endothelial cell nuclei, and at the base of these depressions the openings of the pores, or giant vacuoles, are located.

Vacuolization Cycle

Tripathi suggested that the channel was just one stage in a cycle of vacuolization, as illustrated by Fig. 1.48; in which event it is possible to envisage changes in the resistance to

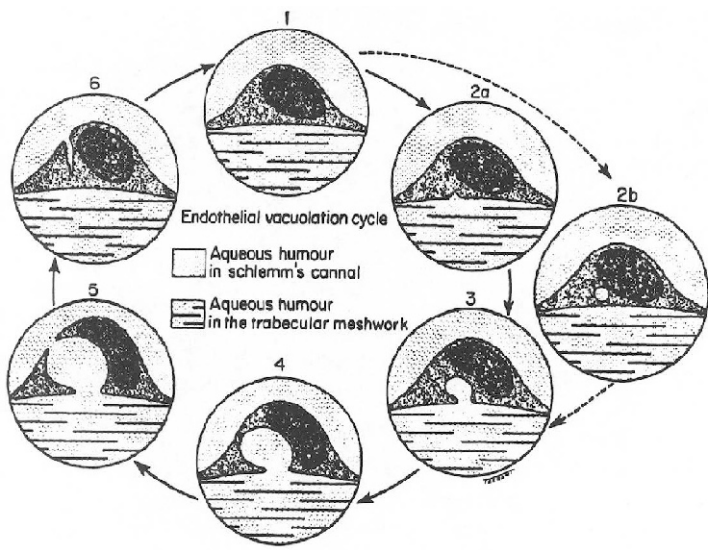

Fig. 1.48 Illustrating hypothetical cycle of vacuolization in an endothelial cell of Schlemm's canal resulting in creation of a temporary channel communicating between the canal and the trabecular meshwork. (Tripathi, *Exp. Eye Res.*)

outflow in accordance with changes in the degree of vacuolization. Cole & Tripathi (1971) calculated that the normal facility of outflow could be accounted for if the life-span of a transcellular channel occupied only one fiftieth of the total life-cycle of the vacuole as depicted in Fig. 1.48.

When particulate matter, such as Thorotrast, ferritin, etc. is introduced into the aqueous humour, it can be identified within the large vacuoles, and even intact blood cells can be seen in them; by contrast, no particulate matter is seen to leak through the intercellular clefts, a route for bulk outflow suggested by Shabo *et al.* (1973), and in fact Bill (1975) has calculated that these clefts would be unable to contribute as much as 1% of the total fluid conductance across the endothelial lining of Schlemm's canal.

The Effects of Pressure

These have been studied by Johnstone & Grant (1973), by Grierson & Lee (1974, 1975a) and Kayes (1975) in primate eyes, and by Grierson *et al.* (1986) in rabbit eyes, using both scanning and transmission electron microscopy. The vulnerable structures were the wall of Schlemm's canal and the tissue immediately adjacent (cribriform meshwork). The general effects may be summarized as a tendency for the tissue to become compressed at low intraocular pressures, reducing the intertrabecular spaces, and for a progressive expansion of the tissue at higher pressures. Thus at 8 mmHg the endothelial meshwork was reduced to less than 10 μm in thickness whilst at 55 mmHg the distension of the endothelial meshwork had led to an expansion to 15–35 mm, so that cell-to-cell contacts were often broken. At zero pressure the endothelial cells and outer corneo-scleral meshworks were very highly compressed. The absence of red blood cells in the inner meshwork, although the canal of Schlemm was packed with them, suggests that the collapsed meshwork adjacent to the canal acts as a filter preventing reflux from the canal (Johnstone & Grant, 1973). The changes in appearance of the meshwork with pressure are illustrated schematically by Fig. 1.49.

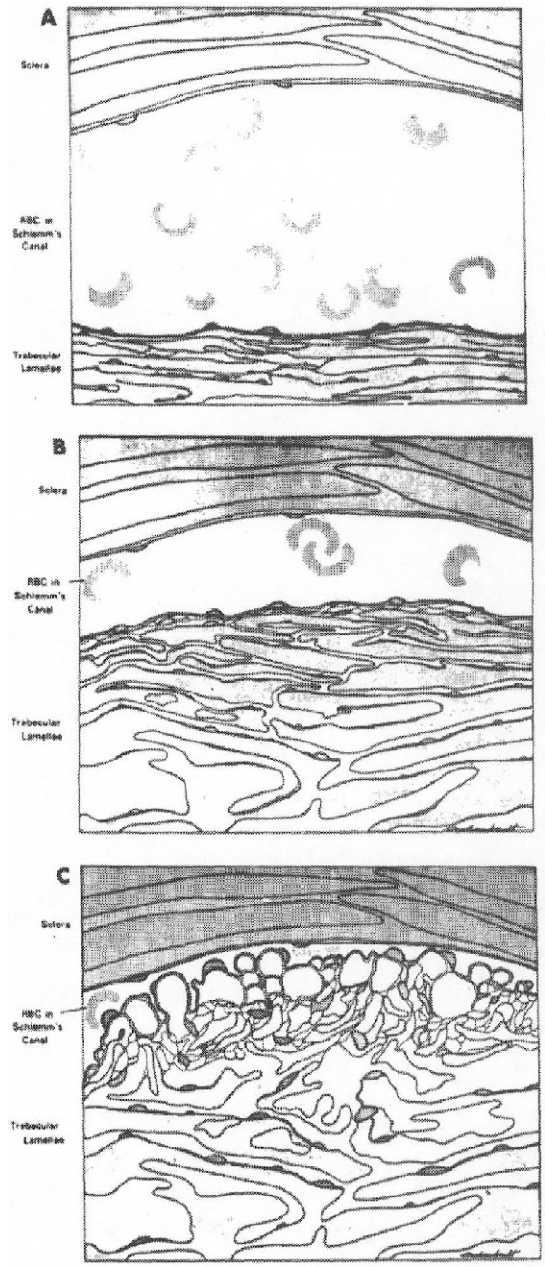

Fig. 1.49 Composite schematic drawing of the trabecular meshwork and Schlemm's canal of the human eye. (A) with intraocular pressure less than the episcleral venous pressure; (B) with equal intraocular and episcleral venous pressures; (C) with intraocular pressure 30 or 40 mmHg greater than episcleral venous pressure. (Johnstone & Grant, *Amer. J. Ophthal.*)

VACUOLES

At the low intraocular pressure of zero there were no giant vacuoles (Johnstone & Grant, 1973), and as pressure was raised there was a progressive increase in the numbers of vacuolated cells, and an increase in size and length of the vacuoles within individual cells, so that it appears that vacuole formation does depend on a positive intraocular pressure; this, of course, does not prove that at high pressures there are more transcellular channels, since the increased vacuolation may not be accompanied by increased numbers of openings into the canal lumen. This is important since many studies have indicated a nearly linear relation between pressure and flow-rate, indicating a resistance to flow that was independent of pressure so that Poiseuille's Law would apply. If rising pressure were accompanied by lowered resistance due to

increased numbers of channels, then flow would rise steeply with increasing pressure. At the highest pressure the number of vacuoles decreased, so that the increases in resistance to flow observed at high intraocular pressures by Ellingsen & Grant (1971) in experiments on enucleated human eyes, may have been due to the reduction in vacuolization as well as the herniation of the canal of Schlemm that also occurs.[25]

EXTRACELLULAR MATERIAL

In the normal and low-pressure eyes the characteristic extracellular material covering the endothelial cells, and probably consisting of mucopolysaccharides, was distributed normally; at the raised pressures this tended to disappear; thus at 22 mmHg it became focally aggregated and usually in limited regions close to the endothelium lining the canal; at 30 mmHg the material was still further reduced and in some areas could not be detected.[26]

Escape of Particulate Matter

Particulate matter of diameter around 1.5 and 3.0 μm, when injected into the anterior chamber, escapes into the blood-stream; even erythrocytes; introduced into the anterior chamber with care not to alter the intraocular pressure, disappear and may be recovered in the blood when appropriately labelled; the rate of escape is not so rapid as that of serum albumin, showing that there is some obstruction to passage; moreover, if the cells are left in the anterior chamber and the eye is allowed to adopt its true pressure, this rises due to a partial obstruction of the outflow routes (Bill, 1968a). The passage of particulate matter has been visualized in the electron microscope, e.g. by Inomata *et al.* (1972) in the monkey. Thorotrast (10 nm diameter), 0.1 μm latex spheres and blood cells (about 6 to 7 μm) readily entered Schlemm's canal, but fewer 0.5 μm and 1.0 μm latex spheres were found, indicating some selection at these sizes. Thorotrast penetrated every space of the trabecular meshwork, except areas with very fine fibrils, and it entered each vacuole in the endothelium lining the canal; as Tripathi also found, Thorotrast particles did not enter micropinocytotic vesicles in the endothelial cells lining Schlemm's canal, nor did they pass between adjacent cells lining the canal. The large latex spheres of 0.5 to 1.0 μm diameter reached the endothelial meshwork adjacent to the canal but most were trapped by its long cytoplasmic processes, which thus acted as a sieve. The escape of erythrocytes is due to their great deformability, so that although 6 to 7 μm in diameter, they were able to squeeze through 2.5 to 3.5 μm diameter pores. The exit vacuole has a smaller diameter than the inlet (1.0 to 1.8 μm compared with 2.5 and 3.5 μm), so that erythrocytes that entered a pore tended to remain there.

PIGMENTARY GLAUCOMA

It has been suggested that the high intraocular pressure in the condition of pigmentary glaucoma in which pigment lost from the iris accumulates in the meshwork, is a consequence of blockage of drainage channels by the pigment. Epstein *et al.* (1986) have discussed the evidence; experimentally they prepared a suspension of ciliary body and iris pigment particles and perfused it through the anterior chamber of the monkey. Acutely there was a 64% decrease in facility, but within a week this had become normal due to phagocytic removal of the particles.

Locus of Outflow Resistance

The actual locus of the main resistance to outflow from the anterior chamber has been implicitly accepted as the trabecular meshwork and endothelial lining of the canal, as opposed to the resistance to flow from the canal

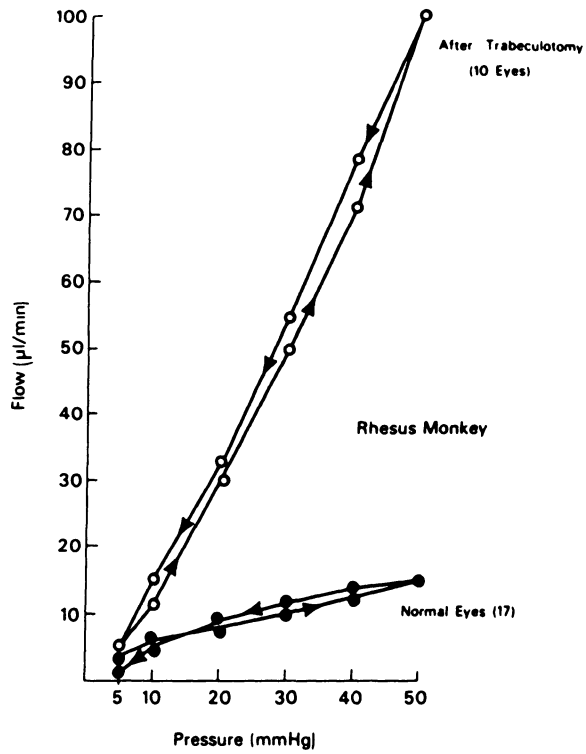

Fig. 1.50 Steady-state intraocular pressures and corresponding aqueous perfusion flow rates in enucleated monkey eyes in which the anterior and posterior chambers were in free communication, showing the difference between normal control eyes and eyes that had internal trabeculotomy of one quadrant. The measurements were made at a series of steady states as the pressure was raised stepwise to 50 mmHg and again as pressure was reduced, in the sequence indicated by the arrowheads. (Ellingsen & Grant, *Invest, Ophthal.*)

through the collector channels and vessels of the scleral plexuses. This viewpoint is supported by the experiments of Grant (1958; 1963) and Ellingsen & Grant (1971) on the trabeculotomized eye, the resistance in this eye being only some 25% of normal. The change in resistance on trabeculotomy is strikingly illustrated by Fig. 1.50; in the monkey some 83% to 97% of the resistance was eliminated by trabeculotomy compared with some 75% in human eyes (Ellingsen & Grant, 1971).

Computed Resistance

Bill & Svedbergh (1972) estimated the probable number of open pores in the canal of Schlemm and their dimensions by examining the tissue in the scanning electron microscope. They computed a resistance at the endothelium of the canal of 0.16 to 0.25 mmHg min μl^{-1}, comparing with actual resistances of 3 to 5 mmHg min μl^{-1} (Grant, 1958). Thus the channels are more than adequate to permit the observed flow. Ethier *et al.* (1986) emphasize that most of the resistance is probably at the juxtacanalicular meshwork, compared with the uveal and corneoscleral tissues. On the basis of a model, they computed that the framework of channels in the tissue would have to be filled with a matrix material to provide the observed resistance.[27]

Glycosaminoglycans and Resistance

Experimentally it has been found that, when the anterior chamber is perfused with an artificial aqueous humour, the facility of drainage tends to decrease with time, a phenomenon attributed to the washing out of material that tended to resist drainage—the *wash-out effect*[28]—and various changes were made in the artificial aqueous humour in efforts to prevent this (see, for example, Gaasterland *et al.*, 1979). That the material responsible for the resistance to drainage was a glycosaminoglycan was suggested by Bárány & Scotchbrook's (1954) observation that incorporation of hyaluronidase in the perfusion fluid increased facility[29], and a number of morphological studies have demonstrated the presence of several of these complex polysaccharides in the meshwork, where they are apparently synthesized since ^{3}H-labelled glucuronic acid and $^{35}SO_4$ are incorporated into material within the meshwork (Knepper *et al.*, 1983); the isolated material contained hyaluronic acid, chondroitin sulphate, dermatan sulphate, keratan sulphate and heparan sulphate (Acott *et al.*, 1985).[30] The exact localization of the material has been established by autoradiography after ^{35}S- and ^{3}H-labelling (Ohnishi & Taniguchi, 1983), or by the use of colloidal iron or thorium as electron-dense stains (Grierson & Lee, 1975; Armaly & Wang, 1975) or, for light-microscopy, ruthenium red (Richardson, 1982). In general the material is on the surface of the meshwork cells and endothelial cells of the canal, and in close association with connective tissue elements. Interestingly, the giant vacuoles were lined by a continuous layer of polysaccharide, thus confirming their origin as invaginations of cell membrane which carried with it its external coating. Thus the transmembrane channels are apparently lined with glycosaminoglycans, which might well influence resistance to flow of aqueous humour. So far as morphological changes at the angle, following prolonged perfusion of the anterior chamber, are concerned, these are serious, to produce wider inter- and intratrabecular spaces; the cribriform layer was so distended as almost to occlude the lumen of Schlemm's canal (McMenamin & Lee, 1986).

Sulphydryl Agents

Epstein *et al.* (1981) showed that perfusion of the anterior chamber with fluid containing iodacetamide caused an increase in facility unrelated to any change in lactate production of the trabecular meshwork, so that its effect could not be attributed to a non-specific interference with metabolizing cells; it was therefore suggested that the reagent might be attacking SH-groups on cell membranes in the tissue. A similar effect was found with *N*-ethylmaleimide (Epstein *et al.*, 1982). Morphologically, there was enlargement of the subendothelial space within the juxtacanalicular meshwork and a disruption of the continuity of the inner wall of Schlemm's canal (Lindenmayer *et al.*, 1983; Freddo *et al.*, 1984), changes that might account for the increase in facility of outflow. Glutathione is present in the meshwork (Kahn *et al.*, 1983), but the sulphydryl reagents do not exert their effects by reacting with this substance, since depletion of glutathione has no effect on facility. Glutathione may well function to remove peroxides from the aqueous humour through the glutathione peroxidase catalysed reaction:

$$H_2O_2 + 2GSH \rightarrow 2H_2O + GSSG$$

(Scott *et al.*, 1984).[31]

Calcium

Removal of calcium from the environment of a tissue tends to inhibit cell adhesion, and it was found by Hamanaka & Bill (1987) that perfusion of the anterior chamber with Na_2EDTA, a calcium chelator, caused an increased facility associated with a loss of cell processes in the meshwork, ballooning of the juxtacanalicular region and the inner wall of Schlemm's canal into the canal itself, and actual rupture of the inner wall. After interruption of the perfusion and resumption with normal artificial aqueous homour, facility returned to normal, although the morphology of the angle remained the same. The authors

assumed that extravasated platelets from the blood blocked up the holes caused by the experimental insult.

Colchicine

This drug specifically attacks cytoplasmic processes dependent on the aggregation and disaggregation of intracellular tubules. Bhattacherjee & Eakins (1978) found a dose-dependent lowering of intraocular pressure in rabbits after topical or intravitreal colchicine or vinblastine. Since Ritch *et al.* (1981) found no effect on rate of flow of aqueous homour, the fall in pressure may be attributed to a decrease in resistance to drainage. However, Williams *et al.* (1983) measured both flow and resistance and found that flow decreased from 3.68 ± 0.09 μl min^{-1} to 1.8 ± 0.034 $\mu l\, min^{-1}$ after a dose of 40 μg of colchicine; the effect was dose-related. There was an increase in facility from 0.39 ± 0.03 to 0.49 ± 0.03 $\mu l\, min^{-1}\, mmHg^{-1}$. Thus the tubule-disruptive effect of colchicine apparently extends to decreasing secretion and increasing facility; the effect on secretion is also seen in milk secretion and hormone release. When ^3H-colchicine was administered, this was taken up by the ciliary processes, and found bound to a microtubule fraction of an iris-ciliary body homogenate (Williams & Bhattacherjee, 1982).

Cytochalasin

This interferes with the microfilament system of cells and thus modifies their structure; such modifications might be important for the drainage process, taking place as it does by passing through a complex system of trabecular tissue. Kaufman & Bárány (1977) found a 150% increase in facility in cynomolgus monkeys; the same effect occurred in animals with disinserted ciliary muscles, so that an effect of ciliary muscle contraction could be ruled out. Morphological studies by Svedbergh *et al.* (1978) and Johnstone *et al.* (1980) revealed quite widespread damage to the tissues in the angle; thus the uveal and corneoscleral meshworks separated, and there were degeneration and disappearance of endothelial cells. Damage to the endothelial lining of Schlemm's canal was rendered visible by reflux of blood into the canal. When cytochalasins B and D were compared, the latter was some 25 times more effective; maximal effects of both practically doubled facility (Kaufman & Erickson, 1982). In spite of the severe morphological changes, repair was rapid, so that after 6 days the structures in the angle were normal. As one might expect, pilocarpine did not increase facility when cytochalasin was exerting its maximal effect (Kaufman, 1987).

Cultured Cells

The cytology of cultured meshwork cells was examined by Ryder & Weinreb (1986) who confirmed the presence of microfilaments, microtubules and intermediate filaments; cytochalasin B caused rounding up of endothelial cells, whereas colchicine had no marked influence on cell structure (Weinreb *et al.*, 1986).

Protein Profiles

Since primary open-angle glaucoma is an age-related disorder, and since the aetiology of the rise in intraocular pressure is clearly related to an increased resistance to drainage, senile changes in the composition of the meshwork are of interest. Millard *et al.* (1987) have summarized the literature relating to the protein composition of the meshwork, and in their own work have examined the protein profiles of the extracted proteins from tissue taken from eyes aged 5 months to 87 years. Significant changes with age were observed, notably a reduction in the prominence of a protein assumed to be G-actin, and an increase in that of the alpha I and II components of Type IV collagen. Thus "molecular ageing" occurs in the meshwork, and the problem will be to ascertain the changes that lead to increased resistance.

Uveoscleral Drainage

Bill (1964) deduced from his studies on the passage of albumin from blood into the uveal tissue that there must be some route for drainage additional to that provided by Schlemm's canal. By perfusing the anterior chamber of the monkey's eye with a mock aqueous humour containing labelled albumin, he was able to divide the losses of protein into two components, the one appearing in the blood and doubtless having been drained through Schlemm's canal, and the other that remained in the uveal tissue, having presumably passed directly into the tissue of the anterior uvea. The average 'uveo-scleral drainage' was 0.44 μl/min compared with a conventional drainage of 0.80 μl/min; thus the rate of formation of aqueous humour, the sum of these, was 1.24 μl/min. In the cat, the rate of secretion was 14.4 μl/min and only 3% of this passed by uveoscleral routes. In man, Bill (1971) demonstrated the uveoscleral flow by autoradiography, iodinated albumin passing through the anterior uvea and along the suprachoroidal space to reach, eventually, the posterior pole of the eye. In rabbits, Cole & Monro (1976) perfused eyes with fluorescein-labelled dextrans and were able to demonstrate that these high-molecular weight compounds found their way to suprachoroid, scleral limbus and iris, and, by quantitative analysis of the material in the dissected eye, it was shown that the amounts recovered were in this order.

The Actual Route

There is no complete endothelial layer lining the anterior surface of the ciliary body which faces the anterior chamber between the cornea and iris; there is also no delimitation of the spaces between the trabecular sheets and the spaces between the bundles of the ciliary muscle so that fluid can pass from the chamber-angle into the tissue spaces of the ciliary muscle, and these spaces in turn open into the suprachoroidal space from which fluid can pass across the sclera or along the perivascular spaces of the large vessels penetrating the sclera. Under normal conditions the pressure in the suprachoroid is less than that in the anterior chamber by a few mmHg (Bill, 1975), and thus the conditions for a flow along this 'unorthodox channel' are present.[32]

ELECTRON-MICROSCOPY

Inomata *et al.* (1972b) followed the passage of particulate matter (Thorotrast of 10 nm diameter and latex spheres of 0.1, 0.5 and 1.0 μm diameter) from anterior chamber along the unconventional route. As others had found, the anterior surface of the iris allowed passage of all sizes of particles into the stroma; the pupillary zone appeared less permeable. All sizes of particles also passed into the intertrabecular spaces, penetrating the corneoscleral and uveoscleral meshwork and thence into the spaces between bundles of the ciliary muscle; the spaces between muscle cells allowed the smaller Thorotrast particles to pass, exluding the latex spheres. All sizes of particles appeared in the suprachoroid and even the largest particles passed along this as far as the macular region in three hours. The compact sclera, as one might expect, allowed only the smaller (Thorotrast) particles to penetrate, and these in relatively small amount. In a later study, the passage of particulate matter was followed through the sclera in the loose connective tissue surrounding the blood vessels piercing this coat (Inomata & Bill, 1977).[33]

Effects of Ciliary Muscle Contraction

Bill & Wàlinder (1966) found in monkeys that, although drugs such as pilocarpine, which cause contraction of the ciliary muscle, increase facility of outflow, they actually decrease uveoscleral flow, and this is clearly because of the reduction in the spaces between ciliary muscle bundles. A similar effect was found in human eyes (Bill, 1971).[34]

THE INTRAOCULAR PRESSURE

We have had occasion to refer to this pressure when considering both the secretion and the drainage of the aqueous humour, since this pressure is governed by the rate of secretion and the resistance to drainage; as indicated earlier, it is governed by the simple formula:

$$P_i - P_e = \text{Flow} \times R \qquad (3)$$

P_i being the intraocular pressure and P_e the pressure of the blood vessel into which the aqueous humour drains, the episcleral venous pressure. R is the resistance, its reciprocal being the facility.

Measurement

On inserting a hypodermic needle into the anterior chamber the aqueous humour flows out because the pressure within is greater than atmospheric; we may define the intraocular pressure as that pressure required just to prevent the loss of fluid. Manometric methods have been developed that permit the measurement of this pressure with a minimal loss of fluid, this being necessary since, as we shall see, loss of fluid *per se* may upset the normal physiology of the eye.

Manometry

The general principle of the manometric methods employed for measuring the intraocular pressure is illustrated by Fig. 1.51. The fluid-filled chamber is connected to a reservoir, R, which is of variable height, and also to the hypodermic needle. The end of the chamber is covered by a membrane, and it is essentially the movements of the membrane, caused by changes in pressure, that are recorded. The membrane may be made of metal to act as the plate of a condenser, as in the Sanborn electromanometer, or it may be connected to a transducer valve, i.e. a valve whose anode may be moved from outside, so that a change in its position is converted into a change of voltage. The reservoir serves to fill the system with a

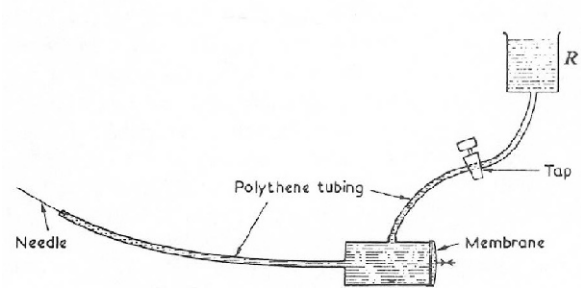

Fig. 1.51 Illustrating the general principle on which manometric measurement of the intraocular pressure is based. The reservoir serves to fill the system with saline. When the needle is in the anterior chamber, and the tap is closed, changes in pressure cause movements of the membrane.

saline solution and may be employed to calibrate the recorded changes in terms of pressure.

Tonometry

For studies on man, the introduction of a needle into the anterior chamber is rarely permissible, so that various *tonometers* have been developed permitting an indirect measure of the pressure within the eye. With the *impression type* of tonometer, such as the Schiøtz instrument, the depth to which a weighted plunger applied to the cornea sinks into the eye is measured, whilst with the *applanation tonometer* the area of flattening of the cornea, when a metal surface is applied with a controlled force, is measured. The two principles are illustrated schematically in Fig. 1.52; the greater the intraocular pressure the smaller will be the depth of impression, or area of applanation.

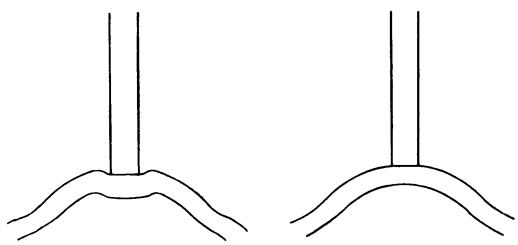

Fig. 1.52 Illustrating the principles of impression tonometry (*left*) and applanation tonometry (*right*).

SCHIØTZ TONOMETER

This is the classical instrument based on indentation, and for this reason merits a brief description although it has been supplanted by other types. The footplate, F, is curved to fit the average curvature of the human cornea. The weighted plunger, P, passes through the footplate; movements of this plunger operate on the hammer, H, which converts vertical movements into readings of the pointer on the scale. This scale reads from 0 to 20, the greater the indentation the lower the intraocular pressure and the *larger* the scale-reading. The frame, Y, serves to hold the instrument upright on the eye, and because the footplate can move freely within the cylindrical part of the frame, the actual weight resting on the eye is that of the plunger, footplate, hammer and scale (17.5 g), the frame being held by the observer. With the smallest weight on the plunger, the total effective thrust on the eye amounts to 5.5 g, and the readings made with this are referred to as the '5.5 g readings'. By using heavier weights the thrust may be increased to 7.5 or 10 g, thereby allowing the instrument to give reasonable scale-readings at higher levels of intraocular pressure. The calibration of the instrument, whereby the scale-readings indicate true pressure within the eye in the absence of the instrument's resting on it, is a complex procedure and need not be entered into. An important parameter, defined by Friedenwald (1957) as the *rigidity coefficient*, makes allowance for different mechanical features of the eye. But this must be assessed for any individual eye, and with its aid and the measured scale-reading, a pressure may be read off from a set of tables. Because of the difficulties in accurate calibration, the Schiøtz instrument is being superseded by an applanation type, since with the latter the deformation of the eye is very small, with the result that calibration is independent of scleral distensibility, i.e. of the rigidity coefficient.

APPLANATION TONOMETER

This measures, in effect, the force required to produce a fixed degree of applanation when a flat surface is pressed against the cornea. The earliest instrument (Maklow) consisted of a cylindrical piece of metal with a flat base weighing 5 to 15 g. A drop of a concentrated dye-solution was spread over the cornea, the instrument was allowed to rest a moment on the corneal surface and a print of the area of contact between cornea and metal was obtained by placing the foot of the instrument on a piece of paper. Goldmann's (1955) instrument is a refinement on this procedure, in which the degree of applanation is kept fixed and the instrument indicates the force required to produce this. Thus the applanation surface is a piece of transparent plastic 7 mm in diameter, and it may be forced against the cornea by turning a knob which operates a spring; the reading on the knob indicates mmHg directly. The point at which applanation occurs is detected optically by observation through a slit-lamp microscope to which the instrument is attached. The amount of fluid displaced from the eye to give applanation was only 0.5 μl compared with some 15–20 μl for the Schiøtz instrument, so that ocular rigidity is not an important factor.

PNEUMATIC TONOMETER

Durham *et al.* (1965) described an instrument illustrated schematically by Fig. 1.53; a diaphragm is applied to the eye and the force applied to it increased until applanation is achieved. The pressure operating against the diaphragm is derived from a gas cylinder, the gas passing into the central chamber and escaping to the exhaust channels through an annular opening that becomes constricted as the diaphragm is pressed more and more firmly against the eye. In this way the applied pressure increases as the instrument is pressed against the eye. The instrument may be applied to the sclera, so that anaesthesia is unnecessary. Walker & Langham (1975) have modified the instrument by introducing a pneumatic bearing, which allows the sensor to float freely on a cushion of gas. Application to the eye results in the development of a pneumatic force which gently holds the sensor against the

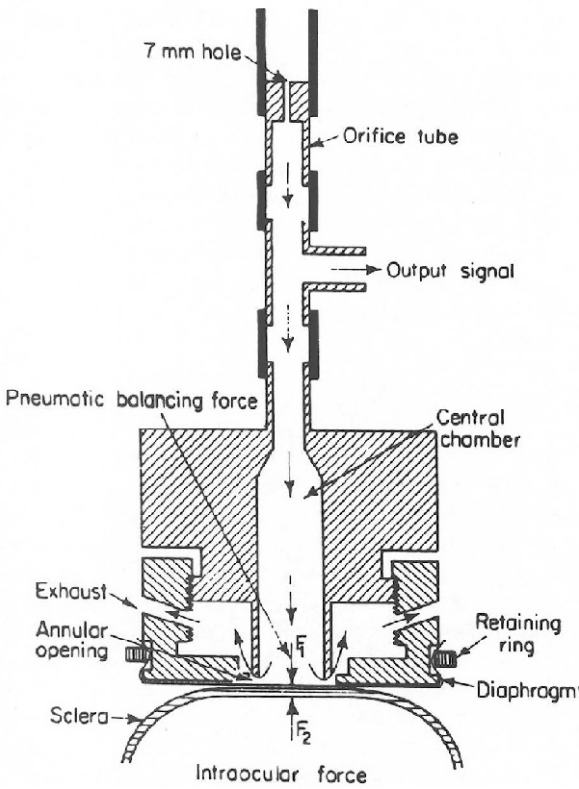

Fig. 1.53 Schematic illustration of the pneumatic applanation tonometer. The more forcibly the diaphragm is pressed against the eye, the greater will be the resistance to escape of air to the exhaust tubes, and thus the greater the pressure, F_1, exerted on the diaphragm to cause applanation. (Durham *et al.*, 1965.)

eye with a constant force. With this arrangement, records of pressure could be obtained over much longer times than when employing the hand-held version.

The Normal Intraocular Pressure

Figure 1.54 illustrates the results of a study of 13 861 apparently healthy human eyes, based on the Schiøtz tonometer (Leydhecker *et al.* 1958). This suggests that 95.5% of all healthy eyes have a pressure lying between 10.5 and 20.5 mmHg; a pressure above 20.5 mmHg may thus be a sign of abnormality. Between the ages of 10 and 70 there is no significant change in mean intraocular pressure, and no difference between the sexes is found. In newborn infants likewise the pressure falls within the normal adult range, the mean value found by Hörven being 16.5 mmHg with limits of 10.9 and 24.2 mmHg. In experimental animals the intraocular pressure may well be of the same order; thus in cats Davson & Spaziani

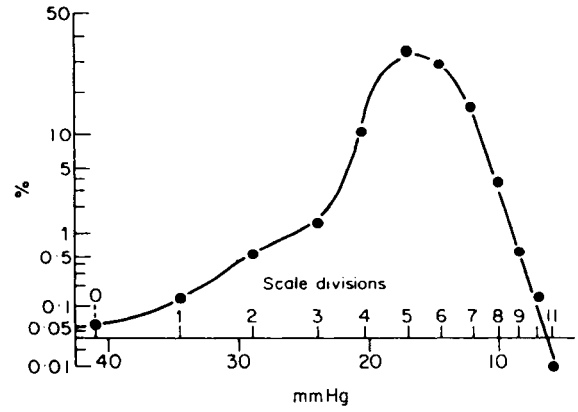

Fig. 1.54 The intraocular pressure in normal individuals. Ordinate: percentage of individuals having pressure indicated on abscissa. (Leydhecker *et al.*, 1958.)

(1961) reported a mean value of 16.5 mmHg, whilst Langham (1958) found 20 mmHg in this animal and 20.5 mmHg in the rabbit.[35]

Circadian Rhythm

A diurnal variation in human intraocular pressure has been recognized for a long time, the pressure being at its highest early in the morning and lowest at about midnight (Köllner, 1916). The fluctuation is on the average some 6 mmHg. According to more recent studies, the lowest intraocular pressure occurred at about 3 a.m. and not in the afternoon; thus Fig. 1.55 from Henkind *et al.* (1973) illustrates the course throughout the 24 hours. Glaucomatous eyes also exhibited variation, so that in a case of unilateral glaucoma, at about 3 a.m. the two eyes had about the same pressure, because of the pronounced diurnal change in the glaucomatous eye. The diurnal change may be related to the plasma levels of cortisol, with, however, a 3 hour phase shift (Weitzman *et al.*, 1971). In the rabbit there are both diurnal and seasonal variations (Bar-Elan, 1984; Vareilles *et al.*, 1977) but there

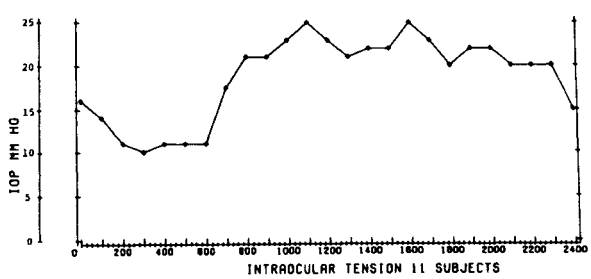

Fig. 1.55 Variation in intraocular pressure of normal human subjects during 24 hr. (Henkind *et al.*, *Invest. Ophthal.*)

is little agreement amongst authors as to the times of peak or low pressure.

Thus, according to Vareilles *et al.*, pressure is highest in winter and lowest in summer, and highest in the day and lowest at night (Katz *et al.*, 1975). According to Bar-Elan (1984) there were both summer and winter peaks of 20.2 mmHg, with lowest values in spring and autumn. Johnson & Maurice (1984) observed a fall in rate of secretion of aqueous humour at night, which would correspond with the low pressures recorded at this time.

Factors Affecting the Intraocular Pressure

General Considerations

The simple relationship between flow-rate of aqueous humour, F, and the pressure-drop, mentioned above, may be rewritten:

$$P_i = F \times R \times t + P_e \qquad (4)$$

where P_i is the intraocular pressure, F is the volume of aqueous humour drained during time t, R is the resistance and P_e is the episcleral venous pressure. With the aid of this relationship some of the factors determining the intraocular pressure may be easily appreciated. Thus an increase in resistance to flow will increase the intraocular pressure, provided that the rate of formation of fluid does not decrease in proportion. The factors determining the rate of production of fluid are not completely understood. As we have seen, the fluid is formed by a process of secretion and, when comparable systems are studied, e.g. secretion of saliva, it is found that the process can operate against very high pressures, so that the secretion of aqueous humour may be assumed to occur at a constant rate independent of fairly wide fluctuations in the pressure. If a process of passive filtration from the vascular bed contributes to flow—and as we shall see this seems to be true of some species—then this contribution will be reduced at higher pressures (p. 52). We shall not go far wrong, however, if we conclude that intraocular pressure varies inversely with resistance to flow. Alterations in episcleral venous pressure, P_e, may likewise be expected to be reflected in predictable alterations in intraocular pressure.

Episcleral Venous Pressure

The episcleral venous pressure, P_e, representing as it does the pressure of the blood into which the aqueous humour drains, is an important experimental parameter, and its measurement has been studied by Brubaker (1967) and Gaasterland & Pederson (1983). In experimental animals the pressure is most accurately measured by a cannulation technique, the cannula being inserted so that its tip is at a Y-junction; the pressure in the cannula is raised until flow of blood into the cannula just ceases. In humans, a non-invasive technique must be employed, consisting in a transparent pressure-chamber, the pressure being raised until flow of blood through the vein is interfered with. The exact end-point for this technique has been examined by Gaasterland & Pederson (1983); the value closest to that given by cannulation, namely 11.3 ± 0.5 mmHg, is obtained when the end-point is a barely detectable indentation of the wall of the vein, and not an intermittent or sustained collapse of the vein.

Variations in Venous Pressure

In man there is a good correlation between intraocular pressure and P_e, whilst in cats Macri (1967) showed the same thing when he varied the intraocular pressure experimentally. Acute changes of venous pressure will influence the intraocular pressure in a twofold manner. First, by affecting drainage as just indicated, and second, by a direct transmission of the changed venous pressure across the easily distensible walls of the intraocular veins. The expansion of the veins will be eventually compensated by a loss of aqueous humour from the eye, so that the rise due to this cause may be more or less completely compensated, but the effect on drainage should last as long as P_e is elevated. Experimentally the effects of changed venous pressure may be demonstrated by administering amyl nitrite; the peripheral vasodilatation causes a general increase in venous pressure and leads to a considerable rise in intraocular pressure in spite of a lowered arterial pressure. Again, ligation of the vortex and anterior ciliary veins causes large rises in intraocular pressure, as we should expect. Finally, destruction of the aqueous veins, by restricting the outlets of aqueous humour, may cause quite considerable rises in intraocular pressure in rabbits, according to Huggert (1958).

Arterial Pressure

The arterial pressure can influence the intraocular pressure through its tendency to expand the intraocular arteries; since these are not easily distensible, however, relatively large changes in arterial pressure will be required to produce measurable changes in intraocular pressure. That the arterial pressure does affect the intraocular pressure in this way is manifest in the *pulse* shown in records of the intraocular pressure; the amplitude of this pulse is small, about 1 mmHg, and coincides with cardiac systole. Thus a change of about 20 mmHg, which is the pulse-pressure in an intraocular artery according to Duke-Elder (1927), causes a change of only 1 mmHg in the intraocular pressure.

In the rabbit, ligation of one common carotid artery lowers the intracranial arterial pressure on the side of the

ligation, whilst the pressure on the other side rises above normal; hence we may study the effects of lowered arterial pressure on one eye, using the other as a control. Wessely in 1908 found a small lowering of the intraocular pressure on the ligated side and Bárány found that after 24 hours the pressure had returned to normal. The immediate effect of the ligation is undoubtedly the result of the fall in arterial pressure which leads to a reduced volume of blood in the eye. As Fig. 1.56 shows, there is a tendency to compensate for this since alternate clamping and unclamping of the artery leads to an overshoot on release of the clamp, suggesting that there has been some vasodilatation which would partly compensate for the reduced flow caused by the fall in pressure. The compensation is not complete, however, since Linnér found a 19 per cent decrease in the rate at which blood escaped from a cut vortex vein on the side of the ligature.

Bill (1970c), working on the monkey, found at normal mean arterial pressure of 119 mmHg a rate of flow of aqueous humour of 2.64 μl min; this was unaffected by lowering the blood pressure, through haemorrhage, to 70 to 90 mmHg; however, when the pressure was reduced to 60 to 40 mmHg there was a sharp fall to as little as 0.5 μl min, presumably due to lowered blood-flow through the ciliary processes.

Rate of Flow of Aqueous Humour

Other things being equal, we may expect changes in rate of secretion of fluid to produce changes in intraocular pressure in the same sense, but the effects are not likely to be large. Thus, if the intraocular pressure, P_i is 16 mmHg, and the episcleral venous pressure, P_e, is 12 mmHg, the pressure drop, $P_i - P_e$, is 4 mmHg. If the rate of flow is doubled the pressure-drop must be doubled too, in which case it becomes 8 mmHg, and if P_e remains the same this means that the intraocular pressure, P_i rises from 16 to 20 mmHg. Thus doubling the rate of secretion causes only a 25% increase in intraocular pressure. In practice it is not easy to vary the rate of secretion; as we have seen, the carbonic anhydrase inhibitor, Diamox, reduces the rate, and this is accompanied by a fall in intraocular pressure; the same is true of digitalis compounds, according to Simon *et al.* (1962).

By injecting saline continuously into the anterior chamber we may experimentally increase the flow of fluid through the eye and test the applicability of the simple equation relating flow-rate to pressure-drop; Langham (1960) found that the equation did not hold, the rise in pressure for a given increase in flow being smaller than predicted, and his results suggested some homeostatic mechanism that decreased the resistance to flow as the intraocular pressure rose. Section of the cervical sympathetic, or ligation of the common carotid, caused the relationship between flow and pressure to become linear, i.e. to follow the simple equation:

$$\text{flow} \times \text{resistance} = \text{pressure drop}$$

and this suggested that the adaptation was largely vascular. The situation is apparently complicated, however, by the effects of pressure on the rate of production of aqueous humour. Thus Bill & Bárány (1966) found a linear relation between flow-rate and pressure, but they also showed that the rate of secretion diminished with higher pressures, so that the linear relation found between flow-rate out of the cannula and pressure means that the actual flow through Schlemm's canal was not linearly related to pressure, a rise in pressure producing too small a flow, and thus suggesting an increased resistance at the higher pressure.

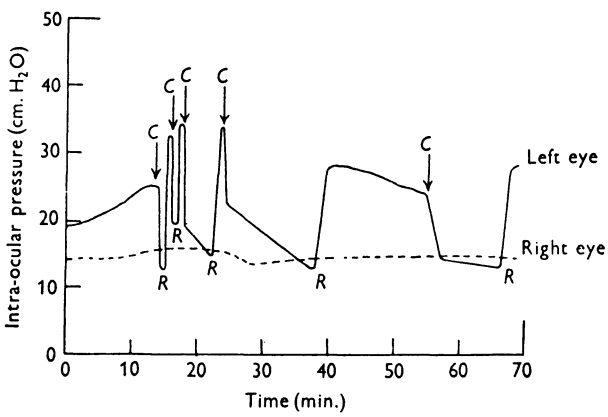

Fig. 1.56 Intraocular pressure of the rabbit. At points marked C the left common carotid artery was clamped, and at points marked R the clamp was released. (Davson & Matchett, *J. Physiol.*)

Pseudofacility

If raising the intraocular pressure reduces the production of fluid, this means that, when facility is determined by measuring the flow of fluid from a cannula in the anterior chamber under an applied pressure, a reduction in fluid production caused by the raised pressure will make room for some fluid from the reservoir and so give too high a measure of the extra flow through Schlemm's canal; the extra fluid entering for a given rise in pressure can be expressed as a 'pseudofacility' (Bill & Bárány, 1966). This may be defined as the decrease in rate of flow, ΔF, divided by the increase in pressure, ΔP_i, i.e. $\Delta F/\Delta P_i$. Bárány (1963) deduced that pseudofacility, C_{pseudo}, was related to C_{gross} by the expression:

$$C_{pseudo} = C_{gross} \times \left(1 - \frac{\Delta P_i}{\Delta P_e}\right) \qquad (5)$$

Where ΔP_i is the change in intraocular pressure when the episcleral pressure is changed by ΔP_e.

Experimental Determination

Brubaker & Kupfer (1966) determined C_{gross} by perfusion of the monkey's eye at constant pressure. They then raised P_e by inflating a cuff round the monkey's neck and determined C_{gross} for the new steady state; P_i and P_e at the new pressures were also determined, to give $\Delta P_i/\Delta P_e$.

Mean values for the monkey were:

$$P_i = 12.7 \text{ mmHg}$$
$$P_e = 9.0 \text{ mmHg}$$
$$C_{gross} = 0.63 \ \mu l \ min^{-1} \ mmHg^{-1}$$
$$C_{pseudo} = 0.19 \ \mu l \ min^{-1} \ mmHg^{-1}$$

Thus in this species, pseudofacility was 30% of the total. In human subjects Goldmann (1968) found a value of 20%.

Effects of Blood Osmolality

Aqueous humour and blood plasma are approximately isosmolal, and this is to be expected in view of the rapid exchanges of water across the blood-ocular fluid barriers (Kinsey *et al.*, 1942) compared with the much slower exchanges of solutes. Raising the osmolality of blood artificially causes a fall in intraocular pressure because of the osmotic outflux of water (Davson & Thomassen, 1950; Auricchio & Bárány, 1959); clinically an acute fall in intraocular pressure may be induced by oral urea, this being chosen because it is not rapidly excreted from the blood and its passage across the blood-ocular barriers is slow; mannitol is less effective presumably because its renal excretion is greater (Galin *et al.*, 1963).

Human Studies

The study of intraocular pressure in man must be made with the tonometer; this permits both the measurement of pressure and facility of outflow. The measurement of episcleral venous pressure, P_e, in humans by Kupfer and his colleagues has permitted the assessment of the pseudofacility, an important parameter since, without a knowledge of the pressure-dependent flow into the eye—and out of it when the pressure is high—no accurate notion of the true facility is obtainable, and without this, of course, no true notion of rate of secretion is obtainable. Kupfer & Ross (1971) measured total facility, using a modified Grant equation that corrects for ocular rigidity, and pseudofacility was determined by measuring change in intraocular pressure, ΔP_i, with change in episcleral venous pressure ΔP_e, in accordance with Equation 5. The flow out of the eye, F, is given by the equation:

$$F = C_{true} (P_i - P_e) \qquad (6)$$

C_{true} being equal to $C_{total} - C_{pseudo}$.

The Normal Values

Average normal values derived from ten determinations of right and left eyes of the same subject are given in Table 1.6, and average results on four separate human subjects are shown in Table 1.7. It emerged that the errors

Table 1.6 Parameters of the right and left eyes of a human subject. (Kupfer & Ross, 1971)

	P_i	P_e	C_{total}	C_{true}	C_{pseudo}	P_k	*Flow*
Right eye	13.8	9.2	0.328	0.256	0.072	31.6	1.19
	±	±	±	±	±	±	±
S.E.M.	0.36	0.14	0.014	0.010	0.006	2.5	0.13
Left eye	14.0	9.0	0.288	0.226	0.062	33.6	1.14
	±	±	±	±	±	±	±
S.E.M.	0.33	0.12	0.016	0.012	0.006	2.3	0.11

Mean of ten determinations.
Pressure mmHg; C in μl min mmHg. Flow in μl/min. (Kupfer and Ross, 1971.)

Table 1.7 Similar to Table 1.6, but results of four human subjects averaged. (Kupfer & Ross, 1971)

	P_i	P_e	C_{total}	C_{true}	C_{pseudo}	P_k	*Flow*
	13.3	8.4	0.285	0.224	0.061	31.0	1.09
	±	±	±	±	±	±	±
S.E.M. ±	0.21	0.26	0.008	0.006	0.002	0.59	0.030

were not very high, so that it is practicable, using these techniques, to study the effects of drugs and to analyse them in terms of changed flow-rate and facilities.

The Critical Intraocular Pressure

Goldmann (1968) pointed out that if the intraocular pressure was caused to rise, e.g. by raised episcleral venous pressure, the pressure-dependent flow would decrease and finally reverse, and that there was a theoretical intraocular pressure, P_k, at which net flow through the eye would be zero, the secretory inflow being balanced by the pressure-dependent outflow. This becomes clear from Fig. 1.57 where intraocular pressure, P_i, is abscissa and the ordinate is flow through the eye. Line II represents the constant (pressure-independent) secretion, S, and line I is the pressure-dependent flow, which is positive at lower values of P_i but becomes negative at higher values. The relationship is probably linear and the slope measures the pseudofacility, $C_{pseudo} = \Delta F / \Delta P_i$. Line III is the sum of lines I and II and represents the net flow through the eye and becomes zero at P_k. It is clear that the slope of line III also represents the pseudofacility.

P_k is given by:
$$P_k = \frac{P_{i_2} P_{e_1} - P_{e_2} P_{i_1}}{\Delta P_i - P_e} \qquad (7)$$

where the numbered suffices indicate the pressures before and after a change in P_e.

Flow-curves

Experimentally, then, so-called flow-curves may be constructed based on tonographic measurements of flow-rate and the influence of altered P_e on P_i. The effects of drugs etc. might then be revealed as an altered slope of the flow-curve, indicating a changed pseudofacility, whilst an altered flow-rate, with unchanged pseudofacility, would give a new line parallel to the first. Kupfer *et al.* (1971) have carried out an elaborate study on human subjects based on this approach, and have shown that a drug, such as acetazolamide, affects pseudofacility as well as rate of secretion, so that the true inhibition of secretion is actually larger than would be deduced from a simple measurement of flow-rate.

Breakdown of the Blood-aqueous Barrier

Under certain pathological and experimental conditions, the blood-aqueous barrier breaks down, so that substances such as proteins, that are normally almost completely excluded from penetration, now appear in the aqueous humour in large amounts, and their presence gives rise to the so-called 'flare' caused by scattering light in the slit-lamp beam. The breakdown is usually, but not always, accompanied by a rise in intraocular pressure which may be spectacular—up to 60–80 mmHg. The vascular engorgement within the eye and its adnexae suggests that the prime action is on the blood vessels. A typical agent is the hydrochloride of nitrogen mustard—methyl bis(β-chloroethyl) amine (Davson & Quilliam, 1947; Davson & Huber, 1950). When this is applied topically to the eye the intraocular pressure rises rapidly (Fig. 1.58) and simultaneously protein enters the aqueous humour, and the pupil constricts. The peripheral irritative effect is manifest as chemosis of the conjunctiva. In general, then, we may define a syndrome of raised intraocular pressure, constricted pupil and breakdown of the blood-aqueous barrier, often associated with migration of

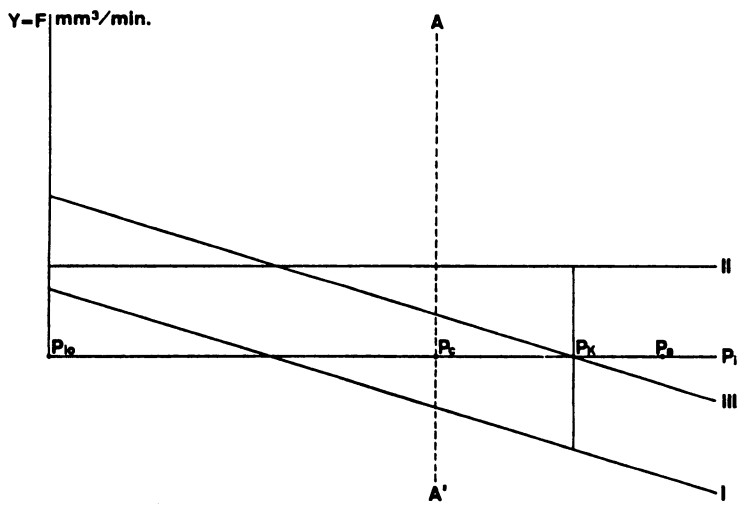

Fig. 1.57 Illustrating significance of the theoretical pressure, P_k, such that flow through the eye is zero, the secretory inflow being balanced by the pressure-dependent outflow, P_i is the abscissa and the rate of inflow is ordinate. Line II represents the pressure-independent influx (secretion), whilst Line I represents the pressure-dependent component, being positive (inflow) at lower values of intraocular pressure (P_i) and negative (outflow) at higher values. Line III is the algebraic sum of I and II. It is clear that total rate of flow is linearly dependent on intraocular pressure and becomes zero at P_k. (Goldmann, *Bibl. Ophthal.*)

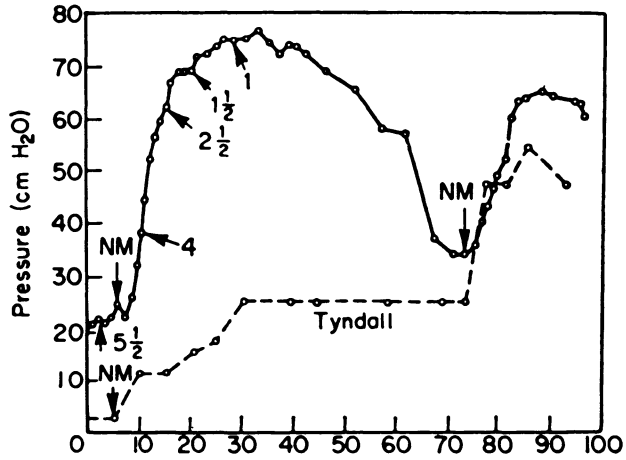

Fig. 1.58 Rise in IOP and intensity of the Tyndall beam in the aqueous humour after subconjunctival injection of nitrogen mustard in the rabbit's eye. At points marked NM the injection was made. Numbers applied to the pressure curve indicate diameter of the pupil in mm. (Davson & Huber, *Ophthalmologica.*)

cellular elements into the aqueous humour as well as protein.

Fluorescein Test

The dye, fluorescein, normally penetrates the blood-aqueous barrier very slowly, but to a measurable extent because, in the intact eye, it may be detected by the fluorescence it causes in the slit-lamp beam. When the blood-aqueous barrier is broken down, the rate of appearance of fluorescein increases, and the change in rate, measured by some simple fluorimetric device such as that devised by Amsler & Huber (1946) or Langham & Wybar (1953), is used as a measure of the breakdown. Clinically this has been found useful in the diagnosis of uveitis, an inflammatory condition associated with breakdown of the barrier.

Paracentesis

There are a variety of insults applied to the eye that cause a breakdown of the blood-aqueous barrier; of especial interest is the effect of removal of aqueous humour from the anterior chamber—paracentesis. After removal, a fluid is re-formed, but now it is no longer normal, the concentration of proteins being raised. The fluid is described as *plasmoid.* The breakdown of the barrier following paracentesis was attributed by Wessely (1908) to the sudden fall in intraocular pressure, causing an engorgement of the blood vessels of the uvea that led to dilatation of the epithelial linings and escape of protein into the anterior or posterior chamber.

OVERSHOOT

The return of the intraocular pressure to normal after paracentesis is often associated with an overshoot, bringing the pressure as high as 70 mmHg (Seidel, 1918; Kahn & Loewenstein, 1922), an overshoot that has been commonly attributed to blockage of the drainage channels by the fibrin in the plasmoid aqueous humour, but the release of prostaglandins (p. 56) and vasodilator substances, such as substance P, bradykinin and histamine, may also be involved.

Antagonism of Breakdown

Wessely (1900) showed that the breakdown could be prevented by sympathetic stimulation or treatment of the eye with epinephrine, and more recently Cole (1961) showed that the anti-inflammatory agent, polyphoretin, which has a direct action on capillaries, also prevented breakdown. It must be emphasized, however, that the degree of breakdown after paracentesis varies with the species, being very pronounced in the rabbit but much less in primates.

Physiological Significance

According to Bito (1982), the escape of proteins, including fibrinogen, into the anterior chamber serves to seal the anterior chamber after puncture by clotting of the re-formed aqueous humour. The source of the newly formed plasmoid aqueous humour is presumably the ciliary body and iris[36]; certainly the rate of refilling of the eye is much greater than can be accounted for by a normal secretion, so that a large part is simply a plasma exudate; thus the concentration of chloride in the newly formed fluid approximates that in a plasma filtrate rather than in normal aqueous humour (Davson & Weld, 1941).

Different Experimental Procedures

A breakdown of the blood-aqueous barrier may be brought about by a large variety of procedures, which

Table 1.8 Experimental procedures producing a breakdown of the blood-aqueous barrier (Eakins, 1977)

Trauma	*Endogenous mediators*
Mechanical injury to iris, lens	Histamine
Contusions	Bradykinin
Paracentesis	Prostaglandins
	Serotonin
Chemical irritants	Acetylcholine
Nitrogen mustard	
Formaldehyde	*Miscellaneous*
Acid burns	Bacterial endotoxins
Alkali burns	X-ray irradiation
	Laser irradiation
Nervous activity	
Stimulation of trigeminal nerve	
Immunogenic mechanisms	
Bovine serum albumin	

may be summarized by Table 1.8. The common causative feature in the rise of intraocular pressure may well be irritative dilatation of the blood vessels of the anterior uvea; the dilatation *per se* would cause an acute rise in pressure, increasing the intraocular contents and promoting a passive filtration of plasma, carrying with it a variable amount of protein. A rise in episcleral venous pressure would also contribute, since the aqueous veins fill with blood (Cabanas & Ugidos, 1954). The importance of vasodilatation is manifest in the observation that polyphloretin phosphate usually prevents the manifestations of breakdown of the barrier (Cole, 1961).

Reactive Hypotonia

The phase of acute rise in intraocular pressure usually gives way, after a short time, to a prolonged phase of lowered intraocular pressure (Larsson, 1932).

Prostaglandins

Ambache (1957) extracted a substance from the iris that he called irin; this seemed to be responsible for the pupillary constriction that followed stroking the iris or mechanical stimulation of the trigeminal nerve (Maurice, 1954), insults that are associated with barrier-breakdown. Subsequent work showed that irin belonged to a class of lipids given the general name of prostaglandins, and derived from arachidonic acid, a fatty acid derived from breakdown of membrane phospholipids. Figure 1.59 illustrates the cyclo-oxygenase catalysed synthetic pathway for one, namely prostaglandin E_2 (PGE_2).

A second pathway, catalysed by lipogenase, gives rise to another group of active compounds; this enzyme is also present in the iris of most species, and gives rise principally to 12-HETE, which is chemotactic for leucocytes; 5-HETE, and 5,12-di-HETE (leukotriene). Thus leucocyte infiltration, often seen with barrier-breakdown, is induced by lipoxygenase products. The specific inhibitor for this pathway is BW 755, whereas those for the cyclo-oxygenase pathway are aspirin and indomethacin.

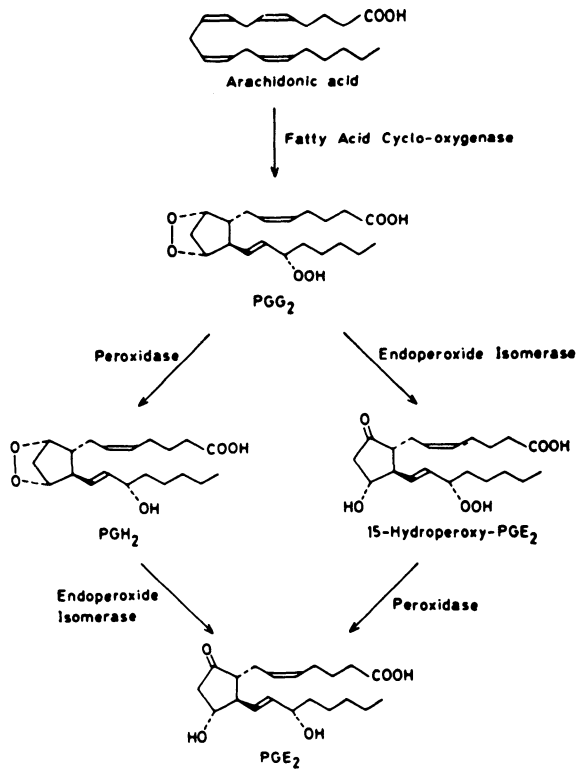

Fig. 1.59 Pathways of biosynthesis of PGE_2 from arachidonic acid. (Eakins, *Exp. Eye Res.*)

Effects on Eye

Waitzman & King (1967) injected prostaglandins E_1 and E_2 into the anterior chamber of the rabbit's eye and obtained a sustained rise in intraocular pressure accompanied by a contracted pupil; the effect on facility of outflow was slight, so they concluded that the influence was on the production of fluid; these authors stated that the protein content of the aqueous humour was not raised significantly, but Beitch & Eakins (1969) found a considerable increase. As Cole had found with breakdown induced by nitrogen mustard, the effects of prostaglandin could be blocked by polyphloretin. Prostaglandin synthetic enzymes are present in the ocular tissues (Bhattacherjee & Eakins, 1974) and the precursor of prostaglandins, arachidonic acid, is effective in causing breakdown of the barrier.

Inhibitors of Prostaglandin Synthesis

The synthesis of prostaglandins is inhibited by aspirin and indomethacin (Ferreira *et al.*, 1971), and the breakdown of the barrier caused, for example, by paracentesis, may be largely inhibited by these agents (Unger *et al.*, 1975).

Synthesis

Prostaglandin synthetic enzymes are present in the eye tissues (Bhattacherjee & Eakins, 1974; 1983), whilst incubation of iris and retina of the rabbit with arachidonic acid gives rise to PGs E_2, $F_{2\alpha}$, 6-keto-$F_{1\alpha}$, thromboxane (Tx) B_2 and LTB_4. The main product of the iris is PGE_2 and LTB_4, this latter stimulating chemotaxis and therefore likely to be involved in this response to injury, whilst PGE_2 reproduces most of the features of ocular inflammation (Preud'homme *et al.*, 1985).[37]

Aqueous Humour Concentrations

In the normal aqueous humour prostaglandins may be assayed, the predominant ones being PGs E_2, F_2 and D_2, with minor amounts of 6-keto-$PGF_{1\alpha}$ and thromboxane B_2. In the laser-treated eye these amounts increased, especially that of PGE_2 which rose from 87 pg/ml to 5.5 mg/nl (Weinreb *et al.*, 1985). The release of PGs into the aqueous humour, caused by injury, is blocked by indomethacin (Miller *et al.*, 1973). When different prostaglandins were compared for activity in raising the intraocular pressure, Beitch & Eakins (1969) found the order:

$$E > E_2 > F_{2\alpha} > F_{1\alpha}$$

Species Variations

The cynomolgous monkey's eye is much less sensitive to PGs than the rabbit's, and in this species Kelly & Starr (1971) found that the changes in protein concentration in the aqueous humour were unrelated to the rise in intraocular pressure, suggesting that something more than a breakdown of the barrier was involved in the rise in pressure. In this connection it is worth noting that Bito & Klein (1981) have shown that the lagomorph (rabbit) is apparently uniquely sensitive to doses of X-rays that induce cataract; they exhibited a full-blooded inflammatory response, including hyperaemia of the iris and ciliary body and cellular infiltration. All other species tried failed to respond in this way, and it was suggested that, in the rabbit, X-rays triggered activity in enzymes that led to the synthesis of PGs and related derivatives of arachidonic acid, whereas they failed to do so in other species.

Nervous Versus Chemical Influences

The rise in intraocular pressure and breakdown of the barrier caused by nitrogen mustard are not inhibited by pretreatment of the animal with aspirin, in contrast with the inhibition of the effects of paracentesis (Neufeld *et al.*, 1972). In further contrast, the effects of nitrogen mustard can be partially inhibited by retrobulbar anaesthetics, such as lidocaine, as indeed Davson & Huber (1950) had found, and the effects are completely blocked by retrobulbar alcohol or tetrodotoxin, whereas these sensory blocks had no effect on the breakdown due to paracentesis (Jampol *et al.*, 1975). A similar discrepancy is found with the breakdown associated with stimulation of the trigeminal nerve. Thus Perkins (1957) showed that stimulation of N V, especially if brought about mechanically, caused a marked rise in intraocular pressure accompanied by dilatation of the intraocular blood vessels and a breakdown of the blood-aqueous barrier. This is presumably an antidromic response to sensory nerve stimulation causing a primary vasodilatation in the anterior uvea. These effects are not blocked by aspirin (Cole & Unger, 1973); again, the breakdown due to formaldehyde is not inhibited by aspirin-like drugs (Cole & Unger, 1973). Finally, laser irradiation, a process that is used clinically to cause lesions in the iris allowing communication between anterior and posterior chambers (laser iridotomy), causes a transient breakdown of the barrier with pupillary constriction (Unger *et al.*, 1974). These effects are only partially blocked by indomethacin, but the residual effect is blocked by tetrodotoxin, indicating the operation of a nerve-mediated influence similar to that caused by nitrogen mustard (Unger *et al.*, 1977). Thus we must distinguish two main effects of the various modes of causing barrier-breakdown, the one caused by liberation of prostaglandins and the other by nervous activity, which is probably mediated by an axon-reflex through N V, involving, perhaps, the liberation of Substance P, since a combination of indomethacin and the SP-inhibitor, (D-arg^1, D-pro^2, Dtrp^{7,9}, leu^{11})SP, practically abolished all the effects of Substance P (Stjernschantz *et al.*, 1986).

Substance P

Stjernschantz *et al.* (1979) observed, with electrical stimulation of N V, a miosis, increased uveal blood-flow, increased protein in the aqueous humour, and an 80% increase in intraocular pressure. They suggested that at least one of the factors involved was Substance P, which would cause vasodilatation and miosis. This peptide is probably the transmitter released by a sensory nerve at its synapse in the central nervous system; it is also, apparently, released at the nerve's peripheral endings (Olgart *et al.*, 1977). Stjernschantz *et al.* (1979) and Bill *et al.*

(1979) measured a release of Substance P-like immunoreactivity into the aqueous humour following stimulation of N V. When Substance P was introduced into the anterior chamber in doses of 1–150 ng, there was a strong miosis with no effect on intraocular pressure or protein in the aqueous humour; with higher doses (0.8–11 μg) there were also a rise in pressure and protein in the aqueous humour. There was, however, no correlation between the protein content and rise in pressure. When Substance P was given intravitreally, a less traumatic method than intracameral, there was no rise in protein in the aqueous humour. The authors concluded that the release of Substance P by stimulation of N V would produce the observed miosis, but that the rise in pressure and protein were due to some other agent.[38]

Species Differences

Unger & Tighe (1984) point out that the rabbit eye is much more sensitive to damage than the primate eye; they have shown that there are striking species differences with respect to sensitivity of the isolated iris to Substance P; preparations from rabbit, pig and cow showed strong responses, whilst those from cat, dog, baboon and human eyes were unresponsive. Bito (1982) has suggested that animals with laterally directed eyes, like the rabbit, have developed a high sensitivity to irritation, in the sense that miosis and breakdown of the barrier are amplified, the breakdown of the barrier especially preventing excessive leakage of aqueous humour by the clotting that occurs. Animals with frontally directed eyes do not employ this protective measure, perhaps because they are not so liable to injury.

DEPENDENCE ON SENSORY INNERVATION

Butler & Hammond (1980) unilaterally destroyed N V diathermically and found a lowered intraocular pressure on the affected side; their striking finding, however, was that the action of intracameral PGE_1 and bradykinin on intraocular pressure, etc., was greatly reduced or abolished. With Substance P there was extreme miosis. Thus the responses to PGE_1 and bradykinin depend on an intact sensory nerve, and the failure to obtain a response in the denervated eye is presumably due to the failure of the sensory nerve to release its transmitter (Substance P). Thus in the intact eye prostaglandin presumably acts on the sensory nerve terminal, causing it to release active material. In the situation where a part of the response is blocked by anaesthesia or nerve destruction (as in laser injury), the blocked part might be due to stopping spread of the stimulus by axon reflexes, whilst the other component, not blocked, would be due to a direct action on nerve terminals.[39]

Calcitonin Gene-related Polypeptide (CGRP)

This novel polypeptide, encoded within the calcitonin gene (Rosenfeld *et al.*, 1983), occurs in the central nervous system (Gibson *et al.*, 1984); and in the eye it is confined to the sensory neurones of the iris and ciliary body. According to Unger *et al.* (1985), it causes breakdown of the blood-aqueous barrier with increased intraocular pressure and vasodilatation after intracameral injection. Oksala *et al.* (1986) have shown that, after stimulation of the trigeminal nerve in rabbits, immunoreactive CGRP could be detected in the aqueous humour, accompanied by hyperaemia, increased intraocular pressure and miosis.

Sympathetic Antagonism

Wessely (1900) observed that sympathetic stimulation reduced the effects of paracentesis, and Davson & Matchett (1951) found a similar effect on the breakdown of the barrier by nitrogen mustard. Again, Waitzman (1970) showed that prostaglandin raised the intraocular pressure more effectively if the superior cervical ganglion was removed. If, as we may assume, the breakdown of the barrier is a consequence of vasodilatory activity, it is not surprising that this should be counteracted by sympathetic stimulation. However, Unger *et al.* (1981) suggested that a part of this effect, which they observed in the laser-irradiated eye, might be due to the increased levels of Substance P in Substance P-immunoreactive nerve fibres observed after ganglionectomy (Zhang *et al.*, 1984).[40]

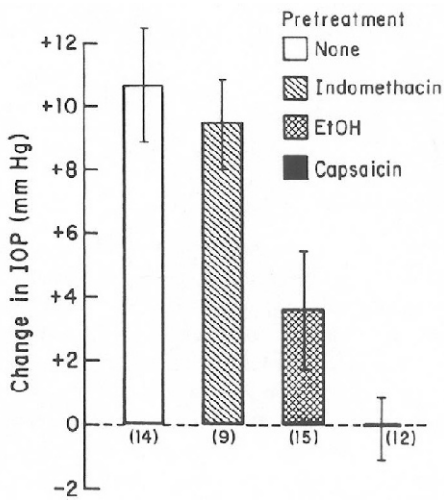

Fig. 1.60 Mean peak change in IOP during the first hour after topical application of nitrogen mustard to normal eyes or to eyes 1 to 3 days after retrobulbar or intracranial pretreatment with capsaicin; 2 to 3 weeks after retrobulbar EtOH injection; or 1 hr after systemic indomethacin pretreatment. The limits represent ±1 S.E.M. Number of eyes in parentheses. (Camras & Bito, *Invest. Ophthal.*)

Biphasic Response to Nitrogen Mustard

Camras & Bito (1980a, b) showed that nitrogen mustard gave rise to a second rise in intraocular pressure after the initial acute rise; this second phase reached its maximum in about 6 hr. The important feature of this second phase is that it was blocked by indomethacin, which also accelerated the return of the pupil-size to normal. Retrobulbar alcohol blocked the initial rise and reduced the peak miosis, leaving the secondary rise in intraocular pressure unaffected; combined indomethacin and ethyl alcohol treatment completely blocked the rise in intraocular pressure, inhibited the aqueous flare and cellular invasion, and the accumulation of prostaglandin in the aqueous humour for at least 12 hr following nitrogen mustard application. They consequently divided the action of nitrogen mustard into three phases: (1) an initial neurogenic irritative response, probably mediated by Substance P; (2) an inflammatory phase at least partially mediated by prostaglandins; (3) a degenerative phase presumably caused by direct cytotoxic effects of nitrogen mustard, leading to coreal opacification, etc. Capsaicin[41] completely blocked the secondary rise in pressure (Fig. 1.60).

Miosis and Inflammation

Bito *et al.* (1982) have emphasized the apparently unique position of miosis in the syndrome of barrier breakdown. They injected PGE_2 intravitreally into the rabbit eye, and observed flare, raised pressure, iridial hyperaemia but minimal miosis. When vasoactive polypeptides were injected, e.g. Substance P, SP-8, eledoisin-related peptide, there was maximal miosis; vasoactive intestinal polypeptide (VIP), bradykinin, and ST gave

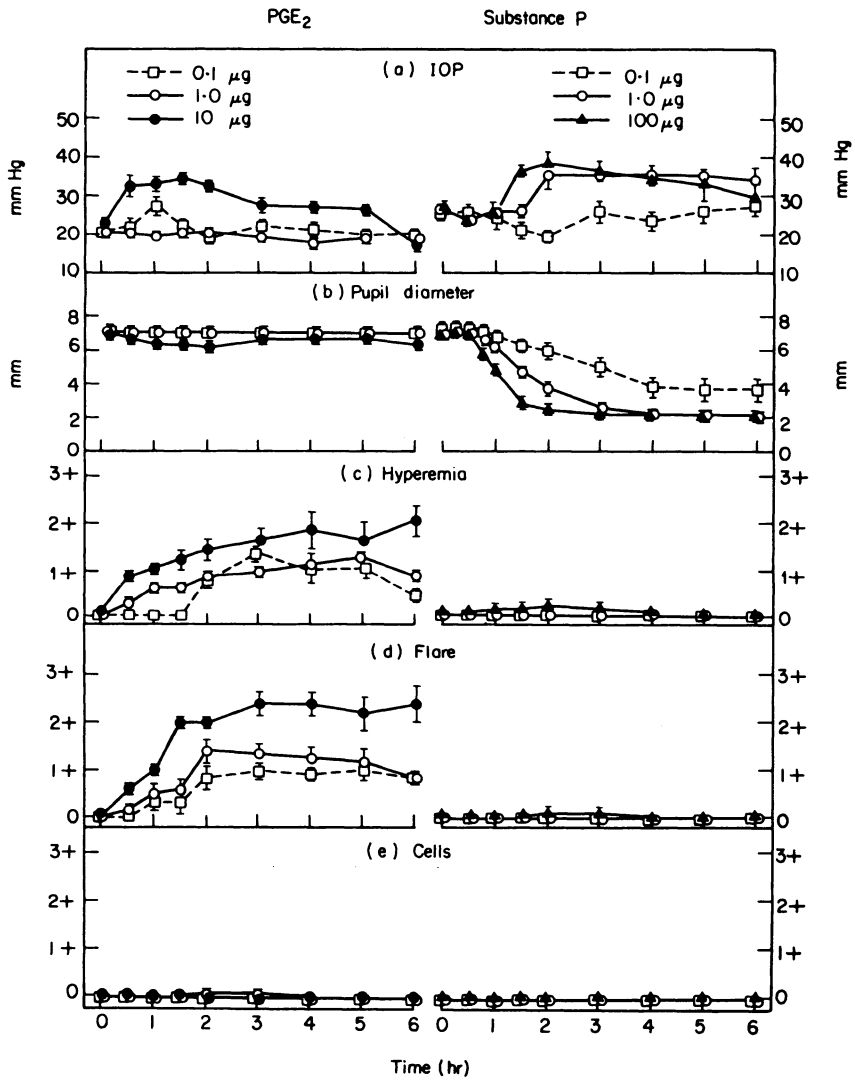

Fig. 1.61 Comparison of the ocular effects of intravitreally injected PGE_2 and Substance P (SP). The points are means obtained from at least four rabbits. The limits are ± S.E.M. (Bito *et al.*, *Exp. Eye Res.*)

submaximal miosis; A II, MSH, poly-DL-alanine gave little or no miosis. None of these peptides gave iridial hyperaemia or cellular invasion (Fig. 1.61) of the anterior chamber. They concluded that the initial, neurogenic effects of chemical irritants, such as nitrogen mustard, could not be entirely due to Substance P since this peptide must be present in concentrations to give maximal miosis if it is to raise the intraocular pressure to high levels, whereas miosis is by no means maximal when the pressure is very high after treatment with nitrogen mustard. Thus some other agent must contribute to the initial response, which is not blocked by indomethacin and therefore presumably not due to prostaglandins. They emphasize, however, that PGE_2 combined with Substance P (Fig. 1.62) gives maximal miosis and all the signs of ocular irritation except cellular invasion, which is probably due to autocoids produced through the lipogenase pathway.

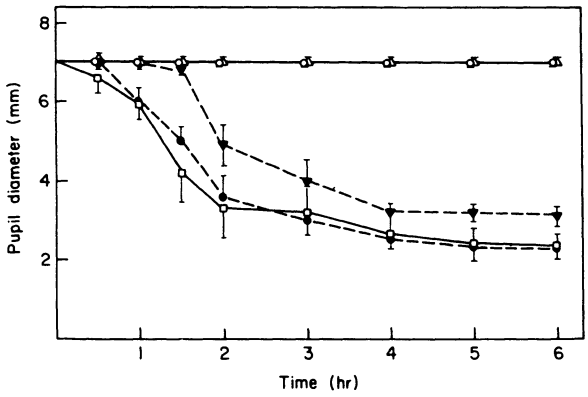

Fig. 1.62 The potentiation of the miotic effect of intravitreally injected SP by low doses of simultaneously injected PGE_2 or arachidonic acid. (○) 0.1 μg PGE_2; (△) 100 μg AA: (▼) 0.1 μg SP; (□) 100 μg AA + 0.1 μg SP; (●) 0.1 μg PGE_2 + 0·1 μg SP. (Bito *et al.*, *Exp. Eye Res.*)

Adrenergic and Serotonergic Block

Uusitalo (1984) found that phentolamine partially blocked the response to corneal application of formaldehyde; since this blocks both adrenergic and serotonergic activity, Krootila *et al.* (1987) applied specific inhibitors, namely methysergide and prazocin to block 5-HT and alpha-adrenergic activity respectively. Both inhibited the peak rise in pressure, but neither inhibited the miosis or breakdown of the barrier, perhaps because these effects are caused by Substance P and calcitonin gene-related peptide (CGRP) respectively (Unger *et al.*, 1985).

Hypotensive Effects of Prostaglandins

Many of the classical workers described a long-lasting hypotonia following the application of drugs or mechanical insults that originally caused a rise in intraocular pressure with breakdown of the blood-aqueous barrier (e.g. Poos, 1937). Starr (1971) found a dose-dependent fall in intraocular pressure on introducing prostaglandin into the aqueous humour, occurring after the initial hypertensive response. When the hypertensive phase was inhibited by the anti-inflammatory drug polyphoretin, this later hypotensive phase was unaffected. The effect could well be mediated through the facility of drainage, since even during the hypertensive phase an increase of this parameter can be measured. Thus Masuda & Mishima (1973) measured rate of secretion, true facility and pseudofacility. At the high pressures due to prostaglandin there was increased flow of aqueous humour accompanied by an increase in pseudofacility, indicating that the increased flow was pressure-dependent, i.e. due essentially to ultrafiltration. Thus there was no apparent increase in true facility or change in resistance at the angle, at any rate so far as the acute phase was concerned. Camras *et al.* (1977), however, found a prolonged fall in intraocular pressure after topical application of PGE_2 to the rabbit's eye; this followed the initial rise and lasted some 15–20 hr. As Fig. 1.63 shows, the associated increase in protein content and fall in ascorbic acid concentration had returned

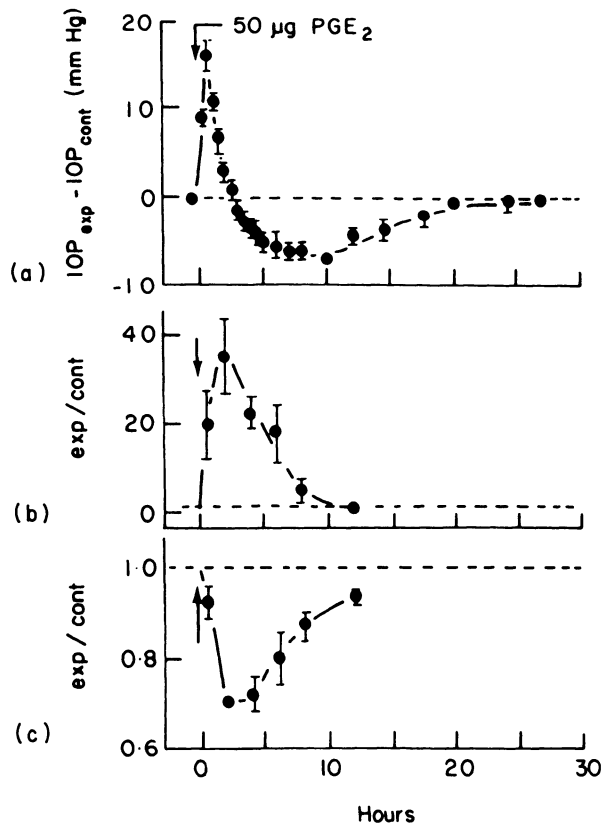

Fig. 1.63 Time-courses of changes in intraocular pressure (A), protein-content (B) and ascorbate content (C) of aqueous humour after topical application of 50 μg of PGE_2 to one eye. (Camras *et al.*, 1977.)

to normal before the pressure had returned to its initial value, suggesting a change in resistance to drainage. With a low dose of PGE_2, insufficient to cause a rise in pressure, the immediate effect was a fall in pressure. This was unaffected by indomethacin, showing that the low pressure is not due to endogenous prostaglandins. In the cat, an initial rise in pressure is only obtained with very high doses, so that with, say, 500 μg the only effect is a fall (Fig. 1.64). Hoyng *et al.* (1986) were able to reduce the initial hypertensive phase due to trauma by pretreatment

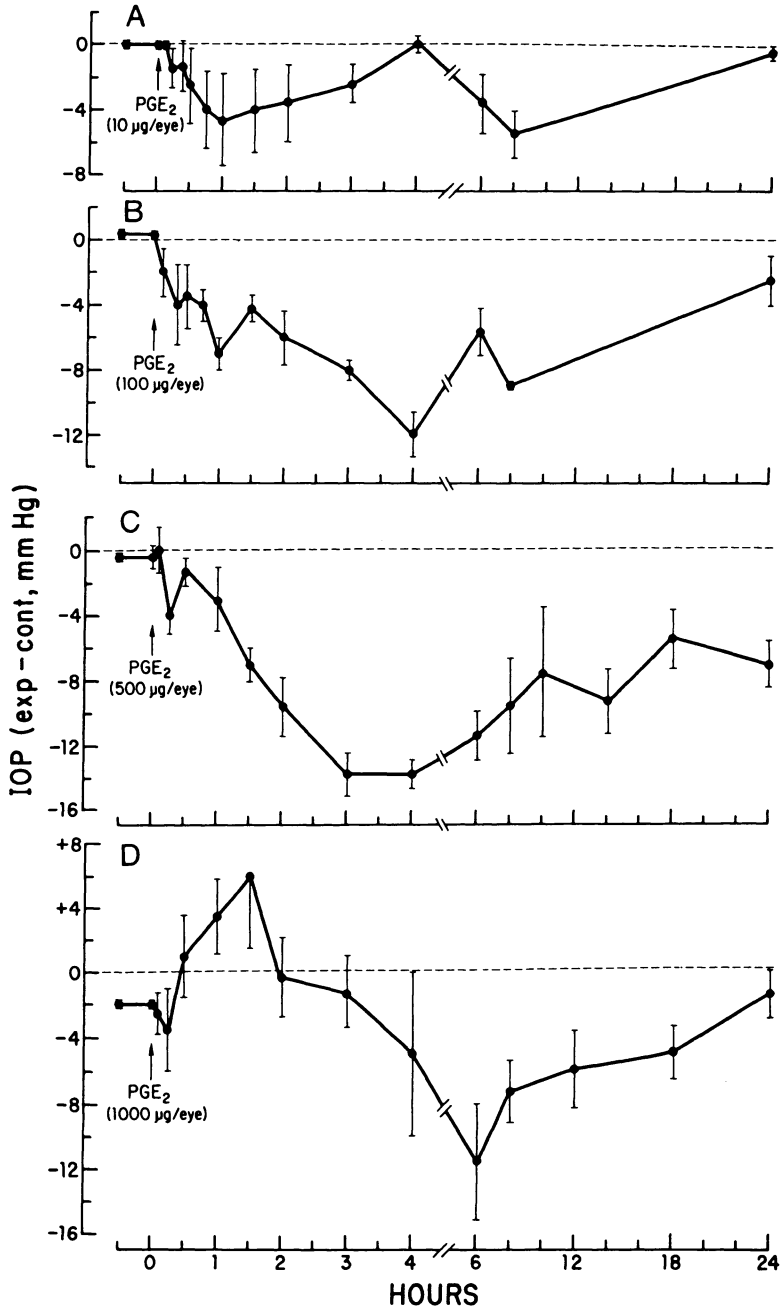

Fig. 1.64 Effects of topical application of 10 to 1000 μg of PGE_2 on the IOP of cats. Points represent the mean IOP values obtained on four (A, B, and D) or five cats (C). The limits represent ± S.E.M. (Stern & Bito, *Invest. Ophthal.*)

of the eye with PGE_1 or PGF_2. Thus the trauma consisted of corneal puncture without loss of aqueous humour so that changes in the composition of the fluid could be estimated at the end of the experiment. The trauma caused a biphasic rise and fall in pressure associated with an increase in protein content of the aqueous humour from 0.5 to 33.5 g/litre; ascorbic acid concentration fell from 29.8 to 17.9 mg/100 ml and PGE_2 rose from 0.04 to 1.6 ng/ml. Pretreatment with PGE_1 or $PGF_{2\alpha}$ reduced the rise and subsequent fall in pressure (Fig. 1.65), and also the rise in protein and fall in ascorbic acid concentrations. Since the authors found no change in facility, they concluded that pretreatment with PGE_1 or $PGF_{2\alpha}$ exerted its effect by virtue of reducing the production of PGE_2 in the eye. Thus, all the effects of the trauma were entirely abolished by indomethacin, so that in this uncomplicated system, anything that reduces the endogenous release of prostaglandins must be expected to reduce these effects, i.e. reduced ascorbic acid and increased protein concentrations.

POSSIBLE CLINICAL APPLICATION

The reduction in intraocular pressure caused by low doses of prostaglandin might well have clinical interest in the treatment of glaucoma, especially if the attack is on the drainage pathway.[42] Since, moreover, in many species, there is no initial hypertensive phase after topical application of prostaglandins, e.g. in the cat and monkey, (Stern & Bito, 1982), it could be that appropriate eucosanoids might be found that could be employed safely. Bito (1984) found that methyl-esters of prostaglandins could be 10–50 times more effective in lowering pressure than $PGF_{2\alpha}$, presumably by virtue of their greater lipid-solubility that permits more rapid diffusion across the cornea (Bito & Baroody, 1987).

Employing a prostaglandin of the A-class, derived from prostaglandins of the E-type by dehydration and isomerization, which had been found to be highly effective in reducing intraocular pressure, producing a much smaller hyperaemia than that of the prostaglandins of the F-class (Bito *et al.*, 1983), Hayashi *et al.* (1987) compared the

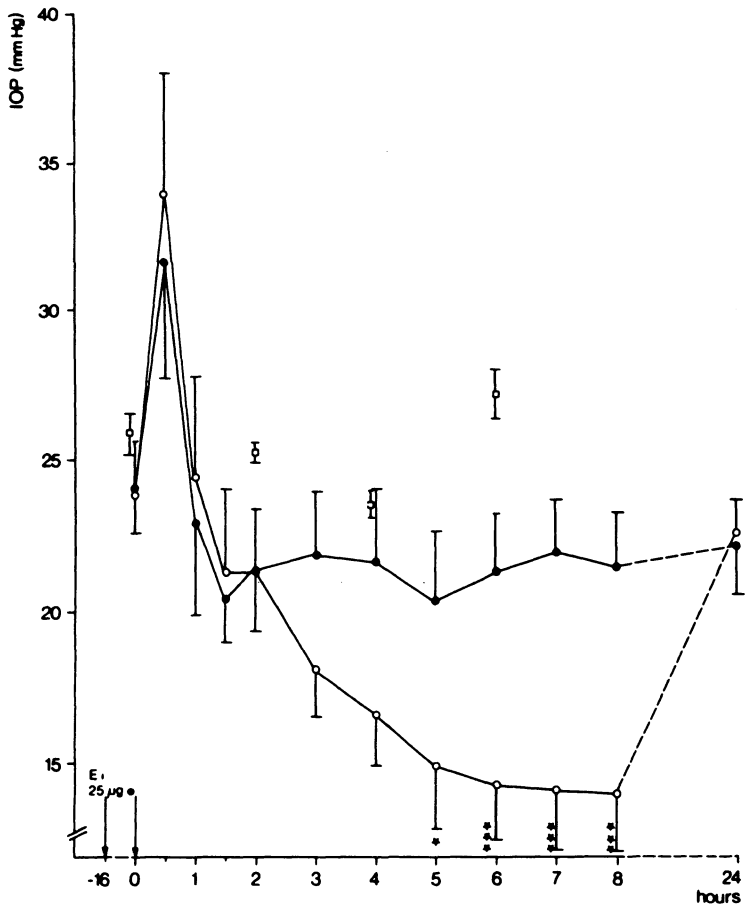

Fig. 1.65 Effect of corneal puncture (0 hr) on intraocular pressure in normal eyes (○—○) and contralateral eyes (●—●) pretreated with topical PGE_1 (25 µg in 30 µl PBS, 16 hr prior to puncture). Baseline IOP measurement is average of values for both eyes (□—□) obtained one day before experiment. The points represent means ±S.E.M. (eight rabbits). (Hoyng *et al.*, *Invest. Ophthal.*)

effects of the esterified derivative of PGF_2 with those of PGA_2 on intraocular pressure; they also measured rate of flow of aqueous humour by fluorophotometry, and facility using tonometry; pressure in the episcleral veins was also measured. Both prostaglandins produced falls in pressure, but these were not associated with change in flow-rate or outflow facility. The authors suggested that the hypotensive effects of prostaglandins were due to increased uveoscleral flow, due presumably to an action on the ciliary muscle. Thus, if contraction of the ciliary muscle reduces this uveoscleral flow by reducing the intercellular channels between ciliary muscle fibres, as suggested by Bill & Walinder (1966; see p. 75) then a relaxation would have the opposite effect, but of course would not favour opening up of the trabecular meshwork. It is of interest, at any rate, that the ocular hypotensive effects of PGF_2 are blocked by pretreatment with pilocarpine (Crawford & Kaufman, 1987).

RELATION TO ADRENERGIC SYSTEM

If the hypotensive response to prostaglandins is, as Bito considers, due to an increased facility of outflow, we are brought to consider the relation of this action to that of adrenergic agents that apparently likewise exert an influence on intraocular pressure through the drainage pathway, in addition to an effect on the secretory process. Thus the low intraocular pressure caused by epinephrine can be blocked by indomethacin (Bhattacherjee & Hammond, 1977), suggesting that prostaglandins form a link between the adrenergic agonist and its target tissue. Again, noradrenaline and other catecholamines stimulate the synthesis of prostaglandins in various tissues, including the iris-ciliary body (see, for example, Yousufzai & Abdel-Latif, 1983).

Species Variations

Lee *et al.* (1984) have compared the rabbit, cat, and monkey with respect to the action of PGF_2 on intraocular pressure and rate of flow of aqueous humour. In the rabbit and monkey a biphasic response was obtained, but in the cat only a fall in pressure. Monkeys showed no breakdown of the barrier whereas the rabbit and cats showed some. The miosis was strongest in the cat. Aqueous flow was unaffected in all apecies. Earlier Stern & Bito (1982) had compared the effects of PGs E_2 and F_2 in the cat and monkey. E_2 caused a fall in intraocular pressure of the cat with no pupillary constriction or flare, whereas F_2 caused profound constriction. In the monkey both prostaglandins produced hypotension without any pupillary constriction. Thus, in general, doses of PGE_2 and F_2 that reduce the intraocular pressure of the monkey fail to cause pupillary constriction or flare. In the cat this is true for PGE_2 but not for F_2 which causes pupillary constriction. When rabbit and monkey are compared they behave similarly with respect to intraocular pressure, but with the rabbit, breakdown of the barrier occurs with very low doses.

Tachyphylaxis

In the monkey, Bito *et al.* (1983) found tachyphylaxis with multiple dosing of PGF_2; Camras *et al.* (1987) applied the prostaglandin to one eye of monkeys for two weeks and measured a sustained lowering of intraocular pressure of some 10 mmHg by the seventh dose. The contralateral eye had a reduction of some 6 mmHg. There was no change in aqueous flow-rate, as measured fluorophotometrically, so it was assumed that resistance to drainage had been reduced.

Morphology of the Breakdown

The early studies of Smelser & Pei (1965) and Bairati & Orzalesi (1966), employing electron microscopy of the anterior segment of the rabbit after paracentesis, demonstrated changes in the pigmented layer of the ciliary epithelium, the intercellular spaces being dilated to form large vacuoles or 'cysts', changes that had been described in the light microscope by Greeff (1894). In spite of this the cells retained their attachments both to the basement membrane and the non-pigmented layer. In man, where the effects of paracentesis are not so great, there were only slight dilatations of the intercellular spaces.

IRIS

The literature contains discordant results as to the involvement of this tissue in barrier breakdown, perhaps due partly to species variations (Shakib & Cunha-Vaz, 1966; Raviola, 1974; Szalay *et al.* 1975). According to Cole's (1974) study, employing vasodilator drugs to cause breakdown, the escape of fluorescein occurred primarily into the posterior chamber, implicating the ciliary body; the drugs caused escape of carbon particles from the blood capillaries of the ciliary body but not from those of the iris.

CILIARY PROCESSES AS MAIN SITE

Cole (1974) emphasized that this obvious increase in ciliary body capillary permeability is not the whole mechanism, since in the normal eye there is some escape of proteins through the ciliary capillaries (Bill, 1968b), further progress being prevented by the ciliary epithelium. Thus a breakdown of the occluding junctions between ciliary epithelial cells is also necessary, and this may be the mechanical consequence of the oedematous condition of the ciliary processes, or it may be that the primary cause of the breakdown affects capillary endothelium and ciliary epithelium together. Extending this work to the situation of paracentesis, Unger *et al.* (1975), using the same techniques of fluorescein angiography and colloidal carbon labelling, showed that the breakdown was indeed primarily in the ciliary processes; these were highly congested, whilst carbon particles were deposited

in the walls of their blood vessels, by contrast with those of the iris, which appeared normal.

PROSTAGLANDINS AND SODIUM ARACHIDONATE

In strong contrast to the effects of paracentesis, these substances, applied topically to the eye, caused increased permeability of the iris vessels, so that fluorescein appeared to come primarily from the anterior surface of this tissue rather than from the posterior chamber. Thus the effects of paracentesis are probably twofold; first, a release of prostaglandins which attack mainly the iris vessels, and secondly, because of the mechanical strains due to the fall in intraocular pressure, the ciliary body vessels are affected (Bhattacherjee & Hammond, 1975).

PARASYMPATHETIC STIMULATION

Uusitalo *et al.* (1974) studied the breakdown of the barrier, following N III stimulation, in the electron microscope. Horseradish peroxidase injected into the blood escaped into the stroma of the ciliary body; it no longer remained accumulated here between the two epithelial layers but presumably, because of the electrical stimulation, was able to pass into the aqueous humour between the epithelial cells at points where the tight junctions had opened. There was no evidence of a vasodilatation in the ciliary body, in that there was no extravasation of red cells into the stroma, and the capillaries seemed to be intact; and this is consistent with the studies of Perkins (1957) and Bill (1962). The ciliary epithelium of the stimulated eyes showed striking changes; in the pigmented layer there were saccular dilatations filled with slightly electron-dense material; these dilatations appeared to be intracellular and thus were giant vacuoles which projected into the intercellular space between pigmented and non-pigmented cells, interrupting this. In the non-pigmented layer there were also dilatations at the lateral borders of the cells, dilatations that seemed to contain electron-dense material.

GREEFF VESICLES

In so far as it allowed the comparison of stimulated and unstimulated eyes in the same animal, this study, although not very instructive as to the nature of the dilatations, i.e. as to whether they were inter- or intracellular, does confirm the fact that breakdown of the barrier is, indeed, associated with the appearance of 'vesicles' probably the same as the Greeff vesicles described so long ago in the light-microscope. That nervous stimulation alone, apparently not producing vasodilatation, can produce these morphological changes is of great interest and could mean some nervous influence on the intactness of the blood-aqueous barrier.

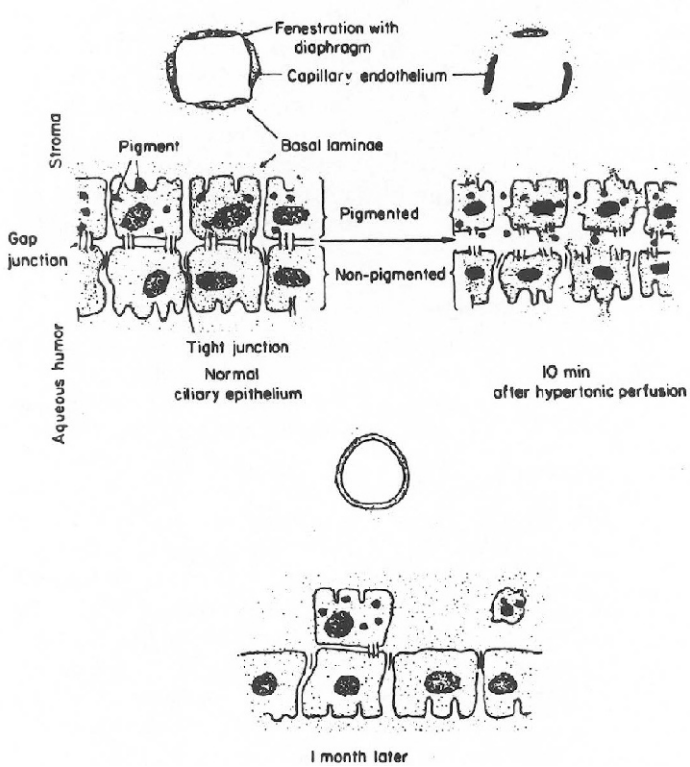

Fig. 1.66 Summary of structural changes in the ciliary epithelium as a consequence of an internal carotid perfusion of hypertonic solution for 20–30 s. (Rapoport, *Exp. Eye Res.*)

Osmotic Agents

Infusion of a hypertonic solution into the internal carotid and ophthalmic arteries causes a rapid and reversible breakdown of the blood-aqueous and blood-vitreal barriers, as manifest by fluorescein penetration (Laties & Rapoport, 1976). Quantitatively the increase has been measured by Ennis & Betz (1986) in a simultaneous study of blood-retinal and blood-brain barriers; it amounted to a factor of about four. The effect is presumably due to shrinkage of the endothelial cells of the vascular system causing an opening of tight junctions. In bilayered ciliary epithelium the hypertonic solutions produce permanent structural changes, by contrast with the pigment epithelium adjacent to the retina where increased fluorescein permeability is not accompanied by any obvious structural change. As illustrated by Fig. 1.66, the pigmented layer of ciliary epithelium separates from the nonpigmented layer and eventually some 50% to 80% of the cells in this layer are lost; the structure of the nonpigmented layer rapidly returns to normal after separating from the pigmented cells, being connected at their basal tight junctions. The intraocular pressure is low immediately after infusion and ultimately returns to normal after 4 to 6 weeks indicating that *normal secretion of aqueous humour can occur in the virtual absence of the pigmented layer of ciliary epithelium.*

MONKEY

More recently Gaasterland *et al.* (1983) have examined the changes in the monkey, after an intracarotid bolus of mannitol, in greater detail. Within 1 hr, pigmented cells and proteins appear in the aqueous humour, and hypotony develops in 1 day. Within 2 weeks the flare in the aqueous humour has cleared, and intraocular pressure has returned to normal within 8–12 weeks. At the end of this period the ascorbic acid concentration in the aqueous humour is a little low but much greater than that in the plasma, indicating the power of actively accumulating this substrate despite permanent damage to the pigmented layer of the ciliary epithelium.

EFFECTS OF NERVOUS SYSTEM ON SECRETION AND PRESSURE

On theoretical grounds, nervous mechanisms may be expected to influence the steady-state intraocular pressure primarily by affecting either the resistance to outflow or the rate of secretion of aqueous humour. Temporary, non-steady-state, changes can be brought about by alterations in the volume of blood in the eye or mechanical compression brought about by the extraocular musculature. A direct influence of the nervous system on the secretory process is a possibility, whilst inhibition by drugs is well proven; alternatively, the secretory process may be limited by blood-flow in the ciliary body, in which event secretion could be controlled by an influence on the vasculature. The resistance of the angle of the anterior chamber could well be affected by the ciliary muscle, as originally suggested by Fortin (1929), since the trabecular meshwork is the insertion of the meridional fibres; a contraction of these fibres should open up the meshwork and promote percolation of fluid through the holes in the lamellae. An effect on the meshwork itself could be brought about by a shrinkage or swelling of the endothelial cells lining the trabeculae, and possibly through an alteration of the size of the vacuolar system in the inner wall of the canal of Schlemm. Finally the pressure within the blood vessels into which the aqueous humour drains—the episcleral venous pressure—may be influenced by nervous activity, either local or through the general vascular pressures.

Pharmacological Approach

The study of the effects of the nervous system on a physiological parameter, such as the intraocular pressure, is carried out predominantly by a study of the pharmacological actions of substances that are either identified as the transmitters liberated at nerve endings, such as acetylcholine and noradrenaline, or by substances that mimic these actions, e.g. pilocarpine for the parasympathetic system, or epinephrine, phenylephrine, isoproterenol for the sympathetic system, or exert a specific blocking action. This blocking action requires that the blocking agent have a strong affinity for the receptive sites of the agonist, e.g. curare or atropine for the acetylcholine-sensitive sites or phenoxybenzamine and propranolol for adrenergic sites, as on the heart or peripheral blood vessels. It is important to appreciate therefore that both agonist, e.g. acetylcholine, and antagonist, have affinities for the same site, or receptor, on the tissue being studied, the blocking action of the antagonist being due to its very high affinity that competitively prevents the agonist from gaining access. In the parasympathetic system we recognize two types of receptor to which acetylcholine or its synthetic analogues have access, the so-called *nicotinic* receptors, characteristic of the skeletal muscle neuromuscular junction and junctions within the sympathetic ganglia, etc., and the *muscarinic* receptors that are involved in excitation of many glands, smooth muscle, and so on.

Adrenergic Receptors

These are more complex; thus we may distinguish alpha- and beta-types of receptor which, in the same organ, usually exert antagonistic effects. Nerves of the sympath-

etic system liberate at their endings noradrenaline, or norepinephrine, whilst the adrenal secretion is adrenaline, or epinephrine. Noradrenaline excites predominantly alpha-receptors, with a small beta-action; adrenaline also has a mixed action, but excites beta-receptors more strongly. Synthetic agonists belonging to the two classes are, for example, phenylephrine (alpha-) and isoproterenol (beta-), whilst they are blocked by phentolamine and isoproterenol respectively. To complicate matters, the beta-receptors have been found to fall into two categories, $beta_1$, typically concerned with the heart-beat and excited by noradrenaline from sympathetic nerves, and $beta_2$, typically concerned with vasodilatation and relaxation of the lung, and excited by adrenaline but not by noradrenaline. Similarly, alpha-receptors are classified as $alpha_1$- and $alpha_2$- (Berthelsen & Pettinger, 1977; Fain & Garcia-Sainz, 1980). The $alpha_1$-receptors, according to their original definition, were the typical postsynaptic receptors at nerve endings, activation of which, for example, causes constriction of vascular smooth muscle, or mydriasis in the eye, whilst $alpha_2$-receptors were said to act presynaptically on sympathetic nerve endings, controlling release of transmitter. This morphological distinction is probably invalid (Mittag & Tormay, 1985), and the two are best characterized in terms of their agonists or antagonists. Thus clonidine is an $alpha_2$-agonist, and yohimbine and phentolamine are its blockers. Methoxamine and phenylephrine are $alpha_1$-agonists with their action blocked by prazocin. Figure 1.67 summarizes the relative $alpha_1$- and $alpha_2$-potencies of a number of agonists. Beta-activity is exerted by action on the enzyme adenylate cyclase, catalysing synthesis of cyclic AMP, which acts as 'second messenger'; according to Fain & Garcia-Sainz (1980), $alpha_2$-receptors inhibit adenylate cyclase, and thus inhibit beta-activity.[43]

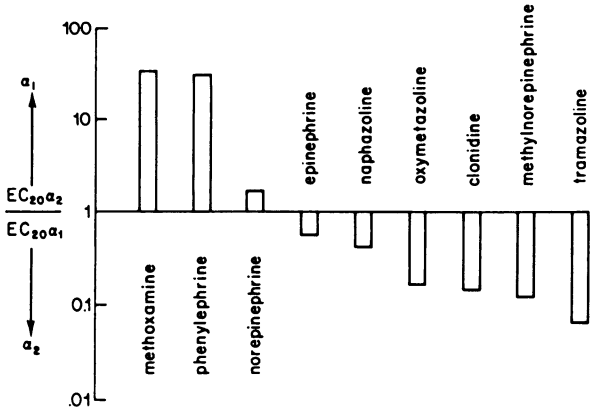

Fig. 1.67 Spectrum of agonist selectivity for α_1 versus α_2 receptors. $EC_{20}\alpha_2$ is the concentration of alpha agonist which causes 20% of maximal inhibition of electrically stimulated ^{3}HNE release from pulmonary artery segments *in vitro*. $EC_{20}\alpha_1$ is the concentration of the alpha agonist which causes 20% of maximal contraction of pulmonary artery strips *in vitro*. Thus, an agonist having a ratio $EC_{20}\alpha_2/EC_{20}\alpha_1$ greater than one is selective for the vascular α_1 receptor. A ratio of less than one indicates selectivity for the presynaptic α_2 receptor. (Berthelsen & Pettinger, *Life Sci.*)

COMPLEXITY

In general, especially with the adrenergic system, the action of drugs on the intraocular pressure will be complex and hard to resolve into specific components because so few of the drugs employed experimentally have a highly specific action on a given type of receptor so that, like the hormone epinephrine, it may have both alpha- and beta-actions. Moreover, as we have enumerated above, the intraocular pressure can, at least theoretically, be influenced by several parameters all of which need not necessarily be controlled by the same agonist.

For these, and other reasons, the analysis of adrenergic influences on the eye has not led to clear-cut conclusions; and this is revealed by the inconclusive nature of such reviews that have appeared (e.g. Kaufman, 1984; Potter & Rowland, 1981). To quote Mittag *et al.* (1985): 'The multiplicity of sites of action and of receptor types for the alpha-adrenergic drugs makes detailed analysis of their mechanisms of action in the iris-ciliary body particularly difficult'.

LOCALIZATION OF RECEPTORS

Specific receptors can be localized in tissue by causing them to react with a ligand that especially binds to them, and may be visualized histochemically, or may be assayed quantitatively. Visually, Dafna *et al.* (1979), for example, identified beta-receptors mainly on the ciliary epithelium by employing the fluorescent 9-amino-acridin-propalol, in albino rabbits. Trope & Clark (1982) used ^{125}I-HYP (iodohydroxybenzyl pindolol) and measured the ability of various known beta-blockers to displace this from the ciliary processes. Practolol with no $beta_1$-action was most effective indicating that the receptors governing adrenergic activity at the ciliary processes, and therefore influencing secretion of aqueous humour, were probably mainly, if not exclusively $beta_2$. If the iris was included in the preparation, some $beta_1$ activity was present.[44] In a study that included both alpha- and beta-receptors, Mittag & Tormay confirmed the predominance of $beta_2$-receptors on the iris-ciliary body cell membrane preparation; using ^{3}H-prazocin and WB-4101 to identify $alpha_1$-, and ^{3}H-yohimbine for $alpha_2$ receptors. Both types were found in the preparation, the total alpha-population being rather less than the beta-. Prazocin-reactive sites indicated the presence of $alpha_1$–sensitivity probably mediating a vasoconstrictor action in the ciliary body. Prazocin, applied to the eye, apparently reduced rate of

secretion (Krupin *et al.*, 1980) of aqueous humour, without affecting the alpha-constriction of the pupil, suggesting a specific set of alpha-receptors active on the blood vessels of the anterior uvea and possibly influencing rate of secretion of fluid. Alpha$_2$-sites were as numerous as alpha$_1$; these were presumably postsynaptic, being attached to cell membranes, and their presence may account for the effect of a typical alpha$_2$-agonist, clonidine, and alpha-methylnorepinephrine in reducing intraocular pressure (Innemee & Van Zwieten, 1979; Langham, 1982).

ADENYLATE CYCLASE

Beta-activity is considered to operate through the second messenger, cyclic AMP, so that activation of beta-receptors will excite adenylate cyclase. Nathanson (1980) isolated adenylate cyclase from an iris-ciliary body preparation and showed that its activity was increased by (−)-isoproterenol; the order of effectiveness of agonists was:

Isoproterenol > Epinephrine > Norepinephrine > Phenylephrine

which is the order expected of a beta$_2$-receptor, e.g. in trachial smooth muscle.

Sympathetic System

Stimulation of the peripheral end of the cut cervical sympathetic trunk in the rabbit causes a constriction of the uveal vessels associated with a marked fall in the intraocular pressure. This is accompanied by a considerable fall in blood-flow through the uvea; thus Alm & Bill (1973), working on the cat, and Alm (1977) on the monkey, measured blood-flow with radioactive microspheres. Results on the monkey are shown in Table 1.9, where a sympathectomized eye is compared with one where the cervical sympathetic on the non-sympathectomized side was stimulated for one minute. The effect on retinal blood-flow was small and probably insignificant, and this is consistent with a correspondingly small effect on cerebral blood-flow; presumably constriction of the retinal artery is compensated by the autoregulatory mechanism peculiar to the central nervous system.

Section of the Cervical Sympathetic

This, or extirpation of the superior cervical ganglion has, in general, remarkably little immediate effect on the normal intraocular pressure (Greaves & Perkins, 1952; Langham & Taylor, 1960), although occasionally quite large rises, lasting for thirty minutes, can be observed (Davson & Matchett, 1951). Twenty-four hours after ganglionectomy the intraocular pressure is definitely lower than normal, and a study of the dynamics of flow of aqueous humour suggested that this was due to a diminished outflow resistance, since P_e was said to be unaffected by the procedure. Tomar & Agarwal (1974) confirmed in rabbits the fall in pressure, reaching a maximum at about 24 hr; by 3 to 4 days, however, it had returned to normal. The fall in pressure was associated with an increased facility of outflow and the return to normal pressure was accompanied by a return to normal facility.

Chronic Stimulation

Langham & Rosenthal (1966) found that prolonged stimulation in anaesthetized rabbits reduced intraocular pressure, rate of secretion and blood-flow through the ciliary processes. Working on conscious rabbits Belmonte *et al.* (1987) used implanted electrodes; Fig. 1.68 illustrates the fall in pressure followed by a gradual return to normal in spite of the maintained stimulation. Rate of aqueous flow, measured by fluorophotometry, remained normal for as long as 120 min but

Table 1.9 Blood-flow through eye of monkey on sympathectomized side, and effects of sympathetic stimulation (Alm, 1977)

Tissue	*Blood flow in whole tissue* (mg/min) (sympathectomized side)	*Blood flow* (g/min/100 g tissue) (sympathectomized side)	*Percent reduction of blood flow on stimulated side*	*Significance level*
Retina	33±2		8±4	
Iris	4±1		52±7	$P<0.001$
Ciliary body	79±4		22±3	$P<0.001$
Choroid	558±59		30±6	$P<0.005$
Ciliary processes		120±18	23±8	$P<0.025$
Ciliary muscle		176±10	29±5	$P<0.001$
Anterior sclera		2±1	52±21	$P<0.05$

The weights for the ciliary processes and muscle are calculated from the dry weight on the assumption that dry weight/wet weight ratio is 0.20 (see Alm & Bill, 1972).

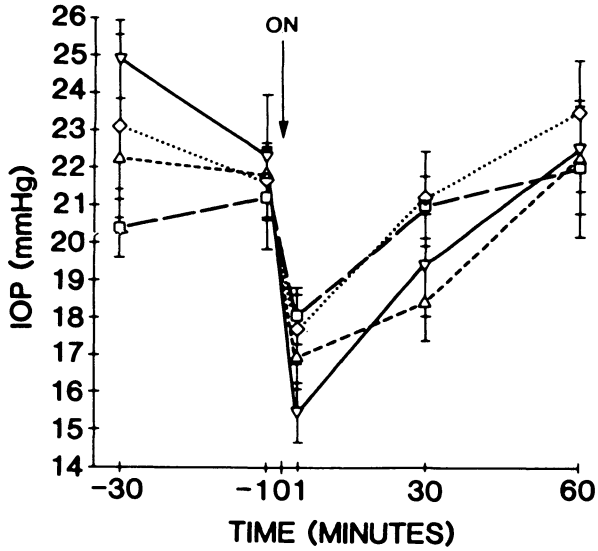

Fig. 1.68 The recovery of intraocular pressure during electrical stimulation of the cervical sympathetic at different frequencies in conscious rabbits. □, 3 Hz; ◇, 6 Hz; △, 9 Hz; ▽, 12 Hz. All points are means ± S.E.M. $n = 5$–11. (Belmonte *et al., Invest. Ophthal.*)

then showed a small decline. The alpha-blocker, phentolamine, reduced pressure itself, and so tended to obscure any effects of electrical stimulation; timolol, a beta-blocker, caused the electrically induced fall in pressure to reverse, to give a rise above normal.

CATECHOLAMINE RELEASE

The effect of ganglionectomy is definitely due to destruction of the postganglionic neurones, since preganglionic sympathotomy is without effect (Langham & Fraser, 1966). It is well known that denervation of a tissue causes hypersensitivity, and it was argued by Sears & Bárány (1960) that the resistance to flow was governed by an adrenergic mechanism which became hypersensitive after denervation, whilst the liberation of catecholamines from the degenerating terminals produced the adrenergic effect. The slow release of the catecholamines would account for the slow onset of the change, and the subsequent return of the intraocular pressure to normal would be accounted for by the eventual release of all stored catecholamines. The effects of reserpine and adrenergic blocking agents generally confirmed the hypothesis. This view is supported by the observation that the ganglionectomy effect was blocked by previous treatment of the animal with reserpine or guanethidine, and reduced by the alpha-blocker, phentolamine (Bárány, 1962). Moreover, robbing the animal of its adrenergic system by reserpine treatment caused a reduced resistance to flow.

INCREASED SENSITIVITY TO CATECHOLAMINES

The increased facility following ganglionectomy is attributable not only to release of adrenergic transmitter into the eye, but an increased sensitivity of the eye to adrenergic agents—the classical denervation hypersensitivity due to an increased formation of receptor sites normally held in check by the nerve terminals. Thus the resistance to outflow was shown by Sears & Sherk (1964) and Eakins & Ryan (1964) to be decreased to a much greater extent by intracamerally injected norepinephrine on the side of ganglionectomy in the unilaterally operated animal.

Effects of Topically Applied Adrenergic Agents

Classical studies, e.g. Poos (1931), reported a fall in intraocular pressure following application of epinephrine, a mixed alpha- and beta-agonist. That a contribution to this could be due to a change in resistance at the angle was shown by Sears & Sherk (1964), who found values for facility as high as 0.9 $\mu l\ min^{-1}\ mmHg^{-1}$ compared with 0.2–0.3 for control rabbits. In the monkey, Bill (1970a) attributed a similar increase in facility to beta-action. In Fig. 1.69 are shown the responses of the rabbit's intraocular pressure and pupil diameter to topically applied epinephrine. The two effects—mydriasis and hypotension—do not follow the same time-course, suggesting that the effect on intraocular pressure is more complex, perhaps involving both β- and α-activity. A β-blocker, propanolol, reduced the hypotensive effect by 17 per cent, indicating some β-action; a much larger reduction in the effect was produced by an α-blocker, e.g. phenoxybenzamine, indicating the predominantly α-action in the hypotensive response.

Salbutamol is a drug that has a purely β-action by contrast with the mixed effects of epinephrine; as Fig. 1.70 shows, it had no effect on pupillary diameter, but it produced an initial rapid fall in intraocular pressure which was over in 5 hr, by contrast with the more prolonged action of epinephrine (Fig. 1.69). It would seem, then, that the powerful and prolonged effects of epinephrine are due to its combined α- and β-actions working in the same direction. It is unusual for α- and β-actions on an effector to work in the same direction, the one usually inhibiting the other; it would seem, then, that the catecholamines can act at two sites, presumably at those influencing the rate of formation of fluid and the facility of outflow. Langham & Diggs (1974) concluded that the rapid beta-action was, in effect, a reduction in secretion rate, whilst the more prolonged alpha-action was due to an effect on facility. This could be achieved by reduction of blood-flow through the intrascleral plexus, leaving more room for aqueous flow in the mixed channels.

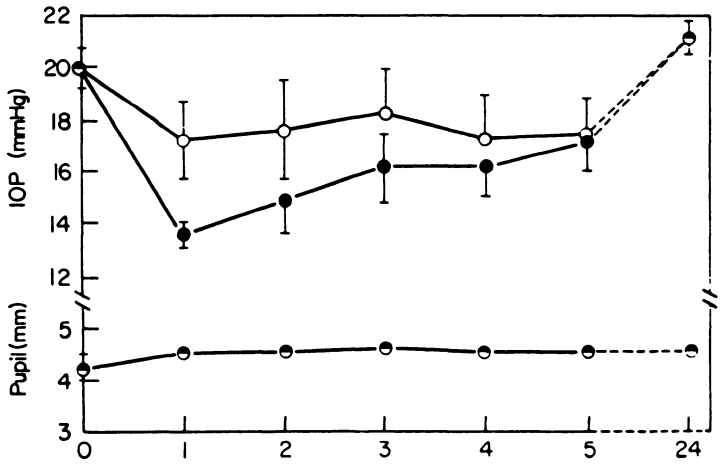

Fig. 1.69 The mean pupillary and intraocular pressure responses to a 2% solution of epinephrine. 25 μl of solution was applied topically to 1 eye (●—●) of 8 conscious rabbits at T = 0, 2 and 4 min. The contralateral eyes (○—○) were untreated. The vertical bars represent ±standard error of the mean. (Langham *et al.*, *Exp. Eye Res.*)

A similar conclusion had been reached by Innemee & Van Zwieten (1982), who pointed out that noradrenaline had no beta$_2$-activity, by contrast with adrenaline, and since adrenaline was more effective in reducing pressure, they concluded the effect must be beta$_2$. By employing the lipid-soluble dipivalyl adrenaline they built up higher intraocular concentrations and produced a much larger hypotensive effect than that produced by either adrenaline or noradrenaline. These authors argued that, since beta$_2$-blockers inhibited secretion, the beta$_2$-agonist could not lower intraocular pressure by an action on secretion, so they concluded on an action on the drainage mechanism, although it would be unlikely to act on receptors in the meshwork since, according to Kaufman & Bárány (1981) adrenaline and noradrenaline were equally effective in affecting facility, whilst noradrenaline does not affect beta$_2$-receptors.

SECRETION OF AQUEOUS HUMOUR

The predominant location of beta-receptors on the ciliary epithelium led to the suggestion that the hypotensive action of the beta-agonist, salbutamol, was due to an inhibition of rate of secretion, but as indicated above, this brings one into conflict with the well established inhibition of secretion by the *beta-blocker*, timolol. Thus Katz *et al.* (1976) showed, surprisingly, that the beta-*blocker*, timolol, reduced intraocular pressure in glaucomatous and normal human subjects; thus agonist and antagonist have the same effect on pressure. The blocker did not affect facility, and so presumably reduced rate of secretion

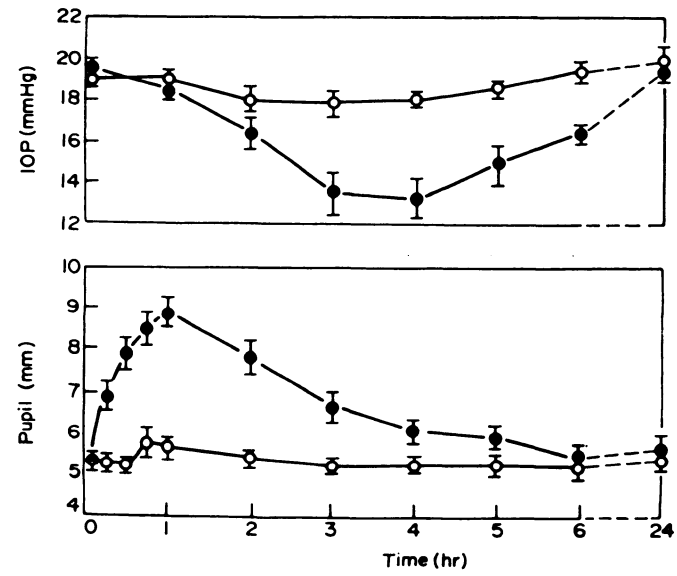

Fig. 1.70 The average time courses of the pupillary and intraocular pressure responses of conscious rabbits to salbutamol ascorbate applied topically. Twenty-five microlitres of a 2% solution (pH 6.5) were applied to one eye (●—●) of individual rabbits at 0, 2 and 4 min. The contralateral eyes (○ - - - ○) were not treated. (Langham & Diggs, *Exp. Eye Res.*)

(Zimmerman & Kaufman 1977; Sonntag *et al.*, 1978), a reduction confirmed by direct measurement of secretion rate by the fluorescein-method of Jones & Maurice (1966) by Coakes & Brubaker (1978) and Yablonski *et al.* (1978).[45] In the rabbit, there seems to be very little, if any, hypotensive effect of timolol or propranolol (Rowland & Potter, 1980).

Experimental studies on rate of secretion under the influence of beta-agonists have given no clear-cut evidence, probably because of the difficulty in making precise estimates in the intact eye, with the consequent resort to techniques involving anterior chamber puncture. Thus in humans Nagataki & Brubaker (1981) concluded that it was impossible to detect any significant change in aqueous flow with epinephrine, and the same was true for isoproterenol (Brubaker & Gaasterland, 1984). Employing the fluorescein technique of Johnson & Maurice (1984), a non-invasive and therefore reliable method, Araie (1985) found a biphasic effect of epinephrine, an initial 20% increase in flow with a subsequent decline over 5 hr to a 5% fall; both effects were abolished by the alpha-blocker, phentolamine. Salbutamol, the beta-agonist, caused falls of 22, 16 and 9% at 1, 2, and 4 hr respectively, effects that were blocked by timolol. By contrast, when intracameral infusion of fluorescein was used to measure secretion rate, salbutamol increased rate by 38%; timolol reduced it by 36%, and simultaneous administration of agonist and blocker gave no effect (Miichi & Nagataki, 1983).

CONTRALATERAL EFFECTS

In numerous studies of topically applied drugs, an effect on the contralateral eye has been described; if this happens, then, of course, the contralateral eye is a poor control for the effect of the drug. This is true of the beta-blocker, timolol, and has been variously attributed to a secondary effect of the drug on the cardiovascular system, cross-over to the contralateral eye through the systemic circulation in spite of the great decrease in concentration that results from passage out of one eye into the general circulation, or to a centrally mediated phenomenon (Radius *et al.*, 1978). In the rabbit, Woodward *et al.* (1987) compared the effects of intravenously administered timolol with those of topically applied doses to the eye; a distinct decrease in heart-rate was observed with topical application; in the contralateral eye virtually complete beta-blockade was established, in that the response to isoproterenol was abolished. The authors emphasize that the clinically employed concentrations of timolol (often as high as 1%) are far higher than those required to establish beta-blockade, since they found that a concentration of 0.01% was adequate to block the effects of isoproterenol on the ipsilateral eye.

Biphasic Response to Epinephrine

Before the obvious fall in intraocular pressure induced by epinephrine, there is usually an initial hypertensive phase, described by Kronfeld in humans (1971) and Norton & Viernstein (1972) in rabbits. Using an improved method of measuring rate of secretion, Johnson & Maurice (1984) were able to associate the initial rise in pressure caused by epinephrine with an initial rise in rate of secretion. The subsequent fall in pressure was accompanied by a fall in rate of secretion. The initial rise in pressure is mimicked by the almost pure alpha-agonist, norepinephrine, whereas the decline in pressure is reproduced by salbutamol, a beta-agonist. According to Woodward *et al.* (1986), the hypotensive response in rabbits is due to a $beta_2$-action; thus Fig. 1.71 shows the effects of L-isoproterenol (1), salbutamol and terbutalin, and (3) prenaterol, which are in this order which is the order of action on $beta_2$-agonists, prenaterol being a selective $beta_1$-agonist with very little $beta_2$-activity. Timolol and pindolol, $beta_2$-blockers, suppressed the effects whereas the $beta_1$-antagonists, metaprolol and betaxol, were ineffective over the same range of concentrations.[46]

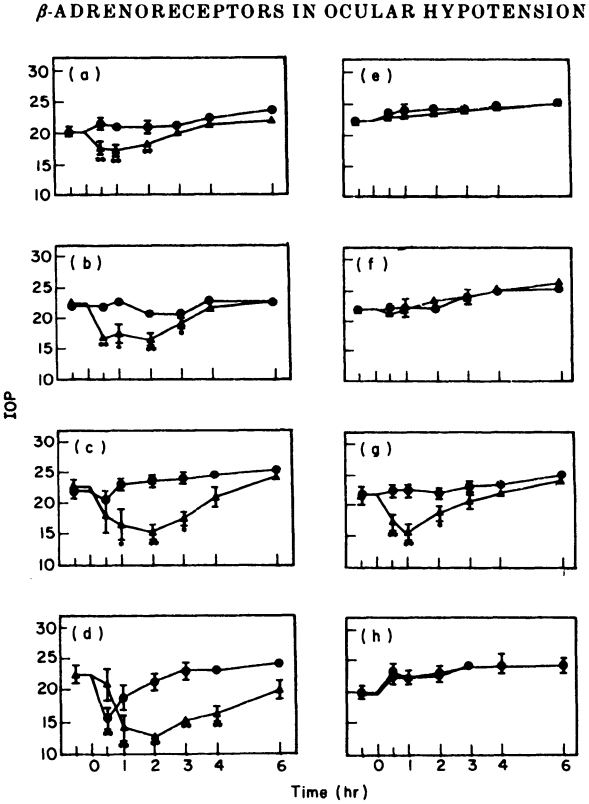

Fig. 1.71 Effect of graded doses of L-isoproterenol and D-isoproterenol on intraocular pressure. Eyes that received L-isoproterenol (a) 0.001%, (b) 0.01%, (c) 0.1% (d) 1% or D-isoproterenol (e) 0.001%, (f) 0.01% and (g) 0.1% are represented by (▲—▲). Contralateral eyes that received the diluent only are represented by (●—●). Intraocular pressure recordings in a vehicle-treated. control group that received diluent in both eyes are depicted in (h). $*P<0.05$. $**P<0.01$ indicate significant decreases from baseline (−0.5 h) intraocular pressure: $n=9$. (Woodward *et al.*, *Exp. Eye Res.*)

Effects of Catecholaminergic Agents on Microvasculature

Funk & Rohen (1987a) have made an elaborate study of the microvasculature of the rabbit's ciliary body and iris, based on scanning electron microscopy of plastic casts; they have applied the technique to measure changes in diameter of the vessels after treatment with adrenergic agents, and described differences in the responses of the three vascular territories, namely iridial, major and minor ciliary processes (p. 16). Epinephrine caused the most pronounced constriction of the iridial vessels, the greatest effect being on the terminal arterioles supplying each territory. If the most anterior (iridial) segment is principally concerned with secretion of aqueous humour, then a constriction of its blood supply, reducing the capillary filtration, might well reduce secretion.

Some Clinical Studies

Potter & Rowland (1978) examined selective beta-agonists from the point of view of their clinical use as ocular hypotensive agents; in view of the general stimulatory effects of $beta_1$-agonists, $beta_2$-agonists were considered preferable. In fact, these were more effective anyway, isoethamine, metaproterenol, terbutaline, carbuterol, salbutamol, quinterenol, and sulfonterol, all $beta_2$-agonists, being effective. The authors frequently found contralateral effects, which may have been a reflection of a fall in arterial pressure due to absorption into the blood stream. The same authors (Rowland & Potter, 1980) raised the intraocular pressure of rabbits by water-loading (60 ml/kg) and demonstrated the efficiency of $beta_2$-agonists, e.g. terbutaline, in lowering the intraocular pressure.

Cyclic AMP

As indicated, this 'second messenger' is intimately involved in beta-adrenergic transmission.

The neurotransmitter activates the enzyme, adenylcyclase, thereby increasing the concentration of cAMP, which then mediates the adrenergic action. Physiological responses to cAMP-assisted reactions can be antagonized by beta-blockers but not by alpha-blockers, such as phentolamine. Waitzman & Woods (1971) prepared a particulate fraction from ciliary processes and showed that it had adenylate cyclase activity, which was accelerated by epinephrine, an effect that was blocked by propranolol, a beta-blocker, but not by phenoxybenzamine.

As Fig. 1.72 shows, the effects of adrenergic agonists, both α- and β-, are accompanied by a rise in aqueous humour cAMP concentration; the falls in intraocular pressure run parallel with the rises in cAMP, suggesting a causal relationship; interestingly, the effects of the β-agonist, isoproterenol, were not blocked by propanolol; thus isoproterenol reduced intraocular pressure but the fall was not blocked by propanolol, whilst the rise in cAMP was also not blocked. These findings were essentially confirmed by Radius & Langham (1973) using norepinephrine, a predominantly α-agonist, as the adrenergic agent; this caused a rise in cAMP in the aqueous humour associated with a fall in intraocular pressure; the α-blocker phenoxybenzamine itself actually increased the concentration of cAMP in the aqueous humour; a further increase was achieved by subsequent application of norepinephrine, whilst the pressure and pupillary responses to norepinephrine were blocked by phenoxybenzamine. Thus it would appear that both α- and β-agonists are able to stimulate adenylcyclase activity in the eye and, through the raised cAMP, to exert a hypotensive effect, but of

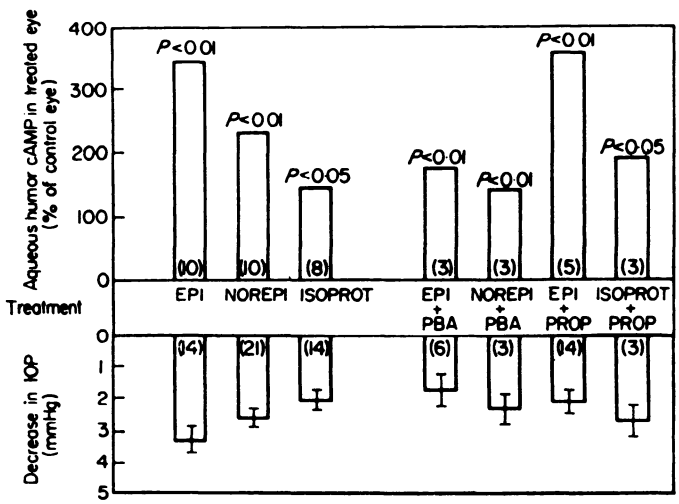

Fig. 1.72 The effects of adrenergic agonists and antagonists on intraocular pressure and cyclic-AMP in the aqueous humour. Agonists: EPI = 1% 1-epinephrine, NOREPI = 1% 1-norepinephrine, ISOP = 2% 1-isoproterenol, were administered topically to one eye, the control vehicle (1 mM HCl) to the other eye. Antagonists: PBA = 30 mg/kg phenoxybenzamine, PROP = 5 mg kg propanolol, were administered, intravenously. The change in intraocular pressure is expressed as the mean ± S.E.M. of the difference between the two eyes. The cyclic-AMP content of the aqueous humour in the drug-treated eye is expressed as the mean per cent of the contralateral eye. The '*P*' values were obtained from the mean ± S.E.M. of the cyclic-AMP levels of the drug treated and control eyes. The numbers of observations are in parentheses. (Neufeld *et al.*, *Exp. Eye Res.*)

course the precise mechanism or mechanisms of the hypotensive effect remain to be discovered.[47]

TOPICAL APPLICATION

Direct application of cAMP to the eye caused an increased facility in both rabbits and monkeys (Neufeld *et al.*, 1975; Neufeld & Sears, 1975). The increased facility occurred in monkeys whether or not the iris had been removed by iridectomy (Kaufman, 1986). Moreover, intracameral epinephrine caused the same increase in facility whether the iris was present or not, so that it is unlikely that the iris contributes in any way to the increased facility, either by producing cAMP or by contributing, by its muscular action, to open the meshwork (Kaufman & Rentzhog, 1981). So far as the ciliary processes are concerned, and therefore secretion of aqueous humour, Cepalik & Cernohorsky (1981) isolated adenylate cyclase from rabbit ciliary processes; this was activated by beta$_2$-adrenergic agonists. A similar localization on ciliary processes was described by Palkama *et al.* (1986) using $SrCl_2$ as a trapping agent and finally precipitating lead phosphate, which could be visualized. It was on the cell membranes of non-pigmented ciliary epithelium.

CHOLERA TOXIN

The pathological effects of this toxin are considered to be due to the stimulation of adenylate cyclase, so that the resulting raised levels of cAMP promote copious intestinal secretion. Gregory *et al.* (1981) found that cholera toxin, administered either topically or by close arterial injection, caused a reduced rate of secretion of aqueous humour, as measured by the rate of disappearance of fluorescein injected into the anterior chamber. Thus, after an intravitreal injection, the rate was 1.1 μl min^{-1} compared with a control rate of 2.4 μl min^{-1}. The intraocular pressure fell from a control value of 14 mmHg to 10 mmHg in about 5 hr (Fig. 1.73). By contrast, Bartels *et al.* (1981), who combined a phosphodiesterase inhibitor (isobutyrylmethylxanthine, IBMX) with the toxin, found only a small decrease in intraocular pressure associated with an increased facility of drainage.

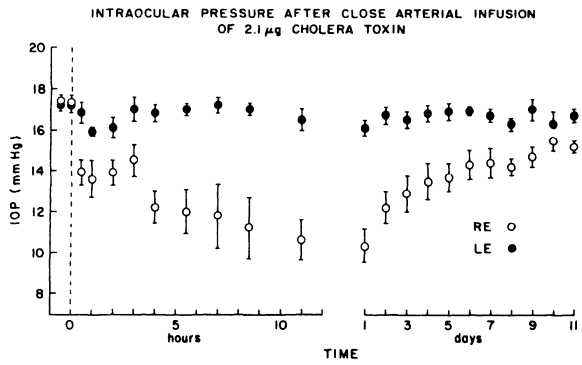

Fig. 1.73 Effects of infusion of cholera toxin (2.1 μg) via the right internal maxillary artery on the intraocular pressure of six rabbits. (Gregory *et al.*, *Invest. Ophthal.*)

FORSKOLIN

This drug is a strong activator of adenylate cyclase, raising cAMP levels in beta-adrenergically activated tissues often as much as that due to maximal nerve stimulation. According to Neufeld *et al.* (1983), it causes a fall in intraocular pressure in the rabbit, due apparently to a doubled facility of outflow. The drug was administered by direct injection into the anterior chamber, but according to the authors the blood-aqueous barrier was unaffected. In a more elaborate study Caprioli *et al.* (1984) found that forskolin reduced intraocular pressure in rabbit, monkey and man; this was definitely attributable to a reduced rate of flow of aqueous humour; measured by the fall in fluorescein concentration after intravitreal injection; the fall was 46% compared with 44% for acetazolamide. Comparable results were described by Lee *et al.* (1984) in the monkey as shown in Table 1.10; here rate of flow was measured from the fall in concentration of fluorescein after iontophoretic introduction through the cornea. Finally, in humans, Burstein *et al.* (1984) found a 34% reduction in rate of flow of aqueous, whilst Seto *et al.* (1986) found a rather smaller effect in the same direction.

COMBINED ACETAZOLAMIDE AND FORSKOLIN EFFECTS

Caprioli & Sears (1984) found that forskolin alone inhibited secretion in the rabbit by 51%, compared with

Table 1.10 Effects of topically applied forskolin on eye parameters in the cynomolgus monkey (Lee *et al.*, 1984)

	IOP (mmHg)	*Facility* (μl min^{-1} mmHg^{-1})	*Flow* (μl min^{-1})
Control	16.9 ± 0.4	0.54 ± 0.07	1.76 ± 0.07
Forskolin	14.1 ± 0.7	0.57 ± 0.06	1.28 ± 0.11
	($P < 0.001$)		($P < 0.01$)

45% by acetazolamide; when the two treatments were combined, there was some addition, to give 72%; this suggests that the two mechanisms of inhibition are different.

WHY REDUCED SECRETION?

Cholera toxin and other stimulants to cAMP production usually increase rate of secretion, e.g. in the gut, cochlea and choroid plexus; Caprioli *et al.* suggest that the opposite effect observed with the eye may be due to the eversion of the ciliary epithelium, so that the basal aspects of the unpigmented cells, where most of the adenylcyclase activity is located, point away from the posterior chamber. Thus the stimulus might favour a backward secretion into the stroma of the tissue.

Resistance to Drainage

A nervous effect on the drainage angle is not inconceivable, especially in view of the ample innervation of the tissue here (Holland *et al.*, 1956, 1957; Laties & Jacowitz, 1966), although the extent of this varies considerably. Thus in subprimates the number of adrenergic terminals varies from very many in the guinea pig to very few in rabbit, rat and mouse. In primates, fibres are only in the uveal portion of the tissue but the density varies from none in cynomolgus and vervet monkeys, through few in owl and squirrel monkeys, to modest in cebus and the baboon (Potter, 1981).[48] By influencing the uveal portion of the tissue the adrenergic system might control the degree of uveoscleral drainage. The subject has been reviewed by Kaufman (1984) who concludes that any effects are largely mediated by alpha-receptors; in his own studies he took care to eliminate effects on the ciliary muscle by disinsertion and retroplacement. Kaufman & Bárány (1981) and Kaufman (1986) concluded that epinephrine and norepinephrine both increased facility in the cynomolgus monkey, probably not through any influence on vascular pressures, i.e. the episcleral venous pressure, since ergotamine and angiotensin had no effect. The interesting finding was that, although facility in monkeys varied by a large factor in different animals, the actual reduction was a constant fraction of the initial value, so that the adrenergic agents were acting on that factor that was responsible for the individual variations. They considered that the effects were too large to be exerted on uveoscleral drainage or pseudofacility, as these constitute too small a fraction of the whole in the monkey.

Alpha$_1$- Versus Alpha$_2$-Actions

Certain alpha-agonists cause a lowering of intraocular pressure, e.g. clonidine and α-methylnorepinephrine; according to Innemee *et al.* (1982) this is probably due to a specific alpha$_2$-action. Thus these authors compared the effects of pure alpha$_1$- and alpha$_2$-agonists on the intraocular pressure of rabbits. The main effect of phenylephrine or St587, alpha$_1$-agonists, was a transient rise in pressure associated with mydriasis. With the alpha$_2$-agonist, B-HT90, the intraocular pressure fell immediately (Fig. 1.74) with no mydriasis; thus mydriasis is a peculiarly alpha$_1$-response. The fall in intraocular pressure was associated with marked falls in the contralateral eye when high concentrations were employed; the effects were blocked by yohimbine. The contralateral effect was presumably due to a central action, since a primary mode of action of alpha$_2$-agonists, e.g. clonidine, is through alpha-adrenoceptors in the pontomedullary area, stimulation causing a decrease in sympatheticone in the body generally and thus accounting for the value of clonidine as a hypotensive agent. The fact that at low doses the effect of the pure alpha$_2$-agonist, B-HT90, was confined to the treated eye suggests that a part of the effect is directly on the eye. When clonidine, a mixed alpha-agonist, is applied to one eye, we may expect any contralateral effect to be due to alpha$_2$-action on the pontomedullary region, since the receptors here are purely alpha$_2$ (Berthelsen & Pettinger, 1977). The effect on the treated eye may well be the result of opposing alpha$_1$ (raising IOP) and alpha$_2$ (hypotensive), the predominant effect being hypotensive; thus the drug has actually been introduced in the treatment of glaucoma (Harrison & Kaufman 1977).

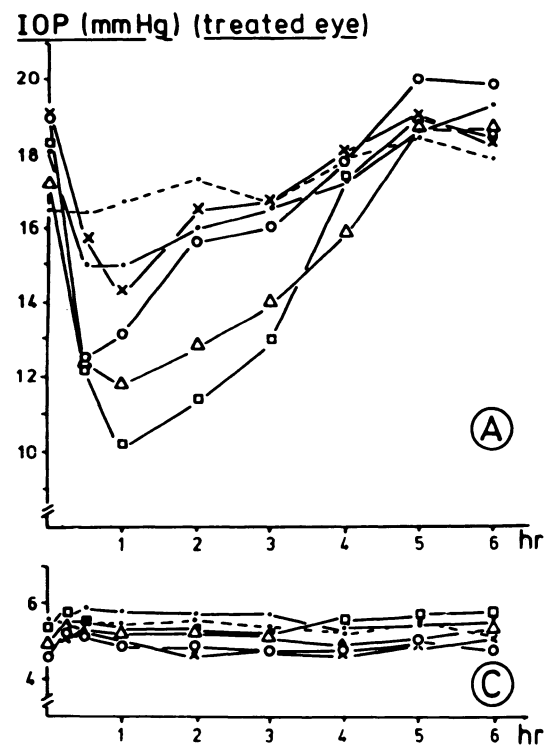

Fig. 1.74 Effects of the alpha$_2$-agonist B-HT 920 on intraocular pressure (A) and pupil diameter (C) after topical administration of 50 μl to conscious rabbits. ·— — —· = saline; ·——· = 0.01%; ×——× = 0.03%; O——O = 0.1%; △——△ = 0.3%;——— = 1%. Symbols represent mean values ($n = 6$), S.E.M. < 10%. Pupil diameters in mm. (Innemee *et al.*, *Doc. Ophthal.*)

The Basis of Alpha$_1$ Hypertension

One of the earliest studies on the effects of sympathetic stimulation of the cervical sympathetic showed a transient rise in intraocular pressure, attributed to a contraction of the smooth muscle of the orbit. It may well be that the hypertensive alpha$_1$-action has a muscular origin (Innemee & Van Zweiten, 1978) since it is antagonized by muscle relaxants and abolished by transection of the three major extraocular muscles (Rowland & Potter, 1980). Thus, as with mydriasis (Gherezghiher & Koss, 1979), the hypertensive effect of alpha-agonists is probably mediated by specific alpha$_1$-receptors.

Prazocin

This is an alpha-blocker and, when applied topically, caused a fall in intraocular pressure, an effect that was blocked by previous application of another alpha-blocker, phentolamine (Krupin *et al.*, 1980). This puzzling finding may find an explanation on the basis of the alpha$_1$- and alpha$_2$-separation. Thus prazocin is a specific alpha$_1$-blocker, and so allows any tonic alpha$_2$-action to manifest itself, especially as the alpha$_2$-receptor is predominant in the rabbit iris-ciliary body preparation. In this way it may cause a hypotensive response. Phentolamine, a non-specific alpha-blocker, would inhibit this release of alpha$_2$-activity.

Binding Affinity and Blocking

Mittag *et al.* (1985) measured the affinities of six alpha-blockers with different specificity for alpha$_1$- and alpha$_2$-, and compared these with their effectiveness in lowering intraocular pressure in the rabbit. Disappointingly, they were all equally effective when applied topically; thus the highly specific rauwolscine alpha$_2$-blocker compared with prazocin and thymoxamine, both specific alpha$_1$-blockers, and with WB 4101 and coryanthin with mixed alpha$_1$- and alpha$_2$-activities. They concluded that both classes of alpha-agonist contributed to lowering intraocular pressure.

Clonidine

Hasslinger (1969) observed that topical application of catapresan, or clonidine, to glaucomatous patients lowered intraocular pressure; this was confirmed by Harrison & Kaufmann (1977). The drug inhibits the release of noradrenaline peripherally, besides having a central effect. Intra-arterial injection in cats and monkeys caused a fall in intraocular pressure on the same side, which was due to a reduced blood-flow within the intrascleral venous plexus, the main drainage route in the cat (Bill & Heilmann, 1975). The authors emphasize the danger in employing a drug that reduces blood flow in the treatment of glaucoma, owing to the possibility of reducing flow to the optic nerve head, which is largely derived from the choroid (Hayreh, 1969).

Parasympathetic

Intraocular Pressure and Blood-flow

The reports on the effects of stimulation of the parasympathetic supply to the eye on intraocular pressure are contradictory; and this may be largely due to the uncertainty as to the nerve fibres actually stimulated, e.g. when an electrode is placed on the ciliary ganglion (Armaly, 1959) or by stereotactic location intracranially (Stjernschantz, 1976a, b). The various studies have been summarized by Stjernschantz & Bill (1976) who have described experiments on rabbits stimulated intracranially. The mean decrease of 1.8 mmHg in intraocular pressure was not statistically significant, and this was associated with a barely significant increase in outflow facility; the mean increase in flow-rate was not significant. Stimulation of N III causes a breakdown of the blood-aqueous barrier, which might be expected to raise intraocular pressure by increasing flow of abnormal aqueous humour from the ciliary body, and such an increased production of fluid has been described by Macri & Cevario (1973) in perfused enucleated cat's eyes. In the rabbit Stjernschantz & Bill (1976) found an actual decrease in blood-flow through the iris and ciliary body, as measured with radioactive microspheres; this was accompanied by an increased flow in the choroid. Thus the equivocal effects on intraocular pressure, as with catecholaminergic agents, are probably the results of opposing actions on the various parameters that go to make up the intraocular pressure.

Resistance to Outflow

Direct stimulation of the oculomotor nerve as it emerges from the brainstem in the monkey causes a fall in resistance to outflow, whilst cutting the nerve unilaterally causes the resistance to be higher on the same side (Tornqvist, 1970).

Parasympatheticomimetic Agents

Drugs that mimic the effects of parasympathetic stimulation, e.g. pilocarpine and eserine, are used in the treatment of glaucoma, and their hypotensive effect has been regarded as largely exerted through the pull of the ciliary muscle on the trabecular meshwork. Atropine, the cholinergic blocking agent, may raise the pressure in glaucoma. In the normal human eye the effects of pilocarpine and atropine are usually negligible, but this does not mean that the drugs are without effects on all the parameters that go to determine the intraocular pressure.

PILOCARPINE

Thus there seems little doubt that pilocarpine causes a decreased resistance to outflow, and Bárány (1967) has shown that the effect is so rapid that it occurs before sufficient of the drug has reached the aqueous humour to enable it to exert any direct effect on the meshwork; its action is therefore on the ciliary body and/or iris; and we may presume that it is exerted through the ciliary muscle. The effects obtained were just as large as any obtained through intracameral injection, so it is unlikely that the

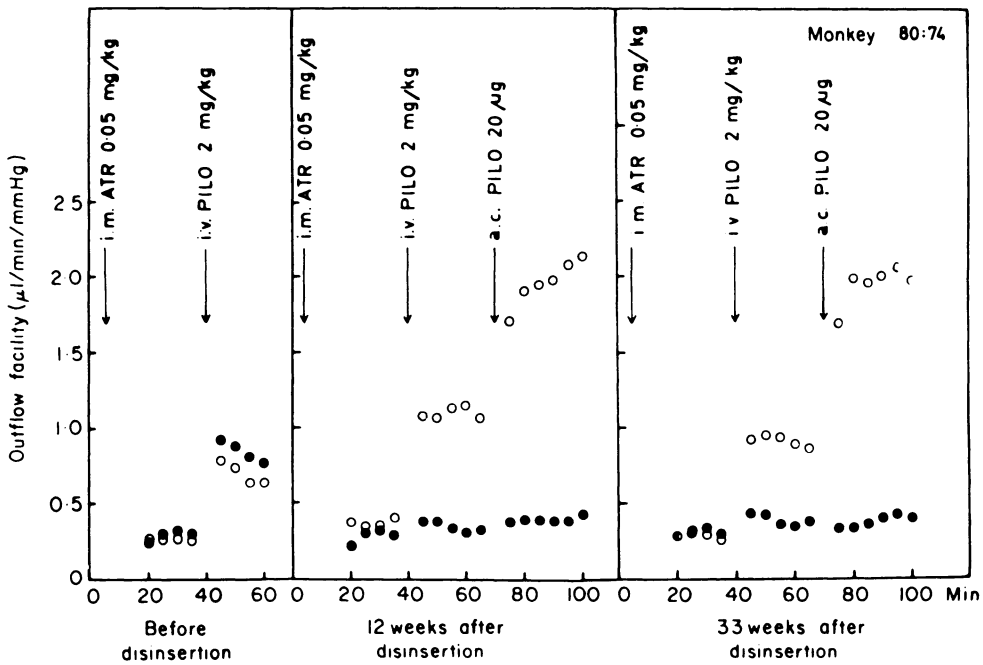

Fig. 1.75 Outflow facility responses to intravenous and intracameral pilocarpine-HCl (i.v. PILO; a.c. PILO) before and after unilateral ciliary muscle disinsertion in a typically bilaterally iridectomized monkey. Intramuscular atropine sulphate (i.m. ATR) was given before each perfusion to minimize systemic effects of intravenous pilocarpine. Note absence of facility increase following intravenous and intracameral pilocarpine in the iridectomized + 'disinserted' eye (solid circles), as opposed to the large facility increases in the opposite iridectomized only eye (open circles). (Kaufman & Bárány, *Exp. Eye Res.*)

drug influences the trabecular meshwork directly. Further proof that the increased facility is a mechanical response to contraction of the ciliary muscle is provided by Kaufman & Bárány (1976) who disinserted the monkey's ciliary muscle and showed that the acute effects of pilocarpine were abolished (Fig. 1.75).

Morphology of Pilocarpine Action Grierson *et al.* (1978) working on human eyes given four doses of pilocarpine before enucleation, found that the contraction of the ciliary muscle pulled the scleral spur posteriorly and internally, so that the angle formed by the scleral spur and sulcus was greater. This produced a widening of the spaces between corneoscleral trabeculae and distended the endothelial meshwork (Fig. 1.76). Similar results were found in the baboon (Grierson *et al.*, 1979) after perfusion of the eye with artificial aqueous humour containing pilocarpine. In the electron microscope the changes were confined to the endothelial meshwork, and the number of vacuoles was increased.

Rate of Secretion Miichi & Nagataki (1983) measured rate of production of aqueous humour by the dilution of labelled dextran perfused through the anterior chamber; they found a 50% reduction in rate with pilocarpine; it must be emphasized, however, as the authors did themselves, that the blood-aqueous barrier is abnormal during this type of perfusion.

Uveoscleral-Schlemm Canal Switch

Some of the complexities in the study of the effects of drugs on intraocular pressure are well revealed by the studies of Bill & Walinder (1966), who showed that, in macaque monkeys, pilocarpine increased the intraocular pressure; this was associated with a fall in rate of secretion of aqueous humour from a control value of 1.60 μl/min to 1.05 μl/min. The reason for the rise in pressure was an almost complete blockage of the uveoscleral drainage route, so that drainage was confined to the canal of Schlemm (Fig. 1.77).

BLOOD-FLOW

We have seen that stimulation of NIII causes a decreased blood-flow through the anterior uvea (of rabbits); the effects of parasympathetic potentiators such as eserine

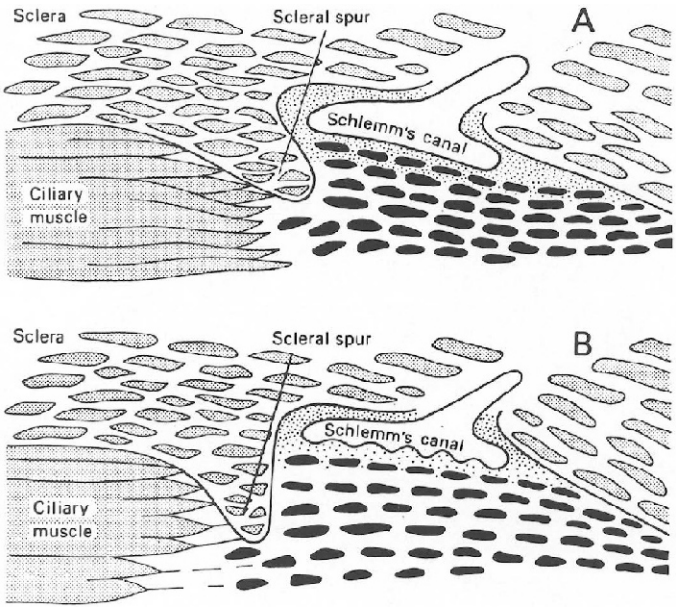

Fig. 1.76 Diagrams to illustrate the effects of pilocarpine-induced contraction of the ciliary muscle on the scleral spur and the trabecular tissues. A, untreated; B, treated. (Grierson *et al.*, *Brit. J. Ophthal.*)

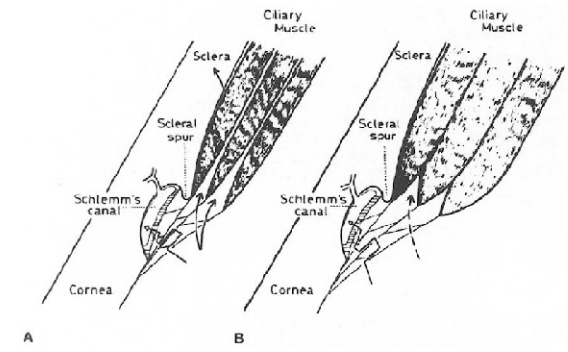

Fig. 1.77 (A) Ciliary muscle is relaxed, spaces between lamellae of uveal and corneoscleral meshwork are narrow, and interstitial spaces between muscle bundles of ciliary muscle are wide. Aqueous humour leaves the anterior chamber via Schlemm's canal and via interstitial spaces of ciliary muscle. (B) Ciliary muscle is contracted, spaces in different parts of meshwork are relatively wide, and interstitial spaces between muscle bundles have almost disappeared. Aqueous humour leaves the eye almost entirely via Schlemm's canal. (Bill, *Physiol. Rev.*)

and DFP are opposite, however, doubling the blood-flow through the anterior uvea (Alm *et al.* 1973), whilst in humans Wilke (1974) found dilatation of superficial blood vessels associated with increased episcleral venous pressure.

Central Control of Intraocular Pressure

Possible Hypothalamic Centre

Attempts to locate a centre controlling the intraocular pressure have been made by v. Sallmann & Loewenstein and Gloster & Greaves, by inserting stereotactically controlled stimulating electrodes into different parts of the brain. The parts of the brain from which effects on intraocular pressure could be obtained were in the hypothalamus, but since this region contains many centres controlling the autonomic system generally, it is important to distinguish primary effects on the intraocular pressure from the secondary consequences of stimulating these autonomic centres. Thus many stimulated points gave rise to rises or falls in intraocular pressure that were obviously associated with corresponding rises or falls of arterial pressure. Nevertheless, other points could be found where a rise or fall of intraocular pressure, independent of general vascular changes, resulted from stimulation; the falls in intraocular pressure were probably mediated by the sympathetic, since they could be prevented by section of the sympathetic trunk. It is possible, then, that there is a co-ordinating centre in the hypothalamus capable of influencing the intraocular pressure, and subject to afferent impulses carried in the long ciliary nerves. The evidence for this is not completely convincing, however, and we must bear in mind the possibility that there is no central control, local homeostatic mechanisms being adequate to keep the intraocular pressure within a narrow range.

If there is a 'centre' controlling the intraocular pressure, we may expect to find evidence of a sensory system capable of keeping the centre informed of the state of the intraocular pressure at any moment. Studies from the laboratories of Vrábec and v. Sallmann have shown that the trabecular meshwork is richly provided with fine nerve fibres.

Sensory Input

TRIGEMINAL

Using electron microscopy and nerve degeneration, Ruskell (1976) showed that fibres from N V terminate in the meshwork. (Sympathetic terminals were also identified by the presence of granular vesicles in terminal varicosities, and these might well be concerned with some of the effects of adrenergic substances on intraocular dynamics.) Bergmanson (1977) has examined the innervation of the uvea in monkeys before and after lesions of the ophthalmic division of N V. It appeared that the choroid was probably not innervated, the fibres running in the suprachoroid having terminals in the anterior uvea; similarly the origin of the ciliary muscle lacked sensory innervation, as also did the individual ciliary muscle fibres. The subepithelial stroma of the ciliary processes was well innervated and it seemed that the fibres terminated in the stroma as the adjacent tissue either had none or very few. It could be these terminals in the ciliary body stroma that gave rise to the action potentials described by Tower (1940) when pushing on the front surface of the lens in cats. According to Bergmanson's study, there are few or no sensory terminals in the monkey's iris; this is surprising in view of the painful nature of iridectomy without retrobulbar anaesthesia.

Thus the source of sensory input from the uvea is apparently largely the stroma of the ciliary processes and the iris root, and we may presume that if such afferent information is concerned in responses to raised or lowered intraocular pressure, then these fibres carry the information. The absence of sensory fibres in the ciliary muscle rules out the trigeminal nerve as a source of muscle proprioception.

AFFERENT DISCHARGES

Belmonte *et al.* (1971) recorded discharges in ciliary nerves of the cat; lowering the intraocular pressure by steps progressively reduced the discharge-frequency.

Efferent Impulses

THE FACIAL NERVE (N VII)

The uveal blood vessels are partly innervated by postganglionic fibres of N VII derived from the pterygopalatine ganglion (Ruskell, 1971) which constitute part of the parasympathetic innervation of the eye. Thus Ruskell (1971) identified a non-myelinated supply to the choroid that was different from the larger myelinated nerve fibres in the suprachoroid; they were related to blood vessels, especially arterioles. After removal of the superior cervical ganglion some of these fibres remained, suggesting a non-sympathetic origin; damage to the pterygopalatine ganglion caused degenerative changes in many of these fibres, indicating a N VII origin; he concluded that, because the sympathetic innervation was vasoconstrictor, these parasympathetic fibres would be vasodilator.

Stimulation Preganglionic stimulation of N VII causes a moderate rise in intraocular pressure (Gloster, 1961), which is probably caused entirely by the associated increase in uveal blood flow; thus in the rabbit Stjernachantz & Bill (1980) measured a 200% increase in choroidal blood-flow, and increases in the iris and ciliary body; with maximal stimulation the IOP rose by 6 mmHg. A more extensive study on cats, monkeys and rabbits, in which blood-flow in different parts of the uvea was measured by the microsphere technique, generally confirmed the rise in blood-flow, varying from 122% in the monkey to 148% and 152% in the rabbit and cat; ganglionic blockade with hexamethonium abolished the effect. In general, choroidal blood-flow was increased to a greater extent than that of the anterior uvea. In all species pressure was raised from 1–11 cm H_2O, the rises being about the same as those in the intrascleral vein. Interestingly, the effect was only partially inhibited by muscarinic blockers, suggesting that an additional transmitter to acetylcholine was involved in this parasympathetic pathway. Such a transmitter could be vasoactive intestinal polypeptide (VIP) which mediates the action of N VII in the cat's tongue. (Lundberg *et al.*, 1982), and is a transmitter that apparently coexists in some parasympathetic cholinergic neurones (Lundberg *et al.*, 1980).

VIP-Fibres By immunofluorescence, the presence of neurones containing a VIP-like material can be visualized in the ocular and orbital structures (Uddman *et al.*, 1980; Uusitalo *et al.*, 1984). Intraocularly the fluorescent fibres are seen in the ciliary processes, the posterior third of the ciliary muscle, and around the small-to-medium blood vessels of the choroid; they were apparently absent from vessels of the anterior uvea, however. Extirpation of the pterygopalatine ganglion resulted in the loss of all fluorescent fibres, and the VIP-content of the choroid and anterior uvea was abolished (Butler *et al.*, 1984). According to Terenghi *et al.* (1982), the choroid of the guinea pig contains the cell bodies of VIP-containing neurones, indicating an intrinsic supply, which would escape destruction by coagulation of the pterygopalatine ganglion.

EFFECTS OF VIP

In the rabbit Nilsson & Bill (1984) showed that intravenous infusion of VIP caused a rise in choroidal blood-flow associated with a rise in intraocular pressure. In the monkey Nilsson *et al.* (1986) measured an increase in aqueous flow-rate from 0.98 ± 0.07 to $1.35 \pm 0.08\ \mu l\ min^{-1}$; this latter effect was not accompanied by a rise in pressure, so that facility must also have increased. When VIP was introduced into the anterior chamber there was an increase in pressure, maximally by about 7.5 cm H_2O, accompanied by an increased flow of aqueous humour from 0.90 ± 0.11 to $1.35 \pm 0.08\ \mu l\ min^{-1}$. Intravenous atropine, surprisingly, abolished the rise in flow-rate.[49] The rise in intraocular pressure of 7.5 cm H_2O was much too high to be accounted for by the increased flow of aqueous humour, which should only have caused a rise of some 1–2 cm H_2O, so presumably the major effect of the VIP was on the pressure in the veins into which the aqueous drained; and it is interesting that the actual rise in pressure with VIP was about the same as that obtained with maximal stimulation of N VII.

VIP RECEPTORS

Stone identified VIP-immunoreactive nerve fibres in the ciliary bodies of rat, guinea pig, cat and monkey; they were also in the aqueous outflow channels, with the exception of the monkey. The source of the nerves seems to be the pterygopalatine ganglion, and many fibres were found in the lacrimal, Harderian and tarsal glands (Uddman *et al.*, 1980).

ADENYL CYCLASE ACTIVITY

The ciliary processes of the rabbit contain a high density of VIP-binding sites; moreover, the processes exhibit a high degree of acceleration of their cyclase activity by VIP, so that VIP- and beta-adrenergic agonists must be closely related in their activities, although, as we have seen, beta-agonists seem to reduce rate of secretion (Mittag *et al.*, 1985).

Hormonal Influences on Intraocular Pressure

Corticosteroids

François (1954) observed that the prolonged use of topical cortisone in the treatment of uveitis sometimes led to a rise in intraocular pressure; patients undergoing systemic corticosteroid therapy for rheumatic conditions also showed raised intraocular pressure. Bernstein & Schwartz (1962) showed that the cause was a decreased facility of outflow, which was reversible when the dose of corticosteroid was reduced. In human subjects, Anselmi *et al.* (1968) found no change in rate of secretion, although the intraocular pressure was high. With glaucomatous subjects Becker & Mills (1963) found an invariable large rise in pressure on systemic treatment; similarly Polansky *et al.* (1985) measured the diurnal variation in intraocular pressure and blood plasma cortisol in glaucomatous subjects; administration of 3 mg of cortisol caused a rise in the free plasma cortisol level and a rise in intraocular pressure imposed on the diurnal variation. With normal human subjects, it would appear that there is a genetic factor disposing to the hypertensive response; thus Becker & Hahn (1964) found a response in only 30% of 'normals', who might have been heterozygous carriers of a genetic defect. On this basis Becker (1965) considered that a given population should exhibit three types, namely those with no or very little response to corticosteroids being phenotypes that relate to homozygous 'poor responders'; those with moderate response, being heterozygous responders, and those with a large response being homozygous 'responders'. Armaly (1963) actually found that his subjects fell into three groups; patients with open-angle glaucoma gave altogether stronger responses (Fig. 1.78).

MECHANISM OF ACTION

We may presume that cortioosteroids influence the state of the glycosaminoglycans in the meshwork (François,

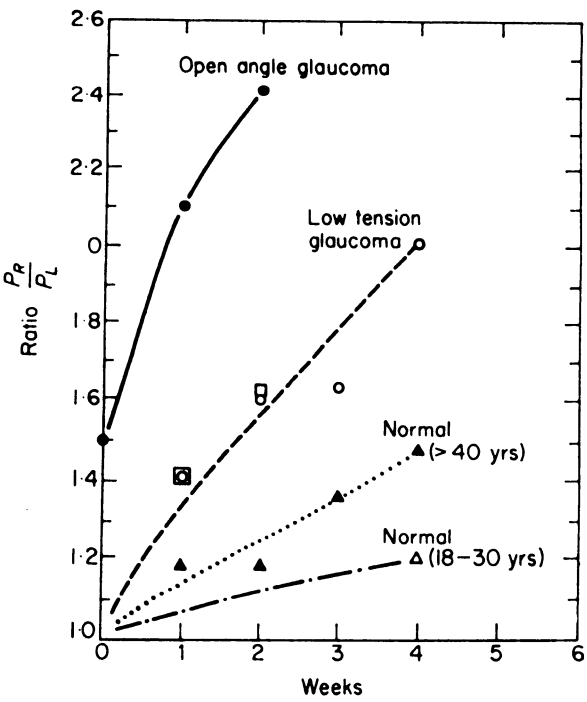

Fig. 1.78 Effects of topical treatment of right eye with dexamethasone on intraocular pressure of normal and glaucomatous human subjects. The ordinate gives the ratio of the pressure in right and left eyes. (Armaly, *Arch. Ophthal.*)

1975). Certainly Rohen *et al.* (1973) found a widening and densification of the tissue adjacent to Schlemm's canal in patients treated with eye-drops for several years and who had developed glaucoma. However, analysis of the tissue has led to no very convincing evidence for an increase in glycosaminoglycans; thus in rabbits Knepper *et al.* (1978) found a decrease in hyaluronic acid, with an increase in chondroitin sulphate.[50]

Vasopressin

Cole & Nagasubramanian (1972) produced some evidence suggesting that this antidiuretic hormone increased rate of flow of aqueous humour; however, Niederer *et al.* (1975) measured an actual decrease; this would be consistent with its inhibitory action on secretion of the cerebrospinal fluid (Davson & Segal, 1970).

Glaucoma

The intensive study of the dynamics of fluid formation and drainage has been largely motivated by the requirement of an understanding and treatment of the condition of chronic simple, or open-angle, glaucoma, a condition in which the intraocular pressure rises to the point of damaging the retina and its nervous outflow. There is little doubt that the raised pressure is due to an increase in resistance to outflow, and non-surgical treatment has been directed to reducing this resistance as well as reducing the rate of secretion. The modes of action of some hypotensive drugs have been discussed earlier, and it would seem that, whereas cholinergic agonists, such as pilocarpine, act primarily, if not exclusively, on the drainage pathway through a mechanical action of the ciliary muscle, the adrenergic drugs may well act on both systems, reducing rate of secretion and resistance to flow. Thus the morphology of open-angle glaucoma is of some interest; Rohen & Witmer (1972) (reviewed in Rohen, 1983) examined trabecular tissue from some 400 patients in whom trabeculotomy had been performed. In normal meshworks Rohen emphasized the character of the layer of tissue immediately adjacent to the endothelium of Schlemm's canal, the cribriform pathway, illustrated schematically by Fig. 1.78; presumably filled with extracellular material. In cases of exfoliation glaucoma these cribriform pathways were apparently obstructed by randomly exfoliated fibrils, the same effect being observed by treatment of eyes experimentally with α-chymotrypsin, which breaks down the zonular fibres, which then accumulate in the drainage pathway. In cases of simple glaucoma, however, it was not exogenous material that accumulated but material derived from the meshwork itself, material that he originally described as 'plaques'. The material peculiar to simple glaucoma was fibrillar, with a characteristic banding comparable with that in collagen or elastin fibres, and presumably derived from basement membranes. Rohen considered that the gradual deposition of this extracellular material, which could be removed by glycosaminoglycan hydrolytic enzymes, such as hyaluronidase and chondroitinase, tended to thicken the 'plates' formed by the 'cribriform plexus' of elastic fibres that underlay the endothelial cells of the canal of Schlemm. Such a thickening would, of itself, increase resistance to flow of aqueous humour, and it would also diminish the separation of these plates that Rohen considered to follow contraction of the ciliary muscle.

Contractile Protein

On the basis that the presence of actin filaments (Gipson & Anderson, 1979; Grierson & Rahi, 1979) within the endothelial cells of the meshwork might provide the mechanism for a change in facility, Tripathi & Tripathi (1980) examined these filaments in normal and glaucomatous eyes; the filaments were present in both but the frequency of occurrence was less in the glaucomatous eyes.

Again Tripathi *et al.* (1987) observed, in trabecular tissue of normotensive eyes, only a sparse amount of ferritin-reactive sialic acid residues on the basal aspects of the endothelial cells, compared with a high density of these in tissue from primary open-angle glaucomatous subjects. They suggested that the paucity of these sites at the basal aspect of the cell reflected the ability of the cell to form giant vacuoles; thus a high density of these might have interfered with vacuole formation by a defective transmembrane interaction of the surface glycoproteins (fibronectin and laminin) with the cytoskeleton of the cells lining Schlemm's canal.[51]

Experimental Glaucoma

Gaasterland & Kupfer (1974) created an experimental glaucoma in monkeys by repeated photocoagulation of the trabecular meshwork; the rise in intraocular pressure was associated with a decreased facility of drainage with trabecular scarring and obliteration of Schlemm's canal.[52] There were cupping of the disc and a loss of ganglion cells. Koss *et al.* (1984) distinguished an initial acute rise in pressure, due apparently to cellular debris in the meshwork entrapped by a fibrin net. This was not seen in later-enucleated eyes. Gherezghiher *et al.* (1986) obtained a glaucomatous condition with buphthalmos in 13/30 rabbits; facility was 0.06 compared with a normal

0.18 $\mu l\,min^{-1}\,mmHg^{-1}$. Forskolin, timolol and pilocarpine all lowered intraocular pressure. Similarly, Siegel *et al.* (1987) found that the ergoline derivative, pergolide, reduced the high intraocular pressure induced in monkeys by laser coagulation of the trabecular meshwork, from some 34 mmHg to some 24–26 mmHg.

BLOCKAGE OF THE DRAINAGE ANGLE

Quigley & Addicks (1980a, b) injected autologous fixed erythrocytes into the anterior chambers of monkeys, and produced lengthy periods of raised intraocular pressure during which they were able to examine the pathology of the optic nerve.

Notes

1. In the rabbit, this is not true; the major circle deriving its blood entirely from the long posterior ciliary arteries (Ruskell, 1964; Morrison *et al.*, 1987a; Funk & Rohen, 1987). Morrison & Van Buskirk (1984) have confirmed the anastomosis of the anterior and posterior ciliary arteries in the primate.
2. *Iris processes* are made up of an occasional lamina of the uveal meshwork that crosses posteriorly to attach to the root of the iris.
3. According to Inomata *et al.* (1972a), the endothelial cells of the inner wall of Schlemm's canal, i.e. that facing the meshwork, have no basement membrane, the cells resting on very fine, unevenly distributed fibrillar material embedded in a homogeneous ground substance. This is in contrast to the cells of the outer layer, adjacent to the corneo-sclera, which rest on a well defined basement membrane. These cells lack vacuoles (p. 41).
4. The stout strands extending from the root of the iris to the inner aspect of the peripheral cornea have been likened to an inverted comb and hence the name pectinate ligament. These strands are most prominent in ungulates.
5. Leber (1903) first noted the intramuscular circle; Morrison & Van Buskirk emphasize its importance as an anastomotic connection between anterior and posterior ciliary arteries; it supplies a large portion of the ciliary muscle's capillary bed, and most of the recurrent ciliary arteries passing back to the anterior choroid, in addition to the major circle. The authors comment on the finding of Talusan & Schwartz (1981), suggesting that the anterior ciliary arteries fill from inside the eye (p. 18); they suggest that the large-calibre muscular circle can permit bidirectional flow.
6. Morrison *et al.* (1987b) have described the microvasculature of the ciliary processes of a number of non-primate mammals; there are some interesting variations. An excellent picture of the capillary supply to this important region of the eye is provided by their scanning electron micrographs of castings; this is true also of the study of Funk & Rohen (1987) on the rabbit.
7. In their table Gaasterland gave concentrations in aqueous humour in mM/kg; I presume they meant μM/kg. They give individual values for some 21 amino acids. We may note that with the exception of the amino acids, serum concentrations have been given per litre of fluid, but for comparison with aqueous humour, all results should have been expressed in terms of the water content of the fluid.
8. Thus Bill (1968a, b), measured the penetration of labelled myoglobin, serum albumin and gammaglobulin from blood into the stroma of the ciliary body and choroid; the turnover rates in the tissue were 25%, 3.9% and 1.6% per minute respectively, showing that the capillaries were exerting a sieve-like action. Bill estimated that the albumin concentration in the stroma was some 55% to 60% of that in plasma, so that the oncotic pressure of the tissue is relatively high.
9. For a more detailed study the reader may be referred to my *Physiology of the Ocular and Cerebrospinal Fluids*, or to a more modern account by Cole in *The Eye*, Vol. 1.
10. Kappelhof *et al.* (1987), employing what they considered to be the best fluorophotometer, obtained a mean value for inward permeability of 5.5 ± 1.8 nm/sec in human subjects; they quote earlier values in the literature ranging from 0.7 to 1.8 nm/sec. Zeimer *et al.* (1983) have described the use and evaluation of results obtained from the new fluorophotometer.
11. Sellner (1986a) found a net transport of leucine from the retinal to the choroidal side of an isolated pigment epithelium when it separated two solutions of equal concentration. In the absence of Na^+ the transport was partially reduced. In a more extended study (1986b) an asymmetrical transport of several other amino acids was established, but not for glucose, choline or ethanolamine. Sellner estimated the probable concentration of leucine in the subretinal fluid as about one eighth that in the plasma, as with cerebrospinal fluid. We may note that cultured retinal pigment epithelial cells of the cat accumulate ascorbate actively in a Na^+-dependent manner. This could be a sign of active transport across the epithelium, but in which direction cannot be said (Khatami *et al.*, 1986).
12. Uusitalo *et al.* (1973) point out that the ciliary epithelium on the ciliary processes and pars plana does allow some horseradish peroxidase to pass between its non-pigmented cells, so that it is possible that the small amounts of protein entering the aqueous humour are carried through these regions.
13. There seem to be species variations, which have been summarized by Szalay *et al.* (1975); thus gap-junctions seem to be predominant in rat, cat and pig, whilst in mouse, monkey and man the junction is of the occluding type (Smith, 1971; Vegge & Ringvold, 1969). However, it would be of interest to determine whether these species differences are reflected in differences in the blood-aqueous barrier.
14. As Steinberg & Miller (1973) emphasized, this retinal layer is analogous with the epithelium lining the choroid plexuses of the ventricles, an epithelium that secretes cerebrospinal fluid, both epithelia being derived from neuroectoderm lining the central canal of the neural tube, and both being backed by a rich vascular bed. The apices of the epithelial cells face cavities, the ventricles on the one hand and the subretinal space on the other. Control of the composition of this subretinal fluid, which is the extracellular medium surrounding the receptors, is vitally important for maintaining the resting potentials of these receptors, and the current flowing across them (Chapter 10).
15. Raviola & Butler (1983) have described an apparent unidirectional vesicular transport of horseradish peroxidase from the vitreous body of the monkey and rabbit into the retinal blood vessels, comparable with that described for iris vessels. Vesicles laden with peroxidase were concentrated at the basal region of the endothelial cell, and occasionally one

was seen discharging its contents into the lumen of the capillary.

16. The potential of opposite polarity found by Cole was due to the absence of bicarbonate from his medium.
17. The distribution of carbonic anhydrase in the human eye has been described recently by Wistrand *et al.* (1986). There are four isoenzymes CA I–IV, three of which are in the cytoplasm and CA IV is membrane bound and perhaps concerned with ion transport. CA II, however, is the dominant isoenzyme in the nonpigmented ciliary epithelium with high activity adjacent to the basolateral membranes. Wistrand *et al.* emphasize this strong localization close to membranes, although 99% of activity is said to be in the cytoplasm. Histochemical localization at the lateral and apical membranes of the ciliary epithelium of rabbits has been described by Lutjen-Drecoll & Lönnerholm (1981) and Hansson (1968).
18. Pederson (1982) has measured the hydraulic conductivity of the ciliary epithelium in the totally iridectomized monkey eye, by perfusing the anterior chamber with an artificial aqueous containing albumin. This came out at $0.027\ \mu l\ min^{-1}\ mmHg^{-1}$, from which he deduced a value of $1200\ \mu l\ min^{-1}\ mosm^{-1}\ cm^{-2}$. On this basis he concluded that, at normal intraocular pressure, filtration would amount to $0.2\ \mu l\ min^{-1}$; with a total production of $1–2\ \mu l\ min^{-1}$, this would represent 10–20% of the total production, a more reasonable estimate than the earlier ones.
19. Lasansky & De Fisch (1966) pioneered this type of study; more recent are those of Steinberg & Miller (1973) and Miller & Steinberg (1976, 1977), Miller *et al.* (1978), Oakley *et al.* (1978) and Miller *et al.* (1982). Pascuzzo *et al.* (1980) have described some of the electrical characteristics of the sheep isolated epithelium. The potential was 6.3 mV (retinal side positive).
20. Matsumoto *et al.* (1986) have shown that beta-blocking agents, such as timolol and befunolol are accumulated by the isolated iris-ciliary body of the rabbit, suggesting an active transport of these out of the eye; after intraocular injection of a mixture of labelled timolol and sucrose, timolol was eliminated at a rate of 36% per hr whilst sucrose at only 5%.
21. We may note that reserpine and propanolol both reverse and inhibit the effects of vanadate on the intraocular pressure of the rabbit (Delamere & Williams, 1985). The same authors (1986) suggest that vanadate acts by potentiating adrenergic influences on the eye, which are generally to reduce rate of secretion of aqueous humour (p. 69).
22. Various photometric devices for measuring the concentration of fluorescent dye in cornea, aqueous humour and vitreous body have been described, all based on directing a beam of light through the eye and measuring the intensity of fluorescence at different depths. The most sophisticated is that of McLaren & Brubaker (1985); an argon laser beam is mechanically scanned through the target area, the fluorescent light being measured with a photomultiplier. A single antero-posterior scan required 100 msec divided into 33 periods of 3 msec, and 30 antero-posterior scans are made within 3 sec. Thus the concentrations in different regions are recorded simultaneously.
23. Coakes & Brubaker (1979) have provided a valuable analysis of the various methods of deducing rate of flow and corneal endothelial permeability, from the basic measurements of concentration of fluorescein in aqueous humour as a function of time, together with that in cornea at a fixed time. Altogether five different analyses of the same study on humans were carried out; the computed mean rates were: 2.9 ± 0.5, 2.7 ± 1.0, 3.0 ± 0.5, 2.9 ± 0.4, and $2.9 \pm 0.4\ \mu l\ min^{-1}$. Araie & Matsumoto (1983) have described a method based on computer fitting of the bi-exponential equation of Jones & Maurice to the time-course of the concentration in the aqueous humour after topical application of fluorescein.
24. Langham & Edwards (1987) have recently described determination of facility in rabbits using the pneumatic tonometer (p. 50). Mean values for intraocular pressure and facility were 20.5 ± 0.2 mmHg and $0.17 \pm 0.01\ \mu l\ min^{-1}\ mmHg^{-1}$ respectively.
25. These authors discuss in some detail the effects of pressure on resistance, as measured by cannulation of the eye and determining the relation between pressure and flow from a reservoir; an important pitfall is the variation in resistance with changing angle of the anterior chamber; thus if no deepening is allowed to take place, facility tends to decrease with increasing pressure, whereas if deepening occurs with raised pressure, then facility tends to remain nearly constant with increasing pressure.
26. Essentially similar results were obtained by Grierson *et al.* (1986) on the rabbit; for a good description of the angle of this animal's anterior chamber the interested reader is referred to this paper. At low pressures the ciliary cleft collapses, and as pressure rises this expands and ruptures the meshwork tissue.
27. Johnson & Kamm (1983) set up a model of the drainage system based on a series of springs that kept the walls of Schlemm's canal apart, the distance apart affecting the resistance to flow in the channel. Because the resistance does not change much with intraocular pressure, it was concluded that any change in diameter of the canal was relatively unimportant, so that the resistance across the inner wall was most important.
28. Ruben *et al.* (1985) have summarized the literature on the 'wash out' effect, and emphasize the probable importance of fibrinolysis, a process that would remove fibrin from the angle; thus Pandolfi & Kiwaan (1967) found plasminogen-activation activity in the outflow channels, whilst perfusion of the enucleated or *in situ* monkey eye with plasmin increased facility (Pandolfi & Astrup, 1966; Perkins and Saiduzzer, 1969). Ruben *et al.* showed that the antifibrinolytic agent, ε-aminocaproic acid (EACA) reduced the wash-out effect in rabbits. We may note that Knapper *et al.* (1984) found that *Streptomyces* hyaluronidase which completely removed hyaluronic acid from the angle, was much more effective than the testicular hyaluronidase employed by Bárány & Scotchbrook. Other glycosaminoglycans were not lost. These authors consider that the glycosaminoglycans are too firmly bound to structural proteins to be amenable to washing out, so that although they are important for the resistance to drainage, the wash-out effect is due to removal of something else.
29. Grant (1963) was unable to repeat this in human eyes; Melton & De Ville (1960) compared dogs, cats, rabbits and guinea pigs with respect to the wash-out effect and susceptibility of facility to hyaluronidase. Cats and dogs showed a large wash-out effect; rabbits and guinea pigs very little. Hyaluronidase improved flow in rabbits and guinea pigs but not in cats and dogs.
30. Schachtschabel *et al.* (1977) have cultured explants of trabecular meshwork and shown that they synthesize glycosaminoglycans consisting of mainly hyaluronic acid and the sulphated glycans, chondroitin-4-sulphate and dermatan sulphate.
31. Epstein *et al.* (1987) found a 115% increase in facility with ethacryinic acid when this was included in the anterior chamber perfusion fluid; this was prevented by cysteine.
32. The proportion of uveoscleral drainage seems to depend on

the size of the ciliary muscle; thus in the cat it is considerable although less than in primates; in the rabbit with its very poor ciliary muscle it is negligible (Bill, 1966).

33. So long as the estimation of the amount of fluid escaping by the uveoscleral route depends on the amount of tracer found in the uveoscleral tissue, the exact determination of uveoscleral flow relies on the assumption that none of the tracer is carried away by the vascular circulation. This may well vary, according as the anterior uvea is normal or inflamed. Toris *et al.* (1987) suggested that a tracer with molecular weight of about 40000 might well be optimal, too small a tracer escaping through blood vessels, and too large a one being inhibited from passage through the congested tissue.
34. The operation of cyclodialysis for relief of high intraocular pressure consists in insertion of a spatula through a corneoscleral incision and separation of part of the ciliary body-iris from the scleral wall. Suguro *et al.* (1985) have shown, in the monkey eye, that the basis of the lowering of pressure is the opening up of a uveoscleral drainage route as measured by the escape of a fluorescent tracer into the tissues.
35. Manometric methods usually demand the use of a general anaesthetic, so that the figures given may not be true of the normal unanaesthetized animal; according to Sears (1960) and Kupfer (1961), the normal unanaesthetized value for rabbits is 19 mmHg; with urethane it was 16.8 mmHg, with paraldehyde, 20.4 and aprobarbital, 17 mmHg.
36. Scheie *et al.* (1943) found that the protein concentration in the fluid formed after paracentesis in the cat was reduced to about a half if the animal was completely iridectomized, and they attributed to the iris a major role in production of the newly formed fluid. However, as Unger *et al.* (1975) point out, iridectomy removes a major source of prostaglandins which, as we shall see, are mainly, if not entirely, responsible for the breakdown of the barrier.
37. Bhattacherjee *et al.* (1979) showed that a microsomal pellet from rabbit ocular tissue would synthesize PGI_1 (prostacyclin) and TxA_2 (Thromboxane), as well as conventional prostaglandins E_2, $F_{2\alpha}$, and D_2. Kulkarni & Srinvasan (1983) showed that rabbit conjunctiva and anterior uvea would produce lipogenase-catalysed material as well, e.g. 12-HETE, 5-HETE, and 5,12-DiHETE, where HETE indicates hydroxyeicosotetraenoic acid. Human tissue has been shown to produce lipoxygenase products from arachidonic acid, notably 15- and 5-HETE (Kulkarni *et al.*, 1984). These compounds exhibit leukotactic activity. In cultured human trabecular meshwork cells, however, Gerritson *et al.* (1986) found little lipoxygenase activity, PGE_2 being the main product.
38. The miotic effect of Substance P on the isolated rabbit iris was demonstrated by Soloway *et al.* (1981) with doses of 10^{-9} to 10^{-7} M. The presence of Substance P in the nerves of the anterior segment of several species was demonstrated by Stone *et al.* (1982). As might be expected, high concentrations were found in the iris sphincter, but also in blood vessels. There were immunoreactive fibres in the structures of the drainage angle, suggesting the possibility of an influence on resistance to drainage; also the ciliary processes contained reactive fibres. With electrocoagulation of the ophthalmic branch of N V, Substance P disappeared from the iris and cornea (Miller *et al.*, 1981).

    Again Tervo *et al.* (1982) showed that, with intracranial maxillary and ophthalmic neurotomy, Substance P-reactive fibres disappeared except those in the retina, which are associated with amacrine cells.
39. Somewhat paradoxically, Substance P causes the liberation of arachidonic acid from membrane lipids, which thus form the substrate for prostaglandin synthesis (Yousufzai *et al.*, 1986).
40. Kessler *et al.* (1983) observed that after superior cervical ganglionectomy the amount of Substance P in the iris increased, an effect that was abolished by N V ablation; Substance P was present in the superior cervical ganglion but it does not migrate into the sympathetic terminals, so presumably subserves some intraganglion function. Whether the increase in the iris tissue is a result of proliferation of fibres or increase per fibre is a matter of conjecture.
41. Capsaicin is the pungent principle of red pepper; it is itself strongly irritant presumably by causing release of Substance P from sensory nerve terminals; with prolonged application it finally desensitizes the nerve presumably by depletion of its Substance P. Bynke (1983) reduced the effects of infra-red irradiation of the iris by previously giving a retrobulbar injection of capsaicin. The response to PGE_2 was also reduced. Capsaicin itself causes an inflammatory reaction which subsides after 2–4 days, after which the test with infrared radiation was made.
42. Kaufman (1986) has reviewed the literature dealing with the effect of prostaglandins on facility; he points out that the prostaglandin might act directly on the smooth muscle of the ciliary body, causing increased facility in this way. When he disinserted and retrodisplaced the muscle, he found no effect on facility in the monkey, however.
43. Adrenaline excites α_1, α_2, β_1 and β_2 receptors, whereas noradrenaline excites only α_1, α_2, and β_1 (Innemee & Van Zwieten, 1982).
44. Earlier Bromberg *et al.* (1980) separated the iridial processes from the rabbit iris-ciliary body preparation (equivalent to ciliary processes in the primate), and using the ^{125}I-HYP displacement technique, demonstrated a predominantly beta-type of receptor. Adenylcyclase was recovered from the same fraction as that containing the binding sites.

    Wax & Molinoff (1987) used ^{125}I-iodopindonol to characterize beta-receptors on membranes separated by isopycnic sedimentation from rabbit iris-ciliary body homogenates. Competitive studies indicated a predominantly beta-innervation, ciliary processes, ciliary body and iris having about equal numbers of receptors.
45. The combined effects of epinephrine and timolol have been examined by Ohrström & Pandolfi (1980) and Thomas & Epstein (1981); the former found a cancellation, whilst the latter found some addition, especially if epinephrine was given first; they provide a plausible explanation for the similar effects of beta agonists and blockers.

    Partamian *et al.* (1983) showed that levobunol, a $beta_1$- and $beta_2$-blocker, reduced intraocular pressure in humans; Yablonski *et al.* (1987) found a 29% decrease in aqueous flow together with a 36% decrease in pressure; it seemed unlikely that drainage-facility was affected.
46. Employing their newly developed technique of microendoscopy of the ciliary-process vasculature in albino rabbits, Funk & Rohen (1987b) have described similar responses to epinephrine and phenylephrine; isoproterenol produced a vasodilatation in the same territories. Substance P exerted a constrictive action on the terminal arterioles of the iridial processes and the anterior portion of the major processes.
47. Boas *et al.* (1981) have largely confirmed these studies on adrenergic action in relation to cAMP appearance in the aqueous humour; however, there was some dissociation between cAMP appearance and intraocular pressure changes, and they have suggested that cAMP levels in the aqueous humour may have no relationship to changes in ocular pressure.
48. Akagi *et al.* (1981) examined the sympathetic innervation of the anterior segment in monkeys after treatment with 5-

hydroxydopamine, which accumulates in terminal vesicles and allows identification. Terminals were only in the posterior region of the meshwork by Schlemm's canal; cholinergic terminals was also here. Terminals were present in the subepithelial tissue of the ciliary body, possibly exerting an influence on secretion. They suggested that the sympathetic might affect the secretion of glycoproteins in the meshwork, affecting its porosity. In human tissue Jampel *et al.* (1987), employing an *in vitro* labelling technique using ^{125}I-cyanopindolol, identified beta-receptors, probably of the beta$_2$-subtype; similar labelling occurred with cultured trabecular cells, suggesting that the receptors were localized to the endothelium.

49. Suzuki & Kobayashi (1983) found that VIP had no effect on the resting tension of the ciliary muscle *in vitro*, nor on its response to the cholinergic agonist, carbachol, but it did increase the effect of N III stimulation; thus it apparently acted presynaptically to increase the release of transmitter. This effect was abolished by atropine. This might explain the effect of atropine on the VIP-response described by Nilsson *et al.*
50. Weinreb *et al.* (1983) showed that dexamethasone inhibited the synthesis of prostaglandins by cultured human trabecular cells in a dose-related manner. If the predominant effect of prostaglandins, such as PGE_2 and $F_{2\alpha}$, is to lower intraocular pressure (p. 62), then this effect of corticosterone acquires significance. Studies on the incorporation of radioactive proline and glucosamine by cultured meshwork explants suggest a decrease in collagen and glycosaminoglycan synthesis in response to dexamethasone (Hernandez *et al.*, 1983; 1985).
51. Thus these sialic acid-containing sites are absent at functional sites of the cell involved in such processes as endocytosis (De Bruyn, 1979).
52. According to Radius & Pederson (1984), however, the pathology of laser-induced glaucoma consisted of adhesion of the iris to the cornea, so that Schlemm's canal was intact.

References

Acott, T. S., Westeott, M., Passo, M. S. & Van Buskirk, E. M. (1985) Trabecular meshwork glycosoaminoglycans in human and cynomolgus monkey eye. *Invest. Ophthal.* **26**, 1320–1329.

Akagi, Y., Nojyo, Y. & Itoi, M. (1981) The localization of sympathetic nerve terminals in the ciliary body and the trabecular meshwork of the monkey. *Jap. J. Ophthal.* **25**, 395–406.

Alm, A. (1977) The effect of sympathetic stimulation on blood flow through the uvea, retina and optic nerve in monkeys (*Macaca irus*). *Exp. Eye Res.* **25**, 19–24.

Alm, A. & Bill, A. (1972) The oxygen supply to the retina. II. *Acta Physiol. Scand.* **84**, 306–319.

Alm, A. & Bill, A. (1973) The effect of stimulation of the cervical sympathetic chain on retinal oxygen tension and on uveal, retinal and cerebral blood flow in cats. *Acta physiol. Scand.* **88**, 84–94.

Alm, A., Bill, A. & Young, F. A. (1973) The effects of pilocarpine and neostigmine on the blood flow through the anterior uvea in monkeys. A study with radioactively labelled microspheres. *Exp. Eye Res.* **15**, 31–36.

Ambache, N. (1957) Properties of irin, a physiological constituent of the rabbit's iris. *J. Physiol.* **135**, 114–132.

Amsler, M. & Huber, A. (1946) Methodik und erste klinische Ergebnisse einer Funktionsprüfung der Blut-Kammerwasser-Schranke. *Ophthalmologica, Basel*, **111**, 155–176.

Anselmi, P., Bron, A. J. & Maurice, D. M. (1968) Action of drugs on the aqueous flow in man measured by fluorophotometry. *Exp. Eye Res.* **7**, 487–496.

Araie, M. (1985) Time change of rabbit aqueous flow under influence of adrenergic drugs. *Exp. Eye Res.* **40**, 391–403.

Araie, M. & Matsumoto, S. (1983) Analysis of fluorescein dynamics in the plasma after intravenous injection and calculation of the blood-aqueous barrier. *Nippon Ganka Gakkai Zaschi* **87**, 403–409.

Armaly, M. F. (1959) Studies on intraocular effect of orbital parasympathetic. *Arch. Ophthal., N.Y.* **62**, 117–124.

Armaly, M. F. (1963) Effects of corticosteroids on intraocular pressure and fluid dynamics. I and II. *Arch. Ophthal.* **70**, 482–491, 492–507.

Armaly, M. F. (1964) Aqueous outflow facility in monkeys and the effect of topical corticoids. *Invest. Ophthal.* **3**, 534–538.

Armaly, M. F. & Wang, Y. (1975) Demonstration of acid mucopolysaccharides in the meshwork of the rhesus monkey. *Invest. Ophthal.* **14**, 507–516.

Ascher, K. W. (1942) Aqueous veins. Preliminary note. *Am. J. Ophthal.* **25**, 31–38.

Ascher, K. W. (1961) *The Aqueous Veins*. Springfield: Thomas.

Ashton, N. (1951) Anatomical study of Schlemm's canal and aqueous veins by means of Neoprene casts. *Br. J. Ophthal.* **35**, 291–303.

Auricchio, G. & Bárány, E. H. (1959) On the role of osmotic water transport in the secretion of the aqueous humour. *Acta physiol. Scand.* **45**, 190–210.

Bairati, A. & Orzalesi, N. (1966) The ultrastructure of the epithelium of the ciliary body. *Z. Zellforsch.* **69**, 635–658.

Bárány, E. H. (1962) Transient increase in outflow facility after superior cervical ganglionectomy in rabbits. *Arch. Ophthal.* **67**, 303–311.

Bárány, E. H. (1967) The immediate effect on outflow resistance of intravenous pilocarpine in the vervet monkey, *Cercopithecus ethiops*. *Invest. Ophthal.* **6**, 373–380.

Bárány, E. H. (1972) Inhibition by hippurate and probenecid of *in vitro* uptake of iodipamide and o-iodohippurate. *Acta physiol. Scand.* **86**, 12–27.

Bárány, E. H. (1963) A mathematical formulation of intraocular pressure as dependent on secretion, ultrafiltration, bulk outflow, and osmotic reabsorption of fluid. *Invest. Ophthal.*, **2**, 584–590.

Bárány, E. H. & Scotchbrook, S. (1954) Influence of testicular hyaluronidase on the resistance to flow through the angle of the anterior chamber. *Acta physiol. Scand.* **30**, 240–248.

Bar-Elan, A. (1984) Diurnal and seasonal variations in intraocular pressure in the rabbit. *Exp. Eye Res.* **39**, 175–181.

Bar-Elan, A., Pessah, N. I. & Maren, T. H. (1984) The effect of carbonic anhydrase inhibitors on aqueous humor chemistry and dynamics. *Invest. Ophthal.* **25**, 1198–1205.

Bartels, S. P., Roth, H. A. & Neufeld, A. H. (1981) Effect of intracitreal cholera toxin on adenosine 3',5'-monophosphate, intraocular pressure and outflow facility in rabbits. *Invest. Ophthal.* **20**, 410–414.

Baurmann, M. (1930) Über die Ciliar-Fortsatz-Gefässystem. *Ber. dtsch. ophth. Ges.* **48**, 364–371.

Becker, B. (1965) Intraocular response to topical corticosteroids. *Invest. Ophthal.*, **4**, 198–205.

Becker, B. (1967) Ascorbate transport in guinea pig eye. *Invest. Ophthal.*, **6**, 410–415.

Becker, B. (1980) Vanadate and aqueous humor dynamics. *Invest. Ophthal.* **19**, 1156–1165.

Becker, B. & Constant, M. A. (1955) The effect of the carbonic anhydrase inhibitor acetazolamide on aqueous flow. *Arch. Ophthal. N.Y.* **54**, 321–329.

Becker, B. & Hahn, K. A. (1964) Topical corticosteroids and heredity in primary open-angle glaucoma. *Amer. J. Ophthal.* **57**, 543–551.

Becker, B. & Mills, D. W. (1963) Corticosteroids and intraocular pressure. *Arch. Ophthal.* **70**, 500–507.

Beitch, B. R. & Eakins, K. E. (1969) The effects of prostaglandins on the intraocular pressure of the rabbit. *Brit. J. Pharmacol.* **37**, 158–167.

Bellhorn, R. W., Burns, M. S. & Benjamin, J. V. (1980) Retinal vessel abnormalities of phototoxic retinopathy in rats. *Invest. Ophthal.* **19**, 584–595.

Belmonte, C., Bartels, S. P., Liu, J. H. K. & Neufeld, A. H. (1987) Effects of stimulation of the ocular sympathetic nerves on IOP and aqueous humor flow. *Invest. Ophthal.* **28**, 1649–1654.

Belmonte, C., Simon, J. & Gallego, A. (1971) Effects of intraocular pressure changes on the afferent activity of ciliary nerves. *Exp. Eye Res.* **12**, 342–355.

Bergmanson, J. P. G. (1977) The ophthalmic innervation of the anterior uvea in monkeys. *Exp. Eye Res.* **24**, 225–240.

Bernstein, H. N. & Schwartz, B. (1962) Effects of long-term systemic steroids on ocular pressure and tonographic values. *Arch. Ophthal., N.Y.* **68**, 742–753.

Berthelsen, S. & Pettinger, W. A. (1977) A functional basis for classification of α-adrenergic receptors. *Life Sci.* **21**, 595–606.

Betz, A. L. & Goldstein, G. W. (1980) Transport of hexoses, potassium and neutral amino acids into capillaries isolated from bovine retina. *Exp. Eye Res.* **30**, 593–605.

Bhattacherjee, P. & Eakins, K. E. (1974) Inhibition of prostaglandin synthetase systems in ocular tissues by indomethacin. *Brit. J. Pharmacol.* **50**, 227–230.

Bhattacherjee, P. & Eakins, K. E. (1974) A comparison of the inhibitory activity of compounds on ocular prostaglandin biosynthesis. *Invest. Ophthal.* **13**, 967–972.

Bhattacherjee, P. & Eakins, K. E. (1978) The intraocular pressure lowering effect of colchicine. *Exp. Eye Res.* **27**, 649–653.

Bhattacherjee, P. & Eakins, K. E. (1983) Biosynthesis of lipogenase products by ocular tissue. *Exp. Eye Res.*, **36**, 397–402.

Bhattacherjee, P. & Hammond, B. R. (1975) Inhibition of increased permeability of the blood-aqueous barrier by non-steroidal anti-inflammatory compounds as demonstrated by fluorescein angiography. *Exp. Eye Res.* **21**, 499–505.

Bhattacherjee, P. & Hammond, B. R. (1977) Effect of indomethacin on the ocular hypotensive action of adrenaline in the rabbit. *Exp. Eye Res.* **24**, 307–313.

Bhattacherjee, P., Kulkarni, P. S. & Eakins, K. E. (1979) Metabolism of arachidonic acid in rabbit ocular tissues. *Invest. Ophthal.* **18**, 172–178.

Bill, A. (1962) The drainage of blood from the uvea and the elimination of aqueous humour in rabbits. *Exp. Eye Res.* **1**, 200–205.

Bill, A. (1964) The albumin exchange in the rabbit eye. *Acta physiol. Scand.* **60**, 18–29.

Bill, A. (1966) The routes for bulk drainage of aqueous humour in rabbits with and without cyclodialysis. *Doc. Ophthal.*, **20**, 157–169.

Bill, A. (1966) The routes for bulk drainage of aqueous humour in the vervet monkey (*Cercopithecus ethipos*). *Exp. Eye Res.*, **5**, 55–57.

Bill, A. (1966) Conventional and uveo-scleral drainage of aqueous humour in the cynomolgus monkey (*Macaca irus*). *Exp. Eye Res.*, **5**, 45–54.

Bill, A. (1968a) The effect of ocular hypertension caused by red cells on the rate of formation of aqueous humour. *Invest. Ophthal.* **7**, 162–168.

Bill, A. (1968b) Capillary permeability to and extravascular dynamics of myoglobin, albumin and gammaglobulin in the uvea. *Acta physiol. Scand.* **73**, 204–219.

Bill, A. (1968c) A method to determine osmotically effective albumin and gammaglobulin concentrations in tissue fluids. *Acta physiol. Scand.* **73**, 511–522.

Bill, A. (1970a) Effects of norepinephrine, isoproterenol and sympathetic stimulation on aqueous humour dynamics in vervet monkeys. *Exp. Eye Res.* **10**, 31–46.

Bill, A. (1970b) Scanning electron microscopy of the canal of Schlemm. *Exp. Eye Res.* **10**, 214–218.

Bill, A. (1970c) The effect of changes in arterial blood pressure on the rate of formation of aqueous humour in a primate (*Cercopithecus ethiops*). *Ophth. Res.* **1**, 193–200.

Bill, A. (1971) Uveoscleral drainage of aqueous humour in human eyes. *Exp. Eye Res.* **12**, 275–281.

Bill, A. (1974) The role of the iris vessels in aqueous humor dynamics. *Jap. J. Ophthal.* **18**, 30–36.

Bill, A. (1975) Blood circulation and fluid dynamics in the eye. *Physiol. Rev.* **55**, 383–417.

Bill, A. & Bárány, E. H. (1966) Gross facility, facility of conventional routes, and pseudofacility of aqueous humour outflow in the cynomolgus monkey. *Archs. Ophthal., N.Y.* **75**, 665–673.

Bill, A. & Heilmann, K. (1975) Ocular effects of clonidine in cats and monkeys (*Macaca irus*). *Exp. Eye Res.* **21**, 481–488.

Bill, A., Stjernschantz, J., Mandahl, A., Brodin, E. & Nilsson, G. (1979) Substance P: release on trigeminal nerve stimulation, effects in the eye. *Acta Physiol. Scand.* **106**, 371–373.

Bill, A. & Svedbergh, B. (1972) Scanning electron microscopic studies of the trabecular meshwork and the canal of Schlemm—an attempt to locate the main resistance to outflow of aqueous humor in man. *Acta ophthal.* **50**, 295–320.

Bill, A. & Walinder, P.-E. (1966) The effects of pilocarpine on the dynamics of aqueous humour in a primate (*Macaca irus*). *Invest. Ophthal.* **5**, 170–175.

Bito, L. Z. (1970) Steady-state concentration gradients of magnesium, potassium and calcium in relation to the sites and mechanisms of ocular cation-transport processes. *Exp. Eye Res.* **10**, 102–116.

Bito, L. Z. (1972) Accumulation and apparent active transport of prostaglandins by some rabbit tissues *in vitro*. *J. Physiol.* **221**, 371–387.

Bito, L. Z. (1977) The physiology and pathophysiology of the intraocular fluids. *Exp. Eye Res.* **25**, Suppl. 273–289.

Bito, L. Z. (1982) The components of the ocular irritation and inflammatory responses and the diversity of their expression in vertebrates. *5th. Int. Congr. Eye Res. (Eindhoven).*

Bito, L. Z. (1984) Comparison of the ocular hypotensive efficacy of eiconasoids and related compounds. *Exp. Eye Res.* **38**, 181–194.

Bito, L. Z. & Baroody, R. A. (1987) The ocular pharmacokinetics of eicosanoids and their derivatives. I. *Exp. Eye Res.* **44**, 217–226.

Bito, L. Z. & Davson, H. (1964) Steady-state concentrations of potassium in the ocular fluids. *Exp. Eye Res.* **3**, 283–297.

Bito, L. Z., Davson, H., Levin, E., Murray, M. & Snider, N. (1965) The relationship between the concentrations of amino acids in the ocular fluids and blood plasma of dogs. *Exp. Eye Res.* **4**, 374–380.

Bito, L. Z., Draga, A., Blanco, J. & Camras, C. B. (1983) Long-

term maintenance of reduced intraocular pressure by daily or twice daily topical application of prostaglandins to cat or monkey eyes. *Invest. Ophthal.* **24**, 312–319.

Bito, L. Z. & Klein, E. M. (1981) The unique sensitivity of the rabbit eye to X-ray-induced ocular inflammation. *Exp. Eye Res.* **33**, 403–412.

Bito, L. Z., Nichols, R. R. & Baroody, R. A. (1982) A comparison of miotic and inflammatory effects of biologically active polypeptides and prostaglandin E_2 on the rabbit eye. *Exp. Eye Res.* **34**, 325–337.

Bito, L. Z. & Salvador, E. V. (1970) Intraocular fluid dynamics. II. *Exp. Eye Res.* **10**, 273–287.

Bito, L. Z. & Salvador, E. V. (1972) Intraocular fluid dynamics. III. The site and mechanism of prostaglandin transfer across the blood intraocular fluid barriers. *Exp. Eye Res.* **14**, 233–241.

Bito, L. Z. & Wallenstein, M. C. (1977) Transport of prostaglandins across the blood-brain and blood-aqueous barriers and the physiological significance of these absorptive transport processes. *Invest. Ophthal.* Suppl. 229–243.

Blair, N. P., Tso, M. O. M. & Dodge, J. T. (1984) Pathologic studies of the blood-retinal barrier in the spontaneously diabetic BB rat. *Invest. Ophthal.* **25**, 302–311.

Boas, R. S., Messenger, M. J., Mittag, T. W. & Podos, S. M. (1981) The effects of topically applied epinephrine and timolol on intraocular pressure and aqueous humor cyclic-AMP in the rabbit. *Exp. Eye Res.* **32**, 681–690.

Bonting, S. L. & Becker, B. (1964) Inhibition of enzyme activity and aqueous humor flow in the rabbit eye after intravitreal injection of ouabain. *Invest. Ophthal.* **3**, 523–533.

Brodwall, J. & Fischbarg, J. (1982) The hydraulic conductivity of rabbit ciliary epithelium *in vitro*. *Exp. Eye Res.* **34**, 121–129.

Bromberg, B. B., Gregory, D. S. & Sears, M. L. (1980) Beta-adrenergic receptors in ciliary processes of the rabbit. *Invest. Ophthal.* **19**, 203–207.

Bron, A. J. & Easty, D. L. (1970) Fluorescein angiography of the globe and anterior segment. *T.O.S.U.K.* **90**, 339–367.

Brubaker, R. F. (1967) Determination of episcleral venous pressure in the eye. *Arch. Ophthal.* **77**, 110–114.

Brubaker, R. F. (1970) The measurement of pseudofacility and true facility by constant pressure perfusion in the normal rhesus monkey eye. *Invest. Ophthal.* **9**, 42–52.

Brubaker, R. F. & Gaasterland, D. (1984) The effect of isoprotorenol on aqueous humor formation in humans. *Invest. Ophthal.* **25**, 357–359.

Brubaker, R. F. & Kupfer, C. (1966) Determination of pseudofacility in the eye of the rhesus monkey. *Arch. Ophthal., N.Y.* **75**, 693–697.

Burstein, N. L., Fischbarg, J. & Liebovitch, L. (1984) Electrical potential, resistance, and fluid secretion across isolated ciliary body. *Exp. Eye Res.* **39**, 771–779.

Burstein, N. L., Sears, M. L. & Mead, A. (1984) Aqueous flow in human eyes is reduced by forskolin, a potent adenylate cyclase activator. *Exp. Eye Res.* **39**, 745–749.

Butler, J. M. & Hammond, B. R. (1980) The effects of sensory denervation on the responses of the rabbit eye to prostaglandin E_1, bradykinin and substance P. *Brit. J. Pharmacol.* **69**, 495–502.

Butler, J. M., Ruskell, G. L., Cole, D. F., Unger, W. G., Zhang, S. Q., Blamk, M. A., McGregor, G. P. & Bliom, S. R. (1984) Effects of VIIth (facial) nerve degeneration on vasoactive intestinal polypeptide and substance P levels in ocular and orbital tissues of the rabbit. *Exp. Eye Res.* **39**, 523–532.

Bynke, G. (1983) Capsaicin pretreatment prevents disruption of the blood-aqueous barrier in the rabbit eye. *Invest. Ophthal.* **24**, 744–748.

Cabanas, J. L. del Rio & Ugidos, C. C. (1954) Estudio sobre las venas acuosas y laminares en ojos con tension intraocular normal. *Arc. Soc. oftal. hisp.-amer.* **14**, 489–509.

Camras, C. B. & Bito, L. Z. (1980a) The pathophysiological effects of nitrogen mustard in the rabbit eye. I. The biphasic intraocular pressure response and the role of prostaglandins. *Exp. Eye Res.* **30**, 45–52.

Camras, C. B. & Bito, L. Z. (1980b) The pathophysiological effects of nitrogen mustard in the rabbit eye. II. The inhibition of the initial hypertensive phase by capsaicin and the apparent role of substance P. *Invest. Ophthal.* **19**, 423–428.

Camras, C. B., Bito, L. Z. & Eakins, K. E. (1977) Reduction of intraocular pressure by prostaglandins applied topically to the eye of conscious rabbits. *Invest. Ophthal.* **16**, 1125–1134.

Camras, C. B., Podos, S. M., Rosenthal, J. S., Lee, P.-Y. & Severin, C. H. (1987) Multiple dosing of prostaglandin $F_{2\alpha}$ or epinephrine on cynomolgus monkey eyes. I. Aqueous humor dynamics. *Invest. Ophthal.* **28**, 463–469.

Cantley, L. C., Resh, M. D. & Guidotti, G. (1978) Vanadate inhibits the red cell (Na^+,K^+) ATPase from the cytoplasmic side. *Nature* **272**, 552–554.

Caprioli, J. & Sears, M. (1984) Combined effect of forskolin and acetazolamide on intraocular pressure and aqueous outflow in rabbit eyes. *Exp. Eye Res.* **39**, 47–50.

Caprioli, J., Sears, M., Bausher, L., Gregory, D. & Mead, A. (1984) Forskolin lowers intraocular pressure by reducing aqueous flow. *Invest. Ophthal.* **25**, 268–272.

Čepalik, J. & Cernohovsky, M. (1981) The effects of adrenergic agonists and antagonists on the adenylate cyclase in albino rabbit ciliary processes. *Exp. Eye Res.* **32**, 291–299.

Chu, T.-C. & Candia, O. A. (1987) Electrically silent Na^+ and Cl^- fluxes across the rabbit ciliary epithelium. *Invest. Ophthal.* **28**, 445–450.

Coakes, R. L. & Brubaker, R. F. (1978) The mechanism of timolol lowering intraocular pressure. *Arch. Ophthal.* **96**, 2045–2048.

Coakes, R. L. & Brubaker, R. F. (1979) Method of measuring aqueous humor flow and corneal endothelial permeability using a fluorophotometry nomogram. *Invest. Ophthal.* **18**, 288–302.

Cole, D. F. (1960) Rate of entrance of sodium into the aqueous humour of the rabbit. *Br. J. Ophthal.* **44**, 225–245.

Cole, D. F. (1961) Electrochemical changes associated with the formation of the aqueous humour. *Br. J. Ophthal.* **45**, 202–217.

Cole, D. F. (1961) Electrical potential across the ciliary body observed *in vitro*. *Br. J. Ophthal.* **45**, 641–653.

Cole, D. F. (1961c) Prevention of experimental ocular hypertension with polyphloretin phosphate. *Brit. J. Ophthal.*, **45**, 482–489.

Cole, D. F. (1966) Aqueous humour formation. *Doc. Ophthalmol.* **21**, 116–238.

Cole, D. F. (1974) The site of breakdown of the blood-aqueous barrier under the influence of vaso-dilator drugs. *Exp. Eye Res.*, **19**, 591–607.

Cole, D. F. (1977) Secretion of the aqueous humour. *Exp. Eye Res.* Suppl., 161–176.

Cole, D. F. (1984) Ocular fluids. In *The Eye*, Vol. 1A, 3rd. Ed., Ch. 2, Ed. H. Davson. Academic Press: London and New York.

Cole, D. F. & Monro, P. A. G. (1976) The use of fluorescein-labelled dextrans in investigation of aqueous humour outflow in the rabbit. *Exp. Eye Res.* **23**, 571–585.

Cole, D. F. & Nagasubramanian, S. (1972) The effect of natural and synthetic vasopressins and other substances on active transport in the ciliary epithelium of the rabbit. *Exp. Eye Res.* **13**, 45–57.

Cole, D. F. & Tripathi, R. C. (1971) Theoretical consideration on

the mechanism of the aqueous outflow. *Exp. Eye Res.* **12**, 25–32.

Cole, D. F. & Unger, W. G. (1973) Prostaglandins as mediators for the responses of the eye to trauma. *Exp. Eye. Res.* **17**, 357–368.

Copeland, R. L. & Kinsey, V. E. (1950) Determination of the volume of the posterior chamber of the rabbit. *Arch. Ophthal., N.Y.* **44**, 515–516.

Cousin, J. L., Motais, R. & Sola, F. (1975) Transmembrane exchange of chloride with bicarbonate ions in mammalian red blood cells: evidence for a sulphonamide-sensitive carrier. *J. Physiol.* **253**, 385–399.

Crawford, K. & Kaufman, P. L. (1987) Pilocarpine antagonizes PGF_2-induced ocular hypotension in monkeys. Evidence for enhancement of uveoscleral outflow by $PGF_{2\alpha}$. *Arch. Ophthal.* (in press; quoted by Hayashi *et al.*, 1987).

Cunha-Vaz. J. G. & Maurice, D. M. (1967) The active transport to fluorescein by the retinal vessels and the retina. *J. Physiol.* **191**, 467–486.

Dafna, Z., Lahav, M. & Melamed, E. (1979) Localization of β-adrenoceptors in the anterior segment of the albino rabbit eye using a fluorescent analog of propranolol. *Exp. Eye Res.* **29**, 327–330.

Davson, H. (1953) The penetration of large water-soluble molecules into the aqueous humour. *J. Physiol.* **122**, 10P.

Davson, H. (1956) *Physiology of the Ocular and Cerebrospinal Fluids.* London: Churchill.

Davson, H. (1969) The intra-ocular fluids. The intra-ocular pressure. In *The Eye*, Ed. Davson, pp. 67–186, 187–272. London: Academic Press.

Davson, H. & Duke-Elder, W. S. (1948) The distribution of reducing substances between the intraocular fluids and blood plasma, and the kinetics of penetration of various sugars into these fluids. *J. Physiol.* **107**, 141–152.

Davson, H. & Hollingsworth, J. R. (1972) The effects of iodate on the blood-vitreous barrier. *Exp. Eye Res.* **14**, 21–28.

Davson, H. & Huber, A. (1950) Experimental hypertensive uveitis in the rabbit. *Ophthalmologica, Basel*, **120**, 118–124.

Davson, H. & Luck, C. P. (1956) A comparative study of the total carbon dioxide in the ocular fluids, cerebrospinal fluid, and plasma of some mammalian species. *J. Physiol.* **132**, 454–464.

Davson, H. & Matchett, P. A. (1951) The control of the intraocular pressure in the rabbit. *J. Physiol.* **113**, 387–397.

Davson, H. & Quilliam, J. P. (1947) The effect of nitrogen mustard on the permeability of the blood-aqueous humour barrier to Evans blue. *Br. J. Ophthal.* **31**, 717–721.

Davson, H. & Segal, M. B. (1970) The effects of some inhibitors and accelerators of sodium transport on the turnover of ^{22}Na in the cerebrospinal fluid and the brain. *J. Physiol.* **209**, 131–153.

Davson, H. & Segal, M. B. (1975) *Introduction to Physiology.* Vol. 1. London: Academic Press.

Davson, H. & Spaziani, E. (1960) The fate of substances injected into the anterior chamber of the eye. *J. Physiol.* **151**, 202–215.

Davson, H. & Spaziani, E. (1961) The effect of hypothermia on intraocular dynamics. *Exp. Eye Res.* **1**, 182–192.

Davson, H. & Thomassen, T. L. (1950) The effect of intravenous infusion of hypertonic saline on the intraocular pressure. *Br. J. Ophthal.* **34**, 355–359.

Davson, H. & Weld, C. B. (1941) Studies on the aqueous humour. *Amer. J. Physiol.* **134**, 1–7.

Deane, R. & Segal, M. B. (1985) The transport of sugars across the perfused choroid plexus of the sheep. *J. Physiol.* **362**, 245–266.

De Bruyn, P. P. H. (1979) The role of sialated glycoproteins in endocytosis, permeability and transmural passage in the myeloid endothelium. *J. Hist. Cyt.* **27**, 1174–1176.

Delamere, N. A. & Williams, R. N. (1985) Detoxification of hydrogen peroxide by the rabbit iris-ciliary body. *Exp. Eye Res.*, **40**, 805–811.

Delamere, N. A. & Williams, R. N. (1985) The influence of reserpine and propranolol upon IOP response to vanadate in the rabbit. *Invest. Ophthal.* **26**, 1442–1445.

Delamere, N. A. & Williams, R. N. (1986) Modulation by vanadate of the adrenergic characteristics of the iris, ileum, and vas deferens. *Invest. Ophthal.*, **27**, 1336–1341.

Di Mattio, J., Degnan, K. J. & Zadunaisky, J. A. (1983) A model for transepithelial ion transport across the isolated retinal pigment epithelium of the frog. *Exp. Eye Res.* **37**, 409–420.

Di Mattio, J. & Streitman, J. (1986) Facilitated glucose transport across the retinal pigment epithelium of the bullfrog (*Rana catesbiana*). *Exp. Eye Res.* **43**, 15–28.

Di Mattio, J. & Zadunaisky, J. A. (1981) Glucose transport into the ocular compartments of the rat. *Exp. Eye Res.* **32**, 517–532.

Di Mattio, J. & Zadunaisky, J. A. (1983) Reduced ocular glucose transport and increased non-electrolyte permeability in rats with retinal degeneration (RCS). *Exp. Eye Res.* **37**, 217–223.

Drance, S. M. (1960) The coefficient of scleral rigidity in normal and glaucomatous eyes. *Arch. Ophthal. N.Y.* **63**, 668–674.

Duke-Elder, W. S. (1927) The pressure equilibrium in the eye. *J. Physiol.* **64**, 78–86.

Duke-Elder, W. S. (1932) *Textbook of Ophthalmology.* Vol. 1. London: Kimpton.

Duke-Elder, S. & Wybar, K. C. (1961) *System of Ophthalmology.* Vol. II: *The Anatomy of the Visual System.* London: Kimpton.

Durham, D. G., Bigliano, R. P. & Masino, J. A. (1965) Pneumatic applanation. tonometer *Trans. Am. Acad. Ophthal. Oto-lar.* **69**, 1029–1047.

Eakins, K. E. (1977) Prostaglandin and non-prostaglandin mediated breakdown of the blood-aqueous barrier. *Exp. Eye Res.* **25**, Suppl. 483–498.

Eakins, K. E. & Ryan, S. J. (1964) The action of sympathetic amines on the outflow of aqueous humour from the eye. *Brit. J. Pharmacol.* **23**, 374–382.

Ellingsen, B. A. & Grant, W. M. (1971) Influence of intraocular pressure and trabeculotomy on aqueous outflow in enucleated monkey eyes. *Invest. Ophthal.* **10**, 705–709.

Ennis, S. R. & Betz, A. L. (1986) Sucrose permeability of the blood-retinal and blood-brain barriers. *Invest. Ophthal.* **27**, 1095–1102.

Ennis, S. R., Johnson, J. E. & Pautler, E. L. (1982) *In situ* kinetics of glucose transport in normal rats and rats with streptozocin-induced diabetes. *Invest. Ophthal.* **23**, 447–456.

Epstein, D. L., Freddo, T. F., Anderson, P. J., Patterson, M. M. & Bassett-Chu, S. (1986) Experimental obstruction of aqueous outflow by pigment particles in living monkey. *Invest. Ophthal.*, **27**, 387–395.

Epstein, D. L., Freddo, T. F., Bassett-Chu, S., Chung, M. & Karageuzion, L. (1987) Influence of ethacrynic acid on outflow facility in the monkey and calf eye. *Invest. Ophthal.* **28**, 2067–2075.

Epstein, D. L., Hashimoto, J. M., Anderson, P. J. & Grant, W. M. (1981) Effect of iodacetamide perfusion on outflow facility and metabolism of the trabecular meshwork. *Invest. Ophthal.* **20**, 625–631.

Epstein, D. L., Patterson, M. M., Rivers, S. C. & Anderson, P. J. (1982) *N*-Ethyl maleimide increases facility of aqueous outflow of excised monkey and calf eyes. *Invest. Ophthal.* **22**, 752–756.

Erdmann, E., Werdan, K., Krawitz, W., Schmitz, W. & Scholz, H. (1984) Vanadate and its significance in biochemistry and pharmacology. *Biochem. Pharmacol.*, **33**, 945–949.

Ethier, C. R., Kamm, R. D., Polaszewski, B. A., Johnson, M. C. & Richardson, T. M. (1986) Calculations of flow resistance in the juxta canalicular meshwork. *Invest. Ophthal.* **27**, 1741–1750.

Fain, J. N. & Garcia-Sáinz, J. A. (1980) Role of phosphatidylinositol turnover in alpha, and of adenylate cyclase inhibition of alpha$_2$ effects of catecholamines. *Life Sci.* **26**, 1183–1194.

Ferreira, S. H., Moncada, S. & Vane, J. (1971) Indomethacin and aspirin abolish prostaglandin release from the spleen. *Nature, New Biol.* **231**, 237–239.

Fishman, M. C. (1979) Endogenous digitalis-like activity in mammalian brain. *Proc. Nat. Acad. Sci.* **76**, 4661–4663.

Forbes, M. & Becker, B. (1960) *In vivo* transport of iodopyracet (diodrast). *Am. J. Ophthal.* **50**, Pt. 2, 862–867.

Fortin, E. P. (1929) Action du muscle ciliare sur la circulation de l'oeil, etc. *C.r. Seanc. Soc. Biol.* **102**, 432–434.

Frambach, D. A. & Marmor, M. F. (1982) The rate and route of fluid resorption from the subretinal space of the rabbit. *Invest. Ophthal.*, **22**, 292–302.

François, J. (1954) Cortisone et tension oculaire. *Annls Oculist.* **187**, 805–816.

François, J. (1975) The importance of the mucopolysaccharides in intraocular pressure regulation. *Invest. Ophthal.* **14**, 173–176.

François, J. & Neetens, A. (1962) Comparative anatomy of the vascular supply of the eye in vertebrates. In *The Eye*, Ed. Davson, pp. 369–416. London: Academic Press.

Freddo, T. F. (1984) Intercellular junctions of the iris epithelia in *Macaca mulatta*. *Invest. Ophthal.* **25**, 1094–1104.

Freddo, T. F., Patterson, M. W., Scott, D. R. & Epstein, D. L. (1984) Influence of mercurial sulphydryl agents on aqueous outflow pathways in enucleated eyes. *Invest. Ophthal.* **25**, 278–285.

Freddo, T. F. & Raviola, G. (1982) Freeze-fracture analysis of the interendothelial junctions in the blood vessels of the iris in *Macaca mulatta*. *Invest. Ophthal.* **23**, 154–167.

Freddo, T. F. & Raviola, G. (1982) The homogeneous structure of blood vessels in the vascular tree of *Macaca mulatta* iris. *Invest. Ophthal.* **22**, 279–291.

Friedland, A. B. (1983) Relationship between arterial pulsations and intraocular pressure. *Exp. Eye Res.* **37**, 421–428.

Friedenwald, J. S. (1957) Tonometer calibration. An attempt to remove discrepancies found in the 1954 calibration scale for Schiotz tonometers. *Trans. Amer. Acad. Ophthal. Otolaryngol.*, **61**, 108–123.

Frokjaer-Jensen, J. (1984) The plasmalemmal vesicular system in striated muscle capillaries and in pericytes. *Tissue & Cell* **16**, 31–42.

Funk, R. & Rohen, J. W. (1987a) SEM studies on the functional morphology of the rabbit ciliary process vasculature. *Exp. Eye Res.* **45**, 579–595.

Funk, R. & Rohen, J. W. (1987b) Intraocular microendoscopy of the ciliary-process vasculature in albino rabbits: effects of vasoactive agents. *Exp. Eye Res.* **45**, 597–606.

Gaasterland, D. E., Barranger, J. A., Rapoport, S. I., Girton, M. E. & Doppman, J. L. (1983) Long-term ocular effects of osmotic modification of the blood-aqueous barrier in monkeys. *Invest. Ophthal.* **24**, 153–158.

Gaasterland, D. & Kupfer, C. (1974) Experimental glaucoma in the rhesus monkey. *Invest. Ophthal.* **13**, 455–457.

Gaasterland, D. E. & Pederson, J. E. (1983) Episcleral venous pressure: a comparison of invasive and noninvasive measurements. *Invest. Ophthal.* **24**, 1417–1432.

Gaasterland, D. E., Pederson, J. E., MacLellan, H. M. & Reddy, V. N. (1979) Rhesus monkey aqueous humor composition and a primate ocular perfusate. *Invest. Ophthal.* **18**, 1139–1150.

Galin, M. A., Davidson, R. & Pasmanik, S. (1963) An osmotic comparison of urea and mannitol. *Am. J. Ophthal.* **55**, 244–247.

Garg, L. C. & Oppelt, W. W. (1970) The effect of ouabain and acetazolamide on transport of sodium and chloride from plasma to aqueous humor. *J. Pharm.* **175**, 237–247.

Gerritson, M. E., Weinstein, B. I., Gordon, G. G. & Southren, A. L. (1986) Prostaglandin synthesis and release from cultured human trabecular meshwork cells and scleral fibroblasts. *Exp. Eye Res.*, **43**, 1089–1102.

Gherezghiher, T. & Koss, M. C. (1979) Clonidine mydriasis in the rat. *Eur. J. Pharmacol.* **57**, 263–266.

Gherezghiher, T., March, W. F., Nordquist, R. E. & Koss, M. C. (1986) Laser-induced glaucoma in rabbits. *Exp. Eye Res.* **43**, 885–894.

Gibson, S. J. *et al.* (1984) Calcitonin gene-releted immunoreactivity in the spinal cord of man and of eight other species. *J. Neurosci.* **4**, 3101–3111.

Gipson, I. K. & Anderson, R. A. (1979) Actin filaments in cells of human trabecular meshwork and Schlemm's canal. *Invest. Ophthal.* **18**, 547–561.

Gloster, J. (1961) Influence of facial nerve on intraocular pressure. *Br. J. Ophthal.* **45**, 259–278.

Gloster, J. & Greaves, D. P. (1957) Effect of diencephalic stimulation upon intraocular pressure. *Br. J. Ophthal.* **41**, 513–532.

Goldmann, H. (1946) Weitere Mitteilung über den Abfluss des Kammerwassers beim Menschen. *Ophthalmologica Basel*, **112**, 344–349.

Goldmann, H. (1955) Un nouveau tonomètre á aplanation. *Bull. Soc. franc. Ophtal.* **67**, 474.

Goldmann, H. (1968) On pseudofacility. *Bibl. Ophthal.* **76**, 1–14.

Grant, W. M. (1950) Tonographic method for measuring the facility and rate of aqueous outflow in human eyes. *Arch. Ophthal., N.Y.* **44**, 204–214.

Grant, W. M. (1958) Further studies on facility of flow through trabecular meshwork. *Arch. Ophthal., N.Y.* **60**, 523–533.

Grant, W. M. (1963) Experimental aqueous perfusion in enucleated human eyes. *Arch. Ophthal., N.Y.* **69**, 783–801.

Greaves, D. P. & Perkins, E. S. (1952) Influence of the sympathetic nervous system on the intraocular pressure and vascular circulation of the eye. *Br. J. Ophthal.* **36**, 258–264.

Greeff, R. (1894) Befund am Corpus ciliare nach Punktion der vorderen Kammer. *Arch. Augenheilk.* **28**, 178–192.

Green, K. & Pederson, E. (1972) Contribution of secretion and filtration to aqueous humor formation. *Amer. J. Physiol.* **222**, 1218–1226.

Gregory, D., Sears, M., Bausher, L., Mishima, H. & Mead, A. (1981) Intraocular pressure and aqueous flow are decreased by cholera toxin. *Invest. Ophthal.* **20**, 371–381.

Grierson, I. & Lee, W. R. (1974) Changes in the monkey outflow apparatus at graded levels of intraocular pressure: a qualitative analysis by light microscopy and scanning electron microscopy. *Exp. Eye Res.* **19**, 21–33.

Grierson, I. & Lee, W. R. (1975a) The fine structure of the trabecular meshwork at graded levels of intraocular pressure (1) Pressure effects within the near-physiological range (8–30 mmHg) (2) Pressure outside the physiological range (0 and 50 mmHg). *Exp. Eye Res.* **20**, 523–530.

Grierson, I. & Lee, W. R. (1975b) Acid mucopolysaccharides in the outflow apparatus. *Exp. Eye Res.*, **21**, 417–431.

Grierson, I., Lee, W. R. & Abraham, S. (1978) Effects of pilocarpine on the morphology of the human outflow apparatus. *Brit. J. Ophthal.* **62**, 302–313.

Grierson, I., Lee, W. R., & Abraham, S. (1979) The effect of topical pilocarpine on the morpholosy of the outflow apparatus of the baboon (*Papio cynocephalus*). *Invest. Ophthal.* **18**, 346–355.

Grierson, I., Nagasubramanian, S., Edwards, J., Millar, L. C. & Ennis, K. (1986) The effect of various levels of intraocular pressure on the rabbit's outflow system. *Exp. Eye Res.* **42**, 383–397.

Grierson, I. & Rahi, A. H. S. (1979) Microfilaments in the cells of the human trabecular meshwork. *Brit. J. Ophthal.* **63**, 3–8.

Grignolo, A., Orzalesi, N. & Calabria, G. A. (1966) Studies on the fine structure and the rhodopsin cycle of the rabbit retina in experimental degeneration induced by sodium iodate. *Exp. Eye Res.* **5**, 86–97.

Grimes, P. A. & Laties, A. M. (1980) Early morphological alteration of the pigment epithelium in streptotozin-induced diabetes: increased surface area of the basal cell membranes. *Exp. Eye Res.* **30**, 631–639.

Hamanaka, T. & Bill, A. (1987) Morphological and functional effects of Na_2EDTA on the outflow routes for aqueous humor in monkeys. *Exp. Eye Res.* **44**, 171–190.

Hansson, H. P. J. (1968) Histochemical demonstration of carbonic anhydrase activity in some epithelia. *Acta Physiol. Scand.*, **73**, 427–434.

Hara, L., Lutjen-Drecoll, E., Prestele, H. & Rohen, J. W. (1977) Structural differences between regions of the ciliary body in primates. *Invest. Ophthal.*, **16**, 912–924.

Harris, J. E. & Gehrsitz, L. B. (1949) The movement of monosaccharides into and out of the aqueous humour. *Amer. J. Ophthal.* **32**, Pt. 2, 167–176.

Harrison, R. & Kaufmann, C. S. (1977) Clonidine: effects of a topically administered solution on intraocular pressure and blood pressure in open-angle glaucoma. *Arch. Ophthal.* **95**, 1368–1373.

Hart, R. W. (1972) Theory of neural mediation of intraocular dynamics. *Bull. Math. Biophys.* **34**, 113–140.

Hasslinger, C. (1969) Catapresan (2-[2,6-Dichlorphenylamino]-2-imidazolamin hydrochlorid)—ein neues augendrucksenkendes Medikament. *Klin. Mbl. Augenheilk.* **154**, 95–105.

Hayashi, M., Yablonski, M. E. & Bito, L. Z. (1987) Eicosanoids as a new class of ocular hypotensive agents. 2. Comparison of the apparent mechanism of the ocular hypotensive effects of A and F types prostaglandins. *Invest. Ophthal.* **28**, 1639–1643.

Hayreh, S. S. (1969) Blood supply of the optic nerve head and its role in optic atrophy, glaucoma, and oedema of the optic disc. *Br. J. Ophthal.* **53**, 721–748.

Hayreh, S. S. & Scott, W. E. (1978) Fluorescein angiography. I. Normal pattern. *Arch. Ophthal.*, **96**, 1383–1389.

Heath, H. & Fiddick, R. (1966) The active transport of ascorbic acid by the rat retina. *Exp. Eye Res.* **5**, 156–163.

Henkind, P., Leitman, M. & Weitzman, E. (1973) The diurnal curve in man: new observations. *Invest. Ophthal.* **12**, 705–707.

Hernandez, M. R., Weinstein, B. I., Wenk, E. J., Gordon, G. G., Dunn, M. W. & Southren, A. L. (1983) The effect of dexamethasone on the in vitro incorporation of precursors of extracellular matrix components in the outflow pathway region of the rabbit eye. *Invest. Ophthal.*, **24**, 704–709.

Hernandez, M. R., Weinstein, B. I., Dunn, M. W., Gordon, G. G. & Southren, A. L. (1985) The effect of dexamethasone on the synthesis of collagen in normal human trabecular meshwork explants. *Invest. Ophthal.* **26**, 1784–1788.

Holland, M. G. & Gipson, C. C. (1970) Chloride ion transport in the isolated ciliary body. *Invest. Ophthal.* **9**, 20–29.

Holland, M. G., v. Sallmann, L. & Collins, E. M. (1956) A study of the innervation of the chamber angle. *Amer. J. Ophthal.* **42**, (pt 2), 148–161.

Holland, N. G., v. Sallmann, L. & Collins, E. M. (1957) A study of the innervation of the chamber angle. II. The origin of trabecular axons revealed by degeneration experiments. *Amer. J. Ophthal.* **44**, (pt 2), 206–221.

Holmberg, A. (1959) The fine structure of the inner wall of Schlemm's canal. *Archs. Ophthal. N.Y.* **62**, 956–958.

Hörven, I. (1961) Tonometry in newborn infants. *Acta ophthal. Kbh.* **39**, 911–918.

Hoyng, P. F. J., Verbey, N., Thorig, L. & van Haeringen, N. J. (1986) Topical prostaglandins inhibit trauma-induced inflammation in the rabbit eye. *Invest. Ophthal.* **27**, 1217–1225.

Hudspeth, A. J. & Yee, A. G. (1973) The intercellular junctional complexes of retinal pigment epithelia. *Invest. Ophthal.* **12**, 354–365.

Huggert, A. (1958) Experimentally induced increase in intraocular pressure in the rabbit eye. *Acta ophthal. Kbh.* **36**, 750–760.

Hughes, B. A., Miller, S. S. & Machen, T. E. (1984) Effects of cyclic AMP on fluid absorption and ion transport across frog retinal pigment epithelium. *J. gen. Physiol.* **83**, 875–899.

Innemee, H. C., De Jonge, A., Van Meel, J. C. A., Timmermans, P. B. M. W. M., & Van Zwieten, P. A. (1982) Differential effects of selective α_1- and α_2-adrenoceptor agonists on intraocular pressure in the conscious rabbit. *Doc. Ophth.* **52**, 287–295.

Innemee, H. C. & Van Zwieten, P. A. (1978) An increase in intraocular pressure due to clonidine. *v. Graefes Arch.* **207**, 149–156.

Innemee, H. C. & Van Zwieten, P. A. (1979) The influence of clonidine on intraocular pressure. *Doc. Ophthal.* **46**, 309–315.

Innemee, H. C. & Van Zwieten, P. A. (1982) The role of beta-2-adrenoceptors in the IOP-lowering effect of adrenaline. *v. Graefes Arch. Ophthal.* **218**, 297–300.

Inomata, H. & Bill, A. (1977) Exit sites of uveoscleral flow of aqueous humour in cynomolgus monkey eyes. *Exp. Eye Res.* **25**, 113–118.

Inomata, H., Bill, A. & Smelser, G. K. (1972a) Aqueous humour pathways through the trabecular meshwork and into Schlemm's canal in the cynomolgus monkey (*Macaca irus*). *Amer. J. Ophthal.* **73**, 760–789.

Inomata, H., Bill, A. & Smelser, G. K. (1972b) Unconventional routes of aqueous humor outflow in cynomolgus monkey (*Macaca irus*). *Amer. J. Ophthal.* **73**, 893–907.

Jampel, H. D., Lynch, M. G., Brown, R. H., Kuhar, M. J. & De Souza, E. B. (1987) β-Adrenergic receptors in human trabecular meshwork. *Invest. Ophthal.*, **28**, 772–779.

Jampol, L. M., Neufeld, A. H. & Sears, M. L. (1975) Pathways for the response of the eye to injury. *Invest. Ophthal.* **14**, 184–189.

Jocson, V. L. & Sears, M. L. (1968) Channels of aqueous outflow and related blood vessels. I. *Macaca mulatta* (Rhesus). *Arch. Ophthal.*, **80**, 104–114.

Johnson, F. & Maurice, D. (1984) A simple method of measuring aqueous humor flow with intravitreal fluorescinated dextrans. *Exp. Eye Res.* **39**, 791–805.

Johnson, M. C. & Kamm, R. D. (1983) The role of Schlemm's canal in aqueous outflow from the human eye. *Invest. Ophthal.* **24**, 320–325.

Johnstone, M., Tanner, D., Chau, B. & Kopecky, K. (1980) Concentration-dependent morphologic effects of cytochalasin B in the aqueous outflow system. *Invest. Ophthal.* **19**, 835–841.

Johnstone, M. A. & Grant, W. M. (1973) Pressure-dependent changes in structure of the aqueous outflow system of human and monkey eyes. *Amer. J. Ophthal.* **75**, 365–383.

Jones, R. F. & Maurice, D. M. (1966) New methods of measuring the rate of aqueous flow in man with fluorescein. *Exp. Eye Res.* **5**, 208–220.

Kahn, M. G., Giblin, F. J. & Epstein, D. L. (1983) Glutathione in calf trabecular meshwork and its relation to aqueous humor outflow facility. *Invest. Ophthal.* **24**, 1283–1287.

Kahn, R. H. & Loewenstein, A. (1922) Uber die Druckschwankungen im Saugerauge nach teilweise Entleerung der Vorderkammer bei langdauernder manometrischer Messung. *v. Graefes Arch. Ophthal.* **109**, 433–453.

Kappelhof, J. P., van Best, J. A., van Valenberg, P. L. J. & Oosterhuis, J. A. (1987) Inward permeability of the blood-retinal barrier by fluorophotometry. *Invest. Ophthal.* **28**, 665–671.

Karnovsky, M. J. (1967) The ultrastructural basis of capillary permeability studied with peroxidase as a tracer. *J. Cell Biol.* **35**, 213–236.

Katz, I. M., Hubbard, W. A., Getson, A. J. & Gould, A. L. (1976) Intraocular pressure decrease in normal volunteers following timolol ophthalmic solution. *Invest. Ophthal.* **15**, 489–492.

Katz, R. S., Henkind, P. & Weitzman, E. D. (1975) The circadian rhythm of the intraocular pressure in the New Zealand white rabbit. *Invest. Ophthal.*, **14**, 775–780.

Kaufman, P. L. (1984) Aqueous humor outflow. *Curr. Topic Eye Res.* **4**, 97–138.

Kaufman, P. L. (1986) Epinephrine, norepinephrine, and isoproterenol dose-outflow facility response relationships in cynomolgus monkeys with and without ciliary muscle retrodisplacement. *Acta Ophthal.* **64**, 356–363.

Kaufman, P. L (1986) Total iridectomy does not alter outflow facility responses to cyclic AMP in cynomolgus monkeys. *Exp. Eye Res.* **43**, 441–442.

Kaufman, P. L. (1986) Effects of intracamerally infused prostaglandins on outflow facility in cynomolgus eyes with intact or retrodisplaced ciliary muscle. *Exp. Eye Res.* **43**, 819–827.

Kaufman, P. L. (1987) Non-additivity of maximal pilocarpine and cytochalasin effects on outflow facility. *Exp. Eye Res.* **44**, 283–291.

Kaufman, P. L. (1987) Adenosine 3′,5′-cyclic monophosphate and outflow facility in monkey eyes with intact and retrodisplaced ciliary muscle. *Exp. Eye Res.* **44**, 415–423.

Kaufman, P. L. & Barany, E. H. (1976) Loss of acute pilocarpine effect on outflow facility following surgical disinsertion and retrodisplacement of the ciliary muscle from the scleral spur in the cynomolgus monkey. *Invest. Ophthal.*, **15**, 793–807.

Kaufman, P. L. & Bárány, E. H. (1977) Recent observations concerning the effects of cholinergic drugs on outflow facility in monkeys. *Exp. Eye Res.* (Suppl.) 415–418.

Kaufman, P. L. & Bárány, E. H. (1981) Adrenergic drug effects on aqueous outflow facility following ciliary muscle retrodisplacement in the cynomolgus monkey. *Invest. Ophthal.* **20**, 644–651.

Kaufman, P. L. & Erickson, K. A. (1982) Cytochalasin B and D dose-outflow facility response relationships in the cynomolgus monkey. *Invest. Ophthal.* **23**, 646–650.

Kaufman, P. L. & Rentzhog, L. (1981) Effect of total iridectomy on outflow facility responses to adrenergic drugs in cynomolgus monkeys. *Exp. Eye Res.* **33**, 65–74.

Kayes, J. (1967) Pore structure of the inner wall of Schlemm's canal. *Invest. Ophthal.* **6**, 381–394.

Kayes, J. (1975) Pressure gradient changes on the trabecular meshwork of monkeys. *Amer. J. Ophthal.* **79**, 549–556.

Kelly, R. G. M. & Starr, M. S. (1971) Effects of prostaglandins and a prostaglandin antagonist on intraocular pressure and protein in the monkey eye. *Can. J. Ophthal.* **6**, 205–211.

Kessler, J. A., Bell, W. O. & Black, I. B. (1983) Substance P levels differ in sympathetic target organ terminals and ganglion perikarya. *Brain Res.* **258**, 144–146.

Khatami, M., Stramm, L. E. & Rockey, J. H. (1986) Ascorbate transport in cultured cat retinal pigment epithelial cells. *Exp. Eye Res.*, **43**, 607–615.

Kinsey, V. E. (1947) Transfer of ascorbic acid and related compounds across the blood-aqueous barrier. *Amer. J. Ophthal.* **30**, 1262–1266.

Kornblath, W. & Linner, E. (1955) Experimental tonography in rabbits: effect of unilateral ligation of common carotid artery on aqueous humor dynamics as studied by means of tonography and fluorescein appearance time. *Arch. Ophthal.* **54**, 717–724.

Kinsey, V. E. & Palm, E. (1955) Posterior and anterior chamber aqueous humour formation. *Arch. Ophthal., N.Y.* **53**, 330–344.

Kinsey, V. E. & Reddy, D. V. N. (1959) An estimate of the ionic composition of the fluid secreted into the posterior chamber, inferred from a study of aqueous humour dynamics. *Doc. Ophthal.* **13**, 7–40.

Kishida, K., Sasabe, T., Manabe, R. & Otori, T. (1981) Electric characteristics of the isolated rabbit ciliary body. *Jap. J. Ophthal.* **25**, 407–416.

Kitahara, S., Fox, K. R. & Hogben, C. A. M. (1967) Depression of chloride transport by carbonic anhydrase inhibitors in the absence of carbonic anhydrase. *Nature*, **214**, 836–837.

Knepper, P. A., Farbman, A. I. & Telser, A. G. (1984) Exogenous hyaluronidases and degradation of hyaluronic acid in the rabbit eye. *Invest. Ophthal.* **25**, 286–293.

Knepper, P. A., Breen, M., Weinstein, H. G. & Blacik, L. J. (1978) Intraocular pressure and glycosaminoglycan distribution in the rabbit eye: effect of age and dexamethasone. *Exp. Eye Res.* **27**, 567–575.

Knepper, P. A., Collins, J. A., Weinstein, H. G. & Breen, M. (1983) Aqueous outflow pathway complex carbohydrate synthesis *in vitro*. *Invest. Ophthal.* **24**, 1546–1551.

Köllner (1916) Uber den regelmässigen täglichen Schwankungen des Augendrucks und ihre Ursache. *Arch. Augenheilk.* **81**, 120–142.

Kinsey, V. E., Grant, M. & Cogan, D. G. (1942) Water movement and the eye. *Archs. Ophthal., N.Y.* **27**, 242–252.

Korte, G. E., Bellhorn, R. W. & Burns, M. S. (1983) Ultrastructure of blood-retinal barrier permeability in rat phototoxic retinopathy. *Invest. Ophthal.* **24**, 962–971.

Koss, M. C., March, W. F., Nordquist, R. E. & Gherezghiher, T. (1984) Acute intraocular pressure elevation produced by argon laser trabeculoplasty in the cynomolgus monkey. *Arch. Ophthal.* **102**, 1699–1703.

Kozart, D. M. (1968) Light and electron microscopic study of regional morphologic differences in the processes of the ciliary body in the rabbit. *Invest. Ophthal.*, **7**, 15–33.

Kronfeld, P. C. (1971) Early effects of single and repeated doses of L-epinephrine in man. *Amer. J. Ophthal.* **72**, 1058–1072.

Krootila, K., Uusitalo, H. & Palkama, A. (1987) Effect of α-adrenergic and serotonergic blockers on the acute irritative response in the rabbit eye. *Exp. Eye Res.* **45**, 721–729.

Krupin, T., Feitl, M. & Becker, B. (1980) Effect of prazocin on aqueous humor dynamics in rabbits. *Arch. Ophthal.* **98**, 1639–1642.

Krupin, T., Reinach, P. S., Candia, O. A. & Podos, S. M. (1984) Transepithelial electrical measurements on the isolated rabbit iris-ciliary body. *Exp. Eye Res.* **38**, 115–123.

Kulkarni, P. S., Rodriguez, A. V. & Srnivasan, B. D. (1984) Human anterior uvea synthesizes lipoxygenase products from arachidonic acid. *Invest. Ophthal.*, **25**, 221–223.

Kulkarni, P. S. & Srnivasan, B. D. (1983) Synthesis of slow reacting substance-like activity in rabbit conjunctiva and anterior uvea. *Invest. Ophthal.*, **24**, 1079–1085.

Kupfer, C. (1961) Studies on intraocular pressure. I. *Arch. Ophthal.*, **65**, 565–570.

Kupfer, C., Gaasterland, D. & Ross, K. (1971) II. Measurements in young normal subjects using acetazolamide and L-epinephrine. *Invest. Ophthal.* **10**, 523–533.

Kupfer, C. & Ross, K. (1971) Studies of aqueous humour dynamics in man. I. Measurements in young normal subjects. *Invest. Ophthal.* **10**, 518–522.

LaCour, M., Lund-Andersen, H. & Zeuthen, T. (1986) Potassium transport of the frog pigment epithelium: autoregulation of potassium activity in the subretinal space. *J. Physiol.* **375**, 461–479.

Langham, M. E. (1958) Aqueous humour and control of intraocular pressure. *Physiol Rev.* **38**, 215–242.

Langham, M. E. (1960) Steady-state pressure relationships in the living and dead cat. *Amer. J. Ophthal.*, **50**, Pt. 2, 950–958.

Langham, M. E. (1982) Intraocular pressure and pupillary responses to the topical application of α-methyl norepinephrine (αMeNE) and of α-methyl epinephrine (αMeEp). *ARVO Suppl.* **22**, 230.

Langham, M. E. & Diggs, E. M. (1974) β-Adrenergic responses in the eyes of rabbits, primates and man. *Exp. Eye Res.* **19**, 281–295.

Langham, M. E. & Edwards, N. (1987) A new procedure for the measurement of the outflow facility in conscious rabbits. *Exp. Eye Res.* **45**, 665–672.

Langham, M. E. & Fraser, L. K. (1966) The absence of supersensitivity to adrenergic amines in the eye of the conscious rabbit following preganglionic cervical sympathotomy. *Life Sciences* **5**, 1699–1705.

Langham, M. E. & Rosenthal, A. R. (1966) Role of cervical sympathetic nerve in regulating intraocular pressure and circulation. *Am. J. Physiol.* **210**, 786–794.

Langham, M. E. & Taylor, C. B. (1960) The influence of pre-and post-ganglionic section of the cervical sympathetic on the intraocular pressure of rabbits and cats. *J. Physiol.* **152**, 437–446.

Langham, M. E. & Taylor, C. B. (1960) The influence of superior cervical ganglionectomy on the intraocular pressure. *J. Physiol.* **152**, 447–458.

Langham, M. E. & Wybar, K. C. (1953) A fluorophotometer for the study of intraocular dynamics in the living animal. *J. Physiol.* **120**, 5P.

Larsson, S. (1932) Les vaisseaux intra-oculaires du segment antérieur et leur influence sur la pression oculaire. *Ann. d'Ocul.*, **169**, 94–119.

Lasansky, A. & De Fisch, F. W. (1966) Potential current and ionic fluxes across the isolated pigment epithelium and choroid. *J. Gen Physiol.*, **49**, 913–924.

Laties, A. M. & Jacowitz, D. (1966) A comparative study of the autonomic innervation of the eye in the monkey, cat and rabbit. *Anat. Rec.* **156**, 383–395.

Laties, A. M. & Rapoport, S. (1976) The blood-ocular barriers under osmotic stress. *Arch. Ophthal.* **94**, 1086–1091.

Leber, T. (1903) Die Cirkulations- und Ernährungverhältnisse des Auges. In *Graefe-Saemisch Hdb der gesamtes Augenheilkunde*, Saemisch, T. (Ed.) 2nd. Ed. Leipzig: Wilhelm Engelmann. Vol. 2, pt. 2. Ch. 11.

Lee, P.-Y, Podos, S. M., Mittag, T. & Severin, C. (1984) Effect of topicallied forskolin on aqueous humor dynamics in cynomolgus monkey. *Invest. Ophthal.* **25**, 1206–1209.

Lee, P.-Y., Podos, S. M. & Severin, C. (1984) Effect of prostaglandin $F_{2\alpha}$ on aqueous humour dynamics of rabbit cat and monkey. *Invest. Ophthal.* **25**, 1087–1093.

Leydhecker, W., Akiyama, K. & Neumann, H. G. (1958) Der intraokulare Druck gesunder menschlicher Augen. *Klin. Mbl. Augenheilk.* **133**, 662–670.

Li, Z.-Y.,Tso, M. O. M., Wang, H. & Organisciak, D. T. (1985) Amelioration of photic injury in rat retina by ascorbic acid: a histopathologic study. *Invest. Ophthal.* **26**, 1589–1598.

Lindenmayer, J. M., Kahn, M. G., Hertzmark, E. & Epstein, D. L. (1983) Morphology and function of the aqueous outflow system in monkey eyes. *Invest. Ophthal.* **24**, 710–717.

Linnér, E. (1952) Effect of unilateral ligation of the common carotid artery on the blood flow through the uveal tract as mesured directly in a vortex vein. *Acta Physiol. Scand.*, **26**, 70–78.

Litchfield, W. J. & Wells, W. W. (1976) Inhibitory action of D-galactose on phagocyte metabolism and function. *Immunity*, **13**, 728–734.

Lund-Andersen, H., Krogsaa, B., la Cour, M. & Larsen, J. (1985) Quantitative vitreous fluorophotometry applying a mathematical model of the eye. *Invest. Ophthal.*, **26**, 698–710.

Lundberg, J. M., Hokfelt, T., Anggard, A., Kimmel, J., Goldstein, M. & Markey, K. (1980) Coexistence of an avian pancreatic polypeptide (APP) immunoreactive substance and catecholamine in some peripheral and central neurons. *Acta Physiol. Scand.* **110**, 107–109.

Lundberg, J. M. *et al.* (1982) Neuropeptide Y (NPY)-like immunoreactivity in peripheral noradrenergic neurons and effects of NPY on sympathetic function. *Acta Physiol. Scand.* **116**, 477–480.

Lutjen-Drecoll, E. & Lönnerholm, G. (1981) Carbonic anhydrase distribution in the rabbit eye by light and electron microscopy. *Invest. Ophthal.*, **21**, 782–797.

Macri, F. J. (1967) The pressure dependence of aqueous humor formation. *Arch. Ophthal., N.Y.* **78**, 629–633.

Macri, F. J. & Cevario, S. J. (1973) The induction of aqueous humor formation by the use of Ach-eserine. *Invest. Ophthal.* **12**, 910–916.

Maggiore, L. (1917) Struttura, comportamento e significato del canale di Schlemm nell'occhio umano, in condizioni normali e patologische. *Ann. Ottalm.* **40**, 317–462.

Maren, T. H. (1977) Ion secretion into the posterior aqueous humor of dogs and monkeys. *Exp. Eye Res.*, **25** (Suppl), 245–247.

Maren, T. H., Jankowska, L., Sanyal, G. & Edelhauser, H. F. (1983) The transcorneal permeability of sulfonamide carbonic anhydrase inhibitors and their effects of aqueous humor secretion. *Exp. Eye Res.* **36**, 457–480.

Marmor, M. F., Negi, A. & Maurice, D. M. (1985) Kinetics of macromolecules injected into the subretinal space. *Exp. Eye Res.*, **40**, 687–696.

Masuda, K. & Mishima, S. (1973) Effects of prostaglandins on inflow and outflow of the aqueous humor in rabbits. *Jap. J. Ophthal.* **17**, 300–309.

Matsumoto, S., Araie, M. & Takase, M. (1986) Active transport of beta-andrenergic blocking agents in the anterior uvea of albino rabbit. *Jap. J. Ophthal.* **30**, 339–350.

Maurice, D. M. (1954) Constriction of the pupil in the rabbit by antidromic stimulation of the trigeminal nerve. *J. Physiol.* **123**, 45–46P.

McEwen, W. K. (1958) Application of Poiseuille's law to aqueous outflow. *Arch. Ophthal., N.Y.* **60**, 290–294.

McLaren, J. W. & Brubaker, R. F. (1985) A two-dimensional scanning ocular fluorophotometer. *Invest. Ophthal.*, **26**, 144–152.

McMenamin, P. G. & Lee, W. R. (1986) Effect of prolonged intracameral perfusion with mock aqueous humour on the morphology of the primate outflow apparatus. *Exp. Eye Res.* **43**, 129–141.

Melton, C. E. & De Ville, W. B. (1960) Perfusion studies on eyes of four species. *Am. J. Ophthal.* **50**, 302–308.

Miichi, H. & Nagataki, S. (1983) Effects of pilocarpine, salbutamol, and timolol on aqueous humor formation in cynomolgus monkeys. *Invest. Ophthal.* **24**, 1269–1275.

Millard, C. B., Tripathi, B. J. & Tripathi. R. C. (1987) Age-related changes in protein profiles of the normal human trabecular meshwork. *Exp. Eye Res.* **45**, 623–631.

Miller, A., Costa, M., Furness, J. B. & Chubb, I. W. (1981) Substance P immunoreactive sensory nerves supply the rat iris and cornea. *Neurosci. Lett.* **23**, 243–249.

Miller, J. D., Eakins, K. E. & Atival, M. (1973) The release of PGE_2-like activity into aqueous humor after paracentesis and its prevention by aspirin. *Invest. Ophthal.* **12**, 939–942.

Miller, S. & Farber, D. (1984) Cyclic AMP modulation of ion transport across frog retinal pigment epithelium. *J. gen. Physiol.* **83**, 853–874.

Miller, S. S., Hughes, B. A. & Machen, T. E. (1982) Fluid transport across retinal pigment epithelium is inhibited by cyclic AMP. *Proc. Nat. Acad. Sci.* **79**, 2111–2115.

Miller, S. & Steinberg, R. H. (1976) Transport of taurine, L-methionine and 3-*O*-methyl-D-glucose across frog retinal pigment epithelium. *Exp. Eye Res.*, **23**, 177–189.

Miller, S. S. & Steinberg, R. H. (1977) Active transport of ions across frog retinal pigment epithelium. *Exp. Eye Res.* **25**, 235–248.

Miller, S. S. & Steinberg, R. H. (1982) Potassium transport across the frog retinal pigment epithelium. *J. Membrane Biol.* **67**, 199–299.

Miller, S. S., Steinberg, R. H. & Oakley, B. (1978) The electrogenic sodium pump of the frog retinal pigment epithelium. *J. Membrane Biol.* **44**, 259–279.

Mishima, H., Bausher, L., Sears, M., Gochu, M., Ono, H. & Gregory, D. (1982) Fine structural studies of ciliary processes after treatment with cholera toxin or its B subunit. *v. Graefes Arch.* **219**, 272–278.

Mittag, T. W., Serle, J. B., Podos, S. M., Cohen, L. & Liebowitz F. (1984) Vanadate effects on ocular pressure, (Na^+, K^+) ATPase and adenylate cyclase in rabbit eyes. *Invest. Ophthal.* **25**, 1335–1338.

Mittag, T. W. & Tormay, A. (1985) Adrenergic receptor subtypes in rabbit iris-ciliary body membranes: classification by radioligand studies. *Exp. Eye Res.* **40**, 239–249.

Mittag, T. W., Tormay, A., Messenger, M. & Podos, S. M. (1985) Ocular hypotension in the rabbit. *Invest. Ophthal.* **26**, 163–169.

Mittag, T. W., Tormay, A., Severin, C. & Podos, S. M. (1985) Alpha-adrenergic antagonists: correlation of the effect on intraocular pressure and on α_2-adrenergic receptor binding specificity in the rabbit. *Exp. Eye Res.* **40**, 591–599.

Morrison, J. C., De Frank, M. P. & Van Buskirk, E. M. (1987a) Regional microvascular anatomy of the rabbit ciliary body. *Invest. Ophthal.* **28**, 1314–1324.

Morrison, J. C., De Frank, M. P. & Van Buskirk, E. M. (1987b) Comparative microvascular anatomy of mammalian ciliary processes. *Invest. Ophthal.* **28**, 1325–1345.

Morrison, J. C. & Van Buskirk, E. M. (1983) Anterior collateral circulation in the primate eye. *Ophthalmology* **90**, 707–715.

Morrison, J. C. & Van Buskirk, E. M. (1984) Ciliary process microvasculature of the primate eye. *Amer. J. Ophthal.* **97**, 372–383.

Nagataki, S. & Brubaker, R. F. (1981) Early effect of epinephrine on aqueous formation in the normal human eye. *Ophthalmology* **88**, 278–282.

Nathanson, J. A. (1980) Adrenergic regulation of intraocular pressure: identification of β_2-adrenergic-stimulated adenylate cyclase in ciliary process epithelium. *Proc. Nat. Acad. Sci.*, **77**, 7420–7424.

Negi, A. & Marmor, M. F. (1983) The resorption of subretinal fluid after diffuse damage to the retinal pigment epithelium. *Invest. Ophthal.* **24**, 1475–1479.

Negi, A. & Marmor, M. F. (1986) Mechanisms of subretinal fluid resorption in the cat eye. *Invest. Ophthal.*, **27**, 1560–1563.

Negi, A. & Marmor, M. F. (1986) Quantitative estimate of metabolic transport of subretinal fluid. *Invest. Ophthal* **27**, 1564–1568.

Nellans, H. N., Frizzell, R. A. & Schultz, S. G. (1975) Effect of acetazolamide on sodium and chloride transport by *in vitro* rabbit ileum. *Amer. J. Physiol.* **228**, 1808–1814.

Neufeld, A. H., Bartels, S. P. & Lee, S. R. (1983) Forskolin stimulates cyclic AMP synthesis, lowers intraocular pressure and increases outflow facility in albino rabbits. *ARVO Suppl.* **24**, 4.

Neufeld, A. H., Dueker, D. K., Vegge, T. & Sears, M. L. (1975) Adenosine 3′,5′-monophosphate increases the outflow of aqueous humor from the rabbit eye. *Invest. Ophthal.* **14**, 40–42.

Neufeld, A. H., Jampol, L. M. & Sears, M. L. (1972) Cyclic-AMP in the aqueous humor: the effects of adrenergic agents. *Exp. Eye Res.* **14**, 242–250.

Neufeld, A. H., Jampol, L. M. & Sears, M. L. (1972) Aspirin prevents the disruption of the blood-aqueous barrier in the rabbit eye. *Nature* **238**, 158–159.

Neufeld, A. H. & Sears, M. L. (1975) Adenosine 3′,5′-monophosphate analogue increases outflow facility of the primate eye. *Invest. Ophthal.* **14**, 688–689.

Niederer, W., Richardson, B. P. & Donatsch, P. (1975) Hormonal control of aqueous humor production. *Exp. Eye Res.* **20**, 329–340.

Nilsson, S. F. E. & Bill, A. (1984) Vasoactive intestinal polypeptide (VIP): Effects in the eye and on regional blood flows. *Acta Physiol. Scand.*, **121**, 385–392.

Nilsson, S. F. E., Sperber, G. O. & Bill, A. (1986) Effects of vasoactive intestinal polypeptide (VIP) on intraocular pressure, facility of outflow and formation of aqueous humour in the monkey. *Exp. Eye Res.* **43**, 849–857.

Noell, W. K. (1955) Metabolic injuries of the visual cell. *Amer. J. Ophthal.* **40**, Pt. 2, 60–76.

Noell, W. K. (1963) Cellular physiology of the retina. *J. Opt. Soc. Amer.* **53**, 36–48.

Norton, A. L. & Viernstein, L. J. (1972) The effect of adrenergic agents on ocular dynamics as a function of administration site. *Exp. Eye Res.* **14**, 154–163.

Oakley, B., Miller, S. S. & Steinberg, R. H. (1978) Effect of intracellular potassium upon the electrogenic pump of frog retinal pigment epithelium. *J. Membrane Biol.* **44**, 281–307.

Ogura, Y., Tsukahara, Y., Saito, I. & Kondo, T. (1985) Estimation of the permeability of the blood-retinal barrier in normal individuals. *Invest. Ophthal.* **26**, 969–976.

Ohnishi, Y. & Taniguchi, Y. (1983) Distributions of ^{35}S-sulfate and ^{3}H-glucosamine in the angular region of the hamster: light and electron microscopic autoradiography. *Invest. Ophthal.* **24**, 697–703.

Ohrström, A. & Pandolfi, M. (1980) Regulation of intraocular pressure and pupil size by beta-blockers and epinephrine. *Arch. Ophthal.*, **98**, 2182–2184.

Oksala, O., Stjernschantz, J., Wohestedt, C. & Hakanson, R. (1986) Calcitonin gene-related polypeptide: release in the eye. *ARVO Suppl.* **27**, 356.

Olgart, L., Gazelius, B., Brodin, E. & Nilsson, G. (1977) Release of substance-P-like immunoreactivity from the dental pulp. *Acta Physiol. Scand.* **101**, 510–512.

Organisciak, D. T., Wang, H.-M., Li, Z. Y. & Tso, M. O. M. (1985) The protective effect of ascorbate in retinal light damage of rats. *Invest. Ophthal.* **26**, 1580–1588.

Ostwald, T. J. & Steinberg, R. H. (1980 Localization of frog retinal pigment epithelium Na^+-K^+-ATPase. *Exp. Eye Res.* **31**, 351–360.

Page, E. D. & Neufeld, A. H. (1978) Characterization of α- and β-adrenergic receptors in membranes prepared from the rabbit iris before and after development of supersensitivity. *Biochem. Pharmacol.* **27**, 953–958.

Palkama, A., Kaufman, H., Uusitalo, R. & Uusitalo, H. (1986) Histochemistry of adenylate cyclase activity in the anterior segment of the eye: a methodological evaluation with biochemical background. *Exp. Eye Res.* **43**, 1043–1056.

Pandolfi, M. & Astrup, T. (1966) Effect of plasmin on outflow resistance in the primate eye. *PSEBM*, **121**, 139–142.

Pandolfi, M. & Kiwaan, H. C. (1967) Fibrinolysis in the anterior segment of the eye. *Arch. Ophthal.*, **77**, 99–104.

Pappas, G. D. & Smelser, G. K. (1958) Studies on the ciliary epithelium and the zonule. I. *Amer. J. Ophthal.*, **46**, 299–318.

Pappas, G. D. & Smelser, G. K. (1961) The fine structure of the ciliary epithelium in relation to aqueous humour secretion. In *The Structure of the Eye*. Ed. Smelser, pp. 453–467. New York: Academic Press.

Partamian, L. G., Kass, M. A. & Gordon, M. (1983) A dose-response study of the effect of levobunolol on ocular hypertension. *Amer. J. Ophthal.*, **95**, 229–232.

Pascuzzo, G. J., Johnson, J. E. & Pautler, E. L. (1980) Glucose transport in isolated mammalian pigment epithelium. *Exp. Eye Res.* **30**, 53–58.

Pautler, E. L. & Tengerdy, C. (1986) Transport of acidic amino acids by the bovine pigment epithelium. *Exp. Eye Res.* **43**, 207–214.

Pederson, J. E. (1982) Fluid permeability of monkey ciliary epithelium *in vivo*. *Invest. Ophthal.* **23**, 176–180.

Perkins, E. S. (1957) Influence of the fifth cranial nerve on the intraocular pressure in the rabbit eye. *Br. J. Ophthal.* **41**, 257–300.

Perkins, E. S. & Saiduzzar, H. (1969) The effect of plasmin on the facility of outflow in cynomolgus monkeys. *Exp. Eye Res.*, **8**, 386–396.

Peyman, G. A. & Bok, D. (1972) Peroxidase diffusion in the normal and laser-coagulated primate retina. *Invest. Ophthal.* **11**, 35–45.

Peyman, G. A., Spitznas, M. & Straatsma, B. R. (1971) Peroxidase diffusion in the normal and photocoagulated retina. *Invest. Ophthal.* **10**, 181–189.

Podos, S. M., Lee, P.-Y., Severin, C. & Mittag, T. (1984) The effect of vanadate on aqueous humor dynamics in cynomolgus monkeys. *Invest. Ophthal.* **25**, 359–361.

Pohjola, S. (1966) The glucose content of the aqueous humour in man. *Acta Ophthal.* Suppl. 88.

Polansky, J. *et al.* (1985) Cellular sensitivity to glucocorticoids in patients with POAG. Steroid receptors and responses in skin. *Invest. Ophthal.*, **26**, 805–809.

Poos, F. (1931) Uber die histologischen und klinischen Erscheinungen bei akuten, lokalen Capillärkreislaufstörungen am Auge. *J. graefes Arch. Ophthal.* **127**, 489–574.

Poos, F. (1937) Uber das Verhalten des Augendruckes bei akuten intraokularen Gefassreaktionen. *Arch. Augenheilk.* **110**, 499–534.

Potter, D. E. (1981) Adrenergic pharmacology of aqueous humor dynamics. *Pharmacol. Rev.* **33**, 133–153.

Potter, D. E. & Rowland, J. M. (1978) Adrenergic drugs and intraocular pressure: effects of selective β-adrenergic agonists. *Exp. Eye Res.* **27**, 615–625.

Potter, D. E. L. & Rowland, J. M. (1981) Adrenergic drugs and intraocular pressure. *Gen. Pharmacol.* **12**, 1–13.

Preud'homme, Y., Demolle, D. & Boeynaems, J. M. (1985) Metabolism of arachidonic acid in rabbit iris and retina. *Invest. Ophthal.* **26**, 1336–1342.

Quigley, H. A. & Addicks, E. M. (1980a) Chronic experimental glaucoma in primates. I. Production of elevated intraocular pressure by anterior chamber injection of autologous ghost red blood cells. *Invest. Ophthal.* **19**, 126–136.

Quigley, H. A. & Addicks, E. M. (1980b) Chronic experimental glaucoma in primates. II. Effect of extended intraocular pressure elevation on optic nerve head and axonal transport. *Invest. Ophthal.* **19**, 137–152.

Radius, R. L., Diamond, G. R., Pollack, G. R. & Langham, M. E. (1978) Timolol: a new drug for the management of chronic simple glaucoma. *Arch. Ophthal.* **96**, 1003–1008.

Radius, R. L. & Langham, M. E. (1973) Cyclic-AMP and the ocular responses to norepinephrine. *Exp. Eye Res.* **17**, 219–229.

Radius, R. L. & Pederson, J. E. (1984) Laser-induced primate glaucoma. II. Histopathology. *Arch. Ophthal.* **102**, 1693–1698.

Rapoport, S. I. (1977) Osmotic opening of blood brain and blood-ocular barriers. *Exp. Eye Res.* **25**, Suppl. 499–509.

Rapoport, S. I., Fredericks, W. R. & Laties, A. M. (1980) Reversible opening of the retinal pigment epithelium by hypercapnia. *Exp. Eye Res.* **30**, 129–141.

Raviola, G. (1971) The fine structure of the ciliary zonule and ciliary epithelium. *Invest. Ophthal.* **10**, 851–869.

Raviola, G. (1974) Effects of paracentesis on the blood-aqueous barrier—an electron microscope study on *Macaca mulatta* using horseradish peroxidase as a tracer. *Invest. Ophthal.* **13**, 828–858.

Raviola, G. (1977) The structural basis of the blood-ocular barriers. *Exp. Eye Res.* **25**, Suppl. 27–63.

Raviola, G. (1983) Conjunctival and episcleral blood vessels are permeable to blood-borne horseradish peroxidase. *Invest. Ophthal.* **24**, 725–736.

Raviola, G. & Butler, J. M. (1983) Unidirectional vesicular transport mechanism in retinal vessels. *Invest. Ophthal.* **24**, 1465–1474.

Raviola, G. & Butler, J. M. (1984) Unidirectional transport mechanism of horseradish peroxidase in the vessels of the iris. *Invest. Ophthal.* **25**, 827–836.

Raviola, G. & Butler, J. M. (1985) Asymmetric distribution of charged domains on the two fronts of the endothelium of iris blood vessels. *Invest. Ophthal.* **26**, 597–608.

Reddy, D. V. N., Chakrapani, B. & Lim, C. P. (1977a) Blood-vitreous barrier to amino acids. *Exp. Eye Res.* **25**, 543–554.

Reddy, D. V. N. & Kinsey, V. E. (1960) Composition of the vitreous humour in relation to that of the plasma and aqueous humour. *Arch. Ophthal., N.Y.* **63**, 715–720.

Reddy, D. V. N. & Kinsey, V. E. (1963) Transport of amino acids into intraocular fluids and lens in diabetic rabbits. *Invest. Ophthal.* **2**, 237–242.

Reddy, D. V. N., Rosenberg, C. & Kinsey, V. E. (1961) Steady-state distribution of free amino acids in the aqueous humors, vitreous body and plasma of the rabbit. *Exp. Eye Res.* **1**, 175–181.

Reddy, D. V. N., Thompson, M. R. & Chakrapani, B. (1977b) Amino acid transport across the blood-aqueous barrier of mammalian species. *Exp. Eye Res.* **25**, 555–562.

Reese, T. S. & Karnovsky, M. J. (1967) Fine structural localization of a blood-brain barrier to exogenous peroxidase. *J. Cell Biol.* **34**, 207–217.

Richardson, T. M. (1982) Distribution of glycosaminoglycan in the aqueous outflow system in the cat. *Invest. Ophthal.* **22**, 319–324.

Ringvold, A. (1975) An electron microscopic study of the iris stroma in monkey and rabbit with particular reference to intercellular contacts and sympathetic innervation of anterior layer cells. *Exp. Eye Res.* **20**, 349–365.

Ringvold, A., Olsen, E. G. & Flage, T. (1981) Transient breakdown of the retinal pigment epithelium diffusion barrier after sodium iodate: a fluorescein angiographic and morphologic study in the rabbit. *Exp. Eye Res.* **33**, 361–369.

Ritch, R. *et al.* (1981) The effect of colchicine on aqueous humor dynamics. *Exp. Eye Res.* **32**, 143–150.

Robey, P. G. & Newsome, D. A. (1983) Biosynthesis of proteoglycans present in primate Bruch's membrane. *Invest. Ophthal.* **24**, 898–905.

Rohen, J. (1961) Morphology and pathology of the trabecular meshwork. In *The Structure of the Eye*, Ed. Smelser, pp. 335–341. New York: Academic Press.

Rohen, J. W. (1965) *Die Struktur des Auges*. Stuttgart: Schattauer Verlag.

Rohen, J. W. (1969) New studies on the functional morphology of the trabecular meshwork and the outflow channels. *Trans. Ophthal. Soc., U.K.* **89**, 431–447.

Rohen, J. W. (1983) Why is intraocular pressure elevated in

chronic simple glaucoma? Anatomical considerations. *Ophthalmology* **90**, 758–765.

Rohen, J. W., Linner, E. & Witmer, R. (1973) Electron microscopic studies on the trabecular meshwork in two cases of corticosteroid-glaucoma. *Exp. Eye Res.* **17**, 19–31.

Rohen, J. W. & Witmer, R. (1972) Electron microscopic studies on the trabecular meshwork in glaucoma simple. *v. Graefes Arch.* **183**, 251–266.

Rosenfeld, M. G. *et al.* (1983) Production of a novel neuropeptide encoded by the calcitonin gene via tissue-specific RNA processing. *Nature* **304**, 129–135.

Rowland, J. M. & Potter, D. E. (1980) Adrenergic drugs and intraocular pressure: suppression of ocular hypertension induced by water loading. *Exp. Eye Res.* **30**, 93–104.

Ruben, J. B., Moses, R. A. & Gradzki, W. J. (1985) Perfusion outflow facility in the rabbit eye. Stabilization by EACA. *Invest Ophthal.*, **26**, 153–158.

Ruskell, G. L. (1964). In *The Rabbit in Eye Research*, Ed. J. H. Prince. Springfield: Charles C. Thomas, pp. 533–538.

Ruskell, G. L. (1970a) The orbital branches of the pterygopalatine ganglion and their relationship with internal carotid nerve branches in primates. *J. Anat.* **160**, 323–339.

Ruskell, G. L. (1970b) An ocular parasympathetic nerve pathway of facial nerve origin and its influence on intraocular pressure. *Exp. Eye Res.* **10**, 319–330.

Ruskell, G. L. (1971) Facial parasympathetic innervation of the choroidal blood vessels in monkeys. *Exp. Eye Res.* **12**, 166–172.

Ruskell, G. L. (1974) Ocular fibres of the maxillary nerve in monkeys. *J. Anat.* **118**, 195–203.

Ruskell, G. L. (1976) The source of nerve fibres of the trabeculae and adjacent structures in monkey eyes. *Exp. Eye Res.* **23**, 449–459.

Ryder, M. I. & Weinreb, R. N. (1986) The cytostructure of the cynomolgus monkey trabecular cell. I. General considerations. *Invest. Ophthal.* **27**, 1305–1311.

Sakimoto, G. & Schwartz, B. (1984) Decrease of anterior ciliary arterial pressure with increased ocular pressure. *Invest. Ophthal.* **25**, 992–995.

Sallmann, L. von & Loewenstein, O. (1955) Responses of intraocular pressure, blood pressure and cutaneous vessels to electrical stimulation of the diencephalon. *Am. J. Ophthal.* **39**, Pt. 2, 11–29.

Schachtschabel, D. O., Bigalke, B. & Rohen, J. W. (1977) Production of glycosaminoglycans by cell cultures of the trabecular meshwork of the primate eye. *Exp. Eye Res.* **24**, 71–80.

Scheie, H. G., Moore, E. & Adler, F. H. (1943) Physiology of the aqueous in completely iridectomised eyes. *Arch. Ophthal., N.Y.* **30**, 70–74.

Scott, D. R., Karageuzian, L. N., Anderson, P. J. & Epstein, D. L. (1984) Glutathione peroxidase of calf trabecular meshwork. *Invest. Ophthal.*, **25**, 599–602.

Sears, M. L. (1960) Outflow resistance of the rabbit eye: technique and effects of acetazolamide. *Arch. Ophthal.*, **64**, 823–838.

Sears, M. L. & Bárány, E. H. (1960) Outflow resistance and adrenergic mechanisms. *Archs. Ophthal., N.Y.* **64**, 839–849.

Sears, M. L. & Sherk, T. E. (1964) The trabecular effect of noradrenaline in the rabbit eye. *Invest. Ophthal.* **5**, 312–318.

Seidel, E. (1918) Experimentelle Untersuchungen über die Quelle und den Verlauf der intraokularen Saftströmung. *v. Graefes' Arch. Ophthal.* **95**, 1–72.

Seidel, E. (1921) Über den Abiluss des Kammerwassers aus der vorderen Augenkammer. *v. Graefe's Arch. Ophthal.* **104**, 357–402.

Sellner, P. A. (1986a). The blood-retinal barrier: leucine transport by the retinal pigment epithelium. *J. Neurosci.*, **6**, 2823–2828.

Sellner, P. A. (1986b) The movement of organic solutes between the retina and pigment epithelium. *Exp. Eye Res.*, **43**, 631–639.

Serr, H. (1937) Zur Analyse der spontanen Pulserscheinungen in den Netzhautgefässen. *v. Graefe's Arch. Ophthal.* **137**, 487–305.

Seto, C., Eguchi, S., Araie, M., Matsumoto, S. & Takase, M. (1986) Acute effects of topical forskolin on aqueous humour dynamics. *Jap. J. Ophthal.* **30**, 238–244.

Shabo, A. L., Reese, T. S. & Gaasterland, D. (1973) Postmortem formation of giant endothelial vacuoles in Schlemm's canal of the monkey. *Amer. J. Ophthal.* **76**, 896–905.

Shakib, M. & Cunha-Vaz, J. G. (1966) Junctional complexes of the retinal vessels and their role in the permeability of the blood-retinal barrier. *Exp. Eye Res.* **5**, 229–234.

Shiose, Y. (1970) Electron microscopic studies on blood-retinal and blood-aqueous barriers. *Jap. J. Ophthal.* **14**, 73–87.

Shiose, Y. (1971) Morphological study on permeability of the blood-aqueous barrier. *Jap. J. Ophthal.* **15**, 17–26.

Siegel, M. J., Lee, P.-U., Podos, S. M. & Mittag, T. W. (1987) Effect of topical pergolide on aqueous dynamics in normal and glaucomatous monkeys. *Exp. Eye Res.* **44**, 227–233.

Simon, K. A., Bonting, S. L. & Hawkins, N. M. (1962) Studies on sodium-potassium-activated adenosine triphosphatase. II. Formation of aqueous humour. *Exp. Eye Res.* **1**, 253–261.

Simoniescu, M., Simoniescu, N. & Palade, G. E. (1972) Permeability of intestinal capillaries. Pathway followed by dextrans and glycogens. *J. Cell Biol.* **53**, 365–392.

Singh, S. & Dass, R. (1960) The central artery of the retina. *Br. J. Ophthal.* **44**, 193–212, 280–299.

Smelser, G. K. & Pei, Y. F. (1965) Cytological basis of protein leakage into the eye following paracentesis. *Invest. Ophthal.* **4**, 249–263.

Smith, R. S. (1971) Ultrastructural studies on the blood-aqueous barrier I. Transport of an electron-dense tracer in the iris and ciliary body of the mouse. *Amer J. Ophthal.* **71**, 1066–1077.

Smith, R. S. & Rudt, L. A. (1975) Ocular vascular and epithelial barriers to microperoxidase. *Invest. Ophthal.* **14**, 556–560.

Soloway, M. R., Stjernschantz, J. & Sears, M. (1981) The miotic effect of substance P on the isolated rabbit iris. *Invest. Ophthal.* **20**, 47–52.

Sonntag, J. R., Brindley, G. O. & Shields, M. B. (1978) Effect of timolol therapy on outflow facility. *Invest. Ophthal.* **17**, 293–296.

Speakman, J. S. (1960) Drainage channels in the trabecular wall of Schlemm's canal. *Br. J. Ophthal.* **44**, 513–523.

Sperber, G. O. & Bill, A. (1984) A method for near-continuous determination of aqueous humour flow; effect of anesthetics, temperature and indomethacin. *Exp. Eye Res.* **39**, 435–453.

Starr, M. S. (1971) Further studies on the effect of prostaglandin on intraocular pressure. *Exp. Eye Res.* **11**, 170–177.

Steinberg, R. H. & Miller, S. (1973) Aspects of electrolyte transport in frog pigment epithelium. *Exp. Eye Res.* **16**, 365–372.

Stern, F. A. & Bito, L. Z. (1982) Comparison of the hypotensive and other ocular effects of prostaglandins E_2 and $F_{2\alpha}$ on cat and rhesus monkey eyes. *Invest. Ophthal.* **22**, 588–598.

Stjernschantz, J. (1976a) Effect of parasympathetic stimulation on intraocular pressure, formation of the aqueous humour and outflow facility in rabbits. *Exp. Eye Res.* **22**, 639–645.

Stjernschantz, J. (1976b) Increase in aqueous humour protein concentration induced by oculomotor nerve stimulation in rabbits. *Exp. Eye Res.* **23**, 547–553.

Stjernschantz, J. & Bill, A. (1976) Effects of intracranial oculomotor nerve stimulation on ocular blood flow in rabbits: modification by indomethacin. *Exp. Eye Res.* **23**, 461–469.

Stjernschantz, J. & Bill, A. (1980) Vasomotor effects of facial nerve stimulation: noncholinergic vasodilation in the eye. *Acta Physiol. Scand.* **109**, 45–50.

Stjernschantz, J., Geijer, G. & Bill, A. (1979) Electrical stimula-

tion of the fifth cranial nerve in rabbits: effects on ocular blood flow, extravascular albumin content and intraocular pressure. *Exp. Eye Res.* **28**, 229–238.

Stjernschantz, J., von Dickhoff, K., Oksala, O. & Sepps, H. (1986) A study of the mechanism of ocular irritation following YAG laser capsulotomy in rabbits. *Exp. Eye Res.*, **43**, 641–651.

Stone, R. A., Laties A. M. & Brecha, N. C. (1982) Substance P-like immunoreactive nerves in the anterior segment of the rabbit, cat and monkey eye. *Neuroscience* **7**, 2459–2468.

Stone, R. A. & Wilson, C. M. (1982) Fluorescein transport in the anterior uvea. *Invest. Ophthal.*, **22**, 303–309.

Suguro, K., Toris, C. B. & Pederson, J. E. (1985) Uveoscleral outflow following cyclodialysis in the monkey eye using a fluorescent tracer. *Invest. Ophthal.* **26**, 810–813

Suzuki, R. & Kobayashi, S. (1983) Vasoactive intestinal peptide and cholinergic neurotransmission in the ciliary muscle. *Invest. Ophthal.* **24**, 250–253.

Svedbergh, B., Lutjen-Drecoll, E. & Kaufman, P. L. (1978) Cytochalasin B-induced structural changes in the anterior ocular segment of the cynomolgus monkey. *Invest. Ophthal.* **17**, 718–734.

Szalay, J., Nunziata, B. & Henkind, P. (1975) Permeability of iridial blood vessels. *Exp. Eye Res.* **21**, 531–543.

Talusan, E. D. & Schwartz, B. (1981) Fluorescein angiography. Demonstration of flow pattern of anterior ciliary arteries. *Arch. Ophthal.* **99**, 1074–1080.

Taniguchi, Y. (1976) Ultrastructure of newly formed blood vessels in diabetic retinopathy. *Jap. J. Ophthal.* **20**, 19–31.

Terenghi, G. *et al.* (1982) Mapping quantitative distribution and origin of substance P- and VIP-containing nerves in the uvea of the guinea pig eye. *Histochemistry* **75**, 399–417.

Tervo, K. *et al.* (1982) Effect of sensory and sympathetic denervation on substance P immunoreactivity in nerve fibres of the rabbit eye. *Exp. Eye Res.* **34**, 577–585.

Theobald, G. D. (1960) The limbal area. *Am. J. Ophthal.* **50**, 543–557.

Thomas, J. V. & Epstein, D. L. (1981) Study of the additive effect of timolol and epinephrine in lowering intraocular pressure. *Brit. J. Ophthal.*, **65**, 596–602.

Tomar, V. P. S. & Agarval, B. L. (1974) Effect of ganglionectomy on intraocular pressure and outflow facility of aqueous humour, *Exp. Eye Res.* **19**, 403–408.

Törnqvist, G. (1970) Effect of oculomotor nerve stimulation on outflow facility and pupil diameter in a monkey (*Cercopithecus ethiops*). *Invest. Ophthal.* **9**, 220–225.

Toris, C. B., Gregerson, D. S. & Pederson, J. E. (1987) Uveoscleral outflow using different-sized fluorescent tracers in normal and inflamed eyes. *Exp. Eye Res.* **45**, 525–532.

Tower, S. (1940) Units for sensory reception in the cornea; with notes on nerve impulses from sclera, iris and lens. *J. Neurophysiol.* **3**, 486–500.

Tripathi, R. C. (1968) Ultrastructure of Schlemm's canal in relation to aqueous outflow. *Exp. Eye Res.* **7**, 335–341.

Tripathi, R. C. (1969) Ultrastructure of the trabecular wall of Schlemm's canal. *Trans. Ophthal. Soc., U.K.* **89**, 449–465.

Tripathi, R. C. (1971) Mechanism of the aqueous outflow across the trabecular wall of Schlemm's canal. *Exp. Eye Res.* **11**, 111–116.

Tripathi, R. C. (1974) Comparative physiology and anatomy of the aqueous outflow pathway. In *The Eye.* Vol. 5, chap 3 (Ed. Davson, H. & Graham, L. T.) New York: Academic Press.

Tripathi, R. C. (1977) The functional morphology of the outflow systems of ocular and cerebrospinal fluids. *Exp. Eye Res.* **25**, (Suppl.) 65–116.

Tripathi, R. C. & Tripathi, B. J. (1980) Contractile protein alteration in trabecular meshwork in primary open-angle glaucoma. *Exp. Eye Res.* **31**, 721–724.

Tripathi, R. C., Tripathi, B. J. & Spaeth, G. L. (1987) Localization of sialic acid moieties in the endothelial lining of Schlemm's canal in normal and glaucomatous eyes. *Exp. Eye Res.* **44**, 293–306.

Troncoso, M. U. (1942) The intrascleral vascular plexus and its relations to the aqueous outflow. *Amer. J. Ophthal.* **25**, 1153–1162.

Trope, G. E. & Clark, B. (1982) Beta adrenergic receptors in pigmented ciliary processes. *Brit. J. Ophthal.* **66**, 788–792.

Uddman, R., Alumets, J., Ehinger, B., Håkanson, R., Lorén, I. & Sundler, F. (1980) Vasoactive intestinal polypeptide nerves in ocular and orbital structures of the cat. *Invest. Ophthal.* **19**, 878–885.

Unger, W. G., Butler, J. M. & Cole, D. F. (1981) Prostaglandin and an increased sensitivity of the sympathetically denervated rabbit eye to laser-induced irritation of the iris. *Exp. Eye Res.* **32**, 699–707.

Unger, W. G., Cole, D. F. & Hammond, B. (1975) Disruption of the blood-aqueous barrier following paracentesis in the rabbit. *Exp. Eye Res.* **20**, 255–270.

Unger, W. G., Cole, D. F. & Bass, M. S. (1977) Prostaglandin and neurogenically mediated ocular response to laser irradiation of the rabbit iris. *Exp. Eye Res.* **25**, 209–220.

Unger, W. G., Perkins, E. S. & Bass, M. S. (1974) The response of the rabbit eye to laser irradiation of the iris. *Exp. Eye Res.* **19**, 367–377.

Unger, W. G. *et al.* (1985) Calcitonin gene-related polypeptide as a mediator of the neurogenic ocular injury response. *J. Ocul. Pharmacol.*, **1**, 188–199. (Quoted by Krootiula *et al.* 1987.)

Unger, W. G. & Tighe, J. (1984) The response of the isolated iris sphincter muscle in various mammalian species to substance P. *Exp. Eye Res.* **39**, 677–684.

Ussing, H. H. & Zerahn, K. (1951) Active transport of sodium as the source of electric current in the short-circuited isolated frog skin. *Acta physiol. Scand.* **23**, 110–127.

Uusitalo, H. (1984) The effect of autonomic receptor blockers on the ocular response to topical chemical irritation. *Acta physiol. Scand.* **121**, 1–8.

Uusitalo, H., Lehtosalo, J., Palkama, A. & Tovianen, M. (1984) Vasoactive intestinal peptide (VIP)-like immunoreactivity in the human and guinea pig choroid. *Exp. Eye Res.* **38**, 435–437.

Uusitalo, R., Palkama, A. & Stjernschantz, J. (1973) An electron microscopical study of the blood-aqueous barrier in the ciliary body and iris of the rabbit. *Exp. Eye Res.* **17**, 49–63.

Uusitalo, R., Stjernschantz, J. & Palkama, A. (1974) Studies on para-sympathetic control of the blood-aqueous barrier in the rabbit. An electron microscopic study. *Exp. Eye Res.* **19**, 125–134.

Van Buskirk, E. M. (1983) Anterior collateral circulation in the primate eye. *Opthalmology* **90**, 707–715.

Vareilles, P., Conquet, P. & Le Douaree, J.-C. (1977) A method for the routine intraocular pressure (IOP) measurement in the rabbit: range of IOP variation in this species. *Exp. Eye Res.* **24**, 369–375.

Vegge, T. (1971) An epithelial blood-aqueous barrier to horseradish peroxidase in the ciliary processes of the vervet monkey (*Cercopithecus aethiops*). *Z. Zellforsch.* **114**, 309–320.

Vegge, T. (1972a) A study of the ultrastructure of the small iris vessels in the vervet monkey (*Cercopithecus aethiops*). *Z. Zellforsch.* **123**, 195–208.

Vegge, T. (1972b) A blood-aqueous barrier to small molecules in the ciliary processes of the vervet monkey (*Cercopithecus aethiops*). *Z. Zellforsch.* **135**, 483–499.

Vegge, T. & Ringvold, A. (1969) Ultrastructure of the wall of the human iris vessels. *Z. Zellforsch.* **94**, 19–31.

Waitzman, M. B. (1970) Pupil size and ocular pressure after sympathectomy and prostaglandin–catecholamine treatment. *Exp. Eye Res.* **10**, 219–222.

Waitzman, M. B. & King, C. D. (1967) Prostaglandin influences on intraocular pressure and pupil size. *Am. J. Physiol.* **212**, 329–334.

Waitzman, M. B. & Woods, W. D. (1971) Some characteristics of an adenyl cyclase preparation from rabbit ciliary process tissue. *Exp. Eye Res.* **12**, 99–111.

Walker, R. E. & Langham, M. E. (1975) Pneumatic applanation manometer studies. III. Analysis of floating tip sensor. *Exp. Eye Res.* **20**, 167–172.

Wallow, I. H. L. & Geldner, P. S. (1980) Endothelial fenestrae in proliferative diabetic retinopathy. *Invest. Ophthal.* **19**, 1176–1183.

Wax, M. B. & Molinoff, P. B. (1987) Distribution and properties of β-adrenergic receptors in human iris-ciliary body. *Invest. Ophthal.* **28**, 420–430.

Weekers, R. & Prijot, E. (1952) Mesure de la resistance a l'écoulement de l'humeur aqueuse au moyen du tonomètre électronique. II. *Ophthalmologica*, **123**, 114–122.

Weinreb, R. N., Mitchell, M. D. & Polansky, J. R. (1983) Prostaglandin production by human trabecular cells: *in vitro* inhibition by dexamethasone. *Invest. Ophthal.* **24**, 1541–1545.

Weinreb, R. N., Ryder, M. I. & Polansky, J. R. (1986) The cytostructure of the cynomolgus monkey trabecular cell. II. Influence of cytoskeleton-active drugs. *Invest. Ophthal.* **27**, 1312–1317.

Weinreb, R. N., Weaver, D. & Mitchell, M. D. (1985) Prostanoids in rabbit aqueous humor: effect of laser photocoagulation of the iris. *Invest. Ophthal.* **26**, 1087–1092.

Weinstein, P. (1950) New concepts regarding anterior drainage of the eye. *Brit. J. Ophthal.* **34**, 161–168.

Weitzmann, E. *et al.* (1971) The twenty-four hour pattern of the episodic secretion of cortisol in normal subjects. *J. Clin. Endocrin. Metab.* **33**, 14.

Wessely, K. (1900) Über die Wirkung des Suprarenins auf das Auge. *Ber. deutsch. ophth. Ges.* 69–83.

Wessely, K. (1908) Experimentelle Untersuchungen ü. d. Augendruck, sowie über qualitative und quantitative Beeinflussung des intraokularen Flussigkeitswechsels. *Arch. Augenheilk.* **60**, 1–48, 97–160.

Wilcox, L. M., Keough, E. M., Connolly, R. J. & Hotte, C. E. (1980) The contribution of blood flow by the anterior ciliary arteries to the anterior segment of the primate eye. *Exp. Eye Res.* **30**, 167–174.

Wilke, K. (1974) Early effects of epinephrine and pilocarpine on the intraocular pressure and the episcleral venous pressure in the normal human eye. *Acta Ophthal.* **52**, 231–241.

Williams, R. N. & Bhattacherjee, P. (1982) Reduction in intraocular pressure induced by colchicine and related compounds. *Eur. J. Pharmacol.* **77**, 17–24.

Williams, R. N., Cole, D. F. & Bhattacherjee, P. (1983) The effect of colchicine on the rate of formation of aqueous humour and the gross outflow facility in the albino rabbit. *Exp. Eye Res.* **36**, 711–717.

Williams, R. N. & Paterson, C. A. (1987) The influence of topical corticosteroid therapy upon polymorphonuclear leukocyte distribution vascular integrity and ascorbate levels in endotoxin-induced inflammation of the rabbit eye. *Exp. Eye Res.* **44**, 191–198.

Williams, R. N., Paterson, C. A., Eakins, E. K. & Bhattacherjee, P. (1984) Ascorbic acid inhibits the activity of polymorphonuclear leukocytes in inflamed ocular tissues. *Exp. Eye Res.* **39**, 261–265.

Wistrand, P. J., Schenholm, M. & Lonnerholm, G. (1986) Carbonic anhydrase isoenzymes CA I and CA II in the human eye. *Invest. Ophthal.* **27**, 418–428.

Wolff, E. (1968) *Anatomy of the Eye and Orbit* (revised by R. J. Last). London: H. K. Lewis.

Woodward, D. F., Chen, J., Podillo, E. & Ruiz, G. (1986) Pharmacological characterization of β-adrenoceptor subtype involvement in the ocular hypotensive response to β-adrenergic stimulation. *Exp. Eye Res.* **43**, 61–75.

Woodward, D. F., Dowling, M. C., Feldmann, B. J. & Chen, J. (1987) Topical timolol, at conventional, unilateral doses causes bilateral β-blockade in rabbits. *Exp. Eye Res.* **44**, 319–329.

Yablonski, M. E., Novack, G. D., Burk, P. J., Cook, D. J. & Harmon, G. (1987) The effect of levobunolol on aqueous humor dynamics. *Exp. Eye Res.*, **44**, 49–54.

Yablonski, M. E., Zimmerman, T. J., Waltman, S. R. & Becker, B. (1978) A fluorophotometric study of the effect of topical timolol on aqueous humor dynamics. *Exp. Eye Res.* **27**, 135–142.

Yousufzai, S. Y., Akhtar, R. A. & Abdel-Latif, A. A. (1986) Effects of substance P on inositol triphosphate accumulation, on contractile responses and on arachidonic acid release and prostaglandin biosynthesis in rabbit iris sphincter muscle. *Exp. Eye Res.* **43**, 215–226.

Yousufzai, S. Y. K. & Abdel-Latif, A. A. (1983) Effect of norepinephrine and other pharmacological agents on prostaglandin E_2 release by rabbit and bovine irides. *Exp. Eye Res.* **37**, 279–292.

Zeimer, R. C., Blair, N. P. & Cunha-Vaz, J. G. (1983) Vitreous fluorophotometry for clinical research. I. Description and evaluation of new fluorophotometer. II. Method of data acquisition and processing. *Arch. Ophthal.* **101**, 1753–1756, 1757–1761.

Zhang, S. Q., Terenghi, G., Unger, W. G., Ennis, K. W. & Polak, J. (1984) Changes in substance P- and neuropeptide Y-immunoreactive fibres in rat and guinea pig irides following unilateral sympathectomy. *Exp. Eye Res.* **39**, 365–372.

Zimmerman, T. J. & Kaufman, H. E. (1977) Timolol: dose response and duration of action. *Arch. Ophthal.* **95**, 605–607.

2. THE VITREOUS BODY

This is a transparent jelly occupying, in man and most vertebrates, by far the largest part of the globe. As Fig. 1.1 shows, it is bounded by the retina, ciliary body and the posterior capsule of the lens. If the sclera is cut through round the equator, the posterior half with the attached retina comes away from the vitreous body, leaving this suspended from its firm attachments to the ciliary body and pars plana of the retina. To isolate it completely from these attachments careful cutting and scraping are necessary.

Embryonic History

In the early stages, the optic cup is mainly occupied by the lens vesicle (p. 140); as the cup grows, the space formed is filled by a system of fibrillar material presumably secreted by the cells of the embryonic retina. Later, with the penetration of the hyaloid artery, more fibrillar material, apparently derived from the cells of the wall of the artery and other vessels, contributes to filling the space. The combined mass is known as *primary vitreous*. The *secondary vitreous* develops later and is associated with the increasing size of the vitreous cavity and the involution of the hyaloid system. The main hyaloid artery remains for some time but eventually disappears, and its place is left as a tube of primary vitreous surrounded by secondary vitreous; this tube is called *Cloquet's canal*, the contents of which are said by Balazs & Denlinger (1984) to be liquid. The *tertiary vitreous* is the name given to the grossly fibrillar material secreted by the inner walls of the optic cup in the region that will later become the ciliary body; this material eventually becomes the zonule of Zinn or suspensory ligament of the lens. In general it is secreted by the retina, ciliary body and lens, and is essentially the material occupying the space created by growth of the eye (Swann, 1980).

Function

Although the vitreous body has very little resistance to any shearing force, as witnessed by the ease with which its liquid may separate, say when placed on a filter with no suction applied, its solidity and viscous elastic properties, together with its attachment to its lining structures, impart a stability to the eye contents that effectually damps down any strains placed on the retina by sudden eye movements as in saccades. Certainly pathological liquefaction of the body is a first stage in retinal detachment (Foulds, 1975).

Structure

The Basal Lamina[1]

The region of junction between the vitreous gel and its surrounding walls, namely retina and ciliary body, called by classical anatomists the *inner limiting membrane of the retina*, is essentially the basement lamina of the adjacent cells, notably the Müller cells of the retina responsible for secreting the gel, and the epithelial cells of the pars plana of the ciliary body. Its thickness decreases as one proceeds from the basal zone, close to the ciliary body, to the posterior zone close to the optic disc (Foos, 1972). Attachment plaques, or hemidesmosomes, attach the gel to the adjacent Müller cells except in the posterior zone, a circumstance that may account for the prevalence of detachments and preretinal haemorrhages here.[2]

Hyalocytes

In the adult vitreous, these free cells named thus by Balazs (1959) are phagocytic cells belonging to the class of mononuclear cells that become permanently embedded in connective tissue and called more generally histiocytes. In the adult, the cells are embedded in the gel some 20–50 μm away from the basal lamina, forming a single layer of evenly scattered cells. In the developing eye they are located more centrally and, since they are capable of synthesizing the main solid constituents of the vitreous gel, they are presumably concerned with the construction of Cloquet's canal; with the regression of this, they move to the periphery, the site of subsequent growth. According to a study based on nuclear labelling (Gloor, 1973), the large increase in the number of hyalocytes occurring during development must be derived from the blood;

within the vitreous there is some proliferation, but this is very slow.

Chemistry

When discussing the dynamic relationships between aqueous humour and the vitreous body it was considered sufficient to treat the latter as an essentially aqueous medium; and this is justified by the observation that over 99% of the material in this body is water and dissolved salts. The special features of the inorganic composition have been considered earlier, and here we are concerned with the composition in so far as it bears on the structure and stability of the vitreous body as a gel. If the vitreous body is held in a pair of forceps, or placed on a filter, it drips and after a time only a small skin of viscid material remains; this residue was called by Mörner (1894) the *residual protein*, and was considered to constitute the gel-forming material, in essentially the same way that fibrin constitutes the gel-forming material of a plasma clot. The liquid dripping away, or passing through the filter, contains the dissolved crystalloids together with a mucopolysaccharide, *hyaluronic acid*, that imparts to the solution a high viscosity by virtue of its high molecular weight and highly asymmetrical molecules. In addition there is a small percentage of soluble proteins, some of which are peculiar to the vitreous whilst others are identical with plasma proteins (Laurent *et al.*, 1962).[2] In particular, the glycoproteins, containing sialic acid, are in much higher concentration than in plasma. Figures given for the colloidal composition of bovine vitreous body are: Vitrosin, 150 mg/litre, Hyaluronic acid, 400 mg/litre and Soluble proteins 460 mg/litre. Thus the colloidal material constitutes less than 0.1% of the total body.

Residual Protein, Vitrosin, Collagen

Purified residual protein may be solubilized and the separated material examined by the battery of techniques available to the protein chemist; its morphological state *in situ* may be studied in the electron microscope. The protein exists as very fine fibrils, some 7 to 13 nm in diameter[3] and of indefinite length which are apparently anchored to the inner basal lamina; Fig. 2.1 from a paper by Fine & Tousimis (1961), which confirms earlier studies

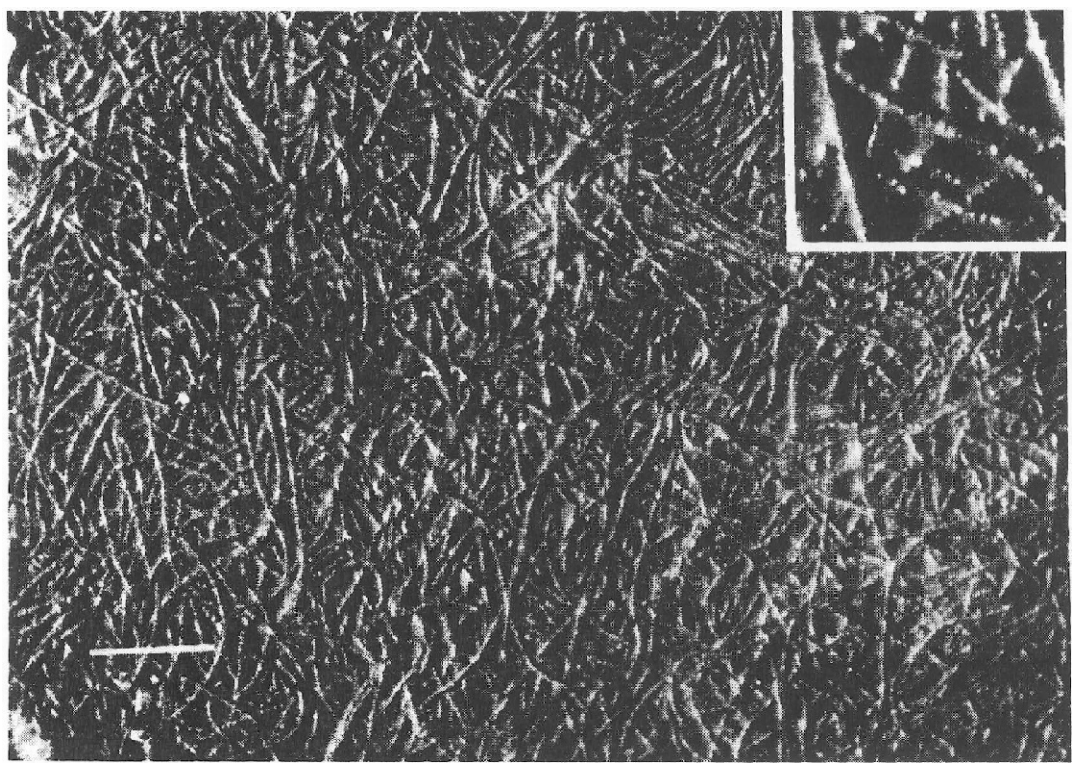

Fig. 2.1 Shadowcast section of posterior vitreous structure. The orientation of the filaments in the plane of the section suggests a tangential cut through a lamella. The filaments are uniform in width and show a distinct periodicity (× 12 000). The enlarged inset (× 38 000) demonstrates periodicity of filaments. (Fine & Tousimis, *Arch. Ophthal.*)

of Schwarz (1956), illustrates the fibrils, which are randomly orientated through the structure. Chemical analysis classified the fibrous protein as a collagen, with the characteristic high proportion of hydroxyproline, glycine, and hydroxylysine amino acids.

COLLAGEN

This is the main structural basis of connective tissues, such as skin, cartilage, cornea, sclera, and so on. There are several types, but all are based on a triple helix of polypeptide chains, which are of two fundamental types called α1 and α2 or A and B. The proportion of either type of chain can vary, e.g. $(\alpha 1)_3$; $(\alpha 1)_2\alpha 2$, and so on. In addition, the chains can vary in their amino-acid composition, retaining, however, certain common properties, such as glycine as every third residue, high concentrations of proline, hydroxyproline and hydroxylysine. Thus the collagens have been described as Type I, Type II, etc., and within the type there are variations in the proportions of α1 and α2. The most ubiquitous collagen is Type I, indicated by $(\alpha 1(I))_2\alpha 2$, which has a chain distribution of two α1 and one α2 in its triple helix. The molecules have a molecular weight of some 95 000 daltons, and arrange themselves to form fibres, an arrangement that leads to a typical 'banding' created by the alignment of specific groups; in the native fibril; this has a periodicity of 67 nm. At least five types have been described, Types I to V; in addition, an EC collagen, derived from the basement-membrane material synthesized by cultured endothelia, has been described by Benya (1980); this is easily separable from Type IV, also associated with basement membranes.

Mucopolysaccharides

This is the name commonly given to a group of polysaccharides containing an amino sugar, and widely distributed throughout the animal body where they may act as lubricants in the joints and saliva, as the anticoagulant called heparin, as blood-group substances on the surface of red cells, as ground substance of connective tissue, as cement between cells, and so on. Strictly speaking the term mucopolysaccharide should be applied, however, only to the combination between this type of polysaccharide and a protein, the reaction of the complex being predominantly polysaccharidic, whilst the term *mucoprotein* is applied to a complex between protein and carbohydrate where the behaviour is predominantly protein in character.[4]

HYALURANIC ACID

Perhaps the best known of the polysaccharides is *hyaluronic acid*, it consists of large asymmetrical molecules (weight of the order of a million or more) made up by the polymerization of N-acetylglucosamine and glucuronic acid, linked together as follows:

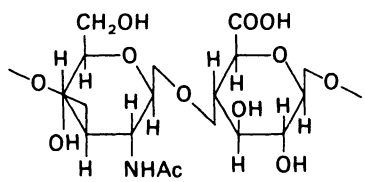

Hyaluronic acid

Hyaluronic acid is specifically broken down by the enzyme, *hyaluronidase*, isolated from streptococci and pneumococci. Chondroitin sulphate was first found in the cornea but also occurs in cartilage; it is built up by the polymerization of N-acetylgalactosamine, glucuronic acid and sulphate, as below:

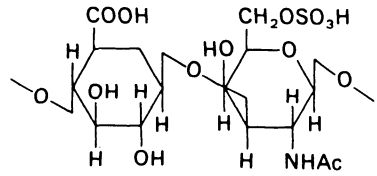

Chondroitin sulphate

SULPHATED GLYCANS

Chondroitin is the desulphated chondroitin sulphate, whilst the latter has been found in three different forms, called chondroitin sulphate A, B and C, the differences being not so much due to differences in the sugar moieties as in the nature of the linkages.

HISTOCHEMISTRY

Histochemically these polysaccharides are identified by their so-called *metachromatic staining* with toluidine blue, whereby the stain acquires a different colour than it had in free solution. The *periodic acid-Schiff test* (P.A.S.) is also characteristic for the chondroitins although there is some doubt as to whether hyaluronic acid reacts positively. The polysaccharides react easily with proteins to form *proteoglycans*, and it is probably in this form that they associate with the collagen fibres of connective tissue.

Vitreous Collagen

Vitreous collagen was shown to be similar to that in cartilage, consisting of three alpha$_1$-chains, and described as Type II. Elaborate comparisons between cartilage- and vitreous collagens (e.g. Swann *et al.*, 1972; Swann, 1980) have revealed some differences, however, and it has been suggested that, perhaps in the non-helical region of the fibril, additional peptides were added. In view of the ectodermal origin of vitreous, as against the mesodermal origin of cartilage, some differences would not be surprising.

The most striking feature of the vitreous body, to the physical chemist, is the remarkably small concentration of the fibrous scaffolding material, vitrosin or collagen, that must be at the basis of its coherent structure, namely 150 mg/litre. Optically this is a highly satisfactory feature since transparency is perfect in spite of the random arrangement of the 10 nm fibrils.

Vitreous Hyaluronic Acid

This polysaccharide, made up of equal proportions of glucuronic acid and glucosamine, was first isolated by Meyer & Palmer (1934) from bovine vitreous body; it is hydrolysed by hyaluronidase, and is characteristically present in synovial fluid where its peculiar molecular features permit it to act as a lubricant. When the gel structure of the vitreous is broken down, as in filtration, the hyaluronic acid passes into the liquid phase and contributes significantly to its viscosity. The most recent[5] determinations of molecular weight are those of Laurent & Granath (1983); from the rabbit it was $2–3 \times 10^6$; in adult bovine, $5–6 \times 10^5$, and the newborn calf 3×10^6.

Basic Structure

An early model, based largely on physicochemical experiments, suggested that the vitreous body was a gel made up of a framework of 'residual protein' fibrils, separated from each other by a space of some 10 nm, and filled with hyaluronic acid and water. It was postulated that the stability of the structure depended critically on the state of the hyaluronic acid (Duke-Elder *et al.*, 1936). All subsequent work has confirmed this picture, which may be illustrated by Fig. 2.2 from Balazs (1961).

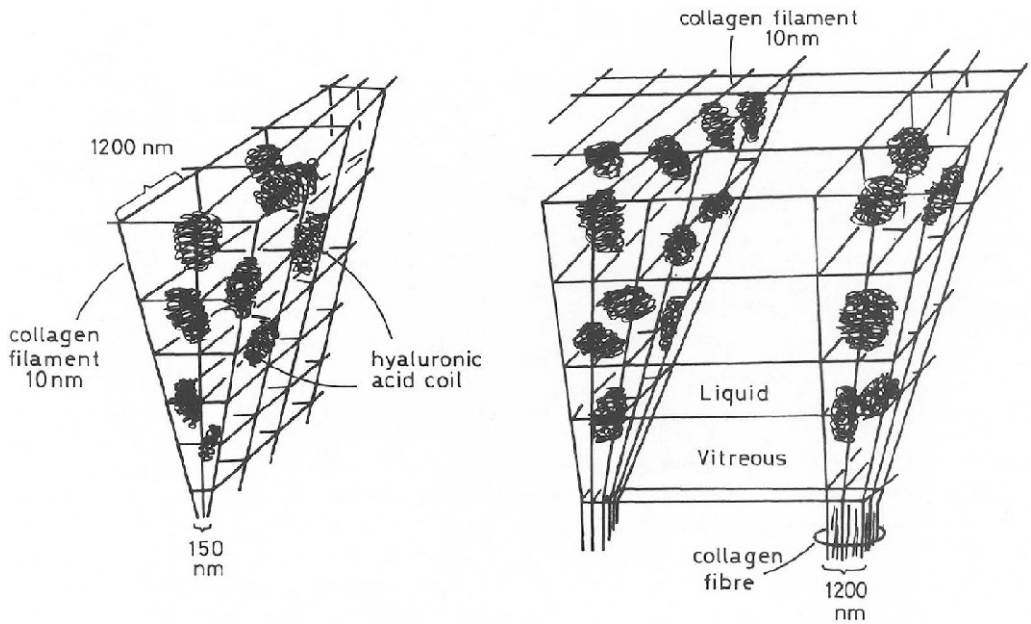

hyaluronic acid molecules. *Left*: random distribution of the structural elements. *Right*: formation of liquid pool and partial collapse of the network. (Balazs, in *Structure of the Eye*.)

The hyaluronic acid component probably exists as a randomly kinked coil entraining large quantities of water so that in solution it occupies some 1000 times the volume it occupies in the dry state. The individual molecules probably entangle with each other to form a continuous three-dimensional network, which would stabilize the collagen skeleton, imparting to the gel its characteristic visco-elastic properties. Its chemical relations to proteins have been discussed at length by Swann (1980) who concludes that it is most unlikely to be linked by covalent bonds.[6]

Regional and Species Variations

PHASE-CONTRAST MICROSCOPY

In the phase-contrast microscope, which permits the resolution of structures in the natural state, Bembridge *et al.* (1952) described three characteristic differentiations; in the anterior portion, definite fibres of relatively large diameter were found, whilst in the bulk there were much finer, but still optically resolvable, fibres. Chemically the large fibres were different from the fine fibres in that they were not attacked by collagenase whereas the fine fibres were; by contrast the protease trypsin attacked the thick fibres but not the thin. On the surface they described a 'hyaline membrane' which would include the basal lamina of the electron microscopists. The large fibres, with diameters in the region of 1 to 2 μm, i.e. 1000 to 2000 nm, must be regarded as aggregates of the basic 10 nm microfibril, although the different vulnerability to enzymes between the thick and fine is due to the difference in protein structure, typically seen with the zonule (p. 102).

THE THREE ZONES

Bettelheim & Balazs (1968) and Bettelheim & Wang (1976) suggested that the fine fibrillar component of the vitreous gel was organized into sheets forming cylindrical layers around Cloquet's canal; they pointed out that collagen and hyaluronic acid varied in concentration as one passed posteriorly from the anterior layer to the retinal layer. Thus, the order of concentrations was: Anterior > Centre < Retina, the central region containing least; the order for hyaluronic acid was: Anterior < Centre < Retina. The visco-elastic properties of the vitre-

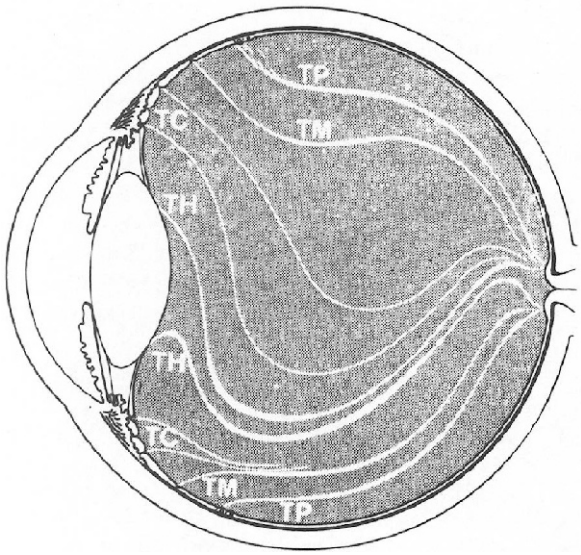

Fig. 2.3 Diagram of the vitreous tracts: TP, preretinal tract; TM, median tract; TC, coronary tract; TH, retrolental ('hyaloid') tract. (Eisner, *Trans. Ophthal. Soc. U.K.*)

ous body varied with direction of compression. Eisner (1971, 1975a, b), on the basis of optical studies of human vitreous described four funnel-shaped structures ('tracts'), as illustrated by Fig. 2.3; changes in these occurred with age, so that in the infant the vitreous was relatively homogeneous except for Cloquet's canal. In late age, 'destruction holes', or regions of liquefaction, became obvious.

These tracts resulted from the successive synthesis of layers of gel by the adjacent retina; thus photocoagulation of a small area of retina in the developing eye caused the appearance of 'holes' in the vitreous immediately above the damaged retina (Eisner, 1978); naturally occurring holes occur above the papilla, fovea, ora serrata, etc. The solid nature of these tracts became clear when it was found that foreign particles, such as erythrocytes, followed a definite channel, e.g. the tractus intermedius, rather than sinking vertically (Eisner, 1971).

Gel and Liquid

Balazs & Denlinger (1984) have emphasized a fundamental distinction between a solid cortical layer and a greater or less amount of liquid material in the central region; the proportions vary with species, so that in the owl monkey the great bulk is a liquid contained within an outer cortex of gel only some 100 μm thick. In birds, on the other hand, the whole structure is uniformly solid. Corresponding with these structural differences, we find the concentration of collagen highest in the solid regions and that of hyaluronic acid least, and vice versa (Swann & Constable, 1972). In most mammals, including some species of monkeys, liquid vitreous does not form, but in humans and rhesus monkeys there is a progressive central liquefaction with age (Eisner, 1976; Denlinger *et al.*, 1980a), presumably due to syneresis of the gel, the fluid contents escaping from the collagenous network, which shrinks but retains its collagen.[7]

Cloquet's Canal

As indicated above this is the remnant of the hyaloid artery and its branches running from the optic nerve to the posterior lens capsule. Its changes during regression in the fetal and neonatal animal have been described by Jack (1972a, b) and Bloom *et al.* (1980). After regression the only remains of the vessel are the vestiges of its muscular sheath, or media, these vestiges being described as multilayered fenestrated sheaths that previously surrounded the muscle cells (Österlin & Balazs, 1968). The canal may be removed easily by pulling, in the 2–3 months-old calf; the absence of strong adhesion being due to the fact that the collagen fibrils lining the canal run parallel with it whereas the adjacent fibres of vitreous are randomly orientated. There is a strong attachment to the lens capsule by a dense collagen fibrillar network (Wieger's ligament) and this is responsible for complications in cataract surgery since the anterior cortical gel may break during separation of the capsule and thus open up the central pool of liquid vitreous, which then has access to the anterior chamber.

Metabolic Aspects

It is generally accepted that there is little, if any, turnover of the vitreous collagen; as indicated, the secondary vitreous is synthesized by the Müller cells of the retina and the epithelia of the ciliary body and lens. During development, the relative amounts of activity change. Thus Newsome *et al.* (1976) measured the synthetic activity of the tissues adjacent to the vitreous of the developing chick at different stages. In the earliest stages studied (26–27 and 29–30), the neural retina produced at least ten times more collagen than the other portions, and this was mainly $(\alpha 1)_3$ collagen; an interesting feature was that there was a high proportion of α_2-chain collagen in these other portions. At stage 40 the major source of α_1-collagen was the vitreous, the retina producing only one fifth of the vitreous collagen, whilst the proportion of its α_2- increased; the lens still only produced a small amount, with a high proportion of α_2-. It would appear, then that the hyalocytes of the vitreous produce collagen as well as hyaluronic acid.

Transport through Vitreous Body

The kinetics of transport across the blood-vitreous barrier are adequately described on the basis of free diffusion through the vitreous, which behaves as a relatively unstirred medium. A significant bulk-flow of fluid through the gel is unlikely with the small pressure-gradients present (Fowlks, 1963). When the eye, as a whole, is subjected to a large osmotic stress, however, the picture is different; thus infusion of hypertonic solutions intravenously causes a loss of water (Robbins & Galin, 1969), due to the semipermeability of the blood-retinal barrier that leads to osmotic withdrawal of subretinal fluid into the blood. The power of the vitreous to retain its water (essentially its swelling pressure) is negligibly small (Duke-Elder *et al.*, 1936; Goedbloed, 1937), so that it will give up water to the subretinal space and ultimately to the blood.

Control of Vascularization

ANGIOGENIC INHIBITOR

In the fetus the vitreous body is vascularized, but in the neonatal animal the system degenerates and is phagocytosed leaving the body avascular with a vestigial Cloquet's canal indicating where the main hyaloid artery was located. We may presume that this devascularization, and the subsequent avascularity, are brought about and maintained by some inhibitory substance, as in cartilage. Since tumours and retinal extracts contain a factor of the opposite type, namely angiogenic excitation, we may test the capacity of vitreous extracts to inhibit angiogenesis by studying their action on angiogenic factors. Felton *et al.* (1979) implanted tumour-tissue, together with a vitreous extract, in corneal stroma and showed, not only that vitreous contained an inhibitor of neovascularization in the cornea, but also an exciter of it, so that, when implanted alone, vascularization was considerable; with the tumour implant plus vitreous extract, vascularization was less than with tumour alone.[8] In a similar way, using a chorioallantoic membrane assay technique, Lutty *et al.* (1983) showed that a vitreous extract would antagonize the effects of an angiogenic factor extracted from retina. (Glaser *et al.* (1980) and Raymond & Jacobson (1981) extracted a factor with molecular weight 62 000 daltons that stimulated growth of endothelial and smooth muscle cells in culture. They argued that the material was synthesized by hyalocytes, since a medium incubated with these cells had similar effects.) Macrophages, to which the hyalocyte is allied, have a similar inhibitory effect on tumour cells, and it is interesting that the lowest density of hyalocytes is at the optic disc, the region where vascular proliferation begins in retinopathy. They suggest, also, that the bullous keratopathy that may follow prolapse of the vitreous on to the corneal endothelium (vitreo-corneal touch) might be due to the hyalocyte factor which, in high concentration, is injurious to cells.

Vasoproliferative Activity

Vascularization of avascular tissues occurs pathologically, as with the cornea (p. 130), and may be regarded as a step in wound healing. When retinal regions are undergoing vascular dystrophy, as in diabetic retinopathy or retrolental hyperplasia, the necrosis of the retinal tissue seems to provoke proliferation of the capillary bed; and it has been suggested (Michaelson, 1948) that the autolysing tissue releases a vasogenic factor, a release that may be terminated by killing the tissue, as with photocoagulation. Glaser *et al.* (1980) extracted material from mammalian retina that stimulated capillary growth in the chick chorioallantoic membrane and also growth of cultured endothelial cells. The material was non-dialysable, indicating a molecular weight of greater than 10 000–12 000 daltons, and its activity was destroyed by heating to 100°C. A similar non-dialysable factor was described by Raymond & Jacobson (1981), the amount of activity obtained increasing with the time the eye was allowed to remain in the enucleated state, suggesting that the factor was liberated by tissue autolysis.[8]

The Normal Condition

Whatever the origins of the opposing vascular factors, it is clear that since both are present in the vitreous body, the maintenance of a normally avascular vitreous depends on a balance between them. In embryogenesis, the regression of the hyaloid arterial system is associated with aggregation of hyalocytes in the region that is to become Cloquet's canal; later the hyalocytes take up a peripheral station.

Antiprotease Activity

The growth of new vessels into a tissue must involve breakdown of the host structure, presumably mediated by proteases; thus an anti-protease factor might well act as an anti-angiogenic factor. However, Jacobson *et al.* (1985) although separating an anti-trypsin factor from vitreous humour, with a molecular weight in the region of 10 000 to 13 000 daltons, showed that this was different from their low-molecular weight anti-angiogenic factor. Earlier, Sorgente & Dorey (1980) had shown that the endothelial growth inhibitor extracted from cartilage was different from the anti-tryptic factor also present.

Proliferative Vitreoretinopathy

This condition, ultimately leading to retinal detachment, is characterized by the growth of cells in the vitreous gel

and on the surface of the retina, presumably as a result of migration of pigment epithelial and glial cells into the vitreous where they acquire the characteristics of myofibroblasts. Wiedemann *et al.* (1985) have shown that vitreous contains a thermolabile factor that stimulates proliferation of porcine retinal pigment epithelial cells. They considered that the mitogenic factor was not derived from leakage into the vitreous of circulating fibroblast epidermal or platelet-derived growth factor.

The Zonule

Macroscopic Appearance

The zonule, or suspensory ligament of the lens, may be regarded as an extreme instance of differentiation of the vitreous body, its fibrous parts being composed presumably of the same material as that making up the large fibres of the vitreous body, described by Bembridge *et al.*, since they are both dissolved by the enzyme trypsin; the difference between the two is essentially that the zonular fibres have found attachment to the lens capsule whilst the coarse fibres of the vitreous attach to the ciliary body. In the fresh specimen the zonule appears as a thick band-shaped structure attached internally to the equatorial region of the lens capsule; the anterior surface runs straight from the lens to the anterior region of the ciliary processes (Fig. 1.4). The surfaces of the zonule show a marked striation running in a general sense from the lens to the ciliary body; these striations probably represent fibres of highly condensed residual protein; between them is a perfectly homogeneous transparent gel which gives the surface a membrane-like appearance. The space between the anterior and posterior surfaces is criss-crossed by strands of fibrous material, the spaces so formed being once again filled by transparent homogeneous jelly.

Fine Structure

In the electron microscope the fibres are seen to consist of bundles of microfibrils of 11–12 nm diameter analogous with the corresponding microfibrils of the vitreous gel; according to Raviola (1971) they bear a striking resemblance to elastic fibres with a typical longitudinal banding of 490 nm. The fibrils are essentially extensions of the internal basement membrane of the ciliary epithelium on which the basal regions of the pigmented cells rest; the fibrils run from here into the epithelium itself and take a tangential path between the epithelial layers emerging from the ciliary valleys and pars plana. At their insertion on the lens capsule, the fibrils fuse with the surface, in the rabbit, but in humans they go deeper towards the epithelium and fibres, forming a continuous mat over the equatorial surface.

Chemistry

Zonular fibres are not attacked by collagenase but they are by trypsin[9] whilst their amino acid composition differs from that of collagen, especially in the absence of hydroxyproline and hydroxylysine and the presence of large amounts of cysteine; this may have some pathological interest for the Marfan syndrome associated with homocystinuria, i.e. the incomplete formation or tearing of the zonular fibres leading to ectopia lentis. The presence of some 9% of carbohydrate indicates that the material is a glycoprotein, i.e. a protein rich in sialic acid, hexoses and hexosamine (Buddecke & Wollensak, 1966).

ELASTIN SYSTEM

The dissimilarity in amino acid composition between zonule and vitreal collagen has suggested to Streeten & Licari (1983) that the structural element of the zonule might be more closely related to elastin, although elastin, as such, is absent. They point to the similarity ultrastructurally between the tubular microfibrils of the zonule and the microfibrils connecting the main elastin elements of the skin with the epidermis, which, according to them, do not contain elastin and are described classically as oxytalan fibrils. Thus Ross & Bornstein (1969) showed that the microfibrillar layer surrounding the amorphous core of the typical elastin fibre was chemically different from elastin, having a higher proportion of SH-amino acids; and they concluded that the microfibrils were neither elastin nor collagen. In their own analysis, Streeten *et al.* (1983) found a similar amino-acid composition in the zonule fibres to that in the microfibrils of the elastic microfibrils of the calf ligamentum nuchae. When the material was solubilized, a unit of 70 000 daltons was dominant, a similar sized unit being found in the ligamentum nuchae of the calf. Thus, according to Streeten, the zonule is made up of similar material to the non-elastin material surrounding the core of the typical elastic fibre. Carbohydrate analysis suggested that the glycoconjugates included a sialofucose-containing glycoprotein and a xylose-containing proteoglycan.

Notes

1. Foos (1972) has recommended that the term inner limiting *membrane* be dropped, and the term inner limiting *lamina* be substituted, and emphasized its analogy with the basement membranes, or basement laminae, of cells in general, the basal lamina proper consisting of a *lamina densa*, some 600 nm thick made up of a fibrous feltwork embedded in an amorphous matrix, the filaments being similar to collagen, and separated from the cell membrane by a *lamina rara*. Filaments anchor the lamina to the adjacent collagenous stroma. The

basal membrane of the light microscopists includes the basal lamina and other neighbouring components.

2. Kohno *et al.* (1987a, b) suggest that the extracellular glycoproteins, laminin and fibronectin, might be concerned with adhesion of the vitreous body to the retina, so that its presence in the vitreous body would be of interest in the study of retinal detachment. Both are present, although fibronectin was barely detectable. The immunofluorescence for laminin became stronger in older subjects. The diabetic eye gave a more intense fluorescence than normal.
3. The diameters of the vitrosin fibrils have been given by Snowden & Swann (1980); they gave the following figures: ox, 10 ± 2; sheep, 12.5 ± 1; human, 12.8 ± 1; dog, 12.0 ± 2; rabbit, 7 ± 1 nm. They have discussed the conditions for revealing typical collagen banding, with a major 62 nm period and segment long-spacing crystals. They emphasize the analogy with cartilage Type II collagen, on this ultrastructural basis.
4. The term *glycosaminoglycan* is recommended for a polysaccharide containing a hexosamine; more specifically, *glucosaminoglycan* is a polysaccharide containing glucosamine; *galactosaminoglycan*, one containing galactosamine, and so on.
5. Gherezghiher *et al.* (1987) have described an assay of hyaluronic acid involving high-performance liquid chromatography on amino-bonded silica columns. Concentrations in aqueous and vitreous humours of owl monkey and the ox ranged between 0.8 to 3.8 and 237 to 280 $\mu g\ ml^{-1}$ for owl monkey, and 3.8 to 6.7 and 402 to 610 $\mu g\ ml^{-1}$ for the ox. In pathological liquefaction of the vitreous, the surgeon seeks to replace the fluid with a new gel; so far, a highly purified hyaluronic acid preparation has been employed that is well tolerated (Denlinger & Balazs, 1980; Denlinger *et al.*, 1980b; Graue *et al.*, 1980).
6. The presence of vitreous-specific proteins, not present in plasma, has been discussed by Swann (1980); proteoglycans, i.e. proteins covalently linked to a glycan through serine SH-groups, are the dominant sulphated constituents of connective tissue, and probably account for the sulphate present in vitreous. Lipids are associated with the 'residual protein' fraction of vitreous, but most of the phospholipids of blood are probably restrained by the blood-vitreous barrier from accumulating here (Kim & Cotlier, 1976). Nguyen & Fife (1986) have found a protein of 550 kd, hitherto thought to be peculiar to hyaline cartilage, in human vitreous; it shares the same antigenic properties, and may have some bearing on eye disease related to rheumatic disorders.
7. Denlinger *et al.* (1980a) found some 0.26 ml of liquid vitreous in 1–5-year-old monkeys; in young adults this was 0.85 ml and in old adults, 1.18 ml, the fluid being in a central pocket surrounded by dense cortical gel. They state that in human less than 4-year-old, there is no liquid; between the ages of 16 to 20 the liquid volume slowly increases so that between 20 and 35 it amounts to 20% of the whole, to reach a figure of 50% in old age.
8. Chen & Chen (1982) extracted a vascular growth factor from retina, vitreous body and serum of fetal calves, as assayed on cultured fetal calf aortic endothelial cells; quite a large proportion was dialysable; and this dialysable material was stable to heating at 100°C. Chromatographically three fractions were separated, one of which was missing from the vitreous extract. The authors suggest that the dialysable material in retina and vitreous body was derived from the blood.
9. This forms the basis of loosening the lens capsule from its attachments during cataract surgery (Barraquer, 1958).

References

Balazs, E. A. (1959) The vitreous body. Scientific exhibit at XVIII International Congress of Ophthalmology, Brussels, pp. 1–10. (Quoted by Balazs & Denlinger, 1984.)

Balazs, E. A. (1961) Molecular morphology of the vitreous body. In *The Structure of the Eye*. Ed. Smelser, pp. 293–310. New York: Academic Press.

Balazs, E. A. & Denlinger, J. L. (1984) The vitreous. In *The Eye*, Ed. H. Davson, Vol. IA, 3rd Edn, pp. 533–588.

Barraquer, J. (1958) Totale Linsenextraktion nach Auflösung der Zonula durch α-Chymotrypsin = enzymatische Zonulyse. *Klin Mbl. Augenheilk.* **133**, 609–615.

Bembridge, B. A., Crawford, C. N. C. & Pirie, A. (1952) Phase-contrast microscopy of the animal vitreous body. *Br. J. Opthalmol.* **36**, 131–142.

Benya, P. D. (1980) EC collagen: biosynthesis by corneal endothelial cells and separation from Type IV without pepsin treatment or denaturation. *Renal Physiol.* **3**, 30–35.

Bettelheim, F. A. & Balazs, E. A. (1968) Light scattering patterns of the vitreous humor. *Biochim. Biophys. Acta* **158**, 309–312.

Bettelheim, F. A. & Wang, T. J. Y. (1976) Dynamic viscoelastic properties of bovine vitreous. *Exp. Eye Res.* **23**, 435–441.

Bloom, G. D., Balazs, E. A. & Ozanics, V. (1980) The fine structure of the hyaloid arteriole in bovine vitreous. *Exp. Eye Res.* **31**, 129–145.

Buddecke, E. & Wollensak, J. (1966) Zur Biochemie der Zonulafaser des Rinderauges. *Z. Naturf.* **21b**, 337–341.

Chen, S. C. & Chen, C.-H. (1982) Vascular endothelial cell effectors in fetal calf retina, vitreous, and serum. *Invest. Ophthal.* **23**, 340–350.

Denlinger, J. L. & Balazs, E. A. (1980) Replacement of the liquid vitreous with sodium hyaluronate in monkeys. I. Short-term evaluations. *Exp. Eye Res.* **31**, 81–99.

Denlinger, J. L., Eisner, G. & Balazs, E. A. (1980a) Age-related changes in the vitreous and lens of rhesus monkeys (*Macaca mulatta*). *Exp. Eye Res.* **31**, 67–69.

Denlinger, J. L., Mofty, A. A. M. & Balazs, E. A. (1980b) Replacement of liquid vitreous with sodium hyaluronate in monkeys. II. *Exp. Eye Res.* **31**, 101–117.

Duke-Elder, S., Davson, H. & Benham, G. H. (1936) The swelling pressures of normal and glaucomatous vitreous bodies. *Brit. J. Ophthal.* **20**, 520–527.

Eisner, G. (1971) Autoptische Spaltlampenuntersuchung des Glaskorpers. I–III. *Graefes Arch.* **182**, 1–7, 8–22, 23–40.

Eisner, G. (1975a) Zur Anatomie des Glaskörpers. *v. Graefes Arch. Ophthal.* **193**, 33–56.

Eisner, G. (1975b) Clinical examination of the vitreous. *T.O.S.U.K.* **95**, 360–363.

Eisner, G. (1976) The anatomy and biomicroscopy of the vitreous body. In: *Documenta Ophthalmologica Proceedings Series, New Developments in Ophthalmology*, pp. 87–104. Junk, The Hague. (Quoted by Balazs & Denlinger, 1984.)

Eisner, G. (1978) Lichtkoagulation und Glaskörperbildung. *v. Graefes Arch. Ophthal.* **206**, 33–38.

Felton, S. M., Brown, G. C., Felberg, N. T. & Federman, J. L.

(1979) Vitreous inhibition of tumor neovascularization. *Arch. Ophthal.* **97**, 1710–1713.

Fine, B. S. & Tousimis, A. J. (1961) The structure of the vitreous body and the suspensory ligaments of the lens. *Arch. Ophthal., Chicago* **65**, 95–110.

Foos, R. Y. (1972) Vitreoretinal juncture: topographical variations. *Invest. Ophthal.* **11**, 801–808.

Foulds, W. S. (1975) The vitreous in retinal detachment. *T.O.S.U.K.* **95**, 412–416.

Fowlks, W. L. (1963) Meridional flow from the corona ciliaris through the pararetinal zone of the rabbit vitreous. *Invest. Ophthal.* **2**, 63–71.

Gherezghiher, T., Koss, M. C., Nordquist, R. E. & Wilkinson, C. P. (1987) Analysis of vitreous and aqueous levels of hyaluronic acid: application of high-performance liquid chromatography. *Exp. Eye Res.* **45**, 347–349.

Glaser, B., D'Amore, P. A., Michels, R. & Patz, A. (1980) Stimulation of neovascularization and endothelial cell proliferation by human intraocular fluid. *ARVO Supp.*, 137–138.

Gloor, B. P. (1973) Zur Entwicklung dea Glaskörpers und der Zonula. III. *v. Graefes Arch. Ophthal.*, **187**, 21–44.

Goedbloed, J. (1937) Studien am Glaskörper. V. Uber den Expansionsdruck des entsalzten Glaskörpers. *v. Graefes Arch. Opthhal.* **137**, 127–130.

Graue, E. L., Polack, F. M. & Balazs, E. A. (1980) The protective effects of Na-hyaluronate to corneal endothelium. *Exp. Eye Res.* **31**, 119–127.

Jack, R. L. (1972a) Regression of hyaloid vascular system. *Amer. J. Ophthal.* **74**, 261–272.

Jack, R. L. (1972b) Ultrastructure of the hyaloid vascular system. *Arch. Ophthal.* **87**, 555–567.

Jacobson, B., Dorfman, T., Basu, P. K. & Hasary, S. M. (1985) Inhibition of vascular endothelial cell growth and trypsin activity by vitreous. *Exp. Eye Res.* **41**, 581–595.

Kim, J. O. & Cotlier, E. (1976) Phospholipid distributions and fatty acid composition of lysophosphatidylcholine and phosphatidylcholine in rabbit aqueous humor, lens and vitreous. *Exp. Eye Res.* **22**, 569–576.

Kohno, T., Sorgente, N., Goodnight, R. & Ryan, S. J. (1987b) Alterations in the distribution of fibronectin and laminin in the diabetic human eye. *Invest. Ophthal.* **28**, 515–521.

Kohno, T., Sorgente, N., Ishibashi, T., Goodnight, R. & Ryan, S. J. (1987a) Immunofluorescent studies of fibronectin and laminin in the human eye. *Invest. Ophthal.* **28**, 506–514.

Laurent, U. B. & Granath, K. A. (1983) The molecular weight of hyaluronic acid in the aqueous humour and vitreous body of rabbit and cattle eyes. *Exp. Eye Res.*, **36**, 481–492.

Laurent, U. B. G., Laurent, T. C. & Howe, A. F. (1962) Chromatography of soluble proteins from the bovine vitreous body on DEAE-cellulose. *Exp. Eye Res.* **1**, 276–285.

Lutty, G. A., Thompson, D. C., Gallup, J. Y., Mello, R. J., Patz, A. & Fenselau, A. (1983) Vitreius: an inhibitor of retinal-extract induced neovascularization. *Invest. Opthhal.* **23**, 52–56.

Meyer, K. & Palmer, J. W. (1934) The polysaccharide of the vitreous humor. *J. Biol. Chem.* **107**, 629–634.

Michaelson, I. C. (1948) The mode of development of the vascular system of the retina with some observations on its significance for certain retinal diseases. *T.O.S.U.K.* **68**, 137–180.

Mörner, C. T. (1894) Untersuchungen der Proteinsubstanzen in den lichtbrechenden Medien des Auges. *Hoppe-Seyl. Z.* **18**, 61–106.

Newsome, D. A., Linsenmayer, T. F. & Trelstad, R. L. (1976) Vitreous body collagen. *J. Cell Biol.* **71**, 59–67.

Nguyen, B. Q. & Fife, R. S. (1986) Vitreous contains a cartilage-related protein. *Exp. Eye Res.* **43**, 375–382.

Österlin, S. E. & Balazs, E. A. (1968) Macromolecular composition and fine structure of the vitreous in the owl monkey. *Exp. Eye Res.* **7**, 534–545.

Raviola, G. (1971) The fine structure of the ciliary zonule and ciliary epithelium. *Invest. Ophthal.* **10**, 851–869.

Raymond, L. & Jacobson, B. (1981) Isolation and identification of stimulatory and inhibitory growth factors in bovine vitreous. *Exp. Eye Res.* **34**, 267–286.

Robbins, R. & Galin, M. A. (1969) The effect of osmotic agents on the vitreous body. *Arch. Ophthal.* **82**, 694–699.

Ross, R. & Bornstein, P. (1969) The elastic fibre. *J. Cell Biol.* **40**, 366–381.

Schwarz, W. (1956) Elektronenmikroskopische Untersuchungen an Glaskörperschnitten, *Anat. Anz.* **102**, 434–442.

Snowden, J. M. & Swann, D. A. (1980) Vitreous structure. V. *Invest. Ophthal.* **19**, 610–618.

Sorgente, N. & Dorey, C. K. (1980) Inhibition of endothelial cell growth by a factor isolated from cartilage. *Exp. Cell Res.* **128**, 63–71.

Streeten, B. W. & Licari, P. A. (1983) The zonule and the elastic microfibrillar system in the ciliary body. *Invest. Ophthal.* **24**, 667–681.

Streeten, R. W. *et al.* (1983) The protein composition of the ocular zonules. *Invest. Ophthal.* **24**, 119–123.

Swann, D. A. (1980) Chemistry and biology of the vitreous body. *Int. Rev. Exp. Path.* **22**, 1–64.

Swann, D. A. & Constable, I. J. (1972) Vitreous structure. I. Distribution of hyaluronate and protein. *Invest. Ophthal.* **11**, 159–163.

Swann, D. A., Constable, I. J. & Harper, E. (1972) Composition of bovine vitreous collagen. *Invest. Ophthal.* **11**, 735–738.

Wiedemann, P., Ryan, S. J., Novak, P. & Sorgente, N. (1985) Vitreous stimulates proliferation of fibroblasts and retinal pigment epithelial cells. *Exp. Eye Res.* **41**, 619–628.

3. THE CORNEA

STRUCTURE

The cornea is illustrated by the meridional section in Fig. 3.1; the great bulk (up to 90% of its thickness) is made up of the *stroma* which is bounded externally by Bowman's membrane and the epithelium, and internally by Descemet's membrane and the endothelium. The total thickness in man is just over 0.5 mm in the central region; towards the periphery it becomes some 50% thicker.

Epithelium

This may be regarded as the forward continuation of the conjunctiva; it is a squamous epithelium consisting of some five or six layers of cells with a total thickness of 50 to 100 μm. The cells at the base are columnar, but as they are squeezed forward by new cells they become flatter so that three layers are recognized: *basal*, *wing-shaped*, and *squamous cells*. The more superficial cells do not show keratinization, as with skin, the process of shedding being accompanied by the breaking up of the cell into fragments (Teng, 1961). Replacement of cells occurs by mitotic division of the basal layer, the average life of a cell being some 4 to 8 days. Junctional complexes between cells in the various layers seem to be mainly of the desmosome type, not involving fusion of adjacent membranes. Nevertheless, because the permeability of the corneal epithelium as a whole is low, we must postulate tight junctions or zonulae occludentes between the cells of at least one layer, possibly the basal layer; according to Pedler (1962) these cells show extensive lateral interdigitation of plasma membranes. The surface layer of cells may be examined by the scanning electron microscope; viewed in this way the anterior surfaces of this outermost layer are covered by villous projections (Blümcke & Morgenroth, 1967). Amongst the cells a special, possibly secretory, type has been described by Teng; it may be that it secretes the basement membrane upon which the epithelium rests; this latter is a layer some 10 to 30 nm thick resolved into an anterior apparently lipid layer and a reticular fibre meshwork in contact with Bowman's membrane.

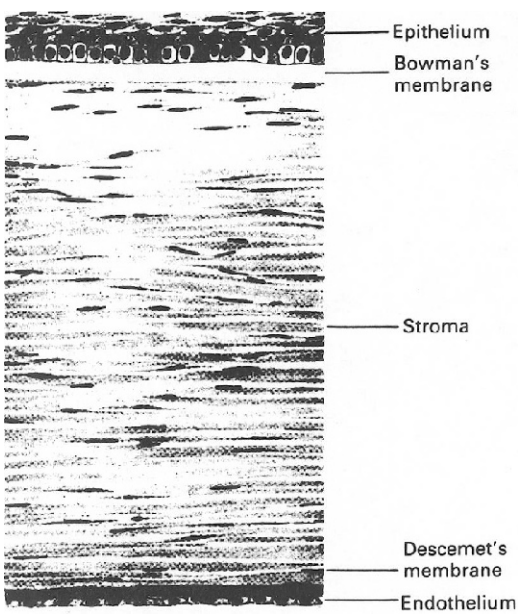

Fig. 3.1 Meridional section through the human cornea. (Wolff, *Anatomy of the Eye and Orbit.*)

Stroma and Bowman's Membrane

The Lamellae and Fibrils

In meridional section the stroma appears as a set of lamellae, running parallel with the surface, and superimposed on each other like the leaves of a book; between the lamellae lie the *corneal corpuscles*, flattened in the plane of the lamellae; they are equivalent to fibrocytes of other connective tissue. The lamellae are made up of microscopically visible *fibres*, which run parallel to form sheets; in successive lamellae the fibres make a large angle with each other. In lower animals the lamellae extend over the whole surface of the cornea and the fibres in adjacent laminae are at right-angles to each other; in mammals and man the lamellae are said to be made up of bands some 90 to 260 μm wide; there is apparently no

interweaving of these bands, however, so that essentially the structure consists of layers of fibres arranged parallel with themselves in any given lamella.

The lamellae in man are some 1.5 to 2.5 μm thick, so that there are at least 200 lamellae in the human cornea. The fibrous basis of the lamellae is made up of collagen which constitutes some 80% of the solid matter of the cornea; by submitting the cornea to ultrasonic vibrations in order to break down its structure into its elementary components, Schwarz (1953) observed typical collagen fibrils of 25 to 33 nm diameter, and having the characteristic 64 nm periodicity (p. 98); the fibrils isolated in this way were covered by a dense layer of cement substance which was presumably the mucopolysaccharide. The fibrils were remarkably homogeneous in regard to diameter, in marked contrast to those of the sclera where the diameter varied from 28 to 280 nm, and where the amount of ground substance was very much less. As we shall see, this uniformity in diameter is important for the transparency of the cornea by contrast with the opacity of the sclera. With the development of thin-sectioning techniques, the fibrillar structure of the individual laminae was firmly established, e.g. by Jakus (1961), the fibrils running parallel with each other in any lamina and at right-angles to those in adjacent laminae. This regularity is clear in the electron micrograph of Fig. 3.2. The stromal cells in the human cornea appeared to lie within, rather than between, the laminae.

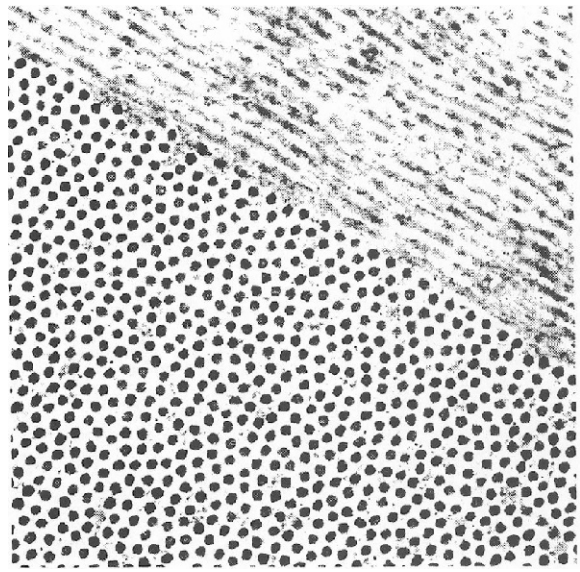

Fig. 3.2 Electron micrograph of normal human cornea. Note regularity of the fibres. (Giraud *et al.*, *Exp. Eye Res.*) (Courtesy of Pouliquen.)

Comparison with Sclera

The basic difference in structure between cornea and sclera consists in the much larger and more variable diameters of the scleral collagen fibrils and their much less dense packing. These differences are strikingly shown by Fig. 3.3; of interest is the transition zone, or limbus, where the changes occur very steeply. The regularity of fibre diameter in the cornea, and its gradual deterioration on passing through the limbus, are also manifest by the increasing size of the standard deviation shown by the vertical lines. The mean diameter in the central cornea found in this study (Berscheding *et al.*, 1975) was 29.6 nm; in the limbal areas adjacent to the sclera the size was 105.4

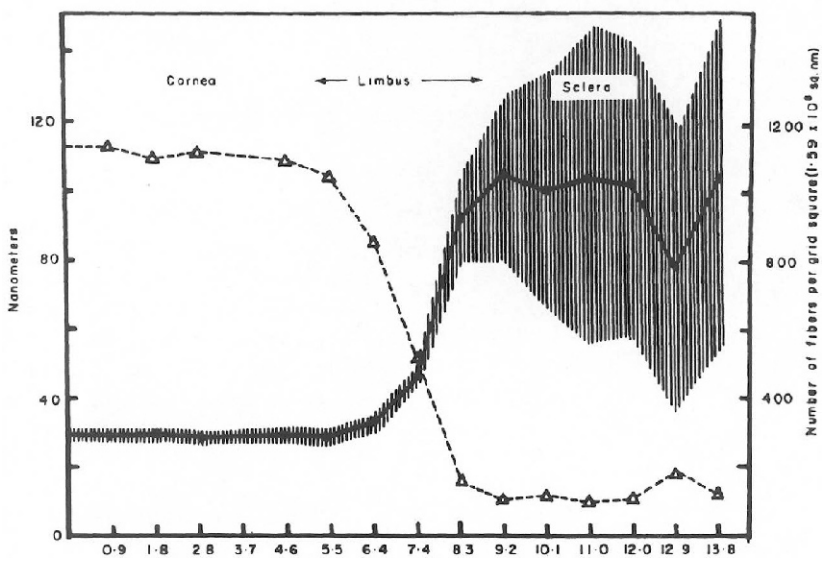

Fig. 3.3 Comparison of the average number of collagen fibres per unit area (△ - - - △) with the mean fibre diameter (●—●) ±s.d. (shaded area) as a function of distance from mid-cornea. Note steepness of change at limbus. (Berscheding *et al.*, *Exp. Eye Res.*)

$\pm$36.5 nm and in the sclera proper the mean was about the same.

Bowman's Membrane

Immediately next to the epithelium, the classical histologists described a layer with no resolvable structure, some 8 to 14 μm thick in man—*Bowman's membrane*[1] (Fig. 3.1). In the electron-microscope it became evident that Bowman's membrane is only a less ordered region of the stroma; thus, according to Jakus, and Kayes & Holmberg (1960), the stroma immediately beneath the basement membrane of the epithelium consists of collagen fibrils closely but randomly packed into a felt-like layer which is not sharply differentiated from the remainder of the stroma beneath it. It should therefore be described as *Bowman's layer* rather than Bowman's membrane.

Descemet's Membrane

This is some 5 to 10 μm thick in man and is revealed as a characteristic differentiation of the stroma in the electron-microscope, although in man the organization is not so precise as in the ox cornea. The collagen is different, having an axial period of 117 nm in place of the usual banding at intervals of 64 nm, and the carbohydrate is also different but similar chemically to that in the lens capsule (Dohlman & Balazs, 1955). Descemet's membrane is secreted by the endothelium.

According to Jakus (1946) there is a hexagonal ultrastructure that differentiates Descemet's membrane from the underlying stroma. Thus a tangential section revealed a hexagonal two-dimensional array of granular nodes connected by fine fibrils, the whole membrane being made up of a series of these two-dimensional grids. Descemet's membrane is a true basement membrane of the endothelium, synthesized by its cells; cultured endothelium will secrete a new basement membrane on which the endothelial cells become organized. It is thicker, however, than the usual basement membranes, being some 10 μm compared with 0.1 μm.

The Endothelium

This is a layer of flattened cells some 5 μm high and 20 μm wide. In the light-microscope the cells may be seen to form a regular mosaic (Fig. 3.4) with perfect contact between them.

Specular Microscopy

The posterior surface of the cornea gives rise to a reflection that allows the outlines of the endothelial cells to be made out when illuminated by the slit-lamp. By appropriate optical devices, the endothelium can be visualized with magnifications of up to 500-times (Maurice, 1968). Yee *et al.* (1987) have summarized the literature on this aspect of corneal morphology, so important for the study of corneal function. They examined the corneas of a range of vertebrates, from the dogfish to man. According to their analysis, the change from an aquatic to an aerial environment has led to the greater importance of the corneal endothelium, as a membrane controlling hydration; and this is reflected in the structure of the endothelium.

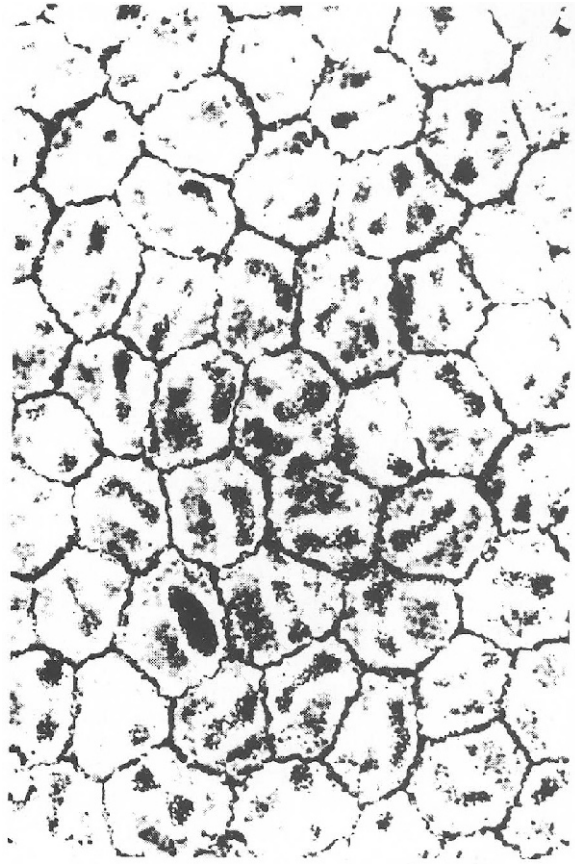

Fig. 3.4 Aspect of normal rabbit cornea after silver impregnation. The cells form a regular mosaic, with perfect contact between them. (Hirsch *et al.*, *Exp. Eye Res.*) (Courtesy of Pouliquen.)

Intercellular Junctions

As we shall see, the endothelium acts as a permeability barrier capable of actively transporting ions, so that on physiological grounds we should expect the individual cells to be closely apposed, with their adjacent membranes forming junctional complexes comparable with

those in the ciliary epithelium for example. However, electron microscopical studies, notably of Kaye *et al.* (1973), Leunberger (1973), Kreutziger (1976), Hirsch *et al.* (1977) and Ottersen & Vegge (1977), lead to the conclusion that, although there are junctional complexes apparently closing up the clefts, these are never of the zonula occludens type, forming a complete belt of fusion between adjacent cell membranes, as found in the corneal epithelium. The most common type is the gap-junction, with a 2 nm channel between membranes; where fusion has taken place, this is of the spot-weld type that does not completely close the cleft, allowing lanthanum to pass from one side of the endothelium to the other.

Cell Division

Division of endothelial cells, when it occurs, is mitotic, but significant division is only seen during repair or during growth of the eye, but even in the latter situation division is restricted, so that the increased area of endothelium is achieved, partly, by expansion of existing cells (Laing *et al.*, 1976). Thus Murphy *et al.* (1984) have described morphological changes in the endothelium from prenatal eyes to those of people over 98 years old. The human cornea reaches maximal growth in about 2 years after birth; the cellularity, i.e. the number of cells per unit area, decreases by about the same factor as the increase in area, about 1.5 compared with 1.4. The endothelial cells expand in size during this time. Between the ages of two and 98 years, cellularity decreases by some 0.56% per year, so that at 100 years some 56% of cells are lost; in this time the remaining cells have increased their area by a factor of 2.6.

^{3}H-Thymidine Incorporation

Experimentally, Simonsen *et al.* (1981) demonstrated some incorporation of ^{3}H-thymidine, indicating DNA synthesis, by endothelial cells in human eye-bank corneas subjected to injury and incubated in a medium. In normal, uninjured corneas there was a little, but much less, incorporation; and this agrees with the rarity with which cell-division is seen in human endothelium (Kaufman *et al.*, 1966).[2]

CHEMISTRY

The cornea contains some 22% of solid matter, and is thus quite obviously built on a more rigid plan than the vitreous body; this solid matter is mainly collagen, but in addition there are mucopolysaccharides, other proteins than collagen, and crystalloids of which salts make up the bulk.

Figures given by Maurice (1969) are as follows:

	per cent
Water	78.0
Collagen	15.0
Other proteins	5.0
Keratan sulphate	0.7
Chondroitin sulphate	0.3
Salts	1.0

Development

The manner in which the corneal collagen fibrils are laid down to give the regular spacing of about 600 Å (60 nm), with the orthogonal arrangement in the successive layers, is of some general interest, especially since it seems to be related to the type of glycosaminoglycan (GAG) present in the cornea; and it has been argued that, during the laying down of collagen, the arrangement is, in fact, governed by the nature of the GAG in association with the collagen, both being synthesized by the secreting cell and subsequently ejected into the extracellular space.

Development of Chick Cornea

The process has been studied in detail by Coulombre and Hay and their collaborators in the chick. At 3 days of development, the newly formed lens of the developing chick induces the overlying epithelium to start producing the primary corneal stroma; and by 4 days (Stage 22) this cellular stroma consists of about 15 layers of collagen with the characteristic orthogonal arrangement of fibrils in successive layers; the fibrils are embedded in a glycosaminoglycan which has also been synthesized by the corneal epithelium. Thus the primary cornea, by contrast with the later-developed or secondary cornea, is a product of *epithelial*, or ectodermal, synthesis; a similar situation prevails in the vitreous body. Between 4.5 and 5 days the corneal endothelium moves into place and by 5.6 to 6 days (Stages 27 to 28) it forms a continuous layer separating the corneal stroma from the lens.[3]

Mesenchymal Invasion

The invasion of this stroma by mesenchymal tissue takes place during this period, and this is preceded by a swelling due to increased hydration of its hyaluronic acid matrix, secreted by the endothelium, a process that is presumably necessary to permit this invasion of mesenchyme. Subsequently thickness decreases as the cornea becomes transparent, and this is associated with a decrease in the hyaluronic acid, brought about by the transitory appearance of the enzyme hyaluronidase (Toole & Trelstad, 1971). Thus the function of hyaluronic acid seems to be that of favouring dispersal of collagen fibrils, and this is especially manifest in the vitreous body where the spacing is of microscopic dimensions.

COLLAGEN SYNTHESIS

The secretion of the collagen by the epithelium and the nature of its GAG are of especial interest, since it seems that these primary layers act as the scaffolding, or template, on which successive

layers are laid down by the invading mesenchymal tissue. Trelstad & Coulombre (1971) showed that the fully formed primary cornea is identical in pattern to the secondary cornea, and they suggested that the fusiform mesenchymal cells, synthesizing collagen, use the primary cornea as a scaffold, a process made easier by the primary collagen being organized in bundles, not sheets. Trelstad *et al.* (1974) showed that the outer primary epithelium produced sulphated glycosaminoglycans, chiefly chondroitin sulphate, which was distributed in the basement membrane of the basal epithelial cells in an ordered pattern. A second sulphated GAG was heparan sulphate (Meier & Hay, 1973).

Primary Cornea as Template

It would seem that the chondroitin sulphate appears at critical periods in morphogenesis, and, in the case of the cornea, when the primary cornea has to be laid down in a pattern that will act as a template for the later-formed material of mesenchymal origin. Thus the 'corneal epithelial cell, by controlling the stoichiometry of syntheses (of GAG and collagen), by the intracellular packaging and timing of the mode of excretion into the extracellular space would play a very direct role in extracellular matrix morphogenesis, and the self-assembly of the macromolecules in the extracellular space would occur, in part, because suitably interactive molecules were deposited at the correct morphogenetic site at the appropriate time' (Trelstad *et al.*, 1974).

Human Cornea

In a study of the human fetus of 5 to 9 months gestation, Breen *et al.* (1972) compared the appearance of the different GAG's in skin, sclera and cornea. In the human the differentiation of these tissues is virtually complete at 5 months, and after this the skin, for example, becomes more compact, and this is associated with a decrease in hyaluronic acid and an increase in sulphated GAG (dermatan sulphate). In the sclera there was very little change in the amounts of GAG's, the much tighter packing of collagen being associated with the presence of dermatan sulphate and some chondroitin sulphate. In the fetal cornea there was a striking change in the total GAG's by 33% at 7 months, when it remained constant. In general, the main change from early fetal to newborn and adult was the increased proportion of keratan sulphate together with chondroitin.

Corneo-scleral Transition Zone

The cornea and sclera differ markedly in structure and in glycosaminoglycan composition, as we have seen; it is therefore of interest to study the topographical variation in composition on moving from corneal centre to the limbus and sclera. Berscheding *et al.* (1975) analysed the acidic glycosaminoglycans in cornea and sclera at successive distances from the corneal centre, and found, as with corneal diameter that the major areas of transition lay between central and peripheral cornea and between corneolimbus and sclerolimbus; in both cases the decrease in ordered arrangement and increase in size of collagen fibrils (Fig. 3.3) coincided with decreases in the concentration of keratan sulphate and the appearance of more highly sulphated galactosaminoglycans (chondroitin sulphate and dermatan sulphate). Thus chondroitin is found primarily in the central cornea, and chondroitin sulphate in the periphery (Fig. 3.5), possibly because the central cornea is unable to derive sufficient sulphate to convert the precursor, chondroitin, to the sulphated form.

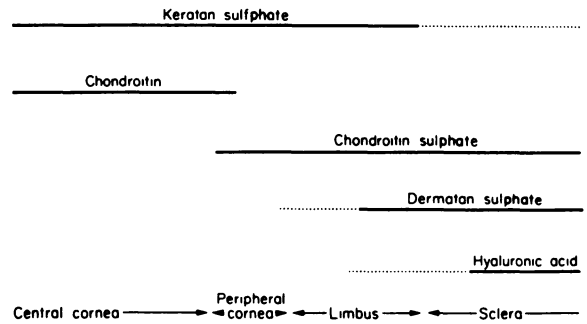

Fig. 3.5 Distribution of acidic glycosaminoglycans from mid-cornea to sclera in the human eye. Dotted line indicates presence of detectable quantities. (Berscheding *et al.*, *Exp. Eye Res.*)

The Glycosaminoglycan Coat

It seems unlikely that the corneal collagen fibrils are held apart by covalently bound cross-linkages (Hodson, 1971) although ruthenium red-stainable filaments are seen between collagen fibrils of many other connective tissues, such as aorta (Myers *et al.*, 1973). As Berscheding *et al.* point out, however, the mere presence of a coating of a proteoglycan containing acidic glycosaminoglycans, especially the highly negatively charged keratan sulphate, might be sufficient. Their protein cores would orientate themselves perpendicular to the long axis of the collagen fibre, like bristles on a brush, so as to create a negative field around each fibre that would maintain the spatial separation; the greater negative charges of chondroitin sulphate in peripheral cornea would increase the interfibre distance. Sclera, in contrast to cornea, contains less proteoglycan of different type, molecular size and shape, and thus a different arrangement of fibres is achieved.

Collagen Types

In the mature cow the proportions of Types I, V, and III are 84.7%:15.3%:1%, so that Type I is the dominant collagen. The types were evenly distributed from centre to limbus, and throughout the depth except for a higher proportion of Type III in Bowman's layer and Type IV in Descemet's membrane (Lee & Davison, 1984). The presence of Type V was demonstrated by Linsenmayer *et al.* (1984), as revealed by a monoclonal antibody technique, but, except in Bowman's membrane, it is in a masked form, in the sense that it can be revealed by acid treatment; its chain basis is ($1V\alpha_2 2V\alpha_1$) and it is synthesized by corneal fibroblasts. The presence of a high proportion of Type V is an unusual feature of a connective tissue, and Birk *et al.* (1986) have suggested that it is concerned in restricting the thickness of the fibres. Itself, it can form thin 22 nm filaments, so it might be used to anchor the limiting membranes, epithelium and endothelium, to their collagen substrates.[4]

Development

The earliest collagen formed in the primary stroma is Type I, but later Type II appears. With the invasion by fibroblasts to produce the secondary stroma, the collagen produced is mostly Type I; Type II persists in the subepithelial and subendothelial stromas. Type IV, typically found in basement membranes, is under the epithelium and endothelium. Lee & Davison (1984) found a progressive decrease in the proportion of Type I to Type V in fetal calves. Thus at 3 months the proportions were: Type I 86.7%, Type V 8.8%, Type III 4.5%. At term the proportions were 89.8%:10.2%:1%. In the mature animal they were those indicated above.

Descemet's Membrane

Because of its special function as a basal lamina, the study of Descemet's membrane collagen has attracted a lot of interest with some conflicting results, partly due to species differences and probably, too, to different methods of analysis, and to the circumstance that the material produced by cultured endothelium, used often as starting material, may not be identical with that produced *in vivo*, i.e. the gene expressing the synthesis of the peptide chains may not be phenotypically stable (Kenney, *et al.*, 1981). Thus Labermeier & Kenney (1983) found no Type III collagen in bovine Descemet's membrane, separated from the cornea, whereas cultured bovine endothelium produces, apparently, Type III and also Type I (Teng *et al.*, 1981) with very little Types IV and V. The collagen, described by Labermeier & Kenney (1983) from *in vivo* synthesized Descemet's membrane, contained Type IV and EC collagens, similar to the situation in rabbit.[5]

HYDRATION AND TRANSPARENCY

Swelling

If an excised eye is kept at, say, 4°C in the refrigerator for 24 hours or more the cornea will be seen to have lost some of its transparency, becoming 'smoky' in appearance; associated with this optical change there is found an increase in thickness due to absorption of aqueous humour. Thus, with an ox eye, there is an increase of water-content from 77.3 to 82%. Expressed in this way the increase in water-content is not impressive, but expressed as the amount of water per gramme of solid matter the increase is from 3.4 g H_2O/g solids to 4.55 g/g, i.e. an increase of 33%. The increase in water is associated with an increase in the salt content and corresponds to an uptake of aqueous humour rather than the selective absorption of water (Davson, 1949). If an excised cornea is placed in saline the same increase in water-content, with absorption of salt, is observed; if the epithelium is removed the uptake is just the same, if somewhat more rapid, so that it is clear that we are dealing with an increased hydration of the stroma, which is behaving similarly to many of the inanimate gels studied by the colloid chemists; like these gels the cornea shows a swelling pressure, which may be measured by exerting a contrary pressure to prevent uptake of fluid; it amounts to 75 to 85 g/cm^2 in the normal cornea; as the cornea takes up water, the pressure it can exert decreases, whilst it increases as water is withdrawn (see, for example, Fatt & Hedbys, 1970).

Effect of Temperature

This uptake of fluid by the dead cornea, and its associated loss of transparency, was considered by Cogan & Kinsey (1942) to result from the removal of the normal osmotic pressures of tears and aqueous humour that were supposed, in the living eye, to remove water continuously from the cornea as fast as it entered. In the first edition of this book the present author showed the theoretical inadequacy of this model and subsequent experimental studies have confirmed this criticism. Thus, to quote a crucial experiment, on the basis of the Cogan–Kinsey theory the swelling of the dead cornea should be much more rapid and extensive if the eye were kept at body-temperature than in the refrigerator, yet if the two eyes of a rabbit are excised and the one is kept at 4°C and the other in a moist chamber at the normal temperature of the aqueous humour, namely 31°C, it is found that the eye kept in the warm is almost completely normal, with good transparency, and water-content only slightly different from the average normal figure. Clearly, by cooling the eye we are robbing the corneal tissue of its power of excluding fluid, and this is presumably due to reducing the metabolism of the eye. In other words, the cornea is probably using metabolic energy to resist the intrusion of fluid from the aqueous humour To understand the factors concerned, let us turn now to the fluid and salt relationships between cornea, on the one hand, and aqueous humour and tears on the other (Davson, 1955).

Stroma-Aqueous Humour-Tears

Analysis of the salt content of the cornea and aqueous humour suggests the simple Gibbs–Donnan type of equilibrium between the stroma and the outside fluids, the stroma containing a high concentration of ionized colloid and being separated from the outside fluids, aqueous humour and tears, by membranes that allow movements of ions and water but not of the colloid. To quote Otori's (1967) figures for the rabbit, the concentrations of Na^+, K^+, and Cl^- in meq/kg H_2O are as follows:

	Aqueous humour	*Stroma*
Na^+	144.0	171
K^+	4.9	22
Cl^-	103.0	108

The high concentration of K^+ in the stroma is doubtless due to the presence of keratocytes, whilst the high concentration of Na^+ is presumably due to the presence of ionized collagen and mucopolysaccharide; on this basis, it is to be remarked, however, that the concentration of Cl^- should be lower in the stroma than in the aqueous humour, and it may be that the bicarbonate ion is not at equilibrium (Hodson, 1971).

Swelling Tendency

The general picture of the relationships between the corneal stroma and the aqueous humour and tears is illustrated schematically in Fig. 3.6. The stroma, being a mixture of collagen and its associated mucopolysaccharides, may be treated as a gel, and largely by virtue of the polysaccharide this gel has a tendency to take up water.[6] It is separated from the two fluids from which this water is obtainable by membranes, the epithelium and endothelium. These membranes are permeable to salts and water (Maurice, 1951) so that the swelling tendency of the gel must be resisted by some active process on the part of either the endothelium or epithelium or both. Removal of the epithelium or endothelium in the intact eye causes a rapid uptake of fluid (Maurice & Giardini, 1951). As Fig. 3.6 indicates, at the limbus the stroma may take up fluid and salts from the pericorneal capillary plexus, since there is no reason to believe that there would not be filtration from these capillaries as in other parts of the body.

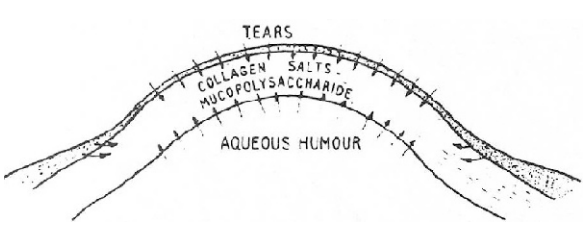

Fig. 3.6 Illustrating the tendency for the stroma of the cornea to hydrate by virtue of the inward movement of water and salts from aqueous humour, tears and limbal capillaries.

SWELLING PRESSURE

This may be defined as the pressure that must be exerted on the cornea to prevent it from increasing in volume when placed in saline; studies on experimental animal corneas agree on a value of some 75–85 $g\,cm^{-2}$; as the cornea swells this pressure falls. Olsen & Sperling (1987) working on human material found a linear relation between the logarithm of corneal thickness and swelling pressure. Their mean value at normal thickness was some 88 mmHg.[7]

Reversal of Swelling

If the cornea of the excised eye is allowed to swell by keeping it for some time at 4°C, the process may be reversed by transferring the eye now to a moist chamber at 31°C (Davson, 1955) so that either the epithelium or endothelium has actively removed the salts and water that entered at the low temperature. Harris & Nordquist (1955) showed that this 'temperature-reversal effect' would still occur when the epithelium was removed, so that the 'pump' that removes fluid as it enters must be located in the endothelium. More recent studies have confirmed the importance of the endothelium; e.g. Green & Otori (1970) showed that the isolated cornea swelled up rapidly on removal of the endothelium, although when the endothelium was intact it could be maintained at normal thickness for hours provided glucose was in the incubation medium.

Again, if a layer of plastic is implanted intralaminarly, it is the region *above* the implant that becomes oedematous whilst that below retains its normal thickness. Finally, Doane & Dohlman (1970) have actually maintained the cornea *in vivo* at normal thickness after total removal of the epithelium by sealing a plastic contact lens over the denuded surface. Maurice & Giardini had shown that removal of the epithelium caused a rapid increase in thickness of the cornea, and the fact that this does not occur when the surface is sealed means that an intact epithelium is important largely or only because it restrains the passive influx of salts and water from the tears and the limbal blood vessels, i.e. the influx becomes too great for the endothelium to deal with.

Active Process

As to the nature of the active process, it was early assumed that this could be achieved by the active transport of sodium from stroma to aqueous humour across

the endothelial membrane, or from stroma to tears across the epithelium. The salt so transferred would carry with it its osmotic equivalent of water. Such an active transport, if it occurred, should be detectable by modern isotopic methods in which the fluxes of ^{24}Na are measured together with the potential across the cornea.

The Potential

The potential between the tears and the aqueous humour sides of the cornea may be measured in the excised tissue using the cornea to separate two chambers of fluid containing electrodes, as in the Ussing technique (Fig. 1.34), or it may be measured *in vivo* as the difference in potential between an electrode on the surface of the cornea and another dipping, say, in a pool of saline in the animal's ear, which makes effective electrical contact with the inside of the eye by way of the blood. In the isolated corneal system, Donn *et al.* (1959) found a potential of some 10 to 40 mV, the tears-side being negative to the aqueous humour-side, and similar potentials were found *in vivo* by Potts & Modrell (1957) and Maurice (1967). By splitting the cornea so that the potential across the epithelium alone could be measured, or by inserting a micro-electrode through the epithelium into the subjacent stroma, it was found that this trans-epithelial *potential* was the same, within experimental error, as the total transcorneal potential; thus the stroma appeared to be at the same potential as the aqueous humour (Fig. 3.13). As we shall see, however, there is a significant difference of potential between the stroma and the aqueous humour, but small enough to escape measurement in this earlier work.

Active Transport

A potential of this polarity, with the stroma positive, would suggest an active transport of Na^+ from tears into the stroma, associated with a passive influx of negative ions; alternatively the potential could be the manifestation of an active transport of Cl^- or HCO_3^- out of the stroma into the tears, associated with passive flux of Na^+. In the latter event the active process might represent the salt-pump driving salt out of the stroma and as a consequence of the associated flow of water to maintain isotonicity, helping to maintain the cornea in its normal state of hydration. An active transport of Na^+ in the opposite direction would, on the other hand, contribute to corneal hydration and so be valueless as a fluid-pump. In fact, Donn *et al.* found that the measured fluxes of isotopic Na^+ indicated an active transport of this ion *into* the cornea, so that, in the rabbit at any rate, we must look to the endothelium for an active transport mechanism that would constitute the basis for the fluid-pump.[8]

The Endothelial Pump

Maurice (1972) allowed a rabbit's cornea to swell by cooling for a definite period; after this, it was mounted in such a way that the aqueous humour-side could be perfused with an artificial aqueous humour[9] whilst the epithelial side, after denuding it of epithelium, was covered with oil. In spite of the absence of epithelium, the cornea lost fluid to the perfusing fluid and returned to its normal thickness (Fig. 3.7). An estimate of the rate of transport of fluid out of the swollen stroma was obtained by covering the outer—epithelium-denuded—surface of the cornea with a layer of artificial aqueous humour and placing above this a layer of silicone oil, as in Fig. 3.8; the cornea, during its deturgescence, removes fluid from its stroma into the artificial aqueous humour and this is replaced by fluid from above, and the decrease in thickness of the layer of fluid can be measured with a microscope. A value of 5.0 μl/hr/cm^2 was found, and this occurred against a positive pressure in the artificial aqueous humour, and so must have resulted from an active transport of salt followed by water across the endothelium. The rate of transport was such that each endothelial cell was actually transporting its own volume every 5 minutes. When the cornea is treated with ouabain, which specifically inhibits active transport of Na^+, it is found to swell (Trenberth & Mishima, 1968) the rate of

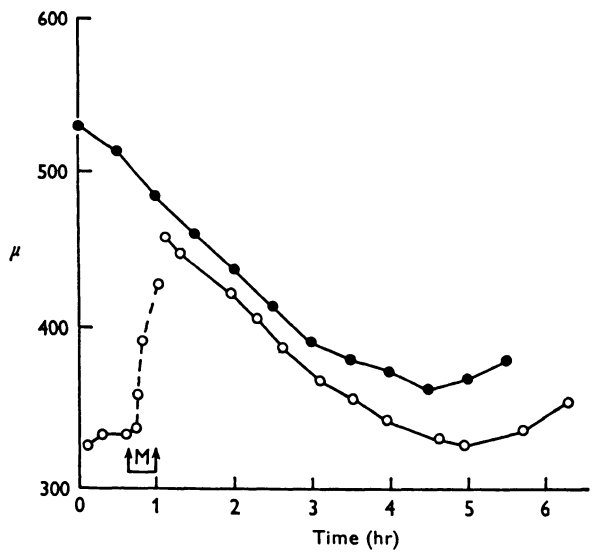

Fig. 3.7 Thinning of a cornea in the absence of epithelium. Open circles: cornea, without epithelium, swollen by application of perfusion fluid to bare surface of cornea at time M, first arrow. At second arrow perfusion fluid replaced by oil. Filled circles: temperature reversal of intact second eye of pair on next day. Vertical displacement of curves corresponds to thickness of scraped-off epithelial layer, 40 μm (Maurice *J. Physiol.*)

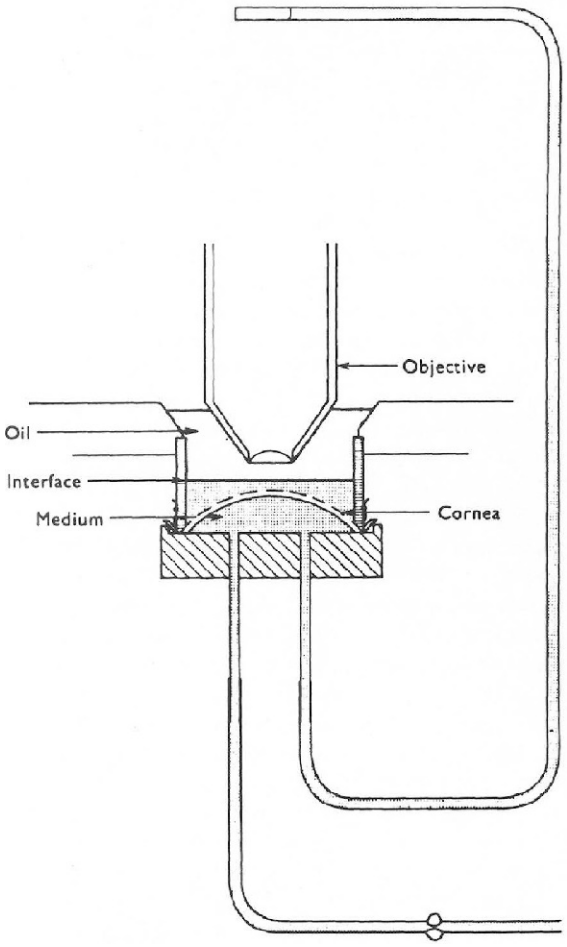

Fig. 3.8 Method of determining flux of fluid across corneal endothelium. The cornea is mounted after the removal of its epithelium and is just covered with the same medium that bathes its inner surface. A thick covering of silicone oil is then poured over the watery layer. Fluid movement is determined by focusing the microscope in turn on the oil–water interface and on the endothelial surface. (Maurice, *J. Physiol.*)

increase in thickness being some 45 μm/hr; the rate of fluid movement measured by Maurice corresponded to an ability to thin the cornea at a rate of 60 μm/hr, indicating that the active pump, before being inhibited, was capable of maintaining the cornea in its normal state, pumping fluid out as fast as it entered passively from the tears.

Endothelial Active Transport

The transport of water in biological systems requires the transport of solute, usually a salt, as a primary step, the water following passively along osmotic gradients. Thus modern work has been concerned with the nature of the solute that must be actively transported out of the stroma, and the possibility that this transport gives rise to a difference of potential between stroma and aqueous humour. As we have seen, the transcorneal potential, i.e. that across tears to aqueous humour, is quantitatively equal to the transepithelial potential, i.e. that between tears and stroma, so that any difference of potential between stroma and aqueous humour, i.e. across the endothelium, must be smaller than the experimental error in the studies.

ENDOTHELIAL POTENTIAL

However, Fischbarg (1972) found a consistent potential across the endothelium, the aqueous humour side being negative by some 500 μV, and subsequent studies have confirmed this; for example Lim & Ussing (1982) found a value of 0.76 ± 0.03 mV; when adenosine is added to the medium the potential is consistently higher at about 1 mV. The potential is reduced to zero by ouabain, indicating that its source is an active Na^+-K^+-ATPase mediated pump; if it is to make the stroma positive in respect to aqueous humour, then the Na^+ must be directed towards this medium; i.e. the active transport of Na^+ must be working against the salt transport process that is driving salt and water out of the stroma into the aqueous humour.[10] Now there is no doubt that, in its normal state, there is a net flux of sodium from stroma into aqueous humour; this was firmly established by Lim & Ussing (1982); it amounted to 2.3 ± 0.04 μeq cm^{-2} hr^{-1}, a flux that would account for the flow of water out of the stroma. This was not accompanied by a net flux of Cl^-, but Hull *et al.* (1977) measured a net flux of HCO_3^- in the same direction, about equal to that of Na^+. We are thus confronted with two active processes, both involving Na^+, but working in opposite directions across the endothelial cell. If we assume that the pump driving Na^+ into the stroma is creating the measured potential, whilst the pump driving Na^+ out is non-electrogenic, the transport of Na^+ and HCO_3^- being 'coupled' in some way, then we have a clear picture of the main events taking place across the endothelium (Fig. 3.9); the potential is abolished by ouabain because the pump facing the stroma is ATPase-dependent and is responsible for the whole potential. Diamox reduces the potential by about 30%, presumably by interfering with anion transport; thus an impediment to the HCO_3^--ion, as it accompanies the Na^+ secreted from stroma to aqueous humour, would make this pump electrogenic, creating a positivity in the aqueous humour that would tend to cancel out the positivity of the stroma-facing ouabain-sensitive pump.

OSMOLALITY OF TRANSPORTED FLUID

All the evidence indicates that the fluid entering the cornea, when it swells, is isotonic; and the same is true for that expelled by the endothelial pump, so that for each

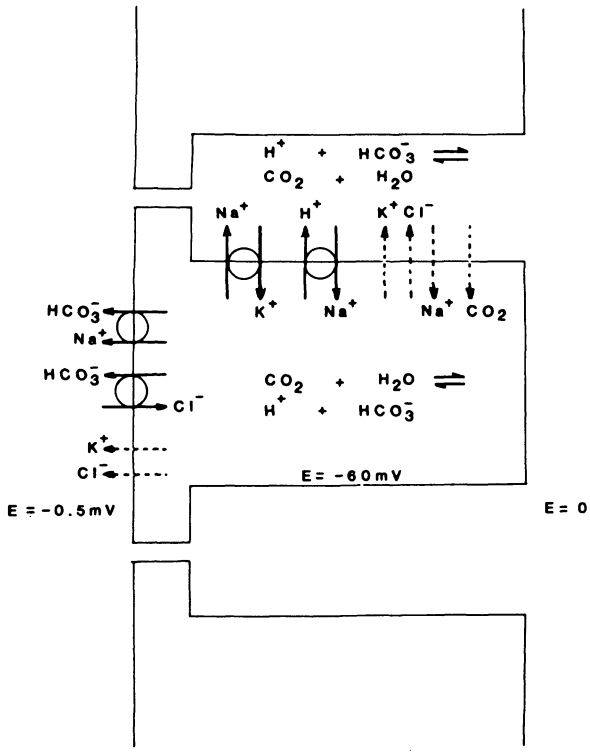

Fig. 3.9 Possible ionic transport mechanisms across the apical and basolateral membranes of the corneal endothelium. Solid lines represent either active transport or coupled movements. Dashed lines represent passive movements. Electrogenic effects could arise from the activity of the Na^+ pump shown at the lateral membrane and the bicarbonate sodium symport shown at the apical membrane. (Fischbarg & Lim, *Curr. Topics Eye Res.*)

equivalent of ions transported, water must be transported with it to maintain a fixed isotonic concentration. We have encountered the same problem with the formation of aqueous humour; and the general mechanisms whereby a membrane may transport a salt and allow water to follow so rapidly that the osmotic pressure-difference, driving it, is immediately dissipated, have been discussed by general physiologists for a long time (Diamond & Bossert, 1967). In general, the measured permeability of the transporting membrane to water appears too small to allow this to happen, if transport of both ions and water occurs at the same site. The standing gradient hypothesis of Diamond & Bossert represents a model to avoid this difficulty, salt being transported into or out of the intercellular clefts of the transporting epithelium or endothelium. Simply on the basis of the measured permeabilities of the corneal endothelium to ions and water, Lim & Ussing (1982) concluded that the transported fluid would have to be hypertonic (see also Fischbarg & Lim, 1984). However Hodson & Wigham (1983) and Hodson & Lawton (1987) have shown that the permeability of the corneal endothelium to water is very much higher than originally thought, whilst that to ions, such as Na^+ and Cl^-, is very low.

MEMBRANE RESISTANCE

Thus, to consider the ions first, the endothelium as a whole has been described as 'leaky' with a low electrical resistance of some 12–13 ohm cm^2, suggesting a relatively high permeability to ions; and this might be expected of a cellular sheet lacking tight junctions sealing intercellular clefts. However, by measuring the electrical resistance across an individual cell membrane, this was found to be so high that a resistance of the whole membrane would have been 1300 ohm cm^2, instead of 12–13 as found. Thus the resistance must have been confined to the intercellular clefts, and only if 99% of transport occurred by this paracellular route, could the low resistance be explained, the ions passing through narrow channels not completely sealed by tight junctions (p. 29) but instead having gap-type constrictions of 2 nm diameter and thus very large compared with ionic diameters. By contrast, the permeability to water, measured either by transport of ^3H_2O, or by the bulk flow under an osmotic gradient, was very high, because water penetrated across the cells as well as through the clefts. Thus the reflexion coefficient, which is governed by the relative permeabilities of ions and water, is effectively unity, and means that for every equivalent of ions transported water will be transported to give an isotonic fluid. Thus transport of water out of the cornea by the endothelium is a highly efficient process in spite of the leakiness of its intercellular clefts, the actively transported ions being accompanied by the isotonic equivalent of water. Hence the net flux of salt measured should be also a measure of the transport of water.[11]

Relation of Fluid Transport to Potential

Hodson (1971) showed that the fluid-pump required, for its full activity in maintaining the cornea dehydrated, the presence of Na^+ and HCO_3^-, and subsequent studies, in which the fluid-transporting capacity of the endothelium was compared with the electrical or ionic-pump characteristics, have shown a remarkably good correlation which definitely implicates the potential, or rather the ionic movements that create it, with the fluid-transport. For example Fig. 3.10 compares the effects of reducing the concentration of Na^+ on the transendothelial potential and on the rate of fluid transport respectively. As a result of a thorough study of fluid transport and potential, Fischbarg & Lim (1974) constructed Table 3.1; it will be seen that the carbonic anhydrase inhibitors tended to block fluid-transport, just as with the aqueous humour, but they failed to influence the potential, suggesting that

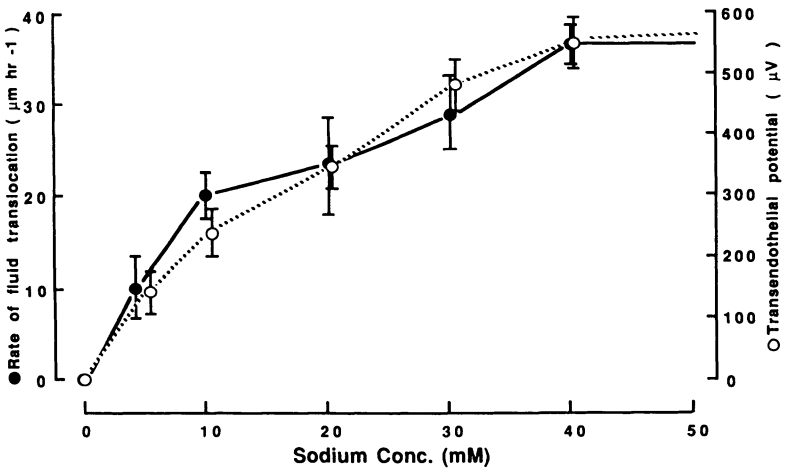

Fig. 3.10 Transendothelial potential (○—○) and rate of fluid translocation (●—●) as a function of sodium concentration in the bathing medium. (After Hodson, *J. Physiol.*)

Table 3.1 Relation between potential difference across endothelium and fluid transport (Fischbarg & Lim, 1974)

Factor	*Effect on p.d.*	*Effect on fluid transport*
$[HCO_3]$ decrease	Reversibly decreased following behaviour similar to that of fluid pump	Decreases or arrests; reversibly decreases
$[Na^+]$ decrease	Reversibly decreases	Arrests
K^+ absence	Reversibly decreases	Reversibly arrests
$[H^+]$ increase	Reversibly decreases	Arrests
Temperature decrease	Decreases	Arrests
Ouabain	Abolishes	Arrests
Carbonic anhydrase inhibitors	No effect	Reduces by half; reduces
Cyanide	Abolishes	Arrests
Iodoacetate	Abolishes	Arrests
Cytochalasin B	Reversibly decreases	Arrests?

the electrogenic stage in the pumping process preceded another stage that could be promoted by carbonic anhydrase and presumably involved hydration of CO_2. Fischbarg & Lim were reluctant to suggest a simple anion-pump, e.g. one based on active transport of bicarbonate linked to that of Na^+, since total removal of bicarbonate, although it abolished fluid-transport, left a residual potential; so they suggested a model requiring secretion of H^+-ions as well as active transport of Na^+ by an ouabain-sensitive mechanism.

Green *et al.* (1981) found that reduction of the Na^+ in the medium reduced net transport of bicarbonate across the rabbit endothelium, whereas there was no chloride dependence. These results, according to them, add support to the thesis that sodium and bicarbonate transport are closely linked to fluid movement. Interestingly, carbonic anhydrase addition to the medium enhanced bicarbonate transport, perhaps by maintaining a high level of bicarbonate in the unstirred layer of fluid immediately adjacent to the endothelium. This would, of course, explain the influence of carbonic anhydrase inhibitors on bicarbonate transport and potential.[12]

POTENTIAL AND WATER-FLUX

Barfort & Maurice (1974) measured transendothelial potential and water-flux in the excised cornea simultaneously and were thus able to correlate the two more accurately; as Fig. 3.11 shows, there is a positive correlation between the magnitude of the potential and water-flux; and it is interesting that the potential measured by these authors was larger, from 0.6 to 1.7 mV with a median of 1.3 mV. As Fischbarg (1973) had found, the correlation extended to the effects of various inhibitors, including cooling, ouabain and antimycin, the blocking of fluid transport being accompanied by reduction of the potential to zero. These authors have discussed in some

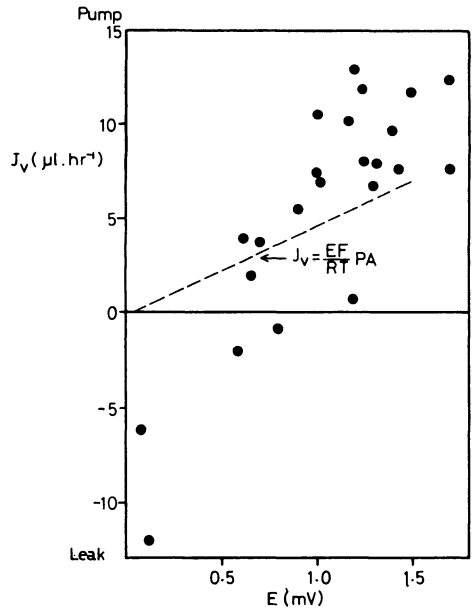

Fig. 3.11 Illustrating correlation between magnitude of potential, E, across the corneal endothelium, and the magnitude of the water-flux, 'Pump' and 'Leak' represent water-flow against and with hydrostatic gradient. The line represents the flow when there is maximal coupling between ion pump and water. (Barfort & Maurice, *Exp. Eye. Res.*)

detail the way in which this potential could cause, or reflect, fluid transport.

Temperature Fluctuations

The cornea can undergo much larger fluctuations in temperature than those in deeper structures of the eye. Hodson (1975) has discussed the effects of temperature on the corneal system; a lowering of temperature decreases the efficiency of the endothelial pump; and this is seen by the slower rate of thinning of a previously swollen cornea when the temperature is reduced from 35°C to 25°C, but the same final condition of normal turgescence is reached. To compensate for the reduced pumping capacity we have the reduced tendency for the corneal stroma to swell, due to the lowered permeability of the endothelium to ions.

Hibernation

An extreme example of the response to lowered corneal temperature is given by the hibernating animal. Bito *et al.* (1973) have drawn attention to the normal state of hydration of the hibernating wood-chuck in spite of its corneal temperature being maintained at 9.4°C for days on end; moreover, if the enucleated eyes are maintained at this temperature in a moist chamber, they increase their hydration in the same way that rabbit corneas do. Working on the frog, however, Bito & Saraf (1973) did find considerable swelling when it was maintained at 0°C. Klyce & Russell (1979), however, consider that these effects of cold may be interpreted on the basis of the endothelial pump; they applied their theoretical equations to the situation, taking probable values for the temperature coefficients of the kinetic processes as well as of the energy-supplying metabolism. They calculated that for the marmot the increase in the thickness would be only 17%, a change that might not have been noticed. Comparisons with the excised eye they consider are not necessarily valid when quantitative considerations are concerned.

Corneal ATPase

Active transport of Na^+ across cell membranes is usually inhibited by ouabain, which acts by inhibiting an enzyme that specifically hydrolyses ATP in the presence of appropriate proportions of Na^+ and K^+ and Mg^{2+}; it is generally referred to as a Na^+-K^+-activated ATPase. The enzyme's localization can be revealed by histochemical techniques, since fixation of the tissue does not inhibit the enzyme, but as Tervo & Palkama (1975) have emphasized in their study of the corneal enzyme, great care must be employed to avoid spurious results. According to these authors, who have summarized earlier studies, both corneal epithelium and endothelium of the rat contain the enzyme in association with their cell membranes; in the epithelium the enzyme was located on the membranes, especially those of the basal cells in the region of their interdigitations, the surfaces facing the basement membrane being unstained. Similarly, the endothelial cell membranes were stained in the region of lateral cell apposition, the anterior and posterior faces being free from reaction-product (Fig. 3.12).

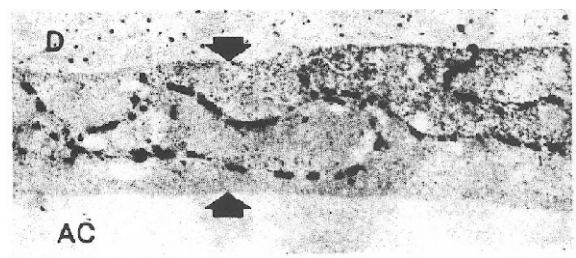

Fig. 3.12 Na-K-ATPase reaction in the corneal endothelium. Note that the enzyme activity is located mainly in the adjoining cell membranes. On the other hand, no activity can be seen on those parts of the cell membrane that face either Descemet's membrane (D) or the anterior chamber (AC) (arrows) (× 11 340). (Tervo & Palkama, *Exp. Eye Res.*)

More recently Geroski & Edelhauser (1984) have measured the density of 'pump-sites' from the uptake of labelled ouabain by the endothelium; some 20.7 fmoles were taken up per mm^2 of cell surface, corresponding to 3×10^6 sites per cell. Estimates of the area of the lateral cell membranes indicated that this was much greater than the minimum required to accommodate these sites.

Activity of the Epithelium

The initial observations of the effects of stripping the epithelium from the cornea on its subsequent hydration suggested that the epithelium was responsible for the water-pump (Maurice & Giardini, 1951; Davson, 1955). As we have seen, however, Donn *et al.* (1959) demonstrated a transport of Na^+ into the stroma rather than out of it.

Amphibian Cornea

In the amphibian, nevertheless, Zadunaisky (1966, 1969) measured a potential between tears and aqueous humour of 10 to 60 mV, the aqueous humour being positive; this was due to the active transport of Cl^- from stroma to tears and could be abolished by removing this ion from the cornea. By splitting the cornea, the separate effects of epithelium and endothelium could be examined, and in this case it was the epithelium that reproduced the behaviour of the whole cornea. There was no evidence for active transport by the endothelium. When the transparency had been allowed to decrease by imbibition of fluid at a low temperature, the partial reversal of this by warming was accompanied by enhanced active transport of Cl^-; moreover the temperature-reversal effect was prevented by substitution of Cl^- by SO_4^{2-}, and this also blocked the short-circuit current (Zadunaisky *et al.*, 1971). Bromide would substitute for Cl^- but not iodide.

Furosemide, a typical inhibitor of active chloride transport in the kidney, inhibited the frog's corneal chloride-pump when applied to the endothelial side (Candia, 1973). The existence of a Na^+-pump, transporting this ion from epithelium to stroma, as in the rabbit, was demonstrated by Candia & Askew (1968); its contribution to the total short-circuit current was only 10%.

Rabbit

Klyce *et al.* (1973) found that epinephrine and theophylline placed on the isolated rabbit corneal epithelium caused a rapid rise in short-circuit current; the current itself they interpreted as an expression of an active chloride-pump contributing to, and dominating, the transepithelial potential causing, by the inward movement of this ion, the tears to become positive in relation to stroma (p. 118). The rise in short-circuit current was accompanied by an increase in net transport of Cl^- from the tears to stromal side; there was no effect of the drugs in a Cl^--free medium. A rise in short-circuit current was also caused by cAMP and DBcAMP, which was reflected in an increase in net transport of Cl^- to the tears side of the epithelium. Removal of Cl^- from the medium prevented these changes. Topical application of 2% epinephrine to the cornea decreases the density of adrenergic receptors in the cornea as measured by uptake of the radioactive ligand, ^{3}H-dihydro-alprenolol. Romero & Axelrod (1974), working on the pineal gland, had shown that, as the density of beta-adrenergic receptors decreased, so did the response to beta-adrenergic stimulation, in this case synthesis of melatonin. Candia & Neufeld (1978) found that this loss of receptors was associated with a complete loss of the ability of the cornea to respond to epinephrine with increased chloride-transport.[13]

ANION-PUMP AND CORNEAL THINNING

That this chloride-pump can contribute to corneal thinning was shown by Klyce (1975), using a cornea with endothelium removed, the endothelial side of the stroma being bathed with silicone oil; a swollen cornea treated in this manner showed some thinning, due to the intact epithelium, and this was increased by theophylline, the rate being predictable from the rate of salt transport. Klyce considered that under normal conditions the two epithelial pumps balanced each other; theophylline, by accelerating the Cl^--pump and leaving the Na^+-pump unaffected, would cause net transport of salt and fluid out of the cornea and promote thinning.

The Epithelial Potential Profile

By moving a micro-electrode from the tears into the epithelium by steps of a few microns at a time, the potential between the tears and successive depths of epithelium and stroma may be measured. Figure 3.13 shows the results of a study by Klyce (1972) where A is a schematic outline of the structural make-up of the epithelium with the important transition points indicated, and B gives the potential, *referred to the stroma as zero*, at successive depths. C indicates the changes of resistance at critical sites. The total transcorneal potential is V_c and here represents the potential between stroma and tears, i.e. before the micro-electrode has penetrated; in this example it is about 15 mV negative in respect to the stroma. On penetrating the squamous cell, *s*, there is a jump of negativity corresponding to the resting potential of the squamous cell, and this is indicated by V_s, the membrane potential of the outer membrane of the squamous cell. On pushing the electrode further into the

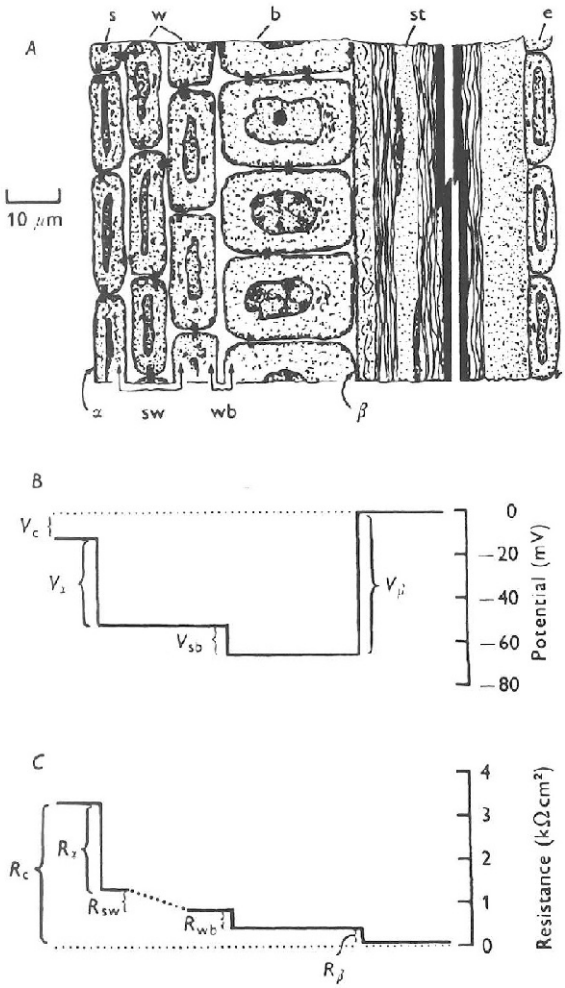

Fig. 3.13 (A) Schematic illustration of the cornea showing the epithelium, a portion of the stroma (st) and the endothelium (e). On the basis of the dye study, the following regions in the electrical profiles were identified: α, the outer membrane of the squamous cell; β, the inner membrane of the basal (b) cell; sw, the region between squamous (s) and wing (w) cells; and wb, the transition region between wing and basal cells. (B) The average potential profile for the epithelium. The extracellular gradient in potential from the sub-epithelial stroma to the aqueous humour was less than 1 mV. (C) The average resistance profile for the epithelium. The stroma and endothelium contributed only a few per cent to total corneal resistance. (Klyce, *J. Physiol.*)

epithelium, no significant change occurs until the space (*wb*), separating the inner wing cell (*w*) and the basal cell (*b*), has been crossed and the electrode has entered the basal cell. There is then a further increase in negativity, V_{sb}, and now the maximal negativity has been reached so that further movement through the basal cell produces no change. When the stroma-facing membrane of the basal cell has been penetrated, the potential swings to zero—the stromal potential—which is positive in relation to the tears. Approximately, then, the corneal potential can be described as that of a giant cell with tears-facing membrane, α, and stroma-facing membrane, β, but the transition between the wing cell and basal cell shows that coupling between these cells is not perfect, by contrast with that between squamous and wing cells; and this is indicated by the resistance-profiles of Fig. 3.13C.

PERMEABILITY

The general problem of the permeability of the cornea to different solutes is a matter of considerable clinical interest, since it is the cornea (and to some extent the sclera) that must be crossed in order that topically applied drugs reach their target tissues and build up an adequate concentration in the face of losses that will occur by drainage of aqueous humour back into the blood, and uptake into the vascular system of the anterior uvea, and loss by flow of tears. The subject has been reviewed by Mishima (1981) under the general title of the 'pharmacokinetics of the eye'.

General Considerations

The membranes separating the stroma from its surrounding media are formed by layers of closely packed cells; lipid-soluble substances may be expected to pass easily into the cornea because they may pass easily into and out of the cells of these membranes; lipid-insoluble substances, including ions, may be expected to penetrate with difficulty; moreover, the endothelium, with its single layer of cells, might be expected to be the more permeable membrane.

Tight Junctions

However, the essential factor in permeability of such cellular layers is the extent to which the intercellular clefts are closed by zonulae occludentes or tight-junctions. If these clefts, or the majority of them, are not closed by the fusion of adjacent membranes, we may expect a high degree of permeability extending to such large molecules as inulin and serum albumin, and this permeability will be relatively unselective because the large diameter of the intercellular clefts will not permit any selective sieve action on the various solutes commonly studied. In general, the qualitative studies of Swan & White (1942), and Cogan & Hirsch (1944) confirm these general principles. Where the substance is an organic base or acid, such as atropine or salicylic acid, the degree of dissociation is an important factor since the undissociated molecule

penetrates more rapidly than the ion; hence the permeability of the cornea to these substances is influenced by pH.

Epithelium and Endothelium

More recent quantitative measurements, carried out mainly by Maurice, Mishima & Trenberth, and by Thoft and his collaborators, have allowed separate estimates of the permeabilities of the epithelium and endothelium. Thus *in vivo* Maurice (1951) showed that the endothelium was 100 times more permeable to the Na^+-ion than the epithelium; this does not mean that the endothelium offers no restraint to the passage of this ion, however; it means, rather, that the permeability of the epithelium is very low, so that for many practical purposes the epithelium may be treated as a 'semipermeable membrane', being permeable to water but effectively impermeable to the solutes of the tears. Maurice (1969) has calculated that, with Na^+, the endothelium offers some 1700 times the resistance to diffusion than would be offered by the same thickness of water; with sucrose it was 2000 times, with fluorescein, 4200, inulin 4400 and serum albumin greater than 100 000.

Thoft & Friend (1975) studied an amino acid analogue, α-aminoisobutyric acid (AIB), a non-metabolizable sugar, 3-0-methylglucose, and mannitol. The calculated epithelial permeabilities were 0.000 97, 0.0013 and 0.0015 cm/hr respectively; these values are equivalent to about 3.10^{-7} cm/sec, which are rather higher than the 1.10^{-7} cm/sec obtained by Maurice in his study. Freshly regenerated epithelium had rather higher permeabilities, 0.0044, 0.0021 and 0.0025 cm/hr respectively. As Maurice had found, endothelial permeability was some 100 times greater, values of 0.36, 0.17 and 0.08 cm/hr being obtained; the difference between mannitol, on the one hand, and the sugar and amino acid on the other, is consistent with the notion of facilitated transport for amino acids and sugars; such a carrier mechanism would not be available for mannitol. These authors stress the extreme inefficiency of any attempt to increase available sugar or amino acid to the cornea by application to the corneal surface.

Endothelium

Kim *et al.* (1971) and Mishima & Trenberth (1968) studied the permeability of the endothelium in isolation by removing the epithelium from the excised cornea; in effect, of course, they were measuring in addition the permeability of Descemet's membrane and the stroma, but these do not impose a significant barrier to diffusion, so that the process was governed by passage across the endothelium. The results of Kim *et al.*'s study are shown in Table 3.2. In general, permeability decreased as molecular weight or radius increased, in fact a linear relation between molecular radius and permeability was found, suggesting that the passage was through large water-filled pores, such as those constituted by the gap-junctions described earlier.

Table 3.2 Permeability coefficients (cm/sec) of corneal endothelium. (Kim *et al.*, 1971)

Solute	*Permeability*	*Mol. wt*
Cl^-	2.2×10^{-5}	35·5
Mannitol	7.0×10^{-6}	182
Sucrose	4.5×10^{-6}	342
Inulin	1.1×10^{-6}	5200
Dextrin A	5.8×10^{-7}	15 000–17 000
PVP	2.9×10^{-7}	40 000–50 000
Dextrin B	8.1×10^{-8}	60 000–80 000

Facilitated Transport

Where metabolically important substances are concerned, however, permeability may be much greater than anticipated on the basis of molecular radius; thus glucose and amino acids are examples, the permeability of alpha-amino isobutyric acid being some 5×10^{-5} cm/sec, which is more than 112 times that of mannitol of comparable molecular radius (Thoft & Friend, 1972), and the same is true of glucose (Hale & Maurice, 1969). With these metabolically important substances the pathway is through the endothelial cells as well as through the gap-junctions, passage through these being significant because of the carrier-mediated facilitated transport across the cell membranes.

Water

As with practically all cellular layers, the permeabilities of epithelium and endothelium to water are large; thus for epithelium Donn *et al.* (1963) found a value of 3×10^{-5} cm/sec, comparing with 1×10^{-7} cm/sec for Na^+. The measurements of permeability to water of the endothelium have been discussed in some detail by Fischbarg & Lim (1984) in relation to the theoretical tonicity of the fluid secreted by the endothelial pump (p. 114). By refining techniques for measuring movements of the endothelial cell membrane under an osmotic gradient, Fischbarg & Montoreano (1982) estimated a value of $1420 \pm 160\ \mu m\ sec^{-1}$ for the apical membrane, and of the whole membrane about one half this. As indicated earlier, Hodson & Wigham (1983) derived a value of $1.27\ \mu m\ hr^{-1}\ mmHg^{-1}$ for the osmotic permeability, i.e. the transport in response to an osmotic gradient; they computed that the stroma, itself, offered a rather higher resistance to water-flow.

PRESSURE-FLOW

Hydraulic water permeability may be measured by the amount of fluid flowing across the endothelium under an established hydrostatic pressure; using this technique, Baum *et al.* (1984) found a linear relation, with an intercept on the flow-axis of some 68 $\mu l\,hr^{-1}$ when the line was extrapolated to zero pressure-difference, and this is approximately equal to the pump-rate of the endothelial pump. At 0°C flow is some 2.12 times less, and this can be accounted for by the increase in viscosity of water; as would be expected, the intercept is now at zero, indicating cessation of the water-pump.

Fluorescein

An accurate knowledge of the permeability of the endothelium is of value for clinical studies, and the ability to measure the concentrations of this solute in cornea and aqueous humour in the living eye has made the study of this, and other fluorescent molecules, of peculiar interest. Measurement of corneal endothelial permeability is required for assessment of the rate of flow of aqueous humour, and the subject has been discussed earlier. An important consideration is the metabolic change of fluorescein while circulating in the blood, a change that alters the molecule's fluorescence. Araie & Maurice (1983) have made a re-evaluation of previous estimates in the light of the known change in fluorescein when circulating in the blood. By substituting an intravitreal injection for systemic injection when measuring the steady-state distribution between cornea and aqueous humour, they avoided this difficulty and the correct ratio was 0.25 ± 0.06, and the permeability coefficient, $k_{c.ca}$, of the endothelium was $5.13 \pm 1.64 \times 10^{-4}\,cm\,min^{-1}$, this value being considerably greater than earlier estimates (Jones & Maurice, 1966; Coakes & Brubaker, 1979).

Pharmacokinetics

The clinician is interested in how much of a drug can be caused to enter the eye after being instilled into the conjunctival sac, a cavity with a capacity of about 7–9 μl of tears which flow away at about $1\,\mu l\,min^{-1}$. The principal factors governing availability by target tissue are the drug kinetics in the *cul-de-sac*, the permeability of the cornea, and the rate of elimination from the eye. It is not feasible in this book to give a detailed account of the theoretical and experimental studies reviewed by Mishima (1981, 1982); instead we may consider a few fundamental approaches based on the model of Fig. 3.14, the parameter $k_{c.dc}$ representing the rate of transport from tears to cornea, α the rate of loss from the tears; k_c represents rate of loss from the cornea, and C is the corneal concentration. The effective concentration in the

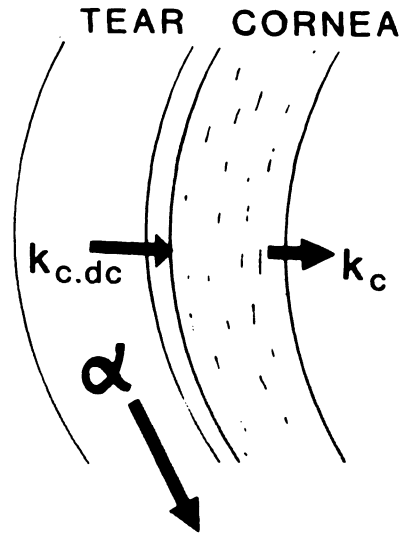

Fig. 3.14 Model of drug uptake by the cornea from the tears. For explanation of symbols, see text. (Mishima, *Invest. Ophthal.*)

tears will be that in a small stagnant precorneal tear-film (Chapter 23) some 7–9 μm thick, and its concentration will depend on blinking, a process that tends to favour drainage of the tears and thus loss of the applied drug. It is estimated that saturation of this film never occurs, so that the effective concentration of drug available to the cornea is about half that in the applied drop (Sugaya & Nagataki, 1978). Increasing the volume of the applied dose has little effect, so that usually 20 μl is enough, an important consideration when side-effects of the drug due to systemic absorption are taken into account. Oil-based vehicles are of value in increasing the time of residence in the *cul-de-sac*, and thus the maximum concentration in the cornea, which is a critical factor. Experimentally, using fluorescein in humans, or by direct analysis in animal eyes, the course of concentration changes in cornea and aqueous humour may be measured and compared with predicted values. An example is shown in Fig. 3.15, the theoretical equation being:

$$C_a = \frac{M_0 k_{c.ca}}{V_a(B-A)}\left[e^{-At} - e^{-Bt}\right] \qquad (1)$$

A and B are elimination and absorption rate-constants which may be derived from the experimental curves.

Since the eye's response, e.g. pupil change, depends on aqueous humour concentration, C_a, the relation between the response, called the response parameter, and time will be similar (Yoshida & Mishima, 1975). Since usually the coefficient B, the absorption factor from cornea, is much larger than A, the elimination factor from aqueous hum-

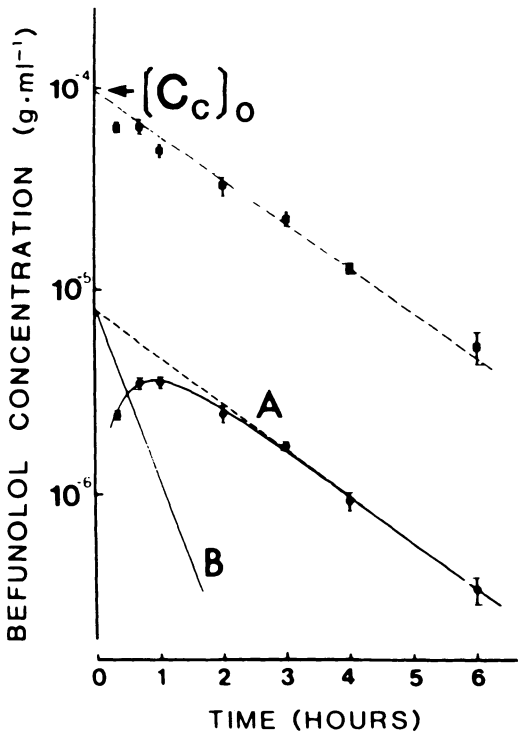

Fig. 3.15 Time courses of the concentration changes of the drug in the cornea (*upper curve*) and in the anterior chamber (*lower curve*) after instillation of 50 μl of 1% ^{14}C-befunolol in the albino rabbit eye. Extrapolation of the corneal concentration curve gives $[C_c]_0$. From the anterior chamber curve, the apparent absorption constant, B, and the apparent elimination rate constant, A, are obtained. (Mishima, *Invest. Ophthal.*)

our, the relation between response and time becomes a simple logarithmic one, i.e.

$$\text{Response} = Xe^{-At} \qquad (2)$$

The steady-state concentrations in tears C_d and aqueous humour, C_a, which are the desired parameters for estimating drug efficiency are given by the equation:

$$[C_a]_s = \frac{K_c Q}{V_0 k_0}[C_d]_s \qquad (3)$$

where K_c is the overall permeability of the corneal layers, Q is the corneal area, V_a is the distribution volume in the anterior chamber, k_0 is the coefficient of loss from the anterior chamber, and the suffix, s, means steady state. Applying measured values for these permeability parameters, Mishima deduced the relationship for pilocarpine as:

$$[C_a]_s = 2.3 - 1.1 \times 10^{-3}[C_d]_s$$

Two experimentally measured physiological parameters of clinical interest are the sensitivity of the cornea to touch after local anaesthesia, and the state of the pupil after topical application of miotics or mydriatics. Both are measurable with precision in the human.

Corneal Anaesthesia

Matsumoto *et al.* (1981) made measurements of sensitivity as a function of time after application of lidocaine, etc. Theoretically the duration, T, would be a simple logarithmic function of applied concentration, C:

$$\log C - \log C_{min} = Tk_e/2.3$$

where C_{min} is the concentration required to give minimal effect and k_e is the elimination constant from the epithelium, and is dominated by the loss from the tears. As Fig. 3.16 shows, the relationship between log-drug concentration and duration of effect is linear; it indicates that drug concentration must be increased logarithmically to produce a linear increase in time of effect.

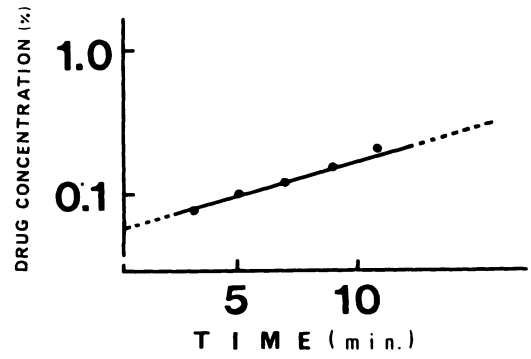

Fig. 3.16 Relationship between the logarithm of benoxinate concentration and the duration of anaesthetic effect. (Mishima, *Invest. Ophthal.*, from Matsumoto *et al.*, 1981.)

Pupil Response

Levy (1964) showed how to calculate drug elimination constants from the decline in mydriatic response to intravenous administration. In the human Yoshida & Mishima (1975) made a corresponding analysis of pupillary response to topically applied pilocarpine (miosis) and tropicamide (mydriasis); the response parameter, RP, which is a measure of the physiological response, was shown to vary with time after topical application in accordance with the equation (1) developed to describe penetration of drug into the aqueous humour from the cornea, being governed by the elimination and absorption constants A and B.

Bioavailability

Finally we may mention the concept of 'bioavailability', defined as the integrated concentration of the topically applied drug in the aqueous humour, i.e. the area under the concentration–time curve. Sugaya & Nagataki (1978) found that the bioavailability of pilocarpine, measured by miosis, increased with increasing drop-size over the range 5 to 20 μl, but beyond this it was not augmented by further increase. Increasing the viscosity of the vehicle increased bioavailability by some three times, as did application in ointment form; in this latter situation its effects showed delays, which were due to slow release from the fatty phase.[14]

TRANSPARENCY OF THE CORNEA

Scattering of Light

By transparency we mean rather more than the ability of a material to transmit light, we are concerned with the manner in which it is transmitted; thus dark glasses may reduce the transmission to 10% of the incident intensity yet the optical image remains perfect; on the other hand an opal screen may reduce the intensity much less, but because of the *scattering* of the light no image is possible. Thus diffraction, or scattering, of light is the important factor for transparency; and in this respect the cornea is very highly transparent, less than 1% of the light being scattered. The question arises as to how this transparency is attained in an inhomogeneous medium consisting of fibres embedded in a matrix of different refractive index; and furthermore, why the transparency should be affected by increases in hydration of the cornea and changes in intraocular pressure, as when haloes are seen during an acute attack of glaucoma.

Lattice Theory

In general, when light strikes a small discontinuity in the medium the latter acts as origin for new wavelets of light travelling in all directions; hence a large number of discontinuities in a transparent medium will give rise to wavelets of light passing backwards as well as forwards and thus making the medium opaque. A solution of very small particles, such as NaCl, remains transparent in spite of these discontinuities in the medium; this is because the discontinuities are small compared with half the wavelength of light. When the particles are of comparable size or greater, the diffraction becomes important, and the question arises as to why the cornea, built up of fibrils with a diameter greater than the wavelength of visible light, should in fact be transparent. The problem has been examined in detail with considerable acumen by Maurice (1957) who has shown, from an analysis of the birefringence[15] of the cornea, that the size of the fibrils, and the difference of refractive index between them and the ground-substance in which they are embedded, are such as to lead one to expect a highly opaque structure, due to scattering of incident light. He has shown, nevertheless, that this scattering may be avoided if the fibres are of relatively uniform diameter and are arranged in parallel rows; in this event the diffracted rays passing forwards tend to cancel each other out by destructive interference, leaving the normal undiffracted rays unaffected. In this way the opacity of the sclera is also explained, since there is no doubt from Schwarz' study that the prime distinction between the two tissues is the irregularity in arrangement and diameter of the scleral fibres.

CONFIRMATION OF THEORY

Although Maurice's explanation was questioned, e.g. by Smith (1969), subsequent theoretical and experimental studies, notably those of Cox *et al.* (1970), Benedek (1971), Farrell *et al.* (1973) and Twersky (1976), have amply confirmed the contention that transparency depends on an ordered arrangement of the collagen fibrils; this ordering need not be so regular as that found in a crystal lattice, so that the short-range ordering actually found, in which regularity of spacing does not extend over many wavelengths in any given region, is adequate (Hart & Farrell, 1969).

Swollen Cornea

An important tool in the analysis of the structure is the dependence of scattering on wavelength; thus the inverse third power dependence of scatter on wavelength found by these authors allowed them to conclude that the ordering was short ranged. When the cornea was grossly swollen the relationship changed to a second power dependence indicating the presence of an inhomogeneous fibril distribution. Electron microscopy of the swollen corneas showing this relationship revealed lakes in which fibrils had apparently disappeared. In analysing the basis for the loss of transparency, Farrell *et al.* (1973) considered the two main factors, namely the disruption in the ordering of the fibrils, and the decreased difference in refractive index between fibrils and surrounding medium, an effect that increases the 'scattering cross-section' of the fibril. They showed that the disorientation effect is by far the most significant.

METABOLISM

Pathways

The metabolic energy of the cornea is derived from the breakdown of glycogen and glucose; since the cornea

utilizes oxygen, which it derives from the atmosphere, through the tears, and from the aqueous humour, at least some of the energy is derived from oxidative mechanisms; the high concentration of lactate in the cornea indicates that aerobic glycolysis is an important pathway for the breakdown of glucose. According to a study of Riley (1969) on the perfused cornea, 85% of the glucose utilized is converted to lactate and only 15% is oxidized. The lactate so formed is carried away into the aqueous humour and thus the cornea contributes to the high concentration of this anion in the fluid.

Oxygen Tension

Langham (1952) used the concentration of lactate in the cornea as a measure of its 'oxygen-deficit', on the assumption that a greater availability of O_2 would be reflected in a lowered concentration of lactate in the cornea. In this way he was able to show that the corneal metabolism was affected by the tension of O_2 in the atmosphere, so that replacing air with O_2 decreased the lactate concentration in the cornea, whilst replacement with N_2 increased the concentration. When one eye was kept closed, the lactate concentration of this cornea increased, but not so much as in an eye exposed to N_2, so that it seems that the conjunctival blood vessels can provide some O_2.

Dependence on Atmosphere

Because of this dependence on the atmosphere, under normal conditions, because of utilization, there is a gradient of oxygen-tension from tears, 155 mmHg, to the aqueous humour, 55 mmHg (Fatt & Bieber, 1968); thus the endothelium can apparently function normally at a relatively low oxygen tension. The question arises as to the extent to which the endothelial layer depends on the atmospheric supply, and the extent to which O_2 is derived from the aqueous humour. Barr & Roetman (1974) found a very steep gradient of O_2-tension sloping away from the endothelium when they measured the tension at different depths in the aqueous humour (Fig. 3.17), and this suggests that the cornea is, in fact, supplying the aqueous rather than vice versa. Barr *et al.* (1977), employing an ingenious experimental set-up in which the cornea was mounted on a layer of agar-gel, determined the tendency of O_2 to diffuse from aqueous humour to cornea as a function of gradient of O_2-tension in the agar, by a suitable mathematical derivation. They found that, when the cornea was exposed to air at an O_2-tension of 155 mmHg, O_2 tended to diffuse out of the cornea when the P_{O_2} in the aqueous humour was 95.9 mmHg and into the cornea when it was 107 mmHg, whilst there was zero net flux at an aqueous humour tension of 102.5 mmHg. Thus, under normal conditions, the tendency is for oxygen to diffuse out of the cornea so that all depths of the cornea receive their oxygen from the atmosphere.

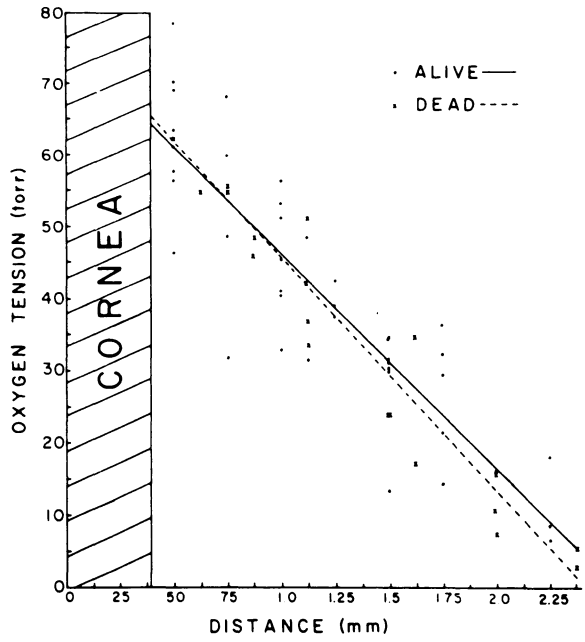

Figure 3.17 Oxygen tension in anterior chamber versus distance behind the corneal surface. Living and dead rabbits. (Barr & Roetman, *Invest. Ophthal.*)

Minimum Atmospheric Oxygen Tension

Polse & Mandell (1970) found that a partial pressure of 11–19 mmHg was adequate to prevent swelling, but a more recent study of Holden *et al.* (1984) on eight human subjects, indicated much higher levels, an average being 74 mmHg or 10.1%. There was considerable variation over the range 55 mmHg to 157 mmHg.

Contact Lenses

When access of oxygen to the outside of the cornea is prevented by a contact glass, or by keeping the eyes closed, the O_2-tension falls from 32 mmHg to 9 mmHg (Barr & Silver, 1973), and this is one of the causes for the corneal haziness that accompanies the wearing of contact lenses for some time (Smelser & Ozanics, 1953).

Utilization by Component Layers

Freeman (1972) developed a rapid polarographic technique for measuring O_2-consumption and applied it to the cornea finding that the relative consumption-rates of endothelium, stroma, and epithelium were as 21:40:39. On the basis of volume of tissue, the epithelium consumed

O_2 ten times faster than stroma; interestingly, its rate was only a fifth of that of the endothelium, on this basis of tissue-volume.

Reserves

The excised cornea, or the cornea in the excised eye, can maintain normal metabolic function for many hours, and this is because of the reserves of glycogen in the epithelium as well as the lactate and glucose in the tissue (and aqueous humour of the intact eye).

Supply of Materials

Glucose

The supply to the cornea of materials required for metabolism, notably glucose, is theoretically possible by three routes; namely diffusion from the limbus, where there is a capillary network; diffusion from tears across the epithelium, and diffusion from aqueous humour. Maurice (1969) has examined the relative significance of these pathways and has shown that, because there is no significant flow of fluid through the stroma from limbus to central region, the transport by simple diffusion will be very inefficient. This is because, while the material diffuses slowly from limbus to central region, it will be exposed to concentration gradients from stroma to aqueous humour and tears (Fig. 3.18). Thus, with a small molecule or ion, if the concentration at the limbus is put equal to 100, the concentration at 6 mm from the limbus will be only 1 when a steady-state has been reached. On the other hand, where diffusion out into the aqueous humour and tears is restricted, as with plasma proteins, then a significant supply from the limbus is practicable, and would account for their presence in the cornea, as well as that of numerous enzymes. The supply of glucose, then, must be from aqueous humour and tears; however, the significance of the tears as a supply is probably negligible since, according to Giardini & Roberts (1950) the concentration in this fluid is very small, whilst the permeability of the epithelium is low. A large number of experiments involving intralamellar implantation of plastic material in the cornea have shown that such a procedure leads to degeneration of the tissue above the layer of plastic, thereby emphasizing the importance of the diffusion of material from the aqueous humour; analysis of the epithelium showed that it had become deficient in glucose, glycogen and ATP (Turss *et al.*, 1970). Again, if the epithelium is removed we may place a cup on the stromal surface and measure diffusion of solutes from the aqueous humour into this fluid in the cup. Thoft *et al.* (1971b) measured a diffusion of glucose equal to 110 $\mu g/hr/cm^2$, which compares with a consumption of 38 to 83 $\mu g/hr/cm^2$. When the aqueous humour was replaced with silicone oil, the flux was decreased very considerably, indicating the importance of the aqueous humour as a source of glucose, in fact it was computed that the epithelium derived 80% of its glucose from the aqueous humour and 20% from the limbus (Thoft *et al.*, 1971b).

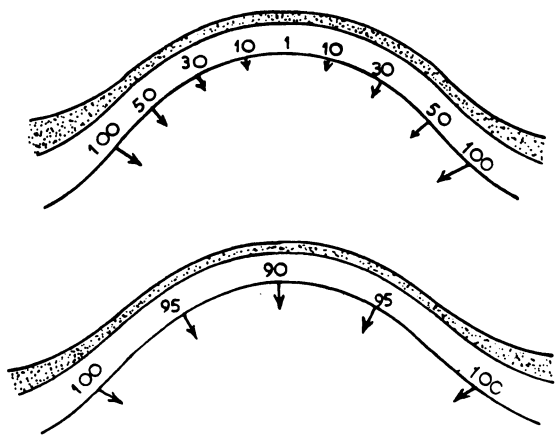

Fig. 3.18 Illustrating the effects of diffusion from cornea into aqueous humour on the transport of material from limbus to corneal centre. *Above*: diffusion into aqueous humour is rapid, so that at the corneal centre the effective concentration is low. *Below*: diffusion out is slow, so that a relatively high concentration can be built up at the corneal centre.

REPAIR OF DAMAGE

Damage to the cornea occurs primarily at the epithelium, so that its regenerative capabilities are of fundamental interest; more serious injuries, including those involved in surgical manoeuvres such as lens extraction, involve the whole thickness of the cornea, including the endothelium. Thus the subject of wound repair in the cornea has excited, and still does excite, a great deal of interest.

Epithelium

Regeneration After Complete Removal

When the epithelium is stripped off from the underlying Bowman's membrane there is a rapid regeneration, so that within 24 hours the surface may be completely covered by a new layer of epithelial cells derived from multiplication of the conjunctival cells at the periphery (Fig. 3.19). This single layer subsequently develops to give, within several weeks, a complete epithelium 4 to 6 cells thick. According to Thoft & Friend (1977), the epithelial cells making up this new epithelium retain the biochemical characteristics of conjunctival cells and only

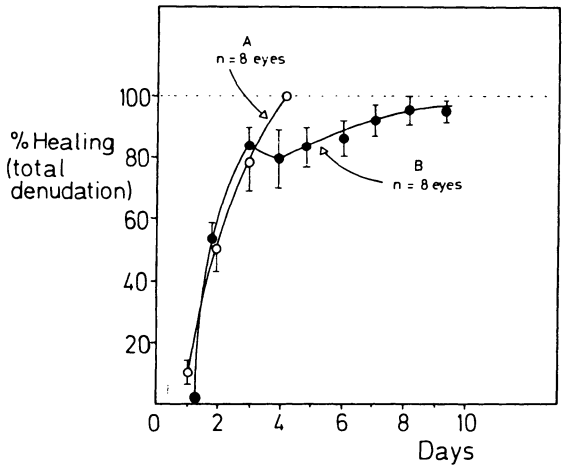

Fig. 3.19 Re-epithelialization of the completely denuded cornea either by knife blade (B) or by a rough stone (A). The response to denudation by knife was apparently biphasic. (Srinivasan *et al.*, *Exp. Eye Res.*)

gradually assume the characteristics of corneal epithelium; morphologically and histologically the regenerated epithelium is indistinguishable from the old in some 6 weeks. Even then there are subtle differences in protein composition, according to Harris *et al.* (1985) who have followed the composition of protein fractions throughout the period of renewal. They found that the process of regeneration took place in three phases, namely one of de-differentiation (24–72 hr after epithelial removal), a period of reorganization (72 hr to 1 week), and a period of differentiation (1–6 weeks).[16]

Smaller Wounds

Smaller lesions are repaired by sliding of the adjacent epithelial cells into the denuded region. Thus Kuwabara *et al.* (1976) made small cuts into the surface of the cornea and examined the behaviour of the adjacent epithelial cells over the subsequent several days. The cells begin to slide into the wound about one hour after the event, the main sliding cells being the wing cells, although the flat superficial (squamous) cells regain the cytoplasmic constituents of the younger cell and slide in a similar fashion. The basal cell also participates, becoming flatter and sliding less. The tight interdigitations between cells are broken down but the cells are held together by desmosomes of extended cytoplasm and never become entirely free of attachments to underlying cells. The cells that have slid on to the surface of the stroma attach firmly to the adjacent cells, and some more distant cells slide over these recently attached cells. The cells on the surface of the denuded area begin to increase in height within 24 hours and acquire the appearance of basal cells.

Time Relations

Crosson *et al.* (1986) made limited circular lesions and measured the time required for the hole in the epithelium to fill; the epithelium was removed mechanically, leaving the basement membrane intact, an important consideration. They noted a quiescent phase of some $5\frac{1}{2}$ hr during which the adjacent epithelial cells were quiescent in terms of cell movement, but there was an extensive cellular and subcellular reorganization going on, including increased desquamation of surface cells, the loss of the columnar appearance of basal cells, formation of processes around the wound edges, and a breakdown of the hemidesmosomes that normally attached epithelial cells to the basal membrane. This was followed by a linear phase of healing, when the average rate of cellular movement was constant at $64\ \mu m\ hr^{-1}$, independent of wound size. Light-microscopy showed that the 'leading edge'[17] was a single layer, but immediately behind this the epithelium was two or more cells thick. Tight junctions, normally associated between superficial cells were absent, so that the migrating cells were more like wing and basal cells. Polymorphonuclear leucocytes were not conspicuous, probably because the epithelium had been carefully scraped away from the basal lamina, leaving little debris to be cleared. Only when the denuded region has been completely covered does mitosis, which ceased in cells adjacent to the wound, resume, leading to the reassumption of full epithelial thickness (Jumblatt & Neufeld, 1986).

Basal Membrane

In most studies of epithelial regeneration, care has been taken to leave the basal lamina of the cornea intact; serious injuries caused by alkalis or acids, or thermal cautery, require the resynthesis of this lamina, which however, is preceded by re-epithelialization through cell migration. Kenyon *et al.* (1977), working on monkeys, found that re-epithelialization after thermal cautery required at least 7 days. Regeneration of basement membrane began at one week with the appearance of short discontinuous segments of basement membrane-material with hemisdesmosomal attachments to Bowman's layer. A total of 6 weeks were required for complete regeneration; and this coincided with the development of a tight adhesion of the epithelial layer to the stroma; before this, it was easy to lift the regenerated epithelium off.

Adhesion

This aspect of the regenerated epithelium was studied first by Khodadoust *et al.* (1968) in the rabbit; thus with a scrape lesion, leaving the basal lamina intact, it was found that the regenerated epithelium could be easily lifted off

the cornea, tearing occurring only at the junction with normal cornea; by the 6th to 7th day, however, it was impossible to wipe or pull off the new epithelium. With keratectomy, where the basal lamina and some subjacent stroma were removed, the regenerated epithelium was only loosely adherent up to 5–7 weeks. Interestingly, the epithelium became thicker than normal, a change that helped to maintain the normal corneal curvature. Examination of the cornea some months later revealed, in the electron microscope, a resynthesized basal lamina.

HEMIDESMOSOMES

Cells are held together mechanically in an epithelium by desmosomes, or attachment zones, where both membranes of adjacent cells participate in the junction. Attachment to a basal lamina is through hemidesmosomes, whose structure has been described by Kelly (1966); the hemisdesmosome apparently contains a large number of fine 10 nm filaments that serve to attach the cell membrane to the basal lamina. Buck (1982) has described the changes in the desmosomes during corneal wound closure. In the normal epithelium the hemidesmosomes are seen in tangential sections as chains running parallel with the radial axis of the cell, occupying some 14% of the total area of the basal lamina. With small epithelial denudations, the cells peripheral to the lesion show these chains organized parallel to the direction of migration of the sliding epithelial cells; that is, parallel to the radius as in the normal situation. Cells covering the area being resurfaced showed no hemidesmosomes; and this was true of the small area of normal cells close to the defect. With large areas of denudation, the situation was different, the cells resurfacing the epithelium forming attachments which seemed to be points of attachment of very fine cellular filaments, points that might indicate a different form of movement; in the small lesion, the cells are probably pushed over the denuded area, whereas with the large area of denudation the cells may use their own inherent power of migration by extension of processes that need points of attachment.

FIBRONECTINS

This is one of the names given to a surface glycoprotein with molecular weight 440 kd intimately concerned with the cell's adhesiveness to surfaces, possibly through a connection with the microfilament system within the cell since it is organized on the surface in filaments parallel to the long axis of the cell like the microfibrils inside (Yamada & Olden, 1978). The associated oligosaccharides are linked to the asparagine molecule of the polypeptide chain through an N-glycosidic link; there are 4 to 6 oligosaccharides linked to a single protein molecule with terminal galactose, sialic acid and fucose residues. Fujikawa *et al.* (1981) found that fibronectin was released beneath regenerating corneal epithelium, and Nishida *et al.* (1982) found it emerging from or synthesized by cut blocks of cornea. When applied topically to damaged corneal epithelium *in vivo*, it increased the rate of wound healing, as measured by the covering of denuded cornea, from 1.3 to 1.6 $mm^2\ hr^{-1}$ (Nishida *et al.*, 1984). In two cases of trophic ulcers in humans, Nishida *et al.* (1983) obtained cures when conventional treatment had failed by applying homologous fibronectin from the patient's own plasma.

LECTINS

Lectins, such as concavalin A bind with the sugar moieties of glycoproteins and inhibit their activity; and Gipson & Anderson (1980) reversibly slowed epithelial migration in rat cornea by blocking glucose, mannose and glucosamine sites on the cell's glycoproteins.

PROTEIN SYNTHESIS

Synthesis of glycoproteins, as measured by incorporation of ^{14}C-leucine and ^{3}H-glucosamine, increased by a factor of about three during epithelial sheet movement, returning to its normal value at wound-closure (Gipson & Kiorpes, 1982). Protein synthesis was studied by Dieske & Gipson (1986); from the incorporation of glucosamine they concluded that a new 100 kd glycoprotein was being produced, possibly concerned with cell migration. Tunicamycin antibodies, which inhibit synthesis of asparagine-linked glycoproteins, reduced the rate of sheet movement (Gipson *et al.*, 1984).[18]

LAMININ

This is another glycoprotein, consisting of two chains of 220 and 444 kd linked by disulphide bonds and considered to be intimately related to cell adhesion and migration (Timpl *et al.*, 1979). Gospodarowicz *et al.* (1981) found both fibronectin and laminin in cultured corneal endothelial cells; laminin was localized to the basal regions of the cells, whereas fibronectin was distributed over the apices as well. Basement membrane is resolved into a lamina lucida and a lamina densa; laminin is present in the lamina lucida, whilst Type IV collagen is in the lamina densa. When basement membrane, secreted by the endothelium, is exposed to endothelial cells in culture, they immediately adhere tightly to it; this is followed by cell migration and spreading. If cultured cells were placed on a plastic surface, proliferation would only proceed with the aid of fibroblast growth factor (Gospodarowicz & Ill, 1980).

CYTOCHALASIN AND COLCHICINE

Migration of cells relies on shape-changes involving, probably, the microfibril system of cytoplasm, and possibly also synthesis and breakdown of tubular structures. Microfibril activity is inhibited by cytochalasins B and D,

and these inhibited initiation and continuation of epithelial cell migration of cultured rat corneal epithelium, whereas colchicine, which blocks microtubule assembly, had no effect. Cytochalasins only affected the ultrastructure of cells at the leading edge of the migrating epithelium, causing blebs, or zeiotic processes, to appear, while actin microfilaments accumulated in the cytoplasm under the blebs (Gipson *et al.*, 1982; Gipson & Keezer, 1982).

Epidermal Growth Factor

This heat-stable protein of molecular weight about 15 000 daltons, was isolated from submaxillary gland and found to promote growth of incisor teeth (Cohen, 1962); when applied to rabbit corneas with epithelial abrasions it increased rate of healing (Frati *et al.*, 1972; Savage & Cohen, 1973) and, initially, produced new epithelium with some 10–15 cell layers in contrast with the normal 4–6 layers. In clinical conditions, such as abrasion, healing was accelerated (Daniele *et al.*, 1979). Nakagawa *et al.* (1985) showed that it promoted synthesis of fibronectin in migrating corneal epithelium.

EYE-DERIVED GROWTH FACTOR

Thompson *et al.* (1982) found that a growth factor derived from corneal tissue accelerated repair of epithelial wounds caused by iodine vapour, a lesion that leaves the basal lamina and keratocytes intact; however, weight-for-weight, it was much less effective than the standard growth factor.

Regeneration of the Endothelium

After damage to the endothelium the intact cells at the edge of the damaged region begin to migrate over those cells that have been destroyed, whilst an intense regeneration, or mitosis, area develops, providing new cells with which to cover the denuded Descemet's membrane. Experimentally, a localized destruction of the endothelium may be achieved by application of a freezing probe to the cornea; this leads to complete destruction of the endothelium covering the frozen region, leaving Descemet's membrane intact.

Changes in the Rabbit

These have been described in some detail by Hirsch *et al.* (1976, 1977) in the rabbit; essentially, the process is revealed by the presence of zones; namely a ring of uninjured cells; next a *regenerative zone* divided into a *transition zone* and a *zone of intense proliferation* abutting on the denuded area. Some 5–6 days after a 1 cm diameter lesion, Descemet's membrane was completely covered by an apparently normal endothelium. Using the specular microscope, the process can be examined *in vivo*. Matsuda *et al.* (1985) have described this in the rabbit; within 3 hr, the most obvious change is the remarkable elongation of the cells adjacent to the damaged area; the migrating cells seemed to move in a body, retaining their contacts, although there were positional changes of the moving cells in relation to each other. The cells during movement were large, pleiomorphic, and most of them showed mitotic figures. As they assumed the hexagonal shape, in about 120 hr, they became smaller and uniform.

Rat

Figure 3.20 illustrates a specular microscopic view of the rat's endothelium adjacent to a wound; the change in shape of the new cells is well shown, a change that permits the covering of the wound, if it is small, by existing cells rather than production of new ones. Tuft *et al.* (1986) found complete covering of the denuded area in 48 hr; an increased DNA synthesis indicated the production of new cells.

Primate Cornea

It is generally recognized that the regenerative capacity of the rabbit's endothelium is greater than that of the primate, so that experimental studies on this class are preferable if results are to be extended to man. Van Horn & Hyndiuk (1975) made freezing lesions in monkey corneas, which led to denudation of Descemet's membrane over the frozen area; this was accompanied by rapid doubling of corneal thickness; as time progressed the cornea regained its normal thickness, indicating endothelial repair, but there was very little evidence of cell division so that the new endothelium was apparently created by migration and enlargement of the uninjured more peripheral endothelial cells.

Fibroblast Growth Factor

In vitro studies on corneal endothelial cells have shown that fibroblast growth factor stimulates proliferation (Gospodarowicz *et al.*, 1977). Landshman *et al.* (1987) produced experimental endothelial lesions in the cat's cornea and examined the effects of a fibroblast growth factor, prepared from brain, on the regeneration of the corneal endothelium. Regeneration of the endothelium was undoubtedly accelerated by the factor, and this was associated with a reduced corneal thickness of the treated corneas.

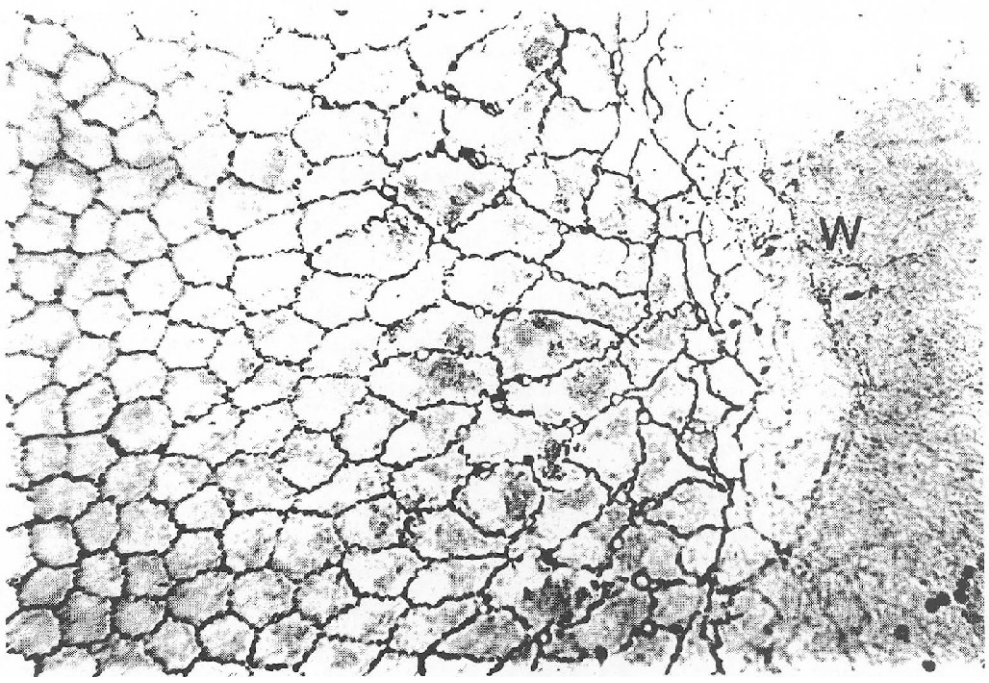

Fig. 3.20 Corneal wholemount stained with silver, 12 hr after injury, showing cell enlargement and slide to cover the wound (W) (× 2000). (Tuft *et al.*, *Invest. Ophthal.*)

Relation to Corneal Thickness

Khodadoust & Green (1976) followed the regeneration of the endothelium, and related this to the deturgescence of the cornea. Thus, after the damage, the cornea above the damaged endothelium swelled; although the damaged area was completely covered after 3 days, the corneal thickness was nearly twice normal, but as the number of cells in the denuded area increased over Days 3 to 8, oedema decreased, indicating that the large flattened cells that first replace the old endothelium are inadequate to function completely; only when the number has increased to permit a less flattened morphology is full physiological function possible, presumably because now the establishment of junctional complexes between the cells becomes possible. Thus five days after injury, when corneal thickness is returning to normal, the junctional contacts appear to be normal (Hirsch *et al.*, 1976).

Monkey Cornea

This correlation between morphological change and functional activity has been more thoroughly investigated by Tsuru *et al.* (1984), who measured endothelial permeability by fluorophotometry, corneal thickness, and examined the state of the endothelium by specular microscopy. Damage to the endothelium resulted in an increased endothelial permeability to fluorescein (Fig. 3.21) which later returned to normal; the course of change correlated with that of corneal thickness (Fig. 3.22). The destroyed area, which was about 50% of the total, was completely resurfaced in 5–6 days, but it was only after some 4 weeks that the junctional complexes

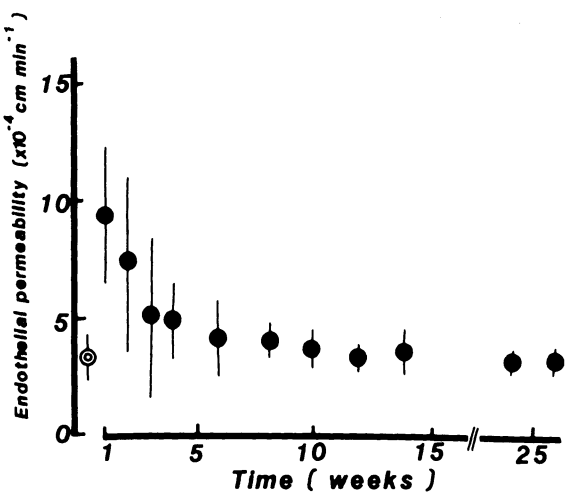

Fig. 3.21 Changes in permeability coefficient of endothelium after cryodestruction, mean and SD of 7 eyes. Open double circle: normal average and SD. (Tsuru *et al.*, *Jap. J. Ophthal.*)

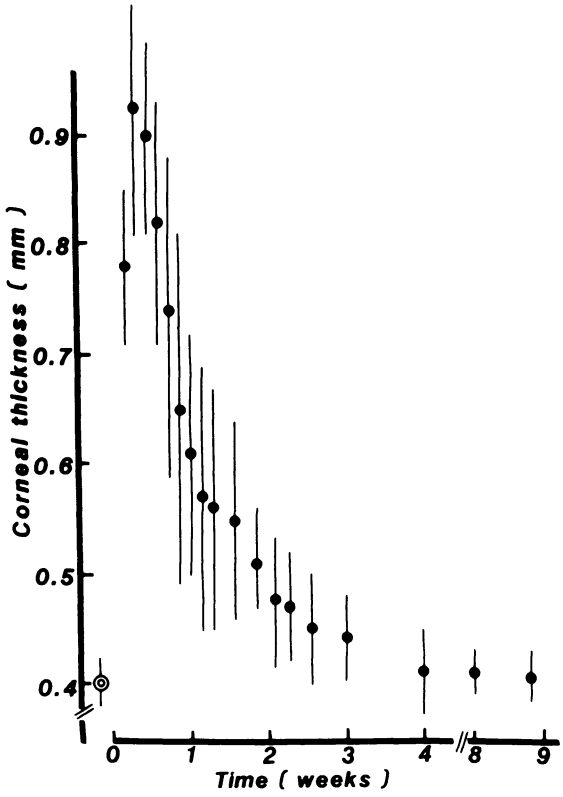

Fig. 3.22 Changes in corneal thickness after cryodestruction, mean and SD of 7 eyes. Open double circle: normal average and SD. (Tsuru *et al.*, *Jap. J. Ophthal.*)

appeared normal, and at this stage corneal thickness and endothelial permeability were almost normal. The study emphasizes that merely covering the denuded area is not sufficient; a much longer period than that is required for the endothelium to recover completely.

Endothelial Pump

Yee *et al.* (1985) correlated the restoration of corneal thickness in rabbits with the return of endothelial Na^+-K^--ATPase, measured histochemically by labelling the tissue with ^{3}H-ouabain. The phase of most rapid dehydration was that during which 'pump density' was increasing most rapidly. As one would expect, permeability of the endothelium to inulin decreased, after having risen as a result of the injury. In the specular microscope it was found that full recovery of pump density required not simply that an intact cellular layer be formed, but that it assume the regular polygonal array; and this was true of barrier-function, as measured by inulin permeability. In the specular microscope, correlations between changes in cell function and morphology could be made; it would seem that, at the end of Stage II, when a complete layer of cells has formed over the denuded area and the cells have nearly acquired their original polygonal shape, with appropriate intercellular attachments, it is only during the final Stage III that a complete return to normal is achieved (Fig. 3.23).[19]

STAGE	DAY	STATE OF HEALING	CORNEAL THICKNESS	PUMP	BARRIER	MORPH-OLOGY
	0-1 day	wound present	++	---	----	
I	1-2 days	cells sliding, mitosis wound ↓ in size	++++	----	---	
	3 days	wound completely covered	+++	---	--	
II	4-6 days	establishment of monolayer	++	-	-	
	7 days		+	NL	NL	
III	8-30 days	remodeling of monolayer	NL	NL	NL	

Fig. 3.23 Summary of the stages of endothelial wound healing and correlation between corneal thickness, pump site density, permeability, and morphology after transcorneal freezing (changes relative to prefreeze values are expressed as follows: ↓ and − = decrease; + = increase; NL = normal, i.e. no change). (Yee *et al.*, *Invest. Ophthal.*)

Polymorphonuclear Leukocytes

During wound repair these cells invade aqueous humour where they have access to the endothelium, and the stroma of the cornea where they probably exert an influence through the release of inflammatory mediators and enzymes (Meyers-Elliott & Chitjian, 1981). Kay *et al.* (1984) found that polymorphs would convert endothelial cells into apparent fibroblasts, irreversibly changing their collagen synthesis from that of Type IV to Type I, and in a later study the collagen fractions produced by normal keratocytes and the transformed endothelial cells were measured quantitatively. Normal keratocytes produced 92–96% Type I, Type III 2–6% and Type V 2% to 5%. The collagen produced by the abnormal cells changed with age of culture, thus at Day 2 Type I accounted for only 57%, Type III for 37.5% and Type V for 5.5%. Later Type I reached a stationary level of 80%. Thus behaviour is typical of wound healing in other tissues.

PROSTAGLANDINS

These agents, intimately connected with inflammatory reactions, are likely to be concerned in leukocytic invasion of the cornea; when leukotriene B_4 was implanted in the cornea it was the most potent in causing invasion, other lipoxygenase products, such as 5HETE, and cyclooxygenase products, such as PGE_2 and PGE_1 being less effective. The lipoxygenase inhibitor, Bay 08276, accelerated re-epithelialization of the denuded cornea whilst it inhibited polymorph chemotaxis and degranulation (Rochels & Busse, 1983, 1984). So far as an influence on endothelial wound healing is concerned, Neufeld *et al.* (1986) showed that inhibition of PG synthesis by indomethacin converted the cells into spindle shapes whilst this was prevented by addition of PGE_2, which thus seems necessary for maintenance of normal shape. Epidermal growth factor (EGF) stimulates proliferation (Gospodarowicz *et al.*, 1977); it similarly promoted elongation, acting additively with indomethacin (Neufeld *et al.*, 1986; Raymond *et al.*, 1986).

CORNEAL VASCULARIZATION

Under conditions of metabolic stress, for example, after injury, when the tissue may be invaded by leucocytes and fibrocytes, the nutritive supply and metabolic reserves may become inadequate, with the result that vessels sprout from the limbal plexus and grow into the stroma—*corneal vascularization.* It is likely that the effects of vitamin deficiency fall into the same category of metabolic stress; thus riboflavine deficiency is associated with corneal vascularization, whilst deficiencies of essential amino acids, such as tryptophan, lysine and methionine, will also produce the condition.

Stimulus to Vascularization

It has been argued that the prime factor leading to ingrowth of vessels is the loosening of the corneal tissue resulting from the oedema associated with inflammation of the adjacent conjunctival tissue. This is doubtless a prime requirement, since vascularization is often, if not invariably associated with corneal oedema, but the fact that, after tissue repair, the vessels may well regress before the subsidence of the oedema, suggests that an additional factor is necessary (Langham, 1953).

Leukocytic Invasion

Fromer & Klintworth (1975) cauterized rat corneas to induce vascularization, and showed that, if leukocytic invasion of the cornea was prevented by previous exposure of the rats to X-rays, thereby making them leukopenic, vascularization was inhibited. However, Sholley *et al.* (1978), and Eliason (1978), were able to induce corneal vascularization in leukopenic rats, so that leukocytic infiltration seems not to be critical, although, if oedema is an ancillary factor, then the finding that in guinea pigs made leukopenic, the oedema following infection with *Pseudomonas aeroginusa* was much less than in normal animals, helps to explain the contradictory results from the different laboratories.

Tissue Factor

We have had occasion to discuss the behaviour of antivascularizing and neovascularizing substances in relation to the vitreous body and retina, and the question arises as to whether the cornea releases a factor in response to injury that promotes vessel growth into it as a requirement of repair processes.

Campbell & Michaelson (1949) found that, if the injury to the cornea occurred too far from the periphery, vascularization failed to take place; and it was argued that a vascularization factor had to diffuse from the point of injury to stimulate vessel growth. Maurice *et al.* (1966) concluded from their own experiments on rabbits that, whereas oedema was a necessary precondition for vascularization, an additional factor was required; and their observations were consistent with the notion of a factor, liberated by the cells of the tissue, that had to diffuse to the limbus to provoke ingrowth of the vessels. Thus they implanted fine tubes, running radially in the stroma, and found that an injury to the centre of the cornea would provoke the growth of vessels inside the tube provided this was open at both ends; if the end nearest the pole of the cornea had been occluded, there was no ingrowth. Again, vascularization was more certain to occur if the aqueous humour was replaced by silicone oil, and it could

be argued that this was because loss of the factor had been reduced.

EPITHELIAL EXTRACTS

Eliason (1985) argued, from his observation that vascularization of cornea would occur in neutropenic rabbits, that the only cells available to provide a stimulus to vascularization were the epithelial cells in the neighbourhood of the injury. By very slow injection of extracts of epithelium into the cornea of normal rabbits he was able to induce vascularization in 13 out of 13 animals, whilst this occurred in only 3 out of 21 animals injected with saline only. The material in the extract was heat-labile, and produced vascularization in leukopenic as well as normal animals.

Non-specific Factors

Tissue injury causes the liberation of a number of pharmacologically active substances such as histamine, 5-hydroxytryptamine and bradykinin; and Zauberman *et al.* (1969) showed that the growth of vessels into tubes implanted in the cornea was more likely to occur if these tubes contained acetylcholine, histamine and 5-hydroxytryptamine, although bradykinin had no effect.

Nervous Supply

The innervation of the cornea is probably entirely sensory, mediated by the ophthalmic division of the trigeminal by way of the ciliary nerves. According to Zander & Weddell (1951) the fibres travel towards the limbus mainly in the perichoroidal space, and enter the substance of the cornea from three levels, scleral, episcleral and conjunctival. Most of the bundles entering the cornea are arranged radially and give rise, by subdivision, to a plexus in the stroma from which fibres supply the different regions. So great is the branching of any nerve fibre during its course in the cornea that a single axon may innervate an area equivalent to a quadrant. The endings are free, similar to those of pain fibres in other parts of the body; those reaching the epithelium are extremely fine, and send loops between the cells to within one cell-layer of the surface; similarly in the endothelium, the terminations are very fine.

Modalities of Sensation

Since v. Frey's time it has been categorically stated that the cornea is sensitive only to pain, in the sense that all forms of stimulus in man arouse only this sensation. According to Lele & Weddell (1956), however, the sensation of touch, as distinct from that of pain, may be evoked by gentle application of a nylon thread; again, a copper cylinder, maintained at 1.5°C above or below the corneal temperature, evoked a sensation of warmth or cold. By recording from the ciliary nerves of the cat, Lele & Weddell (1959) found action potentials in the myelinated fibres in response to both thermal and mechanical stimuli, and it appeared that the same fibres responded to

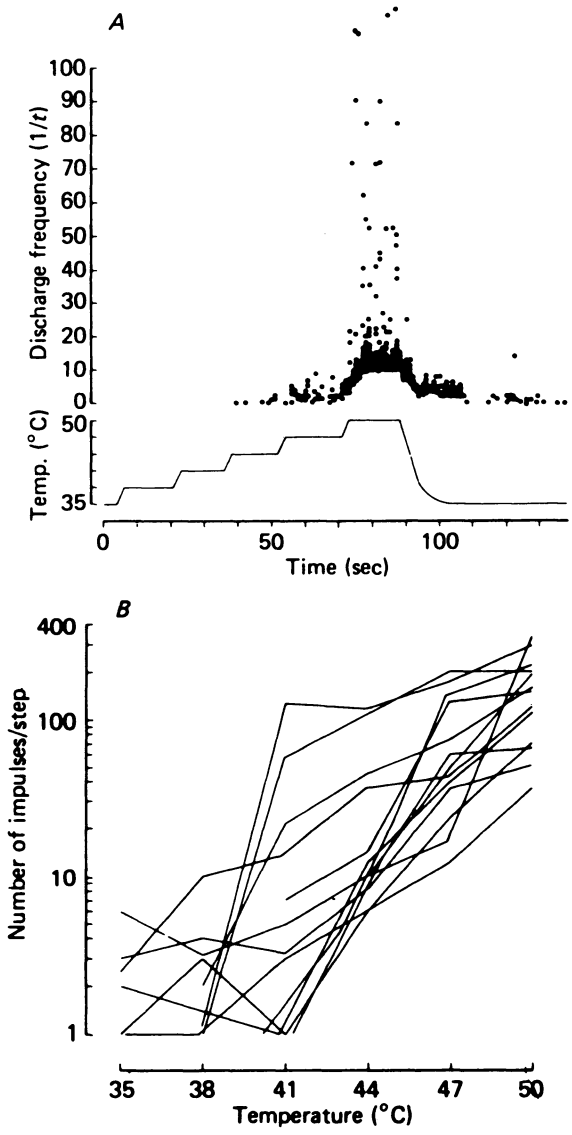

Fig. 3.24 Response of corneal receptors to stepwise heating. *A*, the instantaneous frequency of the discharge evoked in a corneal unit (upper trace) and the stimulus temperature (lower trace) are plotted versus time. The mechanical threshold of this unit was 27 mg and its conduction velocity 4.3 m/s. *B*, stimulus–response relations for thirteen corneal units stimulated with stepwise heating as shown in *A*. The number of impulses evoked during each 15 s step is plotted versus the temperature. Note the logarithmic scale in the ordinates. (Belmonte & Giraldez, *J. Physiol.*)

both types of stimulus. Giraldez *et al.* (1979) obtained similar results. Thus, apparently in contradiction to Müller's Law of Specific Nerve Energies, the sensory fibres of the cornea were able to mediate both thermal and touch sense. According to Kenshalo (1960), however, the sensations evoked by thermal stimulation of the human cornea are not those of warmth and cold but are of different types of 'irritation'; thus the nerve endings are *sensitive* to thermal change as well as mechanical stimuli, but the sensations evoked with the different stimuli belong to the same modality. Essentially similar conclusions were reached by Beuerman & Tanelian (1979).

Polymodal Nociceptors

Belmonte & Giraldez (1981) pointed out that Burgess & Perl (1973) had described skin receptors that were best described as polymodal nociceptors, having different characteristics from the conventional low-threshold touch-receptor, and responding to mechanical and other stimuli. They recorded from cat long and mixed ciliary nerves in response to mechanical and thermal stimuli. The response to a square-wave indentation consisted usually in a brief phasic discharge at threshold; high intensities evoked both a dynamic and sustained discharge. The receptors responded to raised temperature with a threshold at about 38°C, and increasing their discharge monotonically with increasing temperature as in Fig. 3.24. Damage by scratching elicited a high-frequency discharge followed by a long-lasting after-discharge. The responding fibres were described as A-delta, with conduction velocity of 5.4 m/sec. Belmonte & Giraldez (1981) have emphasized the similarity of these corneal fibres to those described as polymodal skin receptors by Bessou & Perl (1969), which may be innervated by either A-delta or unmyelinated C-fibres. Quantitatively the effective mechanical and thermal stimuli were similar to those required to evoke discomfort or pain in the human.

Regeneration of Fibres

When the cornea is cut through, as in making a section for cataract extraction, there is a loss of sensibility of the affected region, followed by a return associated with the growth of new fibres from the cut bundles proximal to the scar; there is no sprouting of adjacent uninjured neurones, however, since Rexed & Rexed (1951) repeatedly renewed a cut in the periphery and found no recovery of sensibility in the area supplied by the cut fibres.[20]

Notes

1. In many lower mammals, such as the rabbit and mouse, Bowman's membrane is absent, so that only the basement membrane, which is common to all species, separates the epithelium from the stroma proper.
2. Bahn *et al.* (1986) have compared the postnatal changes in the endothelium in several mammalian species including man. In all species, the area of the cornea increases with age after birth, but in humans this is only some 15%; nevertheless, there is a considerable loss of cells, of about 40%, indicating an increase in area of those remaining, since in other species the number of cells increased, although cell-density declined; this means that in non-humans some cell replication persists. Ikebe *et al.* (1986) have shown that the very large cells appearing in aged endothelia are polyploid, so that mitosis has occurred without cell division.
3. The evidence favouring an epithelial synthesis of the primary cornea has been summarized by Hay *et al.* (1979); thus cultured isolated epithelium has been shown to synthesize collagen in an otherwise cell-free medium (Dodson & Hay, 1971, 1974; Linsenmeier *et al.*, 1977). We may note that the endothelium is responsible for producing Descemet's membrane, whilst the epithelium secretes Bowman's membrane when this is present (it is absent in the rabbit). Thus Dodson & Hay (1971) described collagen fibres synthesized by the isolated chick embryonic epithelium.
4. The collagen of human sclera has been studied by Keeley *et al.* (1984); it is predominantly Type I with little evidence for the presence of other types. The authors have reviewed the situation in other species.
5. Labermeier & Kenney (1983) have summarized the various claims regarding collagen types in Descemet's membrane; Kenney *et al.* (1981) have summarized the types of collagen in the different parts of the eye. We may note that these last authors showed that subcultures of rabbit endothelium retained a stable phenotype in that they produced only those types found *in vivo*, namely Type IV and EC.
6. It seems well proved that it is the mucopolysaccharide that is responsible for the hydration tendency; thus the fibrils of a swollen cornea are no larger than normal when examined in the electron-microscope (François *et al.*, 1954); again, extraction of the mucopolysaccharides from the cornea reduces its tendency to take up water (Leyns *et al.*, 1940).
7. The physical basis of the swelling pressure has been discussed in some detail by Maurice (1984) and Olsen & Sperling (1987).
8. Midelfart (1987b) has studied the changes in Na^+-concentration in epithelium and stroma when the concentrations of Na^+ on the tear- and aqueous humour-sides were varied, either symmetrically, or asymmetrically. Lowering the concentration in the aqueous with normal concentration in the tears produced drastic lowering of epithelial and stromal concentrations; by contrast, with the reverse orientation of concentration-difference, there was little change. Amiloride decreased the Na^+-content of the epithelium associated with a significant increase in K^+. Midelfart discusses her results in relation to the pumps responsible for normal hydration and in relation to her finding that amiloride completely blocks the transport pump (Midelfart, 1987a).
9. Dikstein & Maurice (1972), in their study of the most suitable medium for maintaining an excised cornea, found that glutathione considerably enhanced fluid transport; Andersen *et al.* (1974) have shown that the effective molecule is oxidized glutathione, and have discussed the effects in relation to the maintenance of adequate supplies of ATP in the endothelium.

10. Riley (1977) demonstrated the presence of an ATPase in the rabbit's corneal endothelium that is dependent, for its activity, on the presence of anions in the medium, including bicarbonate; the enzyme was not inhibited by ouabain, but it was by thiocyanate and cyanate, both of which tend to reduce the ability of the endothelium to pump water out of the swollen cornea.
11. Hodson & Wigham (1983) showed that a simple analysis of the anatomy of the intercellular clefts of the corneal endothelium permitted a prediction of its ionic permeability, restrictions to movement being governed entirely by the restricted pore-sites through which the ions may pass. The actual constriction from the usual diameter of 20 nm to one of 2 nm at the gap-junctions is irrelevant. Only if the average width is greater than 40 nm would a significant increase in permeability over the measured one of $0.185\ cm\ hr^{-1}$ be calculated.
12. Jentsch *et al.* (1984) have studied the intracellular potentials of cultured bovine endothelial cells, their large size permitting microelectrode penetrations. It is impossible, of course, to interpret effects of the ionic environment on these potentials in terms of the secretory process taking place across the whole endothelial cell. Of interest is a tightly coupled Na^+–HCO_3^- co-transport inhibitable by SITS, a typical inhibotor of anion transport. In the isolated human cornea Fischer *et al.* (1978) found a net Na^+-flux from the aqueous humour to the tear side, with no detectable net Cl^--flux; however, when the process was stimulated with cAMP Na^+-flux increased and a net Cl^--flux was measurable. Reinach & Kirchberger (1983) have isolated particulate extracts from rabbit and frog corneal epithelia containing catecholamine-stimulated adenylate cyclase.
13. We may note that serotonin (5-HT) caused a stimulation of the rabbit corneal epithelial short-circuit current from 2.7 ± 0.2 to $3.4 \pm 0.2\ \mu A\ cm^{-2}\ hr^{-1}$; with no Cl^- in the bathing medium serotonin had no effect. The net Cl^--flux from aqueous humour to tears was $44 \pm 11\ nEq\ cm^{-2}\ hr^{-1}$ which rose to 119 ± 10 with 5-HT. Neufeld *et al.* (1982) found that 5-HT increased the level of cAMP in the rabbit cornea; the half-maximal effect was at $1.5\ \mu M$.
14. The interested reader is referred to Mishima's valuable article for further details respecting the value of these theoretical approaches to drug action in the eye, such as the use of soft contact lenses soaked in the drug; inserts containing the drug that is slowly released over long periods; and responses of intraocular pressure. di Mattio (1984) has measured uptake in aqueous, vitreous, cornea and lens of glucose analogues after a single intravenous bolus; penetration into cornea and lens is clearly secondary to penetration of the blood-aqueous and blood-vitreous barriers. The fact that concentrations in the cornea may exceed those in aqueous humour is of no great significance and simply indicates that, later in the exchange processes, the concentrations in plasma and aqueous humour are falling more rapidly than those in cornea. We may note that Antoine *et al.* (1984) have measured transport of phenylephrine across the cornea in the isolated and *in vivo* condition. The elaborate study of Maren *et al.* (1983) of transport of topically applied carbonic anhydrase inhibitors has been discussed in the section on aqueous humour (p. 38); it represents an excellent illustration of the value of bioavailability studies in a clinical situation.
15. The ordered arrangement of the collagen fibrils makes the velocity of light in one plane different from that in one at right-angles; this leads to double refraction or birefringence. From the magnitude and character of this birefringence important information regarding the orientation of the fibrils in the cornea may be obtained (Stanworth & Naylor, 1953; Maurice, 1957).
16. Shapiro *et al.* (1981) define 5 stages in repair taking place over 5–6 weeks: (1) a new epithelium, 2 layers thick, with no goblet cells; (2) goblet cells appear; (3–4) goblet cells become uniformly distributed and then recede to the limbus; (5) normal appearing epithelium, with no fluorescein staining. By sealing the periphery after complete covering, the central epithelium thinned whilst the periphery thickened, suggesting that, even when the cornea is covered, there is continued migration from the periphery. Conjunctival cells are differentiated from corneal epithelium by the presence of the secretory component of IgA on their surface; in the layer covering the denuded cornea derived from conjunctival cells this component disappears, so that the gene responsible for its synthesis is switched off (Liu *et al.*, 1981).
17. Gipson & Keezer (1982) define the 'leading edge' as those cells adjacent to the wound that are flattened with their long axes orientated parallel to the basal lamella. At the tip, it is one-cell thick, but in the major portion it is 2–4-cells thick. Only these cells had an arrangement of microfilaments that suggested that they were capable of movement. These actin filaments have been described in detail by Gipson & Anderson (1977) in migrating cells.
18. The glycoproteins of stationary and migratory epithelial cells during wound repair were separated through their binding to lectins; concavalin A bound two glycoproteins, of 155 kilodaltons and 70 kilodaltons, which were found in 2.9- and 4.0-fold greater amounts in migrating than stratified epithelium (Zieske *et al.*, 1986).
19. An essentially similar study has been described by Minkowski *et al.* (1984) in the rabbit, permeability being measured by fluorophotometry and thickness by pachymetry. They observed a lag between recovery of permeability and the return to normal thickness, this last requiring some 21 days. The authors describe changes in the intercellular contacts, such as the development of long finger-like interdigitations, with a return to normal at about 28 days.
20. A vegetative innervation of the cornea has been postulated and denied; the technique developed by Falck for identifying adrenergic fibres by virtue of their fluorescence has permitted the identification of this type of fibre in the anterior layers of the stroma of the embryonic cornea; in primates these fibres disappear after birth but in most other mammals they remain (Laties & Jacobowitz, 1964; Ehinger, 1966).

References

Andersen, E. I., Fischbarg, J. & Spector, A. (1974) Disulfide stimulation of fluid transport and effect on ATP level in rabbit corneal endothelium. *Exp. Eye Res.* **19**, 1–10.

Antoine, M. E., Edelhauser, H. F. & O'Brien, W. J. (1984) Pharmacokinetics of topical ocular phenylephrine HCl. *Invest. Ophthal.* **25**, 48–54.

Araie, M. & Maurice, D. M. (1983) A reevaluation of corneal endothelial permeability to fluorescein. *Exp. Eye Res.* **41**, 383–390.

Bahn, C. F. *et al.* (1986) Postnatal development of corneal endothelium. *Invest. Ophthal.* **27**, 44–51.

Barfort, P. & Maurice, D. (1974) Electrical potential and fluid transport across the corneal endothelium. *Exp. Eye Res.* **19**, 11–19.

Barr, R. E., Hennessey, M. & Murphy, V. G. (1977) Diffusion of oxygen at the endothelial surface of the rabbit cornea. *J. Physiol.* **270**, 1–8.

Barr, R. E. & Roetman, E. L. (1974) Oxygen gradients in the anterior chamber of anesthetized rabbits. *Invest. Ophthal.* **13**, 386–389.

Barr, R. E. & Silver, I. A. (1973) Effects of corneal environment on oxygen tension in the anterior chambers of rabbits. *Invest. Ophthal.* **12**, 140–144.

Baum, J. P., Maurice, D. M. & McCarey, B. E. (1984) The active and passive transport of water across the corneal endothelium. *Exp. Eye Res.* **39**, 335–342.

Belmonte, C. & Giraldez, F. (1981) Responses of cat corneal sensory receptors to mechanical and thermal stimulation. *J. Physiol.* **321**, 355–368.

Benedek, G. B. (1971) Theory of transparency of the eye. *Appl. Optics* **10**, 459–473.

Berggren, L. & Lempberg, R. (1973) Neovascularization in the rabbit cornea after intracorneal injections of cartilage extracts. *Exp. Eye Res.* **17**, 261–273.

Bessou, P. & Perl, E. R. (1969) Response of cutaneous sensory units with unmyelinated fibres to noxious stimuli. *J. Neurophysiol.* **32**, 1025–1043.

Beuerman, R. W. & Tanelian, D. L. (1979) Corneal pain evoked by thermal stimulation. *Pain* **7**, 1–14.

Bito, L. Z., Roberts, J. C. & Saraf, S. (1973) Maintenance of normal corneal thickness in the cold *in vivo* (hibernation) as opposed to *in vitro*. *J. Physiol.* **231**, 71–86.

Bito, L. Z. & Saraf, S. (1973) The effects of cold on corneal thickness and on aqueous humor and blood composition of *Rana pipiens*. *Exp. Eye Res.* **16**, 315–325.

Birk, D. E., Fitch, J. M. & Linsenmeyer, T. F. (1986) Organization of collagen types I and V in the embryonic chicken cornea. *Invest. Ophthal.*, **27**, 1470–1477.

Blümcke, S. & Morgenroth, K. (1967) The stereo ultrastructure of the external and internal surface of the cornea. *J. Ultrastr. Res.* **18**, 502–518.

Boerscheeding, M. S. *et al.* (1975) Proteoglycans and collagen fibre organization in human corneoscleral tissue. *Exp. Eye Res.* **21**, 59–70.

Breen, M., Johnson, R. L., Sittig, R. A., Weinstein, H. G. & Veis, A. (1972) The acidic glycosaminoglycans in human fetal development and adult cornea, sclera and skin. *Conn. Tissue Res.* **1**, 291–303.

Brown, S. I. (1973) Dry spots and corneal erosions. *Int. Ophthal. Clinics* **13**, 169–185.

Buck, R. C. (1982) Hemidesmosomes of normal and regenerating mouse corneal epithelium. *Virch. Arch.* **41**, 1–16.

Burgess, P. R. & Perl, E. R. (1973) Cutaneous mechanoreceptors and nociceptors. In *Handbook of Sensory Physiology*. Ed. Iggo, A., Vol. 2, pp. 29–78. Berlin: Springer.

Campbell, F. W. & Michaelson, I. C. (1949) Blood-vessel formation in the cornea. *Br. J. Ophthal.* **33**, 248–255.

Candia, O. A. (1973) Short-circuit current related to active transport of chloride in frog cornea: effects of furosemide and ethacrynic acid. *Biochim. biophys. Acta* **298**, 1011–1014.

Candia, O. A. & Askew, W. A. (1968) Active sodium transport in the isolated bullfrog cornea. *Biochim. biophys. Acta* **163**, 262–265.

Candia, O. A. & Neufeld, A. H. (1978) Topical epinephrine causes a decrease in density of β-adrenergic receptors and catecholamine-stimulated chloride transport in the rabbit cornea. *Biochim. biophys. Acta* **543**, 403–408.

Coakes, R. L. & Brubaker, R. F. (1979) Method of measuring aqueous humor flow and corneal endothelial permeability using a fluorophotometry nomogram. *Invest. Ophthal.* **18**, 288–302.

Cogan, D. G. & Hirsch, E. D. (1944) The cornea. VII. Permeability to weak electrolytes. *Arch. Ophthal., N.Y.* **32**, 276–282.

Cogan, D. G. & Kinsey, V. E. (1942) Transfer of water and sodium by osmosis and diffusion through the excised cornea. *Arch. Ophthal., N.Y.* **27**, 466–476.

Cohen, S. (1962) Isolation of a mouse submaxillary gland protein accelerating incisor eruption and eye-lid opening in the newborn animal. *J. biol. Chem.* **237**, 1555–1562.

Coulombre, A. J. & Coulombre, J. E. (1961) The development of the structural and optical properties of the word. In: *The Structure of the Eye*. Ed. G. K. Smelser. Academic Press: N.Y. and London, pp. 405–420.

Cox, J. L., Farrell, R. A., Hart, R. W. & Langham, M. E. (1970) *J. Physiol.* **210**, 601–616.

Crosson, C. E., Klyce, D. & Beuerman, R. W. (1986) Epithelial wound closure in the rabbit cornea. *Invest. Ophthal.* **27**, 464–473.

Daniele, S., Frati, L., Fiore, C. & Santoni, G. (1979) The effect of epidermal growth factor (EGF) on the corneal epithelium in humans. *v. Graefes Arch. Ophthal.* **210**, 159–165.

Davson, H. (1949) Some considerations on the salt content of fresh and old ox corneae. *Br. J. Ophthal.* **33**, 175–182.

Davson, H. (1955) The hydration of the cornea. *Biochem. J.* **59**, 24–28.

Diamond, J. M. & Bossert, W. H. (1967) Standing gradient osmotic flow. A mechanism for coupling of water and solute transport in epithelia. *J. Gen. Physiol.* **5**, 2061–2083.

Dieske, J. D. & Gipson, I. K. (1986) Protein synthesis during corneal epithelial wound healing. *Invest. Ophthal.* **27**, 1–7.

Dikstein, S. & Maurice, D. (1972) The metabolic basis to the fluid pump in the cornea. *J. Physiol.* **221**, 29–41.

Doane, M. G. & Dohlman, C. H. (1970) Physiological response of the cornea to an artificial epithelium *Exp. Eye Res.*, **9**, 158–164.

Dodson, J. W. & Hay, E. D. (1971) Secretion of collagenous stroma by isolated epithelium grown *in vitro*. *Exp. Cell Res.* **65**, 215–220.

Dodson, J. W. & Hay, E. D. (1974) Secretion of collagen by corneal epithelium. II. Effect of the underlying substratum on secretion and polymerization of epithelial products. *J. Exp. Zool.*, **189**, 51–72.

Dohlman, C. H. & Balazs, E. A. (1955) Chemical studies on Descemet's membrane of the bovine cornea. *Arch. Biochem. Biophys.* **57**, 445–457.

Donn, A., Maurice, D. M. & Mills, N. L. (1959) The active transport of sodium across the epithelium. *Arch. Ophthal., N.Y.* **62**, 748–757.

Donn, A., Miller, S. & Mallett, N. (1963) Water permeability of the living cornea. *Arch. Ophthal., Chicago* **70**, 515–521.

Ehinger, B. (1966) Adrenergic nerves to the eye and to related structures in man and in the cynomolgus monkey (*Macaca irus*). *Invest Ophthal.* **5**, 42–52.

Eliason, J. A. (1978) Leukocytes and experimental corneal vascularization. *Invest. Ophthal.* **17**, 1087–1095.

Eliason, J. A. (1985) Angiogenic activity of the corneal epithelium. *Exp. Eye Res.* **41**, 721–732.

Farrell, R. A., McCally, R. L. & Tatham, P. E. R. (1973) Wavelength dependencies of light scattering in normal and cold swollen rabbit corneas and their structural implications. *J. Physiol.* **233**, 589–612.

Fatt, I. & Bieber, M. T. (1968) The steady-state distribution of oxygen and carbon dioxide in the *in vivo* cornea. I. *Exp. Eye Res.* **7**, 103–112.

Fatt, I. & Hedbys, B. O. (1970) Flow conductivity of human corneal stroma. *Exp. Eye Res.* **10**, 237–242.

Fischbarg, J. (1972) Potential difference and fluid transport across rabbit corneal endothelium. *Biochim. biophys. Acta* **288**, 362–366.

Fischbarg, J. (1973) Active and passive properties of the rabbit corneal endothelium. *Exp. Eye Res.* **15**, 615–638.

Fischbarg, J. & Lim, J. J. (1974) Role of cations, anions and carbonic anhydrase in fluid transport across rabbit corneal endothelium. *J. Physiol.* **241**, 647–675.

Fischbarg, J. & Lim, J. J. (1984) Fluid and electrolyte transport across corneal endothelium. *Curr. Topics Eye Res.* **4**, 201–223.

Fischbarg, J. & Montoreano, R. (1982) Osmotic permeability of corneal endothelial cell membrane and endothelial and epithelial layers. *ARVO Suppl.* **32**, 102.

Fischer, F. H., Schmitz, L., Hoff, W., Schartl, S., Liege, O. & Wiederholt, M. (1978) Sodium and chloride transport in the isolated human cornea. *Pflüg. Arch. ges. Physiol.*, **373**, 179–188.

François, J., Rabaey, M. & Vandermeersche, G. (1954) Etude de la cornée et de la sclérotique. *Ophthalmologica, Basel* **127**, 74–85.

Frati, L., Daniele, S., Delogu, A. & Covelli, I. (1972) Selective binding of the epidermal growth factor and its specific effects on the epithelial cells of the cornea. *Exp. Eye Res.* **14**, 135–141.

Freeman, R. D. (1972) Oxygen consumption by the component layers of the cornea. *J. Physiol.* **225**, 15–32.

Fromer, C. H. & Klintworth, G. K. (1975) An evaluation of the role of leukocytes in the pathogenesis of experimentally induced corneal vascularization. II. *Amer. J. Path.* **81**, 531–544.

Fujikawa, L. S., Foster, C. S., Harrist, T. J., Lanigan, J. M. & Colvin, R. B. (1981) Fibronectin in healing rabbit corneal wounds. *Lab. Invest.* **45**, 120–129.

Geroski, D. H. & Edelhauser, H. F. (1984) The quantitation of Ns/K ATPase pump sites in the rabbit corneal endothelium. *Invest. Ophthal.*, **25**, 1056–1060.

Giardini, A. & Roberts, J. R. E. (1950) Concentration of glucose and total chloride in tears. *Br. J. Ophthal.* **34**, 737–743.

Gipson, I. K. & Anderson, R. A. (1977) Actin filaments in normal and migrating corneal epithelial cells. *Invest. Ophthal.*, **16**, 161–166.

Gipson, I. K. & Anderson, R. A. (1980) Effect of lectins on migration of the corneal epithelium. *Invest. Ophthal.* **19**, 341–349.

Gipson, I. K. & Keezer, L. (1982) Effects of cytochalasins and colchicine on the ultrastructure of migrating corneal epithelium. *Invest. Ophthal.* **22**, 643–650.

Gipson, I. K. & Kiorpes, T. C. (1982) Epithelial sheet movement: protein and glycoprotein synthesis. *Dev. Biol.* **92**, 259–262.

Gipson, I. K., Kiorpes, T. C. & Brennan, S. I. (1984) Epithelial sheet movement: effects of tunicamycin on migration and glycoprotein synthesis. *Dev. Biol.* **101**, 212–220.

Gipson, I. K., Westcote, M. J. & Brooksby, N. G. (1982) Effects of cytochalasins B and D and colchicine on migration of the corneal epithelium. *Invest. Ophthal.* **22**, 633–642.

Giraldez, F., Geijo, E. & Belmonte, C. (1979) Response characteristics of corneal sensory fibres to mechanical and thermal stimulation. *Brain Res.* **177**, 571–576.

Gospodarowicz, D., Greenburg, G., Foidart, J. M. & Savion, N. (1981) The production and localization of laminin in cultured vascular and corneal endothelial cells. *J. Cell Physiol.* **107**, 171–183.

Gospodarowicz, D. & Ill, C. (1980) The extracellular matrix and the control of proliferation of corneal endothelial and lens epithelial cells. *Exp. Eye Res.* **31**, 181–199.

Gospodarowicz, D., Mescher, A. L. & Birdwell, C. R. (1977) Stimulation of corneal endothelial cell proliferation *in vitro* by fibroblast and epidermal growth factors. *Exp. Eye Res.* **25**, 75–89.

Green, K. & Otori, T. (1970) Studies on corneal physiology *in vitro*. *Exp. Eye Res.* **9**, 268–280.

Green, K., Simon, S., Kelly, G. M. & Bowman, K. A. (1981) Effects of [Na^+], [Cl^-], carbonic anhydrase and intracellular pH on corneal endothelial bicarbonate transport. *Invest. Ophthal.* **21**, 586–591.

Hale, P. N. & Maurice, D. M. (1969) Sugar transport across the corneal endothelium. *Exp. Eye Res.* **8**, 205–215.

Harris, J. E. & Nordquist, L. T. (1955) The hydration of the cornea. I. Transport of water from the cornea. *Am. J. Ophthal.* **40**, 100–110.

Harris, T. M., Berry, E. R., Pakurar, A. S. & Sheppard, L. B. (1985) Biochemical transformation of bulbar conjunctiva into corneal epithelium: an electrophoretic analysis. *Exp. Eye Res.*, **41**, 597–605.

Hart, R. W. & Farréll, R. A. (1969) Light scattering in the cornea. *J. opt. Soc. Amer.* **59**, 766–774.

Hay, E. D., Linsenmeyer, T. F., Trelstad, R. L. & Von der Mark, K. (1979) Origin and distribution of collagens in the developing avian cornea. *Curr. Topics Eye Res.* **1**, 1–35.

Hay, E. D. & Revel, J. P. (1969) Fine structure of the developing avian cornea. *Monogr. Dev. Biol.*, **1**, 1–144.

Hirsch, M., Renard, G., Faure, J.-P. & Pouliquen, Y. (1976) Formation of intracellular spaces and junctions in regenerating rabbit corneal endothelium. *Exp. Eye Res.* **23**, 385–397.

Hirsch, M., Renard, G., Faure, J.-P. & Pouliquen, Y. (1977) Study of the ultrastructure of the rabbit corneal endothelium by the freeze-fracture technique: apical and lateral junctions. *Exp. Eye Res.* **25**, 277–288.

Hodson, S. (1971) Evidence for a bicarbonate-dependent sodium pump in corneal endothelium. *Exp. Eye Res.* **11**, 20–29.

Hodson, S. (1974) The regulation of corneal hydration by a salt pump requiring the presence of sodium and bicarbonate ions. *J. Physiol.* **236**, 271–302.

Hodson, S. (1975) The regulation of corneal hydration to maintain high transparency in fluctuating ambient temperatures. *Exp. Eye Res.* **20**, 375–381.

Hodson, S. A. & Lawton, D. M. (1987) The apparent reflexion coefficients of the leaky corneal endothelium to sodium chloride is about one in the rabbit. *J. Physiol.* **385**, 97–106.

Hodson, S., Miller, F. & Riley, M. (1977) The electrogenic pump of rabbit corneal endothelium. *Exp. Eye Res.* **24**, 249–253.

Hodson, S. & Wigham, C. (1983) The permeability of rabbit and human corneal endothelium. *J. Physiol.* **342**, 409–419.

Holden, B. A., Sweeney, D. F. & Sanderson, G. (1984) The minimum precorneal oxygen tension to avoid corneal edema. *Invest. Ophthal.* **25**, 476–480.

Hull, D. S., Green, K., Boyd, M. & Wynn, H. R. (1977) Corneal endothelium bicarbonate transport and the effect of carbonic anhydrase inhibitors on endothelial permeability and fluxes and corneal thickness. *Invest. Ophthal.* **16**, 883–892.

Ikebe, H., Takamatsu, T., Itoi, M. & Fujita, S. (1986) Age-dependent changes in nuclear DNA content and cell size of presumably normal human corneal endothelium. *Exp. Eye Res.*, **43**, 251–258.

Jakus, M. (1946) The fine structure of Descemet's membrane. *J. Biophys. biochem. Cytol.* **2**, Suppl., 243–252.

Jakus, M. (1961) The fine structure of the human cornea. In *Structure of the Eye*, ed. Smelser, pp. 343–366. New York: Academic Press.

Jentsch, T. J., Keller, S. R., Koch, M. & Wiederholt, M. (1984) Evidence for coupled transport of bicarbonate and sodium in cultured bovine corneal endothelial cells. *J. Membrane Biol.* **81**, 189–204.

Jones, R. F. & Maurice, D. M. (1966) New methods of measuring the rate of aqueous flow in man with fluorescein. *Exp. Eye Res.* **5**, 208–220.

Jumblatt, M. W. & Neufeld, A. H. (1986) A tissue culture assay of corneal epithelial wound closure. *Invest. Ophthal.* **27**, 8–13.

Kaufman, H. E., Capella, J. A. & Robbin, J. E. (1966) The human corneal endothelium. *Amer. J. Ophthal.* **61**, 835–841.

Kay, E.-D. P., Nimni, M. E. & Smith, R. E. (1984) Modulation of endothelial cell morphology and collagen synthesis by polymorphonuclear leukocytes. *Invest. Ophthal.* **25**, 502–512.

Kaye, G. I., Sibley, R. C. & Hoefle, F. B. (1973) Recent studies on the nature of and function of the corneal endothelial barrier. *Exp. Eye Res.* **15**, 585–613.

Kayes, J. & Holmberg, A. (1960) The fine structure of Bowman's layer and the basement membrane of the corneal epithelium. *Am. J. Ophthal.* **50**, 1013–1021.

Keeley, F. W., Morin, J. D. & Vesely, S. (1984) Characterization of collagen from normal human sclera. *Exp. Eye Res.* **39**, 533–542.

Kelly, D. E. (1966) Fine structure of desmosomes, hemidesmosomes, and an adepidermal globular layer in developing newt epidermis. *J. Cell Biol.* **28**, 51–72.

Kelly, G. & Green, K. (1980) Influence of bicarbonate and CO_2 on rabbit corneal transendothelial bicarbonate fluxes. *Exp. Eye Res.* **30**, 641–648.

Kenney, M. C., Benya, P. D., Nimms, M. E. & Smith, R. E. (1981) Stability of the collagen phenotype and decreased collagen production in serial subcultures of rabbit corneal endothelial cells. *Exp. Eye Res.*, **33**, 131–140.

Kenshalo, D. R. (1960) Comparison of thermal sensitivity of the forehead, lip, conjunctiva and cornea. *J. app. Physiol.* **15**, 987–991.

Kenyon, K. R., Fogle, J. A., Stone, D. L. & Stark, W. J. (1977) Regeneration of corneal epithelial basement membrane following thermal cauterization. *Invest. Ophthal.* **16**, 292–301.

Khodadoust, A. A. & Green, K. (1976) Physiological function of regenerating endothelium. *Invest. Ophthal.* **15**, 96–101.

Khodadoust, A. A., Silverstein, A. M., Kenyon, K. R. & Dowling, J. E. (1968) Adhesion of regenerating corneal epithelium. The role of basement membrane. *Amer. J. Ophthal.* **65**, 339–348.

Kim, J. H., Green, K., Martinez, M. & Paton, D. (1971) Solute permeability of the corneal endothelium and Descemet's membrane. *Exp. Eye Res.* **12**, 231–238.

Klyce, S. D. (1972) Electrical profiles in the corneal epithelium. *J. Physiol.* **226**, 407–429.

Klyce, S. D. (1975) Transport of Na, Cl, and water by the rabbit corneal epithelium at resting potential. *Amer. J. Physiol.* **228**, 1446–1452.

Klyce, S. D., Neufeld, A. H. & Zadunaisky, J. A. (1973) The activation of chloride transport by epinephrine and Db cyclic AMP in the cornea of the rabbit. *Invest. Ophthal.* **12**, 127–139.

Klyce, S. D. & Russell, S. R. (1979) Numerical solution of coupled transport equations applied to corneal hydration dynamics. *J. Physiol.* **292**, 107–134.

Kreutziger, G. O. (1976) Lateral membrane morphology and gap junction structure in rabbit corneal endothelium. *Exp. Eye Res.* **23**, 285–293.

Kuwabara, T., Perkins, D. G. & Cogan, D. G. (1976) Sliding of the epithelium in experimental corneal wounds. *Invest. Ophthal.* **15**, 4–14.

Labermeier, U. & Kenney, M. C. (1983) The presence of EC collagen and Type IV collagen in bovine Descemet's membrane. *Biochem. Biophys. Res. Comm.* **116**, 619–620.

Laing, R. A., Sandstrom, M. A., Berrospi, A. R. & Leibowitz, H. M. (1976) Changes in the corneal endothelium as a function of age. *Exp. Eye Res.*, **22**, 587–594.

Landshman, N., Belkin, M., Ben-Hanan, I., Ben-Chaim, O., Assia, E. & Savion, N. (1987) Regeneration of cat corneal endothelium induced *in vivo* by fibroblast growth factor. *Exp. Eye Res.* **45**, 805–811.

Langham, M. E. (1952) Utilization of oxygen by the component layers of the living cornea. *J. Physiol.* **117**, 461–470.

Langham, M. E. (1953) Observations on the growth of blood vessels into the cornea. *Brit. J. Ophthal.*, **37**, 210–222.

Laties, A. & Jacobowitz, D. (1964) A histochemical study of the adrenergic and cholinergic innervation of the anterior segment of the rabbit eye. *Invest. Ophthal.* **3**, 592–600.

Lee, R. I. & Davison, P. F. (1984) The collagens of developing bovine cornea. *Exp. Eye Res.* **39**, 639–652.

Lele, P. P. & Weddell, G. (1956). The relationship between neurohistology and corneal sensitivity. *Brain* **79**, 119–154.

Lele, P. P. & Weddell, G. (1959) Sensory nerves of the cornea and cutaneous sensibility. *Exp. Neurol.* **1**, 334–359.

Leuenberger, P. M. (1973) Lanthanum hydroxide tracer studies on rat corneal endothelium. *Exp. Eye Res.* **15**, 85–91.

Levy, G. (1964) Relationship between elimination rate of drugs and rate of decline in their pharmacologic effects. *T. Pharmaceut. Sci.*, **53**, 342–343.

Leyns, W. F., Heringa, C. & Weidinger, A. (1940) Water binding capacity of the cornea. *Acta brev. Nederland. Physiol.* **10**, 25–26.

Lim, J. J. & Ussing, H. H. (1982) Analysis of presteady-state Na^+ fluxes across the rabbit corneal endothelium. *J. Membrane Biol.* **65**, 197–204.

Linsenmeyer, T. F., Fitch, J. M. & Mayne, R. (1984) Extracellular matrices in the developing avian eye: type V collagen in corneal and neocorneal tissues. *Invest. Ophthal.* **25**, 41-47.

Linsenmeier, T. F., Smith, G. N. & Hay, E. D. (1977) Synthesis of two collagen types by embryonic chick corneal epithelium in vitro. *Proc. Nat. Acad. Sci.*, **74**, 39–43.

Liu, S. H., Tagawa, Y., Prendergast, R. A., Franklin, R. M. & Silverstein, A. M. (1981) Secretory component of IgA: a marker for differentiation of ocular epithelium. *Invest. Ophthal.* **20**, 100–109.

Maren, T. H., Jankowska, L., Sanyal, G. & Edelhauser, H. F. (1983) The transcorneal permeability of sulfonamide carbonic anhydrase inhibitors and their effects on aqueous humor secretion. *Exp. Eye Res.* **36**, 457–480.

Matsuda, M., Sawa, M., Edelhauser, H. F., Bartels, S. P., Neufeld, A. H. & Kenyon, K. R. (1985) Cellular migration and morphology in corneal endothelial wound repair. *Invest. Ophthal.* **26**, 443–449.

Matsumoto, S., Hayashi, K., Tsuchisaka, H. & Araie, M. (1981) Pharmacokinetics of surface anesthetics in the human cornea. *Jap. J. Ophthal.* **25**, 335–340.

di Mattio, J. (1984) *In vivo* entry of glucose analogs into lens and cornea of the rat. *Invest. Ophthal.* **25**, 160–165.

Maurice, D. M. (1951) The permeability to sodium ions of the living rabbit's cornea. *J. Physiol.* **122**, 367–391.

Maurice, D. M. (1957) The structure and transparency of the cornea. *J. Physiol.* **136**, 263–286.

Maurice, D. M. (1967) Epithelial potential of the cornea. *Exp. Eye Res.* **6**, 138–140.

Maurice, D. M. (1968) Cellular membrane activity in the corneal endothelium of the eye. *Experientia* **24**, 1094–1095.

Maurice, D. M. (1969) The cornea and sclera. In *The Eye.* Ed. Davson, Vol. I, pp. 489–600. London: Academic Press.

Maurice, D. M. (1972) The location of the fluid pump in the cornea. *J. Physiol.* **221**, 43–54.

Maurice, D. M. (1984) The cornea and sclera. In *The Eye.* Vol. IB, Ed. H. Davson, 3rd. Edn. pp. 1–158. New York: Academic Press.

Maurice, D. M. & Giardini, A. A. (1951) Swelling of the cornea *in vivo* after the destruction of its limiting layers. *Brit. J. Ophthal.* **35**, 791–797.

Maurice, D. M. & Riley, M. V. (1970) The cornea. In *Biochemistry of the Eye.* Ed. Graymore, C., pp. 1–103. London: Academic Press.

Maurice, D. M., Zauberman, H. & Michaelson, I. C. (1966) The stimulus to neovascularization in the cornea. *Exp. Eye Res.* **5**, 168–184.

Meier, S. & Hay, E. D. (1973) Synthesis of sulfated glycosaminoglycans by embryonic corneal epithelium. *Dev. Biol.* **35**, 318–331.

Meyers-Elliott, R. H. & Chitjian, P. A. (1981) Immunopathogenesis of corneal inflamation: role of polymorphonuclear leukocyte. *Invest. Ophthal.* **20**, 784–798.

Midelfart, A. (1987a) The effects of amiloride, ouabain and osmolality on sodium transport across bovine cornea. *Pflugers Arch.* **408**, 243–248.

Midelfart, A. (1987b) The effect of amiloride on Na, K and water in bovine corneal epithelium. *Exp. Eye Res.* **45**, 751–762.

Minkowski, J. S., Bartels, S. P., Delari, F. C., Lee, S. R., Kenyon, K. R. & Neufeld, A. H. (1984) Corneal endothelial function and structure following cryo-injury in the rabbit. *Invest. Ophthal.* **25**, 1416–1425.

Mishima, S. (1981) Clinical pharmacokinetics of the eye. *Invest. Ophthal.* **21**, 504–541.

Mishima, S. (1982) Clinical investigations on the corneal endothelium. *Amer. J. Ophthal.* **93**, 1–29.

Mishima, S. & Trenberth, S. M. (1968) Permeability of the corneal endothelium to nonelectrolytes. *Invest. Ophthal.* **7**, 34–43.

Murphy, C., Alvarado, J., Juster, R. & Maglio, M. (1984) Prenatal and postnatal cellularity of the human corneal endothelium. *Invest. Ophthal.* **25**, 312–322.

Myers, D. B., Highton, T. C. & Rayns, D. G. (1973) Ruthenium red-positive filaments interconnecting collagen fibrils. *J. Ultrastr. Res.* **42**, 87–92.

Nakagawa, S., Nishida, T. & Manabe, R. (1985) Actin organization in migrating corneal epithelium of rabbits *in situ. Exp. Eye Res.* **41**, 335–343.

Neufeld, A. H., Jumblatt, M. M., Malkin, E. D. & Raymond, G. M. (1986) Maintenance of corneal endothelial cell shape by prostaglandin E_2: effects of EGF and indomethacin. *Invest. Ophthal.* **27**, 1437–1442.

Neufeld, A. H., Ledgard, S. E., Jumblatt, M. M. & Klyce, S. D. (1982) Serotonin-stimulated cyclic AMP synthesis in the rabbit corneal epithelium. *Invest. Ophthal.* **23**, 193–198.

Nishida, T., Nakagawa, S., Nishibayashi, C., Tanaka, H. & Manabe, R. (1984) Fibronectin enhancement of corneal epithelial wound healing in rabbits *in vivo. Arch. Ophthal.* **102**, 455–456.

Nishida, T., Nakagawa, S., Ohashi, Y., Awata, T. & Manabe, R. (1982) Fibronectin in corneal wound healing: appearance in cultured rabbit cornea. *Jap. J. Ophthal.* **26**, 410–415.

Nishida, T., Ohashi, Y., Awata, T. & Manabe, R. (1983) Fibronectin. A new therapy for corneal trophic ulcer. *Arch. Ophthal.* **101**, 1046–1048.

Olsen, T. & Sperling, S. (1987) The swelling pressure of the human corneal stroma as determined by a new method. *Exp. Eye Res.*, **44**, 481–490.

Otori, T. (1967) Electrolyte content of the rabbit corneal stroma. *Exp. Eye Res.* **6**, 356–367.

Ottersen, O. P. & Vegge, T. (1977) Ultrastructure and distribution of intercellular junctions in corneal endothelium. *Acta Ophthal.* **55**, 69–78.

Pedler, C. (1962) The fine structure of the corneal epithelium. *Exp. Eye Res.*, **1**, 286–289.

Polse, K. A. & Mandell, R. B. (1970) Critical oxygen tension at the corneal surface. *Arch. Ophthal.* **84**, 505–508.

Potts, A. M. & Modrell, R. W. (1957) The transcorneal potential. *Am. J. Ophthal.* **44**, 284–290.

Raymond, G. M., Jumblatt, M. M., Bartels, S. P. & Neufeld, A. H. (1986) Rabbit corneal endothelial cells *in vitro*: effects of EGF. *Invest. Ophthal.* **27**, 474–479.

Reinach, P. S. & Kirchberger, M. A. (1983) Evidence for catecholamine-stimulated cyclase activity in frog and rabbit corneal epithelium and cyclic AMP-dependent protein kinase and its protein substrates in frog corneal epithelium. *Exp. Eye Res.*, **37**, 327–335.

Rexed, B. & Rexed, V. (1951) Degeneration and regeneration of corneal nerves. *Br. J. Ophthal.* **35**, 38–49.

Riley, M. V. (1969) Glucose and oxygen utilization by the rabbit cornea. *Exp. Eye Res.* **8**, 193–200.

Riley, M. W. (1977) Anion-sensitive ATPase in rabbit corneal endothelium and its relation to corneal hydration. *Exp. Eye Res.* **25**, 483–494.

Rochels, R. & Busse, W. D. (1983) Experimentelle Untersuchungen zum Einflusz von Prostaglandin- und Leukotrien-Synthesehemmern auf die Epithelregeneration der Hornhaut. *v. Graefes Arch. Ophthol.*, **220**, 74–78.

Rochels, R. & Busse, W. D. (1984) In vivo evidence for the chemotactic activity of cyclooxygenase- and lipoxygenase-dependent compounds using a corneal implantation technique. *Ophthal. Res.*, **16**, 194–197.

Romero, J. A. & Axelrod, J. (1974) Pineal β-adrenergic receptor: diurnal variation in sensitivity. *Science* **184**, 1091–1092.

Savage, C. R. & Cohen, S. (1973) Proliferation of cornea epithelium induced by epidermal growth factor. *Exp. Eye Res.* **15**, 361–366.

Schwarz, W. (1953) Elekronenmikroskopische Untersuchungen uber den Aufbau der Sklera und der Cornea des Menschen. *Z. Zellforsch.* **38**, 20–49.

Schwarz, W. & Keyserlingk, D. G. (1966) Uber die Fienstruktur der menschlichen Cornea, mit besonderer Berüchsichtigung des Problems der Transparenz. *Z. Zellforsch.* **73**, 540–548.

Shapiro, M. S., Friend, J. & Thoft, R. A. (1981) Corneal re-epithelialization from the conjunctiva. *Invest. Ophthal.* **21**, 135–142.

Sholley, M. M., Gimborne, M. A. & Cotran, R. S. (1978) The effect of leukocytes depletion on corneal neovascularization. *Lab. Invest.* **38**, 32–44.

Simonsen, A. H., Sørensen, K. E. & Sperling, S. (1981) Thymidine incorporation by human corneal endothelium during organ culture. *Acta Ophthal.* **59**, 110–118.

Smelser, G. K. & Ozanics, V. (1953) Structural changes in corneas of guinea pigs after wearing contact lenses. *Arch. Ophthal.*, **49**, 335–340.

Smith, J. W. (1969) The transparency of the corneal stroma. *Vision Res.* **9**, 393–396.

Srinivasan, B. D., Worgul, B. V., Iwamoto, T. & Eakins, K. E. (1977) The reepithelialization of rabbit cornea following partial and complete epithelial denudation. *Exp. Eye Res.*, **25**, 343–351.

Stanworth, A. & Naylor, E. S. (1953) Polarized light studies of the cornea. *J. exp. Biol.* **30**, 164–169.

Sugaya, M. & Nagataki, S. (1978) Kinetics of topical pilocarpine in the human eye. *Jap. J. Ophthal.* **22**, 127–141.

Swan, K. C. & White, N. G. (1942) Corneal permeability. *Am. J. Ophthal.* **25**, 1043–1058.

Teng, G. C. (1961) The fine structure of the corneal epithelium and basement membrane of the rabbit. *Am. J. Ophthal.* **51**, 278–297.

Teng, S. C. G., Savion, N., Gospodarowicz, D. & Stern, R. (1981) Characterization of collagens synthesized by cultured bovine corneal endothelial cells. *J. biol. Chem.* **256**, 3361–3365.

Tervo, T. & Palkama, A. (1975) Electron microscopic localization of adenosine triphosphatase (NaK-ATPase) activity in the rat cornea. *Exp. Eye Res.* **21**, 269–279.

Thoft, R. A. & Friend, J. (1972) Corneal amino acid supply and distribution. *Invest. Ophthal.* **11**, 723–727.

Thoft, R. A. & Friend, J. (1975) Permeability of regenerated corneal epithelium. *Exp. Eye Res.* **21**, 409–416.

Thoft, R. A. & Friend, J. (1977) Biochemical transformation of regenerating ocular surface epithelium. *Invest. Ophthal.* **16**, 14–20.

Thoft, R. A., Friend, J. & Dohlman, C. H. (1971a) Corneal glucose concentration. *Arch. Ophthal.* **85**, 467–472.

Thoft, R. A., Friend, J. & Dohlman, C. H. (1971b) Corneal glucose flux. II. *Arch. Ophthal.* **86**, 685–691.

Thompson, P., Desbordes, J. M., Giraud, J., Pouliquen, Y., Barritault, D. & Courtois, Y. (1982). The effect of an eye derived growth factor (EDGF) on corneal epithelial regeneration. *Exp. Eye Res.* **34**, 191–199.

Timpl, R., Rohde, H., Robey, P. G., Rennard, S. I., Foidart, J.-M. & Martin, G. R. (1979). Laminin—a glycoprotein from basement membranes. *J. biol Chem.* **254**, 9933–9937.

Toole, B. P. & Trelstad, R. L. (1971) Hyaluronate production and removal during corneal development in the chick. *Dev. Biol.* **26**, 28–35.

Trelstad, R. L. & Coulombre, A. J. (1971) Morphogenesis of the collagenous stroma in the chick cornea. *J. Cell Biol.* **50**, 840–858.

Trelstad, R. L., Hayashi, K. & Toole, B. P. (1974) Epithelial collagens and glycosaminoglycans in the embryonic cornea. *J. Cell Biol.* **62**, 815–830.

Trelstad, R. L. & Kang, A. H. (1974) Collagen heterogeneity in the avian eye: lens, vitreous body, cornea and sclera. *Exp. Eye Res.* **18**, 395.

Trenberth, S. M. & Mishima, S. (1968) The effect of ouabain on the rabbit corneal endothelium. *Invest. Ophthal.* **7**, 44–52.

Tsuru, T., Araie, M., Matsubara, M. & Tanishima, T. (1984) Endothelial wound healing of monkey cornea: fluorophotometric and specular microscopic studies. *Jap. J. Ophthal.*, **28**, 105–125.

Tuft, S. J., Williams, K. A. & Coster, D. J. (1986) Endothelial repair in the rat cornea. *Invest. Ophthal.* **27**, 1199–1204.

Turss, R., Friend, J. & Dohlman, C. H. (1970) Effect of a corneal fluid barrier on the nutrition of the epithelium. *Exp. Eye Res.* **9**, 254–259.

Twersky, V. (1976) Transparency of pair-correlated, random distributions of small scatterers, with application to the cornea. *J. opt. Soc. Amer.* **65**, 524–530.

Van Horn, D. L. & Hyndiuk, R. A. (1975) Endothelial wound repair in primate cornea. *Exp. Eye Res.* **21**, 113–124.

Yamada, K. M. & Olden, K. (1978) Fibronectins—adhesive glycoproteins of cell surface and blood. *Nature* **275**, 179–184.

Yee, R. W., Edelhauser, H. F. & Stern, M. E. (1987) Specular microscopy of vertebrate corneal endothelium: a comparative study. *Exp. Eye Res.* **44**, 703–714.

Yee, R. W., Geroski, D. H., Matsuda, M., Champeau, E. J., Meyer, L. A. & Edelhauser, H. F. (1985) Correlation of corneal endothelial pump site density, barrier function, and morphology in wound repair. *Invest. Ophthal.* **26**, 1191–1201.

Yoshida, S. & Mishima, S. (1975) A pharmacokinetic analysis of the pupil response to topical pilocarpine and tropicamide. *Jap. J. Ophthal.*, **19**, 121–138.

Zadunaisky, J. A. (1966) Active transport of chloride in frog cornea. *Am. J. Physiol.* **211**, 506–512.

Zadunaisky, J. A. (1969) The active chloride transport of the frog cornea. In *The Cornea.* Ed. Langham, M. E., pp. 3–34. Baltimore: Johns Hopkins Press.

Zadunaisky, J. A., Lande, M. A. & Hafner, J. (1971) Further studies on chloride transport in the frog cornea. *Amer. J. Physiol*, **221**, 1832–1836.

Zander, E. & Weddell, G. (1951) Observations on the innervation of the cornea. *J. Anat. Lond.* **85**, 68–99.

Zauberman, H., Michaelson, I. C., Bergman, F. & Maurice, D. M. (1969) Stimulation of neovascularization of the cornea by biogenic amines. *Exp. Eye Res.* **8**, 77–83.

Zieske, J. D., Higashijima, S. C. & Gipson, I. K. (1986) Con A- and WGA-binding glycoproteins of stationary and migratory corneal epithelium. *Invest. Ophthal.* **27**, 1205–1210.

4. THE LENS

DEVELOPMENT AND STRUCTURE

The lens is a transparent biconvex body (Fig. 4.1); the apices of its anterior and posterior surfaces are called the *anterior* and *posterior poles* respectively; the line passing through the lens and joining the poles is the *axis*, whilst lines on the surface passing from one pole to the other are called *meridians*. The *equator* is a circle on the surface at right-angles to the axis (Fig. 4.1). Structurally, the lens is divided into the *capsule*, an elastic envelope capable of moulding the lens substance during accommodative changes (Sect. 4), and by which the attachment to the zonule is made; the *epithelium*, extending as a single layer of cells under the anterior portion of the capsule as far as the equator; and the *lens substance* made up of fibres and interstitial cement material. The significance of the intimate structure of the lens substance can only be appreciated with knowledge of its embryonic and later development.

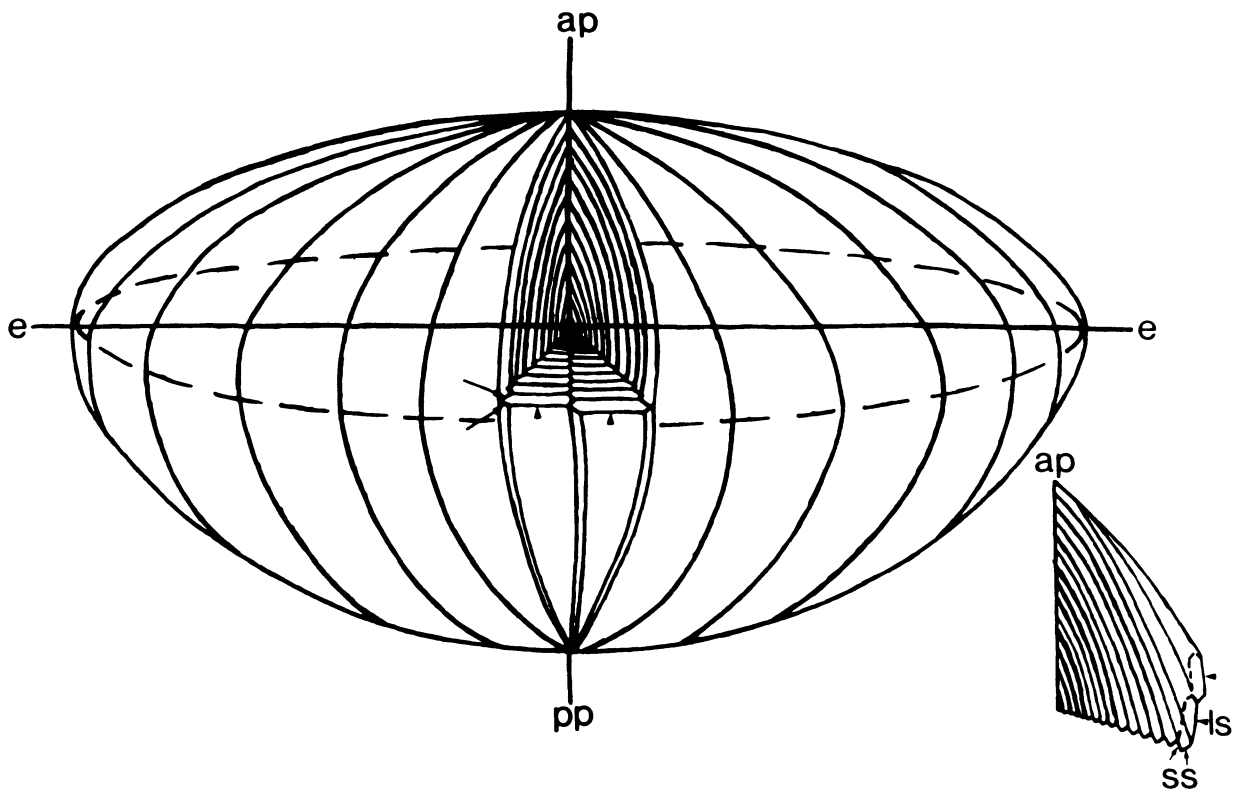

Fig. 4.1 Schematic diagram of a 3-month-old chick lens demonstrating the anteroposterior axis, from the anterior to the posterior pole (ap, pp), and the equatorial axis (e). A wedge of the lens has been removed to show the crescentic fibre shape in longitudinal section (anteroposterior axis) and the hexagonal fibre shape in cross section (equatorial axis). Note that the hexagonal fibres have two long sides (ls, arrowheads), orientated parallel to the lens surface, and four short sides orientated circumferentially. (Kuszak *et al.*, *Amer. J. Anat.*)

Embryology

The lens vesicle, on separation from the surface ectoderm, is a sphere whose wall consists of a single layer of epithelium. On their outer aspect the cells of this epithelium secrete a structureless hyaline membrane, the capsule; the cells of the posterior wall and the equatorial region, moreover, undergo marked differentiation and from these the adult lens is formed. The cells of the posterior wall differentiate first, becoming primitive fibres by a process of elongation (Fig. 4.2): their nuclei ultimately disappear and they remain as an optically clear *embryonic nucleus* in the centre of the mature lens. At the equator, meanwhile, epithelial cells likewise elongate to become fibres; the anterior end of each passes forward towards the anterior pole, insinuating itself under the epithelium, whilst the posterior end passes backwards towards the posterior pole. This process continues, and since each new fibre passes immediately under the epithelium it forces the earlier formed fibres deeper and deeper; successive layers thus encircle the central nucleus of primitive fibres.

Fibre Formation

The actual process whereby the developing lens fibres force themselves over less recently formed ones may now be described. The epithelial cells at the equator tend to become arranged in meridional rows (Fig. 4.3); they assume a pyramidal shape and finally their inner parts elongate and turn obliquely to run under the epithelium of the anterior capsule; the cell is now a young fibre and its inner end, which must now be referred to as its anterior end, grows forward whilst its outer (posterior) end is pushed backwards by a similarly developing cell immediately in front. As the cells grow into the lens substance, the nuclei gradually recede with them, becoming arranged in a wide bend which curves round anteriorly as the process of elongation proceeds; this configuration is termed the *nuclear* or *bow zone.*

At a certain stage the nucleus disappears—*denucleation*—so that the fibres in the less superficial layers are non-nucleated cells.

SUTURES

A recently formed lens fibre thus has its centre approximately at the equator, whilst the two limbs pass forward and backward towards the anterior and posterior poles respectively to meet the limbs of another cell developing from an 'antipodeal' position. If the system were completely symmetrical, the meeting point would be the same for all cells, as illustrated schematically in Fig. 4.4A. In fact, no such complete symmetry exists and the fibres meet each other in quite complicated figures which are called *sutures*; the simplest is probably the line-suture of the dogfish (Fig. 4.4B) and other lower vertebrates, whilst the human embryonic and adult nuclei have Y- and four-pointed stars respectively (Fig. 4.4C and D).

THE LENS FIBRES

The superficial lens fibres are long, prismatic, ribbon-like cells some 8 to 10 mm long, 8 to 12 μm broad, and 2 μm thick. An equatorial section of the lens cuts these fibres transversely, since they run in a generally anteroposterior direction; the appearance of such a section is shown in Fig. 4.5, the orderly development of layer after layer of

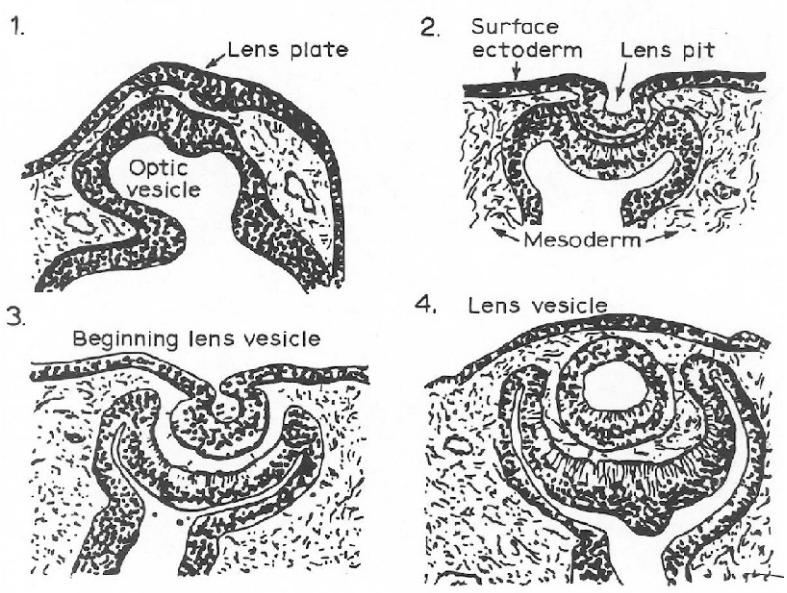

Fig. 4.2 Development of the human lens. (Bellows, *Cataract and Anomalies of the Lens.*)

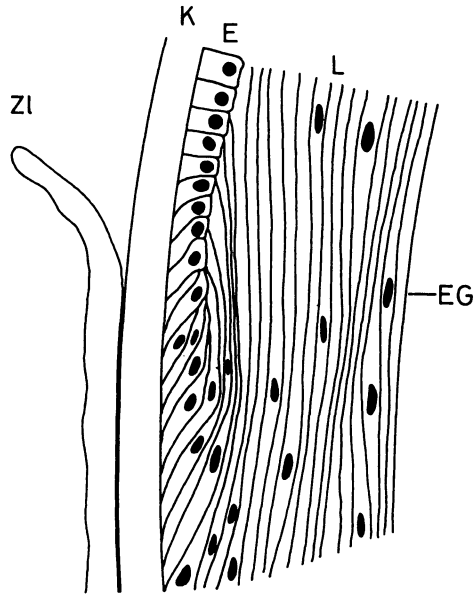

Fig. 4.3 Meridional section of adult human lens, illustrating the formation of meridional rows and the elongation of the epithelial cells. Zl, zonular lamella; K, lens capsule; E, lens epithelium; EG, level of epithelial border. (After Salzmann, *Anatomie u. Histologie d. menschlichen Augapfels.*)

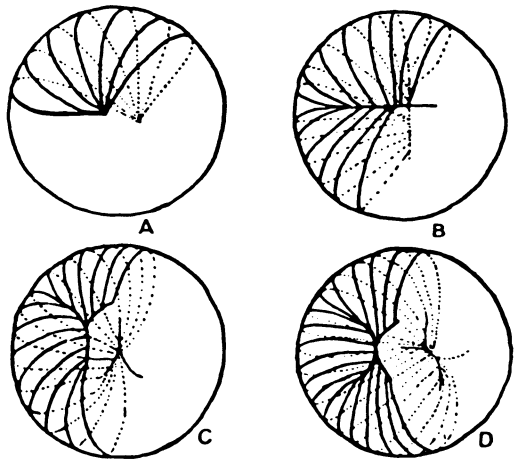

Fig. 4.4 Diagram showing the formation of lens sutures. A, simple arrangement with no sutures; B, linear sutures only; C, the Y-sutures of the human embryonic nucleus; D, four-pointed star of human adult nucleus. (Mann, *Development of the Human Eye.*)

fibres from the cells of the meridional rows leading to a lamellar appearance, the so-called *radial lamellae*. A meridional section, on the other hand, cuts the fibres longitudinally, giving the so-called 'onion-scale' appearance (Fig. 4.3).

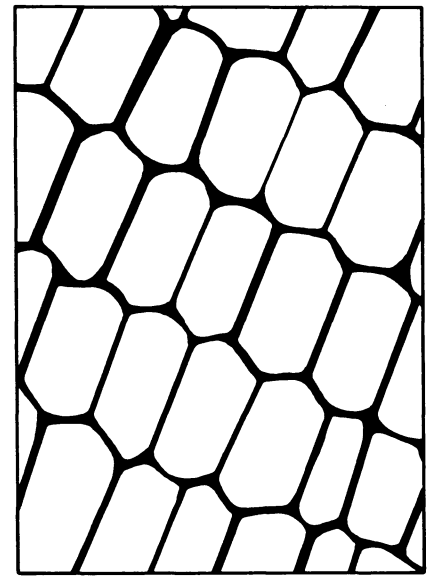

Fig. 4.5 Drawing after phase-contrast micrograph of equatorial section of guinea-pig lens. Haematoxylin-eosin (× 3300). (Hueck and Kleifeld, *v. Graefe's Arch. Ophthal.*)

CORTEX AND NUCLEUS

Since the oldest fibres become more sclerosed and less translucent than the more recently formed ones, the lens is not optically homogeneous; it may be broadly differentiated into a central core—the *nucleus*—and a softer *cortex*. With the slit-lamp the nucleus can be further differentiated into zones, which correspond with the periods at which their fibres were laid down.

The lens grows throughout life, increasing from an average weight of 130 mg at 0 to 9 years to 255 mg at 80 to 89 years. The relative thickness of the cortex increases continuously until in old age it represents a third of the total. As a result of this growth the curvature of the outer zone progressively decreases, i.e. the lens becomes flatter; the decrease in dioptric power that would otherwise ensue is prevented by the simultaneous increase in the refractive index of the nucleus. When the increase in refractive index fails to keep pace with the flattening of the surface, the eye becomes hypermetropic; in early cataract the nucleus becomes excessively sclerosed so that the eye becomes myopic.

Development of the Lens Fibres

Because of the continual growth throughout life, the lens cells differ in morphology, and the differences reveal the successive stages in the life-cycle of the lens cell from the relatively undifferentiated anterior lens cell—*epithelial*

cell—through the young fibre immediately beneath the epithelium in the bow zone, to the mature cortical cells, whilst the innermost *nuclear* cells reveal the size and shape of the earliest formed embryonic and fetal fibres. In discussing the ultrastructure of the lens fibres, then, it is probably best to consider this in relation to the process of development.[1]

Epithelial Cell

Kuwabara (1975) has described the changes in the epithelial cell that lead to its ultimate detachment from the basal lamina to become a lens fibre. In describing, first, the epithelium he points out that this layer is different from many other covering layers in that the apices of the cells face inwards, and that their main function is to produce lens fibres and synthesize the lens proteins, so that the rough endoplasmic reticulum is the only predominant organelle, whilst the profound lateral interdigitations may represent the anlage for the characteristic lateral junctions of the mature lens fibres, interdigitations that probably subserve a structural role. In its early developmental stage, the anterior cell begins to contain a fine granular substance, the lens proteins, and this feature is maintained throughout life.

Young Cells in Bow Zone

The elongation of the anterior lens (epithelial) cells that have migrated to the equator leads to a bow configuration of the nuclei in nearby fibres, because the nuclei retain their central configuration whilst adjacent fibres show different degrees of elongation. The basal ends of these cells remain firmly attached to the basement membrane (capsule) and the apical ends extend towards the anterior of the lens. The cells in the innermost zone of the bow area appear to attach at the posterior pole with their anterior ends at the anterior pole.

Sutures

Cells in the deeper cortex maintain apical junctions with cells extending from the other side, the junction line being the *anterior suture*. The basal ends of the cells detach from the basement membrane at the posterior pole when the cells expel their nuclei, and thus they are free to be pushed deeper into the lens. This area is seen as the Y-shaped *posterior suture*; the basal ends of the cells from opposite sides, forming the suture, seem to be only loosely joined, by comparison with the anterior apical junctions. In the monkey, the nucleated bow cells form a layer averaging 300 to 500 μm thick; the lateral interdigitations seen in the original epithelial cell become protrusions in the extended fibre, forming socket-and-ridge junctions.

Loss of Organelles

Maturation of the lens fibre is associated with loss of protein synthetic power, and this is revealed by a gradual loss of the typical organelles, such as ribosomes, mitochondria and rough-surfaced endoplasmic reticulum, which is manifest even in the cells of the meridional rows (Rafferty & Esson, 1974).

Denucleation

Kuwabara & Imaizumi (1974) followed the process of denucleation in the deeper zones of the bow; the loss of organelles goes hand in hand with the loss of chromatin from the nucleus, which gradually disappears with no signs of degeneration; the membrane finally breaks up into a set of vesicles and the outline becomes Feulgen-negative indicating the loss of all DNA. It would seem that the loss of organelles and nucleus is brought about by phagolysosomes (Gorthy *et al.*, 1971).

Mature Lens Fibres

These cells have lost their attachment to the basement membrane and may be described as band-like structures appearing, on cross-section, as hexagons with four short and two long faces (Fig. 4.1).

Nuclear Cells

These, the oldest cells, are essentially similar in morphology to the cortical cells, but are smaller and more tightly packed; cell membranes can be seen although these appear poorly defined in the electron microscope. Figure 4.6 summarizes the changes in cell structure, as revealed by differences in location.

Relation to Capsule

When viewed in the scanning electron microscope, the surfaces of the cells facing the basal lamina—capsule—show characteristic indentations, whilst the overlying basal lamina shows serpentine bodies on its surface which probably represent the counterparts of these indentations, or craters, and doubtless these maintain adhesions between the cell and the basal lamina. When the basal lamina is peeled away and the cellular surface is compared with the lamina surface, filamentous processes can be seen to have been torn from the epithelial cells giving a pattern of the ridges of the cells indicating attachments at cell borders, perhaps similar to the interdigitations between cells laterally. By contrast, the developing lens fibres, immediately beneath the epithelium, shows a relatively smooth surface, so presumably during development the attachments to the basal lamina are

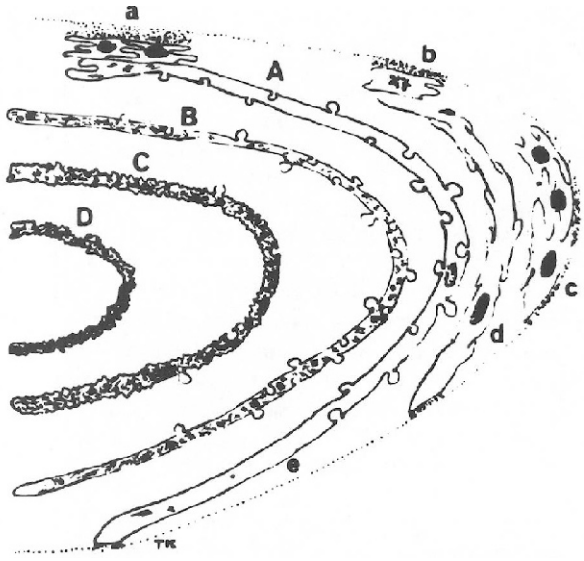

Fig. 4.6 Diagram to show distribution of the cells in various maturation stages and cytological appearances. Broken lines on the left indicate the areas proportionally. A, anterior cells and bow cells; B, cortex; C, deep cortex; D, lenticular nucleus. Sizes of cells shown on the right are not in proportion. Young lens cells, a–e, which occupy only a thin superficial layer, A, contain nuclei and attach to the basement membrane. Matured cells B and C occupy the majority of the lens. These cells have no basal attachment but they have unique apparatus in joining to each other by socket and fine ridge joints. Ridges become more numerous towards the centre. Older cells, D, form the lenticular nucleus. Transition between C and D is gradual. (Kuwabara, *Exp. Eye Res.*)

broken. According to Kuwabara (1975) the epithelial cells are attached by numerous gap-junctions to superficial lens fibres.

Epithelium

This single layer of cells covers only the anterior surface of the lens and should be regarded more as a source of cells, produced by mitotic division near the equator, that produce the lens fibres, rather than as a covering epithelium devoted to selective transport. As seen in the electron microscope, the epithelial cells show marked lateral interdigitations (Fig. 4.7) on which characteristic epithelial junctional apparatuses are found. There is some disagreement as to whether the junctions are exclusively of the gap-type or whether there are also some of the occluding type, and this may be because of species differences. Goodenough *et al.* (1980), working on the mouse, found that horseradish peroxidase penetrated into the lens-substance, passing between epithelial cells; freeze-fracture studies of junctions showed them to be of the gap-type. In the chick lens, however, tight junctions

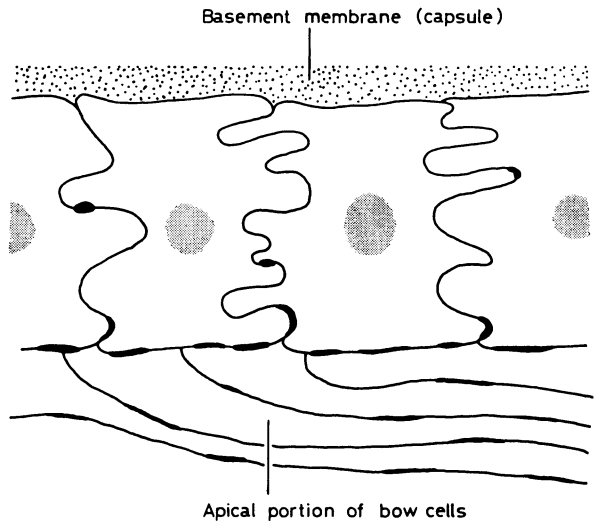

Fig. 4.7 Diagrammatic illustration of lateral interdigitations between lens epithelial cells, with junctional complexes. (Kuwabara, *Exp. Eye Res.*)

were said to be present. Labelled amino acids and sugars passed into the epithelial cells and were apparently transmitted from these to the underlying cortical lens fibres, so that they penetrated to greater depths than did sucrose, which was unable to pass into the epithelial cells. In human and frog lenses Lo & Harding (1983) identified tight junctions through which horseradish peroxidase could not pass; however, it did cross the epithelium into the underlying spaces, presumably through intercellular clefts not sealed in this way.

Interfibre Connections

The lens is a tightly packed mass of cells, and the relations between individual cells are of considerable interest on two main grounds. First, for the maintenance of optical transparency a regular geometrical arrangement of the cells, with a minimum of discontinuity of refractive index between them, is a necessary prerequisite, as we have seen when discussing a similar problem with the cornea. Secondly, this large mass of metabolizing tissue is isolated from the vascular system, its metabolic needs being met by the aqueous humour and vitreous body; cells deep in the lens will be a considerable distance from these fluids, so that an efficient means of transport through the lens is required. This latter requirement is met by an elaborate system of intercellular junctions, of the gap-type, that permit ready diffusion from one cell to the other. The same elaborate system of gap-junctions, together with other junctional arrangements that are peculiar to the lens, contribute to the maintenance of a rigid geometrical

uniformity, maintained in spite of the changes in shape of the lens that take place during accommodation. The metabolic aspect has been discussed at length by Goodenough and his colleagues, and the latter by Kuszak and his colleagues.

Interlocking Junctions

These are formed during fibre maturation (Kuwabara, 1975; Harding *et al.*, 1976), and are particularly evident in young fibres. A study of the lens in the developing chick eye reveals the changes with maturation in some detail, and have been described by Kuszak *et al.* (1980). The interlocking junctions in this species are of three types, namely ball-and-socket, flaps and imprints, and finger-process fitting into fingerprint. Ball-and-socket junctions are illustrated schematically in Fig. 4.8, the balls being formed as extensions of the fibres where two short sides of the hexagons come together. They consist of short cytoplasmic stalks, about 0.6 μm in diameter, that expand to form a 1.1 μm diameter dome that embeds in a complementary depression in the adjoining fibre. The fibres thus interlocked may be of different age, i.e. between two long sides, or they may be of the same age, i.e. between short sides. Flaps are discrete tongue-like extensions elaborated along the angle of short and long sides, repeated regularly along the length of the fibre; they embed into complementary imprints formed on the short sides of neighbouring fibres. A third type of interlocking device, described in the chick lens, is a finger-like process fitting into a complementary fingerprint; the finger-like processes were found in the posterior segment of the concave long sides of the fibres, and they were embedded into fingerprints on the convex long surfaces.

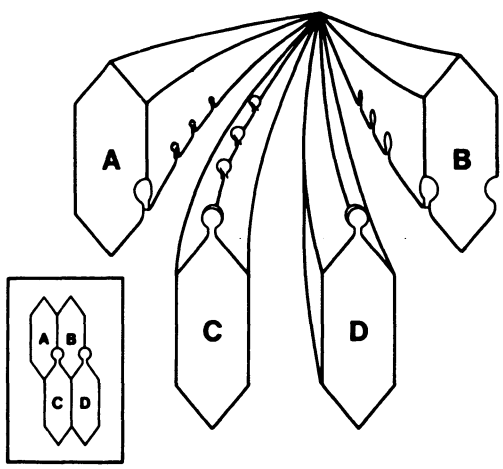

Fig. 4.8 Schematic diagram of the interlocking scheme of short-side balls and sockets. For the sake of clarity, not all balls and sockets are indicated. (Kuszak *et al.*, *Amer. J. Anat.*)

Gap-junctions

The long sides of the fibres had smaller ball-and-socket joints, and their most striking feature was the large number of gap-junctions. These, in addition to serving as intercellular diffusion pathways, probably also contribute to structural rigidity. Thus they are so numerous on the long sides as to eliminate effectively the intercellular space, creating a single refracting surface. The importance of the gap-junction in this respect was demonstrated by Kuszak *et al.* (1980) who showed that the developing chick lens first became transparent on Day 5, and this coincided with the appearance of more than 40% of the long sides being covered by these junctions. In the mature fibre they have been described by Kuszak *et al.* (1978) as ranging in area from 0.02 to 12.5 μm^2, and occupying some 64% of the total fibre surface.[2]

RELATION TO BALL-AND-SOCKET JOINTS

This was investigated by Kistler *et al.* (1985, 1986) by labelling the fibres with fluorescent antibodies that were apparently specific for the membrane protein in gap-junctions, MP70, and one to the membrane of ball-and-socket regions, namely wheat-germ agglutenin. Fluorescence of MP70 was concentrated on the broad sides of lens fibres, as would be expected if it were revealing sites of gap-junctions. Gap-junctions were also demonstrated in ball-and-socket joints.

SWITCH MECHANISM

Goodenough (1979) has argued that the lens gap-junction is different from that in other cells in lacking a switch-mechanism that converts the junction from a low- to a high-resistance state, a switch that operates when a cell is damaged, in intense secretory activity, or when differentiating. Morphologically the change is revealed in a crystallization of the 'connexons', the cylindrical subunits that span both plasma membranes of the participating cells and a narrow 2–3 nm extracellular gap. In the unswitched state the connections are in a disordered morphology. The interesting feature of the lens is that the connexons retain their disordered morphology under conditions where those of a liver cell, for example, would crystallize.

The Posterior Surface

Kuwabara has emphasized that the posterior surface of the lens is essentially similar to the anterior surface, being made up of epithelial cells, with the difference simply that the cells attached to the basement membrane at this side are elongated whilst their nuclei are situated only in the bow zone; they appear not to produce basement membrane to the same degree as the anterior (epithelial cells).

The attachment of these posterior portions of the lens cells to the basal lamina (capsule) is rather loose, and their gap-junctions are sparse. By contrast, the anterior (epithelial) cells are attached to the underlying superficial cortical cells tightly by numerous gap-junctions.

The Capsule

In the electron microscope this appears as a regularly laminated structure, having been formed by the successive deposition of basement-membrane material by the underlying cells. This synthesis was demonstrated by Young & Ocumpaugh (1966) by administering ^{35}S-labelled sulphate and ^{3}H-glycine to young rats and following their appearance into the epithelium and overlying capsule. As with Descemet's membrane, the main basis is collagen with specific chemical and electron-microscopical appearance that differentiates it from the collagen of connective tissue; and it is classed as Type IV. The strong PAS-positivity indicates the presence of sugar-residues, which have been identified as mainly glucosylgalactosylhydroxylysine and galactosylhydroxylysine (Spiro & Fukushi, 1969). The capsule is obviously divided into two layers, the zonular fibres being attached to the outer one, which is therefore called the *zonular lamella.*

TRANSPARENCY

The transparency of this densely packed mass of cells, containing very high protein concentrations that give the whole a high refractive index, probably results from a special character of the lens proteins—*crystallins*—which permits very high concentrations without separation of large aggregates that would cause scatter. In addition, the loss of nucleus and other intracellular organelles, and the dense packing of the fibres that reduces the intercellular spaces to very small values, are contributory factors. Thus the main discontinuities of refractive index are presumably the cell membranes separating the individual fibres; at any rate the X-ray diffraction pattern indicates a spacing of about 7 μm which might well correspond to the separation of membranes by the cytoplasm, and it is likely that the scattering of light by the lens, which makes it visible in the slit-lamp, is due to these discontinuities and could be responsible for the haloes around bright objects (Simpson, 1953).

Birefringence

The uniform distribution of protein in the lens fibre described by Philipson (1969; 1973) is consistent with an absence of optical anisotropy revealed by a negligible birefringence (Bettelheim, 1975); however, this author has suggested that the absence of birefringence is due to cancellation of a negative form-birefringence, governed by the orderly spacing of the lens membranes at right-angles to the optic axis, and a positive intrinsic birefringence, due to an ordered arrangement of macromolecules in the cytoplasm; and it may be that the special feature of the lens crystallins that permits this orientation of aggregates is an adaptation that allows cancellation of the form birefringence to give increased transparency.

THE LENS AS A FUNCTIONAL UNIT

Regional Variations

The essentials of the chemical composition of the lens are shown in Table 4.1. Because of its history, however, we may expect to find differences in composition according to (*a*) the total age of the lens and (*b*), in a given lens, according to the region selected. Thus the average water-content of the calf lens, containing a high percentage of young fibres, was found by Amoore *et al.* (1959) to be 2.1 grammes of H_2O per gramme of dry weight (g/g), comparing with 1.8 g/g for ox lens. Again by carefully peeling off concentric zones and analysing them, Amoore *et al.* found the following values from without inwards: 3.67, 2.86, 2.32, 1.79, 1.51 and 1.28 g/g respectively; thus the water-content of the innermost zone is less than half that of the outermost zone including the capsule. In the human, however, although there is a difference in water-contents between nucleus ($63.4 \pm 2.9\%$) and cortex ($68.0 \pm 4.3\%$) there seems to be no tendency for the water-content to decrease with age (Van Heyningen, 1972; Fisher & Pettet, 1973).

Table 4.1 Chemical composition of the lens

	Young	*Old*
Water (per cent)	69.0	64.0
Protein (per cent)	30.0	35.0
Sodium (meq/kg H_2O)	17.0	21.0
Potassium	120.0	121.0
Chloride (meq/kg H_2O)	27.0	30.0
Ascorbic acid (mg/100 g)	35.0	36.0
Glutathione (mg/100 g)	2.2	1.5

Sodium and Potassium

The lens is essentially a cellular tissue, so that we may expect a high concentration of potassium and a low concentration of sodium; this is generally true since the figures given by Amoore *et al.*, for example, indicate a value of approximately 20 m-molar for the concentration

of sodium in the tissue-water and 120 m-molar for potassium. If this sodium is largely extracellular, whilst the potassium is largely intracellular, we may compute an extracellular space for the lens of about 13%.[3]

Extracellular Space

Direct measurements based on the distribution of large molecular weight extracellular markers, such as inulin, indicate a much smaller space, perhaps as low as 4 to 5% for the mammalian lens (Thoft & Kinoshita, 1965; Paterson, 1970), but the situation is complicated by the low diffusibility of inulin within the tissue compared with, say, mannitol, so that Yorio & Bentley (1976), for example, found values of 7% and 12% respectively using inulin and mannitol; and unless some mannitol enters the cells the value of 12% should be the correct one. However, a great deal of this space seems to be provided by the capsule and perhaps a small pool of fluid immediately beneath, since, when Yorio & Bentley removed the capsule, the inulin-space fell to 1.3%; a similar but smaller influence of removing the capsule was described by Paterson (1970). A small value for the extracellular space is consistent with the histology of the tissue which shows the lens fibres to be tightly apposed to each other. This is especially true of the nucleus of the lens where even the presence of intact cell membranes is difficult to establish in the electron microscope. Rae & Stacey (1979) allowed two typical extracellular markers to diffuse into the lens substance, namely $La(NO_3)_3$ and Procion yellow; both markers passed through the extracellular spaces; interestingly, however long the lens was bathed with the Procion yellow solution, this never became demonstrable in the nucleus, even if the cortical layer had been removed first. This suggests that the intercellular spaces have become too narrow to allow passage of this molcule.

Na^+-K^+-Pump

In tissues such as nerve and muscle, where we also have a mass of cells with high internal potassium and high external sodium, these gradients of concentration are maintained by active processes, in the sense that a part of the metabolic energy of the cells is directed towards 'pumping out' any excess of sodium that penetrates into the cells; this Na^+-pump is linked to transport of the K^+-ion so that extrusion of Na^+ from the cell is accompanied by penetration of K^+, and a steady state is attained with the passive leaks of Na^+ in and K^+ out being compensated by active extrusion of Na^+ and an accumulation of K^+. This type of pump is specifically inhibited by cardiac glycosides, such as ouabain, which is also a specific inhibitor of an ATPase closely connected with the supply of metabolic energy for the pump.

MEMBRANE POTENTIAL

The high internal concentration of K^+ and low concentration of Cl^- are associated with a resting, or membrane, potential across the cell membrane, as illustrated by Fig. 4.9, the inside of the cell being negative, and under ideal conditions, being governed by the Nernst Equation:[4]

$$E = -\frac{RT}{zF}\ln\left(\frac{C_i}{C_o}\right)$$

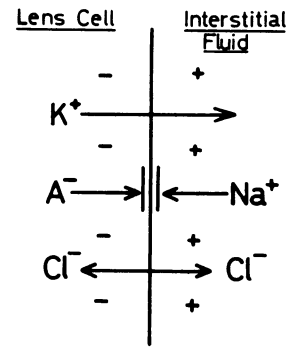

Fig. 4.9 Possible basis of potential across a lens fibre.

An important point to appreciate is that the K^+ and Cl^+ ions are, under these conditions, at equilibrium, although there are large concentration gradients; and this is because the potential operates in the opposite direction to the concentration gradient, so that the two ions are said to be at *equal electrochemical potential* across the membrane. By contrast, the Na^+-ion is not in equilibrium, both the concentration gradient and the electrical potential favouring passage into the cell, and it is the pumping action that prevents the attainment of equilibrium, leaving the concentrations in their steady-state values.

NON-ELECTROGENIC PUMP

An important point to appreciate is that the action of the Na^+-pump does not give rise to the potential directly, but only secondarily by allowing the K^+ to remain accumulated in the cell; thus, poisoning the pump will initially have no effect on the potential, and it will only fall in the course of time as the outside Na^+ penetrates the cell and K^+ leaks out in exchange, and the value of the Nernst-ratio becomes smaller. Thus the pump is said not to be *electrogenic*, by contrast with the corneal and frog-skin pumps where the active transport of Na^+ causes a local accumulation of positive charge on one side of the skin, or cornea, that leads to a passive movement of an anion (Fig. 3.3).

LENS FIBRE

It may be that the situation in the lens is similar to that in muscle or nerve in that the tissue consists of a mass of fibrous cells each enclosed in a membrane capable of sustaining a resting potential associated with a high internal K^+-concentration and low Na^+-concentration; the situation would be represented schematically by Fig. 4.10, where a single fibre represents the total; it is surrounded by extracellular fluid of about the same composition as the vitreous and aqueous humours, these latter fluids being presumably in some sort of dynamic equilibrium with the extracellular fluid since there is no doubt that the capsule is freely permeable to small crystalloids (Friedenwald, 1930).

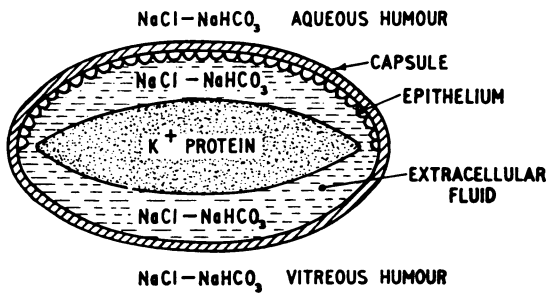

Fig. 4.10 Illustrating the salt and water relationships of the lens fibres, extracellular space, aqueous humour and vitreous body. For simplicity the lens fibres are represented as a single one containing predominantly potassium and protein. The actual volume of the extracellular fluid may be very small indeed, since the fibres are very tightly packed.

EPITHELIUM

A complicating feature is, of course, the layer of epithelial cells on the anterior surface, but it must be appreciated that any activities exerted by these in pumping ions into or out of the extracellular fluid of the lens will be largely vitiated by free exchanges across the posterior surface where there is no epithelial layer unless, of course, a layer of fibres on the posterior surface has become differentiated to permit it to function as an active membrane comparable with the epithelium.

ACTIVE ION TRANSPORT

The importance of metabolism for the maintenance of the normal sodium, potassium and chloride relationships has been demonstrated by several studies; thus Langham & Davson (1949) found that within a few hours *post mortem* the chloride concentration in the lens began to rise; indicating, presumably, an absorption of aqueous humour; again, Harris & Gehrsitz (1951) found that cooling the lens *in vitro*, thereby inhibiting its metabolism, caused the potassium concentration to fall and that of sodium to rise, processes that could be reversed by re-warming.

An obvious interpretation of these findings is that the individual lens fibres maintain their high internal K^+-concentration and low Na^+ by virtue of active pumps; cooling deprives the pumps of metabolic energy and allows K^+ to escape, and Na^+ and Cl^- to enter the fibres; the lost K^+ would diffuse from the extracellular space into the ambient medium.

Duncan Model

Thus by treating the lens as a mass of cells insulated from each other by selectively permeable membranes, and surrounded by an extracellular fluid in free communication through the capsule with the aqueous and vitreous humours, we can account for the basic chemical composition of the lens and its response to environmental changes. However, a number of experimental studies have suggested that this picture is inadequate and that a better picture would be given by the system indicated schematically by Fig. 4.11 in which the fibres are viewed as a syncytium, in the sense that there are gap-type junctions between adjacent fibres permitting free diffusion of ions from one cell to the next. On this basis, it has been argued that the outermost layers of lens fibres would constitute a cellular barrier, beneath the capsule, that would act as a single membrane sealing the contents of the lens fibres from the outside medium. This, which we may describe as the Duncan hypothesis, is a view that seemed to be demanded by the measured electrical potential between the inside of the lens and the adjacent vitreous humour, or aqueous humour, first described by Brindley.

Lens Potential

'Giant Cell'

Brindley (1956) impaled the amphibian lens with a microelectrode; as soon as the capsule was penetrated a potential, inside negative, of 63 to 68 mV, was registered; this was decreased if the external concentration of K^+ was raised. By fitting the Goldman equation to the potentials obtained when the external ion concentrations were varied, Brindley found that the potential could be accounted for by a system consisting of a 'giant cell' containing a high concentration of K^+ separated from aqueous or vitreous humour, containing low K^+ and high Na^+, by a membrane with relative permeabilities to Na^+ and K^+ in the ratio 0.03, comparable with that found in nerve. In the rabbit the potential was somewhat lower (-66 mV). Brindley found, moreover, that the potential across the anterior surface of the lens was the same as that measured across the posterior surface, so that it is unlikely that the potential was due to activity of

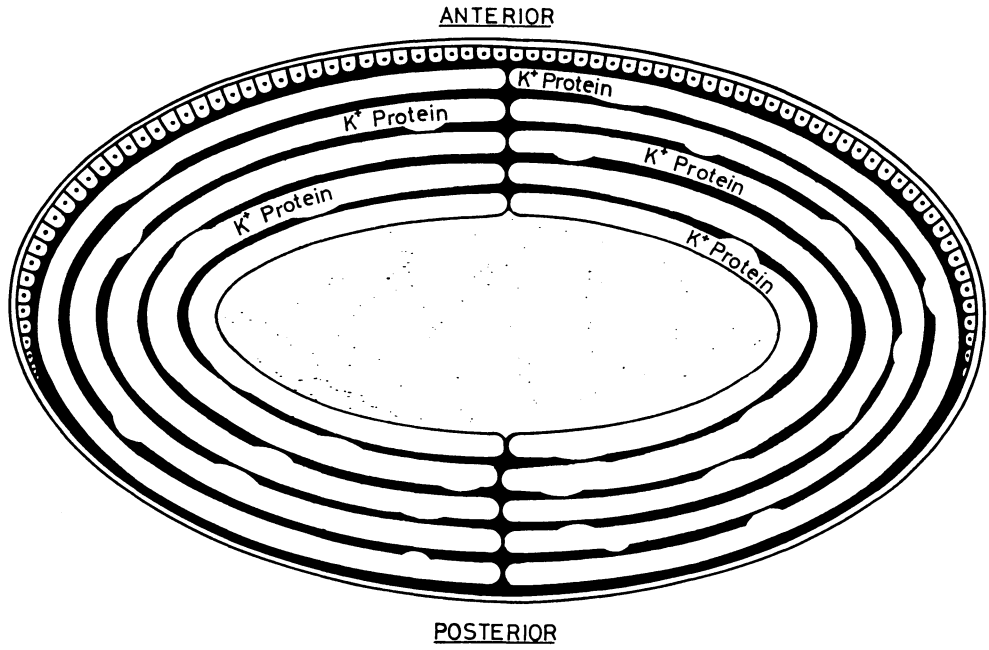

Fig. 4.11 Duncan's hypothesis to account for the lens potential, based on a syncytial organization of the lens fibres so that the system acts as a giant cell with high internal concentrations of potassium and protein.

the epithelial layer, i.e. it was unlikely to be due to an electrogenic pump comparable with that seen in the cornea.

Importance of Fibres

This point was subsequently stressed by Duncan (1969a–c) who found that the potential of the toad lens, measured with a micro-electrode, remained the same however deep it penetrated. Furthermore, Andrée (1958) had found that the removal of the capsule and underlying epithelium only abolished the potential temporarily, so that after some hours it was re-established to reach a value of 68 mV compared with an initial one of 74 mV. Again, Duncan (1969c) found that the changes in potential, measured between an electrode in the lens and one in the outside medium, caused by altering the concentration of K^+ in the outside medium, took place far too rapidly for the altered concentration of K^+ to have reached the internal electrode, so that the change of potential must have occurred at the surface of the lens and been transmitted electrically through the lens-substance to the electrode; if the electrode had been in a lens fibre insulated from adjacent fibres by a high-resistance membrane, then the effects of altered external concentration of K^+ would have had to wait on diffusion from the medium up to the fibre. If this fibre were connected to the surface through low-resistance pathways, as envisaged by the concept of a syncytial arrangement of Fig. 4.11, then the effects would be transmitted rapidly, as indeed they are.

Ionic Concentrations and Permeabilities

In a more definitive study Delamere & Duncan (1977) have developed this concept of the lens potential further and applied it to both amphibian and mammalian lenses as well as to an invertebrate (*Sepiola*) lens. Table 4.2 shows the computed internal ion concentrations and also the Nernst potentials that would arise were the potential governed exclusively by the concentration difference of a given ion; thus if it were governed by K^+ alone it would be 90 mV in the frog compared with a measured value of 63 mV; the fact that the measured potential is less than the Nernst K^+-potential means that there is a significant permeability to Na^+ and Cl^-, and by measuring the

Table 4.2 Concentrations of ions in lenses of different species (mmole/kg lens H_2O) (Delamere & Duncan, 1977)

Lens	Na	K	Cl
Frog	14.7 ± 1.1	90.3 ± 3.1	17.7 ± 2.0
Sepiola	62.4 ± 2.9	124.9 ± 2.8	235.1 ± 5.6
Bovine	30.0 ± 3.1	142.0 ± 3.4	32.8 ± 2.1

The concentrations are given as the mean $\pm$ S.E. of thirty lenses in each case.

effects of altered concentrations of all three ions on the potential and applying the Goldman or Kimizuka–Koketsu equations, estimates of the relative permeabilities of the limiting membrane responsible for the potential could be obtained. Since the electrical resistance of this membrane is a function of permeability to the ions and their concentrations, a function that is predictable on the basis of the above equations, estimates of the resistance or its reciprocal, conductance, were obtained and compared with those measured directly. As Table 4.3 shows, there is reasonable agreement between the two, suggesting that the basic concept of Duncan is correct.[5]

Table 4.3 Computed internal ion concentrations, Nernst potentials and measured lens potentials (Delamere & Duncan, 1977)

	Na^+	K^+	Cl^-	E_{Na}	E_K	E_{Cl}	E_m (mV)
Frog	9.4	94.9	12.8	+62	−90	−54	−63.0±1.4
Sepiola	39.9	131.0	219.3	+61	−63	−22	−63.3±1.2
Bovine	24.7	149.0	26.9	+43	−84	−44	−23.1±0.9

The ion concentrations (mmole/kg lens water) were calculated assuming a value of 5% for the extracellular space.

Membrane Resistance

A very important aspect of Duncan's treatment is the finding that, not only is the potential independent of position of the micro-electrode in the lens, but also that the resistance between an electrode inside the lens and one in the outside medium is also independent of position of the micro-electrode. Such an independence would be very unlikely were each individual fibre encased in a membrane of high electrical resistance, and this would be the case were the electrode within a lens fibre, or in the extracellular space, since the cells are so tightly packed together than the conducting pathway through the space would be tortuous and the resistance would be greater the greater the depth of the electrode in the tissue. Thus the independence of depth indicates an electrical coupling of the lens fibres such as that given by gap-junctions.

MEASUREMENT

In order to measure the resistance, Duncan placed a 'resistance electrode' within the lens and the potential between this and an external electrode was measured. A second 'current-passing' electrode was placed in the lens and the effect on the potential, due to a pulse of current through this current-passing electrode, was measured; and from this the resistance across the lens was computed. Later workers, e.g. Rae & Blankenship (1973) obtained conflicting results, but a thorough theoretical treatment of the problem of current-spread within a cell from a micro-electrode, and a re-examination of the situation within the lens, has confirmed Duncan's conclusion (Eisenberg & Rae, 1976) to the effect that the resistance of the lens is, in effect, dominated by a single membrane at the surface; the resistance to flow of current within the tissue is rather high, namely 625 Ω cm compared with 130 Ω cm measured in cytoplasm, but the difference could be due to the resistance through the gap-junctions, i.e. it would depend on the effectiveness of the cell coupling.

Capacitance

The estimate of membrane capacitance, C_m was very high if the total area was equated to the area of the lens, so that it is likely that the area of membrane charged by the current pulses was much larger, and represented many individual fibre-membranes in the neighbourhood of the electrode.

Potential Profiles

A basic question pertinent to the hypothesis of Duncan is 'Where is his micro-electrode located during measurements of potential and current flow?' If the individual fibres maintain high internal concentrations of K^+ they should individually have membrane potentials across them such that the inside of each fibre is negative to the extracellular space. If an electrode enters a given fibre the measured potential is, in effect, the resting potential of this fibre (Fig. 4.12a), i.e. the potential between the inside and extracellular fluid which we may presume is in equilibrium with the aqueous humour and vitreous.

If the electrode within the fibre were pushed a little further so as just to emerge into the extracellular fluid, then a fall in potential should be recorded and, if there is free communication between the extracellular space and the surrounding medium, the potential should fall to zero. Rae (1974) argued that potential jumps should be measured on pushing a micro-electrode gently through the lens tissue, and furthermore that the frequency of the jumps should vary according to the angle at which the lens penetrated a given region; for example if it penetrated at right-angles to the long axis it would emerge from a fibre sooner than if it penetrated more obliquely. Rae's experimental study indicated that there were, indeed, successive changes in the frog's potential as indicated by Fig. 4.12b suggesting that each fibre does, indeed, maintain a potential difference between itself and the extracellular fluid. However, the potential does not fall to zero, indicating that the extracellular fluid is negative in respect to the bathing medium, but the general concept of a coupling between the fibres is sustained although not proved, and Rae emphasized that more direct evidence on this point would be valuable; thus he found (1974c) that the dye, Procion yellow, injected into a single fibre, was not confined to this but passed from cell to cell, probably

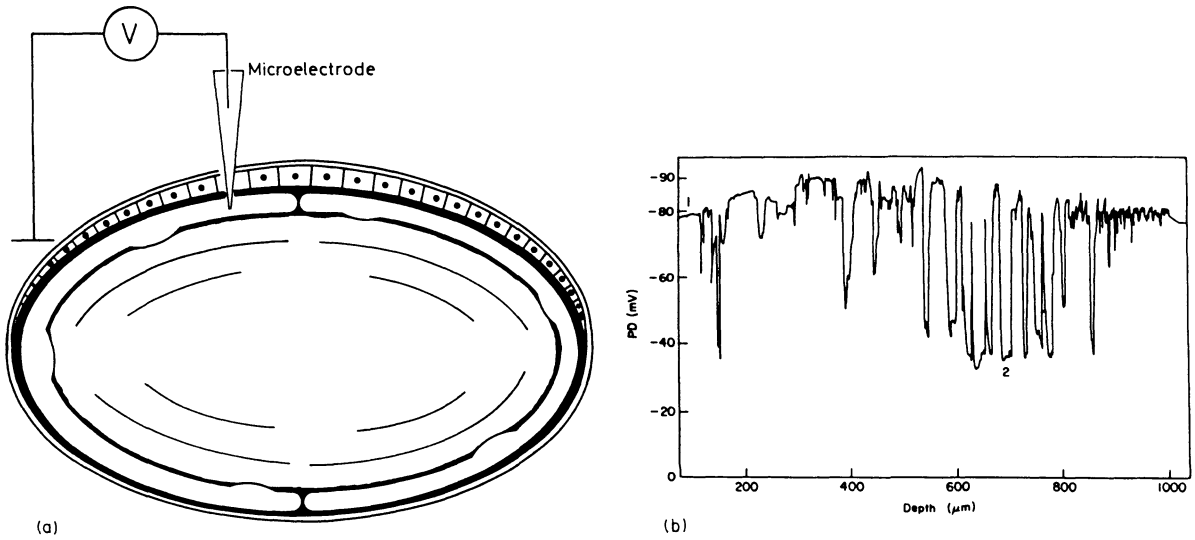

Fig. 4.12 (a) A microelectrode is measuring the potential across the membrane of the fibre it is impaling. (b) Indicating successive jumps in potential between a recording microelectrode pushed into the lens substance and the outside medium, presumably resulting from penetration of successive fibres. (Rae, *Exp. Eye Res.*)

through gap-junctions similar to those that couple the photoreceptors (p. 305). Tentatively, then, we may assume that the potentials recorded by micro-electrodes normally register the potential within the fibre system; whether the difference of potential between the lens and its medium is entirely governed by the fibre-membrane potential of the surface-layers, as suggested by Duncan, or whether there is an additional step leaving the extracellular fluid negative in respect to the outside medium, awaits further investigation.[6]

Asymmetry Potentials

When examined *in vivo*, or in the excised lens surrounded uniformly by a bathing medium, the lens shows the same difference of potential across both anterior and posterior faces; however Candia *et al.* (1970), by mounting a lens in an apparatus illustrated by Fig. 4.13, in which the whole lens separates two compartments, found that there was a difference of potential between anterior and posterior faces of about 26 mV, the front face being positive with respect to the back face. Thus the separate trans-lens potentials were −57 mV for the anterior face and −31 mV for the posterior face, leading to this *asymmetry potential* of 26 mV. *In vivo* this difference of potential would be short-circuited by the suspensory ligament, and *in vitro*, when completely immersed, by the bathing solution. Thus the potential, as normally measured, would be governed by the separate potentials short-circuited, and from estimates of the appropriate electrical parameters Duncan computed that the toad potential

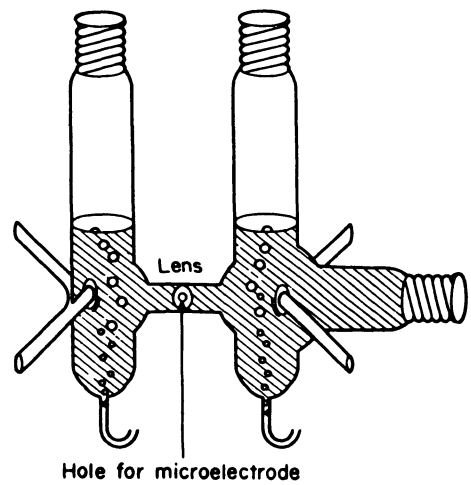

Fig. 4.13 Measurement of asymmetry potential of lens. (Candia, *Exp. Eye Res.*)

would be −49 mV, considerably less than that actually found when totally immersed, namely 59 mV. Later, Duncan *et al.* (1977) improved on the experimental study of the asymmetry potential, pointing out that the lens capsule itself represents a short-circuiting medium in the double-chamber system of Candia *et al.* This was avoided by immersing the lens in liquid paraffin and making separate electrical contacts with agar-bridges to obtain the trans-lens asymmetry potential, while micro-electrodes inserted into the anterior and posterior faces

measured the separate potentials. In the ox lens studied by them, the potentials were smaller, as indicated in Table 4.4, to give a trans-lens potential of only 6.3 mV. In general, each trans-membrane potential, i.e. that across the anterior and posterior faces respectively, responded to changed ion concentrations in the external medium, but not identically, so that the limiting membranes governing the separate potentials are not the same; and it is interesting that the posterior membrane, presumably made up of a layer of lens fibres, had the higher resistance although the epithelium on the anterior surface might have been expected to provide additional resistance.

Table 4.4 Potential differences (mV) in bovine lens (Duncan *et al.*, 1977)

Lens	*I–A*	*I–P*	*A–P*
In situ	-30.0 ± 2.0	-30.3 ± 2.0	0.3 ± 0.4
Under oil	-28.7 ± 1.4	-21.7 ± 1.4	6.3 ± 0.4

I refers to inside of lens; *A* = anterior medium; *P* = posterior medium. Note that the trans-lens potential difference *in situ* is not significantly different from zero, whereas the potential difference for the excised lens, measured under oil, is significantly different.

The Pump-leak Hypothesis

Kinsey and his colleagues have made a series of studies of transport of solutes from the external medium into the lens and interpreted them on the basis of active transport mechanisms, operating across the lens epithelium, associated with passive leak of the actively transported materials at the posterior surface where there is no epithelium. Thus the exchange of K^+ between medium and lens has been described by an active accumulation across the epithelium from the aqueous humour associated with a passive diffusion of the accumulated K^+ into the posterior chamber and vitreous body. The distributions of K^+ between these fluids are not necessarily inconsistent with this view (Bito & Davson, 1964), whilst a kinetic study of the uptake of K^+, Rb^+ and Cs^+ by Kinsey & McLean (1970) was also consistent with the pump-leak hypothesis, in the sense that the measured uptakes could be made to fit the solutions to simple equations based on a primary accumulation process at the epithelium, showing competitive inhibition between the three cations, and a passive diffusion process at the posterior capsule.[7]

Sodium

So far as the exchanges of Na^+ are concerned, Kinsey (1973) has applied the pump-leak hypothesis to experimental measurements of Na^+-fluxes on the basis of an assumed passive diffusion of Na^+ through the posterior surface of the lens and an active transport out through the anterior surface, mediated through the lens epithelium. As with the other ions studied, the curves of uptake and efflux of isotopic Na^+ could be made to fit theoretical ones by appropriate choice of parameters. However, as Duncan has emphasized, the difficulty with the pump-leak hypothesis is that it implies a low-resistance posterior membrane compared with that of the actively transporting anterior membrane (epithelium), but the separate study of resistances, and of variations of potential with ionic concentrations, all indicate a basic similarity between the two membranes, with the posterior membrane the more highly resistant. Nevertheless, the pump-leak hypothesis, by emphasizing the capabilities of the epithelium, has been of value, and it may well be that this active transport contributes to the postulated extracellular potential of Sperelakis & Potts (1959) and of Rae (1974b).

Effects of Ouabain

In this connexion, the effects of this inhibitor of Na^+-pumps on the lens potentials is of some interest. Kinsey & McGrady (1971) found that ouabain caused a relatively rapid fall in the anterior face potential, from -40 to -20 mV in the rabbit lens, this being followed by a much slower change towards zero. In the toad-lens, too, Bentley & Candia (1971) found a decrease in the short-circuit current, measured by short-circuiting the anterior and posterior faces, when ouabain was in contact with the anterior face, by contrast with a negligible effect on the posterior face. The effect was slow, as shown by Table 4.5. As we have indicated earlier, mere inhibition of a Na^+-pump in a tissue like muscle or nerve need not affect the potential immediately, since this depends primarily on the concentration differences of K^+. Inhibition of the Na^+-pump leads, after a time, to a leak of K^+ out of the cell and of Na^+ in, and thus the concentration difference of K^+ falls and hence the potential. Thus, if the lens potential were governed completely by the K^+ concentration gradient, ouabain should only have a slow effect as the concentration of K^+ fell.

Table 4.5 Effects of ouabain on toad-lens short-circuit current (Bentley & Candia, 1971)

	Short-circuit current				
	2 hr	*4 hr*	*6 hr*	*8 hr*	*12 hr*
Control	93	81	73	68	70
Ouabain ant. face	70	45	36	29	9
Ouabain post. face	89	80	71	62	44

Electrogenic Pump

Hence the rapid decline described by Kinsey & McGrady, and later by Paterson *et al.* (1975), could be directly associated with inhibition of the Na^+-pump, so that the pump would be *electrogenic*, possibly accelerating Na^+ out of the lens across the epithelium, as suggested by Kinsey's pump-leak hypothesis; if this acceleration is associated with a slower passive diffusion of Cl^- or HCO_3^- we have the condition for an electrogenic pump comparable with the frog skin or corneal epithelium. Superimposed on this would be the activities of the lens membranes at anterior and posterior faces; these need not

be electrogenic, the extrusion of Na^+ merely maintaining the high internal K^+-concentration which gives the potential. Duncan *et al.* (1977) measured the effects of ouabain on both faces of the lens; after 90 min the trans-lens asymmetry potential was abolished, due to the much slower fall in potential of the posterior surface than that of the anterior, and this would be consistent with the operation of an electrogenic pump by the epithelium, which would be rapidly inhibited.

Subsequently Duncan *et al.* (1980), working on the frog lens, confirmed the depolarization by about 9 mV brought about by ouabain; this occurred with a half-life of about 2 min and also occurred in a Na^+-free medium, a finding that convinced them that the depolarization was, indeed, due to abolition of an electrogenic pump, rather than to a mere accumulation of ions due to blockage of the pump accumulating K^+ and extruding Na^+ at the epithelium.

LOCALIZATION OF ATPase

Palva & Palkama (1974) found, in their initial study, that the enzyme was confined to the epithelial cell membranes; however, in their later (1976) study they found it on the cortical elongating fibres. Gorthy & Anderson (1980), using electron microscopy, found the enzyme between the apicolateral epithelial plasma membranes, along the apical epithelial border, and extending into the lens cortex along fibre-cell margins. In the posterior polar region it was located along the apposed surfaces of superficial fibres, but not at the borders adjoining the capsule.

Human and Rabbit Lenses

Fundamental studies on the electrical characteristics of the lens have been based strongly on the amphibian eye, so that a study by Platsch & Wiederholt (1981) on the rabbit and human is of interest. Using an Ussing-type chamber they separated anterior and posterior faces and measured translenticular potential, resistance and short-circuit current. The potential of the human lens was only some 7.5 mV, and this was reduced to 5.7 mV by application of 5×10^{-5} M ouabain to the anterior surface. Correspondingly there was a reduction in short-circuit current by about 30%, which could also be brought about by removal of Na^+ from the medium. In this work a dependence of the short-circuit current on the presence of HCO_3^- in the medium was described, in contrast with studies on amphibian and rabbit lenses. In Table 4.6 the electrical characteristics of the lenses of several species have been summarized.

Steady Outward Current

We shall see that, because of a difference in resting potential across different parts of the photoreceptor, a local current flows from the more highly polarized part to the less polarized part. A similar situation occurs with the lens fibres, so that by using an appropriate probe, the existence of a steady current flowing from the equator to the poles of the lens has been established (Robinson & Patterson, 1983; Parmelee, 1986). The current density at the anterior pole is some 3–4 times that at the posterior pole; the system behaves as though the central part of the lens fibre were most strongly polarized giving a strong surface positivity, and that the ends of the fibres were less polarized, the ends at the anterior pole being more strongly depolarized than those at the posterior pole. By raising the external concentration of K^+ to 150 mM the currents were blocked, presumably because now the fibres were uniformly depolarized. Translated into ion-movements, these currents would represent a tendency for K^+ to leak out of the fibres at the equator while Na^+ would tend to enter at the poles; thus the outward current would be said to be a K^+-current and the inward current a Na^+-current. In a Ca^{2+}-free medium the current was increased reversibly, but not in a Na^+-free medium (Parmelee *et al.*, 1985). Since permeability to Na^+ is apparently increased in a Ca^{2+}-free medium, we may conclude that the steady current does, indeed, depend on the greater tendency of the poles of the fibres to depolarize, through high permeability to Na^+, than the central parts at the equator.

Effects of Ca^{2+} Removal

The Ca^{2+}-balance of the lens is involved in maintenance of its transparency, so that the influence of changes in the

Table 4.6 Electrical properties in isolated lens preparations of various vertebrate species (Platsch & Wiederholt, 1981)

Species	p.d. (mV)	*SCC* ($\mu A\ cm^{-2}$)	$R(k\Omega\ cm^2)$	*References*
Toad	25	28	—	Candia *et al.*
	27	33	0.8	Candia *et al.* (1971)
	25	30	0.8	Yorio & Bentley (1976)
	17	15	1.2	Yorio & Bentley (1978)
Bovine	6	—	—	Duncan *et al.* (1977)
	4	—	0.6	Delamere & Duncan (1979)
Rabbit	23	—	—	Kinsey & McGrady (1971)
	24	22	1.2	Present paper
Human	7	5	1.5	Present paper

concentration in the surrounding medium are of interest. Delamere & Paterson (1978) found a rapid fall in translens potential and resistance associated with a two-fold increase in K^+-efflux, as deduced from efflux of ^{86}Rb, from the frog lens when this was suspended in a calcium-free EGTA medium. The effect could be attributed entirely to an increased permeability of the lens to Na^+ caused by the Ca^{2+}-free medium. Candia (1980) studied the effects of Ca^{2+}-free medium separately at both lens faces; at the anterior face the potential fell from 67 to 51 mV, and at the posterior face from 49 to 36 mV; these changes were accompanied by a fall in transmembrane resistance. The effects on the total translens potential was the algebraic sum of the effects on the two surfaces. Candia concluded, from the effects of Na^+-free medium, that the effects at the anterior surface were due to an increased Na^+-permeability of the epithelial cells; the effects on the posterior surface seemed to be due to a more generalized increase in permeability to ions. Finally, Jacob & Duncan (1981), also working on the frog, measured a rise in conductance across the lens membranes due to a rise in permeability to Na^+; and this was associated with a depolarization of 30 mV, a degree of depolarization that was far too great to be accounted for by a possible abolition of the Na^+-pump, since this contributes only about 8–10 mV to the potential.[8]

Volume Regulation

Cells and tissues respond to alterations in osmolality of their surrounding medium by losses or gains of water; to some extent these volume changes are resisted by adjustments of the internal osmolality of the cells—volume regulation. The lens is no exception, losing K^+ and amino acids in a hypotonic medium and gaining Na^+ in a hypertonic medium (Patterson, 1979–1981).

METABOLISM

Lens Culture

The metabolism of the lens is most conveniently studied *in vitro*, and since Bakker in 1936 first maintained a lens in an artificial medium for several days with normal transparency, there have been frequent studies of the best medium for the purpose and the most suitable index of viability; outstanding in this respect has been the work of Kinsey and, more recently, Schwartz, and their collaborators. In general, the medium must contain a suitable ionic composition similar to that of the aqueous humour, whilst in order to allow for consumption of glucose and production of lactic and other acids, the medium must be changed regularly. As criterion of normal viability the best is probably the mitotic activity of the epithelium, the cells of which, it will be recalled, are continually dividing to produce new fibres (Kinsey *et al.*, 1955). Besides imitating the aqueous humour with regard to ionic make up, a variety of amino acids and vitamins, together with inositol, lactate and glutathione, were added. By using a constant flow of this solution, Schwartz (1960) kept a lens transparent for some 40 hours, but at the end of this time it was not completely normal, having a higher lactic acid content, for example, than when it began.

Metabolic Pathways

Glycolysis

The lens utilizes glucose as its source of metabolic energy; since the O_2-tension of the aqueous humour is low, most of this metabolism is anaerobic, the Q_{O_2} being only 0.1; thus the main pathway for the utilization of glucose is by way of the Embden-Meyerhof or glycolytic reactions leading to pyruvic acid, which is largely converted to lactic acid; the latter is carried away in the aqueous humour. The enzyme lactic dehydrogenase is involved in this process, together with the coenzyme $NADH_2$:

$$\text{Glucose} + 2\text{Pi} + 2\text{ADP} \rightarrow 2\ \text{Lactate} + 2\text{ATP} + 2\text{H}_2\text{O}$$

Pentose Phosphate Shunt

As with the cornea, Kinoshita & Wachtl (1958) have shown that the pentose phosphate shunt contributes significantly to the oxidative breakdown pathway, in addition to the ordinary glycolytic pathway; this involves the coenzyme NADP.

Sorbitol

Finally Van Heyningen (1959) has shown that the lens contains sorbitol and fructose, together with enzymes capable of converting glucose to fructose by way of sorbitol. Thus the metabolic events in the lens may be summarized by the scheme of Fig. 4.14.

ATP

Glycolysis, the pentose phosphate shunt and the Krebs cycle all lead to the generation of ATP which acts as substrate, or phosphate donor, in a variety of endergonic reactions, e.g. the synthesis of protein and fatty acids, the active transport of ions, and so on. The pentose phosphate shunt is concerned with the production of a variety of intermediates in synthesis, e.g. nucleic acids; it also leads to the production of $NADPH_2$, the coenzyme concerned with many syntheses, especially of fatty acids.

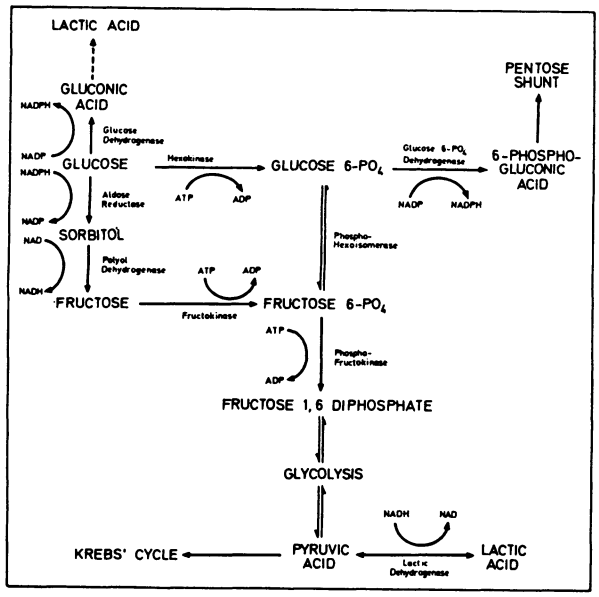

Fig. 4.14 Some of the possible metabolic routes of glucose in the lens. (After Spector, *Arch. Ophthal.*)

Sorbitol Pathway

The significance of the sorbitol pathway, which converts glucose, via sorbitol, to fructose, is not clear; the enzymes concerned are aldol reductase, $NADPH_2$ and polyol reductase:

$$\text{Glucose} + NADPH_2 \rightarrow \text{Sorbitol} + NADP$$

Aldol reductase

$$\text{Sorbitol} + NAD \rightarrow \text{Fructose} + NADH_2$$

Polyol reductase

The same pathway allows xylose to be converted to xylitol, but dulcitol and arabitol, formed from galactose and arabinose by aldol reductase, are not metabolized further.

Oxidative Phosphorylation

Molecular oxygen is used in biological reactions by way of the cytochrome system, which is contained in the mitochondria; this seems to be confined to the epithelium, according to Kinsey & Frohman (1951), so that it may be that respiration, as contrasted with glycolysis, is confined to this cellular layer. Because of the relative insignificance of O_2 in metabolism, keeping a lens anaerobically has no effect on transparency, nor on its power to retain its high K^+ and low Na^+; if glucose is absent from the medium, however, anaerobiosis causes a drastic deterioration in the state of the lens, presumably because, in the absence of glucose, O_2 is utilized to oxidize other substrates than glucose (Kinoshita, 1965).

Control

Control over the rate at which a given metabolic process takes place is generally exerted through inhibition of one or more key enzymes; in the case of the lens these are hexokinase and phosphofructokinase, the former catalysing the conversion of glucose to glucose 6-phosphate and the latter the phosphorylation of fructose 6-phosphate to fructose 1,6-diphosphate:

$$\text{Glucose} + \text{ATP} \rightarrow \text{Glucose 6-phosphate} + \text{ADP}$$
$$\text{Fructose 6-phosphate} + \text{ATP} \rightarrow \text{Fructose 1,6-diphosphate} + \text{ADP}$$

Thus ATP inhibits phosphofructokinase activity whilst glucose-6-phosphate inhibits hexokinase activity; as a result, increasing the concentration of glucose in the lens does not increase lactate production or the level of glucose 6-phosphate. Increasing the level of glucose does, however, stimulate the sorbitol pathway, a finding of significance for the interpretation of diabetic cataract (p. 180).

Protein Synthesis

As indicated earlier, there is a smaller turnover of protein in the adult lens; in addition, new fibres are being laid down throughout life, requiring further synthesis. The total amount of protein synthesized per day is, nevertheless, small, and this, together with an extremely efficient amino acid accumulating mechanism that maintains the concentrations of amino acids in the lens far above those in the aqueous humour and blood plasma, is presumably why the lens remains normal and continues to grow when the level of amino acids in the blood is so low as to inhibit body-growth entirely.

Amino Acid Accumulation

The active accumulation of amino acids by the lens was demonstrated by Kern (1962) and Reddy & Kinsey (1962), and is illustrated in Fig. 1.23; the process seems similar to that described in other cells (Brassil & Kern, 1967) and ensures that protein synthesis will not be limited by availability of amino acids. We may note that the lens, like the brain, may synthesize certain amino acids from glucose, namely glutamic acid and alanine (see, e.g. Van Heyningen, 1965).

Nucleic Acids

Protein synthesis occurs in association with nucleic acids by mechanisms that are now well understood and need not be repeated here. All the evidence indicates that synthesis in the lens is in every way similar; the loss of the nucleus from the lens fibre, like that of the reticulocyte, presumably demands that the template messenger RNA be longer-lived than that in nucleated cells; in this case protein synthesis will not be inhibited completely by actinomycin D as is, indeed, found (Zigman & Lerman, 1968).

Ascorbic Acid

Ascorbic acid (vitamin C) is present in the aqueous humour in high concentration in many species; when this occurs it is also concentrated in the lens, but its significance is not clear since in scurvy the lens shows no defect; furthermore, the *in vitro* preparation seems quite stable without it.

THE PROTEINS

The lens is highly transparent yet its cells contain a very high concentration of proteins, so high that unless these were specially adapted for their specific purpose, which is presumably to create a medium of high optical density and therefore high refractive index, they would impart to the lens a milkiness that would militate against the formation of distinct images.

As summarized by Clayton (1978), the function of the lens is to provide a transparent structure which focuses light on the retina and which will continue to do so accurately as the eye increases in size; this will require a fall in the refractive index of the lens from centre to periphery, which is associated with a parallel fall in protein concentration. The earliest formed, central fibres eventually have the highest protein concentration, and in order to sustain this and maintain transparency it appears that they have a different array of proteins from those in the outer fibres formed later. Certain of the crystallins are successively replaced during ontogeny, while other crystallins are synthesized throughout life, and it would seem that the high refractive index, and therefore high concentration of protein, of the nucleus are made possible by the preferential synthesis of proteins that are capable of entering into closer molecular packing than those in the more peripheral cells (Clayton, 1970; 1974).

Because of these special features of the lens proteins, or *crystallins* as they are called, their isolation and characterization have been studied in great detail, and any exhaustive review of these studies, which at any rate would be more appropriate to a textbook of the biochemistry of the eye, cannot be attempted here, so we must concentrate on those features that bear most directly on the changing composition with ontogeny and the relation to loss of transparency in cataract.

The Main Fractions

When the lens fibres are homogenized we may separate a water-soluble fraction containing the soluble cytoplasmic proteins, and a water-insoluble 'albuminoid' consisting of the cytoskeleton and plasma membranes with their incorporated proteins. By extraction with urea, the cytoskeletal proteins may be solubilized,[9] and by appropriate treatment with detergents, the membrane-associated proteins may be separated from the lipids. The soluble proteins are called crystallins and represent some 86.5% of the total proteins; they fall into three classes, namely alpha-, beta- and gamma-crystallins, and their proportions are given in Table 4.7, whilst some of their physicochemical features are indicated in Table 4.8. Figure 4.15 illustrates the separation of the three types on the basis of molecular weight by Sephadex column filtration. It will be seen that β-crystallin is resolved into two quite distinct components, β_H and β_L. Within any class, modern refinements of technique have often permitted the isolation of sub-classes, whilst treatment with hydrogen-bond breaking agents, such as urea, has permitted the dissociation into small sub-units and their subsequent reassociation after removal of the dissociating agent.

Table 4.7 Protein fractions as described by Mörner

Protein	*per cent*
Insoluble albuminoid	12.5
α-Crystallin	31.7
β-Crystallin	53.4
γ-Crystallin or albumin	1.5
Mucoprotein	0.8
Nucleoprotein	0.07

Low-molecular Weight Crystallins

The Gamma-crystallins

The gamma-crystallin fraction is separated on the basis of its moving most slowly in electrophoresis and, more effectively, by gel-filtration on the basis of its low molecular weight, in the region of 20000. Björk (1964a) has separated four distinct proteins from the gamma-crystallin fraction; their molecular weights are very close, in the region of 19000 to 20000; three of the fractions were

Table 4.8 Characteristics of the main classes of soluble proteins from mammalian lens (Harding & Dilley, 1976, after Waley, 1969)

Property	*Class* α	β	γ
Electrophoretic mobility (towards the anode, at pH 8–9)	High	Medium	Low
Range of isoelectric points shown by proteins	pH 4.8–5.0	pH 5.7–7.0	pH 7.1–8.1
Molecular weight	Over 5×10^5	4 to 20×10^4	About 2×10^4
Molecular form	Aggregates	Aggregates	Monomers
Thiol content	Low	High	High
N-terminal amino acid	Masked	Masked	Free; glycine or alanine

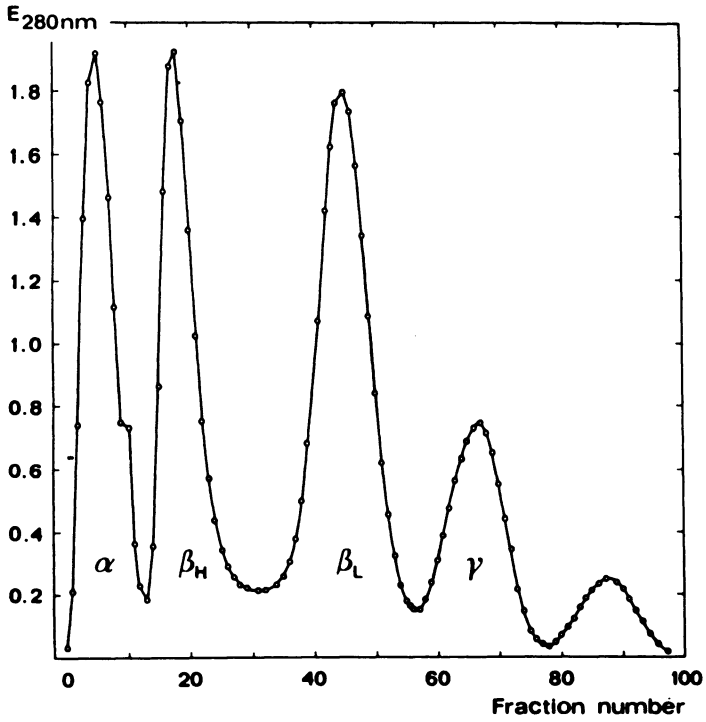

Fig. 4.15 Illustrating the different water-soluble fractions separated from an extract of calf lenses on a Sephadex column. (Bloemendal & Herbrink, *Ophthal. Res.*)

immunologically identical with each other whilst the fourth was only partially identical with these. Thus their differences reside in the amino acid composition, differences that presumably arose by mutations on specific parts of the gene during evolution, but since these mutations did not affect the transparency of the lens they were not eliminated by selection. The protein shares with the beta-crystallin fraction the feature of a high cysteine content, which may be a significant feature in the genesis of a cataract if, as has been suggested, this results from an oxidation of thiol-groups (Dische & Zil, 1951). Subsequent fractionation has shown that Björk's fractions III and IV could be separated into IIIa, IIIb and IVa, and IVb.

AMINO ACID SEQUENCE

The amino acid sequence of calf-lens Fraction II was established by Croft (1972) working with a crystallized preparation. It consists of a chain of 165 amino acids; an irregular spacing of the cysteine residues was a feature of this Fraction II, four being in the N-terminal region; this distinguished Fraction II from other fractions, and might account for its greater stability against denaturation through oxidation of SH-groups, which is a prominent feature of the other fractions.

MODEL

X-ray analysis of the crystals at high resolution permitted the construction of a model for gamma$_{II}$; on the basis of

this it was concluded that the molecules would have a low tendency to bind water, which would make the gamma-crystallins useful for residing in the nuclear region, and it was suggested that their presence might stabilize the polymeric alpha- and beta-crystallin aggregates. Thus alteration in the surface properties of gamma-crystallin might produce a catastrophic change in the crystallin aggregates and so cause light-scatter (Wistow *et al.*, 1983).

RAT LENS

According to Zigman *et al.* (1970) practically the whole of the urea-soluble protein in the lens of rat (and dogfish) is gamma-crystallin, by contrast with the human and bovine lenses where the predominant species is alpha-crystallin. By isoelectric focussing Zigman *et al.* (1970) identified seven separate components, and showed that there were differences in amino-acid composition; notably the fractions with high isoelectric points were rich in SH-groups and those at the lower end had few SH-groups but twice as many disulphide groups.

CAUSE OF HETEROGENEITY

The variety of gamma-crystallins, revealed by modern techniques of separation, could be due to the synthesis of many types, or, more probably, to metabolic alterations in the originally synthesized proteins, so-called post-translational changes. Zigman *et al.* (1971) concluded from their study of ageing rat lenses that the changes in the character of the gamma-crystallin fraction were due to post-translational changes. One of these changes is doubtless deamidation, a change that would affect the isoelectric point of the protein, and be revealed as a heterogeneity during isoelectric focussing (Slingsby & Croft, 1973).[10]

EMBRYONIC CRYSTALLIN

Rabaey (1962) considered that synthesis of gamma-crystallin was confined to the embryonic lens; discussing the matter with respect to the calf lens, Slingsby & Croft (1973), who found some synthesis of Fractions II and III in the calf lens, concluded that, if there were an embryonic protein, it would be Fraction IV of the gamma-crystallins.

mRNAs

Shinohara *et al.* (1982) studied synthesis of proteins by cell-free preparations containing mRNAs of lens in normal and cataractous rats, and showed that synthesis could be measured. When they fractionated the mRNAs by cDNA cloning they identified at least four separate mRNAs some 840 ± 100 nucleotides long.

HUMAN LENS

There is good reason to believe that changes in the nature of gamma-crystallin are involved during the development of senile cataract (Zigler *et al.*, 1985), so that the characterization of this group of proteins and their changes with age are especially interesting. In general, the heterogeneity encountered in extracts of young lenses is much less than that from old lenses (Ringens *et al.*, 1982a, b), and this, heterogeneity has been studied in more detail by Zigler *et al.* (1985).[11]

They found that by, using very young human lenses, the heavy fraction of Kabasawa and others resolved into two, with molecular weights of 24 and 21 kd; in older lenses the 21 kd fraction was still present but this was screened by the much larger amount of the 24 kd occurring with age. A third peak indicated a lighter fraction of molecular weight 19 kd, similar to that of the adult lens. All three fractions were identified immunologically as gamma-crystallins. By isoelectric focussing the heterogeneity within fractions could be demonstrated, and all three showed similar patterns of change, notably a tendency for the more acidic isoelectric points to increase at the expense of the lens, which might well reflect a progressive deamidation of the amino acids with age.

CORTEX AND NUCLEUS

Papaconstantinou (1965) found that the soluble proteins of the lens epithelium contained no gamma-crystallin either in the adult or calf. In the fibres gamma-crystallin was present in adult, calf, and embryonic lens, so that he concluded that it was the *initiation of differentiation* that was accompanied by synthesis of gamma-crystallin.[12] Thus the embryonic and adult nucleus both had gamma-crystallin of similar electrophoretic properties; however, the cortical gamma-crystallin of the adult lens was different, so that it seemed that the type of gamma-crystallin that was synthesized during cell differentiation depended on the age of the animal.

Beta$_s$-CRYSTALLIN

Thus Van Dam (1966) isolated from adult cow lenses, a protein with molecular weight 28 000 and a mobility between those of alpha- and gamma-crystallins, and it was named beta$_s$-crystallin. Kabasawa *et al.* (1974) confirmed that the elution pattern of gel-filtration of calf and adult lens extracts differed strongly, the adult extract being more complex with the appearance of a peak corresponding to beta$_s$-crystallin whilst the gamma-fraction following this is different from the adult gamma-fraction. In general, they found a gamma-crystallin of molecular weight 24 000 belonging to the adult lens cortex, and a gamma-crystallin of molecular weight 20 000 common to the adult nucleus and both cortex and nucleus of the calf. Thus, according to this study, ageing was accompanied by the appearance of a new gamma-crystallin of M.W. 24 000 as well as of beta$_s$-crystallin. In a later study these findings were confirmed and the molecular weight of beta$_s$-crystallin of cattle cortex was given as 28 000, this being characterized by the absence of a

terminal free amino acid; all three proteins were immunochemically distinct with different amino acid compositions. It thus appears that in the cattle lens cortex, gamma-crystallin in the newer fibres is different immunochemically, in charge, and molecular weight from the gamma-crystallins found in the young lens (Kabasawa *et al.*, 1977). As to whether $beta_s$-crystallin may be classed as a beta- or a gamma-crystallin, this has been discussed by Harding & Dilley (1976), Harding & Crabbe (1984) and Kabasawa *et al.* (1977). In spite of similarities in amino acid composition, there is little doubt that $beta_s$ is different from gamma-crystallin isolated from the same lens parts (Bindels *et al.*, 1981) but, as Harding & Crabbe have emphasized, the affinities between gamma- and beta-crystallins are so strong as to make it necessary, in future, to discuss the two as subclasses of a single beta–gamma class.

Thus the principal chain of beta-crystallin, $beta_p$, shows duplication of its two halves, in the sense that the amino-acid sequence of the N-terminal half is homologous with that of the C-terminal half; when these halves were compared with the sequences of other crystallins, it was gamma-crystallin that showed a strong homology, Fraction II of the gamma being some 25% homologous with $beta_p$. This degree of homology would not be sufficient to produce an immunological cross-reactivity between $beta_p$ and gamma-crystallin, but it suggests that the beta- and gamma-genes originated from a common ancestor coding for at most 100 residues. Later both beta- and gamma-genes have presumably duplicated repeatedly, resulting in the presence of multiple beta- and gamma-crystallin chains in all present-day vertebrate species (Driessen *et al.*, 1980; Clayton, 1974).

Beta-crystallins

This class constitutes a larger proportion of the total soluble lens proteins than either the alpha- or gamma-crystallins in the adult; in the embryonic and fetal lens, however, the alpha-proteins are most prominent constituting 62% of the total; this decreases sharply so that at 4 months prenatal it is only 35%, the same as in the postnatal bovine lens; the beta-crystallins represent only 17% in very young embryonic lenses but increase to 40% (Van Kamp *et al.*, 1974).

Heavy and Light Fractions

By gel-filtration the beta-crystallin fraction is separated into a heavy, $beta_H$, and a light, $beta_L$-fraction of molecular weights 210 kd and 52 kd respectively (Zigler & Sidbury, 1973). Under certain conditions the light fraction can be resolved into two, $beta_{L1}$ and $beta_{L2}$ (Asselbergs *et al.*, 1979) also called $beta_L^3$ and $beta_L^2$ (Bindels *et al.*, 1981).[13] When treated with dissociating agents, such as urea, the main components are broken down into smaller subunits with molecular weights in the region of 20–30 kd; thus the difference between $beta_{L1}$ and $beta_{L2}$ is that these are trimer and dimer respectively of basic units, whereas the heavy, $beta_H$, is oligomeric being made up of 7–8 subunits (Bindels *et al.*, 1981). Thus $beta_H$ develops from aggregation of the smaller $beta_L$ fraction; most of the newly synthesized beta-crystallin appears as $beta_L$. These subunits exist in dynamic equilibrium with the heavy polymer, the association–dissociation equilibrium being determined by hydrophilic factors, notably concentration, ionic strength, temperature and medium density (Bindels *et al.*, 1981).

CHARACTERIZATION OF THE SUB-UNITS

Zigler & Sidbury (1973) separated altogether 6 fractions of differing molecular weights; their amino-acid composition was similar but sufficiently different to indicate their separate nature; by a more elaborate analysis, Herbrink *et al.* (1975) concluded that there were, in fact, at least 4 subunits, being common to the light and heavy fractions, and these were named beta-B_2, beta-B_4, beta-B_5 and beta-A, the numbers referring to the order in which the fractions were eluted from a DEAE column, and B and A referring to the basic and acidic character of the units as determined by their isoelectric points. A still more elaborate study carried out in Bloemendal's laboratory (Berbers *et al.*, 1982) led to a more definitive characterization of the subunits. These authors fractionated the subunits, and compared them with synthetic polypeptides produced from lens mRNA. Nine subunits were separated from the native crystallins by dodecyl sulphate gel-electrophoresis and subsequent isoelectric focussing, as indicated in Table 4.9; those fractions marked with an asterisk were apparently identical with primary gene products, as indicated by mRNA synthesis; thus, in all, there seem to be at least 7 primary polypeptides, the rest being formed by post-translational changes. For example, beta-B_{1b} is

Table 4.9 Subunits derived from beta-crystallins and synthesized from lens mRNA (After Berbers *et al.*, 1982)

Subunit	M_r	p*I*
Beta B_{1a}^*	33 000	8.5
Beta B_{1b}	31 000	8.0
Beta B_p^*	25 000	7.1
A*	26 000	6.9
B*	23 000	6.9
C	23 000	6.7
D*	26 000	6.2
E*	23 000	6.1
$Beta_s^*$	22 000	7.0

Subunits marked by asterisk were also synthesized in a medium containing calf lens polyribosomes in a reticulocyte cell-free system.

definitely derived from beta-B_{1a} (Zigler, 1978). The principal subunit of the beta-crystallins was early described as beta-B_p, this being common to both the heavy and light fractions. Beta-L_2 is a dimer, and is made up of Beta-B_p and one or other of Chain A and Chain B. The trimer arises from adding acidic chains D or E. $Beta_H$, containing up to 8 chains, originates from $beta_{L1}$ and $beta_{L2}$ by a combination with the basic $beta_1$-chains and addition of acidic chains D and E.[14] Berbers *et al.* (1982) concluded that most of the beta-chains in a species are produced by a family of genes originating by repeated evolutionary processes of gene duplication. It seems probable that the main subunit, beta-B_p, is the same in all vertebrate species (Clayton & Truman, 1974; Raemaekers *et al.*, 1982). Thus the beta-crystallins are remarkably conservative proteins, their basic structure being maintained through several hundreds of millions of years of vertebrate evolution (Zigler & Sidbury, 1977).

Human Beta-crystallins

These have been characterized by Zigler *et al.* (1980); three fractions described as $beta_1$, $beta_2$ and $beta_3$ were separated, all having very similar secondary and tertiary structures, as indicated by ultraviolet circular dichroism, and they were very closely related immunochemically. Like the beta-crystallins of other species, they were very heterogeneous; they differed from other, non-human, lenses in having a polypeptide, or group of polypeptides, with a molecular weight of about 43 kd.

Re-assembly of Subunits

Berbers *et al.* (1982) showed that the dissociated subunits, produced by 6 M urea, would re-assemble to their original dimeric or polymeric condition by controlled reduction of the urea concentration, showing that the tendency to aggregate was reversible and inherent in the primary structures of the polypeptide units. The heavy $beta_H$ could be re-aggregated from a mixture of beta-B_{1a} and beta-B_{1b}.

Alpha-crystallin

This has the largest molecular weight of the crystallins, with values between 600 and 4000 kd; this wide variation is due to a tendency for aggregation of subunits to greater or less extent. In the electron microscope this heterogeneity is especially manifest. By gel-filtration, or in the ultracentrifuge, alpha-crystallin may be separated into two main fractions, Fraction I, called high-molecular weight alpha-crystallin (HMα), with individual weights varying between 900 and 4000 kd, and Fraction II, or low-molecular weight alpha-crystallin (LMα), with individual weights varying between 600 and 900 kd (Spector *et al.*, 1971b) in the calf preparation. Further analysis of the low-molecular weight fraction shows that it can be resolved into two, so that we may speak, generally, of three size-populations, namely 700–1000 kd, 1000–5000 kd, and greater than 15 000 kd (Siezen *et al.*, 1978). A similar range of molecular weights was found by Horwitz (1976) in human lenses. In general, it has emerged that, because of small changes in the primary structure of its individual subunits taking place after its original translation in the cell, alpha-crystallin cannot be isolated as a homogeneous protein. Thus, through random association of the different subunits, it can be estimated that there are as many as 1000 different hybrids in native alpha-crystallin (Siezen *et al.*, 1978).

Transformation to Fibre

Alpha-crystallin is of special interest in the study of the physiology of the lens since it is the protein that seems to be specifically concerned with transformation of the epithelial cell into a lens fibre; this was made clear by Delcour & Papaconstaninou (1972), who calculated the rate of synthesis of the proteins of the cultured lens by measuring the amount of incorporation of labelled leucine in a given period. In the epithelial cell the rate of synthesis of alpha-crystallin was seven times higher than in a cortical fibre, indicating a large decrease in rate of synthesis on transformation to a fibre. However, the ratio for the non-alpha-crystallins was much higher, namely 41 : 1, so that although total protein synthesis falls, the proportional rate for alpha-crystallin increases, indicating the importance of alpha-crystallin for the fibre, so that fibrogenesis involves a quantitative biochemical specialization in addition to the qualitative specialization for initiation given by gamma-crystallin synthesis.

The Subunits

The preparation described by Bloemendal *et al.* (1962) had a molecular weight of some 810 000; on addition of hydrogen-bond breaking agents, such as 7 M urea, the molecular weight was reduced drastically to around 26 000, suggesting the breakdown into subunits. When the purified alpha-crystallin was examined in the electron microscope spherical molecules of about 150 Å diameter were observed, and these appeared to be made up of smaller subunits. Björk (1964b) examined the chemical character of the subunits and their reaggregation brought about by removing the urea and increasing the ionic strength of the medium. The subunits were definitely not identical chemically; moreover, complete reaggregation to the original alpha-crystallin was never achieved.

VARIATIONS IN SUBUNITS

Subsequent work on the subunit composition of native alpha-crystallin has demonstrated the existence of a variety with nearly the same molecular weights, in the region of 20 kd, but differing primarily in their isoelectric points, so that they are best separated by isoelectric focussing. It would appear that the two main subunits, designated A_2 and B_2, are the primary gene products from which all alpha-crystallins are derived. Thus A_1 and B_1 subunits, described by Waley (1969), are, in fact, post-translational products, being formed by deamidation of the corresponding A_2 and B_2 subunits. In addition, more drastic changes occur, leading to the shortening of the polypeptide chains at the C-terminus, so that, for example, a shortened subunit, designated as A_2^{1-151} has been described. The main number of subunits is embraced by these five, so that other chains, such as B_0, B_2^{1-170} and A_1^{1-151} are relatively rare.

The amino acid sequences of αA and αB subunits have been determined by Van der Ouderaa *et al.* (1973; 1974); the αA_2 consists of a single chain of 173 residues giving a molecular weight of 19 832 daltons, and αB_2 has 175 residues, giving a molecular weight of 20 070 daltons. There is a high degree of homology between the two, about 57%, indicating an origin from a common ancestral alpha-crystallin gene.

CHANGES WITH CORTICAL DEPTH

Since the altered subunits occur after synthesis of the original gene products, we may expect changed proportions as we go deeper into the cortex of the lens, and this was indeed found, Van Kamp *et al.* (1973) and Van Kleef *et al.* (1974) describing a continuous increase in the proportions of A_1 and B_1 and to a lesser extent of A_2^{1-151} and A_1^{1-151} in successive concentric layers of cortex, with corresponding decreases in the primary gene products, A_2 and B_2. In bovine lenses the A:B ratio is almost uniformly the same throughout the different molecular-weight fractions; this was originally thought to be 2:1, but in fact, according to Siezen *et al.* (1978), it is closer to 3:1.

Molecular Weight

An elaborate study of the molecular weight of native alpha-crystallin by Andries *et al.* (1982) has given a most probable mean value of 785 kd; hydrodynamic studies suggested almost spherical molecules of about 16 and 13 nm diameter, roughly agreeing with the electron-microscopically measured values, if allowance was made for shrinkage (Siezen & Berger, 1978).

Quaternary Structure

The building up of the subunits to give this large molecule, i.e. its quaternary structure, was examined by Bindels *et al.* (1979), and their model is illustrated by Fig. 4.16, based on the relative accessibility of the subunits to attack. It consists of a central core of about 12 subunits, surrounded by an inner concentric layer of about 14 subunits, and an outermost concentric layer containing at most 24 subunits. As initially synthesized, this outer layer contains only 16 chains, making a total of 43, but with places still unoccupied in the outermost layer. The filling up of these free spaces by more subunits would lead to an increase in molecular weight to give the heavier of the 'low-molecular weight fractions', namely about 1.0–1.1 $\times 10^6$ daltons found for nuclear, as opposed to cortical alpha-crystallin. Further aggregation would now only be achieved by the alignment of complete monomers. The failure to reassociate subunits to give the original 43-unit structure might be due to the failure of the outer layer to assemble, i.e. the dissociation of the outermost layer is, so far, irreversible (Siezen *et al.*, 1980).

ELECTRON-MICROSCOPY

Three classes of alpha-crystallin—mono-, oligo-, and polymeric aggregates, have been demonstrated electron microscopically by Siezen *et al.* (1979). The oligomeric aggregate was seen as a mixture of mono-, di-, tri- and tetrameric clusters of spherical units. The polymeric fraction consisted of very irregularly shaped aggregates with a largest dimension of about 200 nm. The mode of assembly of the polymers took the form of branching chains, so that, with really large aggregates, it is likely that a three-dimensional network would be built up. There was a higher proportion of shortened chains in the larger aggregates, suggesting that at least one factor favouring aggregation was the splitting off of amino acids from the originally synthesized polypeptide chains.[15]

Evolutionary Changes

Van der Ouderaa *et al.* (1974) computed, on the basis of the known rate of substitution of amino acids during evolution, which amounts to a substitution of 1 in 100 every 40 to 50 million years, that, with only 57% homology, the production of the two alpha-subunits with separate genes would have occurred long before the appearance of the lowest vertebrates some 450 million years ago, so that we may expect to find invertebrate alpha-crystallins homologous with the vertebrate protein. So far as the conversion of alpha-A_2 to alpha-A_1 is concerned, the amino-acid sequencing revealed the conversion of one glutamine to glutamic acid, i.e. the change consisted of deamidation (Bloemendal *et al.*, 1972).

THE PHYLOGENETIC TREE

De Jong *et al.* (1980) pointed out that, because of its organ specificity, the crystalline lens provides a valuable subject for study of evolutionary changes, and for the establishment of relationships between existing species. On the basis of sequence-analysis of the alpha-A chains of some 41 species of mammals, and the approximate sequences of chick, frog and dogfish, a family tree was established that conformed well with trees established on other bases; in fact it permitted the assignment of the place of the ardvark (De Jong *et al.*, 1981).

Alpha$_m$-crystallin

Bindels *et al.* (1978) found that their preparation of alpha-crystallin, which, as is common in protein studies, was made on

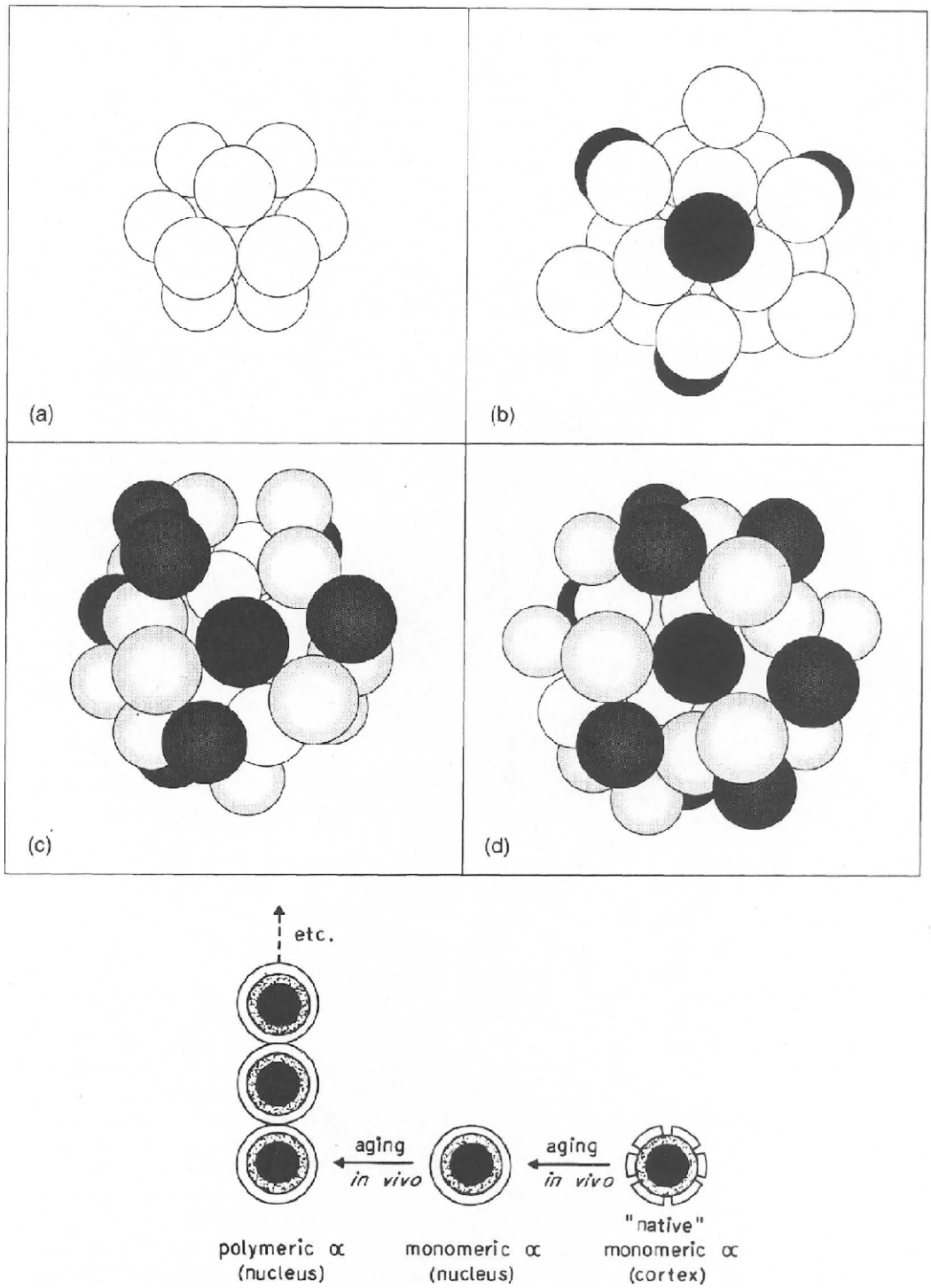

Fig. 4.16 Above. Model for the architecture of bovine α-crystallin successively composed of (a) a core of 13 A chains; (b) 14 not fully solvent-exposed subunits (10 A chains and 4 B chains); (c) an outer layer of 8 A and 8 B chains which are maximally solvent-exposed (this model holds 43 subunits, the average number for calf cortical α-crystallin); (d) additional subunits in the outer layer to occupy the open places in c (this model holds 51 subunits). Below. Schematic illustration of effects of aging to produce polymeric aggregates of α-crystallin. (Bindels *et al.*, *Ophthal. Res.*, and Siezen *et al.*, *Eur. J. Biochem.*)

material kept at a low temperature, was irreversibly changed by maintaining at the normal temperature of the lens, namely 37°C. Thomson & Augusteyn (1983) suggested, therefore, that the material prepared at low temperature, which they called alpha$_c$, was an artefact. By keeping the extract at 37°C they obtained a smaller protein, alpha$_m$, of molecular weight 320 000, with otherwise identical properties with those of alpha$_c$, so far as amino-acid analysis, secondary and tertiary structures, and immunochemistry were concerned. They suggested that their alpha$_m$-crystallin was the true form of alpha-crystallin in the lens, and that the larger alpha$_c$ was an aggregate produced by cooling. The phenomenon was not confined to the bovine lens.

Re-assembly from Subunits

Removal of the dissociating agent permits the subunits to aggregate to form a higher molecular weight protein; in general, the work of Spector and his colleagues indicated that the reassociation was never perfect, in the sense that the molecular weight of the aggregate was smaller than that of the 'native' alpha-crystallin from which the subunits had been derived; and Spector suspected that a low molecular weight material, formed during dissociations, was lost during the subsequent manipulations (Li & Spector, 1972). When Spector *et al.* (1971b) allowed single subunits to re-aggregate, e.g. alpha-B, proteins were formed, once again with a smaller molecular weight; and subsequent studies, based on the re-aggregation of preparations of individual subunits, as well as of mixtures of these, have all pointed to the possibility of producing polymers of the type (beta-A)$_n$, (alpha-B)$_n$, or more complex aggregates, although the sedimentation coefficient was always less than that of the untreated alpha-crystallin (Li & Spector, 1973). When different mixtures of A and B subunits were made, Van Kamp *et al.* (1974) found that all the products, with differing proportions of A and B in their make-up, had identical sedimentation coefficients of 12 S, compared with 18 S for the starting material: the re-aggregated products, however, did not reflect the proportions of A and B present in the mixture, and often pure B aggregates appeared out of a mixture of A and B. Only when the ratio of A/B was 4/6 or less were all B chains accepted completely.

Neoproteins

Manski & Malinowski (1980) labelled either the A or the B subunits derived from alpha-crystallin and measured the proportions in which the subunits reassembled when differing proportions of the two were used in the starting mixture. The products were examined to see whether they maintained their original quaternary structure, a procedure made possible by developing antibodies reactive only to alpha-crystallin when in its normal conformation. When the ratio of A:B was greater than 2:1, assembly was strictly governed by the availability of B subunits to give normal alpha-crystallins with 2A to 1B. The excess A aggregated to give polymers in solution. When the ratio of A:B was less than 2:1 no alpha-crystallin was formed, instead the A and B subunits assembled in a 1 to 1 ratio forming, in low yield, molecules with different quaternary structure from that of native alpha-crystallin. More interestingly, not only did excess of B subunits prevent formation of alpha-crystallin, but addition of re-aggregated B subunits to native alpha-crystallin caused a complete loss of quaternary structure of the alpha-crystallin molecule, as determined by its failure to react to antibodies that distinguished this feature of the molecule. The new protein produced by adding excess of B subunits to A subunits, or to native alpha-crystallin, was described as a neoprotein. In this latter condition they found that, when excess B subunits were added to alpha-crystallin, each A subunit in the latter took up some 495 B subunits. This reactivity of the B subunits is in contrast with that of the A subunits, which, when added to alpha-crystallin, had no effect, a difference of reactivity that might be due to the presence of SH-groups in the A subunit; at any rate carboxymethylation of the SH-groups in the A subunit gave neoproteins on assembly with B subunits, having the subunits in the proportions 1A:5B; 2A:1B and 5A:1B (Malinowski & Manski, 1984). It was found that retention of some quaternary structure was possible only if less than 23% of the SH-groups of alpha-crystallin had been altered, and this percentage is the same as that of readily accessible SH-groups, i.e. on the surface of the crystallin molecule (Siezen *et al.*, 1980). Thus the quaternary structure of alpha-crystallin depends on the presence of these surface SH-groups.

PRESENCE IN INTACT LENS *IN VIVO*

Manski & Malinowski (1985) showed that, *in very young lenses*, neoproteins were absent but they later appeared, mainly in the albuminoid fraction. In human senile cataracts the amount of neoprotein actually exceeded that of normal alpha-crystallin in both the water-soluble and insoluble fractions.

Re-assembly from Dissociated Mixtures of Crystallins

When all the soluble proteins were dissociated together and the resulting subunits were allowed to re-aggregate, some hybridization between alpha- and beta-crystallin subunits occurred, so that when the re-aggregated material was submitted to a new gel-filtration most of the beta$_H$ had disappeared and the α-peak had increased appropriately (Bloemendal *et al.*, 1975). It seemed that gamma-crystallin subunits did not participate in this hybridization. In the electron microscope the re-aggregated α-fraction appeared as molecules of different size and shape. However, when the dissociated protein preparation was strongly diluted, and association allowed, the pattern obtained by gel-filtration was virtually identical with that of the normal preparation. One difference was observed, however, namely that the reconstituted alpha-crystallin molecules were smaller, as seen in the electron microscope, and the difference was confirmed by ultracentrifugation when it was found that, whereas the sedimentation coefficients for the beta- and gamma-crystallins were unaffected by dissociation and re-aggregation, that of alpha-crystallin had decreased from 18.2 to 12.3 Svedberg units.

The Hybrids

Hybridization was recognized by reactions of the re-aggregated material immunoelectrophoretically to both alpha- and beta-antisera, and also by the large sedimentation coefficients, ranging from 30 to 70 S; in the electron microscope rod-like molecules made their appearance by contrast with the spherical shapes of alpha- and beta-crystallins; and it may be assumed that they represent aggregates of alpha and beta subunits.[16]

Newly Synthesized Alpha-crystallin

By incubating a calf lens in a nutritional medium to which radioactively labelled leucine was added, Spector *et al.* were able to separate from the alpha-crystallins a 'highly-labelled fraction' (NS) representing material that had been synthesized during the incubation. The molecular weight was remarkably homogeneous and corresponded with the minimum molecular weight of ordinary preparations; the amino acid composition was basically similar, with the exception of a greater percentage of free amino groups, suggesting that the terminal acetylation had not been completed. In a later study, Stauffer *et al.* (1974) found a molecular weight of 7.4×10^5 and only traces of A_1 and B_1 subunits; the actual relative amounts of the subunits are compared with those in LMα-crystallin as follows:

Subunit	NS alpha	LM alpha
B_2	32	24
B_1	3	11
A_2	56	40
A_1	9	24

Very little radioactivity was associated with the A_1 and B_1 fractions, so that it is unlikely that any of these were synthesized directly. Thus it is reasonable to assume that LM alpha is directly derived from NS alpha through intracellular modification of the A_2 and B_2 chains.

Human Lens

When they extended this work to the human lens, Spector *et al.* (1976) found the isolated labelled alpha-crystallin to contain 3 subunits, one equivalent to the bovine B_2 and two others slightly different from bovine A chains; the molecular weight was 4.9×10^5 compared with 7×10^5 for the bovine material; the amino acid composition was similar. The proportion of A to B was 3:1 by comparison with 2:1 for bovine alpha-crystallin.

Rat Lens

As this species is employed most in the study of experimental cataract, it is important that its lens proteins be examined with the same care as that expended on the bovine organ. A subunit in rat's alpha-crystallin with MW 24 kd, called alpha-X, differentiates this species from the ox; this has been subsequently called alpha-A^{ins}, since its greater molecular weight is due to the insertion of an amino-acid sequence into its primary structure. Cohen *et al.* (1978) showed that rat mRNA directs the synthesis of both the usual alpha-A and this alpha-A^{ins}; immunochemically they are similar but there is no apparent precursor–product relation. With ageing, Raemaekers *et al.* (1982) found a relative decrease in $beta_H$- and gamma-crystallins and an enhancement of alpha- and $beta_L$-crystallins, the opposite to that found in the ox.

Capsular Protein

As indicated earlier, the structural protein of the capsule is collagen; it is hydrolysed by collagenase and has the characteristic proportion of hydroxyproline residues. The high proportion of carbohydrate differentiates it from the collagen of skin, and the fluorescent antibody-staining experiments of Roberts (1957) show that the material is analogous with the basement membrane material characteristically seen surrounding capillaries; embryologically it would seem to arise as a condensation of the basement membranes of lens cells (Cohen, 1965). The major sugar moiety is a sialohexosaminoglycan containing galactose, mannose, fucose and neuraminic acid; some sulphated esters are also present, an unusual feature for a connective-tissue glycan, possibly connected with the need for transparency of the capsule (Dische & Zelmenis, 1966).

FM-Crystallin

This was called by Van Dam pre-alpha-crystallin since it migrated in an electric field more rapidly than alpha-crystallin; however, Van den Broek *et al.* (1973) have shown that it has no relation to alpha-crystallin so far as amino acid content is concerned; its molecular weight is 14 500 daltons and it has been renamed 'fast-moving' or FM-crystallin.

Membrane Proteins

It will be recalled that, after extracting a lens homogenate with the usual buffer solutions, there is left a water-insoluble fraction (Mörner's albuminoid). Most of this material can be solubilized with hydrogen-bond rupturing agents, such as 6 M urea, to give the cytoskeletal proteins. The urea-insoluble residue (UIS) represents cell membranes (Lasser & Balazs, 1972; Maisel, 1977). These membranes have proteins associated with the basic lipid skeleton, proteins that may be separated by the use of detergents or chloroform–methanol. Less drastic treatment, designed to loosen proteins bound through Ca^{2+}-linkage, namely extraction with EDTA, separates a protein-fraction consisting of several polypeptides with molecular weights in the region of 30–35 kd, which have been designated as EEP (EDTA extractable proteins); they are reversibly associated with the lipid part of the cell membranes through a Ca^{2+}-linkage (Van den Eijnden-Van Raaij *et al.*, 1985a, b). Extraction with lipid solvents releases

proteins that are probably buried deep in the cell membrane, one of which is described as 'membrane intrinsic protein (MIP)' (Broekhuyse *et al.*, 1976). The MIP extracted from calf lens has a molecular weight of about 26 kd, and is referred to as MP 26. Broekhuyse & Kuhlmann (1978) suggested that MIP was embedded in the lipid bilayer, extending partly into the cytoplasm, as in Fig. 4.17, so as to be able to bind to the cytoplasmic matrix. Trypsin treatment converted MP 26 into a smaller polypeptide of approximately 22 kd, presumably by splitting off the portion protruding from the lipid bilayer (Broekhuyse & Kuhlmann, 1978).

Human Intrinsic Protein

The situation here is more complex; Roy *et al.* (1979) found two main proteins, a major one of 26 kd and a minor one of 22 kd. With ageing, the 22 kd component became more prominent so that in the aged lens its amount exceeded that of the 26 kd component. In cataract, the components were about equal in quantity. Again, Broekhuyse & Kuhlmann (1980) found two MIPs, described as A and B, with molecular weights of 27 and 23 kd respectively. Trypsin treatment of the MP 27 converted it into a component, MP 22, i.e. smaller than the B component, MP 23. However, trypsin also converted MP 23 into MP 22, and it seems very likely that MP 23 was derived from MP 27 by proteolysis. Immunochemical studies of the relation between MP 26 and MP 22 indicated that a part of the MP 22 was derived from the MP 26; however, the remainder showed no reaction to anti-MP 26 antibodies, so it must be assumed that at least one other 22 kd protein is present in the human lens (Garner *et al.*, 1982).[17]

Water-extractable Proteins

Broekhuyse & Kuhlmann (1978) extracted a number of fractions from urea-treated membranes, with molecular weights in the bands 54, 47, 27, 19 and 16 kd, the major component being the 47 kd material, which may be described as the *main extrinsic polypeptide* of the membrane, probably located at the inner side of the plasma membrane and acting as a nucleation site for aggregation of crystallins to high-molecular weight aggregates (Garner *et al.*, 1979).[18]

In Vitro Synthesis

RNA extracts of lens usually do not cause synthesis of MIP 26 when incubated with the appropriate polyribosome preparation; this seems to be because the polyribosomes responsible for its synthesis are attached to the skeletal protein of the cell, probably in close association with the cell membrane. Treatment of the lens extracts with DNAase I, which specifically depolymerizes actin filaments, released the ribosomes capable of synthesizing MIP 26 in a cell-free preparation. The location of the ribosomes on the actin filaments probably ensures accurate incorporation of MIP, which doubtless subserves important functions in transport across the fibre membrane (Raemaekers *et al.*, 1980).

RELATION TO GAP JUNCTIONS

The proteins associated specifically with the gap-junction region of intercellular contact have been separated from other membrane proteins, and in the case of the hepatocyte it is the main intrinsic protein, MIP, that occurs here, and here only. In the lens, however, this is not true, the gap-junction protein being different from the MIP 26, having a molecular weight of 28 kd

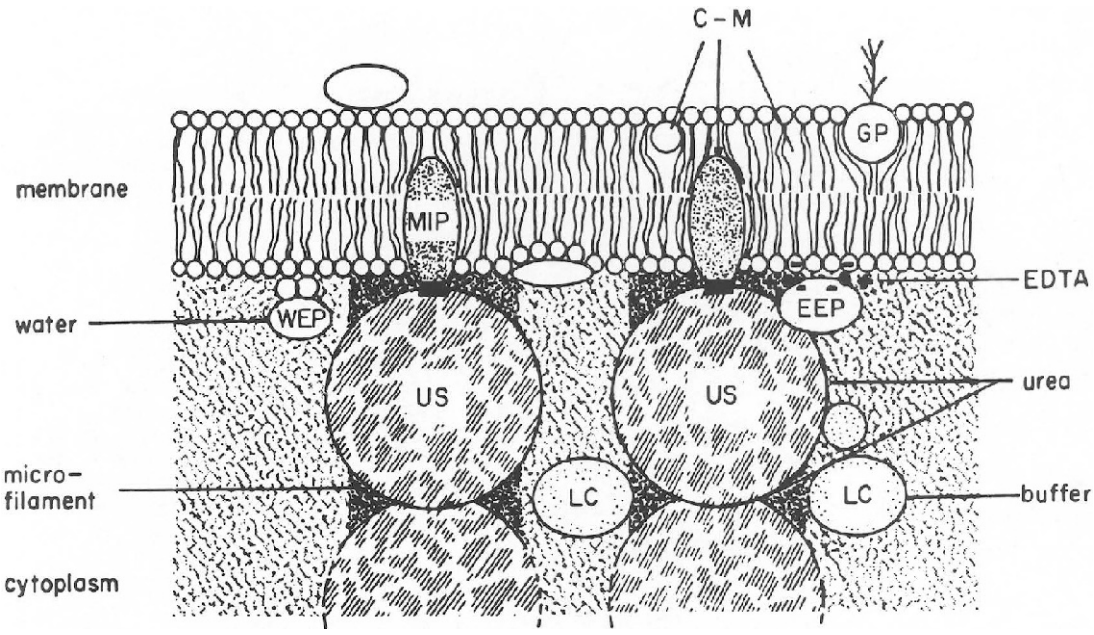

Fig. 4.17 Hypothetical structure of the plasma membrane of the lens fibre. MIP is embedded in the lipid bilayer and both are chloroform–methanol (c–m) soluble. GP; glycoprotein: US, urea-soluble matrix-crystallin bound to microfilament; LC, buffer soluble lens crystallin. EEP is via CA^{2+} ions bound to the membrane and is EDTA-extractable. (Broekhuyse & Kuhlmann, *Exp. Eye Res.*)

(Nicholson *et al.*, 1983); moreover MIP 26 of the lens fibre membrane is not confined to the gap-junctions (Fitzgerald *et al.*, 1983; Fitzgerald & Goodenough, 1986). It is not present in the lens epithelium, however, so that in cultured epithelium it only appears when lentoid structures develop. The fibres so formed have a few gap-junctions, and are electrotonically coupled (Fitzgerald & Goodenough, 1986).

Proteases

An excised lens, maintained under sterile conditions, eventually undergoes autolysis, i.e. non-bacterial decomposition. This is due to the activity of certain proteases that are normally suppressed. In general, because of the extremely slow turnover of the lens protein—not greater than 3% per month according to Waley (1964)—proteolytic activity is not great; nevertheless the study of the lens proteinases, and the factors that normally hold them in check, is important from the point of view of the maintenance of the correct protein composition and the removal of precipitated material. Moreover it is likely that the subtle post-synthetic changes in the lens crystallins are brought about by proteases, for example the shortening of the A and B chains of alpha-crystallin that occurs post-translationally.

Neutral Peptidase

Van Heyningen & Waley (1962) described a proteinase, associated with alpha-crystallin, that cleaved all three crystallin species (Wagner *et al.*, 1982). The finding that autolysis of lens proteins occurred more rapidly if the reaction was allowed to proceed in a dialysis sac, allowing the products of digestion to escape, suggested that these products were inhibitory, and thus restricted the degree of autolysis that would occur in the lens (Blow, 1974; Van Heyningen & Trayhurn, 1976).

LYSOSOMAL SEGREGATION

The segregation of autolytic enzymes in lysosomes, however, would provide another mechanism for holding autolysis in check, and the studies of Swanson (1966, 1977) and Roelfzema *et al.* (1974) have shown that many of the typical enzymes required in tissue breakdown (acid phosphatase, cathepsin C, etc.) are contained within cytoplasmic organelles within the lens epithelium and fibres. Thus, in a recent study of the rat lens, Gorthy & Azari (1987) showed that the lysosomal proteolytic enzyme, dipeptidyl peptidase II (DPP II) was present in lens sections, revealed by a fluorescence technique, most intensively in the epithelium and bow region. Another lysosomal enzyme, cathepsin B, was also demonstrated biochemically in lens[19] extracts.

Lens Endopeptidases

Of especial interest is the mechanism whereby the A and B chains of alpha-crystallin are shortened during the ageing process, a shortening involving the removal of terminal polypeptides that requires an endopeptidase, such as trypsin, for its catalysis. Tse & Ortwerth (1980) considered that such proteinases were present in lens but their activity was obscured by the presence of intrinsic inhibitors.

Trypsin Inhibitor

Tse & Ortwerth (1980a) showed that extracts of bovine lens cortex, but not nucleus, would inhibit trypsin hydrolysis of the typical trypsin substrate N-benzoyl-arginine p-nitroanilide (BAPNA); after making allowances for non-specific effects of protein binding, a true inhibitory activity amounting to a maximum of 30% of total activity was shown. This was associated with material of molecular weights 3×10^5 and $1.5–2.0 \times 10^4$ daltons; in rabbit extracts there was a single peak eluting with the beta-crystallins at 5×10^4 daltons. As indicated, nuclear extracts were inactive, but treatment with EDTA revealed some activity, suggesting inactivation by Ca^{2+}. Wagner *et al.* (1979) were unable to detect any trypsin-like activity in lens extracts, but this may have been due to the presence of inhibitor; thus the nucleus, being devoid of inhibitor, should exhibit trypsin activity, and Tse & Ortwerth found that it did indeed do so, an activity that could be inhibited by soybean trypsin inhibitor. When lens extracts were incubated at 55°C, inhibitory activity was destroyed, and now the extracts acted as substrate for trypsin. The absence of inhibitor in the epithelium suggested that its synthesis by the lens fibre was a feature of lens cell differentiation, necessary to hold in check proteolysis in cells that were about to lose most of their synthetic abilities. Trypsin activity could be demonstrated in lens extracts if inhibitor was destroyed by ultra-violet irradiation (Tse & Ortwerth, 1980b) and also in the alpha-crystallin fraction but only after an activation period of 15–20 hr (Tse & Ortwerth, 1981). The release of the proteinase from alpha-crystallin showed that it consisted of three fractions, designated BAPNA I–III; BAPNA III was considered to be the complex between protease and inhibitor, from which a lower molecular weight free protease was liberated on incubation, which represented BAPNA I; high cation levels favoured release, the order of effectivity being $Mg > Ca > Na, K$. Thus BAPNA III co-elutes with alpha-crystallin, but it can be separated from this by gel-filtration (Tse & Ortwerth, 1982). By purification procedures a 25 kd serine proteinase was separated, free of its inhibitor; it had optimum activity on the alkaline side of neutrality; it was inhibited by most of the recognized trypsin inhibitors. Of the crystallins, only alpha-crystallin was cleaved by the protease by contrast with the neutral protease of Van Heyningen & Waley (1962), which cleaved all three crystallins (Wagner *et al.*, 1982). So far as its state in the lens was concerned, Srivastava & Ortwerth (1983b) concluded that it was probably associated with alpha-crystallin in the outer shell of polypeptides (Siezen *et al.*, 1980), from which salt solutions would gradually release it, in the same way that alpha-subunits are removed from this outer shell.[20]

Calpain

Anderson (1965) showed that autolysis of lens was activated by mono- and divalent cations, and Yoshida *et al.* (1984) suspected that the proteolytic agent might be calpain, a Ca^{2+}-dependent cysteine proteinase ubiquitously distributed throughout mammalian and avian tissues. There are two calpain enzymes, I and II, and their activity is apparently controlled by an endogenous inhibitor, calpastatin. They purified a calpain II from bovine lens that was specific for alpha-crystallin, attacking both A and B subunits to give polypeptide fragments of 18 and 19.5 kd. In cataract the concentration of Ca^{2+} may rise to concentrations that would activate calpain II. They argued that, since there is no carboxypeptidase in lens, the removal of the carboxy-terminal amino acids from alpha-crystallin, found in ageing lenses, must be due to a neutral proteinase, probably calpain. Both calpain I and II were found in bovine capsule, epithelium, and cortex but

not in the nucleus, the concentration of calpain I being much greater than that of calpain II (Yoshida *et al.*, 1985).[21]

LIMITED CLEAVAGE

As indicated above, calpain cleaved only limited portions of the A and B chains, leaving large fragments; this could well be analogous with the limited cleavage of A and B alpha-crystallin chains found *in vivo*. The actual sites of cleavage were identified (Yoshida *et al.*, 1986); in both A- and B-chains they were at the carboxy-terminal, and one of the two sites for the B-chain was the same, namely the Arg^{163}–Glu^{164} bond, as occurs *in vivo*. Thus the actual peptides split off were probably polypeptides of 10 and 11 amino acids, about what would be expected of the changes in molecular weight with ageing.

RAT

David & Shearer (1986) purified a calpain II from rat lens, requiring 400 μM Ca^{2+}, a reducing agent and a pH of 7.7 for maximal activity; it degraded alpha-, beta- and insoluble crystallins and intrinsic membrane proteins but not gamma-crystallin. The degradation of beta-crystallin was interesting since a similar degradation was found in selenite-induced cataract in rats (David & Shearer, 1984), and a similar proteolysis is found in the Nakano mouse cataract (Roy *et al.*, 1982) and Philly mouse (Piatigorsky *et al.*, 1980). David & Shearer suggest that calpain II may well function in the normal ageing process of lens fibres, breaking down their cytoskeletons and membranes; cataract might result from over-activity.

The Cytoskeletal Proteins

The solid fibrous framework within the lens fibre is of some interest in view of the structural alterations that take place during development from the epithelial cell. Three types of ultrastructural elements are usually found in a variety of non-muscle cells, which may be visualized by appropriate fluorescent antibodies to their proteins. Thus antibodies to actin reveal the *microfilaments*, presumably involved in locomotion and elongation; antibodies to tubulin reveal displays of *microtubules*, and antibodies to vimentin, prekeratin or desmin reveal different classes of *intermediate filaments*. The type of intermediate filament seems to depend on the cell's origin and differentiation.

Epithelial Cell

Longchamps *et al.* (1976) have described microfilaments, microtubules and intermediate filaments in lens epithelial cells electron microscopically. Raemaekers *et al.* (1980b), in a more elaborate study of these structures and their characteristic proteins, have emphasized a striking difference between epithelioid cells from lens and many other epithelioid types, in so far as the lens cells contained an abundance of vimentin-type intermediate filaments, whereas filaments containing prekeratin-like proteins (cytokeratins) and desmin filaments were not found in them, and this correlates with the absence of typical tonofilaments and desmosomes in lens-forming cells. Thus epithelioid cells fell into two classes on this basis; cells of epidermis, cornea, respiratory tract, etc. had intermediate filaments of the prekeratin type and desmosomes, but these were absent in lens cells and also germ epithelium of the testis and endothelium. Included in this category are cells of the iris epithelium and ciliary processes. The vimentin filaments are probably closely associated with the plasma membrane since freshly synthesized vimentin rapidly attaches to isolated plasma membranes (Raemaekers *et al.*, 1982).

Lens Fibre

As described by Bradley *et al.* (1980) in the scanning electron microscope the cytoskeleton of the chick lens fibre consists of a network of beaded and unbeaded microfilaments that criss-crossed the interior of the cell (Fig. 4.18). The unbeaded filaments were the characteristic intermediate filaments.

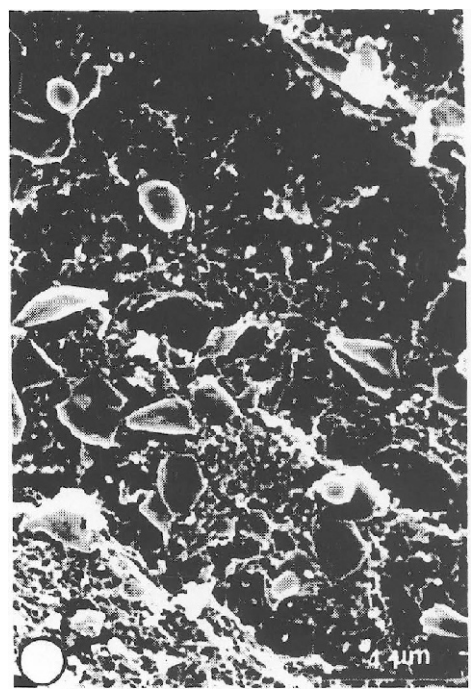

Fig. 4.18 Scanning electron micrograph of cortical fibre cells after treatment with deoxycholate. The cytoskeletal network of three fibre cells is seen, as well as areas of remaining plasma membrane. (Bradley *et al.*, *Exp. Eye Res.*)

Changes During Differentiaiton

When an epithelial cell differentiates into a mature fibre a number of morphological and biochemical changes are observed in addition to elongation, namely synthesis of

crystallins, loss of organelles, and so on. So far as the cytoskeleton is concerned, the act of elongation may involve actin filaments since, according to Beebe *et al.* (1979), epithelial cells will elongate in the presence of an inhibitor of microtubule assembly, nocodazole, whilst cytochalasins, which inhibit microfilament-based activity, inhibit cell differentiation (Mousa & Trevithick, 1977). Raemaekers *et al.* (1981) have described a change in microfilament assembly during development of bovine fibres suggesting a shift in the balance between G- and F-actin. After complete differentiation, as the fibre passes deeper to the nucleus, the total amount of actin in the cell decreases. So far as intermediate filaments are concerned, these are prominent in epithelial cells, and in newly formed cortical fibres, but disappear at later stages (Ellis *et al.*, 1984) so that vimentin is absent from the lens nucleus (Nasser *et al.*, 1980). The protein is very rapidly oxidized, when it forms higher-molecular weight aggregates linked by disulphide bridges, and these aggregates may contribute to the material that appears in the cataractous lens described by Spector & Roy (1978).

Beaded-chain Filaments

According to Ireland & Maisel (1984) the appearance of these in the lens fibre is a characteristic of the differentiation process, similar to the accumulation of MP 26 and the change in crystallins. Thus these filaments are not found in the epithelial cells (Maisel & Perry, 1972). Concurrently with the appearance of these beaded filaments there is the appearance of two cytoskeletal proteins CP 95 and CP 49 that are a part of the filaments. Their function is not known, but it may be that they form attachments for the synthesized crystallins.[22]

Non-beaded Filaments

Ireland *et al.* (1983) isolated a highly pure actin fraction from chick lens and by use of appropriate antibody showed that actin microfilaments were closely associated with the plasma membranes of fibre cells. However, they consider that beaded microfilaments represent a different population of cytoskeletal elements which are not dissociated under conditions where actin would be, and this is true of bovine as well as chick fibres, although Bloemendal *et al.* (1979) considered that the beaded filaments in their bovine preparations were made up of actin (see, also; Ireland & Maisel, 1983).

Organ specificity

As long ago as 1903 Uhlenhuth showed that the immunological characteristics of the lens were unusual. Thus if we inject an extract of, say, ox muscle into a rabbit, the rabbit produces antibodies in its serum that will react with this extract if injected again, to produce the so-called *immune reaction*; if the reaction is carried out *in vitro*, there will be a precipitation of the proteins by the antiserum. This reaction is on quite a strictly species basis, so that the rabbit's serum will not react to sheep muscle for example. If an ox antiserum is prepared to ox lens, by injecting a lens extract into a rabbit, it is found that this antiserum reacts to lens extracts of all other mammalian species, as well as to those of fishes, amphibians and birds (but not to that of the octopus). The lens is said, therefore, to be *organ*—rather than species—specific and we may conclude that the lens proteins that are responsible for this antigenicity are all built on a very similar plan in the lenses of different species. It was thought for some time that it was only the α-crystallin that behaved as an antigen, but by the technique of immuno-electrophoresis, for example, it has been shown that all three groups of crystallins are antigenic. Thus, when a rabbit antiserum was prepared to human lens, this serum was shown to react with some nine components of the lens proteins, two in the alpha-, four in the beta- and three in the gamma-crystallin groups. In the fish there were only five, and in the squid none. According to Manski, *et al.* (1960), the origin of this organ-specificity lies in the retention, by the lens, of its evolutionary history; thus the mammalian lens can produce anti-bird, anti-amphibian, and anti-fish antibodies because it contains proteins common to these classes; the fish lens, on the other hand, cannot produce anti-bird or anti-mammal antibodies. Clayton *et al.* (1968) have shown, along with earlier workers, that many of the antigens in lens are not organ specific in so far as they react with antibodies to other tissues; and they conclude that the real finding is that the concentrations of certain antigens are very much higher in the lens than in other tissues. This is understandable, since the lens contains many enzymes, such as lactic dehydrogenase, that are common to the whole body; thus organ specificity is a tendency rather than an absolute fact, a tendency promoted by the isolated position of the lens.[23]

Comparative Aspects

This account of lens proteins, and for that matter, of the physiology of the crystalline lens, has been largely confined to the mammal owing to limitations on space. The wide variations in structure and physiology of this organ throughout the phylogenetic tree demand many variations in lens composition, and this has been achieved by changes in the character of the crystallins that allow of certain specializations, e.g. softness in eyes that accommodate strongly, high refractive index in short-sighted eyes, and so on. The subject has been discussed at length by Clayton (1974).

Changes in Lens Protein Composition with Age

We have seen, from the brief description of the origin and development of the lens, that, in the adult and senile human, its structure, and presumably its protein composition, reflect the succession of changes that have occurred, in this continuously growing organ, throughout the pre-, post-natal, and later years. If we regard the primary requirement of the lens as that of maintaining transparency, and high refractive index, in the face of dis-

continuities of structure that take place as successive layers of fibres are laid down, then an exact knowledge of changes in protein composition becomes essential. It could be, for example, that a protein appearing in the early stages of lens development, and thus being present on the surface layers, might be unsuitable for maintaining transparency of these same fibres some fifty years later when they are buried deep in the nucleus.

Modes of Study

Since the nucleus of the lens is produced before the cortex, and since synthesis of proteins within the nuclear fibres does not take place in significant amounts, a comparison of cortex with nucleus will reveal changes with age, which, in short-lived animals, may cover a brief span of time, although in the human it could well cover periods of fifty years or more. Alternatively, the protein composition of embryonic, neonatal, juvenile, adult and senile lenses may be studied. The bovine lens has been the most popular subject, and usually calf and adult animal eyes are compared, on the one hand, and cortex and nucleus on the other. In the human, embryonic and fetal lenses are available from aborted material, whilst eye-bank material has supplied lenses of different post-natal age.

Bovine Embryonic and Fetal Lenses

Van Kamp *et al.* (1974) have examined the soluble proteins from bovine lenses from embryos and fetuses from the age of 6 weeks to 9 months; as Fig. 4.19 shows, the proportion of alpha-crystallin is highest in the earliest stages (62%) but as the proportion of beta-crystallin increases, the proportion of alpha-crystallin falls to reach the postnatal value of 35% at 4 months. It will be seen, also, that gamma-crystallin occupies about the same percentage throughout prenatal life. So far as the subunit composition of the alpha-crytallin is concerned, remarkable changes take place; alpha A_2 and alpha B_2 were always present and presumably represent the 'essential' subunits; in the early embryonic lenses two specific subunits, not found in postnatal lenses to any extent, appear; these have been designated as A_x and B_x; after 6 months B_x has disappeared but A_x is still present; in the 3 months post-natal lens only traces of A_x are found. At $2\frac{1}{2}$ months B_1 appears and at $3\frac{1}{2}$ months the first trace of A_1 is seen.

Nucleus Versus Cortex

In the bovine lens Spector *et al.* (1971a) found changes in the proportions of high- and low-molecular weight proteins (HMW and LMW) in cortex and nucleus of calf and steer as follows:

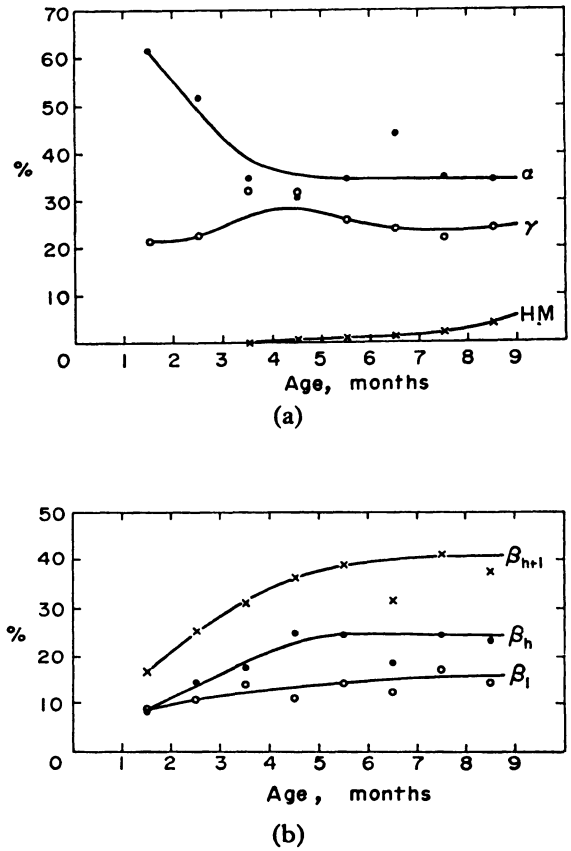

Fig. 4.19 (a) Distribution of alpha- and gamma-crystallins and the high-molecular weight fraction (HM) in prenatal bovine lenses. (b) Distribution of beta-crystallins in prenatal bovine lens. (Van Kamp *et al.*, *Comp. Biochem. Physiol.*)

	High MW	Low MW
Calf cortex	30	70
Calf nucleus	45	55
Steer cortex	43	57
Steer nucleus	70	30

Thus, in the adult animal, the percentage of HMW in the nucleus had become 70 compared with 45 in the calf nucleus and only 30 in the calf cortex.

Combined Approach

Bessems *et al.* (1986) compared the soluble crystallin contents of different portions of the same lens by dividing it into an outer cortex and an inner cylinder, and then the inner cylinder was divided into anterior and posterior cortex and nucleus. Thus, in any given lens, the effects of ageing could be measured. Lenses were taken from

animals ranging in years from 0.3 to 33.7 years, in ten age-groups. The extracts were submitted to high-pressure gel permeation chromatography (HPGTC) permitting separation on the basis of molecular size, and to high-pressure ion-exchange chromatography (HPIEC), which separated on the basis of charge. In general, the trends with age, reflecting changes in synthetic activity as well as post-translational changes in the proteins, confirmed the trends described earlier but in less detail. Results are summarized in Fig. 4.20 where the changes in crystallin distribution in equator, cortex and nucleus with age are plotted. We may note that in Fig. 4.20 the gamma-crystallins have been characterized as heavy and light, $gamma_H$ and $gamma_L$. $Gamma_H$ is otherwise known as $beta_s$ (p. 157). Quax-Jeuken *et al.* (1985) have determined the amino-acid sequence of $beta_s$ and postulated its tertiary structure; it has a molecular weight of 20 773 (177 amino acid residues) and a blocked terminal serine. They conclude that it is more closely related to the monomeric gamma-crystallins than to the oligomeric beta-crystallins, and we may note that the differences between cortex and nucleus found by Slingsby & Croft (1973) are similar to those found by Bessems *et al.* for their $gamma_H$.[24]

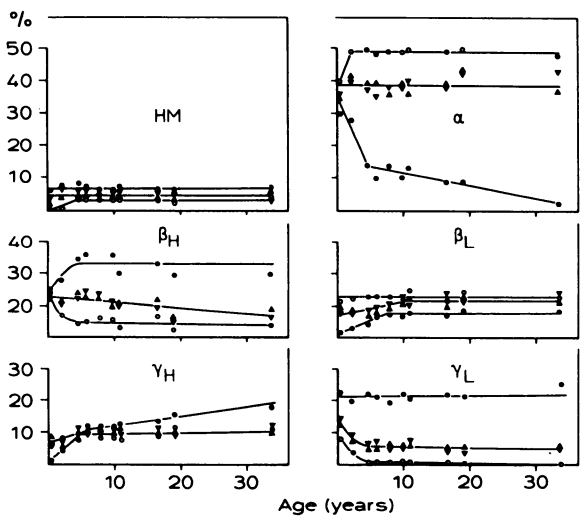

Fig. 4.20 Proportions of the crystallins (with respect to total soluble proteins) in aging bovine lens parts. ○—○, equator; △—△, anterior cortex; ▽—▽, posterior cortex; ●—●, nucleus. (Bessems *et al.*, *Exp. Eye Res.*)

Changes in the Subunits

The demonstration that the primarily synthesized chains for alpha-crystallin are the A_2 and B_2 subunits, the A_1 and B_1 subunits being the result of post-translational changes, indicates that, so far as alpha-crystallin is concerned, changes in composition with age will be reflected in increases in the percentage of the A_2- and B_2-fractions. The work of Delcour & Papaconstantinou (1970) fully confirmed this prediction. They found mainly aggregates of A_2 and B_2 in the epithelium, with only small amounts of A_1 and B_1, whereas in the fibres A_1 and B_1 had become the major constituents of alpha-crystallin. By dividing the lens into nine layers from epithelium to nucleus, a trend towards increasing proportions of A_1 and B_1 fractions became obvious

SHORTENED SUBUNITS

We have seen that the change from alpha A_2 to alpha A_1 results from removal of an amino group from glutamine. De Jong *et al.* (1974) found, during their determinations of the amino acid sequences of the subunits, that a small fraction lacked some amino acid residues at the C-terminal end, and they showed that this fraction was derived from the alpha A chain; it was called alpha A^{1-168} since it was missing the last 5 amino acids of the 173 residues in normal alpha A. Both alpha A_2 and alpha A_1 exhibited the shortened version. The actual residues removed were: Ser-Ala-Pro-Ser. When layers of lens were analysed, the proportion of this degraded subunit increased progressively from epithelium to nucleus as we should expect of a process occurring after initial synthesis of the subunits; interestingly, though, the very high proportion that was found in early embryonic lenses declined rapidly with increasing fetal and post-natal age; thus it seems that the alpha A^{1-168} is further degraded during life, in fact Van Kleef has described a subunit missing the terminal 22 residues.

VARIETY OF POLYPEPTIDE CHAINS

Using the technique of isoelectric focussing, which permits accurate resolution, Van Kleef *et al.* (1974) have identified nine chains which include alpha A_2^{1-151} and alpha A_1^{1-151} lacking two terminal amino acids (Van Kleef *et al.*, 1974a). They point out that, on the basis of subunit composition, there is as great a difference between alpha-crystallin from calf cortex and cow cortex as there is between alpha-crystallin from cortex and nucleus. When the subunit composition of the alpha LM and alpha HM fractions of any given extract were examined, e.g. cortex or nucleus, there was very little difference, indicating a direct aggregation of alpha LM to alpha HM in any given situation; by contrast there were large differences in subunit pattern when different extracts were compared, e.g. calf cortex, cow cortex, calf nucleus, cow nucleus. As these different extracts represent different ages, this means that subunit composition is very definitely a function of age of the synthesized protein.

Human Studies

We have seen that the alpha-crystallins are separated into high- and low-molecular weight fractions, the difference being determined by the aggregation of smaller units. The pioneering studies of Dilley & Harding (1975) and Spector & Sigelman (1974) emphasized the increase in HMW at the expense of LMW material with change from fetal to senile lens, the rise in the nucleus being especially great. In a more exhaustive study, in which the change from pre- to post-natal state was studied with care, Ringens *et al.* (1982) examined molecular weight distribution, the nature of the N-terminal amino acids of the LMW fraction, and the presence of gamma-crystallin. Some of their results are shown in Table 4.10. The striking feature of the low-molecular weight proteins is the rise in the gamma-fraction after 16 weeks of gestation, whilst there was a considerable decrease in the low-molecular weight beta-crystallins. So far as alpha-crystallin was concerned, the LMW material appeared first in development between the 8th and 16th weeks of gestation; in the 14-year-old nucleus it had nearly disappeared, and in 76- and 46-year old lenses no well-separated LMW peak was seen.

Table 4.10 Relative percentages of the various crystallin populations of different ages (Ringens *et al.*, 1982)

	HM	α	β	γ
76 year nucleus	28.7	—	50.8	20.5
cortex	23.9	7.6	45.9	22.6
40 year nucleus	28.8	—	47.0	24.3
cortex	17.5	6.5	51.4	24.7
14 year nucleus	19.0	4.9	45.8	30.3
cortex	10.0	16.9	52.7	20.5
3 days	—	21.3	53.7	25.0
16–30 weeks of gestation	—	19.3	50.9	29.8
8–16 weeks of gestation	—	27.2	53.6	19.1

Note that this table illustrates changes in crystallin composition and does not reflect real proportions.

SUBUNIT COMPOSITION

When the proteins were examined with respect to their subunits, i.e. with SDS-polyacrylamide electrophoresis, changes in subunit composition were observed. In the adult lens alpha-crystallin is composed of a main band around 20 kd and minor chains with lower molecular weights. Beta-crystallin has main bands around 20 and 25 kd and gamma-crystallin polypeptides between 19 and 24 kd and some 10 kd material. Changes in the proportions of all these subunits become evident during development, probably corresponding to post-translational changes in the subunits described in other studies (Delcour & Papaconstantinou, 1972; Strous *et al.*, 1974; Spector *et al.*, 1971a). Most interesting was the pattern for gamma-crystallin, where only 2–3 major polypeptides appeared after the first 30 weeks of gestation, whilst a complex band-pattern appeared later, as revealed by isoelectric focussing, and presumably due to post-translational changes, possibly deamidation (Fig. 4.21). Thus the band at pH 7.0, by which gamma-crystallin is distinguishable from other low-molecular weight crystallins, is already present in the very early fetal stage, and should therefore be typical for the gamma-fraction. The band at pH 7.4 increases during development but disappears completely at some time after birth. Between the first and second trimester of fetal development, a switch to the production of a more basic chain (p*I* 7.5) occurs; this also disappears after birth. These were named gamma$_a$-, gamma$_b$- and gamma$_c$ respectively by Ringens *et al.* Figure 4.21 illustrates strikingly the emergence of many more acid chains in the adult. In general, Ringens *et al.*

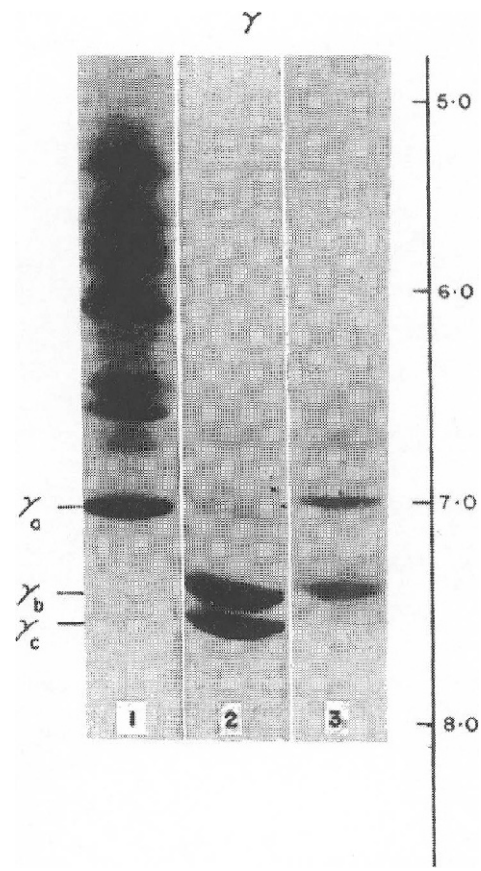

Fig. 4.21 Isoelectric focussing gel patterns of the various human lens crystallins at different ages: (1) adult; (2) fetus, 16–30 weeks; (3) fetus, 8–16 weeks. (Ringens *et al.*, *Exp. Eye Res.*)

(1982a),[25] commenting on their observed changes in the water-soluble and water-insoluble proteins with development, emphasize that many age-dependent changes have already taken place in a 14-year-old lens, so that direct comparisons between human lenses and those from shorter-lived species should not be made. Their studies showed that a typical aged pattern of lens proteins does not correlate with diminished transparency. Thus in comparing, say, 20- with 80-year-old lenses one only compares one, already aged, sample with another, even more aged, sample.

PRIMARY POLYPEPTIDE CHAINS

In a comparable study of pre- and neonatal human lenses, Thomson & Augusteyn (1985) emphasized the probable simplicity of the polypeptide chain composition of the lens crystallins when first synthesized, alpha-A_2, alpha-B_2, beta-B_p and beta$_s$ representing over 75% of the postnatal lens proteins. The great diversity in polypeptide composition found in later ages is the result of post-translational changes, such as deamidation, processes that presumably contribute to the stability of the aggregates that are a feature of development. Thus, by the end of the first year of life, about one third of the total lens polypeptides have been deamidated, whilst about 80% of the beta$_p$-chain has been deamidated by this time. Aggregation also begins early, so that the high-molecular weight alpha-crystallin fraction represents about 7% of the total alpha-crystallin in the neonatal lens. Thomson & Augusteyn separated the lens proteins into four classes on the basis of molecular weight, namely HMalpha, alpha, intermediate (IMW) and low molecular weight (LMW). They emphasized that the IMW group would contain many non-crystallin proteins that might be characteristic of the early life of the cell, so that the decrease in the IMW fraction with age might have no special significance, except to indicate the change in metabolic activity in the lens fibre as it becomes a non-reproducing cell with diminished metabolic activity. From their study, Thomson & Augusteyn concluded that the main changes in synthetic activity taking place around birth were an increase in the proportion of alpha-B subunits synthesized, so that early alpha-aggregates are more acid than those later formed. There is an explosive increase in beta$_s$ synthesis soon after birth associated with cessation of gamma synthesis (Fig. 4.22). Thus it appears that beta$_s$ replaces gamma-crystallin after birth as the main low-molecular weight crystallin.

CLEAVAGE OF BETA-CRYSTALLIN

By making polyclonal antisera to short (10–15 amino acid residues) synthetic peptides corresponding to known terminal sequences of a crystallin, the process of splitting off of these sequences may be followed by radioimmunoassay. Takemoto *et al.* (1987) have applied this technique

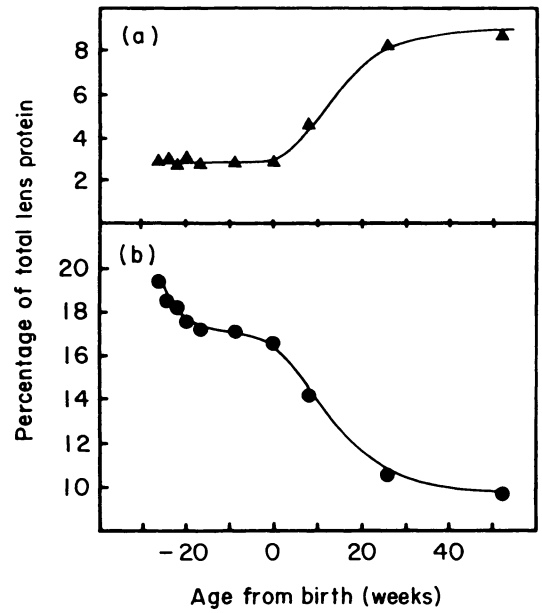

Fig. 4.22 Proportions of (a) beta$_s$-crystallin and (b) total gamma-crystallins, expressed as percentages of total lens proteins. (Thomson & Augusteyn, *Exp. Eye Res.*)

to follow the changes in beta basic principal polypeptide (beta-Bp), the major beta crystallin species of bovine lens and also present in human lens (McFall-Ngai *et al.*, 1986). In the human lens there is progressive cleavage from a 26 000 to a 22 000 dalton form, and by use of antisera to the C- and N-terminal sequences, Takemoto *et al.* (1987) have shown that the site of proteolysis is the N-terminal region. Only the two forms are found in human lens, suggesting that once cleavage begins it proceeds rapidly.

Rat Lens

McAvoy (1978a) examined the developing rat lens with a view to correlating morphological changes with synthesis of crystallins. He emphasized that the rat lens may be differentiated into two functionally distinct compartments, namely a proliferative and an elongation zone, the point of separation between the two being the ciliary body which separates the anterior and posterior portions of the lens (Fig. 4.23). He pointed out, too, that the posterior, elongation zone, was exposed to vitreous body and thus to the influence of retina-produced growth factors that might be responsible for this proliferation. In one-day-old lenses all cells, epithelial and fibre, immunofluoresced to anti-alpha crystallin, as in the bovine. Beta-crystallins were absent from the epithelium but present in those cells belonging to the elongation zone, a situation different from that in the bovine lens. Gamma-crystallin was restricted to fibre cells and appeared later in the

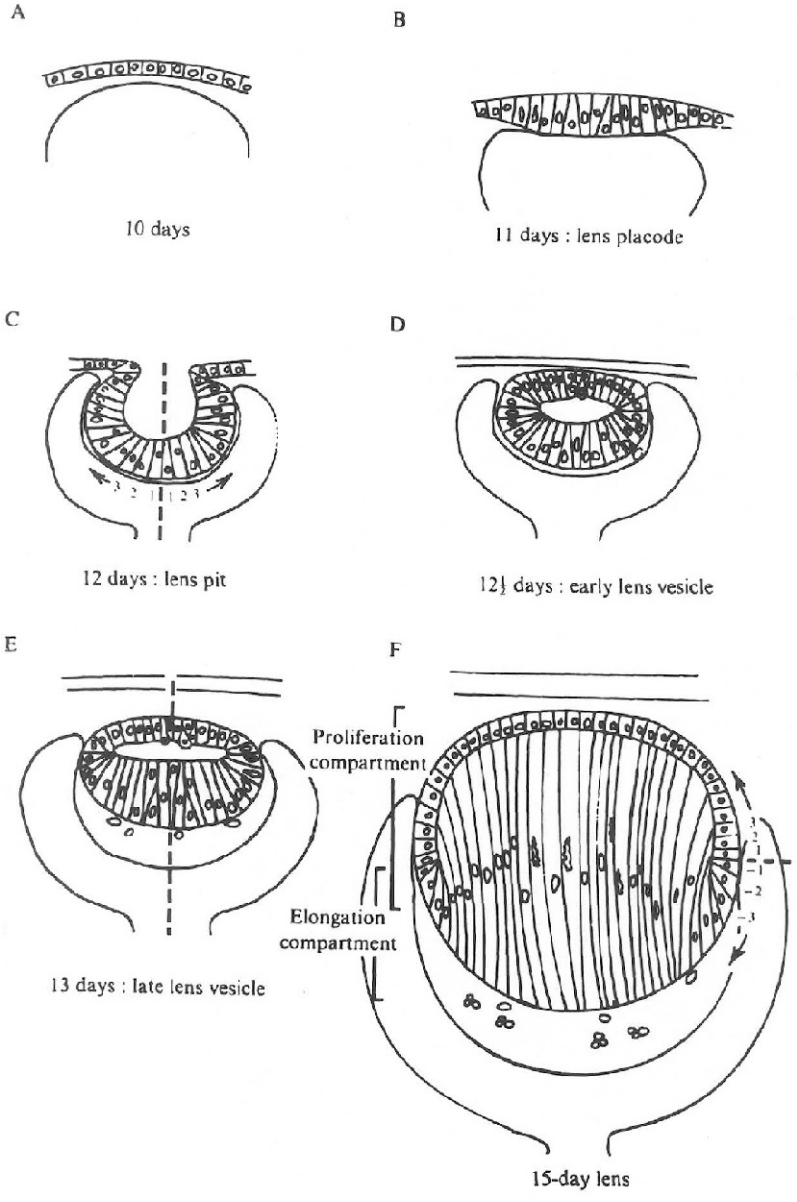

Fig. 4.23 Diagrams of sagittal sections of the main stages in lens development. Numbers indicate mode of indicating positions of cells. The diagrams are schematic and only a small proportion of the cells are represented. (McAvoy, *J. Embryol. Exp. Morph.*)

elongation process, and thus behaved in rat and bovine lens similarly.[26]

Epithelial Explants

Profiting from his finding that retinal extracts will stimulate lens epithelial explants to develop into fibres, McAvoy and his colleagues (Walton & McAvoy, 1984; Campbell & McAvoy, 1984) studied the changes in crystallin synthesis during the early stages of development, comparing their findings with a similar study on developing rat lens *in vivo*. Table 4.11 summarizes their

Table 4.11 Crystallin composition of protein labelled in lens epithelial explants (Walton & McAvoy, 1984; Campbell & McAvoy, 1984)

	Class of crystallin (% of protein synthesis)		
Days of culture	*Alpha*	*Beta*	*Gamma*
0	3.7±1.3	0	0
6	12.8±4.0	4.4±1.0	0.5±0.3
10	16.0±4.5	5.6±2.0	3.7±0.4

Development of the explants was initiated by addition of retinal extract to the medium.

results, where it will be seen that, initially, synthesis of beta-crystallin is more vigorous than that of gamma-crystallin. So far as alpha-crystallin was concerned, the interesting feature was the change in subunit composition; thus the epithelial protein consisted of 2 A to 1 B, but at the end of 10 days' growth the ratio had changed to 9:1. By contrast, the subunit composition of beta-crystallin remained relatively constant.

CATARACT

By cataract we mean any opacification of the lens, which may be a highly localized 'spot' or a complete loss of transmission throughout the substance; it may occur as a senile change; as a result of trauma, which presumably injures the capsule and the underlying epithelium; as a result of metabolic or nutritional defects; or as a consequence of radiation damage.

Morphology

NUCLEAR VERSUS CORTICAL CATARACTS

The histology of the cataractous lens has been described in some detail by v. Sallmann (1951, 1957), and by Cogan (1962). The *nuclear cataract* in which the nucleus of the lens becomes yellow or brown, is probably an exaggeration of the normally occurring senile changes. The cortical cataracts, on the other hand, represent opacities developing in the more recently laid-down lenticular fibres, and thus reflect the response to some abnormality in metabolism.

Cortical Cataracts

The gross morphology of these cortical cataracts consists in the appearance of aberrant forms of epithelial cells, which become large and round and are called 'balloon cells'; again, lens fibres may become fused into discrete masses, called morgagnian globules; if this process goes far enough the whole cortex becomes a milky liquid mass, and material may escape from the lens into the aqueous humour and vitreous body.

Of more interest, of course, are the early changes which, in the nature of things, must be examined in experimental forms of cataract in animals. In galactose cataract, Kuwabara *et al.* (1969) have shown, in the electron microscope, that the first change is a vacuolization of the epithelial and superficial cortical lens cells; also the intercellular spaces between cortical fibres are expanded to form cysts. All these changes were reversible by returning the animals to a normal diet. After 7 days the lenses were opaque, and now the intercellular cysts had enlarged and become vacuoles; the membranes of individual lens fibres had broken and the cells had liquefied. After 10 to 15 days the lens was densely opaque, and the whole cortex had liquefied whilst the epithelium was irregular and showed regions of cell proliferation. Thus the early feature seems to be the appearance of vacuoles in the cells and enlargements of the extracellular space to form cysts; if this process is not held in check there is irreversible rupture of lens fibres.

Human Cortical Cataract

In the human lens the cortical cataracts characteristically begin as localized points of opacity in surrounding transparent material in the subcapsular or supranuclear regions (Nordmann, 1962). In the electron microscope Philipson (1973) found essentially the same changes, consisting of an initial loss or damage to cell membranes leading to cellular dissolution with formation of large intercellular spaces or vacuoles. By microradiography, which permitted the estimate of local protein concentrations, the localized opacities were shown to be associated with a decrease in protein concentration accompanied by abrupt reduction in refractive index, and such localized refractive index transitions would act as scatter sources for light.

Nuclear Cataracts

Nuclear cataracts were completely different, the early stages being essentially a lenticular sclerosis accompanied by yellowing and a diffuse scattering of light with no large foci of scatter. In the advanced stages, usually associated with yellow-brown pigmentation, the electron-microscopical picture was normal so far as extracellular spaces were concerned, but in the dense whitish nuclear cataracts large aggregates of intracellular matrix of diameter 50 to 100 nm became obvious; such particles would be capable of scattering light and might account for the nuclear opacity (Benedek, 1971).

The different appearances of nuclear and cortical cataracts are illustrated by Fig. 4.24 from Garner & Spector (1980).

Sensile Cataract

CLASSIFICATION[27]

Pirie (1968a) classified senile cataracts on the basis of colour, or 'sclerosis' (Chylack *et al.*, 1984a), ranging from uniform pale yellow (I) to pale cortex with deep brown nucleus (IV). An improvement on this was made by Duncan & Bushell (1979) and Marcantonio *et al.* (1986) who included the sodium- and protein-contents of the lens as diagnostic features. Thus total soluble protein decreased with rise in sodium-content; for example, lenses with 50 mg of soluble protein had a Na^+-content of 20–40 mM/kg lens H_2O, whilst those with 5 mg protein had Na^+-contents of 180–220 mM/kg lens H_2O. By far the most

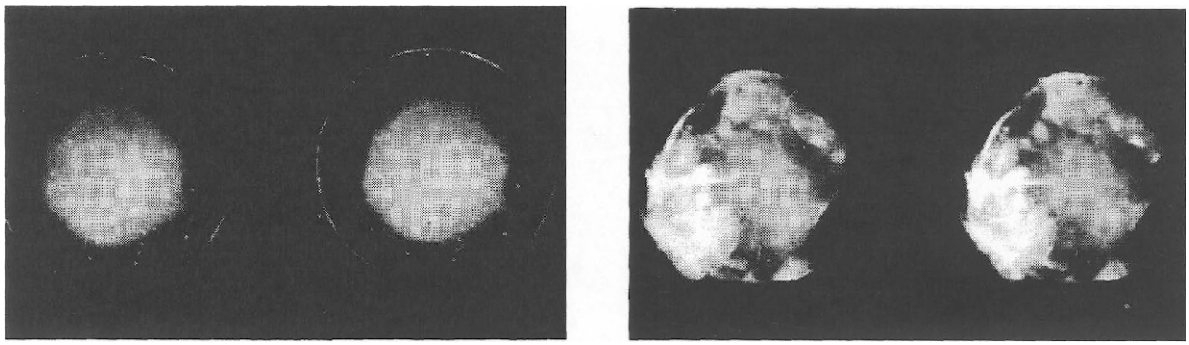

Fig. 4.24 Photographs of anterior views of nuclear (left) and cortical (right) cataracts. (Garner & Spector, *Exp. Eye Res.*)

elaborate classification is that initiated by Chylack (1978), and developed with his colleagues and adopted by the American Cooperative Cataract Research Group (CCRG). Immediately after intracapsular extraction, lenses are photographed against dark and bright backgrounds, and then the colour, degree of opacity in nucleus and six cortical regions (Fig. 4.25) are recorded together with the preoperative visual acuity. This, of course, produces a very large number of classes, but they may be simplified into smaller groups that may be employed where the particular biochemical parameter being studied is taken into account (Chylack *et al.*, 1984b). In general, Chylack *et al.* (1983, 1984a) reject nuclear colour as a basis for classification; thus colour increases with age of lenses, but this does not necessarily mean increased light-scattering, so that even with very dark nuclei loss of visual acuity may be the result of absorption of light rather than light-scatter.

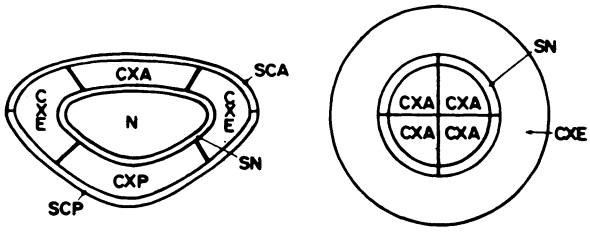

Fig. 4.25 Diagrammatic representation of the separate zones of opacification in human senile cataract: equatorial cortical opacity (CXE), anterior cortical opacity (CXA), posterior cortical opacity (CXP), anterior subcapsular cataract (SCA), posterior subcapsular cataract (SCP), supranuclear opacity (SN), and nuclear opacity (N). (Chylack *et al.*, *Invest. Ophthal.*)

Light-scatter

The opacity of a cataractous lens is due to the scattering of light that occurs when it passes through the medium that has become optically inhomogeneous partly as a result of the presence of large aggregates of protein in the individual lens fibres, but also, on a macromolecular scale, by discontinuities due to cell disruption, vacuole formation, and so on. Bettelheim and his colleagues (Bettelheim *et al.*, 1981; Siew *et al.*, 1981a) have measured scattering of polarized light as a function of the angle of the light-beam in order to be able to classify cataractous lenses in terms of physically measurable parameters. On the basis of a model with protein aggregates with high refractive index randomly distributed in a surrounding medium of lower refractive index, and cytoskeletal elements whose optic axes have preferential alignments and which are dispersed in a surrounding without optical anisotropy, this classification has been successful. If this mode of analysis is correct, then Siew *et al.* (1981b) have established that the essence of the normal ageing process is a gradual increase in the refractive index-difference between protein aggregates and their surroundings, i.e. in a syneresis of these aggregates.

Protein Changes

We have seen that the characteristic feature of the ageing lens is the increase in percentage of 'insoluble albuminoid', which represents an aggregation of lower molecular weight species, with HMW proteins as an intermediate form on the way to complete water-insolubility. The increase is much more prominent in the nucleus so that there are appreciable amounts even in the young animal's nucleus.

In the cataractous lens the process of aggregation goes farther, so that the fraction of high-molecular weight material in the soluble fraction is higher than in normal lenses of the same age. As Table 4.12 shows, the ageing process is accompanied by a decrease in the absolute amount of protein in the lens from 64 to 47 mg/100 g; in cataract this process is enhanced so that in the age-group 40 to 86 the content is 50.2 mg/100 g compared with 44.0 mg/100 g in cataractous lenses, and the percentage of soluble proteins falls from 81% to 51.4%.

The loss of proteins probably represents an escape of intact crystallins through the capsule since Sandberg & Closs (1979) found that the normal levels of alpha- and gamma-crystallins increased in the aqueous humour in cortical cataracts. With nuclear cataracts alpha increased and gamma decreased.

DISULPHIDE LINKAGES

Probably the most important advance in understanding the process of pathological aggregation of lens crystallins

Table 4.12 Effects of age on protein content of human lenses (After Mach, 1963)

Age (years)	Weight (mg)	Protein content (mg/100 g lens) Total	Soluble	Insoluble	% Soluble
0–10	122	64.0	61.0	2.3	96.3
10–20	122	63.0	59.0	3.8	94.1
21–30	140	62.8	57.3	5.5	91.1
30–40	153	57.6	51.7	5.9	90.2
40–50	170	55.6	49.7	5.6	89.2
50–60	212	50.7	43.3	7.6	84.9
60–70	230	49.7	39.5	10.3	79.4
70–80	215	47.0	37.0	10.0	78.6
>80	269	47.6	36.0	11.5	75.9
		Cataract			
Normal (40–86)	297	50.2	41.4	9.1	81.7
Cataract	190	44.0	23.4	19.9	51.4

to form large water-insoluble aggregates was the finding that these are probably brought about by cross-linking of sulphur-containing amino acids, especially cysteine, to form disulphide bonds (Harding, 1973). These bonds, being covalent, are not broken by hydrogen-bond breaking agents such as 6 M urea, so that they remain as a urea-insoluble residue. They are broken by mercaptoethanol, so that on treatment of a cataractous lens with this reagent the gel-filtration profile showed a loss of the high molecular weight peak occurring in cataractous lenses, but had no effect on a smaller peak in a normal lens extract, indicating that the normal high MW fraction is not aggregated by S–S-linkages. Subsequent studies from Spector's laboratory have amply confirmed the importance of the S–S-link; thus Roy & Spector (1978) isolated a high molecular-weight fraction from the water-insoluble fraction of a cataractous lens which, on the basis of light-scattering, had a molecular weight in the region of 1×10^6, i.e. large enough to cause light-scattering if randomly scattered in the cell (Benedek, 1971). On reduction of the S–S links, polypeptides of 60, 43 and 20 kd were separated. Examination of the state of oxidation of S-containing proteins in normal and cataractous lenses showed that, in severe cataract, some 60% of their methionine in membrane-associated material was methionine sulphoxide, and most of the cysteine was oxidized to cystine; mixed disulphides with glutathione were also observed (Garner & Spector, 1980).

MEMBRANE PROTEIN

The involvement of the lens membrane and its proteins in aggregate formation is suggested by several clues, notably the presence of the 43 kd polypeptide considered to be the human extrinsic membrane protein, in aggregates from cataractous lenses but absent in young lenses; complete immunochemical identity of this protein derived from cataract aggregates and its water-soluble counterpart in normal lenses (Garner *et al.*, 1979), and its morphological identification close to fibre membranes by use of a fluorescent antibody to the 43 kd polypeptide (Farnsworth *et al.*, 1981) in normal and human cataractous lenses all support the notion that this extrinsic membrane protein is closely connected with disulphide linked aggregate formation, along the lines suggested by Fig. 4.26.[28]

CORTEX VERSUS NUCLEUS

Garner *et al.* (1981) made three fractions from nucleus and cortex of cortical and nuclear cataracts, namely water-soluble (WS), water-insoluble-non-membrane, and WIS-membrane. They found that transparent regions, e.g. the cortex of nuclear cataracts, exhibited sulphur oxidation as well as the opaque regions, but the interesting finding was that only in the cataractous nucleus was the S–S-aggregated material associated with intrinsic membrane material; thus the insoluble S–S-linked aggregates in the cortex of cortical cataracts was not in the membrane associated fraction, and it was suggested that aggregation had occurred through the 43 kd polypeptide and had come away from the membrane with this, whereas in the cortical cataracts the association with membrane was retained.[29]

CROSS-LINKING AMINO ACID

The disulphide cross-linkage is undoubtedly the most important type so far as aggregation of crystallins is concerned. The question as to the existence of other cross-linkages has been discussed by Kanayama *et al.* (1987). Buckingham (1972) found, in advanced (Group III) cataractous lenses, that 15 to 20% of the protein was in a form resistant to dissociation by hydrogen-bond breaking agents and by reduction of S–S linkages with dithioerythritol; and he concluded that this (nuclear) material was linked by some other covalent bond than the disulphide link. Fujimoto *et al.* (1982) described a cross-linking amino acid, histidino-alanine, in connective tissue proteins with the following structure:

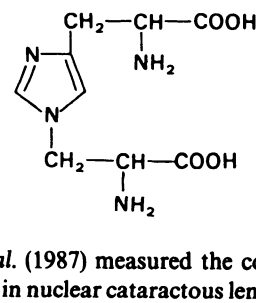

Kanayama *et al.* (1987) measured the concentrations of this amino acid in nuclear cataractous lenses, classified on the basis of colour (Pirie, 1968a). There were large increases with increasing depth of colour, suggesting that

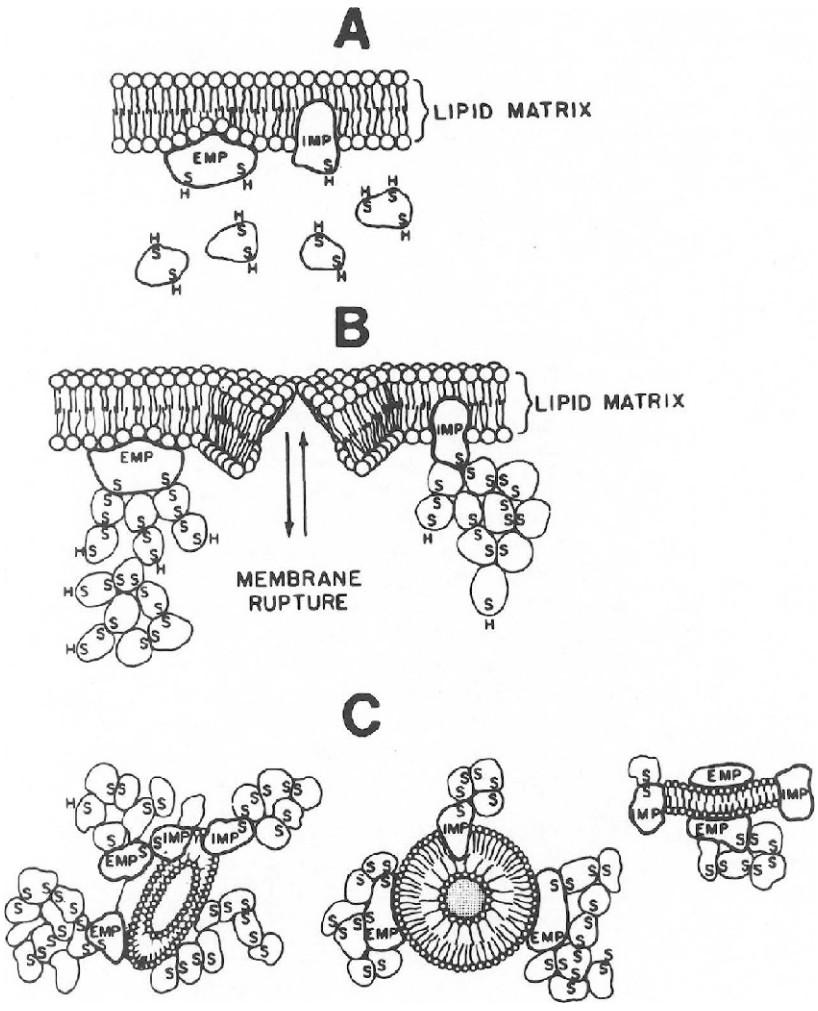

Fig. 4.26 Model of proposed membrane alterations occurring during the development of cataract. EMP, extrinsic membrane protein; IMP, intrinsic membrane protein; other molecules are cytoplasmic polypeptides. (*A*) Normal fibre; (*B*) cataractous fibre, formation of high M_r S–S aggregate and breakdown of membrane; (*C*) membrane disintegration. (Garner *et al.*, *Proc. Nat. Acad. Sci.*)

histidino-alanine is concerned with the linkage of proteins in nuclear cataract.

GAMMA-CRYSTALLIN

Garner *et al.* (1981) found that the major polypeptide released from membrane-associated S–S-linked aggregates from the cataractous lens was material of about 24 kd molecular weight, and amino-acid analysis revealed a remarkable similarity to a gamma-component found in the water-soluble fraction; immunochemical studies confirmed this close relation to gamma-crystallins, and showed that it was present in all cataractous aggregates, thus confirming an earlier suggestion of François *et al.* (1965), based on their observation of a decrease in low-molecular weight material with relative constancy of α-crystallin.

LANTHIONINE LINKED POLYPEPTIDES

Cysteine gives rise to cystine, so that two crystallin molecules can be linked by the disulphide bridge in cystine. Cystine itself can be oxidized to a symmetrical di-ether which could also act as an interpolypeptide link in the insolubilization process. Bessems *et al.* (1987) have demonstrated the presence of this molecule in hydrolysates of the 'yellow protein' extracted from human cataracts, namely the material that remains after urea-DTE extraction and delipidation. It was not present in the urea-soluble material from the same lenses. Lanthionine and cystine were isolated from the yellow protein in the ratio of 5.3 to 2.6, and there was one molecule of lanthionine to four polypeptide units of MW 20 kd.

GAMMA-GLUTAMYL-LYSINE LINKAGE[30]

Lorand *et al.* (1981) have suggested that some protein aggregates in the cataractous lens, not dissociated by disulphide rupturing agents, could be linked by γ-glutamyl-ε-lysine side-chain linkages, catalysed by transglutaminase. They isolated such material from the polymeric fraction of human cataract tissue, and pointed out that the lens contains a Ca^{2+}-dependent transglutaminase that might well be triggered by excess Ca^{2+}.

MOLECULAR WEIGHTS OF THE AGGREGATES

Takemoto & Azari (1977) found a range of 2 to 33 kd from advanced cataracts. These aggregates are not large enough,

however, to cause the scattering of light postulated by Benedek (1971), which would require weights of 50 or more kd.

FLUORESCENT MATERIAL

The yellow material derived from the nucleus of the cataractous lens contains fluorescent substances that are described as a-typical, because the flurorescence does not arise from the aromatic amino acids normally present in lens crystallins. The composition of this material has been examined by Spector and his colleagues, and has proved to be highly complex, presumably derived from photo-oxidation of amino acids such as tryptophan, e.g. kynurenine and beta-carboline (Dillon *et al.*, 1976). Two other compounds, namely bityrosine and anthranilic acid have also been isolated (Garcia-Castineiras *et al.*, 1978). By treatment of the yellow cataractous material with endopeptidases, Dillon *et al.* (1984) prepared an endopeptidase-resistant material (EPRF), which consisted of polypeptides with a fairly uniform molecular weight of around 3000 daltons, and contained most of the atypically fluorescent material. After acid-hydrolysis the cleavage products contained oxindoyl alanine and kynurenine, which could have resulted from photo-oxidation of tryptophan.

Water and Electrolyte Balance

Leaky Membranes

The pathology of the cataractous lens suggests that the cell membranes have broken, and if this is true we may expect the normal electrolyte balance, with the high internal concentration of K^+ and low concentrations of Na^+ and Cl^-, to be upset as with any other tissue, so that initially Na^+ will leak into the cells and K^+ leak out; so long as the exchange is one-for-one there will be little change in internal osmotic pressure, but, because of the Donnan-distribution imposed by a high internal concentration of negatively charged protein, ultimately the cells should swell and the final situation, if all the cells lost their membrane selectivity, would be a swollen lens with low internal K^+ and high internal concentrations of Na^+ and Cl^- (Duncan & Croghan, 1969).

Cortical Versus Nuclear Cataracts

A number of early studies on cataractous lenses showed an increase in Na^+ and fall in K^+ with increase in percentage of water; however, an important study of Maraini & Mangili (1973) emphasized the distinction between the cortical[31] and nuclear forms of cataract; it was only lenses with cortical opacities that showed an increased water-content, expressed as percentage of lens weight, the nuclear cataracts being normal in this respect. As Fig. 4.27 shows, the K^+-Na^+ and Cl^--contents of purely nuclear cataracts are the same as in normal lenses, whereas the large rise in Na^+ and fall in K^+ are peculiar to the cortical cataract. In more elaborate studies, Duncan & Bushell (1975) found the same general picture, those cataractous lenses with high K^+ and low Na^+, comparable with normal lenses, having mainly nuclear opacities; a smaller number of lenses had a moderately raised Na^+ and moderately lower K^+, and another, large, group had very high Na^+ concentrations, considerably higher than that in the aqueous humour.

Three Categories

Thus three broad categories of cataract were established: A, B and C as in Table 4.13, Group A being purely nuclear, Group B a mixed type, and Group C containing mostly purely cortical cataracts. As Maraini & Mangili had found, the percentage of water was high in the cortical cataracts, which had also lower total solid matter per lens; thus the cortical cataract not only gains water but loses solid matter—protein.

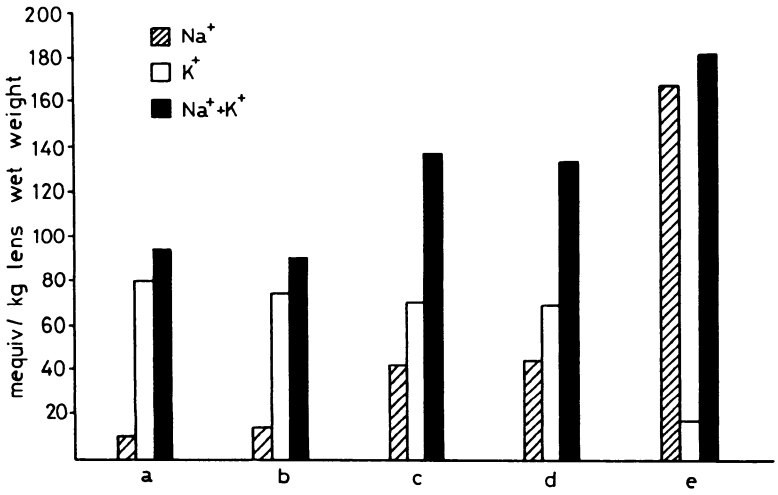

Fig. 4.27 Content of sodium and potassium ions of senile human normal and cataractous lenses: a, normal lenses; b, pure nuclear cataracts; c, nuclear cataracts with early cortical involvement; d, early cortical cataracts; e, complete cortical cataracts. (Maraini & Mangili, *Ciba Symp.*)

Table 4.13 Ionic concentrations in lenses, given as mequiv/kg lens H_2O. The figures marked with an asterisk are taken from Maraini & Mangili (Duncan & Bushell, 1975)

Lens type	*Sodium*	*Potassium*	*Calcium*	*Magnesium*	*Chloride*	*% Water*	*Dry weights* (mg)
Group A	24.7	139.6	1.8	11.6	36.4	68.2	74.5
Group B	52.2	105.7	5.6	10.4	40.0	67.4	66.1
Group C	171.7	24.2	32.4	10.4	88.7	70.9	54.3
Normal bovine	25.0	120.0	0.6	10.4	35.0	67	—
Normal human*	14.5	113.5	—	—	—	70	—
Nuclear*	21.2	113.2	—	—	—	68	—
Early cortical*	67.7	106.1	—	—	—	67	—
Complete cortical*	210.6	21.4	—	—	—	79	—

High Na^+-concentration

The high concentration of Na^+ over that in the aqueous humour in cortical cataract may be accounted for by the high protein content of the tissue; a similar high Na^+-concentration occurs in cornea (Davson, 1949) and is due to a similar cause, but in the case of the lens this is normally prevented by the Na^+-pumps that exclude Na^+ and replace it with K^+; failure of the Na^+-pump allows an equilibrium to be established with a part of the Na^+-ions neutralized by protein anions. When the fibre membranes were damaged by freezing and thawing, a similar uptake of Na^+ and Cl^- and loss of K^+ were observed (Duncan & Bushell, 1976), and the final levels reached were consistent with a Gibbs–Donnan equilibrium so far as these three ions were concerned.

The Calcium Content

Great interest has attached to the Ca^{2+} content of the lens, since it is known that interference in the general calcium metabolism of the organism, as with parathyroidectomy or rickets, can be associated with the development of cataract.

NORMAL LENS

The concentration of Ca^{2+} in the rabbit lens has been studied exhaustively by McGahan *et al.* (1983); expressed in terms of lens-H_2O, it was some 0.09 meq/l compared with 0.7 and 1.1 meq/l in aqueous humour and vitreous body respectively. The concentration was less in nucleus than the whole lens. Only about 45% of the Ca^{2+} is readily exchangeable with ^{45}Ca in the medium, suggesting either slow diffusibility or strong binding. The same authors have examined the Mg^{2+} concentration which is present in considerably higher concentration than in aqueous humour or vitreous body (see, also, Baldwin & Bentley (1980) for a study of amphibian lens).

Jacob (1983), using a Ca^{2+}-sensitive electrode found an 8-fold gradient of concentration along the optic axis, the concentration being greatest at the posterior surface; he concluded that only 0.4% of the total Ca^{2+} of the lens existed as free ions. Raising the external concentration caused penetration leading to opacification; this was associated with an uncoupling of the lens fibres, so that gap-junctions were apparently closed, a process described first by Rose & Loewenstein (1975). This must be regarded as a protective response to local cell damage.

CALCIUM PUMP

As with other cell systems, we may postulate an active transport of Ca^{2+} out of the lens fibres, but the effects of metabolic poisons on efflux are conflicting (Hightower *et al.*, 1980; McGahan *et al.*, 1983; Paterson & Delamere, 1983). Delamere & Paterson (1985) found that lowering the concentration of Ca^{2+} in the medium surrounding the lens increased ^{45}Ca-uptake, showing that calcium influences membrane permeability to itself and probably to other ions, as with, say, the erythrocyte.

Ca-ATPase

According to Hightower *et al.* (1980) the Ca^{2+}-pump that maintains a low internal concentration of the ion, is catalysed by a Ca^{2+}-activated ATPase, which may be inhibited by lanthanum. Iwata *et al.* (1984) only detected Ca-ATPase activity if it was stimulated by calmodulin; inhibition of calmodulin by W-7 caused lens opacity with elevated internal Ca^{2+} and Na^+, and lowered K^+.

CATARACTOUS LENS

The values for the ionic concentrations in cataractous lenses, shown in Table 4.13, indicate a rise in Ca^{2+}-content with severity of cataract, and a more elaborate study, with this ion in mind by Hightower & Reddy (1982a) in which the severity of cataract was assessed by the CCRG classification, amply confirmed this. Thus Hightower & Reddy found values of 0.18–0.56 mM in immature cataracts and 3.4–9.1 mM in mature cataracts. As Duncan & Bushell have pointed out, the normal concentration of Ca^{2+} in the lens is very much less than that in the aqueous humour, so that the lens fibre shares

with many other cells, such as the neurone, this feature of a low internal concentration of calcium, which must be maintained by an active pump since there is an electrical potential favouring influx of positive ions from aqueous humour to lens. Duncan & Bushell (1975) found that a high lens calcium was only associated with those cataractous lenses that had high Na^+ and low K^+, i.e. with the Group C lenses (Table 4.13).

The very high concentration of Ca^{2+} within the cataractous lens cannot be merely the consequence of an increased membrane permeability, having regard to the aqueous humour concentration of about 1.7 mM. Clearly, the Ca^{2+} is at least partly bound to proteins, just as some 50% of this in plasma is bound and unable to diffuse through porous membranes used in dialysis. Of this bound Ca^{2+} some is found associated with the water-insoluble proteins, including the membrane fraction (Hightower & Reddy, 1982b) and the remainder with the water-soluble proteins. The proportion between the two, ca. 15% to 85%, remains the same as Ca^{2+}-content rises, but the absolute amount associated with the insoluble aggregates, characteristic of cataract, increases; and it has been supposed that this divalent cation is closely concerned in the aggregation process. This view is supported by the finding of Jedziniak *et al.* (1972) that the aggregation of bovine alpha-crystallin is favoured by high concentrations of Ca^{2+} in the medium. This is illustrated by the curve of Fig. 4.28 showing the diffusion coefficients of the aggregates against concentration of calcium in which the aggregation took place. At a critical concentration of 4×10^{-3} molar (4 mM) and above, aggregates as high as 300×10^6 to greater than 2×10^9 daltons molecular weight, computed from the diffusion coefficient, were obtained. The aggregation was not brought about by disulphide linkages, and belonged to α-crystallin and not to β or γ. Removal of the calcium with EDTA reversed the process, so that the turbid suspensions containing the highly aggregated material became transparent. In human lens material calcium also caused aggregation, but this was not reversible with EDTA or EGTA, indicating a much firmer binding (Jedziniak *et al.*, 1973).[32]

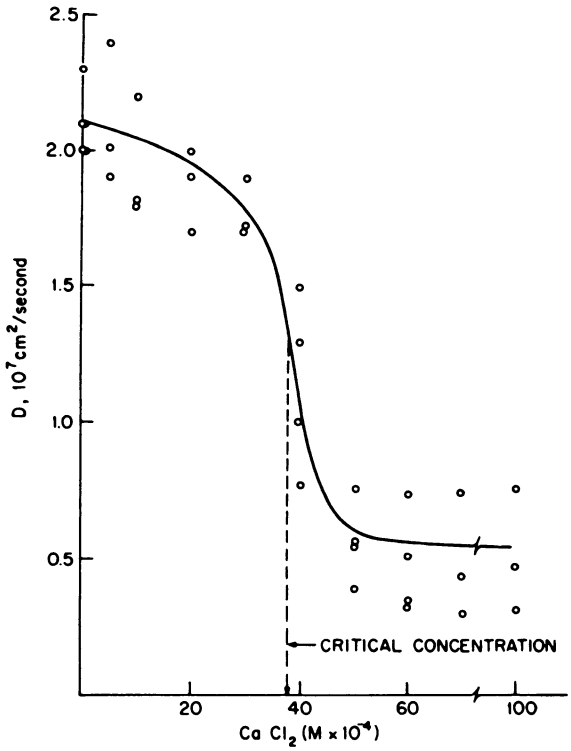

Fig. 4.28 The effects of increasing the concentration of calcium ions on the diffusion coefficient of alpha-crystallin. (Jedziniak, *Invest. Ophthal.*)

Ca^{2+} AND LENS PROTEINS

Giblin *et al.* (1984) induced cataracts in excised rabbit lenses by incubating in 20 mM Ca^{2+}; earlier they had shown that Ca^{2+} induced aggregation of crystallins in solution, and they now found that in the intact lens, too, the HMW fraction was some five-times normal, both alpha- and beta-crystallins being present; the linkage was not covalent, however. When cataracts were induced by X-rays, the concentration of Ca^{2+} was raised, but this time the aggregates contained S–S-linkages, and it was argued that X-rays, besides causing raised Ca^{2+}, might also produce oxidizing free radicals that would assist aggregation by forming S–S-links (Hightower *et al.*, 1983).

MONO- VERSUS DIVALENT CATIONS

The association between raised Na^+ and cataractous signs, such as loss of lens crystallins and opacity, emphasized by Duncan & Bushell, may well obscure the importance of Ca^{2+}, which also increases. Thus Boutros *et al.* (1984), studying an experimental cataract induced by photodynamic action of 8-methoxysporalen (Koch *et al.*, 1982), considered that the loss of transparency was more closely correlated with the rise in Ca^{2+} than that of Na^+. Marcantonio *et al.* (1986) compared the effects of EGTA and strophanthidin on the isolated bovine lens; both caused swelling, the one due to reduced free external Ca^{2+} and the consequent increase in ionic permeability (Delamere & Paterson, 1979; Jacob & Duncan, 1981) and the other due to inhibition of the Na^+-K^+-ion pump. The lens-Ca^{2+} rose only with strophanthidin treatment, and in these lenses crystallin aggregation increased, as measured by increased incorporation of ^{14}C-tyrosine, the presumptive linking agent. Associated with this aggregation there was loss of transparency and loss of soluble crystallins, mainly $beta_L$-, into the culture medium.

PROTEIN SYNTHESIS

Hightower (1983) found that mere interference with the Na^+-K^+-pump of the lens, which increased its Na^+- and decreased its K^+-content, failed to influence protein synthesis, as measured by incorporation of ^{14}C-histidine; raising the internal concentration of Ca^{2+}, however, with A 23187 or high external concentration reduced this considerably; thus with an internal concentration of 1.9 mM the rate fell to 50% of normal.

CALCIUM AND CATARACT

To conclude, then, it seems that failure of the membrane-pumps that occurs in mature cortical cataracts necessarily leads to uptake of calcium as well as Na^+ and Cl^-. The binding capacity of the lens proteins means that the concentration of calcium finally reached in the abnormal lens fibres is greater than would be expected of a passive distribution: however, the very high concentrations found in cataractous lenses do suggest that there has been an alteration in the binding capacity of the lens proteins in the cataractous condition. It is tempting to suggest, along with Spector, that the failure of the cataractous lens to exclude calcium leads to aggregation of lens proteins, an aggregation that leads to the much tighter binding of the calcium that is actually observed.

IONOPHORES

These substances become incorporated into the cell membrane and facilitate exchanges of ions, such as Na^+ and K^+, thereby altering the normal ionic relations between cell and environment. Nogericin and valinomycin, added to the incubation medium of the isolated rabbit lens, caused losses of K^+ with gains of Na^+, associated with cloudiness. There was very little change in hydration as the ionic changes balanced each other (Iwata & Horiuchi, 1980). The causative factor was, in fact, the increase in Ca^{2+}-content, at any rate with valinomycin, since, on incubating the lens with this ionophore but a low Ca^{2+} concentration in the medium, opacity did not develop (Hightower & Harrison, 1982).

Metabolic Defects

Although metabolic activity in a large portion of the lens is probably at a low level, reproduction of cells being limited to a small region and protein turnover being very small, the lens is a living organ so that interference with metabolism may result in cataract.

Toxic Cataracts

A number of drugs will cause opacities in the lens; one that has been studied experimentally in some detail is naphthalene, which is converted in the body to, among other substances, naphthalene diol; according to Van Heyningen & Pirie (1967), this can be converted in the eye to 1-2-dihydroxy-naphthalene, which is probably responsible for the blue fluorescence in the eye of the naphthalene-fed rabbit. This is oxidized to β-naphthaquinone (Rees & Pirie, 1967) and is highly reactive; for example, it reacts with ascorbic acid to form H_2O_2 which is toxic. This reaction converts ascorbic acid into its oxidized product, dehydroascorbic acid; and it is interesting that the concentration of ascorbic acid in the lens actually increases in the naphthalene-fed rabbit; it has been suggested by Van Heyningen (1970) that the dehydroascorbic acid, which readily penetrates the lens, is reduced there to ascorbic acid from which it cannot escape so easily, being less lipid-soluble than dehydroascorbic acid. The actual means whereby β-naphthaquinone causes cataract has not so far been clarified. In addition to naphthalene, many drugs, often used therapeutically at one time, such as dinitrophenol, myeleran, dimethyl sulphoxide, will cause cataracts but not necessarily in man in therapeutic doses; for example dimethyl sulphoxide has not reportedly caused eye damage in man although in experimental animals, such as the dog, doses of 5 g/kg will cause cataract, albeit of an unusual type (Rubin & Barnett, 1967). Such knowledge as we have of the mode of action of a variety of drugs has been summarized by Van Heyningen (1969), whilst Pirie (1968b) has described the early pathology of naphthalene lesions in lens and retina.

Sugar Cataracts

A persistent raised blood-sugar, as in diabetes mellitus, can lead to cataract, due presumably to the high concentration in aqueous and vitreous humours (Davies *et al.* 1984); experimentally, a cataract may be induced in rats by causing diabetes with streptozotocin, or by feeding galactose. Thus addition of this sugar to the diet causes the development of a clinical opacity by the 3rd day, and by the 10th day the lens is completely opaque. Depending on the time of feeding the diet, the opacity is at least partially reversible on returning the animal to a normal diet. The only metabolic pathway common to all the cataractogenic sugars is the production of a polyhydric alcohol, e.g. sorbitol in the case of a high blood-glucose, dulcitol with high blood galactose, etc. Van Heyningen (1959) observed that feeding these sugars led to accumulation of the alcohols in the lens; and it was suggested by Kinoshita *et al.* (1962) that the primary event was, indeed, the intracellular accumulation of the alcohol, which, not being able to escape from the lens fibres, caused an increased osmolality leading to osmotic swelling.

SWELLING OF LENS FIBRES

Figure 4.29 shows changes in water- and dulcitol-content of rat lenses when the animals were maintained on a

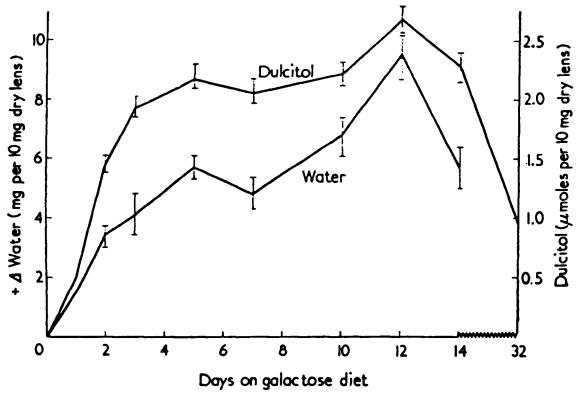

Fig. 4.29 The accumulation of dulcitol and water in lenses during development of galactose cataract in rats. (Kinoshita *et al., Exp. Eye Res.*)

galactose diet. *In vitro*, also, exposure of the lens to galactose caused corresponding increases in hydration and alcohol concentration. When an aldose reductase inhibitor was added to the galactose medium, the formation of dulcitol was prevented, and likewise the increase in hydration (Kinoshita *et al.*, 1968). The same inhibition of cataract development has been described for streptozotocin-diabetic rats, employing the powerful aldose inhibitor sorbinil[33] (D-6-fluoro-spiro(chroman-4,4′-imidazolamine-2′,5′-dione), cataract being prevented and the increased hydration of the lens being reduced (Fukushi *et al.*, 1980).

Na^+-K^+-ATPase As to the ultimate steps leading to the mature cataracts, Kinoshita considered that the swelling of the lens fibres induced secondary changes that reduced the efficacy of their cation pumps, thereby allowing the accumulation of sodium leading to ultimate bursting of the fibres, a process that undoubtedly occurs (Kuwabara *et al.*, 1969) leading to the formation of intercellular cysts that may be as large as 100 μm across. If swelling of the fibres, of itself, caused an increased permeability of their membranes to ions, then the effect would be enhanced, a defective pump having to contest with an increased rate of leakage of K^+ and uptake of Na^+; and in fact Jacob & Duncan (1980) have described such an increase, as measured by membrane conductance.

A decrease in Na^+-K^+-ATPase was described by Fournier & Patterson (1971) and this was confirmed by Unakar & Tsui (1980a, b) on the basis of cytochemical and biochemical studies; reversal of the cataract by return to a normal diet was accompanied by a gradual return of ATPase activity to normal. When rats were fed galactose and the aldose-reductase inhibitor, sorbinil, at the same time, there was not only no cataractous change in the lens, as shown in the electron microscope, but also Na^+-K^+-ATPase activity remained normal (Unakar & Tsui, 1980b).

REVERSAL

Return of a galactose-fed rat to a normal diet causes at least a partial reversal of the cataractous changes, so that even with a 'mature' cataract, the cortical region can become clear leaving only a nuclear opacity (Fournier & Patterson, 1970; Hu *et al.*, 1983; Unakar *et al.*, 1978), the re-establishment of clarity proceeding in the same order as development of opacity, i.e. from the equator to the poles. In view of the obvious destruction of fibres in the cataractous condition, it is clear that reversal of cataract consists in generation of new fibres, and so we may expect this to occur in the equatorial region first, and this is true (Fournier & Patterson, 1970). According to Unakar *et al.* (1978), the clear regions of reversed cataract also show evidence of repair to previously damaged fibres.

BIOCHEMICAL CHANGES

Reddy *et al.* (1976) showed that, after return to a normal diet, the glutathione and amino acid contents of the lenses, which fell during development of cataract, returned to normal. However, the Na^+-content, indicating fibre swelling, remained some four-times normal, and the water-content did not recover completely.

Myoinositol Studies on diabetic nerve indicate that the myoinositol level falls, and since this vitamin is concerned in Na^+-K^+-ATPase regulation (Greene *et al.*, 1985), this fall may be related to the reduced conduction velocity. Kawaba *et al.* (1986) showed that lenses, incubated with galactose, lost myoinositol, an effect that was abolished by sorbinil. This was probably the consequence of the increased membrane permeability due to polyol accumulation.[34]

CRYSTALLIN SYNTHESIS

After 6 days of a 50% galactose diet, crystallin synthesis is severely retarded in rat lenses, and nearly absent after 12 days (Kador *et al.*, 1979). Crystallin synthesis can return to normal after return to a galactose-free diet. Shinohara *et al.* (1982) have measured the mRNA content of galactose-fed rats and shown that after 6 days the lens fibre-cells possessed the full complement of mRNAs for synthesis of the crystallins, but after 12 days, cortical fibre-cells had lost about half, and nuclear fibre-cells had lost all of their mRNA. During reversal, the nuclear fibre-cells did not recover their ability to synthesize crystallins, whereas the cortical fibre-cells did, with a corresponding increase in mRNA content. The authors concluded that a decreased efficiency of utilization of mRNA was a factor in defective crystallin synthesis, as well as degradation of the existing mRNA.

PEROXIDES[35]

It has been suggested that light might induce the formation of peroxides in the lens which, if not reduced, would oxidize SH-groups, promoting crystallin aggregation. Thus there are oxidants derived from the univalent reduction of O_2 in tissues that are highly reactive, including the superoxide radical $O_2^{\cdot -}$, H_2O_2, and the hydroxyl radical ($^{\cdot}OH$). It is considered that they may play a role in a variety of pathological conditions including radiation injury. Tissues have defence mechanisms against these oxidants, notably superoxide dismutase (SOD), catalase and glutathione reductase. Giblin *et al.* (1976) found reduced Na^+-K^+-activated ATPase in the lens after treatment with butyl hydroperoxide, and this was accompanied by penetration of salts and water, suggesting a failure of the cation pumps. Again Varma *et al.* (1979) caused failure of the pump by exposure of the lens to light in the presence of riboflavine, a failure that was prevented by the presence of ascorbic acid. According to Spector & Garner (1981), the mean concentration of H_2O_2 in normal human aqueous humour was 24 μM, and in cataractous patients it was 69 μM. Garner *et al.* (1983) found that concentrations of 250 μM H_2O_2 in the medium surrounding the excised lens caused inhibition of Rb^+-uptake comparable with that caused by 0.1 μM ouabain; however, there was no effect of H_2O_2 on hydrolysis of ATP by ATPase, and no effect on membrane permeability, as assessed by a normal extracellular space, so that the effect was probably due to an uncoupling of the ATPase from its ion-pump.[36]

CATALASE

Bhuyan & Bhuyan (1977) inhibited catalase in the eye of the rabbit with 3-amino-triazole, producing increased concentrations of H_2O_2 in both aqueous and vitreous humours by some 2–3-fold; earlier they had shown that regular feeding of rabbits with the drug induced cataract. Apparently the enzyme is synthesized in the iris-ciliary body, being found in the cytosol (Delamere & Williams, 1985).[37]

Superoxide Dismutase This enzyme is present in the cornea, lens, etc., its major lens activity being in the epithelium; it is inactivated by H_2O_2, and is apparently protected *in vivo* from this oxidant by catalase, since 3-amino-triazole, a catalase inhibitor, potentiates the action of H_2O_2 on the dismutase (Bhuyan & Bhuyan, 1978).

Role of Glutathione

This tripeptide, glutamyl-cysteinyl-glycine, is accumulated in the lens to a concentration some 1000 times that in the aqueous humour, and it has been suggested (Augusteyn, 1979) that it is responsible for maintaining the reduced state of the SH-groups of the lens crystallins and thus prevents the oxidation that leads to aggregates in cataract. He showed that glutathione could, indeed, cleave the disulphide bonds that linked proteins in cataractous lenses. In all forms of cataract the fall in concentration of glutathione is striking. Glutathione constitutes a redox system:

$$2GSH + \tfrac{1}{2}O_2 \rightleftharpoons GSSG + H_2O_2$$
$$NADPH + GSSG + H^+ \rightleftharpoons 2GSH + NADP$$

In the glutathione redox cycle the oxidation of reduced glutathione (GSH) by H_2O_2 is catalysed by glutathione peroxidase. The peroxidase reaction is coupled with the regeneration of GSH from oxidized glutathione, GSSG, by glutathione reductase and NADPH and also with the regeneration of NADPH from $NADP^+$ by the activity of the hexose monophosphate shunt (Giblin & McCready, 1983). Thus exposure of the lens to H_2O_2 stimulates the activity of this shunt.

HEXOSE MONOPHOSPHATE SHUNT (HMPS)

Giblin & McCready (1983) exposed rabbit lenses to increasing concentrations of H_2O_2 and found that HMPS activity increased linearly, indicating the detoxication of the H_2O_2 through the glutathione reductase system. When the concentration of H_2O_2 was raised above 0.06 mM (the normal aqueous humour concentration) there was a sharp decrease in HMPS activity, and accumulation of oxidized glutathione occurred, indicating injury to the enzymes. BCNU, an inhibitor of glutathione reductase, blocked the increase in HMPS activity due to low concentration of H_2O_2. Thus detoxication of H_2O_2 is linked to the metabolism of glutathione. Giblin *et al.* (1985) compared cultured lens epithelium with cultured fibroblasts with respect to responses to H_2O_2; the epithelial cells were able to maintain normal concentrations of reduced glutathione in the face of H_2O_2 uptakes that would have oxidized the whole GSH content every 2 min. By contrast, the fibroblasts were much more vulnerable. As with the whole lens, HMPS activity increased in the presence of 0.04–0.05 mM H_2O_2.

In a further study, Giblin *et al.* (1987) examined the effects of the inhibitor of glutathione reductase (BCNU) in more detail; exposure of isolated rabbit lens to the inhibitor resulted in significant accumulation of oxidized glutathione in the lenses when incubated with 0.05 mM H_2O_2; this was associated with gross disturbances in electrolyte balance. The authors concluded that there was a link between normal glutathione reductase activity and the control of ionic transport within the lens.

NON-SPECIFIC ACTIONS

Rogers & Augusteyn (1978) described a fall in glutathione reductase activity in mature cortical cataracts, but even though

the activity in the nucleus was decreased to one third, there was still enough to keep all the glutathione of the lens in the reduced state. Thus loss of enzyme activity in cataract may be a non-specific consequence of cell damage shared by other enzymes too.[38] The partial failure of the Na^+-K^+-pump observed by treatment of the lens with oxidizing agents might be attributed to oxidation of glutathione, but as Cheng *et al.* (1984) emphasized, a variety of metabolic enzymes are also open to attack by oxidizing agents; they depleted lenses of glutathione specifically by feeding 1-chloro-2,4-nitrobenzene; however, there was no oxidized glutathione nor glutathione-linked protein in the lenses, although Rb^+-uptake was decreased, indicating a defect in the Na^+-K^+-pump. They concluded that the influence of the drug was exerted non-specifically on glucose metabolism.

MULTIPLE ENZYME STUDY

Fecondo & Augusteyn (1983) measured the activities of glutathione peroxidase, catalase, and superoxide dismutase in cataractous lenses; Type I lenses, with no nuclear involvement, were compared with nuclear cataracts of increasing degree of severity as classified by colour (Pirie, 1968). Catalase activity was unaffected by nuclear cataract; glutathione peroxidase activity, on the other hand, showed a precipitate decrease with onset of nuclear cataract, so that in the Type IV nucleus there was no activity. With superoxidase activity this likewise decreased in cataract, more in the nucleus than cortex. The authors considered that the decline in glutathione peroxidase activity might easily be the determinant in allowing excess H_2O_2 to accumulate in the cataractous lens; the reduced amounts of glutathione reductase, and of reduced glutathione, would indicate that the glutathione peroxidase activity *in vivo* was even less than that measured *in vitro* under optimum conditions.

ARTIFICIALLY RAISED GLUTATHIONE LEVELS

Spector *et al.* (1987), arguing that decreased levels of glutathione reduced the lens's power of resisting the action of oxidizing agents, studied the effects of raised concentration in the isolated bovine lens epithelium brought about by incubation with glutathione ethyl ester. Epithelial cells were exposed to H_2O_2, and the protective effect of the elevated glutathione concentration was investigated. Short periods of exposure had to be employed because of the rapid oxidation of the glutathione by the H_2O_2, which tended to bring the concentration back to normal. Lenses were tested for accumulation of ^{86}Rb, the concentration of ATP, which decreases after exposure to the peroxide, and the activity of glyceraldehyde-3-phosphate dehydrogenase, involved in the metabolism of glucose to pyruvic acid, which is greatly decreased by H_2O_2. The results failed to indicate any obvious benefit to the epithelial cells, examined with respect to these three parameters; however, the fact that decreased levels of glutathione reduce the lens's ability to withstand oxidative insult does not rule out the value of this substance in maintaining normal transparency.[39]

H_2O_2-TREATMENT OF LENS PROTEINS

McNamara & Augusteyn (1984) exposed extracted lens proteins to H_2O_2 in concentrations of 100–1000 μM; changes in solubility were observed but these were preceded by oxidation of all free SH-groups; moreover there was no evidence for S–S-linkages of polypeptides in the insoluble aggregates.

CORRELATION OF H_2O_2 AND ASCORBIC ACID CONCENTRATIONS

It would appear that the prime source of H_2O_2 in the aqueous humour, and thus possibly in the lens, is the ascorbic acid, whose accumulation in the aqueous humour of many species is so striking (p. 20); thus Giblin *et al.* (1984) showed a good correlation between the two concentrations, as occurring normally; when the ascorbic acid concentration was reduced by a deficient diet, the concentration of H_2O_2 fell in parallel. Ascorbate can protect the eye against the much more toxic superoxide anion by the reaction:

$$O_2^- + \text{Ascorbate} + 2H^+ \rightarrow 2H_2O_2 + \text{Dehydroascorbate}$$

and we may presume that the less toxic H_2O_2 is removed by another system, perhaps the glutathione one.

ROLE OF LENS EPITHELIUM

Giblin *et al.* (1985) considered that the lens epithelium would be the main site of defence against oxidants by virtue of its catalase activity and its active glutathione redox cycle in contrast to the much weaker activities in the lens substance.[40]

X-radiation Cataract

The lens is especially subject to damage by ionizing radiations, as with X-ray exposure, because the epithelial cells in the multiplicative zone are undergoing mitosis throughout life. Thus interference with the formation of new fibres must be a feature of the cataracts that develop on exposure of the eye to X-rays. If the radiation is confined to the central area of the lens, by screening the equatorial region, no cataract develops (Goldmann & Leichtl, 1938). The sequence of events leading to the development of a mature cataract is still a matter of conjecture.

Biochemical Changes

The basic biochemical and morphological changes resulting from X-irradiation of the eye have been summarized by Liem-The *et al.* (1975), who have described their own studies on the rabbit. Earlier work had emphasized the reduction in reduced glutathione (Pirie *et al.*, 1953) and accumulation of insoluble albuminoid probably resulting from cross-linkage of crystallins through disulphide bonds (Dische, 1966). Liem-The *et al.* assumed that errors in metabolism might lead to synthesis of abnormal

polypeptide chains causing aggregation to unusual high-molecular weight material. The content of the urea-soluble fraction increased some tenfold.

In general, the cataractous lens cortex tended to approach the normal lens nucleus in its crystallin composition, a large peak of HM-crystallin appearing in the chromatogram of the cataractous cortex; a further feature was the decrease in beta-globulin content of the cataractous lens, which might well be accounted for by its incorporation into the HM-fraction.

Absence of Gamma-crystallin

Giblin *etal.* (1978) isolated a high-molecular weight protein aggregate of greater than 4×10^6 daltons, representing some 18% of the total soluble lens proteins in the cataractous cortex and nucleus. By reducing the disulphide linkages that were involved in the aggregation, they isolated alpha- and beta-, but not gamma-crystallins.

Rapid Onset of Cataract

Giblin *et al.* remarked that their cataracts, in the rabbit, formed rapidly, often overnight, and were marked by complete opacification and swelling. Again, Matsuda *et al.* (1981) found that their X-ray induced cataracts developed some 8 to 9 weeks after the exposure, retaining their normal hydration and exhibiting only a posterior subcapsular haziness until shortly before the rapid onset of the mature cataract.

Permeability Changes

The efflux of ^{86}Rb from the previously loaded lenses was increased, the effect coming on slowly and reaching a maximum at about 7 weeks. Similarly, irradiation was followed by a fall in Na^+-K^+-ATPase activity and an increased permeability to cations. Hydration of the lens, i.e. increased water-content, did not increase appreciably above control values until about the onset of mature cataract in about 7–8 weeks. Figure 4.30 illustrates the changes in wet weight, dry weight and hydration of control and irradiated lenses. Since the increased permeability and inhibition of ATPase occur much sooner than the increased hydration, it may be assumed that increases in Na^+-content are accompanied by losses of K^+, so that total $(Na^+ + K^+)$ remains the same until, finally, the increases in Na^+ can no longer be compensated, and the fibres swell. This, in fact, was the situation (Matsuda *et al.*, 1982), the onset of mature cataract coinciding with a rapid increase in $(Na^+ + K^+)$ (Fig. 4.31).

Free Radicals

It has been suggested that in the rabbit, at least, the effects of X-irradiation can be attributed to general effects on the

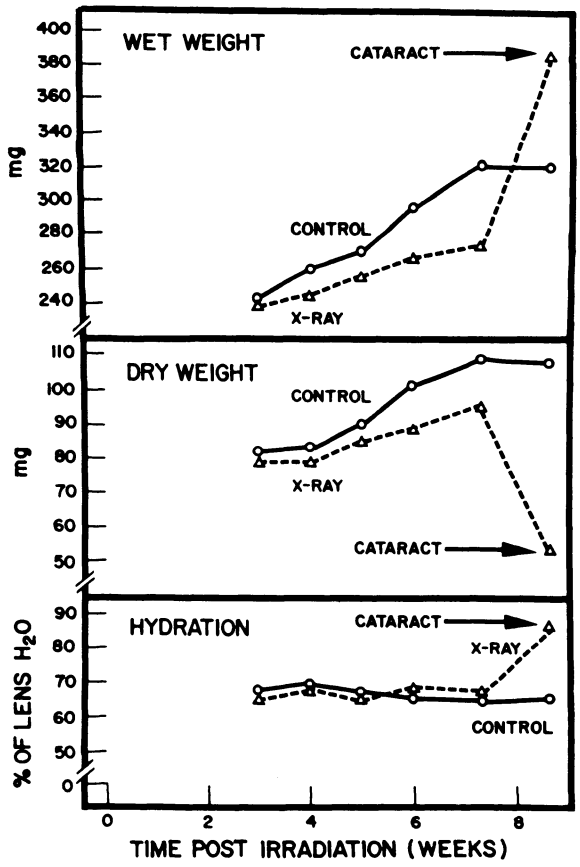

Fig. 4.30 The effect of X-irradiation on wet weight, dry weight, and hydration of rabbit lens. Means ±S.D. for 3–11 experiments. (Matsuda *et al.*, *Invest. Ophthal.*)

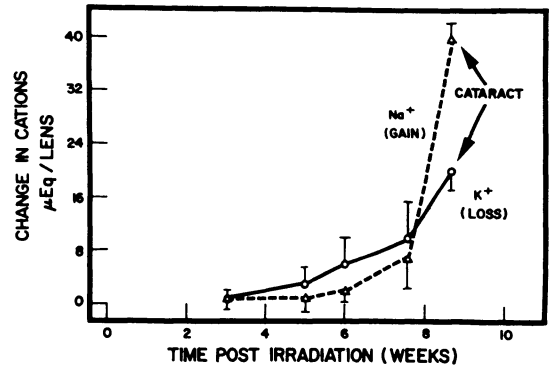

Fig. 4.31 Effect of X-irradiation on levels of Na^+ and K^+ in rabbit lens. (Matsuda *et al.*, *Invest. Ophthal.*)

fibre population that might well involve the appearance of highly reactive free radicals. Thus Kodama *et al.* (1983) reduced the X-ray lens damage in mice by feeding galactose, which does not induce a sugar-cataract in this

species, an effect they attributed to the free-radical scavenging properties of this sugar (Litchfield & Wells, 1976). However, X-ray induced free radicals have a short life, so that if given later the galactose should be ineffective, and Taura *et al.* (1985) found that the protective effect was just as effective if given before or after X-ray irradiation.[41]

Glassblower's Cataract

Exposure of the eyes to strong infra-red radiation causes cataract and this was shown by Goldmann in 1933 to be due to the high temperature to which the lens was raised by the absorption of heat; absorption of light by the ciliary body and iris, if sufficiently intense, will also raise the temperature of the lens and cause cataract (Langley *et al.*, 1960).

Microwave-induced Cataract

Clearly the main cause of this form of cataract is the raised temperature of the lens; thus Kramer *et al.* (1975) concluded that a lenticular temperature of 41°C was a threshold value for lens pathology; however, the studies of Carpenter *et al.* (1977) suggested that temperature, alone, was not a sufficient cause. The matter is of some practical importance so far as the determination of safety standards is concerned. Creighton *et al.* (1987) have reviewed the literature, and in their own experiments on the isolated lens, have shown that, because the same amounts of energy delivered continuously or in a pulsed form produced greatly different degrees of damage, in addition to simple thermal damage, thermoelastic expansions and contractions of the lens-fibres were an additional factor. Thus the pulse-driven energy is a more hazardous form than continuously supplied energy.

Hereditary Cataracts

Vision in the mouse is relatively unimportant, its vibrissae being its main sensory organ during its nocturnal activities; thus congenital forms of blindness, such as that due to cataract, do not necessarily impair survival, and so viable strains, with cataract, have been found. Of these the Nakano (Nakano *et al.*, 1960) and the Philly mouse have been studied in some detail.

Nakano Mouse

This has an inherited defect leading to spontaneous cataract formation some 3–4 weeks after birth. As described by Hamai *et al.* (1974), an important feature was the failure of the lens fibres to lose their organelles including the nucleus, a loss that is a normal feature of transformation from epithelial cell to mature fibre. Iwata & Kinoshita (1971) showed that the development of cataract was accompanied by a rise in Na^+-content at about 25 days postnatal. The rate of loss of $^{86}Rb^+$ from the lens increased at this time, suggesting an increase in membrane permeability that overloaded the normal potassium-accumulating mechanism, catalysed by Na^+-K^+-ATPase. The measured ATPase activity fell by 50% at 13–15days, i.e. before the cataract had manifested itself.[42]

PROTEIN SYNTHESIS

If, as emphasized by Piatigorsky (see, for example, 1980a), the pattern of protein synthesis is affected by the ionic constitution of the fibre cytoplasm, then we may expect to find changes in the proteins of the heriditary cataractous lens, perhaps comparable with those found in senile cataract. Fukui *et al.* (1976) found a decreased rate of incorporation of ^{35}S-methionine into lens crystallins in the Nakano mouse and Roy *et al.* (1982) found that the major changes in the character of the lens proteins were similar to those of the human cataractous lens. For example, the disulphide-linked membrane protein to cytosol polypeptides occurred in the Nakano mouse just as in human cataract; the increase in water-insoluble protein was such that its percentage in the 18–19 days Nakano mouse was the same as that in the 40–50 days normal mouse; at this time the changes in cation balance, hydration and transparancy become manifest (Fukui *et al.*, 1978).

MEMBRANE ALTERATIONS

Tanaka *et al.* (1980) observed a decrease in the number of gap-junctions linking lens fibres in the Nakano mouse; at 29 days the 26 kd membrane intrinsic protein had decreased in amount compared with normal mice, and this was associated with the decrease in gap-junctions. On this basis, the authors considered that the 26 kd membrane protein was peculiar to the gap-junction, but this is not true (p. 164).

POSSIBLE CATARACTOGENIC AGENT

If the prime factor in the cataractous state of the Nakano mouse is a defect in Na^+-K^+-ATPase activity, then some inhibitor may be suspected. Fukui *et al.* (1978) have separated a factor from lens extracts that inhibits this enzyme, prepared from calf lens or retina. The factor was heat-stable but inactivated by carboxypeptidase A and leucine aminopeptidase, indicating its peptide character. It did not compete with Na^+ or K^+, so that it is unlike ouabain.

Philly Mouse[43]

This, derived from the Swiss-Webster strain, develops a cataract visible to the naked eye some 5–6 weeks after

birth. The slit-lamp appearance of the lens has been described by Kador *et al.* (1980); changes begin in the periphery (subcapsular area) and culminate in a dense nuclear opacity by the 45th day. The critical period for changes in the chemistry of the lens appeared to be about 30 days, when hydration increased, associated with a rise in Na^+ and fall in K^+ (Fig. 4.32). Total Ca^{2+} increased from some 0.5 meq/kg lens to over 2.0 whilst glutathione declined from about 5 μmol/g to 1.5 at 40 days. The level of ATP in the lens fell, whilst the ability of the isolated lens to accumulate ^{86}Rb declined. Thus the Philly lens cataract is probably an 'osmotic cataract' in the sense that the first change is a swelling of the lens fibres, due, presumably, to inhibition of the cation-pumps.

PROTEIN SYNTHESIS AND DEGRADATION

Piatigorsky *et al.* (1980b) sought to confirm their hypothesis that altered concentrations of cations in the lens would affect protein synthesis and degradation, thus providing the link between altered transport characteristics and lens opacification. They showed, in the Philly mouse, that the reduced content of soluble protein was due to reduction in synthesis, as measured by the incorporation of ^{35}S-methionine, and to the degradation of alpha- and beta-crystallins.

According to the studies of Zigler *et al.* (1981) the changes are more complex, however; thus the percentage of gamma-crystallin fell from 49% to 12% as cataract developed; correspondingly there was an increase in the percentage of alpha-crystallin from 28 to 74%. Thus, in the 10- and 40-day-old Philly mouse the percentages were as follows:

	Alpha-	Beta-	Gamma-
10 days	26	24	49
40 days	71	16	12

In the normal mouse some 95% of the protein was soluble, but in the Philly mouse this decreased to 90% at 10 days and to 40% at 40 days. indicating an aggregation process as in other types of cataract. There was some leakage into the aqueous humour, however, gamma- and beta-crystallins being found in this fluid in the cataractous eye. The main beta-crystallin polypeptide of 27 kd molecular weight, was absent from the Philly mouse lens; this, in the normal mouse, is first detected 5–10 days after birth and is probably important for maintenance of transparency in the cortical fibres (Carper *et al.*, 1985). Carper *et al.* (1982) found that the mRNA that directed the synthesis of this crystallin in a reticulocyte lysate was present in the 10-day-old normal mouse but absent from the Philly mouse. Heterozygous mice produced some beta-crystallin, but less than normal, whilst onset of cataract was delayed.

MORPHOLOGICAL CHANGES

These have been described by Uga *et al.* (1980). Initial cataractous signs appeared about the 10th day as a diffuse opacity in the anterior subcapsular zone. Cloudiness increased to reach a maximum at about the 40th day. Microscopically the defect seemed to be a failure of the replicating cells in the bow zone to become true fibres, so that they retained their intracellular organelles; thus, in the bow zone, nucleated fibres were observed deep in the cortex. This failure was accompanied by a marked increase in hydration of the fibres.

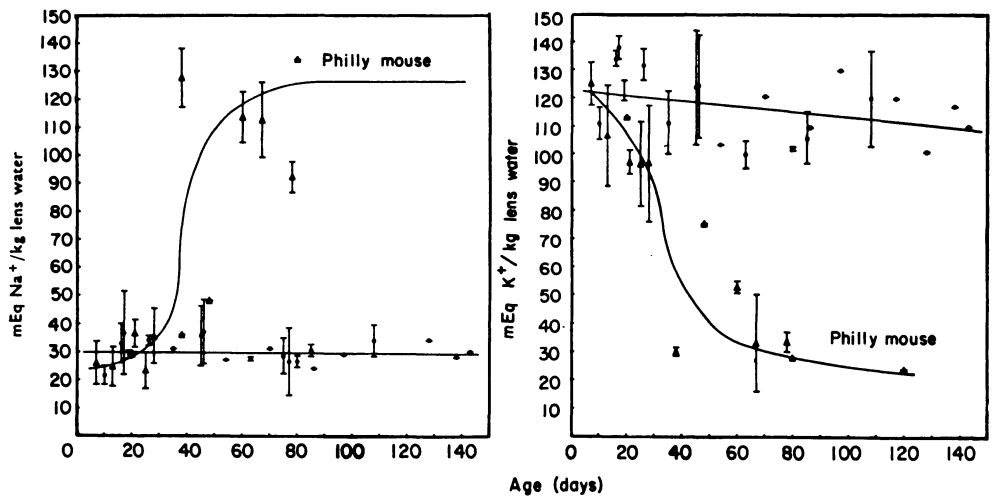

Fig. 4.32 Relationship between the lenticular levels of Na^+ and K^+ and age for Philly (△) and control (●) lenses. $n = 1$–5 mice. (Kador *et al.*, *Exp. Eye Res.*)

Traumatic Cataract

Repair of Injury

Mechanical damage to the lens, such as that caused by entry of a foreign body, initiates a repair process, but, as with the cornea, this repair is usually insufficient to maintain transparency in the injured region, leading to a subcapsular cataract; this is especially true of man. Healing consists, essentially, in the formation of new epithelium and replacement of lost fibres, so that the first sign is rapid mitosis in the epithelial cells adjacent to the injured region. As described by Uga (1981) for the mouse, in response to a needle-stab the capsule everted and lens fibres protruded through the hole in the epithelium, the anterior ends of the fibres showing numerous projections. Mitosis began by 18 hr and the whole injured area was covered with epithelium by the 5th day to give a continuous epithelial layer by the 7th day. By the 30th day the cells had formed a tissue meshwork, basal lamina, filamentous material and collagen fibres. After this there was gradual removal of cells, so that the wound was finally covered by a regularly arranged epithelium by the 4th month, and then the capsule was formed on this. In this species, no severe opacity developed after a lesion of about 100 μm diameter. The initial processes of healing occurred *in vitro*, as well as *in vivo*, so that the healing process seems to be intrinsic to the lens.[44]

CELLULAR INVASION

Associated with the epithelial regeneration process there is a prominent invasion of the site by cells, such as fibrocytes, which embed in a fibrin clot over the surface of the lesion and beneath the epithelial layer. In a pigmented eye, such as that of the squirrel described by Rafferty & Goossens (1984), the appearance of pigmented cells was striking; they were of three types, and the authors were fairly certain that these had not been carried into the wound by the knife-stab as they did not appear until 12 hr after making the wound. Some were definitely iris stromal melanocytes. So far as lens fibres were concerned, there was initial degeneration with formation of Morgnani globules, but after 8 weeks new fibres were reconstituted and abutted tightly to the epithelium, only a slight irregularity in arrangement allowing the wounded area to be identified.

SUBCAPSULAR OPACITIES

Because of the peculiarity of the lens' fibrous structure, whereby each fibre stretches from a central position near the equator to the two poles of the lens, damage at the anterior face will injure cells whose extremities are in the posterior region, at the sutures. Thus subcapsular opacities are found rapidly in the posterior polar region and extend from pole to pole to envelop the whole nucleus, which may or may not be involved. By employing their quantitative microradiographic technique, Fagerholm & Philipson (1979a, b) showed that the spread of opacity was associated with loss of solid material, and this was due to breakdown of fibres with a corresponding increase in extracellular space, as measured by Procion yellow. Recovery, leading to some reversal of opacity, begins in the equatorial region where new fibres are formed and extends to the posterior pole by migration of cell fibres.

CHANGES IN LENS FIBRES

In the scanning electron microscope Nelson & Rafferty (1976) observed an initial flattening of the fibres adjacent to the wound, whilst the ball-and-socket joints were maintained between fibres; by four days the transformed fibres had assumed a wavy outline, freely inderdigitating through lateral appendages that had appeared, suggesting a release from the rigid ordering of the normal fibres in favour of a more fluid interlocking arrangement. By 8 days the original strictly hexagonal structure had been resumed. The authors commented on the fact that transforming fibres could undergo alterations in shape that were limited to discrete regions, the remainder of a given fibre appearing normal.

Experimental Ischaemic Cataract

In the rabbit a subcapsular cataract can be induced by cauterization of the long posterior ciliary arteries, which reduces the glucose supply to the lens and produces a condition similar to that induced by hypoglycaemia (Fagerholm & Chylack, 1982). The superficial lens fibres swell, presumably due to failure of their ionic pumps, and later retract to form a ditch. Lens epithelial breakdown also occurs. Since the capsule is uninjured in this type of insult, the subsequent repair processes are brought about entirely by activity of the lens fibres, which become elongated epithelioid in type, producing a new capsule continuous with the original capsule in the equatorial region, whilst enclosed between the two capsules were epithelioid cells dispersed in a fibrous matrix. Beneath the new capsule new lens fibres were formed. In the cortex amongst swollen and broken-down fibres electron-dense material was found which consisted of calcium-containing crystals, probably hydroxy-apatite.[45]

Cold Cataract

When a young animal, such as a rat, is cooled, cataracts may appear, which disappear on rewarming. They are due to a reversible precipitation of gamma-crystallin (Balazs & Testa, 1965) which the physicochemical studies

of Clark & Benedek (1980) have characterized as a phase-separation, comparable with that described for polymers. At given temperatures and concentrations of total protein, two phases separate out, the one with a high and the other with a low concentration of the protein. Figure 4.33a illustrates the phase-diagram; at all points outside the curve the system is stable and transparent; within the curve separation occurs, and the solid points indicate the concentrations in the two phases when they separate. T_c is defined as the temperature at which there is a 10% loss of light-transmission, and the plot of T_c against concentration is called a co-existence curve. Figure 4.33b shows the curves for gamma-crystallins II, III and IV. It is clear that gamma-IV will give phase separation at higher temperatures than the others, and it is this fraction that, in fact, separates out during development of cold cataract (Siezen *et al.*, 1985). These authors showed that only some 0.1% of the total gamma-crystallins formed sufficiently large aggregates to be capable of scattering light strongly, but this was sufficient to give the observed nuclear cataracts. Cold cataract only develops in the perinatal period; this is partly due to ability of the older animal to maintain a normal eye-temperature during body-cooling, but also to a change in the population of gamma-crystallins (Siezen *et al.*, 1985).

Other Forms of Cataract

Steroids

Treatment of transplant patients with steroids during a rejection crisis can lead to a cataract (Spencer & Andelman, 1965). Experimentally Creighton *et al.* (1983) induced cataracts in rat lenses maintained *in vitro* by addition of 3.8×10^{-9} to 3.8×10^{-6} M solumedrol; at the lowest concentration 5 out of 12 lenses were opaque after 48 hr, and at the highest, all. Opacity began at the anterior pole and spread subcapsularly. Vitamin E reduced the damage. The cataracts were reminiscent of those produced by cytochalasin D, elevated glucose and hygromycin B.

Inhibitors of Cholesterol Synthesis

Drugs that inhibit synthesis of cholesterol late in the pathway, namely the step involving conversion of desmosterol to cholesterol, are known to cause cataracts in rats (von Sallmann *et al.*, 1963) and in humans (Kirby *et al.*, 1962). The cause was supposed to be an accumulation of desmosterol in the lens fibres, but the low concentration of this molecule in cataractous lens after

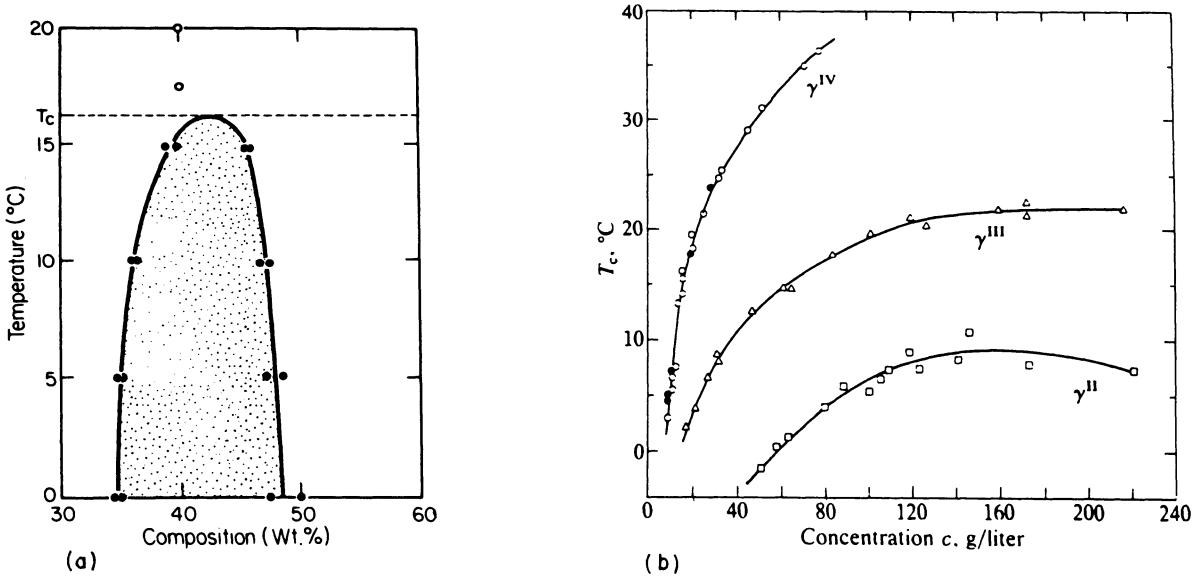

Fig. 4.33 (a) Phase diagram of lens cytoplasm. The coexistence curve for the isolated cytoplasmic homogenate is similar to that of a phase separation in a binary polymer solution. The shaded area represents the conditions of temperature and composition where phase separation occurs and the cytoplasm is opaque. The area outside the curve represents the conditions for transparency of lens cell cytoplasm. The concentration of protein in the homogeneous transparent material was approximately 40% dry weight (open circles). The concentrations measured in the separated phases of the opaque cytoplasm are plotted as solid circles. (Clark & Benedek, *Biochem. Biophys. Res. Comm.*) (b) Coexistence curves for isolated γII- (□), γIII- (△) and γIV-crystallin (○, ●) at pH 7.0 (ionic strength, 0.11). Open symbols designate phosphate buffer; closed symbols designate Tris buffer. These coexistence curves can be shifted upward or downward by variations of pH or ionic strength and by the addition of various chemical reagents. For example, 1 mM reducing agent (dithiothreitol or glutathione) shifts the coexistence curve of γIV down by about 2 °C. (Siezen *et al.*, *Proc. Nat. Acad. Sci.*)

triparanol treatment suggests some other mechanism of cataract formation. Cenedella & Bierkamper (1979) studied an inhibitor of enzymatic reduction of desmosterol to cholesterol, U18666A (3-Δ(2-diethylaminoethoxy)-androst-5-en-17-one hydrochloride) that is recognized as a cataractogenic drug. They studied ion concentrations in the lens as well as synthesis of lens proteins and concentration of lens sterols. The cataracts were nuclear and developed at between 15 and 25 days of age if the drug was administered subcutaneously from birth. Synthesis of gamma-crystallin, the main crystallin of rat lens, was inhibited, and the cause was attributed to the loss of ion balance that was early manifest. Thus if, as Piatigorsky has argued, lens protein synthesis is strongly influenced by intracellular concentrations of K^+ and Na^+, then the effects of this drug could be attributed to membrane changes rather than accumulation of desmosterol which, in the present study, was not detected in opaque lenses until long after their first appearance.

Selenite Cataract

A single subcutaneous dose of the essential trace mineral, selenium, causes the development of a predominantly nuclear cataract in suckling rats (Ostadolova *et al.*, 1978). The primary insult may well be interference with epithelial cell division; thus incorporation of ^{3}H-thymidine into the epithelial cells was reduced by at least 60% (Cenedella, 1987) and Anderson *et al.* (1986) reported a suppression of entry into prophase and mitosis. In the slit-lamp, the primary changes are revealed as a swelling of lens fibres with an initial subcapsular cataract, which only later becomes nuclear (Shearer *et al.*, 1983). In the electron microscope Russell *et al.* (1984) described large intra-fibre aggregates. The most obvious biochemical change was a decrease in glutathione and the NADPH pool, due to a selenium-catalysed oxidation with acceleration of the hexose monophosphate shunt (Bunce & Hess, 1981). Bunce *et al.* (1984) showed that there was an increase in lens Ca^{2+}, perhaps due to inhibition of a Ca^{2+}-ATPase pump comparable with that caused by lanthanum (Hightower & Reddy, 1982).

Retinal Degeneration

An association between posterior subcapsular cataract and retinal degenerative disease, such as retinitis pigmentosa, has been recognized. Zigler & Hess (1985) have related the degeneration of rod outer segments in Royal College of Surgeons rat, caused by a failure of the pigment epithelium to phagocytose the outer segments, to the accumulation of lipid peroxidation products in the vitreous, and thence to the development of cataracts. Thus cataract formation was linked temporally with the accumulation of lipid peroxidation products, which may have caused an increased passive permeability of the lens membranes.

Notes

1. The development of the lens fibre may also be followed by study of the cultured epithelium derived usually from the chick embryonic lens, the whole process being studied within as few as six days (Menko *et al.*, 1984). The same approach has been made with rodent lens, made possible by the discovery that the process was facilitated by retinal extracts (Campbell & McAvoy, 1984). Space will not permit a detailed description of the stages in maturation leading to the production of what Okada *et al.* (1973) and Piatigorsky *et al.* (1973) called 'lentoids', small aggregations of cells some 25 times as long as broad, able to synthesize γ-crystallin, and showing no incorporation of labelled thymidine into the DNA. Fitzgerald & Goodenough (1986) found that the fibres of the lentoid were electrotonically coupled through gap-junctions.
2. Kuszak *et al.* (1980) have discussed the variations in these structures among different species; thus the fingerprints described in the chick are probably equivalent to the ridges seen on the fibre sides of human and monkey lenses described by Kuwabara (1975) and Dickson & Crock (1972). In their work they were able to expose broad areas of long sides so that they could examine the interlocking devices on all six sides of the fibre. The elaboration of such an extensive system of junctions between fibres is considered to be a reflection of the need to maintain adequate orientation during the large changes in shape that may occur in accommodation. In the chick the posterior portion of the lens changes little in shape, by contrast with the lenticonus of the anterior part, and it may be that the concentration of finger-like extensions on the posterior part of the lens fibres provides the rigidity that prevents a marked shape-change here.
3. The pH of the lens interior, measured by an internal electrode, was 6.89 comparing with that of the vitreous body close to the lens which was 7.25 (Bassnett & Duncan, 1985). This agrees with an earlier estimate by Greiner *et al.* (1981) of 6.9, based on nuclear magnetic resonance.
4. The Nernst equation describes the potential for an ion at equilibrium; in most biological systems the given ions are rarely at equilibrium, and a more appropriate equation to describe the potential across a membrane is that of Goldman which takes into account the permeabilities of the membrane to other relevant ions, namely Na^+ and Cl^-, as well as K^+:

$$E = \frac{RT}{F} \ln \frac{P_K[K]_o + P_{Na}[Na]_o + P_{Cl}[Cl]_i}{P_K[K]_i + P_{Na}[Na]_i + P_{Cl}[Cl]_o}$$

   where the P's are relative permeability coefficients and the terms in square brackets are concentrations.
5. Paterson *et al.* (1974) have determined the activity of K^+ within the lens fibres by micro-electrode penetration, using a K^+-sensitive electrode; the activity was 83.6 mM which was converted to concentration by employing an activity coeffi-

cient of 0.77 to give 110 mM; this agreed with the values obtained by flame-photometry, assuming an extracellular space of 4.5%, but it is higher than the value for frog shown in Table 4.3.

6. Rae (1974b) described two distinctly different compartments in the frog lens according as the potential measured in the one was high (−70 mV) and the other low (−30 mV). He has discussed in detail the possibility that the low potential represents that obtained when the electrode is in the extracellular compartment.
7. The estimated transfer coefficients for the epithelium were 0.095, 0.056 and 0.024 hr^{-1} for K^+, Rb^+ and Cs^+ respectively; this means that passage is not through a simple water-filled pore, which would be unable to exert this kind of selectivity.
8. Patmore & Duncan (1979) described a voltage-dependent K^+-channel across the lens membranes such that depolarization of the membrane caused increased permeability to this ion; this channel could be blocked by TEA, as in excitable tissue. The depolarization in a Ca^{2+}-free medium would tend to open this channel, contributing to the rise in membrane conductance. Reszelbach & Patterson (1985) have described an apparatus that permits measurements of fluxes separately across the equatorial region of the lens in addition to the anterior and posterior surfaces; their results on fluxes of ^{86}Rb and ^{22}Na and the effects of ouabain and a Ca^{2+}-free medium seem consistent with Duncan's model.
9. Ortwerth *et al.* (1986) have shown that the mechanical sonication of the water-insoluble fraction will bring as much protein into solution as extraction with urea; the material so solubilized seems to be the same as that solubilized with urea; the authors emphasize that sonication would not disrupt S–S- or Ca^{2+}-induced aggregates.
10. The immunological properties of the rat's gamma-crystallins have been studied by Vornhagen *et al.* (1982) after separation into some 7–11 fractions by isoelectric focussing. The fraction they described as $gamma_1$ was homogeneous and equivalent to calf gamma-crystallin. Other fractions showed immunological heterogeneity.
11. Earlier Zigler *et al.* (1981) had resolved the final peak in gel-filtration, described as gamma-crystallin, or more correctly as low MW crystallin, into 4 components of 24, 21, 19 and 10 kd. Of these, only the 19 kd material could be unequivocally identified, immunochemically, as gamma-crystallin; the heavier 24 and 21 kd material was probably beta-crystallin, and the major effect of age was to increase the proportion of 24 kd material.
12. Bours *et al.* (1979) have produced some evidence, based on immunoelectrophoresis of lens proteins against an anti-gamma antibody, that bovine epithelium contains some gamma-crystallin.
13. The nomenclature of Bindels *et al.* indicates, by the superscript, the number of subunits in the molecule.
14. The authors emphasize that $beta_H$ is not an artefact, formed by aggregation during preparation, since when lenses are incubated with labelled amino acids, no label appears in $beta_H$ whereas there is a great deal in $beta_L$. If the $beta_H$ were formed subsequent to synthesis there would be equal amounts of label in both fractions.
15. The possibility that polymerization would involve oxidation of cysteine residues, as suggested by Harding & Dilley (1976), was examined by Siezen *et al.* This would involve the presence of some beta- and/or gamma-crystallins, i.e. hybridization, which was thought not to occur in bovine lenses. They did find faint bands in SDS-gels in the 24 000–30 000 dalton range of beta-crystallin polypeptides in their bovine preparation.
16. Manski *et al.* (1979) employed immunological techniques in the analysis of the crystallin complexes in the water-insoluble fractions of cortex and nucleus. Polymers of MW greater than 300 kd were separated and shown to be aggregates of alpha- and beta-crystallins when derived from cortex, whereas nuclear material contained complexes of alpha-, beta- and gamma-crystallins, the beta-crystallin apparently acting as the link between gamma- and alpha-crystallins.
17. Horwitz *et al.* (1979) described 26 and 23 kd fractions, the 23 kd material increasing with age; thus, in a 55-year-old lens the 23 kd fraction was more abundant than the 26 kd fraction in the nucleus, but the reverse was true of the cortex. Alcala *et al.* (1980) found 27 and 25 kd phospholipid-containing proteins in human lens membranes; with age the 25 kd preponderated. Alpha-crystallin subunits of 20 and 22.5 kd were consistently associated with these membrane fractions.

    Bouman *et al.* (1981) have compared the lens fibre membranes from bovine, pig, sheep and chicken lenses; all mammalian species had the characteristic MIP 26 and EDTA extractable proteins of 35 and 32 kd, whilst the chicken had an MIP 27, and EEP's of 35, 32 and 44 kd. The observed differences amongst the mammalian MIP and chicken MIP, and between calf or sheep EEP, pig EEP and chicken EEP, are readily explained as a result of evolutionary relationships between the species, just as with the crystallins.
18. Roy (1981) has described an EDTA-extractable protein from human lens with a molecular weight of 22 kd, i.e. similar to that of the smaller intrinsic membrane polypeptide. Immunologically there was no reactivity with alpha- and beta-crystallins; reactivity with gamma-crystallin could not be ruled out. Kistler *et al.* (1985) made monoclonal antibodies to a number of lens membrane proteins, notably MIP, MP57, MP70, MP82 and MP100. Of these it was MP70 that showed a large age-related change, the amount in nucleus being much less than in cortex.
19. The changes in the amounts of the neutral endopeptidase in the rat lens with age have been described by Fleshman & Wagner (1984); using cortical-nuclear differences as a measure, there was a decrease in specific activity and thermal stability with age, i.e. from epithelium to nucleus. The specific activity of the cortex decreased with the animal's age, whilst that of the nucleus was constant. In the epithelium there was no correlation with age. Swanson *et al.* (1981) have examined the activities of some exopeptidases, i.e. enzymes that attack the terminal regions of a polypeptide, in normal and cataractous lenses. Dipeptidyl peptidase II is lysosomal, and dipeptidyl peptidase III is cytosolic; both are in the lens.
20. The differences between this endopeptidase and that described by Van Heyningen & Waley (1962) have been categorized by Tse & Ortwerth (1981). Srivastava & Ortwerth (1983a) have described the changes in distribution of their inhibitors with age.
21. Calpain also degrades vimentin and actin, cytoskeletal proteins, so it might well be involved in transformation of epithelial cells to fibres (Yoshida *et al.*, 1984).
22. Bagchi *et al.* (1985) found synthesis of vimentin in the epithelial cells of the organ-cultured rabbit lens, the epithelial and cortical fibre cells of the organ-cultured adult chicken lens, and the epithelial cells of the rabbit lens grown in tissue culture. The rate of turnover of vimentin was high, in contrast to the crystallins whose turnover is small.
23. Mehta *et al.* (1964) found that it was the β- and γ-crystallins that showed species specificity, so that organ specificity was peculiar to α-crystallin.

24. Bessems *et al.* (1986) described the appearance of a novel fraction in the ageing lens with a molecular weight of about 39 kd, probably arising from the major $beta_L$-crystallin species. It is probably a dimer of beta B_p and a 15 kd subunit.
25. In their earlier study (Ringens *et al.*, 1982a) the SDS-PAGE patterns of developing human water-soluble and water-insoluble proteins have been presented; in both groups of proteins the greater sharpness of the patterns in the very young lenses is striking, suggesting post-translational changes in the proteins with age. Most of the cytoskeletal proteins, myosin, actin, vimentin and alpha-actinin, had disappeared from the nucleus of 14-year-old lenses.
26. In a later study (McAvoy, 1978b) the embryonic lens of the rat was examined in a similar way; by 14 days the proliferating and elongating zones were definitely separated, elongating cells having ceased to divide. At this time all cells contained alpha-crystallin. Beta- and gamma-crystallins appeared at $12\frac{1}{2}$ days, and later became restricted to the elongating compartment. Carper *et al.* (1985) found that three of the beta-crystallins were not synthesized in the embryonic rat lens, and at least one of these had no functional mRNA to direct its synthesis until after the first post-natal day. The 27 kd polypeptide, one of the main constituents of the rat beta-crystallin fraction, was only detected after the first 5 days post-natal, and there was no functional mRNA for this. Thus it would appear that this polypeptide is important for the adequate function of the adult lens, but not for the embryo.
27. Koch (1979), discussing the importance of basic research on the lens for the elucidation of cataract, emphasizes the importance of its classification before biochemical or other studies are made: 'All research conducted on unclassified "senile cataract" lenses in utterly worthless.' The features that he considered as defining were: fluid clefts and spokes; wedge-shaped cortical opacities; nuclear (tumescent) cataract; polychromatic crystal-like deposits; posterior subcapsular opacities.
28. Farnsworth *et al.* (1981) showed that the 43 kd material was absent from epithelial cells. In immature fibres in the bow region it is present in the cytoplasm as well as in membrane, and only by the 40th cell layer in the bow region do we get a predominance in membrane-associated location. In the fetal first trimester it is distributed uniformly throughout the lens; by the second the distribution is as in the adult.
29. Garner *et al.* (1981) showed that in normal lenses of any age the intrinsic membrane polypeptides were 26 kd and 22 kd, and more than 80% of the membrane lipid was found in the fraction containing these components. There was no covalently linked aggregate involving intrinsic membrane, extrinsic membrane and cytoplasmic polypeptides in clear normal lenses at 60–75 years. In cataract, intrinsic membrane polypeptide was found in the non-membrane component of the extract with a concomitant loss of lens membrane lipid, indicating unequivocally the fragmentation of the lens membrane in cataract.
30. McNamara & Augusteyn (1980) have shown that the yellow material in senile cataracts does not contain aggregates linked by 3,3'-dityrosine; there was some material linked in this way in the capsule.
31. Dilley & Pirie (1974) have discussed the meaning to be attributed to the lens 'nucleus' in experimental studies; the term probably includes all the material formed before birth —embryonic and fetal—although biomicroscopically the infantile and adult regions are also distinguished. In practice the central approximately 100 mg of the mature human lens is employed for extraction of the proteins.
32. Harding *et al.* (1983) identified crystalline deposits in 14 out of 406 cataractous lenses which, on analysis, proved to be calcium oxalate. Another group had a high P/S ratio, and probably consisted of membrane aggregates. The technique of Energy Dispersal X-Ray Analysis (EDXA) permits the characterization of these deposits, which must be distinguished from the more amorphous protein aggregates (Harding *et al.*, 1982).
33. The penetration of sorbinil into aqueous humour and lens, either topically or orally administered, is of interest if human diabetic cataract is to be treated by an aldose-reductase inhibitor. Crabbe *et al.* (1985) have demonstrated such a penetration in patients undergoing cataract extraction. Diabetic cataract can be prevented by a high fat and protein diet (Patterson *et al.*, 1965); Creighton *et al.* (1985) have shown that the antioxidant, vitamin E, partially inhibits galactose cataract *in vitro*, but not *in vivo*. Glutathione, likewise, will prevent the cataractous changes occurring in the isolated rat lens by exposure to high concentrations of glucose; the same is true for the *in vivo* treatment of diabetic rats (Ross *et al.*, 1983). The authors emphasize that polyol levels in the high-glucose lenses are as high in the treated as untreated lenses, so that, as Patterson & Bunting, (1966) claimed, an additional factor to osmotic stress must be invoked to describe the whole chain of events leading to a sugar cataract. Williams & Odom (1987) have shown that activity in the sorbitol pathway of the lens may be revealed non-destructively by the use of nuclear magnetic resonance spectroscopy; in this way they have been able to rank the potency of inhibitors of aldose reductase.
34. Galactokinase deficiency has been implicated in the development of early cataract in humans; the subject has been reviewed recently by Stambolion *et al.* (1986) in the light of their own study on patients heterozygous for this deficiency. They concluded that a heterozygous subject was at risk.
35. The proceedings of the 1st International Symposium on Light and Oxygen Effects on the Eye (*Current Eye Res.* 3 (1) (1984)) contain a wealth of information on this aspect of lens damage.
36. Delamere *et al.* (1983) found increased Na^+-, Ca^{2+}-, and H_2O-contents in excised rabbit lenses exposed to 1 mM H_2O_2, with a fall in K^+-content. Efflux of ^{86}Rb and membrane conductance were increased, suggesting an increase in passive membrane permeability. The lens could still be depolarized by ouabain, so that the electrogenic Na^+–K^+-ion pump was at least partially active.
37. Srivastava *et al.* (1980) made a strain of catalase-deficient mice deficient in glutathione superoxidase by selenium-deficiency; no cataracts developed, even after challenge with a superoxide producing drug, phenyhydrazine.
38. Latta & Augusteyn (1984) purified human lens glutathione reductase; they found that it was incapable of splitting mixed disulphides, a feature that would be necessary to protect crystallins from aggregation.
39. Spector *et al.* point out that glutathione may react with certain quinones to form relatively stable free-radical singlets, capable of causing oxidative damage; thus elevated glutathione levels might well be deleterious on their own account.
40. Cyanate causes cataract when its level in the blood rises, as in acute diarrhoea or renal failure (Harding & Rixon, 1980). According to Lewis *et al.* (1986), cyanate raises the phase-separation temperature from 20.3 to 26.4°C; this may be prevented by bendazan, which inhibits the binding of cyanate to lens proteins. In an *in vitro* study of the lens crystallins allowed to react with cyanate, Beswick & Harding (1987) have shown that it is the carbamylated beta L-crystallin that acts as a centre for aggregation of the other crystallins; if the

beta L-crystallin unfolds as a result of carbamylation, the exposure of SH-groups would permit aggregation through disulphide linkages.

41. Zintz & Beebe (1986) have described X-ray induced cataracts in the rat, which develop 10–16 weeks after irradiation; increased hydration does not occur, and it was considered that defective epithelial cell transformation to fibre was the root cause.
42. Heterozygous mice do not develop cataract; they likewise do not have deficient ATPase (Iwata & Kinoshita, 1971).
43. Named after its home-town, Philadelphia.
44. Miller & Riley (1987) have studied the effects of X-irradiation on the ability of epithelial cells to recover from a wound stimulus; as we should expect, the regenerative process, involving as it does DNA synthesis, is impaired by the radiation, but this impairment is only temporary so that by 28 days the wound-response is normal. When half of the lens was shielded from the irradiation, then the recovery of the irradiated half was much more rapid, showing that the unirradiated half contributed to recovery of the irradiated half. Thus complete recovery of the cellular response of partially irradiated lenses occurred in 4 days by contrast with 28 days for the wholly irradiated lenses.
45. In view of the use of the laser-beam in anterior segment surgery, such as iridotomy, the effects of the beam on the lens are of interest. They have been described by Gona *et al.* (1985); there is rupture of the capsule with protrusion of fibres. Closure of the wound was associated with ingrowth of a variety of cell-types which may have contributed to subsequent lens repair.

References

Alcala, J., Valentine, J. & Maisel, H. (1980) Human lens fiber cell plasma membrane. *Exp. Eye Res.* **30**, 659–677.

Amoore, J. E., Bartley, W. & van Heyningen, R. (1959) Distribution of sodium and potassium within cattle lens. *Biochem. J.* **72**, 126–133.

Anderson, E. I. (1965) Dual cation activation of bovine lens autolysis. *Invest. Ophthal.* **4**, 181–186.

Anderson, R. C., Shearer, T. R. & Claycomb (1986) Selenite induced epithelial damage and cortical cataract. *Curr. Eye Res.* **5**, 53–61.

Anderson, R. S., Britton, J. L. & Palmer, E. A. (1983) Early development of selenium-induced cataract: slit-lamp evaluation. *Exp. Eye Res.* **36**, 781–788.

Andries, C., Backhovens, H., Clauwaert, J., De Block, J., De Voeght, F. & Dhont, C. (1982) Physical-chemical studies on bovine eye lens proteins. I. *Exp. Eye Res.* **34**, 239–255.

Asselbergs, F. A. M., Koopmans, M., van Venroolj, W. J. & Bloemendal, H. (1979) Improved resolution of calf lens β-crystallins. *Exp. Eye Res.* **28**, 223–228.

Augusteyn, R. C. (1979) On the possible role of glutathione in maintaining human lens protein sulphydryls. *Exp. Eye Res.* **28**, 665–671.

Bagchi, M., Caporale, M. J., Wechter, R. S. & Maisel, H. (1985) Vimentin synthesis by ocular lens cells. *Exp. Eye Res.* **40**, 385–392.

Bakker, A. (1936) Eine Methode, die Linsen erwachsener Kaninchen ausserhalb des Körpers am Leben zu erhalten. *v. Graefes' Arch. Ophthal.* **135**, 581–592.

Balazs, E. A. & Testa, M. (1965) The cryoproteins of the lens. *Invest. Ophthal.* **4**, 944.

Baldwin, G. F. & Bentley, P. J. (1980) Some observations on the magnesium metabolism of the amphibian lens. *Exp. Eye Res.*, **31**, 665–671.

Bassnett, S. & Duncan, G. (1985) Direct measurement of pH in the rat lens by ion-sensitive microelectrodes. *Exp. Eye Res.* **40**, 585–590.

Beebe, D. C., Feagans, D. E., Blanchette-Mackie & Nau, M. E. (1979) Lens epithelial cell elongates in the absence of microtubules: evidence for a new effect of colchicine. *Science* **206**, 836–838.

Bellows, J. G. (1944) *Cataract and Anomalies of the Lens.* London: Kimpton.

Benedek, G. B. (1971) Theory of transparency of the eye. *Appl. Optics.* **10**, 459–473.

Bentley, P. J. & Candia, O. A. (1971) Effects of some metabolic inhibitors on the electrical potential difference and short-circuit current across the lens of the toad *Bufo marinus. Invest. Ophthal.* **10**, 672–676.

Berbers, G. A. M., Boerman, O. C., Bloemendal, H. & De Jong, W. W. (1982) Primary gene products of bovine β-crystallin and reassociation behavior of its aggregates. *Eur. J. Biochem.* **128**, 495–502.

Berns, T. J. M., Schreurs, V. V. A. M., van Kraaikamp, M. W. G. & Bloemendal, H. (1973) Synthesis of lens proteins *in vitro*, *Eur. J. Biochem.* **33**, 551–557.

Bessems, G. J. H., de Man, B. M., Bours, J. & Hoenders, H. (1986) Age-related variations in the distribution of crystallins within the bovine lens. *Exp. Eye Res.* **43**, 1019–1030.

Bessems, G. J. H., Rennen, H. J. J. M. & Hoenders, H. (1987) Lanthionine, a protein cross link in cataractous human lenses. *Exp. Eye Res.* **44**, 691–695.

Beswick, H. T. & Harding, J. J. (1987) High-molecular-weight crystallin aggregate formation resulting from non-enzymic carbamylation of lens crystallins: relevance to cataract formation. *Exp. Eye Res.* **45**, 569–578.

Bettelheim, F. A. (1975) On the optical anisotropy of lens fiber cells, *Exp. Eye Res.* **21**, 231–234.

Bettelheim, F. A., Siew, E. L. & Chylack, T. L. (1981) Studies on human cataracts. *Invest. Ophthal.* **20**, 348–359.

Bhuyan, K. C. & Bhuyan, D. G. (1977) Regulation of hydrogen peroxide in eye humors. *Biochim. Biophys. Acta* **497**, 641–651.

Bhuyan, K. C. & Bhuyan, D. K. (1978) Superoxide dismutase of the eye. *Biochim. Biophys. Acta* **542**, 28–38.

Bindels, J. G., Koppers, A. & Hoenders, H. J. (1981) Structural aspects of bovine crystallins: physical characterization including dissociation–association behavior. *Exp. Eye Res.* **33**, 333–343.

Bindels, J. G., Siezen, R. J. & Hoenders, H. J. (1978) Effects of elevated temperatures on the structure of alpha-crystallin from calf lens. In: Hockwin, O. (Ed.). *Lens Ageing and Development of Senile Cataracts.* Karger: Basel. pp. 253–260.

Bindels, J. G., Siezen, R. J. & Hoenders, H. J. (1979) A model for the architecture of α-crystallin. *Ophthal. Res.* **11**, 441–452.

Bito, L. & Davson, H. (1964) Steady-state concentrations of potassium in the ocular fluids. *Exp. Eye Res.* **3**, 283–297.

Björk, I. (1964a) Studies on γ-crystallin from calf lens. II. *Exp. Eye Res.* **3**, 254–261.

Björk, I. (1964b) Studies on the subunits of α-crystallin and their recombination. *Exp. Eye Res.* **3**, 239–247.

Bloemendal, H. (1979) Lens proteins as markers of terminal differentiation. *Ophthal Res.* **11**, 243–253.

Bloemendal, H. & Herbrink, P. (1974) Growing insight into the structure of β-crystallin. *Ophthal. Res.*, **6**, 81–92.

Bloemendal, H., Berns, T. J. M., Van der Ouderaa, F. & De Jong, W. W. W. (1972) Evidence for a 'non-genetic' origin of the A 1 chains of α-crystallin. *Exp. Eye Res.* **14**, 80–81.

Bloemendal, H., Bont, W. S. & Benedetti, E. L. (1965) On the subunits of α-crystallin. *Exp. Eye Res.* **4**, 319–326.

Bloemendal, H., Bont, W. S., Jongkind, J. F. & Wisse, J. H. (1962) Splitting and recombination of α-crystallin. *Exp. Eye Res.* **1**, 300–305.

Bloemendal, H., Zweers, A., Benedetti, E. L. & Walters, H. (1975) Selective reassociation of the crystallins. *Exp. Eye Res.* **20**, 463–478.

Bloemendal, H. *et al.* (1977) Nomenclature for the polypeptide chains of lens plasma membranes. *Exp. Eye Res.* **24**, 413–415.

Bloemendal, H. *et al.* (1979) Is the cytoskeleton–plasma membrane complex involved in lens protein synthesis? *Mol. Biol. Rep.* **5**, 99–103.

Blow, A. M. J. (1974) PhD. Thesis, Oxford.

Bouman, A. A., de Leeuw, A. L. M. & Broekhuyse, R. M. (1981) Lens membranes. XIII. Comparative study of biochemical characteristics of the fiber membrane polypeptides from bovine, pig, sheep and chicken lenses. *Exp. Eye Res.* **32**, 491–500.

Bours, J., Zauzig, H.-D. & Rink, H. (1979) Crystallin composition of the bovine lens epithelium related to aging. *Ophthal. Res.* **11**, 351–354.

Boutros, G., Koch, H.-R., Jansen, R., Jacob, J. J. C. & Duncan, G. (1984) Effect of 8-methoxysporalen on rat lens cations, membrane potential and protein levels. *Exp. Eye Res.* **38**, 509–513.

Bradley, R. H., Lo, W.-K., Kuszak, J. & Maisel, H. (1980) The cytoskeleton of the chicken lens fiber cells: a scanning and ultrastructural analysis. *Exp. Eye Res.* **31**, 487–494.

Brassil, D. & Kern, H. L. (1967) Characterization of the transport of neutral amino acids by the calf lens. *Invest. Ophthal.* **7**, 441–451.

Brindley, G. S. (1956) Resting potential of the lens. *Br. J. Ophthal.* **40**, 385–391.

Broekhuyse, R. M. & Kuhlmann, E. D. (1978) Lens membranes. IV. *Exp. Eye Res.* **26**, 305–320.

Broekhuyse, R. M. & Kuhlmann, E. D. (1980) Lens membranes. XI. Some properties of human lens main intrinsic protein (MIP) and its enzymatic conversion into a 22000 dalton polypeptide. *Exp. Eye Res.* **30**, 305–310.

Broekhuyse, R. M., Kuhlmann, E. D. & Stols, A. L. H. (1976) Lens membranes. II. *Exp. Eye Res.* **23**, 365–371.

Buckingham, R. H. (1972) The behaviour of reduced proteins from normal and cataractous lenses in highly dissociating media: cross-linked protein in cataractous lenses. *Exp. Eye Res.* **14**, 123–129.

Bunce, G. E. & Hess, J. L. (1981) Biochemical changes associated with selenite-induced cataract in the rat. *Exp. Eye Res.* **33**, 505–514.

Bunce, G. E., Hess, J. L. & Batra, R. (1984) Lens calcium and selenite cataract. *Curr. Eye Res.* **3**, 315–320.

Campbell, M. T. & McAvoy, J. W. (1984) Onset of fibre differentiation in cultured rat lens epithelium under the influence of neural retina-conditioned medium. *Exp. Eye Res.* **39**, 83–94.

Candia, O. A. (1980) The influence of calcium-free media on the electrical properties of the isolated toad lens. *Exp. Eye Res.* **30**, 193–201.

Candia, O. A., Bentley, P. J., Mills, C. D. & Toyofuku, H. (1970) Asymmetrical distribution of the potential in the toad lens. *Nature* **227**, 852–853.

Carpenter, R. L., Hagen, G. J. & Donovan, G. L. (1977) Are cataracts thermally caused? In *Symposium on Biological Effects and Measurements of Radio Frequency/Microwaves*, pp. 352–379. Rockville. (Quoted by Creighton *et al.*, 1987).

Carper, D., Russell, P., Shinohara, T. & Kinoshita, J. H. (1985) Differential synthesis of rat lens proteins during development. *Exp. Eye Res.* **40**, 85–94.

Carper, D., Shinohara, T., Piatigorsky, J. & Kinoshita, J. H. (1982) Deficiency of functional messenger RNA for a developmentally regulated β-crystallin polypeptide in a hereditary cataract. *Science* **217**, 463–464.

Cenedella, R. J. (1987) Direct chemical measurement of DNA synthesis and net rates of differentiation of rat lens epithelial cells *in vivo* applied to the selenium cataract. *Exp. Eye Res.* **44**, 677–690.

Cenedella, R. J. & Bierkamper, G. G. (1979) Mechanism of cataract production by 3-β(2-diethylaminoethoxy) androst-5-en-17-one hydrochloride, U 1866 A: an inhibitor of cholesterol biosynthesis. *Exp. Eye Res.* **28**, 673–688.

Cheng, H.-M., von Saltza, I., Gonzalez, R. G., Ansari, N. H. & Srivastava, S. K. (1984) Effect of glutathione deprivation on lens metabolism. *Exp. Eye Res.* **39**, 355–364.

Chylack, L. T., Ransil, B. J. & White, O. (1984a) Classification of human senile cataractous change by the America Cooperative Cataract Research Group (CCRG) method. II. The association of nuclear color (sclerosis) with extent of cataract formation, age, and visual acuity. *Invest. Ophthal.* **25**, 174–180.

Chylack, L. T. (1978) Classification of human cataracts. *Arch. Ophthal.* **96**, 888–892.

Chylack, L. T. (1983) Classification of human senile cataractous changes by the American Cooperative Cataract Research Group (CCRG). I. Instrumentation and technique. *Invest. Ophthal.* **24**, 424–431.

Chylack, L. T., White, O. & Tung, W. H. (1984b) Classification of human senile cataractous changes by the American Cooperative Cataract Research Group (CCRG). III. Staged simplification of cataract classification. *Invest. Ophthal.* **25**, 166–173.

Clark, J. I. & Benedek, G. B. (1980) Phase diagram for cell cytoplasm from the calf lens. *Biochem. Biophys. Res. Comm.* **95**, 482–489.

Clayton, R. M. (1970) Problems of differentiation in the vertebrate lens. *Curr. Top. Develop. Biol.* **5**, 115–180.

Clayton, R. M. (1974) Comparative aspects of lens proteins. In *The Eye.* Eds Davson, H. and Graham, L. T. Vol. 5, pp. 399–494. Academic Press: New York.

Clayton, R. M. (1978) Divergence and convergence in lens cell differentiation: regulation of the formation and specific content of lens fibre cells. In *Stem Cells and Hameostasis.* Ed. Lord, Potten & Cole. pp. 115–138. C.U.P.

Clayton, R. M., Campbell, J. C. & Truman, D. E. S. (1968) A re-examination of the organ specificity of lens antigens. *Exp. Eye Res.* **7**, 11–29.

Clayton, R. M. & Truman, D. E. S. (1974) The antigenic structure of chick β-crystallin subunits. *Exp. Eye Res.* **18**, 495–506.

Cogan, D. G. (1962) Anatomy of lens and pathology of cataracts. *Exp. Eye Res.* **1**, 291–295.

Cohen, A. I. (1965) The electron microscopy of the normal human lens. *Invest. Ophthal.* **4**, 433–446.

Cohen, L. H., Westerhuis, W., De Jong, W. W. & Bloemendal, H. (1978) Rat α-crystallin. A chain with an insertion of 22 residues. *Eur. J. Biochem.* **89**, 259–266.

Crabbe, M. J. C., Petchey, M., Burgess, S. E. P. & Cheng, H. (1985) The penetration of sorbinil, an aldose reductase inhibitor, into lens, aqueous humour and erythrocytes of patients undergoing cataract extraction. *Exp. Eye Res.* **40**, 95–99.

Creighton, M. O., Ross, W. M., Stewart-De Haan, J. R., Sanwal,

M. & Trevithvick, J. R. (1985) Modelling cortical cataractogenesis. VII. Effects of vitamin E treatment on galactose-induced cataracts. *Exp. Eye Res.* **40**, 213–222.

Creighton, M. O., Sanwal, M., Stewart-De Haan, J. R. & Trevithick, J. R. (1983) Modeling cortical cataractogenesis. V. Steroid cataracts induced by solumedrol partially prevented by vitamin E *in vitro*. *Exp. Eye Res.* **37**, 65–75.

Creighton, M. O. *et al.* (1987) *In vitro* studies of microwave-induced cataract. II. Comparison of damage observed for continuous wave and pulsed microwaves. *Exp. Eye Res.* **45**, 357–373.

Croft, L. R. (1972) The amino acid sequence of γ-crystallin (Fraction II) from calf lens. *Biochem. J.*, **128**, 961–970.

David, L. L. & Shearer, T. R. (1984) Calcium-activated proteolysis in the lens nucleus during selenite cataractogenesis. *Invest. Ophthal.* **26** (Suppl.), 160.

David, L. L. & Shearer, T. R. (1986) Purification of calpain II from rat lens and determination of endogenous substrates. *Exp. Eye Res.* **42**, 227–238.

Davies, P. D., Duncan, G., Pynsent, P. B., Arber, D. L. & Lucas, V. A. (1984) Aqueous humour glucose concentration in cataract patients and its effect on the lens. *Exp. Eye Res.* **39**, 605–609.

Davson, H. (1949) Some considerations on the salt content of fresh and old ox corneae. *Br. J. Ophthal.* **33**, 175–182.

De Imaldi, A. P. & Corazza, J. P. (1979) Perinatal cataract in the rat. I. Development, influence of temperature, ultrastructure. *Exp. Eye Res.* **29**, 145–153.

De Jong, W. W., Van Kleef, F. S. M. & Bloemendal, H. (1974) Intracellular carboxy-terminal degradation of the αA chain of α-crystallin. *Eur. J. Biochem.* **48**, 271–276.

De Jong, W. W., Zweers, A. & Goodman, M. (1980) Trends in the molecular evolution of α-crystallin. *Protides of Biol. Fluids. 28th. Coll.* Ed. H. Peters. Vol. 28, pp. 161–164.

De Jong, W. W., Zweers, A. & Goodman, M. (1981) Relationship of aardvark to elephants, hyraxes and sea cows from α-crystallin sequences. *Nature*, **292**, 538–540.

Delamere, N. A. & Duncan, G. (1977) A comparison of ion concentrations potentials and conductances of amphibian, bovine and cephalopod lenses. *J. Physiol.* **272**, 167–186.

Delamere, N. A. & Paterson, C. A. (1978) The influence of calcium-free EGTA solution upon membrane premeability in the crystallin lens of the frog. *J. Gen. Physiol.* **71**, 581–593.

Delamere, N. A. & Paterson, C. A. (1979) The influence of calcium-free solutions upon permeability characteristics of the rabbit lens. *Exp. Eye Res.* **28**, 45–53.

Delamere, N. A. & Paterson, C. A. (1985) Characteristics of ^{45}Ca uptake by the rabbit lens. *Exp. Eye Res.* **41**, 11–17.

Delamere, N. A., Paterson, C. A. & Cotton, T. R. (1983) Lens cation transport and permeability changes following exposure to hydrogen peroxide. *Exp. Eye Res.* **37**, 45–53.

Delamere, N. A. & Williams, R. N. (1985) Detoxification of hydrogen peroxide by the rabbit iris-ciliary body. *Exp. Eye Res.* **40**, 805–811.

Delcour, J. & Papaconstantinou, J. (1970) A change in α-crystallin subunit composition in relation to cellular differentiation in adult bovine lens. *Biochem. Biophys. Res. Comm.* **41**, 401–406.

Delcour, J. & Papaconstantinou, J. (1972) Synthesis and aggregation of α-crystallin subunits in differentiating lens cells. *J. biol. Chem.* **247**, 3289–3295.

Dickson, D. H. & Crock, G. W. (1972) Interlocking patterns on primate lens fibres. *Invest. Ophthal.* **11**, 809–815.

Dilley, K. J. & Harding, J. J. (1975) Changes in proteins of the human lens in development and aging. *Biochim. Biophys. Acta* **386**, 391–408.

Dilley, K. J. & Pirie, A. (1974) Changes to the proteins of the human lens nucleus in catarat. *Exp. Eye Res.* **19**, 59–72.

Dillon, J., Castineiras, S. G., Santiago, M. A. & Spector, A. (1984) The endopeptidase-resistant protein fraction from human cataractous lenses. *Exp. Eye Res.* **39**, 95–106.

Dillon, J., Spector, A. & Nakanashi, K. (1976) Identification of β carbolines isolated from fluorescent human lens protein. *Nature* **259**, 422–423.

Dische, Z. (1966) Alterations of lens proteins as etiology in cataracts. In *Biochemistry of the Eye.* Symposium Tutzing Castle. p. 413, Karger, Basel/N.Y.

Dische, Z. & Zelmenis, G. (1966) The sialohexosaminoglycan of the bovine lens capsule. *Doc. Ophthal.* **20**, 54–72.

Dische, Z. & Zil, H. (1951) Studies on the oxidation of cysteine to cystine in lens proteins during cataract formation. *Amer. J. Ophthal.* **34**, 104–113.

Driessen, H. P. C., Herbrink, P., Bloemendal, H. & de Jong, W. W. (1980) The β-crystallin β_p chain is internally duplicated and homologous with γ-crystallin. *Exp. Eye Res.* **31**, 243–246.

Duncan, G. (1969a) Relative permeabilities of the lens membranes to sodium and potassium. *Exp. Eye Res.* **8**, 315–325.

Duncan, G. (1969b) The site of the ion restricting membranes in the toad lens. *Exp. Eye Res.* **8**, 406–412.

Duncan, G. (1969c) Kinetics of potassium movement across amphibian lens membranes. *Exp. Eye Res.* **8**, 413–420.

Duncan, G. (1970) Movement of sodium and chloride across amphibian lens membranes. *Exp. Eye Res.* **10**, 117–128.

Duncan, G. & Bushell, A. R. (1975) Ion analysis of human cataractous lenses. *Exp. Eye Res.* **20**, 223–230.

Duncan, G. & Bushell, A. R. (1976) The bovine lens as an ion-exchanger: a comparison with ion levels in human cataractous lenses. *Exp. Eye Res.* **23**, 341–353.

Duncan, G. & Bushell, A. R. (1979) Relationship between colour, sodium and protein content in individual senile cataractous lenses. *Ophthal. Res.* **11**, 397–404.

Duncan, G. & Croghan, P. C. (1969) Mechanisms for the regulation of cell volume with particular reference to the lens. *Exp. Eye Res.* **8**, 421–428.

Duncan, G., Delamere, N. A., Paterson, C. A. & Neville, M. C. (1980) Contribution of an electrogenic pump to the electrical characteristics of frog lens membranes. *Exp. Eye Res.* **30**, 105–107.

Duncan, G., Juett, J. R. & Croghan, P. C. (1977) A simple chamber for measuring lens asymmetry potentials. *Exp. Eye Res.* **25**, 391–398.

Duncan, G. & Van Heyningen, R. (1977) Distribution of non-diffusible calcium and sodium in normal and cataractous human lenses. *Exp. Eye. Res.* **25**, 183–193.

Eisenberg, R. S. & Rae, J. L. (1976) Current voltage relationships in the crystalline lens. *J. Physiol.*, **262**, 285–299.

Ellis, M., Alousi, S., Lawniczak, J., Maisel, H. & Welsh, M. (1984) Studies on lens vimentin. *Exp. Eye Res.* **38**, 195–202.

Fagerholm, P. & Chylack, L. T. (1982) Regional sensitivity to hypoglycemia within the rabbit lens epithelium. *ARVO Suppl.* **22**, 153.

Fagerholm, P. P. & Philipson, B. T. (1979a) Experimental traumatic cataract. I. A quantitative microradiographic study. *Invest. Ophthal.* **18**, 1151–1159.

Fagerholm, P. P. & Philipson, B. T. (1979b) Experimental traumatic cataract. II. A transmission electron microscopy and extracellular tracer study. *Invest. Ophthal. Ophthal.* **18**, 1160–1171.

Farnsworth, P. N., Spector, A., Lozier, J. R., Shyne, S. E. & Garner, W. H. (1981) The localization of a 43K polypeptide in normal and cataractous lenses by immunofluorescence. *Exp. Eye Res.* **32**, 257–264.

Fecondo, J. V. & Augusteyn, R. C. (1983) Superoxide dismutase, catalase and glutathione peroxidase in the human cataractous lens. *Exp. Eye Res.* **36**, 15–23.

Fisher, R. F. & Pettet, B. E. (1973) Presbyopia and the water content of human crystallin lens. *J. Physiol* **234**, 443–447.

Fitzgerald, P. G., Bok, D. & Horwitz, J. (1983) Immunocytochemical localization of the main intrinsic polypeptide (MIP) in ultrathin frozen sections of rat lens. *J. Cell Biol.* **97**, 1491–1499.

Fitzgerald, P. G. & Goodenough, D. A. (1986) Rat lens cultures: MIP expression and domains of intercellular coupling *Invest. Ophthal.* **27**, 755–771.

Fleshman, K. R. & Wagner, B. J. (1984) Changes during aging in rat lens endopeptidase activity. *Exp. Eye Res.* **39**, 543–551.

Fournier, D. J. & Patterson, J. W. (1970) Lens regeneration after mature galactose cataract formation. *Proc. Soc. Exp. Biol. Med.* **135**, 377–379.

Fournier, D. J. & Patterson, J. W. (1971) Variations in ATPase activity in the development of experimental cataracts. *Proc. Soc. Exp. Biol. Med.* **137**, 826–832.

François, J., Rabaey, M. & Stockmans, L. (1965) Gel filtration of the soluble proteins from normal and cataractous human lenses. *Exp. Eye Res.* **4**, 312–318.

Friedenwald, J. S. (1930) Permeability of the lens capsule. *Arch. Ophthal.*, **3**, 182–193.

Fujimoto, D., Hirama, D. & Iwashita, T. (1982) Histidinoalanine, a new cross-linking amino acid, in calcified tissue collagen. *Biochem. Biophys. Res. Commun.* **104**, 1102–1106.

Fukui, H. N., Merola, L. O. & Kinoshita, J. H. (1978) A possible cataractogenic factor in the Nakano mouse lens. *Exp. Eye Res.* **26**, 477–485.

Fukui, N., Obazawa, H. & Kinoshita, J. H. (1976) Lens growth in the Takano mouse. *Invest. Ophthal.* **15**, 422–425.

Fukushi, S., Merola, L. O. & Kinoshita, J. H. (1980) Altering the course of cataracts in diabetic rats. *Invest. Ophthal.*, **19**, 313–315.

Garcia-Castineiras, S., Dillon, J. & Spector, A. (1978) Non-tryptophan fluorescence associated with human lens protein: apparent complexity and isolation of bityrosine and anthranilic acid. *Exp. Eye Res.* **26**, 461–476.

Garner, M. H., Roy, D. & Spector, A. (1982) Immunochemical characterization of the main intrinsic proteins of the human lens membrane. *Exp. Eye Res.* **34**, 781–788.

Garner, M. H. & Spector, A. (1980) Sulfur oxidation in selected human cortical cataracts and nuclear cataracts. *Exp. Eye Res.* **31**, 361–369.

Garner, M. H. & Spector, A. (1980) Selective oxidation of cysteine and methionine in normal and senile cataractous lenses. *Proc. Nat. Acad. Sci.* **77**, 1274–1277.

Garner, W. H., Garner, M. H. & Spector, A. (1979) Comparison of the 10000 and 43000 dalton polypeptide populations isolated from the water soluble and insoluble fractions of human cataractous lenses. *Exp. Eye Res.* **29**, 257–276.

Garner, W. H., Garner, M. H. & Spector, A. (1981) Gamma-crystallin, a major cytoplasmic polypeptide disulfide linked to membrane proteins in human cataract. *Biochem. Biophys. Res. Comm.* **98**, 439–447.

Garner, W. H., Garner, M. H. & Spector, A. (1983) H_2O_2-induced uncoupling of bovine lens Na^+, K^+, ATPase. *Proc. Nat. Acad. Sci.* **80**, 2044–2048.

Giblin, F. J., Chakrapani, B. & Reddy, V. N. (1976) Glutathione and lens epithelial function. *Invest. Ophthal.*, **15**, 381–393.

Giblin, F. J., Chakrapani, B. & Reddy, V. N. (1978) High molecular weight protein aggregates in X-ray-induced cataract. *Exp. Eye Res.* **26**, 507–519.

Giblin, F. J., Hightower, K. R., Ragatzki, P. A. & Reddy, V. N. (1984) Calcium-induced high molecular weight proteins in the intact rabbit lens. *Exp. Eye Res.* **39**, 9–17.

Giblin, F. J. & McCready, J. P. (1983) The effect of inhibition of glutathione reductase on the detoxification of H_2O_2 by rabbit lens. *Invest. Ophthal.* **24**, 113–118.

Giblin, F. J., McCready, J. P., Kodama, T. & Reddy, V. N. (1984) A direct correlation between the levels of ascorbic acid and H_2O_2 in aqueous humor. *Exp. Eye Res.* **38**, 87–93.

Giblin, F. J., McCready, J. P., Reddan, J. R., Dziedzic, D. C. & Reddy, V. N. (1985) Detoxification of H_2O_2 by cultured rabbit lens epithelial cells: participation of the glutathione redox system. *Exp. Eye Res.* **40**, 827–840.

Giblin, F. J., McCready, J. P., Schrimscher, L. & Reddy, V. N. (1987) Peroxide-induced effects on lens cation transport following inhibition of glutathione reductase activity *in vitro*. *Exp. Eye Res.* **45**, 77–91.

Goldmann, H. (1933) Genesis of heat cataract. *Arch. Ophthal.*, **9**, 314.

Goldmann, H. & Leichtl, A. (1938) Experimentelle Untersuchungen über die Genese des Röntgenstars. *Graefes Arch. Ophthal.*, **138**, 722–736.

Gona, O., White, J. H. & Obenauer, L. (1985) Wound healing by the rat lens after neodymium YAG laser injury *Exp. Eye Res.* **40**, 251–261.

Goodenough, D. A. (1979) Lens gap junctions: a structural hypothesis for non-regulated low-resistance intercellular pathways. *Invest. Ophthal.* **18**, 1104–1122.

Goodenough, D. A. (1980) Lens gap junctions: structural evidence for non-regulated low resistance intercellular pathways. *Invest. Ophthal.* **18**, 1104–1122.

Goodenough, D. A., Dick, J. S. B. & Lyons, J. E. (1980) Lens metabolic cooperation: a study of mouse lens transport and permeability visualized with freeze-substitution autoradiography. *J. Cell Biol.* **86**, 576–589.

Gorthy, W. C. & Anderson, J. W. (1980) Special characteristics of the polar regions of the rat lens: morphology and phosphatase histochemistry. *Invest. Ophthal.*, **19**, 1038–1052.

Gorthy, W. C. & Azari, P. (1987) Biochemical and histochemical evidence for lysosomal proteases in rodent lenses. *Exp. Eye Res.* **44**, 747–753.

Gorthy, W. C., Snavely, M. R. & Berrong, N. D. (1971) Some aspects of transport and digestion in the lens of the normal young adult rat. *Exp. Eye Res.* **12**, 112–119.

Greene, D. A., Lattimer, S., Ulbrecht, J. & Carroll, P. (1985) Glucose induced alterations in nerve metabolism. *Diabetes Care* **8**, 290.

Greiner, J. V., Kopp, S. J., Sanders, D. R. & Glonek, T. (1981) Organophosphates of the crystalline lens: a nuclear magnetic resonance spectroscopic study. *Invest. Ophthal.* **21**, 700–713.

Hamai, Y., Fukui, N. & Kuwabara, T. (1974) Morphology of hereditary mouse cataract. *Exp. Eye Res.* **18**, 537–546.

Harding, C. V., Chylack, L. T., Susan, S. R., Lo, W.-K. & Bobrowski, W. F. (1982) Elemental and ultrastructural analysis of specific human lens opacities. *Invest. Ophthal.* **23**, 1–13.

Harding, C. V., Chylack, L. T., Susan, S. R., Lo, W.-K. & Bobrowski, W. F. (1983) Calcium-containing opacities in the human lens. *Invest. Ophthal.* **24**, 1194–1202.

Harding, C. V., Susan, S. & Murphy, H. (1976) Scanning electron microscopy of the adult rabbit lens. *Ophthal. Res.* **8**, 443–455.

Harding, J. J. (1973) Disulphide cross-linked protein of high molecular weight in human cataractous lens. *Exp. Eye Res.* **17**, 377–383.

Harding, J. J. & Dilley, K. J. (1976) Structural proteins of the mammalian lens: A review with emphasis on changes in development, aging and cataract. *Exp. Eye Res.* **22**, 1–73.

Harding, J. J. & Crabbe, M. J. C. (1984) The lens: development,

proteins, metabolism and cataract. In *The Eye* Vol. 1 B. Ed. Davson, H. pp. 207–492. N. Y., London: Academic Press.

Harding, J. J. & Rixon, K. C. (1980) Carbamylation of lens proteins: a possible factor in cataractogenesis in some tropical countries. *Exp. Eye Res.* **31**, 567–571.

Harris, J. E. & Gehrsitz, L. B. (1951) Significance of changes in potassium and sodium content of the lens. *Am. J. Ophthal.* **34**, Pt. 2, 131–138.

Herbrink, P., Van Westreenen, H. & Bloemendal, H. (1975) Further studies on the polypeptide chains of β-crystallin. *Exp. Eye Res.* **20**, 541–548.

Hightower, K. R. (1983) The influence of calcium on protein synthesis in the rabbit lens. *Invest. Ophthal.* **24**, 1422–1426.

Hightower, K. R., Giblin, F. J. & Reddy, V. N. (1983) Changes in the distribution of lens calcium during development of X-ray cataract. *Invest. Ophthal.* **24**, 1188–1193.

Hightower, K. R. & Harrison, S. E. (1982) Valinomycin cataract: the relative role of calcium and sodium accumulation. *Exp. Eye Res.* **34**, 941–943.

Hightower, K. R., Leverenz, V. & Reddy, V. N. (1980) Calcium transport in the lens. *Invest. Ophthal.* **19**, 1059–1066.

Hightower, K. R. & Reddy, V. N. (1982a) Calcium content and distribution in human cataract. *Exp. Eye Res.* **34**, 413–421.

Hightower, K. R. & Reddy, V. N. (1982b) Ca^{++}-induced cataract. *Invest. Ophthal.* **22**, 263–267.

Horwitz, J. (1976) Some properties of the low molecular weight α-crystallin from normal human lens: comparison with bovine lens. *Exp. Eye Res.*, **23**, 471–481.

Horwitz, J., Robertson, N. P., Wong, M. M., Zigler, J. S. & Kinoshita, J. H. (1979) Some properties of lens plasma membrane polypeptides isolated from normal human lenses. *Exp. Eye Res.* **28**, 359–365.

Hu, T.-S., Datiles, M. & Kinoshita, J. H. (1983) Reversal of galactose cataract with sorbinil in rats. *Invest. Ophthal.* **24**, 640–644.

Ireland, M. & Maisel, H. (1983) Identification of native actin filaments in chick lens fiber cells. *Exp. Eye Res.* **36**, 531–536.

Ireland, M. & Maisel, H. (1984) A cytoskeletal protein unique to lens fiber cell differentiation. *Exp. Eye Res.* **38**, 637–645.

Ireland, M., Lieska, N. & Maisel, H. (1983) Lens actin: purification and localization. *Exp. Eye Res.* **37**, 393–408.

Iwata, S. & Horiuchi, M. (1980) Studies on experimental cataracts induced by ionophores: *in vitro* effects of nigericin and valinomycin on the lenses of mice. *Exp. Eye Res.* **31**, 543–551.

Iwata, S. & Kinoshita, J. H. (1971) Mechanism of development of hereditary cataract in mice. *Invest. Ophthal.* **10**, 504–512.

Iwata, S., Shirasawa, E. & Takehana, M. (1984) Activation of Ca^{2+}-transport in the lens. *Curr. Eye Res.* **3**, 717–721.

Jacob, T. J. C. (1983) Raised intracellular free calcium within the lens causes opacification and cellular uncoupling in the frog. *J. Physiol.* **341**, 595–601.

Jacob, T. J. C. & Duncan, G. (1980) Osmotic influences on lens membrane characteristics. *Exp. Eye Res.*, **31**, 505–512.

Jacob, T. J. C. & Duncan, G. (1981) Calcium controls both sodium and potassium permeability of lens membranes. *Exp. Eye Res.* **33**, 85–93.

Jedziniak, J. A., Kinoshita, J. H., Yates, E. M., Hocker, L. O. & Benedek, G. B. (1972) Calcium-induced aggregation of bovine lens alpha crystallins. *Invest. Ophthal.* **11**, 905–915.

Jedziniak, J. A., Kinoshita, J., Yates, E. M., Hocker, L. O. & Benedek, G. B. (1973) On the presence and mechanism of formation of heavy molecular weight aggregates in human normal and cataractous lenses. *Exp. Eye Res.* **15**, 185–192.

Kabasawa, I., Kinoshita, J. H. & Barber, G. W. (1974) Aging effects on the bovine lens γ-crystallins. *Exp. Eye Res.* **18**, 457–466.

Kabasawa, I., Tsunematsu, Y., Barber, G. W. & Kinoshita, J. H. (1977) Low molecular weight proteins of bovine lenses. *Exp. Eye Res.* **24**, 437–448.

Kador, P. F., Fukui, H. N., Fukushi, S., Jernigan, H. M. & Kinoshita, J. H. (1980) Philly mouse: a new model of hereditary cataract. *Exp. Eye Res.* **30**, 59–68.

Kador, P. F., Zigler, J. S. & Kinoshita, J. H. (1979) Alterations of lens protein synthesis in galactosemic rats. *Invest. Ophthal.*, **18**, 696–702.

Kanayama, T., Miyanaga, Y., Horiuchi, K. & Fujimoto, D. (1987) Detection of the cross-linking amino acid, histidinolamine, in human brown cataractous lens protein. *Exp. Eye Res.* **44**, 165–169.

Kawaba, T., Cheng, H.-M. & Kinoshita, J. H. (1986) The accumulation of myoinositol and rubidium ions in galactose-exposed rat lens. *Invest. Ophthal.* **27**, 1522–1526.

Kern, H. L. (1962) Accumulation of amino acids by calf lens. *Invest. Ophthal.* **1**, 368–376.

Kinoshita, J. H. (1965) Pathways of glucose metabolism in the lens. *Invest. Ophthal.* **4**, 619–628.

Kinoshita, J. H., Dvornik, D., Kraml, M. & Gabbay, K. H. (1968) The effect of an aldose reductase inhibitor on the galactose-exposed rabbit lens. *Biochim. biophys. Acta*, **158**, 472–475.

Kinoshita, J. H., Merola, L. O. & Dikmak, E. (1962) Osmotic changes in experimental galactose cataracts. *Exp. Eye Res.* **1**, 405–410.

Kinoshita, J. H. & Wachtl, C. (1958) A study of the C^{14}-glucose metabolism of the rabbit lens. *J. biol. Chem.* **233**, 5–7.

Kinsey, V. E. (1973) Studies on the crystallin lens. XIX. *Exp. Eye Res.* **15**, 699–710.

Kinsey, V. E. & Frohman, C. E. (1951) Distribution of cytochrome, total riboflavin, lactate and pyruvate and its metabolic significance. *Arch. Ophthal., N.Y.* **46**, 536–541.

Kinsey, V. E. & McGrady, A. V. (1971) Studies in the crystalline lens. XVII. *Invest. Ophthal.* **10**, 282–287.

Kinsey, V. E. & McLean, I. W. (1970) Characterization of active transport and diffusion of potassium, rubidium, and cesium. *Invest. Ophthal.* **9**, 769–784.

Kinsey, V. E. & Reddy, D. V. N. (1965) Studies on the crystalline lens. XI. *Invest. Ophthal.* **4**, 104–116.

Kinsey, V. E., Wachtl, C., Constant, M. A. & Camacho, E. (1955) Mitotic activity in the epithelia of lenses cultured in various media. *Am. J. Ophthal.* **40**, Pt. 2, 216–223.

Kirby, T. J., Anchor, R. W. P., Perry, H. O. & Winkelmann, R. K. (1962) Cataract formation after triparonol therapy. *Arch. Ophthal.* **68**, 486–489.

Kistler, J., Gilbert, K., Brooks, H. V., Jolly, R. D., Hopcroft, D. H. & Bullivant, S. (1986) Membrane interlocking domains in the lens. *Invest. Ophthal.*, **27**, 1527–1534.

Kistler, J., Kirkland, B. & Bullivant, S. (1985) Identification of a 70000-D protein in lens membrane junctional domains. *J. Cell. Biol.* **101**, 28–35.

Kodama, T., Reddy, V. N., Giblin, F. J., Kinoshita, J. H. & Harding, C. (1983) Scanning electron microscopy of X-ray-induced cataract in mice on normal and galactose diet. *Ophthal. Res.*, **15**, 324–333.

Koch, H.-R. (1979) Basic research on the crystallin lens and its importance for clinical ophthalmology. *Ophthal. Res.* **11**, 254–263.

Koch, H.-R., Beitzen, R., Kremer, F., Choralia, G., Baurmann, H., Megaw, J., Gardner, K. & Lerman, S. (1982) 8-methoxysporalen and long ultraviolet effects on the rat lens: experiments with high dosages. *Graefes' Arch. Ophthal* (Quoted by Boutros *et al.*, 1984).

Kramar, P. O., Emery, A. F., Guy, A. W. & Lin, J. C. (1975) The ocular effects of microwaves on hypothermic rabbits: a study

of microwave cataractogenic mechanisms. *Ann. N.Y. Acad. Sci.* **247**, 155–163.

Kuszak, J., Alcala, J. & Maisel, H. (1980) The surface morphology of embryonic and adult chick lens fiber cells. *Amer. J. Anat.* **159**, 395–410.

Kuszak, J., Maisel, H. & Harding, C. V. (1978) Gap junctions of chick lens fiber cells. *Exp. Eye Res.* **27**, 495–498.

Kuwabara, T. (1975) The maturation of the lens cell: a morphologic study. *Exp. Eye Res.* **20**, 427–443.

Kuwabara, T. & Imaizumi, M. (1974) Denucleation process of the lens. *Invest. Ophthal.* **13**, 973–981.

Kuwabara, T., Kinoshita, J. H. & Cogan, D. G. (1969) Electron microscopic study of galactose-induced cataract. *Invest. Ophthal.* **8**, 133–149.

Langham, M. & Davson, H. (1949) Studies on the lens. *Biochem. J.* **44**, 467–470.

Langley, R. K., Mortimer, C. B. & McCulloch, C. (1960) The experimental production of cataracts by exposure to heat and light. *Arch. Ophthal., N.Y.* **63**, 473–488.

Lasser, A. & Balazs, E. A. (1972) Biochemical and fine structure studies on the water-insoluble components of the calf lens. *Exp. Eye Res.* **13**, 292–308.

Latta, K. & Augusteyn, R. C. (1984) The purification and properties of human lens glutathione reductase. *Exp. Eye Res.* **39**, 343–354.

Lerman, S., Kuch, J. F., Borkman, R. *et al.* (1976) Acceleration of an aging parameter (fluorogen) of the ocular lens. *Ann Ophthal.* **8**, 558–561.

Lewis, B. S., Rixon, K. C. & Harding, J. J. (1986) Bendazan prevents cyanate binding to soluble lens proteins and cyanate-induced phase-separation opacities *in vitro*: a possible mechanism by which bendazan could delay cataracts. *Exp. Eye Res.* **43**, 973–979.

Li, L.-K. & Spector, A. (1972) Studies on the reaggregation of isolated subunits of calf lens α-crystallin. *Exp. Eye Res.* **13**, 110–119.

Li, L.-K. & Spector, A. (1973) The reaggregation of purified subunits of alpha-crystallins. *Exp. Eye Res.* **15**, 179–183.

Liem-The, K. N., Stols, A. L. H., Jap, P. H. K. & Hoenders, H. J. (1975) X-ray induced cataract in rabbit lens. *Exp. Eye Res.* **20**, 317–328.

Litchfield, W. J. & Wells, W. W. (1976) Inhibitory action of D-galactose on phagocyte metabolism and function. *Immunity*, **13**, 728–734.

Lo, W.-K. & Harding, C. V. (1983) Tight junctions in the lense epithelium of human and frog: freeze-fracture and protein tracer studies. *Invest. Ophthal.* **18**, 1104–1122.

Longchamps, M. O., Laurent, M., Courtois, Y., Trenchev, P. & Hughes, R. C. (1976) Microtubules and microfilaments of bovine lens epithelial cells: electron microscopy and immunofluorescence staining with specific antibodies. *Exp. Eye Res.* **23**, 505–518.

Lorand, L., Hsu, L. K. H., Siefring, G. E. & Rafferty, N. S. (1981) Lens transglutaminase and cataract formation. *Proc. Nat. Acad. Sci.* **78**, 1356–1360.

Mach, H. (1963) Untersuchungen von Linseneiweiss und Mikroelektrophorese von Wasserlöslichem Eiweiss im Altersstar. *Klin. Mbl. Augenheilk*, **143**, 689–710.

Maisel, H. (1977) The nature of the urea-insoluble material of the human lens. *Exp. Eye Res.* **24**, 417–419.

Maisel, H. & Perry, M. M. (1972) Electron microscope observations on some structural proteins of chick lens. *Exp. Eye Res.*, **14**, 7–12.

Malinowski, K. & Manski, W. (1984) Modification of α-crystallin subunit chains and formation of α-neoprotein molecules: role of SH-groups. *Arch. Biochem. Biophys.* **232**, 721–728.

Mann, I. (1949) *The Development of the Human Eye.* London: B.M.A. (2nd ed.).

Manski, W., Auberach, T. P. & Halbert, S. P. (1960) The evolutionary significance of lens organ specificity. *Am. J. Ophthal.* **50**, Pt. 2, 985–991.

Manski, W. J. & Malinowski, K. C. (1980) Regulatory effect of A to B cattle lens α-crystallin subunit ratios on the quaternary structure of macromolecules formed by their assembly. *J. Biol. Chem.*, **255**, 1572–1576.

Manski, W. & Malinowski, K. (1983) Interaction between the constitutent A and B lens α-crystallin subunits leading to formation of α-neoprotein molecules. *Arch. Biochem. Biophys.*, **226**, 531–538.

Manski, W. & Malinowski, K. (1985) Alpha neoprotein molecules in normal lenses from animals of different ages and in cataractous lenses. *Exp. Eye Res.* **40**, 179–190.

Manski, W., Malinowski, K. & Bonitsis, G. (1979) Immunochemical studies on lens protein–protein complexes. I. *Exp. Eye Res.* **29**, 625–635.

Maraini, G. & Mangili, R. (1973) Differences in proteins and in the water balance of the lens in nuclear and cortical types of senile cataract. In *The Human Lens in Relation to Cataract.* Eds. Elliott, K. M. & Fitzsimmons, D. W. Ciba Symp. No. 19. Elsevier Excerpta Medica: Amsterdam, London, N.Y. pp. 79–97.

Marcantonio, J. M., Duncan, G. & Rink, H. (1986) Calcium-induced opacification and loss of protein in the organ-cultured bovine lens. *Exp. Eye Res.* **42**, 617–630.

Matsuda, H., Giblin, F. J. & Reddy, V. N. (1981) The effect of X-irradiation on cation transport in rabbit lens. *Exp. Eye Res.* **33**, 253–265.

Matsuda, S., Giblin, F. J. & Reddy, V. N. (1982) The effect of X-irradiation on Na–K ATPase and cation distribution in rabbit lens. *Invest. Ophthal.* **22**, 180–185.

McAvoy, J. W. (1978a) Cell division, cell elongation and distribution of α-, β- and γ-crystallins in the rat lens. *J. Embryol. Exp. Morph.* **44**, 149–165.

McAvoy, J. W. (1978b) Cell division, cell elongation and the coordination of crystallin gene expression during lens morphogenesis in the rat. *J. Embryol. Exp. Morph.* **45**, 271–281.

McFall-Ngai, M., Horwitz, J., Ding, L.-L. & Lacey, L. (1986) Age-dependent changes in the heat-stable crystallin, β Bp of the human lens. *Curr. Eye Res.* **5**, 387–394.

McGahan, M. C., Chin, B. & Bentley, P. J. (1983) Calcium metabolism of the rabbit lens. *Exp. Eye Res.* **36**, 57–66.

McNamara, M. K. & Augusteyn, R. C. (1980) 3-3′-Dityrosine in the proteins of senile nuclear cataracts. *Exp. Eye Res.* **38**, 45–56.

McNamara, N. & Augusteyn, R. C. (1984) The effect of hydrogen peroxide on lens proteins: a possible model for nuclear cataract. *Exp. Eye Res.* **38**, 45–56.

Mehta, P. D., Cooper, S. N. & Rao, S. S. (1964) Identification of species-specific and organ-specific antigens in lens proteins. *Exp. Eye Res.* **3**, 192–197.

Menko, A. S., Klukas, K. A. & Johnson, R. G. (1984) Chicken embryo lens cultures mimic differentiation in the lens. *Dev. Biol.* **103**, 129–141.

Miller, R. C. & Riley, E. F. (1987) Recovery of rat lens epithelial cells after total or partial X-irradiation. *Exp. Eye Res.* **45**, 407–418.

Mörner, C. T. (1894) Untersuchung der Proteinsubstanzen in der lichtbrechenden Medien des Auges. II. *Z. physiol. Chem.* **18**, 233–256.

Mousa, G. Y. & Trevithick, J. R. (1977) Differentiation of rat lens epithelial cells in tissue culture. II. *Devel. Biol.*, **60**, 14–25.

Nakano, K. Yamomoto, S., Kutsukako, G., Ogawa, H.,

Nakajima, A. & Takano, E. (1960) Hereditary cataract in mice. *Japn. J. Clin. Ophthal.* **14**, 1772–1776.

Nasser, S., Bradley, R., Alcala, J. & Maisel, H. (1980) Regional differences in the composition of the bovine lens urea-soluble protein. *Exp. Eye Res.* **30**, 109–113.

Nelson, K. J. & Rafferty, N. S. (1976) A scanning electron microscopic study of lens fibers in healing mouse lens. *Exp. Eye Res.* **22**, 335–346.

Nicholson, B. J., Tekemoto, L. J., Hunkapiller, M. W., Hood, L. E. & Revel, J.-P. (1983) Differences between liver gap junction protein and lens MIP 26 from rat: implication for tissue specificity of gap junctions. *Cell* **32**, 967–978.

Nordmann, J. (1962) Acquisitions récentes dans le domaine de la biologie du crystallin. *Progr. Ophthal.* **12**, 1–264.

Okada, T., Eguchi, G. & Takeichi, M. (1973) The retention of differentiated properties by lens epithelial cells in clonal cell culture. *Dev. Biol.* **34**, 321.

Ortwerth, B. J., Olesen, P. R. & Sharma, K. K. (1986) Solubilization of the lens water-insoluble fraction by sonication. *Exp. Eye Res.* **43**, 955–963.

Ostadolova, I., Babický, A. & Obenberger, J. (1978) Cataract induced by administration of a single dose of sodium selenite to suckling rats. *Experientia* **34**, 222–223.

Palva, M. & Palkama, A. (1974) Histochemically demonstrable sodium-patassium activated adenosine triphosphatase (Na-K-ATPase) activity in the rat lens. *Exp. Eye Res.* **19**, 117–123.

Palva, M. & Palkama, A. (1976) Electron microscopical, histochemical and biochemical findings on the Na-K-ATPase activity in the epithelium of the rat lens. *Exp. Eye Res.* **22**, 229–236.

Papaconstantinou, J. (1965) The γ-crystallins of adult bovine, calf and embryonic lenses. *Biochim. biophys. Acta* **107**, 81–90.

Parmelee, J. T. (1986). Measurement of steady currents around the frog lens. *Exp. Eye Res.* **42**, 433–441.

Parmelee, J. T., Robinson, K. R. & Patterson, J. W. (1985) Effects of calcium on the steady outward currents at the equator of the rat lens. *Invest. Ophthal.* **26**, 1343–1348.

Paterson, C. A. (1970) Extracellular space of the crystalline lens. *Am. J. Physiol.* **218**, 797–802.

Paterson, C. A. & Delamere, N. A. (1983) An analysis of ^{45}Ca fluxes in the rabbit lens. *Curr. Eye Res.* **2**, 727–734.

Paterson, C. A., Neville, M. C., Jenkins, R. M. & Cullen, J. P. (1975) An electrogenic component of the potential difference in the rabbit lens. *Biochim. biophys. Acta* **375**, 309–316.

Paterson, C. A., Neville, M. C., Jenkins, R. M. & Nordstrom, D. K. (1974) Intracellular potassium activity in frog lens determined using ion specific liquid ion-exchange filled microelectrodes. *Exp. Eye Res.* **19**, 43–48.

Patmore, L. & Duncan, G. (1979) A TEA-sensitive component in the conductance of a non-excitable tissue (amphibian lens). *Exp. Eye Res.* **28**, 349–352.

Patterson, J. W. (1979) Effects of amino acid loading on lens amino acids, cations and water. *Exp. Eye Res.* **28**, 689–698.

Patterson, J. W. (1980) The effect of incubation medium electrolyte concentration on lens volume. *Ophthal. Res.* **12**, 97–110.

Patterson, J. W. (1981) Lens volume regulation in hypertonic medium. *Exp. Eye Res.* **32**, 151–162.

Patterson, J. W. & Bunting, K. W. (1966) Sugar cataracts, polyol levels and lens swelling. *Doc. Ophthal.* **20**, 64–72.

Patterson, J. W., Patterson, M. E., Kinsey, V. E. & Reddy, D. V. N. (1965) Lens assays on diabetic and galactosemic rats receiving diets that modify cataract development. *Invest. Ophthal.* **4**, 98–103.

Philipson, B. (1969) Distribution of protein within lenses with X-ray cataract. *Invest. Ophthal.* **8**, 271–280.

Philipson, B. (1969) Galactose cataract: changes in protein distribution during development. *Invest. Ophthal.* **8**, 281–289.

Philipson, B. (1973) Changes in the lens related to the reduction in transparency. *Exp. Eye Res.* **16**, 29–39.

Piatigorsky, J. (1980a) Intracellular ions, protein metabolism and cataract formation. *Curr. Topics Eye Res.* **3**, 1–39.

Piatigorsky, J. (1980b) Differential synthesis and degradation of protein in the hereditary Philly mouse cataract. *Exp. Eye Res.* **30**, 59.

Piatigorsky, J., Kador, P. F. & Kinoshita, J. H. (1980) Differential synthesis and degradation of protein in the hereditary Philly mouse cataract. *Exp. Eye Res.* **30**, 69–78.

Piatigorsky, J., Rothschild, S. S., Milstone, M. L. M. (1973) Differentiation of lens fibers in explanted embryonal chick lens epithelia. *Dev. Biol.*, **34**, 334–345.

Pirie, A. (1968a) Color and solubility of the proteins of human cataracts. *Invest. Ophthal.* **7**, 634–650.

Pirie, A. (1968b) Pathology of the eye of the naphthalene-fed rabbit. *Exp. Eye Res.* **7**, 354–357.

Pirie, A., van Heyningen, R. & Boag, J. W. (1953) Changes in lens during the formation of X-ray cataract in rabbits. *Biochem. J.* **54**, 682–688.

Platsch, K. D. & Wiederholt, M. (1981) Effect of ion substitution and ouabain on short circuit current in the isolated human and rabbit lens. *Exp. Eye Res.* **32**, 615.

Quax-Jeuken, Y., Driessen, H., Leunissen, J., Quax, J., DeJong, W. & Bloemendal, H. (1985) β_s-Crystallin, structure and evolution of a distinct member of the βγ-superfamily. *EMBO J.* **4**, 2597–2602. (Quoted by Bessems *et al.*, 1986).

Rabaey, M. (1962) Electrophoretic and immunoelectrophoretic studies on the soluble proteins in the developing lens of birds. *Exp. Eye Res.*, **1**, 310–316.

Rae, J. D. (1974a) Potential profiles in the crystalline lens of the frog. *Exp. Eye Res.* **19**, 227–234.

Rae, J. L. (1974b) Voltage compartments in the lens. *Exp. Eye Res.* **19**, 235–242.

Rae, J. L. (1974c) The movement of procion dye in the crystalline lens. *Invest. Ophthal.*, **13**, 147–150.

Rae, J. L. & Blankenship, J. E. (1973) Bioelectric measurements in the frog lens. *Exp. Eye Res.*, **15**, 209–217.

Rae, J. L. & Stacey, T. (1979) Lanthanum and Procion yellow as extracellular markers in the crystalline lens of the rat. *Exp. Eye Res.* **28**, 1–21.

Raemaekers, F. C. S., Boomkens, T. R. & Bloemendal, H. (1981) Cytoskeletal and contractile structures in bovine lens cell differentiation. *Exp. Cell. Res.* **135**, 454–461.

Raemaekers, F., Dodemont, H., Vorstenbosch, P. & Bloemendal, H. (1982) Classification of rat lens crystallins and identification of proteins encoded by rat lens mRNA. *Europ. J. Biochem.* **128**, 503–508.

Raemaekers, F. C. S., Dunia, I., Dodemont, H. J., Benedetti, E. L. & Bloemendal, H. (1982) Lenticular intermediate-sized filaments: biosynthesis and interaction with plasma membrane. *Proc. Nat. Acad. Sci.* **79**, 3208–3212.

Raemaekers, F. C. S., Selten-Versteegen, A. M. E., Benedetti, E. L., Dunia, I. & Bloemendal, H. (1980a) *In vitro* synthesis of the major lens protein. *Proc. Nat. Acad. Sci.* **77**, 725–729.

Raemaekers, F. C. S., Osborn, M., Schmid, E., Weber, K., Bloemendal, H. & Franke, W. W. (1980b) Identification of the cytoskeletal protein in lens forming cells, a special epithelial type. *Exp. Cell Res.* **127**, 309–327.

Rafferty, N. S. & Esson, E. A. (1974) An electron-microscope study of adult mouse lens: some ultrastructural specializations. *J. Ultrastr. Res.* **46**, 239–253.

Rafferty, N. S. & Goossens, W. (1984) Lens wound healing and cataractogenesis in a pigmented eye. *Exp. Eye Res.* **38**, 267–277.

Reddy, D. V. N & Kinsey, V. E. (1962) Studies on the crystalline lens. Quantitative analysis of free amino acids and related compounds. *Invest. Ophthal.* **1**, 635–641.

Reddy, V. N., Schwass, D., Chakropani, B. & Lim, C. P. (1976) Biochemical changes associated with the development and reversal of galactose cataracts. *Exp. Eye Res.* **23**, 483–493.

Rees, J. R. & Pirie, A. (1967) Possible reactions of 1,2-naphthaquinone in the eye. *Biochem. J.* **102**, 853–863.

Reszelbach, R. & Patterson, J. W. (1985) Localization of potassium and sodium fluxes in the rat lens. *Invest. Ophthal.* **26**, 945–952.

Ringens, P. J., Hoenders, H. J. & Bloemendal, H. (1982a) Effect of aging on the water-soluble and water-insoluble protein pattern in normal human lens. *Exp. Eye Res.* **34**, 201–207.

Ringens, P. J., Hoenders, H. J. & Bloemendal, H. (1982b) Protein distribution and characterization in the prenatal and postnatal human lens. *Exp. Eye Res.* **34**, 815–823.

Roberts, D. St. C. (1957) Studies on the antigenic structure of the eye using the fluorescent antibody technique. *Br. J. Ophthal.* **41**, 338–347.

Robinson, K. R. & Patterson, J. W. (1983) Localization of steady current in the lens. *Curr. Eye Res.* **12**, 843–847.

Roelfzema, H., Broekhuyse, R. M. & Veerkamp, J. H. (1974) Subcellular distribution of sphingomyelinase and other acid hydrolases in different parts of the calf lens. *Exp. Eye Res.* **18**, 579–594.

Rogers, K. M. & Augusteyn, R. C. (1978) Glutathione reductase in normal and cataractous human lens. *Exp. Eye Res.* **27**, 719–721.

Rose, B. & Loewenstein, W. R. (1975) Permeability of cell junction depends on local cytoplasmic calcium activity. *Nature* **254**, 250–252.

Ross, W. M., Creighton, M. O., Trevithvick, J. R., Stewart-De Haan, P. J. & Sanwal, M. (1983) Modelling cortical cataractogenesis. VI. Induction by glucose *in vitro* or in diabetic rats: prevention and reversal by glutathione. *Exp. Eye Res.* **37**, 559–573.

Roy, D. (1981) Characterization of a divalent cation-linked polypeptide fraction of human lens proteins. *Exp. Eye Res.* **32**, 533–539.

Roy, D., Garner, M. H. & Spector, A. (1982) Investigations of Nakano lens proteins. *Exp. Eye Res.* **34**, 909–920.

Roy, D. & Spector, A. (1978) Human insoluble lens proteins. I and II. *Exp. Eye Res.* **26**, 429–443, 445–459.

Roy, D., Spector, A. & Farnsworth, P. (1979) Human lens membrane: comparison of major intrinsic polypeptide from young and old lenses isolated by a new methodology. *Exp. Eye Res.* **28**, 353–358.

Rubin, L. F. & Barnett, K. C. (1967) Ocular effects of oral and dermal application of dimethyl sulfoxide in animals. *Ann. N.Y. Acad. Sci.* **141**, 333–345.

Russell, N. J., Royland, J. E., McCawley, E. L. & Shearer, T. R. (1984) Ultrastructural study of selenite-induced nuclear cataracts. *Invest. Ophthal.* **25**, 751–757.

Sandberg, H. O. & Closs, O. (1979) The alpha and gamma crystallin content in aqueous humor of eyes with clear lenses and with cataract. *Exp. Eye Res.* **28**, 601–610.

Schwartz, B. (1960) Initial studies of the use of an open system for the culture of the rabbit lens. *Arch. Ophthal.*, **63**, 634–659.

Shearer, T. R., Anderson, R. S., Britton, J. L. & Palmer, E. A. (1983) Early development of selenium-induced cataract: slit-lamp evaluation. *Exp. Eye Res.* **36**, 781–788.

Shinohara, T., Piatigorsky, J., Carper, D. A. & Kinoshita, J. H. (1982) Crystallin synthesis and crystallin mRNAs in galactosemic rat lenses. *Exp. Eye Res.* **34**, 39–48.

Shinohara, T., Robinson, E. A., Appella, E. & Piatigorsky, J. (1982) Mulitple γ-crystallins of the mouse lens: fractionation of mRNAs by cDNA cloning. *Proc. Nat. Acad. Sci.* **79**, 2783–2787.

Siew, E. L., Bettelheim, F. A., Chylack, L. T. & Tung, W. H. (1981a) Studies in human cataracts. *Invest. Ophthal.* **20**, 334–347.

Siew, E. L., Opalecky, D. & Bettelheim, F. A. (1981b) Light scattering of normal human lens. II. Age dependence of the light scattering parameters. *Exp. Eye Res.* **33**, 603–614.

Siezen, R. J. & Berger, H. (1978) The quaternary structure of bovine α-crystallin. *Eur. J. Biochem.* **91**, 397–405.

Siezen, R. J., Bindels, H. G. & Hoenders, H. J. (1978) The quaternary structure of bovine α-crystallin. *Eur. J. Biochem.* **91**, 387–396.

Siezen, R. J., Bindels, J. G. & Hoenders, H. J. (1979) The interrelationship between monomeric, oligomeric and polymeric α-crystallin in the calf lens nucleus. *Exp. Eye Res.* **28**, 351–567.

Siezen, R. J., Bindels, J. G. & Hoenders, H. J. (1980) The quaternary structure of bovine α-crystallin. *Eur. J. Biochem.* **111**, 435–444.

Siezen, R. J., Fisch, M. R., Slingsby, C. & Benedek, G. B. (1985) Opacification of γ-crystallin solutions from calf lens in relation to cold cataract formation. *Proc. Nat. Acad. Sci.* **82**, 1701–1705.

Simpson, G. C. (1953) Ocular haloes and coronas. *Brit. J. Ophthal.* **37**, 450–486.

Slingsby, C. & Croft, L. R. (1973) Developmental changes in the low molecular weight proteins of the bovine lens. *Exp. Eye Res.* **17**, 369–376.

Spector, A., Freund, T., Li, L.-K. & Augusteyn, R. C. (1971a) Age-dependent changes in the structure of alpha crystallin. *Invest. Ophthal.* **10**, 677–686.

Spector, A. & Garner, W. H. (1981) Hydrogen peroxide and human cataract. *Exp. Eye Res.* **33**, 673–681.

Spector, A., Li, L.-K., Augusteyn, R. C., Schneider, A. & Freund, T. (1971b) α-crystallin. The isolation and characterization of distinct macromolecular fractions. *Biochem. J.* **124**, 337–343.

Spector, A., Li, S. & Sigelman, J. (1974) Age-dependent changes in the molecular size of human lens proteins and their relationship to light scatter. *Invest. Ophthal.* **13**, 795–798.

Spector, A. & Roy, D. (1978) Disulfide-linked high molecular weight protein associated with human cataract. *Proc. Nat. Acad. Sci.* **75**, 3240–3248.

Spector, A., Stauffer, J., Roy, D., Li, L.-K. & Adams, D. (1976) Human alpha-crystallin. I. The isolation and characterization of newly synthesized alpha-crystallin. *Invest. Ophthal.* **15**, 288–296.

Spector, A. *et al.* (1987) Does elevated glutathione protect the cell from H_2O_2 insult? *Exp. Eye Res.* **45**, 453–465.

Spencer, R. W. & Andelman, S. Y. (1965) Steroid cataracts. *Arch. Ophthal.* **74**, 38–41.

Sperelakis, N. & Potts, A. M. (1959) Additional observations on the bioelectric potentials of the lens. *Am. J. Ophthal.* **47**, 395–409.

Spiro, R. G. & Fukushi, S. (1969) The lens capsule. Studies on the carbohydrate units. *J. Biol. Chem.*, **244**, 2049–2058.

Srivastava, O. P. & Ortwerth, B. J. (1983a) Age-related and distributional changes in the trypsin inhibitor activity of bovine lens. *Exp. Eye Res.* **36**, 695–709.

Srivastava, O. P. & Ortwerth, B. J. (1983b) Isolation and characterization of a 25 K serine proteinase from bovine lens cortex. *Exp. Eye Res.* **37**, 597–612.

Srivastasa, S. K., Lal, A. K. & Ansari, N. H. (1980) Defense system of the lens against oxidative damage: effect of oxidative challenge on cataract formation in glutathione peroxidase deficient acatalasemic mice. *Exp. Eye Res.* **31**, 425–433.

Stambolion, D., Scarpino-Myers, V., Eagle, R. C., Hodes, B. &

Harris, H. (1986) Cataracts in patients heterozygous for galactokinase deficiency. *Invest. Ophthal.* **27**, 429–433.

Stauffer, J., Rothschild, C., Wandel, T. & Spector, A. (1974) Transformation of alpha crystallin polypeptide chains with aging. *Invest. Ophthal.* **13**, 135–146.

Strous, G. J. A. M., Van Westreenen, H., Van der Logt, J. & Bloemendal, H. (1974) Synthesis of lens proteins *in vitro*. The lens cell-free system. *Biochim. Biophys. Acta* **353**, 89–98.

Swanson, A. A. (1966) The identification of lysosomal enzymes in bovine lens epithelium. *Exp. Eye Res.* **5**, 145–149.

Swanson, A. A. (1967) Histochemical identification of lysosomal enzymes in lens epithelial cells. *Exp. Eye Res.* **6**, 351–355.

Swanson, A. A., Davis, R. M., Albers-Jackson, B. & McDonald, J. K. (1981) Lens exopeptidases. *Exp. Eye Res.* **32**, 163–173.

Takemoto, L. J. & Azari, P. (1977) Isolation and characterization of covalently linked, high molecular weight proteins from human cataractous lens. *Exp. Eye Res.* **24**, 63–70.

Takemoto, L., Takemoto, D., Brown, G., Takehana, M., Smith, J. & Horwitz, J. (1987) Cleavage from the N-terminal region of Bp crystallin during aging of the human lens. *Exp. Eye Res.* **45**, 385–392.

Tanaka, M., Russell, P., Smith, S., Uga, S., Kawabara, T. & Kinoshita, J. H. (1980) Membrane alterations during cataract development in the Nakano mouse. *Invest. Ophthal.* **19**, 619–629.

Taura, T., Giblin, F. J. & Reddy, V. N. (1985) Further observations on the effect of galactose on the development of X-ray-induced cataract in mice. *Exp. Eye Res.* **41**, 527–543.

Thoft, R. A. & Kinoshita, J. H. (1965) The effect of calcium on rat lens permeability. *Invest. Ophthal.* **4**, 122–128.

Thomson, J. A. & Augusteyn, R. C. (1983) α_m-crystallin: the native form of the protein? *Exp. Eye Res.* **37**, 367–377.

Thomson, J. A. & Augusteyn, R. C. (1985) Ontogeny of human lens crystallins. *Exp. Eye Res.* **40**, 393–410.

Tse, S. S. & Ortwerth, B. J. (1980a) The distribution of trypsin inhibitor proteins in bovine lens: a possible factor in preventing *in vivo* proteolysis. *Exp. Eye Res.* **31**, 411–423.

Tse, T. T. & Ortwerth, B. J. (1980b) Inactivation of the bovine lens trypsin inhibitor by ultraviolet irradiation. *Exp. Eye Res.* **31**, 313–325.

Tse, S. S. & Ortwerth, B. J. (1981) Activation of proteinases with trypsin-like specificity from bovine and human lenses. *Exp. Eye Res.* **32**, 605–614.

Tse, S. S. & Ortwerth, B. J. (1982) Activation and release of a trypsin-like proteinase from bovine lens α-crystallin. *Exp. Eye Res.* **34**, 659–674.

Uga, S., Kador, P. F. & Kawabara, T. (1980) Cytological study of the Philly mouse cataract. *Exp. Eye Res.* **30**, 79–92.

Uga, S. (1981) Wound healing in the mouse lens. *Exp. Eye Res.* **32**, 175–186.

Uhlenhuth, P. T. (1903) Zur Lehre von der Unterscheidung verschiedener Eiweissarten mit Hilfe spezifischer Sera. In *Koch Festschrift*. p. 49, Jena: G. Fischer.

Unakar, N. J., Genyea, C., Reddan, J. R. & Reddy, V. N. (1978) Ultrastructural changes during the development and reversal of galactose cataracts. *Exp. Eye Res.* **26**, 123–133.

Unakar, N. J. & Tsui, J. Y. (1980a) Sodium-potassium-dependent ATPase. I. Cytochemical localization in normal and cataractous rat lenses. *Invest. Ophthal.* **19**, 630–641.

Unakar, N. J. & Tsui, J. Y. (1980b) Sodium-potassium-dependent ATPase. II. Cytochemical localization during the reversal of galactose cataracts in rat. *Invest. Ophthal.* **19**, 378–385.

Unakar, N. J. & Tsui, J. Y. (1983) Inhibition of galactose-induced alterations in ocular lens with sorbinil. *Exp. Eye Res.* **36**, 685–694.

Van Dam, A. F. (1966) Purification and composition studies of β_s-crystallin. *Exp. Eye Res.* **5**, 255–266.

Van den Broek, W. G. M., Leget, J. N. & Bloemendal, H. (1973) FM-crystallin: a neglected component among lens proteins. *Biochim. biophys. Acta* **310**, 278–282.

Van den Eijnden-Van Raaij, A. J. M., Leeuw, A. L. M. de & Broekhuyse, R. M. (1985a) *In vitro* reassociation of EDTA-extractable proteins with calf lens fiber membranes. *Exp. Eye Res.* **40**, 327–334.

Van den Eijnden-Van Raaij, A. J. M., Leeuw, A. L. M. de & Broekhuyse, R. M. (1985b) Complex formation of EDTA-extracted proteins from calf lens fiber membranes with calcium and acidic phospholipids. *Exp. Eye Res.* **40**, 477–487.

Van der Ouderaa, F. J., De Jong, W. W. & Bloemendal, H. (1973) The amino-acid sequence of the αA_2 chain of bovine α-crystallin. *Eur. J. Biochem.* **39**, 207–222.

Van der Ouderaa, J., De Jong, W. W., Hilderink, A. & Bloemendal, H. (1974) The amino-acid sequence of the $\alpha\beta_2$ chain of bovine α-crystallin. *Eur. J. Biochem.* **49**, 157–168.

Van Heyningen, R. (1959) Formation of polyols by the lens of the rat with 'sugar' cataract. *Nature, Lond.* **184**, 194–195.

Van Heyningen, R. (1965) The metabolism of glucose by the rabbit lens in the presence and absence of oxygen. *Biochem. J.* **96**, 419–431.

Van Heyningen, R. (1969) The Lens Metabolism and Cataract. In *The Eye*, Ed. Davson, H. Vol. I, pp. 381–488. London: Academic Press.

Van Heyningen, R. (1970) Ascorbic acid in the lens of the naphthalene-fed rabbit. *Exp. Eye Res.* **9**, 38–48.

Van Heyningen, R. (1972) The human lens. III. Some observations on the post-mortem lens. *Exp. Eye Res.* **13**, 155–160.

Van Heyningen, R. & Pirie, A. (1967) The metabolism of naphthalene and its toxic effect on the eye. *Biochem. J.* **102**, 842–852.

Van Heyningen, R. & Trayhurn, P. (1976) Proteolysis of lens proteins (autolysis). *Exp. Eye Res.* **22**, 625–637.

Van Heyningen, R. & Waley, S. G. (1962) Search for a neutral proteinase in bovine lens. *Exp. Eye Res.* **1**, 336–342.

Van Kamp, G. J., Schats, L. M. M. & Hoenders, H. J. (1973) Characteristics of α-crystallin related to fiber cell development in calf eye lenses. *Biochim. biophys. Acta* **295**, 166–173.

Van Kamp, G. J., Struyker Boudier, H. A. J. & Hoenders, H. J. (1974) The soluble proteins of the prenatal bovine eye lens. *Comp. Biochem. Physiol.* **49B**, 445–456.

Van Kamp, G. J., Van Kleef, F. S. M. & Hoenders, H. J. (1974) Reaggregation studies on the polypeptide chains of calf lens α-crystallin. *Biochim. biophys. Acta* **342**, 89–96.

Van Kleef, F. S. M., Nijzink-Maas, M. J. C. M. & Hoenders, H. J. (1974a) Intracellular degradation of α-crystallin. *Eur. J. Biochem.* **48**, 563–570.

Van Kleef, F. S. M., Nijzink, M. J. C. M. & Hoenders, H. J. (1974b) Nine polypeptide chains in α-crystallin. *Exp. Eye Res.* **18**, 201–204.

Varma, S. D., Kumas, S. & Richards, R. D. (1979) Light-induced damage to ocular lens cation pump: prevention by vitamin C. *Proc. Nat. Acad. Sci.* **76**, 3504–3506.

Vornhagen, R., Bours, J. & Rink, H. (1982) Immunologic properties of rat lens gamma-crystallins. I. Characterization of the major components. II. Characterization of the low molecular weight components. *Ophthal. Res.* **14**, 298–304, 305–312.

V. Sallmann, L. (1951) Experimental studies on early lens changes after roentgen irradiation. *Arch. Ophthal., N.Y.* **45**, 149–164.

V. Sallmann, L. (1957) The lens epithelium in the genesis of cataract. *Am. J. Ophthal.* **44**, 159–170.

V. Sallmann, L., Grimes, P. & Collins, E. (1963) Triparonol-induced cataract in rats. *Trans. Amer. Ophthal. Soc.*, **61**, 49–60.

Wagner, B. J. & Fu, S.-C. J. (1978) Characterization of lens proteins. II. γ-crystallins of normal and cataractous rat lenses. *Exp. Eye Res.* **26**, 255–265.

Wagner, B. J., Margolis, J. W., Farnsworth, P. N. & Fu, S.-C. (1982) Calf lens neutral proteinase activity using calf lens crystallin substrates. *Exp. Eye Res.* **35**, 293–303.

Wagner, B. J., Margolis, J. W., Fu, S.-C. J., & Lai, C. Y. (1979) Specificity of the calf lens neutral proteinase. *Invest. Ophthal.* (Suppl), 236–237.

Waley, S. G. (1964) Metabolism of amino acids in the lens. *Biochem. J.* **91**, 576–583.

Waley, S. G. (1965) The problem of albuminoid. *Exp. Eye Res.* **4**, 293–297.

Waley, S. G. (1969) Nomenclature of the polypeptide chains of α-crystallin. *Exp. Eye Res.* **8**, 477–478.

Walton, J. & McAvoy, J. (1984) Sequential structural response of lens epithelium to retina-conditioned medium. *Exp. Eye Res.* **39**, 217–229.

Williams, W. F. & Odom, J. D. (1987) The utilization of ^{13}C and ^{31}P nuclear magnetic resonance spectroscopy in the study of the sorbitol pathway and aldose reductase inhibition in intact rabbit lenses. *Exp. Eye Res.* **44**, 717–730.

Wistow, G. *et al.* (1983) X-ray analysis of the eye lens protein γ II crystallin at 1.9° resolution. *J. Mol. Biol.* **170**, 175–202.

Yorio, T. & Bentley, P. J. (1976) The effects of hyperosmotic agents on the electrical properties of the amphibian lens *in vitro*. *Exp. Eye Res.* **22**, 195–208.

Yorio, T. & Bentley, P. J. (1978) Phospholipase C-induced 'Na-channels' in the crystalline lens. *Exp. Eye Res.*, **26**, 165–176.

Yoshida, H., Murachi, T. & Tsukahara, I. (1984) Limited proteolysis of bovine lens α-crystallin by calpain, a Ca^{2+}-dependent cysteine proteinase, isolated from the same tissue. *Biochim. Biophys. Acta* **798**, 252–259.

Yoshida, H., Murachi, T. & Tsukahara, I. (1985) Distribution of calpain I, calpain II and calpastatin in bovine lens. *Invest. Ophthal.* **26**, 953–956.

Yoshida, H., Yumoto, N., Tsukahara, I. & Murachi, T. (1986) The degradation of α-crystallin at its carboxyl-terminal portion by calpain in bovine lens. *Invest. Ophthal.*, **27**, 1269–1273.

Young, R. W. & Ocumpaugh, D. E. (1966) Autoradiographic studies on the growth and development of the lens capsule in the rat. *Invest. Ophthal.* **5**, 583–593.

Zigler, J. S. (1978) Age-related changes in the polypeptide composition of beta crystallin from bovine lens. *Exp. Eye Res.*, **26**, 537–546.

Zigler, J. S., Carper, D. A. & Kinoshita, J. H. (1981) Changes in lens crystallins during cataract development in the Philly mouse. *Ophthal. Res.* **13**, 237–251.

Zigler, J. S. & Hess, H. H. (1985) Characteristics in the Royal College of Surgeons rat: evidence for initiation by lipid peroxidation products. *Exp. Eye Res.* **41**, 67–76.

Zigler, J. S., Horwitz, J. & Kinoshita, J. H. (1980) Human β-crystallin. I. Comparative studies on the β_1, β_2 and β_3-crystallins. *Exp. Eye Res.* **31**, 41–55.

Zigler, J. S., Horwitz, J. & Kinoshita, J. H. (1981) Studies on the low molecular weight proteins of human lens. *Exp. Eye Res.* **32**, 21–30.

Zigler, J. S. & Sidbury, J. B. (1973) Structure of calf lens β-crystallins. *Exp. Eye Res.* **16**, 207–214.

Zigler, J. S. & Sidbury, J. B. (1977) Studies on lens proteins from the smooth dogfish. Evidence for evolutionary conservation in vertebrate β-crystallin. *Ophthal. Res.*, **9**, 92–98.

Zigler, J. S. *et al.* (1985) Partial characterization of three distinct populations of human γ-crystallins. *Invest. Ophthal.* **26**, 525–531.

Zigman, J., Schultz, J. & Yuls, T. (1970) Isoelectric focusing of γ-crystallins. I. Characterization of rat lens components. *Biochim. Biophys. Acta* **221**, 576–582.

Zigman, S. & Lerman, S. (1965) Properties of a cold-precipitable protein fraction in the lens. *Exp. Eye Res.* **4**, 24–30.

Zigman, S. & Lerman, S. (1968) Effect of actinomycin D on rat lens protein synthesis. *Exp. Eye Res.* **7**, 556–560.

Zigman, S., Schultz, J. & Yuls, T. (1971) Isoelectric focusing of γ-crystallins. II. Aging variations in the rat lens. *Ophthal. Res.* **2**, 110–115.

Zintz, C. & Beebe, D. C. (1986) Morphological and cell volume changes in rat lens during the formation of radiation cataracts. *Exp. Eye Res.* **42**, 43–54.

Section 2

THE MECHANISM OF VISION

5. RETINAL STRUCTURE AND ORGANIZATION

In this section we shall be concerned with the peripheral mechanisms in the visual process. When light strikes the retina, physical and chemical changes are induced that lead eventually to a discharge of electrical impulses in the optic nerve fibres. The 'messages' in these nerve fibres are a record of the events taking place in the retina; because of the variety of sensations evoked by visual stimuli, these records must be of almost fantastic complexity when even a simple image is formed on the retina. The aim of investigators in this field of eye physiology is to disentangle the skein; their approaches are various but may be classed generally as psychophysical, chemical, and electrophysiological. Remarkable progress has been made, especially in recent years, but there is still a long way to go before anything approaching an exact picture of the retinal processes can be elaborated. The following description is designed more to show the modes of approach to the various problems than to present a theoretical picture of the 'mechanism of vision'.

STRUCTURE

Sensory Pathways

The retina is a complex nervous structure made up of a number of layers (Fig. 5.1) whose significance is best understood by recalling that in other parts of the body, for example the skin, the nervous elements involved in the transmission of sensory impulses to the cerebral cortex consist of:

1. a specialized arrangement of cells called a receptor-organ, e.g. a Pacinian corpuscle sensitive to pressure
2. a neurone connecting the receptor to the spinal cord and medulla (neurone I) with its cell body in the posterior root ganglion
3. a connector neurone to the thalamus (neurone II) with its cell body in the nucleus cuneatus or gracilis
4. a neurone to transmit the impulses to the cortex (neurone III) with its cell body in the thalamus.

With the vertebrate eye, not only are the specialized receptor cells, the *rods* and *cones*, in the retina, but also the cell bodies and connecting fibres of neurones I and II so that the nerve fibres leading out of the eye, which constitute the optic nerve, are the axons of neurone II, called the ganglion cell; the majority of the fibres run to the lateral geniculate body where the impulses, initiated in the rods and cones, are relayed to the occipital lobe of the cerebral cortex. The analogy between the two systems is demonstrated in Fig. 5.2.

The Retinal Layers

We may thus expect to differentiate in the retina a layer of receptors (*layer of rods and cones*), a layer of cell bodies of neurone I, the *bipolar cells* (*inner nuclear layer*) and a layer of cell bodies of neurone II, the *ganglion cells* (*ganglion layer*) (Fig. 5.1). The rods and cones are highly differentiated cells, and their orderly arrangement gives rise to a *bacillary layer*, consisting of their outer segments; an *outer nuclear layer* containing their cell bodies and nuclei; and an *outer plexiform layer* made up of their fibres and synapses with the bipolar cells. The region of synapse between bipolar and ganglion cells is the *inner plexiform layer*. Two other types of nerve cell are present in the retina, namely the *horizontal* and *amacrine* cells, with their bodies in the inner nuclear layer; the ramifications of their dendritic and axonal processes contribute to the outer and inner plexiform layers respectively; their largely horizontal organizations permits them to mediate connections between receptors, bipolars and ganglion cells. Besides the nerve cells there are numerous *neuroglial cells*, e.g. those giving rise to the radial fibres of Müller, which act as supporting and insulating structures.

The Rods and Cones

The photosensitive cells are, in the primate and most vertebrate retinae, of two kinds, called *rods* and *cones*, the rods being usually much thinner than the cones but both being built on the same general plan as illustrated in Fig. 5.3. The light-sensitive pigment is contained in the *outer segment*, *o*, which rests on the pigment epithelium; the other end is called the *synaptic body*, *s*, and it is through this that the effects of light on the receptor are transmitted to the bipolar or horizontal cell. In the rods

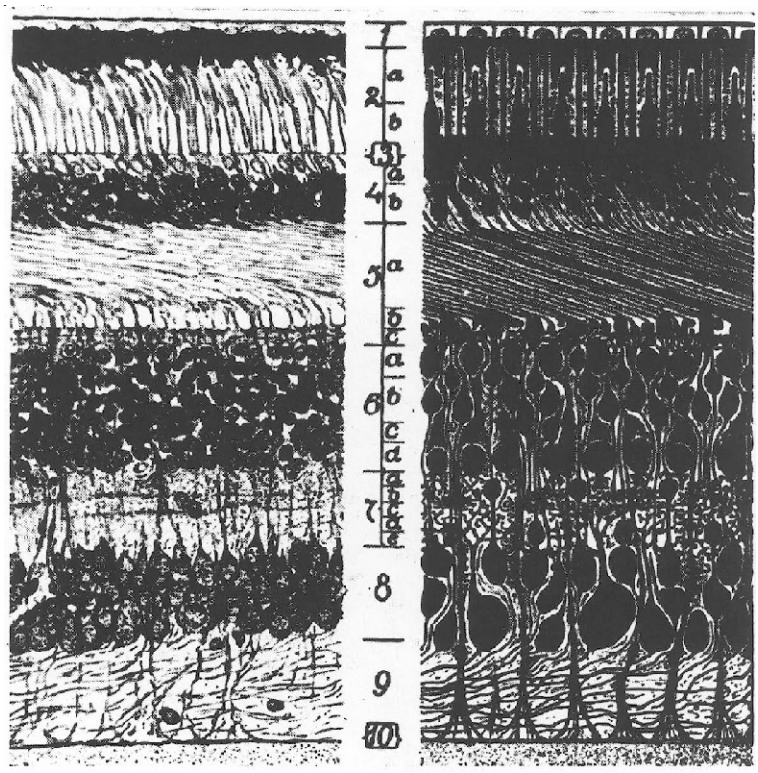

Fig. 5.1 Cross-section through the adult human retina in the periphery of the central area, showing details of stratification at a moderate magnification. The left-hand figure shows the structures as they appear when stained with a non-selective method (e.g. haematoxylin and eosin). The right-hand figure reproduces schematically the same view as it would appear from a study with an analytical method such as Golgi's or Ehrlich's, using many sections to get all details. (1) Pigment epithelium; (2) bacillary layer; (2-*a*) outer segments and (2-*b*) inner segments of the thinner rods and the thicker cones; (3) outer limiting membrane; (4) outer nuclear layer; (4-*a*) outer zone of the outer nuclear layer chiefly composed of the cone nuclei; (4-*b*) inner zone of the outer nuclear layer composed exclusively of the rod nuclei; (5) outer plexiform layer; (5-*a*) outer zone of the outer plexiform layer composed of the inner rod and cone fibres and of the corresponding portions of Müller's 'radial fibres' enveloping the first (here only one shown, beginning with the outer limiting membrane encasing the body and the fibre of a cone and continuing through ventral layers down to the inner limiting membrane); (5-*b*) middle zone of the outer plexiform layer composed of the rod spherules and cone pedicles; (5-*c*) inner zone of the outer plexiform layer made up of the expansions of the nerve cells and of Müller's supporting 'radial fibres' whose bodies and nuclei reside in the sixth layer; (6) inner nuclear layer with its four zones: 6-*a*, 6-*b*, 6-*c* and 6-*d*; (7) inner plexiform layer with its five zones: 7-*a*, 7-*b*, 7-*c*, 7-*d*, and 7-*e*; (8) layer of the ganglion cells; (9) layer of the optic nerve fibres; (10) inner limiting membrane, next to the vitreous. (Polyak, *The Retina.*)

this is called the *rod spherule*, and in the cone the *cone pedicle*. The human rod is some 2 μm thick and 60 μm long; the cones vary greatly in size and shape with their position in the retina, becoming long and thin and not easily distinguished from rods in the most central portion.

Organization of the Retina

Details of the synaptic relations between the various cellular elements of the retina, photoreceptors, bipolar, horizontal, ganglion and amacrine cells, will be con-

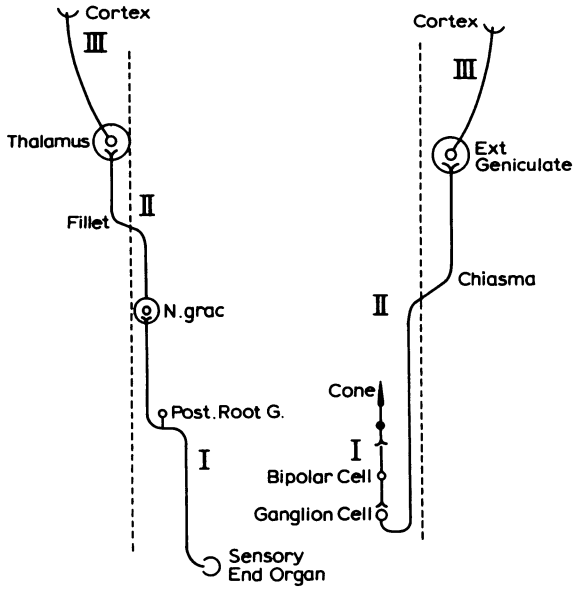

Fig. 5.2 Illustrating the analogy between a typical cutaneous afferent pathway and the visual pathway. Note the cone has not been treated as a neurone.

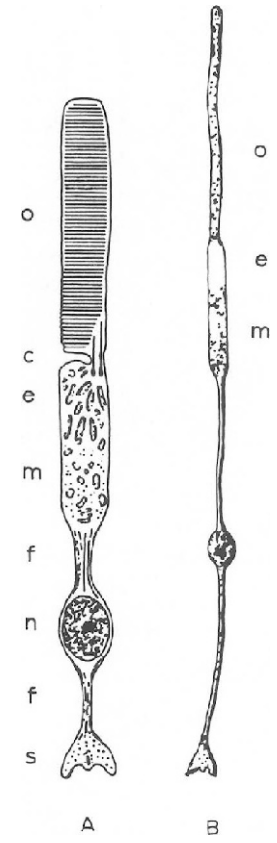

Fig. 5.3 Diagrammatic representation of retinal photoreceptor cells. A is a schematic drawing of a vertebrate photoreceptor, showing the compartmentation of organelles as revealed by the electron microscope. The following subdivisions of the cell may be distinguished: outer segment (*o*); connecting structure (*c*); ellipsoid (*e*) and myoid (*m*), which comprise the inner segment; fibre (*f*); nucleus (*n*); and synaptic body (*s*). The scleral (apical) end of the cell is at the top in this diagram. B depicts a photoreceptor cell (rod) from the rat. (Young, *J. Cell Biol.*)

sidered in some detail in a later chapter, and at present we shall confine attention to the basic principles of organization that permit the effects of the visual image, projected on to the photoreceptors, to be transmitted to higher centres of the brain.

Lateral Spread

The main organization of the retina is on a vertical basis, in the sense that activity in the rods and cones is transmitted to the bipolar cells and thence to the ganglion cells and out of the eye into higher neural centres—the lateral geniculate body, and so on. However, a given receptor may well activate many bipolar cells, and a single bipolar cell may activate many ganglion cells, so that the effect of a light-stimulus may spread horizontally as it moves vertically. The connections brought about by the horizontal and amacrine cells further increase the possibilities of horizontal spread and interaction, so that the problem of the analysis of the pathways of activity in the retina is highly complex, and only a beginning has so far been made in its solution.

Vertical Organization

The basic picture of a vertical retinal organization, as conceived by Polyak (1957), is illustrated by Fig. 5.4; according to this, the bipolar cells are of two main classes, namely *midget bipolars*, *h*, which connect only to a cone, and the diffuse type, which makes synaptic relations with several receptors, *d*, *e* and *f*. Similarly, the ganglion cells fall into two classes, the *midget ganglion cell*, connecting only with a single midget bipolar cell, and the diffuse type connecting with groups of bipolar cells. On this basis, then, convergence of receptors on ganglion cells would be largely achieved by the diffuse types of bipolar and ganglion cells, whilst a virtual one-to-one relationship would exist between those cones that made a connection with a midget bipolar cell. As the figure indicates, however, this relationship is not strictly one-for-one, since a cone, connected to a midget bipolar, also connects with a

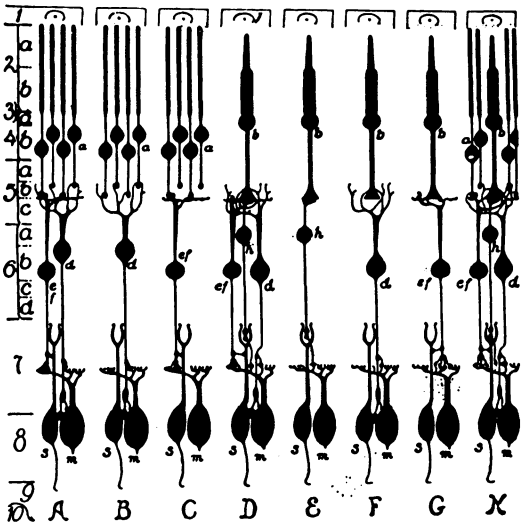

Fig. 5.4 Some of the types of receptor-bipolar synapses in the retina. *a*, rod; *b*, cone; *d*, *e*, *f*, bipolars that make several synaptic relationships with receptors; *h*, midget bipolar; *s*, midget ganglion cell; *m*, parasol ganglion cell (used here to typify the type that makes several synaptic relationships with bipolars). (Polyak, *The Retina.*)

diffuse type of bipolar, and so its effects may spread laterally.

More Modern Picture

More recent studies on the primate retina, notably that of Boycott & Dowling (1969), have largely confirmed Polyak's view, and have corrected some errors. We shall defer the detailed description of their work, but we may present here their illustration of the organization of the retina (Fig. 5.5), since it includes the horizontal and amacrine cells, which contribute to the lateral spread of input from the photoreceptors. Thus the dendritic processes of horizontal cells in the outer plexiform layer make contacts with the photoreceptors and bipolar cells, in a synaptic arrangement called the *triad* illustrated schematically by Fig. 5.6 so that the output from the photoreceptor can be transmitted sideways to the horizontal cells as well as forwards to the bipolar cell.

The forward transmission from bipolar cells occurs through the inner plexiform layer, where synapses are made with ganglion and amacrine cells, the latter behaving similarly to horizontal cells in transmitting sideways, spreading the bipolar input to many ganglion cells, but also concentrating the effects of many bipolar cells on to a single ganglion cell, giving rise to the centre-surround relationship that is such a characteristic feature of the responses of the ganglion cells to a spot of light.

The Retinal Zones

The retina is divided morphologically into two main zones, the *central area* (containing Regions I–III) and the *extra-areal periphery* (containing Regions IV–VII).

Fovea

Region I, the *central fovea* (Fig. 5.7), is a small depression, shaped like a shallow bowl with a concave floor, on the vitreal face of the retina, caused by the bending away of layers 5 to 9 and a thickening of the bacillary and outer nuclear layers. From edge to edge it is some 1500 μm across in man and thus subtends about 5° at the nodal point of the eye; the floor of the fovea is about 400 μm across. The fovea, described in this way, is generally referred to as the *inner fovea*, the word 'inner' being used to denote the aspect from which the depression is regarded; the *outer fovea*, some 400 μm across, represents a depression in the opposite sense, i.e. a cupping of the outer limiting membrane from outwards inwards (Fig. 5.7), and corresponds roughly in extent to the floor of the inner fovea; it is caused by the lengthening of the cones in the bacillary layer, the cone proper increasing in length more than the remaining portion. The outer fovea is thus the central portion of the inner fovea; here the receptor elements consist entirely of cones which, as we have seen, are longer and thinner than elsewhere in the retina, being some 70 μm long and 1.5 μm thick at the base and 1 μm thick at the tip. The '*rod-free territory*' is actually rather greater in extent than the outer fovea, being some 500 to 600 μm across and containing some 34 000 cones. Beyond this limit rods appear and their proportion to cones increases progressively. The total number of cones in the territory of the inner fovea amounts to 115 000. As we shall see, the most central, rod-free, portion of the retina is concerned with the highest degree of visual acuity since it is here that the obstruction to light caused by the nerve fibres and other layers is reduced to a minimum and the density of receptors is highest; vision mediated by this portion of the retina is thus spoken of as 'foveal vision'; it must be emphasized, however, that the fovea proper embraces both this zone and the walls of the inner fovea where obstructions to the passage of light are not removed, where the cone density is considerably less, and where rods are present, so that it is inaccurate to speak of foveal vision when what is meant is vision mediated by the rod-free area or perhaps even a more restricted central zone (the 'central bouquet of cones', for example, some 50 to 75 μm across).

Macula

Mention may be made here of the *yellow spot* or *macula lutea*; this is an ill-defined area of the central retina

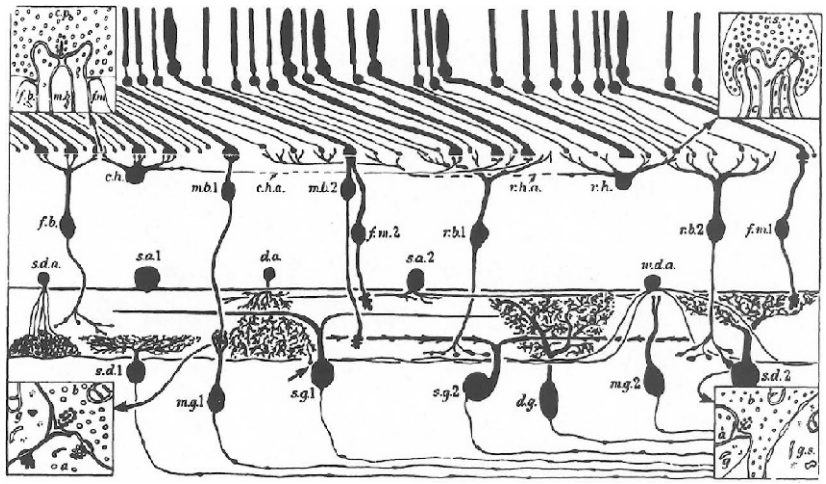

Fig. 5.5 The main kinds of nerve cell identified in the primate retina. *Inset, top left* shows how the cones (c.p.) contact their nerve cells. The *inset, top right* shows how nerve cell processes invaginate into a rod spherule (r.s.). The *inset, lower left* represents a dyad in which a bipolar cell *b* is presynaptic to a ganglion cell dendrite *g* and an amacrine cell process *a*. The amacrine cell process has a reciprocal contact back on to the bipolar terminal and an amacrine to ganglion cell dendrite synapse. The *inset, lower right* shows that the rod bipolar cell axosomatic contacts may consist of 'close contacts' on to the ganglion cell perikaryon (g.s.) (though which types of ganglion cell is unknown). This inset also shows that these same bipolar terminals have dyad contacts. *c.h.* and *r.g.* are horizontal cells considered to connect cones and rods to each other respectively; more recent work shows that horizontal cells only connect cones to rods, however; *f.b.*, flat bipolar making contact with several cones; *m.b.*1 and *m.b.*2 are midget bipolars; *f.m.*1 and *f.m.*2 are flat midget bipolars, making contact with only the base of the cone pedicle by contrast with the *m.b.*s which invaginate into the triad. *r.b.*1 and *r.b.*2 are rod bipolars whose dendrites make the central elements of the rod spherule. (*Upper right inset*). *s.a.*1 and *s.a.*2 are unistratified amacrine cells whose processes ramify immediately under the inner nuclear layer, *d.a.* and *s.d.a.* are amacrine cells with branches extending much deeper; *d.a.* may be seen making an axo-somatic contact with the ganglion cell *s.g.*1. *w.d.a.* indicates a wide-field diffuse amacrine cell, with little or no ramification of the main branches as they run to the ganglion cell perikarya. Midget ganglion cells, *m.g.*1 and *m.g.*2 have a single dendrite branching at its tip to embrace the terminal of a midget bipolar cell. *s.g.*1 and *s.g.*2 are unistratified ganglion cells, the dendrites branching in a single plane, while the diffuse ganglion cell, *d.g.* has dendrites branching in planes throughout the inner plexiform layer. *s.d.*1 and *s.d.*2 are stratified diffuse ganglion cells corresponding to Polyak's 'parasol ganglion cell'. (Boycott & Dowling, *Phil. Trans.*)

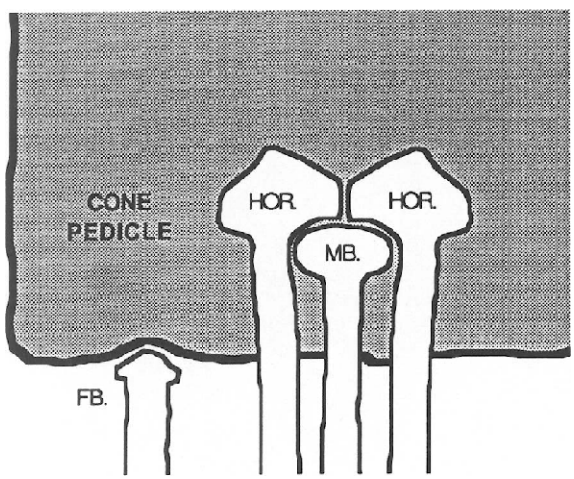

Fig. 5.6 The triad. Dendritic terminals of two horizontal cells (HOR) and one midget bipolar (MB) invaginate into a cone pedicle. A contact-type of synapse is made by a flat bipolar (FB).

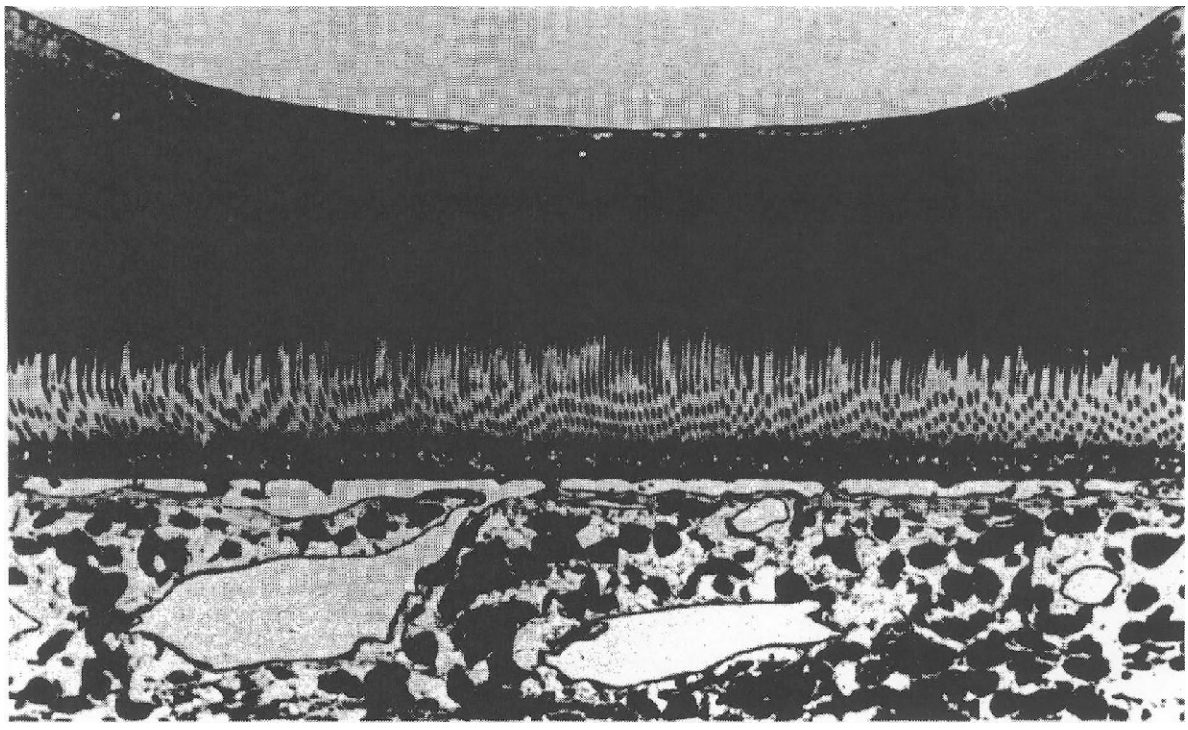

Fig. 5.7 Transverse section through the primate fovea. Note in the central region, the absence of ganglion cell layer, inner nuclear layer and retinal capillaries, the thickening of the outer nuclear layer and the long slender cones (G.A./OsO_4 fixed, toluidine blue stained × 285). (Courtesy of R. C. Tripathi.)

characterized by the presence of a yellow pigment in the nervous layers; in actuality the region extends over the whole of the central area (Regions I–III) but the intensely pigmented part is limited to the fovea (Region I); the central portion of the fovea (outer fovea) is only slightly pigmented in man, since the pigment is associated with layers beyond number 4 which, as we have seen, are very much reduced or absent here.

Parafovea and Perifovea

Regions II and III are the *parafoveal* and *perifoveal* regions respectively, the outer edge of the former being 1250 μm from the centre of the fovea and that of the latter 2750 μm from the centre, the diameter of the entire central area being thus about 5000 to 6000 μm. The cone density is considerably diminished in these regions whilst that of the rods is increased, so that in Region III there are only some twelve cones per 100 μm (compared with some fifty per 100 μm in the outer fovea) with two rods between each pair of cones. The *extra-areal periphery* (Regions IV to VII) is associated with a further decrease in the density of cones and an increase in the proportion of rods. In the whole human retina there are said to be about 7 million cones and 75 to 150 million rods.

References

Boycott, B. B. & Dowling, J. E. (1969) Organization of the primate retina: light microscopy. *Phil. Trans. Roy. Soc.* **B225**, 109–184.

Polyak, S. L. (1957) *The Vertebrate Visual System.* Chicago: University Press.

Young, R. W. (1967) The renewal of receptor cell outer segments. *J. Cell Biol.* **33**, 61–72.

6. MEASUREMENT OF THE STIMULUS AND DIOPTRICS OF THE HUMAN EYE

PHOTOMETRY

Visible Light

Visible light consists of electromagnetic vibrations limited to a certain band of wavelengths—the *visible spectrum*. The limits are given classically as 400 nm and 760 nm, wavelengths shorter than 400 nm being described as ultraviolet, and longer than 760 nm as infrared.[1] As we shall see, however, the retina is sensitive to wavelengths shorter and longer than these limits. Light is a form of energy and, as such, is amenable to quantitative measurement in absolute units, namely ergs. For physiological purposes, however, that subjective quality of light we call 'brightness' or 'luminosity' is the one that is of greatest interest, and since this is not uniquely determined by the energy content of the light, but varies widely with the wavelength (p. 395), it has been considered desirable to base measurements of light on a somewhat arbitrary 'luminosity basis'. Thus, on a luminosity basis, two sources of light are said to be of equal intensity when they produce equal sensations of brightness when viewed by the same observer under identical conditions.

Luminous Intensity

The luminous intensity (I) of a source of light is measured in terms of an arbitrarily chosen standard source of light-energy. Classically, this was a sperm-wax candle made to burn at a certain rate, and it gave rise to the term *candle-power*, a source of light appearing x times as bright as the standard candle having x candlepower. The modern *candela* (abbreviated cd) is fixed in terms of a standard filament lamp. It is such that one square centimetre of the surface of a full radiator at the temperature of solidification of platinum has a luminous intensity of 60 cd in the direction normal to the surface. In effect it has about the same value as the classical candle.

If two sources of light illuminate a screen under identical conditions, to produce identical degrees of illumination they are said to be of equal intensity. An observer may easily determine whether two identical screens, side by side, are equally illuminated; if they are not equally illuminated (i.e. if one appears brighter than the other) he is unable to state exactly how much more intensely illuminated one is than the other, so that in comparing intensities of illumination recourse is had to the photometer, one type of which utilizes as its basis the law that the intensity of illumination of a screen, placed normal to the rays from a point source of light, varies inversely as the square of its distance from the source. Thus, if we have two sources of light, of intensities I_1 and I_2 and at distances r_1 and r_2 from a screen such that they illuminate it equally, we can say:

$$I_1/I_2 = r_2^2/r_1^2.$$

Hence, if one of the light sources (I_2) is the standard candle, the intensity of the other is given by:

$$I_1 = r_2^2/r_1^2 \text{ candelas.}$$

Intensity of Illumination

In introducing the measurement of the intensity of a light source, we have mentioned the *degree of illumination*; this is, of course, determined entirely by the amount of light falling on a surface and hence by the intensity of the light source, the distance of this source from the object, and the angle the surface makes with the direction of the incident light. Thus, if we have a screen perpendicular to the direction of the light incident from a point source of intensity I, we may define the *intensity of illumination*, E, by the equation:

$E = I/r^2$, where r is the distance from the source.

When I equals unity, i.e. one candela, and r equals 1 foot, E is unity and is called 1 *foot-candela*. If r is expressed in metres, the unit of illumination is the *metre-candela* or *lux*; expressed in words, it is the illumination of a surface, normal to the incident rays from a source of 1 candela one metre away. The *centimetre-candela* is called a *phot*. If a surface, normal to the incident rays from a source, has an illumination E, its illumination when the surface is inclined at an angle θ to the rays is given by $E \cos\theta$.

Luminance

The illumination of the surface does not necessarily define its intensity of a stimulus, since the latter depends on the light entering the eye and so is determined by the light reflected from the surface and the direction of view. If, however, we imagine a white surface that reflects all the light it receives and is, moreover, a 'perfect diffuser' in the sense that it appears equally bright from all directions, then the *luminance* of a surface may be defined in terms of its illumination from a standard source. Thus, on the so-called *Lambert system*, a perfectly diffusing surface, normal to the incident light from a source of 1 candela 1 centimetre away, has a luminance of 1 *lambert*. This unit is too large for most purposes and the *millilambert* (mL) represents a thousandth of a lambert; for studies of light thresholds (p. 219) the log micro-microlambert scale is often used. A luminance of 3 log micro-microlamberts means a luminance of $10^3 \times 10^{-12} = 10^{-9}$ lamberts or a millionth of a millilambert; 2 log micro-microlamberts are equivalent to $10^2 \times 10^{-12} = 10^{-10}$ lamberts, and so on. The *equivalent foot-candela*, or *foot-lambert*, is the luminance of a similar screen distant 1 foot from the source.

Surface Intensity

This mode of defining the luminance of a surface in terms of the light incident on it is limited by the ideal nature of a perfectly diffusing surface; a definition that does not involve this would be superior from many points of view. Such a definition is given by describing the luminance in terms of the light emitted by the surface, i.e. we can treat the surface as a luminous source, whether it is self-luminous as in the case of a hot body, or whether its luminosity depends on reflected light. Thus if 1 square foot of a surface emits the same amount of light in a given direction as a source of 10 candelas, for instance, we may define the *luminous intensity of the surface* as 10 candelas; the subjective brightness of the surface and hence its intensity as a stimulus will clearly depend on the area from which this light emanates; if it all comes from a small area the brightness will be greater than if it came from a large area. The luminance is thus defined in terms of the candlepower of the surface per unit area, e.g. candelas per square foot or candelas per square centimetre. We may then calculate the luminance, in candelas per square foot, of a perfectly diffusing surface illuminated by a source of 1 candela at a distance of 1 foot; this turns out to be $1/\pi$ candelas per square foot, i.e. $1/\pi$ *candelas per square foot* = 1 *equivalent foot-candela*. Similarly $1/\pi$ candelas per square centimetre = 1 lambert.

Effectively Point Source

The definition of the luminance of a surface in terms of its candlepower *per unit area* has an obvious physiological basis. By the luminance of a surface we wish to express in a quantitative manner the intensity of the stimulus when its image falls on the retina. An illuminated surface of given area forms an image of a definite area on the retina and the sensation of brightness, or rather the stimulus, depends on the amount of light falling on this area of the retina. If the surface is moved closer to the eye, the amount of light entering the eye is increased in accordance with the inverse square law, but the surface does not appear brighter because the size of the image has increased, also in accordance with an inverse square law, and consequently the actual *illumination* of the retina has not altered. Thus the subjective brightness of an extended source is independent of its distance from the observer. It may be argued that the brightness of a lamp decreases as it is moved away from the eye and eventually becomes so faint that it disappears if it is moved far enough away. This, however, is a consequence of the fact that at a certain distance from the eye the lamp becomes an 'effectively point source', i.e. its image on the retina is of the same order of size as that of a receptor element; consequently, when it is moved further away still, although its image on the retina becomes smaller, the amount of light per receptor element now begins to fall in accordance with the inverse square law. Thus the definition of luminance in terms of candles per unit area of necessity implies that the surface has a finite area; when this surface becomes effectively a point from the aspect of the size of its image on the retina, its power of stimulating the retina will be determined only by its total luminous intensity, i.e. its candlepower, and its distance from the observer. The limiting angle, subtended by an object at the eye, below which it behaves as an effectively point source depends on the particular visual effect being studied and the conditions of observation; for the study of absolute thresholds in the dark it is as big as 30 to 60 minutes of arc.

Retinal Illumination

We have indicated that the characterization of the luminance of an extended surface by its candlepower per unit area is a sound one physiologically in so far as it indicates the illumination of the retina; the retinal illumination is not, however, completely defined by the candlepower per unit area of the surface being viewed, since the amount of light falling on unit area of the retina depends also on the pupil size; thus from Fig. 6.1 it is clear that the pencils of light that form the image of AB on the retina are larger in the case of the larger pupil. Hence the stimulus required

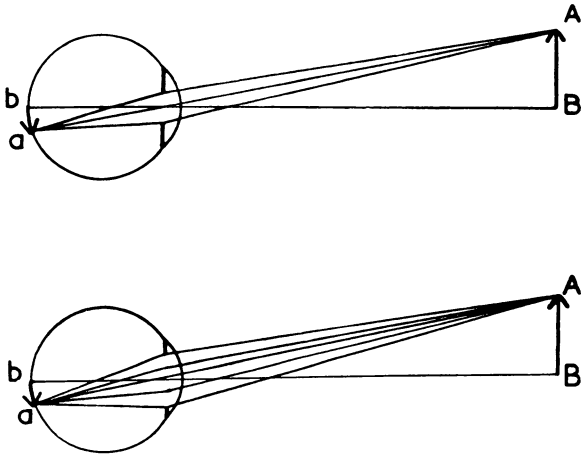

Fig. 6.1 Illustrating the importance of the size of the pupil in defining the stimulus. *Above*: The pupil is small and only a thin pencil of light from A enters the eye. *Below*: The pupil is large, permitting a large pencil to enter the eye. AB = object, ab = image.

to produce a definite sensation in the eye must be defined in terms of both the luminance, in candles per unit area, and pupillary area. The unit of retinal illumination suggested by Troland[2] and now given his name is defined by the statement: A troland is that intensity of stimulation that accompanies the use of a pupillary area of one square millimetre and an external stimulus surface luminance of one candela per square metre. It is to be noted that although the troland is referred to as a unit of 'retinal illumination,' it is not truly so, but is rather an indication of this quantity that is independent of the size of the observer's pupil. To define a stimulus in terms of true retinal illumination we must know the magnification and transmission of the optical media of the eye. On the basis of a value of 16.7 mm for the distance of the nodal point from the retina, the true retinal illumination is given by:

$$D = 0.36\tau_\lambda sB$$

where B is the luminance of the extended source of light, s is the area of the pupil in cm^2 and τ_λ is the *transmission factor*, being the ratio of the intensities of light falling on the retina over the light falling on the cornea. This depends on wavelength, varying from 0.1 in the extreme violet where absorption by the yellow pigment of the lens is important, to 0.7 in the deep red; on average with white light it is about 0.5 indicating 50% loss of light (Ludvigh & McCarthy, 1938).

When the stimulus in question is due to an effectively point source the pupillary area is of course important, and the stimulus is defined by the candlepower of the source, its distance from the eye and the pupillary area, i.e. by the total light flux entering the eye, which is given by the illumination of the pupil multiplied by its area.[3]

In view of the importance of the adequate definition of the stimuli used in experimental studies of vision, it is worth recapitulating the substance of the last few paragraphs. The luminance of an extended source is defined as its candlepower per unit area; its value as a stimulus is independent of its area and of its distance from the observer. For a given pupillary area it is an indication of the retinal illumination; the troland is a measure of retinal illumination which is independent of the observer's pupillary area; the true retinal illumination may be derived from the troland if the magnification and transmission characteristics of the eye are known. If the stimulus is due to an effectively point source, it is sufficient to characterize it by the total light flux entering the eye.

Light Flux

Lumen

For the sake of simplicity, we have so far made our definitions without introducing the concept of *light flux*; this is defined as the amount of visible light energy passing any plane in unit time; its relationship to the luminous intensity of a point source will be clear from the following.

Suppose we have a point source of light of I candlepower; let us imagine the point to be the centre of a sphere of radius r (Fig. 6.2). The light energy from a point source travels in all directions uniformly through space, and we may think of the sphere being occupied by energy passing through it at a definite rate. The flux, considered thus, is defined in relation to the unit of luminous intensity by saying that 4π times the candlepower is the flux emitted by the source, expressed in *lumens*:

$$4\pi \times I(\text{candelas}) = \text{flux(lumens)}$$

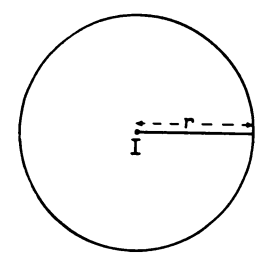

Fig. 6.2 A source of I candlepower at the centre of a sphere of radius r. $4\pi I$ lumens are emitted per second and spread over a surface of $4\pi r^2$; the flux density is I/r^2.

E, the intensity of illumination of the inner surface of the sphere, as defined before, is:

$$E = I/r^2$$
$$= 4\pi I/4\pi r^2.$$

Now $4\pi I$ represents the number of lumens of flux falling on the surface of the sphere, and $4\pi r^2$ is the area of its surface. Hence E may be expressed as the ratio of the flux emitted by the source of light over the area on which it falls: flux per unit area, or *flux density*. The units of illumination may therefore be, besides the foot- or metre-candela, a lumen per square foot or a lumen per square metre. Thus:

1 foot-candela = 1 lumen/sq ft
1 metre-candela = 1 lumen/sq m

In Table 6.1 the illuminations recommended for different tasks are shown; in Table 6.2 some luminance levels commonly encountered are presented, and in Tables 6.3 and 6.4 some conversion factors for different units of illumination and luminance.

Table 6.1 Some recommended illuminations

	foot-candela
General stores	2–4
Classroom	5–10
Billiard table	20
Type-setting	35–50
Operating table	100

Table 6.2 Some commonly encountered luminances

	candela/sq. ft
Starlit sky	0.00005
Moonlit sky	0.002
Full moonlight on snow	0.007
Ploughed land at noon in average daylight	130
Clear sky at noon	1 000
Sun's disk	150 000 000

Photopic and Scotopic Lumens

The lumen is an arbitrary unit of power, based on the candela; it may be converted into absolute units on the basis of the light-energy emitted by the standard source of light; if this is the standard black body of absolute temperature $T = 2042°K$, then the conversion factor is 679.6 lumens per watt. It must be appreciated that the lumen is a unit in whose measurement the human eye is involved, so that the spectral sensitivity curve of the human eye must be taken into account, the luminance of the standard source being governed by the subjective luminances of the gamut of wavelengths of which the source is made up.

This is because the concept of the lumen as a unit of stimulus has been extended to cover any source of light; for example we may have a lumen of violet light in a narrow wavelength band close to 420 nm and a lumen of green light in a narrow wavelength band centred on 530 nm. If the two lumens are to be equal from the point of view of their subjective effects it is not correct for their flux-energies, in absolute units, to be equal; if they were, they would not match in the human eye, the green lumen being considerably brighter than the violet lumen; to be the same, we must know the relative sensitivities of the eye for the different wavelengths, i.e. we must have the *photopic luminosity curve* (Fig. 6.3) for a 'standard observer' and adjust the energy equivalents of the lumen in the different bands of the spectrum. Thus the conversion factor for the lumen, based on the standard white source, is 679.6 lumens per watt of energy-flux, and is the sum of the contributions of all the wavelengths contributing to stimulate the 'standard human eye', weighted according to their contributions to subjective brightness. This is called a *photopic lumen* because the relative brightness scale is based on a high level of illumination. A *scotopic lumen* would be different because the relative sensitivities of the eye to different wavelengths are different when viewing very weak lights (p. 239), and the *scotopic luminosity curve* (Fig. 6.3) must be used for assessing the contributions to the standard source of white light. The conversion factor for the *scotopic lumen* is 1745 lumen per watt. In effect this means that the standard source would appear equally bright to two eyes, the one with relative sensitivities to the different wavelengths governed by the photopic luminosity curve, and the other by the scotopic

Table 6.3 Conversion factors. Illumination. (Value in unit in left-hand column times conversion factor = value in unit at top of column; e.g. 3 foot-candela = $3 \times 1.08 \times 10 = 32.4$ metre-candela.)

	Foot-candela	*Centimetre-candela*	*Metre-candela*
Foot-candela	1	1.08×10^{-3}	1.08×10
Cm-candela (Phot)	9.29×10^{2}	1	1×10^{4}
Metre-candela (Lux)	9.29×10^{-2}	10^{-4}	1

Table 6.4 Conversion factors. Luminance. (Value in unit in left-hand column times conversion factor = value in unit at top of column.)

	Candela/ft²	*Equiv. fc.*	*Candela/cm²*	*Millilambert*
Candela/ft²	1	3.14	1.08×10^{-3}	3.38
Equiv. fc.	3.18×10^{-1}	1	3.43×10^{-4}	1.076
Candela/cm²	9.3×10^{2}	2.92×10^{3}	1	3.14×10^{3}
Millilambert	2.96×10^{-1}	9.29×10^{-1}	3.18×10^{-4}	1

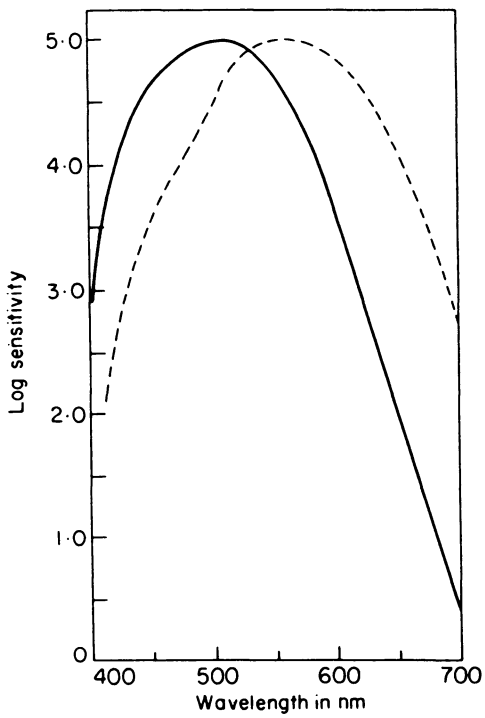

Fig. 6.3 Internationally standardized spectral sensitivity curves for the dark (——) and light (- - -) adapted eye respectively. The curves were recognized as standard in 1951 and 1931 respectively. (Ripps & Weale, *The Eye.*)

luminosity curve, provided the energy fluxes from the light source were in the proportion of 1745:679.6. For convenience the two luminosity curves, whose significance will be discussed later (p. 327), are presented here. Tables 6.3 and 6.4 provide useful conversion factors for units of illumination and luminance.

DIOPTRICS

Refracting Surfaces

The basic dioptrics of the eye have often been likened to those of a simple convex lens, and this is true to the extent that the formation of an image of external objects can be approximately described by drawing rays from a point on the object through a 'centre' and another parallel to the optic axis which passes through a 'focus'. In fact, of course, refraction by the eye is the result of bending light at several surfaces, in particular as it passes from air to the cornea, from aqueous humour to lens, and from lens to vitreous body, since it is at these surfaces that significant changes of refractive index take place.

Schematic Eye

A system of several refracting surfaces, sharing a common axis, can be analysed by the Gaussian treatment, which gives two *principal planes*, two *nodal points*, and two *principal foci*; and the result is described as the *schematic eye* based on measurements of the curvatures of the surfaces (cornea, lens) refractive indices and positions of the surfaces (Fig. 6.4).

Reduced Eye

Since the principal planes and nodal points of the human eye are quite close to each other, a mean position for each is taken, to give a single principal plane 1.5 mm behind the anterior surface of the cornea, and a single nodal point, 7.2 mm behind the anterior surface of the cornea. This gives the *'reduced eye'* of Fig. 6.5, with an anterior focal length of 17.2 mm, measured from the single principal plane, and a posterior focal length of 22.9 mm, measured from the same plane. In the 'emmetropic' eye the pole of the retina coincides with the second principal focus, F_p.

Image Construction

On the basis of this reduced eye, image-formation may be carried out by the usual constructions, the undeviated ray of a pencil passing undeviated through the single nodal point, and parallel rays converging to the second focal plane, or retina (Fig. 6.6).

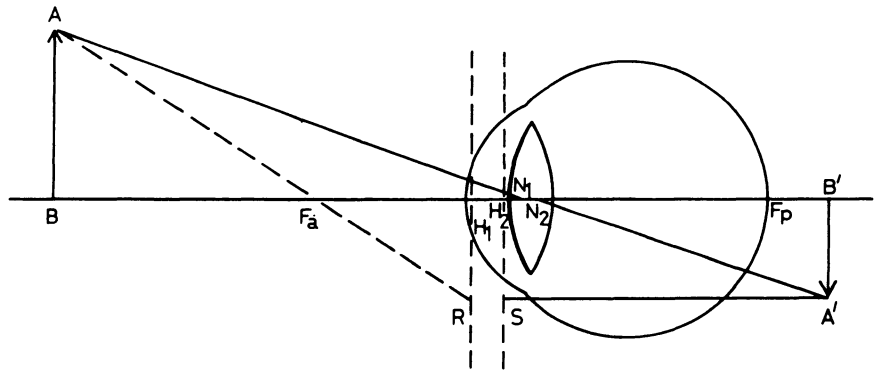

Fig. 6.4 The schematic eye. F_a and F_p are the principal foci; N_1 and N_2 the nodal points, and H_1 and H_2 are the principal planes. A ray from A strikes the first principal plane at R and leaves the second principal plane at S.

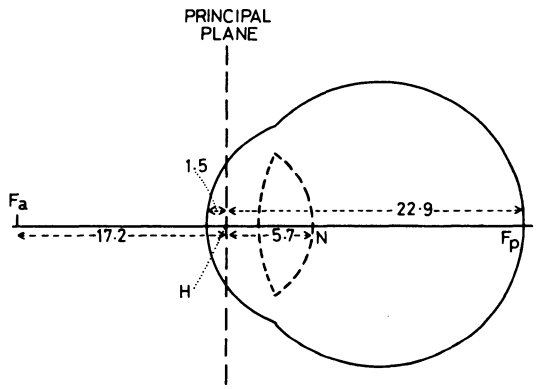

Fig. 6.5 The reduced eye. F_a and F_p = anterior and posterior principal foci respectively. N = nodal point. The optic axis intersects the principal plane at H.

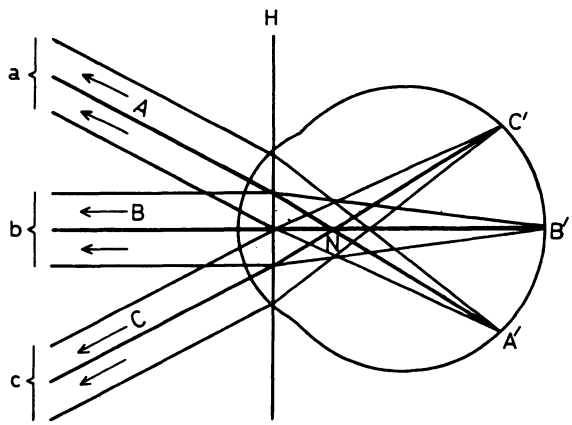

Fig. 6.6 The image of a distant object, ABC, forms an image on the retina, A′B′C′ of the emmetropic eye. H = principal plane. N = nodal point. a, b and c = pencils of light from A, B and C respectively.

ACCOMMODATION

When the object is closer than infinity, the usual image-construction leads to the formation of the image behind the retina (Fig. 6.7), and this means that the reduced eye of Fig. 6.5 is based on the dioptric characteristics of an eye 'focussed for infinity', or 'unaccommodated'. Focussing the image of distant objects on the retina clearly requires a shortening of the focal length, so that the posterior focus moves to F'_p, i.e. it requires an increase in dioptric power of the system. The mechanism of this accommodation will be described in Section 4.

Hypermetropia and Myopia

Failure of the second or posterior focus to coincide with the pole of the retina leads to a blurring of the image of distant points; in myopia (Fig. 6.8) the focal length is too short and in hypermetropia it is too long. The myopic eye is said to be too powerful for its axial length, and this may be due to a more-than-average curvature of the refracting surfaces, or to a longer-than-average axis; and the opposite conditions describe the hypermetropic eye.

Far Point

The myopic eye can focus images of near objects distinctly on the retina, and a *far point* or *Punctum Remotum* is defined as that position on the optic axis that allows the formation of a distinct image on the retina of the unaccommodated eye (Fig. 6.9a). The myopia can be corrected by reducing the vergence of rays reaching the cornea by interposing a diverging lens, as in Fig. 6.9b; now rays from infinity are made to diverge before reaching the cornea, and if they diverge from the Far Point they will come to a focus on the retina of the relaxed, unaccommodated eye.

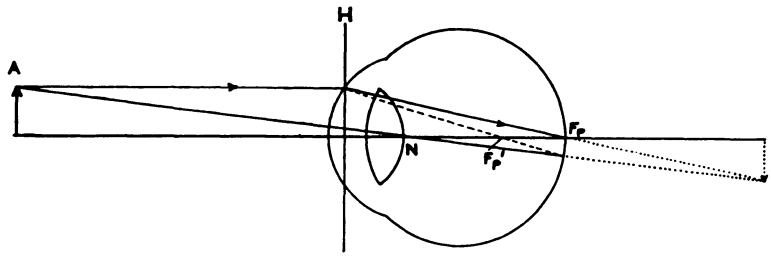

Fig. 6.7 With an object not 'infinitely far away' the image would fall in a plane behind the retina. H = principal plane. N = nodal point. F_p = posterior principal focus in relaxed eye. F_p' is that for the accommodated eye.

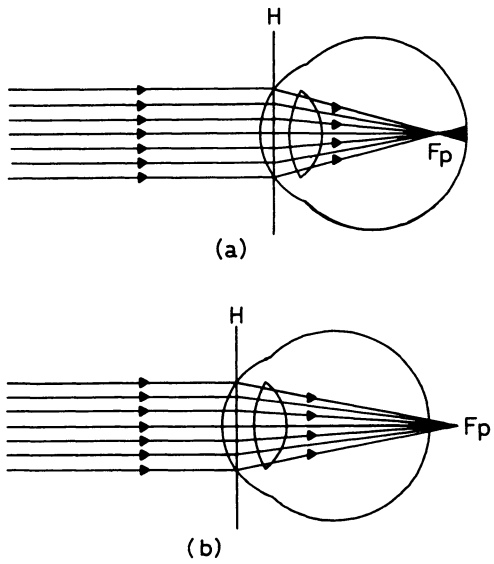

Fig. 6.8 Blurring of the image of a distant point due to myopia (a) and hypermetropia (b). H = principal plane. F_p = posterior principal focus.

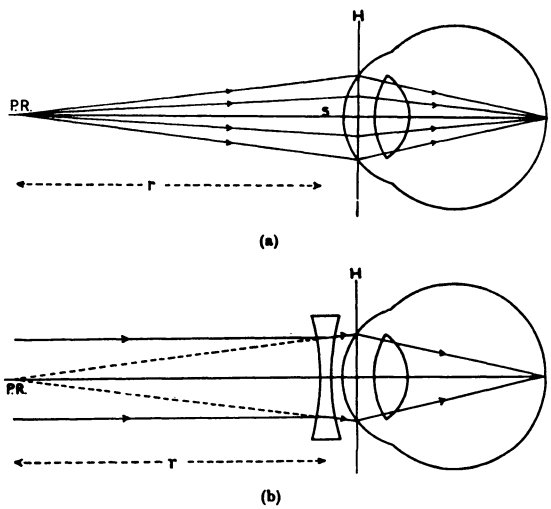

Fig. 6.9 (a) The Far Point in myopia is the point in front of the eye at which an object must be placed for its image to fall on the retina. (b) Correction of myopia by placing a concave lens in front of the eye such that rays from a distant object will diverge from the Far Point. r = the focal length of the lens placed in front of the eye to achieve the necessary correction. PR = Punctum remotum or Far Point. H = principal plane. S = spectacle point.

Hypermetropia

The hypermetropic eye requires an increase in power, which is provided by a converging lens (Fig. 6.10). The hypermetropic subject can, of course, increase the dioptric power of the eye by accommodation, so that it is usually only in middle age, when accommodative power has been reduced or lost entirely, that correction for distant vision becomes necessary.

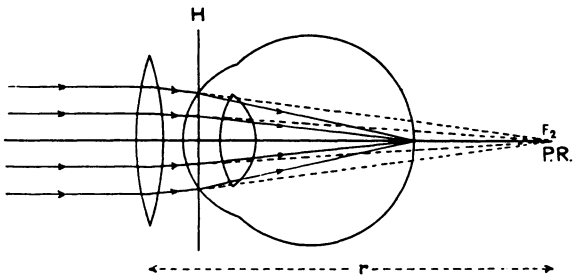

Fig. 6.10 The Far Point (P.R.) in hypermetropia is a point behind the retina to which rays from a distant object must converge in order that the image may fall on the retina. H = principal plane. F_2 = second principal focus of the convex lens which coincides with the Far Point. r = focal length of the convex lens.

Notes

1. The units employed in the earlier literature to define wavelengths were the Ångström Unit (Å), equal to 10^{-8} cm or 10^{-10} m, and the 'millimu' (mμ) equal to 10^{-7} cm or 10^{-9} m. The modern unit is the *nanometre*, equal to 10^{-9} m. Thus 7600 Å = 760 mμ = 760 nm.
2. This unit of retinal illumination was originally called the *photon*, a term that had already been applied to the quantum of light energy. We may note that, in order to convert the luminance of an extended surface, expressed in millilamberts, to trolands of 'retinal illumination', it must be multiplied by $5d^2/2$, where d is the pupillary diameter in millimetres. Because of the different sensitivities of the eye to the different wavelengths, according as it is light- or dark-adapted (p. 264), the equivalent stimuli for white light are not the same under photopic and scotopic conditions, so that we must speak of a *photopic* and *scotopic* troland; the theory behind the estimation of the conversion factor (1 scotopic lumen = 1.4 photopic lumens at a colour-temperature of 2750°C) has been discussed by Schneider & Baumgardt (1966). In terms of energy flux, a scotopic troland is equivalent to 4.46 quanta at 507 nm per square degree of visual field per second, incident on the eye.
3. Stiles & Crawford (p. 423) have shown that pencils of light entering the eye obliquely are less effective as stimuli than those entering the pupil centrally; this effect is not due to aberrations in the optical system but is most likely related to the orientation of the receptors in the retina. A correct definition of the stimulus must therefore take into account the directions of the pencils of light entering the eye.

References

Ludvigh, E. & McCarthy, E. F. (1938) Absorption of visible light by the refractive media of the human eye. *Arch. Ophthal., Chicago* **20**, 37–51.

Schneider, H. & Baumgardt, E. (1966) Sur l'emploi en optique physiologique des grandeurs scotopiques. *Vision Res.* **7**, 59–63.

Walsh, J. W. T. (1953) *Photometry*. London: Constable.

7. SOME GENERAL ASPECTS OF VISION

Photochemical Reaction

The mechanism by which the energy contained in visible light is transmitted to the nervous tissue of the retina in such a way as to produce that change in its structure which we call a stimulus is a fascinating problem and one that lends itself to physicochemical study. There is a group of chemical reactions that derive a part, or all, of their energy from absorbed light—the *photochemical reactions*—a biological instance of this type of reaction is the synthesis of carbohydrate by the green leaves of plants, the pigment chlorophyll absorbing light and transmitting the energy to the chemical reactants. It is thus reasonable to inquire whether there is an analogous chemical reaction at the basis of the response of the retina to light, i.e. whether or not there are substances in the retina that can absorb visible light and, as a consequence of this absorption of energy, can modify the fundamental structure of the rod or cone to initiate a propagated impulse. One such substance, visual purple, was discovered in the retina as long ago as 1851 by H. Müller, but we owe the early knowledge of its function as an absorber of light to the researches of Kühne, described in his classical monograph of 1878. He was the first to obtain this pigment in solution by extracting the retina and he called it '*Sehpurpur*', which has been translated as *visual purple*. As we shall see, thanks to the studies of Dartnall and Wald, the term visual purple must now be used to describe a class of visual pigments rather than a single entity.

Categories of Vision

Before the detailed study of the photochemical and electrical changes in the retina associated with the visual process is entered into, it would be profitable to discuss some of the more elementary phenomena of vision itself and to indicate the experimental methods available for its study. The visual perception of an object is a complicated physiological process, and attempts have been made to resolve it into simpler categories. Thus, it is common to speak of the *light sense*, defined as the appreciation or awareness of light, as such, and of modification in its intensity. Secondly, the *colour sense*, which enables us to distinguish between the qualities of two or more lights in terms of their wavelengths, and finally the *form sense* that permits the discrimination of the different parts of a visual image. For the present we shall preserve this simple classification for its convenience, but modern psychophysicists would hesitate to use the term 'sense' in relation to the discrimination of form.

THE LIGHT SENSE

The Absolute Threshold

The simplest way to study the light sense is to measure the *threshold* to white light, i.e. the minimum light-stimulus necessary to evoke the sensation of light. There are many ways of measuring this, and the general technique will be discussed later. In general, the subject is placed in a completely dark room and the illumination of a test-patch is increased until he is aware of its presence. The patch may be illuminated all the time and its luminance steadily increased, or it may be presented in flashes of varying luminance.

Dark-adaptation

Early attempts to measure the threshold soon showed that, in order to obtain other than very irregular results, the observer must be allowed to remain in the dark for at least half an hour (i.e. he must be *dark-adapted*) before any attempt is made to obtain a definite value. If this is not done, it is found that the threshold luminance of the patch is very high if the test is made immediately after the subject has entered the dark room, and that the threshold falls progressively until it reaches a fairly constant value which may be as small as one ten-thousandth of its initial figure. This effect is demonstrated by Fig. 7.1, in which the illumination of the test patch (in microlux) required to produce the sensation of light in a subject, who had gazed at a bright light for some minutes before entering the dark room, is plotted against time in the dark; the curve is referred to as a *dark-adaptation curve.*

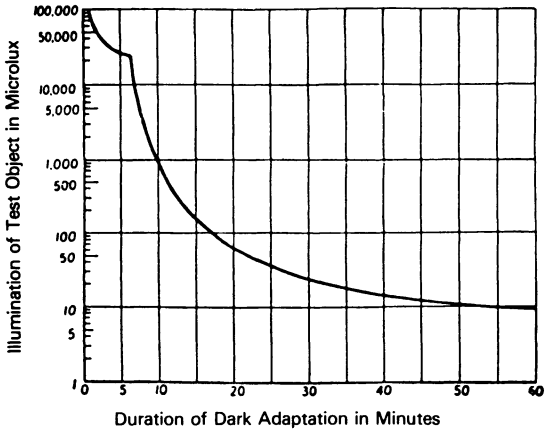

Fig. 7.1 Typical dark-adaptation curve. Ordinate: illumination of the test-patch in microlux. Abscissa: duration of dark-adaptation in minutes. (Kohlrausch, in *Handbuch der Normalen und Pathologischen Physiologie.*)

This extraordinary increase in sensitivity of a sense organ on removing it from its normal background of stimuli has not been met in the study of the other senses, and an inference to be drawn from the dark-adaptation curve is that a second mechanism of vision is being brought into play requiring half an hour, or more, to be established at its full level of efficiency. This inference represents the basis of the *Duplicity Theory of Vision*, a theory which assumes that at luminance levels below a certain value (about 0.01 mL) vision is mediated primarily by one mechanism—*scotopic vision*, involving the rods—and above this value by another mechanism—*photopic vision*, involving the cones; the transition is not abrupt so that there is a range in which the two mechanisms operate together, the *mesopic range.*

Duplicity Theory

Rod Vision

The duplex nature of vision is readily appreciable under conditions of very low illumination. Thus, whereas in daylight, or photopic, vision the subject sees best by direct fixation, so that the image of the object or luminous point he wishes to see falls on the fovea, under night, or scotopic, conditions his best vision is *peripheral*; he must look away from the object he is trying to distinguish so that its image falls on the peripheral retina. Thus, in looking at a dim star one must, as the astronomer Arago said, not look at it; if one fixates it, it disappears. This gives the clue to the anatomical basis of the duplicity theory; the fovea, in its central region specially, contains only cones. Since the fovea is apparently blind at low intensities of illumination, we may conclude that it is the rods that are functional under these conditions. That the rods are indeed responsible for night vision is now well recognized; it was Schultze who put forward this hypothesis on the basis of his comparative studies of animal retinae; thus he found that the nocturnal owl had a preponderance of rods whilst a diurnal bird, such as the falcon, had a preponderance of cones in its retina.

ACHROMATICITY

Another feature of vision at low luminance is its *achromaticity*, i.e. its failure to distinguish colours. Suppose, for example, that the threshold for vision is measured using different wavelengths of light; it is found that these thresholds are different, in the sense that more yellow energy, for instance, is required to give the sensation of light than blue energy, but the 'yellow' and 'blue' lights are both colourless. Only when the intensities are raised well above threshold do colours appear, i.e. when the threshold for stimulation of the *cones* is reached. Thus, on a moonless night colours are not distinguished, whereas in the *mesopic range*, corresponding to around full moonlight, colours may be appreciated but not very distinctly.

LOW VISUAL ACUITY

A very obvious difference between scotopic and photopic vision is the low visual acuity at low luminances; in other words, in spite of the high sensitivity of the eye to light under scotopic conditions, the ability to discriminate detail (e.g. to read print) is very low.

Other features of the duplicity theory will be considered later; for the moment we may say that it is now a well established *principle* rather than a theory. In essence it states that at high levels of luminance the relatively insensitive cones are able to operate, whilst the highly sensitive rods are out of action (perhaps through overstimulation). Vision mediated by the cones is coloured and exhibits high powers of discrimination of detail. When the light available is restricted, the insensitive cones no longer operate whilst the rods, after a period of dark-adaptation as shown by Fig. 7.1, become operative, mediating an achromatic, peripheral, low-acuity type of vision. Over an intermediate range, which may extend up to 1000 times the threshold for cone vision, both rods and cones are operative—the *mesopic range.*

The Differential Threshold or L.B.I.

Instead of using the minimum luminance of a test patch as a means of studying the light sense, we may measure the *differential threshold*—the amount an existing stimulus, which itself produces a sensation of light, must be increased or decreased to produce a change in the sensation.

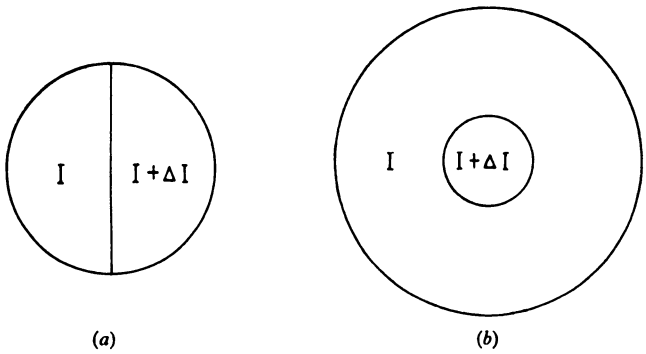

Fig. 7.2 Illustrating the measurement of the liminal brightness increment.

Measurement

Thus the subject may be presented with a luminous field divided into two, as in Fig. 7.2a, the luminances of either being varied independently. Beginning with them both equal at I, the right-hand one may be increased to value $I + \Delta I$, such that the observer can just detect a difference of subjective brightness. The increment, ΔI, is called the *liminal brightness increment* (l.b.i.) or *differential threshold.* Alternatively, as in Fig. 7.2b, the subject may look at a large circular field of luminance I, and a smaller concentric field may be thrown on to this with a variable luminance greater than I. With this experimental technique, the measurements need not be confined to those intensities of illumination in which only scotopic vision is operative, but rather the whole range of intensities may be used.

Weber–Fechner Law

The differential threshold, or l.b.i., varies with the initial value of the prevailing luminance, I; for example if I is 100 mL then ΔI may be in the region of 2 mL; if I is 1000 mL then ΔI is about 20 mL. Over a certain range, however, it may be expressed as a constant fraction of the prevailing luminance, so that the ratio: $\Delta I/I$ is constant. This is the basis of *Weber's Law of Sensation* which applies approximately to all sensory modalities, namely that the difference-limen is proportional to the prevailing stimulus. For example, in the case of the sense of touch or pressure, Weber showed that when two weights resting on the skin differed by about 1 in 30 they could be discriminated as different weights. Thus if an individual could discriminate between a 30 and a 31 g weight he could also discriminate between a 3 and 3.1 g weight; in other words, the *Weber fraction*, $\Delta S/S$, is constant, where S is the prevailing stimulus and ΔS its liminal difference for perception.

Fechner Fraction

Fechner extended Weber's work to the study of visual discrimination, and the fraction $\Delta I/I$ is frequently called the Fechner-fraction. Figure 7.3 represents a more modern study, where the Fechner-fraction, $\Delta I/I$, has been plotted against the intensity level, I. At high intensities, between about 0.1 and 1000 mL, this fraction is fairly constant at about 0.02 to 0.03, indicating that a change of 2 to 3% in luminance can be detected; at low luminances the power to discriminate falls off sharply so that at 0.0001 mL two patches must differ by about 50% in luminance if they are to be discriminated.

THE COLOUR SENSE

By means of the colour sense we become aware of those qualitative characteristics of light that depend on its spectral composition. On passing white light through a

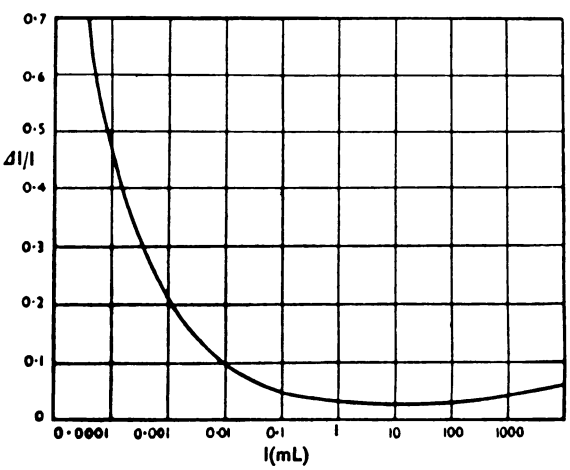

Fig. 7.3 Intensity discrimination curve. The ratio $\Delta I/I$ is the liminal intensity (ΔI) increment divided by the intensity (I). If the Weber–Fechner Law held, this ratio would be independent of the value of I. The curve shows that, over a certain range (0.1 to 1000 mL), this is approximately true. In the scotopic region, however, the ratio increases greatly, i.e. the power to discriminate changes in luminance falls off at low levels.

prism it is resolved spatially into its component wavelengths, and the result is the well-known spectrum; this resolution shows that the sensation of white is evoked by the summated effects of stimuli which, when operating alone, cause entirely different sensations, namely, those of red, orange, yellow, green, etc.

Hue

The spectrum shows a number of characteristic regions of colour: red, orange, yellow, green, blue, indigo and violet; these regions represent large numbers of individual wavelengths; thus the red extends roughly from 750 to 650 nm; the yellow from 630 to 560 nm; green from 540 to 500 nm; blue from 500 to 420 nm, and violet from 420 to 400 nm. Within these bands of colour there are thus a variety of subtle variations, and a spectral colour or *hue*, has been defined somewhat idealistically as the sensation corresponding to a single wavelength. This is too rigid a definition, both because of the limitations to discrimination of the human eye, and the experimental difficulty in obtaining light confined to a single wavelength.

Thus coloured lights may be obtained by the use of filters, which cut out many wavelengths and selectively transmit others; these filters are never sufficiently selective to confine the transmitted light to a single wavelength and at best they transmit a *narrow band* about a mean position. Hence by a green filter of 530 nm is meant a filter that transmits mainly green light with a peak of transmission at 530 nm; transmission at nearby wavelengths is also considerable, however, whilst even at remote wavelengths there may be a little transmission.

Monochromator

A more precise method is by the use of the monochromator, the essential principle of this technique being to select, from a spectrum, just that narrow band of wavelengths that one requires. In practice the band is selected by a movable slit that passes over the spectrum; and its width, in terms of the range of wavelengths, can be reduced by making the slit narrower and narrower. Unfortunately, this decreases the amount of light-energy transmitted, so that once again the experimenter must be content with a band of wavelengths rather than a single one.

Hue-discrimination

The physiological limit to the differentiation of hues is given by the *hue-discrimination curve*, shown in Fig. 7.4. The subject is presented with a split field, the two halves of which may be illuminated independently by lights of equal subjective intensity but differing wavelength. Starting with, say, a red of 700 nm in the left-hand field the wavelength of the light of the right-hand field is shortened till the subject can just discriminate a change in hue, say at 680 nm; the hue-limen is thus 20 nm. With both fields at 680 nm, the righthand field wavelength is again shortened and a new hue-limen obtained. Figure 7.4 shows the results for a normal human observer; discrimination is best at about 500 nm in the blue-green and at 600 in the yellow, but even here the smallest detectable change in wavelength is about 1 nm.[1]

Saturation

In practice, then, coloured lights are not monochromatic, being generally a mixture of different wavelengths; the hue is then said to be *impure*, and in the case when the impurity can be accounted for by an admixture of white light, it is said more specifically to be *unsaturated*, the actual colour being called a *tint* of the hue that has been thus diluted. The percentage saturation of a hue is the percentage contributed by the monochromatic light, estimated on a luminosity basis. By mixing white light with a spectral hue, the latter actually changes; thus red becomes pink, orange becomes yellow, yellow becomes green, green becomes yellow, and violet becomes salmon-pink;

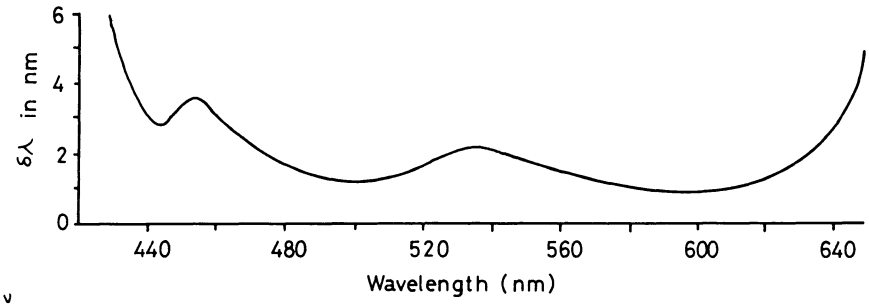

Fig. 7.4 Hue-discrimination curve. At any given wavelength, indicated on the abscissa, there is a certain change in wavelength, $\delta\lambda$, that must be made before the change in hue can be discriminated. (Wright, *Researches on Normal and Defective Colour Vision.*)

the yellow-green does, in effect, remain constant and the blue changes very little.

Limits of the Visual Spectrum

The limits are usually given as 400 nm and 760 nm, wavelengths shorter than 400 nm and longer than 760 nm being characterized as *ultraviolet* and *infrared* respectively. In fact, however, the retina is sensitive to wavelengths well beyond these limits; for example, Wald (1945) showed that the insensitivity of the eye to ultraviolet up to 350 nm is entirely due to absorption by the lens; aphakic subjects are able to see easily with these wavelengths, calling the sensation blue or violet. Again, the failure of early workers to evoke sensation with wavelengths greater than 760 nm was due entirely to their inability to obtain intense enough sources, the retina being so insensitive to red light. Griffin *et al.* (1947) were able to evoke sensation with wavelengths as long as 1000 to 1050 nm, and Brindley (1955) has found that, when compared on an equi-energy basis (p. 395), the far reds are much more orange than the near reds; for example, a red of 887 nm could be matched by an orange of 640 nm.

Just as with white light, we may refer to the luminosity of a given hue and measure it in the same units, and although it may seem somewhat unreal to speak of comparative luminosities of widely different hues, by making use of a suitable colour photometer it is possible to use a scale of luminosity which applies to all the spectral colours in such a way that if all the luminosities of the hues of a spectrum are determined separately, the luminosity of the white light obtained by recombining the spectrum is equal to the sum of these individual spectral luminosities.

The Flicker Photometer

If it is desired to measure the relative luminosities of two differently coloured sources, the most satisfactory instrument to use is the *flicker photometer*. This is represented diagrammatically in Fig. 7.5. It consists of a white screen, A, and a Maltese Cross, C, which is placed at such an angle that light from one of the sources (S_2) is reflected down the viewing tube, T. The screen, A, is likewise placed so that light from the other source (S_1) is reflected down the tube. When the cross is rotated, the eye receives light alternately from S_2 and S_1 by reflection from C and A respectively. If the luminances of the two surfaces are different, a sensation of flicker is experienced which can be made to disappear by adjusting the distances of the two sources from the surfaces which they illuminate. When flicker disappears, the luminances of the two surfaces are equal. If A and C make the same angle with the direction of the incident light, and if their reflection

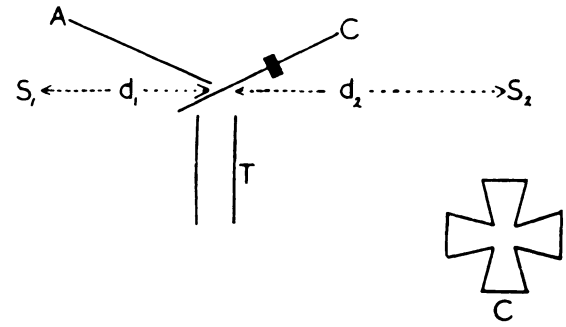

Fig. 7.5 The flicker-photometer. Light from S_1 is reflected from A down the viewing tube, T. Light from S_2 is reflected from the rotating cross, C. When A and C are equally illuminated flicker ceases.

factors are equal, the luminous intensities of S_1 and S_2 will be in the ratio of $d_2^2 : d_1^2$.

Variation of Hue with Intensity

We have seen that hue and saturation are not absolutely independent, since altering the saturation of a yellow, for example, can actually make it into a green. In a similar way, hue is not independent of luminosity. Thus, as the intensity of a coloured light is increased its subjective hue makes a characteristic shift, and ultimately all wavelengths, if made intense enough, appear the same, evoking a yellowish-white sensation. These shifts are described as the *Bezold-Brücke phenomenon*, after their discoverers. On lowering the intensity there are also characteristic changes which will be discussed later in connection with the Purkinje phenomenon, and ultimately the whole spectrum becomes achromatic, in the sense that at sufficiently low intensity levels all wavelengths appear white and indistinguishable from each other qualitatively. It is therefore important to define the level of luminance at which studies of colour vision are made; the value generally chosen is of the order of 2 to 3 mL.

Colour Mixtures

If two colours, not too far apart in the spectrum—say a red and a yellow—are mixed, the resulting sensation is that produced by a single spectral hue of intermediate wavelength. The actual position of the resultant hue in the spectrum is determined by the relative luminosities of the two hues that are mixed; if they are equal, the resultant lies midway between; if the red predominates, the resultant lies towards the red end. As the distance apart of the two hues is increased, the resultant hue is found to become progressively unsaturated, i.e. it can only be matched with an intermediate spectral hue provided that white light is added to the latter. Eventually a

point is reached when the mixture results in white; any two hues that, when combined, give white light are called *complementary colours.* As a result of the classical researches of Young and Helmholtz and more recently those of Wright (1946), the laws of colour mixture have been put on a quantitative basis. In general, it may be stated that any colour sensation, within an average range of intensities, can be produced by a mixture of not more than three *primary spectral wavelengths,* with the reservation that in many cases white light must be added to the comparison colour to obtain a match in saturation as well as in hue. Thus, if it is required to match a given standard colour, say a bluish green, then by varying the intensities of the three primaries it will usually be found that it is impossible to make a perfect match with this standard, the mixture appearing unsaturated by comparison. We must therefore add white to the standard until the two match or, as it is often put, we must subtract white from the mixture to obtain a perfect match in hue and saturation. The three primaries are chosen so that any one cannot be produced by mixing the other two; thus red, green and blue are primaries.[2]

A given hue may thus be expressed in terms of three coefficients, namely:

$$\text{Colour} = \alpha R + \beta G + \gamma B$$

where the latter determine the relative quantities of these arbitrarily chosen primaries. Light is measured on a luminosity basis in most work, so that it would be natural to measure the contributions of the primaries to any given hue in terms of luminosity units, remembering that the luminosity of the hue will be equal to the sum of the separate luminosities of the primaries required to make a match in hue and luminosity. Since the resultant mixture of the primaries will not necessarily correspond in saturation with the given hue to be matched, it is necessary to subtract a certain quantity of white—that is, certain quantities of the three primaries—and this may lead to negative coefficients. There is no particular theoretical objection to negative coefficients, but they can be avoided by choosing certain hypothetical primaries which do not correspond to any spectral hues. Thus we have seen that a mixture of three spectral primaries gives an unsaturated spectral hue; if the amounts of the primaries which must be subtracted from this unsaturated spectral hue, in order to saturate it, are subtracted from the primaries themselves, we obtain a set of hypothetical primaries which give positive coefficients. Thus Wright used hypothetical primaries, R′, G′, B′, defined by the relationship:

$$R' = 1.015\,R - 0.015\,G$$
$$G' = -0.90\,R + 2.00\,G - 0.10\,B$$
$$B' = -0.05\,G + 1.05\,B$$

where R, G, and B were spectral hues of 650, 530, and 460 nm respectively.

TRICHROMATIC UNITS

For ease in manipulation, the quantities of the primaries are often expressed in terms of their contributions to colour quality rather than to luminosity; thus the coefficients are defined by the statement that equal quantities of the primaries make white.

White $= 0.333\,R + 0.333\,G + 0.333\,B$, the units defined in this way being referred to as *trichromatic units,* and since the sum of the coefficients is equal to unity, the equation defining a colour is called a *unit colour equation.* It is a relatively simple matter to transpose from one set of coefficients to another.

The Chromaticity Chart

The unit colour equation is useful because it enables us to express graphically the composition of any hue in terms of the primaries; thus if we construct rectangular coordinates so that the ordinates represent green coefficients and the abscissae red coefficients, then any hue will be given by a point representing its red and green coefficients; since $\alpha + \beta + \gamma = 1$, the blue coefficient will be given by subtracting the red and green coefficients from unity. The locus of spectral hues will be a line (Fig. 7.6) and white, if defined by the equation above, will be

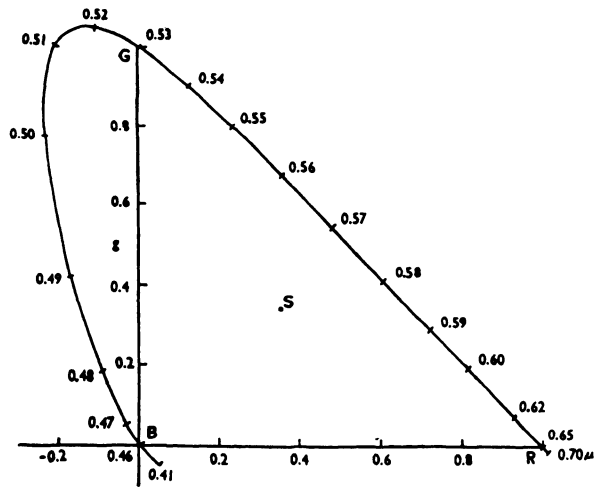

Fig. 7.6 Chromaticity chart. Units of green are indicated on the vertical line; units of red on the horizontal line. The amount of blue in a given mixture is given by the unit colour equation, $R + G + B = 1$. The line joining R to G and continuing as a curved loop to B is called the *spectral locus* and shows how the individual spectral hues can be matched by the three primaries. S is standard white. (Wright, *Researches on Normal and Defective Colour Vision.*)

represented by a point whose ordinate and abscissa are 0.333.

FORM

The form or structure of the visual field is determined by the power to discriminate between two or more separate stimuli in regard to intensity and spatial extension; we perceive the shape of an object by virtue of our ability to integrate our responses to a large number of separate stimuli of varying intensity arising from different positions on its surface.

Resolving Power and Visual Acuity

The power of the eye to discriminate on a spatial basis is studied experimentally by measurements of the *resolving power*, the smallest angle subtended at the nodal point of the eye by two points or lines such that they are appreciated as separate, i.e. the so-called *minimum separable*. The visual acuity is defined as the reciprocal of this angle when it is measured in minutes of arc. Thus, under good experimental conditions, resolving powers of the order of 30 seconds of arc, or half a minute, may be measured, corresponding to a visual acuity of $1/0.5 = 2$.

Measurement

The most commonly used test-objects for measuring resolving power are the Landolt-C and the grating (Fig. 7.7). The Landolt-C can be rotated into eight separate positions which the subject is asked to identify; C's of diminishing size are presented and the errors made in indicating the positions are recorded. Experimentally it is found, as with all psychophysical studies of thresholds, that there is no sharp division between the size of C that can be discriminated and that which cannot; near the 'end-point' we will have a range of sizes where the average number of errors in any set of trials increases with decreasing size of C until eventually the answers are purely random. We must therefore somewhat arbitrarily choose an end-point; Lythgoe (1932) chose that size of C with which 4.5 out of eight answers were correct, and the actual end-point was computed from the errors obtained with several sizes of C by the application of statistical theory. So far as the resolving power of the eye is concerned, it would appear that the ability to detect the position of the break in the C, which distinguishes it from a complete circle, depends on the size of the break, *s*; in fact, the angle subtended at the eye by this distance, *s*, at the end-point, is indeed the measure of the resolving power of the eye. Thus at a distance of 6 metres, under given conditions, the size of the break, *s*, was 3.6 mm, at the end-point; this distance subtended 2 minutes at the eye and so the visual acuity was 0.5.

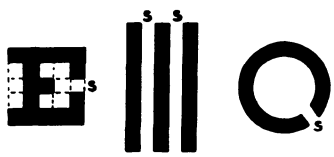

Fig. 7.7 Snellen letter, grating and Landolt-C. In each case the angle subtended at the eye by the distance, *s*, apparently determines whether the gap will be recognized.

GRATING ACUITY

If the grating of Fig. 7.7, consisting of equally spaced black and white lines, is removed sufficiently far from the observer, it appears uniformly grey; at a certain point the lines can be just discriminated and the angle subtended at the eye by the distance *s* once again is said to indicate the resolving power of the eye. According to Shlaer (1937) the limiting size for resolution subtends some 28 seconds of arc at the eye under optimal conditions, corresponding to an acuity of 2.12.

SNELLEN TEST

The clinical *Snellen test* is essentially a resolution test; it is assumed that the average individual can resolve the details of a letter if they subtend one minute of arc at the eye, and the test letters are constructed so that their details (e.g. the gap in a C) subtend this angle, whilst the whole letter subtends five minutes of arc (Fig. 7.7), when they are at a definite distance from the eye. The chart has several rows of these letters, the sizes in the different rows being graded so that their details subtend one minute at different distances, e.g. the smallest letters subtend this angle at 4 metres whilst the largest do so at 60 metres. The subject is placed 6 metres from the chart and the smallest row of letters that can be read correctly is determined. The visual acuity is expressed as the ratio of the distance of the individual from the chart to the distance at which this row of minimum legible letters should be read, assuming a minimum visual angle of one minute. Thus at 6 metres if the individual can read down to the letters whose details subtend one minute when viewed from a distance of 18 metres, his visual acuity is 6/18; if he can read letters so small that they subtend the same angle at only 5 metres, his visual acuity is 6/5, and so on.

Experimental Results

Factors influencing visual acuity will be dealt with in detail later; for the present we need only note that it is markedly influenced by the illumination of the test object,

the state of adaptation of the eye, and the pupil size. Under optimal conditions it has a value in the region between 2 and 3 (i.e. a minimum separable of about 30 to 20 seconds of arc) when a grating or Landolt-C is used as test-object.

VISUAL ACUITY IN ANIMALS

Visual acuity can be measured in animals by training them to choose between alternate pathways marked with a grating or Landolt-C of variable visual angle; selection of the required pathway is rewarded with food. When the choice becomes random the animal is unable to resolve the grating or Landolt-C. Farrer & Graham (1967) found a limiting resolution of 0.5–1.0 minutes of arc in a monkey, indicating a visual acuity as good as that of man; in the rabbit, Van Hof (1967) found values between 10 and 20 minutes, and this corresponds with the absence of a fovea in this animal.

In the cat, Jacobson *et al.* (1976), employing an avoidance technique, found resolving powers as good as 3.5 minutes of arc, comparing with about 5 minutes in Smith's (1936) study. It is possible that the eagle's acuity is, indeed, better than man's (Shlaer, 1972).

INDUCTION

The effect of light falling on a given portion of the retina is generally not confined to the retinal elements stimulated; moreover, the characteristics of those elements that have been stimulated are altered for an appreciable time, so that their response to a second stimulus is modified. The influence of one part of the retina on another is described as *spatial induction*; by *temporal induction* is meant the effect of a primary stimulus on the response of the retina to a succeeding stimulus.

Spatial Induction

Spatial induction, or *simultaneous contrast*, can be demonstrated by comparing the appearance of a grey square, when seen against a black background, with its appearance when seen against a white background; against the black background the grey appears almost white, whereas it appears quite dark when seen against the white background. The white surround apparently depresses the sensitivity of the whole retina, thereby making the grey appear darker; the net effect of this depression in sensitivity is to accentuate the contrast between the grey and the white surfaces. Where coloured lights are concerned the same principle of a reduction in sensitivity of the retina applies, but now this reduction is confined to certain wavebands, and the subjective result is to enhance the appearance of the complementary colour. Thus, if a white and blue light patch are placed side-by-side, the white patch appears yellow; apparently the blue light falling on one half of the retina has depressed the sensitivity of the whole retina to blue light; the white light falling on the retina is now losing some of its 'blueness' because of this loss of blue-sensitivity; removing blue from white leaves a yellow colour, since blue and yellow are complementaries.

Temporal Induction

In a similar way, if the whole retina is stimulated with white light the sensitivity to a given stimulus following this is reduced, so that the second stimulus appears less bright than it would have done had there been no 'conditioning stimulus', as this preliminary, adapting, stimulus is called. This form of induction, which has been called *light-adaptation*, has been studied in detail by Wright in England, and Schouten in Holland.

Binocular Matching

The technique employed was that of binocular matching, based on the principle that the states of adaptation of the two eyes are independent. Thus the observer looks through a binocular eye-piece, each eye seeing the half of a circular patch of light, and these halves have to be matched for equal subjective brightness. If, say, the right eye is exposed to a bright light, we may determine the changes in sensitivity of this eye during its exposure to the bright light by matching its half-field with the left half-field, as seen by the dark-adapted eye. This means varying the intensity of the left half-field until the match is made. It is found that the intensity of the left half-field has to be continuously reduced during exposure of the right eye, until it levels off at a constant value which may be about one-sixteenth of the value at first. This means that the right eye becomes rapidly less sensitive to light from the moment it is exposed to it; this is the phenomenon of light-adaptation and is illustrated by Fig. 7.8. The phenomenon is, of course reversible, so that if the two eyes are now allowed to match fields of moderate luminance, the left field will, at first, have to be made much weaker than the right because the left eye has remained dark-adapted and has remained the more sensitive; very rapidly, however, this matching field will be made stronger until they finally become equal when both eyes are completely dark-adapted.[3]

Practical Demonstration

This adaptation is very easy to demonstrate qualitatively; thus if an observer is instructed to stare at a brilliantly illuminated screen for a few minutes with one eye closed,

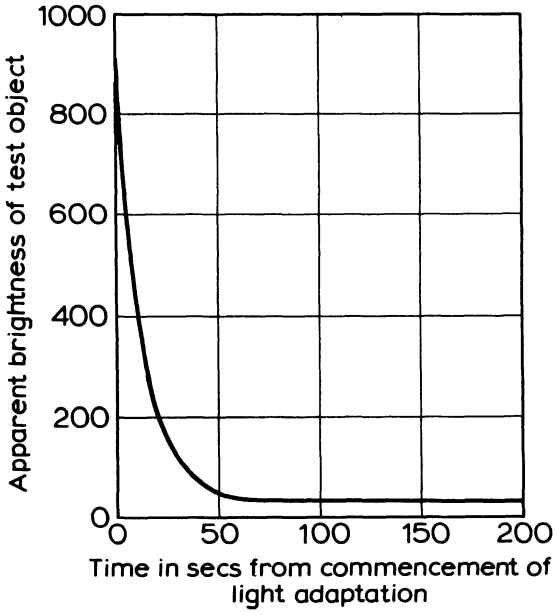

Fig. 7.8 Curve showing the fall in sensitivity of the fovea during exposure to a bright light. The right eye views the bright light whilst the dark-adapted left eye views a patch that must be matched in brightness with the sensation experienced through the right eye. The matching intensity decreases, indicating that the apparent brightness of the light, as seen through the right eye, becomes less and less. (Wright, *Trans. Illum. Eng. Soc.*)

and then this is replaced quickly by one of moderate intensity, he finds, on comparing the subjective brightness of the screen as seen through either eye separately, that the eye that had been kept closed sees the screen as very much brighter. We may note here that the phenomenon of *dark-adaptation*, as revealed by the progressive decrease in the absolute threshold, is a manifestation of temporal induction, in so far as the phenomenon reveals a change in the retina following the cessation of a stimulus, namely of the original bright light to which the observer was exposed before being placed in the dark.

Adaptation to Coloured Lights

The same process of light-adaptation, or successive contrast, is seen with respect to colours; thus with the same binocular matching technique, except that the two fields must be matched for colour rather than subjective brightness, the effects of adapting to a given wavelength of light can be found. The same principle emerges, namely that adaptation of the one eye to, say, green, reduces the sensitivity of this eye to this wavelength, and in order that the other eye may make a match it has to employ much less green than before. Thus two half-fields may be made to match, the right eye viewing a yellow and the left a mixture of red and green, their intensities being adjusted to give the match with the right eye. The right eye is now exposed to an adapting green light for a few minutes and it is found that, on viewing the two fields, the match no longer holds, the right field appearing reddish by comparison with the yellow of the left field. The left field must now be made less green to make the match, and the extent to which the green must be reduced in intensity in this field is a measure of the reduction of sensitivity of the right eye to green.

After-images

When the eye is exposed to a brief flash of light the subjective sensations last for much longer than the stimulus, and are described as a succession of *after-images*. The phenomena may be classed as inductive, in so far as they reveal changes in the retina or its higher pathways following a primary stimulus; although they have attracted a lot of interest, little of fundamental value has emerged from their study and it would be a pity to spend much space on them. As classically described, the responses to a single flash are illustrated schematically in Fig. 7.9 where upward movements indicate sensations of brightness (positive after-images) and downward movements sensations of blackness (negative after-images). If a coloured primary stimulus is used, some of the after-images are coloured, often with the complementary. The events depicted by Fig. 7.9 occur rapidly and are exceedingly difficult to resolve, except by such devices as

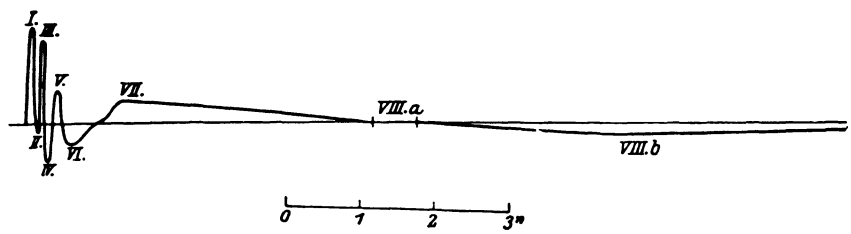

Fig. 7.9 The successive after-images said to be experienced after viewing a bright flash. Time-scale in seconds. (Tschermak, in *Handbuch der Normalen und Pathologischen Physiologie.*)

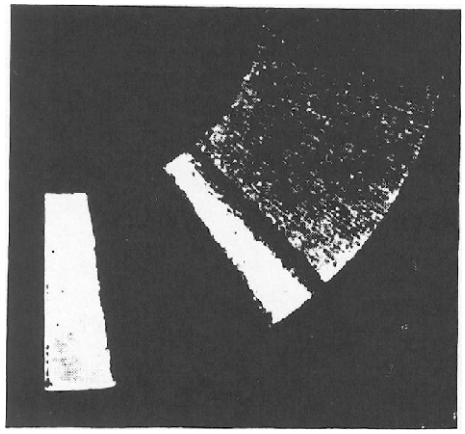

Fig. 7.10 Bidwell's ghost. A black disc with a sector cut out rotates in front of a brightly illuminated opal screen. The after-images of the sector are projected to the left to give the appearance shown. (McDougall, *Brit. J. Psychol.*)

Bidwell's disc, illustrated by Fig. 7.10. Here a disc, with a narrow slit in it, is rotating in front of a bright opal screen, and the after-images are projected on to the black disc to give the appearance of *Bidwell's ghost*. A more slowly developing and longer-lasting after-image is that observed after staring for a few minutes at a bright source and then transferring the gaze to a dimly lit screen. In a little while a 'negative' image of the bright source appears; if the source was coloured this has the complementary colour, e.g. magenta after looking at green; yellow after looking at blue, and so on.

Intermediate Exposures

The after-effects of exposures intermediate in duration between the brief flash and the lengthy gaze have been studied under well controlled conditions by Trezona (1960). Thus, with an exposure of the order of 8 seconds, the after-effects may be classified as follows:

1. *Persistence of vision*, this being the apparent continuation of the stimulus after it has been cut off, and lasting about 1 second at rapidly diminishing subjective brightness.
2. *After-colours*; these may last for seconds or minutes, changing colour frequently. The threshold for these after-colours was very high, of the order of 100 000 trolands of retinal illumination.
3. *After-blueness*; this was a characteristically different effect from the after-colours mentioned above; it lasts for some seconds and remains the same colour. The threshold was much lower, of the order of 100 to 1000 trolands and the effect could only be obtained with peripheral vision, suggesting mediation by the rods.
4. *After-blackness*. This was favoured by long exposures, and consisted of several appearances of the black image of the source.

Liminal Brightness Increment

If a subject was exposed to pairs of bright flashes in the two halves of a test-field, the after-images could be distinguished if the intensities of the flashes differed, the Fechner-fraction, $\Delta I/I$, comparing with that found for direct vision; this was in spite of the fact that with direct vision the two halves of the field could not be distinguished because of the extreme brightness and shortness of the flashes. When the intensities of the flashes became too high, however, there was a fall in discrimination, i.e. a rise in the Fechner-fraction, and this was probably due to excessive bleaching of the cones (Brindley, 1959).

Peripheral Origin

This finding, together with the study of the applicability of Bloch's Law (p. 275) strongly suggests that after-images have a peripheral origin, i.e. are determined by photochemical events in the receptors. Support for this is given by Craik's experiment, in which the eye was temporarily blinded by exerting pressure on the globe. On exposure of the eye to a bright light nothing was seen, but on restoring the circulation an after-image appeared. The possibility that some of the phases have a central origin must not be ruled out, however; thus Brindley was unable to find any regularity in behaviour of his after-images unless he ignored those appearing within the first 15 seconds; after this time they conformed to rules predictable on photochemical grounds.

Value of Contrast

Simultaneous and successive contrast are essentially manifestations of an inductive process that tends to reduce the sensitivity of the retina to an existing stimulus and to enhance its sensitivity to a stimulus of a different kind, e.g. the sensitivity to the complementary of the existing, coloured, stimulus. As a result of simultaneous contrast the contours of an image become better defined and, as a result of successive contrast, the confusion that would result from the mixing of successively presented images is reduced.

Notes

1. Cornu & Harlay (1969) have examined the effects of luminance on hue discrimination, and have summarized the recent literature on this point.
2. There are several ways of expressing the 'Laws of Colour Mixture'. A common one is as follows: given any four lights, it is possible to place three of them in one half of a photometric field and one in the other half, or else two in one half and two in the other, and by adjusting the intensities of three of the four lights to make the two halves of the field indistinguishable to the eye. This appears different from the statement in the text, but is actually the same in so far as it is another statement of the *trivariance* of colour matching, the three variables being the intensities of the three colours that are varied, the fourth remaining constant. The laws governing colour-matching are called *Grassmann's Laws.*
3. These studies of light-adaptation and their reversal are made with foveal vision and are essentially studies of cone vision, i.e. although comparisons are made with a dark-adapted eye, the intensities of the half-fields to be compared are always maintained well above cone-thresholds.

References

Brindley, G. S. (1955) The colour of light of very long wavelength. *J. Physiol.* **130**, 35–44.

Brindley, G. S. (1959) The discrimination of after-images. *J. Physiol.* **147**, 194–203.

Cornu, L. & Harlay, F. (1969) Modifications de la discrimination chromatique en fonction de l'éclairement. *Vision Res.* **9**, 1273–1287.

Ewald, E. & Kühne, W. (1878) Untersuchungen uber den Sehpurpur. *Unters. Physiol. Inst. Heidelberg*, **1**, 248–290.

Farrer, D. N. & Graham, E. S. (1967) Visual acuity in monkeys. *Vision Res.* **7**, 743–747.

Griffin, D. R., Hubbard, R. & Wald, G. (1947) The sensitivity of the human eye to infra-red radiation. *J. opt. Soc. Amer.* **37**, 546–554.

Jacobson, S. G., Franklin, K. B. J. & McDonald, W. I. (1976) Visual acuity of the cat. *Vision Res.* **16**, 1141–1143.

Kohlrausch, A. (1931) Tagessehen, Dämmersehen, Adaptation. *Handbuch der normalen und pathologischen Physiologie.* Bd. XII/2, pp. 1499–1594. Berlin: Springer.

Lythgoe, R. J. (1932) The measurement of visual acuity. *M.R.C. Sp. Rep. Ser.*, No. 173.

McDougall, W. (1904) The sensations excited by a single momentary stimulation of the eye. *Brit. J. Psychol.* **1**, 78–113.

Schouten, J. F. & Ornstein, L. S. (1939) Measurement of direct and indirect adaptation by means of a binocular method. *J. opt. Soc. Amer.* **29**, 168–182.

Shlaer, R. (1972) An eagle's eye: quality of the retinal image. *Science* **176**, 920–922.

Shlaer, S. (1937) The relation between visual acuity and illumination. *J. gen. Physiol.* **21**, 165–188.

Smith, K. U. (1936) Visual discrimination in the cat. IV. The visual acuity of the cat in relation to stimulus distance. *J. Genet. Psychol.*, **49**, 297–313.

Trezona, P. (1960) The after-effects of a white light stimulus. *J. Physiol.* **150**, 67–78.

Tschermak, A. (1929) Licht- und Farbensinn. *Handbuch der normalen und pathologischen Physiologie.* Bd. XII/1, pp. 295–499. Berlin: Springer.

Van Hof, M. W. (1967) Visual acuity in the rabbit. *Vision Res.* **7**, 749–751.

Wald, G. (1945) Human vision and the spectrum. *Science* **101**, 653–658.

Wright, W. D. (1939) The response of the eye to light in relation to measurement of subjective brightness and contrast. *Trans. Illum. Eng. Soc.* **4**, 1–8.

Wright, W. D. (1946) *Researches on Normal and Defective Colour Vision.* London: Kimpton.

8. PHOTOCHEMICAL ASPECTS OF VISION

Introduction

The receptors that mediate vision at night are the rods which, as mentioned earlier, contain a pigment—*visual purple* or *rhodopsin*—responsible for the absorption of light in the primary photochemical event leading to sensation. According to the photochemist, then, the visual process consists of the absorption of light by a specialized molecule, visual purple or rhodopsin. The absorption of light provides the rhodopsin molecule with a supply of extra energy and it is said, in this state, to be 'activated'. In this activated state it is highly unstable and so it will change to a new form, i.e. the molecule will undergo some kind of chemical change by virtue of this absorption of energy. The effects of this change will be to cause an 'excited' condition of the rod as a whole and it will be this excited condition that will ultimately lead to the sensation of light.

Photochemical and Thermal Changes

As we shall see, the effects of light-absorption on the rhodopsin molecule are complex because the new molecule formed is not stable but immediately undergoes a succession of changes, which are called *thermal reactions* to distinguish them from the primary *photochemical* change. From an economic point of view we may expect the photochemical and other changes taking place in the retina to be at least partly reversible, otherwise enormous quantities of rhodopsin would have to be synthesized continuously to keep pace with the material destroyed by light.

Regeneration

In fact, the early investigators who observed the bleaching of visual purple in the retina also observed that it would regenerate if the intact retina was allowed to remain in the dark. Subsequent studies on solutions of rhodopsin have indeed shown that, provided the necessary enzymes are present, the photochemical and subsequent chemical changes are largely reversible. Tentatively, then, the visual process may be represented schematically as follows:

$$\text{Rhodopsin} \rightleftharpoons \text{Activated State} \rightleftharpoons \text{Bleached Products}$$

As we shall see, the 'bleached products' are the results of a highly complex series of changes, so that the rhodopsin molecule alters its 'colour', i.e. its light-absorbing properties, from the original magenta through orange to yellow and ultimately to white, when it has become vitamin A and a protein, *opsin*. In general, when the retina has been kept away from light for some time—i.e. when it has been completely dark-adapted—we may expect to find only rhodopsin in the rods, whilst when the retina is being exposed to light we may expect to find a mixture of rhodopsin with many of its 'bleached products', the relative amounts of each product being determined by the intensity of light and the duration of exposure.

ULTRASTRUCTURE OF THE RODS

Outer Segment

Let us consider the structure of the rod in more detail, as revealed by the electron-microscope. As Fig. 5.3, showed, the rod may be divided into outer and inner segments; since rhodopsin has been shown to be confined to the *outer segment*, the structure of this region is of special interest. Figure 8.1 shows that this part consists essentially of a pile of flattened sacs contained within the limiting plasma membrane, as illustrated schematically by Fig. 8.2. These sacs are formed by deep invaginations of the plasma membrane of the outer segment, the invaginations being ultimately nipped off so that the membranous sac is free in the cytoplasm of the outer segment. As indicated in Fig. 8.3, the invaginations at the base of the outer segment remain continuous with the plasma membrane. When outer segments are treated with trypsin the outer plasma membrane of the segment is digested, liberating the intact discs (Trayhurn & Habgood, 1975).

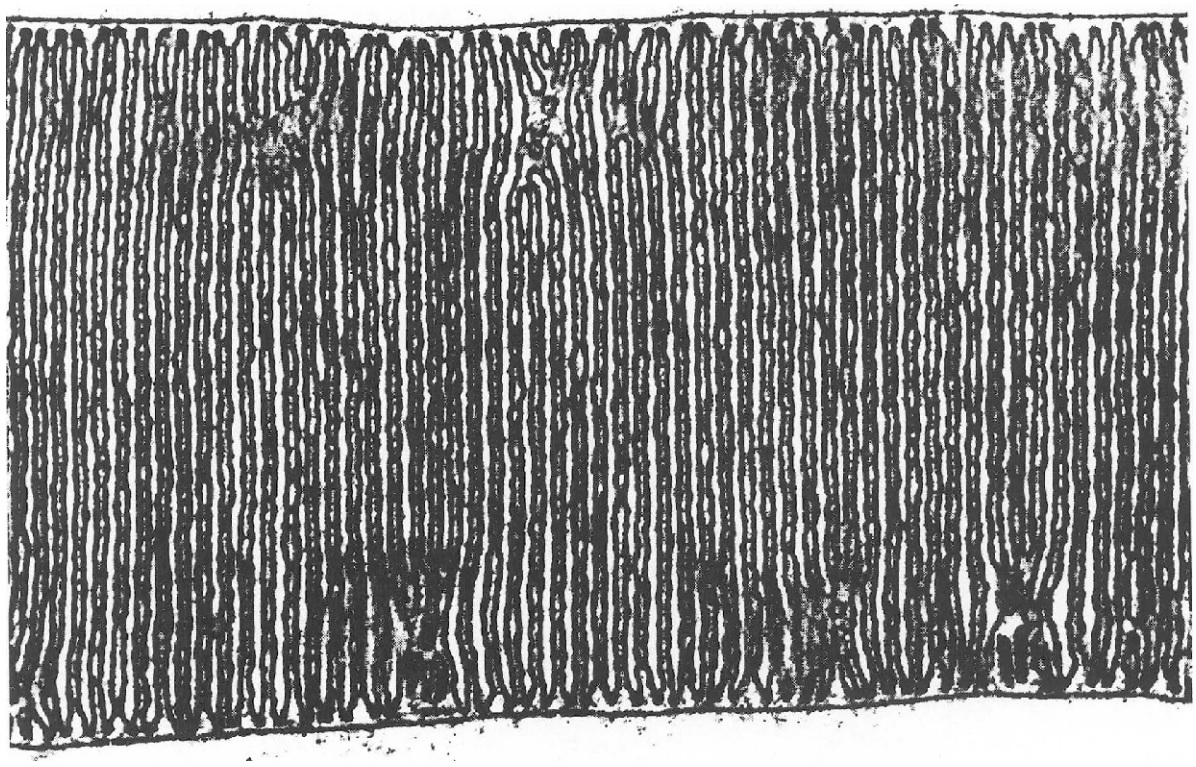

Fig. 8.1 Electron micrograph of a section of a rod outer segment of human retina showing the parallel arrangement of the disc lamellae. Osmium fixed. (×64 000). (Courtesy R. C. Tripathi.)

Inner Segment

The structure of the inner segment is quite different and is comparable with that of many cells, having a nucleus, Golgi apparatus, mitochondria and ribosomes. This part of the rod is thus concerned with the energy-requiring metabolic events, whilst the outer segment is concerned with the absorption of light, since it may be shown, by separating these from the body of the rod, that they contain the light-absorbing pigment, rhodopsin. The outer segment is connected to the inner segment by a cilium (Fig. 8.2B) which suggests that the rod has developed from a primitive ciliated photosensitive cell.

Cilium

The cilium has been examined in some detail by Richardson (1969) who has shown that, in the mammalian rod, it is not the sole connecting link between inner and outer segments; in addition there is a bridge of cytoplasm, and it is through this narrow neck that the products of synthesis within the inner segment may be conveyed to the outer segment.

Protein Synthesis

Thus studies involving radioautography carried out mainly in Young's laboratory (e.g., Young, 1976) have shown that, when tritiated amino acid is incorporated into the rod, it enters into protein synthesis within the myoid region and, within a short time, the radioactive protein may be seen migrating through the connecting cilium and ultimately appearing in the outer segment.

Chemical Composition

The outer segments of rods may be separated easily from the parent rods, and suspensions of these may be purified and analysed. Approximately 60% of the separated membrane material is protein and 40% is lipid, mainly phospholipid. Of the protein about 80% is the visual pigment rhodopsin which, as we shall see, is a chromolipoprotein with retinal linked to it as a chromophore group.

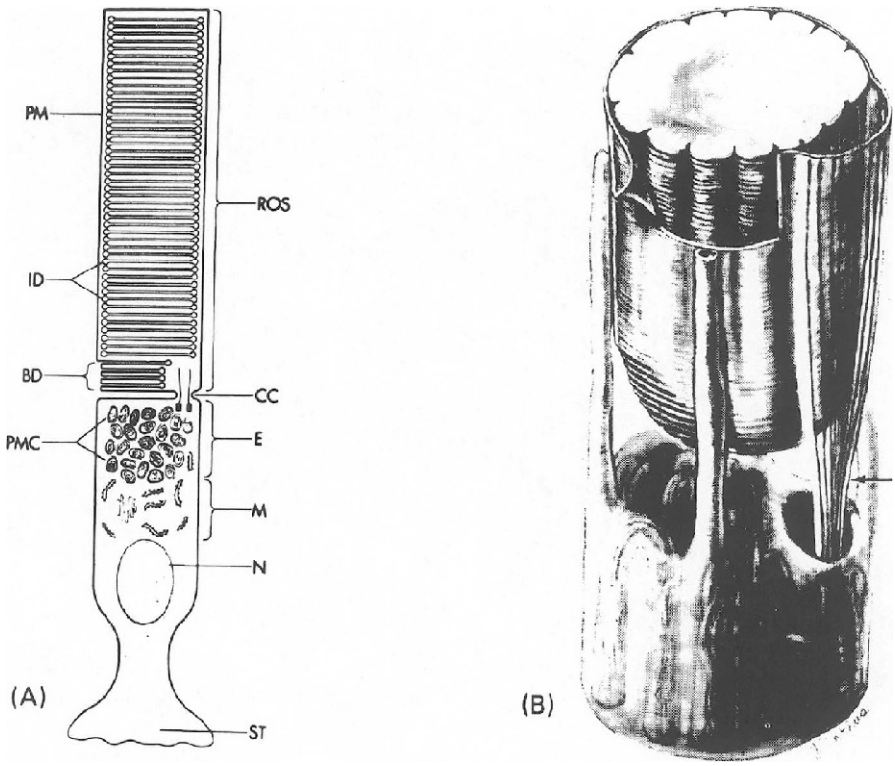

Fig. 8.2 (A) Diagram of frog red rod photoreceptor. ROS, rod outer segment; PM, outer segment plasma membrane; ID, isolated outer segment discs; BD, basal outer segment discs which are continuous with the plasma membrane; CC, connecting cilium; E, mitochondria-rich ellipsoid; PMC, perimitochondrial cytoplasm; M, myoid region containing endoplasmic reticulum and Golgi apparatus; N, nucleus; ST, synaptic terminal. (Basinger *et al., J. Cell Biol.*) (B) Three-dimensional illustration of junction between inner and outer segments of rod. Note scalloped appearance of rod discs. (Young, *Invest. Ophthal.*)

Fig. 8.3 Region at junction of outer and inner segments of rod. Note that the invaginations at the base of the outer segment remain continuous with the plasma membrane. (Young, *Invest. Ophthal.*)

Membrane Structure

The basic structure of the plasma membrane is essentially that postulated by Danielli & Davson (1935), and illustrated schematically in Fig. 8.4, the bilayer of lipid molecules being orientated with their polar groups facing the watery phase and their hydrophobic tails orientated away from the watery phase and attracted to each other. Attached to each outer layer there is a layer of protein molecules.

Rhodopsin

In the case of the discs, the protein attached to the membrane is rhodopsin and X-ray studies of Blasie & Worthington (1969) have indicated that these rhodopsin molecules are arranged in a liquid-like array in the plane of the disc membrane; the X-ray diffraction data indicate an asymmetry, suggesting that the rhodopsin is located only on the inward facing side of the lipid bilayer (Worthington, 1973). There is reason to believe that the rod plasma membrane, and hence that of the discs, is unusually fluid so that the rhodopsin molecules are not

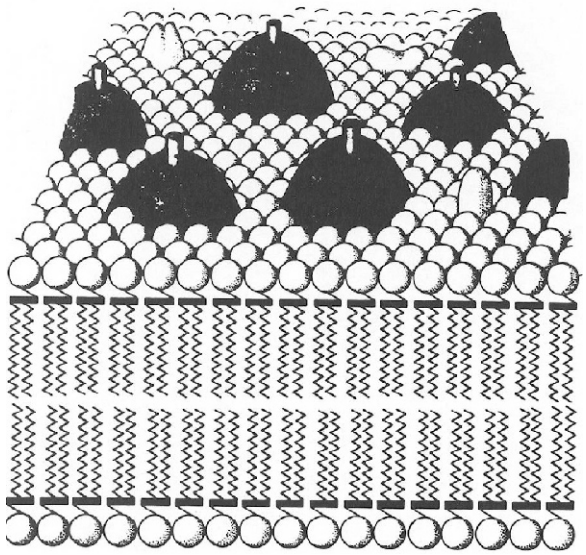

Fig. 8.4 Simplified model of rod outer segment membrane. The basic Danielli–Davson bilayer with its layers of protein on each side constitutes the essential structural element. A perspective view of large rhodopsin molecules, partly immersed in the bilayer, is also shown. The small cylindrical stem attached to each opsin molecule represents its carbohydrate chain. (Young, *Invest. Ophthal.*)

anchored firmly in the lipid bilayer but diffuse readily. This was shown very neatly by Poo & Cone (1973) who measured the change in absorbance of light by single rods when bleached from one side only. At first there was no change in absorbance of the side not exposed to light, but after a time this decreased, indicating diffusion of bleached rhodopsin from the exposed to the non-exposed side of the rod. By contrast, there was no diffusion in a longitudinal direction along the outer segment, and this is understandable since it is well established from Young's work that a rhodopsin molecule, once incorporated in a sac, never leaves this until the sac is finally discarded at the tip of the segment. Since rhodopsin may diffuse within the membrane-material, we may expect it to appear in the outer limiting plasma membrane of the outer segment, diffusing from the innermost set of discs which, as we have seen, are continuous with the outer membrane (Fig. 8.2).

Leucine Labelling

When Basinger *et al.* (1976) labelled rods with tritiated leucine, they found heavy activity in the plasma membrane as well as the basal discs—this could very clearly be seen when, during fixation, the membrane became separated widely from the discs. When the radioactive material was separated and analysed it was over 90% rhodopsin.[1] We shall see that the ultimate effect of light-absorption on the receptor is a change in electrical potential along its length; and it may be that the rhodopsin in the outer membrane, or in the most basal discs with which it is continuous, is important for some phase of the electrical change (p. 286).

Immunocytochemical Localization

Using antibodies to rhodopsin Nir & Papermaster (1983) found highest concentration of opsin in the basal rod discs, compared with those in the plasma membrane of the outer and inner segments; the connecting cilium was almost free, so that there is doubtless some impediment to diffusion back to the inner segment. The authors found some remarkable differences in labelling amongst the different frog receptor types; e.g. red rod outer segments were heavily stained whilst those of green rods were not.

Birefringence

The arrangement of the discs in the rod imparts a form-birefringence to the outer segment, revealed as a difference in refractive index according as the direction of the electric vector of the plane-polarized light is parallel with, or at right-angles to, the long axis of the rod (Fig. 8.5). This *form-birefringence* depends on the difference of refractive index of the disc and the cytoplasm in which it is suspended, and may be abolished by soaking the rod in a solution of refractive index equal to that of the discs. Because the molecules within individual discs are arranged in an ordered

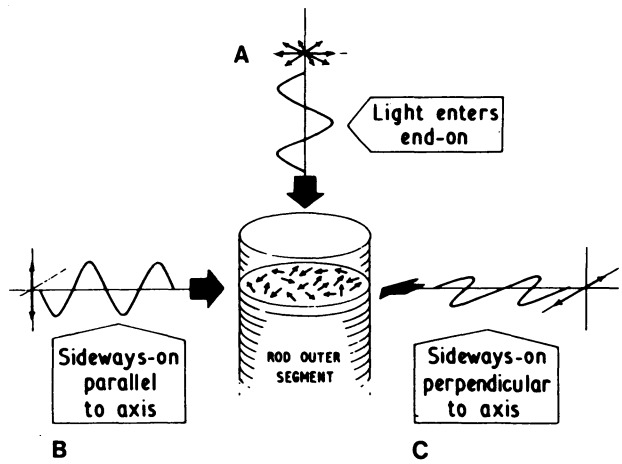

Fig. 8.5 Diagram showing the different ways in which polarized light can pass through a receptor outer segment, and its reaction with the absorption vectors of the pigment molecules (arrows) lying in a particular membrane. (A) Light passing down the receptor is absorbed equally whatever the orientation of its plane of polarization. (B) Light entering the side of the receptor with its plane of polarization *parallel* to the long axis of the receptor is perpendicular to the plane containing the absorption vectors, and is not absorbed. (C) If the plane of polarization is *perpendicular* to the axis, it will also lie in the plane containing the absorption vectors and is strongly absorbed. (Knowles & Dartnall, *The Eye.*)

fashion, the long lipid molecules being orientated at right-angles to the plane of the disc, i.e. along the axis of the rod, the outer segment is said to have, in addition, an *intrinsic birefringence*, and this will remain after abolishing the form-birefringence as described above. The measured birefringence will be the algebraic sum of the negative form- and the positive intrinsic birefringences. Liebman *et al.* (1974) found that, for frog outer segments, the refractive index for light incident side-on, with electric vector parallel to the cell axis, $n_{\parallel}$, exceeded that for light polarized perpendicular to this axis, $n_{\perp}$. Thus for wavelengths greater than 650 nm, the outer segments immersed in saline had a net positive birefringence, $\Delta n = n_{\parallel} - n_{\perp}$ of $+0.0010$. The intrinsic component was $+0.0050$ and the form -0.0040. The measurement becomes of interest when attempting to ascertain the structural consequences of the absorption of light (p. 247) by the rod.

Dichroism

Because the light-absorbing pigment molecules are orientated with their light-absorbing regions predominantly in the plane of the sacs, the absorption of plane-polarized light will be greater when its electric vector is perpendicular to the axis of the rod than when parallel with this, giving rise to what is called *dichroism*. This dichroism was demonstrated by Denton (1959), and when the magnitude of the dichroism, as measured by the optical density difference for light parallel to, and at right angles to, the planes of the discs, was plotted against the wavelength of the light, the curve corresponded with the total retinal optical density as a function of wavelength, indicating that most of the light-absorbing material was, indeed, responsible for the dichroism. When bleaching had been maintained for some time, to give retinol as the final product, the sense of the dichroism reversed, so that it would seem that the retinol (vitamin A) molecules, liberated from rhodopsin, remained in an orientated position but with their axes sticking out of the plane of the disc. A similar dichroism has been measured in single goldfish cones by microspectrophotometry (p. 407), the density for side-illumination of the rods being 2 to 3 times greater when the electric vector of the light was in the plane of the discs than when it was at right-angles (Harosi & MacNichol, 1974).

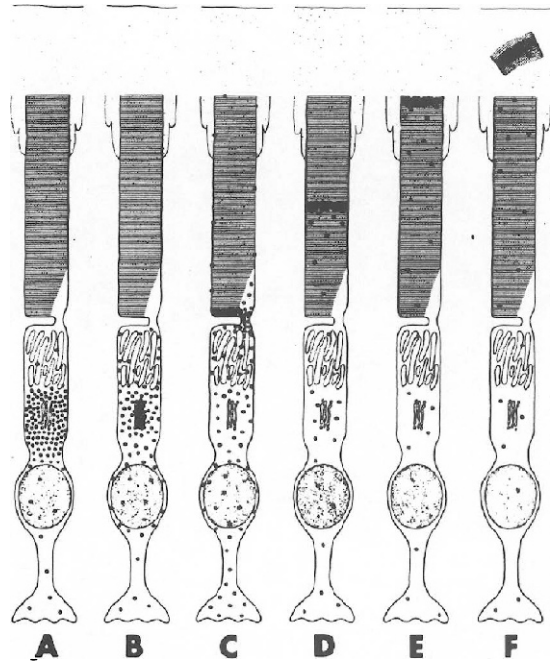

Fig. 8.6 Diagram illustrating the renewal of protein in rod visual cells as it is revealed in autoradiograms after administration of radioactive amino acids. New protein is at first concentrated at its major site of synthesis, the myoid zone of the inner segment (A). The protein molecules then scatter throughout the cell, many of them migrating by way of the Golgi complex, where they are modified by the addition of carbohydrate (B). Much of the new protein traverses the connecting cilium, and is incorporated into growing membranes at the base of the outer segment. Some of the protein diffuses from the new membranes into the outer cell membrane with which they are continuous (C). Detachment of the disc-shaped double membranes from the outer membrane traps labelled protein within the discs. Repeated formation of new membranes displaces the labelled discs along the outer segment (D). Eventually, they reach the end of the cell (E) from which they are shed in small packets. These are phagocytosed by the pigment epithelium (F). (Young, *Invest. Ophthal.*)

TURNOVER OF DISKS

Bairati & Orzalesi (1963) commented on the presence of lamellated bodies within pigment epithelial cells, bodies that resembled phagocytosed receptor disks, and they suggested that the outer segments were in a dynamic state of equilibrium, losing disks at their tips and renewing them at their bases. Young's studies on the incorporation of labelled amino acids into the receptors have confirmed this; thus, when an animal is injected with, say, ^{3}H-leucine, the proteins of the receptors are 'pulse-labelled', in the sense that they incorporate the radioactivity over a limited period of time, and this appears as a band on the autoradiogram. Formation of any new disks after this pulse-labelling will be seen as a displacement of the band towards the apex of the outer segment as in Fig. 8.6.

We may postpone further consideration of the ultrastructure of the photoreceptors until some changes taking place during life, and the preparation of the purified photopigment, have been described together with the amino acid sequence of its polypeptide component.

Pigment Epithelium-receptor Relations

The pigment epithelium is morphologically very intimately related to the photoreceptors. Thus, as described by Young (1971) in the monkey, the surface of the epithelium, facing the outer segments, presents a fringe of delicate cytoplasmic processes, and the rod outer segment is inserted deeply into this meshwork. At or near their origin from the cell body the pigment epithelial processes

form an irregularly fitting cap of flimsy cytoplasm presenting a sort of socket into which the end of the outer segment is loosely fitted. The two cells—receptor and epithelial—are closely apposed but not apparently sealed by any junctional complexes. In the human retina the epithelial processes are of two types, thin slender and broad rampart-like villous extensions encompassing the tips of the outer segments to a depth of about 4 μm (Spitznas & Hogan, 1970).

Phagocytosis

The process of nipping off and subsequent phagocytosis of the rod discs has been followed in the electron microscope; a group of discs at the tip curls or rolls up at the edges, arching in such a way that the convexity faces the remaining rods; the rod cell membrane folds into the zone of separation so formed and finally dissects, or nips off, the packet of discs which remains in the extracellular space wrapped in the outer-segment membrane. Later the packet is seen within the cytoplasm of a pigment epithelial cell as a phagosome. Each pigment epithelial cell engulfs some 2000 to 4000 discs daily (Young, 1971). The process is illustrated schematically in Fig. 8.7 taken from a later study by Steinberg *et al.* (1977) on human cones.

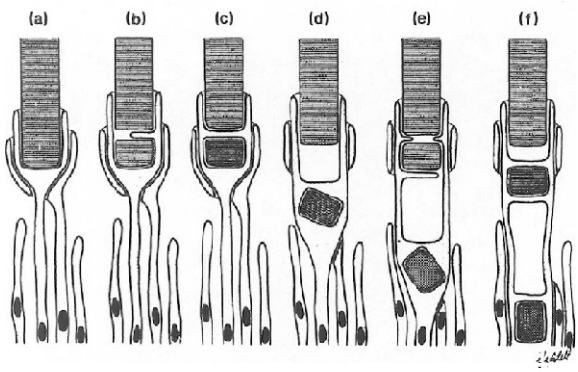

Fig. 8.7 Phagocytosis. Long villus-like pigment epithelial apical processes reach toward the cone from the pigment epithelium. The processes that reach the cone (two are arbitrarily shown) expand to ensheath a portion of the outer segment (*a*). The sequence (*a*)–(*f*) shows the successive phagocytosis of two packets of discs by one apical process. It is assumed that separation of the packet and resealing of outer-segment plasma membrane occurred *before* phagocytosis, (*b*) and (*e*). The forms assumed by apical process pseudopodia—(*b*) and (*e*)—were arbitrarily selected to illustrate several possibilities. The discs in the packets are shown becoming more osmiophilic than those in the outer segment, after they have been phagocytosed. Notice that as the first phagosome ascends in the process, (*d*) → (*f*), the sheath-like region of the process lengthens. Phagocytosis of the second packet of discs might also occur by a different process which, for some reason, displaces the first process. (Steinberg *et al.*, *Phil. Trans.* Drawn by J. Weddell.)

Digestion

Herman & Steinberg (1982) have described the process in the tapetal pigment epithelium of the opossum, a tissue well suited for such a study by virtue of the large size of the cells and the virtual complete absence of pigment in this specialized region. Lysosomes were localized at the basal ends of the pigment epithelial cells, so that the newly engulfed disks had to be carried through the cells to interact with these. On their way the disks underwent some changes, but only in the basal region of the cell was the acid phosphatase activity, characteristic of lysosomal activity, present in the phagosomes, suggesting fusion of the two types of body. Colchicine blocked the movement from apex to base, but not the formation of phagosomes, so that microtubules are concerned in movement within the cell rather than engulfment.

Diurnal Changes

La Vail (1976) observed that shedding of rod disks and the associated accumulation of phagosomes in the pigment epithelium, occurred as a burst some half-hour after onset of light when his rats were maintained on a 12-hour light–dark cycle. Subsequent studies on both rods and cones have confirmed the basic rhythmicity in disk shedding; thus in the pure cone retina of the lizard, the burst of disk shedding occurred during the dark, some

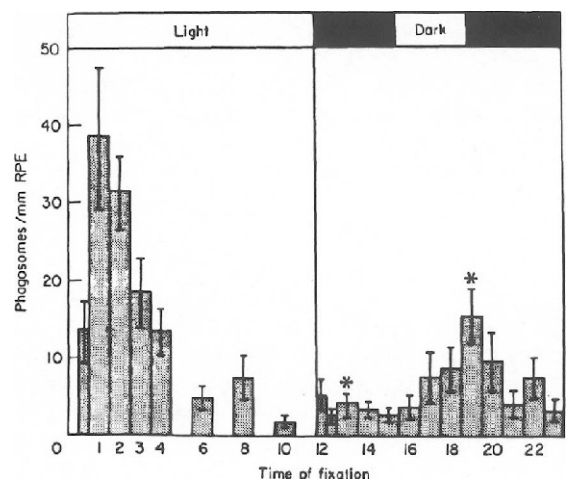

Fig. 8.8 Histogram showing the pattern of photoreceptor disc shedding in light-entrained tree-squirrels over a 24 h light–dark period. Each large vertical bar represents the mean total phagosomes per mm RPE obtained from counts of a single animal killed at hourly intervals except for half-width bars which designate animals killed at 30 min intervals. Error bars = 1 standard deviation of the mean. (*) Two animals killed at each of these times. (Tabor *et al.*, *Exp. Eye Res.*)

2 hr after lights-off (Young, 1972). In the cone-dominated retina of the ground squirrel, Long *et al.* (1986) found a biphasic cone shedding, increases in rate occurring 2–3 hr and 5–6 hr after light-offset.

When mixed retinas were examined, disk shedding, as measured by changes in phagosome content of pigment epithelial cells, occurred biphasically, with maxima in the light and dark cycles corresponding with rod and cone shedding. Thus in a study on the light-entrained tree squirrel, Tabor *et al.* (1980) found maximal phagosome counts 1 hr after light-onset, corresponding to rod shedding, and a less pronounced maximum in the middle of the dark period (Fig. 8.8) due to cone shedding recognized by the accumulation of phagosomes in the pigment epithelial cells close to the cones. Throughout the 24-hr period there was a continuous level of disk shedding on which the cyclical changes were imposed. In the rhesus monkey Anderson *et al.* (1980) measured phagosome counts in pigment epithelium in the foveal and extrafoveal regions, thus comparing cone and rod processes. They identified a morning burst of rod shedding; cone shedding was much less than that of rods, and occurred several hours after onset of light.

Circadian Rhythm

Tabor *et al.* (1979) found that when they kept their grey squirrels in constant darkness, the burst of rod shedding still occurred with a phase delay, so that in this species the rhythm is genuinely endogenous, the light–dark cycle tending to synchronize it. In some species, however, the cycle is entirely light-triggered, as with *Rana pipiens*; in *Xenopus* and the lizard *Sceloporus occidentalis*, on the other hand, the rhythms are circadian, so that constant darkness only advances onset of cone shedding, so that an increase in length of the outer segment can be measured (Bernstein *et al.*, 1984).

Fetal Rhythm

In the late fetal guinea pig the eye is well developed, so that disk shedding and phagocytosis can be examined in the absence of any light-cycle. Huang *et al.* (1982) found that both mother and fetus had a cyclic increase in phagocytosis in the pigment epithelium; that of the mother occurred immediately after light-onset but the fetus was 10 hr out of phase.

Pineal Gland

This is not involved in the rat's cyclical rod disk shedding, pinealectomized-superior cervical ganglionectomized rats shedding at the expected 1 hr after light-onset (Tamai *et al.*, 1978).[2]

ULTRASTRUCTURE OF THE CONES

These are built on the same plan, being made up of an outer and inner segment (Fig. 8.9) but in the cone the sacs are not separated from the plasma membrane, as they are in rods, but remain continuous with this and are thus analogous with the most basal sacs in the rod, remaining, in essence, deep invaginations of the plasma membrane. Development of the outer segment follows the same pattern as that described for the rod, but each invaginated sac moves outwards by a shift of the point of invagination rather than by a movement of the isolated sac (Nilsson, 1964).

Disc Renewal

When Young applied his autoradiographic technique to the study of turnover of the cone sacs he found a very different situation; the labelled amino acid never became concentrated in a band that migrated along the length of the cone outer segment; instead, the radioactivity became diffusely distributed throughout the outer segment. It was surmised, therefore, that the structure of the cone outer segment was more permanent, the incorporation of radioactivity into it representing a renewal of membrane material, including photopigment, in a more piecemeal fashion, old molecules being cast off and replaced with new throughout the whole structure, a process that Young called *molecular replacement* by contrast with *membrane replacement* in the rods.

Phagocytosis

Nevertheless, a number of studies have demonstrated phagocytosis of complete discs derived from cones; thus Hogan & Wood (1974) showed that human cones obviously shed bundles of discs that were enveloped in the plasma membrane of the cone outer segment and, outside this, the membrane of phagosome. Again Anderson & Fisher (1976) have shown that, in several species of squirrel retina, a portion of the outer segment contains, beyond the midpoint, discs that are free-floating in the cytoplasm, as with rods, and in the electron microscope there was clear evidence of a nipping off of bundles of discs by processes from pigment epithelial cells; thus, since there is only diffuse labelling of the outer segment, the absence of a sharp band of labelling is no evidence for the absence of continual replacement of discs.

Finally, Steinberg *et al.* (1977), working on the human retina, observed phagocytosis of cone discs; the process began, as with rods, in a curling of the discs; the packet could be seen still enclosed in plasma membrane of the outer segment, but this membrane pinched at one side. The apical pigment epithelial processes extended along

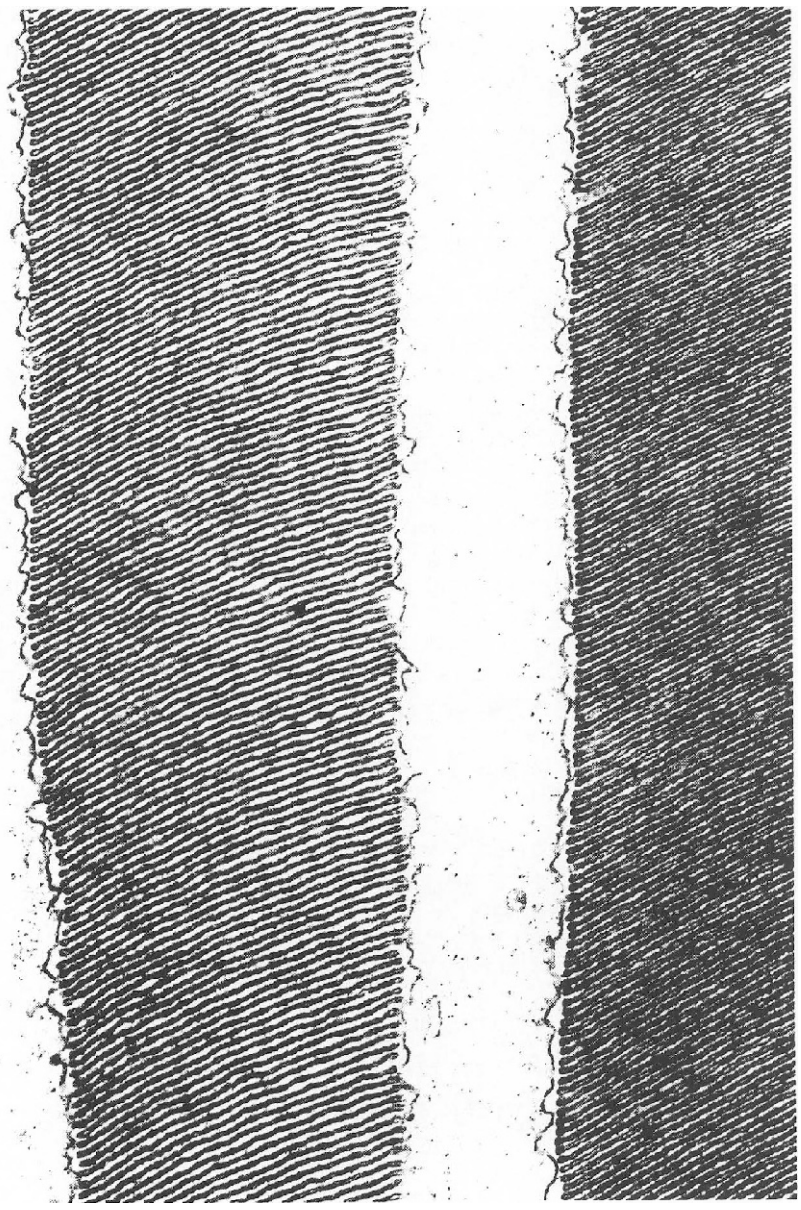

Fig. 8.9 Electron micrographs of outer segments of rhesus monkey cone (left) and rod (right) (× 40 000). (Courtesy R. W. Young.)

both sides of the outer segment but gave no indication that they might soon phagocytose the terminal packet. In other preparations, however, it appeared as though the long apical processes were sending in pseudopods that separated a bundle of terminal discs from the rest, but this process might have been preceded by a pinching off by the outer segment's plasma membrane. Since these processes occurred in eyes spanning a wide age it is unlikely that the phagocytosis was a pathological phenomenon.

Thus diffuse labelling of the discs seems not to be an absolute criterion for determining whether there is casting off and replacement; in this connexion we must note that, in the rod, there is some diffuse labelling similar to, but by no means as intense as, that in the cones (Bok & Young, 1972) indicating, presumably, exchange of newly synthesized protein with that already present in the discs or inter-disc space of the outer segment. Again Ditto (1975) saw no discrete bands of labelling in the developing

salamander's outer segments, yet there must have been a progressive formation of new discs from the base that would be expected to give discrete bands of labelling.

EXTRACTION AND CHARACTERIZATION OF PHOTOPIGMENT

Solubilization

As mentioned earlier, Kühne observed that visual purple in the intact retina went first yellow and then white when exposed to light; on allowing the eye to remain in the dark the changes were reversed. The problem of the photochemist is to extract from the retina the visual purple, and to elucidate its structural chemistry and the changes it undergoes during exposure to light. Extraction of the pigment is achieved by the use of a 'solubilizing agent' such as digitonin or bile salts; these form complexes with the pigment that permit it to form a homogeneous solution. The amount of pigments obtainable from a single retina is so small that special methods for characterizing them, and the changes they undergo, must be employed; of these the study of absorption spectra has been easily the most profitable.

Density Spectra

A solution of a pigment is coloured because the pigment molecules absorb wavelengths more strongly than others, so that white light, after transmission through the solution, has had some of its wavelengths selectively removed. Thus chlorophyll solutions are green because its molecules selectively remove red and blue wavelengths, and hence allow the green and yellow parts of the spectrum to pass through. Visual purple is magenta coloured because its molecules selectively absorb the middle region of the spectrum—blues and greens—allowing a mixture of red and violet lights to pass through with relatively little absorption. The selective absorption of visual purple solutions can be measured by passing a beam of light, whose wavelength can be varied throughout the spectrum at will, through the solution and measuring, with a suitable photocell, the amount of light-energy transmitted. This may be compared with that transmitted through water alone, and the difference gives the light-energy absorbed. The results may be plotted as a density spectrum, as in Fig. 8.10, where the optical density of the solution is plotted against wavelength. It will be seen that the spectrum has a maximum at about 500 nm in the blue-green. It is this *wavelength of maximal absorption*, indicated by λ_{max}, that we may use to characterize a given pigment extracted from the retina.

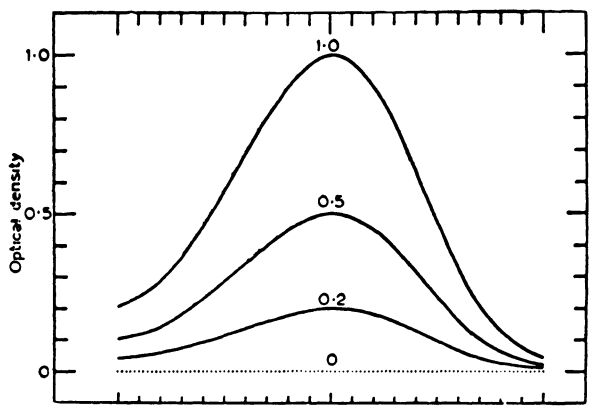

Fig. 8.10 Density spectra of different concentrations of visual purple. Note that as the concentration is reduced the curve becomes flatter although the wavelength of maximum absorption remains the same. (Dartnall, *The Visual Pigments.*)

Optical Density

If the absorption of light obeys Beer's Law, it is determined by the length of a path through which the light travels, and the concentration of pigment, in accordance with the equation:

$$\log_e I_{inc}/I_{trans} = \alpha_\lambda \times c \times l$$

where I_{inc} and I_{trans} are the intensities of the incident and transmitted beams respectively, c is the concentration, l the path-length, and α_λ is the *extinction coefficient* for this particular wavelength. This extinction coefficient is the measure of the tendency for the molecules to absorb light of a given wavelength, so that by plotting α_λ against wavelength the *extinction spectrum* so obtained is a measure of the absorption of the different wavelengths. If logarithms to base 10 are used in the above equation, and the concentration is expressed in moles per litre, the *optical density* or 'absorbance', A_λ, of a solution is defined as:

$$A_\lambda = \log_{10} I_{inc}/I_{trans} = \varepsilon_\lambda \times c \times l$$

where ε_λ is the *molar extinction coefficient*. For a given solution the optical density may be used as the measure of absorption of a given wavelength, and the curve obtained by plotting optical density against wavelength is called a *density spectrum*[3] (Fig. 8.10). It will be clear from the above equations that the extinction coefficients will be independent of concentration of pigments so that extinction spectra will also be independent of this variable; the optical density, on the other hand, increases with increasing concentration, and the shape of the density spectrum will, indeed, vary according to the concentration of the pigment in the solution being studied. Where the concentration of absorbing material is not directly determined, as in studies on the intact retina, then the shape of the density spectrum gives a clue to the actual concentration present. We may note, finally, that if the density for any given wavelength is expressed as a percentage of the maximum density (in the case of rhodopsin 500 nm) then the density spectrum does become independent of concentration, and it may be used to characterize the pigment.

Difference Spectra

It usually happens that visual pigment solutions are contaminated by light-absorbing impurities; if these are unaffected by

light, in the sense that they retain their light-absorbing qualities unchanged after exposure, then the true absorption spectrum of the visual pigment may usually be deduced from the *difference spectrum*, given by measuring the absorption spectrum of the solution before and after bleaching with white light; thus, before the bleaching, the absorption will be due to visual pigment plus impurities; after bleaching it will be due to impurities alone if the visual pigment has become colourless. In many cases, of course, the visual pigment does not become colourless, but allowance can usually be made for this residual absorption.

Purity

Retinal extracts may contain mixtures of visual pigments, in which case it becomes important to decide when any extract is homogeneous or not. Dartnall has developed a technique of partial bleaching with selectively chosen wavelengths that permits of an unequivocal demonstration whether or not the preparation contains more than one visual pigment.

Photosensitivity

The rate at which a simple photochemical reaction proceeds is governed primarily by the rate of absorption of quanta of light and the efficiency with which an absorbed quantum reacts. The rate of absorption will be given by the product of I, the light intensity expressed in quanta per second per unit area, α, the extinction coefficient, and γ, the quantum efficiency of the reaction.

$$\text{Rate of reaction} = \alpha \times \gamma \times I$$

The product $\alpha \times \gamma$ is called the *photosensitivity*; it has units of cm^2 and may be regarded as the effective cross-sectional area of the molecule when bombarded by photons. The *molar photosensitivity*, based on the molar extinction coefficient, ε_λ, can be calculated by multiplying by Avogadro's No. 6.023×10^{23}, by 0.4342 (normal to decadic logs) and by 10^{-3} (cm^3 to litre). $\varepsilon \times \gamma = 2.615 \times 10^{20} \alpha\gamma\ M^{-1}\,cm^{-1}$.

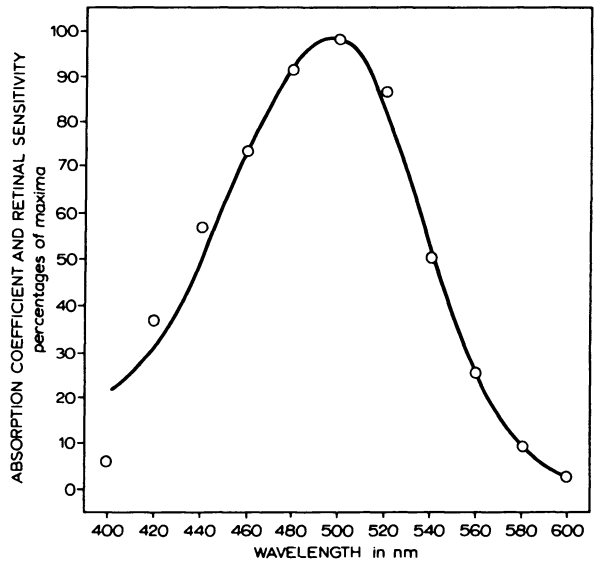

Fig. 8.11 Comparison of human retinal scotopic sensitivity at different wavelengths, as determined by Crawford, with the absorption spectrum of human visual purple. The curve represents the absorption spectrum whilst the plotted points represent human scotopic sensitivity. (Crescitelli & Dartnall, *Nature*.)

Density Spectrum and Scotopic Sensitivity

Human Scotopic Sensitivity

The density spectrum of the pigment extracted from the rods of the dark-adapted retina may be used to determine whether this pigment is, indeed, responsible for night vision, since the efficiency of any wavelength in evoking a sensation of light must be closely related to the efficiency with which it is absorbed by the rods. Clearly, if only 1% of orange light falling on the retina were absorbed, whilst 90% of the blue light were absorbed, we should have to use ninety times as much orange light-energy to evoke the sensation of light. In Fig. 8.11 two things have been plotted; the smooth curve shows the absorption spectrum of visual purple extracted from a dark-adapted human eye, whilst the plotted points are the sensitivities of the dark-adapted human eye to the different wavelengths, the so-called action spectrum of the human eye. As indicated earlier, the dark-adapted eye is achromatic at light intensities in the region of the threshold; the different wavelengths do not evoke the sensation of colour but simply to light, and the experiment consisted of measuring the thresholds for the different wavelengths; the reciprocals of these, measured in quanta, represent the visual efficiencies of the wavelengths. The agreement between the two measurements is striking.

Sensitivity in Animals

In animals, also, the scotopic sensitivity of the eye can be measured; for example, by determining the intensities of different wavelengths required to evoke a *b*-wave of fixed magnitude in the electroretinogram, or to evoke a discharge of fixed frequency in a single optic nerve fibre. The reciprocals of these values give the sensitivities of the retina at the different wavelengths and, when plotted against wavelength, give, usually, the characteristic 'rhodopsin-type' of curve with a maximum in the region of 500 nm. If the light-adapted retina is employed, on the other hand, there is a characteristic shift in the maximum towards, the longer wavelengths to give a maximum in the yellow-green at 560 nm. This is the *Purkinje shift* and represents the change in spectral sensitivity of the eye due to passing from rod to cone vision. Under these conditions, of course, the eye appreciates the colours of the stimuli.

The Nature of Rhodopsin

Lipid Component

The rhodopsin extracted from the retina is a chromoprotein; as characteristically prepared in a digitonin extract, a considerable proportion of the material is phospholipid, but the extent to which this is a genuine part of the rhodopsin molecule is difficult to state since, as we have seen, the molecule is embedded in the membranes of the outer segment, the material of the membrane being largely phospholipid; solubilization by digitonin brings most of the membrane lipid into the micelles. A carbohydrate fraction has also been identified (Heller, 1968). When preparations of rhodopsin are made with a view to characterization of its molecular weight, the lipid fraction is separated, for example by use of a detergent such as Triton X and subsequent removal of the detergent and lipid with toluene (Zorn & Futterman, 1971); in this way the amount of lipid associated with the extracted material is reduced to about 5% of its original amount.

EFFECTS OF LIPID REMOVAL

By employing enzymatic treatments, the amount of lipid can be reduced still more, but when this is reduced to the point that the amounts of phosphatidyl ethanolamine and phosphatidyl serine are reduced to below 0.1 per molecule of rhodopsin there is a loss of absorbance of about 36% at the wavelength of maximum absorbance, namely 500 nm (Borggreven *et al.*, 1972). In fact, considerably smaller losses of lipid are sufficient to affect the absorbing power of the rhodopsin so, although the absorption is due to the chromophore-protein complex, the shape of the complex is presumably stabilized by its association with lipid, as, of course, is the situation in the rod outer segment. The protein would be said to be partially denatured by removal from its normal lipid environment; this denaturation, or loss of shape, presumably affects the chemical interaction between the chromophore and the protein, an interaction that is responsible for its ability to absorb visible light.

Molecular Structure

The complete amino-acid sequence of the polypeptide component of rhodopsin was determined by Ovchinnikov *et al.* (1982), Hargrave *et al.* (1983) and Nathans & Hogness (1983).[4] The polypeptide chain consists of 348 amino acids, many of which undergo post-translational changes such as acetylation, glycosylation and phosphorylation. Of some importance is the distribution of charged amino acids, which occur in tight clusters separated by regions with few or no charged amino acids; in contrast to these, some seven non-polar helical hydrophobic regions were deduced, regions that would most probably be located within the lipid bilayer of the disk membrane, as indicated by Fig. 8.12, the charged, polar,

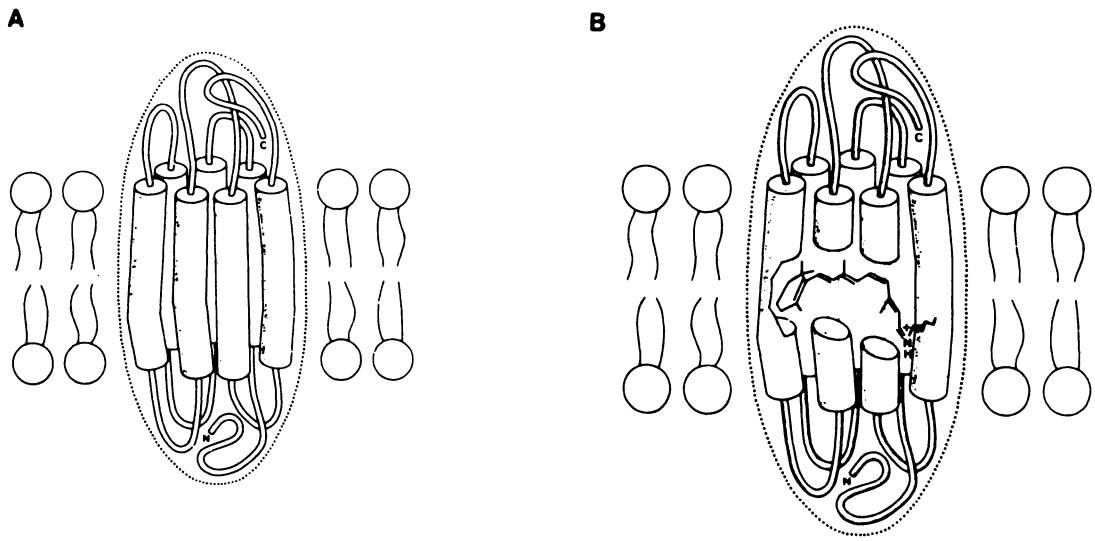

Fig. 8.12 Helical bundle model for rhodopsin. (A) Rhodopsin is hypothesized to consist of an elongated bundle of 7 helices whose connecting regions and chain termini form the aqueous-exposed surface regions. Several of the helices are shown to contain kinks or bends. (B) Parts of helices are cut away to show the retinal (not to scale) attached to the side chain of Lys^{216} midway in Helix VII. The inside surfaces of several helices are shown as providing a binding pocket for the retinal. (Hargrave *et al.*, *Vision Res.*)

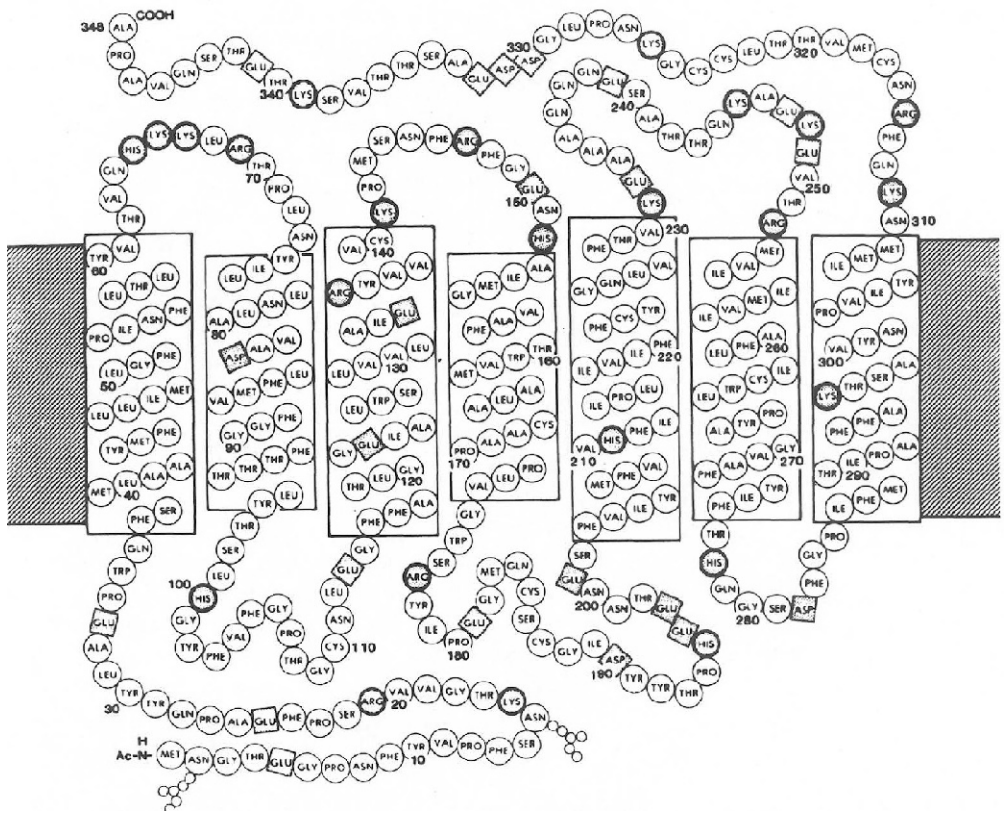

Fig. 8.13 A model for the organization of rhodopsin's polypeptide chain in the lipid bilayer of the disc membrane. The amino-terminal amino acid, Ac-Met, is exposed at the internal aqueous surface of the disc membrane. Rhodopsin's polypeptide chain is shown to traverse the lipid bilayer seven times. The carboxyl-terminal Ala is exposed at the external aqueous surface of the disc membrane. Positively charged amino acids (Lys, Arg, His) are shown as shaded heavy circles, and negatively charged amino acids (Glu, Asp) are shown as shaded squares. Striped areas at each side of the drawing indicate the low polarity portion of the lipid bilayer (the fatty acid side chains and the lower half of the phospholipid head groups). (Adapted from Hargrave *et al.*, 1983.)

sequences projecting into the aqueous phase and being susceptible to enzymatic and other alterations. There are, however, charged residues in the membrane-bound helices; thus Lys^{296} contains the retinal in Schiff's base linkage which occurs midway in Helix 7. Rhodopsin contains oligosaccharide chains, bound at the aqueous, polar, surfaces. A possible model of the three-dimensional structure of rhodopsin is illustrated in Fig. 8.13, where it is seen to consist of a helical bundle whose core is made up of the seven hydrophobic helices, whilst in the aqueous phase we have the interconnecting peptide chains and their terminal residues. As shown in Fig. 8.12B, parts of the helices are cut away to show the retinal attached to the side-chain of Lys^{206} midway in Helix VII. We may assume that the light-induced change in retinal transmits its effects through alteration in the orientation of the helices leading to changes on the surface that allow it to react with transducin thus initiating the cascade of events leading to the photic response of the receptor (p. 291).

PHOSPHORYLATION

All visual pigments have the hydroxy-amino acids serine and threonine well represented in their carboxy-terminal sequences, and thus expose phosphorylation sites to the cytoplasm of the receptor (Thompson & Findlay, 1984). As we shall see, the phosphorylation of photoactivated rhodopsin is an important step in bringing the light-induced excitation of rods to an end.

THE OLIGOSACCHARIDE CHAINS

Rhodopsin is a glycoprotein, the polypeptide chain being covalently linked to a polysaccharide through asparagine residues; the carbohydrate molecules are *N*-acetyl glucosamine and mannose. Fukuda *et al.* (1979) described a major and a minor oligosaccharide, whereas Liang *et al.* (1979) identified three fractions, A, B and C with the structures indicated in Fig. 8.14, A being the same as Fukuda *et al.*'s major component.

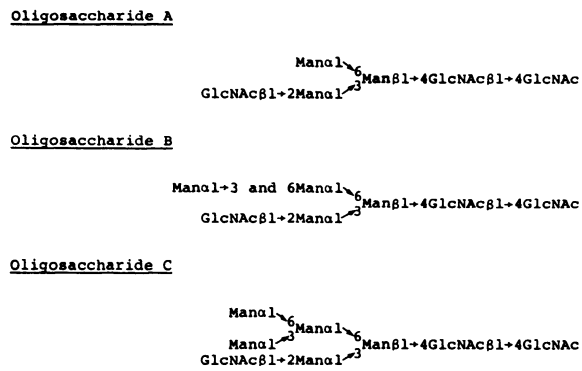

Fig. 8.14 Proposed structures of oligosaccharides A, B and C. (Liang *et al.*, *J. Biol. Chem.*)

SYNTHESIS AND TRANSPORT TO OUTER SEGMENTS

This aspect of rhodopsin metabolism has been reviewed by Bok (1985). As we should expect, rhodopsin is synthesized at the endoplasmic reticulum and carried to the Golgi apparatus in the inner segment of the receptor. The synthetic process includes the glycosylation of the terminal polypeptide chain. Opsin-rich vesicles are then transported towards the apical region of the inner segment into the connecting cilium, where they fuse with the plasma membrane in a specialized region consisting of an array of ridges and grooves called by Peters *et al.* (1983) the *periciliary ridge complex* (Fig. 8.15). In the receptor plasma membrane the opsin diffuses forward towards the outer segment, some inhibitory process preventing backward diffusion along the inner segment membrane.[5]

Incorporation of the Chromophore

Injections of labelled retinol into frog and mice in the dark, under conditions where light-induced changes were excluded, showed that rhodopsin could exchange its chromophore with exogenous material in the dark, thus indicating that assembly of the completed molecule was possible by a reaction between chromophore and opsin (DeFoe & Bok, 1983). Autoradiographic studies indicated that incorporation of labelled retinal occurred

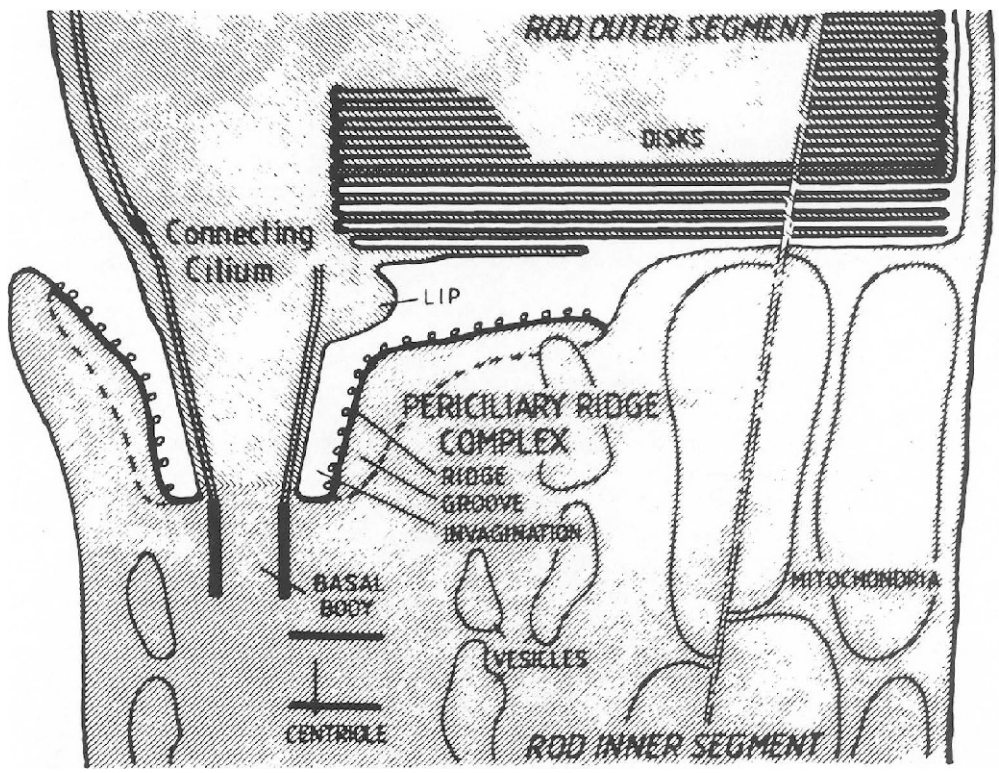

Fig. 8.15 Diagram of the organization of a periciliary ridge complex and of its associated subcellular components in a rod cell of the frog retina. The diagram is restricted to the junctional region between the inner and outer segments of the retinal rod. The width of the cell is shortened as indicated by the gap (dashed lines) in the right half of the diagram. (Peters *et al.*, *J. Cell Biol.*)

exclusively in the outer segments, since after intravenous injection of ^{3}H-retinol bound to RBP and transthyretin, no ^{3}H-retinal was found in the inner segments, and accumulation in the outer segments only became significant after the pigment epithelial cells had become heavily labelled. This would be consistent with the finding that the specific receptor for retinol binding protein, allowing transport of retinol from choroidal blood to the pigment epithelium (p. 252) occurs on the surface of the pigment epithelium (Bok & Heller, 1976).

The Chromophore and Visual Cycle

Each molecule has one light-absorbing chromophore group on it. The nature of this chromophore group, responsible for the colour of the molecule, and thus of its characteristic absorption, and the nature of its linkage to the protein moiety, are the keys to the photochemistry of vision.

When a retina is exposed to light the magenta colour of the visual pigment, rhodopsin, is lost—the retina is said to be bleached, and it was shown by Wald (1935) that, during this bleaching process, the chromophore could be split off, and it was identified as *retinene*, which is vitamin A aldehyde (Fig. 8.16) or, as it has been subsequently called, *retinal*. The remaining colourless protein was called *opsin*, and it was the combination between the two molecules that transformed the yellow retinal into the magenta or purple rhodopsin. Within the retina, retinal could be, and is, indeed, reduced to vitamin A by an alcohol dehydrogenase—retinal reductase. Under appropriate conditions the retinal and opsin could be made to recombine to *regenerate* rhodopsin.

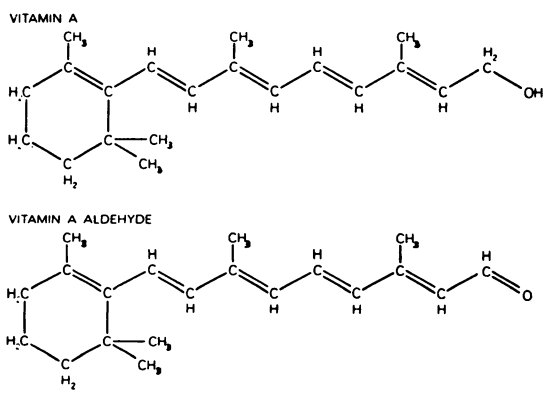

Fig 8.16 Structural formulae of vitamina A, or retinol, and its aldehyde, retinal (retinene).

Thus the basic visual cycle defined by Wald was:

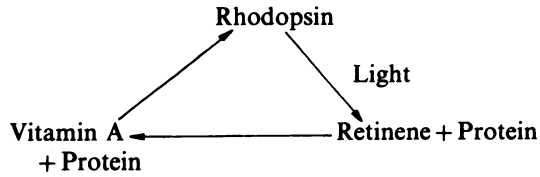

The Shape of the Molecule

Wu & Stryer (1972) found that they were able to attach certain fluorescent markers to the rhodopsin molecule in what seemed to be specific sites, which they called A, B and C, and which were all different from the site of attachment of the retinal. These fluorescent markers were able to transfer their absorbed light-energy to retinal and cause it to emit this, since the λ_{max} of rhodopsin was fairly close to the emission bands of the fluorescent markers. From the efficiency of energy-transfers they computed that the sites were 7.5, 5.5 and 4.8 nm distant from retinal, an arrangement that would correspond to an elongated shape; thus the rhodopsin molecule might well occupy most of the thickness of a disc membrane.

THE RETINAL–OPSIN LINK

According to the studies of Collins & Morton (1950), retinal forms a Schiff-base with amines; thus methylamine reacts with retinal to give retinal methylimine:

$$C_{19}H_{27}.CHO + CH_3.NH_2 \rightarrow C_{19}H_{27}\underset{\displaystyle H}{\underset{|}{C}} = N.CH_3 + H_2O$$

or more generally:

$$C_{19}H_{27}.\underset{\displaystyle H}{\underset{|}{C}} = O + H\text{—}\underset{\displaystyle H}{\underset{|}{N}}\text{—}R \rightleftharpoons C_{19}H_{27} - \underset{\displaystyle H}{\underset{|}{C}} = NR + H_2O$$

Retinal — Amine — Aldimine — Water

The reactions are reversible so that the breakdown of the aldimine to retinal and amine may be described as hydrolysis. The aldimines in neutral solution are pale yellow but in acid solution, when they take on the protonated form, they give a red solution:

$$C_{19}H_{27}C(H)=NCH_3 + H^+ \rightleftharpoons C_{19}H_2.C(H)=\overset{+}{N}(H)-CH_3$$

The protonated form is more stable than the neutral form in the sense that it is not hydrolysed in acid reaction.

N-retinylidene Opsin

By comparing the characteristics of these artificial aldimines with those of partially bleached rhodopsin, where the chromophore group was still attached to the opsin, Collins & Morton concluded that rhodopsin could be described as N-retinylidene opsin (NRO) with the retinal linked to an amino-group of the opsin molecule. Although this conclusion was based on studies of a rhodopsin that had been changed chemically through absorption of light, subsequent studies have confirmed that in its native unbleached state rhodopsin contains retinal linked in the above manner. For example Mathies *et al.* (1976) analysed the Raman spectrum and deduced from the line at 1660 cm^{-1} the presence of a protonated Schiff base.

Isomers of Retinal

Early studies on regeneration of rhodopsin from mixtures of the opsin and retinal formed by bleaching, indicated a far less efficient and complete regeneration than that obtained in the intact retina, and the main cause for this inefficiency turned out to be the necessity for a special isomer of retinene for the combination with opsin (Hubbard & Wald, 1952).

Retinal and vitamin A contain five double-bonds joining C-atoms, and the presence of these gives the possibility of numerous *cis–trans* isomers, due to the fact that rotation about a double bond is not possible, so that a molecule illustrated by Fig. 8.17a is different from that illustrated by Fig. 8.17b. Of the various possible isomers obtained by rotating the molecule about different double bonds Wald found two that were capable of condensing with opsin to give photosensitive pigments. One, neo-b retinal or 11-*cis* retinal (Fig. 8.18), when incubated with

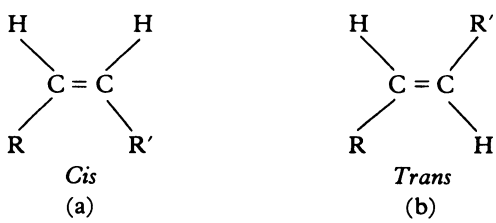

Fig. 8.17 *Cis–trans* isomerism.

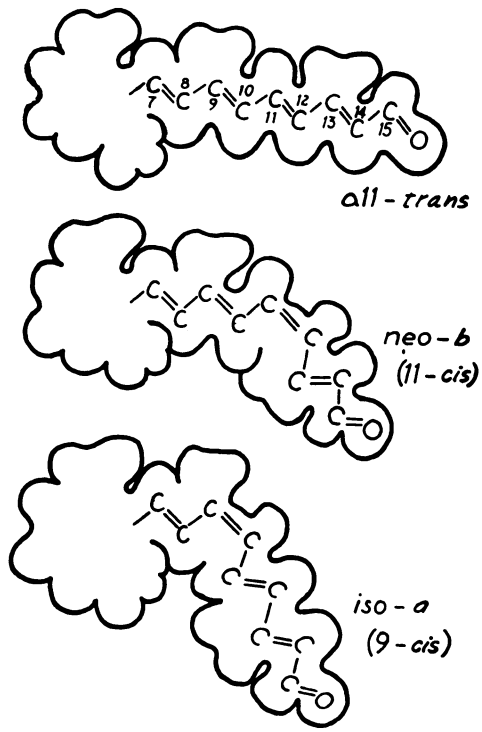

Fig 8.18 Shapes of retinene isomers. The all-*trans* isomer is straight; a *cis*-linkage introduces a bend into the molecule. In addition, the 11-*cis* linkage encounters steric hindrance and therefore twists the molecule out of the plane in the manner not shown in the diagram. (Hubbard & Kropf, *Ann. N.Y. Acad. Sci.*)

opsin gave rhodopsin, whilst the other, isoretinal-a or 9-*cis* retinal (Fig. 8.18) gave a photosensitive pigment, *isorhodopsin*, with λ_{max} of 487 nm.

Isomerization

The reason why reversal of the changes undergone by bleaching is not always possible is because the retinal that splits off from rhodopsin has the all-*trans* form, which is not active for resynthesis; thus retine in the rhodopsin molecule is in the 11-*cis* of neo-b form, but when split off is in the all-*trans* form. In order to be of further use the all-*trans* must be isomerized, a process that can take place in the retina in the presence of an enzyme, *retinal isomerase*, although mere exposure to light also causes isomerization—*photo-isomerization.*

INTERMEDIATE STAGES IN BREAKDOWN TO RETINAL AND OPSIN

It was originally thought that the primary action of light was to split retinal from opsin, but subsequent studies

have emphasized that the photochemical reaction, induced by the absorption of a quantum of light, is only the beginning of a cascade of reactions that ultimately lead to this splitting off of the chromophore, reactions that are no longer dependent on the absorption of light and so are described as thermal. Many of these reactions involve very small changes in internal energy of the various intermediates and may occur so rapidly at body-temperature that their products would escape detection even when employing the changes of absorption spectrum as a means of identifying the various stages. However, by carrying out the initial photochemical reaction at a very low temperature it is possible to arrest the subsequent thermal changes, and the history of the analysis of these thermal changes has depended on the degree of cooling that was employed. Thus Lythgoe & Quilliam (1938) were able to identify an intermediate compound, which they called *transient orange*, because they cooled the rhodopsin to 0°C during irradiation. When the solution was subsequently warmed, a yellow product, which they called *indicator yellow* and is now known as *N-retinylidine opsin*, was produced; subsequent work showed that a further thermal reaction resulted in the splitting of the Schiff base that bound retinal to opsin in N-retinylidine opsin to give retinal and opsin as separate molecules.

Bathorhodopsin

When liquid nitrogen (temperature −195°C) was employed to cool the solution of rhodopsin before and during exposure to light, and the mixture was subsequently warmed in stages, the series of products indicated by Fig. 8.19A was obtained (Abrahamson & Ostroy, 1967); thus the only reaction requiring light-energy was the conversion of rhodopsin to prelumirhodopsin (subsequently called bathorhodopsin), recognized by the change in λ_{max} from 498 nm to 543 nm.

Lumirhodopsin and Metarhodopsins

By warming to −140°C bathorhodopsin is converted to lumirhodopsin, which remains stable at temperatures up

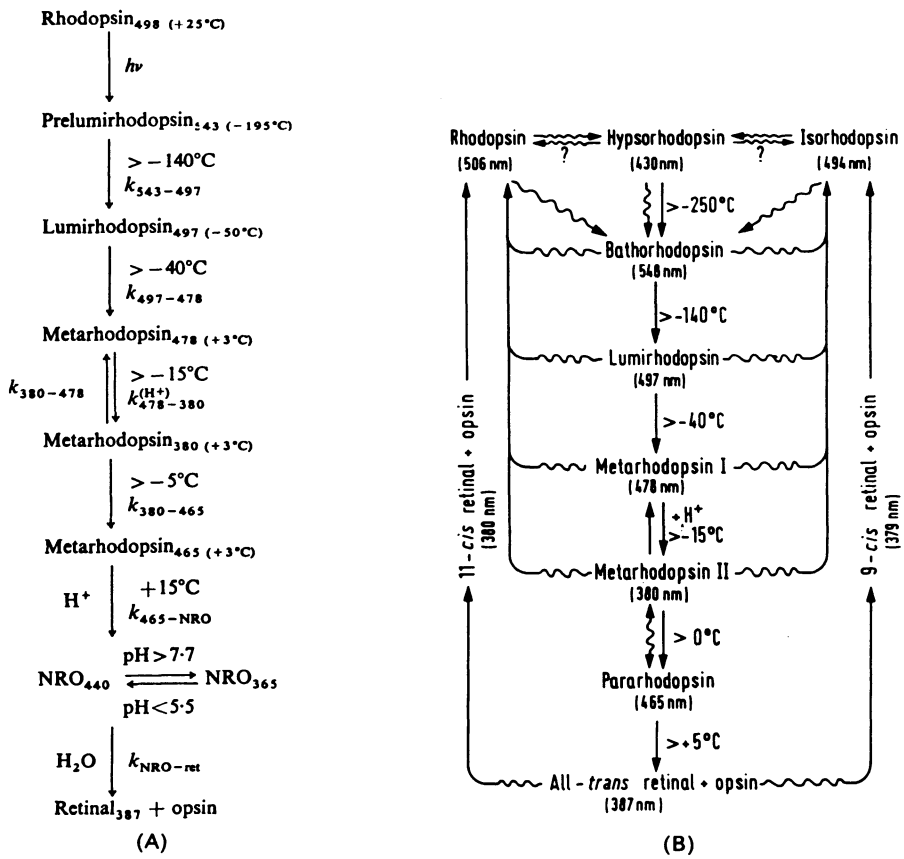

Fig. 8.19 A. Reactions in the thermolysis of rhodopsin after absorption of a quantum of light, according to Abrahamson & Ostroy. (*Progr. Biophys.*) B. Stages in the bleaching of rhodopsin according to Yoshizawa. Photoreactions are symbolized by wavy lines, thermal reactions by straight ones. (*Handbook of Sensory Physiology.*)

to −40°C, above which it is converted to a series of *metarhodopsins*, differing in their λ_{max}, then to N-retinylidene opsin (NRO) previously called *indicator yellow* because of its change of colour with pH, and finally NRO is hydrolysed to retinal and opsin. In all but the last of these successive changes, the rhodopsin molecule has retained its attached chromophore group, retinal, so that the alterations have been essentially changes in the configuration of the whole molecule. The final splitting of the chromophore group from the protein moiety represents the breaking of the Schiff-base link.

Hypsorhodopsin

When liquid helium was employed (temperature −270°C) Yoshizawa (1972) identified an earlier proto-product, which has been called hypsorhodopsin with a λ_{max} at 430 nm; as indicated by the scheme of Fig. 8.19B, this can be converted by a thermal reaction to batho-rhodopsin by warming to −250°C.

Photo-isomerization

The situation becomes much more complex, however, when the effects of light on the reaction mixture at different stages are taken into account, since light can itself bring about many of these conversions. For example, light converts hypsorhodopsin to bathorhodopsin at the temperature of liquid helium; moreover, light can cause regeneration of both rhodopsin and isorhodopsin so that at this low temperature there will be a mixture of four compounds, rhodopsin, isorhodopsin, hypso- and batho-rhodopsin in relative amounts depending on the wavelength of the irradiating light; thus a wavelength of 436 nm favours conversion to bathorhodopsin, whereas at 600 nm there is almost complete reversal to rhodopsin.

Isorhodopsin

As we have indicated above, there are two isomers of retinal, namely 11-*cis* and 9-*cis*, capable of combining with opsin to produce photosensitive pigments, called rhodopsin and isorhodopsin respectively. Photo-isomerization of the products of photolysis of rhodopsin can lead to production of isorhodopsin (λ_{max} = 496 nm) in the retina. The requirement for the initial photo-isomerization is that the chromophore be attached to the opsin moiety. Examination of the products of exposing the eye to very bright and very short flashes of light—*flash photolysis*—has shown that isorhodopsin may, indeed, be formed under these conditions (Bridges, 1961; Frank, 1969; Ripps & Weale, 1969). We may note also that this tendency for photoreversal of the light-induced changes leads to a considerable reduction in the efficiency of bleaching by short flashes of light; thus Hagins (1956) found that brief flashes of light, however intense, were incapable of bleaching all the rhodopsin in the retina, and later Pugh (1975), using a xenon flash, found that no more than 60% of the rhodopsin in the human eye could be bleached.

Metarhodopsins

Metarhodopsin I is stable up to about −15°C, above which it comes into tautomeric equilibrium with meta-rhodopsin II, a change that involves a large change in λ_{max} from 478 to 380 nm, and involves the uptake of an H^+-ion. On warming to a higher temperature, MR II is transformed into *N-retinylidene opsin* (NRO or *indicator yellow*) either directly or through Meta III, which has been called *pararhodopsin*, and is probably equivalent to Lythgoe's & Quilliam's transient orange. N-retinylidene opsin (NRO) has indicator qualities and may be hydrolysed to release the chromophore from opsin.

THE NATURE OF THE CHANGES

Absorption of a quantum of light brings the light-sensitive molecule into an 'excited state' of high potential energy; in this state strains may be introduced in the molecule leading to, perhaps, the rearrangement of chemical bonds or the rupturing of these. These effects are accompanied by changes in the absorbance of the molecule, revealed as a shift in λ_{max}, and also in the shape, of the absorption spectrum. The most important finding of Wald was that the retinal released from rhodopsin had changed its stereo-isomeric configuration from the 11-*cis* to the all-*trans* form; this was certainly true of the released retinal, but the evidence indicated that the very first change following absorption of light consisted in this photo-isomerization of the retinal chromophore *in situ*. Thus, the first effect of the absorption of energy might be regarded as the removing of a linch-pin that held the retinal molecule in the 11-*cis* configuration, the linch-pin consisting of suitable secondary chemical interactions between the retinal and opsin molecules that held the retinal in this particular configuration (Dartnall, 1957).

Hypsorhodopsin and Bathorhodopsin

The conversion of rhodopsin to hypsorhodopsin, or bathorhodopsin, producing considerable shifts in λ_{max}, must be interpreted in terms of a primary conversion of the retinal group to the all-*trans* form, leading to different

side-chain reactions between the prosthetic group and opsin; thus they occur at so low a temperature that it is considered unlikely that any change in the opsin molecule would take place.

Photorhodopsin

By employing picosecond laser photolysis the demonstration of early comers in the photolytic process has been facilitated; thus a precursor to hypso- and bathorhodopsins has been identified, called *photorhodopsin*, with a λ_{max} longer than that of bathorhodopsin. Its probable structure has been discussed by Yoshizawa *et al.* (1984), who conclude that it is, indeed, an intermediate, rather than a singlet excited state (Peters *et al.*, 1977), the retinal being in a twisted all-*trans* state, the Schiff base being probably protonated, as the λ_{max} is greater than that of bathorhodopsin. Two possible routes for the transition are indicated in Fig. 8.20a and b, S_1 being the singlet excited state following absorption of a photon.

Strains in the Chromophore

According to Abrahamson & Wiesenfeld (1972), the position of the λ_{max} of hypsorhodopsin at the short wavelength of 430 nm indicates the absence of significant secondary interaction between the retinal molecule, in its all-*trans* state, and the opsin molecule, since it is these secondary interactions that cause strains in the retinal molecule that enable it to absorb light of longer wavelengths. The position of the λ_{max} of bathorhodopsin, at the longer wavelength of 548 nm, indicates, on the other hand, that new strains have been placed on the retinal molecule owing to secondary interaction with the opsin molecule. Thus, if hypsorhodopsin is an earlier intermediate than bathorhodopsin, the process of photoisomerization may be accounted for as follows: In the excited state, the chromophore, because of the breakdown of secondary linkages with the opsin residue, is potentially able to undergo rotations about both single and double bonds, rotations that would be prevented sterically by its secondary interactions. For example, the rotation about the 11–12 double bond necessary for conversion of the 11-*cis* to the all-*trans* structure, might be preceded by rotation about a single bond (from S-*trans* to S-*cis* or *vice versa*) in order to avoid interference with the opsin structure. Such an isomerization could result in very little interaction with opsin, and this may be the basis for hypsorhodopsin. On absorption of a further photon at the liquid helium temperature, or by raising the temperature to 23°K (−250°C) in the dark, the chromophore might again undergo a rotation about the same, or another, single bond with the consequent establishment of a new side-chain that interacted strongly with opsin to give a highly strained and distorted molecule—bathorhodopsin—absorbing at long wavelengths. The changes through lumirhodopsin to metarhodopsin I, occurring at higher temperature, are thought to involve changes in interaction between the prosthetic group and opsin, this time owing to changes in conformation of the opsin molecule, changes that have become possible through the primary change in the shape of the prosthetic group from the 11-*cis* to the all-*trans* orientation.

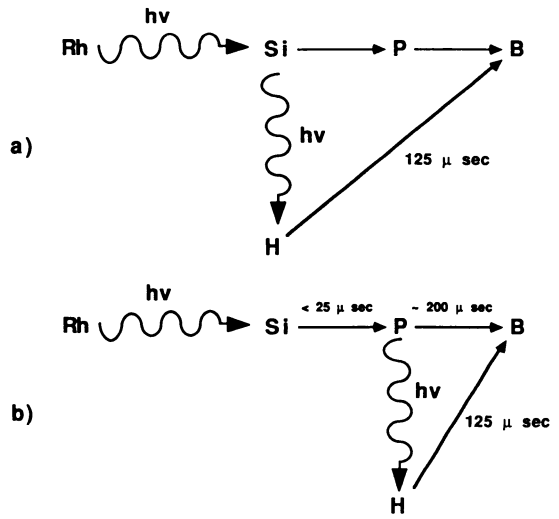

Fig. 8.20 Two possible routes for the transition from rhodopsin to bathorhodopsin. (After Yoshizawa *et al.*, *Vision Res.*)

Hubbard–Kropf Model

In Fig. 8.21 is illustrated the hypothesis of Hubbard & Kropf (1959) that accounts, in a general way, for the successive changes; thus retinal is combined stably with rhodopsin because its 11-*cis* shape enables it to fit into a suitable pocket on the surface of opsin; absorption of light provides the prosthetic group with sufficient energy to break loose from this pocket and thereby assume the all-*trans* configuration, giving rise to hypso- and bathorhodopsins. Subsequent changes are due to alterations in the shape of the opsin pocket that, among other things, reveal chemical groupings that were formerly shielded from the solution, e.g. SH-groups and an H^+-binding group, processes that are manifest as changes in the reactivity of the rhodopsin to SH-reagents and changes in pH of the medium.

Changes in pH

Thus Wong & Ostroy (1973) measured the changes in light absorbance of metarhodopsin at 380 nm during its

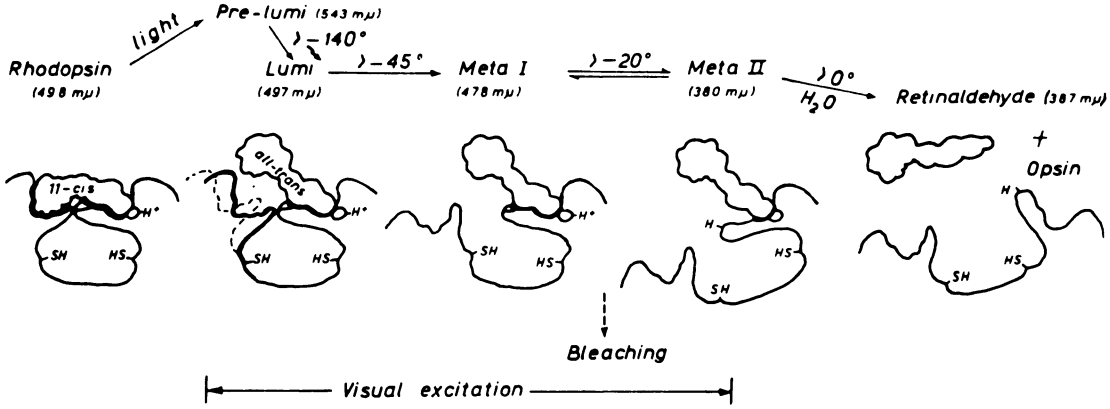

Fig. 8.21 Hubbard-Kropf model of stages in the bleaching of rhodopsin. Rhodopsin has, as a chromophore, 11-*cis* retinal, which fits closely a section of the opsin structure. The only action of light is to isomerize retinal to all-*trans* configuration (prelumirhodopsin). Then the structure of opsin opens in stages (lumirhodopsin, metarhodopsin I and II), until finally the retinaldehyde is hydrolysed away from opsin. Bleaching occurs in the transition from metarhodopsin I and II; and by this stage visual excitation must also have occurred. The opening of the opsin structure exposes new groups, including two —SH groups of one H^+-binding group. The absorption maxima shown are for prelumirhodopsin at −190°C, lumirhodopsin at −65°, and other pigments at room temperature. (Wald, *Proc. Int. Congr. Physiol.*)

conversion to metarhodopsin II at −15°C, and correlated these with the change in pH of the medium as revealed by the change in colour of bromocresol green measured by a change in absorbance at the long wavelength 612.5 nm.

Borohydride Reaction

Another example of changed reactivity is given by treating rhodopsin or metarhodopsin II with borohydride; this substance is a reducing agent that adds hydrogen to the Schiff-base of N-retinylidene opsin:

$$C_{19}H_{27}CH{=}N \times \text{Opsin} + NaBH_4 \rightarrow C_{19}H_{27} \times CH_2 \times NH \times \text{Opsin}$$

It was found that this reduction did not occur with rhodopsin but only when the metarhodopsin II state had been reached, presumably because the CH=N group had become exposed at this stage, being buried in the opsin molecule up to this point.

SH-groups

Again, opsin will react with *p*-chloromercuribenzoate (PCMB) through its SH-groups; Wald & Brown (1952) found that rhodopsin did not react with PCMB, although when rhodopsin is bleached in the presence of the reagent an irreversible change takes place that now prevents the regeneration with 11-*cis* retinal.[6]

The Metarhodopsins

The transitions from lumirhodopsin to NRO are thought to be accompanied by changes in the opsin molecule revealed by changes in the degree of chemical interaction of the chromophore with opsin, and thus changes in the absorption spectrum, and also by changes in the reactivity of the molecule according as reactive groups are exposed. The similarity, in absorption spectra between Meta I and rhodopsin indicates a strong degree of interaction between opsin and chromophore in Meta I but some loosening of the opsin molecule is indicated by its susceptibility to attack by hydroxylamine. The change from Meta I to Meta II is considered to be the key reaction that involves sufficient change in entropy to permit it to alter the rod structure sufficiently to induce chemical changes. The basic reaction is only the addition of an H^+-ion but the entropy change is far greater than would be expected of this. One indication of chemical change is the finding that Meta II can be reduced by sodium borohydride whilst Meta I cannot, presumably because the aldimine bond has now become accessible by unfolding of protein.

Metarhodopsin III and Later

If metarhodopsin II is the form of photolysed rhodopsin that is able to initiate the chemical and physical events in the receptor constituting the light-response—and the evidence for this is compelling—then the subsequent decay and the detailed steps by which this occurs are of

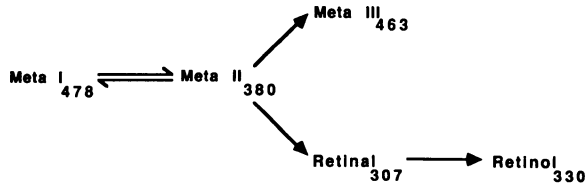

Fig. 8.22 The most likely scheme for the decay of Meta II to retinal and retinol, whereby Meta III may be bypassed. (After Blazynski & Ostroy, *Vision Res.*)

lesser interest and need not detain us long. Meta III, with a λ_{max} of about 470–475 nm, has also been called para-rhodopsin and may be the same as Lythgoe & Quilliam's 'transient orange'. The most likely scheme for decay of Meta II to retinal and retinol is indicated by Fig. 8.22 (Blazynski & Ostroy, 1984), where it is seen that the step to Meta III may be bypassed, so that retinal can be formed in the retina from Meta II_{380} and Meta III_{465}. A direct conversion of Meta III to retinol was disproved by these authors.

N-Retinylidene Opsin (NRO)

This is the indicator yellow of Lythgoe (1937), changing from an orange (λ_{max} = 440 nm) in acid solution to a yellow (λ_{max} = 363 nm) in alkaline solution. At physiological pH the yellow form predominates and, since this is rapidly hydrolysed, the presence of indicator yellow under normal conditions in the retina is difficult to establish, the final product being retinal plus opsin.

An interesting point emphasized by Knowles & Dartnall (1977) is that the absorption spectra of the NRO's from a variety of rhodopsins are essentially similar although their opsins are different; hence in NRO there is no secondary interaction between opsin and chromophore in this molecule.

LINKAGE OF RETINAL

Lysine

The treatment of bleached rhodopsin with borohydride to give the reduced compound:

$$C_{19}H_{27}CH{=}N \times \text{Opsin} \xrightarrow{NaBH_4}$$

$$C_{19}H_{27}CH_2NH \times \text{Opsin}$$

serves to 'freeze' the chromophore on the opsin moiety, and in this state it is feasible to establish the position of the link. Bownds (1967) showed that this link was through the ε-amino group of a lysine residue of opsin, so that unless retinal migrates during the few msec required for conversion of rhodopsin to Meta II, this is the mode of linkage in the unbleached state (Rotmans *et al.*, 1974).

Binding to Phospholipid

However, Poincelot *et al.* (1969) concluded, from their studies on extracting rhodopsin with the lipid solvent methanol, that the binding site in rhodopsin is on the phospholipid moiety as N-retinylidene-phosphatidyl-ethanolamine, and that during bleaching of metarhodopsin I to II the chromophore was transferred from the lipid to the amino-acid skeleton of opsin.

Confirmation of Lysine-linkage

There is little doubt from the work of Fager *et al.* (1972) and DeGrip *et al.* (1973) that the link is to a lysine residue. Fager *et al.* treated rhodopsin with cyanoborohydride, a more specific compound for reacting with protonated Schiff bases and giving a more stable product at acid pH, and found only a lysine-N-retinylidene complex during subsequent chromatography, there being no evidence for the presence of a phosphatido-ethanolamine compound. Again DeGrip *et al.* (1973) amidinated 50 out of the total of 52 primary amino groups (including that attached to retinal) with methylacetimidate:

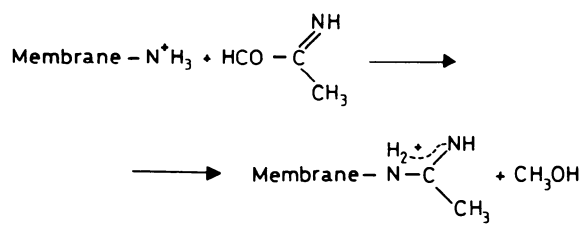

In this condition the rhodopsin was normal to the extent that some 70% could be bleached and regenerated. On subsequent denaturing of this modified rhodopsin, leading to release of retinal, one further ε-lysyl-group of opsin became free; if the rhodopsin was exposed to light before amidination, then one more amido group was taken up and now denaturation did not cause the appearance of one more amino group. DeGrip *et al.* conclude from this study that retinal is unequivocally bound to opsin through a lysyl residue in the unbleached state, and that it is held in this position at least during the important changes of structure—notably those leading to Meta II—during which the visual event presumably takes place.

Protein–lipid Interchange

It would seem that a very facile transfer of the retinal from protein to lipid, or in the reverse direction, can take place, and it is possible that some such retinal-lipid linkage is important in the transfer of liberated retinal to its isomerizing or oxidizing site.

Location of Retinal

Retinal is linked by a Schiff-base to a lysine residue; this residue occupies position 296 in the total sequence, which, on the bais of the model of Hargrave *et al.* (1984) is in a hydrophobic part of a helical region buried in the lipid bilayer. This was confirmed by Davison & Findlay (1986), who treated outer segments with ^{125}I-labelled iodobenzine which, after penetrating lipid bilayers, can be photoactivated by ultra-violet light to produce highly reactive nitrenes thereby labelling the site of linkage. Davison & Findlay showed that the nitrene reacted with Lys^{296}, thus establishing the location of the retinal grouping.

In Vivo *Changes*

The various compounds formed as intermediates in the bleaching of rhodopsin have been identified by optical means in solutions of the pigment or in isolated outer segments, and they have only been identified by the expedient of cooling and thus reducing, or inhibiting, the thermal reactions that occur very rapidly at body-temperature. In view of the extreme lability of the intermediates identified in this way it seems unlikely that significant concentrations of many of the intermediates will build up in the normal retina when exposed to light. There have been a variety of studies on the intact retina, and it would seem that it is metarhodopsin II and pararhodopsin (meta III) that are the main long-lived photoproducts (see, for example, Frank, 1969; Ripps & Weale, 1969; Knowles & Dartnall, 1977, Ch. 9).[7]

A situation approximating some way towards the normal is given by the study of the changes taking place in suspensions of rod outer segments (ROS) where the rhodopsin and its decomposition products remain within the discs and attached, presumably, to the membranes. In general, suspensions of rod outer segments reveal the same sequence of changes, although the stability of the intermediates, e.g. batho- and lumirhodopsins, is less in the receptor than in the digitonin micelles.[8]

REGENERATION OF RHODOPSIN

In the retina the products of bleaching—retinal and opsin—are converted to rhodopsin in the dark—*regeneration*—and this is the basis for dark-adaptation, the recovery of sensitivity to light during the dark (p. 220). This regeneration process must be distinguished from the renewal process that occurs independently of exposure to light or dark, during which packets of rod discs are absorbed by the pigment epithelium whilst new discs, demanding the synthesis of opsin and retinal, are manufactured in the outer segments. Here we need only consider the former, regeneration process, although the continued engulfment of intact rhodopsin molecules by the pigment epithelium will clearly influence the amount of 11-*cis* retinal within its cells at any moment. A basic scheme for the regeneration process, which includes all possible reactions, is illustrated in Fig. 8.23. Thus, as we have seen, retinal, when liberated, is converted to vitamin A or retinol and the relative amounts of retinal and retinol in the retina are governed by the proportions of NADP and NADPH, the coenzyme that cooperates with retinol dehydrogenase in the reversible conversion of retinal to retinol; in the retina the conditions favour production of retinol, so that regeneration from retinol demands a preliminary oxidation of retinol to retinal.

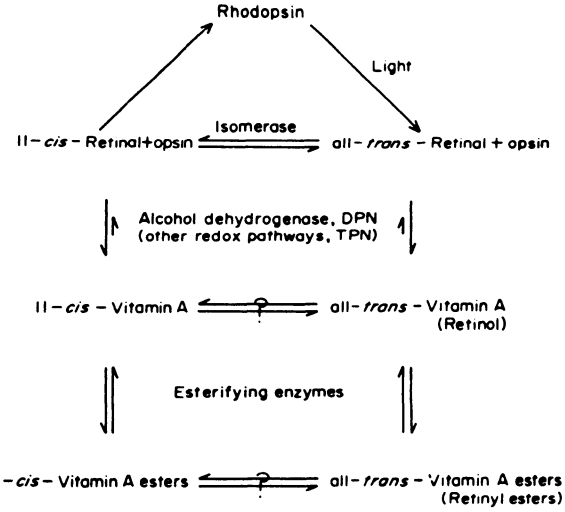

Fig. 8.23 The classical rhodopsin cycle. (Daemen *et al.*, *Exp. Eye Res.*)

Regeneration from Added 11-*cis* Retinal

Breakage of the Retinal Opsin Link

When 11-*cis* retinal is added to a suspension of bleached rod outer segments, rhodopsin is rapidly regenerated (Amer & Akhtar, 1972); a similar regeneration was obtained with bleached isolated retinae (Amer & Akhtar, 1973). An important aspect of this regeneration in the dark is the apparent necessity for the retinal to be

completely split off the opsin molecule, so that if there is a delay in this final step, e.g. if, after illumination, some of the bleached rhodopsin is in the form of metarhodopsins, then regeneration through added 11-*cis* retinal will be delayed until the metarhodopsins have finally been converted to all-*trans* retinal plus opsin (Rotmans *et al.*, 1974; Paulsen *et al.* 1975). Thus Rotmans *et al.* (1974) measured the time-course of release of retinal from the bleached rhodopsin, which reached a plateau level in some 30 to 60 minutes. They also measured the amounts of rhodopsin that could be regenerated by adding pure 11-*cis* retinal to the bleached preparation at different times after the bleach, and they found that the per cent recombination increased with time after the bleach, following the course of the release of the chromophore manifest as loss of metarhodopsin II. This dependence on removal of chromophore doubtless explains the variety of kinetics of regeneration of rhodopsin observed in the intact eye.

Isomerization

In the isolated retina, detached from its pigment epithelium, or in suspensions of rod outer segments, or in solutions of bleached rhodopsin, regeneration has been found either not to occur at all or very inefficiently compared with the intact eye; and the cause of this inefficiency is undoubtedly related to the separation of the receptors from the pigment epithelium. The requirement for regeneration is the availability of a supply of 11-*cis* retinal to replace the all-*trans* retinal split off from the rhodopsin molecule during bleaching. If the all-*trans* retinal is to be re-utilized it must be isomerized to 11-*cis* retinal; moreover, since conversion of retinal to retinol is rapid and may even occur before the final splitting off of the chromophore, then retinol must first be oxidized to retinal by retinol dehydrogenase; finally retinol is esterified so that, as indicated in Fig. 8.23 hydrolysis back to retinol may be necessary. If one or more of these events requires the cooperation of the pigment epithelium, regeneration in the isolated retina will be impaired and rely on local stores of intermediate.

Photo-isomerization

If the chromophore is attached to the opsin molecule, the action of light can cause a photo-isomerization, and thence reversal of the light- and thermally induced changes, to regenerate rhodopsin. During continued light-exposure there is evidence of some regeneration due to this photo-isomerization. The process can lead to the formation of isorhodopsin, due to the conversion of the all-*trans* retinal to the 9-*cis* form; and under experimental conditions isorhodopsin can be demonstrated in the retina. Thus, using very brief flashes—flash-photolysis—permits some of the unstable products of the flash to absorb light before they break down and thus to isomerize. For example, Dowling & Hubbard (1963) found a mixture of 5:1 rhodopsin and isorhodopsin in the flash-irradiated rat retina. Under normal conditions, however, photo-isomerization is a relatively small factor, although it may account for regeneration observed in the frog's isolated retina free from pigment epithelium (Baumann, 1970).

Retinal Isomerase

By far the most important factor for regeneration, however, is the presence of an enzyme, *retinal isomerase*; its presence in the pigment epithelium of the frog, for example, probably accounts for the great fall in power of regeneration observed when the retina was detached from the pigment epithelium, so that it is generally believed that isomerization of the chromophoric group takes place outside the photoreceptor in the pigment epithelial cell, whence it is transferred back to the receptor, either in the form of 11-*cis* retinol or of 11-*cis* retinal.

Retinol

Migration to Pigment Epithelium

An important factor is the rapid conversion of retinal to vitamin A, or retinol, in the retina; this must be converted to retinal before it can react with opsin, and this is carried out by an alcohol dehydrogenase in the visual cells. Retinol formed in the receptor does not remain there but migrates to the pigment epithelium. Thus Jancsó & Jancsó (1936) profited by the fluorescence of vitamin A in ultra-violet light to demonstrate that after maximal light-adaptation there is a high concentration of the vitamin in the pigment epithelium; during full dark-adaptation none could be demonstrated. Again, the chemical studies of Hubbard & Colman (1959) and of Dowling (1960) have confirmed this migration of vitamin A during light- and dark-adaptation, and have shown that the total amount of vitamin A in the eye remains constant, if we include under this title the retinene bound to rhodopsin.

Retinal–Retinol System

The changes in retinal and retinol in retina and pigment epithelium in the rat's eye are illustrated in Fig. 8.24 from a study by Dowling (1960); in the rat, retinol is not stored in the pigment epithelium, by contrast with the frog; thus changes in retinal and retinol content are easy to demonstrate. The figure shows that in the dark-adapted eye there is very little retinol in either pigment epithelium or retina, whilst retinal (as rhodopsin) is in high concentration. With light-adaptation the retinal falls and the retinol

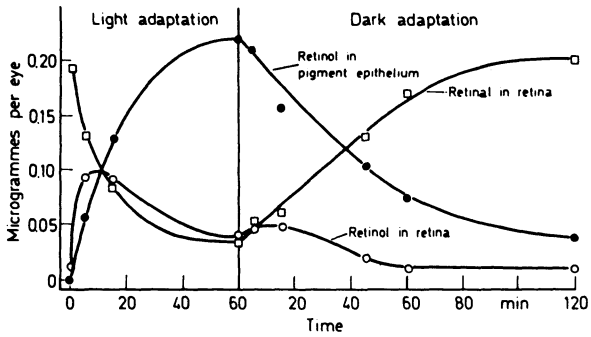

Fig. 8.24 Topographic distribution of retinal and retinol in the eyes of albino rats during light- and dark-adaptation. (Baumann, *Handbook of Sensory Physiology*. From Dowling.)

contents of the retina and pigment epithelium rise; soon the retinol in the retina falls, but that in the pigment epithelium continues to rise. During dark-adaptation the fall in pigment epithelial retinol parallels the rise in retinal in the retina (i.e. rhodopsin content). A similar cycle has been described more recently by Zimmerman (1974).

Oxidation of Retinol

The reduction of retinal to retinol and the reverse oxidation of retinol to retinal are catalysed by a retinene reductase-alcohol dehydrogenase enzyme, requiring NADP as co-enzyme. Daemen *et al.* (1974) and Zimmerman *et al.* (1975) have shown that bovine retinol dehydrogenase only acts on all-*trans* retinol, and if this is true the retinol transported from the pigment epithelium must arrive in the all-*trans* form, be oxidized in the outer segment and then isomerized to 11-*cis* retinal. However, Bridges (1976) was able to show that frog outer segments were capable of regenerating rhodopsin from added 11-*cis* retinol and were thus capable of oxidizing the retinol; this author points to the difficulty in explaining the utility of a small pool of 11-*cis* retinol in the dark-adapted rod outer segments described by him, or yet the decrease in 11-*cis* retinol in the outer segments that takes place during dark-adaptation, unless the outer segments can utilize 11-*cis* retinol.

Esterification of Retinol

Retinol is stored in cells in oil droplets in the form of retinyl esters; in the frog only a few per cent of the total vitamin A is in the form of retinol (Bridges, 1976), and over half of this is in the outer segments, which contain only 0.4% of the total retinyl ester. In dark-adapted frogs between 35 to 47% of the retinyl ester is in the *cis*-form, the remainder being all-*trans*. During light-adaptation the retinol formed passes into the pigment epithelium and is found in the oil-droplets as retinyl ester; thus some 90% of that in the pigment epithelium is esterified and all that in the oil droplets; the esterification apparently takes place in the pigment epithelium so that it is retinol that leaves the outer segments. In fact the outer segment is the predominant site of free retinol; when contact with the pigment epithelium is lost, retinol accumulates in the outer segments which thus lack the ability to esterify retinol.

Site of Isomerization

During dark-adaptation a great deal of the rhodopsin regenerated comes from all-*trans* retinyl ester, and the site of the isomerization has been taken to be the pigment epithelium on the grounds that regeneration of rhodopsin is severely restricted in its absence. Bridges (1976) has discussed this assumption in some detail and raised, also, the question as to the form in which the isomerized material is transferred, i.e. is the returned material 11-*cis* retinal, 11-*cis* retinol, or 11-*cis* retinyl ester. In this last event, the outer segment would have to hydrolyse the ester, and subsequently oxidize it; this latter is certainly possible, as Bridges has shown, whilst Bibb & Young (1974) have observed a transfer of labelled fatty acids from pigment epithelium to outer segments, suggesting a hydrolysis of retinyl esters when they reach the rod outer segment.

Significance of the Shuttle

As Azuma *et al.* (1977) point out, the outer segment-pigment epithelium 'shuttle' makes sense in that detached prosthetic groups are remotely stored for later use, being taken out of the danger zone where they might otherwise combine with opsin at 'wrong' sites. So far as the rate of transport is concerned, if we accept Azuma's figure of a regeneration capability of 12% per minute, it is easy to show from Bridges' (1976) measurements of the traffic between pigment epithelium and rod outer segments, namely 130 molecules per sec per μm^2 of surface, that this would be adequate to maintain regeneration at its maximum rate.

TRANSPORT OF RETINOIDS[9]

These are such water-insoluble substances that transport through the aqueous body fluids must be achieved, as with steroid hormones, for example, by attachment to carrier-protein. Retinol is stored in the liver mainly as retinyl esters, and is released from the hepatocytes as a 1:1 complex of a small 20 kd protein, *retinol binding protein* (RBP). This complex—*holo*-RBP—itself binds to a plasma protein, first called prealbumin, and later transthyretin (TT) with molecular weight of 55 kd. The large

complex, so formed, ensures that the retinol is not lost through glomerular filtration in the kidney; it also strengthens the retinol-RBP link. Retinoids in the free state are highly toxic, damaging cell membranes, so that their transport in a form that allows them to reach their target sites, but not to be indiscriminately released on the way, is important, and release at the pigment epithelium is brought about by exchange of the retinoid at specific receptor sites, identified by labelling with radioactive retinoids (Heller, 1975; Maraini & Gozzoli, 1975).

Heller (1975) described a powerful binding of retinol-complex with RBP to the pigment epithelium surface, but not to that of the rod outer segment. Addition of prealbumin did not affect the binding; the complex of RBP with prealbumin—apo-RBP—was less effective in competing with the pigment epithelium complex than retinol-RBP. Thus, after delivering retinol to the pigment epithelial cell, the apo-RBP can be displaced by another retinol-RBP complex. Hence the delivery of retinol to the cell can be regulated by the relative concentrations of apo- and retinol-RBP and their affinities for the receptor on the pigment epithelial cell.

Tissue Retinoid Binding Proteins

Retinoid-binding proteins, different from that in plasma, have been isolated from retina. Wiggert & Chader (1975) separated from homogenized pigment epithelium or neural retina a protein of about 19 kd; this appeared in the embryonic retina before development of the receptors, and might well play a role during assembly of the outer segment membranes. Heller & Bok (1976) isolated soluble intracellular lipoproteins capable of binding retinol from both pigment epithelial cells and outer segments. Subsequent studies have established the presence of at least three retinoid-binding proteins in retina-pigment epithelium, two of them intracellular and the third localized to the interphotoreceptor space. The intracellular proteins are *cellular retinol binding protein* (CRBP) and *cellular retinal-binding protein* (CRALBP); the latter has been identified immunocytochemically in pigment epithelial and Müller cells, its presence in the latter suggesting a role in the vitamin A metabolism of the retina (Bunt-Milam & Saari, 1983). Cellular retinol-binding protein (CRBP) was localized mainly in the pigment epithelium, with less in the neural retina (Bok *et al.*, 1984). According to Saari *et al.* (1984) and Bok *et al.* (1984) neither of these cellular binding proteins has been identified in the receptors. 11-*cis*-retinal complexes with CRALBP, and on illumination it becomes isomerized to the all-*trans* form. While bound to their binding proteins the retinoids may be esterified, and this reduces their binding so that they may migrate to form oil droplets in the cytoplasm.[10]

Interphotoreceptor Binding Protein (IRBP)

Of especial interest, so far as intraretinal transport of retinoids is concerned, is the discovery of a retinol-binding protein confined to the interphotoreceptor space (Lai *et al.*, 1982; Adler & Martin, 1982). According to Liou *et al.* (1982), it is a glycoprotein of 260 kd molecular weight, the quantity of retinol bound to it being increased when rhodopsin was bleached. They considered that it might be a dimer of 140–145 kd subunits. According to Chader & Wiggert (1984) it binds other retinoids in addition to retinol, so is not so specific as CRBP. Immunocytochemically it was localized to the intraretinal space, bordered by three cell-types, namely pigment epithelium, photoreceptors and Müller cells, a location consistent with a role in transport of retinoids amongst the cells. The heaviest precipitate was found in a line corresponding to the apical surfaces of the pigment epithelial cells; cone outer segments were also positive (Bunt-Milam & Saari, 1983).

SITE OF SYNTHESIS

Wiggert *et al.* (1984) demonstrated synthesis of IRBP by the monkey's neural retina in organ culture, but not in the pigment epithelium. Profiting by the fact that the glycoprotein contained fucose, Hollyfield *et al.* (1985) showed that the primary site of incorporation of the ^{3}H-fucose was the rod inner segment of the human retina. Finally the studies of Gonzalez-Fernandez *et al.* (see, for example, 1985) showed that it was synthesized in the retinas of normal and dystrophic rats, disappearing from the retina of the latter during the phase of rapid cell death of the photoreceptors.

FUNCTION

This has been discussed by Saari *et al.* (1984) who emphasize its transport role in collaboration with CRBP and CRALBP. Most of the 11-*cis* retinol occurs in the retina whilst most of the 11-*cis* retinoid in the pigment epithelium cytosol is in the form of retinal, and they suggest that in the mammalian retina 11-*cis* retinol is generated from all-*trans*-retinol, perhaps in Müller cells, which can be used for rhodopsin regeneration after being transported to the pigment epithelium where it is converted to 11-*cis* retinal and returned to the outer segments. The interphotoreceptor binding protein, IBRP, might be implicated in transporting retinoids between rod outer segments, Müller cells and pigment epithelium. Certainly this last protein is found in five classes of vertebrates and must subserve an important function.[11]

The Esters

Using high pressure liquid chromatography, Alvarez *et al.* (1981) identified the composition and isomeric form

of the retinoid esters. Dark-adapted rabbits had 11-*cis* and all-*trans* retinyl esters, whereas light-adapted albino rats had only the all-*trans* isomer. The rabbit's retinol was esterified almost entirely by palmitic acid, whereas rat had stearic acid esters as well.

Visual Cycle

A visual cycle involving retinol and retinal, suggested by Bridges *et al.* (1984) is shown in Fig. 8.25. According to this, 11-*cis* retinol must be delivered to the pigment epithelium and 11-*cis* retinal returned to the outer segments, IBRP being implicated in transport of 11-*cis* retinol, whereas 11-*cis* retinal is probably carried in some other way. The 11-*cis* retinol not immediately used in the outer segments for regeneration of rhodopsin escapes to the pigment epithelium where it is stored as 11-*cis* esters. In strong illumination all-*trans* retinol passes to the pigment epithelium, where it is stored in this configuration, escaping isomerization. In summary, according to Bridges *et al.* (1984), most of the 11-*cis* retinol in the bovine eye occurs in the neural retina while the 11-*cis* retinoid in the pigment epithelium is principally in the form of 11-*cis* retinal. In the mammalian retina 11-*cis* retinol is generated from all-*trans* retinol but it can only be utilized after transport to the pigment epithelium where it is converted to 11-*cis* retinal and returned to the outer segments.

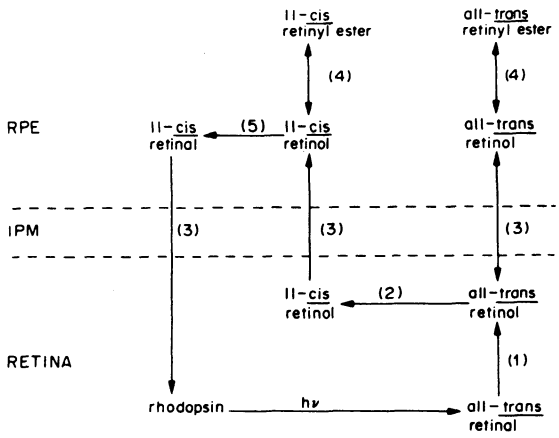

Fig. 8.25 Proposed visual cycle in the mammalian eye. (1) All-*trans* retinol oxidoreductase; (2) isomerase; (3) transport of retinoid through the interphotoreceptor matrix (IPM), possibly bound to IRBP; (4) esterifying enzyme (probably not stereospecific); (5) 11-*cis* retinol oxidoreductase. (Bridges *et al.*, *Vision Res.*)

COMPARATIVE PHYSIOLOGY OF THE PIGMENTS

Rhodopsin and Porphyropsin

Köttgen & Abelsdorff (1896) observed that the 'visual purples' extracted from mammals, birds and amphibians were different from those extracted from various freshwater fishes; the former had the usual maximal absorption near 500 nm whilst the fish pigments had a maximal absorption near 540 nm, and thus appeared more violet. Wald (1939) showed that the retinae of freshwater fishes gave retinene (retinal) and vitamin A (retinol) on bleaching, but it became evident that these were chemically different, having a double bond in the beta ionone ring:

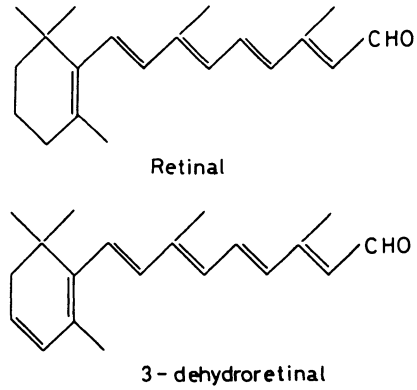

The pigments were called porphyropsins, and the chromophore and its vitamin were called retinene$_2$ and vitamin A$_2$ to distinguish them from the retinene$_1$ and vitamin A$_1$ of the rhodopsins. With the use of the terms retinal and retinol in the place of retinene$_1$ and vitamin A$_1$, the corresponding compounds for the porphyropsins are called dehydroretinal and dehydroretinol.

Marine and Freshwater Fish

In general, the retinae of marine fish contain rhodopsins based on retinal, and we may view the development of porphyropsins, based on dehydroretinal, as an adaptation to permit the fish to make use of the longer wavelengths of light found in freshwater by comparison with sea-water. Euryhaline fish, spending part of their time in freshwater and part in sea-water, contain mixtures of rhodopsin and porphyropsin, the proportion varying with the environment.

Multiplicity of Pigments

Wald's (1939) statement that there were only two scotopic types of pigment, rhodopsin and porphyropsin, has been shown, mainly by Dartnall's work (1957), to be incorrect.

It is true that all the known pigments are based on only two retinals, but presumably because of the widely differing opsins, a very wide range of pigments with characteristic λ_{max} ranging from 563 nm in the yellow to 430 nm in the violet has now been demonstrated; in general those with λ_{max} in the long wavelength region—so-called porphyropsins—are based on retinene$_2$, but there is considerable overlap, so that the carp pigment based on retinene$_2$ has a λ_{max} of 523 nm, whilst the gecko pigment, based on retinene$_1$ has a λ_{max} of 524 nm. Furthermore, some retinae gave extracts containing at least two photosensitive pigments of the scotopic type. Even the typical rhodopsin, moreover, differs significantly according to the species of retina from which it is extracted; thus cattle rhodopsin has a λ_{max} of 499 nm, human 497 nm, squirrel and frog 502 nm.

Relation to Environment

The significance of the wide variations in absorption characteristics of the scotopic visual pigments, found in fish especially, is probably to be sought in the requirements of the animal's habitat. Thus, if maximal sensitivity to the prevailing light is the biological requirement, then we may expect some correlation between the spectral characteristics of the available light and the retinal pigment composition. As Lythgoe (1984) has emphasized, however, maximal sensitivity to the prevailing light may not necessarily be the prime requirement of survival; this, of course, would apply to photopic vision where chromatic features of the environment may be very important.

The Colour of Water

Pure water is blue, partly because of absorption and also due to Rayleigh scatter. The colour can be modified by a variety of influences, such as the proliferation of plankta, vegetable decay, and the general run-off from land, which together impart a green colour to water. Where this contamination is strong, near-infra-red may well be best transmitted (Muntz & Mouat, 1984). In general, water of open oceans and near arid land-masses transmits light maximally at the shorter wavelengths, whereas water close to the shore transmits preferentially at longer wavelengths (Lythgoe, 1984).

Variations with Habitat

Denton & Warren (1956) and Munz (1958) showed that deep-sea fishes, such as the conger eel, had golden coloured pigments that were apparently adapted for the reception of the predominantly blue light of their habitat, and subsequent study has, indeed, shown that the λ_{max} of bathypelagic fishes ranges between 478 and 490 nm, and are based on retinene$_1$. Munz (1958) extended these correlations, so that with surface-pelagic fishes, where the λ_{max} for transmission is about 485 to 495 nm, there is a corresponding λ_{max} of the visual pigments. With rocky coasts, the transmitted light is different from that in the turbid waters near sandy beaches, and there is a corresponding difference in the visual pigments.

Cones

Lythgoe (1984) has emphasized that the cones of some fish exhibit a much better matching of their pigment absorption maxima to their environment than can be seen with the rods. Thus he established two correlations; first, the spread of λ_{max} within the spectrum depended on the bandwidth of the available light, and secondly the most red-sensitive cones containing only 620–625 nm porphyropsins have been found only in fish living in waters relatively rich in red light.

Spread of λ_{max}

The deeper the water, the more limited the range of wavelengths available for useful vision, so that, if environment is to play a role in governing the photopigment content of the retina, we may expect to find that fish living at greater depths will exhibit a narrower range of λ_{max} for the visual pigments. A comparison has shown that species in deeper water do, indeed, show a narrow limit amongst themselves as to their λ_{max}, the values being in the region of 500–550 nm and around 600 nm; fishes living in shallow water have a wider spread of λ_{max} extending from 400 to some 600 nm.

Birds

Their colour discrimination depends largely on the presence of different coloured oil globules, and we may presume that the actual colours are determined by the environment in which the bird lives. Thus night-feeding birds and underwater hunters such as auks, cormorants and penguins, have a very low proportion of red and orange globules, presumably because they utilize long-wavelength light (Bowmaker & Martin, 1984); in fact, so far as the penguin is concerned, it would appear from its oil globule and visual pigment combination that it is highly adapted to give the best colour discrimination in the 400–500 nm waveband, which would fit it for seeing through clear Antarctic waters. By contrast, plunge-diving sea birds have a high proportion of red globules, which might help discrimination of objects just below the water surface (Lythgoe, 1979). Chickens are sensitive to ultraviolet light, and Fager & Fager (1981) have isolated a visual pigment with λ_{max} near 417 nm from their retina.

Evolutionary Processes

In general, then, we may conclude that evolutionary processes have governed the types of visual pigments in the retina, but, as Lythgoe has emphasized, it is not always easy to relate a λ_{max} to a particular habitat. In particular, the Purkinje shift, seen in mammals, is not related to the ambient light of the evening; thus the eye becomes more sensitive in the blue–green region, yet the ambient evening light is actually richer in the longer wavelengths than is daylight (McFarland & Munz, 1975; Lythgoe, 1979).

Labile Scotopic Systems

There is no doubt that with many species the pigment composition of a retina is not an invariable characteristic; this is revealed in the study of diadromous fishes, in the metamorphosis of larvae of some amphibians, and in the variation with the time of the year.

Diadromous Fish

Typical of these are the eels, which are spawned in sea-water, migrate to Europe where they are transformed to elvers or glass eels and begin the ascent of rivers, during which time they become known as yellow eels. Here they undergo a second metamorphosis preparatory to their 3000 to 4000 mile journey back to their spawning grounds, and they become silver eels. Both the American and European species of *Anguilla* have rhodopsin-porphyropsin pigment systems, with λ_{max} at 501 and 523 nm respectively, sharing the same opsin. The immature yellow eels have mixtures of the two pigments in different proportions, but before the migration from the rivers to the sea, all the porphyropsin has been lost, but interestingly, some of the rhodopsin has shifted its λ_{max} towards the short wavelengths to become a 'chrysopsin' of the deep-sea fish. Thus, as Beatty (1975) has emphasized in his study of an American species, *Anguilla rostrata*, the eels are peculiar in making use not only of the rhodopsin-porphyropsin paired system, based on the same opsin and different chromophores, but also, in its transition to sea-water it has utilized the variant employed by marine fishes in their adaptations to deep and shallow water, namely the modification of rhodopsin by a change in its opsin.

SALMONIDS

The salmonids undergo the opposite change in salinity for breeding purposes. Ocean-caught salmon have predominantly rhodopsin in their retinas, but as Fig. 8.26 shows, there is a progressive increase in the proportion of porphyropsin during the pre-spawn return to freshwater. It would seem that, with both eels and salmon, the changeover of pigment takes place before the actual migration to the new environment, and is presumably initiated by some cyclical hormonal action.

Frogs

Wald (1946) showed that in the frog, *Rana catesbiana*, the photopigment was rhodopsin[12] whereas in the tadpole it was porphyropsin, and Wilt (1959), studying the same species, showed that in the tadpole there was a mixture of rhodopsin and porphyropsin based on retinal and dehydroretinal, with a predominance of porphyropsin which is absent in adult frogs. Figure 8.27 illustrates the results of a study on *Rana temporaria* by Muntz & Reuter (1966). When individual rods were examined by microspectrophotometry, the interesting observation was made that

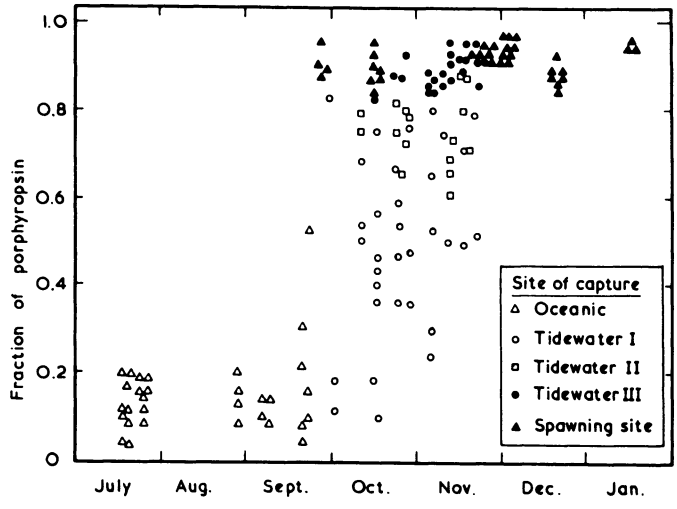

Fig. 8.26 The proportion of porphyropsin in the retinas of individual adult coho salmon, *Oncorhynchus kisutch*, during their return to freshwater spawning grounds. The appearance of the Tidewater Group I fish is identical to ocean-caught fish; Group III fish are nearly identical with those found at the spawning grounds, while Group II are intermediate in appearance. (Knowles & Dartnall, *The Eye*, from Beatty.)

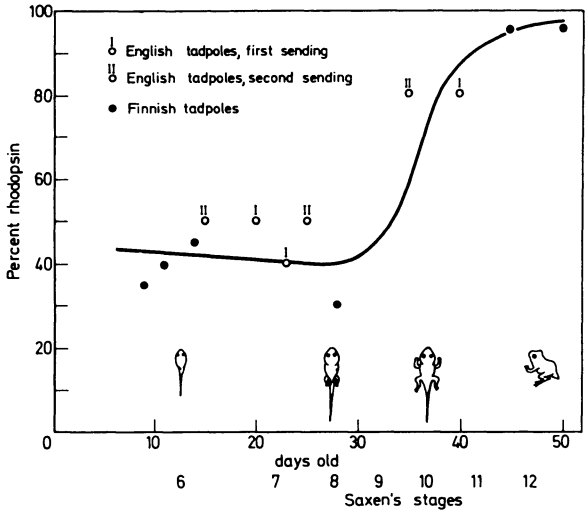

Fig. 8.27 Variations in the proportion of rhodopsin in retinal extracts of *Rana temporaria* during ontogenesis. (Bridges, *Handbook of Sensory Physiology*, from Muntz & Reuter.)

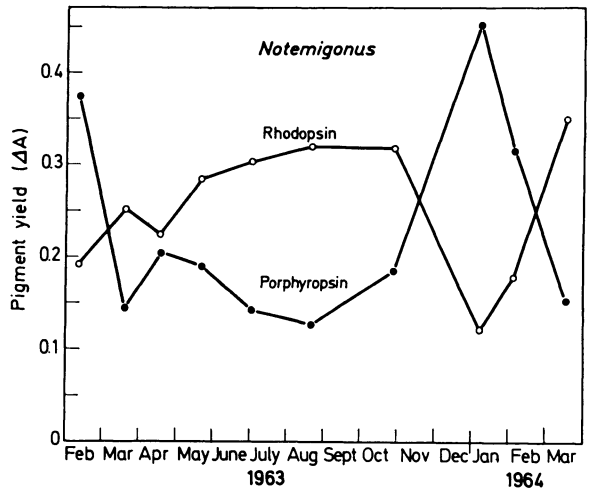

Fig. 8.28 Seasonal reciprocal variation in the amounts of rhodopsin and porphyropsin in *Notemigonus* retinas. ○, rhodopsin; ●, porphyropsin. (Bridges, *Handbook of Sensory Physiology*.)

individual receptors from tadpoles contained mixtures of the pigments.

Synthesis of Vitamin A

It seems generally established that the vitamin A employed by the eye in synthesizing its pigment is determined by synthetic mechanisms in the eye rather than the liver, so that the vitamin A of the liver of freshwater fish is retinol although that of the porphyropsin system is dehydroretinol; the critical enzyme that catalyses the formation of dehydroretinol from retinol is retinol dehydrogenase, the transformation occurring in the isolated eye *in vitro* (Ohtsu *et al.*, 1966), a transformation that is inhibited by thyroxine; thus the hormone that promotes metamorphosis acts directly on the synthetic mechanisms of the eye so far as retinol is concerned.

Dehydrogenation of Retinol

Owing to the rapid conversion of retinal to retinol, any dehydrogenation of retinol would have to occur in the outer segments; the migration of retinol to the pigment epithelium would require the dehydrogenation of this to take place there. We may assume that thyroxine inhibits the dehydrogenase at steps A′ or B; this would limit the supply of dehydroretinaldehyde leading to the predominance of rhodopsin.

Temporal Variations

Dartnall *et al.* (1961) found that, in a given population of rudd, the proportions of the two retinal pigments based on retinal and dehydroretinal varied with time of year, and this was due to the variations in the length of the days; in winter the dominant pigment was that with $\lambda_{max} = 543$ nm based on dehydroretinal$_2$, whilst in summer it was that with $\lambda_{max} = 510$ based on retinaldehyde. By artificially varying the environmental illumination in an aquarium, the proportions of the pigments could be varied, and it became clear that it was the total duration of exposure to light that determined the magnitude of the shift. Figure 8.28 illustrates the seasonal variations in rhodopsin and porphyropsin contents of the freshwater cyprinid *Notemigonus* studied by Bridges (1972), and the important point emerges that there is a reciprocal relation between the contents, suggesting that the one is made at the expense of the other.[13]

Temperature

A change in temperature of a fish's environment may also affect its pigment composition, higher proportions of porphyropsin being associated with winter, suggesting that temperature, as well as photoperiod, has a direct relationship to seasonal changes. Such changes have been described in the golden shiner, *Notemigonus crystolensus*, by Allen & McFarland (1973) and the rainbow trout, *Salmo gairdneri*, by Tsinn & Beatty (1977), the changes taking place regardless of lighting conditions.[14]

Phylogenetic Aspects

Wald considered that the dehydroretinal pigments, his porphyropsins, were exclusively found in fresh-water

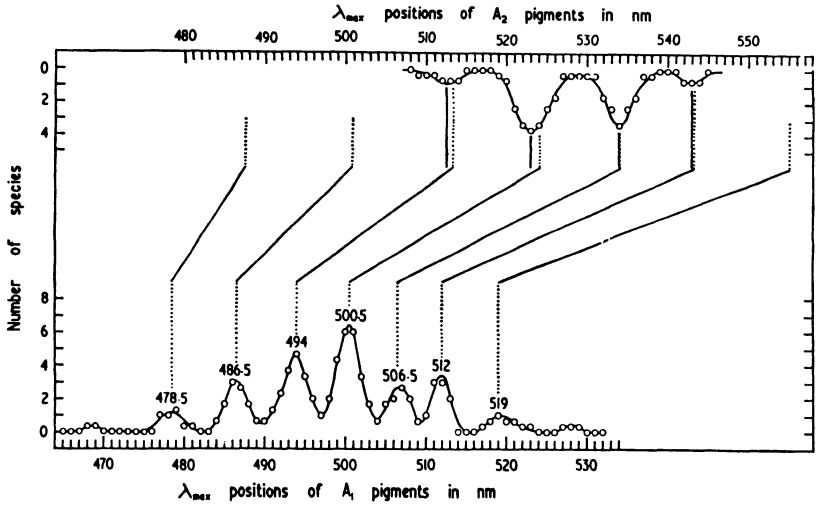

Fig. 8.29 The relationship between the spectral distributions of A_1 and A_2 pigments in teleost fishes. The data for the A_1 pigments are derived from those fishes that possess *only* A_1 pigments; the data for the A_2 pigments are not restricted: *i.e.* they include all fishes that possess A_2 pigments, some of which have A_1 pigments as well. (Dartnall & Lythgoe, *Vision Res.*)

fishes; and this was the basis for some interesting phylogenetic generalizations. However, there is no doubt from Schwanzara's (1967) study that many fresh-water fishes have a retinal pigment, in fact 35% of those examined had this, unmixed with a dehydroretinal pigment; moreover, mixtures commonly were found in fishes that were not euryhaline. Again, marine fishes did not necessarily have exclusively retinal pigments. Schwanzara found a dominance of dehydroretinal pigments in fresh-water fishes of temperate waters and of retinal pigments in tropical fresh-water fishes; and he attributed this to the different spectral qualities of the light in tropical and temperate fresh-water.

Retinal and Opsin Variations

In general, we can expect two ways of varying the character of visual pigment; first with a given retinene we may vary the opsin part of the molecule; with retinal this gives quite a wide range of possibilities permitting pigments that enable the honey-bee, for example, to make full use of ultra-violet light ($\lambda_{max} = 440$ to 450 nm); the deep-sea fish to have golden retinae with λ_{max} in the region of 480 nm; mammals to have pigments with λ_{max} around 500 and so on up to the chicken's pigment, iodopsin, with λ_{max} on the long-wavelength side in the region of 560 nm. Another series of pigments may be obtained by varying the opsins attached to dehydroretinal Fig. 8.29 shows the results of studies by Dartnall & Lythgoe (1965) and of Bridges (1964) on the λ_{max} of pigments extracted from a variety of fishes based on

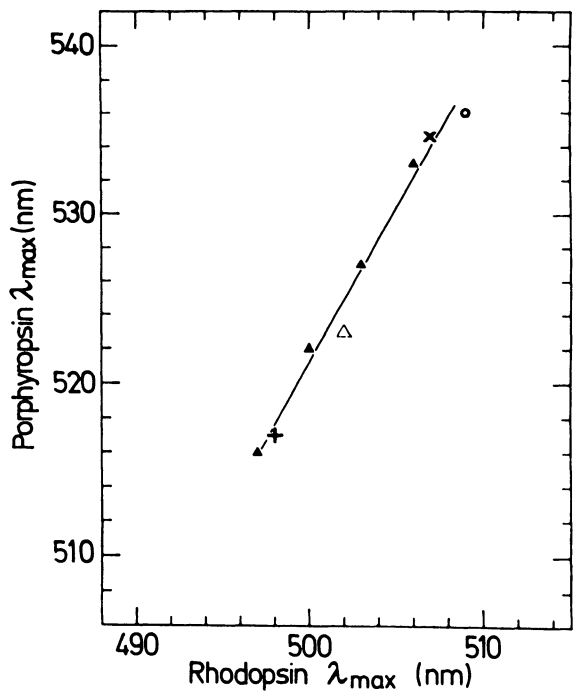

Fig. 8.30 Relationship between the λ_{max} of rhodopsins and their corresponding porphyropsins. Different symbols represent different pairs from different species. + represents a synthetic pair based on cattle opsin. (Bridges, *Handbook of Sensory Physiology.*)

dehydroretinal (above) and retinal (below). The figure illustrates, first, that there is considerable overlap between the two types, and it also shows that there is a tendency for the λ_{max} to cluster around certain wavelengths. Dartnall & Lythgoe established an empirical relationship between the λ_{max} of pigments with the same opsin, and retinal or dehydroretinal attached; with the aid of this, they predicted the shifts in λ_{max} of pigments containing retinal that would be obtained if the same opsin were attached to dehydroretinal. It will be seen that the predictions, indicated by the position of the upper vertical dotted lines, agree with actual pigments very well.

Opsins

With retinas containing mixtures of porphyropsins and rhodopsins it might be assumed that the same opsin would serve for both pigments although this would be difficult to prove; Figure 8.30 shows the relationship between the λ_{max} of corresponding pairs from various species, and it is remarkable that when the λ_{max} of one of a pair is plotted against the λ_{max} of the other, a straight line is obtained which includes a synthetic pair namely a rhodopsin 497 and a porphyropsin 517 derived from cattle opsin.

Notes

1. Papermaster *et al.* (1975) have followed the synthesis of rhodopsin and its migration from inner segment to outer segment; at no time in its life was the rhodopsin unattached to membrane, so that the transport could have occurred by movement through the plasma membrane of the rod, or by movement through the cytoplasm in the form of membrane-bound photopigment.
2. In the dystrophic RCS rat, the rod outer segments are not phagocytosed by the pigment epithelium, so that the balance between formation and shedding of disks is upset, leading to photoreceptor degeneration (Bok & Hall, 1971). Cohen & Nir (1983) found an increase in sialic acid residues above normal, and suggested that this might interfere with the engulfment phase of phagocytosis.
3. The *absorption spectrum* is given by plotting the percentage of light absorbed against wavelength. Terminology is loose in this respect, however, so that absorption spectrum and density spectrum are terms used interchangeably.
4. The appropriate references have been given by Hargrave *et al.* (1984).
5. By use of appropriate opsin antibodies the localization of rhodopsin and of cone photopigments in the outer segments of receptors has been visualized; Jan & Revel (1974) found reaction on both sides of the membranes and, since there was only one layer of photopigment in a cell membrane they correctly concluded that the photopigment was buried deep in the membrane. Freeze-fracture of the membranes showed a regular array of intramembranous particles, presumably of photopigment. These particles were examined in more detail by Besharse & Pfenninger (1980); they attach to the P-face of the disc membrane and are seen associated with Golgi membranes and vesicles near the cilium also. Within the inner segment plasma membrane, which, unlike that of the outer segment, does not contain photopigment, the particles were much smaller, except at the periciliary ridge, the site of membrane transport from inner to outer segment.
6. DeGrip *et al.* (1973) have re-examined the exposure of SH-groups during bleaching; when this is done with intact rod outer segment membranes, there is no increase in reactivity with DTNB or N-ethylmaleimide; only if the rhodopsin is solubilized with detergent is the increase, described by Wald & Brown, observable. We may note that the inhibition of regeneration of rhodopsin, from bleached rhodopsin and added 11-*cis* retinal, consequent on treatment with PCMB, described by Wald & Brown, is apparently not due to blockage of SH-groups since Zorn (1974) blocked these with N-ethylmaleimide, instead of PCMB, and found a high degree of regenerability. Thus PCNB has a specific effect—independent of its SH-blocking activity.
7. The lifetime of metarhodopsin II at room-temperature is of the order of milliseconds; it has been identified in the intact eye by Hagins (1956) using reflexion-densitometry (p. 265). Pugh (1975), in his study of flash photolysis in the human eye, calculated a half-life of 1.4 msec.
8. Crescitelli (1985) has described some properties of solubilized human rhodopsin, its λ_{max} at 37°C being 491 nm. He has discussed, in particular, the Meta II to Meta III transformation; the circular dichroism of Meta II is lost after the transformation indicating an altered opsin conformation, a change that might affect the polyene structure of retinal and so account for the changed λ_{max}. He points out that the λ_{max} of metarhodopsins from different rhodopsins, having different λ_{max}, are all the same, showing that opsin is not interacting with retinal in this state. The possible role of Meta III in the retina, identified there by Ripps *et al.* (1981), is also discussed; thus it is present in the retina during the period of rapid dark-adaptation.
9. The special aspects of carriage of retinoids in the eye have been reviewed by Chader *et al.* (1983) to name only one of a number of reviews.
10. In frogs 96% of retinol is in the pigment epithelium, as much as 99% being esterified, with up to 55% in the 11-*cis* form (Bridges, 1976). The value of these stores is uncertain, since they are virtually absent in the albino rat (Dowling, 1960; Zimmerman, 1974). Interestingly, the rabbit was similar to the frog in having some 80% of its retinyl esters in the form of fluorescent oil droplets in the pigment epithelium, which are absent in the rat.
11. The preparation and purification of the interphotoreceptor retinol-binding protein have been described by Adler & Evans (1985); much more endogenous retinol was carried by IRBP in the light-adapted than in the dark-adapted eye; since the amount of the protein in the eye is invariant, this means that bleaching causes more retinol to bind to IRBP. Wiggert *et al.* (1986) have described the protein's localization in the retinae of different species; it was below the limits of detection in turtle and chicken retinae, and in cases of human retinal degeneration, such as retinitis pigmentosa. Vitreous and aqueous humours of the monkey contained some but far the highest concentrations were in a sample of interphotoreceptor matrix taken by a cannulation technique (Pfeffer *et al.*, 1983).
12. In the frog *Rana pipiens*, Liebman & Entine (1968) found either a rhodopsin ($\lambda_{max} = 502$) or a porphyropsin ($\lambda_{max} = 527$) in the frog or tadpole stages respectively, but there was never any evidence of a mixture, before the final stages of metamorphosis.

13. Muntz & Mouat (1984) found an annual variation in retinal pigment in the brown trout, *Salmo trutta*; only A_2-based pigment was present in winter, while A_1 appeared as well in the summer. Fish from one loch had less A_1 than fish in others; and this was associated with greater depth of penetration of long-wavelength light.

14. In the goldfish, *Carassius auratus*, Tsinn & Beatty (1978) discovered the presence of a hitherto unsuspected rhodopsin, P 499_1, in addition to what was considered its only rod pigment, P 522_2, based on dehydroretinal. It is likely that the temperature at which the fish were maintained led to synthesis of the rhodopsin.

References

Abrahamson, E. W. & Ostroy, S. E. (1967) The photochemical and macromolecular aspects of vision. *Progr. Biophys.* **17**, 181–215.

Abrahamson, E. W. & Wiesenweld, J. R. (1972), The structure, spectra, and reactivity of visual pigments. *Hdb. Sensory Physiol.* **7/1**, 69–121.

Adler, A. J. & Evans, C. D. (1985) Some functional characteristics of purified bovine interphotoreceptor retinol-binding protein. *Invest. Ophthal.* **26**, 273–282.

Adler, A. J. & Martin, K. J. (1982) Retinol binding proteins in bovine interphotoreceptor matrix. *Biochem. Biophys. Res. Commun.* **108**, 1601.

Allen, D. M. & McFarland, W. N. (1973) The effect of temperature on rhodopsin–porphyropsin ratios in a fish. *Vision Res.* **13**, 1303–1309.

Alvarez, R. A., Bridges, C. D. B. & Fong, S.-L. (1981) High-pressure liquid chromatography of fatty acid esters of retinol isomers. *Invest. Ophthal.* **20**, 304–313.

Amer, S. & Akhtar, M. (1972) The regeneration of rhodopsin from all-trans retinal: Solubilization of enzyme system involved in the completion of the visual cycle. *Biochem. J.* **128**, 987–989.

Amer, S. & Akhtar, M. (1973) Studies on the regeneration of rhodopsin from all-*trans* retinal in isolated rat retinae. *Nature* **245**, 221–223.

Anderson, D. H. & Fisher, S. K. (1976) The photoreceptors of diurnal squirrels; outer segment structure, disc shedding and protein renewal. *J. Ultrastr. Res.* **55**, 119–141.

Anderson, D. H., Fisher, S. K., Erickson, P. A. & Tabor, G. A. (1980) Rod and cone disc shedding in the rhesus monkey retina: a quantiative study. *Exp. Eye Res.* **30**, 559–574.

Azuma, K., Azuma, M. & Sickel, W. (1977) Regeneration of rhodopsin in frog rod outer segments. *J. Physiol.* **271**, 747–759.

Bairati, A. & Orzalesi, N. (1963) The ultrastructure of the pigment epithelium and of the photoreceptor–pigment epithelium junction. *J. Ultrastr. Res.* **9**, 484–496.

Basinger, S., Bok, D. & Hall, M. (1976) Rhodopsin in the rod outer segment plasma membrane. *J. Cell Biol.* **69**, 29–42.

Baumann, C. (1970) Regeneration of rhodopsin in the isolated retina of the frog (*Rana esculenta*). *Vision Res.* **10**, 627–637.

Beatty, D. D. (1975) Visual pigments of the American eel *Anguilla rostrata*. *Vision Res.* **15**, 771–776.

Bernstein, S. A., Breding, D. J. & Fisher, S. K. (1984) The influence of light on cone disk shedding in the lizard, *Sceloporus occidentalis*. *J. Cell Biol.* **99**, 379–389.

Besharse, J. C. & Pfenninger, K. H. (1980) Membrane assembly in retinal photoreceptors I. Freeze-fracture analysis of cytoplasmic vesicles in relationship to disc assembly. *J. Cell Biol.* **87**, 451–463.

Bibb, C. & Young, R. W. (1974) Renewal of glycerol in the visual cells and pigment epithelium of the frog retina. *J. Cell Biol.* **62**, 378–389.

Blasie, J. K. & Worthington, C. R. (1969) Planar liquid-like arrangement of photopigment molecule in frog retinal receptor disk membranes. *J. Mol. Biol.* **39**, 417–439.

Blazynski, C. & Ostroy, S. E. (1984) Pathways in the hydrolysis of vertebrate rhodopsin. *Vision Res.* **24**, 459–470.

Bok, D. (1985) Retinal photoreceptor–pigment epithelium interactions. *Invest. Ophthal.* **26**, 1659–1694.

Bok, D. & Hall, M. D. (1971) The role of the pigment epithelium in the etiology of inherited retinal dystrophy in the rat. *J. Cell Biol.* **49**, 664–682.

Bok, D. & Heller, J. (1976) Transport of retinol from the blood to the retina: an autoradiographic study of the pigment epithelial cell surface receptor for plasma retinol-binding protein. *Exp. Eye Res.* **22**, 395–402.

Bok, D., Ong, D. E. & Chytil, F. (1984) Immunocytochemical localization of cellular retinol binding protein in the rat retina. *Invest. Ophthal.* **25**, 877–883.

Bok, D. & Young, R. W. (1972) The renewal of diffusely distributed protein in the outer segments of rods and cones. *Vision Res.* **12**, 161–168.

Borggreven, J. M. P. M., Rotmans, J. P., Bonting, S. L. & Daemen, F. J. M. (1971) The role of phospholipids in cattle rhodopsin studied with phospholipase C. *Arch. Biochem. Biophys.* **145**, 290–299.

Bowmaker, J. K. & Martin, G. R. (1984) Colour vision in the penguin, *Spheniscus humboldti*: a microspectrofluorometric study. *Vision Res.* **24**, 1702 (Abstr.).

Bownds, D. (1967) Site of attachment of retinal in rhodopsin. *Nature* **216**, 1178–1181.

Bridges, C. D. B. (1961) Studies on the flash photolysis of visual pigments. *Biochem. J.* **79**, 128–134.

Bridges, C. D. B. (1964) The distribution of visual pigments in freshwater fishes. *Abstr. Fourth Internat. Congr. Photobiol., Oxford*, p. 53. Bucks: Beacon Press.

Bridges, C. D. B. (1972) The rhodopsin–porphyropsin system. In: *Handbook of Sensory Physiology*. VII/1, pp. 417–486. Springer: Berlin.

Bridges, C. D. B. (1976) Vitamin A and the role of the pigment epithelium during bleaching and regeneration of rhodopsin in the frog eye. *Exp. Eye Res.* **22**, 435–455.

Bridges, C. D. B., Alvarez, R. A., Fong, S.-L., Gonzalez-Fernandez, F., Lam, D. K. & Liou, G. I. (1984) Visual cycle in the mammalian eye. Retinoid binding protein and the distribution of 11-*cis* retinoids. *Vision Res.* **24**, 1581–1594.

Bunt-Milam, A. H. & Saari, J. C. (1983) Immunocytochemical localization of two retinoid-binding proteins in vertebrate retina. *J. Cell Biol.* **97**, 703–712.

Chader, G. J. & Wiggert, B. (1984) Interophotoreceptor retinoid-binding protein. Characteristics in bovine and monkey. *Vision Res.* **24**, 1605–1614.

Chader, G. J., Wiggert, B., Lai, Y.-L., Lee, L. & Fletcher, R. T. (1983) Interophotoreceptor retinol-binding protein: a possible role in retinoid transport in the retina. *Progr. Ret. Res.* **2**, 163–189.

Cohen, D. & Nir, I. (1983) Cytochemical evaluation of anionic sites on the surface of cultured pigment epithelium cells from normal and dystrophic RCS rats. *Exp. Eye Res.* **37**, 575–582.

Collins, F. D. & Morton, R. A. (1950) Studies on rhodopsin. I–III. *Biochem. J.* **47**, 3–9, 10–17, 18–24.

Crescitelli, F. (1985) Some properties of solubilized human rhodopsin. *Exp. Eye Res.* **40**, 521–535.

Crescitelli, F. & Dartnall, H. J. A. (1953) Human visual purple. *Nature* **172**, 195–196.

Daemen, F. J. M., Rotmans, J. P. & Bonting, S. L. (1974) On the rhodopsin cycle. *Exp. Eye Res.* **18**, 97–103.

Danielli, J. F. & Davson, H. (1935) A contribution to the theory of permeability of thin films. *J. cell. comp. Physiol.* **5**, 495.

Dartnall, H. J. A. (1957) *The Visual Pigments.* London: Methuen.

Dartnall, H. J. A., Lander, M. R. & Munz, F. W. (1961) Periodic changes in the visual pigment of a fish. In *Progress in Photobiology*, pp. 203–213. Amsterdam, Elsevier.

Dartnall, H. J. A. & Lythgoe, J. N. (1965) The spectral clustering of visual pigments. *Vision Res.* **5**, 81–100.

Davison, M. D. & Findlay, J. B. C. (1986) Modification of ovine opsin with photosensitive hydrophobic probe 1-azide-4-[^{125}I] iodobenzene. Labelling of the chromophore-attachment domain. *Biochem. J.* **234**, 413–420.

DeFoe, D. M. & Bok, D. (1983) Rhodopsin chromophore exchanges among opsin molecules in the dark. *Invest. Ophthal.* **24**, 1211–1226.

DeGrip, W. J., Bonting, S. L. & Daeman, F. J. M. (1973) The binding site of retinaldehyde in cattle rhodopsin. *Biochim. biophys. Acta* **303**, 189–193.

DeGrip, W. J., Van de Laar, G. L. M., Daemen, F. J. M. & Bonting, S. L. (1973) Biochemical aspects of the visual process. XXIII. *Biochim. biophys. Acta* **325**, 315–322.

Denton, E. J. (1959) The contribution of the photosensitive and other molecules to the absorption of whole retina. *Proc. Roy. Soc., B* **150**, 78–94.

Denton, E. J. & Warren, F. J. (1956) Visual pigments of deep sea fish. *Nature* **178**, 1059.

Ditto, M. (1975) A difference between developing rods and cones in the formation of the outer segment membranes. *Vision Res.* **15**, 535–536.

Dowling, J. E. (1960) Chemistry of visual adaptation in the rat. *Nature* **188**, 114–118.

Dowling, J. E. & Hubbard, R. (1963) Effect of brilliant flashes on light and dark adaptation. *Nature* **199**, 972–975.

Fager, L. Y. & Fager, R. S. (1981) Chicken blue and chicken violet, short wavelength sensitive visual pigments. *Vision Res.* **21**, 581–586.

Fager, R. S., Sejnowski, P. & Abrahamson, E. W. (1972) Aqueous cyanohydridoborate reduction of the rhodopsin chromophore. *Biochem. Biophys. Res. Comm.* **47**, 1244–1247.

Frank, R. N. (1969) Photoproducts of rhodopsin bleaching in the isolated, perfused frog retina. *Vision Res.* **9**, 1415–1433.

Fukuda, M. N., Papermaster, D. S. & Hargrave, P. A. (1979) Rhodopsin carbohydrate. Structure of small oligosaccharides attached at two sites near the NH_2 terminus. *J. Biol. Chem.* **254**, 8201–8207.

Gonzalez-Fernandez, F., Fong, S.-L., Liou, I. & Bridges, C. D. B. (1985) Interstitial retinal-binding protein (IRBP) in the RCS rat: effect of dark-rearing. *Invest. Ophthal.* **26**, 1381–1385.

Hagins, W. A. (1956) Flash photolysis of rhodopsin in the retina. *Nature* **177**, 989–990.

Hargrave, P. A. *et al.* (1983) The structure of bovine rhodopsin. *Biophys. Struct. Mech.* **9**, 235–241. (Quoted by Hargrave *et al.*, 1984.)

Hargrave, P. A., McDowell, J. H., Feldmann, R. J., Atkinson, P. H., Rao, J. K. M. & Argos, P. (1984) Rhodopsin's protein and carbohydrate structure: selected aspects. *Vision Res.* **24**, 1487–1499.

Harosi, F. I. & MacNichol, E. F. (1974) Visual pigments of goldfish cones. Spectral properties and dichroism. *J. gen. Physiol.* **63**, 279–304.

Heller, J. (1968) Purification, molecular weight, and composition of bovine visual pigment. *Biochem.* **7**, 2906–2913.

Heller, J. (1975) Interactions of plasma retinol-binding protein with its receptor. *J. Biol. Chem.* **250**, 3613–3619.

Heller, J. & Bok, D. (1976) Transport of retinol from the blood to the retina: involvement of high molecular weight lipoproteins as intracellular carriers. *Exp. Eye Res.* **22**, 403–410.

Herman, K. G. & Steinberg, R. H. (1982) Phagosome movement and the diurnal pattern of phagocytosis in the tapetal retinal pigment epithelium of the opossum. *Invest. Ophthal.* **23**, 277–290.

Hogan, M. J. & Wood, I. (1974) Phagocytosis by pigment epithelium of human retinal cones. *Nature* **252**, 305–307.

Hollyfield, J. G., Fliesler, S. J., Rayborn, M. E., Fong, S. L., Landers, R. A. & Bridges, C. D. B. (1985) Synthesis and secretion of interstitial retinol-binding protein by the human retina. *Invest. Ophthal.* **26**, 58–67.

Huang, P. T., Spira, A. W. & Wyse, J. P. H. (1982) Phagocytosis in the fetal pigment epithelium: evidence for cyclic activity. *Invest, Ophthal.* **22**, 428–438.

Hubbard, R. & Colman, A. D. (1959) Vitamin A content of the frog eye during light and dark adaptation. *Science* **130**, 977–978.

Hubbard, R. & Kropf, A. (1959) Molecular aspects of visual excitation. *Ann. N.Y. Acad. Sci.* **81**, 388–398.

Hubbard, R. & Wald, G. (1952) Cis–trans isomers of vitamin A and retinene in the rhodopsin system. *J. gen. Physiol.* **36**, 269–315.

Jancsó, N. & Jancsó, H. (1936) Fluoreszenmikroskopische Beobachtung der reversiblen Vitamin-Bildung in der Netzhaut während des Sehaktes. *Biochem. Z.* **287**, 289–290.

Jan, L. Y. & Revel, J.-P. (1974) Ultrastructural localization of rhodopsin in the vertebrate retina. *J. Cell Biol.* **62**, 257–263.

Knowles, A. & Dartnall, H. J. A. (1977) *The Photobiology of Vision.* Vol. 2B, *The Eye* (Ed. Davson, H.). Academic Press, New York and London.

Köttgen, E. & Abelsdorff, G. (1896) Absorption und Zersetzung des Sehpurpurs bei den Wirbeltieren. *Z. Psychol. Physiol. Sinnesorg.* **12**, 161–184.

Lai, Y.-L., Wiggert, B., Liu, Y. P. & Chader, G. J. (1982). Interphotoreceptor retinol-binding proteins: possible transport vehicles between compartments of the retina. *Nature* **298**, 848.

La Vail, M. M. (1976) Rod outer segment disc shedding in relation to cyclic lighting. *Exp. Eye Res.* **23**, 277–280.

Liang, C.-J., Yamashita, K., Muellenberg, C. G., Sachichi, H. & Kobata, A. (1979) Structure of the carbohydrate moieties of bovine rhodopsin. *J. Biol. Chem.* **254**, 6414–6418.

Liebman, P. A. & Entine, G. (1968) Visual pigments of frog and tadpole (*Rana pipiens*). *Vision Res.* **8**, 761–775.

Liebman, P. A., Jagger, W. S., Kaplan, M. W. & Bargoot, F. G. (1974) Membrane structure changes in rod outer segments associated with rhodopsin bleaching. *Nature* **251**, 31–36.

Liou, G. I., Bridges, C. D. B., Fong, S.-L., Alvarez, R. A. & Gonzalez-Fernandez, F. (1982) Vitamin A transport between retina and pigment epithelium—an interstitial protein carrying endogenous retino (interstitial retinol-binding protein). *Vision Res.* **22**, 1457–1467.

Long, K. O., Fisher, S. K., Fariss, R. N. & Anderson, D. H. (1986) Disc shedding and autophagy in the cone-dominant ground squirrel retina. *Exp. Eye Res.* **43**, 193–205.

Lythgoe, J. N. (1979) *The Ecology of Vision.* Clarendon Press: Oxford.

Lythgoe, J. N. (1984) Visual pigments and environmental light. *Vision Res.* **24**, 1539–1550.

Lythgoe, R. J. (1937) Absorption spectra of visual purple and visual yellow. *J. Physiol.* **89**, 331–358.

Lythgoe, R. J. & Quilliam, J. P. (1938) The relation of transient orange to visual purple and indicator yellow. *J. Physiol.* **94**, 399–410.

Maraini, G. & Gozzoli, F. (1975) Binding of retinol to isolated retinal pigment epithelium in the presence and absence of retinol-binding protein. *Invest. Ophthal.* **14**, 785–787.

Mathies, R., Oseroff, A. R. & Stryer, L. (1976) Rapid flow

resonance Raman spectroscopy of photolabile molecules: rhodopsin and isorhodopsin. *Proc. Nat. Acad. Sci. Wash.* **73**, 1–5.

McFarland, W. N. & Munz, F. W. (1975) The evolution of photopic visual pigments in fishes. *Vision Res.* **15**, 1071–1080.

Muntz, W. R. A. & Mouat, G. S. V. (1984) Annual variations in the visual pigments of brown trout inhabiting lochs providing different light environments. *Vision Res.* **24**, 1575–1580.

Muntz, W. R. A. & Reuter, T. (1966) Visual pigments and spectral sensitivity in *Rana temporaria* and other European tadpoles. *Vision Res.* **6**, 601–618.

Munz, F. W. (1958) Photosensitive pigments from the retinae of certain deep-sea fishes. *J. Physiol.* **140**, 220–235.

Nathans, J. & Hogness, D. S. (1983) Isolation, sequence analysis and intron–exon arrangement of the gene encoding bovine rhodopsin. *Cell* **34**, 807–814.

Nilsson, S. E. G. (1964) Receptor cell outer segment development and ultra-structure of the disk membranes in the retina of the tadpole (*Rana pipiens*). *J. Ultrastr. Res.* **11**, 581–620.

Nir, I. & Papermaster, D. S. (1983) Differential distribution of opsin in the plasma membrane of frog photoreceptors: an immunocytochemical study. *Invest. Ophthal.* **24**, 868.

Ohtsu, K., Naito, K. & Wilt, F. H. (1966) Metabolic basis of visual pigment conversion in metamorphosing *Rana catesbiana*. *Dev. Biol.* **10**, 216–232.

Ovchinnikov, Y. A. *et al.* (1982) The complete amino acid sequence of visual rhodopsin. *Biorg. Khim.* **8**, 1011–1014.

Papermaster, D. S., Converse, C. A. & Siu, J. (1975) Membrane biosynthesis in the frog retina: opsin transport in the photoreceptor cell. *Biochemistry* **14**, 1343–1352.

Paulsen, R., Miller, J. A., Brodie, A. E. & Bownds, M. D. (1975) The decay of long-lived photoproducts in the isolated bullfrog rod outer segment: relationship to other dark reactions. *Vision Res.* **15**, 1325–1332.

Peters, K., Applebury, M. L. & Rentzepis, P. M. (1977) Primary photochemical event in vision: proton translocation. *Proc. Nat. Acad. Sci.* **74**, 3119–3123.

Peters, K.-R., Palade, G. E., Schneider, B. G. & Papermaster, D. S. (1983) Fine structure of a periciliary ridge complex of frog retinal rod cells revealed by ultrahigh resolution scanning electron microscopy. *J. Cell Biol.* **96**, 265–276.

Pfeffer, B., Wiggert, B., Lee, L., Zonnenberg, B., Newsome, D. & Chader, G. J. (1983) The presence of a soluble interphotoreceptor retinoid-binding protein in the retinal interphotoreceptor space. *J. Cell Physiol.* **117**, 333.

Poincelot, R. P., Millar, P. G., Kimbel, R. L. & Abrahamson, E. W. (1969) Lipid to protein chromophore transfer in the photolysis of visual pigments. *Nature* **221**, 256–257.

Poo, M. M. & Cone, R. A. (1973) Lateral diffusion of rhodopsin in *Necturus* rods. *Exp. Eye Res.* **17**, 503–510.

Pugh, E. N. (1975) Rhodopsin flash photolysis in man. *J. Physiol.* **248**, 393–412.

Richardson, T. M. (1969) Cytoplasmic and ciliary connections between the inner and outer segments of mammalian visual receptors. *Vision Res.* **9**, 727–731.

Ripps, H., Mehaffey, L. & Siegel, I. M. (1981) Rhodopsin kinetics in the cat retina. *J. Gen. Physiol.* **77**, 317–334.

Ripps, H. & Weale, R. A. (1969) Flash bleaching of rhodopsin in the human retina. *J. Physiol.* **200**, 151–159.

Rotmans, J. P., Daemen, F. J. M. & Bonting, S. L. (1974) Biochemical aspects of the visual process. XXVI. Binding site and migration of retinaldehyde during rhodopsin photolysis. *Biochim. biophys. Acta* **357**, 151–158.

Saari, J. C., Bunt-Milam, A. H., Bredberg, L. & Garwin, G. G. (1984) Properties and immunocytochemical localization of three retinoid-binding proteins from bovine retina. *Vision Res.* **24**, 1595–1603.

Schwanzara, S. A. (1967) The visual pigments of freshwater fishes. *Vision Res.* **7**, 121–148.

Spitznas, M. & Hogan, M. J. (1970) Outer segments of photoreceptors and the retinal pigment epithelium. *Arch. Ophthal.* **84**, 810–819.

Steinberg, R. H., Wood, I. & Hogan, M. J. (1977) Pigment epithelial ensheathment and phagocytosis of extrafoveal cones in human retina. *Phil. Trans.* **277**, 459–476.

Tabor, G. A., Fisher, S. K. & Anderson, D. H. (1979) Evidence for a circadian rhythm of disc shedding in light-entrained gray squirrels. *ARVO Suppl.* **18**, 81.

Tabor, G. A., Fisher, S. K. & Anderson, D. H. (1980) Rod and cone disc shedding in light-entrained tree squirrels. *Exp. Eye Res.* **30**, 545–557.

Tamai, M., Teirstein, P., Goldman, A., O'Brien, P. & Chader, G. (1978) The pineal gland does not control rod outer segment shedding and phagocytosis in the rat retina and pigment epithelium. *Invest. Ophthal.* **17**, 558–562.

Thompson, P. & Findlay, J. B. (1984) Phosphorylation of ovine rhodopsin. Identification of the phosphorylated sites. *Biochem. J.* **220**, 773–780.

Trayhurn, P. & Habgood, J. O. (1975) The effect of trypsin on the retinal rod outer segments: trypsin digestion as a means of isolating viable discs. *Exp. Eye Res.* **20**, 479–487.

Tsinn, A. T. C. & Beatty, D. D. (1977) Visual pigment changes in rainbow trout in response to temperature. *Science* **195**, 1358–1360.

Tsinn, A. T. C. & Beattey, D. D. (1978) Goldfish rhodopsin: $P499_1$. *Vision Res.* **18**, 1453–1455.

Wald, G. (1935) Carotenoids and the visual cycle. *J. gen. Physiol.* **19**, 351–371.

Wald, G. (1939) The porphyropsin visual system. *J. gen. Physiol.* **22**, 775–794.

Wald, G. (1946) The chemical evolution of vision. *Harvey Lectures* **41**, 148–152.

Wald, G. (1960) The distribution and evolution of visual systems. In *Comparative Biochemistry*, vol. I. New York: Academic Press.

Wald, G. & Brown, P. K. (1952) The role of sulphydryl groups in the bleaching and synthesis of rhodopsin. *J. gen. Physiol.* **35**, 797–821.

Wiggert, B. O. & Chader, G. J. (1975) A receptor for retinol in the developing retina and pigment epithelium. *Exp. Eye Res.* **21**, 143–151.

Wiggert, B., Lee, L., O'Brien, P. J. & Chader, G. J. (1984) Synthesis of interphotoreceptor retinol-binding protein (IRBP) by monkey retina in organ culture: effect of monensin. *Biochem. Biophys. Res. Comm.* **118**, 789–796.

Wiggert, B., Lee, L., Rodriguez, M., Hess, H., Redmond, T. M. & Chader, G. J. (1986) Immunochemical distribution of interphotoreceptor retinoid—bindging protein in selected species. *Invest. Ophthal.*, **27**, 1041–1049.

Wilt, F. H. (1959) The differentiation of visual pigments in metamorphosing larvae of *Rana catesbiana*. *Dev. Biol.* **1**, 199–233.

Wong, J. K. & Ostroy, S. E. (1973) Hydrogen ion changes of rhodopsin. I. Proton uptake during the metarhodopsin I_{478} metarhodopsin II_{308} reactions. *Arch. Biochem. Biophys.* **154**, 1–7.

Worthington, C. R. (1973) X-ray analysis of retinal photoreceptor structure. *Exp. Eye Res.* **17**, 487–501.

Wu, C.-W. & Stryer, L. (1972) Proximity relationships in rhodopsin. *Proc. Nat. Acad. Sci. Wash.* **69**, 1104–1108.

Yoshizawa, T. (1972) The behaviour of visual pigments at low temperatures. *Hdb. Sensory Physiol.* **7**(1), 146–179.

Yoshizawa, T., Schishida, Y. & Matsuoka, S. (1984) Primary intermediates of rhodopsin studied by low temperature

spectrophotometry and laser photolysis. *Vision Res.* **24**, 1455–1463.

Young, R. W. (1971) Shedding of discs from rod outer segments in the rhesus monkey. *J. Ultrastr. Res.* **34**, 190–203.

Young, R. W. (1972) The daily rhythm of shedding and degradation of cone outer segment membranes in the lizard retina. *J. Ultrastr. Res.* **61**, 172–185.

Young, R. W. (1976) Visual cells and the concept of renewal. *Invest. Ophthal.* **15**, 700–725.

Zimmerman, W. F. (1974) The distributions and proportions of vitamin A compounds during the visual cycle in the rat. *Vision Res.* **14**, 795–802.

Zimmerman, W. F., Lion, R., Daemen, F. J. M., & Bonting, S. L. (1975) Distribution of specific retinol dehydrogenase activities in sub-cellular fractions of bovine retina and pigment epithelium. *Exp. Eye Res.* **21**, 325–332.

Zorn, M. (1974) The effect of blocked sulfhydryl groups on the regenerability of bleached rhodopsin. *Exp. Eye. Res.* **19**, 215–221.

Zorn, M. & Futterman, S. (1971) Properties of rhodopsin dependent upon associated phospholipid. *J. biol. Chem.* **246**, 881–886.

9. DARK ADAPTATION AND THE MINIMUM VISUAL STIMULUS

THE DARK-ADAPTATION CURVE

We have seen that, in the dark, the sensitivity of the human eye to light increases until a maximum is reached after about 30 minutes; this gives the dark-adaptation curve showing the progressive fall in threshold. We have already concluded that the curve represents the course of recovery of function of the rods. This curve, however, is not smooth, but shows a 'kink' so that adaptation consists in an initial rapid phase of recovery of sensitivity, which is finished in about 5 to 10 minutes, and a slower phase.

Cone and Rod Portions

The first rapid phase has been shown, by many experiments, to represent the increase in sensitivity of the cones in the dark, so that the threshold during the first few minutes in the dark is determined by the cones, the thresholds of the rods still being higher than those of the cones. Numerous lines of evidence support this conclusion. For example, if the area of the light-stimulus used for measuring the threshold is small, and is concentrated on the fovea, the curve of dark-adaptation consists only of the initial part. As the size of the stimulus is increased, so that overlap on to the parafovea, containing rods, occurs, the dark-adaptation curve shows the typical kink with cone and rod portions (Fig. 9.1). Again, if coloured stimuli are used to test the threshold, during the early portion of the curve the subject appreciates the colour of the threshold stimulus, whilst at the later stages the light is said to be white. Yet again, by varying the state of light-adaptation of the subject before he is placed in the dark, the type of curve may be changed. After a period of weak light-adaptation the cones are nearly at their maximum sensitivity, so that the threshold on going into the dark is very soon determined by the rods; hence the kink comes early or not at all. If the wavelength of the adapting light is varied, the relative extents to which the thresholds of the rods and cones are raised will be different, so that on placing the subject in the dark after adapting him to red light, for instance, his rods will be relatively active—because red light barely influences these—whilst the cones will have a high threshold; the curve for dark-adaptation will therefore have no kink, the rods determining the threshold from the beginning.

Rod Monochromat

Finally, a human subject defective in cone vision, the so-called *rod monochromat*, has a dark-adaptation curve with no kink. This type of subject is useful since he permits the study of the rod thresholds without interference from the cones; thus, immediately on placing the normal light-adapted subject in the dark his threshold is determined by the cones; in other words the rods are less sensitive than the cones and so we cannot tell what their threshold is. In the rod-monochromat, however, we can measure the rod threshold as soon as he is placed in the

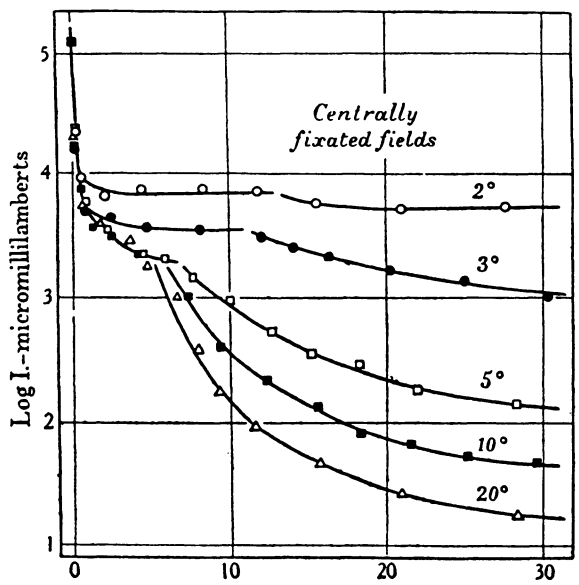

Fig. 9.1 Dark-adaptation curves with centrally fixated field subtending larger and larger angles at the eye. With the larger fields peripheral vision comes into play giving the characteristic break in the curve. (Hecht, *et al.*, *J. gen. Physiol.*)

dark and this is found to be very high; nevertheless the rods are not incapable of being stimulated, so that in ordinary daylight, although their thresholds are higher than those of the cones, they may be responding to light. However, there seems no doubt from Aguilar & Stiles' study, that the rods become 'saturated' at high levels of illumination (2000 to 2500 trolands or 100 to 300 cd/m^2) in the sense that they become incapable of responding to changes of illumination (the l.b.i. is infinitely high); the same was shown by Fuortes *et al.* (1961) on their rod-monochromat who was virtually blind at high levels of illumination; the rods were responding to light, but not to changes, so that there was no awareness of contrast.

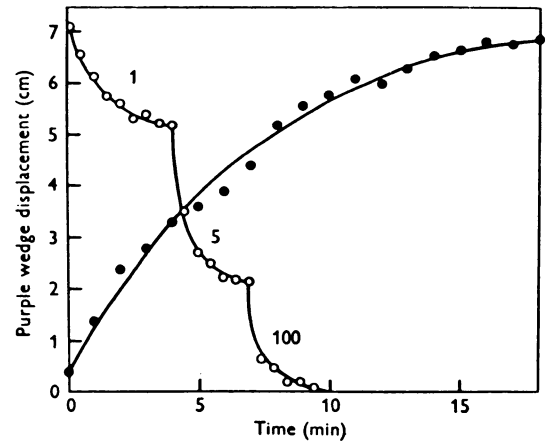

Fig. 9.2 O—O, effect of bleaching the dark-adapted retina with lights of intensities 1, 5 and 100 units (1 unit = 20 000 trolands). ●—●, course of regeneration of rhodopsin. The ordinate indicates the degree of absorption of light in terms of displacement of an optical wedge. (Campbell & Rushton, *J. Physiol.*)

Regeneration of Rhodopsin

Light-adaptation is accompanied by the bleaching of rhodospin as shown by experiments involving extraction of pigment from eyes before and after exposure to light. It seems reasonable to suppose, therefore, that the process of dark-adaptation has as its basis the regeneration of rhodopsin in the rods; and the early studies of Tansley and Peskin certainly showed that the time-course of regeneration, as measured by extraction of frog's retinae after different periods in the dark, corresponded with the time-course of dark-adaptation. By the technique of *reflexion densitometry* the changes in concentration of pigment in the retina have been followed in the intact eye in man and lower animals.

Reflexion Densitometry

The technique is based on the principle of measuring the light reflected from the fundus of the eye; if the retina contains rhodopsin it will absorb blue-green light of 500 nm in preference to red and violet light, hence the light reflected from the fundus will contain less light of 500 nm and more of these other wavelengths. The loss of intensity of light, moreover, will give a direct measure of the degree of absorption, and thus of the optical density of the rhodopsin in the retina. Careful analysis of the changes in amount of light after reflexion showed that they were indeed due, in the dark-adapted eye, to the presence of rhodopsin (Campbell & Rushton, 1955), the degree of absorption of the different wavelengths corresponding approximately with the extinction spectrum of rhodopsin. As Fig. 9.2 shows, exposure to lights of increasing intensity caused decreases in the amount of rhodopsin.

In a later study Alpern & Pugh (1974) compared the action-spectrum for bleaching some 10% of the rhodopsin in a human observer's retina with the scotopic sensitivity of the same observer. Figure 9.3 shows the comparison where the triangles represent the action spectrum

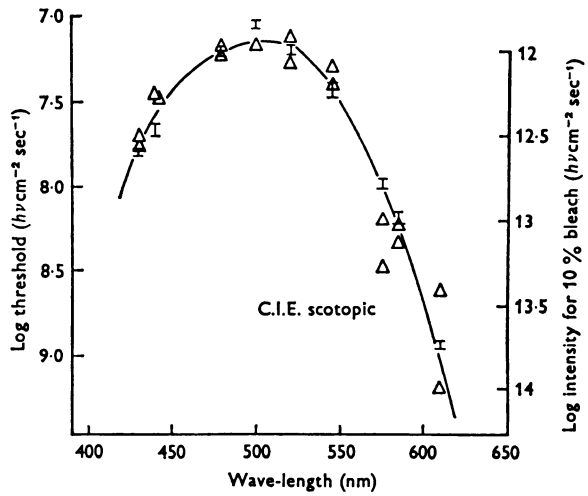

Fig. 9.3 Comparison of the action spectrum for bleaching rhodopsin (triangles and right-hand ordinate) with scotopic sensitivity of the same subject (brackets and left-hand ordinate). The brackets define the geometrical mean ±1 standard error of fifteen determinations of the absolute threshold in a single run. (Alpern & Pugh, *J. Physiol.*)

for the bleach and the brackets determine the geometric mean of fifteen determinations of the absolute threshold at the corresponding wavelengths.

Photosensitivity

An important characteristic of the retinal photopigment *in situ* must be its photosensitivity which defines, in effect,

the rate at which bleaching will take place for a given intensity of retinal illumination (p. 239). The determination *in situ*, as well as that of the optical density of the pigment, given by $\mathrm{Log}_{10} I_i/I_t$, can be carried out by the technique of reflexion-densitometry. The optical density was, on average in human subjects, 0.3, indicating that one out of two quanta incident on the retina was absorbed. The photosensitivity was of the order of 100 000 l.(cm.mole)$^{-1}$, which was two or three times higher than values obtained *in vitro* or in the isolated animal eye, and Alpern & Pugh (1974) suggest that light is being funnelled into the outer segments of rods by the inner segments (Stiles–Crawford effect), although such a funnelling is predominantly a cone phenomenon. We may note that the optical density of rhodopsin in human rods is comparable with that of cone photopigments in the human retina deduced likewise on the basis of reflexion-densitometry.[1]

Rates of Regeneration

After complete bleaching the curve of regeneration is slow, the total regeneration requiring 30 minutes, and thus being equivalent to the time for complete dark-adaptation in man. In the cat, where dark-adaptation is considerably slower, the regeneration, measured in a similar way, takes much longer (Weale, 1953). The half-times (min) for regeneration, determined by reflexion densitometry, in different species are as follows (Bonds & McLeod, 1974):

Man	4.75	Rat	40
Cat	11	Guinea pig	60
Rabbit	24	Skate	60
Frog	25–30		

Rhodopsin Concentration and Retinal Sensitivity

Rushton (1965) observed that the bleaching of only a small amount of rhodopsin caused an inordinate loss of sensitivity; thus exposure to a flash that bleached only 1% of the total rhodopsin in the retina raised the threshold by a factor of ten. Rushton showed that, in the human, there was a logarithmic relation between the rhodopsin content of the eye and the sensitivity, and Dowling (1960), working on the rat, and using the ERG as a measure of light-sensitivity, found a similar relation.[2] Thus the threshold, θ, during dark-adaptation follows the so-called Dowling–Rushton equation:

$$\mathrm{Log}\ (\theta/A) = \alpha B$$

where A is the threshold in complete dark-adaptation, B is the fraction of bleached rhodopsin, and α is a constant of proportionality.

RECEPTOR SENSITIVITY

The important point to appreciate, and brought out by later studies on the electrophysiology of the retina, is that when the eye is exposed to light, long before significant changes in the rhodopsin content of the receptors have taken place, i.e. before the receptor's chance of absorbing a quantum of light has been diminished, there is a profound change in the sensitivity of the receptor. On exposure to lights that bleach significant amounts of rhodopsin and thus reduce the chance of a quantum-catch, sensitivity is further reduced; and this may be established by using an isolated retina in which regeneration of pigment is impossible;[3] under these conditions, although there is considerable dark adaptation after light exposure, sensitivity remains permanently decreased (Donner & Reuter, 1967).

THREE PHASES

Donner & Hemilä (1979) describe three main phases of adaptation as measured in the massed rod response[4] of the isolated frog retina. First there is a fast increase in sensitivity lasting less than 1–2 min at 14°C; if bleaching is less than 0.5% sensitivity returns to the normal dark-adapted value. This they call 'background adaptation'[5] and is clearly unrelated to pigment concentration as far as quantum-catch is concerned. Second, when bleaching is greater than 0.5%, recovery is delayed and slowed and may last 30 min; during the slow phase, sensitivity may increase a hundredfold. The process occurs even if there is no regeneration of visual pigment. This has been called *intermediate adaptation*; finally, there is a slower process directly related to the regeneration of rhodopsin, and is called *opsin adaptation* and is essentially the adaptation described by Rushton and Dowling and is related to the probability of catching a quantum of light. According to Donner & Hemilä, the intermediate adaptation is related to the presence of bleached products in the retina, notably Metarhodopsin II and III, these having sufficiently long lives to exert an effect.

OPSIN ADAPTATION

Grabowski & Pak (1975), using axolotl rods, showed that the value of the maximum hyperpolarization, after greater than 20% bleaching, was proportional to the amount of photopigment remaining; at approximately 100% bleaching the threshold has risen by some 3 log-units, i.e. a thousandfold.

ROLE OF LIGHT-SCATTER

The non-bleaching aspects of light-adaptation are best revealed by the rise in threshold to light of an unexposed part of the retina when another region is exposed to light. However, the course of recovery of sensitivity of the unexposed portion often runs parallel with that of the exposed region, which itself is related to the regeneration

of visual pigment, so that the question arises as to whether the distant effect is due to light-scatter within the eye. This possibility has been discussed by Cicerone & Green (1981) in the light of their experiments with rat's ganglion cells. They showed that the time-constants for recovery in the two regions were, in fact, different; and an analysis of the recovery curves under different conditions indicated that the indirect, or *lateral adaptation*, contained a neural component, presumably mediated by neural interactions within the retina. Thus they estimated that with direct exposure the amount of light required to reduce increment-sensitivity by a given amount was only one-fifteenth of that required by indirect exposure (scattered light). On reducing the light-exposure by a tenth they found that the rate of recovery in the exposed part was considerably more rapid than the rate of recovery in the unexposed half-field when this was exposed to the full illumination, i.e. ten times luminosity. Since rate of recovery decreases with light-exposure, this indicates that the loss of sensitivity at a distance cannot be solely due to light-scatter.

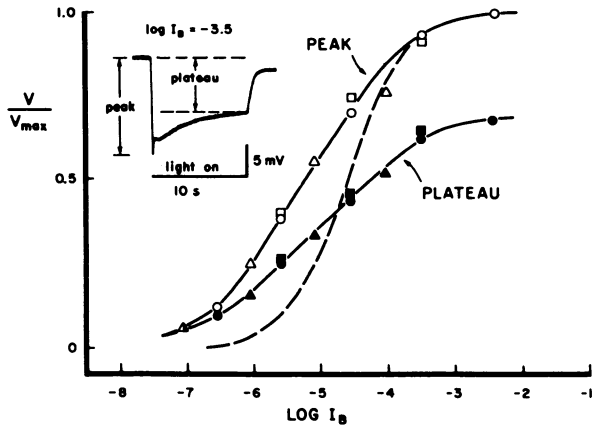

Fig. 9.5 Voltage-intensity functions for peak (open symbols) and the plateau potential (closed symbols) in response to 10 sec flashes. Inset shows how the potentials were assessed. The dashed line corresponds to Fig. 9.4. (Kleinschmidt & Dowling, *J. gen. Physiol.*)

ADAPTATION STUDIES ON SINGLE RECEPTORS

Gecko Rods

Kleinschmidt & Dowling (1975) have made intracellular records from the gecko rods; the hyperpolarizing response to single flashes followed the simple Michaelis-Menten type of curve like that of the turtle cone, and is indicated in Fig. 9.4. When maintained lights of some 10 sec duration are presented, there is an initial rapid transient followed by a slow return to a plateau level. Both peak-voltage and plateau-voltage show a similar relation to the stimulus-intensity (Fig. 9.5) but the plateau shows a shift towards higher intensities indicating that, immediately after the onset of the light, there has been some adaptation leading to a lower hyperpolarization for a given intensity than that which was first obtained. Since there is a limit to the degree of hyperpolarization, any reduction in the presence of a steady background means an increase in the power of the receptor to respond to a brighter stimulus.

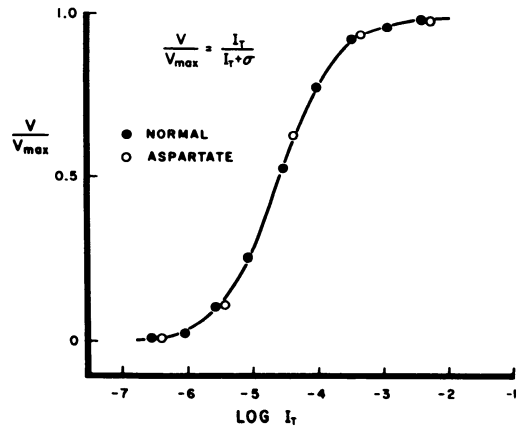

Fig. 9.4 Voltage-intensity function for intracellular responses from two dark-adapted receptors to 0.1 s test flashes in the normal preparation (filled circles) and in the aspartate-treated preparation (open circles). Ordinates are peak responses as fraction of maximum response. Abscissa is logarithm of light intensity, I_T. The solid line plots the function indicated at the top of the graph. (Kleinschmidt & Dowling, *J. gen. Physiol.*)

Increment-thresholds

The adaptive phenomenon is best illustrated by exposing the receptor to backgrounds of increasing intensity and measuring the voltage-intensity relation of the receptor, the voltage being measured as the ratio of the actual voltage to the maximum obtainable in the dark-adapted eye, V_{max}, and the intensity of the stimulus as ΔI. It will be seen from Fig. 9.6 that, as background intensity is increased, the voltage-intensity function shifts bodily to the right. There is also what the authors called a *compression* of the response-range, i.e. a decrease in the maximum amplitude of increment responses available to the receptor; this is due to a combination of two phenomena, namely that the backgrounds induce sustained potentials from which the responses have to arise, and since there is a maximum hyperpolarizing potential, the range is reduced correspondingly; secondly, bright backgrounds lower the actual saturation potential of the receptor.

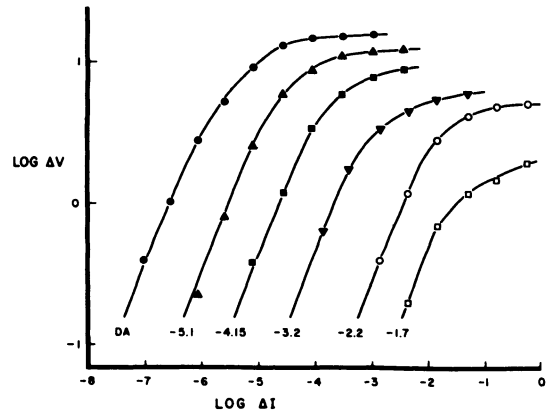

Fig. 9.6 Voltage-intensity functions at different levels of adaptation as indicated by the numbers, which are logarithmic decrements of the standard source (1.3 mW/cm^2). DA = dark-adapted ΔV is the peak amplitude of the response to an increment in intensity, ΔI. (Kleinschmidt & Dowling, *J. gen. Physiol.*)

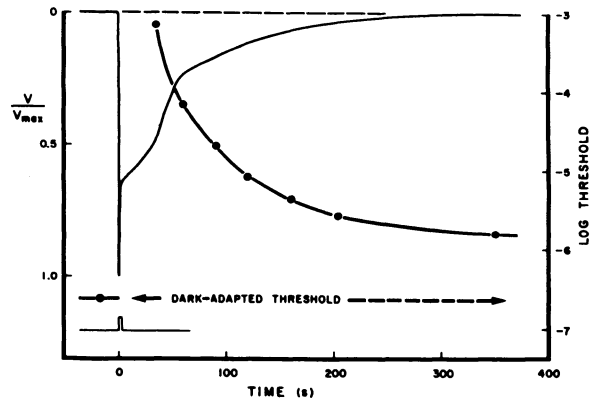

Fig. 9.7 Comparison of temporal change in rod membrane potential, expressed as V/V_{max} (L.H. ordinate) with the change in threshold to a light stimulus, as a function of time in the dark after exposure of the eye-cup to an intense light-adapting stimulus. Note that the threshold was still elevated after the membrane potential had returned to its dark-adapted level. (Kleinschmidt & Dowling, *J. gen. Physiol.*)

Analysis of these responses indicated that the compression phenomenon played very little role in changing the sensitivity at different backgrounds compared with the shift of the voltage-intensity function (Fig. 9.6). In general, however, it must be emphasized that the main effect of light-adaptation is to shift the voltage-intensity function to higher intensities without affecting appreciably the maximum response obtainable. Hence adaptation may be said to decrease the effectiveness of a given isomerization of photo-pigment rather than reduce the number of open channels available, thus Rh*, the number of channels closed per isomerization is decreased. Ultimately, of course, the compression is such that the maximum voltage-change that can be produced by any background is zero, and the threshold becomes infinite; the receptor is now said to be saturated. Interestingly, at this stage, the membrane is still some 5 mV less hyperpolarized than the dark-adapted saturation potential.

Dark-adaptation

Kleinschmidt & Dowling (1975) followed the process of recovery of sensitivity of Gecko rods after exposure to a bright light; as Fig. 9.7 shows, after an initial transient there is a fairly rapid recovery of membrane potential and sensitivity lasting about 5 min. This phase brought the threshold to within 0.8 log units of its dark-adapted value, whilst the membrane potential had returned to its original dark-adapted value. Subsequent recovery of threshold sensitivity lasted much longer and was independent of membrane potential. Kleinschmidt & Dowling suggested that the slow phase was the consequence of a significant bleaching of pigment during the light-adaptation, which reduced the quantum catch, whereas the earlier phase, which can occur when no significant change in bleaching or recovery has taken place, they described as *neural*, and was due to a change in the receptor.

Aspartate Treated Retina

It is possible to block the *b*-wave of the ERG by treating the eye-cup with aspartate, a block due, apparently, to inhibition of synaptic events in the retina which would include horizontal cell feedback on the receptors. Adaptational effects have, in the past, been largely attributed to some such feedback action, so that it is interesting that Kleinschmidt & Dowling (1975) found no influence of aspartate on the main features of the adaptation process in gecko photoreceptors. Thus Fig. 9.8 shows the plot of log-threshold versus log-background intensity for impaled rods; the linear relation over most of the range of backgrounds indicates the application of the Weber law, which implies that the receptors are resetting their dynamic ranges at each new background intensity; at very low scotopic levels there is very little adaptation, in the sense that the value of ΔI does not increase appreciably; at the very highest levels ΔI becomes infinite, indicating saturation of the rod. Aspartate-treated retinae behave similarly to normal, except that the thresholds are slightly lower.

Turtle Cones

In general, cones show much wider dynamic ranges than those of rods, due to their greater powers of adaptation.

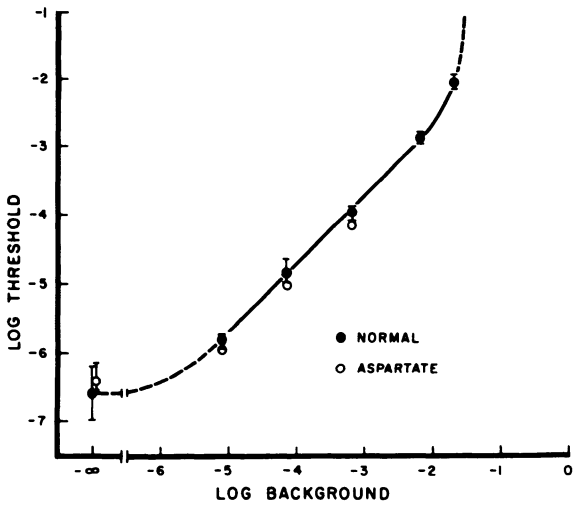

Fig. 9.8 Absence of effect of blocking synaptic transmission in the retina, with aspartate, on the increment threshold of gecko photoreceptors. Threshold criterion was a 0.5 mV incremental response to a 0.1 s flash superimposed on each background, indicated by the abscissa. Note saturation at high background intensities. (Kleinschmidt & Dowling, *J. gen. Physiol.*)

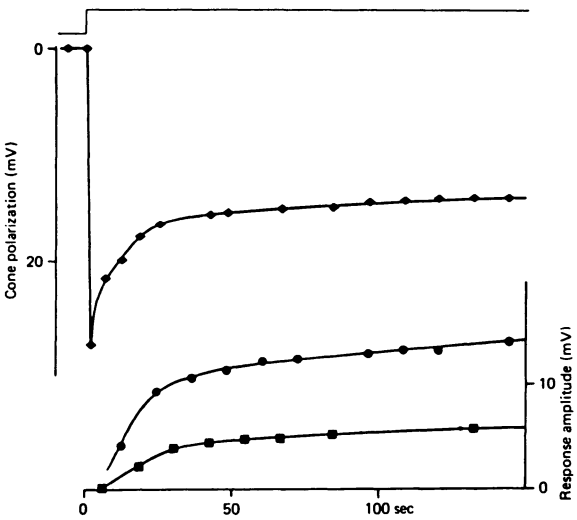

Fig. 9.9 Upper curve shows establishment of plateau-level of polarization during maintained illumination of turtle cone; lower curves show growth of the increment responses (squares) and OFF-responses (circles) as a function of time after the onset of the light-background stimulus. (Normann & Perlman, *J. Physiol.*)

Normann & Perlman (1979) have made intracellular records from turtle cones under various conditions of adaptation. The adaptation during a sustained background is revealed as the establishment of a plateau level, as in Fig. 9.9; during this phase the ability of the cone to respond to an applied flash increases from zero, at the peak of the response, to some 15 mV during the plateau; Fig. 9.9 shows the obvious correlation between the two events indicating a common mechanism, which might be an unblocking of channels initially blocked at the onset of the light. Thus the parallel rise in the increment response illustrated by Fig. 9.9 suggests that the channels that had become unblocked could be reblocked by a further light-stimulus.

Weber Law

The long-term adaptational effects were then studied by maintaining different background intensities and measuring the peak potential as a function of stimulus-intensity (Fig. 9.10); the voltage intensity functions are all shifted to the right at high background intensities so that the dynamic range extends over the same limits of some 3 log units in spite of large changes in background. There is remarkably little compression compared with that observed in rods (p. 267). The condition for strict applicability of the Weber law is that the slope of the intensity-response curves of Fig. 9.10 should be constant when measured about each background intensity, and this is true for these cone responses. Thus, the cone, quite independently of higher neuronal activity, exhibits an adjustment to background-intensity manifest as this Law.

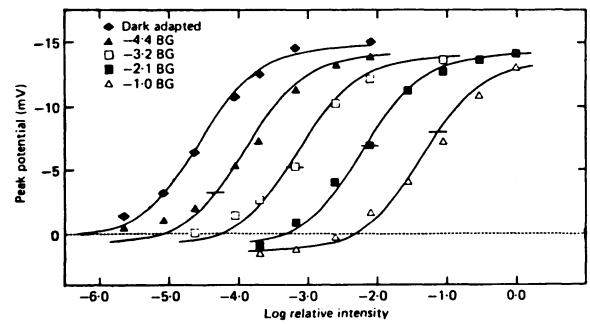

Fig. 9.10 Dependence of intensity-response functions of a red cone on the state of adaptation. The peak response, measured from the dark-adapted potential (dashed line) is plotted as a function of the log of the test-pulse intensity which elicited each response. The steady hyperpolarization produced by each background is indicated by the short horizontal lines on the graphs. (Normann & Perlman, *J. Physiol.*)

Pigment Bleaching

Normann & Perlman measured bleaching of the photopigment under the conditions studied here and showed that it was so small that the decreases in sensitivity, manifest by the shifts in the curves to the right, could not have been due to diminished quantum-catch.

Feedback

Feedback from horizontal cells, which certainly can occur and will diminish the cone response (p. 309) was also ruled out by employing small spot stimuli.

Comparative Aspects of Saturation

In general, cones do not saturate, being able to respond to light-increments at the highest light-intensities; rods of rats, mudpuppy, gecko, and marine toad all saturate, but the rods of the skate form an exception, responding to light-increments even at light-intensities at which over 90% of the rhodopsin is bleached (Dowling & Ripps, 1970). The skate, however, has an all-rod retina, so that this extension of its dynamic range is presumably related to its need to be able to respond at high daylight luminances. (The saturation of rods occurs at light-intensity levels that bleach negligible amounts of their photopigment.) In species that have both rods and cones in the retina, the dynamic range of vision is extended by the presence of cones. The rods seem to fall into two groups, namely those that are capable of adaptation, in the sense of extending their dynamic ranges in response to background illumination, and those that are unable to do this.

Rod Groups

Thus the gecko rods described by Kleinschmidt & Dowling definitely fall into the first category and, according to Fain's (1976) study on the marine toad, the intracellularly recorded responses of these rods show increment-sensitivity to increased background that follows the Weber law over a range of at least 3 log units; in other words, the response-intensity function shifts to regions of higher intensity as background increases. At high enough intensities, however, the toad and gecko rods saturate.[6] The rods of the rat and mudpuppy have been described as essentially non-adapting in so far as the application of the Weber law is concerned, so that there is no shift of the intensity-response function at high background illuminations. The receptors are thus restricted to the narrow dynamic range of their dark-adapted voltage-intensity function, so that they are only capable of responding in the presence of an adapting light if the adapting light is not intense enough to saturate them in their dark-adapted condition. We may say that, at a given adapting, or background, intensity, their response-range has been compressed within a narrower compass (Kleinschmidt & Dowling, 1975; Fain, 1976). The difference between this type of non-adapting rod and the cone is demonstrated in the retina of the mudpuppy, which has both rods and cones that may be recorded from intracellularly.

SOME THEORETICAL CONSIDERATIONS

Dynamic Range

The changes in sensitivity of the eye in response to illumination constitute essentially changes in the dynamic range of the receptors that permit them to operate over a very wide range of luminous intensities. These adaptational changes are by no means peculiar to the eye, but the evolution of the duplex retina, containing two types of receptor with abilities to respond to change in illumination over different ranges, may be regarded as a specialization that enables the eye to respond to changes in intensity of the stimulus over a far wider range than is found, say, with acoustic stimuli. To recapitulate, by dynamic range we mean the range of stimulus-intensities over which the receptor is able to give signals indicating a change, either increase or decrease. Thus, with any receptor, we find that as intensity is increased, as with flashing lights, a value is reached where the receptor is said to be saturated, so that increasing the stimulus-intensity fails to be signalled by a change in response. If the receptor adapts, however, when the maximal or submaximal stimulus is sustained, it is found that what was the maximal stimulus is no longer so, and that an increase will be signalled as an increase in response, e.g. voltage. This adaptation has been measured in many systems, and our psychophysical study of the difference-thresholds obtained by exposing the eye to steady background illuminations, and measuring the threshold increase or decrease in illumination required to give a changed sensation, has implicitly indicated the existence of an adaptation process, since we find that the thresholds, measured as difference-limens, increase as the background intensity increases, the difference-limen being a fraction of the prevailing background illumination, and leading to the well-known Weber–Fechner relationship.

Monkey Cones

Studies on photoreceptors illustrate the phenomenon of adaptation very well; Fig. 9.11 shows that the effect on monkey cones is essentially to shift the intensity-response curves to the right, so that, although we are operating at higher and higher levels of illumination, the dynamic range has remained the same. Adaptation, in this case, has meant that the responsiveness of the receptors has diminished, in the sense that we need stronger and stronger stimuli to produce the same electrical voltage, but that the usefulness of the receptors has not been impaired, since they serve to signal *changes* in light-stimulus. Thus by shifting the separate curves to the left, they can be made to superimpose. The type of adaptation giving this behaviour has been called *cellular adaptation* since it occurs without significant bleaching of the visual pigment. When we move into a range where visual pigment bleaching, by reducing the photon-catch of a given stimulus, produces a diminished responsiveness, but not necessarily a diminution of the dynamic range, once again, the results

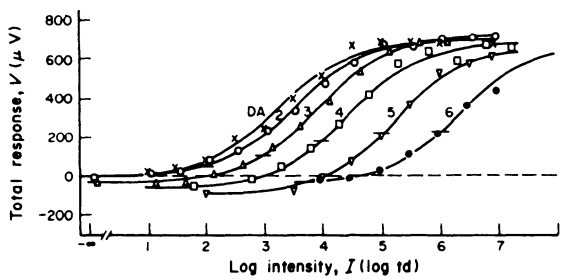

Fig. 9.11 Cone flash response versus intensity curves in the presence of adapting background illumination, from a single experimental run. The background light intensity is indicated by the numbers next to the curves: DA is dark adapted. The response is plotted as total cone response $V = V_R + V_T$. The small horizontal line in each curve indicates the background response level. Responses above this line are increment responses and below this line, decrement responses. (Valeton & Van Norren, *Vision Res.*)

are expressed in a shift of the response-curves to the right (Valeton, 1983).

Finally, there is the factor called 'response compression', which is a consequence of the background adapting light moving the operating point of the receptor up along the operating curve; because of the non-linearity of this operating curve, at higher background intensities the threshold change in intensity, necessary to give a standard response, becomes higher. We may note that, because the initial operating point has been shifted along the response-curve, the dynamic range has been reduced, a phenomenon described as 'response range compression'.

Incident Light Model

Valeton (1983) starts his analysis of adaptation with the basic equation governing the responses of a single receptor at varying intensities of stimulus:

$$\frac{V}{V_m}=\frac{I^n}{I^n+\sigma^n} \tag{1}$$

i.e. the Michaelis-Menten type of equation applicable to a system that 'saturates' at a maximal stimulus, I_m. In most studies, the exponent n is taken as unity. σ, the intensity required to give half-maximal response, is essentially a measure of adaptation, and varies in accordance with the background. The response to a stimulus applied against a background, B, is taken to be the response to the total incident light, the receptor not distinguishing between the two sources. Thus:

$$V_{B+T}=\frac{V_m(I_B+I_T)^n}{(I_B+I_T)^n+\sigma^n} \tag{2}$$

When I_T, the intensity of the test-flash, is zero, we have:

$$V_B=\frac{V_m I_B^n}{I_B^n+\sigma^n} \tag{3}$$

The increment response above a steady background, V_T, to a light-increment, I_T is given by the difference of equations (2) and (3):

$$V_T=V_m\left(\frac{(I_B+I_T)^n}{(I_B+I_T)^n+\sigma^n}-\frac{I_B^n}{I_B^n+\sigma^n}\right) \tag{4}$$

It is assumed that the background changes the value of the parameter σ, which results in a shift of the complete response curve, equation (2), along the intensity axis, which in turn corresponds to a change in sensitivity. The background response, itself, is also affected by a change in I_B, in accordance with equation (3); it is manifest in measurements of receptor response by the initial peak, followed by a 'sag' in the response, e.g. Fig. 10.13, the sag representing the adaptation to the maintained (background) stimulus. Besides shifting the response curve bodily, the background also moves the operating point of the receptor up along the curve, and because this is non-linear, at higher intensities, the responses to given increments of light will become progressively smaller. This is called 'response compression'.[7] Finally, because the operating point has been shifted upwards, the range of response is reduced, i.e. the dynamic range discussed earlier. This has been called 'response range compression'.

By mathematical analysis of equation (4) and assuming that there are two adaptation factors, σ_α and σ_β, corresponding to cellular adaptation and pigment bleaching respectively, Valeton & Van Norren (1983) deduced a theoretical threshold versus intensity function for primate cones, and the relative contributions of response compression, cellular adaptation and pigment bleaching to the adaptation, represented by $\Delta I_L/\Delta I_D$, i.e. the ratio of the light-increment necessary to produce a given voltage-response, 35 μV, at different backgrounds divided by the threshold in the dark. Figure 9.12 illustrates this.

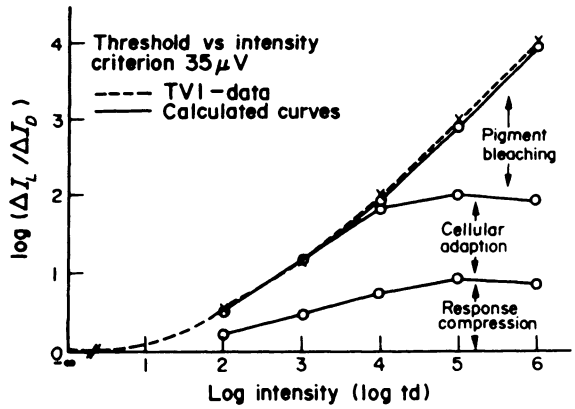

Fig. 9.12 Threshold versus intensity function of primate cones. The thresholds for the backgrounds (ΔI_L) are given relative to the dark adapted threshold (ΔI_D), and hence the ordinate gives log $\Delta I_L/\Delta I_D$. The dashed curve, connecting the crosses, was obtained by determining for each background, the amount of light necessary to elicit a criterion response $\delta = 35\ \mu$V. The three solid lines connecting the open circles show, at each background intensity, the contribution of each of the three sensitivity regulating mechanisms to the total sensitivity loss that occurs in light adaptation. (Valeton & Van Norren, *Vision Res.*)

The curves of Fig. 9.12 are called TVI functions, and are a common method of indicating adaptation, being the change in stimulus intensity required to produce a standard response at different background intensities divided by the threshold intensity in the dark.[8]

THE ABSOLUTE THRESHOLD

Frequency-of-seeing

In the fully dark-adapted state, the minimum stimulus necessary to evoke the sensation of light is called the absolute threshold. It must be appreciated, however, that this threshold is not a fixed quantity but changes from moment to moment, so that if a subject is presented with a luminous screen in the dark, we may find a range of luminance over which there will be some probability, but not certainty, of his seeing it. Experimentally, therefore, the screen must be presented frequently at different luminances and the experimenter must plot the 'frequency-of-seeing' against the luminance, to give the typical 'frequency-of-seeing' curve shown in Fig. 9.13. From

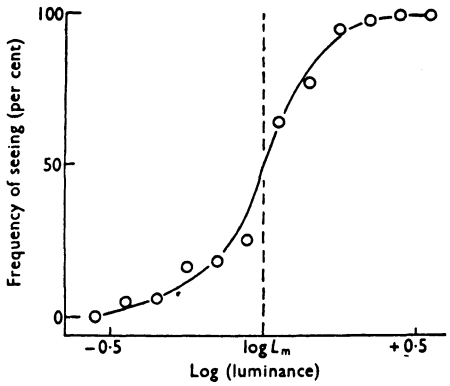

Fig. 9.13 Typical frequency-of-seeing curve for dark-adapted human observer. (Pirenne *et al.*, *M.R.C. Sp. Rep.*)

this curve it is a simple matter to compute a threshold on the basis of an arbitrarily chosen frequency, e.g. 55%.

Thus we may express it as the luminance of a large test-screen, exposed for a relatively long time, e.g. one second. Since the size of the pupil is important, this must be measured, and the threshold expressed in trolands; furthermore the spectral composition of the light must be defined so that, if necessary, the number of quanta falling on unit area of the retina in unit time may be derived. This definition of the threshold stimulus is thus a statement of the *retinal illumination.* Experimentally this type of threshold has been found to be of the order of 0.75×10^{-6} cd/m^2 varying between 0.4 and 2.0×10^{-6} (Pirenne *et al.*, 1957). This is equivalent to a retinal illumination of 4.4×10^{-5} scotopic trolands, and corresponds to the absorption of some 2300 quanta per second by some 13.4 million rods over which the large test-patch fell. Thus, in each second of time, only one rod in 5800 absorbs a single quantum when the eye is being stimulated at threshold intensity.

Minimum Flux of Energy

If an effectively point source of light is used, the image is concentrated on to a point on the retina so that the concept of retinal illumination loses its application; instead, then, we define the threshold as the *minimum flux* of light-energy necessary for vision, i.e. the number of lumens per second or, better, the number of quanta per second entering the eye. Experimentally Marriott *et al.* (1959) obtained a value of 90 to 144 quanta/second.

Minimum Amount of Energy

Finally, if a very brief flash of light is used as the stimulus (less than 0.1 second) we may express the threshold as simply the total number of quanta that must enter the eye to produce a sensation. Thus there are three thresholds, the *minimum retinal illumination*, the *minimum light flux* and the *minimum amount of energy*. Of these, it is the last that interests us most since from this we are able to compute just how many quanta of light a single receptor must absorb to be excited.

Minimum Stimulus

This was determined in 1942 by Hecht *et al.* by the method of presenting short flashes and determining the frequency-of-seeing curves. With a 60% frequency as the end-point for threshold, the amount of energy striking the cornea was 54 to 148 quanta, depending on the observer; after allowing for scattering and absorption by the ocular media the range of useful light-energy was some 5 to 14 quanta. The image of the flash fell on about 500 rods, so that it was unlikely that one rod received more than a single quantum. This might suggest, therefore, that the minimum stimulus consisted of the simultaneous stimulation of some 11 rods, each absorbing a single quantum, their effects being transmitted to bipolar and ganglion cells by convergence. On this basis, then, the excitation of a single rod at threshold levels is not sufficient for vision, the excitatory effect being insufficient to permit conduction through the various synapses on the visual pathway. Only if several rods are excited will their effects be sufficient to break down these synaptic barriers and permit the passage of the excitation along the visual pathway to higher centres in the brain.

Quantum Fluctuations

The threshold varies from moment to moment and, according to Hecht *et al.*, this must be due partly, if not wholly, to fluctuations in the number of quanta that a given flash contains when it is repeated. Thus, when we are dealing with very small amounts of light-energy, the actual number of quanta in any given flash will vary. Hence, according to the *uncertainty principle*, when we speak of a flash having an energy, a, we mean that this is the *average energy* the flash would have if it were repeated a large number of times, and the total number of quanta actually measured were divided by the number of flashes. For any given flash, with a mean energy-content of a quanta, we can only speak of the *probability* that it will contain a given number n, or more, quanta; and this probability may be simply calculated. On raising the stimulus-strength, measured by a, over a range of, say, tenfold, the probability that a flash will have a given number of quanta will increase, and finally become unity. The curve obtained by plotting this probability against the stimulus-strength has a characteristic shape, the steepness depending on the value of n as Fig. 9.14 shows.

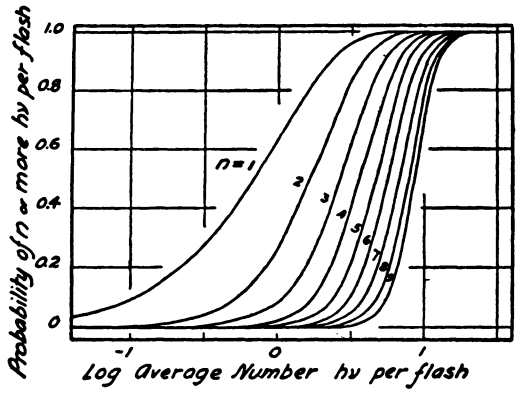

Fig. 9.14 These are probability curves based on quantum theory, showing the chance that a given flash, with average energy shown to the abscissa, will have n quanta in it or more. For example, if we employ curve belonging to $n = 2$, the chance of having 2 or more quanta in a flash is about 0·2 (i.e. 1 in 5) if the average energy of the flashes is 1 quantum (log 1 = 0). (Hecht *et al.*, *J. gen. Physiol.*)

Frequency-of-seeing

Now, if the seeing of a flash depends only on the flash's containing the right number of quanta, say n, clearly the frequency-of-seeing will increase as the strength of the stimulus, measured by a, increases, because the probability that there will be n quanta in a flash increases with increasing value of a. Moreover, the shape of the frequency-of-seeing curve should be similar to the shape of the probability curve. As Fig. 9.15 shows, there is remarkably good agreement between the two, the range of stimulus-strength over which a flash is never seen and always seen being about a factor of tenfold, corresponding with the range over which the probability that a flash has n quanta in it varies from 0 to unity. We may note that the slope of the probability curve depends on the number of quanta, n, required, becoming steeper the greater the number, so that in order that our frequency-of-seeing curve shall match the probability curve we must choose a suitable value of n, the number of quanta required for vision. Hecht *et al.* found that, with different observers, n varied between 5 and 7, a fact suggesting that the absorption of these numbers of quanta corresponded with the stimulus for threshold vision. Direct measurements of the mean amount of quanta in a threshold stimulus gave values ranging from 6 to 17 quanta actually absorbed; since there is reason to believe that only one in two of absorbed quanta are effective—the *quantum efficiency* of the process is said to be 0.5—this would correspond then to 3 to 8 effective quanta.

Later Developments

Since the publication of this study of Hecht *et al.* there have been a number of discussions on the actual minimum number of quanta required to excite vision. There is no doubt that the absorption of one quantum *can* excite a rod, but the phenomena of summation, both temporal and spatial, prove that the excitation of more than one rod is necessary to evoke *sensation*. Thus, it has been found that, within certain limits of area, a given number of quanta in a flash are equally effective if they are concentrated on a small area of retina or spread over a larger one. If only one absorbed quantum was necessary to act as a stimulus, spreading these quanta over a large area should reduce the chance of any one rod absorbing this quantum, so that the threshold should rise. The fact that, within an area subtending some 10 minutes of arc, the stimulus is equally effective, however spread out, means that at threshold more than one rod must be stimulated, their combined effects, transmitted to a bipolar cell, constituting the minimum stimulus for vision. Pirenne inclines to the belief that n is either equal to or greater than 4 although Bouman considers that his own and van der Velden's observations are better fitted by a value of 2.

SIGNAL THEORY

Barlow & Levick (1969) have examined the responses of single ganglion cells of the cat to incremental light-stimuli, with a view to defining a threshold in terms of alteration in the background spike-discharge, the idea being to obtain, from the recorded spike activity before, during, and after a flash, a measurable quantity that would enable the cat to distinguish between a change in retinal illumination and a casual fluctuation in the background spike activity. The prime factor was undoubtedly the quantum/spike ratio, i.e. the extra quanta absorbed required to produce an extra spike in the sampling time, τ. Additional factors are the time-course of the response, so that alterations in this may affect the threshold, as in Bloch's Law; and finally the statistical distribution of the impulses that occur in the time-interval τ in the absence of a stimulus.

COUNTING EVERY QUANTUM

Barlow (1956) discussed the criterion employed for decision as to whether threshold stimulation had been achieved, as against a random variation in 'noise', and emphasized that if the criterion was lowered, i.e. if the observer were to say 'yes' at a trial when he was not absolutely certain of having seen a flash, the threshold

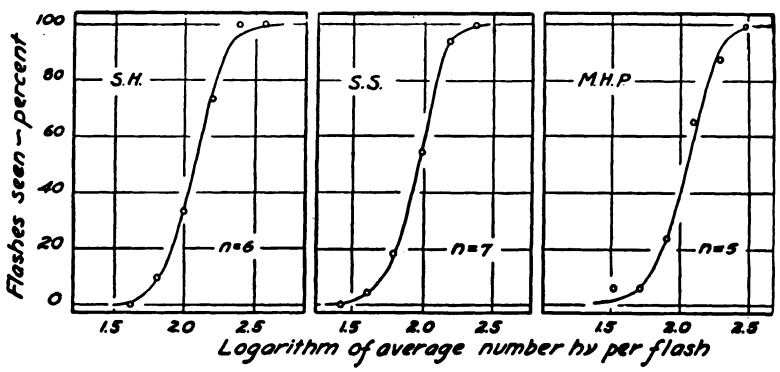

Fig. 9.15 Frequency-of-seeing curves for three human subjects. The number of times the flash was seen is plotted against the logarithm of the average energy per flash. The curves are theoretical ones, based on the theory of quantum fluctuations in the stimulus, and the fact that the experimental points fall on the curves suggests that the failure to see a given flash was largely due to its not having the required number of quanta in it. (Hecht *et al.*, *J. gen. Physiol.*)

would, of course, be lower when the responses of many tests were analysed statistically, but of course the rate of 'false positives' would be increased and the observer would be dismissed as 'untrained' or 'unreliable'. He concluded that at least 2 and probably 10 to 20 excited rods were needed to give a sensation of light and that noise in the optic pathway—e.g. thermal decompositions of rhodopsin molecules—provided the limit to sensitivity. Sakitt (1972) has developed this theme further and emphasized that the choice between 'seen' and 'not seen' is one of several possible choices. Thus, in order to be certain of seeing a flash, an observer chooses a larger signal (or absorbed number of quanta) than if he were allowed to give a less unequivocal statement; his false statements may be more frequent, but statistically he will still be giving meaningful answers and they will be more frequently correct than if answering at random. Thus in 'frequency-of-seeing' tests, subjects are chosen who, in fact, are trained to give no false responses and thus are being trained to use a large signal (large number of absorbed quanta); so that when they deny seeing a flash they may well be ignoring signals from the flash because they are not sufficiently strong—but they would be signals. Sakitt presented observers with three types of stimulus namely a blank, a flash corresponding to 66 photons at the cornea, or one of 55 photons, and the observer was allowed to make 6 types of rating from 0, meaning that he did not see anything, up to 6, indicating a very bright light. When ratings were plotted against number of quanta a linear relation was found, suggesting that the ratings might actually represent numbers of quanta effectively absorbed to give rod-signals greater than the background noise. On this basis he deduced a quantum efficiency of seeing of 0.0274, this being the fraction of quanta falling on the cornea that are actually effective after allowing for absorption in the eye media and the probability of about a half that an absorbed quantum will actually isomerize a molecule of rhodopsin (Hagins, 1955). If the notion that ratings indicated quantum events was correct, the variance in a given rating should follow a Poisson distribution and the result should be a set of 'frequency of seeing curves' as in Fig. 9.16, each being made on the basis of a single, double, triple etc. rod signal. As we should expect, the curve becomes steeper and like the more classical frequency-of-seeing curve when the rating is high; thus if the observer used a criterion of 3 the absolute threshold (50% probability) would correspond to a rod signal of 2.7 and, from the linear relation between this and quanta reaching the cornea,[9] this would correspond to a value of 87 quanta and only one false positive would be made in a hundred trials. If a weaker criterion 2 had been chosen, a, the average number of rod signals, would be 1.7 giving 50 quanta as the threshold stimulus, but 5% of the answers would be false positives. A criterion of 1 would mean a response to as few as 12.6 quanta and would lead to a false-positive rate of 29%, which would be experimentally unacceptable, but the observer would not be answering at complete random. Sakitt concluded, therefore, that his observers were, indeed, 'counting every quantum'.

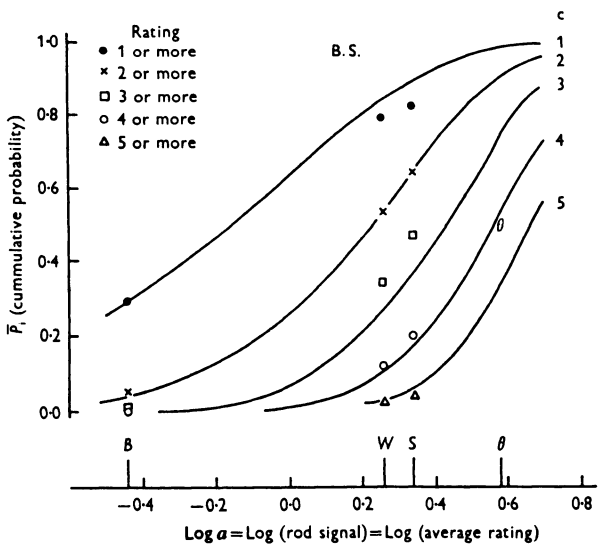

Fig. 9.16 The experimental points are the cumulative probabilities $\bar{P}_i$ for a subject giving a rating i or more. The abscissa is the log of the rod signal which is the same as the log of the average rating. The points labelled B, W and S are at the values of a for the blank, weak and strong stimuli respectively. The symbol θ refers to the absolute threshold. The smooth curves are theoretical cumulative Poisson probabilities $\bar{P}(c, a)$ that c or more rod signals occur when a is the average number occurring. (Sakitt, *J. Physiol.*)

Cat's Sensitivity

Bonds & MacLeod (1974) have studied the *in vivo* bleaching and regeneration of rhodopsin in the cat and have commented on the 'quantum catching' in this animal compared with that in man. They computed that a cat's retina absorbed some 24% of the quanta incident on the cornea compared with only 9% in man, so that the cat's quantum catch is 2.7 times man's on this account; its fully dark-adapted pupil has about 3.2 times the area of that in man, so that man must catch nine times as many quanta as the cat to perceive light.

SPATIAL AND TEMPORAL SUMMATION

The minimum stimulus has been defined in three ways, as we have seen, but the significance of the differences in definition may not be clear unless the importance of spatial and temporal summation is appreciated. It is because of spatial summation that the size of the test-stimulus must usually be stated, and because of temporal summation that the duration of the stimulus acquires significance.

Receptive Fields

Studies on single optic nerve fibres (p. 282) have shown that they have quite extensive 'receptive fields' in the sense that a small stimulus applied over a large number of receptor cells can evoke a response in this single fibre. The anatomical basis for this is the convergence of receptors on bipolar cells and the bipolar cells on ganglion cells, so that a single ganglion cell may have synaptic relationships ultimately with many thousands of rods and cones. Because of this convergence, two spots of light falling within the receptive field may be expected to be more

effective than a single one of the same light-energy, so that if we are measuring thresholds, the luminance of a single test-patch must be greater than that of two test-patches of the same area falling within the receptive field of a single ganglion cell. Our threshold luminance, expressed in terms of retinal illumination, will be smaller, then, the larger the area. If summation is perfect, moreover, we may expect the following relationship to hold:

$$Intensity \times Area = Constant$$

the greater the area of the stimulus the smaller the luminous intensity required to excite.

Ricco's Law

This is *Ricco's Law*. Expressed in terms of the actual number of quanta of energy reaching the retina this means that the threshold is independent of the area of the stimulus; thus if we have two stimuli forming images of 1 mm^2 and 2 mm^2 on the retina, according to Ricco's Law the luminous intensity of the smaller image will be four times that of the larger one at threshold. The *amounts* of energy falling on the two areas of retina in unit time will be equal, however, since the greater area of the one stimulus exactly compensates for its smaller retinal illumination. The area over which Ricco's Law holds varies with position on the retina, being about 30 minutes of arc in the parafoveal region with eccentricity of 4 to 7°, and increasing to as much as 2° at an eccentricity of 35° (Hallett *et al.*, 1962). Over these areas, then, there is complete summation, in the sense that there is no loss of efficiency on spreading the available light-energy over a certain area instead of concentrating it on a much smaller one. When we are determining the minimum amount of energy necessary to excite the sensation of light, then, we must clearly ensure that the area of stimulus is within the limit over which Ricco's Law applies, since beyond this area the summation is only *partial*, in the sense that the larger stimulus will require more quanta than the smaller one, and will therefore have to have a higher luminous intensity. The existence of this partial summation will be indicated by the fact that the *luminous intensity* of the larger stimulus will be less than that of the smaller one, whilst its partial nature will be indicated by the fact that the *number of quanta* required to excite vision will be greater the greater the area over which they are spread.

As we shall see, there are some 'anomalies' in areal summation within the Ricco area that indicate that total summation of quanta falling on a given area is more the exception than the rule; for example, Sakitt (1971) found that presentation of a two-spot stimulus within the Ricco-area defined for a single-spot stimulus did not give total summation, the amount depending on the spatial separation of the spots.

Piper's Law

By Piper's Law is meant the statement that over a certain range of areas, where summation is partial, the relationship:

$$\sqrt{Area} \times Intensity = Constant$$

holds.[10] In practice partial summation extends over large areas, up to about 24°. Beyond this area there is no further summation, so that increasing the area of the stimulus requires no diminution in its intensity for threshold excitation; beyond this area then, the *luminous intensity* of the test-patch is independent of the area. The *amount of energy* entering the eye, of course, increases as the square of the size of the retinal image so that the threshold, expressed as the number of quanta per second required to excite, will increase as the area of test-patch increases.[11]

Probability Summation

Since partial summation extends over large areas of retina, it seems unlikely that convergence can be the sole basis for it, and much more likely that it results from an increased probability that the stimulus will have the necessary number of quanta to stimulate the retina. Thus, we may measure the threshold first with a single patch of light and next with two patches such that their images fall widely apart. If there is any summation at all, the two patches will have a lower luminance than the single one. If we suppose that the two patches are too far apart to permit any convergence of receptors on the same optic nerve fibres, we may nevertheless explain the greater effectiveness of the two patches on a probability basis. Thus, with a single patch the probability of seeing it has a certain value, p, so that the chance that it will not be seen is $(1-p)$. The chance of *not seeing* two patches is $(1-p) \times (1-p)$ which is smaller, so that a lower luminance is necessary for these two patches to have a given 'frequency-of-seeing' than for the single one whose probability of not seeing is only $(1-p)$. We may thus speak of *physiological summation*, when this is due to convergence of retinal elements on optic nerve fibres, and *probability summation*, when the parts of the retina on which the summation occurs may be treated as independent of each other.[12]

Temporal Summation. Bloch's Law

By temporal summation we mean that a stimulus lasting a short time must be stronger in luminance than a stimulus lasting a long time; thus the stimulus with the

longer duration can be considered to be made up of a lot of successively repeated stimuli, and it is these successive stimuli that apparently add their effects. It was found by Bloch in 1885 that, over a period of roughly 100 msec the relationship:

$$I \times t = Constant$$

holds, where I is the threshold luminance in the dark-adapted eye, and t is the duration of presentation. This is the *Bunsen-Roscoe Law* of photochemical reactions and indicates that up to this period of about 100 msec the effective stimulus is only the number of quanta entering the eye, and we may say that the summation is *complete*. On a photochemical basis this complete summation is what one might expect, since the limiting factor in the threshold is presumably the absorption of a definite number of quanta, and the chances that this will happen will increase proportionately with the number of quanta entering the eye.

Partial Summation

Beyond a certain time, which has been called the *action time*, the absorption of a second quantum of light will be of no use to help the effects of the absorption of the first, because these effects, e.g. production of an electrical change, will subside. We can therefore understand the limited period over which the Bunsen-Roscoe Law applies. Beyond this critical period during which summation is complete there is a period of partial summation during which two successive stimuli will add their effects, but not completely, so that some other relationship between I and t holds. On theoretical grounds this may be expected, since the longer the stimulus the greater the probability it will contain a certain minimal number of quanta, and according to Baumgardt (1959) there should be a square-root relationship between the threshold energy and duration of the stimulus. Over a certain range, Baumgardt found the experimental results agreed with this square-root relationship.

Detectability of Signal

On the basis of quantum fluctuation theory, a signal of incremental flux, E, above a background flux, B, due to a distant uniform emitting source subtending area, A and lasting time, T, is given by:

$$d' = \frac{EAT}{(BAT)^{1/2}}$$

or if only a fraction, F, of the available photons are used in the task:

$$d' = \frac{FEAT}{(FBAT)^{1/2}}$$

Implicit in the equation are the deVries–Rose Law ($E \propto B^{1/2}$), Piper's Law ($E \propto A^{1/2}$), and Pieron's Law ($E \propto T^{1/2}$). However, Weber's Law, Ricco's Law and Bloch's Law all indicate the limited applicability of quantum fluctuation theory, although the successful application to the absolute threshold and other measurements indicates that these fluctuations constitute a factor that must be taken into account. Cohn (1976) has applied the theory to detection of foveal luminance changes and shown that results accord with prediction, from which he deduced a quantum efficiency of only 2×10^{-4}, i.e., only one in 10000 of the quanta falling on the cornea are effective in foveal vision. However, when the size of the stimulus was decreased, efficiency increased by a factor of 10, and thus only 3 to 10 times less than that reported for scotopic vision.

Rod-cone Summation

At absolute threshold it is usually assumed that rod function is being measured only; however, according to Drum (1982) there is a summation of rod- and cone-subthreshold responses that is difficult to explain on a basis of probability-summation; the known convergence of rods and cones on horizontal cells might well explain the findings. At supra-threshold levels of stimulation, brightness summation between rods and cones seems also to occur; thus when rod and cone stimuli are combined in the assessment of brightness of a test-flash compared with a white foveal standard, there is summation, not complete but better than the probability summations (Benimoff *et al.*, 1982).

Notes

1. Bonds & MacLeod (1974) found an *in vivo* photosensitivity of about 50000 l.(cm.mole)$^{-1}$ in the cat.
2. In the cat the dynamics of bleaching and regeneration of rhodopsin are well understood (Bonds & MacLeod, 1974): Bonds & Enroth-Cugell (1979) found that the Dowling–Rushton relation applied to recovery of sensitivity, as measured by ganglion cell discharge, after strong bleaching lights. There were exceptions, however.
3. Actually the isolated retina can regenerate some rhodopsin since the receptors have a small store of 11-*cis* retinol in their outer segments; according to Cocozza & Ostroy (1987) the isolated amphibian retina can regenerate some 2.5 to 3% of the bleached rhodopsin. Donner & Hemilä (1979) also observed this; Cocozza & Ostroy discuss the conflicting results of Azuma, claiming a value of 10%, which was probably due to failure to correct for non-wavelength-specific changes in absorbance.
4. The *a*-wave of the ERG is attributed to the layer of receptors: this may be examined in isolated form by treatment of the amphibian retina with aspartate, which blocks synaptic events in the retina.
5. Equivalent to the 'field adaptation' of Rushton.
6. Fain's study on the marine toad's receptors is especially interesting in so far as he compares both rod and cone function in the same retina; a comparison of the increment sensitivity curves shows that rods are light-adapted by backgrounds one thousand times dimmer than those that affect cones. The increment-sensitivity curves of rods and cones cross, so that cones become more sensitive than rods even before the rods begin to saturate. Thus the mesopic range, in which both types of receptor are operative, has very real meaning.

7. Boynton & Whitten (1970) introduced the concept, which has also been described as 'instantaneous non-linearity' by Baylor *et al.* (1974) in their study of single photoreceptor responses. Response compression is not an adaptive process, in the usual sense of the word, since only a change in sensitivity has occurred, with no shift of the operating range. The reader interested in this aspect of sensory physiology should read Valeton's (1983) article.
8. This mode of presentation of results has been called the 'incident light model', because the background and stimulus light are treated together. A common way is to present the results as simple increment curves, the threshold increment over the background being plotted against the background intensity. The two models are not identical, as Valeton points out, and he gives reasons for preferring the incident light model.
9. Thus the relation between a, the average number of rod signals, and Q_e, the average number of quanta falling on the cornea during a flash was:

$$a = 0.0274Q_e + 0.36$$

0.36 is equivalent to the average number of noise events during the flash (Barlow, 1956).
10. According to Baumgardt (1959) this relationship follows from probability theory, but there seems little doubt from Barlow's (1958) studies that no simple law will cover all the phenomena; thus the degree of spatial summation depends on the duration of the stimulus whilst the degree of temporal summation depends on the size of the stimulus. Some of the limitations of studies on area are considered by Hallett *et al.* (1962).
11. At the fovea threshold measurements are those for stimulation of the cones and, as we have seen, in the completely dark-adapted condition the thresholds are much higher. This may well be due, not so much to a lower intrinsic sensitivity of the cone as compared with the rod, but to the much smaller degree of convergence exhibited by cones, so that the area over which complete summation is possible is very small. Hence, as ordinarily measured, the threshold will be in the region of partial or no summation. By reducing the size of the test-stimulus to a substense of 2.7 minutes of arc Arden & Weale (1954) found the threshold intensities to be the same for fovea and parafovea, but their contention that the sensitivities of foveal cones and peripheral rods are equal is probably unsound (Pirenne, 1962, p. 106).
12. An extreme example of probability summation is given by measuring the frequency of seeing a flash, when two observers are employed, with the frequency of seeing when only a single observer is used; from these we may compute thresholds in the usual way and it is found that the threshold for the 'double observer' is less than that for the single.

References

Aguilar, M. & Stiles, W. S. (1954) Saturation of the rod mechanism in the retina at high levels of illumination. *Optica Acta* **1**, 59–65.

Alpern, M. & Pugh, E. N. (1974) The density and photosensitivity of human rhodopsin in the living retina. *J. Physiol.* **237**, 341–370.

Arden, G. B. & Weale, R. A. (1954) Nervous mechanisms and dark-adaptation. *J. Physiol.* **125**, 417–426.

Azuma, K., Azuma, M. & Sickel, W. (1977) Regeneration of rhodopsin in frog outer segments. *J. Physiol.* **271**, 747–759.

Barlow, H. B. (1956) Retinal noise and absolute threshold, *J. opt. Soc. Amer.* **46**, 634–639.

Barlow, H. B. (1958) Temporal and spatial summation in human vision at different background intensities. *J. Physiol.* **141**, 337–350.

Barlow, H. B. & Levick, W. R. (1969) Three factors limiting the reliable detection of light by retinal ganglion cells of the cat. *J. Physiol.* **200**, 1–24.

Baumgardt, E. (1959) Visual spatial and temporal summation. *Nature* **184**, 1951–1952.

Baylor, D. A., Hodgkin, A. L. & Lamb, T. D. (1974) The electrical response of turtle cones to flashes and steps of light. *J. Physiol* **242**, 685–727.

Benimoff, N. I., Schneider, S. & Hood, D. C. (1982) Interaction between rod and cone channels above threshold: a test of various models. *Vision Res.* **22**, 1133 1140.

Bonds, A. B. & Enroth-Cugell, C. (1979) Recovery of cat retinal ganglion cell sensitivity following pigment bleaching. *J. Physiol.* **295**, 47–68.

Bonds, A. B. & MacLeod, D. I. A. (1974) The bleaching and regeneration of rhodopsin in the cat. *J. Physiol.* **242**, 237–253.

Bouman, M. A. (1955) Absolute threshold conditions for visual perception. *J. opt. Soc. Am.* **45**, 36–43.

Boynton, R. M. & Whitten, D. N. (1970) Visual adaptation in monkey cones: recordings of later receptor potentials. *Science* **170**, 1423–1426.

Campbell, F. W. & Rushton, W. A. H. (1955) Measurement of the scotopic pigment in the living human eye. *J. Physiol.* **130**, 131–147.

Cicerone, C. M. & Green, D. G. (1981) Signal transmission from rods to ganglion cells in rat retina after bleaching a portion of the receptive field. *J. Physiol.* **314**, 213–224.

Cocozza, J. D. & Ostroy, S. E. (1987) Factors affecting the regeneration of rhodopsin in the isolated amphibian retina. *Vision Res.* **27**, 1085–1091.

Cohn, T. E. (1976) Quantum fluctuation limit in foveal vision. *Vision Res.* **16**, 573–579.

Donner, K. O. & Hemilä, S. O. (1979) Dark-adaptation of the aspartate-isolated rod receptor potential of the frog retina: threshold measurements. *J. Physiol.* **287**, 93–106.

Donner, K. O. & Reuter, T. (1967) Dark-adaptation processes in the rhodopsin rods of the frog's retina. *Vision Res.* **7**, 17–41.

Dowling, J. E. (1960) Night blindness, dark adaptation and the electroretinogram. *Amer. J. Ophthal.* **50**, 875–889.

Dowling, J. E. & Ripps, H. (1970) Visual adaptation in the retina. *J. gen. Physiol.* **56**, 491–520.

Drum, B. (1982) Summation of rod and cone responses at absolute threshold. *Vision Res.* **22**, 823–826.

Fain, G. L. (1976) Sensitivity of toad rods: dependence on wavelength and background illumination. *J. Physiol.* **261**, 71–101.

Fuortes, M. G. F., Gunkel, R. D. & Rushton, W. A. H. (1961) Increment thresholds in a subject deficient in cone vision. *J. Physiol.* **156**, 179–192.

Grabowski, S. R. & Pak, W. L. (1975) Intracellular recordings of rod responses during dark-adaptation. *J. Physiol.* **247**, 363–391.

Hagins, W. A. (1955) The quantum efficiency of bleaching rhodopsin *in situ*. *J. Physiol.* **129**, 22–23P.

Hallett, P. E., Marriott, F. H. C. & Rodger, F. C. (1962) The relationship of visual threshold to retinal position and area. *J. Physiol.* **160**, 364–373.

Hecht, S., Haig, C. & Chase, A. M. (1937) The influence of light adaptation on subsequent dark adaptation of the eye. *J. Gen. Physiol.* **20**, 831–850.

Hecht, S., Shlaer, S. & Pirenne, M. H. (1942) Energy, quanta and vision. *J. gen. Physiol.* **25**, 819–840.

Kleinschmidt, J. & Dowling J. E. (1975) Intracellular recordings from Gecko photoreceptors during light and dark adaptation. *J. gen. Physiol.* **66**, 617–648.

Marriott, F. H. C., Morris, V. B. & Pirenne, M. H. (1959) The minimum flux of energy detectable by the human eye. *J. Physiol.* **145**, 369–373.

Normann, R. A. & Perlman, I. (1979) The effects of background illumination on the photoresponses of red and green cones. *J. Physiol.* **286**, 491–507.

Pirenne, M. H. (1962) Visual function in man. In *The Eye*, vol. II, chapters 1–11. Ed. Davson. London: Academic Press.

Pirenne, M. H., Marriott, F. H. C. & O'Doherty, E. F. (1957) Individual differences in night-vision efficiency. *Med. Res. Council Sp. Rep. Ser.*, No. 294.

Rushton, W. A. H. (1965) Bleached rhodopsin and visual adaptation. *J. Physiol.* **181**, 645–655.

Sakitt, B. (1971) Configuration dependence of scotopic spatial summation. *J. Physiol.* **216**, 513–529.

Sakitt, B. (1972) Counting every quantum. *J. Physiol.* **223**, 131–150.

Valeton, J. M. (1983) Photoreceptor light adaptation: an evaluation. *Vision Res.* **23**, 1549–1554.

Valeton, J. M. & Van Norren, D. (1983) Light-adaptation of primate cones: an analysis based on extracellular data. *Vision Res.* **23**, 1539–1547.

Weale, R. A. (1953) Photochemical reactions in the living cats retina. *J. Physiol.* **122**, 322–331.

10. ELECTROPHYSIOLOGY OF THE RETINA: RESPONSE TO STIMULATION AND THE TRANSDUCTION PROCESS

THE SENSORY MESSAGE

When a receptor is stimulated, a succession of electrical changes takes place in its conducting nerve fibre. These changes are measured by placing electrodes on the nerve fibre and connecting them to a device for recording rapidly occurring potential differences, an *oscillograph*. A series of electrical variations, called *action potentials* or '*spikes*', is obtained when the receptor is stimulated. The duration of an individual spike is very short (it is measured in milliseconds) and, as the strength of the stimulus is increased, the *frequency* of the discharge (the number of spikes per second) increases, but the size of the individual spikes remains unaltered (*'all-or-none' effect*).

Spike Potentials

Thus the message sent to the central nervous system is in a *code* consisting of a series of spike potentials apparently all with the same magnitude, the frequency being the variable that indicates how strongly the receptor has been stimulated. When the nerve fibres from different receptors are compared, e.g. touch, temperature, vision, hearing, the action-potentials are very similar in magnitude and time-course; and it has not been possible to correlate any given type of action potential with the type of sensation that it is mediating. In other words, it appears that the elements of the message, like the dots and dashes of the Morse code, are the same for all, whether they indicate a change in temperature or the flash of a light, and we must conclude that it is the places where the messages are carried in the brain—the *central terminations*—that determine the character of the sensation. The intensity of the sensation, as indicated above, is determined by the frequency of the spikes, i.e. the number that pass under our recording electrode in unit time.

Recording the Message

The accurate study of the events taking place when a receptor is stimulated demands that the recording electrode should be on or within the receptor or, if this cannot be achieved, on the sensory nerve that makes direct connection with this receptor. Moreover, if a recording from a nerve is to be made, the leads should be taken from a single fibre, otherwise the record of events taking place in the many thousands of fibres of a whole nerve would be a very confused and attenuated picture of the events taking place in the single fibres. With the vertebrate eye, these requirements are very difficult to meet, because the receptors—rods and cones—and the first sensory neurones, the bipolar cells, are buried in the depth of the retina; hence if we wish to record from a reasonably accessible nerve, namely the optic nerve, we will be recording from a second-order neurone, namely the ganglion cell. In its passage through the ganglion cell, the original message from the rod or cone and the bipolar cell has been submitted to a process of what the neurophysiologist calls *re-coding*; unnecessary parts of the message being dropped and other parts being accentuated at their expense. Thus, to understand what happens in the receptor cell, it would be a help if we could place our electrode on or within a rod or cone, or failing that, on a bipolar cell, which makes such intimate relationships with the rods and cones. For this reason the invertebrate eye, built on a simpler plan neurologically, was studied by Hartline (1941/2); and it is to his pioneering studies that we owe so much of our knowledge of sensory mechanisms. Hartline studied the compound eye of the horseshoe crab *Limulus*, the fibres of its optic nerve being, apparently, processes leading away from the retinula cells on which the light impinges. Thus the study of the electrical changes in these fibres brings us close to the electrical changes occurring directly in response to the impinging of light on a light-sensitive cell.

THE INVERTEBRATE EYE

Ommatidium

Essentially the compound eye of insects and crustaceans is an aggregation of many unit-eyes or *ommatidia*, each of these units having its own dioptric apparatus that concentrates light on to its individual light-sensitive surface, made up of specialized *retinula cells*. The facetted appearance of the compound eye is thus due to the regular arrangement of the transparent surfaces of these unit-eyes

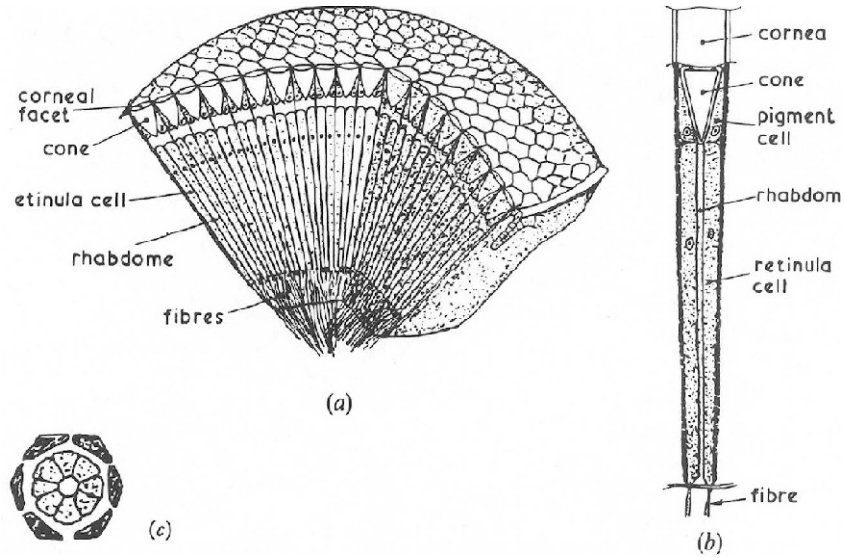

Fig. 10.1 The facetted eye. (*a*) Cut-away view showing the packing of the individual ommatidia; (*b*) longitudinal section of an ommatidium; (*c*) cross-section of ommatidium.

(Fig. 10.1*a*). The *ommatidium* is illustrated schematically in Fig. 10.1*b*; light is focused by the *crystalline cone* on to the highly refractile *rhabdom*, which constitutes an aggregation of specialized regions of the *retinula cells*. These retinula cells are wedge-shaped and are symmetrically arranged around the axial canal like the segments of an orange (Fig. 10.1*c*); the rhabdom is made up of the apical portions of these wedge-shaped cells, the separate portions being called *rhabdomeres*. As illustrated in Fig. 10.2, which shows a cross-section of the *Limulus* (horse-shoe crab) ommatidium, the regions of junction of the retinula cells are characterized by dense staining, so that a cross-section appears like the spokes of a wheel, the axle being the central canal. This canal contains the process of the *eccentric cell*; this is apparently a neurone, with its cell body squeezed between the retinula cells at the base of the ommatidium; its long spear-like process fills the central canal and may be regarded as a dendrite; the central end of the cell consists of a long process that passes out of the ommatidium in the optic nerve.

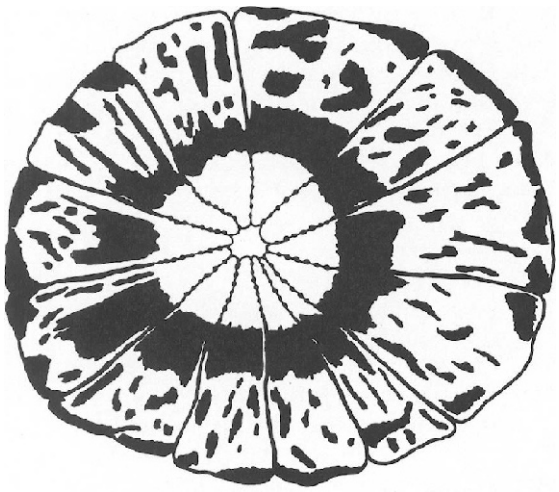

Fig. 10.2 Cross-section of ommatidium of *Limulus*, showing individual retinula cells with the rhabdomeres represented in white. (After Miller, *Ann. N.Y. Acad. Sci.*)

Eccentric Cell

The eccentric cell thus constitutes the nerve fibre of the ommatidium, whilst we may regard the retinula cells, with their specialized rhabdomeres, as the cells responsible for absorbing the incident light. Provisionally, then, we may say that the light-stimulus falls on the rhabdom; as a result of chemical changes taking place in this region, electrical changes are induced in the eccentric cell that culminate in the passage of impulses along the axon-like process of this cell.

Retinula Processes

Actually each retinula cell also has a long proximal process leading out of the ommatidium in the optic nerve; consequently the optic nerve is made up of some 10 to 20 retinula processes to every one eccentric cell process. The significance of these retinula processes is not clear; they do not, apparently, carry action potentials, so that it

would appear that the great majority of the 'optic nerve fibres' of the compound eye are not nerve fibres at all.

The electron-microscope has contributed a lot to the understanding of the structure of the rhabdomere; the spokes illustrated in Fig. 10.2 are apparently made up by innumerable interdigitating villi from the surfaces of contiguous retinula cells; they thus constitute a vast increase in the surface area of the retinula cells and it is here that the photosensitive pigment, responsible for absorbing the energy of the light-stimulus, is apparently concentrated.

Single Fibre Responses

The pioneering study of the electrical responses to light were carried out by Hartline (1941/2) who recorded from single fibres when the eye was exposed to light. Figure 10.3 is a record of responses to two intensities of illumination; as with other receptors, the nervous discharge in response to a continuous stimulus is a discontinuous train of spike-potentials, the frequency being a measure of the intensity of the light-stimulus. The electrical equivalent of dark-adaptation consisted in an increase in frequency of discharge with time after the period of light-adaptation; the latency of the response became shorter as the light-stimulus increased, and the phenomenon of mutual inhibition between neighbouring receptors was demonstrated.

Mechanism of Activation of the Sensory Neurones

Generator Potential

The electrical events following stimulation have been described as a series of spikes, brief changes in potential taking place across the nerve fibre's membrane. Those concerned with the way in which light, or some other stimulus, can provoke this electrical change have studied the events leading up to this spike discharge; and in general it appears that the common feature is the establishment in a sensory cell of what is called a *generator potential*; this is a more slowly developing and longer-lasting electrical negativity of the cell than the brief spike, and is essentially a 'preliminary change' that, if carried far enough, sets off the discharge. The development of this generator potential in the *Limulus* eye was followed by Fuortes (1959), who placed an electrode inside the eccentric cell of an ommatidium; when light fell on this ommatidium the energy was presumably taken up by the rhabdom which, as we have seen (p. 280) surrounds the process of the eccentric cell. As a result of the chemical changes taking place in the rhabdom, the eccentric cell developed a generator potential, becoming negative internally; superimposed on this negativity were the much more rapid and abrupt changes that we call the spikes. This is illustrated by Fig. 10.4 where the ommatidium has been stimulated with three intensities (100, 2.5 and 0.125 units); the generator potential is indicated by the rise in the baseline, and the spikes by the strokes taking off from this; with increasing intensity the generator potential increases, and the spike frequency too.

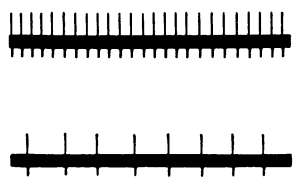

Fig. 10.3 Oscillogram of the amplified potential changes in a single *Limulus* optic nerve fibre due to steady illumination of the eye. Intensity of illumination with upper record 10 times greater than for lower record. Full length of each record corresponds to 1 second. (Hartline, *J. Opt. Soc. Amer.*)

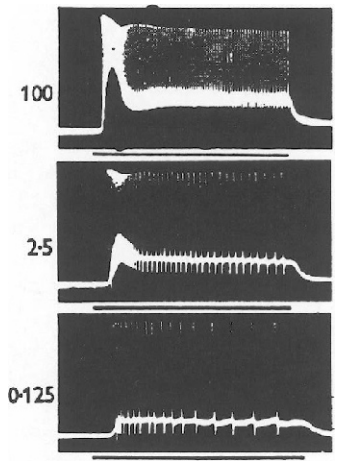

Fig. 10.4 Generator and spike potentials from impaled eccentric cell of *Limulus* ommatidium. Duration of illumination indicated by black lines below records. Intensity of illumination decreases from above downwards. Note that the frequency of the spikes increases with the size of the generator potential. (Fuortes, *J. Physiol.*)

RETINULA AND ECCENTRIC CELLS

Behrens & Wulff (1965) were able to insert microelectrodes into two cells of the same ommatidium and, after recording their responses to illumination, they injected dye so as to be able to identify the types of cell from which records were made. In general, as others had found before, the responses fell into two classes: (*a*) a slow wave of depolarization with superimposed small spikes, and these could be identified with retinula cells; (*b*) a slow wave with large spikes identified with the eccentric cell;

they showed that the retinula responses always preceded, by some 7 to 30 msec, the eccentric cell response; furthermore, the retinula responses, including the small spikes, were always synchronous with each other when two retinula cells were recorded from. Thus the retinula cell's slow potential wave seems to be the initial reaction to light; since the small spikes in this cell are not propagated along its nerve fibre, we may look on these as transmitted effects from the large spikes developed in the eccentric cell. It is possible, then, that the effect of light on the retinula cells is, after some photochemical change, to develop a slow depolarization which acts as a generator potential for the development of a depolarization of the eccentric cell, which finally leads to spike activity. The fact that the electrical changes recorded from the retinula cells of the same ommatidium were always synchronous, indicates an electrical coupling between them, as suggested by Tomita *et al.* (1960) and proved by Smith *et al.* (1965).

SUMMATION

With a subthreshold stimulus there is only a small generator potential, too small to initiate spikes. However, this subthreshold generator potential will add with a second potential, so that one factor in the summation of subthreshold stimuli, observed in psychophysical studies, must be the ability of the generator potentials to add, provided, of course, that the interval between stimuli is not too long.

CHEMICAL TRANSMITTER

According to Fuortes & Hodgkin (1964) the electrical events can be best described on the assumption that the retinula cells (rhabdom) liberate a substance (transmitter) after absorbing light, and it is this chemical transmitter that activates the sensory neurone, in this case the eccentric cell.

VERTEBRATE RESPONSES

It is now time to turn our attention to the messages developed in the vertebrate retina, a system that poses more difficulties to the experimenter because the easily accessible nerve fibres are the axons of the ganglion cells, whose responses are only distantly related to the initial effects of light on the receptors. It will be recalled that the receptors synapse in the outer plexiform later with the bipolar and horizontal cells; the bipolar cells, in their turn, make complex synaptic relations with ganglion and amacrine cells in the inner plexiform layer. It is the axons of the ganglion cells, emerging from the eye, that constitute the optic nerve, and it was the responses in these fibres that were studied in great detail before modern microelectrode techniques permitted recordings from individual rods, cones, bipolar cells, and so on. Logically the description of the visual process, as studied electrophysiologically, should begin with responses in the photoreceptors, but we may take a more historical approach by describing very briefly some of the features of the response in the ganglion cell, or its axon, the optic nerve fibre.

Frog Optic Nerve

The complexities in responses to higher order neurones in the optic pathway were revealed at once in Hartline's (1940) pioneering study of the frog's optic nerve fibres; some gave responses when the light was switched on, the ON-fibres; another group only gave a spike discharge at cessation of illumination, the OFF-fibres, and a third group showed a short discharge at ON and another burst at OFF. It would appear that the initial responses of the receptors to light were being processed so that the retina was responding to change rather than to the incidence of light alone.

Mammalian Ganglion Cells

Hartline's work was extended by Granit (1955) and by Kuffler (1953) and Barlow *et al.* (1957), to the mammalian eye where the same pattern of ON-, OFF-, and ON–OFF-responses was revealed, although the phenomena were even more complex. The mammalian retina shows a background of activity in the dark, so that ON- and OFF-effects were manifest as accentuations or diminutions of this normal discharge. In general, ON-elements showed an increased discharge when the light was switched on, and an inhibition of the background discharge when the light was switched off. Similarly, an OFF-element showed an inhibited discharge when the light was switched on but gave a powerful discharge when the light was switched off. The OFF-effect is thus quite definitely a *release from inhibition.*

Receptive Fields

The number of fibres in an optic nerve is of the order of one million, whilst the number of receptors is of the order of 150 million. This means, in neurophysiological terms, that there is a high degree of *convergence* of the receptors on the ganglion cells, so that a single optic nerve fibre must have connections with many bipolar cells which themselves have connections with many rods and cones. In consequence, the area of retina over which a light-stimulus may evoke a response in a single optic nerve fibre may be quite large; the *receptive field* of a single fibre may be plotted by isolating a single fibre and, with a small

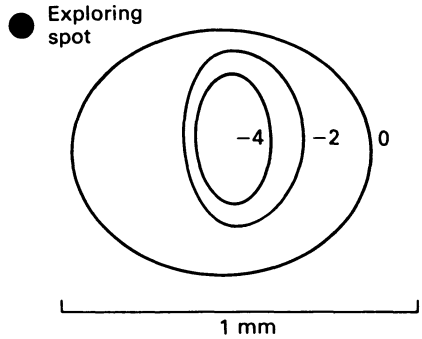

Fig. 10.5 Showing the retinal region with which a single optic nerve fibre makes connections. Each curve encloses the retinal region within which an exploring spot (relative size shown at upper left) produced responses in the fibre at an intensity of illumination whose logarithm is given in the respective curve. Note that the greater the stimulus the greater is the receptive field of the fibre. (Hartline, *J. Opt. Soc. Amer.*)

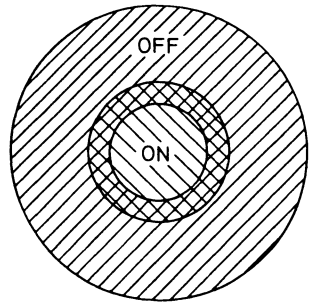

Fig. 10.6 Centre-surround organization of receptive field for a ganglion cell; the centre is excited at ON and the surround is excited at OFF. An intermediate zone may show ON–OFF characteristics.

spot of light, exploring the retina for those parts that will cause a discharge in this fibre. As Fig.10.5 shows, the field increases with the strength of stimulus, so that in order that a light-stimulus falling at some distance from the centre of the field may affect this particular fibre it must be much more intense than one falling on the centre of the field. This shows that some synaptic pathways are more favoured than others.

SUMMATION

As we shall see, this convergence is the anatomical basis for the phenomena of summation: thus a single spot of light falling on the periphery of the receptive field may be too weak to provoke a discharge in the ganglion cell; several spots each too weak to excite will, if presented together in different regions of the field, provoke a discharge. In neurophysiological terms we may say that the ganglion cell requires a certain bombardment by discharges from the bipolar cells, with which it makes synaptic contacts, before it discharges; this bombardment can be provided by a few bipolar cells discharging strongly or by many bipolar cells discharging more weakly. The electrical basis for this summation of effects is essentially the same as that for the summation in the receptors; the ganglion cells develop generator potentials which are this time called *synaptic potentials*; they are not all-or-none, and so can add their effects and ultimately build up to a sufficient height to initiate a spike discharge.

CENTRE AND PERIPHERY

A careful study of the receptive fields in the cat's retina by Kuffler (1953) showed that they were not so simple as had been thought, the more peripheral part of the field giving the opposite type of response to that given by the centre. Thus, if at the centre of a receptive field the response was at ON, the response farther away, in the same fibre, was at OFF, and in an intermediate zone it was often mixed to give an ON–OFF-element as illustrated in Fig. 10.6. In order to characterize an element, therefore, it was necessary to describe it as an *ON-centre* or *OFF-centre* element, meaning thereby that at the centre of its receptive field its response was at ON or OFF respectively. By studying the effects of small spot-stimuli on centre and periphery separately and together, Kuffler demonstrated a mutual inhibition between the two.

NON-RESPONSE TO UNIFORMITY

This opponence between centre and surround of the receptive field, although not universal in the retinae that have been examined exhaustively, is by far the predominant feature. It is continued to further stages in the visual pathway; thus the geniculate neurones exhibit the opponence to the point that centre and surround usually balance each other's effects exactly, so that uniform illumination of the retina usually fails to excite geniculate cells. The physiological significance of this opponence becomes clear if we appreciate that under ordinary conditions of illumination all receptors might be expected to be responding to light, and if these responses were all transmitted to the central nervous system along the million odd optic nerve fibres, this would mean a tremendous bombardment of the higher centres with information; the centre-surround organization means that for the great majority of ganglion cells uniform illumination of their receptive field will produce no, or only a small, effect, the influence of light on the receptors that lie in the centre of the field being balanced by the opposite influence on the receptors that lie in the surround. On the other hand, a spatial discontinuity in the field, given by a bar on a white field, for instance, would activate centre and surround to different extents and so give rise to a message that would enable the perception of form.

THE BASIS OF CENTRE-SURROUND RESPONSIVENESS

Essentially the centre-surround organization of the neurone's response relies on an inhibitory interaction between a given neurone and its neighbours; the detailed organization of this interaction will be discussed later, but as a simple hypothesis we may explain the ganglion cell's responses in terms of Fig.10.7; a group of receptors feed their responses directly to the ganglion cell's dendrites, after relaying at bipolar cells. Adjacent 'surround receptors' excited by light in the receptive-field surround area, are stimulated by light but, because of their synaptic arrangements with bipolar and other neurones, this excitation is converted into an inhibitory action on the ganglion cell. The ganglion cell illustrated in Fig. 10.7 would be described as an ON-centre cell, being excited by a spot of light falling in the centre of its receptive field and inhibited by a peripheral annulus of light. The reverse situation is not difficult to envisage, the peripheral receptors being organized to excite the central receptive field when illuminated and to inhibit themselves; the receptors connecting directly to the ganglion cell's dendrites would inhibit the ganglion cell when illuminated, so

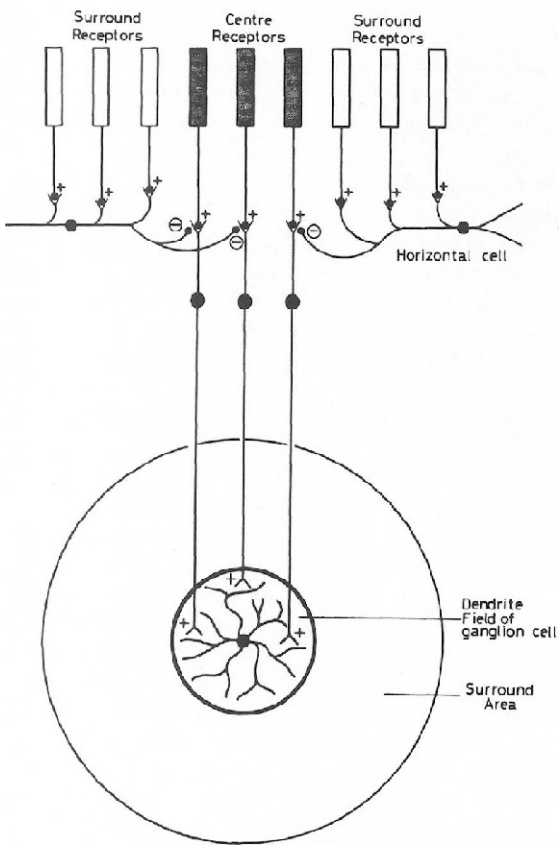

Fig. 10.7 Anatomical basis of the centre-surround organization.

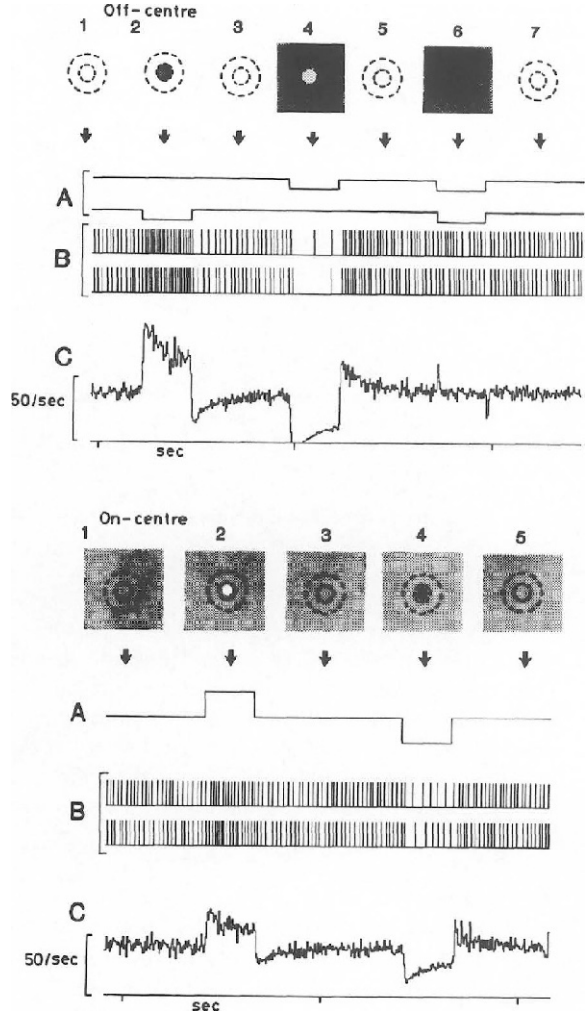

Fig. 10.8 Responses of an ON-centre and OFF-centre ganglion cell to changes in illumination of the receptive-field centre. (Enroth-Cugell & Robson, *Invest. Ophthal.*)

that the ganglion cell would be described as OFF-centre and ON-periphery. The stimulus conditions for ON- and OFF-centre cells are illustrated schematically by Enroth-Cugell & Robson (1984), as in Fig. 10.8.

More Peripheral Responses

The responses recorded from ganglion cells or optic nerve fibres represent activity in third-order cells; as such they provide us with an accurate picture of the messages sent to the brain, but they tell us little of the mode of transduction of the photochemical change in the receptors into an electrical event, the transmission of this change to bipolar and horizontal cells, and finally the

integration of the messages from these second-order cells by the ganglion cells, aided by the amacrine cells. For a long time attempts at intracellular recording of the electrical changes in vertebrate receptors were unsuccessful and the experimenter's only clues to events at this level were provided by analysis of the electroretinogram (p. 313), but even when this was recorded with micro-electrodes placed at different depths in the retina the interpretation was by no means unequivocal. The first records purporting to represent intracellular records of responses to receptors were the S-potentials of Svaetichin, taken from the fish retina on account of its large cones. These will be considered later, but they turned out to be recordings from horizontal cells. With the refinement of micro-electrode techniques and especially with the development of the Procion yellow method for intracellular staining of the cell from which records were taken, enormous strides have been made in the understanding of the primary event in the receptors, especially in those of the fish, turtles and amphibians. The pioneering, and now classical, study is that of Werblin & Dowling (1969) on the retina of the mudpuppy, *Necturus*, and we may profitably begin with a brief description of this.

Intracellular Records from Necturus *Retina*

'WIRING DIAGRAM'

The synaptic structures and relations between retinal cells in *Necturus* are similar to those of the primate retina, but the relations between horizontal cells and receptors and bipolar cells would appear to be different. The 'wiring diagram' of the *Necturus* retina is illustrated schematically in Fig. 10.9, and it will be seen that the horizontal cell is not a mere mixer of rods and cones, since it forms presynaptic relations with bipolar cells, i.e. it transmits from receptor to bipolar cell and thus contributes to vertical transmission. Probably more important, however, is the feedback that allows activity in one receptor to influence activity in its neighbours, thus providing an anatomical basis for surround-on-centre antagonism. In a similar way, the amacrine cell not only links bipolars horizontally but also transmits from bipolars to ganglion cells. Thus there are two pathways from rod to bipolar, and two from bipolar to ganglion, either direct or through a horizontal or amacrine cell.

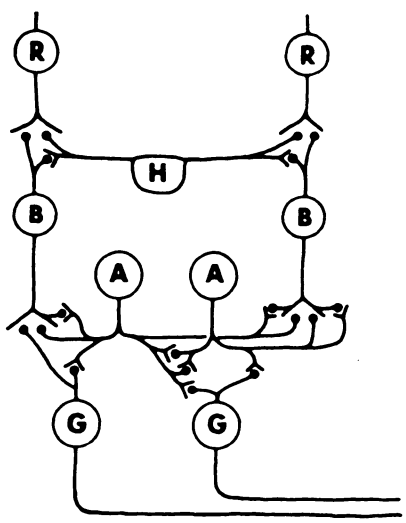

Fig. 10.9 Schematic 'wiring diagram' of the mud-puppy retina. R, receptor; H, horizontal cell; B, bipolar cell; A, amacrine cell; G, ganglion cell. Note that in this retina the horizontal cell influences both receptor and bipolar cell, and the amacrine cell influences both bipolar cell and ganglion cell. (Dowling and Werblin, *J. Neurophysiol.*)

RECORDING

Microelectrodes were inserted into different regions of the retina and intracellular recordings of the responses to light stimuli were made; the stimuli consisted of a small spot or of an annulus, either 250 μm or 500 μm wide, either singly or in combination with the spot. In this way the existence, or otherwise, of opponent responses typical of those described for ganglion cells, could be ascertained. After the recording had been made, the position of the electrode was identified by ejecting Niagara blue from the electrode and subsequent histological examination.

RECEPTOR RESPONSE

The striking feature of the receptor response is that it consists of a hyperpolarization of the cell, rather than a depolarization as found in the invertebrate receptor. The response is graded, like the invertebrate generator potential, but there is no all-or-none spike activity. Annular stimulation did not affect the element, nor did it affect the response to a spot stimulus; thus there was no opponent organization of centre and surround, as found in the ganglion cell.

HORIZONTAL CELL

This cell's response, too, is hyperpolarizing, and comes on with a longer latency than that of the receptor; it is graded and does not lead to spikes, and the effects of light are summated over quite a wide field since a 500 μm annulus of light gave the same response as a 250 μm annulus containing the same number of quanta of energy.

BIPOLAR CELL

Once again, this responds with a slow potential change, graded according to the strength of the stimulus and giving no spikes. The receptive field, however, is concentrically organized in an opponent fashion so that if the centre hyperpolarizes, the periphery causes depolarization, and *vice versa*.

AMACRINE CELL

Responses in these are recorded from the inner plexiform layer; they consist typically of one or two spikes superimposed on a transient depolarizing potential. The transient responses occurred at both ON and OFF. In these cells the effect of variation of intensity of the stimulus was essentially a change in the latency, the number of spikes being independent of the intensity. In some units the receptive field was organized in an opponent fashion, but in others the responses were uniform over the whole area.

GANGLION CELLS

These responded with a spike discharge taking off from an initial depolarization; the frequency of discharge was proportional to the degree of membrane depolarization. ON-, OFF- and ON–OFF-responses were obtained in different cells. Centre-surround antagonism was also a feature of some cells and was similar to that of the bipolar cells; moreover, the extents of the fields were very similar.

RETINAL ORGANIZATION

The central part of the receptive field of the bipolar cell is about 100 μm wide and is surrounded by an annulus of about 250 μm. The dendritic field of a bipolar cell in *Necturus* retina is about 100 μm in diameter, so that the large annular area, stimulation of which gives responses in a single bipolar cell, must transmit its effects through another type of cell that synapses with the bipolar. This other type is presumably the horizontal cell; this receives influences from the receptors in the surrounding annulus and transmits them to bipolar cells connected with the central receptors, exerting an opposite type of action; thus, if the central receptors hyperpolarize the bipolar, the horizontal cell depolarizes it. Hence it is the horizontal cells that organize the contrast-detection, as exhibited in the centre-surround antagonism. The further transformation of the message, which gives it its transient character, is probably done through the amacrine cells; these respond transiently, by contrast with the more sustained responses of bipolar cells, and they thus impose a transient type of response on the ganglion cells; the ganglion cells, driven in this way, presumably are able to carry information about *changes* in the visual field, whilst other ganglion cells, driven by bipolar cells directly, would be better able to carry information about the static character, i.e. contrast.

The Hyperpolarizing Response

The most important finding is clearly the hyperpolarization of the receptor by light, a hyperpolarization that is transmitted to the two types of cell that make synaptic relations with the receptor, namely the bipolar and horizontal cell. If, as is the general rule, depolarization of a nerve cell causes release of a transmitter, we may postulate that the receptor in the dark is continually releasing a transmitter on to the synaptic surfaces of bipolar and horizontal cells, thereby maintaining these in a depolarized state. Light-induced hyperpolarization of the receptor would decrease, or inhibit entirely, the release of transmitter, thereby allowing the bipolar and horizontal cells to become less depolarized, i.e. to *hyperpolarize*. We have therefore to enquire into the mechanism of the hyperpolarizing response in the receptor. The depolarizing responses seen typically in the generator potentials of invertebrate visual cells, or in mechanoreceptors such as the Pacinian corpuscle, are attributable to an increase in permeability of the excitable membrane to certain ions, which is reflected in a decrease in membrane resistance.

Nerve Resting Potential

Thus, in nerve, the resting membrane potential depends on a high internal concentration of K^+ and low concentration of Na^+, the situation being maintained by a low permeability of the membrane to Na^+. Under ideal conditions the potential is given by the Nernst equation:

$$E = \frac{RT}{nF} \ln \frac{[K]_i}{[K]_o}$$

and is described as a K^+-potential, and we may represent the membrane by a simple electrical circuit in which the potential is considered to be due to the action of a battery—the K^+-potential—operating across a capacity and a resistance, or its reciprocal, a conductance.

Sodium Battery

If the ideal situation does not prevail, and the membrane has a significant permeability to Na^+, the membrane potential is lower because the difference in concentrations of Na^+ is capable of acting like a battery working in the reverse direction, so that we must represent the situation as being rather more complex, with two batteries working against each other giving a smaller potential—the membrane is said to be depolarized by the Na^+-battery (Fig. 10.10). If, now, the effect of light is to reduce the permeability to Na^+ by 'blocking Na^+-channels', to use the terminology of Baylor *et al.* (1974), the cell will hyperpolarize.

Gradient of Potential

The observation that the retina exhibited in the dark a gradient of potential such that the tips of the receptors were negative in relation to the synaptic region, and that with light this potential tended to be reversed, suggested

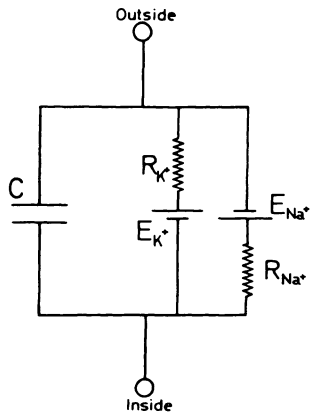

Fig. 10.10 Electrical representation of an excitable cell with batteries due to potassium and sodium differences of concentration working in opposition.

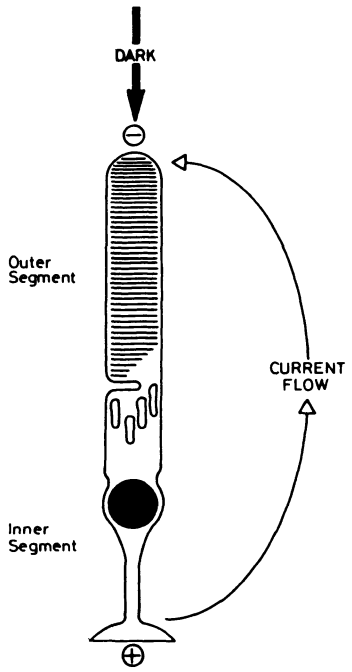

Fig. 10.11 Dark current due to a difference of potential between the outer and inner segments of a rod.

to Bortoff & Norton (1967) that the dark-depolarization of the receptors might be restricted to the outer segments, so that, as indicated by Fig. 10.11, there would be a gradient of potential along the receptor, the tip being less positive (or more negative) than the inner segment, and there would be a flow of positive current through the inter-receptor space, from inner to outer segment, taking place in the dark. Light, by increasing the resistance of the outer segment, would reduce this current and the outer segment would hyperpolarize.

Light-induced Changes

Penn & Hagins (1969) and Hagins *et al.* (1970) placed electrodes at different depths in the retina alongside the receptors and showed that the voltage did, in fact, vary with depth, the electrode becoming progressively more positive as it moved from the receptor tip to the rod synapse, whilst the light-induced voltage increased in parallel. They showed, moreover, when the rod was partially illuminated, that the photocurrent was generated in the zone of the rod outer segment that was illuminated, so that the unilluminated region acted as a sink of current, thus confirming that the effect of light was to reduce a standing dark-current inward at the outer segment and outward along the remainder of each receptor cell. Figure 10.12 shows the membrane current produced by two flashes of light of different intensities at different depths in the retina; the flow of current induced by light is outwards at the outer segments, and this corresponds with a reduction in the dark-current, which occurs in the opposite direction (Fig. 10.11). At the junction of outer and inner segments the current reverses in sign, as we should expect if the flow of current were confined to the receptor, outward flow at one point being accompanied by inward flow at another. The studies of Hagins were on the rods of the rat; when the larger receptors of *Necturus* or the gekko were examined by Toyoda *et al.* (1969), the postulated increase in membrane resistance could be measured with intracellular electrodes.

IONIC CURRENTS

In terms of ionic movements, the flow of current would represent a net penetration of Na^+ into the outer segments and a flow of K^+ out of the inner segments; if this persisted indefinitely, of course, the concentration gradients would disappear and the batteries would run down. We must postulate, as with other neurones, a Na^+–K^+ linked pump that, at the expense of metabolic energy, removes Na^+ and accumulates K^+; such a pump would be inhibited by oubain, and it is interesting that Frank & Goldsmith (1967) found that this ATPase inhibitor rapidly blocked the ERG. Further proof relating to the postulated mechanism of the photocurrents was given by Korenbrot & Cone (1972), who showed that the permeability to Na^+ of isolated rod outer segments was actually decreased by light. That it was the outer (plasma) membrane of the outer segment, rather than the disc membrane, that was affected was shown by Korenbrot *et al.* (1973) and they computed a permeability constant for Na^+ of about 2.8×10^{-6} cm/sec. The dependence of the hyperpolarizing response on external Na^+

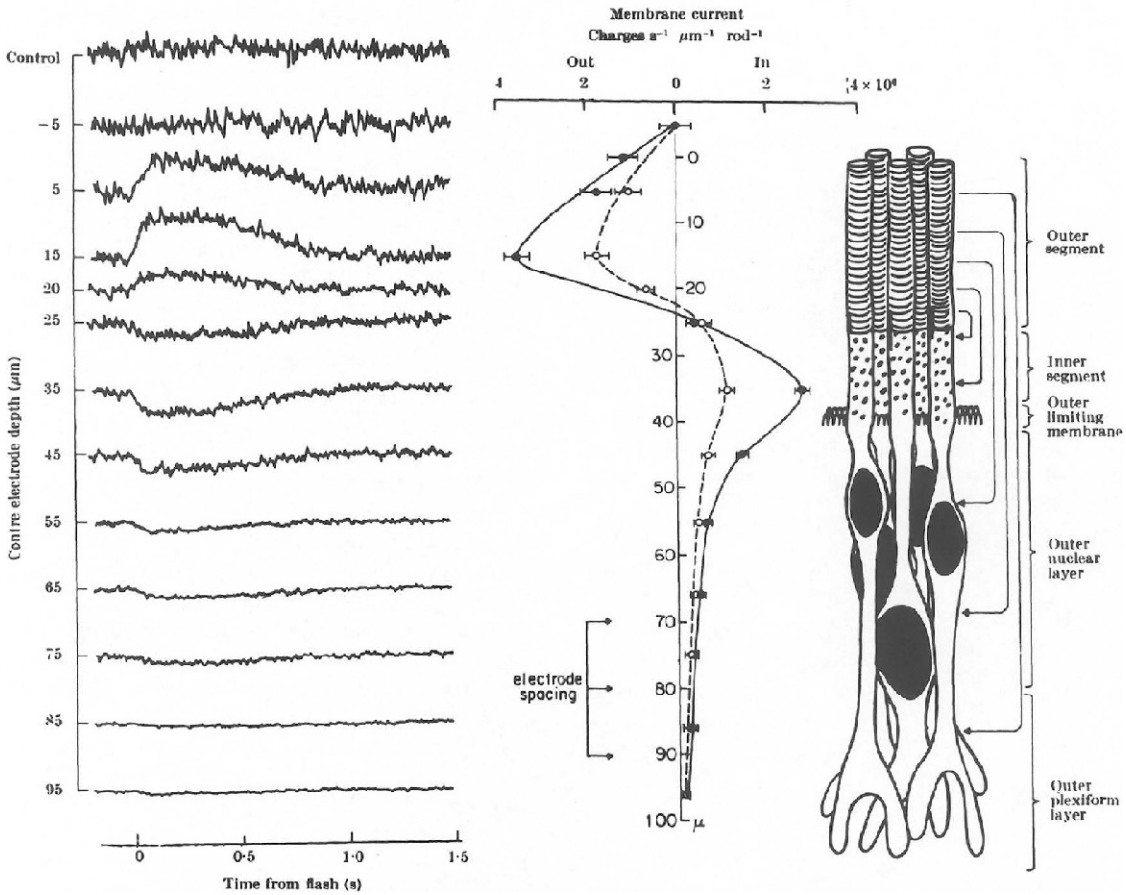

Fig. 10.12 Spatial distribution $\bar{i}_m$ of membrane photocurrent density along rods. Left panel: photocurrent transients against time at electrode depths shown on scale, corrected for radial variations in retinal resistance as described. Each tracing is the average of sixteen responses. Stimuli: 1×10^{11} hV cm^{-2} at 560 nm. Centre panel: peak photocurrent against radial depth of centre electrode of recording triplet. Results from two slices stimulated with 1×10^{11} hV cm^{-2} (○) and 4×10^{11} hV cm^{-2} (●) are shown. Error bars indicate rms noise in current tracings. Right panel: retinal rods of the rat drawn to scale. Pattern of flow of photocurrent indicated by arrows. Outer and inner segments, outer limiting membrane, and outer nuclear and plexiform layers are labelled. (Penn & Hagins, *Nature*.)

was demonstrated by Brown & Pinto (1974) who substituted this ion by choline. Shortly after the replacement the membrane hyperpolarized and the responses to light-stimuli were abolished; after restoration of Na^+ to the medium, the membrane potential returned to its depolarized value, and responses to light returned.

Turtle Cones

Baylor & Fuortes (1970) impaled the large cones of the turtle, *Pseudemys elegans*, and obtained hyperpolarizing responses that increased in size to a maximum of about 12 mV bringing the resting potential from about 25 mV (inside negative) to about 37 mV; the peak potential change at any intensity of illumination, I, was given by the Michaelis-type equation:

$$\frac{V_i}{V_{max}} = \frac{I}{I+\sigma}$$

V_{max} being the potential change recorded at very bright lights and σ the light-intensity when $V_i = \frac{1}{2} V_{max}$. Typical records are shown in Fig. 10.13. The potentials were very similar to the S-potentials derived from horizontal cells in the fish, and they followed a similar equation (Naka & Rushton, 1966). When the size of the spot illumination was increased, there was an apparent summation which the authors considered could be accounted for by scatter from the larger area, but as we shall see, summative interaction between cones does, in fact, occur.

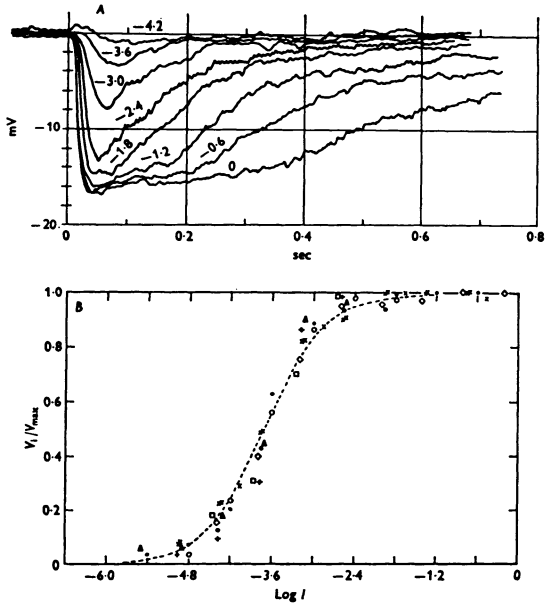

Fig. 10.13 Cone response to flashes of different intensities. *A.* Superimposed tracings of responses to 10 ms flashes of increasing intensity, as indicated (log units), applied at time zero. Potential drop on penetration of cell was 22 mV. Downward deflexion represents hyperpolarization.

B. Peak height of response plotted as a function of light intensity. The symbols plot normalized voltages obtained from ten different cells. As different cells had different sensitivities to light, some shift along the abscissa was necessary to superimpose all points. The largest shift was about 0.6 log unit. The interrupted line follows the Michaelis-type equation. (Baylor & Fuortes, *J. Physiol.*)

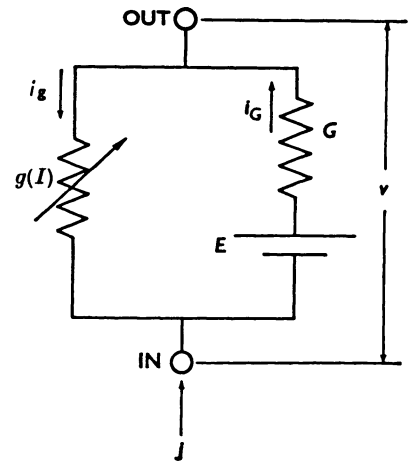

Fig. 10.14 Equivalent circuit of cone membrane. The membrane is represented by a battery having a fixed e.m.f., *E*, and an internal conductance *G*. In parallel with this limb is a conductance *g* whose value is reduced by light. The voltage across the membrane is denoted by *v*. *j* denotes a constant applied current, and i_G and i_g denote currents through conductances *G* and *g* respectively. (Baylor & Fuortes, *J. Physiol.*)

CHANGED MEMBRANE RESISTANCE

If a current is passed through a cone, the change in its potential is governed, other things being equal, by the resistance across its membrane; Baylor & Fuortes observed an increase in this resistance when the light was switched on, and this would correspond to a diminished permeability to Na^+-ions at the outer segment.

EQUIVALENT CIRCUIT

Baylor & Fuortes emphasized that the response to light could be represented by a similar circuit to that proposed to describe the end-plate potential, as in Fig. 10.14, where the membrane is represented by a fixed battery, *E*, a fixed conductance *G*, and another conductance, *g*, which varies with light. In the dark, *g* shunts the battery and causes the voltage, *v*, across the membrane to be less, than *E*. Light reduces *g* and allows *v* to approach *E*. On this basis, it is easy to demonstrate that the light-response will increase with hyperpolarizing, and decrease with depolarizing currents, passed across the receptor membrane. It could be deduced that the response would be zero when the depolarization was 29 mV, i.e. when the cone had been depolarized to give about zero resting potential.

PHOTO-CURRENT

The response to light indicated by Fig. 10.13 is the hyperpolarization of the receptor outer segment so that its internal potential becomes more negative, due to the reduced permeability of some cation, mainly Na^+, of the outer-segment membrane. Such a potential could be produced by driving a current through the outer-segment membrane, so that the response is usually described as a photo-current that blocks the dark-current flowing through the outer-segment membrane. The factor determining the dark current may be described as a conductance, g_{hv}, and the photo-current may be said to result from the closure of the 'g_{hv} gate'.

Carriage of the Dark-current

It was considered by Hagins that Na^+ penetrating the outer segment was responsible for the dark-current; subsequent work has shown that other ions, including Ca^{2+}, are involved, the evidence suggesting an exclusive role of Na^+ being derived from studies in which Na^+ was replaced by other ions, e.g. Li^+, in the outside medium. However, as Bastian & Fain (1982) showed, removal of Na^+ from the outside medium blocks the normal extrusion of Ca^{2+} from the rod outer segment that takes place in the dark to compensate for the steady leak inwards. Thus the extrusion is through a Na^+–Ca^{2+}

exchange pump, which is blocked when Na^+ is removed from the medium. This pump works on the basis of exchange of 3 Na^+ for 2 Ca^{2+}, and is thus electrogenic and contributes to the dark-current (Yau & Nakatani, 1984). According to the study of Yau & Nakatani (1984) and Hodgkin *et al.* (1985) the membrane is not very selective to monovalent cations, the order of permeabilities being:

$$Li^+ : Na^+ : K^+ : Rb^+ : Cs^+ = 1.14 : 1.0 : 0.72 : 0.49 : 0.24$$

Moreover, when the rod is exposed to low Ca^{2+}, very large dark currents can be carried by Ca^{2+}. Since Ca^{2+} internally tends to block the photochannel, g_{hv}, this continual leakage into the receptor must be pumped out, otherwise the receptor would lose its sensitivity to light.[1]

Rod Responses

Microelectrode studies, comparable with those made on cones, have been carried out on turtle (Schwartz, 1973–1976) and amphibian (Cervetto *et al.*, 1977) rods. The basic features of the responses to light have been summarized by Detwiler *et al.* (1980). Some responses are shown in Fig. 10.15. The sensitivity of the rod, when expressed in terms of volts per photoisomerization is 100 to 1000 times greater than that of the cones in the same retina; the responses last several times as long, whilst weak background or adapting lights have a much more striking effect in depressing the response.

COUPLING

The coupling between rods described by Schwartz was striking and was demonstrated by the finding that a large 1000 μm spot of light gave a larger response than that of a small 25 μm spot; although with both stimuli the same number of quanta fell on the retina; the more distant rods were in some way enhancing the response of the central impaled rod. Since fields between 200 μm and 800 μm produced no increase with area, the 'summation area' of the rod was some 200 μm. This is considerably greater than the 40–50 μm for cones.

ENHANCEMENT

The enhancement, manifest in the effects of distant rods on a central one, is easily explained on the basis of a syncytial organization of the rods; thus the current-flow from outer segment to inner segment following a light-stimulus determines the change in potential, recorded as the hyperpolarizing response; this tends to be dissipated by flow into adjacent unstimulated rods by virtue of the syncytial arrangement, and may be mitigated or prevented by simultaneous excitation of adjacent rods. Thus a large stimulus can be more effective than a small one containing the same number of quanta by preventing this dissipation of the voltage.

OUTER SEGMENTS

Baylor *et al.* (1979a, b) isolated single rods by disintegration of the retina with trypsin, and sucked them, or simply their broken-off outer segments, into a micropipette, the projecting end of the outer segment being bathed in Ringer's solution, and the currents passing across the outer segment membrane being recorded. Later modifications of this technique permitted the voltage-clamping of the outer-segment membrane by applying a separate suction microelectrode to the side of the outer segment (patch-clamp), whilst controlling the membrane potential through internal microelectrodes (Bodoia & Detwiler, 1984; Baylor & Nunn, 1986).

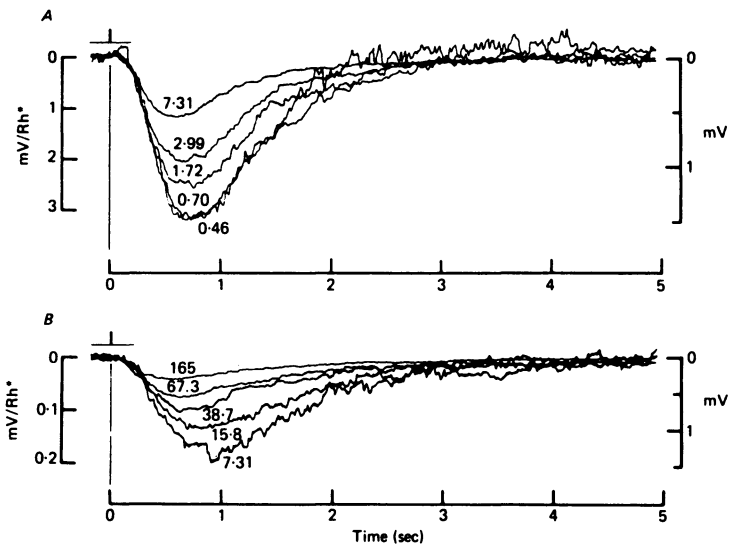

Fig. 10.15 Responses of turtle rod to flashes of different intensities as indicated by the numbers of photoisomerizations per rod (Rh*). These numbers are indicated on the curves. Right-hand ordinate is in millivolts and applies only to the response to the weakest flash. (Detwiler *et al.*, *J. Physiol.*)

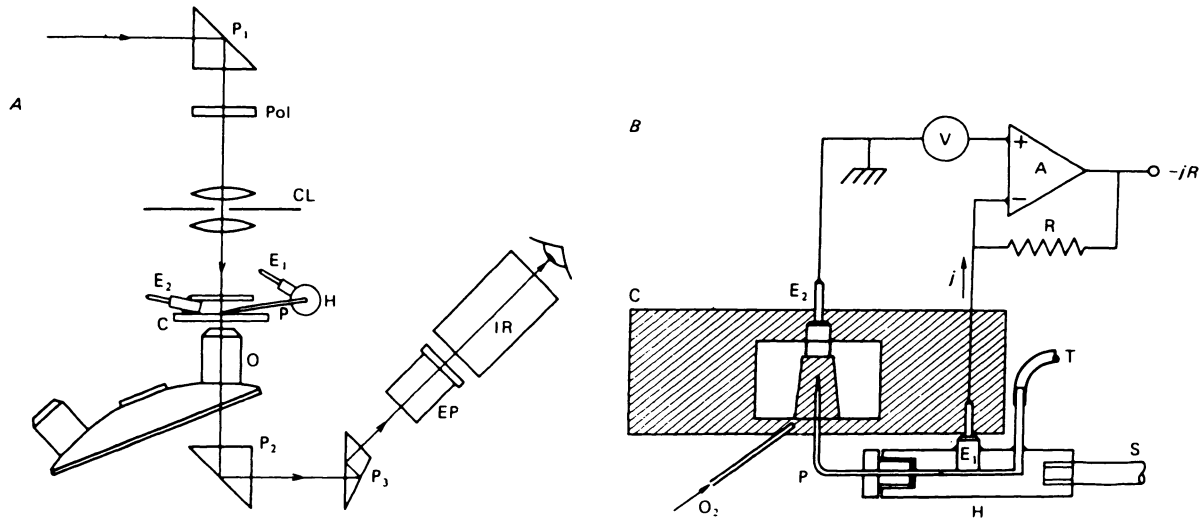

Fig. 10.16 Diagram of the stimulating and recording arrangement. *A*, optical path through the inverted compound microscope. P_1, P_2, P_3, prisms; Pol, polarizer; CL, condensing lens; C, chamber for holding retinal pieces (see *B*); P, pipette; H, pipette holder; E_1, E_2, Ag/AgCl electrodes; O, objective; EP, eye-piece; IR, infra-red image converter. *B*, top view of pipette holder and glass chamber for holding retinal pieces. The chamber, C, consisted of a 25 × 76 mm glass slide with a smaller piece of glass spaced about 4 mm above (see also *A*). This formed a cavity sealed on three sides (stipple), but open at the front, and the Ringer solution containing retinal pieces was held in by surface tension. P, pipette, H, pipette holder; E_1, E_2, Ag/AgCl electrodes; S, shaft for connexion to micromanipulator; T, tubing for connexion to pressure system. O_2, tube for blowing moist oxygen against surface of Ringer solution. The current, *j*, was monitored by amplifier A with feed-back resistance, $R = 100$ MΩ; V, voltage source, variable continuously and stepwise. (Baylor *et al.*, *J. Physiol.*)

Many of the features of the intracellular potential responses to a light-stimulus were reproduced as current changes across the outer segment membrane; thus both showed a response-intensity relation following the rectangular or Michaelis equation (Fig. 10.16), an S-shaped delay involving a series of steps; acceleration of the response by adapting lights and a spectral sensitivity with λ_{max} near 500 nm. A significant difference was the absence of a transient component in the response to bright flashes, so that the conductance change responsible for the intracellular voltage transient was not located in the outer segment but in a more proximal region of the cell.

QUANTAL CURRENT

When very weak flashes were applied, the number of successful flashes, i.e. the number that gave a response, varied with light-intensity in a manner consistent with absorption of a single quantum of light with a quantum-efficiency of about 0.5, similar to that of the absorption of rhodopsin in solution. The actual current due to a single quantum-absorption was 1 pA and this agrees with estimates based on earlier studies on whole rods, e.g. Hagins *et al.* (1970) and Schwartz (1976). This corresponds to a decrease in conductance of 3×10^{-11} S which is close to the conductance of a single acetylcholine channel in the neuromuscular junction (Katz & Miledi, 1972). Since the single photon triggers off a current that rises and falls over a period of time in a smooth manner, we must assume that the absorption leads to release of a number of blocking particles that may block a similar number of channels; on this basis a value of 100 was computed; in fact, the number of channels blocked must be greater than this, as it is unlikely that every particle would be successful in blocking.

LIGHT-SENSITIVITY

At the peak of the response of a rod to light it has been calculated that 3–5% of the 50–70 pA dark-current passing through a rod outer segment is suppressed by a single isomerization of a rhodopsin molecule (Hagins *et al.*, 1970; Baylor *et al.*, 1979, 1984). This very small amount of energy absorption leads to electrical and chemical changes involving much larger amounts of energy, so that the photic process is said to trigger a number of processes, the energy for which must be supplied by the metabolism of the receptor. Thus a simple calculation of the electrical work done in suppressing the dark-current indicates that there has been an amplification of some 100 000-fold.

INTERNAL MESSENGER

The remoteness of the visual pigment from the outer plasma membrane of the receptor, located as it is in discs separated spatially from the cell membrane, demands the activity of a 'messenger' that transmits the primary effects of light, namely photolysis of rhodopsin, to the cell membrane. Thus Hagins suggested that the 'blocking

particles' that were postulated on kinetic grounds to inhibit the dark-current were Ca^{2+}-ions, and a considerable body of experimental evidence was subsequently brought forward in support. For example Yoshikama & Hagins (1973) showed that increasing the external concentration of Ca^{2+} reduced the photocurrent recorded from the isolated rat retina, thus mimicking the effect of light; they also found that the light-intensity required to produce half-maximal photocurrent was increased tenfold when the retina was exposed to a low Ca^{2+} medium. Again, Brown & Pinto (1974) and Lipton *et al.* (1977) lowered the external concentration of Ca^{2+} of the toad's retina and observed a depolarization in the dark, whilst the hyperpolarizing response in the light was increased, the magnitude of the increase being equal to the magnitude of the depolarization. When the outside concentration of Ca^{2+} was raised, there were a steady hyperpolarization and decreased light-response.

Micro-injections Brown *et al.* (1977) injected Ca^{2+} or EGTA into the outer segments of toad rods; injections of Ca^{2+} caused a hyperpolarization, whilst sequestration of Ca^{2+} by EGTA caused depolarization in the dark, a depolarization that was not observed when the rods were in a low-Na^+ medium. This sequestration also reduced the response to light. However, although Bastian & Fain (1979) confirmed the strong similarity in effects of background light and external Ca^{2+}, increased background illuminations produced much larger changes in light-sensitivity than those produced by increases in Ca^{2+}, whilst the background shortened the response, so that they had to conclude either that the effects of a light-stimulus could not be mimicked by altered intracellular Ca^{2+}, or, if they were, there must be two mechanisms, the discs releasing another 'messenger' that altered the state of adaptation of the receptor.

Na^+–Ca^{2+}-pump The most decisive evidence against the Ca^{2+}-hypothesis came from Yau & Nakatani (1984; 1985a) who emphasized the importance of the Na^+–Ca^{2+} exchange pump that kept the outer segment's internal concentration of Ca^{2+} at a low value. Thus the strongest evidence favouring the effect of light as one of increasing internal Ca^{2+} was the finding that light caused an increased efflux of this ion, which was attributed to the liberation of free Ca^{2+} from a bound store. However, Yau & Nakatani (1985a) concluded from their measurements of the photocurrents induced in isolated outer segments that light actually reduced the internal concentration of Ca^{2+}. Bright light completely blocked the normal influx, but the normal pumped efflux continued for a time, and this was what was measured by studies using a Ca^{2+}-sensitive electrode in the outside medium (Gold & Korenbrot, 1980). They predicted an efflux resulting from partial blocking of the Ca^{2+}-channel of 3×10^5 ions per rhodopsin molecule photolysed and this would more than account for the measured efflux of $1–2 \times 10^4$ Ca^{2+} per Rh* estimated by Gold & Korenbrot. By preventing the gain in internal Ca^{2+} that occurs in the dark, Yau & Nakatani (1985a) showed that there was no transient loss during a light flash.

Non-equivalence of light and Ca^{2+} This view was reinforced by a study of Greenblatt (1983) using extracellular recordings across the outer segment layer of the toad retina; they found that lowered external Ca^{2+} desensitized the rods to a flash of light, ten times more light being required for a given response for each tenfold change in $[Ca]_0$ from 10^{-6} to 10^{-9} M. However, the effects on the response kinetics were markedly different; thus background light decreased time-to-peak response and had no effect on latency, whereas decreased Ca^{2+} increased absolute latency and time-to-peak of the flash response. Moreover the effects of background light and altered Ca^{2+} were not additive. The effects of external Ca^{2+} on the photocurrent were large, being reduced to 0.15 of its value on raising the concentration from 1 to 10 mM and increased some 15-fold by decreasing it to 1 μM or less. Thus, if external reflects internal concentration, intracellular Ca^{2+} obviously tends to block the photocurrent. It could do this by holding the channel permanently open, but this is an unlikely mechanism as most of the channels are normally closed in the dark. According to Bodoia & Detweiler (1984), the most likely hypothesis is that the light-sensitive channel is opened by an internal transmitter, e.g. cGMP, and that both open and closed states of the channel are blocked by Ca^{2+}. They showed, moreover, that the effects of alterations in external Na^+ were not simply due to alterations in the current carriers, but also as Bastian & Fain (1982) had postulated, it affected the activity of the Na^+–Ca^{2+} exchange-pump, so that a lowered external Na^+ would reduce the effectiveness of the Ca^{2+}-extrusion process, thereby causing a rise in internal Ca^{2+} with its associated blockage of the photocurrent.

Cyclic Nucleotide

Work in a number of laboratories has emphasized the involvement of cyclic GMP in the phototransduction process. Thus the concentration of cGMP in the rod outer segments is high and decreases when these are exposed to light. A simple hypothesis for the involvement of this substance in transduction could be that the dark-current is maintained by the presence of cGMP in the cytoplasm of the rod outer segment which holds the $g_{h\nu}$ conductance open. If light activated the enzyme that

hydrolyses cGMP, namely phosphodiesterase (PDE), then the conductance gate would be closed and the receptor would hyperpolarize.

Diesterase Activation

The outer segment contains a phosphodiesterase located on the disc membranes; this enzyme is activated by light in the presence of a nucleoside triphosphate, e.g. GTP. This activation will only occur if the diesterase is in the outer segment membrane; when isolated it is not photoactivated (Bignetti *et al.*, 1978). A careful study of the kinetics of the process by Yee & Liebman (1978) has shown that the hydrolysis of cGMP could be a part of a multiplier system whereby a single molecule of bleached rhodopsin serially activated as many as 500 phosphodiesterase molecules, using GTP as an obligatory co-factor. The gain of such a system, measured as the amount of cGMP hydrolysed per bleached rhodopsin, would correspond to 4×10^5/sec and this is comparable with that required of a mechanism mediating visual excitation. The steps postulated by Yee & Liebman were as follows:

Light-dependent

$$Rh + h\nu \rightarrow Rh'$$

Collision binding

$$Rh' + PDE \rightarrow Rh'PDE$$

Nucleotide step

$$Rh'PDE + GTP \rightleftharpoons Rh'PDE\text{-}GTP$$

Catalytic recycling

$$Rh'PDE \times GTP \rightarrow PDE \times GTP + Rh' \text{ (recycled)}$$

Deactivation step

$$GTP \times PDE \text{ (active)} \rightarrow PDE \text{ (inactive)} + GTP$$

As we shall see, the process is rather more complex, involving a specific protein, but the basic concept has been sustained by later research.

Concentration of cGMP

A study of the kinetics of the decrease in cGMP concentration induced by light, as opposed to those of the phosphodiesterase activation, carried out by Woodruff & Bownds (1979) further emphasized the possible involvement of the hydrolytic process in transduction; thus the half-time for completion of the reaction was about 125 msec; light-exposures that bleached less than 100 rhodopsin molecules in each rod outer segment were able to hydrolyse some 10^4 to 10^5 molecules of cGMP per bleached molecule. With continuous illumination, a steady level of cGMP was reached, indicating a balance between hydrolysis and resynthesis; after short bleaches the level of cGMP returned to its original value in 50 to 60 sec.[2]

Effect on Membrane Conductance

Fesenko *et al.* (1985) prepared a suspension of rod outer segments, either separated from the inner segment or intact. By applying a suction patch-electrode they were able to detach a small patch of membrane, which was exposed on its outside to the contents of the patch-pipette and on its cytoplasmic side to the outside medium. Application of cGMP to the cytoplasmic side gave a reversible increase in membrane conductance, which did not require the presence of GTP, showing that no intermediate activation of a protein-phosphorylation step was necessary for this action on the membrane; the most marked change occurred with 20–60 μM cGMP, whilst at 300 μM the system was saturated. Ca^{2+} had no effect on the cGMP effect. That the light-suppressible effect of cGMP was due to the plasma membrane rather than disks was shown by Yau & Nakatani (1985b) using a truncated outer segment lacking disks; they found a large cGMP-induced current, its light-sensitivity depending on the concentration of cGMP in the bath. They computed that a complete suppression of the dark-current would require a very small amount cGMP so that the reduction in concentration in the receptor would be only a few per cent, which would not be detected, thereby explaining Goldberg *et al.*'s (1983) results. Cobbs & Pugh (1985), using a similar technique, confirmed the increase in membrane current caused by cGMP in the cytoplasm of the outer segment, all of which was light-sensitive, whilst the duration of the photocurrent at light-saturation increased tenfold. However, kinetic analysis suggested that cGMP was not simply concerned in keeping the light-sensitive conductance open, but that it might itself affect phosphodiesterase activity. Thus there was no slowing of the rising phase of the photocurrent although this would be expected, after cGMP injection, as there would be more of the cGMP to hydrolyse before the dark-conductance was blocked.[3]

Cones

Haynes & Yau (1985) showed that catfish cones had a light-sensitive conductance induced by cGMP, the half-saturation concentration of cGMP being as low as 35–70 μM.

Permeability Changes

Caretta *et al.* (1979) loaded frog photoreceptor disks with ^{22}Na, ^{42}K, etc. and found an increased rate of outflux on treatment with cGMP. Again, Caretta & Cavaggioni (1983) prepared membrane-bound vesicles by sonication

of rod outer segments; these were loaded with aequorin, and the cytoplasmic sides of the membrane-vesicles were exposed to the outside medium. Addition of cGMP increased the influx of Ca^{2+} by several hundred-fold.

FLUCTUATIONS

Measurements of fluctuations in membrane current can provide useful information as to the events taking place. Three types have been described, attributable to rhodopsin noise, transmitter noise and channel noise. The first probably arises from isomerization of 11-*cis* retinal in the dark–thermal isomerization—occurring about once per 50 sec and having the same amplitude, namely 1 pA, as that of a single photon response. A continuous noise with a smaller amplitude (ca. 0.2 pA) has been attributed to fluctuations in the concentrations of substances involved in the transduction change, following rhodopsin but preceding the sodium channels themselves (Baylor *et al.*, 1980). Finally a higher frequency noise of very small amplitude has been identified using patch-clamps, probably coming from random opening and closing of sodium channels in the dark. It was computed that the channel has a unit current of 4 fA, equivalent to 1.2×10^4 Na^+-ions per sec, and a mean open-time of 2 msec (Gray & Attwell, 1985; Zimmerman & Baylor, 1985). Thus about 24 Na^+-ions travel through the channel while it is open. Light reduces the rate of opening with no effect on rate of closing. Thus a 4 fA unit current means that a 1 pA single-photon response is due to the closure of some 250 channels. In the presence of cGMP it was computed that the average time a channel remained open would be about 5 msec, closing when the cGMP attached to it dissociated, when it would be in a condition to respond to a new cGMP molecule. The longer a channel remained open when attached to a cGMP molecule the less responsive a rod would be to a flash of light. If the open-time were very short, it could be computed from the time required for cGMP to diffuse to the channels that very few channels would be open at any moment with the normal dark concentration of cGMP, and it turns out that the closing rate of the channel is nicely matched to the kinetic characteristics of the light-activated phosphodiesterase system (Stryer, 1986).[4]

Toad Rods

Matthews & Watanabe (1987) obtained single-channel recordings from patch-clamped toad rod outer segments by omitting Ca^{2+} from the medium bathing the extracellular face of the recorded patch; dim light suppressed this activity, but a maintained dim illumination produced large fluctuations in rate of opening and closing, as would be expected on a statistical basis of random photoisomerizations. After recording with the patch in place, the latter was removed, exposing the intracellular face to the outside medium; application of cGMP then produced changes identical with those previously produced by light, thus clinching the proposition that light-sensitive channels were controlled by cGMP.

Monkey Rods

The responses of single rods of the monkey are of great interest since their photoreceptors are similar to those of man as judged by psychophysical experiments (De Valois *et al.*, 1974) and microspectrophotometry (Bowmaker & Dartnall, 1980; Bowmaker *et al.*, 1978, 1980); responses from single outer segments sucked into micropipettes

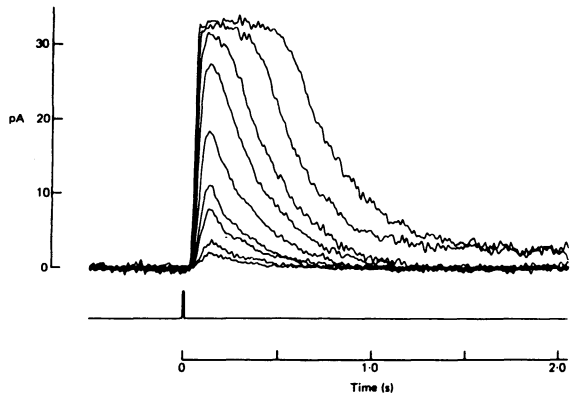

Fig. 10.17 Family of superimposed responses to 11 ms flashes of increasing strength, with outer segment current plotted relative to dark level (outward change in membrane current plotted upwards). Stimulus timing shown by flash monitor below records. Lower traces averaged from up to six responses, uppermost trace is a single sweep. Flash photon densities raised from 1.7 to 503 photons μm^{-2} at 500 nm. Band width 0–50 Hz. (Baylor *et al.*, *J. Physiol.*)

were recorded by Baylor *et al.* (1984). Stimuli of increasing intensity caused greater and greater photocurrents, as illustrated by Fig. 10.17; the saturating photocurrent, when presumably all channels were blocked, was about 30 pA. In this instance the response varied in an exponential fashion with light-intensity:

$$r/r_{max} = 1 - e^{-kri}$$

rather than in the Michaelis fashion as found with cones. It was estimated that the rod saturated, i.e. ceased to increase its response, when the flash intensity was such as to cause some 200 isomerizations per sec, a value that was compatible with human psychophysical measurements on scotopic vision. If this is true, then adaptation involving scotopic (rod) vision could be considered to be purely a function of photoreceptors. The spectral sensitivity curve corresponded well with the human scotopic sensitivity curve of Crawford (1949) (Fig. 10.18) with peak absorption at 2.04 μm^{-1} (wavenumber).

Spatial Spread

By exposing only limited portions of the outer segment to light, the rate and degree of spread of excitation can be measured; from its time-scale the rate of diffusion of the internal transmitter can be estimated, a rate that would be considerably reduced from a true diffusion coefficient measured in an aqueous medium owing to the 'baffling effect' of the stacks of disks round which the transmitter would have to pass. Lamb *et al.* (1981) calculated an effective diffusion coefficient in the region of

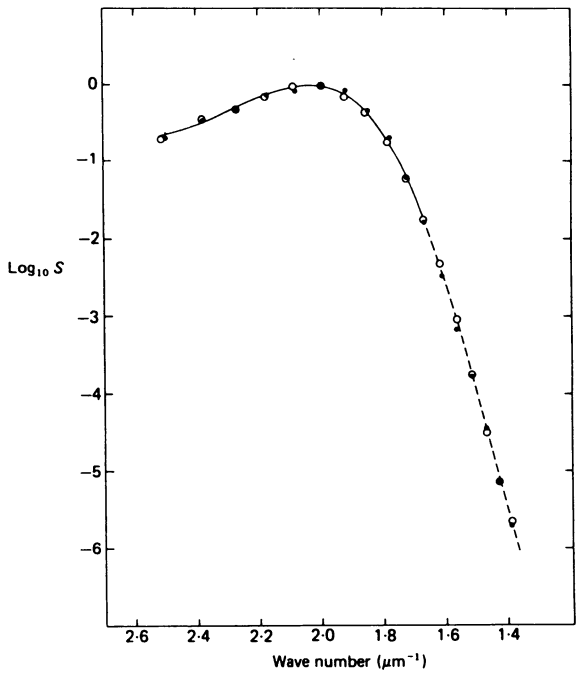

Fig. 10.18 Comparison of averaged spectral sensitivity of monkey rods (○) with corrected human scotopic sensitivity curve of Crawford (1949, ●) and Dartnall nomogram for rhodopsin with peak absorption at 2.04 μm^{-1} (continuous smooth curve). Crawford's results corrected as described in the text for absorption in the lens and self-screening of rhodopsin. Dashed continuation of nomogram drawn by eye. (Baylor *et al.*, *J. Physiol.*)

10^{-7} cm^2 sec^{-1}, much lower than would be expected of a small molecule or ion in a simple medium, and due, as indicated, to the presence of stacks of disks. The actual degree of spread from a limited area of excitation is small, as postulated by Hagins *et al.* (1970), and according to Lamb *et al.* (1981) probably less than 1–2 μm. The same was found by the measured desensitization or adaptation of the rod when exposed to an adapting light-stimulus, agreeing with conclusions of Hemilä & Reuter (1981).

Quantitative Aspects of cGMP Hydrolysis and Regeneration

As summarized by Pugh & Cobbs (1986), in their excellent review of the transduction process, the most serious difficulty encountered when attributing the light-change in conductance to that produced by hydrolysis by PDE, is the failure to measure adequate loss of cGMP after a light-stimulus. The most satisfactory hypothesis, according to them, was the high-affinity binding of cGMP to hypothetical sites, so that the concentration of free cGMP in the dark would be only some 15% of the total measured in the rod outer segment, or about 10% of the total extractable. Associated with this binding would be an on-going guanylate cyclase activity about 1/3000 of the maximal light-stimulated PDE activity, contributing to restore the hydrolysed cGMP utilized in the light-cascade.

PHOSPHODIESTERASE INHIBITION

If the closure of the light-sensitive conductance, g_{hv}, depends on hydrolysis, then clearly inhibition of this hydrolysis by a PDE inhibitor, such as 3-isobutyl-1-methylxanthine (IBMX) should modify the light response; moreover it should increase the dark current, since this is sustained by cGMP. Capovilla *et al.* (1983) showed that these postulates were essentially correct, the increased dark-current or depolarization of the rod in darkness being associated with an enhanced light-response since there were now more open channels to be

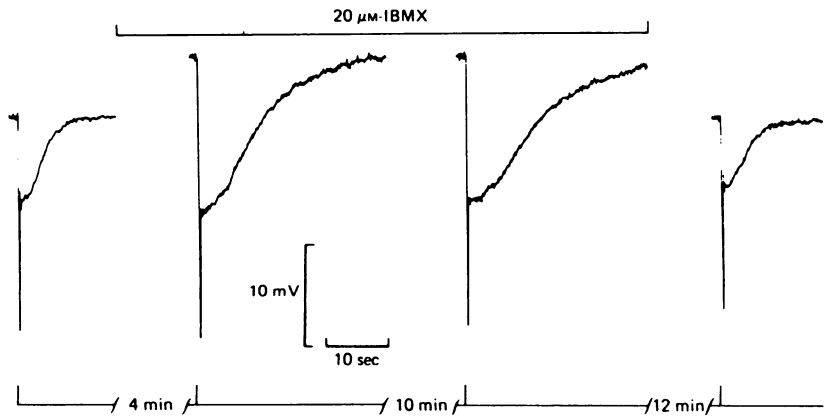

Fig. 10.19 Effect of 20 μM-IBMX on the electrical activity of a rod. 20 μM-IBMX was present in the perfusate during the time indicated by bars at the top. Dark resting potential in control Ringer solution was −40 mV. Bottom trace is light monitor. Monochromatic light of 510 nm; flash duration 20 ms. The flash intensity was equivalent to 6800 photoisomerizations (Rh*)/rod. (Capovilla *et al.*, *J. Physiol.*)

closed by a given flash of light. The time-scale of the response was also altered, the response being slowed down. Figure 10.19 illustrates the effects of 20 μM IBMX on resting potential and photoresponse; the former fell from 40 mV to 34 mV; concomitantly the amplitude of the photoresponse increased and its time-course slowed. The effect was completely reversible on removing the IBMX from the medium.

Information Flow

The studies of Fung & Stryer (1980) and Fung *et al.* (1981) have shown that an important step in the process is the reaction of activated rhodopsin with a regulatory protein—*G-protein* or *transducin*[5]—leading to the activation of phosphodiesterase:

$$R^* \rightarrow T\text{-}GTP \rightarrow PDE^*$$

in which R* denotes photolysed rhodopsin, T-GTP denotes a complex of the regulatory protein with GTP, and PDE* denotes the active form of phosphodiesterase. It was estimated that one photolysed rhodopsin molecule activated some 500 phosphodiesterase molecules. Since a single activated PDE will hydrolyse more than a thousand molecules of cGTP, the amplification of the photoisomerization is such that one photoisomerization can lead to hydrolysis of some 10^5 molecules of GTP.

TRANSDUCIN

Transducin is made up of three subunits (T_α, T_β, and T_γ) of molecular weights 39, 36 and 8 kd respectively (Kuñn, 1980; Stryer *et al.*, 1981). The α-subunit of transducin (T_α) contains the guanyl nucleotide binding site and the site for hydrolysis of GTP to GDP. T_α in the GTP form is the activator of phosphodiesterase, whilst the β- and γ-chains form a $T_{\beta\gamma}$-subunit. T_α and $T_{\beta\gamma}$ are together when GDP is bound but separate when GTP is bound. Thus $T_{\beta\gamma}$ presents T_α to photoexcited rhodopsin so that GTP can be exchanged for GDP, thereby enabling it to activate phosphodiesterase.

CYCLE

The light-activated cycle proposed by Fung *et al.* (1981) is illustrated by Fig. 10.20. In the dark, nearly all transducin is in the T-GDP form; a photoactivated rhodopsin molecule, R*, meets T-GDP in the disk membrane and forms an R*-T-GDP complex. GTP exchanges for GDP in the

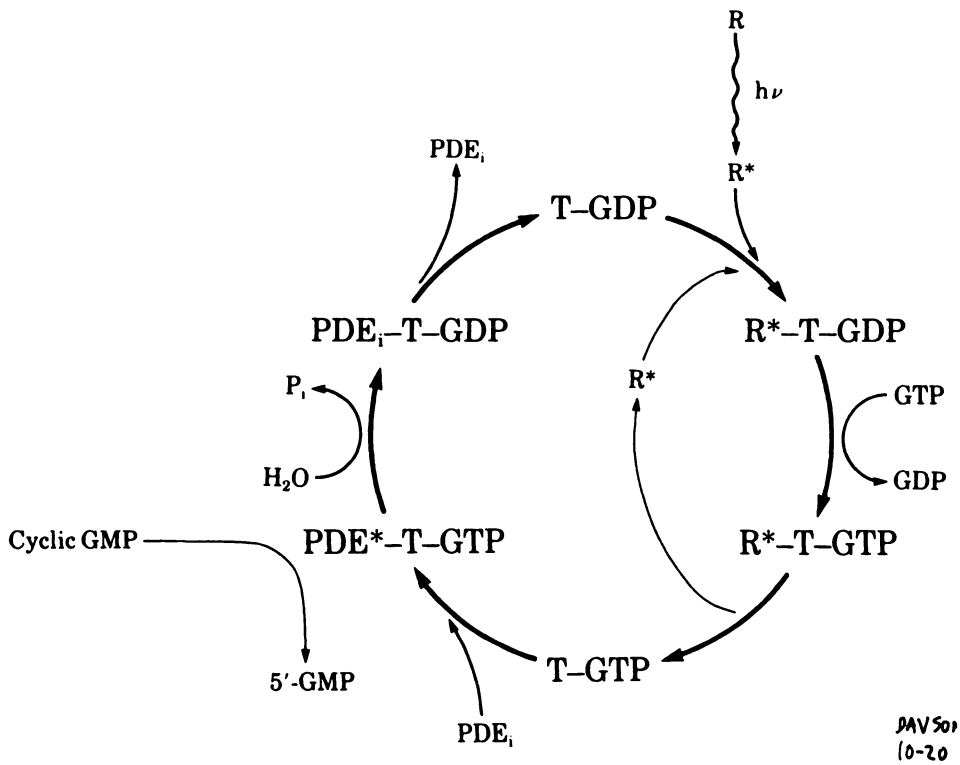

Fig. 10.20 Proposed scheme for the flow of information in the light-activated cyclic nucleotide cascade of vision. PDE, phosphodiesterase; T, transducin; R*, photolysed rhodopsin. (Fung *et al.*, *Proc. Nat. Acad. Sci.*)

complex, so that the role of R* is to release GDP from transducin. The exchange of GTP for GDP diminishes the affinity of R* for transducin; in addition the affinity of T_α for $T_{\beta\gamma}$ is reduced. Thus, because of this reduced affinity, free R* is free to interact with another T-GDP, enabling it to act photocatalytically. T_α-GTP is mobilized so that it can carry the excitation signal to phosphodiesterase, so that in this way some 500 T_α-GTP are formed per R*. T_α-GTP activates the phosphodiesterase by overcoming an inhibitory constraint imposed by one of the subunits of the diesterase. Finally the GTPase-activity inherent in the α-subunit of transducin converts T_α-GTP to T_α-GDP, and this in turn results in the deactivation of phosphodiesterase. T_α-GDP then rejoins $T_{\beta\gamma}$. It is important to appreciate that the energy required for the cGMP cycle is provided by the hydrolysis of GTP and not the photon of energy absorbed by rhodopsin; this became clear when the amplification involved in the initial light event was deduced earlier. Thus in the absence of R* the energy barrier for conversion of T-GDP to T-GTP is too high, and the function of R* is to reduce this activation energy.

ACTIVATION OF PHOSPHODIESTERASE

Phosphodiesterase (PDE) is made up of three subunits, α, β and γ. Limited tryptic digestion increases the normally very low esterase activity, suggesting that removal of one of the subunits releases the enzyme from an inhibition, and this would appear to be brought about by the γ-subunit. Transducin overcomes this inhibition (Fung *et al.*, 1981) and gives the activated diesterase a remarkably high activity, so high that rate of hydrolysis is about limited by the rate at which cGMP can diffuse up to it. As Stryer states: 'PDE has come close to achieving catalytic perfection'. According to Clack *et al.* (1983) injection of activated transducin causes reversible hyperpolarization of the rod outer segment membrane.

METARHODOPSIN II—THE ACTIVATED RHODOPSIN

Of the intermediates in the process of removal of retinal from opsin illustrated by Fig. 8.19, the first likely candidate for initiating the membrane changes leading to hyperpolarization is Meta II; thus the active product must be formed on a millisecond scale, so that products dependent on relatively slow reactions, such as Meta III and later ones, must be ruled out (Wald, 1968). Definitive proof of the role of Meta II was provided by Emeis *et al.* (1982) who profited by the observation that the reaction of photo-activated rhodopsin with the G-protein (transducin) was accompanied by a light-scattering signal due to the turbidity of the solution. They also found that a single flash of light, sufficient to bleach 2% of the rhodopsin, caused the production of only Meta II, whereas an equilibrium mixture:

$$\text{M I} \rightleftharpoons \text{M II}$$

is usually established; with extra flashes, M I appeared, so that it was possible to speak of extra M II produced by single flashes, until after 10 flashes there was no extra M II, the expected equilibrium mixture being attained. By measuring M II formation in response to flashes, and the light-scattering signal, a perfect correlation was found, indicating that the extra M II was being formed because G-protein, or transducin, was reacting with M II, and shifting the equilibrium to the right. Thus the light-scattering signal was related to a stoichiometric binding of G-protein to Meta II:

$$\text{Meta I} \rightleftharpoons \text{Meta II} \rightarrow \text{M II-G}$$

If, in a washed outer segment preparation, there was no G-protein present, there was light-scattering signal, and no extra Meta II; addition of G-protein gave the Meta II signal at the first flash with the light-scattering signal, both being kinetically similar. Addition of GTP-γs, which removes G-protein from its attachments, abolished the effects. The cycle for the events may be represented by Fig. 10.21 (Bennett *et al.*, 1982); Meta-II reacts with GDP, for which it has high affinity; GTP forces an exchange to give a complex of GTP with Meta-II, a process catalysed by GTPase. Meta II has a low affinity for GTP which splits off to complete the cycle, which is energized by the GTP–GDP conversion.[6]

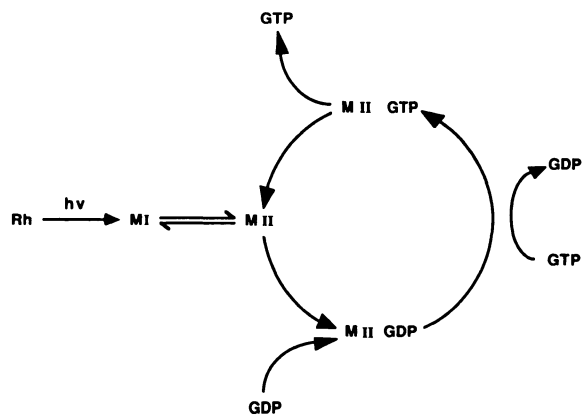

Fig. 10.21 The involvement of metarhodopsins, M I and M II, in the visual cycle. (After Bennett *et al.*, *Eur. J. Biochem.*)

Arrest of the Cascade

An important feature of any excitatory process is that there should be a mechanism for its rapid cessation, on removal of the stimulus, in order that the receptor be in a position to respond again. Two steps are necessary, namely the hydrolysis of T_α-GTP to T_α-GDP, and also the deactivation of R* so that it does not continue to

trigger the conversion of transducin to the GTP-form. The deactivation of R*, which probably represents the metarhodopsin-II condition, is brought about by the final release of all-*trans* retinal and the reassociation with 11-*cis* retinal, but this is a slow process, and a more rapid deactivation must be postulated.

Involvement of ATP

Liebman & Pugh (1980) and Sitaramayya & Liebman (1983a, b) observed that ATP would rapidly quench the photoactivation of phosphodiesterase in rod outer segments. There was some doubt as to whether the effect was rapid enough to permit its involvement in the inhibition of light-activity, since activated phosphodiesterase will continue to hydrolyse cGMP for hours, whilst its inactivation must occur within seconds. Sitaramayya & Liebman (1983a) showed that ATP would not quench phosphodiesterase activity if the kinase concerned in the reaction with ATP were not present, and they showed (1983b) that, provided their rod disk membrane preparations had sufficient kinase present, multiple phosphorylation of rhodopsin by ATP was complete in less than 2 sec compared with the 4 sec required for inactivation of cGMP diesterase under the same conditions.

Zuckerman *et al.* (1983) showed that the formation of Meta-II was associated with a decrease in ATP and a rise in ADP in intact rod outer segments; reversal of the photo-process with blue light caused an increase in ATP. The process was highly amplified, a decrease in cytosol ATP by 2000 molecules occurring per photon absorbed. They suggested that an ATP-binding protein, I_p, competed with T-GTP, the transducin-GTP complex, for the same site on photolysed rhodopsin, so that I_p-ATP would act as an inhibitor of phosphodiesterase inhibition, tending to bring the photo-current to an end. Thus the time-course of activation and inactivation of phosphodiesterase will be determined by the kinetics of formation of T-GTP and I_p-ATP, and by the relative affinities of the two species for the same binding site on Meta-II. The binding protein was subsequently called *arrestin*, Zuckerman *et al.* (1985) having shown that an ATP/ADP exchange could be mediated by arrestin when reconstituted with bleached peripheral protein-stripped rod disk membranes.

Rhodopsin Kinase

Rhodopsin can be phosphorylated, due to the presence of a kinase present in the outer segments, the enzyme being readily extracted from dark-adapted rod outer segments and being a protein of 48 kd (Kühn, 1978). It binds to freshly bleached rods and is slowly released in the dark; while bound, it catalyses the phosphorylation of the serine and threonine residues in the rhodopsin molecule, so that as many as nine phosphate groups per rhodopsin molecule may result from its activation. The actual light-activation process does not consist of an activation of the kinase, however, which is unaffected by light, but rather the activation of the substrate, namely rhodopsin (McDowell & Kühn, 1977). The phosphorylation of rhodopsin together with the action of arrestin, both involving ATP, may well be sufficient to bring the excitatory phase of a light-stimulus to a close.

Relation to Ca^{2+}

At low levels of Ca^{2+} the inhibitory effect of ATP on phosphodiesterase activity is increased (Kawamura & Bownds, 1981), so that if, as we have seen is most probably true, the effect of light is to reduce the internal concentration of Ca^{2+}, we may expect the sensitivity of the receptor to decrease, and this may be a factor in light-adaptation (p. 270).

Binding Region

Figure 8.12, illustrates the basic model for rhodopsin structure when localized in the disk membrane; the binding sites are thought to be on those parts of the protein chains that project out of the membrane bilayer; retinal, the photon-absorbing molecule, is located deeper within the bilayer, the change from 11-*cis* to all-*trans* inducing changes in the configuration of the protein chains that permit the initial binding to transducin.

Analogy with Beta-noradrenergic Receptor Activity

Beta-adrenergic activity is brought about through a cyclic nucleotide-mediated reaction, governed by an initial reaction of the adrenergic drug with its receptor, e.g. on the heart cell. Sequence analysis of the structures of rhodopsin and the beta-adrenergic receptor exhibited strong similarities (Dixon *et al.*, 1986); both systems require an intermediary protein, transducin and G_s, whilst phosphorylation plays an important role with each. The comparison illustrates a remarkable economy in Nature, whereby a single ancestral protein has been adapted to give a protein, rhodopsin, subserving a highly specialized task, whilst another, the adrenergic receptor, is involved in a multiplicity of regulatory functions in the complex organism.

The Role of Ca^{2+}

Although Ca^{2+} has been ruled out as the internal messenger in the phototransduction process, its role in the visual process is a matter of great interest. A recent study of Torre *et al.* (1986) has emphasized the part played by

Ca^{2+} in the control of the adapted state of the receptor, i.e. its responsiveness to a light stimulus in the presence of a background light, an influence that is exerted on the cascade of chemical processes leading to the hydrolysis of cGMP. This apparently takes the form of a feedback control of the 'gain' of the phototransductive process. A second mode of action is through the well established action of internal Ca^{2+} in the control of transmitter release, a rise in internal Ca^{2+} at a nerve terminal promoting the exocytosis of transmitter-laden vesicles.

Influence on Rod Light-response

It will be recalled that Yau & Nakatani (1984) showed that a part of the dark-current was carried by a Ca^{2+}–Na^{+} exchange mechanism, the exchange of 3 Na^{+} for one Ca^{2+} imparting an electrogenicity to the process causing an inward flow of positive current at the outer segment. The effect of light was to close the ionic channels, so that this current decayed, but much more slowly than the abrupt shut-off of the main portion carried by Na^{+}. The decay was associated with a continued pumping out of Ca^{2+}, so that internal Ca^{2+} fell in response to a light-flash, a fall that was subsequently demonstrated by McNaughton *et al.* (1986) using the aequorin method of Ca^{2+} assay.[7] Torre *et al.* (1986) introduced a Ca^{2+}-chelator into the rod inner segment by means of a patch-clamp electrode, thereby preventing the rapid binding of Ca^{2+} by the cytoplasmic proteins that normally maintains the internal concentration at about 0.5 μM. Any effects of altered internal Ca^{2+} would thus be prolonged; such a prolongation is illustrated by Fig. 10.22 which shows the slowing of the Na^{+}–Ca^{2+}-exchange component of the photoresponse in the presence of 2 mM BAPTA, i.e. it slows the fall in internal concentration of Ca^{2+} in response to a light-flash. By studying the effects of BAPTA on the flash-responses as intensity was increased it was shown that the responses to dim flashes were prolonged, the normal acceleration of responses with brighter flashes disappeared, the responses to intense flashes remained saturated for longer, and a pronounced overshoot occurred. At each intensity, the early phases of the rising current were unaffected, suggesting that the initial photoresponse was unaffected by the level of internal Ca^{2+}, but that the recovery phase of the response was prolonged by high Ca^{2+}, i.e. that the return to normal polarization after a flash required rapid removal of Ca^{2+}. With BAPTA, the subsequent recovery of internal Ca^{2+} after a flash should be slowed, and this means that internal Ca^{2+} is being held lower than normal in the dark resting state. If Ca^{2+} influenced the cGMP cascade, the lowered Ca^{2+} would allow cGMP levels to increase rapidly, causing a powerful opening of the light-sensitive channels and thus an overshoot in the response, i.e. a greater-than-normal depolarization of the outer segment. This would give a large circulating current and the required influx of Ca^{2+} to return the internal Ca^{2+}

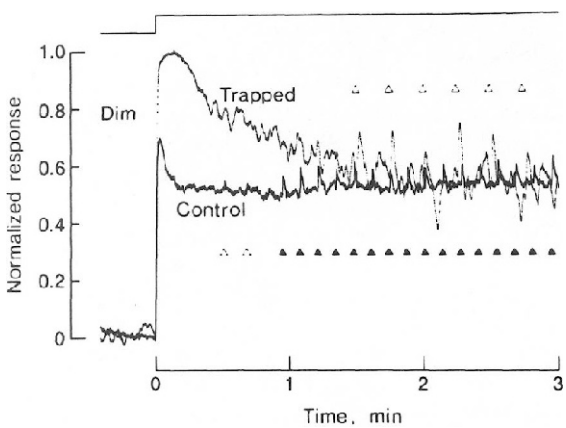

Fig. 10.22 Normalized response under control conditions (heavy trace) and after trapping BAPTA (10 mM in patch pipet, lighter trace), for an intensity of steady illumination (170 isomerizations per sec) sufficient to halve the circulating current. Triangles indicate timing of superimposed test flashes for determining sensitivity, as in Fig. 10.23; lower row, in control case; upper row, in trapped BAPTA. Flashes delivered: △, 70 isomerizations; ▲, 140 isomerizations. Circulating dark current; control, 58 pA; trapped BAPTA, 48 pA. (Torre *et al.*, *Proc. Nat. Acad. Sci.*)

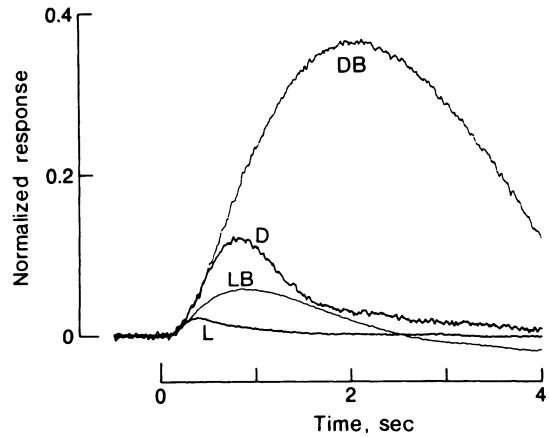

Fig. 10.23 Responses to dim test flashes, normalized with respect to the level of circulating current. Trace D, dark-adapted control; trace L, light-adapted control. Traces DB and LB were obtained in the presence of nominally 10 mM trapped BAPTA, again in darkness (DB) or with the same steady light (LB). In the light-adapted state the test flash intensity was increased to obtain a measurable response, and the traces have been scaled down accordingly. Steady light delivered approximately 330 isomerizations per sec; flashes delivered approximately 17 (D, DB) and 130 (L, LB) isomerizations. Different cell from Fig. 10.22. Circulating current: D, 53 pA; L, 30 pA; DB, 50 pA; LB, 21 pA. Traces are averages of 4–12 responses. (Torre *et al.*, *Proc. Nat. Acad. Sci.*)

rapidly to normal. Studies of the effects of light-adaptation when the changes in internal Ca^{2+} were buffered, or slowed, by BAPTA are illustrated in Fig. 10.23; earlier studies had shown that an increase in light-adaptation did not affect the timing of the initial response but it did shorten the recovery phase, thereby reducing the total response and exhibiting the phenomenon of adaptation, i.e. a reduced response in the presence of a bright light. These points are shown in curves L and D for control receptors; prolonging the change in Ca^{2+} in the outer segment induced by the BAPTA caused a prolongation of the process that brings the response to an end. Thus the reduction of Ca^{2+} that occurs dynamically during the flash-response assists in terminating that response, thereby setting the sensitivity of transduction in both the light- and dark-adapted states.

The essential feature brought out by these experiments is that the light-stimulus decreases internal Ca^{2+} and that this lowering of internal Ca^{2+} is an essential element in bringing the response to an end, thereby leaving the receptor ready to respond to a new stimulus. Alterations of internal Ca^{2+} as a result of continued light or dark influence the subsequent features of the response to another flash.

Mechanism

So far as the mechanism of action of Ca^{2+} in these conditions is concerned, the role of this ion in controlling the cGMP cascade may well be dominant. Thus we have seen that in low Ca^{2+} Kawamura & Bownds (1981) found an increase in the inhibitory effect of ATP on phosphodiesterase activity, an increased inhibition that would reduce the receptor's sensitivity to light.

GUANYLATE CYCLASE

Lolley & Racz (1982) showed that reducing the internal concentration of Ca^{2+} in rat rods stimulated synthesis of cGMP; they assumed that the actual concentration of cGMP was governed by the balance between phosphodiesterase and cyclase activities, and they concluded that Ca^{2+} acted as an inhibitor of guanylate cyclase, most of this activity in the retina being in the visual cells (Farber & Lolley, 1977). If Ca^{2+} were to be able to act as a modulator of the effects of light, Lolley & Racz estimated that the internal concentration in the receptors would have to be less than 10^{-5} M, a reasonable assumption in the light of recent estimates, provided that it is the ionic, and not bound, form of the atom (Hagins & Yoshikami, 1977).[8]

COMBINED EFFECTS

Both of these effects of changed internal concentration of Ca^{2+} combine to give the phenomenon of an increase in dark-current at low levels of Ca^{2+} and a decrease at high levels. Thus the concentrations of Ca and cGMP are reciprocally related in the outer segment, and this can form the basis for a feedback loop. Thus the initial effect of light is to close light-sensitive channels, reducing influx of Ca^{2+}. The lowered internal Ca^{2+} leads to opening of channels through an increase in cGMP and this allows an influx of Ca^{2+} which completes the feedback loop, tending to restore the dark state. Consideration of the influence of injections of cGMP on the light-response (e.g. Cobbs & Pugh, 1985; Matthews *et al.*, 1985) certainly suggested that elevated Ca^{2+} would accelerate phosphodiesterase activity, thereby tending to bring the receptor into the dark state with open channels. Thus injections of cGMP, by increasing the dark-current, would increase internal Ca^{2+} and thus bring any effects of light to a more rapid end.[9]

SYNTHESIS

Schwartz (1985), concluding an authoritative review of the problem of transduction, points out that neither the Ca^{2+} nor the cGMP hypothesis explains all the phenomena, and puts forward a scheme based on four central ideas, namely (1) That cGMP concentration is regulated by a homeostatic feedback system controlled by phosphodiesterase hydrolysis and light, synthesis being controlled by guanylate cyclase, which can be activated by increased concentration of Ca^{2+}. (2) The entry of Ca^{2+} is controlled likewise by a homeostatic mechanism; thus it enters through generator current channels, which are blocked when Ca^{2+} binds at a specific site inside the membrane. (3) cGMP regulates the affinity of the internal site for Ca^{2+}, a fall in cGMP increasing binding. (4) Each absorbed photon transiently upsets the balance created by the systems (1) to (3) and closes all the channels within a short length of outer segment. To summarize his scheme briefly: A photon bleaches a rhodopsin molecule, which then activates some 100 phosphodiesterase molecules, leading to a decline in cGMP concentration, which increases the ability of Ca^{2+} to block generator current channels. Influx of Ca^{2+} and Na^{+} ceases while efflux of Ca^{2+} continues, leading to a fall in internal Ca^{2+} and rise in external Ca^{2+}, as emphasized by Yau & Nakatani (1984; 1985). The lowered internal Ca^{2+} activates guanylate cyclase and decreases activation of phosphodiesterase, both processes acting to decrease the decline in cGMP concentration. An important feature of the system is the control of Ca^{2+}-entry through generator-current channels, acting as part of a feedback system that operates to minimize changes in cGMP concentration.

Notes

1. The reversal potential of the light-sensitive change is nearly zero (Bader *et al.*, 1979; Baylor & Nunn, 1986). If $[K^+]_{In} = [Na]_{Out}$, the theoretical reversal point, V_{re}, is given by: $V_{re} = -(RT/F) \ln b$, where b is the permeability to K^+ related to that to Na^+. The calculated value was 5.6 mV.
2. Goldberg *et al.* (1983), using Ames' isolated rabbit retina preparation, found that the steady-state levels of cGMP in the retina were unaltered appreciably when the level of illumination was changed over a 3-log-fold range; they found, however, that the turnover of cGMP, measured by the incorporation of ^{18}O, was increased greatly, and suggested that the metabolic event, rather than the level of cGMP, somehow provided the light-stimulus. The fact that phosphodiesterase activity was increased meant that the activity of guanylate cyclase would also be accelerated. Stryer (1986), however, rejects this argument in view of the powerful evidence demonstrating the electrical effects of cGMP on rod outer segments. If the free cytosolic level of cGMP is only 5 μM, with the remaining 55 μm bound to sites that do not release cGMP in times of less than a second, the anomalies can be explained.
3. MacLeish *et al.* (1984) found that intracellular injections of cGMP increased the dark current. So far as changes in cGMP concentration are concerned, the contradictions in the literature have been discussed by Cote *et al.* (1984) in the light of their own results, which demonstrated a fall in cGMP concentration in frog rods which preceded a fall in dark current after onset of light. Their preparation consisted in isolated rod outer segments with the ellipsoid still attached, so that enough mitochondria were preserved to enable the cGMP content to remain normal. A flash reduced cGMP concentration by as much as 65% within 200 msec. With a very weak flash the fall in cGMP occurred within 50 msec, before the change in conductance had begun. Meyertholen *et al.* (1986) reduced the internal concentration of cGMP in rods by introduction of buffers; lowered cGMP had the same effect as that of weak light.
4. Gray & Attwell (1985) emphasize that the rod's light-sensitive channel has a smaller conductance than that of any channels so far studied, being some 300 times less than that of acetylcholine receptor at the muscle end-plate. This means that a large number of channels must close for a single response to light, which means that the effects of chance fluctuations in channel-closing will be relatively insignificant, only one in about 10 000 opening by chance at any moment. Secondly, a brief lifetime means that fluctuations that do occur are at frequencies much higher than those of the light-induced signal, so that the effect is filtered out by the membrane capacitance. Thus confusion between light and noise is reduced.
5. Transducin has been called G-protein, GTP-binding protein, and GTPase; Stryer (1986) recommends the use of the term transducin to emphasize its central role in visual transduction and to distinguish it from the G-protein involved in a similar cascade of events leading to hormonal activation of adenylate cyclase, e.g. by epinephrine and glucagon.
6. Kühn *et al.* (1981) described two light-scattering signals in rod outer segment membranes or in a reconstituted system made of purified GTP-binding protein (transducin) and washed disk membranes. Both depended on G-protein. The binding signal occurred in the absence of GTP as an increased turbidity, and was due to binding to photoactivated rhodopsin in a 1:1 molecular ratio. A dissociation signal of the opposite character occurred in the presence of GTP, which was equivalent to the dissociation of the Transducin-R* complex after the GTP–GDP exchange. Thus the binding signal is the binding of GDP to the R*-Transducin complex, R* having a high affinity for the dark-adapted GDP-binding form of the transducin. This signal remains stable for many minutes in the absence of GTP; with GTP added, a rapid exchange with the GDP on the complex occurs, and then dissociation of the complex leading to the new scattering signal.
7. Aequorin, extracted from the chemiluminescent hydromedusa, *Aequoria*, is stimulated to emit flashes of light by Ca^{2+}, and may be used as an assay for this ion. McNaughton *et al.* (1986) deduced an internal concentration of free Ca^{2+} in salamander rods of about 0.5 μM, the limit of sensitivity of the technique. A bright flash reduced this with a time-constant of 0.5 sec. McNaughton *et al.* confirmed Yau & Nakatani's hypothesis concerning the decline of internal Ca^{2+} after a flash, showing that it correlated with the integrated pumping current in the Na^+–Ca^{2+} exchange.
8. If the dark current is increased by lowering the external Ca^{2+}-concentration, the duration of the light response is not increased (Hodgkin *et al.*, 1985), as we should expect, as now the dark-current cannot be carried by Ca^{2+}. Again, an elevated external Ca^{2+}, which undoubtedly raises internal concentration, prolongs the light-response (Hodgkin *et al.*, 1985).
9. We have seen that the response to light in the invertebrate photoreceptor is a depolarization, so that conductance channels may be said to open. A rise in cytoplasmic Ca^{2+} has been implicated in the effects of light (Lisman & Brown, 1972; Brown & Blinks, 1974; Brown *et al.*, 1977), and a 'second messenger' has been proposed to act as a link between photoisomerization of pigment and release of Ca^{2+} from stores (Lisman & Strong, 1979). The possibility that activation of adenylate cyclase is involved has been examined with minute care by Brown *et al.* (1984) in the ventral eye of *Limulus*. The retina contains adenylate cyclase, but all the evidence pointed against an involvement in the excitation mechanism of this eye.

References

Bader, C. R., Macleish, P. R. & Schwartz, E. A. (1979) A voltage-clamp study of the light response in solitary rods of the tiger salamander. *J. Physiol.* **296**, 1–26.

Barlow, H. B., Fitzhugh, R. & Kuffler, S. W. (1957) Change of organization of the receptive fields of the cat's retina during dark adaptation. *J. Physiol.* **137**, 338–354.

Bastian, B. L. & Fain, G. L. (1979) Light adaptation in toad rods: requirement for an internal messenger which is not calcium. *J. Physiol.* **297**, 493–520.

Bastian, B. L. & Fain, G. L. (1982) The effect of low calcium and background light on the sensitivity of toad rods. *J. Physiol.* **330**, 307–328.

Baylor, D. A. & Fuortes, M. G. F. (1970) Electrical responses of single cones in the retina of the turtle. *J. Physiol.* **207**, 77–92.

Baylor, D. A., Hodgkin, A. L. & Lamb, T. D. (1974) The electrical response of turtle cones to flashes and steps of light. *J. Physiol.* **242**, 685–727.

Baylor, D. A., Lamb, T. D. & Yau, K.-W. (1979a) The membrane current of single rod outer segments. *J. Physiol.* **288**, 589–612.

Baylor, D. A., Lamb, T. D. & Yau, K.-W. (1979b) Responses of retinal rods to single photons. *J. Physiol.* **288**, 613–634.

Baylor, D. A., Matthews, G. & Yau, K.-W. (1980) Two components of electrical dark noise in toad retinal rod outer segments. *J. Physiol.* **309**, 591–621.

Baylor, D. A. & Nunn, B. J. (1986) Electrical properties of the light-sensitive conductance of rods of the salamander *Ambystoma tigrinum*. *J. Physiol.* **371**, 115–145.

Baylor, D. A., Nunn, B. J. & Schnapf, J. L. (1984) The photocurrent, noise and spectral sensitivity of rods of the monkey *Macaca fascicularis*. *J. Physiol.* **357**, 575–607.

Behrens, M. E. & Wulff, V. J. (1965) Light-initiated responses of retinula and eccentric cells in the *Limulus* lateral eye. *J. Gen. Physiol.* **48**, 1081–1093.

Bennett, N., Michel-Villaz, M. & Kuhn, H. (1982) Light-induced interaction between rhodopsin and the GTP-binding protein. Metarhodopsin II is the major photoproduct involved. *Eur. J. Biochem.* **127**, 97–103.

Bignetti, E., Cavaggioni, A. & Sorbi, R. T. (1978) Light-activated hydrolysis of GTP and cyclic GMP in the rod outer segments. *J. Physiol.* **279**, 55–69.

Bodoia, R. D. & Detwiler, P. B. (1984) Patch-clamp recordings of the light-sensitive dark noise in retinal rods from lizard and frog. *J. Physiol.* **367**, 183–216.

Bortoff, A. & Norton, A. L. (1967) An electrical model of the vertebrate photoreceptor cell. *Vision Res.* **7**, 253–262.

Bowmaker, J. K. & Dartnall, H. J. A. (1980) Visual pigments of rods and cones in a human retina. *J. Physiol.* **298**, 501–511.

Bowmaker, J. K., Dartnall, H. J. A., Lythgoe, J. N. & Mollon, J. D. (1978) The visual pigments of rods and cones in the rhesus monkey, *Macaca mulatta*. *J. Physiol.* **274**, 329–348.

Bowmaker, J. K., Dartnall, H. J. A. & Mollon, J. D. (1980) Microspectrophotometric demonstration of four classes of photoreceptor in an old world primate *Macaca fascicularis*. *J. Physiol.* **298**, 131–143.

Brown, J. E. & Blinks, J. R. (1974) Changes in intracellular free calcium during illumination of invertebrate photoreceptors: detection with aequorin. *J. Gen. Physiol.* **64**, 643–665.

Brown, J. E., Brown, P. K. & Pinto, L. H. (1977) Detection of light-induced changes of intracellular ionized calcium concentration in *Limulus* ventral photoreceptors using arsenazo III. *J. Physiol.* **267**, 299–320.

Brown, J. E., Coles, J. A. & Pinto, L. H. (1977) Effects of injections of calcium and EGTA into the outer segments of retinal rods of *Bufo marinus*. *J. Physiol.* **269**, 707–722.

Brown, J. E., Kaupp, V. B. & Malbon, C. C. (1984) 3′-5′-cyclic adenosine monophosphate and adenylate cyclase in phototransduction by *Limulus* photoreceptors. *J. Physiol.* **353**, 523–539.

Brown, J. E. & Pinto, L. H. (1974) Ionic mechanisms of the photoreceptor potential of the retina of *Bufo marinus*. *J. Physiol.* **236**, 575–591.

Capovilla, M., Cervetto, L. & Torre, V. (1983) The effect of phosphodiesterase inhibitors on the electrical activity of toad rods. *J. Physiol.* **343**, 277–294.

Caretta, A. & Cavaggioni, A. (1983) Fast ionic flux activated by cyclic GMP in the membrane of the cattle rod outer segments. *Eur. J. Biochem.* **132**, 1–8.

Caretta, A., Cavaggioni, A. & Sorbi, R. T. (1979) Cyclic GMP and the permeability of the discs of the frog photoreceptors. *J. Physiol.* **295**, 171–178.

Cervetto, L., Pasino, E. & Torre, V. (1977) Electrical responses of rods in the retina of *Bufo marinus*. *J. Physiol.* **267**, 17–51.

Clack, J. W., Oakley, B. & Stein, P. J. (1983) Injection of GTP-binding protein or cyclic GMP phosphodiesterase hyperpolarizes retinal rods. *Nature* **305**, 50–53.

Cobbs, W. H. & Pugh, E. N. (1985) Cyclic GMP can increase rod outer-segment light-sensitive current 10-fold without delay of excitation. *Nature* **313**, 585–587.

Cote, R. H., Biernbaum, M. S., Nicol, G. D. & Bownds, M. D. (1984) Light-induced decreases in cGMP concentration precede changes in membrane permeability in frog rod photoreceptors, *J. Biol. Chem.* **259**, 9635–9641.

Crawford, B. H. (1949) The scotopic visibility function. *Proc. Phys. Soc. B* **62**, 321–334.

Detwiler, P. B., Hodgkin, A. L. & McNaughton, P. A. (1980) Temporal and spatial characteristics of the voltage response of rods in the retina of the snapping turtle. *J. Physiol.* **300**, 213–250.

DeValois, R. L., Morgan, H. C., Polson, M. C., Mead, W. R. & Hull, E. M. (1974) Psychophysical studies of monkey vision. I. Macaque luminosity and color vision tests. *Vision Res.* **14**, 53–67.

Dixon, R. A. F. *et al.* (1986) Cloning of the gene and a DNA for mammalian β-adrenergic receptor and homology with rhodopsin. *Nature* **321**, 75–79.

Dowling, J. E. & Werblin, F. S. (1969) Organization of the retina of the mudpuppy, *Necturus maculosus*. I. Synaptic structure. *J. Neurophysiol.* **32**, 315–335.

Emeis, D., Kuhn, H., Reichert, J. & Hofmann, K. P. (1982) Complex formation between metarhodopsin II and GTP-binding protein in bovine photoreceptor membranes leads to a shift of the photoproduct equilibrium. *FEBS Letters* **143**, 29–34.

Enroth-Cugell, C. & Robson, J. G. (1984) Functional characteristics and diversity of cat retinal ganglion cells. *Invest. Ophthal.* **25**, 250–267.

Farber, D. B. & Lolley, R. N. (1977) Light-induced reduction in cyclic GMP of retinal photoreceptor cells *in vivo*: abnormalities in the degenerative diseases of RCS rats and *rd* mice. *J. Neurochem.* **28**, 1089–1095.

Fesenko, E. E., Kolesnikov, S. S. & Lyubarsky, A. L. (1985) Induction by cyclic GMP of cationic conductance in plasma membrane of retinal rod outer segment. *Nature* **313**, 31–313.

Frank, R. N. & Goldsmith, T. H. (1967) Effects of cardiac glycosides on electrical activity in the isolated retina of the frog. *J. Gen. Physiol.* **50**, 1585–1606.

Fung, B. K.-K., Hurley, J. B. & Stryer, L. (1981) Flow of information in the light-triggered cyclic nucleotide cascade of vision. *Proc. Nat. Acad. Sci.* **78**, 152–156.

Fung, B. K.-F. & Stryer, L. (1980) Photolyzed rhodopsin catalyzes the exchange of GTP for bound GDP in retinal rod outer segments. *Proc. Nat. Acad. Sci.* **77**, 2500–2504.

Fuortes, M. G. F. (1959) Initiation of impulses in visual cells of *Limulus*. *J. Physiol.* **148**, 14–28.

Fuortes, M. G. F. & Hodgkin, A. L. (1964) Changes in time scale and sensitivity in the ommatidium of *Limulus*. *J. Physiol.* **172**, 239–263.

Goldberg, N. D., Ames, A., Gander, J. E. & Walseth, T. F. (1983) Magnitude of increase in retinal cGMP metabolic flux determined by ^{13}O incorporation into nucleotide α-phosphoryl compounds with intensity of photic stimulation. *J. Biol. Chem.* **258**, 9213–9219.

Gold, G. H. & Korenbrot, J. I. (1980) Light-induced calcium release by intact retinal rods. *Proc. Nat. Acad. Sci.* **77**, 5557–5561.

Granit, R. (1947) *Receptors and Sensory Perception.* Newhaven: Yale University Press.

Granit, R. (1955) *Receptors and Sensory Perception.* New Haven: Yale University Press.

Gray, P. & Attwell, D. (1985) Kinetics of light-sensitive channels in vertebrate photoreceptors. *Proc. Roy. Soc. B* **223**, 379–388.

Greenblatt, R. E. (1983) Adapting lights and lowered extracellular free calcium desensitize toad photoreceptors by differing mechanisms. *J. Physiol.* **336**, 579–605.

Hagins, W. A., Penn, R. D. & Yoshikami, S. (1970) Dark current and photocurrent in retinal rods. *Biophys. J.* **10**, 380–412.

Hagins, W. A. & Yoshikami, S. (1977) In *Vertebrate Photoreceptors*. Ed. Barlow, H. B. & Fatt, P. Academic Press, London. (Quoted by Matthews *et al.*, 1985.)

Hartline, H. K. (1940) The nerve messages in the fibres of the visual pathway. *J. Opt. Soc. Amer.* **30**, 239–247.

Hartline, H. K. (1941/2) The neutral mechanisms of vision. *Harvey Lectures, Ser.* **37**, 39–68.

Haynes, L. & Yau, K.-W. (1985) Cyclic GMP sensitive conductance in outer segment membrane of catfish cones. *Nature* **317**, 61–64.

Hemilä, S. & Reuter, T. (1981) Longitudinal spread of adaptation in the rods of the frog's retina. *J. Physiol.* **310**, 501–528.

Hodgkin, A. L., McNaughton, P. A. & Nunn, B. J. (1985) The ionic selectivity and calcium dependence of the light-sensitive pathway in toad rods. *J. Physiol.* **358**, 447–468.

Katz, B. & Miledi, R. (1972) The statistical nature of the acetylcholine potential and its molecular components. *J. Physiol.* **224**, 665–699.

Kawamura, S. & Bownds, M. D. (1981) Light adaptation of the cyclic GMP phosphodiesterase of frog photoreceptor membranes mediated by ATP and calcium ions. *J. Gen. Physiol.* **77**, 571–591.

Korenbrot, J. I., Brown, D. T. & Cone, R. A. (1973) Membrane characteristics and osmotic behaviour of isolated rod outer segments. *J. Cell Biol.* **56**, 389–398.

Korenbrot, J. I. & Cone, R. A. (1972) Dark ionic flux and the effects of light in isolated rod outer segments. *J. Gen. Physiol.* **60**, 20–45.

Kuffler, S. W. (1953) Discharge patterns and functional organization of mammalian retina. *J. Neurophysiol.* **16**, 37–68.

Kühn, H. (1978) Light-regulated binding of rhodopsin kinase and other proteins to cattle photoreceptor membranes. *Biochemistry* **17**, 4389–4395.

Kühn, H. (1980) Light- and GTP-regulated interaction of GTPase and other proteins with bovine photoreceptor membranes. *Nature* **283**, 588–590.

Kühn, H., Bennett, N., Michet-Villaz, M. & Chabre, M. (1981) Interactions between photoexcited rhodopsin and GTP-binding protein: kinetic and stoichiometric analyses from light-scattering changes. *Proc. Nat. Acad. Sci.* **78**, 6873–6877.

Lamb, T. D., McNaughton, P. A. & Yau, K. W. (1981) Spatial spread of activation and background desensitization in toad rod outer segments. *J. Physiol.* **319**, 463–496.

Liebman, P. A. & Pugh, E. N. (1980) ATP mediates rapid reversal of cyclic GMP phosphodiesterase activation in visual receptor membranes. *Nature* **287**, 734–736.

Lipton, S. A., Ostroy, S. E. & Dowling, J. E. (1977) Electrical and adaptive properties of rod photoreceptors in *Bufo marinus*. *J. Gen. Physiol.* **70**, 747–770.

Lisman, J. E. & Brown, J. E. (1972) The effects of intracellular iontophoretic injection of sodium and calcium ions on the light response of *Limulus* ventral photoreceptors. *J. Gen. Physiol.* **59**, 701–719.

Lisman, J. E. & Strong, J. A. (1979) The initiation of excitation and light adaptation in *Limulus* ventral photoreceptors. *J. Gen. Physiol.* **73**, 219–243.

Lolley, R. N. & Racz, E. (1982) Calcium modulation of cyclic GMP synthesis in rat visual cells. *Vision Res.* **22**, 1481–1486.

MacLeish, P. R. M. Schwartz, E. A. & Tachibana, M. (1984) Control of the generator current in solitary rods of *Ambystoma tigrinum* retina. *J. Physiol.* **348**, 645–664.

Matthews, G. & Watanabe, S.-I. (1987) Properties of ion channels closed by light and opened by guanosine 3′-5′-cyclic monophosphate in toad retinal rods. *J. Physiol.* **389**, 691–715.

Matthews, H. R., Torre, V. & Lamb, T. D. (1985) Effects on the photoresponse of calcium buffers and cyclic GMP incorporated into the cytoplasm of retinal rods. *Nature* **313**, 582–585.

McDowell, J. H. & Kühn, H. (1977) Light induced phosphorylation of rhodopsin in cattle photoreceptor membranes: substrate activation and inactivation. *Biochemistry* **16**, 4054–4060.

McNaughton, P. A., Cervetto, L. & Nunn, B. J. (1986) Measurement of the intracellular free calcium concentration in salamander rods. *Nature* **322**, 261–263.

Meyertholen, E. P., Wilson, M. J. & Ostroy, S. E. (1986) The effects of HEPS, bicarbonate and calcium on the GMP content of vertebrate rod photoreceptors and the isolated electrophysiologic effects and calcium. *Vision Res.* **26**, 521–533.

Naka, K. I. & Rushton, W. A. H. (1966) S-potentials from colour units in the retina of the fish (*Cypridinae*). *J. Physiol.* **185**, 536–555.

Penn, R. D. & Hagins, W. A. (1969) Signal transmission along vertebrate rods and the origin of the electroretinographic *a*-wave. *Nature* **233**, 201–205.

Pugh, E. N. & Cobbs, W. H. (1986) Visual transduction in vertebrate rods and cones: a tale of two transmitters, calcium and cyclic GMP. *Vision Res.* **26**, 1613–1649.

Schwartz, E. A. (1973) Organization of ON-OFF cells in the retina of the turtle. *J. Physiol.* **230**, 1–14.

Schwartz, E. A. (1974) Responses of bipolar cells in the retina of the turtle. *J. Physiol.* **236**, 211–224.

Schwartz, E. A. (1975a) Responses of single rods in the turtle. *J. Physiol.* **232**, 503–514.

Schwartz, E. A. (1975b) Rod-rod interaction in the retina of the turtle. *J. Physiol.* **246**, 617–638.

Schwartz, E. A. (1975c) Cones excite rods in the retina of the turtle. *J. Physiol.* **246**, 639–651.

Schwartz, E. A. (1976) Electrical properties of the rod syncytium in the retina of the turtle. *J. Physiol.* **257**, 379–406.

Schwartz, E. A. (1985) Phototransduction in vertebrate rods. *Ann. Rev. Neurosci.* **8**, 339–367.

Sitaramayya, A. & Liebman, P. A. (1983a) Mechanism of ATP quench of phosphodiesterase activation in rod disc membranes. *J. Biol. Chem.* **258**, 1205–1209.

Sitaramayya, A. & Liebman, P. A. (1983b) Phosphorylation of rhodopsin and quenching of cyclic GMP phosphodiesterase activation by ATP at weak bleaches. *J. Biol. Chem.* **258**, 12106–12109.

Smith, T. G., Baumann, F. & Fuortes, M. G. F. (1965) Electrical connexions between visual cells in the ommatidium of *Limulus*. *Science* **147**, 1446–1447.

Stryer, L. (1986) Cyclic GMP cascade in vision. *Annu. Rev. Neurosci.* **9**, 87–119.

Stryer, L., Hurley, J. B. & Fung, B. K.-K. (1981) Transducin: an amplifier protein in vision. *Trends Biochem. Sci.* **6**, 245–247.

Tomita, T., Kikuchi, R. & Tanaka, I. (1960) Excitation and inhibition in lateral eye of horseshoe crab. In *Electrical Activity of Single Cells*, Ed. Y. Katsuki, pp. 11–23. Tokyo: I. Shoin.

Torre, V., Matthews, H. R. & Lamb, T. D. (1986) Role of calcium in regulating the cyclic GMP cascade of phototransduction in retinal rods. *Proc. Nat. Acad. Sci.* **83**, 7109–7113.

Toyoda, J., Nosaki, H. & Tomita, T. (1969) Light-induced resistance changes in single receptors of *Necturus* and *Gecko*. *Vision Res* **9**, 453–463.

Wald, G. (1968) The molecular basis of visual excitation. *Nature* **219**, 800–807.

Werblin, F. S. & Dowling, J. E. (1969) Organization of the retina of the mudpuppy, *Necturus maculosus*. II. Intracellular recording. *J. Neurophysiol.* **32**, 339–354.

Woodruff, M. I. & Bownds, M. D. (1979) Amplitude, kinetics, and reversibility of a light-induced decrease in guanosine 3′,5′-

cyclic monophosphate in frog photoreceptor membranes. *J. Gen. Physiol.* **73**, 629–653.

Yau, K. W. & Nakatani, K. (1984) Electrogenic Na–Ca exchange in retinal rod outer segment. *Nature* **311**, 661–663.

Yau, K. W. & Nakatani, K. (1985a) Light-induced reduction of cytoplasmic free calcium in retinal rod outer segment. *Nature* **313**, 579–582.

Yau, K. W. & Nakatani, K. (1985b) Light-suppressible, cyclic GMP-sensitive conductance in the plasma membrane of a truncated rod outer segment. *Nature* **317**, 252–255.

Yee, R. & Liebman, P. A. (1978) Light-activated phosphodiesterase of the rod outer segment. *J. Biol. Chem.* **253**, 8902–8909.

Yoshikama, S. & Hagins, W. A. (1973) Control of the dark current in vertebrate rods and cones. In *Biochemistry and Physiology of the Visual Pigments*, Ed. H. Langer, pp. 245–255. Berlin: Springer.

Zimmerman, A. L. & Baylor, D. A. (1986) Cyclic GMP-sensitive conductance of retinal rods consists of aqueous pores. *Nature* **321**, 70–72.

Zuckerman, R., Buzdygon, B., Philp, N., Liebman, P. & Sitaramayya, A. (1985) Arrestin: an ATP/ADP exchange protein that regulates cGMP phosphodiesterase activity in retinal rod disk membranes (RDM). *Biophys. J.* **47**, 37a.

Zuckerman, R., Schmidt, G. J. & Dacko, S. M. (1983) Rhodopsin-to-metarhodopsin II transition triggers amplified changes in cytosol ATP and ADP in intact retinal rod outer segments. *Proc. Nat. Acad. Sci.* **79**, 6414–6418.

11. ELECTROPHYSIOLOGY OF THE RETINA: FURTHER STUDIES ON COLD-BLOODED RETINA

Because of their larger size the cells of the lower vertebrate retinae have been examined preferentially in the classical studies on intracellularly recorded responses. We may therefore continue with this study by considering further features.

Coupling of Receptors

Stimulation of turtle cones adjacent to that from which records are taken produces responses in this (unstimulated) cone; this spread of effect has a double cause, namely a direct coupling between adjacent cones, through gap-type junctions that permit an electrical change induced in one to be transmitted rapidly to another, and secondly to the cone's synaptic relations with horizontal cells.

The direct cone-cone interaction is demonstrated by passing current into one cone and recording a corresponding, if attenuated, change in nearby cones (Baylor *et al.*, 1971); this interaction extends to a radius of about 50 μm and is probably mediated through lateral processes that extend from one cone pedicle to another, since these have a maximum length of this order (Lasansky, 1971). If a small-radius spot is moved from a central position over an impaled cone, the intensity of the response falls off to each side defining a receptive field which itself defines the extent of the cone-cone interaction (Fig. 11.1), since a small spot-stimulus is unable to exert an appreciable effect on the horizontal cells.

Morphological Basis of Coupling

The physiological studies on inter-receptor coupling suggest that it is electrical through cell-to-cell junctions that permit passage of current from one to another; morphologically these junctions have been characterized—e.g. in epithelia—as gap-junctions and, as such, they have a characteristic appearance in freeze-fractured specimens. Fain (1975a) demonstrated a very powerful interaction between rods of the toad such that a rod could be excited by light that failed to fall on it. The points of contact responsible for this coupling are probably located on the 'fins' or radial processes of the rods, which come into close relations with fins of other receptors. In the electron-microscope rod–rod junctions at these fins are large to give a total area of as much as 1 μm^2 and by freeze-fracture they were shown to have the appearance of characteristic gap-junctions (Fain *et al.*, 1975). These large areas of contact were peculiar to those between red-rods; much smaller points of contact were seen between adjacent rods and cones, and between red and green rods; these apparently do not contribute significantly to mixing of signals from different types of receptor since the spectral sensitivity of red rods

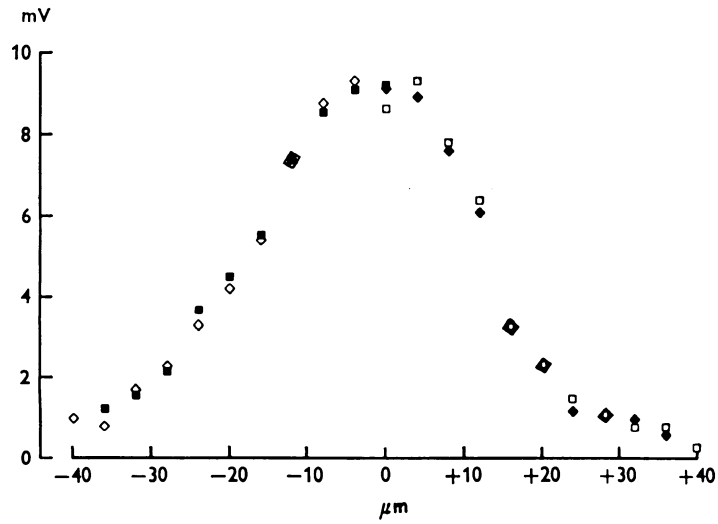

Fig. 11.1 The receptive field of a cone. The peak amplitude of the response is plotted against distance from axis of stimulation light. A flash covering a circle of 4 μm radius was centred on the receptor. The intensity of the flash was adjusted to give a response of about half maximum amplitude. The spot was then moved away from the centre (□ ◇) and then back toward the centre (◆ ■) in 4 μm steps. In this experiment, the retina was quite transparent (decreasing scatter) and at 40 μm from the centre the responses were quite small. (Baylor *et al.*, *J. Physiol.*)

corresponded remarkably closely with that of the toad's rhodopsin, whereas if there had been intermixture with green rods or cones there would have been significant deviations.

In the turtle retina, the cone pedicles have basal processes that may extend laterally as far as 40 nm; these processes end in dyad-structures of other cone pedicles and may well constitute the basis for electrotonic coupling (Lasansky, 1971).

Significance of Coupling

Coupling of receptors, so that they have lost their independence as single units, militates against spatial discrimination (p. 374) although it increases sensitivity to large fields by permitting summation. According to Lamb & Simon (1977), the 'noise' of a single cone, i.e. the spontaneous changes in potential taking place without measurable change in the stimulus conditions, is decreased by exposing the retina to light, a surprising result since one might expect random fluctuations in the number of quanta falling on the retina to introduce more rather than less noise. Lamb & Simon showed that there was a good correlation between the noise, or intrinsic voltage variance, and the tightness of coupling between cones, measured by the so-called space-constant, λ, of a given cone. Thus when a slit of light is moved laterally from its initial position covering the cone there is a falling off in the response. If the cone were not coupled to adjacent cones there would be a very steep falling off as the slit passed off the surface of the cone, a falling off governed entirely by the spread of scattered light to the cone. In fact, the falling off may be quite gentle, due to the coupling between cones so that an electrical change induced in cones, lateral to that from which records are taken, is propagated to this by electrotonic spread of current.

SIGNAL-TO-NOISE RATIO

Lamb & Simon considered that an important function of coupling was the improved 'signal-to-noise' ratio; thus for diffuse illumination the signal is independent of λ but the root mean square noise is inversely proportional to λ, implying that the signal-to-noise ratio increases directly as λ. For a very small spot activating only one cone this is not true since the signal now decreases more rapidly with increasing λ than does the square root of the variance.

BIPOLAR CELLS

It must be emphasized that this averaging, which reduces noise, could be performed, and is, by the bipolar cell which receives, in the peripheral retina where these measurements have been made, input from many cones. It has been well established that the dark noise in the bipolar cell is inhibited by light, but in this case its mechanism is the hyperpolarization of the receptor which reduces the release of transmitter. Thus in the dark the depolarized receptor is continually releasing transmitter, and spontaneous variations in this release would be the cause of the noise comparable with the miniature end-plate potential produced by a motor nerve terminal; hyperpolarization, be it of the motor nerve terminal or of the receptor terminal, would decrease the amplitude and frequency of the miniature potentials.

THE RODS AS A SYNCYTIUM

Schwartz (1973) impaled single rods of the turtle, *Chelydra serpentina*; Fig. 11.2 shows the hyperpolarizing responses to increasing intensities of a spot-stimulus of 100 μm diameter. The gain[1] was some four times that of cones under comparable conditions; this seems a small difference when the much greater sensitivity of the dark-adapted eye is considered, and suggests that in some way the rods can interact with each other, either directly, or through horizontal cells. This interaction was revealed by the greater response obtained by a large 1000 μm field than that of a 25 μm spot, in spite of the fact that both stimuli were adjusted to ensure that the same number of quanta fell on the retina. Fields between 200 μm and 800 μm produced no increase with area so that the summation area in this case is about 200 μm. Unlike the situation with turtle cones, where lateral interaction is probably mediated by horizontal cells, which are certainly activated, the rod interaction was probably mediated by direct rod-rod connections; and a more elaborate study (Schwartz, 1974; 1976) confirmed this, the treatment of the retina with cobalt, which abolishes synaptic activity, being without effect on the response to a large spot of light.

RESOLUTION

The coupling between receptors obviously militates against spatial resolution, since the resolution depends on

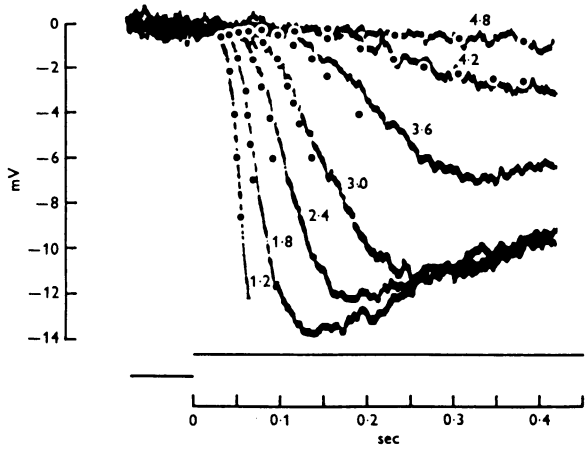

Fig. 11.2 Responses of turtle rods to steps of light of increasing intensity as indicated on the records. The filled circles represent theoretical values calculated on the basis of a model. (Schwartz, *J. Physiol.*)

the ability of the receptor to transmit its message independently of responses in its neighbours (p. 374). Thus this coupling of the rods into a syncytium, extending perhaps over the whole retina, might be expected to destroy resolution; however, Schwartz (1976) calculates that, because of the decay of the potential transmitted laterally to adjacent rods, the effects of a light-stimulus on one rod will be reduced to about 10% at a distance of 20 μm; moreover, the scattering of light within the retina causes considerable spread of the stimulus to adjacent receptors, so that even if the receptors were not electrically coupled they would be affected by a light-stimulus designed to stimulate a single rod; as Fig. 11.3 shows, the spread of the light-stimulus through scatter is comparable in magnitude to the spread of the electrical response of a single receptor through the syncytium.

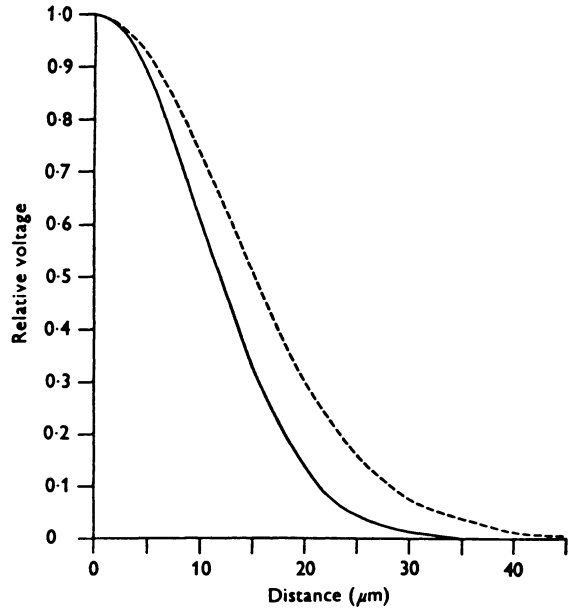

Fig. 11.3 Showing that the scattering of light from a spot source would produce a falling off in response with distance comparable with that predicted with no light-scatter but electrotonic spread through a system of coupled receptors. Ordinate: potential as a fraction of the potential at the site of illumination; abscissa, distance in μm. The continuous line is the result predicted if the rods were not coupled; the dashed line is the result predicted if the rods are coupled. (Schwartz, *J. Physiol.*)

ROD-CONE INTERACTION

The studies on the rods described above were made using a dim green light, calculated to activate rods with a porphyropsin photopigment maximally; when different wavelengths of light were compared, the typical action-spectrum for porphyropsin was obtained provided small spots of light were employed; with large spots there was an increased sensitivity to long wavelengths suggesting that cones were producing an effect (Schwartz, 1975c). This effect could be mediated by horizontal cells but a direct examination of responses in these made this unlikely, and it was suggested that the rod-cone interaction might be direct.

CONE-CONE INTERACTION

This is in marked contrast to the cone-cone interaction, which takes two forms, as illustrated by Fig. 11.4; within a radius of 50 μm they enhance their responses but they also receive a recurrent inhibition from horizontal cells which are electrically coupled so that their receptive fields are very large. The fact that it is the red-sensitive cones that are linked to the rods means that the sensitivity of the retina to red light at dim illuminations is enhanced.

INTERCONNECTION OF RODS

Copenhagen & Owen (1976), also working on the snapping turtle, have examined the summative effects between adjacent rods in considerable detail. They too have ruled out a feedback from horizontal cells. As Fig. 11.5 shows, the amplitude of the response to a flash increased with the size up to a maximum of some 300 μm diameter, and they computed that, when the whole retina was illuminated, the rod's response was only 4% due to absorption of light

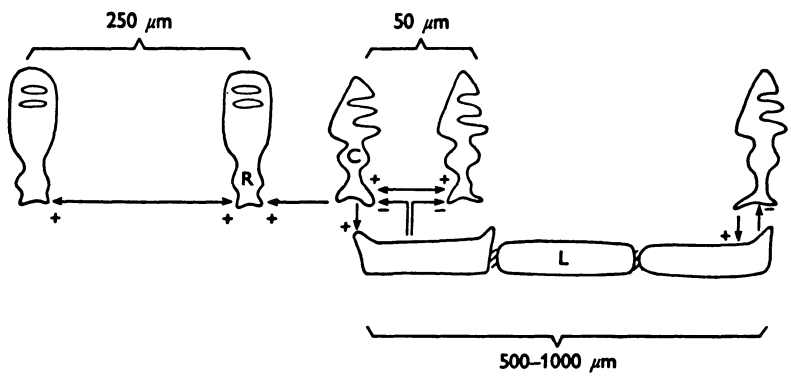

Fig. 11.4 Diagram of the synaptic interactions between rods, R; red-sensitive cones, C; and luminosity horizontal cells, L. + indicates that the pathway preserves the polarity of the presynaptic voltage change; − indicates that it is reversed. The interaction between cones and rods may not be direct but may involve an interneurone.

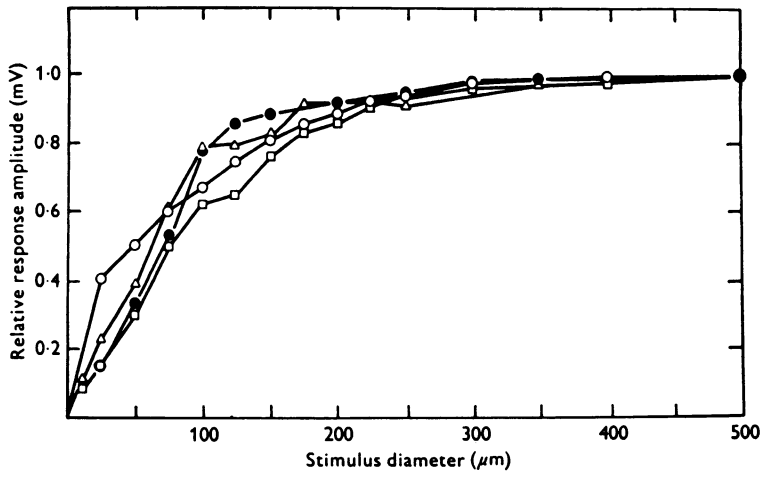

Fig. 11.5 The relative variation in peak amplitude of the rod response as a function of stimulus diameter. Stimuli were flashes of white light, 200 msec in duration, at an intensity approximately 3 log units below saturation. For each of four rods, results are plotted as fractions of the amplitude of the response elicited by the stimulus 500 μm in diameter. (Copenhagen & Owen, *J. Physiol.*)

by itself, the remainder being the result of summative interaction with a total of some 200 rods. In consequence, a rod should, and does, hyperpolarize in response to light absorbed by neighbouring rods even though it fails to absorb light itself. Copenhagen & Owen (1976) have suggested that the interaction is brought about by synaptic connexions through long basal processes extending from the synaptic terminals in the rod spherule, contacting other rods through swellings that might well contain synaptic vesicles, or else the contact points could be gap-junctions mediating an electrical coupling.

The Horizontal Cell[2]

Feedback on Cones

Before discussing the responses of bipolar cells it would be profitable to review some of the properties of horizontal cells. The normal response of a horizontal cell to light falling on the receptors is one of hyperpolarization, and this hyperpolarization *feeds back* on the receptors. Thus when Baylor *et al.* (1971) hyperpolarized a horizontal cell by the injection of current, they found that an impaled cone would exhibit depolarization, indicating an inhibitory action, or negative feedback. Similarly, if the response of a cone to a flash of light was measured, this was depressed by hyperpolarization of the horizontal cell. This horizontal cell-cone interaction extends over wide areas of the retina owing to the junctions between horizontal cells and is of opposite sign to that of direct cone-cone interaction. Thus, if a small spot of light is flashed on to the retina, there is the hyperpolarizing response of the cone, whilst an impaled horizontal cell produces little or no response (Fig. 11.6); as the size of the spot increases the hyperpolarizing response in the cone increases—enhancement—up to about a radius of 70 μm; when the radius of the spot is increased further, there is an

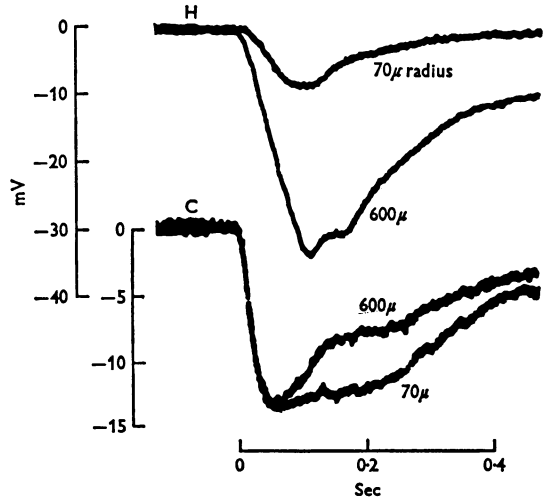

Fig. 11.6 Simultaneous records from a cone (C) and a horizontal cell (H). Superimposed records of responses to stimuli covering different areas. A flash (delivered at a time 0) covering a circle of 70 μm radius produced a small response of the horizontal cell and a large, smooth response of the cone. A second flash of the same intensity but covering a circle of 600 μm radius was then given. The response of the horizontal cell was increased. The response of the cone was the same in its initial phase and peak. Later, however, it developed a depolarizing inflexion. (Baylor *et al.*, *J. Physiol.*)

increased response in the horizontal cell, whilst the hyperpolarizing response in the cone shows a depolarizing deflexion indicating a depolarizing feedback on the cone.

Response of Cone

Thus the response to a large circle of light is complex, and can be described as the '*direct response*' of the cone, an

enhancement due to coupling of cones with each other,[3] and a *negative feedback* due to a depolarizing action of the horizontal cells, this last effect extending over a large radius owing to the electrical coupling of the horizontal cells (Fuortes *et al.*, 1973).

Bipolar Surround

We have seen (p. 285) that the bipolar cell of the mudpuppy exhibits a centre-surround antagonism, like the ganglion cell; and it is likely that the horizontal cell is involved in the activity of the surround, exerting an opposite effect on a group of receptors to that of the light-stimulus falling on these. If it is appreciated that the dendritic field of a bipolar cell rarely exceeds 100 μm, and that bipolar responses can be affected by light falling on the retina at far greater distances, it is clear that we must invoke the horizontal cell to explain these centre-surround interactions.

S-potentials

Historically the horizontal cell is of interest since it was the first cell to be punctured in intracellular recording from the retina (Svaetichin, 1956), and at the time the hyperpolarizing and depolarizing potentials recorded from them were considered to be the responses of receptors. They have been called S-potentials and their main interest at the time was their colour-coding in the sense that some, the C- or chromatic cells, responded with depolarization with one wavelength of light and hyperpolarization with another—opponent-wavelength. Other cells, the L- or luminosity cells, responded in the same way to all wavelengths.

Location

The horizontal cells of the fish and turtle retina occupy a very prominent part of the inner nuclear layer and may constitute as much as two-thirds of the whole; they are organized in layers probably in accordance with function; thus in the goldfish the external layer makes exclusive connexions with cones and the intermediate layer with rod spherules, whilst the internal layer apparently has no distally directed dendrites. In some higher vertebrates horizontal cells receive input from both rods and cones.

Syncytial Behaviour

The striking feature of the horizontal cells of the fish, demonstrated by Naka & Rushton (1966), was their behaviour as a syncytium, they behaved in effect electrically as if they were equivalent to a laminar conducting medium limited by a pair of high-resistance membranes and the whole was thus described as the S-space, extending over the entire retina. As with the syncytium of receptors, the potential at any distance, x, from an applied potential, V_0, was given by:

$$V = V_0 e^{-x/\lambda}$$

where λ is the space-constant, being some 0.25 mm in the tench and 0.5 to 1.0 mm in the catfish.

Electrical Stimulation of Horizontal Cell

It is reasonable, then, to look for the interpretation of the centre-surround organization of the receptive field of the bipolar cell in the behaviour of the horizontal cells. Thus Naka & Witkowsky (1972) showed that, when they penetrated a dogfish horizontal cell with an electrode and applied an extrinsic current through it, either de- or hyper-polarizing it, a slow potential developed in a bipolar cell penetrated at the same time, and this could be associated with a discharge in a ganglion cell. The response-pattern depended on the type of polarizing current passed through the horizontal cell, so that in effect ON- or OFF-responses in bipolar and ganglion-cells could be obtained.

Synaptic Transmission from Receptors

We may assume that, in the dark, the depolarized receptor is releasing an excitatory or depolarizing transmitter at the receptor-horizontal cell synapse (Trifonov, 1968); light, by hyperpolarizing the receptor reduces the transmitter released and thus hyperpolarizes the horizontal cell, a change associated with an increase in resistance indicating, as with the receptor, a decreased permeability to ions such as Na^+ (Toyoda *et al.*, 1969).

EFFECTS OF COBALT

Synaptic transmission is blocked by Co^{2+}, and Fig. 11.7 shows the effect of this ion on the responses of a horizontal cell to flashes of light before, and during, application to the retina. In records *b* the responses of a *cone* to light are shown; these are not blocked, confirming the synaptic effect of the cobalt. La^{3+} facilitates transmitter release, and this caused a strong depolarization of horizontal cells.

Types of L-cell

Horizontal cells, producing only luminosity responses, apparently fall into two classes in lower vertebrate retinas. Thus Lasansky, on morphological grounds, separates one with an obvious soma and long thin dendritic branches, and the other with broad trunk-like main branches with no definite soma. So far as function goes, Simon (1973) described a Type I identified as that with the trunk-like axons, and giving a hyperpolarizing response increasing with the area of the stimulus up to 833 μm

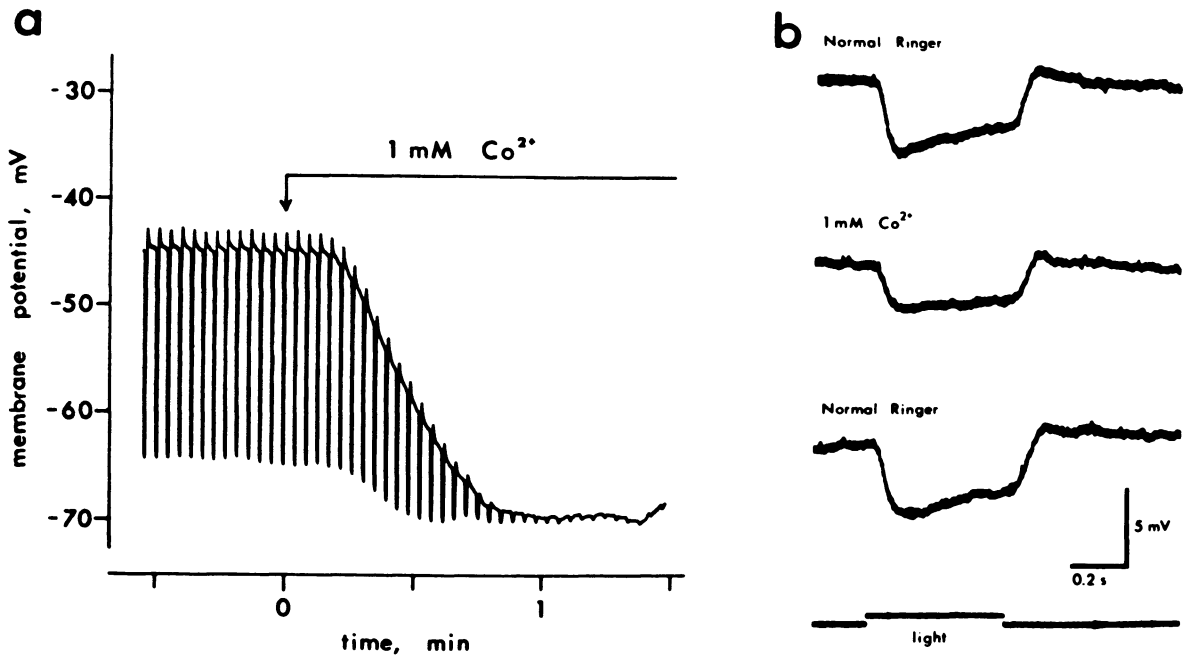

Fig. 11.7 Effect of Co^{2+} on the membrane potential of a cone and a horizontal cell. (*a*) Intracellular recording from a horizontal cell. The perfusing medium was switched, at 0 min, from the standard Ringer to a test solution containing 1 mM Co^{2+}. (*b*) Responses of a red-sensitive cone in normal Ringer (*top*), 2 min after application of Co^{2+} Ringer (*middle*), and 2 min after washing with standard Ringer (*bottom*). Note that horizontal cell responses have already been strongly suppressed 1 min after Co^{2+} application. Red light (620 nm, 3×10^{12} photon/mm^2.s) illuminated the retina diffusely. (Kaneko & Shimazaki, *Cold Spr. Harb Symp. quant. Biol.*)

radius, and a Type II, with a smaller receptive field of 300 μm and corresponding to the cell with soma and thin dendrites. Type I cells were usually coupled, but there was no coupling between Type I and II; he was never able to penetrate two Type II cells and so could not determine whether coupling occurred here. Simon concluded that the morphology of the cell was not the important factor so far as the size of receptive field was concerned, this being governed by the degree of coupling, the Type II cells being presumably poorly coupled and thus not able to operate over large distances. Interestingly, both types had the same action-spectrum with maximal response at about 600 nm, indicating a predominant input from 'red-cones'.

ROD L-CELL

In the carp, Kaneko & Yamada (1972) differentiated L-cells that were obviously related synaptically with rods, their responses appearing in the dark-adapted eye and showing spectral sensitivity corresponding with absorption by the rod pigment, porphyropsin; adaptation with coloured lights failed to influence the shape of the sensitivity curve, indicating the absence of cone input. The penetrated cells were located in the intermediate layer of horizontal cells, and this conforms with the anatomical study of Stell (1967) on the goldfish retina, who found that, whereas the external layer made synaptic contact with cones, the intermediate layer made contacts with rods only. Thus, at the horizontal cell level in these fish, the input from rods is kept separate from that from cones.

TURTLE *GEOCLEMYS*

More recently Ohtsuka (1983) has described the L-type horizontal cell in the turtle (*Geoclemys*) retina. Figure 11.8 illustrates the bipartite nature of the cell as strikingly revealed by horseradish peroxidase injection. The receptive field of the cell body was smaller than that of the axon terminal, confirming the electrical isolation of the two parts, made probable by the length of the thin intervening axon (250 μm). The receptive field diameters exceeded those of the dendritic fields; thus the diameter of the receptive field of a cell body was 1 mm, exceeding the largest receptive field, a difference due to coupling of horizontal cells by gap-junctions.

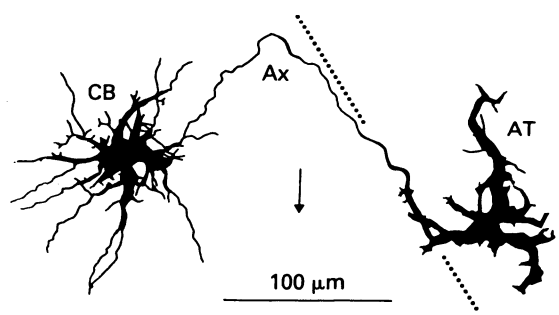

Fig. 11.8 A horseradish peroxide-filled horizontal cell at high magnification. The cell body, CB, and axon terminal, AT, are connected by an axon, Ax. The microelectrode tract (dotted line) indicates that the site of penetration was at a part of the axon terminal. The arrow points towards the location of the optic disk. (Ohtsuka, *J. Comp. Neurol.*)

Leeper & Copenhagen (1979) found apparently two luminosity-type horizontal cells in the turtle, *Pseudomys*, however; L1 was generated by the axon terminal, and was influenced by both red-sensitive cones and rods, whilst L2 was generated by the cell-body, and was influenced by red- and green-sensitive cones. They point out that, in the turtle retina, the axon-terminal is the only horizontal cell-structure contacting rods.[4] Neyton *et al.* (1981) showed that only L2 was involved in feedback to green-sensitive cones.

The Bipolar Cell

Centre-surround Antagonism

The classical study of Werblin & Dowling (1969) showed that the bipolar cells exhibited a centre-surround antagonism, so that a given bipolar cell might respond to a central spot with depolarization and to an annulus with a hyperpolarization—it would be called an ON-centre cell, whilst another bipolar cell might behave in the opposite fashion and be described as an OFF-centre cell, hyperpolarizing in response to a spot and depolarizing in response to an annulus. Figure 11.9 shows the variation in response-amplitude of an impaled goldfish ON-centre cell as a function of spot-size; as the spot-diameter was increased beyond 100 μm there was little change up to 200 μm but beyond this the response declined, indicating the effect of the antagonistic surround, the outer margin of which was of the order of 1 mm. Histological evidence indicated that the size of the centre of the receptive field corresponded with the spread of the bipolar's dendritic tree, whereas the size of the surround obviously exceeds that of any dendritic tree and Kaneko (1973) concluded that horizontal cells were responsible.

In later studies on turtle bipolars by Schwartz (1974) and Richter & Simon (1975), additional features of the bipolar cells' responses have been established. Thus Schwartz showed that the depressant effect of a surround annulus on the response of the centre was associated with a hyperpolarizing response in horizontal cells; moreover he, and Richter & Simon, demonstrated the far greater responses of the bipolar cell to a light stimulus than that in the associated receptors. Thus at an irradiance of about 54 quanta μm^{-2} sec^{-1} the cones produced a response of 1 mV and the bipolar a response greater than 10 mV.

TWO TYPES OF RESPONSE

The bipolar cell quite clearly responds in one of two different manners to a central spot of light, namely by depolarization or hyperpolarization, whilst the surrounding annulus has an opposing influence, reducing the central depolarization or hyperpolarization. We have argued that receptors liberate a depolarizing transmitter in the dark when they are themselves depolarized, so that the onset of light reduces the liberation of transmitter from the receptor and thus causes a hyperpolarizing response in the bipolar cell. How, then, are we to explain the opposite, depolarizing, (or ON-centre) response in the bipolar cell? Either the receptors giving rise to this response liberate a hyperpolarizing transmitter, or all receptors liberate the same transmitter but the post-synaptic membrane of the bipolar cells is different, so that some bipolars are hyperpolarized by the same transmitter that depolarizes others (Fig. 11.10 from Tomita, 1976). We shall see later when considering the actions of transmitters in the mammalian retina, that there is good reason to believe that the photoreceptors liberate only

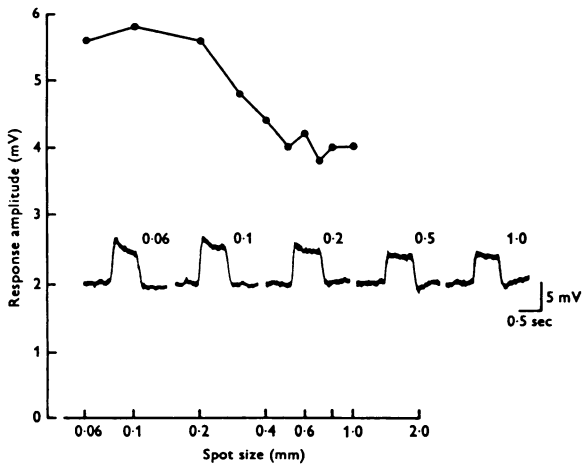

Fig. 11.9 Spatial summation curve of an ON-centre bipolar cell. Response amplitude was measured from the resting level to the peak. Inset: response traces to light spots, sizes of which are indicated in mm on the right upper corner of each trace. D.c. recording, positivity upward. (Kaneko, *J. Physiol.*)

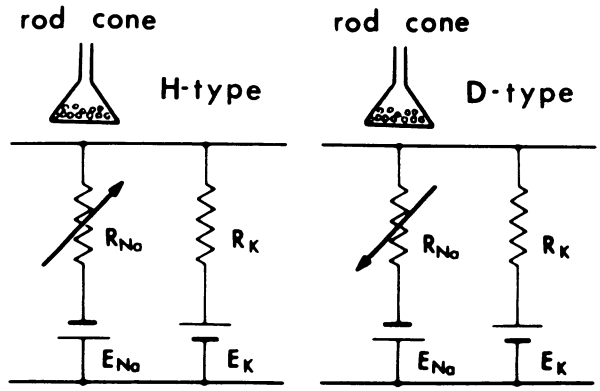

Fig. 11.10 Electrical models of two types of subsynaptic membrane in the ON-centre bipolar cell (left, H-type) and OFF-centre bipolar cell (right, D-type). (Tomita, *Invest. Ophthal.*)

one type of transmitter, so that bipolar cells may depolarize or hyperpolarize in response to this by virtue of different synaptic membrane receptors, using this term in its pharmacological sense.

The Amacrine Cell

Goldfish Retina

Goldfish amacrine cells were classified as transient and sustained types; the transient type always responded with depolarization at both ON and OFF, whereas the sustained type gave a steady hyperpolarization to white light. Only the sustained type showed colour-coding, in the sense that a green stimulus would depolarize the cell and a red stimulus would hyperpolarize (p. 416). When different coloured stimuli were used for the transient type, the responses were qualitatively the same, but of course different wavelengths produced different magnitudes of response in accordance with the efficacy of absorption; the wavelength of maximum sensitivity was 620 nm, suggesting that these amacrine cells received input primarily, if not exclusively, from 'red cones'. In contrast to bipolar cells, there was no centre-surround antagonism. The very large receptive fields encountered, namely 2.5 mm, suggests that there are interconnexions between amacrine cells of similar types (Witkowsky & Dowling, 1969).

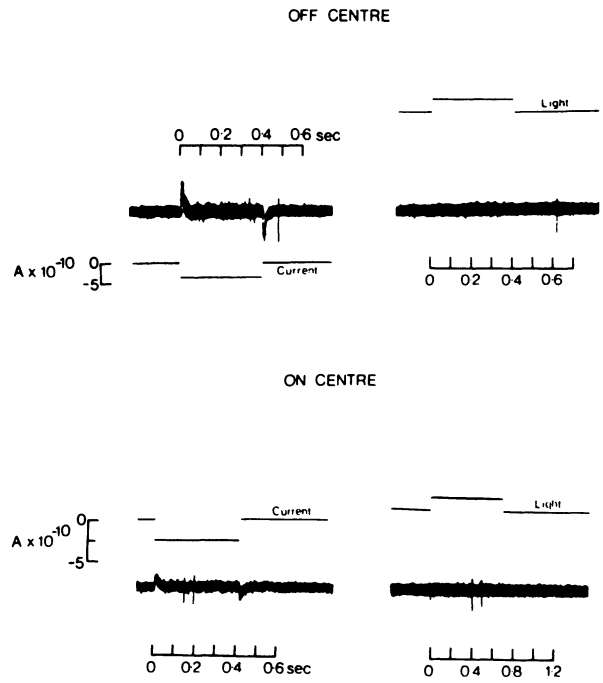

Fig. 11.11 Duplication of the responses of two ganglion cells to light by injection of hyperpolarizing current into red-sensitive cones. The dim, 640 nm, stimulating spot was 60 μm in diameter above and 120 μm in diameter below. (Baylor & Fettiplace, *Cold Spr. Harb. Symp. quant. Biol.*)

CENTRE-SURROUND OF GANGLION CELLS

Both bipolar and amacrine cells feed into ganglion cells, and the similarity in the centres of the receptive fields of ganglion cells and bipolar cells, both with respect to size and chromatic behaviour, leads Kaneko to assume that a bipolar cell feeds directly to the ganglion cell giving it its centre properties, its size being governed by the size of the 'bipolar' cell's dendritic tree. The very large surround of the ganglion cell—up to 5 mm according to Daw (1968)—and the large receptive fields of the amacrine cells, suggest that they are responsible for the surround input—chromatically they behave somewhat similarly.[5]

The Ganglion Cell

Excitation Through Cones

Baylor & Fettiplace (1975b) excited turtle cones electrically and observed the responses in ganglion cells. In this species (*Pseudemys scripta*) the ganglion cells show no spontaneous discharge, and most respond with either a transient discharge at ON or at OFF; the transitoriness of the response is due to the fact that the excitatory synaptic potentials evoked are not maintained during the stimulus. As Fig. 11.11 shows, injection of hyperpolarizing current into a cone could be made to mimic the effects of light; moreover, the response of a ganglion cell to light could be abolished by simultaneous injection of a depolarizing current into a cone, or its effect could be potentiated by injecting a hyperpolarizing current. Of most interest were the time-relations between application of the electrical stimulus to the receptor and the discharge in the ganglion cell; there was a delay of some 75 to 125 msec between switching the current on and the peak probability of obtaining a discharge; the probabilities then fell off rapidly, indicating the absence of any sustained discharge.

MINIMUM STIMULUS

The minimum threshold current in a red-sensitive cone, required to evoke a response in a ganglion cell, was 1.5×10^{-11} amp; this compares with Baylor & Hodgkin's (1973) estimate of the current generated by one photo-isomerization as 1.5×10^{-13} amp, so that the minimum cone stimulus would be equivalent to 100 photo-isomerizations. For rods the value might be 10 photo-isomerizations.[6]

RELATION TO LIGHT RESPONSES

In continuing this study Baylor & Fettiplace (1977) showed that the type of ganglion cell response to electrical stimulation of a cone was related to its response to light: thus an ON-sensitive ganglion cell responded to negative-going electrical current pulses, so that it responded at the make of a hyperpolarizing current or the break of a depolarizing current; OFF-sensitive ganglion cells responded to positive going currents, and ON–OFF cells to both negative- and positive-going currents. The responses to hyperpolarizing currents are indicated in Table 11.1. In general, then, the effects of a hyperpolarization of the receptor can be equated with those of light, and of depolarization as antagonistic to the effects of light. When the effects of a background light on electrical sensitivity were determined, in rods this was equivalent to a simple rise in threshold without change in the membrane resistance, as measured by the current–voltage relationship. In cones, the effect depended on the ON- or OFF-character; thus the threshold of receptors utilizing the ON-pathway was raised by the background light, whereas that of receptors utilizing the OFF-pathway was lowered.

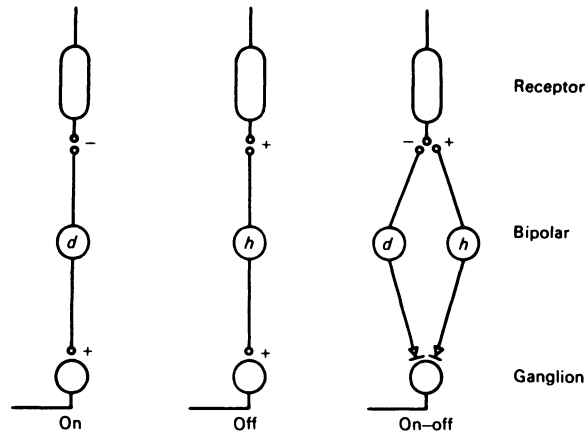

Fig. 11.12 Schematic diagram of proposed connexions between red-sensitive cones and ON, OFF, and ON–OFF ganglion cells. Bipolars depolarized by central illumination denoted by *d*, hyperpolarizing bipolars by *h*. The − indicates a synapse with sign reversal, + a synapse with sign preservation, − ▷| a rectifying synapse which transmits depolarizations but not hyperpolarizations to the postsynaptic cell. (Baylor & Fettiplace, *J. Physiol.*)

CIRCUITS

In general, the experimental results could be best explained on the basis of the circuits illustrated by Fig. 11.12; according to these, an ON-responsive ganglion cell would be connected to a bipolar cell that depolarized in response to the receptor's hyperpolarizing response (synaptic reversal); this depolarization would trigger the ganglion cell through a synaptic depolarization. Thus light at ON would hyperpolarize the receptor, and this would depolarize the bipolar cell giving an ON-response. Bipolar cells responding by hyperpolarization to light (synaptic sign preservation) would inhibit the ganglion cell during ON and excite it at OFF. The ON–OFF ganglion cell would be related to both types of bipolar cell, but an additional factor would have to be introduced if the opposing effects of the two bipolar cells were not to cancel; this additional effect would be a 'rectifying synapse', which transmitted depolarizations but not hyperpolarizations to the postsynaptic cell.

Table 11.1 Patterns of ganglion cell response to light and to hyperpolarizing current in a receptor (Baylor & Fettiplace, 1977)

	Ganglion cell response	
Receptor	*To light*	*To hyperpolarizing current*
Red-sensitive cone	On	Make
	Off	Break
	On and off	Make and break
	On and off	Break
Rod	Off	Break

THE ELECTRORETINOGRAM

The electroretinogram[7] (ERG) is a record of comparatively slow changes of potential that take place across the retina in a radial direction when light falls on it. As classically studied in the intact eye, one electrode is placed on the cornea whilst the other, indifferent, electrode may be placed in the mouth or, in experimental animals, on the optic nerve. A better record may be obtained in experimental animals by placing the active electrode in the vitreous body. It is essentially because the retina is built up of large numbers of extremely well orientated units, arranged in layers, that the successive states of depolarization or hyperpolarization in these units lead to definite changes of polarity across the whole structure.

Typical Record

In Fig. 11.13 is shown a typical example; the first sign of activity is shown as an *a*-wave corresponding to a decrease in the normal positivity of the corneal electrode; this is conventionally recorded as a downstroke on the record, and is called a *negative* wave; it lasts less than 0.1 second. The *a*-wave is followed by a reversal in polarity so that the cornea now becomes strongly positive, and this gives the sharp upward *b*-wave conventionally described

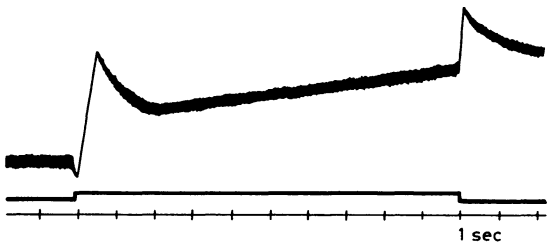

Fig. 11.13 Typical electroretinogram (ERG). Lowest record, time scale; middle record, stimulus; top record, galvanometer deflexion. (Drawn from Hartline, *Amer. J. Physiol.*)

as a *positive* wave; the *c*-wave is a much slower rise in corneal positivity and is terminated, when the light is switched off, by the *d*-wave, or OFF-effect.

Adaptation

According to the type of retina, and the state of adaptation of the eye, the records are qualitatively different; and this is because of the predominance of cones or rods in producing the net record. Thus, when the cones dominate the record, e.g. in the light-adapted mixed retina of the frog or the pure cone retina of the squirrel, the slow rise of the *c*-wave disappears, and the *a*-wave and OFF-effect become prominent. In the dark-adapted state, or in the virtually pure rod retinae of many nocturnal animals, the *a*-wave is not so pronounced whilst the *c*-wave is prominent.

Origin of the ERG

It is well established that the ERG is the record of changes taking place in the retina, and we may ask what is the cause of these fluctuations in potential. Essentially they are changes in potential difference across the retina since they may be best recorded by a pair of electrodes, one on the inner face and the other on the scleral face of the retina. We may recall that a neurone may develop a rapid spike which is reflected in a very brief phase of negativity of an electrode placed exactly at the site of this activity. This change is so rapid, however, that it is unlikely that spike activity on the part of the retinal neurones will have much to do with the ERG.

Slow Potentials

Neurones will also, however, develop a much more slowly occurring change of potential; an example of this is the negativity which has been called the generator potential. In other cases we may record an increase in the normal membrane potential—a hyperpolarization—so that the neurone is said to become *positive*; this change is associated with inhibition of activity. We may assume therefore, that it is this type of change, rather than spike activity, that is at the basis of the ERG and the questions that present themselves are (*a*) What are the actual changes taking place in the retina? and (*b*) Where are they occurring, i.e. in what layer or layers?

Partial or complete answers to these questions have been provided by the studies of Tomita and Brown and their colleagues, based largely on the insertion of microelectrodes to different depths of the retina and noting the changes in the records when the retina was exposed to light. Before describing these, we may consider the classical analysis of Granit.

Granit's Analysis

Granit considered that the ERG was the record of several events taking place very nearly simultaneously, so that the measured potential changes were the algebraic sum, at any instant, of these. On the basis of experiments designed to block some processes, and thus allowing others to appear in a less obscure form, Granit deduced the presence of three 'components', namely PI, PII and PIII. PI is a slowly developing positive component; with strong stimuli, or after light-adaptation, it tends to disappear; it accounts for the secondary rise in positivity, the *c*-

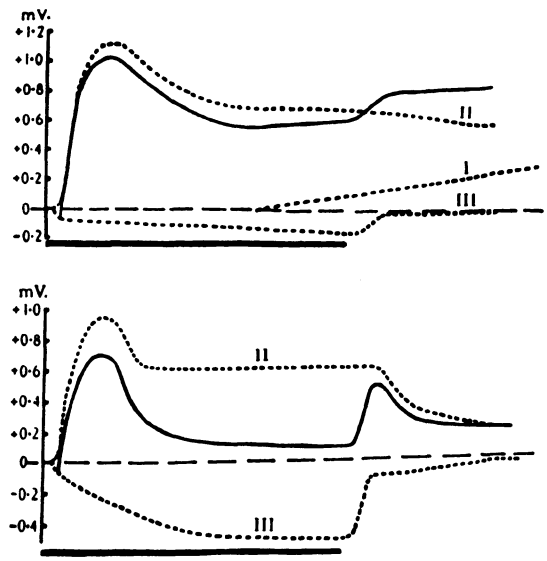

Fig. 11.14 Analysis of the ERG. Above: Dark-adapted frog's eye; PIII component and OFF-effect small. Below: Light-adapted frog's eye; PIII component and OFF-effect large; PI is missing so that the *c*-wave is absent. The black line indicates the duration of the stimulus (0.2 sec). (Granit & Riddell, *J. Physiol.*)

wave. PII is likewise positive but is much more rapid in development and is chiefly responsible for the *b*-wave. PIII is the negative component; it comes on rapidly and is responsible for the initial *a*-wave. The *d*-wave, or 'off-effect', is considered to represent an interference phenomenon resulting from the rapid swing of the negative PIII component back to the baseline; if this occurs more rapidly than the fall of the PI and PII components, it will clearly be reflected in a wave of positivity, the *d*-wave. Figure 11.14 illustrates the analysis for the dark-adapted (above) and light-adapted eye of the mixed frog retina. The dotted lines indicate the probable courses of the pure components acting in isolation, and the full lines the algebraic sums.

E- and I-retinae

The results of numerous experiments by different workers have shown that there is a strong correlation between the magnitude of the negative *a*-wave and the magnitude of the 'off-effect'; thus in the light-adapted frog's eye the *a*-wave and 'off-effect' are both marked (Fig. 11.14); in the dark-adapted frog's eye, or the cat's eye, the *a*-wave and 'off-effect' are small, in fact the latter is just shown as a slight check in the downward trend of positivity. Granit has divided the retinae studied into two groups, *E-* and *I-retinae*, according principally to the predominance of the negative PIII component; thus the retinae of the cat, rat, and guinea pig are all E-retinae with small PIII components in their electroretinograms; the pigeon and light-adapted frog retinae belong to the I-type, with pronounced PIII characteristics. Since those retinae that give the E-type of response contain predominantly rods, whilst the I-type of response is shown either by retinae with predominantly cones, as with the pigeon or tortoise, or by retinae with both types of receptor in which rod function is suppressed (light-adapted frog), it is reasonable to assume that the negative PIII component is mainly associated with cone activity. The available evidence suggests that it is connected with *inhibition* of impulses, as opposed to their initiation.

Excitation

The PII component, on the other hand, is closely associated with the passage of impulses along the optic nerve, i.e. with excitation; thus when the PII component is blocked by ether anaesthesia, simultaneous records of the electrical changes in the optic nerve show that the action potentials here are likewise blocked. So strong, indeed, is the correlation that the height of the *b*-wave has been used as an index to the intensity of the optic nerve response.

Further Developments

In general, Granit's analysis remains essentially valid, in the sense that the record is one of independently generated potential changes, although modifications have been introduced in the light of microelectrode studies.

Records from a Distance

Thus the conventional ERG electrode on the cornea is recording events at a considerable distance from where they take place, and the actual record must be considerably attenuated so that it is, at first thought, surprising that it is not completely extinguished. It is only because the cells of the retina are all so well orientated that a record is possible. Thus, we may suppose the situation to be that illustrated by Fig. 11.15, where the rectangles indicate radially orientated retinal cells; they have become active in the sense that a part of them has become negative in relation to other parts and the rest of the retina. This part would be described as a *sink of current* into which positive current would flow, and it may be shown that a distant electrode, e.g. one on the cornea, or closer still, in the vitreous, would record a phase of *positivity*. If the position were reversed, i.e. if later this cell, or another, became positive, we should expect to record negativity. If different cells showed opposite effects simultaneously we should expect cancellation of effects, so that the magnitude of the changes recorded at a distance might be much smaller than if the electrode were close to the origins of activity. Thus, on causing our electrode to penetrate into the retina we may expect to find larger potential changes; furthermore, when the electrode comes very close to the cells the record changes polarity; the electrode becomes negative when the cell does, and positive when it becomes positive. At the site of electrical activity, then, we may expect to find a *reversal of the ERG*,

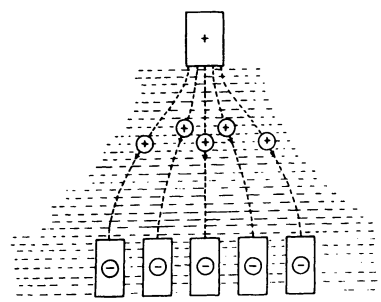

Fig. 11.15 The orientated cells, indicated by the rectangles, have become negative in relation to their surroundings and thus become what is known as a *sink* for positive current; the electrode at the top of the figure, at some distance from the sink, thus becomes positive, i.e. a *source* of positive current which flows into the sink.

or perhaps, if the events take place in different layers, reversal of some components only.

The PIII Component

We may begin with the PIII component, which is the first to manifest itself in the record as a negative downstroke. This was earlier shown to be localized in the region of the outer segments of the receptors (Brown & Wiesel, 1961); a microelectrode was inserted to successive depths, which were later identified; the *a*-wave reached a maximum when the active electrode was some 120 μm from the scleral surface of the retina and this corresponds to the layer of receptors. Again Murakami & Kaneko (1966), using a rather more elaborate recording procedure, identified the origin of the *a*-wave at some 120 μm from the surface, but they noted that at this level there was a considerable *a*-wave, recorded from the receptor layer and the inner surface of the retina, i.e. they identified what they called a proximal component due to activity in the outer plexiform layer. Sillman *et al.* (1969) showed that this component, as well as the *b*-wave, was blocked by aspartate, so that, in the presence of this inhibitor, they were able to record what was probably the pure receptor potential, i.e. the potential change taking place in the outer segments of the receptors. This is illustrated by Fig. 11.16, where the top record shows the normal record, inverted because the retina had been inverted. The lower records show the *a*-wave in isolation after the *b*-wave had been blocked by two concentrations of aspartate.

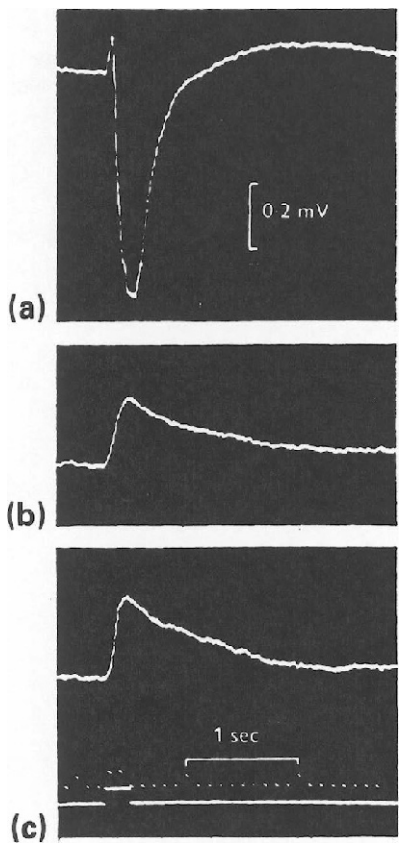

Fig. 11.16 Effect of sodium aspartate on the ERG, recorded from the isolated, inverted frog retina. (a) control, before treatment with aspartate; (b) after washing the retina with 10 mM aspartate-Ringer; and (c) with 110 mM aspartate-Ringer. (Sillman *et al.*, *Vision Res.*)

INTRACELLULAR RECORDS

The unequivocal localization of electrical activity is given by insertion of the recording electrode into the cells responsible for this. We have seen that the response of the receptor of the mud-puppy, *Necturus*, is a wave of hyperpolarization; a similar type of response was found by Tomita (1965) in the large cones of the carp, and by Baylor & Fuortes (1970) in the turtle. Such a change in potential is consistent with the polarity of the *a*-wave, which indicates that the outermost layer of the retina becomes positive in relation to the indifferent electrode outside the eye.

PII Component

The study of Brown & Wiesel (1961) located the maximum amplitude of the *b*-wave at a more proximal site, about half-way through the retina near the inner nuclear layer; by reducing the strength of the stimulus, the interfering effects of the *a*- and *c*-waves were removed. Since it could be abolished by local anaesthetics and anoxia, it was thought to represent synchronized neural activity.

MÜLLER CELLS

Rather surprisingly, at the time, Miller & Dowling (1970) showed that the intracellularly recorded electrical changes in Müller cells showed a much closer parallel to the local ERG than did responses in horizontal, bipolar or amacrine cells (Fig. 11.17). Müller cells have no synaptic relations with retinal neurones, and it was assumed that the changes in extracellular K^+ caused by retinal activity modified the resting potential of the Müller cell, a phenomenon well established with glial cells in other parts of the central nervous system. The actual source of the electrical change was, according to Faber (1969), in Müller cells in the distal part of the inner nuclear layer, the light-induced activity of perhaps bipolar and horizontal cells being responsible. As illustrated schematically in Fig. 11.18, the Müller cell is radially orientated in the retina with terminals at the external and internal limiting membranes, the footplates at the proximal (vitreal) end contributing to the formation of the inner limiting mem-

brane. Laterally processes ramify in the inner and outer plexiform layers, performing a glial function.[8]

Extracellular K^+ (K_0^+) This explanation of the *b*-wave, on the basis of a depolarization of Müller cells has been examined in the light of measurements of the changes in local extracellular K^+-concentration, K_0^+, measured with K^+-sensitive electrodes. Thus Oakley & Green (1976) found two components; a rapid rise in K_0^+ in the proximal retina, i.e. near amacrine or ganglion cells, and a small decrease in the distal retina near the receptors. This latter could have been due to the hyperpolarization induced by light, whilst the proximal increase could have been due to amacrine or ganglion cell[9] activity. Dick & Miller (1978) confirmed the proximal increase in K_0^+ but they also identified a smaller increase in the distal retina which might well have been responsible for the *b*-wave; they used pharmacological agents to separate components of the ERG in order to establish the relation between K_0^+ and potential changes, and they suggested that the distal increase was probably derived from depolarizing bipolars and that it generated the *b*-wave. Thus ethyl alcohol enhanced the *b*-wave and increased the K_0^+ whilst the proximal rise was decreased. Ethyl alcohol depresses activity of most retinal cells, but probably not that of the depolarizing bipolars.

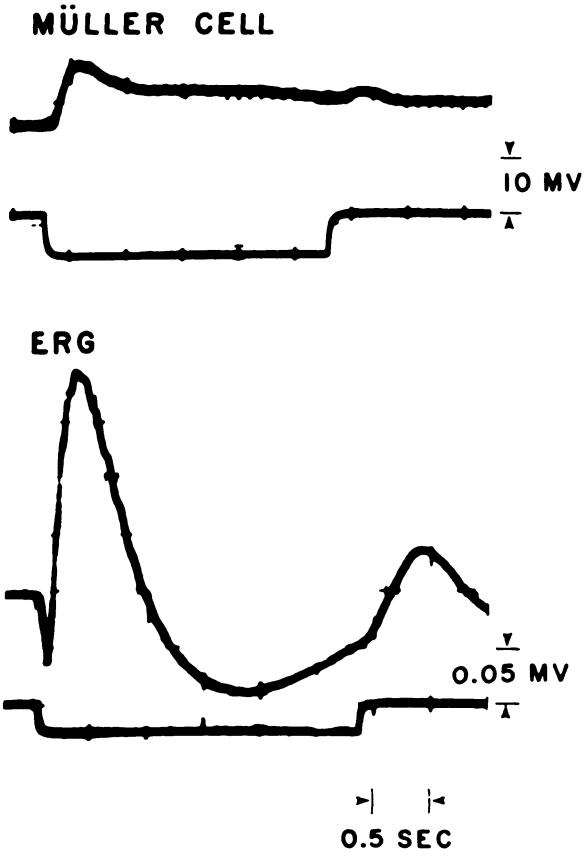

Fig. 11.17 Intracellular response of a Müller cell to a light-flash. (Miller & Dowling, *J. Neurophysiol.*)

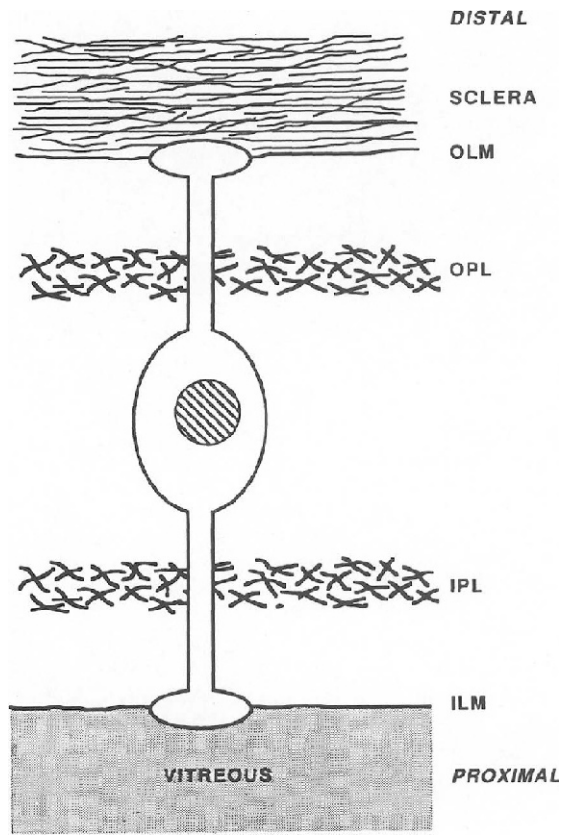

Fig. 11.18 Illustrating the radial orientation of the Müller cell in the retina. (After Uga & Smelser, *Invest. Ophthal.*)

Model of Electroretinogram Newman & Odette (1984) reviewed the objections to the explanation of the *b*-wave based on release of K^+, the chief being the slow time-course of rise and decay of the Müller cell's resting potential compared with those of the *b*-wave. They set up a computer model, based on rises in K_0^+ near the inner and outer plexiform layers respectively, and a decrease in the region of the receptor inner segments (Fig. 11.19); a postulated feature was a high localized K^+-permeability of the Müller cell end-feet at the inner limiting membrane. On the basis of this model they were able to reproduce the local ERG with some accuracy, the brisker feature of the *b*-wave being due to the relatively small influence on the Müller cell of the proximal rise in K_0^+, and thus on the transretinal potential.

Injections of K^+ The Müller cell hypothesis was tested by Fujimoto & Tomita (1981) and Yamagida & Tomita (1982) by localized injections of minute amounts of

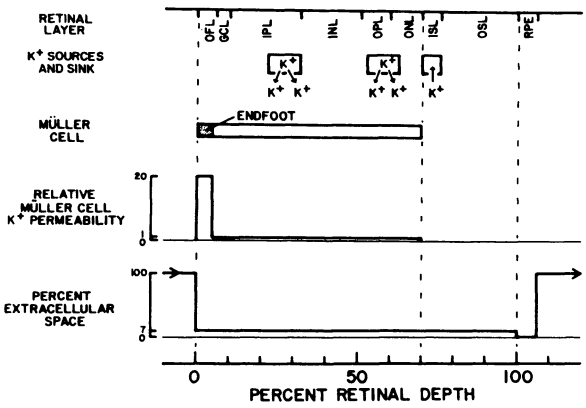

Fig. 11.19 Summary of retinal model. Locations and values of retinal structures and parameters are shown as a function of percent retinal depth. Retinal layers, shown above plots are, from left to right, optic fibre layer, ganglion cell layer, inner plexiform layer, inner nuclear layer, outer plexiform layer, outer nuclear layer, (rod) inner segment layer, (rod) outer segment layer, and retinal pigment epithelium layer. (Newman & Odette, *J. Neurophysiol.*)

75 mM K^+ or K^+-free Ringer and measurement of the potentials developed when the injections were made at different depths. In general, with high K^+, maximal negativity was developed at the site of injection, perhaps due to local depolarization of Müller cells; the potential fell off in both directions but in such a way as to leave the vitreal side positive, as with the *b*-wave. If the Müller cell membrane at the vitreal surface were much more highly permeable to K^+ than elsewhere, this asymmetry of potential could find an explanation. The authors concluded that the effects that they were measuring were, indeed, on Müller cells, and support the view that perhaps two loci of K^+-liberation, proximal and distal, would lead to a current flow such as that described by Newman (1979, 1980), namely two sinks, distal and proximal, which added up to a narrow restricted region bordering the inner limiting membrane.[10]

Proximal Negative Response (PNR)

This is a slow potential change that has often been confounded with features of the ERG, but which Burckhardt (1970) has shown to have a distinct origin, probably representing an extracellular field-potential derived from amacrine cell responses. A careful comparison of the PNR with ganglion cell spike activity and the *b*-wave of the true ERG convincingly demonstrated the separate character of the PNR (thus the *b*-wave increases as the area of the spot-stimulus is extended, whereas the opposite occurs with the PNR). When an electrode was advanced from the vitreal surface into the retina, the *b*-wave was first prominent; a maximal PNR occurred some 50–100 μm deeper, i.e. in the proximal retina by contrast with the *b*-wave which finally becomes zero at 120 μm to become a negative *b*-wave at greater depths; by contrast, the PNR does not reverse polarity with depth. Because the maximal PNR occurred at the junction of the inner nuclear and plexiform layers, Burckhardt concluded that a group of amacrines was responsible; thus its failure to reverse in polarity with depth indicates electrical changes occurring along tangentially orientated cells. Since amacrine cells are depolarized in response to light, we may expect a negative potential in their immediate neighbourhood, agreeing with the negativity of the PNR. Karwoski & Proenza (1978) found that, with small-diameter flashes, the depth-profile of the large increase in K_o^+ in the proximal retina corresponded with the depth-profile of the PNR; thus the maximal increase in K_o^+ occurred at 20% of retinal depth at the boundary of the inner nuclear and plexiform layers, where the maximum of the PNR occurred.

PI Component

This is defined as that responsible for the *c*-wave, and is prominent in the dark-adapted state; microelectrode studies have shown that this, as well as the *a*-wave, is generated close to the scleral surface of the retina; Noell (1954) showed that iodate selectively reduced the *c*-wave and destroyed the pigment epithelium, and he concluded that the *c*-wave was generated by these cells.

Steinberg *et al.* (1970) compared the local ERG obtained with a microelectrode close to the retina with the changes in the intracellular potential of a pigment epithelial cell; as Fig. 11.20 shows, the *c*-wave of the local ERG coincides with a peak in hyperpolarization of the pigment epithelial cell. The effect is not due to the impinging of light on the pigment epithelium, since the action-spectrum is that of the rod pigment (the *c*-wave is absent in a pure cone-retina).

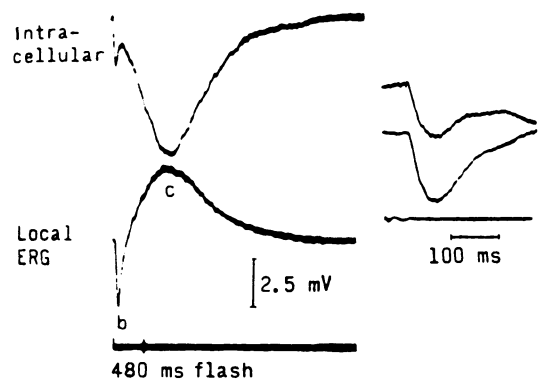

Fig. 11.20 Showing origin of the *c*-wave in the pigment epithelial cells. The intracellular response of a pigment epithelial cell was recorded first; then the microelectrode tip was withdrawn into the photoreceptor layer and the ERG in response to an identical flash was recorded. Records at the right photographed at a faster sweep to illustrate the similar time-course of the *b*-wave of the local ERG (bottom) and the early peak of the intracellular response. Negative responses are displayed downwards. (Steinberg *et al.*, *Nature.*)

RELATION TO $[K^+]$

Simultaneous measurements of the concentration of K^+ in the fluid in immediate contact with the pigment epithelial cells, by a K^+-sensitive electrode, have shown that a considerable fall in this concentration is associated in time with the hyperpolarization (Oakley & Green, 1976). Figure 11.21 shows the relation between the response-amplitude of the *c*-wave and the logarithm of the external K^+-concentration at the peak (Oakley, 1977). On the same graph the changes in transepithelial potential (TEP) have been plotted; the close correspondence with *c*-wave and TEP confirms the origin of the *c*-wave in the pigment epithelium.

D.C. Component

Brown & Wiesel (1961) attribute the OFF-effect, as seen in the cat's ERG, essentially to the cessation of what they called the d.c. component, a phase of negativity that comes on immediately with the light-stimulus and remains at a constant level during this, to fall abruptly when the light is switched off. Thus the d.c. component is a part of what Granit included in his PII, which gives rise not only to the *b*-wave but the sustained negativity during maintained stimulation. Steinberg (1969) has analysed both *b*-wave and d.c. component, and his results tend to confirm the distinction between the two.

Effects of Transmitters

Cunningham & Miller (1980) compared the ERG, PNR and Müller cell responses in the mudpuppy retina; here the ERG consists of a small *a*-wave, a large *b*-wave and a small *d*-wave at OFF. The *d*-wave showed high sensitivity to glycine or taurine, suggesting mediation by hyperpolarizing bipolars which, in the mudpuppy, show high sensitivity to these transmitters. Glycine and taurine also blocked the OFF-response recorded from Müller cells, suggesting these cells as the origin of the *d*-wave as well as the *b*-wave.

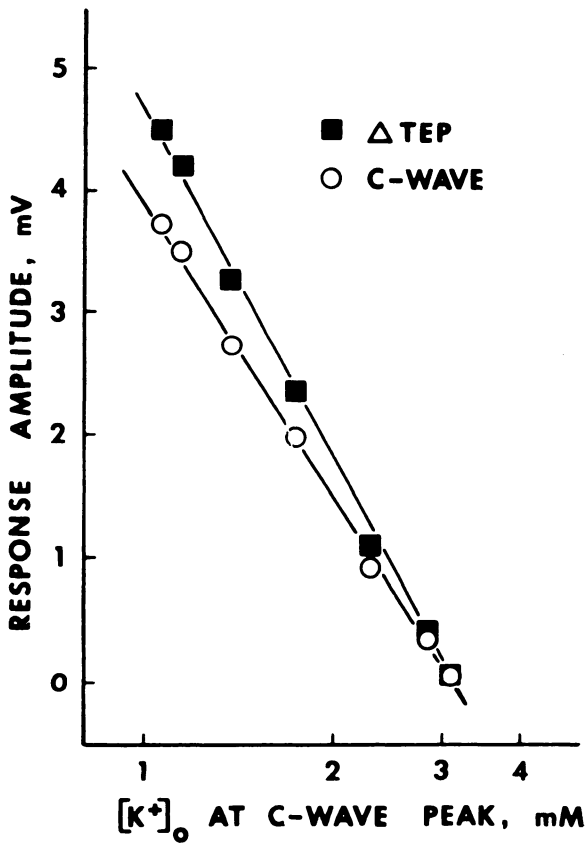

Fig. 11.21 Dependence of the *c*-wave and transepithelial potential (TEP) on the concentration of K^+ in the retinal tissue, measured by a K^+-sensitive electrode, at the peak of the potential change. (Oakley, *J. gen. Physiol.*)

Early and Late Receptor Potentials

Brown & Murakami (1964), when making their ERG records with a microelectrode in the retina, found that the *a*-wave was preceded by a diphasic potential change with no measurable latency; this was obtained with the tip of the electrode in the region of the junction of the outer and inner segments of the receptors. We may therefore speak of an *early* and *late* receptor potential (ERP and RP), the latter being the PIII component of the electroretinogram, and the former being over before this is normally recorded.

Early Receptor Potential

A comparison of the effectiveness of different wavelengths of light showed that, in the virtually all-rod retina of the albino rat, the pigment responsible was rhodopsin (Cone, 1964); however, the early receptor potential is only obtained with intense flashes, the relative amount of energy for late and early potentials being in the ratio of one to a million. The potential is diphasic, beginning with a cornea-positive change (R_1) followed by a cornea-negative change (R_2). R_1 occurs at sub-zero temperatures which abolish R_2. All the evidence indicates that both phases have nothing in common with bioelectric potentials as usually recorded; thus they can be recorded from fixed tissue, and, as indicated, at sub-zero temperatures. Some organization of retinal structure is necessary, however, since the potential vanishes if the eye is heated above 58°C, and this is accompanied by a measurable disorientation of the rhodopsin (Cone & Brown, 1967).

DIPOLE CHANGE

The currently accepted hypothesis is that the potential arises from a change in the orientation, or magnitude, of the electric dipole of the visual pigment molecule dependent on ionized groups. For this change to appear between electrodes in the inside and outside of the retina, it is essential for it to take place within the thickness of the high-resistance membrane separating the receptor interior from the extracellular space, the result being a transient flow of current between the outer and inner segments in one direction and in the opposite direction within the interior of the receptor. The difference in potential measured in the extracellular fluid is the ERP. The first effect of light is to isomerize the 11-*cis* retinal on the rhodopsin molecule (p. 246); in order that rotation of a double-bond may occur, this must be broken, and this will result in the transfer of electrons, and if the transfer is such as to result in a transmembrane movement of current this would account for the difference of potential occurring between outer and inner segments.

INTRACELLULAR RECORDS

Murakami & Pak (1970) compared intra- with extracellular recording of the ERP in the gekko, axolotl and mud-puppy retinae; the amplitude of the intracellular record was 1.7 mV on average, compared with only 0.09 mV extracellularly. The time-course of the intracellular events was slower. These findings are consistent with an initial transfer of electronic charge across the outer segment membrane followed by the spread of potential towards the inner segment, in the same way that an applied potential spreads along the surface of an excitable tissue such as a nerve—the spread is governed by the cable-properties of the receptor membrane—in fact computations of membrane capacitance and resistance, derived from these measurements of receptor potential, are consistent with those in other cells (ca $1\ k\Omega\ m^{-2}$ and $1\ F\ m^{-2}$).

RODS AND CONES

In the mixed retina, it is the cones that determine the early receptor potential in spite of the predominance of the rod pigment; thus the action-spectrum for the monkey retina has a maximum between 535–570 nm (Carr & Siegel, 1970), whilst the recovery of the potential after a flash is at a rate commensurate with cone pigment regeneration rather than that of rhodopsin (Goldstein & Berson, 1969).

It appears from the work of Zanen (1973) and Zanen & Debecker (1975) that the magnitudes of R_1 and R_2 are strongly dependent on the wavelength of light, suggesting that the relative contributions of rods and cones can vary; thus R_1 may well be due to cones entirely, since it is not obtained by violet flashes, whilst R_2 may represent a mixture of rod and cone responses, although the differing sensitivities of the components to temperature would suggest a more fundamental difference in origin.

POLARIZED LIGHT

That rods and cones make separate contributions is also suggested by the effects of light polarized in different planes. Thus, in the cones, the membrane developing the potential is presumably the entire plasma membrane together with that covering the discs which is continuous with it, so that light with its electric vector at right-angles to the discs, i.e., parallel to the outer segments, should be more effective than light with its electric vector at right-angles to this direction. Using a photopic cone-stimulus, the maximal ERP was, indeed, found with the electric vector at right-angles to the discs, giving a dichroic ratio of 1:2; when the retina was bleached with deep red light, the ERP disappeared, indicating a cone phenomenon. When the cone effect was removed, then an opposite dichroic ratio was obtained, and this was presumably by activation of rods, since the active membrane in this case cannot be that in the discs, which are separate, and is probably the plasma membrane, which runs parallel with the outer segments. In the guinea pig, which behaves as a pure rod retina, only one ERP-generating mechanism was obtained and in this the maximal response was to light with its electric vector parallel with the outer segments. If this viewpoint is correct, the predominance of the cone contribution to the mixed retina's ERP is due to its special anatomical feature of continuity of plasma membrane with its infolded discs (Govardovskii, 1975).

DEPENDENCE ON RETINAL PIGMENT

If the ERP depended on an electron charge transfer due to absorption of light, it might depend on the state of the visual pigment at the time of exposure to the intense flash, and Cone & Cobbs (1969) showed that the ERP changed its form at successive intervals following a bleaching exposure, and these changes were correlated with the appearance of Metarhodopsins I, II and pararhodopsin (p. 246). Subsequent work of Zanen (1973) along the same lines certainly indicates that the potentials developed by flashes following an intense bleaching exposure are dependent on the nature of the predominant intermediary of bleaching.[11]

TURTLE'S ERP

Hodgkin & O'Bryan (1977) have extended their studies of intracellular recording of single cone responses to the ERP, which, like those described by Murakami & Pak, consisted of a depolarizing and hyperpolarizing phase. They were able to separate the ERP from the late receptor potential, i.e. from the hyperpolarizing response to light, by imposing the very bright flashes, required to evoke the ERP, on a light of sufficient intensity to saturate the late response. This is possible without serious bleaching of the

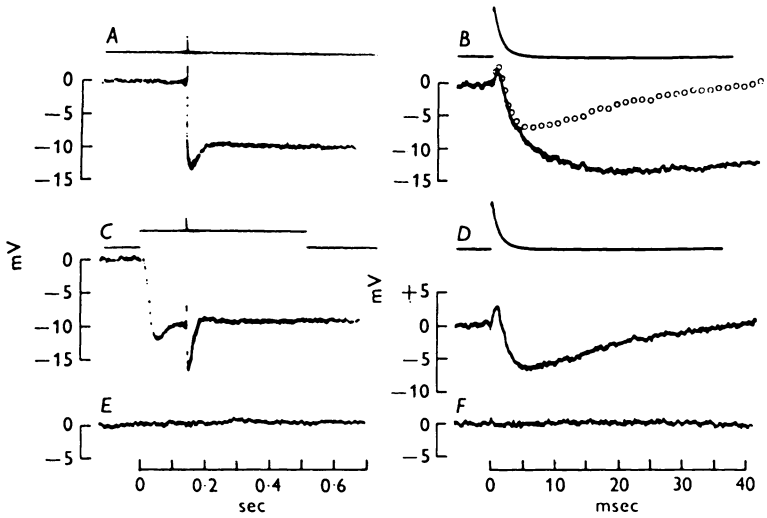

Fig. 11.22 Use of a conditioning step of light to separate ERP from LRP, recorded from a red-sensitive cone with an internal electrode. *A*, effect of unattenuated xenon flash without conditioning light (slow time base). *B*, same but on faster time base. The response is a mixture of ERP (shown by circles obtained from *D*) and LRP. *C*, effect of applying same xenon flash on conditioning step of light which saturates the LRP mechanism. The response to the xenon flash in this record and in *D* is considered to be ERP only. *D*, same as *C* but showing effect of xenon flash on faster time base-expansion of 0.13–0.18 sec of record *C*; the zero on the voltage scale corresponds to −10 mV in *C*. *E*, *F*, same stimulus as in *C* and *D* but recorded with electrode outside cone. (Hodgkin & O'Bryan, *J. Physiol.*)

cone pigment, so that the ERP appears as potential changes imposed on the plateau-response to the conditioning light (Fig. 11.22). A striking difference between the early and late responses was the finding that the shape of the early response was independent of the intensity of the flash, so that, by scaling, responses to weak and strong flashes could be superimposed; this is in contrast with the later response.

SEPARATE CURRENT-GENERATING MECHANISM

All the evidence pointed to the existence of two entirely independent current-generating mechanisms in the early and late receptor potentials; according to theory, the early current is generated by each photo-isomerization of cone pigment whereas the latter is an indirect result of the liberation of a blocking molecule which closes ionic channels and hyperpolarizes the cell to a saturating value. So far as the two components of the ERP are concerned, it may be as Cone & Cobbs (1969) suggested, that the initial depolarizing phase corresponds to the photochemical events leading to the production of metarhodopsin I (or its equivalent cone pigment) and the later hyperpolarization to the conversion of metarhodopsin I to metarhodopsin II.

In contrasting the two receptor potentials, early and late, Hodgkin & O'Bryan (1977) emphasize the basic simplicity of the ERP, which increases linearly with the number of isomerizations brought about by the flash and may be due to a simple molecular rearrangement in the receptor membrane; by contrast, the late potential changes in shape and size as the intensity of the flash is increased in a complex way. Again, there is an enormous difference in the number of photo-isomerizations required to saturate the responses; for the ERP it is half-maximal at 7×10^7 photo-isomerizations per cone, and for the late receptor potential it is half-maximal at only 1000 photo-isomerizations per cone.

TRANSMITTER

Finally, it seems likely that a transmitter action is unnecessary with the ERP, whereas the fact that absorption of a photon by any one of about 10^8 molecules of photopigment can lead to the blockage of about one thousandth of the ionic channels in the outer segment requires some internal transmitter.

ROLE OF PIGMENT EPITHELIUM

Illumination of the eye-cup with the retina removed from its subjacent pigment epithelium gives rise to changes in potential analogous in their time-course to those taking place in the intact eye; Brown & Crawford (1967) showed that these were generated by the pigment epithelium cells with action spectra corresponding to the absorption of light by melanin. The potentials produced in this way will necessarily contribute to the potentials recorded in the intact eye; their contribution has been described non-committally as the *fast photochemical voltage* (*FPV*) and may be assessed by employing sufficiently intense light that effectively bleaches all the visual pigment; the 'photostable residue' of activity is due to the pigment epithelium. Zanen & Debecker (1971), working on human cadavers, showed that the ERP and the photostable fraction occurred in different layers of the retina whilst in the living human eye Debecker & Zanen (1975) found the ERP proportional to flash-intensity up to 130 to 150 μV; they never obtained light-saturation due to the photostable contribution, but they concluded that up to 100 μV the ERP is purely due to visual pigment.

Notes

1. The gain is a measure of the response in terms of voltage and the duration, that permits a comparison between rods and cones when the time-course of the potential change is accurately determined (Schwartz, 1976). Another measure is the *scaled amplitude*, equivalent to the *sensitivity* of Fuortes & Hodgkin, 1964).
2. The main features of the anatomy and physiology of the horizontal cell have been reviewed in an entertaining article by Piccolino (1986).
3. The relations between rods and horizontal cells of the toad *Bufo marinus* have been emphasized by Normann & Pochobradsky (1976), who observed strong oscillations in membrane potential in both types of retinal cell occurring spontaneously and suggesting some feed-back from horizontal cell to rod.
4. In the carp there is interaction between axon terminal and soma, unlike the situation in reptiles and mammals. Stell (1976) found light-evoked responses in both axon and cell body, although the axon terminals had no synaptic contacts with receptors or bipolar cells, suggesting spread of electrical activity from one part of the neurone to the other. The mechanism of this spread is apparently through gap-junctions between adjacent cells, rather than electrotonically along the long thin axon (Yagi, 1986). Cervetto & Piccolino (1974) recorded intracellularly from cones and horizontal cells of the turtle retina; blockage of transmission with low Ca^{2+}, high Mg^{2+} and Co^{2+} hyperpolarized the horizontal cell and suppressed the response to light.
5. About half of the amacrine cells of the carp exhibit centre-surround antagonism, being either OFF-centre or ON-centre (Toyoda *et al.*, 1973). Injection of current into horizontal cells produced responses in about half the amacrine cells studied, the responses being similar to the surround responses to light. These surround effects must be mediated by bipolars, since horizontal cells make no direct connexions with amacrine cells. The changes in resistance suggested that the only input to the amacrine cells was excitatory, no evidence for an inhibitory postsynaptic potential being found. Thus the opposite responses of depolarization and hyperpolarization are brought about by onset and cessation of depolarization. ON–OFF amacrine cells were assumed to have an input from ON- and OFF-bipolar cells, whose effects would tend to cancel out with steady illumination, and thus would only signal at ON and OFF.
6. In their most sensitive pairs of receptor and ganglion cell, the current required to excite was about 2×10^{-11} amp, corresponding to some 130 isomerizations. For rods, the minimum number of isomerizations detectable by a ganglion cell would be about 50, according to this study. Thus detection of a single quantum event is out of the question and the ganglion cell must summate the effects of light falling on the many cones constituting the centre of its receptive field.
7. The 'retinal currents' now called the ERG were first described by Holmgren in 1865 but were independently discovered by Dewar & McKendrick. Kühne & Steiner (1880, 1881) showed that the same electrical changes could be obtained from the retina removed from the eye, whilst the remaining sclera, choroid and pigment epithelium were unresponsive.
8. The electrical characteristics of Müller cells in the turtle retina have been studied by Conner *et al.* (1985); resting potentials were high, but the membrane did not behave like a perfect K^+-electrode, exhibiting some Na^+-permeability. The relatively low membrane resistance measured *in situ*, compared with the high values in isolated cells, indicated the existence of extensive gap-junction coupling, as demonstrated morphologically by Uga & Smelser (1973).
9. Ganglion cell activity must be ruled out so far as contributions to the ERG are concerned, since the ERG is normal when these cells degenerate (Noell, 1954). Cavaggioni *et al.* (1972) showed that light reduced the efflux of ^{42}K from the receptors of the isolated frog retina, a reduction they attributed to the increased resting potentials of the receptors as the result of light; they calculated that an increase of this from 30 to 40 mV would reduce the efflux by 22%, about the difference between efflux in light and dark.
10. In the later study (Yamagida & Tomita, 1982) they concluded that Müller cell depolarization by K^+ contributed to the *b*-wave but that some neuronal activity must also be invoked, as the loci of highest K^+ concentration did not correspond with the loci of high *b*-wave magnitude as determined by Brown & Wiesel (1961). Oakley (1983) has shown that, in the toad, sustained illumination leads to a return of the concentration of K^+ in the extracellular space towards its dark-adapted value, and discusses the mechanism.
11. As we might expect of a process dependent on the absorption of light by photopigment, the appearance of the ERP in embryonic development coincides with the appearance of rhodopsin in the developing chick retina, namely on the 13th day (Hanawa *et al.*, 1976).

References

Baylor, D. A. & Fettiplace, R. (1975a) Light path and photon capture in turtle photoreceptors. *J. Physiol.* **248**, 434–464.

Baylor, D. A. & Fettiplace, R. (1975b) Transmission of signals from photoreceptors to ganglion cells in the eye of the turtle. *Cold Spr. Harb. Symp. quant. Biol.* **40**, 528–536.

Baylor, D. A. & Fettiplace, R. (1977) Transmission from photoreceptors to ganglion cells in turtle retina. *J. Physiol.* **271**, 391–424.

Baylor, D. A. & Fuortes, M. G. F. (1970) Electrical responses of single cones in the retina of the turtle. *J. Physiol.* **207**, 77–92.

Baylor, D. A., Fuortes, M. G. F. & O'Bryan, P. M. (1971) Receptive fields of cones in the retina of the turtle. *J. Physiol.* **214**, 265–294.

Baylor, D. A. & Hodgkin, A. L. (1973) Detection and resolution of visual stimuli by turtle photoreceptors. *J. Physiol.* **234**, 163–198.

Baylor, D. A., Hodgkin, A. L. & Lamb, T. D. (1974) The electrical response of turtle cones to flashes and steps of light. *J. Physiol.* **242**, 685–727.

Baylor, D. A., Hodgkin, A. L. & Lamb, T. D. (1974) Reconstruction of the electrical responses of turtle cones to flashes and steps of light. *J. Physiol.* **242**, 759–791.

Bortoff, A. & Norton, A. L. (1967) An electrical model of the vertebrate photoreceptor cell. *Vision Res.* **7**, 253–263.

Brown, J. E. & Major, D. (1966) Cat retinal ganglion cell dendritic fields. *Exp. Neurol.* **15**, 70–78.

Brown, K. T. & Crawford, J. M. (1967) Melanin and the rapid light-evoked responses from pigment epithelium cells of the frog eye. *Vision Res.* **7**, 165–178.

Brown, K. T. & Murakami, M. (1964) A new receptor potential of the monkey retina with no detectable latency. *Nature* **201**, 626–628.

Brown, K. T. & Wiesel, T. N. (1961) Analysis of the intraretinal electroretinogram in the intact cat eye. *J. Physiol.* **158**, 229–256.

Brown, K. T. & Wiesel, T. N. (1961) Localization of origins of electroretinogram components by intraretinal recording in the intact cat eye. *J. Physiol.* **158**, 257–280.

Burckhardt, D. A. (1970) Proximal negative response of frog retina. *J. Neurophysiol.* **33**, 405–420.

Carr, R. E. & Siegel, I. M. (1970) Action spectrum of the human early receptor potential. *Nature* **225**, 89–90.

Cavaggioni, A., Sorbi, R. T. & Turini, S. (1972) Efflux of potassium from the isolated frog retina: a study of the photic effect. *J. Physiol.* **222**, 427–445.

Cervetto, L. & Piccolino, M. (1974) Synaptic transmission between photoreceptors and horizontal cells in the turtle retina. *Science* **183**, 417–418.

Cone, R. A. (1964) Early receptor potential of the vertebrate retina. *Nature* **204**, 736–739.

Cone, R. A. & Brown, P. K. (1967) Dependence of the early receptor potential on the orientation of rhodopsin. *Science* **156**, 536.

Cone, R. A. & Cobbs, W. H. (1969) Rhodopsin cycle in the living eye of the rat. *Nature* **221**, 820–822.

Conner, J. D., Detwiler, P. B. & Sarthy, P. V. (1985) Ionic and electrophysiological properties of retinal Müller (glial) cells of the turtle. *J. Physiol.* **362**, 79–92.

Copenhagen, D. R. & Owen, W. G. (1976) Functional characteristics of lateral interactions between rods in the retina of the snapping turtle. *J. Physiol.* **259**, 251–282.

Cunningham, R. A. & Miller, R. F. (1980) Electrophysiological analysis of taurine and glycine actions on neurons of the mudpuppy retina. I. Intracellular recordings. II. ERG, PNR and Müller cell recordings. *Brain Res.* **197**, 123–138, 139–151.

Daw, N. W. (1968) Colour-coded ganglion cells in the goldfish retina: extension of their receptive fields by means of new stimuli. *J. Physiol.* **197**, 567–592.

Debecker, J. & Zanen, A. (1975) Intensity functions of the early receptor potential and of the melanin fast photovoltage in the human eye. *Vision Res.* **15**, 101–106.

Dick, E. & Miller, R. F. (1978) Light-evoked activity in mudpuppy retina: its relationship to the b-wave of the electroretinogram. *Brain Res.* **154**, 388–394.

Dowling, J. E. & Werblin, F. S. (1969) Organization of retina of the mudpuppy *Necturus maculosus* I. Synaptic structure. *J. Neurophysiol.* **32**, 315–335.

Faber, D. S. (1969) Analysis of the slow transretinal potentials in response to light. PhD Thesis, University of New York at Buffalo. (Quoted by Miller & Dowling, 1970.)

Fain, G. L. (1975a) Interactions of rod and cone signals in the mudpuppy retina. *J. Physiol.* **252**, 735–769.

Fain, G. L. (1975b) Quantum sensitivity of rods in the toad retina. *Science* **187**, 838–841.

Fain, G. L., Gold, G. H. & Dowling, J. E. (1975) Receptor coupling in the toad retina. *Cold Spr. Harb. Symp. quant. Biol.* **40**, 547–651.

Fujimoto, M. & Tomita, T. (1981) Field potentials induced by injections of potassium into the frog retina: a test of current interpretations of the electroretinographic (ERG) b-wave. *Brain Res.* **204**, 51–64.

Fuortes, M. G. F. & Hodgkin, A. L. (1964) Changes in time scale and sensitivity in the ommatidium of Limulus. *J. Physiol.* **172**, 239–263.

Fuortes, M. G. F., Schwartz, E. A. & Simon, E. J. (1973) Colour-dependence of cone responses in the turtle retina. *J. Physiol.* **234**, 199–216.

Goldstein, E. B. & Berson, E. L. (1969) Cone dominance of the human early receptor potential. *Nature* **222**, 1272–1273.

Govardovskii, V. I. (1975) The sites of generation of early and late receptor potentials in rods. *Vision Res.* **15**, 973–980.

Granit, R. (1947) *Sensory Mechanisms of the Retina.* London: Oxford University Press.

Granit, R. & Riddell, H. A. (1934) The electrical responses of light- and dark-adapted frog's eyes to rhythmic and continuous stimuli. *J. Physiol.* **81**, 1–28.

Hanawa, I., Takahashi, K. & Kawamoto, N. (1971) A correlation of embryogenesis of visual cells and early receptor potential in the developing retina. *Exp. Eye Res.* **23**, 587–594.

Hodgkin, A. L. & O'Bryan, P. M. (1977) Internal recording of the early receptor potential in turtle cones. *J. Physiol.* **267**, 737–766.

Kaneko, A. (1973) Receptive field organization of bipolar and amacrine cells in the goldfish retina. *J. Physiol.* **235**, 133–153.

Kaneko, A. & Shimazaki, H. (1975) Synaptic transmission from photoreceptors to bipolar and horizontal cells in the carp retina. *Cold. Spr. Harb. Symp. Quant. Biol.* **40**, 537–546.

Kaneko, A. & Yamada, M. (1972) S-potentials in the dark-adapted retina of the carp. *J. Physiol.* **227**, 261–273.

Karwoski, C. J. & Proenza, L. M. (1978) Light-evoked changes in extracellular potassium concentration in mudpuppy retina. *Brain Res.* **142**, 513–530.

Kühne, W. & Steiner, J. (1880) Uber das electromotorische Verhalten der Netzhaut. *Unt. physiol. Inst. Univ., Heidelberg*, **3**, 327–377.

Kühne, W. & Steiner, J. (1881) Uber electrische Vorgänge im Sehorgane, *loc. cit.* **4**, 64–168.

Lamb, T. D. & Simon, E. J. (1977) Analysis of electrical noise in turtle cones. *J. Physiol.* **272**, 435–468.

Lasansky, A. (1971) Synaptic organization of cone cells in the turtle retina. *Phil. Trans.* **262**, 365–381.

Leeper, H. F. & Copenhagen, D. R. (1979) Mixed rod-cone responses in horizontal cells of snapping turtle retina. *Vision Res.* **19**, 407–412.

Miller, R. F. & Dowling, J. E. (1970) Intracellular responses of the Müller (glial) cells of mudpuppy retina: their relation to *b*-wave of the electroretinogram. *J. Neurophysiol.* **33**, 323–341.

Murakami, M. & Kaneko, A. (1966) Differentiation of PIII subcomponents in cold blooded vertebrate retinas. *Vision Res.* **6**, 627–636.

Murakami, M. & Pak, W. L. (1970) Intracellularly recorded early receptor potential of the vertebrate photoreceptors. *Vision Res.* **10**, 965–975.

Naka, K. I. & Rushton, W. A. H. (1966) S-potentials from colour units in the retina of fish (*Cypridinae*), *J. Physiol.* **185**, 536–555.

Naka, K. I. & Witkovsky, P. (1972) Dogfish ganglion cell discharge resulting from extrinsic polarization of the horizontal cells. *J. Physiol.* **223**, 449–460.

Newman, E. A. (1979) B-wave currents in the frog retina. *Vision Res.* **19**, 227–234.

Newman, E. A. (1980) Current source–density analysis of the b-wave of frog retina. *J. Neurophysiol.* **43**, 1355–1366.

Newman, E. A. & Odette, L. L. (1984) Model of electroretinogram b-wave generation: a test of the K^+ hypothesis. *J. Neurophysiol.* **51**, 164–182.

Neyton, J., Piccolino, M. & Gerschenfeld, H. M. (1981) Involvement of small-field horizontal cells in feedback effects on green cones of the turtle retina. *Proc. Nat. Acad. Sci.* **78**, 4616–4619.

Noell, W. K. (1954) The origin of the electroretinogram. *Am. J. Ophthal.* **38**, 78–90.

Normann, R. A. & Pochobradsky, J. (1976) Oscillations in rod

and horizontal cell membrane potential: evidence for feedback to rods in the vertebrate retina. *J. Physiol.* **261**, 15–29.
Oakley, B. (1977) Potassium and the photoreceptor-dependent pigment epithelium hyperpolarization. *J. Gen. Physiol.* **70**, 405–425.
Oakley, B. (1983) Effects of maintained illumination upon $[K^+]_o$ in the subretinal space of the isolated retina of the toad. *Vision Res.* **23**, 1325–1337.
Oakley, B. & Green, D. G. (1976) Correlation of light-evoked changes in retinal extracellular potassium concentration with c-wave of the electroretinogram. *J. Neurophysiol.* **39**, 1117–1133.
Ohtsuka, T. (1983) Axons connecting somata and axon terminals of luminosity-type horizontal cells in the turtle retina: receptive field studies and intracellular injections of HRP. *J. Comp. Neurol.* **220**, 191–198.
Penn, R. D. & Hagins, W. A. (1969) Signal transmission along retinal rods and the origin of the electroretinographic *a*-wave. *Nature* **233**, 201–205.
Piccolino, M. (1986) Horizontal cell: historical controversies and new interest. *Progr. Retinal Res.* **5**, 147–163.
Richter, A. & Simon, E. J. (1975) Properties of centre-hyperpolarizing, red-sensitive bipolar cells in the turtle retina. *J. Physiol.* **248**, 317–334.
Schwartz, E. A. (1973) Organization of ON–OFF cells in the retina of the turtle. *J. Physiol.* **230**, 1–14.
Schwartz, E. A. (1974) Responses of bipolar cells in the retina of the turtle. *J. Physiol.* **236**, 211–224.
Schwartz, E. A. (1975a) Responses of single rods in the turtle. *J. Physiol.* **232**, 503–514.
Schwartz, E. A. (1975b) Rod-rod interaction in the retina of the turtle. *J. Physiol.* **246**, 617–638.
Schwartz, E. A. (1975c) Cones excite rods in the retina of the turtle. *J. Physiol.* **246**, 639–651.
Schwartz, E. A. (1976) Electrical properties of the rod syncytium in the retina of the turtle. *J. Physiol.* **257**, 379–406.
Sillman, A. J., Ito, H. & Tomita, T. (1969) Studies on the mass receptor potential of the isolated frog retina. I. *Vision Res.* **9**, 1435–1442.
Simon, E. J. (1973) Two types of luminosity horizontal cells in the retina of the turtle. *J. Physiol.* **230**, 199–211.
Steinberg, R. H. (1969) Comparison of the intraretinal b-wave and d.c. component in the area centralis of cat retina. *Vision Res.* **9**, 317–331.
Steinberg, R. H., Schmidt, R. & Brown, K. T. (1970) Intracellular responses to light from cat pigment epithelium: origin of the electroretinogram *c*-wave. *Nature* **227**, 728–730.
Stell, W. K. (1967) The structure and relationships of horizontal cells and photoreceptor-bipolar synaptic complexes in goldfish retina. *Amer. J. Anat.* **121**, 401–424.
Stell, W. K. (1976) Functional polarization of horizontal cell dendrites in goldfish retina. *Invest. Ophthal.* **15**, 895–908.
Svaetichin, G. (1956) Spectral response curves from single cones. *Acta physiol. Scand.* **39**, Suppl. 134, 17–46.
Tomita, T. (1965) Electrophysiological study of the mechanisms subserving colour coding in the fish retina. *Cold Spr. Harb. Symp. quant. Biol.* **30**, 559–566.
Tomita, T. (1976) Electrophysiological studies of retinal cell function. *Invest. Ophthal.* **15**, 171–187.
Toyoda, J., Nosaki, H. & Tomita, T. (1969) Light-induced resistance changes in single photoreceptors of *Necturus* and *Gekko*. *Vision Res.* **9**, 453–463.
Toyoda, J. I., Hashimoto, H. & Ohtsu, K. (1973) Bipolar amacrine transmission in the carp retina. *Vision Res.* **13**, 295–307.
Trifonov, Y. A. (1968) Study of synaptic transmission between photoreceptors and horizontal cells by means of electric stimulation of the retina. *Biophysika, Moscow* **13**, NS (In Russian).
Uga, S. & Smelser, G. K. (1973) Comparative study of the fine structure of retinal Müller cells in various vertebrates. *Invest. Ophthal.* **12**, 434–448.
Werblin, F. S. & Dowling, J. E. (1969) Organization of the retina of the mudpuppy, *Necturus maculosus*. II. Intracellular recording. *J. Neurophysiol.* **32**, 339–354.
Witkowsky, P. & Dowling, J. E. (1969) Synaptic relationships in the plexiform layer of the carp retina. *Zeit. Zellforsch.* **100**, 60–82.
Yagi, T. (1986) Interaction between the soma and axon terminal of retinal horizontal cells in *Cyprinus carpio*. *J. Physiol.* **375**, 121–135.
Yamagida, T. & Tomita, T. (1982) Local potassium concentration changes in the retina and the electroretinographic (ERG) b-wave. *Brain Res.* **237**, 479–483.
Zanen, A. (1973) Contribution à l'étude électrophysiologique des mécanismes protorecepteurs de l'oeil normale. Thesis, Univ. Brussels.
Zanen, A. & Debecker, J. (1971) Visual pigments and melanin contributions to the fast photovoltage of the human eye. *Vision Res.* **11**, 169–172.
Zanen, A. & Debecker, J. (1975) Wavelength sensitivity of the two components of the early receptor potential (ERP) of the human eye. *Vision Res.* **15**, 107–112.

12. ELECTROPHYSIOLOGY OF THE RETINA: FURTHER ASPECTS

In this chapter we shall examine the responses of ganglion cells to stimulation of the retina in considerable detail, since these responses, provided the stimuli are chosen appropriately, can reveal the extent of the processing of visual information that has taken place after the initial photoprocess in the rods and cones. Adequate interpretation of the ganglion cell's response will clearly depend on knowledge of the synaptic relations between all the neuronal cellular elements of the retina. These have been examined with care in the primate, and more exhaustively, in the cat's retina, largely by Boycott, Kolb and Nelson and their collaborators. We may begin, however, with a description of the responses of the retina, as revealed in ganglion cells, to several types of stimulus, and only later consider the detailed synaptic arrangements, an understanding of which will contribute to the elucidation of the processing that has taken place in the retina.

QUANTITATIVE ASPECTS OF CENTRE SURROUND ORGANIZATION

Determination of Field Size

This is of great interest from the point of view of establishing the relation of the centre- and surround-mechanisms to the underlying retinal morphology. By increasing the size of a spot-stimulus applied to an ON-centre cell, its response will increase due to spatial summation, and the diameter of the spot giving optimal discharge is the diameter of the field-centre; as the size of the spot increases further, the inhibitory action of the surround becomes manifest. The size of the field-surround is best determined by projecting annuli of increasing diameter on to the receptive field; the effects of the annulus on the discharge caused by a small spot projected on to the centre is a measure of the effect of the annulus; if it increases the discharge, the annulus is within the field-centre, if it decreases it, it is within the surround. Figure 12.1 shows a typical example where a discharge of 100 represents that due to the central spot alone; the centre of the field is clearly some 2 degrees in diameter and the surround extends beyond 9 degrees, showing a maximal inhibitory action at about 3.5 degrees.[1]

Effects of Field Size

Rodieck & Stone (1965b) measured the responses of centre and periphery of cat ganglion cell receptive fields to small spots of light, using, as a measure of the response, the summated spikes during the interval of summation; the summation was carried out over small intervals of time and the result presented as a response histogram (Fig. 12.2). Special attention was paid to the sizes of receptive fields, summation within the field, and interaction between centre and surround. In general, the fields were radially symmetrical, and the maximal response of the central region was usually at the geometrical centre,

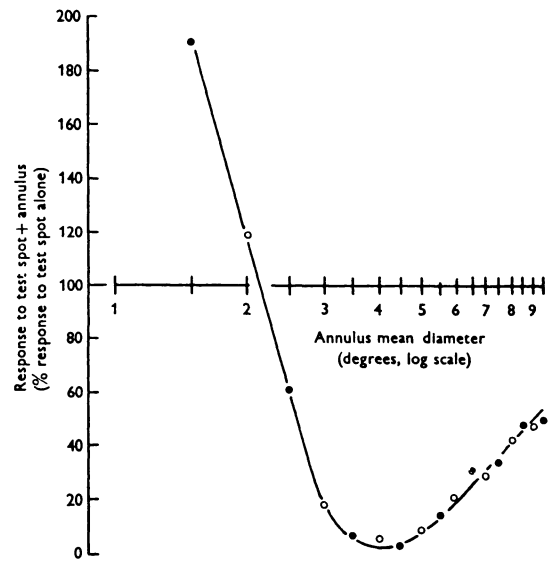

Fig. 12.1 Determination of the size of the receptive field. An annular stimulus is projected on to the retina and the discharge and its effects on the discharge caused by a small centred spot are recorded. A discharge of 100 represents that due to the central spot alone; when combined with annuli of increasing diameter the discharge decreases; annuli of smaller diameter than that of the test spot cause an increased discharge. The diameter of the centre-excitatory field is clearly about 2°, whilst the inhibitory surround extends to beyond 9°, (Hammond, *J. Physiol.*)

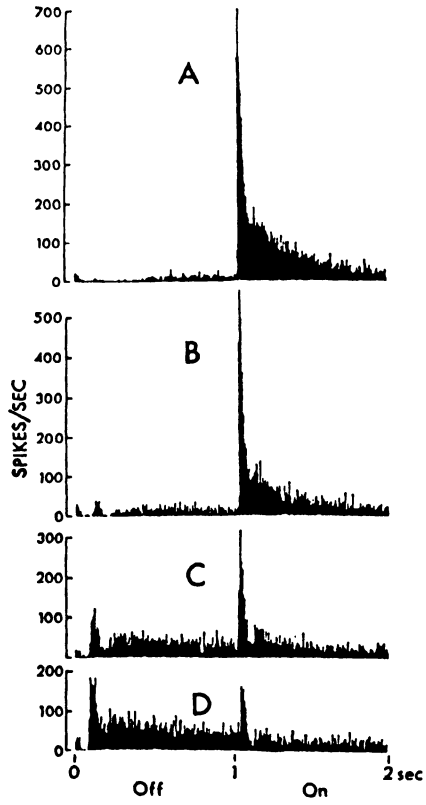

Fig. 12.2 Illustrating the transition from a pure ON-response in A to an ON–OFF response in D. A small spot of light was flashed for 1 sec off and 1 sec on. A shows the prominent ON-response of the centre with suppression of background during the OFF-phase. At B to D the flashes were on more and more peripheral parts of the receptive field. (Rodieck & Stone, *J. Neurophysiol.*)

but not always. The sizes of the central areas varied from 0.5 to 4 degrees. Beyond the centre, the strength of the surround-response increased quickly to a maximum and then gradually decreased until no response could be obtained, the limiting size of the peripheral field being determined by the intensity of the spot stimulus. When the retina was stimulated by a large uniform field, the response of a given unit was that of its centre, i.e. surround and centre did not neutralize each other completely; as Barlow *et al.* (1957) had found, dark-adaptation abolished the surround-effect. Usually a region in the receptive field could be found that gave an ON–OFF response and this was confined to a narrow ring; spot of light flashed 1 second off and 1 second on; it is an ON-centre field and the spot is projected first on the centre (A) and then more and more peripherally, and the transition from a pure ON-response to the ON–OFF response in D is clearly seen. A moving spot was a most effective stimulus, and the response to a small movement varied with the initial position in the receptive field and the direction of the movement; for an ON-centre unit, centripetal movement of the spot anywhere within the border of maximum OFF-surround caused excitation and outside it, inhibition. The converse was true for OFF-centre fields (Rodieck & Stone, 1965a).

CLASSIFICATION OF GANGLION RECEPTIVE FIELD TYPES

Since Kuffler's demonstration of the centre-surround organization of the ganglion cell's receptive field, a variety of subdivisions of these ganglion cells have been made on the basis of special features of their responses in addition to the main classification of ON-centre–OFF-surround and OFF-centre–ON-surround. Additionally, other classes of cells have been described lacking the centre-surround antagonism, such as direction-sensitive units, responding to a spot of light only when it was moved across the retina in a specific direction, and so on.

X- and Y-cells

The first main subdivision was that of Enroth-Cugell & Robson (1966), who used grating stimuli, similar to those employed by Campbell in studies of contrast-sensitivity (p. 381), to characterize the responses of ganglion cells. They found that some cells, their X-cells, behaved as though the responses to individual units of area in the field were linearly additive, the units in the centre adding to give a combined centre-response, and the units in the periphery adding linearly to give a combined surround-response. The final response of a neurone would be determined by subtraction of the combined centre- and surround-responses. A striking example of this linearity of interaction between centre and surround is shown in Fig. 12.3 from a later paper (Enroth-Cugell & Lennie, 1975). The upper straight line shows the increase in firing frequency of an X-cell in response to a spot of light of increasing luminance; the lower line gives the response when an annulus of fixed luminance is present at the same time; at each level of luminance of the central spot, the surround reduces the discharge by a fixed amount.

Null Point

With the *Y-cells* no such linearity was present. Enroth-Cugell & Robson showed that with the linear, or X-cells, two positions of a grating on its receptive field could be found that gave no response (null positions), the positions depending on the phase of the grating in relation to the centre of the field, as illustrated by Fig. 12.4. The existence of these null points means that when the illumin-

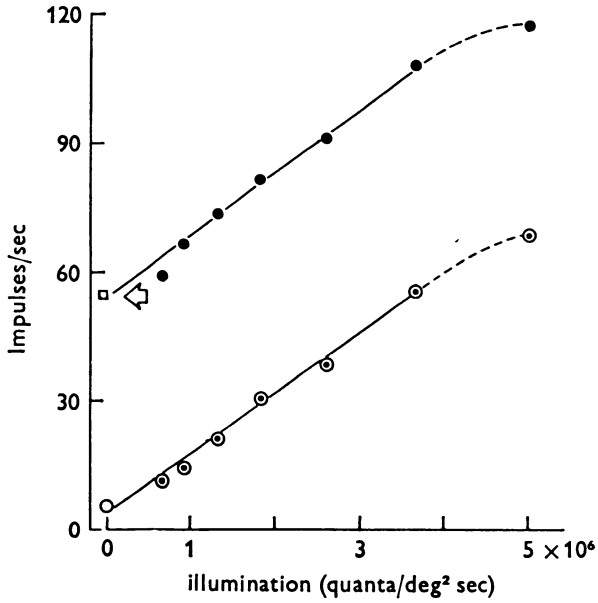

Fig. 12.3 Illustrating the linear summation of centre and surround responses of an X-type ganglion cell. The upper line represents responses to increasing intensities of a spot (0.18°) of light. Open arrow indicates background discharge. Lower curve represents response to same spot but presented with annulus of 1.5–11°. Point for zero spot illumination (open circle) gives the discharge during presentation of the annulus alone. Note how the addition of the annulus uniformly lowered the curve, without change of slope, implying additive combinations of centre and surround responses. (Enroth-Cugell & Lennie, *J. Physiol.*)

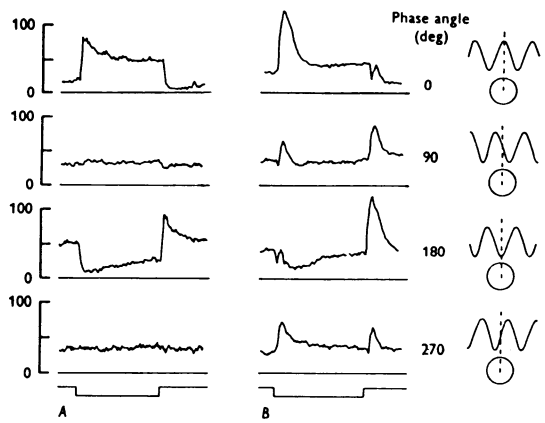

Fig. 12.4 Illustrating the null-point. A is the response of an OFF-centre X-cell; the phases of the grating in relation to the centre of its receptive field are indicated on the right. In order to evoke a response, the contrast was turned on and off, as indicated in the lowest traces where a downward deflection indicates a turning off. Note that with the X-cell there are two positions of the grating that give a null response. B shows the responses for a Y-cell which fails to exhibit a null-point. (Enroth-Cugell & Robson, *J. Physiol.*)

ations over both halves of the receptive field are equal their responses just balance. As Fig. 12.4 shows, no such null-point can be found with the Y-cell due to an absence in linearity of summation of the effects of light and dark. When the grating was caused to drift over the retina in a cyclical fashion—temporal modulation—the X-type of cell responded cyclically in phase with the temporal modulation, but the Y-cell's response was more complex, indicating non-uniformity in response over the receptive field.

Calculated Responses

Rodieck & Stone, on the basis of studies of this sort, computed the effects of stimulating a receptive field by a moving pattern; to do this it was necessary to make assumptions as to the way in which the different regions of a given field interacted, i.e. the manner in which similar portions summated and opposite portions subtracted.

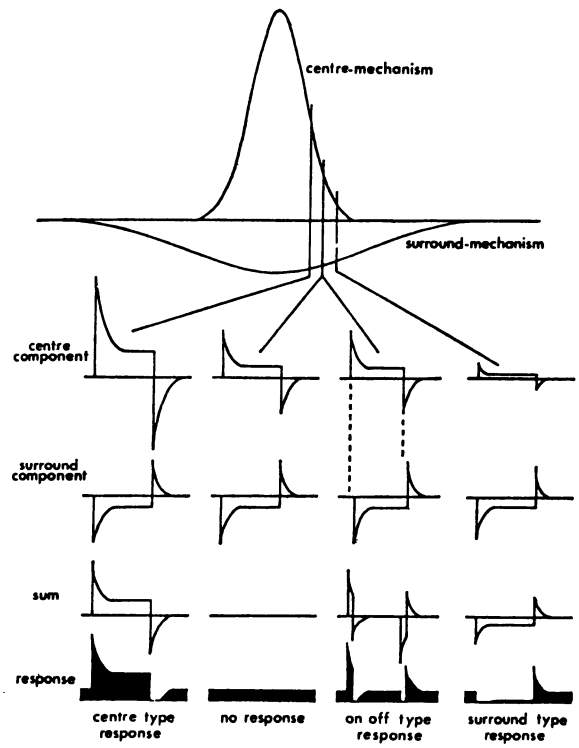

Fig. 12.5 At the top the theoretical responses of the centre and surround mechanisms are depicted, in this case an ON-centre unit with positive response in the centre and a smaller negative response over the whole field. Near the centre of the field, as the left column of hypothetical responses shows, the centre mechanism predominates; a little farther out, centre and surround cancel completely; still farther out the response becomes ON–OFF, and in the extreme periphery of the field the response is that of the surround only. (Rodieck & Stone, *J. Neurophysiol.*)

They accepted the suggestion of Wagner *et al.* (1963) that the surround field, did, in fact, extend into the centre, so that the response to a spot on the centre was really the algebraic sum of centre and 'surround' responses; the situation is illustrated in Fig. 12.5, the curves indicating the relative effectiveness of stimuli falling on different portions of the centre and surround. The centre mechanism has a steep outline whilst that of the surround is altogether broader; the diagrams below indicate the hypothetical results of interaction when stimuli fall in more and more peripheral parts of the field, leading to typical centre-type response, no response, ON–OFF response, and surround-type response. The response of a unit to the movement of a contoured body passing across it will be given by the responses to movement of its leading and trailing edges, and Rodieck (1965) was able to predict these, on the basis of his simple theoretical treatment.

Sustained and Transient

Later, Cleland *et al.* (1971, 1973) classified the cells in accordance with the duration of their responses, *sustained* and *transient*, and these were probably equivalent to X- and Y-cells respectively of Enroth-Cugell & Robson.

Figure 12.6 shows the difference in response to a spot of light centred on the receptive fields of a sustained and transient cell respectively. The responses to gratings, moved steadily across the receptive field, are correspondingly different; thus there were bursts of response as each bar moved across the receptive field; as the spatial frequency of the grating, was increased, i.e. the fineness of the pattern (p. 381), the difference between the two became manifest; the sustained unit continued to modulate its discharge about a mean level until the lines became too fine to allow discrimination, whereas the transient unit's modulations soon ceased, giving an unmodulated increase in discharge while movement continued, and returning to the unstimulated level when movement ceased. With the finest patterns there was only a brief transient discharge when the grid was jerked into motion. Clearly the sustained unit is specifically suited to respond to the spatial pattern of the stimulus, whereas the transient unit seems to represent the initial stage in development of a specific sensitivity to motion, its main responsiveness being to the passage of an object suddenly crossing or moving within the receptive field.

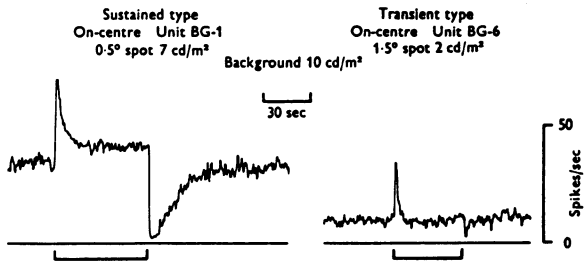

Fig. 12.6 Sustained (left) and transient (right) responses to a spot of light. In each case a centred test spot, adding a luminance of about 10 × threshold, was turned on for the duration indicated by the thick bar beneath each record. (Cleland *et al.*, *J. Physiol.*)

Brisk and Sluggish

Finally Cleland & Levick (1974) introduced a further dichotomy of *brisk* and *sluggish*. Thus, within the centre-surround units there are four subclasses so that, in all, we can characterize eight classes of ganglion cell in accordance with the type of receptive field, the briskness or sluggishness of the response and the transience or sustained nature of the response. A battery of tests was devised to permit the characterization of a given unit; thus the response to standing contrast was measured by projecting a spot of light for ON-centre cells, or unmasking a black disc for OFF-centre cells centred on the receptive field for 20 sec or longer and recording the mean impulse rate. An example is shown in Fig. 12.7 for all eight types of concentrically organized ganglion cells. The response of the sustained brisk cell rose from a moderate level of maintained discharge sharply to a peak, declined a little and was maintained at a high plateau. When the spot was turned off, the discharge ceased but returned slowly to the original maintained discharge. The sluggish sustained ON-centre unit had a lower maintained discharge, which was very regular; when the light was turned on, the discharge accelerated and, with a very small overshoot, reached a plateau which only declined slightly. A characteristic feature of the sluggish maintained ON-centre cell is that the strongest responses were obtained with 1 to 2° spots, whereas the corresponding brisk cells required diameters of 0.3 to 0.7°. This standing contrast-test failed to bring out differences between sluggish and brisk cells of the transient class, so that the use of other tests was necessary. For example, the speed of motion of a spot across the retina was a useful stimulus-parameter, sluggish cells being primarily sensitive to slow movements (about 3°/sec) whilst brisk cells always responded well to rapid movements (*ca.* 100°/sec or greater).

This sensitivity to motion is also manifest in the 'periphery effect' of McIlwain (1964); transient units are weakly excited by stimuli outside the conventionally defined receptive field; the response to the continual movement of a large pattern is an augmentation of the maintained discharge with no relation to the actual movements.

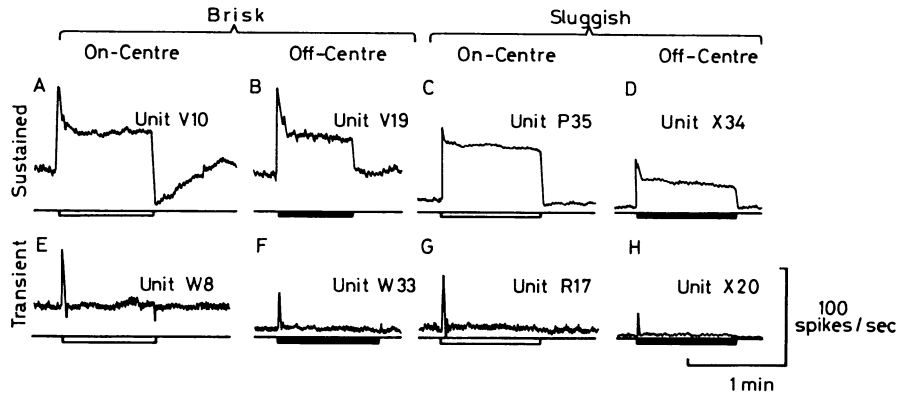

Fig. 12.7 Responses to standing contrast for all eight types of concentrically organized ganglion cells. A projected spot of light was turned on (A, E, G) or a contrasting disk was unmasked at the centre of the receptive field for the duration shown by the signal bar below each base line (□ brightening, ■ darkening); time calibration at lower right. The jagged line traces the mean discharge rate (calibration at lower right). The base line of each record corresponds to zero spikes/sec. A, 0.5° spot, 10 cd/m^2; B, 0.5° black disk; C, 0.8° white disk; D, 1.2° black disk; E, 1.0° spot, 6 cd/m^2; F, 0.5° black disk; G, 0.5° spot, 20 cd/m^2; H, 0.8° black disk. (Cleland & Levick, *J. Physiol.*)

Conduction Velocities

There is little doubt that the transient units have the higher conduction velocities, so that Cleland *et al.* (1971), for example, found a conduction time of 2 to 3 msec to the lateral genicular body compared with 3.4 to 6 msec for sustained cells.

Receptive Fields

Both centre and surround areas of sustained units are smaller than those of transient units.

Units with Non-concentric Surrounds

Cleland & Levick (1974) found some 73 units out of 960 with receptive fields departing from the common centre-surround pattern.

Local Edge Detectors

These have also been called 'excited by contrast' units (Stone & Hoffmann, 1972) and are distinguished from concentric field units by their responses to centripetal and centrifugal movement of small contrast targets. Figure

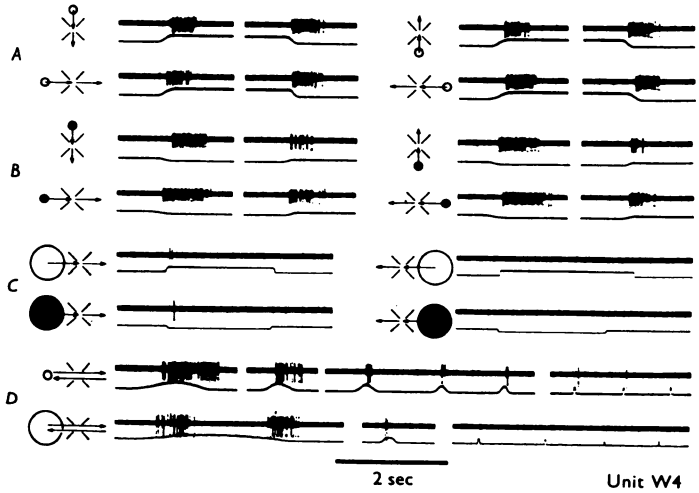

Fig. 12.8 Local edge detector: responses to moving targets. A, 1° white disk moved into centre of receptive field (alignment marks on diagrams to the left of records), stopped, then moved out in the same direction; all four directions (horizontal and vertical) tested. In each record, upper trace is spike record (positivity down) of the cell; lower trace is the output of a photomultiplier receiving light via an optical system from a region 2° in diameter centred on the receptive field (increasing light caused upward deflexion). B, same for 1° black disk. C, 4° white and black disks used. D, 1° white disk (upper row) moved completely across the receptive field at increasing speeds (range 2.3°/sec at left, 75°/sec at right); 4° white disk (lower row) moved similarly (2.2°/sec at left, 430°/sec at right). (Cleland & Levick, *J. Physiol.*)

12.8 illustrates some responses to a white spot; it is moved first into the centre of the field, producing a burst of spikes; on removing it, in the same direction, a second burst occurs, a form of behaviour different from that of an ON-centre unit. A black disc had the same effects. Large spots were much less effective, indicating that an important feature of the stimulus was the establishment of a contrast on the receptive field; when slowly moving targets were used, responses occurred as the leading or trailing edges passed across the receptive field. The surround-field produced no discharge when an annulus of light was presented, but it apparently exerted a strong inhibitory action on the centre, and this meant that discharge could be evoked by moving edges in the centre provided that edges were not moved at the same time in the surround—hence the terms 'local edge detector'.

Direction-sensitive Units

These are much less prominent and selective as to direction than the rabbit units described by Barlow *et al.* (1964) and Barlow & Levick (1965), which will be discussed later.

Colour-coded Units

The responses of units in the visual pathway to different wavelengths of light will be discussed more fully in the section on colour vision. The basis of colour-coding is that the character of the response should vary according to the wavelength of light, a character that does not depend on mere intensity of stimulation. In the cat, Cleland & Levick found very few with this property; they had in common an ON-response to blue light in the centre of their receptive fields and an OFF-response to green and red light. By varying the wavelength of the stimulating light, a 'cross-over point' could be found at which the excitatory (ON) effect of short wavelength light could be balanced by the inhibitory (OFF) effect of longer wavelength light; this occurred at about 509 nm.

Uniformity Detectors

These cells had a brisk maintained discharge which was reduced or abolished by all forms of visual excitation, whether white spots on a dark background or black spots on a light background; moving a grating across the receptive field caused an immediate cessation of discharge, which began again soon after the movement stopped; by continuously moving the grating, the discharge could be suppressed indefinitely. Thus the message conveyed to the brain by discharge in these units is simply: 'No recent temporal or spatial discontinuities over the region covered by the receptive field' and it probably corresponds to the 'suppressed-by-contrast' unit of Rodieck (1967) but is probably different from similarly entitled units described by Stone & Fukuda (1974).

Edge-inhibitory OFF-centre

This is similar to the 'suppressed by contrast' units of Stone & Fukuda (1974), since a grating suppressed discharge not only when moving but also when maintained stationary. Analysis of its receptive field with small spot-stimuli showed that it differed from the classical OFF-centre concentric unit, in fact its field could be considered as being made up of three concentric processes, a central patch which, stimulated in any fashion, caused decrease or abolition of the maintained discharge; a surrounding zone of OFF-responsiveness, and an outermost annulus of ON-responsiveness.

W-cells

Stone & Fukuda (1974) compared the X- and Y-cells with another category, first described by Stone & Hoffmann (1972) and termed W-cells; conduction-velocities were in the order: $Y > X > W$, so that the W-cells were the slowest conducting; as with the Y-cells, their receptive fields were larger than those of the X-cells. They concluded that the W-cells were a very heterogeneous group, but a prominent feature was the maintained discharge when the illumination was sustained, so that they might signal luminosity. According to Fukuda & Stone (1974) W-cells do not project to the lateral geniculate nucleus, but only to midbrain structures such as the superior colliculi (see, however, p. 355).[2]

Directional Sensitivity

As we shall see, neurones within the cerebral cortex were early shown to be sensitive to the direction in which a moving spot passed over the retina; that a single neurone may respond so selectively to the retinal stimulus requires a considerable degree of integration and selection during the transmission of information; thus it has to ignore messages coming from receptors not on this line of movement, and has to take account of the fact that the stimuli in receptors along this preferred direction are sequential, and so on. Barlow *et al.* (1964) showed that, already at the ganglion cell level in the rabbit, this discriminative power is present; they observed many cells with the typical centre-surround arrangement with either ON- or OFF-responses in the centre and OFF- or ON-responses in the surrounds. Others, however, resembled the ON–OFF units of the frog over the whole field, and these showed directional sensitivity in the sense that their maximal response occurred when a moving spot traver-

sed a certain 'preferred' direction, whilst there was no response at all to movement in the opposite, 'null', direction. That inhibition was concerned was suggested by the observation that movement in the null direction would inhibit spontaneous activity; again, very slow motion in the null direction would evoke a response. Thus we may imagine that the bipolar cells related to a series of receptors, located along a certain direction in the retina, all feed their responses into a ganglion cell; these responses are excitatory and inhibitory, the inhibitory effect being transmitted, after a small latency, to the ganglion cell.

Inhibition

The picture that fitted best with the experimental facts is illustrated by Fig. 12.9. Activity roused at either ON or OFF in the receptors C, B, etc., is passed laterally to inhibit the bipolar cell B. $\sim$C', A. $\sim$B' and, so on. This inhibition prevents the excitatory effect on B and A from getting through when the motion of the spot is in the null direction, but arrives too late if motion is in the preferred direction. If the movement is very slow we can imagine easily that the inhibition may not last sufficiently long to inhibit the responses of adjacent elements. On this basis, two stationary stimuli, falling on regions of the retina separated along the preferred direction in sequence, will give a large response when the sequence corresponds with motion along the preferred direction and a smaller response for the null direction. In fact this was found, provided the separation was small; in the null direction sequence, the second stimulus could give no discharge at all (see also, Michael, 1968). Barlow & Levick (1965) postulated that the inhibitory action was mediated by the horizontal cells, and a study of Werblin (1970) on the responses of the different retinal cells—receptors, bipolars, etc.—to moving spots of light are consistent with this inhibitory role of the horizontal cells.

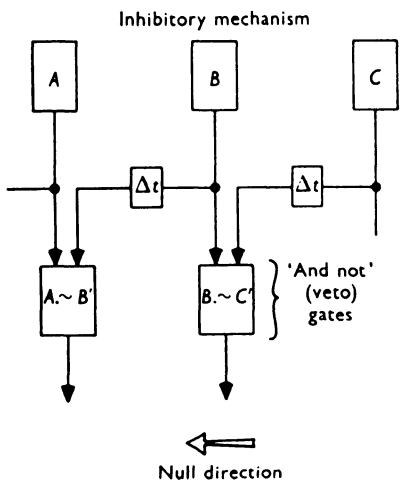

Fig. 12.9 Hypothetical mechanism for direction-sensitive ganglion cell. The receptor elements A, B, C have a direct excitatory influence on bipolar cells and an inhibitory action on adjacent bipolar cells in the null direction, the inhibitory action occurring after a latency of Δt. These are said to act as 'And not' veto gates. A spot of light passing in the null direction, i.e. from right to left, would tend to inhibit its influence on successive receptors. (Barlow & Levick, *J. Physiol.*)

The Preferred Directions

Oyster & Barlow (1967) determined the preferred directions in many units of the rabbit retina and found that they fell into four groups, and these corresponded accurately with the directions of movement of the fixation axis when the four rectus muscles were allowed to act separately; these were not purely horizontal and vertical, but inclined to these by a few degrees. Thus if the retina is to act as a servo-system correcting movements of the eyes, the direction-sensitive units fulfil an obvious role here.

Measurement of Transience

Cleland (1983) measured the responses of his 'brisk transient' class of ganglion cells to a spot of light flashing at 0.5 and 8 Hz; the response was lower at the low frequency, and the ratio of the responses at 0.5 and 8 Hz was used as a measure of 'sustainedness' of the cell. With sustained (X) cells, this did not vary with eccentricity in the retina, whereas with transient (Y) cells, the 'transience' did increase with eccentricity.

Effects of Velocity

As a bar moves across the receptive field, the change in light-flux, which is a measure of the stimulus, increases until the field has been crossed; as velocity is increased there is a steady increase in the light flux that can usefully be employed in generating the stimulus, if the changes fall within the summation-time of the cell. At low velocities the summation-time will be exceeded before the bar has traversed the receptive field, so that increasing velocity will produce larger responses because of the increased light-flux that can be usefully employed. When velocity is increased beyond a certain point, all stimuli fall within the summation time, but the faster the bar moves the less the light-flux falling on the field, so that response declines. Figure 12.10 illustrates the curve for a brisk transient cell of the cat; the cell may be said to be 'tuned' to velocity, and the degree of tuning is conventionally represented by the Tuning Ratio: Upper Velocity $\div$ Lower Velocity at

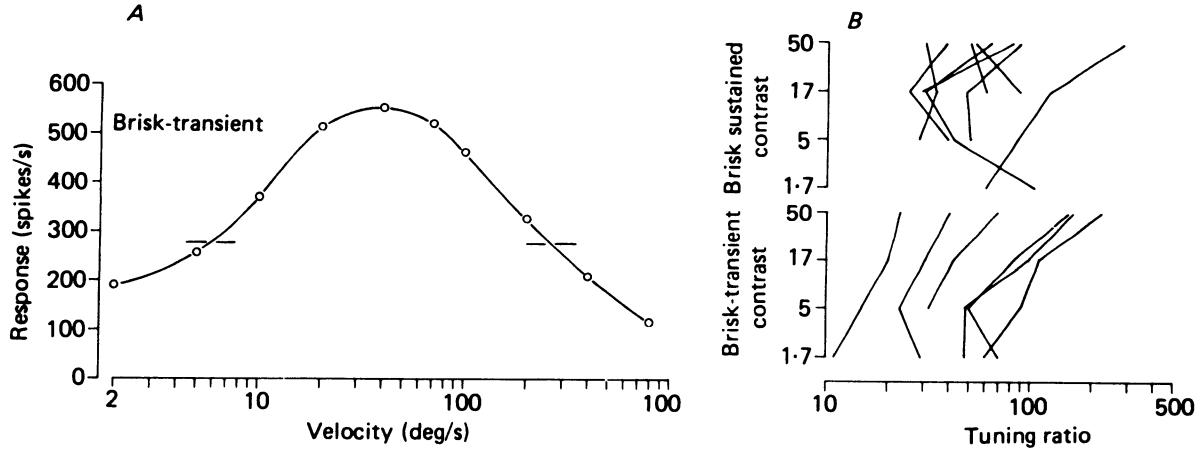

Fig. 12.10 *A*, velocity–response curve for a brisk-transient cell plotted on a linear ordinate scale. The horizontal lines indicate points on the curve at half-height used for determining the tuning ratio (defined as the upper velocity divided by the lower at half-height). The contrast was 17. *B*, tuning ratio for eight brisk-sustained and six brisk-transient cells at a range of contrasts. There is a general trend towards broader turning at high contrasts. (Cleland & Harding, *J. Physiol.*)

half-height of maximal response. Both sustained and transient cells showed about the same tuning of about 70. As we shall see, this figure is much greater than that of the more narrowly tuned cortical cells, of about 20. Within the area centralis, the brisk transient cells responded more readily at high velocities than brisk sustained; in the periphery, however, there was no difference.[3]

Periphery- or Shift-effect

Ikeda & Wright (1972a, b) have shown that there is a region beyond the classical inhibitory surround of an ON-centre ganglion cell, which they describe as disinhibitory. Thus a spot of light was flashed on to the centre of an ON-centre ganglion cell to produce a maximal response; as the spot was made to fall on more peripheral parts of the field, the response decreased, and at about 2 to 2.5° an OFF-response appeared, although the ON-response was larger; on moving to more eccentric positions, the OFF-response disappeared and the ON-response increased; and it was this range, extending from about 3 to 5°, that was described as the disinhibitory zone. When the spike-count for stimulus-ON was plotted against eccentricity, the curve of Fig. 12.11 was obtained, the hump between about 2 and 4° representing the disinhibitory surround. Although harder to demonstrate, a similar surround was found in sustained cells, but because of their much smaller receptive fields, the degree was much less, about 0.6°.

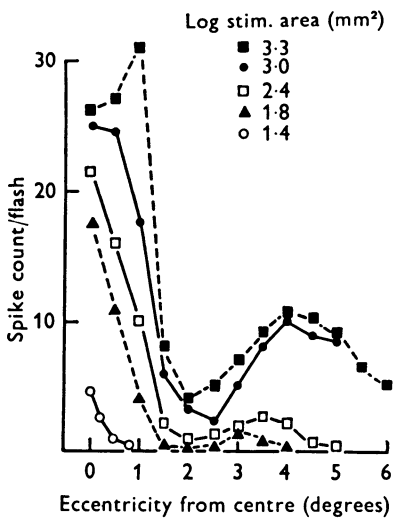

Fig. 12.11 Variation in spike response to a spot of light with eccentricity from the centre. (Ikeda & Wright, *J. Physiol.*)

Centre-surround Interaction

According to Ikeda & Wright the disinhibitory surround of the transient cell may be regarded as part of a zone, concentric with the field-centre, in which interaction between periphery and centre takes place, a zone in which a spot of light will increase the sensitivity of the central spot. Since the transient cell analyses the dynamic aspects of the visual stimulus, this disinhibition might be valuable in signalling movement of the visual stimulus over the retina permitting the fixation-reflex response. With the sustained cells, whose function is concerned with analysis of the spatial characteristics of the visual field, a zone of peripheral disinhibition may contribute to spatial fre-

quency-tuning, but the exact manner in which this can be brought about is by no means clear.

Periphery Effect

This extension of the surround beyond the classical borders is probably merely one example of the more general 'periphery effect' first described by McIlwain (1964, 1966) who stimulated the centre of a receptive field with weak flashes and moved a black disc in the periphery 90° away from the centre of the field; in this case there was an increase in firing rate. The essential feature of the peripheral stimulus was not the change in retinal illumination but the edge of the contrast, and by using a large peripheral grating as in Fig. 12.12, which was moved just the width of a bar of the grating, very powerful discharges were obtained from a ganglion cell whose field had not been exposed to the grating. When the grating was shifted, the ON-centre unit was illuminated at its centre with its surround in darkness and there was a large increase in discharge. If the centre was in darkness and the surround illuminated there was a suppression of discharge (Kruger & Fischer, 1973). With OFF-centre cells the reverse occurred.

Perception of Eye Movement

Ikeda & Wright considered that the periphery or 'shift' effect was purely a function of transient Y-cells, but Barlow *et al.* (1977) could demonstrate it in sustained X-cells and they have suggested that, because it depends quantitatively on the size of retinal field stimulated, it is

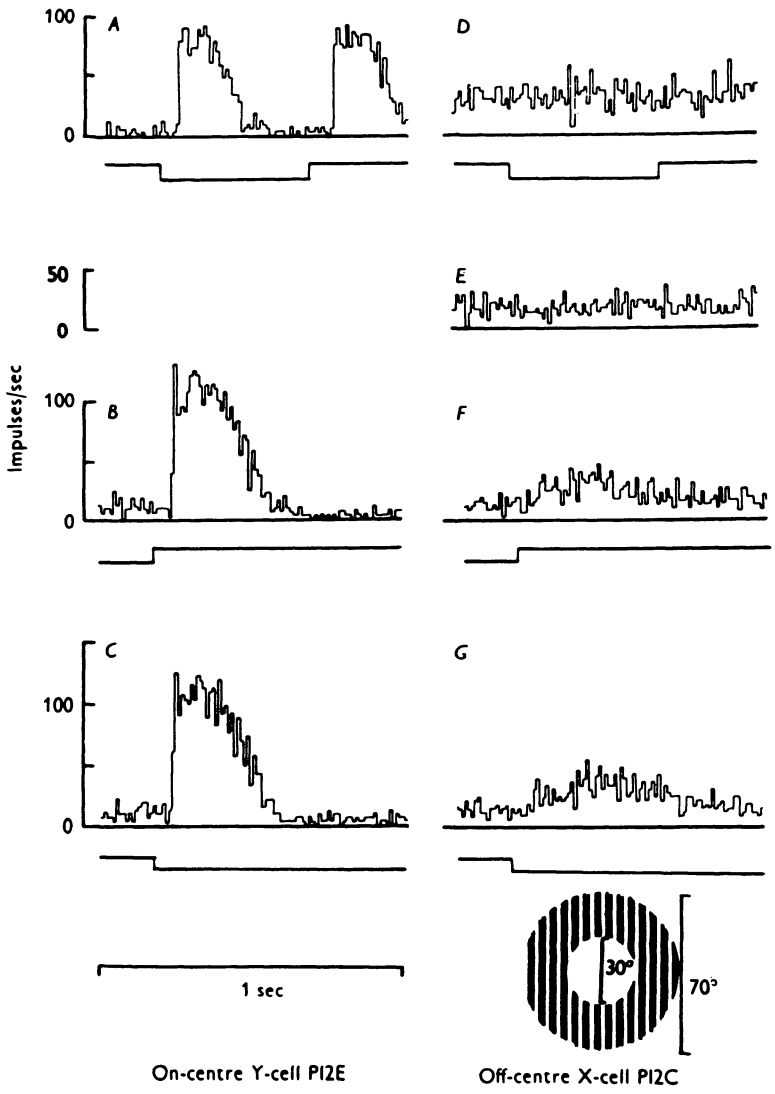

Fig. 12.12 Illustrating the 'periphery effect'. Responses of a typical transient Y-cell (A–C) and a sustained X-cell (D–G) to a shift of the grating shown at the bottom right. The receptive fields were centred in the central 30° disc where the view of the grating was occluded. The grating was moved just the width of a bar, so that the stimulus is essentially a movement of the striped pattern in the far periphery of the receptive field. Note that the sustained X-cell shows some response although much smaller than that of the transient Y-cell. (Barlow *et al.*, *J. Physiol.*)

concerned with signalling a movement of the eye since under these conditions the image of the whole field moves suddenly. Thus, when the eye moves, there is a transient discharge from all ganglion cells that depends on the change in illumination and not on its value at the new position, so that with each movement the pattern of impulse-frequency depends on both the luminous patterns existing in the present position as well as in the new one. Perceptually such a confusing situation is not manifest, and this could be due to the shift-effect which could act to suppress responses during movement thus 'wiping the slate clean' for the next image. During a saccade there is undoubtedly a rise in threshold, and it could be that the movement of the retinal image is the effective stimulus as MacKay's (1970) work suggested (p. 454).

Horizontal and Amacrine Cells

The large extension of the receptive field of ganglion cells (and geniculate cells, McIlwain, 1964) beyond their classical limits clearly indicates the influence of horizontal and amacrine cells which, by synaptic or electrotonic connexions, can transmit horizontally over large distances; and it is interesting that Ikeda & Wright (1972) pointed out that the periphery effects described by McIlwain and Kruger & Fischer were only seen in ganglion cells whose receptive fields did show the continuous expansion with increasing spot size.[4]

SOME MORPHOLOGICAL CORRELATES

Relation to Ganglion Cell Morphology

Boycott & Wässle (1974) characterized the cat's retinal ganglion cells morphologically on the basis of perikaryon size and mode of branching of the dendritic tree; three classes were derived on this basis, namely α, β and γ; it was important to appreciate that there were progressive changes mainly in size as one passed from the central area to more peripheral regions, so that comparison of types must be made at a given retinal point, in fact the variation in, say, the dendritic field size with retinal eccentricity for a given type of cell can give an important clue to its electrophysiological behaviour. Thus Fig. 12.13A shows how the variation in centre-receptive field size of brisk sustained cells correlates with the size of dendritic fields of β cells, leading Cleland & Levick to equate the two. In B there is a corresponding plot for brisk transient cells and α-cells, and in C for sluggish and γ cells. On the basis of this comparison, the correlations indicated in Table 12.1 have been made, sluggish concentric cells corresponding apparently with the γ-cells.[5]

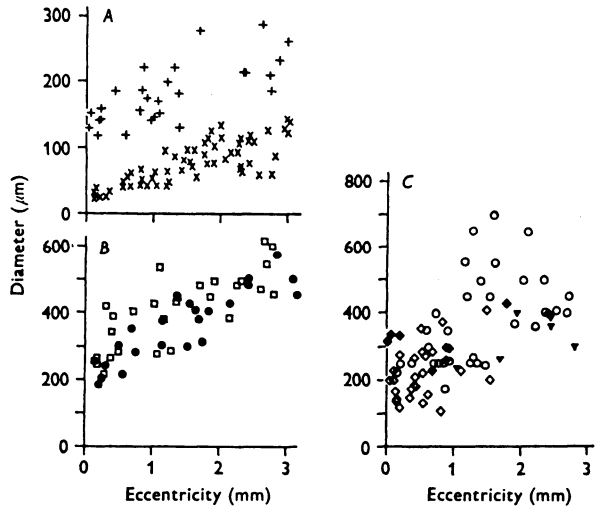

Fig. 12.13 Comparison of receptive field centre sizes with dendritic fields as functions of eccentricity from the *area centralis*. A, Brisk-sustained centres (+) and dendritic fields of β cells (×). B, brisk-transient (□) and α cells (●). C, sluggish (◇, ◆) and γ cells (○ ▽); ◆ signifies members of the subclass; on-centre sustained; ▽ signifies members of the δ subclass. (Cleland & Levick, *J. Physiol.*)

Table 12.1 Receptive fields related to morphology of retinal ganglion cells (Levick, 1975)

Receptive field	*Morphology*
1. Concentric-surround	
(a) Brisk	
(i) Transient	α
(ii) Sustained	β
(b) Sluggish	
(i) Transient	$\gamma(\delta)$
(ii) Sustained	
2. Non-concentric	
(a) Local edge-detector	
(b) Direction-Selective	
(c) Colour-Coded	
(d) Uniformity-Detector	
(e) Edge-Inhibiting OFF-Centre	

Dendritic Tree and Centre Size

It was suggested by Brown & Major (1966) and Leicester & Stone (1967) that the size of the centre of a ganglion cell's receptive field was determined by the size of its dendritic tree, which would govern the number of bipolar cells that could make direct input to the ganglion cell. Peichl & Wässle (1979) pointed out that the dimensions of the dendritic trees were well established, whereas there was ambiguity with respect to the dimensions of the receptive fields, since the determination of these depended

Table 12.2 Receptive-field centre dimensions of cat retinal ganglion cells compared with diameter of the dendritic tree (Peichl & Wässle, 1979)

Reference	*Type*	*Central area*	*1 mm*	*2 mm*	*3 mm*	*4 mm*	*5 mm*
			Diameter of receptive field centre (min of arc)				
Peichl & Wässle (1979)	b.s.	18–23	20–40	30–60	33–60	50–77	—
	b.t.	52	60–100	70–135	80–140	100–150	115–155
			Diameter of the dendritic tree (min of arc)				
Boycott & Wässle (1974)	beta	6	10–25	15–35	20–50	25–60	30–65
	alpha	50	70–110	90–140	100–160	115–180	125–190

on the mode of estimation. By application of several tests they ascertained whether a given cell was an X- or Y-cell, and then proceeded to ascertain the size of its centre by three methods. One such method, finally used routinely, consisted in flashing a small spot of light at different positions in the receptive field, and positions found such that a response could just be detected 50% of the time, this point being taken as the border of the field. In Table 12.2 a comparison of dendritic tree size and receptive field centre is given. The correlation is good; it will be seen that the sustained X-cells (β-cells), presumably involved in spatial discrimination, have smaller receptive fields than those of the transient Y-cells, or α-cells.

LATER STUDIES

Subsequent studies based on more thorough staining of the cell bodies and their dendrites with reduced silver and by retrograde movement of horseradish peroxidase after injections into the lateral geniculate body, carried out in the laboratories of Boycott, Kolb, Peichl, Wässle and Fukuda have established an unequivocal correlation between the morphology of the alpha-cells, with very large cell bodies, and the brisk-transient Y-class of ganglion cells, on the one hand, and the smaller beta-cells with their sustained responses classified as X-cells (Peichl & Wässle, 1981; Wässle *et al.*, 1981a, b). Alpha-, or Y-cells constituted only some 4% of the total population in the cat, and the beta- or X-cells some 55%. In a recent study Fukuda *et al.* (1984) have characterized the receptive fields of more than 400 ganglion cells on the basis of X-, Y- and W-classification, and examined the morphologies of some 21 that were successfully recognized after horseradish peroxide injection. Receptive field sizes of X-, Y-, and W-cells were characteristically different, being 0.2–1.0°, 0.6–2.4° and 0.8–3.7° respectively;[6] axon diameters were greatest with Y-cells, less with X-cells and still less with W-cells, and this corresponds with Hsiao *et al.*'s (1984) study of optic nerve fibres which fell into similar categories. Fukuda *et al.* (1984) also examined their cell-types from this point of view; with X- and Y-cells, with roughly circular or oval dendritic extents the estimate of area was simple; with W-cells, with often very irregular

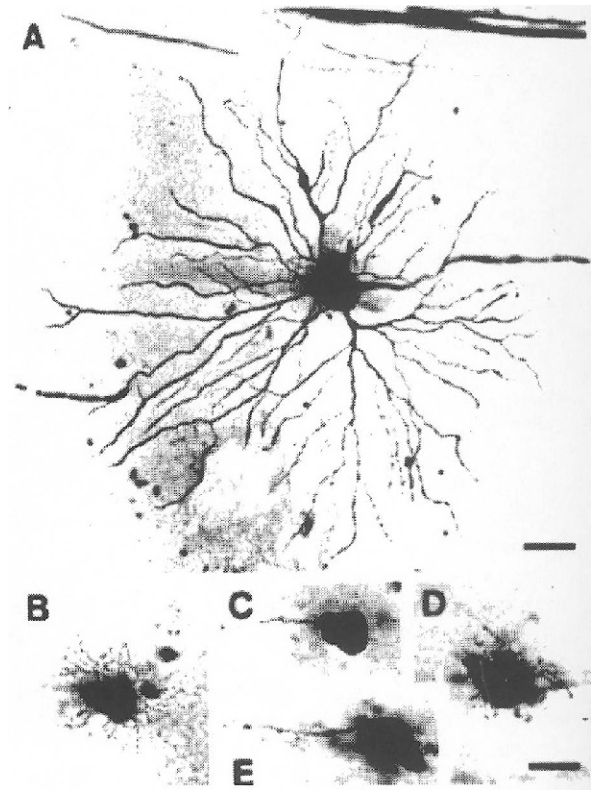

Fig. 12.14 Photomicrographs of a Y-cell (*A*) and two X-cells (*B–E*). Photographs *B* and *C* were taken from the same X-cell at different focal planes. Photographs *D* and *E* show another X-cell also at different focal planes. Bar, 50 μm in *A* and 20 μm in *B–E*. (Fukuda & Stone, *J. Neurophysiol.*)

dendritic trees, a correlation was harder to establish. As Fig. 12.14 shows, however, all three types show a reasonable correlation of receptive field size and dendritic tree. The X-cells reveal a greater field size than expected of their dendritic trees, perhaps due to some convergence through horizontal or amacrine cells. Y-cells, on the contrary, seem to have smaller field-centres than their dendritic fields.

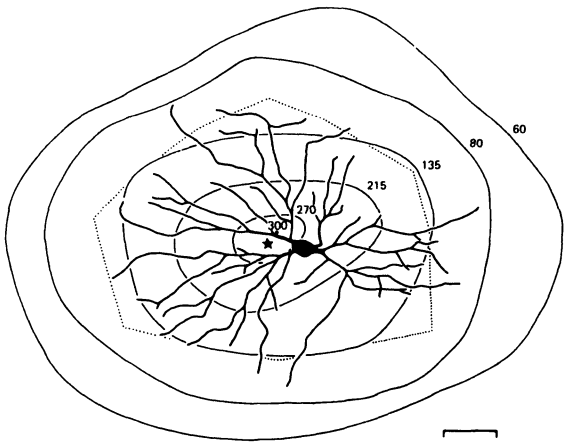

Fig. 12.15 Comparison of the dendritic tree and the receptive field centre of an off-brisk transient cell. The continuous lines are equal response contours and represent peak discharges of 270, 215, 135, 80 and 60 spikes/sec. The maximum discharge of 300/sec is marked by the centre dot. The dotted outline indicates the border, where a clear centre response could be detected on the audiomonitor. The asterisk shows the electrode position. The scale bar represents 100 μm on the retina or 0.5° of visual angle. (Peichl & Wässle, *J. Physiol.*)

The Alpha-cell Peichl & Wässle (1983) made a very elaborate study of the dendritic trees and receptive fields of alpha- or Y-ganglion cells in the cat retina, using a light-stimulus in the mesopic range. An example of the imposition of the receptive field on the dendritic tree is illustrated in Fig. 12.15, where it will be seen that the receptive field exceeds the area of the dendritic tree; specifically they found that always the receptive field of a brisk transient cell had a peripheral zone of some 100–150 μm where the cell was not anatomically present, presumably resulting from the convergence of additional receptors on to the ganglion cell, mediated through amacrine cells.

Multiplicity of Cell Types

The original studies of Boycott & Kolb led to a classification of ganglion cells into three to four types. A more thorough examination of the cat retina by Kolb *et al.* (1981) has revealed an embarrassing variety of neurones contributing processes to the inner plexiform layer; thus eight types of cone bipolars, cb1 to cb8 are pictured, cb7 being a giant bipolar; only one rod bipolar cell was found. In addition to the four types of ganglion cell described by Boycott & Wässle (1974) an additional 19 types were described falling into four groups with respect to cell-body size. Thus the largest, G1, of 30–40 μm were only alpha-cells; the next largest, 20–29 μm included beta- and delta-cells; the medium cells of 15–19 μm included the gamma-cells of Boycott & Wässle. Three pairs of cone bipolars ramified in sublaminae *a* and *b*; one straddled the *a* and *b* regions and one, cb4, was bistratified. Of the 22 or more amacrine cells, some could be paired according as they ramified in *a* and *b* sublaminae, e.g. A1 and A5, A19 and A22, A20 and A21.

SYNAPTIC RELATIONSHIPS AND NEURONAL CIRCUITRY

We may now return to the study of the morphology of the retina, which is, ultimately, the basis of the complex receptive fields of the ganglion cells.

Synaptic Types

If it is the rod or cone that absorbs the light-energy of the stimulus, it is the bipolar and horizontal cells that must transmit any effect of this absorption to higher regions of the central nervous system; consequently the relationship between these cells is of great interest. In general, the relation between receptor and neurone is of the synaptic type, in the sense that the dendrite of the bipolar cell, for example, comes into very close contact with the rod spherule or cone pedicle, whilst fusion of membranes does not occur, a definite synaptic cleft being maintained. The contacts are of two main types, namely an *invaginating synapse*, when the dendritic process penetrates deep into the pedicle or spherule, and a *flat contact*, when the synapse occurs more peripherally. A third type of contact, namely the gap-junction, is common, but in this case there is a cell intercommunication that does not rely on release of a transmitter from synaptic vesicles, but is brought about by so-called electrotonic coupling.[7]

The Triad

This represents a ribbon synapse, and is illustrated by Fig. 12.16, which shows a portion of a cone pedicle, CP, containing many vesicles reminiscent of synaptic vesicles as seen elsewhere in the central nervous system. The triad is formed by the penetration, into the invagination, of a central dendritic process from a bipolar cell, and the bipolar cell is described as an 'invaginatinvg cone bipolar', to distinguish it from a flat bipolar, when the synaptic contact is at the surface, quite frequently contacts being made at both sides of the invagination. The 'ribbon' appearing in the electron microscope as a densely staining lamellar substructure in the presynaptic terminal, is surrounded by a halo of synaptic vesicles, and it has been suggested that it is involved in regulating the supply of vesicles to one or other member of the postsynaptic dendritic processes.

The Dyad

This is another type of ribbon synapse found in the inner plexiform layer where bipolar cells synapse with amacrine

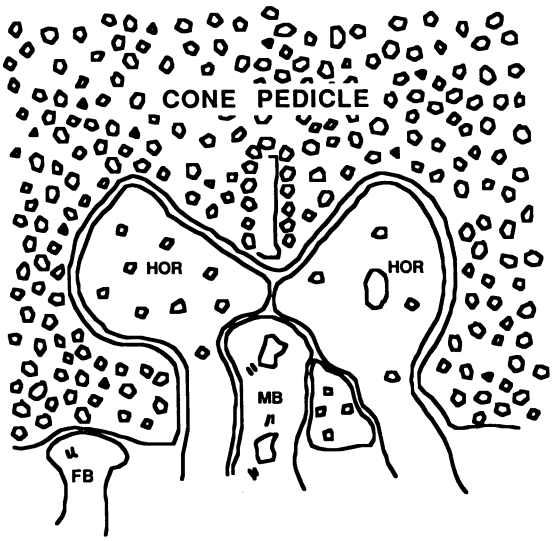

Fig. 12.16 Synaptic junction of the cone pedicle, called a triad. Two processes of horizontal cells (HOR), and a midget bipolar dendrite (MB) invaginate into the cytoplasm of the cone pedicle. (After Dowling & Boycott, *Proc. Roy. Soc.*)

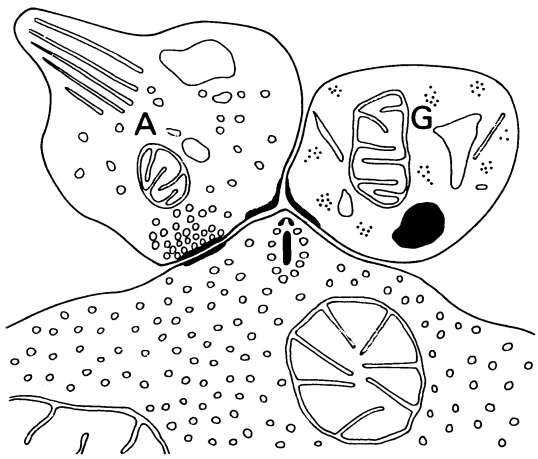

Fig. 12.17 Illustrating the dyad type of synaptic contact of the bipolar terminal with ganglion cell dendrite, G, and amacrine process, A. Frequently the amacrine cell process makes a synaptic contact backwards on to the bipolar terminal, forming a reciprocal contact between bipolar terminal and amacrine process. (Dowling & Boycott, *Proc. Roy. Soc.*)

and ganglion cells. One is illustrated in Fig. 12.17, the element containing the ribbon always being a bipolar cell axon terminal. Two postsynaptic processes are associated with each presynaptic ribbon site. The postsynaptic dyad elements are sometimes both amacrine cells, and at other times consist of one amacrine and one ganglion cell.

Serial Synapses

As described by Kidd (1962) a process is presynaptic to a second process which itself is presynaptic to a third process. Dowling & Boycott (1966), in their study of the primate retina, defined two synapses of this type; in the reciprocal synapse an amacrine cell process in a dyad made a synapse back onto the presynaptic bipolar axon terminal near the ribbon synapse, whilst in the serial synapse, as defined by them, an amacrine cell process was presynaptic to a second amacrine process which itself was presynaptic to a third element, the third being a bipolar terminal, a ganglion cell dendrite, or an amacrine process.[8]

Organization of the Retina

In an earlier chapter the general arrangement of the primate retina, as envisaged by Polyak's study, was described; perhaps the most important point emphasized by Polyak was the distinction between the midget system of bipolar and ganglion cells, providing a direct communication from cone to ganglion cell, and the more diffuse system mediated by diffuse bipolars that allowed for the convergence of many receptors on to a single ganglion cell, on the one hand, and also resulted in divergence of the response of a single receptor to excite many ganglion cells. The more recent studies of Boycott & Dowling (1969) and Boycott & Kolb (1973) on the primate retina have largely confirmed Polyak's presentation, but have corrected some errors. Their more extensive studies on the cat retina, valuable because so much electrophysiological work has been done on this species, reveal some differences from the primate, especially the absence of the midget type of bipolar cell.

Bipolar Cells of the Primate

According to this study, the bipolar cells related to cones are of two types; the *midget*, making a unique type of synapse with the cone, and the *flat* cone bipolar, making connections with some seven cones; the synapses are characteristically different, the dendritic process from the midget bipolar cell penetrating into an invagination of the cone pedicle, whereas the process from the flat cone bipolar makes a more simpler type of contact (Fig. 5.5, *top left inset*). The third type of bipolar is also diffuse, and serves to collect messages from rods, being connected to as many as fifty of these; the synaptic arrangement is one of invagination, as seen in Fig. 5.5, *top right inset*. Bipolars that synapse with both rods and cones, as indicated in Polyak's figure, almost certainly do not occur.

MIDGET BIPOLAR

The midget bipolar has been examined in serial sections by Kolb (1970), and she has shown that a single bipolar may make some twenty-five connections with a single cone pedicle, providing single central dendritic processes for the twenty-five invaginations. Thus, since these twenty-five invaginations constituted the total for the cone pedicle, this proved that the bipolar cell made synapses with only a single cone. In the peripheral retina there were some branched midgets, probably making contact with two cones; whilst in some cases it seemed likely that the pedicle accommodated processes from two midget bipolars. In addition to this connection with a midget, each cone also connected with one or more flat bipolars (Boycott & Dowling, 1969). Kolb also showed that the midget bipolar occurred in two types, the *invaginating midget* as described above, and also a *flat midget*, which at first was mistaken for the invaginating type; in fact, however, its dendritic 'tree-top' consists in a large number of very fine processes that do not enter the invaginations of the pedicle but only make a superficial contact with the base. Thus a cone pedicle contained twenty-five invaginating contacts and some forty-eight superficial contacts. Like the invaginating midget, the flat midget makes contact with only a single cone pedicle.

Horizontal Cells

The dendritic processes of these cells make synaptic contacts with the cone pedicles as lateral processes of the triads (Fig. 12.16); they were considered by Boycott & Dowling (1969) to be of two types, Type A making dendritic connection with cones and Type B with rods (Fig. 5.5); however, Kolb (1970) has shown that both types actually make dendritic connection only with cones; and the only differentiation consists in the numbers of cones with which a single horizontal cell makes contact, the 'small-field' contacting some seven cones and the 'large-field' some twelve.

CONE PEDICLES

A more systematic study (Boycott & Kolb, 1973), in which the synaptic terminals of cone pedicles on the dendrites of horizontal cells were examined, confirmed the unitary character of the primate horizontal cell, but there was a systematic increase in the number of terminal groups on an individual horizontal cell from about 10 near the foveal pit to as many as 40 in the periphery.

ROD AND CONE MIXING

Of greatest interest, of course, is the manner in which the axons of the horizontal cells terminate; thus their arrangement with the cones is post-synaptic, i.e. they receive messages from these; according to Kolb the axon processes terminate exclusively in rod spherules, constituting lateral elements in triads; each rod spherule thereby receives input from two horizontal cells. Thus the horizontal cells in the primate retina apparently mix the rod and cone messages.

Outer Plexiform Layer

In the light of this work, the outer plexiform layer may be illustrated by Fig. 12.18.

Inner Plexiform Layer

Essentially this process of vertical and horizontal connections is repeated in the inner plexiform layer, which consists of axons and terminals of bipolar cells, processes of amacrine cells, and dendrites of ganglion cells. The ganglion cells fall into two main types, namely the midget ganglion cell which connects with a midget bipolar cell and thus has a very close-relationship with a single cone, providing the latter with an exclusive pathway as far as the inner plexiform layer; the other type is diffuse, being connected with many bipolar cells; this type falls into several categories according to the manner in which their

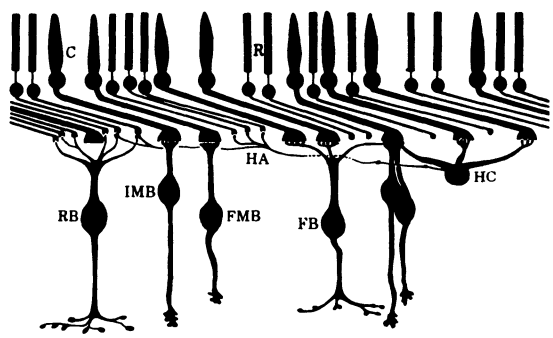

Fig. 12.18 Illustrating organization in the outer plexiform layer of the primate retina. The cells are drawn diagrammatically and do not, except for the midget bipolar cells, show the full extent of their dendritic spread. In general the drawing does not show the overlap of cell types onto their respective receptors, the exception being the third cone from the right, where all the cell types connecting with a single cone pedicle are shown. The rod bipolar (RB) makes contact with rod spherules only. Two or three rod bipolars contact an individual rod, but a single rod bipolar only makes one dendritic contact per rod. Horizontal cell axon terminals (HA) end in rod spherules only. Probably only two axons contribute a terminal to an individual rod. The axon is presented as a dotted line because the direct evidence for axon terminals being connected to the horizontal cell is not yet available. The invaginating midget bipolar (IMB) is connected to a single cone. The flat midget bipolar (FMB) is also exclusive to a single cone pedicle. The flat bipolar (FB) is a diffuse cone bipolar and contacts six to seven cones. Probably six or seven flat bipolars overlap onto a single cone pedicle. The horizontal cell (HC) has dendrites ending in cone pedicles only. (Kolb, *Phil. Trans.*)

dendrites branch. The extent to which a ganglion cell may relay only from rod bipolars or cone bipolars is not clear from the anatomical evidence; physiological evidence indicates that a ganglion cell may respond to both rod and cone stimulation, whilst another may respond exclusively to cone stimulation; the latter is probably of the midget type.

Amacrine Cells

The amacrine cells are of several types with respect to the nature and extent of their ramifications; they may, apparently, receive influences from bipolar cells and from other amacrines, whilst they may transmit influences to other bipolar terminals and to ganglion cells. As we have seen, certain ganglion cells have extremely wide receptive fields (p. 332) in the sense that they may respond to light falling on retinal points that are far remote from each other; this means that the ganglion cell is collecting information from a wide area of rods and cones, and the manner in which their effects are funnelled into the ganglion cell is probably through the amacrine cells. This *convergence* of the retinal message is also assisted by the diffuse type of bipolar and ganglion cells, and it is not surprising that the total number of optic nerve fibres emerging from the human retina, namely about 1 million, is far less than the total number of receptors (7 million cones and 70 to 150 million rods). It is interesting, nevertheless, that in the central retina, there are three times as many bipolar cells as cones.

Synaptic Relations in the Cat

Since so much work has been done on the cat's ganglion cell receptive fields, it is important to learn the retinal circuitry of this animal if one is to be able to interpret the features of the ganglion cells' receptive fields.

Rods

These make dendritic connection with the *rod bipolar*, whose dendritic process is the central element in an invaginating triad. The rod spherule contains two ribbon triads, so that usually two bipolars and three horizontal cells are postsynaptic to a single rod. According to Raviola & Gilula (1973), rods also make gap-junctional contacts with neighbouring cones.

Cones

Cone bipolars of the invaginating type contact some 4–10 cones, with no evidence for a bipolar contacting a single cone, i.e. the cat has no midget system (Boycott & Kolb, 1973). Another type of bipolar, the flat bipolar, makes a superficial contact at the base of the cone pedicle, being postsynaptic to some 8–14 cones. A single cone can have both an invaginating and flat contact synapse. In the central area of the retina the minimum number of cones invaginated by a single bipolar was 4–5, whilst in the periphery the number was some 9–10. Gap-junctions with rods and cones have also been described (Kolb & Famiglietti, 1976).

Horizontal Cells

These have been described in detail by Boycott *et al.* (1978) and Wässle *et al.* (1978a, b). They are of two types, A and B, with and without an axon respectively, as illustrated in Fig. 12.19; this is in contrast to the primate where Kolb found only a single type. The dendrites of the B-cell branch more densely and overlap more frequently than do those of the A-cell; at equivalent points in the retina, the dendritic field of an A-cell is some 1.5 times that of a B-cell. The axon of the B-cell branches at the end of a large axon terminal system. The terminal aggregations of A- and B-type cells are in register with the cone mosaic, and both types are in contact with at least 80% of the cones above their dendritic fields. Thus the different types of horizontal cell cannot be characterized by different types of cone. The A-type contacts some 120–170 cones, and the B-type 60–90. As many as 3000 rods could converge on a single axon-terminal system. So far as synaptic arrangements are concerned, two lateral elements of a cone triad are always occupied by horizontal cell dendrites; since each cat cone pedicle contains some 11 triads, the cone pedicle could synapse with some 20–25 horizontal cells. Thus a single horizontal cell, of either cell type, could not provide all these contacts. So far as rod and cone inputs are concerned, the dendrites of Type B cells contact more cones, whereas the axonal part of the same cell contacts more rods. The interesting feature of the axon-containing horizontal cell (B) is that the ramifications at the axon terminal and at the soma behave separately, owing to the long and tenuous nature of the axon which would not permit electrotonic spread from the one part to the other.[9] Nelson (1977) emphasizes that, in teleosts, entirely separate horizontal cells receive inputs from either rods or cones, whereas in mammals one type receives input from both, but because of the functional separation of the two parts, the one cell can perform rod- or cone-functions.

Bipolar Cells

Cajal's conclusion that rod and cone receptors are connected to separate bipolars was confirmed for the cat by Boycott & Kolb (1973); they are probably the only orthodromic link between the outer and inner plexiform layers, being presynaptic at the outer and postsynaptic at the inner plexiform layer. Rod bipolars are only of one type, the dendrite being the central element in the triad of the rod spherule. The rod bipolar cell is presynaptic only to amacrine cells, where it participates in the dyad type of contact. Their club-shaped axon terminals make contacts only in the innermost sublamina of the inner plexiform layer, participating in dyad contacts where they synapse with AI and AII amacrine cell processes. The important point to appreciate is that rod bipolars do not make contact with ganglion cells, so that they influence these only through amacrine cells. Cone bipolars are of the flat and invaginating type; dendritic trees, contacting cones, typically spread some 30–80 μm according as they are in the area centralis or more peripherally; of the invaginating type, every dendrite terminates in a cone invagination. Flat bipolars make more superficial contacts with the cone pedicle, which may often be at either side of an invaginating contact. The flat bipolar contacts with cone pedicles have often been described as of the gap-junction type (e.g. Levick & Thibos, 1983) but it seems likely

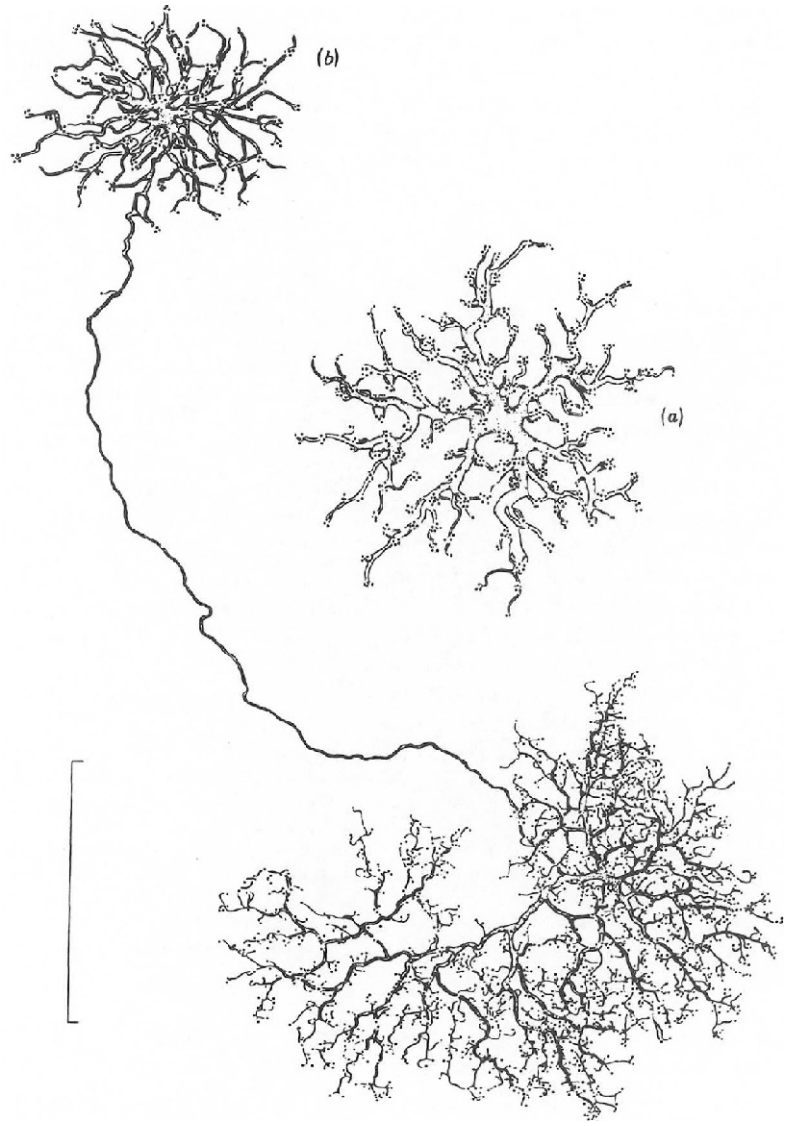

Fig. 12.19 Drawings of representative A- and B-type horizontal cells from a whole mount of Golgi–Colonnier stained cat retina (viewed from the receptor side; eccentricity in (*a*), 4.7 mm; eccentricity in (*b*), 7.3 mm. The scale is 100 μm. (Boycott *et al.*, *Proc. Roy. Soc.*)

that there would also be conventional synapses involving transmitter release, if the flat contact is to represent the only pathway from cone to ganglion or amacrine cell. Kolb (1979) concluded that flat and invaginating cone bipolars had strictly segregated ramifications in the inner plexiform layer.

Amacrine Cells

Kolb & Nelson and Kolb *et al.* (1981) have distinguished more than 20 different types of this cell and they have been given a numerical classification. The AI is involved exclusively in interconnecting rod bipolars; the synaptic arrangement is of the reciprocal type, so that the amacrine is both pre- and postsynaptic to a bipolar cell.

The AII, studied in detail by Famiglietti & Kolb (1975) and Kolb (1979), is unique in having a bistratified vertically organized dendritic tree, the two strata in which ramification occurs being considered to represent the regions where pre- and postsynaptic functions are exercised. Thus the cell body and apical dendrite give rise to processes ramifying in the outer third of the inner plexiform layer, which are presynaptic to ganglion cell dendrites, whilst the dendrites in the inner half of the plexiform layer are postsynaptic at ribbon dyad synapses with rod bipolars.[10]

The Interplexiform Cell

Polyak described centrifugal bipolars that transmitted messages backwards from the inner plexiform layer to the receptors. Although this interpretation of these retinal neurones was questioned, e.g. by Dowling & Boycott (1966) it is now recognized that there are neurones, called *interplexiform cells*, that act as a feedback system between the two plexiform layers (Ehinger *et al.*, 1969). As described by Boycott *et al.* (1975) for the cat and primate, the cell bodies are in the inner nuclear layer and processes run to both inner and outer plexiform layers. They are apparently pre-synaptic to horizontal and bipolar cells in the outer plexiform layer, whilst in the inner plexiform layer they receive and transmit messages. In the goldfish and Cebus monkey, Dowling & Ehinger (1975) described similar dopamine-containing interplexiform cells, and by giving 5,6-dihydroxytryptamine, which characteristically alters terminals of this type of neurone making them recognizable in the electron microscope, they showed that their processes were both pre- and post-synaptic to amacrine cells in the inner plexiform layer and presynaptic to bipolar and horizontal cells in the outer plexiform layer (Fig. 12.20).[11] They obviously subserve a feedback mechanism, perhaps setting the sensitivity of the bipolar cells in adaptational phenomena. Thus they receive input from amacrine cells, which themselves collect input from a wide area of the visual field, and so are well situated to indicate the general state of illumination of the retina (Kolb & Nelson, 1984).

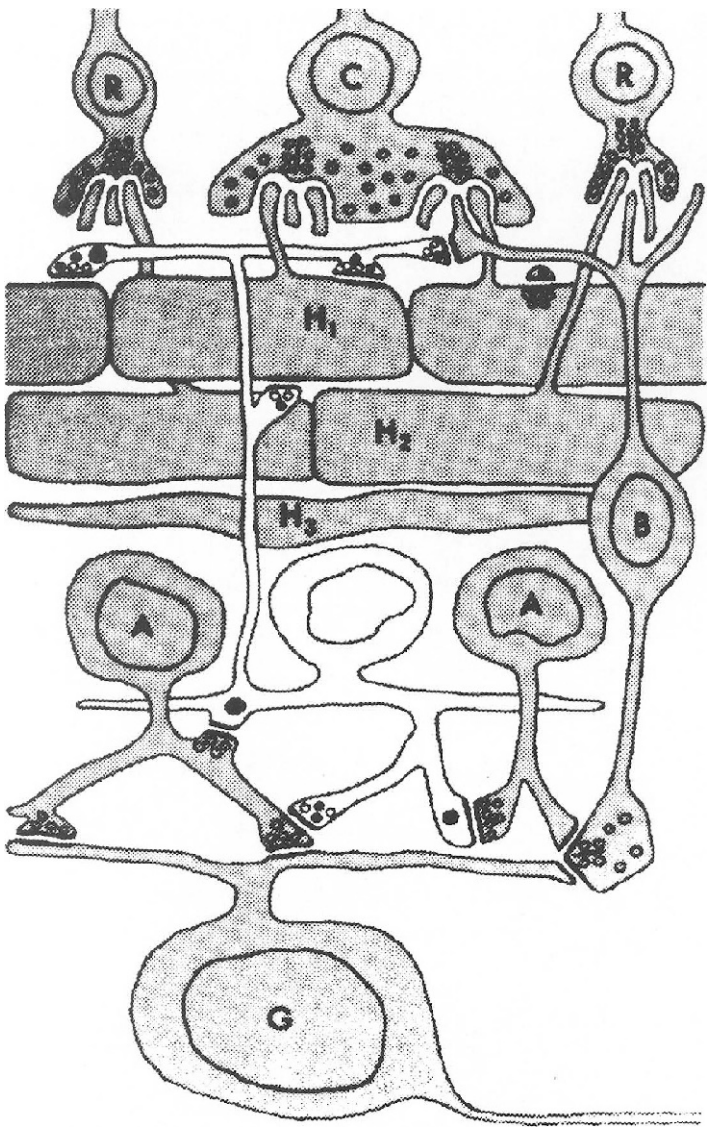

Fig. 12.20 A summary diagram of the synaptic connections of amine-containing interplexiform cells of the goldfish retina. The input to these neurons is in the inner plexiform layer via conventional synapses of amacrine cells (*A*). The interplexiform cell processes have been observed to make conventional synapses onto amacrine cell processes in the inner plexiform layer, but never do they contact the ganglion cells (*G*) or their dendrites. In the outer plexiform layer, the processes of the interplexiform cells make synapses on the perikarya of the external horizontal cells (H_1) and onto bipolar cell (*B*) dendrites. The interplexiform cell processes have never been observed as postsynaptic elements in the outer plexiform layer at either rod (*R*) or cone (*C*) receptor terminal synapses or at the occasional external horizontal cell synapse. No synapses have yet been seen between interplexiform cell processes and elements in the intermediate (H_2) or internal (H_3) horizontal cell layers. (Dowling & Ehinger, *Science*.)

Anatomical Basis for ON- and OFF-centre Units

Famiglietti & Kolb (1976) have shown that ganglion cells may be differentiated on the basis of the layer in the inner nuclear layer in which their dendrites ramify, as illustrated by Fig. 12.21. In layer *a* are to be found the endings of flat cone bipolars and in layer *b* the endings of the invaginated cone bipolars; ganglion cells of Type I (Boycott & Wässle's α) can therefore be subdivided into Ia and Ib according to the layer in which their dendrites ramify; similarly Type II (β) are IIa and IIb. The overlap of dendrites and bipolar terminals in the respective layers is very striking, so that IIa ganglion cells receive major input from flat cone bipolars and IIb from invaginating cone bipolars. From various correlations between the populations of retinal regions and the type of ganglion cell response, the authors concluded that ganglion cells branching in layer *a* will be OFF-centre and in *b* ON-centre. Since flat cone bipolars receive an excitatory synapse from cones their response will be hyperpolarizing and lead to OFF-excitation of ganglion cells with which they synapse. Invaginating cone bipolars apparently do not receive excitatory synapses from cones, these synapses appearing to be of the depolarizing type (Raviola & Gilula, 1975), so that they might well mediate an ON-centre response.

Stratification of Amacrine Cells

Of some interest for retinal circuitry is the observation that the two classes of amacrine cells characterized by their positions in the retina, namely displaced and conventional, have a similar topography in the retinal streak of the rabbit to that of the paired ganglion cells (Vaney *et al.*, 1981). The 'displaced' amacrines are close to the ganglion cell layer and the 'conventional' cells are in the inner nuclear layer. Their cytologies are similar. The displaced amacrines branch in the inner stratum of the inner plexiform layer and may be concerned with the ON-pathway of the ganglion cells, whilst their matching partners could be concerned with the OFF-pathway.

Response Properties and Synaptic Types

Whereas the correlation between the layer of ramification of the ganglion cell's dendrites with the axonal terminals of the bipolar cells in the inner plexiform layer, allowing the classification of ON- and OFF-centre circuits mediated by depolarizing and hyperpolarizing bipolar cells respectively, has proved sound, the attempts to relate the morphology of the synapse of receptor with the bipolar dendrite have not been so successful. Thus the two main types of synaptic type have been classified as *invaginating*, or ribbon, and *basal*; and the original suggestion of Raviola & Gilula, mentioned above, that in the monkey the basal contact was related to an OFF-centre or hyperpolarizing contact, and the reverse for the ribbon-junction, has not been generally confirmed. For example, in the tiger salamander (Lasanky, 1978), catfish (Sakai & Naka, 1983), and carp (Saito *et al.*, 1983) OFF-type bipolars usually made ribbon contacts, and ON-type basal contacts. In the cat, Kolb and her collaborators have described several types of cone bipolar on the basis of their axon ramifications in the inner plexiform layer and their contacts with receptors. By recording from bipolar cells and subsequently injecting horseradish peroxidase, Nelson & Kolb (1983) related response-properties to morphology. Rod bipolars and a cone bipolar cb6 made invaginating ribbon related contacts with photoreceptors and had axons terminating in layer *b* of the

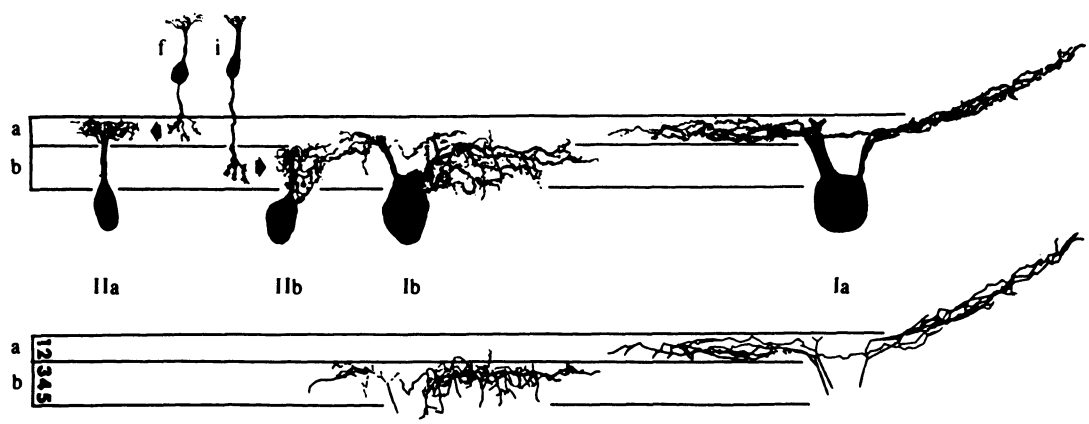

Fig. 12.21 Camera lucida drawings (top) and computer drawings (bottom) of cone bipolar cells and two classes of ganglion cells. Top: Sublamina *a* contains the terminals of flat cone bipolar cells, *f*, and the dendrites of Type Ia and IIa ganglion cells. Sublamina *b* contains terminals of invaginating cone bipolar cells, *i*, and dendrites of Type Ib and Type IIb ganglion cells. For significance see text. (Famiglietti & Kolb, *Science*.)

inner plexiform layer, the layer in which OFF-centre ganglion cells ramify. These bipolar cells hyperpolarized in response to light, likewise being OFF-centre cells.[12] Similarly the axon terminal of another type of cone bipolar, cb2, ended in layer *a* of the inner plexiform layer, and its basal contacts with cones also resulted in a hyperpolarizing response. Another type, cb5, was centre-depolarizing, and ramified in layer *b* of the inner plexiform layer; its synapse with the cone was at a semi-invaginating basal junction, although earlier predictions had been that it would have been of the invaginating type. It made synaptic contacts with both ganglion and amacrine cells as did all other cone bipolars.

The subject has been reviewed by Saito (1987) who concludes that 'hasty generalizations on the relationship between the type of photoreceptor-bipolar synaptic contacts and the sign of synaptic transmission may be inaccurate and misleading'.

TRANSMITTERS IN THE RETINA

In a complex tissue like the retina, the identification of the transmitters released by the various cellular units, receptors, bipolar, horizontal, amacrine and ganglion cells, at their synaptic junctions is difficult and a variety of experimental manoeuvres has been employed to achieve this identification. Thus a tritium-labelled transmitter may be applied to the retina, e.g. by intravitreal injection, and its specific high-affinity uptake by retinal cells determined, e.g. by autoradiography. Again, certain cell types may be separated from the disaggregated retina and their responses to transmitters measured. So far as ganglion cells are concerned, because of their superficial position on the retinal surface, micro-iontophoretic application of transmitters and their specific inhibitors, has yielded a wealth of information (Ikeda, 1985).

The Photoreceptors

The effects of light are transmitted to bipolar and horizontal cells by the terminals of rods and cones. It will be recalled that, in the dark, the photoreceptors, because of their partially depolarized condition, release their transmitter at the synaptic receptors on bipolar and horizontal cells. We have seen that the effects of light, which causes an inhibition of release of transmitter, are split into two pathways. Along the ON-pathway, the effect of light is to depolarize the bipolar cells; thus cessation of transmitter-liberation depolarizes the ON-bipolar cells, and this means that the transmitter must have been hyperpolarizing them, i.e. leading to the *closure* of ionic channels. Along the OFF-pathway the effect of light is to hyperpolarize the bipolar cells, just as it hyperpolarizes the receptors, so that the synaptic effect on the bipolars is said to be 'sign-conserving'. Thus, because light inhibits release of transmitter from the receptors, the hyperpolarizing effect of light on the bipolar cell must be due to the fact that the receptor's action on the bipolar cell was to *depolarize it*, leading to the *opening of channels*. If we accept that the photoreceptors release the same transmitter, the ON-depolarizing and ON-hyperpolarizing effects of light are due to the presence on the postsynaptic cells, e.g. bipolars, of sign-reversing and sign-conserving synaptic receptor sites. Thus, application of the suspected photoreceptor transmitter to the junctional region between it and bipolar and horizontal cells should mimic the action of light, having a dual action according to the type of bipolar cell that is encountered. Moreover, blockade of synaptic transmission, e.g. by the application of cobalt, should have similar effects on the retina as those of light-exposure. Such a blockade was demonstrated by Cervetto & Piccolino (1974) and Dowling & Ripps (1973).

Agonists and Antagonists

The suspected excitatory transmitters released by the photoreceptors are glutamate and aspartate, known to play an excitatory role in other parts of the central nervous system. Thus Cervetto & MacNichol (1972) showed that these dicarboxylic acids mimicked the action of light on the retina, but the main problem remained as to whether the relatively high concentration employed by them could be achieved in the retina.

Four Types of Dicarboxylic Acid Receptors

Just as adrenergic drugs may affect alpha- and beta-receptor sites, and their subclasses, $alpha_1$ and $alpha_2$ and $beta_1$ and $beta_2$, so it has been recognized that there are at least four types of receptors in vertebrates mediating responses to the dicarboxylic acids. Thus, in terms of agonist specificity, sites that prefer kainic acid (KA), quisqualic acid (QQ) and *N*-methyl-D-aspartic acid (NMDA) and 2-amino-4-phosphorus butyrals (APB) have been distinguished. 2-Amino-5-phosphonovaleric acid preferentially antagonizes sites that prefer *N*-methyl-D-aspartic acid; glutamic acid diethylester antagonizes quisqualic acid sites, and γ-D-glutamyl glycine acts as an antagonist at sites preferring either kainic acid or *N*-methyl-D-aspartic acid.

Blocking the Active Uptake

It was suspected that the reason why high concentrations of extrinsic transmitter had to be employed to mimic the action of light was that the active uptake mechanisms at the presynaptic terminals reduced the effectiveness of the applied transmitter. Ariel *et al.* (1984) inserted micro-

electrodes into carp horizontal cells (H), and, by blocking the active uptake of amino acid by saturating it with D-aspartate, they obtained a fifteen-fold increase in sensitivity to glutamic acid. Isolated cells, unaffected by uptake processes, were unresponsive to aspartate, whilst responding actively to glutamate, so the authors concluded that glutamate was the excitatory transmitter. An aspartate analogue, *N*-methyl-D-L-aspartate, was only hyperpolarizing.[13]

Kainic Acid

Slaughter & Miller (1983b) found that this analogue acted as a powerful agonist for all three types of second-order neurones of the outer retina, namely ON- and OFF-bipolars and horizontal cells in the mudpuppy retina. By contrast the action of the aspartate analogue, *N*-methyl-aspartate, was restricted to the inner retina, mimicking the action of light on a group of sustained ON-amacrines. Slaughter & Miller concluded that glutamate, or an analogue (but not aspartate) was the excitatory transmitter liberated by the photoreceptors.

Rabbit Retina

In a study of the rabbit retina, Bloomfield & Dowling (1985) found that both glutamate and aspartate mimicked the effects of light on bipolar and horizontal cells; the glutamate analogues, kainate and quisqualate were just as effective, in fact kainate was much more effective probably because there is no specific uptake mechanism to remove it. It was difficult to decide whether aspartate could also be a transmitter, but on balance the authors concluded in favour of glutamate. The important conclusion, however, was that the mammalian retina behaved similarly to those of amphibians and fish (Ariel *et al.*, 1984) with respect to this stage in transmission, an important point in view of the great mass of work carried out on the cold-blooded retina.

Isolated Photoreceptors

Miller & Schwartz (1983) selectively destroyed the cells of the toad retina, leaving the receptors intact; they then allowed these 'isolated photoreceptors' to accumulate labelled precursors of transmitters, and finally measured release in response to depolarization with high-K^+. Aspartic and glutamic acids were released in this way, but partly by a Ca^{2+}-independent mechanism, suggesting a non-vesicle type of synapse in addition to the conventional type. Putrescine and cadaverine were released by a Ca^{2+}-dependent mechanism. A similar Ca^{2+}-independent release of transmitter, but of GABA by horizontal cells, had been described by Schwartz (1983), and it was suggested that this Ca^{2+}-independent and voltage-dependent release occurred at the flat type of cone contact, whereas the type involving an exocytosis of synaptic vesicles triggered by entry of Ca^{2+} into the synaptic terminal, was confined to the invaginating type of synapse. When Miller & Schwartz measured GABA efflux from 'isolated horizontal cells' they found that aspartic and glutamic acids increased this, whereas putrescine and cadaverine did not.[14]

Blocking the Photoreceptor-second-order Synapse

Slaughter & Miller (1981, 1983a) made two striking discoveries in so far as they were able to block selectively the ON- and OFF-pathways from photoreceptors to bipolar and horizontal cells by use of drugs that presumably had specific affinities for the separate types of postsynaptic receptor postulated for the two different pathways involving the same transmitter.

APB

The glutamic acid analogue, 2-amino-4-phosphonobutyric acid (APB) was found to block only the light-induced ON-responses in mudpuppy retinal neurones including the ganglion cells, leaving the OFF-responses unaffected. The drug had no effect on the receptor cells themselves. Intracellular records showed that APB increased the membrane resistance, i.e. that it closed ionic channels, favouring hyperpolarization. It will be recalled that the ON-response in the bipolar cell is a depolarizing one, due to opening of channels, made possible by inhibition of transmitter release. APB, by hyperpolarizing the bipolar cells, prevented transmission to ganglion cells, a process requiring depolarization at its terminals.

PDA

The excitatory amino acid antagonist, *cis*-2,3-piperidine-carboxylic acid (PDA), had the opposite effect to that of APB, reversibly blocking cone input to OFF-bipolar and horizontal cells of the mudpuppy; it did not block release of transmitter from photoreceptors, since ON-responses in the retina were unaffected. OFF-bipolars and horizontal cells respond to light by hyperpolarization through diminished release of transmitter at their synapses with photoreceptors; application of PDA caused a hyperpolarization of the bipolar and horizontal cells, and thereby prevented light from causing any further hyperpolarization. When centre-surround antagonism was examined, it was found that the light-response of the ON-bipolar was unaffected, but the surround response, relying on hyperpolarization, was eliminated; and this was presumably because the surround-response was mediated by horizontal cells, which behave similarly to OFF-bipolars, both of these being sign-conserving, in the sense that they transfer the hyperpolarizing response of light that they receive from the receptors.

Bipolar Uptake

We may note that Pourcho *et al.* (1983) found two populations of bipolar cells with respect to transmitter uptake, namely cells that took up ^{3}H-GABA and others that took up ^{3}H-glycine.

Horizontal Cells

Because of the complex circuitry, the effects of transmitters applied directly to the retina are hard to analyse. However, the effects of glycine seem straightforward; thus, in the *Xenopus* retina it depolarizes the H1 cell independently of synaptic blockade by Mg^{2+}; this depolarization is inhibited by strychnine (Stone & Witkowsky, 1984).

Rod and Cone Inputs

Horizontal cells of the rabbit retina are of two kinds; the A- (or axonless) cell, and the B-type consisting of functionally independent soma and axon terminal; the B-type axon terminal contacts only rods, whereas the A-type horizontal cell and the B-type soma contact only cones. When transmission was blocked by cobalt, Massey & Miller (1987) found that the somas hyperpolarized, indicating that cones released a depolarizing transmitter; kainic acid and quisqualate now depolarized the somas. The antagonists *cis*-2,3-piperidine dicarboxylic acid (PDA) and kynurenic acid (Kyn) both hyperpolarized the somas and blocked the light-driven responses. It was unlikely that an NMDA receptor was active, since its specific inhibitor, 2-amino-7-phosphonoheptanoate (AP-7), had no action. The rod-dominated axon terminals were depolarized by kainate, whilst the antagonists PDA and Kyn hyperpolarized them and blocked their responses to light. Thus the synaptic receptors that mediate the response of both cone- and rod-dominated horizontal cells seem to be either kainate or quisqualate, suggesting that glutamate is the transmitter released by the rods and cones.

Isolated Cells

A device for studying the effects of suspected transmitters, uncomplicated by synaptic influences, is to isolate the cells by enzyme action on the retina. Lasater & Dowling (1982) and Ariel *et al.* (1984) studied carp horizontal cells isolated in this way. These had resting potentials of -50 to -70 mV; glutamate produced a graded depolarization, accompanied by an increase in membrane resistance which might have been due to a decreased K^+-conductance, since Ca^{2+}-dependent spikes could be fired off, a phenomenon shown by some cells that normally only show graded depolarization in response to their normal stimulus. The concentration of glutamate required to produce these effects was 0.01 mM, comparing with values of 0.5 to 20 mM found in the intact retina (Ariel *et al.*, 1984). Aspartate was without effect. The inhibitory transmitter, GABA, is synthesized and accumulated by H* horizontal cells of goldfish. Ayoub & Lam (1984) isolated horizontal cells from this fish, and found that GABA was released by K^+-depolarization. Thus horizontal cells might exert the surround inhibition of bipolar cells, through this transmitter.

Dopamine

Laufer *et al.* (1981) found that dopamine, applied to the carp retina, modified the centre-response of the so-called S-potentials. This seems to be achieved by reducing electrical communication between adjacent horizontal cells through their gap-junctions, since Teranishi *et al.* (1983) found that the spread of Lucifer yellow from one horizontal cell to adjacent ones, after intracellular injection, was inhibited by previous application of dopamine, an effect that was blocked by the dopamine inhibitor, haloperidol, which also blocked the electrical effects of dopamine. If dopaminergic activity was blocked by injections of 6-hydroxydopamine, the effects of light on the horizontal cell were modified, a wider lateral spread being found with a reduced magnitude of the S-potential.[15]

Amacrine Cells

Because the amacrine cells consist of a very heterogeneous population, it is not surprising to find that a large number of transmitters have been associated with these cells, usually identified by the high-affinity uptake of the ^{3}H-labelled putative transmitter.

Acetylcholine

Acetylcholinesterase was early identified in the retina (Nichols & Koelle, 1968); and Masland & Mills (1979) and Hayden *et al.* (1980) showed that acetylcholine synthesis was confined to amacrine cells, which included the 'displaced' amacrine cells with their somata in the ganglion cell layer and identified as such by their failure to send axons into the optic nerve. It is accepted that the only cholinergic neurones in the retina are amacrines, so that release of acetylcholine from the retina may be attributed to amacrine activity. The exact location of the cholinergic amacrines has been the subject of numerous studies extending over many vertebrate species. The techniques employed to establish the cholinergic activity are several: (1) establishing the presence of the synthetic enzyme, choline acetyl transferase (ChAT); (2) the presence of ^{3}H-labelled cells after presentation of ^{3}H-choline;

(3) the specific staining of cholinergic cells by the fluorescent dye, 4',6-diamidino-2-phenole-indole (DAPI), or (4) establishing the presence of the enzyme that hydrolyses acetylcholine, acetylcholinesterase (AcChase).

'STARBURST-CORONATE' CELLS

In general the ability to synthesize acetylcholine has been shown to be restricted to two bands of amacrine cells located on either side of the inner plexiform layer in a complementary fashion, and ramifying in sublaminae a and b. In the rabbit, the mammalian species in which synthesis is very prominent, these amacrines make up the so-called 'starburst' amacrines, so described by their dendritic appearance (Famiglietti, 1983), which also seem to be identical with the so-called 'coronate' amacrines (Vaney, 1984), with characteristic nuclear morphology and selectively labelled by neurofibrillar methods or with the fluorescent dye 4',6-diamidino-2-phenyl-indole (DAPI). The amacrines synthesizing acetylcholine are thus 'ordinary' amacrines, with cell bodies in the inner nuclear layer, and 'displaced' amacrines, with bodies in the ganglion cell layer, these latter being distinguished from ganglion cells by failure to stain retrogradely from the optic nerve (Masland *et al.*, 1984b). When cholinesterase was used as a marker, the distribution was much more extensive within the inner plexiform layer (Fig. 12.22) and Pourcho & Osman (1986) concluded that this marker stained neurones that were most probably not involved in cholinergic activity.[16]

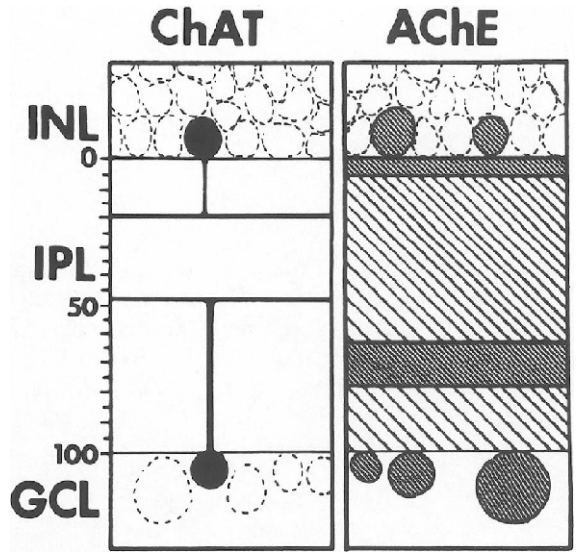

Fig. 12.22 Summary of AChE localization in cat retina as compared with ChAT. ChAT immunoreactivity is limited to amacrine cells in the inner nuclear layer which ramify at a depth level of 20% within the inner plexiform layer (IPL) and to displaced amacrine cells ramifying at a 49% depth level. AChE reactivity was seen throughout the entire IPL with dense bands at 0–6% and 64–78%. Reaction product was seen in two types of amacrine cell in the inner nuclear layer (INL) and in small, medium, and large cells in the ganglion-cell layer (GCL). Percentage depth levels were calculated from measurements made from representative sections. (Pourcho & Osman, *Exp. Eye Res.*)

LIGHT-EVOKED RELEASE

Massey & Neal (1979) and Cunningham & Neal (1983) showed that the light-evoked release of acetylcholine was reduced by GABA, an effect that was blocked by bicuculline; this agent reduced the resting release of acetylcholine in the dark, indicating that there is a tonic inhibitory action of GABA on the amacrine cells. Glycine and taurine also inhibited the light-evoked release, the effect of glycine being blocked by strychnine. Thus GABA-ergic and glycinergic neurones of the retina, which may possibly be other amacrine cells, inhibit cholinergic amacrine activity. Since flashing light is required for release of acetylcholine, it appears that ON- and OFF-bipolars influence amacrine cells. Massey & Redburn (1983) employing the glutamate analogue, 2-amino-4-phosphonobutyric acid (APB) to block the ON-signals arising from depolarizing bipolars, blocked acetylcholine release.

Finally, Masland *et al.* (1984a) measured release of labelled acetylcholine from the incubated rabbit retina in response to flashing light-stimuli. When the ON-stimulus was blocked by APB the release occurred only at cessation of the stimulus. By labelling amacrines with ^{3}H-acetylcholine, it was shown that blocking of the ON-stimulus tended to confine release of transmitter to the dendrites of the displaced amacrine cells, ramifying in the inner part of the plexiform layer. In reviewing earlier studies on the effects of cholinergic agents on responses of ganglion cells (e.g. Masland & Ames, 1976; Ariel & Daw, 1982), Masland *et al.* concluded that a common feature was the influence on motion sensitivity, as revealed by directionally sensitive cells, local edge detectors, etc. They suggested that the detection of motion of a stimulus within the receptive field of the ganglion cell might be mediated by 'units' of amacrine dendrites that would be excited independently and transmit their responses independently, a feature made possible by the non-propagated type of response that is characteristic of many amacrine cells. The mechanism is illustrated by Fig. 12.23.

GABA and Glycine

Pourcho (1980) and Pourcho & Goebel (1983) demonstrated the accumulation of ^{3}H-glycine and ^{3}H-GABA in amacrine cells of the cat; using the GABA-agonist, ^{3}H-muscimol, they identified five classes of amacrine and interplexiform cells that accumulated the agonist; according to Kolb & Nelson's (1981) classification, the amacrines were A2, A10, A13, A17, and A19, providing input

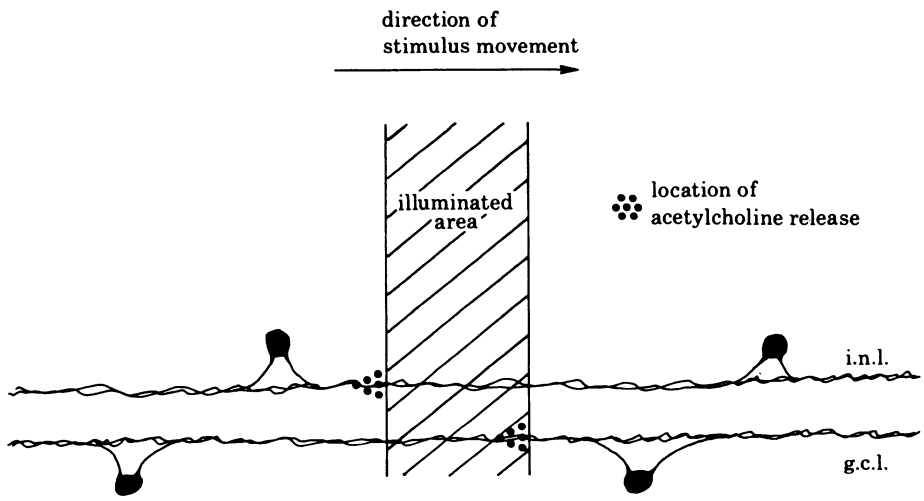

Fig. 12.23 Local dendritic response of the cholinergic amacrine cells to a moving stimulus. (Masland *et al.*, *Proc. Roy. Soc.*)

to all five strata of the inner plexiform layer.[17] Since amacrine cells are involved in ganglion cell surround effects, it is not surprising that GABA mediates inhibitory actions on ganglion cells, as we shall see. So far as the other inhibiting transmitter, glycine, is concerned, Marc & Liu (1984) found ^{3}H-accumulation in two types of amacrine cells in the human retina; the synaptic contacts were almost exclusively of the serial type, receiving both ribbon and conventional inputs and being presynaptic to amacrines, ganglion cells and sometimes bipolar cells. Essentially similar results were obtained by Frederick *et al.* (1984) on the human retina; they found a group of cells in the inner nuclear layer that were probably bipolar cells. As they summarized the position, glycinergic neurones of the human inner nuclear layer were a heterogeneous group sending processes to the inner plexiform layer where input is collected from bipolar and amacrine cells, and output to distal regions of this plexiform layer.

Dopamine

Pourcho (1982) found an accumulation of ^{3}H-dopamine in a subpopulation of amacrine cells whose processes ramified in the outermost strata of the inner plexiform layer; the cells were presynaptic to other labelled cells, and to a population of unlabelled amacrines, but not to bipolar or ganglion cells. There was an extensive input to All cells, which are involved in the rod-to-ganglion cell pathway, so that dopaminergic activity may well play a strategic role in governing rod-activated behaviour (Kolb & Wang, 1985).

SYNAPTIC ORGANIZATION

Dowling & Ehinger (1978) examined the synaptic terminals of dopamine-accumulating cells in the electron microscope; the retina of the rabbit was treated with 6-hydroxydopamine which caused typical changes at the terminals that enable dopaminergic neurones to be identified. The only synapses were with amacrine cells, the processes being restricted to the inner plexiform layer; amacrines not only had dopaminergic input but also they could be presynaptic to other amacrines. Dowling & Ehinger suggested that the role of these neurones might be to modulate the lateral inhibitory actions of amacrine cells, as manifested in surround influences on ganglion cells. In goldfish, apparently dopaminergic interplexiform cells play a similar role.

Ganglion Cells

An early study by Kirby & Enroth-Cugell (1976) demonstrated the value of applied inhibitory transmitters in elucidating the retinal circuitry involved in evolution of the ganglion cell's receptive field characteristics. Thus under scotopic conditions they found that picrotoxin reduced the size of the cat's ON-centre receptive field a little but reduced the size of the surround much more, so that there was a shift in the balance between centre and surround in favour of the centre. If, as is surmised, the centre response is mediated through synapses of bipolar cells on the ganglion cell's dendritic tree, whilst the surround is mediated through bipolar cells that first synapse with amacrine cells, then the shift in favour of the centre can be interpreted as a reduction in the inhibitory

action exerted through GABA-ergic amacrine cells. When strychnine, the antagonist of the inhibition mediated through glycine, was compared with picrotoxin and bicuculline, Kirby (1979) found that this time there was little or no effect on Y-cells whilst in X-cells the shift in balance in favour of the centre occurred. Thus glycine plays a similar role in receptive-field organization of X-cells to that of GABA in Y-cells.

Direction-sensitive Ganglion Cells

Another early study, namely that of Wyatt & Daw (1976) started from the hypothesis that directional-sensitivity in the ganglion cell relied on inhibition; they infused the right internal maxillary artery of the rabbit, with the right lingual, temporal and internal carotid arteries clamped, with picrotoxin, the GABA antagonist. As a result, directionally sensitive ganglion cells became equally responsive to movement in both directions. The effect was reversible. Strychnine, the glycine antagonist, had no effect, although it did influence the responses of edge-detectors. Since amacrine cells were known to contain GABA, the authors concluded that the inhibitory effects required for directionality were derived from amacrine rather than horizontal cells.

ON- and OFF-responses

Ikeda & Sheardown (1983) identified ganglion cell-types in the cat's retina in accordance with their ON- and OFF-centre behaviour and by their sustained (X) and transient (Y) characteristics. They found that acetylcholine excited transient Y-cells whereas aspartate excited sustained X-cells. So far as inhibitory transmitters were concerned, GABA inhibited ON-centre cells, whilst glycine inhibited OFF-centre cells, the two inhibitory processes being mutually exclusive. The actions of antagonists were opposite, so that ON-centre responses were enhanced by bicuculline and those of OFF-centre cells by strychnine (Priest *et al.*, 1985).

Centre versus Periphery

Because the relative amounts of cone and rod input vary from periphery to centre, some differences in pharmacological properties may be expected; Priest *et al.* (1985) examined this point, and found sensitivity of ganglion cells to the transmitters in the central region greater than that of more peripherally located cells, whereas the effects of antagonists were generally uniform. However, they did find that cells from the central fovea were exclusively sensitive to either GABA or glycine, whereas the peripheral cells were less selective.

Diagrammatic Representation

Figure 12.24 illustrates the likely circuits, with their transmitters, involved in cat retinal ganglion cell re-

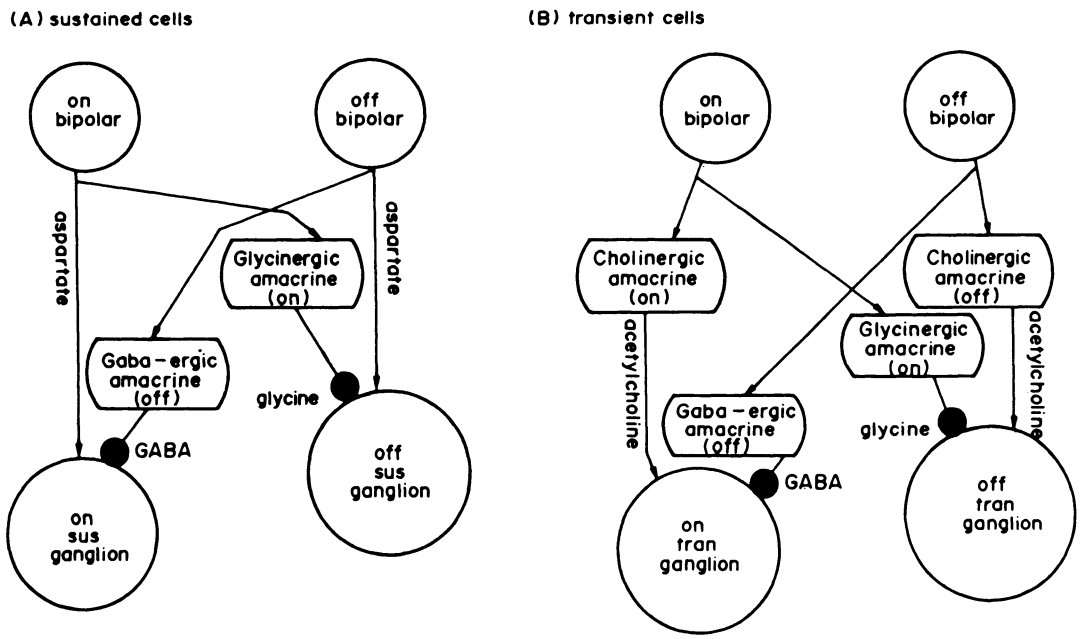

Fig. 12.24 Suggested circuits and their neurotransmitters involved in transmission from bipolars to ganglion cells, based on microiontophoretic application of transmitters. (Ikeda & Sheardown, *Vision Res.*)

sponses, based on elaborate studies of the effects of microiontophoretically applied putative transmitters, namely aspartate, glutamate, acetylcholine, GABA and glycine, and their antagonists 2-amino-5-phosphonovaleric acid (2APV), γ-D-glutamylglycine (γ-DGG), atropine, bicuculline and strychnine. It will be noted that the transient, Y-type, ganglion cell has the more complex input, in the sense that bipolar input is never direct but mediated through amacrine cells.

The existence of different inhibitory transmitters for ON- and OFF-centre ganglion cells makes physiological sense if the function of the retinal ganglion cells is largely to maximize the visual contrast. Thus, the stimuli that excite ON-centre cells must inhibit OFF-centre cells, whilst those that excite OFF-centre cells must inhibit ON-centre cells, in order to enhance the contrast presented by the visual field. If both ON- and OFF-cells received the same inhibitory transmitter, this might lead to inhibition of both types of cell at the same time (Ikeda & Sheardown, 1983).[18]

Contradictory Results

Satisfactory as Ikeda's scheme is intellectually, a recent study of Bolz *et al.* (1985a, b) casts doubt on this segregation of transmitters to ON- and OFF-effects. Using essentially the same techniques of identification and micro-iontophoretic application, they found that GABA suppressed spontaneous and light-evoked activity of all types of ganglion cell. Bicuculline antagonized these effects of GABA (Fig. 12.25), whilst, applied by itself, it enhanced spontaneous and light-evoked activity of ON-centre cells and suppressed the spontaneous activity of most OFF-centre cells. Thus the agonist, GABA, and its antagonist, bicuculline, suppressed maintained firing of OFF-centre cells. The similarity of effects might be due to the types of different types of receptor sensitive to GABA, the one hyper- and the other depolarizing the amacrine cell, as with hippocampal pyramidal cells; alternatively an interneurone might also be involved, releasing a different transmitter from GABA, but being under GABA-ergic influence.[19] When the effects of glycine were studied, an essentially similar picture was observed, suppression of light-evoked discharges of all types of ganglion cell, blocked by strychnine, which, by itself, enhanced light-evoked responses. ^{3}H-glycine labelled a population of amacrine cells in the inner nuclear layer with processes ramifying throughout the inner plexiform layer. GABA-ergic neurones were identified in the inner nuclear and (displaced) ganglion cell layers.

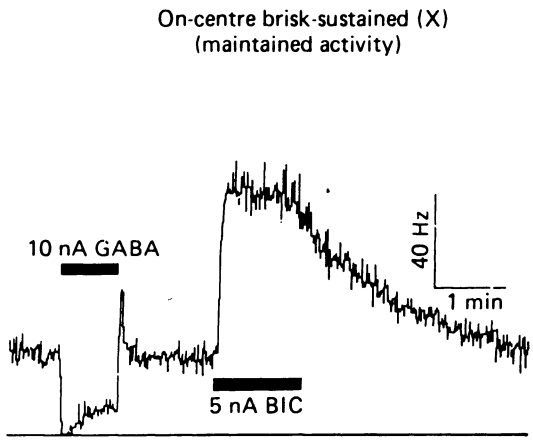

Fig. 12.25 The effects of GABA and bicuculline (BIC) on the spontaneous activity of an on-centre brisk-sustained (X) cell. The continuous record indicates the number of spikes counted in a 1024 ms interval (continuous trace): the bottom horizontal line indicates zero counts. The filled bars show the time intervals of drug application. The strength of iontophoretic current (in nA) and the applied drug are indicated. The background illumination was 5 cd/m^2. (Bolz *et al.*, *J. Physiol.*)

Directional Sensitivity

We have seen that directional sensitivity of ganglion cells may be interpreted on the basis of a lateral inhibition evoked by stimulus-movement in a non-preferred (null) direction. Caldwell *et al.* (1978a, b) showed that directional sensitivity could be blocked by applying picrotoxin to the retina, thus implicating GABA as the inhibitory transmitter. Null inhibition was shown by Ariel & Daw to be overcome by physostygmine, suggesting that light-evoked excitation in the receptive field centre is evoked by acetylcholine. Studying the turtle retina, Ariel & Adolph (1985) confirmed that acetylcholine caused excitation, and GABA caused inhibition, of directionally sensitive ganglion cells, effects that could be obtained in the retina in which synaptic transmission was blocked by low-Ca^{2+}.

Dopamine

The possible role of this transmitter, the most abundant catecholamine of the retina, has been discussed by Jensen & Daw (1983); it is localized in amacrine and possibly interplexiform cells (Ehinger, 1976), and its release from the rabbit retina is increased by light, 40 mM K^+ and MSH (Bauer *et al.*, 1980), whilst there are appropriate receptors of both D1 and D2 kind. Ikeda *et al.* (1986) emphasized the role of dopamine in the rod-dominated retinal pathways. Thus the autoradiographic study of Pourcho (1982) has shown that dopaminergic amacrines do not contact either bipolar or ganglion cells, but make reciprocal contacts with glycinergic and other amacrines. Since glycinergic amacrines, with which dopaminergic

amacrines synapse, receive direct inputs from some thirty rod bipolars, and send output to ganglion cells, we might expect the dopaminergic amacrines to reveal their activity in the rod pathway. Using their micro-iontophoretic technique of drug application, Ikeda *et al.* (1986) found that dopamine reduced spontaneous and light-induced firing of all physiological classes of ganglion cells, the maximal inhibitory effect being at the rod-dominated midperiphery. The inhibitory activity was much smaller than that of GABA and glycine, but was additive with these. Inhibition of dopamine activity by local application of haloperidol had no effect, of itself, on retinal activity, although it did block the effect of locally applied dopamine. Thus dopaminergic receptors are apparently present on ganglion cells but are not activated in normal circumstances.[20] In the rabbit retina, Jensen & Daw (1983) found that dopamine antagonists, haloperidol and fluphenazine, decreased the ON-responses of brisk cells.

Taurine

This sulphur-containing amino acid is present in very high concentration in excitable tissue; in the retina it is concentrated in the receptor layer as well as in Müller and pigment epithelial cells (Voaden *et al.*, 1977), and is released by light-exposure (Pasantes-Morales *et al.*, 1973). In animals like the cat that do not synthesize taurine, a deficiency of this amino acid caused severe retinal degeneration with ultimate disintegration of the photoreceptors. Pourcho (1981) demonstrated accumulation of ^{3}H-taurine by bipolar and some amacrine cells. The retinal degeneration is unaffected by light-exposure during maintenance on a taurine-deficient diet, so that Pasantes-Morales *et al.* (1986) attribute the degeneration to the loss of membrane-protective action of taurine (Pasantes-Morales & Cruz, 1985). Treatment of rod outer segments with taurine increases the ATP-dependent ^{45}Ca-accumulation (Pasantes-Morales, 1982).

Possible Transmitter Role

So far as taurine's role as a transmitter is concerned, this has been discussed by Pasantes-Morales (1982). It may be confidently stated that the actions of exogenous taurine are very similar to those of glycine, a recognized central nervous inhibitory transmitter. Cunningham & Miller (1980) compared taurine and glycine actions on the mudpuppy retina, employing intracellular recording from the different types of cell including Müller cells, as well as studying the ERG. Hyperpolarizing bipolars were depressed by glycine and taurine to a greater degree than by GABA, and the reverse pertained with depolarizing (ON-) bipolars. The effects were blocked by strychnine. The responses of ON–OFF-amacrine cells were blocked by both glycine and taurine; ganglion cells were hyperpolarized by glycine and taurine and the light-responses were blocked. In general the effects of taurine were similar to those of glycine, the latter being the more active.

Bolz *et al.* (1985b) compared the uptake of glycine and taurine by the cat retina, and the effects of micro-iontophoretic application. Like glycine, taurine suppressed light-evoked discharge of all ON- and OFF-centre brisk ganglion cells, an effect blocked by strychnine. A population of amacrine cells was heavily labelled by ^{3}H-glycine, whereas most uptake of taurine was by the outer layers of the retina. Bolz *et al.* emphasize that glycine and taurine probably both act on the same pharmacological receptors, competitively displacing strychnine, but the predominant binding of glycine in the inner plexiform layer probably indicates that this is the transmitter rather than taurine.

5-Hydroxytryptamine

5-Hydroxytryptamine (5-HT, or serotonin) is well established as a transmitter in the central nervous system, and its presence in many retinae has been proved. This is especially true of submammalian species, such as the chicken, but in many mammalian species its chemical assay has been difficult or impossible, so that the possible role of 5-HT in these retinae has been inferred from the ability of neurones to accumulate the metabolic precursor of 5-HT, namely 5,6-dihydroxytryptamine, the formation of 5-HT being recognized by the fluorescence technique of Falck-Hillarp, (Ehinger & Floren, 1979), or by the high-affinity accumulation of ^{3}H-labelled 5-HT, the actual neurones taking it up being recognized by autoradiography (e.g. Holmgren-Taylor, 1982). Employing the isolated bovine retina, Thomas & Redburn (1979) observed a high-affinity uptake of 5-HT, which was blocked by chloriprimine, an inhibitor of monoamine uptake. Reserpine also completely blocked uptake, suggesting that the uptake was into synaptic vesicles, whilst release was favoured by K^{+}-depolarization and Ca^{2+}. In a later study (1980), they showed that 5-HT was, indeed, accumulated in synaptosomes primarily derived from amacrine and bipolar terminals.

Immunofluorescence

Osborne & Patel (1984), employing a monoclonal antibody, identified, by immunofluorescence, amacrine cells that took up exogenous 5-HT in the isolated rabbit retina, although earlier (Osborne, 1982; 1983) endogenous material could not be demonstrated in rabbit and other mammalian tissue. The terminal processes were in the inner plexiform layer. The material taken up by the

cells could be released by high-K^+, a process inhibited by Co^{2+}, and thus suggesting storage in synaptic vesicles.

Electronmicroscopic Autoradiography

Holmgren-Taylor (1982) identified cells that took up labelled 5-HT in the cat's retina as amacrines similar to the AI amacrines of Kolb (1979); they made reciprocal synapses with rod bipolar terminals in sublamina-*b* of the inner plexiform layer, and also in sublamina-*a* with flat cone bipolars.

Developmental Changes

Osborne & Patel (1984) found very low concentrations of 5-HT in the retinae of newborn rabbits; as Fig. 12.26 shows, there was a steep increase from the 10th day. However, a two-day old retina accumulated exogenous 5-HT as efficiently as an adult retina, so that the ability to accumulate the transmitter apparently precedes the ability to synthesize it.

The Actual Transmitter

Florén & Hansson (1980) considered that the actual indoleamine transmitter could not be 5-HT, melatonin or bufotonin; and in their study of the uptake of indoleamine by the horizontal cells of the squirrel monkey, Floren & Hendrickson (1984) came to the same conclusion because, although ^{3}H-5-HT was taken up, the retina contained no intrinsic fluorescence that could be attributed to this indoleamine, so that they argued that the true transmitter was likely to be a non-fluorescent indoleamine. Thus the exogenous indoleamine taken up by the retina was converted to the true, non-fluorescent, transmitter within the cells. The presence of 5-HT decarboxylase, involved in the synthesis of 5-HT, cannot be accepted as evidence for the transmitter function of 5-HT, since the enzyme is also involved in the synthesis of dopamine (Florén & Hansson, 1980). However, Osborne (1984), in his review of the subject, considers that the demonstrable presence of 5-HT in the retinae of many species, including some mammals, makes it likely that it is, indeed, a transmitter.

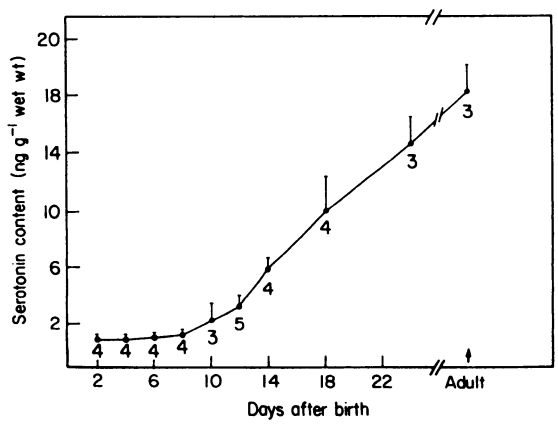

Fig. 12.26 Endogenous level of serotonin in retinas of rabbit from different developmental stages. Each point is the mean ±S.E.M. with the number of determinations shown in each instance. (Osborne & Patel, *Exp. Eye Res.*)

Effects on Ganglion Cells

Thier & Wässle (1984) applied 5-HT and an analogue, 5-methoxy-*N*,*N*-dimethyl tryptamine (MDT), to functionally identified ganglion cells of the cat. The general effect of 5-HT was to suppress ongoing and light-evoked discharge of ON-centre cells and to enhance the responses of OFF-centre cells. There was little distinction between X- and Y-cells. Interestingly, MDT had the opposite effects, possibly because of its preference for presynaptic receptor sites.

Peptides

Brecha *et al.* (1984) have reviewed the literature relating to the identification and localization of biologically active peptides in the vertebrate retina. Eskay *et al.* (1980) have given the concentrations of TRH, somatostatin and substance P in the retinae of several mammals as well as those of chicken, frog and eel. TRH is present in high concentration in the retinae of cold-blooded animals but in negligible concentration in warm-blooded animals. There were significant concentrations of somatostatin (about 50 pg mg^{-1} wet wt.) in mammalian retinae; substance P was also present in mammalian retinae, and in much higher concentration in that of the frog.

Immunocytochemistry

Eriksen & Larsson (1981) identified neurones containing vasoactive intestinal polypeptide (VIP), substance P, somatostatin and gastrin/cholecystokinin in the inner plexiform layer of the rat retina, occupying distinct strata, probably amacrine cells. Karten & Brecha (1983) described a similar lamination in the pigeon retina. Certainly Fukuda *et al.* (1981) found substance P-immunoreactivity in cells throughout the rat retina, most being in the proximal part of the inner nuclear layer with processes directed to the inner plexiform layer, these being amacrine cells; a few in the ganglion cell layer were probably displaced amacrines.[21]

CCK

Cholecystokynin, when applied to ganglion cells of the cat, uniformly suppressed activity, irrespective of re-

ceptive-field type; this is in contrast with CCK activity in other parts of the central nervous system where it is excitatory (Thier & Bolz, 1985).

Neuropeptide Y

Bruun *et al.* (1984) have demonstrated immunoreactive neurones of the guinea pig retina with cell-bodies in the inner nuclear layer and processes in sublamina 1 of the inner plexiform layer.

NEURONAL CIRCUITRY

Having considered the features of the receptive fields of some ganglion cells, the nature of the synaptic arrangements between photoreceptors and higher-order neurones leading to the ganglion cells, together with the nature of their transmitters, we may now proceed to look at some hypothetical circuits in the retina that might account for some of the receptive field features.

Outer Plexiform Layer

Figure 12.27 from Kolb & Nelson (1984) illustrates the basic features of this first region of synaptic contacts involving connections between receptors and bipolars, each receptor type having its specific bipolar cell (rod and cone bipolars, RB, and IB and FB respectively). The rod bipolar of the cat is a single type making an invaginating contact with the rod spherule. Cones make a variety of contacts, as we have seen.[22]

Types of Response

The response of the rod bipolar is one of hyperpolarization, similar to that of the rod. The cone responses are split into two pathways, a hyperpolarizing OFF-centre and a depolarizing ON-centre, handled by different types of bipolar cells. The bipolar cells studied in lower vertebrates, e.g. those of the mudpuppy, have a centre-surround organization, which is considered to be mediated by the horizontal cells, which have large receptive fields.

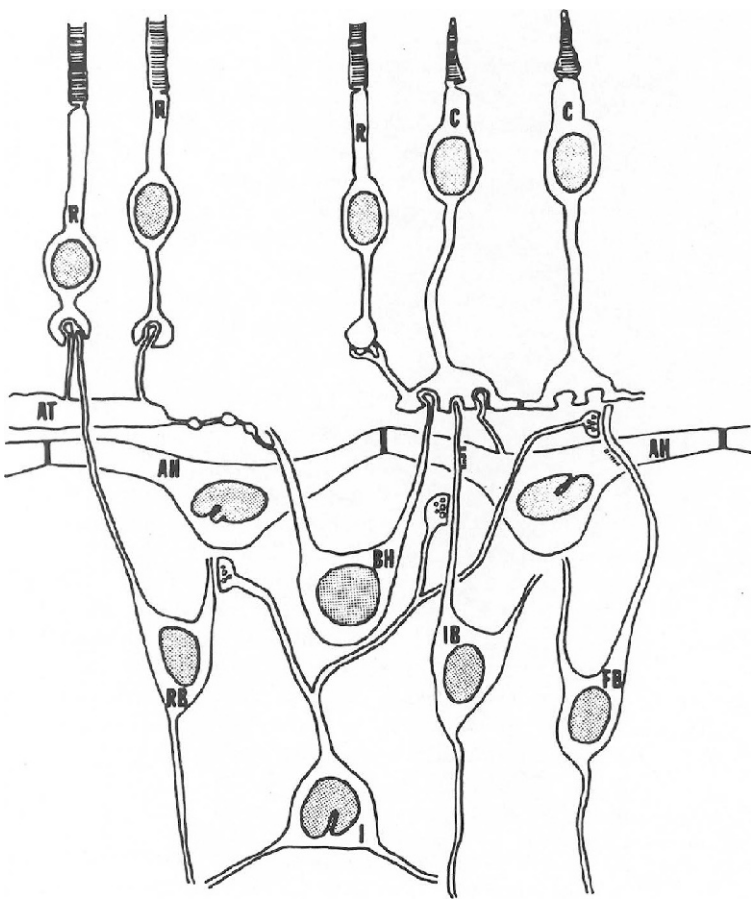

Fig. 12.27 Summary diagram of the neural connections in the outer plexiform layer of the cat retina. At the level of the synaptic terminals, cones (C) have basal processes that make minute gap junctions with rod spherules (R) and larger gap junctions with neighbouring cones. Rod bipolars (RB) connect only to rods while cone bipolars connect only to cones. Each bipolar type is characterized by a particular synaptic arrangement with its photoreceptor type. RB makes invaginating contacts, IB, invaginating contacts and FB, flat contacts, B type horizontal cells (BH) connect with cone pedicles but their axon terminals (AT) contact rod spherules. The axonless horizontal cell (AH) makes exclusive connections with cones and is joined to neighbouring A horizontal cells by gap junctions (thick lines). Specialized junctions (shaded) occur between A horizontal cell dendrites and cone bipolar dendrites. The interplexiform cell (I) extends dendrites into the OPL which are presynaptic to bipolar cell somata and dendrites. (Kolb & Nelson, *Progr. Ret. Res.*)

It will be recalled that in the triad type of synapse formed in the rod spherule or cone pedicle, a dendritic process of a bipolar cell comes into close relation with processes from horizontal cells, and it is easy to envisage the mechanism whereby horizontal cells, collecting input from more peripheral receptors, can influence transmission from more central receptors to give surround-responses. Such a mechanism is necessary, as the receptive-field sizes of rod bipolars far exceed their dendritic spreads, and they exceed that expected of rod-rod coupling (Leeper *et al.*, 1978).

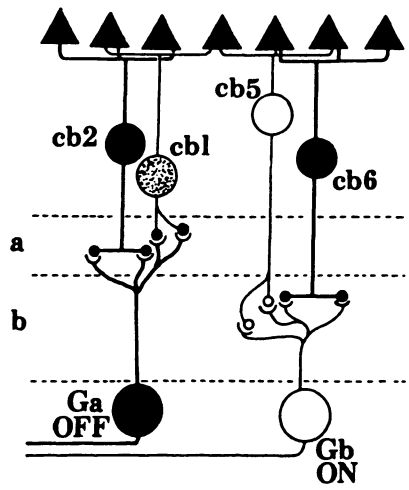

Fig. 12.28 Wiring diagram of the cone bipolar to ganglion cell connections in the cat retina. OFF centre ganglion cells (Ga) have dendrites branching in sublamina *a* of the IPL and receive synaptic input from cb1 and cb2 cone bipolars only. Cb2 is known to give a centre-hyperpolarizing response to light but the response of cb1 is not yet known. ON centre ganglion cells branch only in sublamina *b* of the IPL and receive input from a centre-depolarizing bipolar, cb5 and a centre-hyperpolarizing bipolar cb6. Black symbols represent hyperpolarizing, OFF centre units. Open symbols represent depolarizing ON centre units and stippled symbols have, as yet, unknown response polarities in this and the following wiring diagrams. (Kolb & Nelson, *Progr. Ret. Res.*)

Pathways to the Ganglion Cells

The Inner Plexiform Layer

As just indicated, the cone pathway is split into two, revealed by the ON- and OFF-centre responses of the ganglion cells; in the monkey, two cone midget bipolars are responsible for this dichotomy, being called invaginating and flat midgets in accordance with their types of synaptic contact with cones. The two types differ in the location of their dendritic terminals in the inner plexiform layer, invaginating midgets ending close to ganglion cell bodies, and flat midgets ending close to amacrine cell bodies; and these different levels of ending are associated with different branching levels for midget ganglion cells (Kolb, 1979). Gouras suggested that the two types of midget bipolar and ganglion cells were organized to subserve ON- and OFF-centre ganglion cells. A similar situation, although without midget-type cells, pertains in the cat; and a study of Nelson *et al.* (1978) with intracellular recording from ganglion cells confirmed the surmise of Famiglietti & Kolb (1976) that the ganglion cells with their dendrites ramifying in the a-sublamina of the inner plexiform layer, G_a-cells, subserved OFF-centre responses, and those ramifying in the b-sublamina, the ON-centre responses. This pairing of ganglion cells is shared by the three main types exhibiting centre-surround organization, namely X, Y and W.

Wiring Diagram

This is illustrated by Fig. 12.28 for the direct cone-bipolar-ganglion cell pathway. We may note that the cone bipolar cb6, which is a hyperpolarizing OFF-centre cell, synapses with the ON-centre ganglion cell, indicating that the ON-centre response of the ganglion cell contains an OFF-centre component, which may possibly be inhibitory, contributing to an OFF-inhibition, possibly through a GABA-ergic mechanism. Certainly, according to Ikeda & Sheardown (1983), OFF-inhibition is sensitive to GABA-antagonists.

The Role of Amacrine Cells

These neurones make connections with bipolar and ganglion cells, and may well be the dominant agents in the final centre-surround organization of the ganglion cells. A wiring diagram for one type may be exhibited as an example of the complexities of its synaptic arrangements (Fig. 12.29). Electrical recordings showed it to respond by hyperpolarization to light, with a pronounced OFF-depolarization and spikes. Its receptive field revealed an ON–OFF, depolarizing surround response antagonistic to the centre response. The cell ramifies in two sublaminae of the inner plexiform layer.[23]

The Rod Pathway

The rod connection to the ganglion cell is less direct than that of the cone, involving always an amacrine cell between bipolar and ganglion cell, so that rod bipolars do not synapse with ganglion cells (Kolb & Nelson, 1983). The involvement of the amacrine cells is illustrated in Fig. 12.30. As summarized by Kolb & Nelson (1984), the rod bipolars appear to transmit only a hyperpolarization, in response to light, to the inner plexiform layer; and the separation of the rod response into ON-centre and OFF-

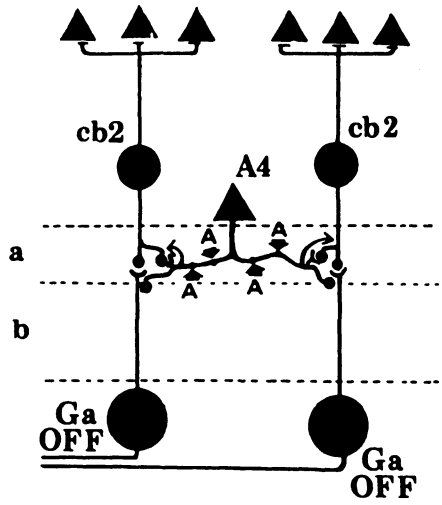

Fig. 12.29 Wiring diagram of connections of A4 as revealed by serial section electron microscopy. The cell is postsynaptic to cb2 bipolar cells in sublamina a of the IPL, makes reciprocal synapses to these bipolars and in presynaptic to OFF centre ganglion cells (Ga). It also receives many synapses from unidentified amacrine cells (A, large arrows). (Kolb & Nelson, *Progr. Ret. Res.*)

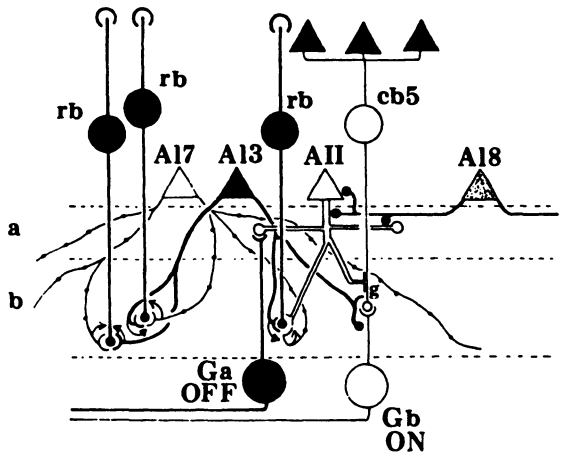

Fig. 12.30 Wiring diagram of the rod pathways of the cat retina. Rod bipolar cells contact rods only in the OPL and have output in the IPL to a number of amacrine cells. A17 amacrine passes amongst groups of rod bipolar axons and makes reciprocal synapses with them. A13 receives synaptic input from rod bipolars, makes reciprocal synapses and is presynaptic to ON centre ganglion cells (Gb). A13 receives synaptic input from rod bipolars in sublamina *b* and is presynaptic to OFF centre ganglion cells (Ga) in sublamina *a*. A11 also makes gap junctions (g) with the axon terminal of cb5 bipolar cells and has input to ON centre ganglion cells (Gb) through the cb5 axon terminal. A18 is the putative dopaminergic amacrine that synapses extensively on A11 amacrine cells in sublamina *a*. (Kolb & Nelson, *Progr. Ret. Res.*)

centre signals is postponed to the inner plexiform layer. Up to that point, the integrative processes have consisted in convergence of large numbers of rod responses on to fewer cells, permitting the amplification of weak light signals that is the dominant feature of rod vision. Thus, according to Nelson & Kolb (1983), by virtue of the synaptic arrangements of the rod bipolar cell, which contacts some 15 rods at triad structures within the rod spherule, where at least two horizontal cells make contact, a single bipolar cell actually integrates the input of at least 2 to 3 thousand rods. Through the integrative activity of amacrine cells the signals are split into ON- and OFF-centre types; the amacrine cells, because of their large receptive fields and amacrine–amacrine interconnections, must also contribute to the increased light-sensitivity of the rod system by promoting convergence of rod signals on to a single ganglion cell.

Three Main Pathways

Levick & Thibos (1983) have constructed retinal circuits, involving three major pathways based on the connectivities of the respective neurones. Thus pathway A (Fig. 12.31) is from cones to OFF-ganglion cells and B from cones to ON-ganglion cells, and C from rods to both ON- and OFF-ganglion cells. According to their analysis, individual ganglion cells, by virtue of their connections along any of the three pathways, are able to convey a unique picture of some spatial, temporal or spectral feature of the visual field, information that is subsequently processed further at higher centres. We may regard the transformation of sensory information from the receptor to higher cortical levels as a process involving the carriage of information from stage to stage employing fewer and fewer sensory neurones; thus Levick & Thibos refer to the 'bottle-neck of the optic nerve', meaning that information, acquired by some 7 million cones and 75 to 150 million rods, has to be carried by some hundred thousand optic nerve fibres. Thus each successive neurone carries a more detailed picture of some aspect of the visual field than the one before it. When we come to study the single units of the visual cortex this amplification of significance will become clear.

X-, Y- and W-pathways

The significance of the apparent separation of retinal information along three pathways mediated through X-, Y- and W-cells has been critically discussed by Levick &

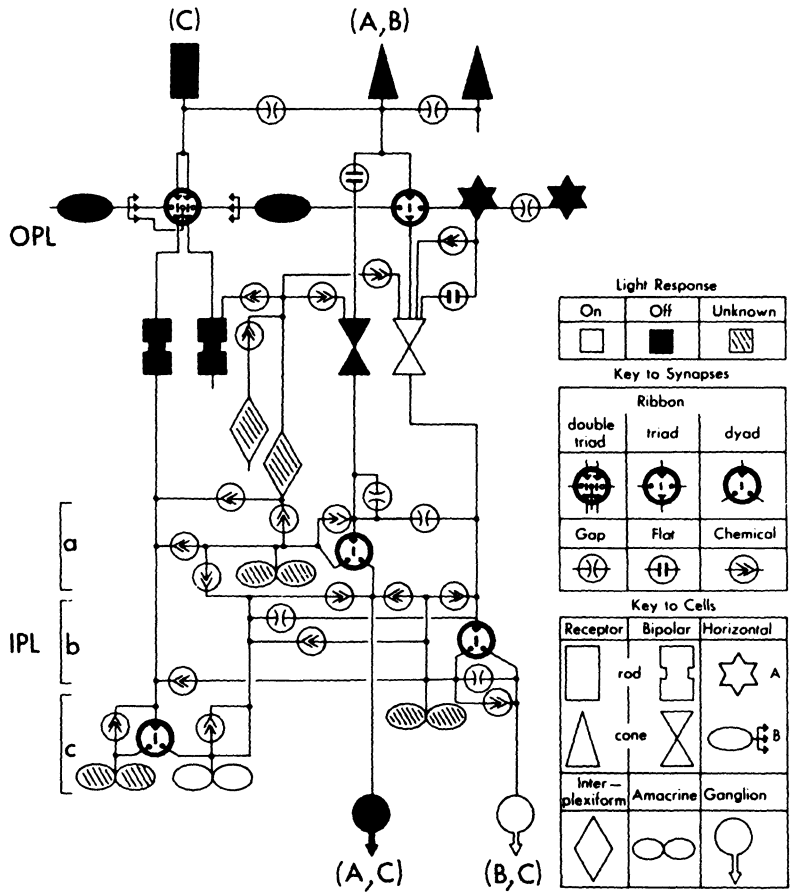

Fig. 12.31 Schematic wiring diagram of the cat retina. Cells provide the electrical pathway for neural signals and synapses provide the link between cells. Pathway (A) is from cones to off-ganglion cells, pathway (B) is from cones to on-ganglion cells and pathway (C) is from rods to both on- and off-ganglion cells. Outer plexiform layer (OPL) is not subdivided further but inner plexiform layer (IPL) has sublaminae a, b, c. At least one example of each type of synaptic interaction known to exist in the cat's retina is shown in the diagram. The existence of chemical synapses from horizontal cells onto bipolar cells is controversial. The on-type amacrine shown post-synaptic to a rod bipolar is of the AII type and the other amacrine of that dyad is of the AI type. Details of the wiring diagram for other morphological types of amacrine cell have not yet been determined but several kinds of synaptic contact involving amacrines have been identified. To keep the diagram uncluttered, these synapses are illustrated by just two other amacrine cells. The axons of B-type horizontal cells and of ganglion cells are indicated by the arrowhead portion of their respective symbols. (Levick & Thibos, *Progr. Ret. Res.*)

Thibos (1983), who call into question the validity of the concept, this being especially germane to the W-cell classification. Thus examination of the basis of this classification reveals the heterogeneity of the W-cell's receptive fields, and also of its morphology, so that, in fact, the only common feature that they hold, not possessed by X- and Y-cells, is the low conduction velocity, the order being: Y > X > W. Thus some W-cells have a concentric field organization and may be classed as either X- or Y-. Their supposedly unique projection to the superior colliculus is not true, as Y-cells also project there, and also some X-cells (Wässle & Illing, 1980). The authors conclude that the best classification is on the basis of conduction velocity, so that a given unit would be said to belong to one of three groups, T_1, T_2 and T_3 of descending conduction velocity and designated accordingly, the earlier classification into Y-, X- and W-cells being dropped, although cells with Y- and X-receptive fields, as originally defined by the tests of Enroth-Cugell & Robson, could still be characterized in this way.

Notes

1. The actual unit shown here is one from the lateral geniculate body the neurones of which have a well defined centre-surround organization (p. 498). Experimentally, annuli of internal and external radii differing by 1 degree were used, and the abscissa is the mean of these two radii.
2. Enroth-Cugell *et al.* (1983) have described a subset of W-cells, which they call Q-cells, that exhibit linear summation, like X-cells; however, when spatial and temporal frequencies of stimulation were varied it was not possible to separate clearly the two features, the response to a given spatial frequency depending on the temporal frequency.

   Stanford (1987) has defined two distinct classes of W-cell in the cat retina, differing in soma size, the phasic W-cells having smaller somas than those of tonic W-cells; axon conduction velocities were in the order: Phasic W < Tonic W < X. The neurones were identified by retrograde transport of HRP from the superior colliculus and the C-laminae of the lateral geniculate nucleus; the phasic W-cells did not project to the C-laminae, but the tonic cells did. The authors suggested that their medium-sized tonic W-cells were equivalent to the Q-cells of Enroth-Cugell *et al.*
3. Earlier Lee & Willshaw (1978) compared the maximal responses of X- and Y-cells to a moving bar; this peaked at 20–40 deg/sec for X-cells and 100 deg/sec for Y-cells. The difference may well reside in the larger receptive field of the Y-cell, so that the moving bar stays longer in the excitatory centre.
4. Ikeda & Wright (1972b) distinguished two aspects of the periphery effect; the *modulated effect* is essentially that described by McIlwain (1966) and is best brought about by moving a grating in the periphery; each shift of the grating produces a modulation in discharge synchronous with the shift. The *unmodulated effect* reflects a more static change in excitability extending over large distances.
5. Boycott & Wässle described a subclass of γ-cells, the δ cells; their perikaryal diameters were larger, and their dendritic morphology was rather similar to that of smaller α-cells.
6. Because of interactions between centre and surround the establishment of the size of the ganglion cell's centre is not always easy; Fukuda *et al.* (1984) have described in detail their own methods for X-, Y- and W-cells. They discuss the divergence of their conclusions regarding Y-cells from those of Peichl & Wässle (1983).
7. The cone-to-cone and cone-to-rod gap junctions described by Raviola & Gilula (1973) were examined by freeze-fracture and were found to be variants on the common form. Thus there were ribbon-like areas of close membrane approximation (but not fusion); on either side of the narrowing intercellular space, Face A (the cytoplasmic leaflet) had a row of particles, with a complementary row of depressions of Face B. These were found in the retinas of monkey, rabbit and turtle. Thus, because of these junctions, the photoreceptors could not be viewed as a strictly independent mosaic of units.
8. Dubin (1970) examined the pattern of synaptic arrangement in species in different places in the phylogenetic tree, namely man, monkey, rat, rabbit, ground squirrel, frog and pigeon. Qualitatively the basic pattern of synaptic arrangement was the same for all, but in the primates the ribbon type of synapse relating bipolar cell to ganglion cell directly was predominant, whilst in the lower vertebrate a more indirect route from bipolar to ganglion cell, via amacrines was usual. Thus a ganglion cell can have three types of bipolar input: direct from the bipolar; indirect through amacrine, exclusively, and indirect through amacrine and direct through bipolar.
9. Nevertheless, because of cone-rod connections in the outer plexiform layer, a horizontal cell can receive a mixed rod-cone message. Thus, although the dendritic terminals of a horizontal cell body contact only cones, and the axon terminals contact only rods, Nelson (1977) was unable to find a horizontal cell driven by cones only, and it turned out that the rod signals came through the cones that made synaptic contact.
10. This is only true of ribbon and conventional synapses; gap-junction types of contact are made with invaginating cone bipolars, whilst the amacrine receives chemical synapses from other amacrines. Nelson (1982) has suggested that, because this amacrine cell makes extensive gap-junctions with invaginating cone bipolars, it may be stimulated rapidly by these elements that are on the direct cone-route to ganglion cells. He concludes from his study of the electrical responses of these AII cells to light that they speed up the responses of ganglion cells. They are relatively insensitive to light, requiring some 200 photoisomerizations at threshold.
11. Mariani (1982) described a 'biplexiform cell' in the primate retina; like ganglion cells it sent dendrites into the inner plexiform layer where it was postsynaptic to bipolars, and it sent its axon into the optic nerve. However, it also sent processes to the outer plexiform layer, where they synapsed with rods. Catecholaminergic neurones are recognized by their fluorescence; the interplexiform cells of teleosts were recognized by this feature. Boycott *et al.* (1975) emphasize that their mammalian interplexiform cells were not catecholaminergic; according to Nakamura *et al.* (1980), they are GABA-ergic.
12. In the turtle retina, Marchiafava & Weiler (1980) described nine different types of bipolar cell, differing in their axon terminations in the inner plexiform layer. Of these, one called B4, was identified as a centre-hyperpolarizing (H-type) bipolar, and another, B6, as a centre-depolarizing bipolar. Kolb & Wang (1985) showed that B4 made wide-cleft striated basal junctions with red and green cone pedicles; B6 made narrow-cleft semi-invaginating basal junctions with cone pedicles; their dendrites did not become central elements at ribbon synapses, although they invaginated towards the synaptic ribbons. Thus, in this particular retina, there are differences between sign-conserving (hyperpolarizing) and sign-reversing (depolarizing) bipolar cells.
13. Marc & Lam (1981) using light-microscope autoradiography, showed that in the isolated goldfish retina the rods accumulated ^{3}H-glutamic acid some thirty times more actively than ^{3}H-aspartic acid; they were more densely labelled by ^{3}H-glutamic acid than were the cones. Red-green sensitive cones exhibited high-affinity uptake for both amino acids but little selectivity; blue-sensitive cones did not show uptake. Thus rods and cones could be distinguished by the selectivity of their dicarboxylic amino acid uptakes. In the human retina Brandon & Lam (1983) found that cones had a specific uptake mechanism for glutamic, but not aspartic, acid; their study, however, was based on immunocytological localization of aspartate aminotransferase, which is also involved in GABA synthesis.
14. Isolation was achieved by incubation with kainic acid and L-α-aminoadipic acid, toxic to horizontal, bipolar and amacrine cells, and with veratrine, toxic to ganglion and amacrine cells. Horizontal cells were isolated by incubation with an anti-photoreceptor immune serum and veratrine.
15. Piccolino *et al.* (1982) found that the GABA antagonists, bicuculline and picrotoxin caused narrowing of the receptive fields of large-field horizontal cells associated with an in-

crease in the coupling resistance between horizontal cells. Since the D1 receptor was involved, it was expected that cAMP would be the 'second messenger', and it was found that forskalin had similar effects (Piccolino, 1985). So far as the role of GABA antagonists is concerned, Piccolino *et al.* (1984) concluded that they acted through dopaminergic neurones; thus the action of bicuculline was blocked by dopamine antagonists, so it may be assumed that GABA is released tonically, reducing the release of dopamine from dopaminergic neurones; bicuculline would relieve this inhibition, thereby promoting increased gap-junction permeability (Piccolino *et al.*, 1983).

16. The literature on localization of cholinergic neurones in the retinae of a variety of species is large; Pourcho & Osman (1986) summarize it well in their paper. We may note that Vaney (1984) suggests that the 'coronate starburst' amacrines be called Type C amacrines, C indicating that their likely transmitter is acetylcholine. Ross *et al.* (1985) measured actual enzyme activity in different layers of the rat retina, and found characteristic peaks in two bands for ChAT whilst esterase activity was more diffusely spread. Also working on the rat, Voigt (1986) identified two layers of amacrines using a monoclonal antibody to ChAT, afterwards revealing their dendritic morphology by intracellular injection of Lucifer yellow. Tauchi & Masland (1984) stained acetylcholine synthesizing cells by intraocular injection of the specific stain (DAPI) and subsequent intracellular injection of Lucifer yellow, thereby revealing the dendritic morphology as typically 'starburst'. Because the cells overlap and branch profusely, a dense cholinergic plexus occurs in the inner plexiform layer of the rabbit.

    Hutchins & Hollyfield (1985) employed the irreversible ligand: ^{3}H-propylbenzilyl choline mustard (PrBCM) to label muscarinic receptors in the human retina; these were located in the inner plexiform layer. There was also some uptake of bungarotoxin that is supposed to label nicotinic receptors, but they question the specificity of the test.

    In a later and more elaborate study of the human retina, using several labelling techniques, Hutchins & Hollyfield (1987) confirmed the presence of a population of cholinergic cells along both margins of the inner plexiform layer. So far as processes in the inner plexiform layer are concerned, the human retina does not display the sublamination that seems to be a feature with other species (see, for example, Voigt, 1986).

17. Agardh *et al.* (1986) found GABA-immunoreactivity in a subset of amacrine cells and in the inner plexiform layer of chicken, guinea pig and rabbit retinae; in the chicken there was also activity in horizontal cells.
18. Schmidt *et al.* (1987) identified ganglion cells by injection of Procion yellow, and studied the effects of acetylcholine in the cat retina. Acetylcholine increased the activity of all brisk cells, the effects on ON-, OFF-, X- and Y-cells being similar; the effects were antagonized by scopolamine, a muscarinic antagonist. DBE, a nicotinic antagonist, raised the firing rate of ON-brisk cells and decreased that of OFF-cells; it blocked the effects of acetylcholine on OFF-centre cells, and reduced that on ON-centre cells. Physostigmine prolonged and enhanced the effects of acetylcholine on all ganglion-cell types, with a relatively greater effect on ON-centre responses. Immunocytochemically they demonstrated two populations of amacrine cells, in the inner nuclear and ganglion cell layers; the dendritic morphology of putative cholinergic amacrine cells, identified by ChAT immunoreactivity, was like that of rat and rabbit 'starburst' amacrines.
19. Bolz *et al.* (1985a, b) discuss the conflict of their results with those of Ikeda & Sheardown (1983) with respect to the ON-, OFF-dichotomy described by them, without reaching a satisfactory explanation. Earlier Belgum *et al.* (1984) showed that the transient inhibitions seen with ON-centre, OFF-centre and ON–OFF-centre mudpuppy ganglion cells were inhibited by strychnine, suggesting that this type of inhibition was mediated by the same transmitter, glycine. Although both GABA and glycine cause hyperpolarization and increases of conductance in all three types of ganglion cell, the inhibitor of GABA, picrotoxin, did not block inhibition of any type. Saito (1983) found a dichotomy with respect to ON-centre responses of the cat's X- and Y-cells, strychnine blocking the surround-inhibition of X-cells, indicating that glycine was its transmitter, whilst bicuculline blocked the surround-inhibition, indicating GABA as the transmitter involved.
20. In Parkinsonism, the visually evoked responses (VER) in the brain are delayed, possibly through delay in the retina; Dyer *et al.* (1981) depleted the retina of the rat of noradrenaline and dopamine with α-methyl-para-tyrosine, and found an increased latency in the early peak of the VER; the delay was definitely associated with the retina, rather than later in the visual pathway.
21. Karten & Brecha (1980) found positive substance P immunoreactivity only in the inner nuclear and plexiform layers of the pigeon retina; it was in the somata of amacrine cells at the border of these layers; on somata in the outer nuclear layer or ganglion cell layer were reactive, nor yet Müller cells. The immunoreactive amacrine cells had a single process that descended directly into the inner plexiform layer and ramified in a narrow band corresponding to Lamina 3 of Cajal.
22. In their description of the cone pathway in the cat's retina, Nelson *et al.* (1981) draw attention to the mixing of rod and cone signals which can occur at the receptor level, as well as at higher-order neurones; thus rod spherules and cone pedicles make contacts, and gives rise to rod-type responses mixed with those of cones (Nelson, 1977). Further mixing occurs at the horizontal and cone-bipolar levels; thus no cone bipolar cell could be found driven exclusively by long-wavelength responsive cones (Nelson, 1980).
23. Kolb & Nelson (1984), in their excellent review of the neural architecture of the cat retina, point out that the lamination of the bipolar terminals, which formed the basis of this concept, has to be modified, the axon terminals of ON- and OFF-bipolars being found at almost any level of the inner plexiform layer. However, the stratification of the dendrites of ON- and OFF-ganglion cells is completely valid.

References

Agardh, E., Bruun, A., Ehinger, B. & Storm-Mathisen, J. (1986) Gaba immunoreactivity in the retina. *Invest. Ophthal.* **27**, 674–678.

Ariel, M. & Adolph, A. R. (1985) Neurotransmitter inputs to directionally sensitive turtle retina ganglion cells. *J. Neurophysiol.* **54**, 1123–1143.

Ariel, M. & Daw, N. N. (1982) Effects of cholinergic drugs on receptive field properties of rabbit ganglion cells. *J. Physiol.* **324**, 135–160.

Ariel, M., Lasater, E. M., Mangel, S. C. & Dowling, J. E. (1984) On the sensitivity of the H 1 horizontal cells of the carp retina to glutamate, aspartate and their agonists. *Brain Res.* **295**, 179–183.

Ayoub, G. & Lam, D. M.-K. (1984) The release of γ-aminobutyric acid from horizontal cells of the goldfish (*Carassius auratus*) retina. *J. Physiol.* **355**, 191–214.

Barlow, H. B., Derrington, A. M., Harris, L. R. & Lennie, P. (1977) The effects of remote retinal stimulation on the responses of cat retinal ganglion cells. *J. Physiol.* **269**, 177–194.

Barlow, H. B., Fitzhugh, R. & Kuffler, S. W. (1957) Change of organization of the receptive fields of the cat's retina during dark adaptation. *J. Physiol.* **137**, 338–354.

Barlow, H. B., Hill, R. M. & Levick, W. R. (1964) Retinal ganglion cells responding selectively to direction and speed of image motion in the rabbit. *J. Physiol.* **173**, 377–407.

Barlow, H. B. & Levick, W. R. (1965) The mechanism of directionally sensitive units in rabbit's retina. *J. Physiol.* **178**, 477–504.

Bauer, B., Ehinger, B. & Åberg, L. (1980) [^{3}H]-Dopamine release from the rabbit retina. *v. Graefes Arch. Ophthal.* **215**, 71–78.

Belgum, J. H., Dvorak, D. R. & McReynolds, J. S. (1982) Sustained synaptic input to ganglion cells of mudpuppy retina. *J. Physiol.* **326**, 91–108.

Belgum, J. H., Dvorak, D. R. & McReynolds, J. S. (1984) Strychnine blocks transient but not sustained inhibition in mudpuppy retinal ganglion cells. *J. Physiol.* **354**, 273–286.

Bloomfield, S. A. & Dowling, J. E. (1985) The roles of aspartate and glutamate in synaptic transmission in rabbit retina. I. Outer plexiform layer. *J. Neurophysiol.* **53**, 699–713.

Bolz, J., Frumkes, T., Voigt, T. & Wässle, A. (1985a) Action and localization of γ-aminobutyric acid in the cat retina. *J. Physiol.* **362**, 369–393.

Bolz, J., Thier, P., Voigt, T. & Wässle, H. (1985b) Action and localization of glycine and taurine in the cat retina. *J. Physiol.* **362**, 395–413.

Boycott, B. B. & Dowling, J. E. (1969) Organization of the primate retina: light microscopy. *Phil. Trans. B* **225**, 109–184.

Boycott, B. B., Dowling, J. E., Fisher, S. K., Kolb, H. & Laties, A. M. (1975) Interplexiform cells of the mammalian retina and their comparison with catecholamine-containing retinal cells. *Proc. Roy. Soc. B* **191**, 353–368.

Boycott, B. B. & Kolb, H. (1973) The connections between bipolar cells and photoreceptors in the retina of the domestic cat. *J. Comp. Neurol.* **148**, 91–114.

Boycott, B. B. & Kolb. H. (1973) The horizontal cells of the rhesus monkey retina. *J. Comp. Neurol.* **148**, 115–140.

Boycott, B. B., Peichl, L. & Wässle, H. (1978) Morphological types of horizontal cell in the retina of the domestic cat. *Proc. Roy. Soc. B* **203**, 229–245.

Boycott, B. B. & Wässle, H. (1974) The morphological types of ganglion cells of the domestic cat's retina. *J. Physiol.* **240**, 397–419.

Brandon, C. & Lam, D. M.-K. (1983) L-Glutamic acid: a neurotransmitter candiatate for cone photoreceptors in human and cat retinas. *Proc. Nat. Acad. Sci.* **80**, 5117–5121.

Brecha, N. C., Eldred, W., Kuljis, R. O. & Karten, H. J. (1984) Identification and localization of biologically active peptides in the vertebrate retina. *Progr. Retinal Res.* **3**, 185–226.

Brecha, N. C., Oyster, C. W. & Takahashi, E. S. (1984) Identification and characterization of tyrosine hydroxylase immunoreactive amacrine cells. *Invest. Ophthal.* **25**, 66–70.

Brown, J. E. & Major, D. (1966) Cat retinal ganglion cell dendritic fields. *Exp. Neurol.* **15**, 70–78.

Bruun, A., Ehinger, B., Sundler, F., Tornqvist, K. & Uddman, R. (1984) Neuropeptide Y immunoreactive neurons in the guinea-pig uvea and retina. *Invest. Ophthal.* **25**, 1113–1123.

Caldwell, J. H. & Daw, N. W. (1978a) Effects of picrotoxin and strychnine on rabbit retinal ganglion cells: changes in centre surround receptive features. *J. Physiol.* **276**, 299–310.

Caldwell, J. H., Daw, N. W. & Wyatt, H. J. (1978b) Effects of picrotoxin and strychnine on rabbit retinal ganglion cells: lateral interactions for cells with more complex receptive fields. *J. Physiol.* **276**, 277–298.

Cervetto, L. & MacNichol, E. F. (1972) Inactivation of horizontal cells in turtle retina by glutamate and aspartate. *Science* **178**, 767–768.

Cervetto, L. & Piccolino, M. (1974) Synaptic transmission between photoreceptors and horizontal cells in the turtle retina. *Science* **183**, 417–419.

Cleland, B. G. (1983) Sensitivity to stationary flashing spots of the brisk classes of ganglion cells in the cat retina. *J. Physiol.* **245**, 15–26.

Cleland, B. G., Dubin, M. W. & Levick, W. R. (1971) Sustained and transient neurones in the cat's retina and lateral geniculate nucleus. *J. Physiol.* **217**, 473–496.

Cleland, B. G. & Harding, J. P. (1983) Response to the velocity of moving visual stimuli of the brisk classes of ganglion cells in the cat retina. *J. Physiol.* **345**, 47–63.

Cleland, B. G. & Levick, W. R. (1974) Brisk and sluggish concentricilly organized ganglion cells in the cat's retina. *J. Physiol.* **240**, 421–456.

Cleland, B. G. & Levick, W. R. (1974) Properties of rarely encountered types of ganglion cells in the cat's retina and an overall classification. *J. Physiol.* **240**, 457–492.

Cleland, B. G., Levick, W. R. & Sanderson, K. J. (1973). Properties of sustained and transient ganglion cells in the cat retina. *J. Physiol.* **228**, 649–680.

Cunningham, R. & Miller, R. F. (1980) Electrophysiological analysis of taurine and glycine action on neurons of the mudpuppy retina. I, II. *Brain Res.* **197**, 123–138, 139–151.

Cunningham, J. P. & Neal, M. J. (1983) Effect of γ-aminobutyric acid agonists, glycine, taurine and neuropeptides on acetylcholine release from the rabbit retina. *J. Physiol.* **336**, 563–577.

Dowling, J. E. & Boycott, B. B. (1966) Organization of the primate retina: electron microscopy. *Proc. Roy. Soc. B* **166**, 80–111.

Dowling J. E. & Ehinger, B. (1975) Synaptic organization of the amine-containing interplexiform cells of the goldfish and cebus monkey retinas. *Science* **188**, 270–273.

Dowling, J. E. & Ehinger, B. (1978) Synaptic organization of the dopaminergic neurons in the rabbit retina. *J. Comp. Neurol.* **180**, 203–220.

Dowling, J. E. & Ripps, H. (1973) Effect of magnesium on horizontal cell activity in the skate retina. *Nature* **242**, 101–103.

Dubin, M. W. (1970) The inner plexiform layer of the vertebrate retina: quantitative and comparative electron microscopic analysis. *J. Comp. Neurol.* **140**, 479–506.

Dyer, R. S., Howell, W. E. & McPhail, R. C. (1981) Dopamine depletion slows retinal transmission. *Exp. Neurol.* **71**, 326–340.

Ehinger, B. (1976) Biogenic amines as transmitters in the retina. In *Transmitters in the Visual Process.* (Ed. Bonting, S. L.) Pergamon, Oxford.

Ehinger, B., Falck, B. & Laties, A. M. (1969) Adrenergic neurons in teleost retina. *Zeit. Zellforsch.* **97**, 285–297.

Ehinger, B. & Florén, I. (1979) Absence of indoleamine-accumulating neurons in the retina of humans and cynomolgus monkeys. *v. Graefes Arch. Ophthal.* **209**, 145.

Enroth-Cugell, C. & Lennie, P. (1975) The control of ganglion cell discharge by receptive field surrounds. *J. Physiol.* **247**, 551–578.

Enroth-Cugell, C. & Robson, J. G. (1966). The contrast sensitivity of retinal ganglion cells of the cat. *J. Physiol.* **187**, 517–552.

Enroth-Cugell, C. & Robson, J. G. (1984) Functional characteristics and diversity of cat retinal ganglion cells. *Invest. Ophthal.* **25**, 250–267.

Enroth-Cugell, C., Robson, J. G., Schweitzer-Tong, D. E. & Watson, A. B. (1983) Spatio-temporal interactions in cat retinal ganglion cells showing linear spatial summation. *J. Physiol.* **341**, 279–307.

Eriksen, E. F., & Larsson, L.-I. (1981) Neuropeptides in the retina: evidence for differential topographical localization. *Peptides* **2**, 153–157.

Eskay, R. L., Long, R. T. & Iuvone, P. M. (1980) Evidence that TRH, somatostatin and substance P are present in neurosecretory elements of the vertebrate retina. *Brain Res.* **196**, 555–559.

Famiglietti, E. V. (1983) 'Starburst' amacrine cells and cholinergic neurons: mirror-symmetric ON and OFF amacrine cells in rabbit retina. *Brain Res.* **261**, 138–144.

Famiglietti, E. V. (1983) ON and OFF pathways through amacrine cells in mammalian retina: the synaptic connections of 'starburst' amacrine cell. *Vision Res.* **23**, 1265–1281.

Famiglietti, E. V. & Kolb, H. (1975) A bistratified amacrine cell and synaptic circuitry in the inner plexiform layer of the retina. *Brain Res.* **84**, 293–300.

Famiglietti, E. V. & Kolb, H. (1976) Structural basis for ON- and OFF-centre responses in retinal ganglion cells. *Science* **194**, 193–195.

Florén. I. & Hansson, H. C. (1980) Investigations into whether 5-hydroxytryptamine in a neurotransmitter in the retinas of rabbit and chicken. *Invest, Ophthal.* **19**, 117–125.

Florén, I. & Hendricksen, A. (1984) Indoleamine-accumulating horizontal cells in the squirrel monkey. *Invest. Ophthal.* **25**, 997–1006.

Frederick, J. M., Rayborn, M. E. & Hollyfield, J. G. (1984) Glycinergic neurons in the human retina. *J. Comp. Neurol.* **227**, 159–172.

Fukuda, Y., Hsiao, C. F., Hara, Y. & Iwama, K. (1981) Properties of ipsilateral retinogeniculate afferents in albino and hooded rats. *Neurosci. Lett.* **22**, 173–178.

Fukuda, Y., Hsiao, C.-F., Watanabe, M. & Ito, H. (1984) Morphological correlates of physiologically identified Y-, X- and W-cells in cat retina. *J. Neurophysiol.* **52**, 999–1013.

Fukuda, Y. & Stone, J. (1974) Retinal distribution and central projections of Y-, X- and W-cells of the cat's retina. *J. Neurophysiol.* **37**, 749–772.

Hammond, P. (1972) Spatial organization of receptive fields of LNG neurones. *J. Physiol.* **222**, 53P–54P.

Hayden, S. A., Mills, J. W. & Masland, R. H. (1980) Acetylcholine synthesis by displaced amacrine cells. *Science* **210**, 435–437.

Holmgren-Taylor, I. (1982) Electron microscopical observations on the indoleamine-accumulating neurons and their synaptic connections in the retina of the cat. *J. Comp. Neurol.* **208**, 144–156.

Hsiao, C. F., Watanabe, M. & Fukuda, Y. (1984) The relation between axon diameter and axonal velocity of Y, X and W cells of the cat retina. *Brain Res.* **309**, 357–361.

Hutchins, J. B. & Hollyfield, J. G. (1985) Acetylcholine receptors in the human retina. *Invest. Ophthal.* **26**, 1550–1557.

Hutchins, J. B. & Hollyfield, J. G. (1987) Cholinergic neurons in the human retina. *Exp. Eye Res.* **44**, 363–375.

Ikeda, H. (1985) Transmitter action at cat retinal ganglion cells. *Progr. Retinal Res.* **4**, 1–31.

Ikeda, H., Priest, T. D., Robbins, J. & Wakakuwa, K. (1986) Silent dopaminergic synapse at feline retinal ganglion cells. *Clin. Vision Sci.* **1**, 25–38.

Ikeda, H. & Sheardown, M. J. (1983) Functional transmitters at retinal ganglion cells in the cat. *Vision Res.* **23**, 1161–1174.

Ikeda, H. & Wright, M. J. (1972a) The outer disinhibitory surround of the retinal ganglion cell receptive field. *J. Physiol.* **226**, 511–544.

Ikeda, H. & Wright, M. J. (1972b) Functional organization of the periphery effect in retinal ganglion cells. *Vision Res.* **12**, 1857–1879.

Jensen, R. J. & Daw, N. W. (1983) Towards an understanding of the role of dopamine in the mammalian retina *Vision Res.* **23**, 1293.

Karten, H. J. & Brecha, N. (1980) Localization of substance P immunoreactivity in amacrine cells of the retina. *Nature* **283**, 87–88.

Karten, H. J. & Brecha, N. (1983) Localization of neuroactive substances in the vertebrate retina: evidence for lamination in the inner plexiform layer. *Vision Res.* **23**, 1197–1205.

Kidd, J. A. (1962) Electron microscopy of the inner plexiform layer of the retina in the cat and pigeon. J. Anat. **96**, 179–187.

Kirby, A. W. (1979) The effect of strychnine, bicuculline, and picrotoxin on X and Y cells in the cat retina. *J. Gen. Physiol.* **74**, 71–84.

Kirby, A. W. & Enroth-Cugell, C. (1976) The involvement of gamma-aminobutyric acid in the organization of cat retinal ganglion cell receptive fields. A study with picrotoxin and bicuculline. *J. Gen. Physiol.* **68**, 465–484.

Kolb, H. (1970) Organization of the outer plexiform layer of the primate retina: electron microscopy of Golgi impregnated cells. *Phil. Trans.* **258**, 261–283.

Kolb, H. (1979) The inner plexiform layer in the retina of the cat: electron microscopic observations. *J. Neurocytol.* **8**, 295–329.

Kolb, H. & Famiglietti, E. V. (1976) Rod and cone pathways in the retina of the cat. *Invest. Ophthal.* **15**, 935–946.

Kolb, H. & Nelson, R. (1981) Amacrine cells of the cat retina. *Proc. Symp. Information Processing in Retina* (Ed. Kafka-Lutzow, A.) Hung. Acad. Sci., Pergamon: Oxford. (Quoted by Kolb *et al.*, 1981.)

Kolb, H. & Nelson, R. (1983) Rod pathways in the retina of the cat. *Vision Res.* **23**, 301–312.

Kolb, H. & Nelson, R. (1984) Neural architecture of the cat retina. *Progr. Ret. Res.* **3**, 21–60.

Kolb, H., Nelson, R. & Mariani, A. (1981) Amacrine cells, bipolar cells and ganglion cells of the cat retina: a Golgi study. *Vision Res.* **21**, 1081–1114.

Kolb, H. & Wang, H. H. (1985) The distribution of photoreceptors, dopaminergic amacrine cells and ganglion cells in the retina of the North American opossum (*Didelphus virginiana*). *Vision Res.* **25**, 1207–1221.

Kruger, J. & Fischer, B. (1973) Strong periphery effect in cat retinal ganglion cells. Excitatory responses in ON- and OFF-center neurones to single grid displacements. *Exp. Brain Res.* **18**, 316–318.

Lasansky, A. (1978) Contacts between receptors and electrophysiologically identified neurones in the retina of the larval tiger salamander. *J. Physiol.* **285**, 531–542.

Lasater, E. M. & Dowling, J. E. (1982) Carp horizontal cells in culture respond selectively to L-glutamate and its agonists. *Proc. Nat. Acad, Sci.* **79**, 936–940.

Laufer, M., Negishi, K. & Drujan, B. D. (1981) Pharmacological manipulation of spatial properties of S-potentials. *Vision Res.* **21**, 1657–1660.

Lee, B. B. & Willshaw, D. J. (1978) Responses of the various types of cat retinal ganglion cells to moving contours. *Vision Res.* **18**, 757–765.

Leeper, H. F., Normann, R. A. & Copenhagen, D. R. (1978) Evidence for passive electrotonic interactions in red rods of toad retina. *Nature* **275**, 234–236.

Leicester, J. & Stone, J. (1967) Ganglion, amacrine and horizontal cells of the cat's retina. *Vision Res.* **7**, 695–705.

Levick, W. R. (1975) Form and function of cat retinal ganglion cells. *Nature* **254**, 659–662.

Levick, W. R. & Thibos, L. N. (1983) Receptive fields of cat ganglion cells: classification and construction. *Progr. Ret. Res.* **2**, 267–319.

MacKay, D. M. (1970) Elevation of visual threshold by displacement of retinal image. *Nature* **225**, 90–92.

Marc, R. E. & Lam, D. M. K. (1981) Uptake of aspartic and glutamic acid by photoreceptors in goldfish retina. *Proc. Nat. Acad. Sci.* **78**, 7185–7190.

Marc, R. E. & Liu, W. E. S. (1984) Glycine-accumulating neurons in the human retina. *J. Comp. Neurol.* **232**, 241–260.

Marchiafava, P. L. & Weiler, R. (1980) Intracellular analysis and structural correlates of the organization of inputs to ganglion cells in the retina of the turtle. *Proc. Roy. Soc. B* **208**, 103–113.

Mariani, A. P. (1982) Biplexiform cells: ganglion cells of the primate retina that contact photoreceptors. *Science* **216**, 1134–1136.

Masland, R. H. & Ames, A. (1976) Responses to acetylcholine of ganglion cells in an isolated mammalian retina. *J. Neurophysiol.* **39**, 1220–1235.

Masland, R. H. & Mills, J. W. (1979) Autoradiographic identification of acetylcholine in the rabbit retina. *J. Cell Biol.* **83**, 159–178.

Masland, R. H., Mills, J. W. & Cassidy C. (1984a) The functions of acetylcholine in the rabbit retina. *Proc. Roy. Soc. B* **223**, 121–139.

Masland, R. H., Mills, J. W. & Hayden, S. A. (1984b) Acetylcholine-synthesizing amacrine cells: identification and selective staining by using autoradioautography and fluorescent markers. *Proc. Roy. Soc. B* **223**, 79–100.

Massey, S. C. & Miller, R. F. (1987) Excitatory amino acid receptors of rod- and cone-driven horizontal cells in the rabbit retina. *J. Neurophysiol.* **57**, 645–659.

Massey, S. C. & Neal, M. J. (1979) The light evoked release of acetylcholine from the rabbit retina *in vivo* and its inhibition by γ-aminobutyric acid. *J. Neurochem.* **32**, 1327–1329.

Massey, S. C. & Redburn, D. A. (1983) The cholinergic amacrine cells of rabbit retina receiver ON and OFF input: an analysis of [^{3}H]-ACh release using 2-amino-4-phosphonbutyric acid (APB) and chloride free medium. *Vision Res.* **23**, 1615–1620.

McIlwain, J. T. (1964) Receptive fields of optic tract axons and lateral geniculate cells: peripheral extent and barbiturate sensitivity. *J. Neurophysiol.* **27**, 1154–1173.

McIlwain, J. T. (1966) Some evidence concerning the physiological basis of the periphery effect in the cat's retina. *Exp. Brain Res.* **1**, 265–271.

Michael, C. R. (1968) Receptive fields of single optic nerve fibres in a mammal with an all-cone retina; I. Contrast-sensitive units. II. Directionally sensitive units. *J. Neurophysiol.* **31**, 249–256, 257–267.

Miller, A. M. & Schwartz, E. A. (1983) Evidence for the identification of synaptic transmitters released by photoreceptors of the toad retina. *J. Physiol.* **334**, 325–349.

Nakamura, Y., McGuire, B. A. & Sterling, P. (1980) Interplexiform cell in cat retina: identification by uptake of γ-[^{3}H]-aminobutyric acid and serial reconstruction. *Proc. Nat, Acad. Sci.* **77**, 658–661.

Nelson, R. (1977) Cat cones have rod input: a comparison of the response properties of cones and horizontal cell bodies in the retina of the cat. *J. Comp. Neurol.* **172**, 109–135.

Nelson, R. (1980) Functional stratification of cone bipolar cells axons in the cat retina. *ARVO Suppl.* 130.

Nelson, R. (1982) All amacrine cells quicken time course of rod signals in the cat. *J. Neurophysiol.* **47**, 928–947.

Nelson, R., Famiglietti, E. V. & Kolb, H. (1978) Intracellular staining reveals different levels of stratification for ON- and OFF-center ganglion cells in the retina of the cat. *J. Neurophysiol.* **41**, 472–483.

Nelson, R. & Kolb, H. (1983) Synaptic patterns and response properties of bipolar and ganglion cells in the cat retina. *Vision Res.* **23**, 1183–1195.

Nelson, R., Kolb, H., Robinson M. M. & Mariani, A. P. (1981) Neural circuitry of the cat retina: cone pathways to ganglion cells. *Vision Res.* **21**, 1527–1536.

Nichols, C. W. & Koella, G. B. (1968) Comparison of the localization of acetylcholinesterase and non-specific cholinesterase in mammalian and avian retinas. *J. Comp. Neurol.* **133**, 1–16.

Osborne, N. N. (1982) Uptake localization and release of serotonin in the chick retina. *J. Physiol.* **331**, 469–479.

Osborne, N. N. (1983) Indoleamines in the eye with special reference to the serotonergic neurones of the retina. In *Progress in Retina Research*, Ed. Osborne, N. N. & Chader, G. A., Vol. 3. Oxford: Pergamon.

Osborne, N. N. (1984) Indoleamines in the eye with special reference to the serotonergic neurones of the retina *Progr. Retinal Res.* **3**, 61–103.

Osborne, N. N., Nesselhut, T., Nicholas, D. A., Patel, S. & Cuello, A. C. (1982) Serotonin-containing neurones in vertebrate retinas. *J. Neurochem.* **39**, 1519–1528.

Osborne, N. N. & Patel, S. (1984) Postnatal development of serotonin-accumulating neurones in the rabbit retina and an immunohistochemical analysis of the uptake and release of serotonin. *Exp. Eye Res.* **38**, 611–620.

Oyster, C. W. & Barlow, H. B. (1967) Direction-selective units in rabbit retina: distribution of preferred directions *Science* **155**, 841–842.

Pasantes-Morales, H. (1982). Taurine–calcium interactions in frog rod outer segments: taurine effects on an ATP-dependent calcium translocation process. *Vision Res.* **22**, 1487–1493.

Pasantes-Morales, H. & Cruz, C. (1985) Taurine and hypotaurine inhibit light-induced lipid peroxidation and protect rod outer segment structures. *Brain Res.* **330**, 154–157.

Pasantes-Morales, H., Dominguez, L., Compomanes, M. A. & Pacheco, P. (1986) Retinal degeneration induced by taurine deficiency in light-deprived cats. *Exp. Eye Res.* **43**, 55–60.

Pasantes-Morales, H., Urban, P. F., Klethi, J. & Mandel, P. (1973) Light stimulated release of [^{35}S] taurine from chicken retina. *Brain Res.* **51**, 375–378.

Peichl, L. & Wässle, H. (1979) Size, scatter and coverage of ganglion receptive field centres in the cat retina. *J. Physiol.* **291**, 117–141.

Peichl, L. & Wässle, H. (1981) Morphology of on- and off-centre brisk transient (Y) cells in the cat retina. *Proc. Roy. Soc. B* **212**, 139–156.

Peichl, L. & Wässle, H. (1983) The structural correlate of the receptive field of α-ganglion cells in the cat retina. *J. Physiol.* **341**, 309–324.

Piccolino, M., Neyton, J. & Gerschenfeld, H. M. (1983) Horizontal cells of turtle retina: a neurotransmitter control of electrical junctions? *J. Physiol. (Paris)* **78**, 739–742.

Piccolino, M., Neyton, J. & Gerschenfeld, H. M. (1984) Decrease of gap junction permeability induced by dopamine and cyclic adenosine 3′:5′-monophosphate in horizontal cells of turtle retina. *J. Neurosci.* **4**, 2477–2488.

Piccolino, M., Neyton, J., Witkowsky, P. & Gerschenfeld, H. M. (1982) γ-Aminobutyric acid antagonists decrease junctional communication between L-horizontal cells of the retina. *Proc. Nat. Acad. Sci.* **79**, 3671–3675.

Pourcho, R. G. (1980) Uptake of [^{3}H] glycine and [^{3}H] GABA by amacrine cells in the cat retina. *Brain Res.* **198**, 333–346.

Pourcho, R. G. (1981) Autoradiographic localization of [^{3}H] muscimol in the cat retina. *Brain Res.* **215**, 187–199.

Pourcho, R. G. (1982) Dopaminergic amacrine cells in the cat retina. *Brain Res.* **252**, 101–109.

Pourcho, R. G. & Goebel, D. J. (1983) Neuronal subpopulations in cat retina which accumulate the GABA agonist, [^{3}H] muscimol: a combined Golgi and autoradiographic study. *J. Comp. Neurol.* **219**, 25–35.

Pourcho, R. G., Goebel, D. J. & McReynolds, J. S. (1983) Autoradiographic studies of [^{3}H]-glycine, [^{3}H]-GABA and [^{3}H]-muscimol uptake in the mudpuppy retina. *Exp. Eye Res.* **39**, 69–81.

Pourcho, R. G. & Osman, K (1986) Cytochemical identification of cholinergic amacrine cells in the cat retina. *J. Comp. Neurol.* **247**, 497–504.

Pourcho, R. G. & Osman, K. (1986) Acetylcholinesterase localization in cat retina: a comparison with choline acetyltransferase. *Exp. Eye Res.* **43**, 585–594.

Priest, T. D., Robbins, J. & Ikeda, H. (1985) The action of inhibitory transmitters, γ-aminobutyric acid and glycine may distinguish between the area centralis and the peripheral retina. *Vision Res.* **25**, 1761–1770.

Raviola, E. & Gilula, N. B. (1973) Gap junctions between photoreceptor cells in the vertebrate retina. *Proc. Nat. Acad. Sci.* **70**, 1677–1681.

Raviola, E. & Gilula, N. B. (1975) Intramembrane organization of specialized contacts in the outer plexiform layer of the retina. *J. Cell Biol.* **65**, 192–222.

Rodieck, R. W. (1965) Quantitative analysis of cat retinal ganglion response to visual stimuli. *Vision Res.* **5**, 583–601.

Rodieck, R. W. (1967) Receptive fields in the cat retina: a new type. *Science* **157**, 90–92.

Rodieck, R. W. & Stone, J. (1965a) Response of cat retinal ganglion cells to moving visual patterns. *J. Neurophysiol.* **28**, 819–832.

Rodieck, R. W. & Stone, J. (1965b) Analysis of receptive fields of cat retinal ganglion cells. *J. Neurophysiol.* **28**, 833–849.

Ross, C. D., Dunning, D. D., Juengel, L. I. & Godfrey, D. A. (1985) Laminar distribution of choline acetyltransferase and acetylcholinesterase activities in the inner plexiform layer of rat retina. *J. Neurochem.* **44**, 1091–1099.

Saito, H.-A. (1983) Pharmcalogical and morphological differences between X- and Y-type ganglion cells in the cat's retina. *Vision Res.* **23**, 1299–1308.

Saito, T. (1987) Physiological and morphological differences between on- and off-center bipolar cells in the vertebrate retina. *Vision Res.* **27**, 135–142.

Saito, T., Kujiraoka, T. & Yanaha, I. (1983) Connections between photoreceptors and horseradish peroxidase-injected bipolar cells in the carp retina. *Vision Res.* **23**, 353–362.

Sakai, H. & Naka, K.-I. (1983) Synaptic organization involving receptor, horizontal and ON- and OFF-center bipolar cells in the catfish retina. *Vision Res.* **23**, 339–351.

Schmidt, M., Humphrey, M. F. & Wässle, H. (1987) Action and localization of acetylcholine in the cat retina. *J. Neurophysiol.* **58**, 997–1015.

Schwartz, E. A. (1983) Calcium-independent release of GABA from isolated horizontal cells of the toad retina. *J. Physiol.* **323**, 211–227.

Slaughter, M. M. & Miller, R. F. (1981) 2-Amino-4-Phosphonobutyric acid: a new pharmacological tool for retinal research. *Science* **211**, 182–184.

Slaughter, M. M. & Miller, R. F. (1983a) An excitatory amino acid antagonist blocks cone input to sign-conserving second-order retinal neurons. *Science* **219**, 1230–1232.

Slaughter, M. M. & Miller, R. F. (1983b) The role of excitatory amino acid transmitters in the mudpuppy retina: an analysis with kainic acid and N-methyl aspartate. *J. Neurosci.* **3**, 1701–1711.

Stanford, L. R. (1987) W-cells in the cat retina: correlated morphological and physiological evidence for two distinct classes. *J. Neurophysiol*, **57**, 218–244.

Stone, J. & Fukuda, Y. (1974) Properties of cat retinal ganglion cells: a comparison of W-cells with X- and Y-cells. *J. Neurophysiol.* **37**, 722–748.

Stone, J. & Hoffmann, K.-P. (1972) Very slow conducting ganglion cells in the cat's retina: a major new functional type? *Brain Res.* **43**, 610–616.

Stone, S. & Witkovsky, P. (1984) The actions of γ-aminobutyric acid, glycine and their antagonists upon horizontal cells of the *Xenopus* retina. *J. Physiol.* **353**, 249–264.

Tauchi, M. & Masland, R. H. (1984) The shape and arrangement of the cholinergic neurons in the rabbit retina. *Proc. Roy. Soc. B* **222**, 101–119.

Teranishi, T., Negishi, K. & Kato, S. (1983) Dopamine modulates S-potential amplitude and dye-coupling between external horizontal cells in carp retina. *Nature* **301**, 243–246.

Thier, P. & Bolz, J. (1985) Cholecystokinin in the cat retina. *Invest, Ophthal.* **26**, 266–272.

Thier, P. & Wässle, H. (1984) Indoleamine-mediated reciprocal modulation of on-centre and off-centre ganglion cell activity in the retina of the cat. *J. Physiol.* **351**, 613–630.

Thomas, T. N. & Redburn, D. A. (1979) 5-Hydroxytryptamine—a neurotransmitter of bovine retina. *Exp. Eye Res.* **28**, 55–61.

Thomas, T. N. & Redburn, D. A. (1980) Serotonin uptake and release by subcellular fractions of bovine retina. *Vision Res.* **20**, 1–8.

Vaney, D. I. (1984) 'Coronate' amacrine cells in the rabbit retina have the 'starburst' dendritic morphology. *Proc. Roy. Soc. B* **220**, 501–508.

Vaney, D. I., Peichl, L. & Boycott, B. B. (1981) Matching populations of amacrine cells in the inner nuclear and ganglion cell layers of the rabbit retina. *J. Comp. Neurol.* **199**, 373–391.

Voaden, M. J., Lake, N., Marshall, J. & Morjarca, B. (1977) Studies on the distribution of taurine and other neuroactive amino acids in the retina. *Exp. Eye. Res.* **25**, 249–257.

Voigt, T. (1984) Cholinergic amacrine cells in the rat retina. *J. Comp. Neurol.* **248**, 19–35.

Voigt, T. (1986) Cholinergic amacrine cells in the rat retina. *J. Comp. Neurol.* **248**, 19–35.

Wagner, H. G., MacNichol, E. F. & Wohlbarsht, M. L. (1963) Functional basis for 'on'-centre and 'off'-centre receptive fields in the retina. *J. Opt. Soc. Amer.* **53**, 66–70.

Wässle, H., Boycott, B. B. & Illing, R.-B. (1981a) Morphology and mosaic of on- and off-beta cells in the cat retina and some functional considerations. *Proc. Roy. Soc. B* **212**, 177–195.

Wässle, H., Boycott, B. B. & Peichl, L. (1978a) Receptor contacts of horizontal cells in the retina of the domestic cat. *Proc. Roy. Soc. B* **203**, 247–267.

Wässle, H. & Illing, R.-B. (1980) The retinal projection to the superior colliculus in the cat: a quantitative study with HRP. *J. Comp. Neurol.* **190**, 333–356.

Wässle, H., Peichl, L. & Boycott, B. B. (1978b) Topography of horizontal cells in the retina of the domestic cat. *Proc. Roy. Soc. B* **203**, 269–291.

Wässle, H., Peichl, L. & Boycott, B. B. (1981b) Morphology and topography of on- and off-alpha cells of the cat retina. *Proc. Roy. Soc. B* **212**, 157–175.

Werblin, F. S. (1970) Response of retinal ganglion cells to moving spots: intracellular recording in *Necturus maculosus*. *J. Neurophysiol.* **33**, 342–350.

Wyatt, H. J. & Daw, N. N. (1976) Specific effects of neurotransmitter antagonists on ganglion cells in rabbit retina. *Science* **191**, 204–205.

13. FLICKER

CRITICAL FUSION FREQUENCY

The sensation of 'flicker' is evoked when intermittent light stimuli are presented to the eye; as the frequency of presentation is increased a point is reached—the *critical fusion frequency*—at which the flicker sensation disappears to be replaced by the sensation of continuous stimulation. The study of flicker has turned out to be a valuable method of approach to the fundamental problems of visual phenomena—it is amenable to fairly accurate measurement and it represents a perceptual process intermediate in complexity between intensity discrimination and form perception.

The Talbot-Plateau Law

This generalization states that, when the critical fusion frequency has been reached, the intensity of the resultant sensation, i.e. the brightness of the intermittently illuminated, but non-flickering, patch, is the mean of the brightness during a cycle. Thus if the subject's view of an illuminated patch, of luminance 5 mL, is interrupted by rotating an opaque disc in front of it from which a sector has been removed, the resultant sensation will be equal to that given by a continuous stimulus of luminance equal to 5 × Area of Sector/Total Area of Disc. This law finds a useful application in many experimental studies in which it is desired to cut down the illumination by accurately determined amounts; by varying the size of the sector in the rotating disc, different average intensities of illumination per cycle may be achieved and, so long as the critical fusion frequency is exceeded, these will appear as different steady luminances.

Effect of Luminance on Fusion Frequency

In general, the greater the luminous intensity of the flickering light, the higher must be its frequency to attain fusion. This is illustrated by Fig. 13.1 where the critical fusion frequency has been plotted against the logarithm of the retinal illumination in trolands. With foveal observation, the relationship is linear over a wide range,

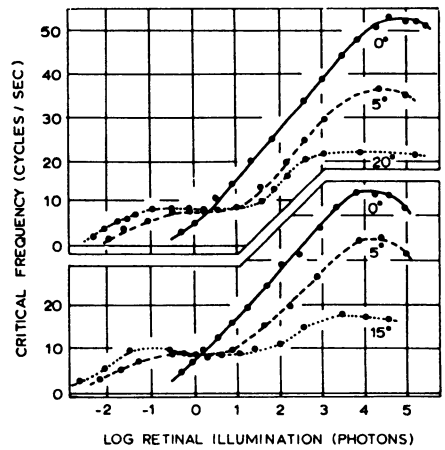

Fig. 13.1 Dependence of critical fusion frequency on the intensity of the stimulus. With foveal fixation (0°), the Ferry-Porter Law holds over a wide range. With eccentric fixation, the curves show discontinuities indicating the activity of the rods. (Hecht, Shlaer & Smith, *Cold Spr. Harb. Symp. quant. Biol.*)

between 0.5 and 10 000 trolands, and this is the basis of the so-called *Ferry-Porter Law* which states that the critical fusion frequency is proportional to the logarithm of the luminance of the flickering patch. At very high luminances the fusion frequency passes through a maximum in the region of 50 to 60 cycles/sec. At very low luminances, in the scotopic range, the fusion frequency is remarkably low, of the order of 5°sec, so that under these conditions the temporal resolution of the fovea is extremely small, a separation of 200 msec between successive stimuli not being discriminated.

Peripheral Vision

With peripheral vision, where use of both rods and cones is possible, there is an obvious discontinuity in the graph, indicating the limited application of the Ferry-Porter Law; by plotting the logarithm of the fusion frequency against the logarithm of the luminance, as in Fig. 13.2, the break in continuity becomes more obvious and may be seen to occur in the region of a retinal illumination of 10

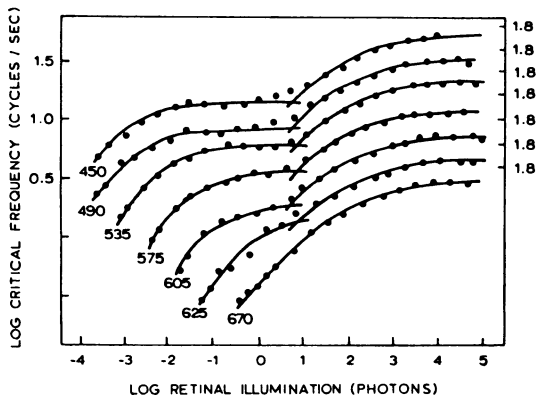

Fig. 13.2 The log of the fusion frequency has been plotted against the log of the stimulus intensity. With red light, no break occurs in the curve. The ordinates to the left apply to the topmost curve; the others have been moved down in steps of 0.2 log units, and their exact positions are indicated to the right. (Hecht, Shlaer & Smith, *Cold Spr. Harb. Symp. quant. Biol.*)

trolands (log 10 = unity), and corresponds to the transition from predominantly cone to predominantly rod vision. In Fig. 13.2 the different curves correspond to the use of different wavelengths of light, and it is seen that no break occurs with a red light of 670 nm, as one would expect since this wavelength tends to stimulate only cones.

Rod Vision

The low fusion frequencies obtainable with rod vision might suggest that these receptors would not give as high fusion frequencies as the cones at high luminances, if they could be studied in isolation. This view of the rods as less discriminating from the point of view of temporal resolution has been amply confirmed by many experiments. Thus Hecht *et al.* (1948) studied a rod monochromat, a subject with apparently non-functional cones. The curve obtained by plotting fusion frequency against log luminance did, indeed, show a break, suggesting the operation of two mechanisms, but it was argued that these corresponded to two types of rod, since the break occurred with red light; the highest fusion frequency measured was only 21°sec so that the rods do, apparently, have less powers of mediating temporal resolution than the cones.

Significance of Ferry-Porter Law

The experimental finding—that to produce fusion the frequency of stimulation must be increased when the intensity of the light stimulus is increased—is, at first thought, surprising. The fact that fusion is possible is clearly dependent on the existence of an 'after-effect' resulting from a single stimulus, so that a succeeding stimulus can fall on the retina while it is still responding positively to the first; on purely photochemical grounds one might expect the after-effect to last longer the more powerful the primary stimulus, since a greater quantity of light-sensitive substance would be decomposed; if this were the case, clearly the minimum time elapsing between this stimulus and the next, such that the latter arrives while the eye is still responding strongly to the first stimulus, will be greater with the more powerful stimulus and therefore the critical fusion frequency should be lowered. The response of the eye to illumination, however, is far too complex to be described simply in terms of a primary photochemical reaction—the latter is the first stage only in a process that is elaborated in the nervous structures of the retina and higher visual centres. The study of the ERG has thrown valuable light on the mechanism of flicker and has emphasized the importance of inhibition, besides excitation, in determining this form of resolution.

THE ERG AND THE INTERPRETATION OF FLICKER

The ERG in response to a single flash of light is a characteristic sequence of potential changes considerably outlasting the duration of the flash; a second flash, falling on the eye during these changes, starts off a new series of events, but the extent to which it will modify the existing state of the retinal potential will depend on how soon it follows; and we may envisage a condition, with rapidly repeated stimuli, such that the potential never falls to its baseline and, moreover, if the frequency is high enough, such that the record appears unbroken and smooth. From the point of view of the ERG we may call this the critical fusion frequency but this need not mean, at any rate without further proof, that the subjective sensation is likewise smooth. Figure 13.3 from Granit & Riddell (1934) illustrates the phenomenon of fusion in the ERG of the light-adapted frog; as the frequency of the intermittent light-stimuli increases, the record becomes smoother, whilst the amplitude of the potential change decreases.

Importance of Inhibition

In the dark-adapted frog's eye, or the rod-dominated retinae of the cat and guinea pig, the fusion frequency was low, and below fusion successive stimuli seemed merely to result in successive *b*-waves imposed on the declining limbs of the previous *b*-wave. In the light-adapted frog eye, or the *I*-type of retina (pigeon, squirrel, etc.), a much higher fusion frequency was obtained, and an analysis of the ERG at frequencies below fusion indicated that the

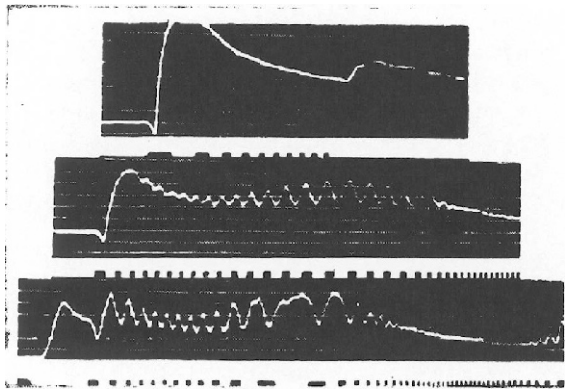

Fig. 13.3 Flicker as shown by the frog's ERG. The light stimuli are shown at the bottom of each record as white rectangles. Top: Dark-adapted eye with no appreciable flicker. Middle and bottom: Light-adapted eye showing flicker with fusion when the stimuli are sufficiently frequent. (Granit & Riddell, *J. Physiol.*)

fluctuations of potential with successive stimuli were now characteristically different, the results of successive stimuli being to impose a negative *a*-wave on the preceding *b*-wave, i.e. the succession of events was *a–b–a–b–a* as opposed to *b–b–b–b–b*.

Granit considered that the *a*-wave represented a state of pre-excitatory inhibition, in which case the greater fusion frequency for cone-vision could be interpreted as a more effective inhibition of the effects of the previous stimulus, leaving the retina free to respond to the next stimulus. The *a*-wave, however, seems to be due to receptor hyperpolarization, a process common to rods and cones, so that its translation into a pre-excitatory inhibition is hardly applicable; it is the light-response of the receptor albeit, in this special case, a cessation of liberation of transmitter. The greater ability to follow a flickering stimulus is to be related to the time-constant of electrical response, hyerpolarization and subsequent depolarization in the cone being a more rapid process than the corresponding events in rods.

Subjective and ERG-flicker

Subjectively, as we have seen, we may obtain fusion frequencies of the order of 60/sec or more by suitably increasing the luminance of the flickering patch; in the early studies of the human ERG, however, the fusion frequency rose to a maximum at about 25/sec, further increases in luminance causing no increase in fusion frequency. The human ERG under photopic conditions, was apparently similar to that given by a rod-dominated retina, so that a smooth record did not correlate with subjective sensation. This could be because the ERG is, in general, the pooled response of all the receptors in the retina, and since rods are in such a huge majority in the human retina the ERG-response to flickering stimuli should be a rod-response. The *subjective sensation*, however, might be determined by the cones, in spite of their numerical inferiority, presumably because, under photopic conditions, their pathway to higher centres are more favoured, or because of their greater cortical representation.

Cone Activity

If this were true it ought to be possible, by adequate amplification of the ERG, and by increasing the intensity of the light stimuli, to bring out the cone activity in the ERG when the rod activity was suppressed. How can we suppress the rod activity, however? The flicker-ERG gives us just this opportunity since, as we have seen, the ERG record becomes smooth at a luminance of about 10 lux with a fusion frequency of about 25/sec. Thus the rod-response can no longer follow the stimuli and any irregularity in the record obtained by increasing the luminance must now be due to cone activity. Dodt in 1951 was able to demonstrate just this; he increased the luminance of the flashes to far greater levels than earlier workers had used, and by employing an opal contact lens that enabled large areas of retina to be stimulated he found that, beyond 10 lux, flicker again appeared on the record, and the curve of fusion frequency against luminance corresponded with the subjective sensation. Fusion frequencies as high as 70/sec were obtained as Fig. 13.4 from Dodt & Wadensten shows. Even in the cat, moreover, Dodt & Walther were able to demonstrate a cone-type of ERG at sufficiently high luminance.

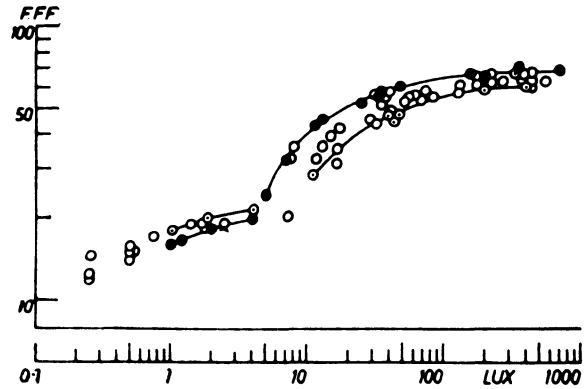

Fig. 13.4 The critical fusion frequency (FFF) as a function of stimulus-intensity as indicated by the human ERG. Ordinate: flashes/second; Abscissa: luminance in lux. Note logarithmic scales. (Dodt & Wadensten, *Acta ophthal. Kbh.*)

GANGLION CELL DISCHARGES

We may ask what takes place in the optic nerve during flicker and fusion; the point was examined in detail by Enroth. It will be recalled that single cells, or optic nerve fibres, respond to a flash of light in different manners and are described as Pure ON-, Pure OFF- and ON–OFF-elements according as they give a burst of spikes at ON, OFF or both at ON and OFF. In the cat the ON–OFF ganglion cells are in the majority so that these were studied most, but the ON-response of such a cell was essentially the same as a pure ON-response from the point of view of flicker, so that the same general principles of behaviour were valid; the same applied to the OFF-responses.

Fusion

To consider the pure ON-element, the first few flashes usually caused a simple spike discharge with no silent period between; this corresponds with the non-flickering period of the ERG. Soon each flash caused a burst of spikes in step with the stimulus (Fig. 13.5); as the frequency of flashing increased, the bursts became shorter but remained in step. At a certain frequency of flashing fusion occurs, in the sense that now the spike discharges, if they occur at all, bear no relationship with the stimuli.

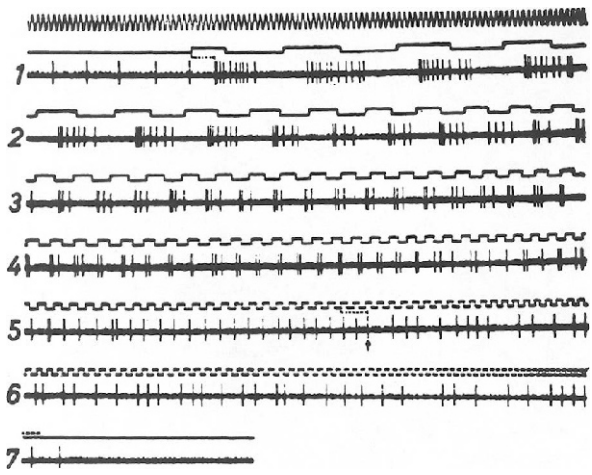

Fig. 13.5 Response of ON-element to repetitive flash stimuli leading to fusion, in the sense that when the flash-frequency reaches a certain value, marked by the arrow, the response is a discharge that bears no relationship to the frequency of flash-stimulation. Before this phase is reached the spike bursts are synchronous with the light flashes, beginning after a latency indicated by the dotted lines on the records marked 1 and 5. Upward movement of signal indicates onset of flash. (Enroth, *Acta physiol. Scand.*)

The unit shown in Fig. 13.5 gave a discharge corresponding to what would be seen with steady illumination, but others (usually OFF- and ON–OFF-elements) remained completely silent during fusion. Decreasing the flash-rate brought about an immediate flicker in the record. With ON–OFF-elements, at low flickering rates the ON- and OFF-discharges behaved independently, each 'flickering' with the ON- and OFF-phases of the light cycle. Usually fusion of the one response occurred before that of the other, so that if, for example, the ON-element fused first, the record was the same as that for a flickering OFF-element.

Ferry-Porter Law

The remarkable feature emerging from this study was the relationship between the fusion frequency for a given ganglion cell and the frequency of its spike discharge in response to a single flash; if the spike discharge had a high frequency the fusion frequency was high, and *vice versa.* Since, usually, spike discharge frequency increases with increasing intensity of light, we have an electrophysiological basis for the Ferry-Porter Law relating fusion frequency with light intensity.

THE VISUALLY EVOKED RESPONSE (VER)

When the sensation of fusion is attained, the organism is unable to utilize, or else it ignores, the information reaching it at the receptor level; an obvious reason for this could be the failure of the receptors, or elements in the conducting pathway, to follow the repetitive stimuli with discrete responses, so that it is of some interest to find where the failure to transmit information occurs. The work with the ERG and ganglion cells suggests that fusion occurs at the retinal level, but a number of studies in which the cortical responses to visual stimuli have been compared with subjective sensation in man, or behavioural responses in animals, indicate that the sensation of fusion may intervene long before the cortical response becomes flat. Thus a repetitive response in the retina is transmitted to the cortex, and may be recorded from its surface as a series of potential changes, of the same frequency as the flash-rate, but this does not necessarily evoke a continuous sensation. The cortical response is referred to as the *visually evoked reponse (VER)*, and will be described in more detail in Section 3. In the rabbit, Schneider (1968) recorded the integrated VER at different frequencies; he found that frequencies that gave fusion, so far as the animal's behaviour was concerned, still gave VER's in phase with the stimuli; only when the flash-rate was some 20 cycles/sec greater than the behavioural critical fusion frequency did the record become smooth.

The amplitude of the VER diminished as the flash rate increased, and it is interesting that behavioural fusion always occurred when the VER had attenuated to 10 to 20% of its maximal value. The attenuation of the VER is due to failure of a proportion of the cortical cells to follow, so that their responses become equivalent to those induced by steady illumination; and examination of individual cortical cells shows that these vary greatly in their power to follow intermittent stimuli (Ogawa *et*

al., 1966). Thus it seems to require a definite number of cortical cells to respond in phase with the stimuli, for flicker to be perceived, or more correctly, a definite amount of cortical activity.

EFFECT OF DARK-ADAPTATION

On the basis of Granit's analysis we may expect the subjective phenomenon of flicker to show marked variations according as the human eye is light- or dark-adapted, i.e. according as the cone or rod mechanism predominates. This is, indeed, the case but the effects are complex for reasons that will become evident.

Let us suppose that a subject is placed in a box and that he looks at a flickering test-patch through a small window; the walls of the box may be illuminated to any desired intensity and thus the subject's state of light- or dark-adaptation may be controlled accurately. The flickering patch may likewise be given any desired luminance, so that we may make two kinds of measurement of the effects of dark-adaptation, i.e. we can make the walls of the box darker and darker and keep the luminance of the test-patch at a level such that rods only will be stimulated; alternatively we may make the walls of the box darker and darker as before, thereby increasing the dark-adaptation, but we can keep the luminance of the flickering test-patch at a level above the threshold for cone vision. It is very important to keep in mind this distinction in experimental approach as the effects of dark-adaptation are greatly different in the two cases. A third method, extensively adopted in the earlier work on this theme, consists in placing the subject in a dark room and varying the luminance of the flickering test-patch from the very highest levels to the lowest, threshold ones; in this case, however, it is very difficult to control the adaptation of the eyes—at the low levels of illumination of the test-patch the eyes will be more or less completely dark-adapted, but at the high levels they will be only partially so, and to different degrees, owing to the effects of the test-patch.

Rod Vision

If the subject is placed in the box and is allowed to view a flickering patch of luminance below the cone threshold, then the effects of dark-adaptation are precisely those we should expect on the basis of the Ferry-Porter Law; as the dark-adaptation proceeds, the test-patch appears brighter and brighter and consequently we may expect the fusion frequency to increase with dark-adaptation—this is the case as Fig. 13.6 (lower curve) shows; the general level of fusion frequency is low (3 to 12 cyc/sec).

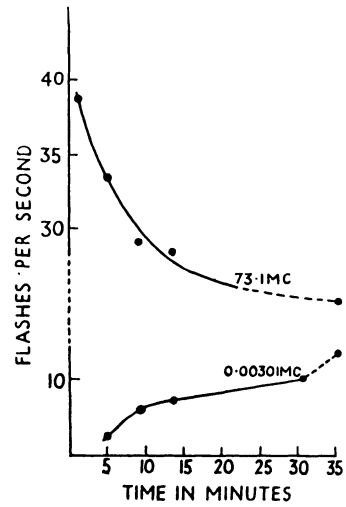

Fig. 13.6 The effect of dark-adaptation on critical fusion frequency. When the patch is of photopic intensity, dark-adaptation decreases c.f.f. when the patch is of scotopic intensity, dark-adaptation increases c.f.f. (10° eccentric fixation). (After Lythgoe & Tansley, *M.R.C. Sp. Rep.*)

Photopic Vision

If, on the other hand, the flickering patch has a high luminance, so that both rods and cones are stimulated, the effect of dark-adaptation (decreasing the illumination of the walls of the box) is in the opposite sense, the critical fusion frequency falling from a value of nearly 40 cyc/sec in the light-adapted eye to about 25 cyc/sec in the completely dark-adapted condition (Fig. 13.6, upper curve). The curves shown in Fig. 13.6 were obtained with 10° eccentric view, i.e. both rods and cones were being stimulated by the test patch; if central vision alone is used, the effects of dark-adaptation are said by Granit to be very small, hence the peripheral cones are apparently behaving differently from foveal cones. The peripheral cones differ in their organization from the foveal ones, in the sense that many share the same bipolar cell with rods, and it is just possible that these effects of dark-adaptation are due to the increased activity of rods that takes place.

Rod–Cone Interaction

In other words, the rods may well inhibit the cones. A particularly good example of this rod–cone interaction was described by Dodt & Heck (1954) in the cat, using the ERG as the criterion of flicker and fusion. Figure 13.7 shows the effects of dark-adaptation on fusion frequency; with a scotopic stimulus, below the cone threshold (1 lux), the fusion frequency increases to a limiting rate of about

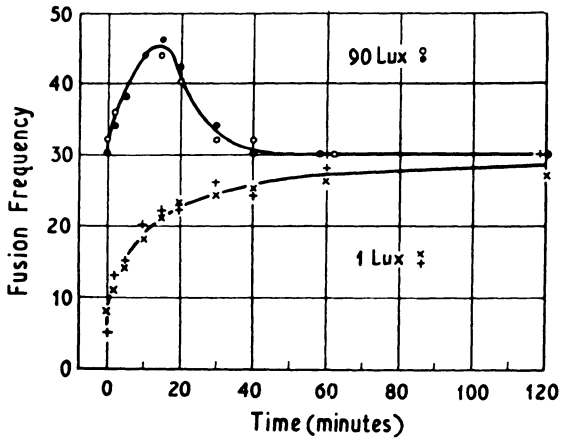

Fig. 13.7 Fusion frequency of cat's ERG. Lower curve shows that with a weak stimulus (1 lux) the fusion frequency increases with dark-adaptation to reach a maximum, characteristic of the rods. Upper curve shows that, with a moderately high intensity of light (90 lux), dark-adaptation causes an increase of fusion frequency, due to cone activity, but after a time the fusion frequency falls to that characteristic of rod vision, presumably because the rods are inhibiting the cones. (Dodt & Heck, *Pflüg. Arch.*)

30/sec, the highest value for rod vision in the cat. This is the effect we have already seen in man. When a moderately high stimulus-intensity is employed (90 lux), the fusion frequency corresponds at first to that of the rods; during dark-adaptation, however, the cones apparently take over, since the fusion frequency rises above the rod limit. After 15 minutes of dark-adaptation, nevertheless, the fusion frequency falls and eventually becomes equal to that obtained with pure rod stimuli; presumably the rods have taken over again and suppressed cone activity.

Rod–Cone Cancellation

MacLeod (1972) has shown that rod and cone signals can interact during the appreciation of flicker in such a way as to cancel the flickering sensation evoked by the one type of receptor. He projected a flickering 3° patch of light on to the parafovea where both rods and cones could be excited; the patch could be illuminated by blue-green light, exciting mainly rods, and yellow light exciting rods and cones. At an alternating-frequency of 7.5 Hz flicker was visible at scotopic levels of intensity and again at photopic levels, but not at the mesopic level when both rods and cones were being excited; the effect was less pronounced at 6.5 Hz and absent at 4.5 Hz. It was postulated that the rod and cone responses were reaching the cortical integrating centre 180° out of phase so that there was no interval of non-stimulation reaching the centre, the cessation of the cone response coinciding with the onset of the rod response. To test this he projected green and deep red light to the test patch; at an alternating frequency of 7 Hz and 100% contrast-modulation, flicker could be appreciated if either coloured light was projected separately, but not if both were projected together; if now a phase-drift of 180° was introduced, so that the maximum red luminance coincided with the minimum green luminance, flicker was obtained.

Recent Studies

More recently the interaction between rods and cones in the perception of flicker has been studied; thus Alexander & Fishman (1984) found that after a whole-field light-adaptation of the retina through which rod-function is extinguished, a minimum value for cone threshold-flicker may be obtained, but as dark-adaptation proceeds, sensitivity to flicker falls off, the unstimulated rods apparently inhibiting cone flicker-sensitivity as they adapt. A similar increase in threshold for cone flicker with dark-adaptation was described by Coletta & Adams (1984); in a later study (1986) they measured sensitivity to a cone-detected flicker of 25 Hz, and found this to increase with increase in background illumination. They showed that the changes were due to two kinds of lateral interaction in the retina. Thus at mesopic levels (0.1–1.0 Td) the cone-mediated resolution of flicker was enhanced by stimulation of surrounding rods; at photopic levels (10 Td) the flicker sensitivity was now improved by stimulation of adjacent cones. The spatial extents of these improvements of flicker acuity differed; thus for a flickering foveal spot of 10 minutes of arc, sensitivity was influenced by cones over a 20′ diameter; the rod effects extended over an annulus of 2° outer diameter and 1° inner diameter centred on the fovea. In this study, then, temporal discrimination is improved by surround illumination, whether rods or cones are being excited.

A similar improvement was found by Goldberg. *et al* (1983); thus a 2° cone-stimulated flickering source of 15–20 Hz was projected some 7° eccentric to the fovea, and a rod-stimulating background of 1 scotopic troland was projected on to this; the cone flicker-threshold was lowered by some 0.7 to 1.0 log units, indicating an increase in temporal discrimination. Conversely they found that cone-mediated flicker sensitivity was decreased by dark-adaptation, during which the rods were not being stimulated as the flickering patch was red. Goldberg *et al.* suggested that the unstimulated rods were releasing more transmitter than when excited by light, and that this transmitter caused amacrine cells to release an inhibitory transmitter at the cones, thus reducing their sensitivity to flicker.

CONE ADAPTATION AND ROD-MEDIATED FLICKER

In a more recent study, Frumkes *et al.* (1986) measured the effects of cone adaptation on rod-mediated flicker. Thus dark-adapted parafoveal flicker was studied using a patch of 2° 20′ surrounded by an annulus of 2.20′ to 7° 30′. A green flickering stimulus, too weak to excite cones was employed; annular stimulation of cones greatly facilitated rod-mediated flicker-sensitivity, especially at greater frequencies than 7 Hz. In a similar way, a *rod–cone* interaction was demonstrated by annular stimulation of rods while measuring cone-mediated flicker. According to Frumkes *et al.*, then, the rod and cone signals summate to produce an absolute threshold of a flicker sensation.

SIZE OF PATCH AND THE GRANIT–HARPER LAW

In general, if the size of the flickering patch is increased, its luminance being held constant, the fusion frequency increases; the effects can be large, so that a retinal area of 10 mm^2 may have a fusion frequency of say 60 cycle/sec whilst an area of 0.001 mm^2 of the same luminance may have just about half this. According to the so-called Granit–Harper Law, the fusion frequency is proportional to the logarithm of area. Varying the stimulus area, however, causes alterations not only in the total number of retinal elements stimulated, but in the relative extents to which peripheral and foveal elements enter into the response, and it would only be accidental if any simple relationship were found to hold over the whole retina. As Landis (1954) states: 'Area as a determinant of fusion frequency is a complicated affair. Not only is the size of the retinal area a determinant, but its position on the retina, its shape, whether it is discrete or composed of several parts, all enter into the areal effect.'

Eccentricity

In this connection studies on the effects of eccentricity of retinal stimulation are relevant. Using a photopic patch of 88.4 degrees^2, Rovamo & Raninen (1984) found an optimal eccentricity for flicker discrimination, in the sense that fusion occurred at about 65 cyc/sec at an eccentricity of 60°, falling to less than 40/sec at the fovea and in the extreme periphery (Fig. 13.8). As the area of summation of light increases with eccentricity (Ricco's Law) allowance was made for this, but then critical fusion frequency decreased with eccentricity; if the area of the stimulus was adjusted so as to keep the cortical area stimulated constant, fusion frequency this time, increased with eccentricity; when both 'corrections' were made, fusion-frequency was invariant at about 35 Hz. A similar study involving both rod- and cone-mediated flicker (Raninen & Rovamo, 1986) showed that this invariability could not be produced by manipulating rod-flicker in this way.

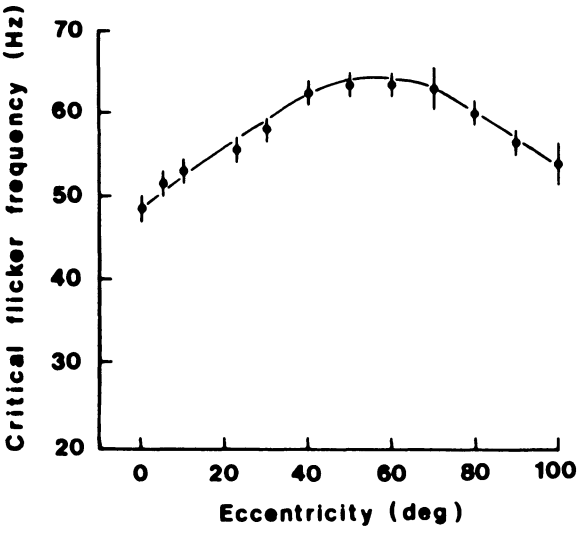

Fig. 13.8 Critical flicker frequency (mean ± SD) as a function of eccentricity in the temporal visual field of the right eye. Stimulus area was 88.4 deg^2, pupillary diameter 8 mm, retinal illuminance 2510 phot. td.

SINUSOIDAL WAVE-FORM

Square-wave Stimulus

The classical studies on flicker have been carried out using what is called a square-wave flickering stimulus, the observed patch being illuminated suddenly and as abruptly quenched, usually by rotating a sectored 'chopper-disc' in front of a constant source. The stimulus is illustrated schematically (Fig. 13.9) and the time-average of the luminance is indicated by the dotted line. This time-average will clearly be governed, not only by the intensity of light falling on the patch—the traditionally employed luminance when discussing the effect of luminance on flicker as in the Ferry-Porter Law—but by the light–dark ratio or more correctly the pulse-to-cycle fraction,[1] or PCF. Thus variation in the PCF will clearly influence the adaptive condition of the eye, and a variety of studies have indicated that the effects of variation of the PCF on c.f.f. are highly complex and apparently unpredictable.

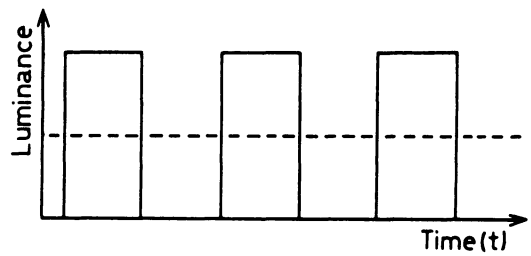

Fig. 13.9 Periodic rectangular waveform used in traditional flicker experiments. The dotted line represents the time-average luminance of the stimulus. (Kelly, *Hdb. Sensory Physiol.*)

Sinusoidal Stimulus

A more promising approach is that of presenting a sinusoidal wave-form whose amplitude varies as well as the mean intensity of the light during a cycle in a manner comparable with that employed in visual acuity studies (p. 380) where a contrast-threshold was determined for a given spatial-frequency of the stimulus. It is impossible to generate a simple sine-wave flicker of the form sin ωt, as this would involve negative values and radiant power is a

non-negative quantity, but a closely related wave-form:

$$f(t) = L(1 + m \sin \omega t)$$

can be generated and is illustrated by Fig. 13.10, where a steady luminance, L, is presented, and this is modulated in a sine-wave fashion, with amplitude, m, and frequency ω. The time-average of the luminance is called the *adaptation level*, and is the luminance parameter that is of much more interest than, say, the maximum luminance. The dimensionless m is called the *modulation*.

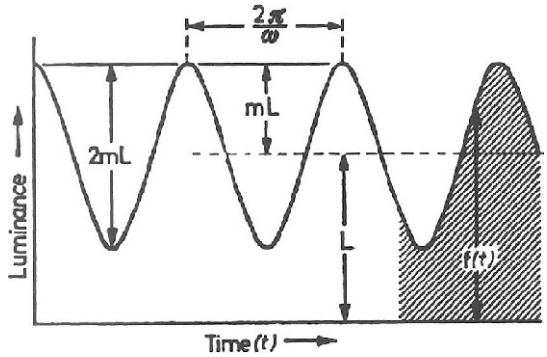

Fig. 13.10 More modern wave-form of stimulus. This is the sum of a sinusoidal component, of amplitude mL, and a constant component, L. The time-average luminance, L, is often called the 'adaptation level', and the dimensionless ratio, m, is called the modulation. (Kelly, *Hdb. Sensory Physiol.*)

C.F.F. Versus Modulation

Experimentally, then, we may fix on a mean luminance, or adaptation-level, and measure the critical fusion frequency (c.f.f.) for various modulations, the greater the modulation the greater the frequency of the wave-form necessary for fusion. Figure 13.11 from Kelly (1972) shows typical values for three different adaptation-levels; they exhibit a peak sensitivity to modulation at 5 to 10 Hz, in the sense that, when the luminance is oscillating at these frequencies, the degree of modulation of light required for the oscillation to be detected is minimal. At lower adaptation-levels the peak disappears and the high-frequency cut-off shifts towards lower frequencies.

First Fourier Component

DeLange (1954) varied the wave-form of the stimulus, as indicated in the figure, but because the Fourier equivalent wave-forms were, in fact, identical, there was no difference in modulation-threshold, the essential features being the first-component modulation and average luminance, i.e. the fundamental was the same, and it is this that determines threshold.

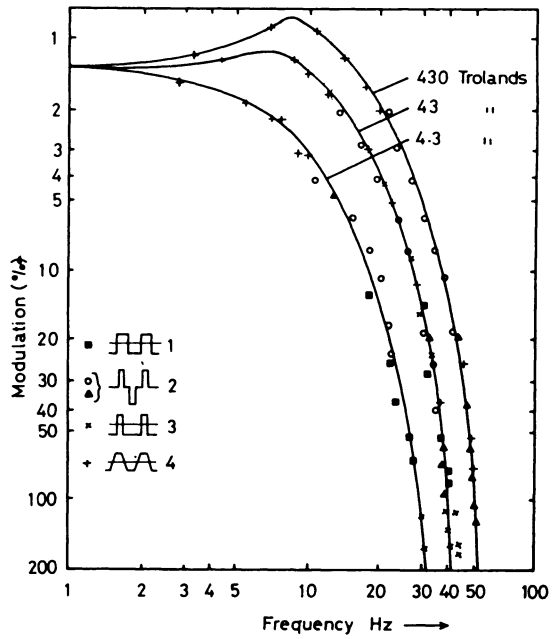

Fig. 13.11 Modulation-threshold curves using the stimulus wave-form illustrated by Fig. 13.10. As the frequency of the wave-form increases the modulation necessary just to perceive flicker is greater. The curves show a peak of sensitivity between 5 and 10 Hertz with a gradual decrease of sensitivity at lower frequencies. (Kelly, *Hdb. Sensory Physiol.*)

Pulse to Cycle Fraction

Because it is the first Fourier component that governs threshold and critical fusion frequency, it is possible to predict the responses to various wave-forms, and these predictions have a bearing on the question of the pulse-to-cycle fraction (PCF). Thus the wave-forms in Fig. 13.12 are, according to Kelly (1964) all equivalent because the product $m_1 L$ is constant.[2] Thus if we pass diagonally from left to right we have three wave-forms with very different PCF's, wave-forms that have been used in many of the classical studies designed to study the effect of PCF. On the basis of this analysis of equivalent wave-forms and estimates of average luminance, Kelly was able to predict the effects of light–dark ratio or PCF on critical flicker frequency. Thus Fig. 13.13 shows his predicted effects of PCF on c.f.f. on the basis of analysis of sine-wave flicker results; the experimental results of Bartley & Nelson (1961) are shown as vertical lines indicating the scatter. Thus the PCF effects are apparently completely predictable from the wave-form and the sine-wave flicker thresholds.

Ferry-Porter Law

So far as Ferry-Porter Law is concerned, this turns out to be somewhat of an accident; thus we may plot log c.f.f.

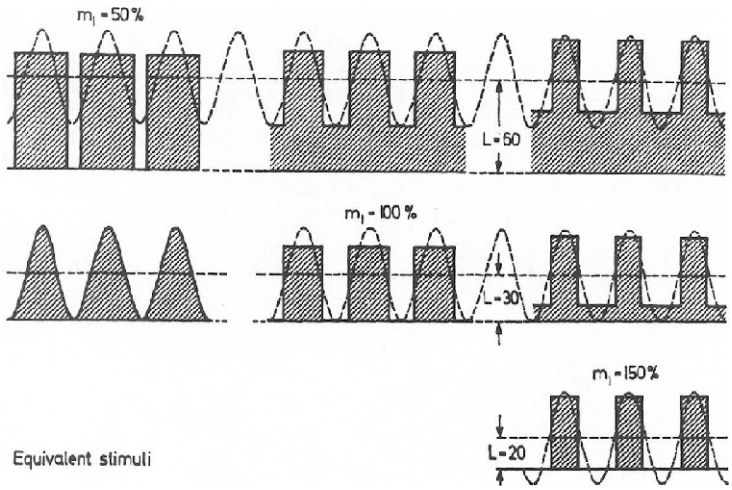

Fig. 13.12 All these wave-forms are equivalent because the product, $m_1 L$, is constant. (Kelly, *Hdb. Sensory Physiol.*)

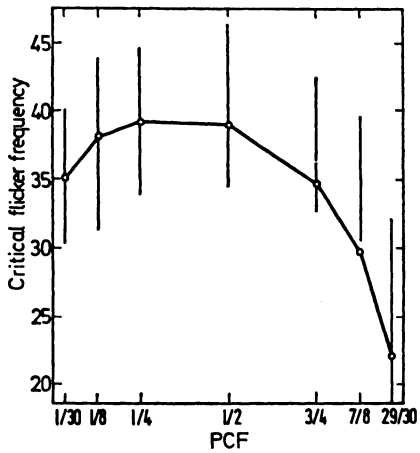

Fig. 13.13 Predicted effects of varying the pulse-to-cycle fraction (PCF) on the critical fusion frequency. The points are calculated whilst the vertical lines represent the total spread of Bartley *et al.*'s (1961) PCF results for five observers. (Kelly, *Hdb. Sensory Physiol.*)

against the time-averaged luminance, L, using m, the modulation, as a parameter, and obtain a set of curves; a straight-line relation occurs over a range of about 2 log units of L when m is high. Thus with high contrast modulation, typical of the black–white alternation in the classical experiments, a logarithmic relation between luminance and c.f.f. is predictable.

Surround Inhibition

Levinson (1964) measured the effect of a subliminal flickering annulus on the modulation-sensitivity of a flickering central spot, varying the phase-relations between the two flickers. The amplitude of the annular modulation was kept below threshold, and it was found that the modulation threshold of the test-spot varied with the relative phase of the annulus in such a way as to indicate inhibition at lower frequencies when the two were in phase. The fact that the interaction only occurred at low frequencies indicated that the channels for spatial interaction integrated more slowly than the channels for transmission of the flicker signal to the brain.

Frequency-labelled Channels

In the studies so far considered, the subject had to state whether flicker existed or not; when working above threshold for flicker sensation, subjects may be asked to state which of two stimuli was modulated at a higher frequency, and an analysis of this type of experiment provides clues as to whether there are 'detectors' in the visual system that operate over a given range of frequencies, as with visual acuity studies. Watson & Robson (1981), working at threshold contrasts, found that at 0 and 2 Hz, discrimination was not perfect whereas at 0 and 8 Hz it was, and they concluded that the range of channels was very limited, only high and low frequencies being accurately discriminated. In a similar type of study, in which the stimuli were moving gratings rather than counterphase modulated (flickering) gratings, Thompson (1983) concluded that there were only two mechanisms operating at detection threshold. With suprathreshold stimuli, once again, the rate of movement was discriminated by two broadly tuned channels.

Mandler (1984) measured difference-thresholds for increasing temporal frequencies and obtained the 'tuning-curve' of Fig. 13.14, which suggests two regions of reasonably good discrimination at about 2 and 5 Hz, and then a

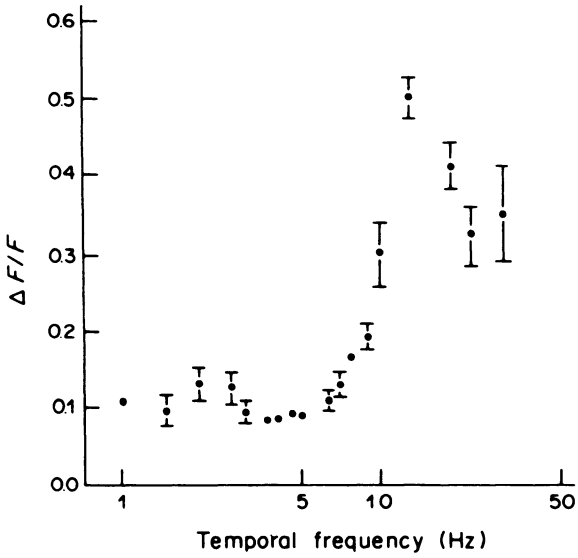

Fig. 13.14 Relative difference thresholds, divided by the base frequency, giving a 'tuning curve' suggesting two regions of good discrimination. (Mandler, *Vision Res.*)

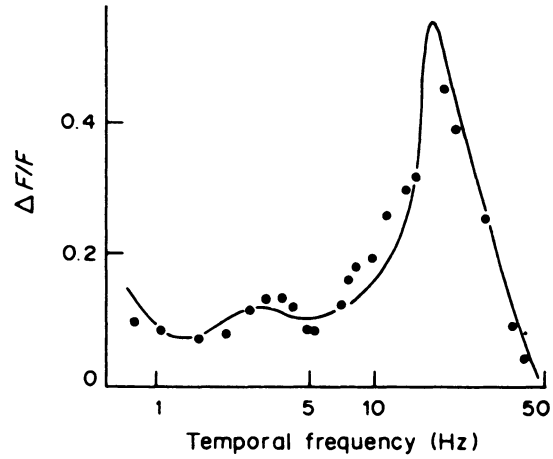

Fig. 13.15 Predicted tuning curve, on the basis of selective channels, the plotted points being those derived by Mandler (1984). (Mandler & Makous, *Vision Res.*)

very pronounced increase in sensitivity at very high frequencies. Mandler & Makous (1984) interpreted the tuning curve on the basis of an assumed three 'channels' with different sensitivity profiles, analogous with three cone systems with their three spectral sensitivity curves. On the assumption that discrimination is best where profiles overlap, they predicted the curve of Fig. 13.15 which fits the experimental points well.

Physiological Significance

The eye is adapted to discriminate small differences in spatial detail, as revealed by grating tests, and the value of this is obvious. The discrimination of temporal change is also an important feature, that enables motion detection; but the assessment of the temporal frequency, i.e. the interval between stimuli, is not so important for the discriminatory tasks that confront higher vertebrates.

Channel Adaptation

The modulation threshold for a given frequency of flicker may be assessed against a steady background luminance; then the subject may be exposed to a flickering stimulus of high modulation, and the sensitivity to the original flickering stimulus measured. The adapting flicker causes a large decrease in sensitivity, the effect of, say, a frequency of 15 Hz being greatest on sensitivity to the same frequency (Smith, 1970).

Notes

1. Gibbins & Howarth (1961) point out that the pulse-to-cycle or light-time fraction (PCF or LTF) is sometimes called the light/dark ratio.

2. More correctly, the stimuli in the horizontal rows, are equivalent since the values of m_1 and L, the first Fourier component, are equal; at high frequencies, the product $m_1 L$, the absolute modulation measured in trolands, becomes the dominant factor and this is equal for all the wave-forms shown in Fig. 13.12.

References

Alexander, K. R. & Fishman, G. A. (1984) Rod–cone interaction in flicker perimetry. *Brit. J. Ophthal.* **68**, 303–309.

Bartley, S. H. & Nelson, T. M. (1961) A further study of pulse-to-cycle fraction and critical fusion frequency. *J. Opt. Soc. Amer.* **51**, 41–45.

Coletta, N. J. & Adams, A. J. (1984) Rod-cone interaction in flicker detection. *Vision Res.* **24**, 1333–1340.

Coletta, N. J. & Adams, A. J. (1986) Spatial extent of rod–cone and cone–rod interactions for flicker detection. *Vision Res.* **26**, 917–925.

DeLange, H. (1954) Relationship between critical flicker frequency and a set of low-frequency characteristics of the eye. *J. opt. Soc. Amer.* **44**, 380–389.

Dodt, E. (1951) Cone electroretinography by flicker. *Nature* **168**, 738.

Dodt, E. & Heck, J. (1954) Einfüsse des Adaptationszustandes auf die Rezeption intermittierender Lichtreize. *Pflüg. Arch.* **259**, 212–225.

Dodt, E. & Wadensten, L. (1954) The use of flicker electroretinography in the human eye. *Acta ophthal. Kbh.* **32**, 165–180.

Dodt, E. & Walther, J. B. (1958) Der photopischer Dominator im Flimmer-ERG der Katze. *Pflug. Arch.* **266**, 175–186.

Enroth, C. (1952) The mechanism of flicker and fusion studied on single retinal elements in the dark-adapted cat. *Acta physiol. Scand.* **27**, Suppl. 100, 67.

Frumkes, T. E., Naarendrop, F. & Goldberg, S. H. (1986) The influence of cone adaptation upon rod mediated flicker. *Vision Res.* **26**, 1167–1176.

Gibbins, K. & Howarth, C. I. (1961) Prediction of the effect of light-time fraction on the critical fusion frequency: an insight from Fourier analysis. *Nature* **190**, 330–331.

Goldberg, S. H., Frumkes, T. E. & Nygaard, R. W. (1983) Inhibitory influence of unstimulated rods in the human retina: evidence provided by examining cone flashes. *Science* **221**, 180–182.

Granit, R. & Riddell, H. A. (1934) The electrical responses of the light- and dark-adapted frog's eyes to rhythmic and continuous stimuli. *J. Physiol.* **81**, 1–28.

Hecht, S., Shlaer, S. & Smith, E. L. (1935). Intermittent light stimuli and the duplicity theory of vision. *Cold Spr. Harb. Symp. quant. Biol.* **3**, 237–244.

Hecht, S., Shlaer, S., Smith, E. L., Haig, C. & Peskin, J. C. (1948) The visual functions of the complete colorblind. *J. gen. Physiol.* **31**, 459–472.

Kelly, D. H. (1964) Sine waves and flicker fusion. *Doc. Ophthal.* **18**, 16–35.

Kelly, D. H. (1964) Sine waves and flicker fusion. *Doc. Ophthal.* pp. 273–302.

Landis, C. (1954) Determinants of the critical flicker-fusion threshold. *Physiol. Rev.* **34**, 259–286.

Levinson, J. (1964) Nonlinear and spatial effects in the perception of flicker. *Docum. Ophthal.* **18**, 36–55.

Lythgoe, R. J. & Tansley, K. (1929) The adaptation of the eye: its relation to the critical frequency of flicker *Med. Res. Council Sp. Rep. Ser.* No. 134.

MacLeod, D. I. A. (1972) Rods cancel cones in flicker. *Nature* **235**, 173–174.

Mandler, M. B. (1984) Temporal frequency discrimination above threshold. *Vision Res.* **24**, 1873–1880.

Mandler, M. B. & Makous, W. (1984) A three channel model of temporal frequency perception. *Vision Res.* **24**, 1181–1187.

Ogawa, T., Bishop, P. O. & Levick, W. R. (1966) Temporal characteristics of responses to photic stimulation by single ganglion cells in the unopened eye of the cat. *J. Neurophysiol.* **29**, 1–30.

Raninen, A. & Rovamo, J. (1986) Perimetry of critical flicker frequency in human rod and cone vision. *Vision Res.* **26**, 1249–1255.

Rovamo, J. & Raninen, A. (1984) Critical flicker frequency and M-scaling of stimulus size and retinal illuminance. *Vision Res.* **24**, 1127–1131.

Schneider, C. W. (1968) Electrophysiological analysis of the mechanisms underlying critical flicker frequency. *Vision Res.* **8**, 1233–1244.

Smith, R. A. (1970) Adaptation of visual contrast sensitivity to specific temporal frequencies. *Vision Res.* **10**, 275–279.

Thompson, P. (1983) Discrimination of moving gratings at and above detective threshold. *Vision Res.* **23**, 1533–1538.

Watson, A. B. & Robson, J. G. (1981) Discrimination at threshold: labelled detectors in human vision. *Vision Res.* **21**, 1115–1122.

14. VISUAL ACUITY

The perception of flicker demands the resolution of two stimuli separated in time; by visual acuity is generally meant the power of the eye to resolve two stimuli separated in space, i.e. it is fundamentally related to the spatial relationships between receptor elements as opposed to the temporal characteristics of the response of a single element.

CENTRAL AND PERIPHERAL VIEWING

As with the other aspects of vision that we have so far considered in detail, the resolving power of the human eye differs markedly according as the conditions of viewing favour rod or cone vision. Thus, visual acuity in the dark-adapted eye with parafoveal vision and scotopic luminous intensities is only a small fraction of that obtained with foveal vision and high luminous intensities. Nevertheless it would be wrong to consider this as a difference in rod and cone functions *per se*, since peripheral vision under photopic conditions gives a low order of visual acuity. This is illustrated by Fig. 14.1, which shows visual acuity as a function of angle of view, foveal acuity being put equal to unity. Thus at 5° the acuity is only about a quarter of that found with foveal vision, and at 15° only about one-seventh.

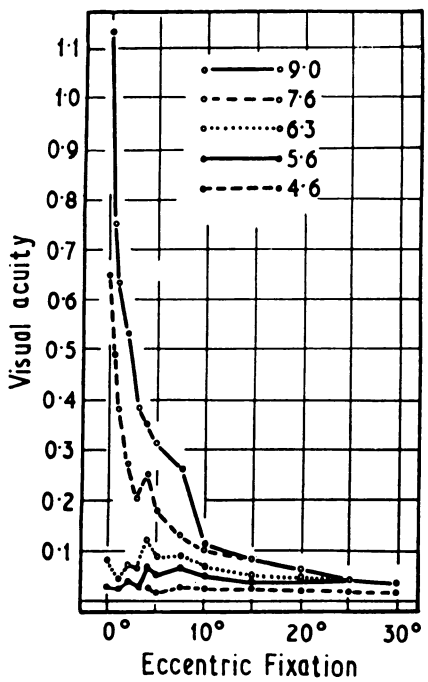

Fig. 14.1 The variation of visual acuity with eccentricity of vision as measured along the horizontal meridian of the temporal retina. Five intensity levels, varying from 9.0 to 4.6 log micromicrolamberts were employed (9.0 log micromicrolamberts = 10^9 micromicrolamberts = 1 mL). At 25° and 30° all the curves, except for 4.6 log micromicrolamberts, practically run together and are designated by single points. (Mandelbaum & Sloan, *Am, J. Ophthal.*)

Cone Density

The fall in visual acuity correlates fairly well with the fall in density of distribution of cones, which become more and more rare as we progress to the periphery of the retina. Density of receptors *per se*, however, is also not the determining factor since the rod density is very high throughout the retina yet visual acuity under scotopic conditions is always less than that under photopic conditions as Fig. 14.1 shows except, perhaps, in the extreme periphery. As we shall see, it is the synaptic organization of the receptors that is the important factor.

EFFECTS OF LUMINANCE OF TEST-OBJECT AND ADAPTATION

If the luminance of the test-object is such as to stimulate the cone mechanism, Lythgoe (1932) has shown that the curve showing the variation of visual acuity with the luminance of the test-object varies according to the experimental conditions; if the subject is placed in a dark box and is allowed to see the test-object through a small window, he can be considered to be in a state of dark-adaptation even though the luminance of the test-object is high enough to stimulate cone vision. In this case the acuity increases up to a maximum at approximately 10 e.f.c. and then begins to fall (Fig. 14.2, A); if the walls of the box are given a luminance of 0.011 e.f.c., i.e. if the subject

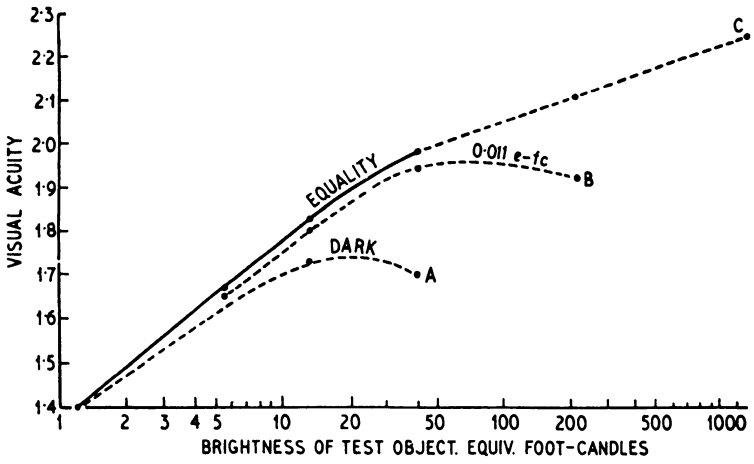

Fig. 14.2 Illustrating the effects of the luminance of the surround (i.e. state of adaptation of the eye) on visual acuity. A, black surround: visual acuity increases with increasing luminance of test-object only up to a certain point. B, surround luminance of 0.11 e.f.c. C, surround luminance varied continuously so as to be equal to that of test-object. (Lythgoe, *Med. Res. Council Sp. Rep.* By permission of the Controller of H.M. Stationery Office.)

is only partly dark-adapted, the acuity continues to increase to a maximum at approximately 50 e.f.c. but then falls off (Fig. 14.2, B). If the luminance of the box is continuously adjusted so that it is equal to that of the test-object, it is found that visual acuity increases progressively with the luminance of the test-object (Curve C). If the luminance of the box is made greater than that of the test-object, generally the acuity is lower than when the luminances are equal. Thus with visual acuity we are confronted again with some form of retinal interaction in so far as the acuity of the central retina is influenced by the general illumination of the eye, i.e. by light-adaptation.

Adaptation

We have seen that dark-adaptation increases visual acuity under scotopic conditions; this effect is doubtless due to the increased sensitivity of the rods; the curves in Fig. 14.2 indicate that light-adaptation, under photopic conditions, increases visual acuity, and consequently dark-adaptation decreases it; since dark-adaptation increases the sensitivity of the cones (although not to the same degree as that of the rods) it is clear that the effect of dark-adaptation on photopic visual acuity is not closely connected with changes in sensitivity of the cones *per se*.

NORMAL VISUAL ACUITY

We have so far considered variations in the visual acuity, but have said little about its absolute magnitude. It is customary to think of the visual acuity being determined by the 'grain' of the retinal mosaic of cones—thus the Snellen letters are constructed on the assumption that the average person can resolve points separated by 1 minute of arc, and this limit has been considered to be roughly determined by the diameter of a single cone. Thus if we consider two white points on a black field, if these are so close together that their images fall on a pair of adjacent cones it is clear that they would not be appreciated as separate since a single, larger, white point would produce the same effect; only if one unstimulated cone is between the two images should the points appear as discrete. If we take Polyak's figure of 1.5 μm for the diameter of the base of a foveal cone, this would permit a resolving power of approximately 20 seconds of arc; the best figure for visual acuity indicates a resolving power of this order. When, however, visual acuity is measured by the power to detect a break in a contour, e.g. with a vernier scale adjustment, or to detect the presence of a single line on a uniform background, a far greater resolving power is found (of the order of 4 seconds of arc for the contour break and 0.5 second for the line), and numerous explanations have been put forward to explain the apparent anomaly.

The 'One-to-one' Relationship

If the individual retinal cones are to be considered as the units on the basis of which resolving power is to be determined, as opposed to groups of cones, there must be a so-called 'one-to-one' relationship between cones and optic nerve fibres; in other words, two adjacent cones must be able to convey their impulses along independent paths; if two cones, close together, were connected to the same bipolar cell, the impulses relayed from this cell would be characteristic of neither cone separately, so that it would be difficult to conceive of a 'local sign' being attached to either cone, and consequently resolving power could not be so fine as to permit the differentiation of stimuli separated by one unstimulated cone.

Midget Cells

The organization of the retina has been discussed earlier, and we have seen that the midget bipolar, whose significance was first emphasized by Polyak (1941), makes a special type of contact with the cone pedicle; furthermore, a given midget bipolar only receives messages from one cone. The same exclusive relationship is found with the midget ganglion cells, so that in this sense a given cone may have an exclusive pathway to the lateral geniculate body, a pathway not shared by another cone. Strictly speaking, however, there is no absolute 'one-to-one' relationship between cones, bipolars, and ganglion cells owing to the fact that cones, even in the central area, make connections with diffuse bipolars besides with a midget; similarly, the same midget bipolar that makes a 'private' synapse with a midget ganglion also makes contact with the diffuse varieties of ganglion cells. The 'one-to-one' relationship thus exists only by virtue of a peculiar synaptical arrangement between a cone and its related midget bipolar and ganglion cells; although a share of the electrical change excited in a cone is directed into collateral channels (diffuse bipolars, horizontal and amacrine cells) the main or specific cone influence seems to remain restricted to this special channel.

Spatial Summation

Thus spatial summation of stimuli, such as is observed with rod vision, could only be mediated in the central (cone) area by means of the subsidiary synaptic connections and it is therefore not surprising that very little evidence of this type of summation by the cones has been obtained. Lythgoe suggested that the increased visual acuity obtained by light-adaptation (*see*, e.g. Fig. 14.2) is due to an inhibition of these subsidiary nervous paths so that the cones, during light-adaptation, tend to react more and more as single units.

Diffraction and Chromatic Aberration

Having established the existence of a 'one-to-one' relationship between cone and optic nerve fibre for the central region of the retina, albeit restricted in scope, we can postulate a certain local sign attached to any foveal cone, so that we have a basis for the differentiation by the higher centres between the stimulation of two adjacent cones and two separated by one unstimulated cone. In the absence of diffraction and aberration effects, then, a figure of 20 seconds of arc could be taken as the anatomical limit of resolution of two points by the most central portion of the fovea. Diffraction and chromatic aberration, however, must certainly be taken into consideration; it is all very well to assume that the image of a grating or Landolt-C will be a clear-cut replica of the original, but let us suppose that the white break in the Landolt-C at the limit of resolution produces an image two, three, or four times its 'geometrical size'; clearly it will stimulate two, three, or four cones so that it will be impossible to localize the break exactly; moreover, the black line of the Landolt-C has the same thickness as its break; if the white points on the inside and outside of the black contour all produce images extending over one or more cones there will be no unstimulated cone on the retina and, on the simple view so far taken, a Landolt-C whose black line subtends only 20 seconds of arc should be invisible.

Diffraction Rings

As a result of diffraction, a point of light produces an image of finite size on the retina; the image consists of a central bright spot surrounded by successive dark and bright rings; with a pupillary diameter of 3 mm and with light of wavelength 555 nm, the central spot will have a diameter of rather more than 3.8 μm, subtending some 47 seconds of arc at the nodal point of the eye; that is, there should be a definite overlapping of cone stimulation even when the stimulus arises from a theoretical point source. In general, the light falling in the bright rings concentric with the central bright disc only amounts to 16% of the whole, so that the much greater overlapping due to these rings can probably be ignored.

Chromatic Aberration

The effects of chromatic aberration are even more serious; the effect is to make the image of a point source into a large disc covering some four cones.

Retinal Image

As a result of these combined effects the image of a grating, for example, will not consist of a series of bright and black patches on the retina; long before the resolution limit of such a grating has been reached, the image will be such that *no cone will be unstimulated*; this is shown by Fig. 14.3 from Hartridge (1947) where the relative luminances of the different parts of the image of a grating on the retina are plotted; in the middle of the geometrical shadow of the black lines, the intensity is some 40% of what it would be if there were no black lines at all; beneath the image of the white bar the intensity is only 60%. In the same figure the distribution of light in the region of the geometrical edge of an extended object is shown; it is seen that there is no clear-cut shadow, light

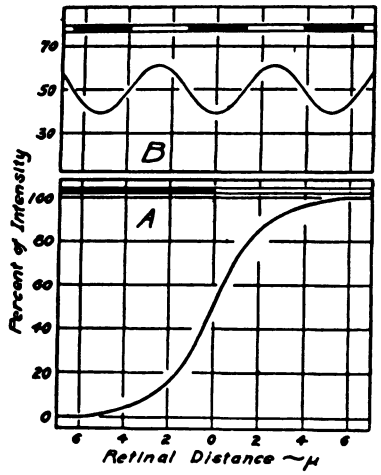

Fig. 14.3 The distribution of light intensity in the image of an edge (A) and a grating (B) on the retina as calculated by Hartridge. (Shlaer, *J. Gen Physiol.*)

falling on the retina several cones' width within the geometrical shadow.

Criterion for Resolution

Clearly the classical conception of the basis of visual acuity—which demands that two resolvable points should be such that their images have an unstimulated cone between them—must be abandoned, since it fails to fit the observed facts of visual acuity. If we adopt Hartridge's criterion of the limit of resolution of two points, namely that their images must be sufficiently far apart so that there is a cone between that is *less stimulated than the rest*, we are not only provided with a way round our difficulty, but we can also explain the extremely high order of visual acuity exhibited in the detection of the break in a contour. Thus although a cone, falling under the geometrical image of a black bar, is stimulated, it receives less light than adjoining cones falling under the geometrical images of the white bars, and there is thus a peripheral basis for the resolution of points closer together than might otherwise have been expected.

Induction Effects

According to Hartridge's analysis, the limit to resolution is determined almost exactly by the 'grain' of the retinal mosaic of cones, i.e. by the diameter of a central retinal cone. It may be mentioned here that local inductive effects, whereby the sensitivity of cones adjacent to the most strongly stimulated one is depressed (Chapter 7), assist in the resolution process. i.e. the inductive effects *amplify* the differences in response of adjoining cones on which the image of a grating falls.

Retinal Mosaic in the Cat

The retina of this mammal has been studied both physiologically and morphologically in far greater detail than that of primates, so that, although visual acuity and colour vision are poorly developed, we must nevertheless rely heavily on experimental studies of the cat's retina.

The Mosaic of Retinal Ganglion Cells

Although it is the mosaic of receptors that ultimately limits the resolving power, when many receptors converge on a single ganglion cell, then the size of the dendritic tree that captures their input is the governing power, rather than receptor spacing; if the ganglion cell spacing is governed by the packing of these dendritic trees, then the spacing of the ganglion cell governs the resolution. Reduced silver stains all the alpha-cells of the cat's retina completely (Wässle *et al.*, 1981a); staining of the beta-cells with sufficient dendritic detail was achieved by retrograde staining with horseradish peroxidase (Illing & Wässle, 1981). By elaborate measurements of the numbers of alpha- and beta-ganglion cells in a given area, and classification of these into ON- and OFF-centre types by their different stratification levels in the inner plexiform layer, Wässle *et al.* (1983) concluded that the retina was covered by a set of mosaics of the different types. So far as the alpha-cells were concerned, the retina was completely covered by what seemed to be the most economical manner, roughly similar to a hexagonal array. ON- and OFF-cells formed separate lattices, so that each retinal point was covered by at least one ON- and one OFF-receptive field. Unlike the alpha-cells, the dendritic fields of beta-cells are completely covered by their immediate neighbours. These small ganglion cells are considered to constitute the basis for the resolution of fine detail, so the high density compared with that of alpha-cells is intelligible. This becomes especially necessary in the cat which, unlike primates or birds, has no midget ganglion cell system. It has been argued that resolving power of the retina is determined by two parameters, the spacing between neighbouring ganglion cells (sampling distance) and the dendritic field diameter of the cells, which acts as a sampling aperture. According to the analysis of Wässle *et al.* (1981b) these two parameters are optimally adjusted for spatial resolution. Thus, in the central area, the beta-cell density is about 5500 cells/mm^2, corresponding to an intercell distance of 20 μm for each of the ON- and OFF-populations, which gives a grating resolving power of 0.18°, corresponding to

a resolution determined behaviourally of 0.2° (Campbell *et al.*, 1973).[1]

Vernier- or Hyper-acuity

The high degree of resolution exhibited in the recognition of breaks in contours, where the limit is of the order of 4 seconds of arc, appears, at first sight to present difficulties in explanation in terms of the retinal mosaic. On the classical view, the limit to detection of a break in a contour would be determined by the break of such a size that the image of the line above the break fell on a row of cones whilst the image of the line below the break fell on another row (Fig. 14.4); the break in the contour would be recognized by the existence of some stimulated and some unstimulated cones in a row. Such a view demands, however, a cone size much too small for the observed resolution.

Fig. 14.4 The break in the contour is recognized, on the classical view, by the fact that the lower cones in the row are stimulated whilst the upper ones are not.

Aberrations

When diffraction and chromatic aberration are taken into account, the image of the contour extends to a considerable distance beyond the geometrical shadow, but the *break* in the contour is accurately reproduced, even though at a considerable distance (Fig. 14.5). Let us imagine that the edge of the shadow falls along a row of cones (Fig. 14.5); at the break in the contour the cones below the break receive less illumination than those above it, but it is impossible, of course, that any number of cones in a row could be unstimulated whilst others were stimulated. The basis for the recognition of the break in the contour must be that in the region of the break some cones will be slightly less strongly stimulated than others. Hartridge has calculated that the variation of luminance in the shadow is sufficiently great to permit a significant difference in stimulus-intensity for the cones in

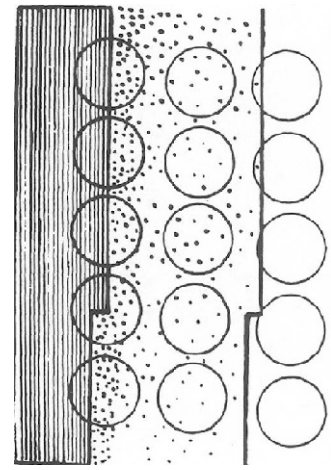

Fig. 14.5 Illustrating how the break in the contour is reproduced accurately in the diffraction shadow, which extends to some distance to the right of the geometrical shadow. Above the break, the shadow is slightly deeper than below, hence the cones above are slightly less strongly stimulated than those below.

the region of the break, even when the latter only subtends an angle of a few seconds at the eye; i.e., by moving along the retina a distance corresponding to 4 seconds of arc, a sufficient change in illumination is obtained to have an effect on the response of the cones. On this view, the edge of the shadow does not have to fall on any line of cones; the shadow varies continuously in luminance from left to right; at any point above the break, the luminance will be always rather less than at any point in the same vertical line below the break. So long as that difference in luminance is adequate to cause a differential stimulation of cones at the two points, we have the basis for the recognition of the break in the contour. Diffraction and aberration, by causing a progressive decrease in luminance of the image of the line to left and right, thus provide the basis for discrimination which would be impossible with a geometrical image.

Vernier-acuity in the Cat

If our argument is correct, the vernier-acuity in the cat should be superior to its grating resolution. Belleville & Wilkinson (1986) quote an average grating resolution of 6 cyc/deg, corresponding to a resolving power of 5 minutes of arc. They found a vernier-acuity of 2.2 to 6.7 minutes of arc, indicating a little improvement over grating resolution, but the difference between the two is clearly not as great as in humans.

GANGLION CELL DISCHARGE

Since ganglion cells have collected and integrated the information contained in the responses of receptors, we

may assume that these cells will contain the information that higher centres will interpret as the offset of a line-image. Shapley & Victor (1986) found a remarkably high sensitivity, a displacement of a line by as little as 1.3 minutes of arc causing a detectable change in discharge-rate, the best result being obtained if the displacement occurred from the null-point. Experimentally the grating-resolution was 2 cyc/deg, or a resolution of 15 minutes of arc, so that, according to this study, the cat manifests hyperacuity of a similar degree to that of the primate, when allowance is made for the much lower grating-resolution of the cat.[2]

Alignment of Dots

Vernier-acuity is most commonly described in terms of separation of lines, but there seems little doubt that the same high degree of resolution is obtained when the subject is asked to determine the alignment of two dots. Westheimer & McKee (1977a) found a resolution of 2–5 seconds of arc when they employed two square spots of light, 1 × 1 min; an optimal vertical separation of 3–6 minutes of arc was found. Again Buck & Schwartz (1979) found a linear increase in threshold from 8 seconds with a 10 minute vertical separation of the spots to 15 seconds at 30 minutes separation. With separations below about 2 min of arc the deterioration presumably is due to blurring of the targets when they are too close; the falling off at larger separations would be expected intuitively; a simple way of expressing it would be that the discrimination at larger separations is one of orientation of the line drawn between the two point-targets and the vertical, in which case, as the distance between them increases, the angle between the two lines becomes smaller, and so the threshold for discrimination becomes larger, i.e. the two points must be separated farther to give the same threshold angle.[3]

Variation of Vernier-acuity with Eccentricity

Just as grating-acuity falls off with peripheral view, so does vernier-acuity. Thus Weymouth (1958) in his classical study, showed that the vernier-threshold increased more rapidly than the minimum separable when plotted as a function of eccentricity, so that, as Fig. 14.6 shows, the lines cross and grating acuity becomes the better. Similar comparisons have been made by Westheimer (1982) and Levi *et al.* (1985); the latter authors analysed the change in vernier-acuity in the light of the 'cortical magnification' or 'scaling' factor (p. 517), concluding that the fall-off is what would be expected of the decreased cortical magnification in the periphery.[4]

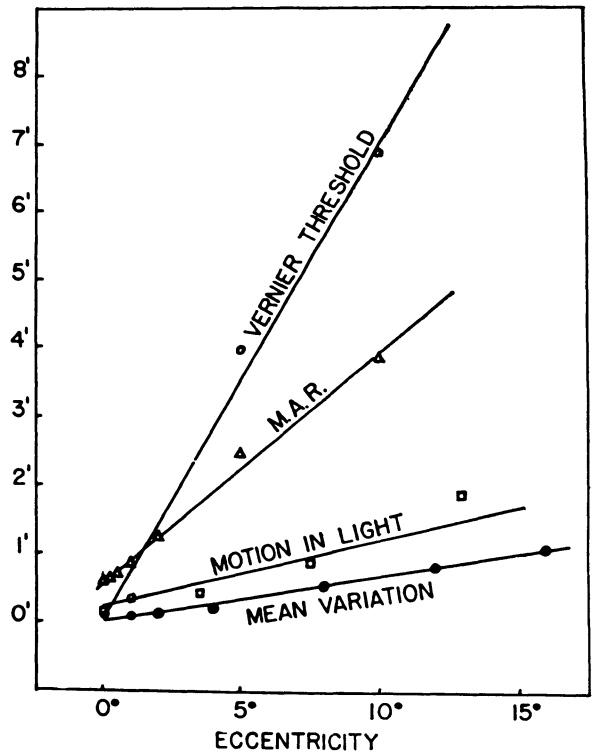

Fig. 14.6 Comparison of vernier threshold, minimal angle of resolution, motion threshold, and mean variation of the settings of horopter rods; all are plotted as functions of retinal eccentricity. Data: vernier threshold, Bourdon; minimal angle of resolution, Ludvigh; motion threshold, Basler; mean variation, Ogle. (Weymouth, *Amer. J. Ophthal.*)

Orientation of Lines

Westheimer (1982) showed that estimation of the orientation of a line may be regarded as another hyperacuity task; thus a subject can detect a difference of orientation of sequentially presented lines as low as 10–20 minutes of arc, a difference corresponding to a relative distance between the ends of the two lines as small as a few seconds of arc.

JUMP TARGET

A bright line may be viewed and its position suddenly changed; the task is similar to a vernier-estimate except that the two lines are perceived successively in time; a similar 'jump acuity' to that of vernier-alignment is found (Westheimer, 1982).

Masking Effect of Line

If, as we have suggested, the detection of a break in a line relies on the integration of input from receptors over

several μm of retina adjacent to the break in the geometrical image, then placing a luminous line beside the test vernier-line may be expected to reduce acuity of detection. This is indeed true, as illustrated by Fig. 14.7A, where it will be seen that a flanking line may increase the vernier-threshold from about 5 sec to nearly 20 sec; there is clearly an optimum distance for maximum effect, namely 2–3 minutes of arc from the test-line. In a rather similar type of experiment Badcock & Westheimer (1985) showed that the flanking line had a tendency to draw the test-line towards it. Thus the vernier-task consisted in saying whether one of two lines on a screen was to the left or right of the other; when 50% of answers consisted in either direction, the subject was said to have aligned the targets. The flanking line increased the errors, but the change was such that the subject tended to judge correct alignment when the test-line was nearer to the flanking line. At a certain distance of the flanking line (about 5 min of arc), however, the reverse took place, the flanking line 'repelling' the testing line (Fig. 14.7B).

Moving Target

A further interesting point brought out by Westheimer & McKee (1977b) is that the same degree of 'hyperacuity' remains if the target moves over the visual field at a rate of 4°/sec. Thus it would seem that over a certain area of the retina the signals indicating spatial separation can be integrated over a time-period. The authors show, moreover, that the phenomenon cannot be explained on a simple basis of sweeping the pattern over a simple 'template' that matches the stimulus offset. Thus the basic feature is the slight difference in illumination of adjacent receptors as the image falls on the retina; if the stimulus-pattern is moving, then different pairs of receptors will continue the signal until the integrated signals are ultimately interpreted.

Resolution of a Single Line

Hecht & Mintz (1939) have shown that a line may be detected against a uniformly bright background when it subtends only 0.5 seconds of arc at the eye; the image of such a line on the retina consists of nothing more than a slight variation in luminance to left and right of the geometrical image; this is so slight that even along the line corresponding to the geometrical shadow the luminance is only 1% less than that in regions unaffected by the line; nevertheless this difference of luminance is considered to be adequate to cause a differential cone stimulation that could be interpreted as a localized change in luminance, i.e. the increment corresponds to the value of $\Delta I/I$ found for the prevailing level of luminance. On this view, it would appear that the limiting factor in the detection of a line is the liminal brightness increment.

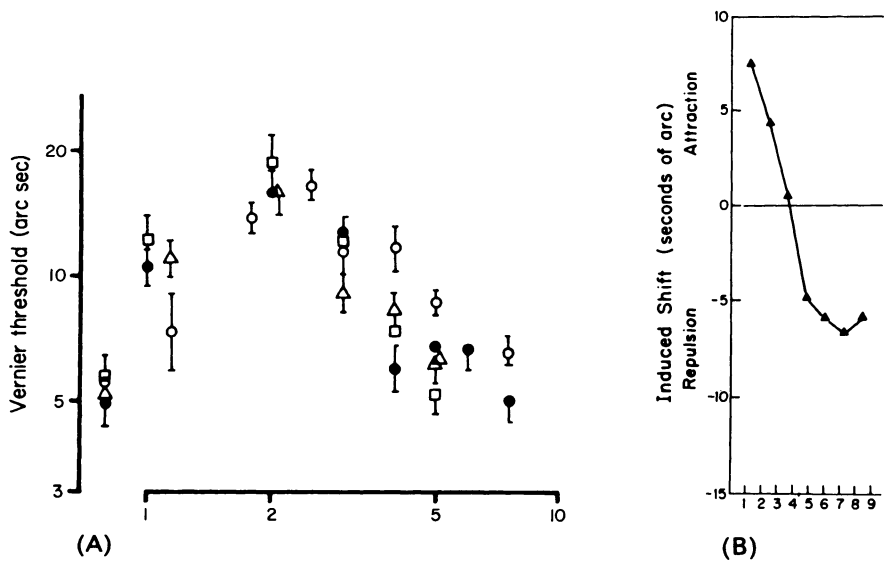

Fig. 14.7 Masking of vernier acuity by a flanking line. A. Vernier threshold as a function of flank separation. B. Induced shift of the mean location of the lower target line in a vernier stimulus as a function of the separation between the target and the flanking line. Abscissa: Target–flank separation in minutes of arc. (Levi *et al.*, *Vision Res.*, and Weymouth, *Amer. J. Ophthal.*)

Effect of Luminance of Test-object

We have seen that visual acuity increases progressively with illumination of the target; the explanation for this is probably not simple, since this improvement is only achieved up to a point unless the surround illumination is increased too (Fig. 14.2). This influence of the surround illumination suggests that neuronal interaction in the retina is also affected by luminance. Hecht (1937) considered that increasing the luminance brought into operation more and more cones, and so the effective mosaic became finer and finer and thereby permitted better and better resolution. In the simple form in which it was presented the theory was inadequate, but as modified by Pirenne (1957–1962) and his colleagues, it may well account for many of the phenomena.

Multiple Unit Hypothesis

Their point of view is best illustrated by a diagram (Fig. 14.8). We have seen that the requirement for maximal visual acuity is the effective one-to-one relationship between cones and optic nerve fibres. Any deviations from this relationship must reduce resolving power. Thus, as Fig. 13.8 shows, a perfect three-to-one relationship would give a visual acuity of one third the maximum, since the effective size of the receptor is three times as large. The visual acuity, other things being equal, must therefore depend on the size of the effective retinal units than can be brought into operation, and Pirenne *et al.* (1957) suggested that it is mainly because increasing the luminance of the test-object brings into operation smaller units, i.e. smaller groups of receptors converging on a single optic nerve fibre, that the basic relationship between visual acuity and luminance pertains.

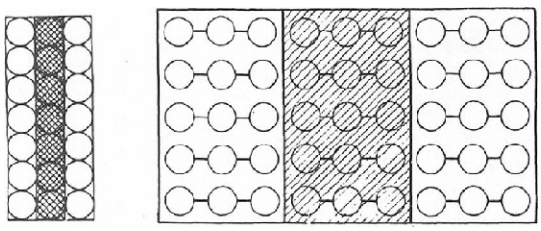

Fig. 14.8 Illustrating the concept of retinal units in defining resolving power. *Left*: The cones behave in a perfect one-to-one manner, so that the effective retinal mosaic for discriminating a grating is constituted by rows of single cones. *Right*: Because of convergence in the visual pathway, three cones behave as units, hence the grating at limiting resolution must be three times as wide.

LIMITING LIGHT-FLUX

Thus the large units are able to summate light-stimuli falling over large areas and therefore their threshold will be lower than that of the smaller units in which summation will be more limited. On this basis we might expect that the flux of light-energy reaching the eye from the white break in the Landolt-C, corresponding to maximal visual acuity, would be the same for the various luminances. Thus under scotopic conditions we might expect it to be equal to the minimum flux necessary for vision, of the order of 150 quanta/sec, and according to Pirenne *et al.* this is roughly true. Similarly, with photopic vision, the minimum flux to excite the cones is of the order of 2.5×10^{-12} lumens/sec, and if the fluxes emitted from the breaks of the Landolt-C's are calculated for different luminances these correspond approximately up to visual acuities of about 2. Beyond this, however, the amount of light entering the eye from the break is well above the threshold flux. As Pirenne has indeed pointed out, it is highly unlikely that this can be a complete explanation since threshold measurements are made under vastly different conditions from measurements of visual acuity, where large parts of the retina are stimulated by the surroundings of the Landolt-C.

Contrast

In considering the luminance of the test object there is an unfortunate tendency to ignore the real factor, namely the contrast between the black details on the white background, or *vice versa*; there is a tendency to treat the black as absolutely black, and not reflecting light from its surface, thereby implying that increasing the luminance will increase the contrast in a parallel fashion. This is not necessarily true, so that it is more logical to express the lighting conditions of the target in terms of its *contrast*. A useful experimental method of establishing gratings with accurately defined contrast is to generate the grating on a cathode-ray oscilloscope screen by means of an appropriate oscillator; in the set-up described by Campbell & Green (1965a) the intensity of emitted light from the screen varied in a sinusoidal manner with distance, as illustrated in Fig. 14.9; the contrast is given by: $(I_{max} - I_{min})/(I_{max} + I_{min})$, and three different contrast-ratios are illustrated for the same grating-frequency. The advantage of this system, besides that of accurately defining the important experimental parameter, namely contrast, is that the average luminance of the screen during a cycle remains the same independently of altered contrast-ratios. We may define the *grating-*, or *spatial, frequency* as the angle subtended at the eye by the distance between two peaks of intensity; when the subject is just able to discriminate the grating, this grating-frequency, in cycles per degree, gives a measure of the resolving power, as usually defined, and its reciprocal is the visual acuity.

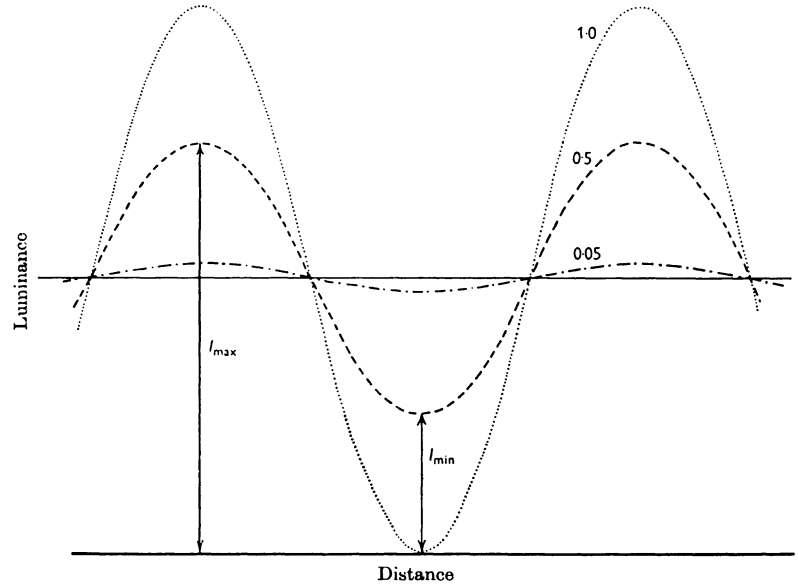

Fig. 14.9 Illustrating the contrast-ratio for a grating generated by a sinusoidal variation in luminance on a cathode-ray screen. Contrast is defined as $(I_{max}-I_{min})/(I_{max}+I_{min})$. Three ratios of 1.0, 0.5 and 0.05 are shown. Note that the mean luminance level remains constant for different contrast-ratios. Spatial frequency is defined as the reciprocal of the angular distance between successive maxima in the sinusoidal distribution. (Campbell & Green, *J. Physiol.*)

Contrast-sensitivity

The subject is presented with a given grating-frequency, and the contrast below which resolution is impossible indicates the threshold; the reciprocal of this contrast is called the *contrast-sensitivity*. The curve through the open circles in Fig. 14.10 shows the relation between contrast-sensitivity and grating-frequency; at low grating-frequencies, i.e. with wide gratings, the contrast-sensitivity is high, i.e. small degrees of contrast are necessary.

Optical Defects in Image

Campbell and Green have applied this technique to assess the extent to which optical defects in the image contribute to a loss of visual acuity; to do this it was necessary to project on to the retina a grating of known contrast on the retina rather than of known contrast on the screen, since the effect of diffraction and aberrations is, by spreading light over the geometrical image of a black line, to reduce contrast. This was achieved by a technique developed by LeGrand in 1937; monochromatic light from two coherent sources was projected into the eye in such a way as to form interference fringes with calculable contrast-ratios, and the width and contrast of these fringes were varied until the subject failed to resolve them. The results have been drawn in Fig. 14.10 as the

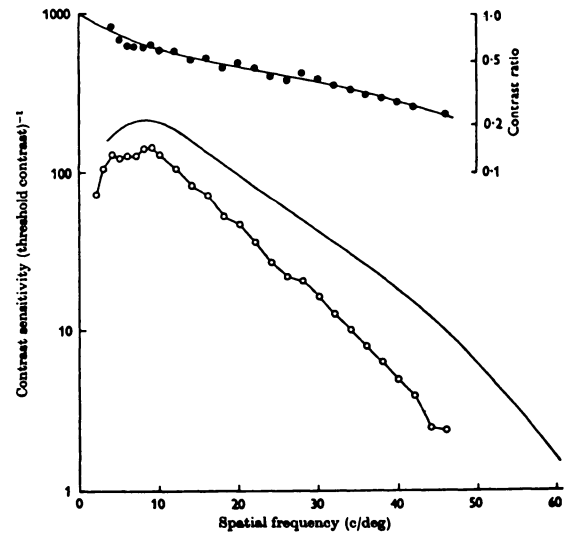

Fig. 14.10 The line through the open circles represents the 'contrast-sensitivity function' of a human observer. As ordinates are plotted the reciprocals of the contrast required to make gratings, of frequencies indicated as the abscissae, just resolvable. The continuous curve is a corresponding function for gratings that have been formed by interference on the retina and thus have suffered no optical defects. The filled circles indicate the ratios of the contrast-sensitivities for the two modes of presentation of the gratings. (Campbell & Green, *J. Physiol.*)

continuous line, whilst the ratios of the contrast-sensitivities are plotted above in solid circles. Essentially these contrast-ratios are a measure of how the optics of the system reduce visual acuity.

Effect of Orientation

The resolution of gratings is better if the lines are arranged vertically or horizontally (Taylor, 1963); Campbell *et al.* (1966) have shown that the effects are similar with high and low spatial-frequency gratings, when they are assessed in terms of contrast-sensitivity (p. 381), so that it is unlikely that optical effects are the cause; and this was confirmed by finding similar orientational effects when the optical system of the eye was by-passed through the formation of interference fringes on the retina.

Vernier Acuity

This form of 'hyperacuity' may also be studied by the contrast-sensitivity technique as adapted by Tyler (1973); thus the typical vernier alignment task consists in a measure of the accuracy with which two line-segments can be aligned, and a periodical version of this employs as a stimulus a wavy line of different spatial frequencies as in Fig. 14.11 and the requirement is that the subject decide whether the line is a straight line or whether it is wavy, and the subject is required to increase the amplitude of the waves until this discrimination can be made. Thus 'line modulation sensitivity' is determined at different spatial frequencies to give characteristic curves, as in Fig. 14.12, the ordinate depicting the threshold amplitude of line modulation; as the scale is marked with displacement amplitude units increasing downwards, sensitivity increases upwards. Peak sensitivity was reached at a spatial frequency of between 2 and 6 c/degree and varied between 6 and 9 seconds of arc. As with the grating-acuity, there was a strong orientational bias, so that sensitivity was reduced by about 30% when oblique patterns were viewed (Tyler & Mitchell, 1977).

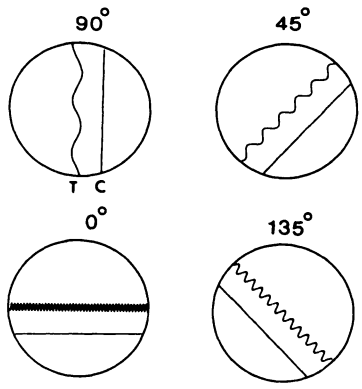

Fig. 14.11 Periodic vernier stimuli, T, are shown with four different spatial frequencies but the same peak-to-peak amplitude of the sinusoid. Clearly, the task of deciding whether the line stimulus is wavy becomes more difficult as spatial frequency is increased. The subject varies the amplitude of the sinusoid waves until discrimination of waviness is just achieved. The figure shows four orientations of the stimulus; a straight line C is situated about 2° to one side of the vernier stimulus acting as a comparison stimulus. (Tyler & Mitchell, *Vision Res.*)

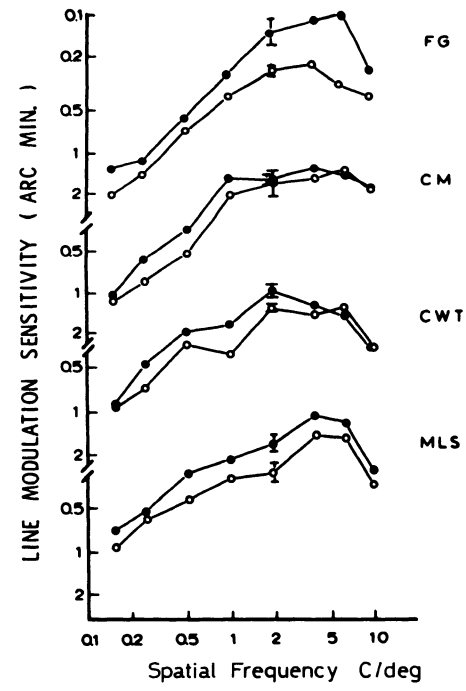

Fig. 14.12 Periodic vernier acuity given by the threshold peak-to-peak amplitude of the sinusoid as a function of the spatial frequency of line modulation. Vertical and horizontal stimuli, filled circles; oblique stimuli, open circles. (Tyler & Mitchell, *Vision Res.*)

Adaptational Effects

Gilinsky (1968) observed that the grating-acuity is lowered by adaptation to an identical pattern and bar-width but of higher mean luminance, an effect that was decreased if the orientation of the two was altered in relation to each other. Blakemore & Campbell (1969) showed that the contrast-threshold for a grating increased by 0.5 logunits after viewing for one minute a high-contrast grating; within a further minute the threshold returned to normal; the greater the contrast of the adapting grating, the greater the rise in threshold. When the effect of a given adapting grating on the contrast-sensitivity function (Fig. 14.10) was studied, it was found that the adaptive effect was limited to a certain range of spatial frequencies, as illustrated in Fig. 14.13 where the effect of a grating of 7.1 cycles/degree is seen to depress contrast sensitivity over only a part of the range of sensitivity, so that when the relative elevation of the threshold is plotted

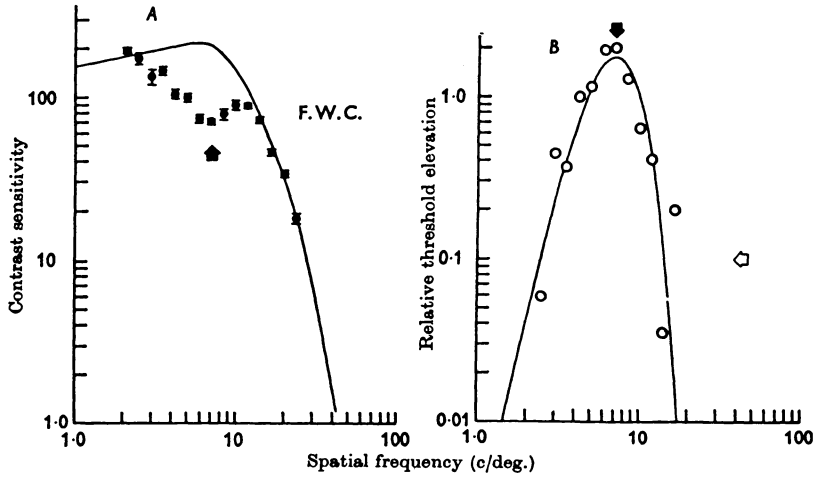

Fig. 14.13 Effect of adaptation to a given grating-frequency on the contrast-sensitivity function. A. The curve shows the contrast-sensitivity function for the observer F.W.C. The plotted points show the effects of adapting to a grating-frequency of 7.1 cyc/deg. B. The relative elevation of the threshold has been plotted against grating-frequency, giving a peak at about 7 cyc/deg. (Blakemore & Campbell, *J. Physiol.*)

against spatial frequency, a narrow curve, peaking at about 7 cycles/degree, is obtained suggesting the preferential depression of some spatial frequency-sensitive channels. When different adapting grating-frequencies were used, different peaks were obtained, except at low spatial frequencies, i.e. wide gratings, when there was only a depression of sensitivity without any change of the peak frequency; thus at 2.5, 1.8, 1.5 and 1.3 cycles/degree the peaks all occurred at 3 cycles/degree. Again, Campbell & Kulikowski (1966) showed that simultaneous viewing of one grating reduced the sensitivity to another, the effect depending on the angles made by the two with each other, falling off to nearly zero over a range of 15 to 20 degrees. An interesting observation was that, not only does adaptation alter the contrast-sensitivity, but it also changes the perceived spatial frequency, so that after adaptation to a given grating, another grating, of about the same spatial frequency appears different, one with bars narrower than those of the adaptation grating appearing even narrower and one with bars wider appearing even wider. Such an effect is predictable if the cortical neurones showing the adaptation effect actually encode the information regarding spatial frequency of the stimulus (Blakemore *et al.*, 1970).

In general, then, it appears that the human visual system is organized in such a way as to give a number of channels tuned to a peak spatial-frequency, and presumably they would operate as size-detectors.[5]

Effects of Displaced Gratings

Takahashi & Ejima (1985) presented subjects with a test-grating, and observed the effects of another grating displaced vertically above the test-grating; when these peripheral gratings were in phase with the test-grating, the threshold contrast was reduced if the peripheral gratings themselves had a low contrast, but was elevated by a high-contrast grating. The effects decreased with distance between the test-grating and the peripheral grating. If the gratings were out of phase, no facilitation of threshold was observed, but the threshold for the test-grating was elevated by low-contrast peripheral gratings.

Importance of Target-width

Below a certain value, the number of cycles of a grating presented for discrimination is important in defining the stimulus; for example, McCann *et al.* (1974) found that with low-spatial frequency gratings of 0.1 to 3 cycles/degree, the visibility depended only on the number of cycles presented and not on the spatial frequency. Hoekstra *et al.* (1974) found that the 'critical number' of cycles necessary for optimal resolution depended on the mean luminance, changing from 2 towards 5 when luminance was increased from 2 to 25 cd/m^2 and at 600 cd/m^2 it reached 10. The subject seems a vexed one, and may well represent a situation in which summation of elements in the visual field plays an important role. Howell & Hess (1978) considered the effects of the lengths of the vertical lines of a grating as constituting one aspect of areal summation in the target area, and then the number of cycles in a grating required to give optimal resolution. They confirmed the existence of a critical number of bars beyond which there was no improvement in resolution; and this could represent a critical area over which summation in the horizontal direction occurred. By keeping the number of bars constant, but changing their length, summation in the orthogonal direction was measured; there was a critical length of bar beyond which there was no improvement in resolution; and this amounted to

the length composed by 10–20 cycles of the grating. If one imagines a number of independent detectors concerned with assessing grating-frequency, the improvement in contrast-sensitivity with target length and width might be predicted on probability theory, and Robson & Graham (1981), on the basis of measurements of grating-acuity as a function of eccentricity from the fovea (an important point when considering the effects of increasing grating-width), concluded that the improvement of contrast-sensitivity with increasing number of cycles was consonant with probability theory.

Bar-length

Wright (1982) found that contrast-sensitivity for a grating increased with the square-root of the length of the bars, up to a critical length equal to the width of 7–14 bars. As an example, a grating of 2 cyc/deg with bars of 1 minute length gave a contrast-sensitivity of about 10, whilst with a bar-length of 120 minutes the contrast-sensitivity was greater than 100.

Ganglion Cell Discharges

Cleland *et al.* (1983) measured the responses of transient (Y) and sustained (X) cat ganglion cells to bars as the length or velocity was increased; with sustained cells, changes in bar-length could be compensated by changes in velocity, indicating that the critical factor was the light-flux that could be usefully employed during the temporal summation-time of the cell. With transient cells. this linear summation was not so evident at low velocities of movement.

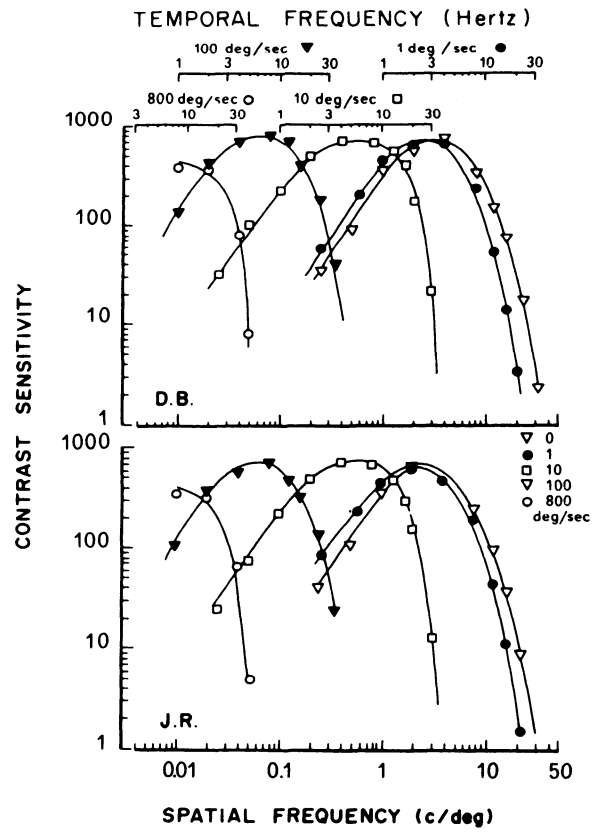

Fig. 14.14 Contrast sensitivity curves for the two observers for sinusoidal gratings drifting at various speeds. The lower abscissa shows the spatial frequency of the gratings, and the upper abscissa the corresponding temporal frequency for each drift speed. Note that at all drift speeds, the curves have the same height, width and general shape. (Burr & Ross, *Vision Res.*)

Effects of Speed of Motion of a Drifting Grating

If a grating moves rapidly across the visual field of a stationary eye, the detection of its discontinuity, i.e. the grating-acuity, obviously diminishes. Thus, when a fine grating moves rapidly over the visual field, a higher contrast is necessary for detection of its motion than when it is moving slowly.

Burr & Ross (1982) asked human subjects to say whether a grating, moving across the visual field, was moving or not, the decision depending on whether a discontinuity in the visual field was detected. Using this approach they plotted contrast-sensitivity functions for different velocities, as in Fig. 14.14. The limiting spatial frequency for detection clearly decreased with increasing speeds, as expected, but the maximal sensitivity was the same, and was simply shifted to lower spatial frequencies, i.e. towards coarser gratings. In effect, motion was making gratings visible that would not have been detected when stationary. An analysis of the curves of spatial frequency against contrast-sensitivity indicated that the detectability of the motion of a grating across the visual field depended entirely on the temporal frequency with which the retina was stimulated; thus a coarse grating would have to be moved faster over the visual field to give the same temporal frequency of stimulation than would a fine grating. Subjectively it is found that very fast velocities, employed for coarse gratings, never appear particularly fast. At all temporal frequencies, which are governed by the speed at which the grating moves and its spatial frequency, the apparent speed of motion remains unchanged with viewing distance, which alters both spatial frequency and velocity but leaves temporal frequency unchanged. Thus perceived velocity is computed from temporal frequency of signal modulation and not retinal velocity, thereby maintaining velocity constancy over a wide range of viewing distances. In general, motion has

two effects; it impairs discrimination of fine gratings, as is seen from the limiting values of the contrast-sensitivity functions of Fig. 14.14, but it emphasizes the low spatial frequency image components, rendering them visible when they would not be distinguishable when stationary.[6]

Variation of Acuity with Eccentricity of View

The decrease in acuity with eccentric view is a matter of common experience; and attempts have been made to relate this to the change in the retinal mosaic, its so-called 'grain'. Thus in the fovea (zero eccentricity) the cones are finest and most closely packed, whilst interference with image-formation is reduced to a minimum by the absence of bipolar and ganglion cells in the immediate light-pathway. As Weymouth (1958) emphasized, the essential factor in reduction in acuity with eccentricity is the change in size of the receptive fields of the ganglion cells; thus at the fovea with a one-to-one midget cell relationship, the receptive field of the midget ganglion cell could be that of a single cone, subtending theoretically some 20–30 sec of arc. In the periphery the convergence of receptors on to single ganglion cells becomes prominent; and this is revealed by the change in ganglion-cell separation (Fig. 14.15) so that, as we have seen when comparing acuity in primates and cats, the mosaic of ganglion cells in the retina provides a fair estimate of the minimum separable. Weymouth has examined this aspect with great acumen, and shown that the fall in acuity can be predicted from the ratio: Cones per min of retina/thresholds per min, which gives the number of cones in a sensory unit; and this varies from one at the fovea (2 cones/min; 2 thresholds/min), to about 8 at 80° in the periphery, which compares with a ratio of acuities of about 9 (Fig. 14.16).

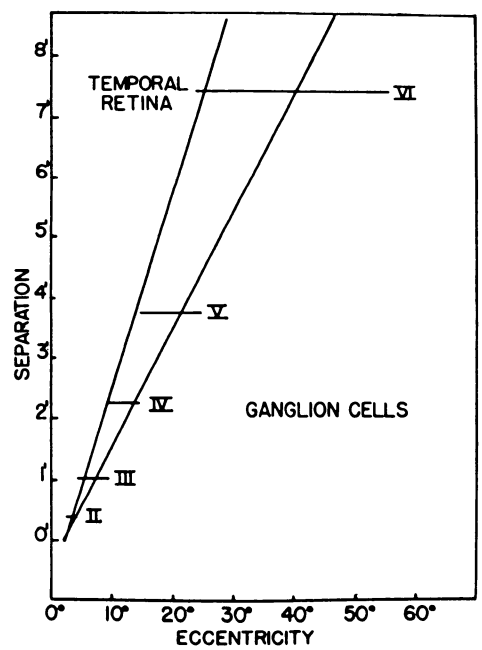

Fig. 14.15 Ganglion cell separation as a function of retinal eccentricity; the two lines represent the two assumptions that the cell counts are characteristic of the inner margins or of the centres of the regions the width of which are represented by the horizontal lines. (Weymouth, *Amer. J. Ophthal.*)

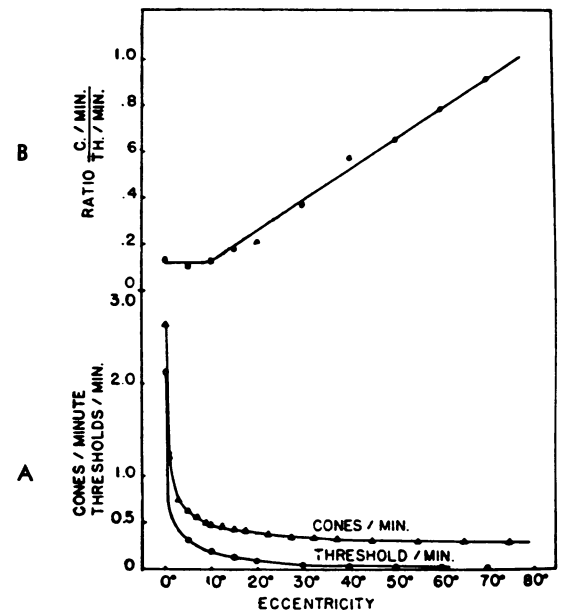

Fig. 14.16 (A) Visual acuity (threshold/minute of arc) and linear cone separation (cones/minute of arc) as functions of retinal eccentricity. Visual acuity data from Fick; cone data from Polyak. (B) Ratio (cones per minute of arc/thresholds per minute of arc) as a function of retinal eccentricity. (Weymouth, *Amer. J. Ophthal.*)

Relation to Cortical Magnification

We shall see in Section 3 that the cortical representation of the fovea occupies a far greater area than that of the peripheral retina, so that a *cortical magnification factor* has been measured, defined as the mm of cortex corresponding to a degree of visual field. Cowey & Rolls (1974) calculated the human magnification factor from the results of a study of Brindley & Lewin (1968) based on induction of a phosphene in blind subjects by a grid of electrodes implanted into the striate cortex. They found that, when the reciprocal of the magnification, $1/M$, was plotted against the minimal resolvable angle at different degrees of eccentricity, they obtained a straight line. Thus a low degree of visual resolution is associated with a

correspondingly small amount of cerebral cortex activated by the minimum separable points. A subsequent study of Rovamo *et al.* (1978) compared contrast-sensitivity functions at different degrees of eccentricity (Fig. 14.17*a*); they then plotted contrast-sensitivity against cycles of grating per mm of cortex, by introducing the cortical magnification, or 'scaling' factor. Not surprisingly, the contrast-sensitivity function was now the same for all eccentricities (Fig. 14.17*b*). This somewhat geometrical exercise indicates the economy of Nature; thus, in peripheral vision, the unit for resolution is a ganglion cell with a large receptive field, i.e. the grain of the retinal mosaic is effectively coarse, and this coarseness increases with degree of eccentricity. Consequently the cerebral cortex requires fewer neurones to handle the messages coming from minimum separable points, and the degree to which this 'scaling' of visual function is successful, i.e. the degree to which a visual function can be expressed in units that give an invariant value with eccentricity, the more economical Nature may be said to be.[7]

Scotopic visual acuity

The essential features of scotopic visual acuity have already been described, and are illustrated by Fig. 14.1; the generally low order is presumably due to the synaptic organization of the rods such that the functional units are large. A study of the completely colour-blind subject with defective cone vision confirms this limitation of the rods; however great the luminance employed the visual acuity could not be improved beyond 0.17, i.e. a value only about one-tenth that found for cone vision in the normal eye. Under mesopic conditions, and with peripheral vision, both rods and cones are active, yet Mandelbaum & Sloan (1947) found that usually the rods dominated the picture, presumably because they were operating far above their thresholds by comparison with the cones.

Pupil-size, Wavelength and Eye Movements

The Effect of Pupil-size

Decreasing the size of the pupil will decrease the effects of aberrations on the optical image, and thus should improve visual acuity; on the other hand, when the pupil becomes sufficiently small, diffraction effects become important. Finally, the smaller the pupil the smaller the amount of light that may enter the eye; under scotopic conditions, at any rate, this must be an important factor. Experimentally it is found that with pupil-sizes below 3 mm the visual acuity is independent of pupil-size because the improvement in the retinal image due to reducing aberrations is compensated by the deleterious effects of diffraction. Increasing the pupil size beyond 3 mm decreases visual acuity at high intensities of illumination, presumably because of the aberrations in the optical image. If a human subject is placed in a room that

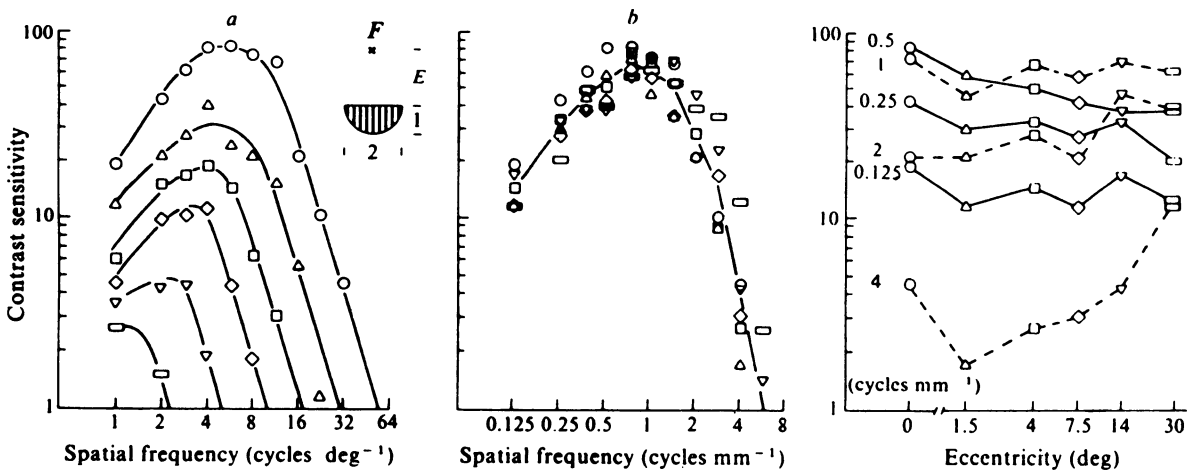

Fig. 14.17 Contrast sensitivity as a function of spatial frequency and eccentricity (*E*) in the lower visual field. *a*, The retinal images of various sinusoidal test gratings were similar at different eccentricities as shown in the inset. Spatial frequency indicates the bar density of gratings in cycles per degree of visual angle and eccentricity refers to the angular distance between the fixation point (*F*) and the nearest edge of the semicircular vertical grating. Curves represent values of *E* as follows: ○, 0°; △, 1.5°; □, 4°; ◇, 7.5°; ▽, 14°; ■, 30°. *b*, Cortical projections of the test gratings were similar at different locations. The symbols are as in *a* regarding eccentricity in the visual field. Spatial frequency indicates the estimated bar density in cycles per mm on the primary visual cortex. *c*, Part of the data of *b* replotted to reveal the expected improvement of sensitivity as a function of *E* at high cortical spatial frequencies. (Rovamo *et al.*, *Nature*.)

is darkened steadily the size of the pupil naturally increases, and it was shown by Campbell & Gregory (1960) that the size attained was, in fact, optimal for visual acuity at this particular luminance. Thus, by using artificial pupils they determined the optimum sizes for given levels of luminance, and they compared these with the actual values that the pupils took up under the same luminances. The results are shown in Fig. 14.18 where the plotted points indicate the optimal pupil-size for different luminance levels, whilst the broken lines indicate the natural pupil-size under the same conditions.

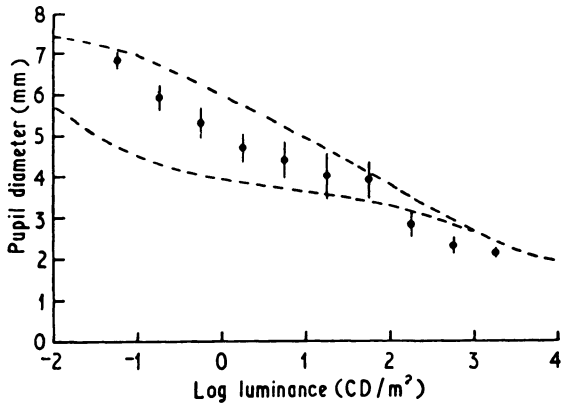

Fig. 14.18 The broken lines indicate the natural pupil-size corresponding with the luminances shown on the abscissa; the points indicate the optimum pupil-sizes appropriate to these luminance levels. (Campbell & Gregory, *Nature*.)

Diffraction

The spread of light from a point source, due to diffraction, is given by $\sin\theta = 1.22\lambda a$, a being the diameter of the entrance-pupil, λ the wavelength of light and θ the angle subtended at the nodal point of the eye by the distance from the centre of the diffraction pattern to the first zero, i.e. the edge of Airy's disc. Westheimer (1964) has discussed the effects of diffraction on the theoretical visual acuity to be expected with varying pupil diameters; his theoretical values are given in Table 14.1, and they represent the limits of a grating that would provide a contrast-ratio between the images of the black and white lines greater than zero. This is obviously a theoretical upper limit, since the ability of the retina to detect this difference must be considered, whilst aberrations in the optical system have been ignored.

Table 14.1 Theoretical Maximal Visual Acuity and Pupil Diameter (Westheimer, 1964)

Entrance-pupil diameter (mm)	*Visual acuity*
0.5	0.5
1.0	1.0
1.5	1.5
2.0	2.0
2.5	2.5
3.0	3.4

Influence of Wavelength

In general, it has been found that the use of coloured lights has little effect on visual acuity, provided that their luminances are adequately adjusted; however, the use of monochromatic, as opposed to white, light should abolish chromatic aberration and thus improve resolution. Cavonius & Schumaker (1966) measured visual acuity using black-and-white gratings and gratings made up of different wavelength-light; they obtained just as good acuity under the two conditions. With short wavelengths, a small difference in wavelength of the bars of a grating was adequate to give high acuity; with long wavelengths, larger differences were necessary. However, in a later study, in which the effects of wavelength were studied systematically, Hilz & Cavonius (1970) found that the dependence on wavelength-difference was strong, so that acuity decreased from 0.8 to zero if one set of bars of a grating were at 660 nm and the other varied from 480 to 660 nm. The best acuity with coloured bars was about 0.6, which could be obtained with a monochromatic contrast of 30–50%.

CONE DENSITY

Mullen (1985) has varied the chromatic composition of her grating stimuli, comparing essentially red-green and blue-yellow gratings. Interestingly, she found that, with low spatial frequencies, sensitivity was greatest when there were colour differences in the stimulus, whereas at higher frequencies, sensitivity was greatest when there was only luminance contrast. At high spatial frequencies, subjects could distinguish gratings, but chromatically they seemed to be homochromatic, whereas at low spatial frequencies, i.e. coarse gratings, colour differences between bars could be detected at threshold. The actual difference in contrast-sensitivity, and thus visual acuity, when a subject viewed blue-yellow or green-red gratings, when compared with a monochromatic grating, e.g. green or yellow, was striking. Thus red-green acuity was only 11–12 cyc/deg compared with a luminance acuity of 34–36 cyc/deg at the same mean luminance. The very low acuity exhibited by the red-green system is surprising in view of the dense distribution of red- and green-sensitive cones in the retina. The low acuity found with the blue-yellow gratings is similar to that shown by the isolated blue-cone mechanism, explained by the sparse distribution of these cones in the retina; however, the fact that it

also occurs with blue-yellow gratings means that some other factor than scarcity of cones is concerned.

Rod–cone Interaction

Under conditions when rods and cones are both active, it is of interest to determine whether signals from both types of receptor contribute to spatial resolution. D'Zmura & Lennie (1986) measured contrast-sensitivity functions when only rods, or rods and cones, were active. When only rods were stimulated, a maximum sensitivity of 50, equivalent to an acuity of 6 cyc/deg was attained at 24 scotopic trolands; then the rod system began to saturate. Over most of the mesopic range, contrast-sensitivity was lower, but the limiting acuity was better, reaching 15 cyc/deg. Within the range of spatial frequencies capable of exciting both rods and cones, a grating that excited only rods was indistinguishable from a grating of the same spatial frequency that excited only cones. The authors concluded that the signals from rods and cones travel together in pathways subserving the detection of low spatial frequencies, i.e. coarse gratings. So far as high spatial frequency gratings were concerned, only the cone system was involved.

The Effect of Eye Movements

The question as to whether involuntary movements of the eyes play a role in determining visual acuity has been agitated repeatedly. As we shall see, the eyes are never absolutely still, so that the contours of the retinal image are repeatedly falling on new sets of receptors; and we may expect the OFF-effects to be just as important as the ON-effects, if not more so, in the interpretation of the retinal image by the brain. Troxler noted that when fixation was maintained by an effort, peripheral images tended to disappear, to reappear immediately on moving the eyes; this is the *Troxler phenomenon*, and suggests that, for peripheral vision at any rate, the eyes must move if the perception of contours is to be maintained.

STABILIZED RETINAL IMAGE

With foveal fixation it requires a special optical device to demonstrate the same effect; Ditchburn & Ginsborg (1952) and Riggs *et al.* (1953), working independently, showed that with a 'stabilized retinal image', such that however the eyes moved the image of a fixated object remained on the same part of the retina, the image would disappear within a few seconds and, if it was of a fine line, would fail to reappear. The actual involuntary movements made by the eye are small, so that it is presumably the renewal of the stimuli at the contour that determines the retention of the visual percept.

The stabilized retinal image has acquired a large literature; the *relative visibility factor* is defined as $t/T \times 100\%$, where t is the time during which the image is visible and T is the total viewing time. If the fading of the image is due to failure to stimulate ON–OFF elements, then a flickering image should increase the visibility factor (Yarbus, 1960) or moving the target in a controlled manner (Ditchburn *et al.*, 1959). West (1968) has studied the effects of target-size, and of position on the retina, on the optimal flicker frequency necessary to give maximal relative visibility factor. Sparrock (1969) has shown that the logarithmic relation between increment threshold and background (Weber's Law) is unaffected by stabilization, so that although the subjective sensation of brightness is reduced the power to discriminate changes has not been affected.

SIGNIFICANCE OF EYE MOVEMENTS

Experimental studies on visual acuity, however, indicate that these movements have little influence on visual acuity. Mandelbaum & Sloan (1947) in the study illustrated by Fig. 14.1 used flash-exposures of their Landolt-C's lasting 0.2 second, so that it is very unlikely that eye movements could have contributed appreciably, yet their recorded visual acuities are not unusually low. Furthermore, if visual acuity were better with long exposures than with short this could be attributed rather to the extra time given the subject to make several tries at resolution rather than to the eye movements; these extra tries would improve resolution on a purely statistical basis. Direct experiments designed to test this point have been carried out by Riggs *et al.* (1953) and Keesey (1960), and both sets of experiments have shown that the involuntary movements are unimportant. Thus Keesey measured visual acuity when the targets were exposed from 0.02 to 1.28 seconds; in one series of experiments the target was viewed normally and in the other as stabilized images; as Fig. 14.19 shows, the curves relating visual acuity to exposure-time are identical.

CONTRAST-SENSITIVITY

We have seen that when visual acuity is measured by the contrast-sensitivity function, there is an optimum spatial frequency at which contrast-sensitivity is maximal, i.e. the threshold contrast is lowest; as spatial frequency is increased, i.e. as the gratings become finer, the contrast-threshold rises, but also as the spatial frequency becomes *smaller*, and below about 10 cycles per degree, contrast-threshold rises. Tulunay-Keesey & Jones (1976) suggested that at these low spatial frequencies movements of the eyes might be important. Figure 14.20 shows the contrast-sensitivity functions of an observer for different exposure-times; as with the more classical study of acuity, reducing exposure-time from 1000 msec to 6 msec caused a rise in threshold, or decrease in sensitivity, but the

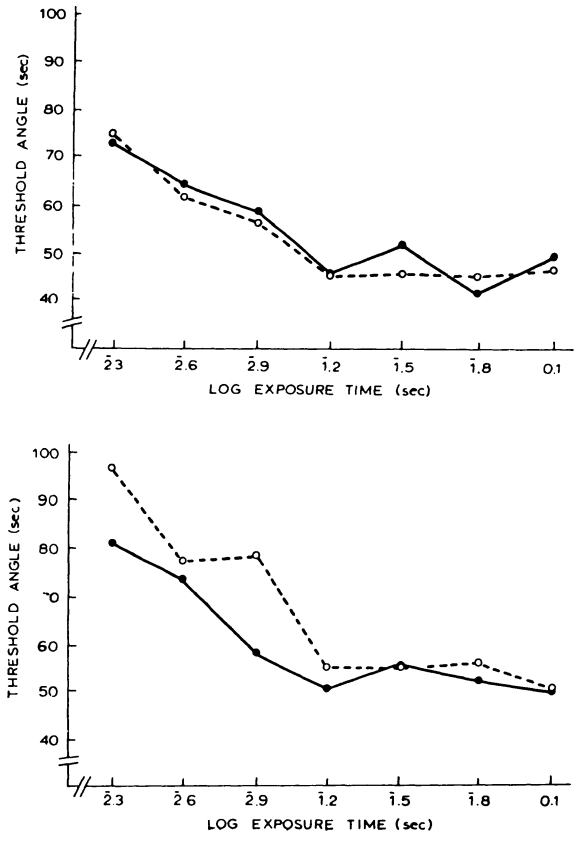

Fig. 14.19 Showing unimportance of involuntary eye movements for visual acuity. Threshold visual angle has been plotted as a function of viewing time, the longer the time the lower the angle subtended by the grating elements at the eye. Dashed lines refer to normal viewing, the full lines to viewing with a stabilized retinal image. Curves for two subjects are shown. (Keesey, *J. Opt. Soc. Am.*)

graphs bring out a significant change in the shape of the sensitivity function, short exposure-times tending to flatten the curves at low spatial frequencies. Thus the sensitivity to coarse gratings tends to remain the same. Once again a stabilized image is without significant influence on contrast-sensitivity.

Bloch's Law

The variation of contrast-sensitivity with exposure-time, such that increasing the exposure increases the probability of detection of a grating, can be viewed as a temporal summation of stimuli comparable with the temporal summation for threshold luminance leading to the relation: $I \times t =$ constant, or Bloch's Law. When log-threshold contrast was plotted against exposure duration as in Fig. 14.21, a critical duration of about 80 to 100 msec was revealed, below which the log-threshold is linearly related to log-duration; a slope of unity for this relationship would indicate perfect temporal summation, and the lines have been drawn with unit slope passing through the time of 70 msec, which we may take as the critical duration. At longer durations there is partial summation and after 1000 msec there is no improvement in sensitivity. The actual slopes to give best fit varied from 0.82 to 0.94 according to the spatial-frequency being studied, and the average for all was 0.88 indicating less than perfect temporal summation. Image stabilization was not completely without effect on contrast-sensitivity; with coarse gratings there was a decrease in sensitivity whereas with gratings of spatial frequencies between 2 and 7.5 c/deg sensitivity increased.[8]

In general, however, the differences were small indicating that movements of the retinal image are of little

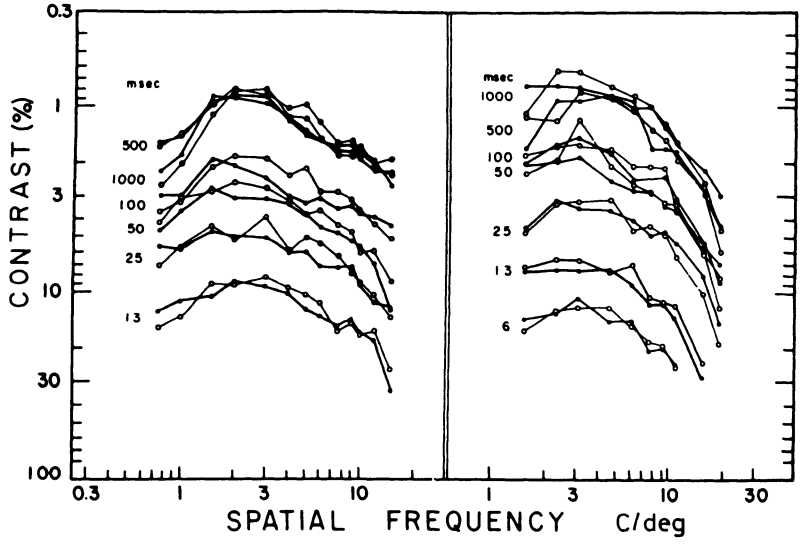

Fig. 14.20 Effects of duration of stimulus on contrast-sensitivity functions for two observers (left and right panels). The closed symbols indicate the unstabilized condition and the open circles the stabilized condition. (Tulanay-Keesey and Jones, *Vision Res.*)

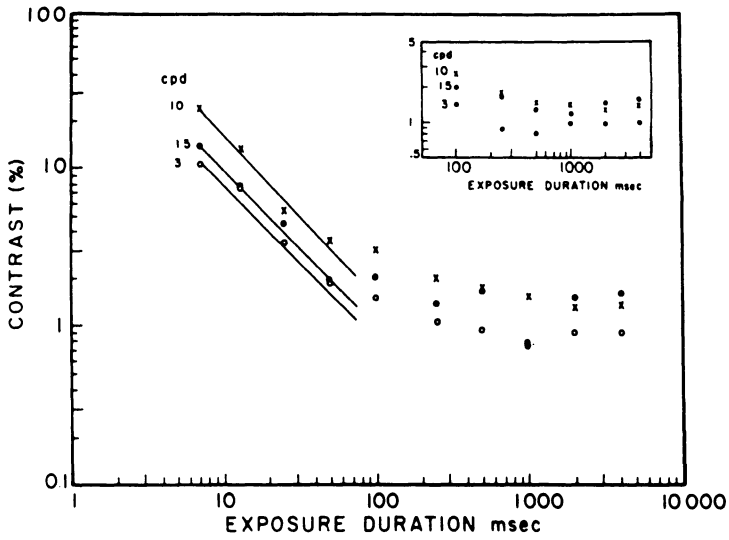

Fig. 14.21 Threshold contrast for recognition of gratings of three spatial frequencies, 1.5, 3 and 10 c/degree. Lines of slope −1 indicating application of Bloch's Law, are drawn through 75 msec. The inset shows the results of an auxiliary experiment in which thresholds were obtained for 1.5, 3 and 10 c/degree and exposures ranging from 100 to 4000 msec. (Tulanay-Keesey & Jones, *Vision Res.*)

value in detecting pattern, although the relief of local adaptation of the retina, preventing disappearance of the image, serves an obvious function.

Binocular Visual Acuity

If the two eyes had identical visual acuity we might, at first thought, expect to find no difference in visual acuity according as monocular or binocular vision were employed. However, in all psychophysical tests one measures, in essence, the probability of a correct answer rather than the certainty that a given grating will be resolved or not. Thus the probability of two eyes giving a correct answer is greater than that of a single eye. Campbell & Green (1965b) treated the matter as a summation of the responses from two eyes, these being fed into a central integrating circuit. If these inputs are 'noisy', the standard error of the sum of n independent measurements of a random noisy process decreases as $\sqrt{n}$; an observer using two eyes would make $2n$ measurements, so that the ratio of visual acuities in binocular and monocular visions should be $\sqrt{2}$. Campbell & Green did, indeed, find experimentally that the ratio was 1.4. The subject has been more thoroughly investigated in later years and the reader may be referred to the reviews of Blake & Fox (1973) and Blake *et al.* (1981). Legge (1984a) measured contrast-detectability of a grating with different contrasts, using a forced-choice procedure, and obtained the curves of Fig. 14.22 for monocular and binocular viewing. From these he calculated a threshold contrast, C', for which detectability, d', was 1, corresponding to 76% correct answers: thus

$$d' = (C/C')^n$$

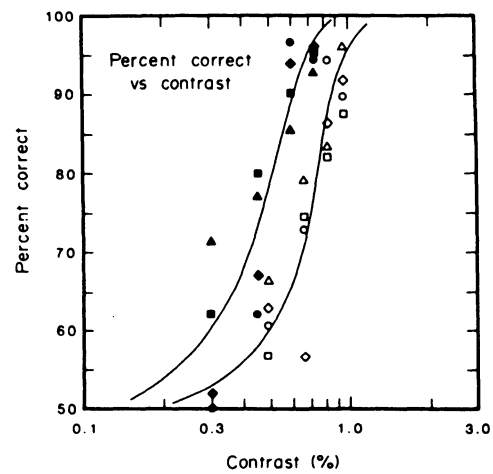

Fig. 14.22 Psychometric functions for 0.5-c/deg grating detection. Monocular and binocular psychometric functions, collected in four sessions from observer D.P., are shown. Each symbol is based on 40–50 forced-choice trials. Corresponding monocular and binocular symbols are based on trials that were interleaved within a single observing session. The per cent correct is plotted as a function of contrast. Open symbols: left eye; solid symbols: binocular. (Legge, *Vision Res.*)

The ratio of the thresholds, C', for monocular over binocular vision was about 1.5, agreeing with Campbell & Green's probability summation estimate. When the subject had to discriminate between two gratings, the threshold ratio was not greatly different.[9]

Visual Acuity in Infants

The determination of visual acuity in infants, as in animals, depends on objective observations of responses

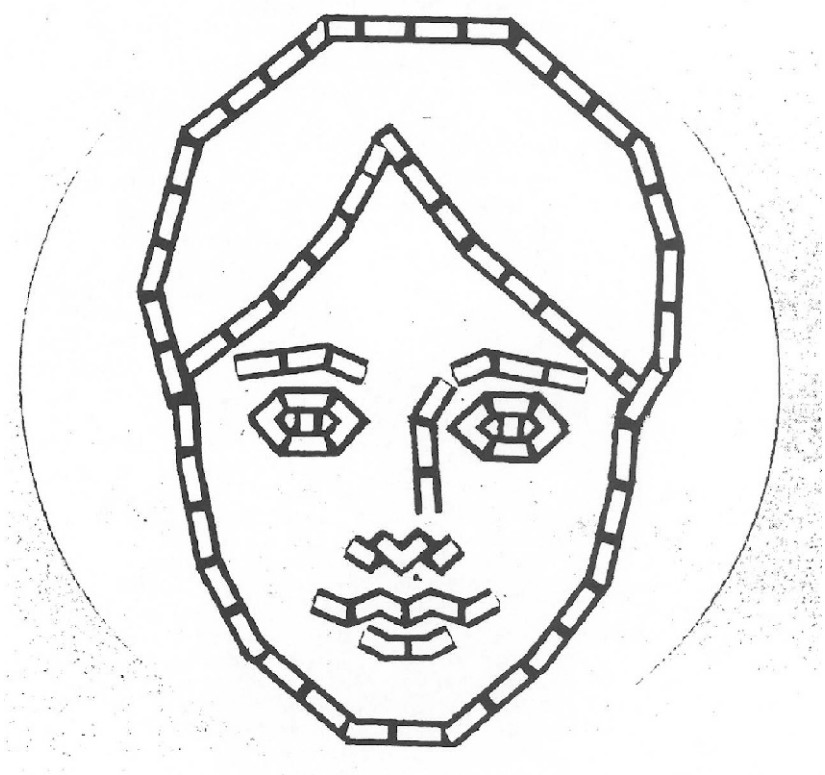

Fig. 14.23 The schematic face pattern. Each face was composed of segments of white lines centred on black lines constructed so that the space-average luminance of the black and white segments equalled the luminance of the grey background. The width of the white lines, which were approximately twice the width of the black lines, was used to denote the stimulus value. Each face figure filled the 9 cm stimulus aperture; the apertures subtended 13° at 31 cm and 9° at 50 cm. (Harris *et al.*, *Invest. Ophthal.*)

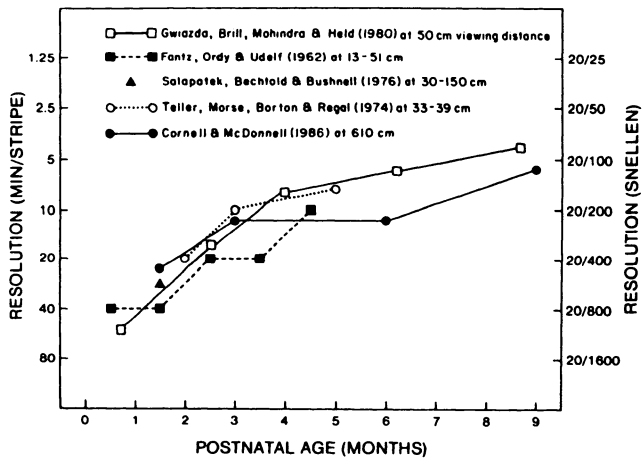

Fig. 14.24 Representative estimates of infants' visual acuity derived from behavioural measures of differential looking. The solid forms represent the minimal stripe width resolved by 75% of the babies in an age group; our estimates are plotted as solid circles. The empty circles represent the stripe width shown to babies when observers were 75% correct in a forced-choice judgement of its location. (Cornell & McDonnell, *Invest. Ophthal.*)

to visual stimuli, for example the optokinetic response to a rotating drum. Modern studies on human infants have employed preferential looking techniques, e.g. presenting the infant with a picture of a face, the resolution of detail being governed by the width of the strips of which it is composed (Fig. 14.23) (e.g. Harris *et al.*, 1984); using this technique Harris *et al.* found a resolution of 16 min at 1 month of age; 8 min at 3 months and 6 min at 5 months. Using the duration of fixation of black-and-white square-wave gratings, compared with the duration for a uniform grey field, Cornell & McDonnell (1986) employing a 20 ft viewing distance, obtained estimates of resolution of infants ranging in age from 6 to 36 weeks postnatal; these have been included in Fig. 14.24 which compares results of other studies, using different distances. Their results indicated that conversion of the minimum resolvable angle to Snellen units (measured at 20 feet) is feasible. The curves show that by nine months, visual acuity is still well below average for adults (20/20 or more).[10]

Notes

1. The resolving power of the eye is measured by the angle subtended at the eye by the minimum separable, i.e. by the line of a grating; the grating-frequency of the system illustrated by Fig. 14.9 is given in cycles per degree subtended at the eye, the angular measure of the cycle being that between peaks of intensity, i.e. twice the angular width of the lines of the grating. Thus with a grating or spatial frequency of 60 cyc/deg, the distance between peaks is 1 minute of arc, and the grating-width is 30 seconds. Thus a resolving power of 60 cyc/deg is equivalent to one of 30 seconds of arc, or a visual acuity of two.
2. Barlow (1979) considers that the improved resolution exhibited in the task of vernier-displacement detection is a function of the lateral geniculate nucleus, where the density of packing of neurones is much greater than that of receptors in the retina. This seems a naive approach, as the geometry of higher-order neurones is of no relevance. As Shapley & Victor point out, the higher brain-centres actually degrade the acuity; thus they estimate that, in the primate eye, vernier-acuity could be about 1 second of arc, instead of the actual 4–6 seconds found in man. They quote the work of Parker & Hawke (1985) showing loss of hyperacuity in cortical neurones.
3. Williams *et al.* (1984) increased two-dot vernier acuity, measured against a dark background, by imposing a background luminance; thus with a 1 minute gap between the points, the threshold against a dark background was some 18 sec, compared with 4.5 sec with the background luminance. We must note that the separation between points was small, well below the optimum of 3–6 min of Westheimer & McKee.
4. Beck & Halloran (1985) found very little effect of retinal eccentricity on vernier-threshold over a range of 8°; however, their dot-separation was large (1°) compared with the optimal, which is of the order of 5 minutes of arc.
5. Studies were usually carried out with gratings designed so that the luminous intensity along the grating varied in a sinusoidal fashion; when a square-wave form was employed, Campbell & Robson (1968) showed that the eye behaved as though it responded to the first higher harmonic, as well as to the fundamental spatial frequency; this is the third, with three times the spatial frequency of the fundamental and one third of the amplitude; it is interesting that Blakemore & Campbell (1969) found that the third harmonic of a square wave did, in fact, produce a substantial elevation of the threshold for a sine-wave grating, in addition to that produced by the fundamental, when the eye was adapted to this square-wave grating.
6. The authors discuss the phenomenon of saccadic suppression; saccades result in movements of the retinal image at over 100 deg/sec, speeds that render fine patterns invisible; gross patterns would, however, become prominent, unless motion-sensitivity were dampened.
7. This geometrical approach to grating-resolution has been developed further by Virsu & Rovamo (1979), and has been applied to a variety of visual functions with greater or less success as summarized by these authors.
8. The Bloch Law applies to the sensation of light and this will be governed by the amount of light-energy entering the eye until further increments fail to summate their effects with the initial input; to compare a discriminatory task with this simple appreciation of brightness is probably misleading; admittedly, the extra light-energy entering the eye with a longer exposure of a grating will be of value, but it is best to view the effect of duration as largely one of increasing the chance of making successive estimates of the visual problem. Baron & Westheimer (1973) showed that, when various gratings were viewed under equal-energy input situations, there was still an improvement of resolution with increased time of exposure.
9. It is well worth consulting this paper, and a succeeding one (Legge, 1984b) for a theoretical treatment of binocular summation.
10. Dobson *et al.* (1985) point out that, employing the operant preferential looking (OPL) technique requires a great deal of time if many different spatial frequencies have to be employed to assess normality of visual acuity in infants. They defined a potential diagnostic grating-frequency for different age-groups of normal children; using a single frequency for a given age-group the examiner could reliably determine whether visual acuity was normal, in the sense that it could be resolved by 90% of children in that group. This spatial frequency was separated by a half to one octave from a frequency that more than 30% of children failed to detect. We may note that Dobson & Teller (1978) have compared results of behavioural and electrophysiological (VER) estimates of acuity in human infants. The VER estimate indicated greater increases of resolution from 0 to 6 months than those based on optokinetic nystagmus and OPL.

References

Alpern, M. & Torii, S. (1968) The luminosity curve of the deutero-anomalous fovea. *J. Gen. Physiol.* **52**, 738–749.

Badcock, D. R. & Westheimer, G. (1985) Spatial location and hyperacuity: the centre-surround localization contribution function has two substrates. *Vision Res.* **25**, 1259–1267.

Barlow, H. B. (1979) Reconstructing the visual image in space and time. *Nature* **279**, 189–191.

Baron, W. S. & Westheimer, G. (1973) Visual acuity as a function of exposure duration. *J. Opt. Soc. Amer.* **63**, 212–219.

Beck, J. & Halloran, T. (1985) Effects of spatial separation and retinal eccentricity on two-dot vernier acuity. *Vision Res.* **25**, 1105–1111.

Belleville, S. & Wilkinson, F. (1986) Vernier acuity in the cat: its relation to hyperacuity. *Vision Res.* **26**, 1263–1271.

Blake, R. & Fox, R. (1973) The psychophysical enquiry into binocular summation. *Percept. Psychophys.* **14**, 161–185.

Blake, R., Sloane, M. & Fox, R. (1981) Further developments in binocular summation. *Percept. Psychophys.* **30**, 266–276.

Blakemore, C. & Campbell, F. W. (1969) On the existence of neurones in the human visual system selectively sensitive to the orientation and size of retinal images. *J. Physiol.* **203**, 237–260.

Blakemore, C., Nachmias, J. & Sutton, P. (1970) The perceived spatial frequency shift—evidence for frequency-selective neurones in the human brain. *J. Physiol.* **210**, 727–750.

Brindley, G. S. & Lewin, W. S. (1968) The sensation produced by electrical stimulation of the visual cortex. *J. Physiol.* **196**, 479–493.

Buck, J. & Schwartz, T. (1979) Vernier acuity with dot test objects. *Vision Res.* **19**, 313–319.

Burr, D. C. & Ross, J. (1982) Contrast sensitivity at high velocities. *Vision Res.* **22**, 479–484.

Campbell, F. W. & Green, D. G. (1965a) Optical and retinal factors affecting visual resolution. *J. Physiol.* **181**, 576–593.

Campbell, F. W. & Green, D. G. (1965b) Monocular versus binocular visual acuity. *Nature* **208**, 191–192.

Campbell, F. W. & Gregory, A. H. (1960) Effect of size of pupil on visual acuity. *Nature* **187**, 1121–1123.

Campbell, F. W. & Kulikowski, J. J. (1966) Orientational selectivity of the human visual system. *J. Physiol.* **187**, 437–445.

Campbell, F. W., Kulikowski, J. J. & Levinson, J. (1966) The effect of orientation on the visual resolution of gratings. *J. Physiol.* **187**, 427–436.

Campbell, F. W., Maffei, L. & Piccolino, M. (1973) The contrast sensitivity of the cat. *J. Physiol.* **229**, 719–731.

Campbell, F. W. & Robson, J. G. (1968) Application of Fourier analysis to the visibility of gratings. *J. Physiol.* **197**, 551–566.

Cavonius, C. R. & Schumacher, A. W. (1966) Human visual acuity measured with colored test objects. *Science* **152**, 1276–1277.

Cleland, B. G., Harding, T. H. & Keesey, U. T. (1983) Response to the length of moving visual stimuli of the brisk classes of ganglion cells in the cat retina. *J. Physiol.* **345**, 27–45.

Cornell, E. H. & McDonnell, P. M. (1986) Infants' acuity at twenty feet. *Invest. Ophthal.* **27**, 1417–1420.

Cowey, A. & Rolls, E. T. (1974) Human cortical magnification factor and its relation to visual acuity. *Exp. Brain Res.* **21**, 447–454.

Ditchburn, R. W., Fender, D. H. & Mayne, S. (1959) Vision with controlled movements of the retinal image. *J. Physiol.* **145**, 98–107.

Ditchburn, R. W. & Ginsborg, B. L. (1952) Vision with a stabilised retinal image. *Nature* **170**, 36–37.

Dobson, V., Salem, D., Mayer, D. L., Moss, C. & Sebris, S. L. (1985) Visual acuity screening of children 6 months to 3 years of age. *Invest. Ophthal.* **26**, 1057–1063.

Dobson, V. & Teller, D. Y. (1978) Visual acuity in human infants: a review and comparison of behavioral and electrophysiological studies. *Vision Res.* **18**, 1469–1483.

D'Zmura, M. & Lennie, P. (1986) Shared pathways for rod and cone vision. *Vision Res.* **26**, 1273–1280.

Fantz, R. L., Ordy, J. M. & Udelf, M. S. (1962) Maturation of pattern vision in infants during the first six months. *J. Comp. Physiol. Psychol.* **55**, 907–917.

Gilinsky, A. S. (1968) Orientation-specific effects of patterns of adapting light on visual acuity. *J. opt. Soc. Am.* **58**, 13–18.

Harris, S. J., Hansen, R. M. & Fulton, A. B. (1984) Assessment of acuity in human infants using face and grating stimuli. *Invest. Ophthal.* **25**, 782–786.

Hartridge, H. (1947) The visual perception of fine detail. *Phil. Trans.* **232**, 519–671.

Hecht, S. (1937) Rods, cones and the chemical basis of vision. *Physiol. Rev.* **17**, 239–290.

Hecht, S. & Mintz, E. U. (1939) The visibility of single lines at various illuminations and the retinal basis of visual resolution. *J. gen. Physiol.* **22**, 593–612.

Hilz, R. & Cavonius, C. R. (1970) Sehscharfe bei Farbenunterschieden ohne Helligkeits Unterschiede. *Vision Res.* **10**, 1393–1398.

Hoekstra, J. H., van der Goot, J., van den Brink, G. & Bilsen, F. A. (1974) The influence of the number of cycles upon the visual contrast threshold for spatial sine wave patterns. *Vision Res.* **14**, 365–368.

Howell, E. R. & Hess, R. F. (1978) The functional area for summation to threshold for sinusoidal gratings. *Vision Res.* **18**, 369–374.

Illing, R.-B. & Wässle, H. (1981) The retinal projection to the thalamus in the cat: a quantitative investigation and a comparison with the retinotectal pathway. *J. Comp. Neurol.* **202**, 265–285.

Keesey, U. T. (1960) Effects of involuntary movements on visual acuity. *J. opt. Soc. Am.* **50**, 769–774.

Kelly, D. H. (1975) How many bars make a grating? *Vision Res.* **15**, 625–626.

Legge, G. E. (1984a) Binocular contrast summation. I. Detection and discrimination. *Vision Res.* **24**, 373–383.

Legge, G. E. (1984b) Binocular contrast summation. II. Quadratic summation. *Vision Res.* **24**, 385–394.

Levi, D. M., Klein, S. A. & Aitsebaomo, A. P. (1985) Vernier acuity, crowding and cortical magnification. *Vision Res.* **25**, 963–977.

Lythgoe, R. J. (1932) The measurement of visual acuity. *Med. Res. Council Sp. Rep. Ser.* No. 173.

Mandelbaum, J. & Sloan, L. L. (1947) Peripheral visual acuity. *Am. J. Ophthal.* **30**, 581–588.

McCann, J. J., Savoy, R. L., Hall, J. A. & Scarpetti, J. J. (1974) Visibility of continuous luminance gradients. *Vision Res.* **14**, 917–927.

Mullen, K. T. (1985) The contrast sensitivity of human colour vision to red–green and blue–yellow chromatic gratings. *J. Physiol.* **359**, 381–400.

Pirenne, M. H. (1957) 'Off' mechanisms and human visual acuity. *J. Physiol.* **137**, 48–49P.

Pirenne, M. H. (1958) Some aspects of the sensitivity of the eye. *Ann. N.Y. Acad. Sci.* **74**, 377–384.

Pirenne, M. H. (1962) Visual acuity. In *The Eye*, vol. II, Chapter 9, Ed. Davson. London: Academic Press.

Pirenne, M. H., Marriott, F. H. C. & O'Doherty, E. F. (1957) Individual differences in night-vision efficiency. *Med. Res. Council Sp. Rep. Ser.* No. 294.

Polyak, S. L. (1941) *The Retina.* Chicago: Chicago University Press.

Polyak, S. L. (1957) *The Vertebrate Visual System.* Chicago: Chicago University Press.

Riggs, L. A., Ratliff, F., Cornsweet, J. C. & Cornsweet, E. F. (1953) The disappearance of steadily fixated visual test objects. *J. opt. Soc. Am.* **43**, 495–501.

Robson, J. G. & Graham, N. (1981) Probability summation and regional variations in contrast sensitivity across the visual field. *Vision Res.* **21**, 409–418.

Rovamo, J., Virsu, V. & Näsanën, R. (1978) Cortical magnification factor predicts the photopic contrast sensitivity of peripheral vision. *Nature* **271**, 54–56.

Salapatek, P., Bechtold, A. G. & Bushnell, E. W. (1976) Infant visual acuity as a function of viewing distance. *Child. Dev.* **47**, 860.

Shapley, R. & Victor, J. (1986) Hyperacuity in cat retinal ganglion cells. *Science* **231**, 999–1002.

Shlaer, S. (1937) The relation between visual acuity and illumination. *J. Gen. Physiol.* **21**, 165–188.

Sparrock, J. M. B. (1969) Stabilized images: increment thresholds and subjective brightness. *J. Opt. Soc. Amer.* **59**, 872–874.

Takahashi, S. & Ejima, Y. (1985) Effects on grating detection of vertically displaced gratings: *Vision Res.* **25**, 129–136.

Taylor, M. M. (1963) Visual discrimination and orientation. *J. opt. Soc. Am.* **53**, 763–765.

Teller, D. Y., Morse, R., Borton, R. & Regal, D. (1974) Visual acuity for vertical and diagonal gratings in human infants. *Vision Res.* **14**, 1433–1439.

Tulunay-Keesey, U. & Jones, R. W. (1976) The effect of micromovements of the eye and exposure duration on contrast sensitivity. *Vision Res.* **16**, 481–488.

Tyler, C. W. (1973) Periodic vernier acuity. *J. Physiol.* **228**, 637–647.

Tyler, C. W. & Mitchell, D. E. (1977) Orientation differences for perception of sinusoidal line stimuli. *Vision Res.* **17**, 83–88.

Virsu, V. & Rovamo, J. (1979) Visual resolution, contrast sensitivity, and the cortical magnification factor. *Exp. Brain Res.* **37**, 475–494.

Wässle, H., Boycott, B. B. & Illing, R.-B. (1981b) Morphology and mosaic of on- and off-beta cells in the cat retina and some functional considerations. *Proc. Roy. Soc. B* **212**, 177–195.

Wässle, H., Peichl, L. & Boycott, B. B. (1981a) Morphology and topography of on- and off-alpha cells of the cat retina. *Proc. Roy. Soc. B* **212**, 157–175.

Wässle, H., Peichl, L. & Boycott, B. B. (1983) A spatial analysis of ON- and OFF-ganglion cells in the cat retina. *Vision Res.* **23**, 1151–1160.

West, D. C. (1968) Flicker and the stabilized retinal image. *Vision Res.* **8**, 719–745.

Westheimer, G. (1964) Pupil size and visual resolution. *Vision Res.* **4**, 39–45.

Westheimer, G. (1982) The spatial grain of the perifoveal visual field. *Vision Res.* **22**, 157–162.

Westheimer, G. & McKee, S. P. (1977a) Integration regions for visual hyperacuity. *Vision Res.* **17**, 89–93.

Westheimer, G. & McKee, S. P. (1977b) Spatial configurations for visual hyperacuity. *Vision Res.* **17**, 941–947.

Weymouth, F. W. (1958) Visual sensory units and the minimal angle of resolution. *Amer. J. Ophthal.* **46** (Suppl), 102–113.

Williams, R. A., Enoch, J. M. & Raphael, S. (1984) Retinal image noise and Vernier acuity. *Vision Res.* **24**, 1735–1738.

Wright, M. J. (1982) Contrast sensitivity and adaptation as a function of grating length. *Vision Res.* **22**, 139–149.

Yarbus, A. L. (1960) Perception of images of variable brightness fixed with respect to the retina of the eye. *Biophysics* **5**, 183–187.

15. WAVELENGTH DISCRIMINATION AND THE THEORY OF COLOUR VISION

The problem of colour vision has attracted the interest and excited the speculation not only of physiologists but of physicists, psychologists, anatomists, philosophers, and poets with the inevitable result that the subject has abounded with theories; in the present treatment we shall confine ourselves to the main experimental findings and show how they are related to the Young–Helmholtz trichromatic theory.

THE PURKINJE PHENOMENON

We may introduce this account by studying the alterations in visual characteristics that take place on passing from scotopic to photopic vision.

Scotopic and Photopic Spectral Sensitivity Curves

Scotopic Sensitivity Curve

As we have seen, the scotopic sensitivity curve is obtained by measuring the absolute threshold of the dark-adapted eye for different wavelengths, and plotting the reciprocals of these thresholds, which measure sensitivity, against the wavelength. In a sense, then, this curve represents the relative luminosities of the different wavelengths so that, if we had a spectrum containing equal energies in all the wavelengths, the blue-green at about 500 nm would appear brightest, and the red and violet darkest. The spectral sensitivity curve is thus sometimes described as the *luminosity curve for an equal-energy spectrum.*

Photopic Sensitivity Curve

The photopic sensitivity curve is the measure of the relative effectiveness of the different wavelengths in exciting the light sense at levels well above threshold; at these levels the lights excite the sensation of colour as well and, since this is mediated by the cones, it would not be surprising if the curve of spectral sensitivities really indicated the relative sensitivities of the cones to different wavelengths. Thus we may take two patches, A and B, of light of different wavelengths and adjust their intensities until they appear equally bright by the method of flicker-photometry (p. 223). We may then compare B with a new patch of light, C, of another wavelength, and so on through the spectrum. The reciprocals of these amounts of energies will be measures of the sensitivity of the eye to the different wavelengths and they give the curve of Fig. 15.1. The maximum occurs at 555 nm in the yellow-green instead of at 500 nm in the blue-green for scotopic vision. On comparing the two sensitivity curves, as in Fig. 15.2, it will be seen that there are characteristic changes in sensitivity of the eye on passing from scotopic to photopic vision, which are given the general name of *Purkinje shift.*

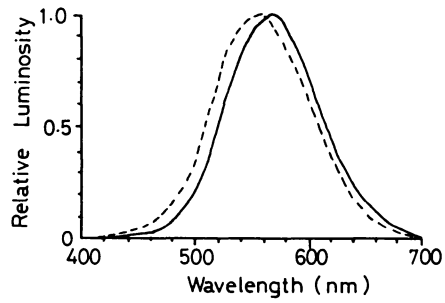

Fig. 15.1 Photopic luminosity curves. The curve in full line is that shown by Jainski whilst that in broken lines is the C.I.E. curve. (Le Grand, *Optique Physiologique.*)

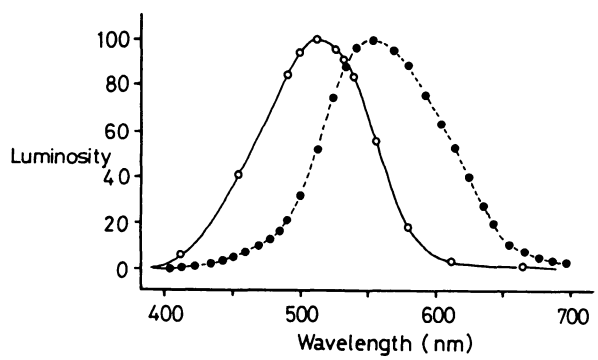

Fig. 15.2 The scotopic luminosity curve (open circles) compared with the photopic curve (full circles). (After Hecht.)

Shift in Sensitivity

Purkinje in 1823 observed that the relative luminosities of hues changed as the luminance was reduced (the *Purkinje shift*), and the nature of the change can be predicted from the curves of Fig. 15.2. Thus let us consider an orange of 650 nm and a yellow-green of 550 nm; under photopic conditions their luminosities are roughly in the ratio of 13:100, the yellow-green being some 8 times brighter than the orange; on referring to the scotopic curve it is seen that the same colours have luminosities in the ratio: 2:56, i.e. the yellow-green is now some 28 times brighter than the orange. In general, the short wavelengths will become brighter in comparison with the long wavelengths as the luminance level is reduced. It should be noted that the Purkinje phenomenon becomes apparent at levels where colour is still perceived, in the mesopic range where both rods and cones are operative; the shift in the apparent luminances of coloured lights is thus due to the superimposition of a rod effect—stimulating only the light sense—on the cone effect. The photopic and scotopic sensitivity curves are thus curves for cones and rods acting essentially alone; at intermediate luminances, where both are operative, the sensitivity curve lies between these limits.

Red Light and Dark-adaptation

We may note from the luminosity curves that red light is much less luminous to the dark-adapted than to the light-adapted eye in comparison with other wavelengths; in fact it is now generally considered that the rods are barely sensitive to the extreme red end of the spectrum, so that the dark-adapted eye may be exposed to fairly high luminance levels of deep red light—bright enough to permit reading with ease and hence to allow the photopic mechanism to function—without serious loss of dark-adaptation. This principle was applied extensively during the war; chartrooms were illuminated with red light and night-fighter pilots wore special red dark-adaptation goggles which permitted them to read in a well-illuminated room and yet maintain a considerable degree of dark-adaptation.

Electrophysiological Aspects

Frog ERG

We may expect the Purkinje effect to be manifest in all mixed retinae, whilst in pure rod (guinea pig) or pure cone (squirrel) retinae it should be absent. The electroretinogram has been a useful tool in the study of this phenomenon; thus we may use the reciprocals of the relative amounts of light-energy to evoke a *b*-wave of fixed magnitude as the index to sensitivity of the retina to different wavelengths; if the light- and dark-adapted eyes are compared in the frog, for example, there is the same characteristic shift in sensitivity to longer wavelengths on passing from dark- to light-adaptation (Fig. 15.3).

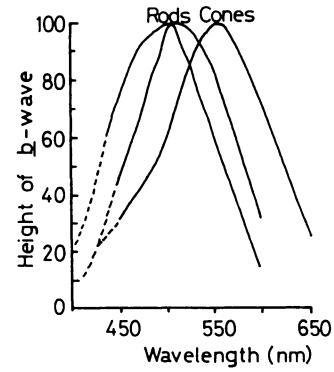

Fig. 15.3 The Purkinje phenomenon in the frog's retina. The curves are luminosity curves and it is seen that the wavelength of maximum luminosity changes from 560 nm to 500 nm on passing from photopic to scotopic conditions. Double contour of rod graph indicates limits of variability. (Granit & Wrede, *J. Physiol.*).

Flicker ERG

Even in the cat, whose retina is very much dominated by rods, a shift in spectral sensitivity can be obtained by employing the flicker method of analysis of the ERG. It will be recalled that the rods are unable to follow a light-stimulus flickering at more than about 25 cycles/sec. With a very strong light, flickering at, say, 50 cycles/sec the responses on the record are thus cone responses, and we may measure the effectiveness of the different wavelengths in producing an electrical effect of fixed magnitude. Under these conditions the maximum sensitivity shifts from 500 nm to 550 nm (Dodt & Walther, 1958). In the pure cone eye of the squirrel there is no Purkinje shift so that only high critical fusion frequencies of flicker are found and the spectral sensitivity shows a maximum in the yellow-green that is barely affected by dark-adaptation (Arden & Tansley, 1955).

Single Fibres

Studies with single fibres of the optic nerve, or of large ganglion cells in the retina, show essentially the same sort of Purkinje shift but, as we shall see, this change belongs to a certain type of element which Granit has called the *dominator*.

Photochromatic Interval

The threshold stimulus for the different wavelengths gives us the scotopic sensitivity curve which, as we have seen, refers only to the light sense since no colour sensation is evoked (except possibly in the deep red). If the threshold stimulus for a given wavelength is increased, at a certain value the sensation of colour is reached (the *specific threshold*). The interval in luminance between the absolute light threshold and the specific threshold is called the *photochromatic interval.* In Fig. 15.4 some results obtained by Dagher *et al.* (1958) on a human subject are shown for the interval between 530 and 630 nm, i.e. over the green-orange-red part of the spectrum. The lower curve represents the absolute thresholds whilst the upper curve represents the specific thresholds. It will be seen that the interval becomes negligibly small at the red end of the spectrum, which means that the threshold for red light corresponds to the threshold for cone vision. At the fovea, too, the photochromatic interval is very small or nonexistent.

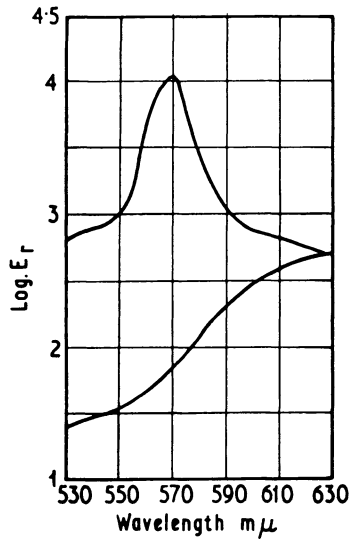

Fig. 15.4 Illustrating the photochromatic interval. The lower curve indicates the thresholds for the sensation of light (absolute thresholds) whilst the upper curve indicates the thresholds for the sensation of colour. Note that the thresholds coincide in the orange-red. (After Dagher *et al.*, *Visual Problems of Colour.*)

Cone Thresholds

Dark-adaptation Curves

As stated above, if the photopic sensitivity curve represents the sensitivities of the cones, then if we can determine the thresholds for cone vision at different wavelengths we may obtain a spectral sensitivity curve which should be similar to that obtained by simple matching techniques. The problem is, of course, to be sure of stimulating only cones when measuring a threshold; in the completely dark-adapted eye this is impossible, except at the extreme red end of the spectrum, because the rods are the more sensitive. Wald (1945) made use of the fact that immediately after light-adaptation the first portion of the dark-adaptation curve (Fig. 7.1) represents cone sensitivity, i.e. under these conditions we may actually measure cone thresholds. By using different wavelengths for the light-stimulus he was able to plot a cone sensitivity curve which had a maximum at 555 nm and was similar in essentials to the C.I.E. curve of Fig. 15.1.

Foveal Thresholds

Again, if vision is confined to the fovea by making use of flash stimuli of small extent, the thresholds should be determined by the cones. Under these conditions the subject usually states that he perceived the colour of the stimulus. By comparing results obtained in this way with those obtained by the dark-adaptation technique, we may compare the sensitivities of foveal and peripheral cones. As Fig. 15.5 shows, the curves are very similar, the foveal cones being less sensitive, except in the red part of the spectrum where they are about the same.

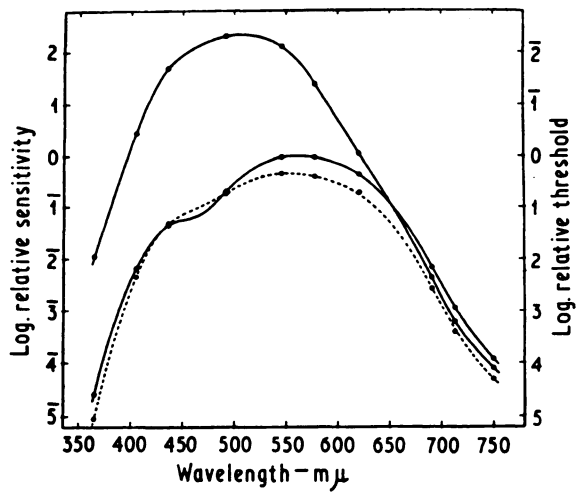

Fig. 15.5 Sensitivity curves for foveal and peripheral cones compared with that for rods. Top curve: rods. Bottom curves: cones. The broken line refers to peripheral cones. (After Wald, *Science.*)

Increment Thresholds

Finally, we may note that measurement of the liminal brightness increment is a measure of the sensitivity of the retina under particular conditions of exposure to light;

and according as to whether the rods or cones are the more sensitive under the particular conditions, the one or other type of receptor will determine this increment, or differential threshold as we have called it. By choosing suitable conditions of light-adaptation it is possible to ensure that the cones will be the more sensitive (e.g. by adapting with blue light to which the rods are so much more sensitive than the cones) and therefore it is possible to measure their thresholds with different wavelengths of light and obtain spectral sensitivity curves. This technique was developed by Stiles & Crawford and has been exploited widely in the measurement of spectral sensitivity curves. As we shall see, the measurements may be so refined that we may determine not only the thresholds of the cones in general, but thresholds of different types of cone (p. 401).

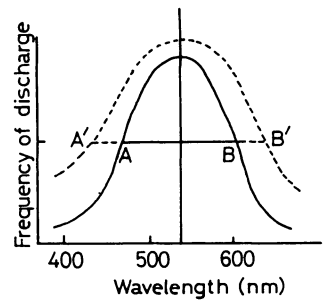

Fig. 15.6 Theoretical wavelength-response curve for a single receptor of *Limulus* retina. The maximum response will occur at 520 nm, the absorption maximum of the retinal pigment. With wavelengths of light corresponding to the points A and B, the responses will be identical, so that no discrimination between these two wavelengths is possible.

WAVELENGTH DISCRIMINATION

As emphasized earlier, the difference between the scotopic and photopic sensitivity curves is not just the shift in maximal sensitivity to a different wavelength described as the Purkinje effect; there is the difference that vision becomes chromatic under photopic conditions, and the subject is able to state not only that light is present but that it belongs to a certain part of the spectrum. Before studying the mechanism of this wavelength discrimination, we may ask why it is that the retina is achromatic under scotopic conditions. The answer is that under scotopic conditions only one type of receptor is operating, the rods, and that these rods are physiologically identical in that they all have the pigment rhodopsin as their photopigment. Such a functionally homogeneous retina cannot act as wavelength discriminator.

Homogeneous Retina

To make this clear we may consider the responses in the optic nerve fibres of *Limulus* which, we may recall, are derived directly from the photoreceptors. A study of their responses to different wavelengths gives a typical sensitivity curve, with maximal sensitivity at 520 nm corresponding to the wavelength of maximum absorption of its photopigment. If we were to plot the intensity of response in a single fibre against wavelength we would obtain a curve roughly like Fig. 15.6. In a sense, then, this receptor, and thus the eye, is showing some wavelength discrimination, in that it is responding with different frequencies of spike discharge to different wavelengths. A little consideration will show, however, that this receptor could not discriminate between changes of wavelength and changes of intensity; and even if we could keep intensity constant its discrimination is limited. Thus, at the points A and B on the curve, the responses are the same but the wavelengths are widely different; by drawing other lines parallel to the abscissa, cutting the curve in two points, many other pairs of spectral hues could be obtained producing identical responses. Moreover, this curve was obtained by keeping the energy content of the stimulus the same; new curves would be obtained by varying the energy content, as indicated by dotted lines, so that in fact with a single wavelength we would be able to mimic the responses of all other wavelengths of the spectrum simply by varying the intensity of this single wavelength. Hence a retina containing a single type of receptor is unable to discriminate changes in both wavelength and intensity.

Multiple Receptor Hypothesis

The position becomes different if we have several types of receptor, with different photosensitive pigments; these would have different response curves and it is not difficult to show that the effects of varying wavelength on the pattern of discharges in the several types might be unique and not matchable by a change in intensity. Thus, for example, with six receptors a green light of wavelength 530 nm might evoke spike responses in these having say, 15, 34, 65, 20, 4, 2 spikes/sec. A yellow light of 600 nm might give a different set of responses, say 35, 65, 45, 20, 15, 7 spikes/sec; and it would be these *patterns* of discharges that would be characteristic of the respective wavelengths for this particular energy level of the stimuli. Increasing the energy would increase the frequencies of discharge, but it could well be that they would be able to maintain a unique pattern that could not be mimicked by other lights however much we varied the intensity. Clearly, the more types of receptor we have, the more certain we will be of having a unique type of response for a given combination of wavelength and intensity. As we shall see, Nature has economized in this respect, since it

appears that only three types of receptor suffice for human wavelength discrimination.

THE YOUNG–HELMHOLTZ THEORY

Trivariance of Colour Vision

We have already seen that colour-matching experiments have led to the generalization that we may match any colour by a mixture of three primary spectral wavelengths provided we admit that the match is not perfect so far as saturation is concerned. Thus if we wish to match a given colour X, we may place it in one half of a photometric matching field and in the other half we may project a mixture of red, green and blue lights; by varying the relative intensities of these we may match our colour from the point of view of chromaticity, but the mixture that we have made will be unsaturated, so we must add some white to X to make the match perfect in respect to both chromaticity and saturation. Thus our mixing equation would take the form:

$$\alpha R + \beta G + \gamma B = X + x\,White$$

or,

$$\alpha R + \beta G + \gamma B - x\,White = X$$

But, since white may be represented by a mixture of red, green and blue, say: $\alpha' R + \beta' G + \gamma' B$, we may subtract these from the left-hand side of the equation, and we are left with an equation that defines our colour, X, in terms of only three variables:

$$(\alpha - \alpha')R + (\beta - \beta')G + (\gamma - \gamma')B = X$$

It is in this sense, then, that we are able to say that colour vision is a *trivariant phenomenon*; we can, in essence, describe any colour-stimulus in terms of three variables; normal human colour vision is thus *trichromatic.*

Spectral Mixture Curves

The trichromaticity of colour vision tells us that *any* colour can be matched in terms of three primary stimuli. If we confine ourselves to matching the spectral colours we may represent this process by the chromaticity chart of Fig. 7.6; alternatively we may plot the individual contributions of our red, green and blue primaries to the different spectral colours as in Fig. 15.7. As abscissae we have the wavelengths of the spectral hues we wish to match, and as ordinates are plotted the amounts of each individual primary required for each match. These *spectral mixture curves* show us at a glance how much of a given primary is required to match a spectral hue; thus a yellow of 600 nm requires some 0.25 units of green and some 0.4 units of red with no blue. A blue-green of 500 nm requires about 0.4 units of green, 0.01 unit of blue[1] and some 'negative red'.

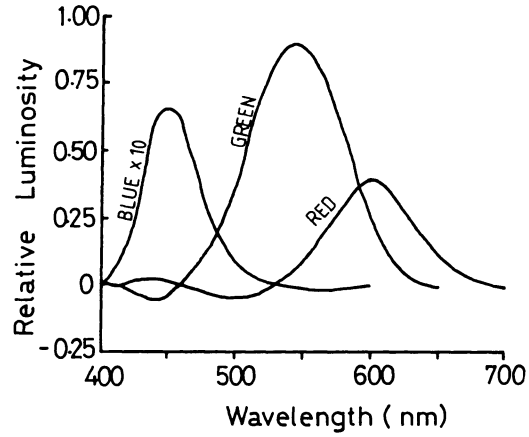

Fig. 15.7 Spectral mixtures curves indicating the relative amounts of the three primaries that are required for matching any spectral wavelength. For example, with a blue of 500 nm the relative contributions are about 0.33 Green, 0.1 (÷10) Blue, and 0.05 Red. (Wright, *Researches on Normal and Defective Colour Vision.*)

Three-receptor Hypothesis

These curves lead naturally to the hypothesis that any colour sensation may be evoked by stimulating three fundamental receptors to varying extents. Thus we see that a yellow sensation may be created either by passing yellow light of, say, wavelength 600 nm into the eye, or we may create exactly the same sensation by passing into the eye a mixture of quite different lights, lights that by themselves would have excited the sensations of green and red respectively. Thus the colour mixing phenomena are essentially phenomena of confusion or failure to distinguish; the light of wavelength 600 nm is physically different from the lights of 530 nm and 650 nm that are used for the match, but the eye cannot distinguish between the light of 600 nm and the mixture. The phenomena illustrate too the economy of Nature; if an eye is to discriminate single wavelengths from mixtures then a large number of receptors must be necessary, but it is very questionable whether this discriminatory power would have much biological survival value, and instead the trivariance of colour sensation suggests that Nature 'makes do' with a very limited number of receptors.

The Fundamental Mechanisms

The three-receptor hypothesis is the essential basis of the Young–Helmholtz trichromatic theory of colour vision;

in essence it has come to mean today that the retina contains three types of cone that respond differently to the same wavelengths; thus a 'blue' cone would respond most prominently to the short end of the spectrum, and only a little to lights of the middle region and perhaps not at all to very long wavelengths; a 'green cone' would respond preferentially to the middle regions, and so on. Each mechanism, or cone-type, may therefore be regarded as having its own spectral sensitivity curve, and we may look on the spectral mixture curves of Fig. 15.7 as being related to the spectral sensitivity curves of the separate mechanisms. Thus, to refer to the figure, we might say that the yellow light of wavelength 600 nm had excited the green mechanism by 0.25 units and the red mechanism by 0.4 units and had failed to excite the blue mechanism at all. Thus the match occurred because the yellow light did exactly what the green and a red lights would have done if they had fallen simultaneously on the retina. On this basis, then, we could plot three sensitivity curves for the three mechanisms, using as ordinates the frequency of discharge, say, in the nerve fibres leading from these fundamental mechanisms as in Fig. 15.8.

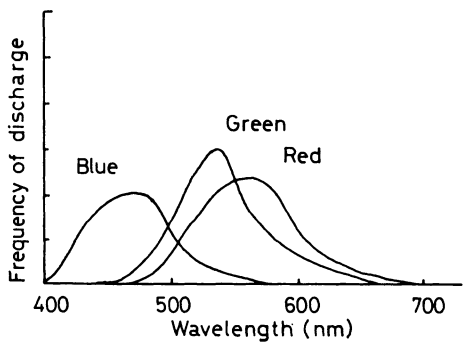

Fig. 15.8 Theoretical wavelength-response curves for three hypothetical receptors maximally sensitive to red, green and blue respectively.

Spectral Sensitivities

The next problem, of course, is to decide on the true spectral characteristics of these mechanisms; the colour-mixing phenomena tell us we can use any three primaries, so we can have an infinite number of sets of spectral mixture curves. Which, if any of these, is the correct set? Various methods were used to derive the true fundamental response curves, as they were called.

ADAPTATION

For example, Wright (1946) used as his criterion the effects of adaptation. He has shown that if the eye is adapted to white light the sensitivity to all wavelengths is depressed in proportion; however, if the adapting light is coloured, there is a certain preferential depression of sensitivity to this colour, so that a subject who has been adapted to red, for instance, requires more red to make a match with white than he did before the adaptation. If the adapting light is yellow, both the red and green sensations are depressed, and so on. Thus if there are, indeed, three fundamental sensations, it should be possible to adapt the eye to at least one or two hues such that sensitivity to these alone is depressed, since these alone should be stimulated. Wright found that a blue of 460 nm and a red of 760 nm behaved in this way, and he suggested that these were two of the primary sensations; violet he concluded was definitely not a fundamental sensation since it was considerably modified by adaptation of the eye to red light. The wavelength corresponding to the third sensation, which from its position cannot be stimulated alone, was deduced to have the value of 530 nm, i.e. in the green. On the basis of this reasoning Wright drew a set of spectral sensitivity curves.

COLOUR-BLIND

Other workers studied the so-called colour-blind, and on the assumption that their colour defect was the consequence of one of the mechanisms' being absent (p. 403), they were able to deduce, from the colour-blind person's matching phenomena, the characteristics of the spectral sensitivity curve of the missing mechanism, and thence that of the remainder.

Two-colour Threshold Technique

Liminal Brightness Increment

Stiles (1959) developed an extremely ingenious technique for the identification of separate cone mechanisms in the human eye. The method is based on the measurement of increment thresholds, or liminal brightness increments (l.b.i.). It will be recalled that the l.b.i. for white light is measured by the extra luminance of a test patch, ΔI, necessary for it to be distinguished against its white background of luminance I. By successively increasing the background luminance, I, we get a series of steps, ΔI, and by plotting $\log \Delta I$ against $\log I$ we find that the graph has a characteristic shape. Thus, over the range of scotopic vision it may be represented by Fig. 15.9; at very low luminance, the increment threshold, ΔI, is approximately constant and equal to the absolute threshold; at a certain point the graph becomes a straight line of slope unity,[2] and finally there is a point where the rod mechanism is said to be saturated.

Rod and Cone Mechanisms

This type of graph is only obtained, however, if a single mechanism is operating over the whole range of luminance, i.e. if the rods only are active; and the type of curve

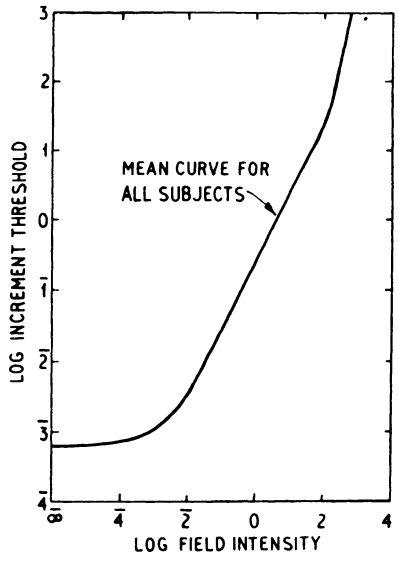

Fig. 15.9 Showing the variation of the liminal brightness increment (l.b.i. or increment threshold) with field intensity. For details see text. (After Aguilar and Stiles, *Optica Acta.*)

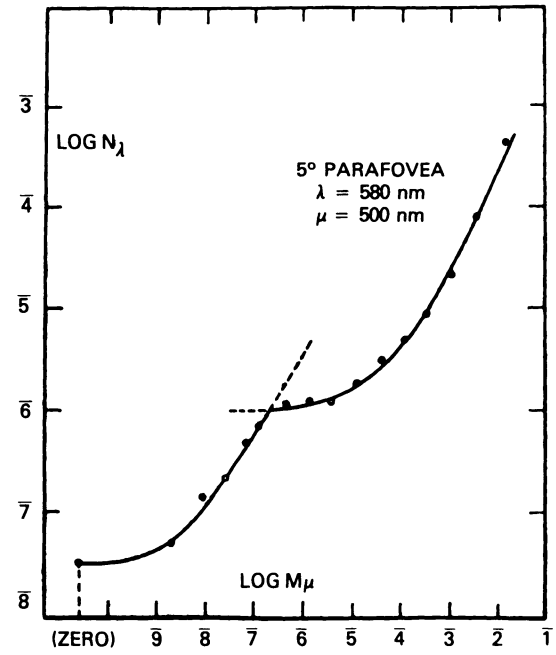

Fig. 15.10 The curve obtained by plotting the logarithm of the liminal brightness increment (Nλ) against logarithm of the background intensity (Mμ). In this case the background was blue-green and the central patch a yellow of 580 nm. The left part of the curve represents increment thresholds for rod vision; at the break and beyond, the increment thresholds are determined by the cones. Nλ and Mμ are expressed as erg sec^{-1} (degree of arc)$^{-2}$. (Stiles, *Proc. Nat. Acad. Sci. Wash*).

shown in Fig. 15.9 could only be obtained by using special techniques to keep the cones from coming into play. In general, then, when the luminance comes up to a certain point the cones become the more sensitive and they now determine the l.b.i., and the graph of $\log \Delta I$ against I shows a characteristic break, or kink, indicating the taking over of the new 'mechanism', in this case the taking over of the threshold by cones in place of rods. This is illustrated by Fig. 15.10. In this way we have identified, then, the operation of a new mechanism. By varying the wavelength of the background, and of the test-stimulus, we may create conditions that favour one or the other mechanism and so study it over a large range of luminance; e.g. by using a red background and measuring the liminal brightness increment with a blue test-stimulus we may suppress cone activity and study rod activity. In this way, then, we may not only identify the presence of rod and cone mechanisms but we may also measure their spectral sensitivities, using the l.b.i. as a measure of threshold for any given wavelength, care being taken that the background and test-stimulus are such that only one of the two mechanisms is operative.

Cone Mechanisms

The same technique can be applied to identify different cone mechanisms, and Stiles found, indeed, that under appropriate conditions of background and test-stimulus the presence of three mechanisms could be established with maximum sensitivities in the red, green and blue. Subsequent studies indicated that the blue mechanism is complex, and can be described as being made up of three, π_1, π_2, and π_3, whilst the green and red mechanisms are called π_4 and π_5 respectively.[3]

COMPOSITE NATURE OF THE MECHANISMS

Since the trivariance of colour vision is so well established, and since, as we shall see, direct experiments on retinal cones indicate unequivocally the presence of only three cone types, the Stiles mechanisms cannot be equated with the fundamental receptors, but rather with a feature of the integrating system. Pugh (1976) has examined the blue-sensitive mechanisms in detail and has shown that, over the short wavelength range of its action-spectrum, it behaves as one would expect of a single blue-sensitive type of cone; over longer wavelengths Grassman's law of additivity fails, indicating the mixing of activity of another type of cone with its region of maximal sensitivity at longer wavelengths. Pugh suggests that the composite π_1 mechanism is generated in the short wavelength-sensitive (blue) cones, but its signal must pass through two gain-stages, the gain in the first stage being controlled by the blue-cones alone and the gain in the second stage being controlled by a signal originating in

the middle (green) or long wavelength (red) cones, or both.

COLOUR-DEFECTS

Since the study of the colour-defective human subject (usually described somewhat inaccurately as the colour-blind) has thrown some light on the more general aspects of colour discrimination, it is right that we devote some space to the main experimental findings at this juncture. In general, a colour-defective subject is one whose powers of discrimination between lights of different wavelengths are more limited than normal; the extent of this defect may range from complete failure of wavelength discrimination—*monochromatism*—through *dichromatism*, where the discrimination is so limited that we must postulate the absence of one of the three fundamental mechanisms, to the *colour-anomalous*, where the defect is a difference from average behaviour, in the sense that the protanomalous uses more red than the average in matching a yellow with a mixture of red and green.

Rod Monochromatism

The more frequently occurring type of completely colour-blind is one whose cones are apparently pathologically defective; the subject is therefore called a *rod monochromat*, and we have already seen that his visual functions are largely what one might expect on the basis of the duplicity theory; thus he shows no Purkinje phenomenon, having a spectral sensitivity curve corresponding only to the scotopic type. Such monochromats occur with a frequency of about one in thirty thousand.

Visual Characteristics

There is by no means complete agreement as to the essential feature, if there is one, of the so-called rod monochromat; being more common than the cone monochromat, the rod monochromat is called 'typical', but various studies indicate that all the features of this condition cannot be forced into a single type. Walls & Heath have emphasized the complexities in some of the visual characteristics of the 'typical' achromat; thus we have already seen that the plot of critical fusion frequency against luminance shows a break, as in normals, suggesting the operation of two types of receptor, and sometimes the dark-adaptation curve also shows a 'kink'. These findings led v. Koenig and later Hecht (1947) to postulate the presence of 'photopic rods' in the retina of the monochromat. In general, we may regard 'typical' achromatopsia as a retinal dystrophy with the following signs, not all of which need be present in any subject: (*a*) achromatic vision; (*b*) low visual acuity, of the order of 0.1 to 0.3, better at moderate luminance than at high; (*c*) no Purkinje shift; (*d*) avoidance of very bright lights; (*e*) nystagmus; (*f*) some signs of macular dystrophy. The post-mortem study of Larsen (1921) showed that cones were indeed present in the retina, with most of them apparently normal.[4]

THREE TYPES

Walls & Heath (1954) suggested that some cases could be accounted for on the assumption of the absence of functional cones together with the presence of rods in the fovea, whilst others could be described as containing, in addition to rods, the 'blue-type' cones postulated by trichromatic theory, the 'red' and 'green' cones being non-functional or absent. More recently Blackwell & Blackwell (1961) have reported on a study of nine subjects whose psychophysical findings allowed them to be placed in three categories: (*a*) typical rod monochromats with all visual functions determined by rods; (*b*) a group with a scotopic luminosity curve very similar to normal except in the blue where sensitivity was low, possibly due to the presence of the yellow xanthophyll macular pigment (they were using central fixation); this suggested that these achromats possessed rods in the fovea. At photopic luminances the sensitivity curve shifted towards the short-wave end of the spectrum, to give a maximum at about 440 nm, suggesting the coming into play of 'blue cones'. The third group were intermediate between (*a*) and (*b*).

Cone Monochromatism

The cone, or atypical, monochromat is extremely rare, occurring with a frequency of only one in a hundred million; in this condition visual acuity is perfectly normal, but there is no discrimination of coloured lights if their luminosities are made equal. It might be thought that the retina, in this condition, contained only one type of cone, but if this were so we should expect the photopic spectral sensitivity curve to be abnormal. Thus, under photopic conditions the sensitivity of the eye to the different wavelengths must be the average sensitivity of the three or more cone mechanisms in the retina; removal of two of the mechanisms would leave the retina with only one type, and now the spectral sensitivity curve should coincide with the sensitivity curve of a single mechanism. In fact, Weale (1953) found the photopic sensitivity curve of the cone monochromat to lie within the normal range. When Weale (1959) applied his foveal bleaching techniques to a cone monochromat (p. 265), he found that the difference-spectrum for light reflected from the fundus indicated the presence of at least two cone mechanisms, and Gibson (1962), using Stiles' incremental threshold

technique, found that three mechanisms were operative. Finally Fincham (1953) showed that a cone monochromat was able to make use of coloured aberration fringes in the accommodation reflex (p. 778), so that all the evidence indicates that the defect is not in foveal pigments but in the central integrating mechanism.

Dichromatism

Colour-matching

The dichromat is one who can match all colours with suitable mixtures of only two, instead of three, primaries. The colour mixing equation will therefore be of the form:

$$C = \alpha A + \beta B$$

where A and B are the primaries; instead of a pair of rectangular co-ordinates being required to represent their colour mixing data (p. 224), these may be exhibited in the form of a straight line where any point on this line corresponds to a definite mixture of the two primaries. It will be clear, without any mathematical analysis, that the range of colours that a dichromat can appreciate as distinct will be very restricted compared with the range of the normal individual, since it is obviously possible to obtain more variations by mixing three things than two.

Missing Mechanisms

According to the classical interpretation, the *protanope* is missing the fundamental red sensation—he is red-blind; the *deuteranope* lacks the green sensation and the *tritanope* the blue. If this viewpoint is correct, we may anticipate the appearance of the spectrum to the protanope, for example, from a consideration of the curves in Fig. 15.7 and imagining that the curve corresponding to the red sensation has been removed. In the region between 760 and about 650 nm no colour sensation should be experienced, i.e. the protanope's spectrum should be shortened; between 650 and about 500 nm the sensation should be that of green only (although it may be called yellow); with the introduction of the blue sensation at about 500 nm, changes in hue should be appreciated and colour discrimination should be approximately normal.

Hue-discrimination Curves

Thus the curve, obtained by plotting the difference in wavelength necessary for a dichromat to appreciate a change in hue, as ordinates, against the wavelength, as abscissae (the hue discrimination curve), should be much simpler than that of a trichromat; in Fig. 15.11 are shown typical curves for the protanope and deuteranope (that of the normal trichromat is shown in Fig. 7.4); it is seen that the maximum discrimination occurs in the region 480 to 500 nm where the blue mechanism is operative. Discrimination falls away rapidly on both sides of this point as we should expect.

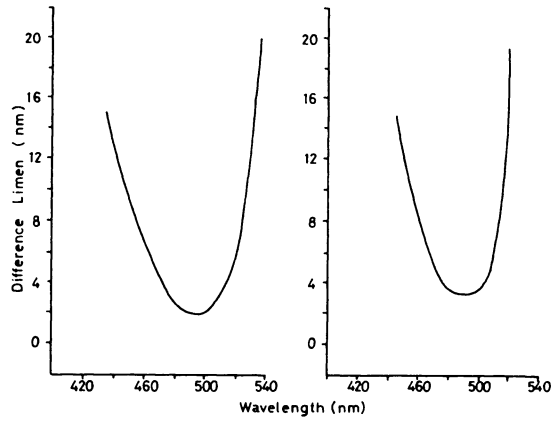

Fig. 15.11 Hue-discrimination curves for deuteranope (left) and protanope (right). The smallest change in wavelength, necessary to produce a change in the sensation of hue, has been plotted against the wavelength. Greatest sensitivity is in the blue-green region. (Wright and Pitt.)

Neutral Point

The dichromat can match all hues (spectral and non-spectral and including white) by appropriate mixtures of two primaries; since white can be formed by a certain mixture of these primaries it follows that there will be a certain point in the spectrum which will appear to the dichromat as white—this point is called the *neutral point* and occurs at 495 nm with the protanope and at 500 nm with the deuteranope.

Iso-colour Chart

We have seen that for the normal trichromat the locus of spectral colours is given by a curved line in the colour chart, where each point represents by its co-ordinates the coefficients in the unit colour equation; by joining the two ends of this curve, to make a closed figure, we get the locus of certain non-spectral hues obtained by mixing blue and red, the purples (Fig. 7.6). All points within this closed figure represent non-spectral hues appreciated by the trichromat. The locus of spectral colours for the dichromat is a straight line only, and since this cannot enclose space, all colours appreciated by the dichromat are spectral hues. This means that for all those numerous hues lying within the normal trichromatic locus, which are appreciated by the trichromat as different, there will

correspond only a few spectral colours in the dichromat's colour range; in other words, to the dichromat, for any given spectral hue there will be a large number of non-spectral hues that are indistinguishable from it.

A determination of the colour-mixing data for dichromats permits the construction of iso-colour charts; in Fig. 15.12 that for a protanope is given. The normal trichromatic spectral locus is drawn in the usual manner, and trichromatic white is indicated by a star. The neutral point of the protanope, i.e. the point on his spectral locus where the mixture of his two primaries gives white, lies at 495 nm; and an iso-colour line can be drawn through this point A, and the star representing trichromatic white, since the latter is appreciated as white by the protanope too. The line cuts the red axis at C, which corresponds to a very reddish purple. All colours represented by this line, ranging from blue to reddish purple, appear to the protanope as identical and white. From the data on the spectral hue discrimination of the protanope (Fig. 15.11), it is possible to mark off points on the spectral locus corresponding to just discriminable differences in hue, and the directions of the iso-colour lines passing through these points may be calculated from colour-mixing data (it will be remembered that between 530 and 760 nm all spectral colours appear the same to the dichromat). The iso-colour lines are drawn in the figure, and they divide the trichromatic colour area into a series of zones; all trichromatic hues represented by points in any one zone are indistinguishable by the dichromat, provided the luminosity is kept constant. For the protanope there are seventeen zones, whilst the deuteranope has some twenty-seven. The iso-colour charts permit one to determine whether any pair of hues can be discriminated by a dichromat, and provide a rational interpretation of the numerous and hitherto uncorrelated facts of dichromatic matching and errors in discrimination.

Luminosity Curves

If dichromatism does, indeed, represent the loss of one of the cone mechanisms we may expect the photopic luminosity curve to be different from normal in dichromatism. The regions of maximum luminosity are, in fact, shifted; that for the protanope lying at about 540 nm and for the

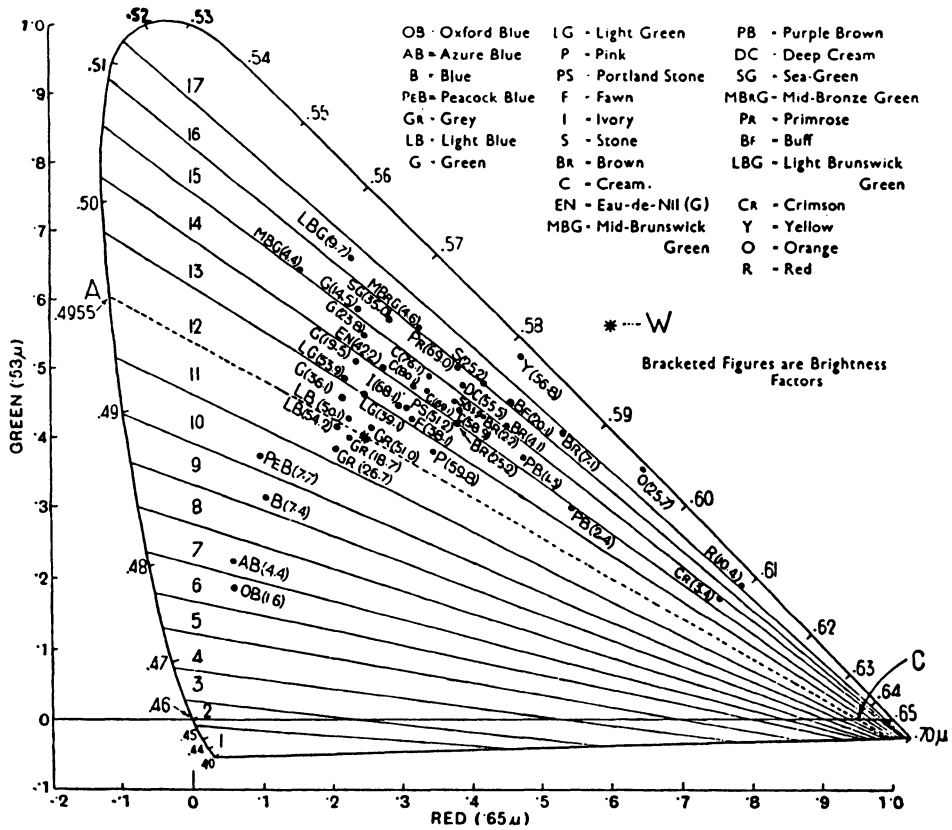

Fig. 15.12 Iso-colour chart for protanope. (Pitt, *Med. Res. Council Sp. Rep.* By permission of the Controller of H.M. Stationery Office.)

deuteranope at about 570 nm. Furthermore we should expect the loss of the red mechanism to cause a shortening of the visible spectrum, and in the protanope this is indeed found, the reds at the end of the spectrum appearing grey. Again the loss of one of the 'colour mechanisms' presumably corresponds to the dysfunction of one group of cones; in this case we may expect a loss of absolute luminosity, i.e. the thresholds for vision in the dichromat should be generally higher than for the trichromat. With the protanope this is very well established in the red end of the spectrum and, according to Hecht, both protanopes and deuteranopes have a general loss of sensitivity over most of the spectrum, the average rise in threshold of the protanope being 49% and that of the deuteranope 39%. Subsequent studies on a uniocular deuteranope, i.e. on a subject with one eye normal and the other deuteranopic, showed that this difference in threshold was quite definite (Graham & Hsia, 1958).

Deuteranope

Pitt's (1935) analysis of deuteranopia suggested, however, that this could not be simply accounted for by the loss of the green mechanism; rather the deuteranope behaved as though he had, in place of the red and green mechanisms, a single one corresponding to a weighted mean of the normal red and green mechanisms; the deuteranope, on this basis, is indeed a dichromat, in the sense that his colour-mixing data can be expressed as a function of only two variables, but he behaves as though his red and green mechanisms are in some way linked so that they cannot act independently. More recent work, however, has shown that the deuteranope does, indeed, lack the green mechanism (p. 406).

Tritanope

The tritanope is rare, constituting, according to Wright (1952), only one in 13 to 65000 of the population by comparison with one in a hundred males for protanopia and deuteranopia. The tritanope seems to lack the blue mechanism, so that his discrimination is good in the red-green part of the spectrum but bad in the blue-green region; the neutral point is in the yellow at 575 nm. By employing Stiles' increment-threshold technique, Cole & Watkins (1967) showed that the tritanope lacked all three of the 'blue mechanisms', namely π_1, π_2 and π_3.

Anomalous Trichromats

Here the subject requires three primaries to match all colours, but uses different proportions from those of the average; frequently this deviation from the average or 'normal' is associated with defective discrimination, but not always, according to Pickford (1951). The abnormalities may be roughly classified as *protans, deuterans* and *tritans*; thus a protan is a trichromat who requires more red to match a yellow than does a normal trichromat. The anomalous trichromat differs from the dichromat in that he will not accept matches that the normal makes; thus the protanope matches a blue-green with white, but he will also accept as white a mixture of this blue-green with red. The protan will match a spectral yellow with an orange, i.e. he requires more red for his match than normal, but he will not accept the normal's red-green mixture as a yellow. Anomalous trichromasy is common, amounting to nearly 6% of the male population.

Cone Photopigments

We have seen that, by the method of reflexion-densitometry, Campbell & Rushton and Weale were able to demonstrate the presence of rhodopsin in the human and animal eye, and to measure the changes that occurred during exposure to light. In the fovea, too, these authors have demonstrated the presence of two pigments absorbing preferentially in the red (*erythrolabe*) and green (*chlorolabe*) parts of the spectrum. The existence of a cone pigment was first established by exposing the eye to a strong orange light, which might be expected to bleach this pigment in preference to rhodopsin; by subsequently measuring the absorption of yellow light after reflexion from the fovea, a curve for regeneration of cone pigment was obtained. This regeneration was much faster than that of rhodopsin, being complete in 5 to 6 minutes.

Erythrolabe and Chlorolabe

A study of the effects of bleaching with different wavelengths indicated the presence of two pigments, and these were isolated by studying a protanope who, according to classical theory, is missing the red mechanism and thus might be expected to have one fewer pigment (Rushton, 1963). The curve of Fig. 15.13 shows the absorption spectrum of what is apparently a single photopigment in the protanope's fovea, and corresponds remarkably well with the photopic spectral sensitivity curve of the protanope, as determined by Pitt (1935).

The peak absorption of this green-sensitive pigment was near 540 nm, and was called *chlorolabe*. In effect the retina of the protanope, under the conditions studied, was behaving as though only one pigment were present, and it was found that lights of different wavelengths, matched by the protanope as equally bright by means of flicker photometry, were, indeed, equally effective in bleaching the foveal photosensitive pigment. The failure to detect

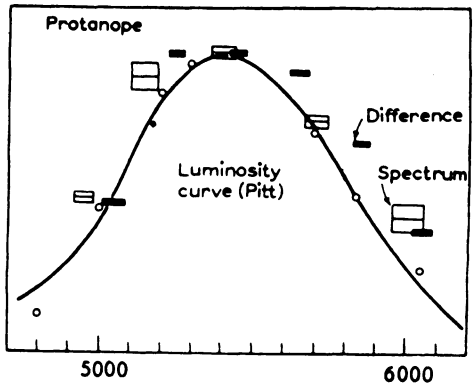

Fig. 15.13 The black and white rectangles represent the difference spectrum of the foveal pigments in the protanope, and presumably therefore correspond to the absorption spectrum of the green-sensitive pigment, chlorolabe. The curve represents the luminosity curve of the protanope as determined by Pitt, whilst the circles represent the actual luminosity curve of one of the subjects studied by reflexion densitometry. (Rushton, *Progress in Biophysics.*)

blue-sensitive pigment was presumably due to the relatively small contribution the blue mechanism makes to luminosity.

The deuteranope, like the protanope, fails to discriminate hues in the red-green part of the spectrum, and his colour-mixing data suggest that he lacks a green mechanism, so that, like the protanope, he has only a single mechanism, or pigment, operating in the red-green part of the spectrum. Rushton (1965) showed that, over this range, only a single pigment absorbed light significantly, and its absorption maximum corresponded reasonably well with the maximum of the deuteranope's luminosity curve. Rushton showed that the effects of bleaching the retina with different coloured lights were not consistent with the presence of a mixture of red- and green-absorbing pigments, as had been at first thought to be the case, so that we can conclude that the deuteranope is red-green blind because he lacks a green-absorbing pigment, *chlorolabe*, and not because, in some way, his red and green cones have become 'mixed'. In the normal eye we may expect to demonstrate the presence of both erythrolabe and chlorolabe; and this was in fact done by Baker & Rushton (Fig. 15.14) with the use of selective bleaching techniques.

Reduction Hypothesis

This so-called 'reduction hypothesis' to account for dichromacy has been generally accepted, although an alternative mechanism of fusion of the red- and green-sensitive mechanisms, either neurally or by their physical presence in the same cone, has been maintained, e.g. by Hurvich (1972). For example, certain deuteranopes have a normal luminosity curve which might be interpreted on this fusion hypothesis. However, Alpern *et al.* (1968) showed that, when a normal luminosity curve was encountered in a deuteranope this was due to a deficiency in macular pigment.

Correct Diagnosis

Alpern[5] has re-investigated this matter, emphasizing that the important point to prove by retinal densitometry is that there is only one pigment active in the medium and long-wavelength regions of the spectrum, compared with two in the normal trichromat. An important point raised by him is the correct diagnosis of dichromacy; the Nagel anomaloscope, by which a subject matches a yellow with different proportions of red and green light, is highly sensitive in discovering dichromacy and anomalous trichromacy but, by itself, it is insufficient, and two addi-

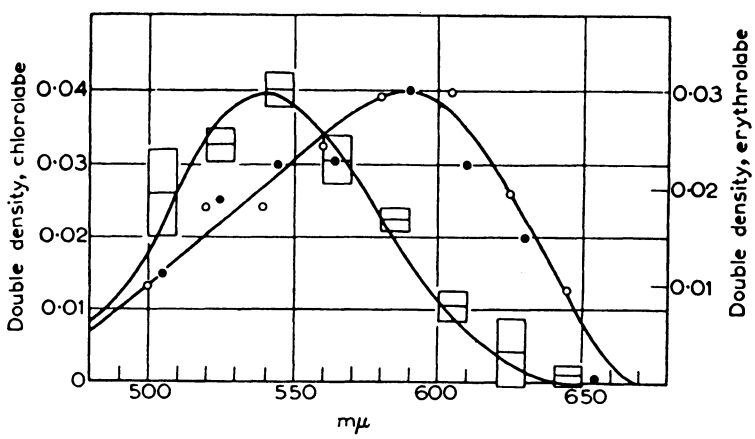

Fig. 15.14 Difference spectra of two pigments in the normal fovea. The left curve represents chlorolabe and the other erythrolabe. (Rushton, *Progress in Biophysics.*)

tional tests, including determining the neutral point, are recommended.

Variability in Red-green Sensitivity

A further point, revealed by the experiments (Alpern & Wake, 1977) is the variability amongst individual protanopes and deuteranopes with respect to the ratio of spectral sensitivities to red and green, as determined on the anomaloscope. Examination of the absorption spectra of the protanope's erythrolabe and the deuteranope's chlorolabe shows that the relative sensitivity to green and red will be very different, the ratio V_{645}/V_{535} being greater for the erythrolabe-containing eye (deuteranope) than for the chlorolabe-containing eye (protanope).

The fact that the ratio varied amongst dichromats suggested that the absorption spectrum of the pigment could vary with individuals, unless, of course, the variation was due to such causes as the presence of colour-filtering pigments in the eye, or to the fact that, in the dichromat, there were varying proportions of the two pigments in the individual cones.[6] By studying the difference-spectra resulting from bleaching with red light, white light, and first red followed by green, Alpern & Wake (1977) confirmed the absence of chlorolabe in the deuteranope.

Anomalous Trichromacy

The generally accepted view of this condition is the presence of one 'abnormal' pigment together with two normal ones; e.g. an 'abnormal' chlorolabe in the deuteranomalous trichromat, the 'deuteranolabe' of Piantanida & Sperling (1973). However, Alpern's study on the colour-matching and hue-discrimination of deuteranomalous subjects indicated that a deuteranomalous subject may have, in both green-sensitive and red-sensitive cones, the same pigment—erythrolabe—but differing in its extinction spectrum. In other words, instead of regarding the visual pigments as invariant molecules with fixed extinction spectra, Alpern suggests the existence of a 'cluster' of erythrolabes, a cluster of chlorolabes and a cluster of cyanolabes. Thus, on this basis, deuteranomaly and deuteranopia would represent the same defect but the deuteranomalous subject would retain a greater sensitivity to the middle wavelengths by virtue of cones containing erythrolabe with λ_{max} closer to the average of the chlorolabe λ_{max}. Thus it is argued that red-green dichromats are merely deutans or protans in whom the long wavelength ('Red') cones have the same pigment as the medium wavelength ('Green') cones, and anomalous trichromats are subjects in whom the spectra of these pigments (always from the same cluster) differ, if ever so slightly.

ABSORPTION SPECTRA OF RECEPTORS

Fish Cones

A more precise characterization of the types of pigment in cones is given by measuring the absorption spectra of individual cones exposed to a minute pencil of light on a microscope slide. The pioneering study was made by Hanoaka & Fujimoto in 1957, using the large fish cones, and it was shown that different cones had different absorption spectra, with maxima in the regions of 500, 535, 575 and 620 nm. More recent studies of Marks (1965), also on fish cones, gave maxima at 455, 530 and 625 nm, i.e. in the blue, green and red parts of the spectrum.

Primate Cones

Subsequent refinements of technique have permitted the study of the smaller human and monkey cones. Thus Brown & Wald (1964), working on human retina, found three cone pigments with λ_{max} at 450, 525 and 555 nm respectively, and Bowmaker & Dartnall (1980) found pigments with λ_{max} at 420, 534 and 563 nm.

Figure 15.15 illustrates the absorption spectra derived from a more recent study by Dartnall *et al.* (1983) on seven humans, exhibiting a rod pigment with λ_{max} at 496.3 $\pm$2.3, and red-, green- and blue-sensitive cones with λ_{max} at 558.4$\pm$5.2, 530.8$\pm$2.5 and 419.0$\pm$3.6 nm respectively.[7] Two patients from whom the eyes were taken exhibited quite a wide difference in their λ_{max} for long

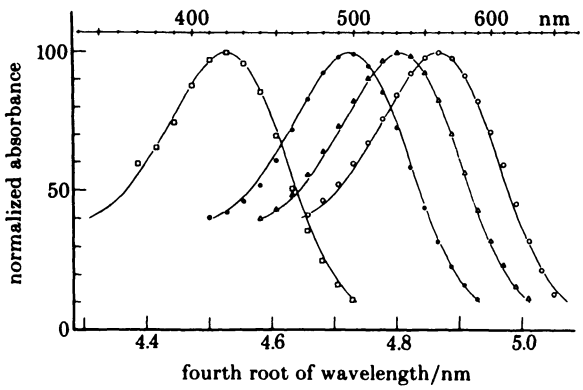

Fig. 15.15 The mean absorbance spectra of the four human photoreceptors. Squares, the blue cones (λ_{max}=419.0$\pm$3.6 nm, mean of 5); filled circles, the rods (λ_{max}=496.3$\pm$2.3 nm, mean of 39); triangles, the green cones (λ_{max}=530.8$\pm$3.5 nm, mean of 45); plain circles, the red cones (λ_{max}=558.4$\pm$5.2 nm, mean of 58). The curves are all of exactly the same shape. Note inset scale of wavelengths. (Dartnall *et al.*, *Proc. Roy. Soc.*)

wavelength cones, namely 561 and 553 nm; as judged by colour-mixing tests they were normal trichromats, yet a careful study of their sensitivities to long wavelengths showed that these were large, and what would be predicted from the different λ_{max}.

Action Spectra of Monkey Cones

Baylor *et al.* (1987) emphasize that measurements of absorption of light of individual cones are restricted by the relatively narrow bands of wavelengths of strong absorption of light; by contrast the electrical responses of receptors can be extended over a wider range; they studied responses in single cone outer segments of the monkey, *Macaca fascicularis*, with a suction electrode and obtained action spectra for three different types of cone with λ_{max} at 430, 531 and 561 nm. Careful analysis of the variations between cones showed a standard deviation for λ_{max} as small as 1.5 nm, ruling out the possibility of subpopulations within any class, the variation being accountable by experimental error. Baylor *et al.* computed theoretical colour-matching curves on the basis of their three cone pigments and compared them with the actual functions given by Stiles & Burch (1959); as Fig. 15.16 shows the agreement is remarkable demonstrating the basic similarity between human and monkey cone mechanisms.

Isolated Cone Pigments

When the relatively pure cone retina of the chicken was extracted Wald *et al.* (1955) obtained a pigment with $\lambda_{max} = 562$ nm, which they called iodopsin. It is based on retinal, and undergoes the same cycle of changes undergone by rhodopsin and thus differs from the latter in the opsin part of the molecule (Yoshizawa & Wald, 1967); by condensing dehydroretinal with the chicken opsin, Wald *et al.* (1955) obtained a new pigment which they called cyanopsin with λ_{max} of 620 nm; this has so far not been extracted from any retina.

Using column chromatography Fager & Fager (1981) separated two new pigments, which they called chicken blue with $\lambda_{max} = 449$ nm and chicken violet of $\lambda_{max} = 417$ nm, in addition to rhodopsin and iodopsin. Again, Yen & Fager (1984) made preparations of rhodopsin and iodopsin which they purified to homogeneity; they performed a partial separation of three further photopigments with λ_{max} in the green, blue and violet, so that, on this basis, the chicken eye has a tetrachromatic system; and this is apparently true of fish retinae, which contain a

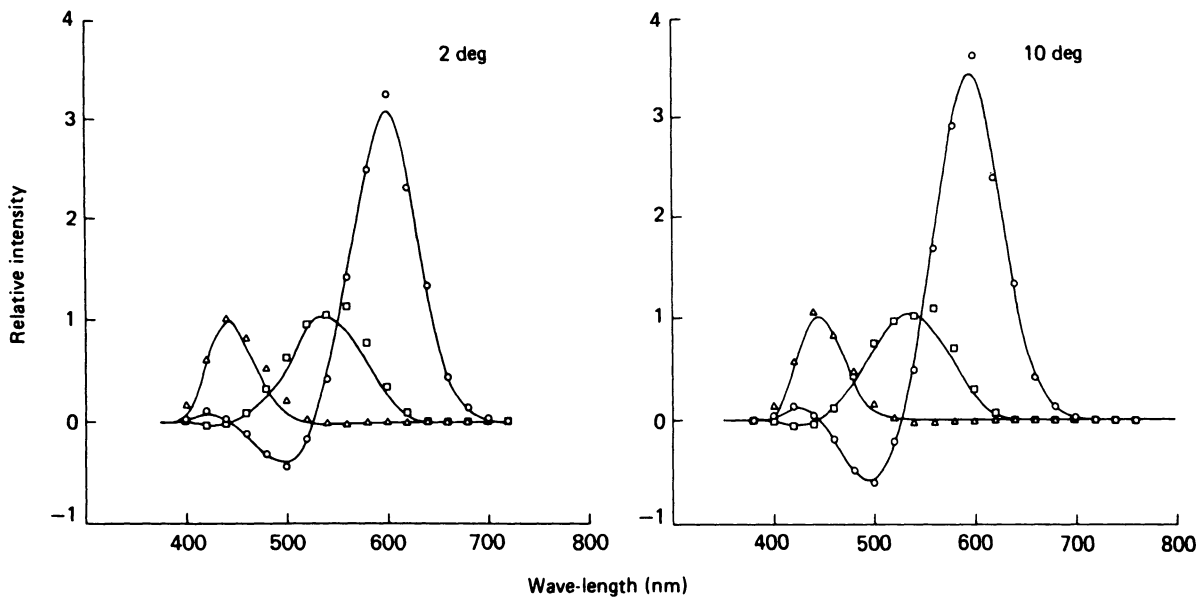

Fig. 15.16 Predicted and actual results from human colour matching experiments. Smooth curves plot the number of photons at each of the three primary wave-lengths required to match a single photon at the wave-length indicated on the abscissa; results obtained from human psychophysical experiments with 2 and 10 deg illumination of the retina (Stiles & Burch, 1959). Tabulated matching function values in Wyszecki & Stiles (1982) were recalculated here for plotting on a quantum basis. Symbols plot the colour matching functions of the long (○), middle (□) and short (△) wave-length primaries produced from the spectral sensitivities after correction for screening by the lens, macular pigment and photopigment. (Baylor *et al.*, *J. Physiol.*)

pigment with λ_{max} in the ultraviolet (Harosi & Hashimoto, 1983).

FISH PIGMENTS

Munz & McFarland (1975) have made a systematic study of extracted pigments from fish retinae in the hope of identifying photopigments responsible for their wavelength-discrimination. They studied more than a hundred marine diurnal tropical fish, extracting photosensitive pigment from light-adapted eyes and thus presumably free from the scotopic visual pigment. In all but two of the species studied, the mixture was a binary one, containing a red-sensitive ($\lambda_{max} = 518$ to 541 nm) and a less red-sensitive pigment ($\lambda_{max} = 500$ nm) differing in λ_{max} by some 20 to 40 nm, the 'less-red' pigment probably being derived from rods. In two species the mixture was ternary containing, in addition, a more blue-sensitive pigment ($\lambda_{max} = 480$ to 500 nm) which was presumably a second cone-pigment. By cutting the retinae, containing these ternary mixtures, into quadrants, containing different proportions of rods to cones, it was established that the cone-poor regions had more of the 'middle pigment' i.e. that with λ_{max} of about 500 nm and between that of the red-sensitive and the blue-sensitive pigments. If the middle pigment is, indeed, a rod pigment, its proportion should be much higher in the dark-adapted retina, and this was indeed the case, as Table 15.1 shows.

Table 15.1 Proportions of the three photopigments extracted from the retina of *Coryphaena* in light- and dark-adapted retina. (Munz & McFarland, 1975)

Light-adapted		*Dark-adapted*	
λ_{max}	*Per cent*	λ_{max}	*Per cent*
521.1	54	521.1	19.8
498.9	31.6	498.9	73.4
469.2	14.4	469.2	68.0

EVOLUTIONARY SIGNIFICANCE

The development of colour vision has survival value in so far as it permits the resolution of contrasts that are not apparent to the monochromat animal. To the predator fish there are two main visual problems according as it hunts from above its prey or not. If viewing its prey from above it is seen in contrast with the down-welling light reaching the depth at which it is hunting; if the absorption of its visual pigment is matched to this surrounding light the contrast provided by its prey is at a maximum and in this way we can explain the shift of λ_{max} to shorter wavelengths in fishes in an environment in which the light is bluish (p. 255). If viewing the target horizontally the target may be brighter or darker than the surroundings, according as the surface is reflecting or non-reflecting, so that a visual pigment with λ_{max} offset from that of the surrounding light will give better contrast for a reflecting surface, whilst a pigment matching the light is better for the non-reflecting prey. The development of a red-sensitive visual pigment may thus be regarded as an adaptation that increases the contrast of a prey that is reflecting the blue light of the underwater environment. These points are illustrated by Fig. 15.17, which shows the contrasts between prey and environment under different conditions and as manifest to eyes with blue-sensitive or red-sensitive visual pigments.

As McFarland & Munz (1975) have pointed out, the development of several photopic visual pigments in the tropical fishes not only represents an evolutionary step towards increasing the perception of contrast but it represents the evolutionary process leading to colour-vision, as such.

ELECTROPHYSIOLOGY OF WAVELENGTH DISCRIMINATION

It is not, of course, sufficient to demonstrate the presence of 'mechanisms' by either subjective or by photochemical methods; the physiologist will only be satisfied when he can tap the messages whereby these mechanisms transmit their separate information. Thus, if there are red-, green- and blue-sensitive cones, these must respond in specific fashions to light of any given wavelength falling on the retina, and somehow these responses must be transmitted to bipolar cells and ganglion cells and pass along the optic nerves to the lateral geniculate bodies. The messages will, of course, be altered, but it is essential to appreciate that the neurones through which they are carried will be unable to *add* anything; the wavelength discrimination must have been carried out at the moment of reception of the light-stimulus, and subsequent alterations in the messages can only be described as a *re-coding* of the information, with perhaps the scrapping of some details and alteration of emphasis of the different parts. Thus, to consider the 'blue mechanisms', there might be three types of 'blue cone', but if their separate messages were all pooled in a single type of bipolar cell, the extra information would be lost. The fact that these mechanisms are shown to exist by psychophysical methods, however, proves that their special messages have indeed survived the re-coding processes so that it is difficult to escape the conclusion that there are several types of cone that are specially sensitive to blue light.

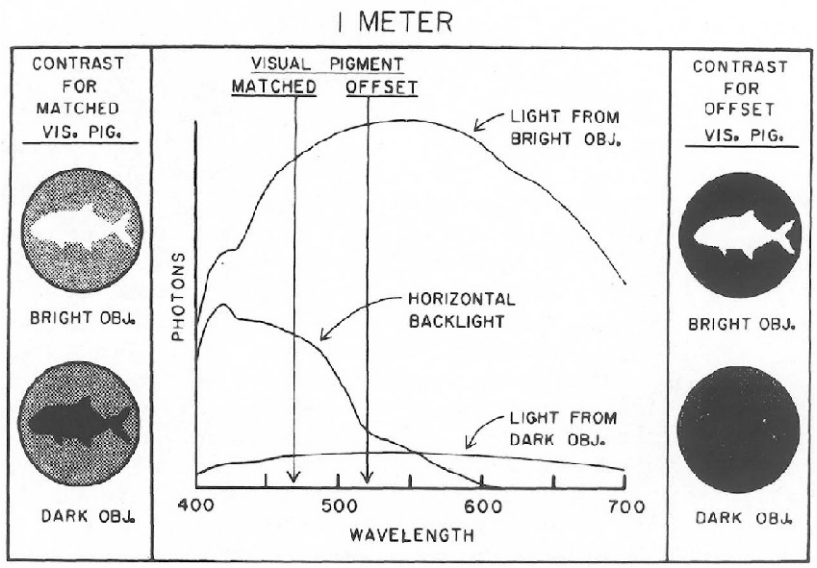

Fig. 15.17 Comparisons of the relative photocontrast of 'bright' (reflective) and 'dark' (nonreflective) objects viewed along the horizontal line of sight at 1 m beneath the surface by fishes with visual pigments matched to (P_{469}) or offset from (P_{521}), the backlight. Both bright and dark targets are assumed to be grey. Light reflected into the horizontal field includes direct reflections of sunlight. Close to the bright objects, reflected light will be 50 to 100 times more intense than the radiance of the horizontal background (scaling not indicated on the ordinate). The insets portray the relative photocontrasts that would be produced by each visual pigment. The matched pigment enhances the contrast of a dark object and the offset pigment results in contrast enhancement of a bright target. (McFarland & Munz, *Vision Res.*)

Intracellular Records from Single Units

S-potentials

In discussing the electrophysiology of the retina earlier, it was indicated that several workers had claimed to have recorded from individual cones by inserting a microelectrode into the retina; some of these showed some interesting chromatic responses, namely the so-called *S-potentials* of Svaetichin in the fish retina;[8] subsequent work has shown that these are derived from horizontal cells, i.e. one step later than the receptors themselves. In general these responses to light were not spike discharges but graded potential responses consisting of either an increase of the normal resting potential, a *hyperpolarization*, or a decrease, *depolarization*. The responses were graded in the sense that the change of potential increased with increasing intensity, whereas a spike potential is all-or-none in character.

L- AND C-TYPES

According to the depth of the electrode in the retina the responses were of two main types; an L-type which responded in the same way with all wavelengths and therefore gave a 'luminosity message' (Fig. 15.18) and a

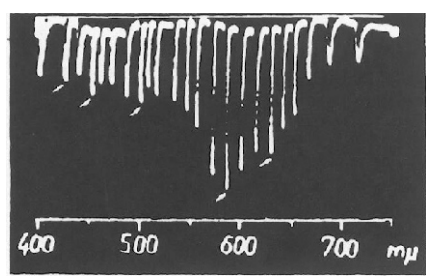

Fig. 15.18 L-type of response of unit in fish retina; the polarity of the electrical change does not alter with varying wavelength of stimulus. (Svaetichin & MacNichol, *Ann. N.Y. Acad. Sci.*)

C-type which gave opposite electrical effects according as the retina was stimulated with red and green or blue and yellow lights (Fig. 15.19*a*,*b*). The messages carried by this second type thus indicated the chromatic nature of the stimulus, and the units were called *chromatic*, or C-units, being subdivided into *R-G* (red-green) and *Y-B* (yellow-blue) categories. Thus the C-potentials exhibit an 'opponent colour' basis so that a given element may be hyperpolarized by one band of wavelengths and depolarized by another band; if hyperpolarization indicates

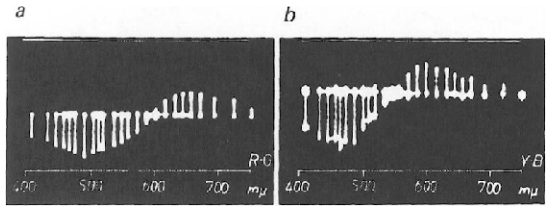

Fig. 15.19 (*a*) C-type of unit, of the red-green variety, giving responses of opposite polarity according as the wavelength of the stimulus lies in the red or green regions of the spectrum. (*b*) C-type, of yellow-blue variety. (Svaetichin & MacNichol, *Ann. N.Y. Acad. Sci.*)

inhibition, and depolarization activation, then these opposite responses may indeed be described as opponent. An interesting characteristic of the S-responses was the very large receptive fields extending across the whole retina; in these fields summation was complete so that Ricco's Law applied perfectly (Norton *et al.*, 1968).

Cone Responses

Carp Retina

Of more interest are the responses of individual cones; and these have been described by Tomita *et al.* (1967) in the carp retina. The response to light was always a hyperpolarization, and when units were examined with light of different wavelengths, regions of maximum sensitivity were obtained in three broad regions in the blue, green and red. Figure 15.20 illustrates the averaged results; the peaks occurred in the following regions:

Blue	*Green*	*Red*	
462±15	529±14	611±23	Carp retina
455±15	530±5	625±5	Goldfish

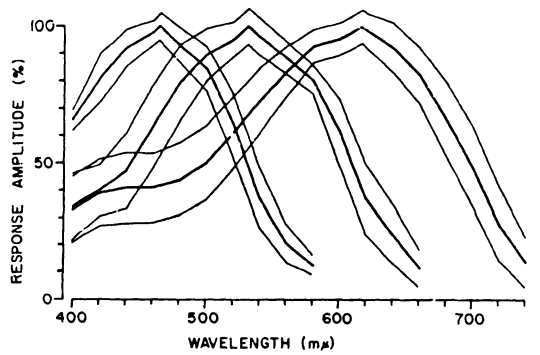

Fig. 15.20 Responses of three types of cone to light of different wavelengths indicating maximum sensitivity in the blue, green and red parts of the spectrum. Thin lines indicate standard deviation curves. (Tomita *et al.*, *Vision Res.*)

These are compared with the absorption maxima of goldfish cones described by Marks (p. 407). The authors point out that their results provide no evidence for cones with maximal responses in the region of 680 nm, as deduced by Naka & Rushton (1966a–c) from their analysis of S-potentials.

Turtle Retina

Baylor & Hodgkin (1973) found three distinct classes of cones on the basis of their spectral sensitivities, with maximal sensitivity at 630 nm (red-sensitive or red cones), 550 nm (green) and 460 nm (blue) respectively. The maximum sensitivity of the green cones, namely 550 nm, was different from that of the rods (520 nm), although both receptors might well have had the same porphyropsin photopigment based on dehydroretinal with λ_{max} of 518 nm (Liebman & Granda, 1971).

OIL DROPLETS

The shift of λ_{max} to the red end of the spectrum in the cone is probably due to the orange oil-droplets in the green cones. Again, variations in wavelength-sensitivity amongst groups of red- and green-sensitive cones could well be due to the extent to which filtering by oil-droplets takes place.

UNIVARIANCE

When small spots of light were used as stimuli, the responses in a given cone were said to be *univariant*, meaning that the response at any wavelength and intensity could be matched by any other wavelength provided the intensity was adjusted appropriately, or more generally, the response at I' and λ_1 could be matched by light of kI' and λ_2 where k is the same for all values of I'. With large spots of light, deviations were observed indicating some coupling of cones.

Coupling of Cones

We have seen that cones are electrically coupled so that the stimulation of one may produce a similar response in cones within a radius of up to about 40 μm; this coupling is manifest in several ways, and Baylor & Hodgkin used the variation in response of a cone to changes in the position of the stimulating light as the criterion. If the cone acts in complete isolation the falling off in response as the light-spot is moved to one or other side of the central position should be symmetrical, whereas coupling results in bumps on the curves; thus Fig. 15.21A shows the sensitivity-profile of a green-sensitive cone, and B that of a red-sensitive cone, and the bump in the profile at $+25\ \mu$m in the one and at $-25\ \mu$m in the other is evidence of coupling with other cones. When the spectral characteristics of the responses were examined, it was

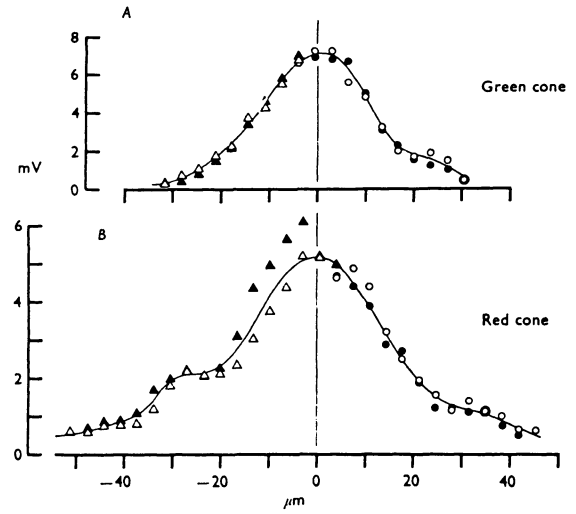

Fig. 15.21 Coupling between cones. A is the profile of spatial sensitivity of a green cone being the response amplitude to a 7 μm spot of light as the spot is moved away from the central position. Light of 559 nm. There is a suggestion of a bump at +25 μm. B is profile of red-sensitive cone. There is a bump in the profile at −25 μm. White light. (Baylor and Hodgkin, *J. Physiol.*)

concluded that coupling of cones must have been amongst cones of the same spectral sensitivity, i.e. green cones with green, red with red, and so on; this is reasonable since it would be pointless to develop specifically sensitive receptors and mix their responses at the very beginning.

However, both electrophysiological (Normann *et al.*, 1985) and morphological (Kolb & Jones, 1985) studies have shown that inter-cone connections can result in considerable mixing of colour signals in the turtle retina. Thus Normann *et al.* (1985) showed that the principle of univariance did not apply to single cones, when response as a function of wavelength was studied, a deviation that could not have been due to horizontal-cell feedback. Kolb & Jones (1985) showed that the turtle cones had sprays of telodendria, some 10–20 μm long, that ended in clusters of terminals. Red- and green-sensitive cones could be distinguished in the electron microscope by virtue of their oil-droplets; and telodendrial connections between green- and red-sensitive receptors were established, their relations appearing to be those of chemical synapses. Thus the telodendria could end as central elements of ribbon-synapses, as basal contacts with cone pedicles, or even as lateral elements in invaginated ribbon-synapses. In addition to these telodendrial connections, gap-junctions between the pedicles of adjacent red- and green-sensitive cones were observed.

Double Cones

In some vertebrates there are, in addition to the three cone types—red-, green- and blue-sensitive—and rods, a fifth type, the double cone. This consists of two tightly joined elements; the 'chief' cone of the turtle, for example, contains an unknown photopigment and an oil droplet in its inner segment and the 'accessory' cone contains pigments 518_2, i.e. the pigment found in the green-sensitive turtle cone (Liebman, 1972). Electrophysiological studies have shown that some retinal cones share electrical properties with both red and green sensitive cones, and since earlier work had shown that direct coupling of cones with each other was only between cones of similar type, it seemed that the receptors responsible for these mixed effects were the double cones. Richter & Simon (1974) made intracellular records from turtle cones, subsequently identifying them as double cones by injection of Procion yellow, which was found in both accessory and principal members. By contrast with single cones, the principle of univariance was not observed indicating the pooling of responses by receptors with different photopigments. The effects of variation of the wavelength of the stimulating light indicated green- and red-sensitive units, and the relative sensitivity to blue light was consistent with the absence of an oil-drop in the accessory cone; the result was a very broad band of spectral sensitivity with peaks in the red and green regions; by adapting with red light, the red peak could be suppressed, and with green light the green peak. The basis for the coupling of the cones could not be established, so that it might be through a chemical synapse or through a gap-junction.

Oil-droplets

In some species, of which the diurnal birds may be chosen as examples, the retinal cones contain, in their inner segments, coloured oil-droplets in such a position that they act as light-filters and therefore modify the spectral characteristics of the light reaching the outer segments. In the chicken there are at least three types, red, orange-yellow and yellow-green, when light-microscopy is employed, but Bowmaker & Knowles (1977), employing microspectrometric measurements, identified in all some six types of oil-droplets.

SPECTRAL CHARACTERISTICS

Figure 15.22 illustrates the spectral characteristics of five of these droplets, and it is evident that, with the exception of the clear droplet, they show a sharp increase in absorbance at specific regions, in fact they are behaving as cutoff filters for shorter wavelengths of light, Type A having a λ_{T-50} (the wavelength at which 50% transmission occurs) at about 454 nm, type C at about 520 nm and the red at about 585 nm; type B_1 has a shoulder and a

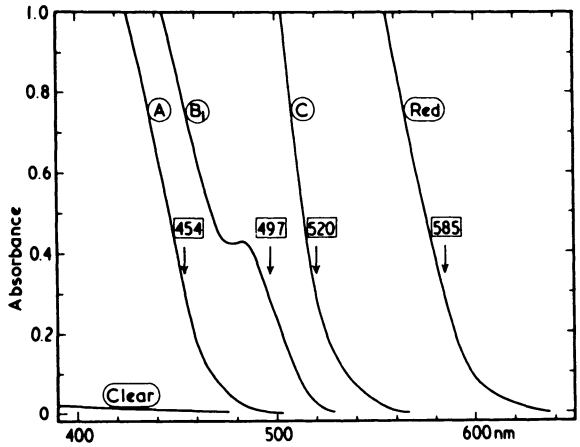

Fig. 15.22 Spectral absorbance of five types of oil-droplet from chicken cones. 'Clear', A, C and Red droplets occur in single cones; B_1 occurs in the chief member of the double cone. (Bowmaker and Knowles, *Vision Res.*)

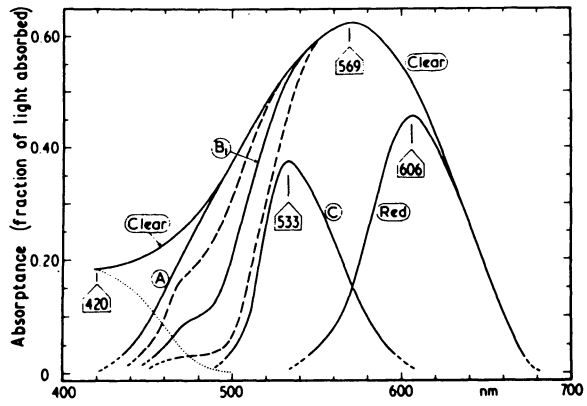

Fig. 15.23 Computed absorptance for the photopigment-oil droplet combinations in the five recognized cone-types. Clear: absorptance of a cone having the clear oil droplet with P_{569} in the outer segment; A: Type A droplet plus P_{569}; B: Type B_1 droplet plus P_{569} (the dashed lines indicate the effect of the range of B_1 droplets found); C: Type C plus P_{497}; Red: Red droplet plus P_{569}. The dotted line indicates the possible response, maximal at 420 nm, derived by interaction between the 'clear' and 'Type A' cones. (Bowmaker and Knowles, *Vision Res.*)

λ_{T-50} of 497 nm. The absorption spectrum of a given cone will depend on the visual pigment it contains together with the cone oil-droplet; according to Bowmaker & Knowles (1977) the chicken cones contain two photopigments with λ_{max} at 569 and 497 nm respectively, so that the absorbance of a given cone may be predicted from the photopigment and oil-droplet it contains. It must be appreciated, moreover, that many cones are double, namely 45%, and these contain the B_1-droplet in the chief member and B_2 in the accessory member; the combined response will presumably be governed by the different absorption characteristics of the cone oil-droplets.

PHOTOPIGMENT AND DROPLET

There was some specificity regarding the association of oil-droplet with photopigment; thus P_{497} contained only Type C droplets, whilst P_{569} cones were associated with red, type A, clear, or type B droplets. On no occasion was either the P_{569} photopigment found associated with type C droplet or the P_{497} photopigment with any other oil-droplet than the Type C. The computed effects of the oil-droplets on the absorptances of photopigment-oil droplet combinations are shown in Fig. 15.23; thus the curve marked *Red* is the absorptance due to a red oil-droplet plus P_{569} giving a λ_{max} at 606 nm, i.e. a shift in sensitivity towards the red. Curve C with λ_{max} at 535 nm is derived from photopigment P_{497} and Type C oil-droplet, once again showing a shift towards the red. A blue-sensitive photopigment has not been identified in the chicken retina, so that blue-sensitivity may depend on interaction of clear oil-droplet cone with Type A cones, a λ_{max} of 420 nm can be predicted if both contain P_{569}.

RELATION TO COLOUR VISION

This study of Bowmaker & Knowles on the chicken and another[9] on the pigeon (Bowmaker, 1977) prove conclusively that colour vision in the bird is not mediated by a single cone photopigment with variable droplet contents of individual cones; thus the oil-droplets *assist* colour discrimination (Muntz, 1972) to the extent that they sharpen the absorptance spectra of the cones, but they are unable to substitute for photopigments.

Opponent Colour Responses in Turtle Horizontal Cells

We have seen that turtle cones show an interaction that depends on feed-back from horizontal cells, this feed-back taking the form of a depolarization, i.e. an electrical change that opposes the primary hyperpolarization in response to the action of light on the cone. As with the fish retina, horizontal cells could be classed as L-cells, showing little variation in response with wavelength of stimulating light, and C-cells which could be classified as R/G (65%) and G/B (35%).

Horizontal Cells

L-cell Responses

As Fig. 15.24 shows, the response is a smooth hyperpolarizing one, and when the total number of quanta

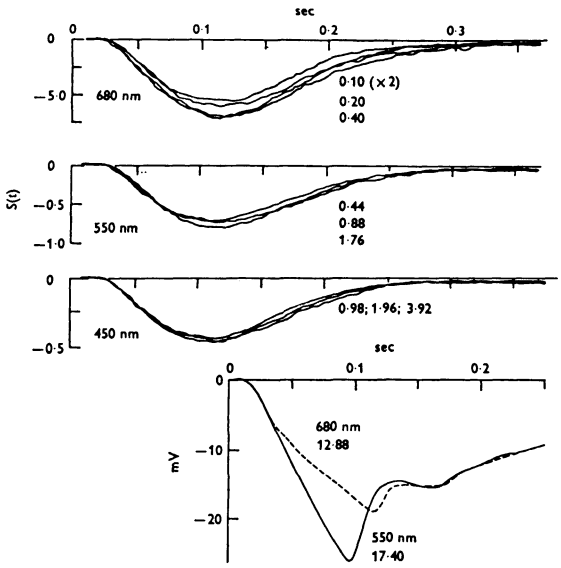

Fig. 15.24 Responses of an L-cell to monochromatic flashes of three different intensities and three different wavelengths. The response is a smooth hyperpolarization and when stimuli are adjusted for equal numbers of quanta there is little variation with wavelength of the stimulating light. Inset: large responses of an L-cell to brighter flashes are clearly different for stimuli of 680 nm (dashes) and 550 nm (continuous). (Fuortes and Simon, *J. Physiol.*)

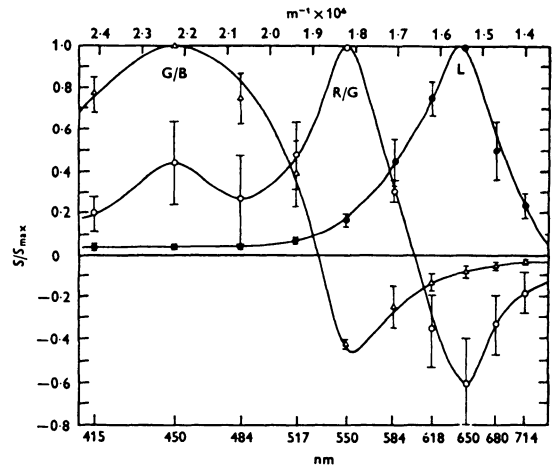

Fig. 15.25 Spectral sensitivity curves of horizontal cells. Hyperpolarizing responses are plotted up and depolarizing responses are down. Results on 23 L-cells, sixteen R/G C-cells and four G/B C-cells. (Fuortes and Simon, *J. Physiol.*)

were adjusted to be the same, the responses varied little with the wavelengths of stimulating light. The responses were not strictly invariant with respect to wavelength, and in some the variation was quite prominent, this was especially true of bright flashes. When the peak response was plotted against wavelength the sensitivity curve was similar to that of red-sensitive cones indicating that the L-cells were predominantly connected with these. By exposing a cone to a background of light that it absorbs strongly its response becomes smaller, faster and often diphasic and its contribution to exciting the L-cell becomes correspondingly smaller. Using this means of suppressing the action of given cones, it was shown that the main input is indeed from red cones but some intermixture of possibly the double cones consisting of two tightly associated cones each containing one pigment-type (Liebman, 1972).

C-cell Responses

With regard to the C-cells, green or blue flashes applied to R/G cells gave smooth hyperpolarizing responses, whereas red flashes gave depolarizing responses; in G/B cells, blue flashes elicited the hyperpolarizing waves and green flashes evoked depolarizing waves. The spectral sensitivities of the three main types of horizontal cell are indicated in Fig. 15.25.

Horizontal Cell Organization in Goldfish

Stell & Lightfoot (1975) have described the cone-horizontal cell connections; the cones consist of double cones, comprising a long and short; two kinds of single long cones, and one short and one miniature. These had specific colour sensitivities, so that it would be their connections with horizontal cells that determined the S-potentials; these were classified as L-type, hyperpolarizing to all wavelengths; biphasic, or C_1 hyperpolarizing to short wavelengths and depolarizing to longer wavelengths, and C_2 or triphasic, hyperpolarizing to long and short wavelengths but depolarizing to intermediate wavelengths. Yang *et al.* (1983) examined the spectral responses of L-type external horizontal cells, with inputs from green- and red-sensitive cones. They explained the L-type of responses on the basis of a negative feedback from them on to the green-sensitive cones, so that the horizontal cell's responses would tend to signal luminosity with high sensitivity to long-wavelength light. Their model is illustrated by Fig. 15.26.

Carp Bipolar Cell

Kaneko & Tachibana (1983) have described a double opponence in the responses of this bipolar cell; thus both the centre and surround exhibit opponence in their responses to different bands of the spectrum. Figure 15.27 illustrates the responses of such an OFF-centre cell; at the

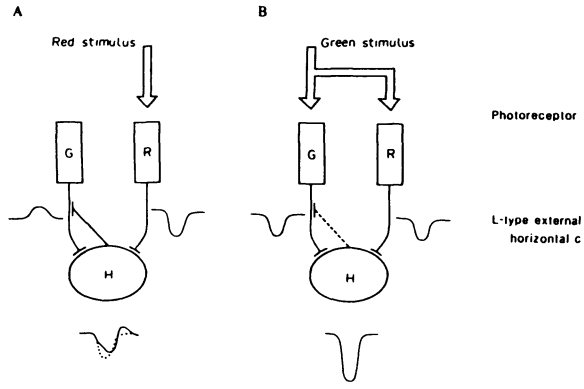

Fig. 15.26 A hypothetical model of synaptic connections between photoreceptors and LEHCs. LEHCs (H) receive inputs directly from red-(R) and green-sensitive cones (G), and, in turn, make inhibitory feedback synapses onto green-sensitive cones. (A) When a red flash is presented, LEHCs receive not only hyperpolarizing input directly from red-sensitive cones, but also a delayed depolarizing feedback input from green-sensitive cones. Waveforms drawn beside photoreceptors schematically represent hyperpolarizing input (right) from red- and depolarizing feedback input (left) from green-sensitive cones to LEHCs, respectively. Waveform drawn by solid line in the lowest row represents the LEHC response, an algebraic sum of the hyperpolarizing input (dotted line) and the depolarizing feedback input. Note that the initial phase of the hyperpolarizing response is not affected by the depolarizing signal. (B) When green flash is presented, the feedback signal is suppressed due to the hyperpolarization of green-sensitive cones, and the LEHC response is an algebraic sum of direct inputs from red- and green-sensitive cones. (Yang *et al.*, *Vision Res.*)

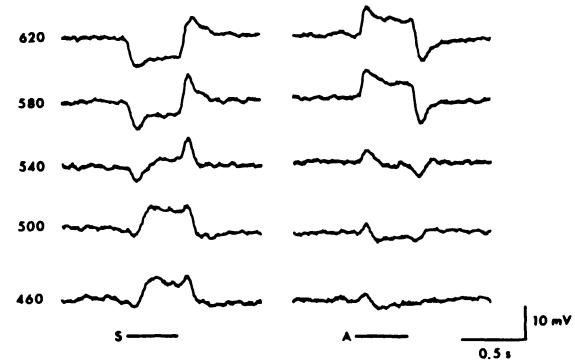

Fig. 15.27 Responses of an off-centre double opponent bipolar cell to spots (left column) which were 100 μm in diameter, and positioned at the most sensitive region of the receptive field centre and annuli (right column) which were 0.5 mm i.d., 3.5 mm o.d., and placed concentric to the spot, at five different wave-lengths (indicated in nm in the far left column) of equal quantal flux. Light intensities were 1.6×10^{12} quanta.cm^{-2}.sec^{-1} (spot) and 2.2×10^{12} quanta.cm^{-2}.sec^{-1} (annulus). The short horizontal bars below each column of records indicate timing of stimulus (duration 400 msec). (Kaneko & Tachebana, *Vision Res.*)

left the responses to spots of different wavelengths projected to the centre of the receptive field are shown. There is a hyperpolarization, settling down to a plateau, followed by an OFF-depolarizing transient. The polarity of this plateau depends on the wavelength, so that at 500 nm it has become depolarizing. Clearly, there are two components to the centre-response, which may be called centre-hyperpolarizing and centre-depolarizing components. Responses of an annulus, surrounding the receptive-field centre, are essentially mirror-images of those of the central spot stimulus. By appropriate adaptations to different wavelengths, the spectral characteristics of the two components responsible for the opponence were derived. It appeared that the main input responsible for the centre-hyperpolarizing component originated in red-sensitive cones; this was counteracted by a centre-depolarizing component with high sensitivity in the short wavelength end of the spectrum, closest to that of the green-sensitive cones of the carp retina, as determined spectrophotometrically. The double opponence revealed at this early stage in information-transfer, is surprising, and reveals the potentialities of the outer plexiform layer in this respect. We may assume that this ready-made double opponence is transferred to ganglion cells in the inner plexiform layer.

Optic Nerve Fibre Response

Dominators and Modulators

Granit (1943) was the first to study the spectral sensitivity of optic nerve fibres. With the dark-adapted frog eye, and scotopic stimuli, the responses were the same whatever unit was picked up, the maximal response corresponding to the wavelength of maximal absorption of rhodopsin, about 500 nm. In the light-adapted frog eye the wavelength-response curves varied with the unit picked up; they fell into two categories described as *dominators* and *modulators*. The dominators were the most common and gave broad sensitivity curves with a maximum at the wavelength for maximal photopic sensitivity as found by the ERG, namely at about 555 nm (Fig. 15.28). The modulators had relatively narrow spectral sensitivity curves confined to one portion of the spectrum, so that it was possible to speak of a red-sensitive modulator whose peak of maximal sensitivity occurred at, say, 600 nm; a green-sensitive modulator with a peak at 530 nm, and so on. Figure 15.29 illustrates the modulators isolated by this electrophysiological method from various eyes.

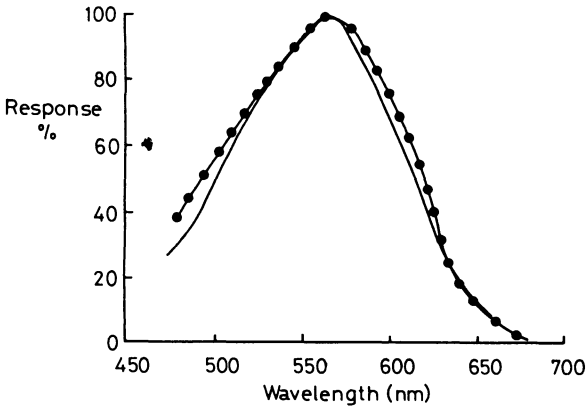

Fig. 15.28 Wavelength-response curves in single fibres of the frog (continuous line) and snake (interrupted line) optic nerve. The greatest response has been put equal to 100. The dominator. (Granit, *Nature*).

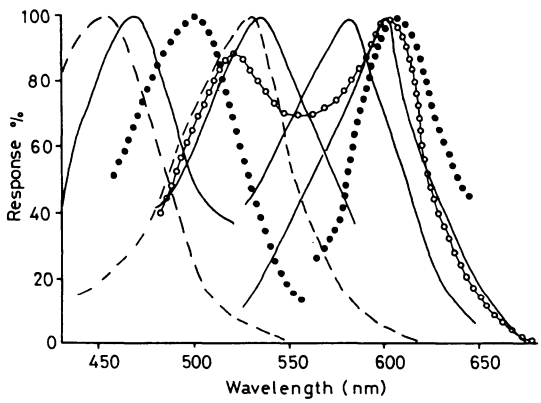

Fig. 15.29 Wavelength-response curves in single fibres of the optic nerve of the rat (dots), guinea pig (broken lines), frog (lines in full) and snake (line interrupted by circles). The modulators. (Granit, *Nature*).

The Optic Nerve Message

Thus, so far as the *message* carried by the ganglion cells to the lateral geniculate bodies is concerned, we may say that it is organized apparently on a dual basis; the dominators indicate, by their frequency of discharge, the intensity of the prevailing light; under scotopic conditions their sensitivities correspond to the absorption of the scotopic pigment; rhodopsin in the case of the frog and mammals, and porphyropsin in the case of many freshwater fishes. In the light-adapted mixed retina the dominator has the sensitivity corresponding to the photopic sensitivity curve. The second half of the message conveys information about the spectral composition; thus the red modulators would respond preferentially to red light falling on the retina, whilst the green and blue modulators would be much less affected, hence the message corresponding to the illumination of the retina with red light at photopic intensity might be a small discharge in the dominator, high discharge in the red modulator and small or negligible discharges in the green and blue modulators.

Opponent-type Responses

We have seen that the receptive fields of optic nerve fibres or of ganglion cells are not simple, but usually organized on a concentric basis, and subsequent work on wavelength-sensitivity of ganglion cells has shown that this concentric organization extends to colour sensitivity of the two components of the receptive field, so that the fields are organized on an opponent basis. Some examples of the types of receptive field are illustrated schematically in Fig. 15.30, thus Type C is relatively simple with no concentric organization, but the type of response, whether ON or OFF, depends on the wavelength of stimulating light. This was called a Type-P by Daw (1968), representing about 5% of the goldfish ganglion cells; the majority, designated as Type-O, gave opponent responses between centre and surround. Where the cen-

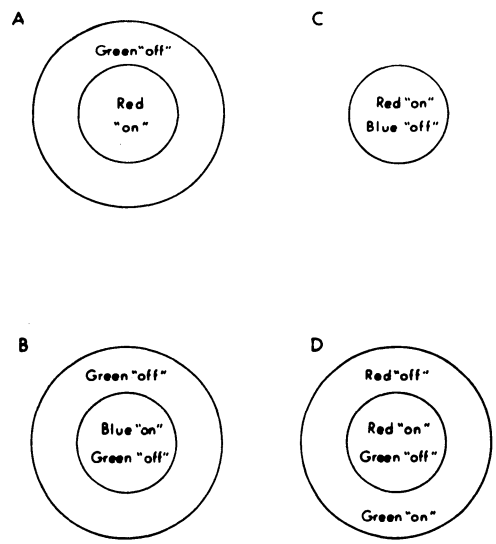

Fig. 15.30 Examples of receptive fields of some colour-coded cells. (A) Centre-surround arrangement with spatial separation of the two colour components. (B) Centre-surround arrangement with overlap of the two colour components. (C) No centre-surround arrangement; complete overlap of the two colour components. (D) Double opponent cell; colour opponency in both centre and surround of the receptive field. (Daw, *Physiol. Rev.*)

tre-surround opponence is between complementary colours, the effects of uniform illumination of the field with white light is to cancel out any response, and this may be a means of reducing the total number of messages sent to the brain when the retina is exposed to uniform white light.

Monkey Ganglion Cells

Hubel & Wiesel (1960), in their study of the receptive fields of monkey ganglion cells, found a small percentage with opponent colour responses, but Gouras (1968) found that the proportion was much higher and consistent with the high proportion of geniculate cells with a similar receptive field organization (p. 587). Gouras (1968, 1969) found two distinct types of ON-centre ganglion cells. Type I received signals from two cone mechanisms, Red and Green, as determined by the effects of selective adaptation to coloured lights. The responses were phasic, and both cone mechanisms excited the centre and surround. They could not be described as colour-coded, since they responded similarly to all wavelengths.

COLOUR-CODED CELLS

The other type was colour-coded, a single cone mechanism Red, Green or Blue exciting the centre with inhibition from the periphery through another cone-mechanism. These units were of the sustained type and were most common near the fovea and so may represent the midget ganglion cells of Polyak; their conduction-velocities were 1.8 m/s compared with 3.8 m/s for the phasic cells, suggesting that colour information was carried by small ganglion cells.

THREE CLASSES

In a more elaborate study, De Monasterio & Gouras (1975) defined three general classes of colour-opponent cells; thus Class I was colour-opponent with concentric fields, so that, for example, the centre responded specifically to one spectral band and the surround to another, represented by G+/R−; Y+/B−, and so on. Class II was colour-opponent but non-concentric, so that the opponence had no spatial element in it. Type III neurones, which were mostly Y-cells, had antagonistic centres and surrounds, but the inputs to both regions were from the same cones; they were called *broad-band* because their action spectra were similar to the CIE photopic luminosity function with maximum at about 560 nm (i.e. they would be described as 'dominators'). These were found most frequently in the peripheral retina. Type IV were Y-cells exhibiting centre-surround colour opponence typically excited by short and medium wavelengths and inhibited by long wavelengths. These were more frequent in the central retina. Types III and IV were similarly distinguished in the magnocellular part of the lateral geniculate nucleus (Wiesel & Hubel, 1966; Dreher *et al.*, 1976). In a more recent study De Monasterio & Schein (1980) showed that Types III and IV Y-cells represented extremes of a continuous variation in chromatic properties of a single class of cells, according as the surround mechanism was supplied by active red- or green-sensitive cones. This variation in type appears as a variation with eccentricity, so that the Type III neurones of the fovea have become Type IV with centre-surround opponence, the surrounds appearing to lack input from the green-sensitive cones, contrasting with Type III neurones with approximately equal inputs of red- and green-sensitive cones to the surrounds, thereby making centre and surround similar and non-opponent.[10]

Tuning

As with spatial and temporal features of the response, so the degree of colour tuning can be assessed by a 'half-bandwidth', namely the full bandwidth of wavelengths at half-maximum sensitivity as illustrated by Fig. 15.31 which shows the tuning of Red-centre–Green-surround ganglion cell units (De Monasterio & Schein, 1982). This tuning allows the assignment of a certain 'signature' to a given ganglion cell that permits identification of its contribution to the input of neurones higher in the visual pathway, the plot of respective bandwidth versus wavelength of peak sensitivity being used as the 'signature'.

Significance of Spatial Opponence

The spatial opponent organization of colour-coded cells may well have little significance for conveying chromatic information to the brain and may simply represent Nature's method of transmitting both contour and colour information; thus the concentric organization of the receptive field of retinal and geniculate neurones, with its further development in simple cortical cells (p. 531), must be regarded as a development permitting the accurate assessment of moving or stationary contours; however, the same cones that are conveying this feature of the environment must be employed in conveying the colour as well; if all types of cone were to converge on single ganglion cells, the centre would lose its chromatic selectivity so that it is understandable that these centres will have preferably a single type of cone input; the input to the surrounds, presumably operating through horizontally organized retinal cells, is usually chromatically opponent so that the response to any spot of light covering the whole receptive field—and this is the usual situation—will be governed by the opposing influences of centre and surround. In the special situation when the receptive field is trichromatically organized, such that centre and surround are sensitive to complementary colours, e.g. Green-Magenta, Blue-Yellow, Red-Cyan, the

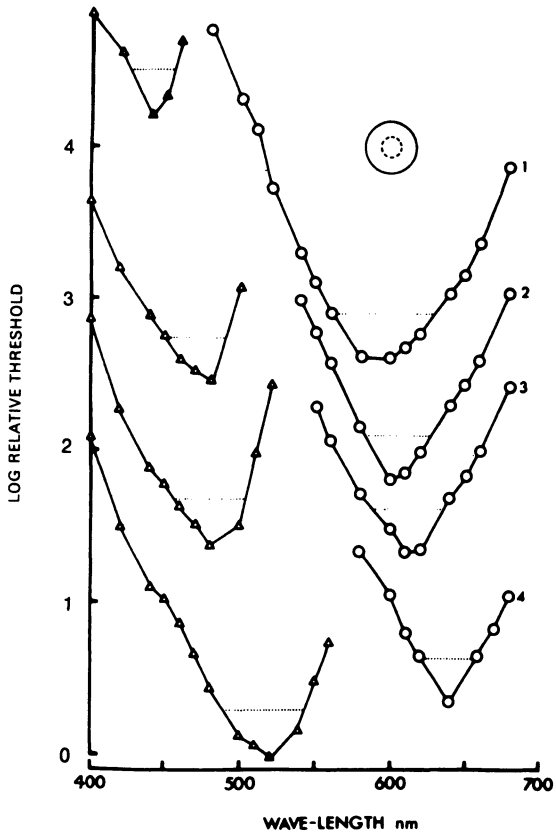

Fig. 15.31 Action spectra of four red-centre, green surround ganglion cells obtained with a 10° spot on a white background; dotted lines indicate full bandwidths at half-maximum. (De Monasterio & Schein, *J. Neurophysiol.*)

ganglion cell may well be irresponsive to white light except when this falls on only a part of the receptive field, as with a contour. Some cortical and geniculate units certainly exhibit trichromatic opponency, and in the retina De Monasterio *et al.* (1975a) identified GM, RC and BY cells, indicating that trichromaticity at the geniculate and cortical levels is not necessarily due to convergence of dichromatic or monochromatic inputs from the lower level.

Concealed Opponence

De Monasterio *et al.* (1975b) have emphasized that many units in the retina, and probably in geniculate and cortex, that are apparently non-opponent, do in effect have some concealed chromatic opponence, which may be revealed by appropriate chromatic adaptation, and fails to be normally evident by the extreme weakness of the surround response on a neutral background. Thus, on a neutral background, these cells behave as luminosity units without capacity to transmit chromatic information.

Further Processing

We must postpone to the next section the study of chromatic responses at higher stages in the visual pathway. Here we may conclude by emphasizing the change in the responses of successively higher-placed units in the retinal pathway, so that the univariant, and thus essentially monochromatic responses of the receptors, have been transformed into responses that differentiate stimuli on a trichromatic basis that confirms the Helmholtz hypothesis. A form of opponence has appeared, however, which provides support for Hering's Theory, a theory considered for a long time to be at variance with the trichromatic one of Young and Helmholtz.

Hering's Theory

According to this, colour vision was mediated by three substances which responded to light by opposite catabolic and anabolic reactions. Thus one substance was broken down by light and regenerated by darkness, or black; equilibrium corresponded to a grey similar to that perceived in complete darkness. A second substance was broken down by red light and regenerated by green, with a neutral point in the yellow, and was unaffected by yellow, its complementary, blue, and mixtures of the two including white. A third substance was broken down by yellow and regenerated by blue, and gave no response to a pure green light, white, or the complementary purple. As Marriott (1976) emphasized, Hering's theory is basically trichromatic, so that a recoding of Helmholtz's primary sensations into an opponent system may be regarded as another way of describing the basic facts of colour vision. Subsequent psychophysical studies of Hurvich & Jameson (1955) and Jameson & Hurvich (1955–1968) have placed the opponent basis of colour vision on a firm experimental basis; and the problem of the physiologist is to determine the manner in which a trichromatic input from cones can be transformed into an opponent system in higher neurones.

INFORMATION THEORY

In this context, Buchsbaum & Gottschalk (1983) have applied modern information theory to the question as to why such a transformation has taken place, and its value. Thus, they accept the three primary mechanisms, with

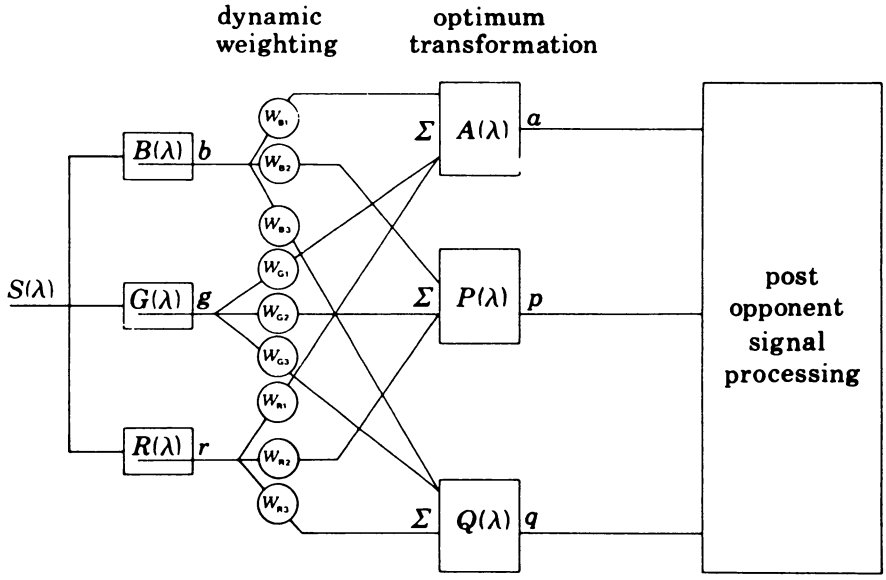

Fig. 15.32 Schematic diagram of colour processing in the visual system. The three initial colour mechanisms $B(\lambda)$, $G(\lambda)$ and $R(\lambda)$ are converted via opponent type processing into the three channels $A(\lambda)$, $P(\lambda)$ and $Q(\lambda)$. This paper considers the issue of the optimal combination of the initial three mechanisms under the criterion of most efficient information transmission. (Buchsbaum & Gottschalk, *Proc. Roy. Soc.*)

outputs in response to different wavelengths of light corresponding to the mixture functions of Fig. 15.8. As illustrated by Fig. 15.32, they feed into three channels with an optimal transformation, a transformation that is necessary because of the strong overlap of the Red and Green mechanisms. Thus there exists a mathematically unique transformation that decorrelates the message components (b, g, r) and enables the best energy distribution (energy compaction) among the transformed components *a*, *p*, *q*, so that there is maximization of the energy in *a*, and in the *a* and *p* combined, so that more resources can be allocated to transmitting the message components that have most of the signal-energy, and less in transmitting those with little energy, without much effect on the error of the perceived signal. Applying this analysis, they showed that the derived opponent signals could be used to describe the change in colour-mixing of the dichromat; and they also deduced that the minimum number of original signals to provide the accuracy of discrimination actually observed, as in the hue-discrimination curve, for instance, was three. Using a different type of analysis Barlow (1982) came to a similar conclusion.

Notes

1. The contribution of blue to any mixture is very small, in terms of luminosity, so that the values have been multiplied by ten in the figure.
2. It is over this range that the Fechner fraction, $\Delta I/I$, is constant; so that we have the relationship:

$$\log \Delta I = \log I + Constant$$

   so that with a logarithmic plot we should have a straight line with slope equal to unity.
3. Stiles' increment-threshold technique is one of several that have been employed to isolate the individual mechanisms; Brindley's studies on adaptation to very strong monochromatic stimuli are described later (p. 440); the blue mechanism may be identified by virtue of its much lower critical fusion frequency for flicker (Brindley *et al.*, 1966), and the greater area over which Ricco's Law applies, (12–18′ compared with 4′ for red and green), suggesting that the blue-sensitive cones are connected to a more diffuse type of bipolar (Brindley, 1954).
4. Glickstein & Heath (1975) found no cones in the fovea of their monochromat with very few in the periphery.
5. Alpern & Wake (1977), Alpern & Pugh (1977), and Alpern & Moeller (1977).
6. Individual variations in colour-mixing function, whether encountered in normal trichromats or in the colour-defective, can often be explained on the basis of variations in transmissivity of the ocular media, etc. (see, for example, Pokorny *et al.*, 1973). The elaborate studies of Alpern, however, have ruled out such an explanation for the variations in computed action-spectra, and therefore of extinction spectra, observed in his colour-defective subjects.
7. Barlow (1982) pointed out that, by plotting absorbance against the fourth root of wavelength, the absorbance curves all had the same shape, so this has been done in Fig. 15.15.

We may note that there was a hint of two subpopulations amongst the red- and green-cone pigments.

8. The fish retina has been studied with micro-electrodes because the cones are very large so that intracellular recording becomes practicable; moreover, the colour vision of fishes has been studied very extensively from a behavioural point of view, and there is no doubt that their colour discrimination is good and similar to that of man (see Svaetichin & MacNichol, 1958, for references).
9. In the pigeon Bowmaker (1977) identified by microspectrophotometry three cone photopigments, P_{567}, P_{514} and P_{461}, in addition to the scotopic rod pigment, P_{503}. Norren (1975), on the basis of ERG measurements, identified two short-wavelength systems in the retinae of pigeon, chicken and daw; these had λ_{max} at 415 and 480 nm. The 480 nm system could be mimicked by a cone-pigment with λ_{max}=460 nm, combined with a yellow oil-droplet; he considered that the system with λ_{max}=415 nm might be based on a violet-sensitive pigment. In the dace, Harosi & Hashimoto (1983) identified some six pigments, two in the violet and ultra-violet-absorbing regions with λ_{max} of 405–415 nm and 350–370 nm. They point out that roach, goldfish, pigeons, humming birds and the chicken are good candidates for having ultraviolet-sensitive cones. The presence of the extra short-wavelength sensitive pigment in the Japanese dace means that its retina operates on a tetrachromatic basis.
10. De Monasterio & Schein discuss the influence of the two types of ganglion cell, both behaving as broad-band dominators, on the psychophysically measured photopic luminosity function of the monkey; the activity of Type IV cells, predominantly in the fovea, would give the luminosity function a protan-like sensitivity, i.e. a reduced sensitivity to long wavelengths. The cat is commonly considered to be colour-blind; as summarized by Ringo & Wohlbarsht (1986) both behavioural and ganglion-cell studies indicate some degree of colour discrimination based on absorbing pigments in the regions 556, 450 and 400 nm. In their own study they found a few ganglion cells with local opponency within either centre or surround of the receptive field. Most had a large-field opponence between centre and surround with partly different cone-inputs. In a behavioural study Loop *et al.* (1987), using essentially Stiles' technique for distinguishing different cone mechanisms, obtained evidence for separate blue and green mechanisms under photopic viewing conditions; there was no evidence for a 500 nm unit in photopic vision.

References

Aguliar, M. & Stiles, W. S. (1954) Saturation of the rod mechanism at high levels of illumination. *Optica Acta* **1**, 59–65.

Alpern, M., Mindel, J. & Torii, S. (1968) Are there two types of deuteranopes? *J. Physiol.* **199**, 443–456.

Alpern, M. & Moeller, J. (1977) The red and green cone visual pigments of deuteranomalous trichromacy. *J. Physiol.* **266**, 647–675.

Alpern, M. & Pugh, E. N. (1977) Variation in the action spectrum of enythrolabe among deuteranopes. *J. Physiol.* **266**, 613–646.

Alpern, M. & Wake, T. (1977) Cone vision in human deutan colour vision defects. *J. Physiol.* **266**, 595–612.

Arden, G. B. & Tansley, K. (1955) The spectral sensitivity of the pure cone retina of the squirrel (*Sciurus carolinensis leucotis*). *J. Physiol.* **127**, 592–602.

Baker, H. D. & Rushton, W. A. H. (1965) The red-sensitive pigment in normal cones. *J. Physiol.* **176**, 56–72.

Barlow, H. B. (1982) What causes trichromacy? A theoretical analysis using comb-filtered spectra. *Vision Res.* **22**, 635–644.

Baylor, D. A. & Hodgkin, A. L. (1973) Detection and resolution of visual stimuli by turtle photoreceptors. *J. Physiol.* **234**, 163–198.

Baylor, D. A., Nunn, B. J. & Schnapf, J. L. (1987) Spectral sensitivity of cones of the monkey *Macaca fascicularis*. *J. Physiol.* **390**, 145–160.

Blackwell, H. R. & Blackwell, O. M. (1961) Rod and cone mechanisms in typical and atypical congenital achromatopsia. *Vision Res.* **1**, 62–107.

Bowmaker, J. K. (1977) The visual pigments, oil droplets and spectral sensitivity of the pigeon. *Vision Res.* **17**, 1129–1138.

Bowmaker, J. K. & Dartnall, H. J. A. (1980) Visual pigments of rods and cones in a human retina. *J. Physiol.* **298**, 501–511.

Bowmaker, J. K. & Knowles, A. (1977) The visual pigments and oil droplets of the chicken retina. *Vision Res.* **17**, 755–764.

Brindley, G. S. (1954) The summation areas of human colour-receptive mechanisms at increment threshold. *J. Physiol.* **124**, 400–408.

Brindley, G. S., Du Croz, J. J. & Rushton, W. A. H. (1966) The flicker fusion frequency of the blue-sensitive mechanism of colour vision. *J. Physiol.* **183**, 497–500.

Brown, P. K. & Wald, G. (1964) Visual pigments in single rods and cones of the human retina. *Science* **144**, 45–52.

Buchsbaum, G. & Gottschalk, A. (1983) Trichromacy, opponent colour coding and optimum colour information transmission in the retina. *Proc. Roy. Soc. B* **220**, 89–113.

Cole, B. L. & Watkins, R. D. (1967) Increment thresholds in tritanopia. *Vision Res.* **7**, 939–947.

Dagher, M., Cruz, A. & Plaza, L. (1958) Colour thresholds with monochromatic stimuli in the spectral region 530–630 μ. In *Visual Problems of Colour. N.P.L. Symp.*, No. 8, pp. 389–398.

Dartnall, H. J. A., Bowmaker, J. K. & Mollon, J. D. (1983) Human visual pigments: microspectrophotometric results from the eyes of seven persons. *Proc. Roy. Soc. B* **220**, 115–130.

Daw, N. W. (1968) Colour-coded ganglion cells in the goldfish retina: extension of their receptive fields by means of new stimuli. *J. Physiol.* **197**, 567–592.

Daw, N. W. (1973) Neurophysiology of color vision. *Physiol. Rev.* **53**, 571–611.

De Monasterio, F. M. & Gouras, P. (1975) Functional properties of ganglion cells of the rhesus monkey retina. *J. Physiol.* **251**, 167–195.

De Monasterio, F. M., Gouras, P. & Tolhurst, D. J. (1975a) Trichromatic colour opponency in ganglion cells of the rhesus monkey retina. *J. Physiol.* **251**, 197–216.

De Monasterio, F. M., Gouras, P. & Tolhurst, D. J. (1975b) Concealed colour opponency in ganglion cells of the rhesus monkey retina. *J. Physiol.* **251**, 217–229.

De Monasterio, F. M. & Schein, S. J. (1980) Protan-like spectral sensitivity of foveal Y ganglion cells of the retina of macaque monkeys. *J. Physiol.* **299**, 385–396.

De Monasterio, F. M. & Schein, S. J. (1982) Spectral bandwidths of color-opponent cells of geniculocortical pathway of macaque monkey. *J. Neurophysiol.* **47**, 214–224.

Dodt, E. & Walther, J. B. (1958) Der photopischer Dominator im Flimmer-ERG der Katze. *Pflüg. Arch.* **266**, 175–186.

Dreher, B., Fukada, Y. & Rodieck, R. W. (1976) Identification, classification and anatomical segregation of cells of X-like and Y-like properties in the lateral geniculate nucleus of old-world primates. *J. Physiol.* **258**, 433–452.

Fager, L. Y. & Fager, R. S. (1981) Chicken blue and chicken violet, short wavelength sensitive visual pigments. *Vision Res.* **21**, 581–586.

Fincham, E. F. (1953) Defects of the colour-sense mechanism as indicated by the accommodation reflex. *J. Physiol.* **121**, 570–580.

Fuortes, M. G. F. & Simon, E. J. (1974) Interactions leading to horizontal cell responses in the turtle retina. *J. Physiol.* **240**, 177–198.

Gibson, I. M. (1962) Visual mechanisms in a cone-monochromat. *J. Physiol.* **161**, 10–11P.

Glickstein, M. & Heath, G. G. (1975) Receptors in the monochromat eye. *Vision Res.* **15**, 633–636.

Gouras, P. (1968) Identification of cone mechanisms in monkey ganglion cells. *J. Physiol.* **199**, 533–547.

Gouras, P. (1969) Antidromic responses of orthodomically identified ganglion cells in monkey retina. *J. Physiol.* **204**, 407–419.

Graham, C. H. & Hsia, Y. (1958) Colour defect and colour theory. *Science* **127**, 675–682.

Granit, R. (1943) A physiological theory of colour perception. *Nature, Lond.* **151**, 11–14.

Granit, R. & Wrede, C. M. (1937) The electrical responses of the light-adapted frog's eyes to monochromatic stimuli. *J. Physiol.* **89**, 239–256.

Hanoaka, T. & Fujimoto, K. (1957) Absorption spectrum of a single cone in carp retina. *Jap. J. Physiol.* **7**, 276–285.

Hárosi, F. I. & Hashimoto, Y. (1983) Ultraviolet visual pigments in a vertebrate: a tetrachromatic cone system in the dace. *Science* **222**, 1021–1023.

Hecht, S. (1947) Colourblind vision. I. Luminosity losses in the spectrum from dichromats *J. gen. Physiol.* **31**, 141–152.

Hubel, D. H. & Wiesel, T. N. (1960) Receptive fields of optic nerve fibres in the spider monkey. *J. Physiol.* **154**, 572–580.

Hurvich, L. M. (1972) Color vision deficiencies. In *Hdb. Sensory Physiol.* VII/4, 607. Springer, Berlin.

Hurvich, L. M. & Jameson, D. (1955) Some quantitative aspects of an opponent colour theory. I–III. *J. Opt. Soc. Amer.* **45**, 546–552, 602–616; **46**, 405–415.

Jameson, D. & Hurvich, L. M. (1955) Some quantitative aspects of an opponent colour theory. I. *J. Opt. Soc. Amer.* **45**, 546–552.

Jameson, D. & Hurvich, L. M. (1956) Some quantitative aspects of an opponent colour theory. III. *J. Opt. Soc. Amer.* **46**, 405–415.

Jameson, D. & Hurvich, L. M. (1968) Opponent response functions related to measured cone photopigments. *J. Opt. Soc. Amer.* **58**, 429–430.

Kaneko, J. A. & Tachibana, M. (1985) A voltage-clamp analysis of membrane currents in solitary bipolar cells dissociated from *Carassius auratus*. *J. Physiol.* **358**, 131–152.

Kolb, H. & Jones, J. (1985) Electron microscopy of Golgi-impregnated photoreceptors reveals connections between red and green cones in the turtle retina. *J. Neurophysiol.* **54**, 304–317.

Larsen, H. (1921) Demonstration mikroskopischer Präparate von einem monochromatischen Auge. *Klin. Mbl. Augenheilk.* **67**, 301–302.

Le Grand, Y. (1948) *Optique Physiologique.* Vol. 2. Paris: Editions de la Revue D'Optique.

Liebman, P. A. (1972) Microspectrophotometry of photoreceptors. In *Hdb Sensory Physiol.* **VII/1**, 482–528. Berlin, Springer.

Liebman, P. A. & Granda, A. M. (1971) Microspectrophotometric measurements of visual pigments in two species of turtle (*Pseudemys scripta* and *Chelona mydas*). *Vision Res.* **11**, 105–114.

Loop, M. S., Millican, C. L. & Thomas, S. R. (1987) Photopic spectral sensitivity in the cat. *J. Physiol.* **382**, 537–553.

Marks, W. B. (1965) Visual pigments of single goldfish cones. *J. Physiol.* **178**, 14–32.

Marks, W. B., Dobelle, W. H. & MacNichol, E. F. (1964) Visual pigments of single primate cones. *Science* **143**, 1181–1183.

Marriott, F. H. C. (1976) Colour vision. In *The Eye*, Ed. H. Davson. Vol. 2A, pp. 475–588. Academic Press: New York.

McFarland, W. N. & Munz, F. W. (1975) The evolution of photopic visual pigments in fishes. *Vision Res.* **15**, 1071–1080.

Muntz, W. R. A. (1972) Inert absorbing and reflecting pigments. *Hdb. Sensory Physiol.* **VII/1**, 529–565.

Munz, F. W. & McFarland, W. N. (1975) Presumptive cone pigments extracted from tropical marine fish. *Vision Res.* **15**, 1045–1062.

Naka, K. I. & Rushton, W. A. H. (1966a) Sopotentials from colour units in the retina of the fish (*Cypridinae*). *J. Physiol.* **185**, 436–555.

Naka, K. I. & Rushton, W. A. H. (1966b) An attempt to analyse colour reception by electrophysiology. *J. Physiol.* **185**, 556–586.

Naka, K. I. & Rushton, W. A. H. (1966c) Sopotentials from luminosity units in the retina of the fish (*Cypridinae*). *J. Physiol.* **185**, 587–599.

Normann, R. A., Perlman, I. & Daly, S. J. (1985) Mixing of color signals by turtle cone photoreceptors. *J. Neurophysiol.* **54**, 293–303.

Norren, D. V. (1975) Two short wavelength sensitive cone systems in pigeon, chicken and daw. *Vision Res.* **15**, 1164–1166.

Norton, A. L., Spekreijse, H., Wohlbarsht, M. L. & Wagner, H. G. (1968) Receptive field organization of the S-potential. *Science* **160**, 1021–1022.

Piantanida, T. P. & Sperling, H. G. (1973) Isolation of a third chromatic mechanism in the deuteranomalous observer. *Vision Res.* **13**, 2049–2058.

Pickford, R. W. (1951) *Individual Differences in Colour Vision.* Routledge and Kegan Paul, London.

Pitt, F. H. G. (1935) Characteristics of dichromatic vision. *Med. Res. Council Sp. Rep. Ser.*, No. 200.

Pokorny, J., Smith, V. C. & Katz, I. (1973) Derivation of the photopigment absorption spectra in anomalous trichromats. *J. opt. Soc. Am.* **63**, 232–237.

Pugh, E. N. (1976) The nature of the π_1 colour mechanism. *J. Physiol.* **257**, 713–747.

Richter, A. & Simon, E. J. (1974) Electrical responses of double cones in the turtle retina. *J. Physiol.* **242**, 673–683.

Ringo, J. L. & Wohlbarsht, M. L. (1986) Spectral coding in cat retinal ganglion cell receptive fields. *J. Neurophysiol.* **55**, 320–330.

Rushton, W. A. H. (1959) Visual pigments in man and animals and their relation to seeing. *Progr. Biophys.* **9**, 239–283.

Rushton, W. A. H. (1963) A cone pigment in the protanope. *J. Physiol.* **168**, 345–359.

Rushton, W. A. H. (1965) A foveal pigment in the deuteranope. *J. Physiol.* **176**, 24–37.

Stell, W. K. & Lightfoot, D. O. (1975) Color-specific interconnections of cones and horizontal cells in the retina of the goldfish. *J. comp. Neurol.* **159**, 473–502.

Stiles, W. S. (1959) Colour vision: the approach through increment-threshold sensitivity. *Proc. Natl. Acad. Sci. Wash.* **45**, 100–114.

Stiles, W. S. & Burch, J. M. (1959) N.P.L. colour-matching investigations: final report (1958). *Optica Acta* **6**, 1–26.

Svaetichin, G. (1956) Spectral response curves from single cones. *Acta physiol. Scand.* **39**, Suppl. 134, 17–46.

Svaetichin, G. & MacNichol, E. F. (1958) Retinal mechanisms for chromatic and achromatic vision. *Ann. N.Y. Acad. Sci.* **74**, 385–404.

Tomita, T., Kaneka, A., Murakami, M. & Pautler, E. L. (1967) Spectral response curves of single cones in the carp. *Vision Res.* **7**, 519–531.

Wald, G. (1945) Human vision and the spectrum. *Science* **101**, 653–658.

Wald, G., Brown, P. K. & Smith, P. H. (1955) Iodopsin. *J. gen. Physiol.* **38**, 623–681.

Walls, G. L. & Heath, G. G. (1954) Typical total colour blindness reinterpreted. *Acta ophthal. Kbh.* **32**, 253–297.

Weale, R. A. (1953) Cone monochromatism. *J. Physiol.* **121**, 548–569.

Weale, R. A. (1959) Photosensitive reactions in fovea of normal and cone-monochromatic observers. *Optica Acta*, **6**, 158–174.

Wiesel, T. N. & Hubel, D. H. (1966) Spatial and chromatic interactions in the lateral geniculate body of the rhesus monkey. *J. Neurophysiol.* **24**, 1115–1156.

Wright, W. D. (1946) *Researches on Normal and Defective Colour Vision.* London: Kimpton.

Wright, W. D. (1952) The characteristics of tritanopia. *J. opt. Soc. Am.* **42**, 509—521.

Wyszecki, G. & Stiles, W. S. (1982) *Color Science. Concepts and Methods.* N.Y.: Wiley. (Quoted by Baylor *et al.*, 1987.)

Yang, X.-L., Tauchi, M. & Kaneko, A. (1983) Convergence of signals from red-sensitive and green-sensitive cones onto L-type external horizontal cells of the goldfish retina. *Vision Res.* **23**, 371–380.

Yen, L. & Fager, R. S. (1984) Chromatographic resolution of the rod pigment from the four cone pigments of the chicken retina. *Vision Res.* **24**, 1555–1562.

Yoshizawa, T. & Wald, G. (1967) Photochemistry of iodopsin. *Nature* **214**, 566–571.

16. THE STILES–CRAWFORD EFFECT, ADAPTATION AND PHOTOPIC SENSITIVITY CURVES

We may conclude this account of modern research devoted to the elucidation of the mechanism of vision with a few special aspects of phenomena that have already been discussed in a more elementary fashion.

DIRECTIONAL SENSITIVITY OF THE RETINA

Pupillary Diameter

Stiles & Crawford (1933) decided to develop an indirect method of measuring pupillary diameter. They argued that the larger the pupil the greater the amount of light that would enter the eye and hence the greater the apparent brightness of a luminous field; the amount of light would increase in proportion to the area of the pupil and this is in proportion to the square of its diameter. They found that the calculated diameter never increased beyond 5.5 mm although the maximum diameter actually measured was about 8 mm. This discrepancy was shown to be due to the circumstance that, as the pupil became larger, the retina received relatively more rays of light that struck it obliquely; if these oblique rays were less efficient than those entering through the centre of the pupil, then the discrepancy could be explained. The effects are large, so that if the subjective brightness of a pencil entering at the very periphery of the pupil is compared with one entering centrally, it may be only 15% of this.

Cone Phenomenon

It was shown that the phenomenon was peculiar to the cones, both foveal and peripheral, and this has provided a valuable method for determining whether rods or cones are concerned in a given visual event. Thus Donner & Rushton (1959), studying the responses of a single ganglion cell in the frog, showed that when it behaved as a scotopic dominator its responses were independent of the direction of incidence of the pencil of light; when it behaved as a photopic dominator, after light-adaptation, it showed directional sensitivity; moreover, in the mesopic range when a hump appears on the sensitivity curve in the blue, this 'blue hump' was shown to be insensitive to direction, and thus to be due to activity of rods, probably of a special type called 'green rods' (Denton & Wyllie, 1955).

Variation with Wavelength

The magnitude of the directional effect varies with wavelength (Stiles, 1937); moreover, if monochromatic light is used there is a change in its subjective hue as the angle of incidence of the rays varies; this is called the Stiles–Crawford effect of the second kind. Brindley (1953) showed that colour-matches could be upset by changing from direct to oblique incidence, so that it would seem that the forms of the fundamental response curves of the cone mechanisms responsible for wavelength discrimination change with angle of incidence of the radiation. Since the shape of an absorption spectrum depends on the density of the pigment in solution, and since the shape of the sensitivity curve presumably depends on that of the absorption spectrum of the cone-pigment, we can conclude that the effective optical density of pigment in the cone varies with direction of incidence.

Wave-guide Theory

The most plausible explanation is that put forward by Wright & Nelson (1936) to the effect that light entering directly along the axis of the cone is more likely to be retained by a series of total internal reflexions than light entering obliquely.

The dense packing of the transverse discs makes the refractive index of the inside of the receptor segment greater than that of the outside medium, and thus promotes total internal reflexion. In addition, the stout outer segments act as light-collectors, funnelling the light into the thinner inner segments (Winston & Enoch, 1971). Such an arrangement would ensure that the pigment was maximally exposed to the incident quanta of light whilst providing the optical isolation of the receptors necessary for resolution (Kirschfeld & Snyder, 1976).

Experiments on Turtle Cone

The theoretical electromagnetic treatment of Snyder & Pask (1973) has confirmed the possibility, whilst recent electrophysiological studies have provided quantitative information respecting its wavelength-dependence in the turtle cone. This cone is interesting because of the presence of oil-droplets in its inner segment, and Baylor & Hodgkin (1973) noticed, in their study of hyperpolarizing responses in individual cones, that there were very wide variations in maximal sensitivity amongst any group, suggesting that the cones were being illuminated at different angles; moreover, there was a positive correlation between the absolute sensitivity of a cone and the reduction in sensitivity when the wavelength was changed from λ_{max} towards the short wavelength. This positive correlation could be explained on the basis of Fig. 16.1; at the left, light enters axially so that it is efficiently absorbed and the cone has a high sensitivity; however, the light passes through the oil-droplet, which absorbs short wavelength light and so there will be a large falling off in sensitivity with short wavelengths. By contrast, at the right the light falls obliquely, less is absorbed by the photosensitive pigment and less passes through the oil-droplet, so that the cut-off at short wavelengths is not so strong. Thus sensitivity and short wavelength cut-off run parallel, as found. In general, many cones showed sharp profiles of sensitivity versus angle of incidence of stimulating light, but this depended very strongly on the wavelength of the stimulating light, as we should expect. Thus with a red-sensitive cone (Fig. 16.2) orange and red lights gave sharp profiles but blue-green light not only showed a low sensitivity but an inverted profile; light entering obliquely, and tending thereby to avoid the blue-absorbing (yellow) droplet, being more efficient.

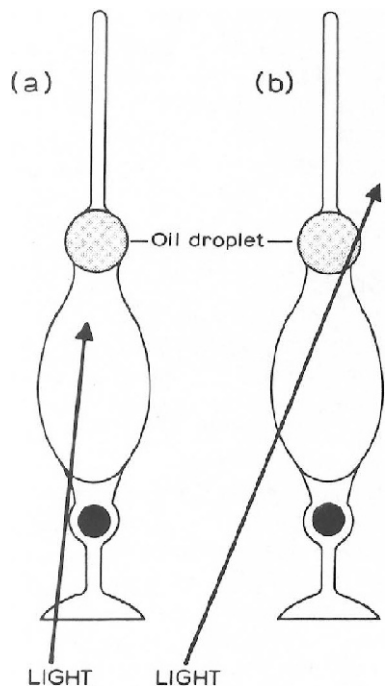

Fig. 16.1 Showing how variation in angle of incidence of light on turtle cone can influence spectral response.

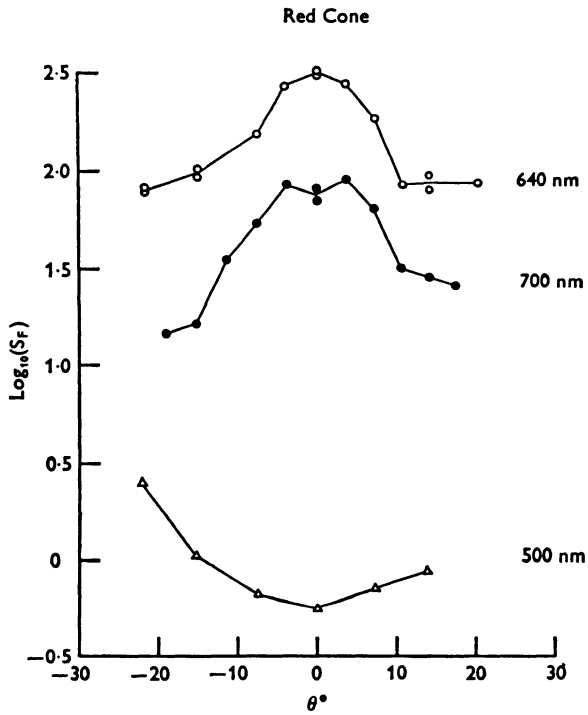

Fig. 16.2 Profiles of angular sensitivity of a red-sensitive turtle cone. The ordinate is the logarithm of the flash-sensitivity to light of the wavelengths indicated on the graphs. Note that with blue light oblique stimuli are more effective (sensitivity greater), and this is because the light avoids the yellow oil-droplets. (Baylor & Fettiplace, *J. Physiol.*)

ORIENTATION OF RECEPTORS

Histological study of the orientation of the receptors revealed that, although the receptors in a given region were aligned parallel with each other, the orientation of the inner segments varied, depending on retinal location, so that at the pole they were at right-angles to the retinal surface and thus pointing into the pupil whereas at the periphery the deviation from perpendicularity could be as great as 60°.

COLLECTION EFFICIENCY

By measuring the amount of light passing through the cones experimentally, a collection efficiency of 0.55 ± 0.05

was obtained where the efficiency E is given by

$$E = \frac{A_1 I_1}{A_1 I_1 + A_2 I_2}$$

A_1 being the cross-sectional area of the spot falling on the base of the outer segment with mean relative intensity I_1, and A_2 is the area of the corresponding inner segment minus A_1, and I_2 is the mean relative intensity in the dark region round the bright spot.

Figure 16.3 shows the directional sensitivity of red-sensitive cones compared with a theoretical curve based on a model cone computed by Winston & Enoch (1971).[1]

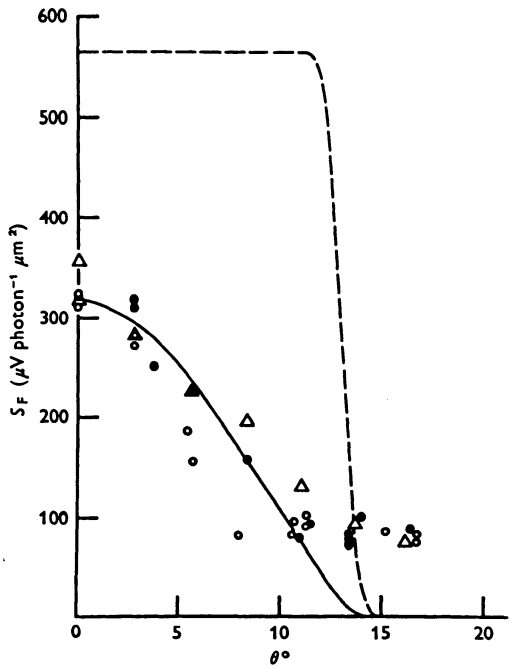

Fig. 16.3 Directional sensitivity of a red-sensitive cone compared with a theoretical curve derived by Winston & Enoch (1971) for a cone with inner and outer segments with diameters in the ratio of 4.5. The dashed line shows the performance of an ideal collector with total internal reflexion and 100% efficiency of collection of light not exceeding θ_{max} of 13°. (Baylor & Fettiplace, *J. Physiol.*)

Rod Vision

Psychophysical studies on man have usually failed to reveal a significant Stiles–Crawford effect for rod vision (see, for example, Flamant & Stiles, 1948) although optical studies on the retinae of several species have indicated wave-guide properties in the rods which, in the goldfish, may be as effective as those of the cones (Tobey *et al.*, 1975). As Van Loo & Enoch (1975) state, the limited angle of acceptance of the rod as a wave-guide, its cylindrical shape, orientated photopigment, its separation from neighbouring cells by interdigitating fibrils from the pigment epithelium, and the higher index of refraction of the cells relative to the surrounding interstitial matrix, indicate that directionality should be present. These authors have re-examined the matter in three human subjects and, as Fig. 16.4 shows, there is directionality, although small compared with that for cone vision.[2]

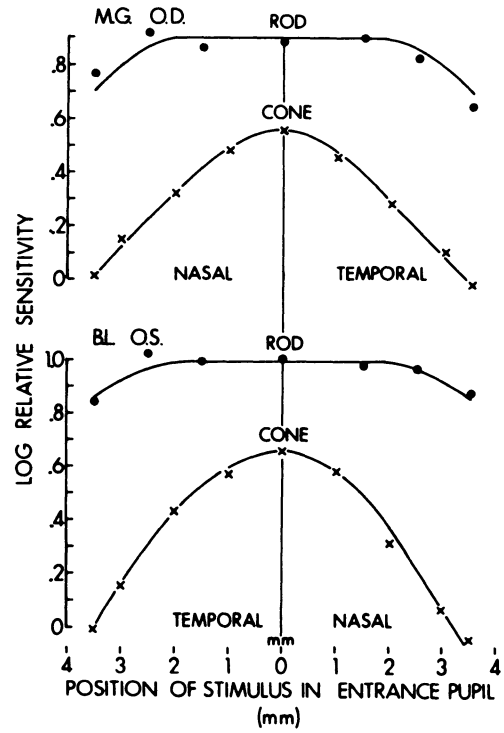

Fig. 16.4 Rod and cone Stiles–Crawford curves for two human observers. (Van Loo & Enoch, *Vision Res.*)

ADAPTATION AND INTERACTION OF LIGHT STIMULI

Rod Adaptation

The main phenomena of adaptation have been already described throughout this section, and here we shall discuss only some special aspects. By dark-adaptation we mean the recovery of sensitivity of the retina following exposure to light; so far as rod vision in man is concerned, there is little doubt that this process is largely determined by the regeneration of rhodopsin, although the relationship between retinal sensitivity and concentration of rhodopsin in the retina is not so simple as had been at first

thought (p. 265), so that the concept of a neural brightness control mechanism has been introduced, a mechanism that behaves like 'dark light' and is apparently governed by signals generated, in the first place, by the amount of unregenerated photopigment in the receptors.

Foveal Adaptation

With human foveal, i.e. cone, vision, Wright (1939) has established the existence of an essentially similar process that takes place far more rapidly however, presumably because cone pigments regenerate more rapidly (p. 405). The reverse process, which we may call foveal light-adaptation, constitutes a decrease in sensitivity of the retina during continued exposure to light; it was studied by Wright with his binocular matching technique, the change in sensitivity of one eye, during exposure to light, being measured by comparing the subjective sensations in the two eyes. The curve of decrease in sensitivity falls over a period of some 50 seconds to reach a plateau with a sensitivity about one sixteenth of the original value (Fig. 7.8).

Alpha-adaptation

A much more rapid adaptive effect was described by Schouten & Ornstein, who measured the effect of a small glare-source of light, stimulating a peripheral part of the retina, on the brightness-sensation experienced by the fovea. Thus the two eyes would view independently the two halves of an illuminated field, and these would be adjusted in luminosity to give a match. The peripheral glare-source, entering one eye only, would now be switched on, and immediately the match would be disturbed, the half of the field seen by the eye with the glare-source appearing much darker. By raising its luminance till a match was obtained the decrease in sensitivity could be determined. This *α-adaptation*, as Schouten & Ornstein called it, is complete within a fraction of a second and was thought to differ from the β-adaptation of Wright in that its effect extended to the whole retina, even though only a small part was stimulated. Provided exposure to the glare-source was short, recovery of sensitivity was rapid. Thus long before Wright, in his binocular matching studies, had made his first measurement of retinal sensitivity, this had presumably decreased by a factor of about five because of this rapid α-adaptive process.

VEILING LUMINANCE

Subsequent work, notably that of Fry & Alpern has shown, however, that the phenomenon is not one of retinal interaction but is due to the scattered light from the glare-source. The effect of this scattered light is to behave as a 'veiling luminance', decreasing the sensitivity of the whole retina. We may regard the phenomenon as one of very rapid adaptation, but not, as originally thought, of inhibition of the whole retina by a stimulus falling on only a part. The rapid change in sensitivity of the retina to light is a very real phenomenon and spatial interaction, although not as marked as originally considered by Schouten & Ornstein, is likewise of considerable importance, and we shall now consider some aspects of temporal and spatial interaction.

Rod-cone Interaction

Where the effects of adapting lights on sensitivity of a given type of receptor are concerned, it is well established that the rod and cone systems of the human eye behave independently, in the sense that an adapting background affecting rods does not influence cone sensitivity, and vice versa. However, later work summarized by Latch & Lennie (1977) has described some exceptions to this rule, which have been tentatively explained on the basis that independence is confined to retinal events, whereas adaptive effects manifest in higher stages of the visual pathway are not independent.

Importance of Field Size

Latch & Lennie examined the situation when the threshold for rod vision in the peripheral retina is raised by a steady background acting through the cones, and showed that the important feature of the stimulus-conditions was the size of the stimulus or the adapting light; thus a large adapting field affected threshold for rods to the extent that the adapting field affected the rods, whereas with a small adapting field, threshold was elevated more by a long-wavelength background than a short-wavelength background although their intensities had been matched for equal effects on rods. Thus the long-wavelength background, stimulating cones, as well as rods, was the more effective background. In a reverse way, a small background-adapting light, affecting rods, could affect also the threshold for a stimulus seen through the cone mechanism. Latch & Lennie suggested that rod-cone interaction took place at a level in the visual pathway where image-size was discriminated, the phenomena described by them being comparable with those in which prolonged exposure to targets of a restricted size leads to reduced sensitivity to targets in this range of sizes but not to targets of different size.

TEMPORAL ASPECTS

Bloch's Law

The limited application of Bloch's Law has already been described; to recapitulate, over a certain action-time two successive stimuli summate completely, so that the product: $I \times t = Constant$ applies. At longer intervals, summation is only partial and at still longer intervals may be characterized as *probability summation*, the two flashes being separated temporally to the extent that they may be considered as independent events, so that there is no question of summation of quanta.

Critical Duration

It becomes of interest, therefore, to ascertain with some precision the critical duration over which Bloch's Law of complete summation holds, and the effects of such stimulus variables as area, eccentricity and wavelength. So far as the minimum period over which the Law applies, Brindley (1952) found that it held down to flash-durations of extreme brevity, at least as short as 4.1×10^{-7} sec when the retinal illumination was 3×10^{8} trolands. In the same study Brindley found that the greatest duration was of the order of 30 msec. The subject has been investigated recently by Saunders (1975) who varied size and eccentricity as well as duration of the flashes required to excite at threshold. Figure 16.5 shows the relative sensitivity of the dark-adapted eye to flashes of increasing duration, where relative sensitivity is the reciprocal of the threshold intensity. When plotted on a log-log basis in this way, the points fall on two straight lines; the initial line represents the application of Bloch's Law and the change to a new relation occurs at the arrow, namely at 80 msec.

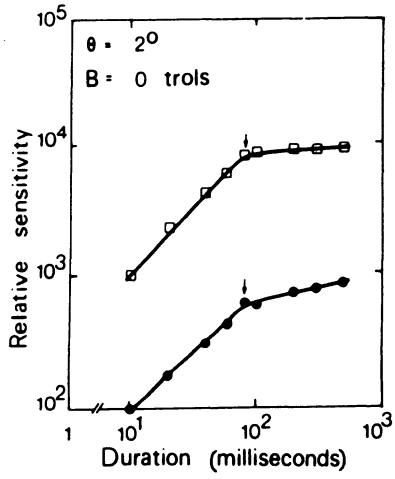

Fig. 16.5 The relative sensitivity of the dark-adapted eye (B = 0 trols) to achromatic stimuli of increasing duration. (●) 3.2 minutes of arc stimulus; (□) 32 minutes of arc. Arrows indicate critical duration below which Bloch's Law applies. (Saunders, *Vision Res.*)

SIZE AND ECCENTRICITY

The two sets of results apply to different sizes of stimulus and the break occurs at the same point indicating no effect of size; similarly, varying the eccentricity of the stimulus was without effect.

BACKGROUND LUMINANCE

When the flash was viewed against a bright background, so that the luminance-increment was being measured, rather than absolute threshold, the critical duration decreased on increasing the stimulus-area, as Barlow (1958) had found. The reason why at high background luminance the critical duration is decreased for large areas of stimulus, i.e. the effective temporal summation is reduced, is probably related to the effects of background on *spatial* summation. Thus the area over which there is complete spatial summation (Ricco's Law) becomes smaller at high background luminance (Barlow, 1958; Glezer, 1965), so that in order to achieve maximal temporal summation the stimulus-area must be smaller than Ricco's summation area when increment threshold measurements are made, by contrast with the situation at absolute threshold when summation-area becomes unimportant. When the Stiles colour mechanisms were studied, using increment thresholds against backgrounds designed to isolate a given mechanism (p. 400), a critical duration of 80 msec was obtained similar to that for achromatic stimuli at threshold, but as we might expect, this was only true of small areas of stimulus as with achromatic increment-thresholds.

Successive Contrast

It is thought that the phenomena of successive contrast, or temporal induction, are associated with the slower β-adaptation described by Wright; here we are dealing with the effects of one stimulus on a succeeding one, both of them falling on the same part of the retina; the phenomena are essentially of an adaptive nature in the sense that the first stimulus depresses the sensitivity of the retina for a succeeding, like stimulus.

Meta-contrast

By *meta-contrast* is meant the inductive effect of a primary light stimulus on the sensitivity of the eye to a previously presented light stimulus on an adjoining part of the retina; it is a combination of temporal and spatial induction, or successive and simultaneous contrast. It is often called the 'flash after-effect' and has been studied by

Baumgardt & Ségal (1946) and Alpern (1953). Baumgardt & Ségal illuminated the two halves of a circular patch consecutively for a brief duration. If the left half only, for example, is illuminated for 10 msec, it produces a definite sensation of brightness. If, now, both are illuminated for the same period, but the right half some 20 to 50 msec later, the left half of the field appears much darker than before, and near the centre may be completely extinguished. The left field has thus been inhibited by the succeeding, nearby, stimulus.

Para-contrast

The right field, moreover, appears darker than when exposed alone—it has been inhibited by the first stimulus (*para-contrast*). Baumgardt & Ségal have shown that, by varying the interval between the presentation of the two halves of the illuminated field, a variety of intermediate degrees of meta-contrast may be achieved; moreover, these may be reproduced as after-images, but in the latter process the time relationships are altered so that if, for example, the left half of the field was dark and the right half bright in the primary sensation, the reverse relationship could be found in the after-image.

Binocular Matching

Alpern (1953) applied the binocular matching technique, whereby the left eye viewed a standard patch and the right eye a test-patch whose luminance could be adjusted by the observer to match the brightness of the left-eye patch. Besides the test-patch, an additional 'contrast-inducing' patch was presented to the right eye at varying intervals before or after the presentation of the test-patch. Figure 16.6 shows the change in apparent brightness of the test-patch as a function of the exposure-asynchrony, a value of zero representing simultaneous presentation. The ordinate is the luminance of the test-patch required for it to appear as bright as the fixed comparison standard seen by the other eye, so that increases represent diminished sensitivity of the right eye. It will be seen that there is a little paracontrast with negative exposure asynchronies (the contrast-inducing patch appearing before the test-patch), and that the maximal meta-contrast occurs at an interval of about 50 msec. The meta-contrast effect operated over only a small area, so that the best effect was achieved if the edges of test and contrast-inducing fields coincided; no effect could be found in the fovea. Alpern's experiments suggested that the para-contrast effect was due to the light scattered within the eye by the preceding contrast-inducing flash.

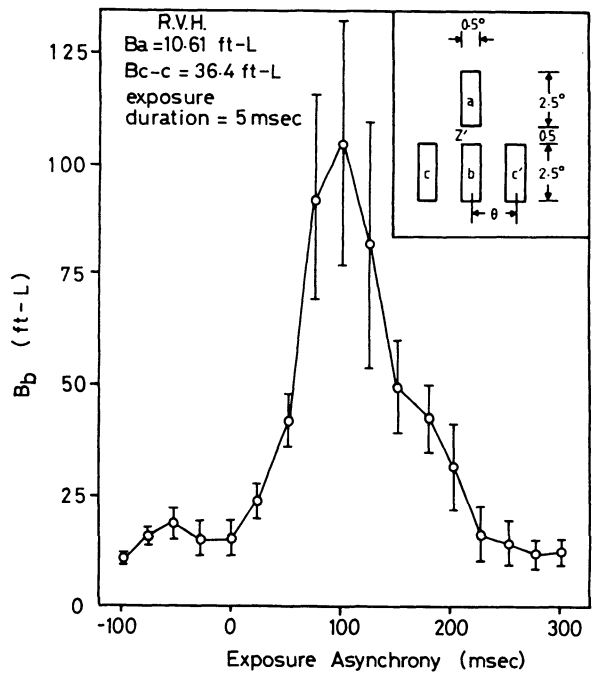

Fig. 16.6 Showing change in apparent brightness of a test-patch as a function of the exposure-asynchrony of two flashes presented in succession. Ordinate is luminance of the test-patch required to give a brightness-match with the comparison standard when the two contrast-inducing patches were flashed at various times before and after the exposure of the test- and comparison-flashes. Abscissa is time-interval between the onset of the test and comparison flashes and that of the contrast-inducing patches. *Inset*: Stimulus pattern. *a* is comparison standard seen with the left eye; *b* is the test patch seen with the right eye; *c*–*c'* are the two contrast-inducing patches also seen by the right eye. The fixation point, *Z'*, is seen singly and binocularly. (Alpern, *J. opt. Soc. Amer.*)

CONE–ROD INTERACTION

In a later study (1965) Alpern considered the possibility that the effect was due to cone–rod interaction, the test patch exciting rods and the contrast-inducing patch exciting cones and, because of the shorter latency of the cone response, the two stimuli being effectively simultaneous. He concluded, however, that meta-contrast was manifest with both rod and cone vision, but that there was no cone-rod interaction, a rod-stimulus being incapable of affecting the cone threshold, and *vice versa.*

π-MECHANISMS

Alpern and Rushton (1965) showed, moreover, that when purely cone excitation was involved in both test- and contrast-inducing stimuli, the cone–cone interaction was highly specific, so that a given Stiles π-mechanism (p. 401) did not affect a test-flash exciting a different π-mechanism.

This degree of specificity is somewhat surprising since we are measuring an adaptive decrease in retinal sensitivity that presumably results from activation of a

gain-control mechanism. Foster (1976) has re-examined the possibility of rod–cone interaction by using a cone-stimulating red test-flash with a rod-stimulating contrast-inducing surround of green; as Fig. 16.7 shows, there is a very definite elevation of threshold for contrast-inducing stimuli that both precede (para-contrast) and follow (metacontrast) the test stimulus.[3]

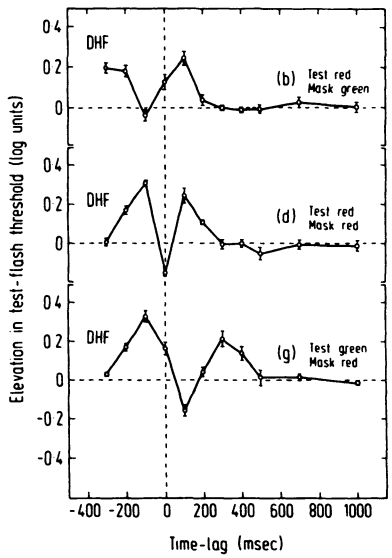

Fig. 16.7 Elevation of threshold for a test-flash by masking stimuli preceding or following the test-flash. (Foster, *Vision Res.*)

Broca–Sulzer Effect

Broca & Sulzer (1902) found that a brief light flash may appear brighter than a steadily maintained light of equivalent luminance.

Growth of Sensation

Thus Fig. 16.8 is a curve of brightness-sensation against time during which a bright light is regarded by an observer, and was redrawn from the classical study of Broca and Sulzer. In effect, the ordinate is the luminance of a long-sustained flash of light necessary to match a brief flash of increasing duration. A number of studies have confirmed and extended this work, e.g. Katz (1964). If we accept, then, that the sensation of brightness builds up rapidly and passes through a maximum, it will be clear from Fig. 16.8 that, if the light had been switched off after 50 msec the sensation, just before switching off, would have been far greater than if it had been maintained for 200 msec or more.

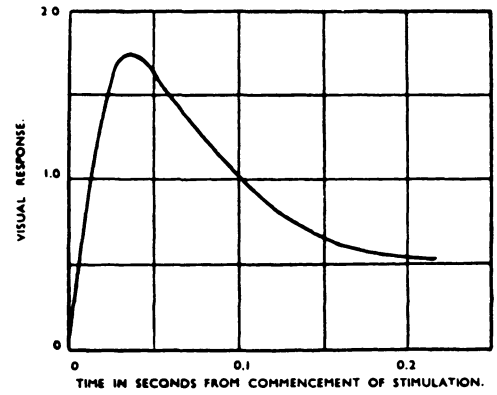

Fig. 16.8 Actual sensation curve during the first 200 msec of stimulation by a bright light. (Wright, from Schouten.)

If, then, we expose one eye to flashes of increasing duration, and we assess the subjective brightness of each flash by matching it with a variable luminance presented to the other eye—the binocular matching technique—the first effect of increased duration will be the temporal summation described by Bloch's Law (p. 275); beyond a critical duration, sensation will not increase appreciably with further duration of the stimulus, and in fact the Broca–Sulzer effect becomes manifest as an actual *decrease* in brightness-sensation until, finally, extending the duration has no effect. This gives the impression that short flashes located in the transition zone between complete temporal summation and duration-independence are brighter than longer flashes.

Dependence on Intensity

The location in time of the Broca–Sulzer effect depends on the flash-intensity, so that Aiba & Stevens (1964), for example, found the maximum effect in the dark-adapted eye decreased from 300 msec to less than 100 msec as the flash-intensity increased.

Rod Vision

By reducing sensitivity of the cones with a red background, the responses of rods could be examined in effective isolation; under these conditions a Broca–Sulzer effect could be demonstrated (White *et al.*, 1976), the maximum effect occurring around 200 to 400 msec. As with photopic vision, the Broca–Sulzer effect depended on the temporal pattern of the flashes so that if both began together there was no effect, but there was one if they finished together or were presented successively.

Finite Response-time

The growth of visual sensation revealed by Fig. 16.8 indicates in effect the finite response-time of the receptors and other elements in the visual pathway; operating against the growth is the development of adaptation or inhibition; the actual range over which the Broca–Sulzer effect will be manifest will be a function of the response-time, and this may be why the rod effect can be seen maximally later than the cone effect.

Backward Masking

It has been known for a long time that a test flash can appear less bright, i.e. be masked, when a more intense flash follows it by a certain period, i.e. there is a retroactive brightness depression. Crawford (1947) examined the phenomenon in some detail; he found that the threshold for a 10 msec 0.5° test-flash was considerably increased if it was followed up by a 524 msec brighter flash subtending 12°, the test flash being within the larger conditioning or masking flash. The period within which this retroactive effect could be elicited was about 100 msec.

Delay-period

Subsequent studies (reviewed by Raab, 1963) have extended the work and the general principle has emerged that there is a delay-period between the two stimuli below which there will be a masking effect, and that this delay-period is governed by the difference in luminance between the two flashes, the dimmer the test-flash in relation to the bright (succeeding) flash, the longer the delay-period.

Latencies of Flashes

If the bright flash is exerting its retroactive effect by an adaptive process—reducing the sensitivity of the retina to the test-flash—then we must assume that its effects reach some brightness-integrating centre before the effects of the weaker test-flash have finished, and the masking effect will be governed by the latencies of the two flashes; thus a weak flash has a longer latency than a brighter one, and this accounts for the fact that the period during which masking can occur is determined by the luminance-difference of test- and bright-flashes. It is interesting that the cortical evoked potential of the masked test-flash is inhibited so that it is, in effect, replaced by the subsequent conditioning flash's response (Donchin *et al.*, 1963).

Rod–Cone Interactions

The Purkinje shift in the scotopic sensitivity curve at mesopic ranges of luminance is an example of rod–cone interaction whereby the relative brightnesses of different wavelengths are influenced by the brightness sensation evoked by rod vision. Frumkes *et al.* (1973) have examined the possible interactions when flash-stimuli are succeeded at different intervals, one flash being such as to stimulate rods only (420 nm) and the other to stimulate cones (680 nm). If, as it seems, the depression of brightness-sensation due to a conditioning flash depends on the difference in latencies for the test and conditioning flashes, then since rods have longer latencies than cones, the maximal effect might be obtained if the rod test-flash preceded the cone flash. As in earlier studies, the threshold began to rise when the test-flash preceded the conditioning flash by about 100 msec, and the effect reached a maximum at an interval of + 10 msec and then it returned to control values. As Fig. 16.9 shows, the effect is manifest when conditioning and test-flashes stimulate different mechanisms. The authors considered that it was unlikely that the interaction occurred at the level of the horizontal cells, since primate horizontal cells receive input from

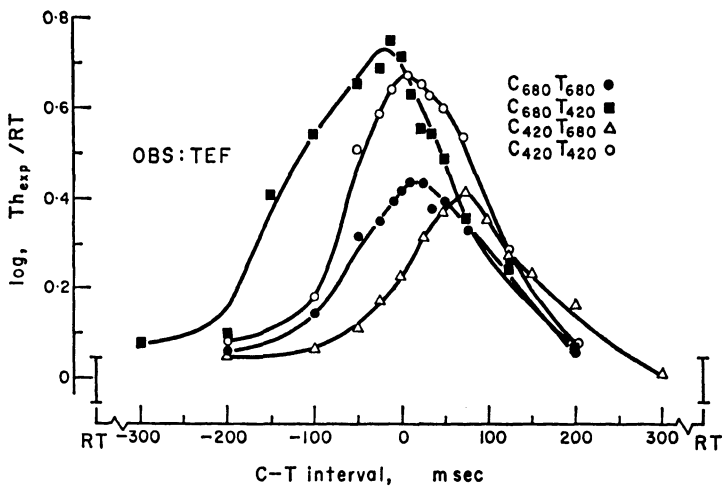

Fig. 16.9 Test threshold as a function of the interval between the test stimulus and the conditioning stimulus (C-T interval). A negative interval indicates that the test precedes the conditioning flash onset. The test and conditioning stimuli are designed to stimulate rod and cones separately. (Frumkes *et al.*, *Vision Res.*)

cones but deliver their output to rods, and not *vice versa*, whereas the interaction described here is reciprocal.

Increments and Decrements of Luminance

Interval Variation

Ikeda (1965) presented the observer with increments or decrements of luminance against a photopic background luminance, and the intervals between successive presentations were varied. Thus Ikeda was examining temporal summation. The two stimuli could be increments (+, +) or both decrements (−, −) or they could be an increment followed by a decrement (+, −) or *vice versa* (−, +). In the +, + case there was complete temporal summation up to about 15 msec and this decreased, i.e. the threshold compared with that for simultaneous presentation increased up to an interval of 53 msec when summation was that expected of probability summation of two independent events. During this period there was evidence for some mutual inhibition of the two stimuli, so that threshold was higher than for a single presentation. As the luminance was decreased, the inhibitory phase was shifted towards longer times and with zero background no inhibition was observed. With the +, − type of stimulation, complete summation was revealed as an absence of sensation of light, and once again the period for complete summation was limited; it emerged that cancellation was good in the time-region where summation of like-stimuli (+, +; −, −) was large; cancellation was also large in the time-region where +, + stimuli tended to inhibit each other. Ikeda concluded that the response to a flash was diphasic, and it was the mutual interaction of these out-of-phase diphasic responses that accounted for the various manifestations. Ikeda's technique was employed by Rashbass (1970); Fig. 16.10 shows the decrease in threshold as the duration of a single increment or decrement of luminance was increased; the line has a slope of unity indicating complete summation, falling off after about 20 msec. At 64 msec, threshold passes through a minimum suggesting some inhibition. In this experiment the change in luminance was brought on abruptly and maintained, so the condition is different from Ikeda's who presented the stimuli as separate flashes; when the same technique was employed Ikeda's result was obtained (Fig. 16.11), indicating failure of complete summation at a much earlier interval, about 10 msec, so once again we see that a patterning of the stimulus—this time a temporal discontinuity—tends to raise threshold.

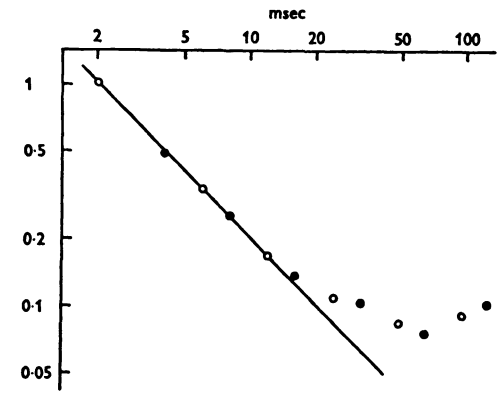

Fig. 16.10 The threshold intensity of rectangular changes of luminance as a function of their duration. Plotted on log-log coordinates, the unit of intensity is the threshold of a 2 msec positive-going flash. The threshold intensity of a 2 msec flash is about 0.18 times the base-line intensity. Circles are positive-going incremental flashes; circles with bars across are negative-going decremental flashes. The line sloping down at 45°, drawn through the 2 msec flash threshold, represents the condition of total summation. (Rashbass, *J. Physiol.*)

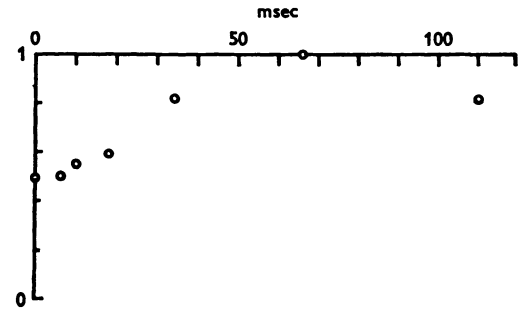

Fig. 16.11 The threshold intensity of two equal 2 msec flashes, as a function of the interval between them. Plotted on linear co-ordinates, the unit of intensity is the threshold of a single 2 msec flash. Thresholds are calculated as the intensity for seeing with a probability of 0.5. Observations on positive-going and negative-going pairs of flashes are grouped together as there is no significant difference between them. (Rashbass, *J. Physiol.*)

Bandpass Filter

Rashbass considered that the visual system contained a bandpass filter that accepted changes in the stimulus occurring at a certain range of frequencies but tended to attenuate those at high frequencies (short intervals between stimuli) and, to a lesser extent, at longer frequencies; on this basis he derived a model that described the phenomena reasonably well.

Subjective Estimates

An interesting point is the subjective unawareness of the direction of luminance-change, so that the subject could not state that a brief decrement in luminance was a decrease or increase in subjective brightness; the stimulus

was recognized as a change without sign. A change lasting 2 msec needs to be four times more intense to obtain any idea that it represents an increase or decrease from the baseline luminance, and as the duration increases the required change becomes smaller.

Brightness Enhancement

Donchin & Lindsley (1965) have described a subjective enhancement of brightness by a flash succeeding the test-flash by longer intervals, i.e. after the depressing effect has subsided. The brightness of the test-flash increased with delays between 100 to 150 msec and, as the delay was shortened, the increase became bigger until the masking effect began; the intervals at which enhancement occurred ranged from 150 to 20 msec depending on the luminance of the test-flash, the lower this the longer the period of enhancement. A satisfactory explanation of this enhancement is not so easy to find; the subject sees the test-flash as a contour different from the succeeding brighter flash and recognizes the period of dark between the two; as Donchin & Lindsley point out, two recognitions are made, namely the contour of the test-flash and its apparent brightness, and what is happening is that the brightness of the later flash is being attributed partly, or wholly, to the contour of the test-flash; thus an asynchrony in the brightness- and contour-messages could well result in the phenomenon.

SPATIAL EFFECTS

Simultaneous Contrast

At the time when the effects of the glare-source described by Schouten & Ornstein were interpreted as being due to an adaptive effect of one part of the retina on the rest, it was natural to assume that this α-adaptation lay at the basis of simultaneous contrast, whereby the apparent brightness of a grey patch is diminished by surrounding it with a white background. However, with the demonstration that the glare-source effect was due to scattered light within the eye, this interpretation becomes suspect. Nevertheless, the fact of simultaneous contrast remains, in the sense that a patch of light appears much darker if surrounded by a white background than if surrounded by a black one; so it may well be that the stimulation of the surrounding retina does, indeed, reduce the sensitivity of the central retina to light.

Steady-state Comparisons

The results of an experiment by Heinemann (1972) are illustrated in Fig. 16.12, where the inset shows the experimental arrangement. The test-field was a spot, T, surrounded by an 'inducing field', I, and the subjective brightness of the test-field was estimated by adjusting its luminance, L_t, to equal that of the comparison spot, $C(L_c)$ when the luminance of I, L_i, was varied. As the luminance of the inducing field, L_i, is increased, the curves at first rise slightly, indicating that the brightness of the test-field increases—i.e. there is *enhancement*. For values of L_i approximately half that of the test-field, the brightness of the test-field is depressed—the classical simultaneous contrast. Near the point where $L_i = L_t$, small increases in L_i make necessary very large decreases in matching luminance, L_c, and when L_i exceeds L_t by only a few hundredths of a log-unit, the brightness of the test-field is so much reduced that a match becomes impossible. It must be emphasized that a depression in test-field brightness can also be induced by an inducing field of smaller luminance than that of the test.

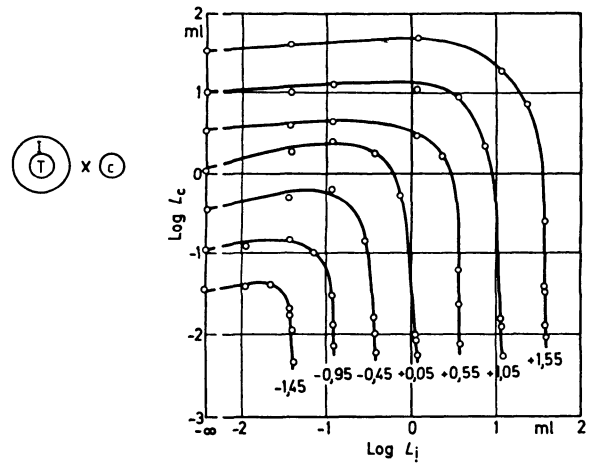

Fig. 16.12 Effects of a surround-field on subjective brightness of a central spot. The experimental arrangement is shown on the left, the central test-spot, T, being matched with a comparison spot, C. The surround luminance is varied. The parameters on the curves are the luminances of the test fields in Log mL. (Heinemann, *Hdb. Sensory Physiol.*)

SCATTERED LIGHT

It would seem, however, from the study of Fry & Alpern (1953) that a great deal of the effects of the inducing stimulus are attributable to the scattered light producing a veiling glare that depresses sensitivity; thus the effect depends strongly on the separation of test and inducing fields, which would be expected of light-scatter. Heinemann (1972) concludes that physiologically transmitted effects at the fovea would not be observed at separations greater than 1.5 to 2°.

Centre-periphery Interactions

The effects of a surrounding annulus of light on the threshold to a test spot have been studied in detail largely by Westheimer, both under scotopic and photopic conditions (Westheimer, 1965, 1967; Westheimer & Wiley, 1970), and finally when both rods and cones were active (Westheimer, 1970). The experimental arrangement is illustrated by Fig. 16.13, the large annulus, surrounding

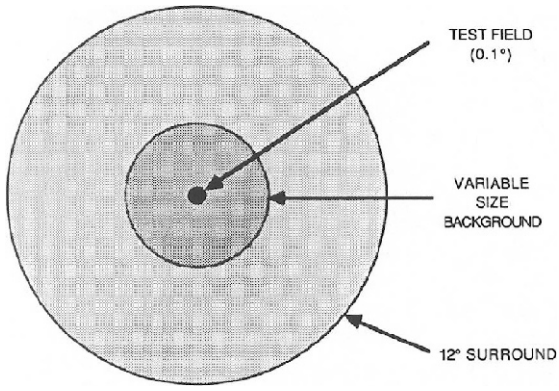

Fig. 16.13 Illustrating the viewing conditions for studying the effects of a variable-size background. (After Westheimer, *J. Physiol.*)

the test-spot of 1 min of arc, whilst a 'background annulus' which varied from 0.6 min to 2.5 degrees, was introduced to prevent the effects of light-scatter from spilling over on to the peripheral regions and giving a flickering sensation when the test-spot was presented at regular intervals. As the size of the small annulus was steadily increased the threshold passed through a maximum; thus below this maximum, threshold increased rapidly with increasing diameter, a process called by Westheimer 'desensitization', the annular light adjacent to the test-patch of retina making the retina less sensitive to light and raising the threshold. Beyond this maximum, threshold falls, a process called 'sensitization'. In general Westheimer considered that the effects were analogous with the centre-surround phenomenon in ganglion cell responses, the sensitization of the retinal test-spot by the periphery being due to excitation of the surround, which was supposed to have an opposite effect on sensitivity to that of centre-stimulation. When curves for rod and cone vision were studied, the critical areas at which sensitization began were different (Fig. 16.14), and when the background conditions were varied, it was concluded that sensitivity-changes of rods were induced by rod, and not cone stimulation, and *vice versa* for cone vision. Moreover, when cone-stimulus conditions were chosen such as to separate the 'red' and 'green' mechanisms, it appeared that effects on red cones were mediated by red cones, and similarly for green cones (McKee & Westheimer, 1970).

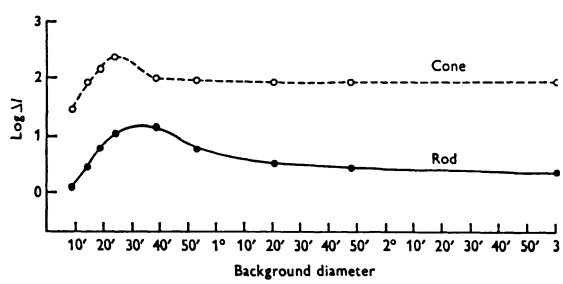

Fig. 16.14 Critical areas at which sensitization begins are different for rods and cones. (Westheimer, *J. Physiol.*)

Contour Effects

A study of Lennie & MacLeod (1973) casts doubt on this interpretation; they studied a small test-flash with backgrounds of varying sizes and concluded that it was the discontinuity in the field-illuminance that affected threshold rather than the absolute amount of light in the surround; thus, as the luminance of the annulus was increased and decreased the threshold, compared with that for a uniform field, increased in both situations (Fig. 16.15). By substituting a windmill for an annulus, they found that, in spite of its much smaller area of the windmill than that of the annulus of the same luminance, the threshold was always higher with the windmill, showing that light, *per se*, was not the important factor in

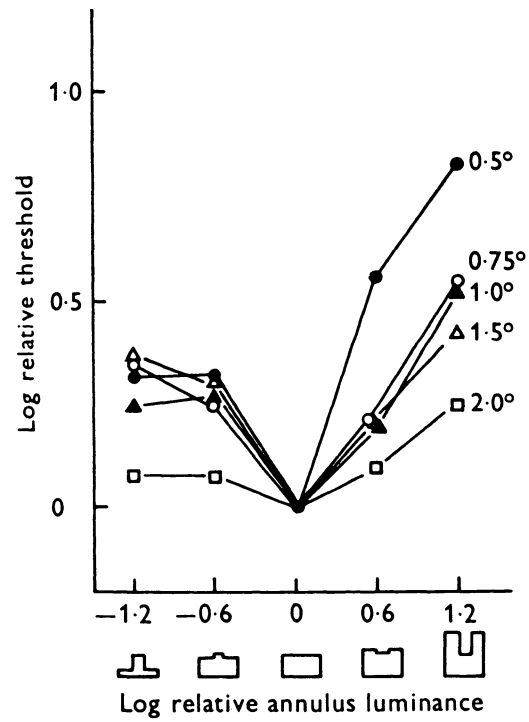

Fig. 16.15 Small backgrounds, of the diameters indicated beside each curve, were encircled by annular surrounds of fixed (8°) outer diameter. The annulus was either equal to the background in luminance (uniform field), or brighter or darker than the background. Curves plot test-spot threshold as a function of annulus luminance. Below each set of points is shown the distribution of light in a cross-section of the display (not to scale). Background luminances: $\bar{1}.3$ log scotopic td. (Lennie & MacLeod. *J. Physiol.*)

raising the threshold. Again, when a thin ring, concentric with the test-flash, was imposed on the system, threshold was raised whether the ring was lighter or darker than background. Finally, when log-reduction in threshold was plotted against background illuminance for a test-spot on a small, 0.5° surround, and against a uniform field, the two curves only separated when the background illuminance was sufficient for the observer to notice a spatial discontinuity in test-flash and surround; thus it was the discontinuity that was creating the change in threshold.[4]

Spatial Summation

Ricco's Law

The existence of an area on the retina—the Ricco area—over which there is complete summation of quanta, has been discussed earlier; the phenomenon may be looked at as a special case of retinal interaction.

RICCO AREA AND STIMULUS PATTERN

Hallett (1963) and Sakitt (1971) have summarized the literature relating to the magnitude of Ricco's area; and the important fact emerges that this is strongly dependent on the pattern of the stimulus. Thus Bouman (1950, 1955) found complete summation for spots of light up to a diameter of 30 minutes of arc, whereas for line-shaped targets the area extended to 32 minutes. Again, when two separate spots are employed, the area in which they must fall for complete summation is much smaller than the Ricco area defined for a single spot. Sakitt measured the threshold as a function of area of stimulus, using a circular spot of increasing diameter; Fig. 16.16 shows the linear relation between log threshold and log area; the slope of the line is -1 for targets less than $\frac{1}{2}$ degree in diameter, indicating complete summation up to a diameter of 30 minutes, the Ricco area for this subject.

When the thresholds for two small squares, separated by a variable distance, were measured it was found that summation was much more limited. Thus the logarithm of the ratio of the two thresholds has been plotted against separation in minutes of arc (Fig. 16.17), for complete summation the ratio of thresholds would be 2 and the logarithm 0.3, and this only applies to the first point on the curve at a separation of centres that was so small that the two squares touched to form a continuous rectangle, whereas the same subject showed complete summation for circular targets up to 30 minutes of arc.

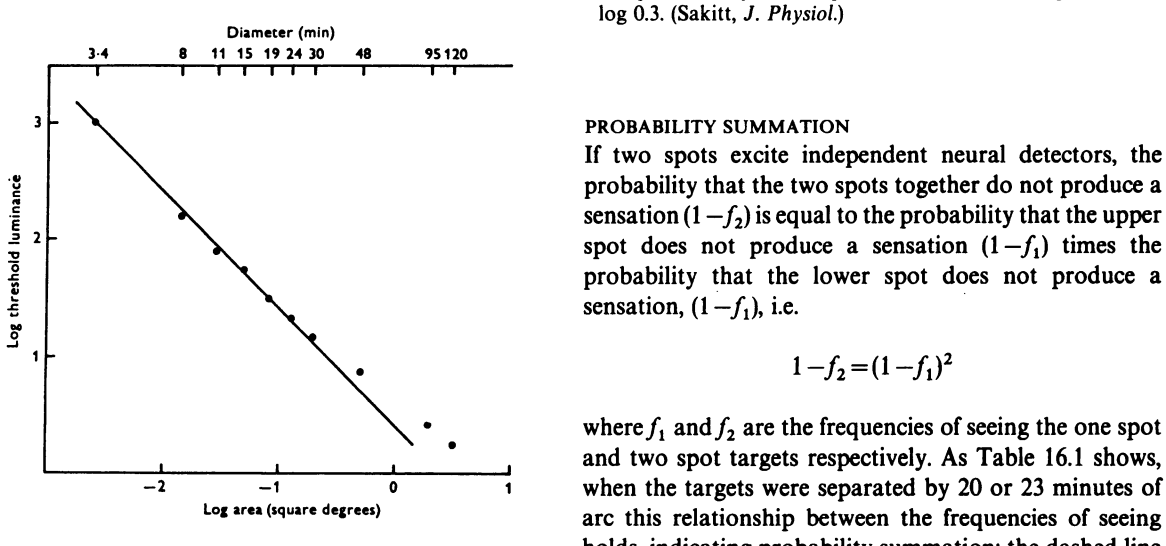

Fig. 16.16 Illustrating spatial summation. The slope of the line has a value of -1 indicating complete summation up to an area of about 30 min of arc. (Sakitt, *J. Physiol.*)

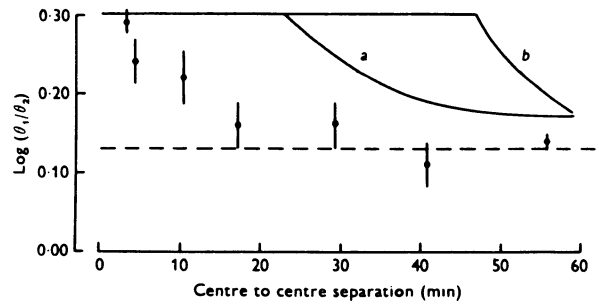

Fig. 16.17 Illustrating reduction in summation when the test-stimuli are separated spatially. As ordinate the log of the ratio of absolute threshold luminance for one 3.4′ square, θ_1, to the absolute threshold luminance of two such squares, θ_2, has been plotted as a function of centre-to-centre separation of the squares. The continuous curves are predicted employing weighting functions. Summation is approximately complete at very small separations, the ratio being 2 and its log 0.3. (Sakitt, *J. Physiol.*)

PROBABILITY SUMMATION

If two spots excite independent neural detectors, the probability that the two spots together do not produce a sensation $(1-f_2)$ is equal to the probability that the upper spot does not produce a sensation $(1-f_1)$ times the probability that the lower spot does not produce a sensation, $(1-f_1)$, i.e.

$$1-f_2=(1-f_1)^2$$

where f_1 and f_2 are the frequencies of seeing the one spot and two spot targets respectively. As Table 16.1 shows, when the targets were separated by 20 or 23 minutes of arc this relationship between the frequencies of seeing holds, indicating probability summation; the dashed line in Fig. 16.17 represents the log of the thresholds for one and two targets when the threshold for two targets is

Table 16.1 Frequencies of seeing one 3.4′ square (f_1) or two such squares (f_2) separated by 20 or 23′ for three subjects. Test duration was 16 msec and the filament image was 1 mm at the pupil. Each entry is based on 120 trials and s_1 and s_2 are the standard errors of the means of f_1 and f_2 (Sakitt, 1971)

Subject	*Separation*	f_1	f_2	s_1	s_2	$(1-f_1)^2$	$(1-f_2)$
L.F.	23′	0.48	0.68	0.05	0.04	0.27	0.32
B.S.	23′	0.18	0.28	0.04	0.04	0.67	0.72
L.F.	23′	0.46	0.68	0.05	0.04	0.29	0.32
C.L.	23′	0.41	0.68	0.05	0.05	0.35	0.32
C.L.	20′	0.39	0.64	0.05	0.05	0.37	0.36
C.L.	20′	0.47	0.73	0.05	0.04	0.28	0.27
C.L.	20′	0.33	0.61	0.05	0.05	0.44	0.39

governed by probability summation, and it will be seen that neural, as opposed to probability, summation ceases at 20 to 30 minutes separation. By increasing the number of spots, more complex patterns of stimulus could be presented and threshold-ratios analysed; and Sakitt concluded that the spatial summation at absolute threshold was configuration-dependent but not uniquely related to a single variable, such as distance of separation. The important point to appreciate is that the introduction of a pattern into the stimulus tends to increase its absolute threshold.

Increments and Decrements

This point was further emphasized by Cohn & Lasley (1975) who presented a subject with two spots of light at arbitrarily chosen separations (Fig. 16.18). The luminance of pairs of spots could both be increased (+ +), both decreased (− −) or there could be a paired increment–decrement (− +; + −). Perfect energy summation when an increment is presented at two separate spots would lead to the prediction that detectability would be independent of the separation, and would be the same as if the spots were superimposed; similarly for a pair of decrements. Secondly, if an increment occurred at one spot and a decrement at another, there should be cancellation and there should be no detectability regardless of separation. In fact, there was no evidence for perfect summation and the results for double increments (+ +, − −) are shown as filled circles in Fig. 16.19, and for paired increment-decrement (+ −, − +) as open squares, detectability being plotted as a function of separation. From these results a *summation index* ψ was computed whose values would vary from −1.0 if the two events to be detected were independent of each other (probability summation) to 0 if the detectability were governed by complete summation of the two stimuli. As Fig. 16.20 shows, there was never complete summation, and this decreased up to

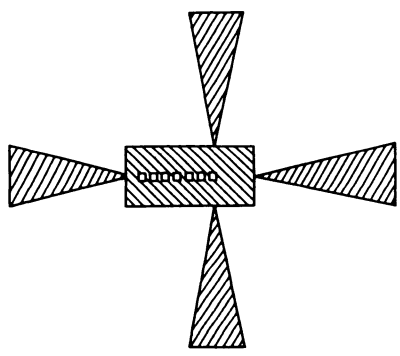

Fig. 16.18 Illustrating the experimental stimulus-conditions. A row of seven light-emitting diodes is continuously lit at about 30 foot-lamberts. The left-most diode (*first spot*) is the fixation point and black arrows point to it to aid fixation. The left-most (first) spot and one of the other six (*second spot*) are the sites of any one of eight possible luminance modulations. (Cohn & Lasley, *Vision Res.*)

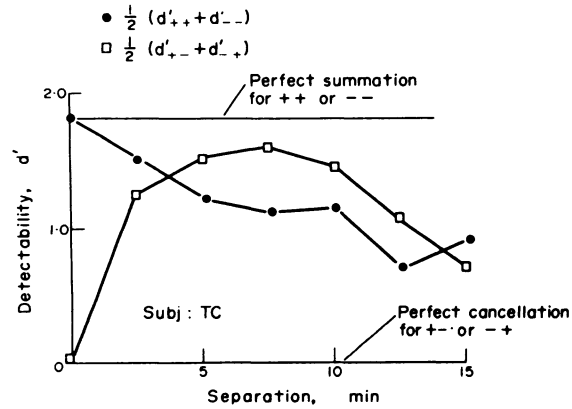

Fig. 16.19 Results of experiments using the experimental set-up of Fig. 16.18. Detectability of double increments or decrements (+ + and − −) and paired increment–decrement (+ − and − +) in luminance of spots one and two are plotted as a function of the separation of the spots. (Cohn & Lasley, *Vision Res.*)

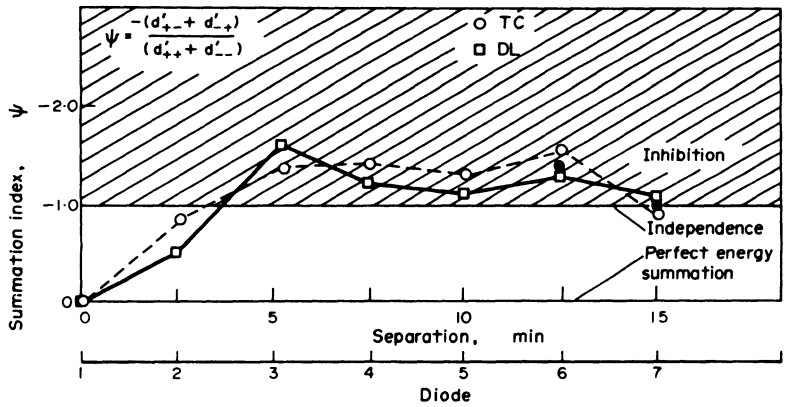

Fig. 16.20 Summation index versus separation plotted for two subjects. Ordinate: Summation index, ψ, computed from $-(d'_{+-}+d'_{-+})/(d'_{++}+d'_{--})$. Negative values plotted upwards. Abscissa: Separation of the two spots in minutes of arc. Shaded area indicates inhibition, $\psi < -1$. d's are detectabilities. (Cohn & Lasley, *Vision Res.*)

a separation of about 4 minutes of arc, when probability summation was reached; at larger separations the index had a larger negative value than -1, indicating mutual inhibition between the two stimuli.

SUMMING AND DIFFERENCING MECHANISMS

Cohn & Lasley interpreted their results on the plausible basis of a summing mechanism that averaged photon flux over the retinal area studied, and a differencing mechanism that detected local contrast. With superimposed stimuli, the differencing mechanism would not be active and summation would be perfect; with increasing separation the differencing mechanism would come into operation. Both mechanisms would be influenced by separation, and at large separations both might become independent (*a*) because, at the fovea especially, summation of photons is limited, and (*b*) because spatial difference-detection is governed by the receptive field of a ganglion cell. Thus, at large separations, the two component stimuli are signalled independently and ψ is unity; at smaller separations there is interaction and it is because of the differencing channel that perfect summation is prevented. In this way we can account for the effects of pattern, for example Kristofferson & Blackwell found lower thresholds for non-circular targets.[5]

Mach Bands

A manifestation of simultaneous contrast or spatial inductive effects is given by the so-called *Mach bands*. If a picture, such as Fig. 16.21, is rotated above the critical fusion frequency in front of the eye, the subject sees a grey surface whose objective luminance varies in accordance with the Talbot-Plateau Law. However, although Fig. 16.21 exhibits no sharp transitions of luminance, the subject sees alternate light and dark stripes on the height axis, adjacent stripes bordering each other at fairly clear lines. The light stripes correspond to the parts of the light-distribution curve that are concave to the height-axis

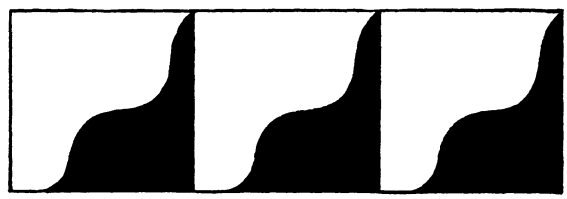

Fig. 16.21 Illustrating the formation of Mach bands. If this figure is rotated on a drum, at a rate above the critical fusion frequency, the subject sees a grey surface with alternate light and dark stripes, although there are no actual sharp transitions of luminance on the figure. (Graham, *Vision and Visual Perception.* John Wiley Inc.)

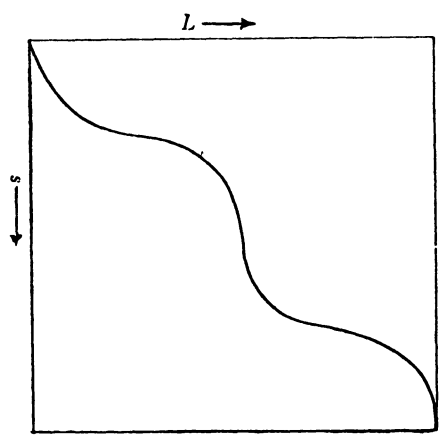

Fig. 16.22 Illustrating the variation of luminance of the picture presented to the eye by Fig. 16.21, when rotated so as to cause fusion of successive images. The luminance is determined, under these conditions, by the Talbot-Plateau Law. (Graham, *Vision and Visual Perception.* John Wiley Inc.)

(Fig. 16.22) and the dark to those that are convex. We may presume that in the regions of fairly rapid change of luminosity, inhibition and facilitation occur, leading to the sharpening of the transition from one level of subjective sensation of greyness to another.

RETINAL ELECTROPHYSIOLOGY AND ADAPTATION

The basic concepts of adaptation have been derived from psychophysical experiments and it becomes of interest to determine to what extent the characteristics of the ganglion cells of the retina determine adaptation phenomena, i.e. the extent to which the retina has processed the spatial and temporal features of the stimulus. Thus the centre-surround antagonism observed with many ganglion cells reveals the possibility of spatial interaction whereby light falling on a part of the retina may inhibit activity in another, but of course this interaction is on a relatively small spatial scale and is unlikely to explain the phenomena described, for example, by Westheimer.

Field Adaptation and its Mechanism

Rushton described the change in sensitivity of the eye following exposures to light that had only a small bleaching action on the retina as field adaptation; it represents a diminished sensitivity of the visual mechanism to light, or to speak in engineering terms, there has been an automatic gain-control.

I/Q Ratio

Enroth-Cugell & Shapley (1973) used as a measure of gain, or rather its reciprocal, the ratio: I/Q, the impulse/quantum ratio, i.e. the number of impulses generated over the background discharge divided by the number of quanta of light effectively absorbed, a ratio which Barlow & Levick (1969) considered to be the most important parameter in determining a response. Figure 16.23 shows a typical increment-sensitivity curve, indicating the extra retinal flux (left-hand ordinates) required to evoke a criterion response of 30 imp/sec at increasing levels of background retinal luminance. The right-hand ordinates give the computed I/Q ratios, which fall with increasing adaptive illumination of the retina. At the lowest levels the curve is flat, i.e. the I/Q ratio is constant and is equivalent to the condition of dark-adaptation. At a particular background level, the I/Q ratio begins to decrease sharply, and the slope has a value of about -0.9 for the log-log plot, indicating that the sensitivity was proportional to the 0.9 power of the background, a relation close to the value expected for strict application of the Weber Law (p. 221). The level of retinal illumination at which the adaptive effect occurs is low, representing absorption of only 0.01 quanta per rod per sec; such absorption could have little effect in saturating the rod from a photochemical point of view, and in fact psychophysical studies of Aguilar & Stiles (p. 400) on man, and equivalent studies on the cat, showed that rod-saturation began only when retinal illumination was of the order of 7500 quanta rod^{-1} sec^{-1}. Thus this field adaptation is certainly a neural rather than a photochemical phenomenon.

Horizontal Cell Feedback

Enroth-Cugell & Shapley presented a model of the adaptive process based on inhibitory feedback to the receptors through horizontal cells,[6] the hyperpolarizing potential of this cell acting as a control on transmission from receptors to bipolars.

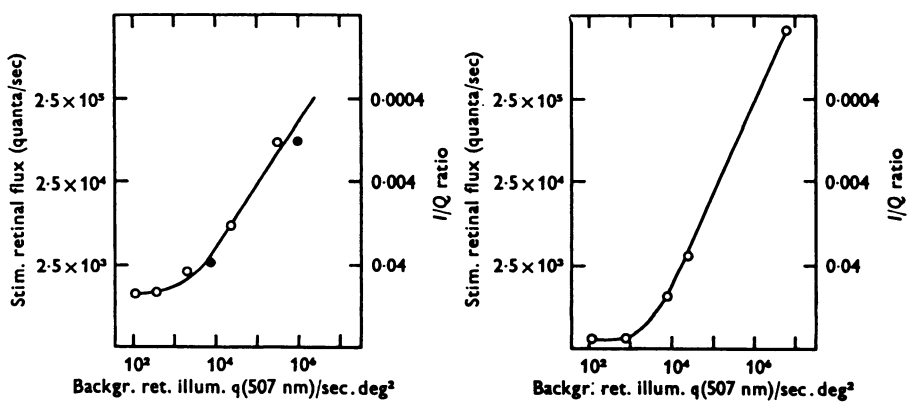

Fig. 16.23 Increment-sensitivity curves of retinal ganglion cells indicating the extra retinal flux (L. H. ordinate) required to evoke a criterion response of 30 imp/sec at increasing levels of background luminance. Right-hand ordinate gives calculated I/Q ratios as defined in text. Open circles are for blue-green stimuli on a red background; filled circles for white stimuli on white background. (Enroth-Cugell & Shapley, *J. Physiol.*)

Importance of Dendritic Field

An important conclusion reached by these authors, was that the sensitivity, or reciprocal of I/Q, for a particular ganglion cell was governed by the amount of light-flux effectively gathered by it through its dendritic field; this is illustrated by Fig. 16.24 which shows the relation between I/Q and background retinal illumination for two ganglion cells with very different central fields, fields that are almost certainly governed by the size of the dendritic spread of the cell. It will be seen that, for the large central area, the transition point occurs at a lower background illumination; and for any given illumination the I/Q ratio is much larger, indicating lower sensitivity.

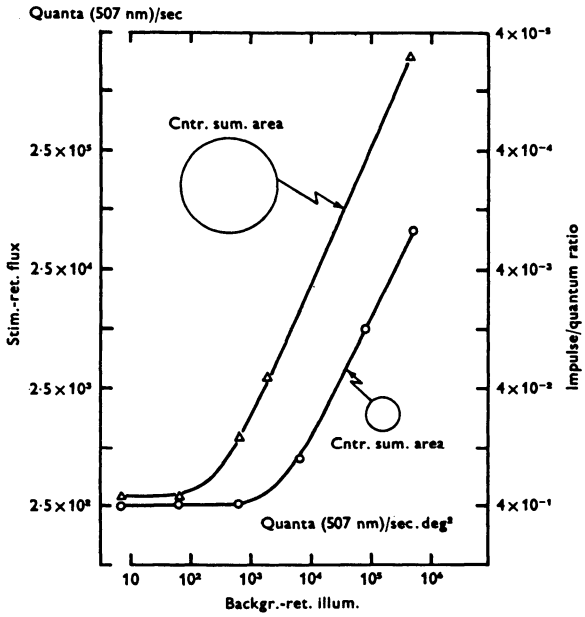

Fig. 16.24 Increment-sensitivity curves for two ganglion cells with different centre-sizes for their receptive fields, as indicated by their summation areas. For the cell with the large central area the transition point occurs at a lower background illumination and for any given illumination the I/Q ratio is much larger, indicating lower sensitivity. (Enroth-Cugell & Shapley, *J. Physiol.*)

Adaptation Pool

Thus the 'adaptation pool' of the cat retina seems to be the receptors that transmit to the ganglion cell, whereas those that are responsible for the surround effects, presumably mediated through amacrine cells, do not contribute to this pool.

If the state of adaptation depends on the size of the receptive field of the ganglion cell, this means that, under many conditions, some cells will be more adapted than others; in general, cells with small fields will be the more sensitive (less adapted) and thus more suited to the detection of small targets.

Characteristics of the Surround

The surround generally antagonizes the central spot-stimulus when the illumination of the retina is diffuse, so that the response to uniform illumination of the retina is small, and such as it is, is due to the different latencies of the centre and surround effects. Enroth-Cugell & Lennie (1975) emphasized the difficulties in determining the true effects of the surround because of the scatter of light from it which may be greater in effect than that on the surround, so that employment of a surround in isolation, i.e. an annulus, to measure its effect on the centre gives results of very doubtful significance. Thus it is necessary to examine the effects of the surround on the centre when the latter is being excited by light, so that the effects of additional scattered light are negligible. Enroth-Cugell & Lennie steadily increased the size of a spot-stimulus until an optimum discharge was obtained; thus, as the size increased, because of summation, the threshold fell until a point was reached when the summational effect of added area was just cancelled by an inhibitory effect from the surround. Having obtained this optimum-spot, they measured the effects of diffuse illumination on the response, but of course the diffuse illumination fell on the centre as well as the surround, so that allowance for this had to be made. The authors found that surround and centre responded in an additive fashion so that the contribution of the surround could be estimated by comparing the ganglion cell's response to diffuse illumination of its receptive field with that to an equiluminous spot which optimally stimulated the centre. When examined in this way, the surround's behaviour with regard to adaptation, etc., was often very similar to that of the centre, although working in opposite directions, with the result that centre and surround tended to balance each other over a wide range of luminances.

Dark Adaptation

However, it will be recalled that Barlow had found that centre-surround antagonism tended to disappear in dark-adaptation, and this is due to different stimulus-response functions of centre and surround at very low luminances, as revealed in Fig. 16.25. Thus in the dark-adapted eye the surround does, indeed, contribute much less than the centre, but the difference is quantitative, not absolute. What is important is that in dark-adaptation the surround is unable to increase the centre discharge of an OFF-centre unit rather than to decrease the discharge of an ON-centre unit at ON.

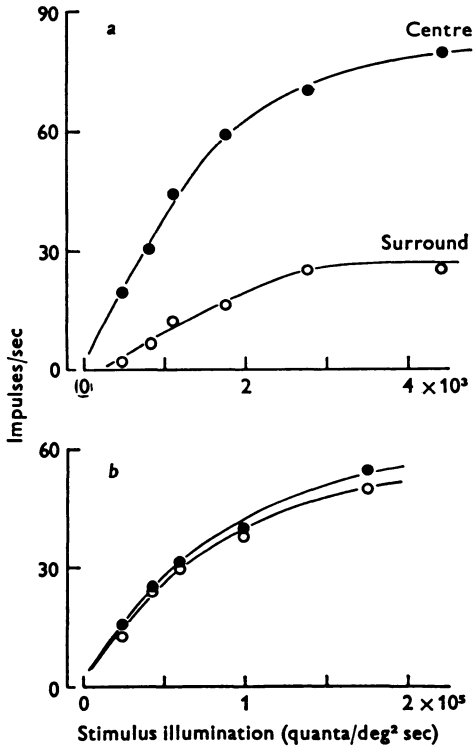

Fig. 16.25 Stimulus-response functions for centre and surround of a ganglion cell under conditions of dark-adaptation (top) and light-adaptation (bottom). Note that under scotopic conditions the response functions of centre and surround are very different. (Enroth-Cugell & Lennie, *J. Physiol.*)

Basis of the OFF-discharge

According to Enroth-Cugell & Lennie (1975) the OFF-discharge is largely the result of delay in establishment of appropriate gain-control in centre and periphery; thus, under steady conditions, centre and surround are fairly closely matched and diffuse illumination produces no significant effect on the maintained discharge. On shifting to a new level, the more sluggish surround fails to adjust its gain in time with the centre, and it is the delay in adjustment that leads to OFF-responses. The same mechanism leads to 'overshoots', in the sense that an ON-centre unit at ON with diffuse illumination gives an initial sharp increase in discharge which declines over some hundreds of milliseconds.

Centre-surround Overlap

According to the treatment of Rodieck & Stone (p. 327) the surround overlaps the centre extensively or completely, so that the rigid separation of the two, employed by Enroth-Cugell, is clearly not absolutely correct; as she points out, however, at any rate where X-cells are concerned, her test of studying the changes in spot-size until qualitatively different responses were obtained meant that, when this qualitative change occurred, she was observing an effect of surround, whereas up to this point the response was entirely due to, or predominated by, the centre. With Y-cells the situation was more complex, the effects of their surrounds being more efficiently masked by those of their centres.

Effects of Steady Illumination of Surround

Westheimer's studies indicated that illumination of one part of the retina depressed the sensitivity of another; the question arises as to whether steady illumination of the surround affects the sensitivity of the centre of a concentric retinal ganglion cell. Sakmann *et al.* (1969) found that, when a receptive field was obtained on the basis of surround antagonism, there was no adaptive centre-surround antagonism, the effects of light on the centre being as effective as on the surround for adaptive suppression of response. This work was confirmed and extended by Enroth-Cugell *et al.* (1975) who measured the sensitivity of the centre of the receptive field to a small spot of flashing light when the field was exposed to a background spot of steadily increasing size from that of the small flashing spot until it extended well beyond the whole centre-plus-surround. Sensitivity decreased (the I/Q ratio fell) by more than a factor of ten as the area of the background spot increased up to the value of the central summation area, A_t, beyond which there was no change. The fall in sensitivity up to A_t was due to light-adaptation which summates within A_t, as shown earlier; the absence of further change indicates the absence of any effect, whether of inhibition or facilitation, of the surround on the sensitivity of the centre.

SENSITIVITY

It must be appreciated that the surround was influencing the ganglion cell, in fact it decreased the maintained discharge; the point is that it failed to alter the *sensitivity* of the centre, as indicated by the number of quanta required to increase the discharge over the steady level by a fixed number of impulses (I/Q). The failure to influence sensitivity indicates that surround signals will either add to, or subtract from, those evoked by the central stimulus. It should be noted that when the surround stimulus was strong, an enhancement of apparent sensitivity was obtained, but this was spurious and due to the reduction of the inhibitory effect of the surround by the adapting surround light; the same effect can be produced by depressing the sensitivity of the centre by an adapting spot.

ADAPTATION AND THE COLOUR SENSE

So far we have considered the effects of adaptation on the light and form senses; we know from the phenomena of spatial and temporal induction that the colour sense can be appreciably affected by adaptation, but it is only comparatively recently that serious quantitative measurements of the specific effects of any given wavelength have been made.

Colour Matches

Wright has applied his binocular matching technique to the problem. For example, the right eye was made to view a yellow patch; the left eye was presented with a patch which could be illuminated by the subject with three primary colours, red, green, and blue, and their proportions and intensities could be varied so that a match, both in hue and intensity, could be made with the yellow viewed by the right eye. The right eye was then exposed to an adapting light for three minutes and both eyes once again viewed their respective test and comparison patches. As a result of the adaptation it was found that the previous match no longer held in respect to either brightness or hue; and the change was measured by adjusting the intensities of the primaries as quickly as possible until a correct match was made. By repeating the matches every thirty seconds the course of recovery from adaptation could be plotted as three separate curves corresponding to the recoveries of the red, green, and blue sensations. In general, it was found that adaptation to any given wavelength had a general and specific effect; there was a general reduction in sensitivity of the eye to all wavelengths, together with a specific reduction in sensitivity to the adapting wavelength. Consequently, a match that holds for one state of adaptation of the eye does not necessarily hold good for another. Thus with a yellow test-colour, a match was made with equal amounts of red and green before adaptation of the right eye to a white light; after adaptation, a match was made with red and green in the proportions of 38:60, i.e. far more green was required by the dark-adapted left eye to match the sensation experienced by the light-adapted right eye, a fact which indicates that an adapting white light depresses the sensitivity to red more than to green.

Colour-mixing Equations

This observation does not, however, indicate that the colour-mixing equations, applicable for one level of luminance, are inapplicable for another; in fact, there is some reason to expect that, in the same eye, matches will hold independently of the condition of this eye, at any rate over a fairly wide range of light-adaptation. Thus if we take a mixture of red and green in one half of a field and match it with a mixture of yellow and white in the other, then the fact that there is a match means that the retina is responding in essentially the same way in the two halves of the field; any change in the retina, caused by adaptation to any wavelength, will influence the receptors receiving both halves of the field in the same way, so that although the subjective sensation will be altered the two halves may be expected to appear the same, and the match will be said to hold in spite of the adaptation of the retina. Thus, presentation of the two halves of the field to the two eyes separately, as in the binocular matching technique, would indicate a failure of the match, but that is because we are comparing two eyes in different states of adaptation. In practice, colour-matches do, indeed, hold under different conditions of adaptation.

Artificial Colour-defectiveness

Nevertheless, if very high adapting luminances are employed, Wright showed that uniocular colour matches may be upset, and the phenomenon was investigated in some detail by Brindley. On the basis of the trichromatic theory, the maintenance of colour matches in spite of adaptation implies that the forms of the three spectral response curves remain unaltered, since it is essentially because of their characteristics that the laws of colour matching are what they are. Thus, to consider the Red and Green response curves and their contribution to Yellow, the matching of Red + Green to equal yellow is represented by Fig. 16.26; here the yellow stimulus matches the mixed Red and Green stimuli because it stimulates the Red by 3 units and the Green by 2 units. If we now adapt to red light so that the shape of the Red curve is altered, then now our yellow radiation is stimulating the Red and Green mechanisms in different proportions and the match may no longer hold. By using very extreme conditions of adaptation such as might be expected to bleach the photopigment specifically from one

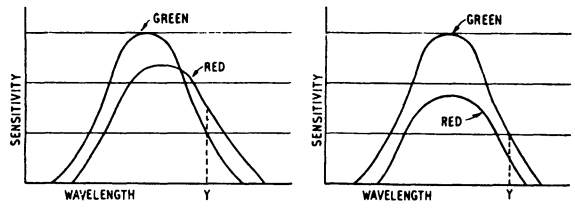

Fig. 16.26 Showing that, if the forms of the fundamental response curves are altered by an adapting light, colour matching will be upset. *Left*: the yellow stimulus, Y, produces responses in the green and red mechanisms in the ratio of 2:3. *Right*: the same yellow stimulus produces responses in the ratio 1:2 because selective adaptation has altered the shape of the red mechanism's response curve.

type of cone completely, we might expect to achieve a state of artificial dichromatism, or, if we put two types of receptor out of action, one of monochromatism. In fact, all these disturbances of colour-matching may be produced (Brindley, 1953). For example, by adapting to a very bright violet light, an artificial tritanopia may be produced so that all spectral wavelengths may be matched by suitable mixtures of only two primaries, a red and a blue. With a very bright red or blue-green light this artificial tritanopia may be converted into an artificial monochromatism, in which large parts of the spectrum can be matched with a single wavelength; thus a 'red monochromatism' was obtained by strong violet and blue-green adaptation, presumably because only the red mechanism was operative. Under these conditions all spectral colours from 500 nm to 700 nm could be matched by suitably varying the intensity of a yellow stimulus of 578 nm. The sensation was that of a very unsaturated red or pink. After adaptation with violet and red, a 'green monochromatism' was obtained, so that all wavelengths between 480 nm and 620 to 630 nm could be matched with a yellow, both fields appearing this time as an unsaturated blue-green.[7] Finally, a 'violet monochromatism' was obtained by adaptation to a bright yellow light; over the range of 400 to 500 nm all wavelengths were matched with violet of 447 nm, both fields appearing as a very saturated violet. Presumably, then, Brindley was putting the fundamental mechanisms out of action selectively, but of course the remaining mechanisms could hardly be called normal since they would have been subjected to quite considerable bleaching, so that the density of pigment in them would be less than that pertaining with normal trichromatic vision.

Bezold-Brücke Phenomenon

When the intensity of a monochromatic light is increased considerably, there is a change of its subjective hue so that it can be matched with a different monochromatic light of lower intensity; this is the Bezold-Brücke phenomenon. The shifts are illustrated in Fig. 16.27 where the lines join wavelengths of the same apparent hue when viewed at ten, and over a thousand, trolands; the arrows indicate the invariant hues, namely a blue of 476 nm, a blue-green of 508 nm and a yellow of 570 nm; thus oranges and reds at high intensities are equivalent to a yellow at moderate intensity, and so on. Peirce in 1877 suggested that these shifts could be explained on the basis of the Young–Helmholtz theory, with the assumption that the three sensitivity curves altered relatively to each other when the intensity-level of stimulation increased. Thus, if an orange at moderate intensity stimulated the red mechanism very strongly and the green mechanism only weakly, then increasing the intensity of the orange might be expected to increase the green's response more strongly than that of the red, and thus to shift the subjective sensation towards the green end of the spectrum, i.e. to make an orange approach a yellow. On this basis, the invariant hues would correspond to the crossing-over points of the three sensitivity curves. This is true of the invariant yellow at 507 nm if we accept Pitt's sensitivity curves, but as Walraven has shown, further assumptions are necessary to account for the other two invariant colours. As presented, the theory of Peirce, and its modification by Walraven (1961), are obviously too naive, but the general principle that the relative shapes of the response curves of the cone mechanisms will alter with intensity is in accordance with what would be expected on electrophysiological grounds.

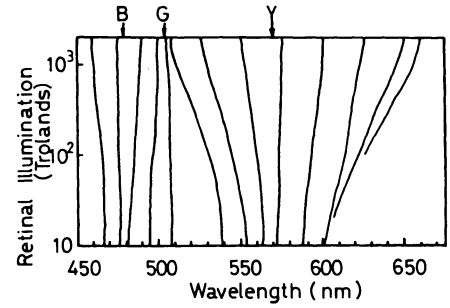

Fig. 16.27 Wavelengths having the same hue at different levels of retinal illumination. For example, an orange of about 600 nm shifts towards the red when the retinal illuminance is increased from 10 to 1000 trolands. The arrows indicate the invariant hues. (Walraven, *J. opt. Soc. Amer.*)

PHOTOPIC SENSITIVITY CURVES

The curves shown in Fig. 15.1 give the relative sensitivities of the light-adapted eye to different wavelengths, i.e. under conditions where the cones apparently determined the sensation. As we have seen, this sensation is mediated by three types of cone, so that one might expect to find discontinuities in the curve in regions where one type of cone tends to 'take over' from another. In fact, as we have seen, Stiles was able to create conditions where the 'taking over' by the separate mechanisms could be demonstrated with some precision, but this required conditions that ensured that he was measuring the threshold for the new mechanism, i.e. by light-adaptation with carefully chosen wavelengths, the mechanisms with which he was not concerned could be depressed in sensitivity sufficiently to allow the single mechanism to manifest itself. Under the ordinary conditions of measurement of photopic sensitivity, where essentially what we are doing is to match different wavelengths for brightness sensation, thereby finding the relative energies required for equal sensation, we may expect all mechanisms to be operative

to some extent, and thus to obtain a smooth curve of spectral sensitivity.

'Humps' on the Curves

By reducing the size of the test-patch, or by using peripheral parts of the retina, however, some evidence for discontinuities, in the form of 'humps' on the sensitivity curves can be obtained; at these humps the retina is presumably specially sensitive to a selected region of wavelengths. For example, Thomson (1951) found evidence for extra sensitivity in three regions of the spectrum, one at 460 nm, another at 520 nm and a third between 580 and 610 nm. Again, by studying the periphery, Weale (1953) found two humps indicating extra sensitivity in the blue at 460 nm and in the green at 540 nm. Using a rather different technique, Auerbach & Wald (1954) identified what they called a violet receptor with maximum sensitivity at 435 nm.

Squirrel

Humps on the sensitivity curve are not peculiar to man; thus Fig. 16.28 shows the mean results for a number of different species of squirrel, animals that are interesting because their retina is a pure cone one. There are two obvious peaks at 535 and 490 nm respectively, and here it is interesting that neither of these coincides with the absorption peaks for the pigments that can be extracted from the squirrel retina, which is actually a rhodopsin with λ_{max} of 502 nm (Dartnall). By selectively adapting the retina with blue or green light the two humps could be selectively depressed, and this suggests that there are different pigments mediating blue and green sensitivity.

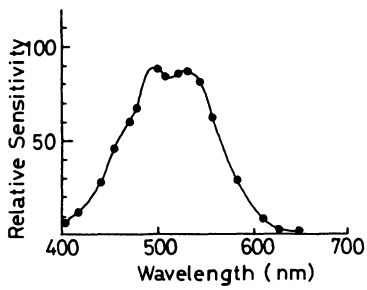

Fig. 16.28 Mean spectral sensitivity curve for several species of squirrel, determined electroretinographically. Ordinate: percentage sensitivity. Abscissa: wavelength in nm of stimulating light. Intensity was adjusted so that at each wavelength the same number of quanta/sec fell on to the retina. (Tansley *et al.*, *Vision Res.*)

Colour Matching

Not only may the sensitivity curves be 'abnormal' under certain conditions but also the phenomena of colour-matching.

Foveal Tritanopia

König, in 1894, discovered that the central fovea is tritanopic, blues and greens, and whites and yellows being confused if the matching fields were kept very small and central fixation was accurately maintained. Later Willmer (1946) rediscovered the phenomenon and suggested that the blue receptor—apparently lacking in the central fovea—was the rod, which behaved as a colour receptor under photopic conditions. However, this tritanopia is probably due, as Hartridge showed, to the use of very small fields *per se*, since a similar dichromacy could be observed in the periphery, provided the field was made small enough. This loss of blue sensitivity may be due to a relative rarity of the 'blue' cones, so that unless the field is large enough an insufficient number are stimulated to permit their effects to be manifested.

Fovea and Periphery

Frequently, however, an increased sensitivity to blue may be demonstrated under suitable conditions; in general, according to Weale (1953), the visual functions of the different regions of the retina may be summarized as in Table 16.2. Thus, in the periphery, the sensitivity to blue seems to be *enhanced.*

MESOPIC SENSITIVITY CURVES

The Purkinje shift has been described as a change in the luminosity curve, or spectral sensitivity function, as one passes from scotopic to photopic levels of luminance; at the intermediate ranges the sensitivity function becomes intermediate between that for rods and that for cones, and it is as though both were contributing to the sense of luminosity at the different wavelengths. When the quantitative aspects of these changes are investigated, however, it may be shown that a given mesopic luminosity curve cannot be constructed by linear addition of the pure scotopic and photopic curves, so that we must envisage interaction between rods and cones at some level in the visual pathway (Hough, 1968). It is interesting that when one studies the successive changes in the luminosity curve as the luminance is increased, it is as though Stiles' blue cone mechanism were coming into play with greater and greater effect, rather than all three cone-types. This was strikingly confirmed by Hough & Ruddock (1969), who found that in the tritanope, whose blue cone mechanism

Table 16.2 Changes in chromatic visual function with retinal fixation area (after Weale, 1953)

Retinal area	*Extent from centre nasally*	*Type of vision*
Foveal centre	50′	Tritanopia
Fovea	2°30′	Trichromatic
Parafovea	4°10′	Trichromatic, with enhanced blue sensitivity
Perifovea	9°10′	Anomalous trichromacy with enhanced blue sensitivity
Inner periphery	14°10′ to	
Intermediate periphery	24°10′	
External periphery	77°35′	Dichromacy with enhanced blue sensitivity

is defective, the Purkinje shift is very defective, the luminosity curve at a mesopic level of 10 photopic trolands being identical with the scotopic luminosity curve, whereas in a normal trichromat the maximum sensitivity had changed from the scotopic 505 nm to some 540 nm. In view of the mixing of rod and cone responses that may occur as a result of the connections of horizontal cells (p. 357), it may well be that the mesopic luminosity curve reveals this interaction.[8]

Plateau-period

During the plateau-period of the dark-adaptation curve of Fig. 7.1, p. 220, the threshold remains constant although the rods are adapting but have not yet come to threshold. During this period, then, we may expect visual function to be governed purely by cones in peripheral vision, so that the mesopic range comes on later than this when cones may be activated by intensities that are sufficient to excite rods, i.e. beyond the break in the curve. Stabell & Stabell (1975, 1976) have shown that the colour-matching functions, and the luminosities of photopic stimuli measured during the period immediately following light-adaptation, remain invariant during the plateau period; thus only when the rod-threshold is exceeded is there rod–cone interaction.

Notes

1. In addition to its capacity as a wave-guide the retinal cone may be described as an 'ideal light collector' by virtue of the ellipsoid, whose structure is such as to favour the funnelling of light from outer to inner segment. An ideal light collector has a completely reflecting inner surface; hence, because the cone relies on total internal reflexion, the collection is reduced on this account (Winston & Enoch, 1971). Tobey & Enoch (1973) passed light backwards through rods and showed that it emerged in a tight cone, so that, on the principle of reversibility of rays, there is a corresponding limitation to the acceptance of light.
2. Alpern and his colleagues (1983) have described an elaborate series of experiments on the Stiles–Crawford effect in human subjects, showing that the different Stiles mechanisms for single cones could be described from measurements of the effect at different wavelengths. They examined also the dependence of colour and subjective brightness of monochromatic lights on the angle of incidence on the retina, and finally they studied the changes in saturation of monochromatic lights with angle of incidence. They reach the somewhat unsatisfactory conclusion: 'Either all unified theories of the Stiles–Crawford effects are wrong or all the effects of oblique incidence operate at a stage in the visual process at which the effects of radiation of different wavelengths are no longer compounded by the simple linear laws.' Their papers contain valuable surveys of the literature.
3. Bowen *et al.* (1977) showed that metacontrast masking failed if, instead of the test- and masking flashes being luminance-transients, i.e. increase or decrease in luminance referred to a steady background, they were colour-transients, i.e. hue-substitutions.
4. The independence of cone and rod influences described by Westheimer was not confirmed by Lennie & MacLeod's work; the threshold for a test-flash, only seen by rods, was decreased by a surrounding cone stimulus. This was confirmed by Frumkes & Temme (1977) and Buck *et al.* (1979), although, with large areas of surround there was independence, when small surrounds were studied cones influenced rod thresholds. Makous & Boothe (1974) showed that the efficiency of a red background in raising rod threshold depended on whether the red beam entered the pupil obliquely or centrally, i.e. on the Stiles–Crawford effect, which is peculiar to cone vision. Stromeyer (1983) found no cone specificity in his study of the effects of small surrounds.
5. Quoted by Cohn & Lasley (1975).
6. Enroth-Cugell & Shapley (1973) discuss some apparent objections to this thesis, but the weight of evidence seems to favour their conclusion that adaptation represents a feedback on the receptors through horizontal cells; thus adaptive inputs from many rods are pooled within horizontal cells which feedback on the rods to set the adaptation level.
7. In a paper published in the *Philosophical Transactions* in 1898, Burch described these 'red' and 'green' monochromatisms after adapting to strong violet + green or violet + red lights. It should be noted that these states last only for a short time, of the order of 10 seconds.
8. Dodt (1967) has described a Purkinje shift in the pure rod eye of the bush-baby, *Galago crassicaudatus*, when the visual response was measured by the height of the *b*-wave of the ERG.

References

Aiba, T. S. & Stevens, S. S. (1964) Relation of brightness to duration and luminance under light- and dark-adaptation. *Vision Res.* **4**, 391–401.

Alpern, M. (1953) Metacontrast. *J. Opt. Soc. Amer.* **43**, 648–657.

Alpern, M. (1965) Rod-cone independence in the after-flash effect. *J. Physiol.* **176**, 462–472.

Alpern, M. & Kitahara, K. (1983) The directional sensitivities of the Stiles' colour mechanisms. *J. Physiol.* **338**, 627–649.

Alpern, M., Kitahara, K. & Tamaki, R. (1983) The dependence of the colour and brightness of a monochromatic light upon its angle of incidence on the retina. *J. Physiol.* **338**, 651–668.

Alpern, M. & Rushton, W. A. H. (1965) The specificity of the cone interaction in the after-flash effect. *J. Physiol.* **176**, 473–482.

Alpern, M. & Tamaki, R. (1983) The saturation of monochromatic lights obliquely incident on the retina. *J. Physiol.* **338**, 669–691.

Auerbach, E. & Wald, G. (1954) Identification of a violet receptor in human colour vision. *Science* **120**, 401–405.

Barlow, H. B. (1958) Temporal and spatial summation in human vision at different background intensities. *J. Physiol.* **141**, 337–350.

Barlow, H. B. & Levick, W. R. (1969) Three factors limiting the reliable detection of light by ganglion cells of the cat. *J. Physiol.* **200**, 1–24.

Baumgardt, E. & Ségal, J. (1946) La localisation du mécanisme inhibiteur dans la perception visuelle. *C. R. Soc. Biol., Paris* **140**, 431–432.

Baylor, D. A. & Fettiplace, R. (1975) Light path and photon capture in turtle photoreceptors. *J. Physiol.* **248**, 433–464.

Baylor, D. A. & Hodgkin, A. L. (1973) Detection and resolution of visual stimuli by turtle photoreceptors. *J. Physiol.* **234**, 163–198.

Bouman, M. A. (1950) Quanta explanation of vision. *Doc. Ophthal.* **4**, 23–115.

Bouman, M. A. (1955) Absolute threshold conditions for visual reception. *J. Opt. Soc. Amer.* **45**, 36–43.

Bowen, R. W., Pokorny, J. & Cacciato, D. (1977) Metacontrast masking depends on luminance transients. *Vision Res.* **17**, 971–975.

Brindley, G. S. (1952) The Bunsen-Roscoe law for the human eye at very short durations. *J. Physiol.* **118**, 135–139.

Brindley, G. S. (1953) The effects on colour vision of adaptation to very bright lights. *J. Physiol.* **122**, 332–350.

Brindley, G. S. (1960) *Physiology of the Retina and Visual Pathway.* London: Edward Arnold.

Broca, A. & Sulzer, D. (1902) La sensation lumineuse en fonction du temps. *J. Physiol. Path. gén.* **4**, 632–640.

Buck, S. L., Pepples, D. R. & Makous, W. (1979) Spatial patterns of rod–cone interaction. *Vision Res.* **19**, 775–782.

Burch, G. (1898) On artificial temporary colour-blindness, with an examination of the colour sensations of 109 persons. *Phil. Trans.* **191 B**, 1–34. (Quoted by Brindley, 1960.)

Cohn, T. E. & Lasley, D. J. (1975) Spatial summation of foveal increments and decrements. *Vision Res.* **15**, 389–399.

Crawford, B. H. (1947) Visual adaptation in relation to brief conditioning stimuli. *Proc. Roy. Soc. B* **134**, 283–302.

Denton, E. J. & Wyllie, J. H. (1955) Study of the photosensitive pigments in the pink and green rods of the frog. *J. Physiol.* **127**, 81–89.

Dodt, E. (1967) Purkinje-shift in the rod eye of the bush-baby, *Galago crassicaudatus. Vision Res.* **7**, 509–517.

Donchin, E. & Lindsley, D. B. (1965) Retroactive brightness enhancement with brief paired flashes of light. *Vision Res.* **5**, 59–70.

Donchin, E., Wicke, J. D. & Lindsley, D. B. (1963) Cortical evoked potentials and the perception of paired flashes. *Science* **141**, 1285–1286.

Donner, K. O. & Rushton, W. A. H. (1959) Rod-cone interaction in the frog's retina analysed by the Stiles-Crawford effect and by dark-adaptation. *J. Physiol.* **149**, 303–317.

Enoch, J. M. (1960) Waveguide modes: are they present, and what is their possible role in the visual system. *J. opt. Soc. Am.* **50**, 1025–1026.

Enoch, J. M. (1961) Visualization of wave-guide modes in retinal receptors. *Amer. J. Ophthal.* **51**, Pt. 2, 1107–1118.

Enroth-Cugell, C. & Lennie, P. (1975) The control of retinal ganglion cell discharge by receptive field surounds. *J. Physiol.* **247**, 551–578.

Enroth-Cugell, C., Lennie, P. & Shapley, R. M. (1975) Surround contribution to light adaptation in cat retinal ganglion cells. *J. Physiol.* **247**, 579–588.

Enroth-Cugell, C. & Shapley, R. M. (1973) Adaptation and dynamics of cat retinal ganglion cells. *J. Physiol.* **233**, 271–309.

Flamant, F. & Stiles, W. S. (1948) The directional and spectral sensitivities of the retinal rods to adapting fields of different wavelengths. *J. Physiol.* **107**, 187–202.

Foster, D. H. (1976) Rod-cone interaction in the after-flash effect. *Vision Res.* **16**, 393–396.

Frumkes, T. E. & Temme, L. A. (1977) Rod-cone interaction in human scotopic vision. II. Cones influence rod increment thresholds. *Vision. Res.* **17**, 673–679.

Frumkes, T. E. *et al.* (1973) Rod-cone interaction in human scotopic vision. I. Temporal analysis. *Vision Res.* **13**, 1269–1282.

Fry, G. A. & Alpern, M. (1953) The effect of a peripheral glare source upon the apparent brightness of an object. *J. opt. Soc. Am.* **43**, 189–195.

Glezer, V. D. (1965) The receptive fields of the retina. *Vision Res.* **5**, 497–525.

Hagins, W. A. (1955) The quantum efficiency of bleaching of rhodopsin *in situ. J. Physiol.* **129**, 22–23P.

Hallett, P. E. (1963) Spatial summation. *Vision Res.* **3**, 9–24.

Heinemann, E. G. (1972) Simultaneous brightness induction. *Hdb. Sensory Physiol.* **VII/4**, 146–169.

Hough, E. A. (1968) The spectral sensitivity functions for parafoveal vision. *Vision Res.* **8**, 1423–1430.

Hough, E. A. & Ruddock, K. H. (1969) The parafoveal visual response of a tritanope and an interpretation of the V_λ sensitivity functions of mesopic vision. *Vision Res.* **9**, 935–946.

Ikeda, M. (1965) Temporal summation of positive and negative flashes in the visual system. *J. opt. Soc. Amer.* **55**, 1527–1534.

Katz, M. S. (1964) Brief flash brightness. *Vision Res.* **4**, 361–373.

Kirschfeld, K. & Snyder, A. W. (1976). Measurement of a photoreceptor's characteristic waveguide parameter. *Vision Res.* **16**, 775–778.

Latch, M. & Lennie, P. (1977) Red-cone interaction in light adaptation. *J. Physiol.* **269**, 517–534.

Lennie, P. & MacLeod, D. I. A. (1973) Background configuration and rod threshold. *J. Physiol.* **233**, 143–156.

Makous, W. & Boothe, R. (1974) Cones block signals from rods. *Vision Res.* **14**, 285–294.

McKee & Westheimer, G. (1970) Specificity of cone mechanisms in lateral interaction. *J. Physiol.* **206**, 117–128.

Raab, D. H. (1963) Backward masking. *Psychol. Bull.* **60**, 118–129.

Rashbass, C. (1970) The visibility of transient changes in luminance. *J. Physiol.* **210**, 165–186.

Sakitt, B. (1971) Configuration dependence of scotopic spatial summation. *J. Physiol.* **216**, 513–529.

Sakitt, B. (1972) Counting every quantum. *J. Physiol.* **223**, 131–150.

Sakmann, B., Creutzfeldt, O. & Schleich, H. (1969) An experimental comparison between the ganglion cell receptive field and the receptive field of the adaptation pool in the cat retina. *Pflüg. Arch. ges. Physiol.* **307**, 133–137.

Saunders, R. McD. (1975) The critical duration of temporal summation in the human central fovea. *Vision. Res.* **15**, 699–703.

Schouten, J. F. & Ornstein, L. S. (1939) Measurements on direct and indirect adaptation by means of a binocular method. *J. opt. Soc. Am.* **29**, 168–182.

Snyder, A. W. & Pask, C. (1973) The Stiles-Crawford effect—explanation and consequences. *Vision Res.* **13**, 1115–1137.

Stabell, U. & Stabell, B. (1975) The effect of rod activity on colour matching functions. *Vision. Res.* **15**, 1119–1123.

Stabell, U. & Stabell, B. (1976) Absence of rod activity from peripheral vision. *Vision Res.* **16**, 1433–1437.

Stiles, W. S. (1937) The luminous efficiency of monochromatic rays entering the eye pupil at different points and a new colour effect. *Proc. Roy. Soc. B.* **123**, 90–118.

Stiles, W. S. & Crawford, B. H. (1933) The luminous efficiency of rays entering the eye pupil at different points. *Proc. Roy. Soc. B.* **112**, 428–450.

Stromeyer, C. F. (1983) Spatial sensitization and desensitization with small adapting fields: interactions of signals from different classes of cones. *Vision Res.* **23**, 621–630.

Tansley, K., Copenhaver, R. M. & Gunkel, R. D. (1961) Spectral sensitivity curves of diurnal squirrels. *Vision Res.* **1**, 154–165.

Thomson, L. C. (1951) The spectral sensitivity of the central fovea. *J. Physiol.* **112**, 114–132.

Tobey, F. L. & Enoch, J. M. (1973) Directionality and waveguide properties of optically isolated rat rods. *Invest. Ophthal.* **12**, 873–880.

Tobey, F. L., Enoch, J. M. & Scandrett, J. H. (1975) Experimentally determined optical properties of goldfish cones and rods. *Invest. Ophthal.* **14**, 7–23.

Van Loo, J. A. & Enoch, J. M. (1975) The scotopic Stiles-Crawford effect. *Vision Res.* **15**, 1005–1009.

Walraven, P. L. (1961) On the Bezold-Brücke phenomenon. *J. opt. Soc. Am.* **51**, 1113–1116.

Weale, R. A. (1953) Spectral sensitivity and wavelength discrimination of the peripheral retina. *J. Physiol.* **119**, 170–190.

Westheimer, G. (1965) Spatial interaction in the human retina during scotopic vision. *J. Physiol.* **181**, 881–894.

Westheimer, G. (1967) Spatial interaction in human cone vision. *J. Physiol.* **190**, 139–154.

Westheimer, G. (1970) Rod–cone independence for sensitizing interaction in the human retina. *J. Physiol.* **206**, 109–116.

Westheimer, G. & Wiley, R. W. (1970) Distance effects in human scotopic retinal interaction. *J. Physiol.* **206**, 129–143.

White, T. W., Collins, S. B. & Rinalducci, E. J. (1976) The Broca–Sulzer effect under scotopic viewing conditions. *Vision Res.* **16**, 1439–1443.

Willmer, E. N. (1946) *Retinal Structure and Colour Vision.* Cambridge: Cambridge University Press.

Winston, R. & Enoch, J. M. (1971) Retinal cone receptor as an ideal light collector. *J. Opt. Soc. Amer.* **61**, 1120–1121.

Wright, W. D. (1939) The response of the eye to light in relation to the measurement of subjective brightness and contrast. *Trans. Illum. Eng. Soc.* **4**, 1–8.

Wright, W. D. (1946) *Researches on Normal and Defective Colour Vision.* London: Kimpton.

Wright, W. D. & Nelson, J. H. (1936) The relation between the apparent intensity of a beam of light and the angle at which the beam strikes the retina. *Proc. Phys. Soc.* **48**, 401–405.

Section 3

VISUAL PERCEPTION

17. VISUAL PERCEPTION: INTRODUCTION

Sensation and Perception

In Section 2 we have investigated the 'mechanism of vision' in the limited sense of attempting to understand the elementary processes in the retina that result in discharges in the optic nerve, and of attempting to correlate these with the sensations. To this end, very simple visual phenomena were chosen—the sensation of luminosity, the discrimination of flicker, colour and form. In respect to this last category, we confined ourselves to the very element of form discrimination—the resolution of points and lines—and in visual acuity studies we indicated that the recognition of letters was an unsuitable basis for the study of resolution since it involved activities at a higher level than those we were immediately concerned with. In this section we must consider some of the manifestations of this higher form of cerebral activity.

The Perceptual Pattern

Essentially we shall be concerned with the modes in which visual sensations are interpreted; the eyes may gaze at an assembly of objects and we know that a fairly accurate image of the assembly is formed on the retinae of the two eyes, and this is 'transferred' by a 'point-to-point' projection to the occipital cortex. This is the basis for the visual sensation evoked by the objects but there is a large variety of evidence, derived from everyday experience, which tells us that the final awareness of the assembly of objects involves considerably more nervous activity than a mere point-to-point projection of the retina on the cortex would require. As a result of this activity we appreciate a *perceptual pattern*; the primary visual sensation, resulting from stimulating the visual cortex, is integrated with sensations from other sources presented simultaneously and, more important still, with the memory of past experience. For example, a subject looks at a box; a plane image is produced on each retina which may be represented as a number of lines, but the perceptual pattern evoked in the subject's mind is something much more complex. As a result of past experience the lines are interpreted as edges orientated in different directions; the light and shade and many other factors to be discussed later are all interpreted in accordance with experience; its hardness is remembered and its uses, and the original visual sensation is *interpreted as a box*, not a series of lines. It is impossible, in practice, to separate the sensation of seeing from the perceptual process; the sensation is essentially an abstraction—what we think would be the result of a visual stimulus if this higher nervous integrative activity had not happened. In the case of a flash of light the influence of higher nervous activity is very small and the sensation is virtually identical with the final perception. With a written word, on the other hand, the final perceptual pattern presented to consciousness is something far different from the bare visual sensation.

We may begin by illustrations of the perceptual process, as revealed by psycho-physical studies, and later we shall consider some electrophysiological studies that illustrate the possible neural basis for some of these higher integrative functions.

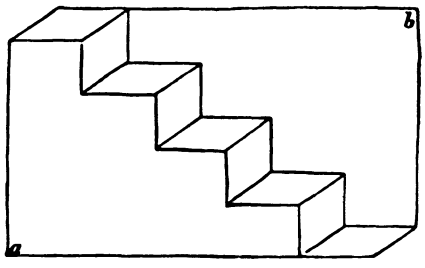

Fig. 17.1 Schroeder's staircase.

HIGHER INTEGRATIVE ACTIVITY

Inadequate Representation

Schroeder's staircase (Fig. 17.1) shows how the same visual stimulus may evoke different meanings in the same subject; to most people the first impression created by Fig. 17.1 is that of a staircase; on gazing at it intently, however, the observer may see it as a piece of overhanging masonry. (If the reader has any difficulty in seeing Fig. 17.1 as a piece of overhanging masonry, he has only to turn the page upside down by slowly rotating the book,

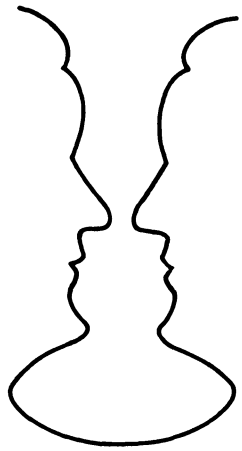

Fig. 17.2 Rubin's vase.

keeping the eyes fixed on the drawing.) *Rubin's vase* (Fig. 17.2) may be seen either as a vase or two human profiles. In general, diagrams of this sort are called *inadequate representations* of the object they are intended to copy, or *ambiguous figures*. The lines, as such, can be interpreted with more or less ease in two different ways and the fact that they are perceived in one or other definite manner emphasizes the arbitrary element of interpretation in the visual process. Helmholtz quotes in this connection the case of a windmill, observed against the night sky; according as the observer fancied that the sails were in front of, or behind, the body of the mill he saw them revolving in different directions. Brown (1962) has described an experimental set-up that simulates the situation described by Helmholtz, the subject observing the shadows cast by a set of six vertical pins arranged in a circle and rotating at constant speed about a vertical axis through the centre of the circle. The stimulus on the screen was two-dimensional, with one set of pins moving left and the other right, but the subject perceived it three-dimensionally, with the apparent direction of rotation of the pins varying. This is because the basic stimulus contains strong depth cues, but without decisive ones concerning the depth relation between the two sets of pins moving in right and left directions.

Careful experimentation with ambiguous figures has shown that, over a period of time, the fluctuations in meaning exhibit a periodicity characteristic of the observer. This is not to deny, however, that with an effort of will, by moving the eyes, blinking, etc., the meaning of the pattern may be made to change. Nevertheless, if the subject merely regards the figure for several minutes and the times during which it is seen in its two meanings are recorded, it is found that the fluctuations are definitely not random in nature. It is interesting that the periodicity may be affected by drugs.

Brown's experimental arrangement described above is particularly suitable for investigation of the rate of change of apparent movement; he found that it increased with viewing time. If this increase had been achieved by monocular observation, then the other eye showed the same increase, so that we may say that there was *inter-ocular transfer* of this adaptational effect, indicating that the process occurs at a higher central level than the retina, namely at some point in the visual pathway common to both eyes.

Reading

The reading process is an instance of the arbitrary attachment of meaning to symbols; with practice the meaning becomes associated not with the complete picture of a word but with its general shape and thus the practised reader can be imposed on easily with misspelt words; the context leads him to expect a certain word and he actually sees it even though it is not on the page. Here the perceptual process is imposing a meaning on the visual stimulus that does not correctly belong to it, and many examples of this arbitrary activity of the higher centres may be cited; for example most people read the word 'vicegerent' as 'viceregent' because the latter is the word they expect even though it does not occur in the dictionary. The filling up of the blind spot and the failure of the hemianopic subject to realize his defect are further instances.

Colour Perception

Colour Constancy

By this term we mean the tendency of the subject to perceive the colour of an object as being the same in spite of large variations in the actual chromaticity of the light emanating from it. The colour becomes one of an object's attributes—its *memory colour*—and there is a strong tendency to perceive this even when the physical conditions have been chosen to make this difficult. For example, a red letterbox may be illuminated with blue light so that far more blue light is reflected off it than red, yet the subject continues to call it red, and his *perception* is that of a red object. If the object, so illuminated, is looked at through a tube, so that its colour may be divorced from its shape, it is said to appear blue. Again, we may place a green filter at arm's length and note that the part of the field of vision seen through the filter acquires a distinct green colour—*colour conversion*—but when the filter is brought close to one eye and the other is closed, the natural colours of the objects viewed are identified readily—*colour constancy*. Thus, as Helmholtz pointed out: '. . . with all coloured surfaces without distinction,

wherever they are in the sphere of the coloured illumination, we get accustomed to subtracting the illuminating colour from them in order to find the colour of the object.' The basis on which the 'discounting of the illuminant colour' is achieved must be an unconscious recognition of the chromaticity of the light reflected off the more highly reflecting objects in the scene, e.g. a piece of white paper.

If we call the colour perceived in an object as the *object colour*, we may refer to these phenomena as examples of *object-colour constancy*. When a coloured light is viewed independently of any object, as through a hole in a screen, then we may call this an *aperture colour*, but it must be appreciated that the perceived aperture colour is by no means invariant for a given chromaticity of its emitted light, and this is largely because of adaptational and contrast effects. Thus, as Helson (1938) showed, it is easily possible to devise a scene in which an object reflecting light of any chromaticity whatsoever is perceived as grey, the main basis for this being the tendency for the subject to see the colour of the illuminant, the colour of the after-image complementary to the illuminant, or achromaticity, depending on the relative reflectances of the surface being viewed and the adaptation reflectance.

These principles, which lead to modifications of the perceived colours of objects, have been formulated quantitatively by Judd (1940), the process of discounting the spectral quality of the illuminant being achieved by defining, on the Maxwellian triangle, a point to correspond with the perception of grey in the object-mode of viewing, this point being close to the chromaticity of the illuminant. The prediction of the hue reported by an observer was given by the vector extending from this achromatic point to the point defining the chromaticity of the light actually emanating from the object.

Two Primary Projections

Interest in colour constancy, and its related phenomena, was revived with the description by Land (1959) of a series of experiments in which he produced, with the aid of only two illuminants, pictures that seemed to give a faithful reproduction of the colours of various scenes—pictures that, on the basis of trichromatic theory, should have required three independent sources of illumination. In general, Land produced two transparent positives of the scene by photographing it first through a red-transmitting filter (585 to 700 nm) and then through a filter transmitting the middle third of the spectrum (490 to 600 nm). The image of one of these positives was usually projected on to a white screen with red light (590 to 700 nm), whilst that of the other usually by an incandescent lamp, the two images being adjusted carefully to be in register. Space will not permit of a summary of the findings, but his Experiment 3 may be quoted as an example: By combining the long-wave picture shown in red light with the middle-wave picture shown in incandescent light, the subject perceived the full colour in a portrait of a blonde girl, i.e. blonde hair, pale blue eyes, red coat, blue-green collar, and strikingly natural flesh tones. For adequate colour representation through photography, a three-primary system is ordinarily employed, and the question to be asked is how this apparently true representation of colours is achieved with only two positives. It must be appreciated, however, that the use of white light in the incandescent illuminant provides the viewer with all colours of the spectrum, and it is essentially the fact that the subject ignores the exact chromatic content of the light reflected off the various parts of the screen that permits him to perceive a fairly true representation of the original. According to Judd's analysis, the perceived colours in this, and in other examples described by Land, are, in fact, predictable on the basis of his earlier quantitative formulation, so that there is no reason to abandon the trichromatic theory of colour perception on the basis of these experiments of Land.

Tone Constancy

Essentially similar phenomena are described for the blacks, greys and whites. A grey wall may be compared with a grey piece of paper on a table reflecting the same amount of light; the wall appears white whilst the paper appears grey, presumably because we associate lightness with the walls of a room. These phenomena are classified under the heading of *tone constancy*, but it must be appreciated that, just as with chromatic vision, the final perception depends on inductive effects taking place at the retinal level. For example, it is argued that the black of this type, seen on a fine day, reflects more light than does the white of the paper in dim illumination, and yet the black is seen as black in both circumstances. The psychologist 'explains' this as tone constancy; the physiologist, however, would merely state that the black sensation is evoked by a certain area of the retina being stimulated less intensely than another, adjoining, area; he would be the last to suggest that there is an absolute black sensation depending on some critical level of retinal stimulation. We know, moreover, that the sensitivity of the retina is enormously affected by light-adaptation (p. 226), so that it is impossible to expect that the same sensation will be evoked by the same stimulus under widely differing states of adaptation. We must therefore be careful of attributing to the activities of higher centres phenomena that properly belong to the retina.

Having clarified our position in relation to the difference between a perception and a sensation, we can now proceed to analyse some of the simple mechanisms concerned in the perceptual processes.

MONOCULAR PERCEPTION

The Projection of the Retina

Objects are perceived in definite positions in space—positions definite in relation to each other and to the percipient. Our first problem is to analyse the physiological basis for this spatial perception or, as it is expressed, the *projection of the retina into space.*

Relative Positions of Objects

The perception of the positions of objects in relation to each other is essentially a geometrical problem. Let us confine the attention, for the present, to the perception of these relationships by one eye—*monocular perception.* A group of objects, as in Fig. 17.3, produces images on the retina in a certain fixed geometrical relationship; for the perception of the fact that A is to the left of B, that B is to the left of C, etc., it is necessary that the incidence of images at *a, b, c* on the retina be interpreted in a similar, but, of course, inverted geometrical relationship. The neural requirements for this interpretation are (*a*) that the retina should be built up of elements which behave as units throughout their conducting system to the visual cortex and (*b*) that the retinal elements should have 'local signs'. The local sign could represent an innate disposition or could result from experience—the association of the directions of objects in space, as determined by touch, etc., with the retinal pattern of stimulation. However they arise, the local signs of the retinal elements provide the complete information as to the relative positions of A, B and C.

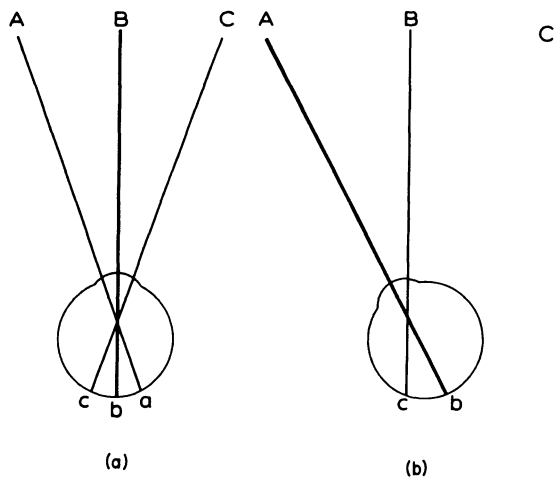

Fig. 17.3 (*a*) A group of objects, A, B, C, produces images on the retina, *a, b, c*; the retinal images are projected outwards in space towards the points evoking them. (*b*) The eye has moved to the left so that the image of A falls on *b*. *b* was previously projected to B but it is now projected to A.

The retinal stimuli at *a, b* and *c* are appreciated as objects outside the eye—the retina is said to be *projected* into space, and the field of vision is thus the projection of the retina through the nodal point. It will be seen that the geometrical relationship between objects and retinal stimuli is reversed; in the retina *a* is to the right of *b*, and so on; it is customary to speak of the 'psychological erection of the retinal image'; this is thoroughly misleading since it suggests an awareness, on the part of the higher centres, of the actual points on the retina stimulated. This of course is untrue; *a* and *c* are projected to the left and right of B, not because the higher centres have learnt the laws of geometrical optics but because such a projection corresponds with experience.

Position in Relation to Observer

The recognition of the directions of objects in relation to the observer is more complex. If the eye (Fig. 17.3*b*) is turned to the left, the image of A falls on the retinal point *b*, so that if *b* were always projected into the same direction in space, A would appear to be in B's place. In practice we know that A is perceived as fixed in space in spite of the movements of the eye; hence the direction of projection of the retinal point is constantly modified to take into account movements of the eye—we may call this '*psychological compensation*'. It will be seen that correct projection is achieved by projecting the stimulated retinal point through the nodal point of the eye. Movements of the eye due to movements of the head must be similarly compensated. As a result, any point in space remains fixed in spite of movements of the eye and head. Given this system of 'compensated projection', the recognition of direction in relation to the individual is now feasible. B may be said to be due north, or more vaguely 'over there'; when the head is turned, since B is perceived to be in the same place, it is still due north or 'over there'.

False Projection

Under some conditions the human subject will make an error in projecting his retinal image so that the object giving rise to this image appears to be in a different place from its true one; the image is said to be *falsely projected.* If the eye is moved passively, for example by pulling on the conjunctiva with forceps, the subject has the impression that objects in the outside world are moving in the opposite direction to the movement of the eye. The exact nature of this false projection is illustrated in Fig. 17.4. The eye is fixated on an object F, whose image falls on the fovea, *f*.[1] The eye is moved forcibly through 30°, so that the image of F falls on a new point, *q* (Fig. 17.4*b*). The correct projection of *q* would be through the nodal point out to F; however, projection takes place as though the eye had not moved. The image falls 30° to the right of the

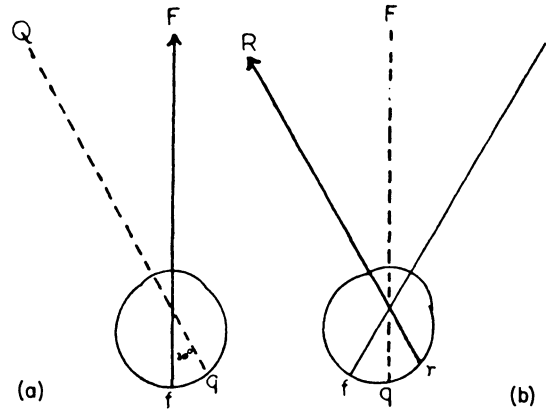

Fig. 17.4 Illustrating false projection resulting from the forcible movement of the eye. (*a*) The point F is fixated. (*b*) The eye has been moved forcibly 30° to the right. The image of F falls on *q*, and the projection of *q* is made on the assumption that the eye has not moved, i.e. towards **R**.

fovea; with the eye in its original position, such a retinal stimulus would correspond to an object 30° to the left, the point Q in Fig. 17.4*a*, so that the stimulus on *q*, in the new position of the eye, is projected 30° to the left, along the line *r*R. Consequently, as the eye is moved to the right, the retinal image of F is projected progressively to the left.

INFORMATION FROM MOTOR DISCHARGE

Quite clearly, under these abnormal conditions, the necessary information as to the position of the eye is not being sent to what we may call a '*space representation centre*' (Ludvigh), so that interpretation of the retinal image is made on the basis of inadequate information. The tension in the spindles and tendon-organs will undoubtedly be altered as a result of this passive movement, and the fact that no use is made of this proprioceptive information indicates that normally the space representation centre employs a different type of information on which to base its estimates of the position of the eye. This information could be provided by the motor discharge from the voluntary and reflex centres controlling the movements of the eyes, as suggested by Helmholtz; thus when the subject moves his eyes to the left to fixate point A in Fig. 17.3, the centre that initiates the motor discharges to the medial and lateral recti, besides sending its impulses to the motor neurones of the nuclei of N III and VI, may also send messages to the space representation centre indicating the intensities of these discharges, and thus the approximate extents of the eye movements. The space representation centre thus interprets the shifting image of A, B and C over the retinae not as movement of these points but as a movement of the eyes to fixate A. The proprioceptive messages from the muscle spindles and tendon-organs operate on a completely unconscious level, simply serving to moderate the strengths of the contractions of individual fibres in accordance with variations in local conditions—the so-called *parametric feedback* (Ludvigh, 1952). In the case of the eye that has been moved passively, the space representation centre has obviously not been informed of the eye movement, and the interpretation of the shifting retinal images is now what would be expected had the eyes remained stationary, i.e. the interpretation is that of a moving of the external objects from right to left, with its consequent false projection. Before examining evidence directly concerning the existence of a collateral supply of information derived from the motor commands—*corollary discharge* of Sperry (1950) *or Efferenzkopie* of v. Holst & Mittelstaedt (1950)—we may consider some phenomena closely related to the simple case of false projection described above.

Perceptual Errors During Pursuit Movements

A number of studies on perceived position of stationary objects while the eye is tracking a moving point suggest that there is very little compensation for the eye movements; for example Stoper (1967) flashed successively two lines while the observer tracked a moving target on a homogeneous ground; if the intervals were short—up to about 300 msec—the subject failed to take account of the eye movement intervening when judging the relative positions of the two lines, which were therefore determined by the retinal pattern with no allowance for the intervening motion; with longer intervals of up to 1.7 sec compensation became manifest but it was on average only 64 per cent. More recently Festinger *et al.* (1976) compared the perceived with the actual paths of spots of light in harmonic motion during the tracking of another spot and concluded that there was little compensation for the tracking movement. Thus, perceptually, the subject is ignorant of the actual speed of his eye movements during slow tracking, but of course practically the control over the eye muscles indicates an accurate adjustment in accordance with speed. Festinger *et al.* suggested that initially, on the basis of perceived motion, tracking commands are initiated and the interpretation of retinal images is based on this primary command, which assumes that a relatively low speed is being utilized almost independently of the actual speed of the target; the actual adjustment of speed to permit accurate tracking is achieved by visual input that is apparently ignored by the perceptual process, thereby leading to considerable perceptual errors.[2]

Control of Eye Position in the Dark

Early studies of the behaviour of the eyes in the dark, when no fixation points are available, indicated that

within a few seconds of extinguishing a luminous target the eyes rapidly wandered from the target; however, when Skavenski & Steinman (1970) examined behaviour during periods of up to two minutes they found that the error in 'fixating' the extinguished target, after increasing rapidly after the target was extinguished increased more slowly and eventually the position of the eye stabilized with an error of about 2°, suggesting that there was some 'extra-retinal' memory and ability to direct the eyes in the light of this memory. In a later study Skavenski (1971) made a correlative study of the apparently random movements under the same conditions and showed that there was a corrective element that led to stabilization of the fixation error. When the position of an eye was changed artificially, without the subject being aware of the manipulation (a pull was exerted on a contact lens attached to the eye), the subject could report the movement correctly more often than not, with a probability of less than 0.001 that the answers could have occurred by chance. Moreover, the subject could also report the position of a target previously seen without the load on the eye that was causing an artificial deviation. Thus it seemed that the subject was correcting for the passive deflexion of the eye in the light of extraretinal *in*flow of information, since the outflow correlative discharge would not provide sufficient information as to the passive deflexion. These experiments indicate that some position-sense remains when the eyes are in the dark, but it is clearly of a very crude nature, and any accurate interpretation of visual images requires more precise information than this extraretinal inflow.

CONSTANT DRIFT

Working over longer periods in the dark, Becker & Klein (1973) described a constant drift, tending to bring the eyes back to the primary position when attempting to maintain any direction of gaze; small corrective saccades were made, of which the subject was unaware, and also larger consciously programmed saccades when the subject felt that the eyes had drifted away from the target. When a subject tried repeatedly to make a given saccade, the size depended on the drift that had taken place during the preliminary fixation in the dark, the larger the drift the smaller the movement, so that the saccade took into account that part of the movement that had already been made by the drift.

Vision During a Saccade

It was shown by Dodge in 1900 that vision was apparently suppressed during a saccade; a convincing demonstration of this was that of Ditchburn (1955) in which a subject fixated a bright spot on a cathode-ray oscillograph, the position of which moved in advance of the eye movement (positive feedback); as a result the spot made rapid flicks whenever the eyes moved, and the subject was unable to see these movements although an observer beside him could. Volkmann (1962) presented 20 μsec flashes to a subject who was told to move his eyes at given times; she found that, during a fixation movement, there was a 0.5 logunit rise in the threshold to the flashes, the change beginning some 40 msec before the beginning of the movement and lasting 80 msec after the end. In addition, the finest gratings that could be resolved by the moving eye were about 1.4 times coarser than those resolved by the fixating eye. Beeler (1967), in confirming the 0.5 logunit rise in threshold, pointed out that this decrease in visual sensitivity would not have been sufficient to prevent Ditchburn's subject from seeing the illuminated spot, so that there must be some other factor operating to prevent detection of movement. He presented a subject with a light-spot and made this move sideways 15 minutes of arc, the movement of the spot being arranged to occur at random intervals after an involuntary saccade; the movement of the spot was too small in extent to cause a fixation movement by the subject. Beeler determined the frequency of seeing the spot when it moved at different intervals after the saccade; and this increased from zero, during the saccade, to 93 per cent if the movement was separated from the flick by more than 100 msec. Thus, during a saccade there is apparently a suppression of target information; Beeler suggested that the cortex investigates the oculomotor system when a movement of the retinal images occurs, for example after a flick; during this time there is no awareness of further motions. If the efferent system has operated, i.e. if the retinal image-movement is due to motor activity and not to actual object movement, then all image-motion is ignored.[3]

'Retinal Smear'

The obvious interpretation of this retinal 'suppression' is that it is responsible for the absence of 'retinal smear' during eye movements. Such a suppression could be achieved by corollary discharge, the command signals to the motor neurones being accompanied by discharge to the visual centres enabling them to interpret the shift in retinal images in terms of eye motion. To have value, of course, such a suppression must distinguish between movement of the image due to movement of the eyes and movement due to movement of the visual environment, since the latter could be of significance and should therefore not be suppressed. MacKay (1970) showed that the increase in threshold to a flash of light could occur by displacement of the visual images on the retina however they occurred, and he suggested that the elevation of threshold was purely determined by the movement of the image, so that the information could not have been provided by corollary discharge. MacKay's results have

been abundantly confirmed, e.g. by Brooks & Fuchs (1975) who have discussed the significance of saccadic suppression in some detail in the light of their studies defining the stimulus parameters necessary for eliciting the phenomenon.[4]

OCULOGYRAL ILLUSION

Another example of false projection is given by the oculogyral illusion described by Graybiel & Hupp in 1946. A subject is seated in a rotatable chair in the dark, and he fixates a small source of light which is attached to the chair and rotates with it. When the chair is rotated the light appears to move in the same direction. In this case the rotation has stimulated the semicircular canals, and the space representation centre has been informed that the body has rotated. The subject is unaware that the fixation light has also moved, so that the stationary retinal image is reinterpreted; clearly, if the head moves whilst the image of a point remains stationary, the point must have moved to the same angular extent as the head. Hence the retinal image is projected as though the object had moved in relation to the observer. Thus, if the chair is rotated to the right, the light will be falsely projected to the right of the observer, although it has remained fixed in relation to him.

AUTOKINETIC ILLUSION

The explorer Alexander von Humboldt in 1799 noticed that after watching a faint star for a short time it would start to move around in various directions. An obvious explanation for this apparent movement may be the occurrence of involuntary eye movements, the space representation centre being inadequately informed of them whilst the relatively uniform background against which the light is viewed fails to provide adequate retinal information of the eye movements. There is still some disagreement as to whether such movements could always account for the phenomenon, so that other factors have been invoked as well. The subject has been reviewed by Grosvenor (1959), whilst the contribution of eccentric vision to the phenomenon has been described by Crone & Verduyn Lunel (1969).

Apparent Movement of an After-image

The apparent movement of an after-image, when the eye moves, is an excellent illustration of psychological compensation. A retinal stimulus, being normally projected through the nodal point, is projected into different points in space as the eye moves; an after-image can be considered to be the manifestation of a continued retinal impulse, and its projection changes as the eye moves. The after-image thus appears to move in the same direction as that of the movement of the eye. Whether or not the gradual drift of an after-image across the field of view is entirely due to eye movements, it is difficult to say. One certainly has the impression that the eye is 'chasing' the after-image.

Figural After-effects

This is the term given by psychologists to a variety of illusions having as their basis the adaptation to prolonged observation of a given figure; thus a subject fixating a curved line for some time sees it as less and less curved, whilst a straight line presented immediately after this prolonged inspection of the curved line appears curved in a direction opposite to that of the original curvature (see, for example, Gibson, 1933). Particularly instructive is Fig. 17.5 from Köhler & Wallach (1944); the subject inspects the fixation cross of the left-hand ensemble for about 40 seconds and then inspects the fixation cross of the right-hand ensemble. As a result of the first period of fixation the right-hand pair of squares look closer to each other in the vertical direction than do the left-hand pair. Thus there is a tendency for the perceived object to be displaced as a result of previous viewing, and the direction of displacement is away from the previously inspected object.

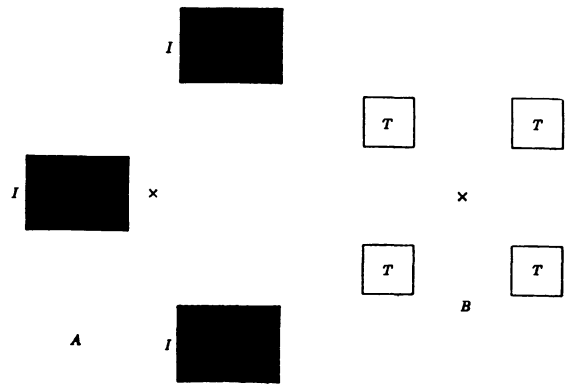

Fig. 17.5 Demonstrating displacement effects. Regard the fixation cross of A at reading distance for about 40 seconds, and then look at the fixation cross of B. After A has been observed, the right-hand squares of B appear nearer the central horizontal axis of this figure than do the left-hand squares. Inspection of the left-hand I-figure in A causes the left-hand squares of B to 'move apart vertically'; and inspection of the right-hand I-figures of A causes the right-hand squares of B to 'move together'. Subjects say that test figures are displaced from the positions of previous inspection figures. (Graham, *Vision and Visual Perception.*)

Visual Estimates

The Directions of Lines

We have so far considered the problem of estimating the positions of points, in relation to each other and to the percipient. The estimate of the directions of lines involves no really new principles, since if two points, A and B, are exactly localized, the direction of the line AB can be appreciated. The perspective distortion, however, and the torsion of the eye resulting from a change in the direction of fixation, can modify the estimate of the direction of a line, referred to a fixed line in space—e.g. the horizontal or vertical—unless some psychological compensatory process is introduced.

RETINAL MERIDIANS

A horizontal line—fixated in the primary position of the eye—is recognized to be horizontal because its image falls on a set of receptor elements on the retina lying on the horizontal meridian. Similarly a vertical line is recognized because its image falls on the vertical meridian. When the eye moves to the right, into a secondary position, a horizontal line still falls on the meridian because there has been no torsion. On looking up and to the right, however, the image of a horizontal line is inclined at a certain fixed angle, depending on the position of the eye, to the horizontal meridian of the retina. Because of the torsion a psychological compensation must be made so that an image, inclined across the horizontal meridian, is perceived as the image of a truly horizontal line. The full significance of Donders' Law (p. 654) now becomes evident. Movements of the eye involve torsion—this cannot be avoided—and torsion involves a disturbance of orientation of lines unless psychologically compensated. The higher centres, in order to compensate, must know the degree of torsion, and this information becomes physiologically simple to acquire if the torsion is characteristic of the position of the eye. Thus the motor innervation bringing about a given position of the eyes is 'reported' to the space representation centre, and this centre, in interpreting the retinal image, works on the assumption that this movement has brought about a characteristic degree of torsion. Donders' Law states that the torsion is a definite quantity for a given position of the eyes; and this regularity is achieved by the eyes rotating about an axis in Listing's plane (Listing's Law, Ch. 24).

VESTIBULAR INFLUENCES

Movements of the head are associated with compensatory reflex movements of the eyes, mainly of vestibular origin, designed to keep the visual fields normally orientated. In man, however, the rolling necessary to compensate for an inclination of the head towards the shoulder is quite inadequate, amounting to only one-tenth to one-fifth of the inclination of the head; since horizontal lines appear horizontal even when the head is strongly inclined, psychological compensation must be involved here; presumably the information required is provided by the labyrinth. That this labyrinthine information is not entirely adequate is shown, however, by *Aubert's phenomenon.* A subject regards a bright vertical slit in a completely dark room; on bending the head over to the side, the slit appears to incline in the opposite direction. When the lights are switched on the slit becomes vertical. If, in the dark, the head is inclined suddenly the slit remains vertical for a while but finally tilts over; it would seem that the abrupt movement stimulates the semicircular canals (p. 677) which cause adequate compensation. If the higher centres have to depend on the tonic receptors only—utricle and proprioceptive neck impulses—the compensatory mechanism becomes inadequate (Merton, 1956). It would appear, therefore, that the tonic receptors must be reinforced by the visual sensation; the observer knows that the bars of the window, for example, are not usually tilted over and so a compensation is initiated.

ACCURACY OF ESTIMATES

The power of appreciating whether a line is horizontal or vertical is very highly developed in man. Volkmann describes experiments in which he repeatedly set a line to what he considered to be the true horizontal; his mean error was only 0.2°; with his left eye, the left-hand end of the line was too low; with his right eye the right-hand end was too low. We may say that Volkmann's '*apparently horizontal meridians*' were slightly inclined to the true horizontal. With vertical lines his error was greater—more than 1°—but it was a constant error indicating an inclination of his '*apparently vertical meridians*'. More recent work, notably that of Gibson, bears out the findings of Volkmann; vertical lines are, on the average, estimated to within 0.28° and horizontal lines to within 0.52°; when an attempt is made to adjust a line to a fixed angle with the vertical, e.g. 60°, the error is much greater (1.74°) a finding which suggests that the vertical and the horizontal act as a frame of reference to which all other directions are referred. A modification of this type of experiment consists in presenting the subject with a short line, AB (Fig. 17.6) at a given angle of slant, α, from the horizontal, and asking him to adjust a dot, some distance away, to a position such that an extension of the line would pass through it. The error is indicated by the angle, β, and the angle $(\alpha+\beta)$ is called the perceived direction. Bouma & Andriessen (1968) found a tendency for the perceived orientation to be closer to the nearest horizontal or vertical than the geometrical slant, α. It was found that β decreased with the length of the short line, AB, up to a subtense of about 1°, so that a foveal line-segment was employed in the estimate; two dots were as effective as a line-segment.

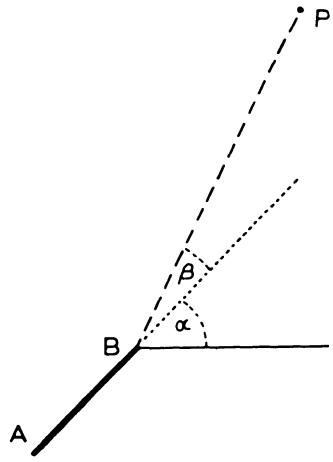

Fig. 17.6 The subject views the line AB and must adjust the position of P such that it appears to coincide with the prolongation of the line AB. (After Bouma & Andriessen, *Vision Res.*)

Comparison of Lengths

The influence of the movements of the eyes in the estimation of length was emphasized by Helmholtz. An accurate comparison of the lengths of the lines AB and CD (Fig. 17.7) can be made, whereas if an attempt is made to compare the lines A'B' and C'D', quite large errors occur. According to Helmholtz, the eye fixates first the point A and the line AB falls along a definite row of receptors, thereby indicating its length. The eye is now moved to fixate C, and if the image of CD falls along the same set of receptors the length of CD is said to be the same as that of AB. Such a movement of the eye is not feasible with the lines A'B' and C'D'. Similarly the parallelism, or otherwise, of pairs of lines can be perceived accurately because on moving the eye over the lines the distance between them must remain the same.

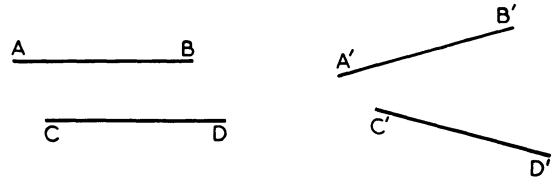

Fig. 17.7 AB and CD, being parallel, can be compared in length with accuracy whereas A'B' and C'D' cannot.

Fairly accurate estimates of relative size may be made, nevertheless, without movements of the eyes. If two equal lines are observed simultaneously, the one with direct fixation and the other with peripheral vision, their images fall, of course, on different parts of the retina; if the images were equally long it could be stated that a certain length of stimulated retina was interpreted as a certain length of line in space. It is probable that this is roughly the basis on which rapid estimates of length depend; a white line stimulating, say, twenty-five retinal elements being considered to have the same length as another line stimulating the same number of elements in another part of the retina. It is easy to show, however, that the matter is not quite so simple; the retina is curved so that lines of equal length in different parts of the visual field do not produce images of equal length on the retina; the distortion in the image resulting from the use of oblique pencils of light also complicates the matter, so that it is unlikely that such a simple relationship between size of image and projected size is achieved. The problem of the estimation of absolute size is closely linked with that of the estimation of distance and will be discussed under that heading.

Estimates of Angles

Two angles may be compared with accuracy if eye movements are permitted and if the sides are parallel. The errors in comparison increase greatly if the sides are not parallel. Essentially we are dealing with the same problem—the superimposition of the retinal pattern on another. In the estimation of right-angles some characteristic errors are encountered. Thus the cross made by the lines *ab* and *cd* (Fig. 17.8) appeared to Helmholtz to be truly rectangular, whereas it is correctly given by the line-segments γ and δ. This error is an expression of the fact that the apparently horizontal and vertical meridians of the retina (p. 456) are not exactly at right-angles. When the cross was turned at an angle of 45° the error in assessing the right-angles became much greater; the true right-angles to the right and left appeared to be 92° whilst those lying above and below appeared to be 88°.

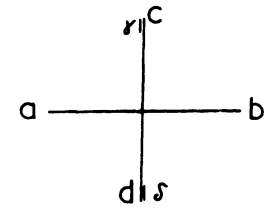

Fig. 17.8 The cross *abcd* appeared correct to Helmholtz, whereas the true cross is given by the line-segments γ and δ.

Optical Illusions

There are innumerable instances in the psychological literature of well-defined and consistent errors in visual estimates under special conditions; there is probably no single hard-and-fast rule by which they can be explained, but an important element may be the tendency for

distinctly perceptible differences to appear larger than those more vaguely perceived. Thus the line AB of Fig. 17.9 has been correctly bisected at C, but because AC is divided into easily perceptible parts, whilst the line CB is not, the former appears longer. The triangles ABC and A′B′C′ are both equilateral but, because of the division of the lines A′B′ and A′C′, the triangle A′B′C′ appears taller and therefore the angles at the base appear greater than 60°. Similarly, ABCD and A′B′C′D′ are squares yet the height of the latter figure appears to be greater than its breadth.

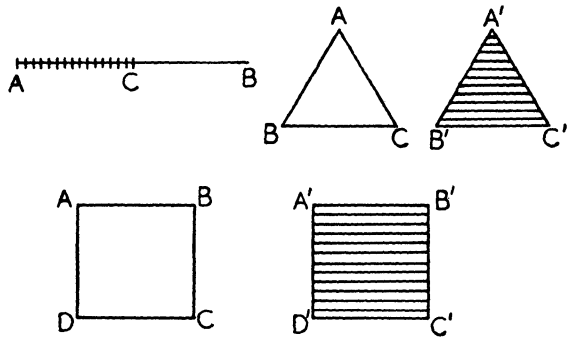

Fig. 17.9 Some optical illusions. AC appears greater than CB. The angles B′ and C′ of the equilateral triangle A′B′C′ appear to be greater than A′. The sides A′D′ and B′C′ of the square A′B′C′D′ appear to be greater than the sides A′B′ and C′D′.

In Fig. 17.10 (after Hering) the lines *ab* and *cd* are truly parallel and yet they appear to converge on each other on moving away from A (above) and diverge on moving away from B (below). It may be shown that the illusion results from the tendency of an angle to appear greater when lines are drawn through it parallel to one of the sides (thus the angles B′ and C′ in the triangle A′B′C′ of Fig. 17.9 appear too large). Blakemore *et al.* (1970) have described a simple experiment in which the influence of one line on the estimated orientation of another is measured; thus the subject views the *Base Line* of Fig. 17.11 and moves the *Comparison Line* so as to appear parallel. The *Angle Line* is moved by the exper-

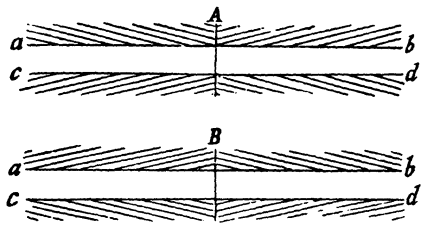

Fig. 17.10 Hering's illusion.

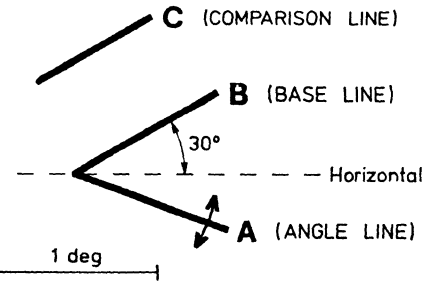

Fig. 17.11 The 'base line' and the 'angle line' meet at the centre of a screen to form an angle so that they appeared to the subject like the hands of a clock. There was a similar 'comparison line', C, with its centre on the normal through the middle of B. During the experiments, B was fixed in the upper right quadrant of the screen at an angle of 30° to the horizontal. Line A was rotated to form various angles with B. (Blakemore *et al.*, *Nature.*)

imenter, and it is found that the subjects make systematic errors in estimating the orientation of the *Bar Line* according to the angle made by the *Angle Line*. The tendency is for the acute angle to appear larger. Blakemore *et al.* have argued that such a result is predictable if the estimate of direction depends on the excitation of orientation-specific cortical neurones whilst other orientation-specific neurones, sensitive to a different orientation, exert an inhibitory action. Such an inhibition would modify the orientation-selectivity of the neurones responsible for determining the orientation of the Bar Line, angling it away from its correct orientation.

Summary

To summarize, we may say that the pattern of objects in the outside world is perceived as a result of the interpretation of the geometrical pattern of the image on the retina. It is not sufficient, however, to know merely the pattern of objects in space, it is useful also to relate *direction* on the retina with certain fixed directions in space. Primarily these are the vertical and the horizontal, the most frequently recurring directions of contours in the outside world. The retina has therefore become specialized by the development of apparently vertical and horizontal meridians; these act as a pair of rectangular coordinates through the fovea to which the position of any point or line is referred. In order that the interpretation of the retinal pattern be independent of the movements of the fixation axis, and of the inclination of the apparently horizontal meridian (torsion), a compensated system of projection into space is necessary. As a result of this compensation, the *absolute* position of an object in space is always correctly interpreted and the directions of lines, in relation to the horizontal and vertical, are also accurately estimated.

There is a great deal of evidence, that the tendency to project the retina is 'innate' although few would deny that accurate projection is only acquired with experience. Presumably the development in evolution of an innate tendency to project the retina in accordance with certain geometrical rules had survival value; the 'rules' turn out to be similar to those that would be followed if the individual learnt to project the retina in accordance with his own experience.

The Monocular Perception of Depth

From purely geometrical considerations, the estimation of the relative positions of objects in three dimensions by a single eye is not feasible; the points A, B and C in space (Fig. 17.12) produces images, *c*, *b* and *a* on the retina which are projected outwards along the lines *c*A, *b*B, and *a*C, but there is nothing in the geometry of this projection system to enable it to differentiate between the points B and B′ for example. The projection of the retinal image of a single eye is thus two-dimensional and objects in space are presented to consciousness as a plane pattern. Nevertheless, the individual may *perceive* depth with a single eye by making use of a variety of clues, whose significance has been ascertained by accumulated experience. These clues are:

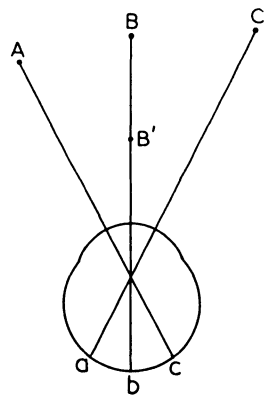

Fig. 17.12 With uniocular projection, the relative positions of B and B′ cannot be distinguished.

'*Aerial Perspective*'

As a result of the scattering of light by the atmosphere the colours of distant objects gave some clue to their distance; the scattered light is predominantly blue and violet and the eye views a distant object through a 'wall' of blue light. The thicker this wall, the bluer will the object appear to be; distant mountains thus appear blue, a fact exemplified in the well-known lines:

'T'is distance lends enchantment to the view
And robes the mountain in its azure hue'.

It must be appreciated, however, that a self-luminous object, such as a lamp, is visible because its own emitted radiations reach the eye; since blue light is scattered preferentially to red, a distant white light appears yellow or red when seen through a hazy atmosphere; the red light penetrates the atmosphere whilst the blue is scattered on the way. It might be objected that a mountain reflects light and that we see it because of this reflected light; this reflected light suffers scattering and so the mountain should appear yellow or red. Distant objects, however, are seen largely through contrast with the brighter sky; it is because they reflect less light than that emitted by the background that they are discriminated; the reflected light is therefore not important in perception and it is the wall of scattered light that determines the colour sensation. (When the brightness of 'wall' plus the brightness of the mountain due to reflected light becomes equal to the brightness of the background, the mountain becomes invisible. For this reason, the visibility of distant points in the landscape constitutes a good measure of the atmospheric haze.)

The scattering of light also blurs the outlines of objects and thus gives another clue to their distance from the observer; the apparent closeness of mountains in a very clear atmosphere is an illusion based on the normal association of clearly defined objects with proximity to the observer.

Relative Sizes of Objects

The apparent size of an object may be represented by the angle it subtends at the nodal point of the eye; thus AB and A′B′ (Fig. 17.13) appear to have the same size because they subtend the same angle and they are the same

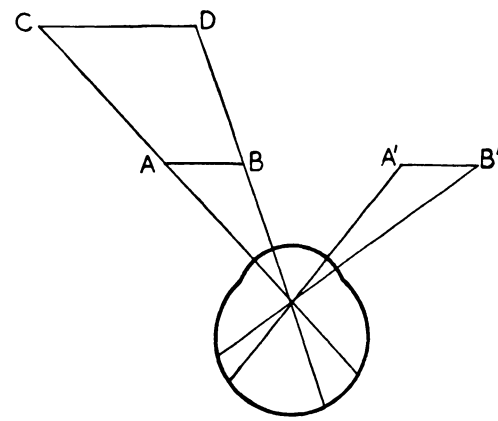

Fig. 17.13 Illustrating the value of relative size in estimating depth.

distance away; CD, moreover, appears as big as AB because it subtends the same angle although its real size is twice as great as that of AB. If the observer knows that CD is twice as large as AB, e.g. if AB is a bicycle and CD is a car, he can say that CD is twice as far away from him as AB, i.e. he can estimate their *relative* distances in the third dimension. A fair estimate of the *absolute* distance away can be made if the object viewed is familiar, e.g. a man or a cottage. When a man walks away from an observer the image on the latter's retina becomes smaller and smaller; this is interpreted as a more and more distant, not as a smaller and smaller, man. In gunnery, the visual estimation of range is made almost entirely on this basis.

The association of size with distance can give rise to common illusions; in a thick fog a figure 'looming up' looks very large because the figure is assumed to be farther away than it actually is. Similarly objects seen through binoculars appear to be very close whereas their images, seen through the instrument, are at infinity.

ABSOLUTE SIZE

The determination of *absolute size* is thus closely interwoven with that of distance; any rigid formulation of this process on the basis of the number of retinal elements stimulated by the image of an object is therefore doomed to failure. A given retinal distance represents an absolute size of an object in space only for one distance of the object from the observer. A change in this distance must necessitate a revaluation of retinal distance. When an object is recognized to be far away, a small retinal distance is interpreted as a certain unit of 'absolute size' in space; if the same object is brought much closer, its image becomes larger so that a larger retinal distance now becomes equivalent to the same unit of 'absolute size' in space. The close linkage between this revaluation process and the acts of convergence and accommodation is shown by the condition of '*paresis micropsia*'. As a result of a defective convergence mechanism, for example, a strong effort of convergence is made in order to fixate a near object; this effort, being out of all proportion to the resulting convergence, is associated with much too great a change in retinal dimension values; the object converged upon appears smaller because it is treated as being much closer and the retinal dimension values have been scaled down too far.

THE MOON ILLUSION

The assignment of a size to objects very far away, such as the sun and moon, must be entirely arbitrary, and so it is not surprising that the assigned size varies, although the reasons for the variations are not apparent. Thus the sun and moon, when seen on the horizon appear very much larger than when viewed at the zenith. It is interesting that the magnitude of the discrepancy between the apparent sizes of a disc viewed horizontally and vertically is much greater in children than in adults; thus in 4 to 5-year-olds a 10-inch disc viewed horizontally was estimated to be of the same size as a 20-inch disc seen vertically; in adults it was considered equivalent to a 16-inch disc (Leibowitz & Hartman, 1959).

Form

The contours of objects give some idea as to their relative positions in the third dimension. Thus in Fig. 17.14 the cottage is in front of the tree which is in front of the windmill which itself is perceived to be in front of the hill, entirely because of the overlapping of the contours.

Fig. 17.14 The value of overlapping contours in the estimation of depth.

Perspective

The projected retinal image of an object in space may be represented as a series of lines on a plane, e.g. a box; these lines, however, are not a unique representation of the box since the same lines could be used to convey the impression of a perfectly flat object with the lines drawn on it, or of a rectangular, but not cubical, box viewed at a different angle. In order that a three-dimensional object be correctly represented to the subject on a two-dimensional surface, he must know what the object is, i.e. it must be familiar to him. Thus a bicycle is a familiar object; viewed flat-on it has the appearance of Fig. 17.15; if it is turned away from the observer it appears as in Fig. 17.16; the wheels, for example, are elliptical and the front one is smaller than the rear one. Because the observer knows that the wheels are actually circular and of the same size he can state that the bicycle is directed into the third dimension, i.e. he perceives depth in a two-dimensional pattern of lines. The perception of depth in a two-dimensional pattern thus depends greatly on experience—the knowledge of the true shape of things when

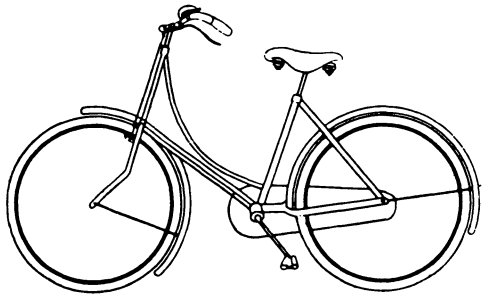

Fig. 17.15 Full side view.

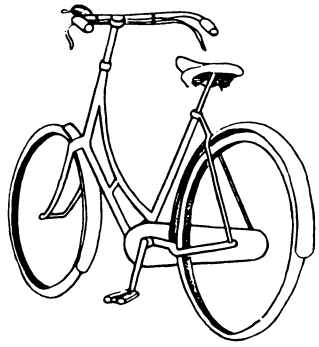

Fig. 17.16 Three-quarters view. The front wheel appears smaller than the back; both appear elliptical.

viewed in a certain way. The limitations of two-dimensional representation become evident when we look at the photograph of an unfamiliar object, such as a complex crystal; the picture is almost meaningless because we have no idea of the actual shapes of its component parts.

Light and Shade

A sphere always appears in a two-dimensional pattern as a circle, however viewed; perspective can therefore give no clue to its solidity. The light and shade on its surface, however, immediately give it a three-dimensional appearance (Fig. 17.17); in general, it is important that the origin of the source of light be known and then the relations of the shadows of objects to each other indicate their mutual arrangement in space. The protective colouring of a large number of animals is designed to offset the appearance of solidity resulting from uneven illumination. Thus the back of an animal receives more light than the belly and if the back reflected the light just as efficiently as the belly it would appear much brighter and convey the impression of solidity (Fig. 17.18). However, the white belly of the donkey, for example, increases the amount of light reflected by it so as to make it approximate in brightness to its back, which is grey. As a result the animal appears, at a

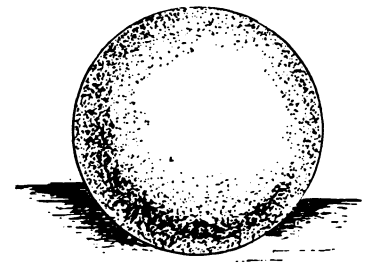

Fig. 17.17 Illustrating the value of light and shade in giving the appearance of depth to a sphere.

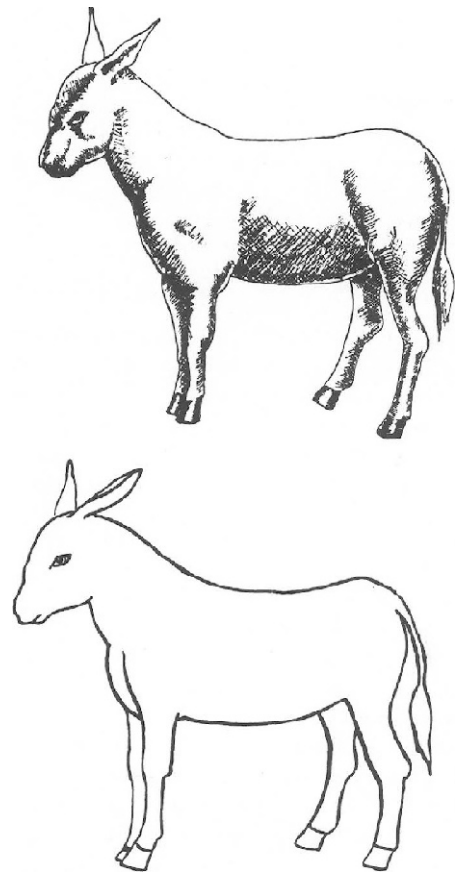

Fig. 17.18 Protective shading of an animal (see text).

distance, to be fairly uniformly bright over its whole surface and therefore appears flat (Fig. 17.18), a characteristic that helps it to merge with its background. Under certain conditions of illumination, light and shade can give valuable clues to the length of a room, for example, in the third dimension; if the source of illumination is close to the observer, the luminance of the walls decreases progressively with their distance away. As a result of the

process that results in 'tone constancy', the walls generally appear to be evenly illuminated, the actual change in luminance being interpreted as an *increase in distance* from the observer. In this case the phenomenon of 'tone constancy' is essentially similar to that of 'size constancy'—the tendency to interpret a diminishing retinal image as an object of constant size moving away from the observer.

Parallactic Displacement

On movement of the head from side to side, the objects nearer to the observer appear to move, in relation to more distant points, in the opposite direction. Similarly, when the observer moves forward, the nearer objects appear to move past him whilst the more distant objects appear to move with him. Helmholtz remarks that if one sits in a wood with one eye closed and the head motionless, the picture presented is quite flat; on moving the head, however, the environment springs to life due to the parallactic displacements, which indicate the essentially three-dimensional nature of the scene.

Accommodation

Within a limited range, the accommodative effort required to see an object clearly might be expected to give a clue as to its absolute distance from the observer, but although opinions differ, it seems safe to conclude that the kinaesthetic sensations from the ciliary muscle do not contribute materially to the power to assess distance, and the same would appear to be true, in binocular vision, for the process of convergence (Zajac, 1960). The extreme difficulty in separating the factor of accommodation from all the other factors concerned reveals that depth perception is a complex process whose components are so interwoven as to make it a somewhat academic exercise to attempt to separate them and measure their individual contributions.

This description of the monocular factors in depth perception shows that there are many ways in which the one-eyed person can perceive depth in his environment; nevertheless his perceptions are grossly inadequate when compared with those of a normal subject, and we may now inquire into the general characteristics of binocular vision.

BINOCULAR PERCEPTION

The two eyes behave, in so far as their motor taxis is concerned, as a single unit; binocular vision is likewise integrated, so that in many respects the perception can be described in terms of a single eye.

'The Cyclopean Eye'

If its two images on the retinae were projected independently into space, an object would appear to be differently orientated in relation to the individual according as its direction was referred to the primary position of one or the other eye. For example, in Fig. 17.19, the point A is fixated by both eyes, and it is correctly projected into space at A; to the left eye, however, it is to the right of the fixation axis in its primary position, whilst to the right eye it is to the left. Since it is symmetrically disposed in regard to the two eyes, the object is considered to be straight ahead of the observer—neither to the right nor to the left—so that binocular projection can be represented by the *'Cyclopean eye'*, as in Fig. 17.19, an imaginary eye in the forehead to which all directions are, in fact, referred. The point A is considered to be straight ahead of the observer because it lies on the fixation axis of the Cyclopean eye in its 'primary' position.

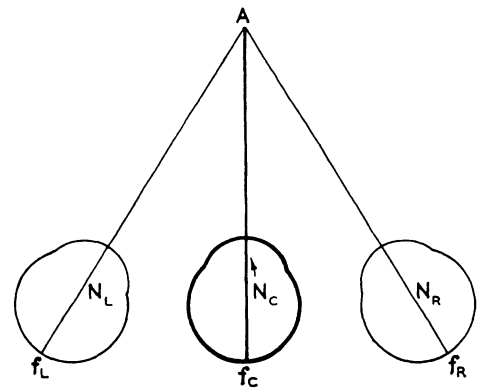

Fig. 17.19 The cyclopean projection.

Binocular Double Vision

The Cyclopean projection is represented by transposing the images on the two retinae to the single, median, eye as in Fig. 17.19. When the images on the two retinae are not symmetrically disposed about the fixation point, however, such a transposition leads to a double projection, and it is found, in fact, that when the same object can be projected in two directions by the Cyclopean eye double vision does actually occur. In Fig. 17.20, the two eyes fixate the point A, as before. A point B, closer to the eye, on the median line, produces images at b_L and b_R; the problem is to determine how the observer projects these images. In Fig. 17.20, the Cyclopean eye, occupying a mean position between the two eyes, is drawn in. The image of A falls on the fovea of each eye and hence its projection by the Cyclopean eye is given by projecting f_C through the nodal point, i.e. it coincides with the true

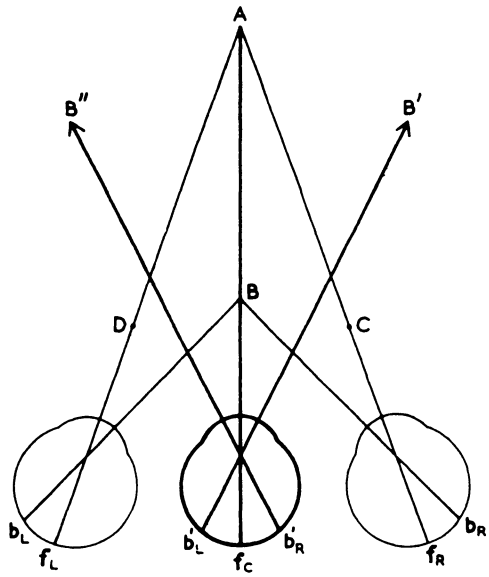

Fig. 17.20 Heteronymous diplopia. B is closer to the eyes than the fixation point. By the left eye the image is projected to B'; by the right eye to B''.

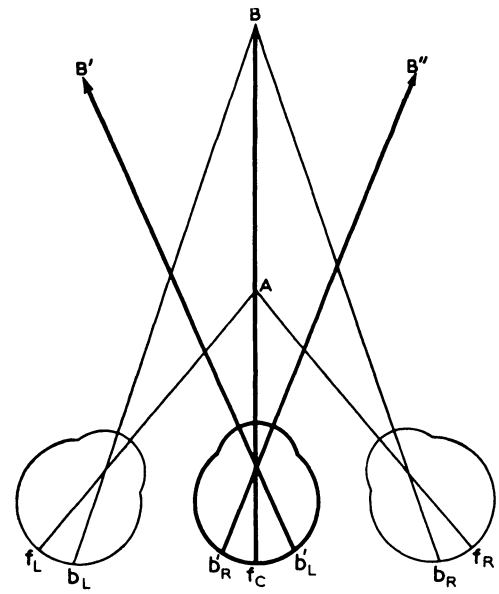

Fig. 17.21 Homonymous diplopia. B is farther away from the eyes than the fixation point, A. By the left eye the image of B is projected to B'; by the right eye to B''.

direction of A. The image of B on the left retina, b_L, occurs to the left of f_L and must be put in a similar position on the Cyclopean retina; b_L is thus projected to B'. On the right retina, B forms an image, b_R, to the right of f_R, which, when transposed to the Cyclopean eye, gives a projection to B''. Since B is projected to B' and B'' at the same time, it is seen double; the diplopia is called *heteronymous diplopia* because on closing one eye the image appears to move away from the fixing eye, e.g. on closing the left eye the image of B appears to be at B'', i.e. away from the right, fixing, eye. The *homonymous diplopia*, caused by an object farther away from the fixation point, is indicated in Fig. 17.21. The normal presence of double images in the binocular field of vision is not usually noticed; they are easily demonstrated, however, by placing a pencil close to the eyes in the median line; when a distant object is fixated, the pencil is seen double.

Binocular Alignment

On a binocular projection, the point B is aligned with the point A, so that if an observer places a pencil in front of him so as to coincide with a distant object when both eyes are open, he really puts the pencil in such a position that its double images lie at equal distances to the left and right of the distant object—B' and B'' of Fig. 17.20. Such a Cyclopean alignment is, in general, not accurate; the careful alignments necessary for sighting a rifle, for example, are made with one eye; if the alignment were made with the right eye a point C, on the fixation axis, would be correctly aligned with A; for the left eye, the point D (Fig. 17.20). (The reader should try rapidly pointing with a pencil at a distant object; keeping the pencil fixed, he should inspect the double images of the pencil while he fixates the distant object; if the latter lies between the double images, the pointing has been carried out on a Cyclopean projection; if, on the other hand, one of the double images coincides with the distant object, the pointing has been carried out on the basis of a monocular projection.)

Diplopia Due to Squint or Prisms

In Fig. 17.20 the point A was seen single, on a Cyclopean projection, because the lines joining it to the nodal point of each eye met the retinae in the foveae. B was seen double because the lines from it through the nodal points met the retinae on opposite sides of the fovea. A similar state of affairs occurs in squint. Figure 17.22 represents a divergent squint. A is fixated by the right eye, but the left visual axis diverges from A; the image of A on the left retina thus falls at a_L. If the images on the two retinae are transposed to the Cyclopean eye, the image of A is projected towards A and towards A', to the right of A. A heteronymous diplopia is therefore caused by this divergent squint.

PRISM

A prism may cause diplopia, provided that the eyes do not compensate for the change of apparent direction of

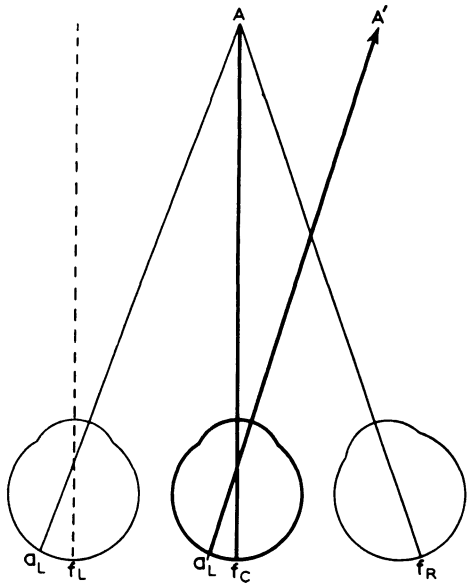

Fig. 17.22 Heteronymous diplopia due to divergent squint. The image of A is correctly projected by the right, fixating, eye to A; by the left eye it is projected to A'.

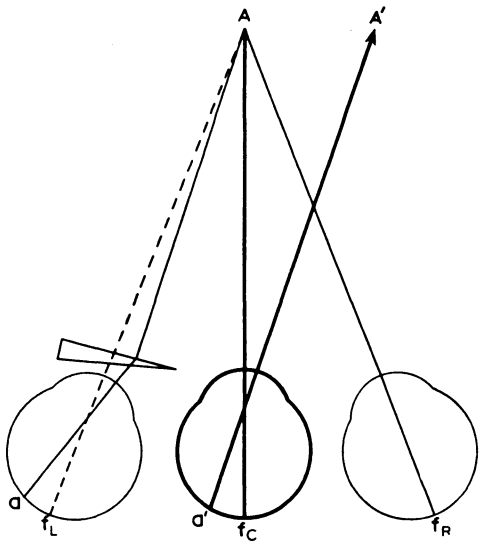

Fig. 17.23 Diplopia due to prism.

the object caused by the prism. In Fig. 17.23, a base-out prism has been placed before the left eye. The image of A falls on f_R the fovea of the right eye, but in the left eye it falls on *a*, to the left of the fovea f_L. On the Cyclopean projection, the images of A are projected in two directions, A and A'. In Fig. 17.24 the eye has compensated for the prism by adducting; both images now fall on the foveae, and the Cyclopean projection indicates single

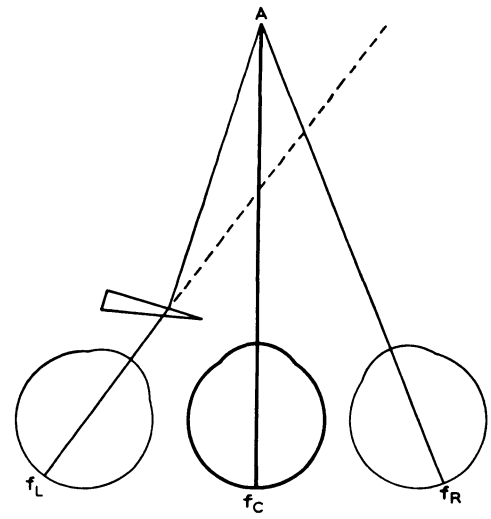

Fig. 17.24 Single vision with prism before one eye.

vision. It is interesting that a single projection is obtained in this instance; the left eye has adducted, so that on the basis of our earlier arguments (p. 453) an image falling on the fovea should be projected through the nodal point—to the right of A. If the left eye, only, were being used, such a projection would occur—a *false projection*, in the sense that the image of A is not projected towards A. The fact that with binocular vision the two images of A are correctly projected to a single point indicates that the Cyclopean projection is determined by the projection of the eye that has not been interfered with.

When prisms are placed in front of both eyes, if the necessary oculo-motor adjustments are possible, single vision is retained, but this time the retinal images of objects are erroneously projected, either closer to, or farther away from, their true position.

The 'False Macula'

The diplopia due to squint is an instance of false projection; the squinting eye fails to project a retinal image through the nodal point, e.g. the stimulated point a_L of Fig. 17.22 is not projected through the nodal point to A but its projection may be described as though the point stimulated were to the left of a_L. The fovea of the squinting eye is likewise projected falsely, an image falling on f_L is projected towards A, the fixation point of the other eye. In many cases the false projection may be corrected by the development of a *'false macula'*, that portion of the retina on which the image of the fixation point, A, of the other eye falls, acquiring some of the characteristics of the fovea. The change is a cortical one—it is impossible for the anatomical characteristics of the retina to alter; the development of a false macula represents a change in the significance of the stimulus falling on it; the stimulus becomes the centre of attention, and that falling on the true macula is suppressed; moreover, the false macula is correctly projected into space. We have seen that projection is essentially a

matter of localization in space of a retinal stimulus; to do this correctly the positions of the eye and head must be known and psychological compensations for movements of the eye and head are an integral part of the projection mechanism. The development of the false macula requires a re-adjustment of this psychological compensation to take into account the abnormal relationship of the visual axes of the two eyes.[5]

Innate Projection

The existence of false projection following squint reveals that the projection of the eye through the nodal point is an innate characteristic, developed doubtless during the early years of life, but nevertheless an inherited quality. The possibility of a development of a false macula reveals, on the other hand, a certain plasticity in the function of the visual cortex. We have already remarked on the rigidity of the relationship between stimulus and sensation in this area of the cortex, a rigidity which differentiates it from other parts of the cerebral mantle, and it is interesting that the relationship may be modified by experience and is therefore not absolute as with processes occurring at lower levels in the brain.

A condition of *monocular diplopia* may arise from the development of a false macula. Thus the stimulus falling on a_L (Fig. 17.22) is originally projected to A'; after the development of a false macula it is correctly projected to A. Sometimes both projections take place simultaneously, so that, as a result entirely of cortical activity (there is clearly only one image on the retina), the point A is seen simultaneously at A and A'.

The development of a '*pseudo-fovea*' may result from hemianopia; in this condition one half of the foveal image is seen, a condition so annoying that the affected person tends to use an adjacent portion of the retina for fixation. With time this point acquires the characteristics of the true fovea—it is correctly projected into space and the images of objects falling on it become the centre of attention and interest.

Convergence

With two eyes we have the geometrical basis for an estimate of the absolute distance of a point from an observer, since the converging power necessary for binocular fixation is uniquely determined by its distance away in the third dimension of space. The relative distances of different objects are likewise determined by the relative degrees of convergence necessary for binocular fixation. That variations in convergence may cause three-dimensional illusions was shown long ago by Meyer in the so-called *wallpaper phenomenon.* As described by Helmholtz, the illusion is brought about by looking at a wallpaper with a vertical line pattern; by making his eyes cross, so that the two eyes were fixating adjacent lines, Helmholtz found that the wallpaper appeared to float out of the wall, whilst if he made his eyes diverge the paper receded into the wall in the region of the fixation points. The crossing or divergence of the eyes caused no apparent diplopia because the fields of view consisted of only vertical lines. As Helmholtz and others have interpreted the phenomenon, the changed convergence *per se* was responsible for the apparent three-dimensionality of the wallpaper; in other words, the act of convergence contributed to the sensation of depth. However, more modern workers are inclined to deny to the convergence *per se* any significant contribution to depth perception (Smith, 1946; 1949; Zajac, 1960); it is because alterations in convergence, by altering the fixation point, change the relative sizes and positions of other objects around the fixation point, that the retinal images are modified and thus the appearance of the fused binocular retinal images. Nevertheless, there is every reason to believe that the act of convergence provides signals to the brain that, in the absence of other clues, are adequate to indicate nearness or farther-awayness with some accuracy; thus Hofsten (1976) exposed two small spots of light to the eyes separately, varying the retinal disparities, and the degree of convergence necessary to fuse the identical images on the retinae provided the cue to apparent depth. The subjects indicated their estimates on a metre-scale seen at the same time. Considerable accuracy was achieved.

STEREOSCOPIC DEPTH PERCEPTION

We have so far considered the geometrical consequences of the use of the two eyes in estimating distance—the system has been treated as a range-finder—and the problem of the fusion of the two images in the separate eyes has not been considered. Not only does the fusion of the images provide a unitary perception of the binocular field of view, but it presents the objects in this field in a three-dimensional pattern that is quite impossible of achievement with monocular vision. In the following pages we shall inquire into those characteristics of the two retinal images that (*a*) permit or favour fusion and (*b*) contribute to the three-dimensional percept.

Corresponding Points and the Horopter

Corresponding Points

We have seen, in our discussion of binocular projection, that a single object in space is projected in two different directions when its images, formed by the two eyes, do not both fall on the foveae (Fig. 17.20); this results in diplopia, and single vision is only achieved when the retinal stimuli are projected to the same point in space. The foveae may therefore be described as *corresponding points*; they are points on the two retinae normally projected to the same point in space.

Every point on the retina of each eye is projected into space to give the field of vision; where the projections overlap we have the binocular field of vision; the problem is to determine which points in the binocular field of

vision are seen single or, more correctly, which pairs of points in the retinae of the two eyes are projected to the same point in space. The matter is subject to experimental investigation and the following conclusions were drawn by Helmholtz:

1. The apparently horizontal meridians of the two retinae correspond.
2. The apparently vertical meridians correspond.
3. Points on the apparently horizontal meridians, equally distant from the foveae, are pairs of corresponding points.
4. Points equally distant from the apparently horizontal meridians, which are on the apparently vertical corresponding lines, are a pair of corresponding points.

In so many words, points equidistant from the apparently horizontal and vertical meridians of the retinae were said to be corresponding points.

The Vieth-Müller Horopter Circle

Figure 17.25 represents a horizontal section through the two eyes, fixating the point F. The points a_L and a_R are equally distant from the vertical meridians of the two eyes and are therefore projected to the same point in space through the respective nodal points, namely, to A. The points b_L and b_R, also symmetrically disposed about the vertical meridians, are projected to B. From the geometry of this binocular projection it is evident that A, F and B lie on a circle passing through the fixation point, F, and the nodal points of the eyes. All points in space, lying on this circle, so long as they produce images on the two retinae, produce them on corresponding points provided that the symmetry, postulated by Helmholtz, exists. The circle is called the *Müller* or *Vieth-Müller horopter circle*: it is the locus of points, in a horizontal plane, that produce images falling on corresponding points of the two retinae when the fixation axes are horizontal, and are directed on the point F. Moreover, if the eyes may be considered to rotate about the nodal points instead of their centres of rotation, the fixation point may move to any point on the circle and all other points will still produce images on corresponding points. With this approximation the Müller horopter circle becomes the locus of points, in a horizontal plane, that produce images on corresponding points for a given degree of convergence of the eyes when the retinal horizons are horizontal. The Müller circle only indicates the points in space *in a single plane* that produce images on corresponding points. If the circle is rotated about a line joining the nodal points, the surface so produced gives the locus of all points in space whose images fall on corresponding points, for a fixed degree of convergence of the eyes. This is only true if the two retinae possess strict spherical symmetry and if the corresponding points are symmetrically disposed around the foveae. As the apparently vertical meridians of the retinae are not parallel to each other (p. 456) there is no such perfect symmetry and this Müller horopter surface, as we may call it, is only an approximation.

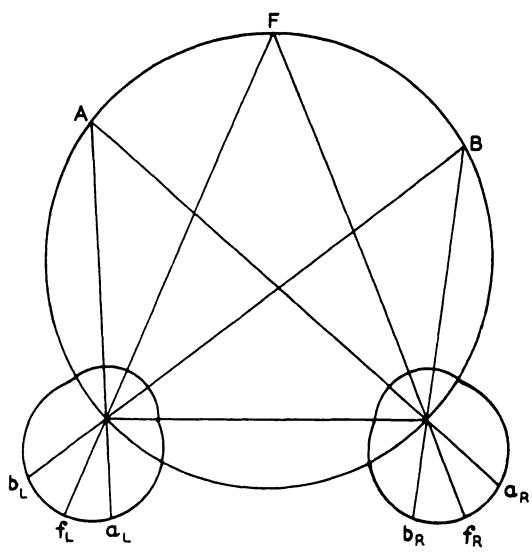

Fig. 17.25 The Vieth-Müller horopter circle. F is the fixation point. If corresponding points are symmetrically distributed about the foveae the points in space, in the fixation plane, whose images fall on corresponding points lie on the circle.

The Horopter

The *horopter* as originally defined is the *locus of points in space whose images fall on corresponding points of the two retinae*, i.e. no proviso is made as to the fixation point or the degree of convergence. The Müller horopter circle must therefore be regarded as a special case of the horopter when the fixation point has been defined. The number of points in space that will produce images on corresponding points, *however the eyes move*, is strictly limited; thus in Fig. 17.26, when the eyes move to a new fixation point not lying on the original Müller circle, e.g. the point F', the images of A do not lie symmetrically with regard to the foveae and are therefore not on corresponding points. Hence, although A lies on the Müller horopter circle when the eyes fixate F, it does not lie on the horopter. The horopter was calculated by Helmholtz from experimental data on the positions of corresponding points and the laws of the eye movements; it is a curve of the third degree (a curve that cuts a plane in three points). Under certain conditions the horopter acquires a simpler form; e.g. if the eyes are looking straight ahead in the primary position, the horopter becomes a horizontal plane passing through the feet, all points on this plane being seen single. When the point of fixation is either in

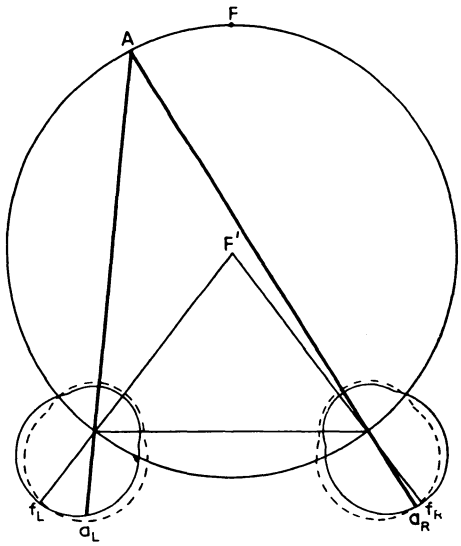

Fig. 17.26 When F was the fixation point, A lay on the horopter-circle; when F′ becomes the fixation point A no longer produces images on corresponding points, so that A is not on the more generally defined horopter.

the median plane of the head or in a horizontal plane with the fixation axes horizontal, the horopter becomes a Müller circle and a vertical line, intersecting in a point.

LONGITUDINAL HOROPTER

For practical purposes, the so-called *longitudinal horopter* is the most useful. For a given fixation point it is the locus of points in a horizontal plane whose images fall on corresponding points of the two retinae. Thus, if Müller's assumptions were correct, it would be his horopter circle. In fact, however, the postulated symmetry about the vertical meridians does not hold good, so that the longitudinal horopter is not a circle.

Hering-Hillebrand Deviation

Thus if we wish to find the point corresponding to a_L (Fig. 17.25) it is, in general, not at a_R such that $f_L a_L = f_R a_R$, but closer to, or farther away from f_R. This so-called *Hering-Hillebrand deviation* causes a characteristic change in the longitudinal horopter, so that not only does it deviate from a circle but its shape changes with the fixation distance. With strong convergence it was found to be concave to the face; at about 2 metres it became approximately a straight line in the frontal plane, whilst beyond this distance it was a curve, convex to the face.

MODERN ANALYSIS

Interest in the horopter, up to 1932, was largely academic; in this year, however, Ogle and his associates drew attention to the implications of the horopter from the point of view of the relative sizes of the retinal images. On the basis of certain assumptions, Ogle showed that the shape of the longitudinal horopter should be an index to the degree of discrepancy between the sizes of the retinal images. His interest in the problem of aniseikonia led to a very thorough investigation of the horopter, both from a practical and theoretical aspect; it is impossible in a brief space to do justice to the results or the conclusions of this study. The mathematical analysis confirmed the general conclusions of Hillebrand on the variation of the shape of the horopter with distance. Thus at a certain distance it coincided with the frontal plane whilst at other distances it was curved. The significance of altered image-size, i.e. of *aniseikonia*, will be discussed later.

The Stereoscope and Depth Perception

The essential feature of stereoscopic perception is the existence on the two retinae of *different images of the same object*; the object is seen in two aspects because of the different viewpoints of the eyes. Thus Fig. 17.27 represents two photographs of a book as it would be seen by the left and right eyes; if these photographs are viewed separately by the two eyes and their images fused, the book is perceived as a three-dimensional object.

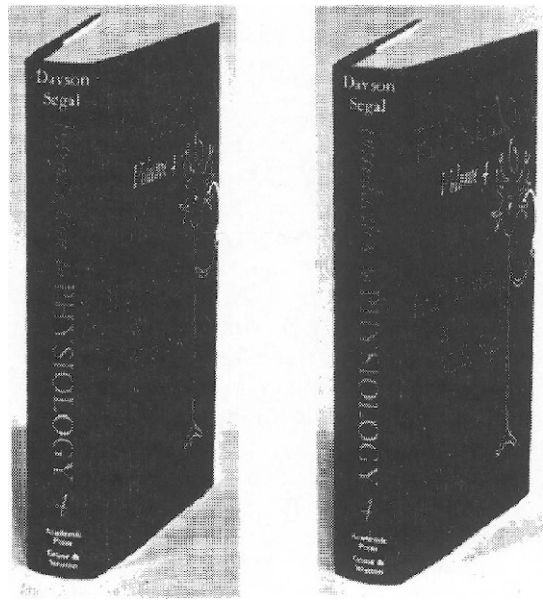

Fig. 17.27 Stereographic photographs of a book.

The Stereoscope

The fusion of the two images can be carried out, with a little practice, by holding them directly in front of the eyes, a piece of cardboard in the median plane being used to keep the fields separate. The conditions are, however, artificial in that the eyes normally converge when near objects are viewed, and a convenient instrument, which permits this convergence when the objects viewed are close to the eyes and directly in front of them, is the *stereoscope*, the optical properties of which are shown in Fig. 17.28. Two pictures, representing different aspects of the same object, AB and CD, are placed about 10 cm from the eyes. They are viewed separately through base-out prisms, so that symmetrically disposed points on the stereograms are projected to the same point, e.g. *a* and *b* are projected to *c*.

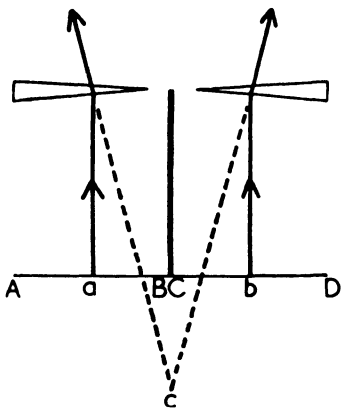

Fig. 17.28 Optical principles of the Brewster stereoscope.

Discrepant Images

If the two identical circles of Fig. 17.29*a* are placed in the stereoscope, their images are fused but no sensation of depth is achieved precisely because the pictures are identical and are such as would, in effect, be presented to the eyes were a flat circle viewed. If the dots are placed in the circles, as in Fig. 17.29*b*, fusion of the images creates the impression that the dot is floating in space in front of the circle, whereas if the dots are placed as in Fig. 17.29*c*, the dots appear to be behind the plane of the circle. The stereograms imitate the appearances to the two eyes of a three-dimensional pattern; thus let us imagine that there is a dot on the surface of a sphere placed symmetrically with regard to the two eyes; viewed with the left eye, the dot appears to the right of the centre of a circle—the outline of the sphere—whilst viewed by the right eye it is to the left. The combined image, as seen in the stereoscope, gives the impression of a point on the surface of the

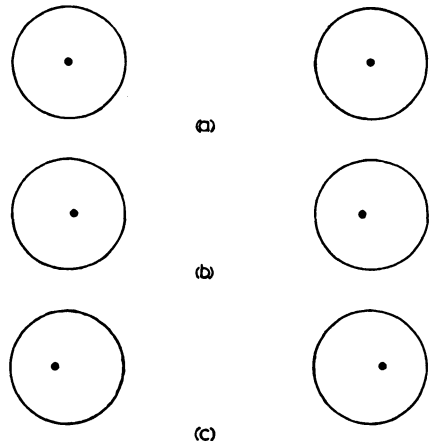

Fig. 17.29 (*a*) The spots are in the centres of the two circles; the fused image is two-dimensional. (*b*) The spots are de-centred nasally. The spot appears, on fusion of the images, to be nearer the observer than the plane of the circle. (*c*) The spots are de-centred temporally. The spot appears, on fusion of the images, to be farther from the observer than the plane of the circle.

sphere. It will be noted that a sphere, viewed from any angle, appears as a circle; the two aspects of a sphere are therefore identical circles and binocular perception of a uniformly bright sphere can give no impression of solidity. It is essentially because a sphere is normally unevenly illuminated, and has light and dark spots on it, that the aspects presented to the eyes are different; the fusion of these aspects places the lights and shades in their true relationships in three dimensions and so creates the appearance of solidity. The importance of light and shade in stereoscopic vision may be seen by examining photographs of unfamiliar objects which reflect light to varying extents on different parts; stereoscopic vision puts the various high lights in their correct positions in the third dimension and so contributes greatly to the intelligibility of the presentation.

Parallax

The difference in the two aspects of the same object (or group of objects) is measured as the *instantaneous parallax*. In Fig. 17.30, B is closer to the observer than A; the fact is perceived stereoscopically because the line AB subtends different angles at the two eyes, and the instantaneous parallax is measured by the difference between the angles α and β. The *binocular parallax* of any point in space is given by the angle subtended at it by the line joining the nodal points of the two eyes; hence the binocular parallax of A is α; that of B is β; the instantaneous parallax is thus the difference of binocular parallax of the two points considered.

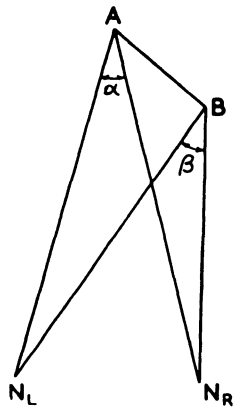

Fig. 17.30 Binocular and instantaneous parallax.

Accuracy and Limits of Stereoscopic Perception

The accuracy of stereoscopic perception is remarkable. Andersen & Weymouth and later, Ten Doesschate, placed three wires in front of an observer; the distance the middle wire had to be moved to appear out of the plane of the other two was measured; the parallax was of the order of four seconds of arc, corresponding to a disparity of the retinal images far smaller than the diameter of a single cone. Other values in the literature range from 1.6 to 24 seconds.

With two editions of the same book, it is not possible, by mere inspection, to detect that a given line of print was not printed from the same type as the same line in the other book. If the two lines in question are placed in the stereoscope, it is found that some letters appear to float in space, a stereoscopic impression created by the minute differences in size, shape, and relative position of the letters in the two lines. The stereoscope may thus be used to detect whether a bank-note has been forged, whether two coins have been stamped by the same die, and so on.

It may be shown, on geometrical grounds, that beyond a certain distance from the eyes, the difference of parallax of objects becomes effectively zero; beyond this point, then objects in the environment appear to be in a single plane; the distance has been computed to be about 450 metres but of course it depends on the figure taken for the smallest perceptible instantaneous parallax.

Effect of Distance

Several studies of the effects of distance on relative depth discrimination have been described. Under these conditions the observer is presented, in the distance, with two similar objects, separated laterally but initially at the same distance from him; one object is moved nearer or farther away until the observer states that he can detect the fact; and the distance between the two objects represents the *linear* depth limen, which may be converted to an angular disparity or parallax. According to Teichner *et al.* (1955), there is an actual improvement in the power to discriminate as the distance increases, although on theoretical grounds we should not expect any change, when the limen is expressed in terms of an angle of parallax. Ogle (1958a) has pointed out, however, that the monocular clue given by difference in perceived size, when the two objects are not equidistant from the observer, becomes relatively more important in depth discrimination as distance increases; and it is for this reason that there is an improvement of depth discrimination, the eye being more sensitive to changes of size than to changes of parallax at large distances. This view was confirmed by Jameson & Hurvich (1959).

Duration of the Stimulus

Dove in 1841 observed that stereopsis could be experienced by viewing pictures in a stereoscope when they were illuminated by an electric spark, proving that the experience did not depend on movements of the eyes, such as those involved in convergence. A more systematic study by Ogle & Weil (1958) has shown that the accuracy of stereopsis increases by a factor of four on increasing the exposure-time from 4 to 1000 msec. This suggested to Ogle & Weil that small nystagmoid movements, by contributing to visual acuity, improved stereoscopic acuity, since there is no doubt that these two parameters are related. That this is not the correct explanation, however, is shown by Keesey's (1960) study on visual acuity with different exposure-times; this did, indeed, improve as the time increased from 20 to 200 msec, but the same improvement was found when the image on the retina was 'stabilized' in such a way that it always remained on the same portion of the retina. Thus the small involuntary scanning movements do not contribute to visual acuity, and the improvement of both visual acuity and stereoscopic acuity with viewing-time implies only that the neural processes concerned with the discrimination require a certain minimum time for their best performance.

Disparate Points and Stereoscopic Perception

Stereoscopic perception results from the fusion of dissimilar images; it follows from this that the fused percept is made up by the integration of stimuli falling on disparate points on the two retinae, i.e. of points which, on a Cyclopean projection, would be seen double. Thus in Fig. 17.31, A′B′C′D′ and A″B″C″D″ are the two aspects of a slab, ABCD, inclined to the median plane. If the lines B′D′ and B″D″ correspond, it is quite clear that the lines A′C′ and A″C″ *cannot*, the line XY corresponding approximately with A′C′. Hence, on a purely Cyclopean

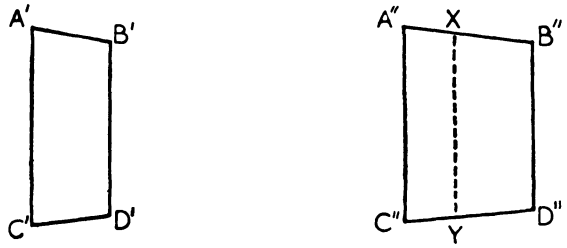

Fig. 17.31 Illustrating the importance of the incidence of images on non-corresponding points in stereoscopic perception.

projection, if the edge of the slab, BD, is seen single, the near edge, AC, is seen double. The fused percept is, nevertheless, that corresponding to a single entity—a slab 'floating in space'. The existence of images of the same point in space on disparate points of the two retinae is, therefore, just as much a characteristic of stereoscopic perception as the existence of images on corresponding points; in fact, if all points on an object produced images on corresponding points, there would be no stereoscopic perception.

Corresponding Points Defined

The facts of stereoscopic perception tell us, therefore, that a pair of corresponding points on the two retinae is not completely defined by the statement that their images are seen single, since disparate points may also be seen single. Let us consider the points A and B of Fig. 17.32. They are on the horopter and their images fall on corresponding points, a_L and a_R; b_L and b_R. Both points are seen single in binocular vision. Let us now consider the points A and B'; if A is the fixation point, B' is not on the horopter and, on a Cyclopean projection, would be seen double. If, however, A and B' are points on an object, seen single as a stereoscopic percept, B' must be seen single although it is not on the horopter; we must find what it is that differentiates its images b'_L and b'_R from the pair b_L and b_R which enables us to say that they are not corresponding points. It will be seen that when A and B are on the horopter, closing either eye fails to alter their apparent relative positions; on the other hand, when A is on the horopter but B' is not, B' is projected in different directions in relation to A according as one or other eye is closed. Thus with the left eye closed, B' appears closer to A than when the right eye is closed. The actual binocular, or stereoscopic, projection of B' in relation to A is, therefore, different from either of the separate projections. It is essentially this difference that is made use of in the most reliable experimental method for assessing the positions of corresponding points (e.g. the so-called *nonius* method). If the fixation point is used for reference, another point will produce images on corresponding points if its binocular projection is identical with the separate projections of the two eyes.

NONIUS METHOD

Experimentally the points on the longitudinal horopter may be determined by an apparatus illustrated schematically by Fig. 17.33. The observer views a fixation point and a vertical horopter-rod through an arrangement of screens that permits both eyes to fixate the fixation point, F, whilst the right eye is able to see only the upper half of the vertical rod, and the left eye only the bottom half. The position of this rod is adjusted so that when the eyes are fixating F, upper and lower halves of the rod appear above and below each other. Under these conditions the

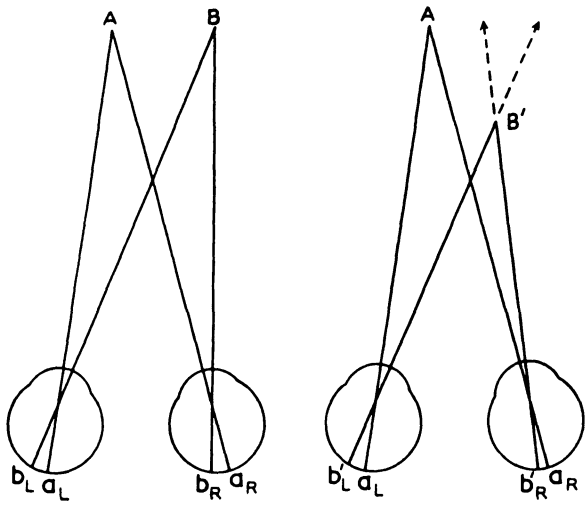

Fig. 17.32 Illustrating the definition of corresponding points.

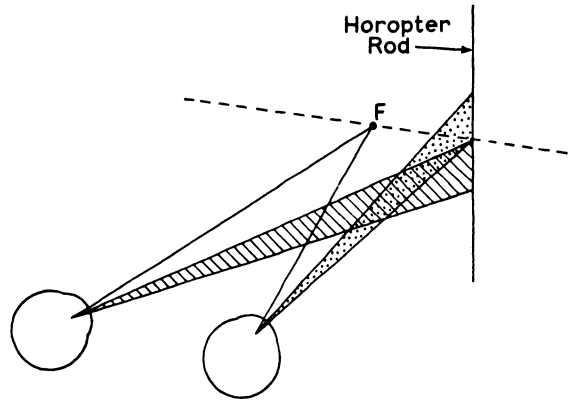

Fig. 17.33 Nonius method for determining corresponding points. Both eyes are able to fixate F, the fixation point, whilst the right eye sees only the upper half of the horopter rod and the left eye only the bottom half. When the rod is on the horopter its upper and lower halves appear in line. (After Ogle.)

retinal direction values of the points stimulated by the rod are the same.

Panum's Area

If the stereograms of Fig. 17.31 are modified so that the lines A'C' and B'D' progressively get closer, whilst the equivalent lines of the right stereogram get progressively farther apart, a point is reached where fusion becomes impossible and double vision takes the place of a stereoscopic percept. There is thus a limit to the disparity of retinal points, beyond which they cannot be fused. Panum attempted to define the limiting degree of disparity beyond which fusion becomes impossible. He stated in general that 'contours resembling each other, depicted on approximately corresponding points, must be fused together'. The circumference that contained those points on the other retina that could be fused with a given point on the first, he called the *corresponding circle of sensation.* This formulation is probably rather too rigid; the ability to fuse contours is determined largely by the possibility of interpreting them as the right- and left-eyed views of a three-dimensional object, and thus the meaning of the final fused percept contributes to some extent to the ability to fuse disparate images. Nevertheless there is reason to suppose that there is a certain contour of finite size such that any point within it will invariably fuse with a single point on the other retina. It is to be noted that the two aspects of any object in space, as seen by the left and right eyes, differ principally in respect to their width, their height being very nearly the same; it is not surprising therefore that it is possible to fuse pairs of vertical parallel lines with quite large discrepancies in their separation, whereas only very small discrepancies in the separation of horizontal lines are tolerated. Panum's 'circle' should thus be described as an ellipse with its long axis horizontal. According to Ogle (1950) the length of the horizontal axis of this ellipse varies from one subject to another and, in a given subject, with the position on the retina at which the measurement is made. In one subject it increased from 5 to 30 minutes of arc on passing from central to peripheral vision, and in another from 10 to 40 minutes. Mitchell (1966), using central vision and flash-presentation of the stimuli so as to preclude fusional eye movements, found that horizontal disparities of 13 to 23 minutes of arc were necessary if two points were to be seen as double; the required vertical disparities were 8.9 to 15.9 minutes of arc.

Double Images in Stereoscopic Perception

If a pencil is placed vertically at arm's length, an inch or two to the side and in front of a thin bar, a unitary stereoscopic percept of the two is obtained, with no double images. The images would be said to fall within the Panum circles. On bringing the pencil closer to the eyes, with the bar as a fixation point, a stage is reached at which the double images of the pencil can be distinguished; nevertheless the pencil and the bar may still be perceived as a unitary pattern because one of the double images is ignored. When the pencil is brought very close to the eyes, no accurate perception of it in relation to the bar may be obtained because the double images have now become too obvious. In this experiment the pencil was not on the horopter, which passes through the fixation point; the farther removed from the horopter the pencil becomes, the less accurate and well defined is the stereoscopic percept; fortunately, however, for the unitary perception of the outside world, the more distant an object from the horopter, the more vaguely is it seen, owing to the limitations in the depth of focus of the eye. Thus objects in the environment may produce retinal images of such gross disparity that, if they were distinctly perceived, a unitary perception would be impossible. The vagueness of the double images, however, permits the ready suppression of one, so that all objects in the binocular field of view appear normally single and it requires a careful examination to reveal the actual existence of double images.

In general, the closer the position of an object to the horopter, the more accurate is depth perception; for example if one pin is placed on the horopter and another very close to it, but off the horopter, the eyes can estimate with extraordinary accuracy the displacement in the third dimension. The farther the pins are off the horopter, the grosser the estimate, a fact following from Weber's psychophysical law.

Range and Scope of Binocular Depth Discrimination

We may ask whether stereoscopic depth perception is achieved when the disparity of retinal images is greater than Panum's area so that an object closer to the fixation point is presented as a pair of double images. Helmholtz was in no doubt that objects could be quite accurately located as being nearer to, or farther from, a given point by virtue of their double images; and it was presumably the crossed disparity in the one case (cf. Fig. 17.20) and the uncrossed disparity in the other (cf. Fig. 17.21) that permitted this. Ogle (1962) investigated the effects of greater and greater disparities in the retinal images on the perception of depth; he confirmed the efficacy of double images in permitting estimates of depth, and divided stereoscopic depth into several parts; for small retinal disparities where fusion takes place, the sensation of depth is compelling and the subject is able to make accurate quantitative estimates of relative depth in accordance with the degree of retinal disparity; beyond this region, where double images may be shown to occur, i.e. where fusion is not real, the experience of depth remains,

but quantitative estimates of relative depth are poor or non-existent. Finally, when the disparity is still larger, the sense of depth disappears and the two images are indefinitely localized.

More recently Blakemore (1970) has made a thorough investigation of the limits of retinal disparity within which estimates of depth can be reliably made, and these turned out to be very large; thus with objects immediately in front of the observer, a convergent disparity as high as 7° could be interpreted as nearness to the observer, and a divergent disparity of 9° could be interpreted as farther awayness. In the periphery the same observer perceived depth with disparities as high as 13 to 14°. Blakemore confirmed that the accuracy of stereopsis, as indicated by the threshold disparity required to permit discrimination of depth, was greatest at the horopter; this is illustrated by Fig. 17.34, where lines indicate contours of isothreshold disparity, the actual values in minutes of arc being indicated by the figures. The filled circles represent the subject's longitudinal horopter, and it is interesting how the contours follow the shape of this horopter and how the range is compressed in the middle of the visual field.

BINOCULARLY STABILIZED VISION

Fender & Julesz (1967) have emphasized the dynamic character of Panum's fusional area; thus when fusion of disparate images was brought about using stabilized images, these images could be pulled apart very much farther than the limits of Panum's fusional area, without the appearance of double images. The fact that the images were stabilized means that no disjunctive movements of the eyes occurred, as would have happened in normal vision. During this pulling apart of the retinal images there was no change in the stereoscopic perception, so that if the images were of a vertical line, its localization in space was unaltered. Thus Fender & Julesz speak of first, a labelling process, operative in Panum's fusional region, which establishes corresponding areas in the left and right images having various disparities, and second a cortical registration process that preserves the labelling of the retinal images of a given point on an object in spite of considerable movements of these images in relation to each other, i.e. in spite of considerable variations in their disparity.

Cyclopean and Stereoscopic Projection

The study of stereoscopic perception has revealed a defect in the Cyclopean system of representing the projection of the two eyes in binocular vision. According to this, the point B of Fig. 17.20 is seen double however close it is to A, whereas we know that, if the separation is not too large, B is seen single. On a *stereoscopic* projection system, therefore, the points b_L and b_R are correctly projected through their respective nodal points to B. The Cyclopean projection of the images of B is unreal, in the

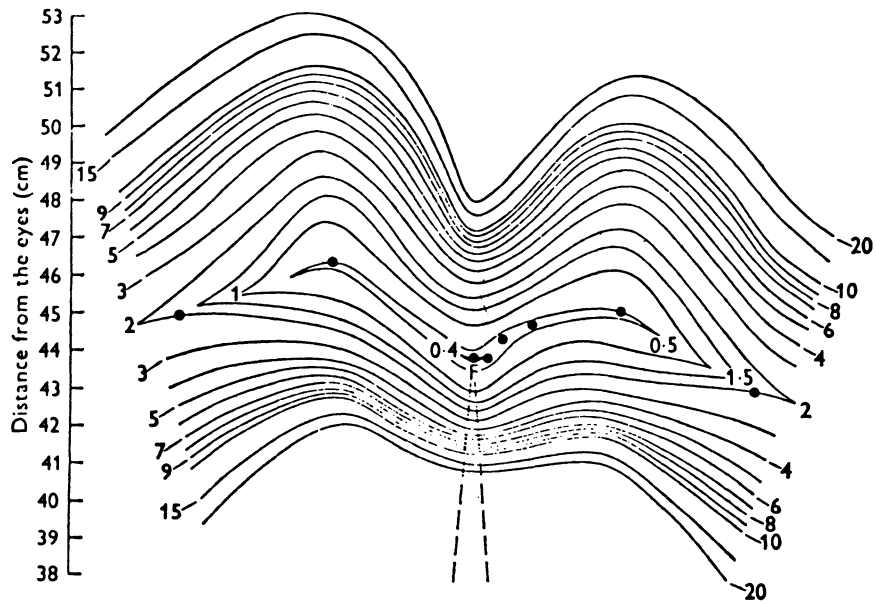

Fig. 17.34 Illustrating retinal disparities that may be fused, as a function of position of the images in relation to the fixation point, F. The disparities are represented on ordinates as distances of the object point from the eyes, causing the disparities. Each smooth line is a contour of iso-threshold-disparity, and the magnitude of that threshold, in minutes, is shown at the end of the contour line. (Blakemore, *J. Physiol.*)

sense that it projects the images of a single object to two different points in space simultaneously; the stereoscopic visual process imposes a truer meaning on the two retinal stimuli, not by suppressing one or the other of the two projected images, but by establishing a single projection that corresponds to the true position of B in relation to A. This process extends to retinal images that fall outside Panum's circle, and, even when double images become apparent, it is found that they tend to be projected into space in a direction much closer to the true position of the point giving rise to them than would be expected on a Cyclopean projection.

The Cyclopean projection is not, nevertheless, to be treated as a useless and academic mode of representing the projections of the two eyes; it tells us how the eyes would combine their separate projections if this combination were a simple additive process; thus in Fig. 17.21 the right eye alone would project its image of B to the right of A, whilst the left eye would project it to the left. The Cyclopean projection is nothing more than an addition of these two projections. By comparing the Cyclopean with the actual stereoscopic projection we can form an idea of the fundamental revaluation of retinal points that must take place to permit single vision as a result of the stimulation of disparate points.

EXPERIMENTAL DEMONSTRATION

An interesting demonstration of this shift in visual directions has been given by Burian (1951) and is illustrated in Fig. 17.35; the subject views a stereogram consisting of a set of three vertically arranged dots. The images of the upper and lower dots fall on corresponding points, whilst those of the middle dots, 2 and 2', do not, being displaced nasally to give a crossed disparity. When viewed, the appearance will be that of the dots 1 and 3 lying in a frontal plane with dot 2 closer to the observer (cf. Fig. 17.29*b*). What is remarkable, is that the three dots will all appear to be in the same vertical line; consequently the visual directions of the retinal points, on which the points marked 2 fall, have been altered because of the stereoscopic effect, since we know that if, in the stereograms, the points 2 were placed immediately under points 1 and 3 they would still appear in the same vertical line, but this time, of course, also in the same fronto-parallel plane.

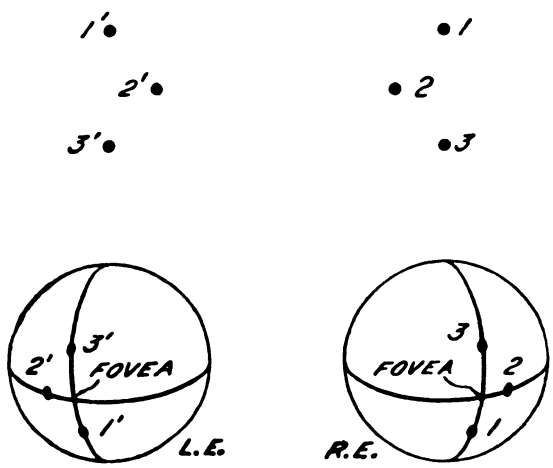

Fig. 17.35 Illustrating the shift in visual direction of a point by virtue of viewing it stereoscopically. The subject views the stereogram consisting of the sets of dots; on fusion the dots appear in a vertical line. (Burian, *Documenta Ophthalmologica.*)

Stereopsis without Familiarity Cues

It has been argued that retinal disparity is not the only, or even the determining, factor in stereopsis; thus with most stereograms familiarity with the figure represented is thought to be an important element, whilst in addition there are often monocular depth cues in the individual stereograms. However, Julesz (1964) has shown that it is possible for the monocularly viewed stereograms to be such that the object, seen in stereopsis, is completely invisible in the individual stereograms. He devised stereograms composed of random dots such that neither had any significance on its own, yet, on viewing these in the stereoscope, the observer saw a central square which could be in front of, or behind, the rest of the field; in Fig. 17.36 it is in front of the background.[6] The manner in which Fig. 17.36 was constructed is too elaborate to permit a detailed description here; suffice it to say that the stereograms are divided into 9×10 picture-elements composed of dots; some of these elements occupy corresponding points whilst others have disparity. It is the organized disparities of certain of these picture-elements that allow the stereoscopic appearance on fusion. This ingenious technique of Julesz allows, now, an unequivocal verification of the interpretation of Dove's experiments with flash-illumination of the stereograms, since it has been argued that fusion under Dove's conditions was only possible because the subjects knew what they were expected to see; with Julesz' stereograms there is 'nothing to see' except a random array of dots. The experiments also dispose of Hering's claim that it is the awareness of double images that determines stereopsis; even if the random elements in Fig. 17.36 were giving double images there could be no awareness of this. Finally, the experiment shows that discrete contours in the left- and right-eye images are not a necessary feature of stereopsis.

ROLE OF EYE MOVEMENTS

Although flash-presentation still permits stereoscopic perception, it is important to note that when Julesz-type patterns are presented to the eyes, i.e. pictures without monocular contours, then perception is greatly reduced

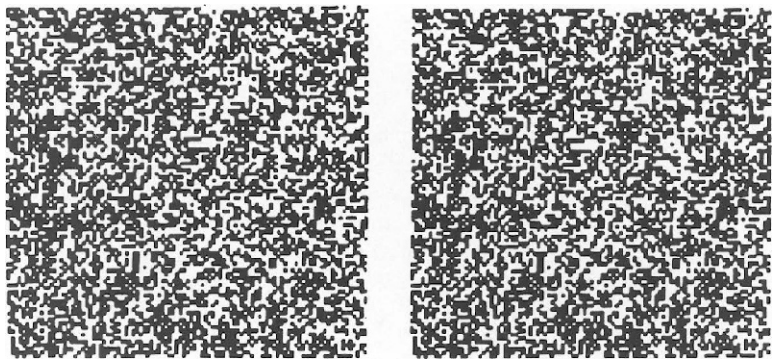

Fig. 17.36 Random-dot stereograms constructed so that the individual pictures reveal no form, yet when viewed in the stereoscope the fused percept is one of a square in front of the background. (Julesz, *Science*.)

and even abolished by flash-presentation. Presumably, when eye movements are allowed, the obscure disparity cues of the Julesz patterns have a better chance of being picked up. As Richards (1977) emphasizes, the Julesz patterns, even under the most favourable conditions, do not permit significant estimates of magnitude of depth implied by the actual disparities of the dots.

Stereopsis and Perception

It has been customary to treat stereopsis as being the result of a higher perceptual process that interprets the separate fields of view of the two eyes. Thus it has been argued that the two fields 'are presented separately to consciousness and that the final percept results from a psychic act'. As Ogle has emphasized, however, the experience resulting from fused disparate images is so immediate and compelling that it is difficult to separate it from a visual sensation, as such, and it might well be more correct to describe the experience simply as the response to the falling of disparate images on the two retinae. Interpretation, in the sense of conscious analysis of the two retinal images, is of course not an element in the experience. The same may be said of stereoscopic lustre (p. 478); for explanatory purposes we may say that the experience results because it is the only way of interpreting the two images of different luminosity, yet once again the experience is so compelling and immediate that we must treat it as the 'response to retinal images of different luminosity'.

Anomalous Contour

The perception of depth created by observing a distant object binocularly, when nearer objects are interposed between the distant object and the observer, provides an example of what the psychologist has called *anomalous contour*; and its contribution to depth perception, apart from the fusion of disparate images, may be investigated by constructing appropriate stereograms that simulate

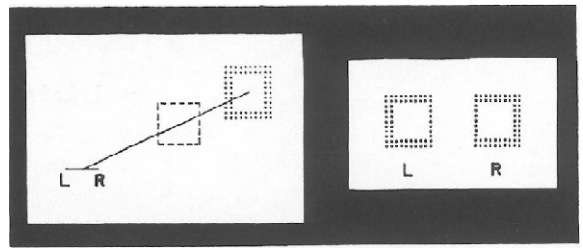

Fig. 17.37 Illustrating depth perception with anomalous contours. The stereogram shown at the right represents the actual situation illustrated at the left, where the view of the squares of dots is interrupted by the white square. (After Lawson & Gulick, *Vision Res.*)

the actual objects viewed. Thus Fig. 17.37, *right* (Lawson & Gulick, 1967), when viewed in the stereoscope, gives rise to the impression of a white square in front of the dots, which lie in a single plane behind. The two pictures are identical except that the right vertical row of dots in the left picture was omitted and the left vertical line of the right picture. The real situation corresponding to the left- and right-eye views could consist of a square frame of dots with a white opaque screen interposed between it and the observer, as illustrated to the left, and this is the 'interpretation' put on the left- and right-eye views. In this case there is no fusion of disparate images of dots since these all appear to lie in a single plane.

Reversal of Relief.

It will be noted by comparing the stereograms of Fig. 17.29*b* and *c*, that the dot in the circle appears to be in front or behind according as it is displaced to the right or left of the centre as viewed by the left eye, and according as the dot is displaced to the left or right of the centre as viewed by the right eye. Thus the pair of stereograms, *c*, is really obtained from the pair, *b*, by interchanging the pictures presented to the left and right eyes. In any pair of

stereograms a *reversal of relief* may be obtained by interchanging the pictures presented to the right and left eyes. Such a reversal implies a knowledge by the higher perceptual centres of the contributions of each retina to the final fused image, and yet it is interesting that we are normally not aware as to which eye sees any object not seen by both eyes in the binocular field of view. Thus Rogers describes the following experiment. A tube, about 2 inches in diameter, is held in front of the right eye and directed towards the far left corner of the room. A piece of white paper is placed in front of the left eye so as to screen this eye from the part of the room seen by the right eye. The impression is obtained of seeing the objects in the room with the *left eye* through a hole in the paper.

Size Effects

Horizontal Magnification

The importance of the sizes of the retinal images in determining space perception can best be described with the aid of an example, in which the size of one retinal image is increased with the aid of a lens that modifies the image-size but leaves the dioptric power of the eye almost unchanged (an aniseikonia glass). In Fig. 17.38 (*left*) we have a line on the longitudinal horopter; it appears to be in the frontal plane and the images on the two retinae are of the same size. In Fig. 17.38 (*right*) a lens has been put in front of the right eye; the lens magnifies in the horizontal meridian only, i.e. it is a cylinder with axis vertical. The retinal image is now formed at a_R and b'_R and is projected through the nodal point. The intersections of the projections of both eyes give the apparent positions of A and B in stereoscopic single vision, namely, at A and B′. It is clear that a considerable distortion of space values has resulted, AB appearing to lie along AB′. AB therefore no longer lies on the 'horopter' of the individual with the aniseikonia glass in front of one eye, and the horopter has thus changed its shape. It has been found that the eye is sensitive to as little as a 0.25 per cent change in the size of one retinal image. This spatial distortion can only be evoked by a magnification in the horizontal meridian; if an ordinary spherical magnifying lens is employed, magnifying in both horizontal and vertical meridians, then the distortion disappears.

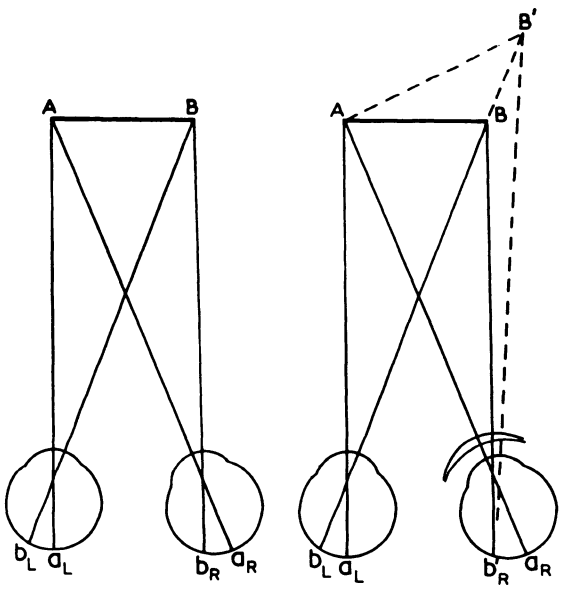

Fig. 17.38 The effect of an aniseikonia glass on depth perception. *Left*: AB is in the frontal plane and may be said to lie on the longitudinal horopter. *Right*: AB is now projected to AB′.

Vertical Magnification

If the magnification is confined to the vertical meridian, then we have what Ogle calls the *induced size effect*. The space dimensions are changed, but in the sense that would have been produced by horizontal magnification of the image in the other eye. It is for this reason that simple over-all magnification of the image in one eye, by a spherical lens, has no effect with regard to spatial distortion. Thus the horizontal magnification in the right eye would give the distortion illustrated by Fig. 17.38, with B appearing at B′; the vertical magnification, by its induced effect, would cause A to move back into the plane of B′, and so the distortion disappears.

INDUCED SIZE EFFECT

The induced effect, which is essentially the effect of producing *vertical disparities* in the retinal images, is a most striking phenomenon. The interpretation put forward by Ogle is difficult to present in a short space and this will not be attempted here; suffice it to say that, as with so many stereoscopic and other illusions, the experience may be regarded as a matter of putting the best interpretation on an anomalous set of stimuli. The experience in ordinary viewing conditions where vertical disparities become prominent is in asymmetrical convergence, one eye fixating a point immediately in front of it, whilst the other converges (see, for example, Fig. 24.25). Under these conditions certain readjustments in spatial orientation are made; if, now, the vertical disparities are introduced artificially, then the adjustments in spatial orientation that would have been appropriate to asymmetrical convergence are carried out, leading to distortion of space values.

The Pulfrich Phenomenon

If a swinging pendulum with a luminous bob is observed simultaneously through a green glass by one eye and a

dark red glass by the other, instead of moving in a plane the pendulum appears to move through an elliptical path. Thus if the left eye wears the red glass, the pendulum on its left-to-right swing appears to move away from the observer and on its reverse swing to move towards him. If the colours are interchanged, the direction of apparent rotation is reversed. Different coloured glasses are unnecessary to evoke the effect, and it is sufficient if the light entering one eye is reduced by placing a neutral filter before it.

Interpretation

The cause of the illusion is the difference in reaction-times of the two eyes in response to the different colours or different luminances. In Fig. 17.39 let us assume for simplicity that the right eye responds instantaneously to the image of the bob at any point in its path, whilst the left eye responds after a delay. In effect, therefore, when the two eyes are fixating the bob, indicated in its true position in black at A, the left eye is seeing it as though it were at A′, i.e. as though its image on the left retina were at *a* instead of at f_L. The disparate images are fused to give a stereoscopic effect, so that the bob is actually projected to a point outside the plane of the pendulum. The disparity is uncrossed, so that the bob on its left-to-right swing appears farther from the observer. The degree of disparity will obviously depend on the speed of the bob, and this passes from zero at the extreme of its swing through a maximum at the bottom of its swing; hence the bob will appear in the plane of the pendulum at the extremes of its swing, and closest to and farthest from the observer at the bottom of its right-to-left and left-to-right swings respectively. In other words, its motion will be elliptical. Careful experimental studies of the Pulfrich phenomenon, for example those of Lit (1960), have confirmed this explanation.[7]

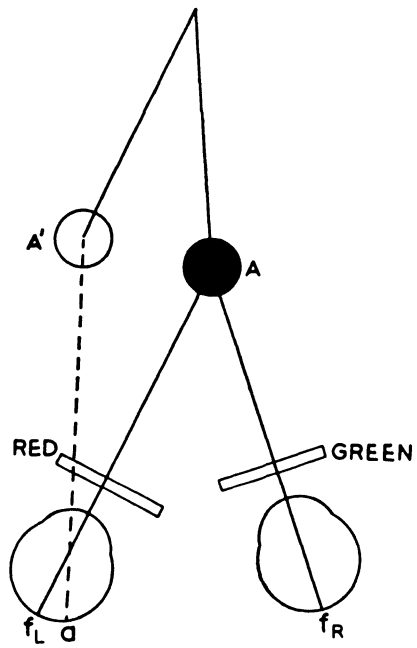

Fig. 17.39 The Pulfrich phenomenon.

FURTHER ASPECTS OF BINOCULAR VISION

Retinal Rivalry and Ocular Dominance

Stereoscopic vision is essentially the response to disparate images on the retinae of the two eyes; if the images are too disparate, as under the artifical conditions of the stereoscope, great difficulty is experienced in obtaining a single fused percept, the double images being so far apart as to force themselves on the awareness and so destroy the unity of the percept. The importance of the *meaning* of the final percept is evident when one attempts to fuse two pictures in the stereoscope; it may be found impossible for a time, but if fusion once takes place to give a three-dimensional representation of some object, then the significance of the two aspects has become clear and the stereograms may be fused rapidly at will.

Retinal Rivalry

If two pictures that cannot possibly be related as two aspects of the same three-dimensional object are presented to the two eyes, single vision *may*, under some conditions, be obtained but the phenomenon of *retinal rivalry* enters. Thus the two letters **F** and **L** of the stereogram in Fig. 17.40, when presented to the two eyes separately, can be fused to give the letter **E**; the letters **F** and **L** cannot, however, by any stretch of the imagination be regarded as left and right aspects of a real object in space, so that the final percept is not three-dimensional and, moreover, it is not a unitary percept in the sense used in this discussion; great difficulty is experienced in retaining the appearance of the letter **E**, the two separate images, **F** and **L**, tending to float apart. We are here dealing with a mode of binocular vision that may be more

Fig. 17.40 The letters F and L in the stereoscope give simultaneous perception to create the impression of the letter E.

appropriately called *simultaneous perception*; the two images are seen simultaneously, and it is by *superimposition*, rather than fusion, that the illusion of the letter **E** is created.

With the stereograms of Fig. 17.41, if both patterns were fused or superimposed, the result would be a criss-cross pattern; in actual fact, however, no such perfect superimposition is achieved and the phenomenon of retinal rivalry becomes strongly evident. In different parts of the field one or other set of lines predominates whilst the opposing set is suppressed; sometimes for a brief interval one set of lines will appear by itself over the entire field; in general the impression is one of fluctuation and Helmholtz stated that the appearance at any moment was largely determined by the attention paid to any aspect, e.g. if the observer started to count the lines of one set the others, in the opposite direction, tended to disappear. Helmholtz deduced from his observation that 'the content of each separate field comes to consciousness without being fused with that of the other field by means of organic mechanisms, and therefore the fusion of the two fields in one common image, when it does occur, is a psychic act'. More recent studies of retinal rivalry, however, indicate that there is a periodicity in the recurrence of one or other field in awareness which appears to be independent of volition; the distinction between fusion by a 'psychic act' and an 'organic mechanism' is, moreover, not one that would be countenanced by the modern physiologist; as we shall see, the fusion of retinal images, when these occur within Panum's area, is brought about by the projection of the evoked nervous discharges from the retinae on to the same cortical neurones. When retinal disparity is so large as to evoke rivalry this projection on to single cortical cells presumably does not occur.

Fig. 17.41 The stereograms do not give a regular criss-cross pattern in the stereoscope.

Ocular Dominance

Retinal rivalry may be viewed as the competition of the retinal fields for attention; such a notion leads to the concept of *ocular dominance*—the condition when one retinal image habitually compels attention at the expense of the other. Whilst there seems little doubt that a person may use one eye in preference to the other in acts requiring monocular vision, e.g. in aiming a rifle, it seems doubtful whether, in the normal individual, ocular dominance is really an important factor in the final awareness of the two retinal images. Where the retinal images overlap, stereoscopic perception is possible and the two fields, in this region, are combined into a single three-dimensional percept. In the extreme temporal fields, entirely different objects are seen by the two eyes and as to which dominates the awareness at any moment depends largely on the interest it arouses; as a result, the complete field of view is filled in and one is not aware of what objects are seen only by one eye. Where the fields overlap, and different objects are seen by the two eyes, e.g. on looking through a window the bars may obscure some objects as seen by one eye but not as seen by the other, the final percept is determined by the need to make something intelligible out of the combined fields. Thus the left eye may see a chimney-pot on a house whilst the other eye sees the bar of a window in its place; the final perceptual pattern involves the simultaneous awareness of both the bar and the chimney-pot because the retinal images only have meaning if both are present in consciousness. So long as the individual retinal images can be regarded as the visual tokens of an actual arrangement of objects, it is possible to obtain a single percept, and there seems no reason to suppose that the final percept will be greatly influenced by the dominance of one or other eye. When a single percept is impossible, retinal rivalry enters; this is essentially an alternation of awareness of the two fields—the subject apparently makes attempts to find something intelligible in the combined presentation by suppressing first one field and then the other—and certainly it would be incorrect to speak of ocular dominance as an absolute and invariable imposition of a single field on awareness, since this does not occur.[8]

When the field of one eye is consistently dominant over that of the other, this generally occurs as a result of a general law that the predominant field along an edge is that field in which the edge lies. Thus if a vertical bar is presented to the left eye and a horizontal bar to the right eye the combined impression may be represented by the cross in Fig. 17.42, although it must be appreciated that the result is by no means so clear-cut as a simple diagrammatic representation would indicate. At the extremes of the fused cross one eye sees only white whilst the other sees the contour, or edge; this eye is 'dominant' and the black bar is seen in preference to the white space. Where the bars overlap there is a mixed state of affairs. To the right eye the field above and below the overlap is white and, since this eye is dominant along the horizontal edge, we may expect white above and below the bar; to the left eye the field to the left and right of the overlap is white and since, in this region, the left eye is also 'dominant' we expect white to the left and right.

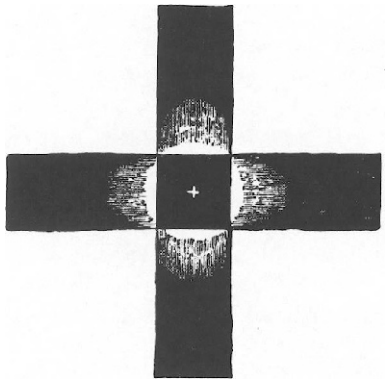

Fig. 17.42 Schematic representation of the simultaneous perception of a vertical and horizontal bar in the stereoscope. (Helmholtz, *Physiological Optics.*)

Optokinetic Nystagmus and Dominance

An interesting situation is provided by allowing the eyes to view a rotating striped pattern through Dove prisms, such that to one eye the pattern is moving, say, to the left and to the other to the right. With the aid of the electro-oculogram it is easy to measure objectively the form of the ensuing nystagmus. This changes repeatedly and the changes are accurately correlated with the subjective dominance of one or other movement-pattern (Fox *et al.* 1975).

Dominance and Handedness

Experimentally the subject of ocular dominance has received more attention than it probably deserves, and attempts have been made to relate it to 'handedness'. Dolman's peephole test consists of a 13 × 20 cm card with a round central hole in it of 3 cm diameter. A target 6 metres away is looked at through the hole held at arm's length. Under these conditions only one eye can actually see the target, and the one that is found to be doing so is adjudged the dominant eye. Walls (1951) has summarized the various tests and placed them in five categories and has stated that in effect they reduce to only two, namely those based on motor control of the eyes and those based on the assessment of subjective visual direction. According to Walls, for instance, the motor taxis of the eyes may be likened to the steering apparatus of a motor car; one wheel is directly attached to the steering rod whilst the other is guided by the track rod. It is difficult to translate this analogy into physiological terms, however; we know that the muscles to both eyes are innervated at the same time in any movement, and it would be quite incorrect to think of the one eye dragging the other along with it, as this view of ocular dominance would require.

Stereoscopic Lustre

If the stereograms of Fig. 17.43 are fused, the impression of lustre is created. By lustre is meant the appearance of a surface when some of its reflected light seems to come from within it; it is as though one sees some of the light from the object *through* the rest of the reflected light. The stereograms of Fig. 17.43 represent the two appearances of a crystal when viewed by the two eyes separately, but the two differ also in being bright and dark at corresponding places. Stereoscopic lustre is therefore the result of stimulating corresponding points of the retinae to different extents, and the phenomenon suggests an explanation for the lustre in real objects. If the two stereoscopic pictures are to be interpreted as tokens of the same object, the surface of the latter must be such that a small change in viewpoint (from left eye to right eye) makes a profound change in the amount of light reflected into the eye. An object with a diffusely reflecting surface could not produce such a change and it therefore appears 'flat'; a strongly reflecting surface, on the other hand, would provide the reflected light with a directional quality such that the amount of light entering the eye varied considerably with the viewpoint; such a surface is, in general, lustrous. The chromatic lustre of a bird's plumage, of a thin film of oil, and so on, is due to the variation in the quantity and *quality* of the light entering the eye with change of viewpoint. It must be pointed out, however, that lustre in objects can be appreciated by *one eye only*; Helmholtz has shown, nevertheless, that the *illusion* of lustre may likewise be produced with a single eye; in these circumstances the illusion is created by rapid changes in the brightness of the points in the retinal image, associated with either movements of the eye or of the object; thus on Helmholtz's view essentially the same impression can be gained in one eye by successive stimuli as is gained in two eyes by simultaneous stimuli. Bartley has confirmed this viewpoint; he has shown that successive monocular presentation of two stereograms of different luminance creates the sensation of lustre. The psychological issues involved in such an equivalence of time and space need not concern us here; the important feature of stereoscopic lustre resides in its demonstration that, wherever this is possible, the higher perceptual

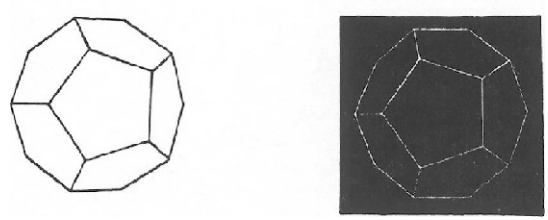

Fig. 17.43 Stereoscopic lustre.

centres will read such a meaning into two retinal images as to make them the tokens of a single object in space; the simultaneous presentation to the two eyes of a light and a dark view of an object is *interpreted* as the single presentation of a lustrous object in three dimensions, and this happens even though both the light and dark views reflect light diffusely. If the two views cannot be regarded as the tokens of a single object, retinal rivalry takes the place of this perceptual process; in the case of stereoscopic lustre this can be shown by presenting differently coloured views of the same object; if the difference in colour is not very pronounced the impression of lustre is gained on fusion; when the difference is made great lustre gives way to retinal rivalry.

The Essential Basis of Stereopsis

The studies of Julesz have prompted several investigations into the nature of stereopsis; for example, the question has been asked whether fusion of disparate images is necessary; whether contours are 'irrelevant', and so on. Thus Kaufman (1964, 1965), in a series of papers has described stereoscopic effects using, instead of random dots, rectangles composed of randomly selected typewriter letters; in one stereogram a block of these letters is shifted to the left or right so as to be out of phase with the identical block in the other stereogram, and as a result this central block appears in depth in relation to the background of surrounding letters. Kaufman concluded that retinal rivalry was present using this type of pattern as well as Julesz' dot patterns, since the binocular percept did not give rise to the density of dots or letters that would have been expected by a simple physical superposition of the two monocular stereograms; instead, the density corresponded with that of single stereogram, as though the percept of depth had been evoked by alternate suppression of one or other stereogram. Kaufman (1965) generalizes correctly when he says that stereopsis will occur when correlated stimuli are out of spatial phase with respect to some reference system. The reference system can be another set of correlated objects or point-arrays, or it may be the edge of the overall half-fields. Any mechanism that can detect the correlation between the binocular stimuli, and also detect a difference in their phase, can yield a representation of depth.

Visual and Objective Unreality

When attempting to steer a way through the rather complex arguments in this field, it is best to keep clearly in mind that the binocular percept, resulting from the presentation of separate and different pictures to the two eyes, will be governed by the relation of these two pictures to reality. How can they be interpreted as left- and right-eyed views of the external world? As indicated earlier, rivalry is the response to *visual* unreality; no object when viewed by left and right eyes simultaneously can appear as a vertical bar and a horizontal bar. *Objective* unreality is given by the formation of double images, e.g. of a pencil held close to the face when viewing a distant point; the double images are real visually in the sense that real objects in space have provoked them, but they are objectively unreal because our sense of touch provides contradictory evidence. Stereopsis is achieved under these conditions, and it is assisted by the suppression of objectively unreal parts of the retinal images. It is probably this ability to suppress parts of the retinal images that permits the development of stereopsis when differently coloured monocular stereograms are presented to the two eyes; according to Treisman (1962), stereopsis is achieved although the colour of one of the fields may be suppressed; thus the brain, under these conditions, was accepting the contours of the stereograms but suppressing the colour of one. Similarly, with many of the random dot and letter stereograms devised by Julesz and Kaufman, the situations presented are often so unreal visually that stereopsis is only achieved by virtue of suppression of parts of the visual fields.

Binocular Aspects of Some Visual Functions

Stereoscopic vision reveals the existence of processes integrating the responses in the two eyes to give a unitary percept quite different from that predictable on the basis of a summation of the separate impressions. Retinal rivalry, on the other hand, provides a condition in which the separate impressions appear, at certain moments, to be unaffected by each other, whilst between these two states we may have a more or less perfect overlap of the visual impressions with, however, dominance of one or other field in certain parts. It is worth inquiring to what extent the simpler aspects of vision discussed in Section 2 are affected by the use of two eyes. There is, unfortunately, disagreement on many points so that the whole subject merits further investigation.

Light Threshold

If there is the possibility of summation between the two eyes, we may expect that the absolute light threshold, i.e. the smallest light stimulus necessary to evoke the sensation of light in the completely dark-adapted eye, will be smaller when the two eyes are employed to view the stimulating patch. Pirenne (1943) found a lower threshold with binocular vision, but attributed this to *probability summation*, a result of the improvement of the possibility of detecting a signal by having two chances using independent detectors; the increase in probability is easily calculated, and Pirenne demonstrated that the lowered threshold conformed to this prediction. However, Thorn & Boynton (1974) examined Pirenne's experiments critically, and questioned the validity of his conclusions; their own experiments showed that, provided the test-stimuli fell on corresponding points of the retinae, there was up to 70–80% summation of responses of the two eyes. Summation was not perfect, as in binaural stimulation in acoustic stimuli.

Brightness Sensation

At higher levels of luminance the position is more complex; when the fields presented to the two eyes are equal, there is no obvious summation—this is evident from

everyday experience, since the closing of one eye does not make a previously binocularly viewed piece of white paper appear significantly darker. When there is a gross discrepancy in the luminance of the two fields, retinal rivalry appears, although it may most frequently manifest itself as ocular dominance, the bright field determining the binocular sensation. (Under special conditions, it will be remembered, the sensation of lustre may be created.) Under intermediate conditions there is a definite fusion of the separate sensations, so that the binocular sensation is compounded of the separate monocular sensations or, to speak more precisely, the binocular sensation is different from that evoked by either eye separately, and is intermediate between these two.

WEIGHTING COEFFICIENTS

Recent experimental studies have been devoted to quantifying the relation between the monocular and binocular stimuli. Thus Levelt (1965) caused subjects to view binocularly two equally illuminated fields; this was the *comparison stimulus*. The sensation of brightness evoked in this way was compared with the *test stimulus*, where the subject once again viewed two monocular fields binocularly, but this time the luminance of one was fixed by the experimenter and that of the other was adjusted by the subject until the binocular sensation of brightness equalled that evoked by the comparison stimulus. An example of the results is given in Fig. 17.44, where the luminance of the left field is plotted as ordinate against that of the right field, the plotted points representing the left and right luminances which, on fusion, gave a binocular sensation of brightness equal to that obtained when both eyes viewed fields of the same luminance of 30 cd/m^2. Over part of the range there is a linear relation between the two field luminances, indicating a weighted averaging of the two; e.g. if the left field was 40 cd/m^2, the right was 16; if the left was 36 the right was 24; if the left was 12 the right was 60, and so on. When the discrepancy between the luminances presented to the two eyes was large, the relation became non-linear and provides the basis for some well known paradoxes. Thus in *Fechner's paradox*: a monocularly viewed white surface appears brighter than when it is viewed binocularly in such a way that one eye views it directly and the other through a dark glass. Thus if we look at Fig. 17.44 we see that if the subject was presented through his left eye with a field of about 40 cd/m^2 it would provoke a considerably brighter sensation than if this field was seen binocularly with a field of about 12 cd/m^2, since the combined sensation for binocular vision is equivalent to that evoked by 30 cd/m^2. In general, Levelt showed that over the linear range, the brightness sensation could be predicted from the weighted mean of the left and right stimuli:

$$W_R E_L + W_R E_R = C$$

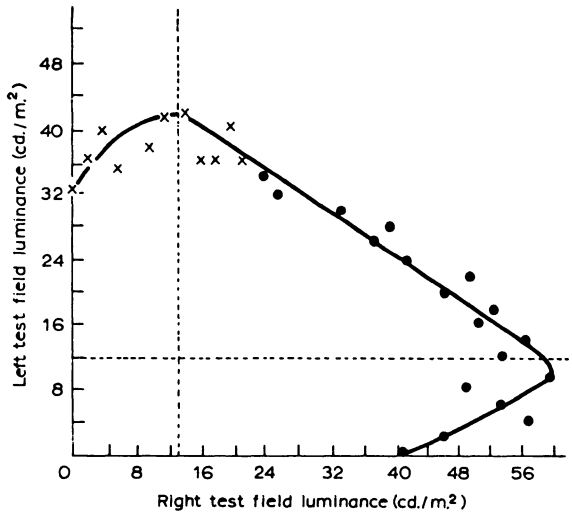

Fig. 17.44 The subject views test fields of different luminances through left and right eyes separately; one field is fixed and the other is varied by the subject so that the combined impression is one of equality with a standard binocularly viewed luminance of 30 cd/m^2. Thus a field of 40 cd/m^2 viewed in conjunction with a right field of about 16 cd/m^2 gave the same subjective sensation as that obtained by viewing fields of 30 cd/m^2 through both eyes. (After Levelt, *Brit. J. Psychol.*)

where the weighting coefficients, W_R and W_L, add up to unity and are constant for a given observer. If a contour was present in one of the binocular fields and not in the corresponding region of the other, then the weighting coefficient for the eye with the contour increased at the expense of that for the other eye. This is demonstrated by viewing Fig. 17.45 stereoscopically; when fused, A appears much brighter than C, although at the centres of the discs the luminances are the same; on the other hand no difference between B and C is observed. Usually, contours in non-corresponding parts of the field give rise to rivalry, and this means, essentially that the contours of one eye dominate the weighting coefficient of this eye when

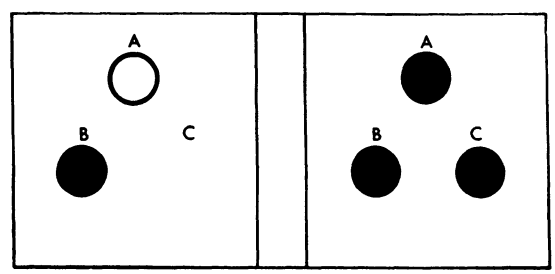

Fig. 17.45 When the left and right figures are fused in the stereoscope, A appears brighter than C although no difference between B and C is noticed. (Levelt, *Brit. J. Psychol.*)

dominant; at another moment, the contour of the other field will become dominant.[9]

Flicker

The classical experiments of Sherrington would indicate a more or less complete independence of the two eyes in respect to the discrimination of flicker. Thus under conditions where flicker is perceptible at 20 cycles/sec, the presentation of separate flickering patches to the two eyes in such a way that the dark period of one eye corresponded to the bright period of the other, did not give fusion although a flicker rate of 40 cycles/sec in one eye would have done. Smith has shown that when one eye views a steady light source and the other an intermittent one, the sensation is one of binocular flicker, i.e. it is impossible to discriminate between the sensation so evoked and that which would be produced by two flickering sources presented separately to the two eyes. In the region of the critical fusion frequency, however, retinal rivalry occurs, so that the flicker sensation alternates with the impression of a stationary source. The critical fusion frequency, under these conditions, is not entirely determined by the luminance of the flickering patch but on the ratio of this luminance to that of the stationary source. The experimental conditions for the study of binocular flicker are clearly essentially the same as those under which retinal rivalry and ocular dominance are studied; where a unitary percept is possible, as in the special case of the two flickering patches being synchronous, we may expect the binocular flicker sensation to be identical with that evoked in either eye separately. When conditions are different in the two eyes, but not too discrepant, retinal rivalry becomes obvious. When the discrepancy is very strong, rivalry gives place to the dominance of one eye. A study of the tendency for dominance, when different pictures are presented in the stereoscope, shows that the picture with the most contours tends to become dominant; in the case of flicker, it is the flickering field that imposes itself on awareness at the expense of the stationary.

Binocular Colour Mixing

When a pair of stereograms consists merely of two coloured pieces of paper, the condition most frequently encountered is that of retinal rivalry, one or other of the colours dominating awareness for a time to give place to the other. A true binocular mixing can be obtained, however, conforming approximately to the laws of monocular colour mixing, if the conditions are suitable. According to some studies by Johannsen, conditions favouring mixture are low absolute luminance and a small separation of the two colours in the spectrum. When rivalry occurs, the longer wavelength tends to dominate, and where there is a difference in luminosity between the colours, dominance occurs with the brighter of the two. The fact that so careful an experimenter as Helmholtz denied the existence of binocular colour mixing reveals that there are large individual differences in the capacity to mix colours binocularly. When red and green stereograms of a three-dimensional object are presented to the eye, it is seen in depth but one or other colour is usually suppressed (Treisman, 1962).

Colour Stereoscopy

The stereoscopic appearance obtained by regarding two differently coloured, but otherwise identical, plane pictures with the two eyes separately, is probably due to chromatic differences of magnification. If the left eye, for example, views a plane picture through a red glass and the right eye views the same picture through a blue glass, an illusion of solidity results.

Adaptation

It would seem from the work of Mandelbaum (1941) that the adaptive state of one eye is unaffected by that of the other; thus the absolute threshold of one eye was not altered by adapting the other to a variety of luminance levels. This is an important finding, since it justifies the use of one eye as a control in adaptation studies, e.g. those of Wright (Ch. 16).

THE PERCEPTION OF MOTION

The perception of motion has two elements in it; there is the direct appreciation of movement in consequence of the gliding of the image over the retina when the eye is still (or as a result of the movement of the eye when the image of the object fixated remains stationary on the retina), and there is the more 'intellectual' recognition of the fact of movement deduced from the observation that an object is projected to a certain point in space at one moment and at another point after a certain interval of time. Thus we recognize that the large hand of a watch is in motion because at one minute it points at 'ten' and at the next minute at 'eleven'; there is, however, no real perception of motion, the threshold rate of movement being too low. In experimental studies the measurements are concerned with the direct perception of movement. The sensitivity of the retina to movement is highest at the fovea, as one might expect, since it is here that discrimination, generally, reaches its acme; nevertheless the periphery shows a high sensitivity in comparison with the low order of visual acuity attainable in this region; in the peripheral retina, so great is the difference between visual acuity and motion acuity, that the existence of objects may often

only enter awareness when they are moved; as soon as they become stationary they are no longer perceived.[10]

Thresholds

The threshold sensitivity to movement can be measured in a number of ways as follows:

1. *The minimum excursion of a moving body necessary for its being in motion to be appreciated.* This minimum depends on the speed of movement, but under favourable conditions it is of the order of 10 seconds of arc. This is an extremely small displacement, so small that if two stationary points were separated by this amount they could not be discriminated as separate. The image of the moving point thus need not move over a whole cone before its movement is appreciated. As a result of diffraction and chromatic aberration, the image of a point covers several cones; these are stimulated to different degrees, since the brightness of the image falls off as the periphery of the blur-circle is approached; a very slight movement of the whole image modifies the distribution of light on the several cones and thus modifies the pattern of discharge in their nerve fibres. A movement much smaller than the diameter of a cone could modify the distribution of light on the cones and so provide the peripheral basis for this high degree of acuity. According to McColgin, the threshold increases with increasing distance from the fovea.
2. *The minimum angular speed of a point.* In the absence of stationary reference points, this of the order of one to two minutes of arc per second.
3. *The minimum duration for a given excursion.* If a point is moved between two stationary points, there is a speed above which the motion cannot be appreciated, i.e. the observer sees the point at all points in its path simultaneously; the moving luminous point becomes a 'streak'. With an excursion of 10°, the minimum duration is of the order of 50 msec, corresponding to a speed of movement of 200°/sec.

Apparent Movement

A common experimental method of inducing the appearance of movement is to present the subject with a given figure or spot for a short period of time and then to present the same figure at a different position in space; if the times and distances fall within certain ranges, the subject reports the perception of movement. This tachistoscopic type of presentation is, of course, the basis of motion pictures. According to Wertheimer's (1912) classical study, when the intervals are less than about 30 msec the two stimuli are reported as occurring simultaneously so that no motion is perceived; with 60 msec, movement is optimal whilst with intervals of 200 msec or more the two stimuli are perceived in succession.

Illusions

A variety of illusions of movement have been described; for example, the apparent movement of the moon behind fast-flying clouds; the apparent backward motion of the water near the shores of a large river if the current is rapid at the middle; the apparent ducking forward of the masts of a ship in passing under a bridge from which it is observed, and so on. If the series of concentric lines in Fig. 17.46*a* is subjected to a slight but rapid circular motion, similar to that used in rinsing a circular dish half-filled with water, an interesting 'propeller-like' motion will appear. Again, if Fig. 17.46*b* is rotated about an axis through its centre, then, if the direction of rotation is that in which the spiral line approaches the centre, the entire surface appears to expand during rotation and to con-

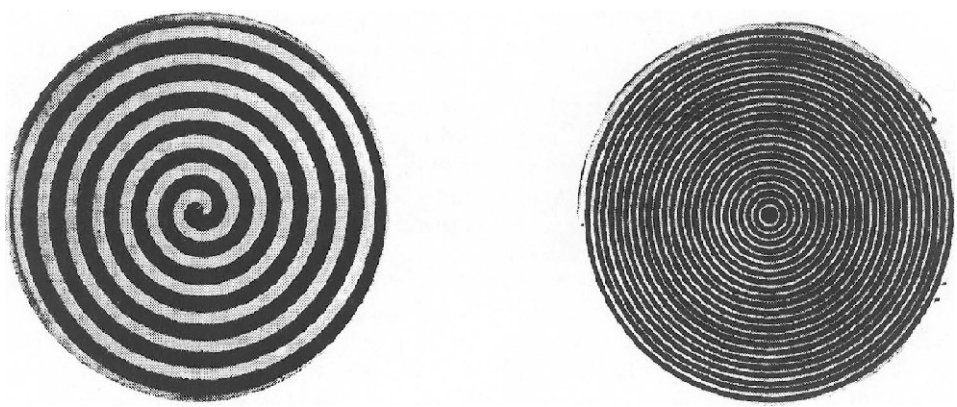

Fig. 17.46 Illustrating illusions of movement. For details see text. (After Bowditch, *J. Physiol.*)

tract after it has ceased, and *vice versa* if the rotation is in the opposite direction (Bowditch & Hall, 1880–2). Alternatively, the prolonged viewing of an object in motion gives rise to a movement-after-image in the opposite direction—the so-called *waterfall phenomenon.* Barlow & Brindley (1963) have shown that there is interocular transfer of the adaptation effect, since if only one eye is exposed to the moving figure, and this eye is subsequently blinded temporarily by exerting pressure on the globe, the after-effect appears in the other eye.

Notes

1. In this chapter the term 'fovea' will be used very loosely to indicate the position of the image of a centrally fixated point; it will be the intersection of the visual axis with the retina.
2. Festinger *et al.* (1976) quote a number of illusions based on failure to correct for eye movements; for example Johannsen reported that if an observer follows a target moving horizontally in simple harmonic motion, a vertically moving spot, 90° out of phase with the horizontally moving spot, is perceived to move in a circle, and this is the path it would sweep out on the retina.
3. Michael & Stark (1967) measured the visually evoked response (VER, p. 365) with scalp electrodes and found that, when saccadic suppression of light-flashes occurred, there was suppression or reduction of some waves on this record. Again, Zuber *et al.* (1966) found that the reduction in pupillary area in response to a flash could be as little as 10 per cent of the control value if the flash occurred during a saccade. Mitrani *et al.* (1970) have demonstrated very neatly that 'retinal smear' is a factor of some significance by showing that the depression of visual acuity was large for vertically orientated gratings, when the eye made a horizontal saccade, but small for horizontally orientated gratings. On the other hand, Collewijn (1969) found depression of the VER in rabbit cortex and colliculus evoked by a flash in one, immobile, eye when the saccade occurred only in the other, non-seeing, eye. The objective measurement of the suppression is well illustrated by the work of Riggs *et al.* (1974) which showed that the phosphene evoked by electrical stimulation of the eye in human subjects required a higher current-intensity during the execution of a saccade; by a suitable calibration of current versus subjective sensation they computed that the threshold rose by some 0.5 log units, or three-fold, as found by others using photic stimulation.
4. Of significance is the failure of thresholds to rise during saccades if these are made in the dark.
5. There is unfortunately a serious danger of confusion arising from the different senses in which 'false projection' is regarded. To the neurologist the macula of the squinting eye is falsely projected because the individual grasps wide of the object whose image falls on it (he 'past-points'). False projection thus means the projection of a retinal image to some other point in space than that occupied by the object evoking it, and this is the sense maintained in this book. To some ophthalmologists, on the other hand, false projection is synonymous with what is called '*abnormal retinal correspondence*'. With the development of a 'false macula', an image, not on the macula of the squinting eye, is projected to the same point in space as the image on the macula of the normal eye; the retinal correspondence (p. 465) has been readjusted to give single binocular vision of an object whose images do not fall on the innate corresponding points of the two retainae. Thus the neurologist would say that the 'false macula' is correctly projected into space, whilst some ophthalmologists would say that it is falsely projected.
6. When the pictures are rotated through 90°, so that the disparities become vertical, stereopsis is lost but the perception of the central square remains, although unrecognizable in either monocular presentation. Thus we must distinguish between the perception of form in depth and form without depth (Kaufman, 1964a).
7. Wist *et al.* (1977) have shown that, if the swinging object is a grating, then the apparent depth during a swing varies with the spatial frequency of the grating, the higher the spatial frequency of the moving grating the smaller the angular speed required to produce a given displacement of its apparent plane of motion. The authors consider that this finding is difficult to reconcile with the interpretation discussed here, but the situation with a vertically striped object must be complex, since now stereopsis is possible by convergence or divergence of the eyes to bring a given stripe on corresponding points, as in the wallpaper phenomenon (p. 465).
8. An interesting observation of Creed's should be recorded here; in studying the retinal rivalry caused by observation in the stereoscope of two postage stamps, differing in colour as well as slightly in design, he noted that the dominance of one colour was not necessarily associated with the dominance of the design belonging to it—thus at a given moment it was quite possible for the design of one stamp to prevail with the colour of the other.
9. Engel (1967) has examined in some detail the manner in which the sensations are combined; his formulation carries that of Levelt farther, invoking a cross-correlation process between the two eyes that allows of an improved prediction of the effects of combining monocular fields.
10. This a somewhat loose way of stating the fact; one becomes aware of an object when it moves in the peripheral field, but this may be an expression of visual acuity rather than motion acuity; owing to adaptation, the awareness of a stationary object in the peripheral field soon ceases, and it requires the stimulation of a new set of receptors to come again into consciousness. The sudden awareness of this fresh stimulation is *interpreted* as a movement of the object, yet experiments seem to show that if the movement of the object is continued there need be no real perception of motion. According to Warden, the direct comparison of visual with movement acuity is beset with difficulties.

References

Andersen, E. E. & Weymouth, F. W. (1923) Visual perception and the retinal mosaic. *Am. J. Physiol.* **64**, 561–594.

Barlow, H. B. & Brindley, G. S. (1963) Inter-ocular transfer of movement after-effects during pressure blinding of the stimulated eye. *Nature* **200**, 1347.

Bartley, S. H. (1941) *Vision. A Study of its Basis.* New York: Van Nostrand.

Becker, W. & Klein, H.-M. (1973) Accuracy of saccadic eye movements and maintenance of eccentric eye positions in the dark. *Vision Res.* **13**, 1021–1034.
Beeler, G. W. (1967) Visual threshold changes resulting from spontaneous saccadic eye movements. *Vision Res.* **7**, 769–775.
Bizzi, E. (1966) Changes in the orthodromic and antidromic response of optic tract during eye movements of sleep. *J. Neurophysiol.* **29**, 861–870.
Blakemore, C. (1970) The range and scope of binocular depth discrimination in man. *J. Physiol.* **211**, 599–622.
Blakemore, C., Carpenter, R. H. S. & Georgeson, M. A. (1970) Lateral inhibition between orientation detectors in the human visual system. *Nature* **228**, 37–39.
Bouma, H. & Andriessen, J. J. (1968) Perceived orientation of isolated line segments. *Vision Res.* **8**, 493–507.
Bowditch, H. P. & Hall, G. S. (1880–82) Optical illusions of motion. *J. Physiol.* **3**, 297–307.
Brooks, B. A. & Fuchs, A. F. (1975) Influence of stimulus parameters on visual sensitivity during saccade eye movement. *Vision Res.* **15**, 1389–1398.
Brown, K. T. (1962) Complete interocular transfer of an adaptation process responsible for perceptual fluctuations with an ambiguous visual figure. *Vision Res.* **2**, 469–475.
Burian, H. M. (1951) Stereopsis. *Doc. Ophthal.* **5–6**, 169–183.
Buttner, U. & Fuchs, A. F. (1973) Influence of saccadic eye movements on unit activity in simian lateral geniculate and pregeniculate nuclei. *J. Neurophysiol.* **36**, 127–141.
Collewijn, H. (1969) Optokinetic eye movements in the rabbit: input–output relations. *Vision Res.* **9**, 117–132.
Creed, R. S. (1935) Observations on binocular fusion and rivalry. *J. Physiol.* **84**, 381–391.
Crone, R. A. & Verduyn Lunel, H. F. E. (1969) Autokinesis and the perception of movement: the physiology of eccentric fixation. *Vision Res.* **9**, 89–101.
Ditchburn, R. W. (1955) Eye-movements in relation to retinal action. *Optica Acta* **1**, 171.
Dodge, R. (1900) Visual perception during eye movement. *Psychol. Rev.* **7**, 454–465.
Engel, G. R. (1967) The visual process underlying binocular brightness summation. *Vision Res.* **7**, 753–767.
Fender, D. & Julesz, B. (1967) Extension of Panum's fusional area in binocularly stabilized vision. *J. Opt. Soc. Amer.* **57**, 819–830.
Festinger, L., Sedgwick, H. A. & Holtzman, J. D. (1976) Visual perception during smooth pursuit eye movements. *Vision Res.* **16**, 1377–1386.
Fox, R., Todd, S. & Bettinger, L. A. (1975) Optokinetic nystagmus as an objective indicator of binocular rivalry. *Vision Res.* **15**, 849–853.
Gibson, J. J. (1933) Adaptation, after-effect and contrast in the perception of curved lines. *J. Exp. Psychol.* **16**, 1–31.
Gibson, J. J. (1952) The relation between visual and postural determinants of the phenomenal vertical. *Psychol. Rev.* **59**, 370–375.
Graham, C. H. (1965) Ed. *Vision and Visual Perception.* New York: Wiley.
Graybiel, A. & Hupp, D. (1946) The oculogyral illusion: a form of apparent motion which may be observed following stimulation of the semicircular canals. *J. aviat. Med.* **17**, 3–27.
Grosvenor, T. (1959) Eye movements and the autokinetic illusion. *Am. J. Optom.* **36**, 78–87.
Helmholtz, H. von. (1925) *Physiological Optics* (translated J. P. C. Southall). Optical Soc. Am.
Helson, H. (1938) Fundamental problems in color vision. *J. Exp. Psychol.* **23**, 439–476.
Holst, E. V. (1957) Aktive Leistungen der menschlichen Gesichtswahrnehmung. *Studien Generale* **10**, 231–243. (Quoted by MacKay, 1973.)
Jameson, D. & Hurvich, L. M. (1959) Note on factors influencing the relation between streoscopic acuity and observation distance. *J. opt. Soc. Am.* **49**, 639.
Judd, D. B. (1940) Hue saturation and lightness of surface colors with chromatic illumination. *J. Opt. Soc. Amer.* **30**, 2–32.
Julesz, B. (1964) Binocular depth perception without familiarity cues. *Science* **145**, 356–362.
Kaufman, L. (1964a) Suppression and fusion in viewing complex stereograms. *Am. J. Psychol.* **77**, 193–205.
Kaufman, L. (1964b) On the nature of binocular disparity. *Am. J. Psychol.* **77**, 393–402.
Kaufman, L. (1965) Some new stereoscopic phenomena and their implications for the theory of stereopsis. *Am. J. Psychol.* **78**, 1–20.
Kaufman, L. & Pitblado, C. (1965) Further observations on the nature of effective binocular disparities. *Am. J. Psychol.* **78**, 379–391.
Keesey, U. T. (1960) Effects of involuntary eye movements on visual acuity. *J. opt. Soc. Am.* **50**, 769–774.
Köhler, W. & Wallach, H. (1944) Figural after-effects: An investigation of visual processes. *Proc. Amer. Phil. Soc.* **88**, 269–357.
Land, E. H. (1959) Color vision and the natural image. Pts. I and II. *Proc. Nat. Acad. Sci.* **45**, 115–129; 636–644.
Lawson, R. B. & Gulick, W. L. (1967) Stereopsis and anomalous contour. *Vision Res.* **7**, 271–297.
Leibowitz, H. & Hartman, T. (1959) Magnitude of the moon illusion as a function of the observer. *Science* **130**, 569–570.
Levelt, W. J. M. (1965) Binocular brightness averaging and contour information. *Brit. J. Psychol.* **56**, 1–13.
Lit, A. (1960) The magnitude of the Pulfrich stereo-phenomenon as a function of target velocity. *J. exp. Psychol.* **59**, 165–175.
Ludvigh, E. (1952) Control of ocular movements and visual interpretation of environment. *Arch. Ophthal.* **48**, 442–448.
MacKay, D. M. (1973) Visual stability and voluntary eye movements. *Hdb. Sensy. Physiol.* **VII/3A**, 307–331.
Mandelbaum, J. (1941). Dark adaptation. Some physiologic and clinical considerations. *Arch. Ophthal.* **26**, 203–239.
McColgin, F. H. (1960) Movement thresholds in peripheral vision. *J. opt. Soc. Am.* **50**, 774–779.
Merton, P. A. (1956) Compensatory rolling movements of the eye. *J. Physiol.* **132**, 25–27P.
Michael, J. A. & Stark, L. (1967) Electrophysiological correlates of saccadic suppression. *Exp. Neurol.* **17**, 233–246.
Mitchell, D. E. (1966) Retinal disparity and diplopia. *Vision Res.* **6**, 441–451.
Mitrani, L., Mateeff, St. & Yakimoff, N. (1970) Smearing of the retinal image during voluntary saccadic eye movements. *Vision Res.* **10**, 405–410.
Ogle, K. N. (1932) Analytical treatment of the longitudinal horopter; its measurement and application to related phenomena, especially to the relative size and shape of the ocular images. *J. Opt. Soc. Amer.* **22**, 665–728.
Ogle, K. N. (1950) *Researches in Binocular Vision.* Philadelphia: Saunders.
Ogle, K. N. (1953) Precision and validity of stereoscopic depth perception from double images. *J. opt. Soc. Am.* **43**, 906–913.
Ogle, K. N. (1958a) Note on stereoscopic acuity and observation distance. *J. opt. Soc. Am.* **48**, 794–798.
Ogle, K. N. (1958b) Present state of our knowledge of stereoscopic vision. *Arch. Ophthal.* **60**, 755–774.
Ogle, K. N. (1962) The optical space sense. In *The Eye*, Ed. Davson, vol. IV, chapters 11–18. London & New York: Academic Press.

Ogle, K. N. & Weil, M. P. (1958) Stereoscopic vision and the duration of the stimulus. *Arch. Ophthal.* **59**, 4–17.

Panum, P. L. (1858) *Physiologische Untersuchungen uber das Sehen mit zwei Augen.* Kiel.

Pirenne, M. H. (1943) Binocular and uniocular thresholds of vision. *Nature* **152**, 698–699.

Richards, W. (1977) Stereopsis with and without monocular contours. *Vision Res.* **17**, 967–969.

Riggs, L. A., Merton, P. A. & Morton, H. B. (1974) Suppression of visual phosphenes during saccadic eye movements. *Vision Res.* **14**, 997–1011.

Skavenski, A. A. (1971) Extraretinal correction and memory for target positon. *Vision Res.* **11**, 743–746.

Skavenski, A. A. & Steinman, R. M. (1970) Control of eye position in the dark. *Vision Res.* **10**, 193–203.

Smith, S. (1946) The essential stimuli in stereoscopic depth perception. *J. exp. Psychol.* **36**, 518–521.

Smith, S. (1949) A further reduction of sensory factors in stereoscopic depth perception. *J. exp. Psychol.* **39**, 393–394.

Stoper, A. E. (1967) Vision during pursuit movements; the role of oculomotor information. *Thesis.* (Quoted by Festinger *et al.*, 1976.)

Teichner, W. H., Kobrick, J. L. & Wehrkamp, R. F. (1955) The effects of terrain and observation distance on relative depth discrimination. *Am. J. Psychol.* **68**, 193–208.

Ten Doesschate, G. (1955) Results on an investigation of depth perception at a distance of 50 metres. *Ophthalmologica, Basel* **129**, 56–57.

Thorn, F. & Boynton, R. M. (1974) Human binocular summation and absolute threshold. *Vision Res.* **14**, 445–458.

Treisman, A. (1962) Binocular rivalry and stereoscopic depth perception. *Quart. J. exp. Psychol.* **14**, 23–37.

Volkmann, A. W. (1863) *Physiologische Untersuchungen in Gebiet der Optik.* Leipzig.

Volkmann, F. C. (1962) Vision during voluntary saccadic movements. *J. opt. Soc. Amer.* **52**, 571–578.

Walls, G. L. (1951) A theory of ocular dominance. *Arch. Ophthal.* **45**, 387–412.

Wertheimer (1912) Quoted by Graham (1965).

Wist, E. R., Brandt, T., Diener, H.-C. & Dichgans, J. (1977) Spatial frequency effect on the Pulfrich phenomenon. *Vision Res.* **17**, 391–397.

Zajac, J. L. (1960) Convergence, accommodation and visual angle as factors in perception of size and distance. *Am. J. Psychol.* **73**, 142–146.

Zuber, B. L., Stark, L. & Lorber, M. (1966) Saccadic suppression of the pupillary light reflex. *Exp. Neurol.* **14**, 351–370.

18. NEUROPHYSIOLOGY OF PERCEPTION: THE HIGHER VISUAL PATHWAYS

THE PRIMARY VISUAL PATHWAY TO THE CEREBRAL CORTEX

Optic Nerve and Tract

The ganglion cells of the retina (p. 205) are the second order neurones in the transmission of retinal impulses to the cerebral cortex; the axons of these cells constitute the *optic nerves* (N II) and *optic tracts*, passing either to the *lateral geniculate bodies* or the *superior colliculi* (the pupillary fibres, it will be remembered, pass to the pretectal region of the midbrain).

Decussation

The general plan of the visual pathway is indicated in Fig. 18.1; the fibres from the nasal halves of the retinae decussate in the *optic chiasma*, so that each optic tract contains fibres from the temporal half of one retina and the nasal half of the other. A visual impulse, arising from the right half of the field, is therefore conveyed exclusively along the left optic tract and thus to the left cerebral hemisphere. Section of the optic tract thus gives rise to what is called *homonymous hemianopia*, or half-blindness—one half of the visual field of each eye, the temporal half of the opposite side and the nasal half of the other, being obliterated. The degree of decussation varies from species to species and is obviously a function of binocular vision; thus in the guinea pig some 99% of the optic nerve fibres cross to the opposite side, leaving only 1% uncrossed; in the rat some 10% remain uncrossed; in the opossum 20%, whilst in the cat and primates, with frontally directed eyes, about equal numbers of fibres are crossed and uncrossed.

PHYLOGENY

Phylogenetically considered, then, the uncrossed fibres are the 'younger' ones and may be expected to subserve primarily stereoscopic perception of depth (Blakemore & Pettigrew, 1970). Thus in an animal with frontally developed eyes, as Fig. 18.1 shows, the temporal half of the retina of one eye is receiving an image of the same region of space as does the nasal half of the other. Hence with both laterally and frontally directed eyes, each cerebral

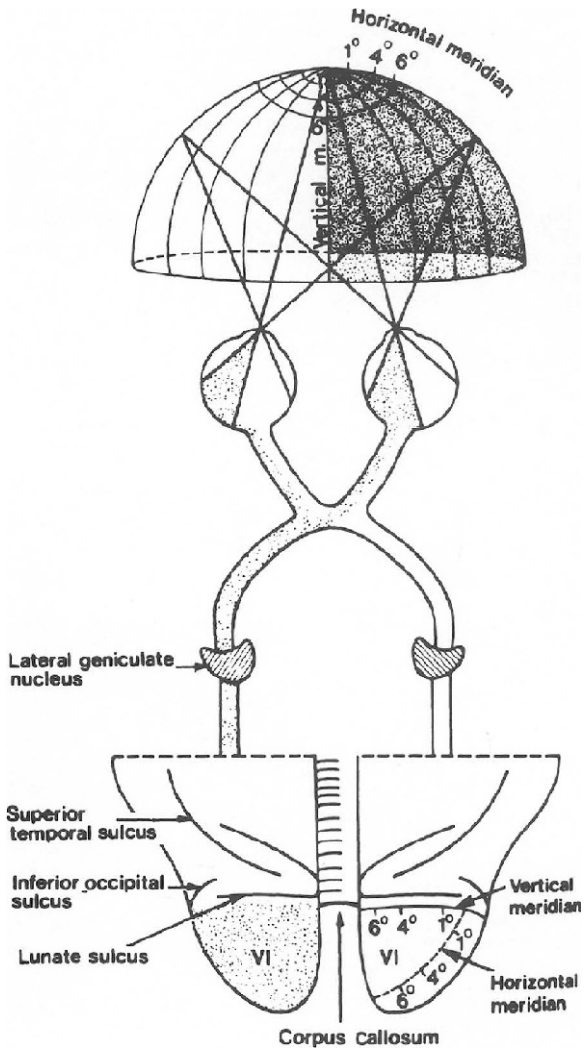

Fig. 18.1 Diagrammatic representation of the projections of the visuals pathway from retina to cortex in the rhesus monkey. The temporal retina of the left eye projects to the left hemisphere, that of the right eye to the right hemisphere. The nasal hemiretinae project to contralateral hemispheres. Regions of vertical meridian representation in the visual areas of the cortex are callosally connected, but these are not shown in the diagram. Only the posterior part of each hemisphere, as viewed from above, is shown. (Zeki, *Nature*.)

hemisphere receives information from the contralateral half of the visual world.

Arrangement of Fibres

The fibres are grouped in the nerve in three bundles according to the retinal fields from which they originate as follows:

1. Uncrossed temporal fibres.
2. Crossed nasal fibres.
3. Macular fibres.

Half of the macular fibres undergo decussation in the chiasma, so that half of the macula is represented in each tract. The relative positions of the bundles in the optic nerve and tract are indicated in Fig. 18.2.

The fibres vary in size, being divided roughly into coarse and fine; since the speed of conduction in a nerve fibre increases with its diameter, this variation in size must be associated with different conduction rates in the visual pathway. It is interesting that in the cat the fine, slowly conducting, fibres pass to the midbrain visual centres whilst the coarse fibres go to the visual cortex. So great is the difference in calibre of the fibres, that a visual impulse can be transmitted to the lateral geniculate body, relayed here to the cortex, and the cortical response may pass to the midbrain before the impulse reaches this region by way of the fine fibres directly. It is theoretically possible, therefore, for midbrain reflex activities to be anticipated and modified by cortical influences initiated by the same stimulus. In fact Doty (1961) states that the evoked potential recorded from the midbrain, in response to a light stimulus, appears some 12 msec after that recorded from the cerebral cortex of the cat.[1]

NON-GENICULATE TARGETS FOR RETINOFUGAL INPUT

In mammals and marsupials there are additional targets for the retinal fibres in addition to those relaying in the lateral geniculate body and thence passing to the cerebral cortex. These may be enumerated as follows:

1. Superior colliculus.
2. Accessory optic system.
3. Hypothalamus.
4. Pretectal complex.[2]

Collicular Fibres

In all species, including man, a portion of the optic tract fibres avoids the lateral geniculate body and goes to the superior colliculus in what has been called the *mesencephalic root of the optic tract* to distinguish it from the *diencephalic root* running to the lateral geniculate body. According to the position of the animal in the phylogenetic scale, the proportion of optic fibres travelling to the midbrain station changes: in birds there is very little cortical representation of retinal impulses, the vast majority of the optic fibres running to the optic tectum, or superior colliculus; in rodents the collicular projection is less, but still very significant, whilst in apes and man it is smaller. The fact that there is a projection of retinal fibres on the superior colliculus in man might suggest that visual responses to light would occur in the absence of an occipital cortex.

For a long time it was considered that ablation of the occipital cortex in primates, including man, led to complete blindness in the hemifield responsible for retinal input, except for pupillary responses, which are mediated by retinal input to pretectal regions. However, more recent studies have indicated that, in monkeys and in man, responses to visual stimuli do occur, mediated presumably by retinal inputs to thalamic nuclei that pass visual information to non-occipital cortex (p. 628).

Accessory Optic System

As described by Hayhow *et al.* (1960), the accessory optic system consists of a group of crossed finely medullated axons of retinal origin which is divided into *inferior* and *superior accessory optic tracts*. The inferior fasciculus is a group of fibres deviating from the course of the main optic tract and terminating in the dorsal portion of a prominent terminal nucleus in the midbrain tegmentum (Fig. 18.3); Hayhow *et al.* (1960) call this the *medial terminal nucleus*

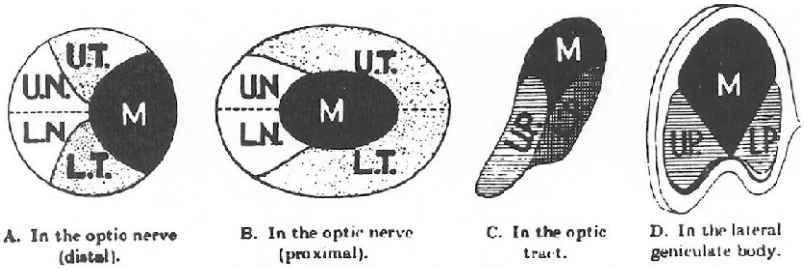

A. In the optic nerve (distal). B. In the optic nerve (proximal). C. In the optic tract. D. In the lateral geniculate body.

The crescents below U.P. and L.P. are the uniocular fibres.

Fig. 18.2 Distribution of the fibres in optic nerve, optic tract, and lateral geniculate body. U.T., upper temporal; U.N., upper nasal; L.N., lower nasal; L.T., lower temporal; U.P., upper peripheral; L.P., lower peripheral. (Wolff, *Anatomy of the Eye and Orbit.*)

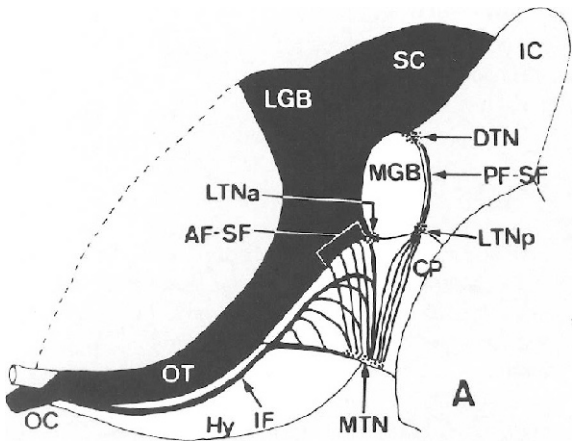

Fig. 18.3 Semischematic representation of the contralateral retinal central pathways in the rat taken by anterograde-filling retinal axons with HRP. The main pathway toward the lateral geniculate body and the superior colliculus, and the accessory optic system consisting of the inferior fasciculus (IF) and the superior fasciculus (SF) are shown by black areas or black lines. The locations of the medial terminal nucleus, the anterior portion of the laterial terminal nucleus, the posterior portion of the lateral terminal nucleus, and the dorsal terminal nucleus are shown by black dots. (Terebayashi & Fujisawa, *J. Comp. Neurol.*)

of the accessory optic system. The superior fasciculus is larger and more diffuse and terminates in the basal portion of the medial terminal nucleus, whilst more posterior fibres of the same fasciculus terminate additionally in two superficially located nuclei, which were called the *dorsal* and *lateral terminal nuclei of the optic tract*. This superior fasciculus includes the classically described *tractus peduncularis transversus* and *the posterior accessory optic tract* of Bochenegg, this latter also being described as *the basal optic root*.

Medial Terminal Nucleus

According to Giolli *et al.* (1984), the projections of this nucleus are of the utmost interest in so far as they show to what extent impulses from the retina, relaying here, are transmitted to lower brainstem regions. They used both antero- and retrograde tracers to follow the pathways, which are summarized in Fig. 18.4. It is clear that through these pathways the retina may influence large portions of the brainstem, and thus become involved in visually guided activity over a large range.

Suprachiasmatic Nuclei

A hypothalamic termination in the suprachiasmatic nucleus of the hypothalamus has been described, reached by what Moore & Klein (1974) describe as the retino-hypothalamic tract. For example, Moore & Lenn (1972) injected ^{3}H-leucine into the rat's eye and subsequently found label in this nucleus bilaterally; the labelling was confined to this hypothalamic nucleus so that the supraoptic nucleus, for example, had no activity. Electron microscopy after removal of the eye showed degenerating terminals on the dendrites of the neurones in the nucleus. The bilaterality of the projection is interesting and occurs even in the albino rat where all the remaining visual input is completely crossed; these authors showed that the hypothalamic projection was common to rat, guinea pig, rabbit, cat and monkey.

Circadian Rhythms

The significance of this hypothalamic projection becomes clear when we consider that, in many mammals, certain bodily functions, controlled by the hypothalamus, such as oestrus, exhibit a circadian rhythm dependent on the light-dark cycle. For example, rearing a rat in continuous light, produces a permanent state of oestrus, and the classical studies of Critchlow (1963) and Butler & Donovan (1971) have shown that these effects may be abolished by a lesion in the suprachiasmatic nucleus. The pineal gland, or epiphysis, is involved in circadian rhythms, but its anatomical location within the skull precludes its being influenced directly by light. Instead, the influence of light must be mediated through the central nervous system, culminating in a sympathetic supply from the superior cervical ganglion. Thus, interruption of this pathway—for example by removing the superior cervical ganglion—completely blocks the responses of the pineal to light or darkness (Wurtman *et al.*, 1964). The gland secretes a hormone, *melatonin*; and the cyclical activity of the gland depends on the cyclical synthesis or activation of the two key enzymes involved in its synthesis, namely hydroxyindole-O-methyltransferase (HIOMT) and serotonin-N-acetyltransferase. Thus the pineal exerts its action on oestrus and other activities through the secretion of melatonin, which inhibits the secretion of pituitary gonadotrophic hormones, the effect of light being to inhibit the secretion of pineal hormones and thus to release the pituitary from inhibitory control.

Retino-hypothalamo-pineal Pathway

The pathway to the hypothalamus apparently leaves the primary optic tracts separately from the accessory optic tracts, as indicated in Fig. 18.5. Moore & Klein (1974) made lesions that sectioned the primary optic tracts (*b*), or the accessory optic tracts (*c*),[3] or sectioned both the primary and accessory optic tracts (*d*) leaving the retinohypothalamic tract intact, and finally one that destroyed the retinohypothalamic tract at the same time as the suprachiasmatic nuclei (*e*). Lesions that involved the

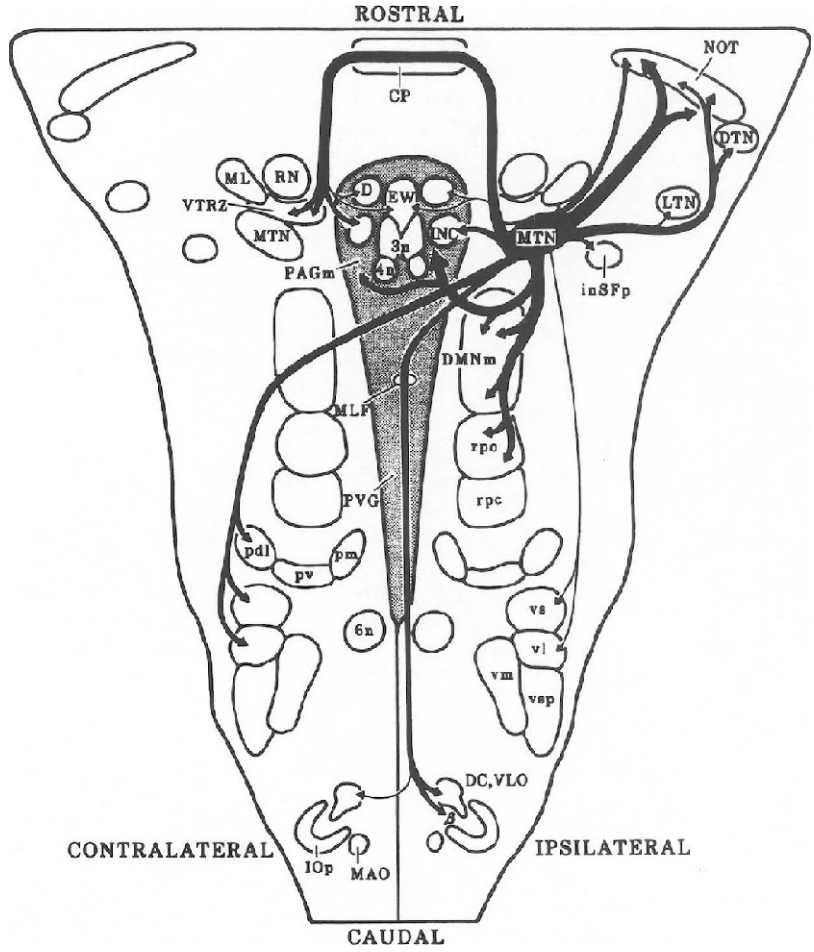

Fig. 18.4 Schematic representation of the brain stem illustrating the projections of the rabbit medial terminal nucleus (MTN). The plane of the section depicted is horizontal, but the nuclei in the ventral midbrain tegmentum, basilar pons, and inferior olive are drawn as in transverse plane. Arrows depict the MTN projections, and arrow thicknesses their relative sizes. The ipsilateral, contralateral and bilateral distributions of these projections are indicated. Principal abbreviations: LTN, DTN: lateral and dorsal terminal nuclei; NOT: nucleus of optic tract; CP: posterior commissure; INC: internal capsule; EW: Edinger-Westphal nucleus; D: Nucleus of Darkschewitsch; DMNm: deep mesencephalic nucleus; rpo: pontine reticular nucleus, pars oralis; rpc: pars caudalis. (Giolli *et al.*, *J. Comp. Neurol.*)

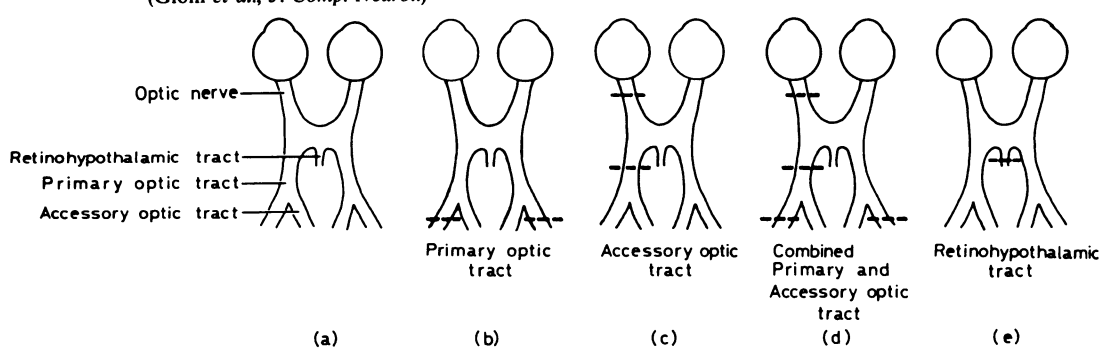

Fig. 18.5 The optic tracts (a) and sections made to elucidate the different pathways. (After Moore & Klein, *Brain Res.*)

suprachiasmatic nuclei and retinohypothalamic pathway completely abolished the rhythmic changes in N-acetyltransferase activity associated with the light-dark cycle. On the contrary, bilateral lesions involving the primary or accessory optic tracts or both were without significant effects. The probable pathway from the suprachiasmatic nucleus to the superior cervical ganglion is indicated in Fig. 18.6.

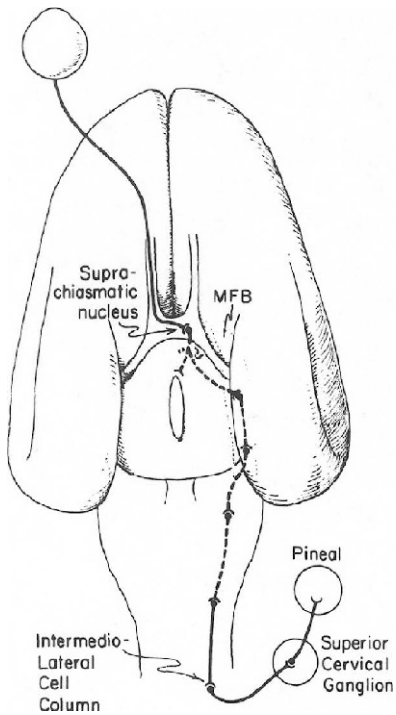

Fig. 18.6 Diagram of proposed central neural pathway regulating pineal N-acetyltransferase activity. Photic input from the eyes traverses the retinohypothalamic tracts to the suprachiasmatic nuclei. From these nuclei information passes through the lateral hypothalamus and brain stem, in unidentified pathways, to the spinal cord and the interomediolateral cell column whose neurons provide preganglionic fibres to the superior cervical ganglia. The dashed lines indicate areas where the exact fibres transmitting information have not been identified with certainty. (Moore & Klein, *Brain Res.*)

Tonic and Rhythmic Light Effects

If it is the retinohypothalamic system that provides the light-information to the circadian rhythm centre, we may ask what function the accessory optic system, terminating in the nuclei of the optic tract, fulfils? Stephan & Zucker (1972) emphasized the distinction between tonic effects of light on bodily function and the rhythmic or phasic effects manifest in circadian rhythms. According to this distinction, the circadian rhythm would be influenced by the light-input through the suprachiasmatic nuclei and pineal gland, whereas the non-rhythmic effects of continuous exposure to light or dark might be influenced by the accessory system.

Pretectal Fibres

These leave the primary optic tract before it enters the lateral geniculate body and relay in a group of midbrain nuclei. The fibres carry the visual input to the pupillomotor and accommodative muscles of the eye, and will be discussed in these contexts.

The Pulvinar

This thalamic nuclear mass is remarkable for its great expansion in primates. Its close connection with the lateral geniculate nucleus, and its projections to cortical regions that may be described as visual, acoustic and somatosensory association areas, suggest an important function in the processing of visual information. Thus Hassler & Wagner (1965) described a case of human congenital anophthalmia in which there was a striking reduction in the size of the inferior pulvinar. As Trojanowski & Jacobson (1976) state, it is a polysensory nucleus relying largely on the *cerebral cortex* for its sensory input and projecting to polysensory areas of cortex, being involved in processing polysensory information a long way removed from the synapses of the primary stimuli.[4]

Visual Thalamic Nuclei

The nomenclature respecting the visual nuclei of the thalamus is confusing and has been clarified, so far as the cat is concerned, by Mason (1978) with special reference to the nuclei of the lateral and posterior thalamic group which includes the pulvinar. Figure 18.7 illustrates the nuclei, based on Niimi & Kuwahara's (1975) cytoarchitectonic study; they may be summarized as follows (Mason, 1978):

Lateral Nuclear Group	Dorsal Lateral Nucleus
	Posterior Lateral Nucleus
Posterior Nuclear Group	Lateral Geniculate Complex
	'Pulvinar Complex'
	Suprageniculate Nucleus

Divisions

The pulvinar complex has been differentiated architectonically into three divisions, namely the *inferior*,

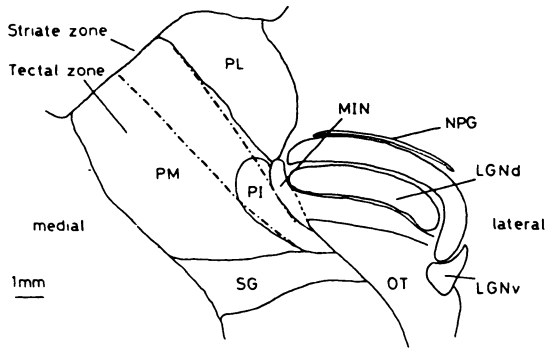

Fig. 18.7 Diagram of the nuclei of the cat's visual thalamus in transverse section (the lateral and posterior nuclear groups and the lateral geniculate complex). PI, inferior pulvinar; PM, medial pulvinar; PL, lateral pulvinar; SG, suprageniculate nucleus; LGNd, dorsal lateral geniculate nucleus; LGNv, ventral lateral geniculate nucleus; MIN, medial interlaminar nucleus; NPG, perigeniculate nucleus; OT, optic tract. (Mason, *Exp. Brain Res.*)

medial and *lateral*, although, as Mason (1978) has emphasized, these architectonic divisions do not correspond strictly with divisions based on cortical and subcortical projections. In phylogenetic development the pulvinar has become larger, and the divisions into inferior, medial and lateral have become more pronounced (Harting *et al.*, 1972).

Further details regarding the projections and neuronal activities of these 'lower visual centres', especially the superior colliculus and the nuclei of the lateral and posterior group of thalamic nuclei, including the pulvinar, will be left until later, and we may proceed to a description of the lateral geniculate pathway.

LATERAL GENICULATE BODY

In primates including man the cells of the dorsal lateral geniculate body, or nucleus, are arranged in six laminae, the four most dorsal being described as parvocellular and the two most ventral magnocellular; the fibres of the optic tract synapse with relay- or principal cells in these laminae. It was shown by Glees & Clark (1941) that the crossed optic fibres end in layers one, four and six, whilst the uncrossed, temporal fibres synapse with cells in layers two, three and five (Fig. 18.8). There thus seems to be a rigid separation of the fibres arriving from the two eyes, so that the fusion of the two retinal images required by binocular vision cannot apparently take place at this level.[5] In this respect, then, we may regard the lateral geniculate body as a sorting centre that rearranges the crossed and uncrossed fibres that had become quite mixed in the optic tract. By noting the distribution of transneuronal atrophies following small retinal lesions,

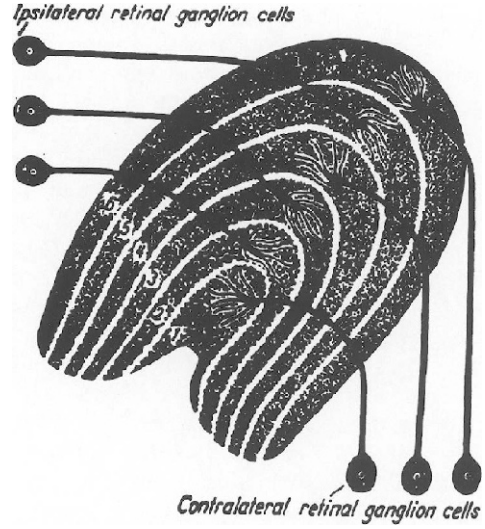

Fig. 18.8 Illustrating the segregation of the optic tract fibres into the separate laminae of the lateral geniculate body in primates. Fibres from the contralateral retina, i.e. the crossed fibres, relay in layers 1, 4 and 6. (Glees, in *The Visual System.*)

Penman (1934) showed that there is a virtual 'point-to-point' representation of the retina in the lateral geniculate body, thereby ensuring that the one-to-one relationship between cones of the fovea, bipolar and ganglion cells is carried through as far as this stage in the visual pathway.

Optic Tract Terminations

Each nerve fibre of the optic tract, after entering its lamina, breaks up into a number of terminals, each ending in a 'bouton' applied to a lateral geniculate body cell; each cell has only one bouton applied to it, so that there is no overlapping of impulses from different retinal receptors. (In the cat, on the other hand, there are a large number of boutons to each cell—in this animal visual acuity is subservient to sensitivity to light.) The terminal branches of each optic tract fibre end on up to thirty lateral geniculate cells. Since each geniculate cell receives a bouton from only one optic tract fibre, there should be some 10 to 30 times as many geniculate cells as optic tract fibres, yet the numbers appear to be about equal.

Lamination in the Cat

The large amount of experimental work on the visual physiology of the cat has required a detailed study of the structure and synaptic arrangements in this thalamic nucleus. The classical study of Thuma (1928) differentiated three layers, described as A, A_1 and B; A and A_1

had strong morphological similarities whilst B was different from the other two; the transneuronal degeneration following removal of one eye suggested A and B received retinal fibres from the contralateral eye, whilst layer A_1 received fibres from the ipsilateral eye; thus A and A_1 would be concerned with the binocular field and would provide a basis for keeping the inputs from the two eyes separate. Peters & Palay (1966) confirmed the lamination, but described thin layers of neurones between the laminae which they called the nucleus interlaminaris centralis, whilst Guillery (1969) has indicated a more complex lamination, layer B being replaced by three layers, C, C_1 and C_2 (Fig. 18.9) differing morphologically mainly by the size of their cells, although transitions between layers are not sharp. Degeneration experiments indicated that layers C and C_1 were analogous with A and A_1, in the sense that they received retinal inputs from contralateral and ipsilateral eyes respectively; and it seemed that C_2 received no retinal input.

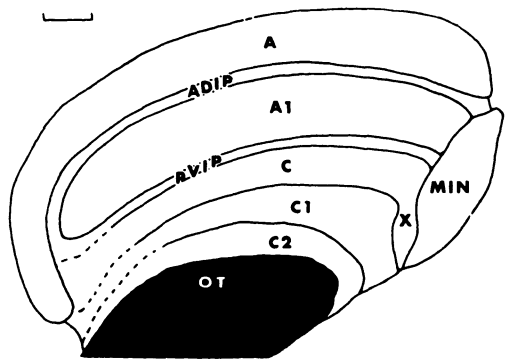

Fig. 18.9 Sketch indicating lamination of cat's dorsal lateral geniculate nucleus as seen in a frontal section through the rostral third. MIN, medial interlaminar nucleus; X shows the part of the lamina, C, that is continuous with the lateral aspect of the medial interlaminar nucleus. ADIP and PVIP indicate the anterodorsal and posteroventral leaflets of the interlaminar plexus. Scale: 500 μm. (Guillery, *J. Comp. Neurol.*)

SUBDIVISION

By employing the axonal transport of radioactive tracer as a marker for fibre terminations, a technique that gives much better definition of terminals so that fibres of passage are easily distinguishable from those of termination (Hickey & Guillery, 1973), it was possible to differentiate four laminae in addition to A and A_1 namely C, C_1, C_2, and C_3, this last having no retinal projection.[6] Laminae A and C and C_2 received afferents from the contralateral eye and laminae A_1 and C_1 received afferents from the ipsilateral eye. There was no evidence of binocular overlap within the nucleus. As indicated by Fig. 18.1, the parts of the retina that are concerned with monocular vision are the extreme nasal areas corresponding to the temporal fields, and electrophysiological evidence indicates that this essentially monocular input is confined to a separate part of the lateral geniculate body, which might be lamina C of Guillery, and might constitute a part of lamina B of Thuma and others.[7]

Medial Interlaminar Nucleus

The lateral geniculate nucleus of carnivores, in addition to the laminated regions just described, contain the medial interlaminar nucleus (MIN; Fig. 18.9). It would seem that, whereas the laminated regions project to Areas 17 and 18 in the cat, MIN projects to Area 19 (Rosenquist *et al.*, 1974) and to other suprasylvian areas. Although categorized as the unlaminated region of the dorsal lateral geniculate nucleus, Guillery *et al.* (1980) and Lee *et al.* (1984) have shown that it is made up of three distinct layers, each receiving inputs from one hemiretina but none representing an entire hemifield. The contralateral field is represented in layers 1 and 2 through the contralateral and ipsilateral eyes respectively, and layer 3 represents the ipsilateral hemifield through the contralateral eye (Guillery *et al.*, 1980). Lee *et al.* (1984) have emphasized that the retinotopic input to this region closely corresponds with that region of the carnivore retina backed by a tapetum, and have suggested that it relays, specifically, input at very low luminances that would be concerned with motion-detection rather than spatial resolution. Its relays to suprasylvian areas, such as the Clare-Bishop area, concerned with motion-sensitivity, would support this view.[8]

Significance of Lamination

The basic function achieved by lamination is clearly to keep the retinal inputs from the two eyes separate; this means that the integration of the inputs from the two eyes, to give a single field of vision, is primarily a function of the cerebral cortex. Although it is customarily stated that it is only in the cortex that neurones are found driven binocularly, this is not strictly true as there are interlaminar connections within the geniculate that permit effects of visual stimulation in both eyes to be transmitted to single geniculate neurones.

Ventral Nucleus

The function of this much smaller and morphologically distinct portion of the lateral geniculate body is by no means clear (Swanson *et al.*, 1974). It receives input from the optic tract through collaterals relaying in the dorsal nucleus, from the superior colliculus (Gilbert & Kelly, 1975) and from the visual and juxta-visual areas of the cerebral cortex, and finally from the dorsal nucleus.

Efferent Connections

Its efferent connections were studied by Swanson *et al.*, using the transport of radioactive leucine as a marker;

these proved to be the pretectal nuclei, the lateral terminal nuclei of the accessory optic system, the ventral portion of the suprachiasmatic nuclei of the hypothalamus, and the superior colliculus; all these regions receive retinal projections and, except for the colliculus, the ventral geniculate input coincides with the retinal. (The ventral geniculate input to the colliculus was confined to the deeper layers.) There was no evidence for a cortical projection.

Pregeniculate Nucleus

The ventral nucleus of the lateral geniculate body of mammals, such as the cat, is clearly separated from the dorsal nucleus by a neurone-free lamina. The equivalent structure in the primate is the pregeniculate nucleus. In man, Preobrazhenskaya (1964) followed the changes in the lateral geniculate body during embryonic and fetal development and described, in the early stages, the separation into ventral and dorsal nuclei; at later stages, after 5 months, the ventral nucleus is no longer seen and its place is taken by a group of small faintly staining cells, the *pregeniculate nucleus* (PrGN), lying over the rostral part of the lateral geniculate body, which has now become a layered structure. In the infant the connexion between the PrGN and the zona incerta is clear, and the author considers that the PrGN, developing as it does in close association with the LGN, is, indeed, part of the visual system and also part of the thalamic reticular formation.

POSSIBLE FUNCTION

The similarity in projections of the retina and the ventral geniculate or pregeniculate nucleus has suggested to Swanson *et al.* that the ventral nucleus might play a centrifugal role, comparable with that played by the isthmo-optic nucleus on the amacrine cells of the pigeon retina; in the case of the mammal, however, the centrifugal effect would be directed to higher brain centres than the retina, such as the superior colliculi, pulvinar, and so on.

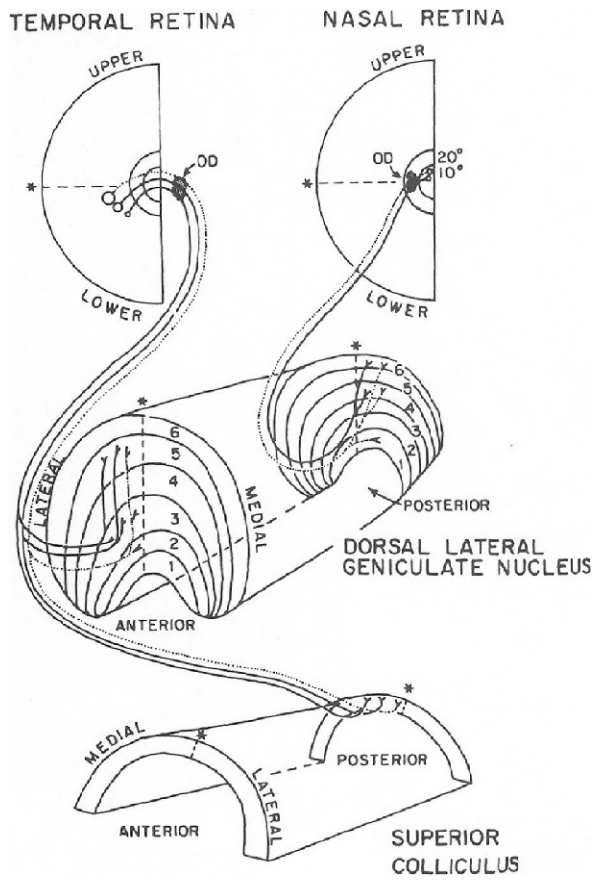

Fig. 18.10 Summary diagram of the organization of the primate visual system. Ganglion cells of all sizes project to the outer four laminae of the dorsal lateral geniculate nucleus, while only the largest cells of the more peripheral retina project to the inner two layers. All ganglion cells of the parafoveal region project to the parvocellular layers, but only some project to the magnocellular layers of the dorsal lateral geniculate nucleus. Scattered ganglion cells of all sizes project to the superior colliculus. * = horizontal meridian; OD = optic disc. (Bunt *et al.*, *J. comp. Neurol.*)

Retinotopic Projection

As we should expect from the orderly projections of fibres from the retina through the optic tracts and their terminations in the laminae of the lateral geniculate bodies, there is a strict retinotopy in the relation of retinal points to given points in the dorsal lateral geniculate nucleus (Bishop *et al.*, 1962). In the primate, Bunt *et al.* (1975) traced the terminations of ganglion cell fibres in the dorsal nucleus by retrograde staining with horseradish peroxidase. Their conclusions regarding retinotopy are illustrated by Fig. 18.10. It will be noted that large Y-cells project to both superior colliculus and geniculate nucleus, a branching that has been established electrophysiologically.

The Decussation

Laterality of Projection

As illustrated in Fig. 18.11 the classical representation of the decussation is such as to split the retinal fields down their centres, so that right-sided events are represented in the left lateral geniculate nucleus; this means that ganglion cells in the temporal half of the retina are ipsilaterally (uncrossed) represented, and the nasal cells are contralaterally (crossed) represented.

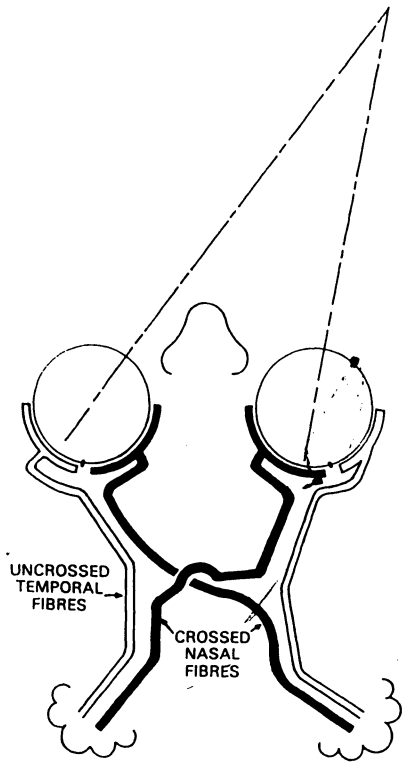

Fig. 18.11 The decussation of the nasal retina fibres results in splitting the visual field through the vertical meridian so that right-sided events in the visual field are represented in the left visual cortex.

Bilateral Strip

Cooper & Pettigrew (1979a) made large injections of horseradish peroxidase into the cat's lateral geniculate nucleus and followed uptake into the retina; in this way the degree of decussation of the geniculocortical pathway is assessed, whereas studies based on optic tract section do not discriminate between this and other projections (Fukuda & Stone, 1974). After injection into one geniculate body a clear line of division along the retinae was found, but it was by no means perfect, and measurements of the relative densities of stained cells in contra- and ipsilateral halves of the retina showed a preponderance of projection in the contralateral retina, suggesting that there was a region of overlap that brought the peak density slightly away from the median edge. In other words there was a strip of bilateral representation running down the centre of the area centralis, as originally suggested by Stone (1966). The median strip of overlap was about 100 μm nasal and 100 μm temporal. Practically all the contralaterally projecting cells in the temporal retina were Y's, so that the decussation of X-cells is strictly at the vertical meridian of the retina (Kirk *et al.*, 1976). It is likely that these retinal Y-cells project to the medial interlaminar nucleus (MIN), the major input to this region being by way of Y-cells (Mason, 1975; Kratz *et al.*, 1978).[9]

Morphological Aspects of Neuronal Circuitry

Neurones of the Dorsal Nucleus

The principal neurones of the dorsal nucleus are the relay-neurones (also called 'principal neurones'), receiving postsynaptic input from the optic tract neurones and transmitting to neurones of the cerebral cortex. Within the nucleus there are also 'intrinsic' neurones, characterized as Golgi Type II, which are interneurones involved in intrageniculate integration of afferent input. In the cat, Dubin & Cleland (1977) described two groups of these interneurones; one group, *intrageniculate*, have cell-bodies within the nucleus and the other, *perigeniculate*, have their cell-bodies immediately above the LGNd at its border with the perigeniculate nucleus. The receptive-field characteristics of the intra- and peri-geniculate cells were characteristically different (p. 506), and Dubin & Cleland suggested the model for organization illustrated by Fig. 18.12, both types of interneurones being respon-

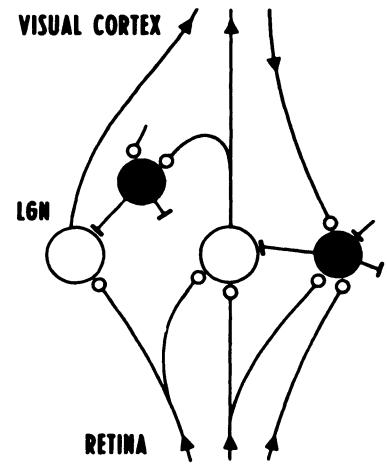

Fig. 18.12 Summary diagram showing principles of organization of the lateral geniculate nucleus. Relay cells (open circles) are shown receiving direct, excitatory retinal inputs as well as inhibitory interneuronal inputs. Interneurones (filled circles) of both types are depicted. An intrageniculate interneurone (right) is placed at the same level as the relay cells to indicate its position within the geniculate laminae. Direct retinal inputs as well as proposed cortical efferent input are shown as being excitatory to such interneurones. A perigeniculate interneurone (left) is placed above the other cells, indicative of its position just above geniculate lamina. A recurrent collateral and other, presently undefined, input is shown exciting such interneurones. (Dubin & Cleland, *J. Neurophysiol.*)

sible for inhibition; the relay-cells, indicated by open circles, are subjected to a feedback inhibition from a perigeniculate neurone and a feed-forward inhibition from an intrageniculate neurone, which probably corresponds to Guillery's Class III neurone.

The Synaptic Glomerulus

Szentagothai (1963) described the electron microscopy of this anatomical unit, which he likened to the glomerulus of the cerebellum in which the terminals of mossy fibres synapse with granule cell dendrites. In the lateral geniculate nucleus it is seen as a group of profiles in the neuropil, relatively isolated from other neuron profiles by glial cell processes and consisting of axodendritic synapses on short dendritic appendages of presumably geniculo-cortical relay cells. According to Peters & Palay (1966), within the glomerulus there was a large centrally placed axon forming an axis about which dendrites, dendritic thorns and peripheral axons are placed, the central axon being presynaptic to all other processes including peripheral axons (Fig. 18.13). Guillery (1969) recognized 4 types of axon, RLP derived from the optic nerve; RSD, derived from the cerebral cortex, and F_1 and F_2, two types of intrageniculate fibre, whose structures were examined in detail by Famiglietti & Peters (1972), and which are presumably axons of the interneurones described functionally by Dubin & Cleland (1977).[10]

ELECTROPHYSIOLOGY OF THE HIGHER VISUAL PATHWAY

Ganglion Cells

Centre-surround Organization

The organization of the receptive fields of the ganglion cells of the retina has been described earlier; to recapitulate, the basic organization is circular, with a central spot and a surrounding annulus responding in opposite fashions; thus we may have a field in which an ON-response occurs when the light stimulus is projected onto this region of retina whilst the surrounding annulus gives an OFF-response, i.e. switching the light on does not excite, in fact it causes inhibition of the background spontaneous discharge if this is present. On switching the light off, there is a prominent OFF-discharge. This unit would be called an ON-centre unit. Quite clearly, then, by the time the responses of the cones or rods have been transmitted through the ganglion cells there has been a considerable elaboration, of which a prominent feature is inhibition. We have seen how this type of unit, acting in conjunction with others, can signal movement and even the specific direction of the movement; in addition, too, the signals of many of the units have become colour-coded in a different manner from the coding found in the receptors themselves, so that a given 'dominator-type' for example, can indicate by its frequency of discharge the prevailing

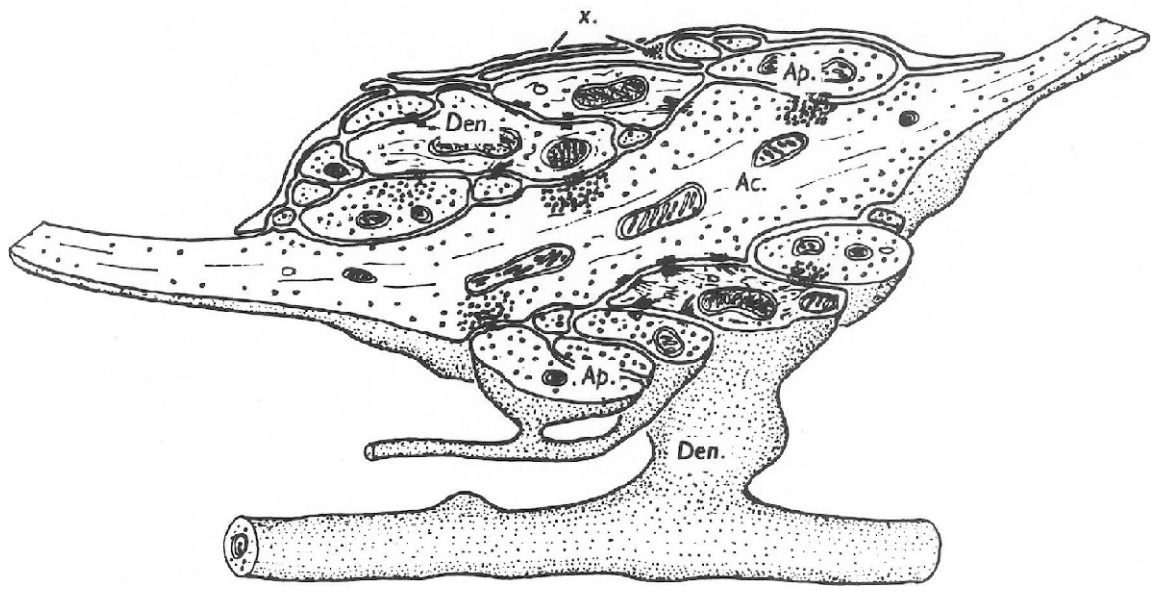

Fig. 18.13 A diagrammatic representation of the structure of a geniculate glomerulus. The central axon terminal (*Ac.*) forms the axis of the structure, and is surrounded by processes of dendrites (*Den.*) and peripheral axon terminals (*Ap.*). The whole is enclosed by astrocyte processes (*x.*) (Peters & Palay, *J. Anat.*)

luminosity independently of the colour of the light, whilst others, modulators, will respond only to a relatively narrow band of wavelengths. Furthermore, the phenomenon of colour-opponence, in various forms, has become manifest.

Geniculate Neurones

X- and Y-cells

Neurones of the dorsal lateral geniculate nucleus exhibit the X-Y-dichotomy seen in the retina, due to specific projections from the ganglion cells.

Retino-geniculate Terminations

Sur & Sherman (1982) and Sur *et al.* (1982) identified the axons of optic tract neurones within the lateral geniculate nucleus and characterized them electrophysiologically as either X- or Y-type. After characterization the axon was injected with horseradish peroxidase and prepared for morphological study.

Figures 18.14 and 18.15 illustrate reconstructions of the terminations of an X- and a Y-cell. Every retinogeniculate axon has the greatest part of its terminal arbour in lamina A or A1 according to whether it is from the contra- or ipsilateral eye. No terminal bouton was found in an inappropriate lamina. The axons, on the way, branch within the optic tract, one branch going to the dorsal lateral geniculate nucleus and the other going medially and rostrally towards the midbrain. Within the geniculate nucleus there is also some branching; thus occasionally an X-axon went to the medial interlaminar nucleus (MIN) and more rarely to the C-laminae; nearly all Y-axons from the retina innervated the MIN and those from the contralateral eye innervated the C-laminae. In general, any Y-axon sent many more terminal boutons to the different regions of the nucleus than did X-axons, so that the Y-pathway tends to diverge more strongly than the X-pathway, the Y-neurones innervating more geniculate neurones and therefore altering the X:Y ratio in their favour by comparison with that in the retina.

Ramifications

The ramifications of an X- and a Y-neurone, injected with horseradish peroxidase, within the layers of the cat's lateral geniculate nucleus are shown in Fig. 18.16. In a comparable study on the primate nucleus, Wilson *et al.* (1984) compared the morphologies of their dendritic complexes and the nature of their synapses. Fine-structural differences between the two types of cell resided entirely in the synaptic arrangements; thus the triadic type of synapse, involving a retinal terminal, is much more frequent on the X-cell dendritic complex. Included in the triad were so-called f_2-terminals with flattened vesicles and probably representing inhibitory input from intrinsic neurones. The total number of dendritic contacts was 4000 on the X-cell and 5000 on the Y-cell.

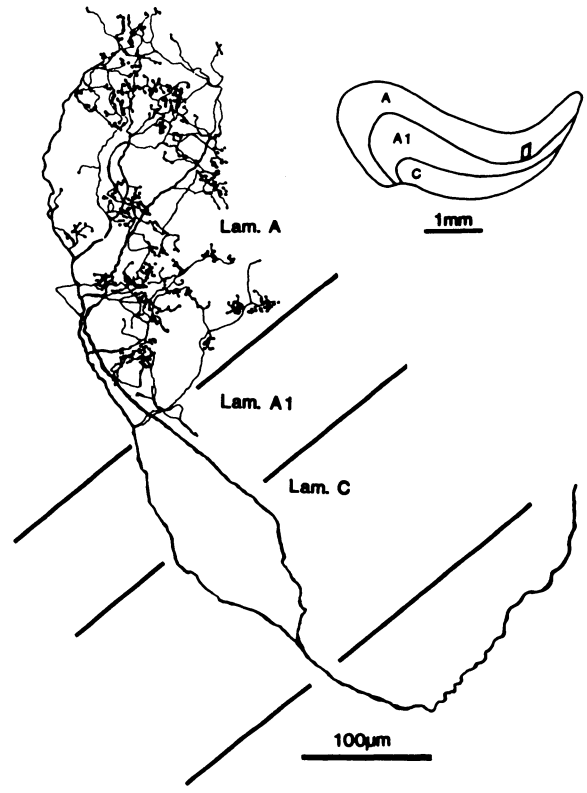

Fig. 18.14 Sagittal view of reconstruction of X-axon from left retina innervating the right lateral geniculate nucleus. Although only lamina A is innervated in the lateral geniculate nucleus, a branch of the axon (not illustrated) continues medially to enter the brachium of the superior colliculus. The box in the *inset* drawing of the lateral geniculate nucleus shows the location of the axon's terminal arbour. (Sur *et al.*, *J. Neurophysiol.*)

W-cells

Stanford *et al.* (1983) have described the morphology of the cat's W-cells, established by the same technique of microelectrode penetration with subsequent injection of horseradish peroxidase. They compared this with that of X- and Y-cells established by the same technique by Friedlander *et al.* (1981) and Friedlander *et al.* (1985). They concluded that the morphology of W-cells was quite distinct from that of X- and Y-cells, and that the dendritic organization of the W-cells might subserve the convergence of large numbers of units to give large receptive fields. They comment on the probably high efficiency of

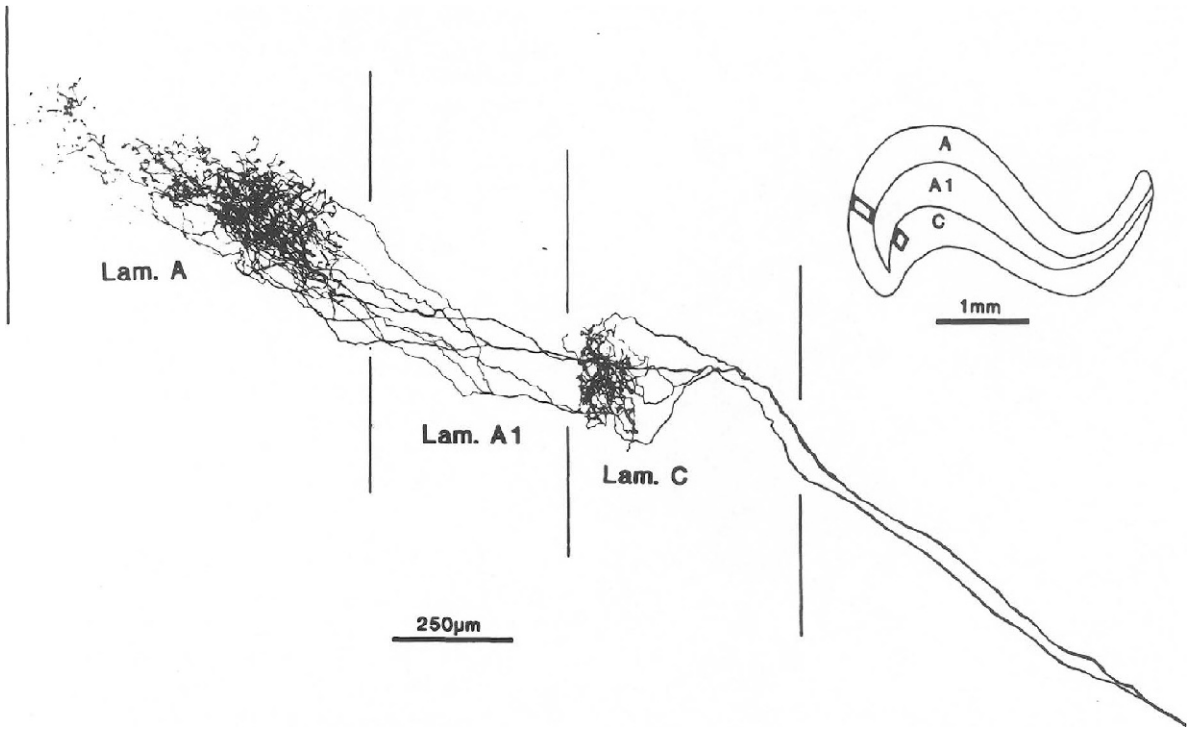

Fig. 18.15 Sagittal view of reconstruction of Y-axon from right retina innervating the left lateral geniculate nucleus; The axon terminates both in lamina A and in the C-laminae, with no boutons in lamina A1. A branch of the axon in the optic tract (not illustrated) courses medially and could not be followed; it may innervate the medial interlaminar nucleus and/or enter the brachium of the superior colliculus. (Sur *et al.*, *J. Neurophysiol.*)

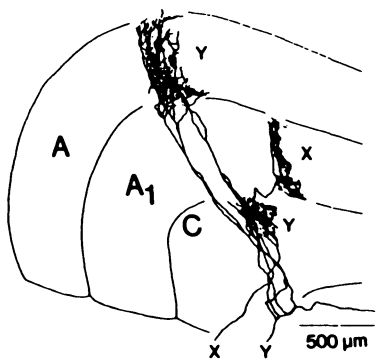

Fig. 18.16 Drawings from a single parasagittal section of two nearby arbours, an X and a Y type, made using a × 100 oil objective. The drawings illustrate the detail that is visible in the sections. They show that X and Y axons differ in the size and shape of their arbours and in the density of their terminal boutons. (Bowling & Michael, *J. Neurosci.*)

synaptic transmission to Y-cells that would make them suitable for transmitting rapidly occurring changes. Figure 18.17 compares X-, Y- and W-cells.

Comparison of Geniculate with Ganglion Cell Responses

A study of the lateral geniculate neurones, e.g. by Hubel & Wiesel (1961), has revealed essentially the same basic organization of receptive fields, characterized by ON-centre–OFF-surround, and *vice versa*. Thus, to a large extent, the geniculate cell is reflecting the input it receives from ganglion cells, an ON-centre type ganglion cell imposing its ON-centre feature on the geniculate cell with which it synapses (Levick *et al.* 1972).[11]

INHIBITION

However, as Hubel & Wiesel emphasized, there is a considerable accentuation of the inhibitory action, revealed typically by the change in response of an ON-centre cell as a spot-stimulus is enlarged. This is illus-

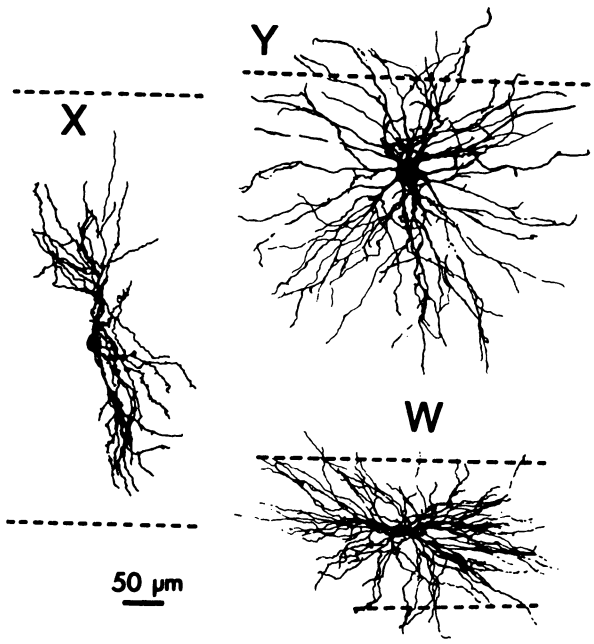

Fig. 18.17 Camera lucida drawings of a W-cell, X-cell, and Y-cell at the same scale for comparison. Laminar borders are indicated by dashed lines. These cells typify many of the morphological differences among classes. The W-cell is located in lamina C2 and/or C3. Some of its dendrites extend ventrally into the optic tract and others extend dorsally into lamina. C1. Its soma is small, its dendrites are thin and varicose, and its dendritic arbour is elongated parallel to the laminar borders. The X-cell soma is located in lamina A1, and its dendrites are entirely confined to that lamina. Its soma is small, its dendrites are thin and have numerous complex, stalked appendages, and its dendritic arbour is elongated perpendicular to the laminar borders. The Y-cell soma is located in lamina A1, and some of its dendrites extend dorsally into lamina A. Its soma is large, its dendrites are thick and have few spinelike appendages, and its dendritic arbour is fairly spherical in shape. (Stanford *et al.*, *J. Neurophysiol.*)

trated by Fig. 18.18 where the microelectrode was recording from an optic tract fibre simultaneously with a geniculate cell. (A) shows the responses to both units when a small light-spot falls on the centre of the receptive field; the optic tract fibre, being on ON-centre one, gives a burst of spikes which are distinguishable from those of the geniculate fibre by their being monophasic and small. The response of the geniculate fibre appears at OFF as large disphasic spikes. Increasing the size of spot, so that the stimulus now falls on the surrounding annulus of opposite response characteristics, has almost completely inhibited the geniculate response, but has had only slight effect on the tract fibre (B). In C the spot has been made much larger, and the geniculate response is virtually abolished and the tract response is reduced. In D only the surround has been stimulated, and now the large diphasic spikes appear first at ON, and the small tract spikes at OFF. Thus the geniculate cells differ quantitatively in the degree of 'surround antagonism'; to such an extent indeed does this occur that diffuse illumination, because it stimulates both centre and surround of the receptive field, has little effect on geniculate cells.

Value of Inhibition Thus, by application of inhibition, Nature has reduced the tremendous bombardment of the visual cortex that would occur continuously as long as the eyes were open in the light; instead, many neurones remain silent and are ready to responsd to what is important in the environment, namely the contrast involved in contours and the effects of a moving stimulus, be it light or dark, which, passing across the concentric receptive fields, has a definite effect.

Sustained and Transient Types

As with the ganglion cells, the geniculate units can be separated into two main types, sustained or X-, and transient or Y-cells. Simultaneous recording from ganglion and geniculate cells showed that there was a functional segregation, so that a given sustained geniculate cell received input from one or more sustained ganglion cells. The similarity extended to conduction-velocities, so that fast-conducting axons from ganglion cells synapsed with fast-conducting geniculate cells (Cleland *et al.*, 1971); this is understandable, since Y-axons conduct more rapidly than the X-axons.

Cleland Classification

When Cleland *et al.* (1976) applied their more elaborate classification to ganglion cells, in an examination of input to lateral geniculate neurones, they were able to extend this classification to these neurones, identifying not only the sustained and transient (X- and Y-) categories but also more rarely encountered sluggish sustained and sluggish transient neurones. As the scatter-diagram of Fig. 18.19 indicates, there is a fair correlation between the cortico-geniculate antidromic latency and the retino-geniculate latency, suggesting that relay to the cortex is carried out by geniculate neurones having the same features as those of the ganglion cells that transmit to them. There were some exceptions, but these could have been due to mixed inputs from retina to geniculate neurone. Finally, we may note that Wilson *et al.* (1976), retaining their W-X-Y-classification, derived the input relations illustrated by Fig. 18.20.[12]

W-CELLS

Sluggish neurones with conduction velocities lower than those of X- and Y-cells, typically found in the C laminae

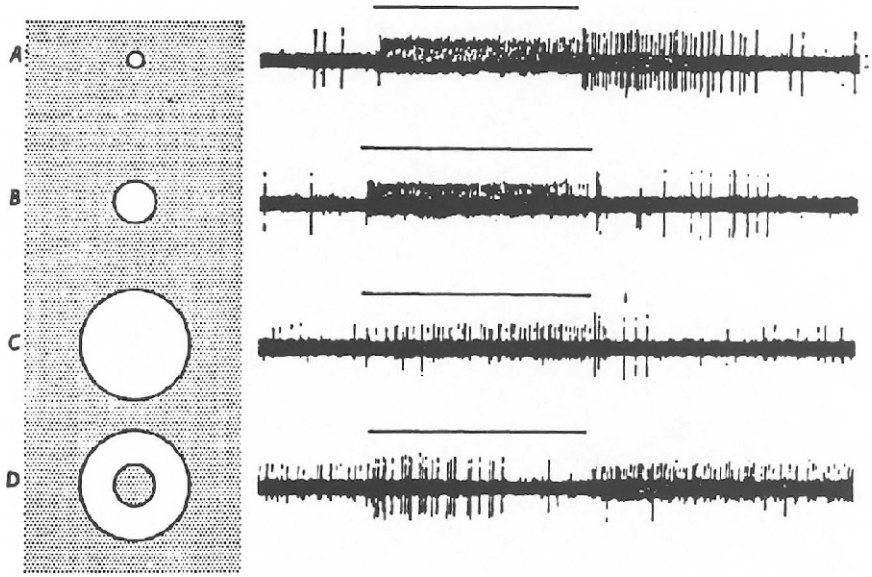

Fig. 18.18 Simultaneous recording from optic tract fibre and from geniculate neurone; the optic tract fibre gives small monophasic spikes. A. The small light-stimulus falls on the centre of the receptive field; the optic tract fibre is excited at ON (it is ON-centre) whilst the geniculate one is excited at OFF (it is OFF-centre). B. The larger stimulus, covering both central region and surrounding region of opposite characteristics, causes almost complete inhibition of the geniculate response. C. The stimulus is larger and has now reduced the optic tract response as well. D. Only the surround is stimulated, and the geniculate neurone has fired at ON and the tract neurone at OFF. Horizontal lines above records indicate duration of light stimulus. (Hubel & Wiesel, *J. Physiol.*)

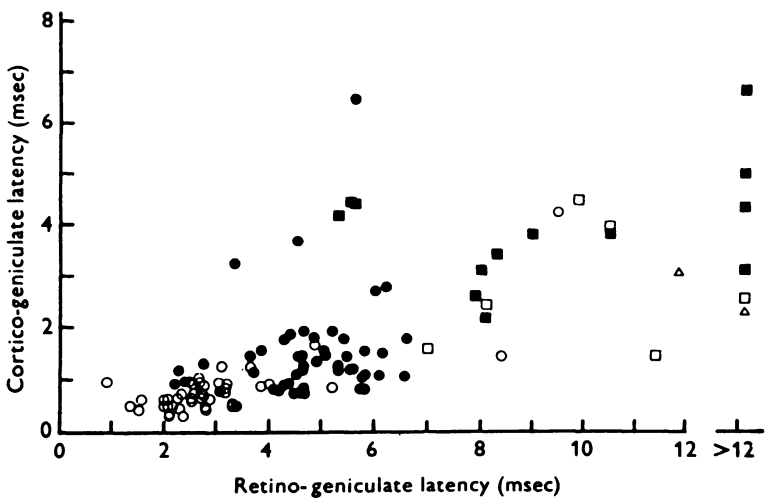

Fig. 18.19 Scatter diagram of corticogeniculate latency (antidromic) against retinogeniculate latency for 115 LGN cells. Symbols indicate class of cell: ○ 'brisk-transient'; ● 'brisk-sustained'; □ 'sluggish-transient'; ■ 'sluggish-sustained'; △ 'local edge-detector'. (Cleland *et al.*, *J. Physiol.*)

of the cat and described as W-cells, have been studied by Sur & Sherman (1982); these gave both linear and non-linear responses to grating stimuli, so that the linearly responding units were comparable with X-cells, and the non-linear with Y-cells. The best contrast-sensitivity of W-cells was, on average only a quarter of that of X- and Y-cells at similar retinal eccentricity.[13]

Organization of the Receptive Fields

A single ganglion cell, synapsing with a geniculate cell, may be expected to transmit its own receptive-field characteristics to the geniculate cell. Thus, an ON-centre X-ganglion cell, with a small receptive field and likely to be concerned with the analysis of spatial characteristics,

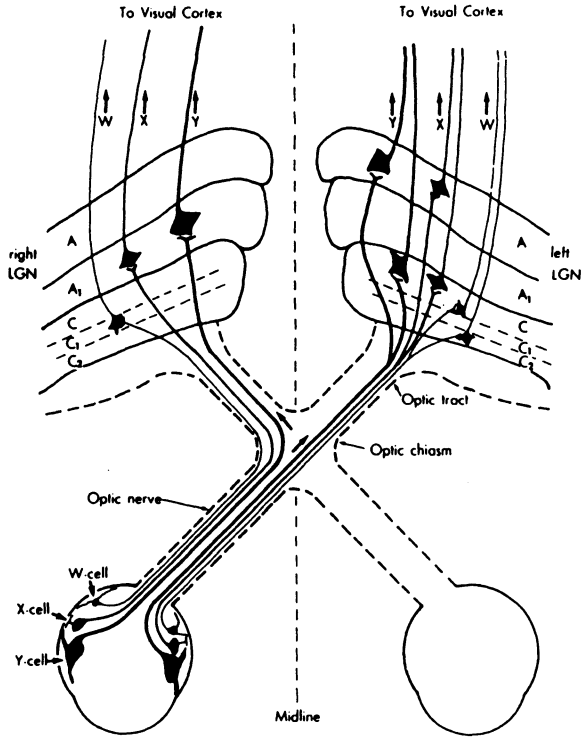

Fig. 18.20 Schematic diagram of the relay of W-, X-, and Y-cells through the LGN. Many of the features represented are derived from earlier studies. Two new features are shown. First, retinal W-cells relay to the visual cortex via cells in laminae C, C_1, and C_2. Second, each type of retinal cell relays through one lamina of the ipsilateral LGN (A_1 or C_1) and through two laminae of the contralateral LGN (X- and Y-cells via laminae A and C, W-cells through C and C_2). (Wilson *et al.*, *J. Neurophysiol.*)

may be expected to give rise to a similar X-type geniculate cell, which would likewise have a small receptive field and be likewise concerned with spatial analysis, provided that this is the only ganglion cell-type with which it synapses and that interactions within the geniculate nucleus, mediated by intrinsic interneurones, may be ignored. When several ganglion cells of the same type converge on a single geniculate cell, then we may expect the same centre-surround organization to be maintained, but that the influence of stimulating the surround will be more complex. We may illustrate the situation by Fig. 18.21 where three ON-centre ganglion cells converge on a single geniculate cell. The central ganglion cell, 1, will presumably determine the centre-response of the geniculate cell; the receptive fields of the adjacent ganglion cells cannot contribute to the geniculate cell's centre-response since the receptors with which they are connected are farther out in the periphery of the centre-stimulus. The surround-response is going to be complex. In the situation described by Fig. 18.21 we may consider the likely responses as a centred spot of light is increased in diameter so that larger and larger regions of the surround are stimulated. The spot moves first into the inhibitory zone of the central ganglion cell 1; when it has exceeded this it moves into a second inhibitory zone provided by the surrounds of ganglion cells 2 and 3; when it has covered these it reaches an excitatory zone, the centres of ganglion cells 2 and 3, so that we may expect a weakening of the inhibition (disinhibition), and finally an increase. If the ganglion cells adjacent to cell 1 are OFF-centre then the first inhibitory phase will give way to disinhibition, and so on. Hammond (1972) projected annuli of larger and larger radii, centred on a geniculate cell's receptive field, and did, indeed, find a region of disinhibition (Fig. 18.22) which was not present in an optic tract fibre with approximately the same centre-size and eccentricity. It must be emphasized, however, that the lateral geniculate nucleus is not a simple relay-centre, there being considerable interaction between geniculate neurones, so that the final receptive field is by no means a simple algebraic sum of ganglion cell input.

INHIBITORY INTERACTION

Stevens & Gerstein (1976) suggested a model based on inhibitory interaction through interneurones of the nucleus. According to this, it is the retinal excitatory surrounds that generate the inhibitory surround of the geniculate neurone's receptive field, as opposed to the retinal centres, as suggested by Singer & Creutzfeldt (1970) and others. Maffei & Fiorentini (1972) observed that both the centre and surround responses of the geniculate cell survived dark-adaptation, by contrast with the ganglion cell, which usually loses its surround response under this condition (Barlow *et al.*, 1957). They argued, on this basis, that the surround of the geniculate cell was determined by input from the centre-mechanisms of ganglion cells. On the other hand, Kaplan *et al.* (1979) found that dark-adaptation greatly affected the response-properties of both ganglion and geniculate cells; they found that both types of cell lost much of their surround-character after dark-adaptation, suggesting a common mechanism for both surrounds, rather than the model suggested by Hammond (1972).

X-, Y- and W-cell Distribution

The manner in which information, carried by X- and Y-type ganglion cells, is transferred to higher structures is a matter of great interest since this dichotomy in receptive-field type suggests a 'parallel processing' throughout the central nervous pathways. Kaplan & Shapley (1982) measured the receptive-field characteristics of neurones in the four parvocellular dorsal layers of the nucleus and in the most ventral two magnocellular layers of the macaque. Some 99% of the units in the parvocellular layers were X-cells; in the magnocellular layers the X-cells were also in a majority, representing some 75% of the total, and the rest were Y-cells. As Kaplan & Shapley point out,

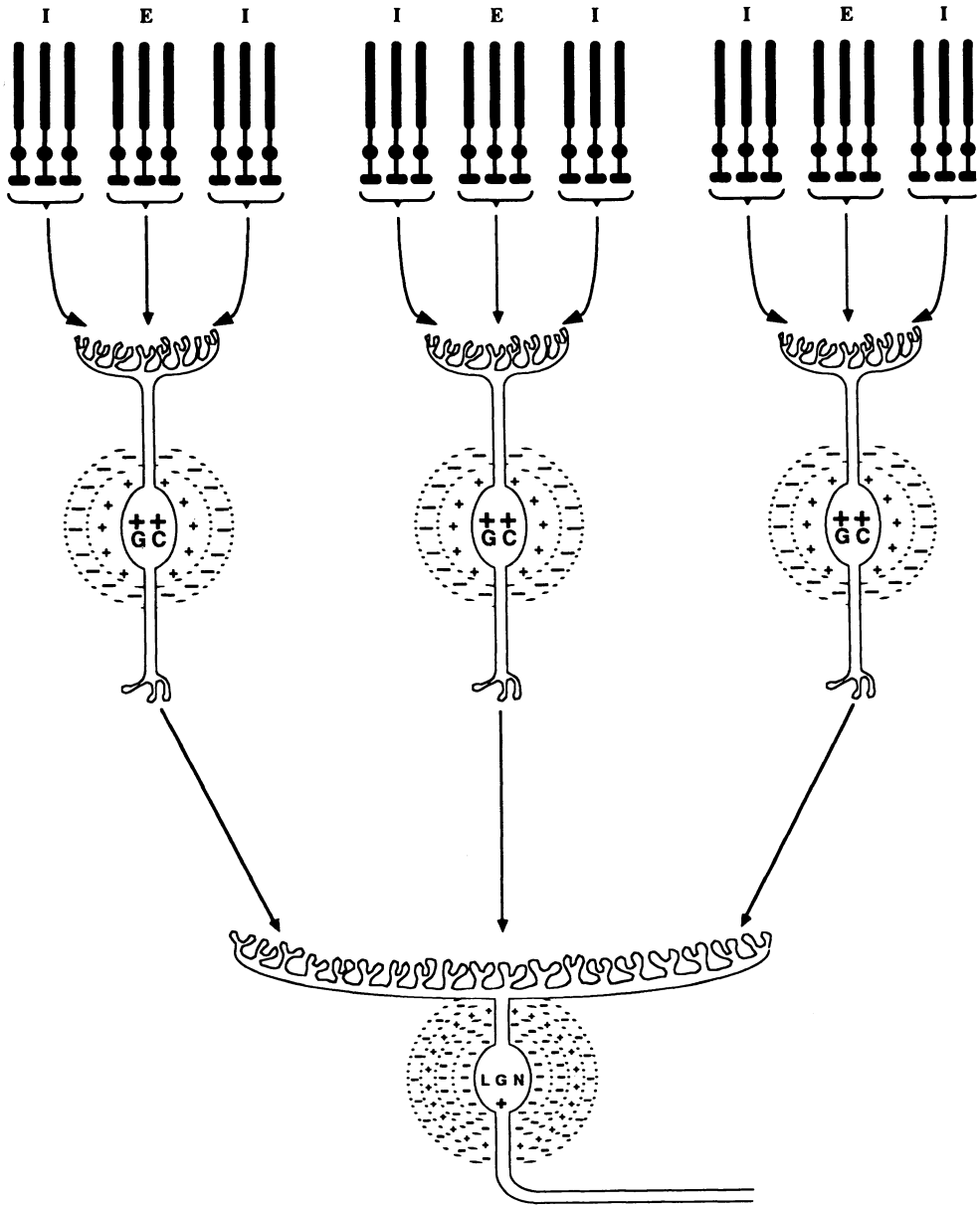

Fig. 18.21 Illustrating the make-up of the receptive field of a geniculate cell receiving input from ON-centre ganglion cells. In this particular situation the geniculate cell becomes ON-centre, but its peripheral field becomes complex.

the neurones of the mecaque nucleus form three groups: X-cells in parvo- and magnocellular layers, and Y-cells restricted to the magnocellular layers.[14] Kaplan & Shapley suggest that the A and Al layers of the cat are homologous with the magnocellular layers of the primate; this would agree with the finding of Rakic (1977) that magnocellular cells are the first to appear in ontogeny of the monkey's lateral geniculate nucleus, whilst Shatz (1983) has shown that cells of the A and A1 layers of the cat have a similar ontogeny.

Importance of Mode of Classification

Marrocco *et al.* (1982b) used the Enroth-Cugell & Robson basis for classifying geniculate neurones in the macaque; they found that some neurones, described as Y-like

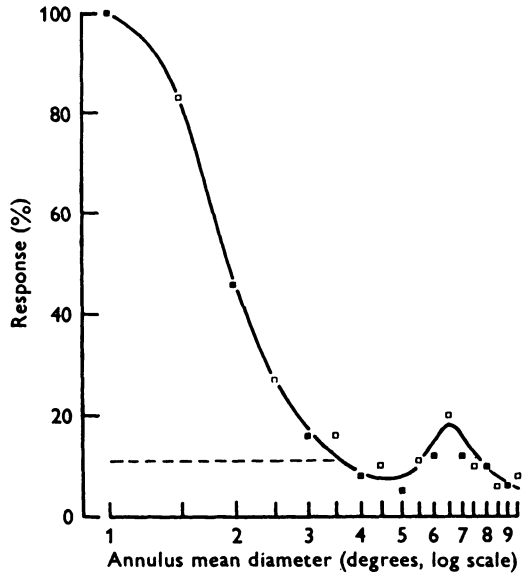

Fig. 18.22 Response variations as a function of mean diameter of the stimulating annulus. Stimulus wavelength was 525 nm presented against an achromatic adapting field. Mean spike counts are presented as percentage of maximum. (■ increasing diameters; □ decreasing diameters.) Spontaneous firing level indicated by dashed line. (Hammond, *J. Physiol.*)

on the basis of conduction latency, were really X-neurones on the basis of linear summation, so that there was no strict segregation of neurones on the basis of their X- or Y-type receptive fields, although most Y-cells were in the magno- and X-cells in the parvocellular layers. Conduction velocity was only partially correlated with receptive-field type, so that the statement of Dreher *et al.* (1976) that all X-like neurones had a latency greater than 1.6 msec and Y-like of less than 1.5 msec could not be sustained. Shapley *et al.* (1981) also found X- and Y-cells in the magnocellular layers.

W-cells

The principal input of W-cells is to the superior colliculi where they presumably exert a role in the control of visually guided movements; according to Stone *et al.* (1979) they also go to parvocellular neurones and the medial interlaminar nucleus of the cat.

ON- and OFF-segregation

In the cat the ON- and OFF-units are intermingled, but in the ferret Stryker & Zahs (1983) have described a distinct sublamination of the retinal input to layers A and Al, each sublamina having a distinct response-type, either ON or OFF. This is true also of the tree-shrew (Conway *et al.*, 1980) and the mink (LeVay & McConnell, 1982).

Y-cells in Laminae A and C

In the cat there are two populations of Y-cells; those in the magnocellular region of lamina C project to areas 17 to 19 and to the posteriormedial lateral suprasylvian area (PMLS) (Tong *et al.*, 1982). A major portion of the cells branch to project to both Areas 17 and 18 (Geisert, 1980). The large cells of A-laminae project to Areas 17 and 18, and only a few to Area 18 alone, and none to Areas 19 and LS. Frascella & Lehmkuhle (1984) have compared the response properties of these two classes of Y-cells; differences were only of a quantitative nature; thus at threshold lamina C cells were the more sensitive to sine-wave gratings, and gave the largest second harmonic response, a feature that is a distinguishing feature of Y-cells (Hochstein & Shapley, 1976), and follows from the non-linearity of the receptive field.

Two Classes of X-cells

Mastronarde (1987) stimulated the cat's eye and recorded from both lateral geniculate cell and the ganglion cell with which it was synaptically related and identified two classes, both of which were activated by a single ganglion cell and sharing the receptive-field characteristics of this cell. The first class, X_S, was typical of X-cells previously studied; the second, X_L, responded after a lag of 40–80 msec behind the X_S-cells and in an anomalous fashion and at times when the X_S- and ganglion cells would not be firing. Responses to a moving bar were characteristically different, the X_S responding when the bar was in the centre of the field and the X_L after it had moved away. Because of the similarity in receptive fields, both types would have the same spatial discrimination, but temporal discrimination would be worse in the X_L-cell because of the lag in its response. Mastronarde concluded that the lag in response was a consequence of internal geniculate circuitry, a circuitry that led to strong post-excitatory inhibition.

Morphology of neurones

Friedlander *et al.* (1981) related the X-, Y-dichotomy of geniculate cells to their morphology, emphasizing that these characteristics were demonstrated on purely electrophysiological considerations. Guillery (1966) had described some four classes of geniculate cells, on the basis of their morphology, classes 1–3 in the A-laminae and class 4 in the C-laminae. LeVay & Ferster (1977) considered that classes 1 to 3 corresponded to Y- and X-principal relay cells, and interneurones respectively; and Wilson *et al.* (1976) considered that class 4 neurones were W-cells, restricted to the C-lamina. Friedlander *et al.* largely confirmed this, but many class 3 neurones were X-cells, and not only interneurones. Interestingly, they found that the proportion of X- to Y-cells in the geniculate was greatly less than in the retina where it was some 10 to 1, and they estimated that one retinal Y-cell might transmit to some 20 geniculate Y-cells, whereas a retinal X-cell projected to only four geniculate X-cells. Thus the Y-pathway is greatly expanded in the lateral geniculate nucleus, an expansion that they considered to be extended to the cortex.

Functional Differences Between X- and Y-cells

Studies on the ganglion cells described earlier have indicated that X-cells are suitable for mediating discrimination of spatial features of the visual field, whilst the Y-cells, with their larger receptive fields and transient responses, would mediate analysis of movement. This view of the dichotomy, so far as geniculate cells are concerned, has been questioned by a number of investigators, some of whose studies will be presented below, but before rejecting the basic concept it is as well to emphasize that spatial resolution must, in the last analysis, be referred back to the receptive fields of the receptors and neurones in the visual pathway; at the ganglion cell level this has been well established, the X-cells, with their small receptive-field centres governing resolving power. The segregation of X- and Y-units is maintained at the geniculate and cortical levels, so that it is difficult to dismiss this as a process subserving analysis of some other characteristic of the visual field than its fine-spatial features. Moreover, the transience of the Y-cell's responses renders it unsuitable for spatial analysis but may well be of value in temporal analysis.

However, the appreciation of spatial features of the environment does not simply depend on the ability to resolve the finest detail, (the classical 'visual acuity'); rather discontinuities, which may be large or small, must be appreciated, so even where simple gratings are concerned the recognition of a low spatial frequency, i.e. a coarse grating, might be better achieved by units with relatively large receptive fields. It is for this reason, as we have seen, that the measurement of contrast-sensitivity functions rather than visual acuity, or resolving power, is of value; the extrapolation of this to high spatial frequencies gives the resolving power, whilst the peak gives the position of the best performance of the unit concerned. So far as geniculate cells are concerned, Y-cells do not show the falling off of sensitivity at low spatial frequencies that is characteristic of X-cells. We shall see later that, at the next stage in the visual pathway, namely the cortical cells of area 17, single units show a tuning with respect to best spatial frequency, and we may regard the successive contrast-sensitivity functions at stages in the visual pathway as steps in 'information transfer' leading to tuning of cortical cells with different optimal spatial frequencies.

Spatial and Temporal Contrast-sensitivity Functions

Lehmkuhle *et al.* (1980a) measured the classical contrast/spatial frequency function (p. 381) and also a contrast/temporal frequency function; thus, having found the optimal spatial frequency for a neurone, this grating was counterphased at a variable frequency, and the contrast required to recognize the temporal fluctuations was assessed for the different frequencies. Figure 18.23 compares the two functions for X- and Y-cells; the X-cells show the characteristic U-shaped curve for spatial sensitivity, with a falling off at low spatial frequencies, i.e. broad gratings, whilst the Y-cells maintain high sensitivity up to the grossest gratings. At the highest spatial frequencies, the two types of cell do not differ strongly. The temporal frequency-functions show that the Y-cells have the higher sensitivity at all frequencies, thus confirming the generally accepted higher sensitivity to temporal change. However, the comparisons of temporal sensitivity are made at the optimum spatial frequencies; if the comparison is made at arbitrarily chosen spatial frequencies, the difference between X- and Y-cells may not be so evident; thus it was found that at the very low spatial frequencies the Y-cells were more sensitive than X-cells to temporal change; at medium spatial frequency the sensitivities were equal, and at the high frequencies the Y-cells were more sensitive than X-cells.

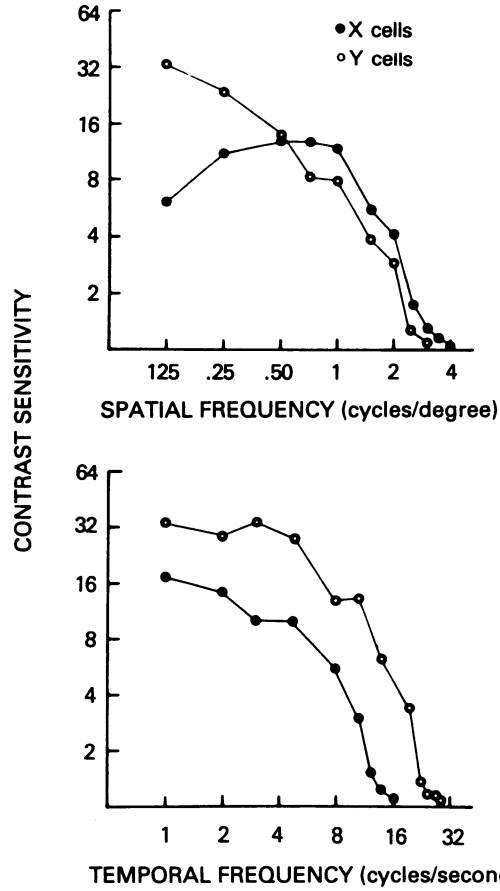

Fig. 18.23 Average spatial and temporal contrast-sensitivity functions for X- and Y-LGN cells. All cells had receptive fields within 10° of the area centralis. (Lehmkule *et al.*, *J. Neurophysiol.*)

Y-CELLS AND SPATIAL RESOLUTION

Thus the pronounced difference in spatial and temporal characteristics between the two types of cell, described earlier, is largely due to the choice of targets that bring out the difference, and Lehmkuhle *et al.* concluded that the Y-cells, because they respond well to a much wider range of spatial frequencies than the X-cells, are essential for spatial resolution; moreover the Y-cells are not very sensitive to the phase of the grating in relation to their receptive fields, because they have no null-point, by contrast with X-cells, so that at high spatial frequencies their responses are virtually phase-independent. The X-cells, with a null-point, are sensitive to the phase of the grating and would thus be kept active by small involuntary eye movements which would bring the patterned visual field through null-points and out of them. According to Lehmkuhle *et al.*, the X-cells would add detail to the analysis of pattern made in parallel by the Y-cells. Thus early visual deprivation in the kitten selectively inactivates Y-cells (Lehmkuhle *et al.*, 1980b) and these animals show a profound loss of spatial pattern vision (Dews & Wiesel, 1970); again, selective removal of X-cell function by removal of visual cortical Area 17 leaves excellent pattern vision in the cat with only 20% loss of visual acuity (Berkley & Sprague, 1979).[15]

Y-cell and the Second Harmonic

So & Shapley (1979) emphasized that the difference between the X- and Y-type geniculate cell had to be based rather on linearity, or otherwise, of summation than on Cleland's 'battery of tests'. They separated cat geniculate cells on the former basis and presented gratings of different spatial frequencies, and these were modulated by contrast-reversal at different temporal frequencies. The X-cells responded with bursts of discharges at the frequency of contrast-modulation, whereas Y-cells responded at this and the second harmonic of this, i.e. twice the frequency. When spatial resolution was compared between the two cell-types, there was no significant difference, provided the response to the second harmonic was used for the Y-cell's performance. Thus both X- and Y-cells responded to fine patterns, but only Y-cells responded well to coarse patterns. In other words by manipulating the temporal features of the stimulus they were able to derive similar sensitivities to spatial frequencies. So & Shapley suggested that, under these conditions, subunits in the Y-cell's receptive field, responsible for the non-linearity of this cell's responses, were acting as independent units in the spatial-frequency resolution. Thus, just as the size of the X-cell's receptive field centre could be deduced from its best spatial frequency, so could the size of the Y-subunit be determined by the Y-cell's best resolution when the second harmonic of the response to a temporally modulated grating-stimulus was taken as an index to sensitivity. It must be emphasized, however, that the Y-cell is only giving this high resolution with a temporally modulated stimulus.[16]

With a stationary grating the variations in the character of a receptive field, leading to non-linear behaviour, cannot be conveyed to higher centres, since the response is confined to a change in intensity of discharge measured as the frequency of spikes. When the grating moves, the lines tend to entrain the bursts of spikes, so that the frequency of these bursts, governed by the motion and the width of the stripes, reflects the movement and the existence of spatial discontinuities of the target. Since visual acuity is independent of motion of the target these discontinuities in the Y cell's field are clearly not being made use of at the limit of resolution, but of course, under normal conditions of visual stimulation, the targets are moving and their movement contributes to the interpretation of the visual field.

Parvo- and Magnocellular Dichotomy

Although most parvocellular units of the primate lateral geniculate nucleus have X-type receptive fields, the segregation into parvo- and magnocellular layers is not on the basis of X- and Y-type units, since X-type units are present in the magnocellular layers. Probably the most important difference between the layers in the primate resides in contrast-sensitivity. Thus Shapley *et al.* (1981) measured the peak contrast-sensitivity of geniculate neurones when a grating of spatial frequencies varying from 0–10 c/deg was allowed to drift over the receptive field. The reciprocal of the contrast required to produce a modulated discharge with an amplitude of 5 imp/sec was the contrast-sensitivity. With parvocellular units the peak sensitivity was 10 whereas with magnocellular units, both X- and Y-types, this was 75, high enough to account for the psychophysically measured sensitivity of the macaque (DeValois & Morgan, 1974). This high contrast-sensitivity was comparable with that found for geniculate cells in layers A and A_1 of the cat. A similarly high contrast-sensitivity of the magnocellular units was also found by Derrington & Lennie (1984), which they attributed to their larger receptive fields and thus higher quantum-catching potential. Parvocellular neurones, amongst which all those with foveal receptive fields were encountered, had low contrast-sensitivity but higher spatial discrimination, reaching a resolution of gratings as high as 40 c/deg, equivalent to that expected of the macaque (DeValois & Morgan, 1974; Harwerth *et al.*, 1980).

Parvocellular and Magnocellular Functional Significance

Marrocco *et al.* (1982a) have discussed the significance of the separation of cell types, as shown by the parvo- and magnocellular layers. They reject the suggestion that it mediates a coding of colour (parvocellular) and luminance (magnocellular) signals postulated by the preponderance of colour-opponent units in the parvocellular layers (p. 587). Such differences as were observed were in the domain of contrast-sensitivity, temporal tuning and conduction latency. The magnocellular layers have a projection from the superior colliculus and brainstem, probably involved in some aspect of the coding of stimulus-information during high velocity stimulus shifts, as when the eyes move. The parvocellular layers might be

better suited for the analysis of the visual scene when static. They point out that the partial segregation of pathways in the lateral geniculate nucleus is similar to that in the superior colliculus; since the visual cortex strongly influences the receptive-field characteristics of collicular neurones, by analogy, they suggest that the magnocellular neurones owe their special features to the predominant cortical input to this layer.

Velocity Sensitivity

Ganglion cells respond to velocity in two ways; there is a simpler type that gives a monotonically increasing response with increasing velocity of target; these are a common feature of many lower vertebrate eyes but may also be found in the cat (Lee & Willshaw, 1978). A second type exhibits a preferred velocity, and is said to be velocity-tuned. In the lateral geniculate nucleus both kinds are found; thus Hess & Wolters (1979) found two thirds of the cells responding monotonically with velocity up to some 100°/sec. The remaining third of the neurones were tuned; an example is shown in Fig. 18.24 in the form of response-histograms, where it will be seen that the neurone is tuned to a velocity of some 3.8°/sec. This process of tuning, as with spatial tuning, is carried further

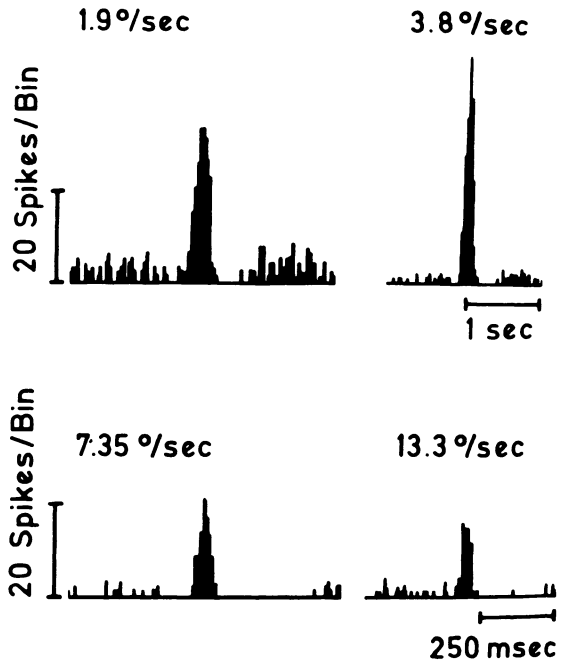

Fig. 18.24 Velocity-tuned responses of an LGN/ON-centre neurone. Response-histograms in the forward direction at four characteristic velocities. Bin-width in upper histograms 20 msec; in lower ones 5 msec. Note increase in peak height from 1.9 to 3.8°/sec and the decrease from 7.35 to 13.3°/sec. (Hess & Wolters, *Exp. Brain Res.*)

in the cerebral cortex. The decrease in response at high velocities that forms the basis of tuning must be due to inhibition, and in this case the X-cell would be the more likely to show tuning; certainly Dreher & Sanderson (1973) showed that it was the Y-cells that exhibited the monotonic increase in discharge with increasing velocity.[17]

Comparison with Ganglion Cells

Frishman *et al.* (1983), in a more elaborate study of the cat's cells, used small lines of about the height of the unit's receptive field and one quarter its width. They confirmed the greater preferred velocity of the Y-cell, and showed that this preferred velocity increased with eccentricity (because of increased field-size) as well as with stimulus-strength. The geniculate Y-cell's preferred velocity was greater than that of a ganglion cell at the same eccentricity, but the reverse was true of X-cells. They attributed the geniculate unit's high preferred velocity to the operation of intrageniculate inhibitory circuits. Thus we have seen that size of the receptive field should determine the ability to respond to a moving target, the larger the field the longer the target will be on it and the greater the summated response. With ganglion cells, receptive-field size explained the X- versus Y-difference; with geniculate cells this was not so; thus the Y-cell's field-size in this case is 2.5 times that of the X-cell, yet the preferred velocity was 5 to 7 times greater. When the height of the moving bar was increased so that it moved into the inhibitory surround, tuning of the Y-unit became sharper and the preferred velocity increased; with X-cells this did not happen, tuning becoming flatter.

Orientation-selectivity

Cortical neurones, as we shall see, respond best to line-stimuli, and exhibit a maximal response when the line is orientated in a given direction—orientation-selectivity. Whilst there is no doubt that this orientation-selectivity can be generated by cortical mechanisms, the extent to which the lateral geniculate nucleus can develop this sensitivity is of interest. Vidyasagar & Urban (1982) showed that geniculate neurones possessed some orientational bias; lesions in cortical areas 17 and 18 did not influence the extent of this, showing that what orientation-selectivity the geniculate cells had was probably not due to a cortical feedback.

Length-tuning

We shall see that a prominent feature of certain visual cortical cells is their sensitivity to the length of a bar in the

receptive field, so that when a critical length is exceeded, inhibition occurs. Ganglion cells show a certain degree of length-sensitivity, and this is accentuated in the geniculate cell, so that it is intermediate in behaviour between ganglion and cortical (hypercomplex) cell (Cleland *et al.*, 1983).

Ventral Nucleus Neurones

The receptive fields of these neurones were studied by Spear *et al.* (1977); these were larger (mean 10.6°) than for dorsal geniculate cells; most were driven by the contralateral eye only, 30% were binocularly driven and 13% by the ipsilateral eye. Only some 20% had concentrically organized receptive fields; some 4% were only movement-sensitive, and an additional 2.5% were directionally sensitive. The generally low conduction-velocities of the ganglion cells synapsing in the ventral nucleus suggested that they were entirely of the W-type, and this would agree with the presence of non-concentric receptive fields in so many of the geniculate cells. As with other regions of brain concerned with visual function, there was good retinotopic spatial representation of the visual field on the ventral nucleus, so that it may be included with the lateral posterior nucleus (LP), pulvinar (PUL), posterior nucleus (PN), medial interlaminar nucleus (MIN), dorsal lateral geniculate nucleus and perigeniculate nucleus (NPG).

Possible Function

Polyak (1957) suggested that the VLG (or pregeniculate nucleus in the monkey) was part of the pathway mediating pupillary constriction in response to light; thus units of the VLG project to the pretectum. In addition its projection from the superior colliculus, which in the cat receives a strong projection from W-cells, suggests a function in relation to the control of eye movements.

Receptive Fields of Interneurones

By electrical stimulation of the cerebral cortex, relay neurones of the lateral geniculate nucleus can be identified by the antidromic spikes that invade their cell-bodies; another group of neurones, not giving an antidromic spike but, instead, being excited synaptically, was recognized by Cleland *et al.* (1976). These neurones were supposed to be interneurones, without axons extending to the visual cortex. The receptive fields of these cells were characteristically different from those of relay-cells, lacking the precise centre-surround organization and giving typical ON-OFF responses. A more careful study showed that these ON-OFF neurones were located just outside the dorsal nucleus, they were the *perigeniculate neurones* described earlier. Another group did have a centre-surround organization and were subdivided into the ganglion cell classification—brisk, sluggish, etc.

By recording simultaneously from the dorsal nucleus and retina, these neurones were shown to have a retinal input, an input that allowed the ganglion-cell type classification (Dubin & Cleland, 1977). The perigeniculate neurones, ON-OFF, were also shown to have retinal input by electrically stimulating the retina, perhaps through recurrent collaterals of relay-cells as suggested by Fig. 18.12. If there were a degree of convergence of input, the receptive fields might lack the precise organization of relay-cells, and it could be postulated that they were involved in more general integrative processes within the visual pathway. So far as the possibility of this recurrent inhibition is concerned, Ahlsén *et al.* (1978) identified relay-cells in the lateral geniculate nucleus by electrical stimulation of the cerebral cortex, which caused antidromic stimulation; they filled the cells with horseradish peroxidase and showed that their axons sent back recurrent branches which probably synapsed with perigeniculate neurones, giving rise to feedback inhibition.[18]

Visual Cortical Influence on Geniculate Neurones

Marrocco *et al.* (1982a) developed a technique for studying the effects of the visual cortex on the response-properties of geniculate neurones. Essentially, the responses to a spot of light were modified by exhibiting a rotating grating in the periphery; cooling the cerebral cortex abolished the effect reversibly. McClurkin & Marrocco (1984) showed that in 20% of geniculate neurones the effect of the visual cortex was excitatory and in 30% inhibitory; there was no effect on the remaining 50%. The effect, so far as receptive-field characteristics were concerned, was to alter the spatial selectivity, so that the effective resolving power of the eye could be modified by cortical activity. Thus spatial selectivity is a dynamic property of the retina and not simply governed by the geometry of the cone mosaic. The authors emphasize that the lateral geniculate body is not a simple relay-nucleus, but an integrating centre.[19]

Synaptic Potentials

Ahlsen *et al.* (1982) stimulated the cat's visual cortex at the border of areas 17 and 18 and recorded intracellularly from principal relay-cells, identified by their monosynaptic excitation through optic tract fibres and antidromic input from the cortex. Both excitatory and inhibitory synaptic potentials were recorded, and although latencies were long, there was little doubt that the geniculate cells were being excited and inhibited monosynaptically

through slowly conducting cortico-geniculate fibres (5.5–9.0 m/sec). Intrageniculate interneurones were also excited monosynaptically, so that it would seem that both centre and surround responses could be modulated by cortical activity.

Inhibition within the Lateral Geniculate Nucleus

Inhibition within the lateral geniculate nucleus was recognized long before the centre-surround organization of its principal neurones had been demonstrated; thus Bishop & O'Leary (1960) described a prolonged decrease in excitability of these neurones after stimulation of the optic nerve, an inhibition attributed by Vastola (1960) to recurrent excitation of an inhibitory interneurone through a collateral of the principal cell's axon.[20] The neurones responsible for the types of inhibition taking place within the nucleus have been described earlier, and the probable circuits, based on Dubin & Cleland's study are indicated in Fig. 18.12. According to this there is a feed-forward inhibition through synaptic connection of an optic tract fibre with an intrageniculate neurone, which then synapses with a principal cell. The disynaptic nature of this was established by Lindström (1982) on the basis of intracellular recordings of synaptic potentials. There is also a feedback inhibition, mediated by a collateral from a principal cell axon synapsing with perigeniculate cells. The feed-forward inhibition is apparently mediated by a different ganglion cell from that exciting a given principal cell, and occurs bilaterally, in the sense that stimulation of the opposite retina will inhibit a geniculate cell excited and inhibited by the homolateral eye.

X- and Y-cell interactions

So far as X- and Y-cell interactions are concerned, it is agreed that the two systems are kept separate with respect to excitatory convergence; however, the situation is different regarding inhibition; thus it is generally agreed that activation of Y-retinal fibres can inhibit both Y- and X-cells but there was doubt as to whether X-cells inhibited Y-cells. Burke *et al.* (1987) selectively blocked the large Y-fibres in the optic nerve by pressure, and found that stimulation of the optic nerve now excited certain X-cells within the nucleus, and this was followed by an inhibition of both X- and Y-cells. The inhibitory interaction of X-cells, concerned in spatial discrimination, is understandable and is doubtless responsible for the strong inhibition of the surround-field of the geniculate X-cell, revealed when a centred spot is increased in diameter (Hubel & Wielsel, 1961), since Y-cells do not show this effect (Fukuda & Stone, 1976). This inhibition of an X-cell by its surround is unlikely to be mediated by Y-cells, since it is maintained at steady illumination. The inhibition of Y-cells by X-cells, through an interneurone, may possibly serve to prevent the Y-neurone from exerting its strong inhibitory action on X-neurones (Burke *et al.*, 1987).

The Inhibitory Transmitter

The transformation of the receptive-field characteristics on passing from ganglion to geniculate cell has been interpreted on the basis of a powerful inhibitory effect of the surround on responses of ON-centre cells, or of the effect of the centre on OFF-centre cells. The presumptive inhibitor is GABA; thus Sterling & Davis (1980) found that about 25% of the A-lamina neurones of the cat's dorsal lateral geniculate nucleus accumulated ^{3}H-GABA or its analogue, ^{3}H-2,4-diaminobutyric acid (DABA), and the GABA agonist ^{3}H-muscimol; the neurones accumulating were small Class III, and the accumulations occurred in the so-called F-terminals which were postsynaptic to retinal terminals and presynaptic to relay-cell dendrites. Similarly Hunt *et al.* (1982), employing a glutamic acid dehydrogenase antibody, stained small neurones in the rat's dorsal nucleus which they considered to be intrinsic inhibitory interneurones. Some stained terminals, in the extraglomerular neuropil, they considered to be derived from the reticular nucleus of the thalamus, known to be GABAergic and to project to the lateral geniculate nucleus. Sillito & Kemp (1983) evoked powerful discharges in geniculate cells by local application of the excitatory transmitter, glutamic acid; visual stimulation of centre or surround regions of the receptive field suppressed this discharge, indicating the inhibitory action of the light-stimulus. These suppressive effects of light were blocked by application of bicuculline, the GABA antagonist. When an ON-centre X-cell was stimulated with flashes of increasing size, there was the characteristic falling off of response due to spread of the stimulus to the surround-inhibitory region (Fig. 18.25); with bicuculline treatment this effect was almost abolished. As the authors point out, the differences in responses in the presence and absence of bicuculline are very similar to the differences in response of ganglion and geniculate cells described by Hammond (1972). Berardi & Morrone (1984a) generally confirmed Sillito & Kemp's work, but by employing grating stimuli they brought out some differences between X- and Y-cells. Thus the normal X-cell shows sharp falls in contrast-sensitivity to gratings at both high and low spatial frequencies; under the influence of bicuculline the low-frequency attenuation was abolished; and it was considered that this attenuation might be mediated by Y-cells, Singer & Bedworth (1973) having demonstrated an interaction of this sort in the cat's lateral geniculate nucleus. With Y-cells there was no low-frequency attenuation so that bicuculline had a relatively small effect (Fig. 18.26).

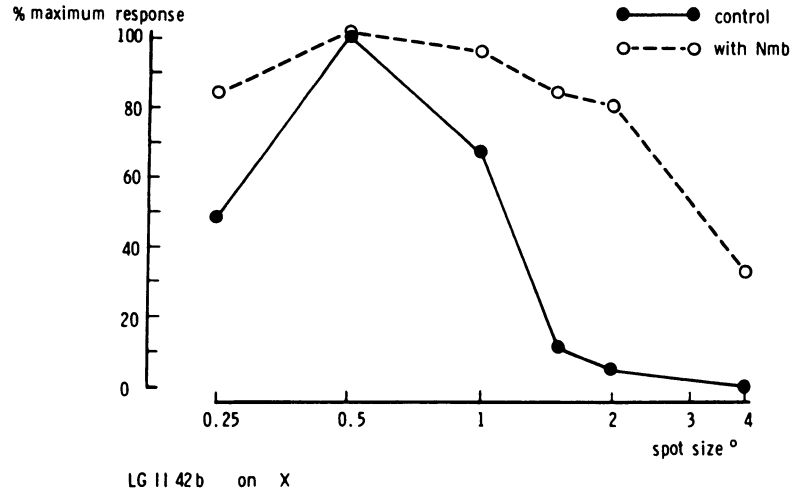

Fig. 18.25 Curves summarizing response of an 'on'-centre 'X' cell to variation in stimulus diameter before and during bicuculline application (Nmb, 60 nA ejecting current). Each point shows average response to 0.5 s flash for 25 trials expressed as percentage of maximum response, ●, control responses; ○, during N-methyl-bicuculline application. (Sillito & Kemp, *Brain Res.*)

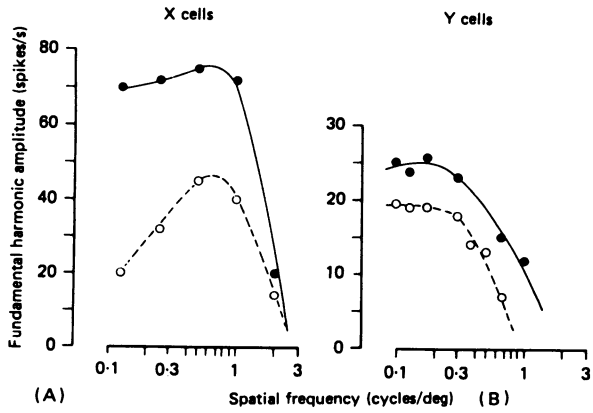

Fig. 18.26 Spatial frequency tuning for X cells and Y cells. Open symbols, normal conditions; filled symbols, bicuculline application. The contrasts used were all approximately 10%, and the temporal frequency was the optimum for each cell. Bicuculline ejection currents: *A*, 60 nA; *B*, 50 nA. (Berardi & Morrone, *J. Physiol.*)

Binocular Interactions

In spite of the segregation of the retinal input within the layers of the geniculate nucleus, most cells do have binocular input, the effect of the dominant eye being excitatory and that of the other being inhibitory. Pape & Eysel (1986) phase-reversed gratings in the non-dominant eye, thereby inducing inhibition in the other. This was blocked by bicuculline. Cortical cooling enhanced the inhibition from the non-dominant eye; similarly, destruction of that part of the retina responsible for the receptive field of a geniculate neurone facilitated the inhibitory action, indicating that excitatory stimulation in the dominant eye antagonized the inhibitory action of the non-dominant eye.

MATURITY

A number of features of the cat's visual system are not fully developed during the early postnatal period; this is true of the inhibitory action revealed, for example, by the low-frequency attenuation of the contrast-sensitivity function; thus it was only after 100 days that curves showing the effect of bicuculline on the contrast-sensitivity function of X-cells could be fully demonstrated (Berardi & Morrone, 1984b).

The Excitatory Transmitter

Kemp & Sillito (1982) have reviewed the evidence relating to the excitatory transmitter released by the optic tract terminals; although acetylcholine exerts an excitatory action on relay-cells of the lateral geniculate nucleus it is generally agreed that this is not the transmitter (e.g. Curtis & Davis, 1963; Phillis *et al.*, 1967). They have re-examined the possibility that the transmitter is an amino acid, such as glutamic or aspartic, by applying specific inhibitors, such as D-α-aminoadipate (D-α-AA), DL-α-ε-diaminopimelic acid (DAP), 1-hydroxy-3-amino-2-pyrolidone (HA 966) and L-glutamate diethyl ester (GDEE). The visual responses of geniculate neurones were reduced; this is illustrated by Fig. 18.27, which shows the responses of a neurone to light, to applied acetylcholine, to glutamate and to DL-homocysteic acid (DLH), all of which are excitatory; D-α-AA reduces the responses to light and to the amino acid transmitters, but has no effect on that of acetylcholine.

Cholinergic Influences

Cholinoceptive neurones are evenly distributed throughout the laminae of the dorsal lateral geniculate nucleus, and Phillis *et al.* (1967) demonstrated an excitatory action on 47% of geniculate neurones, and an inhibitory action

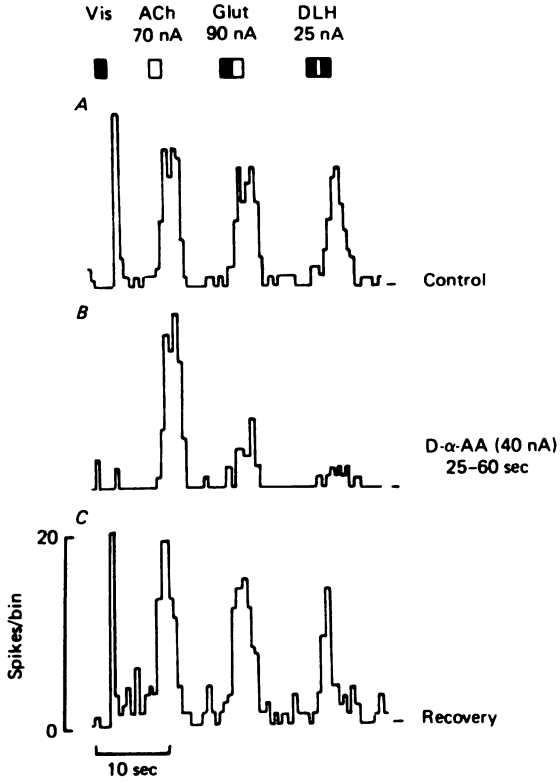

Fig. 18.27 Peristimulus time histograms (PSTHs) illustrating the selective effect of D-α-aminoadipate (D-α-AA) on the responses of a dLGN neurone (LG II, 271) to visual stimulation (vis) and pulsed ionophoretic application of drugs. Visual stimulus is a spot of light flashed within the receptive field centre. Duration of flash and drug pulses is indicated by the symbols above records. Magnitudes of the drug ejection currents are indicated above symbols. Calibration bar on ordinate indicates number of spikes per bin. Calibration of abcissa indicates 10 sec. Bin size 400 msec, one trial, cell type, off X. *A*, control run illustrating responses to visual stimulus, acetylcholine (ACh), L-glutamate (glut) and DL-homocysteic acid (DLH). *B*, responses to the same sequence as in *A* but during ionophoretic application of D-α-AA in a time period after onset of application as indicated to the right of the records. *C*, recovery run after cessation of D-α-AA application. (Kemp & Sillito, *J. Physiol.*)

on 38%; they ruled out the optic tract as a cholinergic pathway to the relay-cells. The suggestion was made, as with cortical cholinergic activity, that cholinergic excitation is mediated by the mesencephalic reticular formation, perhaps originating in the nucleus cuneiformis. Thus Godfraind (1978) described a facilitation of transmission in the lateral geniculate nucleus through somatic stimulation, which he attributed to a disinhibition mediated through the ascending reticular system, and suggested that the perigeniculate neurones were the site of a tonic inhibition; depression of their activity by acetylcholine would reduce their effectiveness.

So far as the direct excitatory action on geniculate neurones is concerned, illustrated by Fig. 18.27, for example, Sillito *et al.* (1983), using their micro-injection technique, showed that all lateral geniculate neurones were excited by acetylcholine whilst perigeniculate neurones were inhibited. The excitatory action extended to both X- and Y-cells, and to ON- or OFF-centre units. Eysel *et al.* (1986) showed that the excitatory effect of applied acetylcholine to the cat's nucleus occurred when the particular region was deafferented by appropriate retinal lesions, thus proving that the effect is truly excitatory and not disinhibitory. The effect was strongly inhibited by barbiturate, which should never be used for studying acetylcholine effects in the central nervous system. However, the long-range inhibition of geniculate neurones, that becomes manifest with localized retinal destruction (Eysel & Ringeler, 1985) was disinhibited by the transmitter.

Notes

1. Studies with the electron microscope have shown that the number of small unmyelinated fibres in the optic nerve is vastly greater than had been estimated on the basis of light-microscopical measurements, so many of these fibres being beyond the limits of resolution of the light-microscope. For example, Maturana has counted some 470 000 unmyelinated fibres in the frog's optic nerve and 12 000 thicker myelinated fibres, whereas earlier counts had shown a total of only about 14 000. Hughes & Wässle (1976) found 193 000 fibres in the cat's optic nerve, with diameters ranging from 0.5 to 13.5 μm; there was a high-density core of fibres, corresponding to the area centralis. The number of ganglion cells in the cat's retina has been estimated at 190 000 by Wässle *et al.* (1975) and 217 000 by Hughes (1975). In the rabbit's optic nerve, Vancy & Hughes (1976) found 349 000 fibres, 98% being myelinated. Diameters ranged from 0.25 to 7 μm with a peak at 0.75 μm. The number of ganglion cells in the retina was 455 000 to 547 000, and the authors suggest that some of these might be displaced amacrine cells.
2. The lateral geniculate body, or nucleus, viewed as a relay-station for visual input to the cerebral cortex, should be described as the *dorsal lateral geniculate nucleus* (LGNd); the *ventral nucleus* of lower mammals (LGNv), and its analogue, the *pregeniculate nucleus* of primates (PGN), receive retinal input that is not relayed directly to the cortes (p. 493).
3. The lesion in (*c*) designed to cut off input through the

accessory optic tracts relies on the complete decussation of these accessory fibres in the chiasma; the same is true for the combined lesions in (*d*).

4. A direct pathway from the retina to the pulvinar has been the subject of debate; that in the cat will be described later. So far as the squirrel monkey is concerned there is apparently no projection but one has been reported for the phalanger (Rockell *et al.*, 1972), tree shrew (Laemle, 1968) and the rhesus monkey and baboon (Campos-Ortega *et al.*, 1970). In the two opossums studied by Royce *et al.* (1976) there were small but distinct retinal projections. In general, however, as we shall see, the pulvinar depends on cortical and tectal input for such integrative visual activities that it mediates.
5. Suzuki & Kato (1969) have discussed the existence of geniculate neurones with binocular input; in the cat there is indeed some overlap of projection, but this occurs only in the interlaminar zone. Electrophysiologically binocular interaction can, and does, occur through intrinsic geniculate interneurones. In their own study they showed that a neurone monosynaptically excited by one eye could be inhibited by a light stimulus from the opposite eye; they proposed an inhibitory feedback from the cortex as the mechanism. However, subsequent work has shown that mechanisms within the nucleus are of greatest importance.
6. According to Gray (quoted by LeVay & Gilbert, 1976) C_3 receives an input from the superior colliculus.
7. The projections of the parvocellular C-laminae of the cat, C1 to C3, have been described by Raczkowski & Rosenquist (1980) on the basis of injections of horseradish peroxidase into different visually responsive areas of the cat's cortex and examining retrograde movement of the tracer. All these regions, namely areas 17, 18, 19, PLLS, MMLS, 20a, 20b and 21a received projections.
8. As described by Guillery *et al.* (1980) the MIN is made up of two layers representing the contralateral eyes, and one, representing the ipsilateral eyes sandwiched between. The neurones are large, probably Y-type, although Dreher & Sefton (1979) described also X- and W-cells, representing some 4.5 and 7.5% respectively of the total population. One lamina represents the nasal retina as a mirror-reversal of the projection of Lamina A; the second the ipsilateral temporal retina as a mirror-reversal of lamina A_1, and the third, close to the optic tract, receiving crossed afferents from the temporal retina. They describe the '*geniculate wing*', which is considered to be part of the pulvinar. Dreher & Sefton (1979) have compared the neurones in the laminate dorsal lateral geniculate nucleus and MIN; in the former 32.5% were Y-cells, 54.5% X-cells and 8.5% W-cells. The great majority of Y-cells, irrespective of their location in the lateral geniculate body, responded orthodromically to stimulation of the superior colliculi, indicating a branching input from the retina. Kratz *et al.* (1978) determined the retinal projection to MIN by anterograde movement of label from the eye; the neurones behave like Y-cells electrophysiologically, as indicated by short-latency conduction from the optic chiasma, non-linearity of receptive fields, etc. These fields were much larger than those of the laminated nucleus, presumably due to the absence of an inhibitory input from the non-dominant eye. The authors considered that the MIN cells should be regarded as a sub-group of the laminar Y-cells.
9. Albino animals often show a genetic error in decussation of their optic nerve fibres; the phenomenon has been studied most exhaustively in the Siamese cat which is often cross-eyed as a consequence. Guillery (1969) and Guillery & Kaas (1971) showed that the defect was due to the fact that many fibres of the temporal retina joined with the nasal fibres to cross to the contralateral geniculate nucleus, leaving only a small number of temporal retinal fibres to pass ipsilaterally.
10. Guillery (1966) described altogether four classes of neurones in the dorsal lateral geniculate nucleus of the cat based on the size of their perikarya, ranging from 25–40 μm (Class 1) to 10–20 μm (Class 3); Class 4, confined to Lamina B, was of medium size. Extrinsic afferent axons were of two types, I and II; Type III were intrinsic.
11. Levick *et al.* (1972) found one to six optic tract fibres relaying with a single geniculate cell of the cat; 8% of units had only one, and the most common number was 2–3. The ON- or OFF-character of the tract-fibre was transmitted to the geniculate cell, as was usually its X- or Y-type. About 10% of cells could be excited binocularly, and some 70% received an inhibitory input from the opposite eye.
12. Shapley & Hochstein (1975) have shown that the best criterion for distinguishing X- and Y-type geniculate neurones, is that of responsiveness to the phase of a grating passing over the receptive field, so that the X-type unit exhibits a null-point whereas the Y-type unit is unaffected by the phase. They found units with transient responses that exhibited null-points, and so should have been classified as X-like.
13. Fischer & Kruger (1974) have described the 'shift-effect' produced by moving a grid far away from the receptive field of geniculate cells, similar to that described for ganglion cells. Kruger (1977) described the effect in the monkey.
14. Earlier workers (Dreher *et al.*, 1976; Sherman *et al.*, 1976; Schiller & Malpeli, 1978) had claimed that there was complete segregation of X- and Y-cells in the monkey lateral geniculate nucleus, probably because there was a tendency to call all magnocellular cells Y-like, on the basis of short-latency, applicable largely in the cat but not in the primate.
15. Troy (1983a) has confirmed the higher sensitivity of Y-cells to temporal fluctuations in a grating stimulus. When spatial contrast-sensitivity was measured at different temporal frequencies, some interaction occurred, i.e. the frequency with which a grating-stimulus was flashed on and off improved the spatial contrast-sensitivity in the region of low spatial frequencies, i.e. with coarser gratings. As to whether these interactions indicated a role of X- and Y-cells in the higher visual pathways, Troy (1983b) was doubtful.
16. Lennie (1980) has reviewed the problem of the X- and Y-cell dichotomy in the light of some simple psychophysical experiments, and concludes that the segregation of visual information into the X- and Y-channels probably subserves some other function than the appreciation of spatial resolution and motion.
17. Lee *et al.* (1979) found that magnocellular units of the monkey gave phasic responses as a moving bar passed across the receptive field, by contrast with a monophasic increase or decrease in firing rate found with the parvocellular units; some of the magnocellular units were sharply tuned to velocity.
18. Geisert *et al.* (1981) have studied the effects of electrical stimulation of the visual cortex on the cat's dorsal geniculate neurones, employing some nine different tests to characterize them, e.g. centre-size, surround-size, and so on. The influences were complex and not easily summarized, both excitatory and inhibitory effects being observed. In the simplest case, a decrease in spontaneous discharge would be found.
19. Geisert *et al.* (1981) studied the effects of areas 18 and 19 on response-characteristics of geniculate neurones by cooling these cortical regions. The main effects were revealed in the intensity of responses to centre and surround stimuli; when these were studied separately in an individual neurone, the

changed response to combined centre-surround stimulation could be predicted from the separate effects. X- and Y-cells were affected equally.

20. Inhibitory activity in the lateral geniculate body was revealed as a slow S-potential recorded excellularly, due to summated postsynaptic inhibitory potentials. These are entirely of ganglion cell origin, and so they may be used as an index to retinal input (Kaplan & Shapley, 1984).

References

Ahlsén, G., Grant, K. & Lindström, S. (1982) Monosynaptic excitation of principal cells in the lateral geniculate nucleus by corticofugal fibers. *Brain Res.* **234**, 454–458.

Ahlsén, G., Lindström, S. & Sylirska, E. (1978) Subcortical axon collaterals of principal cells in the lateral geniculate body of the cat. *Brain Res.* **156**, 106–109.

Barlow, H. B., Fitzhugh, R. & Kuffler, S. W. (1957) Change of organization in the receptive fields of the cat retina during dark adaptation. *J. Physiol.* **137**, 338–354.

Berardi, N. & Morrone, M. C. (1984a) The role of γ-aminobutyric acid mediated inhibition in the response properties of cat lateral geniculate nucleus neurons. *J. Physiol.* **357**, 505–523.

Berardi, N. & Morrone, M. C. (1984b) Development of γ-aminobutyric acid mediated inhition of X cells of the cat lateral geniculate nucleus. *J. Physiol.* **357**, 525–537.

Berkley, M. A. & Sprague, J. M. (1979) Striate cortex and visual acuity functions in the cat. *J. Comp. Neurol.* **187**, 679–702.

Bishop, P. O., Kozak, W. & Vakkur, G. J. (1962) Some quantitative aspects of the cat's eye: axis and plane of reference, visual field co-ordinates and optics. *J. Physiol.* **163**, 466–502.

Bishop, P. O. & O'Leary, J. S. (1960) Electrical activity of the lateral geniculate of cats following optic nerve stimuli. *J. Neurophysiol.* **3**, 308–322.

Blakemore, C. & Pettigrew, J. D. (1970) Eye dominance in the visual cortex. *Nature* **255**, 426–429.

Bowling, D. B. & Michael, C. R. (1984) Terminal patterns of single physiologically characterized optic tract fibers in the cat's lateral geniculate nucleus. *J. Neurosci.* **4**, 198–216.

Bunt, A. H., Hendrickson, A. E., Lund, J. S., Lund, R. D. & Fuchs, A. J. (1975) Monkey retinal ganglion cells: morphometric analysis and tracing of axonal projections, with a consideration of the peroxidase technique. *J. Comp. Neurol.* **164**, 265–286.

Burke, W., Cottee, L. J., Hamilton, K., Kerr, L., Kyriacou, C. & Milosavljevic, M. (1987) Function of the Y-optic nerve fibres in the cat: do they contribute to acuity and ability to discriminate fast motion? *J. Physiol.* **392**, 35–50.

Butler, J. E. & Donovan, B. T. (1971) The effect of surgical isolation of the hypothalamus on reproductive function in the female rat. *J. Endocrinol.* **49**, 293–304.

Campos-Ortega, J. A., Hayhow, W. R. & Cluver, P. F. de V. (1970) A note on the problem of retinal projections to the inferior pulvinar nucleus of primates. *Brain Res.* **22**, 126–130.

Cleland, B. G., Dubin, M. W. & Levick, W. R. (1971) Sustained and transient neurones in the cat's retina and lateral geniculate nucleus. *J. Physiol.* **217**, 473–497.

Cleland, B. G., Lee, B. B. & Vidyasagar, T. R. (1983) Response of neurons in the cat's lateral, geniculate necleus to moving bars of different length. *J. Neurosci.* **3**, 108–116.

Cleland, B. G., Levick, W. R., Morstyn, R. & Wagner, H. G. (1976) Lateral geniculate relay of slowly conducting retinal afferents to cat visual cortex. *J. Physiol.* **255**, 299–320.

Conway, J., Schiller, P. H. & Misler, L. (1980) *Neurosci. Abstr.* **6**, 583. (Quoted by LeVay & McConnell, 1982.)

Cooper, M. L. & Pettigrew, J. D. (1979) The decussation of the retinothalamic pathway in the cat with a note on the major meridians of the cat's eye. *J. Comp. Neurol.* **187**, 285–311.

Critchlow, V. (1963) The role of light in the neuroendocrine system. *Adv. Neuroendocrinol.* 377–402.

Curtis, D. R. & Davis, R. (1963) The excitation of lateral geniculate neurones by quaternary ammonium derivatives. *J. Physiol.* **165**, 62–82.

Derrington, A. M. & Lennie, P. (1984) Spatial and temporal contrast sensitivities of neurones in lateral geniculate nucleus of macaque. *J. Physiol.* **357**, 219–240.

DeValois, R. L. & Morgan, H. C. (1974) Psychophysical studies of monkey vision. I. Macaque luminosity and color vision tests. *Vision Res.* **14**, 53–67.

Dews, P. B. & Wiesel, T. N. (1970) Consequences of monocular deprivation on visual behaviour in kittens. *J. Physiol.* **206**, 437–455.

Doty, R. W. (1961) Remarks on the optic tectum. In *The Visual System.* Ed. Jung & Kornhuber, pp. 215–217. Berlin: Springer.

Dreher, B., Fukada, Y. & Rodieck, R. W. (1976) Identification, classification and anatomical segregation of cells with X-like and Y-like properties in the lateral geniculate nucleus of old-world primates. *J. Physiol.* **258**, 433–452.

Dreher, B. & Sanderson, K. J. (1973) Receptive field analysis: responses to moving visual contour by single lateral geniculate neurones in the cat. *J. Physiol.* **234**, 95–118.

Dreher, B. & Sefton, A. J. (1979) Properties of neurons in cat's dorsal lateral geniculate nucleus: a comparison between medial interlaminar and laminated parts of the nucleus. *J. Comp. Neurol.* **183**, 47–64.

Dubin, M. W. & Cleland, B. G. (1977) Organization of visual inputs to interneurons of lateral geniculate nucleus of the cat. *J. Neurophysiol.* **40**, 410–427.

Eysel, U. T., Pape, H.-C. & Van Schayk, R. (1986) Excitatory and differential disinhibitory actions of acetylcholine in the lateral geniculate nucleus of the cat. *J. Physiol.* **370**, 233–254.

Eysel, U. Th. & Ringeler, U. (1985) Inhibitory periphery effect in geniculate neurons after elimination of specific retinogeniculate excitation. *Neurosci. Lett.* **57**, 119–124.

Famiglietti, E. V. & Peters, A. (1972) Thd synaptic glomerulus and the intrinsic neuron in the dorsal lateral geniculate nucleus. *J. Comp. Neurol.* **144**, 283–332.

Fischer, B. & Krüger, J. (1974) The shift-effect in the cat's lateral geniculate neurons. *Exp. Brain Res.* **21**, 225–227.

Frascella, J. & Lehmkuhle, S. (1984) An electrophysiological assessment of X and Y cells as pattern and flicker detectors in the dorsal lateral geniculate nucleus of the cat. *Exp. Brain Res.* **55**, 117–126.

Friedlander, M. J., Lin, C.-S., Stanford, L. R. & Sherman, S. M. (1981) Morphology of functionally identified neurons in lateral geniculate nucleus of the cat. *J. Neurophysiol.* **46**, 80–129.

Friedlander, M. J., Martin K. A. C. & Vahle-Hinz, C. (1985) The structure of the terminal arborizations of physiologically identified retinal ganglion cell Y axons in the kitten. *J. Physiol.* **359**, 293–313.

Frishman, L. J., Schweitzer-Tong, D. E. & Goldstein, E. B. (1983) Velocity tuning of cells in dorsal lateral geniculate nucleus and retina of the cat. *J. Neurophysiol.* **50**, 1393–1414.

Fukuda, Y. & Stone, J. (1974) Retinal distribution and central projections of Y-, X- and W-cells of the cat's retina. *J. Neurophysiol.* **37**, 749–772.

Fukuda, Y. & Stone, J. (1976) Evidence of differential inhibitory influences on X- and Y-type relay cells in the cat's lateral geniculate nucleus. *Brain Res.* **113**, 188–196.

Geisert, E. E. (1980) Cortical projections of the lateral geniculate nucleus in the cat. *J. Comp. Neurol.* **190**, 793–812.

Geisert, E. E., Langsetmo, A. & Spear, P. D. (1981) Influence of the corticogeniculate pathway on response properties of cat lateral geniculate neurons. *Brain Res.* **208**, 409–415.

Gilbert, C. D. & Kelly, J. P. (1975) The projections of cells in different layers of the cat's visual cortex. *J. Comp. Neurol.* **163**, 81–106.

Giolli, R. A., Banks, R. H. I. & Torigoe, Y. (1984) Pretectal and brain stem projections of the medial terminal nucleus of the accessory optic system of the rabbit and rat as studied by anteriograde and retrograde neuronal tracing methods. *J. Comp. Neurol.* **227**, 228–251.

Glees, P. (1961) Terminal degeneration and trans-synaptic atrophy in the lateral geniculate body of the monkey. In *The Visual System.* Ed. Jung & Kornhuber, pp. 104–110. Berlin: Springer.

Glees, P. & Clark, W. E. LeGros, (1941) The termination of optic fibres in the lateral geniculate body of the monkey. *J. Anat.* **75**, 295–308.

Godfraind, J. M. (1978) Acetylcholine and somatically evoked inhibition on perigeniculate neurones in the cat. *Brit. J. Pharmacol.* **63**, 295–302.

Guillery, R. W. (1966) A study of Golgi preparations from the dorsal lateral geniculate nucleus of the adult cat. *J. Comp. Neurol.* **128**, 21–50.

Guillery, R. W. (1969) The organization of synaptic interconnections in the laminae of the dorsal lateral geniculate nucleus of the cat. *Z. Zellforsch.* **96**, 1–38.

Guillery, R. W., Geisert, E. E., Polley, E. H. & Mason, C. A. (1980) An analysis of the retinal afferents to the cat's medial interlaminar nucleus and to its rostral thalamic extension, the 'geniculate wing'. *J. Comp. Neurol.* **194**, 117–142.

Guillery, R. W. & Kaas, J. H. (1971) A study of normal and congenitally abnormal retinogeniculate projections in cats. *J. Comp. Neurol.* **143**, 73–100.

Hammond, P. (1972) Spatial organization of receptive fields of LGN neurones. *J. Physiol.* **222**, 53–54P.

Harting, J. K., Hall, W. C. & Diamond, I. T. (1972) *Brain Behav. Evol.* **6**, 425–452.

Harwerth, R. S., Boltz, R. L. & Smith, V. R. (1980) Psychophysical evidence for sustained and transient channels in the monkey visual system. *Vision Res.* **20**, 15–22.

Hassler, R. & Wagner, A. (1965) Experimentelle und morphologische Befunde uber die vierfache corticale Projektion des visuellem Systems. *Proc. 8th. Int. Cong. Neurol. III*, pp. 77–96.

Hayhow, W. R., Webb, C. & Jervie, A. (1960) The accessory optic fiber system in the rat. *J. Comp. Neurol.* **115**, 187–215.

Hess, R. & Wolters, W. (1979) Responses of single cells in cat's lateral geniculate nucleus and Area 17 to the velocity of moving visual stimuli. *Exp. Brain Res.* **34**, 273–286.

Hickey, T. L. & Guillery, R. W. (1973) An autoradiographic study of the efferent connections of the ventral lateral geniculate nucleus in the cat and fox. *J. Comp. Neurol.* **156**, 239–253.

Hochstein, S. & Shapley, R. M. (1976) Linear and nonlinear spatial subunits in Y cat retinal ganglion cells. *J. Physiol.* **262**, 265–284.

Hubel, D. H. & Wiesel, T. N. (1961) Integrative action in the cat's lateral geniculate body. *J. Physiol.* **155**, 385–398.

Hughes, A. (1975) A quantitative analysis of the cat retinal ganglion cell topography. *J. Comp. Neurol.* **163**, 107–128.

Hughes, A. & Wässle, H. (1976) The cat optic nerve: fibre total count and diameter spectrum. *J. Comp. Neurol.* **169**, 171–184.

Hunt, S. P., Lieberman, A. R., Ohara, P.T. & Wu, J. Y. (1982) Interneurones in the dorsal lateral geniculate nucleus (LGd) of the adult rat are GABAergic: evidence from immunocytochemistry. *J. Physiol.* **332**, 61P.

Kaplan, E., Marcus, S. & So, Y. T. (1979) Effects of dark adaptation on spatial and temporal properties of receptive fields in the cat lateral geniculate nucleus. *J. Physiol.* **294**, 561–580.

Kaplan, E. & Shapley, R. M. (1982) X and Y cells in the lateral geniculate nucleus of macaque monkeys. *J. Physiol.* **330**, 125–143.

Kaplan, E. & Shapley, R. (1984) The origin of the S (slow) potential in the mammalian lateral geniculate nucleus. *Exp. Brain Res.* **55**, 111–116.

Kemp, J. A. & Sillito, A. M. (1982) The nature of the excitatory transmitter mediating X- and Y-cell inputs to the cat dorsal lateral geniculate nucleus. *J. Physiol.* **323**, 377–391.

Kirk, D. L., Levick, W. R. & Cleland, B. G. (1976) The crossed or uncrossed destination of axons of sluggish-concentric and non-concentric cat retinal ganglion cells, with an overall synthesis of the visual field representation. *Vision Res.* **16**, 233–239.

Kratz, K. E., Webb, S. V. & Sherman, S. M. (1978) Effects of early monocular lid suture upon neurons in the cat's medial interlaminar nucleus. *J. Comp. Neurol.* **181**, 615–626.

Kruger, J. (1977) The shift-effect in the lateral geniculate nucleus of the rhesus monkey. *Exp. Brain Res.* **29**, 387–392.

Laemle, J. K. (1968) Retinal projections of *Tupaia glis. Brain Behav. Evol.* **1**, 473–499.

Lee, B. B., Creutzfeldt, O. D. & Elepfandt, A. (1979) The responses of magno- and parvocellular cells of the monkey's lateral geniculate body to moving stimuli. *Exp. Brain Res.* **35**, 547–557.

Lee, B. B. & Willshaw, D. J. (1978) Responses of the various types of ganglion cells to moving contours. *Vision Res.* **18**, 757–765.

Lee, C., Malpeli, J. G., Schwark, H. D. & Weygand, T. G. (1984) Cat medial interlaminar nucleus: retinotopy relation to tapetum and implications for scotopic vision. *J. Neurophysiol.* **52**, 848–869.

Lehmkuhle, S., Kratz, K. E., Mangel, S. C. & Sherman, S. M. (1980a) Spatial and temporal sensitivity of X- and Y-cells in dorsal lateral geniculate nucleus of the cat. *J. Neurophysiol.* **43**, 520–541.

Lehmkuhle, S., Kratz, K. E., Mangel, S. C. & Sherman, S. M. (1980b) Effects of early monocular lid suture on spatial and temporal sensitivity of neurons in dorsal lateral geniculate nucleus of the cat. *J. Neurophysiol.* **43**, 542–556.

Lennie, P. (1980) Perceptual signs of parallel pathways. *Phil. Trans. B* **290**, 23–37.

LeVay, S. & Ferster, D. (1977) Relay cell classes in the lateral geniculate nucleus of the cat and the effects of visual deprivation. *J. Comp. Neurol.* **172**, 563–584.

LeVay, S. & Gilbert, C. D. (1976) Laminar patterns of geniculocortical projection in the cat. *Brain Res.* **113**, 1–19.

LeVay, S. & McConnell, S. K. (1982) ON and OFF layers in the lateral geniculate nucleus of the mink. *Nature* **300**, 350–351.

Levick, W. R., Cleland, B. G. & Dubin, M. W. (1972) Lateral geniculate neurons of cat: retinal inputs and physiology. *Invest. Ophthal.* **11**, 302–311.

Lindström, S. (1982) Synaptic organization of inhibitory pathways to principal cells in the lateral geniculate nucleus of the cat. *Brain Res.* **234**, 447–453.

Maffei, L. & Fiorentini, A. (1972) Retinogeniculate convergence and analysis of contrast. *J. Neurophysiol.* **35**, 65–72.

Marrocco, R. T., McClurkin, J. N. & Young, R. A. (1982a) Modulation of lateral geniculate nucleus cell responsiveness by visual activation of the corticogeniculate pathway. *J. Neurosci.* **2**, 256–263.

Marrocco, R. T., McClurkin, J. N. & Young, R. A. (1982b) Spatial summation and conduction latency classification of cells of the lateral geniculate nucleus of macaques. *J. Neurosci.* **2**, 1275–1291.

Mason, B. (1975) Cell properties in the medial interlaminar nucleus of the cat's lateral geniculate complex in relation to the transient/sustained classification. *Exp. Brain Res.* **22**, 327–329.

Mason, R. (1978) Functional organization in the cat's pulvinar complex. *Exp. Brain Res.* **31**, 51–56.

Mastronarde, D. N. (1987) Two classes of single-input X-cells in cat lateral geniculate nucleus. I. Receptive field properties and classification of cells. II. Retinal inputs and the generation of receptive field properties. *J. Neurophysiol.* **57**, 357–380, 381–413.

Maturana, H. R. (1959) Number of fibres in the optic nerve and the number of ganglion cells in the retina of anurans. *Nature* **183**, 1406–1407.

McClurkin, J. W. & Marrocco, R. T. (1984) Visual cortical input alters spatial tuning in monkey lateral geniculate nucleus cells. *J. Physiol.* **348**, 135–152.

Moore, R. Y. & Klein, D. C. (1974) Visual pathways and the central neural control of a circadian rhythm in pineal serotonin N-acetyltransferase activity. *Brain Res.* **71**, 17–33.

Moore, R. Y. & Lenn, N. J. (1972) A retinohypothalamic projection in the rat. *J. Comp. Neurol.* **146**, 1–9.

Niimi, K. & Kuwahara, E. (1975) The dorsal thalamus of the cat and comparison with monkey and man. *J. Hirnforsch.* **11**, 303–325.

Pape, H.-C. & Eysel, U. T. (1986) Binocular interactions in the lateral geniculate nucleus of the cat: GABAergic inhibition reduced by dominant afferent activity. *Exp. Brain Res.* **61**, 265–271.

Penman, G. G. (1934) The representation of the areas of the retina in the lateral geniculate body. *T.O.S.U.K.* **54**, 232–270.

Peters, A. & Palay, S. L. (1966) The morphology of laminae A and A_1 in the dorsal nucleus of the lateral geniculate body of the cat. *J. Anat.* **100**, 451–486.

Phillis, J. W., Tebecis, A. K. & York, D. H. (1967) A study of cholinoceptive cells in the lateral geniculate nucleus. *J. Physiol.* **192**, 695–713.

Polyak, S. L. (1957) *The Vertebrate Visual System.* Chicago: University Press.

Preobrazhenskaya, N. S. (1964) Development and functional significance of pregeniculate nucleus in man. *Fed. Proc.* **23** (transl. suppl.), 715–718.

Raczkowski, D. & Rosenquist, A. C. (1980) Connections of the parvocellular C laminae of the dorsal lateral geniculate nucleus with the visual cortex in the cat. *Brain Res.* **199**, 447–451.

Rakic, P. (1977) Genesis of the dorsal lateral geniculate nucleus in the monkey. *J. Comp. Neurol.* **176**, 23–52.

Rockell, A. J., Heath, C. J. & Jones, E. G. (1972) Afferent connections to the diencephalon in the marsupial phalanger and the question of sensory convergence in the 'posterior group' of the thalamus. *J. Comp. Neurol.* **145**, 105–130.

Rosenquist, A. C., Edwards, S. B. & Palmer, L. A. (1974) An autoradiographic study of the projections of the dorsal lateral geniculate nucleus and the posterior nucleus in the cat. *Brain Res.* **80**, 71–93.

Royce, G. J., Ward, J. P. & Harting, J. K. (1976) Retinofugal pathways in two marsupials. *J. Comp. Neurol.* **170**, 391–413.

Schiller, P. H. & Malpeli, J. G. (1978) Functional specificity of lateral geniculate nucleus laminae of the rhesus monkey. *J. Neurophysiol.* **41**, 788–797.

Shapley, R. & Hochstein, S. (1975) Visual spatial summation in two classes of geniculate cells. *Nature* **256**, 411–413.

Shapley, R., Kaplan, E. & Soodak, R. (1981) Spatial summation and contrast sensitivity of X- and Y-cells in the lateral geniculate nucleus of the macaque. *Nature* **292**, 543–545.

Shatz, C. J. (1983) The prenatal development of the cat's retinogeniculate pathway. *J. Neurosci.* **3**, 482–499.

Sherman, S. M., Wilson, J. R., Kaas, J. H. & Webb, S. V. (1976) X- and Y-cells in the dorsal lateral geniculate nucleus of the owl monkey (*Aotus trivirgatus*). *Science* **192**, 475–477.

Sillito, A. M. & Kemp, J. A. (1983) The influence of GABAergic inhibitory processes on the receptive field structure of X- and Y-cells in cat dorsal lateral geniculate nucleus (dLGN). *Brain Res.* **277**, 63–77.

Sillito, A. M., Kemp, J. A. & Berardi, N. (1983) Cholinergic influence on the function of the cat dorsal lateral geniculate nucleus (dLGN). *Brain Res.* **280**, 299–307.

Singer, W. & Bedworth, N. (1973) Inhibitory interactions between X and Y units in the cat lateral geniculate nucleus. *Brain Res.* **49**, 291–307.

Singer, W. & Creutzfeldt, O. D. (1970) Reciprocal lateral inhibition of ON- and OFF-center neurons in the lateral geniculate body. *Exp. Brain Res.* **10**, 311–330.

So, Y. T. & Shapley, R. (1979) Spatial properties of X and Y cells in the lateral geniculate nucleus of the cat and conductance velocities of their inputs. *Exp. Brain Res.* **36**, 533–550.

Spear, P. D., Smith, D. S. & Williams, L. L. (1977) Visual receptive-field properties of single neurons in cat's ventral lateral geniculate nucleus. *J. Neurophysiol.* **40**, 390–409.

Stanford, L. R., Friedlander, M. J. & Sherman, S. M. (1983) Morphological and physiological properties of geniculate W-cells of the cat: a comparison with X- and Y-cells. *J. Neurophysiol.* **50**, 582–608.

Stephan, F. K. & Zucker, I. (1972) Circadian rhythms in drinking behavior and locomotor activity of rats are eliminated by hypothalamic lesions. *Proc. Nat. Acad. Sci.* **69**, 1583–1586.

Sterling, P. & Davis, T. L. (1980) Neurons in cat lateral geniculate nucleus that concentrate exogenous [3H]-gamma-aminobutyric acid (GABA). *J. Comp. Neurol.*, **192**, 737–749.

Stevens, J. K. & Gerstein, G. L. (1976) Spatiotemporal organization of cat's lateral geniculate receptive fields. *J. Neurophysiol.* **39**, 213–238.

Stone, J. (1966) The naso-temporal division of the cat's retina. *J. Comp. Neurol.* **126**, 585–599.

Stone, J., Dreher, B. & Leventhal. A. (1979). Hierarchical and parallel mechanisms in the organization of the visual cortex. *Brain Res. Rev.* **1**, 345–394.

Stryker, M. P. & Zahs, K. R. (1983) On and off sublaminae in the lateral geniculate nucleus of the ferret. *J. Neurosci.* **3**, 1943–1951.

Sur, M., Esguerra, M., Garraghty, P. E., Kritzer, M. F. & Sherman, S. M. (1987) Morphology of physiologically identified retinulogeniculate X- and Y-axons in the cat. *J. Neverophysiol.* **58**, 1–32.

Sur, M., Humphrey, A. L. & Sherman, S. M. (1982) Monocular deprivation affects X- and Y-cell retinogeniculate terminations in cats. *Nature* **300**, 183–185.

Sur, M. & Sherman, S. M. (1982) Retinogeniculate terminations in cats: morphological differences between X- and Y-cells axons. *Science* **218**, 389–391.

Suzuki, H. & Kato, H. (1969) Neurons with visual properties in the posterior group of thalamic nuclei. *Exp. Neurol.* **23**, 353–365.

Swanson, L. W., Cowan, W. M. & Jones, E. G. (1974) An autoradiographic study of the efferent connections of the ventral lateral geniculate nucleus in the albino rat and the cat. *J. Comp. Neurol.* **156**, 143–164.

Szentágothai, J. (1963) The structure of the synapse in the lateral geniculate body. *Acta Anat.* **55**, 166–185.

Terubayashi, H. & Fujisawa, H. (1984) The accessory optic system of rodents. *J. Comp. Neurol.* **227**, 285–295.

Thuma, B. D. (1928) The cytoarchitecture of the corpus geniculatum laterale. *J. Comp. Neurol.* **46**, 173–200.

Tong, L., Kalil, R. E. & Spear, P. D. (1982) Thalamic projections to visual areas of the middle suprasylvian sulcus in the cat. *J. Comp. Neurol.* **212**, 103–117.

Trojanowski, J. Q. & Jacobson, S. (1976) Areal and laminar distribution of some pulvinar cortical efferents in rhesus monkey. *J. Comp. Neurol.* **169**, 371–392.

Troy, J. B. (1983a) Spatial contrast sensitivities of X and Y type neurones in the cat's dorsal lateral geniculate nucleus. *J. Physiol.* **344**, 399–417.

Troy, J. B. (1983b) Spatio-temporal interaction in neurones of the cat's dorsal lateral geniculate nucleus. *J. Physiol.* **344**, 419–432.

Vancy, D. I. & Hughes, A. (1976) The rabbit optic nerve: fibre diameter spectrum, fibre count, and comparison with a retinal ganglion cell count. *J. Comp. Neurol.* **170**, 241–251.

Vastola, E. F. (1960) Monocular inhibition in the lateral geniculate body. *E.E.G. Clin. Neurophysiol.* **12**, 399–403.

Vidyasagar, T. R. & Urban, J. V. (1982) Orientation sensitivity of cat LGN neurones with and without inputs from visual cortical areas 17 and 18. *Exp. Brain Res.* **46**, 157–169.

Wässle, H., Levick, W. R. & Cleland, B. G. (1975) The distribution of the alpha type of ganglion cells in the cat's retina. *J. Comp. Neurol.* **159**, 419–437.

Wilson, J. R., Friedlander, M. J. & Sherman, S. M. (1984) Fine structural morphology of identified X- and Y-cells in the cat's lateral geniculate nucleus. *Proc. Roy. Soc.* **B 221**, 411–436.

Wilson, P. D., Rowe, M. H. & Stone, J. (1976) Properties of relay cells in cat's lateral geniculate nucleus: a comparison of W-cells and Y-cells. *J. Neurophysiol.* **39**, 1193–1209.

Wurtman, H. J., Axelrod, J., Chu, E. W. & Fischer, J. E. (1964) Mediation of some effects of illumination on the rat estrous cycle by the sympathetic nervous system. *Endocrinology* **75**, 266–272.

Zeki, S. M. (1978) Functional specialization in the visual cortex of the monkey. *Nature* **274**, 423–428.

19. NEUROPHYSIOLOGY OF PERCEPTION: CORTICAL PROJECTION

THE VISUAL CORTEX

From the lateral geniculate nucleus the visual impulses are relayed to the cerebral cortex.

Striate and Prestriate Areas

Thus the third-order neurones pass as the *optic radiation* to the surface of the occipital pole, relaying with the cortical neurones in Brodmann's Area 17, or the *striate area*, so called because the axons of the optic radiation form a well-defined *white line of Gennari* on their way to their synapses with the subjacent layer IV, together with axons of association fibres passing to adjacent cortex. The region over which the striate area extends is illustrated in Figs 19.1 and 19.2.

Projection to Prestriate Area

In the primate, the projection from the lateral geniculate nucleus was considered, until recently, exclusively to area 17, or the striate area, so that adjacent visual areas, such

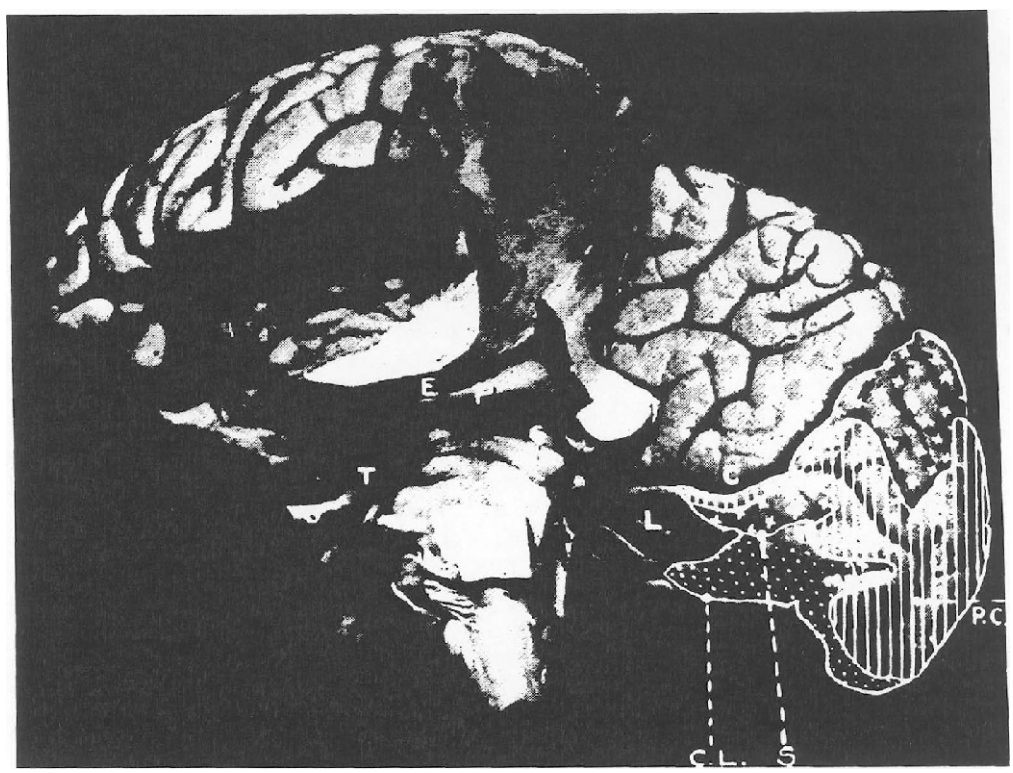

Fig. 19.1 The cortical visual areas. Striate area marked with vertical lines; the parastriate area with crosses and the peristriate area with dots. C, calcarine fissure; C.L., collateral sulcus; S, sagittal sulcus of the gyrus lingualis (L); O, optic nerve; T, optic tract; E, lateral geniculate body; P, pulvinar; S, superior colliculus; *i*, inferior colliculus. (Whitnall, *Anatomy of the Human Orbit.*)

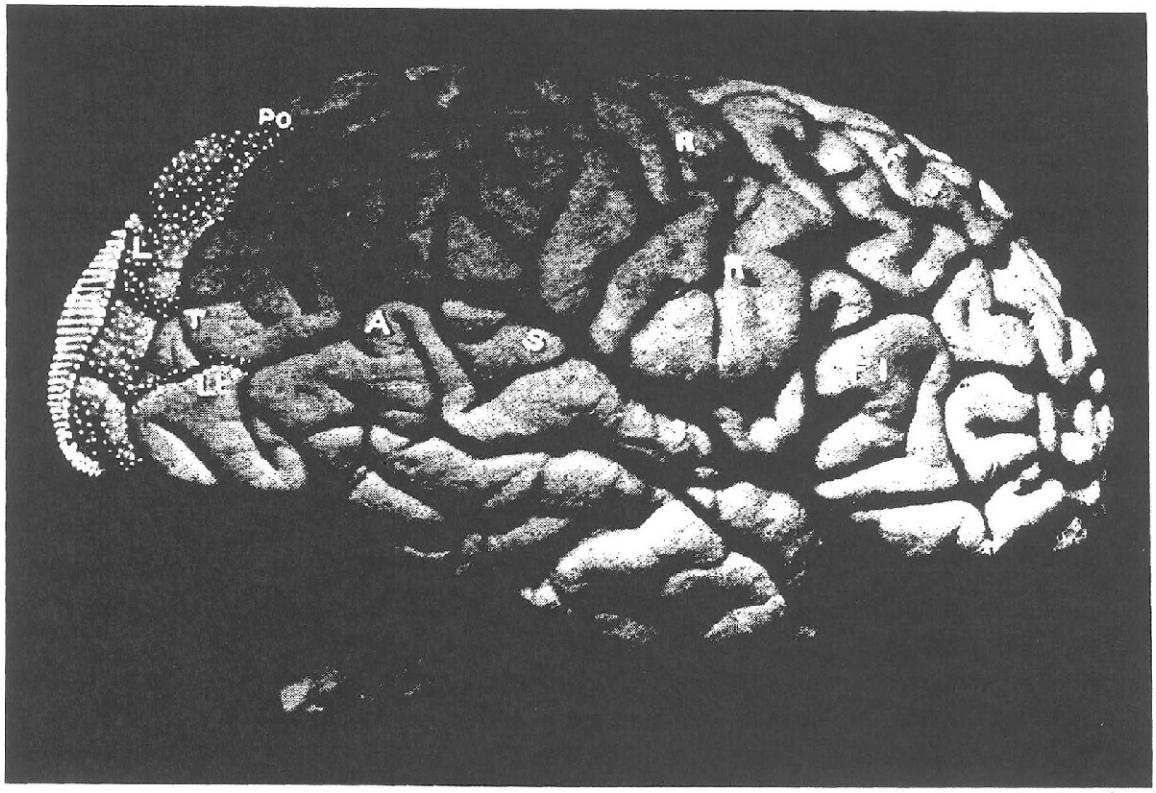

Fig. 19.2 Lateral view of the right hemisphere. Striate area marked with cross lines; the parastriate and peristriate areas by large and small dots respectively. PO, parieto-occipital; L, lunate; T, transverse occipital; Lt, lateral sulcus. A is placed on the angular gyrus, which surrounds the upturned end of the superior temporal sulcus. S, S, S is the lateral cerebral fissure (fissure of Sylvius). R, R is the central sulcus (fissure of Rolando). FS, FM, FI are placed on the posterior parts of the superior, middle and inferior frontal convolutions respectively; between them and the sulcus are the pre-central sulcus and convolution. (Whitnall, *Anatomy of the Human Orbit.*)

as the peristriate and parastriate, or areas 18 and 19,[1] relied on their visual input from area 17. In the cat, however, and some other lower mammals, the prestriate area 18 has been shown to receive a geniculate projection also. In the primate, when retrograde movement of horseradish peroxidase from different visual cortical regions was studied, Yukie & Iwai (1981) demonstrated a relatively small projection to the monkey's prestriate area from the dorsal lateral geniculate nucleus, some of the neurones originating in the interlaminar regions. The neurones projecting to the prestriate area were characteristically different in size and shape from those projecting to the striate area. This projection to area 18, or V2, in the macaque was confirmed by Bullier & Kennedy (1983) who employed a technique involving the retrograde movement of fluorescent dyes, Fast Blue and Diamidino Yellow. The neurones projecting to area 18 were more scattered than those projecting to the striate, or VI, area, and most belonged to the interlaminar S-regions, i.e. regions that did not project to the striate area. The authors emphasized the difference from the cat's projection, which was from the main laminae. The geniculate areas projecting to V2 receive a projection from the superior colliculi, so that in the primate we might expect eye-movement and visual stimulation to be coordinated in V2. However, a similar projection to the striate area has been described (p. 631). In the primate, then, there are two pathways to area 18 or V2, namely direct and through area 17, or V1.

Retinal Projection on the Cortex

Small lesions in the striate area of man lead to blindness in well-defined regions of the visual fields, and a systematic study of the effects of gun-shot wounds in this region of the cortex has led to the definite picture of the projection of the retina on the visual cortex reproduced in Fig. 19.3 from Gordon Holmes (1945). In general the projection may be represented by picturing one half of the

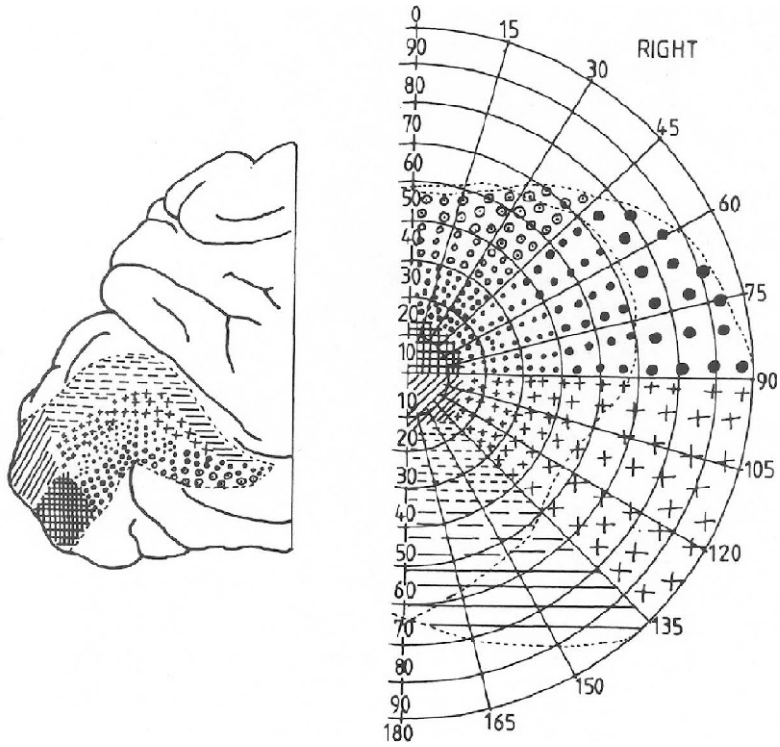

Fig. 19.3 Projection of the retina on the visual cortex. On the left the striate area of the left hemisphere of the brain is shown, the calcarine fissure being opened up to reveal that portion of it that lines its walls. On the right is the right half of one visual field. The correspondence of the markings indicates the representation of different segments of the visual field on the cortex. (Gordon Holmes, *Proc. Roy. Soc.*)

retina spread over the surface of one striate area, the macular region being placed posteriorly, the periphery anteriorly, the upper margin along its upper edge and the lower on its inferior border. The macula, as one might expect, is projected over an area out of all proportion to its size, just as with the motor representation of area 4, where the cortical centres concerned with the hand are much larger than those connected with movements of the proximal segments of the arm. More recent studies of head injuries by Spalding (1952a, b) have largely confirmed the picture presented by Gordon Holmes.

'*Point-to-point Projection*'

Anatomical and physiological investigation has confirmed this general plan of the retinal projection and has brought out the existence of a virtual 'point-to-point' relationship between retinal stimulus and cortical representation. For example, in the monkey, a definite projection map can be plotted by stimulating the retina with a point source of light and determining the exact locus of the electrical potential evoked in the cortex (Talbot & Marshall, 1941). From a strictly anatomical point of view this point-to-point projection, in the sense of a single cone being connected to a single bipolar cell, which is connected to a single ganglion cell, and so on, is not possible; in the retina the one-to-one relationship between cone and optic nerve fibre only holds good in the central fovea, and even here it is only a functional relationship since impulses from a single cone have subsidiary paths which permit a spread of their responses outwards to several ganglion cells. Similarly, as we have just seen, in the lateral geniculate body, although there are no internunciary neurones, each fibre of the tract ends on a number of geniculate cells, and a further dispersion is possible in the cortex by intracortical association cells. The point-to-point relationship is therefore a functional one, in that there is a preferential path from one cone, say, to one cortical cell. In general terms, because of the scattering of receptive field positions of neighbouring cells encountered by an electrode penetrating the cortex, and because of the finite size of each receptive field, a single point on the cortex corresponds, not to a point, but an area of the visual field.

Cortical Magnification Factor

If the retina is projected on to the visual cortex in the way these studies suggest, we may speak of a *cortical magnification factor*; for example, if 1 mm of retina were represented by 3 mm of cortex, the magnification would be 3, or, since 1 mm of retina corresponds to a visual field of about 3.3°, the magnification would be about 1 mm/degree. Daniel & Whitteridge (1959) have extended Talbot &

Marshall's studies on visual cortex of the monkey and baboon and have shown that the magnification decreases evenly from a value of 5.6 mm/degree at the fovea to about 0.1 mm/degree at a visual angle of 60°. Having measured the magnifications along different meridians of the visual field, Daniel & Whitteridge made a map of the striate cortex by applying these magnifications; it was obviously not the simple surface of a sphere, because of the distortion imposed by the variation in magnification. The area of the calculated surface came out at 1320 mm^2. If this was folded twice, once along the horizontal meridian for its anterior half, and vertically at the junction of the posterior and middle thirds, the resulting folded surface corresponded with the actual surface of the calcarine cortex in monkeys and baboons.

WAKING MONKEY

In a more elaborate study on the waking macaque, Dow *et al.* (1981) established a much larger magnification factor at the foveola, namely 30 mm/degree. Essentially the experimenter is measuring the sizes of cortical neurone receptive-fields in relation to position of the stimulating spot of light on the retina. These receptive fields become larger in the periphery and it was generally considered that they increased inversely with the magnification, so that roughly the same number of cortical cells were involved in 'seeing' a point in space, wherever it was located. Dow *et al.* showed, however, that this was not true, the product of magnification and aggregate field-size being greater in central vision than in peripheral vision, a resonable finding in view of the importance of central vision in discriminatory activities such as spatial resolution. Dow *et al.* computed that, with a cortical diameter of 10 mm for the image of a retinal point there would be some 2.65×10^7 cells stimulated for a foveal point, and at 30° eccentricity it would be about 100 times smaller.

In Fig. 19.4 the size of the projection of a point image on the cortex has been plotted against eccentricity; on the same graph is the size of the cortical projection of the minimum resolvable angle expressed as a cortical distance and it will be seen how much larger the image-size is, indicating that resolution depends on discontinuities in the receptive field rather than on the total receptive field, a process achieved by spatial tuning (p. 583).

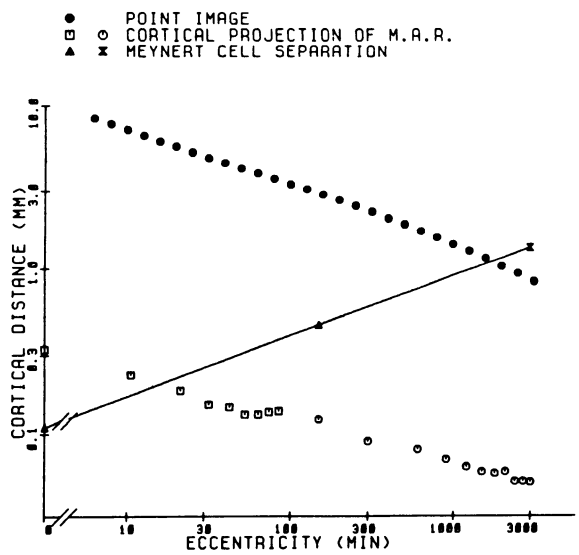

Fig. 19.4 Point image size in monkey striate cortex as a function of eccentricity. Also plotted are minimal angle of resolution (MAR) for man, converted to cortical dimensions, and Meynert cell separation for three eccentricities in the rhesus monkey. ⊡ from Weymouth *et al.* (1928); ⊙ from Wertheim (1894); ▲ from Chan-Palay *et al.* (1974); ⧗ from LeGros Clark (1942). Point image is the product of magnification (M) and aggregate field size (F), where

$$F = 4\sqrt{r^2 + s^2}$$

with r a measure of receptive field scatter and s a measure of receptive field size. r was taken as $0.314f - 0.86$ min. The aggregate field includes two standard deviations on either side of the centre. (Dow *et al.*, *Exp. Brain Res.*)

More Accurate Technique Van Essen *et al.* (1984) have emphasized the difficulties in plotting retinal projection on the striate area since so much of it is buried in the calcarine sulcus; by use of two-dimensional representation, as Daniel & Whitteridge (1959) were the first to do, a planar display is achieved. Van Essen & Maunsell (1983) have considerably increased accuracy of representation by using the outlines of histological sections to construct two-dimensional representations of convoluted regions. Van Essen *et al.* (1984) have applied this technique to a painstaking plotting of the non-foveal retina on the cortex of the macaque monkey. Figure 19.5 illustrates a map based on their main experiment, where the roughly horizontal lines indicate lines of constant eccentricity from the fovea, and the orthogonal lines are those of constant polar angle. The enormous emphasis on central vision is emphasized, more than half of striate cortex being devoted to 10° of central vision. Like earlier workers they assessed the cortical magnification factor,[2] and they confirmed that magnification was roughly predictable from eccentricity, being proportional to the inverse of this; in terms of areas this means that the area of cortex devoted to a given field in the retina is proportional to the inverse square of eccentricity. At large eccentricities they found some deviation. Again, magnification was not independent of the polar angle at any eccentricity, but generally the size of cortex devoted to a given retinal area was higher for fields along the horizontal meridian. By an extrapolation procedure they calculated a factor of 13 mm/deg and 5 mm/deg at 0° and 1° respectively. In general, in the central region, the size of the receptive field of a given cortical point shows a smaller

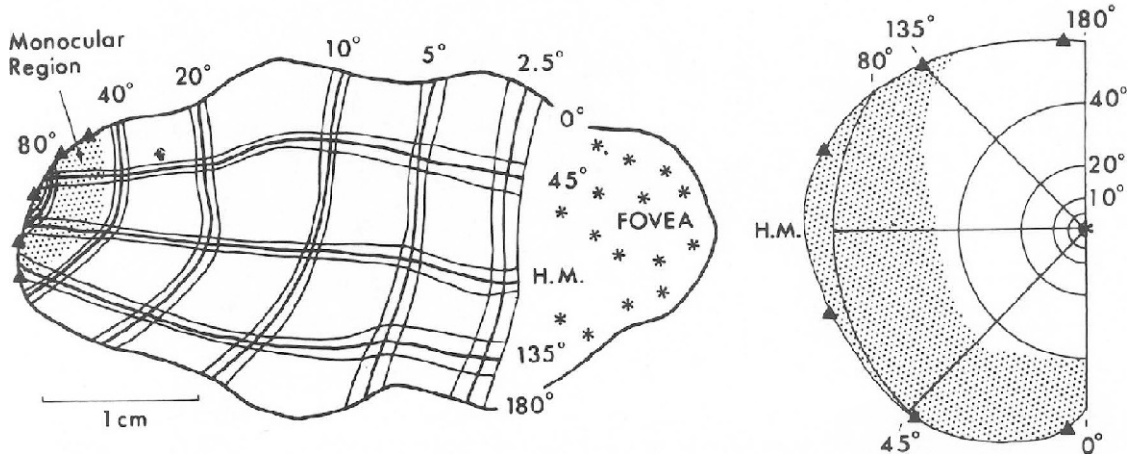

Fig. 19.5 The location of iso-eccentricity and iso-polar contours in striate cortex of the main experiment. The locations of these contours were determined using a computer program to interpolate or extrapolate over limited distances. The computer first searched for all pairs of recording sites separated by less than 8 mm. To determine the location of any given isoeccentricity contour, it then selected all pairs in which one or both receptive fields were within 30% of the desired eccentricity. By interpolation or extrapolation from each pair over a limited distance, the location of a family of points on this contour could be predicted. In making the interpolation or extrapolation, it was assumed that the X-coordinate on the map was proportional to the logarithm of eccentricity and that the Y-coordinate was independent of eccentricity. For iso-polar contours, a similar procedure was carried out, starting by selecting pairs in which one or both receptive fields were within 20° of the desired polar angle. Interpolation and extrapolation were based on the assumption that the Y-coordinate was linearly proportional to the polar angle and the X-coordinate independent of it. None of these assumptions is perfectly true, but it was inferred that they were reasonably accurate, based on the rather limited scatter seen for the points used to predict the various contours. Stippling denotes the region in which exclusively contralateral (left-eye) responses were obtained. This 'monocular region' was determined from recordings while the eyes were directed straight ahead, and it in part reflects the obstruction of the field of view by the nose. The true monocular segment completely lacks anatomical inputs from the ipsilateral eye and cannot be driven binocularly even when the eyes are deviated to the ipsilateral side; it is somewhat smaller than the region indicated here. (Van Essen *et al.*, *Vision Res.*)

dependence on retinal eccentricity than more eccentric regions, so that they plotted separate regression lines for data above and below 5.5° eccentricity, as in Fig. 19.6.

CORTICAL SIZE OF A POINT IMAGE

The extent of cortex activated by a point image on the retina is given by the product of the size of the cortical receptive field covering this point and the magnification. As Dow *et al.*'s (1981) study indicated (Fig. 19.4) this is largest at the fovea and diminishes linearly with eccentricity. In Van Essen *et al.*'s study, because of the more complex relation between receptive field-size and eccentricity, the curve of cortical area of point image versus eccentricity showed two regions. The absolute value of their estimate, 0.1 to 0.6 mm^2, is considerably lower than that obtained by others over the same eccentricity range, namely 1–9 mm^2. The wide range of values hinges largely on the wide range of reported magnification factors from 4.5 mm/deg by Hubel & Wiesel (1974) to 4.30 mm/deg by Talbot & Marshall (1941) and Dow *et al.* (1981), a 50-fold variation. Re-evaluation of earlier work suggested to Van Essen *et al.* a peak value of 15–20 mm/deg, closer to their own estimate and that of Tootell *et al.* (1982) based on deoxyglucose labelling.

GANGLION CELL DENSITY

The steep increase in cortical magnification as the fovea is approached may be compared with the increase in density of ganglion cells in the retina. Thus the magnifications at 1° and 80° eccentricity are in the ratio of about 4400 to 1 so far as cortex is concerned; using the measurements of Rolls & Cowey (1970), Van Essen *et al.* estimated a ratio some 50 times less, thus emphasizing the great extent to which the fovea is favoured by the cortex.

CORTICAL MODULES

We shall see that receptive fields in the striate cortex are arranged in a columnar manner, cortical neurones displaying orientation-sensitivity, for example, being encountered in a vertical penetration of the cortex in regular sequences of slightly changing preference. In general a complete set of orientation columns, called a hyper-

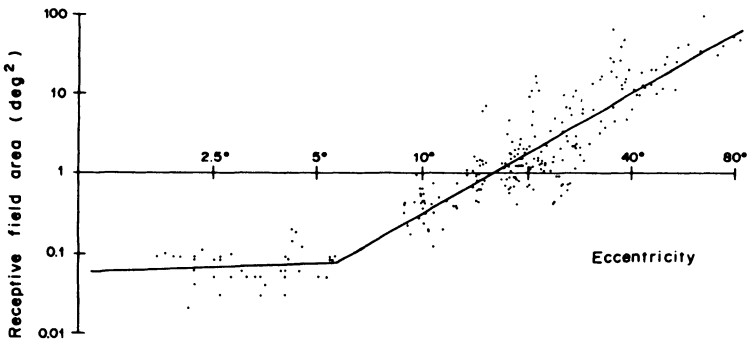

Fig. 19.6 Receptive field area versus magnification. For binocularly driven responses, separate values are plotted for the left and right eyes. Separate regression lines were calculated for the data above and below 5.5° eccentricity. (Van Essen *et al.*, *Vision Res.*)

column, occupied a distance of about 2–3 mm; the estimated cortical size of a point image was likewise of this order, and the conclusion was that these modules contained enough neurones to analyse the spatial features of the points in space covered by their receptive fields. However, the more recent studies of Dow *et al.* (1981) and Van Essen *et al.* (1984) have demonstrated a considerable variability in cortical point-image size, from a minimum of about 0.1 mm^2 to a maximum of 70 mm^2. It is possible, therefore, that more than one module analyses a single point in the retinal field.

Projection of the Lateral Geniculate Nucleus on the Cortex

Geniculate Lesions

Wilson & Cragg (1967) examined the projection of the lateral geniculate body on the visual cortex by the location of degeneration in the cortex following lesions placed in the geniculate bodies. In the monkey they confirmed that the projection was confined to area 17, but in the cat degeneration extended to area 18 (Visual 2); and this agrees with the finding of short-latency responses to light recorded from this area by Berkley *et al.* (1967); responses that survived cutting of the corpus callosum and removal of area 17. A further projection was found on the suprasylvian gyrus. Lesions medial to the lateral geniculate body (pulvinar) caused some degeneration in area 19 (Visual 3), and this may correlate with Suzuki & Kato's (1969) description of cells in the posterior thalamus of the cat responding to photic stimulation of the retina.

Retrograde Labelling

Geisert (1980) examined geniculate projections in the cat to areas 17, 18 and 19 by injections of horseradish peroxidase into the nucleus and studying retrograde movement of the label. Laminae A and A_1 sent 10% of their neurones to areas 17 and 18 by branched axons; 70% to area 17 only and less than 1% to area 18 only. The C lamina sent 50% to areas 17 and 18 by branched axons, 20% to area 17 only and 10% to area 18 only. The medial interlaminar nucleus (MIN) projected to area 17 only, area 18 only, and areas 17 and 18 by branched axons. Injections into area 19 only gave label in MIN and the C-lamina; thus the C-laminae project to areas 17, 18 and 19.

Lamination of the Cerebral Cortex

The sensory cortex of the primate contains six main layers; these are illustrated by Figs 19.7 and 19.8, which not only show the lamination, but some of the types of neurone. In general the, fourth lamina, the so-called granular layer, is the main site of monosynaptic termination of the thalamic input, in this case that of the dorsal lateral geniculate nucleus. Lamina 4 has been divided into a number of sublaminae; geniculate input is segregated so that parvocellular neurones relay in $4C_\beta$ mainly, whilst magnocellular neurones relay in $4C_\alpha$, a segregation that may well be concerned with the parallel processing of visual information through the X- and Y-cell pathways. Lamina 4B is a horizontally orientated band of fibres comprising the major part of the line of Gennari that lends its name to this striate area. As with the other regions of primary sensory cortex, the stellate neurones are able to transmit their inputs vertically by synapsing with the apical dendrites of pyramidal cells, and in this way we obtain the columnar organization that is the dominant feature of primary sensory cortex. In general, the more superficial layers of the cortex are the source of commissural and association connections within the cortex, while the deeper layers are the sources of corticofugal connections. For example, the cells of lamina 5 project to the superior colliculus, and those of lamina 4 to the dorsal lateral geniculate nucleus, thereby providing a reciprocal interconnection between the cortical and subcortical centres.

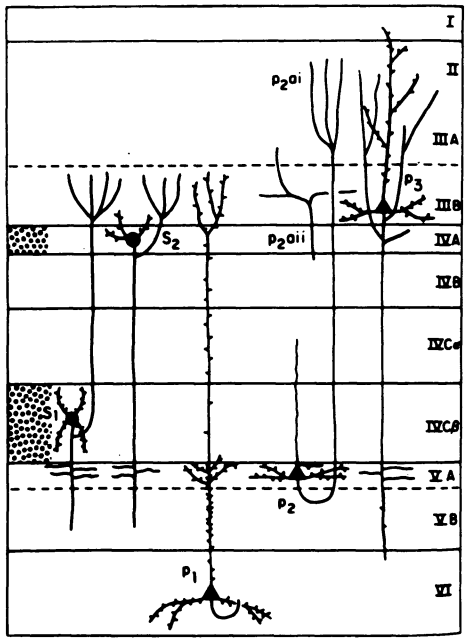

Fig. 19.7 Diagram of spiny stellate and pyramidal neurone relationships to the parvocellular dorsal lateral geniculate projection to area 17. Coarse dots indicate the principal laminae (IVCβ and IVA) receiving parvocellular projection (lamina I projection omitted). The axons of spiny stellate neurones (S1 and S2) lying in laminae IVA and IVCβ project principally to laminae IIIB and VA as well as within IVCβ. One class of lamina VI pyramidal neurone (P1) has apical dendritic branching only in laminae VA and IIIB. Pyramidal neurones with basal dendritic arborization in lamina VA (P2) show a strong axon projection into lamina IIIA (P2ai) or IIIB (P2aii), and those with basal dendritic arborizations in laminae IIIB show principal axonal arborizations in laminae IIIA and VA. (Lund & Boothe, *J. Comp. Neurol.*)

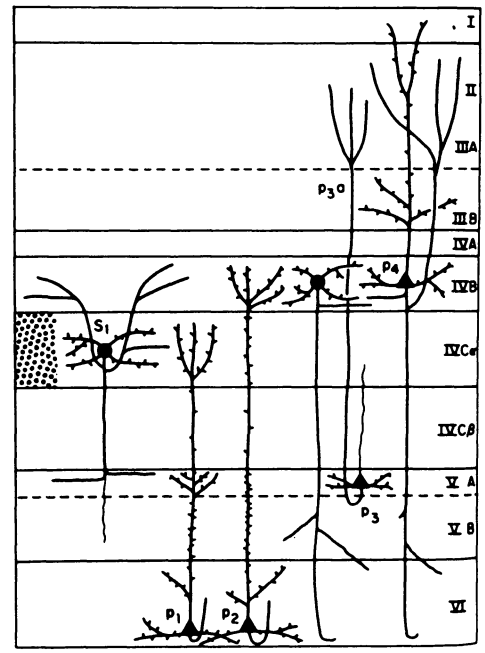

Fig. 19.8 Diagram of spiny stellate (S_1) and pyramidal neurones (P_{1-4}) and their axonal and dendritic ramifications in the laminae of the visual cortex. Coarse dots indicate the principal lamina (IVCα) receiving magnocellular projection. (Lund & Boothe, *J. Comp. Neurol.*)

Projections to the Cortical Laminae

Feline Projections

The specific sensory afferents ramify principally within layer IV of the sensory cortex, and the visual cortex is no exception; the extent to which other laminae are involved in direct projection is a matter on which there is not complete agreement, and there may well be species differences. The modern technique of injecting labelled leucine into a region of the brain, and observing its axonal transport to the projection areas of the neurones taking up the leucine, has enabled more accurate studies of projection. Thus LeVay & Gilbert (1976) injected into the main separate layers A, A_1 and C of the cat's geniculate body and examined the distribution of radioactivity in the visual cortex. With lamina A injections they found uptake in areas 17 and 18 confined to two bands, one occupying layer IV and the bottom of layer III and the other layer VI; injection of layer A_1 gave a similar pattern. No attempt was made to discriminate between the C layers; projection extended not only to areas 17 and 18 but also area 19 and the suprasylvian gyrus. In area 17 the main projection split into two bands, one at the IV/V border and one in the upper part of IVab extending well into layer III; in addition, layer I received a clear projection but there was no projection to layer VI. Thus, according to this study in the cat, the visual projection is distributed more widely than had been suspected, with only the upper parts of layers II + III and the lower part of layer V completely free.

BRANCHED PROJECTION

Stone & Dreher (1973) found that antidromic activation of a given Y-cell in the lateral geniculate body of the cat could be achieved by stimulation of both area 17 and 18, indicating a branching of the Y-cell's axon. The slower-conducting X-cells apparently only projected to area 17.

Primate Geniculate Input

As described by Lund & Boothe (1975), parvocellular laminae project largely to laminae IVC_β and in lamina IVA; these axons probably terminate on spiny stellate neurones. The lamina IVC_β neurones all appear to send

recurrent axons to lamina III where they terminate. Many also project downwards to lamina VA. In general, the bulk of the parvocellular input to lamina IV seems to be transmitted to laminae IIIB and VA. Magnocellular geniculate neurones project to cortical lamina IVC_β, probably to spiny stellate neurones. Axonal projections of these IVC_β neurones are largely recurrent in IVC and in IVB; some descending axons may reach lamina VI. Pyramidal neurones in lamina VI may well transmit this geniculate input, through their apical dendrites, to more superficial laminae, e.g. III and II. In general, magnocellular geniculate information entering lamina IVC appears to be relayed primarily to laminae IVB and VA, whence information is passed to laminae III and II.

SQUIRREL MONKEY

The dorsal lateral geniculate nucleus of the squirrel monkey (*Saimiri sciureus*) consists of two dorsally located parvocellular layers, a pair of more ventral magnocellular layers, and a small pair of S-layers in the hilus adjacent to the inferior pulvinar nucleus. There is also an interlaminar zone between the parvo- and magnocellular pairs of layers, and between the separate pairs. Fitzpatrick *et al.* (1983) studied geniculate projection by antero- and retrograde movements of horseradish peroxidase; they confirmed the segregation of the parvo- and magnocellular geniculate projections in sublaminae of lamina IV, namely IV_β for parvo- and IV_α for magnocellular inputs. They described a third pathway originating in a characteristic group of neurones in the intercalated layers of the nucleus, a region that also has input from the superior colliculus (Harting *et al.*, 1980). These, considered to be W-cells, project to lamina I. This superficial cortical projection may well correspond to the cytochrome oxidase 'puffs' in laminae II–III (Livingstone & Hubel, 1982).

A similar cortical projection to the most superficial lamina I from the interlaminar zones was described by Weber *et al.* (1983), whilst the S-lamina ended in a patch-like fashion in laminae IIIa and IIIb. They considered that both pathways conveyed W-cell information. They emphasized the fact that the projections from the geniculate nucleus to the superficial layers of the cortex provide this region of the brain with information derived from both superior colliculi, concerned with eye-movements, and the retinae, concerned with vision; thus the interlaminar and S-regions are those that received collicular projection (Harting *et al.*, 1980).

Identification by Electrical Recordings

Ferster & Lindström (1983) recorded excitatory and inhibitory postsynaptic potentials in identified cortical neurones within the different layers, resulting from stimulation of afferents from the lateral geniculate nucleus, electrical stimulating electrodes being placed strategically in the optic tract, superior colliculus, lateral geniculate nucleus, and optic radiation. The cortical layer in which the recording electrode was located, for any given cell, was indicated by the character of the field potentials generated by the electrical stimulation. The results of this study are indicated in Fig. 19.9 and may be briefly summarized. All impaled cells in layers, III, IV and VI received direct excitatory connections from the lateral geniculate nucleus, whilst those in layers II and V received visual input only via other cortical neurones. From the point of view of cortical efferent projection, we may say that cortico-geniculate cells receive monosynaptic excitation from the geniculate, so that there is perfect reciprocity leading to feedback on the lateral geniculate nucleus. Corticulo-collicular neurones receive indirect excitation, while cortico-cortical neurones receive either. Interestingly, the connectivity found here for area 17 is similar to that described by Harvey (1980) for area 18 in the cat.

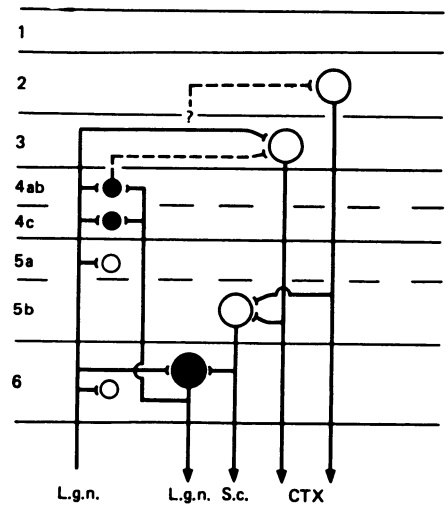

Fig. 19.9 A schematic illustration of excitatory synaptic connexions in area 17. The filled lines represent direct connexions from l.g.n. relay cells and intracortical collateral connections identified by antidromic activation of the presynaptic neurones. The input to layer 3 cells from layer 4ab is suggested on the basis of a disynaptic e.p.s.p. evoked from the l.g.n. and from anatomical evidence (see text). The disynaptic excitatory input to layer 2 cells presumably originates from layer 4c cells. Open and filled circles indicate complex and simple cells; large and small circles represent cells with and without extracortical projection. (Ferster & Lindstrom, *J. Physiol.*)

Layer 4 Cells

Electron microscopical studies of the terminations of geniculate neurones in layer 4 have shown that probably all cortical neurones in this layer synapse with geniculate axon terminals (Davis & Sterling, 1979; Hornung & Garey, 1981); Layer 6 cells send their apical dendrites into

Layer 4 where they branch repeatedly. In general, then, the terminals of geniculate cells do not make contacts indiscriminately with all dendrites in their vicinity, but rather select among them according to functional specificity. Within layer 4, terminals of geniculate afferents are segregated, so that those of Y-cells are in 4ab and of X in 4c. Thus a selective input of this kind could lead to parallel processing of visual input.[3]

Projections from the Visual Cortex

The pathway from cerebral cortex to lower visual centres was investigated by Gilbert & Kelly (1975), who injected horseradish peroxidase into different parts of the brain concerned with vision; this tracer is taken up by nerve endings and passes *retrogradely* to the cell-body and dendrites, where it is identified in the electron microscope. When injected into layers A and A_1 of the lateral geniculate body, the tracer was found in layer VI of the visual cortex, the labelled cells being pyramids. Areas 18 and 19 also contained the tracer, indicating cortico-geniculate pathways from these prestriate areas. Using the opposite technique of axonal transport of ^{3}H-proline from cell body to terminals, Updyke (1975) described projections from areas 17, 18 and 19 to the various laminae of the cat's lateral geniculate body, the most dense projection being from area 17.

Cortical Laminae

The laminar distribution of efferents from the cat's striate area has been studied by several workers, summarized by Lund *et al.* (1979); neurones in lamina VI project to the dorsal LGN whilst lamina VB projects to the superior colliculus and pulvinar through collaterals of giant pyramids. Neurones of VA are intrinsic relay-neurones projecting to upper cortical laminae. Laminae II and III project to the Clare-Bishop area on the medial bank of the lateral suprasylvian sulcus, whilst this area projects back to laminae I and VI. Area 19 (V3) projects to lamina I.

Monkey

In the macaque monkey Lund *et al.* (1975) examined the projections from the striate area by following retrograde passage of horseradish peroxidase. Their results have been summarized in Fig. 19.10. Neurones from the upper half of lamina VI projected to the parvocellular division of the lateral geniculate nucleus and those in the lower half to the magnocellular layers. Projections to the superior colliculi and pulvinar were derived from pyramidal cells in layer VB; the largest neurones gave a branched projection to the lateral geniculate body and superior

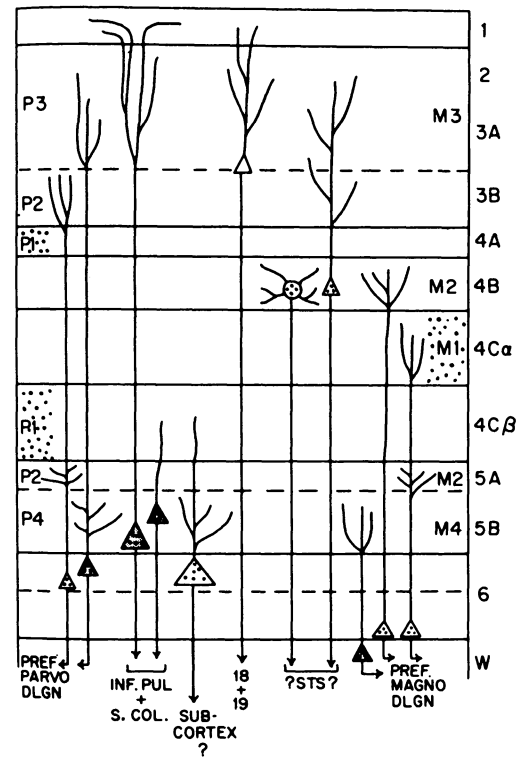

Fig. 19.10 Summary diagram of area 17 correlating the position of efferent cell bodies with the intrinsic organization of the cortex as shown by Golgi studies. The laminar numbering system used here is shown to the right. Laminar stippling indicates primary input from parvocellular (left) and magnocellular (right) divisions of the geniculate. P1 to P4 signify the interlaminar relay of information derived from the parvocellular division of the geniculate; M1 to M4, the interlaminar relay of information from the magnocellular division. Those cells marked by dots have been identified as efferents in this study. Cells for which the destination of the efferents is known have been marked by a shaded cell body when their dendritic tree arborizes in laminae receiving higher order (i.e., P3, P4, M3, M4) connections. The destinations of the pathways marked with queries are unknown. (Lund *et al.*, *J. Comp. Neurol.*)

colliculus. Taken in conjunction with other studies showing that laminae II and III project to areas 18 and 19, the results show that every lamina of the visual cortex of the primate has an extrinsic projection with the exception of those receiving direct thalamic input, namely laminae I, IVA and IVC, each lamina projecting to a different destination.

Horizontal Organization

Lund *et al.* emphasize the horizontal organization of cortical projections, implying marked differences in organization of neurones at different depths of the cortex;

this is in contrast with the physiological studies suggesting a columnar organization of physiological similarity from pia to white matter so far as orientation-specificity is concerned (p. 546).

The Prestriate Cortex

Area 17, the striate cortex, is surrounded by cortex concerned with vision, and this was delineated by Brodmann on a morphological basis; this *prestriate cortex* was designated areas 18 and 19 or the *parastriate* and *peristriate areas* respectively, but there are no obvious cytoarchitectonic features to differentiate the two areas from each other. In order to determine how these areas were interrelated, v. Bonin *et al.* (1942) applied strychnine to localized portions of any one area of the monkey's cortex and studied the 'strychnine spikes' evoked in other regions. Applied to area 17, there was remarkably little spread within this area; spikes appeared in area 18, but not in 19 and never in the contralateral hemisphere, so that the fusion of the two halves of the visual field in any one eye does not take place by direct interhemispheric connections between areas 17. When applied locally to area 18, the parastriate area, there was widespread activity within this area and also in areas 19 and 17. Moreover, activity spread to symmetrical loci in area 18 of the opposite lobe, and also to the temporal lobe (middle and inferior convolutions). Strychninization of area 19 caused only local activity and apparently caused a spreading depression so that spontaneous activity in large areas of the cortex was finally suppressed. Thus area 18, the parastriate area, stands out as the part of the cortex most closely concerned with integrating visual activity in the two hemispheres, and also with activity in the temporal lobe.

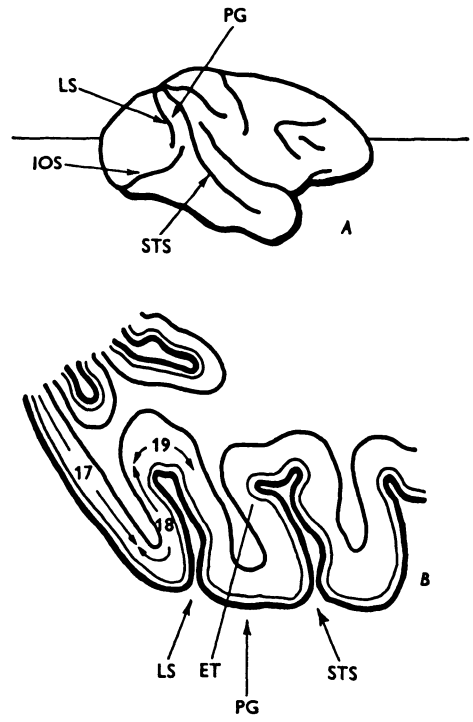

Fig. 19.11 Tracing of a horizontal section through the brain of the rhesus monkey, at the level indicated in *A*. Only the posterior and lateral part of the section is shown in *B*, to indicate the position of the cortex of the posterior bank of the superior temporal sulcus relative to areas 17, 18 and 19 as these have been determined anatomically for regions of central visual field representation in the rhesus monkey. ET = electrode track; LS = lunate sulcus; IOS = inferior occipital sulcus; STS = superior temporal sulcus; PG = prelunate gyrus. (Zeki, *J. Physiol.*)

Prestriate Projection in the Monkey

The projections in the monkey have been examined in detail by Choudhury *et al.* (1965), who confirmed the importance of area 18 in the bilateral response to a visual stimulus; section of the corpus callosum, or cooling of the contralateral projection point on the cortex, extinguished the ipsilateral cortical response in animals with one optic tract cut. More detailed analyses of the primate are those of Meyers (1965), Cragg (1969) and Zeki (e.g. 1969, 1971) based on lesions in the striate area and following degeneration by the Nauta method into the prestriate areas. As we have indicated, there is no clear definition cytoarchitectonically between areas 18 and 19 so that there is some ambiguity as to the limit between the two. As defined by Zeki (e.g. 1974) they are roughly illustrated by Fig. 19.11. Cragg (1969) found projection from the striate area to the posterior wall of the lunate sulcus, but concluded that this did not extend to area 19, although this area received input from the pulvinar and from the corpus callosum, and he emphasized that area 19, as separately defined in the monkey and the cat, could not be considered homologous. Zeki (1969) also placed lesions in the striate area and showed that there are three areas of re-representation of the visual field: at the opercular lip, in the lunate sulcus, and finally the posterior bank of the superior temporal sulcus. Thus any lesion made above the line of representation of the horizontal meridian in the striate cortex leads to a degeneration in dorsolateral prestriate cortex, and any lesion made below the horizontal meridian in the striate cortex leads to degeneration in ventrolateral prestriate cortex.

VERTICAL MERIDIAN

The scheme of projection is illustrated schematically by Fig. 19.12 and anatomically by Fig. 19.13. It will be seen that, as in the cat, the vertical meridian in prestriate

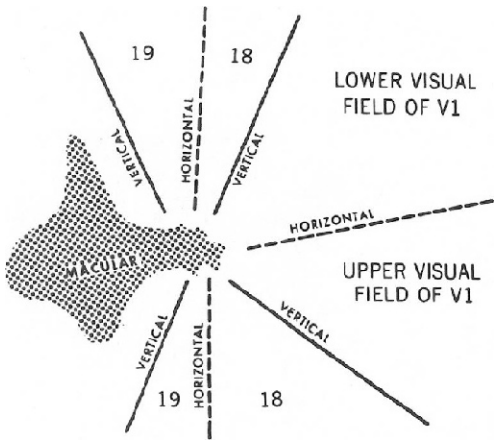

Fig. 19.12 A schematic representation of prestriate cortex and its relation to striate cortex. The prestriate cortex may be completely divided into upper and lower sections, corresponding to the upper and lower retinal quadrants, by an imaginary prolongation of the line of representation of the horizontal meridian in the primary visual cortex (V1). The horizontal meridian rerepresentation in prestriate cortex is almost at right angles to its representation in striate cortex. This horizontal rerepresentation may be considered to form the boundary between the areas 18 and 19, as defined in this study. Note that the areas 18 and 19 of this study are within the lunate sulcus. Points further away dorsally (or ventrally) along the vertical meridian in striate cortex project to more dorsal (or ventral) points in prestriate cortex. Points further peripheral along the horizontal line project to more dorsal or ventral levels, depending on whether they are in the upper or lower visual field representation, the projection from the 2 fields of representation being separate. Not shown is the third vertical and horizontal rerepresentation in the superior temporal sulcus. (Zeki, *J. Physiol.*)

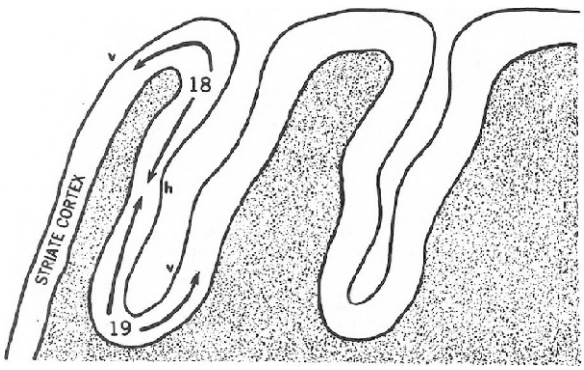

Fig. 19.13 Diagrammatic representations of areas 18 and 19, as defined by Zeki, as they would appear in a horizontal cross-section passing through the lunate (or inferior occipital) sulcus, *v*, area of representation of the vertical meridian; *h*, area of representation of the horizontal meridian. (Zeki, *Brain Res.*)

cortex is represented by the junction between areas 17 and 18; similarly Zeki concluded that the vertical meridian was represented by another line delimiting area 19 from adjacent temporal cortex; as we should expect, these regions are interhemispherically connected.

FOVEAL REPRESENTATION

The foveal area appears to claim a large field of prestriate cortex extending into prelunate gyrus and the later third of the anterior bank of the lunate sulcus, and, in addition, extending ventrally into the inferior occipital gyrus. The large areas of re-representation in prestriate areas suggest that there is some overlap between projections, so that a lesion in area 17 need not necessarily result in two distinct lesions in areas 18 and 19; and this was often found by Zeki (1969) whilst Cowey (1964), applying punctate stimuli to the retina, found prestriate receptive fields larger than those of the striate area and that adjacent points in the striate area projected to overlapping areas in prestriate cortex.

SUPERIOR TEMPORAL SULCUS

In addition to the re-representations of the retina on areas 18 and 19, Zeki observed degeneration in the posterior bank of the superior temporal sulcus but the mode of projection was not clear; frequently lesions in the striate area producing lesions in this area were not accompanied by lesions in areas 18 and 19; there appeared to be no obvious topographical organization so that cortical neurones here might analyse features of the peripheral stimulus independently of the position in space, e.g. on the basis of its colour (p. 595).

Terminology

Zeki compares his subdivisions of the prestriate area with those proposed by Myers (1965); Myers defined four areas, depending on whether they received fibres from striate cortex and from opposite prestriate cortex. His *juxtastriate 18*, the striate-prestriate border, receives striate and contralateral prestriate projections, and projects to the opposite juxtastriate region. In his scheme, the lunate sulcus receives fibres from striate cortex only, with no connexions with the opposite hemisphere, and forms his *striate receptive 19*. This is followed on the surface of the prelunate gyrus by *area 18 proper*, with connexions to the opposite area 18 proper and situated in the posterior part of the prelunate gyrus, and *area 19 proper*, with no connexions with the opposite hemisphere and situated in the anterior part of the prelunate sulcus. On Zeki's scheme, the lunate sulcus and inferior temporal sulcus are divided into at least two areas in which there is an orderly representation from vertical to horizontal and then back to vertical; the areas in which the midline is represented are connected with the opposite hemisphere. Thus the distinction between the two prestriate areas 18 and 19 is made on the basis of the re-representation of the visual fields and not on the basis of whether they are in connexion with the opposite hemisphere or with striate cortex only. Zeki also comments on terminology, suggesting that the terms 'secondary visual cortex' and 'peri-' and 'parastriate cortex' be abandoned. The terms OA and OB should

be used when referring to the subdivisions proposed by Von Bonin & Bailey (1947) but should not be used as synonyms for areas 18 and 19 of Brodmann (1905). The term prestriate cortex may be used as a general term to indicate the cortical field receiving fibres from striate cortex. Areas 18 and 19 defined by Brodmann have been equated with two physiologically distinct areas V2 and V3 in the cat (Hubel & Wiesel, 1965) and it seems likely that the areas 18 and 19 defined by Zeki will have corresponding physiologically defined identities, but he emphasizes that these differ from those defined by Brodmann.

Areas V4 and V4A

The posterior bank of the superior temporal sulcus (Fig. 19.11) receives a convergent projection from area 17, in the sense that lesions in widely distributed points in area 17 produce a single field of degeneration in this region. When examining the projections from areas 18 and 19 to neighbouring parts of the cortex, Zeki (1971) found projections to the posterior bank of the superior temporal sulcus as though there were two routes from striate cortex to here, a direct and more complex. As a result of each projection, the topographical organization becomes blurred. In addition to this projection Zeki found two other areas which he named V4 and V4A. Owing to the changed folding of the cortex V4 and V4A appeared as invaginations into V2 just beyond the lip of the operculum, due to the obliteration of the lunate sulcus and the opening up of the inferior occipital sulcus. In general, the organized topographic projection of the striate area to V2 and V3 breaks down, so that for example, the areas corresponding to horizontal and vertical meridians in V2 and V3 overlap in V4 and V4A.

Re-representations

Zeki's work emphasizes the complex series of steps in analysis of visual input that may take place through these 're-representations' of the visual field; the simple classical picture of projection from area 17 to area 18, from area 18 to area 19 and from area 19 to the so-called 'inferior temporal area' will have to be abandoned and in its place, a rather complex system of 'hierarchical' projections from one cortical region to another substituted (p. 569).

Pathways from V2 to V4 and V5 in the Primate

Most, if not all, the various areas of representation of the visual field on the cerebral cortex receive visual input from subcortical centres, such as the lateral geniculate nucleus and pulvinar. However, if visual information reaching the striate area, V1, is to be further processed in the cortex, projections from here to other areas are important, and the same applies, say, to V2. Shipp & Zeki (1985) have examined the cortical inputs to Areas V4 and V5 from V2; since V2 comprises functionally different subregions, it was of interest to determine whether the pathways leading from these subregions were kept segregated, thereby suggesting a hierarchical processing in V4 and V5. Using the cytochrome oxidase staining technique for defining different regions, they showed that V4 and V5 were, indeed, connected to different regions of V2. Alternating stripes in V2 projected to V4 and V5; thin stripes projected to V4, the colour discrimination region, whilst thick stripes projected to V5, a region characterized by the orientation- and direction-selectivity of its neurones. To determine this, the V4 and V5 neurones were labelled with horseradish peroxidase; the tissue was treated with cytochrome oxidase reagent, and the V4 and V5 neurones were traced back to the cytochrome oxidase strips on V2.

Intracortical Connections in the Cat

In a study largely devoted to the Clare-Bishop area, Sherk (1986) has outlined some of the principal connections between the visual cortical areas of the cat; these are illustrated in Fig. 19.14.

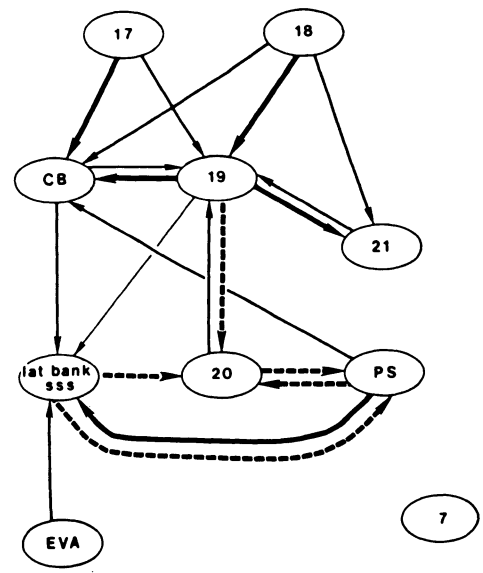

Fig. 19.14 Diagram showing pathways between various visual cortical areas. The thickness of the connecting lines indicates the magnitude of the pathways. A heavy solid line indicates that a projection accounted for 20% or more of the total cortical input to a given area. A medium solid line shows a pathway that made up 10–19% of a given area's input. A thin solid line shows an input accounting for 4–9% of the total to a given area. Dashed heavy lines show pathways that appeared to be quite strong, but that were not assessed quantitatively. In order to simplify the diagram, inputs to, and between, areas 17 and 18 have been left out. (Sherk, *J. Comp. Neurol.*)

Retinotopic Organization in the Cat

According to Tusa *et al.* (1978), there are at least thirteen areas on the cerebral cortex in which visual responses may be recorded, most of these in a retinotopic manner, in the sense that the visual field, or a part of it, may be plotted on the area of cortex.[4] Area 17 is distinguished from the rest (Tusa *et al.*, 1978) by a 'first-order' projection, in the sense that adjacent areas on the retina are represented by adjacent areas on the cortex; with other areas, this adjacency did not apply, so the projection was called 'second-order'. So far as area 17, or striate cortex was concerned, the whole hemifield was strictly mapped on the cortex; magnification was 3.6 mm^2/deg, with 50% of the cortical area devoted to the central 10° of vision; this contrasts with 6.5 mm^2/deg for the primate with 90% of cortex devoted to central vision. Areas 18 and 19 had a single representation of the visual field, exhibiting a distinctive cytoarchitecture; the visual hemifields were nearly mirror-images of each other; magnification was less, and projection was second-order.

Clare-Bishop Area

The lateral suprasylvian area on the banks of the middle and posterior suprasylvian sulcus had six retinotopically organized areas made up of three roughly mirror-symmetrical pairs of images, separated in each case by the fundus of the middle or posterior suprasylvian sulcus. The areas were described as PMLS and PLLS in the middle suprasylvian sulcus; AMLS and ALLS on both banks of the same sulcus, and DLS and VLS on the middle and posterior suprasylvian sulcus (Palmer *et al.*, 1978).

Thalamic Input

The Clare-Bishop area has been compared with area 17 by Tong & Spear (1986) with a view to determining whether the main thalamic input, which is from the lateral division of the lateral posterior complex (LP1), the medial interlaminar nucleus (MIN) and the C-laminae of the dorsal lateral geniculate nucleus (LGNd), is by way of single or branched neurones. They injected the central area of representation in area 17 with one fluorescent dye and the corresponding region in the Clare-Bishop area (PMLS) with another and determined the numbers of double- and single-labelled neurones in the thalamic nucei. The Clare-Bishop area was innervated almost completely by branched axons from the lateral posterior complex (LP1), whilst area 17 was almost exclusively innervated by single neurones from MIN and the lateral geniculate nucleus.[5]

The Corpus Callosum

The brain is organized in such a way that left-sided events are represented in the right cerebral cortex, and right-sided events in the left cerebral cortex. Coordinated activity involving both sides of the body requires a system of interhemispheric connections, of which the corpus callosum is the main pathway. By stimulating discrete points on the cortex, Curtis (1940) recorded electrical responses on symmetrical points of the cortex of the other hemisphere. In primates, the only area that did not give a response was area 17. This seemed reasonable in view of the only partial decussation of the retina, leading to the representation of a complete hemifield on one hemisphere; thus events occurring in the other hemifield, away from the objects of attention, would in general interfere with spatial analysis if projected into awareness at the same time. However, in the midline region, represented by the area 17/18 borders, stereoscopic vision requires fusion of images represented in opposite hemispheres, so that interhemispheric connections in this region are to be expected, and the early anatomical studies of Myers (1962) and Ebner & Myers (1965) left no doubt that it is at the junction of areas 18 and 17 that the great majority of the posterior callosal fibres project in the primate. More recent studies have shown that there are callosal connections between neurones in the primate striate area. Thus Spatz & Kunz (1984), working on both New World and Old World monkeys, injected retrograde tracers into the area 17/18 border, and found labelled neurones in contralateral area 17 as well as area 18. They showed that area 17 not only received callosal neurones but contained neurones projecting through the corpus callosum.

Callosal Connections in the Cat

Segraves & Rosenquist (1982a) followed callosal connections in the cat with horseradish peroxidase; callosal neurones were identified in all the many retinotopically defined areas of the cat's cerebral cortex; the portion of the visual field represented by callosal connections increased from the area 17/18 border to areas 19, 20, 21 and LSA (lateral suprasylvian area). In area 17, regions representing the vertical meridian to 10° of azimuth had callosal neurones; in posterolateral LSA the region extended from the vertical meridian to 60° of azimuth. The widespread distribution of callosal neurones in areas 20, 21 and LSA indicates that large regions of visual field have access to the opposite cortex, a feature important for the callosal transfer of learning. Thus the traditional rule restricting callosal connections to midline representation applies only to areas 17, 18 and 19 but not to others, where receptive fields of single neurones may be found extending well across the midline. In a further study, measuring both afferent and efferent connections,

Segraves & Rosenquist (1982b), using horseradish peroxidase and ^{3}H-leucine, demonstrated precise point-to-point reciprocal connections between retinotopically symmetrical points, not only at the V1/V2 border but between mirror-image points on the peripheral horizontal meridian in right and left posterolateral MLS. This agrees with the finding of Rizzolatti & Camardas (1977) that electrical stimulation of any point in the contralateral PLMS causes inhibition of a corresponding point in the ipsilateral PLMS, operating through the corpus callosum.

More Recent Studies on Primate

Kennedy *et al.* (1986) considered that earlier studies employing retrograde movement of horseradish peroxidase were insufficiently accurate, using as they did, 3,3'-diaminobenzidine as incubation medium. They used horseradish peroxidase, and horseradish peroxidase conjugated with wheat-germ agglutenin; when processed by Mesulam's procedure this is an extremely sensitive anterograde and retrograde neuronal tracer. The V1/V2 border was found to have connections with the contralateral V1 and three other cortical sites in the lunate and superior temporal sulci including V3 and MT. The tangential extent of callosal connections in V1 and V2 was much greater for foveal than peripheral visual fields. The distribution of terminals was patchy, suggesting a columnar organization; patches usually corresponded with areas of high cytochrome oxidase activity. Lamination of cell bodies and terminals followed a regular pattern; thus cell-bodies in V1 were never found in infragranular layers, i.e. deeper than Lamina IV. Labelled terminals, on the other hand, were found in layers III, IVB and V. Thus the callosal projections from V1 to the opposite side are of the feed-forward type, arising from supragranular layers. The terminations within V1, on the other hand, are of the feedback type, avoiding Lamina IV. Thus the lamination of callosal neurones and their regions of termination followed some regularity, although a contrast between feed-forward and feedback was not established. In general the connections of V1 and V2 were reciprocal.

Callosal-free Zones

Van Essen *et al.* (1982) have exploited Zeki's technique for outlining the visuotopically organized cortical regions in the macaque, with a view to specifying more precisely the various visually responsive zones. If the primary hypothesis is correct, namely that the junctions between zones, which share a common representation of the vertical meridian, are innervated by the corpus callosum, then the callosal-free areas are visual areas. These zones are illustrated in Fig. 19.15 and are labelled A to G. A and B

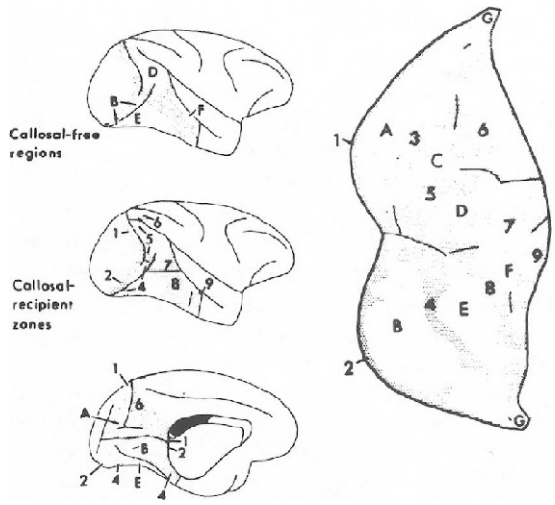

Fig. 19.15 Relationship of extrastriate visual areas to callosal recipient zones and callosal free regions. Major callosal recipient zones (1 to 9) and callosal free regions (*A* to *G*) are designated on the cortical map and on the hemisphere drawings. The borders between callosal recipient zones (*fine lines*) are somewhat arbitrary but, when possible, have been drawn in a manner most likely to reflect the boundaries between visual areas. (Van Essen, *J. Neurosci.*)

contain V2, V3 and the ventral posterior visual area, VP, a broad belt that almost completely surrounds V1 and separated by a narrow callosal zone. They showed that V3 does not adjoin V2 along its whole extent, as previously thought, sharing a common horizontal meridian (Zeki, 1969; Cragg, 1969). Area C is smaller and equivalent to $V3_a$, a region distinct from V3 on the medial side and from V4 on the lateral side. Area 4 contains V4 and MT, mainly on the pre-lunate gyrus and the posterior bank of the superior temporal sulcus. E is one of the largest callosal-free zones, and receives from V2; it is visuotopically organized. In addition to these visuotopically organized regions, there are the inferotemporal, the posterior parietal (area 7 or PG+PE) and visually responsive regions medial to MT. Area G, the prestriate area, is the smallest callosal-free zone and the only one that directly adjoins the striate area without an intervening callosal strip. It is adjacent to the representation of the most peripheral part of the retina, and so would not require callosal connections.

Notes

1. These two areas are often referred to jointly as the prestriate areas.
2. Magnification may be expressed in terms of area, mm^2/deg^2 of visual field, or on a linear basis, mm cortex/deg of visual field. The areal magnification reflects the total amount of cortex devoted to a given part of the visual field, and if thickness and cell density are constant, it indicates the total number of cells employed. Linear magnification is more

complex, as it depends on direction in which it is measured, and is useful as a measure of distortions in cortical representation (Van Essen *et al.*, 1984).

3. Davis & Sterling (1979) identified some seven classes of cortical neurones in layer IV of the cat's area 17 on the basis of their morphology and synaptic terminals; cells in I to VI had geniculate input, but the sites of synapse were different.
4. The various visual areas have been extensively mapped by anatomical and electrophysiological techniques by Palmer *et al.* (1978) and Tusa *et al.* (1978, 1979); the literature on this subject has been quoted by Updyke (1986) in his paper describing additional studies, which include the description of a 'periauditory belt', on the lip of the posterior ectosylvian gyrus, that presumably is concerned with audio-visual co-ordination.
5. Tong & Spear (1986) point out that the Clare-Bishop area, in the middle suprasylvian sulcus, contains several areas on the basis of retinotopic discontinuities in representation (Palmer *et al.* 1978). On the medial bank of the sulcus there are two subdivisions (AMLS and PMLS). They injected horseradish peroxidase in these areas and followed the thalamic projections retrogradely; these were fairly similar in the two subdivisions, and included the C-laminae of the dorsal lateral geniculate nucleus, the pulvinar and centrolateral, lateral posterior and medial interlaminar nuclei. More recently Sherk (1986) has examined the projections to the cat's suprasylvian sulcus in detail; she described an area that occupied most of the medial bank of the suprasylvian sulcus, all or most of its posterior bank, and a small segment of its anterior bank; this area was defined as the Clare-Bishop area, receiving a strong input from area 17.

References

Berkley, M., Wolf, E. & Glickstein, M. (1967) Photic evoked potentials in the cat: evidence for a direct visual input to visual II. *Exp. Neurol.* **19**, 188–198.

v. Bonin, G. N., Garol, H. W. & McCulloch, W. S. (1942) The functional organization of the occipital lobe. *Biol. Symp.* **7**, 165–192.

v. Bonin, G. & Bailey, P. (1947) *The Neocortex of Macaca Mulatta.* University of Illinois Press, Urbana.

Brodmann, K. (1905) Beitrage zur histologischen Lokalisation der Grosshirnrinde. *J. Psychol. Neurol. (Leipzig)* **4**, 176.

Bullier, J. & Kennedy, H. (1983) Projection of the lateral geniculate nucleus onto cortical area V2 in the macaque monkey. *Exp. Brain Res.* **53**, 168–172.

Choudhury, B. P., Whitteridge, D. & Wilson, M. E. (1965) The function of the callosal connections of the visual cortex. *Quart. J. Exp. Physiol.* **50**, 214–219.

Cowey, A. (1964) Projection of the retina on to striate and prestriate cortex in the squirrel monkey, *Samiri sciureus. J. Neurophysiol.* **27**, 366–396.

Cragg, B. G. (1969) The topography of the afferent projections in the circumstriate visual cortex of the monkey studied by the Nauta method. *Vision Res.* **9**, 733–747.

Curtis, H. J. (1940) Intercortical connections of corpus callosum as indicated by evoked potentials. *J. Neurophysiol.* **3**, 407–413.

Daniel, P. M. & Whitteridge, D. (1959) The representation of the visual field on the calcarine cortex of baboons and monkeys. *J. Physiol.* **148**, 33–34P.

Davis, T. L. & Sterling, P. (1979) Microcircuitry of cat visual cortex: classification of neurons in layer IV of area 17, and identification of patterns of lateral geniculate input. *J. Comp. Neurol.* **188**, 599–628.

Dow, B. M., Snyder, A. Z., Vautin, R. G. & Bauer, R. (1981) Magnification factor and receptive field size in striate cortex of the monkey. *Exp. Brain Res.* **44**, 213–228.

Ebner, F. F. & Myers, R. E. (1965) Distribution of corpus callosum and anterior commissure in cat and raccoon. *J. Comp. Neurol.* **124**, 353–365.

Ferster, D. & Lindström, S. (1983) An intracellular analysis of geniculocortical connectivity in area 17 of the cat. *J. Physiol.* **342**, 181–215.

Fitzpatrick, D., Itoh, K. & Diamond, I. T. (1983) The laminar organization of the lateral geniculate body and the striate cortex in the squirrel money (*Saimiri sciureus*). *J. Neurosci.* **3**, 673–702.

Geisert, E. E. (1980) Cortical projections of the lateral geniculate nucleus in the cat. *J. Comp. Neutrol.* **190**, 793–812.

Gilbert, C. D. & Kelly, J. P. (1975) The projection of cells in different layers of the cat's visual cortex. *J. comp. Neurol.* **163**, 81–106.

Harting, J. K., Huerta, M. F., Frankfurter, A. J., Strominger, N. L. & Royce, G. J. (1980) Ascending pathways from the monkey superior colliculus: an autoradiographic analysis. *J. Comp. Neurol.* **192**, 853–882.

Harvey, A. R. (1980) The afferent connexions and laminar distribution of cells in area 18 of the cat. *J. Physiol.* **302**, 483–505.

Holmes, G. (1945) Organization of the visual cortex in man. *Proc. Roy. Soc.* **B 132**, 348–361.

Hornung, J. P. & Garey, L. J. (1981) The thalamic projection to cat visual cortex. *Neurosci.* **6**, 1053–1068.

Hubel, D. H. & Wiesel, T. N. (1965) Binocular interaction in striate cortex of kittens reared with artificial squint. *J. Neurophysiol.* **28**, 1041–1059.

Hubel, D. H. & Wiesel, T. N. (1974) Sequence regularity and geometry of orientation columns in the monkey striate cortex. *J. Comp. Neurol.* **158**, 267–293.

Kennedy, H., Dehay, C. & Bullier, J. (1986) Organization of callosal connections of visual areas V1 and V2 in the macaque monkey. *J. Comp. Neurol.* **247**, 398–415.

LeVay, S. & Gilbert, C. D. (1976) Laminar patterns of geniculocortical projection in the cat. *Brain Res.* **113**, 1–19.

Livingstone, M. S. & Hubel, D. H. (1982) Thalamic inputs to cytochrome oxidase-rich regions in monkey visual cortex. *Proc. Nat. Acad. Sci.* **79**, 6098–6101.

Lund, J. S. & Boothe, R. G. (1975) Interlaminar connections and pyramidal neuron organization in the visual cortex, Area 17, of the macaque monkey. *J. Comp. Neurol.* **159**, 305–322.

Lund, J. S., Henry, G. H., Macqueen, C. L. & Harvey, A. R. (1979) Anatomical organization of the primary visual cortex (Area 17) of the cat. A comparison with Area 17 of the macaque monkey. *J. Comp. Neurol.* **184**, 599–618.

Lund, J. S., Lund, R. D., Hendrickson, A. E., Bunt, A. H. & Fuchs, A. F. (1975) The origin of efferent pathways from the primary visual cortex, area 17, of the macaque monkey as shown by retrograde transport of horseradish peroxidase. *J. Comp. Neurol.* **164**, 287–303.

Myers, R. E. (1962) Commissural connections between occipital lobes in the monkey. *J. Comp. Neurol.* **118**, 1–10.

Myers, R. E. (1965) Organization of visual pathways. In *Function of the Corpus Callosum.* Ed. Ettlinger, G. E., pp. 133–142. Churchill, London.

Palmer, L. A., Rosenquist, A. C. & Tusa, R. J. (1978) Retinotopic organization of lateral suprasylvian visual areas in the cat. *J. Comp. Neurol.* **177**, 237–256.

Rizzolatti, G. & Camarda, R. (1977) Influence of the presentation of remote visual stimuli on visual responses of cat area 17 and lateral suprasylvian area. *Exp. Brain Res.* **29**, 107–122.

Rolls, E. T. & Cowey, A. (1970) Topography of the retina and striate cortex and its relationship to visual acuity in rhesus monkeys. *Exp. Brain Res.* **10**, 298–310.

Segraves, M. A. & Rosenquist, A. C. (1982a) The distribution of the cells of origin of callosal projections in cat visual cortex. *J. Neurosci.* **2**, 1079–1089.

Segraves, M. A. & Rosenquist, A. C. (1982b) The afferent and efferent callosal connections of retinotopically defined areas in cat cortex. *J. Neurosci.* **2**, 1090–1107.

Sherk, H. (1986) Location and connections of visual cortical areas in the cat's suprasylvian sulcus. *J. Comp. Neurol.* **247**, 1–31.

Shipp, S. & Zeki, S. (1985) Segregation of pathways leading from area V2 to areas V4 and V5 of macaque monkey visual cortex. *Nature* **315**, 322–325.

Spalding, J. M. K. (1952a) Wounds of the visual pathway. I. The visual radiation. *J. Neurol.* **15**, 99–107.

Spalding, J. M. K. (1952b) Wounds of the visual pathway. II. The striate cortex. *J. Neurol.* **15**, 169–183.

Spatz, W. B. & Kunz, B. (1984) Area 17 of anthropoid primates does participate in visual callosal connections. *Neurosci. Letters* **48**, 49–53.

Stone, J. & Dreher B. (1973) Projection of X- and Y-cells of the cat's lateral geniculate nucleus to areas 17 and 18 of visual cortex. *J. Neurophysiol.* **36**, 551–567.

Suzuki, H. & Kato, H. (1969) Neurons with visual properties in the posterior group of the thalamic nuclei. *Exp. Neurol.* **23**, 353–365.

Talbot, S. A. & Marshall, W. H. (1941) Physiological studies on neural mechanisms of visual localization and discrimination. *Amer. J. Ophthal.* **24**, 1255–1264.

Tong, L. & Spear, P. D. (1986) Single thalamic neurons project to both lateral suprasylvian visual cortex and area 17: a retrograde fluorescent double-labeling study. *J. Comp. Neurol.* **246**, 254–264.

Tootell, R. B. H., Silverman, M. S., Switkes, E. & De Valois, R. L. (1982) Deoxyglucose analysis of retinotopic organization of primate striate cortex. *Science* **218**, 902–904.

Tusa, R. J., Palmer, L. A. & Rosenquist, A. C. (1978) The retinotopic organization of area 17 (striate cortex) in the cat. *J. Comp. Neurol.* **177**, 213–235.

Tusa, R. J., Rosenquist, A. C. & Palmer, L. A. (1979) Retinotopic organization of areas 18 and 19 in the cat. *J. Comp. Neurol.* **185**, 657–678.

Updyke, B. V. (1975) The patterns of projection of cortical areas 17, 18, and 19 onto the laminae of the dorsal lateral geniculate nucleus in the cat. *J. Comp. Neurol.* **163**, 377–396.

Updyke, B. V. (1986) Retinotopic organization within the cat's posterior suprasylvian sulcus and gyrus. *J. Comp. Neurol.* **246**, 265–280.

Van Essen, D. C. & Maunsell, J. H. R. (1983) Hierarchical organization and functional streams in the visual cortex. *Trends Neurosci.* **6**, 370–375.

Van Essen, D. C., Newsome, W. T. & Bixby, J. L. (1982) The pattern of interhemisphere connections and its relationship to extrastriate visual areas in the macaque monkey. *J. Neurosci.* **2**, 265–282.

Van Essen, D. C., Newsome, W. T. & Maunsell, J. H. R. (1984) The visual representation in striate cortex of the macaque monkey: asymmetries, anisotropies, and individual variability. *Vision Res.* **24**, 429–448.

Weber, J. T., Huerta, M. F., Kaas, J. H. & Harting, J. K. (1983) The projections of the lateral geniculate nucleus of the squirrel monkey: studies of the interlaminar zones and S layer. *J. Comp. Neurol.* **213**, 135–145.

Wilson, M. E. & Cragg, B. G. (1957) Projections from the lateral geniculate nucleus in the cat and monkey. *J. Anat.* **101**, 677–692.

Yukie, M. & Iwai, E. (1981) Direct projection from the dorsal lateral geniculate nucleus to the prestriate cortex in macaque monkeys. *J. Comp. Neurol.* **201**, 81–93.

Zeki, S. M. (1969) Representation of central fields in prestriate cortex of monkey. *Brain Res.* **14**, 271–291.

Zeki, S. M. (1971) Convergent input from the striate cortex (area 17) to the cortex of the superior temporal sulcus in the rhesus monkey. *Brain Res.* **28**, 338–340.

Zeki, S. M. (1974) Functional organization of a visual area in the posterior bank of the superior temporal sulcus of the rhesus monkey. *J. Physiol.* **236**, 549–573.

20. NEUROPHYSIOLOGY OF PERCEPTION: CORTICAL NEURONES

Electrophysiology of Cortical Neurones

We may postpone the consideration of further details of the organization of cortical neurones and their projections until we have considered some properties of these neurones.

Linear Fields

When recordings are taken from neurones in the striate cortex, an entirely different organization of receptive fields appears, the dominant feature being the linear organization of the ON- and OFF-regions, as opposed to the concentric circular organization of the lower neurones. The types of field that are described as 'simple' are illustrated in Fig. 20.1C to G, A and B being the geniculate fields described earlier. Here the ON or excitatory responses are indicated by crosses and the OFF by triangles. The receptive field represented by C consists of a central slit of retina orientated in a definite direction; light falling on this slit, or a spot of light moving along it, produces ON-responses; light falling on the narrow areas to each side gives OFF-responses, whilst light falling on both central slit and the parallel surrounds leads to complete cancellation, so that diffuse illumination of the retina produces no response in these cortical neurones. Summation occurs along the slits, in the sense that a slit of half the length gives a smaller response than one occupying the whole length of the field.

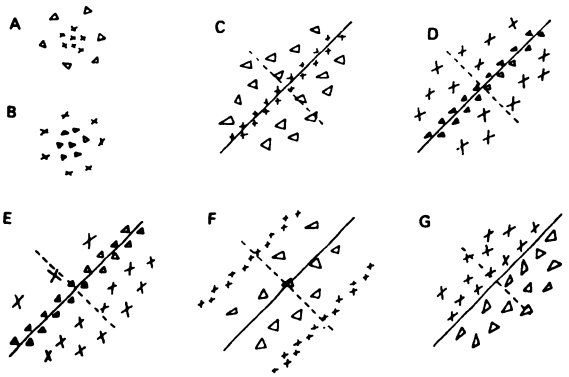

Fig. 20.1 Types of receptive field. Crosses indicate excitatory or ON-responses; triangles indicate inhibitory or OFF-responses. A: ON-centre response typically seen in retina and lateral geniculate nucleus. B: OFF-centre response. C–G: Various arrangements of simple cortical fields. (Hubel & Wiesel, *J. Physiol.*)

Orientation Selectivity

Illumination of both flanks simultaneously produced a larger response than separate illumination of either. The necessary orientation of the slit stimulus to obtain maximal response was quite critical, so that a variation of more than 5 to 10° had a measurable effect. We may assume that these cortical neurones receive their inputs from a number of geniculate cells, each with a circular field, and that the effect of this combination is to give a linear array of these fields that would behave effectively as a unit with a linear receptive field as illustrated in Fig. 20.2. By appropriately arranging geniculate cells the different receptive fields of other types of 'simple' cortical neurones, illustrated in Fig. 20.1, E to G, may be constructed.

To return to Fig. 20.1, D illustrates the mirror-image of field C, the outer flanks being excitatory and the inner slit inhibitory. In both C and D the flanks of the field were more diffuse than the central regions. F illustrates a cell with a more diffuse centre and narrow flanks, and the optimal response was obtained by simultaneously illuminating the two flanks with parallel slits. In G, only two regions could be distinguished; the most effective stimulus, here, was two areas of different luminance placed so that the line separating them fell exactly over the boundary of the fields; this was called by Hubel and Wiesel an 'edge stimulus'. With all these 'simple' units a moving stimulus was always very effective, but it is important that the correct orientation of the slit be maintained, the movement being executed at right-angles to the direction of the slit. Usually the response was the same with forward or backward movement, but in others the responses were very unequal, giving rise to a 'directional sensitivity', measured, customarily, by the difference in response on moving an optimally orientated bar in directions at right-angles to this orientation.

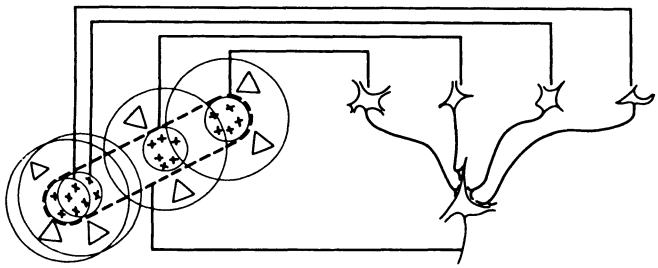

Fig. 20.2 Scheme to explain the organization of the linear cortical receptive field on the basis of summation of circular fields at the geniculate level. (Hubel & Wiesel, *J. Physiol.*)

Simple Units

The fields of these units were described as *simple* because, like retinal and geniculate fields, they were subdivided into distinct excitatory and inhibitory regions; there was summation within the separate excitatory and inhibitory parts; there was antagonism between excitatory and inhibitory regions; and finally because it was possible to predict responses to stationary or moving stimuli of varying shapes from a map of the excitatory areas. Thus, as DeValois *et al.* (1982a) have emphasized, the linearity in the responses of a simple cell make it equivalent to the X-cells of Enroth-Cugell & Robson. The complex cell, on the other hand, is typical of the Y-ganglion cell.

Complex Units

Another class of units showed similarities with the simple ones, but they were called *complex* because their responses to variously shaped stationary or moving forms could not be predicted from a map made with circular spot-stimuli. In general, the fields were larger than those of simple cells, responding poorly to flashes as opposed to movement. The activating region showed no subdivision into spatially separate zones and, when a cell responded to flashes, these elicited responses at both ON and OFF throughout the field. Similarly, a response was obtained to both a bright and dark edge of a moving stimulus. The cells were more often driven binocularly, had greater spontaneous activity, and responded to higher velocities of movement. Hubel and Wiesel suggested that these complex units received input from several simple units, thereby exhibiting a hierarchy of cortical cells (Fig. 20.3).

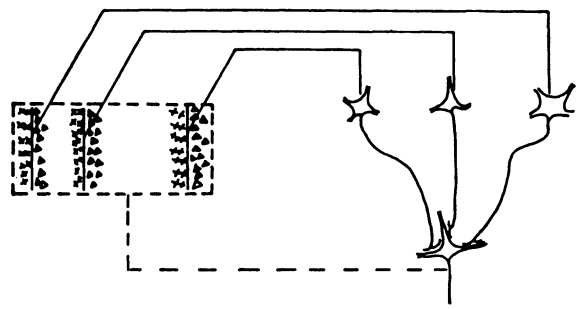

Fig. 20.3 Possible scheme for explaining the organization of complex receptive fields. A number of cells with simple fields, of which three are shown schematically, are imagined to project to a single cortical cell of higher order. Each projecting neurone has a receptive field arranged as shown to the left: an excitatory region to the left and an inhibitory region to the right of a vertical straight-line boundary. The boundaries of the fields are staggered within an area outlined by the interrupted lines. Any vertical-edge stimulus falling across this rectangle, regardless of its position, will excite some simple-field cells, leading to excitation of the higher-order cell. (Hubel & Wiesel, *J. Physiol.*)

Hypercomplex Units

When Hubel & Wiesel (1965a) explored areas 18 and 19 (V2 and V3) they found neurones entirely of the complex type. Furthermore, new degrees of complexity in the receptive fields emerged, so that a further class of 'hypercomplex' cells had to be made, and within this group 'higher order' and 'lower order' cells were described. V2 contained almost entirely complex cells similar to those found in V1, the remainder being hypercomplex, whilst in V3 the majority were hypercomplex. An example of a hypercomplex cell was one that, like the complex cells, could be excited by a line of specific orientation, but this line had to be limited in length in one or both directions to obtain maximal effect. It is essentially this 'end-stopping' that was considered to characterize the 'hypercomplexity' of the neurone.

Orientational Selectivity

Tuning

The characteristic feature of the cortical unit, both simple and complex, is its requirement for a line-stimulus at a definite angle to one of the meridians of the retina; Campbell *et al.* (1969) estimated the orientational selectivity, or 'tuning' of a unit by measuring the response at varying angles of the line, plotted as in Fig. 20.4. The line AB is drawn through the value of half-maximum amplitude of response; bisecting the angle determined by AB

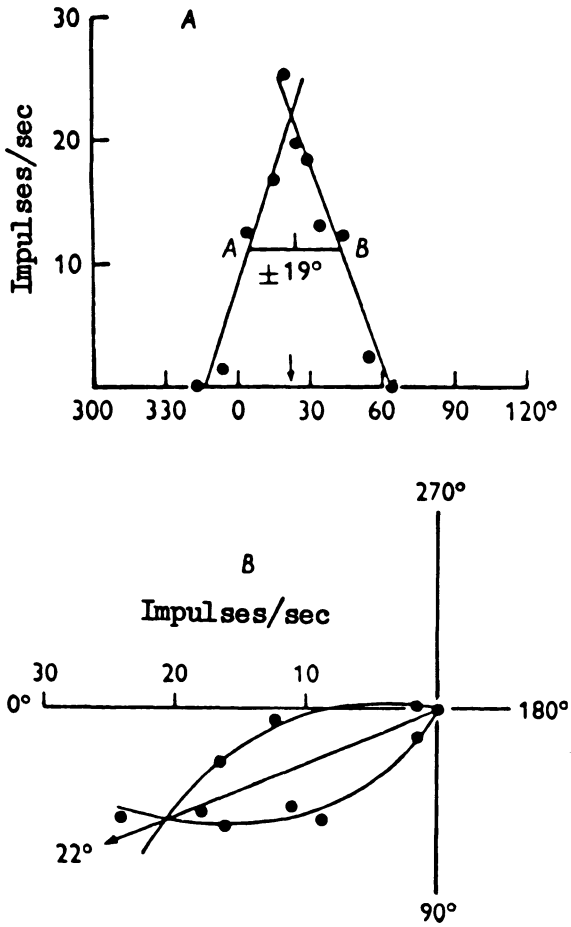

Fig. 20.4 Illustrating sensitivity of a cortical cell to direction of movement of a grating. A. Linear plot of response amplitude (of cortical cell) versus the direction of movement (angle) of the stimulus grating. Their point of intersection is taken as the best estimate of the maximum response amplitude and the preferred angle (arrowed). The horizontal line is drawn at half the maximum response amplitude. Spatial frequency: 0.24 c/deg. Drift frequency: 3.8 c/s. Contrast: 0.7. B. Polar plot of results in A. The arrowed line indicates the preferred angle. 0° = a movement from right to left in the visual field; 90° = a downward movement. (Campbell, *et al.*, *J. Physiol.*)

gives the orientational selectivity, which in the unit illustrated was ±19°.

The sharpness of tuning increases as the length of the test-stimulus is increased in such a way that the line encroaches on the inhibitory regions, flanking the discharge-region, when it moves out of the optimum orientation (Henry *et al.*, 1974). Complex cells are less sharply tuned (±27.5° compared with ±17°), so that a selectivity of ±20° or less almost certainly indicates a complex cell. Simple, hypercomplex I, complex and hypercomplex II cells, in this order, are increasingly sensitive to stimulus orientation (Kato *et al.*, 1978).

Preferred Orientations

Mansfield (1974) found a large preponderance of foveal cortical units with a preference for vertical versus horizontal orientation-specificity compared with oblique angles; this corresponds to the preference of human non-astigmatic subjects for vertical lines. In the parafovea there was no difference. DeValois *et al.* (1982b) found the same vertical-horizontal preference in their monkey units.

The Role of Inhibition

Orientation-selectivity could result simply from the positions of the circular receptive fields of geniculate cells converging on to a cortical cell; if the line-stimulus coincided in direction with the line joining these receptive fields, then there would be maximal summation and the response would be maximal. However, a role for active inhibition has been established by several studies. Thus, although maintained discharge in the absence of a stimulus is rare in cortical cells, DeValois *et al.* (1982a) found a number that did discharge spontaneously; with these, a line-stimulus at the wrong orientation actually produced a decreased discharge rather than having no effect; the maximum effect was not at 90° from the optimum orientation but at about 30° to 40° to either side, i.e. in the inhibitory flank of the cortical cell. Particularly instructive was an experiment in which a cortical cell was stimulated by an optimally orientated line, then by a small square, effectively a spot, on this line at the centre of the receptive field, and finally by the remainder of the line without its central square. The cell responded strongly to the central square alone, in fact its responses were almost as large as those of the line. The responses to the line were never much larger than those to the central square, but at orientations away from the optimal they became smaller. Thus, in this case, the response to the line was 'carved out' of the response to the central square by inhibition from areas when they were in the wrong direction. An important point emphasized by DeValois *et al.* was that maximal inhibition does not occur when the line-stimulus is at right-angles to the preferred direction, but when it is angled just a few degrees from the optimum, a situation one would expect were the main excitatory drive occurring at the centre of the line, and inhibition derived from the flanks of the line.

EFFECT OF LAYER 6 CELLS

These receive direct geniculate input as well as layer 4 cells; the simple cells are characterized by long receptive fields by contrast with layer 4 cells, and it may be that these cells generate the

inhibition through these long fields that provides the end-stopping in layer 4 and elsewhere. The visual claustrum, of the cat is a subcortical region linked almost exclusively to visual cortex, projecting in an orderly fashion to the contralateral hemisphere; it is a prominent structure in carnivores. Most of its visual units are orientation-selective with strikingly long receptive fields; its target-neurones are principally in layer 4 of the striate and parastriate areas (Sherk & LeVay, 1981). When the claustrum was destroyed unilaterally, there was a reduction in the end-stopping of simple cells in area 17 on the same side, this being most marked in layers 2–3 and 4 where end-stopped cells were most abundant. Thus, by analogy, it may be that the units in layer 6 of the striate area, with long receptive fields, exert the end-stopping found in upper layers through inhibition (Sherk & LeVay, 1983).

PHARMACOLOGICAL STUDIES

The orientation-selectivity of simple cells, reflected in the appearance of a maximum discharge when a bar of given orientation was moved orthogonally, was explained by Hubel & Wiesel as a simple consequence of the organization of the receptive fields of the geniculate neurones converging on this simple cell. Essentially, the orientation-selectivity depended on the selectivities of a number of geniculate neurones contributing to the receptive field of the simple cell. Using their micro-iontophoretic injection technique, Sillito *et al.* (1980a) have shown, however, that the orientation-selectivity of a simple cell can be completely abolished by local injection of a GABA-inhibitor, N-methyl-bicuculline. Figure 20.5 illustrates the complete loss of orientation-selectivity of a simple cortical neurone resulting from micro-iontophoretic injection of the GABA inhibitor. The best explanation of this result is that the orientation-specificity of a given simple cell results from an inhibition of the inputs of geniculate units with receptive fields divergent from the direction of the preferred orientation of the simple cell.[1]

Complex Cells

According to the hypothesis of Hubel & Wiesel, complex cells receive their input from simple cells, so that their response-characteristics should be governed by this input. However, a direct geniculate input to complex cells has been established (Hoffmann & Stone, 1971; Singer *et al.*, 1975; Toyama *et al.*, 1977; Tanaka, 1985), so that, in the interpretation of the responses of complex cells to visual stimuli, the direct and indirect inputs to a given cell should be recognized. This ought to be reflected in different responses to a GABA-inhibitor, such as bicuculline, applied locally to the cortex. Thus the complex cell,

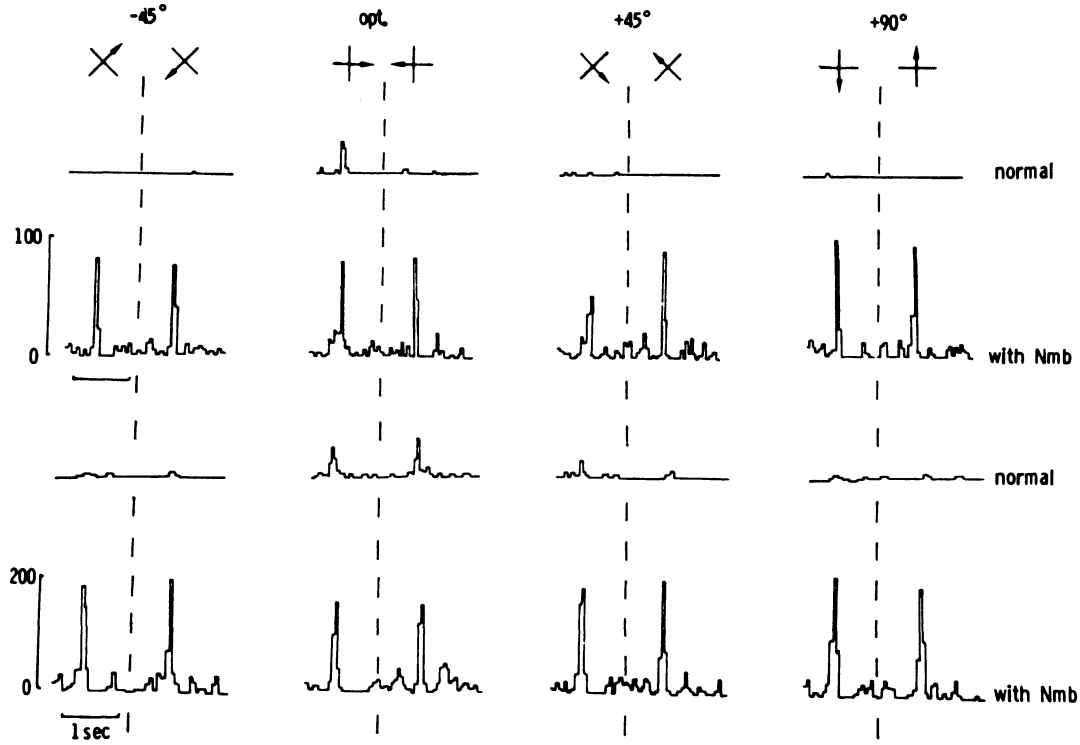

Fig. 20.5 Effects of bicuculline on simple cell orientation-selectivity. Testing orientation and direction of stimulus motion is indicated above each set of PSTHs. Dotted line subdivides records into zones corresponding to the two directions of motion. Optimum orientation is arbitrarily referred to as zero.: −indicates anticlockwise rotation from optima and + clockwise rotation. Vertical calibration indicates number of counts per bin. (Sillito *et al.*, *Brain Res.*)

receiving input from simple cells that were already orientation-selective, and therefore not dependent on cortical inhibition, would be relatively immune from the drug, whilst those receiving input from geniculate units, and therefore relying on cortical inhibition, would be strongly affected. Sillito (1979) found, indeed, two groups of complex cells that were either strongly or less strongly affected by bicuculline, suggesting that some cells had an orientation-specific input whilst others required inhibitory mechanisms either to establish or to sharpen selectivity.

Relation to Hierarchy

In their original description of the visual fields of cortical cells, Hubel & Wiesel suggested that the receptive fields of hypercomplex cells were made up by convergence of complex cells, and those of complex cells by convergence of simple cells, thus defining a 'hierarchy of cortical neurones'. Stone *et al.* (1979), in their detailed analysis of this view, emphasize the importance of these studies on inhibition that would permit the complex and hypercomplex features of a neurone's receptive field to be derived primarily from its geniculate input. This would give a *parallel*, rather than a *serial*, or *hierarchical*, processing.

Directional Selectivity

As indicated earlier, Hubel & Wiesel found many cortical cells that had a preferred direction of movement of an optimally orientated line; in the extreme case the unit would respond to one direction of movement and fail to respond to the opposite direction. Some 72% of simple cells described by Bishop *et al.* (1974) were directionally sensitive, 51% responding to both light and dark edges in the one—preferred—direction and 21% to only one edge. For any given cell the selectivity did not depend on the length of the bar, so that a spot of light was just as directionally selective as a slit. A further point to appreciate is that, although directional selectivity is usually studied by moving a bar at right-angles to its preferred orientation, the selectivity is still manifest if the bar is angled to this preferred orientation, so that the response to movement fails before directional selectivity fails.[2]

Mechanism

The basis of directional selectivity of a ganglion cell is, as we have seen, an inhibitory process that prevents the excitatory process from getting through the ganglion cell when movement is in the preferred direction (p. 330). In the cat and primates ganglion cells do not show the directional selectivity found in the rabbit; and a study of the response-characteristics of geniculate cells led Dreher & Sanderson (1973) to conclude that a mere relaying of their fields would not give the cortical unit directional selectivity without a subsequent intracortical modification. However, Goodwin *et al.* (1975) pointed out that the geniculate unit has a radial directional sensitivity, in the sense that a moving light, swept across the receptive field of an OFF-centre units causes a burst of discharge when it moves away from the unit's receptive field-centre, so that there is a radial directional sensitivity in the geniculate neurone's receptive field; and the problem was to describe how input from several geniculate cells could confer a *lateral* directional sensitivity as the slit-stimulus was moved across the primary borders of the receptive field.

INHIBITION BY SLIT

Goodwin *et al.* (1975) showed that the directional sensitivity of a cortical cell was not a function of the slit-flank type of organization, since a very small movement of a slit within the field's centre was directionally sensitive. Further, a thin slit, or an edge, in the receptive field exerted a strong inhibitory action on the adjacent part of the receptive field, as tested by a second edge or slit-stimulus; thus if the conditioning slit was within about 10 minutes of arc of the test-slit, the response was suppressed; with increasing distance, this suppression became less and finally was converted into a facilitation.

LATERALITY OF INHIBITION

The important finding was that the inhibition could only be evoked from one side of the test-area, namely the side that would be illuminated by a single bright edge as it moved in the non-preferred direction. Thus light on the opposite side of the test-area did not cause inhibition, as manifest by the firing that results when the light moves in the preferred direction over the test area. The inhibition takes time to develop, but if an edge is kept in the field, the inhibition, once developed, remains. Thus the first movement of the edge is, in fact, direction-selective and will remain so however slowly the edge moves. The sustained character might well be due to an X-type of ganglion and geniculate neurones making up the receptive field of the simple cortical cell.

MODEL

The model proposed by Goodwin *et al.* is illustrated by Fig. 20.6 where the circles represent a linear array of geniculate receptive fields; each field has a radial directionality, in the sense that a slit moving away from the centre excites; the inhibitory mechanism blocks off half these fields. The cell would respond to light or dark edges, or to a light bar, only when motion was to the right, away from the centres of the geniculate fields. On moving to the left, in the uninhibited region, the edge would be moving towards the centre of the geniculate fields and, having

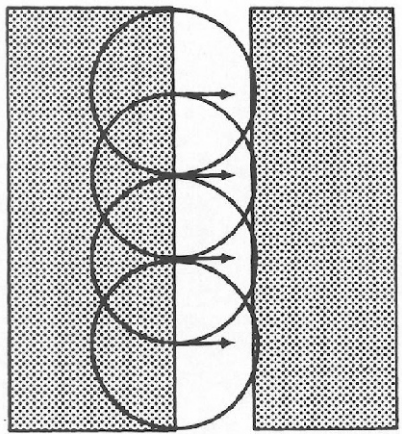

Fig. 20.6 Simple cell receptive field: model for directional selectivity. The simple cell's receptive field is formed by a row of geniculate fields. Cortical directional selectivity is based on the radial directional selectivity of retinal and geniculate receptive fields. Dotted areas indicate inhibitory regions. For details see text. (Goodwin *et al.*, *J. Neurophysiol.*)

moved past the centre, it would be in the inhibited zone. The postulated blanketing inhibition is applied by intracortical circuits.

Complex Cells

Bishop *et al.* (1980) concentrated their attention on directional sensitivity in neurones of the complex classes; about half of those studied were completely directional, in the sense that movement in the null direction provoked no discharge; this absence of discharge was associated with inhibition, revealed by suppression of any ongoing spontaneous activity, or of a driven discharge. The same factors governing the magnitude of the discharge in the favoured direction governed the magnitude of the inhibition in the null direction; e.g. the orientation tuning-curves for maximal excitation and inhibition were the same. Thus inhibition in the null direction is strongly correlated with excitation in the preferred direction. In general, their studies were consistent with the model suggested by Goodwin *et al.* for directional sensitivity.

Velocity Tuning

The assessment of the velocity of a moving object is an important and very necessary feature of the visual system. Movshon (1975) has studied cat's cortical neurones from this aspect and has shown that, just as for spatial frequency of gratings (p. 583) and orientation of lines, the cortical neurones are, in fact, tuned to different bands of velocity, covering a range of velocities of some two-hundredfold from some 0.25 to 64° per sec. Figure 20.7 shows how different types of cortical cells—simple, complex, and hypercomplex—are apparently tuned to different ranges, the complex and some hypercomplex cells being adapted to especially high velocities. Movshon points out that there are two basic ways of developing a system for signalling movement-velocity; units may simply increase rate of discharge monotonically over a wide range of movement, and such seems to be the method employed by the visual neurones of lower vertebrates, and this is also a feature of velocity-sensitive Y-neurones of the cat's lateral geniculate body (Dreher & Sanderson, 1973); the second method is that of multiple-channel analysis, whereby velocity-information is abstracted by determining the most active neural group in a population of such channels, each selective to a narrow range of velocity; and this is the analysis carried out by the cortical units, simple and Type I hypercomplex cells forming a slow group responding optimally to 0.25 to 7.5°/sec, while the fast group is formed by complex and Type II hypercomplex units with preferred velocities of 4 to 50°/sec.

Role of Inhibition

Goodwin & Henry (1978) measured optimal velocities of simple and complex cells; the median value for simple

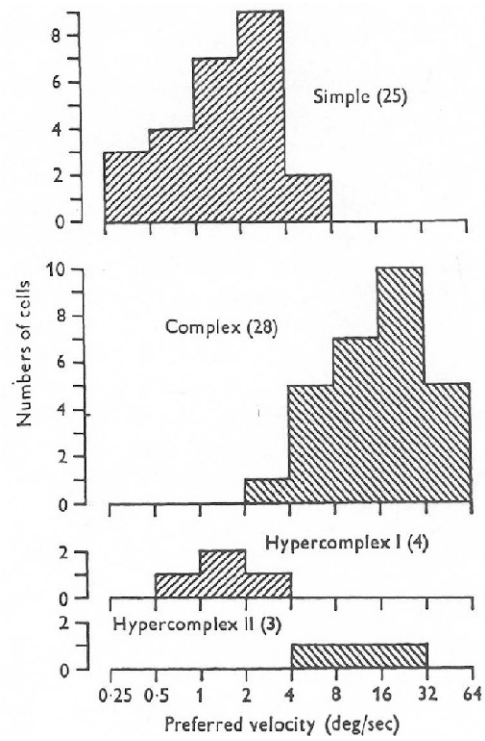

Fig. 20.7 Histograms showing the distributions of preferred velocities for sixty cortical cells of the four major types. (Movshon, *J. Physiol.*)

cells was 2°/sec and that for complex cells 3.1°/sec; they emphasized that the tuning to velocity depended essentially on the cut-off at high velocities, and that this must depend on inhibition as the stimulus passes into the inhibitory flank of a given cortical neurone. Their studies indicated that this inhibition would be retroactive, causing inhibition after the stimulus had reached a given excitatory point. Thus the signals generating inhibition would arrive sooner than those generating excitation.

GABA Block

If inhibition is an important factor, then blocking of the central nervous system inhibitor, GABA, should affect velocity-tuning. Patel & Sillito (1978) applied bicuculline locally to cortical units and found that units that had responded only to low velocities now responded to high velocities; simple and complex cells responded similarly.

Discharge-centres

Bishop *et al.* (1971), by concentrating on the response of cells to moving edges, as opposed to flashing stationary stimuli, brought out an interesting feature of the receptive field, namely its *discharge-centre*, which could be bimodal, in the sense that there were two regions of excitation as an edge moved across the receptive field, separated by a less excitable region. The two types are illustrated in Fig. 20.8, in (a_1) a narrow slit is moved across the receptive field at right-angles to the preferred orientation; as it passes through the discharge-centre, responses are recorded as in the histogram. When a wider slit is passed, two responses are obtained as the leading and trailing edges pass over the discharge-centre. If the two peaks are separated by the width of the slit there is a single discharge-centre (a_2). In (b) the separation between the discharges is greater than the width of the slit, indicating the presence of a second discharge-centre.

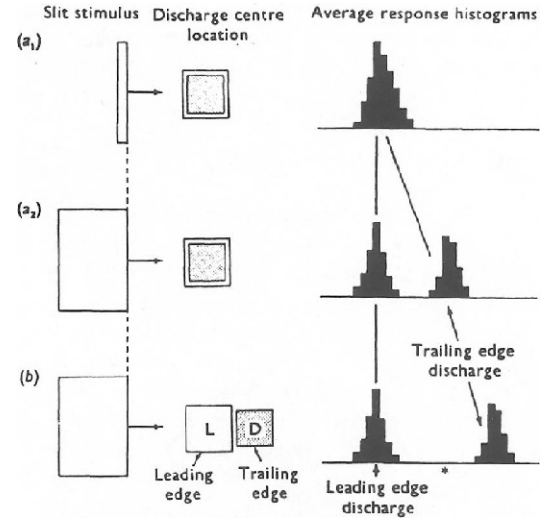

Fig. 20.8 Diagrammatic representation of average response histograms showing the expected locations of discharge peaks in response to the leading and trailing edges of a moving slit of light. With the discharge centres coincident, there is a single discharge peak when the slit is narrow (a_1) and when it is widened there are two peaks separated by a distance equal to the width of the slit (a_2). With spatially separated discharge centres (*b*), the discharge peaks are separated by the width of the slit (i.e. from vertical arrow to asterisk) plus the distance between the discharge centres. Starting position of the leading edge held constant throughout. (Bishop *et al.*, *J. Physiol.*)

Simple versus Complex Cells

This type of response to moving edges permits a fairly accurate distinction between the simple and the complex cell, since, for the simple cell, the recognition of separate light- and dark-edge discharge-regions is equivalent to the recognition of ON and OFF zones to stationary flashing lights; by contrast, cells of the complex type nearly always respond to both light and dark edges over relatively large overlapping discharge-regions in one or both directions of movement (Kato *et al.*, 1978).

Borders and Side-bands

We may define *primary* and *lateral* borders to the receptive field (Bishop & Henry, 1972); thus in Fig. 20.9 the

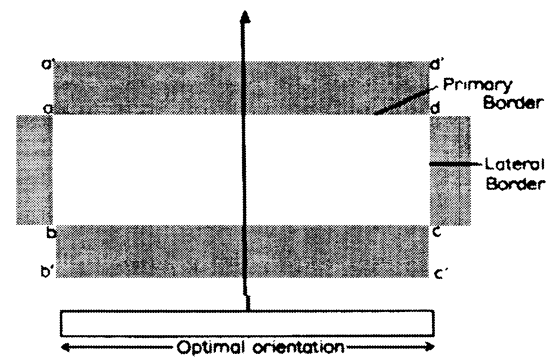

Fig. 20.9 Defining the primary and lateral borders of the receptive field. (Bishop & Henry, *Invest. Ophthal.*)

line-stimulus is orientated parallel with the optimum orientation and, to stimulate the receptive field, it is moved at right-angles to this direction and, if correctly placed, it will move across the *primary borders*, *ad* and *bc*. The *lateral borders* are defined as *ab* and *dc* and may be found by moving a slit placed laterally until positions are reached when a slight movement gives no discharge. Inhibitory side-bands would be indicated by areas *aa'd'd* and *bb'c'c*, to either side of the primary borders, whilst the

lateral or end-zone regions, giving rise to end-stopping, are the areas abutting on the lateral borders and are sometimes called lateral *sidebands.*

Cortical Inhibition and Receptive Field

On the basis of their studies of moving slit-stimuli, Bishop *et al.* (1971, 1973) postulated that an important element in determining the receptive field was the inhibitory interactions taking place at a cortical level, so that the receptive field of a simple cell could not be simply built out of the ON–OFF regions of geniculate neurones as suggested by Fig. 20.2. They emphasized that regions of OFF are not necessarily characterized by inhibition, so that it is possible to inhibit an OFF-response by an appropriate stimulus.

Suppression of Ongoing Activity

Thus inhibition is more correctly defined experimentally by a suppression of ongoing activity; because the simple cell shows little of such spontaneous activity, the inhibitory regions of a receptive field are best detected by studying the effects on the response of the cell to a conditioning stimulus (Henry, 1977; Orban *et al.* 1979).

SIDE-BANDS

In general, there are relatively wide inhibitory bands of about 2° to either side of the discharge-centre of a simple cell's unit, i.e. on the primary borders of the receptive field (Fig. 20.9)[3].

Monkey Units

Schiller *et al.* (1976a–e) have made an elaborate study of cortical neurones in the monkey, classifying their receptive fields on the basis of their discharge-centres, or subfields, along the lines developed by Bishop *et al.*

Seven Classes

Altogether some seven different classes of simple cell were described; complex or CX cells were defined as those with a unified activating region within which a response could be elicited by both light- and dark-increments. A T-type of cell showed no orientation-specificity; many were colour-coded and probably corresponded with Dow's (1974) Class I cells with little transformation of geniculate input. In general, simple, or S-type, cells were more sharply tuned to direction than CX-cells; 88% of CX cells were binocularly activated compared with 49% of S-cells. Directional sensitivity was not organized on a columnar basis, by contrast with orientation selectivity.

End-zone Inhibition

An important feature of Schiller *et al.*'s study was the failure of the hypercomplex cell to emerge as a distinct class. Thus the basic feature of this cell is the 'end-stopping', revealed as a reduction in discharge when the length of a slit exceeds a certain value. Many S- and CX-cells had this feature so that, in so far as hypercomplex cells in area 17 of the monkey are concerned, they are not completely defined by this feature of the stimulus. This feature of the cortical cell has been examined in greater detail by Rose (1977) and Kato *et al.* (1978); Fig. 20.10 illustrates the basic characteristics of end-stopping, namely the rapid rise in spike-response as the length of the slit, orientated optimally and moved across the discharge-region of the unit, is increased. At a certain point, an optimal length is reached—the cell is length-tuned—the slit now entering inhibitory end-zones.[4] The

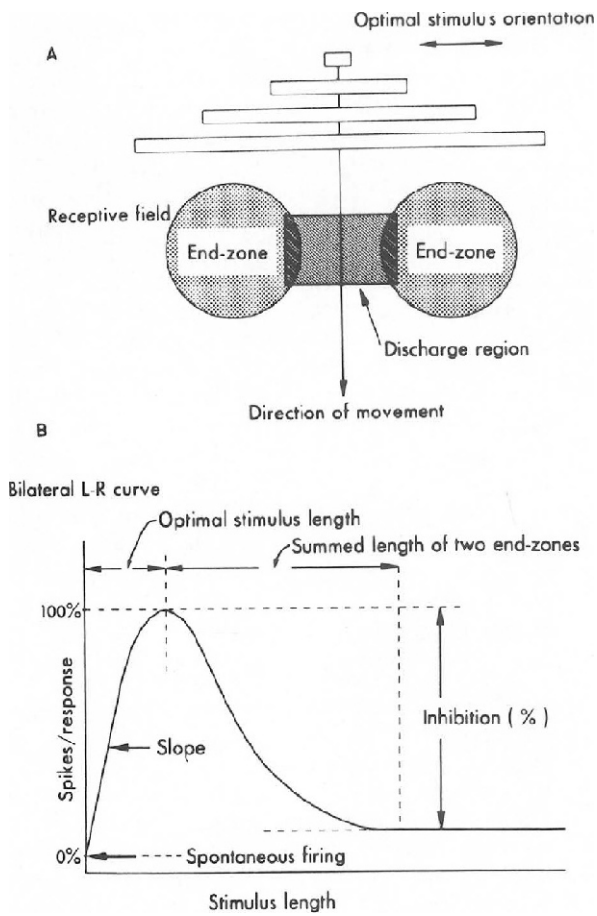

Fig. 20.10 A. Stimulus-configuration used for recording a bilateral length-response curve from a hypercomplex cell. The bar stimulus is centred on the middle of the discharge-region. B. Diagrammatic bilateral length-response curve from a hypercomplex cell to indicate how the various parameters are measured. (Kato *et al.*, *J. Neurophysiol.*)

degree of inhibition is indicated, which may be small or amount to 100% (complete end-stopping). Rose (1977), showed that end-stopping, or end-zone inhibition, was by no means confined to a particular class, so that the hypercomplex cell was only to be described as a cell with either simple or complex character but with extreme 'flanking inhibition', the flanks of the discharge-zone, or lateral borders, being perpendicular to the line of optimal orientation of the stimulus.

SIMPLE VERSUS COMPLEX CELLS

Kato *et al.* plotted the end-zone inhibition, defined by Fig. 20.10, against the optimal stimulus-length for the different classes of cell. On this basis the complex and simple cells fell into one group and the hypercomplex into another, in accordance with the amount of end-zone inhibition and optimal length, but the two classes of hypercomplex cell, i.e. those having simple (I) or complex (II) receptive fields, were not easily distinguished. Thus the most important classification seems to be based on the distinction between simple and complex cells, and Kato *et al.* showed that the proportions of these classes in the cat striate cortex, found by seven groups of workers, were very close to each other, namely some 70:30.

Textured Background

Hammond & MacKay (1977) showed that, whereas simple cells were unresponsive to movement of a textured background over their receptive fields, complex cells were, and for this reason they concluded that complex cells were unlikely to derive their receptive fields from simple cell input. In a further examination of simple cells they found that the response to a simple bar was usually suppressed by the symmetrical movement of a checkerboard pattern; the best effect was when both moved in phase. The effect extended beyond the accepted receptive field and was converted to a facilitation, contrasting with end-stopping. They emphasized that the effect was quite different from the shift-effect manifest in ganglion and geniculate cells. Hammond & McKay considered that this suppressive effect was mediated by complex cells, since they normally respond to a textured stimulus. The suppressive effect has been studied further by Gulyas *et al.* (1987), and was shown to occur with all cortical cell types, probably because the same effect is manifest at the geniculate level. The authors discuss the possibility that this suppressive effect might assist in distinguishing between real movement of an object and apparent movement due to eye movement.

Later Classification of Cortical Neurones

Hubel & Wiesel considered that the transition from simple through complex to hypercomplex neurones represented steps in the serial processing of visual information, so that the complex cell received input from the simple cell, and so on. This 'hierarchical principle' has been disputed by several workers and on several grounds. Before considering these we must consider work carried out in several laboratories in which the basic classification has come under scrutiny and has led to new classifications that better represent basic differences in processing. Thus, until agreement exists as to what are the distinguishing features of a class of neurones, the question as to whether a given type represents a synthesis of input from one or more types, either of cortical or geniculate neurones, cannot be satisfactorily resolved.

Simple Cells

Henry (1977) examined critically the basis of Hubel & Wiesel's classification of simple cells, which, as we have seen, are three, namely spatial summation in ON and OFF areas; mutual antagonism between ON and OFF areas; and prediction of fields from responses to flashing spot-stimuli. He emphasized the inadequacy of these, on the grounds that spatial summation within the discharge-region was not sufficiently distinctive to be treated as a unique classifying property. Again, OFF-regions are not necessarily regions of inhibition, which should be measured rather by suppression of ongoing discharge. Finally, the receptive field cannot be easily predicted on various grounds, in particular because of the limited summation that takes place, in fact, in directions at right-angles to the optimum orientation of the line-stimulus.

Complex Cells

The classification of complex cells, with its subgroups, was also criticized; thus, according to Henry, the three subgroups have little in common except their failure to fit easily into the simple category, while, on the other hand, the responses of each subgroup are distinctive enough to permit their identification. The heterogeneity of this class could be mitigated by taking out the largest subgroup, namely those units with uniform receptive field of mixed ON/OFF discharge constituting 55% of all complex cells (practically the only type in the striate area), and making them a class of their own. Having done this, the other subgroups, namely that with a non-uniform receptive field with distinctive ON- and OFF-regions, but not showing the summation that Hubel & Wiesel considered to be characteristic of the simple cell, and another subgroup responding to a stationary edge rather than to flashing light bars or spots, might be classed with the simple cells.

Hypercomplex Cells

Finally, the features of the hypercomplex cell were supposed to be derived from the input of complex cells, and would thus vary according to the type of complex cell contributing. In the cat's striate cortex they are very rare; however, Henry pointed out that the most common cell with a hypercomplex (end-stopped) receptive field was not included in Hubel and Wiesel's classification; it had the basic features of the simple cell but showed a preference for lines of limited length (end-stopping). In general he considered, in the light of more recent studies, that the term 'hypercomplex' should not be reserved for a class, but should rather indicate this particular (end-stopping) feature of a cell, so that we could have simple cells with and without it.

S-, C- and A-cells

Henry proposed the following nomenclature for the different classes of striate neurones, replacing the 'hierarchical names' with initial letters; thus the simple cell became the S-cell, and the complex the C-cell. S-cells showing end-zone inhibition became S_H-cells, and he proceeded to describe the common properties, discarding spatial summation. The key properties of the C-cell are those of the complex cell with uniform field, whilst the other types of complex cell are excluded; when end-zone inhibition is totally effective in suppressing the driven discharge. the cell is categorized as C_H. In the complex cell, spatial summation occurs along the line of optimal orientation, whilst there is a total absence as a flashing stimulus is widened in the plane perpendicular to the optimal orientation. The A-cell is the complex cell of Hubel and Wiesel with non-uniform receptive field; the presence of discrete ON and OFF areas distinguishes it from the C-cell, whilst the existence of large areas of close-to-maximum discharge, and the larger area of its receptive field, distinguish it from the S-cell. The S_H-cell is similar to the S-cell with the additional feature that inhibition generated from one or both of the end-zones beyond the lateral borders of the discharge-region is capable of total suppression of the discharge.

B-cell

Later (Henry *et al.*, 1978) the category of B-cell was introduced, to include units described by Camarda & Rizzolatti (1976); these had intermediate properties between those of S- and C-cells, sharing the typical C-cell's responsiveness to flashing stimuli, with rather smaller receptive fields ($2° \times 2°$), a preference for slowly moving targets, little or no spontaneous activity, and giving a sustained response when a light was flashed on. If these cells showed end-stopping they became B_H.

Practical Definition of the Simple Cell

For experimental purposes, at any rate, some working definition of a simple cell is necessary; having established this, the investigator can decide just how 'simple' or 'complex' a given unit is. Hammond & MacKay (1981) defined, for this purpose, a simple cell as one with a small receptive field, sharply tuned for orientation, with two adjacent and parallel ON and OFF regions, spatially separate light and dark discharge-centres for moving stimuli, substantial length summation and negligible resting discharge.

Lateral Geniculate Input

Dreher & Sanderson (1973) showed that lateral geniculate cells had discharge-centres, and related them to those of cortical units with which they synapsed. Malpeli *et al.* (1981) inactivated separate geniculate laminae in the monkey by injections of lidocaine and observed the effects on simple cortical neurones. Thus the two dorsal parvocellular layers contain mainly ON-centre X-cells, the two ventral parvocellular layers mainly OFF-centre X-cells, and the two ventral magnocelluar layers a mixture of ON- and OFF-centre Y-cells (Schiller & Malpeli, 1978). Blocking of one or more pairs of these layers might be expected to produce specific effects on the receptive fields of simple cells, or at any rate indicate whether a given cortical cell was driven by a given type of geniculate cell. Convergent input from both magno- and parvocellular layers occurred in some simple cells; others were driven by either a parvo- or magnocellular layer but not by both. A convergent parvo- and magnocellular input was common for complex cells. Neither orientation- nor direction-specificity could be abolished by blocking a single layer of the lateral geniculate nucleus. According to Hubel & Wiesel (1962) the ON- and OFF-regions of the simple cells are determined by convergence of ON-centre and OFF-centre geniculate units on to the simple cell; Malpeli *et al.* found that blocking lamina 6, containing ON-centre cells, blocked the light-edge response of simple and complex cells; again, blocking lamina 4, containing OFF-centre cells, blocked dark-edge responses, in confirmation of Hubel & Wiesel's assumption. Inhibitory input to cortical cells was revealed by facilitation of responses when geniculate layers were blocked.

Sustained Versus Transient Units

Bullier *et al.* (1982) have recorded the responses of geniculate neurones to specific stimuli and followed the corresponding responses in simple cells of lamina 4 in cats. Units were differentiated in respect of the sustained or transient character of their visual responses. They concluded that the receptive fields of their S-cells could have resulted from a major excitatory drive from one or two sets of geniculate neurones, with each set containing a maximum number of as many as 30 elements of the same type. This study, of course, simply indicated the input to the S cells; the actual receptive field exhibited by the S cell, i.e. its orientation-sensitivity, could not be predicted from the excitatory input. When the X- (slow) and Y- (fast) inputs to S-cells were separated, then some clear differences became manifest; thus the width of the receptive fields of slow-input units was less than that of fast-input cells, similar to the X- and Y-difference in receptive fields of ganglion and geniculate cells, suggesting that the X-Y dichotomy extended to cortical units. Cells in lamina 6, monosynaptically activated by geniculate cells, had much wider fields, of 2–6°, compared with about 1° for the lamina 4 units (Mustari *et al.*, 1982).

Cross-correlation Analysis

Tanaka (1983a) recorded from pairs of geniculate and cortical neurones that had similarly located receptive fields; monosynaptic or other connections between the pairs were established by correlating the discharges in

response to photic stimulation. Both simple and complex cortical neurones received monosynaptic geniculate input. When inputs were classified with respect to X-Y and ON-OFF dichotomies, a convergence of types could be demonstrated although many cortical neurones received only a single type. Greater than 10 geniculate cells contributed to simple cells and greater than 30 to complex cells. Complex cells showed the more mixed convergence, ON and OFF centre X and Y cells could all converge on a single complex cell. In general, Tanaka concluded that the X-, Y-dichotomy was continued into the cortex, emphasizing a parallel processing of pathways; they emphasized, too, the fact that complex cells received direct geniculate input, rather than being completely dependent on simple cells, as suggested by Hubel & Wiesel.[5]

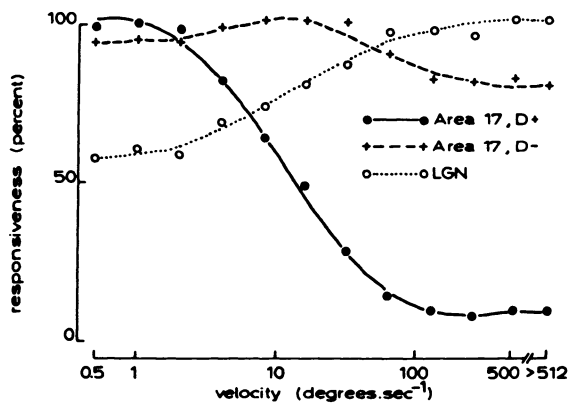

Fig. 20.11 Velocity responsiveness profiles of all duration-sensitive (D^+) and duration-insensitive (D^-) cells in area 17 compared with a similar profile for LGN cells. (Duysens *et al., J. Neurophysiol.*)

Velocity Sensitivity

Hoffmann and his colleagues have compared geniculate and cortical cells of the cat in an effort to determine why there is a large transition from high-sensitivity to velocity in geniculate units to the relatively low sensitivity of cortical units; thus the ubiquitous presence of cells in area 17 only responding to very low speeds of less than 10 °/sec must reflect something additional, in the way of intracortical circuitry, to geniculate input. Area 18 is distinguished from area 17 by its sensitivity to higher velocities; and this was attributed to the projection of Y-cells to this area (in the cat). However, as Orban *et al.* (1985) point out, the difference between the two areas is greater by an order of magnitude than the difference between geniculate X- and Y-cells. Duysens *et al.* (1985a) examined the effects of the lateral surrounds of simple cells on velocity-sensitivity, to see whether the rate of entry and leaving the discontinuities of the receptive field were important. They masked the surrounds of units with symmetrically placed ON- and OFF-fields, and found that many units preferring a low velocity were affected by such a procedure. However, those preferring high velocities did not lose their preference; and, as a result of a further study, Duysens *et al.* (1985b) concluded that with many units the critical factor was the duration of the stimulus required to initiate a response; since this also depended on the intensity, the minimum amount of energy to which the unit could respond limited its sensitivity to high velocities; so that the velocity cut-off was predicted by the minimum duration of a stationary stimulus required to excite the cell. The cells that behaved in this way were called 'duration sensitive' to distinguish them from others that were 'duration insensitive'. Figure 20.11 illustrates the velocity-profiles of the geniculate and two types of cortical unit.[6]

Prestriate Neurones

Most of the features of the receptive fields of cortical neurones have been derived from studies of the striate area; however, as Zeki (1978) has pointed out, the total area of visual representation is extremely large, occupying some fifth of the total neocortex in the primate; this extension from the primary receiving area must be indicative of stages in processing visual information, either in parallel or serially.

Area 18

There have been several studies of neurones in this prestriate area, comparing them with those in area 17. In the cat it must be remembered that area 18 receives a direct geniculate projection by large rapidly conducting Y-axons, so that a difference between the two areas based on, say, velocity-sensitivity might be expected. In the primate, area 18 receives its lateral geniculate input by way of the striate area, so that we might expect that the preliminary processing in the striate area could lead to more complex types of receptive field in area 18 if a 'hierarchical' principle of processing is adopted.

MULTIPLICITY OF CELL TYPES

Hubel & Wiesel (1965a) distinguished only two classes of neurone in the cat's prestriate area 18, complex and lower-order hypercomplex, the latter being complex cells but with end-stopping, and since characterized as hypercomplex II or C_H-cells. However, subsequent work has shown that area 18 contains simple cells (Dreher & Cottee, 1975; Tretter *et al.*, 1975; Orban & Callens, 1977a), and the study of Camarda (1979) has shown that area 18 contains the whole gamut of cortical neurone-

types, simple (S), complex (C) and hypercomplex II (C_H), hypercomplex I (S_H), B- and B_H-cells. Thus all three main cell-types can be end-stopped to give the H-subdivisions defined by Henry (p. 539). Area 18 contains all three main types of cell with their end-stopped counterparts.

MOVEMENT SENSITIVITY

Stone & Dreher (1973) observed that cells in area 18 were exceptionally sensitive to movement,[7] and amongst the fast movement-sensitive cells Orban & Callens (1977a) were able to define two groups, corresponding to simple and complex-type receptive fields. A few cells were described as *amplitude-specific*, which responded only to movements of up to a certain magnitude, beyond which inhibition set in. Orban & Callens (1977b) concluded, from a detailed analysis of the direction-, velocity-, and amplitude-sensitivities of area 18 neurones, that area 18 could, indeed, be regarded as a region where processing of motion-perception is elaborated; thus 94% of the neurones responded to movements, and these were influenced by velocity, in fact velocity was considered to be the analogue of stimulus-intensity for these neurones. Since two other movement-parameters are encoded in area 18 neurones, namely direction and amplitude of movement, all three parameters, together with localization, describe a visual movement. However, as Harvey (1980b) has pointed out, a parallel-processing of information in areas 17 and 18 can be expected to give the area 18 neurones the spatial selectivity found in the area 17 neurones; he has described (1980a) the laminar distribution and afferent connectivities of area 18 neurones in the cat; as others had found, all types of receptive field were represented. Most simple cells were directly driven by geniculate afferents, whereas most (but not all) complex cells were indirectly driven, as deduced by latencies from the optic chiasma and radiation. An important feature is that cells in areas 17 and 18, efferent to the same subcortical site and presumably having completed their processing of visual information, are more closely related than cells in the same cortical area projecting to different subcortical regions. Thus simple and complex cells in both areas project to the dorsal lateral geniculate nucleus and superior colliculus respectively (Harvey, 1980b). Alternatively, it has been suggested by Levick (1977) that the brisk transient system is primarily concerned with the analysis of stimuli close to the animal, so that if area 18 may be regarded, in the cat, as a cortical area selectively processing the Y-stream, the large receptive fields and responsiveness to fast movements characteristic of area 18 neurones would make them suitable for encoding information about objects of this kind.

DEPENDENCE ON AREA 17

Dreher & Cottee (1975) showed that the main features of the cat's area 18 neurone's receptive field were altered little, if at all, by acute electrocoagulation of area 17. They did find that the proportion of cells responding optimally to very high target-velocities increased after the striate lesion, suggesting that area 17 neurones were modulating the area 18 responses; they themselves, with predominantly X-cell input, do not respond to rapidly moving targets.[8]

Area 19

Neurones of this prestriate area in the cat have been examined by Kimura *et al.* (1980), who emphasize that this region, with its large projection from the pulvinar (p. 636), might exhibit differences from areas 17 and 18; moreover, its lateral geniculate projection is mainly from the medial interlaminar nucleus (MIN) and the ventralmost laminae C_1–C_3. They described three classes; A, monosynaptically activated by fast-conducting LGN neurones; B, monosynaptically activated by slowly conducting LGN neurones, and C, polysynaptically activated by slowly conducting neurones. The response persisted after local cooling of areas 17 and 18. In the waking monkey Fischer *et al.* (1981) studied responses of cortical neurones located in a region of the prelunate sulcus belonging to area 19 of Brodmann, comparing them with those in area 17. Of interest was the observation that some area 19 cells apparently received non-sensory signals that reduced the responses to a visual stimulus during rapid eye movements. Thus the presaccadic activation of area 19 units, revealed by this study, suggested to the authors that this prestriate area might be concerned with events related to visually guided changes of direction of gaze.

Posterior Bank of the Superior Temporal Sulcus (STS)

In exploring this region in the monkey, which receives projections from areas 17, 18 and 19, Zeki (1974a) found a portion that could be described as a 'motion area', characterized by neurones that showed a high degree of sensitivity to movement, as such, so that with many cells a moving spot could be more effective than a moving or stationary slit. Many were highly direction-sensitive, giving zero response in the null direction and maximal in the other. The neurones in this region have subsequently been studied in considerable detail since the area is considered to be a stage in the organization of visual information in relation to the spatial, i.e. three-dimensional, aspects of the visual field; they will be considered later.

Structural Correlates of Receptive Fields

Kelly & Van Essen (1974) established the type of receptive field, i.e. simple, complex or hypercomplex, of cortical neurones in the different layers and, after establishing this, they injected Procion yellow through the microelectrode to permit morphological identification. The majority of simple units were stellate cells and the majority of complex and hypercomplex were pyramidal cells; and this accounts for the earlier observations that these last two categories tend to be concentrated in the superficial and deep layers of cortex, whilst the simple cells are more concentrated in the middle layers, where the input from the lateral geniculate body takes place. As Stone *et al.* (1979) point out, the argument drawn from this difference in neurone-type, namely that S-cells are monosynaptically activated by geniculate cells, which synapse with spiny stellate neurones mainly in lamina 4, is not necessarily true; pyramids, with their long apical dendrites, can receive monosynaptic input in most or all laminae, including 4. The identification of the complex cell with the pyramidal cell is reasonable, since these pyramidal cells are those with axons leading out of the cortex; we should expect the neurones in which visual information had been processed to a high degree to be those that would influence other parts of the brain or the periphery. Thus the corticotectal neurones are found predominantly, if not exclusively, in layer 5 and, according to Kelly & Van Essen, these are pyramids. Although simple cells are concentrated in layer 4 and although stellate cells are also concentrated here, Kelly & Van Essen emphasize that they have not provided unequivocal proof that the geniculate input is, indeed, selectively to stellate rather than pyramidal cells; such a situation is demanded by the hierarchical concept of neuronal organization, a concept that has been questioned on several occasions.

Lamination of Cortex

Gilbert (1977) emphasized the importance of assigning cortical cells of a given receptive-field type to a given lamina of the cortex. The principal lateral geniculate input is to spiny stellate cells in lamina 4, which has been divided, in the cat, into sublaminae 4a to 4c, although 4a and 4b are usually considered as a unit.

Pyramidal and Stellate Cells

The cortical neurones are separated into pyramidal and non-pyramidal, or stellate cells. The essential feature of the pyramidal cell is the long dendrite that normally ascends towards the pial surface; it has other primary dendrites to form a basal skirt. The long apical dendrite clearly allows this neurone to collect information from neurones of other layers, finally transmitted through its axon that enters the white matter. The dendrites are spiny. The nonpyramidal or stellate neurones fall into a number of classes characterized by the features of their dendritic trees, the main types being illustrated in Fig. 20.12; on this basis they are described as multipolar, bitufted and bipolar. The dendrites of multipolar cells arise from any part of the somal surface and radiate in all directions. In bitufted cells the dendrites consist of two tufts extending from opposite poles of the cell, whilst bipolar cells have single dendrites originating from opposite poles of the soma to form an elongate and narrow dendritic field. A second criterion for distinguishing nonpyramidal cells is on the basis of spines, neurones being classed as *spiny*, *sparsely spiny*, or *smooth*. As Peters & Regidor (1981) point out, a given type of neurone, characterized by its dendritic tree, may also be characterized by its axonic ramifications, an excellent example being the bitufted cell in layers 2–3 and 4 described as a 'chandelier cell' because the axons end in vertically arranged arrays of boutons. The sparsely spinous and smooth elongate multipolar neurones, with essentially horizontal axons that contribute to form the 'baskets' surrounding the

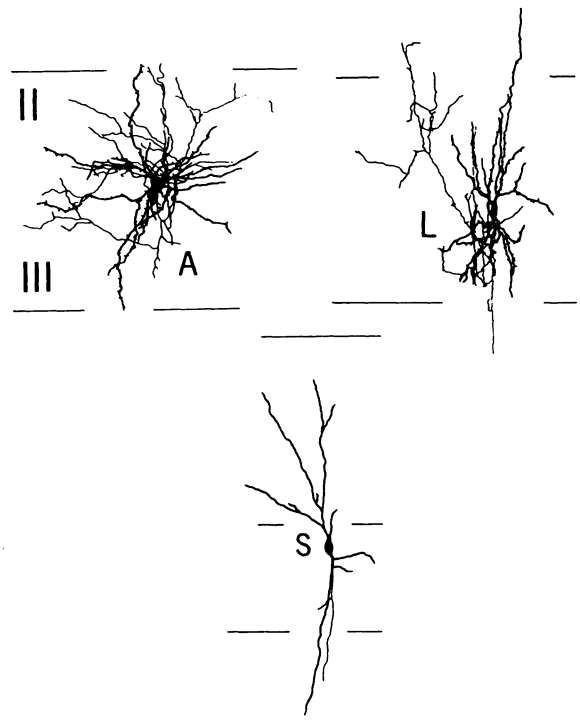

Fig. 20.12 Camera lucida drawings of non-pyramidal cells of cat visual cortex. A: Sparsely spinous, spherical multipolar neurone: L: Sparsely tufted bitufted cell with vertical dendritic tree in layer 2/3. S: Bipolar neurone with vertically orientated dendritic trees. (Peters & Regidor, *J. Comp. Neurol.*)

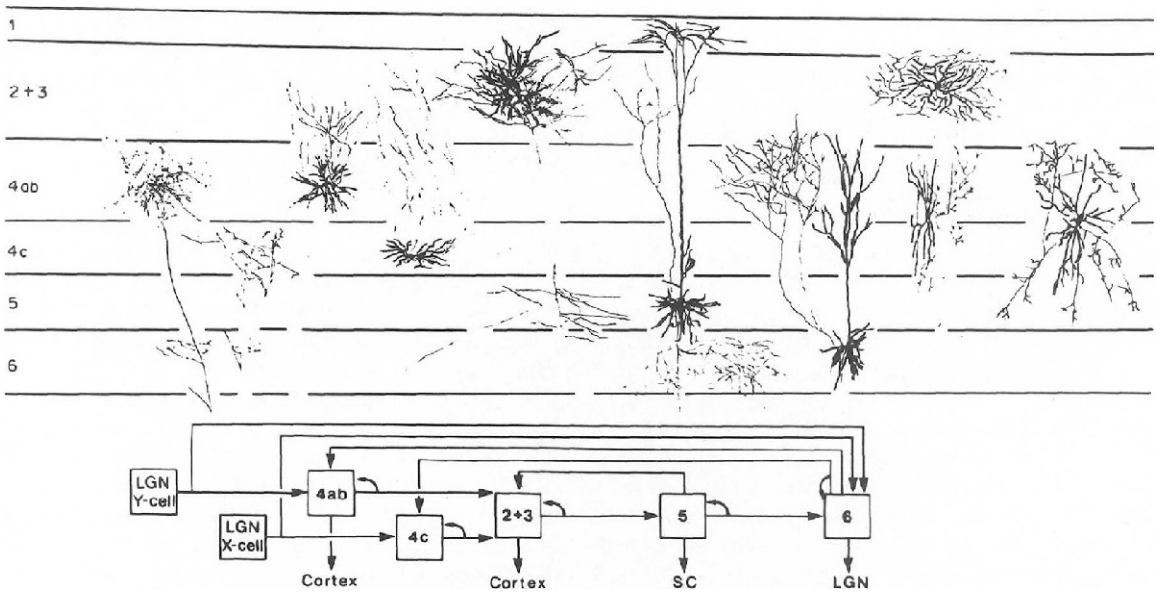

Fig. 20.13 Schematic diagram of the intracortical connections of the cat's striate cortex. The spiny stellate and pyramidal cells are presumably responsible for most of the excitatory connections, and their intracortical and efferent connections are summarized in the block diagram. Smooth stellate cells, several types shown at upper right, are presumed to mediate inhibitory interactions in the cortex. (Gilbert & Wiesel, *Vision Res.*)

perikarya of pyramidal neurones, are likewise distinguished by their terminal axons. Both these types are considered to contribute to inhibitory interactions between cortical neurones, being almost certainly GABA-ergic (Somogyi *et al.*, 1981).[9]

Layer 4 Cells

These had predominantly simple receptive fields; many of these units also showed end-inhibition in the sense that increasing the length of a line beyond a cetain point had an inhibitory effect; this was associated with orientation-tuning. A spiny stellate cell in layer 4ab, with a simple receptive field without end-inhibition, was characterized by extensive axonal ramifications in layers 2+3, presumably contributing to the complex types of receptive field found in these layers (Hubel & Wiesel, 1962; Gilbert, 1977). A complex cell, penetrated in layer 2+3, showed extensive axonal ramifications in its own layer, and its descending axon ramified in layer 5 and finally left the cortex, presumably innervating other regions of cortex. Cells in layer 5 have complex receptive fields but have very large field sizes, and have been divided into two classes, one that shows summation for increased field-length (*standard complex cell*) and one that responds optimally to a small moving slit of light placed anywhere in its large receptive field (*special complex cell*); this shows end-inhibition. A standard complex cell of layer 5 was found to send an axon down to layer 6, spanning an area of cortex representing up to 15° of receptive field, as opposed to its own receptive field of about $2\frac{3}{4} \times 1\frac{3}{4}$ degrees. Layer 6, like layer 4, is one in which geniculate input relays; its cells are a mixture of simple and complex, often requiring long slit-lengths for activation. An injected cell had a basal dendrite branching in the upper parts of layer 6 where the geniculate afferents enter; its axon projected mainly to layer 4 in the region of its apical dendrite. An injected smooth stellate cell had a complex receptive field. On the basis of this and later studies, a scheme for the circuitry of the cat's visual cortex is illustrated by Fig. 20.13 and some of the receptive-field characteristics of cortical neurones have been interpreted provisionally on this basis. Thus the preponderance of complex cells in layers 2+3 would be explained by the projection from layer 4, whilst layer 5 complex cells might have their receptive fields governed by the input from layers 2+3.

X-, Y- and W-streams

The segregation of the three streams of afferent input described in the subcortical centres seems to be maintained within the cerebral cortex. Gilbert & Wiesel (1979) injected horseradish peroxidase into cortical neurones, whose receptive fields had been previously investigated, in order to establish some of the relations between geniculate and intracortical input. They confirmed the claim of Ferster & Levay (1978) that the cortex retained the segregation of the X- and Y-streams, Y-afferents ending in lamina 4ab; X-afferents arborized entirely in

lamina 4c. Some Y-afferents sent collaterals to lamina 6. Figure 20.14 illustrates the scheme of Stone *et al.* (1979); this segregation suggests a continuation, within the cortex, of a parallel processing of information up to the first cortical receiving area. It would seem, moreover, that this parallel treatment extends farther; thus in the cat, and to a limited extent in the primate, area 18, or V2, has a direct geniculate input, as well as area 19, and the inputs are predominantly from X-units to area 17, Y-units to area 18 and W-units to area 19.

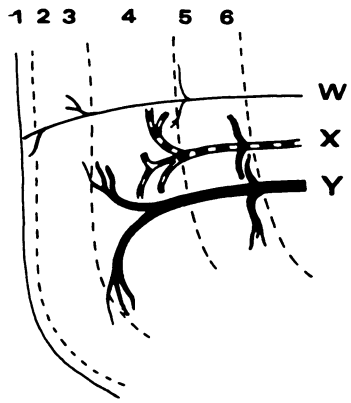

Fig. 20.14 Diagram of laminae of termination of Y-, X- and W-cells in area 17 of the cat. Y- and X-axons terminate at distinct levels within layer 4; both give some branches to layer 6. W-cell axons terminate in lamina 1, lamina 3 and in the region of transition between laminae 4 and 5. This pattern of termination seems consistent with the idea that, at least at the first geniculo-cortical synapse, Y-, X- and W-cell axons activate different subgroups of relay cells. (Stone *et al.*, *Brain Res.*)

SIGNIFICANCE OF THE THREE STREAMS

Stone *et al.* (1979) have suggested that the segregation into streams may subserve the different requirements of foveal and peripheral vision, X-type cells being principally concerned with foveal vision, and Y-type with peripheral vision. A specific role for W-cells, apart from that suggested by the superior collicular input, was difficult to assign. The residual vision found, even in primates, after loss of the striate area, might be mediated through W-cells, projecting as they do mainly to area 19, or V3. So far as the simple-complex dichotomy is concerned, the authors suggest that this should be qualified by assigning neurones to Y-Simple-Y-Complex, X-Simple, and so on, categories.

The Inhibitory Neurones

The intracortical inhibition that has been invoked, and often measured, to account for receptive-field properties has been tentatively ascribed to the *chandelier cell*, a bitufted neurone whose axon-ramifications apparently make specific connections with definite types of cortical cell. Fairén & Valverde (1980) found cells of this type in layers 2–3 mostly, but there were some in layer 4; their synapses were on the initial segment of the postsynaptic neurone's axon, so that they would probably exert a strong action on the output of this cell. The chandelier complex, embracing its postsynaptic neurones, occupied some 200–300 μm across, whilst its vertical space could pass through 2 to 3 cortical layers. The *basket cell*, with its axon ramifying with others to form a basket around a cortical cell's proximal dendrite (DeFelipe & Fairén, 1982) was considered by Fairen & Valverde to contribute to the inhibitory action on a given target cell.

CORTICAL COLUMN DEMARCATION

It has been suggested that basket cells serve, by their inhibitory action, to demarcate cortical columns (Peters & Regidor, 1981; De Felipe & Fairén, 1982). However, Martin *et al.* (1983) identified four basket cells by horseradish peroxidase, after establishing their receptive fields, which were either simple or complex. The ramifications in layers 3, 4b and 5ab, of the axons of a cell in layer 4a gave no suggestion of an organization in columns. i.e., a vertical slab-like arrangement, and they suggested a role of inhibition between columns rather than intracolumnar.

END-INHIBITION

The efferent connection from layer 6, containing simple cells with very long receptive fields, suggested to Gilbert & Wiesel (1985) that the end-inhibition of simple cells in layer 4 might be due to inhibitory inputs from these long-receptive field neurones. Thus a long line-stimulus might activate a layer-6 neurone, which would then activate an inhibitory neurone in layer 4, which would provide an inhibitory input that reduced the discharge of a simple cell as soon as the length of slit to which it was exposed exceeded a certain amount (Fig. 20.15).

Intrinsic Connections

The emphasis on geniculocortical input has been based on a vertical, or columnar, organization (p. 545). Gilbert & Wiesel (1983) have drawn attention to the very wide ramifications of individual cortical neurones on a horizontal basis (up to 4 mm), an interesting feature of which is the appearance of 'clusters' of terminals, repeating with an average periodicity of 1 mm. Thus cells in layers 2–3, 4, 5 and 6 of the striate cortex were penetrated, their receptive fields established, and then they were injected with horseradish peroxidase and their structure was reconstructed, first on a two-dimensional, and then on a

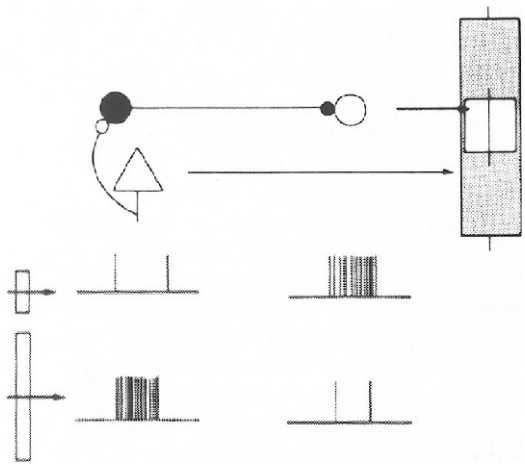

Fig. 20.15 Schematic diagram indicated proposed mechanism underlying end-inhibition Layer 6 cell is indicated by triangle, layer 4 cell by open circle, and layer 4 inhibitory interneurone by filled circle. The responses of these cells to bars of two different lengths is indicated by spike patterns at lower right. The layer 6 (and inhibitory cells) respond poorly to short slits, and very well to long slits. The end-inhibited layer 4 cell responds well to short slit, poorly to long slit. The receptive fields of the layer 6 excitatory and layer 4 inhibitory neurone are indicated by the vertical shaded rectangle; the excitatory portion of the field of the end-inhibited layer 4 cell is indicated by the smaller open square. Here again the orientations of the receptive fields of all three cells correspond. (Gilbert & Wiesel, *Vision Res.*)

three-dimensional basis. The actual areas of cortex included in these widespread ramifications were larger than would be expected from measurements of the excitatory portion of the cell's receptive field; and it was suggested that these cells might contribute to the receptive fields of other cells, either extending these or contributing to their inhibitory surrounds. The clustering of terminals suggests that the given cortical neurone is passing on information to pathways concerned with a specific submodality of vision. Thus, in a simple form, the same occurs with geniculate axon terminals in lamina 4ab; in this case the clustering probably represents the formation of ocular dominance columns. With intrinsic cortical neurones we may be concerned with colour processing, velocity tuning, and so on.

Columnar Organization of Visual Fields

Binocular Fields

The visual fields of animals with frontally placed eyes overlap, and the phenomena of binocular vision indicate that at some stage, or stages, in the visual neuronal pathway, from retina to striate and adjacent cortical areas, there is interaction between the impulses arriving from the separate eyes. When lateral geniculate neurones were examined by Hubel & Wiesel (1961), they found units that could be driven by one or other eye, but they never found one that could be activated by both eyes.[10] With striate neurones the position was different, some 85 per cent responding to stimulation of either eye (Hubel & Wiesel, 1962); furthermore, as we might expect, the receptive fields in the two eyes that stimulated a single cortical neurone were similar in shape and orientation, and they occupied symmetrical positions in the two retinae, i.e. what are called corresponding areas. Summation and antagonism occurred between the receptive fields of the two eyes. For example, if the ON-area of the left eye and the OFF-area of the right eye were stimulated together, the effects tended to cancel each other. In some cases a cell could only respond if both eyes were stimulated together by an appropriately orientated slit.

Dominance

We may speak of the *dominance* of one or other eye, according to its power of exciting a given cortical neurone by comparison with the other eye; thus a neurone excited only by the left eye, i.e. showing no measurable binocular interaction, would be said to be completely left-dominant; between this condition and right-dominance there were many stages. In general, there was a preponderance of contralateral dominance, presumably corresponding with the preponderance of crossed over uncrossed fibres in the cat's optic tracts.

OCULAR DOMINANCE HISTOGRAMS

Hubel & Wiesel devised a scale by which the degree of binocular convergence on a given cortical neurone could be quantified; Fig. 20.16 is an example based on 1256 cells in the macaque striate cortex, cells in lamina 4C being excluded since here the geniculate input is segregated to single eyes and the cortical neurones have, apparently, concentric and simple fields. Cells in groups 1 and 7 are monocularly driven, being excited through the contralateral and ipsilateral eye respectively; cells of group 4 are equally driven by the two eyes; cells in groups 3 and 5 are slightly more strongly driven by the contra- and ipsilateral eyes respectively; and so on.[11]

Cortical Architecture

A columnar organization of cortical neurones in the somatosensory cortex was established by Mountcastle (1957), such that neurones in a column with cross-sectional width about 0.5 mm were excited by the same modality of stimulus.

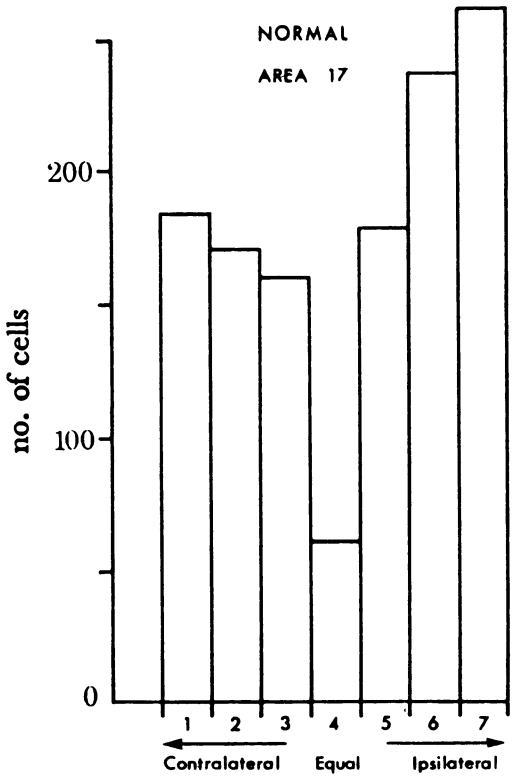

Fig. 20.16 Ocular dominance histograms in normal monkeys. The normal histogram is based on 1256 cells recorded from area 17, cells in layer 4C being excluded. (Hubel *et al.*, *Phil. Trans.*)

ORIENTATION AND DOMINANCE

In the visual cortex Hubel & Wiesel (1962; 1968) defined 'orientation-columns', representing neurones at successive depths in a vertical penetration that had the same, or very similar, preference for line-stimuli orientated at a given angle to the vertical meridian. Classification of units with respect to eye-dominance revealed a similar columnar organization overlapping with columns based on orientation preference. When a slightly oblique penetration of the cortex was made by the recording electrode, there were step-by-step changes in preferred orientation as the electrode crossed different columns. With strongly oblique penetration a very regular shift in preferred orientation was observed, every 25–50 μm shift giving rise to a change of about 10° so that a shift of about 180° occurred in some 600 μm or more. Reversal in the direction of rotation occurred irregularly, roughly one or two to a centimetre, and occasionally the shift could be broken by an abrupt shift of 90°, termed a *fracture*. Ocular dominance, meanwhile, shifted back and forth, apparently quite independently of orientation; first one eye dominated, then the two became roughly equal, and finally the other dominated, a complete cycle occurring roughly every 800 μm. Thus, although the individual subdivisions of the two systems are different in size—25–50 μm for orientation and 400 μm for ocular dominance—a complete set of either type, namely left-plus-right eye or a cycle of 180° of orientation, occupies about the same distance on the cortex, namely 0.5–1 mm.

HYPERCOLUMNS

One complete set of columns of either type was called by Hubel and Wiesel a hypercolumn, as illustrated in Fig. 20.17.

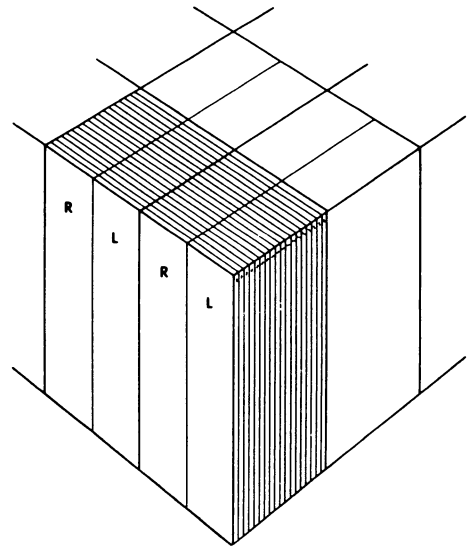

Fig. 20.17 Idealized model of the monkey striate cortex, showing two orientation hypercolumns each covering a full 180°, and two ocular dominance hypercolumns. Here the columnar walls are represented as flat, and the two sets are shown intersecting at right-angles, but the evidence indicates that neither set of walls is flat, and that the intersections are probably random. (Hubel *et al.*, *J. comp. Neurol.*)

LAMINA 4C

In lamina 4c the situation is different since the cells here, relaying directly with the geniculate axons, have no orientation specificity, having the simple centre-surround receptive fields characteristic of geniculate cells. On the other hand these units are strictly monocular, so that in a horizontal penetration there is a strict alternation of eye dominance as the electrode crosses the column borders. A cell above or below lamina 4c presumably receives convergent input from both eyes, relayed from 4c cells, and will thus show dominance rather than complete eye-specificity, the degree of dominance being governed by the region of 4c immediately above or below it.[12]

HISTOLOGICAL DEMONSTRATION

The organization in dominance-columns was demonstrated histologically by taking advantage of the fact that geniculate neurones in a given lamina represent retinal input from one or other eye only; the cortical degeneration following a lesion in this lamina will indicate the mode of projection of one eye, whilst regions of no degeneration in the immediate neighbourhood will represent regions of termination of the other eye. The pattern of degeneration in cortical lamina 4 is illustrated by Fig. 20.18, it occurs in patches, as viewed from above, the shaded regions representing those parts of Lamina 4 receiving from the contralateral eye and unshaded portions from the ipsilateral eye. A similar patchwork of projection was demonstrated by anterograde movement of labelled proline plus fucose from the eye to the cortex. Thus the cortical architecture, based on electrode penetrations at right-angles to, and parallel with, the brain-surface, together with these histological studies, suggest that the cortex is subdivided by two independent sets of partitions perpendicular to the brain surface and the laminae. Moreover, both systems of grouping are probably of the form of parallel vertically disposed sheets. Hubel *et al.* (1978) have exploited the ^{14}C-deoxyglucose technique of Sokoloff *et al.* (1977)[13] to localize histologically the hypothetical orientation columns and sheets. Thus one or both eyes may be exposed to a striped pattern and the increased activity of cortical neurones specifically excited by the stripes of the given orientation may be assessed autoradiographically in terms of the concentrations of the labelled deoxyglucose. The theoretical patterns of cortical activity for eyes stimulated by vertical lines in both eyes (A), the left eye (B) and for the left eye when the section is confined to lamina 4c (C) are indicated in Fig. 20.19. Thus with both eyes stimulated

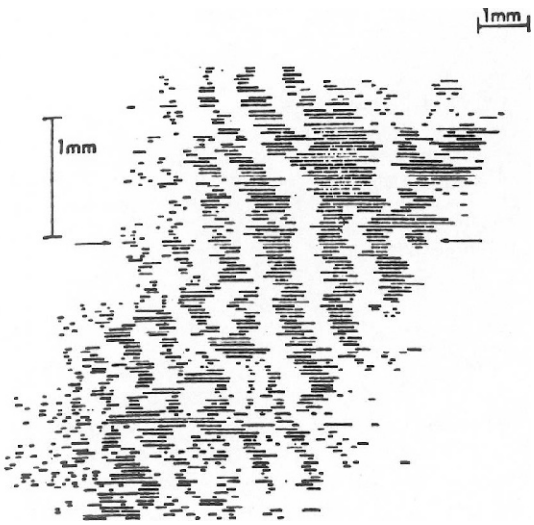

Fig. 20.18 Reconstructed map of regions of fourth layer degeneration in striate area after localized injury to the lateral geniculate body, as they would appear from above. Each horizontal line represents areas of terminal degeneration from one parasagittal section. Shaded areas thus represent those parts of layer 4 receiving input from the contralateral eye; unshaded areas, ipsilateral eye. (Hubel & Wiesel, *Nature.*)

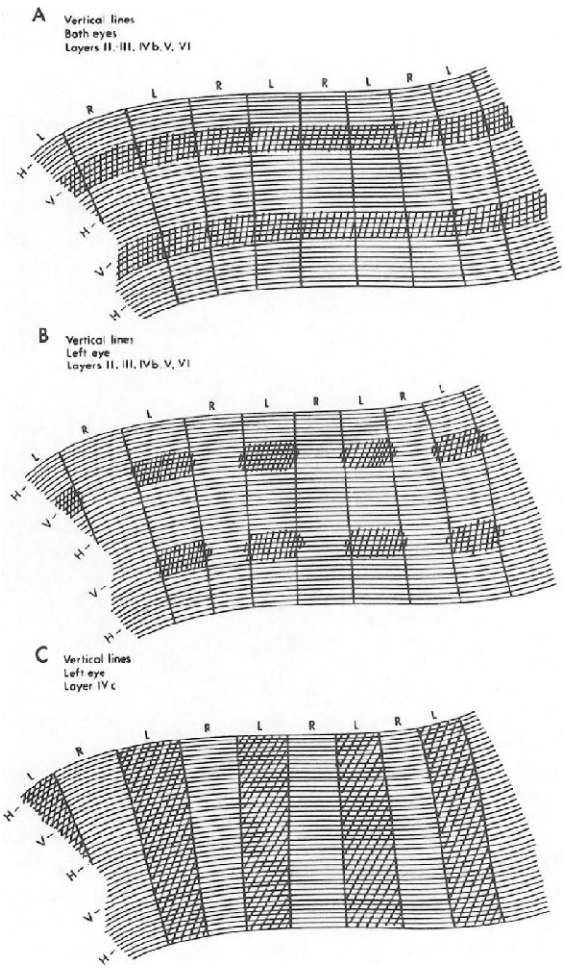

Fig. 20.19 Drawings to indicate the patterns of cortical activity expected from three different visual stimuli. A patch of monkey striate cortex several millimetres in length and width is viewed face-on. The horizontal lines represent boundaries between orientation columns, the vertical lines, boundaries between ocular dominance columns. H and V stand for horizontal and vertical stimulus orientations; L and R, the left and right eyes. As in Fig. 20.17 the column boundaries are very schematic. Shaded areas indicate the regions in which cells are expected to be activated. (Little is known about the response properties of cells in layers 1 or 4a.) A. The pattern expected in layers 2, 3, 4b, 5 and 6 when both eyes are stimulated by vertical lines. B. Activity pattern corresponding to vertical lines stimulating one eye only, in 2, 3, 4b, 5, and 6. C. Activity in layer 4c, in response to vertical-line stimuli to the left eye only. (Hubel *et al., J. comp. Neurol.*)

the stripes will correspond with successive columns representing the vertical orientation of the stimulus within $\pm 10°$. As both eyes are stimulated both dominance columns will be excited. With the left eye stimulated, the stripes will become patches, owing to the failure to excite the right-eye columns of dominance. In layer 4c, where orientation specificity is absent, the left-eye stimulation will give rise to a banding corresponding to the left-eye representation.

In general, these predictions were verified; thus exposure of one eye to stripes presented successively at different orientations through 180° led to the demonstration of dominance columns. When only vertical stripes were presented, the orientation columns, or slabs, could be demonstrated, and they seemed remarkably similar to the dominance columns or slabs, except that there was heavy and continuous staining in lamina 4c, as predicted. The most pronounced staining, indicating a columnar arrangement of orientation-selective neurones, was in lamina 4b, just above 4c, and another deeper in lamina 6. When orientation and dominance columns were separately labelled and compared, the greater simplicity of the dominance pattern became apparent; moreover, there seemed to be no clear geometrical relationship between the two, as suggested schematically by Fig. 20.17. The relation between the two is illustrated by Fig. 20.20. The two sets are certainly not parallel, but neither are they strictly orthogonal, so that the final organization in hypercolumns whereby, over a limited thickness of cortex, all orientations and degrees of dominance are embraced, is achieved by frequent intersections of the two sets of columns.

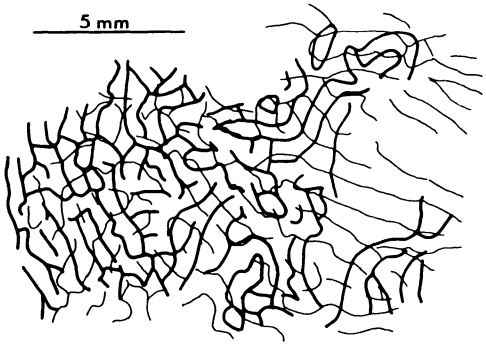

Fig. 20.20 The vertical-orientation columns are traced as thick lines, and the left-eye ocular dominance columns as thin lines. The average widths of the hypercolumns are 770 μm for ocular dominance and 570 μm for orientation. The two sets are certainly not parallel, but neither are they strictly orthogonal. (Hubel *et al.*, *J. comp. Neurol.*)

BASIS OF DOMINANCE

The cortical cells above and below lamina 4c receive input from both eyes with a preference for one or the other; this binocularity is due to input from cortical relay neurones activated by one or other eye; the anatomical connections suggest that a cortical neurone receives input from an area of 1 μm or more in horizontal extent, so that it could receive inputs from two dominance columns, and in accordance with its proximity to one or other column it would have a predominant input from one or other eye.

Inhibitory Interactions That inhibition of the input from one eye contributes to ocular dominance was shown by Sillito *et al.* (1980b), who found that some 50% of the cat's striate cortical neurones showed a change in ocular dominance after treatment with the GABA-inhibitor, bicuculline. Some units, exclusively monocularly driven, were driven by both eyes equally after the treatment.

Aberrant Orientations

There have been several claims indicating that neurones of the same orientation-preference did not traverse a complete column through layers 2 to 6; instead, a discontinuity occurred at the non-selective layer, namely layer 4c (Bauer *et al.*, 1983; Bauer, 1982), so that, in a column, there would be changes in orientation-preference on passing from supra- to infragrular laminae. Such deviations had been noticed by earlier workers, e.g. Hubel & Wiesel, but had been attributed to the electrode track's having moved out of a column. Murphy & Sillito (1986) have made an exhaustive study of numerous penetrations through the cat's striate area, and have concluded that deviations of preference found in a penetration are, in fact, due to the electrode's having passed out of the column.

Direction- and Orientation-preferences

So far as columnar organization of direction-preference is concerned, Berman *et al.* (1987) have found reversal occurring in an orderly fashion within an orientation-column; and, in tangential electrode penetrations, they found that changes in direction-preference did not occur so continuously as those of orientation. Thus the direction-sensitive columns may be said to consist of subunits that are smaller than the units of orientation. They concluded that, in the tangential plane, there were one to two direction-sequences per orientation-sequence, and in the vertical plane there were two direction-selective sequences in each orientation-column. The arrangement is illustrated by Fig. 20.21.

Cytochrome Oxidase Technique

Wong-Riley *et al.* (1978) showed that cortical neuronal activity could be demonstrated by cytochrome oxidase activity; in the visual system changes were reported in

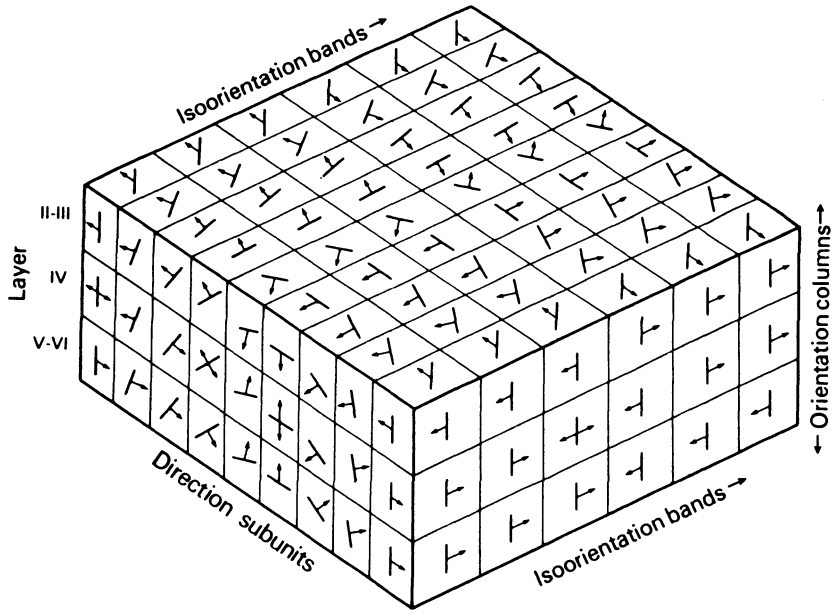

Fig. 20.21 Model of direction and orientation modules. This model illustrates reversals in preferred direction within the orientation columns, the isoorientation bands, and within the orientation sequences. (Berman *et al.*, *J. Neurophysiol.*)

cortex and lateral geniculate nucleus after lid-suture (1979). Using a histochemical stain for this enzyme's activity, several workers (e.g. Horton & Hubel, 1981) have demonstrated a striking pattern of regularly spaced patches, or 'blobs', some 350 μm apart, most obvious in laminae 2 and 3, but also in 1, 4b, 5 and 6, but absent from 4c and 4a, of the primate striate cortex. In V2 a coarser pattern of broad parallel stripes was present, and permitted the accurate delimitation of the two visual areas (Tootell *et al.*, 1983). By using transneuronal radioautography with ^{3}H-proline, given intraocularly, the patches were shown to be coincident with dominance columns. Thus the ^{3}H-proline patches in lamina 4c, the termination layer for geniculate input and therefore delimiting monocularly stimulated cortical neurones, were in exact register with over- and underlying patches of cytochrome oxidase activity (Horton & Hubel, 1981). Apparently each patch sits squarely within a left- or right-eye column (Horton, 1984), as illustrated in Fig. 20.22. If the patch represents a basic module for cortical organization, then this means that the basic module does not contain a complete hypercolumn of each stimulus-parameter; thus a doublet of patches is required to house each dominance hypercolumn. In Fig. 20.23 Horton has adopted a suggestion of Braitenberg & Braitenberg (1979) to the effect that orientation columns were organized around local centres, rather than in parallel slabs. These centres could be the cytochrome oxidase patches, illustrated in Fig. 20.22, and might organize orientation-selectivity in the surrounding cortex[14] but would, themselves, not be orientation-selective. Thus, using the deoxyglucose technique for establishing orientation-columns, they

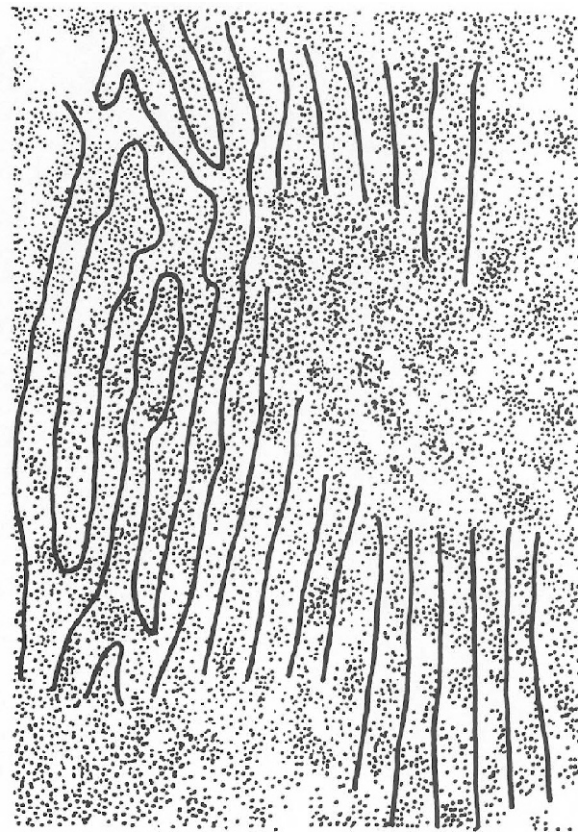

Fig. 20.22 Rows of cytochrome oxidase patches, indicated as clusters of dots, fall squarely within the ocular dominance columns, established by ^{3}H-proline injections into right eye. (After Horton & Hubel, *Nature*.)

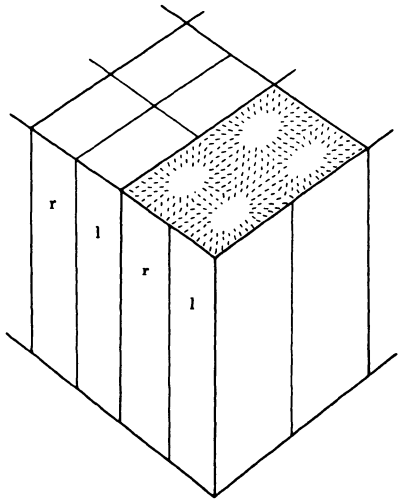

Fig. 20.23 Model of macaque striate cortex showing cytochrome oxidase patches, ocular dominance columns, and orientation columns. Each patch fits within an ocular dominance column, with its long axis orientated parallel to the length of the column. The orientation columns are shown arranged in a radial fashion around each patch, as they might be according to the scheme of Braitenberg & Braitenberg (1979). An electrode passing tangentially through the cortex would encounter long sequences of regular orientation shifts interrupted ocassionally by abrupt discontinuities. Deoxyglucose evidence suggests that the patches may contain cells lacking orientation selectivity. (Horton, *Phil. Trans.*)

found no evidence for orientation selectivity in the cytochrome oxidase patches.[15]

HUMAN VISUAL CORTEX

Using post-mortem material and cytochrome oxidase staining, Horton & Hedley-Whyte (1984) have confirmed the presence of ocular dominance columns in lamina 4c of visual cortex taken from a human subject, previously uniocularly enucleated. They appeared as roughly parallel slabs about 1 mm wide, perpendicular to the area 17/18 border, as in the macaque. Patches were not present in a 6-month fetus, but clearly formed in a 6 month-old baby. Figure 20.24 shows a reconstruction from tissue-sections of the pattern of ocular dominance columns over the medial face of the right hemisphere. There is an overall tendency for the columns to form roughly parallel slabs, about 1 mm wide, orientated perpendicular to the 17–18 border.

Geniculate Control of Receptive Field Properties

The columnar arrangement of neurones in the cortex suggests that the properties of neurones in some layers are determined by influences of neurones in different laminae of the same column. However, Malpeli (1983) found that inactivation of layer A of the cat's dorsal lateral geniculate nucleus, which abolished visually driven activity in layers 4 and 6 of area 17, allowed many of the features of the receptive fields of cells in the supragranular layers

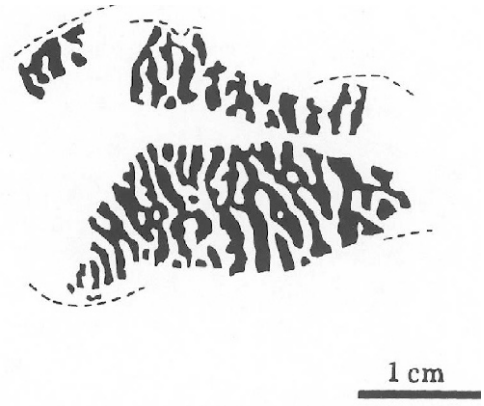

Fig. 20.24 Reconstruction of the pattern of ocular dominance columns over the medial face of the right hemisphere; the region of the photomontage is to the lower right. Dotted lines indicate the 17–18 border; black columns correspond to the intact eye. (Horton & Hedley-Whyte, *Phil. Trans.*)

to survive. In a series of papers describing experiments designed to show the contributions of the different geniculate layers to cortical neurone responses, and of different cortical layers on responsiveness of neurones in nearby layers, Malpeli and his colleagues have shown that, in general, cortical neurones may be placed in two categories constituting two interacting systems. Thus layers 4 and 6 for which the geniculate input is sufficient to define their properties, and the supragranular layers, which integrate information from several geniculate subdivisions and depend on no single subdivision. Thus, in striking contrast with elimination of layer A, which robs layers 4 and 6 of responsiveness to visual stimulation in the contralateral hemifield, elimination of the C layers and MIN did not abolish driven activity, orientation selectivity or directional selectivity of cells in any layer. Thus supragranular neurones rely on input from several geniculate layers. In general, the two groups of cortical neurones develop their receptive-field properties independently of each other, so that neither imposes its characteristics on the other (Malpeli *et al.*, 1987).

INACTIVATION OF SUPRAGRANULAR LAYERS

Schwark *et al.* (1987), continuing this study, found that it was essentially special complex cells in layer 5 that were affected by removal of the supragranular layer activity; thus complex cells are separated into *standard* and *special* by their responses to bars of increasing length; standard complex respond best to long stimuli and special complex to short stimuli; layer 5 cells under the supragranular lesions had the characteristics of standard complex units (Fig. 20.25). Apart from these special complex cells, the receptive-field characteristics of all units in the infragranular layers were normal, so that it would appear that it is only the special complex cell, inhibited by increases in length of the stimulus, that depends on supragranular input.

The Cortical Transmitters

GABA

GABA is well established as an inhibitory transmitter in the visual cortex (Iversen *et al.*, 1971) and we have already

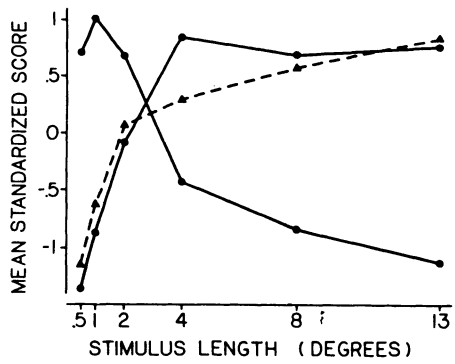

Fig. 20.25 Standardized length response curves for layer 5 cells. The 2 *solid lines* connect the mean values of normal cells classified as special complex ($n = 18$) or standard complex ($n = 21$), and the *dashed line* connects the mean values for layer 5 cells recorded under supragranular layer lesions ($n = 17$). (Schwark *et al.*, *J. Neurophysiol.*)

seen how receptive-field characteristics of visual neurones may be modified by the GABA inhibitor bicuculline. In the cerebral cortex it was identified immunocytochemically by Hendrickson *et al.* (1981) by employment of its labelled precursor. Its presence in the visual cortex of the monkey was established by immunocytochemical localization of the enzyme, glutamic acid decarboxylase (GAD). It was identified in all layers of the macaque striate area; in laminae 2 and 3 the staining revealed a periodic pattern of dots identical with those seen with cytochrome oxidase. The rows of dots ran parallel with ocular dominance columns, suggesting that labelled neurones are preferentially related to each eye. Since GABA-ergic neurones are considered to be highly metabolically active, the relation of GAD-spots to those of cytochrome oxidase suggests that the latter might well reveal inhibitory activity, which of course must be an important factor in determining receptive fields. The distribution of nerve terminals indicated highest concentration in upper laminae 1, 4A and 4C; 2, 3 and 6 were less heavily stained, and laminae 1, 4B and 5 only lightly. Cell bodies were present in all laminae but laminae 5 and 6 exhibited a regular spacing.

Excitatory Transmitters

Shaw & Cynader (1986) studied both inhibitory and excitatory transmitters. They demonstrated powerful binding of the GABA-analogue, ^{3}H-muscimol, especially in lamina 4C of the monkey, as well as in laminae 2, 3 and 4A. The binding of other transmitter analogues is indicated in Table 20.1; it will be noted that, so far as glutamate was concerned, the authors employed ^{3}H-L-glutamate, which labels the major subclasses of receptors, namely NMDA, kainate and quisqualate, within the cortex. Of some interest is the wide distribution of cholecystokinin receptors, suggesting a major role for peptidergic neurones in the cortex.[16] By depolarizing cerebral cortex with a high concentration of K^+, Baughman & Gilbert (1981) caused leakage of endogenous glutamate and aspartate, as well as the inhibitory transmitter GABA. They showed that ^{3}H-labelled glutamate and aspartate, when injected into the lateral geniculate nucleus, passed retrogradely into mainly layer 6 but also to layer 4; thus the projection from the visual cortex back to the lateral geniculate nucleus is mediated by neurones using glutamate or aspartate as a transmitter. Injections into the superior colliculus gave no retrograde labelling.

Tsumoto *et al.* (1986) employed selective antagonists to the three receptor-types, NMDA-preferring, quisqualate-preferring, and kainate preferring, namely γ-D-glutamyl glycine (γ-DGG); *cis*-2,3-piperidine dicarboxylic acid (PDA) and 2-amino-5-phosphonovaleric acid, and kyurenic acid (KYNA). Kynurenic acid (KYNA) was found to be the most effective in blocking visually and glutamate/aspartate induced activity in the visual cortex of the cat, and they used this to explore the excitatory pathway synapses in the visual pathway in area 17. 79/104 cortical simple cells were completely blocked by KYNA, but only 18/68 complex cells and 3/16 special complex cells. Most of the blocked cells were in layers 4ab, 4c and upper layer

Table 20.1 Laminar receptor binding patterns in monkey and cat visual cortex (Shaw & Cynader, 1986)

Receptor	*Monkey*	*Cat*
$GABA_A$	2, 3, 4A, 4C	2, 3, 4
NMDA/kainate/quisqualate	1, 2, 3, 4A	1, 2, 6
Quisqualate ([^{3}H]-AMPA)	1, 2, 6	1, 2, 6
Cholecystokinin	1, 2, 3, 4A, 4C, 5, 6	1, 2, 3
Acetylcholine-muscarinic (high- and low-affinity sites)	1, 2, 3, 4A, 4Cα, 4Cβ	1, 2, 3, 6
Acetylcholine-muscarinic (low-affinity sites)	1, 2, 3, 4A, 4Cβ	1, 2, 3, 5 (upper), 6
Benzodiazepine	2, 3, 4A, 4C	2, 3, 4
A_1-adenosine	2, 3, 4A, 4Cβ	1, 2, 3

6, so that effects were much smaller in other layers. Thus it would seem that glutamate/aspartate are transmitters at the geniculo-cortical synapse.

Cholinergic Activity

Cholinergic axons have been identified in all layers of the visual cortex when immunoreactivity to acetylcholinesterase was used to identify them; the major direction is horizontal and their mainly extracortical origin is demonstrated by the drastic reduction after undercutting the cortex; and it is considered that their main source is the basal nucleus of Meynert (Hendreen *et al.*, 1984). Using a histochemical stain for acetylcholinesterase, Bear *et al.* (1985) confirmed the widespread distribution of axons in all layers, especially 1, lower 3, 4c and 6. In addition they found a population of layer 5 pyramid neurones intensely staining. Undercutting the cortex, or kainate lesions, virtually eliminated all the axons, and kainate lesions showed that the basal forebrain was the sole source of cholinergic axons.[17]

EFFECTS ON CORTICAL NEURONES

The cholinergic system has been implicated in the phenomena of arousal, mediated through the ascending reticular formation; and Livingstone & Hubel (1981) have correlated the response-features of the lateral geniculate nucleus and visual cortex of the cat with the conditions of sleepiness and arousal indicated by the EEG. During slow-wave sleep the ON responses of a geniculate neurone tended to be depressed, whilst they were accentuated during the arousal phase with desynchronized fast waves. OFF-effects were similarly influenced, so that the general effect of arousal was to enhance the responsiveness of geniculate and cortical neurones. There was no effect on such features as end-stopping in cortical units.

LOCAL ACETYLCHOLINE APPLICATION

Sillito & Kemp (1983) found a facilitation of responses to visual stimuli in 61% of cortical neurones in laminae 2 to 6 and a depression in 31% of neurones in laminae 2 to 4. There was no change in the receptive-field characters of the neurones, such as directional sensitivity. In this case the response in the preferred direction increased with no effect on the response, or lack of response, in the opposite direction. The effects of the GABA inhibitor, *N*-methyl bicuculline (Nmb), were quite different, directional sensitivity being abolished and spontaneous activity being increased. In a similar way, orientation-specificity was unaffected by acetylcholine but abolished by Nmb. So far as the depressant action was concerned, this seemed to be a general reduction in responses without changing the receptive-field character; thus the tuning for orientation was the same and the orientation for maximal response was unaltered.

In a comparable study on the cat's visual cortex, Sato *et al.* (1987a, b) confirmed the facilitation of some 74% of neurones and an inhibition of 24%; both effects were blocked by atropine but not by hexamethonium. Reduction in the cholinergic innervation was brought about by injections of kainic acid into the nucleus basalis magnocellularis; they caused a reduction in responsiveness of cortical cells on the lesioned side, and the responses became very variable, but the consistency of response returned after application of acetylcholine. Sato *et al.* considered that the role of the cholinergic innervation was to improve the signal-to-noise ratio for the cortical cells, since the increased responsiveness was not associated with an increase in tonic activity.

Notes

1. Earlier Tsumoto *et al.* (1979) had shown that directional sensitivity, namely the change in response when an optimally orientated line-stimulus was moved in different directions, was completely lost in many simple cells after bicuculline application; orientation-sensitivity was never completely lost, due, as they thought, to the orientation-selectivity of the geniculate input. They found that the excitatory receptive fields tended to become round rather than linear. They noted that a combination of the inhibitor of GABA synthesis, 3-mercaptoproprionic acid (MP), with bicuculline was more effective.
2. Because a slit- or bar-stimulus is moved at right angles to its long axis, the directional sensitivity and the orientation-preference of the cell are confounded, so that, theoretically, it would be best to assess directional tuning by a spot stimulus, but this, of course, tends to exclude simple cells (Henry *et al.*, 1974). Hammond (1978) has substituted for a spot what is called a *random-noise-stimulus*, consisting of 356 × 356 elements subtending 10 × 10° overall. Thus a bar of this display could be moved across the receptive field, and directional tuning compared. Complex cells of area 17 showed stronger directional selectivity with the noise stimuli; however, tuning was sharper with the bar stimulus. Hammond concludes that orientation- and direction-selectivity are mediated by different mechanisms, as suggested by Schiller *et al.* (1976).
3. The detailed features of the receptive fields of the cat's simple and complex striate cortical cells have been examined in much greater detail by Palmer & Davis (1981a, b) making use of the Stevens & Gerstein (1976) technique. Inhibitory regions were established by previous light-conditioning, owing to the usual absence of spontaneous activity in simple cells. It became clear that there were considerable variations in the structure of the receptive fields of simple cells, owing to the different spatial distribution of inhibitory regions; complex cells were more uniform because of the absence of prominent inhibitory regions. Simple and complex cells were distinguished also by the temporal features of their responses, the complex cells giving only transient bursts at ON and OFF, indicating a predominantly Y-cell input.
4. The characteristic 'end-stopping' or length preference of

hypercomplex cells of layers II and III was not greatly affected by bicuculline, suggesting that this feature of the hypercomplex cell's receptive field is built in by its input from length-sensitive units, perhaps cells in layer V (Sillito & Versiani, 1977).

5. This separation into X- and Y-streams was demonstrated very neatly by treating the cortex with the GABA inhibitor, bicuculline; many cortical units developed X-like and Y-like characteristics in consequence, whilst orientation- and directional-selectivities were diminished (Tanaka, 1983a).
6. Complex cells can respond to higher velocities than simple cells; this has been attributed to their larger receptive fields; however, as Duysens *et al.* (1985b) point out, this cannot be the only factor as the velocity cut-off increased by a factor of 25 between retinal eccentricities of 2° and 30°, whereas receptive fields increased by only a factor of 4.
7. The transition from area 17 to area 18 is sharp because of the marked architectonic difference; it is interesting that the transition can be observed by estimating the velocity sensitivity of cortical neurones, but only with respect to foveal representation (Orban *et al.*, 1980).
8. Bilateral removal of area 17 did reduce the number of area 18 cells driven by both eyes from 69% to 42.5%, an effect they attributed to removal of the callosal input to the part of the area 18 from which recordings were made.
9. McGuire *et al.* (1984) described the ramifications of layer 6 pyramidal cells, receiving input from the lateral geniculate nucleus, in layer 4. They injected layer-6 cells with horseradish peroxidase and examined their ramifications in layer 4; the axon terminals made asymmetrical synapses mainly with spiny dendritic shafts; and these were probably excitatory. A large proportion of the postsynaptic dendrites, however, belonged to smooth or sparsely spiny neurones, neurones that are thought to mediate inhibition because they contain glutamic acid dehydrogenase and show specific uptake of ^{3}H-labelled GABA (Somogyi *et al.*, 1981).
10. Although it is generally agreed that neurones in the dorsal nucleus can only be driven by one eye, this does not mean that a given neurone is not binocularly influenced; in fact, a neurone driven by one eye, the dominant eye, will be inhibited by a stimulus in the other eye at a retinal point corresponding with that which excites in the dominant eye (Sanderson *et al.*, 1969; 1971). Thus Singer (1970) stimulated the centre of the receptive field in the dominant eye and simultaneously moved a bar of light across the corresponding point of the other eye, and measured long-lasting inhibitory synaptic potentials in the geniculate neurone. The inhibition described by Sanderson *et al.* (1971) survived removal of areas 17, 18, 19 and the Clare-Bishop area, so it is unlikely that it was cortically mediated; thus interneurones must cross the interlaminar boundaries.
11. Because neurones in lamina 4 are activated by only one eye, a histogram devoted only to neurones in this layer would consist of two columns, 1 and 7. Blakemore *et al.* (1978) separated their histograms into two, lamina 4 and non-lamina 4c.
12. In the cat, the neurones of lamina 4c are orientation-selective, so that the orientation columns are clearly defined even at the base of lamina 4 (Stryker *et al.*, 1977). Orientation columns in the cat's cortex have been mapped, using the Sokolov technique, by Albus (1979) and Flood & Coleman (1979). Albus' orientation subunits appeared as columns in sections perpendicular to the cortical surface. In horizontal sections they appeared as bands, running parallel but sometimes fusing with each other. The distance between subunits centres was 700–1200 μm, agreeing with his physiological observations; the widths of these subunits were 300–600 μm, about twice the value deduced from electrical recordings.
13. 2-Deoxyglucose is phosphorylated by brain cells; metabolism ceases at this point, so that if the sugar is labelled with ^{14}C and injected into the animal, regions of neuronal activity may be localized autoradiographically. Mapping of the blind spot representation in the cortex is possible, using this technique. Thus the spatial extent of cortex where neurones would project if they were in the blind spot, receives no projection from the contralateral eye, but it does receive projection from neurones in the ipsilateral eye, so that with electrode mapping of cortex no blind-spot of cortex would be revealed. However, occlusion of one eye deprives the region of the ipsilateral cortex of all input, and so the blind spot becomes manifest as an ovoid structure extending through the entire thickness of the cortex.
14. Horton emphasizes the analogy between the cytochrome oxidase patches and the 'cortical barrels' representing vibrissal function in somatosensory cortex. These are not present in all animals with vibrissae, in the same way that cytochrome oxidase patches are apparently only present in primate visual cortex, being absent in cat, mink, tree shrew, mouse rat, rabbit and ground squirrel (Horton, 1984).
15. Humphrey & Hendrickson (1983) point out that cytochrome oxidase concentration represents the potentiality for metabolism rather than metabolic rate; deoxyglucose uptake, on the other hand, indicates metabolism, so that changes with neuronal activity are to be expected. Thus, when monkeys were kept in the dark, during deoxyglucose exposure, cytochrome oxidase patches were observed but not deoxyglucose patches: during light-stimulation the two types of patch coincided. Squirrel monkeys do not show the dominance columns revealed by uniocular stimulation in the macaque; and this may be because neurones in lamina 4 are mostly binocular (Hubel & Wiesel, 1978). Humphrey & Hendrickson emphasize that there is a very considerable basal metabolic activity independent of specific retinal stimuli, such as orientation or ocularity; this, moreover, is not uniform but can produce patchy distribution of label that must be allowed for when assessing the effects of specific visual stimuli.
16. The authors discuss in great detail the possible significance of their results in relation to immunocytochemical identification of transmitters; it seems clear that the mere localization of binding sites is unlikely, on its own, to help in unravelling 'chemical circuitry' of the cortex.
17. de Lima & Singer (1986) have emphasized the superior specificity of the immunoreactive staining over that of cholinesterase histochemistry of high-affinity acetylcholine uptake. Using a cloned antibody they found fibres throughout the entire striate cortical thickness, most densely in lamina 1. In this and lamina 4, fibres ran parallel with the pial surface, and in the remaining layers they were randomly distributed. Both pyramidal and non-pyramidal cells were innervated.

References

Albus, K. (1979) ^{14}C-Deoxyglucose mapping of orientation subunits in the cat's visual cortical areas. *Exp. Brain Res.* **37**, 609–613.

Bauer, R. (1982) A high probability of an orientation shift between layer 4 and 5 in central parts of the cat's striate cortex. *Exp. Brain Res.* **48**, 245–255.

Bauer, R., Dow, B. M., Snyder, A. Z. & Vautin, R. (1983) Orientation shift between upper and lower layers in monkey visual cortex. *Exp. Brain Res.* **50**, 133–145.

Baughman, R. W. & Gilbert, C. D. (1981) Aspartate and glutamate as possible neurotransmitters in the visual cortex. *J. Neurosci.* **1**, 427–439.

Bear, M. F., Cames, K. M. & Ebner, F. F. (1985) An investigation of cholinergic circuitry in cat striate cortex using acetylcholinesterase histochemistry. *J. Comp. Neurol.* **234**, 411–430.

Berman, N. E. J., Wilkes, M. E. & Payne, B. R. (1987) Organization of orientation and direction selectivity in areas 17 and 18 of cat cerebral cortex *J. Neurophysiol.* **58**, 676–699.

Bishop, P. O., Coombs, J. S. & Henry, G. H. (1971) Responses to visual contours: Spatio-temporal aspects of excitation in the receptive fields of simple striate neurones. *J. Physiol.* **219**, 625–657.

Bishop, P. O., Coombs, J. S. & Henry, G. H. (1973) Receptive fields of simple cells in the cat striate cortex. *J. Physiol.* **231**, 31–60.

Bishop, P. O., Goodwin, A. W. & Henry, G. H. (1974) Direction-sensitive sub-regions in striate simple cell receptive fields. *J. Physiol.* **238**, 25–27P.

Bishop, P. O. & Henry, G. H. (1972) Striate neurons: receptive field concepts. *Invest. Ophthal.* **11**, 346–354.

Bishop, P. O., Kato, H. & Orban, G. A. (1980) Direction-selective cells in complex family in cat striate cortex. *J. Neurophysiol.* **43**, 1266–1283.

Blakemore, C., Garey, L. J. & Vital-Durand, F. (1978) The physiological effects of monocular deprivation and their reversal in the monkey's visual cortex. *J. Physiol.* **283**, 223–262.

Braitenberg, B. & Braitenberg, C. (1979) Geometry of orientation columns in the visual cortex. *Biol. Cybernetics* **33**, 179–186.

Bullier, J., Mustari, M. J. & Henry, G. H. (1982) Receptive-field transformations between LGN neurons and S-cells of cat striate cortex. *J. Neurophysiol.* **47**, 417–438.

Camarda, R. M. (1979) Hypercomplex cell types in Area 18 of the cat. *Exp. Brain Res.* **36**, 191–194.

Camarda, R. & Rizzolatti, G. (1976) Receptive fields of cells in the superficial layers of cat's Area 17. *Exp. Brain Res.* **24**, 423–427.

Campbell, F. W., Cooper, G. F. & Enroth-Cugell, C. (1969) The spatial selectivity of the visual cells of the cat. *J. Physiol.* **203**, 223–235.

De Felipe, J. & Fairén, A. (1982) A type of basket cell in superficial layers of the cat visual cortex. A Golgi-electron microscope study. *Brain Res.* **244**, 9–16.

de Lima, A. D. & Singer, W. (1986) Cholinergic innervation of the cat striate cortex: a choline acetyltransferase immunocytochemical analysis. *J. Comp. Neurol.* **250**, 324–338.

DeValois, R. L., Yund, E. W. & Hepler, N. (1982a) The orientation and direction selectivity of cells in macaque visual cortex. *Vision Res.* **22**, 531–544.

De Valois, R. L., Albrecht, D. G. & Thorell, L. G. (1982b) Spatial frequency selectivity of cells in macaque visual cortex. *Vision Res.* **22**, 545–559.

Dow, B. M. (1974) Functional classes of cells and their laminar distribution in monkey visual cortex. *J. Neurophysiol.*, **37**, 927–946.

Dreher, B. & Cottee, L. J. (1975) Visual receptive-field properties of cells in Area 18 of cat's cerebral cortex before and after acute lesions in Area 17. *J. Neurophysiol.* **38**, 735–750.

Dreher, B. & Sanderson, K. J. (1973) Receptive field analysis: responses to moving visual contours by single lateral geniculate neurones in the cat. *J. Physiol.* **234**, 95–118.

Duysens, J., Orban, G. A. & Cremieux, J. (1985a) Velocity sensitivity in the cat visual system. II. Independence from interactions between loci. *J. Nuerophysiol.* **54**, 1050–1067.

Duysens, J., Orban, G. A., Cremieux, J. & Maes, H. (1985b) Velocity sensitivity in the cat visual system. III. Contribution of temporal factors. *J. Neurophysiol.* **55**, 1068–1083.

Enroth-Cugell, C. & Robson, J. G. (1966) The contrast sensitivity of retinal ganglion cells in the cat. *J. Physiol.* **187**, 517–552.

Fairén, A. & Valverde, F. (1980) A specialized type of neuron in the visual cortex of cat: a Golgi and electron microscope study of chandelier cells. *J. Comp. Neurol.* **194**, 761–779.

Ferster, D. & LeVay, S. (1978) The axonal arborizations of lateral geniculate neurons in the striate cortex of the cat. *J. Comp. Neurol.* **182**, 923–944.

Fischer, B., Boch, R. & Bach, M. (1981) Stimulus versus eye movements: comparison of neural activity in the striate and prelunate visual cortex (A 17 and A 19) of trained rhesus monkey. *Exp. Brain Res.* **43**, 69–77.

Flood, D. G. & Coleman, P. D. (1979) Demonstration of orientation columns with ^{14}C 2-deoxyglucose in a cat reared in a striped environment. *Brain Res.* **173**, 538–542.

Gilbert, C. D. (1977) Laminar differences in receptive field properties of cells in cat primary visual cortex. *J. Physiol.* **268**, 391–421.

Gilbert, C. D. & Wiesel, T. N. (1979) Morphology and intracortical projections of functionally characterised neurones in the cat visual cortex. *Nature* **280**, 120–125.

Gilbert, C. D. & Wiesel, T. N. (1983) Clustered intrinsic connections in cat visual cortex. *J. Neurosci.* **3**, 1116–1133.

Gilbert, C. D. & Wiesel, T. N. (1985) Intrinsic connectivity and receptive field properties in visual cortex. *Vision Res.* **25**, 365–374.

Goodwin, A. W. & Henry, G. H. (1978) The influence of stimulus velocity on the responses of single neurones in the striate cortex. *J. Physiol.* **277**, 467–482.

Goodwin, A. W., Henry, G. H. & Bishop, P. O. (1975) Direction selectivity of simple striate cells: properties and mechanism. *J. Neurophysiol.* **38**, 1500–1523.

Gulyas, B., Orban, G. A., Duysens, J. & Maes, H. (1987) The suppressive influence of moving textural backgrounds on responses of cat striate neurons to moving bars. *J. Neurophysiol.* **57**, 1767–1791.

Hammond, P. (1978) Directional tuning of complex cells in Area 17 of the feline visual cortex. *J. Physiol.* **285**, 479–491.

Hammond, P. & MacKay, D. M. (1977) Differential responsiveness of simple and complex cells in cat striate cortex to visual texture. *Exp. Brain Res.* **30**, 275–296.

Hammond, P. & MacKay, D. M. (1981) Modulatory influences of moving textured backgrounds on responsiveness of simple cells in feline striate cortex. *J. Physiol.* **319**, 431–442.

Harvey, A. R. (1980a) The afferent connexions and laminar distribution of cells in Area 18 of the cat. *J. Physiol.* **302**, 483–505.

Harvey, A. R. (1980b) A physiological analysis of subcortical and commissural projections of Areas 17 and 18 of the cat. *J. Physiol.* **302**, 507–534.

Hendreen, J. C., Uhle, G. R., Bacon, S. J., Farnbrough, D. M. & Price, D. L. (1984) Acetylcholinesterase-immunoreactive axonal network in monkey visual cortex. *J. Comp. Neurol.* **226**, 246–254.

Hendrickson, A. E., Hunt, S. P. & Yo, J.-Y. (1981) Immunocytochemical localization of glutamic acid decarboxylase in monkey striate cortex. *Nature* **292**, 605–607.

Henry, G. H. (1977) Receptive field classes of cells in the striate cortex. *Brain Res.* **133**, 1–28.

Henry, G. H., Bishop, P. O. & Dreher, B. (1974) Orientation, axis and direction as stimulus parameters for striate cells. *Vision Res.* **14**, 767–777.

Henry, G. H., Lund, J. S. & Harvey, A. R. (1978) Cells of the striate cortex projecting to the Clare–Bishop area in the cat. *Brain Res.* **151**, 154–158.

Hoffmann, K.-P. & Stone, J. (1971) Conduction velocity of afferents to cat visual cortex: a correlation with cortical receptive field properties. *Brain Res.* **32**, 460–466.

Horton, J. C. (1984) Cytochrome oxidase patches: a new cyto-architectonic feature of monkey visual cortex. *Phil. Trans. Roy. Soc. B* **304**, 199–253.

Horton, J. C. & Hedley-Whyte, E. T. (1984) Mapping of cytochrome oxidase patches and ocular dominance columns in human visual cortex. *Phil. Trans. Roy. Soc. B* **304**, 255–272.

Horton, J. C. & Hubel, D. H. (1981) Regular patchy distribution of cytochrome oxidase staining in primary visual cortex of macaque monkey. *Nature* **292**, 762–764.

Hubel, D. H. & Wiesel, T. N. (1961) Integrative action in the cat's lateral geniculate body. *J. Physiol.* **155**, 385–398.

Hubel, D. H. & Wiesel, T. N. (1962) Receptive fields, binocular interaction and functional architecture in the cat's visual cortex. *J. Physiol.* **160**, 106–154.

Hubel, D. H. & Wiesel, T. N. (1963) Receptive fields of cells in striate cortex of very young, visually inexperienced kittens. *J. Neurophysiol.* **26**, 994–1002.

Hubel, D. H. & Wiesel, T. N. (1965) Receptive fields and functional architecture in two non-striate areas (18 and 19) of the cat. *J. Neurophysiol.* **28**, 229–289.

Hubel, D. H. & Wiesel, T. N. (1968) Receptive fields and functional architecture of monkey's striate cortex. *J. Physiol.* **195**, 215–243.

Hubel, D. H. & Wiesel, T. N. (1970) Cells sensitive to nonocular depth in Area 18 of the macaque monkey. *Nature* **225**, 41–42.

Hubel, D. H. & Wiesel, T. N. (1972) Laminar and Columnar distribution of geniculo-cortical fibers in the macaque monkey. *J. Comp. Neurol.* **146**, 421–450.

Hubel, D. H., Wiesel, T. N. & LeVay, S. (1977) Plasticity of ocular dominance columns in monkey striate cortex. *Phil. Trans. B.* **278**, 377–409.

Hubel, D. H., Wiesel, T. N. & Stryker, M. P. (1978) Anatomical demonstration of orientation columns in macaque monkey. *J. Comp. Neurol.* **177**, 361–379.

Humphrey, A. L. & Hendrickson, A. E. (1983) Background and stimulus-induced patterns of high metabolic activity in the visual cortex (Area 17) of the squirrel and macaque monkey. *J. Neurosci.* **3**, 345–358.

Iversen, L. L., Mitchell, J. F. & Srinivasan, V. (1971) The release of γ-aminobutyric acid during inhibition in the cat visual cortex. *J. Physiol.* **212**, 519–534.

Kato, H., Bishop, P. O. & Orban, G. A. (1978) Hypercomplex and simple/complex cell classification in cat striate cortex. *J. Neurophysiol.* **41**, 1071–1095.

Kelly, J. P. & Van Essen, D. C. (1974) Cell structure and function in the visual cortex of the cat. *J. Physiol.* **238**, 515–547.

Kimura, M., Shiida, T., Tanaka, K. & Toyama, K. (1980) Three classes of Area 19 cortical cells of the cat, classified by their neuronal connectivity and photic responsiveness. *Vision Res.* **20**, 69–77.

Levick, W. R. (1977) Participation of brisk-transient retinal ganglion cells in binocular vision—an hypothesis. *Proc. Austral. Physiol. Pharmacol. Soc.* **8**, 9–16. (Quoted by Harvey, 1980.)

Livingstone, M. S. & Hubel, D. H. (1981) Effects of sleep and arousal on the processing of visual information in the cat. *Nature* **291**, 554–561.

Malpeli, J. G. (1983) Activity of cells in area 17 of the cat in absence of input from layer a of lateral geniculate nucleus of the cat. *Neurosci. Lett.* **49**, 595–610.

Malpeli, J. G., Lee, C., Schwark, H. D. & Weyand, T. G. (1987) Cat area 17. I. Pattern of thalamic control of cortical layers. *J. Neurophysiol.* **57**, 1062–1073.

Malpeli, J. G., Schiller, P. H. & Colby, C. I. (1981) Response properties of single cells in monkey striate cortex during reversible inactivation of individual geniculate laminae. *J. Neurophysiol.* **46**, 1102–1119.

Mansfield, R. J. N. (1974) Neural basis of orientation perception in primate vision. *Science* **186**, 1133–1135.

Martin, K. A. C., Somogyi, P. & Whitteridge, D. (1983) Physiological and morphological properties of identified basket cells in the cat's visual cortex. *Exp. Brain Res.* **50**, 193–200.

McGuire, B. A., Hornung, J.-P., Gilbert, C. D. & Wiesel, T. N. (1984) Patterns of synaptic input to layer 4 of the cat striate cortex. *J. Neurosci.* **4**, 3021–3033.

Mountcastle, V. B. (1957) Modality and topographic properties of single neurones of cat's somatic sensory cortex. *J. Neurophysiol.* **20**, 408–434.

Movshon, J. A. (1975) The velocity tuning of single units in cat striate cortex. *J. Physiol.* **249**, 445–468.

Murphy, P. C. & Sillito, A. M. (1986) Continuity of orientation columns between superficial and deep laminae of the cat primary visual cortex. *J. Physiol.* **381**, 95–110.

Mustari, M. J., Bullier, J. & Henry, G. H. (1982) Comparison of response properties of three types of monosynaptic S-cell in cat striate cortex. *J. Neurophysiol.* **47**, 439–454.

Orban, G. A. & Callens, M. (1977a) Receptive field types of Area 18 neurons in the cat. *Exp. Brain Res.* **30**, 107–123.

Orban, G. A. & Callens, M. (1977b) Influence of movement parameters on Area 18 neurons in the cat. *Exp. Brain Res.* **30**, 125–140.

Orban, G. A., Hoffmann, K.-P. & Duysens, J. (1985) Velocity sensitivity in the cat visual system. I. Responses of LGN cells to moving bar stimuli: a comparison with cortical areas 17 and 18. *J. Neurophysiol.* **54**, 1026–1049.

Orban, G. A., Kato, H. & Bishop, P. O. (1979) Dimensions and properties of end-zone inhibitory areas in receptive fields of hypercomplex cells in cat striate cortex. *J. Neurophysiol.* **42**, 833–849.

Orban, G. A., Kennedy, H. & Maes, H. (1980) Functional changes across the 17–18 border in the cat. *Exp. Brain Res.* **39**, 177–186.

Palmer, L. A. & Davis, T. L. (1981a) Receptive-field structure in cat striate cortex. *J. Neurophysiol.* **46**, 260–276.

Palmer, L. A. & Davis, T. L. (1981b) Comparison of responses to moving and stationary stimuli in cat striate cortex. *J. Neurophysiol.* **46**, 277–295.

Patel, H. H. & Sillito, A. M. (1978) Inhibition and velocity tuning in the cat visual cortex. *J. Physiol.* **284**, 113P.

Peters, A. & Regidor, J. (1981) A reassessment of the forms of nonpyramidal neurons in area 17 of the cat visual cortex. *J. Comp. Neurol.* **203**, 685–716.

Rose, D. (1977) Responses of single units in cat visual cortex to moving bars of light as a function of bar length. *J. Physiol.* **271**, 1–23.

Sanderson, K. J., Bishop, P. O. & Darien-Smith, I. (1971) The properties of the binocular receptive fields of lateral geniculate neurons. *Exp. Brain Res.* **13**, 178–207.

Sanderson, K. J., Darien-Smith, I. & Bishop, P. O. (1969) Binocular corresponding fields of single units in the cat dorsal lateral geniculate nucleus. *Vision Res.* **9**, 1297–1303.

Sato, H., Hata, Y., Hagihara, K. & Tsumoto, T. (1987b) Effects of cholinergic depletion on neuron activities in the cat visual cortex. *J. Neurophysiol.* **58**, 781–794.

Sato, H., Hata, Y., Masui, H. & Tsumoto, T. (1987a) A functional

role of cholinergic innervation to neurons in the cat visual cortex. *J. Neurophysiol.* **58**, 765–780.

Schiller, P. H., Finlay, B. L. & Volman, S. F. (1976a–e) Quantitative studies of single-cell properties in monkey striate cortex. I. Spatiotemporal organization of receptive fields. II. Orientation specificity and ocular dominance. III. Spatial frequency. IV. Corticotectal cells. V. Multivariate statistical analyses and models. *J. Neurophysiol.* **39**, 1288–1319, 1320–1333, 1334–1351, 1352–1361, 1362–1374.

Schiller, P. H. & Malpeli, J. G. (1978) Functional specificity of lateral geniculate nucleus laminae of the rhesus monkey. *J. Neurophysiol.* **41**, 788–797.

Schwark, H. D., Malpeli, J. G., Weyand, T. G. & Lee, C. (1987) Cat area 17. II. Response properties of infragranular layer neurons in the absence of supragranular activity. *J. Neurophysiol.* **57**, 1074–1087.

Shaw, C. & Cynader, M. (1986) Laminar distribution of receptors in monkey (*Macaca fascicularis*) geniculostriate system. *J. Comp. Neurol.* **248**, 301–312.

Sherk, H. & LeVay, S. (1981) The visual claustrum of the cat. III. Receptive field properties. *J. Neuroscience* **1**, 993–1002.

Sherk, H. & LeVay, S. (1983) Contribution of the cortico-claustral loop to receptive field properties in area 17 of the cat. *J. Neuroscience* **3**, 2121–2127.

Sillito, A. M. (1979) Inhibitory mechanisms influencing complex cell orientation selectivity and their modifications at high resting discharge levels. *J. Physiol.* **289**, 33–53.

Sillito, A. M. & Kemp, J. A. (1983) The influence of GABAergic inhibitory processes on the receptive field structure of X- and Y-cells in cat dorsal lateral geniculate nucleus (dLGN). *Brain Res.* **277**, 63–77.

Sillito, A. M., Kemp, J. A., Milson, J. A. & Berardi, N. (1980a) A re-evaluation of the mechanisms underlying simple cell orientation selectivity. *Brain Res.* **194**, 517–520.

Sillito, A. M., Kemp, J. A. & Patel, H. (1980b) Inhibitory interactions contributing to the ocular dominance of monocularly dominated cells in the normal cat striate cortex. *Exp. Brain Res.* **41**, 1–10.

Sillito, A. M. & Versiani, V. (1977) The contribution of excitatory and inhibitory inputs to the length preference of hypercomplex cells in layers II and III and of the cat's striate cortex. *J. Physiol.* **273**, 775–790.

Singer, W. (1970) Inhibitory binocular interaction in the lateral geniculate body of the cat. *Brain Res.* **18**, 165–170.

Singer, W., Tretter, F. & Cynader, M. (1975) Organization of cat striate cortex: a correlation of receptive-field properties with afferent and efferent connections. *J. Neurophysiol.* **38**, 1080–1098.

Sokoloff, L. M. *et al.* (1977) The [^{14}C]-deoxyglucose method for the measurement of local cerebral glucose utilization: theory, procedure, and normal values in the conscious and anesthetized albino rat. *J. Neurochem.* **28**, 897–916.

Somogyi, P., Freund, T. F., Halász, N. & Kisvárday, Z. F. (1981) Selectivity of neuronal [^{3}H]GABA accumulation in the visual cortex as revealed by Golgi staining of the labelled neurons. *Brain Res.* **225**, 431–436.

Stevens, J. K. & Gerstein, G. L. (1976) Spatiotemporal organization of cat lateral geniculate receptive fields. *J. Neurophysiol.* **39**, 213–238.

Stone, J. & Dreher, B. (1973) Projection of X- and Y-cells of the cat's lateral geniculate nucleus to areas 17 and 18 of visual cortex. *J. Neurophysiol.* **36**, 551–567.

Stone, J., Dreher, B. & Leventhal, A. (1979) Hierarchical and parallel mechanisms in the organization of visual cortex. *Brain Res. Rev.* **1**, 345–394.

Stryker, M. P., Hubel, D. H. & Wiesel, T. N. (1977) Orientation columns in the cat's visual cortex. *Neurosci. Abstr.* **3**, 1852.

Stryker, M. P., Sherk, H., Leventhal, A. G. & Hirsch, H. V. (1978) Physiological consequences for the cat's visual cortex of effectively restricting early visual experience with oriented contours. J. Neurophysiol. **41**, 896–909.

Tanaka, K. (1983a) Cross-correlation analysis of geniculostriate relationships in the cat. *J. Neurophysiol.* **49**, 1303–1318.

Tanaka, K. (1983b) Distinct X- and Y-streams in the cat visual cortex revealed by bicuculline application. *Brain Res.* **265**, 143–147.

Tanaka, K. (1985) Organization of geniculate inputs to visual cortical cells in the cat. *Vision Res.* **25**, 357–364.

Tootell, R. B. H., Silverman, M. S., De Volois, R. L. & Jacobs, G. H. (1983) Functional organization of the second cortical visual area in primates. *Science* **220**, 737–739.

Toyama, K., Kimura, M., Shiida, T. & Takeda, T. (1977) Convergence of retinal inputs onto visual cortical cells. II: A study of the cells disynaptically excited from the lateral geniculate body. *Brain Res.* **137**, 221–231.

Toyama, K., Maekawa, K. & Takeda, T. (1977) Convergence of retinal input onto visual cortical cells. I. A study of the cells monosynaptically excited from the lateral geniculate body. *Brain Res.* **137**, 207–220.

Tretter, F., Cynader, M. & Singer, W. (1975) Cat parastriate cortex: a primary or secondary visual area. *J. Neurophysiol.* **38**, 1099–1113.

Tsumoto, T., Eckart, W. & Creutzfeldt, O. D. (1979) Modification of orientation sensitivity of cat visual cortex neurons by removal of GABA-mediated inhibition. *Exp. Brain Res.* **34**, 351–363.

Tsumoto, T., Masui, H. & Sato, H. (1986). Excitatory amino acid transmitters in neuronal circuits of the cat visual cortex. *J. Neurophysiol.* **55**, 469–483.

Wong-Riley, M. (1979) Columnar cortico-cortical interconnections within the visual system of the squirrel and macaque monkeys. *Brain Res.* **162**, 201–217.

Wong-Riley, M. T. T., Merzenich, M. M. & Leake, P. A. (1978) Changes in endogenous enzymatic reactivity to DAB induced by neuronal activity. *Brain Res.* **141**, 185–192.

Zeki, S. M. (1974a) Functional organization of a visual area in the posterior bank of the superior temporal sulcus of the rhesus monkey. *J. Physiol.* **236**, 549–573.

Zeki, S. M. (1974b) Cells responding to chaning image size and disparity in the cortex of the rhesus monkey. *J. Physiol.* **242**, 827–841.

Zeki, S. M. (1978) Functional specialization in the visual cortex of the rhesus monkey. *Nature* **274**, 423–428.

21. NEUROPHYSIOLOGY OF PERCEPTION: SPATIAL ANALYSIS

The development of orientation-sensitivity, or tuning, and the spatial-frequency tuning of neurones that we have so far considered may be regarded as modes of analysis of the spatial features of an object in space, leading ultimately to the recognition of shape and texture. Stereoscopic perception adds a third dimension to this analysis, so that we may now proceed to a consideration of the responses of cortical neurones to this feature.

NEUROPHYSIOLOGICAL BASIS OF STEREOPSIS

In looking for electrophysiological correlates of binocular vision involving stereopsis, we must expect to find, as we have indeed, cortical neurones that respond to stimuli in both eyes. Furthermore, as Barlow *et al.* (1967) have put it, the neurone must select those parts of the two images that belong to each other, in the sense that they are images of the same point; secondly, for stereopsis, they must assess the small displacements from exact symmetry that give the binocular parallax.

Minimum Response Fields

Barlow *et al.* recorded from neurones in area 17 of the cat and found, as Hubel & Wiesel had earlier, that binocular stimulation was more effective in stimulating many units than uniocular; if the positioning of the targets was wrong, however, one eye could veto the response of the other as in Fig. 21.1; here a bar moved over the receptive field of the left eye and right eye separately; acting together there was powerful facilitation. When the separate fields were mapped out for each eye, it was found that these 'minimum response fields' did not occupy exactly symmetrical positions in the two eyes, i.e. they were not corresponding areas; instead, for maximal binocular facilitation there had to be a discrepancy; for the unit illustrated by the left part of Fig. 21.1 this was 5.7°; in this case the cat's eyes were divergent by 6.4°, so that the actual disparity corresponded to a convergence of 0.7° for the left unit and 3.1° for the right unit. In general, different neurones required different disparities to obtain maximal facilitation between the two eyes.[1]

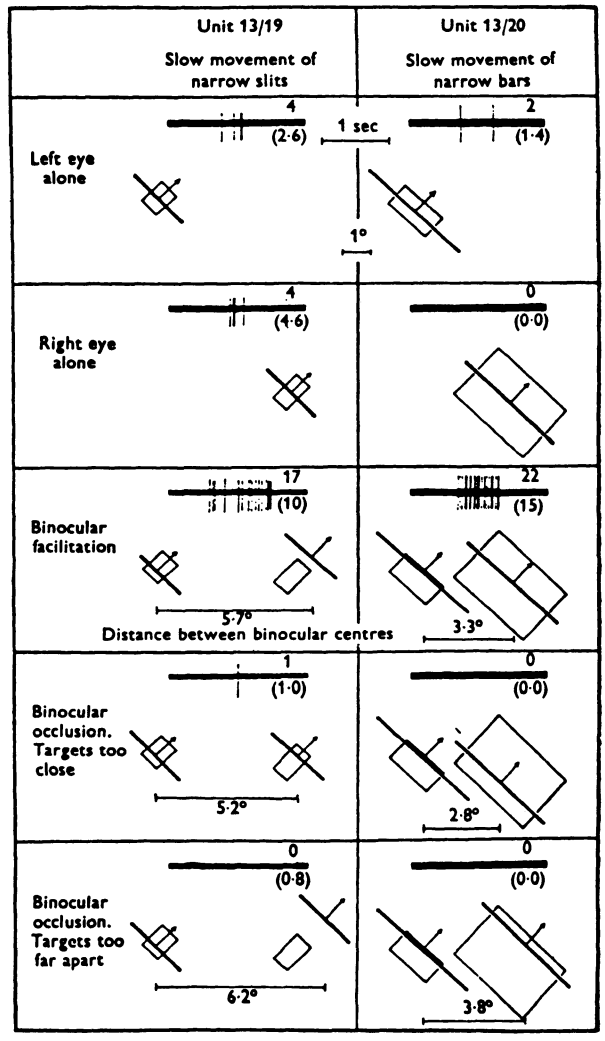

Fig. 21.1 Illustrating responses of two binocularly driven units. Maximal facilitation in binocular stimulation is obtained only when there has been a certain disparity between the stimulated regions in the two retinae. (Barlow *et al.*, *J. Physiol.*)

Detection of Disparity

Pettigrew *et al.* (1968) recorded the summated action potentials from binocularly driven cortical units of the cat when the disparity between left and right-eyed fields was changed by means of a prism. Figure 21.2 shows the evoked response of a unit as a function of prism setting, 0° corresponding to perfect superimposition. The responses of the ipsi- and contralateral eyes are indicated by horizontal bars, and it will be seen that over a certain range of disparities there is facilitation through binocular stimulation. Over the remainder of the range of disparities there is mutual inhibition. The sensitivity of the unit to disparity is high, of the order of 3 minutes of arc (0.1Δ).

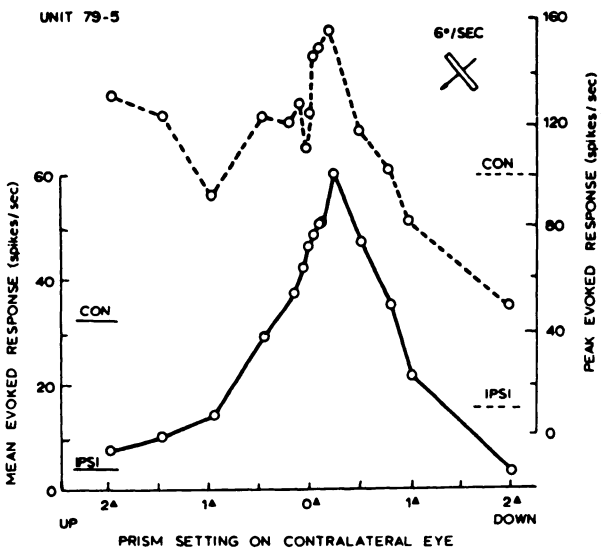

Fig. 21.2 Responses of a cat's cortical neurone to a bar-stimulus applied to both eyes when the degree of retinal disparity was varied by placing prisms in front of the contralateral eye. The bars marked IPSI and CON indicate the responses of ipsi- and contralateral eyes when stimulated alone. Full lines indicate mean evoked response and dashed lines the peak evoked response. (Pettigrew *et al.*, *Exp. Brain Res.*)

Depth and Direction Columns

It will be recalled that Hubel & Wiesel found that the neurones of the striate area were organized in columns according to eye-dominance and according to the direction-preference of the slits required to excite; Blakemore (1970a) examined the effects of recording from striate neurones at successive depths in a column, and he found that, in certain columns, the neurones all had optimal retinal disparities of about the same directon and magnitude; all these neurones were responding, then, to a strip of space at a definite distance from the fixation point. Adjacent columns had disparities differing by about 0.6°. Blakemore called these *constant depth* columns to distinguish them from *constant direction* columns whose neurones showed enormous variations in disparity from unit to unit at successive depths. When the left- and right-eye fields of these units were compared, it was found that for one eye, e.g. the left, the fields of successive units were all superimposed, so that the variation in disparity was due to the variations in the positions of the fields of the right eye. In Fig. 21.3 a spatial plot of the positions of points in space that would give rise to these disparities is shown, and it becomes clear that these units have the common parameter of constant direction in relation to the left eye. Thus the column of neurones is 'peering along a tube of visual space that is lined up along one oculocentric visual direction'. Examination of several direction-columns gave a similar pattern, namely that the superimposable response fields were found in the hemisphere contralateral to the retina in which they were evoked, so that those responsible for the disparities were derived from the ipsilateral retina. It has been pointed out earlier that the

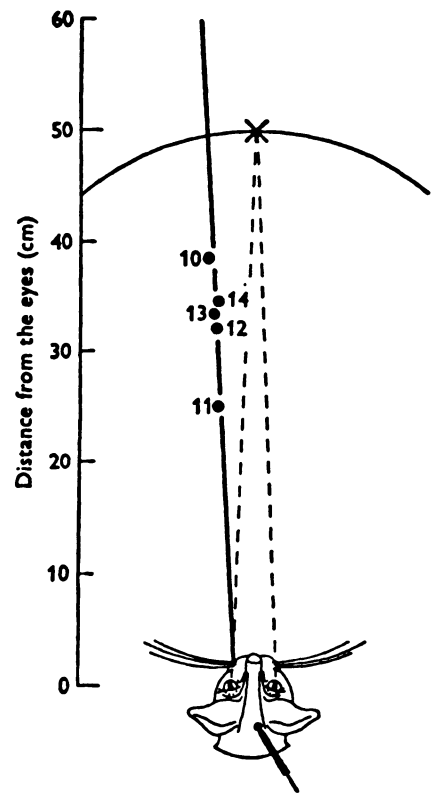

Fig. 21.3 Illustrating the positions in space of points that would give rise to the observed retinal disparities of cortical neurones in a constant direction column. (Blakemore, *J. Physiol.*)

ipsilateral projection of the retina is the phylogenetically newer projection since in lower vertebrates the decussation tends to be complete. It is interesting therefore that it is the ipsilaterally projecting neurones that show the binocular disparities that are essential for stereoscopic vision. Thus in non-stereoscopic vision it would be the direction-columns that were of absolute importance; with the requirements of stereopsis, information both with respect to direction and disparity of retinal images is required, and this is provided by the constant disparity (depth) columns.

Cortical Neurones Required

Blakemore estimated an average of 0.6° difference of horizontal disparity between neighbouring depth-columns, and about 4° of oculocentric visual direction between direction-columns. If the mosaic were maintained across the whole binocular field, and if the total range of disparities were 6°, this would require 500 columns for one orientation of the target. If there were ten to fifteen optimal orientations of the target, this would make a grand total of 8000 to 12 000 columns to encode every orientation and every spatial position, a number that is not impossible anatomically (Blakemore, 1970a).

Stereopsis in the Monkey

By the use of random-dot patterns, as illustrated in Fig. 16.38, such that the individual pictures presented to the eyes in a stereoscope are indistinguishable, it is possible to study the stereoscopic vision of the monkey, training it to respond only when the two pictures give a required stereoscopic depth perception on fusion. In this way Bough (1970) demonstrated that monkeys could discriminate between pictures that, when fused, would give no stereopsis, and those that would. Hubel & Wiesel (1970) have examined the cortical cells of areas 17 and 18 of macaque monkeys and have shown that in area 18 binocularly responding cells are found reacting similarly to complex and hyper-complex cells in area 17; these they called 'ordinary cells of area 18'; they had receptive fields in anatomically corresponding areas; they responded to separate stimulation of the eyes and showed moderate summation when stimulated together. The other half were called 'binocular depth cells', the most common of which gave no response to stimulation of the separate eyes but a brisk response to simultaneous stimulation. Some responded well to stimuli in corresponding points of the retinae, and others exhibited some disparity in their receptive fields. By contrast with the cat, no convincing evidence was found of binocular depth cells in area 17. Thus area 18 has two functions in the monkey, namely linking the two half-fields (as also in the cat), and the elaboration of stereoscopic depth perception.

Bilateral Representation of Retina

Blakemore (1969) has emphasized that if the decussation of the optic nerve fibres splits the visual field exactly into two halves across the vertical meridian, so that all stimuli from the temporal side of the field remain ipsilateral, and all on the nasal side cross over, then, when an object produces disparate images on the retinae, as in Fig. 17.34, a_L. and a_R, the images can fall on the nasal halves of each retina and so their messages are carried to opposite hemispheres of the brain. In this event, the single cortical neurones that receive messages from both of these points on the retinae will have to be connected to a pair of cortical neurones in opposite hemispheres, perhaps through the corpus callosum. Alternatively, of course, we may postulate that over the small regions adjacent to the vertical meridians, where retinal disparities are utilized in binocular stereoscopic vision, the decussation may be incomplete, so that this part of the fovea will be represented, in effect, bilaterally. This might account for the 'sparing of the macula' so-called, but in the primate the evidence against such a bilateral representation through incomplete decussation is preponderant, and callosal connections mediate the necessary integration between the two hemispheres.

Areas 17 and 18

Hubel & Wiesel (1967) recorded from separate units simultaneously in the two hemispheres of the cat, and found some that had receptive fields that overlapped in the middle; these were invariably in the boundary between areas 17 and 18 where the representations of the central vertical meridian in the primary and secondary visual areas are side by side. Blakemore (1969) has examined the response fields of binocularly driven units at the junctions of areas 17 and 18, and has confirmed that some of these overlap, in fact their binocular centres (p. 561) could be on the 'wrong' side of the estimated vertical meridian by a degree or two, as illustrated by Fig. 21.4, where the centres of the response-fields of right eyes have been plotted against azimuth from the vertical meridian. The filled circles indicate responses in the right, or ipsilateral, hemisphere which, in the absence of bilateral representation, should be confined to the left of the Figure, and the open circles indicate respones in the left, contralateral, hemisphere and should be confined to the right of the figure. The 'wrong fields' are indicated by the line joining the points, and this indicates the degree of overlap. This central strip of retina, with a width of about 1.5° and equivalent to horizontal disparities of about twice this, doubtless is the region of bilateral representation that is required for stereopsis in the vertical meridian.

Corpus Callosum

The mechanism of this overlap could be through the corpus callosum, in which event monocularly driven

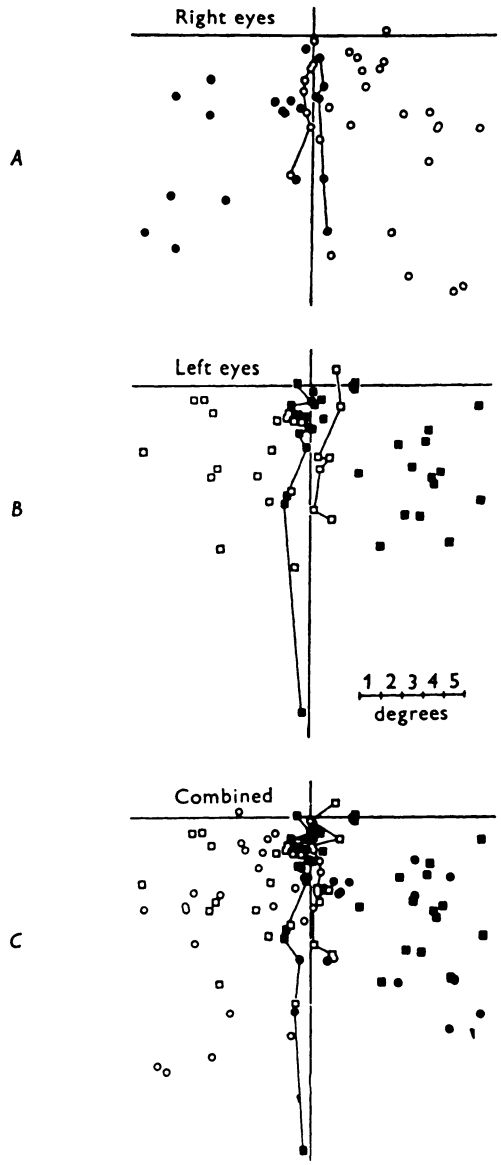

Fig. 21.4 A. Response field centres for four right eyes are pooled by superimposing the true vertical through the middle of the overlap and the horizontal through the estimated area centralis. The open circles are the centres for units recorded in the left (contralateral) hemisphere and the filled circles for units in the right (ipsilateral) hemisphere. B. The field centres for five left eyes are pooled in the same way. The open squares are centres for right (contralateral) hemisphere units and the filled squares for neurones in the left (ipsilateral) hemisphere. C. The data from A and B are combined by lateral inversion of the right eyes' field-centres and the superposition of the verticals and horizontals. Now temporal visual hemifield lies to the left of the vertical meridian and nasal hemifield to the right. The symbols are those used in A and B. All field-centres lying on the 'wrong' side of the vertical meridian (i.e. in the ipsilateral hemifield) are joined to give an indication of the width of the strip of bilateral projection. (Blakemore, *J. Physiol.*)

callosal units should be found, as they apparently are (Berlucchi *et al.*, 1967), whilst cutting the corpus callosum abolishes stereopsis (Mitchell & Blakemore, 1970), of objects in the midline but not, of course, in the periphery since in this event both images are projected to the same hemisphere. The situation is illustrated by Fig. 21.5, which describes the neural arrangements in a human subject with sectioned corpus callosum. To the left, the subject, fixating F, will appreciate the stereopsis created by the positions of A and B because the images fall on the temporal and medial retinae, cortical neurones being binocularly driven by disparate points on the retinae. To the right, the disparities of A and B are such that both the

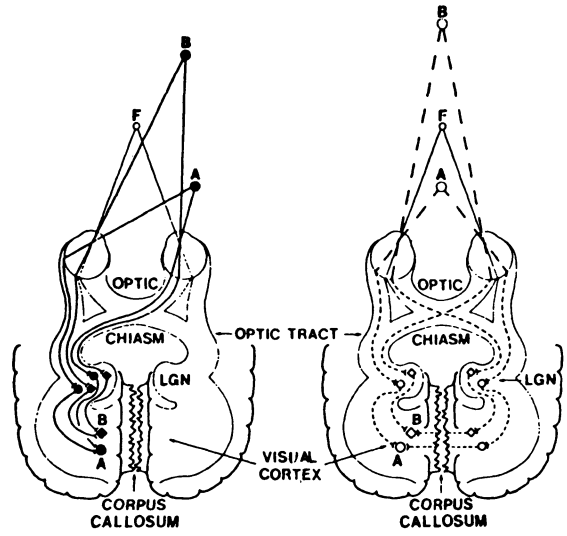

Fig. 21.5 The possible neural system for binocular depth perception in the split-brain human. On the left is the arrangement of neurones which enabled the subject to recognize the depth of the peripheral objects A and B, relative to the fixation point, F. For both objects the image in the right eye falls on nasal retina and that in the left upon temporal, and all the information projects to the left optic tract. The messages from the two eyes remain segregated at the lateral geniculate nucleus (LGN). Solid circles represent neurones within whose receptive field the image of A falls. Solid diamonds are cells to which object B projects. The two binocular cells, A and B, shown as large symbols in the cortex, encode the disparities of the objects. In this case the sectioned corpus callosum is of no hindrance. The binocular information is processed entirely in the left hemisphere and the judgements can therefore be vocalized. In the right diagram objects A and B lie directly in the midline and, therefore, their images fall on temporal or nasal retina, respectively, in *both* eyes. The interrupted lines and open symbols in the visual pathway show the neurones normally responsible for the recognition of the disparity of these objects. The binocular cells A and B in the cortex receive one of their inputs from a fibre from the opposite visual cortex, crossing in the corpus callosum. Section of the commissure has severed this link and binocular integration is impossible. (Mitchell & Blakemore, *Vision Res.*)

images fall on nasal or temporal halves of the retinae, so that a cortical neurone must receive messages from the contralateral hemisphere to integrate the disparate messages. Mitchell & Blakemore found that, whereas the corpus callosum-sectioned subject could discriminate the peripherally placed points A and B in depth, he could not do so when they were in the midline (Fig. 21.5 *right*).

Monkey versus Cat

EFFECTS OF SQUINT

Hubel & Wiesel (1973) commented on the findings of earlier workers on the cat, of remarkably few area 17 neurones with receptive fields falling on corresponding parts of the retina, by contrast with the monkey where all area 17 binocular units had receptive fields in precise register, whilst in area 18 cells they found some 20% of cells with horizontal disparities. They suspected that a serious error in the work on the cat was the failure of the two eyes to be directed at the same point, or failure to detect and correct for this. By using one cortical unit as a reference, while a second electrode explored binocularly driven units, they could tell whether apparent disparities were due to eye-movement or were genuine. Out of 268 binocularly driven cells in area 17, 253 had fields in exact correspondence within 1/4 to 1/2 a degree. With a single reference-cell, random variations of up to 21° in location of the receptive fields of the two eyes could be obtained, which were clearly due to eye-movements in spite of paralysing drugs.

Depth Discrimination

Waking Monkey

Difficulties regarding establishing the real retinal disparity when separate images are presented to the two eyes can be avoided by working on the alert monkey, trained to fixate a point in the visual field, so that images of this point can be said, by definition, to fall on corresponding points. A slit- or bar-stimulus can then be placed closer to, or farther away from, the fixation-point, and the responses of a cortical neurone recorded (Fig. 21.6).

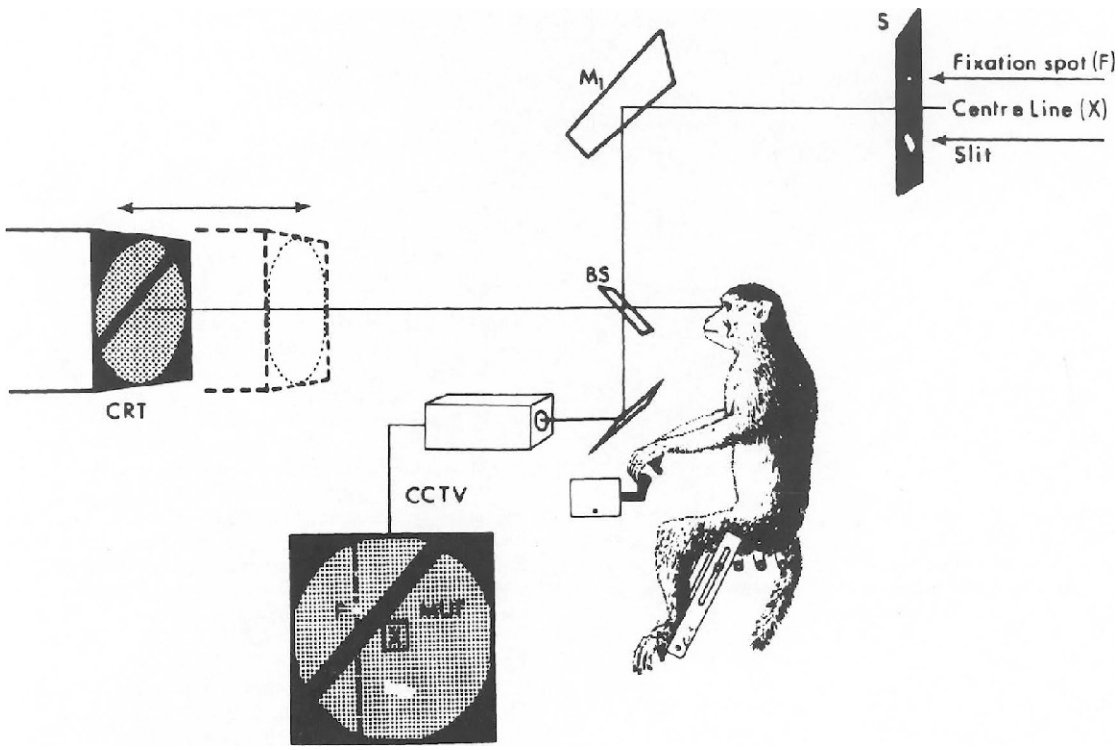

Fig. 21.6 Experimental set-up for studying binocular neurones in the waking monkey. Front (CRT) and rear (S) screens superimposed optically for the monkey's eye and the TV camera (CCTV) by a beam splitter (BS). Depth was introduced by changing the position of the front screen along the centre line of the system. A multiunit field (MUF) is also shown on the TV monitor screen together with the fixation spot (F), the hand-moved slit used to define the field, a stimulating black bar and the vertical meridian. The fixation spot (F) has been shifted in order to centre the MUF at the centre of the system (X). (Poggio & Fischer, *J. Neurophysiol.*)

DEPTH-SENSITIVE CELLS

Poggio & Fischer (1977) made such studies on area 17 and area 18 of the monkey, and found that some 84% of neurones were sensitive to depth, in the sense that their responses were modified by moving the stimulus closer to, or farther away from, the fixation plane. Of 142 cells, 23 gave similar binocular responses at all distances in front of, or behind, the fixation plane, and probably did not signal depth. The remaining 119 were depth-sensitive, and fell into two broad categories, namely *depth-tuned* cells, giving responses that varied symmetrically about some optimal distance from the fixation-plane, and *near-and-far* cells, having asymmetrical depth-profiles, being binocularly activated (or suppressed) by stimuli in front of, and suppressed (or activated) by stimuli behind, the fixation plane.

DEPTH-TUNED CELLS

Depth-tuned neurones were either *tuned excitatory* (T_e) or *tuned inhibitory* (T_i). Thus a tuned excitatory neurone gave weak and unequal monocular responses; with binocular stimulation at the fixation distance (zero disparity) there was a strong response, and at distances of +1 and −1cm (disparities of 0.2°) good responses were obtained; at greater disparities the responses were very small. Most cells had an optimum excitatory distance close to the fixation distance, i.e. at zero-disparity, but not all, so that these were tuned to a certain disparity.

TUNED INHIBITION

A tuned inhibitory unit was one that responded vigorously to one eye, e.g. the left eye, and barely to the other eye, e.g. the right eye. Binocularly the response was dominated by the left eye except when the stimulus came close to the fixation plane, when an inhibitory effect of the right eye became manifest; the range of binocular suppressive activity was small and corresponded to ±0.1° disparity.

PREFERRED DISPARITIES

Figure 21.7 gives the preferred disparities for T_e and T_i units as a function of eccentricity. The occurrence of two neurones activated from the ipsilateral hemifield, and of neurones with non-zero preferred disparities at, or very close to, the vertical meridian indicates a region of overlap between the visual hemifields. The two continuous lines, diverging from the vertical, outline the limits of binocular visual space for an overlap of 0.1°. All the preferred disparities are within this region as emphasized by the dotted lines. The distribution of preferred disparities, indicated at the right, shows that the fixation plane (zero disparity) is most strongly represented.

NEAR-AND-FAR NEURONES

Of 33 falling in this category, 22 responded well to stimuli behind the fixation plane and were suppressed by stimuli in front; the remaining 11 gave the opposite type of response. The disparities involved with these stimuli were large, and it may be that their signals provide the much cruder stereopsis involved with large disparities involving double vision. The fact that the responses of the separate eyes in these cells are usually different, and often strongly dominated by one eye, is a feature that would permit suppression of one of the double images.

CONTROL OF EYE MOVEMENTS

This study, then, provides a reasonable neurophysiological substrate for the observed phenomena of binocu-

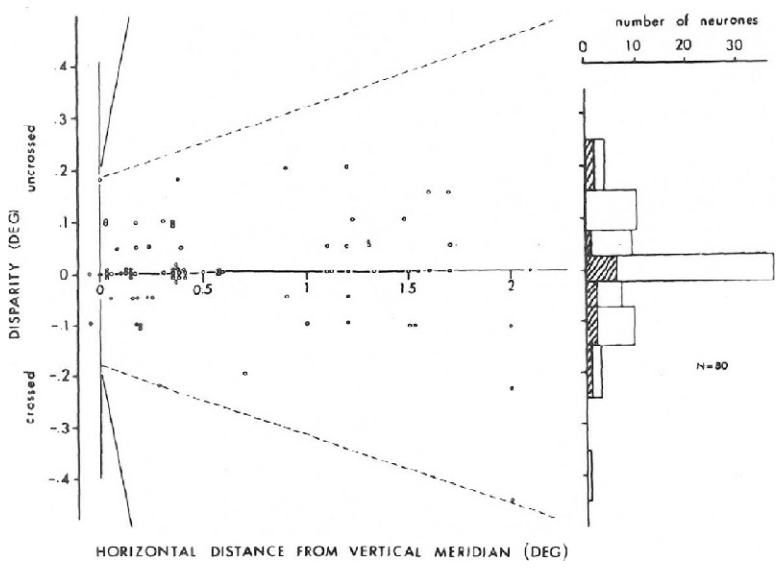

Fig. 21.7 Preferred disparities versus eccentricity of tuned excitatory (○) and tuned inhibitory (●) neurones. The total range observed is given by the two symmetrical dashed lines. The two continuous lines indicate the limits of binocular space for a nasotemporal overlap of ±1.0°. The histogram on the right shows the distribution of neurones over the disparity domain: zero disparity is most densely represented, but about 50% of neurones are tuned to non-zero disparities. Shaded areas represent tuned inhibitory neurones. (Poggio & Fischer, *J. Neurophysiol.*)

lar vision. As Poggio & Fischer suggest, the near-and-far cells might well be of significance in the control of disjunctive eye-movements, as when the eyes converge on a near object. The convergence is initiated by the strong retinal disparities that occur when an object is brought close to the eyes; the opposite divergence would be initiated by the far-response of the same type of cell. Very fine movements, required to maintain accurate fixation of both eyes on a point, might be brought about through the tuned cells.

Further Studies on the Cat

Two Categories

Fischer & Krüger (1979), working on area 18 of the cat, found similar tuned excitatory and inhibitory cells, together with those with asymmetrical disparity-sensitivity corresponding to the near-and-far cells. As with the monkey, only large disparities were effective on the near-and-far cells. The important feature of excitatory disparity-tuning seems to be that both eyes respond nearly equally to separate stimulation, by contrast with the ocular dominance observed with the inhibitory disparity-tuning, and near-and-far cells. Ferster (1981) has avoided the errors in assessing disparity brought about through eye-movements by employing the reference-cell technique of Hubel & Wiesel (1970).[2] As with Poggio and Fischer, he found two categories of depth-sensitive cells, depth-tuned and near-and-far cells.

Tuned Excitatory Units

Figure 21.8 is an example of tuned excitatory cells giving a peak response when the two receptive fields were exactly superimposed on the tangent screen; with small disparities there was an abrupt fall in response to one below that of either eye alone; further increases in disparity gradually separated the two fields completely, and, as a result, the responses rose to an intermediate value. Of 103 cells exhibiting some depth-sensitivity 49 were of this type, with 32 in area 17 and 17 in area 18.

Near-and-far Units

Figure 21.9 shows the response of a near-and far cell; they were most often dominated by one eye and their disparity-response curves showed a broad depression rather than a peak, with a very small, or zero, response at the reference point indicating zero disparity. The disparities involved in this type of cell were very much greater than those for tuned cells, which were of the order of a fraction of a degree, and showed remarkably little scatter from one

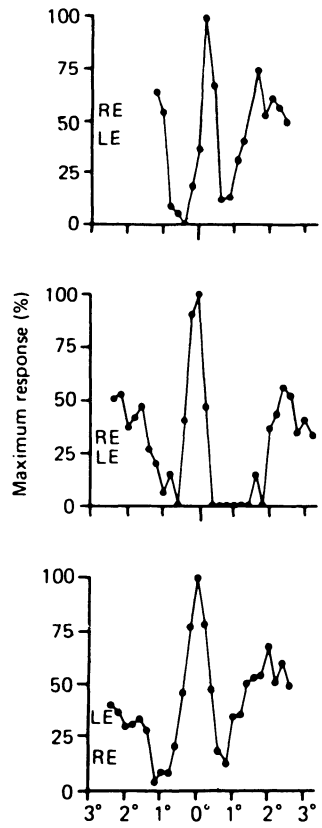

Fig. 21.8 Disparity response curves for three tuned excitatory cells. 0° represents the disparity at which the reference cell receptive fields were superimposed. Disparity was varied in the direction perpendicular to the receptive field orientation, and points were plotted to the left of zero when the horizontal component of the disparity was uncrossed. LE and RE indicate the response of the cell to presenting the stimulus to the left and right eyes alone. (Ferster, *J. Physiol.*)

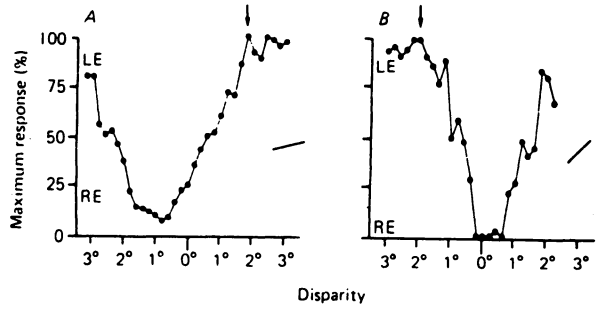

Fig. 21.9 Disparity-response curves for a Near-cell (A) and a Far-cell (B). 0° represents the reference point, and uncrossed disparities are plotted to the left of zero. The short bar to the right of each curve is the orientation of each cell. (Ferster, *J. Physiol.*)

cell to another, suggesting that a small degree of disparity would excite maximally a large number of cells.

Character of Receptive Fields

Ferster paid attention to the features of the receptive fields of cortical neurones in so far as they bore on their binocular responses.

INHIBITORY FLANKS

He showed that all tuned simple cells had a central excitatory zone flanked by strong inhibitory activity; and this applied to the fields of both eyes. If these were exactly superimposed, a moving slit would evoke a maximal response on passing over the excitatory strips; if the fields were displaced a little relatively to each other, the slit-stimulus would fall in the inhibitory sideband of one field while in the excitatory central strip of the other, and this would lead to a reduced response. Thus with simple cells it was easy to predict the reference point, or zero disparity, both excitatory and inhibitory fields are excited, and there is little or no response. The inhibitory region was always larger than the excitatory region of the dominant eye, and the two were slightly displaced with respect to each other at zero disparity. As disparity was increased in one direction, e.g. to give 'nearness', the excitatory and inhibitory regions of the two eyes were separated, and a moving slit would encounter the two regions at different points of its sweep, and inhibition could be reduced. Varying the disparity in the other direction, to give 'farness' would require the excitatory region to cross over the inhibitory region of the other eye before it could become active, giving a trough as in Fig. 21.9. Disparity-insensitive cells, on this basis, should have no strong inhibitory regions in their receptive fields, and this was found.

Area 17 versus Area 18

Ferster found that area 17 contained mostly tuned excitatory cells, and area 18 mostly near-and-far cells; again, cells in area 18 were sensitive to a larger range of disparities than those in area 17.

Prestriate Cortical Neurones

Zeki (see, for example, Zeki 1976) has emphasized the role of different prestriate regions in a parallel processing of the information reaching the striate area 17, a role suggested by Hubel & Wiesel's studies on receptive fields, which indicated that those with complex and hypercomplex fields, and presumably the result of convergence of simple cells, were much more numerous in area 18. Moreover, the ability to discriminate depth through disparity-sensitivity belongs to cortical neurones in area 18 (Hubel & Wiesel, 1970).

Electrode-penetrations

By penetrating through different areas of striate and prestriate cortex Zeki (see, for example, 1976) was able to establish some striking differences in the characteristics of cortical neurones, according as the electrode passed through the several visual areas defined in his earlier anatomical studies. Figure 21.10 illustrates the changes on passing into V2 (area 18) across the lunate sulcus to V4 and finally to V5 the posterior bank of the superior temporal sulcus.

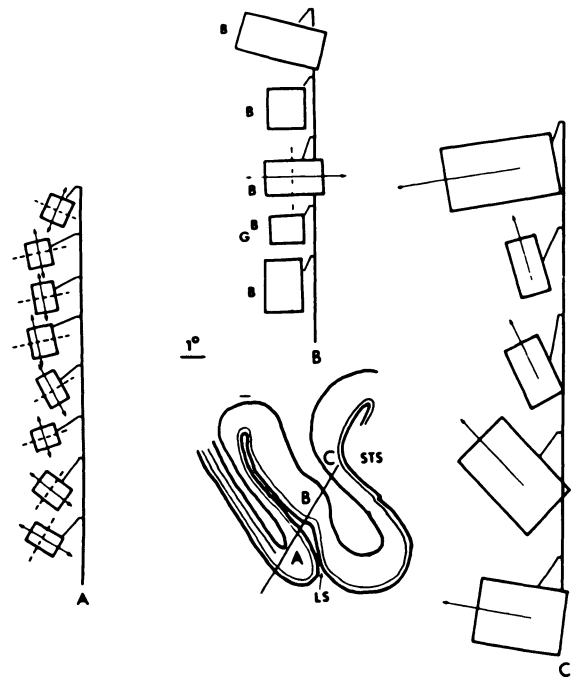

Fig. 21.10 Illustrating changes in character of cortical units during penetration in the manner illustrated. The first cells recorded from (A), (to left of figure) were in V2; they were all binocularly driven, orientation-selective cells without any colour preference. As the electrode crossed the lunate sulcus and hit V4 (B), the cells encountered were colour-coded. They were binocularly driven. In the cortex of the posterior bank of the superior temporal sulcus, the character of the cells changed once again (C, to right of figure). The cells met here were binocularly driven, directionally sensitive for which the form, orientation or colour of the stimulus were irrelevant. Arrows indicate the preferred direction of motion of the stimulus. B, blue; G, green; LS, lunate sulcus; STS, superior temporal sulcus. (Zeki, *Cold Spring Harbor Symposia.*)

Area V2

Cells in V2 were, as Hubel & Wiesel (1970) has found, binocularly driven with well defined orientational preference. Others were disparity-selective (p. 559) and some

colour-coded cells were also found. It seemed that among the functions emphasized in V2 is analysis of the visual fields in terms of binocular disparity, i.e. in depth perception.

Area V4

When the electrode passed into V4 all units examined were colour-coded (Zeki, 1973) responding vigorously to one colour and grudgingly if at all to other wavelengths and to white light; some required a field of a definite shape and position but others were independent of these parameters. In a given penetration successive cells responded to the same wavelength, suggesting an organization in columns, so that with an oblique penetration successive cells responded to different colours. Since colour-coded units in areas 17 and 18 are rare compared with area V4 it may be inferred that V4 is a region for analysis of the stimulus in terms of wavelength. Area 4A contained a wide variety of cells, including colour-coded ones, complex, hypercomplex, and so on. Because of this great variety it is not yet clear what its prime function is.

Area V5

When the electrode passed into the posterior bank of the superior temporal sulcus, V5, the majority of cells were driven from the two eyes with similar receptive fields for either eye, and most cells were equally driven by either eye—i.e. there was little indication of eye-dominance. Of interest were some cells that were similar to the pan-direction units of the superior colliculus their responses being essentially to movement in any direction, rather than to contours. Combined with this appearance of movement-sensitivity, *per se*, there was an increased proportion of direction-sensitive cells compared with areas 17 and 18, so that a specialization for the analysis of movement is clearly a feature of this region. As with area 17, oblique penetrations indicated a columnar organization with an orderly shift in preferred direction of motion when direction-sensitive cells were encountered.

Opposed Movement Cells

In a further study, Zeki (1974b) identified cells that probably signalled movement of an external object closer to or farther away from the subject; thus, as illustrated by Fig. 21.11, movement of the large bar closer to the observer produces two types of signal; as far as an individual eye is concerned the image will expand and can be mimicked by bringing two edges farther apart; as far as both eyes are concerned, the movements of the images are in opposite directions. Cells responding maximally to these types of movement were in fact found, being either monocularly or binocularly driven. Figure 21.12 illustrates the response of a binocularly driven 'opposed movement' hypercomplex cell on stimulation of the ipsilateral eye. The cell responded maximally when two edges moved towards each other along a definite orientation; reducing the length of the edges reduced the response, indicating hypercomplex behaviour. The disparities involved in this type of movement are much larger than those involved in the responses of the disparity-sensitive cells discussed earlier, these latter responding to a fixed disparity whereas the present ones respond to changing disparity. All cells in this region were not selective of wavelength.

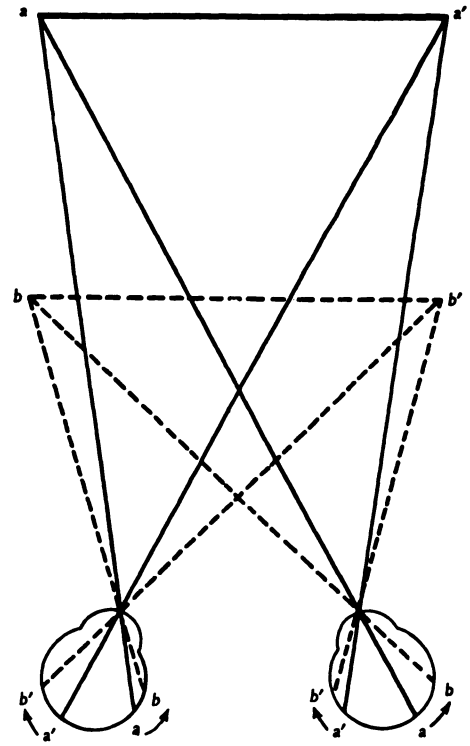

Fig. 21.11 Diagram to show the displacement of the retinal images when a large bar, aa', is moved to bb'. The images will move in opposite directions in each eye. (Zeki, *J. Physiol.*)

Stereoscopic Motion Neurones

Zeki studied responses to movement of an object in a single eye, but, as Cynader & Regan (1978) pointed out, in the natural situation the relative movements of images in the two eyes would be the clues to movement of objects in three-dimensional space. Thus, as Fig. 21.13 shows, movement in the frontoparallel plane gives movements of the retinal images in the same direction and at the same velocity; as the movement enters the third dimension, the relative velocities of retinal movement change; as the

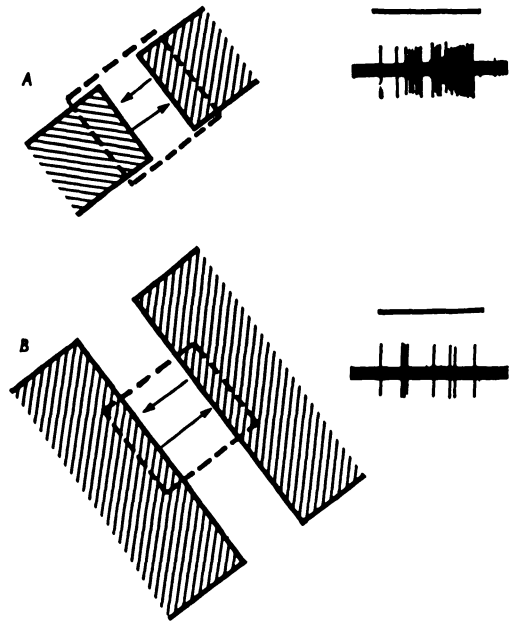

Fig. 21.12 The response of a binocularly driven, opposed movement hypercomplex cell in the cortex of the posterior bank of the superior temporal sulcus to stimulation of the right (ipsilateral) eye. The cell responded when two edges of the appropriate orientation were moved towards each other within the receptive field. Increasing the length of the edges diminished the response (*B*). The cell was 5° × 4° and was located in the lower contralateral quadrant and crossed the midline. (Zeki, *J. Physiol.*)

movement is directed between the eyes movements are in opposite directions.

SIMULATED OBJECT-MOTIONS

The authors simulated these situations in cats, while recording from units in area 18. They oscillated bars from side to side and altered the apparent direction of movement in three dimensions by varying the relative speeds of the bars presented to the separate eyes, and their relative directions of motion. One class of neurone, capable of signalling movement in the frontoparallel plane, was virtually monocular, in the sense that it was excited predominantly through one eye; however, binocular stimulation revealed that the other eye was able to inhibit the response of the dominant eye when movements in the two eyes were in the same direction as in Fig. 21.13 (*top left*). No such effect was obtained when the eyes were stimulated at identical speeds in opposite directions, i.e. as if an object was brought closer to, or farther away from, an observer. In this case the cell responded strongly, indicating a sensitivity to movement towards the cat. Some of these units were tuned so that they only responded to movements that would hit or narrowly miss the cat. Another class showed binocular facilitation when the retinal movements corresponded to those produced by objects that would miss the head, the responses of the two eyes together being greater than the sum of the separate uniocular responses. Finally, a group showed strong facilitation of responses to the two eyes when movements took place at the same speeds and direction in the two eyes. There was strong evidence for a columnar organization of units signalling the same type of information.

VARYING DISPARITIES

In a further study of the cat, Cynader & Regan (1982) extended the scope of stimulation to determine whether neurones tuned for motion in depth, i.e. responding to antiphase image movements in the two eyes at a fixed distance, and thus with one retinal disparity, would maintain the tuning at several disparities; i.e. could the eyes assess motion in depth when both eyes were not fixating the moving target so that, as it moved in depth, the disparity increased? They did, in fact, find such neurones, whilst others changed their tuning systematically with changing disparity. These units contrasted with others that were very selective for disparity, and were most sensitive to sideways movements, i.e. in-phase image movements. This duality in neurone types might be the basis for the observation that some human subjects have regions of visual field sensitive to disparity but 'blind' to motion in depth, and other regions sensitive to motion in depth but 'blind' to disparity (Richards & Regan, 1973).[3]

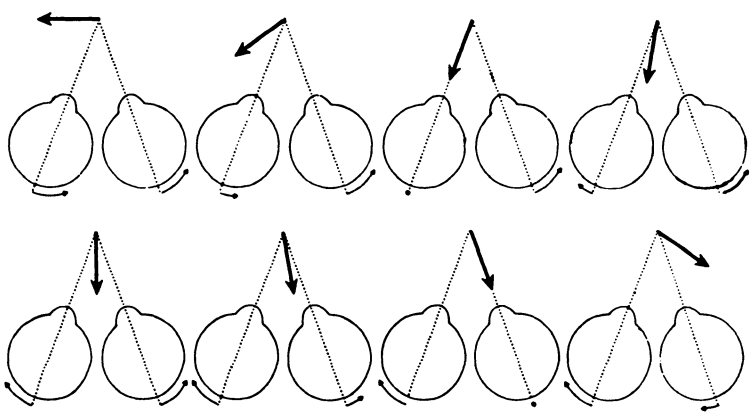

Fig. 21.13 The relative speeds and directions of movement of the retinal images give a sensitive clue to the direction of motion in three dimensions. Motion in opposite directions means that the line of motion passes between the eyes. (Cynader & Regan, *J. Physiol.*)

Waking Monkey

Poggio & Talbot (1981) extended their studies on stereopsis in the waking monkey to the problem of appreciating motion in depth. So far as static stereopsis was concerned they confirmed the existence of units that were tuned to respond to small binocular disparities, exhibiting either binocular facilitation or inhibition. Near- and far-neurones, another class, were capable of analysis of gross disparities when the retinal images were outside Panum's area.

So far as sensitivity to direction in depth was concerned, Poggio & Talbot found that some of their 'tuned excitatory', or Te, neurones that were very sensitive to small retinal disparities were also capable of signalling motion in depth, operating through directional-sensitivity to movement of the retinal images. Some of these were sensitive to motion along sideways trajectories (in phase) and minimally active when stimuli moved towards or away from the head (antiphase). The necessary condition to excite these neurones was some retinal disparity and movement of the retinal images in phase; they signalled direction of movement to the left or right; these movements of the object are not confined to those in the frontoparallel plane but to all trajectories in which the retinal image movements are in phase, i.e. up to a few degrees from the binocular direction of regard. A second group—near- and far-neurones, active in gross stereopsis, also were capable of signalling direction of trajectories that pass wide of the head. Finally there were neurones that responded to retinal images moving in opposite directions in the two eyes; these neurones had excitatory and inhibitory inputs from both eyes and the two inputs had opposite directional sensitivity. Thus selectivity for motion in depth was characterized by binocular facilitation for one direction and inhibition for the other.[4]

STRIATE FUNCTION

Poggio & Talbot emphasize that the neurones studied by them were in the striate area, V1, so that the generally held opinion that analysis of stereopsis was a peculiar feature of prestriate neurones is incorrect, at any rate so far as the primate is concerned.

Section of the Corpus Callosum

It has been commonly accepted that the strip of bilaterally represented visual field on the cerebral cortex is brought about by callosal connections; Leicester (1968) described this overlap of visual fields, and found the same in areas 17 and 18; moreover it survived section of the corpus callosum, so that he considered that the overlap was due to an imperfect decussation in the chiasma. On the other hand, Dreher & Cottee (1975) and later Blakemore *et al.* (1983) showed that the number of binocularly driven neurones in area 17 could be reduced by lesions in the opposite hemisphere, suggesting that binocularity was to some extent a consequence of callosal input.[5] Blakemore *et al.* found that neurones in the supragranular layers 2 and 3 were affected by the transection to a greater extent than those in deeper layers; this would agree with the major termination of callosal outputs from areas 17 and 18 in laminae 1 and 3, whilst the absence of effect on lamina 4 neurones agrees with the absence of callosal terminals there.

Shift in Dominance Spectrum

Payne *et al.* (1980) described a striking shift in the ocular-dominance spectrum of cortical neurones of the cat after callosal section so that classes 1 and 7 were favoured, i.e. monocularly dominated neurones; on average the percentage of binocularly activated neurones decreased from 80% to 37%. The effect depended on eccentricity of the receptive fields, so that at 0–4° the percentage of monocularly driven cells increased from 48 to 60; at 5–9° from 29 to 73; at 10–19° from 17 to 67, whilst at greater than 20° the percentages were about the same.

Temporary and Permanent Changes

Payne *et al.* (1984) found a short-term (3–51 days) reduction in the number of striate neurones driven by both eyes which extended to those with receptive fields extending to some 10° lateral of the midline; in the longer term, however, this reduction only applied to neurones with receptive fields extending 4° laterally. The difference apparently depended on the callosal innervation, the permanent loss of binocularity being due to the absence of reciprocal callosal connections, the striate region containing callosal neurones but not receiving callosal terminations.

Critical Period

Elberger (1981) showed that when the corpus callosum of 13–18 days-old kittens was sectioned there was an increase of monocularly driven striate neurones from 25% to 53%, but the effect depended on the age at which the section was made, and Elberger & Smith (1985) defined the critical period during which callosal section affected binocularity; the earlier the section the greater the effect, so that after 3 weeks callosal section is virtually without effect. They pointed out that this period coincided with the period during which the callosal connections between striate neurones decreased, becoming finally restricted to only neurones with central receptive fields (Innocenti, 1978). Thus only neurones with central fields would be affected by callosal section in the adult cat, and they quoted Timney (1982) to the effect that fine stereopsis in the cat is unimpaired by callosal section.[6]

Eye Alignment

Payne *et al.* (1981) found that callosal section caused a misalignment of the optic axes of the cat, reaching some 5° some 6–8 weeks after the operation. Again Elberger & Hirsch (1982) measured alignment in cats that had been

sectioned neonatally. Neonatally, kittens have a divergent squint which decreases during the second month when adult alignment is achieved. Neonatal section interrupted this process and left the animals with a divergence of some 5–10°, whilst callosal section did not affect alignment in their normal adult cats. Thus it is the development, rather than the maintenance, of alignment that depends on the corpus callosum. The failure to align in these neonatally operated animals was due to a failure of convergence, similar to that seen in normal cats when their eye muscles are paralysed by Flaxedil.

Clare-Bishop Area

Since bilateral removal of areas 17, 18 and 19 in adult or neonatal cats does not affect eye-position (Cynader, 1979; Sherman, 1972) callosal connections between these cortical regions are not responsible for maintenance of eye alignment; Elberger & Smith suggested that the Clare-Bishop area on the suprasylvian cortex might be responsible. So far as binocularity in this region was concerned, they found that neonatal section of the corpus callosum was without effect on the neurones; this would be despite the reduction in binocularity that occurs in area 17, discussed above, so that binocularity in the Clare-Bishop area is independent of corpus callosum and area 17.

Callosal Neurones

In the cat Choudhury *et al.* (1965) found that the receptive fields of cortical units in the medial edge of area 18, just adjacent to area 17, were within a few degrees of the vertical meridian; these responses were recorded when the optic tract of the same side was cut, so that a callosal route from the opposite hemisphere was probably involved, and this was confirmed by cooling the corresponding point on the opposite hemisphere or by complete section of the callosum.

Again, Berlucchi *et al.* (1967) inserted electrodes into the posterior callosum of cats and found axons that gave discharges when the eyes were stimulated with patterns corresponding to those described by Hubel & Wiesel, so that they obtained simple, complex and hypercomplex units (p. 532). In general, it was only when the stimulus was presented close to the vertical meridian that callosal units were excited; three out of seventeen units were driven by both eyes by stimuli located in the same part of the visual field; nine were driven by one eye, and with the remaining five a clear response was obtained with one eye and a weak one with the other. Thus, as Berlucchi *et al.* say, the representation of the visual world is on a continuum, the neurones associated with the vertical meridian and their callosal connections being the hyphen necessary to bring together the two half-fields. Thus the cortical cells connected in this way are at the junction of areas 17 and 18 and it is here that the vertical meridian projects (Choudhury *et al.*, 1965; Bilge *et al.*, 1967), whilst it is here, too, that the great majority of the callosal fibres project (Ebner & Myers, 1965).

Binocular Fields

When the chiasma of the cat was split, so that the visual input from a given eye was entirely homolateral, Berlucchi & Rizzolatti (1968) found 9/70 units driven by both eyes in the visual cortex at the boundary of areas 17 and 18; both receptive fields were very similar and covered the vertical meridian.

THE DOUBLE PATHWAY TO HIGHER VISUAL CENTRES

Multiplicity of Visual Centres

The pioneering studies of Zeki have indicated that the primary visual input to the striate area, V1, is submitted to a series of reprocessing in adjacent cortical regions, a processing that must to some extent be regarded as hierarchical, in the sense that the activity of one centre is transmitted to another in which the receptive-field characteristics of the first have been modified, either by the emphasis of one feature, e.g. chromatic responsiveness or sensitivity to motion, or by combining these characteristics with those of other types of cortical neurones. A parallel processing is, of course, also manifest, the simplest example being the segregation of the X, Y and W streams.[7] Mishkin & Ungergleider (see, for example, Mishkin *et al.*, 1983; Desimone *et al.*, 1985) and Van Essen & Maunsell (1983) have emphasized, first of all, the multiplicity of visual areas, i.e. areas in which neurones responding to visual stimuli predominate, there being perhaps as many as 20. The pathways connecting these are numerous, so that by 1983 at least some 33 had been identified. The positions of some of these in the macaque monkey cortex are illustrated schematically in Fig. 21.14 whilst the hierarchical order of projections is illustrated in Fig. 21.15, horizontal levels indicating equal rank in the hierarchy, and V1 being at the bottom.

Inferior Temporal and Posterior Parietal Regions

Amongst these pathways Mishkin & Ungergleider have separated two (Fig. 21.16) one of which, the inferotemporal (IT), processes the spatial features of the stimulus that lead to recognition of shape and texture and illustrated by Fig. 21.17, and another, a dorsal parietal pathway, which includes the middle temporal area (MT), that processes features of the image that include its

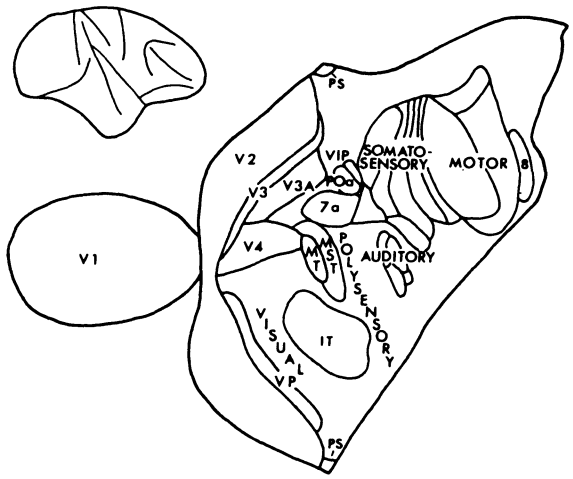

Fig. 21.14 Cortical areas in the macaque monkey. Locations of areas are shown on a lateral view of the right hemisphere (inset) and on a two-dimensional unfolded map of the entire cerebral hemisphere. Visual areas are labelled and coloured individually. A single shade is used for each of the other functional systems (auditory somatosensory and motor), and individual areas are outlined but not labelled on the cortical map. Abbreviations for visual areas: MT (middle temporal); MST (medial superior temporal) VIP (ventral intraparietal); VP (ventral posterior); IT (inferotemporal). Area POa is tentatively split into two subdivisions on the basis of anatomical inhomogeneities. The prostriate area (PS), which is split by an artificial discontinuity, does not have known sensory functions in the macaque. (Van Essen & Maunsell, *Trends in Neurosciences.*)

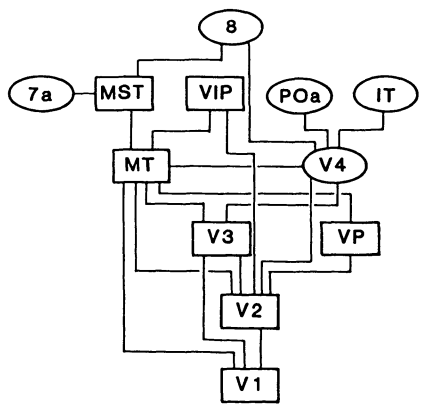

Fig. 21.15 A hierarchy of visual areas in the macaque. Each area is assigned to a specific hierarchical level on the basis of criteria discussed in the text. The majority of pathways indicated on the diagram have been shown to be reciprocal, while the remainder have not been adequately tested. Not shown on the diagram are major inputs to IT from an unnamed region anterior to VP which in turn receives ascending inputs from VP. (Van Essen & Maunsell, *Trends in Neurosciences.*)

motion, thus leading to an appreciation of three-dimensional spatial perception and assisting in visuo-motor control. Broadly speaking, this differentiation was supported by the effects of inferotemporal brain lesions that led to losses of visual discrimination but not to the performance of visuo-spatial tasks, such as object recognition. Posterior parietal lesions, on the other hand, disturbed the performance of visually guided tasks.

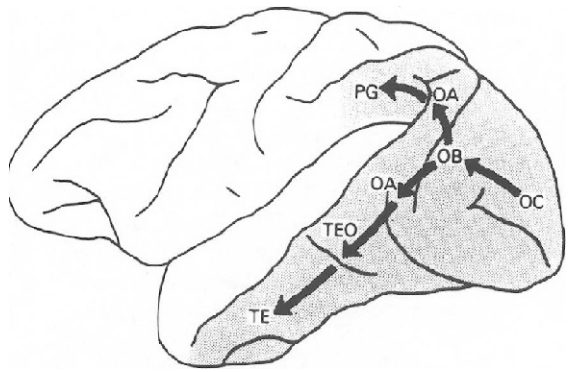

Fig. 21.16 Lateral view of the left hemisphere of a rhesus monkey. The shaded area defines the cortical visual tissue in the occipital, temporal and parietal lobes. Arrows schematize two cortical visual pathways, each beginning in primary visual cortex (area OC), diverging within prestriate cortex (areas OB and OA), and then coursing either ventrally into the inferior temporal cortex (areas TEO and TE) or dorsally into the inferior parietal cortex (area PG). Both cortical visual pathways are crucial for higher visual function, the ventral pathway for object vision and the dorsal pathway for spatial vision. (Mishkin *et al.*, *Trends in Neurosciences*).

The separation of discrimination into two main streams begs the question, of course, as to where they will be finally reintegrated to permit an adequate response to the visual field both from a pattern and spatial aspect. Both systems have projections to the limbic system and the frontal lobe; in the latter there is a region, area 8, in which eye movements are controlled, and it may be here that the final integration takes place.

Inferotemporal (IT) Neurones

Gross *et al.* (1972), working on the anaesthetized monkey, found large receptive fields, the neurones being driven either monocularly or binocularly, with sensitivities to size, shape and direction of movement. Certain neurones had a preference for simian shapes, such as the hand or face.[8]

Size Constancy

Rolls *et al.* (1977), working on the alert monkey, found neurones responding to objects, such as real food and card shapes, and compared their responses with those recorded earlier from the hypothalamus and related satiety centre on the assumption that these cortical

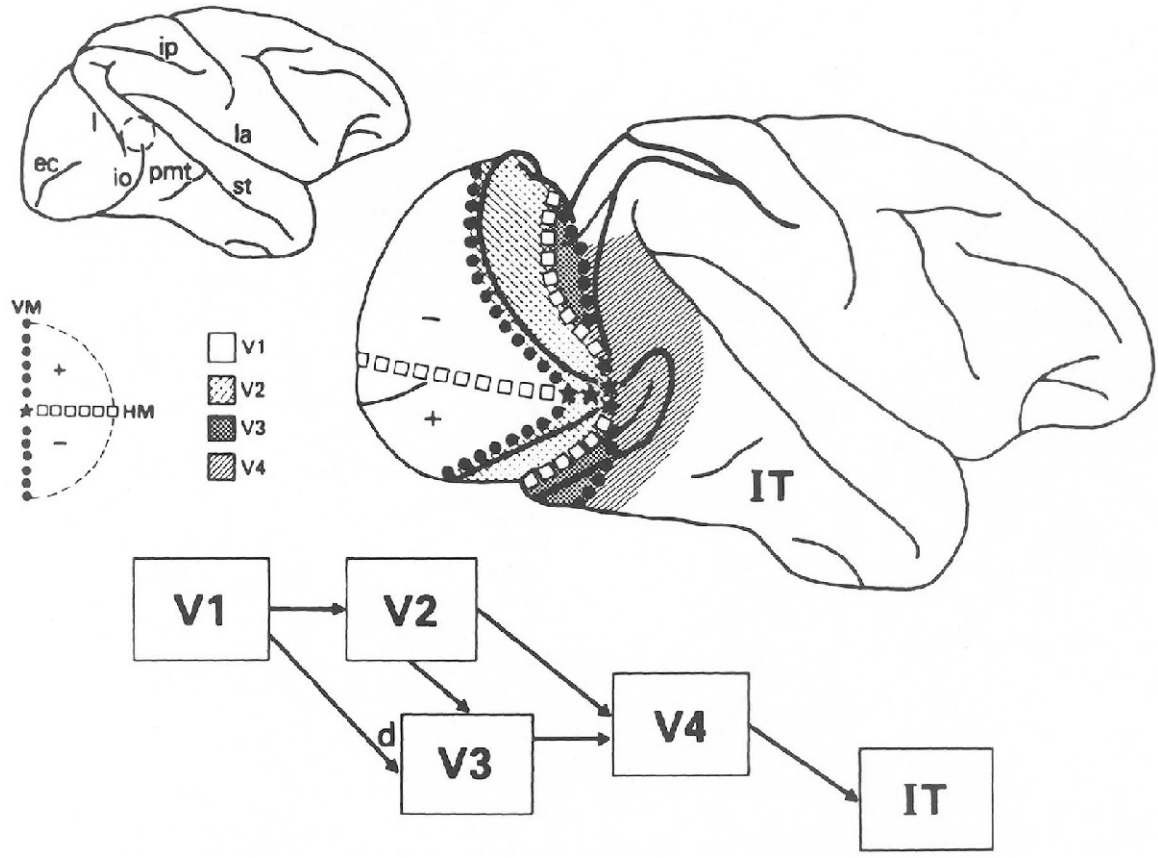

Fig. 21.17 The corticocortical pathway from striate cortex into the temporal lobe. *Top*: Location of V1, V2, V3, V4 and IT shown on lateral view of hemisphere with sulci partially opened. Dashed circle on small brain drawing indicates the location of our recording sites in V4. *Bottom*: Diagrammatic illustration of occipito-temporal pathway. Arrows indicate projections with 'forward' laminar pattern, i.e. terminals concentrated in layer 4. The small 'd' indicates that the striate projection is limited to the dorsal portion of V3. In addition to projections shown, all areas have additional forward projections that do not contribute to the occipito-temporal pathway. Abbreviations: ec, external calcarine sulcus; io, inferior occipital sulcus; ip, intraparietal sulcus; l, lunate sulcus; la, lateral sulcus; pmt, posterior middle temporal sulcus; st, superior temporal sulcus. (Desimone *et al.*, *Vision Res.*)

neurones might be involved in the visual attention required for taking food; however, unlike the latter, the response to the sight of food was independent of the state of satiety, and even of its meaning. When objects of varying shapes based on a Fourier descriptor such as those illustrated in Fig. 21.18 were applied to IT neurones, Desimone *et al.* (1985) found a sensitivity to a specific frequency, as in Fig. 21.19, but this selectivity was unaffected by varying the size of the objects and also by varying the position of the object in the large receptive fields. Since IT neurones appear to maintain their selectivity for textures and colours throughout a large receptive field as well, they could contribute to mechanisms that produce size-constancy when objects vary in position.

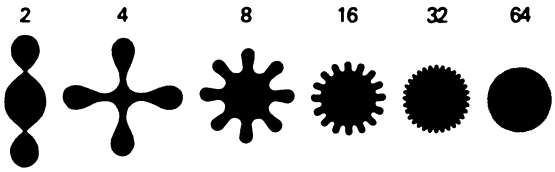

Fig. 21.18 Examples of FD stimuli, which vary in frequency from 2 to 64 cycles per perimeter. Although stimuli are shown in black, the stimuli used in the experiment were normally white on a neutral background. (Desimone *et al.*, *Vision Res.*)

Discrimination Tasks

Sato *et al.* (1980) measured the activity of inferotemporal neurones of monkeys when they were performing tasks requiring the discrimination of simple forms, such as a cross, circle, triangle etc. Neurones were grouped into those that responded to all four patterns, through those that responded to 2 or 3 and those that responded only to

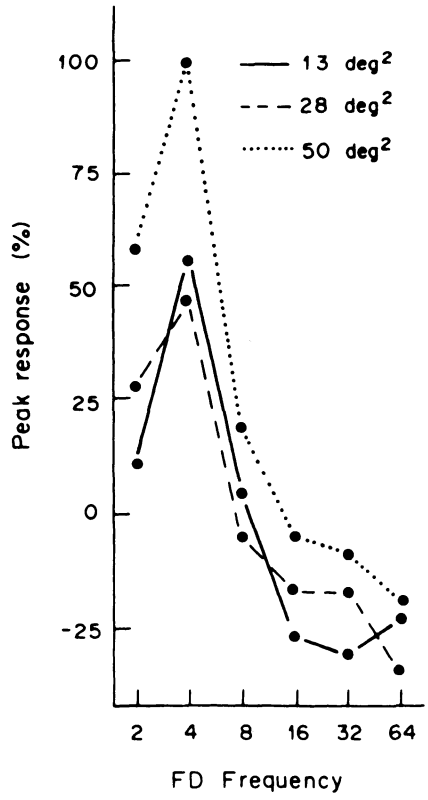

Fig. 21.19 Responses of an IT neuron to FD stimuli of different sizes. All stimuli were confined to the receptive field and were centred on the fovea. Although the absolute response of the neurone varied with stimulus size, the preferred frequency remained 4 cycles per perimeter. (Desimone *et al.*, *Vision Res.*)

one; there were relatively few of these highly selective neurones, and their responses were unaffected by the size, colour or luminance of the pattern. In a later study on the behaving monkey they showed that the responses of inferior temporal neurones could be enhanced when the task to be carried out demanded attention (Richmond & Sato, 1987).

Visual Memory

Discrimination between successively presented objects requires the exercise of memory, an 'imprint' of the first object must be retained and recalled for recognition and discrimination from a new object. Ferster & Jervey (1982) exposed monkeys briefly to a colour, the 'sample', and measured the responses of IT neurones to this and during the presentation of two to four colours subsequently presented. Many cells showed a discharge above background in the interval between presentation of the sample and the choice-task, and during the exercise of the choice the discharge was as high as during initial presentation of the sample. They suggested that retention of the initial response was an important feature of IT neurones, pointing out that, in man, the integrity of inferotemporal cortex was essential for performance of short-term memory tasks. In monkeys Sahgal & Iversen (1978) found that, in tests of colour matching, the ability to retrieve information was impaired with inferotemporal lesions.

Relation to Fixation

Richmond *et al.* (1983) found that IT neurones in the waking monkey responded better to a spot of light if this was presented away from the fixation point than otherwise; if they were trained to expect the fixation point, their response was much less, so that the inferotemporal neurones, with their large receptive fields that include the fixation point, seem to be the sites of interaction between the responses of the point of interest and other points in space.

Dependence on Striate Cortex and Forebrain Commissure

Rocha-Miranda *et al.* (1975) showed that bilateral removal of striate cortex completely abolished the responsiveness of inferotemporal neurones; with unilateral removal, then the neurones in both hemispheres only responded to stimuli arising in the hemifield contralateral to the lesion. After section of the corpus callosum and anterior commissure, the inferotemporal neurones in both hemispheres responded to stimuli arising in the hemifield contralateral to the recording site.

Superior Temporal Sulcus

Perrett *et al.* (1982) described neurones in the fundus of this sulcus that were selectively responsive to faces; the face could be real or the projected image of a human or monkey; they would also respond to simple geometrical shapes or complex three-dimensional objects. Sometimes a real face gave a stronger response than the two-dimensional representation of one. Covering up parts of the face reduced the responses, and it was considered that recognition depended on the integration of responses to different parts, especially the eyes. The authors considered that lesions in this region might be responsible for the condition of *prosopagnosia*, failure to recognize faces (Meadows, 1974; Whiteley & Warrington, 1977). The region receives an input from the inferior temporal cortex and sends efferents to the amygdala, parietal and frontal cortices, areas in which face-responsive neurones have been described, in addition to the inferior temporal (IT) neurones mentioned above.[9]

Area V4 Neurones

Desimone & Schein (1987) have pointed out that, whereas a great deal of work has been done to characterize the contributions of cortical neurones in the striate area, V1, and the inferotemporal area, IT, little has been done to characterize the neurones in intervening areas; they began by a study of V4, originally characterized by Zeki as one devoted to colour discrimination, but shown by Desimone *et al.* (1985) to have considerable spatial selectivity in so far as orientation tuning and peak spatial frequencies were concerned. Desimone & Schein applied a battery of tests to V4 cells designed to demonstrate the degree of spatial processing that had taken place in these cells, and the results showed that most cells were highly selective for the form

of the stimulus; length, width, orientation, etc., and in these respects resembled V1 and V2 cells. Cells could be categorized as simple and complex, using the criteria applied to V1 cells; a characteristic feature was the large suppressive zones surrounding the excitatory receptive field; because of this, many responded poorly to bars or gratings extending beyond the excitatory field; if the cell was colour-selective, the wavelength eliciting maximal excitation also exhibited maximal suppression, so that the cell responded best to a stimulus that stood out well from its environment.

Middle Temporal Neurones

According to the scheme of Mishkin & Ungergleider outlined above, the middle temporal region (MT) is the second region into which the striate neurones funnel their inputs in the analysis of the spatial features of the environment, an analysis relying heavily on the responses to movement that enable a recognition of contours and three-dimensional shape, by contrast with the pattern-discrimination that depends on a static presentation of the visual image. It was described initially as a motion-sensitive region by Dubner & Zeki (1971), its neurones being relatively insensitive to size and shape and lacking pronounced orientation-selectivity, which contrasted them with V1 neurones. Receptive fields were large— 12° × 8°. They considered that the Clare-Bishop area on the suprasylvian sulcus of the cat was an analogous region.

Location in Macaque

As described by Van Essen *et al.* (1981) in the macaque it is a small elliptical area on the posterior bank of the superior temporal sulcus identified by inputs from striate cortex and its heavy myelination. It contains a complete topological representation of the contralateral visual hemifield, a great proportion devoted to the central area, as with V1. The region has a high concentration of direction-sensitive neurones, and it is this that characterizes the MT area from the adjacent region along the lateral border; along its medial border this transition does not occur, but the myeloarchitecture is different, so that Van Essen *et al.* consider that the region has three subdivisions, but it is the heavily myelinated area with V1 projection that represents the functional MT region.

Receptive Fields

These have been exhaustively examined by Maunsell & Van Essen (1983a, b) in both the macaque and owl-monkey; by Albright (1984) and Albright *et al.* (1984) in the macaque and Felleman & Kaas (1984) in the owl-monkey; and Desimone & Ungergleider (1986) in the macaque. Direction-sensitivity was a well defined feature, the response above background to a unit's preferred direction being some 11 times that in the opposite direction. Velocity-tuning was another feature, as illustrated by Fig. 21.20 preferred speeds ranged over some 2 to nearly 500°/sec with a median in the range of 32°/sec. Orientation-selectivity, determined by flashing a bar orientated through 180° in the receptive field, was also a feature of the cells. As Dubner & Zeki (1971) and Zeki (1974a) found colour discrimination was apparently absent.

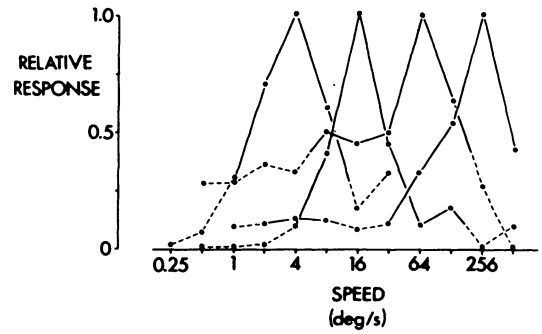

Fig. 21.20 Responses of four units in MT to different speeds of motion in their respective preferred directions. Each curve has been normalized to its greatest average rate of firing response. Portions of curves that are below the background rate of firing for each unit are dashed. Each unit's tuning curve is narrow compared to the range that they covered collectively. Each unit's response fell to background level or showed inhibition at speeds far from the peak. (Maunsell & Van Essen, *J. Neurophysiol.*)

Visual Topography

The retinotopic projection in the macaque has been described by Gattass & Gross (1981); the projection is 'first-order' and represents practically the entire contralateral visual hemifield, the vertical meridian forming the ventrolateral border, and the horizontal meridian running across the floor of the superior temporal sulcus. Receptive field-size and cortical magnification increased with eccentricity in accordance with the same power-function. The authors emphasize the analogy with the similar region in New World monkeys, but point out that in the macaque the area is not in the middle of the temporal lobe.

Columnar Organization

Albright *et al.* (1984) divided their MT units into four categories on the basis of sensitivity to moving targets, 60% responding exclusively to one direction, 24% responding best to one and weakly to the opposite direction; 8% responding equally well to two opposite directions, and 8% responding to all directions of motion.

During penetrations, direction-preference changed systematically from one cell to the next—'sequence regularity'. Discontinuities in the sequences occurred, and were shifts of about 180°. It appeared that cells in columns at right-angles to the surface of the brain had the same preferred axis of motion, although, because of the position of this part of the cortex, penetrations in the required direction were not easily made and deductions from the angle of penetration and rate of change of preferred axis of motion were employed to assess depth. When direction-of-motion preference was compared with axis-of-motion preference, it appeared that cells with the same direction-preference likewise stayed within the same column. On the basis of their results they depict the cortical organization by Fig. 21.21. Thus MT, along with striate cortex, permits the analysis of the motion as well as spatial aspects of the visual image. In the striate cortex some 500 μm of cortex includes cells with receptive fields representing the same portion of the visual field, and these cells include a full complement of preferred orientations. Because of their much larger receptive fields, the MT neurones can span the same region of space in spite of the much larger spatial area of the striate cortex.

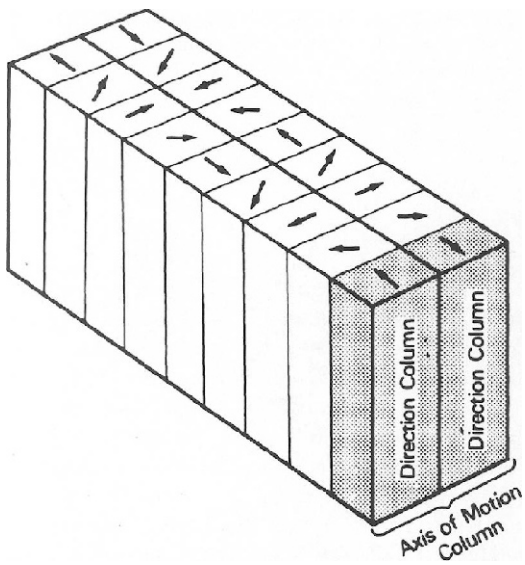

Fig. 21.21 Three-dimensional depiction of a block of cortical tissue containing one configuration of axis and direction of motion columns that is consistent with our data. The vertical dimension represents cortical depth. The long axis of the figure may be viewed as two complete revolutions of axis of motion columns. Moving in this dimension, one would encounter gradual changes in preferred direction. Within each axis of motion column (along the short axis of the figure) the two opposite directions of motion along that axis of motion are represented as adjacent columns. Moving in this dimension, one would encounter frequent 180° reversals in preferred direction, with no change in preferred axis of motion. (Albright *et al., J. Neurophysiol.*)

Orientation Selectivity

Albright (1984), in a study designed to compare the motion-properties of MT units with those of the striate area, V1, found that the percentages of cells with preferred directions, either parallel with, or at right-angles to the preferred orientation were similar in the two areas, suggesting a direct transmission of this feature from V1 to V5.

Owl-monkey

Felleman & Kaas (1984) emphasized the similarity in properties of MT neurones in New and Old World monkeys.[10] They emphasized that neurones were, indeed, sensitive to orientation of bars as well as to direction of motion, and found receptive fields that were very similar to those of complex C2 cells with overlapping ON- and OFF-regions. They pointed out that, in spite of the small size of MT (*ca.* one tenth that of V1), the large receptive fields, some 5–10 times those of V1, meant that the same cortical magnification factor pertained in the two areas, so that a given MT neurone would receive ionput from V1 neurones providing spatial, temporal and chromatic features derived from the same region of space.

Stroboscopic Studies

Akichika *et al.* (1986) used stroboscopic stimuli to simulate motion, varying the spatial and temporal frequencies of a spot of light that would give apparent motion at different speeds. The use of this form of motion-stimulus, rather than the continuous movement of a spot of light over the receptive field, enables the experimenter to measure the state of the receptive field during the apparent motion by interpolating single stimuli between the spatially separated stimuli simulating motion. In this way the sensitivity to a standard flash is tested to determine whether inhibition or facilitation is taking place. Akichka *et al.* concluded that inhibition was the prime mechanism for directional and speed selectivity; thus the response to a flash embedded in a series of flashes moving in the null direction could be completely suppressed. Velocity tuning could be ascribed to a simple summation of responses of subunits, as considered earlier. In a second paper (Mikami *et al.*, 1986) the maximal spatial interval between two flashes that still permitted the simulation of motion was compared in neurones of V1 and MT; this distance was much larger in MT; and it was suggested that the large receptive fields of its neurones permitted the directional interactions over large distances, thereby enabling them to encode directional information at higher speeds of stimulus motion. Finally Newsome *et al.* (1986) compared psychophysical and electrophysiological measurements of apparent motion using identical sequences of flashed stimuli. Thus the same apparent speed can be created by flashes with different spatial and temporal separation, so these two parameters can be systematically varied and the results compared for V1 and MT on the one hand, and the psychophysically determined results on the other. They concluded that MT was responsible for simulated high speeds, whereas both areas could be responsible for slow speeds. The comparisons are illustrated in Fig. 21.22 where the plotted line

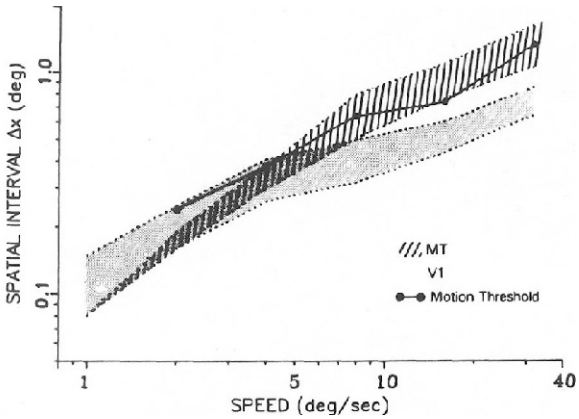

Fig. 21.22 Comparison of composite physiological responses with psychophysical thresholds for apparent motion. *Hatched region* shows the envelope of direction index curves produced for MT neuron. These curves indicate the range of spatial intervals at each apparent speed over which MT neurones, on the average, undergo a transition from directional (*below envelope*) to nondirectional (*above envelope*). *Stippled region* shows the equivalent transition area for directionally selective V1 neurones. The *solid circles* connected by *line segments* show the psychophysical thresholds for perception of apparent motion by human observers. Observers saw motion for spatial intervals and apparent speeds below the line but did not see motion for points above the line. (Newsome *et al.*, *J. Neurophysiol.*)

represents results from human observers, the hatched area for MT neurones, and the stippled area for striate neurones.[11]

Disparity-tuned Units

As we should expect of a centre in which analysis of movement and the spatial features of the environment are developed, Maunsell & Van Essen (1983b) found many units that were tuned to respond to a disparity of the images on the foveae of the two eyes. Units could be classed in the four categories described by Poggio & Fischer (1977) in V1 and V2. The authors considered the likelihood that neurones were sensitive to motion in depth, as such, rather than merely possessing a sensitivity to disparity; thus a neurone specially responding to motion in depth, i.e. following a three-dimensional trajectory, would need to integrate a series of rapidly changing disparities. In fact, they concluded that none of the neurones studied by them in the MT fulfilled this latter requirement. They were all capable of responding to a degree of disparity, but this was limited to a fixed and small range. This is surprising at a station in the central pathway more advanced than V1 and V2 when we consider the large increase in form-selectivity between V1 and IT described by Gross *et al.* (1972) and later workers.

Relation to Cortical Hierarchy

Maunsell & Van Essen (1983b) followed the reciprocal connections of MT with other visual areas by antero- and retrograde movements of tracer (^{3}H-proline and horseradish peroxidase). MT was shown to link with corresponding parts of the visual fields in V1 to V4, and also to two previously unidentified areas, MST (medial superior temporal area) and VIP (ventral intraparietal area). The laminar distributions of the terminals, on the one hand, and the cell bodies, on the other, followed a consistent pattern, and enabled the classification of the connections on a hierarchical basis. Thus MT was considered to be at a higher level than V1 to V3, but at a lower level than MST and VIP. Thus, if a cortical neurone is transmitting its information, after processing, forwards it may be said to be transmitting to a higher region in the hierarchy of the brain; similarly a feedback would indicate transmission to a lower region.

Visuotopical Representations

The early study of Ungergleider & Mishkin (1979), based on lesions, indicated that the whole visual field was represented in the medial temporal zone of the macaque, but it seemed that the peripheral field was represented in regions beyond the heavily myelinated zone that distinguishes MT. Using more modern methods of retro- and anterograde transport of tracers, Ungergleider & Desimone (1986a) have confirmed this; they suggested that the symbol MT be confined to the heavily myelinated area, so that the region of peripheral representation would be MTp. This difference in representation of central and peripheral visual input may be a general feature of parallel processing of retinal input; thus V3A and PO receive inputs predominantly from the peripheral field representations of other visual areas (Zeki, 1980; Colby *et al.*, 1983), whilst V4 receives predominantly from central field representations (Ungergleider *et al.*, 1983). The region received projections from both V1 and V2.

MST as the Main Relay System for Striate Area to Parietal Lobe

Desimone & Ungergleider (1986) and Ungergleider & Desimone (1986b) have described visual areas adjacent to MT and their projections. MST neurones had very large receptive fields and had some visuotopic organization. A posterior parietal area (PP) adjacent to MT had directional-sensitive neurones, but did not receive a direct projection from MT. The area FST, in the fundus of the superior temporal sulcus, received projection from MT; receptive fields were very large, but directional sensitivity was not so frequent as in MT. V4 also received a projection from MT. In general, they concluded that, within this region, successive stages in motion-analysis took place, integrating information over increasingly large areas of retina, whilst inputs from other modalities became involved, as with PO which has somatosensory input. Their general conclusions as to connectivity between striate and temporal regions are illustrated by Fig. 21.23; in general, their conclusions as to feed-forward and feed-backward, derived from the cortical layers of origin and termination of the

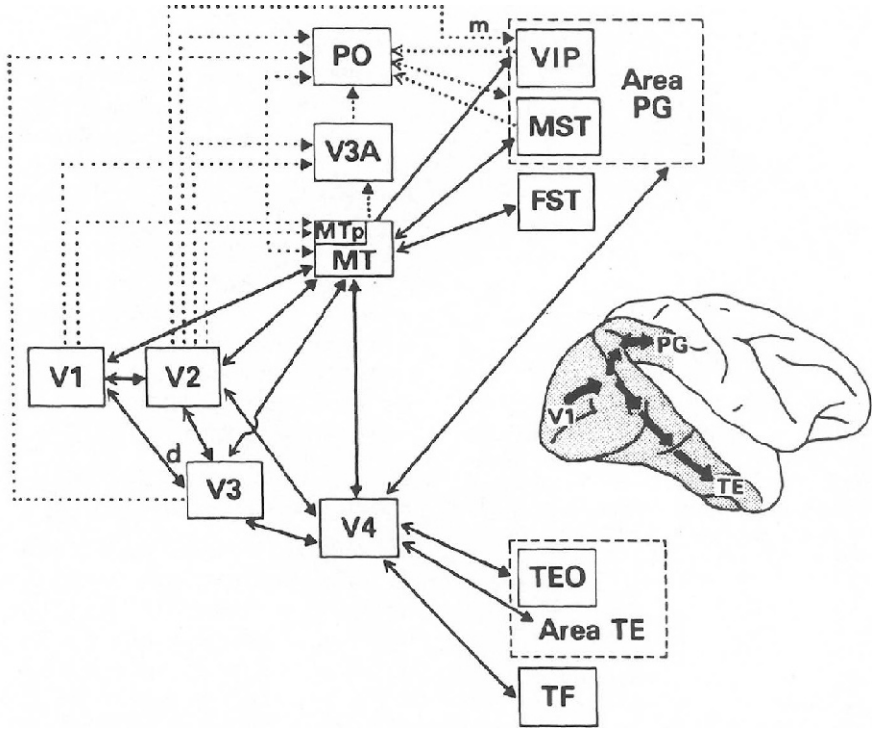

Fig. 21.23 Summary of visual cortical areas and their known connections. Heavy arrowheads indicate 'forward' projections, which terminate predominantly in layer IV, and light arrowheads indicate 'backward' projections, which avoid granular layer IV and terminate instead in the supragranular and infragranular layers. 'Intermediate' projections are indicated by two, reciprocal, heavy arrowheads. The absence of a reciprocal arrowhead does not indicate the absence of a projection but only that it is still unknown. Solid lines indicate projections that arise from both central and peripheral field representations, whereas dotted lines indicate projections that arise exclusively from peripheral field representations. 'd' indicates that the projection from V1 to V3 limited to V3d. 'm' indicates that the projection from V2 to VIP is limited to VIP's medial portion. The projections of Mtp and the connections of V4t are as yet unknown and are therefore not illustrated. The results suggest that MT provides a major route from striate cortex into the parietal lobe. Other potential visual pathways into the parietal lobe include those carrying inputs representing the peripheral visual field. The major route from striate cortex into the temporal lobe is via area V4. (Ungergleider & Desimone, *J. Comp. Neurol.*)

neurones, agree with those of Van Essen & Maunsell (Fig. 21.15). Some interconnections, however, are described as 'intermediate', in so far as projections from MT were spread evenly across cortical layers.

Lesions in the Two Regions

Lesions in the inferior temporal cortex caused loss of pattern discrimination, in the absence of any sensory loss, and were considered thus to be 'visuopsychic'. According to Mishkin (1982) the important inferior temporal region is one called TE (Fig. 21.16) into which visual information is finally channelled. Lesions here cause a loss of the power to store its visual image that is necessary to permit comparisons with other images, so that when subjected to a test involving choice of an object with which subjects have been familiarized, and another that they have not seen before, their performance is severely impaired. Lesions in the posterior parietal area produce a different type of deficit in which the recognition of position in space is impaired, whereas the recognition test that the animal with the inferior temporal lesion failed was passed successfully.

Cat Clare-Bishop Area

This region in the medial bank of the lateral suprasylvian cortex is the analogue of the primate MT region; it receives a direct input from the lateral geniculate nucleus as well as from areas 17, 18 and 19. Toyama *et al.* (1985) have studied the responses to moving objects in three dimensions; in addition, they have

presented disparity-cues equivalent to moving an object nearer or farther away. Neurones were found responding binocularly to approaching (AP), receding (RC) and fronto-parallel movement. When monocular responses of AP cells were examined, a response to a rightward movement in the right eye was observed but none at all with a leftward movement in the left eye. The binocular response was about equal to the combined monocular responses. The same was true for RC cells. An AP cell responded to an increase in size of the object less strongly than to a decrease; when both size-change and motion-disparity were altered simultaneously the strongest response was obtained. There were some differences when comparing their results with those on V2 by Cynader & Regan; thus inputs from the two eyes were balanced compared with the dominance for one eye and inhibition for the other in V2; thus Clare-Bishop cells apparently integrate the excitation of both eyes whereas V2 cells work by inhibitory cancellation.

SPATIAL AND TEMPORAL CHARACTERISTICS

Morrone *et al.* (1986) have compared neurones of the Clare-Bishop area with those of striate cortex; spatial acuity and spatial preferences and selectivity bandwidths were comparable with those of cells in other visual areas, except for area 17 where bandwidths of tuning were about twice; temporal selectivity, however, was as good as anywhere else. Receptive fields were very large, presumably due to convergence of many cortical units, but spatial resolution was better than would be expected were receptive field size the decisive factor. The large fields might be valuable for analysis of stereopsis and motion in depth.

Background Movement

The analysis of motion depends critically on the ability to distinguish apparent movement of the environment caused by eye-movement from real movement. The necessary information must be derived from an input related to extraocular muscle activity. The integrated information will be revealed in the responses of motion-sensitive cortical cells, and the problem is to identify these cells. Tanaka *et al.* (1986) examined directionally sensitive neurones in the middle temporal (MT) and medial superior temporal (MST) regions of the macaque, studying their responses to movement of a bar, of a wide dot-pattern, and to combined movements of these. Most MT cells responded equally well to a bar or patterned stimulus provided that it fell on the excitatory portion of the receptive field. Surround inhibition, revealed by increasing the size of the stimulus, was directionally sensitive, as illustrated by Fig. 21.24 where responses to a bar in the excitatory region are compared with those to simultaneous movements of a patterned surround. Movement in the same direction suppressed the response, whilst in the opposite direction there was some enhancement. In MST a greater variety of response-patterns was encountered; a type unique to this area, called the 'field-type' preferred a wide-field patterned stimulus and hardly responded to a bar-stimulus, and it was considered that it was this type that permitted the detection of real object movement as compared with apparent movements induced by eye-movements. The inhibitory field surrounding the central excitatory, or discharge-region, is reminiscent of the end-stopping of hypercomplex cells; however, in these MT and MST cells the region extends radially; as receptive fields of MST neurones are very large, probably because of convergence of MT cells, they could presumably subserve the analysis of image-motion in large areas of retina. The directionally sensitive inhibition was thought by Tanaka *et al.* to permit the discrimination of real from apparent motion.

Polysensory Region of Superior Temporal Sulcus (STP)

This region lies on the upper bank and fundus of the superior temporal sulcus of the macaque (Desimone & Gross, 1979). Its thalamic afferents are from the medial pulvinar (Burton & Jones, 1976) which in turn receives afferents from the deeper layers of the superior colliculus. It receives cortical projections from the inferior temporal region (IT) and posterior parietal cortex (Jones & Powell, 1970), so that here visual, auditory and somaesthetic inputs converge. The visual properties of the neurones were examined in detail by Bruce *et al.* (1981), since nearly all of them were visually responsive, 41% being exclusively so.

The receptive fields were so large as to make the concept meaningless, extending as they did across large areas and often the whole visual field. Most neurones had little or no preference for size, shape, orientation or contrast of the visual stimulus; of some interest was an apparent preference for a face, as illustrated in Fig. 21.25 where it will be seen that the responses to a hand, or random pattern, were negligible compared with those to different faces. It could be that the neurones are part of a cortical system specialized for the recognition of faces or facial expression; thus lesions at the occipitotemporal junction are associated with a selective impairment of the recognition of faces (prosopagnosia), according to Meadows (1974). A feature held in common with those of striate and prestriate cortical neurones is directional selectivity; thus the Class 2 neurones of Bruce *et al.* were selective for movement in depth, similar to those described by Zeki in the posterior bank of the superior temporal sulcus; the Class 3 neurones, however, were selective for directions radially symmetrical about the centre of gaze; such neurones are not encountered in striate and prestriate areas, although they have been in the posterior parietal cortex (Motter and Mountcastle, 1979).

Roles of Striate Cortex and Superior Colliculus

Bruce *et al.* (1986) considered that most cells in this area exhibited receptive-field features reminiscent of a system

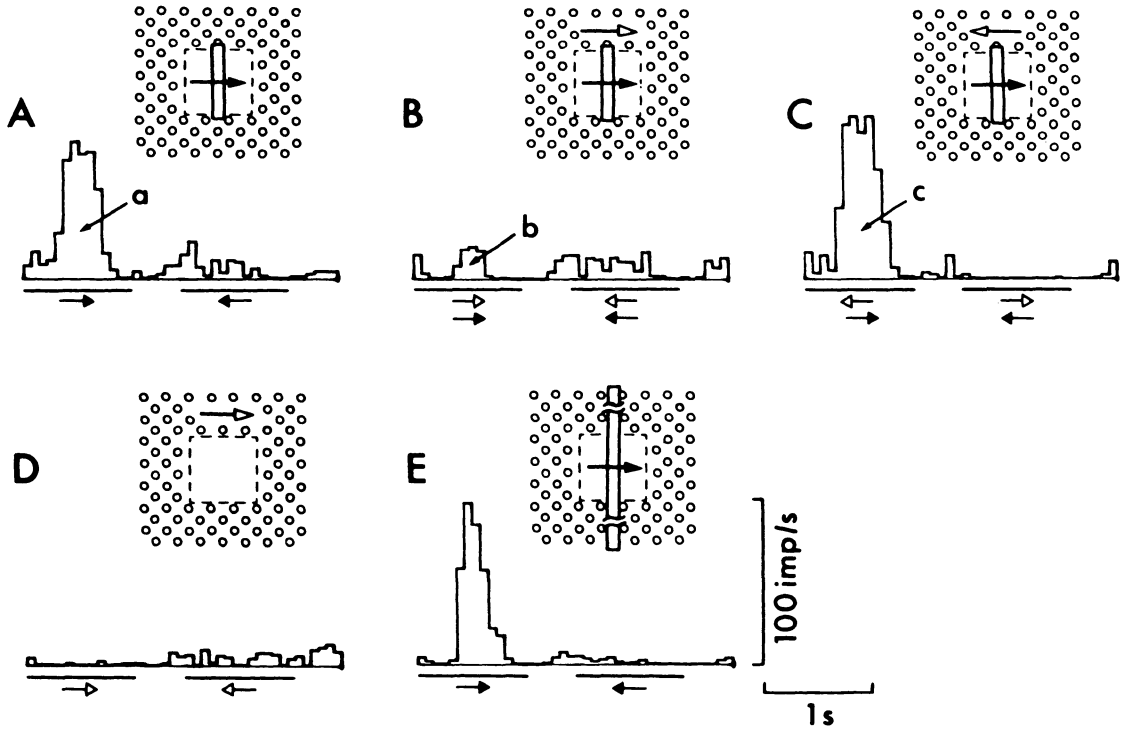

Fig. 21.24 Properties of surround inhibition observed in a MT cell. *A*, Response to a bar movement with a dot pattern held stationary. *B*, *C*, Response to the bar movement was suppressed by 84% when the dot pattern moved in the same direction with the bar (*B*), but was facilitated by 35% when the dot pattern moved in the opposite direction (*C*). Therefore, the inhibition was directionally selective. *Filled arrows*, Direction of the bar movement; *open arrows*, direction of the dot-pattern movement. *D*, The dot-pattern movement by itself never evoked excitatory response. This was also true when the dot pattern moved while a bar remained stationary at the centre of the excitatory field. *E*, Lengthening of the bar caused only slight suppression of response (−16%). Field size, 7.5° × 7.5°; bar size, 1° × 3°; amplitude of movement, 20°. (Tanaka *et al.*, *J. Neurosci.*)

dominated by the superior colliculus, being concerned with 'spatial vision', i.e. vision related to the three-dimensional character of the environment. They studied the effects of unilateral lesions of the striate area and superior colliculus on the neurones; since these neurones respond to both hemifields, it is possible to compare neurones with normal and deprived inputs from the two regions. After complete unilateral removal of area 17, visual responses were still obtained in nearly half the cells in the hemifield contralateral to the lesion. Thus these STP neurones are not completely dependent on striate input for their visual responses, although their response-features were abnormal, directional and form-sensitivity being lost. When both striate area and superior colliculus were removed on the same side, responses in the hemifield contralateral to the lesions were now abolished, whilst nearly 80% of neurones in the hemifield ipsilateral to the lesions were responsive. Unilateral removal of the superior colliculus only had a small effect. Thus the striate area is critical for STP function, whilst the superior colliculus is responsible for visual responses that survive the loss of the striate input, and thus contribute to the visually guided behaviour that may be retained after striate lesions in monkeys.[12]

ELECTROPHYSIOLOGICAL ASPECTS OF VISUAL ACUITY

Although the resolving power of the retina depends in the last analysis on the size and density of packing of the receptors in the retina, we must remember that it is the neural organization of these receptors, to give receptive fields of higher order neurones such as the ganglion cell, that determines whether or not the maximal theoretical resolving power is attainable.

Contrast-sensitivity Function

We have seen that the perception of detail may be characterized quantitatively by the contrast-sensitivity

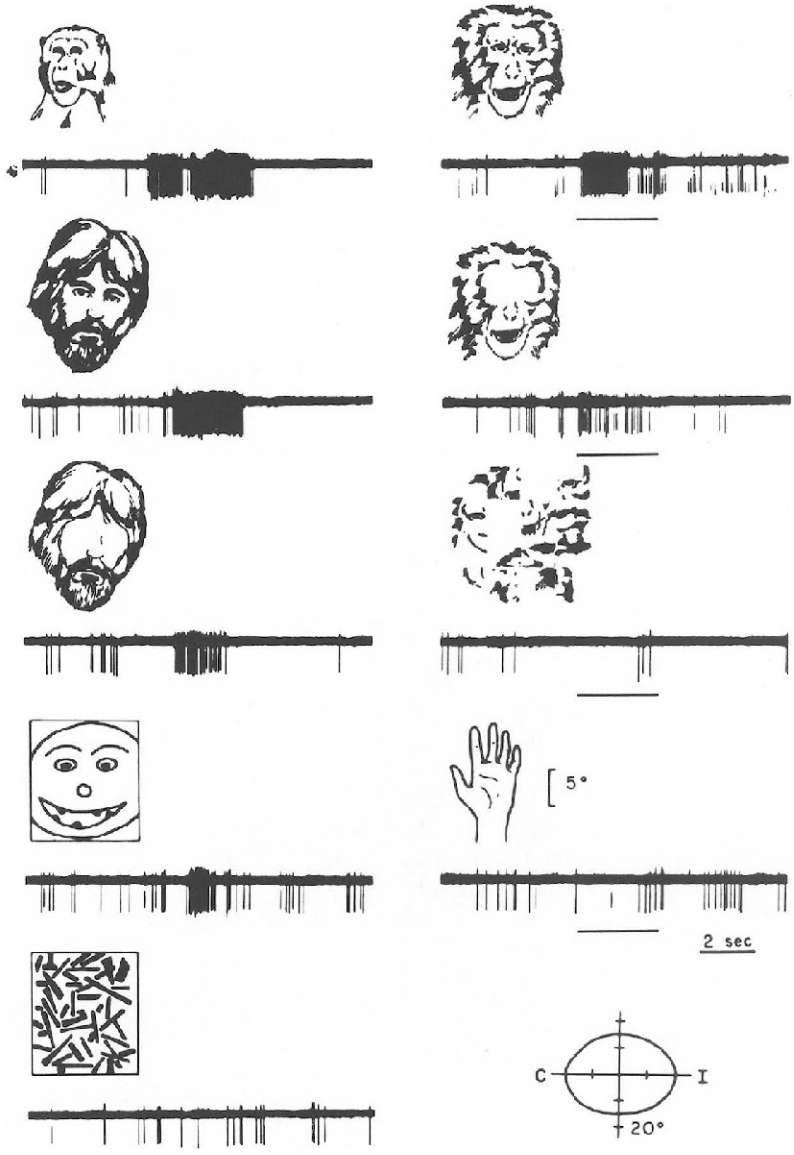

Fig. 21.25 Responses of an STP unit that responded better to faces than to all other stimuli tested. Removing eyes on a picture or representing the face as a caricature reduced the response. Cutting the picture into 16 pieces and rearranging the pieces eliminated the response. Stimuli represented on the left were traced from a colour photograph (monkey face), black and white photographs (human face) and drawings (caricature and random pattern), which were swept across the fovea at 10°/sec. Stimuli presented on the right were traced from colour slides, which were projected on the fovea for 3 sec, as indicated by the horizontal bars. (Bruce *et al., J. Neurophysiol.*)

function (Fig. 14.10)[13] derived from measuring the threshold light contrast required to resolve gratings of increasing spatial frequencies, an approach developed by Campbell and his colleagues. This type of stimulus has been applied to ganglion cells and higher-order neurones, the employment of which allowed Enroth-Cugell & Robson (1966) to establish the X- and Y-dichotomy in the visual pathway. In the lateral geniculate nucleus this dichotomy has been continued, and we have discussed the values of the two types of neurone in resolving spatial and temporal features of the visual scene. Where visual acuity is measured as the ability to resolve the finest detail, i.e. at

the limit of the spatial-contrast-sensitivity function, the small size of the X-cell's receptive field demands that this resolution be mediated by it; in regions of grosser spatial detail the greater sensitivity of the Y-cell suggests that it would be involved in resolution, whilst its transient responses would fit it for the resolution of temporal changes in the visual scene, as during movements of the eyes. Thus, according to Cleland *et al.* (1971) the transient type of ganglion cell represents the initial stage in the development of a specific sensitivity to motion, by virtue of its responsiveness to movement of large objects in the periphery of its receptive field—*periphery effect*—and to objects of any size suddenly crossing or moving within the receptive field. With small objects moving slowly, both types of neurone can provide information that *localizes* the stimulus—in the sense that the response-magnitude increases as movement is towards the centre of the field—and *identifies* the stimulus, in the sense that the response depends on lightness or darkness of its image.

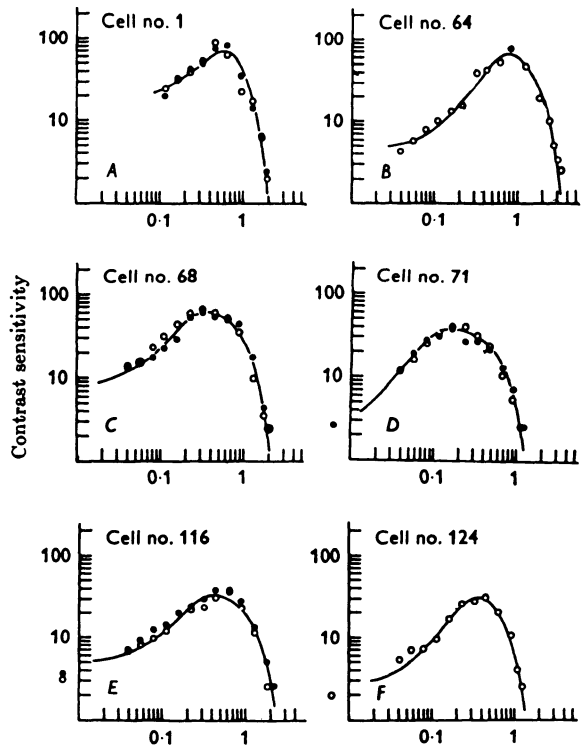

Fig. 21.26 Contrast-sensitivity functions of five ON-centre X-cells (A–E) and one OFF-centre X-cell (F). Gratings of different frequencies drifted over the receptive field at a frequency of *c* cyc/sec, and the contrast was altered until the observer could detect a modulation of the discharge-frequency at 1 cyc/sec (i.e. synchronously with the temporal luminance modulation). (Enroth-Cugell & Robson, *J. Physiol.*)

Psychophysical Studies

Kulikowski & Tolhurst (1973) have carried this distinction further with pyschophysical studies on humans in which grating stimuli were modulated spatially—i.e. the spatial frequency was altered, as in the determination of the contrast-sensitivity function of Fig. 21.26, and the stimuli were also modulated temporally, either being flashed on and off at varying frequencies, or being 'alternated', in the sense that bars that were black at one moment became white, and *vice versa*; in this latter case the change in contrast of the adjacent bars was twice that when the grid was just switched on and off. Figure 21.27 shows a typical experiment where contrast-sensitivity has been plotted against spatial frequency as before. The interesting point is that at high spatial frequencies—i.e. with fine stripes—there is no difference in sensitivity to the two modes of stimulation, although, on the basis of temporal sequence of events, the retina is being exposed to twice the contrast during alternation. At lower spatial frequencies (wider gratings) a difference in sensitivity becomes manifest, and below 2.5 c/degree the predicted doubling of sensitivity is obtained. The results might suggest that different ganglion cells were being utilized for conveying the message; at the high spatial frequencies (fine lines) the retina would not be taking notice of the temporal sequence of stimuli and would be responding as though the receptors were being stimulated continuously with the contrast appertaining to a static presentation. Thus, it might be the sustained type of ganglion cell, with small receptive field, that was responsive. With the wider gratings the retina would be taking note of the alternation (which is equivalent to a movement of the grating backwards and forwards 3.5 times per sec) and this permits a greater effective contrast-sensitivity, since the retina is working on a basis of doubled contrast.

FLICKER SENSATION

The difference is manifest in a difference of sensation at threshold; thus, with alternating spatial frequencies of greater than about 4/sec, and in the region where alternation was not being recognized, the gratings appeared stationary, whereas at the lower spatial frequencies—broader stripes—there was a definite sensation of motion, or flicker, i.e. the subject was recognizing the temporal, as well as the spatial, features of the stimulus. In the experiment illustrated by Fig. 21.27, the subject was required to say whether or not he considered that the stimulus appeared to be flickering at his threshold; if not, he was required to increase the contrast until the flicker was just apparent—the *flicker-threshold.* It is clear from Fig. 21.27 that the flicker-threshold and stimulus-detection threshold are the same for wide stripes, but differ with fine gratings so that the contrast must be increased in order to detect flicker as well as contrast. It is evident

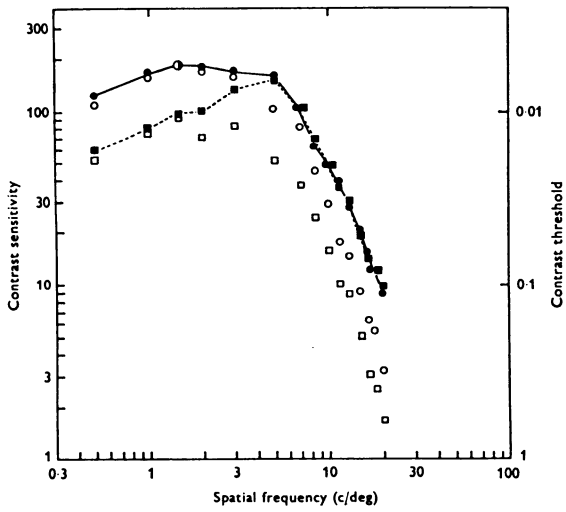

Fig. 21.27 Contrast sensitivity to sinusoidal gratings alternated in phase and switched on and off at 3.5 Hz. The filled symbols show the sensitivity for detecting a stimulus irrespective of its appearance: alternating (●) and on/off (■). The open symbols show the sensitivity for detecting that the stimuli were flickering: alternating (○) and on/off (□). The alternating grating was seen better than the corresponding on/off grating only when the alternating grating appeared to be flickering. Mean luminance 7 cd/m^2. (Kulikowski & Tolhurst, *J. Physiol.*)

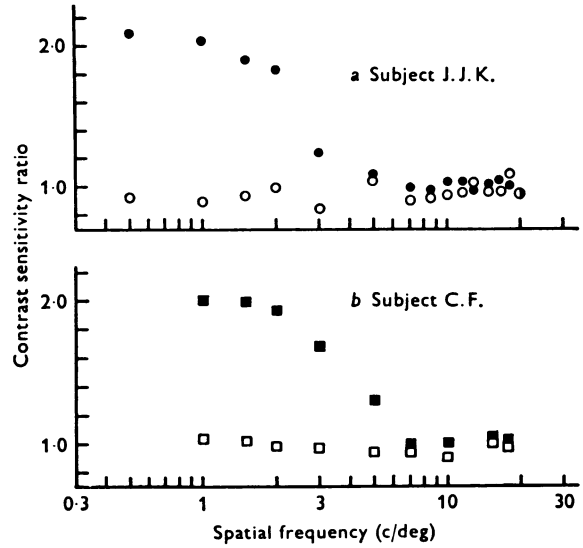

Fig. 21.28 The sensitivity ratio for pattern recognition as a function of spatial frequency. The filled symbols represent the sensitivity ratio for detecting the stimulus irrespective of the appearance. The open symbols show the the ratio for the pattern recognition task; it is close to 1 over the whole range of spatial frequency. (Kulikowski & Tolhurst, *J. Physiol.*)

from Fig. 21.27, as well, that when the contrast has been raised so as to appreciate flicker it must be more for ON-OFF presentation than for alternation. Thus, under these conditions, namely recognition of flicker, the retina is taking notice of alternation and utilizing the greater contrast provided by this method of stimulation. As indicated, the ratio of contrast-sensitivities for the two types of presentation is theoretically 2, but varies from this to unity according to the spatial frequency, or fineness, of the pattern.

FLICKER VERSUS PATTERN

When a subject is asked to use, as threshold, the contrast necessary to appreciate pattern and, again, the contrast necessary to detect the stimulus either through its flickering or its pattern, two types of graph are obtained (Fig. 21.28) where the ordinate is the sensitivity-ratio for the two types of presentation, i.e. for ON-OFF flashing and alternation. With pattern recognition, the ratio is unity at all spatial frequencies, but when the temporal features of the stimulus are recognized, the ratio rises to two at low spatial frequencies (broad stripes).

These studies emphasize, then, the operation of two separate mechanisms for recognition of the spatial and temporal characteristics of the stimulus and Kulikowski & Tolhurst argue that they are mediated through sustained and transient ganglion cell types.

LINE STIMULUS

The above results applied to sinusoidal gratings; Keesey (1972) observed the same phenomenon with a flickering line-stimulus subtending 4 minutes of arc at the eye on a background of a 1° diameter field; at the visual contrast-threshold, only a diffuse flickering sensation was perceived and only at a higher contrast could the pattern perception of a well localized line be perceived. King-Smith & Kulikowski (1975) have examined the respective features of the pattern and flicker detectors; for example the receptive field of the most sensitive flicker detector is about twice as broad as that for pattern detection. They noticed that the vertical test line, modulated at frequencies of 3 Hz or more, produced a strong sensation of lateral motion at threshold comparable with that described for modulated gratings. Thus, it is likely that the flicker-sensitive cells are really motion sensitive; as we have seen, there are cells in the cerebral cortex that are specifically sensitive to moving targets (Zeki, 1974).

ADAPTATION

Blakemore & Campbell's (1969) study on adaptation by gratings of different spatial frequency indicated the existence of separate 'channels' for analysis of this type of image. Tolhurst (1973) has extended his studies on flickering gratings to the effect of adaptation and shown that, at low spatial frequencies, where Blakemore & Campbell had been unable to detect specific channels on the basis of stationary targets, these could be detected when the target was moved; then it was found that the contrast-sensitivity was unaffected by adaptation to stationary targets.

Value of Grating Adaptation

Adaptation to luminance has the value of extending the working range of the receptors over a very wide range of luminance so

that the response of retinal ganglion cells to a fractional change in luminance. $\Delta I/I$, is roughly the same whether the eye is exposed to a luminance of 1 or 100. This is achieved by a decrease in contrast-sensitivity as retinal illumination increases, so that the maintained discharge in the ON-centre ganglion cells remains fairly constant. Lateral inhibition is another feature of the adaptive process, increasing sensitivity to high spatial frequencies compared with low, and finally there is the greater sensitivity to flicker or temporal resolution at high luminances. All these effects of adaptation have obvious value in enabling the eye to convey information to the brain. Barlow *et al.* (1976) pose the question as to the value, if any, of the adaptive effects of gratings; since these adaptive effects on one eye transfer to the other it is concluded that the mechanism is cortical rather than retinal. Their studies indicated, however, that there was no improvement in discriminating changes of spatial frequency or orientation of gratings.

MONKEY PSYCHOPHYSICAL STUDIES

In view of the great similarity in visual function between monkey and man, Harwerth *et al.* (1980) considered that psychophysical studies that supplemented electrophysiological ones would be of value. They studied the reaction-time[14] for near-threshold gratings as a function of spatial frequency; contrast-sensitivity as a function of viewing duration and spatial frequency, and finally the reaction-time as a function of contrast for suprathreshold frequencies. Essentially they were combining spatially and temporally modified stimuli and attempting to establish a dichotomy indicating twin mechanisms for the analysis of spatial and temporal features. The contrast-sensitivity function for a monkey is illustrated in Fig. 21.29 comparable with the human and indicating a limiting visual resolution of about 20 cycles/degree. In general all three approaches indicated the operation of two processes over a certain range of spatial frequencies. Thus Fig. 21.30 illustrates contrast-sensitivity as a function of viewing time. With low spatial frequencies a time is soon reached where further viewing time causes no improvement, suggesting a transient mechanism. At high spatial frequencies the contrast sensitivity continues to improve indefinitely, suggesting the operation of a sustained mechanism. When reaction-times were measured, there was a sharp transition between spatial frequencies of 1 and 2 cycles/degree; with the lower frequencies, i.e. coarser gratings, reaction times were distributed bimodally, whilst at high frequencies they were unimodally distributed. The transition point between 1 and 2 cyc/deg corresponds to a human transition point; thus the threshold for detection of flicker is lower than that for detection of pattern at 1 cyc/deg, and the reverse becomes true at 2 cyc/deg (Harwerth *et al.*, 1979).

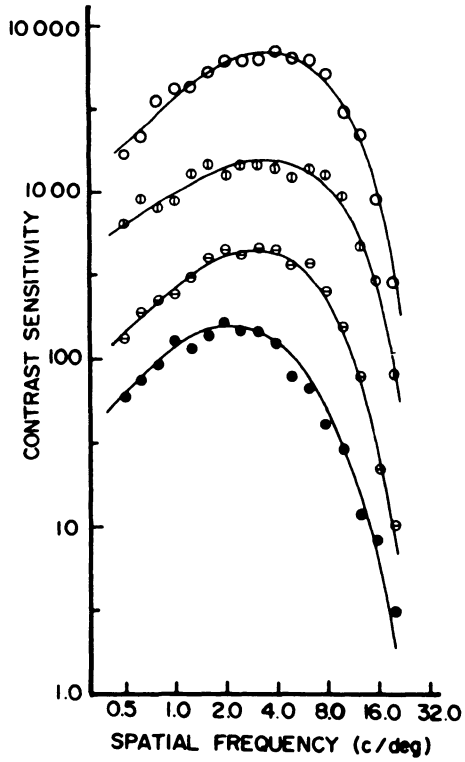

Fig. 21.29 Contrast sensitivity functions with a 500 msec viewing duration for each of the 4 monkeys used in the experiments. The data for subject 7508 (solid circles) are correctly positioned while the data for 7722 (circles with horizontal bars), 7721 (circles with vertical bars) and 7512 (open circles) have been successively displaced upward by 0.5 log unit for clarity of presentation. (Harwerth *et al.*, *Vision Res.*)

Lateral Geniculate and Cortical Units

Campbell *et al.* (1969) compared geniculate and cortical units in the cat and obtained characteristic contrast-sensitivity functions with sharp cut-off points such that a small change in spatial frequency of the grating caused an abrupt decrease in sensitivity; the 'attenuation points' varied from about 0.2 to 1.5 cycles/degree for cortical cells and 0.3 to 4 cycles/degree for geniculate cells. By human standards the grating discrimination displayed by these cells, is low, indicating a low visual acuity in the cat. Later Maffei & Fiorentini (1973) measured the amplitude of response of simple cortical units as a function of the spatial frequency of gratings moved in the preferred direction; Fig. 21.31 shows that the units responded over separate and narrow ranges of spatial frequency; and comparison with curves for ganglion cells and lateral geniculate units indicated that there was a progressive narrowing of the range of sensitivity, indicating the development of spatial frequency analysers that may well constitute the basis for the psychophysical results of Campbell and his colleagues (p. 381). The maximal resolution, of which these cat cortical analysers were capable, was 0.2°, which is comparable with the resolving

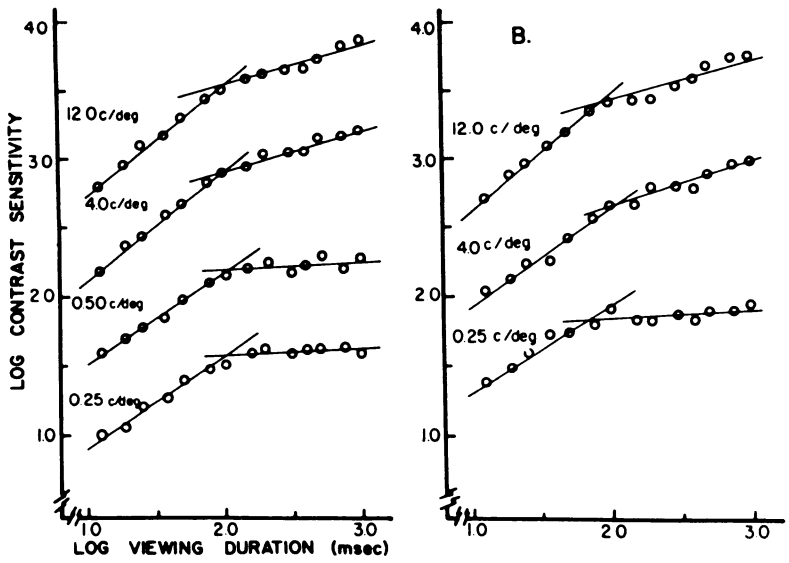

Fig. 21.30 Contrast sensitivity as a function of viewing duration for subjects 7512 and 7508. The spatial frequencies of the stimuli are indicated beside the plot. The data are arbitrarily displaced along the abscissa for clarity of presentation. (Harwerth *et al.*, *Vision Res.*)

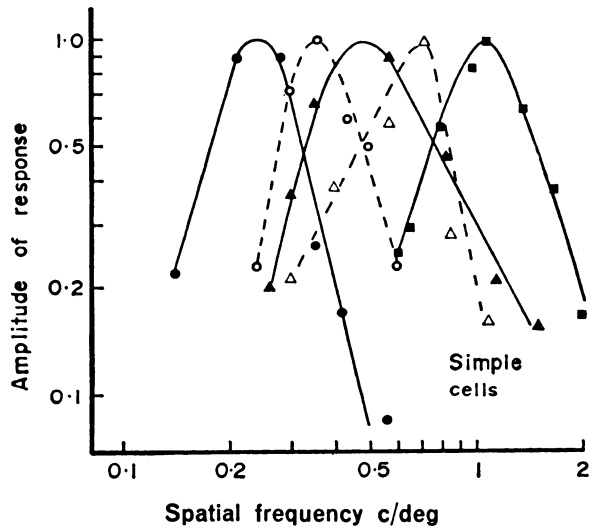

Fig. 21.31 Response of simple cortical cells to a sinusoidal grating, as a function of spatial frequency. Filled circles: unit with an ON-centre region of 1.2° width, flanked by two OFF-regions. Total width of the receptive field 5°. Open circles: unit with a receptive field of the same type as the previous one, but with very weak OFF-flanks. ON-centre region of 1° width. Filled triangles: unit with a bipartite receptive field consisting of an ON-region of 1.3° flanked by one OFF-region of 0.7° width. Open triangles: unit with a bipartite receptive field of total width 0.9°. Filled squares: unit with a bipartite receptive field of total width 0.6°. (Maffei & Fiorentini, *Vision Res.*)

power of the cat determined through the visually revoked response (Campbell *et al.*, 1973).[15] Complex cells did not show such narrow ranges of frequency-selection, so that resolution of spatial detail was never greater than 1°.

Monkey Units

DeValois *et al.* (1982a,b) measured contrast-frequency functions of macaque cortical units with a view to establishing quantitative relations between spatial-frequency tuning and other aspects of the cortical cell, notably its orientation-tuning. Cells were differentiated as X- or Y- on the basis of linearity of summation along the lines of Enroth-Cugell & Robson (1966). In general, cells tuned to a high spatial frequency tended to be tuned to a narrow band of orientation. Interestingly, they found that whenever a cortical cell could be categorized as an X-cell it was likewise categorized as a simple cell, as would be expected of the linear summation originally described by Hubel & Wiesel, the well defined excitatory and inhibitory regions producing a modulated discharge in response to a drifting grating (Fig. 21.32). A cell categorized as Y-type, giving a poorly modulated discharge, could be described as complex, and this fits with the original description as that of a cell that fires similarly to a stimulus regardless of its location within the receptive field. DeValois *et al.* failed to confirm the difference in the narrowness of spatial frequency tuning between simple and complex cells described by Maffei & Fiorentini; they found that both cell-types had a wide range of bandwidths varying from 0.6 to over 2.5 octaves, and the difference in tuning widths on average was barely significant. However, simple cells had a lower peak tuning frequency (mean 3 c/deg) than complex cells (mean 4.4 c/deg); this is in spite of the apparent predominantly Y-type of input to the complex cell, with the larger receptive fields; however, it is argued that, where cortical cells are concerned, a simple relation between receptive-field size and peak tuning frequency need not be expected.[16]

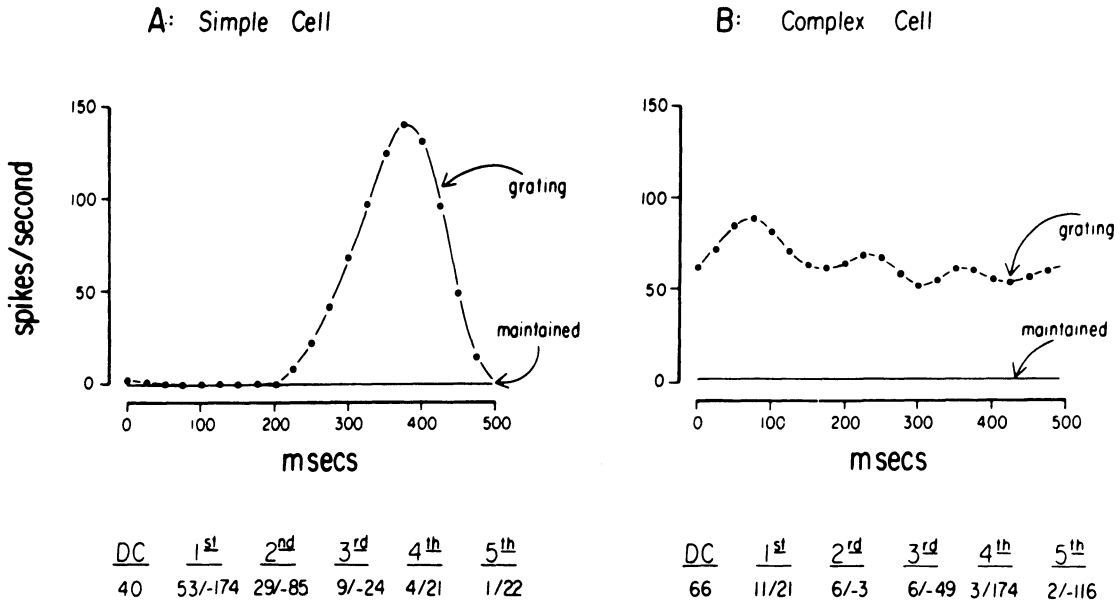

Fig. 21.32 Response patterns of a representative simple cell (A) and complex cell (B) to gratings drifted across their receptive fields. The response (peri-stimulus time histogram, PSTH) averaged over 20 repetitions of the sinusoidal stimulus is shown above a printout of the d.c. (mean rate of firing) and the first five harmonic components (amplitude/phase). The average maintained discharge in the absence of any visual stimulus is also displayed for each cell. Note that the simple cell's response to the drifting grating shows a discharge pattern which modulates in synchrony with the fundamental temporal cycle of the stimulus, therefore most of the power appears in the 1st harmonic. The complex cell's response, on the other hand, shows an overall increase in the mean rate of firing with little modulation; therefore the response appears in the d.c. component with little power in the harmonics. (DeValois *et al.*, *Vision Res.*)

Cat

Bradley *et al.* (1987) measured orientation-tuning and spatial resolution of striate units of the cat, estimating from these the minimum changes that produced reliable cortical signals; these were compared with published behavioural studies. The average values, namely a difference of 6.4° for orientation and 21.3% for spatial frequency, were considerably higher than the cat's discrimination, as measured behaviourally. However, the most selective neurones were capable of performing the required discrimination. The authors point out, though, that many other stimulus-changes can produce comparable discharges in single units, so that a single unit could not uniquely signal the particular stimulus-change being studied.[17]

Double-field Simple Cell

A possible candidate for spatial frequency selectivity, according to Bishop *et al.* (1973) is the double-field simple cell in which both sub-fields respond to the same direction of movement, with one region responsive to a dark edge and the other to a light edge (S_2 type of Schiller *et al.*). The optimal response would be obtained when the moving bar had a width equal to the centre-to-centre separation of the two subfields, when the two subfields would be excited simultaneously by the opposite contrasts. An alternate, or additional, mechanism in which inhibitory discharges arising when edges of non-optimal bar-widths impinged on inhibitory regions of the receptive field would probably be far more effective in governing selectivity, since it is possible to envisage no response at all to bars of widths exceeding a certain critical value.

Spatial-frequency Tuning in Complex Cells

The tuning of the simple cell's receptive field, so that it responds maximally to a certain spatial-frequency with a sharp cut-off at higher frequencies (Fig. 21.27), seems to be a feature of the width of the receptive field, units with narrow fields being able to signal higher spatial frequencies (thinner bars) than those with wider fields; in fact, as we have seen, the visual acuity of a cat can be assessed in terms of the width of its simple cell receptive fields. Pollen & Ronner (1975) examined the receptive fields of complex cells of the cat by moving a fine slit at the correct orientation across the field; they found a periodic series of peaks in the response-histograms, most having five principal peaks but one cell located near the border of areas 17 to 18 had as many as thirteen. The response-pattern to the moving slit remained the same while velocity was varied, although the magnitudes of the responses showed some dependence. Thus these cells are capable of analysing a spatial pattern of stripes moving across the visual field, independently of its movement, and they could well be responsible for the spatial frequency-analysis examined psychophysically by Campbell and his colleagues. Moreover, if the complex cell received input from simple cells, the receptive field characteristics could be the result of this input.

The spatial frequencies of the individual cells varied from 0.4 to 5.0 cycles per degree, so that a half-period as small as 0.1

degree could be achieved; in general, the periodicity of the receptive field, in cycles per degree, was inversely related to the width of the receptive field, a wide field representing a coarser pattern. As we should expect from earlier studies, simple cells showed no such periodicity in response. Pollen & Ronner projected a slit of varying width symmetrically on the receptive field of a simple cell; the response increased as slit-width increased to about 1°, where it peaked and fell to about zero at 2°; each width of slit could be represented as a spatial-frequency by taking the reciprocal of twice the width, and so a spatial-frequency-response curve comparable with those described by Maffei & Fiorentini (1973) was obtained.[18]

Sustained and Transient Cortical Responses

Ikeda & Wright (1975) compared contrast spatial frequency sensitivity functions of simple and complex cells of cat striate neurones and found no difference, but in both classes there was a difference between 'sustained' and 'transient' units, the former being sharply tuned with a low-frequency cut-off, whereas the transient units had a shallow low-frequency cut-off. There was a difference in temporal frequency tuning, the transient units having the sharper low-frequency cut-off. They concluded that the X- and Y-dichotomy was continued into the striate cortex to give a parallel processing of visual information that was apparently equally shared by simple and complex cortical cells. They noted that sustained units were most common in the central retina. Movshon *et al.* (1978) found, however, that when their electrode penetrations were strictly confined to area 17 to which, in the cat, mainly, if not exclusively, X-cells project, then not only was there no difference in spatial and temporal tuning between simple and complex units, but also there was no 'sustained-transient' dichotomy. When area 18 was penetrated, however, there was a pronounced shift in the spatial and temporal tuning of the units. Moreover, only now did transient units appear, suggesting that Y-cells projected only to area 18, or at any rate were rare in area 17, having regard to the bifurcation of Y-geniculate cells to give branches in both areas. In general, Movshon *et al.* concluded that area 17 in the cat could be a region for pattern-discrimination and area 18 for movement-discrimination. They pointed to human and cat psychophysical studies suggesting the existence of two classes of discriminators (Tolhurst, 1973; Kulikowski & Tolhurst, 1973; Blake & Camisa, 1977).[19]

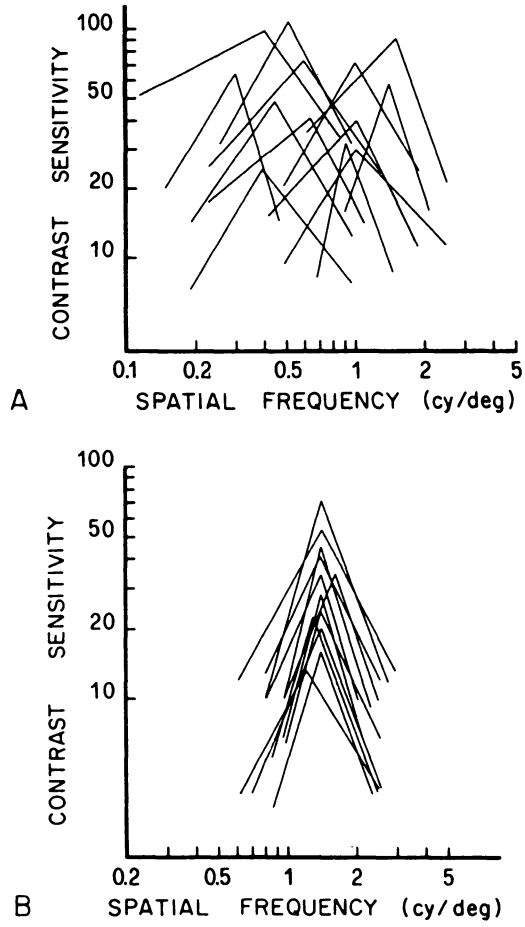

Fig. 21.33 A, contrast sensitivity curves for a sample of 13 out of 27 neurones recorded in a penetration perpendicular to the cortical surface in area 17. All the cells had approximately the same preferred stimulus orientation (vertical). B, contrast sensitivity curves of 12 neurones recorded in a tangential penetration perpendicular to the medial plane in area 17 (layer IV). (Maffei & Fiorentini, *Vision Res.*)

Cortical Columns

It will be recalled that, during a vertical penetration, at right-angles to the surface of the cortex, the preferred orientation of cortical units remains the same within a few degrees, whereas with tangential penetration there are successive changes in preferred orientation. So far as spatial frequency-tuning of cortical cells is concerned, there is an opposite relationship, so that during a depth-penetration Maffei & Fiorentini (1977) found a changing spatial-frequency optimum with different depths (Fig. 21.33A), whereas with a tangential penetration the spatial frequency optima were the same within ±20% over a length of 2 mm (Fig. 21.33B). Thus cells in a column have the same preferred direction; they also have the same area of receptive field so that they 'look' at the same area of visual field. If we assume that the cortex analyses the spatial features of the visual field, we may expect an orientation-column to contain all the tools required for processing visual information contained in the area of visual space the column is 'looking' at. Each column should therefore have cells tuned to a variety of spatial frequencies spread over a sufficiently wide range of frequency spectra, and in fact this was found, a range of about ten-fold, or 1 log-unit, in spatial frequencies being measured in a depth-penetration. Thus the neurones in a column contain all the spatial information necessary to describe any object in a given orientation.

DEOXYGLUCOSE MAPPING

Tootell *et al.* (1981) presented cats with gratings of given spatial frequency repeatedly at all orientations. Labelled

deoxyglucose revealed columns, the distance between them being some 0.8 to 1 mm, about the same for the ocular dominance and orientation columns revealed by the same technique. Control animals exposed to a wide variation of spatial frequencies gave no indication of columnar pattern. High spatial frequencies were represented only within 5° of the area centralis, thus confirming the single-unit studies of Movshon *et al.* (1978).

Velocity Dependence

Tolhurst & Movshon (1975) found that the spatial-frequency tuning of area 17 cells was unaffected by the rapidity with which a grating moved across the receptive field, so that the psychophysically observed enhanced detectability of low spatial frequencies by movement (or temporal modulation) must be explained in terms of the responses of some other type of neurone. In view of Movshon *et al.*'s (1978) report that area 18 neurones exhibited strong sensitivity to movement, Bisti *et al.* (1985) investigated these neurones in greater detail in the cat. They found a shift of the spatial tuning curves as velocity of movement was changed. As Fig. 21.34 shows, there is a shift in the maximum of the response-curve to lower spatial frequencies as the temporal frequency changes, i.e., as the speed of movement of the grating increases. This was in contrast to units in area 17, a difference they attributed to the different subcortical inputs to the two areas. Bisti *et al.* suggested that area 18 tends to supplement the processing of area 17 so far as perception of detail is concerned, taking over analysis of form when motion is sufficiently rapid to prevent the recognition of fine detail, i.e. when resolution of only low spatial frequencies can be attempted. Thus with a rapidly moving object, area 17 neurones cease to respond to its detail and area 18 neurones take over the analysis which is largely to determine where the object is and its gross shape.[20]

Inhibitory Process

Sharp tuning of spatial-frequency units requires the operation of inhibitory processes; to some extent this is achieved in the lateral geniculate nucleus and earlier at the high spatial-frequency range but, as we have seen, there is little selectivity at the low-frequency range so that geniculate cells are often described as low-pass filters. DeValois & Tootell (1983) examined the role of intracortical inhibition by measuring the effects of different spatial-frequency gratings on the responses to a given grating, i.e. they were examining the adaptation-effects of gratings. Thus the cell's response to its optimal spatial-frequency, f, and to combinations with gratings of $\frac{1}{4}$, $\frac{1}{3}$, $\frac{1}{2}$, 2, 3 and $4f$ were measured. 97% of simple cells showed some inhibition of f by one or more of the other frequencies; 34 out of 38 were maximally inhibited by a higher frequency and 3 out of 38 by a lower frequency. Only 38% of the complex cells studied showed inhibition.

Analysis of Space

Cortical tuning for orientation and spatial frequency may be considered to be the basis for analysis of spatial detail, and we may presume that it is the cells with narrowest tuning that become involved in the finest tasks. Since the band-widths of tuning vary greatly, we may assume, either that those with wide bands represent earlier stages in cortical processing, or else fulfil a role in the analysis of coarser detail. So far as foveal and parafoveal differences were concerned, DeValois & Tootell (1983) found very little difference, with the exception that foveal units had the narrowest spatial frequency tuning. An interesting feature of cortical neurone sensitivity is that these are more narrowly tuned to sine-wave than square gratings (Schiller *et al.*, 1976a–e; Albrecht *et al.*, 1980). The broad tuning to square waves, however, follows from the nature of a square wave which can be resolved into a fundamental frequency and its odd harmonics, so that a cell tuned

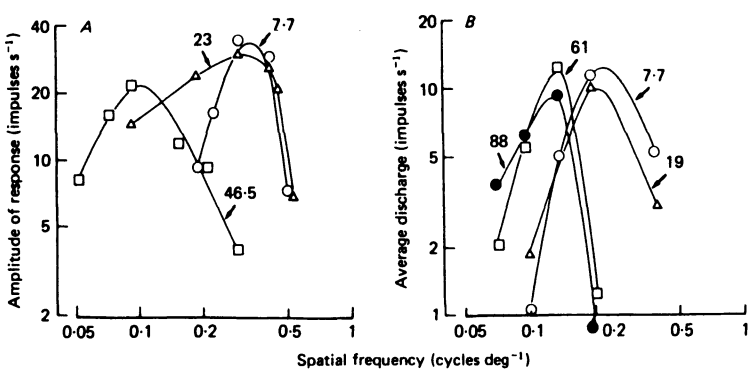

Fig. 21.34 Spatial-frequency tuning curves of a simple-like cell (*A*) and a complex cell (*B*) of area 18. Each curve is obtained with drifting gratings of constant velocity. Numbers in the figure indicate the velocities in deg s^{-1}. *A*, velocity: ○, 7.7 deg s^{-1}; Δ, 23 deg s^{-1}; □, 46.5 deg s^{-1}. Contrast 0.17. *B*, velocity: ○, 7.7 deg s^{-1}; Δ, 19 deg s^{-1}; □, 61 deg s^{-1}; ●, 88 deg s^{-1}. Spontaneous firing rate 0.2 impulses s^{-1}. Contrast 0.4. Mean luminance 7 cd m^{-2}. (Bisti *et al.*, *J. Physiol.*)

to a square-wave pattern of 2c/deg would also respond to higher frequencies, whereas a sine-wave pattern has ideally only a single frequency; if the brain is analysing patterns on a basis of sine-waves, then it is clear that cells must be developed with narrow tuning to sine-waves, since those are the units of its measurement (DeValois *et al.*, 1982).

COLOUR DISCRIMINATION

The responses of individual units in the visual pathway to differences in wavelength of the stimulus have been followed from those of the receptors to those of the ganglion cells. At the earliest stage a single receptor is unable to transmit an unequivocal message as to the wavelength composition of the stimulus because it cannot distinguish changes of intensity from changes in frequency, it being always possible to match a stimulus of one wavelength with a stimulus of another wavelength but different intensity. When the three separate cone mechanisms are integrated, however, as in the ganglion cells, then, over a wide range of light-intensities, a message specific for the wavelength composition of the stimulus is achieved. During and after this development the phenomenon of opponence has appeared, a cell responding positively to one band of wavelength and oppositely to another; this opponence extends to the centre-surround organization of the ganglion cell's receptive field.

Chromatic Features of Lateral Geniculate Neurones

DeValois (1960), working with the monkey, demonstrated the presence of modulator-type neurones in the lateral geniculate body; some showed colour-opponence, in the sense of an inhibition of the ON-response by short wavelengths and an increased discharge at long wavelengths. Some pure OFF-elements were of the dominator type with maximal sensitivities at 510 and 550 nm, presumably corresponding to scotopic and photopic mechanisms. At any rate, Jacobs (1964), studying the squirrel-monkey in which behavioural experiments had given the scotopic and photopic sensitivity curves, found reasonable concordance with the corresponding wavelength-sensitivity curves of dominator units of the lateral geniculate nucleus.

Concentric Stimuli: Spatial Opponences

DeValois used large light-stimuli and so he examined the overall effects of stimulating all the receptors in the receptive field of a given geniculate cell. Wiesel & Hubel (1966) showed that, like the ganglion cell units, the geniculate units were also spatially organized, having opposing centre and periphery effects with white light; when spectral sensitivity was studied a number of types were identified. The Type I unit gave an ON-response at its centre with a limited range of wavelengths whilst the surround gave an OFF-response to the complementary band, e.g. the commonest was a Red ON-centre, Green OFF-surround. These corresponded with DeValois' ON-OFF elements since he illuminated the whole receptive field. At a certain wavelength, the *neutral point*, the opposing effects of centre and surround just balanced; thus at 540 nm a large spot of light had no effect. There were relatively few Blue ON-centre-Green-OFF-surround, and no Blue-Red units. With this Type-I, then, it appears as though the geniculate cell is connected to two types of cone, one of which inhibits and the other excites, or *vice versa*. When the intensity of the light-stimulus was reduced, a Purkinje-shift in sensitivity could be obtained with some Type I units, indicating connections with rods as well as cones.

The Type II units showed no centre-surround organization and consisted of a receptive field of some $\frac{1}{2}$ degree; the responses to different wavelength-bands were opposite in character, e.g. ON to blue and OFF to green, with a neutral point of 500 nm, ON to red and OFF to green with a neutral point of 600 nm, and so on. This type obviously receives input from two populations of cones, one excitatory and the other inhibitory, and the two types are distributed uniformly throughout the $\frac{1}{2}$ degree field. No Purkinje-effect was observed with these.

Type III units revealed no opponent colour effects; they had the centre-surround organization, the periphery usually suppressing the centre, but the responses were similar at all wavelengths. In these the representation of cone types was the same for inhibitory and excitatory areas of the field.

All these types were found in the dorsal layers of the lateral geniculate body; in the ventral layers an additional type was found, Type IV; they were organized on a centre-surround basis and were characterized by the very effective inhibition exerted by the surround.

LUMINOSITY UNITS

Like the ganglion cells with wide spectral sensitivity curves, similar to the luminosity curves of the intact animal, Wiesel and Hubel's Type III units may be classed as luminosity units. However, a much more thorough examination of the responses to different wavelengths under different degrees of chromatic adaptation would be necessary to decide whether there is no opponence in the responses. This point was emphasized by Padmos & Norren (1975) who showed, by selective adaptation, that many geniculate units that would have been classed as non-opponent did, in fact, have some concealed opponence with antagonistic green-red cone interactions, as

revealed by the altered responses when adapted to different wavelength bands. This opponence might have been suspected from the deviation of the spectral sensitivity curve from the mean CIE curve; however, when many such units are averaged the average sensitivity is that of the CIE observer so that, as Padmos & Norren (1975) have argued, it could be that luminosity is not signalled by specific ganglion or geniculate cells, but rather through averaging this type of unit with antagonistic green and red inputs. In a similar way many cells that would have been characterized as having dichromatic input, e.g. Green-ON-Red-OFF by their response patterns on a neutral background could be shown to have a trichromatic input, in conflict with DeValois' generalization that all monkey geniculate cells had only dichromatic input.

Silent Substitution Technique

Derrington *et al.* (1984) defined the chromatic and luminosity characteristics of their stimuli in a systematic and highly precise fashion, representing them as points in three-dimensional space with coordinates representing the contribution of a Blue-mechanism and its opponent Red+Green mechanism, on the one hand, and the luminosity as the third coordinate. Thus all points in an 'isoluminent plane', containing the B- and R+G coordinates, would, if there were linear summation of cone-effects, produce equal responses in a selected geniculate cell, so that substitution of one stimulus for another, confined to this plane, would produce no change in the cell's discharge. The authors compared parvo- and magnocellular responses. They concluded that magnocellular units had chromatically opponent receptive fields in which the antagonistic mechanisms were segregated spatially, so that their results did not support the separation into Type III, spatially but not chromatically opponent, from Type IV, spatially opponent with surround specially sensitive to long wavelengths. Parvocellular neurones, i.e. those in the dorsal four layers, fell into two groups: R−G, receiving opposed inputs from R and G cones; the other, B−(R+G), receiving inputs from blue-sensitive cones opposed by variously weighted red-plus-green sensitive cones. In general, the analysis of cone contributions to the receptive fields suggested no principle by which the cells might be grouped, and it was concluded that only the parvocellular neurones had the chromatic properties for colour vision.

It appeared that cells with Red and Green input could subserve the evaluation of contrast-sensitivity, and therefore act as luminance detectors; they could be doing 'double duty' in detecting both luminance and chromaticity, whilst further analysis of the encoded messages would require activity in cortical neurones. A group of parvocellular neurones, with Blue−(Red+Green) opponence would play an important role in colour discrimination, but their rarity and very low sensitivity to black-and-white gratings would make them useless for accurate spatial discrimination. So far as the role of magnocellular cells is concerned, Derrington *et al.* (1984) emphasize their probable role in movement detection; thus they have very high contrast-sensitivity and sensitivity also to the flicker-type of stimulus (temporal intensity variation) would favour this role. From their site of termination in area 4c they project, via layer 4b to the middle temporal region which contains neurones well suited to analyse motion (Movshon *et al.*, 1984).[21]

Colour-coding of Cortical Units

Early Studies

Motokawa *et al.* (1962) recorded from single neurones in the striate cortex of the monkey; many of these gave simple ON-responses to illumination with maximal responses to one part of the spectrum; the regions of maximum response were 600 to 640, 520 to 540 and 460 nm, i.e. the red, green and blue; others gave opponent type responses, similar to those described by DeValois for the lateral geniculate body, the wavelengths for maximum ON- and OFF-responses being in different regions, e.g. in the red and blue. Some units gave ON-OFF responses to light over the whole range of wavelengths with maximum effect at 500 nm; these were presumably related to rods, but their sensitivity to light was low suggesting an inhibitory activity in the pathway. With other units there was no clear-cut peak over the whole spectrum, whilst with still others there were peaks at the two ends, suggesting connections with two types of cone; as the intensity of the stimulus was reduced the peaks diminished and a new peak at 500 nm emerged, indicating that rods and cones were converging on the same cortical neurone; in the light of the studies on geniculate cells this was to be expected.

Importance of Receptive Field

These pioneering experiments on cortical cells were carried out before the work of Hubel & Wiesel had drawn attention to the special spatial characteristics of the receptive fields of cortical neurones. Thus, in order to excite most of these neurones with white light it is necessary to choose a stimulus of a particular orientation, a particular length, a particular direction of movement, and so on. Hence a thorough examination of the chromatic characteristics of cortical cells would require that first the special spatial and temporal features of the receptive field be determined with white light, and then, having categorized the cell in terms of these—simple, complex, direction-sensitive, and so on—to ascertain the effects of different wavelengths on the responses.

Simple versus Complex Cells

Hubel & Wiesel found that some 6 out of 25 simple cells showed chromatic sensitivity; they responded to long narrow fields with greatest sensitivity to long wavelengths; these fields were flanked by a more inhibitory area with blue-green sensitivity. Thus the cortical cell behaved as though it were connected with a set of Type I Red-ON-centre Green-OFF-surround geniculate cells organized in a linear fashion. Twelve out of 177 complex

cells showed chromatic preference; these could be stimulated by a blue slit orientated in a specific direction; they did not respond to white; other units were similar but favoured longer wavelengths. Since this study, several workers, notably Dow & Gouras (1973), and Poggio *et al.* (1975), have examined the monkey's cortical neurones from this aspect, the monkey possessing good colour vision characteristic of a human trichromat (DeValois & Morgan, 1974) by contrast with the cat on which so many studies of cortical neurones have been carried out.

Monkey Fovea

Dow & Gouras (1973) paid special attention to striate units representing the fovea of the monkey; 34% showed chromatic sensitivity whilst 42% were highly orientation-selective but had little chromatic sensitivity, being driven by all three types of cone so that the action-spectrum had a maximum at about 550 nm.

CO-EXTENSIVE OPPONENT FIELDS

Colour-opponence was manifest in some 24% of the units examined, in the sense that they could be excited by one band of wave-lengths and inhibited by another; however, the opponence was not spatial, as with the centre-surround opponence in geniculate cells, so that the receptive fields for the opponent responses were coextensive.

SPATIAL COLOUR CELLS

Another group, however, combined spatial and chromatic specificities and were described as *spatial colour cells*, in the sense that a slit stimulus, optimally orientated, would produce an ON- or OFF-response according to the wavelength, e.g. Red-ON and Green-OFF. When a very narrow slit was employed pure Red or Green responses could be obtained, suggesting that the opponent response was derived from the flanking region; however, the flanking region was not necessarily sensitive to a different wavelength-band, so that a thin red slit could be inhibited by a flanking red. Double-opponent cells, with centre and flanks each exhibiting opponent responses, analogous with those seen in ganglion cells were not observed. Thus a slit-flank antagonism, involving the same wavelength-band, seems to be a new feature emerging in the cortex.[22]

Luminosity Units

Poggio *et al.* (1975), in their study of the monkey, considered that the cortical units showing unselective chromatic behaviour were luminosity-units analogous with the dominators of Granit; they constituted nearly half the units isolated and presumably received inputs from all three types of cone, to give an action-spectrum equivalent to the photopic luminosity function with a maximum in the yellow-green.

Colour-tuned Units

Units exhibiting some chromatic selectivity, Poggio *et al.* described as colour-tuned; Fig. 21.35 shows action-spectra for a luminosity unit, a blue-green tuned unit and a red-tuned unit.

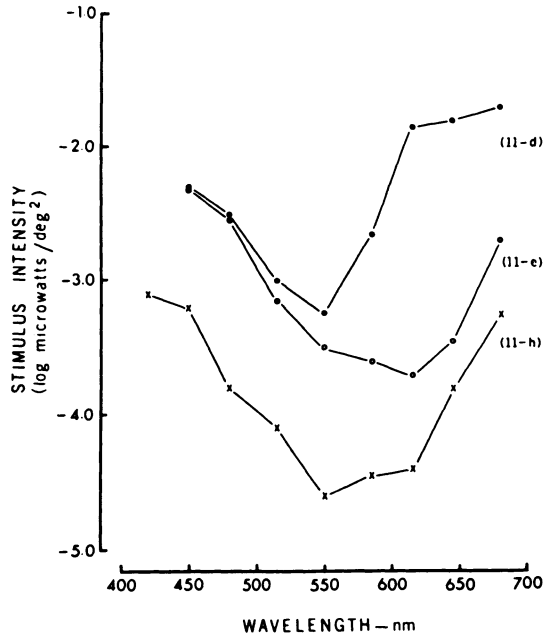

Fig. 21.35 Action spectra for a luminosity-unit (11-h), a blue-green tuned unit (11-d) and a red tuned unit (11-e) in the monkey's visual cortex. (Poggio *et al.*, *Brain Res.*)

Colour-opponent Units

Other units exhibited colour-opponence, the nature of this depending on the shape of the receptive fields. If these were uniform, a short wavelength stimulus could evoke, say, an ON-response, and a long-wavelength stimulus an OFF-response; middle wavelengths were either ineffective or evoked ON–OFF responses at high intensities. Units with bipartite fields, e.g. a slit with flanking surrounds, or concentric centre-surround, had opponent responses from centre and surround, e.g. a centre response to blue-green and a surround response to red. Some of these were double-opponent, so that the centre might be Red-ON-Green-OFF and the surround Red-OFF-Green-ON.

Continuum of Types

Poggio *et al.* considered that their tuned units might well be the same as some of the opponent units described by Dow & Gouras, the tuned units representing the interaction of two systems, one of which did not manifest its action directly, either due to its intrinsic weakness or to its inhibition by an opponent system. Thus the two categories of tuned and opponent neurones could cover the continuum of spectrally selective properties from evident and unbalanced opponence, through opponence with one system dominant, to tuned.

Stages in Chromatic Processing

The studies so far alluded to have been principally on units of area 17 that could be described as simple cells. Michael (1978a, b, c; 1979) has examined the chromatic sensitivities of cortical neurones that he considers to be successive stages in processing of visual information, namely cortical neurones with concentric receptive fields, simple, complex and hypercomplex neurones, all of these being located in the monkey's striate cortex.

CELLS WITH CONCENTRIC FIELDS

These units, presumably representing the first relay with geniculate neurones, were always located in lamina 4 and were monocularly driven. They were dual-opponent of the Red-Green type, e.g. Red-ON-Green-OFF Centre/Green-ON-Red-OFF surround, or the reverse arrangement. No Blue-Yellow combinations were seen. Figure 21.36 illustrates the spectral sensitivity of a Red-ON-Green-OFF centre unit with peaks at 500 nm and 600–620 nm for ON- and OFF- respectively. The cross-over, or neutral, point occurred at 540 nm so that at this wavelength excitation was balanced by inhibition.

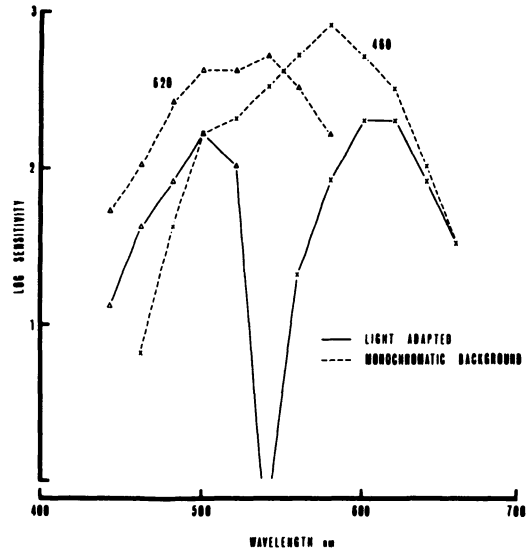

Fig. 21.36 Spectral sensitivity of a Red-ON and Green-OFF centre cell of monkey striate cortex. Crosses designate ON-responses; triangles, OFF-responses. At the cross-over point of about 540 nm excitation was balanced by inhibition and there was no response. Dashed curves represent sensitivity after adaptation to 620 or 460 nm monochromatic spots on the centre. During each chromatic adaptation, a single receptor-process controlled the centre response. (Michael, *J. Neurophysiol.*)

Geniculate Fibre and Cortical Cell Responses Sometimes simultaneous responses from the afferent fibre and cortical neurone could be recorded. The fibre and cell centre always had the same opponent colour properties and the same spectral sensitivity. Thus Michael never saw a Red-ON-Green-OFF fibre associated with a Green-ON-Red-OFF centre cortical cell. A second type of relationship was found in which both fields were concentrically organized and coincided. The fibre could be ON-centre-OFF-surround or the reverse, and it was activated by only one type of cone, so that there was no chromatic opponence. Fibre and neurone never received from opposite types, so that a combination of Green-OFF-centre fibres plus Red-OFF-centre-Green-ON centre cell was not possible. Figure 21.37 is an example; the cortical cell is described as $\left.\begin{matrix}\text{Green-OFF}\\ \text{Red-ON}\end{matrix}\right\}$-centre and $\left.\begin{matrix}\text{Red-OFF}\\ \text{Green-ON}\end{matrix}\right\}$-surround, whilst the fibre is Green OFF-centre-Green-OFF-surround. A green spot on the centre elicted an OFF-response from both; a red spot on the centre elicited an OFF-response from the fibre but an ON-response from the cortical cell. A green annulus had the same effect on both whilst a red annulus had opposite effects. A diffuse monochromatic light had no effect on the cortical cell but produced an OFF-effect on the geniculate fibre. Spectral sensitivities of the fibre and the concentric cortical cell indicated that the cell was activated by two types of cone whilst the fibre probably by only one.

LAMINAR DISTRIBUTION

Most of the concentrically organized cortical cells were in lamina 4C with fewer in laminae 3 and 5. There were none in laminae 1, 2 and 6.

SIMPLE CELLS

Michael (1978b) recorded from chromatically sensitive simple cortical units with linearly organized receptive fields that were insensitive to white light. Usually the field consisted of a central oblong or rectangular strip with one Red-Green opponent colour system (e.g. Red-ON-Green-OFF) and two antagonistic flanks with the reverse opponent arrangement. An example is illustrated in Fig. 21.38 which shows the responses to simple bars of monochromatic light flashed on or off the centre and flanks. The field consists of a Red-ON-Green-OFF central band

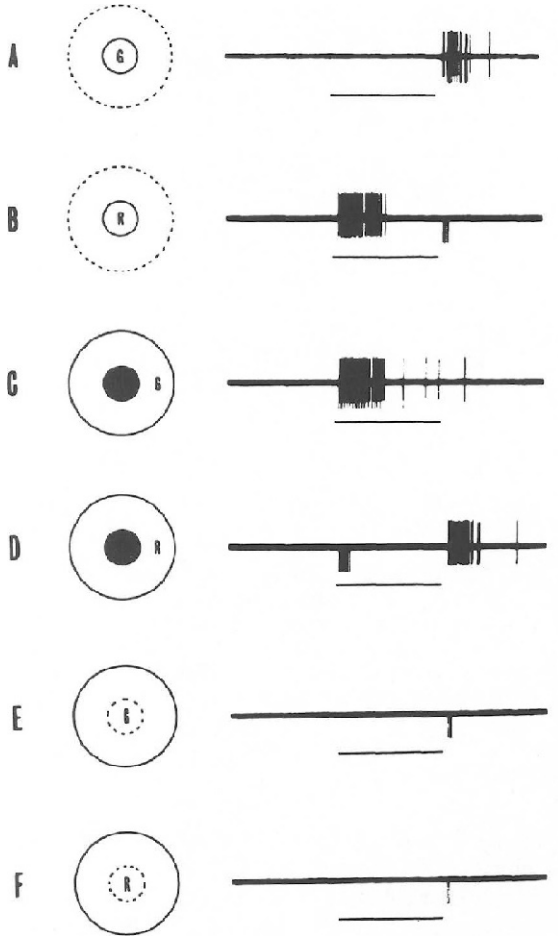

Fig. 21.37 Simultaneous recordings from a concentric cortical cell (left-hand group of spikes) and a geniculate fibre. The receptive field of the cell was Green-OFF, Red-ON (centre) with the reverse surround. The fibre was Green-OFF (centre), Green-OFF (surround). Both neurones gave OFF-responses to a centred green spot (A). The cell responded with an ON-discharge to a Red spot while the fibre again gave an OFF-response (B). Green annuli had the same ON-effect for both units (C), but red annuli had reverse influences on them (D). Large spots produced OFF-responses from the fibre but did not activate the cortical cell (E, F). (Michael, *J. Neurophysiol.*)

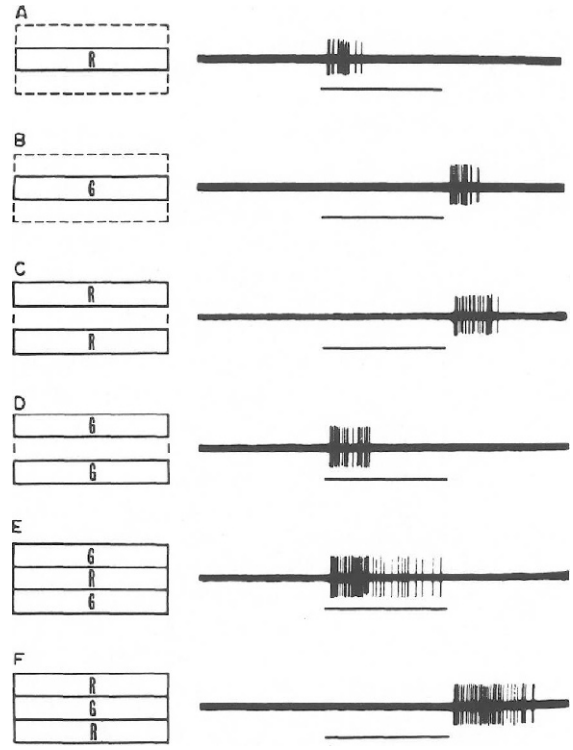

Fig. 21.38 Responses of a light-adapted simple cell to monochromatic bars of light. The central band was 0.5° wide and 3° long, the overall receptive field was 1.5° wide. The stimulus bars were 0.5° wide and 3° long; they were orientated horizontally along the receptive-field axis of the cell (9:00–3:00 o'clock). A: a red bar covering the central strip produced an on-discharge. B: a green bar, an off-discharge. C: two red bars covering the antagonistic flanks evoked an off-response. D: two green bars, an on-response. E: a red bar flanked by two green ones elicited a strong, maintained on-response. F: a green bar flanked by two red ones, a vigorous off-discharge. The 1 sec stimulus duration is indicated by the black bar below each oscilloscope trace. (Michael, *J. Neurophysiol.*)

with opposite type of flanks; the unit is a double-opponent cell, and because of this spatial arrangement it is most sensitive to the simultaneous presentation of two different colours, one falling in the central strip and the other on the flanks. Thus a maintained ON-discharge was obtained by a central red bar flanked by two green ones (Fig. 21.38E) while a green bar between two red ones evoked a very strong OFF-discharge (Fig. 21.38F).

White Light These cells never responded to diffuse light of any wavelength, nor to white light since diffuse colours simultaneously stimulated an ON-region in one part of the field and an OFF-region in another whilst white light stimulates the antagonistic chromatic mechanisms at any point in the field.

Spectral Sensitivities of ON- and OFF-Responses Spectral sensitivities for the ON- and OFF-responses of the Red-ON-Green-OFF central field exhibited maxima at about 620 and 480 nm for the ON- and OFF-responses respectively; the cross-over point was at 540 nm, and light of this wavelength failed to have a response.

Orientation Selectivity Dow & Gouras (1973) observed that in simple cells that responded to narrow

wavelength-bands their orientation-selectivity was independent of the wavelength of light, so that the spatial inhibition responsible for this orientation-specificity must involve interactions between units with a common cone mechanism. Michael found a similar independence.

Afferent Input Frequently Michael was able to record simultaneously from two units that were clearly related, in the sense that the simple cell received input from the other cell which was often a concentrically organized cortical cell. In these cases the concentric field's centre was always in register with the simple cell's central strip and never overlapped into the antagonistic flanks, whilst both centre and strip had the same colour-opponence and the same spectral sensitivities.

Ocular Dominance The concentrically organized cortical cells described earlier were all driven by one eye only; of the simple cells exhibiting chromatic opponence the great majority were likewise driven by one eye only, more being driven by the contralateral eye (73 versus 58 units). In all cases of multiple recordings from a simple plus concentric cell, the simple cell was driven by only one eye, and that, of course, was the same as that driving the concentric unit.

Laminar Distribution The simple cells were located almost exactly as the concentric cells with the great majority in laminae 4A and 4C.

Model Michael suggested a model for input from a row of concentrically organized double-opponent cortical cells on to a single simple cell in a manner similar to that proposed by Hubel and Wiesel to account for the spatial features of the simple cell as derived from the geniculate cell.

COMPLEX CELLS

Pursuing his study of the sequential processing of chromatic information in the cortex, Michael identified complex cells with rectangular or square receptive fields that could not be mapped out by stationary stimuli, and did not have antagonistic subdivisions; they responded only to moving monochromatic bars or edges of the proper orientation and width; the length was not critical. They did not respond to a white bar. When different wavelengths of stimulus, equated to equal luminosity, were employed, different spectral sensitivity curves were obtained amongst different cells; Fig. 21.39 is an example; in the light-adapted state the response is restricted to short wavelengths with a maximum of about 500 nm; however, if the retina is previously adapted to a red light, the spectral sensitivity-curve shifts into longer wavelengths and becomes similar to that of the monkey's green-sensitive cone. Thus the complex cell's response is

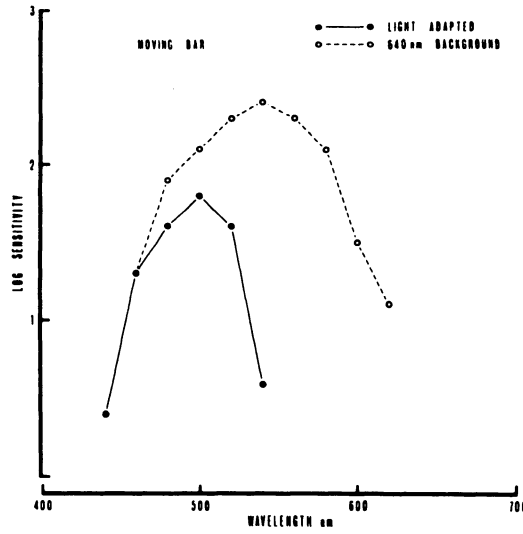

Fig. 21.39 Spectral sensitivity curves for colour-sensitive complex cell in white-light adapted condition (full lines) and after adaptation to monochromatic 640 nm light (dashed lines). Peak sensitivity is at 500 nm which changed to 540 nm after adaptation to orange (640 nm) light, i.e. it has the sensitivity of the monkey's green-sensitive cone. (Michael, *J. Neurophysiol.*)

apparently subject to inhibition by red-sensitive cones, an inhibition that is removed by prior adaptation of the retina to red light. In general, the peak-sensitivities of complex units varied from 490 to 640 nm, with two populations centred on 500 and 600 nm respectively. The effects of dark-adaptation indicated that rods were not involved in these responses; and this was true of the simple and concentric units studied earlier.

Colour-contrast Some units showed a striking sensitivity to a two-colour edge, e.g. red adjacent to green; a single coloured edge failed to excite. The unit is clearly sensitive to colour-contrast, as such, and is presumably involved in the perception of simultaneous contrast.

Model A synaptic model based on the convergence of several double-opponent simple cortical cells was suggested; if correct this would represent the third stage of cortical processing of the geniculate input.

Laminar Distribution Very few complex cells were encountered in lamina 4, the great majority being found in laminae 2, 3, 5 and 6; although cells in laminae 2 and 3 project to areas 18 and 19; in lamina 5 to the colliculus, and in lamina 6 to the lateral geniculate nucleus, no obvious distinctions in type of receptive field were observed between cells in different laminae.

HYPERCOMPLEX CELLS

These cells were specifically excited by an orientated monochromatic bar or edge; their receptive fields were end-stopped and consisted of a central excitatory region flanked by inhibitory regions; these regions all had the same spectral sensitivities for a given cell; and the effects of adaptation to chromatic stimuli indicated that they were activated by both red and green cones; there was no evidence for blue cone activity. Once again the orientation-selectivity was a result of antagonism between cones with the same spectral properties rather than through colour-opponent mechanisms.

Comparison with Complex Cells Multiple unit recordings involving simultaneous recordings from complex and hypercomplex cells showed that the complex unit's field was always in register with either the activating area or one of the antagonistic flanks of the hypercomplex cell's field. Both units had the same axis orientation, directional sensitivity, and spectral sensitivity. Most of the colour-sensitive hypercomplex cells were driven by both eyes, with the majority falling in Category 4, being equally influenced by either eye. The dominance-distribution was, in effect, similar to that of complex cells; and when recordings were made from both complex and hypercomplex cell simultaneously, the two almost always belonged to the same dominance category. Once again the major concentrations of these cells were in the superficial and deep laminae.

Synaptic Model A synaptic model based on the input of groups of three separate complex cells, or groups of complex cells, to the three separate areas of the hypercomplex receptive field was put forward, one complex cell being excitatory to the central part of the hypercomplex field and the other two inhibitory to the flanks.

COLUMNAR ORGANIZATION

Several authors described a clustering of colour-selective units in the cortex, but it remained for Michael (1981) to demonstrate a truly columnar organization of colour units, defined by his criterion that they should be irresponsive to white but responsive to monochromatic light. An example of a penetration nearly at right-angles to the cortical surface, giving rise to recordings from successive colour-coded units is shown in Fig. 21.40. Complex (CX), hypercomplex (H) and simple (S) cells occur as well as units with concentric centre-surround organization (circles). Preferred orientations are indicated by the lines and dominance by the type of line. All these cells responded exclusively to coloured stimuli; the two simple cells and the three concentric neurones were double opponent, the field centres being Red-ON-Green-OFF. The remaining cells had single spectral sensitivity curves peaking at about 610 nm, with shapes very similar to those of the red

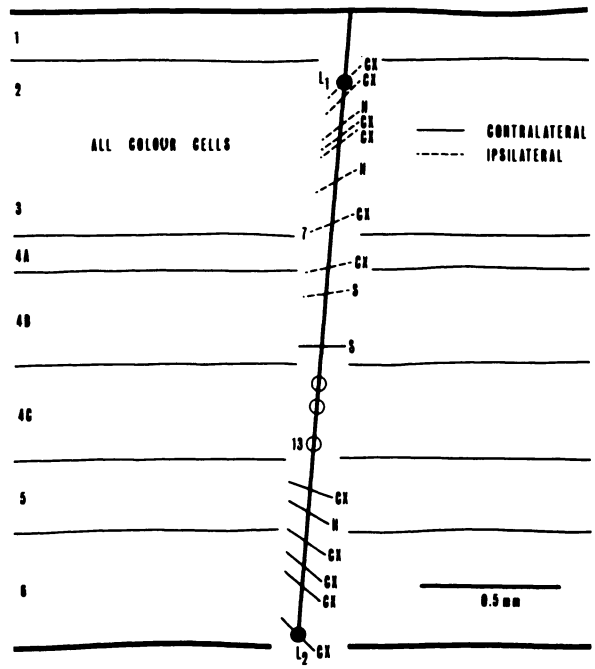

Fig. 21.40 Illustrating colour column in monkey's striate cortex. Reconstruction of a microelectrode penetration made in the right striate cortex. The electrode's path was close to perpendicular and passed through all of the layers. Positions of the 19 units encountered along the penetration are indicated by circles or short lines intersecting the electrode track. Circles represent concentric cells; the other three cell types are indicated by letters to the right of the short lines (S, simple; CX, complex; H, hypercomplex). The angle of each short line represents the axis orientation of each cell's receptive field. Two small lesions (ca. 50–75 μm; L_1, L_2) were made in the penetration: one at the site of the first cell studied and one at the site of the last unit in the track. All 19 units were responsive only to colour stimuli; the electrode stayed within a single colour column throughout its entire path. The axis orientations of the successively studied cells rotated clockwise in an orderly fashion from 45 to 135°. The first nine cells were in an ipsilaterally dominated eye-preference column, while the remainder were controlled by the contralateral eye. Scale, 0.5 mm. (Michael, *J. Neurophysiol.*)

component of the concentric and simple cells. So far as orientation-selectivity and dominance were cocerned, it is clear that this penetration crossed numerous orientation columns and two dominance columns, but stayed within a single colour column throughout its length. With other penetrations, the units could be confined to a single dominance, and varying orientation, or, in some cases, to a single dominance and orientation indicating coincidence of the three types of column. Oblique and horizontal penetrations gave evidence for the random arrangement of colour columns, or slabs, in relation to the dominance and orientation columns. In one case an oblique penetration was made in which all the units were

colour coded, the electrode having passed along a path that was parallel to the straight walls of this particular colour slab. The penetration passed through innumerable orientation columns and eight dominance columns. The view that the concentric, simple, complex and hypercomplex colour cells are related synaptically, developed in Michael's earlier papers, receives strong support from the columnar organization described here, since in a column the simple, complex and hypercomplex units show similar spectral characteristics. Thus, within a column, the simple and concentric cells always had the same double opponent-colour organization; the complex and hypercomplex cells always had single spectral sensitivity curves which peaked at about the same wavelength as that of the ON-component of the concentric and simple field-centres.[23]

Cytochrome Oxidase Activity

We have seen that groups of neurones sharing a common feature may be revealed by their cytochrome oxidase activity, revealed by an appropriate staining technique. In this way Horton & Hubel (1981) and Humphrey & Hendrickson (1983) described 'blobs', appearing most conspicuously in layers 2 and 3. The cells within the blobs, although quite unselective regarding orientation of a line-stimulus, did exhibit colour-selectivity, however (Livingstone & Hubel, 1984). The cells included those with broad-band responses, responding vigorously to all wavelengths but maximally to a given range; the most common was the double opponent unit, having a central portion of the receptive field excited by, say, red, and inhibited by green, whilst the surround had the opposite pair of colour preferences. In general, the double opponent inputs were equally matched, so that a white stimulus produced little or no response.

Colour-contrast Responses

Gouras & Krüger (1979) commented on the infrequency with which units in the striate cortex with chromatic sensitivity were encountered, and suggested that an important feature was the cell's responsiveness to colour-contrast, which might be obscured by the existing luminance-contrast. A stimulator designed to project colour-contrasts, keeping luminance-contrast zero, was employed, and with this many units with receptive fields in the monkey's fovea were found at the junction between areas 17 and 18. Thus a unit may be found that responds to luminance-contrast, the response diminishing with decreasing contrast until a null-point is reached with no response; the responsiveness is now restored by introducing chromatic contrast. These cells that can discriminate luminance from chromatic contrast might be ultimately important in making colour-vision independent of luminance.

Laminar Segregation

Michael (1985) made horizontal penetrations into monkey striate cortex, endeavouring to confine the electrode-track to one or more sublaminae of layer 4. Thus layers 4A and $4C_\beta$ both receive parvocellular input; cells in layer $4C_\alpha$ receive input from the magnocellular layers and, in turn, project to layer 4B. It is of interest, therefore, to determine the chromatic features of neurones in the different sublaminae. When a penetration ran through all the subdivisions of layer 4, some nine concentric units were first encountered in lamina 4A, occurring in two clusters of double-opponent colour-coded units. On passing through 4B, there was no colour-coding, the units being orientation-selective with complex or simple receptive fields. Cells in the next sublamina, $4C_\alpha$, were all broad-band, being neither double opponent nor colour-selective. In the last part of the track, $4C_\beta$, colour-coding was renewed, the receptive fields being mainly concentric. The results were consistent with the strong parvocellular input to 4A and $4C_\beta$, and the exclusive innervation of $4C_\alpha$ by magnocellular fibres (Hubel & Wiesel, 1972; Blasdel & Lund, 1983). Thus the magnocellular geniculate layer contains mainly broad-band units, and the parvocellular units are predominantly colour-opponent (Wiesel & Hubel, 1966; Schiller & Malpeli, 1978). When an electrode-track was confined almost entirely to sublamina $4C_\beta$, twenty-eight out of thirty-four cells had concentric fields and no orientation-selectivity; five clusters of cells had colour-opponence, those in a given cluster sharing the common response-sign and spectral properties, e.g., in one cluster the cells were Red-ON-Green-OFF centre, with their surrounds of the opposite character. The next cluster had the opposite organization. Parvocellular neurones project to 4A as well as $4C_\beta$, and it is interesting that an electrode track along 4A gave clusters of units similar to those of $4C_\beta$. A tract confined to $4C_\alpha$, to which magnocellular geniculate cells project, exhibited two layers of cell-type, but none had significant colour coding, all being described as broad-band. Predominantly simple cells were at the top and concentric at the bottom. The transition from $4C_\alpha$ to $4C_\beta$ was striking, the units of $4C_\alpha$ being essentially Y-type neurones with transient responses and large contrast-sensitivity and receptive fields with no colour coding, and those of $4C_\beta$ being essentially X-type cells with small fields and colour-coding. Figure 21.41 illustrates penetrations confined to layers 2 and 3, 5 and 6 and $4C_\beta$; the comparison illustrates strikingly the predominance of concentric fields in the C-lamina of layer 4, and the predominance of complex and hypercomplex units in the layers above and below, colour-coding being frequent in all three penetrations.

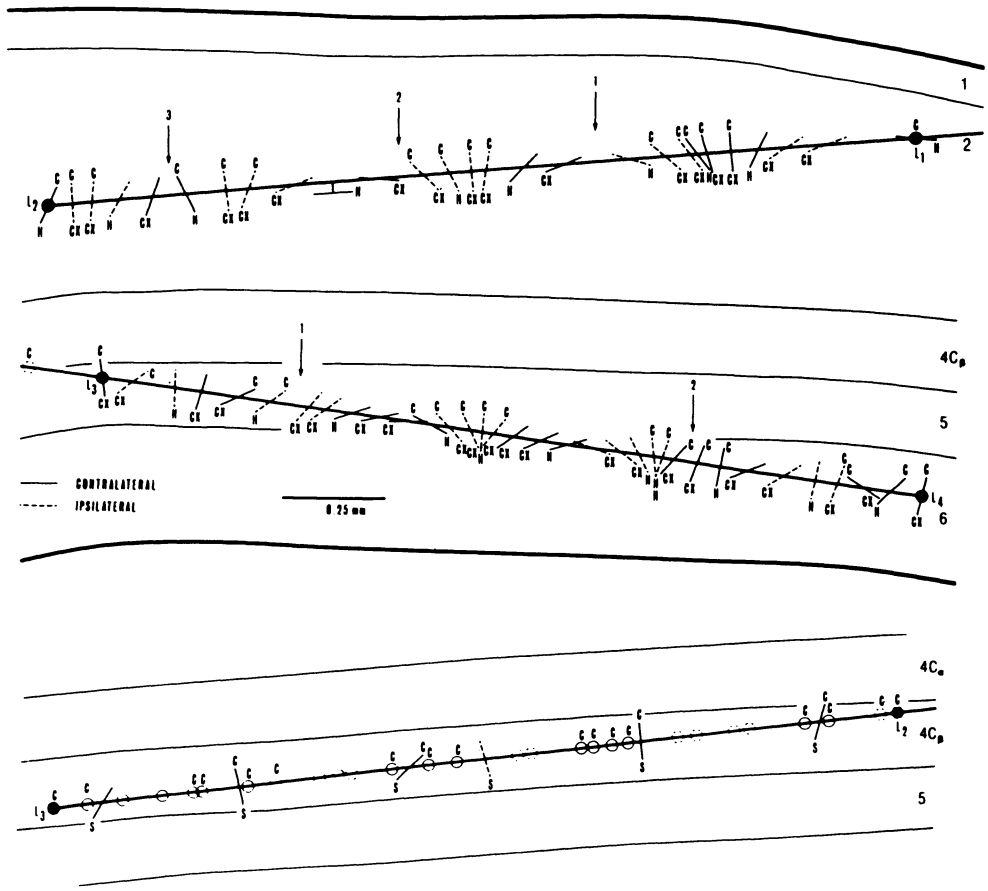

Fig. 21.41 Oblique electrode tracks through the visual cortex. Receptive field orientation of each cell is indicated by a short line. Cells dominated by contralateral eye, solid lines; ipsilateral eye interrupted lines. CX = complex cell; H = hypercomplex cell. The letter C denotes that the cell did not respond to white light in any form, that it was excited only by monochromatic light and that it had a relatively narrow spectral sensitivity. Cell given no label always responded to white light; they were also excited by monochromatic light but less strongly; they had relatively broad spectral sensitivities. Concentric cells are indicated by circles. (Michael, *Vision Res.*)

Prestriate Cortex

VISUAL 4

Zeki (1973) noticed, with penetrations into the monkey's prestriate cortex, that when his electrode passed across the lunate sulcus from V2 to V4, the neurones encountered were predominantly colour-coded, by contrast with the neurones in V2, which were predominantly orientation-selective binocularly driven cells without any colour preference. This area was characterized as V4 on anatomical grounds (Zeki, 1971) lying on the anterior bank of the lunate sulcus dorsally and, because of the complicated gyral changes, emerging ventrally in the posterior bank of the inferior occipital sulcus. All 77 units responded to coloured stimuli, vigorously to one wavelength and grudgingly to another, or not at all. They were arranged in columns with receptive fields varying from the complex to the hypercomplex type with colour as an additional requirement for excitation. Some could be described as successive contrast units, responding maximally when the receptive field was flooded with light of one wavelength and changed to light of another wavelength. Since no colour-specific units had been described in areas 18 and 19 (V2 and V3) Zeki presumed that the input to V4 was from the striate area (V1).

Limits of V4 In a later study (Zeki, 1977) the region of prestriate cortex exhibiting heavy concentrations of colour-coded cells was defined more accurately, a region that turned out not to be homogeneous but being subdivided into separate anatomical and functional zones. As Fig. 21.42 shows, the region extends to the posterior bank of the superior temporal sulcus up to the region described as the 'movement area'. Thus, according to Zeki, no colour-coded cells were encountered in his 'movement area' of STS (p. 542), and only 13/500 cells in

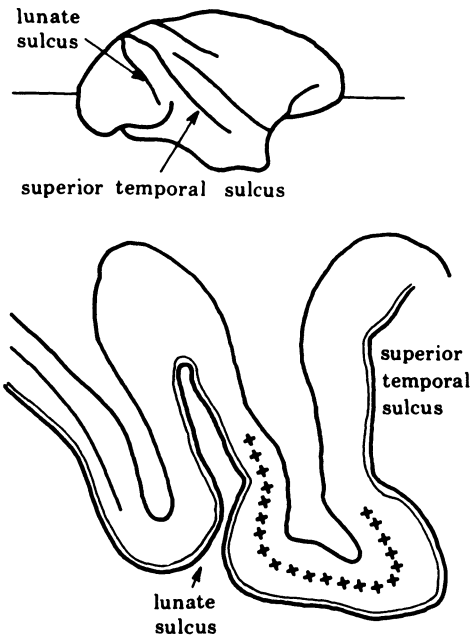

Fig. 21.42 Tracing of a horizontal section through the brain of the rhesus monkey, at the level indicated in *A*. Only the posterior and lateral part of the section is shown in *B*, to indicate the position of the cortex of the posterior bank of the superior temporal sulcus relative to areas 17, 18 and 19 as these have been determined anatomically for regions of central visual field representation in the rhesus monkey. ET = electrode track; LS = lunate sulcus; IOS = inferior occipital sulcus; STS = superior temporal sulcus; PG = prelunate gyrus. (Zeki, *J. Physiol.*)

V3 were colour-coded; in area 18 (V2) only some 8 per cent of cells were colour-coded. Thus colour processing seems to be a special feature of this area. An important feature of the cells described by Zeki in this region of prestriate cortex is the sharpness of colour-tuning. As to whether the area V4, as originally defined lying on the anterior bank of the lunate sulcus and extending on to the prelunate sulcus, is separate from the region extending on to the bank of the superior temporal sulcus, as illustrated in Fig. 21.42, it is not easy to say (Zeki, 1977).

Afferent Projection An important point is that the projection from the striate cortex to this visual area is from regions of high concentration of colour-coded units, notably the region of foveal representation, which receives purely cone input; however, V2, containing some colour-coded units, also projects to V4 as well as the pulvinar, and the final features of the V4 units are doubtless compounded of these several inputs.

V4 as Chromatic Processing Centre

Doubt has been expressed as to the description of V4 as a chromatic processing centre. Thus Schein *et al.* (1982) in work designed to define the spectral characteristics of V4 cells were surprised to find that colour-selective cells, with either colour-biased or colour opponent properties constituted only some 20% of units encountered, no greater than in a corresponding foveal region in V2. Most of these colour-selective cells were biased towards wavelengths longer than 580 nm, i.e. to red, or shorter than 460 nm, i.e. to blue and violet; green-biased units were not found. One fourth of V4 cells could not be stimulated visually and presumably responded to extraretinal signals. In general it was difficult to find a characteristic of V4 cells that suggested a specific processing of visual input. Again, Desimone *et al.* (1985) concluded from their studies on 200 V4 cells that they were by no means sharply tuned to wavelength, responding well to white light, and exhibiting no colour opponence; they behaved, essentially, like a white-sensitive cell stimulated by white light passing through coloured glass. As the authors point out, such colour-filter cells may or may not be classified as colour-selective, according to the criteria used to define colour selectivity, and may account for differences in claims regarding colour selectivity in this cortical region. As they emphasize, whatever their spectral features, the cells are also spatially selective.

Spectral Bandwidths

De Monasterio & Schein (1982) have used the half bandwidth as a measure of tuning of colour-opponent ganglion cells. They have compared these with those in lateral geniculate and cortical neurones, and have concluded that 'the retinal spectral information is preserved as centrally as the striate cortex without significant tuning of information'. Examination of Zeki's (1980a) report of spectral bandwidths for V4 cells led them to conclude that the probable half-bandwidths of these cells, averaging about 23 nm, were not significantly narrower than that of cells at lower stages in the pathway.

Clustering of Peak Sensitivities

Zeki (1980a) found that wavelengths of peak sensitivity for the opponent receptive fields of colour-coded cells fell into three clusters, peaking apparently at the loci of the pure hues, red, green and blue. This claim is disputed by De Monasterio & Schein (1982), however, thereby reinforcing their view that colour-tuning at higher stages in the visual pathway is little different from that in the retina, so that the final awareness of colour depends ultimately on a simple integration of messages elaborated in the retina.

Colour Constancy

By this term we mean the tendency for an observer of coloured objects to continue to recognize their colours in the face of varying composition of the light reflected from their surfaces. Thus a red letter box is said to appear red when illuminated by light from which the red has been filtered. Essentially, because of the specific reflectance of the red object, the light reflected off it, and from objects surrounding it, stimulates the retinal receptors, i.e. red, green- and blue-sensitive cones, in such a manner that only a red object would excite the sensation of red, and this is in spite of the paucity of red light reflected from the object. The retina and higher pathways are thus integrating, not only the effects of the reflected light off the coloured object but also that reflected from its surrounds. In deciding that the object is red it is stating that a green object, submitted to the greenish light that falls on it and its surrounds, would not excite the retinal cones similarly to the red object, also reflecting green light; and therefore the integrated response would not be that of a green object. By the same process other possible colours of the red object are excluded, and it appears that the only interpretation of the spectral composition of the light reflected from the object and the surrounds is that the object is red. Zeki (1980a) has described colour-coded non-opponent units in V4, which reveal this power of taking note of the composition of the total light falling in the receptive field in determining the response to a given hue. Thus a red-sensitive neurone, when exposed to a red matte paper illuminated by a mixture of red, blue, and green lights, was excited strongly, although, when the patch was illuminated by red light alone, the response was negligible.

Notes

1. Nikara *et al.* (1968) have made comparable studies in the cat, studying the vertical and horizontal disparities between receptive fields of binocularly represented units of area 17. The disparities were in the range of $\pm 1.2°$ in both horizontal and vertical directions. The significance of vertical disparity is that it permits single vision of points when the directions of regard of the two eyes are in error due to random movements of the fixation axes in relation to each other.
2. The technique has been described in detail by Ferster (1981), and the interested reader is referred to his paper. The important feature is that the measurements of altered disparity are accurately assessed by ensuring that the eyes are in the same relative positions during the measurement.
3. Ohzawa & Freeman (1986) have examined binocular interaction in cortical cells using less highly specific criteria for interaction as stereoscopic acuity, and so on. They simply assessed the degree to which inputs from the two eyes could interact when the stimuli were presented dichoptically, i.e. separately to the two eyes. Thus gratings were presented to the two eyes, drifting over the receptive fields of a cortical neurone at different phases, and they found that the binocular response could be greater, or less than the monocular responses according to the phase-discrepancy. They concluded that a linear summation of the responses of each eye would account for interaction, dominance being unimportant.
4. The authors point out some differences between Cynader & Regan's neurones, said to be sensitive to motion in depth, and their own; the choice of target-motion may have been the cause.
5. Blakemore *et al.* (1983) wonder why callosal connections are necessary; thus in the cat the partial decussation is far from complete, each optic tract containing input from the part of the ipsilateral hemifield close to the vertical meridian, mainly contributed by ganglion cells in the temporal retina that join in the decussation. Leicester (1968) has shown that sectioning the corpus callosum does not lead to the receptive fields of cortical cells being confined precisely to the contralateral hemifield.
6. Payne *et al.* (1984) quote several studies showing that callosal neurones are rather ineffective excitants of the neurones with which they synapse, producing synaptic potentials that often do not lead to firing. Elberger & Smith (1985) discuss the contradiction between their results and those of Payne and others. They suggest that their effects were those of a non-specific post-surgical depression of activity due to failure to allow sufficient time for recovery from surgery.
7. Van Essen & Maunsell (1983) have objected to the polarity in reasoning with regard to hierarchical and parallel processing, whereby some argue for an exclusively hierarchical and others an exclusively parallel processing. Clearly both processes occur, both within any cortical region, as in vertical columns, and from one region to another.
8. Pollen *et al.* (1984) found no such neurones in the posterior inferotemporal area of the New World owl-monkey. They showed that the preferred spatial frequency (0.2 to 0.6 c/deg) was the same throughout the large receptive field, suggesting input from a single cortical neurone tuned to this frequency.
9. The authors suggest that the region in the fundus of the inferior temporal sulcus studied by them is the same as Bruce *et al.*'s (1981) polysensory area; however, the cells described by them were not polysensory but purely visual. They suggest that the failure to react to faces in the Kluver-Bucy syndrome is due to destruction of the amygdala, which receives face-responses from the temporal cortex.
10. Zeki (1980b), in his description of neurones in the occipito-parietal region of the owl-monkey, a region lying dorsolaterally in the occipito-parietal area at the posterior end of the superior temporal sulcus, described by Allman & Kaas (1971), has questioned the equivalence of this area, containing direction-specific neurones, with the V5 area of the macaque, stating that the differences between neurones in the two areas were as great as the similarities.
11. Baker & Cynader (1986) have made a similar study of directional sensitivity in simple and complex units of the striate cortex, working, however, with only two flashes separated by a variable distance, and determining the optimal distance, D_{opt}, that gave the maximal directional response, in the sense that responses in the preferred and null

directions were maximally distinct. These measurements were related to the spatial features of the receptive field, as measured by responses to flashed lines of varying separation presented simultaneously. In this way they deduced a wavelength for the separation of subunits in the receptive field, a wavelength that might be related to D_{opt}. It was found that the ratio of D_{opt} to the wavelength was 1/10 to 1/4, agreeing with theoretical predictions (Marr & Poggio, (1979).

12. The inferior temporal (IT) visual area projects to STP, but the receptive-field properties of the two areas are so different that it is unlikely that STP processes information from IT; since IT neurones cease to respond to visual stimuli after loss of the striate area (Rocha-Miranda *et al.*, 1975), it is unlikely to provide the residual vision. However, the form-selectivity, so prominent in STP, could be due to projection from IT. We may refer the reader to an excellent discussion of the effects of cortical lesons on residual visual behaviour in the Discussion of Bruce *et al.*'s paper.
13. The contrast-sensitivity is a measure of the ability of the cell to respond to a grating-stimulus; thus, in general terms, a higher contrast is required to discriminate high-spatial frequency stimuli, i.e. fine gratings, than for lower spatial frequencies, i.e. coarse gratings. The resolving power of a ganglion cell will be given by extrapolating the contrast-sensitivity curve to the highest spatial frequency. In general, we may expect a cell with high contrast-sensitivity to have a high resolving power, but the two cannot be equated, so that it is quite possible to have two units with the same average contrast-sensitivities but strongly differing spatial resolving powers.
14. Tolhurst (1975a) has analysed the reaction-times to different grating-frequencies and shown that they can be accounted for on the basis of probability summation. So far as gratings are concerned, if a transient channel is employed in detection, the reaction-times will be governed by the fact that the system will respond at the beginning and at the end of the flashed presentation; with a sustained channel the responses would last during the whole time of presentation. At low spatial frequencies the reaction-times were, indeed, clustered round the onset and offset of the flash, but with high spatial frequencies the reaction-times were unimodally distributed. Tolhurst (1975b) also studied the effects of a maintained subliminal grating on the human subject's response to a flash, arguing that, if the subliminal grating was influencing a transient channel, its effect would cease before the test-stimulus was presented. Once again the operation of sustained and transient mechanisms was demonstrated. The author refers to earlier studies of Ikeda & Boynton (1965), Rashbass (1970) and Battersby & Schuckman (1970) involving uniform flashes and leading to the conclusion that the flashes were detected by channels with transient step-responses. Legge (1978) showed that, with coarse gratings, the effects of prolonging viewing-time on sensitivity were more restricted than with fine gratings, a dichotomy of behaviour that could be reduced by adaptation with appropriate gratings that reduced sensitivity to given spatial frequencies.
15. Campbell *et al.* (1973) emphasize that the falling-off in contrast-sensitivity with wide gratings found in the human (p. 381) is shifted towards wider gratings in the cat, so that, although its resolution of fine gratings is far inferior to man's, the cat is able to discriminate gross patterns better. In an extremely interesting comparison, these authors point out that the cat's vision is not comparable with the blurred vision a man would have if his acuity were reduced artificially with a blurring lens of +3D, so that the comparison might be better with a man viewing through binoculars the wrong way round, i.e. distinct vision with lower resolution.
16. DeValois *et al.* (1982a) have described an elaborate study of the relation between orientation-tuning and sensitivity to direction of motion of a line-stimulus lying at the optimum orientation. They found that, with every cell tested, the orientation of the line was critical for excitation rather than direction of motion. They suggested three models of receptive field build-up from geniculate input, and discussed them in relation to the responses of cortical cells to changes in orientation.
17. In a second study (Skottun *et al.*, 1987) the authors have compared the effects of varying contrast on these two discriminations made by human observers and cat cortical units. Cortical units that saturated at moderate contrasts might account for the psychophysically determined relative insensitivity of the discrimination abilities to raised contrast, once a maximum was reached of about 10%; other cortical units, however, did not saturate, and so improved their discrimination up to high contrasts.
18. Maffei & Fiorentini reported broader-band tuning of complex cells using their grating stimuli by contrast with the much more selective tuning revealed by Pollen & Ronner's study; these latter authors suggest that Maffei & Fiorentini were, in fact, measuring an average receptive field *shape*, rather than the periodic component revealed here. In their more recent and exhaustive study Schiller *et al.* (1976c) found very little difference between the two types of cortical cell; however, a very clear difference was manifest in the temporal modulation of the cell's discharge as a grating was moved over the field; the S-cells showed a sharp burst to each cycle that traversed the field whereas the CX cell responded in a rather continuous fashion, and this feature provides a reliable means of classifying S and CX cells. The difference in response to moving gratings is equivalent to the difference between the responses of X-ganglion cells, which show phasic bursts of impulses linked to the movement of the grating over the receptive field, and Y-cells that show no such locking.
19. The effects of adaptation to high-contrast gratings on the responses of cortical cells to a grating have been examined by Albrecht *et al.* (1984); as we should expect, responses are depressed. The authors have discussed the possible extension in dynamic range of cortical neurones resulting from this adaptation.
20. Burr & Ross (1982) measured contrast-sensitivity functions of human observers, presented with gratings of different spatial frequency moving across their visual field. They had to decide whether the grating was moving, or not, a decision depending on the recognition of a discontinuity in the visual field, i.e. the presence of a grating or not. As velocity increased, there was a shift to lower spatial frequencies for the maximum contrast-sensitivity, but the maximum sensitivity was the same.
21. Earlier Schiller & Colby (1983) compared parvo- and magnocellular units in the monkey's lateral geniculate nucleus; they found that broad-band magnocellular units could not be silenced by appropriate substitution, contrasting with parvocellular units. They suggest that this feature, along with other features of the magnocellular system, including its projection eventually to the superior colliculus, contributes to its value in detection of contours rather than pattern discrimination.
22. A feature of Dow & Gouras' study was the tendency for colour-coding to be separate from spatial-coding, so that many colour-coded neurones did not require a strict alignment of a slit-stimulus for excitation. However, Bertulis *et al.*

(1977), studying mainly foveal cones of the vervet monkey, found that most cells responding to only a narrow band of the spectrum, and thus being described as colour-coded, did require a precisely orientated slit in order to respond. These authors, moreover, failed to observe the colour-opponence between surround and centre.

23. Michael is of the opinion that the chromatic units of the simple type were units receiving only, or predominantly, X-cell input; in this event the separation of the two streams—X and Y—may be regarded as a mode of segregating colour-coded from non-chromatic information.

References

Akichika, M. T. A., Newsome, W. T. & Wurtz, R. H. (1986) Motion selectivity in macaque visual cortex. I. Mechanisms of direction and speed selectivity in extrastriate area. *J. Neurophysiol.* **55**, 1308–1327.

Albrecht, D. G., DeValois, R. L. & Thorell, L. G. (1980) Visual cortical neurons: are bars or gratings the optimal stimuli. *Science* **207**, 88–90.

Albrecht, D. C., Farrar, S. B. & Hamilton, D. B. (1984) Spatial contrast adaptation characteristic of neurones recorded in the cat's visual cortex. *J. Physiol.* **347**, 713–739.

Albright, T. D. (1984) Direction and orientation sensitivity of neurons in visual area MT of the macaque. *J. Neurophysiol.* **52**, 1106–1130.

Albright, T. D., Desimone, R. & Gross, C. G. (1984) Columnar organization of directionally sensitive cells in visual area MT of the macaque. *J. Neurophysiol.* **51**, 16–31.

Allman, J. M. & Kaas, J. H. (1971) A representation of the visual field in the caudal third of the middle temporal gyrus of the owl monkey *(Aotus trivergatus). Brain Res.* **31**, 85–105.

Allman, J. M. & Kaas, J. H. (1975) The dorsomedial visual area: a third tier area in the occipital lobe of the owl monkey (*Aotus trivirgatus*). *Brain Res.* **100**, 473–487.

Baker, C. L. & Cynader, M. S. (1986) Spatial receptive-field properties of direction-selective neurons in the cat striate cortex. *J. Neurophysiol.* **55**, 1136–1152.

Barlow, H. B., Blakemore, C. & Pettigrew, J. D. (1967) The neural mechanism of binocular depth perception. *J. Physiol.* **193**, 327–342.

Barlow, H. B., Macleod, D. I. & van Maeteren, A. (1976) Adaptation to gratings: no compensatory advantages found. *Vision Res.* **16**, 1043–1045.

Battersby, W. S. & Schuckman, H. (1970) The time-course of temporal summation. *Vision Res* **10**, 263–273.

Berlucchi, G., Gazzaniga, S. & Rizzolatti, G. (1967) Microelectrode analysis of transfer of visual information by the corpus callosum. *Arch. Ital. Biol.* **105**, 583–596.

Berlucchi, G. & Rizzolatti, G. (1968) Binoculary driven neurons in visual cortex of split-chiam cats. *Science* **159**, 308–310.

Bertulis, A., Gold, G. C. & Lennox-Buchtal, M. A. (1977) Spectral and orientation specificity of single cells in foveal striate cortex of vervet monkey, *Cercopithecus aethiops. J. Physiol.* **268**, 1–20.

Bilge, M., Bingle, A., Seniviratne, K. N. & Whitteridge, D. (1967) A map of the visual cortex in the cat. *J. Physiol.* **191**, 116–117P.

Bishop, P. O., Coombs, J. S. & Henry, G. H. (1973) Receptive fields of simple cells in the cat striate cortex. *J. Physiol.* **231**, 31–60.

Bisti, S., Carmignole, G., Galli, L. & Maffei, L. (1985) Spatial frequency characteristics of neurones of area 18 in the cat: dependence on the velocity of the visual stimulus. *J. Physiol.* **359**, 259–268.

Blake, R. & Camisa, J. M. (1977) Temporal aspects of spatial vision in the cat. *Exp. Brain Res.* **28**, 325–333.

Blakemore, C. (1969) Binocular depth discrimination and the nasotemporal division. *J. Physiol.* **205**, 471–497.

Blakemore, C. (1970a) The representation of three-dimensional visual space in the cat's striate cortex. *J. Physiol.* **209**, 155–178.

Blakemore, C. (1970b) The range and scope of binocular depth discrimination in man. *J. Physiol.* **211**, 599–622.

Blakemore, C. & Campbell, F. W. (1969) On the existence of neurones in the human visual system selectivity sensitive to the orientation and size of retinal images. *J. Physiol.* **203**, 237–260.

Blakemore, C., Diao, Y., Pu, M., Wang, Y. & Xiao, Y. (1983) Possible functions of the interhemispheric connexions between visual cortical areas in the cat. *J. Physiol.* **337**, 331–349.

Blasdel, G. G. & Lund, J. S. (1983) Termination of afferent axons in macaque striate cortex. *J. Neurosci.* **3**, 1389–1413.

Bradley, A., Skottun, B. C., Ohzawa, I., Sclar, G. & Freeman, R. D. (1987) Visual orientation and spatial frequency discrimination: a comparison of single neurons and behavior. *J. Neurophysiol.* **57**, 755–772.

Bruce, C., Desimone, R. & Gross, C. G. (1981) Visual properties of neurons in a polysensory area in superior temporal sulcus of the macaque. *J. Neurophysiol.* **46**, 369–384.

Bruce, C. J., Desimone, R. & Gross, C. G. (1986) Both striate cortex and superior colliculus contribute to visual properties of neurons in superior temporal polysensory area of macaque monkey. *J. Neurophysiol.* **55**, 1057–1075.

Burr, D. C. & Ross, J. (1982) Contrast sensitivity at high velocities. *Vision Res.* **22**, 479–484.

Burton, H. & Jones, E. G. (1976) The posterior thalamic region and its cortical projection in new world and old world monkeys. *J. Comp. Neurol.* **168**, 249–302.

Campbell, F. W., Cooper, G. F. & Enroth-Cugell, C. (1969) The spatial selectivity of the visual cells of the cat. *J. Physiol.* **203**, 223–235.

Campbell, F. W., Maffei, L. & Piccolino, M. (1973) The contrast sensitivity of the cat. *J. Physiol.* **229**, 719–731.

Choudhury, B. P., Whitteridge, D. & Wilson, M. E. (1965) The function of the callosal connections of the visual cortex. *Quart. J. Exp. Physiol.* **50**, 214–219.

Cleland, B. G., Dubin, M. W. & Levick, W. R. (1971) Sustained and transient neurones in the cat's retina and lateral geniculate nucleus. *J. Physiol.*, **217**, 473–496.

Colby, C. L., Gattass, R., Olson, C. R. & Gross, C. G. (1983) Cortical afferents to visual area PO in the macaque. *Soc. Neurosci. Abstr.* **9**, 152. (Quoted by Ungergleider & Desimone, 1986.)

Cynader, M. (1979) Role of visual cortex in interocular alignment. *Invest. Ophthal.* **18**, 742–751.

Cynader, M. & Regan, D. (1978) Neurones in cat parastriate cortex sensitive to the direction of motion. *J. Physiol.* **274**, 549–569.

Cynader, M. & Regan, D. (1982) Neurons in cat visual cortex tuned to the direction of motion in depth: effect of positional disparity. *Vision Res.* **22**, 967–982.

De Monasterio, F. M. & Schein, S. J. (1982) Spectral bandwidths of color-opponent cells of geniculostriate pathway of macaque monkeys. *J. Neurophysiol.* **47**, 214–224.

Derrington, A. M., Krauskopf, J. & Lennie, P. (1984) Chromatic mechanisms in lateral geniculate nucleus of macaque. *J. Physiol.* **357**, 241–265.

Desimone, R. & Gross, C. G. (1979) Visual areas in the temporal cortex of the macaque. *Brain Res.* **178**, 363–380.

Desimone, R. & Schein, S. J. (1987) Visual properties of neurons in area V4 of the macaque: sensitivity to stimulus form. *J. Neurophysiol.* **57**, 835–868.

Desimone, R., Schein, S. J., Moran, J. & Ungergleider, L. G. (1985) Contour, color and shape analysis beyond the striate cortex. *Vision Res.* **25**, 441–452.

Desimone, R. & Ungergleider, L. G. (1986) Multiple visual areas in the caudal superior temporal sulcus of the macaque. *J. Comp. Neurol.* **248**, 164–189.

DeValois, R. L. (1960) Colour vision mechanisms in the monkey. *J. Gen. Physiol.* **43** (Suppl. 6), 115–128.

DeValois, R. L., Yund, E. W. & Hepler, N. (1982a) The orientation and direction selectivity of cells in the macaque visual cortex. *Vision Res.* **22**, 531–544.

DeValois, R. L., Albrecht, D. G. & Thorell, L. G. (1982b) Spatial frequency selectivity of cells in macaque visual cortex. *Vision Res.* **22**, 545–559.

DeValois, R. L. & Morgan, H. C. (1974) Psychophysical studies of monkey vision. I. Macaque luminosity and color vision tests. *Vision Res.* **14**, 53–67.

DeValois, K. K. & Tootell, R. B. H. (1983) Spatial-frequency-specific inhibition in cat striate cortex cells. *J. Physiol.* **336**, 359–376.

Dow, B. M. & Gouras, P. (1973) Color and spatial specificity of single units in rhesus monkey striate cortex *J. Neurophysiol.* **36**, 79–100.

Dreher, B. & Cottee, L. J. (1975) Visual receptive-field properties of cells in area 18 of cat's cerebral cortex before and after acute lesions in area 17. *J. Neurophysiol.* **38**, 735–750.

Dubner, R. & Zeki, S. M. (1971) Response properties and receptive fields of cells in an anatomically defined region of the superior temporal sulcus in the monkey. *Brain Res.* **35**, 588–532.

Ebner, F. F. & Myers, R. E. (1965) Distribution of corpus callosum and anterior commissure in cat and raccoon. *J. Comp. Neurol.* **124**, 353–365.

Elberger, A. J. (1981) Ocular dominance in striate cortex is altered by neonatal section of the posterior corpus callosum in the cat. *Exp. Brain Res.* **41**, 280–291.

Elberger, A. J. & Hirsch, H. V. B. (1982) Divergent strabismus following neonatal callosal section is due to a failure of convergence. *Brain Res.* **239**, 275–278.

Elberger, A. J. & Smith, E. L. (1985) The critical period for corpus callosum section to affect cortical binocularity *Exp. Brain Res.* **57**, 213–223.

Enroth-Cugell, C. & Robson, J. G. (1966) The contrast sensitivity of ganglion cells in the cat. *J. Physiol.* **187**, 517–552.

Felleman, D. J. & Kaas, J. H. (1984) Receptive field properties of neurons in middle temporal visual area (MT) of owl monkeys. *J. Neurophysiol.* **52**, 488–513.

Ferster, D. (1981) A comparison of binocular depth mechanisms in Areas 17 and 18 of the cat visual cortex. *J. Physiol.* **311**, 623–655.

Fischer, B. & Krüger, J. (1979) Disparity tuning and binocularity of single neurons in cat visual cortex. *Exp. Brain Res.* **35**, 1–8.

Gattass, R. & Gross, C. G. (1981) Visual topography of striate projection zone (MT) in posterior temporal sulcus of the macaque. *J. Neurophysiol.* **46**, 621–638.

Gouras, P. & Krüger, J. (1979) Responses of cells in foveal visual cortex of the monkey to pure color contrast. *J. Neurophysiol.* **42**, 850–860.

Gross C. G., Rocha-Miranda, C. E. & Bender, D. B. (1972) Visual properties of neurons in inferotemporal cortex of macaque. *J. Neurophysiol.* **35**, 96–111.

Harwerth, R. S., Boltz, R. L. & Smith, E. L. (1980) Psychophysical evidence for sustained and transient channels in the monkey visual system. *Vision Res.* **20**, 15–22.

Harwerth, R. S., Smith, E. L. & Levi, D. L. (1979) Binocular interactions for grating patterns. *Percept. Psychophys.* (Quoted by Harwerth *et al.*, 1980.)

Horton, J. C. & Hubel, D. H. (1981) Regular patchy distribution of cytochrome oxidase staining in primary visual cortex of macaque monkey. *Nature* **292**, 762–764.

Hubel, D. H. & Wiesel, T. N. (1967) Cortical and callosal connections concerned with the vertical meridian of visual fields in the cat. *J. Neurophysiol.* **30**, 1561–1573.

Hubel, D. H. & Wiesel, T. N. (1968) Receptive fields and functional architecture of monkey striate cortex. *J. Physiol.*, **195**, 215–243.

Hubel, D. H. & Wiesel, T. N. (1970) Stereoscopic vision in macaque monkey. *Nature* **225**, 41–42.

Hubel, D. H. & Wiesel, T. N. (1972) Laminar and columnar distribution of colliculocortical fibers in the macaque monkey. *J. Comp. Neurol.* **146**, 421–450.

Hubel, D. H. & Wiesel, T. N. (1973) A re-examination of stereoscopic mechanisms in Area 17 of the cat. *J. Physiol.* **232**, 29–30P.

Humphrey, A. L. & Hendrickson, A. E. (1983) Background and stimulus-induced patterns of high metabolic activity in the visual cortex (Area 17) of the squirrel and macaque monkey. *J. Neurosci.* **3**, 345–358.

Ikeda, M. & Boynton, R. M. (1965) Temporal summation of positive and negative flashes in the visual system. *J. Opt. Soc. Amer.* **55**, 1527–1534.

Ikeda, H. & Wright, M. J. (1975) Retinotopic distribution, visual latency and orientation tuning of 'sustained' and 'transient' cortical neurones in area 17 of the cat. *Exp. Brain Res.* **22**, 385–398.

Innocenti, G. M. (1978) Postnatal development of interhemispheric connections of the cat visual cortex. *Arch. Ital Biol.* **116**, 463–470.

Jacobs, G. H. (1964) Single cells in squirrel monkey lateral geniculate nucleus with broad spectral sensitivity. *Vision Res.* **4**, 221–232.

Jones, E. G. & Powell, T. P. S. (1970) An anatomical study of converging sensory pathways within the cerebral cortex of the monkey. *Brain* **93**, 793–820.

Keesey, U. (1972) Flicker and pattern detection: a comparison of thresholds, *J. Opt. Soc. Amer.* **62**, 446–448.

King-Smith, P. E. & Kulikowski, J. J. (1975) The detection of gratings by independent activation of line detectors. *J. Physiol.* **247**, 237–271.

Kulikowski, J. J. & Tolhurst, D. J. (1973) Psychophysical evidence for sustained and transient detectors in human vision. *J. Physiol.*, **232**, 149–162.

Legge, G. E. (1978) Sustained and transient mechanisms in human vision: temporal and spatial properties. *Vision Res.* **18**, 69–81.

Leicester, J. (1968) Projection of the visual vertical meridian to cerebral cortex of the cat. *J. Neurophysiol.* **31**, 371–382.

Livingstone, M. S. & Hubel, D. H. (1984) Anatomy and physiology of a color system in the primate visual cortex. *J. Neurosci.* **4**, 309–356.

Maffei, L. & Fiorentini, A. (1973) The visual cortex as a spatial frequency analyser. *Vision Res.* **13**, 1255–1267.

Maffei, L. & Fiorentini, A. (1977) Spatial frequency rows in the striate visual cortex. *Vision Res.* **17**, 257–264.

Marr, D. & Poggio, T. (1979) A computational theory of human stereo vision. *Proc. Roy. Soc. B* **204**, 301–328.

Maunsell, J. H. R. & Van Essen, D. C. (1983a) Functional properties of neurons in middle temporal visual area of the macaque monkey. I. Selectivity for stimulus direction, speed

and orientation. II. Binocular interactions and sensitivity to binocular disparity. *J. Neurophysiol.* **49**, 1127–1147, 1148–1167.

Maunsell, J. H. R. & Van Essen, D. C. (1983b) The connections of the middle temporal visual area (MT) and their relationship to a cortical hierarchy in the macaque monkey. *J. Neurosci.* **3**, 2563–2586.

Meadows, J. C. (1974) The anatomical basis of prosopagnosia. *J. Neurol. Neurosurg. Psychiat.* **37**, 489–510.

Michael C. R. (1978a) Color vision mechanisms in monkey striate cortex: dual-opponent cells with concentric receptive fields. *J. Neurophysiol.* **41**, 572–588.

Michael, C. R. (1978b) Color vision mechanisms in monkey striate cortex: simple cells with dual opponent-color receptive fields. *J. Neurophysiol.* **41**, 1233–1249.

Michael, C. R. (1978c) Color-sensitive complex cells in monkey striate cortex. *J. Neurophysiol.* **41**, 1250–1266.

Michael, C. R. (1979) Color-sensitive hypercomplex cells in monkey striate cortex. *J. Neurophysiol.* **42**, 726–744.

Michael, C. R. (1981) Columnar organization of color cells in monkey's striate cortex. *J. Neurophysiol.* **46**, 587–604.

Michael, C. R. (1985) Laminar segregation of color cells in the monkey's striate cortex. *Vision Res.* **25**, 415–423.

Mikami, A., Newsome, W. T. & Wurtz, R. H. (1986) Motion selectivity in macaque visual cortex. II. Spatiotemporal range of directional interactions in MT and V1. *J. Neurophysiol.* **55**, 1328–1339.

Mishkin, M. (1982) A memory system in the monkey. *Phil. Trans. B* **298**, 85–95.

Mishkin, M., Ungergleider, L. G. & Macko, K. A. (1983) Object vision and spatial vision: two cortical pathways. *Trends Neurosci.* **6**, 414–417.

Mitchell, D. E. & Blakemore, C. (1970) Binocular depth perception and the corpus callosum. *Vision Res.* **10**, 49–54.

Morrone, M. C., Stefani, M. Di & Burr, D. C. (1986) Spatial and temporal properties of neurons of the lateral suprasylvian cortex of the cat. *J. Neurophysiol.* **56**, 969–986.

Motokawa, K., Taira, N. & Okuda, J. (1962) Spectral responses of single units in the primate visual cortex. *Tohoku J. Exp. Med.* **78**, 320–337.

Motter, B. C. & Mountcastle, V. B. (1979) Afferent visual signals for directed visual attention. *Soc. Neurosci. Abstr.* **5**, 118.

Movshon, J. A., Thompson, I. D. & Tolhurst, D. J. (1978) Spatial summation in the receptive fields of simple cells in the cat's striate cortex. *J. Physiol.* **283**, 53–77.

Newsome, W. T., Mikami, A. & Wurtz, R. H. (1986) Motion selectivity in macaque visual cortex. III. Psychophysics and physiology of apparent motion. *J. Neurophysiol.* **55**, 1340–1351.

Nikara, T., Bishop, P. O. & Pettigrew, J. D. (1968) Analysis of retinal correspondence by studying receptive fields of binocular single units in cat striate cortex. *Exp. Brain Res.* **6**, 353–372.

Ohzawa, I. & Freeman, R. D. (1986) The binocular organization of simple cells in the cat's visual cortex. I. and II. *J. Neurophysiol.* **56**, 221–242, 243–259.

Padmos, P. & Norren, D. V. (1975) Increment spectral sensitivity and colour discrimination in the primate studied by means of graded potentials from the striate cortex. *Vision Res.* **15**, 1103–1113.

Payne, B. R., Berman, N. & Murphy, E. H. (1980) Organization of direction preference in cat visual cortex. *Brain Res.* **211**, 445–450.

Payne, B. R., Berman, N. & Murphy, E. H. (1981) A quantitative assessment of eye alignment in cats after corpus callosum transection. *Exp. Brain Res.* **43**, 371–376.

Payne, B. R., Pearson, H. E. & Berman, N. (1984) Role of corpus callosum in functional organization of cat striate cortex. *J. Neurophysiol.* **52**, 570–594.

Perrett, D. I., Rolls, E. T. & Caan, W. (1982) Visual neurons responsive to faces in the monkey temporal cortex. *Exp. Brain Res.* **47**, 329–342.

Pettigrew, J. D., Nikara, T. & Bishop, P. O. (1968) Binocular interaction on single units in cat striate cortex: simultaneous stimulation by single moving slit with receptive fields in correspondence. *Exp. Brain Res.* **6**, 391–410.

Poggio, G. F., Baker, F. H., Mansfield, R. J. W., Sillito, A. & Grigg, P. (1975) Spatial and chromatic properties of neurons subserving foveal and parafoveal vision in rhesus monkey. *Brain Res.* **100**, 25–59.

Poggio, G. F. & Fischer, B. (1977) Binocular interaction and depth sensitivity in striate and prestriate cortex of behaving rhesus monkey. *J. Neurophysiol.* **40**, 1392–1405.

Poggio, G. F. & Talbot, W. H. (1981) Mechanisms of static and dynamic stereopsis in foveal cortex of the rhesus monkey. *J. Physiol.* **315**, 469–492.

Pollen, D. A., Nagler, M., Daugman, J., Kronauer, R. & Cavanagh, P. (1984) Use of Gabor elementary functions to probe receptive field substructure of posterior inferotemporal neurons in owl-monkey. *Vision Res.* **24**, 234–241.

Pollen, D. A. & Ronner, S. F. (1975) Periodic excitability changes across the receptive fields of complex cells in the striate and parastriate cortex of the cat. *J. Physiol.* **245**, 667–697.

Rashbass, C. (1970) The visibility of transient changes of luminance. *J. Physiol.* 210, 165–186.

Richards, W. & Regan, D. (1973) A stereo field map with implications for disparity processing. *Invest. Ophthal.* **12**, 904–909.

Richmond, B. J. & Sato, T. (1987) Enhancement of inferior temporal neurons during visual discrimination. *J. Neurophysiol.* **58**, 1292–1308.

Richmond, B. J., Wurtz, R. H. & Sato, T. (1983) Visual responses of inferior temporal neurons in awake rhesus monkey. *J. Neurophysiol.* **50**, 1415–1432.

Rocha-Miranda, C. E., Bender, D. B., Gross, C. G. & Mishkin, M. (1975) Visual activation of neurons in inferotemporal cortex depends on striate cortex and forebrain commissures. *J. Neurophysiol.* **38**, 475–491.

Rolls, E. T., Judge, S. J. & Sanghero, M. K. (1977) Activity of neurons in the inferotemporal cortex of the alert monkey. *Brain Res.* **130**, 229–238.

Sahgal, A. & Iversen, S. D. (1978) Categorization and retrieval after selective inferotemporal lesions in monkeys. *Brain Res.* **146**, 341–350.

Sato, T., Kawamura, T. & Iwai, E. (1980) Responsiveness of inferotemporal single units to visual pattern stimuli in monkeys performing discrimination. *Exp. Brain Res.* **38**, 313–319.

Schein, S. J., Marrocco, R. T. & MeMonasterior, F. M. (1982) Is there a high concentration of color-selective cells in area V4 of monkey visual cortex? *J. Neurophysiol.* **47**, 193–213.

Schiller, P. H. & Colby, C. L. (1983) The responses of single cells in the lateral geniculate nucleus of the rhesus monkey to color and luminance contrasts. *Vision Res.* **23**, 1631–1641.

Schiller, P. H., Finlay, B. L. and Volman, S. F. (1976a–e) Quantitative studies of single-cell properties in monkey striate cortex. I. Spatiotemporal organization of receptive fields. II. Orientation specificity and ocular dominance. III. Spatial frequency. IV. Corticotectal cells. V. Multivariate statistical analysis and models. *J. Neurophysiol.* **39**, 1288–1319, 1320–1333, 1334–1351, 1352–1361, 1362–1374.

Schiller, P. H. & Malpeli, J. G. (1978) Functional specificity of lateral geniculate nucleus laminae of the rhesus monkey. *J. Neurophysiol.* **41**, 788–797.

Sherman, S. M. (1972) Development of interocular alignment in cats. *Brain Res.* **37**, 187–203.

Skottun, B. L., Bradley, A., Sclar, G., Ohzawa, I. & Freeman, R. D. (1987) The effects of contrast on visual orientation and spatial frequency discrimination: a comparison of single cells and behavior. *J. Neurophysiol.* **57**, 773–786.

Tanaka, K., Hikosaka, K., Saito, H.-A., Yukie, M., Fukada, Y. & Iwai, E. (1986) Analysis of local and wide-field movements in the superior temporal visual areas of the macaque monkey. *J. Neurosci.* **6**, 134–144.

Timney, B., Elberger, A. & Vandewater, L. (1982) Binocular depth perception in cats following neonatal section of the corpus callosum. *Soc. Neurosci. Abstr.* **8**, 628. (Quoted by Elberger & Smith, 1985.)

Tolhurst, D. J. (1973) Separate channels for the analysis of the shape and movement of a moving visual stimulus. *J. Physiol.* **231**, 385–402.

Tolhurst, D. J. (1975a) Reaction times in the detection of gratings by human observers: a probabilistic mechanism *Vision Res.* **15**, 1143–1149.

Tolhurst, D. J. (1975b) Sustained and transient channels in human vision. *Vision Res.*, **15**, 1151–1155.

Tolhurst, D. J. & Movshon, J. A. (1975) Spatial and temporal contrast sensitivity of striate cortical neurones. *Nature* **257**, 674–675.

Tootell, R. B., Silverman, M. S. & De Valois, R. L. (1981) Spatial frequency columns in primary visual cortex. *Science* **214**, 813–815.

Toyama, K., Komatsu, Y., Kasai, H., Fujii, K. & Umetani, K. (1985) Responsiveness of Clare-Bishop neurons to visual cues associated with motion of a visual stimulus in three-dimensional space. *Vision Res.* **25**, 407–414.

Ungergleider, L. G. & Desimone, R. (1986a) Projections to the superior temporal sulcus from the central and peripheral field representation of V1 and V2. *J. Comp. Neurol.* **248**, 147–163.

Ungergleider, L. G. & Desimone, R. (1986b) Cortical connections of visual area MT in the macaque. *J. Comp. Neurol.* **248**, 190–222.

Ungergleider, L. G., Gattass, R., Sousa, A. P. B. & Mishkin, M. (1983) Projections of area V2 in the macaque. *Soc. Neurosci. Abstr.* **9**, 152. (Quoted by Ungergleider & Desimone, 1986.)

Ungergleider, L. G. & Mishkin, M. (1979) The striate projection zone in the superior temporal sulcus of *Macaca mulatta*: location and topographic organization. *J. Comp. Neurol.* **188**, 347–366.

Van Essen, D. C. & Maunsell, J. H. R. (1983) Hierarchical organization and functional streams in the visual cortex. *Trends Neurosci.* **6**, 370–375.

Van Essen, D. C., Maunsell, J. H. R. & Bixby, J. L. (1981) The middle temporal visual area in the macaque: myeloarchitecture, connections, functional properties and topographic organization. *J. Comp. Neurol.* **199**, 293–326.

Whiteley, A. M. & Warrington, E. K. (1977) Prosopagnosia: a clinical, psychological, and anatomical study of three patients. *J. Neurol. Neurosurg, Psychiat.* **40**, 395–403.

Wiesel, T. N. & Hubel, D. H. (1966) Spatial and chromatic interactions in the lateral geniculate body of the rhesus monkey. *J. Neurophysiol.* **29**, 1115–1156.

Zeki, S. M. (1971) Convergent input from the striate cortex (area 17) to the cortex of the superior temporal sulcus in the rhesus monkey. *Brain Res.* **28**, 338–340.

Zeki, S. M. (1973) Colour coding in rhesus monkey prestriate cortex. *Brain Res.* **53**, 422–427.

Zeki, S. M. (1974a) Functional organization of a visual area in the posterior bank of the superior temporal sulcus in the rhesus monkey. *J. Physiol.* **236**, 549–573.

Zeki, S. M. (1974b) Cells responding to changing image size and disparity in the cortex of the rhesus monkey. *J. Physiol.* **242**, 827–841.

Zeki, S. M. (1976) The functional organization of projections from striate to prestriate visual cortex in the rhesus monkey. *Cold. Spr. Harb. Symp. Quant. Biol.* **40**, 591–600.

Zeki, S. M. (1977) Colour coding in the superior temporal sulcus of rhesus monkey visual cortex. *Proc. Roy. Soc. B* **197**, 195–223.

Zeki, S. (1980a) The representation of colours in the cerebral cortex. *Nature* **284**, 412–418.

Zeki, S. (1980b) The response properties of cells in the middle temporal area (area MT) of owl monkey visual cortex. *Proc. Roy. Soc. B* **207**, 239–248.

22. NEUROPHYSIOLOGY OF PERCEPTION: DEVELOPMENTAL ASPECTS OF VISUAL FIELD CHARACTERISTICS

VISUAL DEPRIVATION

The consequences of failure to use an eye in childhood (*amblyopia ex anopsia*) are well known as clinical manifestations of squint or of the operated congenital cataract (Von Noorden, 1960). In the human infant, the deprivation must apparently extend for several years, and the loss of vision exhibits some degree of reversibility if the disuse has not lasted too long. In the cat, Hubel & Wiesel (1963, 1965, 1970) carried out pioneer investigations into the requirements of previous visual experience for the features of the receptive field of cortical neurones; and the subject has been subsequently investigated in great depth by Blakemore and his colleagues.

Dominance and Orientation Specificity

The two features that have excited most interest are the degree of dominance by a given eye, revealed by the dominance histogram, and the orientation-specificity, of simple cells, the question posed being, essentially, whether these features of the cortical cells are innately determined at birth and, if so, to what extent they may be modified by visual experience as soon as the eyes are capable of responding to light and a patterned environment. In this respect it must be appreciated that about seven days must elapse in the kitten before the eyes open and even then the optical quality of the retinal image is poor until the pupillary vascular membrane disintegrates (Freeman & Marg, 1975), whereas the eye of the newborn monkey is open and optically clear. A newborn kitten, kept in the dark or with its eyes sutured for several weeks after birth, is completely blind; but this does not mean that its cortical cells are unresponsive, so that the orientation-specificity and ocular dominance of given cortical cells may be determined, and compared with those of normally reared animals or with those in the newborn.

Bilateral Deprivation

Although it has been stated that, at the time of the kitten's lid-opening, most of its cortical neurones have bilateral input, giving an adult histogram (Hubel & Wiesel, 1963), the studies of LeVay *et al.* (1978) have shown that intraocular injection of labelled amino acid at 2 weeks gives rise to a uniform band of labelling in cortical lamina 4 in both sides of the brain, indicating a continuous non-columnar distribution of geniculate afferents. By three weeks, periodicity becomes apparent, and is complete in 6 weeks. The binocularity of the cortical neurones in bilaterally deprived kittens shows abnormalities but is quite evident.

Unilateral Deprivation

When only one eye is sutured, however, there is a striking change in the dominance histogram, as seen in Fig. 22.1 which shows the histogram for normal cats (A) and for kittens that had been reared with the ipsilateral eye occluded (C). It will be seen that a negligible number of cells are driven by the ipsilateral eye (Group 1) and practically all by the contralateral eye. Clearly, this robbing the animal of visual experience has resulted in a diminution of the effective input from the deprived eye, either through a physical loss of synapses or a decreased efficiency of transmission.

COMPETITION

The fact that these striking changes in function only occurred when one eye was deprived of vision and the other was active suggested that, in normal development, the layers of geniculate neurones providing axons representing each eye competed for synapses at the cortical level. If vision in both eyes was prevented, the competition would remain, but if only one eye was deprived, the other eye took over synapses that would have belonged to the deprived eye (Hubel *et al.*, 1977).

CORTICAL STRIPE-SIZES

Hubel *et al.* (1976) injected tritiated fucose and proline into the experienced eye of a monocularly deprived monkey and made autoradiographs of the cortex; the average total width of the left- plus right-eye stripes, indicating terminations in the cortex, was unchanged, but the relative sizes of the two indicated expansion by the experienced eye at the expense of the deprived eye. Since the cell-bodies had not shrunk, the altered width of the

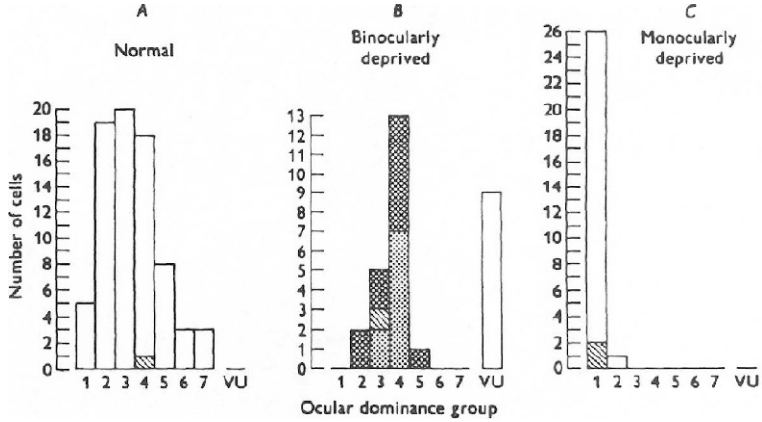

Fig. 22.1 Histograms, showing the number of neurones, their ocular dominance groups and the types of receptive fields classified on the basis of responses in the eye dominating the cell. Cells in groups 1 and 7 are monocularly driven, being excitable only through the contralateral (left) eye or ipsilateral (right) eye respectively. Cells of group 4 are equally driven by the two eyes. Group 3 and 5 cells are slightly more strongly driven by the contralateral and ipsilateral eyes respectively; group 2 and 6 neurones are very strongly dominated by the contralateral and ipsilateral eyes respectively. Receptive field types: *orientation selective* = open blocks; *orientational bias* = cross-hatched blocks; *pure direction selective* = diagonally striped blocks; *non-oriented* = stippled blocks; *visually unresponsive* = open blocks under a separate column labelled V.U. *A*, seventy-six neurones from three normal kittens aged 3 to 5 months. *B*, thirty neurons from a kitten binocularly deprived until recording at 8 weeks. *C*, twenty-seven neurones from a kitten monocularly deprived by suturing the right (ipsilateral) eyelids until recording at 5 weeks. (Blakemore & Van Sluyters, *J. Physiol.*)

stripes indicated changes in synaptic development. That the change is due to competition is indicated by the fact that, in regions of the cortex representing the extreme temporal crescent area, and thus receiving input from only one eye, there was no change in the width of the stripes representing the deprived eye.

In a similar study of the Old World monkey, Blakemore *et al.* (1978) described the same striking loss of dominance of the deprived eye when lid-suture was carried out between 2 to $5\frac{1}{2}$ weeks. This is illustrated by Fig. 22.2 where lamina 4c neurones have been considered separately from the remainder. There is a suggestion that the proportion of units dominated by the deprived eye remained higher within lamina 4c than those outside it. Thus representation of the deprived eye seems to persist as shrunken but otherwise normal columns in layer 4c, whilst its influence on the other layers in the column is reduced or obliterated. When occlusion was delayed to 11 to 16 months there was very little effect, although it appeared that the non-deprived eye had a higher proportion of dominant units. They did not measure stripe widths morphologically, but deduced these from the results of near-horizontal electrode penetrations; they arrived at a ratio for non-deprived over early-deprived of about 2.8, similar to that measured directly by Hubel *et al.* (1977).

EXCITATORY CONNECTIONS

Tsumoto & Suda (1978) measured responses of cortical neurones representing the deprived eye to electrical stimulation; they found that, although 91% failed to respond to a visual stimulus, this percentage fell to some 66% on the basis of electrical stimulation. There was evidence from the intracellular recording that inhibitory circuits from the deprived eye were present in addition to the excitatory.

MONOCULAR AND BINOCULAR CORTICAL REGIONS

If competition between the eyes governs the effects of deprivation, then cortical regions representing the monocular segments of the retinae should have a weaker response to monocular lid-closure. Wilson & Sherman (1977) confirmed this expectation when they compared regions of 0–30°, 30–45° and 45–90° of retinal eccentricity; however the extreme peripheral representation was not entirely normal, suggesting non-competitive effects.

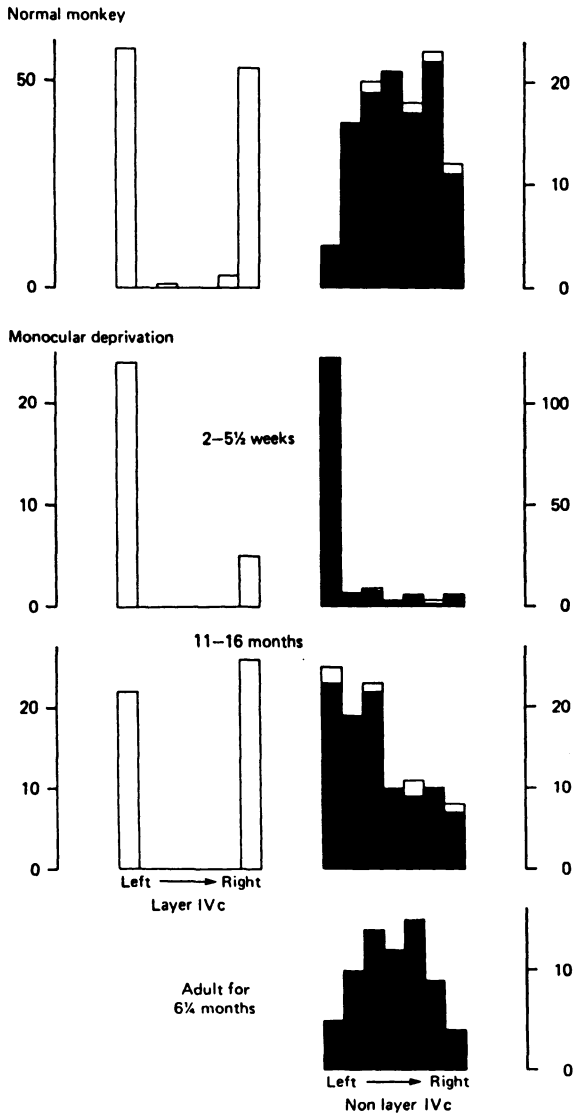

Fig. 22.2 Ocular dominance histograms for 'non layer 4c' and 'layer 4c' units for the normal animal and three animals monocularly deprived in the right eye. Results from the two hemispheres are pooled and plotted as if they all came from the right hemisphere (group 1 units are dominated by the left eye, group 7 by the right). No results are shown for layer 4c for the monocularly deprived adult, since only three non-orientated cells, all driven by the left eye alone, were recorded in this animal. (Blakemore *et al., J. Physiol.*)

Period of Susceptibility

Induction Index

Occlusion of a single eye in the adult cat has no influence on ocular dominance, as measured in electrode penetrations, so that it is of interest to determine the period during which the synaptic connexions remain plastic, and the extent to which any changes, due to modifying the kitten's visual environment, are reversible. Figure 22.3 summarizes the results of Hubel & Wiesel, where the ordinate is the *induction index*, defined as the ratio of the number of cells dominated by the experienced eye over the total number of cells; thus the value of about 0.3, represented by the dashed horizontal line, corresponds to the normal adult value; the horizontal bars indicate the periods during which the contralateral eye was held closed; and it will be seen that, to achieve an index of unity, the closure must occur at an early state in development, whilst the total sensitive period is of the order of fifteen weeks. The period of susceptibility begins rather suddenly at about the beginning of the fourth week; it is very high during that week, and it begins to fall between the sixth and eighth week and has disappeared at the end of the third month.

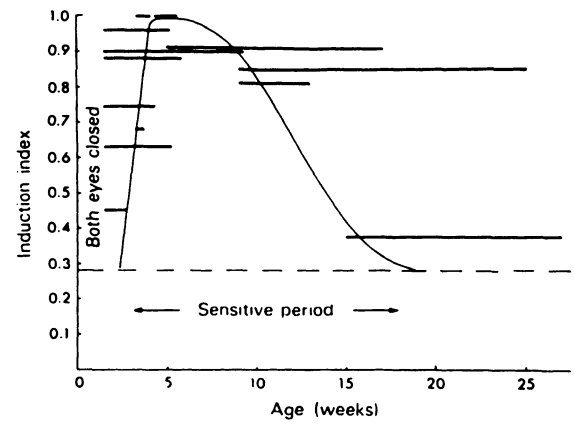

Fig. 22.3 Time-course of the sensitive period for changes in ocular dominance in kitten cortical cells, induced by monocular visual deprivation. (Blakemore from Hubel & Wiesel, *Brit. med. Bull.*)

Rapidity of Effect

Hubel & Wiesel (1970), examining kittens at the most sensitive period to monocular deprivation (3 to 5 weeks old), found definite abnormalities in the histogram after only three days whilst after 6 days the picture was similar to that of an animal monocularly deprived for a long time. Again, Olson & Freeman (1975) found definite changes in the ocular dominance-pattern after 1 day of monocular deprivation of a 4-week-old kitten; they pointed out that it was unnecessary to keep the kittens in the dark before imposing the monocular deprivation. When the sensitivity of the cortex to exposure to stripes of a given orientation was examined, Blakemore & Mitchell (1973) found that exposure of as little as 1 hour to vertical

stripes produced cortical neurones with receptive fields predominantly sensitive to the vertical by comparison with control animals similarly reared in the dark but with no visual experience. When the criterion was a change in the dominance histogram, then 6 to 20 hours of monocular vision on the 29th day of lid suturing was sufficient to shift dominance towards the experienced eye (Peck & Blakemore, 1975).

Primate

LeVay *et al.* (1980), in their study designed to determine the sensitive period, began by following the development of dominance columns during the first 6 weeks. In the first week there was a mixing of inputs from the two eyes in lamina 4c although a basic columnar pattern was becoming evident. By the third week the segregation of inputs to separate groups of neurones according to eye-origin was almost complete, and at 6 weeks it was complete. They then studied monkeys subjected to monocular lid-closure at ages ranging from 2 days to adult and allowed to live for long periods before final examination. With suture at 2 days it was found that the afferents from the open eye expanded their realm of termination to widen the size of the columns in lamina 4c, whilst afferents from the closed eye shrank and became fragmented. In the layers above and below 4c the open eye was completely dominant. With eye-suture at 10 weeks the morphological effects in lamina 4c were milder, but there was still a change of dominance in favour of the open eye. Lid-closure at 7–14 months produced no morphologically observable change although there was still some change in dominance. Lid-closure in the adult, or monocular enucleation had no effects. The authors pointed out that the completion of segregation of eye-inputs by no means puts an end to susceptibility to the effects of deprivation, as had been supposed, so that some other process puts an end to the critical period, for example, the development of myelination of the terminal arborizations of the geniculate afferents, which is a gradual process continuing after segregation has ceased. Alternatively, the increase in the number of dendritic spines on the cortical cells receiving geniculate input that takes place during the first two postnatal months (Boothe *et al.*, 1979) might account for the increase in synaptic input from the geniculate cells.[1]

RATE OF DEVELOPMENT OF EFFECT

With very early lid-closure the afferents to the cortex continue their segregation process to give dominance columns at the normal rate, but the effect is to give the abnormal dominance distribution already described. At 3–4 weeks, a short period of closure (nine days) also produced marked effects, and at 5–7 weeks a short period could still produce a mild effect. Thus it appeared that monocular suture, performed after about 5 weeks, requires a longer time to produce its anatomical effects in lamina 4c than does closure soon after birth.

EFFECTS OF PRENATAL ENUCLEATION

Rakic (1981) enucleated one eye from two- and three-month monkey embryos and examined their lateral geniculate bodies some $5\frac{1}{2}$ months after term, after injections of ^{3}H-labelled proline or fucose into the surviving eye. Label occupied the whole of the lateral geniculate nucleus, so that the ganglion cell axons were invading regions that would have been occupied by the other eye; moreover, the six laminae were reduced to two, with one interlaminar fibre-band separating them, which contained parvo- and magnocellular neurones in their respective laminae. Ocular dominance columns failed to develop in the visual cortex. Thus the development of the laminated geniculate body depends on a competition that takes place long before birth in the primate.

Development of Pattern Sensitivity

Visual Acuity

The visual acuity of the kitten, measured in terms of resolvable spatial frequency, increases rapidly from about the start of the fourth week, at about the same time as the sensitive period for exhibiting effects of deprivation comes to an end (Freeman & Marg, 1975). At the 23rd day it was about 0.3 cycles/degree or 20/200; at Day 33 it was 1 cycle/degree or 20/600, and between Days 33 to 100 it reached 3 cycles/degree or 20/200. In the primate, as we have seen, visual acuity in the early postnatal infant is low, namely 0.5 to 1.0 c/deg, i.e. some 50 to 100 times less than that of the adult; and the full development may well take nearly a year.

Requirements for Patterned Vision

The development of patterned vision requires the specialization of cortical cells so that they respond to, or are triggered by, highly specific visual stimuli, such as the orientation of a line, the direction and velocity of movement, to the polarity of an edge, to the angular width of a bar, and so on; and there is no doubt that these qualities, as well as the ability to respond to visual stimuli in both eyes, can be considerably modified by visual experience or its absence.

Bilateral Deprivation

The effects of monocular occlusion, revealing as they do the competition between the two eyes for cortical rep-

resentation, have attracted more attention than the effects of simple dark-rearing or binocular lid-suture. There is no doubt that long-term binocular deprivation has severe effects on cortical neurones; and this is revealed in their receptive-field characteristics, many features of these depending on visual experience.

Development of Specific Sensitivities

Pettigrew (1974), in his study of disparity-tuning (p. 559), made observations on orientation- and direction-specificity of cortical cells in the developing kitten, and compared the relative proportions of sensitive cells in the adult with those in the visually deprived animal. It is clear from Fig. 22.4 that the picture in the deprived kitten is not much different from that of the normal kitten in its second week, when good pattern vision first becomes feasible, whereas in the fifth week the visually experienced kitten has a nearly normal pattern of sensitive neurones, by contrast with the binocularly deprived animal. In general, Pettigrew concluded that, whereas binocularity and motion-sensitivity are innately specified, visual experience is essential for development of orientation- and disparity-specificities. Hirsch & Spinelli (1970) reared kittens in an environment such that one eye viewed vertical stripes and the other horizontal stripes, and found that the preferred directions of simple cortical cells matched the direction to which the eye had been exposed. Again, Blakemore & Cooper (1970) exposed kittens to a variety of directional stripes and, after five months, examined their behaviour; they were obviously blind to lines at right-angles to those of their environment if tested by a visual placing reaction on to a lined surface; Fig. 22.5 shows the preferred directions of the cortical neurones examined some 7–8 months after the visual testing.

Receptive Field Types

In a more elaborate study of the effects of visual experience on cortical neurones Blakemore & Van Sluyters (1975)[2] have made a study of receptive fields of over 700 cortical neurones in normal kittens with ages ranging from 9 days to 22½ weeks, and the effects of depriving the kitten of visual experience on the receptive fields. The receptive fields were defined as follows: *Non-orientated*, responding to moving stimuli but with no clear preference for direction of movement or any orientation of edge. *Pure direction-sensitive*, the receptive field having a clear axis, movement in one (preferred) direction exciting and in the reverse (null) direction, not; they are comparable to Barlow's direction- selective ganglion cells in the rabbit; *Orientation-bias*; here the cell responds to movement in all directions but shows a preference for one axis; this cell is rare in the adult cat, but has been identified in the rabbit (Van Sluyters & Stewart, 1974a); *Orientation-selective* with a clear preferred orientation for a linear stimulus, with no discharge for movement along the orthogonal axis; these are the cells described by Hubel & Wiesel (p. 531) and are subdivided into simple, complex and hypercomplex categories.

Orientation-selectivity

Blakemore & Van Sluyters (1975) found that kittens older than about 4 weeks, brought up in a normal environment, were virtually adult in their cortical physiology, and even the youngest studied (19 days) was surprisingly mature, so that despite the cloudy optics, the majority of neurones were distinctly orientation-selective, narrowly tuned for orientation, and binocularly driven. This orientation-selectivity could be demonstrated by flashing a bright bar with an appropriate orientation, and so was differentiated

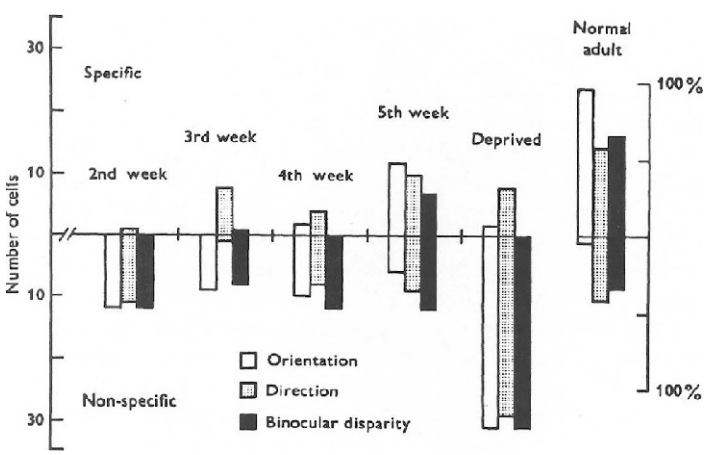

Fig. 22.4 The numbers of cortical cells responding specifically (above horizontal) to orientation, direction and binocular disparity are shown during development of the normal kitten; included in the diagram are the numbers in binocularly deprived kittens aged 2 to 6 weeks. The proportion of specific cells increased with age and visual experience, particularly with respect to orientation and disparity. No cells were found in binocularly deprived cortex that were specific for disparity and very few showed orientation selectivity. Directional sensitivity was seen at all ages irrespective of visual experience. (Pettigrew, *J. Physiol.*)

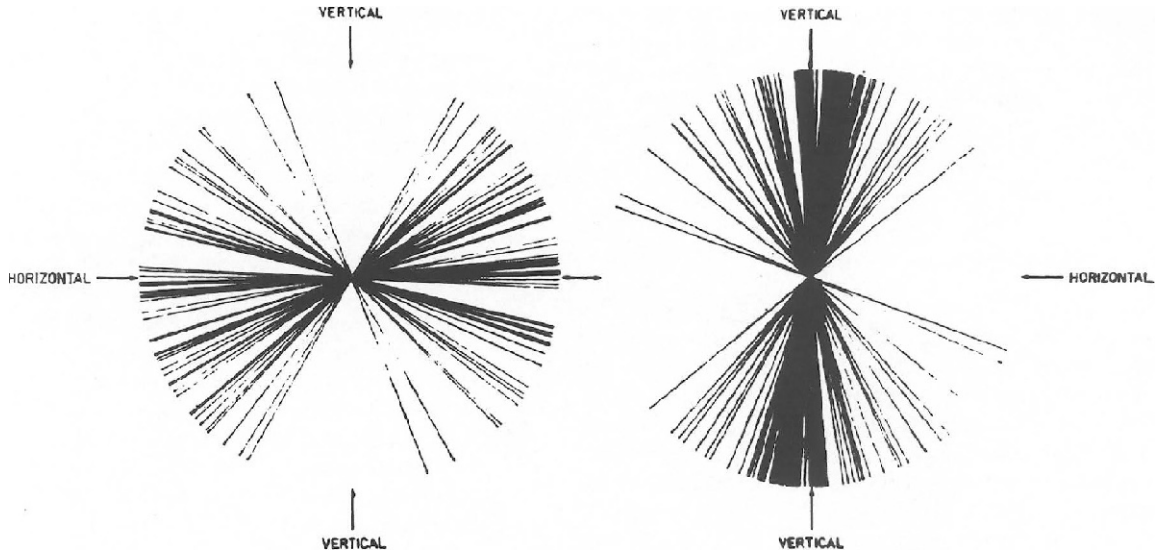

Fig. 22.5 These polar histograms show the distributions of optimal orientations for 52 neurones from a horizontally experienced cat on the left, and 72 from a vertically experienced cat on the right. The slight torsion of the eyes, caused by the relaxant drug, was assessed by photographing the pupils before and after anaesthesia and paralysis. A correction has been applied for torsion, so the polar plots are properly orientated for the cats' visual fields. Each line shows the optimal orientation for a single neurone. For each binocular cell the line is drawn at the mean of the estimates of optimal orientation in the two eyes. No units have been disregarded except for one with a concentric receptive field and hence no orientational selectivity. (Blakemore & Cooper, *Nature*.)

from the *direction-sensitive* neurone that required motion to excite. The dependence on visual experience is illustrated by Fig. 22.6 where the initial point represents a nine-day-old kitten that had just opened its eyes and was, indeed, visually inexperienced. The curves indicate changes due to visual experience, but the existence of orientation-selectivity in the nine-day-old kitten is remarkable. The ocular dominance pattern for this kitten was normal.[3]

REQUIREMENTS OF VISUAL EXPERIENCE

Blakemore & Van Sluyters varied the type of visual experience in a variety of ways and measured the proportions of cortical neurones exhibiting given receptive field-types. The results emphasized the importance of lines, and, as had been found earlier, if the lines were in a given orientation the orientation-selective units were sensitive to this direction. The main change in the character of the receptive field after birth was in orientation-selectivity, a characteristic that is poorly developed at birth and requires a patterned environment for its development.

More Comprehensive Study In a more comprehensive study involving over 600 cortical neurones in kittens ranging in age from 6 to 24 days, Albus & Wolf (1984) confirmed the importance of visual experience in determining orientation-selectivity; thus at 2–3 days after lid-opening they found a proportion of orientation-selective neurones about the same as found by Blakemore & Van Sluyters (1975) in the dark-reared kitten. However, the initial generation of orientation-selectivity takes place well before lid-opening, so that the connections of these cells are obviously genetically determined. The authors did not find a predominance of vertical and horizontal orientation preferences, as had been described by Frégnac & Imbert (1978).[4] As we should expect, the cortical laminae receiving direct geniculate input, namely 4 and 6, exhibited earlier maturity of function, so far as orientation-selectivity was concerned. So far as the adult type of receptive field was concerned, such as that classically described for simple, complex and hypercomplex cells, all these took time to develop, so that at the earliest stages in development the presence of excitatory and inhibitory regions adjacent to each other was not observed; instead, the responses were described as unimodal, responding exclusively to ON or OFF. Up to the end of the second week no complex fields were encountered. These unimodal neurones were strikingly similar to those described by Hoffmann & Cynader (1977) in uniocularly deprived eyes, after reverse suture. Lamina 5 was striking in that visually responsive neurones were not encountered during the first two postnatal weeks, although in the adjacent laminae 4 and 6 they were numerous; this layer projects to the superior colliculus, and it is interesting that devel-

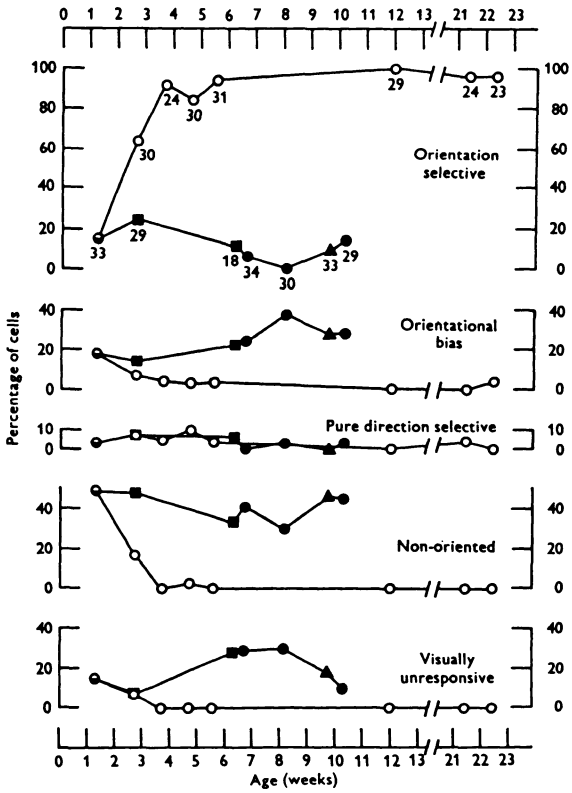

Fig. 22.6 Comparison of the effects of binocular deprivation with those of normal visual experience. The five pairs of curves show the percentages of each type of receptive field for 397 cells recorded from seven normal kittens (open circles) and six binocularly deprived kittens (filled symbols) of various ages. In each case the two curves originate from points representing the data for the 9-day-old kitten recorded at the time of natural eye opening. For the binocularly deprived kittens: *Lid suture* = filled circles; *dark reared* = filled squares; *nictitating membrane suture* = filled triangle. The numbers beneath the data points for the top pair of curves indicate the total number of cells recorded in each animal. (Blakemore & Van Sluyters, *J. Physiol.*)

opment of its directional selectivity, which depends on cortical input, does not begin until the second postnatal week (Stein & Gallagher, 1981).

Development of Disparity Specificity

Disparity Tuning

We have seen (p. 559) that cortical neurones show an optimal binocular response when the points on the two retinae that are excited have a certain disparity; within this range there is facilitation of responses from either eye, but when this range is exceeded, greater disparities lead to mutual inhibition, as revealed by Fig. 21.2. In very young kittens, the optic axes diverge strongly (as much as 30° in a 2-week-old animal), but during the critical period there is a rapid decrease in this retinal disparity running parallel with other features already discussed. In these very young kittens it is possible to evoke binocular responses in cortical neurones, provided the optic axes are brought into alignment by means of prisms, but there is none of the disparity-selectiveness, or tuning, that is characteristic of the adult where 63% of cortical neurones exhibit this sharp tuning (Pettigrew *et al.*, 1968). Thus in kittens of 16 days, for example, a neurone could be found sensitive to binocular stimulation so that nearly three times more spikes were elicited on stimulating both eyes than by stimulating the contralateral eye; however, this facilitation of one eye by the other extended over a wide disparity (over 6° in the ipsilateral retina), and the characteristic inhibition at high disparities, and peak response at a minimum disparity, were not present.

MATURATION

It was concluded that development to adult was manifest as a reduction in *facilitation*, and an increase in *inhibition*, to produce the highly tuned binocular disparity-selector.

Effects of Deprivation That the development of this selectivity depended on visual experience rather than on an inherent tendency to maturation, was shown by binocular deprivation experiments; an example is given in Fig. 22.7 which shows the disparity-response curve for a 6-week-old kitten reared normally (lower curve) and for a kitten with lids sutured during this period; the binocularly deprived neurone shows facilitation over a wide range of disparity similar to an immature neurone, although the optimum is fairly well defined. In contrast, the normal neurone exhibits facilitation over a narrow range and, at non-optimal disparities, the binocular response is depressed below monocular levels.

Development of Inhibition Thus inexperienced binocular neurones tolerate a wide range of retinal disparity, and this range is narrowed by age and visual experience; hence disparity-detection, which is the basis of stereoscopic vision, results from a refinement of the interaction of the two eyes on a given cortical neurone, a refinement that would be very difficult to develop in an innate fashion in view of the variations in the directions of the optic axes of growing kittens. The development is one of inhibition, and another example of inhibitory interactions in visually experienced animals has been described by Sherman & Sanderson (1972) whilst Lund & Lund (1972) have shown, in the visually inexperienced rat, the failure of development in the superior colliculus of F-type terminals, presumed intrinsic inhibitory connections.

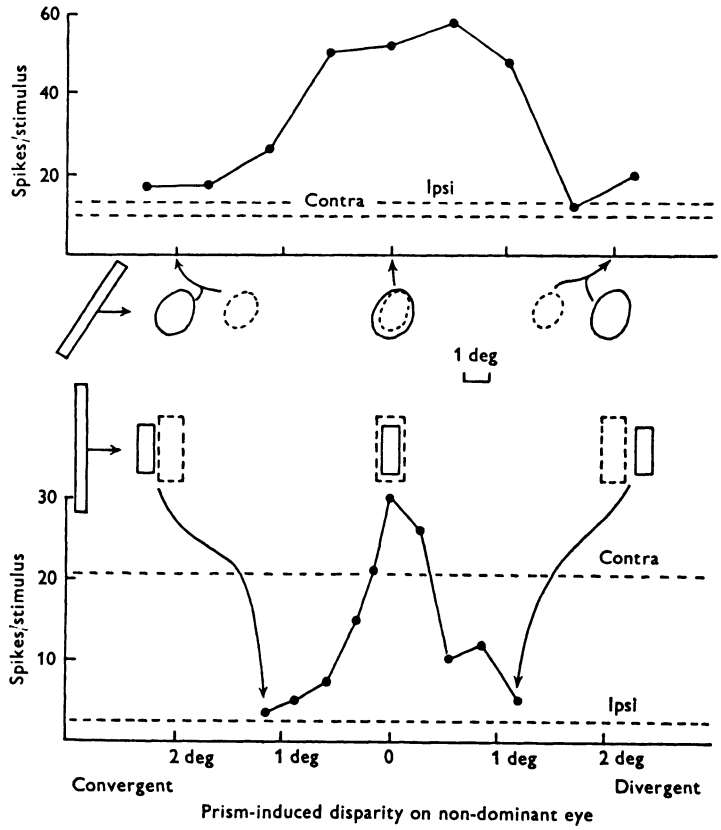

Fig. 22.7 Most selective binocular response curves found in visual cortex of binocularly deprived (upper curve) and of normal (lower) kittens at 6 weeks. Both neurones were well matched in terms of receptive field size and both were located less than three degrees from the area centralis. Despite comparable accuracy in their detection of the retinal position of a stimulus presented to one eye alone, the two cells differ markedly in their ability to detect the relative retinal positions of the two images of the same stimulus presented to both eyes. The binocularly deprived neurone gave a binocular response which is much greater than the monocular response levels (indicated by dashed lines) and it was independent of disparity over a wide range; binocular facilitation was still evident when the stimulus passed over the two receptive fields successively (contralateral field—continuous outline, ipsilateral field—interrupted outline). The normal neurone gave a facilitatory binocular response over a very narrow range of disparity; the binocular response was suppressed below the monocular level when the two receptive fields were offset by a fraction of their width. (Pettigrew, *J. Physiol.*)

BINOCULAR AND MONOCULAR CORTICAL SEGMENTS

Watkins *et al.* (1978) re-examined the effects of bilateral lid-suture on the cortical neurones of cats at the time they had become adult. They could classify cortical neurones into three types: *mappable*, with clearly defined receptive fields (49%); *unmappable*, with diffuse receptive fields (31%) and *inexcitable* (20%). Less than 12% of the total sample could have been described as normal simple or complex cells. Orientation-selectivity was observed in 12% of the neurones, all of them characterized as mappable, whilst the unmappable had no neurones exibiting this feature. There was an abnormally low proportion of binocularly activated mappable units, whereas in the unmappable units there was no abnormality in this respect. Strong inhibitory side-bands to the receptive fields were absent in mappable units. Interestingly, the effects observed were the same in monocular and binocular regions of cortical representation, supporting the notion of binocular competition.

Reversal of Some Effects of Deprivation

Reverse-suturing

Merely opening the previously sutured eye after a long period of monocular deprivation fails to reverse the changes in the cortical neurones.[5] If recovery depended on a competitive recapture of synapses lost during deprivation, then depriving the experienced eye while the deprived eye was open might favour the process. Blakemore & Van Sluyters (1974) sutured one eye of newborn kittens for five weeks and established the binocular histogram which, as we have seen, indicates complete monocularity. With other kittens the sutured eyes were opened after periods ranging from 5 to 14 weeks, and the previously open eyes were sutured (*reverse-suturing*) and, after allowing the kitten to use its previously deprived eye for 9 weeks, its cortical neurones were examined. When reverse-suturing was carried out at 5 weeks, there was a complete reversal of the dominance pattern, the previously sutured eye losing its dominance and transferring it to the newly opened eye, whilst few or no cells were binocularly driven. As the time for reverse-suturing was delayed, the reversal became less and less effective so that reversal at 14 weeks left the dominance distribution similar to that in the animal deprived for five weeks without reverse-suturing; at intermediate periods, e.g. reverse-suturing at 6 weeks, a fair number of cells were binocularly driven.

PREFERRED ORIENTATION

In these cells, which had never had binocular visual experience, there was a remarkable difference in preferred orientation for line-stimuli according to the eye being

stimulated, preferred orientations differing by as much as 70° by contrast with normal kittens where there is a strong correlation between preferred orientations in the two eyes when binocularly driven neurones are studied. This change is shown by Fig. 22.8 from a later study by Movshon (1976a), which compares histograms of preferred orientation-differences in the two eyes of binocularly driven cortical neurones; visual inexperience alone widens the spectrum, and reverse suturing not only fails to re-establish the normal situation but widens the spectrum still further. This emphasizes the importance of binocular visual experience for maintaining this similarity in orientation-preference, so essential for fusion of retinal images.

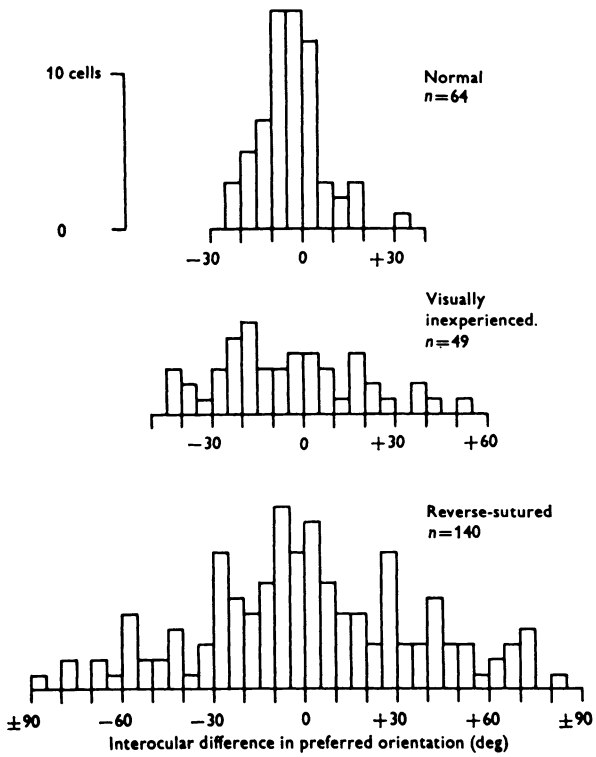

Fig. 22.8 Showing the effects of binocular deprivation and subsequent reverse suturing on the differences in preferred orientation between the two receptive fields of given binocular neurones. In the normal eye the preferred orientations are close to each other in the majority of cells (top histogram). In the visually inexperienced kittens much larger differences occur, widening the spectrum; reverse suturing widens the spectrum still further so that direction sensitive units could have preferred orientations differing by as much as 90° in the two eyes. Differences of positive sign occur when the receptive field of the right eye is tilted clockwise with respect to that in the left eye; negative differences are anticlockwise. (Movshon, *J. Physiol.*)

SENSITIVE PERIOD

The sensitive period during which reversal of the effects of deprivation can be effected coincides fairly closely with the sensitive period for producing some effect of deprivation, so that the sensitive period is one of plasticity during which synaptic connexions may be broken and re-established.

RECOVERY OF VISUAL FUNCTION

Behaviourally, the kitten after 5 weeks of monocular deprivation was blind in the sutured eye, but after reverse suturing at 5 to 8 weeks there was considerable recovery of visual function in the newly opened eye; when reverse suturing was delayed to 8 to 14 weeks there was some vision through both eyes with progressively less in the newly opened eye.[6]

DOMINANCE COLUMNS

Monocular deprivation, as we have seen, makes a striking change in ocular dominance so that on a given side of the cortex virtually all neurones are driven by the eye contralateral to lid-suture; the same columnar arrangement of neurones is, however, maintained, so that ocular dominance-columns become larger when projected to the surface of the cortex; Movshon (1976a) showed that, during reversal of dominance, there was a strong correlation between the reversal index[7] and the column size (Table 22.1).

Table 22.1 Reconstructed column sizes in reverse-sutured kittens. The extent of each defined ocular dominance column is given in millimetres projected to the cortical surface in twelve kittens. The animals are arranged in order of increasing reversal index, their rearing conditions are indicated in the left-hand column as: age (weeks) at reverse-suturing + days of reversed suture. The left eye was the contralateral, initially experienced eye in all cases (Movshon 1976a).

		Column sizes	
Animal	*Reversal index*	*Left-eye*	*Right eye*
7+6	0.25	1.6	0.3
5+3	0.26	0.4	0.5, 0.5
7+9	0.32	1.2	0.6
6+6	0.36	0.5	0.5
5+6	0.38	1.4, 0.9	0.5
7+24	0.40	0.9	0.6
7+63	0.48	0.6, 0.4	0.5
6+9	0.49	0.4	0.4
4+3	0.63	0.1, 0.4	0.5
6+63	0.65	0.7, 0.3	0.7
6+12	0.75	0.2, 0.3	0.7
5+9	0.77	0.3, 0.6	1.4

STUDIES ON THE PRIMATE

Blakemore *et al.* (1978; 1981) found that reverse-suturing of monkeys that had been lid-sutured monocularly at 2 to 5½ weeks led to a return to an apparently normal ocular dominance histogram for neurones outside lamina 4c. Figure 22.9 illustrates an example of a monkey reverse-sutured at 5½ weeks after the initial suture; the ocular dominance sequence is the mirror-image of that in the monocularly deprived animal, so that reverse-suture has done more than bring about the status quo; the previously deprived eye is now behaving as an undeprived eye after monocular lid-suture. Moreover, the receptive-field properties of the neurones were normal. The later the reverse-suturing the smaller the degree of recapture, so that at 8 weeks roughly equal numbers of neurones were dominated by each eye. Reverse-suturing at 38½ weeks had no effect.

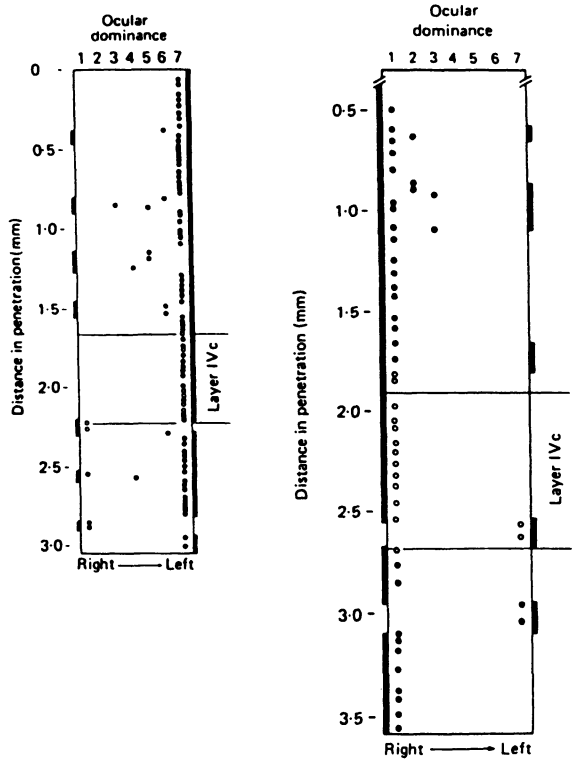

Fig. 22.9 *Left.* Reconstruction of penetration through cortex of animal deprived in the right eye from 2–5½ weeks of age. The sequence of preferred orientations was particularly striking in the first part of the track, moving through a total range of more than 360° at a surface-parallel rate of about 360°/mm. *Right.* Reconstruction of penetration of animal that was deprived in the right eye until 5½ weeks, then reverse sutured and recorded 4 months later. Compare the ocular dominance sequence with that shown on left. (Blakemore *et al.*, *J. Physiol.*)

Combined Morphological and Physiological Studies

Physiological studies on deprivation and reverse-suturing have led to the view of a definite shrinkage and re-expansion of the regions of synaptic contact with cortical neurones. This re-expansion has been demonstrated by LeVay *et al.* (1980); thus, with a monkey monocularly sutured at 2 days and reverse-sutured at 3 weeks of age, there was a great expansion of the sublamina 4c, so that the appearance was that of the non-deprived region of a monocularly occluded animal, reverse-suturing not only reversing the shrinkage but causing an expansion into the territory of the formerly non-deprived eye. Sublamina 4cβ is the site of termination of the parvocellular geniculate neurones; the situation in sublamina 4cα the area of termination of magnocellular neurones was entirely different, the region remaining shrunken. Examination of the lateral geniculate nucleus revealed somewhat equivocal results; the parvocellular laminae regained their original size and were actually some 25% larger than those innervated by the late-sutured eye; cells in the magnocellular laminae were about the same size in the originally deprived and non-deprived laminae.[8] Essentially similar results have been described in a series of papers from Blakemore's laboratory in which electrophysiological measurements of dominance columns were combined with anatomical studies based on anterograde movement of labelled amino acid from the eye to the cortex. In the operculum, the region representing central vision, they did not observe an expansion of the stripes of the previously deprived eye to beyond their normal width; in the calcarine cortex, on the other hand, the area occupied by the originally deprived eye in lamina 4c expanded from 24% to around 88%. Swindale *et al.* calculated, from the rate of re-expansion of the cortical stripes, that new synapses might be formed at the rate of some 100 per hr per axon; on this basis they considered that some of the very rapid changes in dominance might be explained on the basis of formation of new synapses.

EFFECTS OF EYE ENUCLEATION

Studies on geniculate input from the deprived eye have shown that it is abnormal, especially in relation to Y-cells; nevertheless, there is undoubtedly some input, so that the 100% loss of response of cortical neurones to the deprived eye suggests that there is some inhibitory input from the non-deprived eye that reduces the effectiveness of that from the deprived eye. This was confirmed by Kratz *et al.* (1976) who enucleated the non-deprived eye; there was an increase of cortical responding cells from 5% to over 30%, the effect appearing within hours of the enucleation. The cells responding usually had abnormal receptive fields, lacking both directional and orientation-selectivity, suggesting abnormal excitatory inputs from the deprived eye. The time at which enucleation was

carried out was important; thus Spear *et al.* (1980) found that enucleation during the critical period caused the number of cortical units responding to the deprived eye to rise from about 10% to 65%, nearly the same as those responding to the non-deprived eye. If enucleation was postponed till 9 weeks the proportion fell precipitately, to rise again to about 30% at 21 weeks; beyond this there was no further improvement.

COMPARISON WITH REVERSE-SUTURING

Hoffmann & Cynader (1977) studied the reversal of the effects of monocular lid-closure, by reverse-suture or enucleation, on the lateral geniculate nucleus, the visual cortex and the superior colliculus. Reverse-suture brought the proportion of Y-cells in the geniculate nucleus back to normal, whilst enucleation actually increased the percentage of Y-cells from normal to 61%. When cortical units were studied, however, reverse-suture had very little effect on binocularity, only a few units being driven by the deprived eye. With enucleation, they found many more units driven by both eyes, and the authors concluded that interaction between eyes leading to competition might well be the consequence of interaction in the lateral geniculate nucleus, rather than a competition for synapses in the cortex.

SPEED OF EFFECT

Reverse-suturing requires several days for its effect to become manifest, whereas enucleation exerts its effect in a few hours. A further difference is that reverse-suturing is effective on animals lid-sutured from the time of eye-opening until 4–5 weeks, whereas enucleation is effective for longer periods of deprivation. Blakemore & Hawken (1982) considered that, in both cases, the non-deprived eye was exerting some inhibitory effect on the cortical neurones that had formerly been activated by the deprived eye. After deprivation, the input from the deprived eye is too weak to excite the cortical neurone; removal of the inhibitory input from the non-deprived eye thus permits some recovery of cortical function. Blakemore *et al.* (1982) produced evidence for a subthreshold input from the deprived eye.

EFFECTS OF PRIOR VISUAL EXPERIENCE

Blasdel & Pettigrew (1978) deferred monocular deprivation for periods of 3–5 weeks, thereby allowing the kittens some visual experience before deprival. The effects of reverse-suture were then studied. The degree of recovery was proportional to the length of visual experience; kittens reared in the dark for 4–5 weeks before unilateral lid-closure showed little reversal after reverse-suture. The authors considered that at least a part of the effect of experience was the absence of a squint that usually occurs in dark-reared animals. Van Sluyters (1978) obtained similar results, achieving complete reversal of the dominance histogram in 14 days after reverse-suture (Fig. 22.10); the receptive fields of the cortical neurones were normal and matched those of the previously non-deprived eye, a matching that was presumably due to the early visual experience.[9] Blakemore & Hawken (1982) found that, when lid-suture was carried out before eye-opening and lasted for some five weeks, the reduction in binocularity was not influenced by enucleation of the non-deprived eye.[10] However, if lid-suture was performed at 5 weeks and lasted some three or more days, enucleation, or just blocking of the optic nerve with local anaesthetic, allowed a substantial recovery, so that some 78% of units were responsive to the deprived eye. This was strikingly shown by comparing responsiveness of cortical cells in a descending track of the electrode and subsequently in the ascending withdrawal; between the two operations the non-deprived eye was removed. Thus visual experience lasting a few weeks after lid-opening, a period during which there is massive synaptogenesis in the kitten's visual cortex (Cragg, 1975), seems to lead to a consolidation of organized input to the cortical neurone.

Visual Defects following Deprivation

Bilateral Deprivation

The kitten deprived of visual experience bilaterally for some months after birth is said to be behaviourally blind (Ganz & Hirsch, 1972), but according to Sherman (1974) there is improvement after eye-opening, and the initial behaviour may be the consequence of complete absence of visuomotor experience during deprivation. Sherman used a perimetric technique, whereby he introduced new objects into a definite segment of the visual field and observed the visuomotor response. Both his binocularly deprived cats seemed totally blind at first, then visual placing, and the following of moving objects and reaching with a forepaw, returned after 17 days, in one, and 5 days in the other. The perimetric tests indicated that the binocular field of vision was fairly normal, but the responses to appearance of a new object indicated that the cats were ignoring the contralateral field of view when tested monocularly, responding only to objects in the ipsilateral hemifield.[11] Kalil (1978) compared visuomotor behaviour and cell growth in the lateral geniculate nucleus of dark-reared cats. After 8, 12, and 16 weeks they appeared blind, but within 4 weeks visuomotor behaviour was normal; the visual field defects, as measured perimetrically, were attributed to the squint that remained. During the first 3 months of dark-rearing, the geniculate cell growth was retarded; the maximum difference from normal was at the 12th week, and then growth caught up and by the fourth month there was no abnormality. Visual experience after periods of 8, 12 and 16

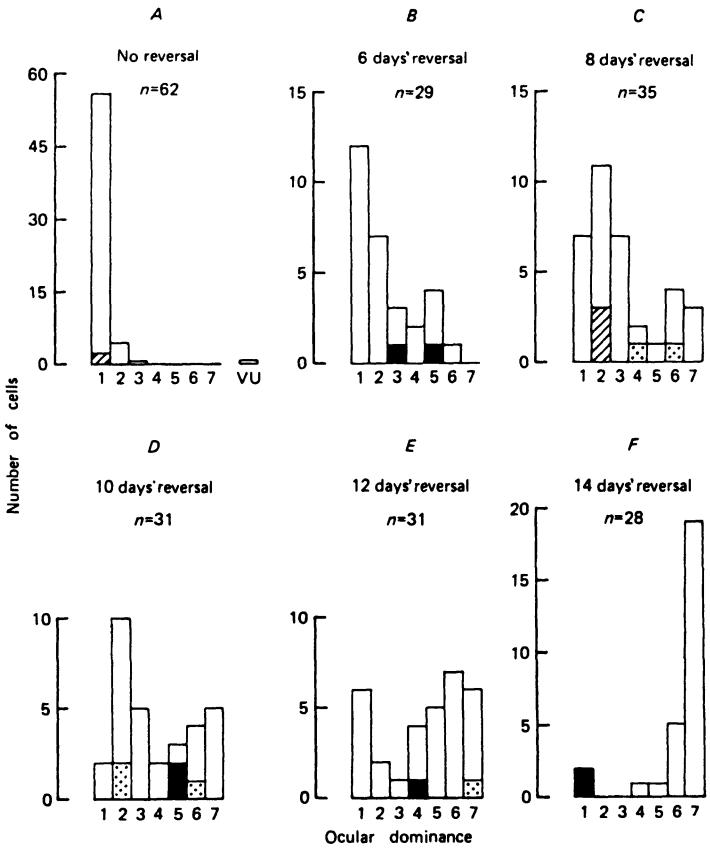

Fig. 22.10 Ocular dominance histograms for the five reverse-sutured kittens. *A*, comparison data from three kittens monocularly deprived from day 32 to day 42 and not reverse sutured; *B*, histogram for the kitten deprived from day 32 to day 42 and allowed 6 days of deprivation reversal; *C*, 8 days of deprivation reversal; *D*, 10 days of deprivation reversal; *E* 12 days of deprivation reversal; *F*, 14 days of deprivation reversal. Receptive field types: *orientation selective* = unfilled blocks; *orientational bias* = stippled blocks; *pure direction selective* = diagonally striped blocks; *non-oriented* = filled blocks; *visually unresponsive* = unfilled blocks in a separate column labelled VU. (Van Sluyters, *J. Physiol.*)

weeks of dark-rearing led to normal cells, so that reversal occurs in light or dark.

Monocular Deprivation

Dews & Wiesel (1970) compared the behaviour of kittens monocularly deprived, when the deprived eye was open and the undeprived eye was closed, and *vice versa*. They concluded that, for kittens sutured after birth and opened after 4 months, the animal had no visuomotor control when using only the deprived eye. However, Sherman (1973, 1974), using his perimetric technique, showed that monocularly deprived cats responded to objects in the monocular segment of the ipsilateral visual field and ignored the binocular segments, as illustrated by Fig. 22.11. We may presume, then, that the monocularly deprived kitten makes use of such monocularly driven cortical neurones as are available. When Dews & Wiesel deferred lid-suture until days 8 to 15 after birth, and lid-opening was allowed at about 110 to 145 days, there was some evidence of response to light, but not to patterned stimuli. As date of lid-suture was advanced, the response to performance-tests improved and, in general, the effects of timing of lid-suture on the degree and permanence of visual defects paralleled the changes in the cortical neurones with respect to ocular dominance.[12]

Species Differences

Monkey

Hubel & Wiesel (1970) found, in monkeys, that two weeks of monocular closure during the first five weeks produced at least temporary blindness in the eye that had been closed, and an absence of responses of cortical cells to stimulation of that eye. Again, Von Noorden *et al.* (1970) deprived monkeys of form-vision, but not of light, and found a critical period of up to three months of deprivation from birth when no recovery of form vision was obtained, as tested with a Landolt-C. If deprivation occurred after 3 months of form experience there was no effect. Later Baker *et al.* (1974) showed that the sensitive period begins at birth and may continue up to 8 weeks. They were able to correlate the low visual acuity following deprivation or strabismus with the paucity of cortical cells driven by the deprived eye.

Rabbit

In the rabbit Van Hof (1969) found no abnormality in the ability of young animals to discriminate patterns when they were deprived of vision for six weeks after birth. So far as binocularly

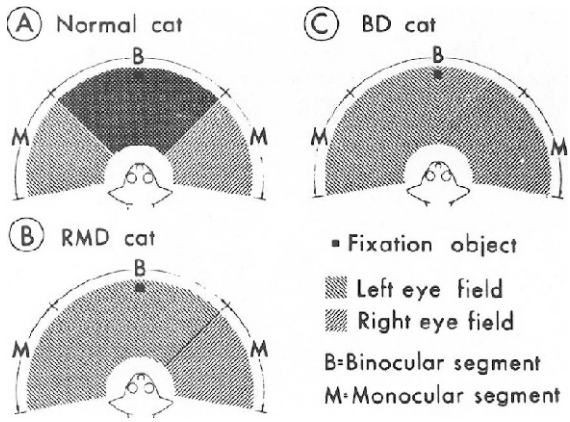

Fig. 22.11 Monocular and binocular segments of cat's visual field when both eyes are aligned on the fixation object. A, *Normal cats.* The binocular field extends between about 100° on either side. The monocular fields each extend from about ipsilateral 100° to contralateral 45° which delineates the *binocular segment* of visual field as bounded bilaterally by about 45° on either side and the *monocular segment* on each side as extending from about 45° to about 100°. B, *Monocularly deprived (MD) cats.* The binocular field has a normal extent as in A. Also, the non-deprived eye monocular field is normal but the deprived eye monocular field includes only the monocular segment. C, *Binocularly deprived (BD) cats.* The binocular field has a normal extent as in A, but each monocular field includes only the ipsilateral hemifield. (Sherman, *Brain Res.*)

driven cortical neurones were concerned, monocular deprivation had only a small effect on dominance, skewing it towards the ipsilateral eye when the contralateral eye was sutured. Deprivation did affect some other characteristics of the receptive fields such as the clustering of preferred directions around horizontal and vertical meridians and increasing the number of binocularly driven cells with non-identical receptive fields (Van Sluyters & Stewart, 1974b).

Changes in the Visual Pathway

A defect in the responsiveness of ganglion cells of the retina of the deprived eye would, of itself, reduce the degree of dominance of that eye on the cortical neurones. Similarly with lateral geniculate neurones.

Ganglion Cells

Sherman & Stone (1973) found a completely normal histology of the retina of the monocularly deprived kitten eye; as studies on the lateral geniculate nucleus had shown that any defects due to deprivation were manifest principally in Y-cells, they measured the number of these, deduced from the antidromic latencies which, because of the large axon size, are smallest in Y-cells. The relative numbers of Y- and X-cells deduced in this way were quite normal (13% Y, 67% X and 20% W). Kratz *et al.* (1979a) found no change in the spatial resolution of ganglionic X-cells, as shown in Fig. 22.12 in contrast with lateral geniculate cells. In a similar way Cleland *et al.* (1980), using their brisk transient and sustained classification, found no change in the cut-off frequencies for contrast-sensitivity such as to indicate a decrease in spatial resolution in the deprived ganglion cells; thus the highest cut-off frequencies in the area centralis were in the region of 9 cyc/deg, well within the normal range.[13] Against these studies we have that of Leventhal & Hirsch (1983) who found a diminution in cell-size of X- and Y-cells in the retinal regions of monocularly deprived kittens involved in binocular vision, Y-cells being more affected than X-cells. In the regions of monocular representation there was no difference, so that competition between the eye inputs to the lateral geniculate nucleus affects the size of the ganglion cells of the deprived eye, their size being reduced, perhaps because they do not have to sustain as many synapses in the lateral geniculate nucleus.

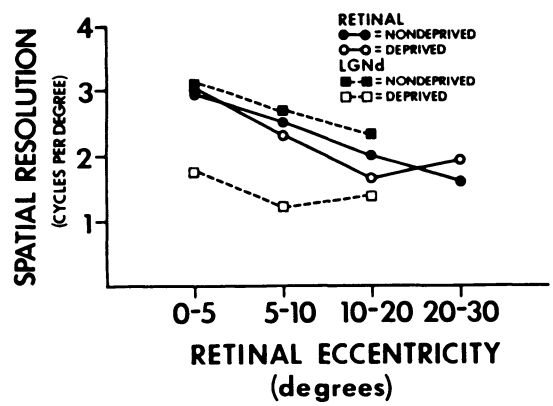

Fig. 22.12 Mean spatial resolution of normal, non-deprived and deprived retinal and geniculate (LGNd) X-cells plotted as a function of eccentricity groups; eccentricity is indicated as visual angle from area centralis. (Kratz *et al.*, *Brain Res.*)

Development of the Lateral Geniculate Nucleus

Winfield & Powell (1980) and Winfield *et al.* (1980) have followed the development of the synaptic organization of the kitten's lateral geniculate body. They observed a remarkable increase in the percentage of glomerular synapses between the 20th and 40th postnatal days, i.e. during the period of susceptibility to monocular suture; this was associated with a corresponding decline in percentage in the neuropil. As Fig. 22.13 shows, the changes were unaffected by monocular lid-suture, showing that the synaptic organization, from this aspect at any rate, was not dependent on visual experience.

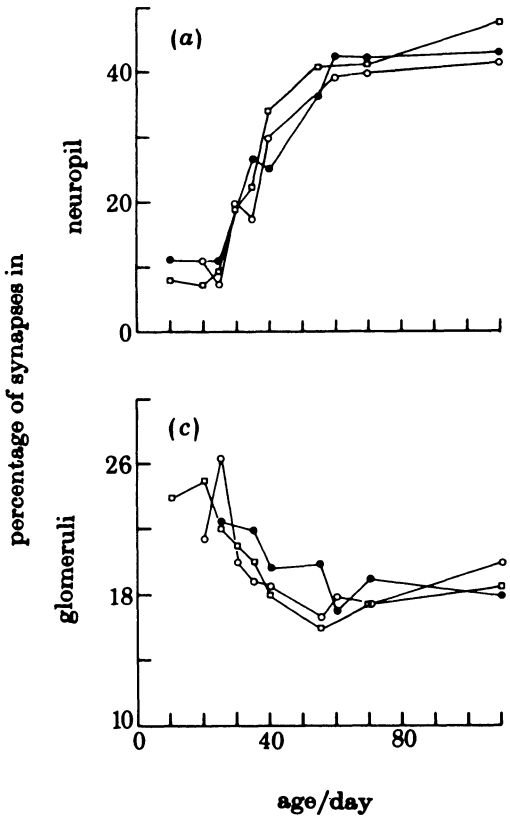

Fig. 22.13 The changes in the proportions of symmetrical synapses with age in glomerulus (a) and extraglomerular neuropil (c) of the binocular parts of lamina A in the normal kitten (□) and in kittens with unilateral eyelid closure (○, undeprived; ●, deprived). (Winfield *et al.*, *Proc. Roy. Soc.*)

POSTNATAL EXPANSION OF RETINAL INPUT

Friedlander *et al.* (1985) have shown that, although laminar segregation is complete at birth in the kitten, there are considerable changes in growth and reorganization within the laminae postnatally; thus the number of terminal boutons on the axon ramifications in the nucleus increases some threefold, a factor that may account for the increased number of Y-cells encountered with age (Mangel *et al.*, 1983). If the Y-characteristic of a geniculate neurone depends on its retinal input, rather than any inherent characteristic of the neurone, then clearly an increased Y-input, made possible by expansion of synapses in the geniculate laminae, will increase the proportion of Y-cells encountered in any electrophysiological study. Thus the effects of monocular occlusion, so evident with respect to the Y-pathway, could be due to arrest of the expansion of synaptic contacts occurring postnatally.

LAMINAR SEGREGATION OF INPUTS

This was examined by Shatz (1983) in kittens, using anterograde movement of label; by embryonic (E) day 32 label from the ipsilateral eye had invaded the anlage, whilst the contralateral eye invaded on E35 (gestation in the cat is 55 days). Initially the pattern was uniform but by E47 gaps appeared contralaterally, indicating that inputs were beginning to separate. By E54 it was possible to identify unambiguously layers corresponding to the separate eyes, and at birth the efferent inputs had the adult appearance; cellular lamination, however, had just begun, lagging behind the afferent segregation by 2 weeks. Shatz emphasized the early invasion by the contralteral eye, and suggested that the view that segregation resulted from some simple competition seemed unlikely; they suggested that the early invasion of lamina A by the contralateral eye might leave the adjacent lamina A1 free for the ipsilateral eye, a form of 'biased competition' that would lead to accurate segregation.

GENICULATE NEURONES

Blakemore & Vital-Durand (1986) have emphasized the value of studying the development of the primate visual resolution postnatally, since the optical media are clear at birth. They emphasize, too, the poor resolution at birth, namely some 5 c/deg, compared with the adult value of 30 c/deg in the adult, and the slow improvement, so that it may require a year before adult acuity is achieved. Physical factors, of course, must be important, namely the degree of emmetropia achieved, which depends on curvatures of the refractive surfaces and the size of the eye. They investigated in detail the properties of lateral geniculate neurones in the Old World monkey. Figure 22.14 shows the maturation of visual resolution of geniculate X-type neurones, which parallels that of behavioural acuity, although resolution determined in this manner usually lags behind the best resolution of the geniculate neurones; thus shortly after birth the monkey can only resolve 1–2 c/deg whilst geniculate neurones resolve 5 c/deg probably because of defective accommodation. The neural factors, i.e. those not depending on optics, etc., involved in the improvement of resolving power of the monkey, and of its geniculate cells, probably depended on the reduction in the size of the receptive fields of X-like cells, deduced from the shift towards higher spatial frequencies in the high-frequency cut-off of the curves of response versus spatial frequency illustrated by Fig. 22.15.

SHRINKAGE OF LAMINAE

Wiesel & Hubel (1963a, b) and Garey *et al.* (1973) found no morphological changes in the lateral geniculate nucleus of bilaterally deprived eyes; however, with the unilaterally deprived eye, with monocular suture, there was a large shrinkage of the laminae to which the deprived eye projected, due to a diminution of cell-size. This difference between mono- and binocular deprivation

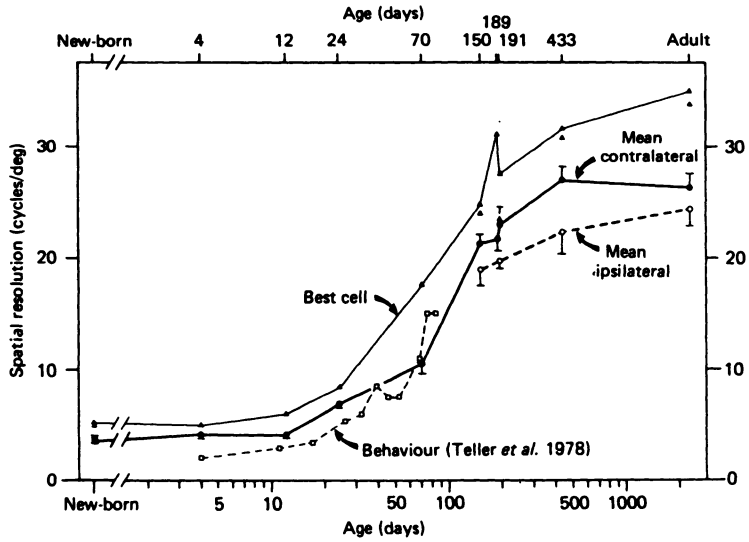

Fig. 22.14 Spatial resolution (linear scale) is plotted against age (logarithmic). The data all come from visually experienced laminae of the l.g.n. The filled circles, joined by thick lines, show the mean resolution (+ or −1 S.E. of mean) for all l.g.n. X cells connected to the contralateral (left) eye, with receptive fields centred within 2° of the middle of the fovea. For the animals that were not monocularly deprived (new-born, 150, 191, 433 days and adult) there are corresponding open circles joined by dashed thick lines, showing the mean resolution for similar samples of central receptive fields connected to the ipsilateral (right) eye. The triangles (filled for the left eye, open for the right) show the acuity for the best cell in each sample. The highest points are joined by a thin line, this being the upper envelope of performance for this series of animals. For comparison, the open squares, joined by interrupted thin lines, replot behavioural determinations of visual acuity (square-wave gratings, binocular viewing, preferential-looking technique) for an individual pigtail monkey (F2) studied by Teller *et al.* (1978). (Blakemore & Vital-Durand, *J. Physiol.*)

suggested that there might be a competition for synapse-formation at the geniculate or cortical stations, so that monocular deprivation would not simply lead to reduction of synapses by the deprived neurones, but an increase obtained at the expense of the deprived eye by the non-deprived eye.

RELATIVE CELL SIZES

Vital-Durand *et al.* (1978) made measurements of cell-size in the deprived and non-deprived laminae of the monkey's lateral geniculate nucleus; within 6 weeks of monocular deprivation the neurones in the deprived laminae were some 15% smaller than in the other laminae; reverse suture led to a restoration of the status quo rather than a relative increase in the reverse-sutured eye at the expense of the previously non-deprived laminae. They noted that the effects on cell size could be manifest as early as 3 days postnatal, whereas in kittens the period was longer, slightly before 3 weeks (Garey *et al.*, 1973).

MONOCULAR AND BINOCULAR SEGMENTS OF LGN

As indicated by Fig. 22.16 the extreme nasal retina of one eye has no corresponding projection from the other eye, so that this area, in both eyes, will be monocularly represented in the lateral geniculate nucleus. When the monocular and binocular segments of the cat's lateral geniculate body were compared, the importance of competition for control became evident. Thus in the ipsilateral portion of lamina A thinning was restricted to the medial portion, which has a binocular input; no thinning occurred in the lateral part of lamina A, which is uniocular in representation, receiving its input from the extreme nasal crescent of the retina (Guillery & Stelzner, 1970).

AXON TERMINALS

Sur *et al.* (1982) described changes in the axon terminals from ganglion cells innervating the A laminae of the cat's lateral geniculate nucleus resulting from monocular deprivation; this was true of both X- and Y-retinogeniculate terminations; thus many X-cells from the deprived eye had unusually broad terminal fields; some also densely innervated the medial interlaminar nucleus, normally associated with Y-input. Many Y-axons had shrunken terminal fields in lamina A and the MIN. At the ultrastructural level, however, Winfield & Powell (1980) were surprised to find no difference in the lateral geniculate

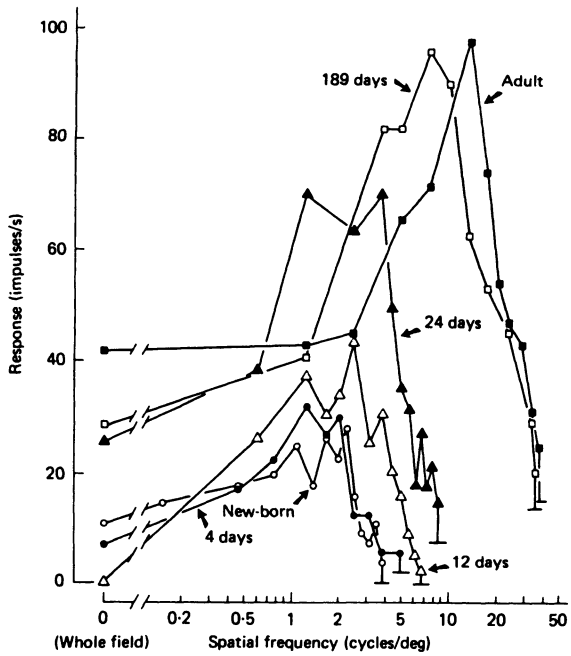

Fig. 22.15 These curves show the way in which the discharge rate for a drifting, high-contrast grating varied with spatial frequency, for representative cells from animals of different ages. Each symbol (different for each cell) represents the average impulse frequency over the three 7 ms bins centred on the bin containing the largest number of spikes in the averaged discharge histogram. A line is extrapolated from the data point for the highest spatial frequency tested, down to a horizontal bar that indicates the mean spontaneous firing rate of the cell (measured from discharge histograms collected with no pattern on the screen). The points plotted above zero spatial frequency represent responses to whole field modulation of the screen. With age, not only does the resolution of l.g.n. cells improve dramatically but spontaneous activity and peak discharge frequency tend to increase considerably. There is also a tendency for the band width of the response functions to narrow amongst these examples, which were typical of the more narrowly 'tuned' cells seen at each age. (Blakemore & Vital-Durand, *J. Physiol.*)

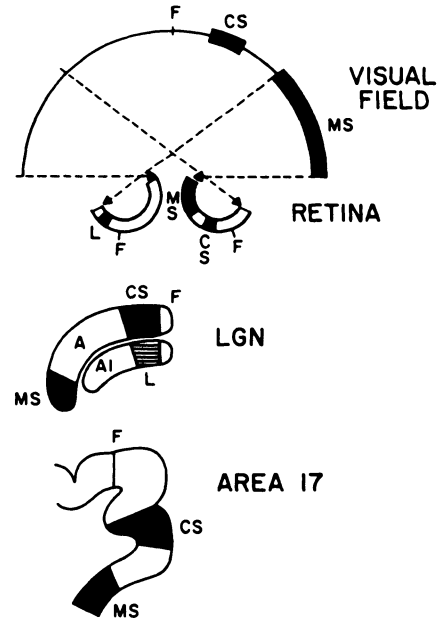

Fig. 22.16 Natural and artificial monocular segments (MS and CS, respectively) illustrated for right eye and left half of brain. Natural monocular segment includes a peripheral region of right visual field that can be viewed only by right eye, because nasal retina in right eye extends beyond homonymous representation of temporal retina in left eye. Because of precise retinotopic representation of visual field in lateral geniculate nucleus (LGN) and cortical area 17, monocular segments of these structures can be readily identified. This segment has not yet been identified for study in cortical area 18. Same relationships apply to monocular segment in left hemi-field. Finally, if a small retinal lesion is placed in left retina, an artificial monocular segment is created for homonymous region of right retina, and this region is retinotopically represented in each central structure. F, fixation point in visual field and its representation in each neuronal structure; L, retinal lesion and its representation in lateral geniculate nucleus. (Sherman & Spear, *Physiol. Rev.*)

cells related to the monocularly deprived eye; no neurones showed signs of degeneration, and it was not possible to determine which cells were deprived at the magnifications employed, with the exception of a slight diminution in the endoplasmic reticulum in the deprived cells. There were no marked changes in the synaptic organization of the nucleus, and this might agree with the fact that such morphological and physiological changes that occur in the deprived neurones are confined to the Y-cells, which may not be associated with the glomeruli examined in Winfield & Powell's study. In a quantitative study of the synaptic contacts in glomeruli and extra-glomerular neuropil, Winfield *et al.* (1980) confirmed that there were no differences between normal and monocularly deprived kittens.

PROPORTION OF X- TO Y-CELLS

Sherman *et al.* (1972) compared binocularly with monocularly deprived cats submitted to eye-suture from the 8th postnatal day. With bilateral lid-closure there was some loss of Y-cells throughout all laminae of the nucleus. With monocular closure the loss was much more severe; this occurred in the 'binocular segments' of the deprived laminae, whereas there was no loss in the 'monocular segments'. However, Shapley & So (1980) used the linearity of summation in receptive fields as the criterion for categorizing geniculate cells as X- or Y-type. They found the proportions of the two types to be normal after

monocular deprivation; and this agrees with the finding of Eysel *et al.* (1979) that the proportions of the two types of axon in the optic radiation passing to area 17 were normal.

MEDIAL INTERLAMINAR NUCLEUS (MIN)

The neurones of this part of the lateral geniculate body are almost exclusively Y-cells; Kratz *et al.* (1978) found no change in the electrical properties of neurones of the non-deprived regions. So far as the deprived regions were concerned, after monocular lid-suture prior to eye-opening about half as many as normal were activated per mm of electrode penetration, and these had abnormal receptive fields and response properties. The mean cell size, measured by injections of ^{3}H-proline into the eye, was 34% smaller in the deprived region, with apparently no difference in packing density. Essentially, Kratz *et al.* found no difference between the MIN and the laminated regions of the nucleus, so far as change in Y-cells was concerned.

STRUCTURE-FUNCTION RELATIONSHIP

Friedlander *et al.* (1982) identified geniculate neurones electrophysiologically and then injected horseradish peroxidase, and characterized them microscopically. Ten out of 24 neurones encountered had abnormalities and were identified as Y-cells; 13 out of 24 were normal, 12 being X-cells and one a Y-cell.

The abnormal Y-cells had small somata, exhibited poor responsiveness, and showed thin tortuous dendrites. One Y-cell had abnormal morphology but behaved like a normal X-cell, and this might well be a neurone accepting X-ganglion cell input rather than Y-input. The authors concluded that the reduced size of the deprived laminae was due, essentially, to reduced cell-size, rather than numbers of Y-cells; a reduction in size that was associated with poor responsiveness, leading to failure of Y-determined cortical responses, as in flicker responses (Jones & Berkley, 1977).

In a further study, made necessary by the contradictory claims of Shapley & So (1980), Friedlander & Stanford (1984), employing fine-tipped electrodes,[14] confirmed their earlier measurements; thus in the normal nucleus the proportion of X- to Y-cells was 2:1; they found fewer X- and Y-cells in the deprived laminae, but after allowing for the thinning of these laminae, they concluded that only Y-cells were affected. Figure 22.17 illustrates their comparison of work from four laboratories.[15]

PRIMATE GENICULATE NUCLEUS

Blakemore & Vital-Durand (1986) deprived Old World monkeys monocularly from birth for periods up to 27 weeks, and binocularly in one monkey for about a year. In the monocularly deprived geniculate nucleus the cells in the deprived layers were obviously smaller, but there was no difficulty in recording from them, and their response-properties seemed completely normal including their spatial-frequency resolution. So far as the vexed question as to whether there was a decrease in the number of Y-cells relative to X-cells was concerned, they mentioned that, in the primate, the Y-type cell is rare in the nucleus, so that it would have been difficult to detect a change. Blakemore & Vital-Durand concluded that the deficiencies in visual performance in the visually deprived eyes must result from changes in neurones central to the lateral geniculate nucleus, i.e. in the cortical neurones.

CYTOCHROME OXIDASE STUDY

The staining for this enzyme indicates loci of higher than usual oxidative metabolism (p. 549), and the technique is being increasingly employed to detect functional changes in the central nervous system. Kageyama & Wong-Riley (1985) differentiated

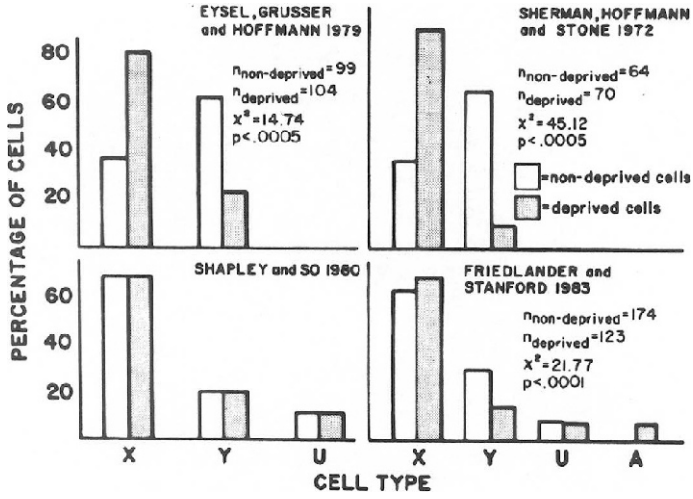

Fig. 22.17 Comparison of the percentages of cells encountered with recordings in the A-laminae of monocularly deprived cats in three previous studies and in that of Friedlander & Stanford (1984). (Friedlander & Stanford, *Exp. Brain Res.*)

W-, X- and Y-cells by their different reactivities. Thus Y-cells are normally darkly reactive, X-cells mediumly so, and W-cells lightly. The authors found (1986a) that, after early postnatal monocular suture, the reduced oxidase activity found in the neuropil of laminae A and A1 was primarily due to a loss of Y-cells. In regions where there was no binocular interaction, the effect was not so strong. When uniocular lid-suture was followed at 2 months by removal of the other eye, in order to remove the effects of binocular competition, the changes were similar to those seen with uniocular enucleation alone, as described by Wong-Riley (1979), the deafferented laminae becoming narrow with reduced staining. The monocularly deprived laminar regions, however, were now normal.[16]

GAD-POSITIVITY

Cells exhibiting glutamic acid dehydrogenase reactivity are GABA-ergic, and thus probably inhibitory neurones in the lateral geniculate nucleus. Robson & Martin-Elkins (1985) considered that, if the supposed binocular competition, manifest in the lateral geniculate nucleus and cortex, were of cortical origin, the inhibitory interneurones would not be affected by uniocular lid-closure; in fact they found no diminution in the size of the GAD-positive neurones.

SPATIAL AND TEMPORAL SENSITIVITY

Lehmkuhle *et al.* (1980) measured contrast-sensitivity functions of geniculate neurones; in monocularly deprived laminae; the X-cells, most commonly encountered, had a change in cut-off frequency (Fig. 22.18) indicating reduced resolving power, or visual acuity, in these cells. The few Y-cells encountered behaved normally; there was no effect on temporal frequency sensitivity. They considered that the loss in resolution at high spatial frequencies would be unlikely to cause the visual behaviour deficits of the monocularly deprived eye, and suggested that these deficits were attributable to loss of Y-cell function, visually guided behaviour being assisted by sensitivity to low spatial frequencies, as in distinguishing contours of objects in the visual field. Thus Berkley & Sprague (1979) found that lesions of area 17 that eliminated X- but not Y-pathways, produced a relatively mild loss of visual acuity; similarly, as Hess & Woo (1978) have argued when discussing vision through the cataractous lens, deprivation leading to absence of experience for low spatial frequencies and thus to Y-cell loss, causes severe loss of visual acuity; in milder visual experience deficits, as in strabismus, anisometropia, or astigmatism, there are X-cell deficits that only produce deficits at high spatial frequencies, i.e., under conditions requiring very fine discrimination.

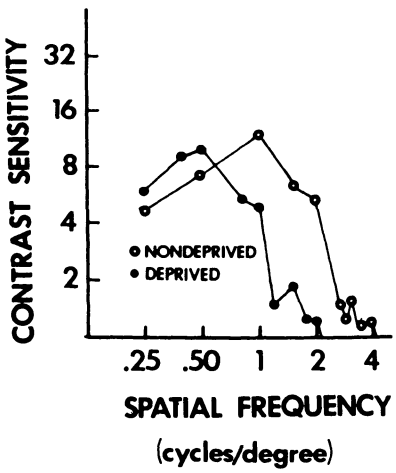

Fig. 22.18 Spatial contrast sensitivity functions of deprived X-cells. Average functions for 17 deprived and 11 nondeprived X-cells with receptive fields within the area centralis. Open circles denote the average sensitivities for the nondeprived X-cells; filled circles; deprived X-cells. (Lehmkuhle *et al.*, *J. Neurophysiol.*)

Signal Transmission

Eysel *et al.* (1979) recorded from the optic tract, lateral geniculate nucleus and optic radiation of the cat, distinguishing the X- and Y-characteristics of the axons by the evoked wave-amplitudes in the cortex, distinguished by r_1 for Y-axons and r_2 for more slowly conducting X-axons. The responses from the deprived eye were smaller than normal but the ratio of the two was the same, indicating no change in the relative numbers of X- and Y-neurones in the visual pathway. The maintained activity of ganglion and geniculate units was actually larger than normal in the deprived eye, suggesting that effects in the cortex were not due to reduced input; however, they emphasized that the patterned vision, which is defective in the deprived eye, depends on a complex series of bursts and synchrony between left and right eyes, rather than simply the efficiency of signal transmission.

Influence of Cortex

The inability of the deprived eye to drive the superior colliculus is due to a suppression exerted by areas 17 and 18 (Wickelgren & Sterling, 1969; p. 632), a suppression that is abolished by removal of cortex (Berman & Sterling, 1974). However, removal of areas 17 and 18 in monocularly deprived cats failed to remedy the loss of Y-cells, which according to their study fell from 39 to 18% of geniculate units encountered in the deprived laminae.

Retinal Damage

If the effects of monocular deprivation can be attributed principally to competitive action on the part of the non-deprived eye, then localized retinal damage in the non-deprived eye should reduce the severity of monocular deprivation; in fact Sherman *et al.* (1974) found this; behaviourally cats would respond to visual signals reaching the retina of the deprived eye provided they fell in a region corresponding to the damaged region of the retina. Morphologically the beneficial effect of retinal damage was seen in better growth of geniculate neurones in the region of the binocular segment of the deprived eye that had no input from the damaged retinal region.

Laterality of Effect

Sherman *et al.* found that about 20% of units could be activated by the deprived eye in the contralateral cortex, whereas ipsilat-

erally only 5%. In normal cats there is no marked contralateral dominance in the cortex, so that the contralateral effect of deprivation is the weaker.

Strabismus

The visual defects associated with strabismus in the young are so important, from the clinical aspect, that a great many studies have been carried out on animals with an artificially induced squint produced by sectioning of appropriate eye-muscle tendons. From the experimenter's point of view, however, the situation is far more complex than that provided by simple monocular lid-suture, since both eyes are receiving visual input, and the deficiencies arise from the absence of appropriate binocular stimulation.[17]

Ocular Dominance

When squints were induced from birth by section of a rectus muscle, there was no obvious visual defect, but when the distribution of ocular dominance amongst cortical cells was examined, this was found to be grossly abnormal (Fig. 22.19) Groups 1 and 7 predominating at the expense of bilaterally driven neurones; under these conditions each eye is receiving experience, and this experience is permitting it to pre-empt cortical neurones at the expense of the other. Thus, for a neurone to be binocularly driven, both eyes must apparently view the same object or patterned environment at the same time, and on corresponding parts of the two retinae. Hence any method of robbing the cortical neurones of congruent signals from the two eyes may be expected to reduce binocularity.

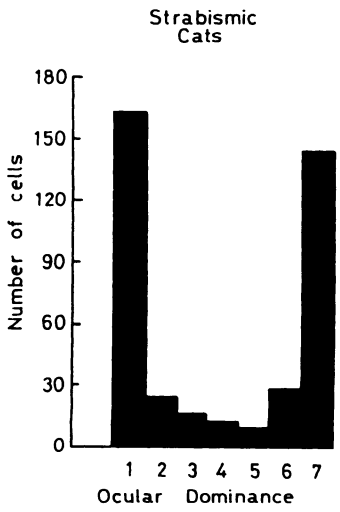

Fig. 22.19 Ocular dominance histogram for kittens reared with artificial strabismus. (Blakemore from Hubel & Wiesel, *Brit. med. Bull.*)

Striped Environments

Blakemore (1976) established squints in the young kittens surgically, and reared these in the dark except at intervals when they were exposed to a striped environment. Under these conditions there was no significant loss of binocularity since, although the eyes were squinting, the retinal images overlapped sufficiently to permit simultaneous activation of cortical cells by the two eyes. If, however, a squinting kitten was exposed to horizontal stripes through one eye and vertical stripes through the other, binocularity was impaired (Hirsch & Spinelli, 1970, 1971; Blakemore, 1976).

Alternating Monocular Occlusion

Hubel & Wiesel (1965) found that exposing only one eye at a time to a patterned environment, by alternately occluding one eye, had a similar effect to that produced by strabismus. The essential feature of the treatment is, once again, robbing the cortical cells of simultaneous congruent signals from both eyes. The importance of simultaneity was demonstrated by exposing dark-reared kittens for periods to a striped environment with alternating occlusion; thus they received the same retinal image through each eye but never simultaneously; and binocularity was reduced to the same extent as through simple alternating monocular occlusion. Thus the necessary condition for the maintenance of binocularity is that cortical neurones should be stimulated by patterned retinal images with contours of approximately the same orientation, falling simultaneously on the receptive fields of the two eyes (Blakemore, 1976).

Geniculate Neurones

Ikeda & Wright (1976) studied the receptive-field characteristics of lateral geniculate neurones, representing central vision, in the cat reared with a convergent squint, the spatial resolution of these cells being poor compared with geniculate cells representing the non-squinting eye. Ikeda *et al.* (1976) correlated the defective responsiveness of the geniculate cells with morphological changes, similar to those observed in cells representing the monocularly deprived eye, but they also observed that these morphological defects extended beyond the regions of representation of the area centralis of the squinting eye, suggesting that the visual defects were not confined to central vision.

NASAL VISUAL FIELD

In a more elaborate study, Ikeda *et al.* (1977) measured the spatial resolution of cells in different parts of the lateral geniculate body of kittens reared with a convergent strabismus; the regions were chosen so as to represent central and more and more peripheral parts of the retina, and the units responding were compared with corresponding areas for the non-squinting eye. In general it was found that, in each lateral geniculate body of the normal kitten, cells with normal receptive fields were equally common in layers A and A1, whereas in kittens with over 23.5° of squint no briskly functional cells could be recorded from layer A1 of the left lateral geniculate body where the squinting eye's *nasal visual field* projects. In addition to this restriction in the visual field, it was found that cells representing the area centralis of the squinting eye, although responsive, had much lower spatial resolution; the degree of loss did not depend on the degree of squint, whereas the restriction of the nasal field did do so. In general, there was a graded deterioration in the function of cells fed by the squinting eye, ranging from minor alterations in the receptive field properties in the temporal visual field projection zones, and the loss of spatial resolution at the central retinal projection zone leading to complete loss of function at the extreme nasal field projection zone. Morphologically a gradation in defect could also be established, in that there was a diminution in the mean perikaryal size; shrinkage in this occurred in all regions representing the squinting eye, the effect being greatest in the extreme nasal field. An examination of the visual fields of the normal and squinting left eyes, as in Fig. 22.20, reveals that a portion of the nasal field of the squinting eye is restricted by the bridge of the nose thus preventing stimulation. Thus the defects are essentially those due to disuse, and they will be graded because the shadow of the bridge of the nose does not create a sudden occlusion, the effects depending on the degree of eye movement and the angle of incident light. The defects in the neurones fed by the area centralis, and giving rise to low spatial resolution in central vision, are not due to disuse but to inappropriate stimulation of non-corresponding areas of the two retinae during development.

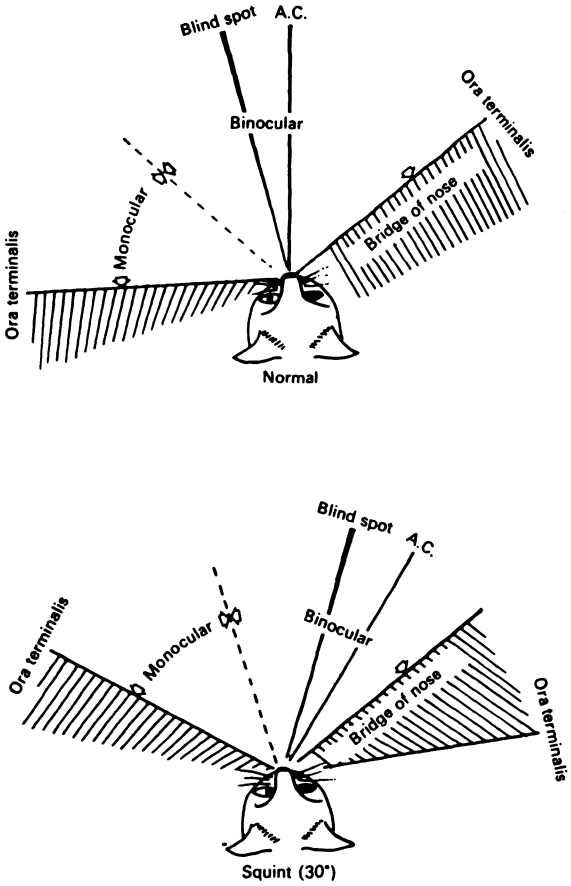

Fig. 22.20 The limit of the visual field of a cat seen by a normal left eye (upper diagram) and that seen by a left eye with a convergent squint of 30° (lower diagram). Note that the convergent squint of 30° results in approximately 30° of the temporal retina, which should receive inputs from the peripheral nasal field, being hidden behind the bridge of the nose, thus preventing stimulation. (Ikeda *et al.*, *J. Physiol.*)

Geniculate Amblyopia, Cell Shrinkage and Cortical Dominance

Tremain & Ikeda (1982) showed that cats with the greater loss of spatial resolution in their geniculate cells driven by the area centralis as a result of squint also showed the greater degree of cell shrinkage and a greater proportion of cortical neurones driven by the control eye. However, all cats had a loss of binocularly driven cells regardless of geniculate changes, but if these changes were present, then binocularity was inversely proportional to the degree of geniculate deficit.

More Recent Studies

Jones *et al.* (1984), in contrast with Ikeda *et al.* (1977), found no changes in the characteristics of the neurones representing the peripheral nasal field of the deviated eye, a contradiction they attributed to a difference in surgical techniques employed to establish the strabismus. In general, Jones *et al.* (1984) conclude that the behavioural abnormalities of squinting cats are to be attributable to cortical rather than geniculate deficiencies. However, so far as spatial-resolution was concerned, Jones *et al.* agreed with Ikeda & Tremain's (1978) finding that spatial resolution was some 2.1 cyc/deg in the deviated eye's

neurones compared with a normal of 3.1 cyc/deg. This was not due to an overall reduction in contrast-sensitivity, but was specific for high spatial-frequencies, with no loss at frequencies lower than 0.7 cyc/deg. Jones *et al.* compared the effects of strabismus on geniculate with those on cortical cells, where there is an apparent loss of contrast-sensitivity at all spatial-frequencies, as described by Chino *et al.* (1983) for cortical neurones, and Freeman *et al.* (1983) for cortically evoked potentials.

GANGLION CELLS

Cleland *et al.* (1982) have confirmed the reduction in visual resolution, measured behaviourally, of cats with surgically induced strabismus. However, when they investigated the claim of Ikeda & Tremain (1979) that the spatial resolution of brisk sustained ganglion cells was reduced in the region of the area centralis of the deviating eye, they found that the spatial resolution, measured with horizontal and vertical gratings, was normal in the amblyopic eyes; especially there was no deficit in ganglion cells of the area centralis.[18]

Notes

1. Von Noorden (1973) measured the effects of deprivation on visual acuity in monkeys; the work suggested that a detectable and persistent loss of acuity only occurred if deprivation began before about 2 months of age.
2. The requirement of experience for the development of orientation-selectivity in cortical neurones has been questioned in more than one study; Hubel & Wiesel, in their original studies on binocular deprivation, found orientation-selective neurones, but Blakemore & Mitchell (1973) and Imbert and Buisseret (1975) were unable to do so. Sherk & Stryker (1976) sutured kittens from first lid-opening and examined them at 22 to 29 days old. Ninety out of 98 cortical cells responded to a moving bar stimulus at an appropriate orientation, and a similar columnar organization of the orientation-selective units to that in the adult was found.
3. An interesting exception amongst the visually deprived kittens was one that had been kept in a diffusely illuminated cylinder which showed a strong preference for vertical or near-vertical lines, in contrast with another kitten with its nictitating membranes sutured and thus similarly exposed to diffuse uncontoured light; however, it turned out that there were, in fact, some low-contrast contours visible to the kitten in the cylinder, e.g. a distinct vertical seam where the sheet of white card lining the walls of the cylinder was joined together.
4. The study of Frégnac & Imbert (1978) is interesting; it confirmed that those cortical neurones in the young kitten that are orientation-specific have this specificity independently of visual experience. They emphasize that, in early stages of development, cortical neurones are driven by only one—the contralateral—eye, so that their subcortical input does not involve any competition, and because of this, their selectivity remains. At stages where binocularity appears, then receptive-field features are now subject to competition, and therefore require visual experience to be maintained. Kittens reared in the dark develop binocularity, but because this is not accompanied by visual experience, the initial orientation-selectivity is lost; being interfered with by input from the other eye that, presumably, has a different orientation preference
5. This is not true of kittens, however, since Mitchell *et al.* (1977), Blasdel & Pettigrew (1978) and Olson & Freeman (1978) found partial recovery by merely reopening the sutured eye. In monkeys, both LeVay *et al.* (1980) and Blakemore *et al.* (1981) have found no recovery at all. In Mitchell *et al.*'s study, for example, the kittens appeared blind through the deprived eye immediately on opening, but, within one to twelve days of opening, normal visual acuity of some 5 cyc/deg was attained; if deprivation was extended from 45 to 60 days, recovery was not complete. They also obtained some recovery of dominance.
6. In a more elaborate study of the recovery of visual function after cross-suturing, Movshon (1976b) established that, unless the previously deprived eye had recovered control over an appreciable proportion of cortical neurones, it was unable to perform reliably the more demanding visually controlled tasks such as placing or following. He points out that Spear & Ganz (1975) have shown that recovery depends on the presence of the visual cortex, so that ablation prevents this.
7. By this is meant the proportion of visually responsive neurones dominated by the initially deprived eye.
8. Hoffmann & Hollander (1978) found no increase in average size of lateral geniculate cells in the deprived regions after reverse-suture, although the chance of recording from Y-cells had returned to normal.
9. The authors point to common clinical experience with interruption of vision in one eye for a long enough period to produce defects in binocular visual performance; the prognosis for full recovery is good if the period of disruption is relatively brief, and even better if preceded by a period of normal binocular vision.
10. Kratz *et al.* (1976) did obtain some reversal after enucleation in eyes that had been sutured at the time of eye-opening; Blakemore & Hawken discuss the difference from their results, which might be due to difference in depth of anaesthesia; Kratz *et al.*'s cortical neurones that recovered were weakly driven and had lost most of their receptive-field specificity.
11. Blakemore & Van Sluyters (1974), in discussing the amblyopia in a squinting eye, have pointed out that children with extreme astigmatism that defocusses one meridian, by contrast with the orthogonal one, are often left with a meridional amblyopia, acuity for contours being poor when these are in the out-of-focus meridian.
12. Van Hof-Van Duin (1976) compared visual performance of cats, monocularly deprived but subsequently reverse-sutured. They concluded that visuo-motor responses were permanently impaired, whereas spatial discrimination of gratings at different orientations became normal after 4 weeks of reverse-suture. Ganz & Haffner (1974) have emphasized that many tests applied to cats are too simple, so that they fail to reveal defects depending on some degree of generalization. They found better performance in reverse-sutured animals compared with those monocularly deprived for 3 months.
13. Ikeda & Tremain (1978) had described a loss of ganglion cell resolution in the area centralis of monocularly deprived cats.
14. Shapley & So (1980) emphasize the importance of employing fine tipped microelectrodes in making these counts.
15. In dark-reared kittens Kratz *et al.* (1979b) found only a few normal Y-cells in either the monocular or binocular segments of the lateral geniculate nucleus; there was no reversal by a subsequent period of 1–2 years in the light; the authors

considered that, as the cell bodies appeared normal in the dark-reared kittens, many of the Y-cells had become X-cells.

16. Kageyama & Wong-Riley (1986b) have followed the staining for cytochrome oxidase in postnatal kittens; in the cortex there is heavy staining in lamina 2 in the first two postnatal weeks, and during this period there is a large geniculostriate projection here; it originates mainly from the geniculate C-laminae; the appearance and disappearanceof this staining coincide with this cortical staining. There is some geniculostriate afferent input to lamina 4 at birth giving some staining; there is a prominent increase of staining in this lamina around the fourth week corresponding to the increase in geniculate projection; and this corresponds to the beginning of the 'critical period' and time of geniculocortical afferent segregation (LeVay *et al.*, 1978).
17. The literature on artificial squint has expanded as rapidly as that on controlled ocular deprivation; limitations of space have led me to concentrate principally on the effects of occlusion, and its reversal, because of the certain knowledge of the nature of the visual stimuli reaching the eyes under these experimental conditions.
18. Siamese cats are often cross-eyed and this may follow from an unusual projection from the retina on to the lateral geniculate body, since Guillery (1970) has shown that many fibres that should, in the normal animal, have crossed in the chiasm, failed to do so, with the result that parts of the ipsilateral visual field were represented on the lateral geniculate body and thence on to the cortex. Hubel & Wiesel (1971) showed that this projection from the contralateral eye relayed in layer A_1, which in the normal cat receives input from the ipsilateral eye. This aberrant projection resulted in the appearance on the cortex of regions represented by the ispilateral field inserted between regions representing the contralateral field. Interestingly, no cortical cells were driven by both eyes, as found with kittens brought up with artificially created squints. Later Kaas & Guillery (1973) described two different types of abnormality in American bred Siamese cats; in one type the relays from layers A_1 and C_1 were suppressed, whereas in the other there was a rearrangement with a reversal of input from these segments. Chino *et al.* (1978) found that ganglion cells were abnormal, only 14% being Y-cells compared with 35% in the common cat; the greater the squint, the lower the percentage of Y-cells, as measured in the optic tract fibres.

References

Albus, K. & Wolf, W. (1984) Early post-natal development of neuronal function in the kitten's visual cortex: a laminar analysis. *J. Physiol.* **348**, 153–185.

Baker, F. H., Grigg, P. & Von Noorden, G. K. (1974) Effects of visual deprivation and strabismus on the response of neurons in the visual cortex of the monkey, including studies on the striate and prestriate cortex in the normal animal. *Brain Res.* **66**, 185–208.

Barlow, H. B. (1975) Visual experience and cortical development. *Nature* **258**, 199–204.

Berkley, M. A. & Sprague, J. M. (1979) Striate cortex and visual acuity functions in the cat. *J. Comp. Neurol.* **187**, 679–702.

Berman, N. J. & Sterling, P. (1974) Immediate reversal of eye dominance in the superior colliculus of the monocularly deprived cat following cortical removal. *Anat. Rec.* **178**, 310.

Blakemore, C. (1974) Development of functional connexions in the mammalian visual system. *Brit. Med. Bull.* **30**, 152–157.

Blakemore, C. (1976) The conditions required for the maintenance of binocularity in the kitten's visual cortex. *J. Physiol.* **261**, 423–444.

Blakemore, C. & Cooper, G. F. (1970) Development of the brain depends on the visual environment. *Nature* **228**, 477–478.

Blakemore, C., Garey, L. J. & Vital-Durand, F. (1978) The physiological effects of monocular deprivation and their reversal in the monkey's visual cortex. *J. Physiol.* **283**, 223–262.

Blakemore, C. & Hawken, M. J. (1982) Rapid restoration of functional input to the visual cortex of the cat after brief monocular deprivation. *J. Physiol.* **327**, 463–487.

Blakemore, C., Hawken, M. J. & Mark, R. F. (1982) Brief monocular deprivation leaves subthreshold synaptic input on neurones of the cat's visual cortex. *J. Physiol.* **327**, 489–505.

Blakemore, C. & Mitchell, D. E. (1973) Environmental modification of the visual cortex and the neural basis of learning and memory. *Nature* **241**, 467–468.

Blakemore, C. & Van Sluyters, R. C. (1974) Reversal of the physiological effects of monocular deprivation in kittens: further evidence for a sensitive period. *J. Physiol.* **237**, 195–216.

Blakemore, C. & Van Sluyters, R. C. (1975) Innate and environmental factors in the development of the kitten's visual cortex. *J. Physiol.* **248**, 663–716.

Blakemore, C. & Vital-Durand, F. (1986) Effects of visual deprivation on the development of the monkey's lateral geniculate nucleus. *J. Physiol.* **380**, 493–511.

Blakemore, C., Vital-Durand, F. & Garey, L. J. (1981) Recovery from monocular deprivation in the monkey. I. Reversal of physiological effects in the visual cortex. *Proc. Roy. Soc. B* **213**, 399–423.

Blasdel, G. G. & Pettigrew, J. D. (1978) Effect of prior visual experience on cortical recovery from the effects of unilateral eyelid suture in kitten. *J. Physiol.* **274**, 601–619.

Boothe, R. G., Greenough, W. T., Lund, J. S. & Wrege, K. (1979) A quantitative investigation of spine and dendrite development of neurons in visual cortex (Area 17) of *Macaca nemestrina* monkeys. *J. Comp. Neurol.* **186**, 473–489.

Chino, Y. M., Shansky, M. S. & Hamasaki, D. L. (1978) Properties of X- and Y-type retinal ganglion cells in Siamese cats. *Brain Res.* **143**, 459–473.

Chino, Y. M., Shansky, M. S. & Hamasaki, D. I. (1980) Development of receptive-field properties of retinal ganglion cells in kittens raised with convergent squint. *Exp. Brain Res.* **39**, 313–320.

Chino, Y. M., Shansky, M. S., Janowski, W. L. & Banser, F. A. (1983) Effects of rearing kittens with convergent strabismus on development of receptive-field properties in striate cortex neurons. *J. Neurophysiol.* **50**, 265–286.

Cleland, B. G., Crewther, D. P., Crewther, S. G. & Mitchell, D. E. (1982) Normality of spatial resolution of retinal ganglion cells in cats with strabismic amblyopia. *J. Physiol.* **326**, 235–249.

Cleland, B. G., Mitchell, D. E., Gilliard-Crewther, S. & Crewther, D. P. (1980) Visual resolution of retinal ganglion cells in monocularly deprived cats. *Brain Res.* **192**, 261–266.

Cragg, B. G. (1975) The development of synapses in the visual system of the cat. *J. Comp. Neurol.* **160**, 147–166.

Dews, P. B. & Wiesel, T. N. (1970) Consequences of monocular deprivation on visual behaviour in kittens. *J. Physiol.* **206**, 437–455.

Eysel, U. T., Grüsser, O.-J. & Hoffmann, K.-P. (1979) Monocular deprivation and the signal transmission by X- and Y-neurons of the cat lateral geniculate nucleus. *Exp. Brain Res.* **34**, 521–539.

Freeman, D. N. & Marg, E. (1975) Visual acuity development coincides with the sensitive period in kittens. *Nature* **254**, 614–615.

Freeman, R. D., Sclar, G. & Ohzawa, I. (1983) An electrophysiological comparison of convergent and divergent strabismus in the cat. *J. Neurophysiol.* **49**, 227.

Frégnac, Y. & Imbert, M. (1978) Early development of visual cortical cells in normal and dark-reared kittens: relationship between orientation selectivity and ocular dominance. *J. Physiol.* **278**, 27–44.

Friedlander, M. J., Martin, K. A. C. & Vahle-Hinz, C. (1985) The structure of the terminal arborizations of physiologically identified retinal ganglion cells. *J. Physiol.* **359**, 293–313.

Friedlander, M. J. & Stanford, L. R. (1984) Effects of monocular deprivation on the distribution of cell types in the LGNd: a sampling study with fine-tipped micropipettes. *Exp. Brain Res.* **53**, 451–461.

Friedlander, M. J., Stanford, L. R. & Sherman, S. M. (1982) Effects of monocular deprivation on the structure–function relationship of individual neurons in the cat's lateral geniculate nucleus. *J. Neurosci.* **2**, 321–330.

Ganz, L. & Haffner, M. E. (1974) Permanent perceptual and neurophysiological effects of visual deprivation in the cat. *Exp. Brain Res.* **20**, 67–87.

Ganz, L. & Hirsch, H. V. B. (1972) The nature of visual deficits in visually deprived cats. *Brain Res.* **44**, 547–568.

Garey, L., Fisher, R. A. & Powell, T. P. S. (1973) Effects of experimental deafferentation on cells in the lateral geniculate nucleus. *Brain Res.* **52**, 363–369.

Guillery, R. W. (1970) An abnormal retinogeniculate projection in Siamese cats. *Brain Res.* **14**, 739–741.

Guillery, R. W. & Stelzner, D. J. (1970) The differential effects of unilateral lid closure upon monocular and binocular segments of the dorsal lateral geniculate nucleus in the cat. *J. Comp. Neurol.* **139**, 413–422.

Hess, R. & Woo, G. (1978) Vision through cataracts. *Invest. Ophthal.* **17**, 428.

Hirsch, H. V. B. & Spinelli, D. N. (1970) Visual experience modifying distribution of horizontally and vertically oriented receptive fields in cats. *Science* **168**, 869–871.

Hirsch, H. V. B. & Spinelli, D. N. (1971) Modification of the distribution of receptive field orientation in cats by selective visual exposure during development. *Exp. Brain Res.* **12**, 509–527.

Hoffmann, K.-P. & Cynader, M. (1977) Functional aspects of plasticity in the visual system of adult cats after early monocular deprivation. *Phil. Trans. B* **278**, 411–424.

Hoffmann, K.-P. & Hollander, H. (1978) Physiological and morphological changes in cells of the lateral geniculate nucleus in monocularly-deprived and reverse-sutured cats. *J. Comp. Neurol.* **177**, 145–157.

Hubel, D. H. & Wiesel, T. N. (1963) Receptive fields of cells in striate cortex of very young, visually inexperienced kittens. *J. Neurophysiol.* **26**, 994–1002.

Hubel, D. H. & Wiesel, T. N. (1965) Binocular interaction in striate cortex of kittens reared with artificial squint. *J. Neurophysiol.* **28**, 1041–1059.

Hubel, D. H. & Wiesel, T. N. (1970) The period of susceptibility to the physiological effects of unilateral eye closure in kittens. *J. Physiol.* **206**, 419–436.

Hubel, D. H. & Wiesel, T. N. (1971) Aberrant visual projections in the Siamese cat. *J. Physiol.* **218**, 33–62.

Hubel, D. H., Wiesel, T. N. & LeVay, S. (1976) Functional architecture of Area 17 in normal and monocularly deprived macaque monkeys. *Cold Spr. Harb. Symp. Quant. Biol.* **40**, 581–589.

Hubel, D. H., Wiesel, T. N. & LeVay, S. (1977) Plasticity of ocular dominance columns in monkey striate cortex. *Phil. Trans. B* **278**, 377–409.

Ikeda, H., Plant, G. T. & Tremain, K. E. (1976) Morphological changes in the dorsal lateral geniculate nucleus of kittens raised with surgically produced squint. *J. Physiol.* **258**, 70–71P.

Ikeda, H., Plant, G. T. & Tremain, K. E. (1977) Nasal field loss in kittens reared with convergent squint—neurophysiological and morphological studies of the lateral geniculate nucleus. *J. Physiol.* **270**, 345–366.

Ikeda, H. & Tremain, K. E. (1978) The development of spatial resolving power of LGN cells and its susceptibility to blur and strabismus. *Arch. Ital. Biol.* **116**, 375–384.

Ikeda, H. &Tremain, K. E. (1979) Amblyopia occurs in retinal ganglion cells in cats reared with convergent squint without alternating fixation. *Exp. Brain Res.* **35**, 559–582.

Ikeda, H. & Wright, M. J. (1976) Properties of LGN cells in kittens reared with convergent squint: a neurophysiological demonstration of amblyopia. *Exp. Brain Res.* **25**, 63–77.

Imbert, M. & Buisseret, P. (1975) Receptive field characteristics and plastic properties of visual cortical cells in kittens reared with or without visual experience. *Exp. Brain Res.* **22**, 25–36.

Jones, K. R. & Berkley, M. A. (1977) Distribution and temporal response characteristics of evoked potentials in the visually deprived cat. *Brain Res.* **130**, 572–578.

Jones, K. R., Kalil, R. E. & Spear, P. D. (1984) Effects of strabismus on responsivity, spatial resolution, and contrast sensitivity of cat geniculate neurons. *J. Neurophysiol.* **52**, 538–552.

Kaas, J. H. & Guillery, R. W. (1973) The transfer of abnormal visual field representations from the dorsal lateral geniculate nucleus to the visual cortex in Siamese cats. *Brain Res.* **59**, 61–95.

Kageyama, G. H. & Wong-Riley, M. (1985) An analysis of the cellular localization of cytochrome oxidase in the lateral geniculate nucleus of the adult cat. *J. Comp. Neurol.* **242**, 338–357.

Kageyama, G. H. & Wong-Riley, M. (1986a) Differential effect of visual deprivation on cytochrome oxidase levels in major cell classes of the cat LGN. *J. Comp. Neurol.* **246**, 212–237.

Kageyama, G. H. & Wong-Riley, M. (1986b) The localization of cytochrome oxidase in the LGN and striate cortex of postnatal kittens. *J. Comp. Neurol.* **243**, 182–194.

Kalil, R. (1978). Dark rearing in the cat: effects on visuomotor behavior and cell growth in the dorsal lateral geniculate nucleus. *J. Comp. Neurol.* **178**, 451–468.

Kratz, K. E., Mangel, S. C., Lehmkuhle, S. & Sherman, M. (1979a) Retinal X- and Y-cells in monocularly lid-sutured cats: normality of spatial and temporal properties. *Brain Res.* **172**, 545–551.

Kratz, K. E., Sherman, S. M. & Kalil, R. (1979b) Lateral geniculate nucleus in dark-reared cats: loss of Y-cells without change in cell size. *Science* **203**, 1353–1355.

Kratz, K. S., Spear, P. D. & Smith, D. C. (1976) Post-critical period reversal of effects of monocular deprivation on the striate cortex in cats. *J. Neurophysiol.* **39**, 501–511.

Kratz, K. E., Webb, S. V. & Sherman, S. M. (1978) Studies of the cat's medial interlaminar nucleus: a subdivision of the dorsal lateral geniculate nucleus. *J. Comp. Neurol.* **181**, 601–614.

Lehmkuhle, S., Kratz, K. E., Mangel, C. & Sherman, M. (1980) Spatial and temporal sensitivity of X- and Y-cells in dorsal lateral geniculate nucleus. *J. Neurophysiol.* **43**, 520–541.

LeVay, S., Stryker, M. P. & Shatz, C. J. (1978) Ocular dominance columns and their development in layer IV of the cat's visual cortex: a quantitative study. *J. Comp. Neurol.* **179**, 223–244.

LeVay, S., Wiesel, T. N. & Hubel, D. H. (1980) The development of ocular dominance columns in normal and visually deprived monkeys. *J. Comp. Neurol.* **191**, 1–51.

Leventhal, A. G. & Hirsch, H. V. B. (1983) Effects of visual deprivation upon the morphology of retinal ganglion cells

projecting to the dorsal lateral geniculate nucleus of the cat. *J. Neurophysiol.* **33**, 332–344.

Lund, R. D. & Lund, J. S. (1972) Development of synaptic patterns in the superior colliculus of the rat. *Brain Res.* **42**, 1–20.

Mangel, S. C., Wilson, J. R. & Sherman, S. M. (1983) Development of neuronal response properties in the cat dorsal lateral geniculate nucleus during monocular deprivation. *J. Neurophysiol.* **5**, 240–264.

Mitchell, D. E., Cynader, M. & Movshon, J. A. (1977) Recovery from the effects of monocular deprivation in kittens. *J. Comp. Neurol.* **176**, 53–63.

Movshon, J. A. (1976a) Reversal of the physiological effects of monocular deprivation in the kitten's visual cortex. *J. Physiol.* **261**, 125–174.

Movshon, J. A. (1976b) Reversal of the behavioural effects of monocular deprivation in the kitten. *J. Physiol.* **261**, 175–187.

Olson, C. R. & Freeman, R. D. (1975) Progressive changes in kitten striate cortex during monocular vision. *J. Neurophysiol.* **38**, 26–32.

Olson, C. R. & Freeman, R. D. (1978). Monocular deprivation and recovery during sensitive period in kittens. *J. Neurophysiol.* **41**, 65–74.

Peck, C. K. & Blakemore, C. (1975) Modification of single neurons in the kitten's visual cortex after brief periods of monocular visual experience. *Exp. Brain Res.* **22**, 57–68.

Pettigrew, J. D. (1974) The effect of visual experience on the development of stimulus specificity by kitten cortical neurones. *J. Physiol.* **237**, 49–74.

Pettigrew, J. D., Nikara, T. & Bishop, P. O. (1968) Binocular interaction on single units in cat striate cortex: simultaneous stimulation by single moving slit with receptive fields in correspondence. *Exp. Brain Res.* **6**, 391–410.

Rakic, P. (1981) Development of visual centers in the primate brain depends on binocular competition before birth. *Science* **214**, 928–931.

Robson, J. A. & Martin-Elkins, C. L. (1985) The effects of monocular deprivation on the size of GAD+ neurons in the cat's dorsal lateral geniculate nucleus. *J. Comp. Neurol.* **239**, 62–74.

Shapley, R. & So, Y. T. (1980) Is there an effect of monocular deprivation on the proportions of X- and Y-cells in the cat lateral geniculate nucleus? *Exp. Brain Res.* **39**, 41.

Shatz, C. J. (1983) The prenatal development of the cat's retinogeniculate pathway, *J. Neurosci.* **3**, 482–499.

Sherk, H. & Stryker, M. P. (1976) Quantitative study of cortical orientation selectivity in visually inexperienced kitten. *J. Neurophysiol.* **39**, 63–70.

Sherman, S. M. (1973) Visual field defects in monocularly and binocularly deprived cats. *Brain Res.* **45**, 25–45.

Sherman, S. M. (1974) Permanence of visual perimetry deficits in monocularly deprived cats. *Brain Res.* **73**, 491–501.

Sherman, S. M., Guillery, R. W., Haas, J. H. & Sanderson, K. J. (1974) Behavioral, electrophysiological and morphological studies of binocular competition in the development of the geniculo-cortical pathways of cats. *J. Comp. Neurol.* **158**, 1–18.

Sherman, S. M., Hoffmann, K.-P. & Stone, J. (1972) Loss of a specific cell type from dorsal lateral geniculate nucleus in visually deprived cats. *J. Neurophysiol.* **35**, 532–541.

Sherman, S. M. & Sanderson, K. J. (1972) Binocular interaction on cells of the dorsal lateral geniculate nucleus of visually deprived cats. *Brain Res.* **37**, 126–131.

Sherman, S. M. & Spear, P. D. (1982) Organization of visual pathways in normal and visually deprived cats. *Physiol. Rev.* **62**, 738–855.

Sherman, S. M. & Stone, J. (1973) Physiological normality of the retina in visually deprived cats. *Brain Res.* **60**, 224–230.

Spear, P. D. & Ganz, L. (1975) Effects of visual cortex lesions following recovery from monocular deprivation in cat. *Exp. Brain Res.* **23**, 181–201.

Spear, P. D., Langsetmo, A. & Smith, D. C. (1980) Age-related changes in effects of monocular deprivation on cat striate cortex neurons. *J. Neurophysiol.* **43**, 559–580.

Stein, B. E. & Gallagher, H. L. (1981) Maturation of cortical control over superior colliculus cells in cat. *Brain Res.* **223**, 429–435.

Sur, M., Humphrey, A. L. & Sherman, S. M. (1982) Monocular deprivation affects X- and Y-cell retinogeniculate terminations in cats. *Nature* **300**, 183–185.

Swindale, N. V., Vital-Durand, F. & Blakemore, C. (1981) Recovery from monocular deprivation in the monkey. III. Reversal of anatomical effects in the visual cortex. *Proc. Roy. Soc. B* **213**, 435–450.

Teller, D. Y., Regal, D. M., Videen, T. O. & Pulos, E. (1978) Development of visual acuity in infant monkeys (*Macaca nemestrina*) during the early postnatal weeks. *Vision Res.* **18**, 561–566.

Timney, B. (1981). Development of binocular depth perception in kittens. *Invest. Ophthal.* **21**, 493–496.

Tremain, K. E. & Ikeda, H. (1982) Relationship between amblyopia, LGN cell 'shrinkage' and cortical ocular dominance in cats. *Exp. Brain Res.* **45**, 243–252.

Tsumoto, T. & Suda, K. (1978) Evidence for excitatory connections from the deprived eye to the visual cortex in monocularly deprived kittens. *Brain Res.* **133**, 150–156.

Van Hof, M. W. (1969) Discrimination of striated patterns of different orientation in rabbits deprived of light after birth. *Exp. Neurol.* **23**, 561–565.

Van Hof-Van Duin, J. (1976) Early and permanent effects of monocular deprivation on pattern discrimination and visuomotor behavior in cats. *Brain Res.* **111**, 261–276.

Van Sluyters, R. C. (1978) Reversal of the physiological effects of brief periods of monocular deprivation in the kitten. *J. Physiol.* **284**, 1–17.

Van Sluyters, R. C. & Stewart, D. L. (1974a) Binocular neurons of the rabbit's visual cortex: receptive field characteristics. *Exp. Brain Res.* **19**, 166–195.

Van Sluyters, R. C. & Stewart, D. L. (1974b) Binocular neurons of the rabbit's visual cortex: effects of monocular sensory deprivation. *Exp. Brain Res.* **19**, 196–204.

Vital-Durand, F., Garey, L. J. & Blakemore, C. (1978) Monocular and binocular deprivation in the monkey: morphological effects and reversibility. *Brain Res.* **158**, 45–64.

Von Noorden, G. K. (1960) Pathophysiology of amblyopia: diagnostic principles in pleoptics. *Amer. Orthopt. J.* **10**, 7–16.

Von Noorden, G. K. (1973) Experimental amblyopia in monkeys. Further behavioral observations and clinical correlations. *Invest. Ophthal.* **12**, 721–726.

Von Noorden, G. K., Dowling, J. E. & Ferguson, J. E. (1970) Experimental amblyopia in monkeys. I. *Arch. Ophthal.* **84**, 206–214.

Watkins, D. W., Wilson, J. R. & Sherman, S. M. (1978) Receptive field properties of neurons in binocular and monocular segments of striate cortex in cats with binocular lid suture. *J. Neurophysiol.* **41**, 322–337.

Wickelgren, B. G. & Sterling, P. (1969) Influence of visual cortex on receptive fields in the superior colliculus of the cat. *J. Neurophysiol.* **32**, 16–23.

Wiesel, T. N. & Hubel, D. H. (1963a) Effects of visual deprivation on morphology and physiology of cells in the cat's lateral geniculate nucleus. *J. Neurophysiol.* **26**, 978–993.

Wiesel, T. N. & Hubel, D. H. (1963b) Single cells responses in striate cortex of kittens deprived of vision in one eye. *J. Neurophysiol.* **26**, 1003–1017.

Wilson, J. R. & Sherman, S. M. (1977) Differential effect of early monocular deprivation on binocular and monocular segments of cat striate cortex. *J. Neurophysiol.* **40**, 891–903.

Winfield, D. A., Hiorns, R. W. & Powell, T. P. S. (1980) A quantitative electron-microscopical study of the postnatal development of the lateral geniculate nucleus in normal kittens and in kittens with eyelid suture. *Proc. Roy. Soc. B* **210**, 211–234.

Winfield, D. A. & Powell, T. P. S. (1980) An electron-microscopical study of the postnatal development of the lateral geniculate nucleus in the normal kitten and after eyelid suture. *Proc. Roy. Soc. B* **210**, 197–210.

Wong-Riley, M. T. T. (1979) Changes in the visual system of monocularly sutured or enucleated kittens demonstrable with cytochrome histochemistry. *Brain Res.* **171**, 11–28.

23. NEUROPHYSIOLOGY OF PERCEPTION: NON-GENICULOSTRIATE PATHWAYS AND THE NEURONES OF THEIR CENTRAL STATIONS

The lateral geniculate body is the major processing nucleus for retinal information; however, in 1961 Altman and Carpenter drew attention to the thalamic projection from the superior colliculi; these bodies receive a powerful retinal projection, so that this collicular projection reveals an indirect access of visual information to the cerebral cortex. The target-areas of the ascending collicular projections are mainly within the pulvinar posterior system of the thalamus (PUL-PO), which, in turn, receives a strong projection from the visual cortex. Besides the colliculus, the adjacent pretectal region contains nuclei receiving retinal input; thus the circuitry for this subsidary processing system may be indicated crudely by Fig. 23.1. We shall see that the cortical influence on the colliculi is profound, so that their receptive-field characteristics become very similar to those of certain cortical cells.

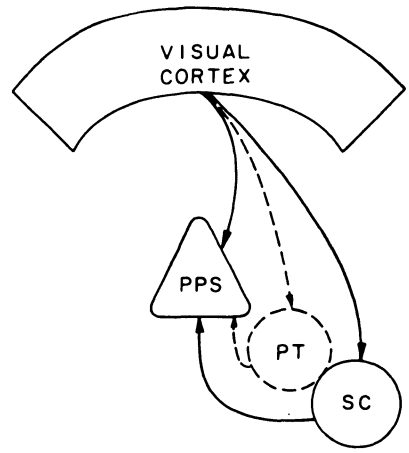

Fig. 23.1 Schematic summary of extrageniculate pathways to visual cortex. PPS, pulvinar posterior system; PT, pretectal region; SC, superior colliculus. (Graybiel, *Invest. Ophthal.*)

THE SUPERIOR COLLICULI

Species Variations

These midbrain centres have long been associated with vision; in orders below the mammals they are the end-stations for visual input and are described as the optic lobes. In mammals their prominence varies greatly from species to species; they are highly developed in flying lemurs, squirrels and tree shrews, animals exhibiting rapid motion and requiring accurate association of vision with this; in insectivores and prosimians, closely related to tree shrews phylogenetically, the colliculus is smaller and less differentiated (Casagrande & Diamond, 1974).

Structure and Projections

Each colliculus is composed of several layers, namely, from without inwards, the *stratum zonale*, *superior grey* (s. superficiale griseum), *optic grey*, *intermediate grey*, *intermediate white*, *deep grey* and *deep white* (see, for example, Kanaseki & Sprague, 1974). Functionally the colliculus has been divided into *superficial layers*, receiving projections from the optic tract and visual cerebral cortex, and *deeper layers* with no obvious retinal input but with afferent input from acoustic, and somatosensory systems in addition to visual cortical input. According to Stein *et al.* (1976), the intermediate layers combine visual, somatic and acoustic inputs, whilst the deepest layers are non-visual and the somatosensory organization suggests an arrangement that favours coordination of visual with motor activity in the limbs.

Retinotectal Projection

In primates and many other mammals the visual fields are organized similarly to those of the lateral geniculate body, so that each hemifield of visual space is represented on the contralateral colliculus as a result of a partial decussation of the optic nerves. In the cat and tree shrew, however, a portion of the ipsilateral hemifield, in addition to the whole contralateral hemifield, is represented in each colliculus, indicating a crossing of some fibres from the temporal half-retina in the chiasma (Harting & Guillery, 1976), together with a failure of some nasal retinal fibres to cross (Fig. 23.2). In the monkey, however, the half-fields are strictly segregated (Cynader & Berman, 1972).

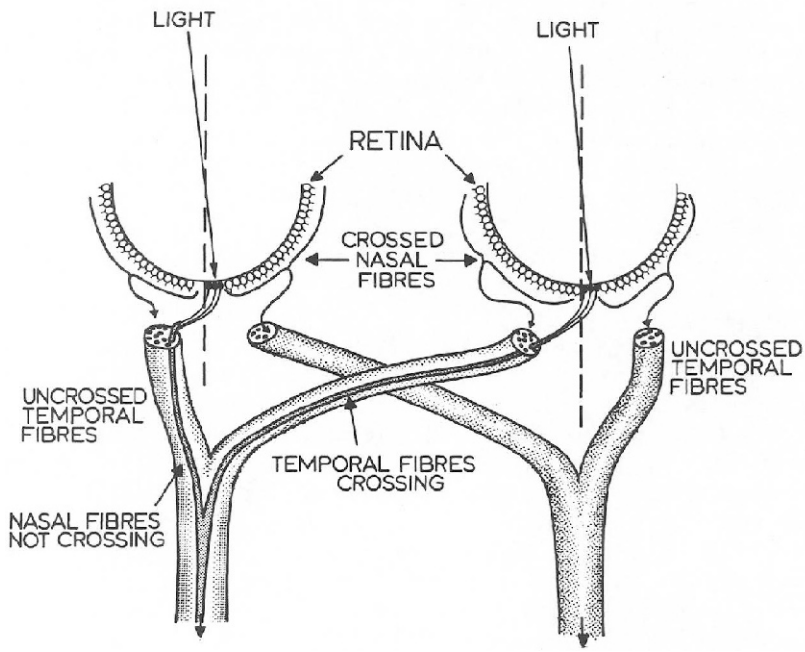

Fig. 23.2 Showing how a portion of the ipsilateral visual hemifield is represented in the superior colliculus, in addition to the whole contralateral hemifield, as a result of the crossing of some fibres from the temporal retina in the chiasma together with the failure of some nasal fibres to cross.

COLLICULAR MAP

Figure 23.3 relates the positions of the receptive fields in space to position on the superior colliculus; the periphery of the contralateral half-field is represented on the most posterior part, the upper fields on the medial part and the lower on the lateral part. The area centralis has a disproportionately large area of representation. Localized electrical stimulation caused eye-movements directed to definite points in space, and it is interesting that the point in space to which the eye was directed was that from which a visual stimulus would evoke a response on the same stimulated point (Robinson, 1972; Cynader & Berman, 1972).

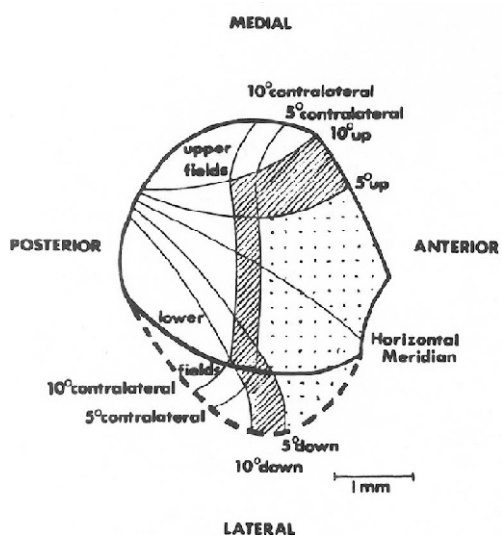

Fig. 23.3 Representation of the visual field on the surface of the right colliculus (as viewed from above in the Horsley-Clarke plane). The stippled area represents parts of the contralateral visual field within 5° of the fovea. Striped and stippled areas combined represent parts of the contralateral visual field within 10° of the fovea. (Cynader & Berman, *J. Neurophysiol.*)

Anterograde Labelling Graybiel (1975) followed the anterograde movement of labelled fucose or proline after injections into the eye of the cat. The interesting feature of the projection in the superficial layers, observed by this technique, was what she called the 'puffs' and 'holes', as manifested in the density of radiation in restricted portions of the colliculus, suggesting a fairly strict segregation of ipsi- and contralateral inputs, similar to that observed more precisely in the lateral geniculate body. Hubel *et al.* (1975) used a similar technique in the macaque monkey and observed that, contrary to previous reports, all layers of the colliculus were labelled, including an anterolateral region to which the fovea projects. This foveal projection is of special interest since it has been claimed that the foveal region of representation on the superior colliculus receives its entire projection exclusively from the visual cortex, rather than the retina directly (Wilson & Toyne, 1970).[1] This would be in marked disagreement with the physiological observation of a strong response to foveal stimulation when the visual cortex is put out of action by cooling or ablation (Schiller *et al.*, 1974). In addition, the authors noted a marked

tendency in regions of binocular representation for projections from ipsi- and contralateral eyes to be segregated; in the temporal crescents of the visual field there was only a continuous labelling from the contralateral eye. In general, in or near the foveal projection, a predominantly superficial input was found, with an apparent alternation between the two eyes; in regions representing more peripheral parts of the retina there was a tendency for the contralateral input to be confined to the superficial level of the upper grey with the ipsilateral input displaced to a deeper level in clumps. Still further posteromedially in the colliculus, where the temporal crescent of the visual field is represented, the ipsilateral input disappears and there is only a continuous layer of contralateral input. Although the ipsilateral eye is represented in the superior colliculus of the monkey, this representation seems subservient to the contralateral projection, by contrast with the lateral geniculate body and visual cortex, where, in the regions of binocular overlap, the two eyes are virtually equally represented; in the cat this parsimony in representation of the ipsilateral eye is much more striking (Cynader & Berman, 1972; Kanaseki and Sprague, 1974; Graybiel, 1975).

Cortical Projections to Colliculus

According to Kawamura *et al.* (1974), the cat's visual areas 17, 18 and 19 project to the superior colliculus, in particular to the superficial lamina 2, but also to layers 4, 5 and 6. All the other visual cortical areas (20, 21, 7 and Clare-Bishop), i.e. areas receiving indirect, as opposed to geniculostriate, projections, project to the deep layers only. As we might expect, points on the visual cortex receiving input from a given point in space project to corresponding points in the superficial layers, an arrangement that permits integration of two visual inputs, for example, in the interests of guided movements of the eyes. As we shall see, moreover, the cortical input to tectal neurones has a profound influence on their response-characteristics. In monkeys, Leichnetz *et al.* (1981) injected horseradish peroxidase into the superior colliculus and observed retrograde movement into the frontal eye-field (Brodmann's area 8, or area 'a and dorsal area 45 of Walker, or area FD and dorsal FD of v. Bonin & Bailey) homolaterally. An anterograde study, involving injection into the frontal eye-field, combined with this retrograde study showed that the projection was topographically organized in the stratum intermedium.

CONTRALATERAL PROJECTION

Since the visual cortex and superior colliculus cooperate, it is reasonable to presume that the projection of the cortex would be ipsilateral. However Powell (1976) has described, in the cat, contralateral projections from striate cortex and also from non-visual cortical areas. Distel & Fries (1982), using retrograde labelling in the monkey, showed that most of the projection came from area 6 homotopically on both sides; very little of the projection was from the frontal eye-fields, area 8. However, it was pointed out that a part of the frontal eye-fields is included in area 6 of Brodmann.[2]

Efferent Projections

The superior colliculus does not project directly to the cerebral cortex; nevertheless, it projects to subcortical visual centres which then relay visual information to the cortex. Thus the stratum griseum superficialis projects to the posterior thalamus (n. lateralis posterior—LP—and the pulvinar) the C-laminae of the dorsal lateral geniculate nucleus, to the ventral LGN, the pretectal nucleus, and to deeper collicular layers, whilst the deeper layers project to the brainstem and intralaminar thalamic nuclei.[3] For convenience, the main afferent and efferent projections of the primate superior colliculus have been summarized in Table 23.1, after Wurtz & Albano (1980); these have been segregated according as the superficial or deeper layers of the colliculus are concerned.

Table 23.1 Connections of the layers of the superior colliculus (after Wurtz & Albano, 1980).

Afferent connections	*Efferent connections*
Superficial layers	
Retina	*Thalamus*:
	Dorsal lateral geniculate (magnocellular, interlaminar)
Visual cortex:	
Striate & Prestriate	Pregeniculate (Ventral lateral geniculate)
Other cortical areas:	Inferior pulvinar
Frontal eye fields	
Midbrain:	*Midbrain*:
* Parabigeminal	Parabigeminal
* Pretectum	Pretectum
Intermediate and deep layers	
Striate and prestriate cortex	Ascending
	Intralaminar nuclei
Frontal eye fields	Suprageniculate nucleus
Pregeniculate nucleus	Pretectal nuclei
Pretectum	Descending (Ipsilateral)
Substantia nigra	Parabigeminal
Locus caeruleus	Inferior colliculus
n. Pontis caudalis, oralis	Reticularis tegmenti pontis
Cerebellum	Reticularis pontis oralis
Lateral cervical nucleus	Descending (Contralateral)
	Reticularis tegmenti pontis
	Abducens, perioculomotor regions
	Cervical spinal cord

Neurone-types and Retinotectal Projection

Hoffmann & Stone (1973) described three main pathways from the retina in the cat, namely a direct pathway involving W-cells, transmitting to some 73% of collicular cells; a direct pathway carried by axons of Y-cells and transmitting to some 9% of the cells; and an indirect pathway, involving a cortical loop, consisting of retinal Y-cell, geniculate Y-cell, and a cortical complex cell which sends its axon through the corticotectal descending pathway.

Branched Axons

At least a part of the retinotectal pathway results from branching of the retinogeniculate fibres, since electrical stimulation of the colliculus produces antidromic spikes in the optic tract which interfere with spikes antidromically activated from the lateral geniculate body (Hayashi *et al.*, 1967). Alternatively, orthodromic impulses reach the lateral geniculate nucleus when the colliculus is stimulated, travelling in axon-reflex manner.

Conduction-velocities

The study of Hoffmann (1973) is in essential agreement; he identified the retinal neurone-types by their conduction-velocities, Y-, X- and W-cell axons conducting at 35–45, 20–25 and 3–15 m/sec respectively. Y-ganglion cells supplied the colliculus directly, through a branched axon, and indirectly after relaying in the visual cortex monosynaptically. W-cells had a direct input to the colliculus. X-cells did not communicate with the colliculus, either directly or indirectly.

Velocity and Direction

Collicular neurones driven by Y-axons responded to high velocities of movement ($> 200°$/sec) whilst those driven by W-cells preferred slower movement ($< 100°$/sec). 61% of these were directionally sensitive. Axons of cells in the visual cortex, projecting to the colliculus, had complex receptive fields and responded to high stimulus-velocity and were directionally sensitive. Thus directional selectivity seems to be a property of the cortical cell imposed on the collicular neurones. However 61% of the cells driven from the retina by W-cells were directionally specific.[4]

Monkey

In the monkey it appears that X-cell projection does not occur, the retinotectal fibres corresponding to Wiesel & Hubel's broad-band Y-type cell and W-cells.

Geniculostriate Projection

Schiller *et al.* (1979) examined the geniculostriate projection to the colliculus, making use of the known segregation of X- and Y-cells in the lateral geniculate nucleus, Y-cells being confined to the ventral magnocellular layers 1 and 2. The separation is maintained in the visual cortex, the parvocellular layers going to layers 4A and 4cβ and the magnocellular layers to layer 4cα (Hubel & Wiesel, 1972; LeVay & Gilbert, 1976). Schiller *et al.* (1979) reversibly inactivated parvo- or magnocellular layers in the lateral geniculate nucleus by microinjections of lidocaine or $MgCl_2$. Inactivation of the magnocellular layer disrupted the visually driven activity of neurones in the superior colliculus corresponding topographically with those in the geniculate nucleus, but not in the superficial areas, which receive a direct retinal projection in the monkey and are not dependent on cortical input so far as being driven visually is concerned (Schiller *et al.*, 1974). Inactivation of the parvocellular layers had no effect on visually driven collicular activity. Thus the indirect activation of the colliculus by way of the geniculostriate system is mediated by the broad-band Y-system. If, as seems true of the monkey, the colour-opponent X-cells do not project directly to the colliculus, the absence of a geniculostriate projection through X-cells indicates that truly colour-coded information probably does not reach the colliculus.[5]

Y-cell Function

If, as has been suggested, a prominent role for the large fast-conducting Y-neurones is in establishing the location of a visual target in space, a function for the superior colliculus would be that of directing attention and the eyes to a target in visual space; this view is certainly in keeping with the effects of collicular lesions which manifest themselves as loss of attention to visual stimuli (p. 634).

Receptive Fields

Cat

According to Sterling & Wickelgren (1969) the receptive fields of the cat's collicular neurones have much in common with those of cortical cells, especially the complex and hypercomplex varieties, the fields being elliptical rather than circular and surrounded usually by an inhibitory area; and this undoubtedly reflects the projection of the visual cortex on the colliculus as will be described below. Thus an optimal size could be found such that a bar just did not overlap with the inhibitory region. The units were not so highly orientation-specific, so that a

change of at least 30° was necessary to cause a reduction in response. Whereas fine jittery movements were suitable for evoking responses in cortical units, large sweeps across the receptive field were best for the collicular units. Preferred orientations of collicular units were mainly horizontal, by contrast with cortical units where these were distributed uniformly throughout 360°. In general, Sterling & Wickelgren's study, and later ones by Cynader & Berman (1972), emphasize the collicular neurone's sensitivity to motion, and to direction and speed of motion. Thus responses to stationary flashes are relatively weak by comparison with those of geniculate and cortical cells. As Hoffmann & Dreher (1973) showed, a bar of optimal width passing across its receptive field, is the best stimulus for a collicular neurone.

Monkey Units

These have been studied by Cynader & Berman (1972) and Marrocco & Li (1977) among others; the units in the superficial layers could be classified into two groups with regard to their directional sensitivity, namely those that were and were not sensitive to the direction of a moving target.

PAN-DIRECTIONAL UNITS

The non-directionally sensitive units were divided into a subgroup containing the majority of collicular units which responded to ON-OFF stimuli of appropriate size, and to moving stimuli in any direction; these may be called *pan-directional cells* (Goldberg & Wurtz, 1972).

JERK DETECTORS

The other subgroup, called by Schiller & Koerner (1971) *jerk detectors*, responded poorly or not at all, to smooth movements, but well to rapid jerky movements.

DIRECTIONAL SENSITIVITY

The great majority of directionally sensitive units—a small percentage of the total of visually responsive units—did not respond to ON and OFF stimuli (Goldberg & Wurtz, 1972).

Preference for Moving Target Moors & Vendrik (1979), working on anaesthetized monkeys, recorded from 135 units in the superficial layers; every one was pan-directional and, of these, none could be described as a 'jerk detector'. They compared responses to stationary flashing stimuli with those to moving ones, in an attempt to explain the great preference of collicular units for moving stimuli. They found that stationary flashing stimuli did, indeed, evoke transient ON- and OFF-responses in the field-centres of these pan-directional cells, whilst the surrounds were inhibitory, suppressing light-evoked responses or spontaneous activity. Moving stimuli evoked transient-responses as the leading and trailing edge of the target passed over the receptive field-centre, and these were attenuated by concurrent inhibition by the surround. In general, the authors confirmed that collicular units 'prefer' a moving stimulus but this depended on the velocity of movement and the size of the receptive field, so that with a small field and high velocity of movement the stationary flashing response might be greater. Thus the stimulus yielding the strongest response in a collicular cell was a small spot moving slowly through the receptive field and having a diameter at which the excitatory input was maximum or at its saturation level, since the authors found that spatial summation in the centre tended to saturate at large areas, by contrast with summation of the inhibitory surround; in fact, this contrasting effect of summation in centre and surround permitted the elaboration of a model that could explain many of the features of the collicular neurone's responses to moving stimuli.

Complex Stimuli

Updyke (1974) noted that collicular units in New World monkeys responded particularly well, and sometimes exclusively, to complex stimuli such as three-dimensional objects. Rizzolatti *et al.* (1980), working on the macaque, found two groups of collicular neurones: Type I, in the superficial layers, with what may be called characteristic response-types, and a Type II, driven very poorly by stationary or smoothly moving conventional targets but well to unconventional targets. For example, one neurone gave very small responses to square spots of light and discharged very strongly to a pink plastic bottle, a small brown bottle with a red label, and a yellow plastic cap. The meaning of the object was not significant since articles of food did not arouse any special response. The authors suggested that Type I neurones might serve to direct the eyes to the object stimulating the retina, whilst Type II drew attention of the cerebral cortex to the stimulus for examination in greater detail. Thus the most obvious effect of collicular ablation is the lack of attention to visual stimuli (p. 634).

Cortical Influences on Collicular Neurones

If the cerebral cortex is imposing its influence on collicular neurones, we may expect to see changes in their receptive-field characteristics after cooling or ablating the visual cortex. The collicular neurones can be imagined to be responding to a contralateral retinal stimulus directly, and to an ipsilateral retinal stimulus indirectly through the visual cortex (Fig. 23.4). Removal of the ipsilateral cortex in the cat produced a great change in the collicular units, so that they became highly responsive to stationary

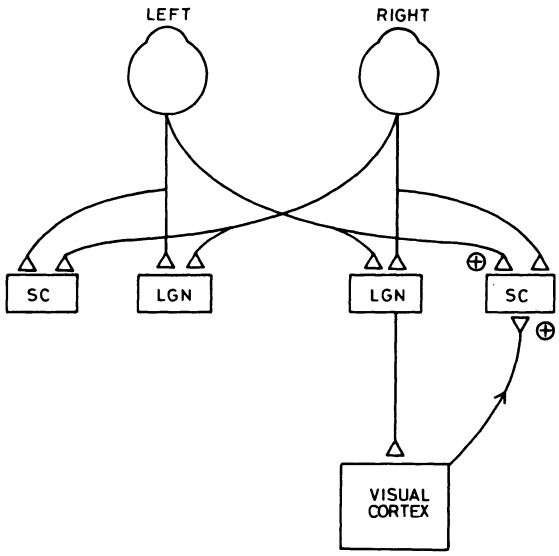

Fig. 23.4 The right superior colliculus responds directly to the contralateral eye and indirectly to the ipsilateral eye by way of the lateral geniculate nucleus (LGN) and visual cortex.

targets, lost their directional sensitivity, and were driven only by the contralateral eye.

Monocular Occlusion

Since monocular occlusion in the kitten makes the contralateral visual cortex unresponsive to visual stimuli, it was not surprising to find that the effects of monocular occlusion were similar to those of removal of the contralateral visual cortex. Thus Hoffmann & Sherman (1974) visually deprived kittens monocularly and showed, by electrical stimulation, that the indirect pathway from retina to the colliculus through the visual cortex, mediated by Y-neurones, was eliminated. Moreover, collicular neurones in the lower superficial layers, where the cortical neurones terminate, were driven by the deprived eye much less frequently. The ocular dominance and directional sensitivity of collicular neurones were impaired by this monocular deprivation.

Inhibition

The strong directional sensitivity of collicular neurones suggests an inhibitory influence that prevents the neurone from responding when the target moves in the null direction. According to Dreher & Hoffmann (1973), this inhibition could be mediated through complex cortical neurones with preferred directions in the collicular neurone's null direction; these would provide the null-direction inhibition; other, excitatory, neurones, with preferred directions the same as those of the collicular neurone, would provide the excitatory influence.

OCULAR DOMINANCE

The same inhibitory processes might account for the absence of ipsilateral response in the cat's colliculus, and this would account for the loss of ocular dominance in the collicular neurones after cortical ablation or monocular occlusion. Thus Fig. 23.5 shows the dominance distribution, the majority of cells being driven by both eyes; the distribution is similar to the cortical one but skewed more to the contralateral eye. After removal of the ipsilateral cortex, collicular units responded only to the contralateral eye. A similar effect was shown in kittens reared with monocular occlusion where almost all neurones are now driven by the experienced eye, and the experiments of Berman & Sterling (1976) suggest strongly that, under these conditions, the experienced eye is inhibiting responses through the deprived eye. Thus Fig. 23.6 (left) shows the ocular-dominance distribution of a kitten after monocular deprivation; the shift in dominance to the ipsilateral (experienced) eye is striking. After a lesion in areas 17 and 18 the dominance-pattern was measured again and, as Fig. 23.6 (right) shows, the situation has been completely reversed.

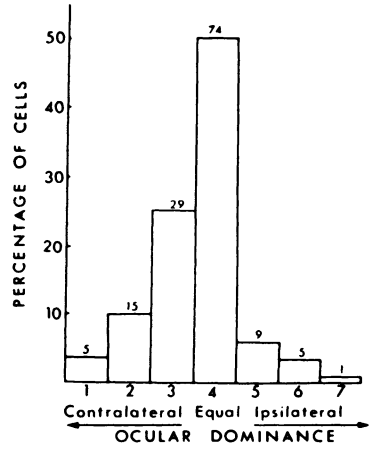

Fig. 23.5 Ocular dominance distribution of 138 units in superior colliculus. Number over each bar gives absolute number of cells in this category. Group 1 cells are driven only by the contralateral eye; Group 4 cells are driven about equally by each eye. Group 7 respond only to the ipsilateral eye. (Sterling & Wickelgren, *J. Neurophysiol.*)

Corticotectal Neurones

These neurones are located in layer 5 of the striate area; Palmer & Rosenquist (1974) found, in the cat, that all cortical neurones that responded antidromically to

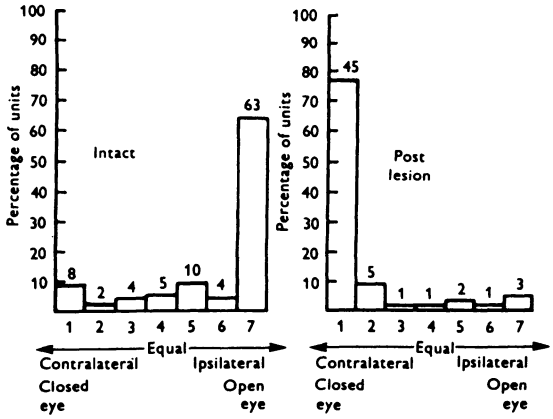

Fig. 23.6 Ocular dominance distribution of units in the superior colliculus contralateral to the deprived eye in five animals before and immediately following removal of visual cortex. Groups 1–7 on the abscissa represent a contralateral to ipsilateral trend in ocular dominance with units in group 1 driven only by the contralateral eye, units in group 4 driven equally by either eye, and units in group 7 driven only by the ipsilateral eye. The numbers above each bar represent the number of units in that group. (Berman & Sterling, *J. Physiol.*)

stimulation of the colliculus belonged to the complex and hypercomplex varieties, or as they are now more commonly described, complex and special complex, the latter showing end-stopping in a marked degree. They have been examined in greater detail by Weyand *et al.* (1986a, b), who studied the effects of increasing the length on the responses, and confirmed that they fell into the two groups of complex and special complex units. Orientation-selectivity varied widely, the standard complex cells being more sharply tuned; directional sensitivity varied from sharp tuning to complete unselectivity. The predominant preferred direction for collicular cells is away from the centre of gaze; this was by no means true of the corticotectal cells, however, and, generally speaking, it was not easy to relate the orientation- and direction-selectivities of cortical and collicular neurones.

TWO SYSTEMS

Ogasawa *et al.* (1984) selectively cooled cortical regions in the cat and exposed two apparently independently developed corticotectal systems that individually produce similar types of receptive field; the one system is in areas 17–18, acting on superficial lamina cells, and the other in the Clare–Bishop area in the posterior regions of the suprasylvian cortex, influencing deep lamina cells. Thus inactivation of each cortical area reduced sensitivity to motion, directional selectivity, binocularity, and velocity-sensitivity. The segregation of collicular units, influenced by the two cortical areas, was not complete, so that units in the more superficial layer were found to be influenced by elimination of both cortical inputs, but even here there was some segregation, so that cells influenced by area 17–18 were located 100–300 μm below the pial surface, whereas most of the cells affected by the suprasylvian cortex were located in the *stratum opticum* and sublamina II_3 of the *stratum griseum superficiale*. The authors ruled out the possibility that effects of the suprasylvian cortex were mediated through areas 17–18. In the deep laminae the cortical effects seemed to be solely mediated by the suprasylvian cortex.

Effects of Lesions

The effects of lesions in the superior colliculi are not easily defined, and they doubtless depend critically on the extent of the lesion since the projections to the superficial and deep layers are fundamentally different. The effects have been summarized by Sprague (1972). In the cat, for example, total extirpation produces an inattention to visual stimuli, but the ability to follow objects and localize them visually is not seriously impaired. In the monkey, too, no serious defects in visual guidance were evident, and the emphasis has been on inattention rather than any precise defect. Wurtz & Goldberg (1972) have pointed to the grossness of the movement-fields of collicular neurones, so that these neurones are unlikely to be responsible for the highly accurate movements of fixation. These fields were of the order of 5°, whereas errors in a saccade are of the order of 0.5°. Casagrande & Diamond (1974) made elaborate studies of visually directed behaviour in the spider monkey after lesions that invaded different extents of the superior colliculi. Many of the visual defects could not have been accounted for by failure of attention, and they concluded that the superior colliculus should be regarded as a double organ, its superficial layers, receiving the direct retinal and visual cortical inputs, might be responsible for some degree of pattern vision, whilst the deeper layers, with their more extensive and complex inputs, would be responsible for visual attentiveness, lesions here causing a remarkable degree of inattention to visual stimuli. Thus the projections from the deep layers descend to motor areas of the brainstem and ascend to thalamic areas not usually associated with vision, such as the posterior nuclei, the intralaminar complex, and regions of the subthalamus. The main problem, however, is how the deeper layers receive the visual input necessary to permit the visually guided behaviour that was clearly present in the absence of the superficial layers; Casagrande & Diamond quote some work indicating a visual input to the deeper layers.

In general, then, it seems that the superior colliculus acts at a very early stage in eye-movement processing, whilst other inputs must be available to the oculomotor system that permit adequate control in the presence of collicular lesions.

Comparison with Striate Cortex

Wurtz & Mohler (1976a, b) emphasize the great power of the striate cortex to analyse the visual stimulus in terms of contour, motion and colour, and they contrast this with the poor behaviour of the colliculi in these respects but their excellent ability to assess the significance of the visual stimulus in relation to the individual. Thus the cortical neurones do not distinguish between movement of the object in space from the similar movement of the retinal image that takes place when the eye moves (Wurtz, 1969), although the collicular neurones do (Robinson & Wurtz, 1975). The enhancement of the collicular neurone is selective to the movement, in the sense that it is greatest when the movement is directed towards the centre of the receptive field of the collicular neurone and falls off with distance from here; this selectivity clearly allows the collicular cell to signal movement to a specific point in space, whereas such enhancement as was seen in striate cortical neurones was unspecific and might have been related to general alerting. Hence, as Wurtz & Mohler state, 'at these early stages in processing, the cortical and the collicular areas stand in a nearly reciprocal relation: the cortex is an excellent analyser of stimulus characteristics but a poor evaluator of stimulus significance, while the colliculus is an excellent evaluator but a poor analyser'.

THE PULVINAR

The relation of the pulvinar to other thalamic nuclei is illustrated in Fig. 18.7. As indicated earlier, this thalamic nuclear mass has evolved from a rudimentary structure in rodents to become one of the largest thalamic nuclei in primates and the largest in man; its inputs and outputs in primates suggest that it plays an important role in man's cognitive functions that depend on symbolic cognitive thinking and language.

Subdivisions

Cytoarchitectonically, the pulvinar has been divided into inferior, medial, and lateral and oral subgroups. The main sources of input are non-retinal, through the superior colliculus, pretectum and visual cortical areas.

Retinal Projection

In the cat, Berman & Jones (1977) described a retinal projection to the pulvinar, employing anterograde flow of labelled leucine and proline from the retina; a similar projection was demonstrated by Itoh *et al.* (1979) using horseradish peroxidase.

Slabs of Projection

The projection described by Berman & Jones consisted of a thin sagitally orientated but interrupted sheet of radioactivity extending through the greater part of the anteroposterior extent of the lateral posterior-pulvinar complex. The projection was the most lateral of four slabs of non-overlapping projection from the colliculus, visual cortex, pretectum and retina. Each slab projected to different visual cortical areas, the collicular slab to area 20, the visual cortical slab diffusely to several areas of the lateral and suprasylvian gyri and to the lateral geniculate nucleus of the same side. The pretectal slab to area 21; the projection of the retinal slab is not known, but may be adjacent to area 21. This retinal projection would provide a more direct pathway from retina to the extrastriate regions of the cerebral cortex than that passing through the colliculus and lateral posterior nucleus. Berson & Graybiel (1978) found adjoining slabs of projection to the lateral-posterior pulvinar complex of the cat receiving distinct inputs as follows: (1) from the retina; (2) from the pretectum; (3) from the visual cortex; (4) from the superior colliculi; (5) from the insular cortex. The cortical projections were all reciprocal and included areas 17, 18, 19 and the Clare-Bishop region. The retinal terminations were related to the different slabs so that they ended in *striate-recipient* and *colliculus-recipient* zones.

Divisions

So far as the three divisions of the pulvinar are concerned, the respective projections have been summarized by Mason (1978). Thus the striate receptive area is in the inferior and medial divisions, whereas the tectal projection is confined to the medial division—the tectal recipient zone. The projection from area 18 overlaps that of area 17, as might be expected of the cat where area 18 represents a primary visual centre. Areas 19 and 21 project to the medial pulvinar, overlapping with the tectal projection, and to the lateral pulvinar, overlapping with the pretectal recipient zone (Kawamura *et al.*, 1974; Graybiel, 1972).

Primate Retinal Projections

In the monkey and baboon Campos-Ortega *et al.* (1970) found degeneration in the inferior pulvinar after optic tract section, indicating some retinal input. More recently Itaya & Van Hoesen (1983) measured anterograde transport of horseradish peroxidase from retina to the inferior and medial pulvinar nuclei of the Old World monkey; there was a bilateral projection to the inferior subnucleus and only contralateral to the posterior. Again Nakagawa & Tanaka (1984), after reviewing the controversy as to whether there is, indeed, a retinal projection on the

pulvinar, studied the anterograde movement of ^{3}H-proline and ^{3}H-leucine from the retina, examining the projection autoradiographically. They found two groups of terminations; a more rostral one in the inferior pulvinar nucleus immediately ventral to the parvonuclear portion of the dorsal lateral geniculate nucleus, extending back to the area between the brachium of the superior colliculus and the lateral geniculate nucleus. A second projection was at the caudal pole of the lateral geniculate nucleus. Thus there were two groups of terminals bilaterally in the inferior pulvinar, most in the rostral region. They found no terminals in the medial pulvinar.

Cat Cortical Projections

In this species projections from pulvinar are to a wide range of areas; thus according to Raczowski & Rosenquist (1983) the connections include areas 19, 20a, 21a, 21b, 5 and 7; they distinguished between projections from the lateral and medial divisions of the lateral posterior nucleus and compared these with that of the medial interlaminar nucleus (MIN). Only X-cells projected to the cortex by a geniculate route, the W- and Y-cells projecting by extrageniculate routes.[6]

Primate Cortical Projections

The projections to and from the monkey's visual cortex have been examined by several authors, using both anterograde and retrograde movement of tracers. Whilst it is generally agreed that the primate pulvinar has reciprocal connections with the parastriate regions, areas 18 and 19, the relations between striate area and pulvinar are not so clear, although a projection *from* the striate area to the pulvinar is well established (Campos-Ortega & Hayhow, 1972; Spatz & Erdmann, 1974). However, Ogren & Hendrickson (1976), by injecting mixtures of ^{35}S-methionine and horseradish peroxidase into the macaque striate area, demonstrated a reciprocal projection from area 17 to and from the inferior and lateral pulvinar nuclei. There was a clear topography in the projections, in the sense that the different quadrants of the contralateral visual hemifield were projected to give a retinotopic map, the vertical meridian being represented at the common boundary between the inferior and lateral divisions. No projection was observed to the medial pulvinar, in agreement with Campos-Ortega & Hayhow (1972). Benevento & Davis (1977) followed anterograde movement of labelled amino acid, injected into the prestriate areas and temporal, frontal and parietal regions known to have visually responsive cells. They found parallel projections from areas 18 and 19 to the inferior and adjacent ventral lateral pulvinar; in addition there were projections to the remaining portions of lateral and medial pulvinars and other dorsal group nuclei, regions, that project to cortical regions other than the occipital cortex. For example, the rostral lateral portion of the medial pulvinar projects to orbital cortex and the frontal eye-fields (area 8); the dorsal and rostral portions of the lateral pulvinar project to the parietal cortex; and the lateral portion of the caudal pulvinar projects to inferotemporal cortex.

Dual Cortical Relations

Thus Benevento & Davis emphasize the dual relations between the pulvinar and the cerebral cortex: first there are the reciprocal connections to the visual cortex proper, and secondly there are these connections that may be regarded as constituting the corticothalamic half of cortico-thalamo-cortical projections that connect the occipital cortex with the temporal, parietal and frontal cortices. Figure 23.7 gives a summary of the projections from the three pulvinar nuclear divisions derived from antero- and retrograde labelling (Trojanowski & Jacobson, 1976); according to this representation, there is no projection to any *primary* sensory area—visual, auditory or somatosensory—so that in respect of area 17 Trojanowski & Jacobson's results are at variance with those of Ogren and Hendrickson.[7]

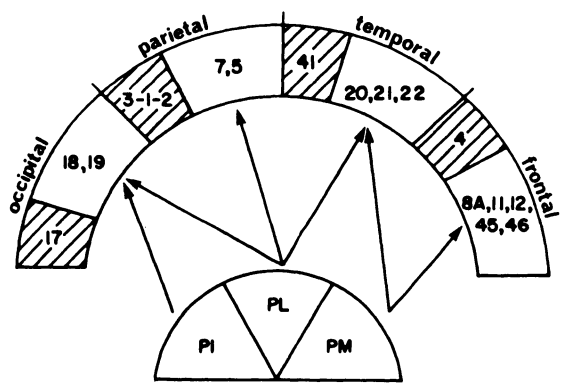

Fig. 23.7 Schematic diagram of the relationship of the pulvinar to the cerebral cortex based on results of Trojanowksi & Jacobson. PI, PL and PM are the inferior, lateral and medial pulvinar nuclei. (Trojanowski & Jacobson, *J. comp. Neurol.*)

Laminar Terminations

Benevento and Rezak (1976), in their elaborate description of the projections from the inferior and lateral pulvinars, have shown that laminae 1 and 6 receive these projections; the caudal extension of the lateral pulvinar projects to areas 20 and 21 (inferotemporal areas). The pulvinar projection to the striate area corresponds with

that of the dorsal lateral geniculate nucleus, but the laminae to which these nuclei project are different.[8]

Tectal and Pretectal Projections

The projections of the superior colliculus on the pulvinar have been reviewed by Partlow *et al.* (1977), who have examined the terminations of collicular fibres in the pulvinar. The projection is to the inferior pulvinar (Benevento & Rezack, 1976); and the synaptical terminals on the pulvinar dendrites are typical of those seen in characteristic relay-synapses, suggesting that the colliculus is able to influence pulvinar neurones strongly. The projection was retinotopic, in the sense that regions of the colliculus responding to input from a given quadrant of the visual field projected to a corresponding region in the pulvinar.

Benevento & Standage (1983) have used modern antero- and retrograde tracer techniques to define the projections of both pretectal and tectal nuclei to the pulvinar, distinguishing between retina-recipient and non-recipient zones in these midbrain nuclei. They concluded that there were some five 'extrageniculate pathways' to the cerebral cortex, passing from the midbrain nuclei to the thalamic nuclei and onwards. As a result, visuomotor and polysensory information can be passed to visually responsive association cortex. Thus retinal information can not only be relayed via retino-tectal-geniculate and retino-tectal-inferior pulvinar routes, but also by retino-tectal-lateral pulvinar, retino-tectal-parabigeminal-pulvinar, and retino-pretectal-lateral pulvinar routes. In addition, visuomotor and polysensory information can be relayed by the deep tectal layers to the medial pulvinar route to the cortex. As a result of these numerous projections, it is possible for a great deal of visual information to be processed throughout large regions of visual cortex independently of direct cortico-cortical connections.

Overlapping Cortical and Tectal Projections

Both the superior colliculus and the striate cortex project to the pulvinar, and since each of these regions receives a direct retinal input, it seemed that most of the characteristics of the visually responsive pulvinar neurones might be determined by one or both of these inputs. Itaya & Van Hoesen (1983) suggested that this convergence of inputs would allow the integration of the motor aspects of vision, due to the movements of the eyes, with the purely sensory aspects, and considered that the two regions of projection would overlap. Horseradish peroxidase studies confirmed this overlap, and they found neurones in these regions of overlap that responded to electrical stimulation of both area 17 and the superior colliculus.

Visuotopic Organization

When the relation of the receptive field of a neurone to position on the pulvinar was examined, some degree of visuotopic organization was apparent in the inferior pulvinar, in the sense that the central azimuths were arranged medially and the peripheral laterally; the horizontal meridian was represented superiorly whilst successively lower meridians were represented inferiorly. In the medial pulvinar, visuotopic organization was present and more complex, and the authors emphasized that perhaps the correct means of establishing visuotopic organization would be to examine the neurones in the striate and tectal-receiving zones separately, zones that are not equivalent to the architectonic divisions represented by inferior and medial pulvinar. Thus, when penetrations were confined to the striate-recipient zone, delineated by retrograde movement of horseradish peroxidase, visuotopic organization was better defined. On this basis, the tectal-recipient zone exhibited a much cruder visuotopic organization.

Macaque Visuotopic Organization

Bender (1981) has used electrophysiological methods to map the retinotopic organization within the inferior and lateral pulvinar of the macaque monkey, regions where, according to him, there is little or no direct retinal connection but where there are extensive connections with other parts of the visual system. He has shown that there are two separate projections of the contralateral hemifields; the first within the inferior and a small part of the lateral pulvinar, and the second entirely within the lateral pulvinar. The two projections show analogy with the respective projections on the striate (V1) and prestriate (V2) cortices, which have been described as first- and second-order transformations (Allman & Kaas, 1974a, b). In the first-order transformation, adjacent points in the hemifield are adjacent on the cortex, whereas in the second-order transformation, as in V2, the hemifield is split along most of the horizontal meridian, and upper and lower quadrants are represented in non-adjacent regions of cortex. The two patterns are juxtaposed to share a common representation of the vertical meridian, and the visuotopic organization reverses across the common border, so that V1 and V2 are roughly mirror images. In the pulvinar projections, the reversal occurred at the common boundary between the inferior and lateral maps, at the representation of the vertical meridian, a region that could be recognized with myelin-stained sections, showing a prominent fibre system filling

the outer half of the lateral pulvinar. In both representations the sizes of receptive fields varied progressively from about 1° centrally to some 10° in the periphery. According to Bender, the retinotopic map on the inferior pulvinar could be due to the striate and tectal projections, with the possible exception of the central (foveal) portion, so far as tectal projection was concerned.

INFERIOR AND LATERAL PULVINARS COMPARED

The analogy between the inferior and lateral pulvinars, on the one hand, and the striate and prestriate cortices (V1 and V2) on the other has been discussed by Bender, and it has been suggested that a common feature is that both are the targets of geniculostriate projections and that both project to wide areas of the occipital lobe. As such, each represents an alternative path, in addition to the transcortical route, by which striate cortex can influence a number of visual cortical areas. However, only one of these routes, that via the inferior pulvinar, is subject to direct influence from the colliculus, so that the inferior pulvinar has a unique role in integrating visual and ocular motor inputs.

Unit Responses

Some elaborate studies on single-unit responses in the cat's pulvinar have been described by Mason (1978) and Chalupa & Fish (1978). Movement-sensitive cells responded to velocities of target between 5–10 deg/sec up to more than 120 deg/sec. Direction-sensitive cells had preferred directions of movement, usually in one direction, although some responded to two directions 180° apart; in some, definite evidence of suppression in a null-direction was apparent.

Primate Unit Responses

Mathers & Rapisardi (1973) recorded visually evoked responses in neurones of the squirrel monkey pulvinar; most were monocularly driven from the contralateral hemifield; they had large receptive fields (100 square degrees compared with about 10 for the lateral geniculate nucleus). There were no polymodal units in spite of the reciprocal connections with areas adjacent to the auditory and somatosensory receiving areas. They demonstrated a retinotopic organization of the responses on the inferior pulvinar, the lower visual quadrant being represented on a rostromedial portion and the upper quadrant on a caudolateral portion. The horizontal meridian continued laterally to divide the dorsal lateral geniculate nucleus similarly. Gattass *et al.* (1978), working on another New World monkey, *Cebus*, described the receptive fields of pulvinar neurones, finding a great diversity; areas varied greatly from 0.8 to 1592 square degrees, with a median of 69. Although a part of the receptive field could extend ipsilaterally beyond the vertical meridian, the centres were always in the contralateral visual hemifield. Units could be classified in terms of eye dominance, as with cortical units. The regions in which the units were found corresponded to the inferior pulvinar and the ventrolateral portion of the lateral pulvinar. In general, the characteristics of a receptive field could be related to those of the cortical and subcortical brain regions projecting on the pulvinar; thus units with a concentric centre-surround organization with small and exclusively contralateral receptive fields doubtless reflected features of the lateral geniculate nucleus, since a projection from here to the pulvinar has been established in the rhesus monkey (Trojanowski & Jacobson, 1976).

RECEPTIVE FIELD CHARACTERISTICS

Bender (1982) has described the characteristics of the receptive fields of macaque inferior pulvinar neurones; their diameters were from 1 to 5°; two thirds of the units were sensitive to orientation of a line-stimulus, and many of these were directionally sensitive, being excited by one direction and inhibited by the reverse movement. Most cells showed pronounced moment-to-moment fluctuations in sensitivity that were often correlated with the state of arousal. Most units responded strongly to unicocular stimulation, by contrast with prestriate neurones that preferred binocular stimulation.[9]

BEHAVING MONKEY

Petersen *et al.* (1985) defined three retinotopically organized areas that were not strictly confined to the architectonically defined regions; these were PI (inferior), PL (lateral) and Pdm, dorsal and medial to these areas. Most cells were only broadly tuned or non-selective for direction and orientation, although a few in Pdm were directionally selective. In these waking animals they were able to study the effects of attention and saccades on responses; in the Pdm the response was enhanced when the stimulus was the target for attention or a saccadic movement, as opposed to a simple passive fixation, so it was considered that this region might be responsible for selective visual attention; thus lesions in this region might be responsible for the visual defects after pulvinar destruction. Petersen concluded that the contribution of the superior colliculus to the receptive-field properties of pulvinar neurones was very small, compared with that due to the cerebral cortex.

Lesions in the Pulvinar

Pattern Discrimination

Chalupa *et al.* (1976) showed that lesions in the monkey's inferior pulvinar impaired the post-operative learning of

a simple pattern-discrimination, namely between the letters N and Z; lesions in the medial and lateral divisions had no effect. A further impairment of learning was obtained if distracting stimuli, such as the imposition of a grid on the pattern, were presented.

Eye Movements

The lesions produced by Ungergleider & Christensen (1977) left pattern discrimination normal but apparently interfered with the coordination of eye movements with visual input; thus during visual discrimination training they observed phases of prolonged fixation or 'visual capture' suggesting a disturbance of the processes that co-ordinate visual input with the eye-movements necessary to acquire or retain fixation on a target.

Cortical and Collicular Lesions

That the primate's pulvinar neurones are predominantly controlled by striate input was shown by Bender (1983) who compared the effects of either unilateral striate or collicular lesions on the receptive fields of pulvinar neurones. Collicular lesions had virtually no effect whereas, striate lesions left some 85% of neurones which, on retinotopic grounds were likely to be involved in the field-deficit, completely unresponsive. The 15% of responsive cells behaved like collicular neurones, but they did not survive long after the lesion.

Role of Pulvinar

As summarized by Berson & Graybiel (1983) in their study devoted to the striate recipient zone, the cat's striate recipient zone seems an ideal region in which to study the circuitry of the 'association thalamus', the cortico-thalamo-cortical loop, by which visual information, reaching the visual cortex by the geniculate route, is transmitted to the extrastriate cortex and from one extrastriate region to another. Both ascending and descending projections are massive and may well serve to define the response properties of many cortical cells.

Cerebellum

The cerebellum is a centre closely involved in all bodily movements, including those of the eyes; thus the retinal pathway to this part of the brain is of great interest. This is indirect, and derived from the visual cortex, neurones in layer 5 projecting to the cerebellar relay-nuclei in the rostral pons. These pontine nuclei also receive visual input by way of the superior colliculus and the ventral lateral geniculate nucleus. The pathway to the cerebellum is apparently mainly, or exclusively, through the middle cerebellar peduncle, terminating as mossy fibres.

Cortical Projections

Kawamura & Chiba (1979) injected horseradish peroxidase into the pons and observed retrograde staining in the cortex; layer 5 neurones throughout the cortex took up the tracer, the cells being small and medium-sized pyramidal neurones; these were different from corticotectal and corticoreticular neurones, so that, although corticopontine fibres are known to branch to supply the tectum and lateral geniculate nucleus, it would seem that a direct input from specific corticopontine cells is present.[10] The extent of the cortical origins was described by Albus *et al.* (1981), likewise on the basis of retrograde movement of horseradish peroxidase injected into the pons; these included areas 17, 18, 19 and the lateral suprasylvian area of the cat, the projections overlapping in the anterior half of the basal pons; interestingly, the regions of central retinal representation sent fewer axons than those representing the periphery.

Area 18 Neurones

Baker *et al.* (1976) found that the receptive fields of pontine cells, receiving input from area 18, were quite different from area 18 neurones, having no orientation-selectivity and being very large; they were directionally sensitive, however. Baker *et al.* (1983) identified area 18 cells projecting specifically to the pons, by antidromic stimulation, and showed that their receptive fields were similar to those of the pontine cells to which they projected, the fields being some 485 deg^2 compared with 59 deg^2 for non-corticopontine cells, responding well to multiple spots, a stimulus preferred by pontine cells; orientated slits were not the best stimuli, and direction-preference was marked, especially so in the downward direction.

Projections to the Cerebellum

Mower *et al.* (1980) investigated the separate projections of visual neurones from pontine neurones receiving input from the cortex and those receiving from the colliculus, these pathways terminating in distinct and non-overlapping regions of the pons, their cells having different receptive-field properties (Baker *et al.*, 1976; Mower *et al.*, 1979). By antidromic stimulation, they showed that cells in the median pontine visual area, receiving input from the visual cortex, transmitted to the contralateral cerebellar hemisphere, whilst cells in the dorsolateral pontine visual area, receiving input from the colliculus, transmitted to the vermis and ipsilateral cerebellar hemisphere. These connections were largely confirmed by horseradish

peroxidase labelling. It is considered that the cerebellar vermis is concerned with the control of whole-body movements, whereas the hemispheres control ipsilateral limbs; it may be that the separate collicular and cortical projections to the cerebellum subserve different functions, i.e. different types of visually guided movement. Since the cerebellar hemispheres receive principally from the contralateral visual pontine area and also from the ipsilateral dorsolateral nucleus, and since both cortically driven pontine cells and tectal-receiving pontine cells in the dorsolateral pons respond to visual stimuli in the contralateral visual hemifield, it follows that the cerebellar hemispheres receive visual input from the entire visual field. As Mower *et al.* point out, this complete representation of the visual fields in both sides of the cerebellar cortex helps to explain the finding that animals can still guide a limb visually even though the motor centres controlling that limb appear to be entirely disconnected from visual input by optic tract or chiasma section and division of all the brain commissures, the uncrossed pontocerebellar pathway being the critical neuronal pathway that was spared.

Notes

1. Cowey & Perry (1980) have pointed out that the interpretation of the functions of colliculi versus cerebral cortex hinges on the claimed lack of a direct foveal representation of the retina. They injected horseradish peroxidase into the monkey's colliculus and found a definite retrograde uptake by ganglion cells. They discuss the failure of Lund *et al.* to observe foveal uptake of horseradish peroxidase.
2. Powell points out that this may help to understand the connections remaining between hemispheres even after section of the corpus callosum and other forebrain commissures; thus the colliculus projects to the lateral geniculate nucleus which projects back to the ipsilateral cortex.
3. Harting *et al.* (1980) have examined projections of the middle and deeper collicular layers to the dorsal thalamic nuclei, using anterograde labelling after injections into the colliculus; from these projections, further passage to cortical regions was predicted from the known connections. For example, they gave access to the prefrontal eye-fields, area 8, and the inferior parietal lobule, area 7, both regions that contain neurones with functionally similar characteristics to those of the deep superior colliculus. So far as a projection to the dorsal lateral geniculate nucleus was concerned, this was demonstrated in the squirrel monkey by anterograde movement of tracer from the superficial laminae. The projection linked the same visuotopic regions of colliculus and geniculate nuclei; the interlaminar zones were regions of high extraretinal input, especially that of striate neurones. The suggestion was made that both tectal and cortical projections to the lateral geniculate nucleus were involved in binocular interactions.
4. Additional details regarding retinotectal projection in relation to the W-, X-, Y-classes of ganglion cell are provided in the paper by Fukuda & Stone (1974). Y-cells behaved as a separate group, many or all of the nasal cells passing to the contralateral lateral geniculate body and superior colliculus, presumably by branched axons; most of those in the temporal retina likewise passed to both colliculus and geniculate body, but ipsilaterally, and presumably by branched axons. A minority of the Y-cells in the temporal retina joined the decussating nasal fibres to terminate in the contralateral geniculate nucleus and colliculus. This input by branched axons of the retinogeniculate pathway may be universal, since Bunt *et al.* (1975) injected horseradish peroxidase in the cat's lateral geniculate body and found that all superior collicular neurones had taken up the marker, presumably carried retrogradely along the branched axons.
5. The geniculostriate projection to the colliculus in the cat is likewise supplied by Y-type units (Hoffmann & Straschill, 1971; Hoffmann & Sherman, 1974). Although the study of Schiller *et al.* (1979) suggests that corticotectal cells receive input only from magnocellular cells of the dorsal lateral geniculate nucleus, according to Lund *et al.* (1975) the pyramidal cells of layer 5B act as a source of input to the corticotectal cells of area 17, and these pyramidal cells receive from both parvo- and magnocellular layers of the lateral geniculate nucleus.
6. The reader is referred to a more recent study of the projections to and from the striate recipient zone of the cat by Berson & Graybiel (1983) in which modern antero- and retrograde techniques have been used; the zone may be identified by its relatively weak staining for acetylcholinesterase. A striking feature was the reciprocity of all corticothalamic projections, and the large amount of projection to extrastriate zones, such as area 19 and the Clare-Bishop zone, from the striate-recipient region. The authors emphasize the role of this pulvinar area in establishing connections between the striate and other visual areas independently of transcortical projections.
7. Ogren & Hendrickson (1976) have discussed the failure of earlier workers to find a projection from the pulvinar to the striate area. By employing a more reactive horseradish peroxidase, they were able to detect a projection from the lateral pulvinar to the striate area in *Saimiri* (squirrel monkey) as well as in the macaque.

   Livingstone & Hubel (1982) in the course of a study of thalamic projections to the visual cortex of monkeys, injected ^{3}H-proline into the pulvinar and found labelling of area 18 leading to a banding of label at right-angles to the 17/18 border. If injections were confined to the lateral geniculate nucleus, there was little or no labelling of area 18.

   According to Rezak & Benevento (1979), the inferior pulvinar and an immediately adjacent portion of the lateral pulvinar project to both striate and prestriate areas of the primate, terminating in layers above the geniculate terminations in layers 1, 2 and 3 that overlie those of the geniculate projection in layer 4A. In prestriate cortex, terminations are in layers 4, 3 and 1.
8. The cortical projections on the pulvinar of other primates have been reviewed by Bender (1981); a retinotopic map on the inferior nucleus, comparable with that in the macaque, is present in two New World monkeys, *Cebus* (capuchin monkey) and the owl monkey (Gattass *et al.*, 1978; Allman *et al.*, 1972; Lin & Kaas, 1979), whilst topographical projections from striate and prestriate cortex and superior colliculus have been demonstrated in the owl monkey. On the basis of striate projections, a retinotopically organized projection area exists in the inferior pulvinar of the bush baby, *Galago*, although this part of the pulvinar lacks a collicular

input (Glendenning *et al.*, 1975). The possibilities of a second visuotopically organized area in these primates is suggested by striate projections. Harting *et al.* (1972) have compared the pulvinar projections in hedgehog, tree shrew and bush baby, indicating an evolutionary increase in size and complexity of the pulvinar from the ancestor of the placentals to the prosimian bush baby.

9. Benevento & Miller (1981) have emphasized the difference between the rostral region of the pulvinar complex, both inferior and lateral portions of which contain retinotopical representations of the contralateral hemifield, and the caudal region where retinotopy is poor; this region has input to the inferior temporal cortex (IT), and apparently acts to link this with other associational cortical areas. They have described the receptive fields of this caudal region.
10. Baker *et al.* (1983) stimulated electrically the rostral visual pontine area and excited, antidromically, neurones in area 18 and the Clare-Bishop area; two-thirds of these could also be excited by antidromic stimulation from the superior colliculus. Thus, if we agree that the superior colliculus is mainly concerned with visual control of eye movements, a cortical input to this and the cerebellum by the same neurones permits the cerebellum to superintend the execution of eye movements primarily initiated by the colliculus.

References

Albus, K., Donate-Oliver, F., Sanides, D. & Fries, W. (1981) The distribution of pontine projection cells in visual and association cortex of the cat: an experimental study with horseradish peroxidase. *J. Comp. Neurol.* **201**, 175–189.

Allman, J. M. & Kaas, J. H. (1974a) The organization of the second visual area (V II) in the owl monkey: a second order transformation of the visual hemifield. *Brain Res.* **76**, 247–265.

Allman, J. M. & Kaas, J. H. (1974b) A crescent-shaped cortical visual area surrounding the middle temporal area (MT) in the owl monkey (*Aotus trivirgatus*) *Brain Res.* **76**, 247–265.

Allman, J. M., Kaas, J. H., Lane, R. H. & Miezin, F. M. (1972) A representation of the visual field in the inferior nucleus of the pulvinar in the owl monkey (*Aotus trivirgatus*). *Brain Res.* **40**, 291–302.

Altman, J. & Carpenter, M. B. (1961) Fiber projections of the superior colliculus in the cat. *J. Comp. Neurol.* **116**, 157–177.

Baker, J., Gibson, A., Glickstein, M. & Stein, J. (1976) Visual cells in the pontine nuclei of the cat. *J. Physiol.* **225**, 415–433.

Baker, J., Gibson, A., Mower, G., Robinson, F. & Glickstein, M. (1983) Cat visual corticopontine cells project to the superior colliculus. *Brain Res.* **265**, 227–232.

Bender, D. B. (1981) Retinotopic organization of macaque pulvinar. *J. Neurophysiol.* **46**, 672–693.

Bender, D. B. (1982) Receptive-field properties of neurons in the macaque inferior pulvinar. *J. Neurophysiol.* **48**, 1–17.

Bender, D. B. (1983) Visual activation of neurons in the primate pulvinar depends on cortex but not colliculus. *Brain Res.* **279**, 258–261.

Benevento, L. A. & Davis, B. (1977) Topographical projections of the prestriate cortex to the pulvinar nuclei in the macaque monkey: an autoradiographic study. *Exp. Brain Res.* **30**, 405–424.

Benevento, L. A. & Miller, J. (1981) Visual responses of single neurons in the caudal lateral pulvinar of the macaque monkey. *J. Neorosci.* **1**, 1268–1278.

Benevento, L. A. & Rezak, M. (1976) The cortical projections of the inferior pulvinar in the rhesus monkey (*Macaca mulatta*): an autoradiographic study. *Brain Res.* **108**, 1–24.

Benevento, L. A. & Standage, G. P. (1983) The organization of projections of the retinorecipient and nonretinorecipient nuclei of the pretectal complex and layers of the superior colliculus to the lateral and medial pulvinar in the macaque monkey. *J. Comp. Neurol.* **217**, 307–336.

Berman, N. & Jones, E. G. (1977) A retino-pulvinar projection in the cat. *Brain Res.* **134**, 237–248.

Berman, N. & Sterling, P. (1976) Cortical suppression of the retinocollicular pathway in the monocularly deprived cat. *J. Physiol.* **255**, 263–273.

Berson, D. M. & Graybiel, A. M. (1978) Parallel thalamic zones in the LP-pulvinar complex of the cat identified by their afferent and efferent connections. *Brain Res.* **147**, 139–148.

Berson, D. M. & Graybiel, A. M. (1983) Organization of the striate-recipient zone of the cat's lateralis posterior-pulvinar complex and its relations with the geniculostriate system. *Neuroscience* **9**, 337–372.

Bunt, A. H., Hendrickson, A. E., Lund, J. S., Lund, R. D. & Fuchs, A. J. (1975) Monkey retinal ganglion cells: morphometric analysis and tracing of axonal projections, with a consideration of the peroxidase technique. *J. Comp. Neurol.* **164**, 265–286.

Campos-Ortega, J. A. & Hayhow, W. R. (1972) On the organization of the visual cortical projections to the pulvinar in *Macaca mulatta*. *Brain Behav. Evol.* **6**, 394–423.

Campos-Ortega, J. A., Hayhow, W. R. & Cluver, P. F. deV. (1970) A note on the problem of the retinal projections to the inferior pulvinar nucleus of primates. *Brain Res.* **22**, 126–130.

Casagrande, V. A. & Diamond, I. T. (1974) Ablation study of the superior colliculus in the tree shrew (*Tupaia glis*). *J. Comp. Neurol.* **156**, 207–238.

Chalupa, L. M., Coyle, R. S. & Lindsley, D. B. (1976) Effect of pulvinar lesions on pattern discrimination in monkeys. *J. Neurophysiol.* **39**, 354–369.

Chalupa, L. M. & Fish, S. E. (1978) Response characteristics of visual and extravisual neurones in the pulvinar and lateral posterior nuclei of the cat. *Exp. Neurol.* **61**, 96–120.

Cowey, A. & Perry, V. H. (1980) The projection of the fovea to the superior colliculus in rhesus monkeys. *Neuroscience* **5**, 53–61.

Cynader, M. & Berman, N. (1972) Receptive field organization of monkey superior colliculus. *J. Neurophysiol.* **35**, 187–201.

Distel, H. & Fries, W. (1982) Contralateral cortical projections to the superior colliculus in the macaque monkey. *Exp. Brain Res.* **48**, 157–162.

Dreher, B. & Hoffmann, K.-P. (1973) Properties of excitatory and inhibitory regions in the receptive fields of single units in the cat's superior colliculus. *Exp. Brain Res.* **16**, 333–353.

Fukuda, Y. & Stone, J. (1974) Retinal distribution and central projections of Y-, X- and W-cells of the cat's retina. *J. Neurophysiol.* **37**, 749–772.

Gattass, R., Oswaldo-Cruz, E. & Sousa, A. P. B. (1978) Visuotopic organization of the *Cebus* pulvinar: a double representation of the contralateral hemifield. *Brain Res.* **152**, 1–16.

Glendenning, K. K., Hall, J. A. & Diamond, I. T. (1975) The pulvinar nucleus of *Galago senegalensis*. *J. Comp. Neurol.* **161**, 419–457.

Goldberg, M. E. & Wurtz, R. H. (1972) Activity of superior colliculus in behaving monkey. I. Visual receptive fields of single neurons. *J. Neurophysiol.* **35**, 542–559.

Graybiel, A. M. (1972) Some extrageniculate visual pathways in the cat. *Invest. Ophthal.* **11**, 322–332.

Graybiel, A. M. (1975) Anatomical organization of retinotectal afferents in the cat: an autoradiographic study. *Brain Res.* **96**, 1–23.

Harting, J. K. & Guillery, R. W. (1976) Organization of retinocollicular pathways in the cat. *J. Comp. Neurol.* **166**, 133–144.

Harting, J. K., Hall, W. C. & Diamond, I. T. (1972) Evolution of the pulvinar. *Brain Behav. Evol.* **6**, 425–452.

Harting, J. K., Huerta, M. F., Frankfurter, A. J., Strominger, N. L. & Royce, G. J. (1980) Ascending pathways from the monkey superior colliculus: an autoradiographic analysis. *J. Comp. Neurol.* **192**, 853–882.

Hayashi, Y., Sumitomo, I. & Iwama, K. (1967) Activation of lateral geniculate neurons by electrical stimulation of superior colliculus in cats. *Jap. J. Physiol.* **17**, 638–651.

Hoffmann, K.-P. (1973) Conduction velocity in pathways from retina to superior colliculus in the cat: a correlation with receptive-field properties. *J. Neurophysiol.* **36**, 409–425.

Hoffmann, K.-P. & Dreher, B. (1973) The spatial organisation of the excitatory region of receptive fields in the cat's superior colliculus. *Exp. Brain Res.* **16**, 354–370.

Hoffmann, K. P. & Sherman, S. M. (1974) Effects of early monocular deprivation on visual input to cat superior colliculus. *J. Neurophysiol.* **37**, 1276–1286.

Hoffmann, K.-P. & Stone, J. (1973) Central termination of W-, X- and Y-type ganglion cell axons from cat retina. *Brain Res.* **49**, 500–501.

Hoffmann, K.-P. & Straschill, M. (1971) Influences of corticotectal and intertectal connections on visual responses in the cat's superior colliculus. *Exp. Brain Res.* **12**, 120–131.

Hubel, D. H., LeVay, S. & Wiesel, T. N. (1975) Mode of termination of retinotectal fibers in macaque monkey: an autoradiographic study. *Brain Res.* **96**, 25–40.

Hubel, D. H. & Wiesel, T. N. (1972) Laminar and columnar distribution of geniculo-cortical fibers in the macaque monkey. *J. Comp. Neurol.* **146**, 421–450.

Itaya, S. K. & Van Hoesen, G. W. (1983) Retinal axons to the medial terminal nucleus of the accessory optic system in old world monkeys. *Brain Res.* **269**, 361–369.

Itoh, K. *et al.* (1979) Cerebello-pulvino-cortical and retino-pulvino-cortical pathway in the cat as revealed by the use of anterograde and retrograde transport of horseradish peroxidase. *J. Comp. Neurol.* **187**, 349–357.

Kanaseki, T. & Sprague, J. M. (1974) Anatomical organization of pretectal nuclei and tectal laminae in the cat. *J. Comp. Neurol.* **158**, 319–337.

Kawamura, K. & Chiba, M. (1979) Cortical neurons projecting to the pontine nuclei in the cat. An experimental study with the horseradish peroxidase technique. *Exp. Brain Res.* **35**, 269–285.

Kawamura, S., Sprague, J. M. & Niimi, K. (1974) Corticofugal projections from the visual cortex to the thalamus, pretectum and superior colliculus in the cat. *J. Comp. Neurol.* **158**, 339–362.

Leichnetz, G. R., Spencer, R. F., Hardy, S. G. P. & Astruc, J. (1981) The prefrontal corticotectal projection in the monkey; an anterograde and retrograde study. *Neuroscience* **6**, 1023–1041.

LeVay, S. & Gilbert, C. D. (1976) Laminar patterns of geniculocortical projection in the cat. *Brain Res.* **113**, 1–19.

Lin, C. S. & Kaas, J. H. (1979) The inferior pulvinar complex in owl monkeys: architectonic subdivisions and patterns of input from superior colliculus and subdivisions of the visual cortex. *J. Comp. Neurol.* **187**, 655–678.

Livingstone, M. S. & Hubel, D. H. (1982) Thalamic inputs to cytochrome oxidase-rich regions in monkey visual cortex. *Proc. Nat. Acad. Sci.* **79**, 6098–6101.

Lund, J. S., Lund, R. D., Hendrickson, A. E., Bunt, A. W. & Fuchs, A. F. (1975) The origin of efferent pathways from the primary visual cortex, Area 17, of the macaque monkey as shown by retrograde transport of horseradish peroxidase. *J. Comp. Neurol.* **164**, 287–303.

Marrocco, R. T. & Li, R. H. (1977) Monkey superior colliculus: properties of single cells and their afferent inputs. *J. Neurophysiol.* **40**, 844–860.

Mason, R. (1978) Functional organization in the cat's pulvinar complex. *Exp. Brain Res.* **31**, 51–66.

Mathers, L. H. & Rapisardi, S. C. (1973) Visual and somatosensory receptive fields of neurons in the squirrel monkey pulvinar. Brain Res. **64**, 65–83.

Moors, J. & Vendrik, A. J. H. (1979) Responses of single units in the monkey superior colliculus to stationary flashing stimuli. *Exp. Brain Res.* **35**, 333–347.

Mower, G., Gibson, A. & Glickstein, M. (1979) Tectopontine pathways in the cat: laminar distribution of cells of origin and visual properties of target cells in dorsolateral pontine nucleus. *J. Neurophysiol.* **42**, 1–15.

Mower, G., Gibson, A., Robinson, F., Stein, J. & Glickstein, M. (1980) Visual pontocerebellar projections in the cat. *J. Neurophysiol.* **43**, 355–366.

Nakagawa, S. & Tanaka, S. (1984) Retinal projections to the pulvinar nucleus of the macaque monkey: a re-investigation using autoradiography. *Exp. Brain Res.* **57**, 151–157.

Ogasawa, K., McHaffie, J. G. & Stein, B. E. (1984) Two visuocortical systems in cat. *J. Neurophysiol.* **52**, 1126–1245.

Ogren, M. & Hendrickson, A. (1976). Pathways between striate cortex and subcortical regions in *Macaca mulatta* and *Saimiri sciureus*: evidence for a reciprocal pulvinar connection. *Exp. Neurol.* **53**, 780–800.

Palmer, L. A. & Rosenquist, A. C. (1974) Visual receptive fields of single striate cortical units projecting to the superior colliculus in the cat. *Brain Res.* **67**, 27–42.

Partlow, G. D., Colonnier, M. & Szabo, J. (1977) Thalamic projections of the superior colliculus in the rhesus monkey, *Macaca mulatta*. A light and electron microscope study. *J. Comp. Neurol.* **171**, 285–318.

Petersen, S. E., Robinson, D. L. & Keys, W. (1985) Pulvinar nucleis of the behaving rhesus monkey: visual responses and their modulation. *J. Neurophysiol.* **54**, 867–886.

Powell, T. P. S. (1976) Bilateral cortico-tectal projection from the visual cortex in the cat. *Nature* **260**, 526–527.

Raczkowski, D. & Rosenquist, A. C. (1983) Connections of multiple visual cortical areas with the lateral posterior-pulvinar complex and adjacent thalamic nuclei in the cat. *J. Neurosci.* **3**, 1912–1942.

Rezak, M. & Benevento, L. A. (1979) A comparison of the organization of the dorsal lateral geniculate nucleus, the inferior pulvinar and adjacent lateral pulvinar to primary visual cortex (area 17) in the macaque monkey. *Brain Res.* **167**, 19–40.

Rizzolatti, G., Buchtel, H. A., Camarda, R. & Scandolara, C. (1980) Neurons with complex visual properties in the superior colliculus of the macaque monkey *Exp. Brain Res.* **38**, 37–42.

Robinson, D. A. (1972) Eye movements evoked by collicular stimulation in the alert monkey. *Vision Res.* **12**, 1795–1808.

Robinson, D. A. & Wurtz, R. H. (1975) Superior colliculus neurons distinguish between stimulus movement and self-induced stimulus movement. *ARVO Suppl.*

Schiller, P. H. & Koerner, F. (1971) Discharge characteristics of single units in superior colliculus of the alert rhesus monkey. *J. Neurophysiol.* **35**, 920–936.

Schiller, P. H., Malpeli, J. G. & Schein, S. J. (1979) Composition of geniculostriate input to superior colliculus of the rhesus monkey. *J. Neurophysiol.* **42**, 1124–1133.

Schiller, P. H., Stryker, M. Cynader, M. & Berman, N. (1974) Response characteristics of single cells in the monkey superior colliculus following ablation or cooling of visual cortex. *J. Neurophysiol.* **37**, 181–194.

Spatz, W. B. & Erdmann, G. (1974) Striate cortical projections to the lateral geniculate and other thalamic nuclei: a study using degeneration and autoradiographic tracing methods in the marmoset *Callithrix*. *Brain Res.* **82**, 91–108.

Sprague, J. M. (1972) The superior colliculus and pretectum in visual behavior. *Invest. Ophthal.* **11**, 473–482.

Stein, B. E., Magalhaes-Castro, B. & Kruger, L. (1976) Relationship between visual and tactile representation in cat superior colliculus. *J. Neurophysiol.* **39**, 401–419.

Sterling, P. & Wickelgren, B. G. (1969) Visual receptive fields in the superior colliculus of the cat. *J. Neurophysiol.* **32**, 1–15.

Trojanowski, J. Q. & Jacobson, S. (1976) Areal and laminar distribution of some pulvinar cortical efferents in rhesus monkey. *J. Comp. Neurol.* **169**, 371–392.

Ungergleider, L. G. & Christensen, C. A. (1977) Pulvinar lesions in monkeys produce abnormal eye movements during visual discrimination training. *Brain Res.* **136**, 189–196.

Updyke, B. V. (1974) Characteristics of unit responses in superior colliculus of the Cebus monkey. *J. Neurophysiol.* **37**, 296–309.

Weyand, T. G., Malpeli, J. G., Lee, C. & Schwark, H. D. (1986a) Cat area 17. III. Response properties and orientation anisotropies of corticotectal cells. *J. Neurophysiol.* **56**, 1088–1101.

Weyand, T. G., Malpeli, J. G., Lee, C. & Schwark, H. D. (1986b) Cat area 17. IV. Two types of corticotectal cells defined by controlling geniculate inputs. *J. Neurophysiol.* **56**, 1102–1108.

Wilson, M. E. & Toyne, M. J. (1970) Retino-tectal and cortico-tectal projections in *Macaca mulatta*. *Brain Res.* **24**, 395–406.

Wurtz, R. H. (1969) Comparison of effects of eye movements and stimulus movements on striate cortical neurons of the monkey. *J. Neurophysiol.* **32**, 987–994.

Wurtz, R. H. & Albano, J. E. (1980) Visual motor function of the primate superior colliculus. *Ann. Rev. Neurosci.* **3**, 189–226.

Wurtz, R. W. & Goldberg, M. E. (1972) Activity of superior colliculus in behaving monkey. III and IV. *J. Neurophysiol.* **35**, 575–586, 587–596.

Wurtz, R. W. & Goldberg, M. E. (1972) The primate superior colliculus and the shift of visual attention. *Invest Ophthal.* **11**, 441–450.

Wurtz, R. W. & Mohler, C. W. (1976a) Organization of monkey superior colliculus: enhanced visual response of superificial layer cells. *J. Neurophysiol.*, **39**, 745–765.

Wurtz, R. W. & Mohler, C. W. (1976b) Enhancement of visual response in monkey striate cortex and frontal eye fields. *J. Neurophysiol.* **39**, 766–772.

Section 4

THE MUSCULAR MECHANISMS

24. THE EXTRAOCULAR MUSCLES AND THEIR ACTIONS

Apart from its importance in the treatment of squint, an adequate knowledge of the movements of the eyes, and their neuromuscular control, is of considerable value in understanding the physiological mechanisms concerned with the maintenance of posture; moreover, it would seem that our perceptions of objects, and particularly of their spatial relationships, are determined in part by the laws governing the movements of the eyes.

The Muscles

The Recti

The muscles concerned with the eye movements are six in number: the *medial* and *lateral recti*, which determine sideways movements; the *superior* and *inferior recti* causing primarily upward and downward movements, and the *superior* and *inferior obliques*, which, when acting alone, primarily cause the eye to twist around its antero-posterior axis.

The insertions of the rectus muscles are indicated in Fig. 24.1, and since the muscles arise from a common origin at the apex of the orbit, their main actions of elevation, depression, adduction (i.e. pulling towards the nose) and abduction, are not difficult to appreciate.

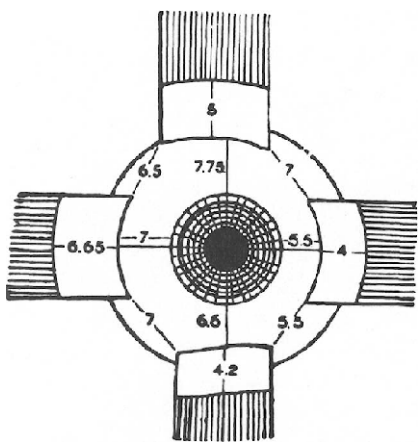

Fig. 24.1 Insertions of the rectus muscles. The medial rectus is to the right of the diagram. (Duke-Elder, *Textbook of Ophthalmology*.)

The Obliques

The superior oblique (Fig. 24.2) likewise arises from the apex of the orbit but after running above the medial rectus almost to the orbital margin, it becomes tendinous as it passes through a cartilaginous pulley, the trochlea, and turning sharply backward, downwards, and laterally over the eye it is inserted into the postero-lateral aspect of

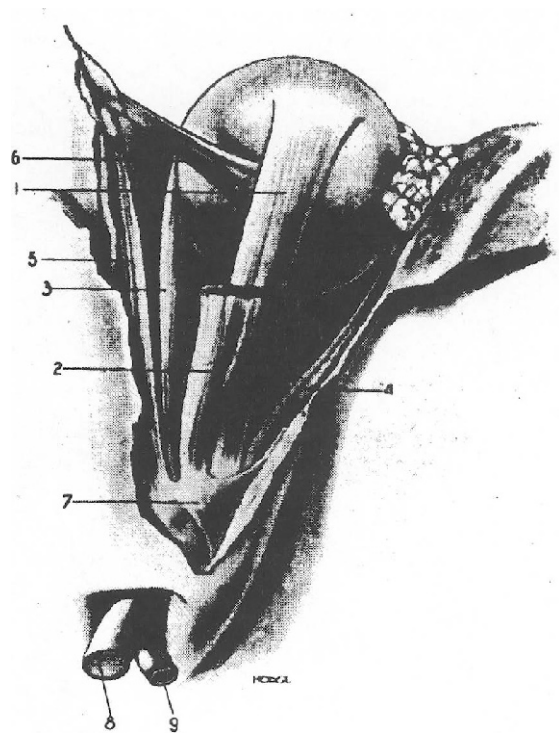

Fig. 24.2 Extrinsic muscles of the eye from above. 1, superior rectus; 2, levator palpebrae superioris; 3, medial rectus; 4, lateral rectus; 5, superior oblique; 6, reflected tendon of the superior oblique; 7, annulus of Zinn; 8, optic nerve; 9, ophthalmic artery. (Duke-Elder, *Textbook of Ophthalmology*.)

the sclera. Since the muscle pulls from above on an attachment behind the equator of the eye, it acts as a depressor.

The inferior oblique (Fig. 24.3) arises from the anterior part of the orbit, in the antero-medial corner of its floor. It passes laterally and backwards beneath the inferior rectus and is inserted into the posterolateral aspect of the globe. Pulling from below on an attachment behind the equator the inferior oblique thus acts as an elevator.

Defining the Movements

Axes of Rotation

In describing the actions of the muscles, we are concerned with changes in the direction in which the eye is 'pointing' i.e. the orientation of the *fixation axis* (defined as a line joining the point of fixation with the centre of rotation of the eye; Fig. 24.4). As a *primary position* or starting point, we may consider that position in which the eye is looking straight ahead when the head is erect. If the fixation axis swings horizontally, the eye is said to *adduct* or *abduct*, according as it swings towards or away from the nose; if the fixation axis swings vertically, the eye is *elevated* or *depressed*. After any purely horizontal or vertical movement of the fixation axis from the primary position, the eye is said to have reached a *secondary position*. If the eye executes a movement which causes both a horizontal and vertical displacement of the fixation axis (e.g. if the eye looks up and to the right) it is said to adopt a *tertiary position*.

Experiment has shown that the movements of the eye in general can be approximately described as rotations about a fixed point,[1] the *centre of rotation*, situated some 13.4 mm behind the anterior surface of the cornea. To define a movement it is, of course, not sufficient to indicate the centre of rotation, but an *axis*, passing through the centre, about which the eye turns, must be given; thus adduction or abduction is achieved by rotation about a vertical axis, the *z-axis* (Fig. 24.5); elevation or depression by rotation about a transverse horizontal axis, the *x-axis*. The fixation axis can be made to point in any direction by rotating the eye first about one axis and then about the other—alternatively the necessary position of the eye can be attained by a single rotation about an axis intermediate between the *x*- and *z*-axes. It is worth noting that when the eye is in the primary position the *x*- and *z*-axes are in a vertical frontal plan—called *Listing's plane* (Fig. 24.5)—and that any direction of the fixation axis can be obtained by rotating the eye about an axis lying in this plane.

Torsion or Rolling

The physiologist is concerned not only with the direction of the fixation axis—which tells him where the eye is pointing—but also with the orientation of a certain fixed plane in the eye—the *retinal horizon* (Fig. 24.6).

Imagine the eye in the primary position looking straight ahead; a horizontal plane through the pole of the cornea is the retinal horizon and the image of any point in space lying on this plane falls on a horizontal line on the retina—the *horizontal meridian*. The retinal horizon, being fixed in relation to the eye, moves with it. Now we shall see that the appreciation of direction—of a line for example—depends in large measure on the directions the

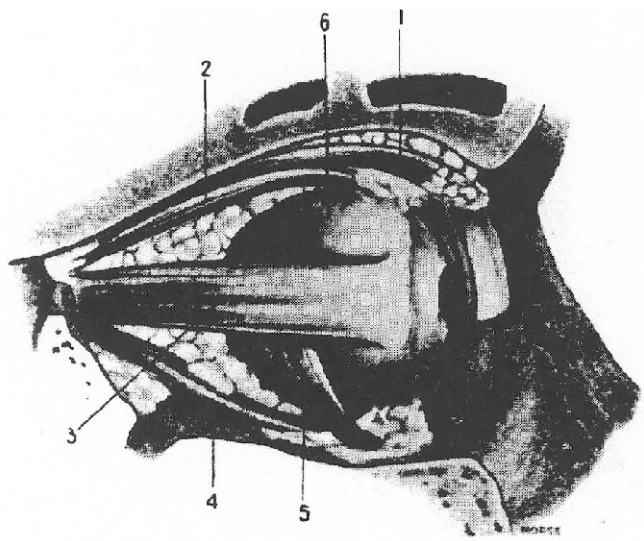

Fig. 24.3 Extrinsic muscles of the eye. Lateral view. 1, levator palpebrae superioris; 2, superior rectus; 3, lateral rectus; 4, inferior rectus; 5, inferior oblique; 6, superior oblique. (Duke-Elder, *Textbook of Ophthalmology*.)

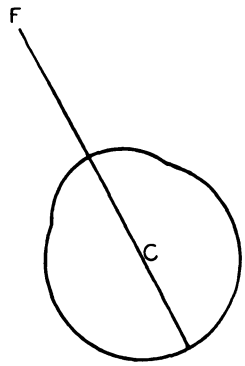

Fig. 24.4 The fixation axis.

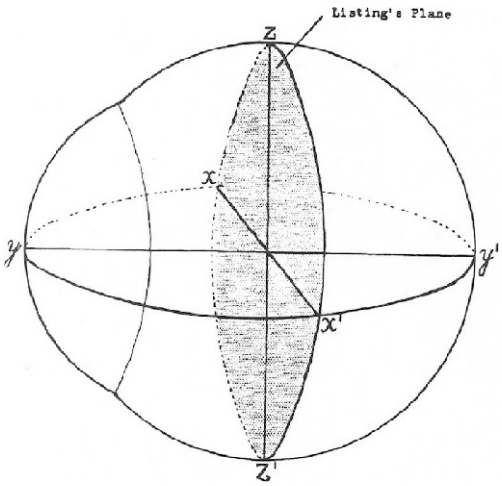

Fig. 24.5 The primary axes of rotation and Listing's plane. *xx'*, transverse horizontal, giving elevation and depression; *yy'*, antero-posterior, giving rolling or torsion; *zz'*, vertical, giving adduction or abduction.

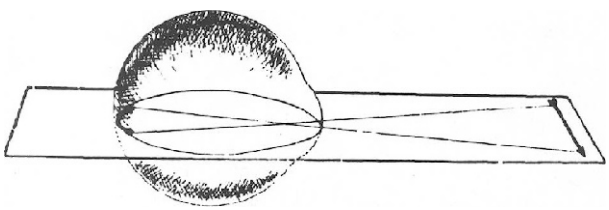

Fig. 24.6 The retinal horizon. The image of the arrow, fixated in the primary position of the eye, falls on the horizontal meridian.

images of external objects make on the retina, and if the orientation of the retina is upset, estimates of direction can become erroneous. Thus a horizontal line is appreciated as such because its image falls on, or is parallel to, the horizontal meridian; if the retina is twisted round, the horizontal line appears to be inclined unless the twist is compensated psychologically (p. 456).

We have thus to take into account the influence of movements of the eye on the orientation of the retina, or what amounts to the same thing, the orientation of the retinal horizon. So long as this plane keeps a definite orientation in space the images of horizontal lines in a frontal plane fall on the horizontal meridian or are parallel to it; the problem is how to define a position of the retinal horizon which we may consider normal—i.e. where there is no 'twist' of the retina; for the primary position of the eye this is easy, the retinal horizon must be horizontal and, if the eye rotates about its antero-posterior axis (the *y*-axis) from this position, the retinal horizon becomes inclined to the horizontal and the eye is said to have *rolled* or to have attained an *angle of rolling* or *torsion*. For other positions of the eye we cannot use the horizontal as our reference plane, e.g. if the eye is directed vertically upwards the retinal horizon is not twisted round but it is not horizontal. The normal position of the retinal horizon can be defined in relation to a fixed plane in space—the *median plane*, a vertical plane through the nose (Fig. 24.7); so long as the retinal horizon remains perpendicular to this, its position is normal and there is no torsion. Thus in Fig. 24.8 the eye is represented as looking up and to the right; the retinal horizon is inclined upwards, but it remains at right-angles to the median plane; there is no torsion and a horizontal line on the wall is parallel with the retinal horizon. In Fig. 24.9 the retinal

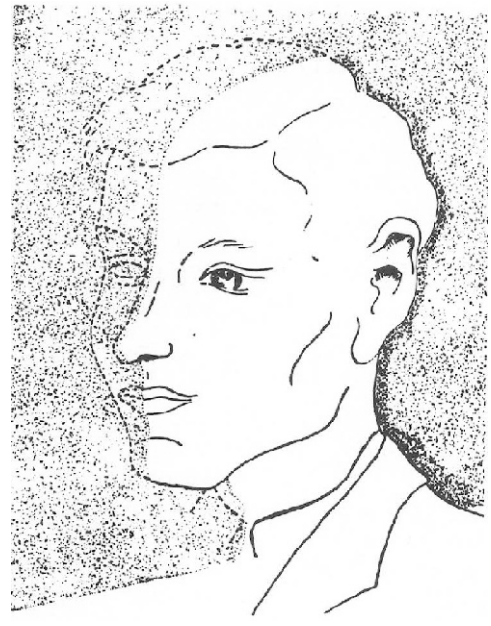

Fig. 24.7 The median plane.

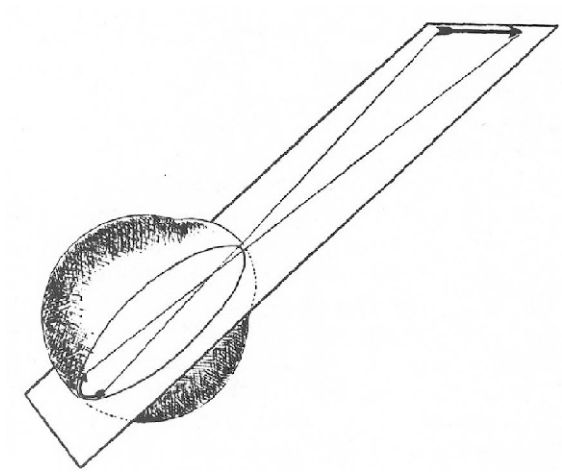

Fig. 24.8 The eye is inclined up and to the right. No rolling has occurred, and the arrow produces an image coinciding with the horizontal meridian.

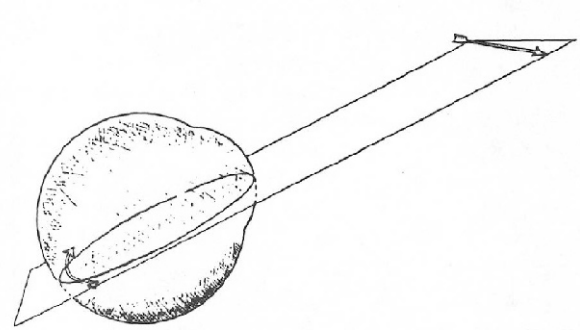

Fig. 24.9 The eye is inclined up and to the right. Torsion has occurred, so that the horizontal arrow produces an image inclined across the horizontal meridian.

horizon has been twisted, i.e. there has been torsion; it is now no longer at right-angles to the median plane and a horizontal line on the wall is not parallel with the retinal horizon; its image on the retina is therefore not parallel with the horizontal meridian.[2]

Rotations about Intermediate Axes

Rolling is brought about by rotation of the eye around its antero-posterior axis; it is not difficult to see that a combined elevation and rolling can be achieved by rotating the eye first about the x-axis and then about the y-axis, or alternatively by rotating about a horizontal axis intermediate between the two. A motion consisting of all three types, e.g. elevation, adduction, and rolling, can be obtained by choosing an axis with components along each of the three primary x-, y-, and z-axes.

Actions of the Individual Muscles

We are now in a position to analyse the actions of the individual muscles.

The Medial and Lateral Recti

In Fig. 24.10 is shown a horizontal meridional section through the eye; the medial and lateral recti are indicated by the heavy lines; they run over the surface of the globe but the pull takes place where the muscle is tangential to this surface, at T, the *tangential point*, and the direction of pull is a long the *tangential line of force*, TT'. The *muscle plane* is defined as the plane containing the tangential line of force, TT', and the centre of rotation C, i.e. it is the plane of the paper in Fig. 24.10. If C, the centre of rotation, is to remain fixed in space, a pull along TT' must result in a rotation about an axis through C projecting vertically through the paper; in general we may state that *any muscle will rotate the eye about an axis perpendicular to the muscle plane concerned.* The muscle planes of the medial and lateral recti may be taken as horizontal and they thus rotate the eye about a vertical axis through C which has already been defined as the z-axis. Such a rotation leads, as we have seen, to a simple movement of adduction or abduction.

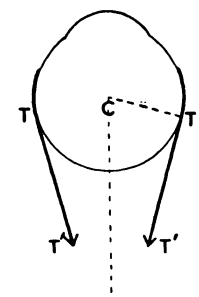

Fig. 24.10 The actions of the medial and lateral recti T, tangential point; TT', tangential line of force; C, centre of rotation. The muscle plane is the plane of the paper.

The Superior and Inferior Recti

The muscle planes of the superior and inferior recti are vertical and approximately identical; however they do not pass through the antero-posterior axis of the eye but are inclined at about 23° to it. The axis of rotation for these muscles is perpendicular to this plane and therefore lies horizontally but, as a result of this inclination, it does not correspond with the transverse horizontal x-axis but is inclined 23° away from it. The position is indicated in Fig. 24.11 which shows a horizontal section through a right eye. The vertical muscle plane intersects this section

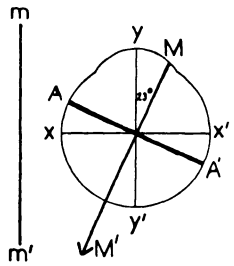

Fig. 24.11 Actions of the superior and inferior recti (right eye). The muscle plane intersects the horizontal section of the eye in MM'. AA' is the axis of rotation; mm' is the intersection of the median plane with the plane of paper.

in the line MM' inclined at an angle of 23° to the anteroposterior axis, *yy'*. The axis of rotation is the line AA' inclined at an angle of 23° to the transverse horizontal axis, *xx'*.

Rotation of the eye about *xx'* causes pure elevation or depression; rotation about *yy'* causes pure rolling; hence rotation about the intermediate axis AA' causes a movement involving both these effects; thus the superior rectus causes a rotation such that M rises out of the paper and its action is therefore *elevation and inward rolling*, the movement of the retinal horizon being clockwise; the inferior rectus causes *depression and outward rolling.*

ADDUCTION

Besides causing elevation (or depression) and rolling, the superior and inferior recti act as adductors, causing the fixation axis to move towards the median plane. This is not immediately evident since it is clear that there can be no rotation about the vertical *z*-axis, the axis of rotation AA' being perpendicular to it; this third action results from referring the orientation of a fixed direction in the eye—the fixation axis—to a plane outside the eye—e.g. the median plane through the head.

Thus in Fig. 24.11 let us imagine that the superior rectus acts; *yy'* corresponds to the fixation axis, which in the primary position remains parallel to the median plane, *mm'*; when the eye is elevated, *y* moves out of the plane of the paper and moves through a circle which is clearly not parallel to *mm'*; hence *y* becomes closer to *mm'* whilst *y'* moves farther away, and this can only result in the line *yy'*, the fixation axis, being directed towards the median plane, *mm'*, i.e. the superior rectus causes adduction. The inferior rectus causes *y* to move downwards, but it still moves towards *mm'* whilst *y'* moves away; hence both superior and inferior recti cause adduction.

The difficulty arises from the physiological necessity of referring a direction in the eye, the fixation axis for example, to a plane outside it, the median plane; if the axis of rotation is parallel with, or perpendicular to, this plane of reference the inclination of this direction in the eye is unchanged during rotation; thus rotation about *xx'* gives pure elevation because the axis of rotation is at right angles to the reference plane, *mm'*; similarly rotation about *yy'* causes pure rolling because *yy'* is parallel to *mm'*; AA', the axis of rotation for the superior and inferior recti, is neither parallel with, nor perpendicular to *mm'*, hence the inclination of the fixation axis to *mm'* must alter during rotation, i.e. adduction must occur.

MODEL EXPERIMENT

The problem becomes very much clearer with a model; a tennis ball may be used; a point is marked to represent the pole of the cornea and a knitting needle is inserted through the centre to represent any desired axis of rotation. If the needle is passed vertically through the ball, rotation causes adduction or abduction; a horizontal needle through the equator permits elevation and depression; a horizontal one through the pole of the cornea causes pure rolling. A horizontal needle passed in a direction intermediate between these two positions, which gives us the axis of rotation for the superior and inferior rectus muscles, causes both rolling and elevation or depression, and it will be seen also that the direction in which the pole of the cornea points, referred to a vertical plane parallel to the original direction of the fixation axis, changes during the rotation. It becomes quite clear that this change of direction is not brought about by rotation about a vertical axis since the knitting needle is held horizontally all the time.

The Superior and Inferior Obliques

The muscle planes of the superior and inferior obliques may be considered to be vertical, as with the recti, but to run at an angle of about 50° to the anteroposterior axis, and on the opposite side, as in Fig. 24.12. The axis of rotation, AA', is likewise inclined at 50° to the transverse horizontal axis. Contraction of the inferior oblique causes rotation about AA' such that *y* moves up out of the paper; the eye is thus elevated and rolled outwards; moreover, since the axis of rotation is inclined towards the median plane, the direction of the fixation axis, *yy'*, does not remain constant in respect to this median plane; as *y* comes up out of the paper it clearly moves away from *mm'*

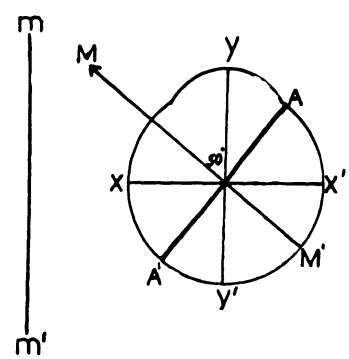

Fig. 24.12 Actions of the obliques (right eye). AA' is the axis of rotation.

and thus the inferior oblique causes *abduction*; the superior oblique causes depression, inward rolling and abduction.

Summary

The individual actions of the muscles, thus deduced, may be summarized in Table 24.1.

Combined Actions of Muscles

As we shall see, a given movement involves activity in, or inhibition of, several if not all of the six extraocular muscles. It is therefore important to consider their combined actions. Furthermore, we have so far only discussed the direction of pull of a muscle from the primary position of the eye; since this must change frequently as the eye moves out of the primary position, the theoretical axis of rotation must also alter.

EFFECT OF CHANGED POSITION OF EYE

The simplest example of the effects of moving out of the primary position on the action of a muscle is given by Fig. 24.13 which illustrates the effects of abduction of the right eye on the direction of pull of the superior rectus. Obviously the rolling and adduction will decrease as the antero-posterior axis of the eye approaches the plane of the muscle, whilst the elevating action will increase. An exactly reverse relationship must exist with the obliques. The variations in the degree of elevation or depression exerted by the superior and inferior rectus, according as the eye is caused to adduct or abduct before the muscle acts, are shown in Fig. 24.14 after Boeder. Here we imagine that we are looking into a sphere concentric with the left eye, and the lines are those that would be traced out by the fixation axis when the superior or inferior rectus acted alone, and caused a rotation of 50° about the axis of rotation. It is seen that, as the initial position becomes more and more one of adduction, the elevation caused by a given degree of rotation about the axis of rotation becomes smaller and smaller, whilst it increases with abduction.[3]

Diagnostic Directions of Gaze

These essentially theoretical considerations on the change in the direction of pull with adduction and abduction, according to which the superior and inferior recti become more efficient in abduction whilst the inferior and superior obliques become more efficient in adduction, have led to the clinical concept of the *diagnostic directions of gaze*. In most movements of elevation and depression the obliques and the recti cooperate; thus a pathologically reduced ability to elevate could be due to paresis of either the superior rectus or the inferior oblique. If, however, the defect is accentuated when the eye is caused to abduct to the extent that the elevating action of the inferior oblique is very small, then the superior rectus is probably the defective muscle. As Boeder has shown, however, because the axes of rotation of the eyes, due to single muscle-pairs, vary so considerably as elevation or depression takes place, this simple view may well be illusory, so that in fact the superior and inferior recti probably always contribute more to elevation and depression than their synergistic obliques. According to Boeder's calculation, their proportionate contractions remain always in the ratio of about three to two. This is borne out by the observations of Breinin (1957a) and of Tamler *et al.* (1959) that when the eye is looking upwards in strong adduction and then moves horizontally to abduction, e.g. if the left eye starts by looking up and to the right and then looks up and to the left, the superior rectus actually shows increased activity in the electromyogram although, on the classical view, the reverse would be expected since the eye is passing into a position where the action of the superior rectus becomes more and more efficient and therefore, presumably, requires less powerful contraction of its fibres.

Torsion and Listing's Law

We have indicated (p. 649) that a rolling movement of the eye—e.g. by rotation about its antero-posterior *y*-axis, would upset the individual's estimate of direction in space unless psychologically compensated. It has been seen that the associated actions of the superior oblique with the inferior rectus tend to cancel out any rolling motion, and

Table 24.1 Individual actions of the extraocular muscles

Muscle	*Main action*	*Secondary action*
Lateral rectus	Abduction	None
Medial rectus	Adduction	None
Superior rectus	Elevation	Inward rolling and adduction
Inferior rectus	Depression	Outward rolling and adduction
Inferior oblique	Outward rolling	Elevation and abduction
Superior oblique	Inward rolling	Depression and abduction

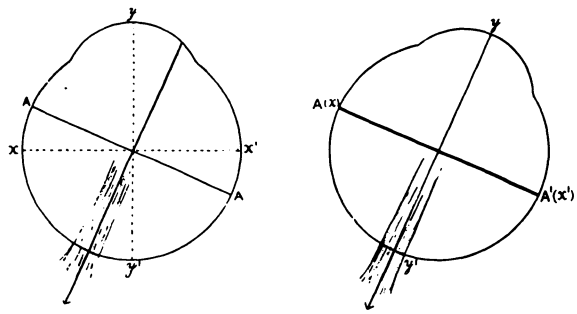

Fig. 24.13 Illustrating the effect of abduction on the action of the superior rectus. Abduction causes the *x*-axis of the eye to approach the axis of rotation, AA', so that rolling and adduction are decreased.

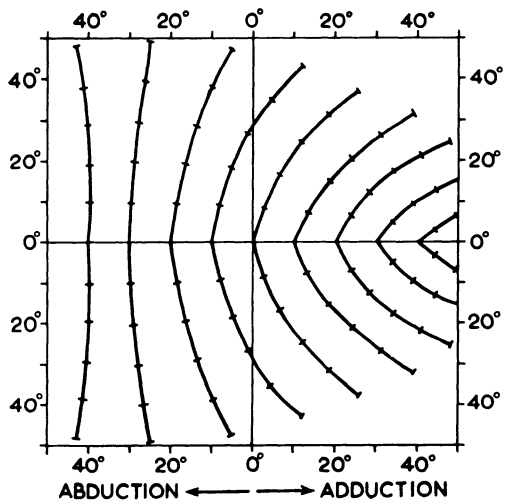

Fig. 24.14 Trace of line of fixation on a sphere concentric with the eye when the superior and inferior recti act individually from positions of adduction or abduction. If we imagine we are viewing inside the sphere, the diagram corresponds to a left eye. Each complete curve represents rotation of 50° about the axis of rotation. Small cross-lines indicate cyclotorsion with respect to the objective vertical at every 10° of rotation. (After Boeder, *Amer. J. Ophthal.*)

in actual fact a study of the movements of the eyes shows that they are executed in such a way as, in general, if not to exclude rotations about the anteroposterior axis, to reduce them to a minimum. This is the basis of *Listing's Law* which will be enunciated more exactly later; for the moment we need only note that since rotations about this third, antero-posterior, axis are apparently excluded, there are virtually only two degrees of freedom in the motions of the eyes, i.e. the motions can be resolved into rotations about the horizontal *x*- and vertical *y*-axes. Can we conclude, therefore, that there is no torsion during all movements of the eyes, so that the image of a horizontal line in the frontal plane always falls on the horizontal meridian or parallel with it? We have seen, in the analysis of the actions of the superior and inferior recti, that the latter adduct the eye even though they rotate it about an axis perpendicular to the vertical, i.e. in spite of the fact that there is no rotation about the vertical *z*-axis, and it can be shown that rolling or torsion will occur in spite of the exclusion of rotations about the antero-posterior axis.

Torsion in the Tertiary Position

In Fig. 24.15 a vertical section through the equator of the eye in the primary position is shown, so that the plane of the paper corresponds to Listing's plane; *xx'* is the transverse horizontal axis, rotation of the eye about which causes pure elevation or depression; *zz'* is the vertical axis, rotation about which causes adduction or abduction. *xx'* coincides in direction with the horizontal meridian and may be considered as the intersection of the retinal horizon with the plane of the paper; it is at right-angles to the median plane, *mm'*, coming out of the plane of the paper; in this, the primary position, there is no torsion and, so long as the retinal horizon, passing through *xx'*, remains at right-angles to this plane, torsion will be absent.

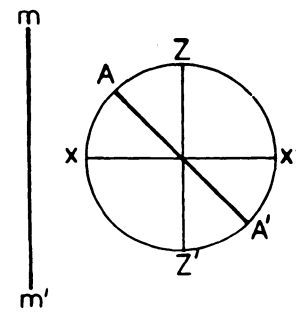

Fig. 24.15 Illustrating torsion. A vertical frontal section through the right eye. Rotation about AA' brings *z* nearer to *mm'* and takes *z'* farther away.

Rotation about *xx'* obviously does not alter its inclination, and therefore that of the retinal horizon, to *mm'*, so that with pure elevation from the primary position there is no torsion; similarly, rotation about *zz'*, causing adduction or abduction, does not change the inclination of the retinal horizon to the plane *mm'*.

Rotation about the intermediate axis, AA', lying in the plane of the paper (Listing's plane), causes a combined movement of adduction and depression or abduction and elevation; during this rotation the point *x'*, for example, moves in a circle which is obviously not parallel with the plane *mm'* nor at right angles, to it, consequently the retinal horizon passing through *xx'* becomes inclined to

the plane *mm'* and the eye experiences torsion in spite of the fact that the axis of rotation, AA', is in Listing's plane, at right-angles to the antero-posterior axis. If we imagine that we are looking into the eye from behind, a rotation that brings *x'* up out of the paper corresponds to looking up and to the right; in this event the inclination of the retinal horizon towards *mm'* follows an anti-clockwise direction and if the eye is a right eye it may be said to have undergone inward rolling. (It is perhaps easier to visualize the events by considering a median plane through *zz'*, corresponding to the vertical meridian of the retina; on rotation about AA' *z* clearly moves closer to *mm'*.)

TORSION AND ROLLING

Thus rotation of the eye about an axis intermediate between the horizontal and vertical, whereby the eye passes from the primary position to a tertiary one, results in an angle of torsion; it is customary, but confusing, to draw a distinction between the two general ways of producing this deviation of the retinal horizon from perpendicularity to the median plane; if this is caused by rotation about the antero-posterior axis, or an axis with a component along this direction, it is said to be due to *rolling*; if it is a consequence of rotation about an axis in Listing's plane, it is called *torsion* or *false torsion*. No one has suggested a similar differentiation between adduction or abduction caused by rotation about a vertical axis and that caused by rotation about an axis perpendicular to this (p. 651), and the differentiation between the two processes is entirely unnecessary; the physiologist is chiefly concerned with the position of the retinal horizon in respect to the median plane, and the degree to which it deviates from perpendicularity may be called the angle of torsion or angle of rolling indifferently. Rather than increase the already existing confusion, however, it is probably advisable to retain the distinction; thus, with Quereau (1955) we may define rolling as a rotation about an antero-posterior axis and torsion (or false torsion as it is often called) as the consequence of oblique rotations about an axis in Listing's Plane.

So long as the head is vertical and no torsion has occurred, the retinal horizon will intersect a vertical frontal plane, e.g. the wall of a room, in a horizontal straight line (Fig. 24.8); if the eye fixates any horizontal line in this plane, therefore, its image will fall on the horizontal meridian of the retina so long as no torsion has been experienced during the movement of fixation.

Donders' Law

The position of the horizontal meridian of the eye in relation to the median plane, i.e. the degree of torsion present, can be ascertained by after-image experiments. If the eye, in the primary position, is directed at a horizontal straight line, the image of the latter falls on the horizontal meridian; if the stimulus is strong, an after-image may be evoked and the sensation is projected outwards, so that wherever the gaze is directed the line is perceived in the position it must have if its image is to fall on the horizontal meridian. If this projected after-image coincides with a true horizontal line, it can be said that the truly horizontal line produces an image on the horizontal meridian, i.e. that no torsion is present. If, on the other hand, torsion has occurred, the projection of the horizontal meridian appears inclined to a truly horizontal line, and the angle between the after-image and the horizontal gives the angle of torsion.

With the eye in the primary position, a black horizontal line is fixated for a time and the eye is then moved over a screen with horizontal lines on it. If the eye moves vertically upwards or downwards, or horizontally to the left or right, the after-image is found to coincide with the lines on the screen, indicating that there is no torsion. If the eye is moved to a tertiary position, the after-image no longer coincides with the horizontal lines; e.g. if the eye looks up and to the right, or down to the left, the after-image is inclined over to the left, as we should expect if rotation took place about an intermediate axis in Listing's plane. The actual directions, in which the projected after-image lies for different movements are indicated in Fig. 24.16. It is found that no matter how the eye is moved to any position-whether in several steps or as a result of a single rotation—the torsion is the same; this is the basis of *Donders' Law* which states: '*When the position of the line of fixation is given with respect to the head, the angle of torsion will have a perfectly definite value for that particular adjustment; which is independent not only of the volition of the observer but of the way in which the line of fixation arrived in the position in question.*'

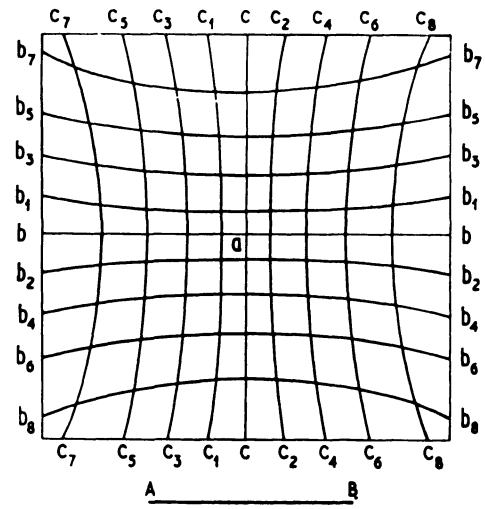

Fig. 24.16 The inclination of the projection of the after-image of a horizontal line, fixated in the primary position of the eye, on moving the latter into various other positions. *a* is the original fixation point and AB represents the relative distance of the eye from this point. (Helmholtz, *Physiological Optics.*)

Projection of Vertical Lines

With vertical lines, the position is more complicated; a vertical after-image is found to be inclined as though the eye had twisted in the opposite sense, i.e. on looking up

and to the right the vertical line after-image is tilted over to the right instead of to the left; since the eye cannot exhibit torsion in two ways at once, and since the twist of the horizontal line agrees with theory, this apparent torsion in the opposite sense must be due to some other cause. Suppose now the eye is moved from the primary position upwards and to the right, and the torsion is corrected by an appropriate rolling movement. The after-image of a horizontal line, fixated in the primary position, now corresponds in direction with the truly horizontal line through the new point of fixation; the vertical meridian of the retina is at right angles to the retinal horizon so that we might expect that its projection outwards would be at right angles to a horizontal line on the wall, coinciding with a vertical line. This, however, is not true; the retinal horizon is inclined upwards and to the right, and a line perpendicular to it—which represents the projection of the vertical meridian in the absence of torsion—is inclined over to the right when projected on the screen (Fig. 24.17).

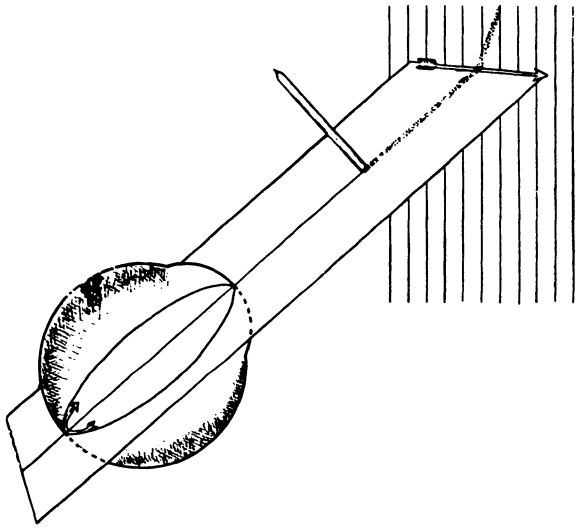

Fig. 24.17 Illustrating the projection of the vertical meridian of the retina. The eye is looking up and to the right, and it is supposed that torsion has been corrected. The image of the pencil thus falls on the vertical meridian of the eye; its projection against the frontal plane is nevertheless inclined over to the right.

We are now in a position to explain the opposite appearances of horizontal and vertical after-images; due to torsion the horizontal and vertical meridians are tilted over to the left in the case examined. Owing to the characteristics of the projection of the vertical meridian on a vertical frontal plane in space, the after-image of a vertical line, fixated in the primary position, appears tilted over to the right, and more so than the tilt to the left due to torsion.

As a result of these combined effects, therefore, the after-image of a cross, fixated in the primary position, will have the appearances shown in Fig. 24.18 when the eyes are moved into various tertiary positions.

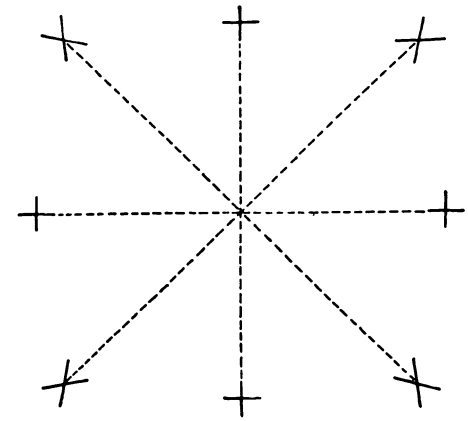

Fig. 24.18 Approximate appearances of the projections of the after-image of a cross, fixated in the primary position of the eye, for various directions of the fixation axis.

Listing's Law

It is clear that if, during a rotation of the eyes from the primary position, there is to be no component of rolling about the antero-posterior axis, then the axis of rotation must be perpendicular to this axis, i.e. it must lie in Listing's plane (Fig. 24.5). According to Listing this is, indeed, true so that movements of the eye are confined to two, instead of three, degrees of freedom. Given this limitation—which is the basis of Listing's Law—the experimental finding of Donders that the torsion of the eye is characteristic for its position however this was achieved, follows at once, since the torsion due to rotation about an axis in Listing's plane is predictable on geometrical grounds.

More recent experimental studies have shown that Listing's Law is only an approximation. Most recently Ferman *et al.* (1987a) have measured the rotation of the globe, using an electromagnetic coil device, in relation to the objective vertical. Figure 24.19 is an example of the mean effective torsions determined in this way for various positions of the left eye. In a second paper (1987b) they measured torsion under dynamic conditions.[4]

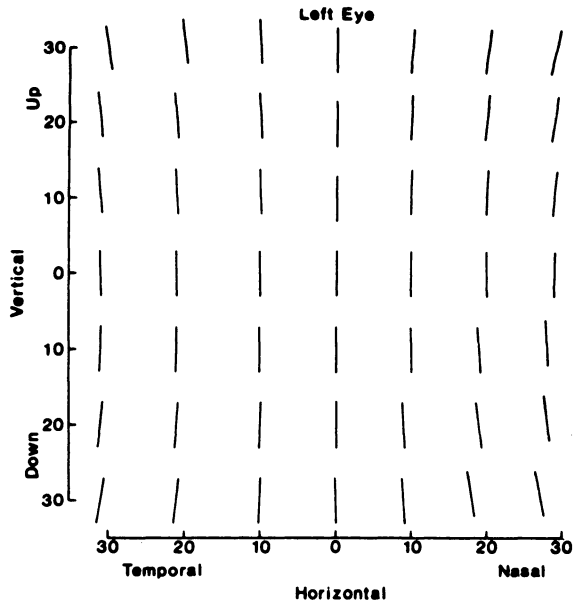

Fig. 24.19 Plotted lines in the figure represent the means of effective torsion values of the left eye of all subjects corresponding to all 49 target positions at the various horizontal and vertical eccentricities. Angles with the vertical made by the lines are actual torsion angles. Upper pole of line tilted clockwise: intorsion; upper pole of line tilted anti-clockwise: extorsion. All values in degrees. (Ferman *et al.*, *Vision Res.*)

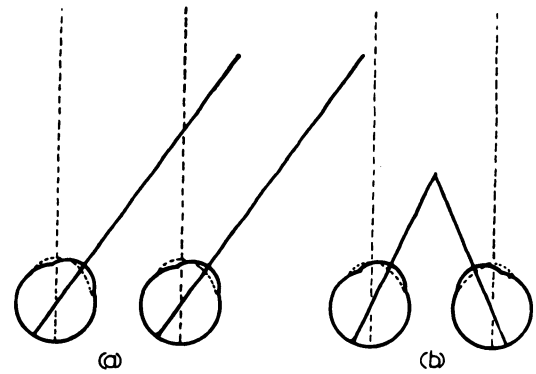

Fig. 24.20 Conjugate (*a*) and disjunctive (*b*) movements of the eyes.

BINOCULAR MOVEMENTS

Hering's Law

The movements of the two eyes are so co-ordinated as to permit them to operate as a single entity; this unity in behaviour is the basis for *Hering's Law of the Ocular Movements* which states: '*The movements of the two eyes are equal and symmetrical*'.

A movement is said to be *conjugate* when the fixation axes are parallel and the movements of the separate eyes are equal in all respects (Fig. 24.20*a*). When the fixation axes are not parallel, as in convergence or divergence, the movement is said to be *disjunctive* (Fig. 24.20*b*); in this case the movements of the two eyes are symmetrical, and, as we shall see, they may well be equal in extent even though it can appear that one eye does not move at all (e.g. when converging on a point directly in front of one eye).

The Position of Rest

We have so far defined a primary position of the eyes as a reference point from which movements may be described; when the eyes are free from any stimulus determining their mutual orientation (accommodation, fusion of images, etc.) they adopt the so called *fusion-free position* or *physiological position of rest* and it generally happens that in this position the fixation axes diverge slightly (physiological heterophoria) and are thus not in their primary positions; hence, even for a distant point, the act of fixation requires a tonic action of the extraocular muscles whereby the fixation axes are maintained parallel. As we shall see, this 'tonic' action is the result of the operation of the fixation reflex that ensures that both eyes will fixate a given point accurately and thereby prevent the diplopia that would occur were this accurate binocular fixation not maintained (p. 464). To determine this fusion-free position various optical devices are employed to remove the tendency to binocular fixation; thus if a red spot on a green background is viewed by one eye through a red glass and by the other through a green one, the two eyes see quite different pictures and there is no tendency to fuse these, so that the fixation reflex is not operative and the eyes adopt their 'natural positions'. The muscle balance of the eyes would be said to be perfect if the two eyes maintained accurate alignment with the same point; if they tended to converge they would be said to be *esophoric*; if they diverged *exophoric*, and so on.

Conjugate Movements

Conjugate Innervation

In conjugate binocular movements both eyes must move to the same extent if diplopia is not to result from any shift of the gaze, and it is therefore reasonable to suppose that there is some sort of conjugate innervation of the principal actors in any binocular movement, in the sense that the passage of impulses to one is accompanied by the facilitated passage of impulses to the other. Broadly

speaking we may expect that for a conjugate deviation to the right the left medial rectus will be associated with the right lateral rectus; for a movement up and to the right, the right superior rectus (the elevator with the stronger action in abduction) will be associated with the left inferior oblique (the elevator with the stronger action in adduction). The muscles of the two eyes may thus be classified in pairs, or 'associates', such that in any general type of movement a pair may be designated as the chief actors. The clinician makes use of this classification in order to assess a muscle deficiency; the 'diagnostic directions of gaze', classified below, are chosen so that any defect in binocular fixation may be related to the muscle associates chiefly acting (Table 24.2). That this linkage is real is proved by the phenomenon of the secondary deviation of a squinting eye. For example, if the left lateral rectus is partially paralysed, when the eyes look left the eyes squint because the left eye fails to make the necessary movement (Fig. 24.21*b*). If, however, a special effort is made by the left eye to fixate the point, then the right eye, by overaction of its medial rectus, squints, giving what is called a *secondary deviation* (Fig. 24.21*c*).

Table 24.2 Diagnostic positions of gaze

Diagnostic direction	*Chief actors*	
	R.E.	*L.E.*
Right	L. rectus	M. rectus
Left	M. rectus	L. rectus
Up and right	S. rectus	I. oblique
Up and left	I. oblique	S. rectus
Down and right	I. rectus	S. oblique
Down and left	S. oblique	I. rectus

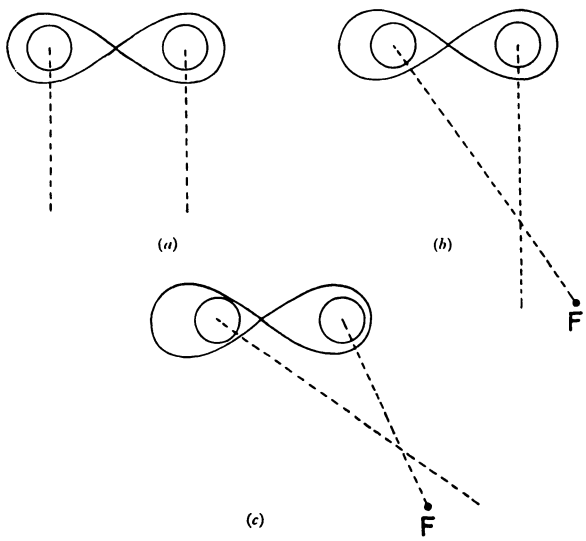

Fig. 24.21 Illustrating primary (*b*) and secondary (*c*) deviations due to paresis of left lateral rectus.

Limits of Movements

For practical purposes, the limits of binocular conjugate movements are given by the *field of binocular single vision*, i.e. one determines the position, for any direction of the gaze, at which one eye can no longer keep pace with the other, as evidenced by an insuperable diplopia. Duane's measurements have shown that this field extends to at least 40° in any given direction and usually up to 50° or more, in fact he states that most individuals retain binocular single vision up to the very limits of the excursions of the eyes, so that it may happen that the binocular field of single vision is larger than either monocular field of fixation taken separately. Thus it appears that, no matter what the maximum excursion of each eye separately is, the excursion of both together is, in normal cases, such that one eye keeps pace with the other and diplopia is avoided even in extreme deviations of the eyes.

Disjunctive Movements

Converging Power

When a near object is fixated, the eyes converge as a result of the combined contractions of the medial recti. There is, of course, a limit to which the fixation axes can be deviated inwards so that if, for example, a pencil in the median line is moved closer and closer to the eyes, a point is reached where the two eyes can no longer fixate the pencil and it appears double. This point, the nearest consistent with single vision, is called the *near point of convergence* (Fig. 24.22); in 80% of normal individuals it lies between 5 and 10 cm in front of the eyes and is not greatly affected by age as with the near point of accommodation. The *far point of convergence* is given by the point of intersection of the fixation axes in the physiological position of rest; since the eyes in this condition are

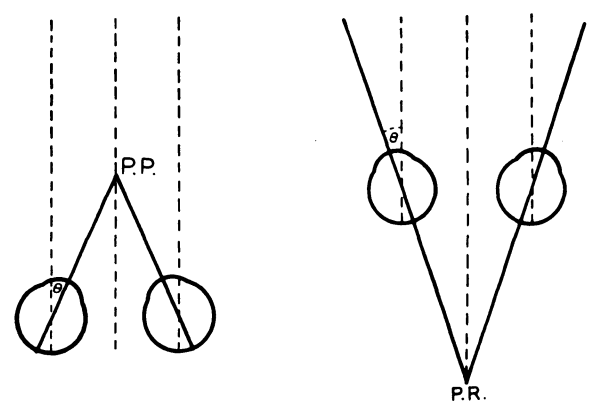

Fig. 24.22 The near point (P.P.) and far point (P.R.) of convergence.

usually divergent, this point is generally behind the eyes (Fig. 24.22), its distance being given a negative value.

METRE-ANGLE

By the *converging power* of the eyes, for any given point of fixation in the median line, is meant the angle through which *either* fixation axis moves from the primary position when the convergence takes place (Fig. 24.22); this angle can, of course, be represented in degrees but Nagel introduced the *metre-angle* as a convenient unit. The metre-angle is the angle through which each eye has rotated from the primary position in order to fixate an object 1 metre away in the median line. If the eyes converge on an object 2 metres away, clearly the angle is approximately halved, and the convergence of each eye is said to be 0.5 metre-angle; if the object is 10 cm away the angle is approximately ten times as large and the convergence is 10 metre-angles. In general, the converging power of each eye is given by the reciprocal of the distance of the fixation point in metres. For an average interpupillary distance of 6 cm the metre-angle corresponds to the convergence angle of 1.7°. It will be noted that the accommodative power in dioptres for any point is given by the same reciprocal (p. 767), so that in some respects this is a convenient notation; nevertheless, because the actual angle of convergence depends on the interpupillary distance, this equality can be misleading. Thus for an emmetrope converging on a point $\frac{1}{3}$ metre away the convergence and accommodation are respectively 3 metre-angles and 3 dioptres. With interpupillary distances of 5, 6 and 7 cm the actual convergences are, however, 15, 18 and 21 prism-dioptres respectively. This is an important point when considering accommodative convergence (Breinin, 1957b).

AMPLITUDE OF CONVERGENCE

The *amplitude of convergence* is given by the difference in the converging powers of the eyes for the near and far points; hence with a near point of +8 cm and a far point of −1 metre, the amplitude is:

$$1/0.08 - 1/-1 = 12.5 + 1 = 13.5 \text{ metre-angles}$$

A prism alters the apparent direction in which an object is seen; if it is base-out, the object appears to be deviated inwards and the eye adducts in order to fixate it (a base-out prism is called an *adducting prism*). Theoretically, then, the near point of convergence may be determined by placing pairs of base-out prisms in front of the eyes until a distant object can no longer be seen single (Fig. 24.23). The strength of the prisms required to achieve this could be converted into metre-angles of convergence by the formula:

$$\textit{Strength of prism in dioptres} = \textit{No. of metre-angles} \times \tfrac{1}{2}\ \textit{interpupillary distance in cm.}$$

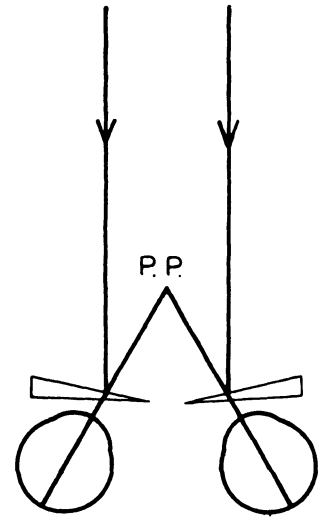

Fig. 24.23 The use of adducting prisms to cause maximum convergence. (P.P., near point of convergence.)

Thus with a near point of 12.5 m. a. and an interpupillary distance of 6 cm the prism strength would be given by:

$$\text{Prism strength} = 12.5 \times 3 = 37.5\Delta \text{ (or } 18.75\,^{\circ}\text{d)}.^{5}$$

In practice, however, this would be an unreliable measure of convergence-power since the ability to converge in response to prisms varies from moment to moment, and with practice.

FUSION SUPPLEMENT

It is stated that the desire for fusion permits a stronger convergence than that obtained without this stimulus; if an object is fixated at the near point of convergence and one eye is then covered up, the other deviates a little; the extra degree of convergence obtained when the stimulus for fusion is present is called the *fusion supplement.*

'See-saw' Movements

Disjunctive vertical movements—'see-saw' movements —in which one eye moves up and the other down, are not normally produced voluntarily; in the interests of single vision, however, the eyes are able, on the average, to overcome the effects of a 2Δ prism base-up or base-down in front of one eye, i.e. they can exhibit a 'supervergence' of 1°.

Convergence as a Function of the Two Eyes

It must be appreciated that disjunctive movements are a function of both eyes so that if a distant object in the

median line is fixated and the strongest tolerated adducting prism is put in front of one eye, on placing a prism, however weak, in front of the other, diplopia results, i.e. no further convergence is possible. The near point of convergence is thus measured by half the strength of the strongest prism tolerated by one eye (when the other has none) or the strength of equal prisms tolerated by both eyes. The explanation for this, according to Hering, was that both eyes shared in the convergence although the direction of one fixation axis might remain finally unchanged. Thus in Fig. 24.24 the fixation axes of the left and right eyes were initially parallel; a prism has been placed in front of the left eye so that it adducts maximally towards P. The right eye, during this process, was said not to remain fixed and the motions of the two eyes were analysed into an initial convergence to a point P′, such that the convergence of each eye is half the angle necessary for the left fixation axis to move through to fixate P, followed by a conjugate deviation to the right through the same angle; this leaves the right fixation axis pointing in its original direction, whilst the left is directed at P.

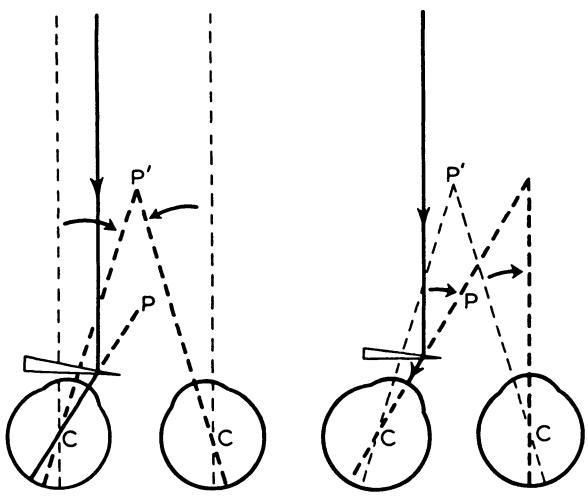

Fig. 24.24 The fixation axes were originally parallel. A strong adducting prism has been placed in front of the left eye so that it must be directed to P if it is to maintain fixation of the distant point. Both eyes converge to P′ and then make a conjugate deviation to the right. As a result, the left eye is directed to P, whilst the right eye re-assumes its original direction of fixation.

In a similar way the asymmetrical convergence to a point P, on the fixation axis of one eye when it is looking straight ahead (Fig. 24.25), was said to be achieved by an initial convergence to a point P′ in the median line, followed by a conjugate deviation. Since convergence is equally shared by the two eyes, we can obtain the convergence of *each* eye for any position of the fixation point by halving the sum of the angles moved through by the two fixation axes from their primary positions.

EXPERIMENTAL EVIDENCE

The asymmetrical convergence illustrated by Fig. 24.25 need not take place in the gross steps illustrated, and the process may consist in a series of convergence and conjugate lateral movements that may escape observation in the absence of an accurate means of measuring either the movements of the eyes or activity in their muscles. Alpern & Wolter (1956), employing the electrooculogram (EOG, p. 660) to record the eye movements, found that they were, indeed, compound, but apparently the conjugate movement preceded the convergence, i.e. the eyes tended to look to the right of P and subsequently to converge on it. As Alpern & Wolter emphasized, the speed of the conjugate type of movement, namely about 400°/sec, is so much greater than that of convergence (about 25°/sec) that the former might be missed. By measuring the eye movements by photographing the light reflected from the cornea, Westheimer & Mitchell (1956) were able to confirm Hering's view exactly, the asymmetrical convergence consisting of a rapid 'saccade', i.e. a conjugate version, followed by convergence.[6]

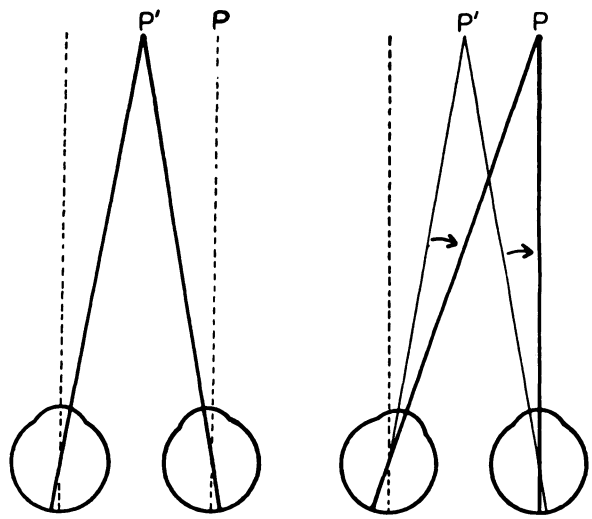

Fig. 24.25 Illustrating asymmetrical convergence to point P. The two eyes converge on the point P′, and then make a conjugate movement to the right. The direction of the right fixation axis is thus finally unchanged.

Rolling

When the eyes are in the primary position they cannot be rolled voluntarily; however, the stimulus for fusion can cause such a movement. It is possible, with the aid of 90°

prisms placed in front of one eye, to cause the image of an object on the retina to rotate about the fixation axis, e.g. the image of a cross may be tilted over. The two eyes are thus presented with different images that can only be fused if the eyes are rolled in opposite directions; the stimulus for fusion causes such a rolling, which may amount to as much as 10° to 14°, divided between the two eyes, but is generally much smaller.[7] Convergence is said to be associated with a certain degree of outward rolling of the two eyes, so that their vertical meridians make an angle with each other which, in extreme instances, may amount to as much as 25°. This rolling must produce a rotation of the two retinal images in respect to each other, so that points in space formerly seen single might now be seen double (p. 463); on converging on a line of print, for example, diplopia should result from this asymmetrical torsion; in practice this does not occur so that it would seem, as Harms has pointed out, that when there is stimulus for fusion, rolling does not take place during convergence; only when the object fixated has adequate symmetry about the fixation axis, so that its retinal image is not seriously modified by rotation about this axis, does rolling occur. For example, if an individual fixated a circle binocularly, rolling of one or both eyes would make no difference to the two retinal images; with a cross, on the other hand, the images would tilt in opposite directions and the individual would have to fuse dissimilar images; the rolling that occurs during convergence is therefore probably largely countered by a corrective fusion movement. As we shall see, the eyes execute a conjugate rolling movement when the head is tilted towards the shoulder; this is a reflex response to the altered pull of gravity on the head, and to the stretch of neck muscles (p. 682).

Analysis of the Movements

It was Dodge in 1903 who made the first serious quantitative attempt to analyse the movements of the eyes; subsequent work has depended for its fruitfulness on improvements in the technique for recording eye movements. Probably the most satisfactory method consists of reflecting light from the cornea, or a contact glass fitting snugly on the eye, and focusing it on to a moving photographic film. By suitable calibration the movements of the reflected light may be converted into angular movements of the eye quite accurately.

Electro-oculogram

When an electrode is placed on the cornea and another on the posterior pole of the eye or elsewhere on the head, a 'standing potential' is recorded of about 1 mV, the cornea being positive. Illumination of the eye gives alterations of this standing potential which we call the electroretinogram (ERG); thus the ERG is really superimposed on the 'standing potential'. Because of this potential the eye behaves like a dipole orientated along its antero-posterior axis, and if electrodes are placed at right-angles to this axis, e.g. in the two canthi, then movements of the eye will cause changes of potential between the electrodes because the dipole's orientation with respect to these electrodes changes. This is the basis of *electro-oculography* (EOG), an indirect method of recording eye movements, which can be employed even with the eyes closed. Methods specially adapted to record the small involuntary movements that take place during maintained fixation are those of Rashbass (1960) and Ginsborg & Maurice (1959).

In experimental animals, such as the monkey, Fuchs & Robinson (1966) have implanted a fine wire coil under the conjunctiva; this was joined to a connector fixed to the skull. The animal's head was exposed to two alternating magnetic fields in spatial and phase quadrature, and signals could be made to indicate horizontal and vertical eye motions.

TYPES OF MOVEMENT

The conjugate movements of the eyes may be classified as *saccades* and *smooth following*, or *tracking*, movements. Saccade was the name originally given by Dodge to the rapid movements between fixation-pauses that occur in reading, but it is now applied more generally to the conjugate shifts of gaze from one fixation point to another. The very small saccades, occurring during steady fixation, as described later, are now called *micro-saccades* or *flicks*. The movements of the eyes during convergence take place so much more slowly than the conjugate movements that a separate effector system has been postulated (Alpern & Wolter, 1956).

The Saccade

The mechanics of the saccade were first seriously investigated by Westheimer (1954), the subject being told to fixate a light whose position could be suddenly changed. He found a reaction-time of some 120 to 180 msec, after which both eyes simultaneously moved; the maximum velocity attained varied with the magnitude of the saccade, being 500°/sec for a 30° movement and 300°/sec for 10°.

Pre-emphasis

Subsequent studies of Robinson (1964), in which he measured both the eye movements and the tensions

developed in the extraocular muscles, showed that the eye was impulsively driven in a saccade by a brief burst of force much greater than necessary to maintain the eye in its final position; it is essentially this 'pre-emphasis', or excess force, that allows the saccade to be executed so rapidly, permitting a 10° saccade to occur within 45 msec after its beginning.

Damping

The deceleration of the eye that brings it to rest at the end of the saccade is not achieved by any checking action of the antagonistic muscle, but relies entirely on the viscous-elastic damping of the muscles and orbital connective tissue, a finding that has been amply confirmed by EMG and single unit studies of the eye motor nuclei (p. 690). It is this orbital stiffness, of course, that requires that the muscles contract when the eyes deviate from their primary positions, the greater the angular deviation the greater the force of contraction.[8]

Accuracy

In general, the saccadic movement matches that of the target to about 0.2° (Rashbass, 1961) but sometimes it does not, in which case it is followed, after a new reaction-time, by a second saccade; in some subjects there may be three or four saccades, each separated by one reaction-time, before the final fixation is reached. Rashbass also observed that there was a threshold target displacement, so that a movement of 0.25 to 0.5° is usually not accompanied by a response.

Control-mechanism

Young & Stark (1963) showed that the control mechanism during the saccadic type of target-following could be described as a 'sampled data system', in the sense that the brain made discontinuous samples of the position of the eyes in relation to the target, i.e. of the 'error', and corrected this. Proof of such discontinuity was provided by Westheimer who showed that, if the target was caused to step aside and return to its original position within 100 msec, the eye nevertheless made a saccade 200 msec later.

LARGE SACCADES

According to Becker & Fuchs (1969) a saccade of over 15° occurs in two pre-packaged stages; the first saccade brings the eyes short by about 10% of the target, and after a reduced latency (130 instead of 230 msec) a second saccade brings the eyes on target.

ERROR-SIGNAL

It seems unlikely, however, that the secondary saccade, subserving the obvious function of correcting the first, should be executed in a pre-programmed fashion but rather in the light of visual information that provides the error-signal. Prablanc & Jeannerod (1975) showed that the secondary corrective saccade failed if the visual input was no longer present, i.e. if the target was extinguished before the end of the primary saccade. Interestingly, they showed that the error for the primary saccade increased as the duration of presentation of the target decreased, so that it was only 1° for a 200 msec presentation and was 3° for a 20 msec presentation. Thus time is required to weigh up the situation and programme the saccade with accuracy.

LATENCY

So far as the latency of the second corrective saccade was concerned, Prablanc and Jeannerod found that it depended on conditions; when they presented the signal twice at the same place, e.g. two 20 msec pulses separated by greater than 50 msec, then after the first saccade there was a small corrective saccade with a latency of 176 msec, which is less than that for the primary saccade of some 217 msec. An important condition for this reduced latency is the error in the primary saccade; if this is greater than 4°, then the latency is not reduced, presumably because a completely new decision has to be made; with a smaller error it appears that the execution of the first saccade in some way speeds up the computation of the motor discharge necessary for the secondary saccade.

VISUAL INPUT

Hallett & Lightstone (1976a, b) studied the responses of subjects to presentation of a target during the execution of a saccade, to determine the extent to which information derived from the eyes could be utilized during the eye movement. A target was presented, inducing a saccade, S_0, and the eye-movement triggered a new target movement before S_0 was completed; after the target had made its new movement it was exinguished so that the new saccade, S_1, required to fixate it, was made while it was invisible. It was found that the saccade, S_0, occurred with its normal latency, usually undershooting its target, but it was never followed by the expected corrective saccade, showing that this requires visual input; after a further more or less normal latent period, the usual response was a primary saccade, S_1, towards the target in its second position; even though it was not lit throughout the latent period, the timing and accuracy were more or less normal. Thus the cancellation of the corrective saccade and the occurrence of S_1 indicate the effectiveness of visual input during the saccade.

Smooth Pursuit or Tracking Movements

Under these experimental conditions the fixated spot of light is caused to move at a constant velocity in a given direction; if this movement does not exceed a certain speed, namely about 30 to 40 °/sec, the eyes move with the same speed, so that the image remains effectively stationary on the retina. As we should expect, the smooth pursuit movement is usually, itself, compound; thus, because of the reaction-time of some 150 msec before the smooth movement begins, and because it takes at least 400 msec for the eye to reach the target speed, the pursuit movement, by itself, would inevitably leave the point of fixation of the eye trailing behind the target unless a saccade intervened; and this in fact happens. Figure 24.26 from Robinson (1965) shows the four main types of following movement, that marked 1 being the most common; here, after a delay of 125 msec, the eye accelerates at a mean value of 60°/sec^2 to reach a velocity of 6.1°/sec and a displacement of 0.38° in 112 msec before the interruption of a saccade; this has an amplitude of 1.24 °, so that an error of 0.7° remains. The eye leaves the saccade at a smooth velocity of 12.2°/sec, i.e. it has overshot the target velocity; it maintains this excessive velocity until the error is nearly zero, when the velocity slackens off to become equal to that of the target. Figure 24.26 also illustrates the development of tension in the horizontal recti associated with the movement; as with the saccade, there is an initial 'pre-emphasis', this time on the rate of change of tension.

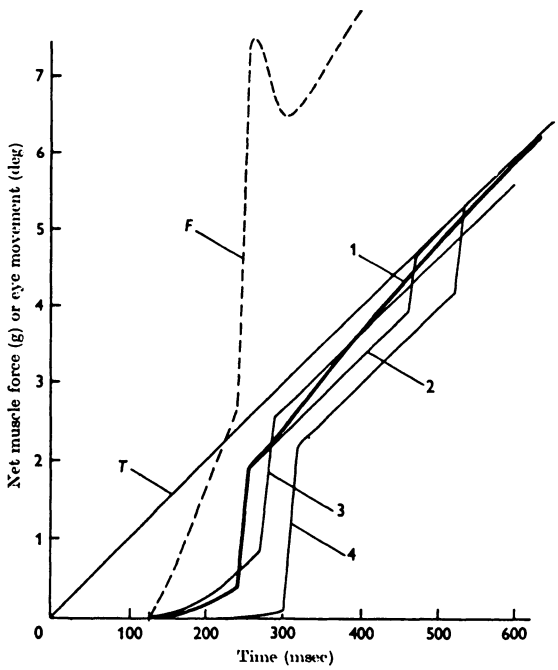

Fig. 24.26 A composite graph to show the various types of eye-movement responses to a 10°/sec ramp target motion, T. Response 1 is the mean of fourteen responses of the most common type, and F is the net isometric muscle tension in the horizontal recti associated with it. Responses 2, 3 and 4 illustrate variations in overshoot and temporal spacing between smooth and saccadic components. (Robinson, *J. Physiol.*)

Control

Young and Stark considered that smooth pursuit movements were also controlled by a sampled data system, the data utilized being the positions of the retinal image only. The studies of Rashbass and of Robinson, however, indicate that the control is continuous, presumably of the feed-back type, the eye responding to disparity, *per se*, and to the rate of change of position on the retina, i.e. there is response to both position and velocity, the latter being the dominant influence. Thus Rashbass' experiments have provided a number of interesting examples of the independence of the systems of control of saccades and pursuit movements. For example, if a target is given an initial rapid displacement of, say, 3 ° to the left, followed immediately by movement at uniform velocity to the right (step-ramp stimulus), a saccade is made to the left, after which the pursuit movement to the right occurs. Hence the saccade, because of the reaction-time, begins during the smooth movement of the target in the opposite direction; in this case, then, the position stimulus has taken precedence over the velocity stimulus. If the initial step-displacement is reduced to 1 °, then the saccade fails, and the eye starts moving, after a longer-than-normal latency of 150 msec, in the same direction as the target. In this case the eye begins a smooth pursuit movement in response to target velocity even though the movement is away from the target position at this time. Thus the pursuit movement is primarily responsive to target velocity rather than position.

Young & Stark (1963) assumed that a retinal image-error exceeding 0.2 ° was adequate stimulus for a saccade, but the step-ramp experiment of Rashbass shows the inadequacy of this picture; similarly in curve 1 of Fig. 24.26, after the initial saccade, an error of 0.7 ° remained but no saccade was elicited, the velocity overshoot being adequate for ultimate correction. Thus, the decision as to whether a saccade is to be made, as well as the determination of its magnitude, are functions of both retinal image-error and its rate of change, and it may be that the ganglion cells described by Barlow *et al.* (1964) (p. 330), sensitive to direction of image-motion, are involved here.

Disjunctive Movements

Convergence

The disjunctive movement of convergence is altogether slower than the conjugate movement, although the reaction-time of about 160 msec is of the same order. The movement takes place with a constant velocity, which is a function of the magnitude of the stimulus;[9] this velocity falls off asymptotically, with a total movement-time of about 800 msec. Even with a sudden change of vergence of the target, it is possible for control to be continuous rather than of the sampled data type; and according to Rashbass & Westheimer (1961a) this is true, so that, when momentary changes in the vergence stimulus are introduced during the execution of a movement, these are responded to after a reaction-time; thus disjunctive eye movements can be modified during their progress, and information concerning disparity can be assimilated during the reaction-time as well as during movement.

Version Plus Vergence

When the following of a target involves simultaneous conjugate and disjunctive movements, then, along whatever path the target moves, the movement of the eyes is resolved into two components corresponding to mean target position and target vergence, respectively, and appropriate responses to these components are made by two independent systems of control (Rashbass & Westheimer, 1961b).

MOVEMENTS DURING STEADY FIXATION

It has been known for a long time that the eyes do not maintain a steady fixation of a point for any length of time; instead, fixation is interrupted by rapid jerks at irregular intervals. The actual movements that take place have been analysed by several workers using modern methods of recording, usually employing the reflexion of light from the cornea.[10]

Three Types

They have been resolved into three types, as follows:

1. Irregular movements of high frequency (30 to 70/sec) and small excursion, namely some 20 sec of arc; these are described as *tremor*.
2. Flicks or microsaccades of several minutes of arc, occurring at irregular intervals of the order of 1 sec.
3. Between flicks there are slow irregular drifts extending up to 6 minutes of arc. Fig. 24.27 illustrates the region

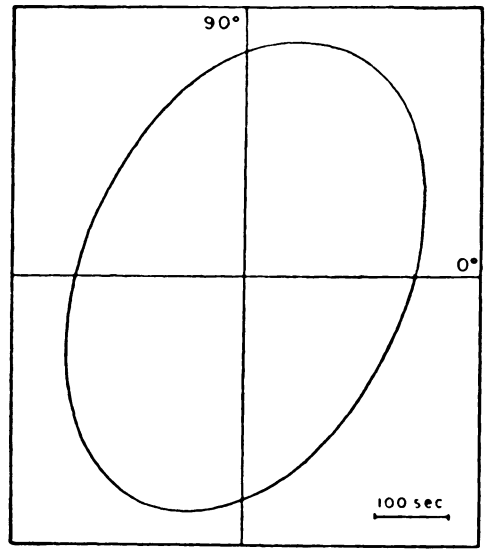

Fig. 24.27 Indicating probable range of movements of the eye over a period of steady fixation. The solid line bounds the region within which a point retinal image will be found projected in space 68 per cent of the time during 30-sec fixation intervals. (After Nachmias, *J. Opt. Soc. Amer.*)

in which the fixation point would be 68 per cent of the time during a 30 seconds fixation period, and it will be seen that the range of excursion is not large, certainly not large enough to bring the image of the fixated point off the fovea.

Corrective Saccade

Most workers are agreed that the flick is a corrective movement that brings the image back when, as a result of a drift or previous saccade, it is in danger of moving off the central fovea. This is deduced from statistical studies that show that the chance of a flick occurring in a given direction correlates well with the degree of deviation from central fixation.[11]

Binocular Fixation

When the involuntary movements in the two eyes are studied together during binocular fixation, it is found that the slow drifts take place independently in the two eyes, leading to small degrees of fixation-disparity; i.e. if the eyes are looking at a distant point the fixation axes will tend to converge or diverge at random. On the other hand, the rapid saccades take place simultaneously and in the same direction, and corrections for convergence-errors result from the circumstance that the saccades in the two eyes are not always equal in extent. According to Krauskopf *et al.* (1960), the eyes apparently behave as

independent detectors of fixation error, and in correcting their own errors they cause conjugate movements of the other eye that may not necessarily be in the right direction for correction of this eye's error. Since the chance of initiating a saccade by either eye is proportional to the magnitude of its fixation error, we may expect the eye with the larger error to initiate the corrective saccade; if the movement of the other eye in this saccade is a little smaller than that of the initiator, then on a statistical basis we may expect a reasonably accurate binocular fixation. Thus it appears that it is not the error in convergence that is detected, and corrected for, but simply the error of fixation by either eye acting as an independent unit from the viewpoint of detection.

A more exhaustive study by St.-Cyr & Fender (1969) of both monocular and binocular fixation, in which the corrective effects of flicks and drifts were examined statistically suggests, however, that retinal disparity, as such, can act as a stimulus for corrective movements; furthermore, the drifts seem to be the movements responsible for these vergence corrections. Another point brought out by this work is the large individual variations in the character of the fixation movements, and the dependence of their direction on the type of target fixated; thus a vertical line tended to cause the flicks to take an upward direction.

Steady Fixation in the Cat and Rabbit

The Cat

Winterson & Robinson (1975) found that cats, with their heads fixed, when allowed to fixate objects of their own choosing, maintained a steady fixation by a slow control mechanism exclusively, in the sense that eye-drift, which occurred, was not corrected by microsaccades, as frequently seen in man, but by equal and opposite slow drifts, which ensured that the mean eye position did not change. Thus, when looking about, they make saccades, but these are maintained by the above slow control process. The stability of fixation was remarkably good, in fact as good as that of a human when told to fixate a given point. The stability relied on visual input since it was lost in the dark. Its basis is apparently the optokinetic reflex (p. 675), manifest experimentally in the slow movement of optokinetic nystagmus. Thus the drifts, which occur spontaneously, are being corrected by slow optokinetically induced compensatory movements. The latency is about 150 msec, and since a feedback system tends to oscillate with a frequency given by the reciprocal of twice the delay, the prominent frequency component of the drifts of 3 sec is intelligible on the basis of visual correction. Winterson & Robinson emphasize that this slow control is not peculiar to lower animals, in fact, when fixation patterns of man, rabbit and monkey were studied, a similar slow control was observed, the slow drifts being corrected by opposite slow drifts. So far as man is concerned, this does not mean that the microsaccades described above are not corrective, but that when an effort is made to prevent the microsaccade a slow drift-type of correction can replace this.

Rabbit

The remarkable immobility of the rabbit's eye, when its head is fixed, is only apparent, and in fact it is the consequence of a stabilized fixation process, operating through visual feedback since, as soon as the rabbit is placed in the dark, large drifts take place. Collewijn & Van der Mark (1972) experimentally separated visual input from oculomotor response by the expedient of clamping one eye (the seeing eye) and covering the other (moving) eye. Under these conditions the seeing eye was providing no feedback because it was unable to drift, so that the covered, moving, eye exhibited the instability seen when both eyes were in the dark. By providing the seeing eye with suitable information regarding the moving eye, it was possible to enable the rabbit to stabilize its moving eye. This was achieved by using a servo-driven striped *optokinetic* drum whose rotation was steered by the position-signal of the moving eye; thus any movement of the eye caused a movement of the striped drum which induced an optokinetic correction in the moving, unseeing, eye. By making the drum rotate in the opposite direction to that which permitted stability, there was a positive feedback leading to very much enhanced instability, the drift being enhanced and interspersed with fast movements so that the movements assumed the character of a nystagmus. It is interesting that when single step-movements of the drum were made, as opposed to continuous rotations, there was no response of the eyes, so that the servosystem was velocity-sensitive rather than position-sensitive.

Notes

1. This is, indeed, an approximation; it would seem from the most recent work on this subject that the 'centre of rotation' varies within a range of about 2 mm according to the nature of the eye movement; in Van der Hoeve's view, this variability permits a more accurate adjustment of the eyes than would be possible with a fixed centre of rotation.
2. The definition of the primary position can now be modified to take into account the orientation of the retina; it is the position when the eye is looking straight ahead with head erect and the retinal horizon horizontal.

3. This assumes of course that the insertion of the muscle remains the same during abduction; in fact the effective insertion of an extraocular muscle varies very little because it is wide with its tendinous fibres fanning out; hence the axis of rotation tends to remain in the same *position in space* and therefore different in respect to the antero-posterior axis of the eye.
4. The reader interested in following this rather confusing subject farther would be advised to read the papers by Ferman *et al.* (1987) who have shown that the meaning of torsion depends on the choice of coordinates with which to define movements of the fixation axis.
5. The terminology of convergence is so varied that it is also necessary to be able to convert a convergence distance into an angle of convergence; the formula supplied by Duane is:

$$\text{Convergence angle} = \frac{\text{I.P.D. (mm)} \times 25}{\text{Convergence distance}} + 1.5°.$$

6. As summarized by Zuber (1971) the evidence on this point is conflicting, and a great deal depends on the mode of presentation of the asymmetrical convergence stimulus, especially on whether or not the fusional mechanism is activated.
7. According to Kertesz & Jones (1970), however, when cyclovergence is measured objectively under these conditions, it is negligible so that, in fact, fusion of the rotated images has taken place without rolling of the eyes, i.e. disparate images are fused.
8. The mechanical studies of Childress & Jones (1967), in which they caused adduction by a mechanical pull on the eye and observed the responses to quick releases, have generally confirmed Robinson's assessment of the eye in its socket as a high-inertia heavily damped system. Fuchs (1967) has studied the eye movements of the monkey, which are qualitatively similar in so far as the differentiation between saccades and pursuit movements is concerned; quantitatively the monkey differs in being able to follow more rapidly moving targets, and in executing the saccades more rapidly.

   Fuchs (1967) has discussed the length of the sampling time; he suggests that the sample may be taken over half a reaction time, a position-correction decided on the basis of the information collected, and the correction effected without change half a reaction time later. Such a system would be described as *semi-discrete*, to distinguish it from smooth pursuit behaviour.
9. Crone (1969) has emphasized the kinetic aspects of the retinal disparity that provokes a convergent fusional movement; the rate at which a fusional movement is brought about is, indeed, a linear function of the magnitude of the disparity.
10. Of the contributors to this subject mention may be made of Riggs and his colleagues (Ratliff & Riggs, 1950; Cornsweet, 1956; Riggs & Niehl (1960); Krauskopf *et al.* 1960); Barlow (1952); Ditchburn & Ginsborg (1953); Drischel & Lange (1956); Nachmias (1959).
11. Cunitz & Steinman (1969) have pointed to some remarkable similarities between the flicks that occur during steady fixation and the larger saccades occurring during reading. Thus the intersaccadic intervals are remarkably similar; further-more, during the reading pauses, the number of flicks is very small compared with a similar period of steady fixation, and they have argued that the flick, like the reading saccade, is a scanning mechanism. They point out that when a subject is asked to 'hold' rather than to fixate a target, flicks are very rare (Steinman *et al.*, 1967). Zuber *et al.*, (1965) have shown that, when maximum velocity is plotted against amplitude, the values for flicks fall on the same graph as those for the larger saccades in voluntary fixation movements.

References

Alpern, M. & Wolter, J. R. (1956) The relation of horizontal saccadic and vergence movements. *Arch. Ophthal.* **56**, 685–690.

Barlow, H. B. (1952) Eye movements during fixation. *J. Physiol.* **116**, 290–306.

Barlow, H. B., Hill, R. M. & Levick, W. R. (1964) Retinal ganglion cells responding selectively to direction and speed of image motion in the rabbit. *J. Physiol.* **173**, 377–407.

Becker, W. & Fuchs, A. F. (1969) Further properties of the human saccadic system: eye movements and correction saccades with and without visual fixation points. *Vision Res.* **9**, 1247–1258.

Boeder, P. (1961) The co-operation of extraocular muscles. *Am. J. Ophthal.* **51**, 469–481.

Breinin, G. M. (1957a) Quantitation of extraocular muscle innervation. *Arch. Ophthal.* **57**, 644–650.

Breinin, G. M. (1957b) The nature of vergence revealed by electromyography. *Arch. Ophthal.* **58**, 623–631.

Childress, D. S. & Jones, R. W. (1967) Mechanics of horizontal movement of the human eye. *J. Physiol.* **188**, 273–284.

Collewijn, H. & Mark, F. van der (1972) Ocular stability in variable visual feedback conditions in the rabbit. *Brain Res.* **36**, 47–57.

Cornsweet, T. N. (1956) Determination of the stimuli for involuntary drifts and saccadic eye movements. *J. Opt. Soc. Am.* **46**, 987–993.

Crone, R. A. (1969) The kinetic and static function of binocular disparity. *Invest. Ophthal.* **8**, 557–560.

Cunitz, R. J. & Steinman, R. M. (1969) Comparison of saccadic eye movements during fixation and reading. *Vision Res.* **9**, 683–693.

Ditchburn, R. W. & Ginsborg, B. L. (1953) Involuntary eye movements during fixation. *J. Physiol.* **119**, 1–17.

Dodge, R. (1903) Five types of eye movement in the horizontal meridian plane of the field of regard. *Amer. J. Physiol.* **8**, 307–329.

Drischel, H. & Lange, C. (1956) Uber unwillkürliche Augapfelbewegungen bei einäugigen Fixieren. *Pflug. Arch.* **262**, 307–333.

Ferman, L., Collewijn, H. & Van den Berg, A. V. (1987a, b) A direct test of Listing's law. I and II. *Vision Res.* **27**, 929–938, 939–951.

Fuchs, A. F. (1967) Saccadic and smooth pursuit eye movements in the monkey. *J. Physiol.* **191**, 609–631.

Fuchs, A. F. & Robinson, D. A. (1966) A method for measuring horizontal and vertical eye movement chronically in the monkey. *J. appl. Physiol.* **21**, 1068–1070.

Ginsborg, B. L. & Maurice, D. M. (1959) Involuntary movements of the eye during fixation and blinking. *Br. J. Ophthal.* **43**, 435–437.

Hallett, P. E. & Lightstone, A. D. (1976a) Saccadic eye movements towards stimuli triggered by prior saccades. *Vision Res.* **16**, 99–106.

Hallett, P. E. & Lightstone, A. D. (1976b) Saccadic eye movements to flashed targets. *Vision Res.* **16**, 107–114.

Helmholtz, H. von (1925) *Physiological Optics*, vol. III, ed. Southall. Optical Soc. Am.

Kertesz, A. E. & Jones, R. W. (1970) Human cyclofusional response. *Vision Res.* **10**, 891–896.

Krauskopf, J., Cornsweet, T. N. & Riggs, L. A. (1960) Analysis of eye movements during monocular and binocular fixation. *J. opt. Soc. Am.* **50**, 572–578.

Nachmias, J. (1959) Two-dimensional motion of the retinal image during monocular fixation. *J. opt. Soc. Am.* **49**, 901–908.

Prablanc, C. & Jeannerod, M. (1975) Corrective saccades: dependence on retinal reafferent signals. *Vision Res.* **15**, 465–469.

Quereau, J. V. D. (1955) Rolling of the eye around its visual axis during normal ocular movements. *Arch. Ophthal.* **53**, 807–810.

Rashbass, C. (1960) New method for recording eye movements. *J. opt. Soc. Am.* **50**, 642–644.

Rashbass, C. (1961) The relationship between saccadic and smooth tracking eye movements. *J. Physiol.* **159**, 326–338.

Rashbass, C. & Westheimer, G. (1961a) Disjunctive eye movements. *J. Physiol.* **159**, 339–360.

Rashbass, C. & Westheimer, G. (1961b) Independence of conjugate and disjunctive eye movements. *J. Physiol.* **159**, 361–364.

Ratliff, F. & Riggs, L. A. (1950) Involuntary motions of the eye during monocular fixation. *J. exp. Psychol.* **40**, 687–701.

Riggs, L. A. & Niehl, E. W. (1960) Eye movements recorded during convergence and divergence. *J. opt. Soc. Am.* **50**, 913–920.

Robinson, D. A. (1964) The mechanics of human saccadic eye movement. *J. Physiol.* **174**, 245–264.

Robinson, D. A. (1965) The mechanics of human smooth pursuit eye movement. *J. Physiol.* **180**, 569–591.

Robinson, D. A. (1966) The mechanics of human vergence movements. *J. Pediat. Ophthal.* **3**, 31–37.

St. Cyr., G. T. & Fender, D. H. (1969) The interplay of drifts and flicks in binocular fixation. *Vision Res.* **9**, 245–265.

Steinman, R. M., Cunitz, R. J., Timberlake, G. T. & Herman, M. (1967) Voluntary control of microsaccades during maintained monocular fixation. *Science* **155**, 1577–1579.

Tamler, E., Jampolsky, A. & Marg, E. (1959) Electromyographic study of following movements of the eye between tertiary positions. *Arch. Ophthal.* **62**, 804–809.

Westheimer, G. (1954) Mechanism of saccadic eye movements. *Arch. Ophthal.* **52**, 710–724.

Westheimer, G. (1954) Eye movement responses to a horizontally moving visual stimulus. *Arch. Ophthal.* **52**, 932–941.

Westheimer, G. & Mitchell, A. M. (1956) Eye movement responses to convergence stimuli. *Arch. Ophthal.* **55**, 848–856.

Winterson, B. J. & Robinson, D. A. (1975) Fixation by the alert but solitary cat. *Vision Res.* **15**, 1349–1352.

Young, L. R. & Stark, L. (1963) Variable feedback experiments testing a sampled data model for eye tracking movements. *Int. Elect. Electronics Engineers. Transactions on Human Factors in Electronics.* HFE-4, 38–51.

Zuber, B. L. (1971) Control of vergence eye movements. In *The Control of the Eye Movements.* Ed. Bach-y-Rita, P., Collins, C. C. & Hyde, J. E., pp. 447–471. New York: Academic Press.

Zuber, B. L., Stark, L. & Cook, G. (1965) Microsaccades and the velocity-amplitude relationship of saccadic movements. *Science* **150**, 1459–1460.

25. NERVOUS CONTROL OF THE EYE MOVEMENTS

General Considerations

The activities of the muscles of the neck and trunk are ultimately determined by the discharges in the motor neurones of the ventral horns of the spinal cord, which are described as the *final common path*. These neurones are acted upon by sensory neurones, and by interneurones localized in all levels of the central nervous system, from the various segments of the cord to the cerebral cortex. Thus the activity of any given muscle is determined by nervous activity in practically the whole of the central nervous system; nevertheless the activity of an organism may be resolved into certain stereotyped patterns of behaviour—the *reflexes*—which may be evoked independently of many regions of the central nervous system; thus the flexor reflex may operate in the spinal animal, i.e. the animal whose spinal cord has been severed from the brain; whilst a large variety of reflex responses may be achieved in the decerebrate animal, the animal whose cerebral hemispheres and basal ganglia have been removed. In general, we may say that these patterns of behaviour may be controlled and modified by activity in brain centres that are located higher in the system than those required for the performance of the reflex activity. This is manifest especially in the voluntary control of muscular activity mediated by the frontal motor cortex and along the pyramidal tracts.

The movements of the eyes form no exception to these general principles; well established reflex patterns of behaviour are present and these may be largely controlled, or at any rate influenced, by voluntary activity initiated, it is presumed, also in the frontal cortex. The final common path is given by motor neurones in the brain, rather than the spinal cord, whilst higher coordinating centres are found in the *superior colliculi* and in the *occipital cortex*. These reflex centres are well established; somewhat more problematical are certain regions of the brain stem, notably the tegmentum of the midbrain, pons and medulla, stimulation of which electrically gives rise to well coordinated patterns of eye movement.

Reflexes

In this short, and necessarily somewhat elementary, discussion of the nervous control of the eye movements we shall be concerned with the reflexes and their nervous pathways—the *reflex arcs*. It must be strongly emphasized, however, that most reflexes are only exhibited reproducibly and in the 'pure' form under artificial conditions, for example, in the decerebrate animal; any actual movement in the normal individual represents the final outcome of the antagonistic interplay of numerous reflexes which, in their turn, may be modified to a greater or lesser extent by the voluntary centres. For example, we shall see that a bright light in the periphery of the visual field evokes a *fixation reflex* whereby the eyes are turned towards the light so as to bring its image on the fovea; this does not mean, however, that the eyes are invariably turned to any light in the peripheral visual field. The reflex, defined as the response of the individual to a stimulus, must be considered, especially in man, as a component in behaviour; under special conditions it may be elicited with the utmost regularity, whilst in the normal intact animal the response to the same stimulus may be greatly different according to the conditions prevailing.

THE MUSCLE FIBRES AND THEIR INNERVATION

The mammalian extraocular muscles have several structural and physiological features that differentiate them from most other striated muscles, features that they share with some submammalian skeletal muscles and with mammalian intrafusal fibres.

Motor Unit

The motor unit, i.e. the number of muscle fibres supplied by a single motor axon, is remarkably small being probably of the order of 6, although the difficulty in establishing whether a given fibre is sensory or motor may result in some error in the estimate. This compares with some 100 to 150 for limb muscles (Torre, 1953). Because of its short twitch-time the fusion frequency for an extraocular muscle is very high indeed, of the order of 350 impulses per sec, and this permits a large variation in tension—over a range of tenfold—on passing from a single twitch to a fused tetanus. These two features, namely small size of motor unit and small twitch/tetanus

tension ratio, permit a high degree of gradation of the strength of contraction.

Twitch and Slow Fibres

Again the muscles of the frog, for example, fall into two classes, characterized by the structure and innervation of their fibres; the *twitch*, or *fast*, fibres are usually large and innervated by large, rapidly conducting, nerve fibres that make typically a single *en plaque* or *sole-plate* ending on each muscle fibre; this type of muscle is concerned with rapid phasic movements and, on electrical stimulation of its nerve, gives a twitch response. The other type of muscle has thinner fibres with multiple *en grappe* nerve terminals distributed over its whole length; this type is associated with the tonic type of sustained contraction; electrical stimulation of its motor nerve leads to graded mechanical responses without the spread of action potentials. Pharmacologically, the fibres are distinguished by their responses to acetylcholine, the slow fibres giving a substantial contraction whilst the twitch fibres give a single twitch. Structurally there are striking differences between the fibres; Krüger pointed out that the slow fibres lacked the M-band whilst their fibrils were irregularly arranged, being clustered together in clumps to give what he called the *Felderstruktur*, which contrasted with *Fibrillenstruktur* of the twitch fibre, in which the myofibrils were regularly arranged in a more abundant sarcoplasm. Subsequent electron-microscopical studies of Peachey & Huxley (1962) and Page (1965) have emphasized these differences; in the fibrillar, or twitch, type of fibre the myofibrils are surrounded by a well defined system of sarcoplasmic reticulum made up of longitudinal and transverse systems giving rise to the *triads*, which are considered to be developments permitting the rapid transmission of the electrical changes occurring on the surface into the depths of the fibre. In the slow fibres the myofibrils lack regular arrangement, the sarcoplasmic reticulum is scarcer and lacks the transverse system, so that the triads are absent.

Mammalian Skeletal Muscles

In the skeletal muscles of mammals this sharp differentiation into twitch and slow muscles does not occur; nevertheless, it is possible to describe muscles as either fast or slow on the basis of their contraction-times, i.e. the time to reach peak tension after a nerve stimulus; the fast muscles are usually white, capable of rapid action but soon fatiguing, whilst the slow, concerned with sustained postural contractions, are red, having large amounts of myoglobin and usually plentiful mitochondria.[1] More modern techniques, involving fatiguing the muscle with repetitive stimuli, have permitted the easy identification of the twitch-fibre histologically, and have resulted in a classification based on speed of contraction and fatiguability (Burke *et al.*, 1973). According to this, there are three basic types designated as FF (fast-rapidly fatiguable), FR (fast-fatigue-resistant) and S (slow-fatigue resistant).

Extraocular Muscle

Harker (1972a, b) has examined the types of muscle fibre in the sheep's superior rectus and levator palpebrae with histochemical and electron microscopical techniques.

Basic Structure

The basic structure of the superior rectus consists in a central core-layer of mainly large-diameter muscle fibres adjacent to the eyeball, covered dorsally and laterally by an *orbital rim layer* of small muscle fibres; at the origin and insertion ends an additional *peripheral patch layer* surrounds the orbital rim; it contains medium-diameter muscle fibres. (The spindles are distributed peripherally either within the orbital rim or at the junction between this and the peripheral patch layers.)

Fibre Types

On the basis of fibre diameter and histochemical profiles some six types were differentiated, probably corresponding with the three types just outlined and seen in the gastrocnemius, although a group of the slow, or S fibres, called G, had a distributed grape-like innervation by contrast with the plate-endings of the other types.[2] According to Harker's classification, there were three types of C-fibre equivalent to the Fast-Fatigue-resistant category, differing in size and their histochemical features; there were A-fibres, equivalent to the Fast-rapidly fatiguable (FF), and finally B fibres, equivalent to the slow fibres (S) of the gastrocnemius. In the superior rectus there were no B-fibres, so that the G fibres with distributed endings, and probably multiply innervated, provided the slow component. The nerve fibres supplying the end plate-innervated twitch-type muscle fibres (A and C) were larger (4.3 μm) than those supplying the grape-innervated muscle fibres (2.5 μm). In the levator palpebrae, in which there was no distinct layering, all fibres were plate-innervated including the slow B-fibres, which were not represented in the rectus.

TWO MAIN TYPES

In general, then, the early observation of two fundamentally differently innervated types of muscle fibres, apparently peculiar to the extraocular muscles in the mammal, but common in submammalian species, has been sus-

tained; and there is little doubt that the two main types of fibre differ functionally as well as morphologically, the plate-innervated belonging to the fast or twitch-type and the grape-innervated to the slow type; apart from this difference, the many gradations of size, and proportions of aerobic to anaerobic enzymes, are found in the extraocular muscles as with the rest of the skeletal musculature.

Contractile Properties

Phasic and Tonic Responses

The Soviet physiologist, Matyushkin (1961), was the first to demonstrate that the mammalian extraocular muscles contained two types of fibre that responded differently to electrical stimulation of the nerve nucleus; Fig. 25.1 shows intracellularly recorded responses of muscle fibres of the superior oblique to a single stimulus in the trochlear nucleus; the records in (*a*) are responses in a phasic fibre, being spike of 60 to 90 mV amplitude, and duration 1.3 to 1.5 msec, whilst the records in (*b*) are from a tonic fibre of low amplitude (12 to 28 mV) and duration greater than 20 msec. At rest, the phasic fibre was silent whilst the tonic fibre gave small potentials at 20/sec. The longer latent period for the tonic fibre indicated that it was supplied by finer fibres. In a later study (1964), the effects of repetitive stimulation of the nerve supplying the superior oblique indicated the phasic and tonic natures of the two types of fibre; the spikes were associated with the rapid development of tension whilst the small potential changes were only associated with significant tension when repetitive stimulation was maintained.

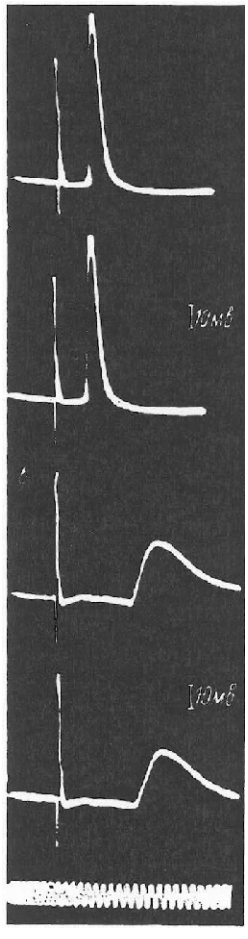

Fig. 25.1 Intracellular recordings of superior oblique muscle fibres in response to trochlear nerve stimulation. a Responses in phasic fibre; b. Responses in tonic fibre. (Matyushkin, *Sechenov Physiol. J.*)

Twitch and Slow

In a comparative anatomical and physiological study, Hess & Pilar (1963) showed that the two types of muscle fibre could, indeed, be classed as twitch and slow, as revealed by their responses to repetitive stimulation. Thus, if the nerve to the superior oblique, for example, is stimulated repetitively at 250 to 300 impulses/sec, maximal tension develops, and this soon falls off due to Wedensky block, but the tension does not fall to zero, remaining at about 30 per cent of the maximum value, whilst records of activity in the muscle fibres now show no evidence of spikes but only the slow monophasic potentials characteristic of the non-propagated type of change occurring in slow muscles (Pilar, 1967).[3]

Single Muscle Units

Lennerstrand (1974) studied single units in the cat's inferior oblique muscle by separating its nerve fibres until only one fibre in the remaining portion activated the muscle fibre under examination. Of the three types of fibre, identified by their electrical responses to nerve fibre stimulation, one (MINC) gave only local electrical responses with no propagated action potential and no twitch; this, representing five out of a total of 60 units studied, was clearly the slow grape-innervated unit similar to those in amphibian slow muscle. Of the other types, SI had a single end-plate, and the MIC had two or more end-plates, but they were both of the twitch-type giving action potentials. The MINC fibres gave no mechanical response to a single stimulus, requiring repetitive stimulation to develop tension; the tetanic fusion-frequencies varied from 50 to 350 impulses/sec, being least with the slow MINC and greatest with the fast singly-innervated SI units. An interesting feature of the units studied by Lennerstrand was the small difference in fatiguability between fast and slow units. Lennerstrand suggested that

the slow twitch units described by Bach-y-Rita might be the end-plate innervated units described as MIC rather than the MINC with grape innervation.

Functional Significance

This differentiation of muscle fibre types into twitch, with propagated action potentials, and slow, with non-propagated action potentials, is of obvious significance in the submammalian species, the former being required for rapid activity as in the jumping of a frog, and the latter for sustained postural activity. In the mammal this difference in function is usually achieved by employing the same type of muscle fibre, so far as innervation is concerned, so that all give an all-or-none action potential, but their mechanical features vary, giving a fairly wide spectrum of speed and fatiguability. It has been argued that the requirements for two very different types of movement, as well as posture, namely the fast saccade and the slow pursuit and vergence movements, have led to the retention of the more primitive submammalian muscle fibre with its grape-like terminations and multiple innervation permitting a more precise control over its tension.

Tonic Component of Contraction

Subsequent work has not left a completely clear picture as to the functional significance of the morphologically identified two main types of muscle fibre; thus Barmack *et al.* (1971), studying the effects of two successive stimuli, found no evidence of a significant contribution of slowly contracting fibres to the total muscle tension in the cat's extraocular muscle, arguing that the slowly contracting fibres should show evidence of interaction between two stimuli separated by, say, a twentieth of a second, but in fact there was no interaction until the stimuli were repeated at 40/sec, double the fusion-frequency for the slow fibres described by Bach-y-Rita & Ito (1966). Similarly, Fuchs & Luschei (1971), working on simian muscle, found no measurable tonic component of contraction when stimulating the abducens nerve, supplying the lateral rectus, at low frequencies (30/sec) adequate to cause tetanic fusion of cat's slow fibres. Again, Close & Luff (1974) found only a very small slow component in the response of the rat's inferior rectus giving what they considered to be a negligible contribution to total tension. An important point to appreciate, however, is the large differences in muscular tension required for different types of activity. If these are taken into account, it might very well be that a small development of tension, capable of being sustained for long periods, would escape measurement in many of the muscles studied.

SELECTIVE STIMULATION OF SLOW FIBRES

Thus Browne (1976) pointed out that the tension in the lateral rectus required to maintain the human eye in the primary position was only 12 to 17 g compared with the 130 g developed in a saccade (Robinson *et al.*, 1969); if the holding tension in the primary position represented activity in slow, slowly-fatiguing fibres, then the demonstration of such tensions in the absence of fast twitch-type muscle activity would confirm the belief in the physiological significance of the obvious morphological difference in muscle fibre-types. Browne profited by the different sizes of nerve fibres supplying the two main types of fibre, employing a technique of electrical stimulation that permitted the blocking of the lower-threshold large nerve fibres supplying the fast fibres, while the high-threshold small fibres transmitted their effects to the muscle. As Fig. 25.2 shows, small-fibre stimulation causes a twitch that is slow by comparison with that due to the whole muscle, and developing only a fraction of the tension (note different calibrations for upper and lower records). With selective repetitive stimulation of the small nerve fibres, the tetanic fusion-frequency was 60 Hertz, but maximal tension was only developed when the frequency of stimulation was raised to 140 Hertz. If it is appreciated that motor neurones to the extraocular muscles are capable of discharging at rates in excess of 700 imp/sec, and when in the primary position the rate is typically 100 imp/sec, it is clear that these slow fibres would be activated nearly maximally. The actual tension developed

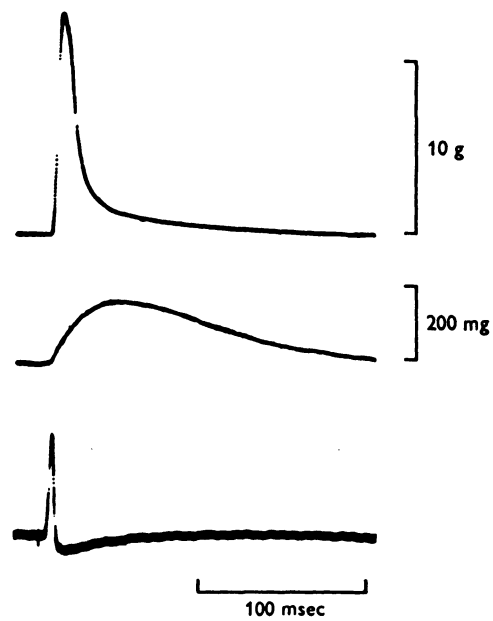

Fig. 25.2 Comparison between the time-course of a whole muscle twitch (upper trace) and a slow fibre contraction (middle trace). The bottom trace shows the late monophasic component of the e.m.g. The stimulus was applied 12 msec after the start of the sweep. (Browne, *J. Physiol.*)

under optimal conditions and maximal frequency of stimulation was some 8 g, compared with 166 g when the whole muscle was activated at an optimal rate of 280 to 320 imp/sec. Consequently it is very likely that the slow fibres, capable of developing some 8 g of tension compared with the 12 to 17 g required for maintaining the primary position, are capable of contributing a large part of the tension necessary for sustaining this tension under conditions where fatigue must not be allowed to intervene. Thus these slow fibres showed very little fall in tension when stimulated for 16 sec (9%) compared with that observed in activation of the whole muscle (49%).

SMOOTHING FUNCTION

An additional function of these slow fibres will be to smooth the activities of the twitch-fibres; these have a tetanic fusion-frequency of 350 to 500 imp/sec, so that when the eye is in the primary position and these twitch fibres are being activated along with the slow fibres, their responses will be twitches instead of smooth tetanic contractions. The simultaneous activation of the slow fibres at frequencies to give a smooth tension will tend to reduce the twitch-like character imparted by the fast muscle fibres.

Length-tension Characteristics

In general, skeletal muscle can increase its isometric tension, when maximally stimulated, if its length is increased above resting length; this gives the characteristic length-tension curve. The extraocular muscles are no exception, and this means, for example, that when the eye is in strong adduction, thereby stretching the lateral rectus, the lateral rectus can command much more tension to execute a lateral saccade than if the movement were initiated from the primary position.[4]

Pharmacology

Acetylcholine Contracture

Duke-Elder & Duke-Elder (1930) observed that mammalian extraocular muscles resembled the slow skeletal muscles of lower vertebrates in responding by a contracture to applied acetylcholine.[5] In the superior rectus of the rabbit, where the slow and fast types of fibre are separated in two layers within the muscle plate, Kern (1965) demonstrated contracture-type responses in the slow fibres. The tension developed during acetylcholine contracture of the superior rectus muscle is about 30% of the maximal tetanic tension, and it is interesting that the tension developed during repetitive stimulation of this muscle settles down to 30% of the maximal tension developed (Pilar, 1967); this corresponds with the situation when the fast fibres have ceased to respond because of Wedensky inhibition, so that the tension finally reached during repetitive stimulation is due to the slow fibres. Suxamethonium is a nicotinic cholinergic drug, and Browne (1976), in his study of the sheep's superior oblique muscle, found that this caused a contracture that developed a tension of 8.0 and 10.6 g in two sheep while the maximal tensions developed by repetitive stimulation of the small nerve were 7.0 and 7.1 g respectively.

Sympathetic

Paralysis of the sympathetic system produces Horner's syndrome consisting of ptosis, due to paralysis of the adrenergic Muller's muscle, miosis due to paralysis of the dilator pupillae, and enophthalmos. The last effect suggests that the extraocular musculature may be influenced by the sympathetic system. Kern (1968) has found that isoproterenol causes relaxation of tension in the monkey's extraocular muscles, an effect that is blocked by DCI, indicating a β-action. Since the amine caused relaxation of tension developed during treatment with acetylcholine, he argued that it was the slow fibres that were sensitive to the sympathomimetic agent. On the same basis, then, the exophthalmos accompanying extreme fear could be due to the β-action of the adrenaline secreted by the adrenal gland under these conditions.

Sensory Innervation

Information regarding the position of the eyes in the orbit is probably utilized during the control of eye-position; thus unilateral section of the ophthalmic division of the trigeminal nerve in the cat causes pendular movements of the eye ipsilateral to the lesion; with vestibularly induced nystagmus (p. 681) the amplitude was reduced in the ipsilateral eye in the dark, but in the light patterns of eye movement were equal in both eyes (Fiorentini & Maffei, 1977).

Muscle Spindle

Muscle spindles were described in the sheep's extraocular muscles as early as 1910 by Cilimbaris, but it was not until 1946 that Daniel described spiral nerve endings surrounding fibres of the human extraocular muscle; he surmised that they were sensory in function, responding perhaps to thickening during contraction. Later Cooper & Daniel (1949) identified definite muscle spindles in human muscles, a single rectus containing as many as 50, a number comparable with those in a lumbrical muscle of the hand; the spindles were concentrated near the origin of the muscle, and that was why they had not been discovered earlier.

STRUCTURE

In general the structure of the spindle was similar to that classically described in other muscles; 2 to 10 fine muscle fibres (intrafusal) are enclosed in a capsule whilst an adjacent nerve trunk sends fibres into the capsule to end on the intrafusal fibres. The innervation is both motor and sensory: thus the gamma efferents—fine motor fibres—by causing the muscle fibres in the capsule to contract are able to increase the sensitivity of the spindle to stretch; whilst the sensory endings are characteristically of the primary, or annulospiral, and secondary, or flower-spray, types supplied by large Group I and smaller Group II fibres respectively.

BAG AND CHAIN FIBRES

The sheep's spindle has been described more recently by Harker (1972) who has compared the superior rectus with the levator palpebrae. The distributions are illustrated in Fig. 25.3, most of them being in the peripheral (orbital rim and peripheral patch) layers. They contained both nuclear bag and nuclear chain fibres and each spindle was innervated by a large Group I primary nerve fibre which divided to supply each intrafusal fibre with annulospiral endings; in addition a spindle could have up to four secondary endings derived from smaller Group II nerves and terminating in irregular spirals mainly on the chain fibres. The nuclear bag fibres have a low alkali-stable ATPase and are similar to slow fibres whilst the nuclear chain fibres have high ATPase activity and are similar in this and other respects to twitch fibres.

MOTOR INNERVATION

These similarities extend to the mode of motor innervation, the nuclear bag fibres having a grape-ending similar to the G-fibres described above, and the nuclear chain a plate ending similar to the C-fibres (Fig. 25.4). An interesting feature is the collateral motor innervation, so that a fibre that activates an extrafusal fibre also activates a spindle intrafusal fibre—the motor innervation thus corresponds to the β-innervation, which is generally regarded as a more primitive type that fails to provide independent control of the two types of fibre, and this doubtless corresponds with the more limited functions of extraocular muscle spindles, which are not involved in any direct servo-type stretch-reflex (p. 689). The levator palpebrae muscle differed from the rectus in having a smaller number of spindles—61 compared with 181—and the motor innervation was different insofar as the grape innervation of the nuclear bag fibres was not shared with extrafusal fibres (it will be recalled the levator does not contain extrafusal G-fibres).

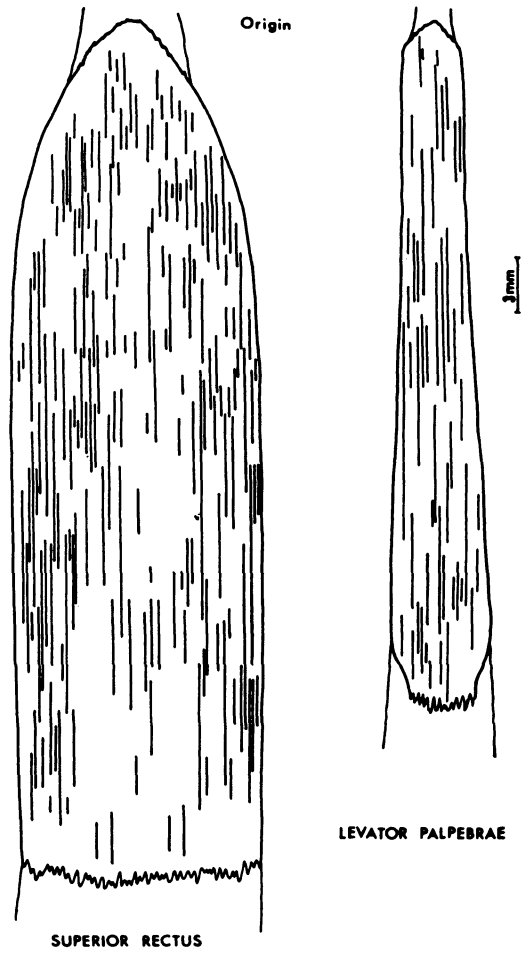

Fig. 25.3 Distribution of muscle spindle capsules in superior rectus and levator palpebrae muscles of the sheep. The capsules are plotted within the limits of a single representative longitudinal section. (Harker, *Invest. Ophthal.*)

Spindle Analogues

In certain species, notably the cat and monkey, no spindles were found but the richness of the innervation of the muscles certainly suggests the presence of simpler organs, perhaps just spirally wound endings encircling single muscle fibres (Cooper & Fillenz).[6] Subsequent work, notably that of Wolter (1955), suggests that the sensory apparatus in the human extraocular muscles is even more varied; in all, he has described some six different types of ending, varying in complexity from the spindle to relatively simple terminations, which may be distinguished from motor endings by the circumstance that they end in connective tissue between fibres.

Sensory Pathway

The evidence relating to the pathway for this sensory information has been summarized by Rogers (1957) and Whitteridge (1960). There seems little doubt that there are

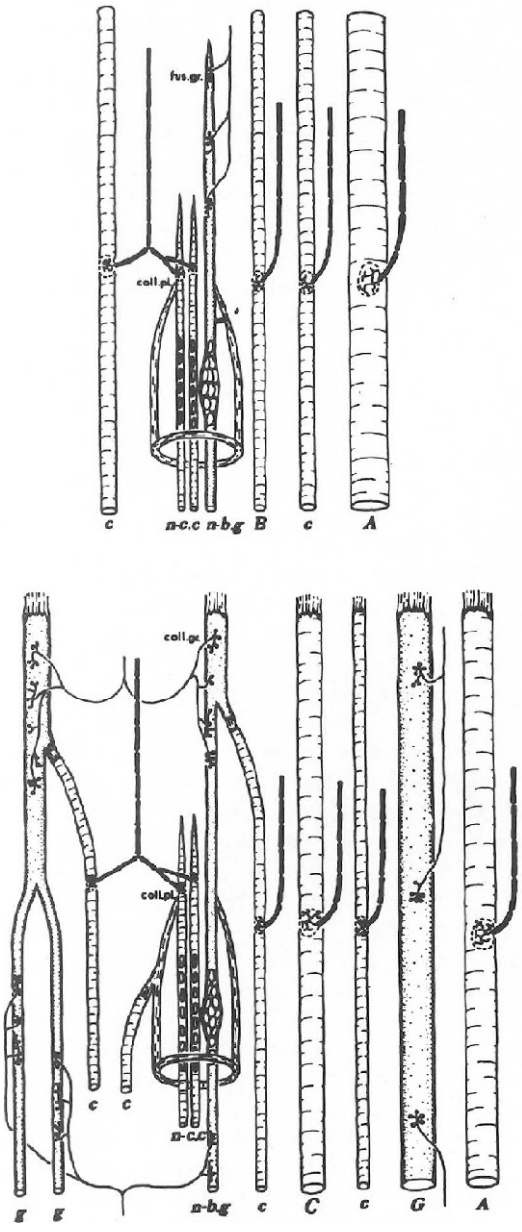

Fig. 25.4 Top: Schematic representation of the pattern of motor innervation in levator palpebrae. Bottom: Superior rectus. A, large A-fibre; B, small B-fibre; C, intermediate C-fibre; c, small C-fibre; *coll. gr.*, collateral grape endings; *coll. pl.*, collateral plate endings; *fus, gr.*, fusimotor grape endings; G, large G-fibre; *g*, small G-fibre; *n-b.g.*, nuclear bag G-fibre; *n-c.c*, nuclear-chain C-fibre. (Harker, *Invest. Ophthal.*)

connections between the muscle-nerves and the trigeminal (N V), often within the orbit; recording from these branches, in the goat, Whitteridge (1955) obtained spindle-responses on stretching the eye-muscle. In the sheep, Manni *et al.* (1967) found a group of neurones in the Gasserian ganglion with a steady discharge of 10 to 20/sec; on stretching an extra-ocular muscle, the discharge-rate suddenly increased to up to 300/sec, finally settling down to 150 to 90/sec when the stretch was maintained. On release of the muscle, the discharge ceased abruptly, and later the steady discharge of 10 to 20/sec was reassumed. This is typical of the behaviour of spindle afferent neurones. Subsequent studies in both sheep and pig leave no doubt that in these species the sensory neurones innervating the spindles are located in the Gasserian ganglion, and not in the mesencephalic root of the trigeminal (Manni *et al.*, 1970b), nor yet in ganglion cells located along the oculomotor nerve (Manni *et al.*, 1970a). The fact that the oculomotor nerve in these species contains sensory fibres is due to the passage of the central processes of the ganglion cells of N V into the central portions of the oculomotor nerve (Fig. 25.5) at the oral portion of the cavernous sinus and thus reaching the midbrain through this nerve (N III). As to where these centrally directed processes terminate, Manni *et al.* (1976) suggest two possibilities: (i) they could end in the rhombencephalic reticular formation, or (ii) they could run directly to the cervical spinal cord in the trigeminal tract and synapse with motor neurones supplying the muscles of the neck. This latter suggestion arises from the circumstance that stretching eye muscles can affect neck muscle activity as recorded by the EMG (Easton, 1971; Manni *et al.*, 1975).[7] In the cat, destruction of the eye-muscle nuclei completely denervated the muscles, according to Corbin & Oliver (1942), so that it may well be that in this species the sensory neurones have migrated from N V to the motor nuclei. Certainly Manni *et al.* (1968) were unable to find neurones in the Gasserian ganglion responding to stretch of eye muscles, as in the

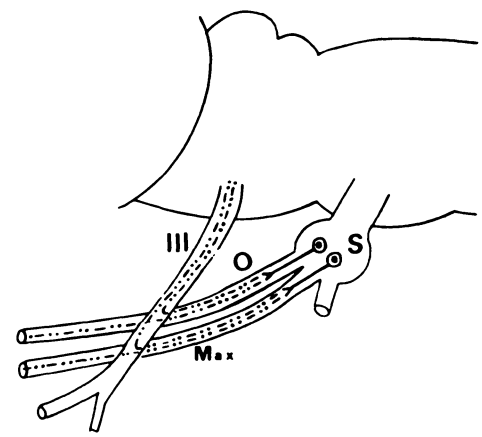

Fig. 25.5 Probable arrangement of the trigeminal fibres contained in the oculomotor nerve. III, oculomotor nerve; O, trigeminal ophthalmic branch; Max, trigeminal maxillary branch; S, semilunar ganglion. (Manni *et al.*, *Exp. Neurol.*)

sheep and pig. However, employing injections of horseradish peroxidase into the medial and lateral recti of cats, Porter & Spencer (1982) found some 90 labelled pseudo-unipolar neurones in the Gasserian ganglion, a number correlating well with the number of proprioceptive terminals on the muscles and the percentage of afferents in the motor nerves.

THE ROLE OF PROPRIOCEPTION IN INTERPRETATION OF THE RETINAL IMAGE

Earlier we have seen that the illusion of movement of the external field of vision, when the eye is moved passively, has suggested that in this instance proprioception from altered tension in the eye muscles is not taken notice of. Nevertheless there are a number of studies indicating a role of proprioception in governing visual activity. For example, Buisseret & Maffei (1977) found that electrical stimulation of the intraorbital part of the branch to the extraocular muscles, where the proprioceptive fibres of the cat run, evoked responses in 25% of striate cortical neurones with a latency of 25–40 msec. Stretch of the muscles also produced multi-unit responses. Again Donaldson & Long (1980) found responses in the superficial layers of both superior colliculi of the cat on stretching extraocular muscles; latencies showed two peaks at 17 and 60–75 msec. These responses interacted with those derived from a visual input through the opposite eye, the effect being either inhibition or enhancement, and depending on the timing of the two stimuli. The authors considered that the extraocular proprioception might permit the distinction between visual stimuli, evoked by real object-movement, and movement of the eyes.[8]

VISUOMOTOR DEVELOPMENT

Hein *et al.* (1979) pointed out that visually naive kittens fixated visual targets but lacked any visuomotor coordination; the animals need exposure to the motion of images, which they relate to movements of the body; if this experience is forbidden, then visuomotor coordination is lost. Thus Hein *et al.* (1970) allowed kittens to move in a stroboscopically illuminated environment, so that movements of their bodies were not associated with moving retinal images, and then found that they did not acquire visuomotor coordination. Hein *et al.* (1979) sectioned nerves III, IV and V unilaterally, thereby immobilizing the eye, and found that this prevented acquisition of visually coordinated behaviour through this eye. In further studies, Trotter *et al.* (1981, 1987) showed that the critical period during which monocular deprivation could affect the binocularity and ocular dominance of cortical neurones coincided with that during which the removal of proprioceptive afferent information exerted its effects.

SOME REFLEXES

Before proceeding further, we may consider some reflexes involved in the control over eye movements, reflexes that form the basis for most experimental studies on eye movements.

Psycho-optical Reflexes

The most important group of reflexes involving eye movements in man are those in which the incidence of light on the retina acts as the primary stimulus; it is as a result of these reflexes that the eyes are (*a*) directed to objects of interest and (*b*) maintained in the necessary orientation to ensure that the images formed by the two eyes fall on the foveae. We are accustomed to think of reflexes as being executed without the intervention of awareness on the part of the individual; these visual reactions, however, definitely involve awareness and are therefore classed as *psycho-optical reflexes*; as we shall see, there can be no doubt of their essentially involuntary nature.

The Fixation Reflex

SACCADE AND MAINTAINED FIXATION

All psycho-optical reflexes may be regarded as manifestations of the more general *fixation reflex*—the reflex which brings the images of an object on to the foveae of the two eyes and maintains them there. The fixation reflex develops early, since an infant a few days after birth will fixate a bright light; binocular fixation, however, does not develop for some months.

The reflex exhibits itself in two aspects—(*a*) the response to a peripheral stimulus and (*b*) the maintenance of fixation; the mechanism involved in the two processes is nevertheless the same. Thus let us imagine that the eyes are stimulated by a bright object in the peripheral field. Attention is aroused and the eyes move so that the images of the object approach the foveae—suppose that the nervous response grows in intensity as the images approach closer and closer to the foveae and reaches a maximum when they fall actually on them. The eye muscles can then be considered to behave as a tuning system, causing movements of the eyes until a maximum nervous response is obtained, just as the knob of a tuning dial is turned to obtain maximum sound from a wireless set. Fixation is thus achieved when maximum nervous discharge is reached. If the head moves slightly, the images are displaced and the nervous response falls off; immediately the tuning mechanism comes into play and the eyes are readjusted to maintain perfect fixation. Thus the same principle, the movement of the eyes to maintain a maximum nervous response, operates both to initiate and to maintain fixation.

MOVEMENTS DURING FIXATION

This principle may also explain the neural basis for the frequent small movements of the eyes that take place even during attempts at steady fixation (p. 663). As studies on the stabilized retinal images have shown (p. 388), the perceived image becomes rapidly indistinct in the absence of a shift of this image on the retina, so that the nervous discharge, postulated above, tends to decrease as the eye remains stationary. The eyes presumably respond to this

falling off with a movement which shifts the images on the retinae sufficiently to excite a new set of cones and the discharge again becomes maximal. The constant, small movements of the eyes in fixation may thus be regarded as the restless groping of the oculomotor centres for a position that gives maximum nervous discharge.

OCULAR NYSTAGMUS

This pendular to-and-fro movement of the eyes may be regarded as an exaggeration of this groping; if fixation is difficult, as in amblyopia, the eyes move excessively in a vain attempt to find a clear image. The nystagmus of miners working for long periods in the dark is a complex syndrome; nevertheless an element in the aetiology must be the necessity for using peripheral vision; under these conditions fixation on the fovea reduces the visual acuity rather than enhances it, so that the 'best position' for the retinal image is much more vaguely defined and this might well result in a ceaseless search for it over relatively large areas of retina to give a pendular type of nystagmus.

SIMPLIFICATION

It must be appreciated, however, that this point of view represents a crude simplification of what must be a more complex process; the factors of attention and meaning cannot be ignored; for example, corrective fusion movements, to be described below, are brought about as a result of a changed orientation of the retinal images, e.g. when one eye rolls, and the intensity of the 'nervous discharge' remains unaltered.

Other Manifestations

Other manifestations of the fixation reflex are given by:

1. The following movements in *optokinetic nystagmus*
2. The *corrective fusion movements* made in the interests of single vision
3. The movements of the eyes concerned with the *visual righting reflexes.*

Optokinetic Nystagmus

This describes the movements of the eyes when the body is in motion and the subject is gazing at the environment, as when he looks out of a railway carriage (train-nystagmus) or alternatively when the subject is still and his environment, or a prominent part of it, moves around him, as in the clinical test when a rotating striped drum is gazed at steadily. The process is divided into a slow movement, during which the eyes follow the moving target, e.g. a stripe on a drum, and a rapid saccade when the eyes flick back to a new position, when the slow movement is resumed. When the drum is stopped, the eyes exhibit an optokinetic after-nystagmus (OKAN), during which the eyes continue making the same movements in the same directions. The slow movement has been categorized as a following movement, but its features do not exactly correspond to those in which a single target is fixated; the fast movement is difficult to categorize.[9]

EXPERIMENTAL METHODS

The optokinetic response can be evoked in three separate ways: (1) when the head is fixed and an external object is moved, retinal slip is induced leading to the opto-kinetic movement. (2) Induced slow eye movements with the head fixed in front of a stationary lighted surround generate a retinal slip. This effect is the basis for the inhibition of the vestibulo-ocular reflex when the head rotates in phase with the surroundings. (3) A retinal slip is produced when the head rotates in front of a lighted surrounding, as in the vestibulo-ocular reflex test; the optokinetic effect is seen by the improvement of the vestibulo-optic reflex when the test is carried out in the light.

AFOVEATE ANIMALS

When one eye of a rabbit or guinea pig is covered, then an optokinetic nystagmus can only be evoked in one direction, namely when the pattern moves from the uncovered to the covered eye, i.e. temporo-nasally (Rademaker & Ter Braak, 1948). Tauber & Atkin (1968) studied a number of species and established that this deficiency was associated with the lack of a fovea, and also with complete crossing of the optic tracts; thus most birds are foveate and give bidirectional responses; the prairie dog is afoveate and is unidirectional.[10]

This finding that optokinetic nystagmus in these animals is unidirectional for a given eye, each eye giving only a response to a temporo-nasal movement of the visual field, means that the bidirectional nystagmus evoked in each eye relies on the combined activities of the separate eyes. Tauber & Atkin related this unilaterality to the fact that the animal with sideways directed eyes uses nystagmus to stabilize vision during forward motion.

RECORD

Figure 25.6 is a record of the slow movements in response to a rotating drum at several speeds; it will be noted that the velocity builds up to a plateau. Here the stimulus is the movement of the image of the fixation point on the retina, the eye responding, during the slow phase of the nystagmus, by movements designed to keep the image on the fovea. At a certain moment, fixation of this point ceases and the eyes make a rapid saccade in the opposite direction, to fixate a new stripe on the drum, and the slow movement begins again. The slow movement is obviously a following movement, but the rapid movement is difficult to categorize. It was originally thought that it occurred

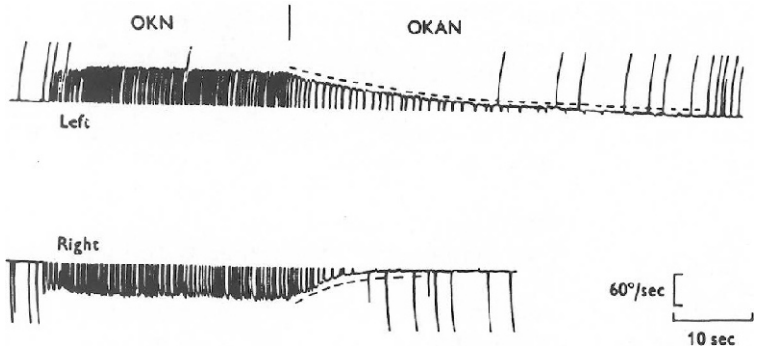

Fig. 25.6 Velocity of slow phases of optokinetic nystagmus (OKN) and optokinetic after-nystagmus (OKAN) induced by full-field rotation at 60°/sec. Note the faster decline of the slow phase velocity during right OKAN. The interrupted lines adjacent to the traces are the exponentials estimating the velocity-declines during OKAN; they were moved by a small amount so as not to be obscured by the experimental records. The time-constants for the declines were 16.2 and 5.3 sec for left and right OKAN respectively. (Cohen *et al.*, *J. Physiol.*)

simply because the eyes were unable to maintain fixation on the fixated stripe, i.e. because the stripe had moved out of the field of binocular fixation. In fact, however, the rapid movement usually takes place long before this limit has been reached; moreover, it is not apparently due to a deliberate attempt to fixate a new stripe appearing in the periphery since optokinetic nystagmus occurs in homonymous hemianopia when, because of a lesion in the visual pathway, the eye is blind to half the visual field (Fox & Holmes, 1926; Pasik *et al.*, 1959). Thus the eye makes a rapid movement into its blind side.

NYSTAGMUS CENTRE

We must conclude, therefore, that the unusual stimulus-condition, namely the apparent rotation of the visual environment, activates a *nystagmus centre* that triggers off these involuntary rhythmical movements (Rademaker & Ter Braak (1948)).[11] The involuntary nature of this movement in man is best revealed when he is surrounded by the moving drum so that practically the whole visual field moves; in this case it is impossible to avoid the nystagmus so long as the eyes are open. When only a small part of the visual field moves, as when the subject looks at a small striped drum, then the subject may avoid the nystagmus by 'looking through' the drum, i.e. by refusing to fixate any given stripe (Carmichael *et al.*, 1956).

CORTICAL AND SUBCORTICAL NYSTAGMUS

In animals, such as the rabbit and dog, an optokinetic nystagmus may be evoked even in the absence of cerebral hemispheres, and for this reason it is called *subcortical*. Visual reactions in man, in the absence of a cortex, are, as we have seen, impossible, presumably because of the relative insignificance of the visual projection to the colliculi. It is unwise, therefore, to transpose studies on lower animals to man, and certainly unwise to speak of a *subcortical nystagmus* as such, although the presence of a nystagmus-centre in the lower parts of the brain is not an unreasonable hypothesis. In man this would be activated by the cortical visual stimuli, but in lower animals the colliculi or pretectum might suffice.

DIRECTIONAL PREPONDERANCE

Under pathological conditions in man, involving lesions in the cerebral hemispheres, optokinetic nystagmus may be impaired, frequently with the appearance of a *directional preponderance*, in the sense that the reflex is normal when the drum moves one way, and reduced when it moves in the other. In the case of optokinetic nystagmus in man the preponderance is seen when the drum rotates away from the affected side, so that the study of this nystagmus may be a valuable diagnostic tool (Fox and Holmes, 1926).

SINGLE MOVING POINT

We may note that when a single object moves across the stationary visual field, there is no optokinetic nystagmus unless the field is otherwise empty; thus according to Rademaker & Ter Braak (1948), we may think of two opposing tendencies, the shifting of the images of stationary objects on the retina, tending to inhibit the following movement, and the shifting of the image of the single moving point that incites to movement. According to the relative preponderance of the moving or fixed field, one or other of the tendencies will determine the result, i.e. whether the eye remains fixed or follows the moving point. This was well demonstrated by Ter Braak who immobilized one eye of a rabbit and examined the movements of the other, which was blinded. Moving a single point across the visual field of the immobilized eye now caused the other eye to give a genuine nystagmus; because the stimulated eye was immobilized, there was no movement of images of stationary objects over its retina, and so the normal inhibition of the nystagmus was released. A similar experiment on a human subject, with one eye immobilized by paralysis of its extraocular muscles, is described by Mackensen (1959).

OPTOKINETIC AFTER-NYSTAGMUS

When a rotating drum is stopped after the subject viewing it has experienced a nystagmus for some time, there is an after-nystagmus, which is best recorded when the animal is in darkness, after the optokinetic nystagmus has lasted some time, and when fixation is prevented. There are generally two phases, the first with the nystagmus in the same direction as that of the original optokinetic nystagmus; this may give way to a nystagmus in the opposite direction. The significance of the after-nystagmus is probably to be seen in its antagonism to the vestibularly evoked after-nystagmus of rotation, which occurs in the opposite direction (Ter Braak, 1936).

TORSIONAL NYSTAGMUS

Brecher (1934) induced an optokinetic torsional nystagmus by causing a subject to view a rotating sectored disc; the nystagmic jerks were of several degrees in amplitude.

Corrective Fusion Movements

The orientation of both eyes so as to produce images of the same object on corresponding parts of the two retinae requires continuous adjustments, which are brought about by this reflex. Here the effective stimulus is diplopia.

Visual Righting Reflexes

In man and the ape the eyes play a very important part in the maintenance of posture. It is quite clear that the movements of the eyes must be closely attuned to the posture of the animal; in lower forms this is achieved by a rigid association of the eye muscles with the vestibular apparatus so that the position of the eyes is completely determined by the orientation of the body in relation to gravity and the parts of the body in relation to each other. Here, then, the labyrinth dominates eye movements. The visual impressions alone, however, can clearly provide information as to the orientation of the head, and therefore the body. Thus if a subject is falling forward, his original point of fixation moves upwards and, as a result of the fixation reflex, his eyes move upwards to maintain fixation; the necessary postural adjustments for recovery can be made in the light of impressions provided by the eyes and their adjustments. In this case proprioceptive impulses from the superior recti demand a movement of the head upwards so that the eyes can re-assume the primary position. The proprioceptive impulses from the neck muscles now demand postural changes that will permit the head to re-assume its normal erect position. In man and the ape posture can be maintained quite adequately by means of the visual righting reflexes when the labyrinths have been destroyed.

VESTIBULAR AND NECK PROPRIOCEPTIVE REFLEXES

The primary stimulus for these reflexes is not visual but arises from the vestibular apparatus or the proprioceptive stretch receptors in the neck muscles. They are classed as *static (or tonic) reflexes* and *kinetic reflexes*; by the first class a definite orientation of the eyes is evoked and maintained for a given position of the head in relation to the trunk and the pull of gravity, whilst by the latter a definite *movement* of the eyes follows a movement or acceleration of the head.

The Vestibular Apparatus

A brief description of the vestibular apparatus would be useful at this point. In man it consists essentially of three semicircular canals in mutually perpendicular planes, and two sacs, the *utricle* and *saccule* (Figs 25.7 and 25.8). Each canal widens at one end into an *ampulla* containing a sense organ—the *crista ampullaris* or *crista acustica*, which bears as an auxiliary structure a jelly-like *cupula*

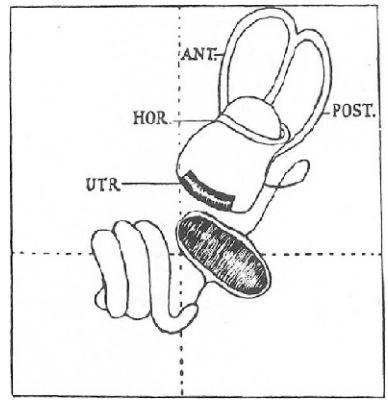

Fig. 25.7 The positions of the semicircular canals in the head viewed from the side.

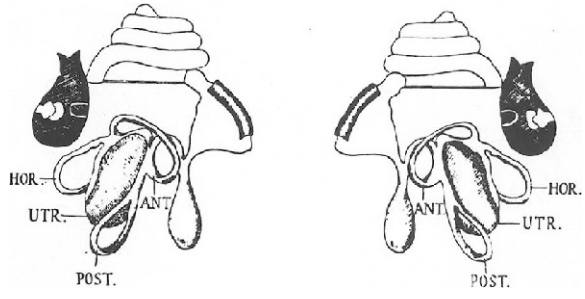

Fig. 25.8 The positions of the semicircular canals in the head viewed from above.

which encloses the sense hairs protruding from the surface of the crista (Fig. 25.9). The utricle and saccule or otolith organs contain sensory organs called *maculae*, with a similar type of sense cell but with shorter hairs. The sense hairs of the macula are embedded in an otolith membrane which is encrusted with numerous concretions of lime crystals (*otoconia*) (Fig. 25.10). The membranous labyrinth, the cavities of which are filled with endolymph, is surrounded by cartilage or bone, the space between it and the surrounding tissues being filled with perilymph.

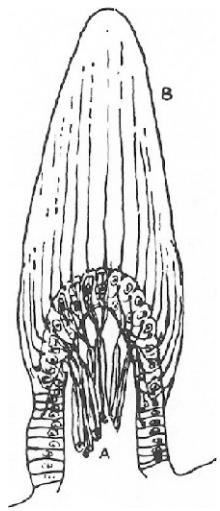

Fig. 25.9 The cupula of the crista ampullaris.

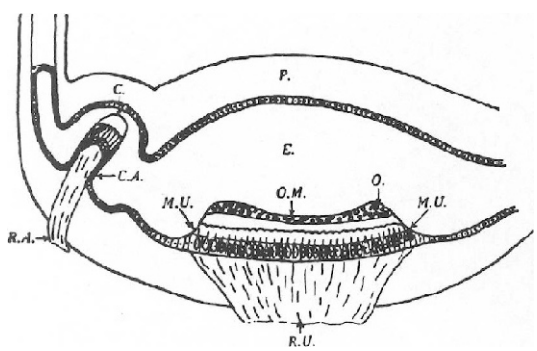

Fig. 25.10 Section through the macula utriculi and the ampulla of a vertical semicircular canal in man. *C*, cupula; *C.A.*, crista ampullaris; *E*, endolymph; *M.U.*, macula utriculi; *o*, otoconia; *O.M.*, otolith membrane; *P*, perilymph; *R.A.*, ramus ampullaris; *R.U.*, ramus utricularis of N VIII. (Lowenstein, after Kolmer, *Biol. Rev.*)

The Utricle and Saccule

The maculae of the otolith organs are stimulated by a gravitational pull on the otolith membrane which alters the tension in the hair cells; the macula of the utricle lies normally in a horizontal plane, and under these conditions the tension is at a minimum; if the head is held upside down the stimulus is at a maximum. The utricle is thus a receptor which can respond to alterations in the orientation of the head in relation to the direction of gravity; it can therefore mediate the static class of reflex, i.e. compensating poses of the eyes, head, etc. It is worth noting, however, that a sudden linear acceleration of the head could exert an inertial pull on the hairs of the macula and give rise to a kinetic type of reflex response. The saccule's macula lies in a plane at right-angles to that of the utricle.

The Semicircular Canals

The semicircular canals are receptor organs responding to acceleration of the head; opinion on the manner in which the crista ampullaris is stimulated by an acceleration has fluctuated, but the experiments of Steinhausen (1933) and Dohlman (1935) have now firmly established the original notion of Mach that it is the inertial movements of the endolymph that deform the cupula and stimulate the hair-fibres embedded in it. As Fig. 25.11 shows, when the head is accelerated the endolymph within the membranous canal tends to be 'left behind' and so produces an inertial force that deflects the cupula, which is thought to move in much the same way as a rotating door. When the acceleration ceases there is an inertial movement of fluid in the opposite direction.

INTEGRATING ACCELEROMETER

The elements determining the dynamic behaviour of the canals are thus the moment of inertia of the ring of fluid in the canal, the viscous drag of the fluid, and the 'spring-stiffness' of the cupula, which always returns to its neutral position in the absence of external forces. It is apparently the viscous drag that is the dominant force; the velocity of flow is proportional to the angular acceleration of the head, so that the position of the cupula, which is the integral of the fluid velocity, is proportional to the angular velocity of the head. Thus the sense organ behaves like an integrating accelerometer, with the result that its neural discharge indicates the angular velocity of the head. If the head movements are too short or too long the viscosity no longer predominates over the inertial or spring forces, and the canal ceases to integrate head acceleration properly (Robinson, 1968). Thus, if the head is accelerated to a definite angular speed and then this speed is maintained, as when a subject is rotated in a chair, at the end of the acceleration the deflexion of the cupula indicates the velocity attained, but now the spring-stiffness asserts itself and the cupula gradually returns to its original position, although the velocity remains the same.

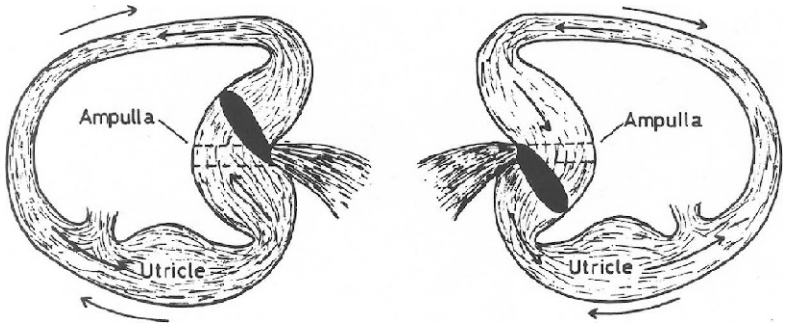

Fig. 25.11 Illustrating movements of the cupula in the ampullae of the horizontal canals on accelerating the head to the right. In the left canal the inertial flow of fluid is away from the ampulla, whilst in the right canal it is towards the ampulla.

The Hair Cells

The sensitive epithelium of the ampulla is called the crista and consists of a sheet of hair-cells; closely related to these are the terminals of vestibular nerve fibres; the hairs on these cells consist of two types, a single kinocilium and a number of stereocilia arranged in a characteristic pattern. As indicated, the stereocilia increase in size as they approach the kinocilium, and as Lowenstein & Wersäll (1959) pointed out, the arrangement of the cilia constitutes the structural basis for the polarization of the hair cell such that a deflexion of the cilia in the direction of the kinocilium, as indicated by the arrow in Fig. 25.12, constitutes an excitatory stimulus whereas a deflexion in the opposite direction constitutes an inhibitory one. In a given ampulla, all the hair-cells are polarized in the same direction so that the response in all the neurones is qualitatively uniform.

ROLE OF KINOCILIUM

Experimentally it has been found that, so far as the horizontal canals are concerned, an ipsilateral acceleration, i.e. an acceleration towards the canal under consideration, causes increased nervous discharge, and a contralateral acceleration a decreased discharge. Examination of Fig. 25.11 indicates that an ipsilateral acceleration leads to an inertial flow of fluid towards the ampulla or the utricle—the deflexion of the cupula is thus ampullipetal or utriculopetal—and Lowenstein & Wersäll pointed out that the kinocilium is placed on the hair-cells in such a way that when it is bent towards the utricle it is excited and when bent away from it—utriculofugal—it is inhibited. In the vertical canals the opposite relation pertains, in the sense that movement of fluid towards the ampulla or the utricle causes *inhibition*; and it is found that the orientation of the kinocilium is now opposite, facing away from the utricle, so that it is utriculo*fugal* displacement that causes excitation.

POLARIZATION IN UTRICLE AND SACCULE

Here the polarization is more complex; in general the otolith membrane shows a characteristic division caused by a denser aggregation of otoconia to form a line, or *striola*; so, as indicated by Fig. 25.12, we may speak of a *pars interna* and *pars externa*, and it is found that the polarization of the cilia varies in a characteristic manner in relation to this dividing line; moreover, in the saccule, the polarization is away from the line and in the utricle towards it. This variation in polarization in a given macula means that the organ is sensitive to gravitational pulls in a large variety of directions, in the sense that there will be individual neurones that are maximally excited by a specific direction of pull; in this way the organ can accurately convey information respecting the position of the head in relation to gravity over a wide range of inclinations. If all the hair-cells were polarized in the same direction there would be only one direction of maximal sensitivity, with a corresponding diminution in the range of useful information.

Vestibulo-ocular Reflex

Acceleration of a human subject by rotation in a chair causes a slow movement of the eyes in the opposite direction, at about the same angular velocity as that of the rotation, with the result that the eyes are able to maintain fixation on a previously fixated point. The response happens in the dark, but in this case some 'phase-error' may be present, in the sense that the compensatory rotation is not completely adequate to maintain the original direction of gaze. Thus the function of the vestibulo-ocular reflex is to permit a stabilization of the retinal image to the extent that only small corrections of fixation need be made by way of the fixation reflex, utilizing visual input.

Efficiency

The vestibularly evoked movement serves to keep the image of an external object on the retina stationary, even when the angular velocity is as high as 300°/sec; the control mechanism may therefore be said to be far more

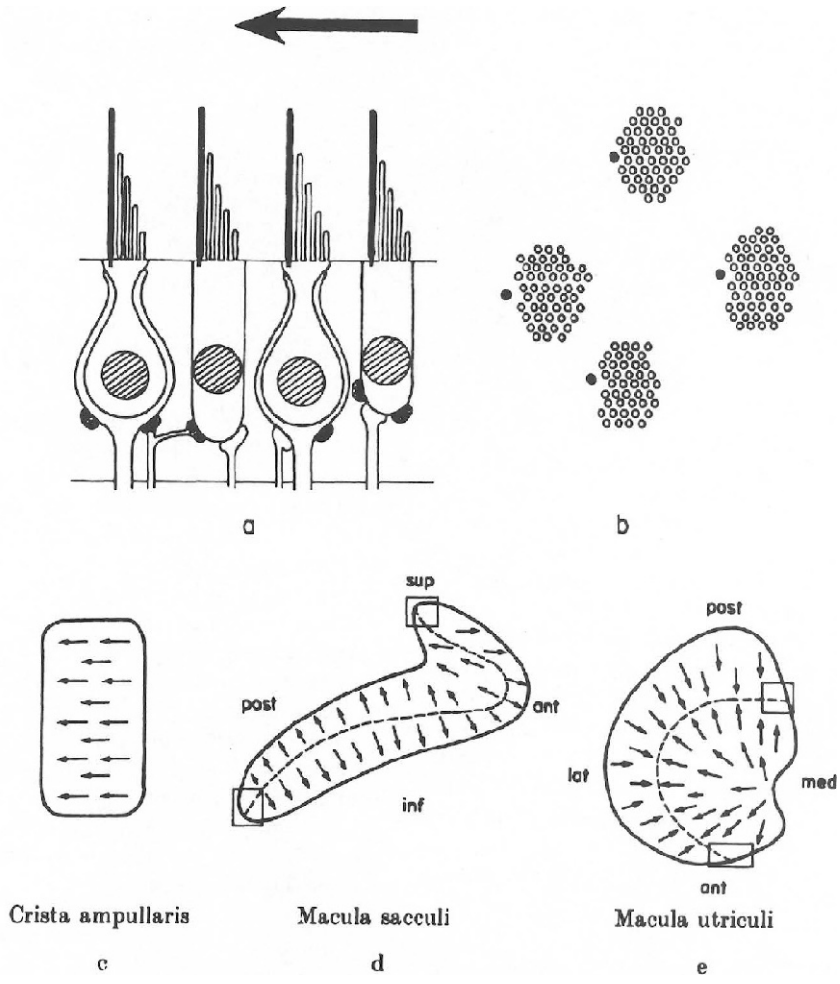

Fig. 25.12 Morphological polarization of the sensory cells and the polarization pattern of the vestibular sensory epithelia. The morphological polarization (arrow) of a sensory cell is determined by the position of the kinocilium in relation to the stereocilia. (*a*) Section perpendicular to the epithelium showing the increasing length of the streocilium as the kinocilium is approached. (*b*) Section parallel to the epithelial surface. Sensory cells on the crista ampullaris (*c*) are polarized in the same direction whereas those on the macula sacculi (*d*) and macula utriculi (*e*) divided by an arbitrary curved line into two areas of opposite morphological polarization, the pars interna and the pars externa. On the macula sacculi the cells are polarized away from the dividing line, on the macula utriculi towards the line. Constant irregularities in the polarization pattern are found in areas corresponding to the peripheral continuation of the striola (rectangles in *d* and *c*). (Lindeman, *Acta otolaryngol.*)

effective than the visual tracking movement, which is only effective up to velocities of 30°/sec.

Arrangement of Canals

As illustrated by Fig. 25.8, the canals are arranged in the head in three mutually perpendicular planes. We may distinguish on each side a horizontal or external canal, both lying in the same plane which, in effect, is not horizontal when the head is erect but slopes backwards at 30°, hence they only come into the horizontal plane when the head is tilted forward through this angle. Rotation of the head about a vertical axis has its main effect on this pair of canals, which we may describe as a *synergic pair.* When the head is rotated about its vertical axis, e.g. when the head looks to the right, the reflex movement of the eyes in the opposite direction that maintains fixation on a point that was originally straight ahead of the eyes will be

mediated by the inertial stimuli in the horizontal canals. The anterior vertical canal of one side is in the same plane as the posterior vertical canal of the other, so that we may distinguish two more synergic pairs, namely left anterior-right posterior, and left posterior-right anterior. When the head is moved forwards and backwards, towards and away from the chest, the compensatory rapid movements of the eyes upwards and downwards are mediated by the synergic pair whose planes lie in a sagittal plane, whilst when the head is moved towards and away from the shoulder the other vertical pair, lying in the frontal plane, parallel to the forehead, will mediate the rolling movement that takes place. In fact, as we shall see, the reflex movements involving vertical and torsional rotations are governed by activities in the ampullae of all four vertical canals.

Vestibular Nystagmus

The mechanism of the semicircular canals is best investigated in the intact animal or man by the study of the nystagmus that occurs on rotating about a given axis. If a human subject is rotated about a vertical axis when he is seated in a rotating chair with his head bending forward to bring his horizontal canals into the plane of rotation, then his eyes go into a *rotatory nystagmus*; it is as though they were making repeated attempts at maintaining fixation of an object in front, but they are not visual responses since they occur when the eyes are closed, the eye-movements being recorded electrically. The nystagmus consists in a slow movement of the eyes in the opposite direction to that of rotation, followed by a rapid saccade in the direction of rotation. The speed of the slow movement is that of the speed of rotation. The direction of the nystagmus is named after the direction of the fast movement; hence the direction of a rotatory nystagmus is the same as that of the rotation. If the rotation is maintained for about 20 to 30 seconds the nystagmus ceases.

Mechanism

Why should the eyes go into a nystagmus on rotation? That is, what is there in the stimulus-conditions that results in this repetitive type of motion? We may answer the last question first. It will be recalled that for any abrupt movement of the head there are an acceleration and a deceleration, and therefore there are two sets of messages sent to the central nervous system, determined by two types of inertial fluid movement. The cupula is deflected one way and then the other. By contrast, when the rotation is sustained, the initial acceleration is not followed by a deceleration, and consequently no inertial force is brought into play to return the cupula to its mid-position. Instead the cupula must rely on its own elasticity, and experiments have shown that it behaves as a heavily damped pendulum, requiring some 20 to 30 seconds to return to its mid-position after maximal deflection, i.e. it requires as long as the nystagmus lasts. Thus a sustained deflection of the cupula, with its accompanying pattern of nervous discharges, gives rise to rhythmic nystagmoid movements, whilst a deflection followed by a rapid return gives rise only to a compensatory deflection of the eyes. Experimentally this was demonstrated by Steinhausen who showed that if he applied a transitory pressure to a canal, through a tube inserted into it, the effect was only a simple movement of the eyes; if he maintained a constant pressure, so that the cupula remained deflected, the eyes went into a nystagmus which lasted as long as the pressure was maintained.

Post-rotatory Nystagmus

We may imagine that our human subject has been rotated at a steady speed for some 20 to 30 seconds; the cupulas have returned to their mid-positions and the rotatory nystagmus has ceased. We now abruptly cease the rotation. There is now an inertial flow of endolymph such as to deflect the cupulas in the opposite direction. Moreover, these deflections will be maintained until the natural elasticity brings the cupulas back to their mid-positions. Hence the conditions are such as to induce another nystagmus, lasting another 20 to 30 seconds, but differing only in the direction; thus the slow component will be in the direction of rotation. It is this nystagmus that is easy to demonstrate; the subject is rotated at an even speed for some 20 to 30 seconds and then the rotation is abruptly stopped and the experimenter observes the nystagmoid movements.

The Vertical Canals

The effects of stimulating the vertical canals are more complex. Studies of the discharges in the nerve fibres from the ampullae indicate that, whereas rotation in the plane of the horizontal canals only stimulates the horizontal ampullae, rotation in other planes causes a complex group of inhibitory and excitatory responses in the ampullae of *all* the canals. The final compensatory movement of the eyes, resulting from a rotation in a plane other than that of the horizontal canals, represents the integrated response to stimuli arising in all the ampullae. It must be appreciated, moreover, that the macula of the utricle may be stimulated by these rotatory accelerations, and thus make its contribution to the general response of the eyes.[12]

Reaction of Labyrinth to Artificial Stimuli

A number of artificial stimuli will upset the normal balance between the tonic activities of the left and right labyrinths; such an upset, if maintained, usually leads to a nystagmus.

Labyrinthectomy

Unilateral labyrinthectomy causes a nystagmus for a few days with the slow phase directed towards the operated side; injection of cocaine has a similar effect. It will be seen that in the normal animal at rest there are tonic discharges from both ampullae of a synergic pair. Accelerations, requiring compensatory movements, cause an imbalance in this system, the discharge from one ampulla increasing and that from the other being inhibited. Clearly, then, extirpation of one labyrinth creates an imbalance that will be interpreted by the central nervous system as an acceleration, and some compensatory movements of the eyes will be initiated. In this way we may explain the effects of extirpation; with irritative lesions in the vestibular apparatus or in its nervous pathway the balance is upset once again, but this time in the opposite sense (see, for example, Cranmer, 1951).[13] After a time the necessary central compensations take place and the nystagmus subsides. When, after the nystagmus due to a lesion in the labyrinth has subsided, the labyrinth on the opposite side is injured, then a new nystagmus occurs with the slow phase now directed towards the newly injured side—the so-called *Bechterew nystagmus.*

Caloric Nystagmus

A current of warm water (40° to 45°) or cold water (22° to 27°) through the auditory meatus causes a nystagmus of vestibular origin; the slow movement is towards the stimulated side, with cold water, and away from this side with warm water. The fact that the nature of the nystagmus depends on the position of the head suggests that the cause is associated with thermal currents in the endolymph.

Electrical Stimulation

Passing a direct current from one ear to the other causes a nystagmus, the slow phase being towards the positive pole. The nature of the nystagmus is independent of the position of the head. In the experimental animal application of repetitive stimuli to an ampulla produces a nystagmus. Thus a single shock, applied to the right vestibular nerve, causes contractions of the left lateral rectus and right medial rectus, leading to a horizontal movement to the left, i.e. away from the stimulated side. If this stimulation is continued the eyes go into a nystagmus with the slow movement away from the stimulated side and a fast movement towards it. Thus the nystagmus may be regarded as a rhythmic interruption in the response to stimulation of one vestibular nerve or ampulla. Experimental reduction in the tonic discharges in a vestibular nerve also induces a nystagmus, this time in the opposite direction.

Static Vestibular Reflexes

These reflexes, mediated by the utricle and saccule, serve to maintain a normally orientated field of vision despite changes in the position of the head. Thus when the body is tilted towards the prone position the eyes move upwards; when the body is inclined sideways, the eyes roll; it should be emphasized, however, that in man the rolling of the eyes by no means compensates entirely for the altered position of the head; psychological adjustments are necessary (p. 456). Movement of the body or the head about a vertical axis will clearly have no influence on the direction of gravitational pull on the otolith membrane, hence any compensatory movement of the eyes that takes place must be mediated by another type of receptor. It is here that the proprioceptive impulses from the neck muscles are involved.

Compensatory Rolling

The rolling of the eyes that takes place when the head is tilted towards the shoulder has attracted considerable interest. It is clear that both otolith and semicircular canals may act as receptors, but if the compensatory rolling is to be sustained for any length of time clearly it is only the otolith, or neck proprioception mechanism, that will operate. Merton's (1956) studies have emphasized the much greater effectiveness of the semicircular canals in producing a rolling. When a subject is swung from side to side on a swing hung from a ball-bearing, such that the axis of rotation corresponds to the visual axis of the eye, then it is found that the eyes roll in the opposite direction to that of the movement of the head; the rolling movement lags behind the head movement, so that the compensation is never complete; in other words, the vertical meridians of the eyes do not remain vertical. The compensation amounts to about a quarter of the actual movement of the head. When a head movement is sustained, however, this partial compensation is not maintained, so that the vertical meridian returns almost completely to the position it would have had if no rotation had occurred. According to Woellner & Graybiel, for example, at a tilt of 15° the rolling is only 1.5°, whilst with a tilt of 70° it is only 4°. As Merton has explained, the partial compensatory movements during rotation are of value in reducing the angular movements of the retina, and thereby permitting a reasonable visual acuity even when the head is swinging through quite large angles.

The Doll-reflex

When a subject is moved in the median plane with his head fixed so that movements of the head in relation to the trunk, evoking neck proprioception, are avoided the vestibulo-ocular reflex tends to make the eyes rotate upwards or downwards through utricular stimulation. If the human subject is rotated in this way in the dark and presented with only a series of vertically arranged fixation points we may estimate the degree to which this so-called doll reflex has operated by asking him to state which

fixation point is directly ahead. Consistent errors are in fact found (Ebenholtz & Shebilske, 1975) indicating some upward and downward movements; the errors followed a sine-function such as would be anticipated of stimuli governed by the pull of gravity on the otolith membrane assuming this to be at an angle of about 30° backwards when the head is vertical. The results of experiments are illustrated by Fig. 25.13; as with the torsional movement the doll-reflex only partially compensates for the tilt, a maximum ocular deviation of about 9° being obtained with a 70° tilt.

Otolith Responses to Acceleration

Although the otolith organs are essentially gravity receptors they are, of course, susceptible to shearing forces developed in other ways than the pull of gravity; thus acceleration of a rabbit forwards should exert shearing forces on the utricular macula and appropriate eye-movements should be recorded, whilst swinging the animal, inducing rhythmic parallel or transverse accelerations, should induce nystagmic types of movement. The responses of a rabbit to simple linear accelerations and to sinusoidal swings have been studied by Baarsma & Collewijn (1975); during transverse swinging vertical eye movements were recorded and during sagittal swinging torsional eye movements. The important feature of these responses was their sluggishness, indicating the unsuitability of the otoliths as acceleration sensors; thus with sinusoidal swings the phase-lag amounted to 180°, and in general the responses took many seconds to develop fully.

Proprioceptive Neck Reflexes

Bending the head forward and backwards towards or away from the chest, besides activating the utricle, will stretch the neck muscles, and it may be shown that the compensatory movements of the eyes that are elicited may be caused by both of these receptive mechanisms. Thus movement of the trunk, keeping the head fixed, gives the same reflex, but by virtue of the stretched neck muscles. Lateral movements in response to moving the head about a vertical axis are mediated exclusively by the neck mechanism. Hence cutting the cord in the cervical region may reduce an animal's ability to maintain orientation (Cohen, 1971).

Movements of Head and Eyes

The great majority of studies of eye movements have been carried out with the head fixed, an unnatural situation and one that obscures the coordination that is necessary to establish fixation when both eyes and head participate in the actual gaze-process.

Saccade and Slow Movement

Bizzi *et al.* (1971) noted that, when a light was presented to a monkey in its peripheral field of view, the response was quite stereotyped, consisting of a saccade followed by a slow movement, in the opposite direction to the head movement, that compensated for this and maintained fixation.[14] Although the eyes actually moved first, EMG activity began first in the neck muscles and only some

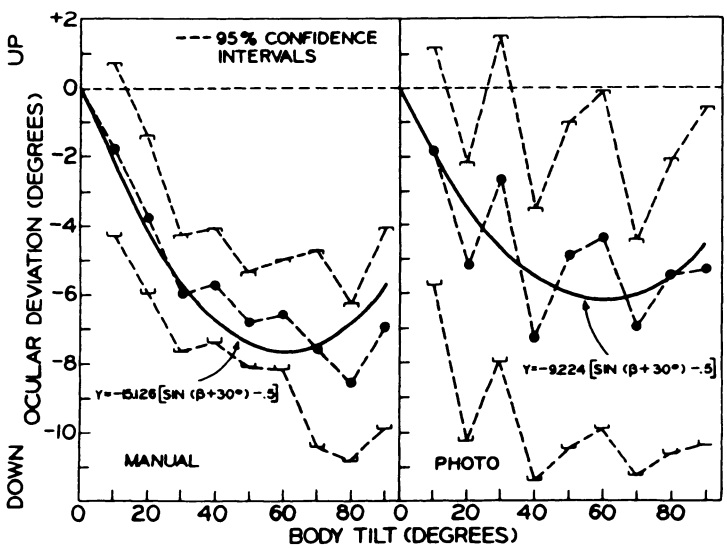

Fig. 25.13 Ocular deviation due to body-tilt in a median plane. The ordinate represents the difference between the subjectively estimated and the true positions of the fixation point. Dashed lines indicate 95% confidence intervals. 'Manual' and photo' indicate different methods of measuring the ocular deviation. (Ebenholtz & Shebilska, *Vision Res.*)

20 msec later in the eye muscles. It appeared that the movements of eye and head were programmed by a central mechanism that works in a stereotyped fashion activating both eye and head muscles nearly simultaneously, the delay in head movement being due to the greater inertia of the head and slower action of the neck muscles. The slow compensatory movement is not programmed, but is a reflex response to the movement of the head. Its reflex nature was demonstrated by placing the head in a rotatable frame provided with a brake, so that movement of the head was brought to a halt immediately after or during the saccade; as Fig. 25.14 shows, the following movement was inhibited.

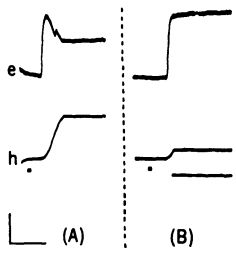

Fig. 25.14 A, coordinated eye (e) and head (h) response to sudden appearance of a target. B, presentation of the same target is followed by application of the brake, preventing head movement (horizontal bar). Note lack of compensatory eye movement. Dots represent onset of luminous target. Calibration: Horizontal bar equals 500 msec; vertical bar equals 15 degrees. (Bizzi *et al.*, *Science.*)

Saccade During Head-turn

Morasso *et al.* (1973) raised the question as to whether, when the head was allowed to move *during* the saccade, so that the goal was reached by a combined saccade and head movement, the saccade would be smaller than if the head had been fixed. Fig. 25.15 shows the record of a saccade made with the head fixed (a) and the records of the saccade and the head movement when both participated in the gaze-process (b); the Curve G represents the sum of the eye (E) and head (H) displacements, and it is seen that this sum exactly matches the saccade in (a); the head movement reduces the size of the saccade. Experiments indicated that there was no preprogramming, so that if the head movement was suddenly stopped just as the saccade began there was no reduction in the amplitude, suggesting that the reduction was carried out in the light of proprioceptive or vestibular input following the head movement. When the animal was bilaterally vestibulectomized, the saccade-amplitude was the same with head fixed or free, so that there was a remarkable overshoot of gaze; the latency for neck proprioceptive responses was shown to be some 50 msec, which was too long to allow neck reflexes to contribute.[15]

LINEAR SUMMATION

These results of Morasso and Bizzi suggest that the vestibulo-ocular reflex is active during gaze-saccades, compensating for the overshoot that would occur were the saccade programmed without allowance for head movement. Such a linear summation has been discussed by Laurutis & Robinson (1986) in the light of conflicting evidence; thus Tomlinson & Bahra (1986) found this to be true only for saccades up to 20°; for saccades above about 40°, the vestibulo-ocular reflex was absent. Laurutis & Robinson worked on human subjects who had to make large shifts of gaze under various conditions. They argued that, with linear summation of the saccade command and the vestibulo-ocular command when the head made a quick movement, gaze-velocity, i.e. the combined eye- and head-velocity, and its duration should be constant; the more slowly the head moves the more rapidly will the eyes move, being released from the vestibulo-ocular reflex. An example is shown in Fig. 25.16, where the subject was told to move the head to fixate a point at a fast (A) and a slower (B) speed. Again, when the subject's head was momentarily stopped during a gaze-saccade, the eyes did not change velocity, in the head, although there had been a considerable deceleration of the head. Clearly the vestibulo-ocular reflex is not operative during gaze-saccades. It was argued that the modification of the eye-saccade signal required by the head-movement was made on the basis of a modification of the duration of the saccade, which cannot be programmed since it occurs

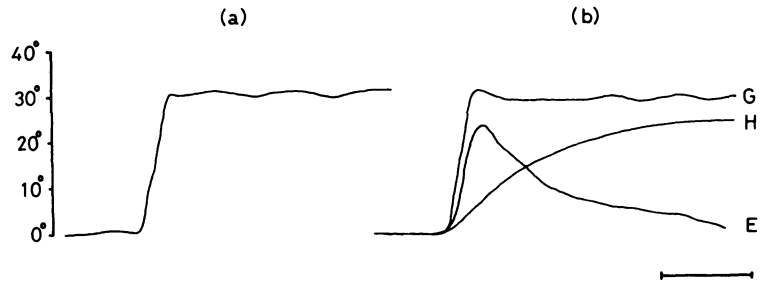

Fig. 25.15 Comparison of saccade with gaze. (*a*) Eye saccade to a suddenly appearing target with head fixed. (*b*) Coordinated eye saccade (E) and head movement (H) to the same target with head free. The gaze movement (G) represents the sum of E and H. Note the remarkable similarity of eye saccade in (*a*) and gaze trajectory in (*b*) as well as reduced saccade amplitude in (*b*). Time calibration, 100 msec. (Morasso *et al.*, *Exp. Neurol*)

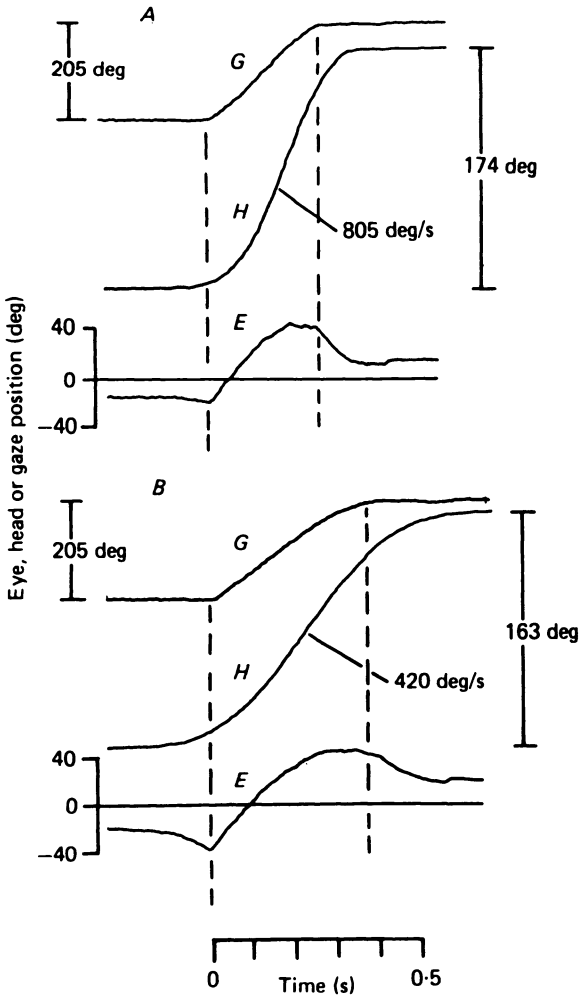

Fig. 25.16 Typical behaviour of eye, *E*, head, *H*, and gaze, *G*, during gaze saccades between targets 205 deg apart. In *B*, the subject deliberately moved the head more slowly. In *A*, the duration (vertical dashed lines) was 250 ms; in *B*, 380 ms. (Larutis & Robinson, *J. Physiol.*)

with sudden interruptions of head-movement, the signal being determined by the comparison of an internal copy of eye position with an internal command for eye position; the difference, the *motor error*, would then be amplified by burst neurones. The model proposed by Laurutis & Robinson thus consisted of that proposed by Zee *et al.* (1976) for simple saccades, with the modification of a contribution of head-position. Their model certainly predicted the behaviour of the eyes during head-movements of gaze-fixation.

Rabbit

Collewijn (1977) employed a technique that permitted the measurement of the absolute position in space of both head and eye at any moment. These experiments revealed a remarkable co-ordination of eye and head movements during normal exploratory behaviour, so that although saccades could be, and often were, initiated before any head movement, the subsequent movement of the head tended to stabilize the direction of gaze or position of the eye in space. All the movements of the eyes in space were saccadic and accompanied by a head movement that tended to stabilize the position of the eye in the head. The head movements were mainly smooth, in perfect coordination with the eye movements, and the head was nearly stable in the intervals. Thus, in general, movements of the eye in the head were limited and transient, so that the rabbit, as with other species, achieves its exploratory and other fixations finally by a changed orientation of the head.

Cat

Guitton *et al.* (1984) have discussed eye-head coordination in the cat, an animal that uses head movements for changes in gaze to a greater extent than the primate; they consider that the rapid eye movements made during a gaze-saccade are generated by the quick phase of the vestibulo-ocular reflex, a condition in which the reflex is disconnected from the control mechanisms, unlike the condition in a programmed saccade (Robinson & Zee, 1981). Eye and head positions were considered to be monitored by a corollary discharge, or efference copy, that yielded an internal representation of gaze. Fuller *et al.* (1983) argued for a compensatory eye-movement that allowed for the head-movement; this was pre-programmed and not generated by the vestibular system.

The Nystagmuses Compared

The analysis of nystagmus is facilitated if the rotating turntable, or the rotating drum, is accelerated in a sinusoidal fashion, rather than at constant velocity; thus in the dark, as we have seen, the rotatory nystagmus soon ceases, due to the return of the cupula to its equilibrium position. The effects of the frequency of these sinusoidal changes are usually described as *Bode plots*, the phase of the eye-position in relation to the head or drum, and the gain, being plotted against frequency. Figure 25.17 shows plots for both types of nystagmus in the alert cat (Godaux *et al.*, 1983).

THE MOTOR NEURONES

The motor neurones activating the eye muscles are derived from the cranial nuclei as follows:

N III. (*Oculomotor nerve*). Superior rectus. Inferior rectus. Medial rectus. Inferior oblique.

N IV. (*Trochlear*). Superior oblique.

N VI. (*Abducens*). Lateral rectus.

These nerves represent essentially the axons of cell bodies collected in the grey matter of the mid-brain and pons—the *eye-muscle nuclei.*

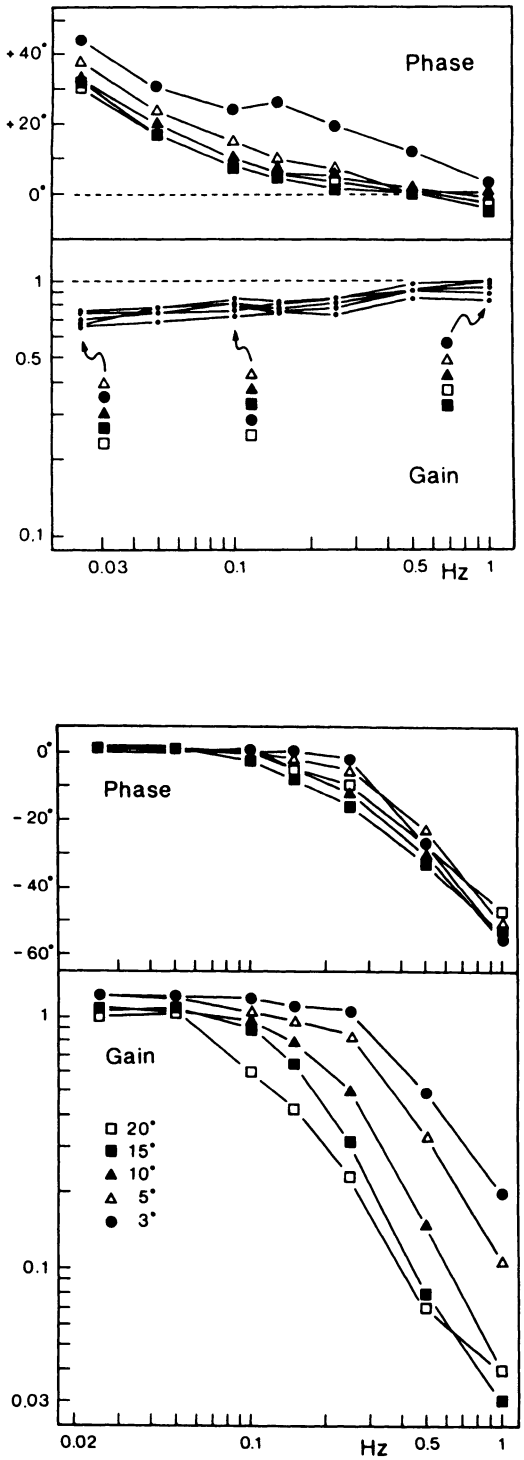

Fig. 25.17 Above. Gain and phase of the vestibulocular reflex as a function of frequency (Bode plot). These values are plotted for the amplitudes 20° (□), 15° (■), 10° (▲), 5° (Δ), and 3° (●). Average values of five experiments on four cats. Below. Gain and phase of optokinetic response. (Godaux *et al., Exp. Neurol.*)

The Nucleus of Nerve III

This lies in the tegmentum in the central grey matter in the upper part of the mid-brain below the superior colliculus, beneath and running parallel to the aqueduct of Sylvius (Fig. 25.18). It is some 5 to 6 mm long and extends between the third and fourth ventricles. It has been conventionally divided into a series of discrete zones each concerned with a pair of muscles; thus according to Brouwer (1918) it is divided primarily into a principal (lateral) nucleus providing the motor neurones to the levator palpebrae and four extraocular muscles; the *median nucleus of Perlia*, considered to be a coordinating centre for activating the medial recti during convergence; and the *Edinger-Westphal nucleus*, containing the autonomic motor neurones controlling the ciliary muscle and sphincter pupillae. The principal lateral nucleus was divided into zones from above downwards (rostrocaudally) each zone representing the motor neurones for the levator, superior rectus, medial rectus, inferior oblique and inferior rectus in this order. Subsequent work, notably that of Warwick (1953), has shown that the organization is not so simple. Thus, although the individual eye muscles are indeed operated by localized groups of neurones within the principal nucleus, the simple rostrocaudal arrangement postulated by Brouwer apparently does not pertain. Instead, the arrangement is that shown in Fig. 25.19 (*right*); it will be seen that the inferior rectus, inferior oblique and medial rectus possess discrete motor pools arranged along the axis of the somatic nucleus in this *dorsoventral* order. The superior rectus, on the other hand, is innervated by neurones scattered along the medial aspect of the caudal two thirds of the main nucleus. Moreover, Warwick (1955) showed that in monkey and man, the two species in which convergence of the eyes is a prominent feature of the movements, the median nucleus of Perlia is difficult to find, and, when present, its neurones are not internuncial, as one would expect of a coordinating centre, but rather they are motor neurones supplying the superior rectus and inferior oblique. Hence

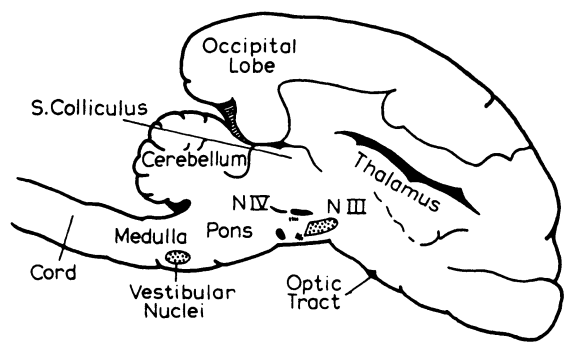

Fig. 25.18 Sagittal section of the cat's brain.

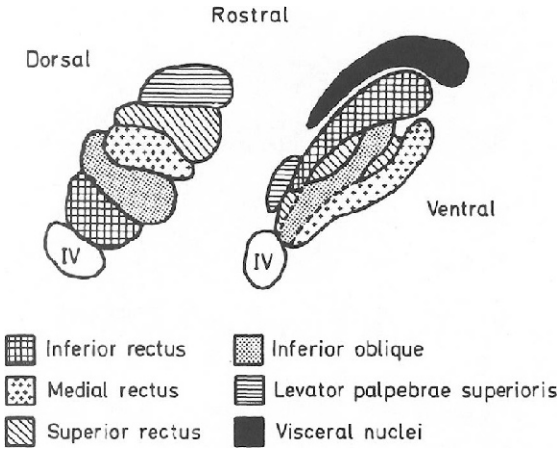

Fig. 25.19 Illustrating Brouwer's (left) and Warwick's (right) views of the organization of the oculomotor nucleus. (After Warwick, *J. Comp. Neurol.*)

we must assume that the act of convergence is organized at a higher level. The Edinger-Westphal nucleus is well established as the autonomic division of the oculomotor nucleus.

The Nucleus of Nerve IV

This is a small clump of cells lying caudally to the nucleus of N III, being situated in the central grey matter in the floor of the aqueduct of Sylvius and at the level of the lower part of the inferior colliculus. The nerve fibres, which represent the motor pathway for the superior oblique, undergo an almost complete decussation in the anterior medullary velum, emerging on the dorsal aspect of the brain stem.

The Nucleus of Nerve VI

This nucleus lies in the pons, in the floor of the fourth ventricle.

Medial Longitudinal Fasciculus (MLF)

A conjugate lateral movement requires a co-ordinated response on the part of the medial rectus of one eye, innervated by N III, and the lateral rectus of the other, innervated by N VI. This coordination was considered by Crosby to be mediated by a group of neurones in a 'parabducens nucleus' close to the abducens nucleus; as illustrated by Fig. 25.20 the interneurone activated the abducens nucleus on the same side and sent a branch through the medial longitudinal fasciculus (also called posterior longitudinal bundle) to synapse with a N III motor neurone activating the medial rectus contralaterally. Evidence for such a connection was derived initially

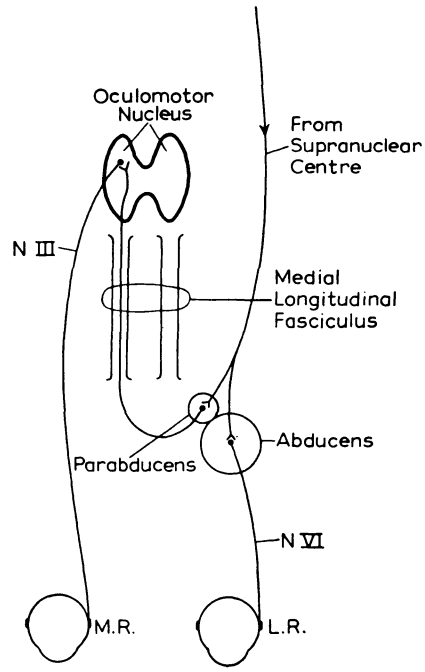

Fig. 25.20 Illustrating the conjugate innervation of the lateral rectus of one side and the medial rectus of the other.

from the observations of so-called internuclear palsy which, as reviewed by Highstein & Baker (1978), was associated with a lesion in the median longitudinal fasiculus, and appeared as a paralysis of both medial recti when making lateral movements, but not when making convergent movements.

Nuclear Interneurones

In their electrophysiological study they confirmed that interneurones of the abducens nucleus sent axons in the median longitudinal fasiculus to the contralateral oculomotor neurones. That these ascending axons were not branches of the abducens motor neurones, but were derived from a special class of interneurones, was shown by Highstein *et al.* (1982) by first identifying motor neurones through antidromic stimulation of N VI, and interneurones by antidromic of the median longitudinal fasiculus, and subsequent morphological study. The internuclear axons crossed the midline at the level of their parent somata and ascended in the MLF towards the nucleus of N III. The two classes of neurone were mixed throughout the abducens nucleus, with the internuclear neurones predominating in the rostral part of the nucleus. About 30% of the internuclear neurones sent collaterals to the prepositus hypoglossi nucleus, a neuronal group associated with the control of saccade eye movements

(p. 697). The internuclear neurones were excited by vestibular nucleus neurones, and so participate in movements induced by the vestibular apparatus (p. 699).[16]

Inhibition

Reciprocal innervation demands that inhibitory impulses pass to the antagonist muscles; in a lateral movement these would be the ipsilateral medial rectus and the contralateral lateral rectus. Highstein *et al.* (1976) recorded excitatory postsynaptic potentials in ipsilateral abducens motor neurones and internuclear neurones, and contralateral disynaptic inhibitory postsynaptic potentials in the contralateral neurones on stimulating higher motor centres, e.g. the pontine reticular formation and the vestibular nuclei.

Internuclear Ophthalmoplegia

Lesions in the median longitudinal fasciculus may well be responsible for the so-called internuclear ophthalmoplegia; the loss of the power to adduct the eye in conjugate lateral movements with its retention in convergence. Certainly this syndrome may be evoked by bilateral section of the fasciculus (Hyde, & Slusher, 1961).

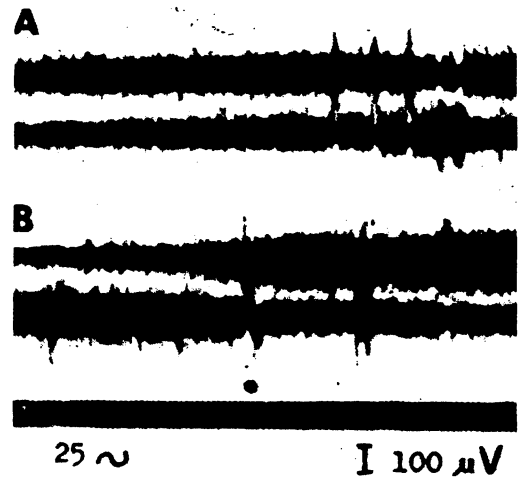

Fig. 25.21 Electromyograms of human medial and lateral recti during steady fixation (A) and a lateral movement (B). The upper record of each pair is from the lateral rectus, the lower is from the medial rectus. A. The gaze is maintained in the straightforward direction; note intense activity in both muscles. B. Slow following movement from 40′ inward to 40° outward showing continuous diminution of activity in medial rectus and corresponding increase in the lateral rectus. The dot below the traces in record B indicates the moment at which the gaze passes the midline. Records read from right to left. (Björk & Kugelberg, *EEG clin. Neurophysiol.*)

ELECTROMYOGRAPHIC STUDIES

Electromyogram

The activity in a muscle may be measured by the action potentials of its muscle fibres recorded from a needle-electrode inserted into the muscle; the more intense the contraction the greater will be the frequency of the spike discharges in individual units and the larger will be the number of units active. Because of the danger of various artefacts, the results of any study must always be interpreted with caution, but in the hands of experienced workers the EMG has been a valuable tool in assessing the contributions of individual muscles to given eye movements.[17]

Reciprocal Innervation

Björk & Kugelberg showed that, when the eye looked straight ahead, a given extraocular muscle gave a steady tonic discharge, single units firing with frequencies as high as 50/sec.[18] This is in marked contrast with skeletal muscles which are usually almost or completely silent during relaxation. With needles in the medial and lateral recti, reciprocal innervation was very well demonstrated; thus on abduction, there was an increased discharge in the lateral rectus associated with a simultaneous inhibition of the tonic discharge in the medial rectus. This is illustrated by Fig. 25.21; the records marked A are obtained with steady fixation, whilst B shows the discharges in the medial (top) and lateral (bottom) recti during a slow following movement from 40° inward to 40° outward, reading from right to left. The gradual diminution in activity in the medial rectus (top record), accompanied by the increase in activity of the lateral rectus, is well brought out. With this slow type of movement there was never a complete inhibition of the antagonist, by contrast with the rapid 'saccade' where the antagonist becomes quite silent.

Co-contraction

The EMG has also permitted a solution of the problem of co-contraction, the simultaneous contraction of agonist and antagonist that is a feature of certain acts involving the skeletal musculature. The phenomenon of reciprocal inhibition shows that in the execution of any movement of the eyes agonist and antagonist do not work against each other, and this applies even to the point at which the movement terminates; thus the movement of abduction, say, is not arrested by activity in the medial rectus, the reciprocal inhibition observed at the beginning and during the course of the movement being maintained to the end, at which time the muscle exhibits a discharge that is characteristic for the particular position of the eye. Thus

the movement is not *ballistic*, as a movement arrested by active contraction of antagonists would be called (Miller, 1958). Nevertheless it might be argued that the movement would be steadied by co-contraction of the elevator and depressor pairs (Boeder), but Breinin (1957a) and later workers have shown that there is no increase over the normal tonic resting activity in these muscle-pairs during a lateral movement; similarly, during a pure elevation or depression, the medial and lateral recti fail to show augmented activity.

THE SENSORY MESSAGES

Effects of Stretch

That sensory information is conveyed from the muscles, during stretch, was shown without doubt by Cooper *et al.* (1955) for the goat where spindles were identified, and also for the cat and monkey in which spindles were not found (Fillenz); action potentials being recorded from the brainstem, or from the nerve supplying the muscle, e.g. the oculomotor nerve (N III), on stretching the inferior oblique (thus proving that this nerve is not purely motor, incidentally). Stretching a muscle activates its spindles and induces a monosynaptic activation of its motor neurons, causing it to contract, thereby resisting the stretch. According to Breinin (1957b) the resting activity of a muscle falls to practically nothing on cutting its tendon, suggesting that the normal resting activity is a reflex response to stretch; however, the failure to augment the discharge on pulling the muscle rather discountenances this view of the origin of *tonic* activity, which is therefore probably central in origin.

Absence of Stretch-reflex

Later studies have tended to confirm the absence of a stretch-reflex in the extraocular muscles. Thus Keller and Robinson (1971), in their study of isolated abducens motor neurones in the intact monkey, failed to observe any increase in discharge on rotation of the eye so as to stretch the lateral rectus. Thus the normal tone of the extraocular muscles, as revealed by their tensions when the eye is in the primary position, is due to centrally controlled discharges to the motor neurones.

Feed-back

The participation of the spindles in a feed-back mechanism is indicated, however, by Breinin's failure to observe the finely graded reciprocal innervation of agonists and antagonists in the muscles of an enucleated eye; thus, under these conditions, the antagonist is abruptly inhibited as soon as the agonist acts instead of showing the gradual decrease illustrated by Fig. 25.21. Sears *et al.* (1959) have shown that pulling on the agonist or on the antagonist during a movement causes a decrease in the spike discharge measured electromyographically, whilst mere cutting the insertion of the muscle had no effect on spontaneous activity. On balance, then, the electromyographic evidence suggests that the motor discharge to the muscles is influenced by sensory messages from the muscles themselves, but more work is obviously required.

Proprioceptive Deafferentation

Graves *et al.* (1987) considered that the development of binocularity in kittens depended on a combination of retinal and extraocular muscle signals as visual experience was acquired; thus section of N V in kittens 4–8 weeks old resulted in a loss of binocularity of cortical cells (Trotter *et al.*, 1981). In behavioural studies, Graves *et al.* showed that section of N V at 6–11 weeks, either uni- or bilaterally, reduced binocular depth perception, whereas in adult cats there was no effect. Earlier Maffei & Bisti (1976) had induced a strabismus in kittens by tenotomy, and also prevented them from using their eyes visually. A loss of binocularity was found, indicating that a muscular imbalance of itself was adequate to reduce binocularity, thereby emphasizing the value of proprioceptive input.

SUSCEPTIBLE PERIOD

Trotter *et al.* (1987) found that the loss of binocularity of cortical neurones as a result of uniocular section of N V depended on a critical period; thus section before 4 weeks or in adulthood had no effect; between 4 and 8 weeks the reduction occurred, and the time-course of susceptibility fell within the period when ocular dominance could be disrupted by closure of one eye.

MOTOR NEURONE DISCHARGES DURING MOVEMENTS

Recording Technique

Fuchs & Luschei (1970) and Robinson (1970) have described the firing of motor neurones in the abducens and oculomotor nucleus respectively in the waking monkey. To make these measurements, in a preliminary operation a coil of wire was implanted on one globe which, used in conjunction with magnetic fields, permitted the recording of eye movements. At the same time stimulating electrodes were implanted in N III so that when, later, the recording electrode was passed through an implanted guide-tube, the position in the oculomotor nucleus could be ascertained by antidromically conducted impulses evoked by stimulating N III.

Saccade and Fixation

Figure 25.22 shows typical discharge activity during fixation and saccadic movements of a unit that was almost certainly one controlling the inferior rectus; with steady fixation there is a steady discharge; with an upward movement (A) this discharge is inhibited, to be resumed at the new fixation point. With a downward movement there is a burst-discharge of very high frequency which increases with the velocity of the saccade; after the saccade the burst did not subside instantaneously but gradually, indicating a continuing contraction of the muscle in spite of the stationary position of the eye and probably necessary to compensate for the slow stress-relaxation of visco-elastic elements in the globe's suspensory tissue. With any given unit we may recognize an ON-direction, such that movement in this direction is associated with a burst-discharge, and an OFF-direction associated with inhibition of the resting fixation discharge; thus with the lateral rectus the ON-direction was an abduction, and so on.

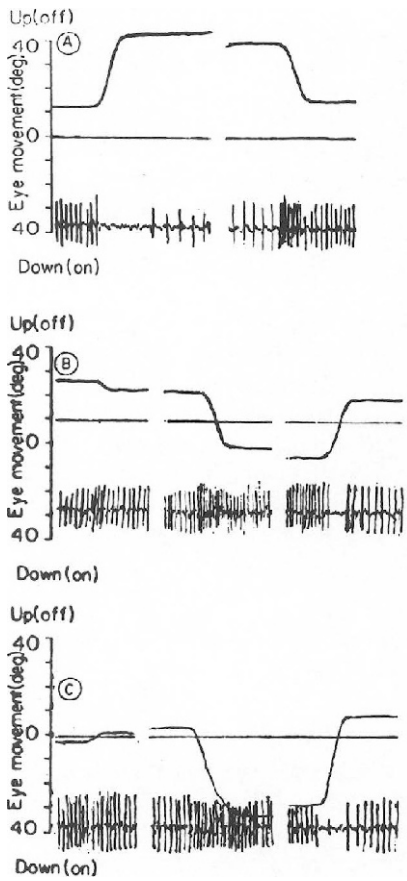

Fig. 25.22 Discharges of single units in the oculomotor nucleus of the intact, alert monkey during fixation and saccadic eye movements. The upper record of each section indicates eye movement, and the lower, unit discharge. The sections were selected from a continuous recording of the activity of a unit associated with downward movements and thought to be a motor neurone of the inferior rectus muscle. (Robinson, *J. Neurophysiol.*)

Discharge During Steady Fixation

The steady discharge during fixation depended on the direction of gaze so that, as this was directed from the primary position more and more into the OFF-direction, the steady discharge decreased and finally could be inhibited completely. There was thus a *threshold direction of gaze*. Figure 25.23 shows the behaviour of a variety of units with different ON-directions; also shown is the percentage of units, out of a pooled population of 35, that were active for a given direction of fixation, and it will be seen that, as the eye moved farther in the ON-direction, units were recruited; thus small angles of deviation from the primary position are achieved by contractions of fewer units, and in a given unit, with a lower frequency of discharge. In general the studies of Fuchs & Luschei and of Robinson indicated that, when the eye was in the

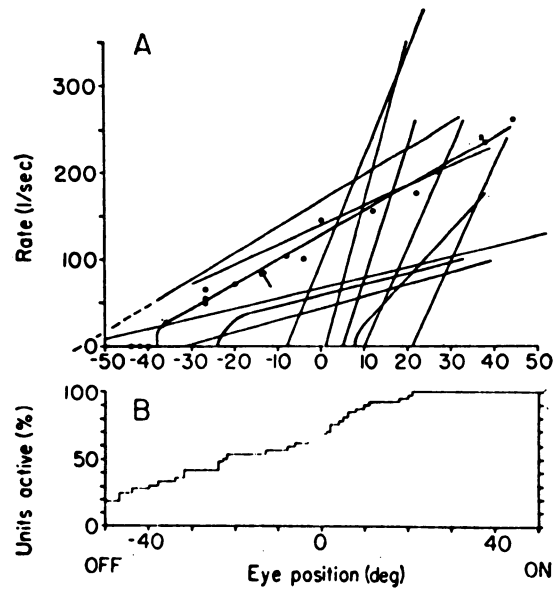

Fig. 25.23 A. Relation between discharge-rate (impulses/sec) and eye position during steady fixation. Responses in single units are shown to indicate the variety of slopes and thresholds. Experimental points for one curve, marked with arrow, are shown to indicate the typical nature of the fit between experimental points and staight-line approximation. B. Percentage of units acitve out of the pooled population of 35 units during fixation at any angle of gaze. The ON-direction could be either up or down, left or right, depending on which extraocular muscle was associated with the unit under study. (Robinson, *J. Neurophysiol.*)

primary position, a considerable discharge, of the order of 100 imp/sec, was maintained indefinitely. This is very high for a tonic postural type of innervation and demands a muscle fibre with a low degree of fatiguability.[19]

Time-relations for a Saccade

These are indicated in Fig. 25.24 from Fuchs & Luschei's (1970) study of abducens units; the burst-discharge definitely precedes the eye movement and ceases before the end, exhibiting a fast decline (d_{fast}) and a slower one (d_{slow}).

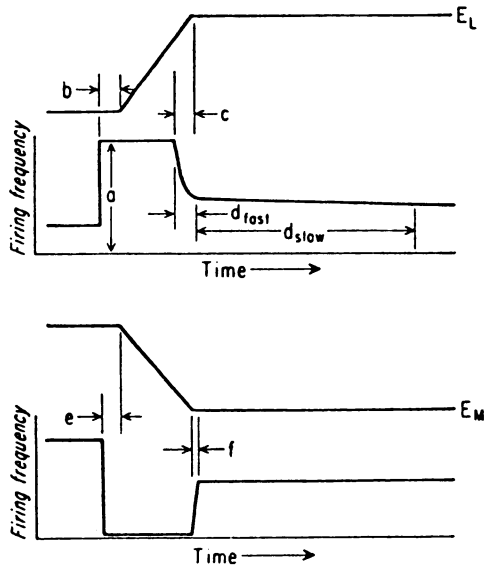

Fig. 25.24 Schematic representation of changes in firing frequency of abducens units during a lateral saccade (E_L) and a medial saccade (E_M). Lower case letters designate measurements used to characterize the unit firing patterns. Upper trace represents EOG; lower trace represents firing frequency. (Fuchs & Luschei, *J. Neurophysiol.*)

High Saccadic Discharge Rates

It has been noted by several workers that, although the tetanic fusion frequency for fast extraocular muscle fibres is high, of the order of 200 imp/sec, the maximum discharge rates during saccades are very much higher, although maximum tension in the fast muscle units is developed at the fusion frequency. Barmack *et al.* (1971) suggested that the *rate* of development of tension might increase at frequencies beyond the fusion-frequency, and this was true, so that the maximum rate of tension-development was achieved at 600 imp/sec although maximum tension was developed at 400/sec (Fuchs & Luschei, 1971). This is shown by Fig. 25.25 where the top curve (A) shows the effects of increasing frequency of stimulation on the development of tension and the lower curve (B) shows the differential of tension with time, i.e. the rate of tension development; and it will be seen that this increased up to 600 imp/sec, so that the maximum rate was about 25% greater at 600/sec than at 400/sec, the fusion frequency, which gave maximum tension.

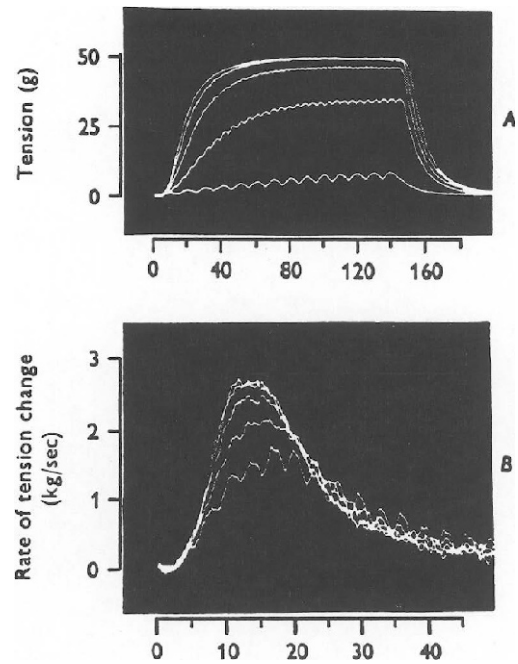

Fig. 25.25 A, isometric tension in the lateral rectus due to a train of supramaximal shocks applied to the abducens nerve. Stimulation frequencies were varied in 100/sec steps from 100 (lower curve) to 500/sec (upper curve). Maximum tension produced by 400 and 500/sec stimuli was identical. B, rate of change of isometric tension obtained by differentiating records similar to those of A. Stimulation frequencies ranged from 300/sec (lower curve) to 700/sec (upper curve) in 100/sec steps. Maximum rate of change of tension was identical at 600 and 700/sec. (Fuchs & Luschei, *J. Physiol.*)

Pursuit Following Movement

When the eyes followed a moving target there was an increase in the rate of discharge of a given unit, over that during fixation on a given point, by an amount that was proportional to the velocity of following. Thus the rate of discharge, D, was related to the angle of view, θ, by:

$$D = k\theta + r\,\mathrm{d}\theta/\mathrm{d}t$$

The ratio r/k is a time-constant, T, with a mean of 198 msec. In terms of force developed, the movement can be characterized by a similar equation:

$$F = K\theta + R\,\mathrm{d}\theta/\mathrm{d}t$$

where F is the force. R/K is likewise a time-constant and has a value of the same order. Figure 25.26 shows the relation between discharge-rate and eye-velocity; as the velocities of following are so much lower than those in a saccade it is not surprising that the discharge rates are very much less (of the order of 100/sec compared with rates as high as 400/sec in a saccade.

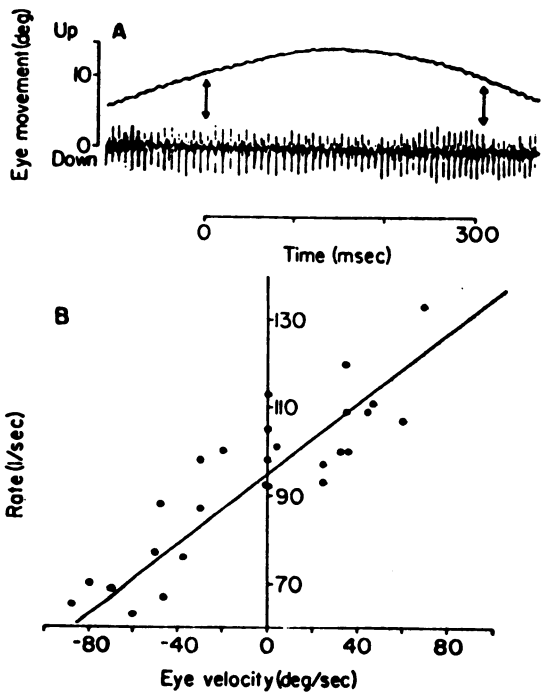

Fig. 25.26 Relation between discharge-rate and pursuit eye-velocity. A. At each arrow the eye position was 10° upwards. The discharge rate for steady fixation at this position was 130/sec but the rate was only 86/sec when the eye was travelling in the OFF-direction at 38°/sec (left arrow) and was 167/sec when travelling in the opposite direction at 49°/sec (right arrow). B. Discharge-rate of another unit plotted against pursuit velocity at instants when the eye passed through a given position when going in the ON-direction (positive abscissae) and the OFF-direction (negative abscissae). (Robinson, *J. Neurophysiol.*)

Robinson noted that all the motor neurones studied were involved in any given type of activity—fixation, saccade and pursuit—so that a separate class of motor neurones is apparently not involved in, say, pursuit. The same applies to vergence movements (Keller & Robinson, 1972; Keller, 1973) in spite of the claim that these are mediated by slow muscle fibres (p. 670), all abducens units participating in vergence movements, decreasing their discharge with convergence and increasing it with divergence. Moreover the value of r in the above equation, deduced from vergence movements, was the same.

Asymmetrical Convergence

We have seen that on Hering's view, when the eyes converge asymmetrically (Fig. 24.25) the apparently motionless eye did, in fact, take part in a convergence which was subsequently balanced by a version to leave its fixation direction the same. Using the electromyograph Tamler *et al.* (1958) showed that the apparently stationary eye in asymmetrical convergence showed activity in both medial and lateral rectus, a *co-contraction* that would balance the version and vergence if the activities were synchronous; this certainly supports Hering's view of conjugate innervation of both medial recti and suggests that, either the tendency for the apparently stationary eye to adduct is balanced by the pull of the lateral rectus, or that the eye does adduct and then abducts in a conjugate version. However, Keller & Robinson (1972) found no evidence, from their studies on single units in the waking monkey, of a co-contraction during asymmetrical convergence and they agreed with Breinin (1957a) that the version and vergence commands required for this type of vergence are summed centrally, with the net result appearing as activity in a shared common path, i.e. the opposing commands simply cancel out in each motor nucleus of the horizontal recti of the non-moving eye.

TENSIONS IN THE EYE MUSCLES

Fields of Action

As we have indicated, a definite tension is developed in the eye muscles even when the eye is in the primary position; this amounts to about 8 g. As the eye moves towards a new fixation point, we may say that it moves into the *field of action* of the muscle that is primarily concerned with the movement, and out of the field of action of its antagonist. For example, the left medial rectus will be active when this eye moves to the right, and the eye would be said to be moving into its field of action and out of the field of the left lateral rectus. Collins *et al.* (1975) implanted microtransducers into the muscles of human subjects and measured the tensions developed at different fixation points, during following movements, and during saccades. As we should predict from the studies on motor neurone discharges (p. 690), the tension developed as the fixation point is moved into the field of action of the muscle increases; the form of the curve relating tension to fixation position is not linear but parabolic. Tension increases in the antagonist as well, but

to a much less extent since this is being inhibited and the tension is the result of passive stretch.

Following Movements

During slow following movements the tensions were close to those attained during steady fixation at any position, although there was some hysteresis, in the sense that, when the eye moved nasally, the right medial rectus developed a greater tension for any given fixation point than when it moved in the opposite direction, i.e. out of its field of action (Fig. 25.27).

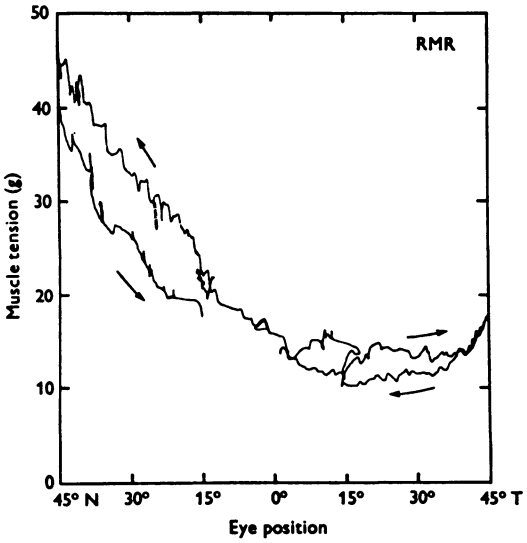

Fig. 25.27 Tensions recorded in a right medial rectus muscle tendon during unrestrained movements by a patient with 30 prism-dioptres of intermittent exotropia. The eye followed a target moving from the primary position to 45° temporal, then to 45° nasal and back toward 15° nasal at 10°/sec. The lower curve closely approximates the static locus of fixation-tensions. (Collins *et al.*, *J. Physiol.*)

Saccades

During the saccade, the tension rose rapidly and isometrically to a peak before the eye had moved; this was followed by an isotonic phase of lowered tension as the eye moved and fixation at the new point was maintained (Fig. 25.28); the antagonist, although being inhibited by reciprocal innervation, showed a sharp peak in tension due to passive stretch, and finished with a higher tension than before, due to this passive increase in length.

Operational Envelope

Collins *et al.* (1975) summarized the mechanical features of the muscular contractions during normal movements by the operational envelope shown in Fig. 25.29.

The lower heavy line indicates the tension in the muscle during fixation, rising steeply as the eye fixates nasally into the field of action of the medial rectus, and more gradually as the eye moves temporally. The upper curve is obtained by adding the force-increment necessary to make a saccade to any new position, the upward arrow indicating the increment as the eye fixates 15° medially; after the fixation the tension falls back to the lower curve along the line with the downward pointing arrow. If the eye moved back to the primary (0°) position the medial rectus would be relaxing and only a small passive increase in tension would occur (horizontal arrow).

COORDINATING CENTRES

Paramedian Pontine Reticular Formation (PPRF)

The nuclei of the motor nerves driving the eye muscles are the final common pathway through which commands for given eye movements are transmitted. Coordinating centres higher in the brain develop these commands; undoubtedly a region in the paramedian pontine reticular formation may be identified as a centre very closely related, both spatially and temporally, to the oculomotor nuclei. Microstimulation in this region with implanted electrodes in waking cats or monkeys causes eye movements, whilst records give discharges that are very closely related to subsequent discharges in the motor neurones and the consequent eye movements. Lesions here lead to paralysis of horizontal gaze towards the side ipsilateral to the lesion; stimulation of the labyrinth, designed to cause lateral movements, led to movements that failed to cross the midline (Cohen & Komatsuzaki, 1968, 1972). Finally, direct neural connections between this pontine region and the abducens nucleus have been demonstrated by retrograde movement of horseradish peroxidase (Baker & Berthoz, 1977).

Types of Neurone Discharge

Of particular interest are the studies of Luschei & Fuchs (1972) and Keller (1974) on alert monkeys with electrodes implanted in the dorsomedial pontine reticular formation close to the abducens (N VI) nucleus. The onset, duration and intensity of the burst firing of these units were tightly correlated with the direction, duration and velocity of saccades, and typically began before the burst of firing in the abducens motor neurones. Altogether four main categories of units were described by Luschei & Fuchs (1972) as follows:

1. *Burst-tonic.* Giving a burst discharge related to a saccade and a tonic discharge related to the steady direction of gaze.

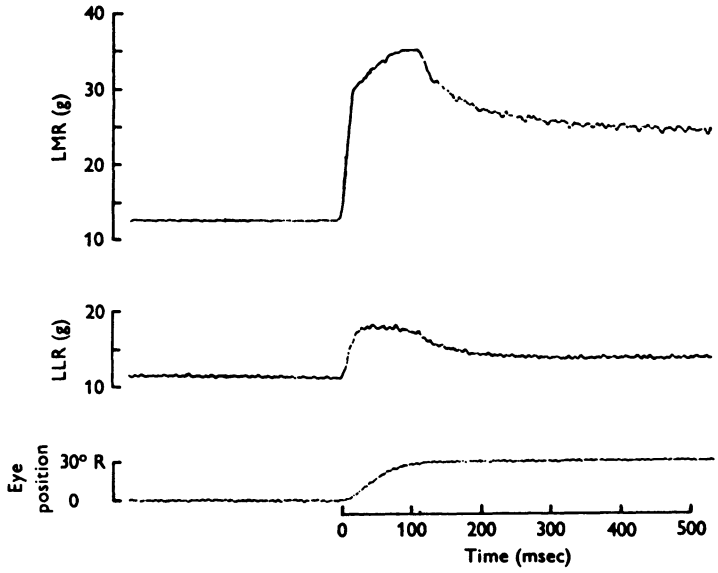

Fig. 25.28 Tensions recorded in a left medial rectus (upper channel) and a left lateral rectus (middle channel) during an unrestrained saccadic movement from primary position to 30° right (indicated on the lower channel). Note the initial isometric tension rise in the agonist left medial rectus before the eye moves appreciably, then a break in the curve as the eye achieves significant velocity. Note also that the tension in the relaxing antagonist left lateral rectus increases during the early stage of the saccade before it assumes the new steady-state fixation level, which is several grams greater than that for the primary position. (Collins *et al.*, *J. Physiol.*)

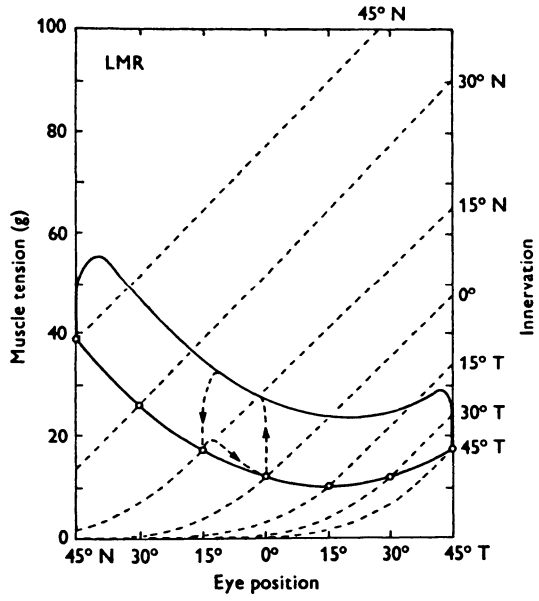

Fig. 25.29 An operational envelope of the normal ranges of extraocular muscle tension for a typical left medial rectus during fixation, following and saccadic movements. Dashed lines in the background represent a family of length–tension curves for each of the innervations shown. The lower curve represents the static locus or the tension required to maintain the eye in each position of horizontal gaze indicated on the abscissa. The upper curve represents the dynamic locus, or force increment producing a saccadic movement. The area between the static and dynamic loci represents the normal operational envelope. The counterclockwise loop between the zero and 15° nasal positions indicates tension changes in the muscle during a saccadic refixation into the muscle's field of action. The small clockwise loop from left to right indicates the passive tension changes occurring in the muscle as an antagonist during saccade. (Collins *et al.*, *J. Physiol.*)

2. *Burst-unit.* Burst related to saccade; usually no tonic activity and if so unrelated to eye position.
3. *Tonic.* Tonic discharge related to eye position. No burst on saccade.
4. *Pausing.* Discharging tonically but pausing when movement occurs in one or several directions. The pause preceded the movement and lasted as long as the saccade.

The lead, defined as the time between first spike of a burst and the beginning of eye movement, varied from as long as 80 msec to only 8 to 9 msec. In some units the burst followed the beginning of the saccade. Keller's (1974) study revealed the same types of unit; however, he was able to divide the tonic units, i.e. those related to the position of the eye in the orbit, into two classes, one, coding eye-position only, and another coding the velocity during smooth following movements. The difference is illustrated by Fig. 25.30; the units coding velocity are obviously involved in the execution of slow pursuit movements, by contrast with the other group that simply encodes eye-position, serving to maintain fixation between saccades.[20]

RELATION TO MOVEMENT AND POSITION VECTORS

Henn & Cohen (1976) described neurones obviously related to saccades and probably the quick phase of nystagmus; they analysed the responses of burst and pause units and were able to ascribe features of them that correlated with position, amplitude of movement and direction. An interesting finding was that units that apparently coded change in position indicated this change by the number of spikes during a burst, whereas with those that coded direction of movement the fre-

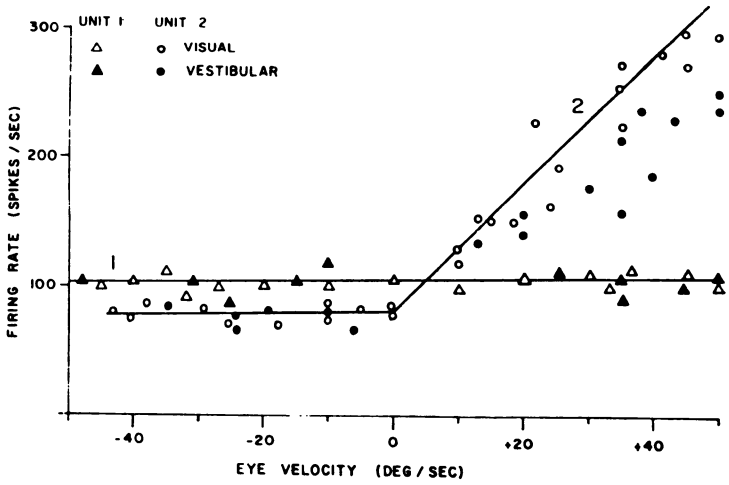

Fig. 25.30 Relationship between unit discharge rate and eye velocity for two tonic units. Discharge rates for visual pursuit velocities (open) and vestibular slow-phase velocities (filled) in both the ipsilateral (+) and contralateral (−) directions at instants when the eye passed through a given position for each unit. (Keller, *J. Neurophysiol.*)

quency of discharge was the parameter that correlated best. Probably the best way of indicating change of position is the number of spikes, a neuronal signal that could be integrated to provide the signal of the actual eye-position after the burst. The authors pointed out that motor neurones not only need instructions with respect to the movement undertaken, but they have to have instructions that will maintain the new point of fixation; this is achieved by the fact that, according to their analysis, the frequency of discharge of pontine neurones to motor neurones during the period of fixation is determined by the parameters that determined the previous fixation response; i.e., the level of steady excitatory output to the motor neurones is equivalent to the integral of the activity that caused the phasic response in the motor neurones.

Push-pull Stimulation of Motor Neurones

In a further quantitative study of abducens and related medium-lead burst neurones of the pontomedullary reticular region of the waking monkey (Van Gisbergen *et al.*, 1981) the evidence suggested that control over the motor neurone was exerted by combined excitation and inhibition; thus inhibition is not necessarily confined to the motor neurones activating the antagonist muscle. The authors showed that this was true especially for small saccades; moreover, when a saccade was in the vertical direction, burst cell activity directed to the laterally pulling eye muscles was found, the excitatory and inhibitory inputs presumably just balancing (Fig. 25.31). Moreover, instantaneous eye velocity did not correlate with instantaneous burst rate but it did with the instantaneous difference between the discharge rate of ipsilateral and contralateral burst neurones.

Relation to Motor Error

Robinson considered that discharge-rate of the burst reticular neurones, which determines the size of the saccade, was governed by an internal estimate of motor error, i.e. the difference between the final and the instantaneous eye position during the saccade. Figure 25.32 illustrates just such a case.

Oculomotor Nerve Nucleus

Although the pontine reticular formation is considered to be involved primarily in horizontal movements,

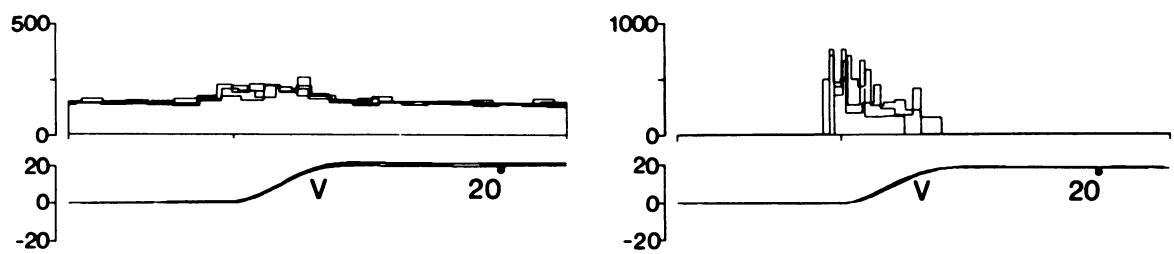

Fig. 25.31 A comparison of the instantaneous discharge rate, during a saccade, of an abducens motor neurone (left) and a burst neurone (right). Note different firing-rate scales. The saccade was vertical. (After Van Gisbergen *et al.*, *J. Neurophysiol.*)

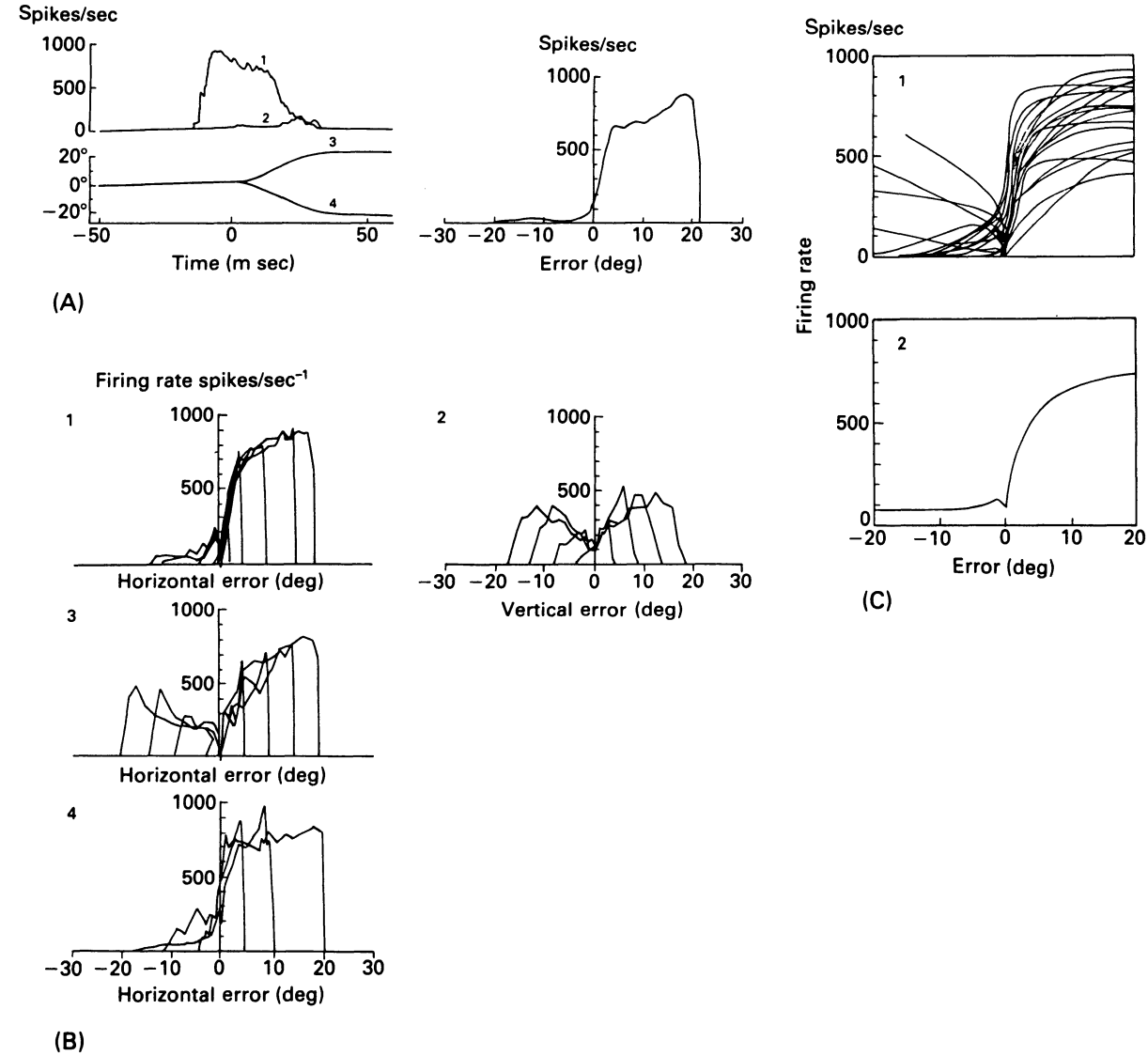

Fig. 25.32 Relationship between the discharge rates B(t) of horizontally acting burst neurones and the motor error, e_m, the distance between instantaneous and final eye position in a saccade. *A*: when B(t) (curve 1) is plotted against e_m, taken from curve 3 and corrected for this cell's lead time (14 ms), a phase plane trajectory, B(e_m), occurs as shown on the right for positive e_m for an on-saccade. *B*: trajectories B(e_m) are shown for three cells for horizontal (curves 1, 3, 4) and vertical (curves 2) saccades for various sizes (equal to initial error). The most common cell type is shown in curves 1 and 2. Note that the trajectories of all horizontal saccades follow the same curve, indicating that B is uniquely specified by e_m. For vertical saccades the cell (unit *2-55-1*) burst at a moderate rate that depended little on saccade size or vertical motor error. *C*: upper part shows smoothed curves B(e_m) drawn by eye for all 18 horizontally acting burst cells for horizontal saccades. The mean of these curves is shown below to represent the curve B(e_m) for the typical burst cell.

Highstein *et al.* (1974) found excitatory postsynaptic potentials in all types of motor neurone in this nucleus, involved in both horizontal and vertical eye movements, when they stimulated the pontine reticular formation; this was not due to stimulation of the vestibular nuclei as there was no occlusion of the responses in the median longitudinal fasciculus, the pontine pathway not making use of this nerve bundle.

Interstitial Nucleus of Cajal

The neurones of this brainstem nucleus end on all motor neurones governing the eye muscles except those activating the medial and lateral recti, and electrical stimulation causes conjugate vertical and rolling movements. By way of the MLF it connects to the vestibular nuclei and so is able to influence vestibularly evoked eye movements.

Markham *et al.* (1966), working on the cat, obtained ipsilateral inhibition of Type I vestibular neurones (p. 704) and activation of Type II neurones. These actions are consistent with a projection from the interstitial nucleus to the medial vestibular nucleus, no other midbrain structure projecting to the vestibular complex. The effect is primarily on the horizontal canals and it is suggested that the interstitial nucleus tends to inhibit lateral canal activity when the vertical canals are active. In the *encéphale isolé* cat, Hyde & Eason (1959) observed a slow movement on electrical stimulation of the nucleus; it was accompanied by rolling. There was no correlation between the initial velocity and the distance to travel.

Nucleus of Darkschewitsch

This nucleus has been invoked as a step in the motor pathway from the superior colliculus to the motor neurones, since there is no direct projection; the work of Carpenter *et al.* (1970), involving discrete lesions, confirmed the connections since these produced lesions in the oculomotor complex bilaterally. Szentagothai & Schab (1956) obtained inhibition of vestibularly evoked eye reflexes by stimulation of the nucleus; this was accompanied by protrusion of the eye-ball suggesting inhibition of tonic contraction of the eye muscles. Carpenter (1972) made lesions in the nucleus that spared the interstitial nucleus of Cajal, and degenerating fibres were found in the interstitial nucleus and the oculomotor complex, so that the pathway may well be through the interstitial nucleus; however, the abducens nucleus showed no degeneration, and the animal showed normal lateral movements with impaired upward movements.

Prepositus Hypoglossi Nucleus

A perihypoglossal region contains three subgroups that are usually treated together, namely the *n. prepositus hypoglossi*, *n. intercalatus* and *Roller's nucleus*; recently the involvement of the prepositus nucleus in control of saccades has been invoked (see, for example, Robinson, 1987). By injecting horseradish peroxidase into the abducens nucleus, Maciewicz *et al.* (1977) demonstrated projections to the prepositus from the vestibular nuclei (ventromedial and ventrolateral). Afferent input to the prepositus is from the flocculus by way of the fastigial nucleus, from the interstitial nucleus of Cajal and cerebral cortex, and perhaps from the paramedian reticular formation.

Unit Recordings

Unit recordings from the prepositus yielded discharges correlated with eye movements, often preceding them (Baker *et al.*, 1975). One class of neurones were typical burst-tonic, the burst preceding saccades, and having a steady firing rate proportional to the position of the eyes; the discharge-rate was proportional to the velocity of the saccade. A second class showed discharges that were correlated with eye-position; thus there was no burst with movement, and the discharge was never modulated until the saccade had been performed. Baker *et al.* (1975) suggested that the prepositus might be the site where input from the superior colliculus interfaced with vestibular information and transformed the result into a command to the motor neurones.[21] The relation to the oculomotor complex was established by Graybiel & Hartwieg (1974) who found labelling after injections into the oculomotor (N III) complex and trochlear (N IV) of the cat. Lopez-Barneo *et al.* (1982, 1984) found, in the alert cat, a group of prepositus neurones whose firing rates were correlated with eye-position or velocity in a horizontal plane; the latency for antidromic stimulation from N III nucleus was as little as 0.6–0.8 msec. The neurones showed an increase in activity with each saccade, but this did not precede the eye movement; when eye movements were induced by vestibular stimulation, e.g. by sinusoidal rotations, the firing rate was clearly related to the horizontal position and velocity of the eyes. The neurones in this centre were not sending direct commands to the oculomotor neurones, but they may well have been involved in neuronal circuits that controlled the actual movements, as suggested by Robinson (1987).[22]

Phase-relationships

We shall see that the phase-relationships between the acceleration of the head, in vestibulo-ocular reflexes, and the discharge in the motor neurones, demand the imposition of a phase-lag on the motor neurone discharge of 180° if the order to the extraocular muscles is to keep pace with the head rotation during a sinusoidal acceleration on a moving chair. Fukushima *et al.* (1977) showed that the phase-lag of interpositus neurones was similar to that of abducens neurones during horizontal head accelerations in the cat, suggesting that these interpositus neurones had carried out the necessary integration required to convert the acceleration signal to a position signal to the motor neurones.

The Nervous Pathways in the Labyrinthine Reflexes

Primary Vestibular Afferents

The labyrinth is supplied by the vestibular branch of N VIII; as with other sensory nerves, the fibres have their cell bodies outside the central nervous system, in this case the *ganglion of Scarpa* (Fig. 25.33). Some primary sensory

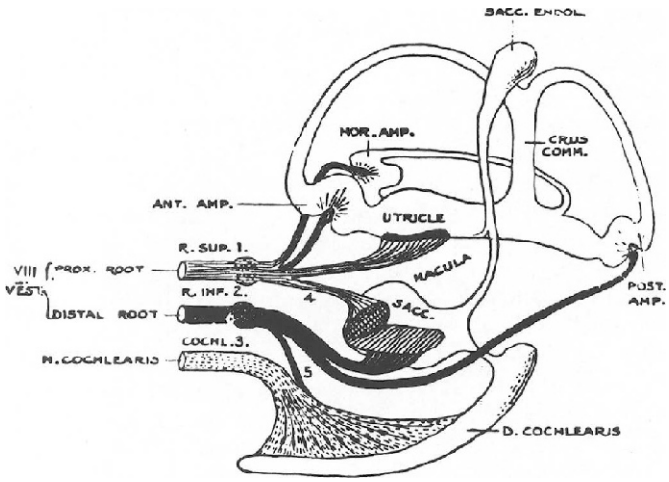

Fig. 25.33 Innervation of the membranous labyrinth.

fibres travel directly to the cerebellum (p. 723) and the rest pass into the medulla to relay in four *vestibular nuclei*, with functionally different afferent inputs and efferent projections.

Vestibular Nuclei

The nuclei are (a) *Deiters'* or the *lateral nucleus*; (b) *Schwalbe's* or the *medial nucleus*; (c) *Bechterew's* or the *superior nucleus* and (d) *Roller's* or the *descending* or *spinal vestibular nucleus.*

Secondary Neurones

Secondary vestibular nucleus neurones project (a) to the spinal cord as the vestibulo-spinal tracts; thus the lateral vestibulospinal tract is derived entirely from neurones of Deiters' nucleus which thus exerts its descending action on the spinal motor neurones, (b) to the cerebellum and cerebral cortex, (c) to the brainstem eye-muscle nuclei mainly by way of the medial longitudinal fasciculus (MLF); another route is by way of the reticular formation where neurones with monosynaptic connexions with vestibular nuclear neurones may be identified, mostly in *n.r. gigantocellularis* in the medulla and in *n.r. pontis caudalis* in the pons.

CONNECTIONS TO MOTOR NEURONES

According to Tarlov (1972), who made discrete lesions in the vestibular nuclei and followed the resulting degeneration to the motor nuclei of the eye muscles, only lesions in the superior and rostral portions of the medial vestibular nucleus caused degeneration in the eye motor nuclei, and Fig. 25.34 illustrates the courses of the oculo-motor fibres, which pass by way of the medial longitudinal fasciculus.

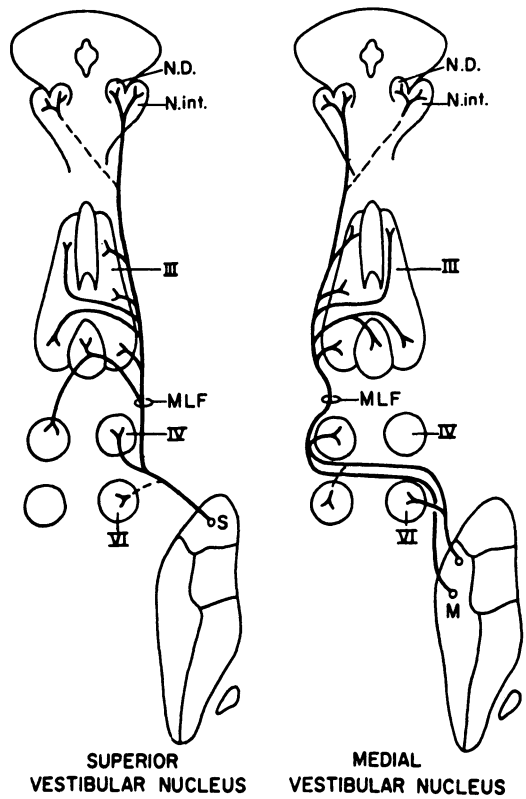

Fig. 25.34 Courses of vestibulo-oculomotor fibres. Ascending fibres from superior vestibular nucleus (left) pass in ipsilateral medial longitudinal fasciculus (MLF) to extraocular muscle nuclei bilaterally. Note that fibres to contralateral IIIrd and IVth nuclei cross midline within the IIIrd nuclei. In contrast, fibres from medial vestibular nucleus (right) decussate between levels of IVth and VIth nuclei, and ascend entirely in contralateral MLF. Dashed lines indicate sparse projections. (Tarlov, *Progr. Brain Res.*)

We must note that McMasters *et al.* (1966) considered that the ascending fibres from Deiters' and the medial nucleus were capable of mediating all patterned eye movements, so that Tarlov's study suggests that the connexions from Deiters' (lateral) nucleus involve an extra synapse, possibly by way of the reticular formation, the interstitial nucleus of Cajal and the nucleus of Darkschewitsch. His results are consistent with Highstein and Ito's electrophysiological study, and the observations of Shimazu *et al.* (1971) that most of the Deiters' neurones are activated by the utricle rather than the semicircular canals, and it is therefore likely that utricular responses in the eye muscles are mediated by a more complex pathway than the semicircular canal responses. This is understandable since these last mediate dynamic responses to acceleration whereas the utricle is mainly concerned with static postural responses tending to maintain poses when speed of execution is not so important.

ADDITIONAL CONNECTIONS

The connections of the vestibular nuclei with the spinal motor neurones, with the eye-muscle motor neurones, with the cerebellum and with the motor nuclei of the reticular formation indicate their possible role as co-ordinators of eye movements with movements of the head and trunk.

The Three-neurone Arc[23]

A variety of anatomical and electrophysiological studies have established the existence of a simple three-neurone arc mediating the vestibulo-ocular reflex, as illustrated in Fig. 25.35.

Specificity of Input to Eye Muscles

Figure 25.36 from Szentagothai (1950), who stimulated different ampullae and measured the predominant motor action in the individual muscles, shows that the lateral ampulla activates the ipsilateral medial rectus and the contralateral lateral rectus to produce a deviation away from the stimulated side. Stimulation of the superior vertical ampulla activated the ispilateral superior rectus and the contralateral inferior oblique; these are a 'linked pair', as we have seen, and thus may be expected to be activated in unison to cause an upward deviation with some rolling. The posterior canal activated the ipsilateral superior oblique and the contralateral inferior rectus producing downward deviation and some rolling. An important feature of the responses was the simultaneous inhibition or relaxation of antagonist muscles, e.g. lateral rectus when medial rectus of the same eye contracts, or if linked pairs are concerned, inhibition of the superior rectus of the opposite side when the inferior oblique of the same side is activated.

PRIME AND SYNERGIC ACTORS

In a more precise study, combining electrical stimulation of individual canal nerves with simultaneous stimulation of pairs, Cohen *et al.* (1964) define the prime actors as well as synergic actors in the response to stimulation of a given nerve; the results are indicated in Table 25.1, where it is seen that a given canal can activate six muscles, three in each eye, and since relaxation of antagonists was also observed this means that even the horizontal canals influence all twelve muscles. As an example we may take the response to stimulating the left anterior vertical canal, having its prime action on the right inferior oblique and left superior rectus; the observed eye movements (Fig. 25.37) were not conjugate, the left eye elevating with a slight counterclockwise rolling and the right giving mainly a counterclockwise rolling and a slight upward movement. When both anterior canal nerves were stimulated conjugate upward eye movements were obtained through activation of the superior recti whilst stimulation of one anterior and one posterior canal of the same side gave a conjugate rolling (Fig. 25.38).

STIMULATION OF CANAL PAIRS

When a pair of canals lying in the same plane were stimulated, e.g. the lateral canals, there was no eye movement; this was true of simultaneous stimulation of the right posterior and left anterior canal; as indicated earlier these lie in the same plane and are normally

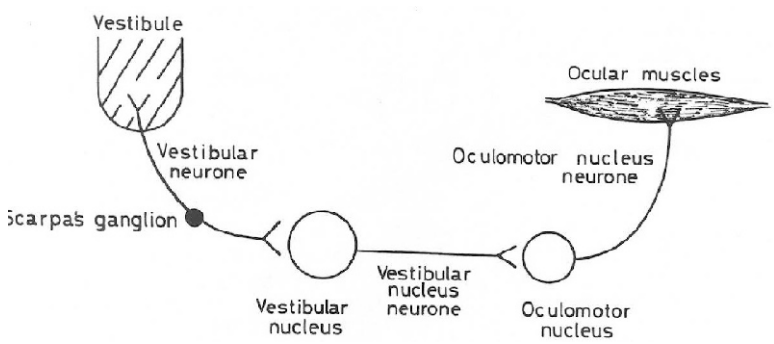

Fig. 25.35 The three-neurone arc mediating vestibulo-ocular reflexes.

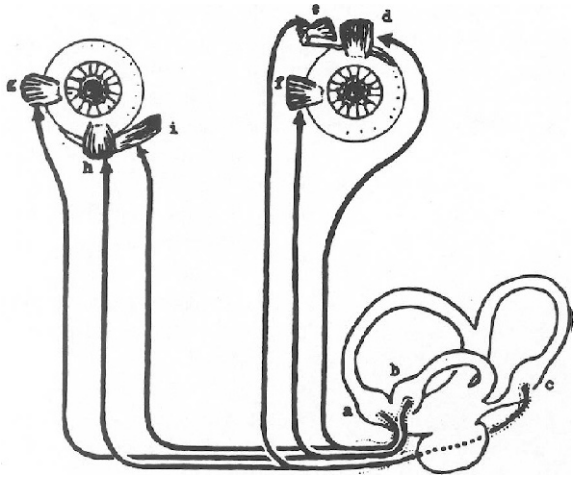

Fig. 25.36 Specificity of connexions of semicircular canals. Ampulla of superior canal (a) is in three-neurone connexion with ipsilateral superior rectus (d) and with contralateral inferior oblique (i); ampulla of horizontal canal (b) with ipsilateral medial rectus (f) and contralateral lateral rectus (g); ampulla of posterior canal (c) establishes three-neurone connexions with ipsilateral superior oblique (e) and contralateral inferior rectus (h). (Szentagothai, *J. Neurophysiol.*)

excited in opposite senses in any movement with a component in this plane; thus activation of one and inhibition of the other is the natural consequence of an acceleration in the plane. Simultaneous activation of both is an artificial situation equivalent to no head movement and thus does not call for any movement of the eyes.

Responses from the Otolith Organs

Compensatory poses in response to head tilts mediated through the gravity receptors involve elevation and depression, and conjugate rolling; lateral movements are evoked by stimulation of neck receptors. When Suzuki *et al.* (1969) stimulated the left utricular nerve of the cat the response was mainly a conterclockwise rolling, with the strongest increase in tension in the ipsilateral superior oblique and contralateral inferior oblique.

UTRICLE

The most thorough study of the electrophysiology of the utricle and saccule is that of Fernandez *et al.* (1972), based on a study of individual nerve fibres in the superior nerve, which innervates the utricle, and the inferior nerve innervating the saccule. They postulated that acceleration of the animal's head in a given plane and direction should activate those fibres related to hair-cells with maximal response to movement in this direction, so they defined the *functional polarization vector* of the given unit as that direction in space that gave the highest response. So far as the utricle was concerned the polarization vectors lay in the horizontal plane and 70% of the units were most sensitive to an ipsilateral roll of the head sideways, and 30% to a contralateral roll. Of those responding preferentially to pitches, equal numbers responded to nose-up and nose-down accelerations. Thus basically the sensitive cells in the macula utriculae fall into four classes with their discharge affected primarily by ipsilateral or contralateral rolls and forward and backward pitches.

SACCULE

With the inferior nerve, innervating the saccule, the polarization vectors tended to lie in the sagittal plane, and this would conform with the orientation of its macula in this plane.

Pathways to the Motor Neurones

The main pathway from the vestibular nuclei to the motor neurones governing the eye muscles is through the medial longitudinal fasciculus (MLF). Although destruc-

Table 25.1 Contractions of extraocular muscles during stimulation of single semicircular canals. (Cohen *et al.*, 1964)

Canal nerve stimulated	*Primary contractions*	*Synergistic contractions*	
		(stronger)	*(weaker)*
left anterior canal	left superior rectus	left superior oblique	left medial rectus
	right inferior oblique	right superior rectus	right lateral rectus
left posterior canal	left superior oblique	left inferior rectus	left lateral rectus
	right inferior rectus	right inferior oblique	right medial rectus
left lateral canal	left medial rectus	left superior oblique left superior rectus	
	right lateral rectus	right inferior oblique right inferior rectus	

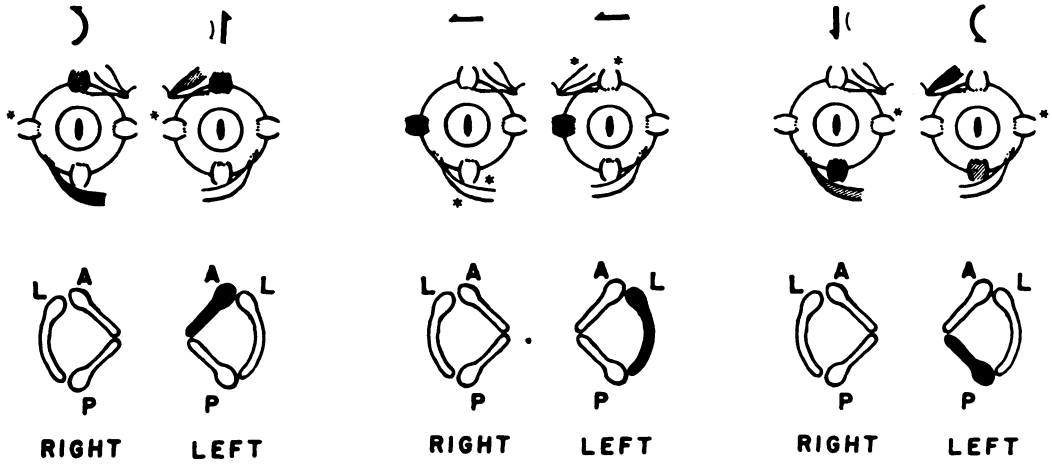

Fig. 25.37 Diagram of the eye movements and eye muscle activity elicited by stimulating ampullary nerves from left anterior canal (left), lateral canal (centre), and posterior canal (right). Anterior (A), lateral (L), and posterior (P) semicircular canals are represented in the diagrams below the eyes. The direction of the evoked eye movement is shown by arrows above the eyes. The canal whose nerve is stimulated and the eye muscles primarily activated are shaded in black. Stronger synergistic activity of eye muscles is shown by cross hatching and weaker synergistic activity by asterisks (see text for details). Muscles that are not excited, relax. (Cohen *et al., Ann. Otolaryngol.*)

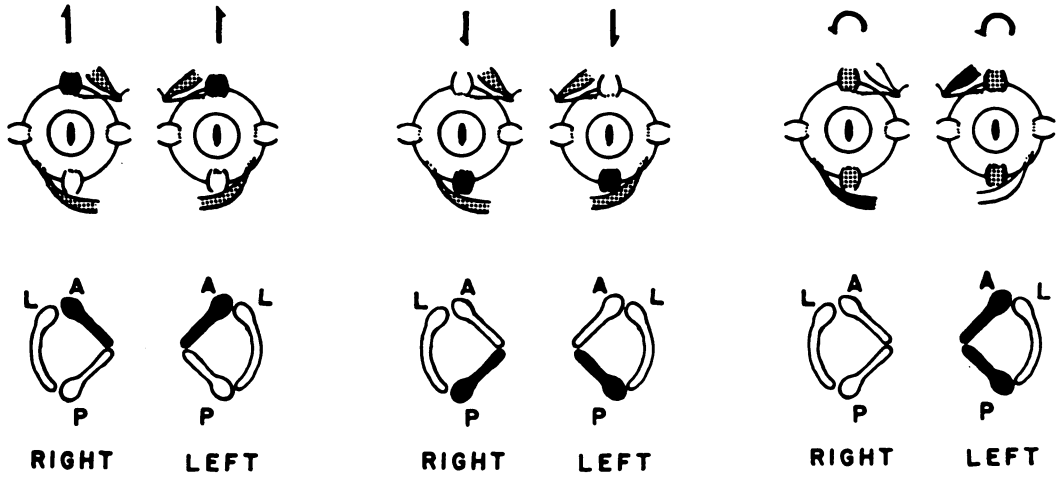

Fig. 25.38 Diagram of eye-movements evoked by simultaneous stimulation of both anterior canal nerves (left), both posterior canal nerves (centre), and the left anterior and posterior canal nerves (right). Scheme as in Fig. 25.37 with exception that muscles activated by stimulation of one canal nerve and partially or completely inhibited during stimulation of more than one canal nerve are shown as dotted. (Cohen et al., *Ann. Octolaryngol.*

tion of the MLF will often abolish vestibular responses in eye muscles, it does not always do so, but only attenuates them. According to Cohen (1971), the semicircular canals may send messages directly through the MLF or alternatively through the reticular formation. An additional route, probably carrying otolith messages, runs via the cerebellum, impulses leaving the inferior vestibular nucleus to reach the fastigial nucleus, whence fastigial neurones send impulses to the motor neurones of the eye muscles.

Input to Neck Muscles

Wilson & Yoshida (1969) found that, whereas a single shock to the labyrinth evoked no monosynaptic responses in motor neurones of the spinal cord activating

the fore- and hind-limbs of the cat, responses in neck motor neurones were obtained; and in a more recent study, Wilson & Maeda (1974) obtained EPSP's and IPSP's in all neck motor neurones on stimulating individual ampullary nerves. The responses were quite stereotyped, e.g. the biventer cervicis and complexus motor neurones were excited by stimulation of two anterior canals and inhibited from two posterior canals. Figure 25.39 illustrates the probable connections which involve, once again, both disynaptic excitation and inhibition of the motor neurone through a three-neurone arc.

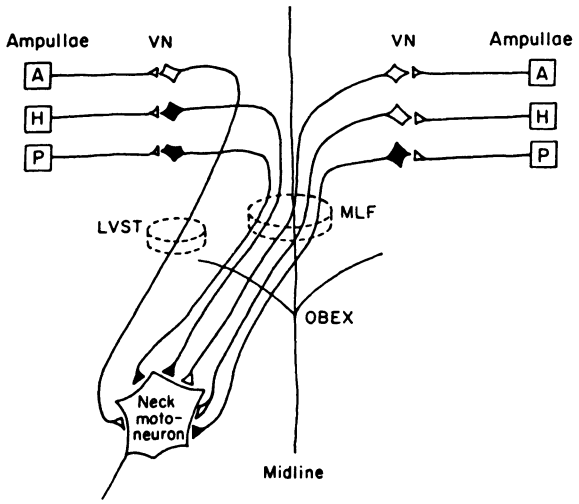

Fig. 25.39 Schematic diagram showing connexions between ipsilateral and contralateral ampullae and neck motor neurones. A, H, P are anterior, horizontal and posterior ampullae; VN, vestibular nuclei. Inhibitory neurones and their terminals are shown in black; excitatory in white. (Wilson & Maeda, *J. Neurophysiol.*)

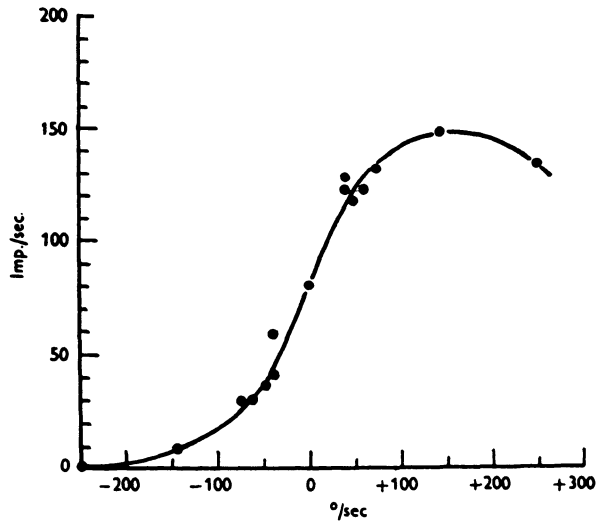

Fig. 25.40 Frequency of discharge of a fibre from the horizontal semicircular canal of the ray plotted as a function of angular acceleration. With zero acceleration there was a resting discharge of 80 imp/sec, which diminished or increased according to the direction of acceleration. (Groen *et al., J. Physiol.*)

Responses in Primary Afferent Neurones

Fish Semicircular Canals

The sensory fibres from the semicircular canals have usually a tonic resting discharge, and this is enhanced when the head is accelerated in one direction and inhibited by acceleration in the opposite direction. A typical response curve for the ray's horizontal semicircular canal is illustrated in Fig. 25.40. It will be seen that at rest, or zero acceleration, there is a tonic discharge of 80 imp/sec; this may be increased or decreased according to the direction of acceleration. When different units were examined the same basic feature was revealed, namely reversed type of response with accelerations in opposite directions, so that we may conclude that the hair-cells of the crista ampullaris of any given canal are polarized in the sense that bending in one direction excites its associated axon, and bending in the other inhibits it. The sign of this polarization is the same for all the hair-cells in a given ampulla, and the positions of ampullae in canal pairs are such that excitation of one set of hair cells is accompanied by inhibition of the opposite set. In this way we see the advantage of a high tonic discharge in the labyrinthine neurones; this permits two signals, namely increase and decrease of discharge indicating acceleration in one or the opposite direction; if the neurones, in the absence of acceleration, were silent, then acceleration in one, the inhibitory, direction would result in no signal since there can be no negative discharge in a neurone.

Mammalian Units

Goldberg & Fernandez (1971) studied responses of monkey units; Fig. 25.41 illustrates the response of a single vestibular nerve fibre to a stimulus-pattern illustrated in Fig. 25.42; this consists of a period, T_1, during which the head is at rest, and the record indicates a tonic discharge of 80 imp/sec. A period of abrupt acceleration, T_2, indicated by the bar on the record, is accompanied by an abrupt increase in discharge. At the end of the period of acceleration, the velocity is held constant over the period T_3, and during this period the discharge steadily wanes, returning to the resting value in about 1 minute. Next the rotation was decelerated over the period T_4, indicated by the second bar, and it will be seen that there is a prompt inhibition of the tonic discharge followed by a return to the basal rate when the animal is stationary.

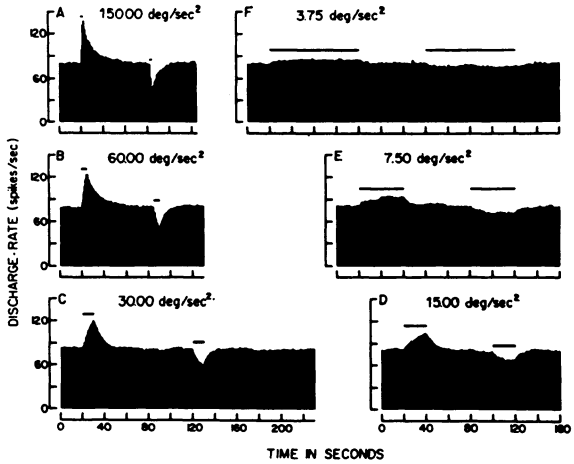

Fig. 25.41 Response of superior canal sensory unit to the velocity trapezoids depicted in Fig. 25.42. Each histogram represents the response to the presentation of a single stimulus. Each histogram column depicts the discharge rate for 1 sec and the horizontal marks denote periods of constant acceleration and deceleration (T_2 and T_4). Accelerations are as stated, all rotations counterclockwise, and maximum velocity always 300/sec. (Goldberg & Fernandez, *J. Neurophysiol.*)

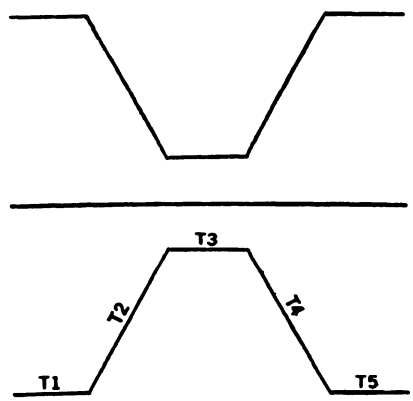

Fig. 25.42 Stimulus pattern used to obtain the responses indicated in Fig. 25.41. Each velocity trapezoid consists of stationary period (T_1), constant acceleration period (T_2), constant velocity period (T_3), constant deceleration period (T_4) and final stationary period (T_5). The signal is proportional to the angular velocity; the upper and lower traces correspond to counterclockwise and clockwise rotation respectively. (Goldberg & Fernandez, *J. Neurophysiol.*)

TORSION-PENDULUM

The period at constant velocity—zero acceleration—represents the period when the cupula is being restored to its resting position under the influence of its own elasticity, and Goldberg & Fernandez showed that the dynamics of the changes in unit discharge conformed with those predicted on the basis of the movement of a heavily damped torsion-pendulum, as earlier described by Van Egmond *et al.* (1949), when they studied the duration of the sensation of giddiness, or Hallpike & Hood (1953) studying the duration and velocity of oculogyral illusion, after attaining a steady velocity.

Adaptive Changes in Vestibulo-ocular Reflex

It is well established that repeated induction of vestibular nystagmus, e.g. by rotation or calorically, leads to a diminution in the amplitude of the response; however, as Gonshor & Melvill Jones (1976) have pointed out, such an attenuation, occurring as a result of everyday head movements, would reduce the value of the reflex; and in their experiments, in which human subjects were repeatedly exposed to sinusoidal rotations at angular velocities that fell within the range expected during normal head movements, there was no attenuation. As a quantitative estimate of the magnitude, or efficacy, of the reflex the gain, G, defined as the ratio of peak eye velocity (ω_e) to peak head velocity (ω_h):

$$G = \omega_e \max / \omega_h \max$$

was employed. In the dark, this normally has a value of 0.7, indicating that the eyes tend to lag behind the head. With eye(s) open, so that the optokinetic reflex can cooperate, the gain becomes about unity, indicating perfect fixation.

Reversed Tracking

When subjects were exposed to a reversed optokinetic tracking task, by causing them to view a mirror-image of the environment as the head was rotated, it was found that there was some attenuation of the reflex—decreased gain—when the subjects were subsequently tested in the dark, so that, on average, a reduction of some 23% in gain was achieved by interposing periods of reverse tracking.

When human subjects were exposed to reversed tracking for long periods of time by wearing, during their waking hours, goggles with reversing prisms, the effects were much more striking. After 7 days the gain fell to a plateau at about 25% of normal, so that when the electro-oculographic records of eye movements during rotation were analysed it was difficult to recognize any sinusoidal component in them.

REFLEX REVERSAL

The more important finding was that there was a phase-change in the eye movements of such a size as to result in a *reflex reversal*, i.e. the vestibular response to a head acceleration was of the opposite character to that normally required, so that the eyes were in fact moving with the

direction of rotation. This means that the central programming device is able to make use of visual information, translating its false into its true meaning so far as head turning is concerned, and influencing the vestibular reflex mechanism appropriately.

Cerebellectomy

A clue to the mechanism of this adaptive change was provided by Robinson (1976), who showed that it was completely abolished in cats by removal of the vestibular portion of the cerebellum. Thus the cat's gain in the dark was 0.90; after wearing reversing prisms for 8 days the gain decreased by 93%; on removal of the cerebellum the gain rose to 1.17, and now there were no plastic changes with reversing prisms. That visual input can influence activities in cerebellar Purkinje cells is well established (p. 725).

The Neurones of the Vestibular Nuclei

The Three-neurone Arc

Studies on the discharges and membrane potentials of individual neurones in the vestibular nuclei during vestibular stimulation have shown unequivocally that both the excitation of the vestibular neurone, revealed usually as an increase in its basic discharge, and the inhibition, revealed as a reduction in discharge, can be mediated by a monosynaptic connexion between the vestibular nerve and the vestibular nucleus neurone. Since, also, the study of the motor neurones, under the same conditions reveals a monosynaptic connexion between these vestibular neurones, the concept of a three-neurone arc—labyrinthine sensory neurone in Scarpa's ganglion, vestibular neurone in medulla, and brainstem motor neurone—is well substantiated both for excitation and inhibition.

Responses of Vestibular Nucleus Neurones

Duensing & Schaefer (1958) carried out the classical study on responses of these neurones to accelerations of the head, and they defined four types according to whether discharge was accelerated or inhibited by ipsi- or contralateral rotation. Thus Type I gave increased discharge on acceleration to the same side and decrease to the opposite side. Type II gave a reciprocal behaviour, giving decreased discharge on ipsilateral turning and increased on contralateral turning. Type II neurones, which were much rarer, were considered by Shimazu & Precht (1966) to be inhibitory vestibular neurones that could mediate the commissural inhibition of Type I vestibular neurones, as suggested by Fig. 25.43, where it is seen that a horizontal ampullary neurone activates Type I neurones, and that one of these activates a contralateral

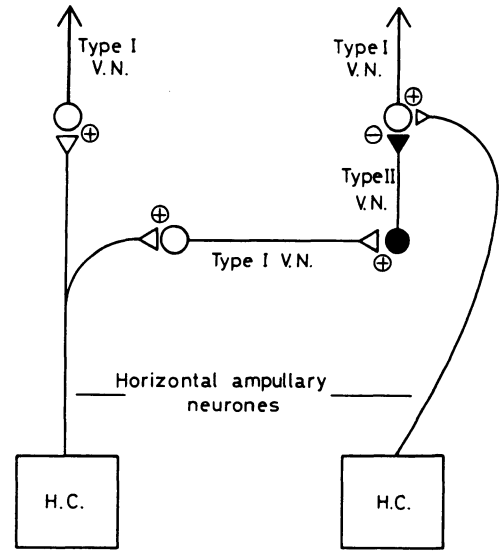

Fig. 25.43 Illustrating mechanism of Type II neurones. A horizontal ampullary neurone activates Type I neurones, one of which activates a contralateral Type II interneurone which then inhibits a Type I vestibular neurone. (After Shimazu & Precht, *J. Neurophysiol.*)

Type II interneurone which then inhibits a Type I vestibular neurone. This inhibition is to be contrasted with the monosynaptic activation of an inhibitory vestibular neurone, V_i, that is responsible for the simultaneous activation of agonists and antagonists seen during vestibularly stimulated eye movements, described by Baker & Berthoz (1974) for example. Thus inhibition of a Type II neurone, if this were spontaneously active, would *disinhibit* a Type I neurone and so facilitate the motor neurone with which it is related.

SPECIFICITY OF INPUT

Wilson & Felpel (1972), working on the pigeon's labyrinth, found that, of the individual neurones studied in the vestibular nuclei, greater than 55% of the responding cells only fired in response to electrical stimulation of a single ampulla; some were influenced by two ampullae, but when allowance was made for electrical spread from one ampulla to another Wilson & Felpel estimated that at least 81% of the responding vestibular neurones were influenced by only one ampulla.

Influence on Motor Neurones

As an example of the postsynaptic potentials observed on direct stimulation of the vestibular nerve, we may cite the study of Baker *et al.* (1969). Intracellular records of abducens (N VI) motor neurones controlling the lateral

rectus revealed the development of hyperpolarizing IPSP's in the ipsilateral neurones, which were probably derived from inhibitory vestibular neurones in the ipsilateral medial vestibular nucleus. Thus stimulation of the ipsilateral vestibular nucleus gave slowly developing IPSP's in the abducens motor neurones. The shortest latency from the ipsilateral vestibular nucleus was 0.65 msec, indicating a mono-synaptic pathway since conduction-time was some 0.2 to 0.3 msec. The latency from the ipsilateral vestibular nerve to the motor neurone was 1.4 to 2.0 msec, giving a latency-difference of 0.9 msec, on average, which could be the time for activation of the inhibitory neurone in the vestibular nucleus. Thus the IPSP is produced disynaptically from the ipsilateral vestibular nerve Fig. 25.44, and the total reflex arc is a 3-neurone one.

TROCHLEAR NEURONES

An essentially similar result was obtained by Baker *et al.* (1973) when studying trochlear (N IV) motor neurones; these receive short-latency excitation (EPSP) from the contralateral labyrinth, and inhibition (IPSP) from the ipsilateral labyrinth. Stimulation of the individual labyrinth nerves from the separate anterior and posterior vertical ampullae revealed a reciprocal activation, the one activating while the other inhibited the trochlear motor neurone. We may note that when Cohen *et al.* (p. 701) stimulated the same pair of canals, there was a strong conjugate torsion caused by powerful activation of the contralateral inferior oblique; at the same time, of course the contralateral superior oblique, innervated by trochlear motor neurones, would be inhibited, so that in a given eye there would be a strong reciprocal activity on a given trochlear motor neurone.

OBLIQUES AND RECTI

In another study (Baker & Precht, 1972), the combined actions of the posterior canal on the obliques and recti were studied; strong activity was evoked in the ipsilateral superior oblique and the contralateral inferior rectus (linked pair) but a weaker excitation was observed in the ipsilateral inferior rectus and the contralateral inferior oblique. The joint action on the eyes was to cause an anticlockwise rotation and a depression of both eyes.

Mechanism of Relaxation of Antagonists

The development of monosynaptically activated IPSP's in the motor neurones indicates the primary mode of inhibition, or relaxation, of antagonists; another process is described as *disfacilitation*, by commissural fibres running from one vestibular nucleus neurone to another on the opposite side; if the neurone with which this commissural neurone synapses is being tonically excited by a vestibular nerve neurone, then inhibition of this excitation by presynaptic activity would be described as disfacilitation, to distinguish it from the inhibition that results from direct synaptic action producing an IPSP.

Study on Waking Monkey

Fuchs & Kimm (1975) pointed out that vestibular neurones were not solely concerned with vestibularly evoked eye movements; thus, as early as 1933, Spiegel showed that eye movements, initiated by occipital cortex stimulation in the cat, were abolished by lesions in the vestibular nuclei, whilst more recent studies on monkeys have shown that vestibular neurones discharge in relation to eye movements, such as saccades, in a way similar to those of the paramedian reticular formation, described by Luschei & Fuchs (1972) and Keller (1974). Moreover, vestibular neurones, responding during the slow movement of nystagmus, could also discharge in relation to the fast-movement saccadic type of movement. By appropriate stimulation procedures in the waking monkey that enabled the separation of vestibularly evoked eye movements from others, they identified four groups of vestibular nucleus neurones, mostly in the median nucleus. Thus about half responded to the vestibular stimulus only, showing no change with eye movement; the remaining

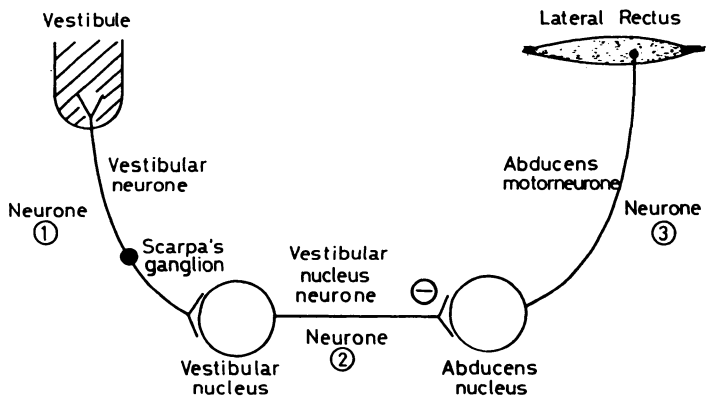

Fig. 25.44 Reflex are for inhibition of an abducens motor neurone.

three groups gave responses that were related to eye movements as well, some usually pausing with saccades; others having discharges related to eye position, and some responding to eye movements alone, behaving like abducens units. Saccade-related units, observed during spontaneous saccades to pause, also paused when the quick movement of nystagmus occurred in the same direction. An example of a vestibular-plus-saccade neurone is shown in Fig. 25.45 with no acceleration (0.0 Hz) the unit has a steady discharge interrupted by pauses during saccades; with vestibular stimulation, the phasic bursts due to acceleration are interrupted by saccades in all directions. Some examples of vestibular and visual interactions will be discussed later, interactions that may be mediated within the vestibular nuclei.[24]

SUPERIOR COLLICULUS

The position of this subcortical visual centre has been described earlier together with its main projections and some of its interactions with the cortical visual centres. There is no doubt that it is closely involved in the encoding of motor signals to the motor neurones of the eye muscles, signals that may well be adequate to direct the eyes to visual targets as well as those governed by other sensory inputs. Its precise role, however, is still a matter of speculation.

Connections

The anatomical basis for a special role in visually directed movements is provided by the fibres from the optic tract terminating directly on tectal neurones in the superficial[25] strata of the bodies, together with a projection from areas 17 and 18 of the cerebral cortex. Projections to the thalamus, particularly the posterior nuclei including the pulvinar, probably permit feedback circuits that allow coordination of all types of sensory information with motor activity through association areas of the cerebral cortex.

Phylogeny

In general, the higher the animal phylogenetically, the larger the proportion of optic tract fibres that pass to the lateral geniculate body and thence to the cerebral cortex. In man and the higher apes, therefore, only relatively few fibres terminate in the colliculi.

Efferent Connections

These have been summarized earlier (p. 630); of interest is the fact that collicular neurones are said not to project directly to the motor neurones of the eye muscles, relaying in brainstem neurones such as those in the pontine reticular formation.[26] In general, as we have seen, the superior colliculus may be divided into superficial layers, projecting to the cortical and thalamic structures, and the intermediate and deep layers with major descending pathways that include those to the control centres for activation of the motor neurones.

IPSILATERAL AND CROSSED TRACTS

Harting (1977), using an autoradiographic analysis of descending pathways from the monkey's superior colliculus, described an ipsilateral tecto-pontine-tecto-bulbar tract, and a crossed tectospinal tract. The ipsilateral tract terminated on the parabigeminal nucleus, the mesencephalic reticular formation, the dorsal lateral pontine gray, the dorsal lateral wing of the nucleus reticularis tegmenti pontis, and the nucleus reticularis oralis. The crossed tectospinal tract had as its most rostral and quite extensive target the paramedian pontine reticular formation (PPRF) also described as the n. reticularis tegmentum pontis (Goebel *et al.*, 1971). Further projections were to the oral and caudal divisions of n. reticularis pontis, the caudate medulla, the medial accessory nuclei and the inferior olivary complex; through this last named nuclear complex there would be access to the cerebellum. The projection to the n. reticularis pontis

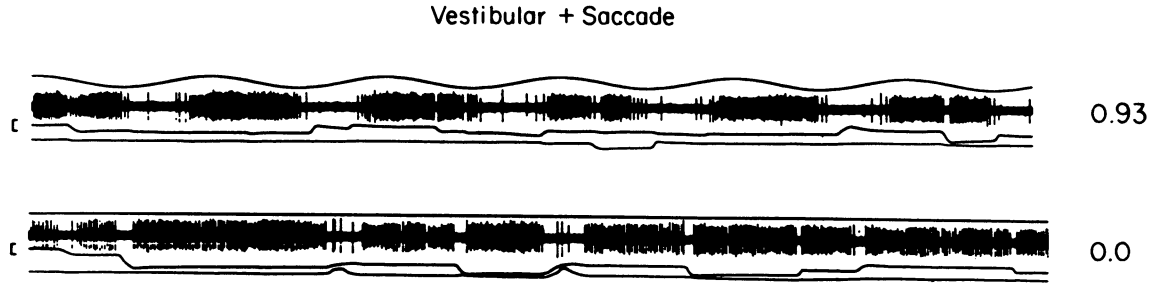

Fig. 25.45 Discharge characteristics of representative vestibular plus eye-movement neurone during vestibular stimulation and eye movement. Vestibular plus saccade unit exhibits an increasing rate for contralateral accelerations (Type II) which is interrupted by saccades in all directions including the vertical (note downward saccade in 4th cycle; 0.93 Hz). In the absence of vestibular stimulation (0.0 Hz), the unit exhibits a relatively constant rate of 62 spikes/s except for the saccadic interruptions. (Fuchs & Kimm, *J. Neurophysiol.*)

oralis may well be the pathway to the spinal cord through which the superior colliculus influences head movements in relation to eye movements, a direct projection to the cervical motor neurones from the superior colliculus not having been demonstrated.

Response to Electrical Stimulation

Electrical stimulation of the superior colliculi with electrodes implanted in the waking and freely moving cat, by Hess' technique, causes a movement of the head towards the opposite side; a careful study of the eyes shows that the movement of the head is preceded by a conjugate movement of the eyes (Burgi, 1957). Usually there is an upward or downward component in the movement according to the part of the colliculus stimulated; and in the rostro-median region a pure upward movement can be obtained. In the alert monkey, electrical stimulation evoked short-latency saccadic movements (Robinson, 1972; Schiller & Stryker, 1972), and the *amplitude*[27] and *direction* of the eye movement were largely determined by the point stimulated, rather than intensity, so that there is an upward component if medial regions are stimulated and downward component on lateral stimulation; if the stimulus is applied to a rostral region the movement is small compared with a caudal stimulus. When a given point was stimulated repeatedly, successive saccades were made from the position reached by the previous one until the limit of movement of the eye was reached.

Foveation

According to Robinson, the electrical stimulation is essentially similar to photic stimulation of a given point on the retina, and the response may be regarded as a 'foveation', but not a goal-directed movement since stimulation of the same collicular point can cause movement to different fixation points whereas in the normal animal allowance would be made for a given movement. Thus the colliculus is responding to a retinal system of coordinates and failing to translate retinal stimuli on to a system of coordinates involving the head.

Tectal Influence on Motor Neurones

According to Precht *et al.* (1974), the pathway from the colliculus to the motor neurones of the eye muscles is at least disynaptic and many of the responses were trisynaptic, as judged by the latency between stimulating the colliculus and the electrical response in the motor neurone. They consider that the pathway is probably by way of the ipsilateral midbrain reticular formation, with a crossing over to the contralateral motor neurones at some point caudal to the midbrain and certainly not within the collicular commissure.

Responses to Light

Eye Movements

In the anaesthetized cat, stimulation of the retina by light does not evoke any eye movements; if, however, the excitability of the superior colliculus is enhanced locally by the application of a crystal of strychnine, then light causes a prompt movement of the eyes directed to a definite spot in space characteristic for the particular region of the colliculus that has been made thus sensitive. By systematically changing the position of the strychninized area, a map of the surface of the colliculus may be plotted indicating regions of the visual field towards which the eyes will be directed when a given point is rendered hypersensitive. Presumably there is a reflex path from the retina through the colliculus that determines that the eyes will move towards the point in the visual field that stimulates the retina; such a concept is the basis of the 'foveation hypothesis' of collicular function (Schiller & Koerner, 1971), a hypothesis that has been questioned by Wurtz & Goldberg (1972).

Discharges in Collicular Neurones

According to the depth of penetration into the colliculus, units may be found that respond to visual stimuli and, in general, the receptive fields of the units, i.e. the regions on the retina or visual space that evoke responses in the given tectal unit, are located in space where electrical stimulation of the unit would direct the eyes (Robinson, 1972; Cynader & Berman, 1972). Figure 25.46 relates the receptive fields of collicular neurones to position on the colliculus; the periphery of the contralateral half-field is represented on the most posterior part, the upper field on the medial part and the lower on the lateral part, and the fovea, or area centralis, has a disproportionately large representation. In the monkey, Cynader & Berman found that the half-fields were strictly segregated to the contralateral colliculus, whereas in the cat some 10 to 12° ipsilateral to the area centralis could be represented.

MOVEMENT FIELDS

Some units produce discharges in relation to eye movements—*movement-related neurones*—the discharge preceding the movement and having a maximal value for a particular direction and amplitude, so that, in addition to the *receptive field* of the tectal unit we may plot a *movement field*, the region in space to which the eyes must be directed to obtain a discharge in the tectal unit.[28]

Recording and Stimulation at Same Sites

Figure 25.47 indicates graphically the correspondence between receptive fields, indicated by contours, of collicu-

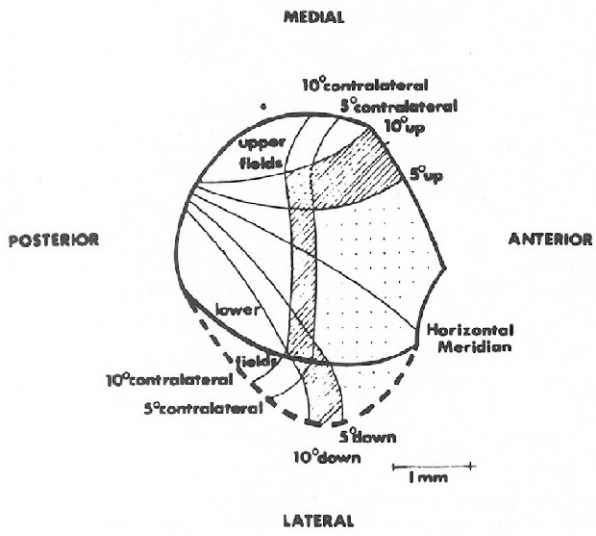

Fig. 25.46 Representation of the visual field on the surface of the right colliculus (as viewed from above in the Horsley-Clarke plane). The stippled area represents parts of the contralateral visual field within 5° of the fovea. Striped and stippled areas combined represent parts of the contralateral visual field within 10° of the fovea. (Cynader & Berman, *J. Neurophysiol.*)

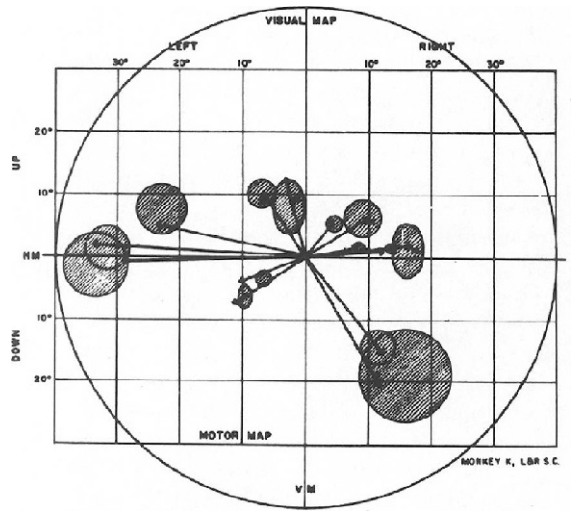

Fig. 25.47 Effects of recording and stimulation in the superficial layers of the superior colliculus. The visual map with the receptive fields of 14 units is superimposed on the motor map with its arrows representing the electrically elicited saccades at each of the 14 sites. The length of each arrow represents the mean length of 8–14 stimulation-elicited saccades; the direction of each arrow represents the mean direction of saccades. HM = horizontal meridian, VM = vertical meridian. (Schiller & Stryker, *J. Neurophysiol.*)

lar neurones and the directions and magnitudes of saccades evoked by stimulation of the particular collicular unit, so that these units, in the superficial layers, elicited saccades that directed the eyes to the point in space that caused an evoked response.[29]

Neck and Eye-muscle Afferent Inputs

If the superior colliculi are to act as integrating centres, controlling movements of both head and eyes, we must expect to find collicular neurones responsive, not only to visual input, but also to proprioceptors from neck and eye-muscles. Thus it is well established that neck-muscle receptors are concerned in tonic neck and eye reflexes in the decerebrate cat (Carpenter, 1972; McCouch *et al.* 1951). Abrahams & Rose (1975) found a powerful projection from the neck-muscles of the cat to the superior colliculus, long-latency responses to neck-muscle afferent stimulation being predominantly in the superficial layer, whilst short-latency responses were found in the intermediate and deep layers, predominating in the tegmentum. Projection from the extraocular muscles constituted the single richest projection, long-latency responses being the most common.

Vestibular Competition

In order that visually and neck-operated responses may act effectively, it might often be necessary to inhibit vestibular reflexes (p. 677) operating in an opposite sense to that required; there is little doubt from the work of Abrahams (1972) that receptors in the neck can inhibit or excite vestibulospinal output.

Colliculo-pontine Relations

Neuronal connections between the superior colliculus and the pontine reticular formation have been demonstrated (Kawamura, 1974; Harting, 1977). Raybourn & Keller (1977) identified units in the pontine reticular formation, characterizing them as those whose discharges could be related in some manner to eye movements or fixation (EMR) and another group that could not (NEMR). Among the eye-movement related (EMR) neurones they found that those that discharged with a long lead (some 50 to 250 msec) to saccade onset were synaptically activated by collicular stimulation, with latencies varying from 2 to 5 msec, indicating mono- and disynaptic activation. Interestingly, any long-lead burst neurone could be activated from all spatial locations within the colliculus, indicating a strong convergence of input. The medium-lead neurones, presumably most directly connected with the motor neurones, could only be activated with strong collicular stimulation, strong enough to evoke saccades directly; and so these medium-lead neurones appeared to be tightly coupled to the occurrence of the saccade but not to direct input from the colliculus. Pause units, namely those that were inhibited before and for the duration of a saccade, were all activated synaptically by the colliculus; latencies were consistent

with monosynaptic activation. That the colliculus was not responsible for maintained activity of pause cells was clear from the fact the some pause units were not affected by collicular stimuli. Tonic and burst-tonic units were activated by the colliculus at latencies excluding monosynaptic activation.

Types of Response and Location of Neurones

The features of the discharges of collicular neurones in relation to visual stimuli that normally led to fixation movements have been described in a series of now classical papers by Wurtz and his colleagues. The basic features of the receptive fields have been described earlier, and our interest here is in the relation of collicular neurones to eye movement, whether induced by visual and other peripheral stimuli, or occurring spontaneously. We may review, here, his study of neuronal activity as related to depth within the colliculus (Mohler & Wurtz, 1976). Neurones in the most superficial layers responded to visual input but did not discharge in association with eye movements. The next, deeper, type was also visually responsive and discharged before movements of the eyes to a restricted part of the visual field, the *movement-field.* This was defined as the outline in space where movement from the fixation point to another point in the visual field is preceded by an increase in rate of discharge. Deeper still, cells responded before eye movements but were usually visually unresponsive. Thus the visually responsive cells are located in the superficial layers, and the movement-related cells in the deeper layers; interestingly, the receptive fields of the superficially located cells are in register with the movement-fields of the deeper neurones; and it has been suggested (Schiller & Koerner, 1971) that efferent impulses from the superficial cells activate the deeper ones; however, according to Edwards (1980), a direct pathway between the two divisions of the colliculus has yet to be demonstrated. As the electrode penetrated deeper amongst the movement-related cells, the interval between the initiation of a saccade and the beginning of the discharge increased from some 50 msec to 150–150 msec. The deeper the cells, moreover, the longer the discharge. Another feature was that the size of the movement-field increased with depth. It was noted that the movement-related cells could also be responsive to visual stimuli, and that the number with both characteristics was highest in the superficial layers.

Visually Triggered Movement-related Cells

At the zone of transition of the two main types of cell, Mohler & Wurtz (1976) found units that discharged before eye movements and which were visually triggered, i.e., they discharged when the monkey made a saccade towards an object presented to the visual field, but they failed to make this discharge when the movement was spontaneous. These cells were thus visually triggered, but they showed two bursts, of discharge, namely an initial burst in response to the appearance of the target—the *visual response*—and the *movement-related discharge.* These visually triggered cells had the smallest movement-fields and had the shortest lead-times; the movement-fields were of about the same size as the visual receptive fields. Experimentally it was possible to dissociate the burst of discharge from the occurrence of an actual eye movement. Thus the monkey would be looking at a fixation point, and a new visual stimulus would be presented at a different point, as in the usual tests. If the fixation point was extinguished, and the visual target was turned on for only 100 to 200 msec and then the fixation point was turned on again, the monkey sometimes made saccades to the target and sometimes not. Even when no saccade occurred, there was a strong discharge which could not have been a simple visual response since this cell showed only a weak visual response. Thus these eye-movement cells could discharge at the time appropriate for association with a saccade, even though no saccade occurred; so that the discharge could easily be looked upon as a command for eye movements. It appeared, too, that the discharge was prominent if the monkey anticipated the requirement for a saccade rather than if this occurred randomly. Thus the characteristics of the movement-cells seem more closely related to the monkey's *readiness* to make a movement than to its actual execution.

Co-ordinators

Mohler & Wurtz suggested that these visually triggered movement-cells were, in fact, co-ordinating visual and movement information, providing some higher centre with this combined information rather than being concerned in the execution of the movement as such. Their anatomical location at the junction between the regions where the purely visually responsive and the 'ordinary' movement-related cells occurred would favour this function; and the similarity in magnitude of receptive fields would be consonant with such a function. It is possible, then, that the visually triggered movement-cell represents the culmination of one line of collicular processing, and it may be an important efferent neurone from the superior colliculus.

This processing would be from above—visual—and below—movement-related—and would represent a convergence of information, the source of the visual input being the retinal and cortical inputs to the superficial layers; the source of the movement-related input is not clear, however, but the fact that their activity begins before that in more superficial layers rules out the superficial collicular cells as the origin. A final possibility is that

of parallel inputs and outputs without vertical interaction in the colliculus.

Enhancement

Wurtz & Goldberg (1972) observed an enhancement of a collicular neurone's tonic discharge if the eyes made a movement towards a light-stimulus rather than being made without this stimulus. This *enhancement* was studied in greater detail by Wurtz & Mohler (1976). It was shown to be highly specific for the direction and extent of the saccade, so that a maximal enhancement was obtained when the eyes fixated the centre of the receptive field of the collicular neurone, and fell off with distance away from here. Wurtz and Mohler concluded that it resulted from an input from the deeper, movement-related, cells; thus if the monkey was trained to make a hand, rather than an eye, response to the visual stimulus the enhancement was not present.

Agent for Readiness

The main problem, of course, is the relation between the processing within the colliculus, as revealed by these visually and movement-related discharges, and the actual discharges to the motor neurones that determine the movement. The visual input apparently induces a readiness to respond in the superficial collicular neurones, mediated possibly through a parallel input to the deeper cells; and as a result, the eyes are finally directed towards a specific region of the visual field. Thus the colliculus is acting as an agent for readiness-to-respond rather than as the initiator, and as such it facilitates eye movements rather than initiates them, so that lesions in the colliculus may increase latency of movements and only slightly decrease the accuracy.

Retinal Error Signal

Schiller & Koerner (1971) suggested that the function of the colliculus was to encode the position of the visual target in relation to the fovea, deriving a retinal error-signal that was transmitted to the saccade-generating system. Since the map of movement-fields in the deeper layers corresponds with the map of the receptive fields of the overlying neurones, it was suggested that the superficial neurones triggered activity in the deeper neurones that led to a retinotopically triggered signal to lower motor centres. We have seen, however, that the error-signal is more complex, requiring not only the retinal position of the target but a knowledge of eye-position in the orbit, so the question arises as to whether this more complex integration process occurs in the colliculus; in which case the motor signals will be encoded on a spatial rather than a retinal basis.

Types of Neurone

Mays & Sparks (1980a) have discussed this problem in the light of their elaborate examination of collicular neurones, studied with stimuli that enabled a separation of visual from movement-induced responses. They categorized neurones as (1) *Visual cells*, responding only to a visual stimulus appearing in their receptive fields; these matched those described by Schiller *et al.* (1974), which were independent of visual cortical activity and were presumably activated directly by the retina. (2) *Saccade-Related Cells* (*SR*); these discharged just prior to a saccade and were not dependent on a visual stimulus and were probably the same as those described by others as discharging before spontaneous saccades in the dark (e.g. Mohler & Wurtz, 1976). Others, described by Mohler & Wurtz (1976), were either partially or completely dependent on a direct saccade target to produce the saccade-related discharge, and called *visually triggered motor cells* (*VTM*). According to Mays & Sparks, this type of neurone only required a brief appearance of a visual target in that part of the visual field that corresponded to the movement-field of the saccade-related neurone. (3) *Long-Lead SR Cells.* These gave sustained activity, preceding saccades by several hundred milliseconds, activity that was not triggered visually. This pre-pulse activity could sometimes be dissociated from any saccade activity, and might have indicated some integrating activity. Finally (4) there were *Quasivisual cells*, being neither purely motor nor visual; they appeared similar to those collicular cells that Wurtz & Mohler (1976) described as 'enhanced', showing an increased visual discharge when the stimulus was also used as a saccade target.

LINKAGE OF VISUAL AND SACCADE ACTIVITY

The few units that were saccade-related but also depended on a visual target might be concerned with the postulated direct link between the superficial and deeper layers, although the connections of the visual cortex with the deeper layers provides a different pathway.

ERROR SIGNALS

Mays & Sparks (1980b) suggested that the colliculus might well contain neurones that could encode not only the retinal error but also the other error-signals that make the saccade reach its target in spite of changed eye-position. Thus the saccade-related (SR) neurones were shown, by using the double-saccade paradigm of Hallett & Lightstone (1976), to have fully encoded eye-position and retinal error signals, so that they were capable of triggering a saccade to the correct position. In a more recent study, Sparks & Porter (1983) confirmed that the

intermediate layers of the colliculus contain neurones that encode the errors due to induced eye movements during a saccade, and are therefore capable of producing saccades that compensate for these movements.

Role of Proprioception from the Neck

Robinson & Jarvis (1974) studied eye and head movements in the monkey when the head was unrestrained; analysis of the records showed that the discharges in the superior collicular neurones that were related to the saccades were quite unrelated to head movements. For example, when the head moved, vestibular inhibition of the eye movement occurred, but the superior colliculus discharge was unaffected, and the actual command was made as though the head had not made a movement in contributing to fixation. Thus the collicular cell discharges in relation to the programmed saccade rather than to the accomplished eye movement, so that the superior colliculus does not receive input that enables it to modify the saccade command, this being done presumably at a lower level.

Lesions

Wurtz & Goldberg (1972) identified collicular neurones in the alert monkey and measured their receptive fields. They then caused the monkey to make saccades into the field, measuring accuracy and latency. An electrolytic lesion was finally made at the recording site and once again saccade measurements were made. The accuracy was unaffected, but latencies increased above the normal average of 300 msec to as much as 500 msec. The latency of a saccade was always larger when it was directed to a point in the receptive field of the lesioned region than when directed to other parts of the visual field.

Periaqueductal Gray Matter (PAG)

Lesions here cause abnormal eye movements (*periaqueductal gray syndrome*). In the monkey, Kase *et al.* (1986) described neurones here that paused during saccades, preceding their onset by some 35 msec. Superior colliculus cells studied under the same conditions showed bursts with average lead-times of some 25 msec, so an involvement of the periaqueductal gray in elaboration of saccade signals was suggested, possibly operating through collicular neurones.

CORTICAL CENTRES

Occipital Cortex

The classical investigators of the function of the cerebral cortex observed contralaterally directed conjugate movements of the eyes in response to stimulation of area 17 in primates, the movements being apparently directed to the parts of the visual field that are projected to the cortex. Later work has largely confirmed this (Crosby & Henderson, 1948; Wagman *et al.*, 1958). According to these last workers, the occipital cortex may be divided into four quadrants by two planes; a midsagittal vertical plane dividing the cortex into a right and left half, and a roughly horizontal plane through the calcarine fissure. Two of these quadrants are illustrated in Fig. 25.48. The movements of the eyes were such as to direct the gaze away from the quadrant stimulated. In man, Foerster obtained eye movements by stimulating area 19.

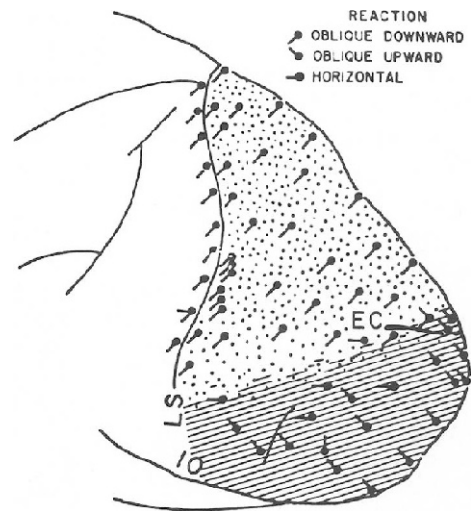

Fig. 25.48 Contralateral eye movements elicited upon stimulation of the dorsal, lateral and lateral inferior surfaces of the occipital lobe of *Macaca mulatta*. The solid circles indicate the points that were actually stimulated, whilst the lines originating at these circles indicate the direction of the contralateral eye movement in response to this stimulation. The dots outline the regions from whcih obliquely downward and contralateral deviations were obtained, whilst the shaded area indicates the region from which obliquely upward and contralateral deviations of the eyes were obtained. (Wagman *et al.*, *J. comp. Neurol.*)

Motor Area?

Wagman *et al.* raise the point as to whether the movement of the eyes is the result of stimulating a sensory region, evoking a sensation of light to which the animal responds, or whether the stimulus does, indeed, activate a motor centre. This question is probably somewhat academic since the modern tendency is to treat many areas of the brain as both sensory and motor. The finding that certain occipital lesions may impair motor activity without impairing vision (Bender *et al.*, 1957), and that in

human subjects eye movements that are not always associated with visual sensation may be evoked by electrical stimulation, suggests that there are, indeed, motor regions in the occipital cortex (Bickford *et al.*, 1953).

Effects of Striate Lesions

Immediately after striate lesions monkeys cannot make visually guided saccades to stationary or moving targets in the contralateral hemifield, although they can make spontaneous and target-searching saccades to all positions (Mohler & Wurtz, 1977).[30] Within a few months the animals recover the ability to make visually guided saccades to stationary targets in their defective hemifields. Tusa *et al.* (1986) found that, when the lesions extended beyond the striate area, the animals never regained this ability, so presumably the geniculostriate system was replaced by other parallel pathways that project to prestriate and other areas; these could be retinal-pretectal-cortical; retinal pulvinar-cortical, or retina-dorsal lateral geniculate nucleus-cortical.[31]

The Frontal Eye Fields

Classical Studies

Classical workers on the effects of cortical stimulation (Grünbaum & Sherrington, 1903; Foerster, 1931; Penfield & Boldrey, 1937) described a region in the frontal cortex close to the precentral gyrus, electrical stimulation of which evoked eye movements, and, in view of the proximity of the area (area 8) to the precentral Rolandic motor area concerned with voluntary somatic muscular control, it was suggested that this was a voluntary gaze centre.

Saccades

Robinson & Fuchs (1969) studied the waking monkey and controlled the stimulus strength whilst recording with precision the eye movements. The great majority of the eye-movements evoked by frontal field stimulation were single contralateral saccades occurring about 25 msec after initiating the stimulation; the amplitude and direction were determined by the position of the stimulating electrode; with continuous stimulation, as with the colliculus, a succession of saccades, spaced about 100 msec apart, took place until the mechanical limit of eye excursion was reached. Directions ranged from horizontal to almost vertical and the amplitudes form 1 to 70° (Fig. 25.49). Centring, smooth pursuit or nystagmus movements were never observed. The saccade had an all-or-none characteristic so that if the stimulus was below a certain strength there was no response; above the critical

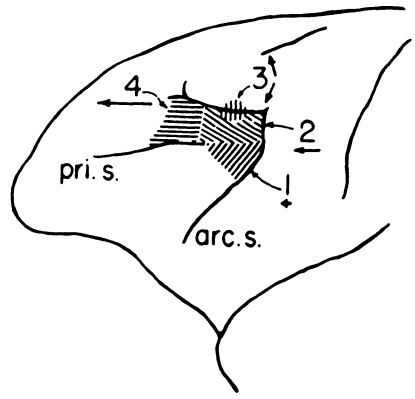

Fig. 25.49 Summary map of amplitude and direction of saccades evoked by stimulation of the frontal eye fields of a rhesus monkey (left cortex shown). Pri. s. = principal sulcus; Arc. s. = Arcuate sulcus. (Robinson & Fuchs, *J. Neurophysiol.*)

strength the size and direction of the saccade varied little with further increases.

COMPARISON WITH BRAINSTEM

In general, there was very little influence of eye position so that if a saccade of 10° to the left was produced by a stimulus when the eye was looking straight ahead, the response when the eye was looking 10° to the right would be such as to bring the eyes straight ahead. This is quite different from the goal-directed type of response to brainstem stimulation, described for example by Hyde & Eason (1959), in which stimulation causes the eyes to be directed to the same final point from any initial point.

ANAESTHESIA

Studies on the effects of anaesthesia, which demanded much larger stimulus currents, indicated that responses such as vergence, slow following type movements, and nystagmus, were due to this agent.

TWO-POINT STIMULATION

When two points, producing by themselves saccades of different direction and amplitude, were stimulated simultaneously the resulting saccade lost its all-or-nothing character, its direction and amplitude depending on the relative stimulus strengths. When bilateral two-point stimulation was employed, the result depended on the time-interval between the two stimuli; if this was less than 30 msec, the two responses interfered with each other, the second tending to cancel, in mid-flight, the first saccade and replacing it by all or a fraction of its own. When the stimuli were simultaneous then a single saccade was evoked which could be graded in size and duration, just as with two-point unilateral stimulation.

CONTROL OF DURATION OF DISCHARGE

The authors emphasize that control over the amplitude of a saccade represents essentially control over the duration of activation of the eye muscles and not over the intensity of stimulation, since the muscular activity is virtually maximum at the beginning of any saccade. The cortical control is determined, not by how many cortical fibres are excited, since once the threshold is exceeded the size of the saccade is unchanged with increasing current-strength and therefore increasing numbers of excited cortical cells. Thus control is governed by *which* cortical cells are excited, and these cells must influence the brainstem neural networks that control the duration of the discharge to the motor neurones. When two cortical points are stimulated, in some way the midbrain circuits are influenced by the two cortical inputs to strike a compromise to produce a pulse-width of discharge intermediate between the two evoked separately.

Activities of Cortical Units

By inserting an electrode into area 8, Bizzi (1967) recorded from single units that altered their discharge-rate when the eyes moved, the final rate of discharge being a function of the direction of gaze; the interesting feature of these cells was that the change of discharge only occurred *after* the movement had been initiated, so that Bizzi postulated that this area of the cortex was only concerned with the tonic control of eye position after a movement had been made. He points out that, in the monkey, ablation of area 8 only leads to paralysis of eye movements for a few days (Pasik & Pasik, 1964). In a later study (1968) these cortical neurones were found to be of two types: *Type I*, which fired during voluntary saccades or the quick phase of nystagmus in a given direction, whilst they were silent during the slow phase; and *Type II*, which discharged during fixation of gaze in a specific direction as well as during smooth pursuit movements. When the head was allowed to move as well as the eyes the same pattern of discharge in Type I and II neurones was observed, so that the slow compensatory following movements that followed the head movement were accompanied by Type II discharge. A further group of neurones were found discharging in association with the head movement, some were specific so far as direction was concerned, others not. Discharge in head neurones occurred *prior* to rotation whilst, as we have seen, the eye neurones discharged after (Bizzi & Schiller, 1970).

Visual Receptive Fields

Mohler *et al.* (1973) described the visual responses to area 8 cortical neurones of the monkey; in their sample, some 47% of recorded neurones responded only to visual stimuli and not in association with saccades. The response was usually a vigorous ON-discharge with latencies of 50–120 msec; there was little tonic discharge and no OFF-response. Receptive fields were always large, usually a whole quadrant or hemifield in the contralateral visual field but extending also into the ipsilateral field. There was no orientation-selectivity and no effect of increasing the size of a stimulus. Clearly the neurones are not concerned in spatial analysis.

Neurones Discharging before Saccades

Bruce & Goldberg (1985) have discussed the early studies of frontal neurones, which seemed to indicate that they were not concerned in initiating saccades; thus those studied by Bizzi (1968) and Bizzi & Schiller (1970) failed to discharge before a saccade. In their own studies on waking monkey neurones in the periarcuate region, they found 54% of neurones that discharged before saccades. Recordings were made on monkeys that had been trained to perform certain tasks involving making a saccade to a spot of light presented in the peripheral field, the signal for making the saccade being the extinguishing of the initial fixation point. These tasks are illustrated in Fig. 25.50; they include the 'no-saccade task' in which the monkey is trained not to fixate the new stimulus, S_2; by testing with the various tasks it was possible to describe a number of different types of presaccadic activity, a given type not necessarily being confined to a single cell. The activities were described as *visual*, in response to visual stimuli whether or not the monkey made saccades; *movement activity* preceded purposive saccades, even those made without visual targets, and *anticipatory activity* preceded even the cue to make a saccade if the monkey could reliably predict what saccade it had to make.

MOVEMENT CELLS

These presaccadic neurones discharged as briskly with and without a visual target, and were only weakly responsive to visual stimuli.

VISUOMOVEMENT CELLS

These discharged most briskly before visually guided movements, but also before purposive eye movements made in darkness, and responded to visual stimuli in the absence of saccades. In this class there was a continuum of features, varying from cells in which visual activity predominated to cells in which movement activity predominated, so that the assignment to a third class may not really be justified.

ANTICIPATORY ACTIVITY

This was revealed when the monkey was presented with a visual stimulus and was rewarded on making a correct saccade to it, by contrast with the situation when the stimulus appeared but it had been trained not to fixate the

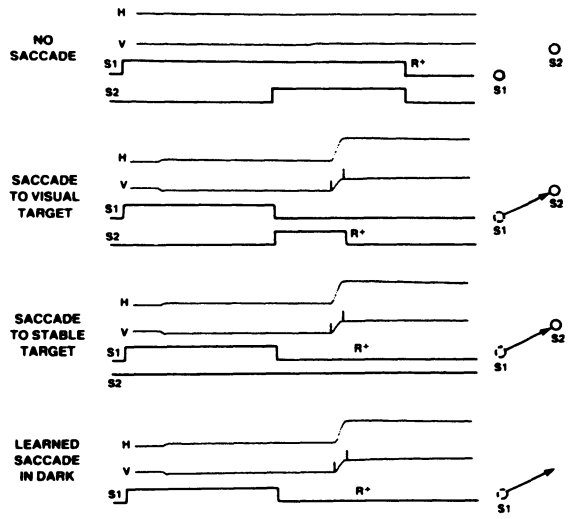

Fig. 25.50 Behavioural paradigms. Horizontal and vertical eye position (H and V) and stimulus traces (S1 and S2) are shown for each of four tasks. In NO SACCADE task S1 appears and remains on. Monkey fixates S1 and does not break gaze to look at S2 when it appears (upward deflection in S2 trace) or disappears (downward deflection). He is rewarded (R+) for either releasing a bar at the dimming of S1 or merely for maintaining proper eye position. Cartoon at the right shows that no eye movement is made. In SACCADE TO VISUAL TARGET S1 disappears when S2 appears and monkey makes saccades to fixate S2, as indicated by *arrow* in cartoon. *Ticks* at saccade beginning and end in vertical eye trace signal computer's on-line recognition of the saccade. In SACCADE TO STABLE TARGET S2 is always on. Signal to saccade from S1 to S2 is the disappearance of S1, indicated by the downward deflection in the S1 trace. Cartoon shows the saccade from S1 to S2. In the LEARNED SACCADE task, monkey makes a saccade to where S2 had been in previous trials. Signal to make eye movement is disappearance of S1. Cartoon shows that saccade is made in absence of a target. (Bruce & Goldberg, *J. Neurophysiol.*)

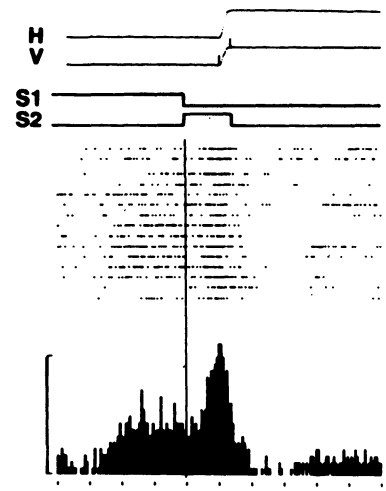

Fig. 25.51 Anticipatory activity of a visuomovement cell showing activity during a series of visually guided saccades. In these trials the monkey was directly rewarded for making the saccade. The trials were synchronized on stimulus-onset. Calibration line at the left of histogram represents a discharge rate of 100 Hz. (Bruce & Goldberg, *J. Neurophysiol.*)

new target. Figure 25.51 illustrates this; the up-movement of S_2 indicates onset of the peripheral spot which occurs as the fixation stimulus is extinguished (downward movement of S1). Strong activity occurs well before the saccade, as indicated by the top trace of H and V. With 'no-saccade' trials, in which the peripheral spot, S_2 appeared but the monkey was trained not to make a saccade, there was very little activity. Figure 25.52A illustrates a visual cell, responding to stimulus onset but not during the saccade. Figure 25.52B illustrates a visuomovement cell, responding at stimulus onset and also during the saccade. Figure 25.52C illustrates a cell that responded with a burst around saccade onset but with no response to the onset of the visual stimulus, a typical movement cell.

DIRECTION AND AMPLITUDE

As we should expect, given neurones exhibited preferential directions so far as the intensity of the presaccadic

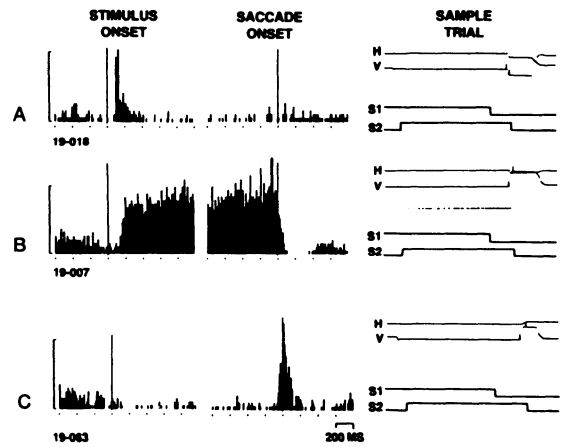

Fig. 25.52 Timing of responses to stimulus onset and eye movement in stable target saccade task. Each row contains a histogram aligned on target onset, a histogram of same trials aligned on saccade onset, and a representative record of a single trial showing eye position (H for horizontal, V for vertical), stimulus position (S1 the original fixation point, S2 the saccade traget), and cell discharge (*dots* between the position and stimulus traces). First row shows a visual cell that discharged in response to stimulus onset, but not in response to movement. Second row shows a visuomovement cell discharging in response to onset, of stimulus and maintaining discharge until eye movement triggered by subsequent disappearance of fixation point. Bottom row shows response of a movement cell that discharged in a burst around movement, and not at all to stimulus. All calibration lines signify a discharge rate of 100 Hz. (Bruce & Goldberg, *J. Neurophysiol.*)

activity was concerned, so that a tuning-index could be computed; this was remarkably broad, indicating that the brain must fashion an adequate saccade by recruiting a precise assembly of neurones rather than depending on the activity of a few highly tuned neurones. A similar broad tuning was observed when amplitudes of saccades were studied; in general, there was an optimal amplitude of saccade that produced maximum presaccadic discharge, but its quantification was more complex than that for direction.

SUPPRESSION OF PRESACCADIC ACTIVITY

A sharp suppression of response following the performance of a saccade was always observed, so sharp as to suggest an inhibitory activity, and this was confirmed.

POST-SACCADIC DISCHARGE

At least 16% of presaccadic neurones exhibited a discharge after the execution of the saccade; this was when the saccade was in a direction opposite to that which had produced the presaccadic discharge; this was not dependent on purposive oculomotor behaviour but also followed spontaneous saccades. Bruce & Goldberg considered that the purely visual responses of frontal eye-field neurones were a reflection of the process of targeting the eyes to a visually perceived point in space, rather than acting to analyse the spatial features of the field; thus, by continuing after the target disappears, the tonic activity could direct the oculomotor centres accurately to produce the eye-movement required. This activity is promptly terminated by the eye movement, a desirable feature. In some respects the visual responses resemble those of the colliculus, having saccade-related enhancement and suppression of activity (p. 710). Presaccadic activity is clearly related to the performance of a purposive saccade, activity that is presumably transmitted to the lower oculomotor centres such as the superior collliculi.[32]

MICROSTIMULATION

Bruce *et al.* (1985) examined the effects of electrical stimulation of neurones that had already been characterized with respect to their discharges during eye movements. They studied one group that showed presaccadic activity, and two other groups that lacked this feature; thus the second group discharged in response to visual targets whether or not the stimuli were saccade targets. In the third group the presence of movement activity was ambiguous. The presaccadically discharging neurones were those of most interest, i.e. visuomovement and movement neurones; thus, thresholds for visual and post-saccadic cells were much higher, and it seemed likely that they were concerned with processing visual information that would be used for developing the final signal for eye movement, whereas the presaccadically discharging neurones would be concerned with passing the saccade signal to lower centres. When the cell was characterized it was stimulated, and the response related to this characterization. This relation was very obvious, as illustrated by Fig. 25.53 where the graphs show the presaccadic discharges evoked in a single unit when the direction of the saccade was varied. The vertical lines indicate the

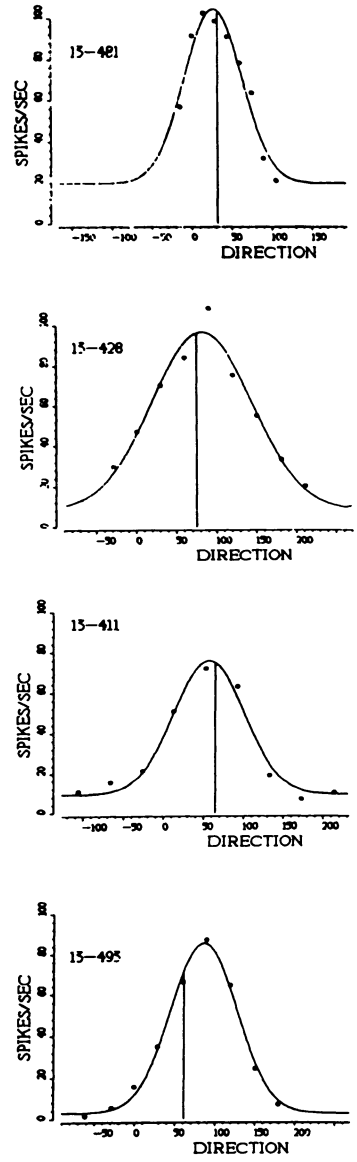

Fig. 25.53 Correlation of movement-fields of neurones with saccades evoked by electrical stimulation at the site of the neurones. The graphs show the relationship between cell discharge and direction of eye movement at the optimum amplitude for each cell. Direction is in degrees of arc, with 0 representing horizontal rightward, by convention. The vertical line through the graph shows the median direction of electrically elicited saccades at the site of the cell. (Bruce *et al.*, *J. Neurophysiol.*)

median direction of electrically elicited saccades at the site of the cell. A similar correlation was found with the amplitude of saccades. With cells responding post-saccadically, no such relationship was observed; and it was concluded that it was presaccadic activity that was most closely related to eye movement, as we should expect of a centre concerned with the planning of a scaccade.

Definition of Frontal Eye Fields On the basis of their microstimulation studies, using low-amperage stimuli ($\leqslant 50\ \mu A$), Bruce *et al.* (1985) defined the limits of the frontal eye fields; the surface projection of the arcuate sulcus in which low-threshold units are found is illustrated by Fig. 25.54; however, the region is largely buried in the anterior bank of the arcuate sulcus and extends only a few millimetres on to the surface of the prearcuate gyrus; it probably encompasses some 80 mm^2 of cortex in each hemisphere. This region is smaller than Brodmann's area 8 and corresponds better with Walker's area 8A and area 45 (Walker, 1940).

Nature of the Saccades Depending on the site of stimulation, practically any saccade could be elicited, both with respect to amplitude ($< 1°$ to $> 30°$) and direction. There was some topographical organization with respect to amplitude, but none with respect to direction. However, this was well organized at a local level, so that, as an electrode penetrated deeper the direction of the saccade shifted systematically, with electrode movements of 0.25 to 0.55 mm.

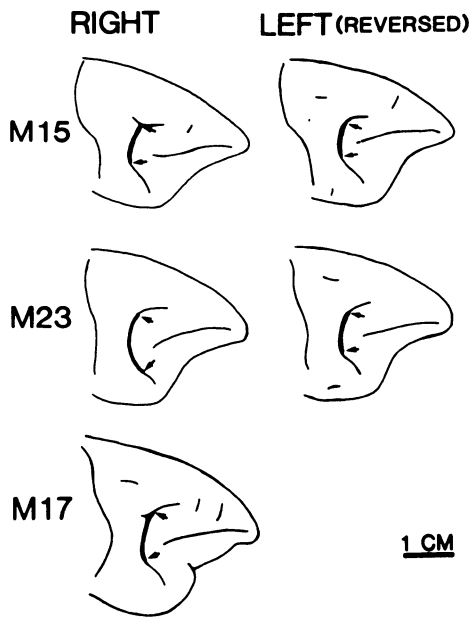

Fig. 25.54 Location of the frontal eye fields. The low-threshold frontal eye fields in five different hemispheres of three cynomolgus monkeys. The surface projection of the arcuate sulcus in which low-threshold saccades were found in the anterior bank is shown as the *darkened line* between two arrows. Each hemisphere is shown in a view looking directly down on the principal sulcus, with the central sulcus shown as the far-left landmark of each drawing, and the front of the brain on the right. (Bruce *et al.*, *J. Neurophysiol.*)

Slow Eye Movements At some sites microstimulation evoked slow eye movements, continuing for the duration of the stimulation; these stimulations might well have been producing, artifiically, slow pursuit movements, since at some of the sites the cells exhibited a discharge during visually guided pursuit movement. In general, Bruce *et al.* concluded that the activity of visuomovement and movement cells constituted the frontal eye-field signal that triggered particular saccades, and that electrical stimulation of the frontal eye field elicited saccades of the same direction and amplitude by exciting these neurones.

Laminar Location of Low-threshold Sites The sites were usually in the infragranular laminae; cortical projections to the superior colliculus, thalamus and brainstem originate in the pyramidal cells of lamine 5 and 6, so that the exciting electrode could well have been here. Whether or not the higher-threshold visual and post-saccadic cells are located in supragranular laminae remains to be proved.

Latencies The variable latencies of responses to electrical stimulation presumably reflect alternate pathways from the frontal eye field to the lower oculomotor centres. In the present work, involving relatively weak stimuli, latencies varied from 20 to 60 msec, with 30–45 msec being typical. These are longer than those found by Robinson & Fuchs (1969), using much higher stimulating currents, presumably because the higher currents were able to stimulate neurones employing more direct routes. The routes, as indicated earlier, are firstly through the massive projection to the intermediate layers of the superior colliculus, and a less direct route to this centre by way of the caudate nucleus and substantia nigra; secondly, the mediodorsal nucleus of the thalamus, and thirdly, the direct projections to several premotor nuclei of the brainstem including the paramedian pontine reticular formation, which is considered to contain the saccade generator of the brainstem (Robinson, 1981).

Projections

The frontal eye fields do not project directly to the motor nuclei of the extraocular muscles, in this way differing from the precentral motor cortex (area 4) which, through pyramidal tract neurones, exerts control over individual somatic muscles. The pathway is independent of the occipital cortex, since ablation of this does not affect eye movements obtained by stimulation of

area 8. Astruc (1971) made limited ablations in area 8 of the monkey and followed degeneration; the superior colliculi and the pretectal area were the main midbrain recipients; pontine nuclei also received projection, as well as certain thalamic regions; there was no projection caudal to the pons. Using autoradiographic techniques, Kunzle & Akert (1977), after injections of ^{3}H-proline into area 8, described cortical uptake of tracer in areas 4 and 9 within a few mm of the injection site; other cortical uptakes were area 7 and area 19 at the caudal end of the sulcus intraparietalis, and on the anterior bank of the superior temporal sulcus, a region they described as the superior temporal sulcus (STS). This region receives a convergent input from auditory, somatic and visual association cortex as well as direct afferents from the striate and prestriate regions. The intraparietal sulcus (IPS) also receives a powerful projection from area 5 and the striate and prestriate regions. Subcortical projections included the superior colliculi, mainly to the stratum zonale, stratum opticum and stratum griseum intermedium, regions corresponding to the striate and retinal projections. Projection to the dorsolateral pontine nucleus puts area 8 in connection with the cerebellum, which is related to the oculomotor muscle nuclei by way of the fastigial nucleus. Leichnetz (1982), using both antero- and retrograde labelling with horseradish peroxidase, emphasized a prominent afferent input from the nucleus of the optic tract and suprageniculate nucleus, the former giving access of visual input by way of the pretectum to area 8. Leichnetz suggested that the projection to the pretectal area might be concerned with pupillary activity, which could accompany, or be independent of, eye movements; there was no direct connection to the Edinger-Westphal nucleus.

PARAMEDIAN PONTINE RETICULAR FORMATION

Of most interest is a projection to this brainstem region so intimately concerned with programming saccade movements. Leichnetz *et al.* (1984a, b) made implants of horseradish peroxidase in this region and showed that a main source of projection was the frontal eye field.

Effects of Lesions

Schiller *et al.* (1980) found only temporary defects in performance of monkeys following frontal eye field ablations; the animals tended to neglect the contralateral visual hemifield, making fewer saccades to peripheral targets. Recovery was virtually complete in 2–4 weeks. Superior colliculus ablations reduced fixation accuracy, saccade frequency and saccade velocity, with little recovery with time. Ablations of both regions caused serious effects on visually triggered movements; the animals could not fixate with accuracy, the range of eye movements was reduced as were the frequency and velocity of saccades. Schiller *et al.* concluded that, for visually triggered saccades, there were two parallel channels, the one involving the superior colliculus and the other the frontal eye field.

STRIATE AND COLLICULAR LESIONS

Mohler & Wurtz (1977) measured the accuracy of saccades made by monkeys to points in the visual field that were represented by corresponding points on the retinotopic maps of cortex and superior colliculus. After ablation of the cortical region corresponding to a given point, then the only defect was the requirement of a stronger light-stimulus to induce the saccade, and within about a month accuracy was normal. With collicular lesions there were defects in accuracy of saccades, and double saccades had usually to be made to fixate the stimulus. With joint lesions the monkey was blind to the spot corresponding to the lesions, so no saccades were made. The authors considered that both visual centres cooperated normally in governing eye movements, rather than viewing the two systems as a mark of redundancy in the nervous pathway.

SUPERIOR COLLICULUS ABLATIONS

The shifts of gaze induced by frontal eye-field stimulation were unaffected by ablation of the superior colliculus in *Macaca fasciculus* (Schiller, 1977). This is in contrast to the responses to striate, prestriate and parietal stimulation, when eye movements were silenced (Keating *et al.*, 1983). The role of the superior colliculus in these occipital and parietal oculomotor pathways has been discussed in this connection; thus although the striate cortex projects to the superior colliculus, this is to the superficial layers, so routes through the frontal eye field or the parietal cortex to the colliculus have been considered but rejected; thus lesions in parietal area 7 did not affect eye-movement responses to striate and prestriate stimulation.

Frontal Dorsomedial Cortex

The cortical activity preceding eye movements described by Bizzi and by Bruce & Goldberg depended on a visual stimulus, being induced typically, in Bruce & Goldberg's experiments, by training the monkey to fixate a spot of light and then to make a saccade to another spot appearing in the periphery. Schlag & Schlag-Rey (1985) asked whether there were a true voluntary centre that operated independently of a visual clue. They considered that the so-called supplementary motor area, distinct from the Rolandic prefrontal motor area, described by Woolsey (1952), might contain a region concerned with eye movements, and they probed frontal dorsomedial cortex outside the frontal eye field, a region said to project to the superior colliculus and other oculomotor centres (Leichnetz, 1980; 1982), and said by Brinkman & Porter (1979) to possess neurones related to vision and movements of the eyes. The area they examined was at the dorsomedial edge of the superior frontal convolution at the antero-posterior level of the superior arcuate sulcus, equivalent to Vogt's area 6a, clearly separated by about 10 mm from the classically defined frontal eye field. They found units that definitely fired before exploratory saccades (Fig. 25.55), and some were active exclusively with

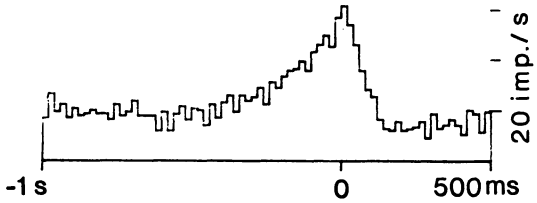

Fig. 25.55 Perisaccadic histogram of frontal eye fields neurone, discharging with increased rate before downward spontaneous saccades. Saccade onset was at time zero. (Schlag & Schlag-Rey, *Exp. Brain Res.*)

spontaneous saccades and not with visually triggered movements.

The Thalamus

There is a region in the thalamus that forms a link between the superior colliculus, cortical frontal eye field and the posterior parietal cortex; this region, in and around the internal medullary lamina, contains neurones that are responsive to visual stimuli and exhibit activity with eye movements (Schlag *et al.*, 1974; Schlag-Rey & Schlag, 1977). Schlag-Rey & Schlag (1984) implanted electrodes in waking monkeys and observed responses of thalamic neurones during spontaneous eye movements; their electrodes were centred on the internal medullary lamina, which comprises n. centralis lateralis (CL), centralis superior lateralis (CSL) and paracentralis (Pc). They suggested that their results indicated that the main function of the thalamic system that they were studying was to provide cortical areas with information on gaze behaviour; in their own ways individual units signalled a particular moment during a shift of gaze, namely when the eye movement was about to begin, when it started, and when it stopped, where the eyes went and whether they stayed in this position. In a study of visually triggered responses (Schlag & Schlag-Rey, 1984) the units were shown to have large receptive fields, and to exhibit presaccadic bursts; and in general it was concluded that the units were concerned largely with holding of gaze. As to the actual mechanism, it was suggested that the thalamic region, by virtue of its widespread reciprocal connections, might be concerned with control signals, as opposed to elaborating specific eye movements which would depend on spatially organized input such as that received by the striate and prestriate cortex, superior colliculus, and so on. The control signals could determine the starting, stopping and distributing tasks in time and space.[33]

Substantia Nigra

This mesencephalic region is of great interest as the source of dopaminergic projections to the striatum (caudate and putamen), deficiencies in which are responsible for Parkinsonism, a disease in which deficiencies of the ability to make voluntary saccades is included in the general syndrome (Teräväinen & Calne, 1980). The part of the substantia nigra involved in this projection is the pars reticulata. The pars reticulata has been recognized recently as being one of the two major outputs of the striatum, the other being the globus pallidum. It receives afferents predominantly from the striatum and projects to the superior colliculus and thalamus, and is thus the major step between the basal ganglia and the thalamus and superior colliculus. The projection is to the intermediate layers of the colliculus, those closely connected with eye movements. In a series of papers, Hikosaka & Wurtz (1983a–d) have described nigral neurones that discharged, or suppressed their discharge, in relation to eye movements, with a variety of experimental paradigms in the monkey. Their experiments showed that neurones in the pars reticulata received visual signals and/or cognitive signals, e.g. those instrumental in execution of visual tasks requiring memory of position of the target; these neurones produced an output leading to saccadic eye movements. The signals are transmitted to the superior colliculus, which presumably is also receiving inputs from the frontal eye field, which then sends a signal to the brainstem oculomotor system.

Relation of Substantia Nigra to Superior Colliculus

The relation between substantia nigra neurones related to visuomotor activity and the superior colliculus was studied by Hikosaka & Wurtz (1983d) in order to prove that substantia nigra units were definitely involved in initiation of eye movements, rather than reflecting activity in other centres. They first identified the visual and oculomotor properties of a given substantia nigra cell; they then stimulated the ipsilateral colliculus at different points until they identified antidromic responses in the nigral cell. Finally they compared the visual and oculomotor properties of both collicular and nigral cell. The low-threshold collicular cell that was most probably related to a nigral cell was usually located in the intermediate layers. The saccade-related activities of pairs of cells located in this manner showed an inverse relationship, the burst of spikes in a collicular cell being associated with a diminution in the spontaneous discharge of the nigral cell. Thus substantia nigra cells show a high rate of spontaneous discharge (Joseph & Boussoud, 1985), probably tonically inhibiting collicular cells; a release of this tonic inhibition would therefore contribute to the generation of a burst of activity in the collicular cells, contributing to the initiation of the saccade. As Hikosaka & Wurtz have shown, however, the relation between the two types of neurone is not automatic, the substantia nigra neurones becoming active only under specific conditions e.g. when the saccade was memory-contingent.[34]

Posterior Parietal Cortex

Ferrier described two separate cortical eye-fields, the frontal one already considered, and a parieto-occipital one on the posterior parietal lobe, area 7a or PG, stimulation of which produced movements of the eyes. Ferrier also described a blink-response on stimulation of the inferior parietal lobule. Clinically, lesions in the posterior parietal region cause disorders of eye movements and loss of blinking in response to visual threat. This region contains several kinds of neurones related to visually guided movements. Thus Hyvärinen & Poranen (1974) found the majority of cells related to sensory function of the opposite side; many cells discharged when the sensory stimulus merely interested the monkey; some were clearly related to movement, and others to visual sensory stimuli. The sensory input, by no means purely visual, was likely to be from ascending sensory systems through cortico-cortical connections, and through the pulvinar. They considered the function of the system was to relate sensory input to motor output.[35] In a more elaborate study Lynch *et al.* (1977) emphasized that, although the majority of area 7 cells were visual, this was not in the usual sense, the cells not being activated directly by light, becoming active when the animal fixed gaze on objects of interest; another class became active while following a moving target, showing directional preference. They appreciated that, in order to define the features of neurones in this part of the brain, more elaborate tasks must be presented to the monkey than the simple ones usually adopted. They suggested that in the parietal lobe, there were mechanisms for directing visual attention, for the fixation of gaze on objects of interest, for maintaining visual grasp of an object if it moved slowly, and for loosening fixation and initiating rapid saccade towards new objects of interest presenting within the visual field. These functions they described as the positive image of the defects shown by lesions in the same cortex.

Types of Neurone

VISUAL FIXATION NEURONES

These accelerated their discharge synchronously with fixation on an object the animal desired, and continued until rewarded and then decreased abruptly. They also discharged while following within the gaze-field; 40% were suppressed during a saccade.

VISUAL TRACKING NEURONES

These were active during tracking of a slowly moving target but not during steady fixation; they were inhibited by a saccade.

SACCADE NEURONES

These discharged before and during a visually evoked, but not a spontaneous, saccade; the lead-time was about 75 msec. So far as the pathway to the eye muscles was concerned, the authors emphasized the similarity of the discharge-properties of paramedian pontine reticular cells; the cerebellum was ruled out as a station directly mediating area 7 activity by a cortico-ponto-cerebellar route.

Target and Background Movement

Visual tracking is a complex process, since in normal circumstances following a target involves both head and eye movements; head movements without appropriate eye movements will cause retinal slip, and this must be interpreted as the result of a head movement; similarly, the following of a small target against a structured background is associated with retinal slip of the main retinal image. Thus neurones with sensitivity to both movement of target and background are of interest; these were described by Sakata *et al.* (1980); again Robinson *et al.* (1978) found neurones in area 7a that responded to visual stimuli while the monkey maintained fixation on a stationary target; these neurones might well be responsible for messages indicating the movements of the background over the retina while the eye was tracking; responses that must be finally interpreted as a stationary background and a moving eye.

Visual Tracking Neurones

Disturbance of smooth pursuit movements is one of the common symptoms of parieto-occipital lesions in man (see, for example, Holmes, 1918). In patients with unilateral lesions, eye movements become saccadic during visual tracking towards the ipsilateral side. Monkeys with bilateral lesions including prestriate cortex showed severe and long-lasting deficits in visual tracking (Lynch, 1980). For this reason Sakata *et al.* (1983) studied these neurones in depth in the waking monkey, choosing as 'true tracking neurones' those that responded to a moving target in the dark and in the light, since a large number of neurones, formerly classified as tracking neurones, were found to be inactive when tracking in the dark. Most were found in the posterolateral part of area 7a, a region not examined in detail by earlier workers. These neurones showed a strong directional sensitivity when tracking, so that activity could be suppressed by movements opposite to the preferred direction. If the eye tracked in the dark, the response would be independent of any background stimulus that must arise through movement of the image of the background across the retina—retinal slip. Most showed a slower rate of discharge in the dark, but a few showed the opposite effect; thus it was concluded that most neurones were affected by the surrounding stimulus, usually inhibited. When the monkey fixated a central spot and maintained fixation in spite of a new moving spot in the periphery, this visual stimulus evoked a response that had a preferred direction, which could be the same as that for tracking—isodirectional—or opposite—antidirectional. Finally, the behaviour of a tracking neurone in the absence of a visual stimulus i.e. when the target was turned off for 0.5–1.0 sec during tracking, was studied; a majority of neurones maintained a significant fraction of their activity, suggesting that non-retinal signals were maintaining tracking, the retinal and non-retinal signals presumably converging on the area 7a neurone, as suggested by Fig. 25.56. In interpreting their results, Sakata *et al.* pointed to the behaviour of the antidirectional neurones; nearly all of these showed larger responses when tracking in the light than when tracking in the dark. This could

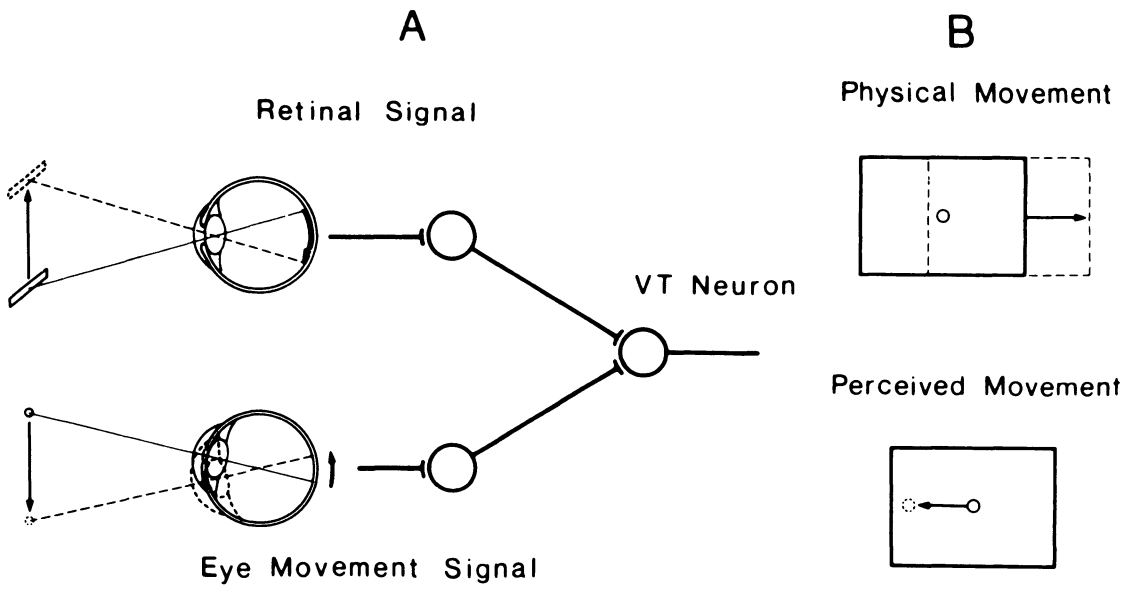

Fig. 25.56 A. Schematic neural circuit that may be involved in order that the retinal signal of image-motion and the extraretinal signal of eye-movement may converge on a single VT neurone of area 7a. B. Diagram to show the visual illusion of induced movement. (Sakata *et al.*, *J. Neurophysiol.*)

be explained by the fact that tracking against a fixed field in the light caused a retinal slip signal that added to the eye movement signal, the two converging on the tracking neurone. This convergence ensures maximum sensitivity to the movement of the target in the light. With the isodirectional neurones, on the other hand, the retinal signal moving in the opposite direction tended to suppress the tracking neurone, so that the response in the light was smaller than in the dark. Sakata *et al.* concluded that the antidirectional units were more likely to be concerned with perceived motion than with the control of eye movement. Thus many of the antidirectional units could be activated by moving a frame around a stationary fixation target; such a procedure induces an illusion of induced movement of the target in the opposite direction (Fig. 25.56B); this type of unit might be the origin of the illusion. Thus the perception of the movement of the pursued object depends both on the eye movement and the movement of the image of the background; antidirectional units are maximally activated under these conditions, and this corresponds with the greater accuracy of perceived movement when tracking across a stationary background. The isodirectional tracking unit was considered to be concerned with control of a smooth pursuit movement, summating the retinal slip response caused by movement of the target with the extraretinal signals indicating eye position, as suggested by Robinson's model (p. 737).

Saccade and Blinking

Shibutani *et al.* (1984) made electrode penetrations into area 7a of the monkey to determine points where saccades and blink-responses occurred as a result of microstimulation; Fig. 25.57 illustrates regions where saccades, blinking, and saccades plus blinking occurred; in a given penetration the directions and amplitudes of saccades were the same, with some shifts in these parameters with depth. Blinking, with a latencey of only 12 msec,

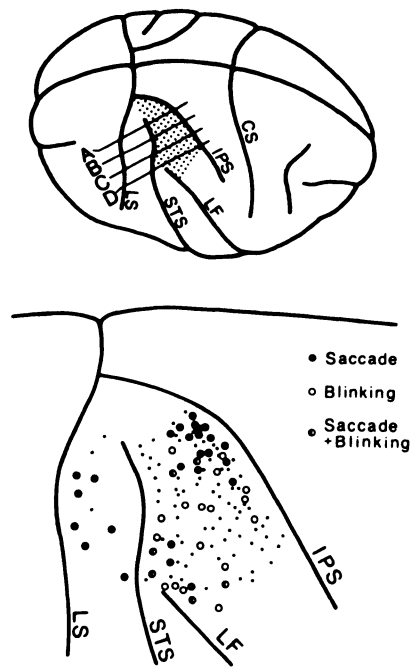

Fig. 25.57 Sites of stimulation in the parieto-occipital cortex. The lower part of the diagram indicates loci of penetrations plotted on the cortical surface. Open circles, filled circles, and half-filled circles indicate penetrations in which blinking, saccades, and both saccades and blinking were evoked, respectively. Small dots are those without effect. (Shibutani *et al.*, *Exp. Brain Res.*)

was a very regular type of response. Most units were also passive visual respone units, whilst many blink-units were sensitive to a plate moving towards the face, i.e. those that respond to a visual threat; lesions in this area abolished this threat-response (Holmes, 1918). Shibutani *et al.* pointed out similarities of these posterior parietal neurones to those of the frontal eye field and superior colliculus; the direction and amplitude of the saccades depended on the site of stimulation but were independent of the intensity of stimulation and the position of the eye. They considered that the parietal neurones probably linked the perception of approaching movement to the motor reaction of blinking. The actual routes for blinking include the frontal eye field (Jampel, 1960), the lateral-posterior pulvinar complex and pretectum (Schlag & Schlag-Rey, 1971) and the cerebellum (Ron & Robinson, 1973).

Object Movement versus Eye Movement

The same movement of the image of an external object on the retina can be achieved by movement of the object or movement of the eye when the object remains stationary. Sakata *et al.* (1985) described a neurone in area 7a of the parietal cortex that responded well to real movement of a slit but, when the eye moved across the stationary slit, failed to respond at all. This means, in essence, that, when eye-movement occurred, the response to movement of the retinal image was suppressed completely. Of some 25 neurones classed as passive visual, responding to movement of an object in space, seven behaved in this manner; eight gave the same response to both types of image-movement, and ten gave a smaller response to the self-induced movement than that with the real movement of the object.

Vestibular and Optokinetic Influences

The influence of vestibular stimuli on tracking was demonstrated by Kawano *et al.* (1984) who found that the responses of a typical visual tracking neurone were the same during pure eye tracking and when the same target moved across the visual field but the monkey was rotated in a chair so that fixation was maintained without significant eye movement. The cancellation of the vestibulo-ocular reflex provided the cortex with the appropriate signals. When monkeys were oscillated in a rotating chair in complete darkness while carrying out a visual tracking task, individual neurones fell into three classes. Of interest are their Class A neurones that were unaffected by these oscillations; they were considered to be analogous with the so-called 'gaze Purkinje cells' of the flocculus, whose firing patterns could be explained by the linear vector addition of components separately encoding velocities of the eyes and head; the weak effects of oscillations would be due to cancellation of the equal but opposite head and eye components

OPTOKINETIC NEURONES

Kawano & Sasaki (1984) defined a number of area 7a neurones as optokinetic because they responded to a rotating drum but did not respond to a small moving target or to saccadic eye movement. These neurones responded to visual tracking during foveal pursuit across a textured background, although they did not respond to foveal tracking in the dark; thus the movement of the background was the adequate stimulus, regardless of whether it was real or induced by eye movements.

Posterior Parietal and Frontal Eye Field Neurones

Goldberg & Bruce (1985) compared the activities of frontal eye field neurones with those of posterior parietal neurones with a view to assessing the importance of attention paid to a visual stimulus; thus lesions in both areas lead to the well known clinical syndrome of 'neglect'; an inability to respond to stimuli in a portion of the visual field (Critchley, 1953; Heilman & Valenstein, 1972). Monkeys were trained to perform tasks involving simple fixation; execution of a saccade, which could be directed to a visible target, or to a remembered target, the latter being executed in complete darkness and with no visual clue. In the peripheral attention task the monkey received a peripheral visual stimulus but maintained fixation on a first, fixation spot. The act of attention was revealed by the pressing of a lever. Finally, there was a hand-reach task, in which the monkey maintained fixation on a central fixation point, and was trained to reach towards a new stimulus without breaking fixation. Single neurones in both cortical regions were examined for the enhancement of their discharge during execution of the tasks, an enhancement that occurs, for example, when a visual stimulus is accompanied by a saccade towards it; thus a neurone will respond to the appearance of the new visual stimulus, but this response will be strongly enhanced if this appearance is followed by a saccade. Figure 25.58 illustrates an experiment in which responses of a frontal and parietal neurone to fixation, saccade, and peripheral attention are shown; it will be seen that the frontal neurone is only enhanced in relation to the saccade, whereas the parietal neurone is enhanced in relation to the peripheral attention task as well. Parietal neurones that showed enhancement in the saccade also showed enhancement with the hand-reach task; the presence and amount of enhancement were cross-correlated across neurones, in the sense that cells tended to be enhanced on all tasks or not enhanced at all. It was also spatially selective in the peripheral attention task (Bushnell *et al.*, 1981), and it was concluded that enhancement in posterior parietal cells is a unitary attentional process found in different neurones to different extents.

In discussing their comparisons between frontal and parietal neurones, Goldberg & Bruce emphasize the joint roles of the two areas in attending to visual stimuli, manifest, with the frontal neurones, in the anticipatory activity described earlier, and, with the parietal neurones, in the experiments just described; however, the frontal neurones are much more closely related to execution of movement; and this is emphasized by the independence of the frontal cortex, and the dependence of the parietal cortex, on the superior colliculus (Schiller 1977; Keating *et al.* 1983) and the fact that electrical stimulation of frontal cortex can produce saccades with very low stimulation currents, as low as 10 μA, whereas very much higher currents of 0.5–3 mA are required to evoke movements from the parietal cortex.

Analysis of Motion in Extrapersonal Space

In reviewing the characteristics of neurones in the posterior parietal region, Hyvärinen (1982) suggested that this cortical area was the site of a neural model of the spatial relationships in an individual's surroundings, surroundings both actual and remembered. Thus the superior colliculus codes eye-position only with respect to an

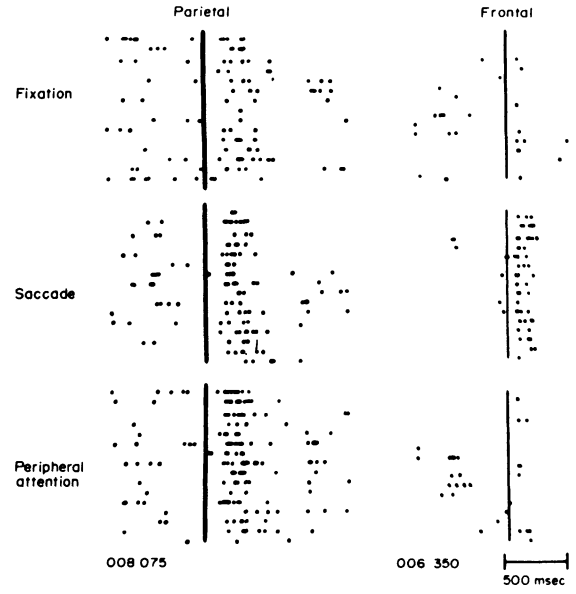

Fig. 25.58 Comparison of enhancement of visual response in parietal and frontal cortex for fixation, saccade, and peripheral attention tasks. Each column shows the responses of a single neurone in the parietal (left column) or frontal (right column) cortex to the onset of a visual stimulus in the fixation task (first row). saccade task (second row) and peripheral attention task (third row). Each dot in the raster diagram corresponds to a neuronal discharge. Each line contains the discharges in a single trial, displayed on a time line. Successive trials are all synchronized on the onset of the visual stimulus, signified by the vertical line. Note that the parietal activity is equivalently enhanced in both the saccade and peripheral attention tasks, but the frontal activity is enhanced only in the saccade task. (Goldberg & Bruce, *Vision Res.*)

oculomotor map of the eye position within the orbit, rather than within coordinates of extrapersonal space (Sparks & Porter, 1983). Hence accurate saccades within extrapersonal space coordinates would involve the integration of a signal based on spatial coordinates from the inferior parietal lobule with the oculomotor coordinate map of the colliculus.

Middle Temporal Area

We have seen that there is a region in the temporal cortex in which neurones are predominantly responsive to motion; this MT area, on the posterior bank of the superior temporal sulcus, contains neurones that encode the direction of movement of a visual stimulus, and, as such, are of obvious interest to the student of eye-movement control in the more complex situations than those usually employed in the study of eye-movements, such as saccadic movements to stationary stimuli or tracking movements of a slowly moving target. Newsome *et al.* (1985) have examined the effects of lesions in this region on oculomotor performance of alert monkeys, the lesions being made by strictly localized injections of the neurotoxin, ibotenic acid, calculated to inactivate those neurones whose receptive fields had been characterized. The monkeys had to fixate a spot of light, which could remain stationary (step-task) or else could be moved as soon as it appeared (step-ramp task). Saccades to stationary targets were unaffected by the lesion, whilst in the step-ramp task the monkey's ability to match the speed of the pursuit was impaired, as well as the accuracy of the saccade to a moving target, the monkey failing to adjust the magnitude of the saccade to the speed of target motion (Fig. 25.59). It was assumed that the visual input occurred

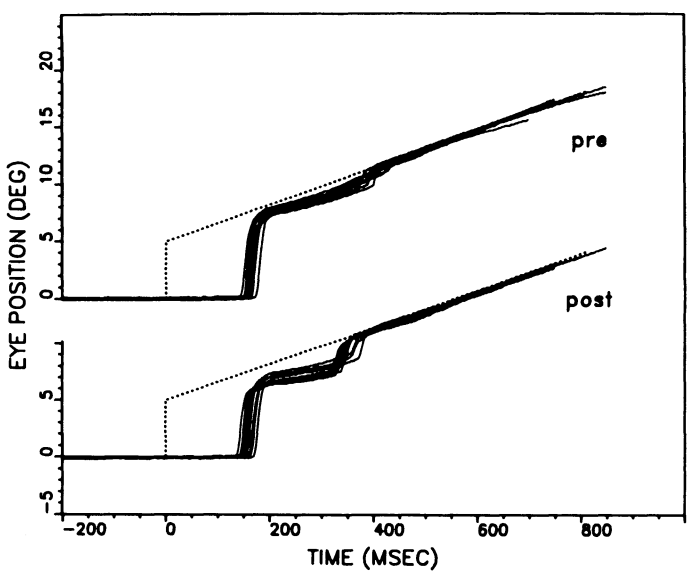

Fig. 25.59 Defect in pursuit initiation following an ibotenic acid lesion of MT. Horizontal eye movements made in response to a pursuit target which underwent a rightward step-ramp displacement. The target stepped 5° to the right and then moved smoothly to the right (dashed line). The top set of traces shows 10 superimposed responses recorded before an injection of ibotenic acid into MT. The bottom set shows impaired responses of the same monkey 24 hr after the injection. (Newsome *et al.*, *J. Neurosci.*)

by way of the striate cortex, since, according to Goldberg *et al.* (1982), permanent deficits in smooth pursuit movement occurred with lesions here.[36]

THE CEREBELLUM

This region of the brain is off the main ascending and descending pathways from cord to midbrain and cortex, and may be regarded essentially as a regulating device for the smooth execution of the motor activity of the organism. It may be described as a 'feed-back centre', in the sense that it receives information from all regions of the body and from the parts of the brain directly concerned in motor activities; because of its reciprocal connections with these parts, including the regions of the cortex concerned with voluntary movements, it is able to modify their activities continuously in the light of this information. The control of the eye movements, both reflex and voluntary, therefore involves activity of this part of the brain. The direct connections of the flocculonodular lobe with the vestibular nuclei in the medulla suggest a very intimate connection between vestibularly evoked eye reflexes and this, the so-called paleocerebellum.

Anatomy and Connections

Figure 25.60 is a schematic drawing in which the cerebellum is supposed to be spread out in one plane. It consists of two main divisions: (1) a smaller *flocculonodular lobe*, consisting of the *flocculi*, the *nodulus* and their peduncles, and (2) a larger *corpus cerebelli*, the two being separated by the posterolateral fissure. The corpus cerebelli is divided by the fissura prima into an anterior and posterior lobe, each further divided into smaller lobules by smaller fissures.

Cortex and Nuclei

We may distinguish an outer layer of gray matter, the cerebellar cortex, and a deeper layer of white matter; beneath this white matter are the deep cerebellar or roof nuclei, which are relay stations for the outwardly directed

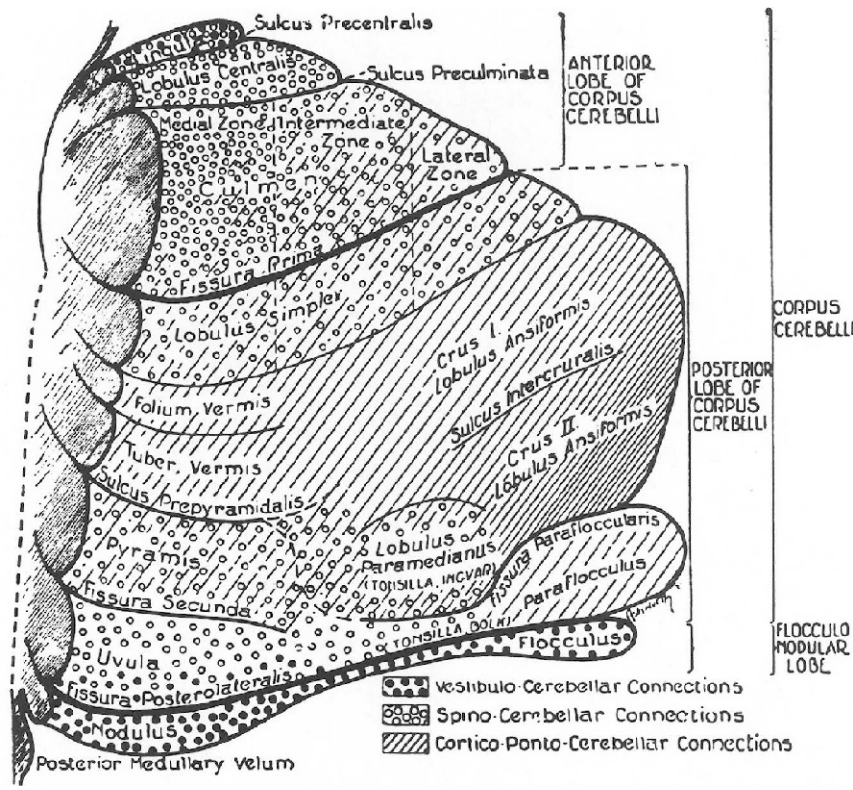

Fig. 25.60 Schema of the cerebellum. The brackets on the right show the divisions according to Larsell's classification. Afferent fibre connexions as determined by oscillographic studies are indicated by the different types of shading. (Dow, *Biol. Rev.*)

cerebellar impulses. They consist of three pairs, the *fastigial*, the *interpositus* and *dentate*.

Modes of Connection

The cerebellar cortex is thrown into laminae, or folia, by the transverse arrangement of the smaller fissures. Its substance shows three layers; outermost is the molecular layer; next a layer of Purkinje cells, and on the inside a granular layer. Beneath this is the white matter (Fig. 25.61).

Purkinje Cells

These are the only neurones with axons passing out of the cortex, and are thus its effector cells, relaying in the roof nuclei, and with their dendrites ramifying in the molecular layer; their chief synaptic input is from the *climbing fibres*, which are the axons of the inferior olivary complex, relaying input from various central regions, such as the cerebral cortex, as well as peripheral input from muscles and skin. It appears that a single climbing fibre is associated with a single Purkinje cell, making numerous synaptic contacts over its dendritic tree and thus making a powerful contribution to its activity. The *mossy fibres*, bringing information from the periphery, and command from the cerebral cortex, relay in the cerebellar glomeruli, synapsing with granule cells (Fig. 25.61); the glomerulus permits the spread of a single mossy fibre's input to several granule cells.

Parallel Fibres

The axons of the granule cells run perpendicular to the cortical surface, and then, in the molecular layer, bifurcate into *parallel fibres* (PF of Fig. 25.61); these fibres make axo-dendritic synapses with numerous Purkinje cells and also with Golgi cells, stellate cells and basket cells. Basket cells make contact with Purkinje cells; thus Purkinje cells receive direct inputs from climbing and parallel fibres, and less direct inputs from parallel fibres by way of basket cells.

Paleocerebellum and Neocerebellum

Phylogenetically and embryologically the cerebellum has

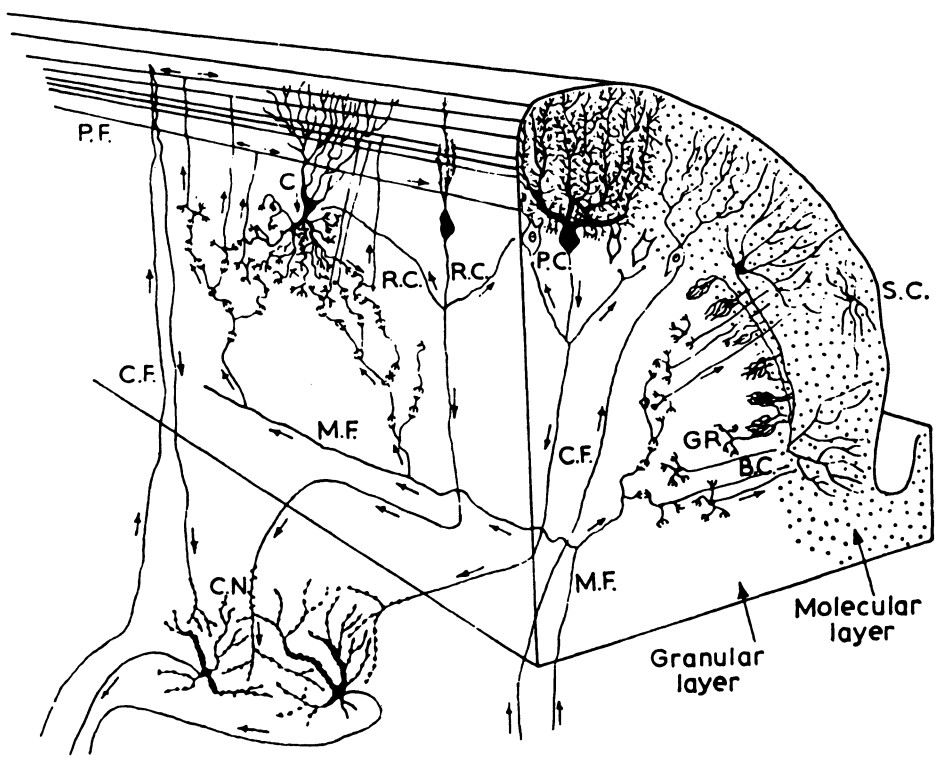

Fig. 25.61 Schematic view of a folium of the cerebellum showing interneuronal connexions of the cortex. B.C., basket cell; C, Golgi cell; C.F., climbing fibre; C.N., deep cerebellar nuclei; GR, granule cell; M.F., Mossy fibre; P.C., Purkinje cell; P.F., parallel fibre; R.C., recurrent collateral; S.C., stellate cell. (After C. A. Fox, in *Correlative Anatomy of the Central Nervous System.*)

developed from the vestibular complex of nuclei in the medulla, and may be expected to be primarily concerned with maintenance of equilibrium. In mammals there are powerful connections with the cerebral cortex, made through the corticopontine system and developing with the posterior lobes, which in higher mammals and primates become the predominant part of the cerebellar cortex. In mammals, therefore, the fissura posterolateralis is considered to be the fundamental landmark in cerebellar physiology, since it separates the flocculonodular lobe from the corpus of the cerebellum. The basic feature of the flocculonodular lobe is its connections with the vestibular apparatus and its medullary nuclei. The corpus is divided by another fissure—the fissura prima—into—a posterior and anterior lobe; the anterior lobe, together with the flocculonodular lobe and parts of the posterior lobe—uvula, pyramis and paraflocculus—has been termed the *paleocerebellum*, whilst the remainder, consisting largely of the hemispheres, has been called the *neocerebellum*. All parts of the cerebellum, except the flocculonodular lobe, receive cortical input (Dow, 1938).

Vermal and Lateral Regions

Chambers & Sprague (1955a,b) emphasized that the separation of the cerebellum into anterior and posterior lobes does not correspond with the functional analysis of its parts, and argued that a division on a longitudinal basis was more appropriate. They described a medial, or *vermal*, cortex associated with the fastigial nuclei; a *paravermal*, or intermediate, cortex, associated with the interpositus nucleus, and a lateral or *hemispheral* cortex associated with the dentate nucleus. Thus vermal portions of both anterior and posterior lobes have essentially the same function. Moreover, vestibular function was not confined to the flocculonodular lobe but was associated with the entire vermal strip. Functionally it is thought that the vermal portion is concerned with the follow-up control of movement on the basis of information from the periphery; the intermediate zone with integration of input from the cerebral cortex with muscular activity, whilst the hemispheral portions are concerned with the execution of highly skilled tasks.

Afferent Input from Eye Muscles

We have seen that the extraocular muscles are well provided with sensory receptors—spindles and comparable bodies—capable of providing information as to the state of tension of their fibres. This information is not utilized directly in a stretch-reflex, and instead is passed to higher integrating centres (Keller & Robinson, 1971). Fuchs & Kornhuber (1969) stretched extraocular muscles of the cat and recorded evoked potentials in the vermian folia of Lobules V, VI and VII; these had a short latency of some 4 msec, and the location of the evoked responses corresponds with the regions of projection of the visual and auditory cerebral cortex, as well as homologous projections from Area 8 as found in the monkey.

Most afferent fibres from the extraocular muscles travel in the trigeminal nerve (N V); Baker *et al.* (1972) stimulated this and observed potentials in mossy and climbing fibre terminals in the same regions of the cerebellum as those that generated field potentials before onset of saccades. Short-latency responses were found at terminations of mossy fibre afferents in the granule layer of lobules V, VI and VII. Longer-latency responses were at terminations of climbing fibres, presumably through the olivo-cerebellar pathway. Again Maekawa & Kimura (1980) examined the floccular region, well known to integrate various sensory signals from vestibule, eyes and neck. In the rabbit they found mossy fibres and Purkinje cells responding to ramp stretches of extraocular muscles; there was no evidence of climbing fibre responses. 21% of Purkinje cells responded with phasic excitation, possibly signalling velocity of eye movement; 36% gave tonic responses, and might have been signalling eve-position.

Visual Input

Maekawa & Simpson (1972, 1973) showed by electrical stimulation that the rabbit's flocculus received ipsilateral visual input mediated by the dorsal part of the accessory optic tract, the central tegmental tract and inferior olive and eventually transmitted to Purkinje cells by climbing fibres; thus the flocculus is informed, through this pathway, of the results of vestibulo-ocular reflexes conducted under its control (Ito, 1972). Using visual stimuli and recording field-potentials resulting from activation of Purkinje cells by climbing fibres, Maekawa & Natsui (1973) defined rather narrow receptive fields; slits, usually vertical, were the most effective visual stimuli; latencies of action potentials were 35–45 msec.[37] Winfield *et al.* (1978) injected horseradish peroxidase into the chinchilla's flocculus and observed retrograde labelling in the medial terminal nucleus of the accessory optic tract; the projection was from the dorsal cap of the inferior olive; thus the medial terminal nucleus was labelled with ^{3}H-labelled amino acid after injections into the retina. They concluded that the medial terminal nucleus also projected directly to the flocculus, giving rise to mossy fibres (Fig. 25.62). Thus the accessory optic system provides the cerebellum with a visual input independently of the geniculostriate pathway.

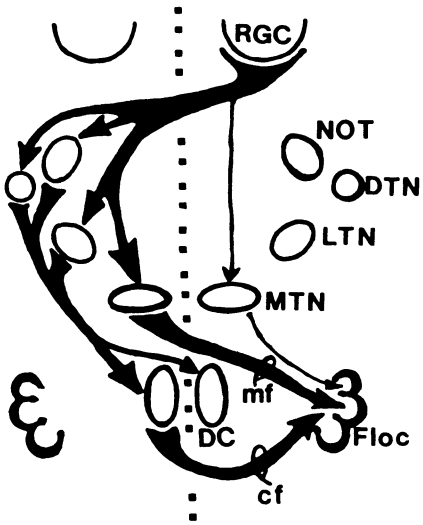

Fig. 25.62 Diagram of visual pathways to the mammalian flocculus of the cerebellum. Note that the predominant visual input to most of the flocculus is from the ipsilateral retina as indicated by heavy arrows, but some contralateral retinal influence can occur at the level of MTN; RGC, retinal ganglion cells; NOT, nucleus of optic tract; DTN, dorsal terminal nucleus; LTN, lateral terminal nucleus and MTN, medial terminal nucleus; DC, dorsal cap of Kooy; Floc, flocculus; mf, mossy fibre pathway; cf, climbing fibre pathway. Dotted line is midline of brain. (Winfield *et al.*, *Brain Res.*)

Electrical Stimulation of Vermis

In the alert monkey Ron & Robinson (1973) obtained direction-specific saccades by stimulation of vermal and hemispheral regions. Both smooth movements and saccades were obtained. With the saccade the response was independent of the visual field, being the same in complete darkness or with a textured field; by contrast, a textured field exerted a strong inhibitory action on the evoked smooth movement.

Stimulation During Saccades

Keller *et al.* (1983) considered that the effects of cerebellar stimulation on the oculomotor system would be best revealed during the performance of a saccade, since between saccades the motor system, or saccade generator, is subject to powerful inhibitory influence from pause cells (Keller, 1974). They stimulated in the region of Purkinje cells, the latency between onset of the saccade and the stimulus being some 4 msec. Contralaterally directed saccades were slowed and made hypometric; thus, in attempting a saccade of 20°, the monkey only reached 13°; lengthening the stimulus had no effect on the change in velocity or hypometria. Ipsilaterally directed saccades were unaffected.

Discharges in Cerebellar Neurones

Kase *et al.* (1980) emphasized the large amount of work that had been carried out on the discharges of neurones in the oculomotor nuclei, the superior colliculus, the prepositus hypoglossal and vestibular nuclei and the flocculus, but the paucity of studies on the cerebellar vermis. In waking monkeys they recorded discharges in relation to eye movements in mossy fibres and Purkinje cells in lobules VI and VII of the posterior vermis. In the mossy fibres they found three groups, described, in accordance with their lead-times. Thus long-lead burst units gave an initial, prelude-discharge, with a lead of 160 msec followed by a burst with average lead of 16 msec. Burst-units started firing some 7.4 msec before saccade-onset, and burst-tonic units had a lead-time of 0.2 msec.

Purkinje cell discharge represents the output from the cerebellum after processing of the input via mossy and climbing fires. The cells showed a high discharge-rate spontaneously, and most showed an increased discharge related to saccades; a few showed pauses. The burst discharge associated with a saccade had an average lead-time of only 0.6 msec. In spite of the temporal relation between burst activity in mossy fibres and Purkinje cells, Kase *et al.* doubted whether this cerebellar activity initiated or pre-programmed the saccades, the lead-times for most Purkinje cells being too short to drive neurones of the oculomotor complex.

Limited Location of Active Neurones

Fujikado & Noda (1987) pointed out that the saccade-related cerebellar neurones encountered by them in the monkey were confined mostly to lobule VII, including a posterior part of lobule VI, whereas reports on microstimulation indicated lobules V–VII as active oculomotor-related sites. The difference may well have been due to the use of very strong stimuli in the earlier studies (Keller *et al.*, 1983; McElligott & Keller, 1984). By confining their stimuli to low currents (less than 30 μA), they confirmed that the oculomotor cerebellar centre was confined to lobule VII in most monkeys, and in the rest it included a posterior part of lobule VI. The responses consisted of quick conjugate eye movements, i.e. saccades; their amplitudes and direction could be increased by extending the duration of stimulation, in contrast with those evoked by collicular or frontal eye field stimulation where the directions and amplitudes depended on sites of stimulation; thus prolonged stimulation in the colliculus produced only a staircase of saccades (Schiller & Stryker, 1972). Another feature of the saccades was their curved trajectories, suggesting an independent control over the horizontal and vertical components; this contrasts once again with natural saccades which are straight, the vertical and

horizontal components of the neuronal drive being adjusted to permit this (see, for example, Van Gisbergen *et al.*, 1985). Fujikado & Noda considered that a given weak stimulus would activate fibres influencing both vertical and horizontal components of a saccade, travelling to separate premotor circuits; the emergent pathway would be through the fastigial nucleus, and thence to the pontine and mesencephalic reticular formation oculomotor centres concerned with horizontal and vertical saccades.

White Matter

Fujikada & Noda and McElligott & Keller (1984) found that the most sensitive parts of the cerebellum were in the white matter; under these conditions mossy and climbing fibres, as well as Purkinje axons, are stimulated; Purkinje cells are essential for obtaining saccades from stimulating the vermis, since after injections of kainic acid, which destroys cell bodies but not axons, Noda & Fujikada (1987) were unable to evoke saccades by stimulation of the kainate-treated regions; only where Purkinje cells remained were responses obtained.[38]

Brainstem Centres

Burst lead-times in vermal mossy fibres correspond with burst activity recorded in several brainstem structures. As summarized by Kase *et al.* (1980), the burst lead-times for the pontine reticular formation (Luschei & Fuchs, 1972), the mesencephalic reticular formation (Büttner *et al.*, 1977), the vestibular nuclei (Miles, 1974), and the prepositus hypoglossal nucleus (Baker, 1977), are all consistent with a primary input from these structures, providing the cerebellum with information as to the ongoing stimulation of the extraocular muscles. It was suggested that the posterior vermis, after receiving saccade-related information from the brainstem saccadic centres, sent feedforward control signals to the oculomotor complex, and possibly feedback signals to the brainstem saccadic centres immediately prior to the initiation of saccades.

Inhibition

Kase *et al.* (1980) found a close temporal relation between the end of a saccade and discharge in certain Purkinje cells; thus Purkinje neurones are inhibitory, so that the high tonic rate of discharge between saccades indicates an inhibition that might maintain fixation steady.

Position Information

In some Purkinje cells, the tonic rate of discharge was proportional to the eye-position in a certain plane; it may be that this information could help in maintaining steady fixation in the absence of visual cues. Ablation of the posterior vermis induced position-dependent dysmetria (Ritchie, 1976), so that it is possible that information from vermal Purkinje cells contributes to the adjustment of saccadic magnitudes with reference to the starting position of the eye. Since position-related discharges occur in mossy fibres, this information is presumably derived by the burst-tonic and tonic fibre channels, but within the cerebellum it undergoes considerable processing leading to a much more sophisticated position-related output in Purkinje cells. We may presume that the extraocular muscle-input to the cerebellum is the source of position-related discharges.

Eye-position Neurones

Central neurones capable of signalling the position of the eyes, as opposed to change in position, are necessary if the visual scene is to be interpreted correctly. Such neurones should be found in the cerebellum, since it is a central region closely concerned with controlling movement in the light of sensory afferent input and efferent motor output, a continuous stream of information serving to update the final motor commands that lead to well coordinated movements. Noda & Warabi (1982) examined the modulation of discharge of Purkinje cells of the monkey's flocculus while it tracked a sinusoidally moving target; the modulation was roughly sinusoidal, with maximal discharge near the maximum of target velocity. These units were clearly signalling eye-velocity. In some units, however, the phases of peak firing and peak velocity varied widely, suggesting a different sort of signal; they displayed a cyclic modulation with smooth pursuit, but with moderate velocities the modulation lagged behind velocity, and it was considered that they were signalling position. As velocity of movement increased, it became harder and harder to separate the position-component in the signal. Mossy fibres showed an essentially similar phenomenon. The authors excluded proprioceptive signals as a cause, on grounds of latency. Visual input was excluded since the signals occurred in the dark. By exclusion, the burst-tonic cells of the brainstem, which have a comparable lead-time, were accepted as a source. The neurones could be in the superior and medial vestibular nuclei, the pontine reticular formation, or the prepositus hypoglossi nucleus.

Smooth Pursuit

Vestibular and visual signals, together with proprioceptive signals, make important contributions to tracking a visual stimulus. Figure 25.63A shows the discharge of a Purkinje cell in relation to tracking of a sinusoidally moving target. When the monkey was trained not to

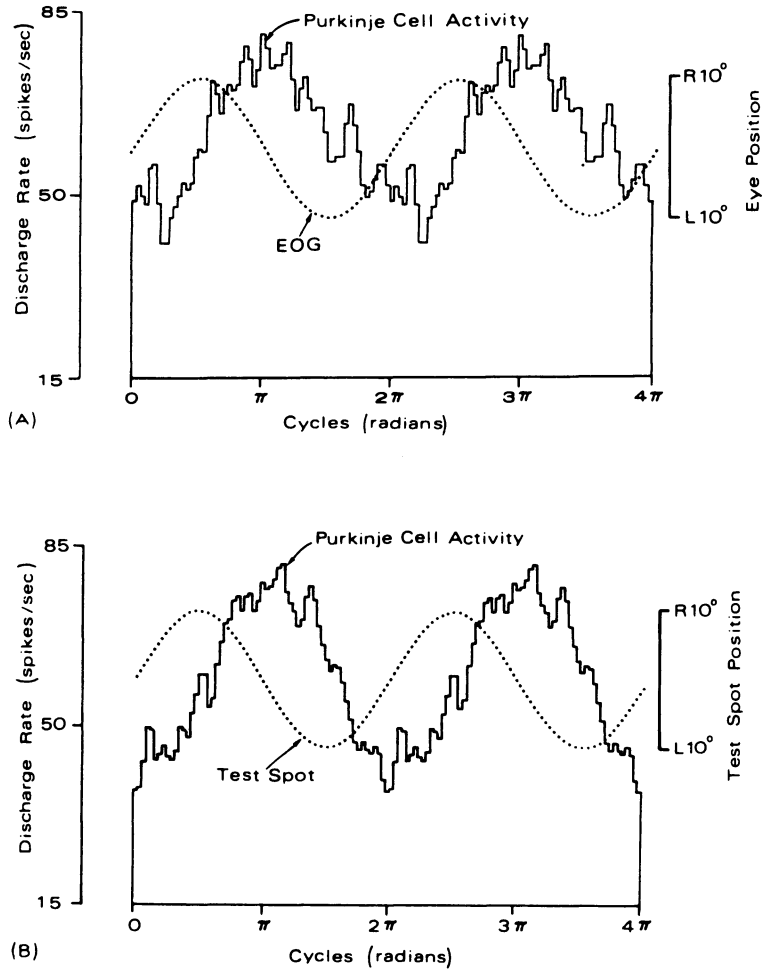

Fig. 25.63 A. Smooth-pursuit eye movement-related Purkinje cell activity. The Purkinje cell discharges associated with ±10-deg, 0.35-Hz pursuit were sampled with a bin width of 45 ms and accumulated over 10 cycles. The resulting histogram was digitally filtered and one average response cycle repeated for clarity. The spontaneous activity level was 52 spikes/s. B. Test spot movement-related Purkinje cell activity. The Purkinje cell discharges associated with ±10-deg. 0.35-Hz test spot movement were sampled with a bin width of 45 ms and accumulated over 10 cycles. The resulting histogram was digitally filtered and one average response cycle repeated for clarity. Spontaneous activity was 52 spikes/s. The activity represented in the histogram was recorded from the same cell associated with the histogram in A. (Suzuki *et al., J. Neurophysiol.*)

follow the target, the response was very similar (Fig. 25.63B), the effective stimulus being clearly retinal slip-velocity. The neurones exhibiting this responsiveness were in lobules VI and VII; and Suzuki *et al.* (1981) concluded that these cerebellar neurones contained all the necessary signals to be concerned with control or monitoring of smooth pursuit.

Role of the Flocculus

This part of the cerebellum, with its close connections with the vestibular nuclei, has been called the vestibular cerebellum, and is phylogenetically related to the close linkage of head and eye position with body muscles. Takemori & Cohen (1974) found that bilateral removal in monkeys failed to influence the vestibulo-ocular reflex in the dark, indicating that the cerebellum does not play an essential role in this reflex; however, they found that, when vestibular and visual reflexes were in conflict, as when the animal is rotated while viewing a stationary object in space, then the well-established suppression of the vestibular reflex (see, for example Koenig *et al.*, 1978) was impaired.

Lisberger & Fuchs (1978a, b) have described responses in Purkinje cells and in mossy fibres during visual track-

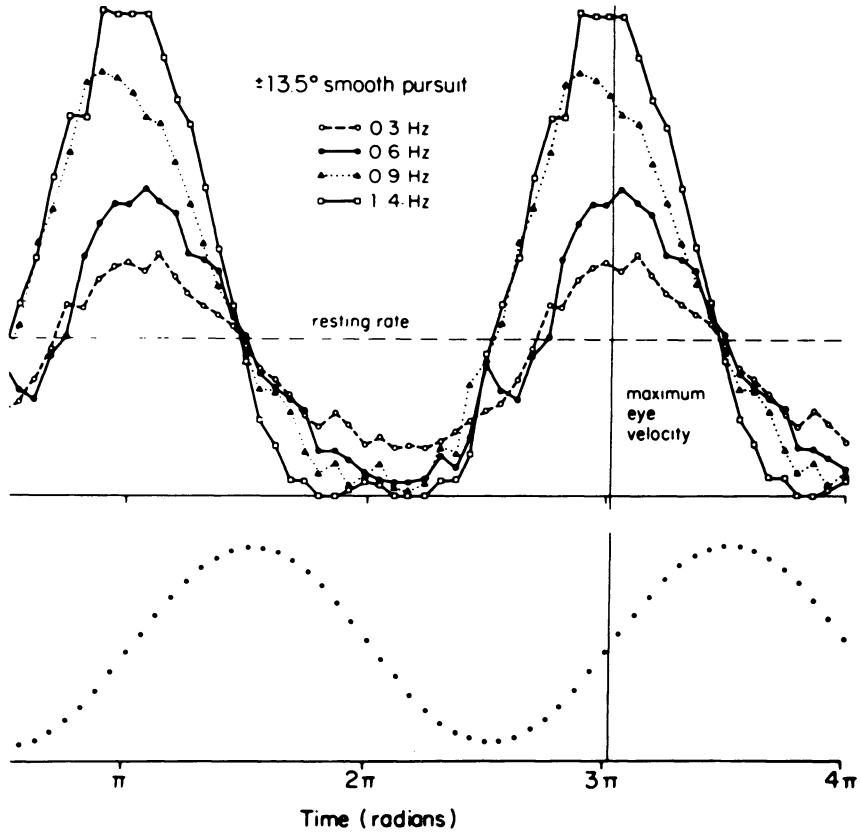

Fig. 25.64 Discharge characteristics of a P-cell averaged over 10 cycles of sinusoidal smooth pursuit. The upper panel shows averages from a P-cell studied during four frequencies of smooth pursuit at a fixed amplitude of ±13.5°. The horizontal dashed line shows the resting rate of 77 spikes/s. The solid vertical line shows maximum ipsilateral eye velocity, which was 26°/s at 0.3 Hz, 57°/s at 0.6 Hz, 77°/s at 0.9 Hz, and 110°/s at 1.4 Hz. An upward deflection of eye position (lower panel) represents ipsilateral eye movement. The time base has been shown in radians to normalize the abscissa for the different frequencies of eye movement. In this figure a single cycle has been repeated to facilitate visualization of the periodic events. (Lisberger & Fuchs, *J. Neurophysiol.*)

ing with or without head movements. Figure 25.64 illustrates simple tracking, maximum discharge occurring at the peak of eye-velocity. When rotation was carried out in the dark the discharges were only weakly modulated; when the monkey fixated a target that moved with it (and thus when the vestibulo-ocular reflex was suppressed) the discharge was deeply modulated in phase with maximal head velocity. Thus neurones exhibited sensitivity to both eye- and head-velocities, and under three conditions when the responses to the two velocities occurred simultaneously the resulting response could be predicted from a vector sum of the individual responses.

Visuo-vestibular Conflict

Lisberger & Fuchs concluded that the flocculus plays a minor role during vestibulo-ocular rotation in the dark but a major role when the conflict between visual and vestibular reflexes requires inhibition of the vestibular component; this can occur transiently, when the head and eyes accelerate quickly to fixate a target, and in the steady state during steady tracking of a visual object. The absence of Purkinje cell modulation during rotation in the dark is probably attributable to a cancellation of the head-velocity input by the eye-velocity input, rather than due to a visual input, *per se*, to the flocculus. On the basis of a schematic circuit, the Purkinje responses to various conditions of experiment could be predicted. Lisberger & Fuchs point out that, on the basis of this circuit, stimulation of the flocculus, and thus of the Purkinje cells, would cause a smooth ipsilateral conjugate movement, as found by Ron & Robinson (1973).[39]

Cerebellar Lesions

Westheimer & Blair (1973) observed a failure to hold gaze in cerebellectomized monkeys; thus, when attempting to

maintain eccentric fixation, the eyes went into a nystagmus. There was an absence of all pursuit movements; saccade movements, and the vestibulo-ocular responses were apparently normal. The authors showed that the smooth eye movements elicited by stimulation of the pontine reticular formation could not be evoked in the cerebellectomized animal.

Dysmetria

Ritchie (1975) made lesions of the cerebellar regions associated with oculomotor activity. The only obvious defect found by him was a dysmetria in saccades in the sense that they resulted in either overshoot or undershoot. The interesting feature of the defect was its dependence on the original position of the eyes, so that the hypermetria was greatest if movement began from an extreme eccentric position; by contrast, if the movement began from the primary position there was hypometria. Moreover, the lesions caused similar errors when the visual stimulus to the saccade was removed. Thus it is unlikely that the normal cerebellum was processing visual information and thereby modifying the motor activity in the light of this information. It is more likely that, in some way, the cerebellum is utilizing proprioceptive information from the extraocular muscles that permits a more accurate match of the burst-frequency and duration with the required eye movement, but it seems clear that the visual information has already been encoded.

Man

Pathologically in humans the oculo-motor errors are similar; as described by Cogan (1954), the ocular hypermetria is greatest when moving from eccentric points to the primary position. Such dysmetria leads to successive corrective saccades until fixation is achieved, thereby giving rise to oscillatory movements; a similar oscillation was observed by Ritchie.

Floccular Lesions

According to Takemori & Cohen (1974a) the most striking feature of floccular lesions was the loss of the ability to reduce the slow-phase velocity in vestibular nystagmus by a visual stimulus; with bilateral floccular lesions the quick phase was abolished. It would appear from this, and other studies, that the cerebellum is critically involved in interactions between the visual and vestibular eye reflex mechanisms, presumably in the vestibular nuclei.[40]

Dorsolateral Pontine Nucleus

This is the major terminus for converging descending pathways from vision- and visuomotor-related structures, and the major source of efferents to the cerebellar regions involved with ocular motility; horseradish peroxidase studies have shown the projection to the vermal lobules VI and VII and to the flocculus. Suzuki & Keller (1984) studied activity in this nucleus in waking monkeys and concluded that it would be able to signal smooth pursuit eye movements, indicating direction and velocity of target image-motion on the retina; thus the responses to a moving spot, or movements of the visual field, indicated that retinal-slip, considered to be an important cue for establishing the magnitude of a saccade, could be signalled through the pontine nucleus. Directional selectivity of neurones might be due to projection from cortical MT (p. 569).

MODELS OF CONTROL

We may complete this subsection by considering some of the models that have been put forward to describe oculomotor movements under certain special conditions. We may begin with a fundamental study of Cohen *et al.* (1977) in which the concept of velocity storage was first mooted, to be developed by Robinson and his colleagues.

Optokinetic Nystagmus. Quantitative Analysis of the Slow Movement

A typical record of optokinetic nystagmus and after-nystagmus is illustrated in Fig. 25.6. From such records Cohen *et al.* measured the velocity of the eye in the slow movement of optokinetic nystagmus, and also in the after-nystagmus, i.e. the movements in the same direction that occur when the optokinetic stimulus has ceased. They pointed out that the after-nystagmus appeared to compensate for vestibular after-responses (Ter Braak, 1936; Mowrer, 1937). Moreover, it is apparently the manifestation of an excitatory state built up during the period of exposure of the subject to the rotating visual field. Cohen *et al.* examined the responses of monkeys to a step-wise imposed stimulus, in the sense that the striped drum was caused to rotate at a constant velocity, the time required to establish this being only some 20 msec. They found that the eyes moved to maintain adequate following of the target in two stages, an initial rapid movement, followed by a slower movement when eye- and target-velocities were equal. Time-constants for the slow rise were estimated to be of the order of 2.6 to 3.0 sec. Once the steady-state velocity was achieved it was maintained for long periods. As velocity of drum-movement in-

creased so did that of the slow eye-movement, as one would expect; above about 180 °/sec, however, the linearity broke down, and the curve finally flattened at a drum-velocity of 240–270 °/sec.

After-nystagmus

There was a rapid initial fall in velocity of the slow phase, followed by a slower decline approaching zero over 20–60 sec. The velocity at the beginning of after-nystagmus depended on the velocity and duration of the preceding optokinetic stimulus. If steady-states of optokinetic nystagmus had been reached, i.e. if the eyes were following the drum perfectly, then the initial velocity of the after-nystagmus was about 0.8 of the velocity of the slow-phase during optokinetic nystagmus; however, at velocities above 90–120 °/sec the peak after-nystagmus velocities saturated, in spite of increases in optokinetic slow-phase velocities. This indicated that the mechanisms for induction of the slow movements of optokinetic nystagmus, and after-nystagmus, were different.

Charging the Mechanisms

Cohen *et al.* (1977) inferred the presence of a central nervous integrator into which was fed information about the movement of the eyes and target, an integrator that operated during the establishment of the optokinetic nystagmus and manifested its activity in the after nystagmus following cessation of the stimulus; it also operated during the build-up of the slow velocity to its steady-state value. Thus the initial rapid eye-movement was considered to be mediated by a direct visual input to motor centres, but at the same time an indirect input went to the integrator whose activity supplemented the direct input, allowing the eye- and target-velocities to match exactly (gain equals unity). The charging and discharging of the integrator were computed by the curves showing build-up of velocity in the initial optokinetic nystagmus and by the build-up of the initial eye-velocity of after-nystagmus achieved by increasing the duration of the initial drum-stimulus. As Fig. 25.65 shows, both processes could be fitted by the same time-constant of 3 sec.

Effects of Fixation

After-nystagmus is best observed in darkness since it is brought to an end fairly quickly if the subject fixates in the light. If fixation occurs for only a short time, then the after-nystagmus is resumed, but with diminished velocity. Figure 25.66A shows the decline in velocity with duration of fixation, and B compares the time-course of loss due to fixation with the time-course of charge of the after-nystagmus mechanism. Clearly the discharge rate is much greater than the charge rate.

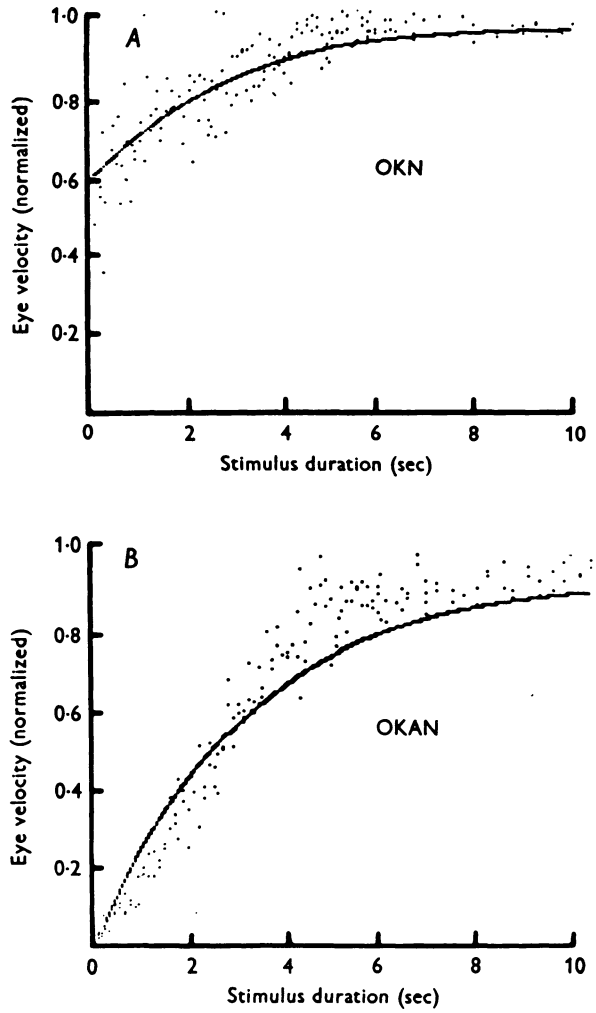

Fig. 25.65 Approximation of results from slow rise of OKN (*A*) and charge of OKAN mechanism (*B*) by exponentials with the same time-constant (3 sec). The stimulus was rotation at 60°/sec for both groups of results. Dots are experimental points and continuous lines are exponential fits to them. (Cohen *et al.*, *J. Physiol.*)

Model

Cohen *et al.* (1977) established a model that accounted for the main features of the build-up and decay of the slow movement, the essential feature being the integrator. This could be short-circuited by a 'fixation switch' which allowed a rapid discharge and so slowed the after-nystagmus. Figure 25.67 illustrates the computed slow-phase velocity as a function of time. According to the model, the after-nystagmus is produced by a subset of the system that produces the nystagmus; this latter is initiated by direct pathways which of themselves are inadequate, so that the integrator contributes more and more until

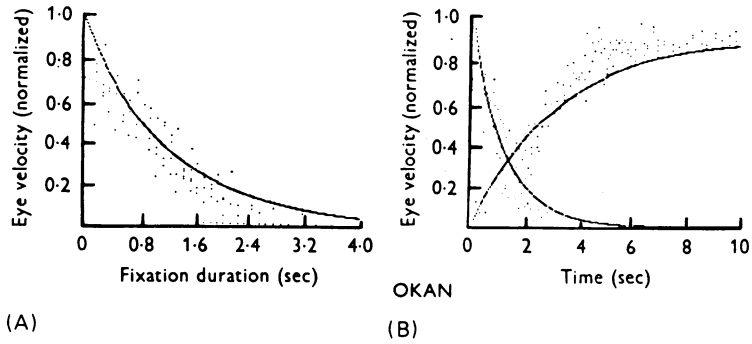

Fig. 25.66 A. Post-fixation OKAN velocity, normalized with respect to pre-fixation velocity (ordinate) as a function of duration of fixation. OKAN was lost after fixations lasting about 3 sec. B. Comparison of the time-course of loss of OKAN activity due to fixation (falling curve) to the time-course of charge of the OKAN mechanism (rising curve). The discharge of activity was about twice as fast as the charge. (Cohen *et al., J. Physiol.*)

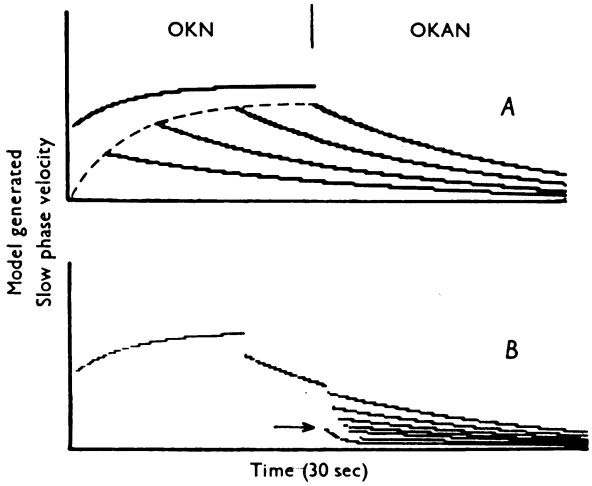

Fig. 25.67 *A*, curves generated by OKN-OKAN model. The input was a step in stimulus velocity of 60°/sec. Slow phase velocity during OKN increases along continuous rising line. The OKAN mechanism charges along dashed rising line. The falling lines show the decay of OKAN slow phase veocity after stimuli of varying durations (Cohen *et al., J. Physiol.*). *B*, curves of discharge of OKAN mechanism caused by periods of fixation.

the correct velocity is achieved. Once the slower pathways are fully active, the rapid pathway becomes inactivated, so that it contributes little to the velocities up to 90–120 °/sec; above this, however, the slower pathways are saturated and the fast pathways are recruited up to 180 °/sec. At these velocities the nystagmus becomes increasingly irregular. This would be expected were the integrator responsible for the accurate adjustment of eye-speed to target velocity, to be inactivated.

Circularvection

When a subject is completely surrounded by the moving field, which thus occupies his whole field of view, within a few seconds of beginning the rotation the perception of movement of the field changes to one of motion of the subject—*circularvection* (Brandt *et al.* 1973). This persists even if the eyes do not make an optokinetic nystagmus. If only the central part of the visual field rotates, then only optokinetic nystagmus is present, but if only the periphery rotates then circularvection dominates. The phenomenon is interesting since the sensation of motion is obtained in the absence of any vestibular stimulation, but of course, if a subject were rotating at constant velocity for any length of time, vestibular stimulation would subside. Thus the stimulus-conditions are, in fact, indistinguishable from rotation in a chair at constant velocity.

CHARGE-TIMES

The charge-times of 5–6 sec and discharge times of 20–30 sec for both after-nystagmus and circularvection are comparable, and they both saturate at about 120 °/sec; on the basis of their model, Cohen *et al.* (1977) described circularvection as the result of monitoring activity in integrators associated with both optokinetic nystagmus and after-nystagmus.

Velocity Storage

In a subsequent study from Cohen's laboratory (Raphan *et al.*, 1979) the process that led to this build-up in velocity-input, typically seen as optokinetic after-nystagmus, and the absence of vestibular after-nystagmus after rotation of the head in the light, was called the *velocity*

storage mechanism, differentiating it from the 'integrator' postulated by Robinson that contributed to the phase-lag of the vestibulo-ocular reflex (p. 736). It would be this process that was responsible for the slow decay of vestibular nystagmus that is observed when the head is rotated at constant velocity in the dark. Thus the mechanics of the cupula suggest that it would return to its equilibrium position when acceleration ceased with a time-constant of 3–5 sec, yet the constant is much larger, of the order of 15 sec (Goldberg & Fernandez, 1971), and may be attributed to a neural factor—velocity storage—that tends to maintain eye-movement in the initial direction, as in optokinetic after-nystagmus.

VESTIBULAR AND OPTOKINETIC INTERACTION

Raphan *et al.* (1979) studied the interaction of vestibular and optokinetic mechanisms. They first measured the relation between eye-velocity and head velocity for rotation in the dark, and found a linear relation as in Fig. 25.68, indicating virtually perfect match, and a gain of unity. They then compared post-rotatory slow-phase velocity after periods of rotation in the dark and light, changes in the curves being an index of interaction of the two types of stimulus. After rotation in the dark the curve for post-rotatory eye-velocity against platform-velocity was similar to that for per-rotatory nystagmus; however, after rotation in the light, the velocity in after-nystagmus was virtually zero up to a platform-velocity of 120 °/sec, after which the curve started to run parallel with the other curve, suggesting that the storage term saturated at platform-velocities of 120 °/sec and greater. By fitting the velocity-curves to polynomials and subtracting them, the curve of Fig. 25.68D is obtained, which suggests that the relation of eye-velocity to platform-velocity in the light, when the velocity storage due to optokinetic nystagmus competes with that induced by the vestibular reflex, can be obtained by subtraction of the two storage-mechanisms, indicating a common basis.[41] In further experiments they rotated the optokinetic drum and the table together so as to assist or inhibit the slow component.

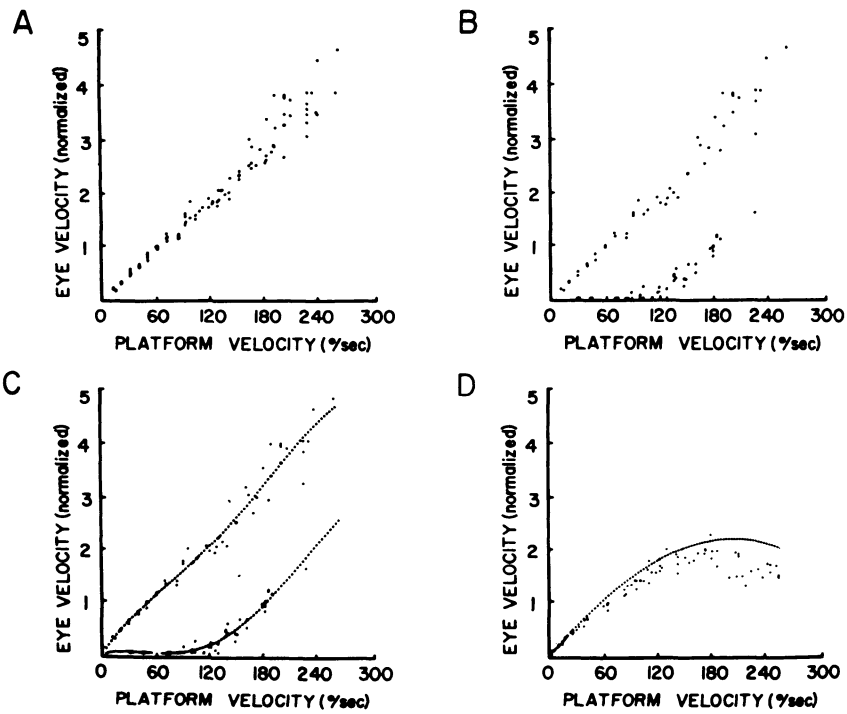

Fig. 25.68 A Peak eye velocity (ordinate) induced by steps of platform velocity in darkness (abscissa). Eye velocity was normalized in relation to values recorded during 60°/s rotation in light. Each dot is the peak velocity of one sample of per- or post-rotatory nystagmus. B Post-rotatory slow phase eye velocities recorded in darkness after rotation in darkness and in light. the points on the left going through the origins are from rotation in dark. Data from post-rotatory responses to steps of velocity in light are below and on the right. The velocity of the nystagmus following rotation in light was less than 10°/s for stimulus velocities up to 120°/s. Above this eye velocity increased linearly parallel to post-rotatory nystagmus in dark. C Data approximated by polynomials. D Comparison of difference between polynomial curves of C (dotted line) with OKAN data from Cohen *et al.* (1977). (Raphan *et al.*, *Exp. Brain Res.*)

Thus, if the drum and the table rotated at the same rate, there was no nystagmus, and the intensity of the after-nystagmus was the same as after rotation in the dark. A model circuit allowed the prediction of slow phase eye-velocity under the various conditions of interaction.

Effects of Occipital Lobectomy

The residual vision in lower primates after occipital lobectomy has been described earlier; optokinetic nystagmus may still be generated (Denny-Brown & Chambers, 1976) but is not normal. In normal nystagmus the slow phase has two components, the immediate jump in velocity described by Cohen *et al.* (1977), and the slower increase that leads to accurate following of the visual target, the *velocity storage component.*

In a study of bilateral ablations, Zee *et al.* (1987) confirmed the recovery, within about a month, of the ability of the monkey to track a moving target with accuracy, although initially the monkeys appeared quite blind. In this initial state, however, a modified form of optokinetic nystagmus was evoked, in which apparently the immediate rapid component was lacking, whilst the velocity storage mechanism was impaired but still present. Thus the residual optokinetic nystagmus was similar to that found in afoveate animals like the rat and rabbit. In these animals the nystagmus is unaffected by occipital lobectomy, and the accessory optic system, through the nucleus of the optic tract (NOT), is considered to be the afferent pathway; in the monkey with cortical ablation we may assume that this system is operative. Thus Kato *et al.* (1986) have shown that lesions in the nucleus of the optic tract in monkeys eliminated the movements of the eyes to the lesioned side when presented with the moving drum, so that no nystagmus was evoked, only voluntary saccades. Nystagmus directed to the unlesioned side was normal. Interestingly, however, tracking of a moving target was apparently normal.

MOTOR PATHWAY

The higher motor centres likely to be concerned in visuomotor activity in the occipitally lesioned animals are the frontal eye field and the region in the superior temporal sulcus characterized as MT and MST (p. 569), together with the posterior parietal area. These areas normally rely on a topographic projection from the striate cortex (Ungergleider *et al.*, 1979; Van Essen *et al.*, 1981; Chapter 21). In the absence of striate cortex we may presume that visual information reaches it by way of the pulvinar. Their descending pathway may be partly through the superior colliculus, the posterior parietal region[42] having a dense projection to the intermediate and deep layers of this body (Lynch *et al.*, 1985), whilst there are intimate relations with the frontal eye fields, (Barbas & Mesulam, 1981).

Nucleus of Optic Tract

This is considered to be an important centre in the execution of optokinetic nystagmus, especially in those lower mammals whose nystagmus is unimpaired by cortical ablation, e.g. the rabbit and rat. From this nucleus the pathway descends to the n. reticularis tegmenti pontis (NRTP), a large midline reticular nucleus whose major efferent projection is to the cerebellum. In the monkey, Keller & Crandall (1981) found no cells responding to optokinetic stimuli in this nucleus, but they did find a more rostral region in the pontine nuclei proper that contained neurones responding to optokinetic stimuli. A large number showed increased discharge with rotation in one—the preferred—direction, and decreased in the opposite direction. When tested in a simple tracking movement, the response was an increase in discharge when moving in the same direction as that preferred in optokinetic nystagmus. After stimulating a neurone at constant velocity for 30/sec and then suddenly stopping the drum and extinguishing the light, the discharge ceased abruptly in spite of an after-nystagmus, suggesting that this nuclear region is not the site of velocity storage. Six out of twenty-one cells also responded to vestibular stimulation. The authors suggested that this pontine nuclear region might be analogous with the n. reticularis tegmenti pontis of lower mammals so far as optokinetic nystagmus was concerned.[43]

LESIONS

Kato *et al.* (1986) destroyed the nucleus of the optic tract unilaterally in the monkey and abolished optokinetic nystagmus towards the lesioned side; however saccades and ordinary tracking movements were unaffected.

RESPONSE CHARACTERISTICS OF NOT NEURONES

In the cat these were studied by Hoffmann & Schoppmann (1975) who made electrode penetrations through the superior colliculus to reach the pretectal region, finding neurones with different characteristics from those of the colliculus. The neurones belonged to the nucleus of the optic tract which was a narrow irregular band of cell nests lying along the dorsomedial edge of the pretectum just lateral to fibres of the brachium of the colliculus. Neurones showed a strong response to slow target motion with directional sensitivity for the temporal to nasal movement; the receptive fields were located in a narrow band of the retinal projections, equivalent to the retinal streak of the rabbit. The neurones were activated by both eyes with a contralateral ocular dominance; the sensitivity to random-dot patterns was reminiscent of complex cortical cells and might account for the binocular input to the neurones. It will be recalled that, in the afoveate rabbit, optokinetic nystagmus can only be evoked by stripes moving in the temporal to nasal direction; al-

though the cat can give a nystagmus with rotation in both directions, it is interesting that when the occipital cortex is ablated, the nystagmus is only evoked in the temporal to nasal direction, the occipitalectomized cat thus behaving like the afoveate animal (Wood *et al.*, 1973).

Vestibulo-ocular Reflex (VOR)

The basis of this reflex is the slow movement that permits the retinal image to remain stable during a movement of the head. When the movement of the eyes becomes too extreme, the slow movement is interrupted by a saccade and the following movement is restarted—thus the experimentally studied vestibular nystagmus is simply a manifestation of the vestibulo-ocular reflex. The visually determined saccade may be viewed as a phylogenetically later developed type of movement that simply borrows the quick movement necessary for efficient use of the vestibulo-optic reflex. The sensory basis of the slow following movement is the stimulation of the semicircular canals by the acceleration, and the problem is to deduce a neural mechanism such that the commands to the extraocular muscles, passing through the motor neurones, ensure that the eye movement is such as to maintain fixation on a stationary target; thus, experimentally it has been found that, over a fairly wide range of frequencies, the eye-movement compensates exactly for the head movement (the gain of the reflex is said to be unity). Thus variations of eye- and head-position are in phase during, say, a rotation in which the acceleration is varied sinusoidally.

Phase-relations

Skavenski & Robinson (1973) emphasized that the vestibular apparatus responded to angular acceleration, whilst the signal required for the motor neurones is one of position. The question was how the acceleration-response in the vestibular neurone was to be converted into a position-command; in mathematical terms this means a double integration with respect to time, and, in the case of the sinusoidal stimulus, there should be a phase-lag of 180° between stimulus and discharge of the motor neurones. The studies of Steinhausen (1933) showed that the displacement of the cupula in the semicircular canal was, in fact, proportional to velocity, so that the first integration is carried out mechanically (Melvill-Jones & Milsum, 1965). Between the vestibular neurone signal and the motor neurone only a single integration has to be carried out; to some extent this is achieved by the elastic features of the extraocular muscles and orbital tissue (Robinson, 1964) and the rest was assumed to be done by a neural circuit. Thus the three factors contributing to phase-lag were designated α, β, and γ. The cupula factor, α, provides 90°; and the neural lag, β, plus the orbital mechanics lag, γ, provide the remaining 90°. The basic signal flow-diagram is illustrated by Fig. 25.69. Skavenski & Robinson made use of the finding of Robinson (1970) that at low frequencies of acceleration γ became very small. In experiments on monkeys they showed that, in pursuit movements, and in the slow movement of vestibular nystagmus, the motor neurone discharged in accordance with the equation already described (p. 691), namely:

$$R = k(\theta - \theta_T) + r\frac{d\theta}{dt} \qquad (1)$$

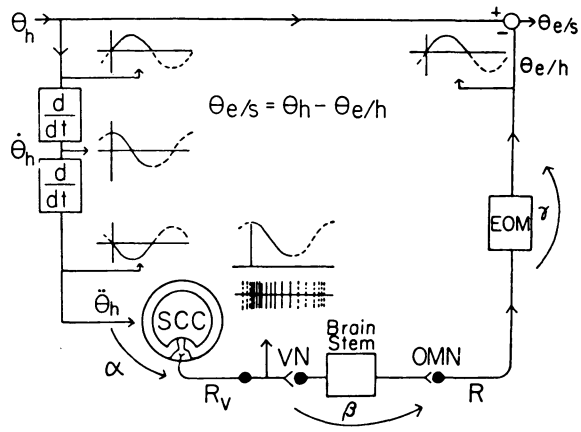

Fig. 25.69 Signal flow diagram illustrating the way in which the vestibuloocular reflex generates changes in eye position with respect to the head, $\theta_{e/h}$, that are opposite to changes of the head position in space, θ_h, and stabilizes eye position in space, $\theta_{e/s}$. Signals are shown for the special case of a sinusoidal head rotation so that a phase shift can be assigned to each signal-processing element. The top path shows the mechanical addition of θ_h and $\theta_{e/h}$ to produce $\theta_{e/s}$. The lower path illustrates that head acceleration, θ_h, stimulates the semicircular canals, SCC, which integrate it ($\int dt$) with phase lag α to produce a frequency-coded signal proportional to head velocity (θ_h) in the neural discharge pattern of the primary vestibular afferents, R_v, and in neurons in the vestibular nuclei (VN). The signal needed to drive the oculomotor neuron (OMN) discharge rate, R, is obtained by neural elements in the brain stem pathways of the vestibuloocular reflex with phase lag β. $\theta_{e/h}$ is produced by R through dynamics of the extraocular muscles, EOM, with a phase lag γ. The negative sign indicates that $\theta_{e/h}$ is opposite to θ_h and is obtained by connecting the appropriate canals and extraocular muscles. Small plots of sinusoids show the difference in form of signals as a function of time at various critical points in the model. (Skavenski & Robinson, *J. Neurophysiol.*)

where the first term denotes the instantaneous position of the eye and the second the velocity of movement; *R* is the rate of discharge of the motor neurone. They deduced from this equation that, with sine-wave eye movement,

the phase-lag between eye position and motor neurone discharge rate is given by:

$$\gamma = \tan^{-1}(\omega \hat{T}) \qquad (2)$$

where ω is the frequency in radians per sec, t is time, and $\hat{T}$ is the time-constant of Eqn. (1), which is the ratio r/k. Values of T, for oculomotor neurones obtained by direct measurements of phase-lag during natural sinusoidal rotations, and those calculated, $\hat{T}$, from the ratio r/k based on the behaviour of motor neurones during fixation and vestibular nystagmus were computed. By substituting these time-constants in Equation (2), it was shown that the orbital mechanics only effectively integrate high frequencies, i.e. only at high frequencies γ becomes 90°; thus at frequencies below 1.0 Hz eye-position lags behind neurone discharge by 45° or less. Direct measurements during sinusoidal rotation confirmed this (Fig. 25.70). In discussing their analysis, in which the commands to the motor neurones will be governed by phase-shifts of different origins according to the frequency of sinusoidal head rotation, Skavenski & Robinson concluded that the operation of the neural circuit would not be adequate without some direct feed-foward of the vestibular neurone's discharge directly to the oculomotor neurones. Thus the model that finally emerged, as a basic description of the control of the smooth movement in the vestibulo-ocular reflex (and also in visual tracking), is that illustrated by Fig. 25.71. The illustration shows, also, the participation of visuomotor systems in the neural circuits, a tentative hypothesis that has been amply confirmed by the studies from Robinson's laboratory.

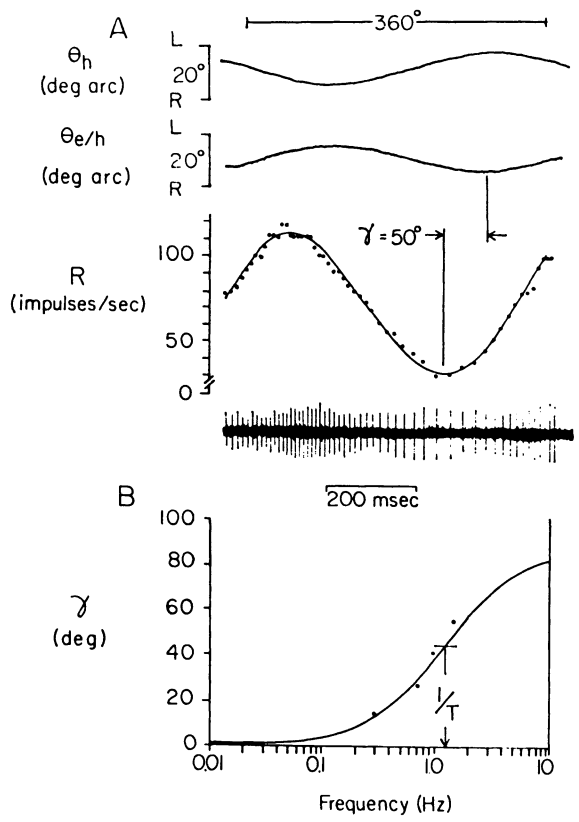

Fig. 25.70 *A*: Illustration of the phase-lag, γ, between eye-position in the head, $\theta_{e/h}$, and the firing of an abducens motor neurone (bottom trace) during sinusoidal rotation of the head in space, θ_h. Neural discharge rate, R, was smoothed over two interspike intervals. *B*: Points (●) show mean phase-lags ($N \geq 4$) between eye-position and abducens discharge rate at four different frequencies for a typical unit Phase lag is plotted upward. (Skavenski & Robinson, *J. Neurophysiol.*)

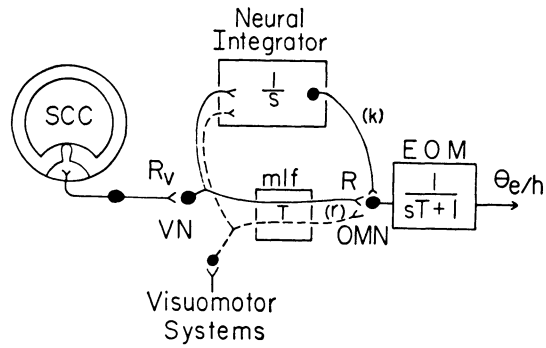

Fig. 25.71 A simplified model of the vestibuloocular reflex showing the role of the direct relay part of the medial longitudinal fasciculus (mlf) in the information transmission pathways between the semi-circular canals and the oculomotor neurons. Symbols are the same as in Fig. 25.69. It is suggested that the direct pathway of the mlf, which provides velocity feed forward with a gain T, is in parallel with a neural network located in the brain stem which integrates head velocity information to provide the OMN with position information. The transfer functions of the integrator and EOM are shown in Laplace transform notation. The suggestion that these vestibular paths are shared by visually driven oculomotor systems is also shown. (Skavenski & Robinson, *J. Neurophysiol.*)

Thus Fig. 25.72 from Cannon & Robinson (1987) is a more complete representation of the position of the integrator, based on the fact that the premotor brainstem neurones send out a velocity command to the system, including those for saccades seen in burst neurones and on gaze-velocity signals from Purkinje cells involved in pursuit, in addition to the vestibular neurones for vestibular and optokinetic movements. All these velocity signals must be converted into combined velocity and position commands through the neural integrator.

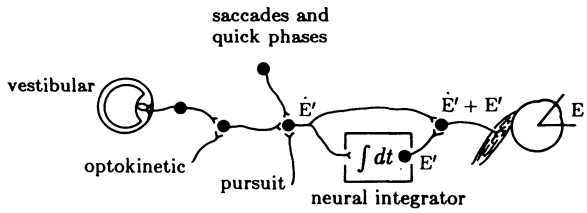

Fig. 25.72 The final common integrator hypothesis. All eye movement commands are initiated as eye-velocity encoded signals. Ė′, which then enter the neural integrator to provide the eye-position encoded signal, E′, present on the motor neurone. The arrangement is schematic and is only intended to show that all eye-velocity signals are passed directly to the motor neurones along with the integrated eye-position signals and is not intended to represent neurones actually involved in this process. (Cannon & Robinson, *J. Neurophysiol.*)

Saccades

In developing a model for the elaboration of the signals to the motor neurones, Robinson (1987) took into account the finding that a saccade, once initiated, could be modified in full flight by an appropriate signal.

Thus Mays & Sparks (1980b) and Sparks & Mays (1983) stimulated the superior colliculus[44] before a saccade that had been evoked by a light-stimulus; the saccade landed on the target in spite of the initial deflection of the eyes caused by the collicular stimulus, indicating that the saccade was spatially, rather than retinocentrically, coded. The saccade must have been localized by recombining retinal error with an extra-retinal eye-position signal. This result was compatible with the spatial view of the saccadic system proposed by Hallett & Lightstone (1976) on the basis of measurement of saccades made when the target jumps to a new position during the execution of a primary saccade. Their results showed that the eyes were making use of visual information during the actual saccade.

Hallett & Lightstone showed that a visual target, flashed during a primary saccade, could elicit a secondary saccade that would accurately fixate the target in spite of the fact that the eye had moved since receiving its visual stimulus; thus the retinal error-signal, alone, could not have been the adequate stimulus for fixation, a knowledge of eye-position in relation to space being necessary as well.

Pulse-step

The basic feature of the discharge, so far as the command to the eye muscles is concerned, is the pulse-step discharge of the motor neurones. Thus the initial burst is followed by a steady discharge that will maintain the eye in its new position against the elastic forces tending to return it to its primary position.

Model Circuit

The model circuit (Fuchs & Kaneko, 1981) is illustrated in Fig. 25.73; the generation of the saccadic pulse in motor neurone discharge being attributed primarily to the burst neurones (EBN) and pause neurones (OPN) within the paramedian pontine reticular formation, this region of the brainstem being associated with the generation of saccades. Thus lesions here cause paralysis of gaze; electrical stimulation activates motor neurones with a latency of less than 3 msec, whilst horseradish peroxidase injections reveal direct connections with the abducens nucleus. Also, as we have seen, the region has neurones correlated with saccades. The pause neurone plays a complementary role, discharging regularly during maintained fixation, or when making smooth following movements in relation to visual or vestibular stimuli. Some 10–12 msec before the saccade, the pause neurone exhibits a reduction or cessation of its discharge, thereby releasing EBN from its inhibition. A third group, the tonic neurones (TN), fire steadily during fixation; these neurones fire at regular rates depending on eye position, so that their integrated discharge provides information as

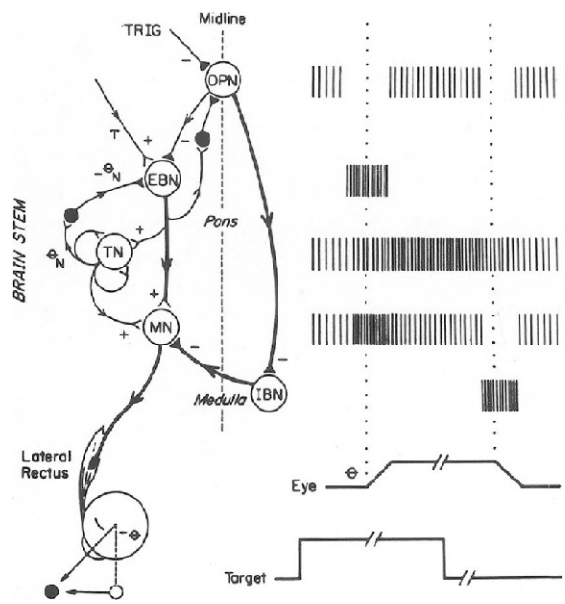

Fig. 25.73 Schematic representation of the circuitry and firing patterns of brainstem neurones involved in the genesis of saccades. At lower left, a target-spot jumps to the side, causing neurones in both the pons and medulla to change their discharge-rates to produce a saccade (θ). The thick connections in the circuit diagram have been verified, whereas the thin connections are from a popular model of the saccade generator. EBN, excitatory burst neurone; IBN, inhibitory burst neurone; OPN, omnidirectional pause neurone; MN, motor neurone; TN, tonic neurone. (Fuchs & Kaneko, *Trends in Neurosci.*)

to just how far the eye has moved at any time during the saccade. In this way it is able to indicate the error i.e. the difference between the required position and actual one, an integration that no longer depends on a visual stimulus but essentially on the computed position of the eye. A third group, the tonic neurones, discharge steadily during fixation, firing at rates that increase linearly as the eye moves into a new position. During a saccade, the tonic neurone changes its firing gradually between the pre- and post-saccadic rates; these neurones could clearly provide the step component that is necessary to maintain the new position of gaze. Luschei & Fuchs considered that the tonic neurone was responsible for the step component of firing rate in motor neurones. In the model, TN is thus seen as feeding forward to the motor neurone, participating in control of the saccade, but also feeding back negatively to turn-off the EBN when the error is zero. As pointed out by Fuchs & Kaneko (1981), the theory predicts that at least some burst neurones will discharge at a rate proportional to the error-signal at any moment; and this has been shown to be true by Van Gisbergen *et al.* (1981); secondly, stimulation of a pause neurone during a saccade should interrupt a saccade in midflight; Baker & Berthoz (1977) found that this was, indeed, true, the duration of the interruption being equal to that of the stimulus. Moreover, the interrupted saccade eventually reached its target, as would be predicted of the feedback model (Becker *et al.*, 1981).

The Error Signal

The position of the eye after the initiation of any movement can theoretically be assessed by counting the number of impulses in the burst discharge of the motor neurones. This integration is achieved, according to the circuit of Fig. 25.73 by feeding the impulses from EBN neurones into the tonic neurones, which provide a neural replica, or efference copy, θ_N, of eye position. A saccade is initiated by an input to the burst neurones which is proportional to the desired position, T, causing the EBN to discharge at its maximum rate. To turn this burst off at exactly the right time the EBN is inhibited by the neural replica of eye-position, so that when the eye reaches the target, and $\theta_N = T$, the inhibitory feedback cancels the excitatory input and the EBN stops discharging. Thus, the basis of the circuit is the control of the saccadic trajectory by an efference copy signalling eye-position, ensuring accurate fixation under a variety of situations. Between saccades, EBN is kept inhibited, a device that allows it to respond, when required, at low threshold, but not to be disturbed by 'noise' in the circuit; this inhibition is carried out by the pause units (OPN), which, just before the saccade, would be inhibited so as to allow the saccade to occur.

Scudder Model

Some of the shortcomings of the Robinson model have been discussed by Fuchs *et al.* (1985) in the light of experiments involving changing target position, e.g. those of Becker & Jurgens (1979), and a new model has been proposed that introduces a further integrating neurone, the long-lead burst neurone, which is directly programmed by the superior colliculus. The superior colliculus, as the study of Sparks & Porter (1983) indicated, takes into account altered position of target or eye-position, presumably, as Keller (1980) proposed, by receiving the neural replica of eye position derived from the integrated efference copy in the reticular formation, and compares this with target position to generate motor error.

The important point is that the motor error is fed directly into the excitatory burst neurones (EBN), as shown in the model, whereas Fuchs *et al.* (1985) argue that this is most unlikely since the superior colliculus, the most likely source of the trigger, T, does not project directly to short-lead burst neurones (Raybourn & Keller, 1977).

Identification of Pontine Neurones

As Fuchs & Kaneko (1981) emphasized, neurones with specific roles in the reticular formation are not usually arranged in anatomically separate groups, so that a functional atlas of the paramedian pontine reticular formation would be difficult to make. In the squirrel monkey Strassman *et al.* (1986) identified saccade-related neurones, and injected horseradish peroxidase to localize their somas and axonic projections. They identified a population of burst-excitatory neurones in the caudal pontine reticular formation, all giving a burst discharge before a saccade. They projected mainly to the abducens nucleus; other projections were to the medial vestibular nucleus, n. prepositus, and regions of the pontine reticular formation rostral, ventral and caudal to the abducens nucleus. They were related to both ipsi- and contralateral saccades, usually with a vertical component, but the firing was unrelated to this. They suggest that the pure horizontal saccades are obtained by a cancellation of excitatory and inhibitory burst neurone discharges directed to the vertical motor neurone pools. Inhibitory burst neurones, associated with reciprocal inhibition of the lateral and medial recti, were located ventrally and caudally to the abducens nucleus, projecting contralaterally to this; other projections were similar to those of the excitatory burst neurones. The mean lead-time was 12.7 compared with 10.4 msec for the excitatory burst neurones. In discussing the role of the superior colliculus in discharges of these medium-lead neurones the authors considered it unlikely that its neurones would activate them directly, and suggested that long-lead neurones in the reticular formation were the more likely to be first activated, as suggested in the model developed by Scudder (Fuchs *et al.*, 1985).

Site of the Integrator

Cannon & Robinson (1987), after reviewing the evidence favouring various brainstem nuclei as the likely locus of the integrator, considered that the nucleus prepositus hypoglossi was the most likely. Lopez-Barneo *et al.* (1982) also reviewed the history of the idea that it was closely concerned in control of eye movements. Thus Hyde & Eliasson (1957) described a hindbrain centre for the control of horizontal gaze caudal and ventral to the

abducens nucleus; Uemura & Cohen (1973) found defects in optokinetic nystagmus and after-nystagmus after lesions there. Nearly every neurone of the nucleus receives from the vestibular nuclei, and prepositus can excite motor neurones monosynaptically. Cannon & Robinson injected neurotoxins, kainate and ibotenate, in the region of the medial vestibular and prepositus nuclei, causing reversible lesions. The time-constant for the integrator was assessed by the velocity of centripetal drift just after an eccentric saccade made in total darkness; thus a perfect integrator would show no leakiness and the stored command should remain intact; in the normal animal this is not always true and a long time-constant of greater than 20 sec was measured. In kainate-treated animals the time-constant was drastically reduced, in the sense that, after a saccade, the eyes drifted back to their null position, giving time-constants for horizontal saccades of about 2.0 sec. Figure 25.74 illustrates the post-saccadic drifts at times after the injection. Essentially similar effects, indicating failure of the integrator, were found when studying the vestibulo-ocular and optokinetic reflexes; thus, instead of receiving velocity signals that led to smooth movements corresponding to the velocity of rotation, the initiation of movement caused a step-change in eye-position. Velocity storage was also damaged. Thus, with the vestibulo-ocular reflex, when the animal was rotated in a chair, there was no slow movement in the opposite direction, but rather there were brief changes in eye position that were attempted saccades.

Velocity Storage

This is the term applied to the change in the time-constant of the vestibular signal that reflects a tendency to counteract the decay of the signal that would occur normally with return of the cupula to its unperturbed position during rotation, or during post-rotation. Its time-constant is increased to some 16–20 sec compared with one expected of decay due to cupula relaxation of about 3–5 sec (Fernandez & Goldberg, 1971). In the kainate-treated animals the head-velocity signal decayed with a time-constant of 6 sec, about that expected of the cupula alone. As with vestibular stimulation, optokinetic nystagmus showed a change in velocity storage; this is normally manifest in the after-nystagmus that occurs, as described by Cohen *et al.* (1977). When the light of the

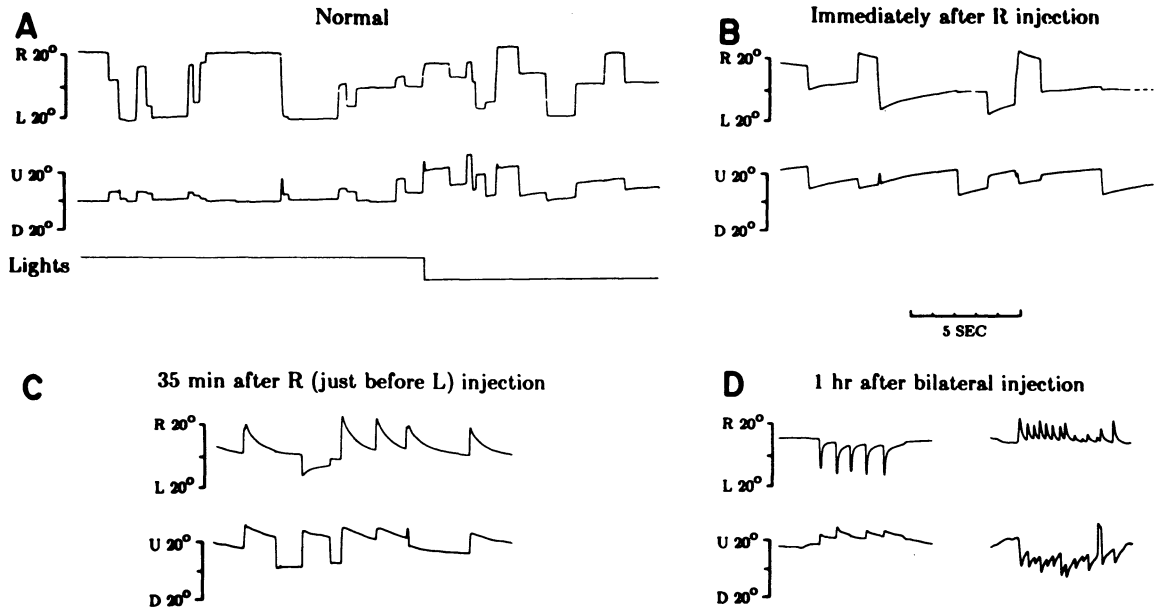

Fig. 25.74 Saccadic eye movements before and after injection. Horizontal eye position is on *upper trace*, vertical on *lower*. *A*: target-directed and spontaneous saccades recorded from a normal monkey. In the first half of the record the fixation target was alternated between right and left 20°. For the second half, spontaneous eye movements were recorded in total darkness. Notice that even in total darkness horizontal gaze holding is steady. The upward drift in darkness is a form of downbeat nystagmus found in many normal rhesus monkeys. *B–D*. each panel shows spontaneous saccades recorded in total darkness from the same monkey as in *A* at various times after the injection of 30 μg of ibotenate as indicated. The records in *D* are 2 excerpts from a continuous record to demonstrate that eye position drifts centripetally after both leftward and rightward saccades. The time constant of the horizontal drift decreases progressively from 2 to 0.6 to 0.2 s in *B-D*. *A–D* were recorded at the same time scale as indicated. R, L, U, D are right, left, up, and down. (Cannon & Robinson, *J. Neurophysiol.*)

rotating drum was switched off in kainate-treated animals the eye did not immediately return to its baseline null-point, indicating the operation of the eye-storage mechanism that would normally have induced an after-nystagmus; however, the time-constant for decay of the velocity storage was abnormally short, 3.5 sec compared with a normal values of about 16 sec.

Pursuit Eye Movements

After the kainate lesion, pursuit of a moving target was materially altered; instead of making a ramp eye movement in which the eyes rapidly matched the velocity of the moving target, the eyes made a step-change in eye position suggesting that a direct command had been made to the motor neurones, bypassing the neural integrator. The similarity in deficits in nystagmus-evoked slow movements and the following movement tends to confirm the belief that the same basic mechanism comes into play in all cases (Robinson, 1981).

Electrolytic Lesions

Cheron *et al.* (1986), making bilateral electrolytic lesions within and around the prepositus nucleus, found defects in saccades and in the vestibulo-ocular reflex that were consistent with the loss of the integrator; thus in the vestibulo-ocular reflex there was a large phase-lead of as much as 90° at low sinusoidal frequencies. A considerable post-saccadic drift was also observed, indicating the failure of the step-mechanism following the burst discharge, the step mechanism being the sustained discharge that maintains the eyes in their new position. According to Robinson's models, the step-command could be obtained by processing the initial pulse-signal in the integrator; thus post-saccadic drift would be expected to follow from the lesions.

OCULAR AND VESTIBULAR INTERACTION

We have seen that ocular and vestibular inputs meet in the vestibular nuclei, an interaction that was described by Ohm (1936). That the vestibular nuclei are not a necessary stage in the circuitry for optokinetic nystagmus was suggested by the observation that, in cases of streptomycin lesions of the vestibular nuclei, severe enough to abolish caloric nystagmus, optokinetic nystagmus could be elicited (Dix *et al.*, 1949). However, optokinetic after-nystagmus and nystagmus are affected by labyrinthectomy, presumably because tonic inputs from the labyrinth are necessary for adequate function of the vestibular nuclei; thus after-nystagmus was permanently lost, suggesting that the vestibular nuclei are concerned in velocity storage (Raphan *et al.*, 1977). The slow rise in slow-phase velocity, succeeding the initial rapid rise in optokinetic nystagmus, is due to velocity storage, and Raphan *et al.* showed that the maximum rise in slow-phase velocity was equal to the initial fast rise in the normal subject. According to the model suggested by Raphan *et al.*, the vestibular and optokinetic mechanisms have their separate routes to the eye muscles, but share an integrator that is responsible for velocity storage. Another integrator, that postulated by Skavenski & Robinson (1973), performs a velocity-to-position transformation in activity to drive the oculomotor musculature.

Torsion-swing Responses

Baarsma & Collewijn (1974) measured the rabbit's responses to sinusoidal yaw movements on a torsion-swing under conditions where the vestibular response could be examined in isolation (eyes closed), when it co-operated with the optokinetic response (eyes open), and when an artificial situation was created in which the visual environment moved in unison with the swing, so that there was conflict between the vestibular reflex, demanding movement of the eyes away from the direction of movement, and the optokinetic reflex which demanded a stationary position of the eyes, since the visual environment had not moved. The variables measured were the *gain*, which in this case was defined as the amplitude of eye movement/amplitude of swing movement, and the *phase-shift* defined as 0° when the eye movement is shifted 180° with respect to the swing movement and in phase with the visual movement of earth-fixed surroundings, i.e. the phase-shift was zero if there was exact compensation. The main results are summarized in Fig. 25.75; the increase in gain on opening the eyes (B compared with A) is obvious.

Non-linearity of Vestibular Response

An important feature of the purely vestibularly evoked response was its non-linearity with respect to frequency of oscillation, so that at low frequencies, and therefore with low velocities and accelerations, the gain was low, and only at high frequency did it reach a maximum of about 0.8; similarly there was a phase-lead which could be as high as 50° at low velocities but reached zero—perfect compensation—at high frequency. This non-linearity was abolished by opening the eyes with an earth-fixed environment (B of Fig. 25.75) where it is seen that, at low and high frequencies of swing oscillation, there is perfect compensation with respect to both gain and phase.

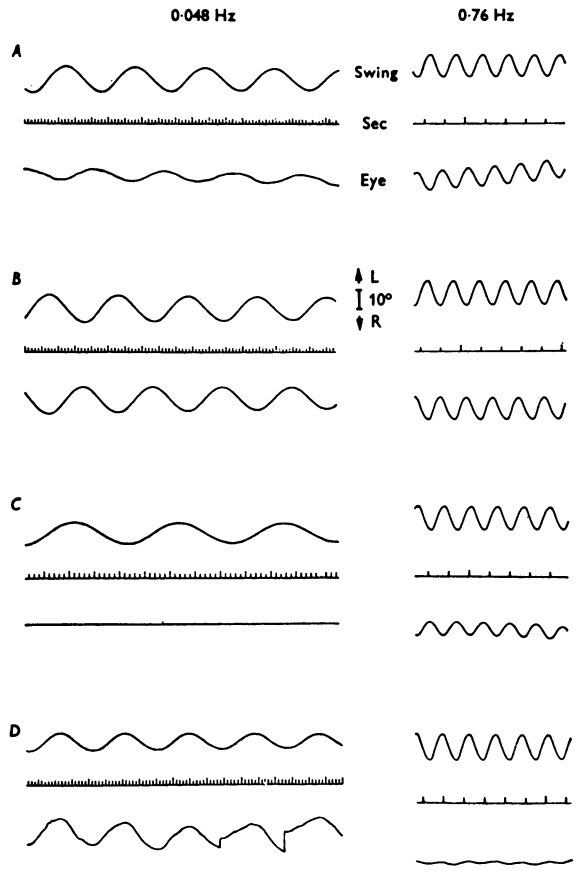

Fig. 25.75 Examples of compensatory eye movements on the torsion swing, for an amplitude of about 5° and frequencies of 0.048 and 0.76 Hz. A: Eyes closed. B: Eyes open, earth-fixed visual surroundings. C: Eyes open, platform-fixed visual surroundings. D: Eyes open, earth-fixed surroundings, labyrinthless animal. Calibrations valid for both swing and eye movements, except that polarity of eye movement recording in D has been inverted. (Baarsma & Collewijn, *J. Physiol.*)

Vestibulectomized Animal

When the optokinetic system is examined in isolation, i.e. in the vestibulectomized animal, it is found that the gain varies *inversely* with the velocity of movement, in marked contrast to the situation with the normal animal in the dark where the gain increases with velocity; thus the *vestibular system is tuned to operate at high velocities* and the *optokinetic system at low velocities*, so that when they both operate, as in Fig. 25.75B, there is a practically constant gain and negligible phase-error. Figure 25.75D illustrates the result with the labyrinthectomized animal; at low swing-frequency, compensation is good but at high frequencies gain is very small.[45]

Abnormal Situation

The abnormal stimulus-situation, with swing-fixed visual environment, caused an accentuation of the non-linearities described above for the animal swung in the dark, so that, as Fig. 25.75C shows, at low frequency there was virtually no eye movement (gain zero); at the higher frequency gain was improved and phase-lead, which could be as high as 70° at low frequency, was reduced.

Human Studies

Koenig *et al.* (1978) quantified the interaction between vestibular and optokinetic nystagmus in human subjects and concluded that the signals created by retinal image stabilization and the vestibular reflex systems combined to a weighted sum within the central nervous system to produce a single slow-phase velocity output. Thus combined rotation and optokinetic stimulation gave a better gain at high accelerations and velocities. They elicited an optokinetic nystagmus with a rotating drum and then accelerated the subject in the opposite direction so that the speed of rotation equalled the speed of the drum; there was an enhancement of the slow-phase movement. Under suitable stimulus-conditions, e.g. 30 deg/sec drum velocity and 12 deg/sec^2 vestibular acceleration, the enhancement could lead to a slow-phase velocity that, over a few seconds, exceeded the pattern-velocity by a few deg/sec. If the chair was rotated at the same speed as the drum, the nystagmic response was reduced to about 13% of its maximum during pure vestibular stimulation.

Neurophysiological Studies

Waespe & Henn (1977) have reviewed early evidence on vestibulo-ocular interactions; in their own quantitative study they identified Type I and Type II vestibular nuclear neurones, and found that all responded to rotation of a striped drum as well as to vestibular stimulation; thus Type I units, excited by acceleration to the ipsilateral side were also excited by optokinetic stimuli in the opposite direction, stimuli that elicit nystagmus in the same direction. The maximum response to optokinetic stimuli was usually about 70% of that obtained with the labyrinthine stimulus. Figure 25.76 illustrates the average responses to vestibular stimulation only; to vestibular stimulation plus viewing the striped drum, and to rotation of the striped drum only. The plateau phases for rotation in the light and rotation of the striped drum are about the same.[46]

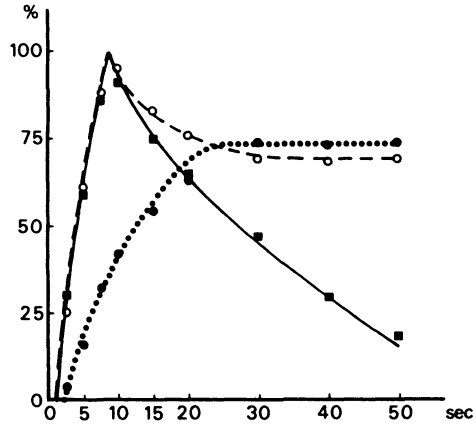

Fig. 25.76 Average frequency responses from 6 neurones (3 type I and 3 type II units) during chair rotation in the dark (solid line), chair rotation in the light (broken line), and cylinder rotation around the stationary animal (dotted line). Abscissa is time in seconds after start of a 7.5 sec acceleration, after which stimulus maintains a constant velocity of 60°/sec. Ordinate is the normalized response. 100% is the maximum activation of units while animals are turned in the dark. Note that initially the response to animal rotation in the dark and the light are similar. During the plateau phase frequencies are not significantly different for turning the animal in the light or turning the cylinder around the stationary monkey. (Waespe & Henn, *Exp. Brain Res.*)

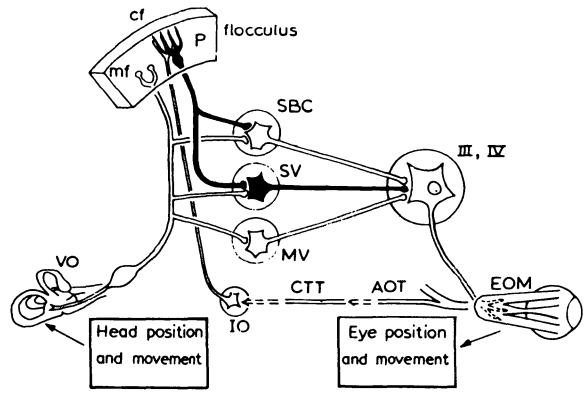

Fig. 25.77 Neuronal diagram for the vestibulo-ocular reflex arc. VO, vestibular organ; SBC, sources of brachium conjunctivum pathways arising from the lateral cerebellar nucleus and the Y group of the vestibular nuclei complex; III, IV, IIIrd and IVth oculomotor nuclei; EOM, extra-ocular muscles; SV, superior vestibular nucleus; MV, medial vestibular necleus; mf, mossy fiber terminal; cf, climbing fiber terminal; P, Purkinje cell; IO, inferior olive; AOT, accessory optic tract; CTT, central tegmental tract. Inhibitory neurones are filled in black. (Ito *et al., Brain Res.*)

Cerebellar Neurones

Ito *et al.* (1974) considered that the visual input to the flocculus operated a feedback from the retina to correct the vestibulo-ocular reflex, thereby improving the stability of the retinal image. In the rabbit they showed that presentation of a slit of light during vestibular nystagmus enhanced the horizontal slow movement; moving the slit in phase with the rotating turntable reduced this enhancement, showing that the enhancement was caused by a retinal-slip stimulus. If the flocculus was destroyed on the left side, the slit failed to enhance movement of the left eye, whereas it did that of the right eye. Ito (1972) suggested a model circuit attached as a side-loop to the primary three-neurone arc of the vestibulo-ocular reflex, as in Fig. 25.77; thus, after making excitatory synapses with the vestibular nucleus relay-neurone, the primary vestibular afferent fibre enters the flocculus and terminates in the cerebellar cortex as a mossy fibre input. The Purkinje cell in the flocculus projects to the vestibular nucleus to make an inhibitory contact on the relay-neurone.

Open and Closed Loops

Ito emphasized the difference between vestibular control of the body musculature through vestibulospinal reflexes, and the vestibular control over the eyes. In the former, the activation of the muscles is associated with direct feedback from these, indicating the position of the limb, or head, to give a closed loop control. By contrast, the eye muscles are activated by the vestibule, but the position of the eyes, required as information for correctional feedback, is derived from the visual, and not from the vestibular apparatus; the control is said to be through an open loop. Ito pointed out that closed loop controls are much more stable, whereas an open-loop one may be easily perturbed; however, the visual information is integrated within the cerebellar cortex which behaves as a computer linked with the open loop control system, eventually leading to an accurate control over eye position. Such a system provides the opportunity for interaction of vestibular and visual reflexes.

Notes

1. It must be appreciated that many muscles are mixed, containing both twitch and slow fibres; in the mammal, for example, Close (1967) described slow and intermediate types of unit in the soleus, whereas the extensor digitorum longus contained only fast fibres.
2. The multiple endings on the slow grape-termination muscle fibres suggest a multiple innervation, although all the grape endings could have been derived from a single fibre; intra-

cellular recordings of these fibres has indicated a multiple innervation (e.g. Hess & Pilar, 1963). Bach-y-Rita & Lennerstrand (1975) have denied the existence of polyneural innervation of cat extraocular muscles, but as Browne (1976) points out, their measurements could only apply to the twitch-type fast fibres.

3. Bach-y-Rita & Ito (1966) disputed this difference between slow and fast fibres and considered that both were of the twitch type, but Pilar (1967) has confirmed, with additional experiments, the qualitative difference between the responses in the two types of fibre. It may be, however, that there are three types of fibre: fast and slow twitch-types, and slow graded fibres (Peachey, 1968). In some extraocular muscles, e.g. the superior oblique studied by Hess & Pilar, the *Felderstruktur* fibres are large and plentiful by comparison with the inferior oblique. Hess (1967) has summarized the similarities and differences between submammalian skeletal and mammalian extraocular muscle fibres.
4. The length-tension diagrams were obtained by holding the muscle of one eye at a fixed length and asking the subject to gaze at points farther and farther in the field of action of the muscle, i.e. more and more nasally for the medial rectus; since the nervous discharge to the muscle increases with increasing size of saccade, this means that graded degrees of 'innervation' of the muscle could be obtained for each artificially maintained length.
5. The effects of several cholinomimetics on the cat's extraocular muscles have been examined by Sanghvi & Smith (1969); spike activity certainly occurs, perhaps due to the twitch fibres only. Muscarine has a smaller effect than that of acetylcholine, which is blocked by atropine, so that the receptors are mainly 'nicotinic'.
6. The responses recorded from N III when the cat's inferior oblique was stretched have been examined in great detail by Bach-y-Rita & Ito (1966), and compared with the responses from true muscle spindles in skeletal muscle. In general, it seems that the receptor-organ of the cat extraocular muscle is simpler, without any gamma-efferent control.
7. As summarized by Manni *et al.* (1974) the central processes of the trigeminal neurones, concerned with proprioception, enter the ipsilateral trigeminal root and run in the descending trigeminal tract to end in the oral part of the descending nucleus and in the main sensory nucleus. Second-order neurones run to the thalamus, tectum and tegmentum.
8. Brindley *et al.* (1976) pointed out that, when the eye muscles are completely paralysed, attempted eye movements failed to give the illusion of object movement, as would be expected of corollary discharge (Siebeck, 1954; Stevens *et al.*, 1976). In their own studies, so long as the eye muscles were completely paralysed, an attempted eye movement involving the paralysed muscles produced no illusion; partial paralysis did. If one eye was completely paralysed and the other not, then an after-image appeared to move with movements of the non-paralysed eye, but there was no movement when movement was attempted involving the paralysed muscle.
9. We may note the danger of confusion according as the direction of the nystagmus is described in terms of the quick component or the direction of rotation of the drum; thus when Carmichael, Dix & Hallpike (1954) say that nystagmus to the healthy side is suppressed, they are referring to the quick phase of the nystagmus, so that there is suppression of nystagmus when the drum rotates away from the healthy side, i.e. towards the lesion.
10. Precht (1981) has described the activities of vestibular neurones in rat and rabbit, with uncrossed visual pathways, under binocular and monocular conditions, with lesions in the pretectum designed to put the nucleus of the optic tract out of action, considered to be the important visual station in the optokinetic pathway. The results on vestibular neurones were consistent with this view; since there are apparently no direct pretectal projections to the vestibular nuclei the n. reticularis tegmenti pontis was suspected as a relay station; response deficits were similar to those found in pretectal lesions. When the vestibular commissure was sectioned transfer of optokinetic signals from one side to the other was abolished.
11. The *rhythm* of the nystagmus will be largely determined by the amplitude of the excursions for a given speed of rotation; the fact that this alters under a variety of experimental conditions is further proof that the initiation of the fast movement, which puts an end to the slow movement, is not due to the eyes reaching the maximal extent of the field of fixation. We may note that, according to Ter Braak (1936), the eyes lag slightly behind the movement of the drum during the slow phase; consequently there is a slight drift of the retinal image over the retina.
12. The effects of electrical stimulation of the ampulla of a single canal have been described by Fluur (1959), but as he points out, this is an exceedingly artificial procedure, since under normal conditions of stimulation, there are reactions in both sides of the head simultaneously. Stimulation of the left lateral canal caused a conjugate movement to the right; of the left anterior vertical canal a conjugate movement upwards, and the left posterior vertical canal a conjugate movement downwards. Combined stimulation of the left anterior and posterior canals caused a conjugate counterclockwise rolling.
13. Because of the involvement of proprioceptive impulses from the neck muscles in eye movements, we might expect irritative lesions in the cervical cord to cause nystagmus; in fact they do. Presumably impulses pass up the cord in the spinovestibular pathways which connect the proprioceptive centres of the cord with the inferior vestibular nuclei; within the vestibular areas there is a transfer of impulses to pathways connecting with the oculomotor nuclei (Crosby, 1953).
14. Barnes (1979), in a careful study of the human, found that the movement of the head in the dark gave rise to a similar initial saccade and slower return towards orbital centre, indicating a role of the vestibular apparatus in the visually directed gaze-movement. With fixating targets offset by more than 60°, there were often large errors, 22% of responses undershooting the target by more than 15°. The author has discussed in some detail the relation between vestibular and visually determined saccades; under normal conditions it is likely that any vestibular command for a saccade would be suppressed by the visual system; with very large head movements, however, Barnes considered that gaze-displacement was generated as an automatic response to head-turning.
15. Dichgans *et al.* (1973) found that this stabilization of the eyes during head movements was just as efficient in the dark as in the light; after labyrinthectomy it was abolished, but there was a remarkable compensation with time, which was retained in spite of de-afferentation of the neck-muscles. In some way, information from the neck-programming centre governing the intended head movement is fed forward to the oculomotor centres.
16. McCrea *et al.* (1986) studied the activities of abducens motor and internuclear neurones during eye movements in the alert squirrel monkey. As with motor neurones, the internuclear neurones gave discharges related to eye-position and velocity. Over 40% of the internuclear neurones gave rise to collaterals, half of these projecting to the intermediate

nucleus of the medial longitudinal fasciculus (MLF) or the adjacent raphe, and the other half to the caudal interstitial nucleus of the MLF. The other sixty per cent gave no collaterals. All terminations in N III were in the division for the medial rectus muscle.

17. The technique and many of the pitfalls in interpretation of the EMG have been described in some detail by Marg *et al.* (1959).
18. This is true of all the extraocular muscles, so that all three antagonistic pairs are constantly pulling against each other at rest; the oblique muscles are less active than the recti. According to Björk & Wahlin (1960) the resting activity is absent in sleep and general anaesthesia.
19. The motor neurones to other muscles, such as the gastrocnemius or soleus, usually discharge at rates far below their maximum possible; this 'stabilization' is due, partly at any rate, to the recurrent negative feedback through Renshaw cells. According to Sasaki (1963), the eye-muscle motor neurones do not show this recurrent inhibition; and this may account for the much higher rates of discharge.
20. Keller (1974), during his study of single units of the medial pontine reticular formation in the waking monkey, stimulated the sites of recording and found a single type of movement, whatever the type of unit—burst, tonic, etc. from which he recorded; this was the constant-velocity type described by Cohen & Komatsuzaki, the eyes accelerating smoothly through a transient phase to reach a constant velocity maintained as long as the stimulation, the velocity varying linearly with frequency of stimulation up to 500/sec.
21. Baker *et al.* (1977) found a weak monosynaptic input to trochlear motor neurones. They considered that the nucleus was concerned with integration rather than producing a direct command to motor neurones, as previously suggested.
22. Hikosaka *et al.* (1978) point out that many prepositus neurones receive reciprocal inputs disynaptically from the vestibular nerve on each side, and they respond to rotation of the head (Fukushima *et al.*, 1977); Hikosaka *et al.* (1978) described Type I_B and Type II_B neurones according as they increased or decreased firing rate with direction of angular acceleration, by analogy with vestibular neurones. The prepositus neurones had an excitatory input to the medial rectus motor neurones during ipsilateral horizontal eye movements; actually an inhibitory input would be expected, so these prepositus neurones were presumably modifying the inhibition, derived more immediately from, say, vestibular or reticular neurones.
23. In an article entitled 'Some thoughts about the three neurons in the vestibular ocular reflex' Baker *et al.* (1981) discuss the more complex relations of the individual neurones to the execution of oculomotor tasks than was envisaged by Llorente de No's original concept.
24. Berthoz *et al.* (1981) have described, in the waking cat, vestibular neurones that discharged in relation to both vestibular stimuli and eye-position signals. They emphasize that vestibular nucleus second-order neurones are not simple relay-neurones but are highly complex neurones integrating a number of signals in order to control eye movement from a premotor level. Thus the nearly complete suppression of the vestibulo-ocular slow-movement discharges during a saccade probably corresponds to the occurrence of rapid saccades when the head makes a rapid gaze movement of fixation, as described, for example, by Barnes (1979).
25. The superficial laminae are exclusively visual in input; the intermediate layers combine visual, somatic and acoustic inputs, whilst the deepest layers are essentially non-visual Stein *et al.*, (1976). Tactile representation in the deeper layers is in register with visual representation in the overlying layers, so that the magnified representation of the visual field overlapped with the tactile representation of the face. In general, the overlap could be described by viewing the visual field as a flexible sheet stretched over the body with the area centralis on the nose and the limbs radiating out at acute angles. Such an overlap would suggest an involvement in coordinating visual input with motor activity in the limbs and face.
26. Grantyn & Grantyn (1976) examined the synaptic actions of tectofugal pathways on abducens motor neurones; from their latencies it was concluded that most excitatory synaptic potentials were disynaptically mediated; however, there were some monosynaptic synaptic potentials, indicating a direct access to the motor neurones, but this might have been through the internuclear neurones. The inhibitory pathway was at least disynaptic and usually trisynaptic. The interneurones on the excitatory pathway lay in the pontine tegmentum on the same side as the motor neurones; ipsilateral stimulation of the n. reticularis pontis oralis evoked excitatory postsynaptic potentials in ipsilateral motor neurones.
27. Straschill & Rieger (1973) working on the cat, found, in contradiction to Robinson, that the magnitude of the saccade was not completely determined by the position of stimulation on the colliculus but that it increased with current strength and suggested that Robinson's weakest stimuli had already saturated the system. Continuous stimulation did not produce a series of saccades, but usually just one with subsequent maintenance of fixation. The final position achieved by the eyes was independent of their initial position so that in the cat the stimulus leads to a *goal-directed* response; consequently only in the primary position does the sensory map match the motor map.
28. Cynader & Berman (1972) point out that the foveal representation of the colliculus, i.e. the region that, when stimulated, directs the eye towards peripheral stimuli that fall on the fovea, receives only a cortical projection (Wilson & Toyne, 1970).
29. Robinson & Jarvis (1974) raised the question as to whether the collicular discharge that precedes an eye movement was due to an intended eye movement or, because the head was fixed in these experiments (e.g. Schiller & Stryker, 1972) it was related to an intended head movement. In their study they were able to dissociate head and eye movements and found a better temporal relation of the saccade to the collicular discharge than the head movement.
30. Sprague (1966) demonstrated an inhibitory action of one superior colliculus on the activity of the other; thus in the cat removal of striate cortex unilaterally prevented visually guided movements; these returned, however, when the contralateral colliculus was removed or the intertectal commissure cut.
31. Tusa *et al.* (1986) point out that so-called blind-sight is difficult to detect in most human subjects with occipital cortical lesions; this could be due to the fact that these are usually due to infarctions that have damaged more than the striate area.
32. Bruce & Goldberg (1985a) show that the frontal eye field discharges could not be regarded as an 'efference copy' of actual command signals, such as that postulated to provide the basis for recognition of eye-position; thus the presaccadic activity occurs when the monkey fails to make the saccade it was trained to make. Postsaccadic activity, however, reliably follows saccades regardless of cause and may well fulfil this role (Bizzi, 1968).
33. Earlier, in the cat, Schlag & Schlag-Rey (1971) obtained

saccadic, conjugate and contraversive eye movements by stimulating a low-threshold region in the internal medullary lamina; these were independent of the cerebral cortex and corpus striatum and were abolished by small caudal lesions, indicating a thalamo-mesencephalic pathway. They discussed the possibility of antidromic stimulation of reticulothalamic neurones that bifurcated and sent a caudal branch to oculomotor neurones. Such a reticular cell could send an 'efference copy' of motor excitation to the thalamus.

34. Unfortunately space does not allow the detailed description of the experiments carried out by these authors, using ingenious experimental paradigms that revealed special features of the visuomotor activity of nigral cells; of special interest are memory-contingent units that were revealed when the monkey was required to remember the position of a briefly presented stimulus, being rewarded if it made a successful saccade to this position when the stimulus was no longer present. The memory-contingent saccade response usually preceded the saccade onset by 70 to 240 msec.
35. According to Hyvärinen & Poranen, in the monkey, sensory processes end in this region of the cortex; in man it is carried further to areas 40 and 39, lesions here giving rise to apractognosia. The authors discuss the terminology of this region as applied to monkey and man; thus area 7 or PF and PG of the monkey can be compared with the same region in human brain variously called area 7, PF and PG, or 40 and 39.
36. A study of Fig. 25.59 shows how important accurate measurement of eye position and velocity are if defects in visual performance are to be demonstrated; thus 400 msec after the step-ramp stimulus the monkeys are following the target perfectly in both the normal and lesioned state; the defects appear in the initial 200–400 msec period.
37. In the rabbit, stimulation of the optic disc caused field potentials in the inferior olive, giving rise to a mossy fibre input to Purkinje cells in addition to their climbing fibre input. The origin of the climbing fibres was studied by Alley *et al.* (1975) with horseradish peroxidase injections; labelling was in the rostral third of the medial accessory olive, the dorsal cap of the principal olive, and also the inferior olive from the nodulus. The double visual input was thought by Maekawa & Takeda (1975) to operate a feedback on the vestibulo-ocular reflex and to account for visual influence on the reflex.
38. McElligott & Keller (1984) produced saccades in monkeys in lobules V–VII, the direction and size depending on the position of the eyes when stimulated. They considered that the saccades arose from antidromic stimulation of mossy fibres emanating from the saccadic burst generator in the brainstem, thereby avoiding cerebellar circuits. Fujikado & Noda (1987) reject this explanation, however; thus the saccades may be blocked by injections of bicuculline, an inhibitor of GABA-ergic inhibitory activity, into the fastigial nucleus, presumably blocking the inhibitory activity of Purkinje cells that releases the oculomotor centres from ongoing inhibition.
39. Lisberger & Fuchs (1978b) compared mossy fibre input to the flocculus with the responses of Purkinje cells; they discuss the possibility that the 'efference copy' of motor activity that is presumed to signal eye-position is carried by these fibres. The necessity for a corollary discharge was demonstrated by Heywood & Churcher (1971) when they showed that smooth tracking eye movements were made during tracking of an after-image where there could have been no retinal error to act as a stimulus.
40. In the chinchilla Hassul *et al.* (1976) showed that the improvement of the gain of the vestibulo-ocular reflex at low frequencies on illuminating the visual field was inhibited by flocculectomy.
41. Robinson (1977) has discussed the mode of summation of vestibular and optokinetic signals; thus Waespe & Henn (1977) examined the transient and sustained responses in the vestibular nucleus neurones with rotation in the dark and light, and concluded that summation must be very non-linear. However, Robinson argued that simple superposition of signals from the two systems should not apply, as the conditions of rotation in dark and light are different, the optokinetic feed-back loop being open in the dark; employing his neural model he was able to fit the experimental results on the basis of a linear addition of signals in the vestibular nuclei. Raphan *et al.* (1977) have discussed the neural site of the storage mechanism; The effects of labyrinthectomy suggest that tonic activity from the labyrinth within the vestibular nuclei is a factor; destruction of the vestibular nuclei is also associated with loss of optokinetic after-nystagmus, the manifestation of storage.
42. Lynch *et al.* (1985) emphasize the different projections of the portion within the inferior bank of the intraparietal sulcus (area POa of Seltzer & Pandya, 1980), and the adjoining part of area PG on the convexity of the hemisphere. It is POa that has the dense projection to the superior colliculus.
43. Keller & Crandall (1983) have reviewed their studies on the NRTP of the monkey, and emphasize the number of neurones that seem to be specifically responsive to movement of small stimuli. The saccade-related cells showed a movement-field organization reminiscent of the deeper superior colliculus cells; on a step movement of a spot-stimulus there was usually a small presaccadic discharge followed by a burst. With a sinusoidal spot movement some neurones modulated their discharge in a tracking-type of response.
44. Schiller & Sandell (1983) showed that a similar compensation for error, induced by prior excitation, could be obtained after stimulation of the frontal eye field; neither centre, however, is necessary for the execution of the compensation since it occurs in the absence of either, bilaterally. According to Guthrie *et al.* (1983) the compensation that corrects for eye-position occurs in the absence of extraocular signals, so that it is apparently the 'efference copy' of the command signals to the eye muscles that is made use of. Sparks *et al.* (1987) asked whether an eye movement, provoked by stimulation of the pontine reticular formation, could be compensated, this being the region thought to be involved in producing the efference copy of the eye-movement signal. Their experiments were equivocal, compensation occurring sometimes but not always; this was in contrast with collicular stimulation where compensation occurred invariably.
45. Godaux *et al.* (1983) have described a comparable study on the cat; many of the features of interaction were similar to those of the rabbit. However, the cat made quick interruptions of the stabilizing (slow) movement, by contrast with the rabbit, presumably because of the virtual lack of a fixation system in the afoveate rabbit; in man this target tracking is even more efficient; thus a cat cannot exceed velocities of 0.6°/sec, whereas man and monkey achieve 20°/sec and 45°/sec respectively. In optokinetic nystagmus the maximum slow-phase velocities are 28, 50 and 120 deg/sec in cat, man and monkey respectively.
46. Waespe *et al.* (1983) removed the flocculus bilaterally and unilaterally; they concluded that the effects were on the rapid phase, so that the velocity-storage mechanism was unaffected. Visual-vestibular interactions were unaffected.

References

Abrahams, V. C. (1972) Neck muscle proprioceptors and a role of the cerebral cortex in postural reflexes in primates. *Rev. canad. Biol.* **31**, Suppl., 115–130.

Abrahams, V. C. & Rose, P. K. (1975) Projections of extraocular, neck muscle and retinal afferents to superior colliculus in the cat: their connections to cells of origin of tectospinal tract. *J. Neurophysiol.* **38**, 10–18.

Alley, K., Baker, R. & Simpson, J. I. (1975) Afferents to the vestibulocerebellum and the origin of the visual climbing fibers in the rabbit. *Brain Res.* **98**, 582–589.

Astruc, J. (1971) Corticofugal connections of area 8 (frontal eye field) in *Macaca mulatta*. *Brain Res.* **33**, 241–256.

Baarsma, E. A. & Collewijn, H. (1974) Vestibulo-ocular and optokinetic reaction to rotation and their interaction in the rabbit. *J. Physiol.* **238**, 603–625.

Baarsma, E. A. & Collewijn, H. (1975) Eye movements due to linear accelerations in the rabbit. *J. Physiol.* **245**, 227–247.

Bach-y-Rita, P. & Ito, F. (1966) Properties of stretch receptors in cat extraocular muscles. *J. Physiol.* **186**, 663–688.

Bach-y-Rita, P. & Lennerstrand, G. (1975) Absence of polyneuronal innervation in cat extraocular muscles. *J. Physiol.* **244**, 613–624.

Baker, B., Gresty, M. & Berthoz, A. (1975) Neuronal activity in the prepositus hypoglossi nucleus correlated with vertical and horizontal eye movements in the cat. *Brain Res.* **101**, 366–371.

Baker, R. (1977) The nucleus prespositus hypoglossi. In *Eye Movements*, Ed. Brooks, B. A. & Bajandas, F. J., pp. 145–178. New York, London: Plenum Press. (Quoted by Kase *et al.*, 1980.)

Baker, R. & Berthoz, A. (1974) Organization of vestibular nystagmus in oblique oculomotor system. *J. Neurophysiol.* **37**, 195–217.

Baker, R. & Berthoz, A. (1977) (Quoted by Fuchs & Kaneko, 1981).

Baker, R., Berthoz, A. & Delgado-Garcia, J. (1977) Monosynaptic excitation of trochlear motoneurons following electrical stimulation of the prepositus hypoglossi nucleus. *Brain Res.* **121**, 157–161.

Baker, R., Evinger, C. & McCrea, R. A. (1981) Some thoughts about the three neurons in the vestibular ocular reflex. *Ann. N.Y. Acad. Sci.* **374**, 171–188.

Baker, R. G., Mano, N. & Shimazu, H. (1969) Postsynaptic potentials in abducens motoneurons induced by vestibular stimulation. *Brain Res.* **15**, 577–580.

Baker, R. & Precht, W. (1972) Electrophysiological properties of trochlear motoneurons as revealed by IVth nerve stimulation. *Exp. Brain Res.* **14**, 127–157.

Baker, R., Precht, W. & Berthoz, A. (1973) Synaptic connections to trochlear motoneurons determined by individual vestibular nerve branch stimulation in the cat. *Brain Res.* **64**, 402–406.

Baker, R., Precht, W. & Llinas, R. (1972) Mossy and climbing fiber projections of extraocular afferents to the cerebellum. *Brain Res.* **38**, 440–445.

Barbas, H. & Mesulam, M.-M. (1981) Organization of afferent input to subdivisions of area 8 in the rhesus monkey. *J. Comp. Neurol.* **200**, 407–431.

Barmack, N. H., Bell, C. C. & Rence, B. G. (1971) Tension and role of tension development during isometric responses of skeletal muscle. *J. Neurophysiol.* **34**, 1072–1079.

Barnes, G. R. (1979) Vestibulo-ocular function during co-ordinated head and eye movements to acquire visual targets. *J. Physiol.* **287**, 127–147.

Becker, W. & Jurgens, R. (1979) An analysis of the saccadic system by means of double step stimuli. *Vision Res.* **19**, 967–983.

Becker, W., King, W. M., Fuchs, A. F., Jurgens, R., Johanson, G. & Kornhuber, H. H. (1981) Accuracy of goal-directed saccades and mechanisms of error correction. (Quoted by Fuchs *et al.*, 1985.)

Bender, M. B. & Cohen, B. (1971) Lesions of the pontine tegmentum and conjugate gaze paralysis. *Arch. Neurol.* **24**, 431–440.

Bender, M. B., Postel, D. M. & Krieger, H. P. (1957) Disorders of oculomotor function in lesions of the occipital lobe. *J. Neurol. Neurosurg. Psychiat.* **20**, 139–143.

Berthoz, A., Yoshida, K. & Vidal, P. P. (1981) Horizontal eye movement signals in second-order vestibular nuclei neurons in the cat. *Ann. N.Y. Acad. Sci.* **374**, 144–156.

Bickford, R. G., Petersen, M. C., Dodge, H. W. & Sem-Jacobsen, C. W. (1953) Observations on depth stimulation of the human brain through implanted electrographic leads. *Proc. Staff Meetings Mayo Clinic* **28**, 181–187.

Bizzi, E. (1967) Discharge of frontal eye field neurons during eye movements in unanesthetized monkeys. *Science* **157**, 1588–1590.

Bizzi, E. (1968) Discharge of frontal eye field neurons during saccadic and following eye movements in unanaesthetized monkeys. *Exp. Brain Res.* **6**, 69–80.

Bizzi, E., Kalil, R. E. & Tagliasco, V. (1971) Eye-head coordination in monkeys: evidence for centrally patterned organization. *Science* **173**, 452–454.

Bizzi, E. & Schiller, P. H. (1970) Single unit activity in the frontal eye fields of unanaesthetized monkeys during eye and head movement. *Exp. Brain Res.* **10**, 151–158.

Björk, A. & Kugelberg, E. (1953) The electrical activity of the muscles of the eye and eyelids in various positions and during movement. *E.E.G. clin. Neurophysiol.* **5**, 595–602.

Björk, A. & Wahlin, A. (1960) Muscular factor in enophthalmos and exophthalmos. *Acta Ophthal.* **38**, 701–707.

Boeder, P. (1961) The co-operation of extraocular muscles. *Amer. J. Ophthal.* **51**, 469–481.

Brandt, T., Dichgans, J. & Koenig, E. (1973) Differential effects of central versus peripheral vision on egocentric and exocentric motion perception. *Exp. Neutol.* **16**, 476–491.

Brecher, G. A. (1934) Die optokinetische Auslösung von Augenrollung und rotorischem Nystagmus. *Pflüg. Arch. ges. Physiol.* **234**, 13–28.

Breinin, G. M. (1957a) Quantitation of extraocular muscle innervation. *Arch. Ophthal.* **57**, 644–650.

Breinin, G. M. (1957b) Electromyographic evidence for ocular proprioception in man. *Arch. Ophthal.* **57**, 176–180.

Brindley, G. S., Goodwin, G. M., Kulikowski, J. J. & Leighton, D. (1976) Stability of vision with a paralysed eye. *J. Physiol.* **258**, 65–66P.

Brinkman, C. & Porter, R. (1979) Supplementary motor area in the monkey: activity of neurons during performance of a learned motor task. *J. Neurophysiol.* **42**, 681–709.

Brouwer, B. (1918) Klinisch-anatomische Untersuchung uber den Okulomotoriuskern. *Z. ges. Neurol. Psychiat.* **40**, 152–193.

Browne, J. S. (1976) The contractile properties of slow muscle fibres in sheep extraocular muscle. *J. Physiol.* **254**, 535–550.

Bruce, C. J. & Goldberg, M. E. (1985) Primate frontal eye fields. I. Single neurons discharging before saccades. *J. Neurophysiol.* **53**, 603–635.

Bruce, C. J., Goldberg, M. E., Bushnell, M. C. & Stanton, G. B. (1985) Primate frontal eye fields. II. Physiological and anatomical correlates of electrically evoked eye movements. *J. Neurophysiol.* **54**, 714–734.

Buisseret, P. & Maffei, L. (1977) Extraocular proprioceptive projection to the visual cortex. *Exp. Brain Res.* **28**, 421–423.

Burgi, S. (1957) Das Tectum opticum. Seine Verbindungen bei der Katze und seine Bedeutung beim Menschen. *Deutsch. Z. Nervenheilk.* **176**, 701–729.

Burke, R. E., Levine, D. N., Tsairis, P. & Zajac, F. E. (1973) Physiological types and histochemical profiles in motor units of the cat gastrocnemius. *J. Physiol.* **234**, 723–748.

Bushnell, M. C., Goldberg, M. E. & Robinson, D. L. (1981) Behavioral enhancement of visual responses in monkey cerebral cortex. I. Modulation in posterior parietal cortex related to selective visual attention. *J. Neurophysiol.* **46**, 755–772.

Büttner, U., Hepp, K. & Henn, V. (1977) Neurons in the rostral mesencephalic and paramedian pontine reticular formation generating fast eye movements. In *Control of Gaze by Brain Stem Neurons*, Ed. Baker, R. & Berthoz, A. pp. 309–318. Amsterdam, New York: Elsevier. (Quoted by Kase *et al.*, 1980.)

Cannon, S. C. & Robinson, D. A. (1987) Loss of neural integrator of the oculomotor system from brain stem lesions in monkey. *J. Neurophysiol.* **57**, 1383–1408.

Carmichael, E. A., Dix, M. R. & Hallpike, C. S. (1956) Pathology, symptomatology and diagnosis of organic affections of the eighth nerve system. *Br. med. Bull.* **12**, 146–152.

Carpenter, M. B., Harbison, J. N. & Peter, P. (1970) Accessory oculomotor nuclei in the monkey: projections and effects of lesions. *J. Comp. Neurol.* **140**, 131–153.

Carpenter, R. H. S. (1972) Cerebellectomy and the transfer function of the vestibulo-ocular reflex in the decerebrate cat. *Proc. Roy. Soc. B* **181**, 353–374.

Chambers, W. W. & Sprague, J. M. (1955a) Functional localization in the cerebellum. I. *J. Comp. Neurol.* **103**, 105–129.

Chambers, W. W. & Sprague, J. M. (1955b) Functional localization in the cerebellum. II. *Arch. Neurol. Psychiat.* **74**, 653–680.

Cheron, G., Godaux, E., Laune, J. M. & Vanderkelen, B. (1986) Lesions in the cat prepositus complex: effects in the vestibulo-ocular reflex and saccades. *J. Physiol.* **372**, 75–94.

Close, R. (1967) Properties of motor units in fast and slow skeletal muscles. *J. Physiol.* **193**, 45–55.

Close, R. I. & Luff, A. R. (1974) Dynamic properties of inferior rectus muscle of the rat. *J. Physiol.* **246**, 259–270.

Cogan, D. G. (1954) Ocular dysmetria: flutter-like oscillations of the eyes, and opsoclonus. *Arch. Ophthal.* **51**, 318–335.

Cohen, B. (1971) Vestibulo-ocular relations. In *The Control of Eye Movements*. Ed. P. Bach-y-Rita & C. C. Collins. Academic Press: N. Y. pp. 105–148.

Cohen, B. & Henn, V. (1972) Unit activity in the pontiné reticular formation associated with eye movements. *Brain Res.* **46**, 403–410.

Cohen, B. & Komatsuzaki, A. (1968) Electroculographic syndrome in monkeys after pontiné reticular formation lesions. *Arch. Neurol.* **18**, 78–92.

Cohen, B. & Komatsuzaki, A. (1972) Eye movements induced by stimulation of the pontiné reticular formation: evidence for integration in oculomotor pathways. *Exp. Neurol.* **36**, 101–117.

Cohen, B., Matsuo, V. & Raphan, T. (1977) Quantitative analysis of the velocity characteristics of optokinetic nystagmus and optokinetic after-nystagmus. *J. Physiol.* **270**, 321–344.

Cohen, B., Suzuki, J.-I. & Bender, M. B. (1964) Eye movements from semicircular canal nerve stimulation in the cat. *Ann. Otol. St. Louis* **73**, 153–169.

Collewijn, H. (1977) Eye and head movements in freely moving rabbits. *J. Physiol.* **266**, 471–498.

Collins, C. C., O'Meara, D. & Scott, A. B. (1975) Muscle tension during unrestrained human eye movements. *J. Physiol.* **245**, 351–369.

Cooper, S. & Daniel, P. D. (1949) Muscle spindles in human extrinsic eye muscles. *Brain* **72**, 1–24.

Cooper, S., Daniel, P. D. & Whitteridge, D. (1955) Muscle spindles and other sensory endings in the extrinsic eye muscles. *Brain* **78**, 564–583.

Cooper, S. & Fillenz, M. (1955) Afferent discharges in response to stretch from the extraocular muscles of the cat and monkey and the innervation of these muscles. *J. Physiol.* **127**, 400–413.

Corbin, K. B. & Oliver, R. K. (1942) The origin of fibres to the grape-like endings in the insertion third of the extraocular muscles. *J. comp. Neurol.* **77**, 171–186.

Cranmer, R. (1951) Nystagmus related to lesions of the central vestibular apparatus and the cerebellum. *Ann. Otol.* **60**, 186–196.

Critchley, M. (1953) *The Parietal Lobes.* London: Edward Arnold.

Crosby, E. C. (1953) Relations of brain centres to normal and abnormal eye movements in the horizontal plane. *J. comp. Neurol.* **99**, 437–479.

Crosby, E. C. & Henderson, J. W. (1948) Pathway concerned in automatic eye movements. *J. comp. Neurol.* **88**, 53–91.

Cynader, M. & Berman, W. (1972) Receptive-field organization of monkey superior colliculus. *J. Neurophysiol.* **35**, 187–201.

Daniel, P. D. (1946) Spiral nerve endings in the extrinsic eye muscles of man. *J. Anat. Lond.* **80**, 189–192.

Denny-Brown, D. & Chambers, R. A. (1976) Physiological aspects of visual perception. II: The subcortical visual direction of behavior. *Arch. Neurol.* **33**, 228–242.

Dichgans, J., Bizzi, E., Morasso, P. & Tagliasco, V. (1973) Mechanism underlying recovery of eye-head coordination following bilateral labyrinthectomy in monkeys. *Exp. Brain Res.* **18**, 548–562.

Dix, M. R., Hallpike, C. S. & Harrison, M. S. (1949) Some observations upon the otological effects of streptomycin intoxication. *Brain* **72**, 241–245.

Dohlman, G. (1935). Some practical and theoretical points in labyrinthology. *Proc. roy. Soc. Med.* **28**, 1371–1380.

Donaldson, I. M. L. & Long, A. C. (1980) Interactions between extraocular proprioceptive and visual signals in the superior colliculus of the cat. *J. Physiol.* **298**, 85–110.

Dow, R. S. (1938) The electrical activity of the cerebellum and its functional significance. *J. Physiol.* **94**, 67–86.

Dow, R. S. (1942) The evolution and anatomy of the cerebellum. *Biol. Rev.*, **17**.

Duensing, F. & Schaefer, K.-P. (1958) Die Activität einzelner Neurone im Bereich der Vestibulariskerne bei Horizontalabsehleuningen unter besonderer Berücksichtigung des vestibularen Nystagmus. *Arch. f. Psychiat.* **198**, 225–252.

Duke-Elder, W. S. & Duke-Elder, P. M. (1930) The contraction of the extrinsic muscles of the eye by choline and nicotine. *Proc. R. Soc. B* **107**, 332–343.

Easton, T. A. (1971) Inhibition from cat eye muscle stretch. *Brain Res.* **25**, 633–637.

Ebenholtz, S. M. & Shebilske, W. (1975) The doll reflex and ocular counterrolling with head-body tilt in the median plane. *Vision Res.* **15**, 713–717.

Edwards, S. B. (1980) The deep cell layers of the superior colliculus. In *The Reticular Formation Revisited.* Ed. A. Hobson & M. Brazier. New York: Raven Press.

Fernandez, C. & Goldberg, J. M. (1971) Physiology of peripheral neurons innervating semicircular canals of the squirrel monkey. II. *J. Neurophysiol.* **34**, 661–675.

Fernandez, C., Goldberg, J. M. & Abend, W. K. (1972) Response to static tilts of peripheral neurons innervating otolith organs of the squirrel monkey. *J. Neurophysiol.* **35**, 978–997.

Fillenz, M. (1955) Responses in the brainstem of the cat to stretch of extrinsic ocular muscles. *J. Physiol.* **128**, 182–199.

Fiorentini, A. & Maffei, L. (1977) Instability of the eye in the dark and proprioception. *Nature* **269**, 330–331.

Fluur, E. (1959) Influences of semicircular ducts on extraocular muscles. *Acta otolaryngol. Suppl.* **149**.

Foerster O. (1931) The cerebral cortex in man. *Lancet (2)*, 309–312.

Fox, J. C. & Holmes, G. (1926) Optic nystagmus and its value in

the localisation of cerebral lesions. *Brain* **49**, 333–371.
Fuchs, A. F. & Kaneko, C. R. S. (1981) A brain stem generator for saccadic eye movements. *Trends Neurosci.* **4**, 283–286.
Fuchs, A. F., Kaneko, R. S. & Scudder, C. A. (1985) Brainstem control of saccadic eye movements. *Ann. Rev. Neurosci.* **8**, 307–337.
Fuchs, A. F. & Kimm, J. (1975) Unit activity in vestibular nucleus of the alert monkey during horizontal angular acceleration and eye movement. *J. Neurophysiol.* **38**, 1140–1161.
Fuchs, A. F. & Kornhuber, H. H. (1969) Extraocular muscle afferents to the cerebellum of the cat. *J. Physiol.* **200**, 713–722.
Fuchs, A. F. & Luschei, E. S. (1970) Firing patterns of abducens neurons of alert monkeys in relationship to horizontal eye movement. *J. Neurophysiol.* **33**, 382–392.
Fuchs, A. F. & Luschei, E. S. (1971) Development of isometric tension in simian extraocular muscle. *J. Physiol.* **219**, 155–166.
Fujikada, T. & Noda, H. (1987) Saccadic eye movements evoked by microstimulation of lobule VII of the cerebellar vermis of macaque monkeys. *J. Physiol.* **394**, 573–594.
Fukushima, Y., Igusa, Y. & Yoshida, K. (1977) Characteristics of responses of medial brain stem neurons to horizontal head angular acceleration and electrical stimulation of the labyrinth in the cat. *Brain Res.* **120**, 564–570.
Fuller, J. H., Maldonado, H. & Schlag, J. (1983) Vestibulo-oculomotor interaction in cat eye–head movements. *Brain Res.* **271**, 241–250.
Godaux, E., Gobert, C. & Halleux, J. (1983) Vestibuloocular reflex, optokinetic response, and their interactions in the alert cat. *Exp. Neurol.* **80**, 42–54.
Goebel, H., Komatsuzaki, A., Bender, M. & Cohen, B. (1971) Lesions of the pontine tegmentum and conjugate gaze paralysis. *Arch. Neurol.*, **24**, 431–480.
Goldberg, M. E. & Bruce, C. J. (1985) Cerebral cortical activity associated with the orientation of visual attention in the rhesus monkey. *Vision Res.* **25**, 471–481.
Goldberg, M. E., Bruce, C. J., Ungergleider, L. & Mishkin, M. (1982) Role of the striate cortex in generation of smooth pursuit eye movements. *Ann. Neurol.* **12**, 113 (Abstr.).
Goldberg, J. M. & Fernandez, C. (1971) Physiology of peripheral neurons innervating semicircular canals of the squirrel monkey. *J. Neurophysiol.* **34**, 635–660; 676–684.
Gonshor, A. & Melvill Jones, G. (1976) Extreme vestibuloocular adaptation induced by prolonged optical reversal of vision. *J. Physiol.* **256**, 381–416.
Grantyn, A. A. & Grantyn, R. (1976) Synaptic actions of tectofugal pathways on abducens motoneurons in the cat. *Brain Res.* **105**, 269–285.
Graves, A. L., Trotter, Y. & Frégnac, Y. (1987) Role of extraocular proprioception in the development of depth perception in cats. *J. Neurophysiol.* **58**, 816–831.
Graybiel, A. M. & Hartwieg, E. A. (1974) Some afferent connections of the oculomotor complex in the cat: an experimental study with tracer techniques. *Brain Res.* **81**, 543–551.
Groen, J. J., Lowenstein, O. & Vendrik, A. J. H. (1952) The mechanical analysis of the responses from the end organs of the horizontal semicircular canal of the isolated elasmobranch labyrinth. *J. Physiol.* **117**, 329–346.
Grünbaum, A. S. F. & Sherrington, C. S. (1903) Observations on the physiology of the cerebral cortex of the anthropoid ape. *Proc. Roy. Soc. B* **72**, 152–155.
Guitton, D., Douglas, R. M. & Volle, M. (1984) Eye–head coordination in cats. *J. Neurophysiol.* **52**, 1030–1050.
Guthrie, B. L., Porter, J. D. & Sparks, D. L. (1983) Corollary discharge provides accurate eye position information to the oculomotor system. *Science* **221**, 1193–1195.
Hallett, P. E. & Lightstone, A. D. (1976) Saccadic eye movements towards stimuli triggered by prior saccades. *Vision Res.* **16**, 99–106.
Hallpike, C. S. & Hood, J. D. (1953) The speed of the slow component of ocular nystagmus induced by angular acceleration of the head: its experimental determination and application to the physical theory of the cupular mechanism. *Proc. Roy. Soc. B* **141**, 216–230.
Harker, D. W. (1972a) The structure and innervation of sheep superior rectus and levator palpebrae extraocular muscles. I. Extrafusal muscle fibers. *Invest. Ophthal.* **11**, 956–969.
Harker, D. W. (1972b) The structure and innervation of sheep superior rectus and levator palpebrae extraocular muscles. II. Muscle spindles. *Invest. Ophthal.* **11**, 970–979.
Harting, J. K. (1977) Descending pathways from the superior colliculus: an autoradiographic analysis in the rhesus monkey (*Macaca mulatta*). *J. Comp. Neurol.* **173**, 583–612.
Hassler, R. & Hess, W. R. (1954) Experimenteller und anatomische Befunde über die Drehbewegungen und ihre nervösen Apparate. *Arch. Psychiat.* **192**, 488–526.
Hassul, M., Daniels, P. D. & Kimm, J. (1976) Effects of bilateral flocculectomy on the vestibulo-ocular relex in the chinchilla. *Brain Res.* **118**, 339–343.
Heilman, K. M. & Valenstein, E. (1972) Frontal lobe neglect in man. *Neurology* **22**, 660–664.
Hein, A., Held, R. & Gower, E. C. (1970) Development and segmentation of visually controlled movement by selective exposure during rearing. *J. Comp. Physiol. Psychol.* **73**, 181–187.
Hein, A., Vital-Durand, F., Salinger, W. & Diamond, R. (1979) Eye movements initiate visual-motor development in the cat. *Science* **204**, 1321–1322.
Henn, V. & Cohen, B. (1976) Coding of information about rapid eye movements in the pontine reticular formation of alert monkeys. *Brain Res.* **108**, 307–325.
Hess, A. (1967) The structure of vertebrate slow and twitch muscle fibers. *Invest. Ophthal.* **6**, 217–228.
Hess, A. & Pilar, G. (1963) Slow fibres in the extraocular muscles of the cat. *J. Physiol.* **169**, 780–798.
Heywood, S. & Churcher, J. (1971) Eye movements and the afterimage. I. Tracking the afterimage. *Vision Res.* **11**, 1163–1168.
Highstein, S. M. & Baker, R. (1978) Excitatory terminations of abducens internuclear neurons on medial rectus motoneurons: relationship to syndrome of internuclear ophthalmoplegia. *J. Neurophysiol.* **41**, 1647–1661.
Highstein, S. M., Cohen, B. & Matsunami, K. (1974) Monosynaptic projections from the pontine reticular formation to the IIIrd nucleus in the cat. *Brain Res.* **75**, 340–344.
Highstein, S. M. & Ito, M. (1971) Differential localization within the vestibular nuclear complex of the inhibitory and excitatory cells innervating IIIrd nucleus oculomotor neurons in rabbit. *Brain Res.* **29**, 363–365.
Highstein, S. M., Karabatas, A., Baker, R. & McCrea, R. A. (1982) Comparison of the morphology of physiologically identified abducens motor and internuclear neurons in the cat: a light microscopical study employing the intracellular injection of horseradish peroxidase. *J. Comp. Neurol.* **208**, 369–381.
Highstein, S. M., Maekawa, K., Steinacker, A. & Cohen, B. (1976) Synaptic input from the pontine reticular nuclei to abducens motoneurons and internuclear neurons in the cat. *Brain Res.* **112**, 162–167.
Hikosaka, O., Igusa, Y. & Imai, H. (1978) Firing pattern of prepositus hypoglossal and adjacent reticular neurons related to vestibular nystagmus in the cat. *Brain Res.* **144**, 395–403.
Hikosaka, O. & Wurtz, R. H. (1983a–d). Visual and oculomotor functions of monkey substantia nigra pars reticulata. I–IV. *J. Neurophysiol.* **49**, 1230–1253, 1254–1267, 1268–1284, 1285–1301.
Hoffmann, K.-P. & Schopmann, A. (1975) Retinal input to

direction selective cells in the nucleus tractus opticus of the cat. *Brain Res.* **99**, 359–366.

Holmes, G. (1918) Disturbances of visual orientation. *Brit. J. Ophthal.* **1**, 506–516.

Hyde, J. E. (1962) Effect of hindbrain lesions on conjugate horizontal eye movements in cats. *Exp. Eye Res.* **1**, 206–214.

Hyde, J. E. & Eason, R. G. (1959) Characteristics of ocular movements evoked by stimulation of brainstem of cat. *J. Neurophysiol.* **22**, 666–678.

Hyde, J. E. & Eliasson, S. G. (1957) Brainstem-induced eye movement in cats. *J. Comp. Neurol.* **108**, 139–172.

Hyde, J. E. & Slusher, M. A. (1961) Functional role of median longitudinal fasciculus in evoked conjugate ocular deviations in cats. *Am. J. Physiol.* **200**, 919–922.

Hyvärinen, J. (1982) Posterior parietal lobe of the primate brain. *Physiol. Rev.* **62**, 1066–1129.

Hyvärinen, J. & Poranen, A. (1974) Function of the parietal association area 7a revealed from cellular discharges in alert monkey. *Brain* **97**, 673–692.

Ito, M. (1972) Neural design of the cerebellar motor control system. *Brain Res.* **40**, 81–84.

Ito, M., Shiida, T., Yagi, N. & Yamamoto, M. (1974) Visual influence on rabbit horizontal vestibulo-ocular reflex presumably effected via the cerebellar flocculus. *Brain Res.* **65**, 170.

Jampel, R. S. (1960) Convergence, divergence, pupillary reactions and accommodation of the eyes from faradic stimulation of the macaque brain. *J. Comp. Neurol.* **115**, 371–397.

Joseph, J. P. & Boussoud, D. (1985) Role of the cat substantia nigra pars reticulata in eye and head movements. I. Neural activity. *Exp. Brain Res.* **57**, 286–296.

Kase, M., Miller, D. C. & Noda, H. (1980) Discharges of Purkinje cells and mossy fibres in the cerebellar vermis of the monkey during saccadic eye movements and fixation. *J. Physiol.* **300**, 539–555.

Kase, M., Nagata, R. & Kato, M. (1986) Saccade-related activity of periaqueductal gray matter of the monkey. *Invest. Ophthal.* **27**, 1165–1169.

Kato, I., Harada, K., Hasegawa, T., Igarashi, T., Koike, Y. & Kawasaki, T. (1986) Role of the nucleus of the optic tract in monkeys in relation to optokinetic nystagmus. *Brain Res.* **364**, 12–22.

Kawamura, S. (1974) Topical organization of the extrageniculate visual system in the cat. *Exp. Neurol.* **45**, 451–461.

Kawano, K. & Sasaki, M. (1984) Response properties of neurons in posterior parietal cortex of monkey during visual-vestibular stimulation. II. Optokinetic neurons. *J. Neurophysiol.* **51**, 352–360.

Kawano, K., Sasaki, M. & Yamashita, M. (1984) Response properties of posterior parietal cortex of monkey during visual-vestibular stimulation. *J. Neurophysiol.* **51**, 340–351.

Keating, E. G., Cooley, S. G., Pratt, S. E. & Kelsey, J. E. (1983) Tactal ablation arrests eye movements electrically evoked from occipital and parietal eye fields. *Abstr. Soc. Neurosci.* **9**, 750.

Keating, E. G., Gooley, S. G., Pratt, S. E. & Kelsey, J. E. (1983) Removing the superior colliculus silences eye movements normally evoked from stimulation of the parietal and occipital eye fields. *Brain Res.* **269**, 145–148.

Keller, E. L. (1973) Accommodative vergence in the alert monkey. Motor unit analysis. *Vision Res.* **13**, 1565–1575.

Keller, E. L. (1974) Participation of medial pontiné reticular formation in eye movement generation in monkey. *J. Neurophysiol.* **37**, 316–332.

Keller, E. L. (1979) Colliculoreticular organization in the oculomotor system. *Progr. Brain Res.* **50**, 725–734.

Keller, E. L. & Crandall, W. F. (1981) Neural activity in the nucleus reticularis tegmenti pontis in the monkey related to eye movements and visual stimulation. *Ann. N.Y. Acad. Sci.* **374**, 249–261.

Keller, E. L. & Crandall, W. F. (1983) Neuronal responses to optokinetic stimuli in pontiné nuclei of behaving monkey. *J. Neurophysiol.* **49**, 169–187.

Keller, E. L. & Robinson, D. A. (1971) Absence of a stretch reflex in intra-ocular muscles of the monkey. *J. Neurophysiol.* **34**, 908–919.

Keller, E. L. & Robinson, D. A. (1972) Abducens unit behavior in the monkey during vergence movements. *Vision Res.* **12**, 369–382.

Keller, E. L., Slakey, D. P. & Crandall, W. F. (1983) Microstimulation of the primate cerebellar vermis during saccadic eye movements. *Brain Res.* **288**, 131–143.

Kern, R. (1965) A comparative pharmacologic-histologic study of slow and twitch fibers in the superior rectus muscle of the rabbit. *Invest. Ophthal.* **4**, 901–910.

Kern, R. (1968) Uber die adrenergischen Receptoren der extraoculären Muskeln des Rhesusaffen. *v. Graefes Arch. Ophthal.* **174**, 278–286.

Koenig, E., Allum, J. H. J. & Dichgans, J. (1978) Visual-vestibular interaction upon nystagmus slow phase velocity in man. *Acta Otolaryngol.* **85**, 397–410.

Krüger, P. (1952) *Tetanus und Tonus der quergestreiften Skelettmuskel der Wirbeltiere und des Menschen.* Leipzig, Acad. Verlag, Geest & Portig.

Kunzle, H. & Akert, K. (1977) Efferent connections of cortical, area 8 (frontal eye field) in *Macaca fascicularis.* A reinvestigation using the autoradiographic technique. *J. Comp. Neurol.* **173**, 147–164.

Laurutis, V. P. & Robinson, D. A. (1986) The vestibulo-ocular reflex during human saccadic eye movements. *J. Physiol.* **373**, 209–233.

Leichnetz, G. (1980) An anterogradely-labeled prefrontal cortico-oculomotor pathway in the monkey demonstrated with HRP gel and TMB neurochemistry. *Brain Res.* **198**, 440–445.

Leichnetz, G. R. (1982) Connections between the frontal eye field and pretectum in the monkey: an anterograde/retrograde study using HRP gel and TMB neurohistochemistry. *Brain Res.* **207**, 394–402.

Leichnetz, G. R., Smith, D. J. & Spencer, R. F. (1984a) Cortical projections of the paramedian tegmental and basilar pons in the monkey. *J. Comp. Neurol.* **228**, 388–408.

Leichnetz, G. R., Spencer, R. F. & Smith, D. J. (1984b) Cortical projection to nuclei adjacent to the oculomotor complex in the medial dien-mesencephalic tegmentum in the monkey. *J. Comp. Neurol.* **228**, 359–387.

Lennerstrand, G. (1974) Electrical activity and isometric tension in motor units of the cat's inferior oblique muscle. *Acta physiol. Scand.* **91**, 458–474.

Lisberger, S. G. & Fuchs, A. F. (1978a,b) Role of primate flocculus during rapid behavioral modification of vestibulo-ocular reflex. I and II. *J. Neurophysiol.* **41**, 733–762, 763–777.

Lopez-Barneo, J., Darlot, C., Berthoz, A. & Baker, R. (1982) Neuronal activity in prepositus nucleus correlated with eye movements in the alert cat. *J. Neurophysiol.* **47**, 329–352.

Lopez-Barneo, J., Ribas, J. & Delgado-Garcia, J. M. (1984) Identification of prepositus neurons projecting to the oculomotor nucleus in the alert cat. *Brain Res.* **214**, 174–179.

Lowenstein, O. (1936) The equilibrium function of the vertebrate labyrinth. *Biol. Rev.* **11**, 113–145.

Lowenstein, O. & Wersäll, J. (1959) Functional interpretation of the electron microscopic structure of the sensory hairs in the cristae of the elasmobranch *Raja clavata* in terms of directional sensitivity. *Nature* **184**, 1807–1808.

Luschei, E. S. & Fuchs, A. F. (1972) Activity of brain stem neurons during eye movements of alert monkeys. *J. Neurophysiol* **35**, 445–461.

Lynch, J. C. (1980) The functional organization of posterior parietal association cortex. *Behav. Brain Sci.* **3**, 485–534.

Lynch, J. C., Graybiel, A. M. & Lobeck, L. J. (1985) The differential projection of two cytoarchitectonic subregions of the inferior parietal lobe of macaque upon the deep layers of the superior colliculus. *J. Comp. Neurol.* **235**, 241–254.

Lynch, J. C., Mountcastle, V. B., Talbot, W. H. & Yin, T. C. T. (1977) Parietal lobe mechanisms for directed visual attention. *J. Neurophysiol.* **40**, 362–389.

Maciewicz, R. J., Eagen, K., Kaneko, C. R. S. & Highstein, S. M. (1977) Vestibular and medullary brain stem afferents to the abducens nucleus in the cat. *Brain Res.* **123**, 229–240.

Mackensen, G. (1959) Untersuchung zur Physiologie des optokinetischen Nachnystagmus. *v. Graefes' Arch. Ophthal.* **160**, 497–509.

Maekawa, K. & Kimura, M. (1980) Mossy fiber projections to the cerebellar flocculus from the extraocular muscle afferents. *Brain Res.* **191**, 313–325.

Maekawa, K. & Natsui, T. (1973) Climbing fiber activation of Purkinje cells in rabbit's flocculus during light stimulation of the retina. *Brain Res.* **59**, 417–420.

Maekawa, K. & Simpson, J. I. (1972) Climbing fiber activation of Purkinje cells in the flocculus by impulses transferred through the visual pathway. *Brain Res.* **39**, 245–251.

Maekawa, K. & Simpson, J. I. (1973) Climbing fiber responses evoked in vestibulocerebellum of rabbit from visual system. *J. Neurophysiol.* **36**, 649–666.

Maekawa, K. & Takeda, T. (1975) Mossy fiber responses evoked in the cerebellar flocculus of rabbits by stimulation of the optic pathway. *Brain Res.* **98**, 590–595.

Maffei, L. & Bisti, S. (1976) Binocular interaction in strabismic kittens deprived of vision. *Science* **191**, 579–580.

Manni, E., Bortolami, R. & Deriu, P. L. (1970a) Superior oblique muscle proprioception and the trochlear nerve. *Exp. Neurol.* **26**, 543–550.

Manni, E., Bortolami, R. & Desole, C. (1967) Relationship of Gasserian cells to extraocular muscle proprioception in lamb. *Experientia* **23**, 230–231.

Manni, E., Bortolami R. & Desole, C. (1968) Peripheral pathway of eye muscle proprioception. *Exp. Neurol.* **22**, 1–12.

Manni, E., Bortolami, R., Pettorossi, V. E. & Callegari, E. (1976) Trigeminal afferent fibers in the trunk of the oculomotor nerve of lambs. *Exp. Neurol.* **50**, 465–476.

Manni, E., Desole, C. & Palmieri, G. (1970b) On whether eye muscle spindles are innervated by ganglion cells located along the oculomotor nerves. *Exp. Neurol.* **28**, 333–343.

Manni, E., Giretti, M. L. & Deriu, P. L. (1974) Eye movements elicited by electric stimulation of the pontiné reticular formation. *Arch. int. Physiol. Biochim.* **82**, 831–842.

Manni, E., Palmieri, E., Marini, R. & Pettorossi, V. E. (1975) Trigeminal influences on extensor muscles of the neck. *Exp. Neurol.* **47**, 330–342.

Marg, E., Jampolsky, A. & Tamler, E. (1959) Elements of human extraocular electromyography. *Arch. Ophthal.* **81**, 258–269.

Markham, C. H., Precht, W. & Shimazu, H. (1966) Effect of stimulation of interstitial nucleus of Cajal on vestibular unit activity in the cat. *J. Neurophysiol.* **29**, 493–507.

Matyushkin, D. P. (1961) Phasic and tonic neuromotor units in the oculomotor apparatus of the rabbit. *Sechenov Physiol. J. USSR* **47**, 960–965.

Mays, L. E. & Sparks, D. L. (1980a) Dissociation of visual and saccade-related responses in superior colliculus neurons. *J. Neurophysiol.* **43**, 207–232.

Mays, L. E. & Sparks, D. L. (1980b) Saccades are spatially, not retinocentrically coded. *Science* **208**, 1163–1165.

McCouch, G. P., Deering, I. D. & Ling, T. H. (1951) Location of receptors for tonic neck reflexes. *J. Neurophysiol.* **14**, 191–195.

McCrea, R. A., Strassman, A. & Highstein, S. M. (1986) Morphology and physiology of abducens motoneurons and internuclear neurons intracellularly injected with horseradish peroxidase in alert squirrel monkey. *J. Comp. Neurol.* **243**, 291–308.

McElligott, J. G. & Keller, E. L. (1984) Cerebellar vermis involvement in monkey saccadic eye movements: microstimulation. *Exp. Neurol.* **86**, 543–558.

McMasters, R. E., Weiss, A. H. & Carpenter, M. B. (1966) Vestibular projection to the nuclei of the extraocular muscles. *Amer. J. Anat.* **118**, 163–193.

Melvill Jones, G. & Milsum, J. H. (1965) Spatial and dynamic aspects of visual fixation. *IEEE Trans. Bio-Med. Eng.* **12**, 54–62. (Quoted by Skavenski & Robinson, 1973.)

Merton, P. A. (1956) Compensatory rolling movements of the eye. *J. Physiol.* **132**, 25–27P.

Miles, F. A. (1974) Single unit firing patterns in the vestibular nuclei related to voluntary eye movements and passive body rotation in conscious monkeys. *Brain Res.* **71**, 215–224.

Miller, J. E. (1958) Electromyographic pattern of saccadic eye movements. *Am. J. Ophthal.* **46**, Pt. 2, 183–186.

Mohler, C. W., Goldberg, M. E. & Wurtz, R. H. (1973) Visual receptive fields of frontal eye field neurones. *Brain Res.* **61**, 385–389.

Mohler, C. W. & Wurtz, R. H. (1976) Organization of monkey superior colliculus: intermediate layer cells discharging before eye movements. *J. Neurophysiol.* **39**, 722–744.

Mohler, C. W. & Wurtz, R. H. (1977) Role of striate cortex and superior colliculus in visual guidance of saccadic eye movements in monkeys. *J. Neurophysiol.* **40**, 74–94.

Morasso, P., Bizzi, E. & Dichgans, E. (1973) Adjustment of saccade characteristics during head movement. *Exp. Brain Res.* **16**, 492–500.

Mowrer, O. H. (1937) The influence of vision during bodily rotation upon the duration of post-rotational vestibular nystagmus. *Acta Otolaryngol.* **25**, 351–364.

Newsome, W. T., Wurtz, R. H., Dürsteler, M. R. & Mikami, A. (1985) Deficits in visual motion processing following ibotenic acid lesions of the middle temporal visual area of the macaque monkey. *J. Neurosci.* **5**, 825–840.

Noda, H. & Fujikada, T. (1987) Involvement of Purkinje cells in evoking saccadic eye movements by microstimulation of the posterior cerebellar vermis in monkeys. *J. Neurophysiol.* **57**, 1247–1261.

Noda, H. & Warabi, T. (1982) Eye position signals in the flocculus of the monkey during smooth pursuit movements. *J. Physiol.* **324**, 187–202.

Ohm, J. (1936) Ueber Interferenz mehrerer Arten von Nystagmus. *Proc. Acad, Sci. Amst.* **39**, 549–558.

Page, S. G. (1965) A comparison of the fine structures of frog slow and twitch fibres. *J. Cell Biol.* **26**, 477–497.

Pasik, P. & Pasik, T. (1964) Oculomotor functions in monkeys with lesions of the cerebrum and the superior colliculi. In *The Oculomotor System*, Ed. M. B. Bender, pp. 40–80. New York: Harper & Row.

Pasik, P., Pasik, T. & Krieger, H. P. (1959) Effects of cerebral lesions upon optokinetic nystagmus in monkeys. *J. Neurophysiol.* **22**, 297–304.

Peachey, L. D. (1968) Muscle *Ann. Rev. Physiol.* **30**, 401–429.

Peachey, L. D. & Huxley, A. F. (1962) Structural identification of twitch and slow striated muscle fibers of the frog. *J. Cell Biol.* **13**, 177–180.

Penfield, W. & Boldrey, E. (1937) Somatic motor and sensory representation in the cerebral cortex of man as studied by electrical stimulation. *Brain* **60**, 389–443.

Pilar, G. (1967) Further study of the electrical and mechanical responses of slow fibers in cat extraocular muscles. *J. gen. Physiol.* **50**, 2289–2300.

Porter, J. D. & Spencer, R. F. (1982) Localization and mor-

phology of cat extraocular muscle afferent neurones identified by retrograde transport of horseradish peroxidase. *J. Comp. Neurol.* **204**, 56–64.

Precht, W. (1981) Visual–vestibular interactions in vestibular neurons: functional pathway of organization. *Ann. N.Y. Acad. Sci.* **374**, 230–248.

Precht, W., Schwindt, P. C. & Magherini, P. C. (1974) Tectal influence on cat ocular motoneurons. *Brain Res.* **82**, 27–40.

Rademaker, G. G. J. & Ter Braak, J. W. G. (1948) On the central mechanism of some optic reactions. *Brain* **71**, 48–76.

Raphan, T., Cohen, B. & Matsuo, V. (1977) A velocity-storage responsible for optokinetic nystagmus (OKN), optokinetic after-nystagmus (OKAN) and vestibular nystagmus. *Developments in Neuroscience*, Vol. 1, Ed. Baker, R, & Berthoz, A. Elsevier: Amsterdam, pp. 37–47.

Raphan, T., Matsuo, V. & Cohen, B. (1979) Velocity storage in the vestibulo-ocular reflex arc (VOR). *Exp. Brain Res.* **35**, 229–248.

Raybourn, M. S. & Keller, E. L. (1977) Colliculoreticular organization in primate oculomotor systems. *J. Neurophysiol.* **40**, 861–878.

Ritchie, L. (1975) Effects of cerebellar lesions on saccadic eye movements. *J. Neurophysiol.* **39**, 1246–1256.

Ritchie, L. (1976) Effects of cerebellar lesions on saccadic eye movements. *J. Neurophysiol.* **39**, 1246–1256.

Robinson, D. A. (1964) The mechanics of human saccadic eye movement. *J. Physiol.* **174**, 245–264.

Robinson, D. A. (1968) Eye movement control in primates. *Science* **161**, 1219–1224.

Robinson, D. A. (1970). Oculomotor unit behavior in the monkey. *J. Neurophysiol.* **33**, 393–404.

Robinson, D. A. (1972) Eye movements evoked by collicular stimulation in the alert monkey. *Vision Res.* **12**, 1795–1808.

Robinson, D. A. (1976) Adaptive gain control of vestibulo-ocular reflex by the cerebellum. *J. Neurophysiol.* **39**, 954–969.

Robinson, D. A. (1977) Linear addition of optokinetic and vestibular signals in the vestibular nuclei. *Exp. Brain Res.* **30**, 447–450.

Robinson, D. A. (1981) Control of eye movements. In: *Handbook of Physiology*, Vol. II, sect. I, Ch. 28, pp. 1275–1320. Bethesda, Md: *Amer. Physiol. Soc.*

Robinson, D. A. (1987) The windfalls of technology in the oculomotor system. *Invest. Ophthal.* **28**, 1912–1924.

Robinson, D. A. & Fuchs, A. F. (1969) Eye movements evoked by stimulation of frontal eye fields. *J. Neurophysiol.* **32**, 637–648.

Robinson, D. A. & Jarvis, C. D. (1974) Superior colliculus neurons studied during head and eye movements of the behaving monkey. *J. Neurophysiol.* **37**, 533–540.

Robinson, D. A., O'Meara, D. M., Scott, A. B. & Collins, C. C. (1969) Mechanical components of human eye movements. *J. appl. Physiol.* **26**, 548–553.

Robinson, D. A. & Zee, D. S. (1981) Theoretical considerations of the function and circuitry of various rapid eye movements. In *Progress in Oculomotor Research*, Ed. Fuchs, A. F. & Becker, W., pp. 3–9. Amsterdam: Elsevier/North Holland. (Quoted by Guitton *et al.*, 1984.)

Robinson, D. L., Goldberg, M. E. & Stanton, G. B. (1978) Parietal association cortex in the primate: sensory mechanisms and behavioral modulations. *J. Neurophysiol.* **41**, 910–932.

Rogers, K. T. (1957) Ocular proprioceptive neurons in the developing chick. *J. comp. Neurol.* **107**, 427–437.

Ron, S. & Robinson, D. A. (1973) Eye movements evoked by cerebellar stimulation in the alert monkey. *J. Neurophysiol.* **36**, 1004–1022.

Sakata, H., Shibutani, H. & Kawana, K. (1980) Spatial properties of visual fixation neurons in posterior parietal association cortex of the monkey. *J. Neurophysiol.* **43**, 1654–1672.

Sakata, H., Shibutani, H. & Kawano, K. (1983) Functional properties of visual tracking neurons in posterior parietal association cortex of the monkey. *J. Neurophysiol.* **49**, 1364–1380.

Sakata, H., Shibutani, H., Kawano, K. & Harrington, T. L. (1985) Neural mechanisms of space vision in the parietal association cortex of the monkey. *Vision Res.* **25**, 453–463.

Sanghvi, I. S. & Smith, C. M. (1969) Characterization of stimulation of mammalian extraocular muscles by cholinomimetics. *J. Pharmacol.* **167**, 351–364.

Sasaki, K. (1963) Electrophysiological studies on oculomotor neurones of the cat. *Jap. J. Physiol.* **13**, 287–302.

Schiller, P. H. (1977) The effect of superior colliculus ablation on saccades elicited by cortical stimulation. *Brain Res.* **122**, 154–156.

Schiller, P. H. & Koerner, F. (1971) Discharge characteristics of single units in superior colliculus of the alert rhesus monkey. *J. Neurophysiol.* **34**, 920–936.

Schiller, P. H. & Sandell, J. H. (1983) Interactions between visually and electrically elicited saccades before and after superior colliculus and frontal eye field ablations in the rhesus monkey. *Exp. Brain Res.* **49**, 381–392.

Schiller, P. H. & Stryker, M. (1972) Single-unit recording and stimulation in superior colliculus of the alert rhesus monkey. *J. Neurophysiol.* **35**, 915–924.

Schiller, P. H., Stryker, M., Cynader, M. & Berman, N. (1974) Response characteristics of single cells in the monkey superior colliculus following ablation or cooling of visual cortex. *J. Neurophysiol.* **37**, 181–194.

Schiller, P. H., Truc, S. D. & Conway, J. L. (1980) Deficits in eye movements following frontal eye-field and superior colliculus ablations. *J. Neurophysiol.* **44**, 1175–1189.

Schlag, J., Lehtinen, I. & Schlag-Rey, M. (1974) Neuronal activity before and during eye movements in thalamic internal medullary lamina of the cat. *J. Neurophysiol.* **37**, 982–995.

Schlag, J. & Schlag-Rey, M. (1971) Induction of oculomotor responses from thalamic internal medullary lamina in the cat. *Exp. Neurol.* **33**, 498–508.

Schlag, J. & Schlag-Rey, M. (1984) Visuomotor functions of central thalamus in monkey. II. Unit activity related to visual events, targeting, and fixation. *J. Neurophysiol.* **51**, 1175–1219.

Schlag, J. & Schlag-Rey, M. (1985) Unit activity related to spontaneous saccades in frontal dorsomedial cortex in monkey. *Exp. Brain Res.* **58**, 208–211.

Schlag-Rey, M. & Schlag, J. (1977) Visual and presaccadic neuronal activity in thalamic internal medullary lamina of cat: a study of targeting. *J. Neurophysiol.* **40**, 156–173.

Schlag-Rey, M. & Schlag, J. (1984) Visuomotor functions of central thalamus in monkey. I. Unit activity related to spontaneous eye movements. *J. Neurophysiol.* **51**, 1149–1174.

Sears, M. L., Teasdall, R. D. & Stone, H. H. (1959) Stretch effects in human extraocular muscle. *Bull. Johns Hopk. Hosp.* **104**, 174–178.

Seltzer, B. & Pandya, D. N. (1980) Converging visual and somatic sensory cortical input to the intraparietal sulcus of the rhesus monkey. *Brain Res.* **192**, 339–351.

Shibutani, H., Sakata, H. & Hyvärinen, J. (1984) Saccade and blinking evoked by microstimulation of the posterior parietal association cortex in the monkey. *Exp. Brain Res.* **55**, 1–8.

Shimazu, H. & Precht, W. (1966) Inhibition of central vestibular neurons from the contralateral labyrinth and its mediating pathway. *J. Neurophysiol.* **29**, 467–492.

Siebeck, R. (1954) Wahrnehmungsstörung und Störungswahrnehmung bei Augenmuskellähmungen. *v. Graefes Arch. Ophthal.* **155**, 26–34.

Skavenski, A. A. & Robinson, D. A. (1973) Role of abducens neurons in vestibuloocular reflex. *J. Neurophysiol.* **36**, 724–738.

Sparks, D. L. & Mays, L. E. (1983) Spatial localization of saccade targets. I. Compensation for stimulation-induced perturbations in eye position. *J. Neurophysiol.* **49**, 45–63.

Sparks, D. L., Mays, L. E. & Porter, J. D. (1987) Eye movements induced by pontiné stimulation: interaction with visually triggered saccades. *J. Neurophysiol.* **58**, 300–318.

Sparks, D. L. & Porter, J. D. (1983) Spatial localization of saccade targets. II. Activity of superior colliculus neurons preceding compensatory saccades. *J. Neurophysiol.* **49**, 64–74.

Spiegel, E. (1933) Role of vestibular nuclei in the cortical innervation of the eye muscles. *Arch. Neurol. Psychiat.* **29**, 1084–1097.

Sprague, J. M. (1966) Interaction of cortex and superior colliculus in mediation of visually guided behavior in the cat. *Science* **153**, 1544–1547.

Stein, B. E., Magalhães-Castro, B. & Kruger, L. (1976) Relationship between visual and tactile representations in cat superior colliculus. *J. Neurophysiol.* **39**, 401–419.

Steinhausen, W. (1933) Uber die Beobachtung der Cupula in den Bodengangasmpullen des Labyrinths des lebenden Hechts. *Pflüg. Arch.* **232**, 500–512.

Stevens, J. K. *et al.* (1976) Paralysis of the awake human: visual perceptions. *Vision Res.* **16**, 93–98.

Straschill, M. & Rieger, P. (1973) Eye movements evoked by focal stimulation of the cat's superior colliculus. *Brain Res.* **59**, 211–227.

Strassman, A., Highstein, S. M. & McCrea, R. A. (1986) Anatomy and physiology of saccadic neurons in the alert squirrel monkey. I. Excitatory burst neurons. II. Inhibitory burst neurons. *J. Comp. Neurol.* **249**, 337–357, 358–380.

Suzuki, D. A. & Keller, E. L. (1984) Visual signals in the dorsolateral pontiné nucleus of the alert monkey: their relationship to smooth-pursuit eye movements. *Exp. Brain Res.* **53**, 473–478.

Suzuki, D. A., Noda, H. & Kase, M. (1981) Visual and pursuit eye-movement-related activity in posterior vermis of monkey cerebellum. *J. Neurophysiol.* **46**, 1120–1139

Suzuki. J. I., Todumasu, K. & Goto, K. (1969). Eye movements from singular utricular nerve stimulation in the cat. *Acto-Otolaryngologica*, **68**, 350–362.

Szentágothai, J. (1950) The elementary vestibulo-ocular reflex arc. *J. Neurophysiol.* **13**, 395–407.

Szentágothai, J. & Schab, R. (1956) A midbrain inhibitory mechanism of oculomotor activity. *Acta physiol. Hung.* **9**, 89–98.

Takemori, S. & Cohen, B. (1974a) Visual suppression of vestibular nystagmus in rhesus monkeys. *Brain Res.* **72**, 203–212.

Takemori, S. & Cohen, B. (1974b) Loss of visual suppression of vestibular nystagmus after flocculus lesions. *Brain Res.* **72**, 213–224.

Tamler, E., Jampolsky, A. & Marg, E. (1958) An electromyographic study of asymmetric convergence. *Amer. J. Ophthal.* **46**, Pt. 2, 174–182.

Tarlov, E. (1972) Anatomy of the two vestibulo-oculomotor projection systems. *Progr. Brain Res.* **37**, 471–491.

Tauber, E. S. & Atkin, A. (1968) Optomotor response to monocular stimulation: relation to visual system organization. *Science* **160**, 1365–1367.

Teravainen, H. & Calne, D. B. (1980) Studies of parkinsonian movement: I. Programming and execution of eye movements. *Acta Neurol. Scand.* **62**, 137–148.

Ter Braak, J. W. G. (1936) Untersuchungen ueber optokinetischen Nystagmus. *Arch. néerl. Physiol.* **21**, 309–376.

Tomlinson, R. D. & Bahra, P. S. (1986) Combined eye-head gaze shifts in the primate: I. Metrics. II. Interaction between saccades and the vestibulo-ocular reflex. *J. Neurophysiol.* **56**, 1542–1557, 1558–1570.

Torre, M. (1953) Nombre et dimensions des unités motrices dans les muscles extrinsiques de l'oeil et, en général, dans les muscles squelettiques. *Schweiz. Arch. Neurol.* **72**, 362–378.

Trotter, Y., Frégnac, Y. & Buisseret, P. (1981) Période de sensibilité du cortex visuel primaire du chat à la suppression unilatérale des afferences proprioceptives extraoculaires. *C.R. Acad. Sci. Paris* **293**, 245–248.

Trotter, Y., Frégnac, Y. & Buisseret, P. (1981) Synergie de la vision et la proprioception extraoculaire dans les mécanismes de plasticité fonctionelle du cortex visuel primaire du chaton. *C.R. Acad, Sci. Paris* **296**, 665–668.

Trotter, Y., Frégnac, Y. & Buisseret, P. (1987) The period of susceptibility of visual cortical binocularity to unilateral proprioceptive deafferentation of extraocular muscles. *J. Neurophysiol.* **58**, 795–815.

Tusa, R. J., Zee, D. S. & Herdman, S. J. (1986) Effect of unilateral cerebral cortical lesions on ocular motor behavior in monkeys: saccades and quick phases. *J. Neurophysiol.* **56**, 1590–1625.

Uemura, T. & Cohen, B. (1973) Acta Oto-Laryngol. *Suppl.* 315.

Van Egmond, A. A. J., Groen, J. J. & Jongkees, L. B. W. (1949) The mechanics of the semicircular canal. *J. Physiol.* **110**, 1–17.

Van Gisbergen, J. A. M., Robinson, D. A. & Gielen, S. (1981) A quantitative analysis of generation of saccadic eye movements by burst neurons. *J. Neurophysiol.* **45**, 417–442.

Van Gisbergen, J. A. M., Van Opstal, A. J. & Schoenmakers, J. J. M. (1985) Experimental test of two models for the generation of oblique saccades. *Exp. Brain Res.* **57**, 321–336.

Waespe, W., Cohen, B. & Raphan, T. (1983) Role of the flocculus and paraflocculus in optokinetic nystagmus and visual–vestibular interactions: effects of lesions. *Exp. Brain Res.* **50**, 9–33.

Waespe, W. & Henn, V. (1977) Neuronal activity in the vestibular nuclei of the alert monkey during vestibular and optokinetic stimulation. *Exp. Brain Res.* **27**, 523–538.

Wagman, I. H., Krieger, H. P. & Bender, M. B. (1958) Eye movements elicited by surface and depth stimulation of the occipital lobe of macaque mulatta. *J. Comp. Neurol.* **109**, 169–193.

Walker, A. E. (1940) A cytoarchitectural study of the prefrontal area of the macaque monkey. *J. Comp Neurol.* **73**, 59–86.

Warwick, R. (1953) Representation of the extra-ocular muscles in the oculomotor nuclei of the monkey. *J. Comp. Neurol.* **98**, 449–503.

Warwick, R. (1955) The so-called nucleus of convergence. *Brain* **78**, 92–114.

Westheimer, G. & Blair, S. M. (1973) Oculomotor defects in cerebellectomised monkeys. *Invest. Ophthal.* **12**, 618–621.

Whitteridge, D. (1955) A separate afferent nerve supply from the extraocular muscles of goats. *Quart. J. exp. Physiol.* **40**, 331–336.

Whitteridge, D. (1960) Central control of the eye movements. In *Handbook of Physiology*, Ed. Field, Magoun & Hall, vol. II, pp. 1089–1109. Washington: Am. Physiol. Soc.

Wilson, M. E. & Toyne, M. J. (1970). Retino-tectal and cortico-tectal projections in *Macaca mulatta*. *Brain Res.* **24**, 395–406.

Wilson, V. J. & Felpel, L. P. (1972) Specificity of semicircular canal input to neurons in the pigeon. *J. Neurophysiol.* **35**, 253–264.

Wilson, V. J. & Maeda, M. (1974) Connections between semicircular canals and neck motoneurons in the cat. *J. Neurophysiol.* **37**, 346–357.

Wilson, V. J. & Yoshida, M. (1969) Comparison of effects of stimulation of Deiters' nucleus and medial longitudinal fasciculus on neck, forelimb, and hindlimb motoneurons. *J. Neurophysiol.* **32**, 743–758.

Winfield, J. A., Hendricksen, A. & Kimm, J. (1978) Anatomical evidence that the medial terminal nucleus of the accessory

optic tract in mammals provides a visual mossy fiber input to the flocculus. *Brain Res.* **151**, 175–182.

Woellner, R. C. & Graybiel, A. (1959) Counterrolling of the eyes and its dependence on the magnitude of gravitation or inertial force acting laterally on the body. *J. app. Physiol.* **14**, 632–634.

Wolter, J. R. (1955) Morphology of the sensory nerve apparatus in the striated muscle of the human eye. *Arch. Ophthal.* **53**, 201–217.

Woolsey, C. N. *et al.* (1952) Patterns of localization in precentral and "supplementary" motor areas and their relation to the concept of a premotor area. *ARNMD* **30**, 238–264.

Wood, C. C., Spear, P. D. & Braun, J. J. (1973) Direction specific deficits in horizontal optokinetic nystagmus following removal of visual cortex in the cat. *Brain Res.* **60**, 231–237.

Wurtz, R. H. & Goldberg, M. E. (1972) Activity of superior colliculus in behaving monkey. III. Cells discharging before eye movements. *J. Neurophysiol.* **35**, 575–586.

Wurtz, R. H. & Mohler, C. W. (1976) Organization of monkey superior colliculus: enhanced visual response of superficial layer cells. *J. Neurophysiol.* **39**, 745–765.

Zee, D. S., Optican, L. M., Cook, J. D., Robinson, D. A. & Engel, W. K. (1976) Slow saccades in spinocerebellar degeneration. *Arch. Neurol.* **33**, 243–251.

Zee, D. S., Tusa, R. J., Herdman, S. J., Butler, P. H. & Gücer, G. (1987) Effects of occipital lobectomy upon eye movements in primate. *J. Neurophysiol.* **58**, 883–907.

26. THE PUPIL

SPHINCTER AND DILATOR MUSCLES

The aperture of the refracting system of the eye is controlled by the iris which behaves as a diaphragm, contracting or expanding as a result of the opposing actions of two muscles of ectodermal origin, namely the *sphincter pupillae* and the *dilator pupillae*. As classically described, the sphincter is an annular band of smooth muscle, 0.75 to 0.8 mm broad in man, encircling the pupillary border, which on contraction draws out the iris and constricts the pupillary aperture. At the pupillary border the muscle is closely associated with the pigment epithelium, so that, on contraction, the latter tends to be drawn on to the anterior surface of the iris. The sphincter is closely adherent to the adjacent connective tissue so that, after an iridectomy, it does not contract up, and the pupil remains reactive to light. Like the sphincter, the dilator muscle is of ectodermal origin, but in the sphincter the ectodermal cells have been transformed into true muscle fibres whereas the cells of the dilator retain their primitive characteristics and are called *myoepithelial cells*. It will be recalled (p. 9) that the ciliary epithelium consists of two layers of cells, an outer pigmented layer and, inside this, the unpigmented layer; these two layers are continued over the posterior surface of the iris, the pigmented layer becoming the layer of myoepithelial cells and the unpigmented layer acquiring pigment and becoming the posterior epithelium of the iris. The myoepithelial cells are spindle shaped with long processes that run radially to constitute the fibres of the dilator, making a discrete layer anterior to that made up by the bodies of the myoepithelial cells; the layer of fibres is called the *membrane of Bruch*. Close to the edge of the pupil the dilator fibres fuse with the sphincter, and at the other end they continue into the ciliary body where they take origin; between the insertion and origin, 'spurs' make connection with adjacent tissue. When it contracts, the dilator draws the pupillary margin towards its origin and thus dilates the pupil.

Innervation

The sphincter is innervated by parasympathetic fibres from N III by way of the ciliary ganglion and the short ciliary nerves; the dilator is controlled by the cervical sympathetic, the fibres relaying in the superior cervical ganglion; post-ganglionic fibres enter the eye in the short and long ciliary nerves (Fig. 1.5).

Functions of the Pupil

A pupil of varying size performs three main functions:

1. It modifies the amount of light entering the eye, thus permitting useful vision over a wide range of luminance levels. The amount of light entering the eye is directly proportional to the area of the pupil; under conditions of night vision the absolute amount of light entering the eye is of great importance and a sixteenfold increase of sensitivity of the eye to light should be obtained by an increase of pupil diameter from 2 to 8 mm. At the other end of the scale, excessive luminance reduces visual acuity; the strong pupillary constriction occurring in these circumstances mitigates this condition and thus extends the range of useful vision. In nocturnal animals this aspect of pupil-size is of greater importance and it is probable that the slit of the fully constricted pupil of the cat is an adaptation permitting a greater restriction of the amount of light penetrating the eye in daylight.
2. As a result of constriction, the pencils of light entering the eye are smaller and the depth of focus of the optical system is increased (p. 771). When the eye is focused for distant objects, the depth of focus is large and the pupil-size is relatively unimportant; when the eye is focused for near objects, on the other hand, the depth of focus becomes small and a constricted pupil contributes materially.
3. By the reduction in the aperture of the optical system aberrations are minimized. In the dark these aberrations are unimportant, since form is only vaguely perceived, so that the advantage accruing from the increased light entering a dilated pupil far outweighs the effects of aberrations; in daylight, however, the reverse is true; and we have already seen how, at varying luminances, the size of the pupil is adjusted to give optimum visual acuity (p. 386).

THE PUPILLARY REFLEXES

The accurate adjustment of the pupil-size to the optical requirements of the eye implies a reflex response to illumination; this is the basis of the *light reflex* under which term we may include the constriction of the pupil when the luminance is increased, and the dilatation when the luminance is decreased. The other important reflex, from the optical point of view, is the *near reflex*, the constriction of the pupil that takes place during the focusing on a near object. Additional reflexes are the *lid-closure reflex*, a constriction in response to closure of the lid, and the *pyscho-sensory reflex*, a dilatation of the pupil in response to a variety of sensory and psychic stimuli.

Experimental Measurement—Pupillography

The experimental study of the size of the pupil—*pupillography*—has been carried out by a variety of techniques; since the pupil responds to visible light the method of measurement must dispense, if possible, with illumination unless this involves flashlight photography where the duration of the flash is so short that the pupil has no time to respond. For continuous studies flash-photography is obviously of no use, since the flashes have their effects, although delayed; by the use of infrared photography, however, a cinematographic record of the pupil in the dark may be obtained and this is the method that has been most commonly employed. More recently Lowenstein & Loewenfeld (1958) have developed a method of 'electronic pupillography' based on infrared scanning of the pupil, the reflected light from the scanned pupil being brought on to an infrared sensitive photo-tube. The scanned image is made visible by the usual television principles, if this is required; alternatively the size of the pupil may be recorded less directly on a cathode-ray screen. Thus when the scanning spot crosses from the iris to the pupil there is an abrupt decrease in the reflected light, and this shows up as a sudden fall in the signal on the oscilloscope. The larger the pupil the longer the portion of a given scan will give the low signal.

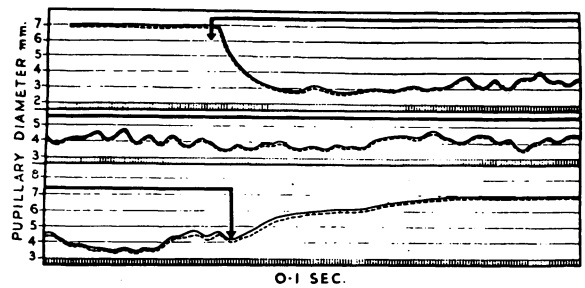

Fig. 26.1 Effect of exposure of right eye to a bright light. Ordinate: pupillary diameter in mm. Abscissa: time of exposure. Record in full line applies to right eye; in broken line to left eye. *First line*: the pupils were large and quiet in darkness. At the arrow the right eye was exposed to a steady illumination. *Second line*: this shows the pupillary oscillations after the right eye had been exposed for 3 min to the light. *Third line*: when the light was turned off, at the arrow, the pupils dilated and the oscillations disappeared. (Lowenstein & Loewenfeld, *Amer. J. Ophthal.*)

The Light Reflex

When the light falling on one eye is increased, the pupil of this eye constricts—the *direct light reflex*; at the same time the pupil of the other, unstimulated, eye also contracts—the *indirect* or *consensual light reflex*. A record of the changes in pupil-size in the two eyes during exposure to a bright light is shown in Fig. 26.1, where the pupil-diameter is given as the ordinate and is plotted against time of exposure. The record is shown in three parts; at the arrow on the top, the light is switched on to illuminate the right eye, whose pupillary diameter is indicated by the full line. Both pupils contract down to about 3 mm, and the sizes oscillate together whilst, as time progresses, there is an increase in size on which the oscillations are imposed; this is seen by the middle record, the mean pupil-size being about 4 mm. At the arrow in the bottom record the light was turned off, and the pupils return slowly to their original diameters. The increase in diameter that occurs during sustained illumination may be regarded as an effect of light-adaptation. On flashing a light into the eye, then, the response is a constriction of the homolateral and contralateral pupils, the extent of the constriction depending on the intensity of the light and the state of adaptation of the eye. If the light-stimulus is prolonged, the pupil dilates slowly and reaches a size which, for a given individual, depends on the intensity of the light. When both eyes are stimulated there is a summation of the individual responses so that both pupils constrict rather more than when one alone is stimulated with the same intensity of light; conversely if, when both are being subjected to a light stimulus, one eye is closed, the contralateral pupil dilates slightly.

Effect of Luminance

The magnitude of the initial constriction caused by a light-stimulus depends, as we should expect, on the intensity of the light. This is demonstrated by Fig. 26.2 where the constriction, in millimetres, is represented by the heights of the black bars, whilst the relative luminances of the stimuli are plotted logarithmically as abscissae. At the arrow marked *a*, the intensity is some millionth of that required to evoke the 3 mm response, and this corresponds to the threshold for colour vision, i.e. the cone threshold. At the arrow marked *b*, the intensity is

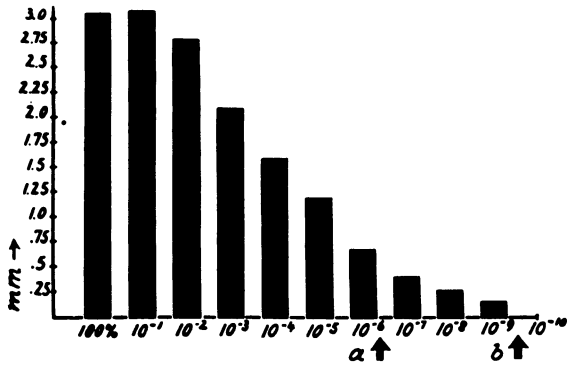

Fig. 26.2 Average extent of pupillary reflexes elicited by light-stimuli of decreasing intensity. The heights of the columns indicate the average degree of constriction, whilst the abscissa shows the intensities of the light-stimuli (duration 1 second). The arrow *a* shows the threshold for colour vision and the arrow *b* the absolute threshold. (Lowenstein & Loewenfeld, *Amer. J. Ophthal.*)

some 10^{-9} to 10^{-10} of that required to produce the 3 mm response; this is the threshold for rod vision, and it will be seen that under the conditions of these experiments the threshold for pupillary response is higher than that for the visual response.

Rods and Cones

The receptors for the pupillary response to light are obviously the rods or cones or both; in fact, many studies have shown that both receptors may bring about the reflex. At threshold intensities for pupillomotor activity the visual sensation is colourless, proving that the rods are mediating the response; on plotting the sensitivity to the different wavelengths a typical scotopic sensitivity curve is obtained with maximum in the region of 500 nm (Schweitzer, 1956).

Spectral Sensitivity

The most thorough investigation of the influence of wavelength on pupillary response is that of Alpern & Campbell (1962), who studied both transient pupillary changes, i.e. the response to rhythmically altered intensities, and steady-state changes. In both cases, the responses to relatively high luminances never gave an uncomplicated photopic luminosity curve comparable with that for vision; instead, the maximum was between 530 and 540 nm, suggesting that, even under highly photopic conditions and foveal stimulation, the rods and cones were both operative, due, presumably, to scatter from the fovea. When the effects of rods were excluded by keeping them adapted to a blue light acting as a background upon which the foveal test-stimulus was imposed, then the action-spectrum gave a curve with a peak at about 560 nm, in reasonable agreement with the C.I.E. standard curve (Fig. 26.3). Analysis of the curve obtained when the maximum was at 530 to 540 nm, on the basis of the different effects of the Stiles-Crawford phenomenon with red and blue lights, suggested that the rod and cone effects were, indeed, simultaneously present, and that their separate contributions to the final pupillary response could be estimated if the measured sensitivity was treated as the weighted mean of the logarithms of the individual rod and cone sensitivities at a given wavelength.[1] If the response of the pupil is plotted against intensity of the light-stimulus, as in Fig. 26.4, there appears an obvious break in the curve when white or blue light is employed, a break corresponding to the transition from rod to cone vision. When red light is employed there is no break, and the threshold is higher because the red

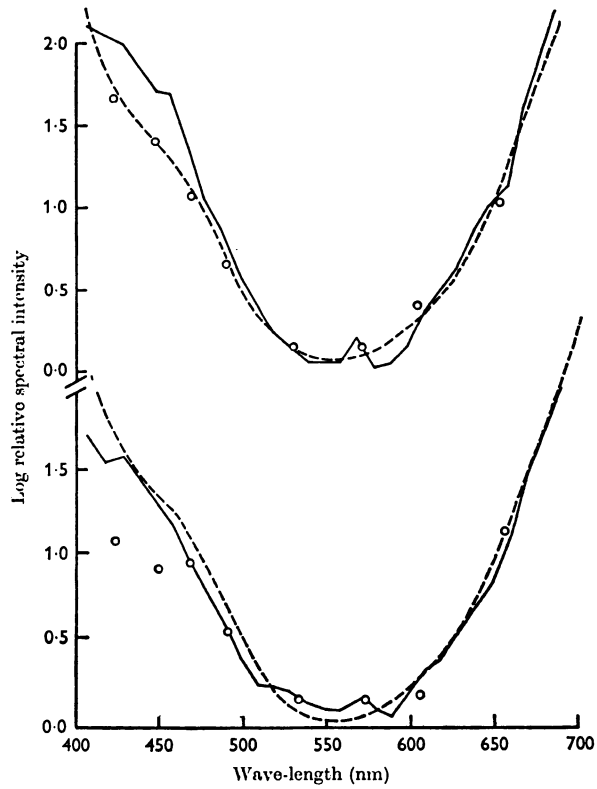

Fig. 26.3 Mean spectral sensitivity curve for the pupil response of two subjects. O, Differential threshold measurements are plotted for 2 sec flashes of a 2° test patch centrally fixated and seen against a continuous blue background approximately 15° in diameter, which produced a retinal illuminance somewhere between 100 and 200 td. Interrupted line, C.I.E. photopic luminosity curve; solid line, mean results of psychophysical measurements of photopic luminosity (flicker photometry) on the same two subjects with the same apparatus. (Alpern & Campbell, *J. Physiol.*)

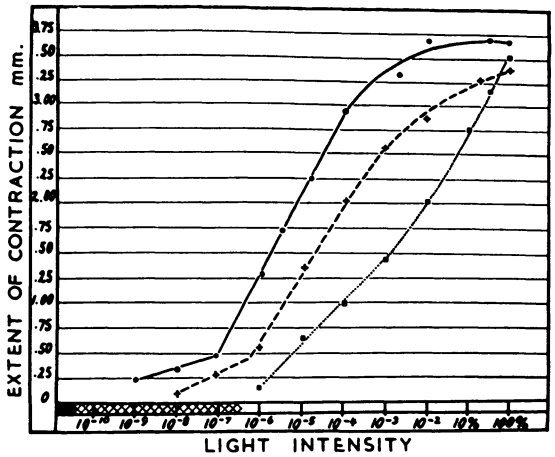

Fig. 26.4 Pupillary contraction as a function of the intensity of the light-stimulus for three different types of light. Solid line and dots: curve for white light. Broken line and crosses: curve for blue light obtained by placing filter in front of white source; the apparent increase in the threshold is due to the absorption of light by the filter. Dotted line and squares: curve for red light obtained by placing red filter in front of the white source. The black bar above the abscissa indicates values below the absolute threshold; the hatched bar indicates the range of scotopic vision. Note that with red light pupillary responses are only obtained at intensity levels corresponding to photopic vision. (Lowenstein & Loewenfeld, *Amer. J. Ophthal.*)

light is very ineffective as a rod stimulator. In general, the cone response to a flash has a shorter latency (0.2 to 0.3 second) and is more rapid and longer-lasting than the rod response, which has a latency of 0.45 to 0.6 second.

Summation

Schweitzer (1956) has studied the effects of increasing the area and duration of the stimulus. It will be recalled that the visual stimulus shows a limited amount of spatial summation, in the sense that if the thresholds for a small patch of light and a larger patch are compared, the threshold is lower for the larger patch; this is due, as we have seen, to the convergence of rods and cones on to ganglion cells. The area over which summation of the visual response occurs is relatively small by comparison with that for the pupillographic response; thus Schweitzer found complete summation up to an area subtending 4° in the periphery and 0.5° at the fovea, whilst partial summation extended over much wider areas. This means that to make the most efficient use of light in the pupillomotor response we must stimulate a large area of retina; when this is done we find that the visual and pupillomotor thresholds are equal, but Schweitzer was unable to push the sensitivity of the pupillomotor response beyond this point, i.e. he could not obtain a contraction of the pupil in the absence of visual sensation.[2] As a result of the operation of the light reflex, the size of the pupil tends to adopt a characteristic value for each level of luminance; according to De Groot & Gebhard (1952) the diameter, d, in mm, is related to the luminance, B, in mL, by the empirical equation:

$$\log d = 0.8558 - 0.000\,401(\log B + 8.1)^3$$

In the completely dark-adapted eye the mean pupillary diameter is given variously as 6.6 to 7.6 mm.

The Near Reflex

By the near reflex is meant the constriction of the pupil accompanying the convergence of the eyes on to a near object; associated with these two actions of convergence and miosis, there is, of course, the act of accommodation, all three being mediated by N III. The response is bilateral and the maximal constriction obtained with this reflex is approximately equal to that obtained with the light reflex; the two reflexes may summate their responses.

The Lid-closure Reflex

This had been classically described as a homolateral pupillary constriction associated with closure of the lid; it was said to be evoked if the lid was held open while the effort to close the eye was made. Lowenstein & Lowenfeld (1969) have pointed out that this latter phenomenon is really an example of the near reflex, since it does not occur if the subject is told to look at a far point all the time. As these authors state, it is best to include all pupillary changes associated with lid-closure in the class of 'lid-closure reflexes', but the variety of conditions under which the lids close means that the pupillary changes will be different and have different mechanisms. Thus, if the lids close to avoid a noxious stimulus, it is probable that the pupils will dilate because of the psycho-sensory reflex; a brief, naturally occurring, blink is associated with dilatation due to the operation of the light-reflex in reverse, i.e. the response to the short period of darkness.

Psycho-sensory Reflex

This is a dilatation of the pupils evoked by stimulation of any sensory nerve or by strong psychical stimuli. Pupillary dilatation thus occurs during the induction stage of anaesthesia, in extreme fear and in pain; in sleep, on the other hand, when these stimuli are lacking, the pupils are generally constricted. The mechanism is clearly a cortical

one and is apparently mediated both by way of the cervical sympathetic, which activates the dilator pupillae, and by way of N III which inhibits the tonus of the sphincter pupillae. The reaction is not seen in the newborn, but appears in the first few days of life, developing fully at the age of six months.

NERVOUS PATHWAYS

Reflex Arc

The receptors of the light reflex are the rods and cones; the afferent pathway is therefore through the optic nerves and tracts; the pupillary fibres leave the optic tract before the lateral geniculate body is reached, and for many years it was thought that they relayed in the superior colliculus. Magoun & Ranson (1953) showed, however, that in cats and monkeys the fibres pass through the medial border of the geniculate body and then run, by way of the brachium of the superior colliculus, into the *pretectal nucleus*, a group of cells occupying a position at the junction of the diencephalon and the tectum of the mid-brain; here they have their first synapse. In the cat the majority of the secondary fibres cross in the posterior commissure and terminate in the Edinger-Westphal nucleus; in primates the crossing is not so extensive. Destruction of the superior colliculus, therefore, leaves the light reflex intact; stimulation of the pretectal area gives a bilateral constriction of the pupils; conversely, destruction of this area gives a dilated and fixed pupil. From the Edinger-Westphal nucleus the pupillo-constrictor fibres pass with the IIIrd nerve fibres to the ciliary ganglion. The reflex arc for the direct and indirect light reflexes is indicated in Fig. 26.5; the diagram indicates quite clearly how a light stimulus, falling on one eye, gives rise to pupillary constriction in both eyes.

Identification of the Neuronal Pathway

Pretectal Complex

The regions of termination of the retinal fibres in the midbrain have turned out to be complex, so that the simple statement that the pupillo-sensory input relays in the 'pretectal nucleus' is misleading; it is possible furthermore that fibres concerned with accomodation relay in a different nucleus from those mediating pupillary responses (Westheimer & Blair, 1973). The subject has been discussed in detail by Scalia (1972) in the light of his own studies, and he has constructed a valuable table indicating the equivalent structures in a variety of mammalian species, and the different terminologies employed by the many anatomists who have described one or more of these.

NUCLEAR MASSES

His own study led to the conclusion that there were four pretectal cell masses or nuclei receiving retinal input, namely: *Nucleus of the Optic Tract* (*NOT*); *Anterior Pretectal Nucleus*; *Olivary Pretectal Nucleus* (*PON*) and *Posterior Pretectal Nucleus.* Some of these nuclei are illustrated in Fig. 26.6 which is an outline drawing of a brainstem section through the most compact portion of

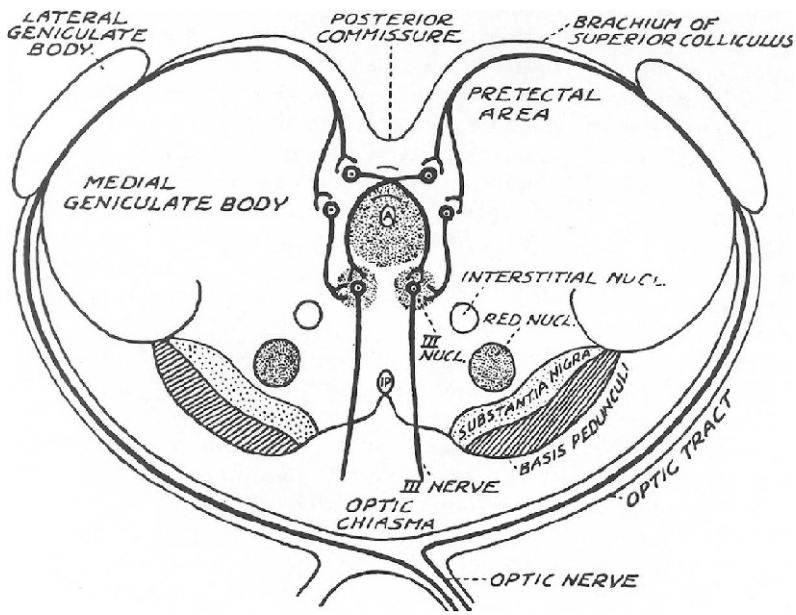

Fig. 26.5 The path concerned in the pupillary light-reflex, according to Magoun & Ranson (*Arch. Ophthal.*).

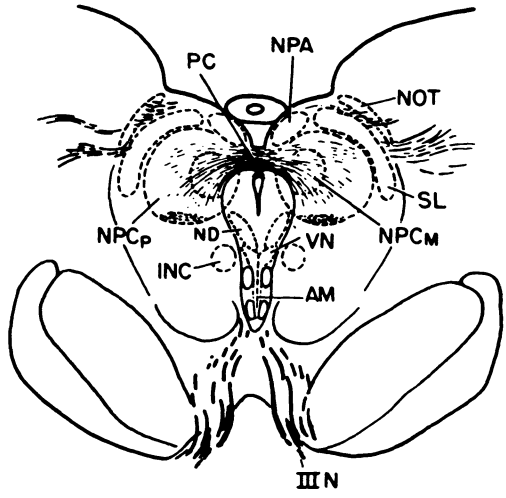

Fig. 26.6 Outline drawing of a brain stem section through the most compact portion of the posterior commissure (PC). At this level, the nucleus of the optic tract (NOT), the sublentiform nucleus (SL), the nucleus of the pretectal area (NPA), and the nucleus of the posterior commissure (NPC) are well developed. The anterior median nucleus (AM) is present, but the dorsal visceral nuclei (VN) of the oculomotor complex have not separated into medial and lateral cell columns. Additional abbreviations: INC, interstitial nucleus of Cajal; ND, nucleus of Darkschewitch; NPCm, nucleus of posterior commissure, pars magnocellularis; NPCp, nucleus of posterior commissure, pars principalis; III N, oculomotor nerve. (Pierson & Carpenter, *J. Comp. Neurol.*)

the posterior commissure. The features common to all species are a heavy retinal projection to the olivary pretectal nucleus and to the nucleus of the optic tract; the posterior pretectal nucleus is present in all species and receives a retinal projection; the retinal projection to the anterior pretectal nucleus is variable amongst species. Of most interest was the re-discovery of the retinal projection to the olivary pretectal nucleus, the high density of retinal terminals indicating an obvious visual function. Later, Pierson & Carpenter (1974) described a similar dense projection to this nucleus in monkeys, and demonstrated, moreover, a projection from the PON to the pregeniculate nucleus. The projections were predominantly contralateral but an ipsilateral projection in addition, giving rise to the possibility of binocular visual input, was found in each of the mammals studied by Scalia, but it depended on the nucleus.

Pregeniculate or Ventral Geniculate Nucleus

The role of this diencephalic nucleus, closely related anatomically and phylogenetically to the thalamus (p. 493), in pupillary or accommodative activity has been discussed by Pierson & Carpenter. There is no doubt that this is a nucleus in which retinal fibres terminate, but these authors were unable to find pupillary misfunction in monkeys with lesions in this nucleus. According to Swanson *et al.* (1974) the ventral nucleus of the lateral geniculate body of cat and rat projects to the pretectal nuclei.

Edinger-Westphal Nucleus

This, the visceral portion of the nucleus of N III, has been described earlier on the basis of Warwick's classical study employing a degeneration technique. More modern techniques of retrograde labelling have led to some disagreement, at any rate so far as the cat is concerned. Toyoshima *et al.* (1980) injected horseradish peroxidase into the ciliary ganglion of the cat and found that the projection was from the large polygonal neurones of the ventral tegmental area related to the Edinger-Westphal nucleus, the central gray, and the caudal half of the anterior-median nucleus. Cells of the Edinger-Westphal nucleus were unlabelled except for those in the periphery, considered by Toyoshima *et al.* to have migrated from the central gray and the ventral tegmental area. According to these authors, then, the Edinger-Westphal nucleus was not involved in the projection to the ciliary ganglion, sending axons to the spinal cord (Loewy *et al.*, 1978; Castiglioni *et al.*, 1978) principally.[3]

PRIMATE

It may well be that there is a difference between the cat and monkey. Thus Akert *et al.* (1980) also using retrograde tracing from the ciliary ganglion, found labelled neurones in a small compact group on the ipsilateral side and dorsal to the somatic cell column of the N III nucleus. The anteromedian nucleus was free of label. Figure 26.7 illustrates the Edinger-Westphal nucleus defined as the area of retrograde labelling from the ciliary ganglion. The preganglionic neurones stood out clearly, being nearly as large as the motor neurones to the extraocular muscles; surrounding cells were smaller and seemed to belong to the reticular formation. Anteromedian cells were quite different, and Akert *et al.* discussed the finding of Jampel & Mindel (1967) that stimulation here produced pupilloconstriction, suggesting that the definition of this group of neurones might vary from one experimenter to another.

Single Unit Activity

Sillito (1968) and Sillito & Zbrożyna (1970) recorded activities of single neurones in the midbrain of cats which discharged in relation to pupilloconstrictor activity. Thus a given neurone discharged at 1/sec when the pupil diameter was 10 mm, at 2.5/sec at 3 mm, 7.5/sec at 0.5 mm

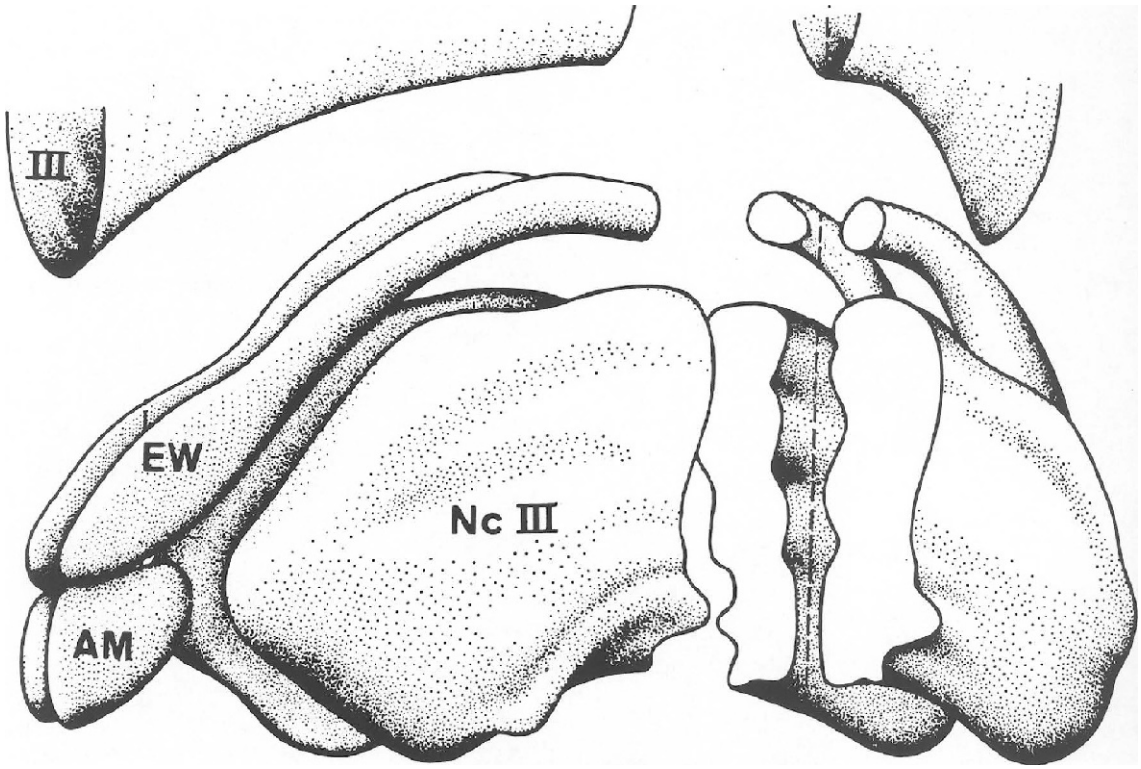

Fig. 26.7 Three-dimensional reconstruction of the oculomotor complex on the basis of Nissl-stained serial sections. The Edinger-Westphal nucleus was identified on the basis of the present experimental work. AM, anteromedian nucleus; EW, Edinger-Westphal nucleus; NcIII, oculomotor nucleus; SGC, substantia grisea centralis; III, third ventricle. (Akert *et al.*, *Brain Res.*)

and at 8.5/sec when the pupil was slit-like. During the light-reflex the rate rose to 8.5 to 12.5/sec and could be as high as 25/sec. When the perifornical region of the hypothalamus (a pupillodilator centre) was stimulated, the discharge of the units was completely silenced.

Midbrain Location

When the regions of the midbrain in which these pupilloconstriction-associated neurones were localized were explored they were found to include a region containing both the cells of the Edinger-Westphal nucleus and of the anteromedian nucleus where they adjoin; the caudal part of the Edinger-Westphal nucleus and the rostral part of the anteromedian nucleus were not involved in pupilloconstrictor activity, so that the distribution of neurones cuts across the traditional basis of division that attributed pupilloconstrictor activity entirely to the Edinger-Westphal nucleus. Sillito & Zbrożyna emphasize, moreover, that the pupilloconstrictor centre is not a paired structure, as represented in Fig. 26.5, for example, but is strictly a group of cells with no midline cleavage; in agreement with this, all pupillomotor responses produced by stimulation of the nucleus, or of supranuclear structures, were strictly bilateral.[4]

The Neuronal Pathway

Hultborn *et al.* (1978a) showed that records of spike activity in the ciliary nerve of the cat in response to electrical stimulation of the optic tract, were manifestations of the pupillomotor reflex. They then recorded from different positions in the central nervous system, measuring the latencies of the responses. Figure 26.8 illustrates their results; latency falls with distance of the stimulating electrode from the ciliary nerve in two steps, corresponding to the posterior commissure and the Edinger-Westphal nucleus.

Dilator Neurones

Smith *et al.* (1970) found neurones some 0.5 to 2.0 mm above and below the Edinger-Westphal nucleus which

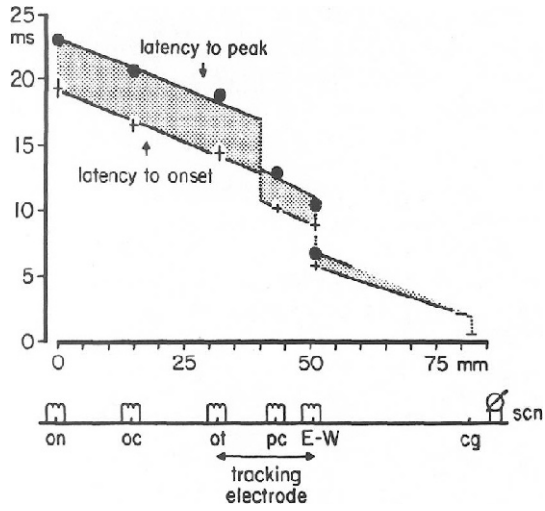

Fig. 26.8 Diagram showing the latency of the 'pupillo-constrictor' short ciliary nerve-response to electrical stimulation along the pathway subserving the pupillary light reflex. Latency (in msec, ordinate) is plotted against the distance along the reflex pathway (from the stimulating electrode on the optic nerve; abscissa). Below the abscissa are indicated the central structures corresponding to the different distances. The horizontal bars indicate mean values for the latency to the onset of the scn-response (and the vertical bars the S.E.M.), while the filled circles indicate the latency to the peak of the same responses. The times-to-peak (from the onset) are thus given by the dotted areas. (Hultborn *et al.*, *Brain Res.*)

discharged at rates related to the degree of dilatation of the pupil; when the brain was stimulated at the recording sites there was pupillary dilatation, and the same occurred when the cervical sympathetic nerves were cut, so that the response was mediated by inhibition of tonically active pupilloconstrictor neurones in the Edinger-Westphal nucleus with their pathway through the ciliary ganglion.

Pretectal Units

Cavaggioni *et al.* (1968) recorded responses to light in single units of the nucleus of the optic tract in the midpontine-trigeminal cat and correlated these with pupillary responses. The feature that differentiated the responses from those in the adjacent superior colliculus was their sustained nature, which was usually an increased rate of discharge maintained as long as the light-stimulus; a short phasic component was completed before the pupil began to constrict and might have been responsible for activating the Edinger-Westphal neurones to initiate the constrictor response to light, whilst the tonic sustained increase augmented the tonic discharges in the Edinger-Westphal neurones maintaining the pupillary constriction at the value for the new light-intensity. The responses of collicular neurones were easily distinguished from the pretectal units, for example in their sensitivity to moving stimuli. Other pretectal units were suppressed by light and gave a prominent OFF-response, and it was suggested that this OFF-discharge was inhibitory, so that the dilatation of the pupil at onset of darkness was not a mere passive return to a relaxed state but was aided by active inhibition of the tonically active Edinger-Westphal neurones; certainly a 'supranuclear inhibition of the light-reflex', not involving the sympathetic pathway and presumably involving inhibition of the Edinger-Westphal nucleus, has been described (Bonvallet & Zbrożyna, 1963; Lowenstein & Loewenfeld, 1969).

Sympathetic Units

Passatore & Pettorossi (1976) measured responses in single fibres dissected from the central end of the cat's cervical sympathetic nerve; as Fig. 26.9 shows, the resting discharge during illumination of the eye was strongly increased with onset and maintenance of darkness, indicating that the response to darkness involves an active process of exciting the dilator pupillae. The effect was stronger in the homolateral eye when the consensual reflex was studied. When painful stimuli were applied to the skin or cornea, discharges were recorded comparable with those obtained on cutting off illumination, and these coincided with pupillary dilatation. Since the same fibres exhibited responses to changes in illumination, we may conclude that the pathways for the light-reflex and the psycho-sensory reflex converge on the same sympathetic neurones (Passatore, 1976).

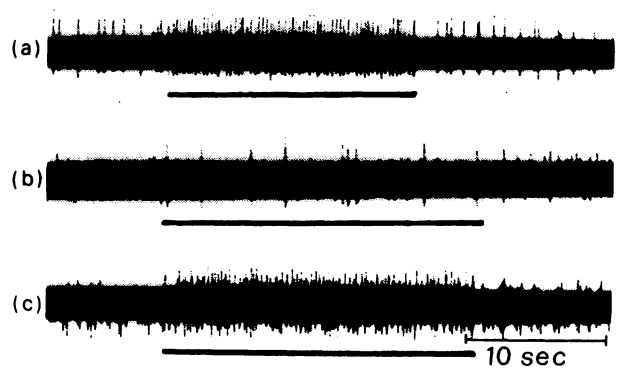

Fig. 26.9 Different response patterns to ON–OFF light-stimulus in fibres dissected from the central end of the cat's cervical sympathetic nerve. Time signal: 10 sec. (Passatori & Pettorossi, *Exp. Neurol.*)

Other Pupillomotor Centres

The sphincter pupillae undoubtedly dominates pupil activity so that the pretectal and cortical pupilloconstrictor centres have received most attention. The strong association of dilatation of the pupil with emotional states would indicate the presence of dilator centres in those parts of the brain that have been shown to be strongly associated with emotional states, namely the hypothalamus and the limbic system generally. In fact, electrical stimulation in the hypothalamus, over quite a wide region, causes dilatation of the pupil (Hess, 1957). The pathway from the brain in dilator responses involves the sympathetic system, the pupillomotor fibres leaving the cord from the first and second thoracic segments and relaying in the superior cervical ganglion. Stimulation of the cord between the VIth cervical and IVth thoracic segments causes dilatation of the pupil and it is customary to speak of spinal dilator centres, but it seems most likely that the stimulus merely activates the sympathetic motor neurones in the cord.

Cerebellar Involvement

Ijichi *et al.* (1977) analysed the pupillomotor responses of the cat when exposed to a sinusoidally varying light-stimulus; the curve for the normal animal, describing phase-lag with frequency, showed a sharp cut-off at high frequencies; in the cerebellectomized animal this cut-off occurred at lower frequencies. They considered that the effect would be mediated by the sympathetic rather than the Edinger-Westphal parasympathetic pathway. Thus in their study of cerebellar influence on accommodation, the stimulation of the interpositus and fastigial nuclei as well as cerebellar cortex caused discharges in the ciliary nerve, but studies on the interaction of these responses with those to optic tract stimulation, and also records from individual cells of the ciliary ganglion, persuaded Hultborn *et al.* (1978b) that the ciliary discharge related to accomodative activity alone. They found no significant changes in pupil-size with cerebellar stimulation.

The Peripheral Mechanisms

Reflex Dilatation

Stimulation of the cervical sympathetic trunk in the neck causes a pronounced dilatation of the pupil. If the sympathetic trunk is cut there is an initial dilatation, due to the irritative effect of the cut, and this is followed by a constriction so that the pupil on the cut side is smaller than the other; this is presumably due to the fact that normally the size of the pupil is determined by a balance of forces between sphincter and dilator; putting the dilator out of action allows the sphincter to take control. The same phenomenon is manifest in the reflex response to light; in the sympathectomized eye the response is generally larger. Reflex dilatation, brought about by some sensory stimulus, is mainly due to active dilatation, mediated by the sympathetic, since when the sympathetic trunk is cut there is only a small dilatation, due to inhibition of sphincter tone. Some time after removing the sympathetic supply to the iris it becomes hypersensitive to adrenaline and this gives rise to what has been called 'paradoxical pupillary dilatation'. Thus a sensory stimulus causes, in this sympathectomized eye, a small dilatation due to relaxation of sphincter tone, and this is followed by a much larger dilatation due, presumably, to the liberation into the blood of adrenaline as a consequence of the sensory stimulus.

Stimulation of N III, or the ciliary ganglion, causes constriction of the pupil; damage to the ciliary ganglion or IIIrd nerve reduces the reflex responses to light very considerably, such constriction as occurs being due to inhibition of sympathetic tone.[5] Weak psycho-sensory stimuli result in reflex pupillary dilatation in both normal and ciliary ganglionectomized eyes, the effect being a little larger in the normal eye, as we should expect.

The Effects of Drugs

The main effects of drugs on the pupil are largely what one would expect of a system innervated by both parasympathetic and sympathetic fibres.

Parasympathetic Drugs

It will be recalled that parasympathetic activity is mediated by the liberation of acetylcholine, so that this substance and drugs with a similar chemical constitution will behave in the same way as parasympathetic stimulation, causing a constriction of the pupil. Thus acetylcholine, pilocarpine, muscarine and many synthetic compounds are *parasympathomimetic*, by virtue of their chemical similarity to the parasympathetic chemical mediator. Another group mimics the parasympathetic by virtue of their inhibitory action on cholinesterase, the enzyme that destroys acetylcholine at its site of action and thus prevents the chemical mediator from acting indefinitely. They are said to *potentiate* the action of acetylcholine. Eserine, physostigmine and many modern synthetic drugs, such as diisopropylfluorophosphate (DFP), act in this way causing a prolonged pupillary constriction by preserving from destruction the acetycholine, liberated by the tonic and reflex activity of the parasympathetic nerve endings. Another group of substances block the action of acetylcholine by competing for its sites of activity on the muscle; an example of this

parasympatholytic action is given by atropine, and various synthetic drugs such as homatropine. These drugs, by blocking the tonic parasympathetic activity, leaving sympathetic activity normal, cause a long-lasting dilatation of the pupil, which is now unresponsive to light.

GANGLION BLOCKERS, ETC.

Since the parasympathetic innervation operates through the ciliary ganglion, we may expect drugs that act specifically on autonomic ganglia to influence the pupil; in fact, hexamethonium and pentolinium block transmission and cause dilatation of the pupil, due to cutting off of tonic action. Transmission through the ganglion is brought about by the liberation of acetylcholine, hence this transmitter, as well as nicotine and tetramethyl ammonium, causes discharge in the postganglionic fibres and thus brings about constriction of the pupil. However, the sympathetic system, causing dilatation of the pupil, also operates through a ganglion, this time the superior cervical, hence the final effect of a blocking agent on the pupil will depend on which division of the autonomic system is having the dominant action at the time of administration of the drug.

Sympathetic Drugs

The sympathetic chemical mediator is noradrenaline, whilst adrenaline, liberated by the adrenal medulla in response to stress, has an essentially similar action, in so far as it mimics many of the actions of the sympathetic system. These substances cause dilatation of the pupil.

INTRAOCULAR INJECTIONS

Bennett *et al.* (1961) injected sympathetic amines into the posterior chamber of rabbits, and the anterior chamber of dogs, measuring the pupillary effects. If the dilatation caused by adrenaline was put equal to 100, that due to noradrenaline was 37 and to isoproterenol 19; the action of isoproterenol was not blocked by DCL, so that we may attribute all three effects to alpha-activity. In these animals, then, pupillary dilatation seems to be dominated by alpha-receptors in the dilator muscle.

Reciprocal Innervation

Although pupillary constriction is effected primarily by parasympathetic activation of the sphincter, associated with inhibition of any tonic sympathetic activation of the dilator muscle, a number of studies have suggested that this reciprocal control is even more exact, the sphincter and dilator muscles each being influenced by excitatory and inhibitory inputs. Some evidence for dual innervation of both muscles has been provided by studies on the effects of cholinergic and adrenergic drugs and antagonists on the contraction of the isolated muscles.

Van Alphen *et al.* (1964), working on the cat, found that, with the dilator, the order of effectiveness in causing contraction was: Adrenaline > Noradrenaline ≫ Isoproterenol. These effects were blocked by phenoxybenzene so that there is little doubt that the main activity is through α-receptors. Some β-activity was demonstrated by the observation that smaller doses of isoproterenol often produced a relaxation, which was blocked by DCI; again, phenoxybenzene not only blocked the contraction due to isoproterenol but could reverse this into a relaxation. With the sphincter, a relaxation of the muscle, previously caused to contract with acetylcholine, was caused by the amines in the order: Isoproterenol ≫ Adrenaline > Noradrenaline, thus indicating mainly β-activity. The action of adrenaline is indicated by Fig. 26.10, at A, contraction was induced with acetylcholine; at E, adrenaline was applied, which caused a relaxation after a brief contraction. When DCI was added (lower trace) the relaxation failed and adrenaline now caused contraction due to its α-action. Thus the cat sphincter is, indeed, influenced by adrenergic amines, the dominant influence being relaxation through β-receptors. Hence the effects of adrenaline in the cat are synergic, the α-activity on the dilator being assisted by the β-relaxation of the sphincter. Essentially similar conditions were found by Van Alphen *et al.* (1965) in the rabbit, and by Patil (1969) in the ox; in the monkey, however, α-activity was strongly predominant in both sphincter and dilator, so that under the action of sympathetic amines there should be antagonism.

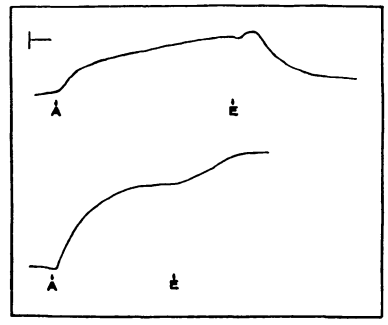

Fig. 26.10 Effects of epinephrine on the iris sphincter. *Top*: At A, contraction was induced by acetylcholine; at E, relaxation was caused by epinephrine. *Bottom*: After treatment with DCI, the contracture induced by acetylcholine is stronger, and the effect of epinephrine is reversed into an additional contraction. (Van Alphen *et al.*, *Int. J. Neuropharmacol.*)

Ultrastructure of Nerve Terminals

The nature of nerve terminals on smooth muscle may be ascertained with some degree of probability by the types

of vesicles within them, as seen in the electron microscope (see, for example, Richardson, 1964). Nishida & Sears (1969a,b) found two types of axon running in the sphincter muscle of the albino guinea pig; 85% belonged to the type containing agranular vesicles characteristic of cholinergic fibres whilst the remaining 15% contained vesicles with a dense core characteristic of adrenergic fibres; these were morphologically identical with the majority of fibres in the dilator muscle. Twenty-four hours after superior cervical ganglionectomy these fibres showed degenerative changes. Thus, so far as the dilator was concerned, it appeared that antagonistic actions were mediated by the sympathetic system through opposed alpha- and beta-activity. With the sphincter, it seemed that antagonism was by way of excitatory parasympathetic and inhibitory sympathetic innervation. However, there is some evidence that the dilator is innervated by inhibitory parasympathetic fibres (Ehinger *et al.*, 1968).

Cholinergic Active Dilator

Thus Suzuki *et al.* (1983) found that carbachol caused a relaxation of isolated bovine iris dilator muscle, an effect that was blocked by atropine. Again, Yoshitomi *et al.* (1985), working on isolated human iris, found that electrical stimulation caused an initial phasic contraction followed by a long-lasting relaxation, suggesting the operation of two nervous actions; the effects were blocked by tetrodotoxin, which blocks nervous conduction. The phasic contraction was blocked by the adrenergic alpha-blocker, phentolamine, whilst the phase of relaxation was blocked by atropine, indicating a cholinergic inhibitory action on the dilator muscle. This cholinergic inhibition would support the miosis due to cholinergic activation of the pupilloconstrictor muscle.

In the dog, Yoshitomi & Ito (1986) studied both sphincter and dilator along the same lines. Electrical excitation of either muscle caused an initial contraction followed by a phase of relaxation; atropine blocked the phasic contraction of the sphincter and the relaxation of the dilator, whilst guanethidine blocked relaxation of the sphincter and contraction of the dilator. Thus it seems that the two iris muscles receive double reciprocal innervation: cholinergic activation contracts the sphincter and relaxes the dilator, whilst activation of the adrenergic nervous system contracts the dilator and relaxes the sphincter to give mydriasis.[6]

Bovine Dilator

Classically we should expect adrenergic agents such as adrenaline to cause contraction of the dilator muscle, but in this species norepinephrine produced only a very slight contraction; by contrast carbachol or acetylcholine produced a strong relaxation that was inhibited by atropine, suggesting that dilatation of the bovine pupil is mediated primarily through cholinergic inhibition of the constrictor; thus pupil-constriction would be brought about by excitatory cholinergic activity on the sphincter muscle associated with cholinergic inhibition of the dilator. Electrical excitation of the dilator caused relaxation of the muscle, an effect completely blocked by atropine and hardly affected by propranolol (Suzuki *et al.*, 1983).

Antidromic Pupilloconstriction

This has been discussed in relation to the breakdown of the blood-aqueous barrier that takes place on antidromic stimulation of N V, and has been attributed to the liberation of substance P at the sensory nerve terminals. The effect is mimicked by capsaicin, which presumably stimulates the release of substance P, capsaicin being dependent on an intact sensory nerve supply. Zhang *et al.* (1984) have shown that capsaicin action is not suppressed by atropine or tetrodotoxin, so that although it needs an intact nerve supply, it does not require axonal activity. Zhang *et al.* have discussed the possibility that substance P is, indeed, the antidromic transmitter, its release being inhibited by morphine, as in the central nervous system.

Other Drugs

Certain drugs act directly on smooth muscle, and since the sphincter is the stronger of the two iris muscles, their action on the pupil is largely determined by whether they cause this muscle to relax or contract. Thus *histamine* causes a powerful miosis which overcomes the mydriasis of atropine. *Morphine* and veratrine cause a miosis by direct action on the plain muscle; the pin-point pupil of morphia addicts is thought to be due, however, to the action of the drug on the central nervous system.

PROSTAGLANDINS

We have seen earlier that irritation of the iris is associated with liberation of prostaglandins into the anterior chamber together with a pronounced miosis. Zhang *et al.* (1982) have discussed the miotic action of prostaglandins, but they themselves found that doses as high as 2.8×10^{-4} molar had no effect on the isolated rabbit sphincter; they conclude that, so far as the rabbit iris is concerned, prostaglandins have no direct action on the sphincter, nor yet an indirect action dependent on sensory innervation.

Pupillary Unrest

It is clear from the above that the state of the pupil at any moment is determined by a variety of synergic and antagonistic nervous influences; in general, external circumstances—light, and proximity of the fixation point—

tend to cause constriction whilst the internal factors of sensation, and psychic activity generally, cause dilatation. The continual interplay between these opposing forces results in a constant state of pupillary activity—the pupil is restless—and the size of the pupil under any given conditions is a fluctuating quantity. The fact that both pupils fluctuate in size in harmony shows that the phenomenon of pupillary unrest is determined centrally, and is not merely an example of the independent rhythmic activity so frequently seen in smooth muscle (Stark *et al.*, 1958). The pathological condition in which this activity is abnormally great is called *hippus*.

Notes

1. Alexandridis & Koeppe (1969) have described the typical Purkinje shift in maximal sensitivity to wavelength on passing from scotopic to photopic stimulation; their sensitivity curves coincided remarkably well with the corresponding sensitivity curves for vision, with maxima at 500 nm and 560 nm.
2. It is commonly stated that the threshold for pupillomotor activity is higher than that for vision, and this is true for small test-fields; thus if this subtended 1° 50′, the ratio of thresholds varied from 8 to 1000; when the Ulbricht integrating sphere was employed, permitting exposure of a very large field, the thresholds became equal because of the greater degree of summation in the pupillomotor response. Temporal summation, whereby two stimuli, following each other rapidly, are more effective than a single one, depends essentially on the photochemical characteristics of the receptors (Bunsen-Roscoe Law) rather than on any neural organization; it is not surprising, therefore, that temporal summation is the same for the pupillomotor and visual responses (Schweitzer, 1956).
3. A cortical projection to the Edinger-Westphal nucleus of the macaque by anterograde movement of tracer after injection into precentral and premotor areas has been described by Hartmann-von Monakow *et al.* (1979).
4. This view differs a little from that of Jampel & Mindel (1967), who placed an electrode exactly in the midline of the monkey's midbrain and, according to its depth, obtained accomodation only, a mixture of this with pupilloconstriction, or only pupilloconstriction. As soon as the electrode was displaced laterally the responses became ipsilateral, so they concluded that there were paired masses close to the midline responsible for pupillary and accommodative activity, cells controlling accommodation being located dorsally and somewhat rostrally to cells innervating the iris.
5. In the cat, in contrast to man and monkey, the sympathetic supply to the iris does not pass through the ciliary ganglion; hence in this animal damage to, or removal of the ganglion does not influence sympathetic activity.
6. Pharmacological studies showed that the sphincter muscle contained alpha$_1$ (excitatory) and alpha$_2$-inhibitory receptors as well as beta-inhibitory receptors, whilst the dilator had alpha$_1$-excitatory and beta-inhibitory receptors.

References

Akert, K., Glicksman, M. A., Lang, W., Grob, P. & Huber, A. (1980) The Edinger–Westphal nucleus in the monkey. A retrograde tracer study. *Brain Res.* **184**, 491–498.

Alexandridis, E. & Koeppe, E. R. (1969) Die spektrale Empfindlichkeit der für den Pupillenlichtreflex verantwortlichen Photoreceptoren beim Menschen. *v. Graefs' Arch. Ophthal.* **177**, 136–151.

Alpern, M. & Campbell, F. W. (1962) The spectral sensitivity of the consensual light reflex. *J. Physiol.* **164**, 478–507.

Bennett, D. R., Reinke, D. A., Alpert, E., Baum, T. & Vasquez-Leon, H. (1961) The action of intraocularly administered adrenergic drugs on the iris. *J. Pharmacol.* **134**, 190–198.

Bonvallet, M. & Zbrozyna, A. (1963) Les commandes reticulaires du système autonome et en particulier de l'innervation sympathique de la pupille. *Arch. Ital. Biol.* **101**, 174–207.

Castiglioni, A. J., Gallaway, M. C. & Coulter, J. D. (1978) Spinal projections from the midbrain in monkey. *J. Comp. Neurol.* **178**, 329–346.

Cavaggioni, A., Madarasz, I. & Zampollo, A. (1968) Photic reflex and pretectal region. *Arch. ital. Biol.* **106**, 227–240.

De Groot, S. G. & Gebhard, J. W. (1952) Pupil size as determined by adapting luminance. *J. Opt. Soc. Am.* **42**, 492–495.

Ehinger, B., Falck, B. & Persson, H. (1968) Function of cholinergic nerve fibres in the cat iris dilator. *Acta Physiol. Scand.* **72**, 139–147.

Hartmann-von Monakow, K., Akert, K. & Künzle, H. (1979) Projections of precentral and premotor cortex to the red nucleus and other midbrain areas. *Exp. Brain Res.* **34**, 91–105.

Hess, W. R. (1957) *The Functional Organization of the Diencephalon.* New York: Grune & Stratton.

Hultborn, H., Mori, K. & Tsukahara, N. (1978a) The neuronal pathway subserving the pupillary light reflex. *Brain Res.* **159**, 255–267.

Hultborn, H., Mori, K. & Tsukahara, N. (1978b) Cerebellar influence on parasympathetic neurones innervating intraocular muscles. *Brain Res.* **159**, 269–278.

Ijichi, Y., Kiyohara, T., Hosoba, M. & Tsukahara, N. (1977) The cerebellar control of the pupillary light reflex in the cat. *Brain Res.* **128**, 69–79.

Jampel, R. S. & Mindel, J. (1967) The nucleus for accommodation in the midbrain of the macaque. *Invest. Ophthal.* **6**, 40–50.

Loewy, A. D., Saper, C. B. & Yamodis. (1978) Re-evaluation of the efferent projections of the Edinger–Westphal nucleus in the cat. *Brain Res.* **141**, 153–159.

Lowenstein, O. & Loewenfeld, I. E. (1958) Electronic pupillography. *Arch. Ophthal.* **59**, 352–363.

Lowenstein, O. & Loewenfeld, I. E. (1959a) Scotopic and photopic thresholds of the pupillary light reflex in normal man. *Am. J. Ophthal.* **48**, pt. 2, 87–98.

Lowenstein, O. & Loewenfeld, I. E. (1959b) Influence of retinal adaptation upon the pupillary reflex to light in normal man. *Am. J. Ophthal.* **48**, pt. 2, 536–550.

Lowenstein, O. & Loewenfeld, I. E. (1969) The Pupil. In *The Eye*, 2nd ed., Ed. Davson, Vol. III, pt. 2. London & New York: Academic Press.

Magoun, H. W. & Ranson, S. W. (1953) The central path of the light reflex. *Arch. Ophthal.* **13**, 791–811.

Nishida, S. & Sears, M. (1969a) Fine structural innervation of the dilator muscle of the iris of the albino guinea pig studied with permanganate fixation. *Exp. Eye Res.* **8**, 292–296.

Nishida, S. & Sears, M. (1969b) Dual innervation of the iris sphincter muscle of the albino guinea pig. *Exp. Eye Res.* **8**, 467–469.

Passatore, M. (1976) Physiological characterization of efferent cervical sympathetic fibers influenced by changes of illumination. *Exp. Neurol.* **53**, 71–81.

Passatore, M. & Pettorossi, V. E. (1976) Efferent fibers in the cervical sympathetic nerve influenced by light. *Exp. Neurol.* **52**, 66–82.

Patil, P. N. (1969) Adrenergic receptors of the bovine iris sphincter. *J. Pharmacol.* **166**, 299–307.

Pierson, R. J. & Carpenter, M. B. (1974) Anatomical analysis of pupillary reflex pathways in the rhesus monkey. *J. comp. Neurol.* **158**, 121–143.

Richardson, K. C. (1964) The fine structure of the albino rabbit iris with special reference to the identification of adrenergic and cholinergic nerves and nerve endings in its intrinsic muscles. *Am. J. Anat.* **114**, 173–184.

Scalia, F. (1972) The termination of retinal axons in the pretectal region of mammals. *J. comp. Neurol.* **145**, 223–245.

Schweitzer, N. M. J. (1956) Threshold measurements on the light reflex of the pupil in the dark adapted eye. *Doc. Ophthal.* **10**, 1–78.

Sillito, A. M. (1968) The location and activity of pupilloconstrictor neurones in the mid-brain of the cat. *J. Physiol.* **194**, 39–40 P.

Sillito, A. M. & Zbrozyna, A. W. (1970) The localization of pupilloconstrictor function within the mid-brain of the cat. *J. Physiol.* **211**, 461–477.

Smith, J. D., Masek, G. A., Ichinose, L. Y., Watanabe, T. & Stark, L. (1970) Single neuron activity in the pupillary system. *Brain Res.* **24**, 219–234.

Stark, L., Campbell, F. W. & Atwood, J. (1958) Pupil unrest: an example of noise in a biological servomechanism. *Nature, Lond.* **182**, 857–858.

Suzuki., R., Oso, T. & Kobayashi, S. (1983) Cholinergic inhibitory response in the bovine iris muscle. *Invest. Ophthal.* **24**, 760–765.

Swanson, L. W., Cowan, W. M. & Jones, E. G. (1974). An autoradiographic study of the efferent connections of the ventral lateral geniculate nucleus in the albino rat and the cat. *J. Comp. Neurol.* **156**, 143–163.

Toyoshima, K., Kawana, E. & Sakai, H. (1980) On the neuronal origin of the afferents to the ciliary ganglion in cat. *Brain Res.* **185**, 67–76.

Van Alphen, G. W. H. M., Kern, R. & Robinette, L. (1965) Adrenergic receptors of the intraocular muscles. *Arch. Ophthal. N.Y.* **74**, 253–259.

Van Alphen, G. W. H. M., Robinette, S. L. & Macri, F. J. (1964) The adrenergic receptors of the intraocular muscles of the cat. *Int. J. Neuropharmacol.* **2**, 259–272.

Westheimer, G. & Blair, S. M. (1973) The parasympathetic pathways to internal eye muscles. *Invest. Ophthal.* **12**, 193–197.

Yoshitomi, T. & Ito, Y. (1986) Pre-synaptic action of noradrenaline on the dog ciliary muscle tissue. *Exp. Brain Res.* **43**, 119–127.

Yoshitomi, T., Ito, Y. & Inomata, H. (1985) Adrenergic excitatory and cholinergic inhibitory innervation in the human iris dilator. *Exp. Eye Res.* **40**, 453–459.

Zhang, S. Q., Butler, J. M., Ohara, K. & Cole, D. F. (1982) Sensory neural mechanisms in contraction of the isolated sphincter pupillae: the role for substance P and the effects of sensory denervation on the response to miotics. *Exp. Eye Res.* **35**, 43–54.

Zhang, S. Q., Butler, J. M. & Cole, D. F. (1984) Sensory neural mechanisms in contraction of the rabbit isolated sphincter pupillae: analysis of the responses to capsaicin and electrical field stimulation. *Exp. Eye Res.* **38**, 153–163.

27. ACCOMMODATION

The emmetropic eye is defined as one whose optical system is such as to cause images of distant objects to be focused on the retina, which is therefore at the second principal focus of the dioptric system. Images of near objects will necessarily be formed behind the retina (Fig. 6.7) so that in order to bring these on to the retina an increase in dioptric power is necessary, and this increase is described as accommodation.

Amplitude of Accommodation

As an object is moved closer and closer to the eye, at a certain point—*the near point of accommodation*—the eye can no longer increase its dioptric power and the object becomes indistinct. The far point of the eye has been defined as the position of an object such that its image is formed on the retina of the completely relaxed eye. Thus in the emmetrope this is infinity. We may define the *amplitude of accommodation*, therefore, as the difference in refracting power of the eye in the two states of complete relaxation and maximal accommodation. Thus if Q is the refracting power of the eye in maximum accommodation, and S its power when completely relaxed, the amplitude, A, is given by:

$$A = Q - S$$

Since the amplitude is a *difference* in refracting power of the eye in two conditions, it is not necessary to know its actual power in either; the amplitude may be calculated from the near and far points quite simply, as follows.

Myopic eye

In Fig. 27.1 the near and far points of a myopic eye are shown. It is required to find how much the power of the eye is increased when an object, formerly at the far point, is seen distinctly at the near point. To do this we can imagine that the eye, instead of accommodating, has remained in the relaxed condition and that the increased dioptric power to permit distinct vision of the object at the near point has been provided by a converging lens. The power of this lens would represent the increase in dioptric power of the eye in maximum accommodation. The completely relaxed eye sees distinctly an object at the far point; the lens must be chosen, therefore, of such a strength that it will form an image of an object, situated at the near point, at the far point. In the lens formula:

$$1/v - 1/u = 1/f$$

$v = r$, where r is the distance of the far point in metres,

$u = p$, where p is the distance of the near point in metres.

Thus $$1/r - 1/p = 1/f$$

If we let $1/r$ in metres be R; $1/p$ be P; the power of the lens, A, is given by:

$$R - P = A$$

R may be called the *dioptric value of the far point distance*; P the *dioptric value of the near point distance*, and A is the amplitude of accommodation, in dioptres.

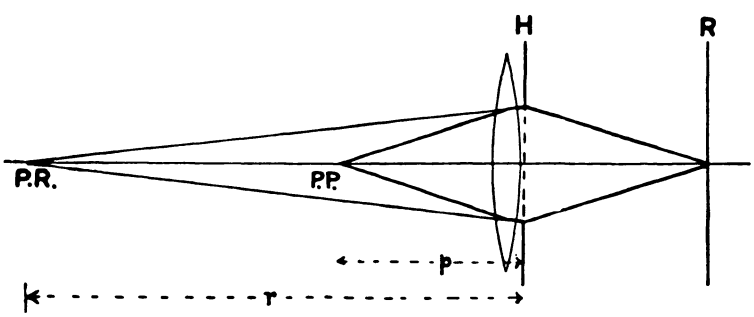

Fig. 27.1 Illustrating the amplitude of accommodation in a myopic subject. At maximum accommodation the extra dioptric power exerted is equivalent to that given by placing a thin lens of focal length p in front of the eye.

This relationship between R, P, and A has been derived from the lens formula, consequently it will only hold if the usual sign convention is applied. Thus in the case of the myope R and P are both negative.

Emmetrope and Hypermetrope

In the emmetrope the Far Point is infinity, so that R is zero and the formula becomes:

$$A = -P$$

so that if the Near Point is, say, 10 cm or 0.1 m, the amplitude is $1/0.1 = 10$ dioptres. In the hypermetrope the Far Point is a fictitious point behind the eye, so that R is positive and the same Near Point-distance of 10 cm would correspond to a greater amplitude than 10 dioptres. This becomes clear when we realize that, in order to see distant objects distinctly, the hypermetrope has to make use of a part of his total amplitude.

THEORY OF ACCOMMODATION

According to the modern theory of accommodation, which is largely based on Helmholtz's ideas, the capsule has sufficient elasticity to mould the lens into a more strongly curved system than is necessary for distant vision. The elasticity of the capsule is held in check by the normal tension in the zonule, so that accommodation consists in a relaxation of the tension in the zonule which permits the capsule to mould the lens into a more strongly curved system. The relaxation of the zonule follows a *contraction* of the ciliary muscle.

The Ciliary Muscle

The Fibre Types

The ciliary muscle is classically described as containing three types of unstriped muscle fibre:

1. *Meridional fibres*, arising from the epichoroid and attaching to the scleral spur.
2. *Radial fibres*, situated more internally and anteriorly, arranged in the manner of a fan.
3. *Circular fibres*, continuous with, and inseparable from the radial fibres, running round the free edge of the ciliary body just behind the root of the iris.

However, Fincham has shown that this formulation is rather too rigid; the fibres take origin from the epichoroid, and in the outer part of the muscle (nearest the sclera) they run a purely meridional course, to be inserted in the scleral spur. More internally, the fibres make up a branching meshwork and it is this part that has been incorrectly called the radial portion—the fibres are not arranged in a regular radial manner but, as indicated, in a reticular meshwork. As a result of the branching of the bundles of fibres, a number acquire a more or less circular direction, a tendency that becomes more pronounced towards the inner edge of the muscle. Thus the innermost edge consists essentially of circular fibres—the so-called *sphincter muscle of Müller*—but they are not to be regarded as making up a separate muscle. The circular elements give off short tufts of fibres which are inserted into a ring of elastic tissue (A of Fig. 27.2) at the base of the iris. Another layer of elastic tissue (B) is situated between the muscle and the pigment epithelium of the ciliary body. The elastic elements presumably resist the tension of the zonule.

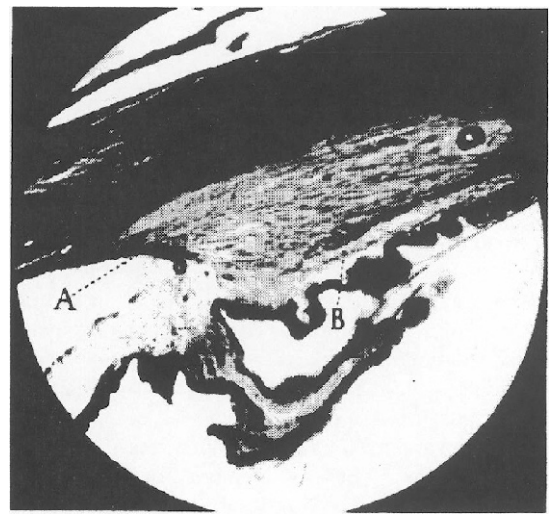

Fig. 27.2 The ciliary muscle as described by Fincham. A and B indicate elastic tissue. (*Brit. J. Ophthal.*)

Effects of Contraction

The general anatomical characteristics of the ciliary muscle indicate that its contraction must relax the zonule; the meridional fibres pull on the epichoroidal tissue and drag the ciliary body forward. The circular fibres, probably the most important in accommodation, must, on shortening, decrease the radius of the circle that they constitute; this can only be achieved by a radial extension of the ciliary body which must reduce the tension in the zonule (Fig. 27.3). These anatomical considerations are confirmed by the observation that during accommodation the external surface of the ciliary body moves forward by 0.5 mm. Moreover, careful observation of the lens during accommodation shows that it becomes tremulous as though its normal taut suspension had been

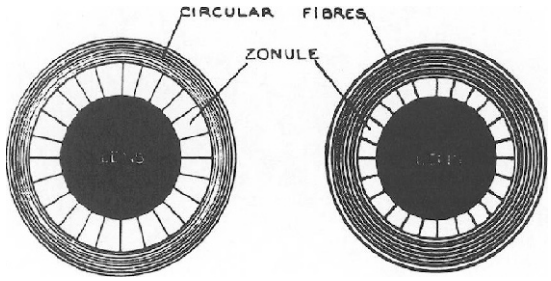

Fig. 27.3 Illustrating the action of the circular fibres in relaxing tension in the zonule.

relaxed; again, the equator of the capsule of the unaccommodated lens shows fine wrinkles, proving that it is held under tension; during accommodation these wrinkles are smoothed out.

The Zonular System

Structure

The actual mechanism whereby contraction of the ciliary muscle affects the tension in the zonular fibres is not completely clear, since the muscle has no direct connections with the fibres. The structure of the human zonule has been examined in some detail by Rohen & Rentsch (1969) with a view to elucidating this point. According to this study, the fibres fall into two classes, the separation into two groups occurring in the middle third of the ciliary body; behind this, the system is a uniform mat of fibres. As indicated in Fig. 27.4 the main system of 'holding fibres', H, runs forward towards the pars orbicularis where the individual fibres split at the *zonular fork*, ZF, and finally both branches insert into the lens capsule. Branching off from the holding fibres is the second system of *tension fibres*, T, inserting into the ciliary epithelium in the orbicularis region of the ciliary body. It seems that it is because of the close relation of these tension fibres to the ciliary epithelium on the ciliary processes, and in the valleys between, that effects of changes in volume of the ciliary body, due to contraction of the muscle, are transmitted to the lens.

Changes with Accommodation

Thus Fig. 27.4 illustrates the postulated changes; below, the muscle is relaxed in the unaccommodated state, and the holding fibres are stretched, maintaining tension on the capsule. Above, the muscle has contracted and the changed shape of the ciliary body has caused the tension fibres to become stretched, and this has permitted the main holding fibres to relax. It is essentially the tension

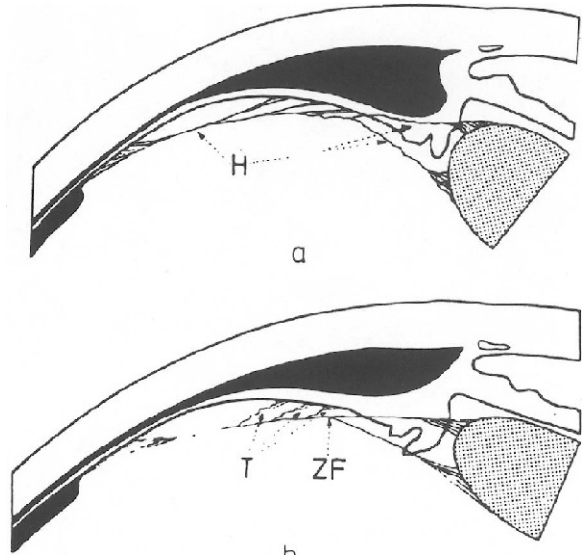

Fig. 27.4 Illustrating Rohen and Rentsch' concept of the structure of the zonular fibres. (a) The accommodated state. (b) The relaxed state. H are the *holding fibres* which split at the *zonular fork*, ZF. Branching from the holding fibres are the *tension fibres*, T, inserting into the ciliary epithelium. (After Rohen & Rentsch, *v. Graefes' Arch. Ophthal.*)

fibres that cause the important change in tension in the capsule, and they do this by virtue of their attachment to the ciliary epithelium, the changed shape of the ciliary body causing a forward and axial pull.

Changes in the Lens

Purkinje Images

The actual changes in the lens during accommodation were studied by Helmholtz by means of the Purkinje images; during accommodation image III, formed by the anterior surface of the lens, became smaller, indicating an increase in the curvature of this surface (Fig. 27.5). Studies on individuals with congenital aniridia have shown that the lens does become smaller (1.25 mm) and thicker (1.3 mm) as Helmholtz's theory would demand.

Slit-lamp Measurements

Fincham's work suggested that the central zone of the anterior surface became more convex in relation to the periphery, the surface becoming what Fincham called 'conoid'. The much more precise studies of Brown (1973, 1974), based on slit-lamp microscopy, confirmed the conoid shape in the adult lens but not in that of a child of 11 years. The actual radii of curvature for the central and

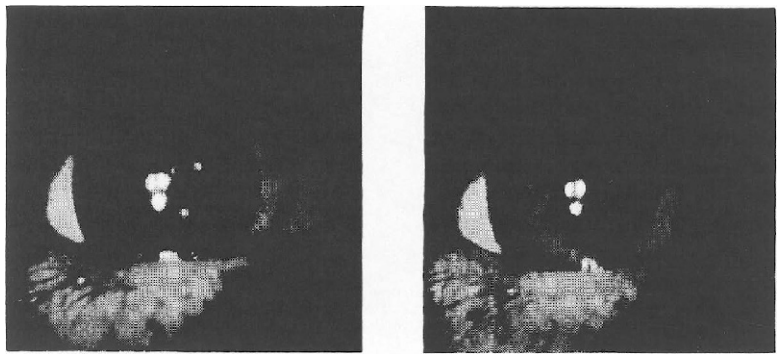

Fig. 27.5 The change in the size of the Purkinje image, formed by the anterior surface of the lens, following accommodation. The object, whose image was formed by the reflecting surfaces of the eye, consisted of three bright lamps arranged in a triangle. Left: unaccommodated eye. Right: accommodated eye. (Fincham, *Brit. J. Ophthal.*)

Table 27.1 Mean radii of central and peripheral lens surfaces in mm ± S.D. (Brown, 1974).

Anterior Central Chord	12.4 ± 2.6
Anterior Peripheral Chord	13.3 ± 3.2
Posterior Central Chord	8.1 ± 1.6
Posterior Peripheral Chord	7.1 ± 1.4

peripheral parts are shown in Table 27.1; and the changes in shape during accommodation are illustrated by Fig. 27.6. Thus the radius of curvature of the central surfaces shortens whilst those of the periphery lengthen; the changes in the anterior surface are more marked. The anterior pole is pushed forward and the posterior backward a little. According to Brown, the accommodative changes are largely brought about by the nucleus, and this is indicated in Fig. 27.6. With age, the volume of nucleus becomes a smaller fraction of the total, and Brown suggested that this change might well be a factor in the reduced accommodative power with age—*presbyopia.*

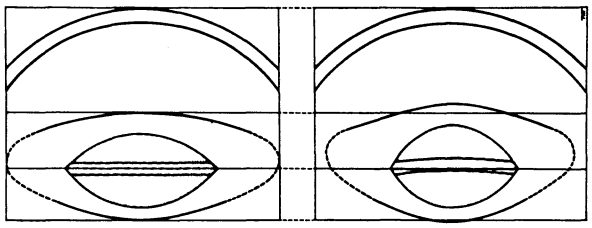

Fig. 27.6 The shape of the whole lens obtained by extrapolation. 29-year-old subject. Left: 0 D accommodation; right: 10 D accommodation. (Brown, *Exp. Eye Res.*)

REARRANGEMENT OF LENS SUBSTANCE

Whatever the exact changes may be, they must involve a rearrangement of the lens substance since this is quite incompressible; the general increase in curvature must mean a decrease in the surface of the lens and this must mean that the shape approaches more closely to that of a sphere (in the sphere we have the condition of maximum volume for minimum area; if we decrease the surface of a body and maintain its volume the same, we must make it more nearly spherical). The effects of this rearrangement may be observed with the slit-lamp microscope when there are mobile opacities in the lens; the movement consists generally of an axial flow from the periphery, as we should expect.

ZONULAR RIDGES

The attachment of the zonular fibres at the equator gives rise to an anterior and a posterior equatorial ridge, the posterior one being visualized by gonioscopy and the anterior in subjects with iris colobomata (Brown, 1974b). The changes in these ridges during stimulation and paralysis of accommodation support strongly the Helmholtz-Fincham hypothesis of accommodation, the ridges becoming more pronounced in the relaxed phase when the tension is expected to be greatest.

EXCISED LENS

It follows from the theory of accommodation that the excised lens must be in a state of maximum accommodation. Hartridge & Yamada (1922) estimated the dioptric power of the cat's eye *in situ* by measuring the magnification of a portion of the fundus observed through a modified ophthalmoscope. On removal of the lens its curvatures were measured and its dioptric power calculated. They showed that the combined power of the cornea and excised lens amounted to 12 dioptres more than the power of the eye *in vivo*, i.e. the lens, with the curvatures it possessed in the excised state, would provide the eye with an extra 12 dioptres of refractive power. However, the experimentally determined amplitude of accommodation in the cat is only about 2D (Ripps *et al.*, 1961); moreover Fisher (1971), from his measurements of Young's modulus of the cat lens, together with the capsular energy, concluded that any change in shape of the lens would be out of the question, and the same was

true of the rabbit.[1] Again Vakkur *et al.* (1963), in their valuable study of the dioptrics of the cat's eye, concluded that there was little or no accommodative power, any change that did occur being more likely to be due to a shift in position of the lens than a change in shape, and they showed that Hartridge & Yamada's conclusion was based on a miscalculation of the power of the eye *in situ*. In fact O'Neill & Brodkey (1969) have measured a linear movement of the anterior pole of the cat's lens associated with increased power when stimulating the ciliary ganglion; the average maximum accommodation exerted was 1.72 D, corresponding to a movement of 0.57 mm.

Depth of Focus of the Eye

In a lens system there is theoretically only one position of the object that will give an image at a definite distance from the principal plane; hence with the eye, where the position of the retina is fixed, there is only one position, for a given state of the dioptric power, where an object will produce a distinct image. For the emmetropic eye, this is at infinity. When the object is brought nearer to the eye, the image of a point on it becomes a 'blur-circle' because the true image is behind the retina. If the blur-circle is not large, however, it is not recognized as differing from a point and the object may thus be brought within a finite distance of the eye before the blur-circle becomes so large that the image is appreciated as 'indistinct'. The extent to which the object may be moved before the points on it appear out of focus is called the *depth of focus*. As Fig. 27.7 shows, the depth of focus obviously depends on the pupil-size. It will also depend on the distance of the fixation point from the eye; if this is large (e.g. 100 m) the point may be moved many metres closer to the eye before it goes out of focus; if it is small (e.g. 25 cm) a movement of a centimetre or two is enough to blur the image. For the human eye the figures obtained by Campbell (1954) were as follows:

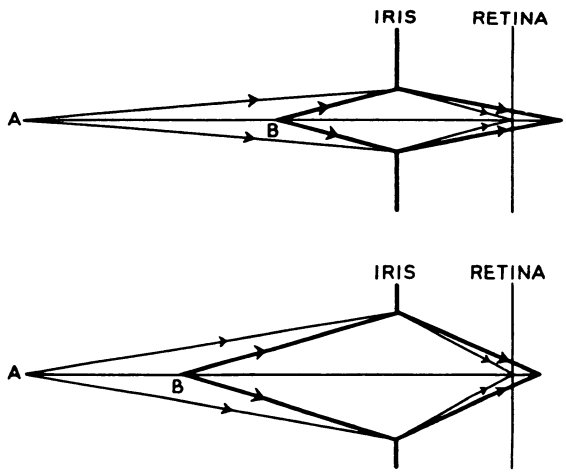

Fig. 27.7 Illustrating the influence of the size of the pupil on the depth of focus. With the small pupil (above) B produces a blur-circle of fixed size when it is closer to the eye than with the large pupil (below). The depth of focus (AB) is smaller with the larger pupil.

Pupil diameter	*Depth at infinity*	*Depth at 1 metre*
1 mm	From infinity to 1.25 m	5.0 m to 56 cm
2 mm	2.33 m	1.8 m to 70 cm
3 mm	2.94 m	1.5 m to 75 cm
4 mm	3.57 m	1.4 m to 78 cm

Visual Acuity

Ogle & Schwartz (1959) presented the subject with a chart and changed the vergence of light from it by means of a lens, keeping the image-size constant. At a certain point the visual acuity was decreased and the change of vergence was recorded. This amounted to 0.6 dioptres and Ogle & Schwartz defined the depth of focus in terms of this amount of vergence. The depth of field, on the other hand, could be defined as the equivalent distance through which the chart would have been moved to produce this change of vergence. The *hyperfocal distance* was defined as the distance of the fixation point at which objects beyond this all appear in focus.

Tolerated Change of Vergence

Adamson & Fincham (1939) measured the change of vergence tolerated by the eye; i.e. if an object was made to appear closer or farther away, by means of lenses, a point was reached when the eye adjusted its accommodation, and this was indicated by a change of its refracting power as measured with an optometer. The average change in vergence tolerated by the eye was found to be ± 0.25 D. An object 1 m away (vergence -1 D) may be moved so that the vergence changes to -0.75 D or to -1.25 D without blurring of the image; i.e. it can be moved to 1.33 m or 0.80 m, giving a depth of focus of 53 cm. If the object is 25 cm away (vergence -4 D) the limits of tolerance are -3.75 D and -4.25 D, representing a depth of focus of 3.0 cm (26.6 $-$23.6 cm). The difference between the values found by Ogle & Schwartz and Fincham depends on their different criteria.[2]

THE CHANGE IN ACCOMMODATION WITH AGE (PRESBYOPIA)

Ciliary Muscle

The amplitude of accommodation decreases progressively with age (Fig. 27.8) falling from some 14 dioptres in a

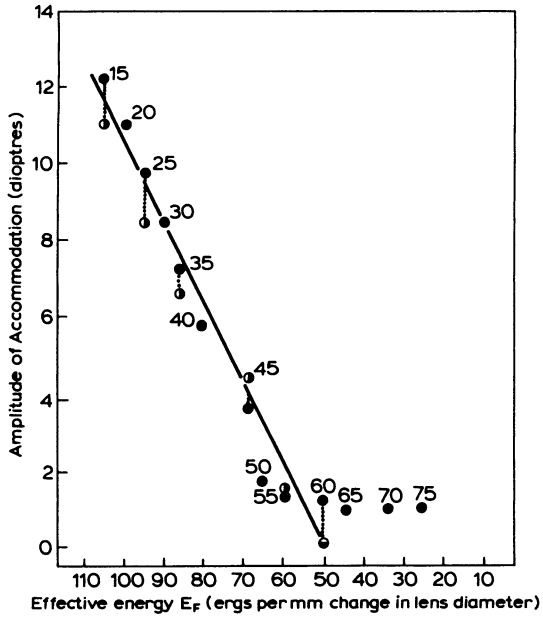

Fig. 27.8 Showing presbyopic changes in amplitude of accommodation and effective energy of the lens capsule. ● Duane's data; ◑ Bruckner's data mean per decade; ◓ Hamasaki's data. Age in years (15 to 75). (Fisher, *J. Physiol.*)

child of ten years to about zero at the age of 52 (Hamasaki *et al.*, 1956). It has been argued that the failure is due to atrophy of the ciliary muscle, but denied by Swegmark (1969), who measured ciliary muscular activity by means of its changes in electrical impedance, measured through four electrodes on the perilimbal region of the eye. Through one pair an alternating current was passed and through the other impedance was measured. The ciliary contractile power, measured in this way, remained the same up to the age of 60 years; Swegmark emphasized, moreover, that a disuse atrophy of the ciliary muscle was extremely unlikely to occur, since the ciliary muscle would be activated during convergence of the eyes—part of the near response (p. 783)—whether or not accommodation took place.

Lens Capsule

Helmholtz's view, that there is a failure of the lens capsule to modify the shape of its contents receives far more support. Thus Fincham observed that the curvature of the excised senile lens was considerably less than that of a juvenile one. This failure could be due to a hardening of the lens material, *sclerosis*, to a decrease in modulus of elasticity, or to a decrease in thickness, of the capsule, or to all three of these factors.

Capsular Surface Tension

In an attempt to assess the importance of the various factors, Fisher (1969b) measured the capsular surface tension, i.e. the energy that unit area of the capsule can exert, at rest and during accommodation; this was computed from the measured changes in outline of the anterior capsule and the force required to stretch it. In Fig. 27.8 the effective energy of the capsule is plotted against the amplitude for lenses taken from different aged eyes; there is a remarkable correspondence between the two since the capsule actually increases in thickness with age up to 60 years; this suggests that the modulus of elasticity, which decreases from some 6×10^7 dynes/cm^2 in childhood to 1.5×10^7 dynes/cm^2 in extreme old age, plays an important role. However, this parallelism does not rule out a significant contribution of increased stiffness of the lens material; it does show, however, that the earlier tendency to attribute presbyopia entirely to lens sclerosis is unjustified.[3]

When the effects of altered elasticity and lens shape[4] were taken into account, the measurements indicated that, in the absence of changed power of the ciliary muscle, about 50% of the loss of accommodative power would be due to lens hardening.

Muscle Force

In a more elaborate study in which lenses of freshly enucleated cadaver eyes were studied with their zonular and ciliary attachments intact, Fisher (1977) was able to deduce, not only the changes in the ability of the lens to alter its shape passively in response to a change in diameter of the ciliary ring, but also to compute the probable changes in muscle tension that took place at different degrees of accommodative effort; and he concluded that the basic concept of Helmholtz was, indeed, correct, namely that presbyopic changes were due to altered physical characteristics of the lens, whilst the actual power of the ciliary muscle to develop tension actually increased with age up to about 45 years old (Fig. 27.9).

CILIARY RING

Fisher placed the lens-ciliary body preparation in an apparatus that enabled him to increase or decrease the radius of the ciliary ring by gentle traction; Fig. 27.10 shows the measured changes in dioptric power of the lens with a given increase in radius of the ciliary ring, and it is immediately evident that in the old lens the dioptric power shows little increase with decreasing radius of the ring, so that contractions of the ciliary muscle that reduce the size of the ring would contribute little to the dioptric power of the eye.

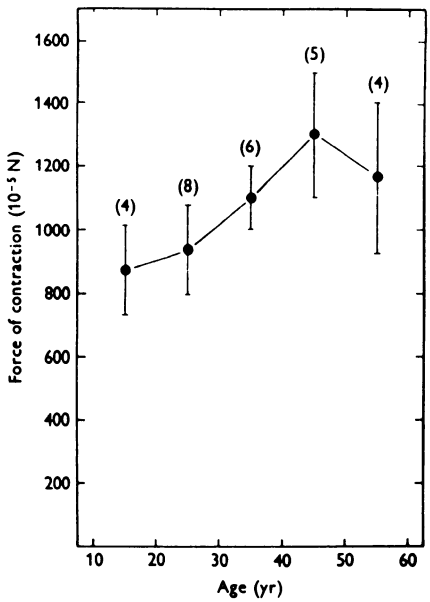

Fig. 27.9 Maximum force of contraction of the entire ciliary muscle plotted against age. Bracketed numbers indicate numbers of subjects. Vertical lines standard deviation per decade. (Fisher, *J. Physiol.*)

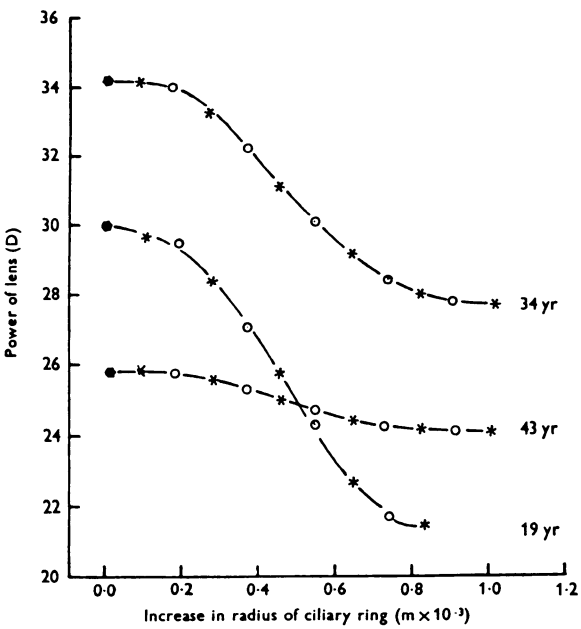

Fig. 27.10 Typical dioptric power/ciliary ring strain curves of human lenses. *Note*: 0.0 radius of ciliary ring corresponds to the unaccommodated state of the lens. *, increase in radius; O, decrease in radius. (Fisher, *J. Physiol.*)

ESTIMATED MUSCLE FORCE

Fisher measured the force required to be exerted on the equator of the capsule to produce a given change of shape, and thus of dioptric power; this was done by spinning the lens around its antero-posterior axis, which has the effect of flattening the lens in a manner comparable to that brought about by tension in the zonule (Fisher, 1971), and by an appropriate calculation he was able to relate a given dioptric change with a change in force, and in this way he computed the force of contraction exerted by the entire ciliary body. The equation used was:

$$F_{CB} = \tfrac{2}{3}\pi a_s^2 \{a_u t_u \Omega_u^2 - a_a t_a \Omega_a^2\} \rho,$$

where $\Omega_a \rightarrow \Omega_u$ is such $st_s = st_a$.

F_{CB} = radial force exerted by the entire ciliary body (N).
a_a = equatorial radius of accommodated lens (m)
a_u = equatorial radius of unaccommodated lens (m)
a_s = equatorial radius of spinning lens (m)
t_u = polar thickness of unaccommodated lens (m)
t_a = polar thickness of accommodated lens (m)
st_a = change in thickness of lens under zonular tension (m)
st_s = change in thickness of lens when spinning (m)
ρ = density of lens substance (kg m^{-3})
Ω_a = equivalent speed of rotation of lens when eye is accommodated (rad sec)
Ω_u = equivalent speeds of rotation of lens when eye is unaccommodated (rad sec^{-1}).

Thus the important experimental parameters were the equivalent speeds of rotation of the lens to produce the shape when the eye is accommodated and unaccommodated. In this way the points in Fig. 27.11 were calculated. Thus to predict the amplitude of accommodation, D, from the force that the ciliary muscle can exert and the forces required to produce a change in shape Fisher gave the equation:

$$D = K_{df}\sqrt{F_{CB}}$$

K_{df} is a dioptric force-coefficient and F_{CB} is the force of contraction of the ciliary muscle; as Fig. 27.11 shows, this coefficient reaches a value of zero between ages 50 and 60.[5]

Theoretical Model

Koretz & Handelman (1982, 1983) and Koretz *et al.* (1984) have applied mechanical considerations to explain the changes in shape of the lens during accommodation, the two parameters necessary for the calculation being Young's modulus and the Poisson ratio. According to their treatment the lens is not being

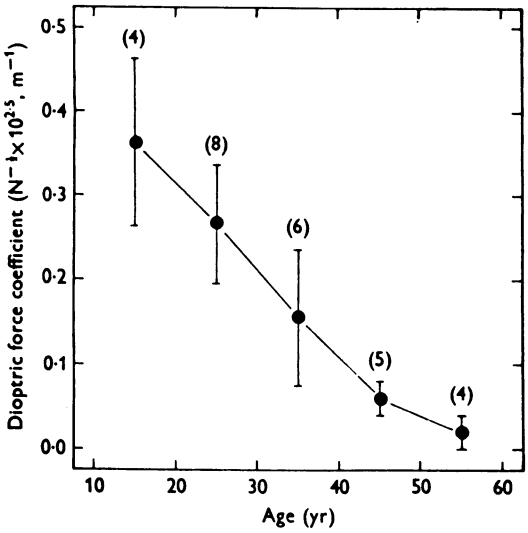

Fig. 27.11 Dioptric force coefficient plotted against age. Bracketed numbers indicate numbers of subjects. Vertical lines, standard deviation per decade. (Fisher, *J. Physiol.*)

moulded by the capsule into the various shapes seen during accommodation since the force exerted on the anterior lens capsule, presumably at the point of zonule attachment, is transmitted to the underlying lens fibres as a uniformly distributed force. It is rather the nature of the fibre organization within the lens that ultimately converts the applied stress to the observed shape-changes.[6]

Depth of Focus

Fisher points out that the computed amplitudes are some 1.25 D less at each age than those obtained *in vivo*, when amplitude of accommodation was measured by the 'blurring technique'. However, if amplitude is measured objectively by retinoscopy a smaller value is obtained (Hamasaki *et al.*, 1956) and, as Fig. 27.8 shows, accommodative power, measured in this way, becomes zero at age 50 about. Thus the 'accommodation' apparently exerted by subjects over 52 years is in fact fictitious and a reflexion of the subject's depth of focus, i.e. the degree of blurring of the optical image he is prepared to accept.

Value of Magnification

Hamasaki *et al.* pose the problem as to why subjects, who have reached the age of 52, with no accommodative power still require stronger presbyopic corrections as they get older. The answer is to be sought in the larger image provided by the increased spectacle power; thus the subject is using the spectacles as a younger subject would use a magnifying glass; in both situations distinct vision is possible with the eye closer to the object being viewed, and this means an effective increase in magnification.

Accommodation for Near Vision

The amount of accommodative power for near vision, as in reading, is about 3.5 D when measured by the blur technique, and accepting this value, we may calculate the percentage of the total ciliary muscle force available required for near vision at different ages; in the young person this is small, namely about 5%, but with age this percentage increases rapidly to 100, indicating that, with onset of presbyopia, it is likely that the subject is using maximal ciliary muscle power, a condition that might produce 'eye-strain' rendering the use of spectacles desirable before near vision is impossible. However, as Fisher emphasizes, the extra muscle force that becomes available due to hypertrophy with age, indicated by Fig. 27.9 is only sufficient to provide 0.6 D of extra accommodative power.

Changes in Lens Shape with Age

Using his slit-lamp microscopy technique, Brown (1974a) has studied these in great detail and they are summarized by Fig. 27.12; the author failed to confirm the oft-repeated statement that, in advanced age, the peripheral lens becomes flatter, thus apparently explaining the hypermetropia of old age. In fact the curvature increases, due to a greater increase in sagittal width than in transverse diameter.

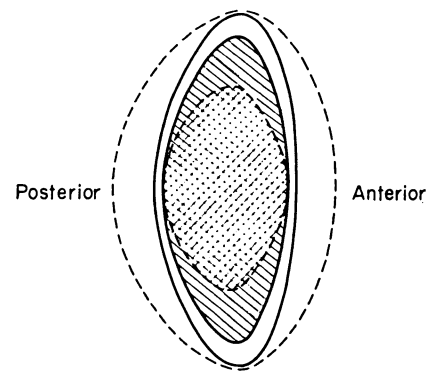

Fig. 27.12 Comparison between the shape of a 10-year-old lens (continuous line), with that of an 82-year-old (interrupted line). The nucleus of the 10-year-old is shown by single hatching, and that of the 82-year-old by cross hatching. (Brown, *Exp. Eye Res.*)

The Capsule

Fincham, in attempting to explain the large change of curvature of the anterior surface suggested that it was due to the greater thickness of the capsule at the periphery. However Fisher & Pettet (1972) showed that this peri-

pheral thickening occurred only at an advanced age when accommodative power had been lost. The post-natal changes in the dimensions of the capsule were measured, and are illustrated by Fig. 27.13; the posterior polar region retains about the same thickness through life, probably due to the lack of synthetic power of the lens fibres adjacent to it; the anterior polar region does increase in thickness. Fisher & Pettet, in commenting on these changes, suggest that when the eye focuses a near object the thicker equatorial zone of unrestrained capsule is that which deforms the lens substance. With distant vision the influence of the equatorial capsule is decreased and the much thinner polar portion of the capsule may assist the backward movement of the lens. The posterior capsule is so much thinner that it is unlikely to exert any appreciable force on the lens substance.

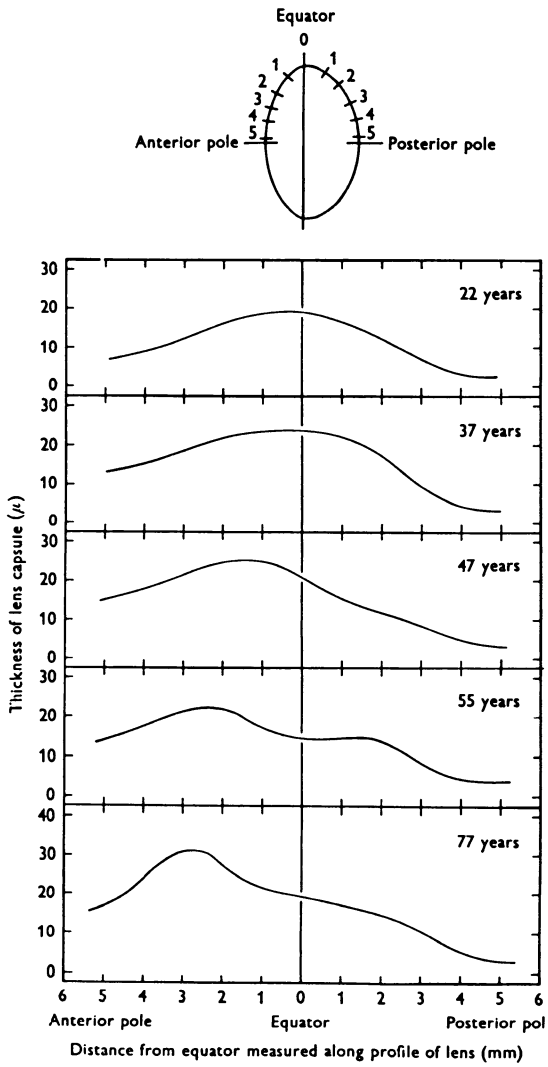

Fig. 27.13 Changes of capsular thickness with age in typical human lenses. (Fisher & Pettet, *J. Anat.*)

Presbyopia in the Monkey

Bito *et al.* (1982), in seeking an animal model for human presbyopia examined, the accommodative power of monkeys ranging in age from less than 0.5 to greater than 30 years. The amplitude of accommodation, induced by cholinomimetics, such as pilocarpine, was measured as a function of age; Fig. 27.14 shows the comparison with humans, using different age-scales to allow for the more rapid maturity of the monkey. The parallelism is remarkable and shows that the monkey is indeed, a useful animal in which to study presbyopia. In further studies (Koretz *et al.*, 1987a, b) various dimensions[7] of the monkey's eye, e.g. anterior chamber depth, lens thickness, and so on, were measured as a function of age in the resting state, and then during accommodation. With increasing accommodation both the surfaces became more sharply curved, the lens thickened causing a bulging of the anterior surface into the anterior chamber while the posterior surface remained fixed in relation to the anterior surface of the cornea (Fig. 27.15). The authors noticed the remarkable similarity between Brown's (1974) study of lens thickness and shape in humans as a function of age. Thus Brown found an age-dependent shallowing of

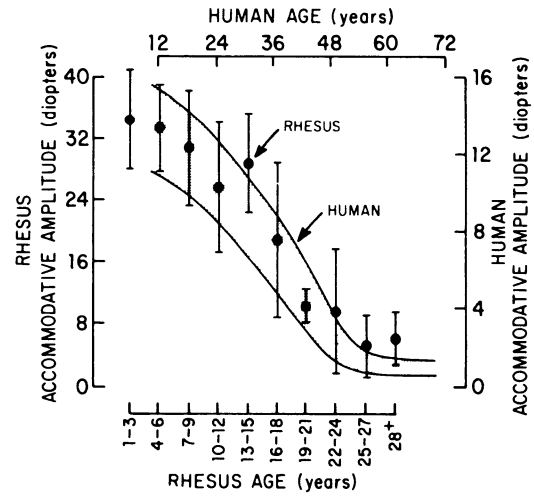

Fig. 27.14 Human and rhesus patterns of age-dependent loss in accommodative amplitude. The mean (±S.D.) rhesus monkey accommodative amplitude for each age group (3 year intervals), superimposed on the time curve of decrease in accommodative amplitude in humans, reveals a remarkable similarity in the patterns of age change in the two species. The curves representing human accommodative capacity (*shaded area*) were taken from figures constructed by Duane to include most 'normal' cases. (Bito *et al.*, *Invest. Ophthal.*)

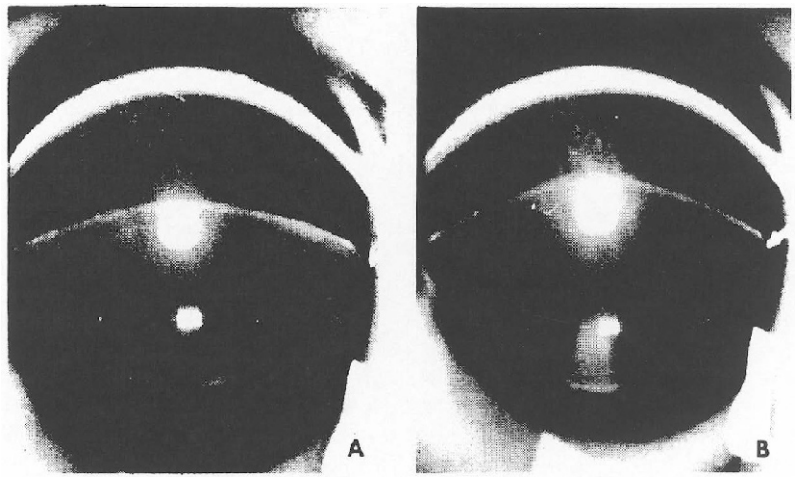

Fig. 27.15 Slit-lamp photographs of an 8-year-old rhesus eye (A) before CARB stimulation (refractive error = −4.10 D) and (B) at maximum accommodative amplitude (refractive error = −18.7 D). It is clear that the anterior chamber has become shallower, the lens has become thicker along the polar axis and more sharply curved on both surfaces, and that there has been little or no change in the location of the posterior lens surface relative to the cornea. (Koretz *et al.*, *Exp. Eye Res.*)

the anterior chamber, and an increase in lens thickness; and he estimated that both surfaces of the lens increased their curvature with age; in their studies of the monkey similar changes occurred with age. However, the slopes of change of the individual lens surface curvatures as a function of age were very different in the human, that for the anterior surface being some ten times that for the posterior, so by the age of 75 to 80 years both curvatures were equal; by contrast, in the monkey, the slopes were about the same so that the posterior surface remained more sharply curved than the anterior at all ages.

THE NERVOUS MECHANISM

Parasympathetic

Contraction of the ciliary muscle is brought about by the activity of the parasympathetic fibres of N III, with their origin in the Edinger-Westphal nucleus; the fibres relay in the ciliary ganglion. Stimulation of N III causes an increase in the refractive power of the eye (the eye becomes myopic), an effect that is inhibited by blocking the ciliary ganglion or by the application of atropine to the eye. Eserine, which potentiates the action of acetylcholine, and pilocarpine, which mimics its action, cause a spasm of accommodation, that by the former being due to failure to hydrolyse the transmitter liberated as a result of tonic action of the nerve.

Alternate Pathway

Westheimer & Blair (1973) found, in the monkey, that painting the ciliary ganglion with nicotine reduced, but did not abolish, the accommodative response to stimulation of N III intra-orbitally; furthermore, when they stimulated N III at high frequency (440 Hz) they obtained full accommodation although at this frequency transmission through the ganglion would be impaired or blocked. They concluded, therefore, that fibres to the ciliary muscle passed through the ciliary ganglion without relaying. However, Ruskell & Griffiths (1979) showed that after intracranial section of the oculomotor nerve in monkeys, thus robbing the ciliary ganglion of its preganglionic input, the appearance of the postganglionic neurones was normal; short ciliary nerves were sectioned and these appeared normal, although a few scattered fibres were degenerated. In the electron microscope the ciliary muscle fibres were normal and nerve terminals were as numerous as in control eyes. Thus the claim that nerves serving accommodation, in contrast to those serving pupilloconstriction, pass through the ganglion cannot be sustained; by far the greatest number of parasympathetic fibres passing into the eye subserve accommodation (Warwick, 1954), so that most of the fibres in the ciliary nerve should have degenerated after oculomotor section.

Sympathetic

Opinions have varied as to whether the sympathetic plays any role in accommodation (see, e.g. Cogan, 1937; Toates,

1972); the action of the ciliary muscle is antagonized by the elasticity of the capsule, and fine adjustments are therefore possible by means of the interplay of these opposing forces; an antagonistic muscle, innervated by the sympathetic, whose contraction tightens the zonule and therefore flattens the lens, may be thought to be unnecessary in man on this account. Some studies of Olmsted & Morgan and their colleagues have suggested, however, that the sympathetic nerves might cause an active flattening of the lens, insults likely to cause generalized sympathetic stimulation, such as a tap on the nose of a rabbit, being said to cause an increase of the animal's normal hypermetropia by about 1 D; stimulation of the cervical sympathetic in the anaesthetized cat and dog caused large changes in refractive condition, especially if the parasympathetic division to the eye was cut.

In primates Törnqvist (1966, 1967) has shown that stimulation of the cervical sympathetic causes a small decrease in the dioptric power of the eye; this becomes greater if the stimulation is carried out against a background of parasympathetic activity, either by pretreatment of the eye with pilocarpine or by stimulation of the oculomotor nerve; it was never greater than 1.5 to 2.0 D, however. He pointed out that the responses were so slow, taking some 5 to 10 seconds to begin and 10 to 40 seconds to reach a maximum, that they are unlikely to have physiological significance. The sympathetic innervation of the ciliary muscle has been described by Ruskell (1973).

Excised Muscle

Studies on excised strips of ciliary muscle leave little doubt that sympathetic amines are active, but the effect varies with the species; in the cat the order of increasing effectiveness in causing relaxation is Isoproterenol $\gg$ Noradrenaline > Adrenaline, an order indicating a β-action of the sympathetic, especially since the relaxation due to isoproterenol is blocked by DCI. That there are also α-receptors is indicated by the fact that the relaxation caused by adrenaline and noradrenaline is converted to contraction when the β-activity is blocked by DCI (Bennett *et al.*, 1961). In the monkey, sympathetic activity is exclusively β whilst in the rabbit the action is mainly α with a little β.

DOG'S CILIARY MUSCLE

Yoshitomi & Ito (1986) investigated the effects of adrenergic agents and their inhibitors on contraction of isolated dog ciliary muscle elicited by electrical and chemical stimulation, noting that application of beta-blockers to the eye produced a myopic shift in the resting point of accommodation (Gilmartin *et al.*, 1984)[8] whilst phenylephrine, an alpha-adrenomimetic, decreased the near point without affecting the resting point (Garner *et al.*, 1983). Noradrenaline reduced the amplitude of contraction induced by electrical stimulation, but not when it was caused by carbachol, suggesting that the action of noradrenaline was on the presynaptic terminals of the parasympathetic nerve, i.e. that it was exerting an alpha$_2$-action. This was confirmed by the reduction in junctional potentials and the finding that the effects of noradrenaline were blocked by yohimbine, but not by timolol or prazocin.

Midbrain Neurones

Bando *et al.* (1984a) measured accommodation in cats using the infra-red optometer of Campbell & Robson (1959); they probed the midbrain to discover neurones discharging in relation to accommodation in the cat, identifying them by antidromic stimulation of preganglionic fibres of the ciliary ganglion and electrical stimulation of the cerebellar interpositus nucleus. Thus, earlier, it had been shown that accommodation was affected by stimulation of the interpositus nucleus but not pupillomotor activity. The accommodation-related neurones were mostly located laterally and dorsally to the Edinger-Westphal nucleus, and not within it. Thus, in the cat at any rate, the preganglionic neurones that excite the ciliary ganglion neurones during accommodation, seem to be situated outside the Edinger-Westphal nucleus.

Cortical Neurones

Jampel (1960) stimulated the posterior bank of the superior temporal sulcus in monkeys and obtained pupillary and accommodative responses. In the cat, Bando *et al.* (1984b) examined the discharges of units in the posterior lateral suprasylvian area of cats in relation to accommodation; they considered that the area studied, surrounding the suprasylvian sulcus, corresponded to the area on the posterior bank of the superior temporal sulcus of the monkey, equivalent to that studied by Jampel, a region also concerned with motion-sensitive units (p. 524). They found some 48 units discharging before accommodation, with a lead-time of some 360 msec, 95% being related to an increase in refractive power. 67% of the neurones were activated antidromically from the superior colliculus and/or pretectum. The activities of the units were not affected by cooling of the cerebellum.

The Stimulus for Accommodation

It might be thought that the effective stimulus for accommodation would be the blurring of the retinal image, but

if this were the only clue, the centre responsible would be unable to determine whether the object had come nearer or moved farther away, since in both cases the image would be blurred. We should therefore expect the eye to 'grope' for the correct change in power, whereas it was found by Fincham (1951) that when the eye observes an object, and the vergence[9] of the light is altered, the accommodative effort is correct; that is, if the vergence is changed so that the object is apparently closer, the eye increases its power, and *vice versa*. There is no oscillation, as we should expect in an instrument unable to distinguish the nature of the vergence-change. Moreover, if too large a degree of blurring is induced through lenses, then no attempt at accommodation is made (Heath, 1956). As to the actual stimulus, this has been debated for a long time, and the arguments and experiments in their support have been reviewed by Toates (1972). Thus Alpern (1958) and Campbell *et al.* (1959) emphasized the small fluctuations in accommodative power occurring normally, and suggested that such fluctuations would 'sample' the state of the image, indicating the direction in which change should occur to obtain perfect focus. However, accommodation is rarely perfect; thus Fig. 27.16 illustrates schematically the average response to objects at different distances; only at the dark-focus point is accommodation exact (p. 780), so that a system oscillating about 0.2 D would not tolerate such errors.

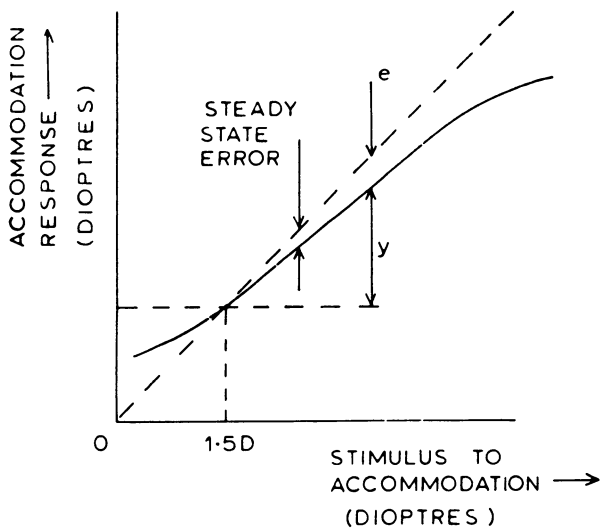

Fig. 27.16 Typical stimulus-response curve. Broken line indicates relationship on basis of equality between input and output. Continuous line is actual relationship found. Distance *y* is magnitude of output measured from resting point, which is at 1.5 D. Steady-state error *e* is the difference between input and output. (Toates, *Physiol. Rev.*)

Aberrations

What then is the stimulus? Fincham's experiments indicated that in many subjects the chromatic aberration of the retinal image provided the necessary clue, the aberration rings being theoretically different according to the nature of the out-of-focus image. Thus, if the object were too close, the image of a point would be a light disc surrounded by a red fringe, whilst if it were too far away the disc would be surrounded by a blue fringe. By using monochromatic light many subjects were unable to make correct adjustments. A certain number of subjects were able to do so, however, and it would seem that spherical aberration provides a clue (Campbell & Westheimer, 1959) since reducing the spherical aberration of the eye reduced the subject's accuracy in accommodating in monochromatic light.[10] Thus, under essentially laboratory conditions, when other clues are excluded, it is likely that chromatic aberration is a dominant factor. In ordinary life, however, changes in size of an object contribute (Ittelson & Ames, 1950) as well as changes in convergence (Alpern, 1958), but neither of these can be sole determinants; thus Campbell & Westheimer (1960) moved targets towards or away from an observer, without allowing the apparent size to change, and they still obtained accommodation.

Cones

Campbell (1954) showed that the intensity of illumination of an object had to be above the threshold for cone vision in order to initiate accommodation; moreover, this was a function of foveal vision. Thus Fincham (1953) found that blue-green light was not such an effective stimulus as a red-green mixture, presumably because of the relative insensitivity of the central fovea to blue light.

Control Mechanisms

Toates (1972) has emphasized that accurate accommodation must require a control system with feedback from the retina; the finding that error is always, or nearly always, present indicates that the feedback is proportional to the error, rather than its integral; Toates has suggested a model (Fig. 27.17) based on a feedback control of this nature, the defocus of the image driving the accommodative effort. Incorporated into the model is a factor involving pupil-size, since, with a small pupil, a larger error is required to produce a given degree of accommodation (Ripps *et al.*, 1962). Finally, a factor allowing for the effects of convergence on accommodation is included.

CYCLOPLEGIA

Inhibition of accommodation by homatropine caused an increased accommodative convergence, presumably

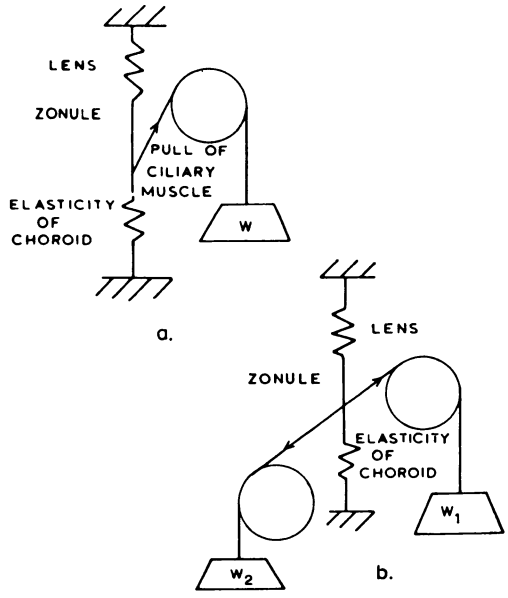

Fig. 27.17 Mechanical models of accommodation. *a*: Single innervation; effort is proportional to weight *W*. *b*: Dual innervation; parasympathetic effort is proportional to W_1 and sympathetic effort is proportional to W_2. (Toates, *Physiol. Rev.*)

because of the more powerful central drive on the accommodative mechanism (Christoferson & Ogle, 1956); expressed in terms of Toates' model, the accommodative stimulus is normally inhibited by the response of the lens; when the lens is unable to respond, i.e. change its shape, this inhibition is missing and convergence is increased.

Fluctuations

When a subject views a near object steadily his accommodation fluctuates through a range of about 0.25 D with a dominant frequency of the order of 2 cycles/sec (Campbell *et al.*, 1959); this is presumably analogous with pupillary unrest, and with the high-frequency tremor in the eye movements although here the frequency is in the range of 75 cycles/sec. Since the unrest is considerably reduced when the subject views an empty field it is possible that these oscillations are determined by variations in the clarity of the image—retinal feedback.

The Resting Point of Accommodation

On the classical view, e.g. that of Helmholtz, the emmetropic subject's relaxed state of accommodation, when there is no stimulus to evoke it, is zero, i.e. adjusted for infinity. If, as the studies of Olmsted and others have suggested, the accommodative state is due to a balance struck between the opposing sympathetic and parasympathetic activations of the ciliary muscle, the resting position might not necessarily be at zero accommodation (Fig. 27.17). Alternatively, in the absence of a sympathetic activation, a tonic parasympathetic activity might lead to a resting myopic condition. In fact, a variety of studies have indicated a resting myopic condition averaging some 1.5 to 2.0 D. For example, Hennessy *et al.* (1976) allowed subjects to view objects, at different distances, through artificial pupils of smaller and smaller size. The increased depth of focus provided by the small pupils reduces the necessity for accommodation on nearer objects, so that by extrapolation it could be estimated what state of accommodation the eye would take up when there was no necessity to accommodate. Figure 27.18 illustrates some results; the theoretical line indicates the amounts of accommodation required for the different distances, and the filled circles are the experimental values for an emmetropic subject with normal pupils; the slopes are similar indicating, as we should expect, the adoption of appropriate increases in dioptric power with proximity of the target, and extrapolating to about 6 metres for zero accommodation. As the pupil is reduced in size, there is the expected flattening of the line, indicating smaller accommodation for a given fixation-distance; and at the lowest pupillary size the state of accommodation is nearly constant at the value required for 1 metre viewing-distance, suggesting that this, indeed, is the true relaxed condition.[11] Again, Leibowitz & Owens (1978) determined the state of refraction of the eye using a laser optometer[12], an instrument that does not depend on the

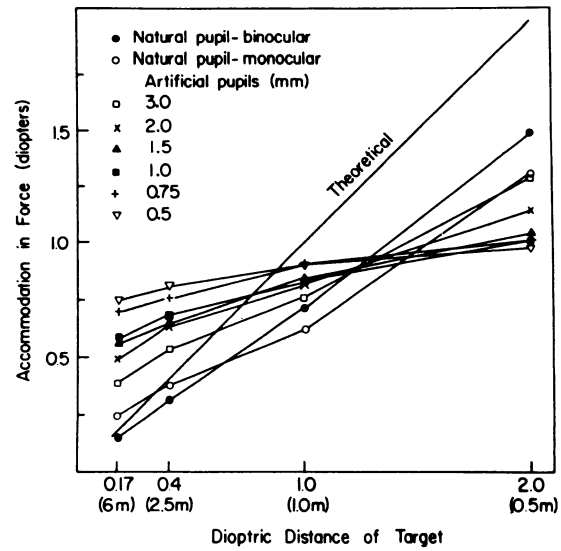

Fig. 27.18 Accommodation as a function of dioptric distance for various sized artificial pupils. The theoretical line indicates values expected if accommodation corresponded to target distance. (Hennessy *et al.*, *Vision Res.*)

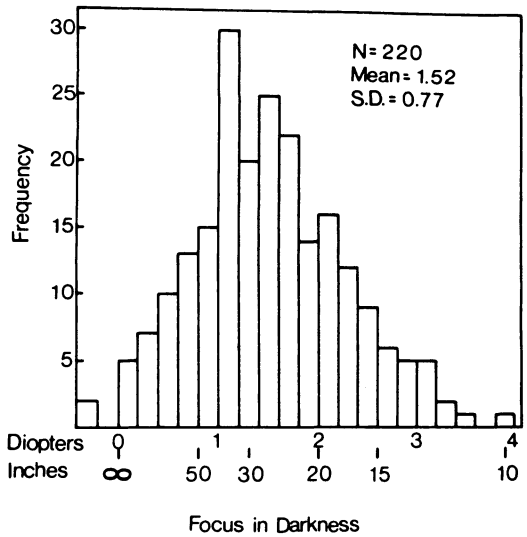

Fig. 27.19 Frequency distribution of the magnitude of the focus in total darkness, as measured with the laser optometer, for 220 college-age observers. (Leibowitz & Owens, *Doc. Ophthal.*)

formation of a precise retinal image that would influence accommodation. Figure 27.19 illustrates the frequency-distribution of the magnitude of the focus in total darkness, giving a mean of 1.52 D.

Anomalous Myopias

The myopia developing in complete darkness—night myopia—is analogous with a similar myopia when viewing a structureless field (Whiteside, 1952), and when using instruments such as microscopes or binoculars that have an adjustable focus (Schober *et al.*, 1970)—*instrument myopia*—or when the retinal image is degraded with lenses, or simply by changing the spatial frequency of a grating to zero frequency (Charman & Tucker, 1977). Leibowitz & Owens, in the same study, examined 20 observers under four conditions, namely (1) while viewing a distant outdoor scene through a neutral-density filter that reduced the daylight luminance by a factor of 16 000 (night myopia), (2) a bright uniform field produced by positioning a table-tennis ball hemisphere before the eye (empty-field myopia), (3) a grating through a microscope that had been focussed by the subject (instrument myopia, Hennessy, 1975) and (4) in complete darkness (the dark-focus). All three anomalous myopias correlated well with the dark focus.[13]

VISUAL ACUITY AND DISTANCE

Theoretically, visual acuity, measured in angular terms, should be independent of distance; actually Johnson (1976), who measured visual acuity and accommodation at different distances, showed that best visual acuity was obtained at a distance corresponding to the observer's dark-focus over a wide range of luminances.[14] Under these conditions there was no refractive error; under other conditions the degree of accommodation was the result of a balance struck by the subject's dark-focus and the retinal stimulus; in consequence, visual acuity was diminished due to an effective refractive error of myopia or hypermetropia according to the distance of the object.

Notes

1. With this technique, which avoids the damaging procedure of compression, Fisher (1971) showed that the lens is a truly elastic body and therefore repeated deformations, as in accommodation, will not tend to 'set' the lens in a given shape. The technique permitted the calculation of Young's modulus of elasticity in the polar and equatorial regions. A necessary condition for the attainment of ellipsoidal shapes at different degrees of flattening (accommodation) is that the strain at the pole should be twice that at the equator, and the finding that the ratio of polar to equatorial elasticities was, in man, 0.62 indicates that the human lens is adapted to permit this; by contrast, the cat and rabbit had ratios of about 3.
2. Campbell & Westheimer (1958) prevented their subjects from accommodating with atropine and they were asked to recognize the rhythmic blurring of the image of an object brought nearer to and farther from the eye; when this rhythmic excursion was too small, no change was experienced, and on increasing it a point was reached when the rhythmical changes were noted. The average 'sensitivity to difference of focus' was 0.2 D. Oshima (1958) found a much higher sensitivity, 0.02–0.06 D.
3. The difficulty in accepting lens sclerosis as the sole cause of presbyopia is that the condition begins essentially in childhood, when it is unlikely that 'senile' changes in the lens fibres would have occurred.
4. The effective energy of the capsule, in relation to its power of altering refractive power, depends on the shape of the lens as well as on the modulus of elasticity; the flatter human lens allows the capsule to exert a greater moulding pressure for a given modulus of elasticity than the more spherical lenses of the cat and rabbit; to some extent, then, the differences in accommodative power of these species are attributable to this since their elasticities are not greatly different: 0.9 and 2.5×10^7 dynes/cm^2 respectively.
5. An earlier study (Fisher 1973) led to the same conclusions regarding the cause of presbyopia; here a 'lens coefficient' was computed from the elasticities of capsule and lens substance and the dimensions of the lens in accommodated and unaccommodated states; this gives a measure of the ability of the capsule to overcome the forces preventing the lens from assuming a more spherical shape. The line relating this coefficient to age coincided well with that relating accommodation to age. The three factors leading to presbyopia are thus the decreased elastic modulus of the capsule,

the increased modulus of the lens substance, and a flattening of the lens.

6. Koretz *et al.* (1984) attribute a role to the vitreous body in accommodation; however Fisher (1983) compared the accommodative power in the separate eyes of a human subject who had had a vitrectomy in one eye. The amplitudes were 9.7 ± 1.05 and 8.9 ± 0.51 D in the eyes without and with vitreous, and the respective movements of the anterior pole of the lens were 0.14 ± 0.04 and 0.15 ± 0.04 mm. Clearly the vitreous plays no significant role.
7. Dimensions were measured by two independent methods with remarkably good agreement between them, namely using slit-lamp Scheimpflug photographs and A-scan ultrasonography. Accommodation was induced with carbachol or electrical stimulation of the Edinger-Westphal nucleus.
8. Gilmartin *et al.* (1984) measured tonic accommodation in the dark, tonic vergence and pupil diameter; the beta-blocker, timolol, caused a myopic shift of tonic accommodation of 0.85 D, so that they concluded that tonic accommodation was mediated by a beta-adrenergic *inhibition* of the ciliary muscle. Ruskell (1973) had shown that about 1% of the nerve terminals on the ciliary muscle had small granular vesicles typical of sympathetic endings.
9. By *vergence*, in this context, is meant the degree of divergence or convergence of the rays of light in a pencil as they strike the principal plane of a refracting system; the closer an object, the greater the vergence of its rays, hence the reciprocal of its distance from the principal plane may be used as a measure of vergence; if this is in metres the unit of vergence is the dioptre; thus the vergence of the light from an object is the *dioptric value of the object-distance*. We may note that the term vergence is also applied to the degree of convergence or divergence of the fixation axes; this often leads to ambiguities and confusion. Thus by 'vergence-induced accommodation' a writer could mean accommodation induced by convergence or by changed light-vergence.
10. Fincham (1951) observed that if a subject, who failed to accommodate correctly in monochromatic light, was allowed to scan the object in view, correct accommodation became possible, and he pointed out that when the eye turns through a small angle from the point of fixation the rays of light at the opposite sides of the blur-circles on the retina acquire different degrees of obliquity to the surface, this difference being opposite in direction when the image is out of focus due to being too close and too far away. The different degrees of obliquity will be translated into different sensations of brightness by the operation of the Stiles-Crawford effect.
11. More recently Ward & Charman (1985) have improved on the technique employed by Hennessy *et al.* by measuring the accommodative responses in the eye studied, rather than the fellow eye; they have also taken into account the different refractive changes occurring with smaller pupils. In general, they confirmed the conclusion of Hennessy *et al.*, and analysed their results in terms of the possible response of the accommodative system to the presence of a blur-circle on the retina whose diameter is a linear function of the dioptric difference between the magnitude of the stimulus and the accommodative resting state.
12. Laser refraction depends on the speckle pattern produced by interference of reflected coherent laser light; the subjective appearance is 'speckled'. The laser light is reflected into the eye and when the reflecting surface or the observer's head moves, the speckles appear to move in a direction determined by the eye's refractive state. If the receptor plane is precisely conjugate with the reflecting surface the speckles remain stationary or move randomly during any head or surface motion.
13. Krumholz *et al.* (1986) have studied variations in 'tonic accommodation' of subjects in darkness and in daylight; in the day it varied between 0.5 and 1 D; in continual darkness there was much greater variation, between 0.6 and 2.5 D.
14. Leibowitz & Owens (1978) have discussed the relevance of dark-focus to night driving; with poorly illuminated road-signs, drivers tended to accommodate to a position about half-way between the correct amount and the subject's own dark-focus.

References

Adamson, J. & Fincham, E. F. (1939) The effect of lenses and convergence upon the state of accommodation of the eye. *Trans. Ophthal. Soc. U.K.* **59**, 163–179.

Alpern, M. (1958) Vergence and accommodation. *Arch. Ophthal.* **60**, 358–360.

Bando, T., Tsukuda, K., Yamamoto, N., Maeda, J. & Tsukara, N. (1984a) Physiological identification of midbrain neurons related to lens accommodation in cats. *J. Neurophysiol.* **52**, 870–878.

Bando, T., Yamomoto, N. & Tsukahara, N. (1984b) Cortical neurons related to lens accommodation in posterior lateral suprasylvian area in cats. *J. Neurophysiol.* **52**, 879–891.

Bennett, D. R., Reinke, D. A., Alpert, E., Baum, T. & Vasquez-Leon, H. (1961) The action of intraocularly administered adrenergic drugs on the iris. *J. Pharmacol.* **134**, 190–198.

Bito, L. Z., De Rousseau, C. J., Kaufman, P. L. & Bito, J. W. (1982) Age-dependent loss of accommodation amplitude in rhesus: an animal model for presbyopia. *Invest. Ophthal.* **23**, 23–31.

Brown, N. (1973) The change in shape and internal form of the eye on accommodation. *Exp. Eye Res.* **15**, 441–459.

Brown, N. (1974a) The change in lens curvature with age. *Exp. Eye Res.* **19**, 175–183.

Brown, N. (1974b) The shape of the lens equator. *Exp. Eye Res.* **19**, 571–576.

Campbell, F. W. (1954) Accommodation reflex. *Brit. Orthop. J.* **11**, 13–17.

Campbell, F. W. & Robson, J. G. (1959) High-speed infra-red optometer. *J. Opt. Soc. Amer.* **49**, 268–272.

Campbell, F. W., Robson, J. G. & Westheimer, G. (1959) Fluctuations in accommodation under steady viewing conditions. *J. Physiol.* **145**, 579–594.

Campbell, F. W. & Westheimer, G. (1958) Sensitivity of the eye to difference in focus. *J. Physiol.* **143**, 18P.

Campbell, F. W. & Westheimer, G. (1959) Factors influencing accommodation responses of the human eye. *J. opt. Soc. Am.* **49**, 568–571.

Campbell, F. W. & Westheimer, G. (1960) Dynamics of accommodation responses of the human eye. *J. Physiol.* **151**, 285–295.

Charman, W. N. & Tucker, J. (1977) Dependence of accommodation response on the spatial frequency spectrum of the observed object *Vision Res.* **17**, 129–139.

Christoferson, K. W. & Ogle, K. N. (1956) The effect of homatropine on the accommodation-convergence association. *Arch. Ophthal.* **55**, 779–791.

Cogan, D. G. (1937) Accommodation and the autonomic nervous system. *Arch. Ophthal.* **18**, 739–766.

Erickson-Lamy, K. A., Polansky, J. R., Kaufman, P. L. & Zlock, D. M. (1987) Cholinergic drugs alter ciliary muscle response and receptor content. *Invest. Ophthal.* **28**, 375–383.

Fincham, E. F. (1937) The mechanism of accommodation. *Br. J. Ophthal.* Mon. Suppl. No. 8.

Fincham, E. F. (1951) The accommodation reflex and its stimulus. *Br. J. Ophthal.* **35**, 381–393.

Fincham, E. F. (1953) Defects of the colour sense mechanism as indicated by the accommodation reflex. *J. Physiol.* **121**, 570–580.

Fisher, R. F. (1969a) Elastic constants of the human lens capsule. *J. Physiol.* **201**, 1–19.

Fisher, R. F. (1969b) The significance of the shape of the lens and capsular energy changes in accommodation *J. Physiol.* **201**, 21–47.

Fisher, R. F. (1971) The elastic constants of the human lens. *J. Physiol.* **212**, 147–180.

Fisher, R. F. (1973) Presbyopia and its changes with age in the human crystalline lens. *J. Physiol.* **228**, 765–779.

Fisher, R. F. (1977) The force of contraction of the human ciliary muscle during accommodation. *J. Physiol.* **270**, 51–74.

Fisher, R. F. (1983) Is the vitreous necessary for accommodation in man? *Brit. J. Ophthal.* **67**, 206.

Fisher, R. F. & Pettet, B. E. (1972) The postnatal growth of the capsule of the human crystalline lens. *J. Anat.* **112**, 207–214.

Fleming, D. G. & Olmsted, J. M. D. (1955) Influence of cervical ganglionectomy on the lens of the eye. *Am. J. Physiol.* **181**, 664–668.

Garner, L. F., Brown, B., Baker, R. & Colgan, M. (1983) The effect of phenylephrine hydrochloride on the resting point of accommodation. *Invest. Ophthal.* **24**, 393–395.

Gilmartin, B., Hogan, R. E. & Thompson, S. M. (1984) The effect of timolol maleate on tonic accommodation, tonic vergence, and pupil diameter. *Invest. Ophthal.* **25**, 763–770.

Hamasaki, D., Ong, J. & Marg, E. (1956) The amplitude of accommodation in presbyopia. *Amer. J. Optom.* **33**, 3–14.

Hartridge, H. & Yamada, K. (1922) Accommodation and other optical properties of the eye of the cat. *Brit. J. Ophthal.* **6**, 481–492.

Heath, G. G. (1956) Components of accommodation. *Amer. J. Optom.* **33**, 569–579.

Hennessy, R. T. (1975) Instrument myopia. *J. opt. Soc. Am.* **65**, 1114–1120.

Hennessy, R. T., Iida, T., Shina, K. & Leibowitz, H. W. (1976) The effect of pupil size on accommodation. *Vision Res.* **16**, 587–589.

Ittelson, W. H. & Ames, A. (1950) Accommodation, convergence and their relation to apparent distance. *J. Psychol.* **30**, 43–62.

Jampel, R. S. (1960) Convergence, divergence, pupillary reactions and accommodation of the eyes from faradic stimulation of the macaque brain. *J. Comp. Neurol.* **115**, 371–397.

Johnson, C. A. (1976) Effects of luminance and stimulus distance on accommodation and visual resolution. *J. Opt. Soc. Amer.* **66**, 138–142.

Koretz, J. F., Bertasso, A. M., Neider, M. W.,True-Gabelt, B. & Kaufman, P. L. (1987b) Slit-lamp studies of the rhesus monkey eye: II. Changes in crystalline lens shape, thickness and position during accommodation and aging. *Exp. Eye Res.* **45**, 317–326.

Koretz, J. F. & Handelman, G. H. (1982) Model of the accommodative mechanism in the human eye. *Vision Res.* **22**, 917–927.

Koretz, J. F. & Handelman, G. H. (1983) A model for accommodation in the young human eye: the effects of lens elastic anisotropy on the mechanism. *Vision Res.* **23**, 1679–1686.

Koretz, J. F., Handelman, G. H. & Brown, N. P. (1984) Analysis of human crystalline lens curvature as a function of accommodative state and age. *Vision Res.* **24**, 1141–1151.

Koretz, J. F., Neider, M. W., Kaufman, P. L., Bertassp, A. M. De Rousseau, C. J. & Bito, L. Z. (1987a) Slit-lamp studies of the rhesus monkey eye. I. Survey of the anterior segment. *Exp. Eye Res.* **44**, 307–318.

Krumholz, D. M., Fox, R. S. & Ciuffreda, K. J. (1986) Short-term changes in tonic accommodation. *Invest. Ophthal.* **27**, 552–557.

Leibowitz, H. W. & Owens, D. A. (1978) New evidence for the intermediate position in relaxed accommodation. *Doc. Ophthal.* **46**, 133–147.

Morgan, M. W., Olmsted, J. M. D. & Watrus, W. G. (1940) Sympathetic action in accommodation for far vision. *Am. J. Physiol.* **128**, 588–591.

Ogle, K. N. & Schwartz, J. T. (1959) Depth of focus of the human eye. *J. opt. Soc. Am.* **49**, 273–280.

Olmsted, J. M. D. & Morgan, M. W. (1939) Refraction of the rabbit's eyes in the unexcited and excited state. *Am. J. Physiol.* **127**, 602–604.

Olmsted, J. M. D. & Morgan, M. W. (1941) The influence of the cervical sympathetic nerve on the lens of the eye. *Am. J. Physiol.* **133**, 720–723.

O'Neill, W. D. & Brodkey, J. S. (1969) Linear regression of lens movement with refractive state. *Arch. Ophthal.* **82**, 795–799.

Oshima, S. (1958) Studies on the depth of focus of the eye. *Jap. J. Ophthal.* **2**, 63–72.

Ripps, H., Breinin, G. M. & Baum, J. L. (1961) Accommodation in the cat. *Trans. Am. Ophthal. Soc.* **59**, 176–193.

Ripps, H., Chin, N. B., Siegel, I. M. & Breinin, G. M. (1962) The effect of pupil-size on accommodation, convergence and the AC/A ration. *Invest. Ophthal.* **1**, 127–135.

Rohen, J. W. & Rentsch, F. J. (1969) Der konstruktive Bau des Zonulaaparatus beim Menschen und dessen funktionelle Bedeutung. *v. Graefs' Arch. Ophthal.* **178**, 1–19.

Ruskell, G. L. (1973) Sympathetic innervation of the ciliary muscle in monkeys. *Exp. Eye Res.* **16**, 183–190.

Ruskell, G. L. & Griffiths, T. (1979) Peripheral nerve pathway to the ciliary muscle. *Exp. Eye Res.* **28**, 277–284.

Schober, H. A. W., Dehler, H. & Kassel, R. (1970) Accommodation during observation with optical instruments. *J. Opt. Soc. Amer.* **60**, 103–107.

Swegmark, G. (1969) Studies with impedance cyclography on human ocular accommodation at different ages. *Acta ophthal.* **47**, 1186–1206.

Toates, F. M. (1972) Accommodation function of the human eye. *Physiol. Rev.* **52**, 828–863.

Törnqvist, G. (1966) Effect of cervical sympathetic stimulation on accommodation in monkeys. *Acta physiol. Scand.* **67**, 363–372.

Törnqvist, G. (1967) The relative importance of the parasympathetic and sympathetic nervous systems for accommodation in monkeys. *Invest. Ophthal.* **6**, 612–617.

Vakkur, G. J., Bishop, P. O. & Kozak, W. (1963) Visual optics in the cat, including posterior nodal distance and retinal landmarks. *Vision Res.* **3**, 289–314.

Ward, P. A. & Charman, W. N. (1985) Effect of pupil size on steady state accommodation. *Vision Res.* **25**, 1317–1326.

Warwick, R. (1954) The ocular parasympathetic nerve supply and its mesencephalic sources *J. Anat.* **88**, 71–93.

Westheimer, G. & Blair, S. M. (1973) The parasympathetic pathways to internal eye muscles. *Invest. Ophthal.* **12**, 193–197.

Whiteside, T. C. D. (1952) Accommodation of the human eye in a bright and empty visual field. *J. Physiol.* **118**, 65P.

Yoshitomi, T. & Ito, Y. (1986) Pre-synaptic action of noradrenaline on the dog ciliary muscle tissue. *Exp. Brain Res.* **43**, 119–127.

28. THE NEAR RESPONSE

CONVERGENCE, ACCOMMODATION AND MIOSIS

When a near object is focused, three events occur simultaneously—convergence, accommodation and pupillary constriction (miosis). The motor pathway for all three activities is through the nucleus of N III, accommodation and miosis being mediated by the autonomic division of this motor nucleus—the Edinger-Westphal nucleus; and there is no doubt that these pathways, along the oculomotor nerve, are separate since the three reactions may be abolished selectively by appropriate treatment of the nerve or ciliary ganglion. As we have seen, the central coordination of this triad of responses is probably at a higher level of the brain, in the cerebral cortex. The question naturally arises as to the extent to which these responses to the near stimulus are independent of each other. Is it possible to converge without accommodating? Can one accommodate without converging? If the answers to these questions are yes, is pupillary constriction tied preferentially to the convergence or the accommodation? These questions, so important for the theory of squint, have been examined and discussed intensively, whilst in recent years Fincham in England and Alpern in America have submitted them to exact quantitative study.

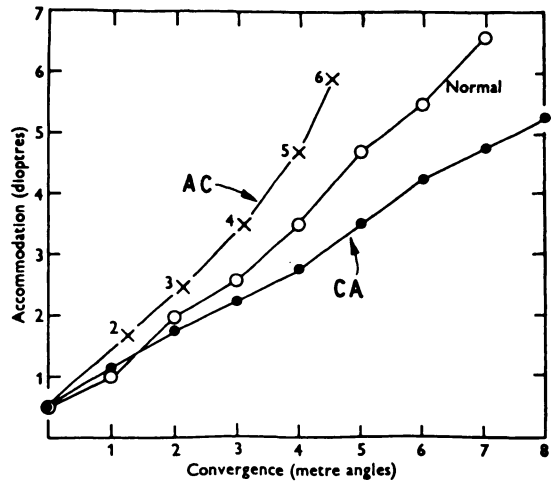

Fig. 28.1 The relation between accommodation and convergence. The curve marked AC represents accommodative convergence, i.e. the convergence that takes place when the eyes accommodate under conditions where altered convergence does not lead to diplopia. The curve marked CA represents the accommodation that takes place when the eyes converge, the arrangement being such that altered accommodation does not lead to blurring of the image. (Fincham & Walton, *J. Physiol.*)

Accommodation and Convergence

Suppose first we examine a normal young subject and measure his accommodation, by means of an objective optometric test, whilst he converges on an object that is brought closer and closer to his eyes. Clearly, if he is to see single and distinctly, the convergence and accommodation must 'match', 1 dioptre of accommodation occurring with 1 metre-angle of convergence. The results of such a measurement are shown by the line marked 'normal' in Fig. 28.1; it will be seen that accommodation does not match exactly; and since diplopia does not occur, we may attribute this to an 'accommodation lag', the eye tolerating a certain degree of blurring of the image that is important for depth of focus (p. 774).[1] The line marked 'normal' of Fig. 28.1 thus gives us a standard of reference, telling us how convergence and accommodation go together when the stimuli for these responses match, and presumably reinforce each other.

Accommodative Convergence

Next we may allow the two eyes to view separate objects independently by a haploscopic device; under these conditions there is no compulsion for fusion and the eyes may adopt any degree of convergence without experiencing diplopia. The apparent nearness of the test-chart, seen by the right eye, is now varied by means of lenses, so that in order for it to be seen distinctly the right eye must accommodate. The line in Fig. 28.1 marked AC shows that the eyes converge as a result of the accommodation of the right eye; this *accommodative convergence* matches

the accommodation over a certain range; but not exactly, so that with 6 dioptres of accommodation the convergence is only a little over 4 metre-angles.[2]

Convergence-induced Accommodation

Next, we may measure the changes of accommodation that take place when the eyes are *made* to converge whilst the object remains at the same apparent distance—the *vergence* of the light is said to be fixed.[3] The *convergence-induced accommodation* is indicated in the line of Fig. 28.1 marked CA. Once again the linkage between the two processes is manifest, and in this case, too, the accommodation lags behind the convergence. This is because of the age of the subject who was 32 years old, and the lag is a sign of presbyopia, subjects under 24 years old showing an almost perfect match between convergence and accommodation. *In a young subject, therefore, the stimulus to convergence automatically induces an accommodation of the right order of magnitude for distinct vision.*

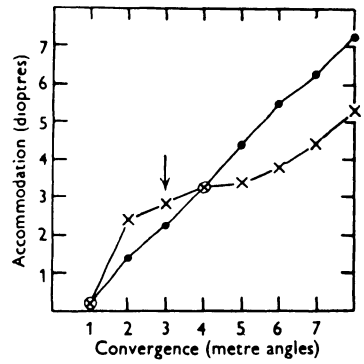

Fig. 28.2 Illustrating the convergence-induced accommodation that occurs when alterations of accommodation will lead to blurring of the image. The line through the circles shows the normal relationship between accommodation and convergence, whilst the line through the crosses shows the convergence-induced accommodation taking place when the subject views an object 0.33 m away whilst the degree of convergence is varied by a haploscopic device. (Fincham & Walton, *J. Physiol.*)

Conflict Between Reflexes

In the experimental arrangements so far employed there has been no conflict between the two stimuli, an alteration in the degree of convergence, for example, being compatible with single vision over the whole range. If we cause a subject to fixate a test-chart some 0.33 metres away, his accommodation for distinct vision is 3 D whilst his convergence is 3 metre-angles. By means of prisms, or other devices, we may make it necessary for him to converge further, or diverge, in order to maintain single vision. We may ask: What happens to his accommodation? If the linkage were still maintained, an increase in convergence would be accompanied by an increased accommodation, but since the vergence of the light has not been altered the chart would become blurred by the unnecessary increase in power. There would be thus a conflict between the accommodation reflex, which demands that the accommodation remain unchanged, and the convergence-induced accommodation that operates through the link. Figure 28.2 shows that the link has some flexibility. The line through the circles shows the convergence-induced accommodation that occurred under the earlier conditions where there was no compulsion to maintain any degree of accommodation. The curve through the crosses shows the convergence-induced accommodation during the present experiment; the arrow indicates the initial condition, the subject converging on an object 0.33 m away, showing 3 metre-angles of convergence and 3 D of accommodation. As convergence increases, accommodation does indeed follow it, but to a much smaller extent, an increase of convergence from 3 to 7 metre-angles being associated with an increase of only about 1 D, by contrast with an increase of 3 D that would have occurred under the 'free conditions'. Thus some blurring of the image has occurred, but this has acted as a 'brake' on the convergence-induced accommodation. This experiment thus reveals, once again, the presence of a link between convergence and accommodation, but also demonstrates that the link is not rigid and may be relaxed when its effects militate against distinct vision.

Relative Amplitude of Accommodation

The converse experiment is carried out by fixing the convergence and placing lenses in front of the eyes to alter the degree of accommodation. Any accommodative convergence, under these conditions, will cause diplopia, so that the compulsion for fusion operates as an inhibitor of this linked convergence. In fact we do indeed find that convergence is maintained to give single vision over quite a wide range of accommodation, but the conflict between the two requirements leads to a restriction of the amount of accommodation that can be exercised, in other words the *relative amplitude of accommodation* is less than the amplitude when the eyes are free to converge and diverge in accordance with the nearness or farness of the object.

Convergence–Accommodation Link

In general, then, we may conclude that accommodation and convergence are linked together by a common ner-

vous mechanism that activates the two together. Because the stimulus of diplopia is more effective than that of blurred vision, we may consider that the response to nearness is primarily one of convergence; in a young person the associated activation of the accommodation mechanism is accurate enough to make the image fairly distinct, whilst the fine adjustment is provided by the accommodation reflex *per se*, which adjusts the focal power of the eye more exactly, using as clues the alterations of chromatic aberration etc. that take place when the image is not accurately focussed. In older persons the convergence-induced accommodation is less adequate and the reflex response must be larger.

Behaviour in Darkness

Kotulak & Shaw (1986) measured accommodation and eye vergence of human subjects in the dark; cross-correlation studies of the spontaneous variations of the two parameters showed that they were not linked, or at any rate the correlation was very small. In most cases accommodation trailed vergence changes, suggesting that vergence-variations, on open loop, induced accommodative changes. Fincham (1962) had shown that the link between accommodation and convergence was weak in the absence of a retinal image.

Pupillary Response

Finally we may ask how the pupillary reflex is involved. When the eyes are made to converge, with accommodation kept fixed, there is usually some pupillary constriction, but very small by comparison with that which would occur were accommodation permitted to occur to match the convergence (Knoll, 1949). Thus the inhibition of the convergence-induced accommodation has been associated with inhibition of the near pupillary reflex. By contrast, the relationship with accommodation is very strong (Marg & Morgan, 1950), in fact, according to Alpern *et al.* (1958), the pupil continues to constrict even when the amplitude of accommodation has been exceeded; thus the increased effort to accommodate is apparently sufficient to cause pupillary constriction. In a similar way, with presbyopic subjects, the stimulus to accommodation is sufficient to cause pupillary constriction, so that presenting a near object, even if accommodation is inadequate, causes a constriction of a magnitude that would be expected had the accommodation taken place (Alpern *et al.*, 1961).

Notes

1. It has been argued, e.g. by Ogle *et al.* (1949), that a certain degree of 'fixation disparity' is tolerated, in which case, of course, the failure of accommodation to match convergence could be due to errors in binocular fixation, the resultant physiological diplopia (p. 463) being in some way suppressed or tolerated. Not all workers are willing to accept the existence of a significant fixation disparity, however.
2. The ratio of the accommodative convergence, indicated by AC, over the accommodation, indicated by A, is called the AC/A ratio, and is considered a valuable diagnostic measurement. It has been examined in great detail by Alpern and his collaborators.
3. Convergence was stimulated by bringing the object closer, but the effective vergence of the light was held constant by the use of very narrow pencils of light so that the rays entering the eye were effectively parallel for all distances of the object from the eye.

References

Alpern, M. (1958) Vergence and accommodation. I and II. *Arch. Ophthal.* **60**, 355–357, 358–359.

Alpern, M., Ellen, P. & Goldsmith, R. I. (1958) The electrical response of the human eye in far-to-near accommodation. *Arch. Ophthal.* **60**, 595–602.

Alpern, M. (1969) Movements of the eyes. In *The Eye.* Ed. Davson, vol. III, 2nd ed. pt. 1. London and New York: Academic Press.

Alpern, M., Mason, G. L. & Jardinico, R. E. (1961) Vergence and accommodation V. Pupil size changes associated with changes in accommodative convergence. *Am. J. Ophthal.* **52**, pt. 2, 762–766.

Fincham, E. F. (1962) Accommodation and convergence in the absence of retinal images. *Vision Res.* **1**, 425–440.

Fincham, E. F. & Walton, J. (1957) The reciprocal actions of accommodation and convergence. *J. Physiol.* **137**, 488–508.

Knoll, H. A. (1949) Pupillary changes associated with accommodation and convergence. *Am. J. Optom.* **26**, 346–357.

Kotulak, J. C. & Schor, C. M. (1986) Dissociability of accommodation from vergence in the dark. *Invest. Ophthal.* **27**, 544–551.

Marg, E. & Morgan, M. W. (1950) The effect of accommodation, fusional convergence and the proximity factor on pupillary diameter. *Am. J. Optom.* **27**, 217–225.

Ogle, K. N., Mussey, F. & Prangen, A. de H. (1949) Fixation disparity and the fusional process in binocular single vision. *Amer. J. Ophthal.* **32**, 1069–1087.

29. THE PROTECTIVE MECHANISM

The eyes are protected from mechanical insults by two mechanisms—blinking and the secretion of tears; by the latter process irritating particles and fumes are washed away from the sensitive cornea, and the surface of the globe is maintained in a normally moist condition. Blinking, besides its obvious protective function, also operates to prevent dazzle by a blinding light, to maintain the exposed surface of the globe moist by spreading the lacrimal secretions and, during sleep, by preventing evaporation. Finally the act of blinking assists in the drainage of tears. The pathological condition of *keratitis sicca* may thus result from either defective lid closure or defective lacrimal secretion.

BLINKING

Orbicularis Oculi

Closure of the eyes is brought about by contraction of the orbicularis oculi muscle, associated with a reciprocal inhibition of the levator palpebri of the upper lid. The orbicularis oculi is an oval sheet of concentric striped muscle fibres extending from the regions of the forehead and face surrounding the orbit into the lids (Fig. 29.1). Although a single muscle, with its origin mainly in the medial canthal region of the orbit, it is customary to divide it into a number of separate muscles, or parts, the main divisions being the *pars orbitalis* and *pars palpebralis*. The pars palpebralis is divided itself into the upper and lower pretarsal and upper and lower preseptal muscles (Fig. 29.2). All the palpebral muscles insert into the lateral palpebral raphe and thus, by contracting, act as tensor muscles to the lids, moving the nasal end of each lid towards the nose.

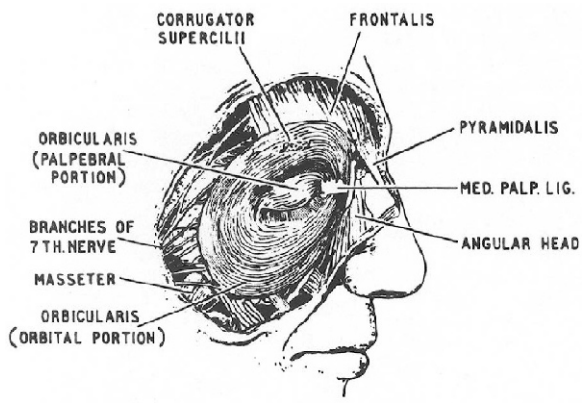

Fig. 29.1 Illustrating the orbicularis oculi muscle. (After Wolff, *Anatomy of the Eye and Orbit.*)

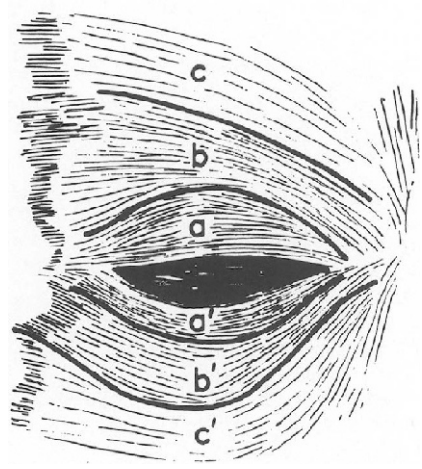

Fig. 29.2 Illustrating the subdivisions of the orbicularis muscle. *c* and *c'* represent the pars orbitalis; *b* and *b'* are the pretarsal, and *a* and *a'* the preseptal muscles. (After Jones, *Trans. Amer. Acad. Ophthal.*)

Orbital Portion

The orbital portion of the muscle is not normally concerned with blinking, which may be carried out entirely by the palpebral portion; however, when the eyes are closed tightly, for example in the blepharospasm consequent on a painful stimulus, then the skin of the forehead, temple and cheek is drawn towards the medial side of the orbit; the radiating furrows caused by this action of the orbital portion eventually lead to the 'crow's feet' of elderly persons. The two portions can be activated independently; thus the orbital portion may contract, causing

a furrowing of the brows that reduces the amount of light entering from above, e.g. in strong sunshine, whilst the palpebral portions remains relaxed and allows the eyes to remain open.

Levator Palpebrae

Opening of the eye is not just the result of passive relaxation of the orbicularis muscle; the upper lid contains the *levator palpebrae superioris*, which takes origin with the extraocular muscles at the apex of the orbit as a narrow tendon and runs forward into the upper lid as a very broad tendon, the *levator aponeurosis*, which inserts into the anterior surface of the tarsus and the skin covering the upper lid. Contraction of the muscle will obviously cause elevation of the upper eye-lid, and it is interesting that the nervous connections of this muscle are closely related to those of the superior rectus, required to elevate the eye, so that when the eye looks upwards the upper eyelid moves up in unison.

Müller's Muscle

The orbicularis and levator are striped muscles under voluntary control; the lids contain, in addition, unstriped muscle fibres deep to the septum orbitale; they take origin among the fibres of the levator in the upper lid and the prolongation of the inferior rectus in the lower, whilst they are inserted into the attached margins of the tarsal plates. They are described as the *superior* and *inferior palpebral muscles* respectively. The muscles are activated by the sympathetic division of the autonomic system and tend to widen the palpebral fissure by elevation of the upper, and depression of the lower, lid.

Accessory Muscles of Lid-closure and Lid-opening

In addition to the muscles already described, we may note that other, facial, muscles often cooperate in the acts of lid-closure or opening; thus the *corrugator supercilii* muscles pull the eyebrows towards the root of the nose, making a projecting roof over the medial angle of the eye and producing characteristic furrows in the forehead; they are used primarily to protect the eye from the glare of the sun. The *pyramidalis*, or *procerus*, muscles occupy the bridge of the nose; they arise from the lower portion of the nasal bones and, being inserted into the skin of the lower part of the forehead on either side of the midline, they pull the skin into transverse furrows. In lid-opening, the *frontalis muscle*, arising midway between the coronal suture of the scalp and the orbital margin, is inserted into the skin of the eyebrows; contraction therefore causes the eyebrows to rise and opposes the action of the orbital portion of the orbicularis; the muscle is especially used in gazing upwards. It is also brought into action when vision is rendered difficult, either by distance or the absence of sufficient light.

Analysis of the Blink

Doane (1980) analysed the blink using high-speed photography, his interest being mainly to relate the blink to the requirement of maintaining the stability of the tear-film which tends to break some 15–30 sec after a blink (Brown, 1973). The upper eyelid accelerates rapidly as it descends to reach a maximum by the time it crosses the visual axis; it then decelerates to come to rest before making contact with the lower lid. Most blinks were not complete, in the sense that complete eye-closure was not attained. The primary movement of the lower lid is horizontal in the nasal direction, sometimes with a downward movement of 1–2 mm. The time-relations of the two movements are illustrated by Fig. 29.3, and may be summarized as follows:

Duration	Closing phase	82 msec
	Opening phase	176 msec
Total		258
Maximum Closing Velocity:		18.7 cm sec^{-1}
	Opening Velocity:	9.7 cm sec^{-1}

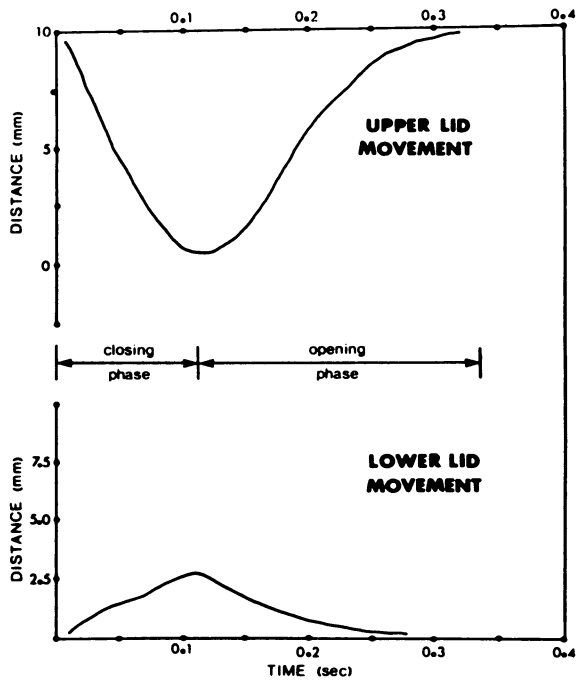

Fig. 29.3 Upper eyelid motion (down, then up) and lower eyelid motion (nasal, then temporal) for the same blink. (Doane, *Amer. J. Ophthal.*)

EMG Analysis

Evinger *et al.* (1984) have analysed the blink in greater detail, measuring eyelid position and velocity and the electromyograms of the orbicularis oculi and superior

and inferior recti. In general, the metrics of blinking were the same in man, rabbit and guinea pig, although in man these were a little slower than those of the guinea pig. The down phase was shorter, and had higher velocities than the up phase (eye-opening). The orbicularis oculi muscle always participated in blinking, but, interestingly, did not actively contribute to the lid movements accompanying downward saccadic eye movements (Fig. 29.4); thus closing the eyes and holding them closed exhibited sustained orbicularis activity, whereas lid movements of nearly equal amplitude but not causing complete eye closure caused no activity; this confirmed earlier observations, e.g. those of Björk & Kugelberg (1953) and Esteban & Salinero (1979). The levator palpebri muscle, on the other hand, plays a purely passive role; prior to the blink, the tonically discharging EMG of the levator ceases discharging and the orbicularis produces a burst of activity pulling the lid down. When the orbicularis ceases discharging, the levator resumes its tonic activity, and the upper lid returns to its initial position. In saccadic movements, it is now the levator that plays a prominent role; since the orbicularis is the only muscle producing downward lid movement, a constant downward passive tension must exist on the upper lid such that relaxation of the levator allows the lid to fall, gravity itself being inadequate, since subjects standing on their heads exhibit normal lid movements during saccades (Sewall, 1933). The force probably arises from the mechanics of the lid system (Kennard & Smyth, 1963).[1] Upward movement results from a pulse discharge coincident with that to the superior rectus; whilst cessation results from pause neurones, so that we have the pulse-step command similar to that of extraocular muscle control for saccades.

Movements of the Eyes

A variety of studies have shown that there is a strong association between the act of blinking and the actions of the extraocular muscles, an association first mentioned by Bell's (1823) study of the palsy named after him. Before considering some of the modern studies relating blinks to eye movements, we may emphasize that the blink is a disruptive activity that interferes with the appreciation of the outside world, albeit for only a short time, but it also interferes with oculomotor control, so that, to minimize the potentially disruptive effect of a blink on ongoing extraocular muscle activity, the oculomotor system regulates the occurrence of blinks (Evinger *et al.*, 1984). Thus smooth pursuit movements result in the almost total suppression of blinks (Tada, 1978), whilst saccadic movements are usually accompanied by blinks (Zee *et al.*, 1983), and blinks almost always accompany rapid eye and head movements. In general, the oculomotor system regulates blinking by suppressing it at times when its effects would be most deleterious, and initiating it at times when it would be least disruptive.

Rotation and Retraction

The clinical literature contains frequent allusions to an upward movement of the eye during a blink, originally described by Bell and again by Miles (1931). However, more modern studies have shown that the direction, from the primary position, is downwards and inwards; when the eye is not in the primary position, Ginsborg & Maurice (1959), using an ingenious technique for the study of random eye movements, showed that the eyes tended to move towards the primary position during a blink. Subsequent work has amply confirmed this diagnosis of the eye movement made by Ginsborg & Maurice; thus Evinger *et al.* (1984), in a comparative study on humans, guinea pigs and rabbits confirmed the movement in man as a return to the primary position rather than as a movement in any particular direction; in the rabbit and guinea pig, the movements were upward and abducting rotations.

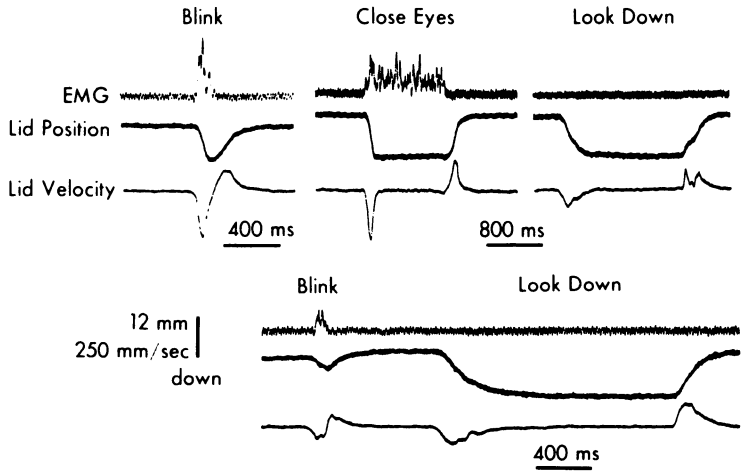

Fig. 29.4 Human orbicularis oculi EMG activity associated with blinking, closing the eyes, and looking down. The EMG activity was rectified and low-pass filtered. (Evinger *et al.*, *J. Neurophysiol.*)

In a more thorough study devoted only to the nature of the eye movements during blinks, Collewijn *et al.* (1985) showed that, from the primary position, an initially downward and nasalward motion of the eye invariably accompanied a blink. The amplitude varied between 1 and 5° according to the amplitude of the blink. Closing one eye with tape did not affect the trajectory of the other. When the lids of one eye were held open by a retractor, the blink eye movements became somewhat more horizontal but remained of about the same size in both eyes. Thus the eye movements are not generated by sliding the lid across the eye.

Retraction of the Eyeball

Doane, while failing to confirm the upward eye movement during blinks, observed a retraction of the eye into the orbit amounting to some 0.7–1.6 mm. This may be measured photographically, as shown by Fig. 29.5, which also illustrates the time-relations between retraction and lid-closure. Figure 29.6 from Riggs *et al.* (1987) shows the greater degree of retraction when a powerful blink was made. Using the persistence of vision of a moving spot to determine the eye movement, Riggs *et al.* showed that a blink from the primary position tended to cause a movement of the eye inwards and downwards.

CO-CONTRACTION OF EXTRAOCULAR MUSCLES

The strong association of retraction with rotation of the eye towards the primary position suggests that it is essentially the co-contraction of the extraocular muscles that leads to the rotation, the co-contraction pulling the eye into the orbit—retraction—but, through imbalance, causing eye rotation, the degree of imbalance probably being a function of the initial position of the eye. Thus, if the eye is looking down, the inferior rectus is already active and may receive less activation during the blink than the superior rectus, leading to a partial return towards the primary position (Evinger *et al.*, 1984; Riggs *et al.*, 1987).

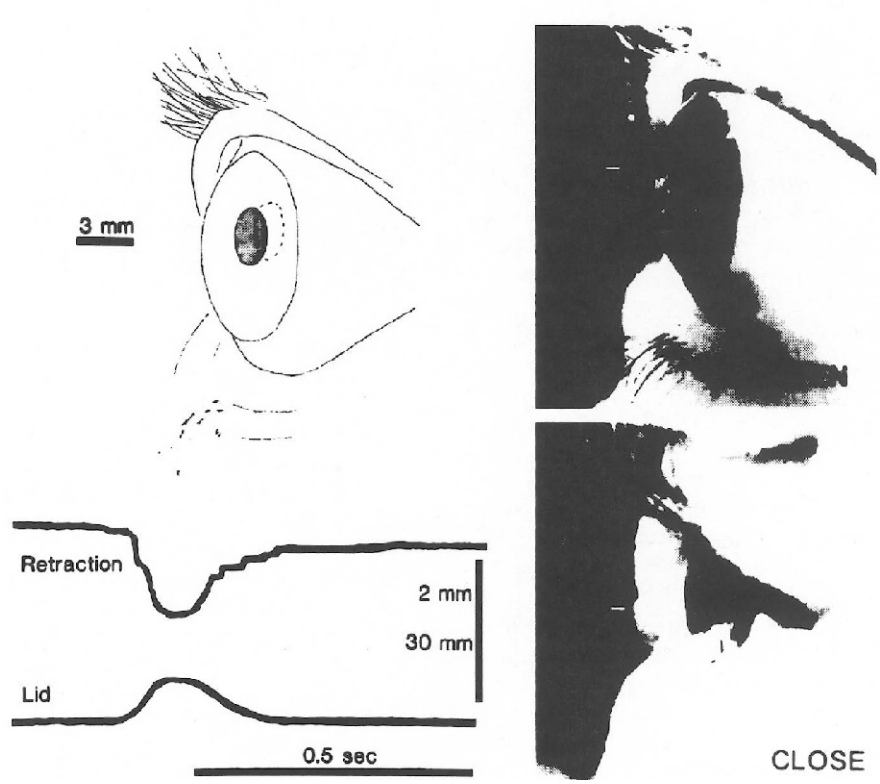

Fig. 29.5 Movements of the human eye during eyelid closure. Photographs show the left eye in profile with both eyes (open) and when instructed to close eyes (close). Tape attached to margins of eyelids held the left eyelid open and away from the globe. The eye retraction may be seen by comparing the distance from the pupil to the bridge of the nose (bar) in the two pictures. Superimposed tracings of the two pictures also show the retraction. The shaded pupil is the eye-open condition; the dotted pupil is the eye-closed condition. The individual record demonstrates dynamics of the eye retraction during a blink. The 2-mm calibration refers to the retraction trace. (Evinger *et al.*, *J. Neurophysiol.*)

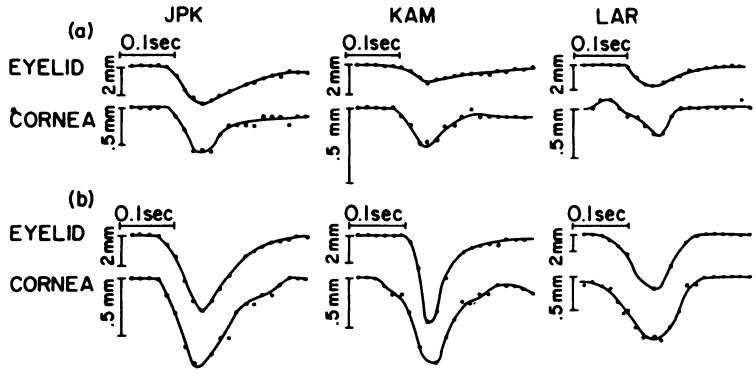

Fig. 29.6 Photographic measurements (64 frames/sec) of eyeball retraction during small blinks (upper) and larger blinks (lower). Size of blink indicated by amplitude of upper eyelid lowering. Eyeball retraction indicated by inward motion of the cornea. Measurements are based on film records showing an oblique view of the cornea and eyelids from below and to the side of the eye. The true excursions are thus slightly larger than indicated in this figure. (Riggs *et al.*, *Invest. Ophthal.*)

Eye-position Information

The coordination of lid movements with eye movements during changes in gaze could well be governed by the nervous apparatus required for execution of the eye rotation alone, since this is shared by the levator palpebrae; we have seen how the orbicularis oculi does not play an active role in lid movements associated with eye movements, so we need not expect the facial nucleus to receive information regarding eye-position to alter lid-position with changes of gaze. However, in the cat and rabbit, the facial nucleus does receive this information from vestibular nucleus neurones, which send collaterals to the nucleus (Shaw & Baker, 1983).

Prolonged Lid Closure

Eye movements associated with long, e.g. 2 sec, voluntary closures were entirely different from those associated with blinks. In one example, during lid closure the eye showed a transient downward movement but this was followed by a slow and tonic deviation upward. On opening the eye the consequent downward movement was much faster. Tonic elevation, corresponding with Bell's description, was not found in all cases; thus in three out of six subjects the tonic vertical movement was downwards. The size of the vertical components was from 5–20° but was governed by the initial angle of gaze. When the eyes were held open with a retractor, then subjects that gave an upward tonic movement with prolonged closure also gave it; however, with subjects that gave a downward tonic movement, then with lid-opening the eye movement was upwards, a situation analogous with Bell's palsy.[2]

Visual Suppression

Volkmann *et al.* (1980) pointed out that in normal life the interruption of vision associated with a blink is barely noticed, and certainly not to the extent as a black-out of illumination during the same period would cause. They considered that during a blink the brain generated an inhibitory signal that would diminish the effect of the interruption of vision, perhaps equivalent to the saccadic suppression already described. They stimulated the eye by light carried into the roof of the mouth by a fibre-optical system; during blinks the subjects detected a brief decrement in the apparent brightness of the light; the loss began before the onset of the blink and recovered well before the lid had covered the pupil. In a later study, Volkmann *et al.* (1982) confirmed the early depression of retinal sensitivity at the time of the blink, the loss being equally extensive if the eyes remained closed. They concluded that it was the act of closure that caused the suppression, presumably as a result of corollary discharge accompanying the command to the blink-centre. They considered that the blink-suppression was equivalent to the saccadic suppression already described (p. 454). Thus if the lids were held closed, there was little change in sensitivity on opening the eyes; it was essentially the act of closure that induced the change.

Reflexes

Reflex blinking may be caused by practically any peripheral stimulus but the two functionally significant reflexes are (*a*) that resulting from stimulation of the endings of N

V in the cornea, lid or conjunctiva—the *sensory blink reflex*, or *corneal reflex*, and (*b*) that caused by bright light—the *optical blink reflex*. The corneal reflex is rapid (0.1 second reflex time) and is the last to disappear in deepening anaesthesia; it is mediated by N V, impulses being relayed from the nucleus of this nerve to N VII. The reflex is said to be under the control of a medullary centre. The optical reflex is slower and, in man, the nervous pathway includes the visual cortex; the reflex is absent in children of less than nine months.

The blink- or wink-responses to a tap on the face, for example on the supra-orbital region, have been described as a group of *facial reflexes* to which various names, after their discoverers, have been attached (McCarthy, v. Bechterew, etc.). The name *orbicularis oculi reflex* has been suggested to cover them all since their reflex paths are essentially the same, and they apparently consist of two phases—a *proprioceptive* response due to stretch of the facial musculature, followed by a *nociceptive* response which may be regarded as protective in function (Rushworth, 1962).

Normal Rhythm

In the waking hours the eyes blink fairly regularly at intervals of two to ten seconds, the actual rate being a characteristic of the individual. The function of this is to spread the lacrimal secretions over the cornea, and it might be thought that each blink would be reflexly determined by a corneal stimulus—drying and irritation. As a result of extensive studies by Ponder & Kennedy (1928) on human subjects, it would appear that this view is wrong; the normal blinking rate is apparently determined by the activity of a 'blinking centre' in the globus pallidus of the caudate nucleus. This is not to deny, however, that the blink-rate is modified by external stimuli, particularly through N V and N II, and also by the emotional state of the individual; Ponder's work shows this most clearly—for example, the blink-rate of an individual in the witness-box went up markedly during cross-examination; that of another decreased on ingestion of a large dose of alcohol, and so on; the fact remains, however, that when any given route for sensory impulses is blocked, e.g. by cocainization of the cornea, the blink-rate is, on the average, unchanged, i.e. characteristic of the individual.

LACRIMATION

The surface of the globe is kept moist by the tears, secreted by the lacrimal apparatus, together with the mucous and oily secretions of the other secretory organs and cells of the conjunctiva and lids.

Lacrimal Glands

The lacrimal gland, proper (Fig. 29.7) lies in the upper and outer corner of the orbit, just within the orbital margin. It is divided by the lateral horn of the aponeurosis of the levator muscle into two lobes, *orbital* and *palpebral*. About twelve ducts gather the secretion of the entire gland and open through the palpebral conjunctiva, some 4 to 5 mm above the upper border of the tarsus. It has a typical serous gland structure, and is supplied mainly by the lacrimal branch of the ophthalmic artery, the lacrimal vein draining the blood into the superior ophthalmic vein. The glands are supplied by the *lacrimal nerve*, which is the smallest terminal twig of the ophthalmic division of the trigeminal (Fig. 29.15).

Histology

The microscopical appearance of the gland has been described by Scott & Pease (1959), Kühnel (1968) and Ruskell, (1975). The basic structure, as with the salivary glands with which it has been compared, is the acinus, opening into the tubule. The cells

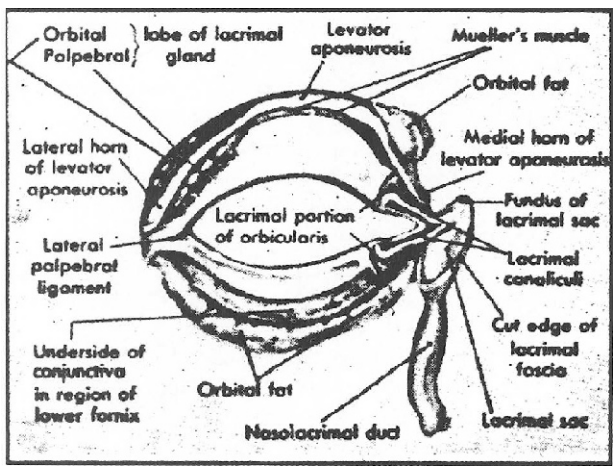

Fig. 29.7 Tarsal plates and lacrimal system. (Kronfeld *et al.*, *The Human Eye in Anatomical Transparencies.*)

constituting the acinus are of two main types, as characterized by the types of granule within their cytoplasm, and on this basis they have been described as mucous (with clear granules, Type A or K) and another serous (dense granules, Type B or G). According to the histochemical study of Allen *et al.* (1972), the type A, or mucous cell, granules stain similarly to the granules in the Paneth cell, which contain lysozyme, whilst the type B or serous cell granules contain either neutral or acid glycoprotein. Thus the mucous and serous cell types are responsible for secretion of the glycoprotein and lysozyme of tears respectively. The myoepithelial cells are the third type, and these presumably serve to compress the acini, expelling the secretion into the ducts.

Accessory Lacrimal Glands

In addition to the lacrimal gland, there are numerous microscopical *accessory lacrimal glands* in the conjunctiva—the glands of Krause and Wolfring—structurally organized in an essentially similar fashion but on a very much smaller scale.

Sebaceous and Mucous Secretions

An oily fluid is secreted by the glands of Zeis and the Meibomian glands, in the eyelids, whilst goblet cells in the conjunctiva secrete mucus.

The Precorneal Film

The fluid layer on the cornea is called the precorneal film and consists of three layers; thus closest to the epithelial surface there is a thin film of mucus, or mucin, that follows the contours of the epithelial surface; next there is a layer of tears and, on the surface a thin film of lipid that serves to reduce evaporation from the surface (Mishima & Maurice, 1961) as well as preventing overflow at the lid margin. The film is illustrated by Fig. 29.8.

The Mucus Layer and Surface Epithelium

Nichols *et al.* (1983, 1985) have described the light- and electron-microscopical appearances of the corneal and conjunctival epithelial surfaces with their associated mucus layer. The corneal epithelium was covered by microvilli and microplicae, the surface projections varying from 150 to more than 300 nm at the centre and periphery respectively. A filamentous cell coat, or glycocalyx, extended some 300 nm, and it is this that binds the mucus layer to the cells. This layer was seen as a dense black precipitate about 8 μm thick after precipitation with tannic acid. Examined by freeze-substitution, it was seen to form a layer filling the irregularities of the cornea and conjunctiva.

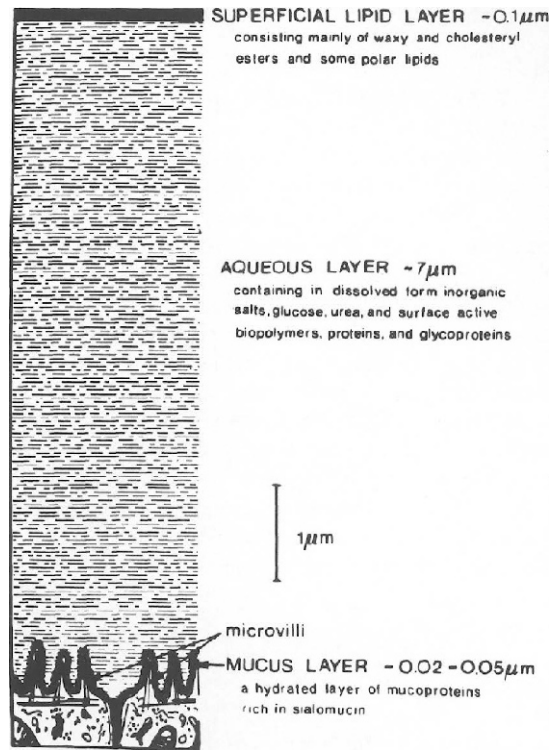

Fig. 29.8 Structure and composition of the tear film. (Holly & Lemp, *Survey Ophthal.*)

Wetting and Stability of the Film

The factors governing the wetting of the cornea by the tears have been discussed by Holly (1973) and Holly & Lemp (1977). They are characterized by a spreading coefficient, S, determined by the surface tensions indicated in Fig. 29.9. Expressed in words, the film will remain stable when the sum of the surface tension of the fluid film and the interfacial tension at the solid-fluid boundary is smaller than the surface tension of the bare solid. The surface tension of the tear-film is determined by the film pressure, i.e. the depression of surface tension, caused by the superficial lipid layer; and the magnitude of this depends on the palpebral fissure width. Thus the more the film is compressed by the lid, the lower its surface tension becomes.[3] The tear-epithelium surface tension is kept low by the presence of mucus.[4]

Re-forming the Film

When the eyes close, the superficial layer of lipid is actually swept off the mucinous surface and compressed to the small area between the lid edges. When the eyes open, a new lipid film must be spread over the surface, and it is important that this remain stable for some time.

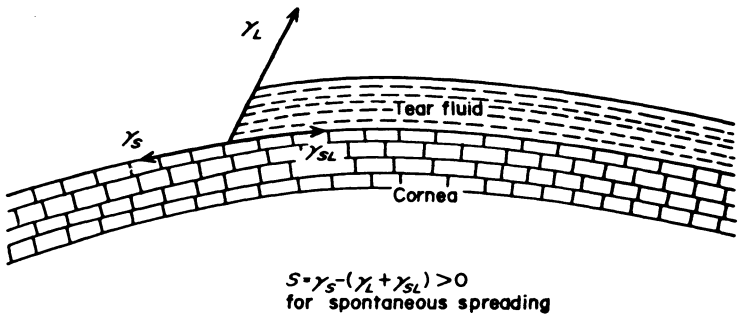

Fig. 29.9 Interfacial tensions determining the spread of tear fluid over the cornea. (Holly, *Exp. Eye Res.*)

According to Holly, the breakdown of the new film provides the stimulus for the next blink. Thus, when blinking is prevented, the tear-film ruptures in 15 to 40 sec to produce dry spots, which are regions of non-wetting and not of localized drying caused by discontinuities in the superficial lipid layer as was formerly believed. The period between a blink and the appearance of the first dry spot—the breakup time—is usually greater than the interval between two consecutive blinks, and is a clinical parameter of some value. As Holly & Lemp (1977) point out, an excess of lipid may very well tend to break up the tear film owing to a disturbance in the surface forces; thus, if it passes into the aqueous phase it can lower the surface tension at the solid epithelium-liquid interface and so cause instability of the film, and this, according to Holly, is the ultimate cause of the dry spot which, if not repaired by a blink, can extend over the whole corneal surface, e.g. during forced lid-opening.[5]

Removal of Lipid-mucus

The lipid removed by the lid when it sweeps over the surface is carried away with mucus to form threads in the inner canthus. It is this material that is collected for study of the mucus composition. Figure 29.10 illustrates the mechanism for removal of lipid-contaminated mucus. It

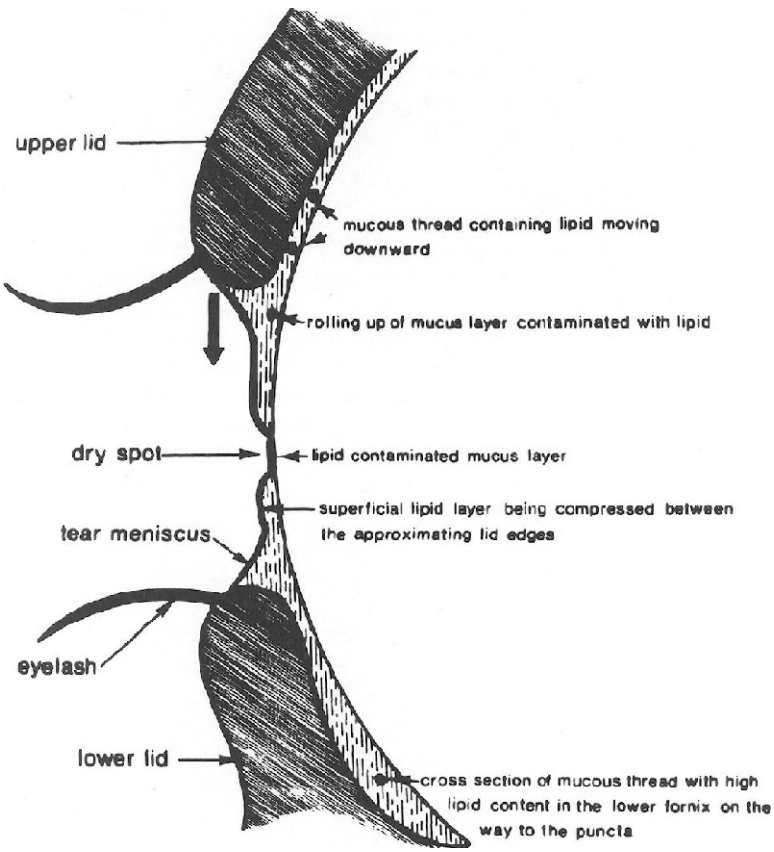

Fig. 29.10 Tentative mechanism for removal of lipid-contaminated mucus layer. (Holly & Lemp, *Survey Ophthal.*)

also illustrates some features of the corneal film; thus at the lid margins there is a reservoir of tear-fluid, exhibiting the tear-meniscus which, because of capillarity, tends to retain fluid so that at the junction between it and the tear film, a *black line* is observed in the slit-lamp indicating that, here, fluid has become unavailable for tear film formation (McDonald & Brubaker, 1971). Figure 29.11 illustrates this process in more detail; blinking of the eyes is said by these authors to act as a 'subsurface vacuum cleaner', resulting in renewal of the aqueous phase of the tears, while lipid is spread over the outer surface.

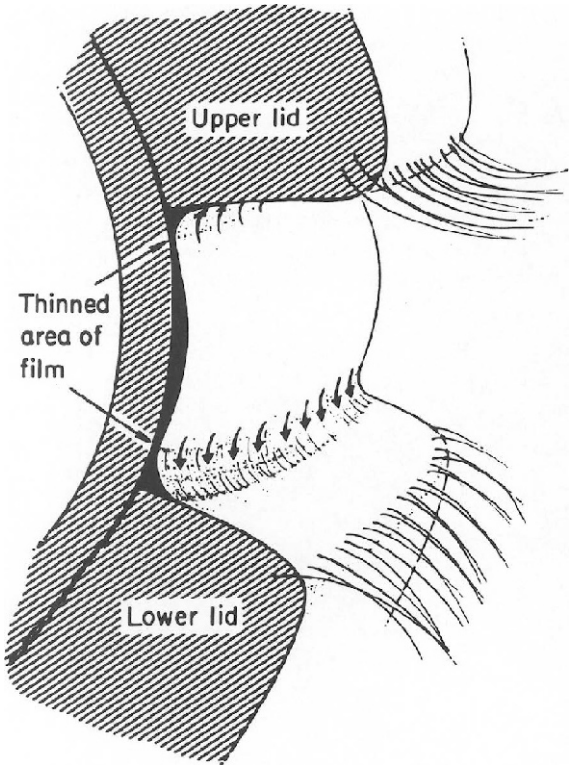

Fig. 29.11 Negative pressure in the meniscus thins the adjacent tear film. The blinking of the eyelids acts as a surface vacuum cleaner resulting in renewal of the aqueous phase of the tears. (McDonald & Brubaker, *Amer. J. Ophthal.*)

New Film

As the eyelids open, an aqueous-air interface of high surface tension is formed; and this is immediately followed by spreading of lipid; the gradually thinning tear-meniscus exerts a greater and greater pull on the aqueous fluid, and it ceases to spread at the black line.

Normal Output of Tears

This is not easy to measure, largely because the steps taken to estimate it may easily cause reflex increase in secretion (Jordan & Baum, 1980); to avoid this, the surface of the cornea may be anaesthetized but this may introduce complications. Schirmer, in 1903 devised a test based on the absorption on to a strip of filter-paper hooked over the lower lid margin and measuring the length of wetting that occurred in a fixed time; this has played a prominent role in diagnosis although its value has been questioned. Schirmer made quantitative estimates in subjects with the lacrimal ducts and sacs removed; the time for a drop to form was measured and, after allowing for evaporation, he deduced a rate of 0.5 to 0.75 g in 16 hr, i.e. 0.5 to 0.8 μl/min. Mishima *et al.* (1966) estimated the volume of tears normally present by determining the dilution of a drop of fluorescein instilled into the eye, using a spectrofluorophotometer; the rate of flow could be measured by the decline in concentration; this occurred in two phases, an initial rapid decline, due to dilution by stimulated secretion, and a slower decline due, it was thought, to drainage. The mean rate was 1.2 μl/min with limits of 0.5 and 2.2 μl/min. The initial dilution of fluorescein gave a bad measure of tear volume because of the stimulated flow, but by extrapolating the slow decline back to zero-time a more accurate measure was obtained, namely 6.2 ± 2.0 μl. Maurice (1973) pointed out that Mishima *et al.* did not allow for absorption of fluorescein into the cornea; when corrected for this, the rate of production was about half, namely ca. 0.6 μl/min.

Basic Flow-rate

Jordan & Baum (1980) made a more elaborate study and obtained a basic flow-rate of 1 μl/min; the rate decreased with age as others had found (e.g. Van Bijsterveld, 1969); basic tear-volumes were 7.4 ± 1.3 and 6.6 ± 2.3 μl in young and old subjects respectively; when eyes were anaesthetized, however, volumes were much less, namely 2.1 ± 0.4 and 2.6 ± 1.3 μl in young and old persons; this decrease was confirmed by measurement of the meniscus-height which decreased over a period of 4 minutes. When the lower lid margin was touched gently with filter-paper in the topically anaesthetized eye, there was a 300% increase in rate of flow. Thus, even in the anaesthetized eye, the Schirmer test is unlikely to be of value as an estimate of 'basic flow-rate'; in fact Jordan & Baum question the concept of such a flow.

Chemistry of the Lacrimal Secretion[6]

The fluid collecting in the lacus lacrimalis is a mixture of mucus and secretions of the lacrimal glands—the tears

Table 29.1 Ionic composition of human tears collated from the literature by Van Haeringen (1981).

	Concentration in mmol/l					
	Na^+	K^+	Ca^{2+}	Mg^{2+}	Cl^-	HCO_3^-
Tears	120–170	6–26	—	—	118–138	—
	80–161	6–36	—	—	106–130	—
	145	24	—	—	128	26
	134–170	26–42	0.5–1.1	0.3–0.6	120–135	—
	—	—	0.4–0.8	—	—	—
	—	—	0.4–1.0	0.5–1.1	—	—
	—	—	0.4–1.1	—	—	—
	—	—	0.3–2.0	—	—	—
Serum	140	4.5	2.5	0.9	100	30

proper—and is thus slightly opalescent. The ionic composition is shown in Table 29.1 from Van Haeringen (1981).

Osmolality

According to Krogh *et al.* (1945) the tears are isosmolal with blood plasma, but the precise relationship between the two fluids will obviously depend on the degree of evaporation that the fluid undergoes before collection, and, in addition, the rate of secretion may affect the total concentration of solutes secreted into the ducts; thus Giardini & Roberts (1950) found the concentration of chloride to fall from 135 mM to 110 mM as the rate of secretion was increased by exposing the human eye to larger and larger concentrations of tear-gas. To avoid complications due to evaporation, Gilbard & Dartt (1982) collected tears directly from the rabbit's duct, and varied rate of secretion by intra-arterial injections of acetylcholine. At a low flow-rate of less than 0.11 μl/min, osmolality was 334 ± 4 milliosmoles per litre; as rate increased to a maximum of 13–19 μl/min, the osmolality decreased to 294 ± 2.

Vitamin A (Retinol)

The cornea has a requirement for retinol, deficiency leading to xerophthalmia (see, for example, Van Horn *et al.*, 1980). Retinol is present in the tears of rabbits and humans (Ubels & MacRae, 1984) from which it might be carried into the cornea. Ubels *et al.* (1986) cannulated the lacrimal gland ducts of rabbits and rats and identified retinol in the collected fluid. Secretion was stimulated by cholinergic drugs and by vasoactive intestinal polypeptide (VIP) in manners analogous with the stimulated secretion of protein by these agents.

Proteins

The concentration of proteins in tears is low, being of the order of 1–6 mg/ml compared with about 70 mg/ml for serum. Modern separative techniques have resolved the proteins into some 60-odd types (Gachon *et al.*, 1979) most of which are common to serum and probably derived from this by leakage across the blood-tear barrier or from the conjunctival capillaries. The principal proteins are specific tear prealbumin, lysozyme, lactoferrin, peroxidase and some immunoglobulins, principally IgA.

BACTERICIDES

Of especial interest is the bactericide, lysozyme, first described by Fleming (1922) and considered to be responsible for the low bacterial count of normal human tears. Lysozyme is a strongly basic protein, of molecular weight 14 000 to 25 000 daltons; with an iso-electric point of 10.5 to 11.0 it has a net positive charge at physiological pH and thus migrates to the cathode by contrast with the other proteins which have a net negative charge. It is an enzyme, and owes its bactericidal activity to its power of dissolving the mucopolysaccharidic coats of certain bacteria. It is not peculiar to human tears, being widely distributed in the plant and animal kingdoms, egg-white and fig-tree latex being rich sources, for example.

Other Bactericides Iron-binding proteins are thought to play a role in protecting mucosal surfaces from infection; Broekhuyse (1974) noted that Sapse *et al.* (1969) had identified several proteins in human tears including ceruloplasmin, lysozyme and transferrin. Again Friedland *et al.* (1972) had identified a non-lysozymal bactericide in human tears, its activity against *M. lysodiektus* being some 200 times that expected of the lysozyme present in the tear sample; the material was destroyed by heating to 100 °C and had a molecular weight of about 5–6 kd. However Broekhuyse suspected that the main bactericidal activity, in addition to that of lysozyme, might be due to another iron-complexing protein, *lactoferrin*, first identified by Sørensen & Sørensen in 1939 in bovine milk and described as a red protein. This protein is present in polymorphonuclear leukocyte specific granules (Masson *et al.*, 1969), and has been identified in a number of

external secretions such as saliva, bronchial mucus, hepatic bile, etc., including tears (Masson *et al.*, 1964). By immunoelectrophoresis Broekhuyse separated lactoferrin from tears and by dodecylsulphate electrophoresis estimated its molecular weight at 82 kd. Its concentration was 1.45 mg/ml. Some transferrin was found, but he considered that this had escaped from the serum. Broekhuyse emphasized that lactoferrin was quite different from the factor described by Friedland *et al.* (1972). In a later study Kiljstra *et al.* (1983) measured mean total concentration of protein in human tears at 9.6 mg/ml and of lactoferrin 2.4 mg/ml; thus some 25% of the human tear proteins are made up of lactoferrin.[7]

Bactericidal versus Bacteriostatic Actions Iron-chelating substances may act bacteriostatically by depriving bacteria of iron; growth resumes when sufficient iron is added to the medium. There is little doubt, however, that lactoferrin is truly bactericidal; thus according to Arnold *et al.* (1982) it may kill bacteria when the concentration of lactoferrin in the medium is far too small to chelate all the iron in the medium.[8]

Three Distinct Components Selsted & Martinez (1982) isolated and purified three distinct bactericidal factors from human tears by gel filtration and exchange chromatographic methods. They collected tears either emotionally or onion-stimulated, and confirmed that the three major proteins were lactoferrin, specific tear prealbumin and lysozyme in order of decreasing molecular weight. In addition to lysozyme there were two other bactericidal components; one called bactericidal glycoprotein, and the other migrating electrophoretically with specific tear prealbumin. The purified materials were tested on *B. subtilis*, both with respect to bactericidal action and with respect to interference with RNA and protein synthesis; and Fig. 29.12 shows the effects on incorporation of ^{14}C-uracil by the three preparations; lysozyme was by far the most effective inhibitor. Gram-negative bacteria were unaffected by all three factors, whereas Gram-positive organisms, such as *B. subtilis* and *L. momocytogenes*, were all killed by the three factors.[9] As to the nature of these two additional bactericidal factors, previously unreported, further work is necessary for their complete characterization.

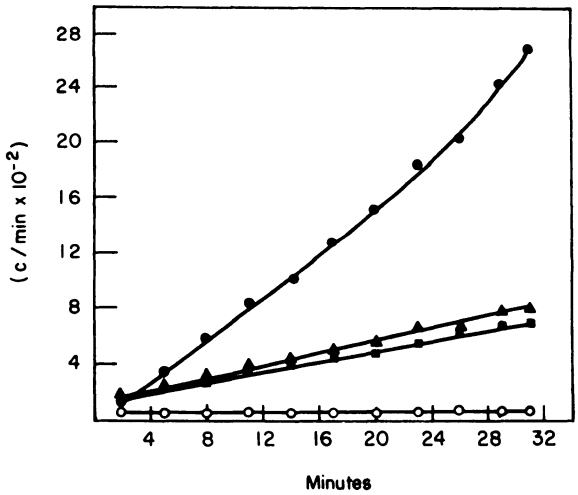

Fig. 29.12 Effects of tear bactericides on incorporation of ^{14}C-uracil by *B. subtilis*. Incorporation of TCA precipitable counts by 3.7×10^6 cells/ml treated with (●) buffer, (■) 135 μg/ml tear bactericidal protein, (▲) 175 μg/ml specific tear prealbumin, (○) 2.0 μg/ml lysozyme. (Selsted & Martinez, *Exp. Eye Res.*)

TEAR-SPECIFIC PREALBUMIN

Bonavida *et al.* (1969) pointed out that the major component of the tear proteins migrated more anodally than serum albumin and thus behaved like prealbumin or transferrin, the iron-complexing protein of plasma. However, they showed that this prealbumin was different, moving more rapidly during electrophoresis and having a molecular weight of 15–20 kd compared with 61 kd for serum prealbumin. They excluded lysozyme as its possible identity; it was not present in milk or other secretions, thereby excluding lactoferrin. In cultured lacrimal gland, labelled amino acid was secreted, and after electrophoresis of the synthetic products, labelled material was found at the spot where the specific prealbumin would have been.[10]

IMMUNOGLOBULINS

Bacterial and viral pathogens frequently colonize mucosal surfaces, which are bathed in mucous fluids containing specific immunoglobulin and innate host factors. The predominant immunoglobulin in external secretions is secretory IgA, and this is true of the tears. In the lacrimal gland IgA is synthesized by interstitial plasma cells and, after entry into the intercellular spaces, it is coupled to an additional antigenic fragment, the secretory component, SC, and secreted as secretory IGA (IGA-SC) through the blood-tear barrier involving intracellular transport by acinar cells into the lumen (Franklin *et al.*, 1973). The mechanism is illustrated by Fig. 29.13, based on Franklin *et al.*'s electron microscope study. Although IgA is the main immunoglobin of tears IgG, IgM and IgF have all been identified in cells within the lacrimal gland.[11] According to McClellan *et al.* (1973) the average concentrations of IgA and IgG in human tears are 1.7 and 1.4 mg/ml respectively; the concentrations are very strongly correlated with each other, perhaps because variations are due to evaporation and dilution. The proportions of IgG to IgA were 54:1 in serum but 1:1 in tears. The authors found no IgM in normal tears, but it appeared in inflammatory conditions of the conjunctiva.

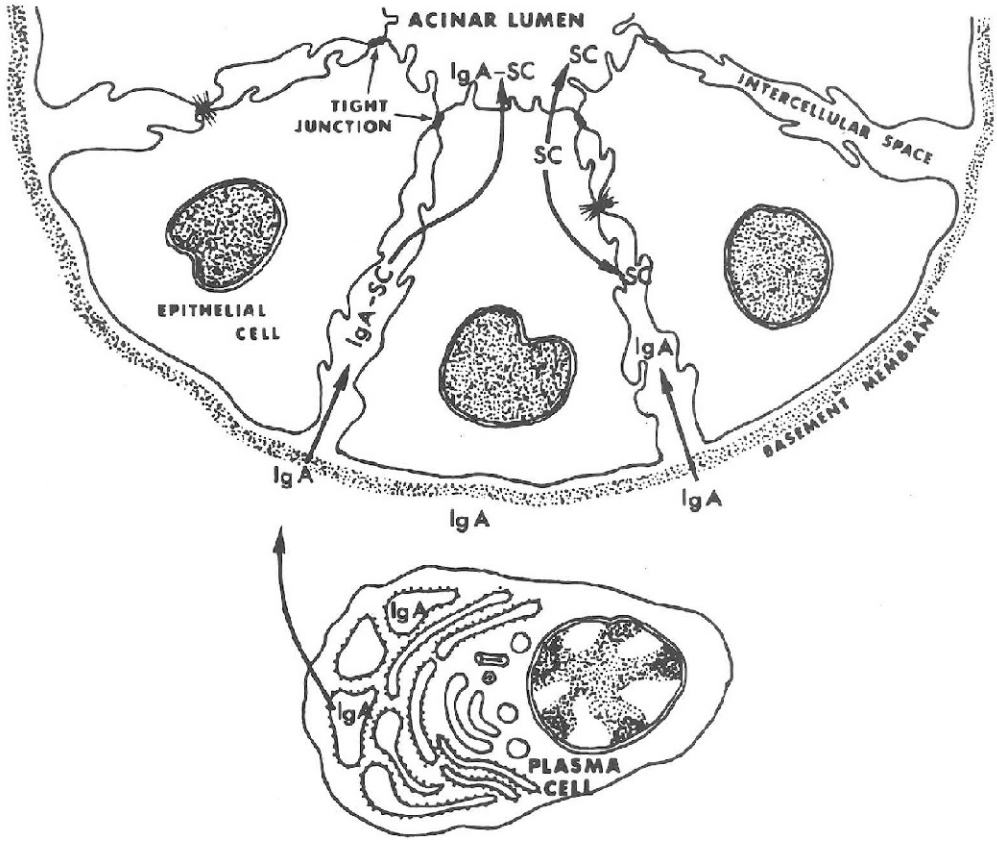

Fig. 29.13 Diagrammatic representation of human lacrimal gland depicts synthesis of IgA by interstitial plasma cells, entry of IgA into acinar intercellular spaces, and passage of IgA-SC through epithelial cells into acinar lumen. (Franklin *et al.*, *J. Immunol.*)

COMPLEMENT

The complement system is one of the main effector mechanisms of the humoral immune response; Yamamoto & Allansmith (1979) stated that tears contained haemolytic complement activity suggesting the presence of all components from C1 to C9. Subsequent work, however, has failed to confirm this; in fact Kiljstra & Veerhuis (1981) found that tears contained an anti-complement factor due to the presence of lactoferrin (Kijlstra & Jeenssen, 1982). The formation of EAC4 was not affected but the next step in the chain, the formation of EAC142 was markedly inhibited. In a quantitative study, (Veerhuis & Kijlstra, 1982), it was shown that, in a concentration of 4.8 μg/ml, isolated tear lactoferrin could inhibit by 50% the haemolytic complement activity present in diluted serum containing 1.5 total complement units. Thus lactoferrin, besides its known bactericidal properties, is able to control the complement system, and conceivably play an anti-inflammatory role with respect to the surface of the eye.

In a study of different species, Kijlstra *et al.* (1984) found very high activity in the tears of rat and mouse; in the goat, guinea pig, rabbit and monkey the activity was about equal to that of human tears; in the chicken and cat it was very weak.

The Mucus

We have seen that a layer of mucus separates the surface of the corneal and conjunctival epithelial cells from the overlying fluid of the precorneal tear-film. This material is necessary for the stability of the tear-film; some may be secreted by the epithelial cells themselves, whilst the bulk is probably contributed by the goblet cells; the mucus material in the tear secretion, collected directly from the lacrimal gland, indicates a source here too.

Basic Features of the Mucus Proteins

The biochemical and histochemical nomenclature of mucus has been described by Reid & Clamp (1978); thus

mucin is the generic name for substances consisting of carbohydrate covalently linked to non-carbohydrate material, e.g. lipid or protein. There are two different types of carbohydrate-linked protein, namely proteoglycans and glycoproteins; the proteoglycans have been considered in relation to the cornea, and consist of long branched-chain carbohydrates (glycosaminoglycans) mostly with repeating disaccharide units, e.g. the hexuronic acid-hexosamine repeat. The glycoproteins contain smaller carbohydrate units, with an average of less than 10 monosaccharide residues; the units are thus described as oligosaccharides, usually branched and not containing hexuronic acid. The mucus glycoproteins are distinguished from the plasma proteins, which are also glycoproteins, in having very large molecular weights of several million daltons, with a carbohydrate content of over 50%; the small carbohydrate units are attached to about every third amino-acid residue, to give the so-called 'lampbrush' structure, but there are some naked regions that permit aggregation through disulphide linkages. The linkage between carbohydrate and protein in the mucus proteins is through an oxygen-atom (*O-glycosidic*), the monosaccharide involved in the linkage being *N*-acetylglucosamine, which is attached to either serine or threonine. The linkage in the plasma glycoprotein is through a nitrogen-atom from *N*-acetylglucosamine to asparagine, the linkage being called *N*-glycosidic.

Ocular Mucus

This accumulates in the inner canthus and may be collected experimentally by wiping with moistened cotton-wool. Pioneering studies on its composition were made by Moore & Tiffany (1979; 1981); in unreduced mucus, i.e. without breaking disulphide linkages, they found a GP1 with molecular weight of 2×10^6 daltons and GP3, of 200000 daltons.[12] Reduction gave GP1, GP2 and GP3, whereas in tears they found only a GP3 (GP3T). GP2 was considered to be a reduction product from GP1. Immunofluorescence studies showed that GP2, and hence GP3M, was derived from goblet cells of the conjunctiva and not from the lacrimal gland. Thus the glycoprotein in the secretory granules of the lacrimal gland, described by Allen *et al.* (1972) may be the tear glycoprotein GP3T of relatively low molecular weight observed in this study. This tear glycoprotein did not cross-react with the GP2 from mucin (Moore & Tiffany, 1979).[13]

Human Lacrimal Gland Explants

Chao *et al.* (1980) obtained three major fractions of protein material synthesized by gland explants; these had molecular weights of 580, 100 and 39 kd; amino acid compositions were similar but they differed in their carbohydrate moieties; the percentage of carbohydrate was from 8 to 26 so that the products were typical of plasma glycoproteins; IgA, IgG, albumin, transferrin and ceruloplasmin were also synthesized. Thus no mucous glycoprotein was synthesized by the gland.

According to Chao *et al.* (1983a) the glycoproteins are bound to lipids in the high molecular weight fraction of greater than 10^5 daltons. Their studies were in general agreement with those of Moore & Tiffany in so far as the high sugar content was concerned; they considered that, in contradiction to Iwata & Kabasawa (1971), their glycoprotein was not of the plasma type; thus mucus-type glycoproteins contain predominantly *O*-glycosidic linkages whereas the plasma glycoprotiens contain predominantly *N*-glycosidic linkages.

In a separate study, Chao *et al.* (1983b) demonstrated that the linkage between carbohydrate and protein in the high-molecular weight material prepared from human mucus was of the *O*-glycosidic type; at least 22% of the total peptide-bonded hydroxyamino acid residues were linked *O*-glycosidically.

Lacrimal Gland Mucosubstances

Jensen *et al.* (1969) identified strongly PAS-positive material in the acini of the human lacrimal gland histochemically; the material was resistant to hyaluronidase but highly sensitive to neuramidase, indicating the presence of sialic acid, so they suggested that the lacrimal gland secreted mucinous material. Biochemically, Falbe-Hansen *et al.* (1969) showed that an extract from the gland, designed to prepare mucoprotein, contained material with a protein content of 46%; hexosamine, 13%; hexose, 7% and sialic acid 40%. The material was clearly a mucus-type glycoprotein. Working on the rabbit, Kreuger *et al.* (1976) cannulated the orbital lacrimal gland duct, this being analogous with the human orbital duct, and they compared the sialic acid contents of fluid collected from here with that collected at the same time from the material, secreted by the other glands, that collected in the conjunctival sac. They found sialic acid in both fluids, the concentration increasing with pilocarpine stimulation. It would seem, therefore, that the lacrimal gland secretion contributes to production of the mucus material that is probably so important for maintaining the stability of the precorneal film.

Age-related Changes

Liakos *et al.* (1984) have followed the concentrations of lysozyme, lactoferrin, ceruloplasmin, IgA and IgG, together with the rate of tear formation, in human subjects with ages ranging from 20 to 80 years. There was a linear decline in rate of production of tears after the age of 40 years. Lysozyme and lactoferrin concentrations declined

over the 60-year period, but ceruloplasmin rose; the immunoglobulins changed very little.

Origins of the Proteins

The 60-odd proteins identified by modern separative techniques in tears may be divided into three groups (Janssen & Van Bijsterveld, 1983), namely those that are present in both serum and tears, those that are present only in tears, and those present in the epithelial cells of the cornea and conjunctiva. The presence of these last in the tears may be attributed to epithelial damage during collection, as with the filter-paper method (Van Haeringen & Glasius, 1976a); and their presence in the cells may be detected by immunofluorescence. Those synthesized by the lacrimal gland, principal or accessory, may also be identified by immunofluorescence, the most important of this class being lysosome, lactoferrin, tear-specific prealbumin, the secretory component and immunoglobulins (Franklin *et al.*, 1973; Gillette *et al.*, 1980; Janssen & Van Bijsterveld, 1981), or else in cultured transplants of the gland as with the tear glycoproteins (Chao *et al.*, 1980).[14]

BLOOD ORIGIN

The large number of serum proteins found in tears may be assumed to be derived from the blood directly by leakage through the conjunctival capillaries; thus Van Bijsterveld & Janssen (1981) deduced, from the high levels during hyperaemia, and the reduction by application of dobesilate—an agent that reduces capillary permeability—that the blood was the source.

ROLE OF EPITHELIAL DAMAGE

In an exhaustive study of human tear proteins, in which the effects of different sampling methods were compared in order to assess the contribution of epithelial damage, Janssen & Van Bijsterveld (1983) showed that serum albumin was definitely not present in the lacrimal secretion, collected with a glass pipette close to the exit of the lacrimal duct. Thus albumin concentrations were negligible in this fluid whereas they reached levels as high as 1–2 mg/100 ml in fluid collected from the conjunctival fluid by filter-paper. This concentration was too high to be accounted for entirely by epithelial damage, and must have been due to leakage from capillaries.

Lipids

These have been examined by Andrews (1970), Ehlers (1965), and Van Haeringen & Glasius (1975); remarkable is the large concentration of cholesterol (3 to 6.6 mM); as Van Haeringen and Glasius emphasize, it is unlikely that such large concentrations would be derived from the lacrimal gland, especially as the transport requires a β-lipoprotein, the low protein concentration in lacrimal secretion being incompatible with this. It is likely that the cholesterol is derived from the Meibomian secretion, as suggested by Ehlers (1965), who found no evidence of lipids in the lacrimal glands, goblet cells, or glands of Wolfring, whereas the lipids of the Meibomian secretion corresponded with those in the precorneal film.

MEIBOMIAN SECRETION

Tiffany (1979) has described the main lipid constituents of the rabbit's Meibomian secretion; these are limited in number by contrast with the wide variety in human secretion (Tiffany, 1978). In a later study Tiffany & Marsden (1982) have further characterized the lipids from the rabbit secretion; as they point out, the identification of the principal lipids involved in the formation of the tear-film is of great practical importance for understanding the pathology of the cornea caused by defective lipid film, which would promote loss of fluid by evaporation.

Metabolic Enzymes

Van Haeringen & Glasius (1974; 1976a,b) have described a variety of enzymes in human tears, notably the hydrolases associated with breakdown of tissue, such as acid and alkaline phosphatase. It seems likely that when enzymes concerned in carbohydrate metabolism, such as lactate dehydrogenase, are found in the tears collected from the conjunctival sac they are derived from the corneal epithelium through trauma, so that when fluid is collected by a glass cannula these enzymes are absent. The metabolic condition of the cornea varies according to the degree of anoxia it undergoes, and such changes are reflected in the proportion of lactate to malate dehydrogenase activity in tears; thus changes in the ratio are observed diurnally, LDH activity being very high at 6 a.m. after the prolonged lid-closure of sleep (Pullard & Carney, 1984). Moreover, the subunit composition of LDH varies in accordance with metabolic state of the cornea (Kahan & Ottovay, 1975).

LYSOSOMAL ENZYMES

These enzymes, essentially concerned with breakdown of unwanted material, such as alpha-galactosidase, beta-galactosidase, beta-hexosaminidase, beta-glucuronidase, acid phosphatase, alpha-L-fucosidase and alpha-D-mannosidase have been examined by Van Haeringen & Glasius (1976) and Van Hoof *et al.* (1977), and more recently by Kitoaka *et al.* (1985). Lysosomal tear activities were higher than in serum, but otherwise their characteristics were similar.

Drainage of Tears

When the secretion of tears exceeds the loss due to evaporation the excess fluid, if it is not to overflow—

epiphora—must be drained away. The passage for this drainage consists of the *canaliculi*, the *lacrimal sac* and the *naso-lacrimal duct*. The lacrimal *puncta* are the openings of the canaliculi in the lid-borders of the inner canthus; the canaliculi course at first vertically and then more or less horizontally to the lacrimal sac, which is continued inferiorly as the nasolacrimal duct emptying into the inferior meatus of the nose (Fig. 29.7). The sac and the duct may be regarded as essentially a continuous structure, the term 'sac' really applying to *that part of the duct lying within the orbit*. Any theory of the mechanism of conduction of the tears must take into account the common experience that the act of blinking favours drainage and prevents overflow; thus paresis of N VII prevents orbicularis action, and also impairs drainage. Certainly the dimensions of the canaliculi and puncta are so small (about 0.5 mm diameter) as to make it unlikely that an adequate drainage could be maintained by the unassisted action of gravity (siphoning would of course be necessary for the upper canaliculus).

The Lacrimal Pump

The mechanism has been analysed by Jones (1958) and is described by him as the *lacrimal pump*. Essentially the pumping action consists in an alternate negative and positive pressure in the lacrimal sac caused by the contraction of the orbicularis muscle. Because of the anatomical relationships of this muscle, in particular that part called Horner's muscle, to the palpebral ligament and lacrimal sac, contraction during blinking causes a dilatation of the sac. At the same time, the muscular contraction also causes the canaliculi to become shorter and broader. Finally contraction of the orbicularis also tends to invert the lower lid, thus ensuring that the punctum dips in the lacus lacrimalis. Negative pressure in the nose during inhalation, and gravity, are also factors in emptying the sac. However, after Toti's operation, drainage still occurs.

Pressure Changes

Rosengren (1973) emphasized that any mechanism of drainage must take into account two clinical observations, namely that facial paresis, involving loss of action of the orbicular muscles, prevents drainage whilst Toti's operation, dacryocystectomy, allows drainage to continue. Thus an active suction by the lacrimal sac cannot be a requisite. Rosengren inserted a cannula into the sac by way of the nose and connected this to a liquid manometer; the column of fluid in this rose with each blink, indicating a positive pressure; each blink caused expulsion of 1.8 mm^3 of fluid. The rise in pressure was about 7 mmHg. Measurements of the pressure in the cannaliculi revealed a rise with blinking, showing that fluid could be forced into the system by contraction of the canalicular muscle. Rosengren's manometer was of a primitive type, depending on fluid-flow; using a sensitive manometer Maurice (1973) found a steady negative pressure in the sac after passing a cannula through the upper canaliculus; this pressure rose with blinking, suggesting a compression of the sac. The steady negative pressure in the sac between blinking agrees with the observation of Frieberg (1951), confirmed by Rosengren (1973) and Maurice (1973) that, in the absence of blinking, there is a steady flow of tears into the sac, which may be seen in the slit-lamp microscope after introduction of a carbon-particle suspension.[15]

High-speed Cinematography

Reference has been made to Doane's study of the blink in human subjects, using high-speed cinematography when describing the main features of the process. Doane observed the rapid mixing of a drop of fluorescein after a single blink; he considered that mucus would be carried down by the upper lid and moved towards the inner canthus by the lateral movement of the lower lid. In a continuation of this study, Doane (1981) examined the blink with a view to elucidating the mechanism of drainage. He noted that the punctal openings elevated themselves permitting their muscular occlusion before the completion of the blink. Completion of lid-closure would force fluid through the drainage system by compression of the canaliculi and sac. He considered that the elastic expansion of the canaliculi during the opening phase formed a suction holding the lid margins at the punctal region together as the lids open until they broke apart, allowing fluid to be drawn through the puncta. Lemp & Weiler (1983) used a slow-speed (64 versus 500 frames/sec) and studied the movement of black polystyrene microspheres instilled into the sac. The spheres rushed into the puncta immediately on completion of the blink, confirming the negative pressure in the canaliculi; there was some regurgitation. Krebiel-flow was observed. Lemp & Weiler found that the superior punctum could carry out the drainage when the lower one was occluded; this was confirmed with a patient with atresia of the inferior punctum who exhibited no epiphora. Thus, if one wishes to alleviate the signs of keratitis sicca, both puncta must be occluded (Dohlman, 1978; Jones, 1957).

As summarized by Maurice (Fig. 29.14), when tear-flow is stimulated the canaliculi fill quickly with about 2 mm^3 of fluid; after this the negative pressure in the sac assists flow; with a blink the rise in pressure drives the fluid into the lacrimal sac and thence into the nose; probably some sphincter mechanism prevents back-flow into the puncta. Under normal conditions of unstimulated tear-flow, the small amount of fluid secreted is sucked into the puncta,

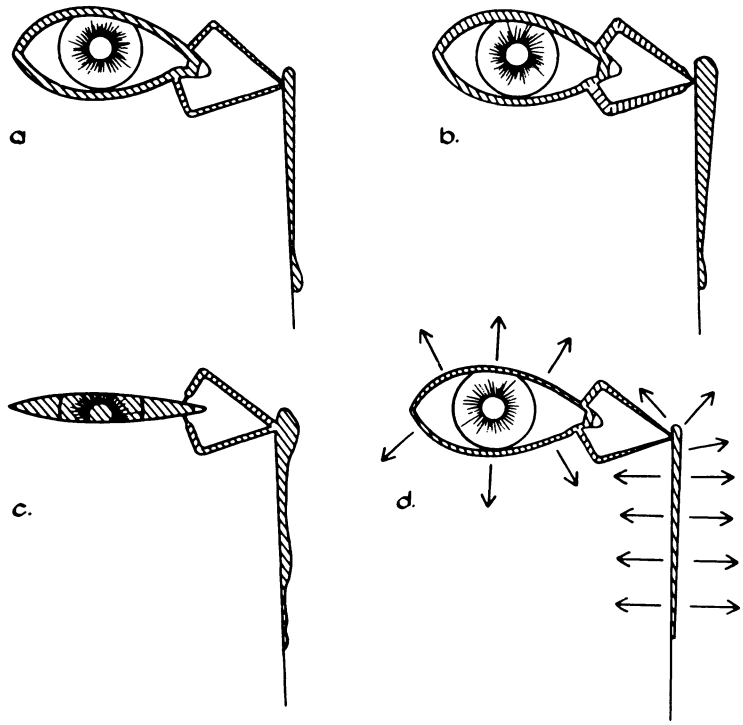

Fig. 29.14 Proposed tear drainage mechanism (a, b and c, tear flow; d, basal lacrimation). (a) Immediately after blink, canaliculi empty. (b) After a brief period, expansion of canaliculi causes them to fill with fluid from lacrimal strip; one-way valve at nasal end prevents regurgitation from sac. When canaliculi are filled, they act as conduits through which sac can imbibe tear fluid directly from lacrimal strip. (c) On blinking, canaliculi squeeze fluid into sac; sphincter or other mechanism obstructs puncta. At same time, sac presses fluid down nasolacrimal duct. (d) During slow lacrimation, fluid largely absorbed over mucosa of conjunctiva and lacrimal system. (Maurice, *Int. Ophthalmic Clinics.*)

and on each blink both the canaliculi and sac expel a little fluid, and the system remains virtually empty at all times.

The Nervous Mechanism

Tears are secreted reflexly in response to a variety of stimuli, e.g. irritative stimuli to the cornea, conjunctiva, or nasal muscosa; thermal stimuli, including peppery foods, applied to the mouth and tongue; bright lights, and so on. In addition it occurs in association with vomiting, coughing and yawning. The secretion associated with emotional upset is described as *psychical weeping*. Section of the sensory root of the trigeminal prevents all reflex weeping, leaving psychical weeping unaffected; similarly the application of cocaine to the surface of the eye, which paralyses the sensory nerve endings, inhibits reflex weeping, even when the eye is exposed to potent tear-gases. The afferent path in the reflex is thus by way of N V. The motor pathway to the main lacrimal gland is more complex.

Parasympathetic

The parasympathetic supply is from the *facial nerve* (N VII); preganglionic fibres arise from the *lacrimal nucleus* in the pons; they run in the *nervus intermedius*, through the *geniculate ganglion* (without relaying), to the *sphenopalatine ganglion* as the *greater superficial petrosal nerve*. Post-ganglionic fibres enter the *zygomatic nerve* and thence the *lacrimal* (Fig. 29.15). The sympathetic pathway is by way of the *deep petrosal nerve* which arises from the cervical sympathetic plexus; it joins the greater superficial petrosal nerve to form the *nerve of the pterygoid canal*, or *Vidian nerve*, which ends in the sphenopalatine ganglion; thence the fibres run with the parasympathetic as described above. Other fibres reach the gland by way of the lacrimal artery.

Nerve Terminals

The nerve terminals in the gland have been examined by Ruskell (1968, 1975) in the monkey and Tsukahara &

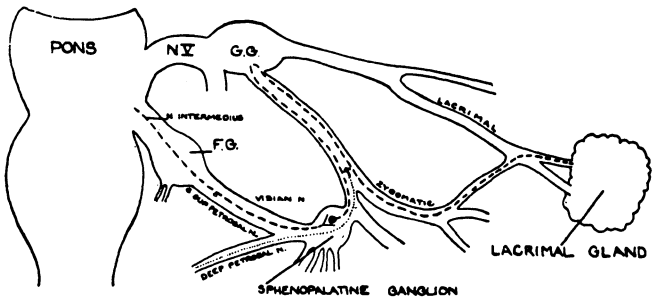

Fig. 29.15 Innervation of the lacrimal gland, G.G., Gasserian ganglion; F.G., facial ganglion. (After Mutch, *Brit. J. Ophthal.*)

Tanishima (1974) in man, with a view to their identification as either adrenergic or cholinergic. Although Tsukahara & Tanishima found catecholamine fluorescence, they were unable to identify the characteristically cored vesicles of adrenergic terminals, and they concluded that, in man, there was little adrenergic innervation. Cholinergic terminals were identified, and these were related to the myoepithelium. In the monkey, Ruskell found both sympathetic and parasympathetic terminals, but the sympathetic innervation seemed to be confined to the interstices of the gland, whilst the parasympathetic fibres ended in relation to acini and ducts, most being adjacent to myoepithelial cells, as in man. If the myoepithelial cells are responsible for forcing the secretion along the ducts, then the fibres ending in relation to these would be responsible for this mechanical aspect of secretion of tears, whilst the actual elaboration in the acini would be controlled by the fibres making relation to acinus cells.[16]

Sympathetic

The function of the sympathetic in the secretion of tears is problematical; section of the superficial petrosal nerve—a procedure often concomitant with operative removal of the Gasserian ganglion—or blocking of the sphenopalatine ganglion, causes a failure of reflex and psychical lacrimation, suggesting that the parasympathetic only is concerned with reflex secretion. Furthermore, there is no apparent interference with weeping as a result of bilateral section of the cervical sympathetic. According to Whitwell (1961), therefore, it is the sympathetic innervation that is responsible for a tonic secretion adequate to keep the eye moist, but the possibility must be considered that the main gland is normally at rest, whilst the accessory glands operate continuously and independently of any innervation. Nevertheless there is some evidence of sympathetic activity in relation to the lacrimal glands.

GUINEA PIG AND RAT

Physiological studies involving adrenergic agonists and stimulation have shown that acinar cells may be stimulated to secrete through the sympathetic; Nikkinen *et al.* (1985) have used a histological fluorescence technique to identify adrenergic terminals in the extra- and intra-orbital glands of the guinea pig and rat. Blood vessels and secretory acini of the guinea pig had a rich innervation, whereas in the rat the innervation was sparse and apparently confined to blood vessels. Ipsilateral extirpation of the superior cervical ganglion eliminated the fluorescence.

Isolated Gland

Protein secretion by the isolated rabbit lacrimal gland was stimulated by both adrenergic and cholinergic agonists; the former were inhibited by propranolol and phentolamine and the latter by atropine. The nature of the proteins secreted in response to these agents seemed to be the same with either type (Bromberg, 1981).

Role in Tear Formation

So far as the actual production of tears is concerned, studies on control of synthesis of specific elements, such as proteins, may not be relevant; the synthetic machinery may be modulated, but the actual secretion of tears, as such, may be independent of sympathetic innervation.

However, Botelho *et al.* (1973) demonstrated increased flow through the cannulated rabbit lacrimal duct in response to adrenergic agonists, the strongest effect being with isoproterenol and the least with noradrenaline; the effects were prevented by beta-blockers. However, in a subsequent paper, Botelho *et al.* (1976) argued that, because the rabbit's acini are not adrenergically innervated, the effects of adrenergic stimulation might be related to blood-flow; electrical stimulation of the preganglionic sympathetic trunk inhibited pilocarpine-induced flow, presumably through vasoconstriction; there was a post-stimulus increase in secretion, presumably due to a reactive vasodilatation.

Vasoactive Intestinal Polypeptide (VIP)

According to Lundberg *et al.* (1981), this neuroactive polypeptide is probably localized in cholinergic neurones controlling exocrine gland activity. Thus it is present in

some 98–99% of the perikarya of neurones in the pterygopalatine ganglion; with removal of the ganglion the choline acetyltransferase and VIP activity of the innervated tissue (nasal mucosa) fall together. Since the activity of VIPergic cells is not blocked by atropine, separate receptors are presumably involved in their activity. Dartt *et al.* (1984) measured the effects of VIP on the protein secretion by isolated acinar cells from the rat lacrimal gland; in concentrations of 1×10^{-10} to 1×10^{-7} M it stimulated synthesis in a dose-dependent manner; the synthesis was also stimulated by carbachol; atropine had no effect on VIP-induced synthesis but did inhibit that stimulated by carbachol. Immunohistochemical examination revealed VIP-reactive nerve fibres throughout the gland, most fibres being associated with the acini.[17]

Substance P

Nikkinen *et al.* (1984) searched for VIP- and Substance-P-fibres in the rat and guinea pig lacrimal glands. They confirmed the presence of VIP-nerve fibres in the lacrimal glands of both species, apparently concentrated around the acini; substance P-fibres were present and dominant around the ducts. It is likely that the substance P-fibres were sensory.

Drugs

As one would expect of a parasympathetic-dominated process, intravenous pilocarpine produces a large and prolonged increase in flow-rate of tears; according to a study of Goldstein *et al.* (1967) there may be an elevenfold increase, in the rabbit, lasting for 33 minutes. Intravenous noradrenaline increased flow in this animal some threefold for two minutes; it inhibited the increased flow due to pilocarpine, however, perhaps because of its vasoconstrictive action.

Crocodile Tears

Some human subjects lacrimate strongly when eating, and the syndrome has been given the name of 'crocodile tears'. The mechanism has been discussed by Golding-Wood (1963), and he concludes that the prime cause is a degeneration of the greater superficial petrosal nerve which provokes sprouting of fibres from the lesser superficial that normally subserves salivary secretion; as a result, the salivary secretory fibres stimulate the lacrimal gland. He found that intracranial section of the glossopharyngeal nerve relieved the condition.

Newborn

Innervation of the lacrimal gland is not always complete at the time of birth; thus Sjögren found a complete lack of reflex secretion of tears in 13% of normal full-term babies and in 37% of premature babies during the first three days of extra-uterine life. Since this condition was not associated with any dryness of the cornea—keratitis sicca—it might be suspected that normally the secretions of the accessory lacrimal glands, which are not involved in reflex secretion, are adequate to keep the cornea moist. This suggestion is supported by the relative absence of corneal symptoms after complete removal of the lacrimal gland. Thus the reflex secretion may be regarded as an emergency response.

Notes

1. Lesions of the facial nerve result in abnormal lid movements during attempted eye closure, when the orbicularis oculis muscle is involved, and normal lid movements with saccadic eye movements, when only the levator palpebrae, innervated by N III, is involved.
2. Collewijn *et al.* (1985) discuss their results in connection with those of Allik *et al.* (1981), where a different method of measuring eye position was employed; the upward eye movements recorded by them might have been a reflection of retraction, the time-course for their change being similar to that for retraction described by Collewijn *et al.* We may note that Hall (1936) examined the eye movement during attempted lid-closure when the lid was held open manually in 1250 normal people. 90% of his subjects showed upward movement. This is consistent with Collewijn *et al.*'s finding that prevention of lid-closure converts a downward into an upward movement.
3. Surface tension is the tendency for the liquid to resist expansion; lipid, on the surface of water, will reduce this resistance to expansion; when the lipid is compressed the tendency to expansion will be greater, and the surface tension is said to be decreased, whilst the surface-pressure, the tendency for the surface to expand, will increase.
4. The value of a mucin derived from bovine submaxillary gland in affecting the contact-angle of a tear solution at the corneal surface was demonstrated by Lemp *et al.* (1970); it was far more effective than tear proteins.
5. The situation with contact lenses has been discussed in detail by Holly & Lemp (1977); they emphasize that the corneal damage is much more likely to be due to interference with the precorneal film under the lens than to oxygen-lack, as originally thought; thus the exchange of tears trapped under the lens by a pump mechanism, driven by the blink, is considered more important than oxygen permeability *per se*. The restraint to renewal of the sub-lens film is imposed by the non-equilibrium meniscus formed at the edge of the lens producing a large 'black line'.
6. Van Haeringen (1981) has reviewed the clinical aspects of the biochemistry of the tears.
7. Boonstra & Kijlstra (1984) have discussed the relative roles of transferrin and lactoferrin in the secretions of different species; thus lactoferrin is the main iron-binding protein of human milk whereas in rabbit and rat milk it is transferrin, considered to be exclusively a serum iron-binding protein. In

the rabbit tears they found transferrin as the main iron-binding protein, by contrast with human tears where lactoferrin is predominant. Ballow *et al.* (1987) have measured the levels of lactoferrin in patients with inflammatory ocular disease; there was a reduced level in vernal conjunctivitis and giant papillary conjunctivitis. The normal concentration was 1.73 ± 0.46 mg/ml. Arnold *et al.* (1977) described the bactericidal effect of lactoferrin.

8. Ford *et al.* (1976) considered that the non-lysozymal factor in tears described by Friedland *et al.* (1972) was beta-lysin, a bactericidal factor found in platelets, serum and other body fluids; they stated that the concentrations of beta-lysin in tears and aqueous humour were greater than that in plasma or serum although there are no platelets in tears or aqueous humour. However, beta-lysin is a peptide of some 2 kd molecular weight; this would be dialysable through commercial membranes, whereas the factor described by Ford *et al.* was said not to be (Selsted & Martinez, 1982).
9. Carroll & Martinez (1979) have shown that in the rabbit, beta-lysin is more important than lysozyme in bactericidal activity.
10. Sapse *et al.* (1969), in a publication from the same laboratory, described seven proteins, identified immunologically, in the tears, emphasizing that one, specific tear prealbumin, was peculiar to tears and absent from serum. They noted, also, that the IgA from tears had a different antigenic moiety from that of serum; other proteins were ceruloplasmin, serum albumin, transferrin, IgG and lysozyme. Subsequent work has shown that transferrin and serum albumin in tears are derived from serum.
11. Franklin *et al.* (1973) have quoted the literature in which the presence of all these immunoglobulins in human tears is described. Gregory & Allansmith (1986) have examined the possibility that the naturally occurring IGA-SC in tears and other external secretions is ultimately derived from a common mucosal immune system through antigen ingestion and stimulation; this appears to be true although local activity induces greater clonal expression and results in higher levels of IGA-SC than if the particular secretory system had not been exposed to the antigen.
12. Iwata & Kabasawa (1971) described three fractions from rabbit lacrimal mucus with molecular weights of about 400, 50 and 14 kd; the carbohydrates were fucose, galactose, *N*-acetylglucosamine and sialic acid; the carbohydrate: protein ratios were 0.10, 0.14 and 0.23, which would be low for mucus-type glycoproteins.
13. Moore & Tiffany (1979) emphasize that the mucus collected from the eye contains the products of the tear glands, so that it is not feasible to use the carbohydrate content of tears to diagnose keratitis sicca; e.g. Dohlman *et al.* (1976) found that the lowering of the sugar levels in tears from dry-eyes patients was insufficient to account for tear-film instability. Thus only about 10% of carbohydrate is in GP3T, the tear glycoprotein, so that a change of mucus production would not be adequately identified by assay of tear carbohydrate.
14. Covey *et al.* (1971) measured the concentrations of lysozyme in tears and serum of human subjects and found no correlation between the two, the serum level varying from 2–14 μg/ml and that in tears from 1100–2200 μg/ml; they concluded from this that lysozyme was synthesized by the gland. Gillette *et al.* (1980) found the same proteins in the main and accessory glands using histological and immunohistological techniques; they remarked that the proteins were in myoepithelial cells, which were also present in the accessory glands; since Ruskell (1975) had shown that the parasympathetic innervation was concentrated at myoepithelial cells, they argued that the accessory gland secretion would also be controlled by the parasympathetic. We may note that Janssen & Van Bijsterveld (1981) have compared four techniques for analysis of tears and recommend the SDS polyacrylamide gel electrophoretic mode of separation.
15. This flow is described as 'Krebiel flow' after its discoverer (Rosengren, 1973). We may note that Frieberg (1951) described the canaliculi and lacrimal sac as a suction-pressure pump; the compressive action of the canaliculi was considered to dominate the situation, the caruncle passively transmitting the contractile effects of the orbicularis muscle to the lumen of the canaliculi.
16. In the sheep's gland Yamauchii & Burnstock (1967) found that the myoepithelial cells covering the acini were very prominent, and bare axons could be seen in grooves on their cytoplasm. These authors suggest that all axons might well be innervating myoepithelial, rather than acinar, cells.
17. Uddman *et al.* (1980) have described the distribution of VIP-reactive neurones in intra- and extra-ocular structures of the cat's eye; they were numerous in the lacrimal glands, and somewhat less numerous in the Harderian and tarsal glands. The nerves surrounded glandular acini and small blood vessels.

References

Allen, M., Wright, P. & Reid, L. (1972) The human lacrimal gland. *Arch. Ophthal.* **88**, 493–497.

Allik, J., Rauk, M. & Leuk, A. (1981) Control and sense of eye movement behind closed eye lids. *Perception* **10**, 39–51.

Andrews, J. S. (1970) Human tear film lipids. I. Composition of the principal non-polar component. *Exp. Eye Res.* **10**, 223–227.

Arnold, R. R., Cole, M. F. & McGhee, J. R. (1977) A bactericidal effect for human lactoferrin. *Science* **197**, 263–265.

Arnold, R. R., Russell, J. E., Champion, W. J., Brewer, M. & Gauthier, J. J. (1982) Bactericidal activity of human lactoferrin: differentiation from the stasis of iron deprivation. *Inf. and Immun.* **35**, 792–799.

Ballow, M., Donshik, P. C., Rapacz, P. & Samarino, L. (1987) Tear lactoferrin levels in patients with external inflammatory ocular disease. *Invest. Ophthal.* **28**, 543–545.

Baum, J. L. (1973) Systemic disease associated with tear deficiencies. *Int. Ophthal. Clinics* **13**, 169–185.

Bell, C. (1823) On the motions of the eye, an illustration of the uses of muscles and nerves of the orbit. *Trans. Roy. Soc. Lond.* **111**, 166–186. (Quoted by Evinger *et al.*, 1984.)

Björk, A. & Kugelberg, E. (1953) The electrical activity of the muscles of the eye and eyelids in various positions and during movements. *E.E.G. Clin. Neurophysiol.* **5**, 595–602.

Bonavida, B., Sapse, A. T. & Sercarz, E. E. (1969) Specific tear prealbumin: a unique lachrymal protein absent from serum and other secretions. *Nature* **221**, 375–376.

Boonstra, A. & Kijlstra, A. (1984) The identification of transferrin, an iron-binding protein in rabbit tears. *Exp. Eye Res.* **38**, 561–567.

Botelho, S. Y., Goldstein, A. M. & Martinez, E. V. (1973) Norepinephrine-responsive beta-adrenergic receptors in rabbit lacrimal gland. *Amer. J. Physiol.* **224**, 1119–1122.

Botelho, S. Y., Martinez, E. V., Pholpramool, C., Van Prooyen,

H. C., Janssen, J. T. & de Palau, A. (1976) Modification of stimulation lacrimal gland flow by sympathetic nerve impulses in the rabbit. *Amer. J. Physiol.* **230**, 80.

Brienen, J. A. & Snell, C. A. R. D. (1969) The mechanism of the lacrimal flow. *Ophthalmologica, Basel* **159**, 223–232.

Broekhuyse, R. N. (1974) Tear lactoferrin: a bacteriostatic and complexing protein. *Invest. Ophthal.* **13**, 550–554.

Bromberg, A. B. (1981) Autonomic control of lacrimal protein secretion. *Invest. Ophthal.* **20**, 110–116.

Brown, S. I. (1973) Dry spots and corneal erosions. *Int. Ophthal. Clin.* **13**(1), 149–156.

Carroll, S. F. & Martinez, R. J. (1979) Role of rabbit lysozyme in *in vitro* serum bactericidal reactions against *Bacterium subtilis*. *Inf. & Immun.* **25**, 810–819.

Chao, C. C. W., Vergnes, J. P. & Brown, S. I. (1983a) Fractionation and partial characterization of macromolecular components from human ocular mucus. *Exp. Eye. Res.* **36**, 139–150.

Chao, C. C. W., Vergnes, J. P. & Brown, S. I. (1983b) O-Glycosidic linkage in glycoprotein isolates from human ocular mucus. *Exp. Eye Res.* **37**, 533–541.

Chao, C.-C. W., Vergnes, J.-P., Freeman, I. L. & Brown, S. I. (1980) Biosynthesis and partial characterization of tear film glycoproteins. Incorporation of radioactive precursors by human lacrimal gland explants. *Exp. Eye Res.* **30**, 411–425.

Collewijn, H., Van den Steen, J. & Steinman, R. M. (1985) Human eye movements associated with blinks and prolonged eye closure. *J. Neurophysiol.* **54**, 11–22.

Covey, W., Perillie, P. & Finch, S. C. (1971) The origin of tear lysozyme. *Proc. Soc. Exp. Biol. Med.* **137**, 1362–1363.

Dartt, D. A., Baker, A. K., Vaillant, C. & Rose, P. E. (1984) Vasoactive intestinal polypeptide stimulation of protein secretion from rat lacrimal gland acini. *Amer. J. Physiol.* **247G**, 502–509.

Doane, M. G. (1980) Interaction of eyelids and tears in corneal wetting and the dynamics of the normal human eyeblink. *Amer. J. Ophthal.* **89**, 507–516.

Doane, M. G. (1981) Blinking and the mechanics of the lacrimal drainage system. *Ophthalmology* **88**, 844–851.

Dohlman, C. H. (1978) Punctal occlusion in keratoconjunctivitis sicca *Ophthalmology* **85**, 1277–1281.

Dohlman, C. H., Friend, J., Kalevar, V., Yagoda, D. & Balazs, E. (1976) The glycoprotein (mucus) content of tears from normals and dry eye patients. *Exp. Eye Res.* **22**, 359–365.

Ehlers, N. (1965) The precorneal film. *Acta Ophthal., Kbh.* Suppl. 81.

Ehlers, N., Kessing, S. V. & Norn, M. S. (1972) Quantitative amounts of conjunctival mucous secretion and tears. *Acta Ophthal.* **50**, 210–213.

Esteban, A. & Salinero, E. (1979) Reciprocal reflex activity in ocular muscle implications in spontaneous blinking and Bell's phenomenon. *Eur. Neurol.* **18**, 157–165.

Evinger, C., Shaw, M. D., Pech, C. K., Manning, K. A. & Baker, R. (1984) Blinking and associated eye movements in human, guinea pigs and rabbits. *J. Neurophysiol.* **52**, 323–339.

Falbe-Hansen, E., Jensen, O. A. & Degn, J. K. (1969) Mucosubstances of the acini of the human lacrimal gland (orbital portion). II. Biochemical identification. *Acta Ophthal.* **47**, 620–624.

Fleming, A. (1922) On a remarkable bacteriolytic element found in tissues and secretions. *Proc. Roy. Soc. B* **93**, 306–317.

Ford, L. C., De Lange, R. J. & Petty, R. W. (1976) Identification of a nonlysozymal bactericide factor (beta lysin) in human tears and aqueous humor. *Amer. J. Ophthal.* **81**, 30–33.

Franklin, R. M., Kenyon, K. R. & Tomasi, T. B. (1973) Immunohistologic studies of human lacrimal gland: localization of immunoglobulins, secretory component and lactoferrin. *J. Immunol.* **110**, 984–992.

Frieberg, T. (1951) Uber den Anteil des Tränensackes und der Caruncula lacrimalis am Tränenabflussmechanismus. *Ophthalmologica* **122**, 193–206.

Friedland, B. R., Anderson, D. R. & Forster, R. K. (1972) Nonlysozyme antibacterial factor in human tears. *Amer. J. Ophthal.* **74**, 52–59.

Gachon, A. M., Verrelle, P., Betail, G. & Dastugue, B. (1979) Immunological and electrophoretic studies of human tear proteins. *Exp. Eye Res.* **29**, 539–553.

Giardini, A. & Roberts, J. R. E. (1950) Concentration of glucose and total chloride in tears. *Br. J. Ophthal.* **34**, 737–743.

Gilbard, J. P. & Darth, D. A. (1982) Changes in rabbit lacrimal fluid osmolarity with flow rate. *Invest. Ophthal.* **23**, 804–806.

Gillette, T. E., Allansmith, M. R., Greiner, J. V. & Janusz, M. (1980) Histologic and immunohistologic comparison of main and accessory lacrimal tissue. *Amer. J. Ophthal.* **89**, 724–730.

Ginsborg, B. L. & Maurice, D. M. (1959) Involuntary movements of the eye during fixation and blinking. *Brit. J. Ophthal.* **43**, 435–437.

Golding-Wood, P. H. (1963) Crocodile tears. *Br. med. J.* (i), 1518–1521.

Goldstein, A. M., de Palau, A. & Botelho, S. Y. (1967) Inhibition and facilitation of pilocarpine-induced lacrimal flow by noradrenaline. *Invest. Ophthal.* **6**, 498–511.

Gregory, R. L. & Allansmith, M. R. (1986) Naturally occurring IgA antibodies to ocular and oral microorganisms in tears, saliva and colostrum: evidence for a common mucosal immune system and local immune response. *Exp. Eye Res.* **43**, 739–749.

Hall, A. J. (1936) Some observations on the acts of closing and opening the eyes. *Brit. J. Ophthal.* **20**, 257–295.

Holly, F. J. (1973) Formation and rupture of the tear film. *Exp. Eye Res.* **15**, 515–525.

Holly, F. J. & Lemp, M. A. (1977) Tear physiology and dry eyes. *Survey Ophthal.* **22**, 69–87.

Iwata, S. & Kabasawa, I. (1971) Fractionation and chemical properties of tear mucoids. *Exp. Eye Res.* **12**, 360–367.

Janssen, P. T. & Van Bijsterveld, O. P. (1981) Comparison of electrophoretic techniques for the analysis of human tear fluid proteins. *Clin. Chim. Acta* **114**, 207–218.

Janssen, P. T. & Van Bijsterveld, O. P. (1983) Origin and biosynthesis of human tear fluid proteins. *Invest. Ophthal.* **24**, 623–630.

Jensen, O. A., Falbe-Hansen, I., Jacobsen, T. & Michelsen, A. (1969) Mucosubstances in the acini of the human lacrimal gland (orbital portion). I. Histochemical identification. *Acta Ophthal.* **47**, 605–619.

Jones, L. T. (1957) Epiphora. II. Its relation to the anatomie structures and surgery of the medial canthal region. *Amer. J. Ophthal.* **43**, 203–212.

Jones, L. T. (1958) Practical fundamental anatomy and physiology (of lacrimal apparatus). *Trans. Am. Acad. Ophthal.* **62**, 669–678.

Jordan, A. & Baum, J. (1980) Basic tear-flow. Does it exist? *Ophthalmology* **87**, 920–930.

Kahan, I.-L. & Ottovay, E. (1975) The significance of tears' lactate dehydrogenase in health and external eye diseases. *v. Graefes Arch. Ophthal.* **194**, 267–276.

Kennard, D. W. & Smyth, G. L. (1963) The causes of downward eyelid movement with changes of gaze, a study of the physical factors concerned. *J. Physiol.* **166**, 178–190.

Kijlstra, A., Jeenssen, S. H. M. & Koning, K. M. (1983). Lactoferrin levels in normal human tears. *Brit. J. Ophthal.* **67**, 199–202.

Kijlstra, A., Jeenssen, S. H. M. & Koning, K. M. (1984) Comp-

lement inhibitors in tears of different species. *Exp. Eye Res.* **38**, 57–62.
Kijlstra, A. & Veerhuis, R. (1981) The effect of an anticomplementary factor on normal human tears. *Amer. J. Ophthal.* **92**, 24–27.
Kitaoka, M., Nakazawa, M. & Hayasaka, S. (1985) Lysosomal enzymes in human tear fluid collected by filter paper strips. *Exp. Eye Res.* **41**, 259–265.
Kreuger, J., Sokoloff, N. & Botelho, S. Y. (1976) Sialic acid in rabbit lacrimal gland fluid. *Invest. Ophthal.* **15**, 479–481.
Krogh, A., Lund, C. G. & Pedersen-Bjergaard, (1945) The osmotic concentration of human lacrymal fluid. *Acta physiol. Scand.* **10**, 88–90.
Kühnel, W. (1968) Menschliche Tränendrüse. *Z. Zellforsch.* **89**, 550–572.
Lemp, M. A., Holley, F. J., Iwata, S. & Dohlman, C. H. (1970) The precorneal tear film. I. Factors in spreading and maintaining a continuous tear film over the corneal surface. *Arch. Ophthal.* **83**, 89–94.
Lemp, M. A. & Weiler, H. H. (1983) How do tears exit? *Invest. Ophthal.* **24**, 619–622.
Liakos, G. M., Goulding, N. & Seal, D. V. (1984) Normal tear protein profiles and age-related changes. *Brit. J. Ophthal.* **68**, 316–320.
Lundberg, J. M., Ånggård, A., Emson, P., Fahrenkrug, J. & Hökfelt, T. (1981) Vasoactive intestinal polypeptide and cholinergic mechanisms in cat nasal mucosa: studies on choline acetyltransferase and release of vasoactive intestinal polypeptide. *Proc. Nat. Acad. Sci.* **78**, 5255–5259.
Masson, P. L., Heremans, J. F. & Dive, C. (1964) An iron-binding protein common to many external secretions. *Clin. Chim. Acta* **14**, 735–739.
Masson, P. L., Heremans, J. F. & Schonne, E. (1969) Lactoferrin, an iron-binding protein in neutrophilic leukocytes. *J. Exp. Med.* **130**, 643–656.
Maurice, D. M. (1973) The dynamics and drainage of tears. *Int. Ophthal. Clinics* **13**, 103–116.
McClellan, B. H., Whitney, C. R., Newman, L. P. & Allansmith, M. R. (1973) Immunoglobulin in tears. *Amer. J. Ophthal.* **76**, 89–101.
McDonald, J. E. & Brubaker, S. (1971) Meniscus-induced thinning of tear films. *Amer. J. Ophthal.* **72**, 139–146.
Miles, W. R. (1931) Elevation of the eye-balls on winking. *J. Exp. Psychol.* **14**, 311–332.
Mishima, S., Gasset, A., Klyce, S. D. & Baum, J. L. (1966) Determination of tear volume and tear flow. *Invest. Ophthal.* **5**, 264–276.
Mishima, S. & Maurice, D. M. (1961) The oily layer of the tear film and evaporation from the corneal surface. *Exp. Eye Res.* **1**, 39–45.
Moore, J. C. & Tiffany, J. M. (1979) Human ocular mucin. Origins and preliminary characterization. *Exp. Eye Res.* **29**, 291–301.
Moore, J. C. & Tiffany, J. M. (1981) Human ocular mucus. Chemical studies. *Exp. Eye Res.* **33**, 203–212.
Mutch, J. R. (1944) The lacrimation reflex. *Br. J. Ophthal.* **28**, 317–336.
Nichols, B. A., Chiappino, M. L. & Dawson, C. R. (1985) Demonstration of the mucous layer of the tear film by electron microscopy. *Invest. Ophthal.* **26**, 464–473.
Nichols, B., Dawson, C. R. & Togni, B. (1983) Surface features of the conjunctiva and cornea. *Invest. Ophthal.* **24**, 570–576.
Nikkinen, A., Lehtsalo, J. I., Uusitalo, H., Palkama, A. & Panula, P. (1984) The lacrimal glands of the rat and the guinea pig are innervated by nerve fibers containing immunoreactivities for substance P and vasoactive intestinal polypeptide. *Histochemistry* **81**, 23–27.
Nikkinen, A., Uusitalo, H., Lehtosalo, J. I. & Palkama, A. (1985) Distribution of adrenergic nerves in the lacrimal glands of guinea-pig and rat. *Exp. Eye Res.* **40**, 751–756.
Ponder, E. & Kennedy, W. P. (1928) On the act of blinking. *Quart. J. exp. Physiol.* **18**, 89–110.
Pullard, R. J. & Carney, L. G. (1984) Diurnal variation in human tear enzymes. *Exp. Eye Res.* **38**, 15–26.
Reid, L. & Clamp, J. R. (1978) The biochemical and histological nomenclature of mucus. *Brit. Med. Bull.* **34**, 5–8.
Riggs, L. A., Kelly, J. P., Manning, K. A. & Moore, R. K. (1987) Blink-related eye movements. *Invest. Ophthal.* **28**, 334–342.
Rosengren, B. (1973) On lacrimal drainage. *Ophthalmologica* **164**, 409–421.
Rushworth, G. (1962) Observations on blink reflexes. *J. Neurol. Neurosurg. Psychiat.* **25**, 93–108.
Ruskell, G. L. (1968) The fine structure of nerve terminations in the lacrimal glands of monkeys. *J. Anat.* **103**, 65–76.
Ruskell, G. L. (1969) Changes in nerve terminals and acini of the lacrimal gland and changes in secretion induced by autonomic denervation. *Z. Zellforsch.* **94**, 261–281.
Ruskell, G. L. (1975) Nerve terminals and epithelial cell variety in the human lacrimal gland. *Cell Tiss. Res.* **158**, 121–136.
Sapse, A. T., Bonavida, B., Stone, W. & Secarz, E. E. (1969) Immunoelectrophoresis in human tears. I. Immunoelectrophoretic patterns. *Arch. Ophthal.* **81**, 815–819.
Schirmer, O. (1903) Studien zur Physiologie und Pathologie der Tränenabsonderung und Tränenabfuhr. *v. Graefes' Arch. Ophthal.* **56**, 197–291.
Scott, B. L. & Pease, D. C. (1959) Electron microscopy of the salivary and lacrimal glands of the rat. *Amer. J. Anat.* **104**, 115–161.
Selsted, M. E. & Martinez, R. J. (1982) Isolation and purification of bactericides from human tears. *Exp. Eye Res.* **34**, 305–318.
Sewall, E. C. (1933) Decompression of the facial nerve. *Arch. Otolaryngol.* **18**, 746–752.
Shaw, M. D. & Baker, R. (1983) Direct projections from vestibular nuclei to facial nucleus in cats. *J. Neurophysiol.* **50**, 1265–1280.
Sjögren, H. (1955) The lacrimal secretion in newborn, premature and fully developed children. *Acta ophthal. Kbh.* **33**, 557–560.
Sørensen, M. & Sørensen, S. P. L. (1939) The proteins in whey. *C. R. Trans. Lab. Carlsberg* **23**, 55.
Tada, H. (1978) Spontaneous blinking during a visual tracking performance. *Fukushima J. Med. Sci.* **25**, 91–100.
Tiffany, J. M. (1978) Individual variations in human meibomian lipid composition. *Exp. Eye Res.* **27**, 289–300.
Tiffany, J. M. (1979) The Meibomian lipids of the rabbit. I. Overall composition. *Exp. Eye Res.* **29**, 195–202.
Tiffany, J. M. & Marsden, R. G. (1982) The Meibomian lipids of the rabbit. II. Detailed composition of the principal esters. *Exp. Eye Res.* **34**, 601–608.
Tsukahara, S. & Tanishima, T. (1974) Adrenergic and cholinergic innervation of the human lacrimal gland. *Jap. J. Ophthal.* **18**, 70–77.
Ubels, J. L., Foley, K. M. & Rismondo, V. (1986) Retinol secretion by the lacrimal gland. *Invest. Ophthal.* **27**, 1261–1268.
Ubels, J. L. & MacRae, S. M. (1984). Vitamin A is present as retinol in the tears of rabbits and humans. *Curr. Eye Res.* **3**, 815–822.
Uddman, R., Alumets, J., Ehinger, B., Hakanson, R., Loren, I. & Sundler, F. (1980) Vasoactive intestinal peptide nerves in ocular and orbital structures of the cat. *Invest. Ophthal.* **19**, 878–885.
Van Bijsterveld, O. P. & Janssen, P. T. (1981) The effect of calcium dobesilate on albumin leakage of the conjunctival vessels. *Curr. Eye Res.* **1**, 425. (Quoted by Janssen & Van Bijsterveld, 1983.)

Van Haeringen, N. J. (1981) Clinical biochemistry of tears. *Survey Ophthal.* **26**, 84–96.

Van Haeringen, N. J. & Glasius, E. (1974) Lactate dehydrogenase in tear fluid. *Exp. Eye Res.* **18**, 345–349.

Van Haeringen, N. J. & Glasius, E. (1975) Cholesterol in human tear fluid. *Exp. Eye Res.* **20**, 271–274.

Van Haeringen, N. J. & Glasius, E. (1976a) The origin of some enzymes in tear fluid, determined by comparative investigation with two collection methods. *Exp. Eye Res.* **22**, 267–272.

Van Haeringen, N. J. & Glasius, E. (1976b) Characteristics of acid hydrolases in human tear fluid. *Ophthalmic Res.* **8**, 367–373.

Van Hoof, F., Libert, J., Aubert-Tulkens, G. & Serra, M. V. (1977) The assay of lacrimal enzymes and the ultrastructural analysis of conjunctival biopsies. *Metab. Pediatr. Ophthalmol.* **1**, 165–171.

Van Horn, D. L., Schutten, W. H., Hyndiuk, R. A. & Kurz, P. (1980) Xerophthalmia in vitamin-deficient rabbits. *Invest. Ophthal.* **19**, 1067–1079.

Veerhuis, R. & Kijlstra, A. (1982) Inhibition of hemolytic complement activity by lactoferrin in tears. *Exp. Eye Res.* **34**, 257–265.

Volkmann, F. C., Riggs, L. A., Ellicott, A. G. & Moore, R. K. (1982) Measurement of visual suppression during opening, closing and blinking of the eye. *Vision Res.* **22**, 991–996.

Volkmann, F. C., Riggs, L. A. & Moore, R. K. (1980) Eye blinks and visual suppression. *Science* **207**, 900–902.

Whitwell, J. (1961) Role of the sympathetic in lacrimal secretion. *Br. J. Ophthal.* **45**, 439–445.

Yamamoto, G. K. & Allansmith, M. R. (1979) Complement in tears from normal humans. *Amer. J. Ophthal.* **88**, 758–763.

Yamauchii, A. & Burnstock, G. (1967) Nerve-myoepithelium and nerve-glandular epithelium contacts in the lacrimal gland of the sheep. *J. Cell Biol.* **34**, 917–919.

Zee, D. S., *et al.* (1983) Blink-saccade synkinesis. *Neurology* **33**, 1233–1236.

INDEX*

Abducena nerve 5, 685
ISPSs in 704
nucleus 687, 705
unit discharges in saccade 691
Abduction 648, 650
by obliques 651
Aberrations
accommodation and 778
pupil and 754
Abnormal retinal correspondence 483[5]
Absolute threshold 271
quantum absorption and 273
relation to rhodopsin 265
summation and 274
Absorption spectrum 259
compared with scotopic sensitivity 239
of cones 255, 407
oil-droplets and 255
variability of 254–259
AC/A ratio 785[2]
A-cell 540
Accessory cone 412
Accessory lacrimal glands 792
Accessory optic system 487
and cerebellum 725
Accommodation 767–781
amplitude of 767
effect of age on 771–775
control model 778
and convergence 783
cortical influence 777
depth perception and 462
fluctuations of 779
hypermetropia and 216, 768
nervous mechanisms 776
optics of 216
presbyopia and 771
relative amplitude of 784
resting position of 779
stimulus to 777
Accommodative convergence 783
Acetazolamide (Diamox)
effects on i.o.p. and aqueous secretion 34
combined with forskolin 72
local action of 38
Acetylcholine
as amacrine transmitter 345–346
effect on cortical neurones 553
effect on extraocular muscles 671
effect on LGN 508
effect on pupil 762
effect on vascularization 131
release from retina 346
Acetylcholinesterase, in retina 345, 346
Actin
in lens epithelium 166
in meshwork 79
Action potentials 279
cortical cells 531
flicker fusion and 279
ganglion cells 282, 286
LGN 496
Limulus fibres 281
relation to generator potential 281
superior colliculus 707
wavelength discrimination and 411
Action spectra, cones 408
Action time 276
Active transport
aqueous and 31
cornea and 112
lens and 146
out of eye 37
potentials 32
Adaptation
alpha- 426
beta- 426
colour and 227, 440
contralateral threshold and 481
ERG and 314
field 437
flicker and 366
foveal 426
grating 382
line orientation 382
visual acuity and 374
see also Dark-adaptation, Light-adaptation
Adaptation pool 438
Adducting prism 658
Adduction 648, 650
due to superior and inferior recti 651
Adenylate cyclase
effect of alpha- and beta-agonists on 71
in iris-ciliary body 67, 72, 78
Adrenaline (epinephrine)
effect on i.o.p., etc 68
effect on pupil 763
see also Epinephrine
Adrenergic drugs
effect on ciliary muscle 776
effect on i.o.p. 68
effect on pupil 763
Adrenergic receptors 66
Aequorin, in Ca^{2+}-assay 301[7]
Aerial perspective 459
After-colours 228
After-images 227
apparent movement of 455
torsion and 654
After-nystagmus 677
Ageing of lens 167–173
refractive power and 770–776
proteins and 157, 167–173
Albumin, penetration into ciliary body 23
Albuminoid 155
Aldimines 243
Alignment
binocular 463
of dots 378
All-*trans* retinal 244, 247
Alpha-crystallin 159–163
changes during development 160, 168
LM and HM 159, 170
molecular weight 160
neoproteins 162
newly synthesized 163
percentage of total protein 155
phylogeny and 160
quaternary structure 160
subunits 159
post-translational changes 160, 169
reassembly 162
shortened 169
Alpha$_m$-crystallin 162
Amacrine cells 205
accumulation of 5-HT 350
bipolar connections in cat 353
directional sensitivity and 348
dopamine and 347
GABA and 346
glycine and 346
responses in 286, 312
rod pathway to 353
surround to ganglion cell and 339
transmitters of 345–347
triad and 337
types in cat 340
Ambiguous figures 450
Amblyopia ex anopsia 603
astigmatism and 623[11]
Amino acids
aqueous humour 19, 20
lens 20
transport in 154
vitreous 20, 28
2-Amino-5-phosphonovaleric acid 343
Amphibian cornea 117
lens 147
Amplitude of accommodation 767
cat's 770

*Superior numbers after page numbers refer the reader to the note on that page.

Amplitude of accommodation – *cont.*
change with age 771
relative 784
Amplitude of convergence 658
Ampulla 677
electrical stimulation of 699
Ampullipetal flow 679
Anaerobiosis, on lens 154
Angiogenic factor 101
Angiogenic inhibitor 101
Angle of anterior chamber 10–15
Ångström unit 218^{1}
Angular aqueous plexus 14
Angular meshwork 15
Anion pump
ciliary 33–35
corneal 117
pigment epithelium 37
Aniseikonia 467, 475
Annulospiral endings 672
Anomaloscope 406
Anomalous contour 474
Anomalous trichromat 405, 407
Anterior aqueous humour 27
Anterior chamber 3
Anterior ciliary arteries 7, 10, 16, 18
Anterior ciliary veins 8, 10
Anterior epithelium of iris 30
Anterior pretectal nucleus 758
Anteromedian nucleus of oculomotor complex 760
Anticipatory cortical neurones 713
Antidirectional neurones 719
Antidromic pupilloconstriction, capsaicin and SP 764
Antiprotease 101
Antitrypsin factor 101
APB 343
block of AcCh release 346
block of ON-pathway 344
Aperture colour 451
apo-RBP 253
Apparent movement 482
Apparently horizontal meridian 456
Apparently vertical meridian 456
Applanation tonometer 49
Apractognosia 745^{35}
Aqueous humour 3–48
anterior and posterior 7, 27
dynamics of 26
chemical composition of 18, 27
drainage of 10–46
primary 23
proteins of 18, 23
secretion of 31–38
rate of 39
adrenergic agents on 69
diurnal variations of 39
pilocarpine on 75
volume of 7, 40
Aqueous veins 40
Arachidonic acid 56
Area of test-field
effect on c.f.f. 368
effect on dark-adaptation curve 264
effect on threshold 275
Area 6, superior colliculus projection to 630
Area 6a 717
Area 7 717
Area 7a (PG) 719
blinking and 720
self-induced movement and 721
Area 8 (frontal eye fields) 712
ablation of 713, 717
afferent projection to 717
comparison with posterior parietal cortex 721
effect of stimulation on eye movements 712
projections from 716
projections to colliculi 630, 640^{3}
responses before saccades 713
routes to motor neurones 716
stimulation of 715
tectal projection via dorsolateral nucleus of pulvinar 640^{3}
unit discharges in 713
visual responses in 713
Area 17 (striate area, V1) 515
cortical projections from 523–525
lesions and eye movements 717
LGN projection 520–523
monocular and binocular segments 618
pattern discrimination 585
projection to pulvinar 635
retinal projection 516
role in binocular perception 560
stereopsis and 568
tuned excitatory cells 565
unit discharges in 531 *et seq.*
X- and Y-cell dichotomy 523
Area 18 (parastriate, V2)
cell types 541
cortical projections to 523–525
effects on LGN neurones 510^{18}
LGN projection to 520
meridians and 525
movement-sensitive neurones 512, 585
near-and-far cells 565
pathway to V4 and V5 526
projection to pons and cerebellum 639
projection to pulvinar 635
role in binocular perception 560, 565
Area 19 (peristriate, V3)
cortical projections to 523–525
effect on LGN neurones 510^{18}
meridian and 525
projection of LGN to 520
response features of neurones 542
Areas V4 and 4A 526
colour coding in 566
form selectivity 572
Arrestin 298
Arterial pressures in eye 16
effect on i.o.p. 51
Ascorbate
accumulation in aqueous 20, 27
concentration in aqueous after PG 60
related to H_2O_2 183
species variations 22
concentration in lens 145
cataractous 180
concentration in retina 21
Aspartate
effect on adaptation 268
on ERG 316
transmitter action 343, 344
Asymmetrical convergence 659
unit discharges in 692
Asymmetry potential of lens 150
ATP, effect on photoactivation 298
ATPase
ciliary epithelial 34
vanadate and 39
corneal 116
and repair 129
lens 152
and cataract 181
Atropine
effect on accommodation 776
effect on i.o.p. 74
effect on pupil 763
Aubert's phenomenon 456
Autokinetic illusion 455
***a*-Wave**, of ERG 314
origin of 377
relation to flicker 363
Axes of rotation 648
Axon terminal, of horizontal cell 310

Bacillary layer 205
Background adaptation 266
Background movement, neurone response to 719, 721
Backward masking 430
Bactericidal glycoprotein 796
Bactericides, in tears 795
Ball-and-socket junctions 144
Ballistic type of movement 689
Balloon cells 173
BAPTA, effect on photocurrent 299
Basal cells of cornea 105
Basal lamina
of cornea 107
epithelial regeneration and 123
of lens 142
of vitreous 96
Basal nucleus of Meynert 553
Basal optic root 488
Basket cells
cerebellar 724
cortical 545
Bathorhodopsin 245
Bathypelagic fishes 255
B-cell 540
Beaded chain filaments 167
Bechterew's nucleus 698
Beer's law 238
Bell's palsy 788
Beta-action
on extraocular muscles 777
on i.o.p. 70, 71
on pupil 763

Beta adaptation 426
Beta adrenergic receptors, analogy with rhodopsin 298
Beta-blockers, and i.o.p. 69
Beta$_1$- and beta$_2$-receptors 66
Beta B_p-crystallin 158
Beta-crystallin 158–159
assembly of subunits 159
changes with age 168, 171
human 159
Philly mouse and 186
subunit composition 158
Beta$_s$-crystallin 157, 169
Beta-ganglion cells 334
mosaic of 376
Beta innervation 672
Beta-naphthaquinone 180
Bezold-Brücke phenomenon 441
Bicarbonate
in aqueous 21
effect of acetazolamide on 35
effect on ciliary potential 33
effect on corneal transport 115
species variations 21
Bicuculline, effects of
on dominance columns 549
on ganglion cells 348, 349, 356[15]
on LGN cells 507
on orientation selectivity 534
on X- and Y-units 554[5]
Bidwell's ghost 228
Bilateral strip, of retinal representation in LGN 494
Binocular alignment 463
Binocular colour mixing 481
Binocular cortical units 558–568
Binocular depth cells 560
Binocular diplopia 462
Binocular fixation 663
Binocular flicker 481
Binocular luminance 479
Binocular matching 226
Binocular movements 656
Binocular parallax 469
Binocular segment, of LGN 618
Binocular threshold 479
Binocular vision 462
Binocular visual acuity 390
Binocularity, and proprioception 689
Bioavailability 122
Biplexiform cell 356[11]
Bipolar cells 205, 208
circuitry 352
flat 337, 339–340, 352
invaginating 338, 352
kainic acid and 344
midget 337
opponent-type responses in 414
responses in 285
surround effects on 286, 311
spatial summation in 354
synapse with receptor 337, 339
Birds, visual pigments 255
Birefringence
of cornea 122
of lens 145
of rods 233
Black line 794
Blind sight 744[31]
Blind spot, cortical representation 554[13]
Blinking 786–791
centre 791
corneal film and 792
drainage of tears and 799
oculomotor relations and 788
posterior parietal cortex and 719, 720
reflexes 790
time-relations of 787
visual suppression and 790
Bloch's law 275
contrast-sensitivity and 390
critical duration 427
Blood–aqueous barrier 22
breakdown of 54–65
morphology of 28–30
Blood-flow
and ascorbate 21
and parasympathetic stimulation 75
and stimulation of N VII 77
and sympathetic stimulation 67
Blood–retinal barrier 24
capillaries and 31
diabetic retinopathy and 25
iodate on 25
PCO_2 on 25
Blood–vitreous barrier 24
Blue mechanisms 401
in tritanope 405
Bode plots 685
Borohydride reaction 248, 249
Bow zone 140, 142
Bowman's membrane 105, 107, 110
Bradykinin, corneal vascularization and 131
Breakdown of blood–aqueous barrier 54–65
laser and 56
methods of study 56
morphology of 63
nitrogen mustard and 54
osmotic 65
paracentesis and 55
parasympathetic and 64
polyphloretin and 55
prostaglandins and 56
sympathetic and 58
Break-up time 793
Brewster stereoscope 468
Brightness enhancement 432
Brightness summation 480
Brisk ganglion cells 328
Broca–Sulzer effect 429
Bromacetazolamide 38
Bruch's membrane 4, 7, 754
composition of 26
Bunsen–Roscoe law 276
Burst discharge
of abducens unit in saccade 691
cerebellar 726
and motor error 695
Burst neurones (EBN) 737
in PPRF 693, 694
in prepositus hypoglossi nucleus 697
***b*-Wave of ERG** 315
flicker and 363
P II and 315

Cadaverine, release by receptors 344
Calcitonin gene-related polypeptide 58
Calcium
in aqueous 19, 20, 27
drainage facility and 46
hyperpolarizing response and 290, 292, 294
as second messenger in 301[9]
in lens 178
bound 179
cataract and 180
protein synthesis and 180
in tears 795
in vitreous 27
Calcium–ATPase pump 178
effect of selenium on 189
Calcium-free medium, on lens current, etc 152
Calcium oxalate, in cataract 191[32]
Callosal-free zones 528
Calmodulin 178
Caloric nystagmus 682
Calpain in lens 165
Canal of Schlemm 10
comparative anatomy of 14
drainage route and 11–15
endothelium of 13
giant vacuoles in 41
relation to aqueous vein 41
resistance to flow in 45
Canaliculi 791, 800
pressure in 800
Candela 211
Capacitance, lens 149
Capsaicin, pupil and 764
Capsule, lens 139
changes in accommodation 770, 774
with age 774
extracellular space and 146
protein of 163
structure of 145
surface tension of 772
Young's modulus of 773
Carbonic anhydrase
distribution in the eye 81[17]
effect of, on HCO_3^--transport 115
Carbonic anhydrase inhibitors
and aqueous formation 34
local action 38
and corneal pump 114
Cardiac glycosides
effect on corneal pump 112
effect on formation of aqueous 34
effect on lens potential 151
effect on pigment epithelium 36
Carotid ligation 151
Cat
amplitude of accommodation 770
colour discrimination 420[10]
fixation movements 664

Cat – *cont.*
grating acuity 376
minimum visual stimulus 274
retinal circuitry 339
vernier acuity 377
visual cortical areas 526
Catalase
effect of inhibition of 182
in cataract 183
in iris, ciliary body 21
Cataract 173–189
calcium and 178
cold 187
cortical 173
morphology of 173
crystallin synthesis and 181
cysteine and 175
desmosterol and 189
disulphide bonds in 174
enzyme activities in 183
free radicals and 184
galactose 180
glassblowers' 185
glucose in aqueous and 20
glutathione and 182
heriditary 183
ionic concentrations in 178
ischaemic 187
light-scatter and 174
membrane proteins and 175
metabolism and 180
morphology 173
Nakano mouse 185
naphthalene 180
nuclear *vs.* cortical 173
Philly mouse 183
proteins in 173, 174
radiation 183
reversible 187
selenite 189
senile 173
sodium–potassium ATPase and 29
steroid 188
sugar 180
superoxides and 181
toxic 180
traumatic 187
Catecholamines, on i.o.p. 68
Cavernous sinus 7
C-cells 410, 414, 540
Cellular adaptation 270
Cellular RALBP 253
Cellular RBP 253
Cellularity, of corneal endothelium 108
Central artery
of optic nerve 8
of retina 4, 7, 8
Central fovea 208
Central retinal vein 8
Centre of rotation 648
Centre–periphery interaction, psychophysical 432
Centre-surround relations
adaptation and 439
anatomical basis 284
bipolar cell 311
colour and 416
ganglion cells 283, 325
effect of dark-adaption 438
LGN cells 499, 500
mechanism of 438
Centrifugal bipolars 341
Cerebellectomy, and reflex reversal 704
Cerebellum 639, 723
control of eye movements 641^{10}, 723
eye-muscle afferents 725
glomerulus 724
lesions in 729
medial terminal nucleus and 725
muscle stretch and 725
proprioceptive input 730
pupil responses in 762
retino-cortical projections 639
retino-tectal projection 639
stimulation of 726
superior collicular projection 630, 706
vestibular afferents 701
vestibulo-ocular reflex and 743
visual input 725
Cerebral cortex 515
lamination 520
neurone types 521
topography 515
Ceruloplasmin, in tears 795
Chandelier cell 543, 545
Channels in receptors 286, 294
Chemotaxis, PGs and 57
Chief cone 412
Chloride
active transport by cornea 117
blood-aqueous barrier to 26
concentration in aqueous 19–22, 27
concentration in cornea 111
concentration in lens 145, 148
concentration in tears 795
Chlorolabe 405
Cholera toxin 72
Choline acetyltransferase (ChAT), in retina 357^{16}
Cholinergic activity
in cortex 553
in LGN 509
Chondroitin 98
Chondroitin sulphate 108, 109
Choriocapillaris 7
Choroid 3, 4, 7
Choroid plexus 80^{80}
Chromatic aberration
and accommodation 778
and visual acuity 375
Chromaticity chart 224
Chrysopsin 256
Ciliary body 3, 4, 8
structure of 4, 8
Ciliary capillaries 29
Ciliary cleft 5, 15
Ciliary epithelium 9, 10
electrical resistance of 36
junctions of 29
paracentesis and 63
Ciliary ganglion 5, 6
accommodation and 776
pupil and 758
Ciliary muscle 3
anatomy of 768
excised 777
forces of 773
presbyopia and 772
sympathetic innervation of 777
Ciliary nerves 5, 6
Ciliary processes 4, 5
angioarchitecture 17
area of 8
iridial 8
microvasculature of 80^{6}
number of 8
posterior principal 8
site of barrier breakdown 63
Cilium of rod 231, 242
Circadian rhythm 488
of disc-shedding 236
Circle of Zinn (or Haller) 8
Circular fibres, of ciliary muscle 768
Circularvection 732
Circulation, vascular, of eye 15–18
***cis*-2,3-piperidine-carboxylic acid (PDA)**, effect on OFF-pathway 344
11-*cis*-retinal 244
***cis-trans* isomers** 244
Clare–Bishop area
analogy with MT 573, 576
binocularity and 569
callosal projection 528
comparison with V1 577
influence on superior colliculus 634
motion sensitivity in 577
retinotopic organization in 527
subcortical projections to 527
visual cortical connections to 526, 527, 528
Cleft of Fuchs 9
Climbing fibres 724
Clonidine 73, 74
Cloquet's canal 96, 100, 101
Closed loop control 742
Cobalt, effect on horizontal cell responses 309, 343
Co-contraction 688
Co-existence curves 188
Colchicine
resistance to drainage and 47
rod phagocytosis and 235
Cold-cataract 187
Collagen 98
capsular 145
corneal 106, 108, 110
synthesis of 130
vitrosin and 97, 98, 100
Collagen types 110, 120
Collagenase, effect on vitreous 99
Collection efficiency 425
Collectors 10, 11, 15
Colour-coded neurones
cortical 588–597
colour constancy and 597
colour opponence 589
colour tuning 589
columnar organization 593
complex cells 592
geniculate fibres compared 590

hypercomplex cells 593
laminar distribution 592, 594
ON-OFF spectral sensitivity 591
V4 neurones 595
ganglion 330, 416, 417
geniculate 587
and superior colliculus 631
Colour coefficients 224
Colour constancy 450
Colour conversion 450
Colour defectiveness 402
anomalous trichromats 405, 407
artificial 440
dichromats 403
monochromats 402
Colour matching 223, 399
adaptation and 440
binocular 481
dichromat's 403
foveal 442
Colour-opponent neurones
cortical 589
ganglion 416
horizontal cell 413
LGN 587
Colour stereoscopy 481
Colour-tuned units 589
Colour vision 221, 395
abnormalities of 402
adaptation and 227
cone pigments and 408
cone responses and 397
electrophysiology of 409, 587–590
evolutionary significance of 409
Hering theory 418
oil-droplets and 255, 411
S-potentials and 410
trivariance of 399
Young–Helmholtz theory 399
Columnar organization of cortical neurones 546–551
colour-coding and 593
spatial frequency and 585
Competition between eyes 604, 620
Complement, in tears 797
Complementary colours 224
contrast and 226
Complex (CX) cells 532
collicular units and 634
definition of 539
directional sensitivity of 536
effect of textured background on 539
orientation tuning 533
pyramidal cells as 543
spatial frequency tuning in 584
Complex stimuli, and superior colliculus 632
Compound eye 279
Compression of response 267
Concavalin A 126, 133[18]
Concealed opponence 418
Conductance
cGMP on 293
light-sensitive 289, 291
Conduction velocity, of ganglion cells 329, 330, 355
Cone(s) 205
absorption spectra of 407
coupling of 305, 411
density and visual acuity 376
diameter of 374
disc, renewal of 236
distribution in retina 208
double 412
electrical stimulation of 312
hyperpolarizing response in 288, 293
mechanisms 401
pedicle 206
pigments of 408, 409
receptive fields of 305
spectral sensitivity curves of 397, 411
structure 236
threshold 397
total number of 210
visual pigments of 255
Cone-bipolar cells 339, 352, 353
connections to ganglion cells 353
Cone–cone interactions 307
Cone-ERP 320
Cone monochromat 402
Conger eel visual pigment 255
Conjugate eye movements 656
Conjugate innervation 656
Conjunctiva 4
goblet cells of 492
Conjunctival cells, and corneal epithelium renewal 124
Conjunctival plexus 10
Conjunctival sac 4
Connecting cilium 231–232, 242
Conoid shape of lens 769
Consensual light reflex 755
Constancy
colour 450
tone 451
Constant depth columns 559
Constant direction columns 559
Constant velocity neurones 744[20]
Contact lens, effect on cornea 123, 803[5]
Contour effects 433
Contralateral effects on i.o.p. 70
Contrast 380
meta- 427
simultaneous 226, 432
successive 226, 427
Contrast ratio 380
Contrast-sensitivity 381
adaptation to gratings and 382
bar length and 384
exposure time and 388, 389, 583
ganglion cell and 580
LGN units and 503
compared with cortex 582
monkeys and 582, 583
velocity of motion and 384
Contrast-temporal frequency function 503
Convergence
accommodation and 783, 784
amplitude of 658
darkness and 785
depth perception and 465
far point of 657
near point of 657
rolling and 660
speed of 663
symmetrical 659
Converging power 657
Cornea 3, 105–132
amphibian 117
anion transport across 35
sulphonamides and 35
ATPase of 116
chemistry of 108
corpuscles 105
development of 108
endothelium 107
cellularity of 108
permeability of 111
potential and fluid transport across 114, 115
pump 112
regeneration of 105
removal of 111
resistance of 114
epithelium 105
effect of removal 11, 117
permeability of 111
regeneration of 124–127
fibrils 106
hydration 110
innervation 131
lamellae 106
metabolism 122
oxygen tension of 123
permeability of 118
potential 112, 117
stroma 105
structure 105
swelling 110
tear film of 792
transparency 122
vascularization 130
Corneal reflex 791
Corneoscleral meshwork 11, 12
Corona ciliaris 4
Coronary tract 100
Corpus callosum 527
connections through 527
relation to stereopsis 540
section of 561, 568
critical period and 568
single units of 569
Corpus cerebelli 723
Corrective fusion movements 675, 677
Corresponding circle of sensation 471
Corresponding points 465
definition of 470
determination of 470
Corrugator supercilii 786, 787
Cortex
cerebral 515
lens 141
Cortical architecture 546
Cortical barrels 554[14]
Cortical cataract 173
Cortical control, of eye movements 711
Cortical magnification factor 517
relation to visual acuity 385
Cortical module 519
Cortical neurones 521, 531–641

Cortical neurones – *cont.*
binocular 558
classification of 539
colour-coding of 588–597
columnar organization of 545
contrast-sensitivity functions 582
directional sensitivity 533–536
discharge centres 537
laminar organization of 520
LGN input to 540, 541
orientation selectivity 531
receptive fields 531
borders defined 537
end-stopping 532–545
structural correlates of 543
stereopsis and 559–568
velocity tuning of 536, 541
visual deprivation and 603–621
X-, Y-dichotomy 544
Cortical zone of vitreous 100
Cortico-pulvinar projection 630
Cortico-tectal projection 630
Cortico-thalamo-cortical loop 639
Corticosteroids, effect on i.o.p. 78
Coupling
between cones 305, 411
between rods 290, 305
Cribriform meshwork 14
Crista acustica 677
Crista ampullaris 677, 680
Critical duration, for summation 276
Critical fusion frequency 362
light–dark ratio and 369
Critical intraocular pressure 54
Critical period 605
corpus callosal section and 568
for loss of binocularity through N V section 689
for retinal disparity changes 609
for reversal 611
for visuomotor coordination 674
Crocodile tears 803
Cross-correlation analysis 540
Crow's feet 486
Crystallins 155–172
synthesis and cataract 181
see also **alpha-**, **beta-**, etc
C-type responses 410
Cupula 677
as torsion pendulum 681
time-constant of 733
velocity proportionality 735
***c*-Wave of ERG** 314
PI component and 314
pigment epithelium and 318
CX-cells 532
Cyanate, and cataract 191[40]
Cyanopsin 408
Cyclic AMP
adrenergic drugs and 71
aqueous humour and 71
ciliary processes and 71
effects of application on corneal s.c.c. 117
Cyclic GMP
on facility 72
and phototransduction 292, 293, 296
Cyclopean eye 462
and stereopsis 472
Cyclotorsion, with superior and inferior recti 652
Cysteine, in gamma-crystallin 156
Cytochalazin
corneal regeneration and 115
transport and 115
resistance to drainage and 47
Cytochrome oxidase technique 549, 551
post-natal kittens and 624[16]
Cytoskeletal proteins 166

DABTA 507
Dacryocystectomy 800
DAP, effect on LGN 508
Dark, eye position in 453
Dark-adaptation 219, 264
area of field and 264
curves of 220, 264
ERG and 314
flicker and 366, 367
gecko rods 268
phases of 266
pigment bleaching and 265
retinal-retinol distribution and 265
rod monochromat 264
visual acuity and 374
Dark current 287, 289
effect of IBMX on 295
Dark focus 780
Darkschewitz nucleus 489
D.C. component 319
Decussation of optic pathway 3, 4, 486, 493
in superior colliculus 628
Deep petrosal nerve 801
Deep-sea fish, visual pigments of 255
Dehydro-ascorbic acid, and cataract 180
Dehydro-retinal 254
Deiters' neurones and utricle 699
Deiters' nucleus 698
Delta-ganglion cells 334
Dendritic fields
of bipolar cells 309
of ganglion cells 334–336
in relation to sensitivity 438
Density (absorption) spectrum, of rhodopsin 238
Dentate nuclei 724
Deprivation, visual 603–621
bilateral 603, 606
binocularity and 603
cortical ablation and 620
cortical morphology and 612
cortical unit changes in 603–613
disparity specificity and 609
effects of enucleation on changes 612
ganglion cells and 615
inhibition and 609, 612
LGN changes in 606, 615–631
monocular 603–606
rabbit 614
retinal damage and 620
reversal of effects 610–613
spatial and temporal sensitivity of LGN cells and 620
unilateral 603–606
alternating 621
visual defects following 613
X- and Y-cells and 618, 619–621
Depth of focus 754, 771
presbyopia and 774
Depth perception 459
accuracy of 469
convergence and 465
monocular 459
range of 471
stereoscopic 465–479
Depth-sensitive cells 563
Depth-tuned cells 563, 564
inhibitory flanks of 565
Dermatan sulphate 109
Descemet's membrane 11, 13, 107, 110
Desensitization 433
Desmosome 29
Desmosterol, and cataract 189
Detectability of signals 276
Deuteran 405
Deuteranope 403
difference spectra of 406
hue-discrimination curve 403
missing mechanism 405
De Vries–Rose Law 276
Dexamethasone, effect on i.o.p. 78
DFP, effect on uveal flow 76
Diabetic cataract 180
Diabetic retinopathy 25
Diadromous fish pigments 256
Diagnostic directions of gaze 652, 657
Diamox (acetazolamide)
effects on corneal endothelial potential 112
on i.o.p. and aqueous secretion 34
combined with forskolin 72
local action of 38
Dichroism of rods 234
Dichromat 403
artificial 441
colour mixing of 403
reduction hypothesis 406
thresholds of 405
Diencephalic root 487
Difference spectrum 238
Differential threshold 220
Diffraction
corneal 122
visual acuity and 375
Diffusion coefficient, of rod internal transmitter 294
Dilator innervation 763
Dilator, isolated 764
Dilator pupillae 754
Dinitrophenol (DNP)
cataract due to 180
effect on transport of Na 34
Diodrast, transport by ciliary body 37
Dioptric force-coefficient 773
Dioptrics of eye 215–218
Diplopia
heteronymous 463
homonymous 463

monocular 465
squint and 463
stereopsis and 471
Direction columns 559
Directional preponderance 559
Directional sensitivity
of collicular cells 631, 632
of cortical cells 535, 549, 566
development of 607
of ganglion cells 330
effects of GABA and AcCh on 349
effects of physostigmine on 349
effects of picrotoxin on 348, 349
of LGN cells 535
of retina 423
Discharge centres 537, 540
Discrepant images 468
Disfacilitation, of motor neurones 705
Disinhibiting surround 332
Disinsertion, of ciliary muscle 75
Disjunctive eye movements 656, 657
Disks of rods and cones 230, 236
shedding of 234–236
Disparate points 469
Disparity-detector neurones 559
development of 609
Displaced amacrine cells 342, 509[1]
cholinergic nature of 346
Disulphide cross-linkages 174
Diurnal changes, in disk-shedding 235
in i.o.p. 50
DLH, effect on LGN 508
Dobesilate 799
Doll reflex 682
Dolman's peephole test 478
Dominance columns 547
demonstration by cytochrome oxidase 550
deprivation and 603–610
reversal of 610–614
GABA effect on 549
histological demonstration 548
prenatal enucleation and 606
squint and 621
Dominance histogram 546
Dominance, ocular 477, 546
collicular units and 633
cortical units and 546
effects of deprivation on 603–606
reversal of 610
effects of squint on 621
Dominators 415, 417
Donders' law 654
Dorsal parietal pathway 569
Dorsal terminal nucleus 488
Double cones 412
Double-field simple cell 584
Double images (diplopia) 463–471
Double opponent cell 416
Dowling–Rushton equation 266
Drainage
of aqueous humour 10, 40
aqueous veins and 40
comparative aspects of 14
rate of 40
resistance to 39
uveoscleral 31, 47, 48
of tears 799
Drift of eye position 663
Dry spots 793
Dulcitol, in lens 180
Duplicity theory 220
Duration sensitivity 541
***d*-Wave of ERG** 314
Dyad 336, 340
Dynamic range 270
of rods and cones 270
Dysmetria and cerebellectomy 730
Dystrophic rats
IRPB in 253
outer segment renewal in 253

Eagle, visual acuity of 226
Early receptor potential (ERP) 319–321
in embryonic development 322[11]
Eccentric cell 280
generator potential in 281
Edge-inhibitory OFF-centre cell 330
Edinger–Westphal nucleus 489, 686
accommodation neurones 777
cortical projections to 765[3]
dilator neurones 761
non-ciliary ganglion projection 759
Eel visual pigments 256
EEP-protein 163
Effectively point source 212
Efference copy 453, 738, 744[32, 33], 745[39, 44]
Elastin and zonule 102
Electrical resistance
of ciliary epithelium 36
of lens fibres 147, 152
Electrochemical potential 146
Electrogenic pump 146
Electromyogram (EMG) 688
Electronic pupillography 755
Electro-oculogram (EOG) 660
Electroretinogram (ERG) 313
component analysis 314
dark-adaptation and 314
d.c. component of 319
flicker and 363
Purkinje effect and 396
Ellipsoid 207
Embryonic and fetal lens proteins 157, 168
Embryonic nucleus 140
Emmetrope, and accommodation 768
Endolymph 678
Endopeptidase of lens 165
Endothelial meshwork 13, 43
Endothelial pump 112
Endothelium
of cornea 107
permeability of 111
post-natal changes in 132[2]
potential of 113
regeneration of 127–130
swelling and 111–116
of Schlemm's canal 11, 42
Enhancement 290, 308
of collicular discharge 710
of cortical discharge 721
Enophthalmos 671
Epidermal growth factor 127, 130
Epinephrine (adrenaline)
agonist selectivity of 66
effect of, on cornea 117
on i.o.p. 68–70
on microvasculature 71
Epiphora 800
Episcleral circle 16
Episcleral plexus 10
Episcleral venous pressure 51
influence on i.o.p. 51
Epithelium
ciliary 9, 10
corneal 105
permeability of 111
potential profile of 118
regeneration of 124
lens 140, 142, 143
cytoskeleton of 166
retinal pigment 25, 31
Equatorial ridges 770
Equivalent foot-candela 212
E-retina 315
Error-signal 710
Erythrolabe 405
Eserine
effect on accommodation 776
effect on pupil 762
effect on uveal flow 76
and i.o.p. 74
Esophoria 656
Esterification of retinol 252
Ethacrynic acid, effect on facility 81[31]
Euryhaline fish, retinoids 254
Exophoria 656
Extinction coefficient 238
Extra-areal periphery 208
Extracellular space of lens 146
Extraocular muscles 4, 647
actions of 658
activity during blink 789
anatomy of 647, 668
cerebellum and 725, 730
combined actions of 652
effects of stretch of 689
in cerebellum 725
fibre types 668
innervation of 685
motor neurone discharges to 689
motor unit of 667
role of proprioception in 671–674
spindles in 671
stretch-reflex 711
tension developed in 692
vestibular stimulation and 699
Extrapersonal space, and eye movements 722
Extraretinal memory 454
Extreme nasal segment of LGN, and deprivation 617
Eye-derived growth factor 127
Eye-position cerebellar neurones 727

Faces, responses to 572, 577
Facetted eye 280

Facial ganglion 802
Facial nerve (N VII) 5
effect of, on i.o.p. 77
innervation of uvea 77
Facial reflex 791
Facilitated transfer 23
corneal 119
Facilitation, binocular 559
Facility of outflow 39
adrenergic agents and 73
cAMP and 72
forskolin and 72
normal human 53
pilocarpine and 74
prostaglandins and 82[42]
False macula 464
False projection 452, 464
False torsion 654
Far point 216
of convergence 657
Fast fibres 668
Fast photochemical voltage 321
Fastigial nuclei 724
Fechner fraction 221
Felderstruktur 668
Ferry–Porter law 362, 365, 369
Fetal disk shedding 236
Fetal lens proteins 168
Fibres of lens 140
development of 141
structure and connections 142–145
Fibrillenstruktur 668
Fibroblast growth factor 127
Fibronectin 79, 103[2]
corneal 126, 127
Field of action 692
Field adaptation 276[5]
Field of binocular single vision 657
Figural after-effects 455
Finger junctions 144
First-order projections, pulvinar 637
Fish photopigments
absorption spectra 407
extracted 409
Fissura prima 723
Fixation
EMG during 688
movements during 663
unit activity during 690
Fixation axis 648
Fixation disparity 785[1]
Fixation reflex 674
Flap junctions 144
Flash after-effect 427
Flash photolysis 251, 259[7]
Flat bipolar 209, 337, 339–340
midget 338, 353
Flick 663
Flicker 362–371
binocular 481
channel adaptation 371
cone 364
eccentricity and 368
effect of adaptation on 366
ERG and 363
frequency-labelled channels 370
ganglion discharges and 365
light–dark ratio and 369
rod 363
sinusoidal stimulus 368
surround-inhibition 370
VER and 365
Flicker-photometer 223
Flicker-threshold, and grating frequency 580
Flocculonodular lobe (flocculus) 723
electrical stimulation of 729
vestibular function and 728, 742
visual pathway 725
Floor of fovea 208
Flow of aqueous humour 39
effect of adrenergic agents on 68
effect of arterial pressure on 52
effect of forskolin on 72
effect of intraocular pressure on 52
effect of VIP on 78
facility and 39
rate of 52
Flow-curves, of aqueous humour 54
Flower-spray endings 670
Fluctuations, in membrane current 294
Fluid pump, corneal 114
Fluorescein
blood-vitreal barrier 25
rate of aqueous secretion and 39
Fluorescein-test 55
Fluorophotometry 39
Fluphenazine, on ganglion cells 350
FM-crystallin 163
Foot-candela 211
Formaldehyde, and blood-aqueous barrier 56, 57, 60
Form-birefringence of rods 233
Forskolin 72, 80
on ganglion cells 357[15]
Fourier analysis and flicker 369
Fourier descriptor stimuli 571
Fovea 3, 208
cortical representation of 517
dark-adaptation at 264
structure of 208
threshold at 397
Foveal adaptation 425
Foveal tritanopia 443
Foveation 707
Free-radicals, and cataract 184
Freeze-fracture of receptor membrane 259
Frequency-of-seeing curve 271
Freshwater fishes, porphyropsins 254
Frog
optic nerve responses of 282
photopigments of 256
Frontal dorsomedial cortex, and saccades 717
Frontal eye-fields 712
compared with posterior parietal cortex 721
delineation of 716
Frontalis muscle 787
Fructose, in lens 153
Fundamental response curves 400
effect of adaptation on 400
Furosemide, and cornea 117
Fusion-free position 656
Fusion supplement 658

GABA
cortical localization 552
cortical tuning 537
inhibition of AcCh release 346
of ganglion cells 348, 349
of LGN cells 507
release from horizontal cells 345
uptake by amacrine cells 346, 349
uptake by bipolar cells 345
uptake by LGN cells 507
Gain
of receptor response 306[1]
of reflex 703, 735, 740
Galactokinase activity, and cataract 191[34]
Galactose cataract 180, 181
Galactose, free radical scavenging 184
Galvanic nystagmus 682
Gamma-crystallin 155
age of lens and 157, 169, 170
cataract and 187
molecular weights 155
per centage of total proteins 155
synthesis by explants 172
Gamma$_H$-crystallin 169
Gamma-DGG, effect on cortical cells 552
Gamma-efferents 672
Gamma-ganglion cells 334
Gamma-globulin, penetration into ciliary body 23
Ganglion blockers, effect on pupil 763
Ganglion cells 207
action of transmitters and their inhibitors on 347–352
alpha-, beta-, and gamma-types 334
broad-band 415
colour-coded 330, 415
cone pathways to 353, 354, 355
dendritic fields of 334–336
density and eccentricity 519
deprivation effects 615
directional sensitivity 330, 423
excitation through cones 312
flicker in 365
grating resolution of 378
minimum stimulus 312
mosaic of 376
Necturus 286
number in retina 509[1]
opponent type responses in 416
periphery effect 332
receptive field 282, 325
response-types 326
rod-pathway to 354, 355
shift effect 332
sustained-transient classification 328
turtle 312
visual acuity and spacing 376
W-cells 330
X- and Y-cells 326
Ganglion of Scarpa 697
Ganglionectomy effect 67, 82[40]

Gap-junctions 29
between Müller cells 322^{8}
between receptors 305
ciliary 29
lens 143, 144
effects of Ca^{2+} on 178
proteins of 164
switch mechanism 144
synapses and 336
Gasserian ganglion 5, 802
muscle innervation through 673, 674
Gaze Purkinje cell 721
Gaze saccade 684
Generator potential 281
Geniculate ganglion 801
Giant vacuoles 41
Gibbs–Donnan Equilibrium 19
Glands of Krause and Wolfring 792
Glassblowers' cataract 185
Glaucoma
dexamethasone and 78
experimental 79
trabecular tissue in 79
Glucose
in aqueous 20, 27
cataractous 20
corneal supply of 124
facilitated transfer of 23
transport across pigment epithelium 25
Glutamate
excitation of LGN cells 507
as cortical transmitter 552
block by KYNA, etc 552
as receptor transmitter 343, 349
Gamma-D-Glutamyl glycine 343
Glutathione
cornea and 132
lens and 145, 181–183, 189
meshwork and 46
Glutathione peroxidase 182
Glutathione reductase 182, 183
Glycocalyx 792
Glycogen, corneal 122
Glycolysis, by lens 153
Glycoproteins
corneal 126
definition of 798
Glycosaminoglycans (GAG)
in cornea 109
in meshwork 46
***N*-glycosidic linkage** 798
***O*-glycosidic link** 798
Goblet cells 792
glycoproteins of 798
Goldfish, horizontal cells of 414
Goldfish retina 341
Goldman equation 189^{4}
G-protein 296
reaction with Meta II 297
Granit–Harper law 368
Granular layer 724
Grape-like terminations 668
Grassmann's laws 229
Grating acuity 225
cat's 377
Grating adaptation 382, 581
Grating frequency 380
flicker threshold and 580
ganglion cell responses and 580
LGN and cortical cells and 582
Pulfrich phenomenon and 483^{7}
Gravity reflexes 678, 682
Greeff vesicles 63, 64
Green rods 423
Growth of sensation 429
GTP, activation of PDE in rods 293
Guanylate cyclase, inhibition by Ca^{2+} 300

HA, effect on LGN 508
Haloperidol, effect on ganglion cells 350
Haploscopic device 783
Harmonics of gratings
and c.f.f. 370
and visual acuity 392^{5}
Head movements and saccades 683
Hemianopia 486
OKN and 676
Hemidesmosomes, corneal 126
Heparan, of cornea 109
Hereditary cataracts 185
Hering after-image 248
Hering–Hillebrand deviation 467
Hering opponent colour theory 418
Hering's law 656
Heteronymous diplopia 463
Hexamethonium, on pupil 763
Hexose monophosphate shunt 182
Hibernation, and cornea 116
Hierarchical processing 535, 569
Hippus 165
Histamine
miosis due to 764
vascularization and 131
Holding fibres 769
Holo-RBP 252
Homonymous diplopia 463
Homonymous hemianopia 486
optokinetic nystagmus and 676
Horizontal cells 205
A- and B-types 345, 352
axon terminals 310
C-cells 414
depolarization by glycine 345
directional sensitivity and 331
effect of Co^{2+} on 309
effect of dopamine on 345
effect of glutamate on isolated 345
effect of kainic acid on 344, 345
effect of quisqualate on 345
electrical stimulation of 309
feedback on cones 308
GABA release from 345
L-potentials and 309, 310
Necturus responses 285
release of GABA by 344
S-potentials of 285, 309, 410
synapses of 285, 338, 339, 352
turtle responses 308, 411, 413
Horizontal, estimate of 456
Horizontal magnification 475
Horizontal meridian 648
cortical representation 525
objective horizontal and 456
pulvinar representation 637
Horner's muscle 800
Horner's syndrome 671
Horopter 466
longitudinal 467
Horseradish peroxidase
choroidal transport 31
iris transport 30
Hubbard–Kropf model 247
Hue 222
variation with intensity 223, 441
Hue discrimination curve 222
dichromat's 403
Hyaline cartilage protein 103^{6}
Hyalocytes 96, 100
Hyaloid artery 96
Hyaluronic acid 97
corneal 108
vitreous 97, 98, 100
replacement therapy 103^{5}
Hyaluronidase
effect on hyaluronic acid 98
effect on resistance to flow 46
Hybrid crystallins 162, 163
Hydration of cornea 110
Hydraulic conductivity, of ciliary epithelium 36
Hydrogen peroxide
aqueous 182
related to ascorbic acid 183
effect of, on lens proteins 183
effect of, on Rb^{+} uptake by lens 183
5-Hydroxytryptamine (serotonin, 5-HT)
accumulation in retina 350
corneal vascularization and 131
effect of, on ganglion cells 351
transmitter action 351
Hyperacuity 377
Hypercolumns 547
Hypercomplex cells 532
collicular units and 539
definition of 539
end-stopping of 532
opposed movement 566
velocity tuning in 536
Hyperfocal distance 771
Hypermetropia 216
accommodation and 768
Hyperpolarizing response
cones 288
mechanism of 286
Necturus receptors 285
rods 290
Hypertonic injections, and i.o.p. 28
Hypotensive effect of PGs 60
Hypothalamus
i.o.p. and 76
pupil and 762
visual pathway and 487, 488
Hypothermia, and cataract 187
Hypothetical primaries 224
Hypsorhodopsin 245

IBMX, effect on dark current 295
Ibotenic acid lesions 722
Immunoglobulins, in tears 796

Immunology, of lens proteins 167
Impression tonometer 49
Imprint junctions 144
Inadequate representation 449
Incident light model 271
Increment thresholds 397
and cone mechanisms 401
Indicator yellow 245
Indomethacin 57, 62
effect on corneal healing 130
Induced size effect 475
Induction 226
Induction index 605
Inferior accessory optic tract 487
Inferior oblique 647, 648
abduction by 651
actions of 651
innervation 685
Inferior occipital sulcus 524, 526
Inferior olivary complex 724
route from superior colliculus to cerebellum 706
Inferior orbital vein 7
Inferior palpebral muscle 787
Inferior rectus 648
actions of 650
innervation of 685
Inferotemporal cortex (IT)
dependence on V1 572
neurones of 570
pathway 569
pulvinar connections 641^{9}
size-constancy and 571
visual memory and 572
Information theory, and colour vision 418
Infra-red, sensitivity to 223
Inhibition
collicular cells and 633
of cones by rods 366
cortical cells and 533
binocular 559
development of 609
directional sensitivity and 331
dominance and 549
flicker and 363
GABA and 346–349, 507
LGN units and 507
orientation selectivity and 533
P III component and 315
velocity tuning and 536
vestibular of N III and N IV neurones 702
within receptive field 283
Inner fovea 208
Inner limiting membrane 96, 206
Inner nuclear layer 205
ramification of ganglion cell dendrites in 342
Inner plexiform layer 338
cholinergic distribution in 346
glycinergic cells and 347
pathway to ganglion cells 353
Inner segment 231
Innervation of e.o. muscles 685
Insertion of e.o. muscles 647
Insoluble albuminoid 155
Instantaneous parallax 468
Instrument myopia 780
Integrating accelerometer 678
Intensity of illumination 211
Interlocking junctions 144
Intermediate adaptation 266
Intermediate filaments 166
Internal medullary lamina, eye movement control and 718
Internal messenger 291
Internuclear neurones 687
Internuclear ophthalmoplegia (palsy) 687, 688
Interphotoreceptor binding protein (IRBP) 253
Interplexiform cell 341, 347
Interpositus nucleus 724
accommodation and 777
Interstitial nucleus of Cajal 696
Intracranial pressure 8
Intrafusal fibre 671
Intrageniculate neurones 494
Intramuscular circle 16
Intraocular pressure 7, 48–80
breakdown of blood–aqueous barrier and 55
critical 54
diurnal variations of 50
effects of
adrenergic agents on 68
arterial pressure on 51
blood osmolality on 53
carbonic anhydrase inhibitors on 34
corticosteroids on 78
on drainage channels 44
flow of aqueous on 52
ganglionectomy on 68
nervous activity on 65–80
parasympathetic drugs on 74
prostaglandins on 60
vanadate on 38
vasopressin on 79
venous pressure on 51
measurement of 48
normal 50, 53, 81^{24}
Intrascleral plexus 10
Intrinsic birefringence of rods 234
Inulin-space of lens 146
Invaginating midget bipolar 338, 353
type of synapse 336
Invariant hues 441
Invertebrate eye 279
responses in 281
transduction process in 301^{9}
Involuntary eye movements 663
depth perception and 469
visual acuity and 388
Iodate, effect on blood–vitreous barrier 25, 28
Iodide, active removal of 38
Iodopsin 408
***I/Q* ratio** 437
I-retina 315
and flicker 363
Iridectomy, and paracentesis 82^{36}
Iridial processes 17
Irin 56
Iris 3, 9
anterior lining of 9
breakdown of barrier and 63, 64
capillaries of, and blood–aqueous barrier 23, 30
crypts 11
diaphragm action of 754
major circle of 7
structure of 9, 30
Iris-process 80^{2}
Iso-colour chart 404
Isodirectional neurones 720
Isolated retina, rhodopsin regeneration in 266, 276^{3}
Isomerization of retinal, and rhodopsin regeneration 250
Isomers of retinal 244
Isoproterenol
effect on ciliary muscle 777
effect on extraocular muscles 671
effect on pupil 763
Isoretinal-a 244
Isorhodopsin 246, 251

Julesz stereograms 474
Jump acuity 378
Junctional complex 29
ciliary epithelial 30
corneal endothelium 108
and repair 128
lens 143
Junctions, interlocking 144

Kainic acid 343
as agonist 344
effect of, on velocity storage 739
Keratan sulphate, corneal 108, 109
Keratitis sicca 786
glycoproteins in tears and 804^{13}
puncta occlusion and 800
Kinetic reflexes 677
Kinocilium 679
Krause glands 792
Krebiel flow 800, 804^{15}
Kyurenic acid (KYNA), effect on cortical cells 552

Labyrinth, membrous 677
Labyrinthectomy
and eye–head movements 743^{15}
and torsion swing 741
Labyrinthine reflexes
nervous pathways 697
see also Vestibular reflexes 677
Lacrimal gland 791
innervation of 801
isolated 798, 802, 803
Lacrimal nerve 6, 791, 801
Lacrimal nucleus 801
Lacrimal pump 800
Lacrimal puncta 800
Lacrimal sac 791, 800
pressure in 800

Lacrimal secretion 792
chemistry of 794
rate of 794
effect of adrenergic agents on 802
effect of age 798
see also Tears
Lacrimation 791–804
in newborn 803
Lactate
in aqueous 19, 27
in cornea 123
in vitreous 27
Lactic dehydrogenase, in tears and cornea 799
Lactoferrin, in tears 797
anti-complement 797
Lambert 212
Lamellae
corneal 106
radial, of lens 141
zonular, of lens 141
Lamina vitrea 4, 7
Lamina 4C
dominance in 604
units of 547
Laminated aqueous vein 41
Lamination
of cerebral cortex 520, 716
neuronal types and 543
of LGN 491
of superior colliculus 628
Laminin 79, 103[2]
corneal 126
Landolt-C 225
Land's experiments 451
Lanthanum hydroxide 29
Laser irradiation
effect on blood–aqueous barrier 56, 57
effect on lens 192[45]
Laser optometer 778, 781[12]
Late receptor potential 319
Lateral border of cortical reticular formation 537
Lateral geniculate nucleus (LGN) 486, 491
bilateral strip 494
binocular effects 554[16]
input 508
cholinergic activity in 509
chromatic features of responses 587
control of cortical neurones 551
cortical stimulation and 510[18]
corticofugal input to 506
discharge centres 540, 606, 613
ganglion cell terminations in 496–497
interneurones of 506
intrageniculate 491
perigeniculate 494, 506
lamination of 491
ontogeny and 616
length-tuning in 506
maturity and 615
occlusion and reverse-suturing and 613, 616
shrinkage of laminae 616
orientation selectivity 505
parvo- and magnocellular units 522
cortical projections 616
colliculi and 631
post-natal changes 616
pre-natal enucleation and 606
projections to cortex 521
projections to pulvinar 638
receptive fields 500, 501
squirrel monkey 522
superior collicular projection to 630
synaptic glomerulus 495
transmitters
excitatory 509
inhibitory 507
velocity-sensitivity 505
ventral nucleus 492
receptive fields of units 506
X-, Y-, W-cells 496–498, 502
Lateral palpebral ligament 791
Lateral palpebral raphe 786
Lateral pulvinar nucleus 635, 636
Lateral rectus 647, 648
action of 650
innervation of 685
Lateral suprasylvian area, callosal connections 527
Lateral terminal nuclei 488
Lateral vestibular nucleus (Deiters') 698
Lattice theory of transparency 122
Laws of Colour Mixture 223, 399
L-cells 309, 310, 413
Leading edge 125, 133[17]
Lectins, corneal 126
Lengths, comparison of 457
Length-tension 671
Length-tuning 538
LGN units and 506
Lens, crystalline 1, 139–192
amino acids in 20
asymmetry potential 150
capacitance 149
capsule 139, 142, 145
cataract and 173–189
changes in accommodation 769
changes in shape with age 774
chemistry of 145
culture of 153
embryology of 140
epithelial cells 140, 142, 143
cytoskeleton of 166
extracellular space of 146
fibres 140
cytoskeleton of 165
development of 141
junctions between 144
ionic composition of 145, 148
ionophore action on 180
metabolism of 153
potassium 189[5]
potential 147–151
proteases 165
proteins 155–172
pump-leak hypothesis 151
repair of injury 187
resistance 149
structure of 139
sutures 140, 142
transparency 145
volume-regulation 153
water-content 145
weight of 141
Lens proteins 155–172
ageing and 167
cataract and 174–177
characteristics of 156
cortex vs. nucleus 168
crystallin fractions 155
cytoskeletal 166
evolutionary changes 160
membrane 163, 164
organ specificity of 167
post-translational changes 171
see also Alpha-, Beta- and Gamma-crystallins
Leucine, pigment epithelial transport of 80[11]
Leukocytic invasion, of cornea 130
Leukotriene B_4, effect on cornea 130
Levator palpebrae superioris 648, 787
activity during blink 788
aponeurosis of 787
spindles in 672
Lid-closure reflex 757
Light-adaptation 226
alpha- and beta- 426
colour and 227, 240
effect of, on visual acuity 374
Light-and-shade 461
Light–dark ratio 369
Light flux 213
Light reflex 755
effect of luminance on 755
neuronal pathway 758–760
spectral sensitivity and 756
supranuclear inhibition 761
threshold 756
Light sense 219
Limbus 3, 106, 109
Liminal brightness increment 220
cone sensitivity and 400
detection of line and 379
Limits of visual spectrum 223
***Limulus* eye**, optic nerve discharges in 281
Line modulation sensitivity 382
Line, resolution of 379
Linear depth limen 469
Lipid film, corneal 792
Lipid-solubility
and blood–aqueous barrier 22
and corneal permeability 118
Lipids, of tears 799
Listing's law 653, 655
Listing's plane 648, 653
Local edge detectors 329
Local sign 452
Long ciliary nerves 4, 6
Long posterior ciliary arteries 7, 16
Longitudinal horopter 467
determination of 470
L-type responses 410, 413, 414
Lumen 213
photopic and scotopic 214
Luminance 212

Luminosity curves 395
dichromat's 404
Luminosity units
cortical 589
ganglion cell 416
geniculate 587
Luminous intensity 211
Lumirhodopsin 245
Lustre 478
Lux 211
Lymphatic capillary 11
Lysosomal enzymes, in tears 799
Lysosomal segregation, of proteases 165
Lysozyme 792

Mach Bands 436
Macula 208
false 464
projection on cortex 517
Macula sacculi 678, 680
Macula utriculi 678, 680
Magnesium
in aqueous 19, 27, 28
in lens 178
in tears 795
in vitreous 27
Magnocellular and parvocellular layers, of LGN 491
relation to colliculus 631
Main extrinsic polypeptide 164
Major ciliary process, vasculature 17
Major circle of iris 7, 11, 16
Mannitol space of lens 146
Manometry 48
Mappable cortical neurones 610
Marfan syndrome 102
Marine fishes, rhodopsins 254
Maturation
of cortical cells 609
of LGN cells 508
Maxillary fibres 5
nerve 6
Medial interlaminar nucleus (MIN) 492
effects of deprivation on 619
projection to cortex 520
Medial longitudinal fasciculus 492
lesion of 698
vestibular fibres in 698, 700
Medial rectus 647
action of 650
innervation of 685
Medial superior temporal (MST) area 570
relay centre for V1 to parietal lobe 575
Medial terminal nucleus 487, 488
pathway to cerebellum 725
Medial vestibular nucleus 697, 698
Median nucleus of Perlia 686
Median plane 649
Median tract 100
Meibomian gland 792
cholesterol secretion by 799
Melatonin 488
Membrane of Bruch 4, 7
Membrane currents, receptor 291
Membrane proteins of lens 163
in cataract 175
Membranous labyrinth 677
nervous pathways 697
Memory-colour 450
Memory-contingent units 745^{34}
Meridional fibres of ciliary muscle 768
Meridional rows 140
Mesencephalic reticular formation, projection on LGN 509
Mesencephalic root, of optic tract 487
Mesopic range 220, 276^{6}
flicker and 367
Purkinje shift and 396
sensitivity curves 442
visual acuity and 386
Metabolism
of cornea 122
of lens 153
Metachromatic staining 98
Meta-contrast 427
Metamorphosis, and visual pigments 256
Metarhodopsin II 245
life-time of 259
role in transduction 297
Metarhodopsins 245, 248, 259^{8}
***S*-Methoxysporolan**, and cataract 179
***N*-Methyl-D-L-aspartate (NMDA)** 343, 344
Methysergide, and blood–aqueous barrier breakdown 60
Metre-angle 658
Metre-candela 211
MIC fibre 669
Microendoscopy 82^{46}
Micropsia 460
Microsaccade 660
Microvasculature, of eye 10, 16
adrenergic influences on 71
Microwave cataract 185
Middle temporal (MT) area 569
directional sensitivity 577
inhibition in 574
lesions and oculomotor control 722
location in macaque 573
motion columns 574
receptive fields 573
route from V1 to parietal lobe 576
Midget bipolar 337
Midget cells and visual acuity 375
Midget ganglion cell 207
Millilambert 212
MINC fibre 669
Miners' nystagmus 675
Minimum amount of energy 272
Minimum flux 272
Minimum response fields 558
Minimum retinal illumination 272
Minimum separable 225
Minimum stimulus
to cone to excite ganglion cell 312
to excite vision 272–274
Minor circle of the iris 17
Miosis
and blood–aqueous barrier breakdown 54, 59
and near response 783
and Substance P 82^{38}
MIP of lens 164
Modulation of flicker stimulus 369
Modulation sensitivity 369
Modulators 415
Molar extinction coefficient 238
Molecular layer 724
Monochromatism 402
artificial 441
cone 402
rod 264, 363, 402
Monochromator 222
Monocular deprivation (occlusion) 614–621
alternating 621
Monocular diplopia 465
Monocular perception 452–464
of depth 459
Monocular segments, of LGN 618
Moon illusion 460
Morgagnian globules 173
Morphine, effect on pupil 764
Mosaic, retinal 376
ganglion cells 376, 385
Mossy fibres 724
Motion
illusions of 482
MT neurones and 574
perception of 481
sensitivity of collicular cells to 632
Motion area 542
Motion columns 574
Motion neurones 566
Motor error, and burst discharge 695
Motor neurones, of eye muscles 685
discharges during asymmetrical convergence 692
discharges during movements 690
PPRF connections 693
PSPs in 704
superior collicular connections 707
vestibular connections 698
Motor root of ciliary ganglion 5
Movement cells 713
Movement fields 707, 709
Movement illusion 482
Movement-related cells, of colliculus 709
Movement sensitivity, of cortical cells 542
area 8 713
Movements of the eyes: mechanical aspects 647–665
disjunctive movements 657
fixation movements 663
muscles 647
rotations of globe 648
saccades 660
torsion 652
tracking 662
Movements of the eyes: nervous control 667–745
cerebellum 723
cerebral cortex 711–723
frontal eye-fields 712–718, 721
occipital 711

posterior parietal 719–723
models of control 730–742
paramedian pontine reticular formation 693
prepositus hypoglossi nucleus 697
proprioceptive reflexes 683
spindles 671
substantia nigra 719
superior colliculi 706–711
thalamus 718
vestibular control 697–706
vestibular reflexes 677–683
Mucin 798
Mucopolysaccharides, of cornea 108, 109
and swelling 132[6]
Mucoprotein 98
Mucous cells, of lacrimal gland 792
Mucus layer, of cornea 792
composition of 797
threads 797
Mudpuppy retina 285
Müller horopter circle 466
Müller's cells 96
origin of P II and 316
vitreous secretion by 100
Müller's muscle 787, 791
Müller's radial fibres 205
Muscarinic receptors 65
Muscimol
accumulation by amacrine cells 346
accumulation by LGN cells 507
Muscle pairs 657
Muscle plane 650
Muscle spindle 671
Mydriasis, and pharmacokinetics 121
Myoepithelial cells
iris 754
lacrimal gland 802, 804
Myoglobulin, penetration into ciliary body 23[8]
Myoid 207
Myoinositol, and galactose cataract 181
Myopia 216
accommodation and 767, 779, 780

N V (trigeminal), and reflex weeping 801
N VII (facial)
lesions and blinking 803[1]
paresis and tear draining 800
Nakano mouse cataract 185
ATPase activity and 185
Nanometre 218[1]
Naphthalene cataract 180
Naso-ciliary nerve 5, 6
Naso-lacrimal duct 791
Near-and-far cells 563, 564
Near point
of accommodation 767
of convergence 657
Neck muscles
N V and 673
superior collicular input 707
vestibular control of 702
Neck reflexes 683
***Necturus* retina** 285
Negative after-image 228
Negative colour-coefficient 399
Negative feedback on cones 308
Neglect syndrome 721
Neo-b-retinal 244
Neocerebellum 724
Neoproteins 162
Neovascularizing substances
corneal 130
vitreous 103[8]
Nernst equation 146
Nerve of pterygoid canal 6, 801
Nervous supply
of extraocular muscles 685
of eye 6
of lacrimal gland 801
of pupil 758
Nervus intermedius 801
Neural integrator 737
site of 738
Neuronal circuitry of retina 352–355
Neutral peptidase 165
Neutral point 403
***N*-glycosidic linkage** 798
Nicotinic receptors 65
Night myopia 780
Nitrogen mustard
biphasic effects of 59
on blood–aqueous barrier 54
nervous influence on 57
***N*-Methyl-D-L-aspartate (NMDA)** 343, 344
Nociceptors, in cornea 132
Nodal point 215
Non-geniculate pathways 628
Non-geniculate targets 487, 628
Nonius method 470
***N*-Retinylidine opsin** 244, 245, 249
Nuclear bag fibres 672
Nuclear cataract 273
compared with cortical 273
Nuclear chain fibres 672
Nuclear zone 140
Nucleic acids, in lens 155
Nucleus of Darkschewitz 697
Nucleus intercalatus 697
Nucleus of N III 686, 760
Nucleus of N IV 687
Nucleus of N VI 687
Nucleus of the optic tract (NOT) 489
and OKN 734
and pupillary activity 761
Nucleus of Perlia 686
projection from area 8 717
Nucleus prepositus hypoglossi 698
locus of integration 738
Nucleus reticularis oralis 706
Nucleus reticularis tegmentum pontis (NRTP) 706
and OKN 734
Null direction 331
Null position, of X-cell 326
Nystagmus
caloric 682
central 672
galvanic 682
ocular 670
optokinetic (OKN) 675
directional preponderance 676
post-rotatory 681
rotatory 681
subcortical 676
torsional 677
vestibular 681

Object colour 451
Object- vs eye-movement responses 721
Occipital area 515
see also Striate cortex, etc
Occipital motor centre 711
Occlusion of eyes 603–624
bilateral 603, 606
binocularity and 603
cortical ablation and 620
cortical morphology and 612
cortical unit changes in 603–613
disparity specificity and 609
effects of enucleation 612
ganglion cells and 615
inhibition and 609, 612
LGN changes in 606, 615–631
monocular 603–606
rabbit 614
retinal damage and 620
reversal of effects 610–613
spatial and temporal sensitivity of LGN cells and 620
unilateral 603–606
alternating 621
visual defects following 613
X- and Y-cells and 618, 619–621
Ocular dominance 477
and handedness 478
see also Dominance, ocular
Ocular nystagmus 675
Oculogyral illusion 455, 703
Oculo-hypotensive effects of $PGF_{2\alpha}$ 60
effect of pilocarpine on 63
Oculomotor complex 760
Oculomotor nerve (N III) 5, 6, 685
discharges during eye movements 689–692
effect of stimulation on aqueous flow 74
innervation of extraocular muscles 685
of ciliary and iris muscles 489, 686, 777
sensory messages 673, 689
Oculomotor nucleus 686, 760
neurone discharges of 689–692
relation to n. prepositus 697
OFF-centre field 284
anatomical basis of 342
OFF-direction 690
OFF-effects, ERG 314
OFF-elements 283
and colour 416
lateral geniculate 497
OFF-pathway
blocking of 344, 348
in cat retina 353

O-Glycosidic link 798
Oil droplets, cone 255, 411
and Stiles–Crawford effect 424
Oligosaccharides of rhodopsin 241
Olivary pretectal nucleus 758
Ommatidium 279
ON-centre field 283
anatomical basis of 342
ON-direction 690
ON–OFF elements 285
and colour 416
responses 326
LGN units 506
One-to-one relationship 374
Open-loop control 742
Operant preferential looking (OPL) technique 392[10]
Operational envelope 693
Ophthalmic artery 7
pressure in 16
Ophthalmic nerve 6
Opponent-type responses
in cortical cells 588–596
in ganglion cells 416–419
in horizontal cells 410
in LGN cells 587
Opposed movement cells 566
Opsin 242
variations in 258
Opsin adaptation 266
Optic chiasma 3, 486
Optic foramen 3
Optic nerve(s) 3, 486
blood vessels of 8
decussation of 486
fibres in 487, 509[1]
invertebrate 280
single fibre responses in 282
vertebrate single fibre responses 282, 325–334
wavelength and 415, 416
Optic radiation 515
Optic tracts 3, 486
mesencephalic root 487
Optical blink reflex 791
Optical density 238
of retinal pigments 266
Optical illusions 457
Optokinetic after-nystagmus (OKAN) 676, 731
Optokinetic neurones in area 7a 721
Optokinetic nystagmus (OKN) 675
afoveate animals and 675, 734
cortical ablation and 734
directional preponderance 559
dominance and 478
integrator 731
interaction with vestibular reflexes 740–742
labyrinthectomy and 740
maximum following speeds 745[45]
NOT and 734
NRTP and 734
quantitative analysis of 730
torsional 677
velocity storage and 732, 739
vestibular nystagmus and 733
Ora serrata 3, 4, 5
Orbicularis oculi 786
activity during blink 788
tear drainage and 800
Orbicularis oculi reflexes 791
Orbital rim layer 668
Organ specificity 167
Orientation columns 547
Orientation of gratings, and resolution 382
Orientation of lines, estimates of 378
Orientation-selectivity, cortical neurones 531
and behavioural study in cat 584
cytochrome oxidase and 551
development of 605
effect of GABA inhibition on 534
in LGN units 505
role of inhibition in 533
superior colliculus units and 631
visual experience and 607–609
Osmolality
of aqueous humour 53
of transported fluid from cornea 113
of tears 795
Osmotic agents
effect on blood–aqueous barrier 65
effect on i.o.p. 53
Otoconia 678
Otolith membrane 678
Otolith organs 678
response to acceleration 678, 683
Ouabain
effect on aqueous formation 35
effect on corneal pump 112, 115
effect on ERG 287
effect on lens potential 151
effect on pigment epithelium potential 36
short-circuit current 33
Outer fovea 208
Outer limiting membrane 206
Outer nuclear layer 205
Outer plexiform layer 205
synaptic arrangements in 338, 352
Outer segment 207, 230
a-wave and 316
disk turnover in 234–238
patch-clamp responses 291
ultrastructure 230, 236
Owl monkey, vitreous 100
Oxygen consumption of cornea 123
Oxygen tension in cornea 123
Oxytalan fibrils 102

P I component of ERG 314, 318
P II component of ERG 314, 316
P III component 314, 316
Paleocerebellum 724
Panum's area 471
Para-aminohippurate, transport out of the eye 37
Parabducens nucleus 687
Paracentesis 55
breakdown of blood–aqueous barrier and 56, 63
Parabigeminal nucleus 706
Para-contrast 428
Paradoxical pupillary dilatation 762
Parafovea 210
Parallax
binocular 468
instantaneous 468
monocular depth perception and 462
Parallel fibres 724
Parallel processing 535
Paramedian pontine reticular formation (PPRF) 693
abducens connections 737
area 7 cells and 719
area 8 projection to 717
lesions in 737
role in saccade generation 737
tectospinal connections 706
unit discharges in 693
Parametric feedback 453
Pararhodopsin 246
Parasol ganglion cell 208
Parastriate area (area 18) 524
Parasympathetic 5
effect on accommodation 776
effect on blood–aqueous barrier 74
effect on blood flow 74
effect on i.o.p. 74
effect on pupil 762
effect on resistance to outflow 74
effect on secretion of tears 801
Parasympatholytic drugs 763
Parasympathomimetic drugs
effect on accommodation 776
effect on i.o.p. 74
effect on pupil 762
Paresis micropsia 460
Parieto-occipital lesions 719
Pars orbitalis 786
Pars palepebralis 786
Pars plana 3
Partial bleaching 239
Partial summation 275
Particulate matter, escape from aqueous 45, 48
Parvo- and magno-cellular dichotomy in LGN 504
Patch-clamp of rods 290
Pattern, and development of visual acuity 606
Pause neurones, (OPNs) 737
and saccade 738
Pausing units in PPRF 694
PDA
effect on cortical neurones 552
effect on OFF-pathway 344
Pectinate ligament 80[4]
Pentose phosphate shunt 153
Perceived direction 456
Periaqueductal gray syndrome 711
Periauditory belt 529[4]
Pericilliary ridge complex 242
Perifovea 210
Perigeniculate neurones 494
Perilymph 678
Period of susceptibility to occlusion 605
Periodic acid Schiff test 95

Peripheral patch layer 668
Periphery effect 332
Peristriate area (area 19) 524
Perlia's nucleus 686
Permeability constant
of blood–aqueous barrier 24
of rod outer segment 287
Permeability of cornea 118
and endothelial repair 128
Peroxides, and GSH 46
cataract and 182
Perspective 460
aerial 459
pH of lens interior 189
pH changes and bleaching 248
Phagocytosis, of cones 236
Pharmacokinetics 118, 120, 121
Phase-error 679
Phase-lag
in motor neurone discharge 697
in VOR 735
Phasic fibre 669
Phentolamine, and breakdown of blood–aqueous barrier 60
Phenylephrine, effect on i.o.p. 73
Phosphodiesterase
and hyperpolarizing response 293
inhibition of 295
subunits of 297
Phot 211
Photochromatic interval 397
Photocurrent 289
after BAPTA 299
Photo-isomerization 244, 246, 251
Photometry 211
Photopic lumen 214
Photopic pigments 255
cone 408, 409
Photopic sensitivity curve 395, 441
cone monochromat's 402
dichromat's 404
humps on 442
Photopic troland 218^2
Photopic vision 220
Photopigments 240–259
comparative physiology and variations 254–259
fish 409
oil-droplets and 413
Photoreceptors, transmitters 343
Photorhodopsin 247
Photosensitivity 239, 266
Phylogeny
and crystallins 160
and retinal pigments 257
Physiological heterophoria 656
Physiological position of rest 656
Physiological summation 275
Picrotoxin
effect on directional sensitivity 349
effect on ganglion cell receptive fields 347, 348
Pieron's law 276
Pigeon photopigments 420^9
Pigment epithelium
ciliary body 9, 10
junctions in 10, 30
iris 9, 30
retinal 206
c-wave and 318
electrical characteristics 36
ERP and 321
junctions in 31
phagocytosis by 235
RBP in 251
rhodopsin regeneration and 251
transport across 25
Pilocarpine
effect on accommodation 776
effect on i.o.p. 74
effect on oculohypotensive effect of PGF_2 63
effect on pupil 762
effect on tears 803
effect on uveoscleral flow 48
Pineal gland 488–490
Piper's law 275
Plasmoid aqueous humour 55
Plate endings on extraocular muscles 668
Plexuses of anterior segment 10, 14
Pneumatic applanation tonometer 49
Point image, cortical projection of 518
Point-to-point projection 517
Polarized light, and ERP 320
Polymodal nociceptors, in cornea 132
Polyol reductase 154
Polyphloretin 55, 60
PON (olivary pretectal nucleus) 758, 759
Pontine reticular formation, saccade-related neurones 738
Pontine visual neurones 639
and superior colliculus 708
Pore area 13
Pore tissue 13
Porphyropsin 254
Position information, cerebellar 727
Position sense of eyes 454
Posterior accessory optic tract 488
Posterior aqueous humour 27
Posterior bank of STC, units of 566
Posterior chamber 3
Posterior ciliary arteries 7, 16
Posterior epithelium, of the iris 30
Posterior parietal cortex
compared with frontal cortex 721
compared with superior colliculus 722
eye movements and 719
Posterior pretectal nucleus 75^8
Posterior principal processes 8
Posterior thalamus, collicular projection to 630
Posterolateral fissure 723
Post-rotatory nystagmus 681
Post-saccadic drift 739, 740
Potassium
aqueous humour concentration 19, 20, 27
corneal concentrations 111
lens concentrations 145, 148, 189^4
cataractous 177, 178
retinal changes 317
subretinal fluid concentration 37
tear concentration 795
transport across retinal pigment epithelium 36
vitreous concentration 27
Potassium channel, in lens 190^8
Potential
ciliary 33
corneal 112
amphibian 117
endothelial 113
fluid transport and 115
profile in epithelium 117
lens 147–151
Prairie dog, afoveate 675
Prazocin
effect on breakdown of blood–aqueous barrier 60
effect on i.o.p. 74
Pre-albumin 252
in tears 795, 796
Pre-corneal film 792
Pre-emphasis 661, 662
Preferred disparities 563
Preferred orientation
reverse suturing and 611
visual deprivation and 607
Pregeniculate nucleus 493
PON projection to 758
Prelumirhodopsin 245
Prenatal enucleation 606
Prepositus hypoglossi nucleus 698
internuclear neurones and 687
lesions in 740
projections of 697
unit responses in 697
Preretinal tract 100
Pre-saccade cortical neurones 714
discharges related to direction 715
Presbyopia 770, 771–776
miosis in 785
monkeys and 775
Preseptal muscle 786
Pressure, intraocular 7, 48–80
effect of, on vacuolization 44
in lacrimal sac 800
swelling 101, 111
vascular 16
Prestriate cortex (areas 18, 19; V2, V3) 524
definition of 525
neurones of 565
relation to striate cortex 524, 525
retinal projection to 515, 524
Pretarsal muscle 786
Pretectal complex (nucleus) 487, 628, 758
fibres 490
NOT neurones of 734, 758
projection to pulvinar 637
projection from superior colliculus 635
projection to VLG 506, 759
role in pupillary reflex 758
unit activity in 761
Primary aqueous humour 22
Primary border, of cortical receptive field 537

Primary cornea 108, 109, 132[3]
Primary deviation 657
Primary position 648
Primary spectral wavelengths 224
Primary vitreous 96
Principal foci of eye 215
Principal lateral nucleus of N III 686
Principal neurones of LGN 494
Principal plane 215
Principal points 215
Prism
diplopia due to 463
use of, in measuring convergence 658
Probability curves 273
Probability summation 275, 434, 479
Probenecid 38
Procerus muscle 787
Projection, false 452, 464
Projection of retina
cortical 493, 516
into space 452
Proliferative retinopathy 101
Propranolol 70
Proprioception from eye muscles 671–674
cerebellum and 725, 730
false projection and 453
role of 674, 711
Proprioceptive de-afferentation 689
Proprioceptive neck reflexes 453
Prosopagnosia 572, 577
Prostaglandins
biosynthesis of 57
breakdown of blood–aqueous barrier and 54
cyclo-oxygenase pathway of 56
effect of catecholamines on 63
effect of, on cornea 30
effect on i.o.p. 56, 60
species variations 63
tachyphylaxis 63
effect on iris 64
lipogenase pathway 56
transport of, in eye 37
Protan 405
Protanope 403
isocolour chart 403
luminosity curve 404
reflexion densitometry 406
Proteases, of lens 165
Protective mechanism 786–804
Protective shadowing 461
Proteins
in aqueous 18, 23
lens 155–172
after paracentesis 55
tears 795
Proteoglycans
corneal 109
tears 798
vitreous 103[6]
Proximal negative response 318
Pseudo-facility 52
effect of PGs on 60
Pseudo-fovea 465
Psychical weeping 801
Psychological compensation 452
Psycho-optical reflexes 674
Psycho-sensory reflex 757
Pterygoid canal 6
Pterygopalatine ganglion 6, 77
VIP in 803
Pulfrich phenomenon 475
Pulse, in i.o.p. 15
Pulse-to-cycle fraction 369
Pulvinar 490
collicular projection to 630, 637
collicular-recipient zone 635
cortical projections to 636
inferior and lateral compared 638
lesions of 638
LGN projection to 638
overlapping cortical and tectal projections to 637
phylogeny and 635, 641[8]
posterior system 628
pretectal projection to 637
retinal projection to 635
slabs of projection 635
striate lesions and 639
striate-recipient zone 635
subdivisions of 635
tectal projection to 637
unit responses in 638
receptive-field areas 638
Pump-leak hypothesis 151
Pump-site density, corneal 129
Puncta, lacrimal 800
Pupil 754–765
blood–aqueous barrier breakdown and 54
cerebellum and 762
dilator neurones in Edinger–Westphal complex 760
Edinger–Westphal complex and 758–760
effects of accommodation and convergence on 780
of drugs 121, 762
of epinephrine 69
of salbutamol 69
innervation of 754
pretectal 506
reciprocal 763
reflexes 755
lid-closure 757
light 755
near 757
psychosensory 757
spectral sensitivity 756
ventral nucleus of LGN and 506
Pupillary unrest 764
Pupillography 755
Pupil-size
and depth of focus 771
and directional sensitivity 423, 756
and luminance 757
and retinal illumination 213
and visual acuity 386
Purkinje cells
effects of electrical stimulation 729
inhibitory action on saccades 727
response to muscle stretch 725
Purkinje shift 239, 256, 395
pupil and 765[1]
tritanope and 442
Purkinje–Sanson images 769
Pursuit movement (tracking) 660
effect of kainate 740
neural mechanisms 660
velocity storage and 740
Push–pull stimulation 695
Putrescine, release by receptors 344
Pyramidal cortical cells 521
complex and hypercomplex 543

Q-ganglion cells 356[2, 3]
Quanta, minimum for vision 272
Quantal currents, rods 291
Quantum efficiency 273
Quantum fluctuations 272
Quisqualic acid 343

Rabbit
directional sensitivity of ganglion cells 330
steady fixation 664
Radial fibres of Müller 205
Radial lamellae 141
Radiation cataract 183
Rami oculares 5
Rami orbitales 5
Random-dot stereograms 474
Random noise stimulus 553[2]
Range of stereoscopic vision 469
RCS-rats, blood–vitreous barrier of 25
Reactive hypotonia 56
Reading, and saccades 665[11]
Real and apparent motion, MT neurones and 577
Receptive fields 282
calculated 327
centre-surround organization 283, 325
collicular 708
colour-coded 330, 416, 417, 587, 588–597
cone 305
cortical neurones 531–551
deprivation and 603–621
ganglion cells 282, 325
classification 326
dendritic trees and 334, 335
null point 326
LGN neurones 500, 501
minimum stimulus and 274
W-, X-, Y-cells 326, 330, 335, 502, 503, 631
Receptor responses
cone 288
ERG and 316
hyperpolarizing 286
Limulus 281
Necturus 285
rods 290
Receptors, structure of 207, 230, 280
Reciprocal innervation 688
pupil 763
Rectifying synapse 313
Rectus muscles 647
Reduced eye 215

Reduction hypothesis 406
Reflex control, of eye movements 674
fixation reflex 674
psycho-optical reflexes 674
vestibular 677
Reflex reversal 704
Reflexion densitometry 265
cone pigments 406
Refraction by eye 215
Regeneration
of corneal endothelium 127–130
related to corneal thickness 128
of corneal epithelium 124
of corneal nerves 132
of rhodopsin 250
dark-adaptation and 265
rate of 266
Relative amplitude of accommodation 784
Relative positions of objects 452
Relative visibility factor 388
Relay-neurones of LGN 494
Renshaw-inhibition, and extraocular muscles 744[19]
Repair
corneal 124
lens 187
Residual protein 97
Resistance, electrical
of cones 289
of corneal endothelium 114
of corneal epithelium 118
of lens 149
Resistance to flow 39
adrenergic influences on 72
calcium and 46
calculated 46
colchicine and 47
ganglionectomy and 67, 82[40]
glycosaminoglycans and 46
location of 45
measurement of 52
parasympathetic effect on 74
pilocarpine effect on 74
prostaglandins and 60
sulphydryl agents and 46
Resolving power 225
grating-frequency and 381, 392[1]
Response compression 271
Response range compression 271
Retina 3
detachment of 96
projection to cortex 486, 516
projection to LGN 486, 491
projection to non-geniculate targets 487, 628
structure of 205
synaptic organization of 208, 352
zones of 208
Retinal (retinene) 243
dehydroretinal 254
incorporation into rhodopsin 242
isomerase 244, 251
isomers of 244
link with opsin 243, 249
–reductase 243
–retinol relations 252
Retinal artery 7
pressure in 16
Retinal binding protein (RLBP) 253
Retinal capillaries 31
isolated 26
Retinal circulation 8
Retinal disparity 469
limits for fusion 471
Retinal error signal 710
Retinal horizon 648
Retinal illumination 212
Retinal meridian 648
Retinal pigment epithelium 206
c-wave and 318
ERP and 321
junctions in 31
phagocytosis by 235
RBP in 251
rhodopsin regeneration and 251
transport across 25
Retinal rivalry 476
Retinal sensitivity, adaptation and 266
Retinal smear 454
Retinal uptake index 25
Retinal vein 8
pressure in 16
Retinitis pigmentosa
cataract in 189
IRBP in 259
Retino-hypothalamic tract 488, 489
Retinoid esters 254
Retinol (Vitamin A) 243
deficiency of 795
esterification of 252
oxidation of 252
pigment epithelium and 251
relation to retinal 243
in tears 795
transport of 252
Retinol-binding protein (RBP) 252
cellular 253
interphotoreceptor 253
Retinol–retinal visual cycle 254
Retino–pretectal–pulvinar projection, to cortex 637
Retino–tectal–pulvinar projection, to cortex 637
Retinula cell 280
***N*-Retinylidine opsin** 244, 245, 249
Retrolental tract 100
Retro-orbital plexus 5
Reversal index 611
Reversal potential, of photocurrent 301[1]
Reversal of relief 474
Reversal of swelling, of cornea 111
Reverse tracking 703
Reverse suturing 610
visual performance after 623[12]
Reversible cataract 187
Rhabdom 280
Rhabdomere 280
Rhodopsin 232
activation of PDE 293
carbohydrate of 241
changes on exposure to light 244–249
cycle 250
dark-adaptation and 265
density-spectrum 238
and scotopic sensitivity curve 239
kinase 298
linkage of retinal 249
lipid of 240
localization of retinal 250
oligosaccharide of 241
phosphorylation sites 241
polypeptide chains of 240
position in rod 240, 259[5]
regeneration of 250
and dark-adaptation 265
synthesis and transport of 242
variation with species 254
Rhodopsin noise 294
Ribbon synapse 336
Riboflavine deficiency 130
Ricco's law 275
and background luminance 427
and stimulus pattern 434
Righting reflex 675, 677
Rigidity coefficient 49
RNA in lens 157
Rod(s) 205
distribution in retina 208
fusion frequency of 363
hyperpolarizing response in 290
increment threshold of 398
pathway to ganglion cells 354, 355
photopigments of 254–259
saturation of 265, 270, 294
spectral sensitivity of single 294
structure of 230
synaptic relations of 338, 339
threshold 264
and pupillary reflex 756
total number of 210
Rod-bipolars 338, 339
Rod–cone cancellation 367
Rod–cone interaction 307, 357[22], 388, 426, 429, 430, 443
Rod-free territory 208
Rod monochromat 402
c.f.f. of 363
dark-adaptation curve of 264
visual acuity of 386
Rod–rod interaction 307
Rod saturation 265, 401
Rod spherule 206
Rod vision 220
and Stiles–Crawford effect 425
Roller's nucleus 697, 698
Rolling 648, 649
caused by convergence 660
caused by head movement 682
caused by prism 659
caused by superior and inferior recti 654
Roof nuclei 723
Rotatory nystagmus 681
Rubin's vase 450
Rudd, photopigment variation 257

Saccade 660
area 7a neurones and 720
area 8 neurones and 713

Saccade – *cont.*
cerebellar neurones and 726
stimulation and 726
control mechanisms 661
corrective 661, 663
EMG in 688
error-signal 661, 711, 737
head turning and 683
latency of 660
mechanics of 660
neural model 737
occipital neurones and 711
Purkinje cell inhibition 727
superior colliculi and 707
tension during 693
unit discharges in 680
velocity of 660
vision during 454
Saccade-related neurones 737, 738
Saccadic suppression 392^{6}, 454
Saccule 677
macula of 680
polarization vector of 700
Salbutamol, effect on i.o.p. 68
Salmonid photopigments 256
Sampled data system 662
Saturation
of colours 222
of rods and cones 265, 270, 294
S-cells 540
Scaled amplitude 322^{1}
Scarpa's ganglion 697
Scattering of light
corneal 122
depth perception and 459
Schematic eye 215
Schiotz tonometer 49
Schirmer test 794
Schlemm's canal 10
as drainage route 11–15
giant vacuoles in 41
relation to aqueous vein 41
Schroeder's staircase 449
Schwalbe's ring 698
Schwalbe's nucleus 698
Sclera 3
fibrils of 106
opacity of 122
Scotopic lumen 214
Scotopic sensitivity curve 395
and action spectrum of bleaching retina 265
and density spectrum of rhodopsin 239
pupillary 756
Scotopic troland 218^{2}
Secondary deviation 657
Secondary position 648
Secondary vitreous 96
Second-order projection
of prestriate cortex 527
of pulvinar 637
Secretory component (SC) 796
See-saw movements 658
Selenite cataract 189
Semicircular canals 677
discharges in primary afferents 702
electrical stimulation of 699
input to muscles 699
mechanism of 678
Semi-discrete control system 665^{8}
Senile cataract 173
Sensitive period
for deprivation 605
for reversal 611
Sensitization 433
Sensory blink reflex 791
Sensory innervation
of e.o. muscles 673
of uvea and meshwork 77
Serial processing 535
Serial synapse 337
Serotonin (5-HT), accumulation by retina 350
Serous cells, of lacrimal gland 792
SH-groups
and assembly of subunits 162
and cataract 174
and rhodopsin 248, 259^{6}
Short ciliary nerves 4, 6
pupillo-constrictor reflex responses 761
Short-circuit current
ciliary 33
corneal 117
lens 151, 152
Short posterior ciliary arteries 7
Sialic acid 79, 102, 798
Siamese cats 510^{9}, 624^{18}
Signal-to-noise
and coupling 306
effect of AcCh on 553
Sign-conserving synapse 313, 343, 356^{12}
Sign-reversing synapse 313, 356^{12}
Simple cells 532
definition of 539, 540
stellate cells and 543
velocity tuning in 536
versus complex cells 539
X-cells as 583
Simultaneous contrast 226, 432
Simultaneous perception 477
Size
and depth perception 459
estimates of 456
Size constancy neurones 571
Size effects 475
Size of LGN neurones, and deprivation 617, 619, 623^{8}
Slow fibres 668, 669
Slow-wave sleep, and LGN neurones 553
Sluggish ganglion cells 328
Smooth following movement (tracking) 660, 662
blinking and 788
control of 662
Smoothing function, of slow fibres 671
Snellen letters 225
Sodium
active transport
by ciliary body 31
effects of DNP on 34
effects of ouabain on 35
by cornea 112
by lens 146
by rod outer segment 287
blood–aqueous barrier to 22, 26
concentration
in aqueous 19, 20, 27
in cornea 111
in lens 145, 148
cataractous 173, 178, 184, 186
in tears 795
hyperpolarizing response and 287
Sodium pump 32
Sodium-battery, receptor 286
Sodium–calcium pump 289, 292
Sodium–potassium ATPase
lens and cataract 181
Nakano mouse 185
Philly mouse 186
see also ATPase
Solumedrol, cataract 188
Sorbinil, effect on galactose cataract 181
Sorbitol in lens 153
cataract and 180
Sorbitol pathway 154
Space-constants
of cone 306
of horizontal cell 309
Space representation centre 453
Sparing of the macula 560
Spatial frequency 381
selectivity of cortical cells 583–587
selectivity of ganglion cells 378
in squint 622, 623
selectivity of LGN cells 503
Spatial induction 226
Spatial opponence 416
Spatial resolution (visual acuity) 373–392
Spatial summation 275
pupillary 757
Spatial tuning curves 583
effect of velocity of grating 586
inhibition of 586
simple vs. complex cells 586
Special complex cells 544, 551, 634
Specific threshold 397
Spectral mixture curves 399
predicted from cone action spectra 408
Spectral sensitivity curves 215, 395
cone 397
pupillary 756
Spectrum 211
limits of visual 211
Specular microscopy 107
Sphenopalatine ganglion 801
blocking of 802
Spherical aberration, and accommodation 778
Sphincter muscle of ciliary body 769
Sphincter pupillae 754
isolated 764
Spinal vestibular nucleus 698
Spindles, in eye muscles 671
Spiny stellate cell 521
Split-brain animal 569

S-potentials 285, 309
colour vision and 410
in LGN 511[20]
Spreading coefficient 792
Squamous cells of cornea 105
Squint (strabismus) 621
dominance histograms in 621
ganglion cells and 623
LGN cells and 621
prisms and 463
projection of image in 463
secondary deviation in 651
see also Strabismus
Squirrel monkey, dLGN 522
Squirrel retina 396
Stabilized retinal image 388
fusion and 472
Standard complex cell 544, 551
Standing gradient 32
Starburst-coronate amacrines 346
Static reflexes 677
Steady current, lens 152
Steady fixation
eye movements and 663
motor neurone discharges in 690
Stellate cells 521
simple cells and 543
Stereocilia 679
Stereoscope 467
Stereoscopic lustre 478
Stereoscopic vision 465–479
accuracy of 469
corpus callosum and 540
development of 607
double images and 471
duration of stimulus and 469
electrophysiology of 558
limits of 469
motion neurones and 566
random-dot stereograms 473
Steroid cataract 188
Stiles–Crawford effect 469
and accommodation 781[10]
Strabismus (squint) 621
effect on dominance columns 621, 623
effect on ganglion cells 623
effect on LGN cells 621, 622
effect of striped environment on 621
Siamese cats and 624[18]
simultaneous congruent signals and 621
visual resolution, cats 623
see also Squint
Stratum zonale 628
Streptomycin, and OKN 740
Streptozotocin diabetes
blood–vitreous barrier and 25
cataract and 180
Stretch receptors 671
Stretch–reflex 689
responses in collicular neurones 674
responses in striate neurones 674
Striate cortex (Area 17, Visual cortex V1)
cortical projections from 523–525
lesions and eye movements 717
LGN projection 520–523
monocular and binocular segments 618
pattern discrimination and 585
projection to pulvinar 635
retinal projection 516
role in binocular perception 560
stereopsis and 568
tuned excitatory cells 565
unit discharges in 531, *et seq.*
X- and Y-cell dichotomy 523
Striola 679
Stripes, cortical 603
Stroma, of cornea 105
Strophanthidin, and cataract 179
Strophanthin G, and Na influx to aqueous 34
Strychnine, effect of, on ganglion cells 348, 349
Subcapsular opacities 187
Subretinal fluid, absorption of 37
Substance P
and breakdown of blood–aqueous barrier 57, 59
compared with PGE_2 59
species variations 58
Substance P fibres, and lacrimal gland 803
Substantia nigra, and eye movements 718
Subunits of alpha-crystallin 159
shortened 169
Successive contrast 226
Sugar (glucose)
barrier to 23
cataract due to 180
concentration
in aqueous 20, 27
in vitreous 27
Sulphonamides, effect on anion transport 31
Sulphydryl-groups
and assembly of subunits 162
and cataract 174
and rhodopsin 248, 259[6]
Summation, and minimum stimulus 275
between rods 307
of generator potentials 282
neuronal basis of 283
physiological 275
probability 275, 434, 479
rod-cone 276
spatial 275
in pupillary reflex 757
temporal 275
Bloch's law and 275
critical duration for 276
Summation area 290
Summation index 435
Superior accessory optic tract 487
Superior bank of STC (V5) 566
Superior cervical ganglion 5
Superior cervical ganglionectomy 67, 82[40]
Superior collicular unit discharges 707
colour-coding and 631
cortical ablation and 632
directional sensitivity of 631
enhancement 710
geniculo-striate influence on 631
jerk detectors 632
monocular occlusion and 633
motion sensitivity of 632
movement fields of 707
pan-directional units 632
receptive fields of 631
related to depth in tissue 709
role in control of saccade 738
saccade-related cells 710
visually triggered cells 710
Superior colliculi 487, 628
ablation of 717
area 8 projection 717
comparison with striate cortex 635
cortical projections 630
descending pathways 706, 707
effects of lesions in 634, 711
e.o. muscle projections to 708
intertectal inhibition 744[30]
lamination and connections 706[25]
LGN input 402, 628
maturation of 609
pontine reticular formation projection to 708
projection to cortex 630
projection to pulvinar 635, 637
stimulation of 707
structure of 628
subcortical projections 630
substantia nigra and 718
vestibular reflexes and 708
W-cell input 502
Y-cell input 502
Superior oblique muscle 647, 648
abduction due to 651
actions of 651
innervation of 685
Superior palbebral muscle 787
Superior rectus 684
abduction and 652
action of 650
innervation of 685
Superior temporal sulcus (STS) 524, 525
motion area 542
polysensory region 577
face preference 577
lesions in V1 and colliculus on neurones 578
pupillary and accommodation responses from 777
responses to faces 572
Superior vestibular nucleus 698
Superoxides and cataract 182
Supervergence 658
Suppressed-by-contrast units 330
Suppression of vision during saccade 392[6]
Suprachiasmatic nuclei and tract 488
Suprageniculate nucleus 490
projection from area 8 717
Supragranular layers 551
Surface intensity 212
Surface tension and tear film 792
Susceptible period 605

Sustained cells (X-cells)
cortical 544
ganglion 328
LGN 496–504
Sutures, lens 140, 142
Suxamethonium, effect on e.o. muscles 671
Swelling of cornea 110, 111
and endothelial repair 128
Swelling pressure
corneal 111
vitreal 101
Sympathectomy, effect of
on i.o.p. 67
on pupil 762
on tear secretion 802
Sympathetic
accommodation and 776
breakdown of blood–aqueous barrier and 58
effects of stimulation
on i.o.p. 67
on blood-flow 67
extraocular muscles and 671
palpebral aperture and 787
pupillomotor control 761
supply to eye-ball 5
supply to lacrimal gland 802
Sympathetic root 6
Synapses in retina 336
Synaptic body 205
Synaptic glomerulus 495
Synaptic ribbon 336
Synaptic sign
preservation 313
reversal 313
Synaptic type, and response properties 342

Tadpole photopigments 256
Talbot–Plateau law 362
Tangential line of force 650
Tangential point 650
Tapetum and MIN 492
Target width and visual acuity 383
Taurine
accumulation by bipolars and amacrine cells 350
blockage of AcCh release by 346
effect on Ca^{2+}-accumulation by r.o.s. 350
effect on ERG 319, 350
possible transmitter action 350
transport across pigment epithelium 25
Tears 792–804
age and 799
composition of 794
drainage of 799
enzymes of 799
glycoproteins 798
lipids of 799
meniscus 793
mucus 797
normal output of 794
proteins of 795
synthesis by gland explants 798
Tear-specific prealbumin 796
Tectopontine–tectobulbar tract 706
Tectospinal tract 706
Temperature, effect on photopigment composition 257
Temperature-reversal effect 111, 117
Temporal crescent of visual field 604
superior colliculus and 630
Temporal induction 226
Temporal summation 275
Bloch's law and 275
critical duration for 276
increments and decrements 431
Temporal variations, in photopigment composition 257
Tenon's capsule 4
Tension in eye muscles 692
Tension fibres 769
Terminal nucleus of the optic tract 488
Tertiary position 648
torsion in 653
Thalamic nuclei 490
Thalamus, role in control of eye movements 718
Theophylline, effect on cornea 117
Thorotrast, escape from aqueous 44, 45, 48
Three-neurone arc 699, 704
Threshold
absolute 271
binocular 479
dichromat's 405
differential 220
foveal 264, 277[11]
motion 482
pupillary 756
specific 397
Threshold direction of gaze 690
Thromboxane B_2 57
Thymidine, corneal endothelial 108
Thyroxine, and retinol 257
Tight junctions
in ciliary epithelium 29
in corneal epithelium 108
in lens epithelium 143
Timolol
on accommodation 781[8]
on aqueous dynamics, etc 69, 70, 81[20], 82[45]
Tint 222
Tolerated change in vergence 771
Tone constancy 451
Tonic fibre 669
Tonic reflexes 677
Tonic units in PPRF 694, 737
Tonography 39
Tonometer 49
Torsion 648, 649
false 649, 654
in tertiary position 653
Torsion pendulum, cupula as 703
Torsion swing 740
Torsional nystagmus 677
Toti's operation 800
Trabecular meshwork 11, 13
actin in 79
effects of corticosteroids on 781
effects of cytochalazins 47
effects of pilocarpine on 74
effects of pressure on 44
glaucomatous 79
glycans in 46
laser coagulation of 79
nerve fibres of 73, 77
proteins of 47
age and 47
resistance of 45
Trabeculotomy 46
Tracking (smooth pursuit) 660
area 7a neurones and 719
cerebellectomy and 729
control of 662
EMG and 688
neural mechanisms 691
parieto-occipital lesions and 719
Purkinje cells and 727, 729
striate lesions and 723
tension during 662, 693
unit discharges during 691
velocity storage and 740
vestibular influences on 721
Transcellular channels 42
Transducin 296
hyperpolarization due to 297
Transduction of light 286–300
Transferrin, in tears 795
Transient (Y-) ganglion cells 328
LGN cells 540
Transient orange 245
Transmission factor, for optical media 213
Transmitter noise 294
Transmitters
excitatory
in cortex 552
in LGN 508
inhibitory
in cortex 552
in LGN 507
retinal 343–352
Transparency
of cornea 122
of lens 145
Transthyretin 252
Trauma, and i.o.p. 56
effects of PGs 61
Traumatic cataract 187
Tremor 663
Triads
muscle 668
synaptic 208, 336
Trichromatic theory 399
Trichromatic units 224
Trifluoromethazolamide 38
Trigeminal nerve (N V) 5
effect of section on i.o.p. etc 58
effect of section on weeping 801
effect of stimulation on cerebellum 725
effect of stimulation on i.o.p. 57
eye muscle afferents and 671
supply to cornea 131
supply to meshwork 77

Trian 405
Tritanopia 403, 405
artificial 441
foveal 442
Purkinje effect in 442
Trivariance, of colour vision 399
Trochlea 641
Trochlear nerve 5
motor neurones 685
PSPs in 705
Trochlear nucleus 687
and nucleus prepositus 697
Troland 213
Troxler phenomenon 388
Trypsin
effect on vitreous 99
effect on zonule 102
Trypsin inhibitor, in lens 165
Tuned excitatory unit 563, 564
Tuned inhibitory unit 563
Tuning curves
for flicker 370
for saccades 714
Tuning ratio
colour 417
velocity 331
Turnover of disks 234
Turtle cones
responses in 288
Stiles–Crawford effect and 424
TVI functions 271
Twitch fibres 668, 669
Twitch-tetanus ratio 667
Two-colour threshold technique 400
Type I vestibular cells 697
Types I and II vestibular cells 704

Ultrafiltration, and aqueous formation 35
Ultraviolet light, sensitivity to 35, 255
Uncertainty principle 272
Uniformity detector 330
Unit colour equation 224
Univariance 411
Unmappable cortical neurones 610
Urea
in aqueous 19
effect of hypertonic solutions of 53
Urea-soluble lens proteins 155
Utricle 677
Deiters' neurones and 699
functional polarization vector 700
macula of 678
response to swing 683
Utricular nerve, stimulation of 700
Utriculofugal flow 679
Utriculopetal flow 679
Uvea 7
Uveal meshwork 11, 12
Uveoscleral drainage 31, 47
route for 48
Schlemm's canal switch 75

Vacuoles (giant) 41
Vacuolization cycle 43
Vanadate, effect on i.o.p. 38
Vascular circulation of eye 7
ciliary processes 17, 18
optic nerve 8
pressures in 16
pulses in 15
Vascular coat 4
Vascularization
corneal 130
vitreal 101
Vasoactive intestinal polypeptide (VIP), effect of
on ciliary muscle 83[49]
on i.o.p., etc 78
on tear secretion 795, 802
fibres in uvea 77
Vasopressin, effect on secretion of aqueous 79
Veiling luminance 426
Velocity dependence of spatial tuning 586
Velocity storage 732, 733
decay constants 739
effect of kainate 739
GABA block and 537
Velocity tuning
of cortical cells 536
of ganglion cells 331
of LGN cells 505
compared with cortical units 541
of MT units 573
Venous circulation of eye 8
pressures in 16
Ventral nucleus of LGN 492
collicular projection 630
pretectal projection 759
Vergence of light 781[9]
and accommodation 771
Vermis 725
electrical stimulation of 725
unit discharges in 726
Vernier acuity 377–379
contrast-sensitivity and 382
Vertical canals 677, 681
Vertical, estimates of 456
Vertical meridian
cortical neurones and 533
representation on cortex 486, 525, 569
Vesicular transport, iris 30
Vestibular apparatus 677
nervous connections 697–702
specific inputs
to cerebellum 701
to eye muscles 699
to neck muscles 702
Vestibular cerebellum 728
Vestibular nerve discharges 702
Vestibular nuclei 698
types of response in 697, 704
related to movements, etc 706
Vestibular nystagmus 681
interaction with OKN 733
Vestibular reflexes 677
nervous pathways in 697–699, 704
Vestibulectomy and torsion swing 741
Vestibulo-ocular reflex 679
analysis of 735
flocculus and 728, 742
interaction with OKN 733, 740
neuronal model 736
phase-lag and 735
Vidian nerve 801
Vieth–Müller horopter circle 466
Vimentin filaments, in lens 166
Visual acuity 225, 373
adaptation and 374
in animals 226
binocular 390
contrast and 380
cortical magnification factor and 385
deprivation and 606, 614
diffraction and aberrations and 375, 387
eccentricity and 373
electrophysiology of 578
exposure time and 388
eye movements and 388
in infants 390
luminance and 373, 380
measurement of 225
one-to-one relationship and 374
pupil size and 386
in rod monochromat 386
rod–cone interaction and 388
scotopic 386
surround luminance and 374, 380
target-width and 383
viewing time and 388
wavelength and 386
Visual capture 639
Visual claustrum 534
Visual cortex (area 17, etc) 486, 515
ablation of 620
electrophysiology of 531, *et seq.*
projections from 523
projections to superior colliculi 633
LGN projection to 520–523
retinal projection 515
superior colliculi compared 635
Visual cycle, retinoid 243, 250, 254
Visual deprivation 603–621
bilateral 603, 606
cortical changes in 612
LGN changes 606, 615–635
rabbit 614
reversal of effects 610–613
unilateral 603, 606
visual defects following 613
recovery from 610–613
Y-cells and 504
Visual field, cat 615
Visual memory 572
Visual pathways 486–495
non-geniculate 628–641
Visual pigments 240–259
comparative physiology and 254–259
Visual purple 219, 238–259
see also Rhodopsin
Visual righting reflexes 675, 677
Visual thalamic nuclei 490
Visually evoked response (VER) 365
catecholamine depletion and 357[20]
flicker and 365

Visually evoked response (VER) – *cont.*
saccade and 483[3]
visual acuity and 392[10]
Visually triggered movement related cells 709
Visuomotor coordination, development of 674
Visuomovement cells, area 8 713
Visuotopic projections
pulvinar 637
striate cortex 516
superior colliculi 629
Visuo-vestibular conflict 729
Vitamin A (retinol) 243
deficiency of 795
relation to retinal 243
in tears 795
transport of 252
visual cycle and 254
Vitreous body 3, 96–104
accommodation and 781[6]
angiogenic factor in 101
blood-barrier 24
chemistry of 97
compared with aqueous 20, 27
embryonic history 96
lactate and pyruvate in 21
primary 96
secondary 96
structure of 99
tertiary 96
vascular growth factor 103[8]
Vitrosin 97
Volume regulation of lens 153
Voluntary centre for eye movements 712, 717
lesions in 717
Vortex veins 7, 8

Wallpaper phenomenon 465
Wash-out effect 46, 81[29]
Water
colour of 255
exchanges of, in eye 28
permeability of cornea to 119
Water-content
of cornea 110
of lens 145
cataractous 178
Waterfall phenomenon 483
Wave-guide theory 423
Wavelength discrimination (colour vision, etc) 395–420
Wavelength, and visual acuity 386
Wavelength-response curves
cones 397
cortical cells 588–597
ganglion cells 330
geniculate cells 587
horizontal cells 410, 416, 417
optic nerve fibres 416
theoretical 398
W-cells 330
cortical 544
heterogeneity of 355
LGN 498, 499
ventral nucleus 506
receptive field sizes 335
retino-geniculate terminations 496
superior colliculi and 631
W-, X-, Y-cells, and collicular projection 640[4]
Weber–Fechner law 221, 269, 270
Wettability 792
White line of Gennari 515
Wing-shaped cells of cornea 105, 118
Wiring diagrams
amacrine cells 354
cat bipolar–ganglion cell connections 353
cat retina 355
mudpuppy retina 285
Wolfring glands 792

X-cells, ganglion 326
absence of collicular projection 631
contrast-sensitivity functions 503
effect of aspartate on 348
effect of glycine on 5
LGN terminations 496, 503
as pattern sensors 581
Xerophthalmia 795
X-radiation cataract 183
X–Y-dichotomy
cortical input layer 4, 523
cortical receptive fields 540, 544, 585
functional significance 503
ganglion cells 326
LGN cells 496, 503
inhibition and 507

Y-cells
ganglion 326
bilateral retinal strip 494
branched axons 631, 640[4]
contrast-sensitivity functions 503
effects of AcCh on receptive field 348
effects of GABA 348
projection to LGN and superior colliculi 493, 496
second harmonic and 504
LGN units 496
superior colliculus units 502, 631
visual deprivation and 504
Yellow spot 208
Young–Helmholtz theory 399
Young's modulus of lens 773

Zeis glands 792
Zinn, circle of 8
Zonula occludens (tight junction)
in ciliary epithelium 29
in corneal epithelium 108
in lens epithelium 143
Zonular fork 769
Zonular lamella 145
Zonule 3, 96, 102
chemistry of 102
relaxation in accommodation 769
structure of 102, 769
Zygomatic nerve 801